Fitness-For-Service

API 579-1/ASME FFS-1, JUNE 5, 2007
(API 579 SECOND EDITION)

The American Society of Mechanical Engineers

energy API

API 579-1/ASME FFS-1 2007 Fitness-For-Service

FOREWORD

This standard is based on and supercedes the American Petroleum Institute's Recommended Practice 579, Fitness-For-Service.

In contrast to the straightforward and conservative calculations that are typically found in design codes, more sophisticated assessment of metallurgical conditions and analyses of local stresses and strains can more precisely indicate whether operating equipment is fit for its intended service or whether particular fabrication defects or in-service deterioration threaten its integrity. Such analyses offer a sound basis for decisions to continue to run as is or to alter, repair, monitor, retire or replace the equipment.

The publication of the American Petroleum Institute's Recommended Practice 579, Fitness-For-Service, in January 2000 provided the refining and petrochemical industry with a compendium of consensus methods for reliable assessment of the structural integrity of equipment containing identified flaws or damage. API RP 579 was written to be used in conjunction with the refining and petrochemical industry's existing codes for pressure vessels, piping and aboveground storage tanks (API 510, API 570 and API 653). The standardized Fitness-For-Service assessment procedures presented in API RP 579 provide technically sound consensus approaches that ensure the safety of plant personnel and the public while aging equipment continues to operate, and can be used to optimize maintenance and operation practices, maintain availability and enhance the long-term economic performance of plant equipment.

Recommended Practice 579 was prepared by a committee of the American Petroleum Institute with representatives of the Chemical Manufacturers Association, as well as some individuals associated with related industries. It grew out of a resource document developed by a Joint Industry Program on Fitness-For-Service administered by The Materials Properties Council. Although it incorporated the best practices known to the committee members, it was written as a Recommended Practice rather than as a mandatory standard or code.

While API was developing Fitness-For-Service methodology for the refining and petrochemical industry, ASME also began to address post-construction integrity issues. Realizing the possibility of overlap, duplication and conflict in parallel standards, ASME and API formed the Fitness-For-Service Joint Committee in 2001 to develop and maintain a Fitness-For-Service standard for equipment operated in a wide range of process, manufacturing and power generation industries. It was intended that this collaboration would promote the widespread adoption of these practices by regulatory bodies. The Joint Committee included the original members of the API Committee that wrote Recommended Practice 579, complemented by a similar number of ASME members representing similar areas of expertise in other industries such as chemicals, power generation and pulp and paper. In addition to owner representatives, it included substantial international participation and subject matter experts from universities and consulting firms.

This publication is written as a standard. Its words *shall* and *must* indicate explicit requirements that are essential for an assessment procedure to be correct. The word *should* indicates recommendations that are good practice but not essential. The word *may* indicates recommendations that are optional.

Most of the technology that underlies this standard was developed by the Joint Industry Program on Fitness-For-Service, administered by The Materials Properties Council. The sponsorship of the member companies of this research consortium and the voluntary efforts of their company representatives are acknowledged with gratitude.

The committee encourages the broad use of the state-of-the-art methods presented here for evaluating all types of pressure vessels, boiler components, piping and tanks. The committee intends to continuously improve this standard as improved methodology is developed and as user feedback is

received. All users are encouraged to inform the committee if they discover areas in which these procedures should be corrected, revised or expanded. Suggestions should be submitted to the Secretary, API/ASME Fitness-For-Service Joint Committee, The American Society of Mechanical Engineers, Three Park Avenue, New York, NY 10016, or SecretaryFFS@asme.org.

This standard is under the jurisdiction of the ASME Board on Pressure Technology Codes and Standards and the API CRE Committee and is the direct responsibility of the API/ASME Fitness-For-Service Joint Committee. The American National Standards Institute approved API 579-1/ASME FFS-1 2007 on June 5, 2007.

Although every effort has been made to assure the accuracy and reliability of the information that is presented in this standard, API and ASME make no representation, warranty, or guarantee in connection with this publication and expressly disclaim any liability or responsibility for loss or damage resulting from its use or for the violation of any regulation with which this publication may conflict.

SPECIAL NOTES

This document addresses problems of a general nature. With respect to particular circumstances, local, state, and federal laws and regulations should be reviewed.

Nothing contained in this document is to be construed as granting any right, by implication or otherwise, for the manufacture, sale, or use of any method, apparatus, or product covered by letters patent. Neither should anything contained in this document be construed as insuring anyone against liability for infringement of letters patent.

Neither API nor ASME nor any employees, subcontractors, consultants, committees, or other assignees of API or ASME make any warranty or representation, either express or implied, with respect to the accuracy, completeness, or usefulness of the information contained herein, or assume any liability or responsibility for any use, or the results of such use, of any information or process disclosed in this document. Neither API nor ASME nor any employees, subcontractors, consultants, or other assignees of API or ASME represent that use of this document would not infringe upon privately owned rights.

This document may be used by anyone desiring to do so. Every effort has been made to assure the accuracy and reliability of the data contained herein; however, API and ASME make no representation, warranty, or guarantee in connection with this document and hereby expressly disclaim any liability or responsibility for loss or damage resulting from its use or for the violation of any requirements of authorities having jurisdiction with which this document may conflict.

This document is published to facilitate the broad availability of proven, sound engineering and operating practices. This document is not intended to obviate the need for applying sound engineering judgment regarding when and where this document should be utilized. The formulation and publication of this document is not intended in any way to inhibit anyone from using any other practices.

Classified areas may vary depending on the location, conditions, equipment, and substances involved in any given situation. Users of this Standard should consult with the appropriate authorities having jurisdiction.

Work sites and equipment operations may differ. Users are solely responsible for assessing their specific equipment and premises in determining the appropriateness of applying the Instructions. At all times users should employ sound business, scientific, engineering, and judgment safety when using this Standard.

Users of this Standard should not rely exclusively on the information contained in this document. Sound business, scientific, engineering, and safety judgment should be used in employing the information contained herein.

API and ASME are not undertaking to meet the duties of employers, manufacturers, or suppliers to warn and properly train and equip their employees, and others exposed, concerning health and safety risks and precautions, nor undertaking their obligations to comply with authorities having jurisdiction.

Information concerning safety and health risks and proper precautions with respect to particular materials and conditions should be obtained from the employer, the manufacturer or supplier of that material, or the material safety data sheet.

CONTENTS

ANNEX B1 - STRESS ANALYSIS OVERVIEW FOR AN FFS ASSESSMENT

PART 1

INTRODUCTION

PART CONTENTS

1.1 Introduction

1.1.1 The ASME and API new construction codes and standards for pressurized equipment provide rules for the design, fabrication, inspection and testing of new pressure vessels, piping systems, and storage tanks. These codes do not provide rules to evaluate equipment that degrades while in-service and deficiencies due to degradation or from original fabrication that may be found during subsequent inspections. API 510, API 570, API 653, and NB-23 Codes/Standards for the inspection, repair, alteration, and rerating of in-service pressure vessels, piping systems, and storage tanks do address the fact that equipment degrades while in service.

1.1.2 Fitness-For-Service (FFS) assessments are quantitative engineering evaluations that are performed to demonstrate the structural integrity of an in-service component that may contain a flaw or damage. This Standard provides guidance for conducting FFS assessments using methodologies specifically prepared for pressurized equipment. The guidelines provided in this Standard can be used to make run-repair-replace decisions to help determine if pressurized equipment containing flaws that have been identified by inspection can continue to operate safely for some period of time. These FFS assessments are currently recognized and referenced by the API Codes and Standards (510, 570, & 653), and by NB-23 as suitable means for evaluating the structural integrity of pressure vessels, piping systems and storage tanks where inspection has revealed degradation and flaws in the equipment.

1.2 Scope

1.2.1 The methods and procedures in this Standard are intended to supplement and augment the requirements in API 510, API 570, API 653, and other post construction codes that reference FFS evaluations such as NB-23.

1.2.2 The assessment procedures in this Standard can be used for Fitness-For-Service assessments and/or rerating of equipment designed and constructed to the following codes

a) ASME B&PV Code, Section VIII, Division 1

b) ASME B&PV Code, Section VIII, Division 2

c) ASME B&PV Code, Section I

d) ASME B31.1 Piping Code

e) ASME B31.3 Piping Code

f) API 650

g) API 620

1.2.3 The assessment procedures in this Standard may also be applied to pressure containing equipment constructed to other recognized codes and standards, including international and internal corporate standards. This Standard has broad application since the assessment procedures are based on allowable stress methods and plastic collapse loads for non-crack-like flaws, and the Failure Assessment Diagram (FAD) Approach for crack-like flaws (see Part 2 , paragraph 2.4.2).

a) If the procedures of this Standard are applied to pressure containing equipment not constructed to the codes listed in paragraph 1.2.2, then the user is advised to first review the validation discussion in Annex H. The information in Annex H, along with knowledge of the differences in design codes, should enable the user to factor, scale, or adjust the acceptance limits of this Standard such that equivalent FFS in-service margins can be attained for equipment not constructed to these codes. When evaluating other codes and standards the following attributes of the ASME and API design codes should be considered:

   1) Material specifications
   2) Upper and/or lower temperature limits for specific materials
   3) Material strength properties and the design allowable stress basis
   4) Material fracture toughness requirements
   5) Design rules for shell sections
   6) Design rules for shell discontinuities such as nozzles and conical transitions
   7) Design requirements for cyclic loads
   8) Design requirements for operation in the creep range
   9) Weld joint efficiency or quality factors
   10) Fabrication details and quality of workmanship
   11) Inspection requirements, particularly for welded joints

b) As an alternative, users may elect to correlate the pressure-containing component's material specification to an equivalent ASME or API listed material specification to determine a comparable allowable stress. This approach provides an entry point into the ASME or API codes (refer also to Annex A) wherein the pressure-containing component is reconciled or generally made equivalent to the design bases assumed for this Standard. Hence, general equivalence is established and the user may then directly apply the acceptance limits of the Fitness-For-Service procedures contained in this Standard. Equivalent ASME and ASTM material specifications provide a satisfactory means for initiating reconciliation between the ASME and API design codes and other codes and standards. However, the user is cautioned to also consider the effects of fabrication and inspection requirements on the design basis (e.g., joint efficiency with respect to minimum thickness calculation).

1.2.4 The Fitness-For-Service assessment procedures in this Standard cover both the present integrity of the component given a current state of damage and the projected remaining life. Assessment techniques are included to evaluate flaws including: general and localized corrosion, widespread and localized pitting, blisters and hydrogen damage, weld misalignment and shell distortions, crack-like flaws including environmental cracking, laminations, dents and gouges, and remaining life assessment procedures for components operating in the creep range. In addition, evaluation techniques are provided for condition assessment of equipment including resistance to brittle fracture, long-term creep damage, and fire damage.

1.2.5 Analytical procedures, material properties including environmental effects, NDE guidelines and documentation requirements are included in the Fitness-For-Service assessment procedures in this Standard. In addition, both qualitative and quantitative guidance for establishing remaining life and in-service margins for continued operation of equipment are provided in regards to future operating conditions and environmental compatibility.

1.2.6 The Fitness-For-Service assessment procedures in this Standard can be used to evaluate flaws commonly encountered in pressure vessels, piping and tankage. The procedures are not intended to provide a definitive guideline for every possible situation that may be encountered. However, flexibility is provided to the user in the form of an advanced assessment level to handle uncommon situations that may require a more detailed analysis.

1.3 Organization and Use

The organization, applicability and limitations, required information, analysis techniques and documentation requirements are described in Part 2 of this Standard. In addition, an overview of the acceptance criteria utilized to qualify a component with a flaw is provided. First time users of the Fitness-For-Service assessment technology in this Standard should carefully review Part 2 prior to starting an analysis.

1.4 Responsibilities

1.4.1 Owner-User

The Owner-User of pressurized equipment shall have overall responsibility for Fitness-For-Service assessments completed using the procedures in this Standard, including compliance with appropriate jurisdictional and insurance requirements. The Owner-User shall ensure that the results of the assessment are documented and filed with the appropriate permanent equipment records. Many of the Owner-User responsibilities are given to the Plant Engineer (see paragraph 1.4.3.3).

1.4.2 Inspector

The Inspector, working in conjunction with the NDE engineer, shall be responsible to the Owner-User for determining that the requirements for inspection and testing are met. In addition, the Inspector shall provide all necessary inspection data required for a Fitness-For-Service assessment in accordance with the appropriate part of this Standard, and be responsible for controlling the overall accuracy of the flaw detection and sizing activities. In some instances, as determined by the Owner-User, the Inspector may also be responsible for the Fitness-For-Service assessment (Level 1 Assessment, see Part 2 , paragraph 2.4).

1.4.3 Engineer

1.4.3.1 The Engineer is responsible to the Owner-User for most types of Fitness-For-Service assessments, documentation, and resulting recommendations. The exception is that a Level 1 Assessment (see Part 2, paragraph 2.4) may be performed by an Inspector or other non-degreed specialist; however, in these cases the Engineer should review the analysis.

1.4.3.2 In the context of this Standard, the term Engineer applies to the combination of the following disciplines unless a specific discipline is cited directly. A Fitness-For-Service assessment may require input from multiple engineering disciplines as described below.

a) *Materials or Metallurgical Engineering* – Identification of the material damage mechanisms, establishment of corrosion/erosion rates, determination of material properties including strength parameters and crack-like flaw growth parameters, development of suitable remediation methods and monitoring programs, and documentation.

b) *Mechanical or Structural Engineering* – Computations of the minimum required thickness and/or $MAWP$ (MFH) for a component, performance of any required thermal and stress analysis, and knowledge in the design of and the practices relating to pressure containing equipment including pressure vessel, piping, and tankage codes and standards.

c) *Inspection Engineering* – Establishment of an inspection plan that is capable of detecting, characterizing, sizing flaws or damage, and selection and execution of examination procedures in conjunction with available NDE expertise.

d) *Fracture Mechanics Engineering* – Assessment of crack-like flaws using the principles of fracture mechanics.

e) *Non-Destructive Examination (NDE) Engineering* – Selection and development of methods to detect, characterize, and size flaws or quantify the amount of damage, and the analysis and interpretation of inspection data.

f) *Process Engineering* – Documentation of past and future operating conditions, including normal and upset conditions, and identification of the contained fluid and its contaminant levels that may affect degradation of the component being evaluated.

1.4.3.3 Plant Engineer

In the context of this Standard, the term Plant Engineer applies to an engineer with knowledge of the equipment containing the component requiring the FFS Assessment. The Plant Engineer may perform both a Level 1 Assessment and Level 2 Assessment and typically has certain knowledge of the engineering disciplines, or access to personnel with the necessary engineering disciplines knowledge required for the FFS Assessment to be performed, described in paragraph 1.4.3.2.

1.5 Qualifications

1.5.1 Education and Experience

The level or amount of education and experience of all participants shall be commensurate with the complexity, rigor, requirements and significance of the overall assessment. All individuals involved shall be able to demonstrate their proficiency to the satisfaction of the Owner-User.

1.5.2 Owner-User

The Owner-User (see paragraph 1.4.1) shall understand the overall process, the importance of each piece of equipment to that process, and the failure consequences of each piece of equipment such that the Owner-User can assume overall responsibility for the results of the Fitness-For-Service assessment performed. The Owner-User shall have the ability and experience to recognize potentially damaging operations or equipment conditions and to take remedial steps.

1.5.3 Inspector

The Inspector (see paragraph 1.4.2) shall be qualified and certified in accordance with the applicable post-construction Code, API 510, API 570, API 653, ANSI/NB-23, or other post-construction code or standard required by the jurisdiction. Nondestructive examination personnel responsible for data used in a Fitness-For-Service assessment shall be certified to at least Level II in accordance with industry standards such as the American Society for Nondestructive Testing (ANST) SNT-TC-1A, CP-189, ACCP, or equivalent. The Inspector shall have experience in the inspection, examination, or both, of the type of equipment and associated process that is the subject of the Fitness-For-Service assessment.

1.5.4 Engineer

The Engineer (see paragraph 1.4.3) shall be competent to perform the level of assessment required. The Engineer shall meet all required qualifications to perform engineering work within the applicable jurisdiction and any supplemental requirements stipulated by the Owner-User.

1.6 Definition of Terms

Definitions of common technical terms used throughout this Standard may be found in Annex I.

1.7 References

1.7.1 Throughout this Standard, references are made to various international codes, standards, recommended practices, and technical reports that cover:

a) Design, fabrication, inspection and testing of pressure vessels, piping, and tankage

b) In-service inspection of pressure vessels, piping, and tankage

c) Fitness-For-Service standards applicable to welded components

d) Materials selection and behavior in process plants or other industrial environments

1.7.2 Rules for the use of these codes, standards, recommended practices and technical reports are stated in each part and annex of this Standard. The referenced codes, standards, and recommended practices in this Standard are listed in Table 1.1. The edition of the codes, standards, and recommended practices used in the FFS Assessment shall be either the latest edition, the edition used for the design and fabrication of the component, or a combination thereof. The Engineer responsible for the assessment shall determine the edition(s) to be used. The principles cited in paragraph 1.2.3 and Annex A, paragraph A.2 should be considered when making this determination.

1.7.3 References to other publications that provide background and other pertinent information to the assessment procedures used in this Standard are included in each part and annex, as applicable.

1.8 Tables

Table 1.1
Codes, Standards, Recommended Practices, and Reports

Title	Identification
Pressure Vessel Inspection Code: Maintenance Inspection, Rerating, Repair and Alteration	API 510
Calculation of Heater-Tube Thickness in Petroleum Refineries	API Std 530
Piping Inspection Code: Inspection, Repair, Alteration, and Rerating of In-Service Piping Systems	API 570
Damage Mechanisms Affecting Fixed Equipment In The Refining Industry	API RP 571
Inspection of Pressure Vessels	API RP 572
Inspection of Fired Boilers and Heaters	API RP 573
Inspection of Piping, Tubing, Valves, and Fittings	API RP 574
Recommended Practice for Inspection of Atmospheric and Low Pressure Storage Tanks	API RP 575
Inspection of Pressure Relieving Devices	API RP 576
Recommended Practice for Inspection of Welding	API RP 577
Recommended Practice for Positive Materials Identification	API RP 578
Recommended Practice for Risk-Based Inspection	API RP 580
Base Resource Document – Risk-Based Inspection	API Publ 581
Design and Construction of Large, Welded, Low-Pressure Storage Tanks	API Std 620
Welded Steel Tanks for Oil Storage	API Std 650
Tank Inspection, Repair, Alteration, and Reconstruction	API Std 653
Steels for Hydrogen Service at Elevated Temperatures and Pressures in Petroleum Refineries and Petrochemical Plants	API RP 941
Avoiding Environmental Cracking in Amine Units	API RP 945
National Board Inspection Code	NB-23
Minimum Design Loads for Buildings and Other Structures	ASCE 7
Rules For Construction of Power Boilers	ASME B&PV Code Section I
Boiler and Pressure Vessel Code, Section II, Part A – Ferrous Material Specifications	ASME B&PV Code Section II, Part A
Boiler and Pressure Vessel Code, Section II, Part B – Nonferrous Material Specifications	ASME B&PV Code Section II, Part B
Boiler and Pressure Vessel Code, Section II, Part D – Properties	ASME B&PV Code Section II, Part D
Subsection NH – Class 1 Components in Elevated Temperature Service	ASME B&PV Code Section III, Division 1
Boiler and Pressure Vessel Code, Section VIII, Pressure Vessels Division 1	ASME B&PV Code Section VIII, Division 1

Table 1.1
Codes, Standards, Recommended Practices, and Reports

Title	Identification
Boiler and Pressure Vessel Code, Section VIII, Pressure Vessels Division 2, Alternative Rules	ASME B&PV Code Section VIII, Division 2
Rules For Inservice Inspection Of Nuclear Power Plant Components	ASME B&PV Code Section XI
Alternative Method to Area Replacement Rules for Openings Under Internal Pressure, Section VIII, Division 1	ASME B&PV Code Case 2168
Alternative Rules for Determining Allowable Compressive Stresses For Cylinders, Cones, Spheres and Formed Heads Section VIII, Divisions 1 and 2	ASME B&PV Code Case 2286
Factory-Made Wrought Steel Buttwelding Fittings	ASME B16.5
Manual for Determining the Remaining Strength of Corroded Pipelines	ASME B31G
Power Piping	ASME B31.1
Process Piping	ASME B31.3
Specification for General Requirements for Steel Plates for Pressure Vessels.	ASTM A20
Electric-Fusion-Welded Austenitic Chromium-Nickel Alloy Steel Pipe for High Temperature Service	ASTM A358
Standard Test Methods and Definitions for Mechanical Testing of Steel Products	ASTM A370
General Requirements for Specialized Carbon and Alloy Steel Pipe	ASTM A530
Electric-Fusion Welded Steel Pipe for Atmospheric and Lower Temperatures	ASTM A671
Electric-Fusion Welded Steel Pipe for High-Pressure Service at Moderate Temperatures	ASTM A672
Carbon and Alloy Steel Pipe, Electric-Fusion Welded for High-Pressure Service at High Temperatures	ASTM A691
Standard Practices for Cycle Counting in Fatigue Analysis	ASTM E1049
Standard Test Method for Measurement of Fracture Toughness	ASTM E1820
Test Method For The Determination of Reference Temperature, T_0, For Ferritic Steels In The Transition Range	ASTM E1921
Standard Test Method for Measurement of Fatigue Crack Growth Rates	ASTM E647
Test Methods of Tension Testing of Metallic Materials	ASTM E8
Standard Guide for Examination and Evaluation of Pitting Corrosion	ASTM G46
Specification for Unfired Fusion Welded Pressure Vessels	BS PD 5500
Method for Determination of K_{IC}, Critical CTOD and Critical J Values of Welds in Metallic Materials	BS 7448: Part 2
Code of Practice for Fatigue Design and Assessment of Steel Structures	BS 7608

Table 1.1
Codes, Standards, Recommended Practices, and Reports

Title	Identification
Guide on Methods For Assessing the Acceptability of Flaws in Structures	BS 7910
Guidance on Methods for Assessing the Acceptability of Flaws in Fusion Welded Structures	BS PD 6493
Methods for the Assessment of the Influence of Crack Growth on the Significance of Defects in Components Operating at High Temperatures	BS PD 6539
Design of Steel Pressure Pipes	DIN 2413 Part 1
Design of Steel Bends Used in Pressure Pipelines	DIN 2413 Part 2
Summary of the Average Stress Rupture Properties of Wrought Steels for Boilers and Pressure Vessels	ISO/TR 7468-1981(E)
Guidelines for Detection, Repair, and Mitigation of Cracking of Existing Petroleum Refinery Pressure Vessels in Wet H_2S Environments	NACE Std RP0296
Assessment Procedure For High Temperature Response Of Structures	Nuclear Electric R-5
Assessment Of The Integrity of Structures Containing Defects	Nuclear Electric R-6
Damage Mechanisms Affecting Fixed Equipment In Fossil Electric Power Industry	WRC 490
Damage Mechanisms Affecting Fixed Equipment In The Pulp And Paper Industry	WRC 488
Damage Mechanisms Affecting Fixed Equipment In The Refining Industry	WRC 489
Evaluation Of Design Margins For ASME Code Section VIII and Evaluation Of Design Margins For ASME Code Section VIII, Division 1 And 2 – Phase 2 Studies	WRC 435
A Procedure for Safety Assessment of Components with Cracks – Handbook	SAQ/FoU-Report 96/08
Method of Assessment for Flaws in Fusion Welded Joints with Respect to Brittle Fracture and Fatigue Crack Growth	WES 2805

PART 2

FITNESS-FOR-SERVICE ENGINEERING ASSESSMENT PROCEDURE

PART CONTENTS

2.1 General

2.1.1 This Standard contains Fitness-For-Service *(FFS)* assessment procedures that can be used to evaluate pressurized components containing flaws or damage. If the results of a Fitness-For-Service assessment indicate that the equipment is suitable for the current operating conditions, then the equipment can continue to be operated at these conditions provided suitable monitoring/inspection programs are established. If the results of the Fitness-For-Service assessment indicate that the equipment is not suitable for the current operating conditions, then the equipment can be rerated using the calculation methods in this Standard. . These calculation methods can be used to find a reduced Maximum Allowable Working Pressure *(MAWP)* and/or coincident temperature for pressurized components (e.g. pressure vessels drums, headers, tubing, and piping). The calculation methods can also be used to determine a reduced Maximum Fill Height *(MFH)* for tank components (e.g. shell courses).

2.1.2 The Fitness-For-Service assessment procedures in this Standard are organized by flaw type and/or damage mechanism. A list of flaw types and damage mechanisms and the corresponding Part that provides the FFS assessment methodology is shown in Table 2.1. In some cases, it may be necessary to use the assessment procedures from multiple Parts if the primary type of damage is not evident. For example, the metal loss in a component may be associated with general corrosion, local corrosion and pitting. If multiple damage mechanisms are present, a damage class, e.g., corrosion/erosion, can be identified to assist in the evaluation. An overview of damage classes in this Standard is shown in Figure 2.1. As indicated in this figure, several flaw types and damage mechanisms may need to be evaluated to determine the Fitness-For-Service of a component. Each Part referenced within a damage class includes guidance on how to perform an assessment when multiple damage mechanisms are present.

2.1.3 The general Fitness-For-Service assessment procedure used in this Standard for all flaw types and damage mechanisms is provided in this Part. An overview of the procedure is provided in the following eight steps. The remaining Parts in this Standard utilize this assessment methodology for a specific flaw type or damage mechanism and provide specific details covering Steps 2 through 8 of this procedure.

a) STEP 1 – *Flaw and Damage Mechanism Identification:* The first step in a Fitness-For-Service assessment is to identify the flaw type and cause of damage (see paragraph 2.1.2). The original design and fabrication practices, the material of construction, and the service history and environmental conditions can be used to ascertain the likely cause of the damage. An overview of damage mechanisms that can assist in identifying likely causes of damage, is provided in Annex G. Once the flaw type is identified, the appropriate Part of this Standard can be selected for the assessment (see Table 2.1 and Figure 2.1).

b) STEP 2 – *Applicability and Limitations of the FFS Assessment Procedures:* The applicability and limitations of the assessment procedure are described in each Part, and a decision on whether to proceed with an assessment can be made.

c) STEP 3 – *Data Requirements:* The data required for a *FFS* assessment depend on the flaw type or damage mechanism being evaluated. Data requirements may include: original equipment design data, information pertaining to maintenance and operational history, expected future service, and data specific to the *FFS* assessment such as flaw size, state of stress in the component at the location of the flaw, and material properties. Data requirements common to all *FFS* assessment procedures are covered in this Part. Data requirements specific to a damage mechanism or flaw type are covered in the Part containing the corresponding assessment procedures.

d) STEP 4 – *Assessment Techniques and Acceptance Criteria:* Assessment techniques and acceptance criteria are provided in each Part. If multiple damage mechanisms are present, more than one Part may have to be used for the evaluation.

e) STEP 5 – *Remaining Life Evaluation:* An estimate of the remaining life or limiting flaw size should be made for establishing an inspection interval. The remaining life is established using the FFS assessment procedures with an estimate of future damage. The remaining life can be used in conjunction with an inspection code to establish an inspection interval.

f) STEP 6 – *Remediation:* Remediation methods are provided in each Part based on the damage mechanism or flaw type. In some cases, remediation techniques may be used to control future damage associated with flaw growth and/or material deterioration.

g) STEP 7 – *In-Service Monitoring:* Methods for in-service monitoring are provided in each Part based on the damage mechanism or flaw type. In-service monitoring may be used for those cases where a remaining life and inspection interval cannot adequately be established because of the complexities associated with the service environment.

h) STEP 8 – *Documentation:* Documentation should include a record of all information and decisions made in each of the previous steps to qualify the component for continued operation. Documentation requirements common to all FFS assessment procedures are covered in this Part. Documentation requirements specific to a damage mechanism or flaw type are covered in the Part containing the corresponding assessment procedures.

2.2 Applicability and Limitations of the FFS Assessment Procedures

2.2.1 The FFS assessment procedures in this Standard were developed to evaluate the pressure boundaries of pressure vessels, boiler components, piping, and shell courses of storage tanks with a flaw resulting from single or multiple damage mechanisms. The concepts presented in this Standard may also be used for the assessment of non-pressure-boundary components such as supports. Fitness-For-Service procedures for fixed and floating roof structures, and bottom plates of tanks are covered in Part 2 of API 653.

2.2.2 In the context of this Standard, a component is defined as any part that is designed and fabricated to a recognized code or standard (see Part 1, paragraphs 1.2.2 and 1.2.3), and equipment is defined to be an assemblage of components. Therefore, the *MAWP* for the equipment is the lowest *MAWP* for any component in the assemblage.

2.2.3 For components that have not been designed, or constructed to the original design criteria, the principles in this Standard may be used to evaluate the in-service damage and as-built condition relative to the intended design. FFS assessments of this type shall be performed by an Engineer (see Part 1, paragraph 1.4.3) knowledgeable and experienced in the design requirements of the applicable code.

2.2.4 Each Part in this Standard where a FFS Assessment procedure is described includes a statement of the applicability and limitations of the procedure. The applicability and limitations of an analysis procedure are stated relative to the level of assessment (see paragraph 2.4).

2.3 Data Requirements

2.3.1 Original Equipment Design Data

2.3.1.1 The following original equipment design data should be assembled to perform a FFS assessment. The extent of the data required depends on the damage mechanism and assessment level. A data sheet is included in Table 2.2 to record the required information that is common to all FFS assessments. In addition, a separate data sheet is included with each Part of this Standard to record information specific to the flaw type, damage mechanism, and assessment procedure.

a) Data for pressure vessels and boiler components may include some or all of the following:

1) An ASME Manufacturer's Data Report or, if the vessel or system is not Code stamped, other equivalent documentation or specifications.

2) Fabrication drawings showing sufficient details to permit calculation of the $MAWP$ of the component containing the flaw. If a rerate to a different condition of pressure and/or temperature is desired (i.e. increase or decrease in conditions), this information should be available for all affected components. Detailed sketches with data necessary to perform $MAWP$ calculations may be used if the original fabrication drawings are not available.

3) The original or updated design calculations for the load cases in Table A.1 of Annex A, as applicable, and anchor bolt calculations.

4) The inspection records for the component at the time of fabrication.

5) User Design Specification if the vessel is designed to the ASME Code, Section VIII, Division 2.

6) Material test reports.

7) Pressure-relieving device information including pressure relief valve and/or rupture disk setting and capacity information.

8) A record of the original hydrotest including the test pressure and metal temperature at the time of the test or, if the metal temperature is unavailable, the water or ambient temperature.

b) Data for piping components may include some or all of the following:

1) Piping Line Lists or other documentation showing process design conditions, and a description of the piping class including material specification, pipe wall thickness and pressure-temperature rating.

2) Piping isometric drawings to the extent necessary to perform a FFS assessment. The piping isometric drawings should include sufficient details to permit a piping flexibility calculation if such an analysis is deemed necessary by the Engineer in order to determine the $MAWP$ (maximum safe or maximum allowable operating pressure) of all piping components. Detailed sketches with data necessary to perform $MAWP$ calculations may be used if the original piping isometric drawings are not available.

3) The original or updated design calculations for the load cases in Table A.1 of Annex A, as applicable.

4) The inspection records for the component at the time of fabrication.

5) Material test reports.

6) A record of the original hydrotest including the test pressure and metal temperature at the time of the test, or if the metal temperature is unavailable, the water or ambient temperature.

c) Data for tanks may include some or all of the following:

1) The original API data sheet.

2) Fabrication drawings showing sufficient details to permit calculation of the maximum fill height (MFH) for atmospheric storage tanks and the $MAWP$ for low-pressure storage tanks. Detailed data with sketches where necessary may be used if the original fabrication drawings are not available.

3) The original or updated design calculations for the load cases in Table A.1 of Annex A, as applicable, and anchor bolt calculations.

4) The inspection records for the component at the time of fabrication.

5) Material test reports.

6) A record of the last hydrotest performed including the test pressure and metal temperature at the time of the test or, if the metal temperature is unavailable, the water or ambient temperature.

2.3.1.2 If some of these data are not available, physical measurements or field inspection of the component should be made to provide the information necessary to perform the assessment.

2.3.2 Maintenance and Operational History

2.3.2.1 A progressive record including, but not limited to, the following should be available for the equipment being evaluated. The extent of the data required depends on the damage mechanism and assessment level.

a) The actual operating envelope consisting of pressure and temperature, including upset conditions should be obtained. If the actual operating conditions envelope is not available, an approximation of one should be developed based upon available operational data and consultation with operating personnel. An operating histogram consisting of pressure and temperature data recorded simultaneously may be required for some types of FFS assessments (e.g., Part 10 for components operating in the creep regime).

b) Documentation of any significant changes in service conditions including pressure, temperature, fluid content and corrosion rate. Both past and future service conditions should be reviewed and documented.

c) The date of installation and a summary of all alterations and repairs including required calculations, material changes, drawings and repair procedures, including PWHT procedures if applicable. The calculations should include the required wall thickness and $MAWP$ (MFH for atmospheric storage tanks) with definition and allowances for supplemental loads such as static liquid head, wind, and earthquake loads.

d) Records of all hydrotests performed as part of any repairs including the test pressure and metal temperature at the time of the tests or, if the metal temperature is unavailable, the water or ambient temperature at the time of the test if known.

e) Results of prior in-service examinations including wall thickness measurements and other NDE results that may assist in determining the structural integrity of the component and in establishing a corrosion rate.

f) Records of all internal repairs, weld build-up and overlay, and modifications of internals.

g) Records of "out-of-plumb" readings for vertical vessels or tank shells.

h) Foundation settlement records if corrosion is being evaluated in the bottom plate or shell courses of the tank.

2.3.2.2 If some of these data are not available, physical measurements should be made to provide the information necessary to perform the assessment.

2.3.3 Required Data/Measurements for a FFS Assessment

2.3.3.1 Each Part in this Standard that contains FFS assessment procedures includes specific requirements for data measurements and flaw characterization based on the damage mechanism being evaluated. Examples of flaw characterization include thickness profiles for local corrosion/erosion, pitting depth, and dimensions of crack-like flaws. The extent of information and data required for a FFS assessment depends on the assessment level and damage mechanism being evaluated.

2.3.3.2 The Future Corrosion Allowance (FCA) should be established for the intended future operating period. The FCA should be based on past inspection information or corrosion rate data relative to the component material in a similar environment. Corrosion rate data may be obtained from API Publication 581 or other sources (see paragraph A.2.7 of Annex A). The FCA is calculated by multiplying the anticipated corrosion rate by the future service period considering inspection interval requirements of the applicable inspection code. The FFS assessment procedures in this Standard include provisions to ensure that the FCA is available for the future intended operating period.

2.3.4 Recommendations for Inspection Technique and Sizing Requirements

Recommendations for Non Destructive Examination (NDE) procedures with regard to detection and sizing of a particular damage mechanism and/or flaw type are provided in each Part.

2.4 Assessment Techniques and Acceptance Criteria

2.4.1 Three Levels of assessment are provided in each Part of this Standard that cover FFS assessment procedures. A logic diagram is included in each Part to illustrate how these assessment levels are interrelated. In general, each assessment level provides a balance between conservatism, the amount of information required for the evaluation, the skill of the personnel performing the assessment, and the complexity of analysis being performed. Level 1 is the most conservative, but is easiest to use. Practitioners usually proceed sequentially from a Level 1 to a Level 3 analysis (unless otherwise directed by the assessment techniques) if the current assessment level does not provide an acceptable result, or a clear course of action cannot be determined. A general overview of each assessment level and its intended use are described below.

2.4.1.1 Level 1 Assessment

The assessment procedures included in this level are intended to provide conservative screening criteria that can be utilized with a minimum amount of inspection or component information. A Level 1 assessment may be performed either by plant inspection or engineering personnel (see Part 1, paragraphs 1.4.2 and 1.4.3).

2.4.1.2 Level 2 Assessment

The assessment procedures included in this level are intended to provide a more detailed evaluation that produces results that are more precise than those from a Level 1 assessment. In a Level 2 Assessment, inspection information similar to that required for a Level 1 assessment are needed; however, more detailed calculations are used in the evaluation. Level 2 assessments would typically be conducted by plant engineers, or engineering specialists experienced and knowledgeable in performing FFS assessments.

2.4.1.3 Level 3 Assessment

The assessment procedures included in this level are intended to provide the most detailed evaluation which produces results that are more precise than those from a Level 2 assessment. In a Level 3 Assessment the most detailed inspection and component information is typically required, and the recommended analysis is based on numerical techniques such as the finite element method or experimental techniques when appropriate. A Level 3 assessment is primarily intended for use by engineering specialists experienced and knowledgeable in performing FFS assessments.

2.4.2 Each of the FFS assessment methodologies presented in this Standard utilize one or more of the following acceptance criteria.

2.4.2.1 Allowable Stress

This acceptance criterion is based upon calculation of stresses resulting from different loading conditions, classification and superposition of stress results, and comparison of the calculated stresses in an assigned category or class to an allowable stress value. An overview and aspects of these acceptance criteria are included in Annex B1. The allowable stress value is typically established as a fraction of yield, tensile or rupture stress at room and the service temperature, and this fraction can be associated with a design margin. This acceptance criteria method is currently utilized in most new construction design codes. In FFS applications, this method has limited applicability because of the difficulty in establishing suitable stress classifications for components containing flaws. As an alternative, assessment methods based on elastic-plastic analysis may be used (see Annex B1). Elastic-plastic analysis methods were used to develop the Remaining Strength Factor (see paragraph 2.4.2.2).

2.4.2.2 Remaining Strength Factor

Structural evaluation procedures using linear elastic stress analysis with stress classification and allowable stress acceptance criteria provide only a rough approximation of the loads that a component can withstand without failure. A better estimate of the safe load carrying capacity of a component can be provided by using nonlinear stress analysis to: develop limit and plastic collapse loads, evaluate the deformation characteristics of the component (e.g. deformation or strain limits associated with component operability), and assess fatigue and/or creep damage including ratcheting.

a) In this Standard, the concept of a remaining strength factor is utilized to define the acceptability of a component for continued service. The Remaining Strength Factor (RSF) is defined as:

$$RSF = \frac{L_{DC}}{L_{UC}} \tag{2.1}$$

b) With this definition of the RSF, acceptance criteria can be established using traditional code formulas, elastic stress analysis, limit load theory, or elastic-plastic analysis. For example, to evaluate local thin areas (see Part 5), the FFS assessment procedures provide a means to compute a RSF. If the calculated RSF is greater than the allowable RSF (see below) the damaged component may be placed back into service. If the calculated RSF is less than the allowable value, the component shall be repaired, rerated or some form of remediation can be applied to reduce the severity of the operating environment. The rerated pressure can be calculated from the RSF as follows:

$$MAWP_r = MAWP\left(\frac{RSF}{RSF_a}\right) \qquad for \quad RSF < RSF_a \tag{2.2}$$

$$MAWP_r = MAWP \qquad for \quad RSF \geq RSF_a \tag{2.3}$$

c) For tankage, the RSF acceptance criteria is:

$$MFH_r = H_f + (MFH - H_f)\left(\frac{RSF}{RSF_a}\right) \qquad for \quad RSF < RSF_a \tag{2.4}$$

$$MFH_r = MFH \qquad for \quad RSF \geq RSF_a \tag{2.5}$$

d) The recommended value for the allowable Remaining Strength Factor, RSF_a, is provided in Table 2.3. The values in Table 2.3. have been shown to be conservative (see Annex H). These values may be reduced based upon the type of loading (e.g. normal operating loads, occasional loads, short-time upset conditions) and/or the consequence of failure. For example, a lower RSF_a could be utilized for low-pressure piping containing a flaw that conveys cooling water, or for a shell section containing a flaw subject to normal operating pressure and design wind loads.

2.4.2.3 Failure Assessment Diagram

The Failure Assessment Diagram (FAD) is used for the evaluation of crack-like flaws in components.

a) The FAD approach was adopted because it provides a convenient, technically based method to provide a measure for the acceptability of a component with a crack-like flaw when the failure mechanism is measured by two distinct criteria: unstable fracture and limit load. Unstable fracture usually controls failure for small flaws in components fabricated from a brittle material and plastic collapse typically controls failure for large flaws if the component is fabricated from a material with high toughness. In a FFS analysis of crack-like flaws, the results from a stress analysis, stress intensity factor and limit load solutions, the material strength, and fracture toughness are combined to calculate a toughness ratio, K_r, and load ratio, L_r. These two quantities represent the coordinates of a point that is plotted on a two-dimensional FAD to determine acceptability. If the assessment point is on or below the FAD curve, the component is suitable for continued operation. A schematic that illustrates the procedure for evaluating a crack-like flaw using the Failure Assessment Diagram is shown in Figure 2.2.

b) In the assessment of crack-like flaws, partial safety factors are utilized along with the FAD acceptance criteria to account for variability of the input parameters in a deterministic fashion. Three separate partial safety factors are utilized: a factor for applied loading; a factor for material toughness; and a factor for flaw dimensions. The partial safety factors are applied to the stresses resulting from a stipulated loading condition, the fracture toughness and the flaw size parameters prior to conducting a FAD analysis. The partial safety factors recommended for use with Part 9 of this Standard (see Table 9.2) were developed based upon the results of a series of probabilistic analyses of components with crack-like flaws. Other values for these factors may be used based on a risk assessment where the potential failure modes and type of loading (e.g., normal operating loads, occasional loads, short-time upset conditions) are considered.

c) The in-service margin for a component with a crack-like flaw provides a measure of how close the component is to the limiting condition in the FAD. The in-service margin is defined by how far the assessment point, which represents a single operating condition, is within the failure envelope of the FAD. This point is determined based on the results from stress and fracture mechanics analyses after applying the three partial safety factors discussed above. The in-service margin is defined to be greater than or equal to one when the point resides underneath or on the FAD failure curve. The recommended minimum allowable value for the in-service margin is set at 1.0.

2.4.3 The FFS assessment procedures provided in this Standard are deterministic in that all information required for an analysis (independent variables) are assumed to be known. However, in many instances not all of the important independent variables are known with a high degree of accuracy. In such cases, conservative estimates of the independent variables are made to ensure an acceptable safety margin; this approach can lead to overly conservative results. The following types of analyses can be used to provide insight into the dependency of the analysis results with variations in the input parameters. The deterministic FFS assessment procedures in this standard can be used with any of these analyses.

2.4.3.1 Sensitivity Analysis

The purpose of such an analysis is to determine if a change in any of the independent (input) variables has a strong influence on the computed safety factors. The sensitivity analysis should consider the effects of different assumptions with regard to loading conditions, material properties and flaw sizes. For example, there may be uncertainties in the service loading conditions; the extrapolation of materials data to service conditions; and the type, size, and shape of the flaw. Confidence is gained in an assessment when it is possible to demonstrate that small changes in input parameters do not dramatically change the assessment results; and when realistic variations in the input parameters, on an individual or combined basis, still lead to the demonstration of an acceptable safety margin. If a strong dependence on an input variable is found, it may be possible to improve the degree of accuracy used to establish the value of that variable.

2.4.3.2 Probabilistic Analysis

The dependence of the safety margin on the uncertainty of the independent variables can be evaluated using this type of analysis. All or a limited number of the independent variables are characterized as random variables with a distribution of values. Using Monte Carlo simulation, first order reliability methods or other analytical techniques, the failure probability is estimated. These methods can be used to combine a deterministic FFS assessment model with the distributions prescribed for the independent variable to calculate failure probabilities. Once a probability of failure has been determined, an acceptable level can be established based on multiple factors such as jurisdictional regulations and the consequence of failure.

2.4.3.3 Partial Safety Factors

Partial Safety Factors are individual safety factors that are applied to the independent variables in the assessment procedure. The partial safety factors are probabilistically calibrated to reflect the effect that each of the independent variables has on the probability of failure. Partial safety factors are developed using probabilistic analysis techniques considering a limit state model, distributions of the main independent variables of the model, and a target reliability or probability of failure. The advantage of this approach is that uncertainty can be introduced in an assessment by separately combining the partial safety factors with the independent variables in a deterministic analysis model; the format of the analysis is similar to that used by many design codes. In this Standard, partial safety factors are only utilized in the assessment of crack-like flaws (see Part 9 and paragraph 2.4.2.3.b).

2.5 Remaining Life Assessment

2.5.1 Once it has been established that the component containing the flaw is acceptable at the current time, the user should determine a remaining life for the component. The remaining life in this Standard is used to establish an appropriate inspection interval, an in-service monitoring plan, or the need for remediation. The remaining life is not intended to provide a precise estimate of the actual time to failure. Therefore, the remaining life can be estimated based on the quality of available information, assessment level, and appropriate assumptions to provide an adequate safety factor for operation until the next scheduled inspection.

2.5.2 Each FFS assessment Part in this Standard provides guidance on calculating a remaining life. In general, the remaining life can be calculated using the assessment procedures in each Part with the introduction of a parameter that represents a measure of the time dependency of the damage taking place. The remaining life is then established by solving for the time to reach a specified operating condition such as the $MAWP$ (MFH) or a reduced operating condition $MAWP_r$ (MFH_r) (see paragraph 2.4.2.2.b).

2.5.3 Remaining life estimates will fall into one of the following three general categories.

a) *The Remaining Life Can be Calculated With Reasonable Certainty* – An example is general uniform corrosion, where a future corrosion allowance can be calculated and the remaining life is the future corrosion allowance divided by the assumed corrosion rate from previous thickness data, corrosion design curves, or experience in similar services. Another example may be long term creep damage, where a future damage rate can be estimated. An appropriate inspection interval can be established at a certain fraction of the remaining life. The estimate of remaining life should be conservative to account for uncertainties in material properties, stress assumptions, and variability in future damage rate.

b) *The Remaining Life Cannot be Established With Reasonable Certainty* – Examples may be a stress corrosion cracking mechanism where there is no reliable crack growth rate data available or hydrogen blistering where a future damage rate cannot be estimated. In these examples, remediation methods should be employed, such as application of a lining or coating to isolate the environment, drilling of blisters, or monitoring. Inspection would then be limited to assuring remediation method acceptability, such as lining or coating integrity.

c) *There is Little or No Remaining Life* – In this case remediation, such as repair of the damaged component, application of a lining or coating to isolate the environment, and/or frequent monitoring is necessary for future operation.

2.6 Remediation

2.6.1 In some circumstances remediation should be used (see paragraph 2.5.3). Examples include: where a flaw is not acceptable in its current condition; the estimated remaining life is minimal or difficult to estimate; or the state-of-the-art analysis/knowledge is insufficient to provide an adequate assessment. Appropriate remediation methods are covered within each Part of this standard that contains an FFS Assessment procedure.

2.6.2 Only general guidelines are provided in this Standard; each situation will require a customized approach to remediation. Periodic checks should be made to ensure that the remediation actions have prevented additional damage and can be expected to prevent future damage. The user may need to refer to other standards for detailed remediation procedures; for example, weld repair guidelines can be found in applicable repair codes, such as API 510, API 570, API 653, and ANSI/NB-23.

2.7 In-Service Monitoring

Under some circumstances, the future damage rate/progression cannot be estimated easily or the estimated remaining life is short. In-service monitoring is one method whereby future damage or conditions leading to future damage can be assessed, or confidence in the remaining life estimate can be increased. Monitoring methods typically utilized include: corrosion probes to determine a corrosion rate; hydrogen probes to assess hydrogen activity; various ultrasonic examination methods and acoustic emission testing to measure metal loss or cracking activity; and measurement of key process variables and contaminants. Appropriate in-service monitoring methods are covered within each Part of this standard that contains an FFS Assessment procedure.

2.8 Documentation

2.8.1 A Fitness-For-Service analysis should be sufficiently documented such that the analysis can be repeated later. Documentation requirements specific to a particular assessment are described in the corresponding Part covering the FFS assessment procedure. The following items should be included in the documentation.

a) The equipment design data, and maintenance and past operational history to the extent available should be documented for all equipment subject to a FFS assessment.

b) Inspection data including all readings utilized in the FFS assessment.

c) Assumptions and analysis results including:

   1) Part, edition, and assessment level of this Standard and any other supporting documents used to evaluate the flaw or damage.

   2) Future operating and design conditions including pressure, temperature and abnormal operating conditions.

   3) Calculations of the minimum required thickness and/or $MAWP$.

   4) Calculations of remaining life and the time for the next inspection.

   5) Any remediation or mitigation/monitoring recommendations that are a condition for continued service.

2.8.2 All calculations and documentation used to determine the Fitness-For-Service of a pressurized component should be kept with the inspection records for the component or piece of equipment in the owner-user inspection department. This documentation will be a part of the records required for mechanical integrity compliance.

2.9 Nomenclature

FCA	future corrosion allowance (see Annex A, paragraph A.2.7).
H_f	distance between the bottom of the flaw and the tank bottom.
L_{DC}	limit or plastic collapse load of the damaged component (component with flaws).
L_{UC}	limit or plastic collapse load of the undamaged component.
$MAWP$	maximum allowable working pressure of the undamaged component (see paragraph A.2.1 of Annex A).
$MAWP_r$	reduced permissible maximum allowable working pressure of the damaged component.
MFH	maximum fill height of the undamaged component (see paragraph A.2.1 of Annex A).
MFH_r	reduced permissible maximum fill height of the damaged tank course.
RSF	remaining strength factor computed based on the flaw and damage mechanism in the component.
RSF_a	allowable remaining strength factor (see paragraph 2.4.2.2.d).

2.10 References

1. Ainsworth, R.A., Ruggles, M.B., and Takahashi, Y., "Flaw Assessment Procedure for High-Temperature Reactor Components," *Journal of Pressure Vessel Technology*, Vol. 114, American Society of Mechanical Engineers, New York, May, 1992, pp. 166-170.
2. API, Base Resource Document on Risk-Based Inspection, API Publication 581, American Petroleum Institute, Washington D.C., 1996.
3. Buchheim, G.M., Osage, D.A., Prager, M., Warke, W.R., "Fitness-For-Service and Inspection for the Petrochemical Industry," ASME PVP-Vol. 261, American Society of Mechanical Engineers, New York, 1993, pp. 245-256.
4. Buchheim, G.M., Osage, D.A., Warke, W.R., Prager, M., "Update for Fitness-For-Service and Inspection for the Petrochemical Industry," ASME PVP-Vol. 288, American Society of Mechanical Engineers, New York, 1994, pp. 253-260.
5. Kim, D.S., Reynolds, J.T., "Fitness-For-Service Analysis in Turnaround Decision Making," ASME PVP-Vol. 261, American Society of Mechanical Engineers, New York, 1993, pp. 283-294.
6. Osage, D.A. and Prager, M., "Status and Unresolved Technical Issues of Fitness-For-Service Assessment Procedures for the Petroleum Industry," ASME PVP-Vol. 359, American Society of Mechanical Engineers, New York, 1997, pp. 117-128.
7. Yin, H., Bagnoli, D.L., "Case Histories Using Fitness-For-Service Methods," ASME PVP-Vol. 288, American Society of Mechanical Engineers, New York, 1994, pp. 315-328.

2.11 Tables and Figures

Table 2.1
Overview of Flaw and Damage Assessment Procedures

Flaw or Damage Mechanism	Part	Overview
Brittle Fracture	Part 3	Assessment procedures are provided for evaluating the resistance to brittle fracture of existing carbon and low alloy steel pressure vessels, piping, and storage tanks. Criteria are provided to evaluate normal operating, start-up, upset, and shut-down conditions.
General Metal Loss	Part 4	Assessment procedures are provided to evaluate general corrosion. Thickness data used for the assessment can be either point thickness readings or detailed thickness profiles. A methodology is provided to utilize the assessment procedures of Part 5 when the thickness data indicates that the metal loss can be treated as localized.
Local Metal Loss	Part 5	Assessment techniques are provided to evaluate single and networks of Local Thin Areas and groove-like flaws in pressurized components. Detailed thickness profiles are required for the assessment. The assessment procedures can also be utilized to evaluate individual pits or blisters as provided for in Part 6 and Part 7, respectively.
Pitting Corrosion	Part 6	Assessment procedures are provided to evaluate widely scattered pitting, localized pitting, pitting which occurs within a region of local metal loss, and a region of localized metal loss located within a region of widely scattered pitting. The assessment procedures can also be utilized to evaluate a network of closely spaced blisters as provided for in Part 7.
Blisters and HIC/SOHIC Damage	Part 7	Assessment procedures are provided to evaluate isolated and networks of blisters and HIC/SOHIC Damage. The assessment guidelines include provisions for blisters and HIC/SOHIC damage located at weld joints and structural discontinuities such as shell transitions, stiffening rings, and nozzles.
Weld Misalignment and Shell Distortions	Part 8	Assessment procedures are provided to evaluate stresses resulting from geometric discontinuities in shell type structures including weld misalignment and shell distortions (e.g. out-of-roundness and bulges)).
Crack-Like Flaws	Part 9	Assessment procedures are provided to evaluate crack-like flaws. Solutions for stress intensity factors and reference stress (limit load) are included in Annex C and Annex D, respectively. Methods to evaluate residual stress as required by the assessment procedure are described in Annex E. Material properties required for the assessment are provided in Annex F. Recommendations for evaluating crack growth including environmental concerns are also covered.
High Temperature Operation and Creep	Part 10	Assessment procedures are provided to determine the remaining life of a component operating in the creep regime. Material properties required for the assessment are provided in Annex F. Analysis methods for evaluating crack growth including environmental concerns are also covered.
Fire Damage	Part 11	Assessment procedures are provided to evaluate equipment subject to fire damage. A methodology is provided to rank and screen components for evaluation based on the heat exposure experienced during the fire. The assessment procedures of the other Parts of this publication are utilized to evaluate component damage.
Dent, Gouge, and Dent Gouge Combinations	Part 12	Assessment techniques are provided to evaluate dent, gouge, and dent gouge combinations in components.
Laminations	Part 13	Assessment procedures are provided to evaluate laminations. The assessment guidelines include provisions for laminations located at weld joints and structural discontinuities such as shell transitions, stiffening rings, and nozzles.

Table 2.2
Overview of Data Required for Flaw and Damage Assessment

The following data are required for most types of Fitness-For-Service assessments and it is recommended that this completed table accompany the data table completed for the specific damage type that are located in the respective Part of this standard.

Equipment Identification: _____
Equipment Type: _____ Pressure Vessel _____ Piping Component _____ Boiler Component
_____ Storage Tank
Component Type & Location: _____
Design Code: _____ ASME Section VIII Div. 1 _____ ASME Section VIII Div. 2 _____ ASME Section 1
_____ ASME B31.1 _____ ASME B31.2 _____ API 650 _____ API 620
_____ other: _____
Material of Construction (e.g. ASTM Specification): _____
MAWP or MFH: _____
Minimum Required Wall Thickness: _____
Temperature: _____
Cyclic Operation: _____

Type of Damage
Metal Loss – General: _____
Metal Loss – Local: _____
Metal Loss – Pitting: _____
HIC, SOHIC & Blisters: _____
Misalignment or Out-Of-Roundness: _____
Bulge: _____
Crack-Like Flaw: _____
Creep Damage: _____
Fire Damage: _____
Dent, Gouge & Dent/Gouge Combinations: _____
Laminations: _____

Location of Damage (provide a sketch)
Internal/External: _____
Near weld: _____
Orientation: _____

Environment
Internal: _____
_____
External: _____
_____

Repair and Inspection History (Including any Previous FFS Assessments)
_____
_____
_____

Operations History
_____
_____
_____

Future Anticipated Operations
_____
_____

Table 2.3
Recommended Allowable Remaining Strength Factor Based on the Design Code

Design Code	Recommended Allowable Remaining Strength Factor RSF_a
ASME Section 1	0.90
ASME Section VIII, Division 1 (pre 1999)	0.90
ASME Section VIII, Division 1 (post 1999)	0.90
ASME Section VIII, Division 2	0.90
AS 1210	0.90
BS PD 5500	0.90
CODAP	0.90
ASME B31.1	0.90
ASME B31.3	0.90
API 620	0.90
API 650	0.90

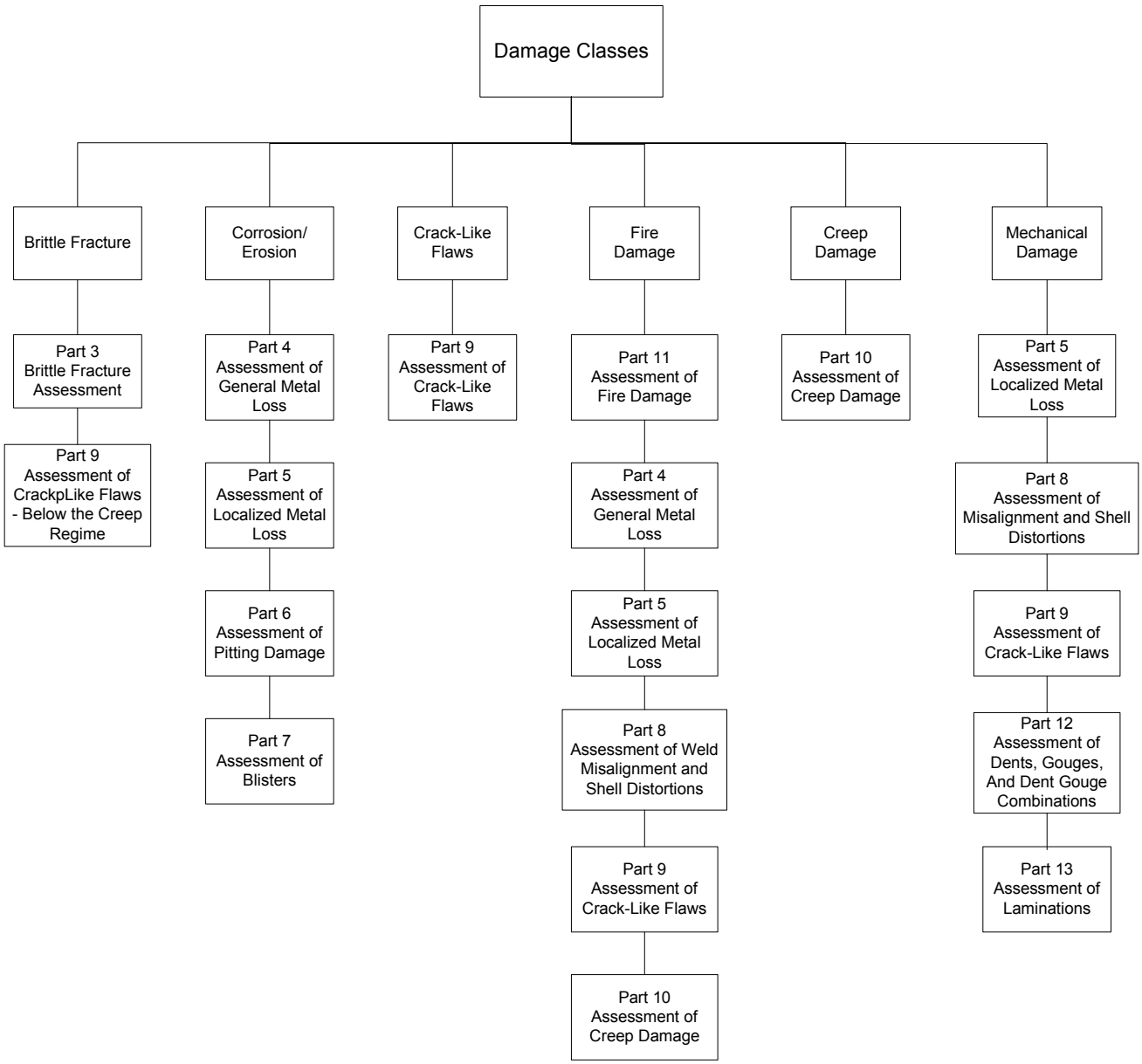

Figure 2.1
FFS Assessment Procedures for Various Damage Classes

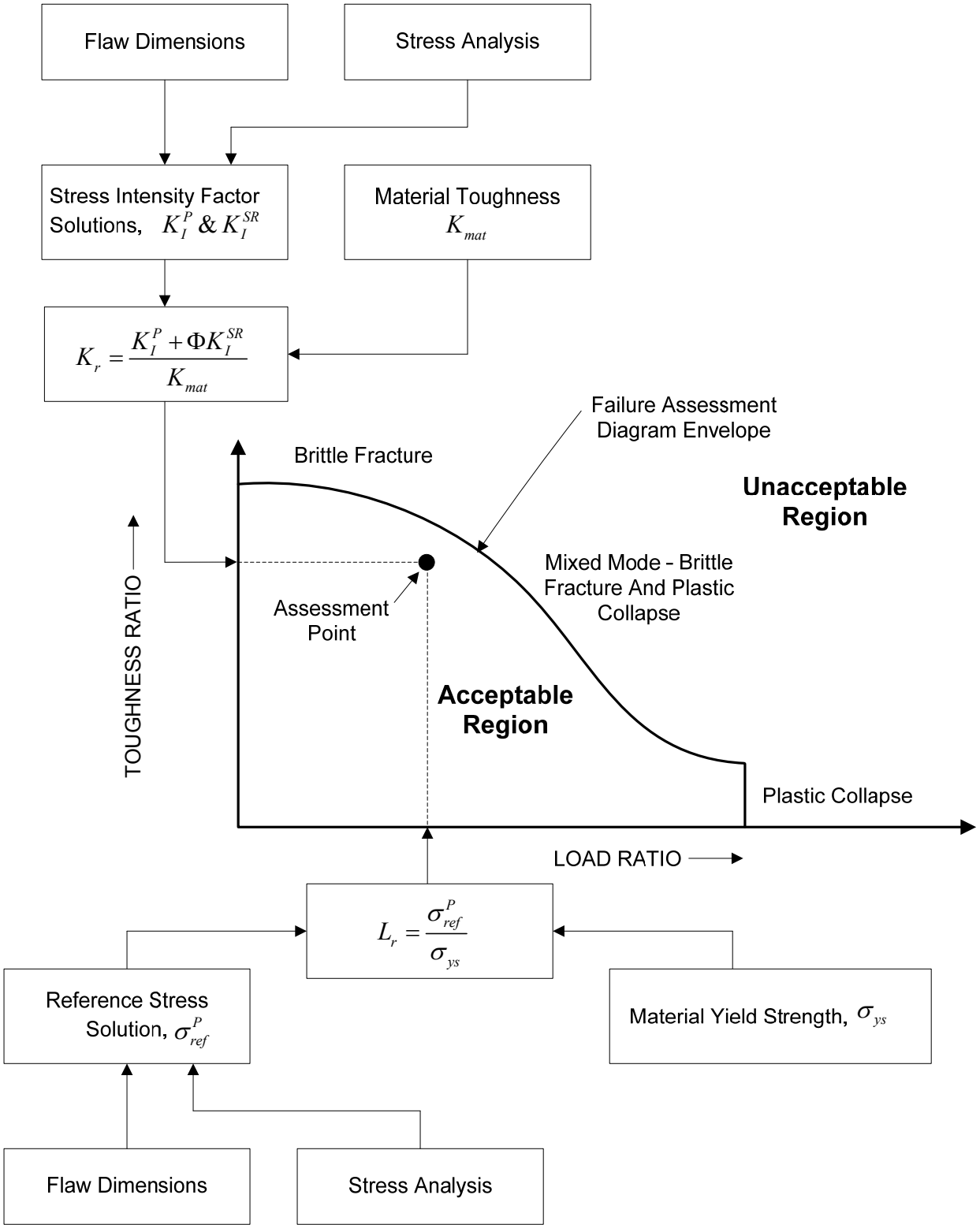

Figure 2.2
Overview of an FFS Analysis for Crack-Like Flaws Using the Failure Assessment Diagram

PART 3

ASSESSMENT OF EXISTING EQUIPMENT FOR BRITTLE FRACTURE

PART CONTENTS

3.1 General

3.1.1 This Part provides guidelines for evaluating the resistance to brittle fracture of existing carbon and low alloy steel pressure vessels, piping, and storage tanks. Other materials that could be susceptible to brittle fracture, such as ferritic, martensitic and duplex stainless steels, are not addressed in this Standard. The principles of some of the methods in Part 3 (e.g. Level 2, Methods B and C and Level 3) can be used to evaluate these materials. However, the user is cautioned that the methodology in Part 3 may not apply to materials that have a transition curve slope that is different from that for carbon and low alloy steels. Boilers and boiler external piping are not included within the scope of this Part. The purpose of this assessment is to avoid a catastrophic brittle fracture failure consistent with the ASME Code, Section VIII design philosophy. It is intended to prevent the initiation of brittle fracture; however, it does not ensure against service-induced cracks resulting in leakage nor does it ensure arrest of a running brittle fracture. Unlike other Parts in this Standard, this Part is used to screen for the propensity for brittle fracture. If a crack-like flaw is found, Part 9 should be used for the assessment. A flow chart for the brittle fracture assessment procedure is shown in Figure 3.1.

3.1.2 A brittle fracture assessment may be required as part of the assessment procedure of another Part in this Standard. In addition, the following circumstances may indicate the need for a brittle fracture assessment:

a) A change in process operating conditions, including startup, shutdown and upset conditions, that increase the possibility of low metal temperatures.

b) A process hazards review indicates that process temperatures, including those during start up, shutdown and upset conditions, could be lower than anticipated in the original design.

c) The equipment item is rerated using a lower design margin.

d) A minimum temperature is needed for a hydrotest.

e) The equipment is expected to be exposed to a general primary membrane tensile stress greater than 55 MPa (8 ksi) at or near ambient temperature and either of the following is true:

   1) The equipment has a wall thickness equal to or greater than 50 mm (2 in.)

   2) The equipment has been subjected to conditions that may cause embrittlement.

The owner/user may identify other circumstances where a brittle fracture assessment of equipment items may be warranted based on operating conditions and/or the condition of the component.

3.1.3 The Critical Exposure Temperature (CET) as used in this Part is defined as the lowest (coldest) metal temperature derived from either the operating or atmospheric conditions at the maximum credible coincident combination of pressure and supplemental loads that result in primary stresses greater than 55 MPa (8 ksi). Note that operating conditions include startup, shutdown, upset and standby conditions. The CET may be a single temperature at the maximum credible coincident combination of pressure and primary supplemental loads if that is also the lowest (coldest) metal temperature for all other combinations of pressure and primary supplemental loads. If lower (colder) temperatures at lower pressures and supplemental loads are credible, the CET should be defined by an envelope of temperatures and pressures (see paragraph 3.3.3). The CET for atmospheric storage tanks constructed to API 650 is defined as the lower of either the lowest one-day mean atmospheric temperature plus 8°C (15°F), or the hydrostatic test temperature. The CET for low-pressure storage tanks constructed to API 620 should be established using the methodology for pressure vessels (see paragraph 3.3.3).

3.1.4 The Minimum Allowable Temperature (MAT) is the lowest (coldest) permissible metal temperature for a given material and thickness based on its resistance to brittle fracture. It may be a single temperature, or an envelope of allowable operating temperatures as a function of pressure. The MAT is derived from mechanical design information, materials specifications, and/or materials data using the guidance in this Part.

3.2 Applicability and Limitations of the Procedure

3.2.1 This Part should be applied only to the following equipment:

a) Pressure vessels constructed in accordance with any edition of the ASME Boiler and Pressure Vessel Code, Section VIII, Divisions 1 and 2; however, the same guidelines may be used for pressure vessels constructed to other recognized codes and standards (see Part 2, paragraphs 2.2.2 and 2.2.3).

b) Pressure vessels constructed in accordance with any edition of the former API or API/ASME Code for Unfired Pressure Vessels for Petroleum Liquids and Gases.

c) Piping systems constructed in accordance with the ASME B31.3 or ASME B31.1 Codes; however, the same guidelines may be used for piping systems constructed to other recognized codes and standards (see Part 2, paragraphs 2.2.2 and 2.2.3).

d) Atmospheric or low-pressure above ground storage tanks that are welded or riveted, non-refrigerated, or operating at atmospheric or low pressure, and constructed in accordance with any edition of API 650 or API 620.

3.2.2 The Level 1 and 2 Assessment procedures in this Part may be applied to components subject to general corrosion, local metal loss and pitting damage provided the assessment criteria in Part 4, Part 5, and Part 6, respectively, are satisfied. Components with known crack-like flaws shall be evaluated using the procedures in Part 9.

3.2.3 The assessment methods in this Part apply only to equipment that has been and will continue to be included in a plant inspection and maintenance program that is consistent with API 510, API 570, API 653, NB 23 or other applicable in-service inspection code. If environmental cracking or a service condition that may result in a loss in the material toughness is possible, the Level 3 procedures of this Part should be utilized in the assessment. For example, low alloy steels such as 2.25Cr–1Mo may lose toughness at ambient temperature if exposed to high temperatures, above 400°C (750°F), for long periods because of thermal aging degradation mechanisms (see API-RP571). Components made from these types of materials require special precautions if a hydrotest or other low temperature pressurization is required.

3.3 Data Requirements

Data that may be needed for a brittle fracture analysis are described in this paragraph. The specific data requirements depend on the type of equipment and the level of the assessment.

3.3.1 Original Equipment Design Data

Mechanical design information, materials of construction, and specific materials properties test data, such as Charpy V-notch and tensile data, if available, should be obtained for all components. These data should be obtained for the base metal, weld metal and heat affected zones, if available. An overview of the original equipment data that may be required for an assessment is provided in Part 2, paragraphs 2.3.1. A summary of the original equipment design data typically used for an assessment is shown in Table 3.1.

3.3.2 Maintenance and Operational History

In addition to original equipment design data, information pertaining to repair history, and past and future operating conditions should be gathered. These data should include a summary of repairs and alterations, and include the current design pressure and temperature as well as the current wall thickness. Previous or proposed operating pressures and temperatures should be included as well as startup, shutdown, transient and/or upset operating conditions, and extreme environmental conditions. These data are used to establish the most severe operating and exposure conditions encountered during the life of the equipment. Information related to environmental exposure will also be needed to determine whether there is a probability of environmental cracking. An overview of the maintenance and operational history information required for an assessment is provided in Part 2 paragraphs 2.3.2. A summary of the maintenance and operational history data typically used for an analysis is shown in Table 3.1.

3.3.3 Required Data/Measurements for a FFS Assessment

The CET loading-temperature envelope should be determined after consideration of all potential operating conditions (including startup, shutdown, upset and standby conditions) using review procedures encompassing hazard analysis or other comparable assessment methodologies. Of special concern with existing equipment is any change in the operation that has occurred after the equipment was placed into service that could result in a lower (colder) CET than accounted for in the original design. In determining the CET, the current process design and safety philosophies should be employed. The CET loading-temperature envelope should consider the following process conditions and ambient factors:

a) The lowest (coldest) one-day mean atmospheric temperature, unless a higher (warmer) temperature is specified (e.g., specifying a minimum required startup temperature and coincident pressure). If a higher (warmer) temperature is specified, it must be confirmed that the system has control capabilities and/or that operating procedures are in place to maintain the higher temperature.

b) The lowest metal temperature under normal operating conditions.

c) The lowest metal temperature associated with startup, shutdown, upset conditions, standby, pressure tightness testing, and hydrotest. The following items should be considered:

   1) Failure of warning and/or shutdown systems (e.g. a pump stops, control valve shuts, etc.).

   2) A colder than expected warming stream.

   3) Reboiler failure or stall (e.g., flow loss of reboiling medium, failure of a control valve, etc.).

   4) The possibility of future field hydrotest.

d) Potential for autorefrigeration due to depressurization, either during operations or due to equipment failure (e.g., a safety relief valve sticks open). In some services where autorefrigeration can occur, equipment can be chilled to a temperature below the CET at an applied pressure less than that defined in paragraph 3.1.3. When this occurs, the possibility of any repressurization of equipment before the material has had sufficient time to warm up to the CET should be considered. The effect of autorefrigeration on the equipment depends upon the state of the process fluid, for example whether the vessel contents are all liquid, all gas, or a mixture and how the vessel may be vented. Autorefrigeration, caused by depressurization, may also occur in a flowing system with a flashing liquid. As the pressure decreases, the temperature will follow the vapor pressure curve. When only vapor is present, the effect of pressure on temperature is small and is governed by Joule-Thompson cooling. However, when a vessel is depressurized through a long line, the gas flowing through the line may be cold because it was autorefrigerated in the vessel.

e) The CET should not be higher than the temperature of the liquid causing the shock chilling. Shock chilling is a rapid decrease in metal temperature caused by the sudden contact of liquid or a two-phase (gas/liquid) fluid with a metal surface when the liquid or two-phase fluid is colder than the metal temperature at the instant of contact by more than 56°C (100°F) or the temperature difference determined from Figure 3.2, whichever is greater. Interpolation may be used for intermediate values of thickness when using Figure 3.2. If the heat transfer properties used in Figure 3.2 are not known, shock chilling should be considered to occur when the liquid or two phase fluid is 56°C (100°F) colder than the metal at the instant of contact. Shock chilling does not typically result from rapid changes in temperature in a flowing liquid, but rather from the sudden contact of a liquid with a hot surface. One example of this is a flare header that receives sub-cooled or flashing liquid from a safety valve discharge.

3.3.4 Recommendations for Inspection Technique and Sizing Requirements

The current component wall thickness is required for all assessments. Methods for establishing this thickness are provided in Part 4, paragraph 4.3.4.

3.4 Assessment Techniques and Acceptance Criteria

3.4.1 Overview

An overview of the assessment levels for pressure vessels and piping is shown in Figure 3.1. A separate assessment procedure is provided for tankage as shown in Figure 3.3. A summary of the three assessment levels is described below.

a) The Level 1 assessment procedures are based on the toughness requirements in the ASME Boiler and Pressure Vessel Code, Section VIII, Divisions 1 and 2. Level 1 can be satisfied based on impact test results or impact test exemption curves. At this Level, a single value for the MAT is determined at the maximum operating pressure. Development of a load (e.g. pressure) vs. temperature envelope in accordance with the Code requires a Level 2A analysis.

b) The Level 2 Assessment procedures for pressure vessels and piping are divided into three methods (see Figure 3.1). In the first method (Method A), equipment may be exempt from further assessment if it can be shown that the operating pressure and temperature are within a safe envelope. In the second method (Method B), equipment may be qualified for continued service based on a hydrotest. In the third method (Method C), equipment may be qualified for continued service based on materials of construction, operating conditions, service environment and past operating experience. A separate assessment procedure is provided for tankage (see Figure 3.3) that is based on a combination of these three methods.

c) A Level 3 Assessment may be used for equipment that does not meet the acceptance criteria for Levels 1 and 2. This equipment must be evaluated on an individual basis with the help of process, materials, mechanical, inspection, safety, and other specialists as appropriate. A Level 3 Assessment normally involves a more detailed evaluation using a fracture mechanics methodology (see Part 9). A Level 3 assessment should include a systematic evaluation of all of the factors that control the susceptibility of the component to brittle fracture: stress, flaw size and material toughness.

3.4.2 Level 1 Assessment

3.4.2.1 Pressure Vessels

a) Assessment Level 1 is appropriate for equipment that meets toughness requirements in the ASME Boiler and Pressure Vessel Code, Section VIII, Division 1 or 2. This can be determined from impact test results, or from the use of impact test exemption curves.

b) Pressure vessels that have a CET equal to or greater than the MAT, as demonstrated by the following procedure, are exempt from further brittle fracture assessment provided conditions do not change in the future. If a change in the operating conditions is made that affects the CET, a reassessment should be done. These vessels require no special treatment other than to continue their inclusion in a normal plant inspection and maintenance program encompassing generally accepted engineering practices such as contained in API 510, NB-23, or other recognized inspection codes.

c) A general procedure for determining the MAT for a component is described below. The MAT for a pressure vessel is the highest value of the MAT for any of its components.

1) STEP 1 – Determine the starting point for the MAT using one of the following two options:

i) Option A – Determine the starting point for the MAT using a governing thickness and the exemption curves shown in Figure 3.4 as described below. These curves are limited to components designed to the ASME Code, Section VIII, Division 1 or 2, and other recognized pressure vessel codes provided the design allowable stress is less than or equal to 172.5 MPa (25 ksi). Alternatively, exemption curves from other recognized codes and standards may be utilized.

I) STEP 1.1 – For the component under consideration, determine the following parameters:

A. Nominal uncorroded thickness at each weld joint, t_n

B. Material of construction

II) STEP 1.2 – Determine the uncorroded governing thickness, t_g, (see paragraph 3.4.2.1.d based on the nominal uncorroded thickness of the component. For formed heads, the minimum required thickness may be used in lieu of the nominal thickness. For components made from pipe, the thickness after subtracting the mill tolerance may be used.

III) STEP 1.3 – Determine the applicable material toughness curve of Figure 3.4. The applicable material toughness curve can be determined from the material specification (see Table 3.2), heat treatment, and steel making practice. If this information is not available, Curve A should be used.

IV) STEP 1.4 – Determine the MAT from Figure 3.4 based on the applicable toughness curve and the governing thickness, t_g (see paragraph 3.4.2.1.d). The MAT for flanges meeting ASME B16.5 or B16.47 shall be set at -29°C (-20°F), unless the MAT determined by the governing thickness at the flange nozzle neck weld joint together with the curve associated with the flange material gives a higher value. The MAT for carbon steel components with a governing thickness of less than 2.5 mm (0.098 inch) shall be -48°C (-55°F). The MAT for carbon steel nuts shall be -48°C (-55°F).

V) STEP 1.5 – The MAT determined in STEP 1.4 can be reduced further using Equation (3.2) if all of the following are true:

A. The component was fabricated from ASME P1 Group 1 or P1 Group 2 material,

B. The component has a wall thickness that is less than or equal to 38 mm (1.5 inches), and

C. The component was subject to $PWHT$ and the status of the $PWHT$ has not been changed because of repairs and/or alterations.

$$MAT = MAT_{STEP1.4} - 17^{o}C\ (30^{o}F) \qquad (3.1)$$

ii) Option B – If impact test results are available for the component, then the MAT may be set at the temperature at which the impact test values required by the ASME Code, Section VIII, Division 1 or 2, as applicable, or other international codes and standards are satisfied. However, the reduction in the MAT for $PWHT$ that is described in STEP 1.5 above shall not be applied to impact tested components.

2) STEP 2 – Repeat STEP 1 for all components that make-up the piece of equipment being evaluated (e.g. pressure vessel or piping system). The MAT for the piece of equipment is the highest value obtained for any component.

d) When determining the MAT, parts such as shells, heads, nozzles, manways, reinforcing pads, flanges, tubesheets, flat cover plates, skirts, and attachments that are essential to the structural integrity of the vessel shall be treated as separate components. Each component shall be evaluated based on its individual material classification (see Table 3.2, Table 3.3, and Figure 3.4) and governing thickness (see Figure 3.5).

1) The uncorroded governing thickness, t_g, of a welded component, excluding castings, is as follows:

i) For butt joints except those in flat heads and tubesheets, t_g is the nominal thickness of the component at the weld joint (see Figure 3.5 (a)),

ii) For corner, fillet, or lap welded joints, including attachments as defined above, t_g is the nominal thickness of the thinner of the two parts joined (see Figure 3.5 (b), (f) and (f)),

iii) For flanges, flat heads, or tubesheets, t_g is the thinner of the two parts joined at a weld, or the flat component thickness divided by 4, whichever is larger (see Figure 3.5 (c), (d) and (e)), and

iv) For welded assemblies consisting of more than two components (e.g., nozzle-to-shell joint with a reinforcing pad), t_g is the largest of the values determined at each joint (see Figure 3.5(b)).

2) The governing thickness of a casting is its largest nominal thickness.

3) The governing thickness of flat non-welded parts, such as bolted flanges (see STEP 1.4 in paragraph 3.4.2.1.c), tubesheets, and flat heads, is the component thickness divided by four (see Figure 3.5 (c)).

e) Vessels constructed to the ASME Code, Section VIII, Division 1 that meet all of the following requirements satisfy the Level 1 assessment. It is not necessary to compute the MAT on a component basis to complete the assessment.

1) The material is limited to P-1, Group 1 or Group 2 as defined in the ASME Code Section IX, and the uncorroded governing thickness, as defined in paragraph 3.4.2.1.d , does not exceed the following:

i) 12.7 mm (1/2 inch) for materials listed in Curve A of Figure 3.4, and

ii) 25.4 mm (1 inch) for materials listed in Curve B, C, or D of Figure 3.4.

2) The completed vessel has been hydrostatically tested per the ASME Code, Section VIII, Division 1, provided the test pressure is at least 1.5 times the design pressure for vessels constructed prior to the 1999 Addendum, or 1.3 times the design pressure for vessels constructed to or after the 1999 Addendum.

3) The design temperature is less than or equal to 343°C (650°F) and the CET is greater than or equal to -29°C (-20°F). Occasional operating temperatures less than -29°C (-20°F) are acceptable when due to lower seasonal atmospheric temperature.

4) Shock chilling or significant mechanical shock loadings are not credible events.

5) Cyclic loading is not a controlling design requirement.

3.4.2.2 Piping Systems

Piping systems should meet the toughness requirements contained in ASME B31.3 at the time the piping system was constructed (or an equivalent piping code if that code contains material toughness requirements). Piping systems should be evaluated on a component basis using the procedures in paragraph 3.4.2.1. The MAT for a piping system is the highest MAT obtained for any of the components in the system. Piping constructed to ASME B31.1 should be evaluated using the toughness requirements contained in ASME B31.3.

3.4.2.3 Atmospheric and Low Pressure Storage Tanks

a) Atmospheric storage tanks constructed to API 650 shall meet the Level 1 Assessment criteria contained in Figure 3.3, as applicable, and the accompanying notes. The Level 1 Assessment criteria require that these tanks meet the toughness requirements contained in API 650 or an equivalent construction code.

b) Low-pressure storage tanks constructed to API 620 shall be evaluated as pressure vessels using the assessment procedures of paragraph 3.4.2.1.

c) The Level 1 and Level 2 procedures are not applicable for atmospheric or low-pressure storage tanks that contain a refrigerated product.

3.4.2.4 If the component does not meet the Level 1 Assessment requirements, then a Level 2 or Level 3 Assessment can be performed.

3.4.3 Level 2 Assessment

3.4.3.1 Pressure Vessels – Method A

a) Pressure vessels may be exempt from further assessment at this level if it can be demonstrated that the operating pressure/temperature is within a safe envelope with respect to component design stress and the MAT.

b) The MAT may be adjusted from the value determined in the Level 1 Assessment by considering temperature reduction allowances as described below. If the Level 1 MAT was determined from impact test values, and if these values exceed the code minimum required values, then the MAT from Level 1 to be used as the starting point for a Level 2 assessment may be set to a lower temperature (see Annex F, paragraph F.4.5). These reductions from the Level 1 value apply to pressure vessels with excess thickness due to lower actual operating stresses at the low temperature pressurization condition. These temperature reductions can also be applied to vessels designed for elevated temperatures that have excess thickness at low-temperature conditions because of the difference in design allowable stresses. A procedure for determining the MAT considering the temperature reductions is shown below. This procedure can only be used for components with an allowable stress value less than or equal to 172.5 MPa (25 ksi); otherwise, a Level 3 Assessment is required.

1) STEP 1 – Determine the starting point for the MAT using one of the following two options:

i) Option A – The MAT is determined using Option A, STEP 1.4 of paragraph 3.4.2.1.c). Do not apply the reduction for PWHT in STEP 1.5.

ii) Option B – The MAT is determined using Option B of STEP 1 of paragraph 3.4.2.1.c).

2) STEP 2 – For the component under consideration, determine the following parameters:

i) All applicable loads and coincident Minimum Allowable Temperatures. A summary of the loads that should be considered is included in Table A.1 of Annex A.

ii) Previous metal loss associated with the nominal thickness, $LOSS$.

iii) Future corrosion allowance associated with the nominal thickness, FCA.

iv) Weld joint efficiencies, E and E^*.

v) Required thickness in the corroded condition for all applicable loads, $t_{\min}$, using the applicable weld joint efficiency.

3) STEP 3 - Determine the stress ratio, R_{ts}, using one of the equations shown below. Note that this ratio can be computed in terms of thicknesses and weld joint efficiencies, applied and allowable stresses, or applied pressure and permissible pressure based on pressure-temperature ratings.

$$R_{ts} = \frac{t_{\min} E^*}{t_g - LOSS - FCA} \qquad (Thickness\ \ Basis) \tag{3.2}$$

$$R_{ts} = \frac{S^* E^*}{SE} \qquad \left(Stress\ \ Basis\right) \tag{3.3}$$

$$R_{ts} = \frac{P_a}{P_{rating}} \qquad \left(Pressure - Temperature\ Rating\ \ Basis\right) \tag{3.4}$$

4) STEP 4 – Determine the reduction in the MAT based on the R_{ts} ratio.

i) If the starting point for the MAT is established using Option A in STEP 1, then:

I) If the computed value of the R_{ts} ratio from STEP 3 is less than or equal to the R_{ts} ratio threshold from Figure 3.7, then set the MAT to $-104^o C\ (-155^o F)$.

II) If the computed value of the R_{ts} ratio from STEP 3 is greater than the R_{ts} ratio threshold from Figure 3.7, then determine the temperature reduction, T_R, based on the R_{ts} ratio using Figure 3.7. The reduced MAT can be calculated using the following equation:

$$MAT = \max\left[\left(MAT_{STEP1} - T_R\right),\ \ -48^o C\,(-55^o F)\right] \tag{3.5}$$

ii) If the starting point for the MAT is established using Option B in STEP 1, then the reduced MAT is determined using Equation (3.6).

$$MAT = \max\left[\left(MAT_{STEP1} - T_R\right),\ \ -104^o C\,(-155^o F)\right] \tag{3.6}$$

5) STEP 5 – The MAT determined in STEP 4 can be reduced further if all of the following conditions are met:

i) the starting point for the MAT in STEP 1 was determined using Option A,

ii) the component was fabricated from P1 Group 1 or P1 Group 2 material,

iii) the component has a wall thickness that is less than or equal to 38 mm (1.5 inches), and

iv) the component was subject to $PWHT$ and the status of the $PWHT$ has not been changed because of repairs and/or alterations.

$$MAT = MAT_{STEP5} - 17^o C\ (30^o F) \tag{3.7}$$

6) STEP 6 – Repeat STEPs 1 through 5 for all components that make-up the piece of equipment being evaluated (e.g. pressure vessel or piping system). The MAT for the piece of equipment is highest value obtained for any component.

c) When evaluating components with a metal thickness below the minimum required thickness, $t_{\min}$, as permitted in Part 4, Part 5 and Part 6, $t_{\min}$ shall be based on the minimum required thickness of the undamaged component at the design conditions.

3.4.3.2 Pressure Vessels – Method B

a) A vessel may be qualified for continued service based on a hydrotest. A minimum acceptable temperature for operating pressures below the hydrotest pressure can be determined using Figure 3.8. This allowance is limited to hydrotest pressures of 125%, 130% and 150% of the design pressure corrected for the ratio of the allowable stress at test temperature to the allowable stress at design temperature (based on the original design code), and to materials with an allowable design stress equal to or less than 172.5 MPa (25 ksi).

   1) The test pressure should be corrected for the difference in allowable stresses between the design and hydrotest temperatures, but the test pressure should be limited to a value that will not produce a general primary membrane stress higher than 90% of the specified minimum yield strength for the steel used in the construction of the vessel. This can provide an additional advantage for vessels designed for elevated temperatures that have a design stress value lower than the allowable stress at ambient temperature.

   2) The metal temperature during hydrotest, rather than water temperature, is the relevant parameter in a brittle fracture assessment. Therefore, it is preferable to measure and use this value directly. Records of the measured metal temperature used in the assessment should be kept.

   3) If the hydrotest is performed at a temperature colder than the MAT as determined by a Level 1 assessment plus 17°C (30°F), it should be noted that a brittle fracture may occur during the hydrotest.

   4) The MAT should not be less than -104°C (-155°F) after adjustments using this procedure.

b) If the vessel is subject to multiple operating conditions, a MAT curve can be established using Figure 3.8 by plotting the pressure versus the permissible temperature.

3.4.3.3 Pressure Vessels – Method C

a) Pressure vessels in which all components have a governing thickness less than or equal to 12.7 mm (0.5 in.), or that meet all of the criteria listed below, may be considered to be acceptable for continued service without further assessment. Vessels that satisfy these criteria should be assigned a MAT consistent with the service experience. Note that the MAT may be a single temperature or a pressure-temperature operating envelope for the vessel.

   1) Pressure vessels fabricated from P-1 and P-3 steels (as defined in the ASME Code, Section IX) where the design temperature is less than or equal to 343°C (650°F). P-4 and P-5 steels may also be evaluated at this level, provided the proper precautions (e.g. preheating prior to pressurization) are taken to avoid brittle fracture due to in-service embrittlement.

   2) The equipment satisfied all requirements of a recognized code or standard (see Part 2, paragraph 2.2.2) at the time of fabrication.

   3) The nominal operating conditions have been essentially the same and consistent with the specified design conditions for a significant period of time, and more severe conditions (i.e., lower temperature and/or higher stress) are not expected in the future.

   4) The CET at the $MAWP$ is greater than or equal to -29°C (-20°F).

   5) The nominal uncorroded governing thickness is not greater than 50.8 mm (2 inches).

   6) Cyclic service as defined in Annex I is not a design requirement.

   7) The equipment is not subject to environmental cracking (see Annex G).

   8) The equipment is not subject to shock chilling (see paragraph 3.3.3.e for a definition of shock chilling).

b) Pressure vessels that are assessed using Method C of the Level 2 Assessment procedure are qualified for continued operation based on their successful performance demonstrated during past operation. However, if a repair is required, the guidelines in paragraph 3.6 should be followed to ensure that the probability of brittle fracture does not increase.

c) A documented pressure and metal temperature combination from the operating history of a component may be extrapolated to a pressure no more than 10% above the documented pressure using Figure 3.6. In no case shall the resulting pressure be higher than the MAWP.

d) A documented pressure and metal temperature combination from the operating history of a component may be used as a basis for developing a MAT pressure-temperature operating envelope as follows:

1) STEP 1 – Determine the stress ratio, R_{ts}, for a series of metal temperatures below the documented temperature from the operating history. The stress ratio, R_{ts}, is the ratio of the general primary stress in the component at the reduced temperature to the general primary stress in the component at the documented metal temperature from the operating history.

2) STEP 2 – Determine the temperature reduction, T_R, based on the R_{ts} ratio from STEP 1 and the R_{ts} ratio threshold from Figure 3.7.

3) STEP 3 – Determine the reduction in the MAT based on the R_{ts} ratio from STEP 1.

i) If the computed value of the R_{ts} ratio from STEP 1 is less than or equal to the R_{ts} ratio threshold from Figure 3.7, then set the MAT to $-104^o C\ (-155^o F)$.

ii) If the computed value of the R_{ts} ratio from STEP 1 is greater than the R_{ts} ratio threshold from Figure 3.7, then determine the temperature reduction, T_R, from Figure 3.7 based on the R_{ts} ratio. The reduced MAT can be calculated using the following equation:

$$MAT = \max\left[\left(MAT_{STEP1} - T_R\right),\ -48^o C\,(-55^o F)\right] \tag{3.8}$$

3.4.3.4 Piping Systems – Method A

Piping systems are acceptable if it can be demonstrated that the operating pressure/temperature is within a safe envelope with respect to component design stress and the MAT. The provisions in paragraph 3.4.3.1 can be applied to piping to lower the MAT when the operating stress level is below the design allowable stress. Assessments should consider component stress due to combined sustained and thermal loads (see Note 5 in Figure 3.9).

3.4.3.5 Piping Systems – Method B

Piping systems are acceptable if it can be demonstrated that the operating pressure and coincident temperature is within a safe envelope with respect to a hydrotest condition. The approach discussed in paragraph 3.4.3.2 that provides for a reduction in the MAT can be applied to piping. Assessments should consider component stress due to combined sustained and thermal loads (see Note 5 in Figure 3.9).

3.4.3.6 Piping Systems – Method C

Piping systems are acceptable if the assessment criteria in Figure 3.9 and the accompanying notes are satisfied. This method is limited to piping components with a thickness of 38 mm (1.5 inch) or less.

3.4.3.7 Atmospheric and Low Pressure Storage Tanks

a) Atmospheric and low-pressure storage tanks that operate at ambient temperature (including those that contain a heated product) shall meet the Level 2 Assessment criteria contained in Figure 3.3.

b) Low pressure storage tanks constructed to API 620 shall be evaluated as pressure vessels using the assessment procedures in paragraphs 3.4.3.1, 3.4.3.2, and 3.4.3.3.

c) The Level 1 and Level 2 procedures are not applicable for Atmospheric or low-pressure storage tanks that contain a refrigerated product.

3.4.3.8 If the component does not meet the Level 2 Assessment requirements, then a Level 3 Assessment can be performed.

3.4.4 Level 3 Assessment

3.4.4.1 Pressure vessels, piping and tankage that do not meet the criteria for Level 1 or 2 assessments can be evaluated using a Level 3 assessment. Level 3 assessments normally involve more detailed determinations of one or more of the three factors that control the susceptibility to brittle fracture: stress, flaw size and material toughness.

3.4.4.2 Part 9 may be used as a basis for a Level 3 Assessment. A risk analysis considering both the probability and potential consequences of a brittle fracture in the specific service should also be considered in a Level 3 Assessment.

3.4.4.3 At this assessment level, the judgment of the engineer involved (see Part 1, paragraph 1.4.1) may be used to apply some of the principles of Levels 1 and 2 without the specific restrictions used at those levels. Examples of some other approaches that may be considered are described below.

a) A heat transfer analysis may be performed to provide a less conservative estimate of the lowest metal temperature that the vessel will be exposed to in service.

b) If loadings are always quasi-static, the additional credits due to the temperature shift between dynamic (e.g., Charpy V-notch) and quasi-static toughness may be considered.

c) Inspection of seam welds and attachment welds to the pressure shell can be made to determine the presence and size of crack-like flaws. Guidance on acceptable flaw sizes based on a flaw assessment (see Part 9) can be used. The extent of subsequent inspections should be based upon the severity of the service considering the conditions given in paragraph 3.3.3. Ultrasonic examination from the outside is permissible if the inside surface cannot be inspected directly.

3.4.4.4 It may be necessary to evaluate stresses using advanced techniques such as finite element analysis. Consideration should be given to all relevant loads including those that produce localized stresses (e.g. forces and moments at nozzles), thermal transient effects, and residual stress. These additional considerations may result in different criteria for different locations within a piece of equipment. Probable locations and orientations of crack-like flaws should be determined to guide the stress analyst.

3.4.4.5 A Level 3 assessment normally relies on a determination of maximum expected flaw sizes at locations of high stresses. In general, these postulated flaws should be assumed to be surface breaking, and to be oriented transverse to the maximum stress. For welded structures, this often implies that the flaw is located within the residual stress field parallel to a longitudinal weld or transverse to a circumferential weld. The maximum expected flaw size should be detectable with standard NDE techniques. The detectable flaw size will depend on factors such as surface condition, location, accessibility, operator competence, and NDE techniquePart 9 can be used to derive limiting sizes for crack-like flaws. In this assessment, the aspect ratio of the assumed flaw should be large enough to ensure that the calculations are not highly sensitive to small variations in flaw depth in the through thickness direction. To reduce this sensitivity, a minimum crack-like flaw aspect ratio of 6:1 is recommended.

3.4.4.6 The use of material toughness data from appropriate testing is the preferred basis for a Level 3 assessment. Where this is not practical, appropriate and sufficiently conservative estimates should be made. Methods for obtaining or estimating fracture toughness are described in Annex F.

3.5 Remaining Life Assessment – Acceptability for Continued Service

3.5.1 Remaining life is not normally an issue associated with equipment's resistance to brittle fracture. Therefore, equipment evaluated using the Level 1 or 2 assessment procedures is acceptable for future operation as long as operating conditions do not become more severe and there is no active degradation mechanism that can result in loss of material toughness or the propagation of a crack-like flaw. If this is not the case, a Level 3 assessment should be performed, and the remaining life associated with the time for a flaw to grow to critical size should be calculated.

3.5.2 Pressure vessels constructed of materials that satisfy the requirements of a Level 1, 2 or 3 assessment are considered acceptable for continued service. Pressure vessels can be fully pressurized within the limits of their design parameters at any metal temperature above the MAT.

3.5.3 Piping systems constructed of materials that satisfy the requirements of a Level 1, 2 or 3 assessment are considered acceptable for continued service. Piping systems can be fully pressurized within the limits of their design parameters at metal temperatures above the MAT. The acceptability of piping systems for continued service can be determined by using similar methods as those to evaluate pressure vessels. There are two facts that distinguish piping from pressure vessels and make piping less likely to experience brittle fracture:

a) A lower MAT is more easily attainable because the component is usually thinner (see Figure 3.4, Note 4); and

b) There is a lower probability that crack-like flaws will be oriented perpendicular to the highest stress direction in piping systems because there are fewer longitudinal weld seams (i.e. seamless pipe).

3.5.4 Atmospheric and low-pressure storage tanks constructed of materials that satisfy the requirements of a Level 1, 2 or 3 assessment are considered acceptable for continued service. A Level 3 Assessment for storage tanks should follow the same general guidelines as used for pressure vessels. However, the analysis must reflect the special design considerations used for storage tanks such as the bottom plate-to-shell junction.

3.6 Remediation

3.6.1 A FFS analysis typically provides an evaluation of the condition of a component for continued operation for a period based upon a degradation rate. In the case of brittle fracture, a component is suitable for continued service as long as the operating conditions do not become more severe and/or there is no active material degradation mechanism that can result in loss of material toughness or the propagation of crack-like flaws. However, in many cases, future degradation rates are very difficult to predict, or little or no further degradation can be tolerated. Therefore, the Owner-User may choose to apply mitigation methods to prevent or minimize the rate of further damage.

3.6.2 Remediation methods are provided below. These methods are not inclusive for all situations, nor are they intended to be a substitute for an engineering evaluation of a particular situation. The Owner-User should consult a qualified metallurgist/corrosion engineer and a pressure vessel engineer as to the most appropriate method to apply for the relevant damage mechanism(s).

3.6.2.1 *Limiting Operation* – The limitation of operating conditions to within the acceptable operating pressure-temperature envelope is the simplest type of remediation effort. This method, however, may be impractical in many cases because of the requirements for stable process operation. The most successful, and effective, technique for limiting operation has been to implement a controlled start-up procedure. This is because many petroleum and chemical processes that undergo this type of assessment for brittle fracture were originally designed for substantially warmer temperatures, above the temperature range where the probability of brittle fracture is of concern.

3.6.2.2 *Postweld Heat Treatment (PWHT)* – If the component has not been subject to $PWHT$, $PWHT$ may be performed to enhance the damage tolerance to crack-like flaws and resistance to brittle fracture. The effects of $PWHT$ are described below.

a) The beneficial effects of $PWHT$ are:

1) A reduction in the residual stresses that contribute to the driving force for brittle fracture.

2) Improvement in the resistance of hard heat affected zones to environmental cracking and a potential improvement in the toughness.

b) The detrimental effects of $PWHT$ are:

1) A potential reduction in the toughness of the heat affected zone

2) The potential for reheat cracking in certain materials (see API-RP571).

3.6.2.3 *Hydrostatic Test* – If the component has not been subject to a hydrotest, then a hydrotest may be performed to enhance the damage tolerance to crack-like flaws and resistance to brittle fracture. The beneficial effect of a hydrotest is that crack-like flaws located in the component are blunted resulting in an increase in brittle fracture resistance. The beneficial effects of a hydrotest can be quantified using a Level 2 assessment (see paragraph 3.4.3.2) or a Level 3 assessment. If a hydrotest is performed, it should be conducted at a metal temperature that will permit plastic flow without the possibility of brittle fracture (i.e. conduct the test at a metal temperature that is in the upper shelf region of the transition curve). A typical hydrotest temperature that has been used is 17°C (30°F) above the MAT.

3.7 In-Service Monitoring

3.7.1 In-service monitoring and control of process conditions, with operating procedures in place to remain within a defined pressure-temperature envelope, can reduce the probability of brittle fracture.

3.7.2 Monitoring for Degradation of Low Alloy Steel Notch Toughness

Certain materials, such as the chromium-molybdenum low alloy steels, experience a loss of notch toughness due to exposure at high temperatures. This degradation may be monitored over the service life by means of sentinel material included within a pressure vessel. Periodically, a portion of this material is removed and tested to monitor for the degradation of material toughness. The degradation of material properties is evaluated against a minimum acceptable brittle fracture criterion that has previously been established. A Level 3 Assessment is usually required to justify continued use when the material no longer meets this criterion.

3.7.3 Monitoring for Criticality of Growing Flaws

Flaws that develop or propagate during the service life of equipment can increase the probability of brittle fracture. The assessment of each type of flaw is prescribed in other Parts of this Standard; see Part 2 for an overview.

3.7.4 Assessment of Non-Growing Flaws Detected In-Service

In-service inspections may result in the detection of flaws that are original material or fabrication flaws. These flaws may or may not be in excess of the requirements of the original design and construction code. While these flaws may have been innocuous relative to the original design code, their presence may affect current or altered design and operating parameters. Alternatively, flaws may have developed or resulted from service exposure, excessive operating conditions, or maintenance-related activities. The influence of such flaws on the increased susceptibility for brittle fracture should be assessed. This assessment generally requires either a Level 2 or a Level 3 analysis.

3.8 Documentation

3.8.1 The documentation for each level of brittle fracture assessment should include the information cited in Part 2, paragraph 2.8 and the following specific requirements:

3.8.1.1 *Level 1 Assessment* – Documentation covering the assessment, the specific data used, and the criteria that have been met by the results obtained from the evaluation.

3.8.1.2 *Level 2 Assessment* – The documentation should address the reason(s) for the assessment, the assessment level used, the engineering principles employed, the source of all material data used, identification of any potential material property degradation mechanisms and their associated influence on the propagation of flaws, and the criteria applied in the assessment procedure.

3.8.1.3 *Level 3 Assessment* – The documentation should cover the reason(s) for performing a Level 3 assessment and all issues pertaining to the Fitness-For-Service assessment. The documentation should also address the engineering principles employed including stress analysis methods and flaw sizing, the source of all material data used, identification of any potential material property degradation mechanisms and their associated influence on the propagation of flaws, and the criteria applied in the assessment procedure.

3.8.2 All documents pertaining to the assessment for brittle fracture should be retained for the life of the equipment in the equipment history file. This includes all supporting documentation, data, test reports, and references to methods and criteria used for such assessments and evaluations. For vessels exposed to identical conditions, a single document with appropriate references is adequate.

3.9 Nomenclature

CET	Critical Exposure Temperature.
α	coefficient of thermal expansion
C_1	55 MPa for SI Units, 8000 psi for US Customary Units
$\Delta T_{\max}$	temperature difference between the liquid and metal temperatures
E_y	elastic modulus
E	joint efficiency (e.g. see Table UW-12 of the ASME Code, Section VIII, Division 1) used in the calculation of t_r. For castings, the quality factor or joint efficiency E, whichever governs design, should be used.
E^*	is equal to E except that E^* shall not be less than 0.80, or $E^* = \max\left[E, 0.80\right]$.
FCA	future corrosion allowance associated with the governing thickness.
h	convective heat transfer coefficient
k	thermal conductivity of the metal
$LOSS$	previous metal loss associated with the governing thickness.
MAT	Minimum Allowable Temperature.
$MAWP$	Maximum Allowable Working Pressure.
ν	Poisson's ratio
P_a	applied pressure for the condition under consideration.
P_I	per cent increase in pressure above the initial point.
P_{rating}	component pressure rating at the MAT.
R_{ts}	stress ratio defined as the stress for the operating condition under consideration divided by the stress at the design minimum temperature. The stress ratio may also be defined in terms of required and actual thicknesses, and for components with pressure temperature ratings, the stress ratio is computed as the applied pressure for the condition under consideration divided by the pressure rating at the MAT.
S	allowable stress value in tension from the applicable code.
S^*	applied general primary stress; for piping systems, the applied general primary stress is computed using the guidelines in Figure 3.9, Note 5.
t	component thickness.

t_g governing nominal uncorroded thickness of the component (see paragraph 3.4.2.1.d.)

t_{gi} governing thickness of the component at weld joint i.

t_n nominal uncorroded thickness of the component. For welded pipe where a mill under tolerance is allowed by the material specification, the thickness after mill under tolerance has been deducted shall be taken as the nominal thickness. Likewise, for formed heads, the minimum specified thickness after forming shall be used as the nominal thickness.

$t_{\min}$ minimum required thickness of the component in the corroded condition for all applicable loads.

T_I increase in temperature above the initial point.

T_{pwht} MAT adjustment for components subject to $PWHT$.

T_R reduction in MAT based on available excess thickness.

T_{RH} reduction in MAT based on the operating-to-hydrotest ratio.

T_S shell metal temperature.

3.10 References

1. McLaughlin, J.E., "Preventing Brittle Fracture of Aboveground Storage Tanks – Basis for the Approach Incorporated in API 653," Proceedings Case Studies: Sessions III and IV of the IIW Conference, Fitness-For-Purpose of Welded Structures, Key Biscayne, Florida, USA, October 23-24, 1991.
2. McLaughlin, J.E., Sims, J.R., "Assessment of Older Equipment for Risk of Brittle Fracture," ASME PVP-Vol. 261, American Society of Mechanical Engineers, New York, N.Y., 1993, pp. 257-264.
3. Findlay, M., McLaughlin, J.E., and Sims, J.R., “Assessment of Older Cold Service Pressure Vessels for Brittle Fracture During Temperature Excursions Below the Minimum Design Temperature,” ASME PVP-Vol. 288, American Society of Mechanical Engineers, New York, N.Y., pp. 297-305.
4. TWI, “Fracture -Safe Designs for Large Storage Tanks,” ed. A.A. Willoughby, The Welding Institute, 1986.

3.11 Tables and Figures

Table 3.1
Overview of Data for the Assessment of Brittle Fracture

Use this form to summarize the data obtained from a field inspection.

Equipment Identification: _____
Equipment Type: _____ Pressure Vessel _____ Storage Tank _____ Piping Component
Component Type & Location: _____
Year of Fabrication: _____

Data Required For A Level 1 Assessment (V – indicates data needed for pressure vessels, P – indicates data needed for piping, and T – indicates data needed for tankage)
Design Temperature {V,P,T}: _____
Original Hydrotest Pressure {V,P}: _____
Product Specific Gravity & Design Liquid Height {T}: _____
Temperature During Original Hydrotest Pressure {V,P,T}: _____
Nominal Wall Thickness of all components {V,P,T}: _____
Critical Exposure Temperature (CET) {V,P,T}: _____
Minimum Allowable Temperature (MAT) {V,P}: _____
$PWHT$ done at initial construction? {V,P,T}: _____
$PWHT$ after all repairs? {V,P,T}: _____

Additional Data Required For Level 2 Assessment (In Addition to the Level 1 Data):
Weld Joint Efficiency (level 2) {V,P,T} : _____
Metal Loss {V,P}: _____
Future Corrosion Allowance {V,P}: _____
Weld Joint Efficiency {V,P}: _____
Maximum Operating Pressure {V,P}: _____
Charpy Impact Data, if available {V,P,T}: _____

Table 3.2
Assignment Of Materials To The Material Temperature Exemption Curves In Figure 3.4

Curve	Material (1), (2), (6)
A	1. All carbon and all low alloy steel plates, structural shapes and bars not listed in Curves B, C, and D below. 2. SA-216 Grades WCB and WCC if normalized and tempered or water-quenched and tempered; SA -217 Grade WC6 if normalized and tempered or water-quenched and tempered 3. The following specifications for obsolete materials: A7, A10, A30, A70, A113, A149, A150 (3). 4. The following specifications for obsolete materials from the 1934 edition of the ASME Code, Section VIII: S1, S2, S25, S26, and S27 (4). 5. A201 and A212 unless it can be established that the steel was produced by a fine-grain practice (5)
B	1. SA-216 Grades WCA if normalized and tempered or water-quenched and tempered SA-216 Grades WCB and WCC for thicknesses not exceeding 2 inches if produced to a fine grain practice and water-quenched and tempered SA -217 Grade WC9 if normalized and tempered SA-285 Grades A and B SA-414 Grade A SA-442 Grade 55>1 in. if not to fine grain practice and normalized SA-442 Grade 60 if not to fine grain practice and normalized SA-515 Grades 55 and 60 SA-516 Grades 65 and 70 if not normalized SA-612 if not normalized SA-662 Grade B if not normalized 2. Except for cast steels, all materials of Curve A if produced to fine grain practice and normalized which are not listed for Curve C and D below; 3. All pipe, fittings, forgings, and tubing not listed for Curves C and D below; 4. Parts permitted from paragraph UG-11 of the ASME Code, Section VIII, Division 1, shall be included in Curve B even when fabricated from plate that otherwise would be assigned to a different curve. 5. A201 and A212 if it can be established that the steel was produced by a fine-grain practice.
C	1. SA-182 Grades 21 and 22 if normalized and tempered. SA-302 Grades C and D SA-336 Grades F21 and F22 if normalized and tempered SA-387 Grades 21 and 22 if normalized and tempered SA-442 Grades 55 < 1 in. if not to fine grain practice and normalized SA-516 Grades 55 and 60 if not normalized SA-533 Grades B and C SA-662 Grade A 2. All material of Curve B if produced to fine grain practice and normalized and not listed for Curve D below

Table 3.2
Assignment Of Materials To The Material Temperature Exemption Curves In Figure 3.4

Curve	Material (1), (2), (6)
D	SA-203 SA-442 if to fine grain practice and normalized SA-508 Class 1 SA-516 if normalized SA-524 Classes 1 and 2 SA-537 Classes 1 and 2 SA-612 if normalized SA-662 if normalized SA-738 Grade A

Notes:

1. When a material class or grade is not shown, all classes or grades are included.
2. The following apply to all material assignment notes.
   a. Cooling rates faster than those obtained in air, followed by tempering, as permitted by the material specification, are considered equivalent to normalizing and tempering heat treatments.
   b. Fine grain practice is defined as the procedures necessary to obtain a fine austenitic grain size as described in SA-20.
3. The first edition of the API Code for Unfired Pressure Vessels (discontinued in 1956) included these ASTM carbon steel plate specifications. These specifications were variously designated for structural steel for bridges, locomotives, and rail cars or for boilers and firebox steel for locomotives and stationary service. ASTM A 149 and A150 were applicable to high-tensile-strength carbon steel plates for pressure vessels.
4. The 1934 edition of Section VIII of the ASME Code listed a series of ASME steel specifications, including S1 and S2 for forge welding; S26 and S27 for carbon steel plates; and S25 for open-hearth iron. The titles of some of these specifications are similar to the ASTM specifications listed in the 1934 edition of the API Code for Unfired Pressure Vessels.
5. These two steels were replaced in strength grades by the four grades specified in ASTM A 515 and the four grades specified in ASTM A 516. Steel in accordance with ASTM A 212 was made only in strength grades the same as Grades 65 and 70 and has accounted for several known brittle failures. Steels in conformance with ASTM A 201 and A 212 should be assigned to Curve A unless it can be established that the steel was produced by fine-grain practice, which may have enhanced the toughness properties.
6. No attempt has been made to make a list of obsolete specifications for tubes, pipes, forgings, bars and castings. Unless specific information to the contrary is available, all of these product forms should be assigned to Curve A.

Table 3.3
Impact Test Exemption Temperature For Bolting Materials

Specification	Grade	Impact Test Exemption Temperature	
		(°C)	(°F)
SA-193	B5	-29	-20
SA-193	B7 $\{Dia \le 63.5\ mm\ (2.5\ in.)\}$	-46	-50
SA-193	B7 $\{Dia > 63.5\ mm\ (2.5\ in.)\}$	-40	-40
SA-193	B7M	-48	-55
SA-193	B16	-29	-20
SA-307	B	-29	-20
SA-320	L7, L7A, L7M, L43	Impact Tested per Specification	Impact Tested per Specification
SA-325	1, 2	-29	-20
SA-354	BC	-18	0
SA-354	BD	-7	+20
SA-449	---	-29	-20
SA-540	B23/24	-12	+10
SA-194	2, 2H, 2HM, 3, 4, 7, 7M, and 16	-48	-55
SA-540	B23/B24	-48	-55
Note: Bolting materials are exempt from assessment due to loading conditions.			

Table 3.4
Equations For The Curves Included In Figures 3.2, 3.4, 3.6, 3.7, 3.8, and 3.10

Figure	Equation
3.2 (Note 1)	$\Delta T_{\max} = \max\left[\frac{C_1(1-\nu)}{E\alpha}\left(1.5+\frac{3.25k}{ht}-0.5\exp\left[\frac{-16k}{ht}\right]\right),\ C_2\right]$
3.4 (Note 2)	**Curve A** $MAT = 18$ for $0 < t \le 0.394$ $MAT = \frac{-76.911+284.85t-27.560t^2}{1.0+1.7971t-0.17887t^2}$ for $0.394 < t \le 6.0$ **Curve B** $MAT = -20$ for $0 < t \le 0.394$ $MAT = \left(\begin{array}{l}-135.79+171.56t^{0.5}+103.63t- \\ 172.0t^{1.5}+73.737t^2-10.535t^{2.5}\end{array}\right)$ for $0.394 < t \le 6.0$ **Curve C** $MAT = -55$ for $0 < t \le 0.394$ $MAT = 101.29-\frac{255.50}{t}+\frac{287.86}{t^2}-\frac{196.42}{t^3}+\frac{69.457}{t^4}-\frac{9.8082}{t^5}$ for $0.394 < t \le 6.0$ **Curve D** $MAT = -55$ for $0 < t \le 0.50$ $MAT = \left(\begin{array}{l}-92.965+94.065t-39.812t^2+ \\ 9.6838t^3-1.1698t^4+0.054687t^5\end{array}\right)$ for $0.50 < t \le 6.0$
3.6 (Note 2)	$P_I = 0.5T_I$
3.7 (Note 2)	$T_R = 100.0(1.0-R_{ts})$ for $R_{ts} \ge 0.6$ (see Note 2) $T_R = \left(\begin{array}{l}-9979.57-14125.0R_{ts}^{1.5}+ \\ 9088.11\exp[R_{ts}]-17.3893\frac{\ln[R_{ts}]}{R_{ts}^2}\end{array}\right)$ for $0.6 > R_{ts} > 0.3$ (see Note 2) $T_R = 105.0$ to 275 for $R_{ts} \le 0.40$ (see Note 2 in Figure 3.6) $T_R = 140.0$ to 275 for $R_{ts} \le 0.35$ (see Note 3 in Figure 3.6) $T_R = 200.0$ to 275 for $R_{ts} \le 0.30$ (see Note 4 in Figure 3.6)

Table 3.4
Equations For The Curves Included In Figures 3.2, 3.4, 3.6, 3.7, 3.8, and 3.10

Figure	Equation
3.8 (Note 2)	$T_{RH} = 52.1971 - 53.3079H_R - 15.7024H_R^2 + \frac{16.7548}{H_R}$ for $H_r > 0.25$ $T_{RH} = 105 \; to \; 275.0$ for $H_R \le 0.25$
3.10 (Note 2)	$T_S = 30$ for $0 < t \le 0.50$ $T_S = 191.03 - 0.48321t^2 - \frac{133.75}{t^{0.5}} + \frac{10.775}{t^{1.5}}$ for $0.50 < t < 0.875$ $T_S = 60$ for $0.875 \le t \le 2.0$

Notes:

1. The SI and US Customary Units for this equation are shown below. Note that the screening curve was developed based on: $K = 2.3 \; BTU/hr - in - F$, $E_y = 29.3E6 \; psi$, and $\alpha = 6.13E-6 \; in/in - F$.

$\Delta T_{\max}$	Temperature difference between the liquid and metal temperatures, °C, °F
C_1	55.2 MPa for SI Units, 8000 psi for US Customary Units
C_2	55.6°C for SI Units, 100°F for US Customary Units
E	Elastic modulus, MPa, psi
α	Coefficient of thermal expansion, mm/mm-°C, in/in-°F
k	Thermal conductivity of the metal, J/s-m-°C, BTU/hr-in-°F
h	Convective heat transfer coefficient, J/s-m2-°C, BTU/hr-in2-°F
t	Component Thickness, mm, in
ν	Poisson's ratio

2. The equations are based on the US Customary units shown below. When working in the SI system of units, the SI units used for input to the equations should be converted to US Customary units to at least four significant figures. Similarly, the US Customary output should be converted back to the SI system.

MAT	Minimum Allowable Temperature in degrees Fahrenheit.
P_I	per cent increase in pressure above the initial point.
T_I	increase in temperature above the initial point in degrees Fahrenheit.
T_R	reduction in MAT based on available excess thickness in degrees Fahrenheit.
T_{RH}	reduction in MAT based on the operating-to-hydrotest ratio in degrees Fahrenheit.
T_S	component metal temperature is in degrees Fahrenheit.
t	component thickness in inches.

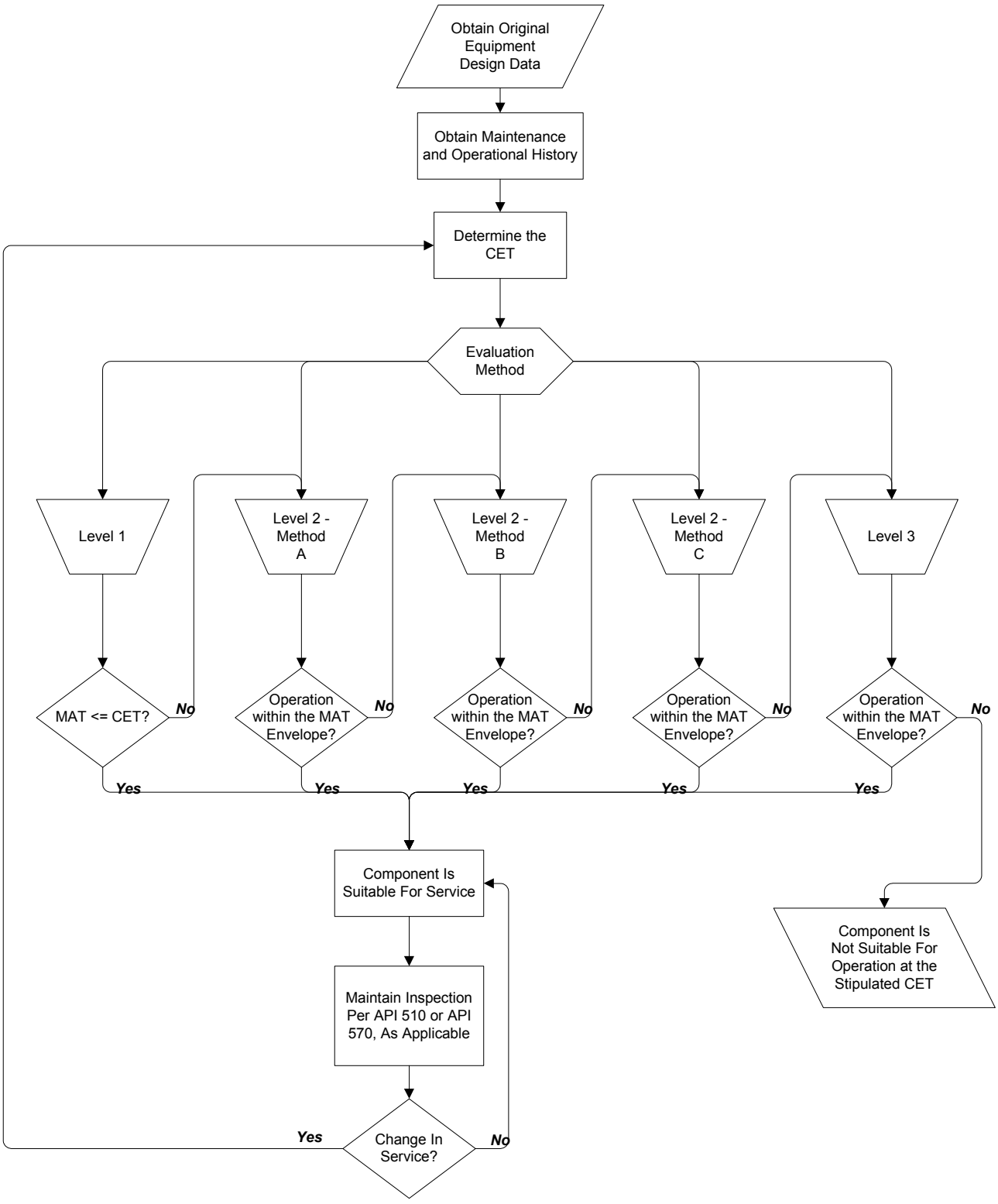

Figure 3.1 – Overall Brittle Fracture Assessment Procedure for Pressure Vessels and Piping

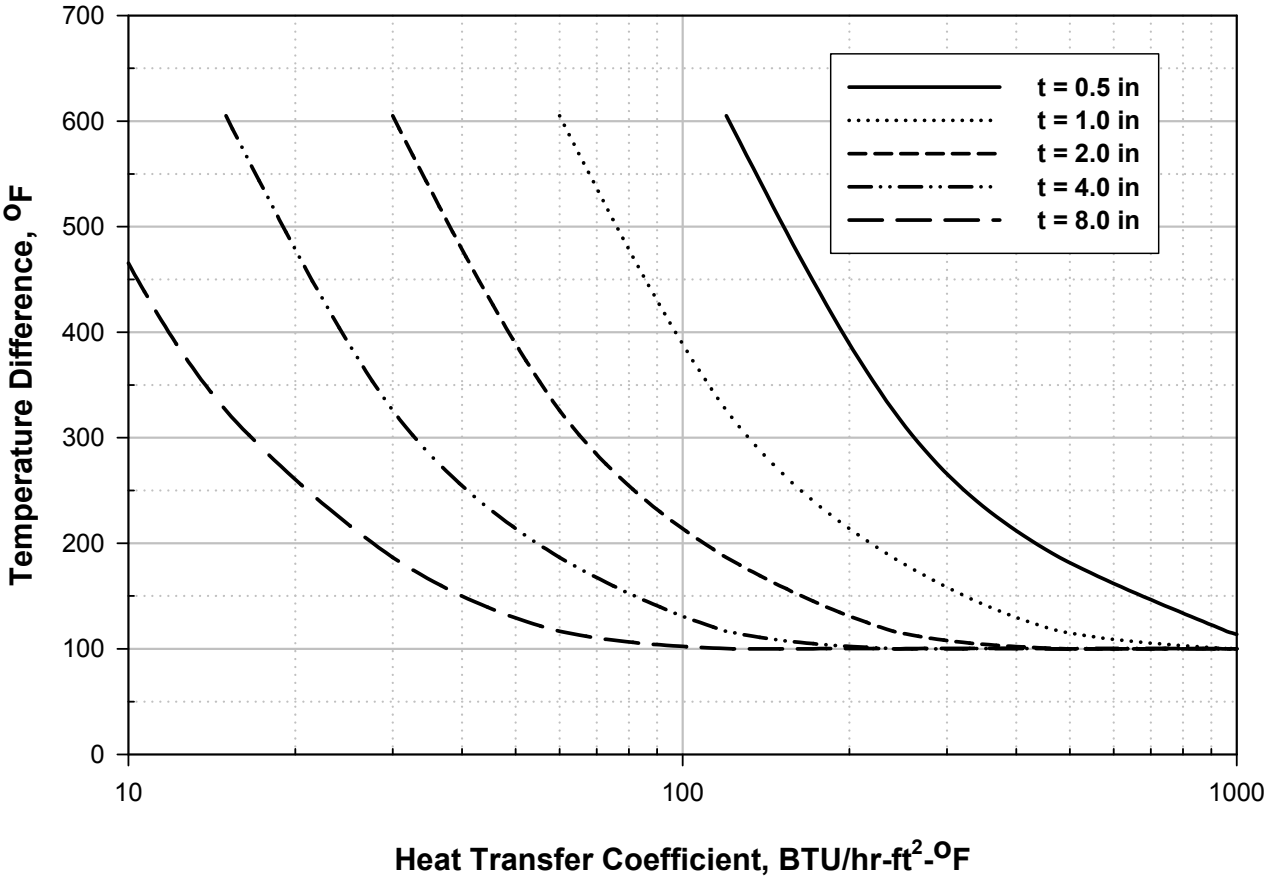

Note: The equations for these curves in this figure are provided in Table 3.4

Figure 3.2 – Definition of Shock Chilling for Carbon and Low Alloy Steels
Conditions Above and to the Right of the Line are Considered to be Shock Chilling

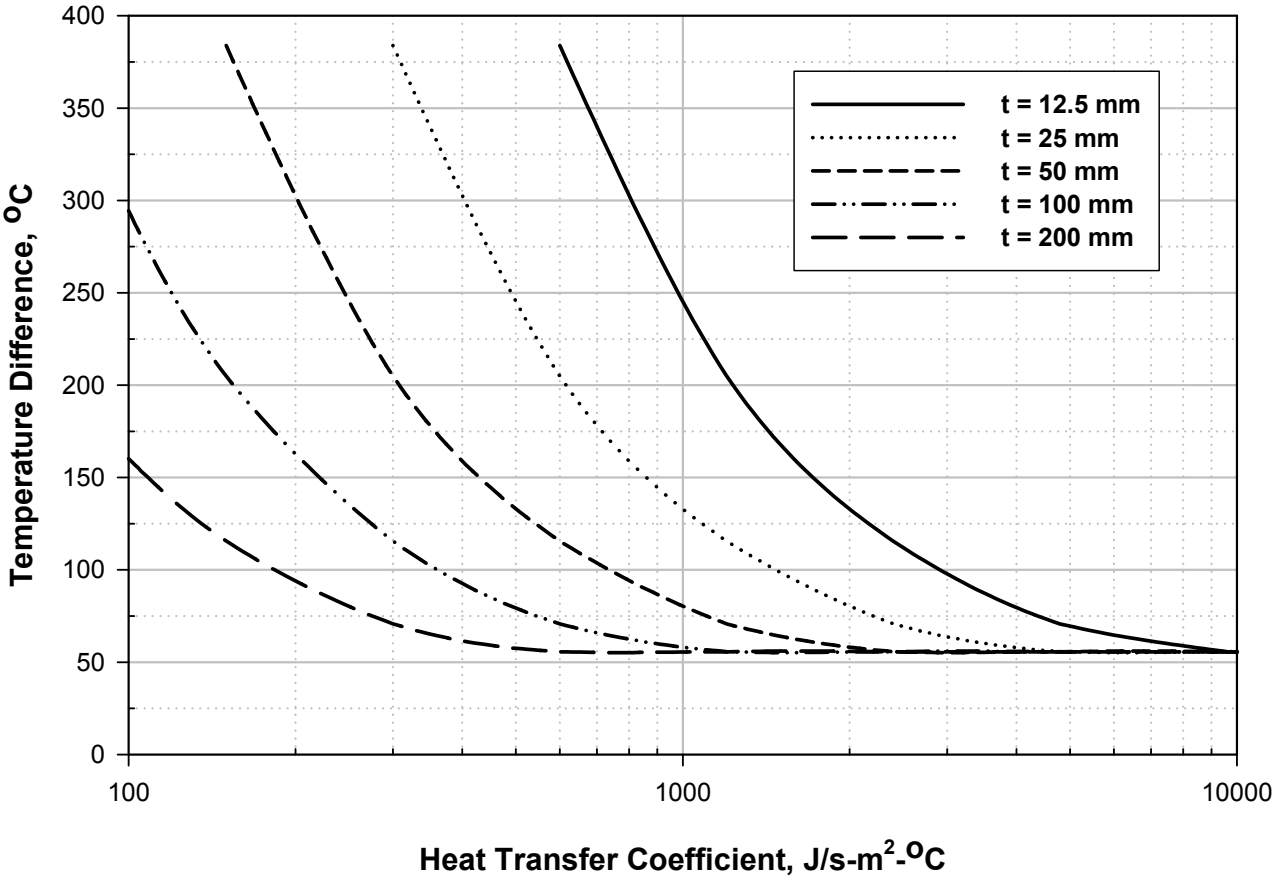

Note: The equations for these curves in this figure are provided in Table 3.4

Figure 3.2M – Definition of Shock Chilling for Carbon and Low Alloy Steels
Conditions Above and to the Right of the Line are Considered to be Shock Chilling

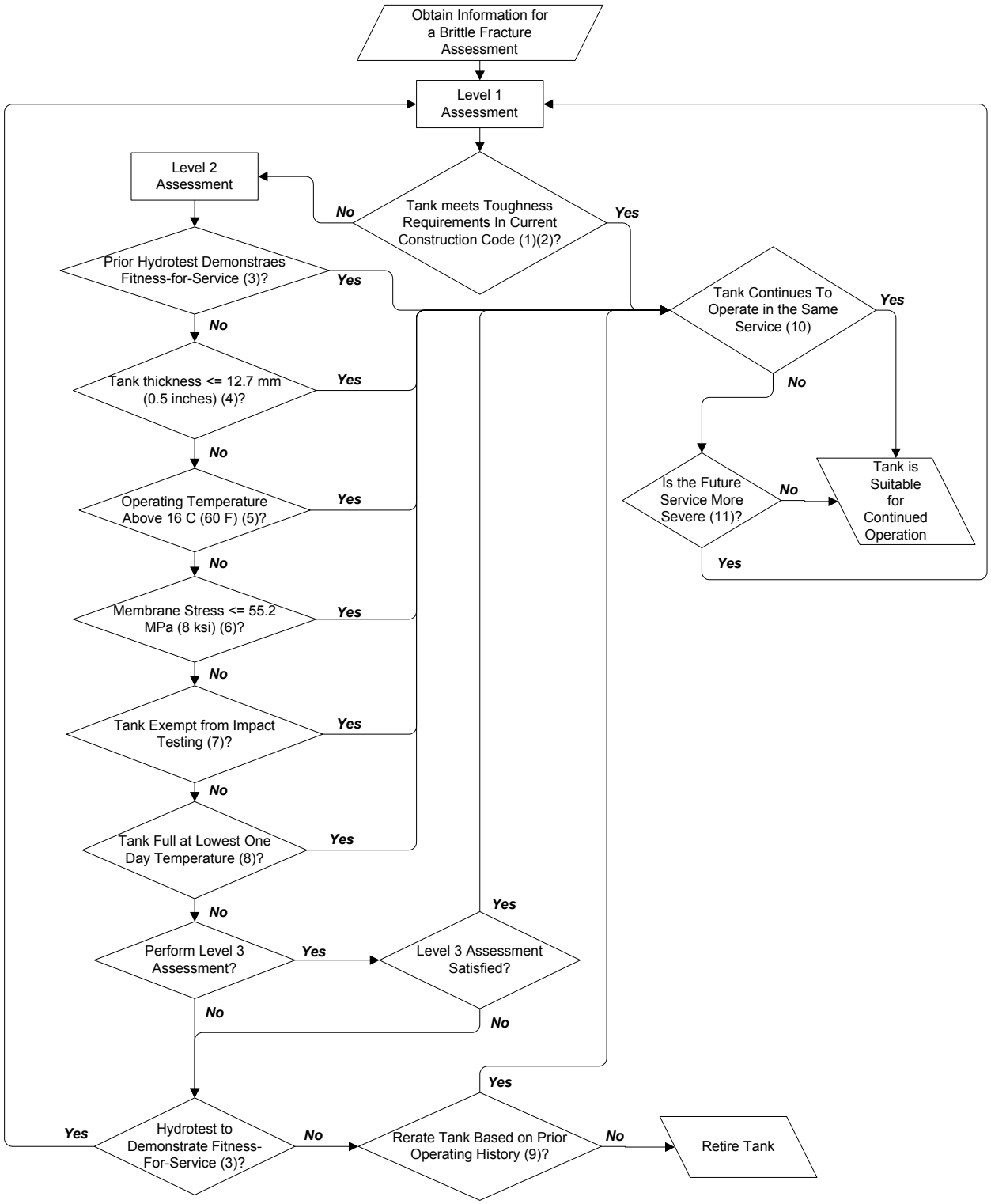

Figure 3.3 – Brittle Fracture Assessment Procedure for Storage Tanks

Footnotes for Figure 3.3

The assessment procedure as illustrated in Figure 3.3 shall be used for Level 1 and Level 2 assessment of aboveground atmospheric storage tanks in petroleum and chemical services. Each of the key steps on the decision tree is numbered corresponding to the explanation provided as follows:

1. Atmospheric storage tanks constructed in accordance with API Standard 650 (seventh edition or later) include requirements to minimize the probability of failure due to brittle fracture. Tanks constructed to earlier version of this Standard may also be shown to meet the API 650 (seventh edition or later) toughness requirements by impact testing coupon samples from a representative number of shell plates.
2. Many tanks continue to operate successfully in the same service that were not constructed to the requirements of API Standard 650 (seventh edition or later). These tanks are potentially susceptible to failure due to brittle fracture and require a Level 2 Assessment.
3. For purposes of this assessment, hydrostatic testing demonstrates that an aboveground atmospheric storage tank in a petroleum or chemical service is fit for continued service and at minimal probability of failure due to brittle fracture, provided that all governing requirements for repair, alterations, reconstruction, or change in service are in accordance with API Standard 653 (including a need for hydrostatic testing after major repairs, modifications or reconstruction). The effectiveness of the hydrostatic test in demonstrating fitness for continued service is shown by industry experience.
4. If a tank shell thickness is no greater than 12.7 mm (0.5 inches), the probability of failure due to brittle fracture is minimal, provided that an evaluation for suitability of service per API 653, Section 2 has been performed. The original nominal thickness for the thickest tank shell plate shall be used for this assessment.
5. No known tank failures due to brittle fracture have occurred at shell metal temperatures of 16°C (60°F) or above. Similar assurance against brittle fracture can be gained by increasing the metal temperature by heating the tank contents.
6. Industry experience and laboratory tests have shown that a membrane stress in tank shell plates of at least 55.2 MPa (8 ksi) is required to cause failure due to brittle fracture.
7. Tanks constructed from steel listed in Figure 2-1 of API Standard 650 can be used in accordance with their exemption curves, provided that an evaluation for suitability of service per Section 2 of API Standard 653 has been performed. Tanks fabricated from steels of unknown toughness thicker than 12.7 mm (0.5 inches) and operating at a shell metal temperature below 16°C (60°F) can be used if the tank meets the requirements of Figure 3.10. The original nominal thickness for the thickest tank shell plate shall be used for the assessment. For unheated tanks, the shell metal temperature shall be the design metal temperature as defined in 2.2.9.3 of API Standard 650.
8. The probability of failure due to brittle fracture is minimal once a tank has demonstrated that it can operate at a specified maximum liquid level at the lowest expected temperature without failing unless repairs or alterations have been made. For the purpose of this assessment, the lowest expected temperature is defined as the lowest one day mean temperature as shown in Figure 2-2 of API Standard 650 for the continental United States. It is necessary to check tank log records and meteorological records to ensure that the tank has operated at the specified maximum liquid level when the one-day mean temperature was as low as shown in Figure 2-2 of API Standard 650.
9. An evaluation can be performed to establish a safe operating envelope for a tank based on the past operating history. This evaluation shall be based on the most severe combination of temperature and liquid level experienced by the tank during its life. The evaluation may show that the tank needs to be rerated or operated differently. Several options exist such as: restrict the liquid level, restrict the minimum metal temperature, change the service to a stored product with a lower specific gravity, or combinations of these options.
10. An assessment shall be made to determine if the change in service increases the probability of failure due to brittle fracture. The service can be considered more severe and creating a greater probability of brittle fracture if the service temperature is reduced (for example, changing from heated oil service to ambient temperature product), or the product is changed to one with a greater specific gravity and thus increasing stresses.
11. A change in service must be evaluated to determine if it increases the probability of failure due to brittle fracture. In the event of a change to a more severe service (such as operating at a lower temperature or handling product at a higher specific gravity) it is necessary to consider the future service conditions in the Fitness-For-Service assessment.

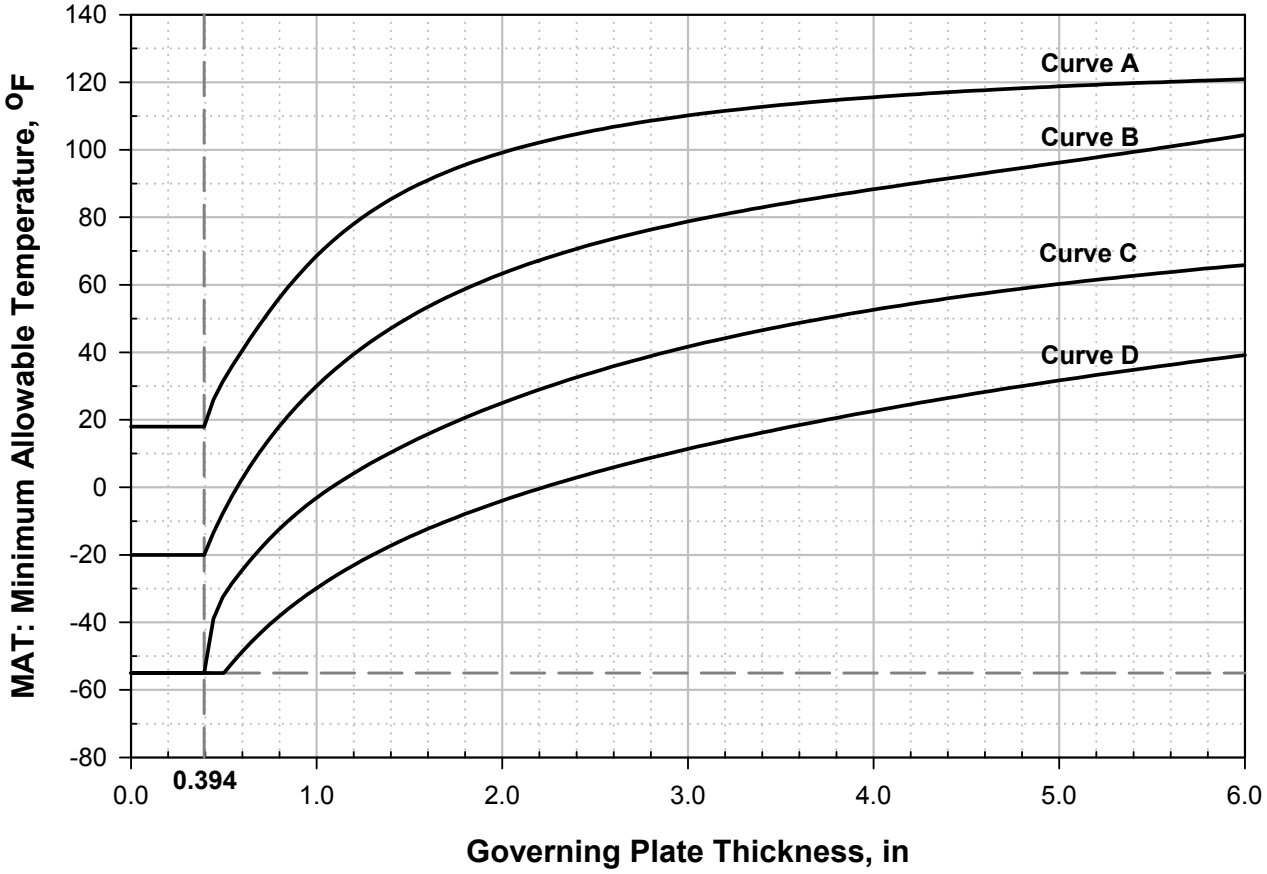

Notes:

1. Curves A through D define material specification classes in accordance with Tables 3.2.
2. This figure is from the ASME Code Section VIII, Division 1, paragraph UCS-66.
3. Curve A intersects the MAT -axis at $18^o F$, Curve B intersects the MAT -axis at $-20^o F$, and Curves C and D intersect the MAT -axis at $-55^o F$.
4. These curves can also be used to evaluate piping components. In this case, Curve B should be shifted to the right so that 0.5 in. corresponds to a temperature of $-20^o F$. To account for this shift in an assessment, an effective governing thickness equal to the actual governing thickness minus 0.106 in. can be used to determine the MAT .
5. The equations for the curves in this figure are provided in Table 3.4.

Figure 3.4 – Minimum Allowable Metal Temperature

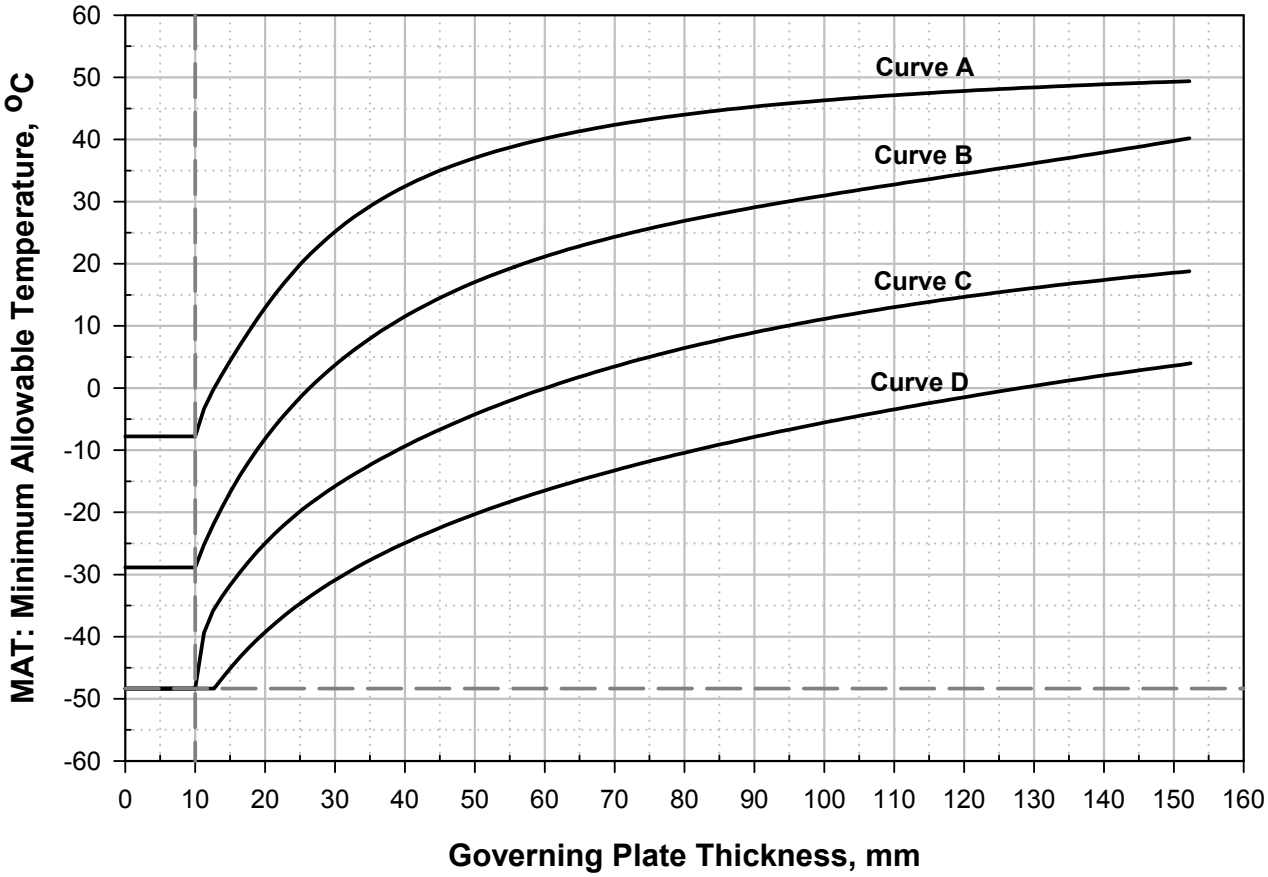

Notes:

1. Curves A through D define material specification classes in accordance with Tables 3.2.
2. This figure is from the ASME Code Section VIII, Division 1, paragraph UCS-66.
3. Curve A intersects the MAT -axis at $-8^{o}C$, Curve B intersects the MAT -axis at $-29^{o}C$, and Curves C and D intersect the MAT -axis at $-48^{o}C$.
4. These curves can also be used to evaluate piping components. In this case, Curve B should be shifted to the right so that 12.7 mm corresponds to a temperature of $-29^{o}C$. To account for this shift in an assessment, an effective governing thickness equal to the actual governing thickness minus 2.69 mm can be used to determine the MAT.
5. The equations for the curves in this figure are provided in Table 3.4.

Figure 3.4M – Minimum Allowable Metal Temperature

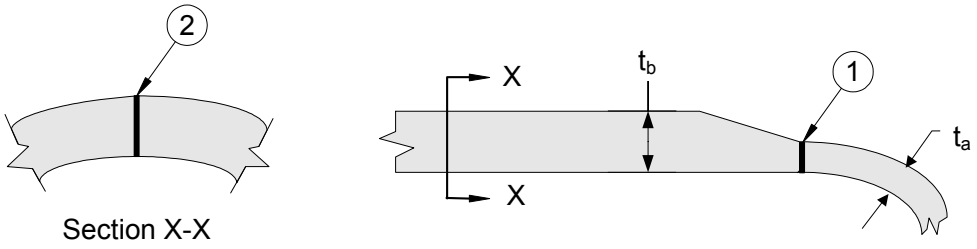

$t_{g1}=t_a$

$t_{g2}=t_a$ (seamless) or t_b (welded)

(a) Butt Welded Components

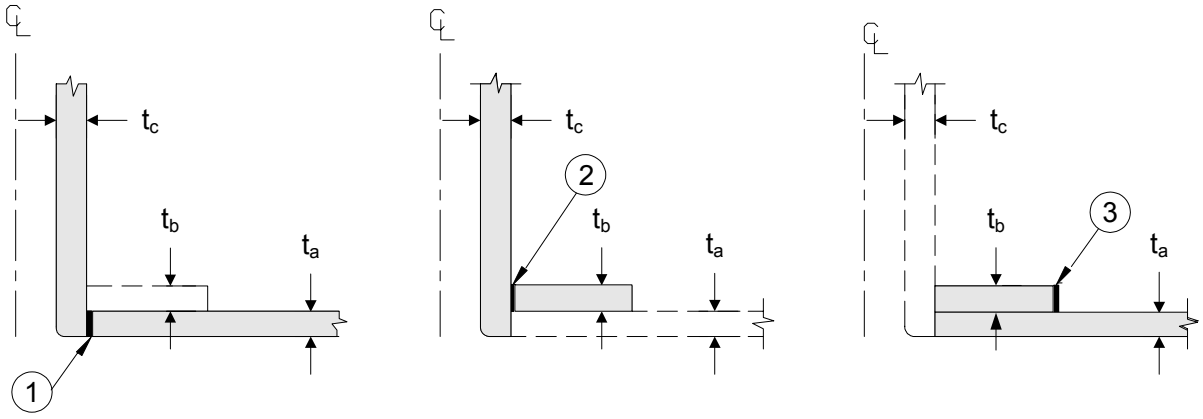

t_{g1}= min (t_b, t_c)

t_{g2}= min (t_b, t_c)

t_{g3}=min (t_a, t_b)

(b) Welded Connection with or without a Reinforcing Plate

Figure 3.5 – Some Typical Vessel Details Showing the Governing Thickness

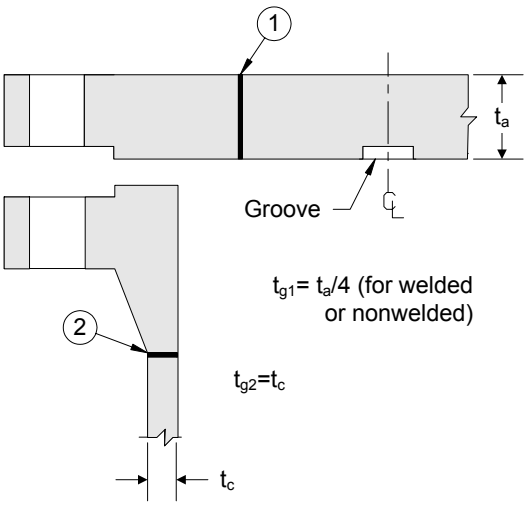

(c) Bolted Flat Head or Tubesheet and Flange

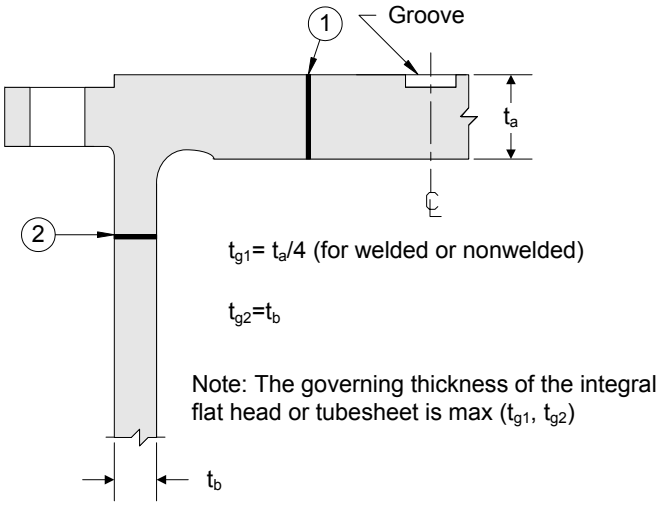

(d) Integral Flat Head or Tubesheet

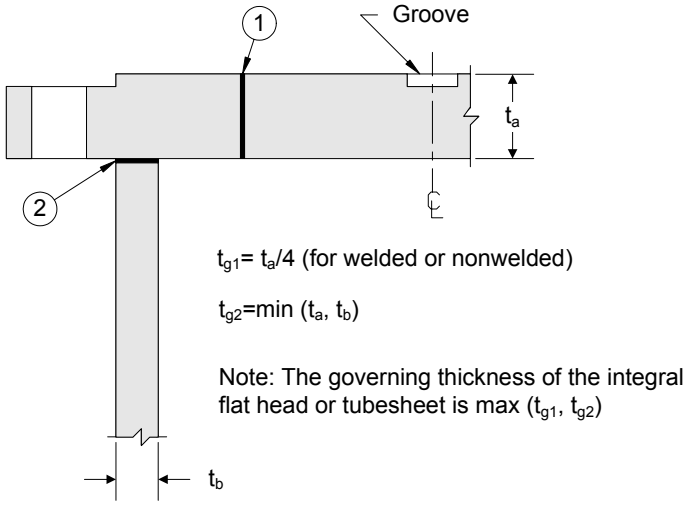

(e) Flat Head or Tubesheet with a Corner Joint

Figure 3.5 – Some Typical Vessel Details Showing the Governing Thickness

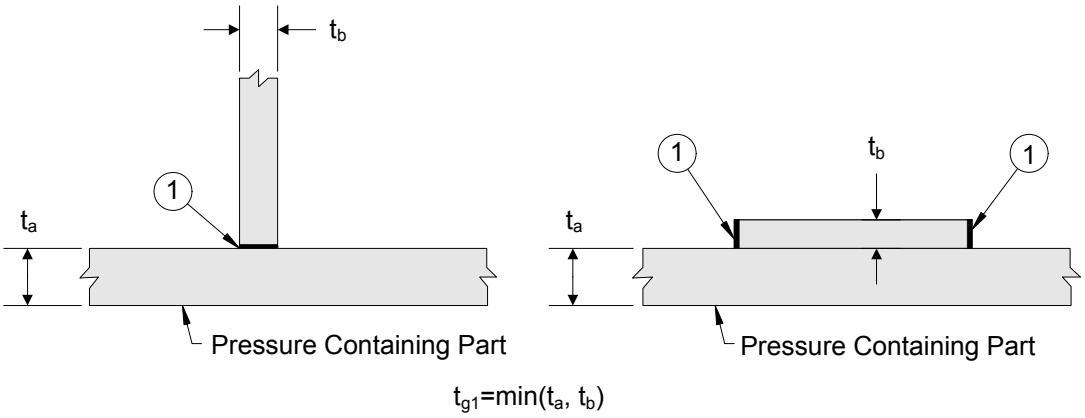

(f) Welded Attachments

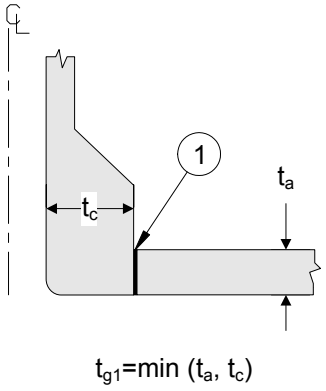

(g) Integrally Reinforced Welded Connection

Notes:

1. In general, the governing thickness is the thinner of the two parts at the welded joint.
2. In Details Figure 3.5(a) to (g), t_{gi}, governing thickness at weld joint i.
3. The MAT of a component is evaluated at each governing thickness, t_{gi}, as applicable.

Figure 3.5 – Some Typical Vessel Details Showing the Governing Thickness

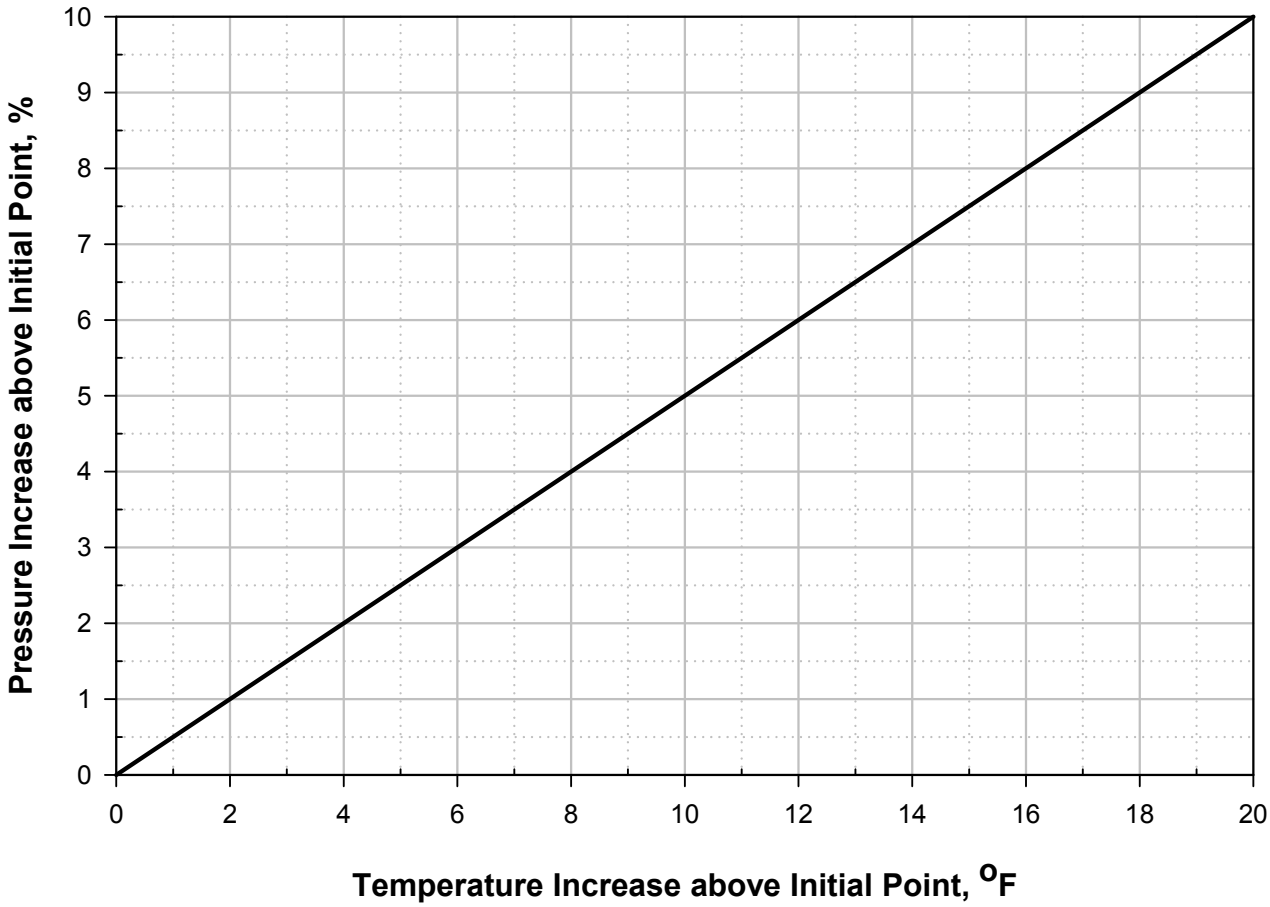

Note: The equation for the curve in this figure is provided in Table 3.4

Figure 3.6 – Pressure-Temperature Curve

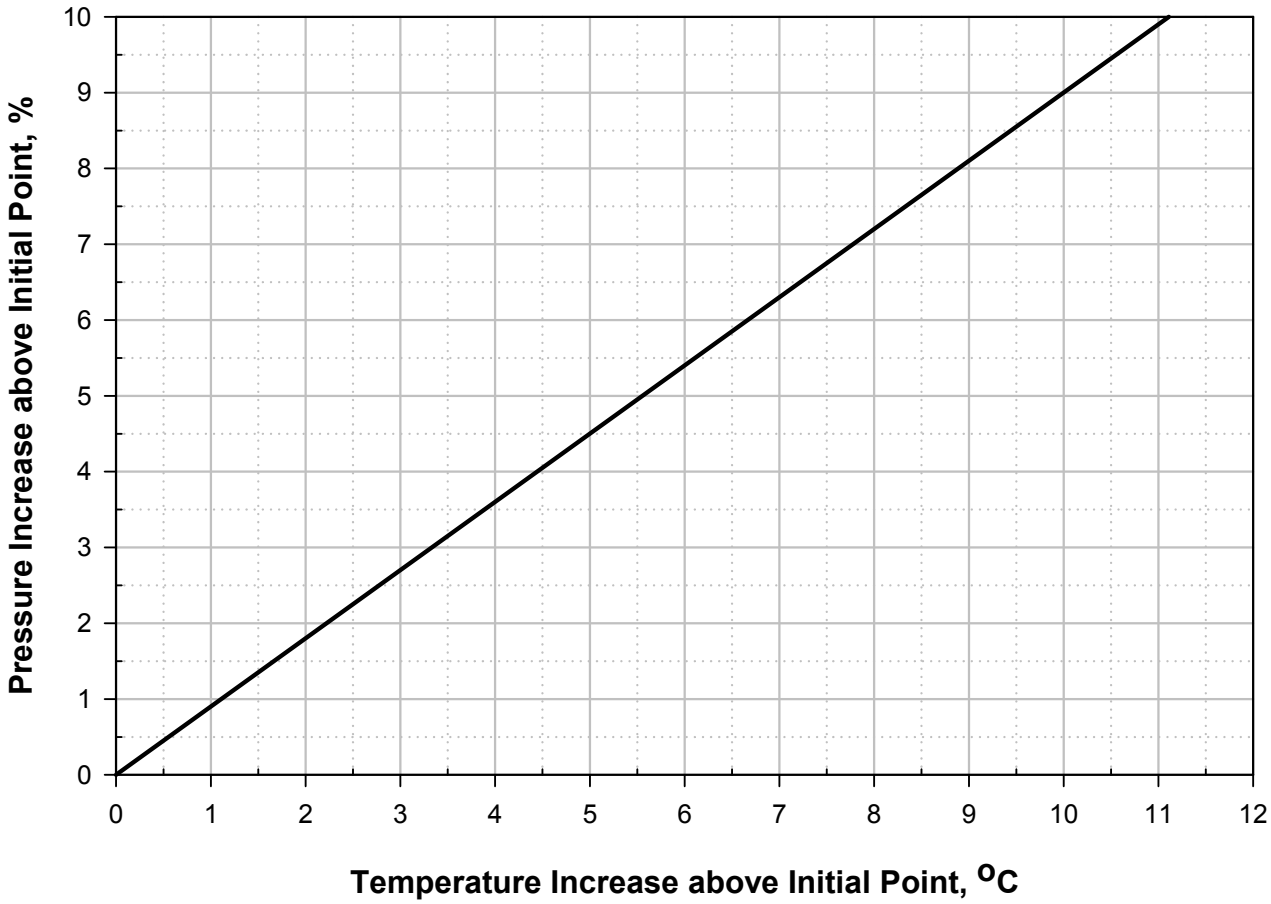

Note: The equation for the curve in this figure is provided in Table 3.4

Figure 3.6M – Pressure-Temperature Curve

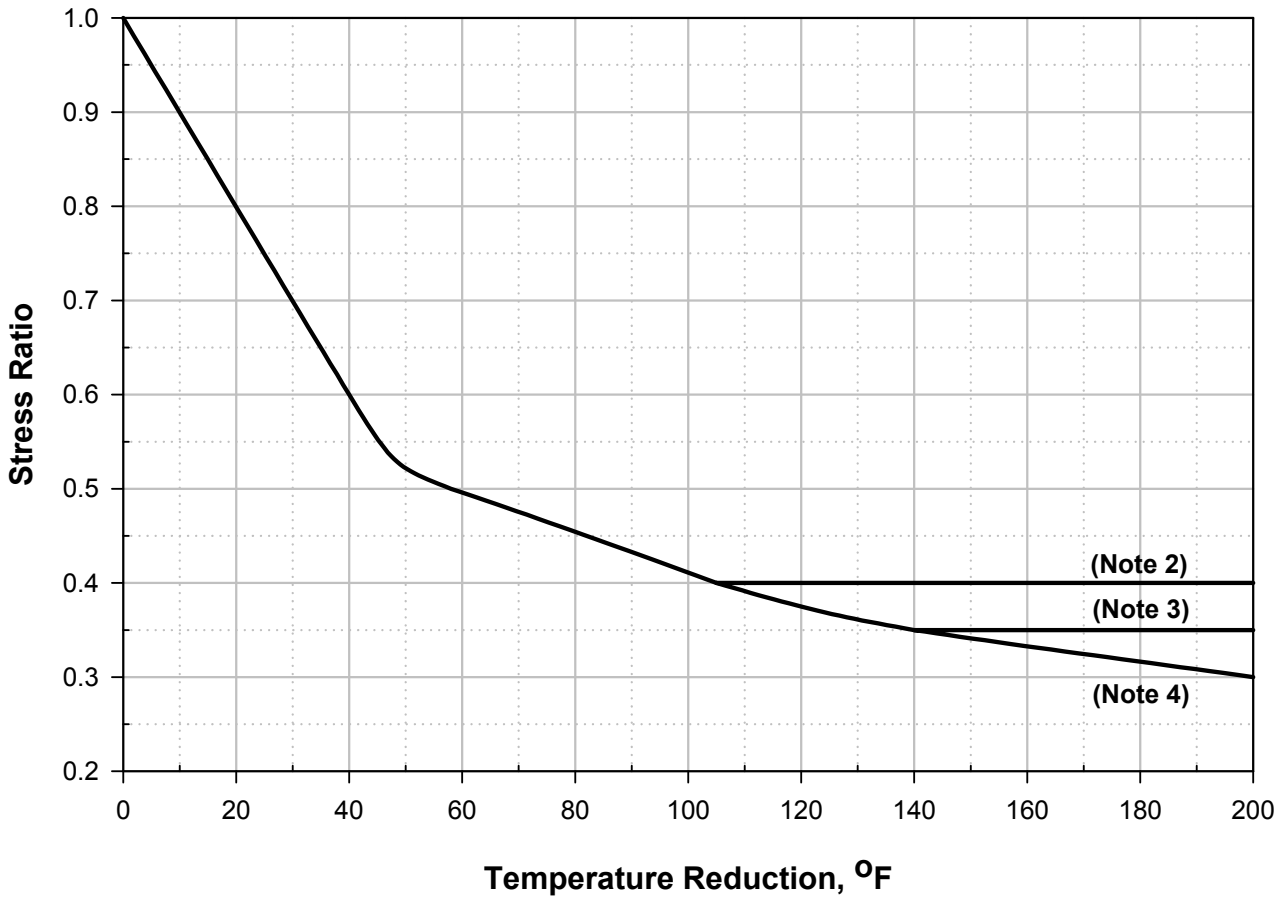

Notes:

1. A definition of the parameters used in this curve is provided in paragraph 3.9.
2. Use this curve for components with a design allowable stress at room temperature less than or equal to 17.5 ksi. This curve can be used for vessels constructed to all Editions and Addenda prior to 1999 of the ASME Code, Section VIII, Division 1; and piping constructed to all Editions and Addenda prior to 2002 of ASME B31.1. The threshold value for this curve is 0.40.
3. Use this curve for components with a design allowable stress at room temperature less than or equal to 20 ksi but greater than 17.5 ksi. This curve can be used for vessels constructed to the 1999 Addenda and later Editions and Addenda of the ASME Code, Section VIII, Division 1; and piping constructed to the 2002 Addenda and later Editions and Addenda of ASME B31.1. The threshold value for this curve is 0.35.
4. Use this curve for components with a design allowable stress at room temperature less than or equal to 25 ksi but greater than 20 ksi. This curve can be used for vessels designed and constructed to the ASME Code, Section VIII, Division 2, and piping designed to ASME B31.3. The threshold value for this curve is 0.30.
5. The equations for the curves in this figure are provided in Table 3.4.

Figure 3.7 – Reduction in the MAT Based On Available Excess Thickness for Carbon and Low Alloy Steel Components

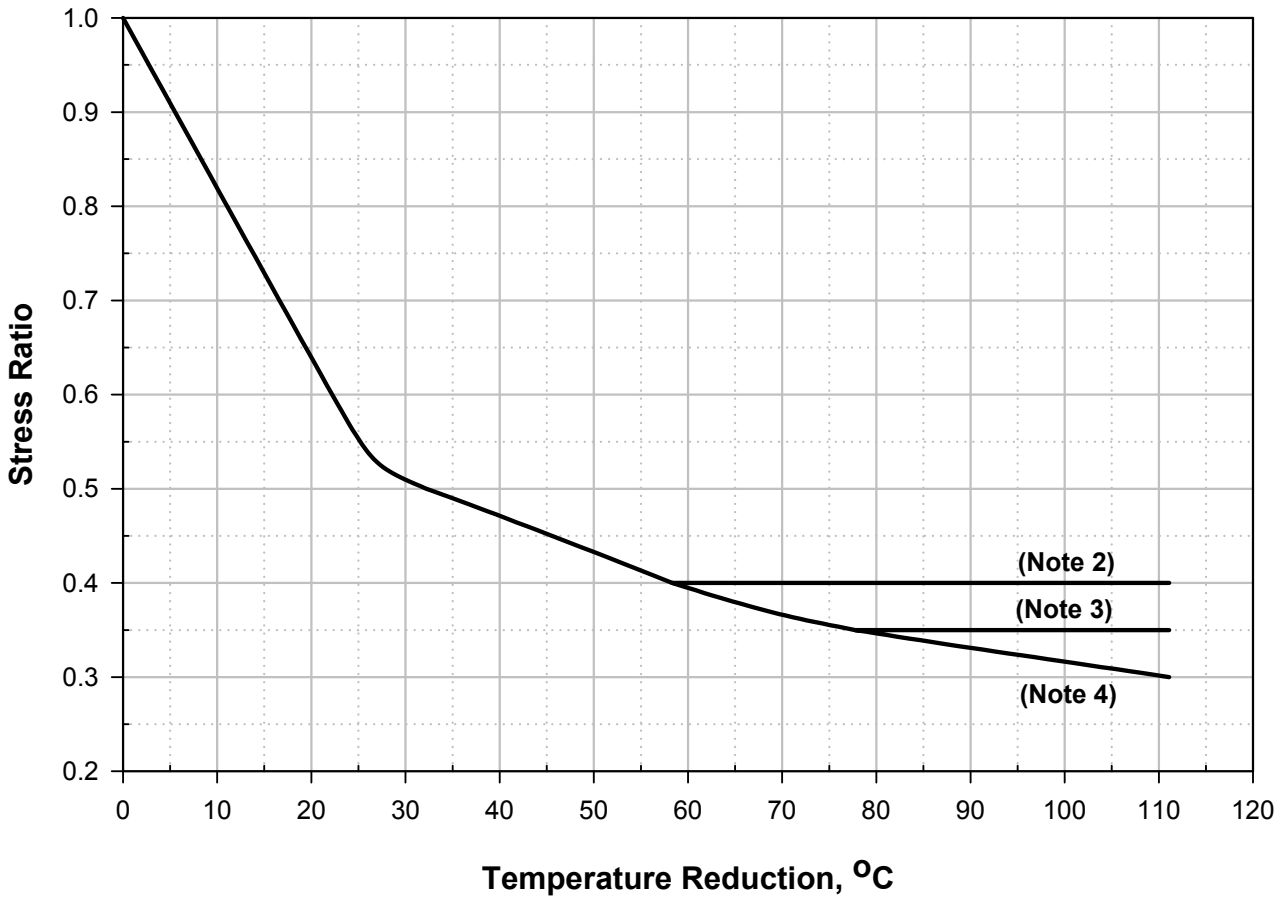

Notes:

6. A definition of the parameters used in this curve is provided in paragraph 3.9.
7. Use this curve for components with a design allowable stress at room temperature less than or equal to 120.8 MPa. This curve can be used for vessels constructed to all Editions and Addenda prior to 1999 of the ASME Code, Section VIII, Division 1; and piping constructed to all Editions and Addenda prior to 2002 of ASME B31.1. The threshold value for this curve is 0.40.
8. Use this curve for components with a design allowable stress at room temperature less than or equal to 137.8 MPa but greater than 120.8 MPa. This curve can be used for vessels constructed to the 1999 Addenda and later Editions and Addenda of the ASME Code, Section VIII, Division 1; and piping constructed to the 2002 Addenda and later Editions and Addenda of ASME B31.1. The threshold value for this curve is 0.35.
9. Use this curve for components with a design allowable stress at room temperature less than or equal to 172.5 MPa but greater than 137.8 MPa . This curve can be used for vessels designed and constructed to the ASME Code, Section VIII, Division 2, and piping designed to ASME B31.3. The threshold value for this curve is 0.30.
10. The equations for the curves in this figure are provided in Table 3.4.

Figure 3.7M – Reduction in the MAT Based On Available Excess Thickness for Carbon and Low Alloy Steel Components

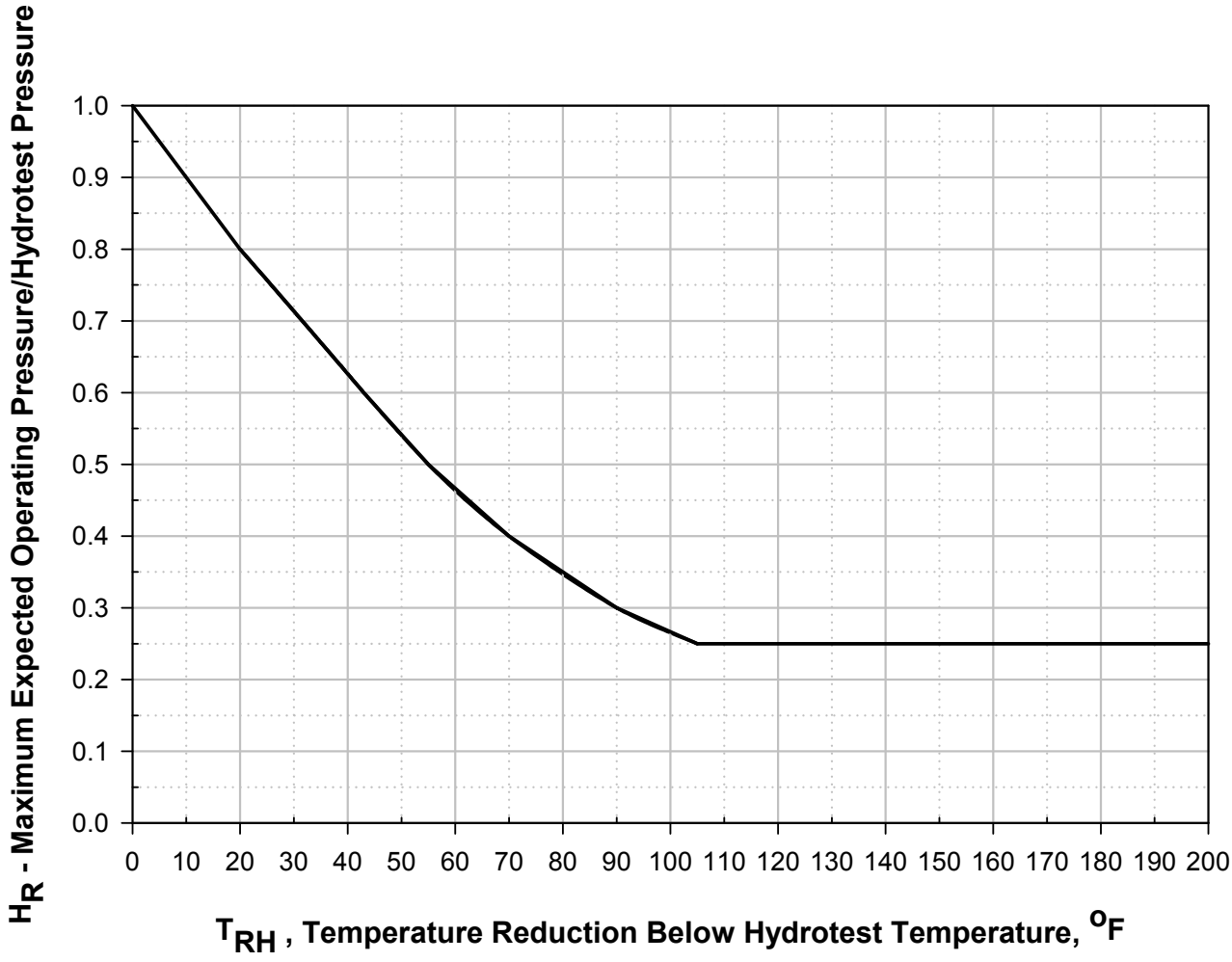

Note: The equations for the curve in this figure are provided in Table 3.4

Figure 3.8 – Allowable Reduction in the MAT Based On Hydrostatic Proof Testing

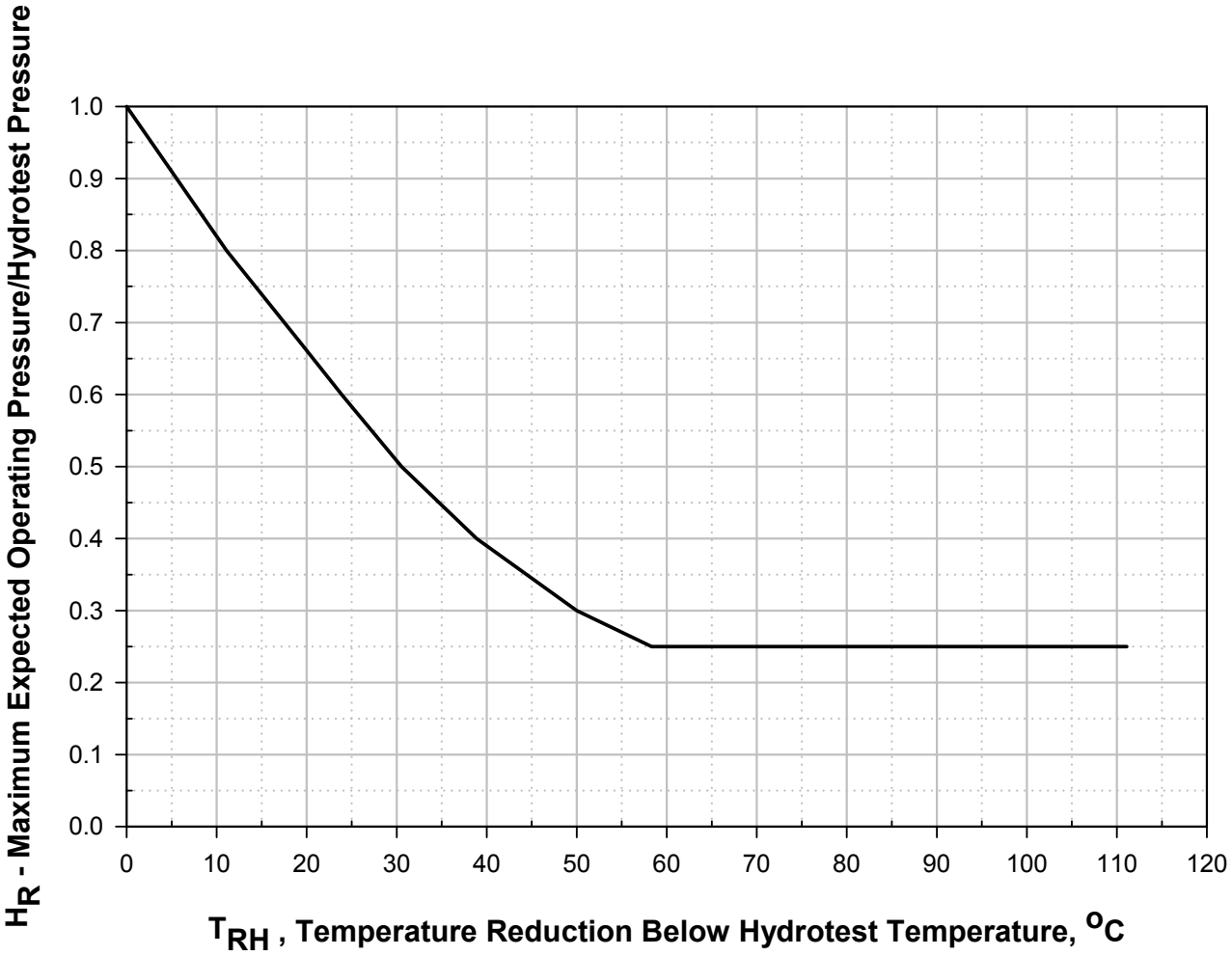

Note: The equation for the curves in this figure are provided in Table 3.4

Figure 3.8M – Allowable Reduction in the MAT Based On Hydrostatic Proof Testing

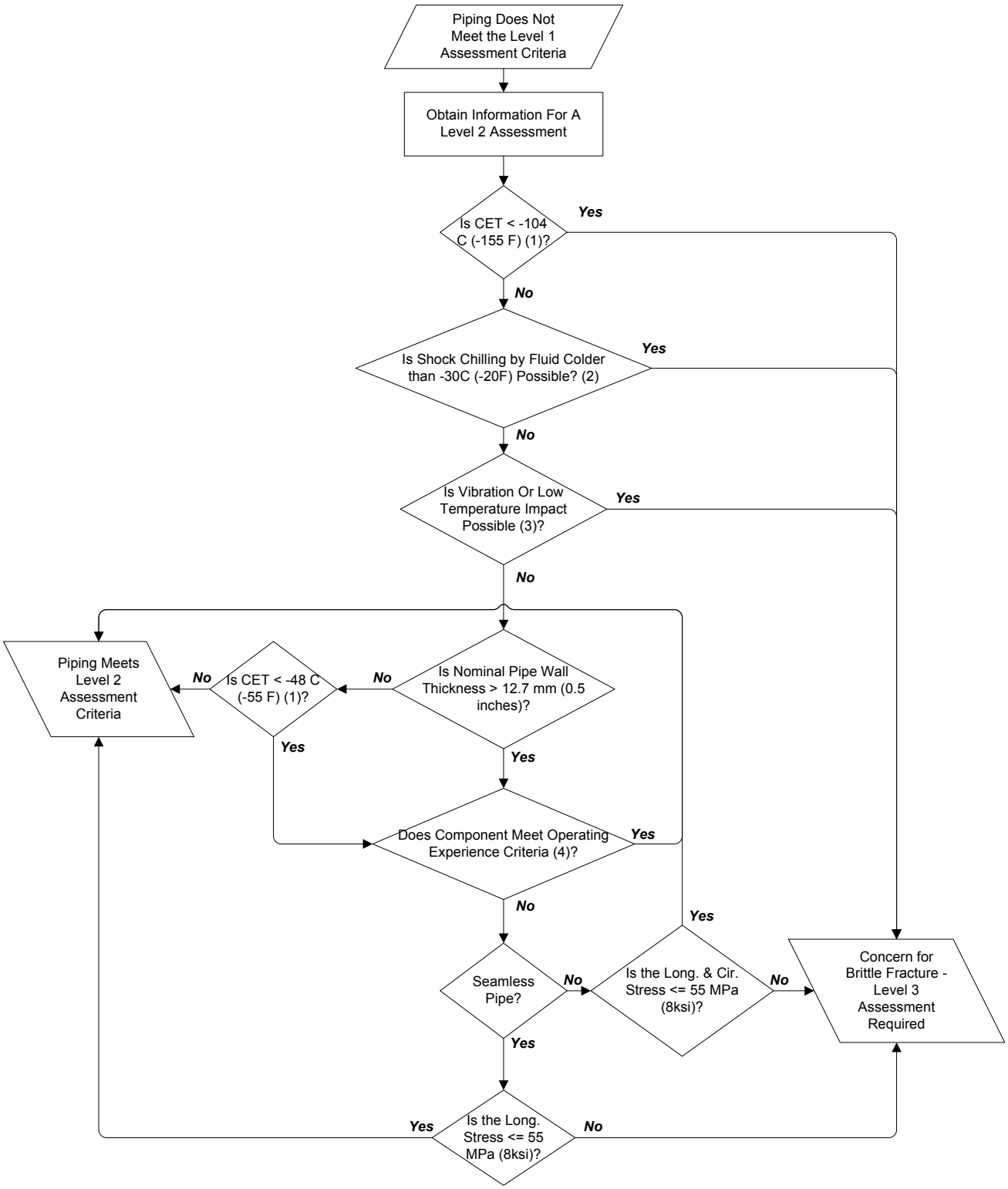

Figure 3.9 – Level 2 Method C Assessment for Carbon Steel Piping

Footnotes for Figure 3.9

1) Experience suggests that brittle fracture of piping is usually associated with unanticipated low temperature excursions.

2) See definition of shock chilling in paragraph 3.3.3 e.

3) Vibrations in a portion of the piping system could initiate cracks that are cause for a high level of concern of brittle fracture. If the system could be subject to cyclic operating or impact load while it is operating below -29°C (-20°F), then an assessment should be made to determine whether the resulting cyclic stresses could result in the initiation and propagation of a crack. If crack initiation and/or propagation are determined to be possible, then a Level 3 Assessment is required. Impact loads include hammering from flow or aggressive repeated strikes from tools or mobile equipment, etc. Minor impact loads from hand tools other than deliberate hammering are not generally a cause for concern.

4) Acceptance based on successful operating experience is based on the following:

   i) The nominal operating conditions have been essentially the same and consistent for a significant period of time and more severe conditions (i.e., lower temperature and/or higher pressure or stress) are not expected in the future. In addition, the maximum design temperature and pressure have not been exceeded for a significant period of time. Note that safety valve discharge lines usually do not meet this criterion, see Note 2.

   ii) The piping is not in a stress corrosion cracking environment such as non-$PWHT$ piping in DEA, MEA, NaOH, or KOH. This restriction does not apply to seamless pipe in wet H_2S service or seamless and welded pipe in anhydrous ammonia service unless there are clear indications of cracking in the piping.

   iii) The piping system is in good condition as determined by an inspection using API 570 or other applicable inspection code or standard.

   iv) The piping system has adequate flexibility by virtue of layout, freedom for thermal growth, and the supports as determined by visual inspection are in good condition.

5) Guidelines for stress calculations are as follows:

   i) The circumferential stress should be calculated based on the nominal wall thickness minus the metal loss, future corrosion allowance, mechanical allowances, and the manufacturing mill tolerance.

   ii) The longitudinal stress should be calculated based on the combined stress resulting from pressure, dead weight, and displacement strain. In calculating the longitudinal stress, the forces and moments in the piping system should be determined using section properties based on the nominal dimensions adjusted for metal loss and future corrosion allowance, and the stress should be calculated using section properties based on the nominal dimensions minus the metal loss, future corrosion allowance, and mechanical allowances. Stress intensification factors associated with pipe bends, elbows, tees, etc., do not need to be included in the longitudinal stress calculation. The thermal stress does not have to consider a full design range, such as would result from a system with a high design temperature. It should best reflect the actual stress imposed at low temperature.

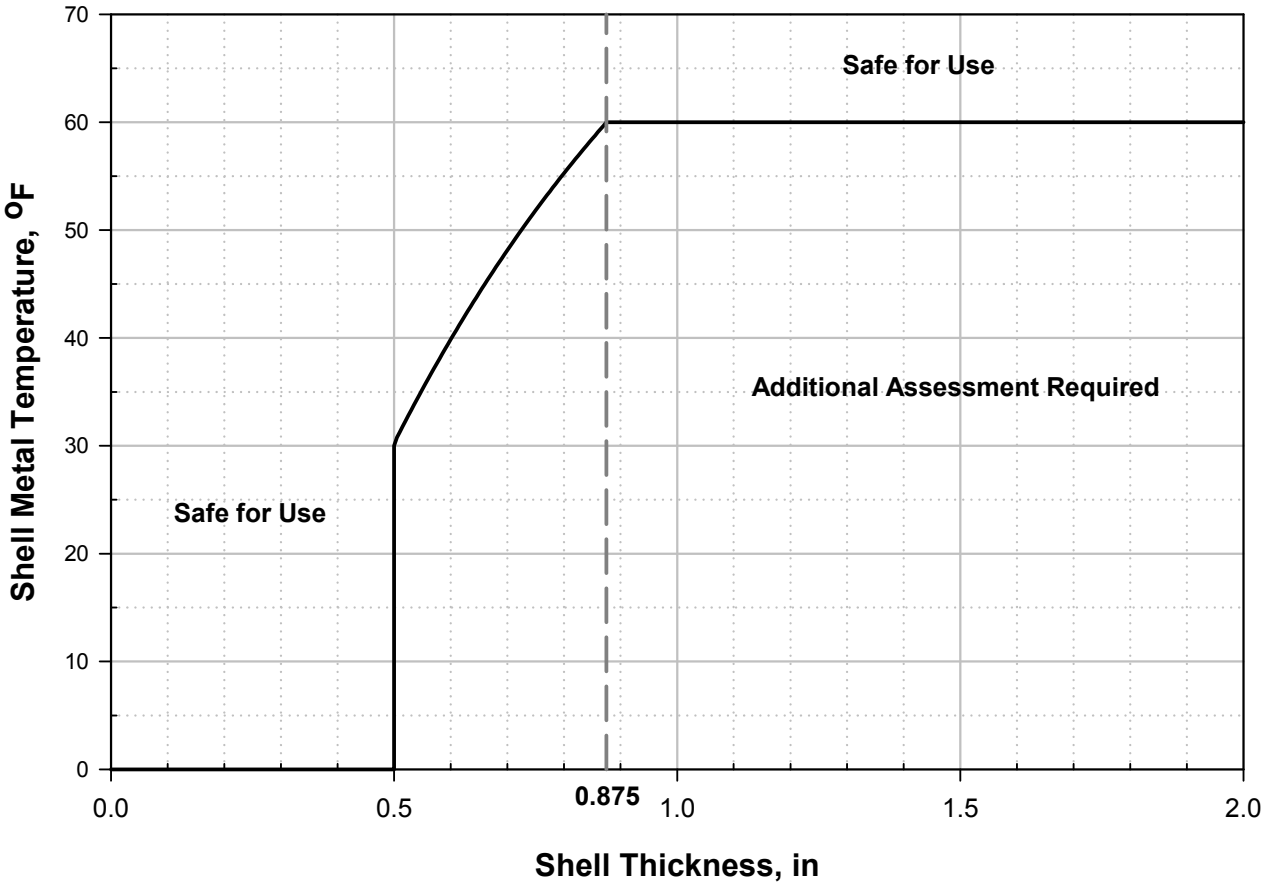

Note: The above exemption curve between 30°F and 60°F is based on Curve A in Figure 3.4. The other parts of the curve were established based on successful operating experience. The equations for the curve in this figure are provided in Table 3.4.

Figure 3.10 – Exemption Curve for Tanks Constructed From Carbon Steel of Unknown Toughness Thicker Than 1/2 inch And Operating at A Shell Metal Temperature Below 60°F

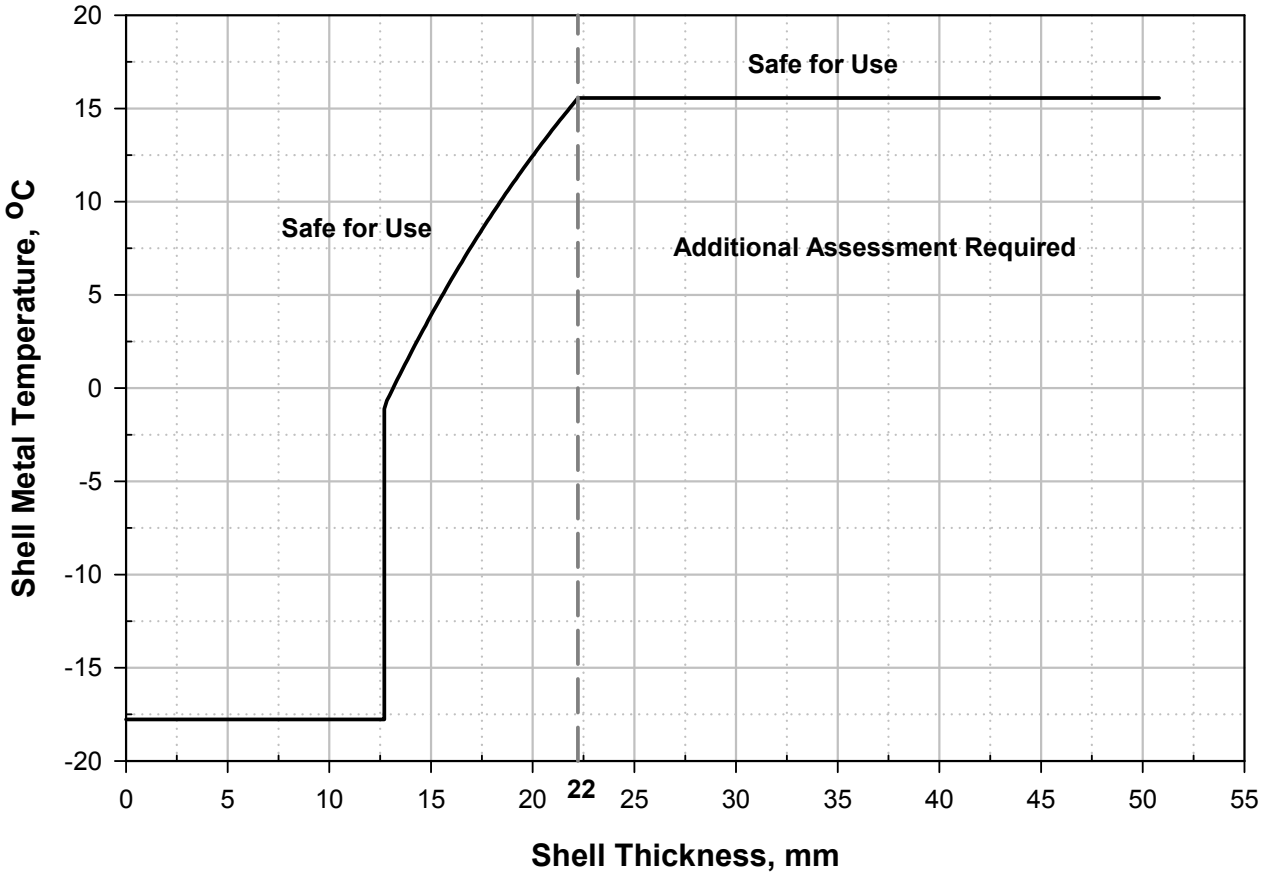

Note: The above exemption curve between -1°C and 16°C is based on Curve A in Figure 3.4. The other parts of the curve were established based on successful operating experience. The equations for the curve in this figure are provided in Table 3.4.

Figure 3.10M – Exemption Curve for Tanks Constructed From Carbon Steel of Unknown Toughness Thicker Than 12.7 mm And Operating at A Shell Metal Temperature Below 16°C

PART 4

ASSESSMENT OF GENERAL METAL LOSS

PART CONTENTS

4.1 General

4.1.1 Fitness–For–Service (FFS) assessment procedures for pressurized components subject to general metal loss resulting from corrosion, erosion, or both corrosion and erosion are provided in this Part. The procedures can be used to qualify a component for continued operation or for rerating. A flow chart for the assessment procedure for general metal loss is shown in Figure 4.1.

4.1.2 The assessment procedures in this Part are based on a thickness averaging approach. If local areas of metal loss are found in the component, the thickness averaging approach may produce conservative results. For these cases, the assessment procedures of Part 5 can be utilized to reduce the conservatism in the analysis. The exact distinction between uniform and local metal loss cannot be made without knowing the characteristics of the metal loss profile. For most evaluations, it is recommended to first perform an assessment using Part 4.

4.2 Applicability and Limitations of the Procedure

4.2.1 The assessment procedures in this Part can be used to evaluate general metal loss (uniform or local) that exceeds or is predicted to exceed the corrosion allowance before the next scheduled inspection. The general metal loss may occur on the inside or outside of the component. Assessment procedures based on point thickness readings and thickness profiles are provided. The assessment procedure to be used in an evaluation depends on the type of thickness data available (point thickness readings or thickness profiles, see paragraph 4.3.3), the characteristics of the metal loss (i.e. uniform or local), and the degree of conservatism acceptable for the assessment. The methodology shown in Figure 4.2 can be used to determine the assessment procedure to be used in the evaluation.

4.2.2 Unless otherwise specified, this Part is limited to the evaluation of metal loss. Other flaw types shall be evaluated in accordance with Part 2, Table 2.1.

4.2.3 Calculation methods are provided to rerate the component if the acceptance criteria in this Part are not satisfied. For pressurized components, the calculation methods can be used to find a reduced maximum allowable working pressure $(MAWP)$. For tank components (i.e. shell courses), the calculation methods can be used to determine a reduced maximum fill height (MFH).

4.2.4 The assessment procedures only apply to components that are not operating in the creep range; the design temperature is less or equal to the value in Table 4.1. The Materials Engineer should be consulted regarding the creep range temperature limit for materials not listed in this table. Assessment procedures for components operating in the creep range are provided in Part 10.

4.2.5 In this Part, the following component definitions are used in determining the permissible assessment level for a component.

a) Type A Components – A component that has a design equation that specifically relates pressure (or liquid fill height for tanks) and/or other loads, as applicable, to a required wall thickness. Examples of Type A components are shown below.
   1) Pressure vessel cylindrical and conical shell sections
   2) Spherical pressure vessels and storage spheres
   3) Spherical, elliptical and torispherical formed heads
   4) Straight sections of piping systems
   5) Elbows or pipe bends that do not have structural attachments
   6) Cylindrical atmospheric storage tank shell courses

b) Type B Components – A component that does not have a design equation that specifically relates pressure (or liquid fill height for tanks) and/or other loads, as applicable, to a required wall thickness. These components have a code design procedure to determine an acceptable configuration, examples are shown below. Type B components typically exist at a major structural discontinuity and involve the satisfaction of a local reinforcement requirement (e.g. nozzle reinforcement area), or necessitate the computation of a stress level based upon a given load condition, geometry, and thickness configuration (e.g. flange design). These rules typically result in one component with a thickness that is dependent upon that of another component. Design rules of this type have thickness interdependency, and the definition of a minimum thickness for a component is ambiguous. Examples of Type B components are shown below.

1) Pressure vessel nozzles, tank nozzles and piping branch connections
2) The reinforcement zone of conical transitions
3) Cylinder to flat head junctions
4) Integral tubesheet connections
5) Flanges
6) Piping systems (see paragraph 4.4.3.3.b.3)

c) Type C Components – A component that does not have a design equation which specifically relates pressure (or liquid fill height for tanks) and/or other loads, as applicable, to a required wall thickness. In addition, these components do not have a code design procedure to determine local stresses. Examples of Type C components are shown below.

1) Pressure vessel head to shell junctions
2) Stiffening rings attached to a shell
3) Skirt and lug-type supports on pressure vessels
4) Tank shell bottom course to tank bottom junction

4.2.6 Specific details pertaining to the applicability and limitations of each of the assessment procedures are discussed below.

4.2.6.1 The Level 1 or 2 assessment procedures in this Part apply only if all of the following conditions are satisfied.

a) The original design criteria were in accordance with a recognized code or standard (see Part 1, paragraphs 1.2.2 or 1.2.3).

b) The region of metal loss has relatively smooth contours without notches (i.e. negligible local stress concentrations).

c) The component is not in cyclic service. If the component is subject to less than 150 cycles (i.e. pressure and/or temperature variations including operational changes and start-ups and shut-downs) throughout its previous operating history and future planned operation, or satisfies the cyclic service screening procedure in Annex B1 paragraph B1.5.4, then the component is not in cyclic service.

d) The following limitations on component types and applied loads are satisfied:

1) Level 1 Assessment – Type A Components subject to internal pressure or external pressure (i.e. supplemental loads are assumed to be negligible).
2) Level 2 Assessment – Type A or B Components (see Part 4, paragraph 4.2.5) subject to internal pressure, external pressure, supplemental loads (see Annex A, paragraph A.2.7), or any combination thereof.

4.2.6.2 A Level 3 Assessment can be performed when the Level 1 and 2 Assessment procedures do not apply, or when these assessment levels produce overly conservative results (i.e. would not permit operation at the current design conditions). Examples include, but are not limited to the following.

a) Type A, B, or C Components subject to internal pressure, external pressure, supplemental loads, and any combination thereof.

b) Components with a design based on proof testing (e.g. piping tee or reducer produced in accordance with ASME B16.9 where the design may be based on proof testing).

c) Components in cyclic service or components where a fatigue analysis was performed as part of the original design calculations; the assessment should consider the effects of fatigue on the Fitness–For–Service calculations used to qualify the component for continued operation.

4.3 Data Requirements

4.3.1 Original Equipment Design Data

An overview of the original equipment data required for an assessment is provided in Part 2, paragraph 2.3.1.

4.3.2 Maintenance and Operational History

An overview of the maintenance and operational history required for an assessment is provided in Part 2, paragraph 2.3.2.

4.3.3 Required Data/Measurements For A FFS Assessment

4.3.3.1 Thickness readings are required on the component where the metal loss has occurred to evaluate general metal loss. An overview of the Level 1 and Level 2 assessment options are shown in Figure 4.2, and are described in paragraph 4.4.

a) Two options for obtaining thickness data are presented:
   1) Point thickness readings - point thickness readings can be used to characterize the metal loss in a component if there are no significant differences in the thickness reading values obtained at inspection monitoring locations.
   2) Thickness profiles – thickness profiles should be used to characterize metal loss in a component if there is a significant variation in the thickness readings. In this case, the metal loss may be localized, and thickness profiles (thickness readings on a prescribed grid) should be used to characterize the remaining thickness and size of the region of metal loss.

b) The thickness quantities used in this Part for the assessment of general metal loss are the average measured thickness and the minimum measured thickness. If thickness readings indicate that the metal loss is general, the procedures in this Part will provide an adequate assessment. However, if the metal loss is localized and thickness profiles are obtained, the assessment procedures of this Part may produce conservative results, and the option for performing the evaluation using the assessment procedures of Part 5 is provided.

4.3.3.2 If point thickness readings are used in the assessment, the assumption of uniform metal loss should be confirmed.

a) Additional inspection may be required such as visual examination, radiography or other NDE methods.

b) A minimum of 15 thickness readings should be used unless the level of NDE utilized can be used to confirm that the metal loss is general. In some cases, additional readings may be required based on the size of the component, the construction details utilized, and the nature of the environment resulting in the metal loss. A sample data sheet to record thickness readings is shown in Table 4.2.

c) If the Coefficient Of Variation (COV) of the thickness readings is greater than 10%, then thickness profiles shall be considered for use in the assessment (see paragraph 4.3.3.3). The COV is defined as the standard deviation divided by the average. A template that can be used to compute the COV is provided in Table 4.3.

4.3.3.3 If thickness profiles are used in the assessment, the following procedure shall be used to determine the required inspection locations and the Critical Thickness Profiles ($CTPs$).

a) STEP 1 – Locate the region of metal loss in the component and determine the location, orientation, and length of the inspection plane(s).

b) STEP 2 – To determine the inspection plane(s) for thickness readings the following shall be considered:
   1) Pressure Vessel Heads and Spheres – Both the circumferential and meridional directions shall be set as inspection plane(s) (see Figure 4.3).
   2) Cylindrical Shells, Conical Shells and Elbows – The critical inspection plane(s) are meridional (longitudinal) if the circumferential stress due to pressure governs, and circumferential if the longitudinal stress due to pressure and supplemental loads governs (see Figure 4.4).

3) Atmospheric Storage Tanks – The critical inspection plane(s) are in the meridional (longitudinal) direction (see Figure 4.5).

4) Low Pressure Storage Tanks – The critical inspection plane(s) are assigned based on the component geometry (see subparagraph 1 and 2 above).

5) If the critical inspection plane(s) for a component are not known at the time of the inspection, a minimum of two planes at right angles to each other should be utilized to record thickness readings.

c) STEP 3 – Mark each inspection plane on the component; the length of the inspection plane for the corroded/eroded region should be sufficient to characterize the metal loss.

d) STEP 4 – Determine the uniform thickness away from the local metal loss at the time of the assessment, t_{rd}.

e) STEP 5 – Measure and record the wall thickness readings at intervals along each inspection plane and determine the minimum measured wall thickness, t_{mm}. The spacing distance for thickness readings should allow for an accurate characterization of the thickness profile.

1) If the corroded surface is not accessible for visual inspection, then the recommended spacing distance for thickness readings along each inspection plane is given by the following equation; however, a minimum of five thickness readings is recommended for each inspection plane(s).

$$L_s = \min\left[0.36\sqrt{Dt_{\min}},\ 2t_{rd}\right] \tag{4.1}$$

2) The above recommended spacing for thickness readings can be modified based on the actual size and extent of the region of metal loss. If visual inspection or NDE methods are utilized to quantify the metal loss, an alternative spacing can be used as long as the metal loss on the component can be adequately characterized. For example, if the region of metal loss is determined to be uniform based on a visual inspection, the spacing utilized to take thickness readings can be increased without a reduction in accuracy in the FFS assessment.

3) A sample data sheet to record thickness readings is shown in Table 4.2. If more than four inspection planes are utilized, additional copies of this sheet can be used to record the thickness profile data.

f) STEP 6 – Determine the CTP in the meridional and circumferential directions. The CTP in each direction is determined by projecting the minimum remaining thickness for each position along all parallel inspection planes onto a common plane as shown in Figure 4.6. The length of the profile is established by determining the end point locations where the remaining wall thickness is greater than t_{rd} in the meridional and circumferential directions.

1) The CTP in the meridional or longitudinal direction is obtained by projecting the minimum thickness at each interval along M1–M5 inspection planes onto a common plane. The length of the metal loss in the longitudinal direction, denoted as s, is determined using the CTP and t_{rd} as shown in Figure 4.6.

2) The CTP in the circumferential direction is obtained by projecting the minimum thickness at each interval along C1–C7 inspection planes onto a common plane. The length of the metal loss in the circumferential direction, denoted as c, is determined using the CTP and t_{rd} as shown in Figure 4.6.

3) If there are multiple flaws in close proximity to one another, then the size of the flaw to be used in the assessment is established considering the effects of neighboring flaws using the methodology shown in Figure 4.7. The final CTP for the flaw, or network of flaws, can be established as shown in Figure 4.8. The thickness profile for both the longitudinal and circumferential planes should be evaluated in this manner.

4) For large regions of metal loss, it may be overly conservative to project the minimum thicknesses on to a single plane to determine a CTP. For these cases, more than one CTP in the longitudinal or circumferential directions may be utilized in the assessment. The number of $CTP's$ to be used in an assessment to achieve an optimum result depends on the uniformity of the metal loss. A sensitivity analysis (see Part 2, paragraph 2.4.3.1) can be performed to evaluate the benefits of using multiple $CTP's$ in the assessment of the longitudinal and circumferential directions.

4.3.3.4 If the region of metal loss is close to or at a major structural discontinuity, the remaining thickness can be established using the procedure in paragraph 4.3.3.2 or 4.3.3.3. However, additional thickness readings should be taken to include sufficient data points in the region close to the major structural discontinuity. This involves taking adequate thickness readings within the zones defined as follows for the components listed below:

a) Nozzle or branch connection (see Figure 4.9 for the thickness zone, L_v, L_{no} and L_{ni})

b) Conical shell transition (see Figure 4.10 for the thickness zone, L_v)

c) Flange connections (see Figure 4.11 for the thickness zone, L_{vh} and L_{vt})

4.3.3.5 Additional thickness readings are required if discrepancies are noted in the reported thickness measurements. For example, if the latest thickness reading is greater than the reading at the time of the last inspection, additional readings may be required to resolve the discrepancies in the data.

4.3.4 Recommendations for Inspection Technique and Sizing Requirements

4.3.4.1 Thickness readings can be made using straight beam ultrasonic thickness examination (UT). This method can provide high accuracy and can be used for point thickness readings and in obtaining thickness profiles (continuous line scans or area scans can also be used to obtain thickness profiles). The limitations of UT are associated with uneven surfaces and access. Examples include measuring the thickness at a weld or the thickness of the shell located underneath a reinforcing pad from the outside of a vessel.

4.3.4.2 Obtaining accurate thickness readings using UT depends on the surface condition of the component. Surface preparation techniques vary depending on the surface condition, but in many cases, wire brushing is sufficient. However, if the surface has a scale build–up or is pitted, grinding may be necessary.

4.3.4.3 All UT thickness readings should be made after proper calibration for the wall thickness, ultrasonic velocity and temperature ranges of the component. Special UT couplants are required if the thickness readings are obtained on high temperature components. It may be preferable to obtain readings with probes less than 12.7 mm (1/2 inches) in diameter to provide greater assurance that pitting/localized corrosion is not present.

4.3.4.4 Radiographic examination (RT) may also be used to determine metal loss; however, accurate thickness data may only be obtained by moving the component containing the metal loss, or moving the source around the component to obtain multiple views. This type of manipulation may not be possible for all pressure-containing components. However, RT examination can be effectively used to qualify the existence, extent and depth of a region of metal loss, and may be used in conjunction with UT to determine whether the metal loss on a component is general or local.

4.4 Assessment Techniques and Acceptance Criteria

4.4.1 Overview

4.4.1.1 If the metal loss is less than the specified corrosion/erosion allowance and adequate thickness is available for the future corrosion allowance, no further action is required other than to record the data; otherwise, an assessment is required.

4.4.1.2 An overview of the assessment levels is provided in Figure 4.1.

a) Level 1 Assessments are limited to Type A components subject to internal or external pressure (i.e. supplemental loads are assumed to be negligible).

b) Level 2 Assessments may be used to evaluate Type A components that do not satisfy the Level 1 Assessment criteria, and may be used to evaluate Type A or Type B components subject to internal pressure, external pressure, supplemental loads or any combination thereof.

c) Level 3 Assessments may be used to evaluate Type A and B components that do not satisfy the Level 1 or Level 2 Assessment criteria, and may be used to evaluate Type C components using stress analysis methods (see Annex B1).

4.4.1.3 If thickness readings indicate that the metal loss is localized and thickness profiles are obtained, the assessment procedures in this Part can still be used for the assessment. However, the results may be conservative, and the option for performing the analysis using the assessment procedures of Part 5 is provided.

4.4.1.4 *FFS* assessments for the components listed below require special consideration because of the complexities associated with the design requirements of the original construction code. In each case, an Engineer knowledgeable and experienced in the design requirements of the applicable code should perform the assessment (see Part 1, paragraph 1.4.3). If the metal loss is in a component that was not subject to special design requirements per the original construction code (i.e. design requirements based on stress analysis), then the Level 1 or Level 2 assessment procedures may be applied. If the corrosion/erosion damage is in a component subject to special design requirements, then the calculations required in the original design to qualify the component should be repeated considering a reduced wall thickness.

a) Pressure Vessels Designed To The ASME Code, Section VIII, Division 2 – A user design specification is required where the operational parameters for the original design were established. In addition, detailed heat transfer and stress calculations, and a fatigue analysis may have been performed to satisfy the design–by–analysis rules required in this code.

b) Low Pressure Storage Tanks Designed To API 620 – The design rules for low–pressure storage tanks contained in API 620 require a thorough knowledge of engineering mechanics in that the required thickness of a shell component is based upon the evaluation of free body diagrams, the development of equilibrium equations, and the consideration of a biaxial stress field to determine an allowable design stress.

c) Piping Designed To ASME B31.3 – Metal loss in piping systems can be evaluated using a Level 1 Assessment by the Inspector if the supplemental loads on the piping system are negligible (see Annex A, paragraph A.2.6). If these loads are not negligible, a piping stress analysis is required. The piping analysis should take into account the relationship between the component thickness, piping flexibility, and the resulting stress (see paragraph 4.4.3.3).

4.4.2 Level 1 Assessment

4.4.2.1 The following assessment procedure shall be used to evaluate Type A Components (see paragraph 4.2.5) subject to internal or external pressure when Point Thickness Reading (PTR) data are used to characterized the metal loss (see paragraph 4.3.3.2).

a) STEP 1 – Determine the minimum required thickness, $t_{\min}$ (see Annex A, paragraph A.2).

b) STEP 2 – Take the point thickness reading data in accordance with paragraph 4.3.3.2. From these data determine the minimum measured thickness, t_{mm}, the average measured thickness, t_{am}, and the Coefficient Of Variation (COV). A template for computing the COV is provided in Table 4.3.

c) STEP 3 – If the COV from STEP 2 is less than or equal to 10%, then proceed to STEP 4 to complete the assessment using the average thickness, t_{am}. If the COV is greater than 10%, then the use of thickness profiles should be considered for the assessment (see paragraph 4.4.2.2).

d) STEP 4 – The acceptability for continued operation can be established using the Level 1 criteria in Table 4.4. The averaged measured thickness or MAWP acceptance criterion may be used. In either case, the minimum thickness criterion shall be satisfied.

4.4.2.2 The following assessment procedure shall be used to evaluate Type A Components (see paragraph 4.2.5) subject to internal or external pressure when Critical Thickness Profile *(CTP)* data are used to characterized the metal loss (see paragraph 4.3.3.3).

a) STEP 1 – Determine the minimum required thickness, $t_{\min}$ (see Annex A, paragraph A.2).

b) STEP 2 – Determine the thickness profile data in accordance with paragraph 4.3.3.3 and determine the minimum measured thickness, t_{mm}.

c) STEP 3 – Determine the wall thickness to be used in the assessment using Equation (4.2) or Equation (4.3).

$$t_c = t_{nom} - LOSS - FCA \tag{4.2}$$

$$t_c = t_{rd} - FCA \tag{4.3}$$

d) STEP 4 – Compute the remaining thickness ratio, R_t.

$$R_t = \left(\frac{t_{mm} - FCA}{t_c} \right) \tag{4.4}$$

e) STEP 5 – Compute the length for thickness averaging, L where the parameter Q is evaluated using Table 4.5.

$$L = Q\sqrt{Dt_c} \tag{4.5}$$

f) STEP 6 – Establish the Critical Thickness Profiles ($CTP's$) from the thickness profile data (see paragraph 4.3.3.3). Determine the average measured thickness t_{am}^s based on the longitudinal CTP and the average measured thickness t_{am}^c based on the circumferential CTP. The average measured thicknesses t_{am}^s and t_{am}^c shall be based on the length L determined in STEP 5. The length L shall be located on the respective CTP such that the resulting average thickness is a minimum.

g) STEP 7 – Based on the values of t_{am}^s and t_{am}^c from STEP 6, determine the acceptability for continued operation using the Level 1 criteria in Table 4.4. The averaged measured thickness or $MAWP$ acceptance criterion may be used. In either case, the minimum measured thickness, t_{mm}, shall satisfy the criterion in Table 4.4.

4.4.2.3 If the component does not meet the Level 1 Assessment requirements, then the following, or combinations thereof, shall be considered:

a) Rerate, repair, replace, or retire the component.

b) Adjust the FCA by applying remediation techniques (see paragraph 4.6).

c) Adjust the weld joint efficiency or quality factor, E, by conducting additional examination and repeat the assessment (Note: To raise the value of E from 0.7 to .85, or from .85 to 1.0, would require that the weld seams be spot or 100% radiographed, respectively, and these examinations may reveal additional flaws that will have to be evaluated).

d) The region of metal loss can be evaluated using the Part 5 Assessment procedures for local metal loss.

e) Conduct a Level 2 or a Level 3 Assessment.

4.4.3 Level 2 Assessment

4.4.3.1 The assessment procedure in paragraph 4.4.2.1 may be used to evaluate Type A Components (see paragraph 4.2.5) subject to the loads defined in paragraph 4.2.6.1.d when Point Thickness Reading (PTR) data are used to characterized the metal loss (see paragraph 4.3.3.2). Note that the Level 2 Acceptance Criteria in Table 4.4 shall be used in conjunction with STEP 4.

4.4.3.2 The assessment procedure in paragraph 4.4.2.2 may be used to evaluate Type A Components (see paragraph 4.2.5) subject to the loads defined in paragraph 4.2.6.1.d when Critical Thickness Profile *(CTP)* data are used to characterize the metal loss (see paragraph 4.3.3.3). Note that the Level 2 Acceptance Criteria in Table 4.4 shall be used in conjunction with STEP 7.

4.4.3.3 The following assessment procedure can be used to evaluate Type B Components (see paragraph 4.2.5) subject to the loads defined in paragraph 4.2.6.1.d.

a) Compute the $MAWP$ based upon the average measured thickness minus the future corrosion allowance $\left(t_{am} - FCA\right)$ and the thickness required for supplemental loads (see Annex A, paragraph A.2.6) for each component using the equations in the original construction. The calculated $MAWP$ should be equal to or exceed the design $MAWP$.

b) The average thickness of the region, t_{am}, shall be obtained as follows for components with a thickness interdependency:

1) Nozzles and Branch Connections – Determine the average thickness within the nozzle reinforcement zone shown in Figure 4.9 (see paragraph 4.3.3.4). The assessment procedures in Annex A, paragraph A.3.11 can be utilized to evaluate metal loss at a nozzle or piping branch connection, respectively. The weld load path analysis in this paragraph should also be checked, particularly if the metal loss has occurred in the weldments of the connection.

2) Axisymmetric Structural Discontinuities – Determine L using Equation (4.5) and L_v based on the type of structural discontinuity listed below. The average thickness is computed based on the smaller of these two distances. If $L < L_v$, then the midpoint of L should be located at t_{mm} to establish a length for thickness averaging unless the location of t_{mm} is within $L/2$ of the zone for thickness averaging. In this case, t_{mm} should be positioned so that it is entirely within L before the average thickness is computed.

i) Conical shell transition (see Figure 4.10 for the zone for thickness averaging and L_v).

ii) Flange connections (see Figure 4.11 for the zone for thickness averaging and L_v). If the flange has a hub, and the metal loss is uniform along the hub, then the average thickness may be proportioned in accordance with the original hub dimensions for the flange calculation. If the metal loss is non-uniform or the flange does not have a hub, then the flange calculation should be performed using a uniform hub section with a thickness equal to the average thickness.

3) *Piping Systems* – Piping systems are Type B Components because of the relationship between the component thickness, piping flexibility, and the resulting stress. For straight sections of piping, determine L using Equation (4.5) and compute the average thickness based on L to represent the section of pipe with metal loss in the piping analysis. For elbows or bends, the thickness readings should be averaged within the bend and a single thickness used in the piping analysis (i.e. to compute the flexibility factor, system stiffness and stress intensification factor). For branch connections, the thickness should be averaged within the reinforcement zones for the branch and header, and these thicknesses should be used in the piping model (to compute the stress intensification factor). An alternative assumption is to use the minimum measured thickness to represent the component thickness in the piping model. This approach may be warranted if the metal loss is localized; however, this may result in an overly conservative evaluation. In these cases, a Level 3 assessment may be required to reduce the conservatism in the assessment (see paragraph 4.4.4.4).

c) The minimum measured wall thickness, t_{mm}, shall satisfy the criterion in Table 4.4

4.4.3.4 If the component does not meet the Level 2 Assessment requirements, then the following, or combinations thereof, can be considered:

a) Rerate, repair, replace, or retire the component.

b) Adjust the FCA by applying remediation techniques (see paragraph 4.6).

c) Adjust the weld joint efficiency factor, E, by conducting additional examination and repeat the assessment (see paragraph 4.4.2.3).

d) Conduct a Level 3 Assessment.

4.4.4 Level 3 Assessment

4.4.4.1 The stress analysis techniques discussed in Annex B1 can be utilized to evaluate regions of general or local metal loss in pressure vessels, piping, and tanks. The finite element method is typically used to compute the stresses in a component; however, other numerical methods such as the boundary element or finite difference method may also be used. Handbook solutions may also be used if the solution matches the component geometry and loading condition. The evaluation may be based on a linear stress analysis with acceptability determined using stress categorization, or a nonlinear stress analysis with acceptability determined using a plastic collapse load. Nonlinear stress analysis techniques are recommended to provide the best estimate of the acceptable load carrying capacity of the component. Guidelines for performing and processing results from a finite element analysis for a Fitness-For-Service analysis are provided in Annex B1.

4.4.4.2 If a component is subject to external pressure and/or other loads that result in compressive stresses, a structural stability analysis should be performed using the methods in Annex B1 to determine suitability for continued service. In addition, methods to evaluate fatigue are also included in Annex B1 if a component is subject to cyclic loading.

4.4.4.3 Thickness data per paragraph 4.3.3 as well as the component geometry, material properties and loading conditions are required for a Level 3 Assessment. The thickness data can be used directly in finite element model of the component. If thickness profile data are available, the thickness grid can be directly mapped into a three–dimensional finite element model using two or three dimensional continuum elements, as applicable. This information can also be used if the component is modeled using shell elements.

4.4.4.4 If the region of local metal loss is close to or at a major structural discontinuity, details of the component geometry, material properties, and imposed supplemental loads (see Annex A, paragraph A.2.6) at this location are required for the assessment. Special consideration is required if there are significant supplemental loads at a nozzle, piping branch connection, or pipe bend. The location and distribution of the metal loss in these components may significantly affect both the flexibility and stress distribution in a manner that cannot be evaluated using the approaches employed in the design. In addition, the localized metal loss may significantly reduce the plastic collapse load capability depending on the nozzle geometry, piping system configuration, and/or applied supplemental loads.

4.5 Remaining Life Assessment

4.5.1 Thickness Approach

4.5.1.1 The remaining life of a component can be determined based upon computation of a minimum required thickness for the intended service conditions, thickness measurements from an inspection, and an estimate of the anticipated corrosion rate. This method is suitable for determination of the remaining life for Type A Components (see paragraph 4.2.5)

$$R_{life} = \frac{t_{am} - Kt_{\min}}{C_{rate}} \tag{4.6}$$

4.5.1.2 The remaining life determined using the thickness–based approach may produce non–conservative results when applied to Type B or Type C Components (see paragraph 4.2.5). For these cases, the remaining life should be established using the $MAWP$ Approach.

4.5.2 MAWP Approach

4.5.2.1 The $MAWP$ approach provides a systematic method for determining the remaining life of Type A, B, and C components [2]. This method is also the only method suitable for determining the remaining life of Type B and C components. In addition, the $MAWP$ approach ensures that the design pressure is not exceeded during normal operation if the future corrosion rate is accurately established.

4.5.2.2 The following procedure can be used to determine the remaining life of a component using the $MAWP$ approach.

a) STEP 1 – Determine the metal loss of the component, t_{loss}, by subtracting the average measured thickness from the time of the last inspection, t_{am}, from the nominal thickness, t_{nom} (see paragraph 4.3.3.2 or 4.3.3.3, as applicable).

b) STEP 2 – Determine the $MAWP$ for a series of increasing time increments using an effective corrosion allowance and the nominal thickness in the computation. The effective corrosion allowance is determined as follows:

$$CA_e = t_{loss} + C_{rate} \cdot time \tag{4.7}$$

c) STEP 3 – Using the results from STEP 2, determine the remaining life from a plot of the $MAWP$ versus time. The time at which the $MAWP$ curve intersects the design $MAWP$ for the component is the remaining life of the component.

d) STEP 4 – Repeat the STEPS 1 through 3 for each component. The equipment remaining life is taken as the smallest value of the remaining life computed for each of the individual components.

4.5.2.3 This approach may also be applied to tanks using the maximum fill height, MFH, instead of the $MAWP$.

4.6 Remediation

4.6.1 A FFS assessment provides an evaluation of the condition of a component for continued operation for a period based upon a future corrosion or degradation rate. However, in many cases, future degradation rates are very difficult to predict, or little or no further degradation can be tolerated. Therefore, remediation methods may be applied to prevent or minimize the rate of further damage.

4.6.2 Remediation methods for general corrosion/erosion as well as local corrosion/erosion and pitting are provided below. These methods may also be suitable for mitigation of crack-like flaws in some process environments. The methods described below are not inclusive for all situations, nor are they intended to be a substitute for an engineering evaluation of a particular situation. The Owner–User should consult a qualified Metallurgist/Corrosion Engineer and Mechanical Engineer as to the most appropriate method to apply for the relevant damage mechanism(s).

4.6.2.1 *Remediation Method 1* – Performing Physical Changes to the Process Stream; the following can be considered.

a) Increasing or decreasing the process temperature, pressure, or both – If the degradation mode is temperature or pressure sensitive, a process change may minimize the progression of the damage. However, the component must be evaluated so that the design still meets the changed conditions. Note that a reduction in the pressure or temperature may result in a reduction of the minimum required wall thickness, thereby increasing the life of the component.

b) Increasing or decreasing the velocity of the stream – Some damage mechanisms, such as erosion, sour water corrosion, under–deposit corrosion, and naphthenic acid corrosion are very velocity sensitive. A slight decrease or increase in stream velocity can change the rate of damage.

c) Installing scrubbers, treaters, coalescers and filters to remove certain fractions and/or contaminants in a stream.

4.6.2.2 *Remediation Method 2* – Application of solid barrier linings or coatings to keep the environment isolated from the base metal that has experienced previous damage.

a) Organic coatings – The coating must be compatible with the service (temperature and stream composition) and must be resistant to all service conditions, including steaming–out. Surface preparation, particularly filling of pits, cracks, etc., is critical to achieve a solid bond. Curing conditions are also very important to assure a reliable lining. These fall into the following general classes:
   1) Thin film coatings – Typically, these include epoxy, epoxy phenolic, and baked phenolic coatings applied in dry film thickness less than 0.25 mm (10 mils).
   2) Thick film coatings – Typically, these include vinyl ester and glass fiber reinforced coatings that are applied in dry film thickness greater than 0.25 mm (10 mils).

b) Metallic linings – These fall into three general classes:
   1) Metal spray linings – Various metal spray processes are available. In general, higher velocity processes such as HVOF (high velocity oxy–fuel) produce denser coatings, which are less susceptible to spalling or undermining. Coatings are often applied in multiple layers, with different compositions in each layer. The coating material in contact with the process environment should be corrosion resistant. Surface preparation is critical in achieving a solid bond. One advantage of metal spray linings is that the base material is not heated to high temperatures as in welding.
   2) Strip linings – Thin strips of a corrosion resistant metal are applied to the area of concern. They are fastened to the backing metal by small welds, which help to minimize the size of the weld heat affected zone. Note that strip linings may crack at the lining attachment-to-component wall weld and may need periodic maintenance. In addition, corrosion of the underlying wall by leaking fluid at these cracks may be difficult to detect.
   3) Weld overlay (see paragraph 4.6.2.4).

c) Refractory linings – Many materials fall into this category. Depending on the damage mechanism, insulating refractories can be used to decrease the metal temperature, erosion resistant refractories can be used for erosion protection, and corrosion resistant refractories can be used to protect the base material. Selection of the refractory type and anchoring system, and curing of the refractory are critical elements for this remediation method. A refractory specialist should be consulted for details.

4.6.2.3 *Remediation Method 3* – Injection of water and/or chemicals on a continuous basis to modify the environment or the surface of the metal. Important variables to consider when injecting chemicals are: the particular stream contaminants, injection point location and design, rate of injection, eventual disposition and any adverse reactions, the effect of process upsets, and monitoring for effectiveness. Examples of this type are as follows:

a) Water washing to dilute contaminants – This strategy is often applied in fluid catalytic cracking light end units and hydrodesulfurization reactor outlet systems. Important variables to consider when stipulating a retrofit water wash installation are location of injection, distribution of water, water rate, water quality, injection point design and disengagement, and monitoring for effectiveness.

b) Injection of chemicals to change the aggressiveness of the solution – Neutralizing chemicals as used in atmospheric distillation unit overheads, polysulfide, and oxygen scavengers all fall into this category. Important variables to consider include; the injection location and design, possible adverse side effects, and monitoring for effectiveness.

c) Injection of filming type chemicals to coat the metal surface – Filming chemicals attach to the metal surface to form a thin barrier that protects the metal. Important variables to consider are; the injection location and design, response to upsets, and monitoring effectiveness.

4.6.2.4 *Remediation Method 4* – Application of weld overlay for repair of the base material or for the addition of a corrosion resistant lining. If weld overlay is applied, the weldability of the base metal considering the effects of the environment should be evaluated (see Annex G). Note that the application of a weld overlay may necessitate a PWHT.

a) Repair of Base Material – Weld overlay with the same chemistry (P–Number) as the base metal of the component is added to the component to provide the necessary increase in wall thickness to compensate for corrosion/erosion. Note that this method does not eliminate/reduce the rate of degradation. The weld overlay may be added either to the inside or outside surface regardless of the surface on which the metal loss is occurring. For some applications, a repair procedure can be developed which permits deposition of the weld overlay while the component is in operation. Since this process changes the geometry of the component, an analysis considering bending stresses should be made to determine the acceptability of the proposed design.

b) Application of corrosion resistant lining – A corrosion/erosion resistant material is applied to the surface of the base material.

4.7 In–Service Monitoring

4.7.1 As discussed above, mitigation methods can be applied, but in some cases, these are not feasible or, if they are applied, it still is important to confirm that they are effective. Therefore, in-service monitoring methods can be applied to monitor directly any further damage or to monitor indirectly conditions that might lead to further damage.

4.7.2 Typical monitoring methods include the use of the following tools or procedures:

a) Corrosion probes

b) Hydrogen probes

c) Retractable corrosion coupons and physical probes

d) Spot UT measurements and scanning

e) Radiographic examination

f) Stream samples for H_2S, Cl, NH_3, CO_2, Fe, Ni, pH, water content, Hg, etc.

g) Infrared thermography

h) Thermocouples

4.7.3 Care must be exercised in defining the in–service monitoring method, determining the required measurement sensitivity of the method based on the environment, and locating monitoring stations on the component to insure that the damage mechanism resulting in the metal loss can adequately be measured and evaluated during operation.

4.8 Documentation

4.8.1 The documentation of the FFS Assessment should include the information cited in Part 2, paragraph 2.8.

4.8.2 Inspection data including all thickness readings and corresponding locations used to determine the average measured thickness, t_{am}, and the minimum measured thickness, t_{mm}, should be recorded and included in the documentation. A sample data sheet is provided in Table 4.2 for this purpose. A sketch showing the location and orientation of the inspection planes on the component is also recommended.

4.9 Nomenclature

A_R	vessel stiffening ring cross–sectional area.
COV	Coefficient Of Variation.
CTP	Critical Thickness Profile.
C_{rate}	future corrosion rate.
CA_e	effective corrosion allowance used to determine a remaining life.
c	extent of the metal loss established using the CTP in the circumferential direction.
D	inside diameter of the shell corrected for $LOSS$ and FCA as applicable.
d_i	current inside diameter of the nozzle including the specified FCA.
E	weld joint efficiency or quality factor.
FCA	Future Corrosion Allowance (see Annex A, paragraph A.2.7).
K	factor depending on the assessment level; for a Level 1 assessment $K = 1.0$, for a Level 2 Assessment; $K = RSF_a$ for pressure vessels and piping components and $K = 1.0$ for shell courses of tanks.
L	length for thickness averaging along the shell.
L_{ni}	length for thickness averaging at a nozzle in the vertical direction on the inside of the shell.
L_{no}	length for thickness averaging at a nozzle in the vertical direction on the outside of the shell.
L_s	recommended spacing of thickness readings.
L_v	length for thickness averaging along the shell at shell discontinuities such as stiffening rings, conical transitions, and skirt attachment locations.
L_{vh}	length for thickness averaging for the flange hub.
L_{vf}	length for thickness averaging for a flange.
$LOSS$	amount of uniform metal loss away from the local metal loss location at the time of the assessment.
$MAWP$	Maximum Allowable Working Pressure.
$MAWP_r$	permissible maximum allowable working pressure of the damaged component.
$MAWP_r^C$	*MAWP* of a conical or cylindrical shell based on the stresses in the circumferential or hoop direction (see Annex A paragraph A.2).
$MAWP_r^L$	*MAWP* of a conical or cylindrical shell based on the stresses in the longitudinal direction.
MFH	Maximum Fill Height.
MFH_r	permissible maximum fill height of the damaged tank course.
Q	factor used to determine the length for thickness averaging based on an allowable Remaining Strength Factor (see Part 2) and the remaining thickness ratio, R_t (see Table 4.5).
R	vessel inside radius corrected for $LOSS$ and FCA as applicable.
R_S	small end radius at a conical transition corrected for $LOSS$ and FCA as applicable.
R_L	large end radius at a conical transition corrected for $LOSS$ and FCA as applicable.
R_t	remaining thickness ratio.
R_{life}	remaining life.
RSF_a	allowable remaining strength factor (see Part 2).
s	extent of the metal loss established using the CTP in the longitudinal direction with $t_{\min}$.

t_{am} average measured wall thickness of the component based on the CTP determined at the time of the inspection.

t_{am}^{c} average measured wall thickness of the component based on the circumferential CTP determined at the time of the inspection.

t_{am}^{s} average measured wall thickness of the component based on the longitudinal CTP determined at the time of the inspection.

t_c corroded wall thickness.

t_{co} furnished cone thickness at a conical transition.

t_e reinforcing pad thickness.

$t_{\lim}$ limiting thickness

t_{loss} metal loss, defined as $(t_{nom} - t_{am})$.

t_L furnished large end cylinder thickness at a conical transition.

$t_{\min}$ minimum required wall thickness of the component(see Annex A, paragraph A.2).

$t_{\min}^{C}$ minimum required thickness of a conical or cylindrical shell based on the stresses in the circumferential or hoop direction (see Annex A, paragraph A.2).

$t_{\min}^{L}$ minimum required thickness of a conical or cylindrical shell based on the stresses in the longitudinal direction (see Annex A, paragraph A.2).

t_{mm} minimum measured thickness determined at the time of the inspection.

t_{nom} nominal or furnished thickness of the component adjusted for mill undertolerance as applicable.

t_n nozzle thickness.

t_{rd} uniform thickness away from the local metal loss location established by thickness measurements at the time of the assessment.

t_S furnished small end cylinder thickness at a conical transition.

t_{sl} required shell thickness for supplemental loads.

t_v furnished vessel thickness.

$time$ time allocated for future operation.

4.10 References

1. Janelle, J.A. and Osage, D.A., “An Overview and Validation of the Fitness-For-Service Assessment Procedures for Local Thin Areas in API 579,” WRC Bulletin 505, Welding Research Council, New York, N.Y., September, 2005.
2. Osage, D.A., Buchheim, G.M., Brown, R.G., Poremba, J., "An Alternate Approach for Inspection Scheduling Using the Maximum Allowable Working Pressure for Pressurized Equipment," ASME PVP–Vol. 288, American Society of Mechanical Engineers, New York, 1994, pp. 261–273.
3. Osage, D.A., Krishnaswamy, P., Stephens, D.R., Scott, P., Janelle, J., Mohan, R., and Wilkowski, G.M., “Technologies for the Evaluation of Non-Crack-Like Flaws in Pressurized Components – Erosion/Corrosion, Pitting, Blisters, Shell Out-Of-Roundness, Weld Misalignment, Bulges and Dents,” WRC Bulletin 465, Welding Research Council, New York, N.Y., September, 2001.

4.11 Tables and Figures

Table 4.1 – Temperature Limit Used To Define The Creep Range

Material	Temperature Limit
Carbon Steel $\left(UTS \le 414MPa\ \left(60\ ksi\right)\right)$	343°C (650°F)
Carbon Steel $\left(UTS > 414MPa\ \left(60\ ksi\right)\right)$	371°C (700°F)
Carbon Steel – Graphitized	371°C (700°F)
C-1/2Mo	399°C (750°F)
1-1/4Cr-1/2Mo – Normalized & Tempered	427°C (800°F)
1-1/4Cr-1/2Mo – Annealed	427°C (800°F)
2-1/4Cr-1Mo – Normalized & Tempered	427°C (800°F)
2-1/4Cr-1Mo – Annealed	427°C (800°F)
2-1/4Cr-1Mo – Quenched & Tempered	427°C (800°F)
2-1/4Cr-1Mo – V	441°C (825°F)
3Cr-1Mo-V	441°C (825°F)
5Cr-1/2Mo	427°C (800°F)
7Cr-1/2Mo	427°C (800°F)
9Cr-1Mo	427°C (800°F)
9Cr-1Mo – V	454°C (850°F)
12 Cr	482°C (900°F)
AISI Type 304 & 304H	510°C (950°F)
AISI Type 316 & 316H	538°C (1000°F)
AISI Type 321	538°C (1000°F)
AISI Type 321H	538°C (1000°F)
AISI Type 347	538°C (1000°F)
AISI Type 347H	538°C (1000°F)
Alloy 800	565°C (1050°F)
Alloy 800H	565°C (1050°F)
Alloy 800HT	565°C (1050°F)
HK-40	649°C (1200°F)

Table 4.2 – Inspection Summary Required For The Assessment Of General Metal Loss

Use this form to summarize the data obtained from a field inspection.

Equipment Identification: _____
Equipment Type: _____ Pressure Vessel _____ Storage Tank _____ Piping Component
Component Type & Location: _____

Data Required for Level 1 And Level 2 Assessment
Future Corrosion Allowance: _____
Inside Diameter: _____
Minimum Required Thickness: _____
Flaw Dimensions (s & c): _____

Enter the thickness data for each of the inspection planes in the table shown below.

Inspection Plane:__		Inspection Plane:__		Inspection Plane:__		Inspection Plane:__	
Location	**Thickness**	**Location**	**Thickness**	**Location**	**Thickness**	**Location**	**Thickness**
t_{mm}		t_{mm}		t_{mm}		t_{mm}	
t_{am}		t_{am}		t_{am}		t_{am}	

Table 4.3 – Template For Calculating The Coefficient Of Variation (COV) For Point Thickness Reading

Location	$Thickness\ Reading$ $t_{rd,i},\ i = 1\ to\ N$	$\left(t_{rd,i} - t_{am}\right)$	$\left(t_{rd,i} - t_{am}\right)^2$
1			
2			
3			
…			
…			
…			
…			
…			
…			
…			
…			
…			
…			
…			
…			
…			
13			
14			
15			
…			
…			
….			
…			
N			
—	$t_{am} = \frac{1}{N}\sum_{i=1}^{N} t_{rd,i} =$		$S = \sum_{i=1}^{N}\left(t_{rd,i} - t_{am}\right)^2 =$

Notes:

1. N total number of thickness readings, the number of thickness readings should be greater than or equal to 15 (see paragraph 4.3.3.2)
2. The equation for the Coefficient of Variation is:

$$COV = \frac{1}{t_{am}}\left[\frac{S}{N-1}\right]^{0.5}$$

Table 4.4– Acceptance Criteria For Level 1 And 2 Assessments

Assessment Parameter	Level 1 Assessment Acceptance Criteria	Level 2 Assessment Acceptance Criteria
Average Measured Thickness from Point Thickness Readings *(PTR)*	• Cylindrical and Conical Shells, and Elbows $t_{am} - FCA \geq t_{\min}$ • Spherical Shells and Formed Heads $t_{am} - FCA \geq t_{\min}$ • Atmospheric And Low Pressure Storage Tanks $t_{am} - FCA \geq t_{\min}$	• Cylindrical and Conical Shells, and Elbows $t_{am} - FCA \geq RSF_a \cdot t_{\min}$ • Spherical Shells and Formed Heads $t_{am} - FCA \geq RSF_a \cdot t_{\min}$ • Atmospheric And Low Pressure Storage Tanks $t_{am} - FCA \geq t_{\min}$
Average Measured Thickness from Critical Thickness Profiles *(CTP)*	• Cylindrical and Conical Shells, and Elbows $t^s_{am} - FCA \geq t^C_{\min}$ $t^c_{am} - FCA \geq t^L_{\min}$ • Spherical Shells and Formed Heads $\min\left[t^s_{am},\, t^c_{am}\right] - FCA \geq t_{\min}$ • Atmospheric And Low Pressure Storage Tanks $t^s_{am} - FCA \geq t_{\min}$	• Cylindrical and Conical Shells, and Elbows $t^s_{am} - FCA \geq RSF_a \cdot t^C_{\min}$ $t^c_{am} - FCA \geq RSF_a \cdot t^L_{\min}$ • Spherical Shells and Formed Heads $\min\left[t^s_{am},\, t^c_{am}\right] - FCA \geq RSF_a \cdot t_{\min}$ • Atmospheric And Low Pressure Storage Tanks $t^s_{am} - FCA \geq t_{\min}$
MAWP or *MFH* from Point Thickness Readings *(PTR)*	• Cylindrical and Conical Shells, and Elbows Compute the $MAWP_r$ based on the thickness $\left(t_{am} - FCA\right)$ Acceptability criteria $MAWP_r \geq MAWP$ • Spherical Shells and Formed Heads Compute the $MAWP_r$ based on the thickness $\left(t_{am} - FCA\right)$ Acceptability criteria $MAWP_r \geq MAWP$ • Atmospheric And Low Pressure Storage Tanks Compute MFH_r based on the thickness $\left(t_{am} - FCA\right)$ Acceptability criteria $MFH_r \geq MFH$	• Cylindrical and Conical Shells, and Elbows Compute the $MAWP^C_r$ based on the thickness $\left(t_{am} - FCA\right)/RSF_a$ Compute the $MAWP^L_r$ based on the thickness $\left(t_{am} - t_{sl} - FCA\right)/RSF_a$ Acceptability criteria $\min\left[MAWP^C_r,\, MAWP^L_r\right] \geq MAWP$ • Spherical Shells and Formed Heads Compute the $MAWP_r$ based on the thickness $\left(t_{am} - FCA\right)/RSF_a$ Acceptability criteria $MAWP_r \geq MAWP$ • Atmospheric And Low Pressure Storage Tanks Compute the MFH_r based on the thickness $\left(t_{am} - FCA\right)$ Acceptability criteria $MFH_r \geq MFH$

Table 4.4– Acceptance Criteria For Level 1 And 2 Assessments

Assessment Parameter	Level 1 Assessment Acceptance Criteria	Level 2 Assessment Acceptance Criteria
MAWP or *MFH* from Critical Thickness Profiles *(CTP)*	• Cylindrical and Conical Shells, and Elbows Compute the $MAWP_r^C$ based on the thickness $\left(t_{am}^s - FCA\right)$ Compute the $MAWP_r^L$ based on the thickness $\left(t_{am}^c - FCA\right)$ Acceptability criteria $\min\left[MAWP_r^C,\ MAWP_r^L\right] \geq MAWP$ • Spherical Shells and Formed Heads Compute the $MAWP_r$ based on the thickness $\left(\min\left[t_{am}^s,\ t_{am}^c\right] - FCA\right)$ Acceptability criteria $MAWP_r \geq MAWP$ • Atmospheric And Low Pressure Storage Tanks Compute the MFH_r based on the thickness $\left(t_{am}^s - FCA\right)$ Acceptability criteria $MFH_r \geq MFH$	• Cylindrical and Conical Shells, and Elbows Compute the $MAWP_r^C$ based on the thickness $\left(t_{am}^s - FCA\right)\big/RSF_a$ Compute the $MAWP_r^L$ based on the thickness $\left(t_{am}^c - t_{sl} - FCA\right)\big/RSF_a$ Acceptability criteria $\min\left[MAWP_r^C,\ MAWP_r^L\right] \geq MAWP$ • Spherical Shells and Formed Heads Compute the $MAWP_r$ based on the thickness $\left(\min\left[t_{am}^s,\ t_{am}^c\right] - FCA\right)\big/RSF_a$ Acceptability criteria $MAWP_r \geq MAWP$ • Atmospheric And Low Pressure Storage Tanks Compute the MFH_r based on the thickness $\left(t_{am}^s - FCA\right)$ Acceptability criteria $MFH_r \geq MFH$
Minimum Measured Thickness	• Pressure Vessel Components $\left(t_{mm} - FCA\right) \geq \max\left[0.5t_{\min},\ t_{\lim}\right]$ $t_{\lim} = \max\left[0.2t_{nom},\ 2.5\ mm\ (0.10\ inches)\right]$ • Piping Components $\left(t_{mm} - FCA\right) \geq \max\left[0.5t_{\min},\ t_{\lim}\right]$ $t_{\lim} = \max\left[0.2t_{nom},\ 2.5\ mm\ (0.10\ inches)\right]$ • Atmospheric And Low Pressure Storage Tanks $\left(t_{mm} - FCA\right) \geq \max\left[0.6t_{\min},\ t_{\lim}\right]$ $t_{\lim} = \max\left[0.2t_{nom},\ 2.5\ mm\ (0.10\ inches)\right]$	

Notes:

1. Procedures to compute the minimum required thickness (i.e. $t_{\min}^C$, $t_{\min}^L$, and $t_{\min}$, as applicable) for pressure vessel components, piping components and atmospheric storage tank shells are provided in Annex A
2. Procedures to compute the maximum allowable working pressure (i.e. $MAWP^C$, $MAWP^L$, and $MAWP$, as applicable) for pressure vessel components and piping components, and the maximum fill height, MFH, for atmospheric storage tank shells are provided in Annex A
3. In the above equations, t_{mm} may be substituted for t_{am}, t_{am}^s, or t_{am}^c to produce a conservative result.

Table 4.5– Parameters To Compute The Length For Thickness Averaging

R_t	Q				
	$RSF_a = 0.90$	$RSF_a = 0.85$	$RSF_a = 0.80$	$RSF_a = 0.75$	$RSF_a = 0.70$
0.900	50.00	50.00	50.00	50.00	50.00
0.895	21.19	50.00	50.00	50.00	50.00
0.875	4.93	50.00	50.00	50.00	50.00
0.850	2.82	50.00	50.00	50.00	50.00
0.845	2.62	29.57	50.00	50.00	50.00
0.825	2.07	6.59	50.00	50.00	50.00
0.800	1.68	3.65	50.00	50.00	50.00
0.795	1.62	3.38	36.82	50.00	50.00
0.775	1.43	2.63	8.01	50.00	50.00
0.750	1.26	2.11	4.35	50.00	50.00
0.745	1.23	2.03	4.01	42.94	50.00
0.725	1.12	1.77	3.10	9.20	50.00
0.700	1.02	1.54	2.45	4.93	50.00
0.695	1.00	1.51	2.36	4.53	47.94
0.675	0.93	1.37	2.05	3.47	10.16
0.650	0.86	1.24	1.77	2.73	5.39
0.625	0.80	1.13	1.56	2.26	3.77
0.600	0.74	1.04	1.40	1.95	2.94
0.575	0.70	0.96	1.27	1.71	2.43
0.550	0.65	0.89	1.16	1.53	2.07
0.525	0.61	0.83	1.07	1.38	1.81
0.500	0.58	0.77	0.99	1.26	1.61
0.475	0.55	0.72	0.92	1.15	1.45
0.450	0.51	0.68	0.86	1.06	1.32
0.425	0.49	0.64	0.80	0.98	1.20
0.400	0.46	0.60	0.74	0.91	1.10
0.375	0.43	0.56	0.70	0.84	1.01
0.350	0.41	0.53	0.65	0.78	0.93
0.325	0.38	0.50	0.61	0.73	0.86
0.300	0.36	0.46	0.57	0.67	0.79
0.275	0.34	0.43	0.53	0.63	0.73
0.250	0.31	0.40	0.49	0.58	0.67
0.200	0.27	0.35	0.42	0.49	0.57

Notes:

1. The equation for Q is:

$$Q = 1.123\left[\left(\frac{1-R_t}{1-R_t/RSF_a}\right)^2 - 1\right]^{0.5} \qquad for \quad R_t < RSF_a$$

$$Q = 50.0 \qquad for \quad R_t \geq RSF_a$$

2. The length for thickness averaging is given by Equation (4.5).

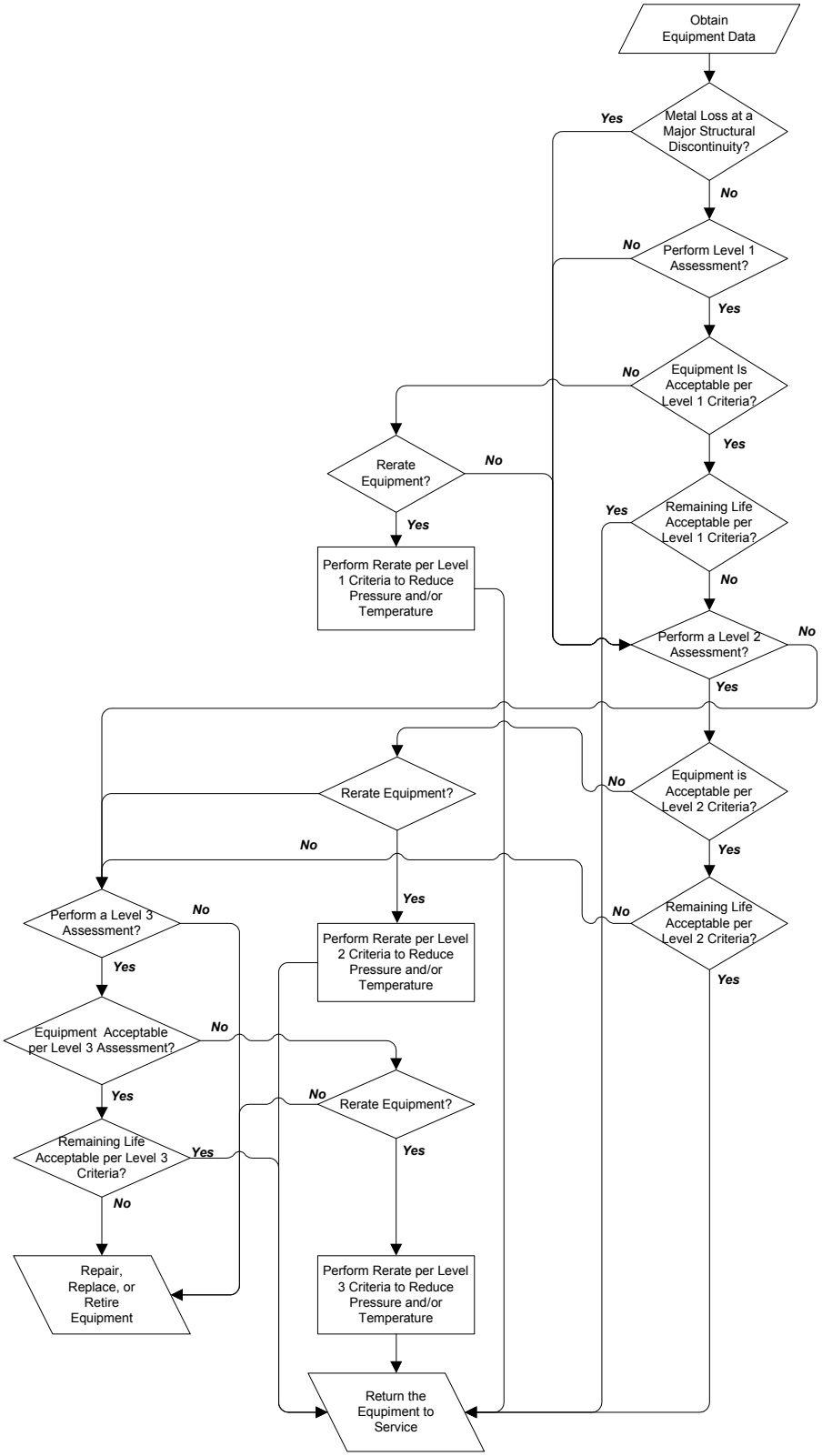

Figure 4.1 – Overview of the Assessment Procedures to Evaluate a Component with General Metal Loss

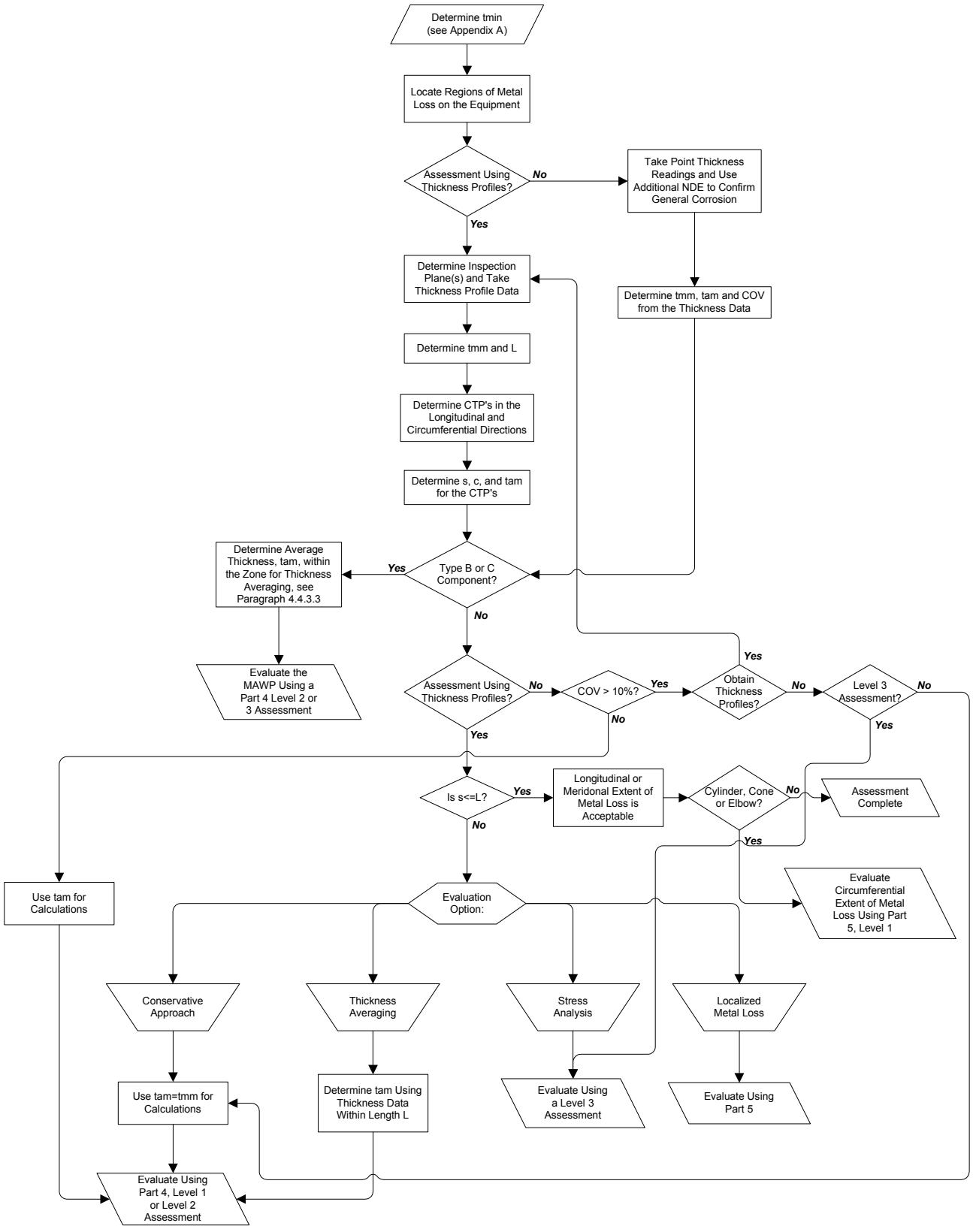

Figure 4.2 – Assessment Procedure to Evaluate a Component with Metal Loss Using Part 4 and Part 5

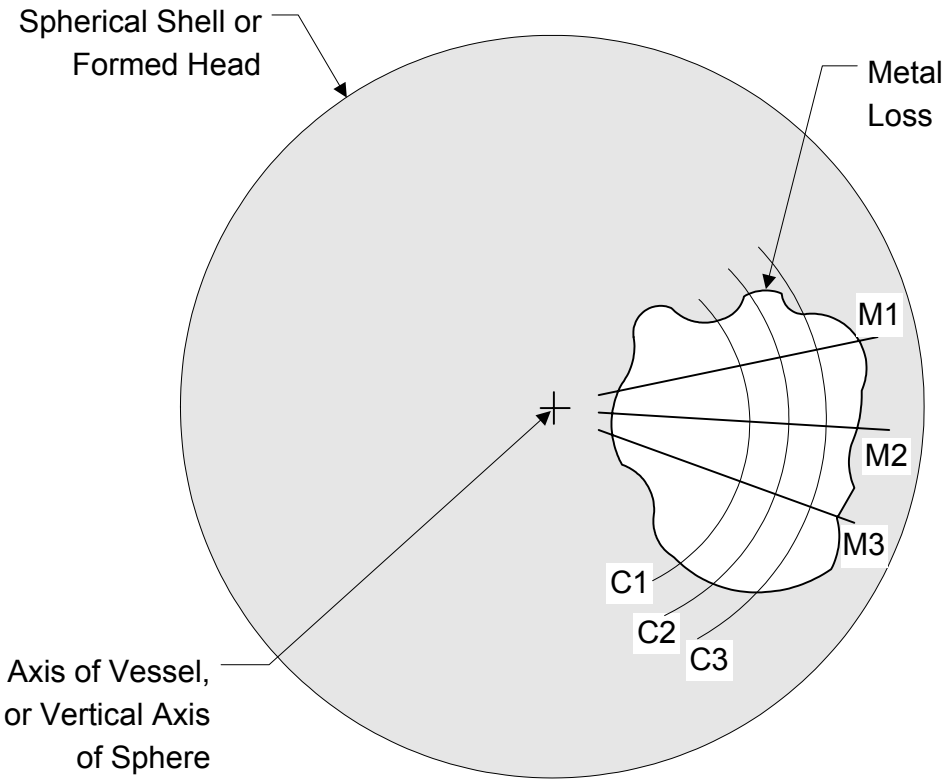

Note: M1 – M3 are meridional inspection planes and C1–C3 are circumferential inspection planes.

Figure 4.3 – Inspection Planes for Pressure Vessel Heads and Spheres

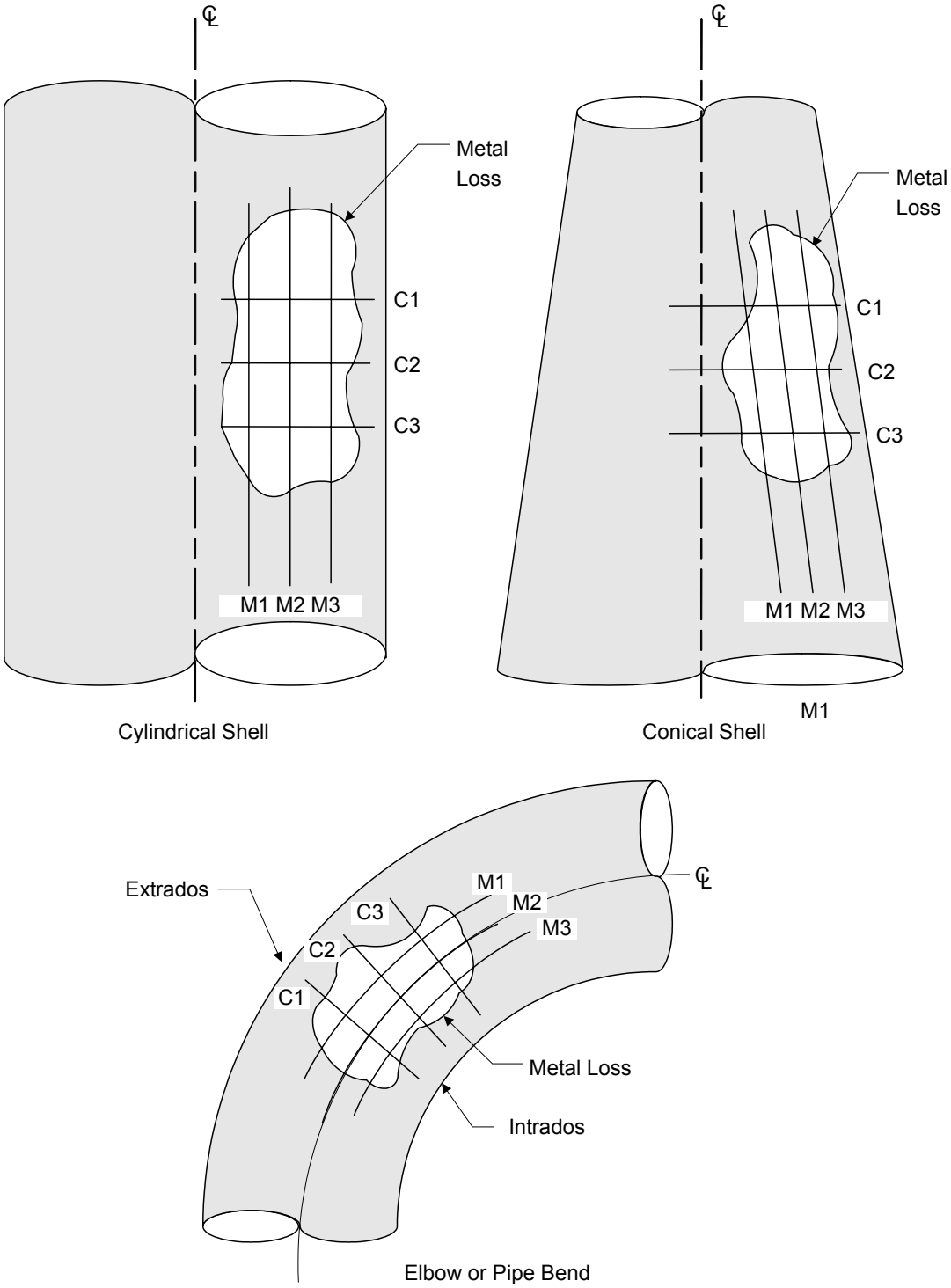

Notes:

1. For cylindrical and conical shells, M1 – M3 are meridional (longitudinal direction) inspection planes and C1–C3 are circumferential inspection planes.
2. For elbows and pipe bends, M1 – M3 are longitudinal inspection planes and C1–C3 are circumferential inspection planes.

Figure 4.4 – Inspection Planes for Cylindrical Shells, Conical Shells, and Pipe Bends

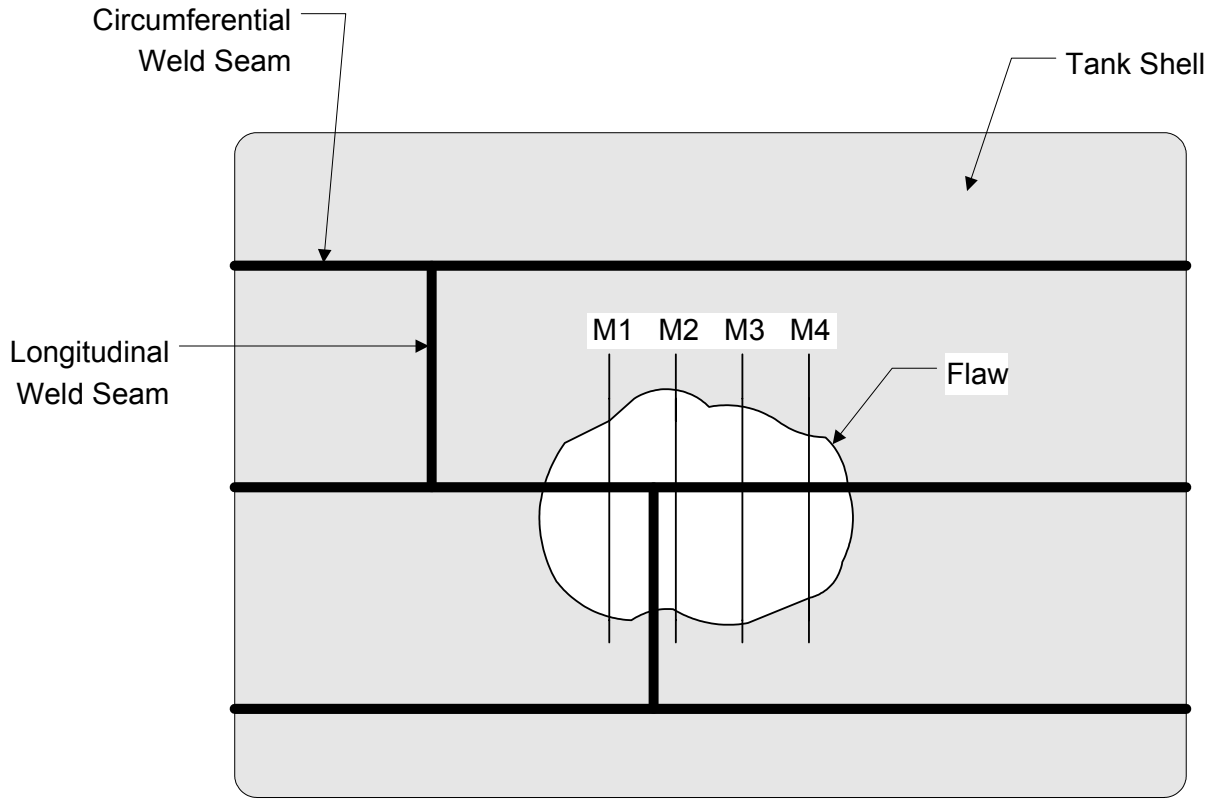

Notes:
1. M1 – M4 are meridional (longitudinal direction).
2. Circumferential inspection planes are not required because the stress normal to this direction is negligibly small and does not govern the design thickness calculation.

Figure 4.5 – Inspection Planes for Atmospheric Storage Tanks

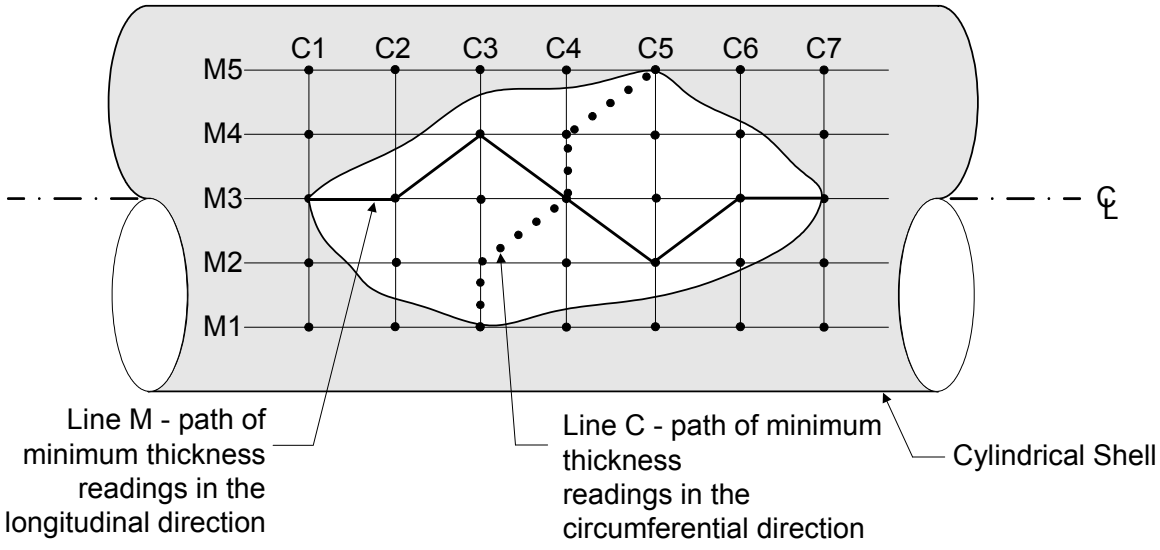

(a) Inspection Planes and the Critical Thickness Profile

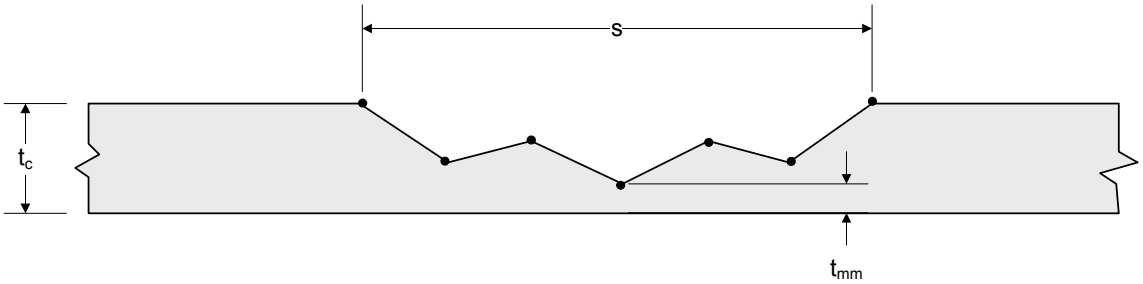

(b) Critical Thickness Profile (CTP) - Longitudinal Plane (Projection of Line M)

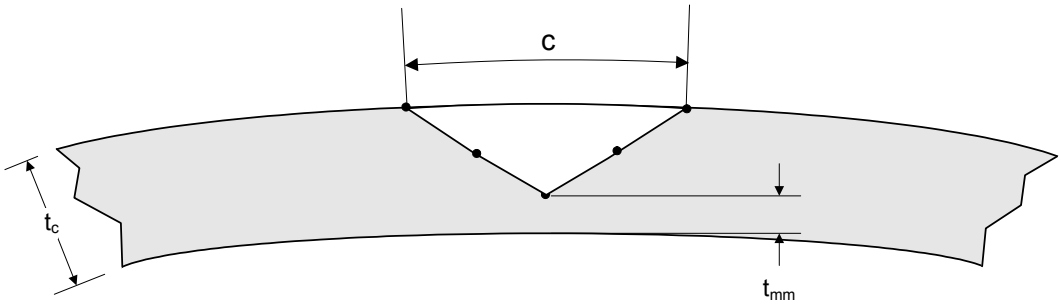

(c) Critical Thickness Profile (CTP) - Circumferential Plane (Projection of Line C)

Notes:
1. M1 – M5 are meridional (longitudinal) inspection planes.
2. C1 – C7 are circumferential inspection planes.

Figure 4.6 – Method for Determining the Plane of Maximum Metal Loss (Critical Thickness Profile)

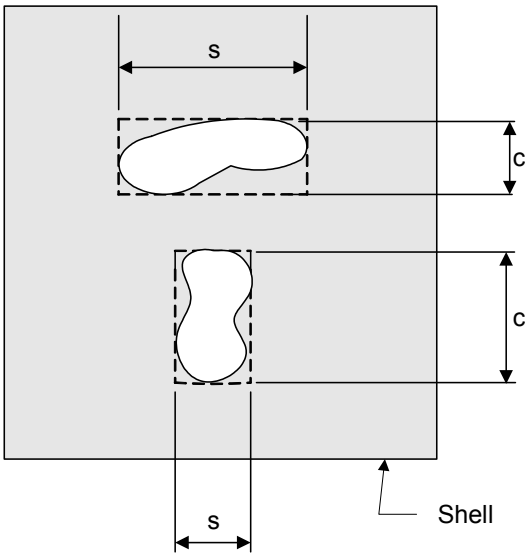

Step 1 - Draw a box that completely encloses each LTA. Measure the maximum longitudinal (axial) extent, s (in. or mm.) and the maximum circumferential extent, c (in. or mm.) of this box. These will be the dimensions of the thinned area used in the assessment.

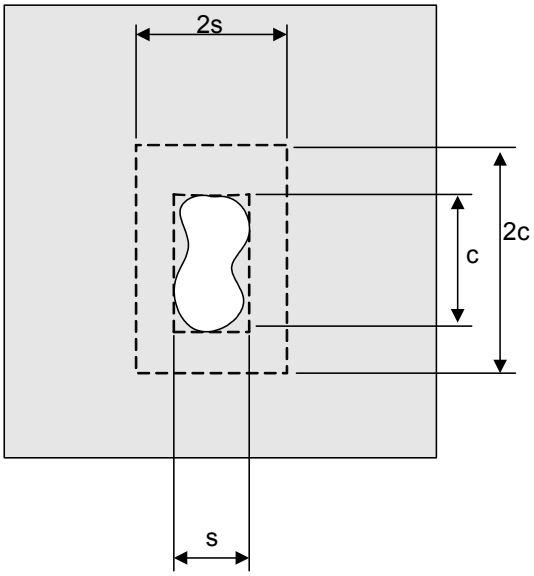

Step 2 - Draw a second box twice the size of the first box (2s x 2c) around each LTA.

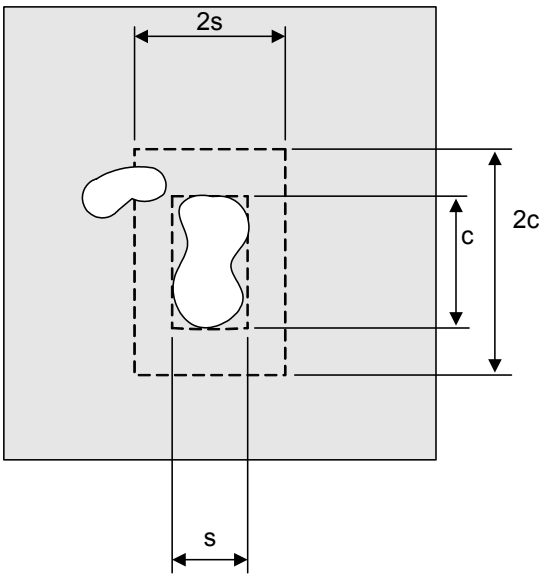

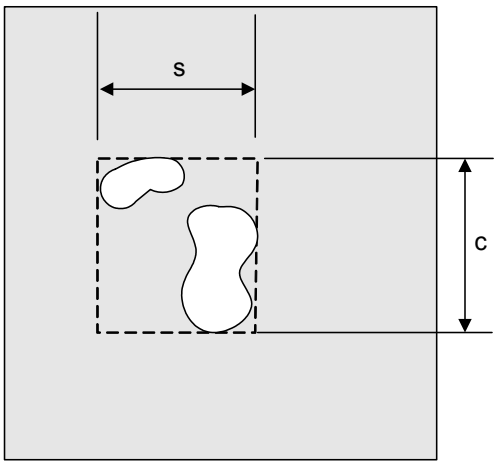

Step 3 - If another LTA is within the larger box, the dimensions s and c should be adjusted to include the additional thinned area. Go back to step 2.

Figure 4.7 – Sizing of a Region with Multiple Areas of Metal Loss for an Assessment

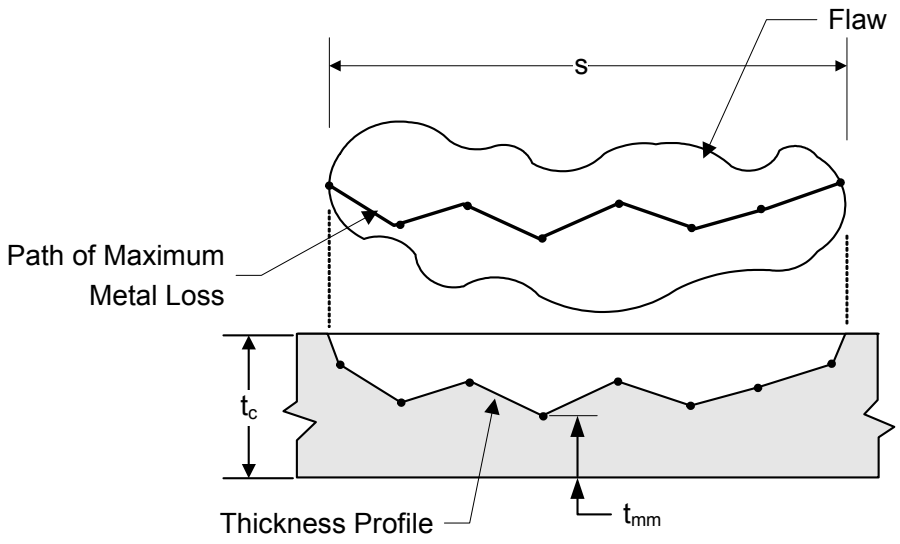

(a) Isolated Flaw

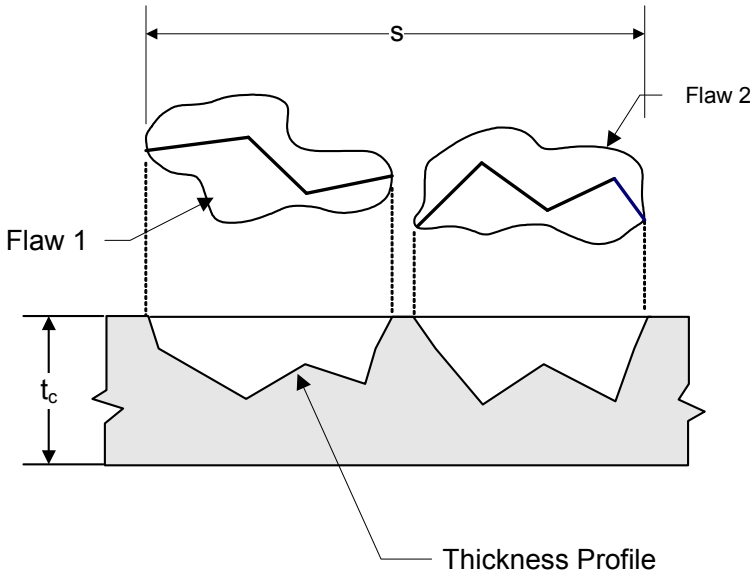

Note: Flaw 1 and Flaw 2 Are Combined Based on the Criterion Shown In Figure 4.7 To Form A Single Flaw For The Assessment

(b) Network Of Flaws

Figure 4.8 – Sizing of an Isolated Metal Loss Region and a Network of Metal Loss Regions

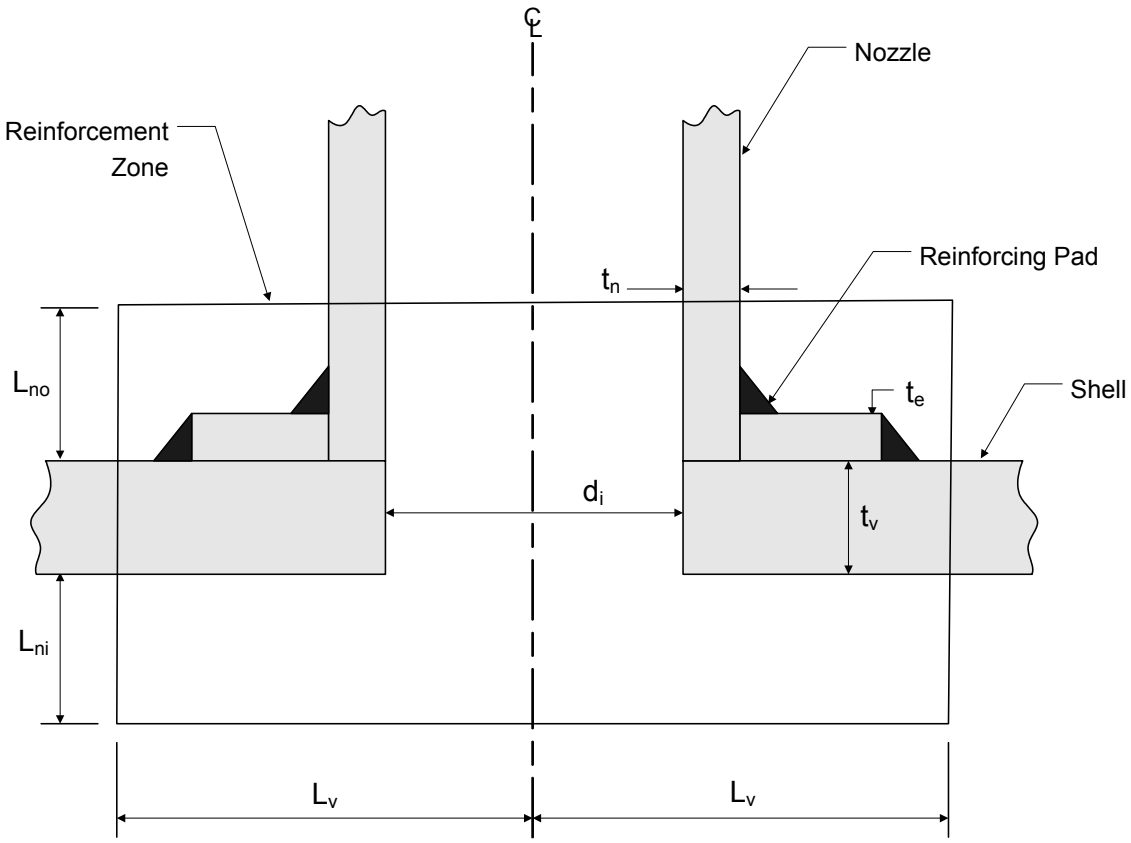

Nozzle with a Reinforcement Element

Notes:

1. $L_v = \max\left[d_i,\ \left(d_i/2 + t_n + t_v\right)\right]$ (thickness averaging zone in the horizontal direction, see paragraph 4.3.3.4.a)
2. $L_{no} = \min\left[2.5t_v,\ \left(2.5t_n + t_e\right)\right]$ (thickness averaging zone in the vertical direction on the outside of the shell, see paragraph 4.3.3.4.a)
3. $L_{ni} = \min\left[2.5t_v,\ 2.5t_n\right]$ (thickness averaging zone in the vertical direction on the inside of the shell, see 4.3.3.4.a)
4. See paragraph 4.4.3.3.b.1 to determine the length for thickness averaging

Figure 4.9 – Zone for Thickness Averaging – Nozzles and Fabricated Branch Connections

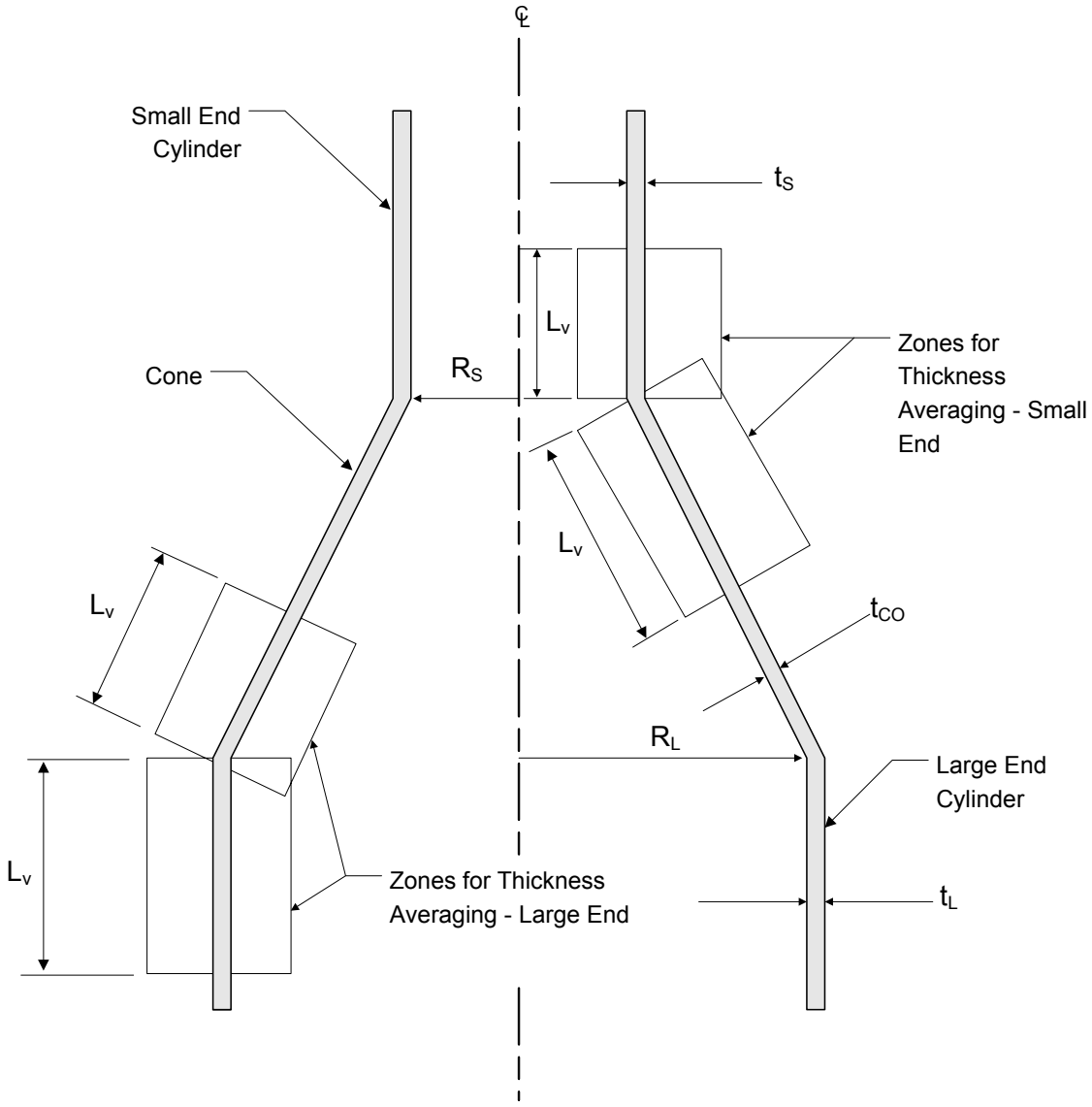

Notes:

1. $L_v = 0.78\sqrt{R_S t_S}$ (thickness averaging zone for the small end cylinder , see paragraph 4.3.3.4.b)
2. $L_v = 0.78\sqrt{R_S t_{CO}}$ (thickness averaging zone for the small end cone see, paragraph 4.3.3.4.b)
3. $L_v = 1.0\sqrt{R_L t_{CO}}$ (thickness averaging zone for the large end cone, see paragraph 4.3.3.4.b)
4. $L_v = 1.0\sqrt{R_L t_L}$ (thickness averaging zone for the large end cylinder, see paragraph 4.3.3.4.b)
5. See paragraph 4.4.3.3.b.1 to determine the length for thickness averaging.

Figure 4.10 – Zone for Thickness Averaging – Conical Transitions

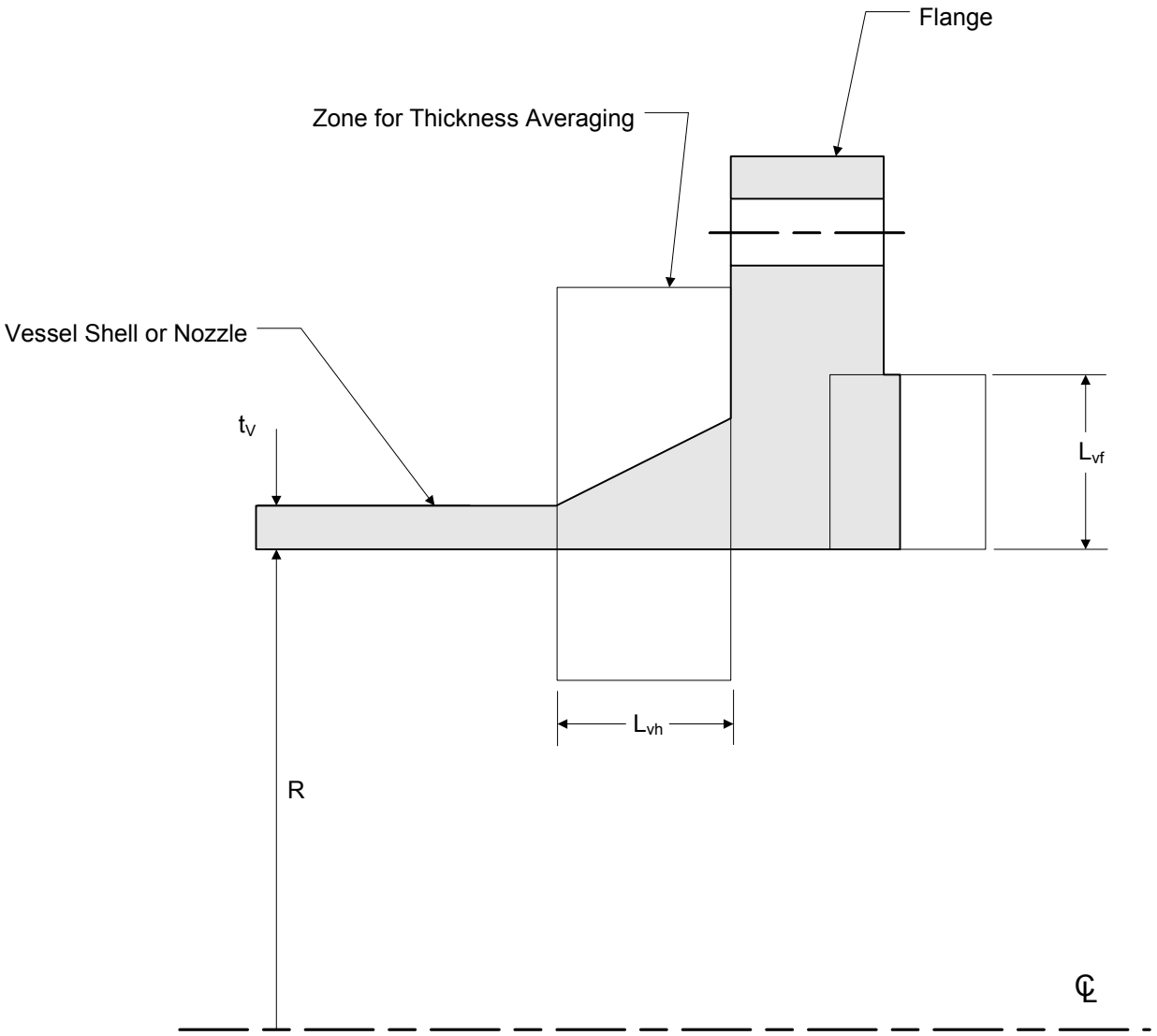

Notes:

1. L_{vh} is thickness averaging zone for the hub.
2. L_{vf} is thickness averaging zone for the flange.

Figure 4.11 – Zone for Thickness Averaging – Flange Connections

PART 5

ASSESSMENT OF LOCAL METAL LOSS

PART CONTENTS

5.1 General

5.1.1 Fitness-For-Service (*FFS*) assessment procedures for pressurized components subject to local metal loss resulting from corrosion/erosion and/or mechanical damage are provided in this Part. These procedures can be used to qualify a component for continued operation or rerating, and can also be used to evaluate regions of local metal loss resulting from blend grinding of crack-like flaws. A flow chart for the assessment procedures for local metal loss is shown in Figure 5.1.

5.1.2 The assessment procedures of this Part are for the analysis of local metal loss whereas the procedures of Part 4 are for general metal loss. The methodology shown in Part 4 Figure 4.2 can be used to determine whether the assessment procedures of Part 4 or Part 5 should be used in the evaluation. For most evaluations, it is recommended to first perform an assessment using Part 4. The assessment procedures for local metal loss in this Part can only be established using thickness profiles because the size of the region of the metal loss is required as well as thickness data for the assessment.

5.1.3 Damage associated with pitting and blisters can also be evaluated using the assessment procedures in this Part in conjunction with the assessment procedures of Part 6 and Part 7, respectively.

5.2 Applicability and Limitations of the Procedure

5.2.1 The procedures in this Part can be used to evaluate components subject to local metal loss from corrosion/erosion, mechanical damage, or blend grinding that exceeds, or is predicted to exceed, the corrosion allowance before the next scheduled inspection. The local metal loss may occur on the inside or outside of the component. The types of flaws that are characterized as local metal loss are defined as follows:

a) *Local Thin Area (LTA)* – local metal loss on the surface of the component; the length of a region of metal loss is the same order of magnitude as the width.

b) *Groove-Like Flaw* – the following flaws are included in this category; a sharp radius may be present at the base of a groove-like flaw.

   1) *Groove* – local elongated thin spot caused by directional erosion or corrosion; the length of the metal loss is significantly greater than the width.

   2) *Gouge* – elongated local mechanical removal and/or relocation of material from the surface of a component, causing a reduction in wall thickness at the defect; the length of a gouge is much greater than the width and the material may have been cold worked in the formation of the flaw. Gouges are typically caused by mechanical damage, for example, denting and gouging of a section of pipe by mechanical equipment during the excavation of a pipeline. Gouges are frequently associated with dents due to the nature of mechanical damage. If a gouge is present, the assessment procedures of Part 12 shall be used.

5.2.2 Unless otherwise specified, this Part is limited to the evaluation of local metal loss. Other flaw types shall be evaluated in accordance with Part 2 Table 2.1.

5.2.3 Calculation methods are provided to rerate the component if the acceptance criteria in this Part are not satisfied. For pressurized components, the calculation methods can be used to find a reduced maximum allowable working pressure *(MAWP)*. For tank shell courses, the calculation methods can be used to determine a reduced maximum fill height *(MFH)*.

5.2.4 The assessment procedures only apply to components that are not operating in the creep range; the design temperature is less or equal to the value in Part 4, Table 4.1. A Materials Engineer should be consulted regarding the creep range temperature limit for materials not listed in this table. Assessment procedures for components operating in the creep range are provided in Part 10.

5.2.5 Specific details pertaining to the applicability and limitations of each of the assessment procedures are discussed below.

5.2.5.1 The Level 1 or 2 Assessment procedures in this Part apply only if all of the following conditions are satisfied.

a) The original design criteria were in accordance with a recognized code or standard (see Part 1, paragraphs 1.2.2 or 1.2.3).

b) The material is considered to have sufficient material toughness. If there is uncertainty regarding the material toughness, then a Part 3 assessment should be performed. If the component is subject to embrittlement during operation due to temperature and/or the process environment, a Level 3 assessment should be performed. Temperature and/or process conditions that result in material embrittlement are discussed in Annex G.

c) The component is not in cyclic service. If the component is subject to less than 150 cycles (i.e. pressure and/or temperature variations including operational changes and start-ups and shut-downs) throughout its previous operating history and future planned operation, or satisfies the cyclic service screening procedure in Annex B1, paragraph B1.5.2, then the component is not in cyclic service.

d) The following limitations on component types and applied loads are satisfied:

   1) Level 1 Assessment – Type A Components (see Part 4, paragraph 4.2.5) subject to internal pressure (i.e. supplemental loads are assumed to be negligible).

   2) Level 2 Assessment – Type A or B Components (see Part 4, paragraph 4.2.5) subject to internal pressure, external pressure, supplemental loads (see Annex A, paragraph A.2.7), or any combination thereof.

e) A flaw categorized as a groove in accordance with paragraph 5.2.1.b has a groove radius that satisfies the requirements in paragraph 5.4.2.2.f.

5.2.5.2 A Level 3 Assessment can be performed when the Level 1 and 2 Assessment procedures do not apply, or when these assessment levels produce conservative results (i.e. would not permit operation at the current design conditions). Examples include, but are not limited to the following.

a) Type A, B, or C Components (see Part 4, paragraph 4.2.5) subject to internal pressure, external pressure, supplemental loads, and any combination thereof.

b) Components with a design based on proof testing (e.g. piping tee or reducer produced in accordance with ASME B16.9 where the design may be based on proof testing).

c) Components in cyclic service or components where a fatigue analysis was performed as part of the original design calculations; the assessment should consider the effects of fatigue on the Fitness–For–Service calculations used to qualify the component for continued operation.

d) The metal loss is located in the knuckle region of elliptical heads (outside of the $0.8D$ region), torispherical and toriconical heads, or in conical transitions.

5.2.5.3 The assessment procedures in this Part can be used to evaluate a region of local metal loss that is created when a crack-like flaw is removed by blend grinding.

5.3 Data Requirements

5.3.1 Original Equipment Design Data

An overview of the original equipment data required for an assessment is provided in Part 2, paragraph 2.3.1. These data can be entered in the form provided in Part 2, Table 2.2, and Table 5.1 for each component under evaluation.

5.3.2 Maintenance and Operational History

An overview of the maintenance and operational history required for an assessment is provided in Part 2, paragraph 2.3.2.

5.3.3 Required Data/Measurements for a FFS Assessment

5.3.3.1 To assess general corrosion/erosion, thickness readings are required on the component in the area where the metal loss has occurred. If the metal loss is less than the specified corrosion/erosion allowance and adequate thickness is available for the future corrosion allowance, no further action is required other than to record the data.

5.3.3.2 The following information is required for a Level 1 and Level 2 Assessment.

a) *Thickness Profiles* – The region of local metal loss on the component should be identified and inspection planes should be established to record thickness data. Based on these inspection planes, Critical Thickness Profiles (CTP) and the minimum measured thickness, t_{mm}, can be established for the flaw types shown below using the procedures in Part 4, paragraph 4.3.3.3.

1) $Local\ Thin\ Area\ (LTA)$ – A grid should be established to obtain thickness readings and to establish the CTP in the meridional (longitudinal direction for a cylinder) and circumferential directions. For an atmospheric storage tank, only the longitudinal CTP is required.

2) *Groove-Like Flaw* – For groove-like flaws oriented in the circumferential and longitudinal directions, a grid similar to that used for an LTA can be utilized. For all other groove-like flaw orientations, the inspection planes of the grid should be located parallel and perpendicular to the groove.

b) *Flaw Dimensions* – The following procedures can be used to establish the flaw dimensions.

1) $Local\ Thin\ Area\ (LTA)$ – The relevant dimensions are s and c (see Figure 5.2) that are defined as the longitudinal and circumferential dimensions, respectively, of the extent of the local metal loss based on the corresponding CTP. The CTP is determined using the procedure in Part 4, paragraph 4.3.3.3.

2) *Groove-Like Flaw* – The relevant parameters are g_l, g_w, g_r, and β, the dimensions that define the length, width, radius and orientation of the *Groove-Like Flaw*, respectively (see Figures 5.3 and 5.4). The flaw dimensions g_l and g_w are based on the corresponding CTP measured parallel and normal to the groove. In the Level 1 and Level 2 Assessment procedures, the Groove-Like Flaw is treated as an equivalent LTA with dimensions s and c established as shown in Figure 5.4. For cylinders and cones, if the groove is orientated at an angle to the longitudinal axis, then the groove-like flaw profile can be projected on to the longitudinal and circumferential planes using the following equations to establish the equivalent LTA dimensions (see Figure 5.4). Alternatively, the flaw may be treated as an LTA with dimensions s and c established using subparagraph 1 above.

$$s = g_l \cos\beta + g_w \sin\beta \qquad for \quad \beta < 90\ Degrees \tag{5.1}$$

$$c = g_l \sin\beta + g_w \cos\beta \qquad for \quad \beta < 90\ Degrees \tag{5.2}$$

c) *Flaw-To-Major Structural Discontinuity Spacing* – The distance to the nearest major structural discontinuity should be determined (see Figure 5.5).

d) *Vessel Geometry Data* – The information required depends on the shell type as summarized in paragraphs 5.4.2 and 5.4.3 for a Level 1 and Level 2 Assessment, respectively.

e) *Materials Property Data* – The information required is summarized in paragraphs 5.4.2 and 5.4.3 for a Level 1 and Level 2 Assessment, respectively.

5.3.3.3 The information required to perform a Level 3 Assessment depends on the analysis method utilized. In general, a limit load procedure using a numerical technique can be used to establish acceptable operating conditions. For this type of analysis, a description of the local metal loss including size and thickness profiles (similar to that required for a Level 2 Assessment) should be obtained along with the material yield strength (see paragraph 5.4.4).

5.3.4 Recommendations for Inspection Technique and Sizing Requirements

5.3.4.1 Recommendations for obtaining thickness measurements to characterize the local metal loss are covered in Part 4, paragraph 4.3.4.

5.3.4.2 The radius at the base of the groove-like flaw can be established by using a profile gauge. Alternatively, a mold can be made of the flaw using clay or a similar material and the radius can be directly determined from the mold.

5.3.4.3 In addition to thickness readings to establish the thickness profile, the following examination is recommended:

a) All weld seams within a *"2s x 2c box"* (see Figure 5.2), and the entire surface of the flaw should be examined using Magnetic Particle (MT), Dye Penetrant (PT), or Ultrasonic (UT) techniques,

b) Any portion of a weld seam with a thickness less than the required thickness, $t_{\min}$, within a *"2s x 2c box"* (see Figure 5.2) should be volumetrically examined with Radiographic (RT) or Ultrasonic (UT) techniques, and

c) If crack-like flaws or porosity not meeting the acceptance criteria of the original construction code are found, they should be repaired or an assessment in accordance with Part 9 should be conducted.

5.4 Assessment Techniques and Acceptance Criteria

5.4.1 Overview

5.4.1.1 If the metal loss is less than the specified corrosion/erosion allowance and adequate thickness is available for the future corrosion allowance, no further action is required other than to record the data; otherwise, an assessment is required.

5.4.1.2 An overview of the assessment levels is provided in Figure 5.1.

a) Level 1 Assessments are limited to Type A Components (see Part 4, paragraph 4.2.5). The only load considered is internal pressure, and a single thickness with one or two surface area dimensions are used to characterize the local metal loss.

b) The Level 2 Assessment rules provide a better estimate of the structural integrity of a component when significant variations in the thickness profile occur within the region of metal loss. More general loading is considered (e.g. net-section bending moments on a cylindrical shell), and rules are provided for the evaluation of local metal loss at a nozzle connection.

c) Level 3 Assessment rules are intended to evaluate components with complex geometries and/or regions of localized metal loss. Numerical stress analysis techniques are normally utilized in a Level 3 assessment.

5.4.2 Level 1 Assessment

5.4.2.1 The Level 1 Assessment procedures can be used to evaluate a Type A Component with local metal loss subject to internal pressure. The procedures can be used to determine acceptability and/or to rerate a component with a flaw. If there are significant thickness variations over the length of the flaw or if a network of flaws is closely spaced, this procedure may produce conservative results, and a Level 2 assessment is recommended.

5.4.2.2 The following assessment procedure can be used to evaluate Type A Components subject to internal pressure (see paragraph 5.2.5.1.d). The procedure shown below is developed for pressurized components where an $MAWP$ can be determined. For an atmospheric storage tank, the same procedure can be followed to determine a MFH by replacing the $MAWP$ with the MFH, and determining the MFH using the applicable code equations for a tank shell.

a) STEP 1 – Determine the CTP (see paragraph 5.3.3.2).

b) STEP 2 – Determine the wall thickness to be used in the assessment using Equation (5.3) or Equation (5.4), as applicable.

$$t_c = t_{nom} - LOSS - FCA \tag{5.3}$$

$$t_c = t_{rd} - FCA \tag{5.4}$$

c) STEP 3 – Determine the minimum measured thickness in the LTA, t_{mm}, and the dimension, s, (see paragraph 5.3.3.2.b) for the CTP.

d) STEP 4 – Determine the remaining thickness ratio using Equation (5.5) and the longitudinal flaw length parameter using Equation (5.6).

$$R_t = \frac{t_{mm} - FCA}{t_c} \tag{5.5}$$

$$\lambda = \frac{1.285s}{\sqrt{Dt_c}} \tag{5.6}$$

e) STEP 5 – Check the limiting flaw size criteria; if the following requirements are satisfied, proceed to STEP 6; otherwise, the flaw is not acceptable per the Level 1 Assessment procedure.

$$R_t \geq 0.20 \tag{5.7}$$

$$t_{mm} - FCA \geq 2.5\ mm\ (0.10\ inches) \tag{5.8}$$

$$L_{msd} \geq 1.8\sqrt{Dt_c} \tag{5.9}$$

f) STEP 6 – If the region of metal loss is categorized as an LTA (i.e. the LTA is not a groove), then proceed to STEP 7. If the region of metal loss is categorized as a groove and Equation (5.10) is satisfied, then proceed to STEP 7. Otherwise, the groove shall be evaluated as an equivalent crack-like flaw using the assessment procedures in Part 9. In this assessment, the crack depth shall equal the groove depth and the crack length shall equal the groove length.

$$g_r \geq (1 - R_t)t_c \tag{5.10}$$

g) STEP 7 – Determine the $MAWP$ for the component (see Annex A, paragraph A.2) using the thickness from STEP 2.

h) STEP 8 – Enter Figure 5.6 for a cylindrical shell or Figure 5.7 for a spherical shell with the calculated values of λ and R_t. If the point defined by the intersection of these values is on or above the curve, then the longitudinal extent (circumferential or meridional extent for spherical shells and formed heads) of the flaw is acceptable for operation at the $MAWP$ determined in STEP 7. If the flaw is unacceptable, then determine the RSF using Equation (5.11). If $RSF \geq RSF_a$, then the region of local metal loss is acceptable for operation at the $MAWP$ determined in STEP 7. If $RSF < RSF_a$, then the region of local metal loss is acceptable for operation at $MAWP_r$, where $MAWP_r$ is computed using the equations in Part 2, paragraph 2.4.2.2. The $MAWP$ from STEP 7 shall be used in this calculation.

$$RSF = \frac{R_t}{1 - \frac{1}{M_t}\left(1 - R_t\right)} \tag{5.11}$$

The parameter M_t in Equation (5.11) is determined from Table 5.2.

i) STEP 9 – The assessment is complete for all component types except cylindrical shells, conical shells, and elbows. If the component is a cylindrical shell, conical shell, or elbow, then evaluate the circumferential extent of the flaw using the following procedure.

1) STEP 9.1 – Determine the circumferential flaw length parameter using Equation (5.12).

$$\lambda_c = \frac{1.285c}{\sqrt{Dt_c}} \tag{5.12}$$

2) STEP 9.2 – If all of the following conditions are satisfied, proceed to STEP 9.3; otherwise, the flaw is not acceptable per the Level 1 Assessment procedure.

$$\lambda_c \le 9 \tag{5.13}$$

$$\frac{D}{t_c} \ge 20 \tag{5.14}$$

$$0.7 \le RSF \le 1.0 \tag{5.15}$$

$$0.7 \le E_L \le 1.0 \tag{5.16}$$

$$0.7 \le E_C \le 1.0 \tag{5.17}$$

3) STEP 9.3 – Determine the tensile stress factor using Equation (5.18).

$$TSF = \frac{E_C}{2 \cdot RSF}\left(1 + \frac{\sqrt{4 - 3E_L^2}}{E_L}\right) \tag{5.18}$$

4) STEP 9.4 – Determine the screening curve in Figure 5.8 based on TSF. Enter Figure 5.8 with the calculated values of λ_c and R_t. If the point defined by the intersection of these values is on or above the screening curve, then the circumferential extent of the flaw is acceptable per Level 1.

5.4.2.3 If the component does not meet the Level 1 Assessment requirements, then the following, or combinations thereof, shall be considered:

a) Rerate, repair, replace, or retire the component.

b) Adjust the FCA by applying remediation techniques (see Part 4 paragraph 4.6).

c) Adjust the weld joint efficiency factor by conducting additional examination and repeat the assessment (see Part 4, paragraph 4.4.2.3.c).

d) Conduct a Level 2 or Level 3 Assessment.

5.4.3 Level 2 Assessment

5.4.3.1 The Level 2 Assessment procedures provide a better estimate of the Remaining Strength Factor than computed in Level 1 for local metal loss in a component subject to internal pressure loading if there are significant variations in the thickness profile. These procedures account for the local reinforcement effects of the varying wall thickness in the region of the local metal loss and ensure that the weakest ligament is identified and properly evaluated. The procedures can also be directly used to evaluate closely spaced regions of local metal loss, and to evaluate cylindrical and conical shells with supplemental loads.

5.4.3.2 The following assessment procedure can be used to evaluate Type A Components subject to internal pressure (see paragraph 5.2.5.1.d). The procedure shown below is developed for pressurized components where a $MAWP$ can be determined. For an atmospheric storage tank, the same procedure can be followed to determine a MFH by replacing the $MAWP$ with the MFH, and determining the MFH using the applicable code equations for a tank shell.

a) STEP 1 – Determine the CTP (see paragraph 5.3.3.2).

b) STEP 2 – Determine the wall thickness to be used in the assessment using Equation (5.3) or Equation (5.4), as applicable.

c) STEP 3 – Determine the minimum measured thickness, t_{mm}, and the flaw dimensions s and c (see paragraph 5.3.3.2).

d) STEP 4 – Determine the remaining thickness ratio, R_t, using Equation (5.5) and the longitudinal flaw length parameter, λ, using Equation (5.6).

e) STEP 5 – Check the limiting flaw size criteria in paragraph 5.4.2.2.e). If all of these requirements are satisfied, then proceed to STEP 6; otherwise, the flaw is not acceptable per the Level 2 Assessment procedure.

f) STEP 6 – If the region of metal loss is categorized as an LTA (i.e. the LTA is not a groove), then proceed to STEP 7. If the region of metal loss is categorized as a groove and Equation (5.10) is satisfied, then proceed to STEP 7. Otherwise, the groove shall be evaluated as an equivalent crack-like flaw using the assessment procedures in Part 9. In this assessment, the crack depth shall equal the groove depth and the crack length shall equal the groove length.

g) STEP 7 – Determine the $MAWP$ for the component (see Annex A, paragraph A.2) using the thickness from STEP 2.

h) STEP 8 – Determine the Remaining Strength Factor for the longitudinal CTP using the following procedure.

   1) STEP 8.1 – Rank the thickness readings in ascending order based on metal loss.

   2) STEP 8.2 – Set the initial evaluation starting point as the location of maximum metal loss, this is the location in the thickness profile where t_{mm} is recorded. Subsequent starting points should be in accordance with the ranking in STEP 8.1.

3) STEP 8.3 – At the current evaluation starting point, subdivide the thickness profile into a series of subsections (see Figure 5.9). The number and extent of the subsections should be chosen based on the desired accuracy and should encompass the variations in metal loss.

4) STEP 8.4 – For each subsection, compute the Remaining Strength Factor using Equation (5.19).

$$RSF^i = \frac{1-\left(\frac{A^i}{A_o^i}\right)}{1-\frac{1}{M_t^i}\left(\frac{A^i}{A_o^i}\right)} \tag{5.19}$$

with,

$$A_o^i = s^i t_c \tag{5.20}$$

The parameter M_t^i in Equation (5.19) is determined from Table 5.2 using $\lambda = \lambda^i$.

5) STEP 8.5 – Determine the minimum value of the Remaining Strength Factors, RSF^i, found in STEP 8.4 for all subsections (see Figure 5.9). This is the minimum value of the Remaining Strength Factor for the current evaluation point.

6) STEP 8.6 – Repeat STEPs 8.3 through 8.5 of this calculation for the next evaluation point that corresponds to the next thickness reading location in the ranked thickness profile list.

7) STEP 8.7 – The Remaining Strength Factor to be used in the assessment, RSF, is the minimum value determined for all evaluation points.

i) STEP 9 – Evaluate the longitudinal extent of the flaw for cylindrical and conical shells. For spherical shells and formed heads evaluate the larger of the circumferential extent and meridional extent of the flaw. If $RSF \geq RSF_a$, then the region of local metal loss is acceptable for operation at the $MAWP$ determined in STEP 7. If $RSF < RSF_a$, then the region of local metal loss is acceptable for operation at $MAWP_r$, where $MAWP_r$ is computed using the equations in Part 2, paragraph 2.4.2.2. The $MAWP$ from STEP 7 shall be used in this calculation.

j) STEP 10 – For cylindrical shells, conical shells, and elbows, evaluate the circumferential extent of the flaw using the following criteria. If supplemental loads are not present or are not significant, then circumferential dimension, c, of the flaw determined from the circumferential CTP should satisfy the criterion in paragraph 5.4.2.2.i. If the supplemental loads are significant, then the circumferential extent of the region of local metal loss shall be evaluated using the procedures in paragraph 5.4.3.4.

5.4.3.3 The following assessment procedure can be used to evaluate cylindrical shells subject to external pressure. If the flaw is found to be unacceptable, the procedure can be used to establish a new $MAWP$.

a) STEP 1 – Determine the CTP (see paragraph 5.3.3.2).

b) STEP 2 – Subdivide the CTP in the longitudinal direction using a series of cylindrical shells that approximate the actual metal loss (see Figure 5.10). Determine the thickness and length of each of these cylindrical shells and designate them t_i and L_i.

c) STEP 3 – Determine the allowable external pressure, P_i^e, of each of the cylindrical shells defined in STEP 2 using $\left(t_i - FCA\right)$ and the total length, L_T, given by Equation (5.21), and designate this pressure as P_i^e. Methods for determining the allowable external pressure are provided in Annex A.

$$L_T = \sum_{i=1}^{n} L_i \tag{5.21}$$

d) STEP 4 – Determine the allowable external pressure of the actual cylinder using the following equation:

$$MAWP_r = \frac{L_T}{\sum_{i=1}^{n} \frac{L_i}{P_i^e}} \tag{5.22}$$

e) STEP 5 – If $MAWP_r \geq MAWP$, then the component is acceptable for continued operation. If $MAWP_r < MAWP$, then the component is acceptable for continued operation at $MAWP_r$.

5.4.3.4 The assessment procedure in this paragraph can be used to determine the acceptability of the circumferential extent of a flaw in a cylindrical or conical shell subject to pressure and/or supplemental loads. Note that the acceptability of the longitudinal extent of the flaw is evaluated using paragraph 5.4.3.2 or 5.4.3.3, as applicable.

a) *Supplemental Loads* – These types of loads may result in a net-section axial force, bending moment, torsion, and shear being applied to the cross section of the cylinder containing the flaw (see Annex A, paragraph A.2.7). Supplemental loads will result in longitudinal membrane, bending, and shear stresses acting on the flaw, in addition to the longitudinal and circumferential (hoop) membrane stress caused by pressure.

1) The supplemental loads included in the assessment should include loads that produce both load-controlled and strain-controlled effects. Therefore, the net-section axial force, bending moment, torsion, and shear should be computed for two load cases, weight and weight plus thermal. The weight load case includes pressure effects, weight of the component, occasional loads from wind or earthquake, and other loads that are considered as load controlled. The weight plus thermal load case includes the results from the weight case plus the results from a thermal case that includes the effects of temperature, support displacements and other loads that are considered as strain-controlled

2) For situations where the results of a detailed stress analysis are unavailable, the following modification may be made to the procedure in subparagraph c.

i) Calculate the longitudinal stress due to pressure and designate this value as S_{lp}.

ii) Subtract S_{lp} from the allowable stress for load-controlled effects, S_{al}, and the allowable stress for strain-controlled effects, S_{as}.

iii) Multiply each of the resulting stress values obtained in subparagraph ii) above by the section modulus of the cylinder in the uncorroded condition to obtain the maximum allowable load-controlled bending moment, M_{al}, and the strain-controlled bending moment, M_{as}.

iv) Calculate the longitudinal stress at point A, σ_{lm}^A, for the two load cases using Equation (5.27) by setting the axial force term, F, to zero and substituting M_{al} for both M_x and M_y to obtain the maximum load-controlled longitudinal stress, and M_{as} for both M_x and M_y to obtain the maximum strain-controlled longitudinal stress.

v) Calculate the longitudinal stress at point B, σ_{lm}^{B}, for the two load cases using Equation (5.28) by setting the axial force term, F, to zero and substituting M_{al} for both M_x and M_y to obtain the maximum load-controlled longitudinal stress, and M_{as} for both M_x and M_y to obtain the maximum strain-controlled longitudinal stress.

vi) Proceed to STEP 6 to evaluate the load-controlled and strain-controlled load cases values of σ_{lm}^{A} and σ_{lm}^{B}. When evaluating the results in STEP 6, set the shear stress, τ, to zero.

b) *Special Requirements For Piping Systems* – The relationship between the component thickness, piping flexibility or stiffness, and the resulting stress should be considered for piping systems.

1) The forces and moments acting on the circumferential plane of the defect resulting from supplemental loads can be computed from a piping stress analysis. The model used in this analysis should take into account the effects of metal loss. Recommendations for modeling piping components are provided in Part 4, paragraph 4.4.3.3.c.3. Alternatively, a maximum value of the moments can be computed using the procedure in paragraph 5.4.3.4.a.2).

2) Special consideration may be required if the local metal loss is located at an elbow or pipe bend (see Part 4, paragraph 4.4.4.4). A Level 3 Assessment using a detailed stress analysis performed using shell or continuum elements may be required in some cases.

c) *Assessment Procedure* – If the metal loss in the circumferential plane can be approximated by a single area (see Figure 5.11), then the following procedure can be used to evaluate the permissible membrane, bending and shear stresses resulting from pressure and supplemental loads. If the metal loss in the circumferential plane is composed of several distinct regions, then a conservative approach is to define a continuous region of local metal loss that encompasses all of these regions (as an alternative, see STEP 6 below).

1) STEP 1 – Determine the Critical Thickness Profiles(s) in the circumferential direction (see paragraph 5.3.3.2).

2) STEP 2 – For the circumferential inspection plane being evaluated, approximate the circumferential extent of metal loss on the plane under evaluation as a rectangular shape (see Figure 5.11).

i) For a region of local metal loss located on the inside surface,

$$D_f = D_o - 2\left(t_{mm} - FCA\right) \tag{5.23}$$

ii) For a region of local metal loss located on the outside surface:

$$D_f = D + 2\left(t_{mm} - FCA\right) \tag{5.24}$$

iii) The circumferential angular extent of the region of local metal loss is:

$$\theta = \frac{c}{D_f} \qquad (\theta \text{ in radians}) \tag{5.25}$$

3) STEP 3 – Determine the remaining strength factor, RSF, the reduced permissible maximum allowable working pressure, $MAWP_r$, and supplemental loads on the circumferential plane. The remaining strength factor and reduced maximum permissible pressure for the region of local metal loss can be established using the procedures in paragraph 5.4.3.2. The supplemental loads are determined in accordance with paragraphs 5.4.3.4.a and 5.4.3.4.b.

4) STEP 4 – For the supplemental loads determined in STEP 3, compute the components of the resultant longitudinal bending moment (i.e. excluding torsion) in the plane of the defect relative to the region of metal loss as shown in Figure 5.11. This will need to be done for the weight and weight plus thermal load cases.

5) STEP 5 – Compute the circumferential stress resulting from pressure for both the weight and weight plus thermal load cases at points A and B in the cross section (see Figure 5.12):

$$\sigma_{cm} = \frac{MAWP_r}{RSF \cdot \cos\alpha}\left(\frac{D}{D_o - D} + 0.6\right) \tag{5.26}$$

6) STEP 6 – Compute the longitudinal membrane stress and shear stress for the weight and weight plus thermal load cases at points A and B in the cross section (see Figure 5.12). All credible load combinations should be considered in the calculation. If the circumferential plane of the metal loss can be approximated by a rectangular area, then the section properties required for this calculation are provided in Table 5.3 (see Figure 5.11). If the metal loss in the circumferential plane cannot be approximated by a rectangular area because of irregularities in the thickness profile, then a numerical procedure may be used to compute the section properties and the membrane and bending stresses resulting from pressure and supplemental loads.

$$\sigma_{lm}^{A} = \frac{M_s^C}{E_C \cdot \cos\alpha}\left\{\begin{array}{l}\dfrac{A_w}{A_m - A_f}\left(MAWP_r\right) + \dfrac{F}{A_m - A_f} + \\ \dfrac{y_A}{I_{\bar{X}}}\left[F\bar{y} + \left(\bar{y} + b\right)\left(MAWP_r\right)A_w + M_x\right] + \dfrac{x_A}{I_{\bar{Y}}}M_y\end{array}\right\} \tag{5.27}$$

$$\sigma_{lm}^{B} = \frac{M_s^C}{E_C \cdot \cos\alpha}\left\{\begin{array}{l}\dfrac{A_w}{A_m - A_f}\left(MAWP_r\right) + \dfrac{F}{A_m - A_f} + \\ \dfrac{y_B}{I_{\bar{X}}}\left[F\bar{y} + \left(\bar{y} + b\right)\left(MAWP_r\right)A_w + M_x\right] + \dfrac{x_B}{I_{\bar{Y}}}M_y\end{array}\right\} \tag{5.28}$$

$$\tau = \frac{M_T}{2\left(A_t + A_{tf}\right)\left(t_{mm} - FCA\right)} + \frac{V}{A_m - A_f} \tag{5.29}$$

where

$$M_s^C = \frac{1 - \left(\dfrac{1}{M_t^C}\right)\left(\dfrac{d}{t_c}\right)}{1 - \left(\dfrac{d}{t_c}\right)} \tag{5.30}$$

$$M_t^C = \frac{1.0 + 0.1401\left(\lambda_c\right)^2 + 0.002046\left(\lambda_c\right)^4}{1.0 + 0.09556\left(\lambda_c\right)^2 + 0.0005024\left(\lambda_c\right)^4} \tag{5.31}$$

$$\lambda_c = \frac{1.285c}{\sqrt{Dt_c}} \tag{5.32}$$

Equation (5.31) is valid for $\lambda_c \le 9$. If the value of $\lambda_c > 9$, then a Level 3 Assessment is required except that if the circumferential extent of the LTA is 360°, then $M_t^c = 1.0$.

7) STEP 7 – Compute the equivalent membrane stress for both the weight and weight plus thermal load cases at points A and B in the cross section (see Figure 5.12):

$$\sigma_e^A = \left[\left(\sigma_{cm}\right)^2 - \left(\sigma_{cm}\right)\left(\sigma_{lm}^A\right) + \left(\sigma_{lm}^A\right)^2 + 3\tau^2 \right]^{0.5} \tag{5.33}$$

$$\sigma_e^B = \left[\left(\sigma_{cm}\right)^2 - \left(\sigma_{cm}\right)\left(\sigma_{lm}^B\right) + \left(\sigma_{lm}^B\right)^2 + 3\tau^2 \right]^{0.5} \tag{5.34}$$

8) STEP 8 – Evaluate the results as follows:

i) Equation (5.35) should be satisfied for either a tensile or compressive longitudinal stress for the weight and weight plus thermal load cases. For the weight case, $H_f = 1.0$, for the weight plus thermal load case $H_f = 3.0$.

$$\max\left[\sigma_e^A, \sigma_e^B\right] \le H_f \left(\frac{S_a}{RSF_a} \right) \tag{5.35}$$

ii) If the maximum longitudinal stress computed in STEP 6 is compressive, then this stress should be less than or equal to the allowable compressive stress computed using the methodology in Annex A, paragraph A.4.14 or the allowable tensile stress, whichever is smaller. When using this methodology to establish an allowable compressive stress, an average thickness representative of the region of local metal loss in the compressive stress zone should be used in the calculations.

9) STEP 9 – If the equivalent stress criterion in STEP 8 is not satisfied, the $MAWP$ and/or supplemental loads determined in STEP 3 should be reduced, and the evaluation outlined in STEPs 1 through 8 should be repeated. Alternatively, a Level 3 Assessment can be performed.

5.4.3.5 The assessment procedure in Part 4, paragraph 4.4.3.3 can be used to evaluate Type B components (see Part 4, paragraph 4.2.5) subject to the loads in paragraph 5.2.5.1.d.

5.4.3.6 If the component does not meet the Level 2 Assessment requirements, then the following, or combinations thereof, can be considered:

a) Rerate (i.e. reduce the $MAWP$ and/or supplemental loads), repair, replace, or retire the component.

b) Adjust the FCA by applying remediation techniques (see Part 4, paragraph 4.6).

c) Adjust the weld joint efficiency factor by conducting additional examination and repeat the assessment (see Part 4, paragraph 4.4.2.3.c).

d) Conduct a Level 3 Assessment.

5.4.4 Level 3 Assessment

The recommendations for a Level 3 Assessment of local metal loss are the same as those for general metal loss (see Part 4, paragraph 4.4.4).

5.5 Remaining Life Assessment

5.5.1 Thickness Approach

5.5.1.1 The remaining life of a component with a region of local metal loss can be estimated based upon computation of a minimum required thickness for the intended service conditions, actual thickness and region size measurements from an inspection, and an estimate of the anticipated corrosion/erosion rate and rate of change of the size of the flaw. If this information is known, or can be estimated, the equations in paragraph 5.4.2.2 or 5.4.3.2 can be solved iteratively with the following substitutions to determine the remaining life:

$$RSF \rightarrow RSF_a \tag{5.36}$$

$$R_t \rightarrow \frac{t_{mm} - \left(C_{rate} \cdot time\right)}{t_{\min}} \tag{5.37}$$

For a LTA or groove-like flaw evaluated as an equivalent LTA;

$$s \rightarrow s + C^s_{rate} \cdot time \tag{5.38}$$

$$c \rightarrow c + C^c_{rate} \cdot time \tag{5.39}$$

5.5.1.2 The rate-of-change in the size or characteristic length of a region of local metal loss can be estimated based upon inspection records. If this information is not available, engineering judgment should be applied to determine the sensitivity of the remaining life of the component to this parameter.

5.5.1.3 The remaining life determined using the thickness-based approach can only be utilized if the region of local metal loss is characterized by a single thickness. If a thickness profile is utilized (Level 2 assessment procedure), the remaining life should be established using the $MAWP$ Approach.

5.5.2 MAWP Approach

The $MAWP$ approach can be used to determine the remaining life of a pressurized component with a region of local metal loss characterized by a thickness profile. To use this approach, the methodology in Part 4, paragraph 4.5.2.2 is applied in conjunction with the assessment methods of this Part. When determining a remaining life with the $MAWP$ approach, the change in the flaw size should be considered as discussed in paragraph 5.5.1.

5.6 Remediation

The remediation methods for general corrosion provided in Part 4, paragraph 4.6 are applicable to local metal loss. Because of the localized damage pattern, it may be necessary in some cases to fill deep areas of metal loss with substances such as caulking, before applying linings.

5.7 In-Service monitoring

The remaining life may be difficult to establish for some regions of local metal loss in services where an estimate of the future metal loss and enlargement of the LTA cannot be adequately characterized. In these circumstances, remediation and/or in-service monitoring may be required to qualify the assumptions made to establish the remaining life. Typical monitoring methods and procedures are provided in Part 4, paragraph 4.7.

5.8 Documentation

5.8.1 The documentation of the FFS assessment should include the information cited in Part 2, paragraph 2.8.

5.8.2 Inspection data including all thickness readings and corresponding locations used to establish the thickness profile and determine and the minimum measured thickness, t_{mm}, should be recorded and included in the documentation. A sample data sheet is provided in Table 5.1 for this purpose. A sketch showing the location and orientation of the inspection planes on the component is also recommended.

5.9 Nomenclature

A^i area of metal loss based on s^i including the effect of FCA (Figure 5.9).

A^i_o original metal area based on s^i.

A_a cylinder aperture cross-section.

A_f cross-sectional area of the region of local metal loss, (the unshaded area labeled “Local Metal Loss” in Figure 5.12).

A_m metal area of the cylinder’s cross-section.

A_t mean area to compute torsion stress for the region of the cross section without metal loss.

A_{tf} mean area to compute torsion stress for the region of the cross section with metal loss.

A_w effective area on which pressure acts.

α cone half-apex angle.

b location of the centroid of area A_w, measured from the $x-x$ axis.

β orientation of the groove-like flaw with respect to the longitudinal axis.

C_{rate} anticipated future corrosion rate.

C^c_{rate} estimated rate of change of the circumferential length of the region of local metal loss.

C^s_{rate} estimated rate of change of the meridional length of the region of local metal loss.

c circumferential extent or length of the region of local metal loss (see Figure 5.2 and Figure 5.11) at the time of the inspection.

D inside diameter of the cylinder, cone (at the location of the flaw), sphere, or formed head; for the center section of an elliptical head an equivalent inside diameter of $K_c D_c$ is used where D_c inside diameter of the head straight flange and K_c is a factor defined in Annex A, paragraph A.3.6; for the center section of a torispherical head two times the crown radius of the spherical section is used. D shall be corrected for $LOSS$ and FCA as applicable.

D_f diameter at the base of the region of local metal loss (see Figure 5.12).

D_o outside diameter of the cylinder, corrected for $LOSS$ and FCA as applicable.

d maximum depth of the region of local metal loss.

E_C circumferential weld joint efficiency.

E_L longitudinal weld joint efficiency.

E_y modulus of elasticity.

F applied net-section axial force for the weight or weight plus thermal load case.

FCA future corrosion allowance applied to the region of local metal loss.

g_l length of the *Groove-Like Flaw.*

g_w width of the *Groove-Like Flaw.*

g_r radius at the base of a *Groove-Like Flaw.*

H_f allowable stress factor depending on the load case being evaluated.

θ angle describing the circumferential extent of the region of local metal loss on the cross section (see Figure 5.11 and Figure 5.12).

I_{LX} moment of inertia of area A_f about a local x-axis (see Figure 5.12).

I_{LY} moment of inertia of area A_f about the y-axis (see Figure 5.12).

I_X cylinder moment of inertia about the x-x axis .

I_Y cylinder moment of inertia about the y-y axis.

$I_{\bar{X}}$ moment of inertia of the cross section with the region of local metal loss about the $\bar{x}$-axis (see Figure 5.12).

$I_{\bar{Y}}$ moment of inertia of the cross section with the region of local metal loss about the $\bar{y}$-axis (see Figure 5.12).

$LOSS$ amount of uniform metal loss away from the local metal loss location at the time of the assessment.

L_i length of the cylinder i that is used to determine the maximum allowable external pressure of a cylindrical shell with an LTA (see Figure 5.10).

L_{msd} distance to the nearest major structural discontinuity.

L_T total length of the cylinder.

λ longitudinal flaw length parameter.

λ^i incremental longitudinal flaw length parameter..

λ_c circumferential flaw length parameter.

M_{al} load controlled bending moment.

M_{as} strain controlled bending moment.

M_T applied net-section torsion for the weight or weight plus thermal load, as applicable (see Figure 5.11).

M_x applied section bending moment for the weight or weight plus thermal load case about the x-axis, as applicable, that is defined as the component of the net-section bending moment that is perpendicular to M_y as shown in Figure 5.11.

M_y applied section bending moment for the weight or weight plus thermal load case about the y-axis, as applicable, that is defined as the component of the net-section bending moment that is perpendicular to M_x as shown in Figure 5.11.

M_t Folias factor based on the longitudinal extent of the LTA for a through-wall flaw (see Annex D, paragraph D.2.3).

M_t^i Folias factor based on the longitudinal extent of the LTA for a through-wall flaw .

M_t^C Folias factor based on the circumferential extent of the LTA for a through-wall flaw.

M_s^C Folias factor based on the circumferential extent of the LTA for a surface flaw.

$MAWP$ maximum allowable working pressure (see Annex A paragraph A.2).

$MAWP_r$ reduced permissible maximum allowable working pressure of the damaged component.

MFH maximum fill height of the tank (see Annex A, paragraph A.2).

P_i^e allowable external pressure of cylinder i that is used to determine the maximum allowable external pressure of a cylindrical shell with an LTA.

R outside radius of area A_f corrected for $LOSS$ and FCA as applicable.

R_t remaining thickness ratio.

RSF computed remaining strength factor based on the meridional extent of the LTA.

RSF^i RSF for the current subsection being evaluated.

RSF_a allowable remaining strength factor (see Part 2, paragraph 2.4.2.2).

s longitudinal extent or length of the region of local metal loss at the time of the inspection.

s^i longitudinal extent or length increment of metal loss (see Figure 5.9).

S_a allowable stress determined based on the component's original construction code.

S_{al} allowable stress determined from the component's original construction code for load-controlled effects.

S_{as} allowable stress determined from the component's original construction code for strain-controlled effects.

S_{lp} longitudinal stress due to pressure.

σ_{cm} maximum circumferential stress, typically the hoop stress from pressure loading for the weight and weight plus thermal load case, as applicable.

σ_{lm}^A maximum longitudinal membrane stress, computed for both the weight and weight plus thermal load cases at Point A (see Figure 5.12).

σ_{lm}^B maximum longitudinal membrane stress, computed for both the weight and weight plus thermal load cases at Point B (see Figure 5.12).

σ_e^A equivalent stress, computed for both the weight and weight plus thermal load cases at Point A (see Figure 5.12).

σ_e^B equivalent stress, computed for both the weight and weight plus thermal load cases at Point B (see Figure 5.12).

t_c corroded wall thickness away from the region of local metal loss.

t_i wall thickness of the cylinder i that is used to determine the maximum allowable external pressure of a cylindrical shell with an LTA.

$t_{\min}$ minimum required thickness for the component that governs the $MAWP$ (MFH) calculation (see Annex A).

t_{mm} minimum remaining thickness determined at the time of the assessment

t_{nom} nominal or furnished thickness of the component adjusted for mill undertolerance as applicable

t_{rd} uniform thickness away from the local metal loss location established by thickness measurements at the time of the assessment.

t_{sl} thickness required for supplemental loads (see Annex A, paragraph A.2).

$time$ time for future operation.

TSF tensile strength factor.

τ maximum shear stress in the region of local metal loss for the weight and weight plus thermal load case, as applicable.

V applied net-section shear force for the weight or weight plus thermal load case, as applicable.

$\overline{x}$ location of the neutral axis (see Figure 5.12).

x_A distance along the x-axis to Point A on the cross section shown in Figure 5.12.

x_B distance along the x-axis to Point B on the cross section shown in Figure 5.12.

$\overline{y}$ location of the neutral axis (see Figure 5.12).

y_A distance from the $\overline{x} - \overline{x}$ axis measured along the y-axis to Point A on the cross section shown in Figure 5.12.

y_B distance from the $\overline{x} - \overline{x}$ axis measured along the y-axis to Point B on the cross section shown in Figure 5.12.

$\overline{y}_{LX}$ distance from the centroid of area A_f to the x-axis (see Figure 5.12).

5.10 References

1. Bubenik, T.A., Olsen, R.J., Stephens, D.R. and Francini, R.B., "Analyzing the Pressure Strength of Corroded Line Pipe," *Offshore Mechanics and Arctic Engineering Symposium*, OMAE Volume V-A, Pipeline Technology, American Society of Mechanical Engineers, pp. 225-231, 1992.
2. Bubenik, T.,A., Rosenfeld, M.,J., "Assessing the Strength of Corroded Elbows," NG-18 Report No. 206, Pipeline Research Committee of the American Gas Association, 1993.
3. Chouchaoui, B.A., Pick, R.J., "A Three Level Assessment of the Residual Strength of Corroded Line Pipe," *Offshore Mechanics and Arctic Engineering Symposium*, OMAE Volume V, Pipeline Technology, American Society of Mechanical Engineers, pp 9-18, 1994.
4. Eiber, ER.J., Maxey, W.A., Duffy, A.R. and Atterbury, T.J., "Investigation Of The Initiation And Extent Of Ductile Pipe Rupture," BMI-1908, Battelle Columbus Laboratories, Ohio, 1971.
5. Folias, E.S., "On the Effect of Initial Curvature on Cracked Flat Sheets," *International Journal of Fracture Mechanics*, Vol. 5, No. 4, December 1969, pp. 327-346.
6. Hantz, B.F., Sims, J.R., Kenyon, C.T., Turbak, T.A., "Fitness For Service: Groove Like Local Thin Areas on Pressure Vessels and Storage Tanks," ASME PVP-Vol. 252, American Society of Mechanical Engineers, New York, 1992.
7. Herter, K.H., Julisch, P., Stoppler, W. and Sturm, D., "Behavior of Pipes Under Internal Pressure and External Bending Moment – Comparison between Experiment and Calculation," Fracture Mechanics Verification by Large-Scale Testing, EGF/E5158, Edited by K. Kussmaul, Mechanical Engineering Publications, London, 1991, pp. 223-241.
8. Janelle, J.A. and Osage, D.A., "An Overview and Validation of the Fitness-For-Service Assessment Procedures for Local Thin Areas in API 579," WRC Bulletin 505, Welding Research Council, New York, N.Y., September, 2005.
9. Kastner, W., Rehrich, E., Schmitt, W. and Steinbuch, R., "Critical Crack Sizes in Ductile Piping," *International Journal of Pressure Vessels & Piping*, 9, 1981, pp. 197-219.
10. Kiefner, J.F., Maxey, W.A., Eiber, R.J., and Duffy, A.R., "Failure Stress Levels Of Flaws In Pressurized Cylinders," ASTM STP 536, American Society for Testing and Materials, 1973, pp. 461-481.
11. Kiefner, J.F. and Vieth, P.H., "A Modified Criterion for Evaluating the Remaining Strength of Corroded Pipe," RPC International Catalog No. L51609, 1989.
12. Leggatt, R.H., Hodgson, A.P., Hayes, B. and Chan, S.W.K., "Safety Factors In Flaw Assessment of Girth Welds," For the American Gas Association, Contract No: PR 164 509, The Welding Institute, 1988.
13. Maxey, W.A., Kiefner, J.F., Eiber, R.J., and Duffy, A.R., "Ductile Fracture Initiation, Propagation, and Arrest In Cylindrical Shells," ASTM STP 514, American Society for Testing and Materials, 1972, pp. 70-81.
14. Osage, D.A., Krishnaswamy, P., Stephens, D.R., Scott, P., Janelle, J., Mohan, R., and Wilkowski, G.M., "Technologies for the Evaluation of Non-Crack-Like Flaws in Pressurized Components – Erosion/Corrosion, Pitting, Blisters, Shell Out-Of-Roundness, Weld Misalignment, Bulges and Dents," WRC Bulletin 465, Welding Research Council, New York, N.Y., September, 2001.
15. Sims, J.R., Hantz, B.F., Kuehn, K.E., "A Basis for the Fitness For Service Evaluation of Thin Areas in Pressure Vessels and Storage Tanks," ASME PVP-Vol 233, American Society of Mechanical Engineers, New York, 1992.

16. Stephens, D.R., Bubenik, T.,A., Francini, R.,B., “Residual Strength of Pipeline Corrosion Defects Under Combined Pressure and Axial Loads,” NG-18 Report No. 216, Pipeline Research Committee of the American Gas Association, 1995.

17. Stephens, D.R., Krishnaswamy, P, Mohan, R., Osage, D.A. and Wilkowski, G., “A Review of Analysis Methods and Acceptance Criteria for Local Thinned Areas in Piping and Piping Components,” 1997 Pressure Vessels and Piping Conference, Orlando, Florida, July, 1997.

18. Strum, D., Stoppler, W. and Schiedermaier, “The Behavior Of Dynamically Loaded Pipes With Circumferential Flaws Under Internal Pressure and External Bending Loads,” *Nuclear Engineering and Design*, 96, 1986, pp. 99-113.

19. Rosenfeld, M.J., Vieth, P.H. and Haupt, R.W., “A Proposed Corrosion Assessment Method And In-Service Safety Factors For Process And Power Piping Facilities,” PVP-Vol. 353, ASME, pp. 395-405, 1997.

20. Rosenfeld, M.J., “Serviceability Of Corroded Girth Welds,” RPC International, Catalog No. L 51742, 1996.

21. Turbak, T.A. and Sims, J.R., “Comparison of Local Thin Area Assessment Methodologies,” ASME PVP-Vol. 288, American Society of Mechanical Engineers, New York, 1994, pp. 307-314.

22. Turbak, T.A. and Sims, J.R., “Fitness-For-Service Local Thin Areas Comparison Of Finite Element Results To Physical Test Results,” ASME PVP-Vol. 315, American Society of Mechanical Engineers, New York, 1995, pp. 285-292.

23. Vieth, V.H. and Kiefner, J.F., “RSTRENG2 User’s Manual”, RPC International Catalog No. L51688, 1993.

24. Vieth, V.H. and Kiefner, J.F., “Database Of Corroded Pipe Tests”, RPC International Catalog No. L51689, 1993.

25. Wang, K.C. and Smith, E.D., “The Effect Of Mechanical Damage On Fracture Initiation In Linepipe Part II – Gouges,” Metals Technology Laboratories, Report MTL 88-16(TR), March, 1988.

26. Wilkowski, G.M. and Scott, P.M., “A Statistical Based Circumferentially Cracked Pipe Fracture Mechanics Analysis For Design Or Code Implementation,” *Nuclear Engineering and Design*, 111, 1989, pp. 173-187.

27. Willoughby, A.A., “A Survey of Plastic Collapse Solutions Used in the Failure Assessment of Part Wall Defects,” The Welding Institute, 1982.

5.11 Tables and Figures

Table 5.1
Data Required for the Assessment of Local Metal Loss

Use this form to summarize the data obtained from a field inspection

Equipment Identification: _____
Equipment Type: _____ Pressure Vessel _____ Storage Tank _____ Piping Component
Component Type & Location: _____

Data Required For A Level 1 And Level 2 Assessment
Future Corrosion Allowance: _____
Inside Diameter: _____
Minimum Required Thickness (t_{min}): _____
Minimum Measured Wall Thickness: _____
Distance to the Nearest Structural Discontinuity (L_{msd}): _____
LTA Dimensions $(s \ \& \ c)$: _____
Groove-Like Flaw Dimensions $(g_l, \ g_r, \ g_w \ \& \ \beta)$: _____

Additional Data Required For A Level 2 Assessment
Distance to the Nearest LTA: _____

The thickness data for each of the inspection planes may be entered in a table as shown below.

Inspection Plane:__		Inspection Plane:__		Inspection Plane:__		Inspection Plane:__	
Location	**Thickness**	**Location**	**Thickness**	**Location**	**Thickness**	**Location**	**Thickness**
t_{mm}		t_{mm}		t_{mm}		t_{mm}	

Table 5.2
Folias Factor, M_t, Based on the Longitudinal or Meridional Flaw Parameter, λ, for Cylindrical, Conical and Spherical Shells

λ	M_t	
	Cylindrical or Conical Shell	Spherical Shell
0.0	1.001	1.000
0.5	1.056	1.063
1.0	1.199	1.218
1.5	1.394	1.427
2.0	1.618	1.673
2.5	1.857	1.946
3.0	2.103	2.240
3.5	2.351	2.552
4.0	2.600	2.880
4.5	2.847	3.221
5.0	3.091	3.576
5.5	3.331	3.944
6.0	3.568	4.323
6.5	3.801	4.715
7.0	4.032	5.119
7.5	4.262	5.535
8.0	4.492	5.964
8.5	4.727	6.405
9.0	4.970	6.858
9.5	5.225	7.325
10.0	5.497	7.806
10.5	5.791	8.301
11.0	6.112	8.810
11.5	6.468	9.334
12.0	6.864	9.873
12.5	7.307	10.429
13.0	7.804	11.002
13.5	8.362	11.592
14.0	8.989	12.200
14.5	9.693	12.827
15.0	10.481	13.474
15.5	11.361	14.142
16.0	12.340	14.832
16.5	13.423	15.544

Table 5.2
Folias Factor, M_t, Based on the Longitudinal or Meridional Flaw Parameter, λ, for Cylindrical, Conical and Spherical Shells

λ	M_t	
	Cylindrical or Conical Shell	Spherical Shell
17.0	14.616	16.281
17.5	15.921	17.042
18.0	17.338	17.830
18.5	18.864	18.645
19.0	20.494	19.489
19.5	22.219	20.364
20.0	24.027	21.272

Notes

1. λ is the longitudinal or meridional flaw length parameter computed using Equation (5.6).
2. Interpolation is permitted for intermediate values of λ, Figure 5.13 may also be used.
3. The equation for the cylindrical shell is shown below. If $\lambda > 20$, then use $\lambda = 20$ in the calculation.

$$M_t = \left(\begin{array}{l} 1.0010 - 0.014195\lambda + 0.29090\lambda^2 - 0.096420\lambda^3 + 0.020890\lambda^4 - \\ 0.0030540\lambda^5 + 2.9570\left(10^{-4}\right)\lambda^6 - 1.8462\left(10^{-5}\right)\lambda^7 + 7.1553\left(10^{-7}\right)\lambda^8 - \\ 1.5631\left(10^{-8}\right)\lambda^9 + 1.4656\left(10^{-10}\right)\lambda^{10} \end{array} \right)$$

4. The equation for the spherical shell is shown below. Note that the value of λ is limited by the inside circumference of the shell.

$$M_t = \left(\frac{1.0005 + 0.49001(\lambda) + 0.32409(\lambda)^2}{1.0 + 0.50144(\lambda) - 0.011067(\lambda)^2} \right)$$

Table 5.3
Section Properties for Computation of Longitudinal Stress in a Cylinder with an LTA

$$I_{\bar{X}} = I_X + A_m \bar{y}^2 - I_{LX} - A_f \left(\bar{y}_{LX} + \bar{y} \right)^2$$

$$I_{\bar{Y}} = I_Y - I_{LY}$$

$$I_X = I_y = \frac{\pi}{64}\left(D_o^4 - D^4 \right)$$

$$I_{LX} = R^3 d \left[\begin{array}{l} \left(1 - \frac{3d}{2R} + \frac{d^2}{R^2} - \frac{d^3}{4R^3} \right) \left(\theta + \sin\theta\cos\theta - \frac{2\sin^2\theta}{\theta} \right) + \\ \frac{d^2 \sin^2\theta}{3R^2\theta\left(2 - d/R\right)} \left(1 - \frac{d}{R} + \frac{d^2}{6R^2} \right) \end{array} \right]$$

$$I_{LY} = R^3 d \left[\left(1 - \frac{3d}{2R} + \frac{d^2}{R^2} - \frac{d^3}{4R^3} \right) \left(\theta - \sin\theta\cos\theta \right) \right]$$

$$\bar{y}_{LX} = \frac{2R\sin\theta}{3\theta} \left(1 - \frac{d}{R} + \frac{1}{2 - d/R} \right)$$

$$A_t = \frac{\left[0.5\pi \left(D + D_o \right) - c \right] \left(D + D_o \right)}{8}$$

$$A_a = \frac{\pi}{4} D^2$$

$$A_m = \frac{\pi}{4}\left(D_o^2 - D^2 \right)$$

Table 5.3
Section Properties for Computation of Longitudinal Stress in a Cylinder with an LTA

For A Region Of Local Metal Loss Located On The Inside Surface	For A Region Of Local Metal Loss Located On The Outside Surface
$A_f = \frac{\theta}{4}\left(D_f^2 - D^2\right)$	$A_f = \frac{\theta}{4}\left(D_o^2 - D_f^2\right)$
$A_w = A_a + A_f$	$A_w = A_a$
$\bar{y} = \frac{1}{12}\frac{\sin\theta\left(D_f^3 - D^3\right)}{A_m - A_f}$	$\bar{y} = \frac{1}{12}\frac{\sin\theta\left(D_o^3 - D_f^3\right)}{A_m - A_f}$
$x_A = 0.0$	$x_A = 0.0$
$y_A = \bar{y} + \frac{D_o}{2}$	$y_A = \bar{y} + \frac{D_f}{2}$
$x_B = \frac{D_o}{2}\sin\theta$	$x_B = \frac{D_f}{2}\sin\theta$
$y_B = \bar{y} + \frac{D_o}{2}\cos\theta$	$y_B = \bar{y} + \frac{D_f}{2}\cos\theta$
$b = \frac{1}{12}\frac{\sin\theta\left(D_f^3 - D^3\right)}{A_a + A_f}$	$b = 0$
$R = \frac{D_f}{2}$	$R = \frac{D_o}{2}$
$d = \frac{\left(D_f - D\right)}{2}$	$d = \frac{\left(D_o - D_f\right)}{2}$
$t_{mm} = \frac{\left(D_o - D_f\right)}{2}$	$t_{mm} = \frac{\left(D_f - D\right)}{2}$
$A_{tf} = \frac{c\left(D_o + D_f\right)}{8}$	$A_{tf} = \frac{c\left(D + D_f\right)}{8}$

Table 5.4
Equations for the TSF Curves in Figure 5.8

TSF	$\lambda_{c-0.2}$	C_1	C_2	C_3	C_4	C_5	C_6
0.7	0.21	9.9221E-01	-1.1959E-01	-5.7333E-02	1.6948E-02	-1.7976E-03	6.9114E-05
0.75	0.48	9.6801E-01	-2.3780E-01	-3.2678E-01	2.0684E-01	-4.6537E-02	3.9436E-03
0.8	0.67	9.4413E-01	-3.1256E-01	-6.9968E-01	6.5020E-01	-2.2102E-01	2.8799E-02
0.9	0.98	8.9962E-01	-3.8860E-01	-1.6485E+00	2.3445E+00	-1.2534E+00	2.5331E-01
1.0	1.23	8.5947E-01	-4.0012E-01	-2.7979E+00	5.0729E+00	-3.5217E+00	9.1877E-01
1.2	1.66	7.8654E-01	-2.5322E-01	-5.7982E+00	1.3858E+01	-1.3118E+01	4.6436E+00
1.4	2.03	7.2335E-01	1.1528E-02	-9.3536E+00	2.6031E+01	-2.9372E+01	1.2387E+01
1.8	2.66	6.0737E-01	9.3796E-01	-1.9239E+01	6.4267E+01	-9.1307E+01	4.8962E+01
2.3	3.35	4.9304E-01	2.1692E+00	-3.2459E+01	1.2245E+02	-2.0243E+02	1.2727E+02

Notes:

1. If $\lambda_c \le \lambda_{c-0.2}$, then $R_t = 0.2$.
2. If $\lambda_{c-0.2} < \lambda_c \le 9$, then the equation to determine R_t for a given TSF value is shown below where the coefficients are defined above.

$$R_t = C_1 + \frac{C_2}{\lambda_c} + \frac{C_3}{\lambda_c^2} + \frac{C_4}{\lambda_c^3} + \frac{C_5}{\lambda_c^4} + \frac{C_6}{\lambda_c^5}$$

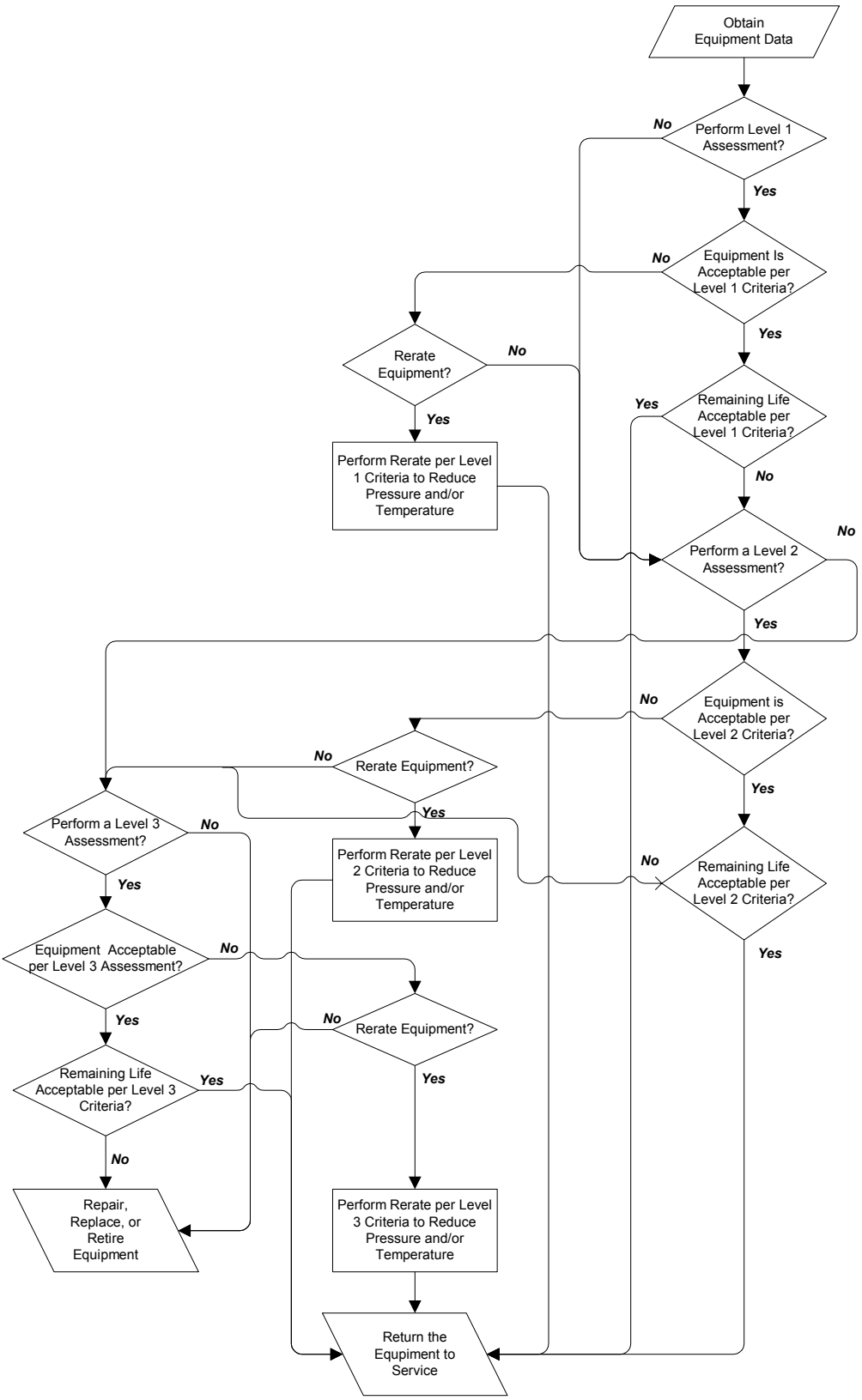

Figure 5.1 – Overview of the Assessment Procedures to Evaluate a Component with Local Metal Loss

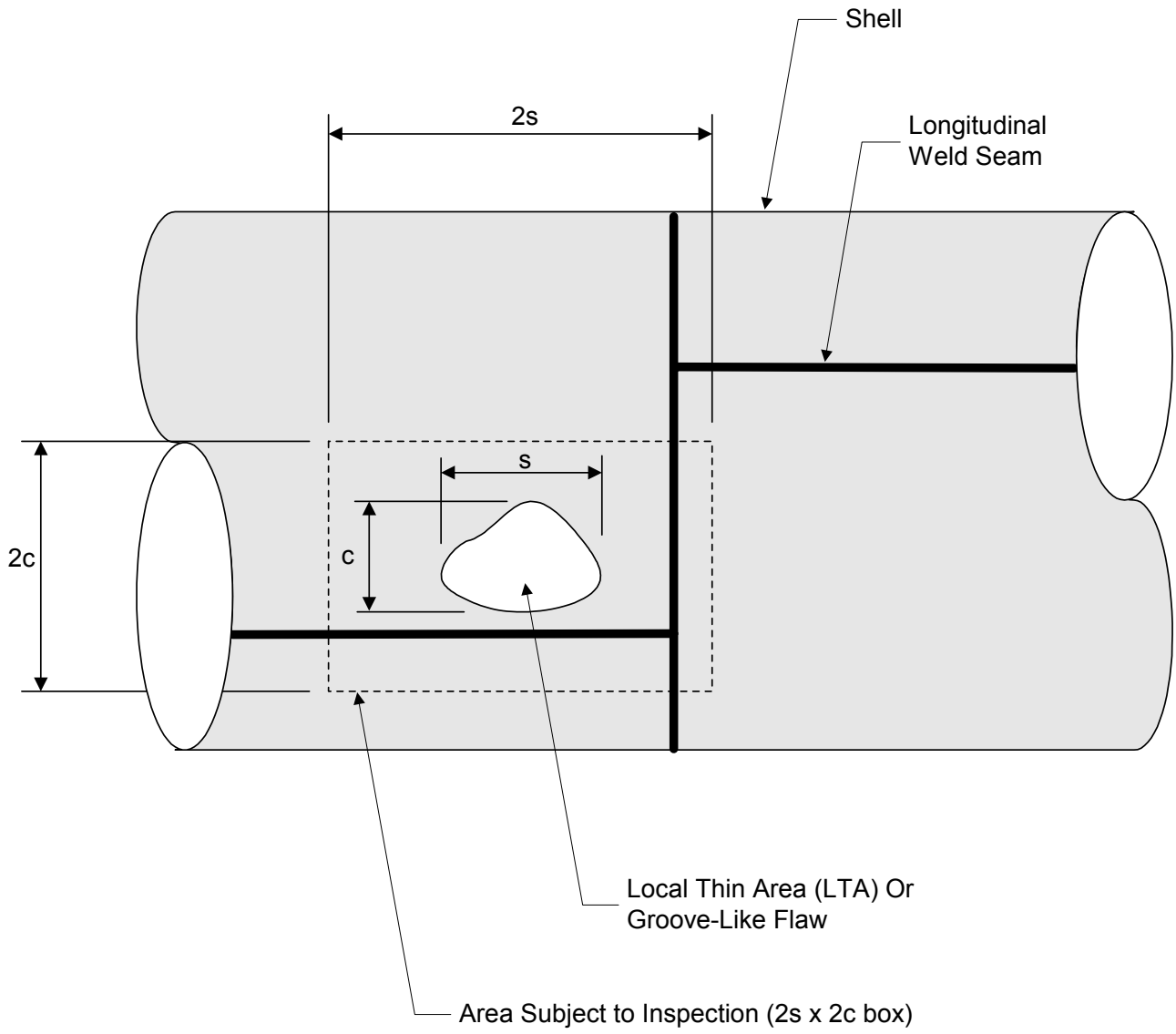

Note: See Part 4, paragraph 4.3.3.3 for the procedure to determine s and c.

Figure 5.2 – LTA Flaw Dimensions

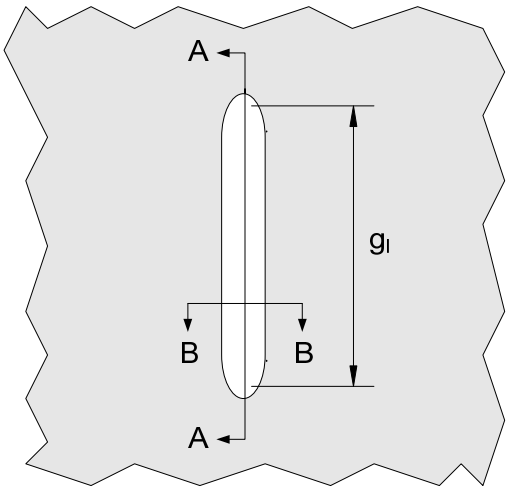

(a) Groove-Like Flaw - Plan View

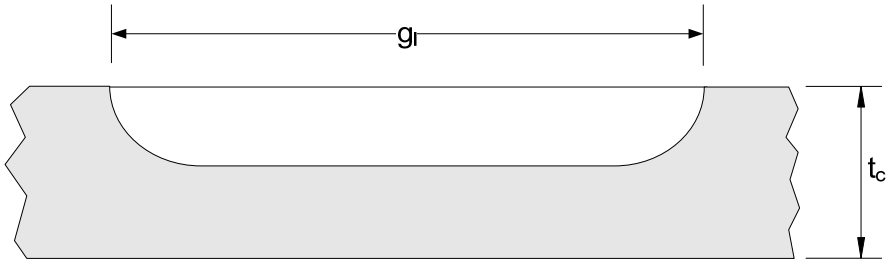

(b) Groove-Like Flaw -Section A-A

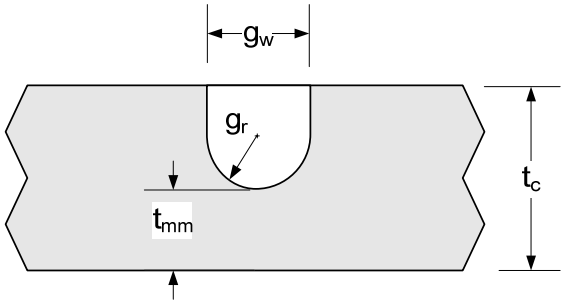

(c) Groove-Like Flaw - Section B-B

Figure 5.3 – Groove-Like Flaw Dimensions – Flaw Profile

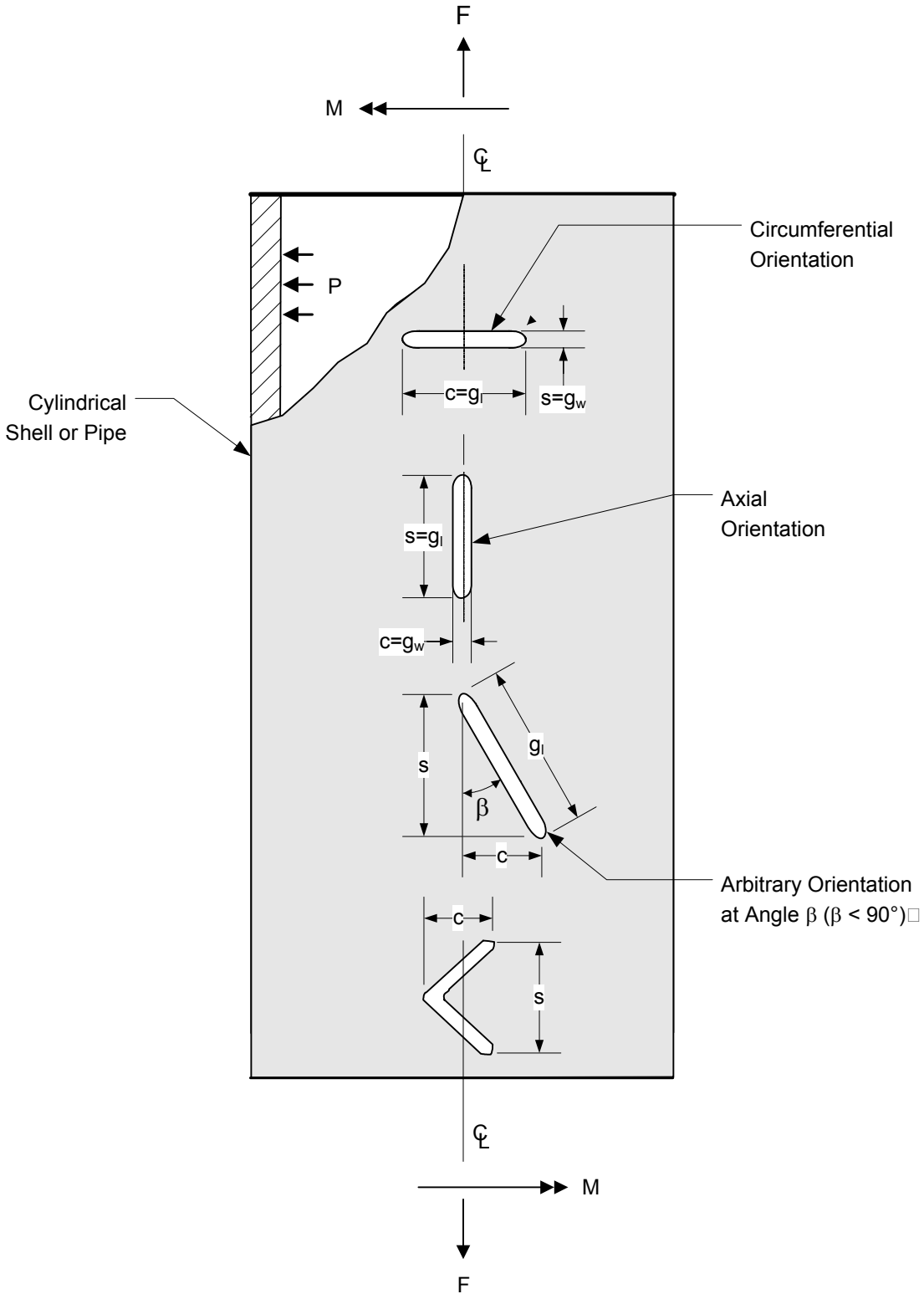

Figure 5.4 – Groove-Like Flaw Dimensions – Flaw Orientation on a Cylindrical Shell

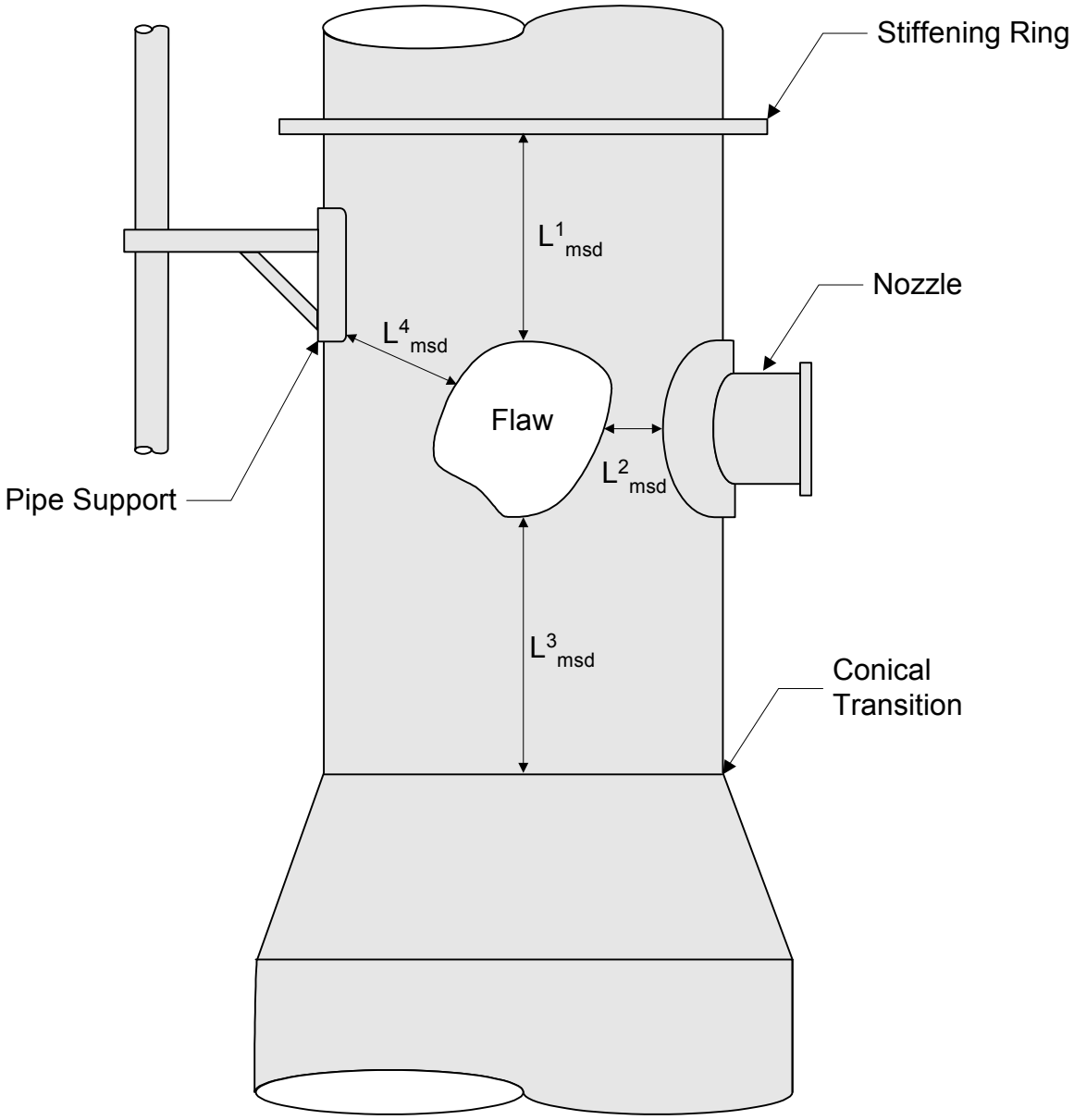

Notes:

1. For the example shown above, the minimum distance to a major structural discontinuity is: $L_{msd} = \min\left[L^1_{msd}, L^2_{msd}, L^3_{msd}, L^4_{msd} \right]$
2. Typical major structural discontinuities associated with vertical vessels are shown in this figure. For horizontal drums, the saddles supports would constitute a major structural discontinuity and for a spherical storage vessel, the support locations (shell-to-leg junction) would constitute a major structural discontinuity. The location of the flaw from these support locations would need to be considered in determining L_{msd} as well as the distances from the nearest nozzle, piping/platform support, conical transition, and stiffening ring.
3. The measure of the minimum distances defined in this figure is from the nearest edge of the region of local metal loss to the nearest weld of the structural discontinuity.

Figure 5.5 – Procedure to Determine L_{msd}

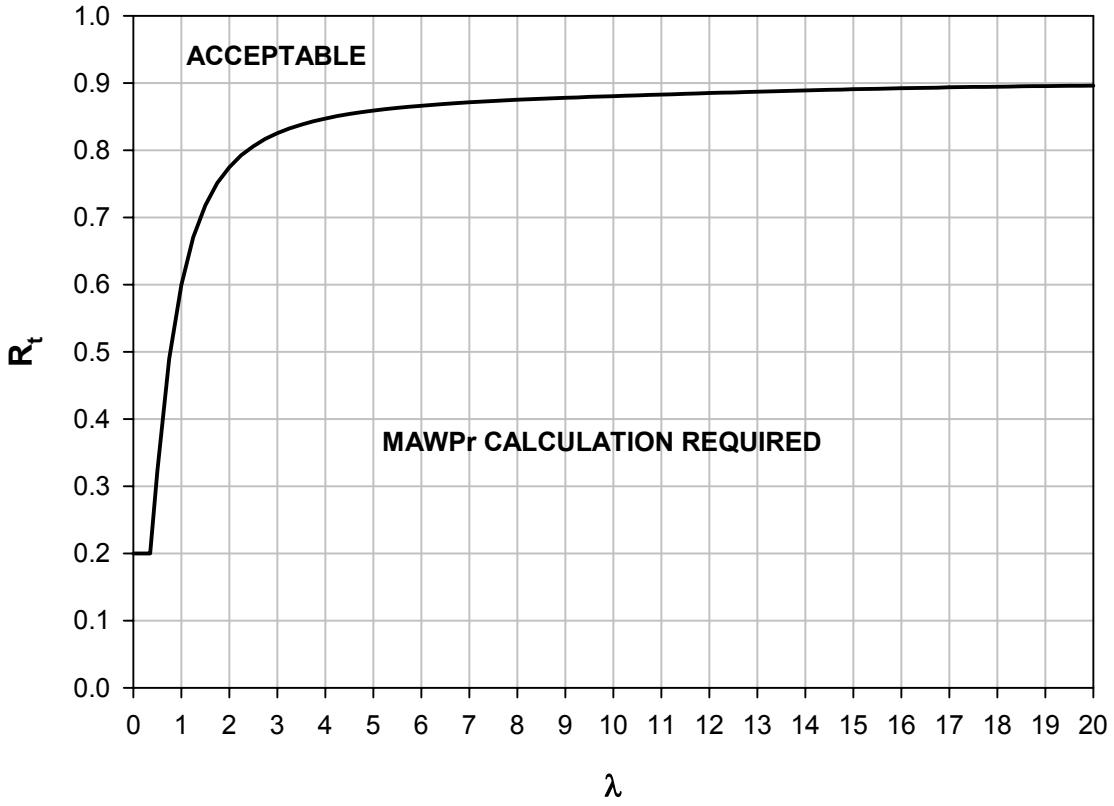

Note: The allowable remaining strength factor for this curve is $RSF_a = 0.90.$ Equations for the curves in this figure are provided below where M_t for a cylindrical shell is determined using Table 5.2.

$$R_t = 0.2 \qquad \lambda \le 0.354 \qquad (5.40)$$

$$R_t = \left(RSF_a - \frac{RSF_a}{M_t} \right) \left(1.0 - \frac{RSF_a}{M_t} \right)^{-1} \qquad 0.354 < \lambda < 20 \qquad (5.41)$$

$$R_t = 0.90 \qquad \lambda \ge 20 \qquad (5.42)$$

Figure 5.6 – Level 1 Screening Criteria for Local Metal Loss in a Cylindrical Shell

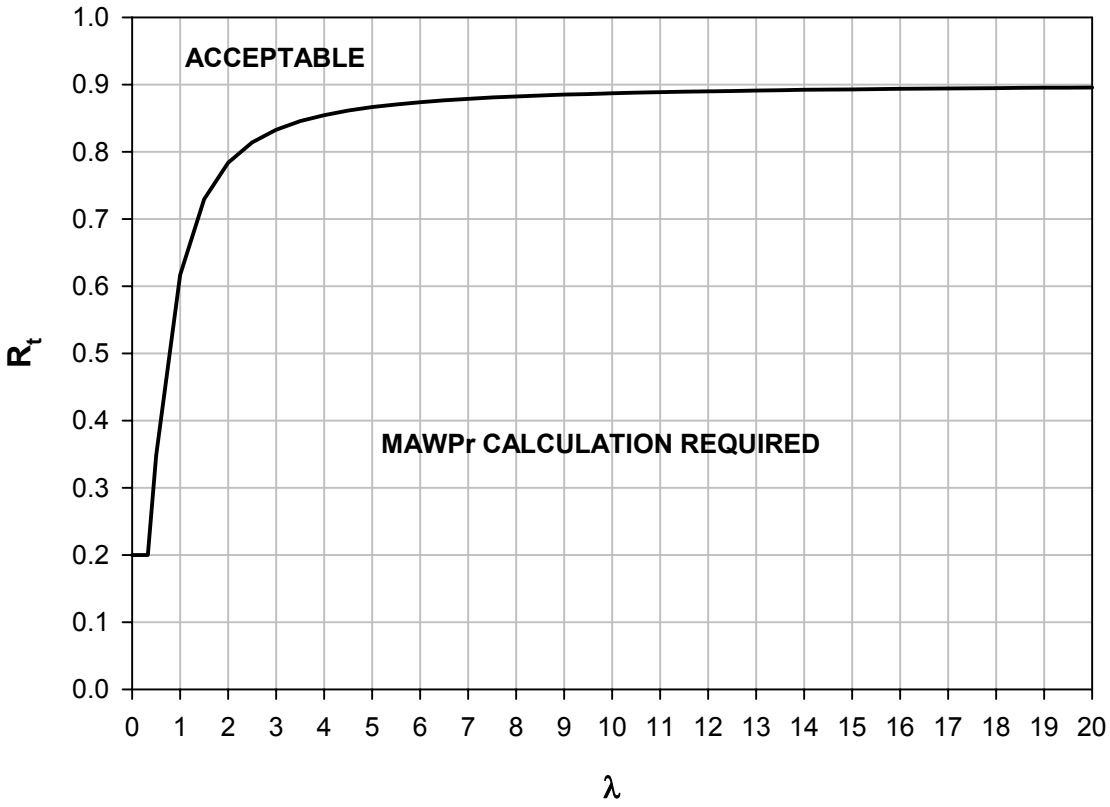

Note: The allowable remaining strength factor for this curve is $RSF_a = 0.90$. Equations for the curves in this figure are provided below where M_t for a spherical shell is determined using Table 5.2.

$$R_t = 0.2 \qquad \lambda \le 0.330 \tag{5.43}$$

$$R_t = \left(RSF_a - \frac{RSF_a}{M_t} \right) \left(1.0 - \frac{RSF_a}{M_t} \right)^{-1} \qquad 0.330 < \lambda < 20 \tag{5.44}$$

$$R_t = 0.90 \qquad \lambda \ge 20 \tag{5.45}$$

Figure 5.7 – Level 1 Screening Criteria for Local Metal Loss in a Spherical Shell

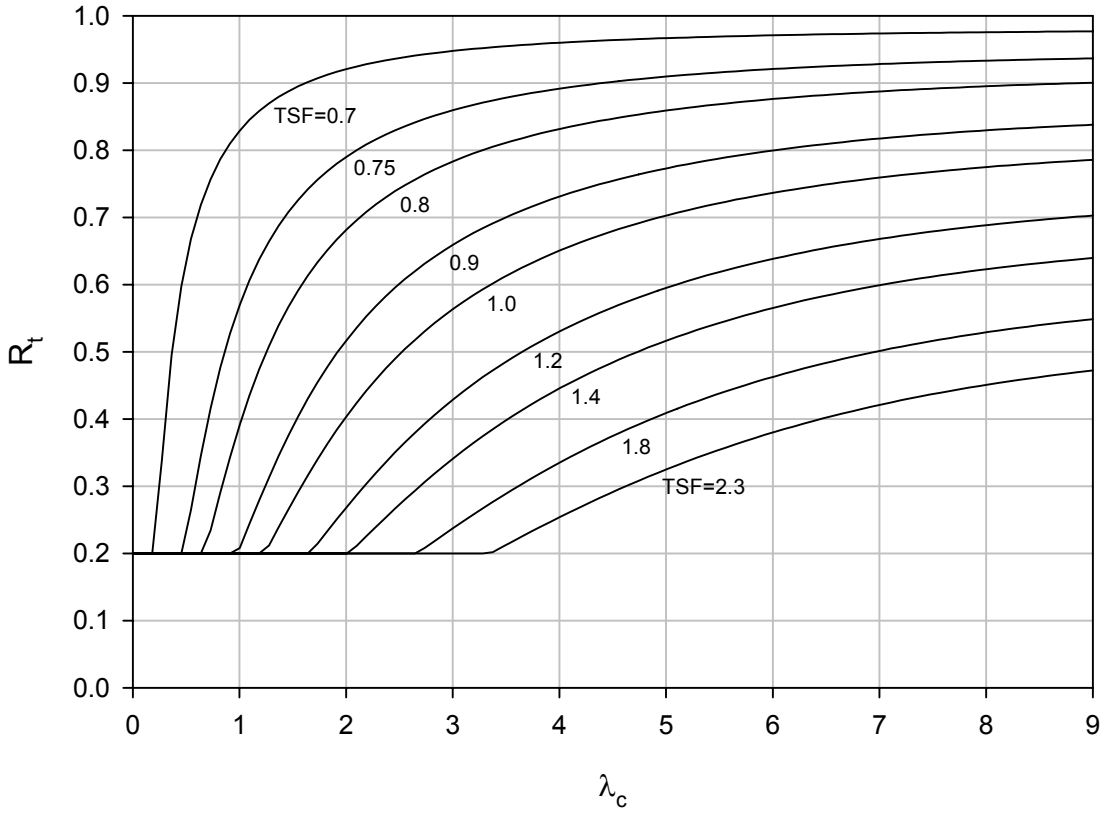

Notes:

1. If the point defined by the intersection of these values is on or above the screening curve, then the circumferential extent of the flaw is acceptable per Level 1 (see paragraph 5.4.2.2).
2. Equations for the TSF curves in this figure are provided in Table 5.4.
3. Interpolation may be used for intermediate values of TSF .

Figure 5.8 – Level 1 Screening Criteria for the Maximum Allowable Circumferential Extent of Local Metal Loss in a Cylinder

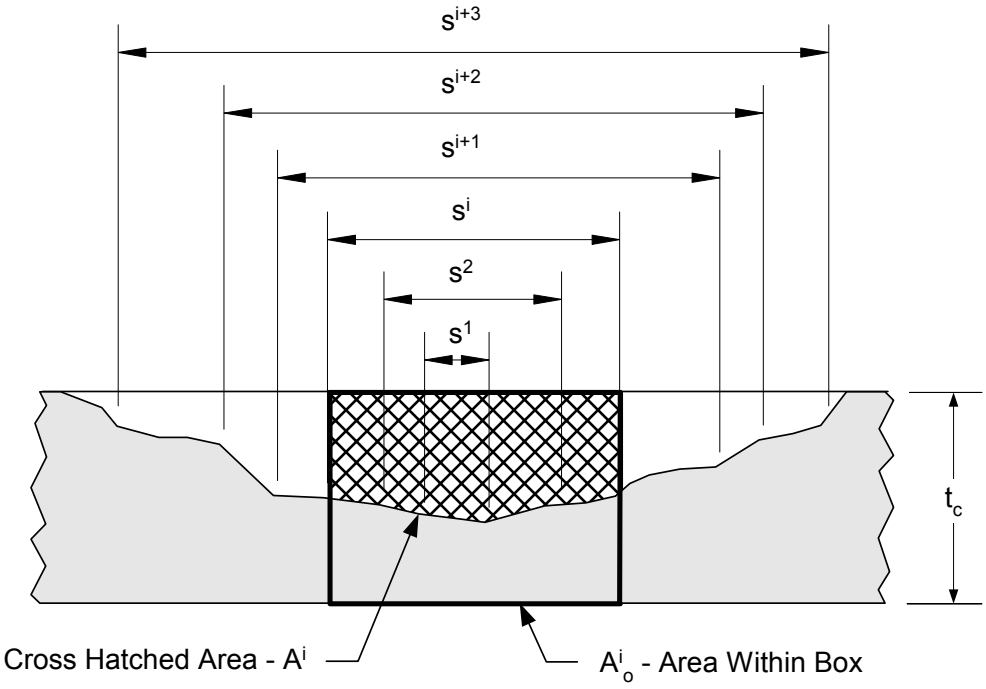

(a) Subdivision Process for Determining the RSF

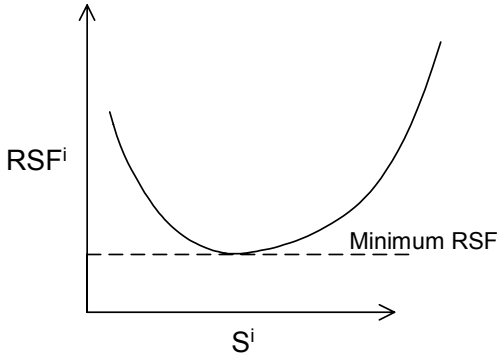

(b) Determining the Minimum RSF Value

Notes:

A^i = Area of metal loss associated with length s^i (cross-hatched area). This area can be evaluated using a numerical integration technique (e.g. Simpson's or Trapezoidal Rule).

A_o^i = Total original area associated with length s^i and thickness t_c, or $A_o^i = s^i t_c$

Figure 5.9 – Definition of Areas Used to Compute the RSF for a Region of Local Metal Loss in a Level 2 Assessment

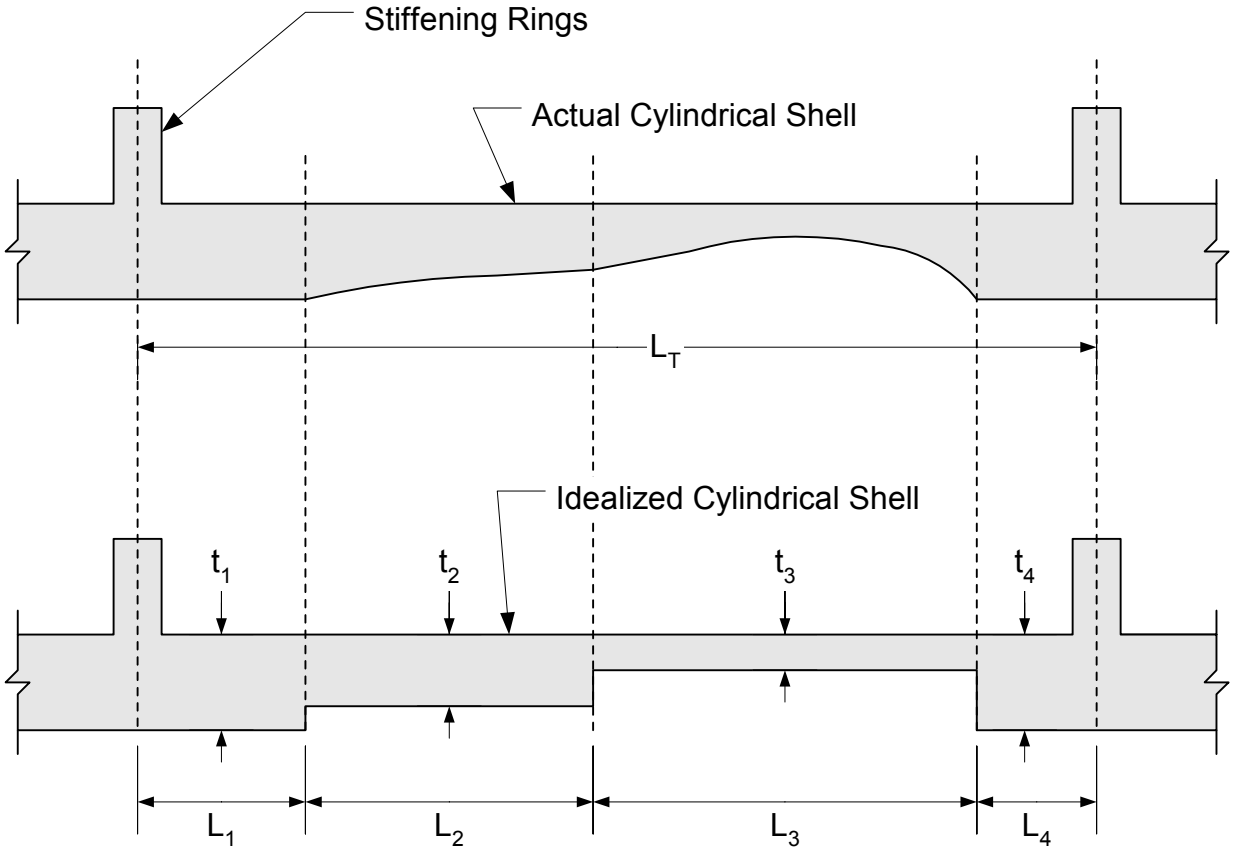

Figure 5.10 – Parameters for Determining the Maximum Allowable External Pressure of a Cylinder with an LTA

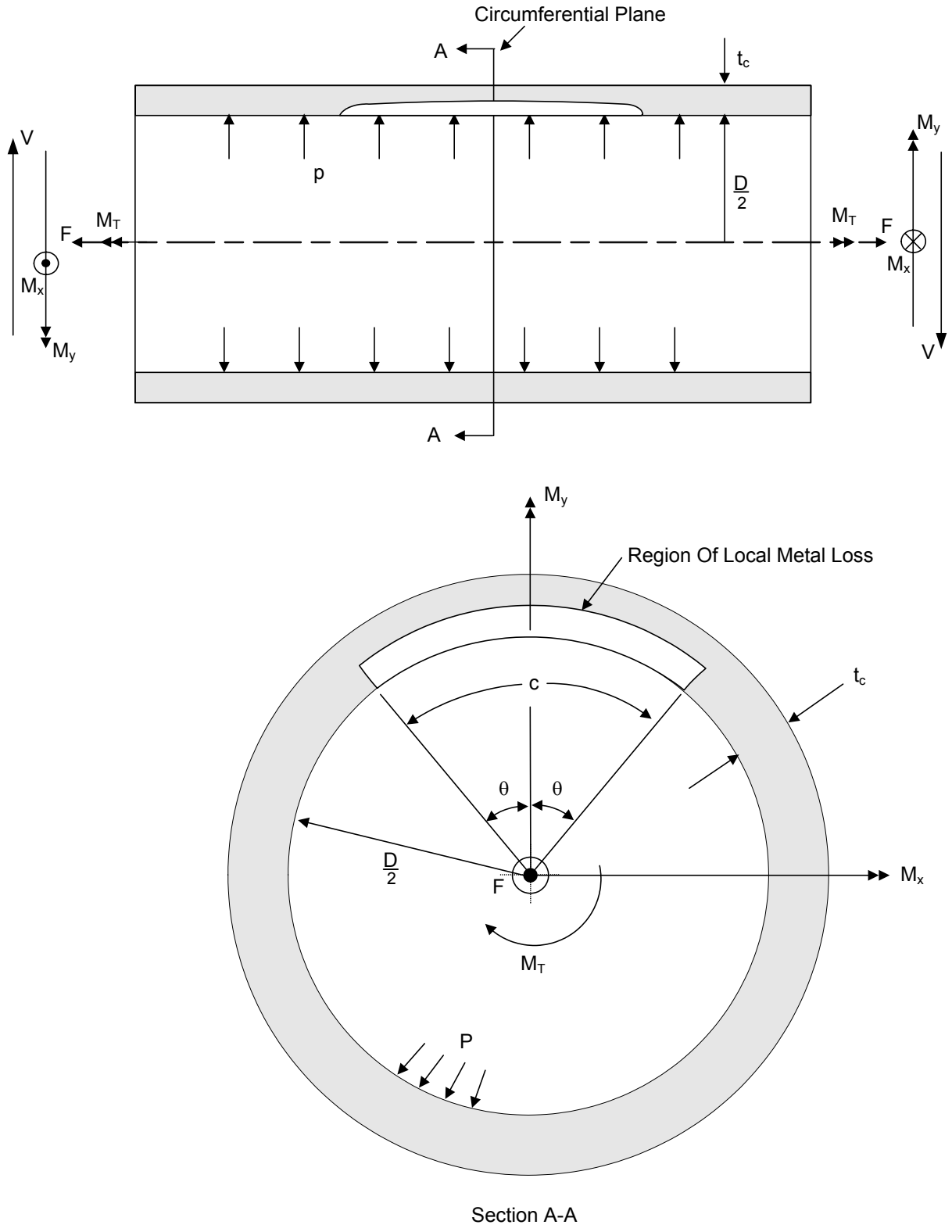

Figure 5.11 – Parameters for Permissible Bending Moment, Axial Force, and Pressure for a Cylinder with an *LTA*

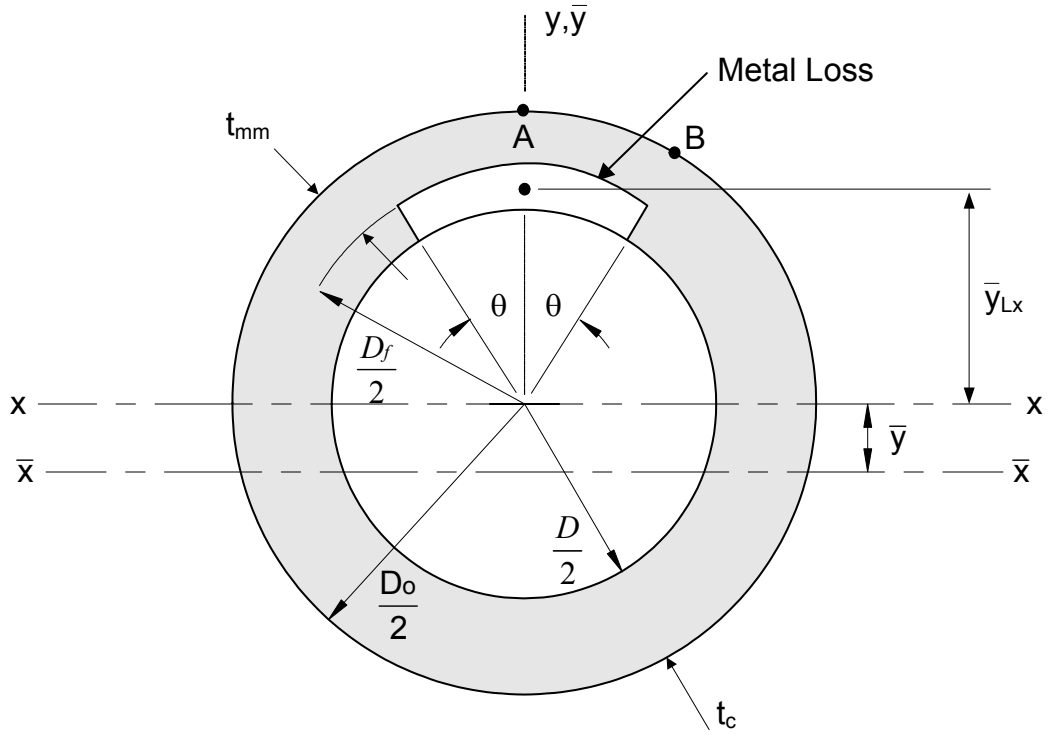

(a) Region Of Local Metal Loss Located on the Inside Surface

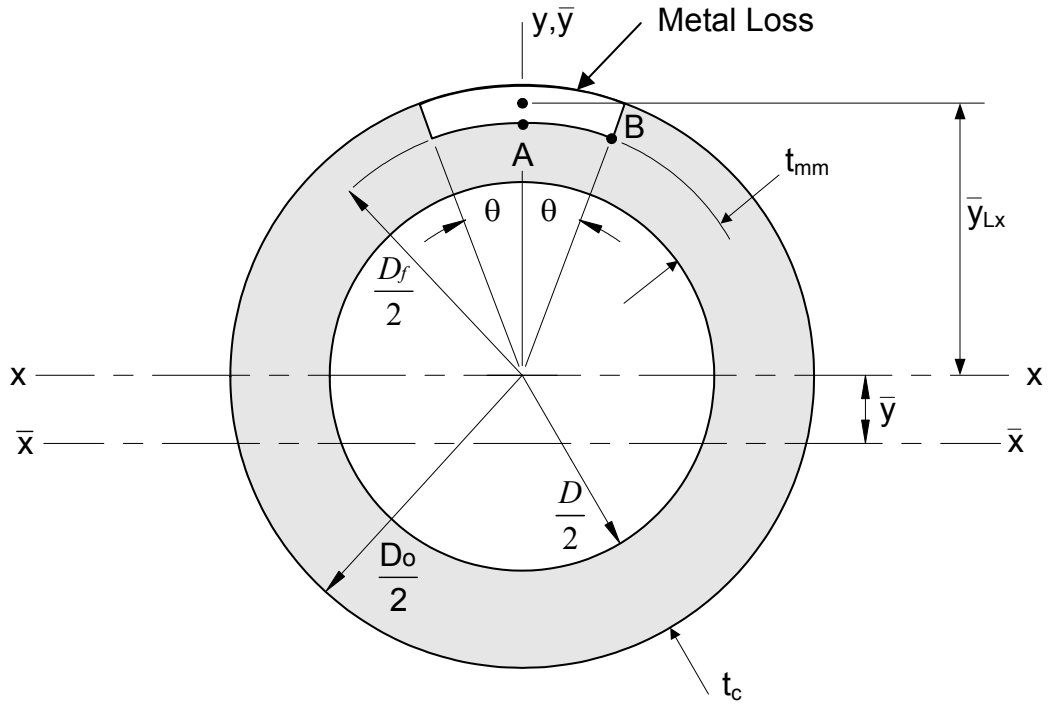

(b) Region Of Local Metal Loss Located on the Outside Surface

Figure 5.12 – Parameters for Determining Section Properties of a Cylinder With An LTA

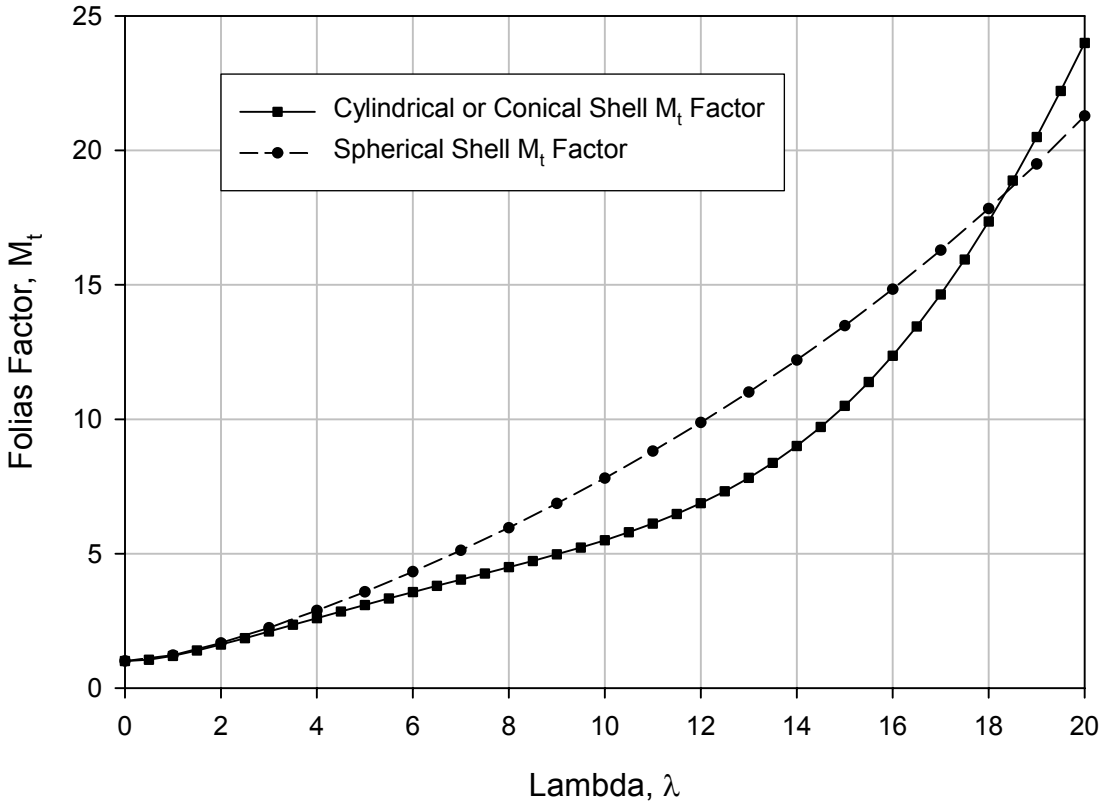

Figure 5.13 – M_t Parameter from Table 5.2

PART 6

ASSESSMENT OF PITTING CORROSION

PART CONTENTS

6.1 General

The assessment procedures in this Part can be utilized to evaluate metal loss from pitting corrosion. Pitting is defined as localized regions of metal loss that can be characterized by a pit diameter on the order of the plate thickness or less, and a pit depth that is less than the plate thickness. Assessment procedures are provided to evaluate both widespread and localized pitting in a component with or without a region of local metal loss. The procedures in this Part can be used to assess an array of blisters as described in Part 7. A flow chart for the evaluation procedure of equipment with pitting is shown in Figure 6.1.

6.2 Applicability and Limitations of the Procedure

6.2.1 The assessment procedures in this Part can be used to evaluate four types of pitting: widely scattered pitting that occurs over a significant region of the component, a local thin area (LTA) located in a region of widely scattered pitting, localized regions of pitting, and pitting confined within a region of a LTA. A flowchart that provides details of the assessment procedures required is shown in Figure 6.2. Depending on the type of pitting damage, either assessment methods in Part 6 or a combination of assessment methods in Part 5 and 6 are used in the evaluation.

6.2.2 Calculation methods are provided to rerate the component if the acceptance criteria in this Part are not satisfied. For pressurized components (pressure vessels and piping), the calculation methods can be used to find a reduced maximum allowable working pressure $(MAWP_r)$ and/or temperature. For tank shell courses, the calculation methods can be used to determine a reduced maximum fill height (MFH_r).

6.2.3 Unless otherwise specified, this Part is limited to the evaluation of pitting damage. Other flaw types shall be evaluated in accordance with Part 2, Table 2.1.

6.2.4 The assessment procedures in this Part shall only apply to components that are not operating in the creep range, i.e. when the design temperature is less or equal to the value in Part 4, Table 4.1. The Materials Engineer should be consulted regarding the creep range temperature limit for materials not listed in Table 4.1.

6.2.5 Specific details pertaining to the applicability and limitations of each of the assessment procedures are discussed below.

6.2.5.1 The Level 1 and 2 assessment procedures in this Part shall apply only if all of the following conditions are satisfied.

a) The original design criteria were in accordance with a recognized code or standard (see Part 1, paragraphs 1.2.2 or 1.2.3).

b) The material is considered to have sufficient material toughness. If there is uncertainty regarding the material toughness, then a Part 3 assessment should be performed. If the component is subject to embrittlement during operation due to temperature and/or the process environment, a Level 3 assessment should be performed. Temperature and/or process conditions that result in material embrittlement are discussed in Annex G.

c) The component is not in cyclic service. If the component is subject to less than 150 cycles (i.e. pressure and/or temperature variations including operational changes and start-ups and shut-downs) throughout its previous operating history and future planned operation, or satisfies the cyclic service screening procedure in Annex B1, paragraph B1.5.2, then the component is not in cyclic service.

d) The following limitations on component types and applied loads are satisfied:

1) Level 1 Assessment – Type A Components (see Part 4, paragraph 4.2.5) subject to internal pressure (i.e. supplemental loads are assumed to be negligible).

2) Level 2 Assessment – Type A or B Components (see Part 4, paragraph 4.2.5) subject to internal pressure, external pressure, supplemental loads, or any combination thereof (see Annex A paragraph A.2.7).

e) Additional requirements for Level 1 Assessments are:

1) The pitting damage is arrested.

2) The pitting damage is located on only one surface (ID or OD) of the component.

3) The pitting damage is composed of many pits; individual pits or isolated pairs of pits should be evaluated using the assessment procedures in Part 5.

f) Additional requirements for Level 2 Assessments are:

1) The pitting damage is characterized by localized regions of pitting, a LTA located in a region of widely scattered pitting, or pitting that is confined within a LTA.

2) The pitting damage is located on either one surface or both surfaces of the component and the pitting damage is not overlapping (see Figure 6.15).

3) The pitting damage is composed of many pits; individual pits or isolated pairs of pits should be evaluated as $LTAs$ using the assessment procedures in Part 5.

6.2.5.2 A Level 2 Assessment should be performed if:

a) An appropriate pit comparison chart cannot be found (see paragraph 6.3.3.1).

b) A more detailed assessment of widespread pitting (e.g. inclusion of the pit-couple orientation) is required.

6.2.5.3 A Level 3 Assessment should be performed where Level 1 and 2 methods do not apply, such as for the component geometry and loading conditions described in Part 5, paragraph 5.2.5.2. In addition, a Level 3 assessment is required if the pitting corrosion is located in a component with a non-uniform through-wall stress distribution (e.g. bending stress).

6.2.6 In Level 2 and 3 assessments, pitting damage shall be assessed at a specific future inspection date, with the available pitting data at the current inspection date. The user shall determine the acceptability of the pitting damage at the future inspection date by performing a series of assessments for various pitting progression rates to simulate the change in pitting depths, diameters, spacing (density) at the specific time interval (see paragraphs 6.3.3.4 and 6.5).

6.2.7 The Future Corrosion Allowance (FCA) shall be based on the projected future metal loss in the pitting region. The FCA is not applied to the depth or diameter of the pits.

6.3 Data Requirements

6.3.1 Original Equipment Design Data

An overview of the original equipment data required for an assessment is provided in Part 2, paragraph 2.3.1.

6.3.2 Maintenance and Operational History

An overview of the maintenance and operational history required for an assessment is provided in Part 2, paragraph 2.3.2.

6.3.3 Required Data/Measurements for a FFS Assessment

6.3.3.1 In a Level 1 Assessment, a measure of the surface damage in terms of pitted area and the maximum pit depth are used to quantify the extent of pitting damage. The measure of surface area damage is determined using standard pit charts (see Figures 6.3 to 6.10) by comparing the actual damage on the component to the damage represented on the pit chart. A pit chart is found by comparing the surface damage (black areas) to the surface damage on the actual component. This chart along with an estimate of the corresponding maximum pit depth is used to directly determine acceptability. Therefore, the data required for an assessment should include a photograph (with a reference scale) and/or rubbing of the surface of the damaged component with an estimate of the maximum pit depth. A cross sectional UT thickness scan can also be performed to determine the pitting profile. Guidelines for determining the maximum pit depth are included in paragraph 6.3.4.1.

6.3.3.2 In a Level 2 Assessment, the measure of damage used to evaluate pitting is the pit-couple. A pit-couple is composed of two pits separated by a solid ligament (see Figure 6.11). The metal loss of each pit in a pit-couple is modeled as an equivalent cylinder. To define a pit-couple, the diameter and depth of each pit, and the distance between the pit centers are required. The orientation of the pit-couple in the biaxial stress field may also be included in the assessment (see Figure 6.11). The depth and diameter of a pit should be carefully measured because of the variety of pit types that can occur in service (see Figure 6.12). If the pit has an irregular shape, a diameter and depth that encompasses the entire shape should be used in the assessment.

a) The occurrence of pits and their relative size in a region of a component are typically random. User discretion is required to select a population of pits that adequately represents the damage in the component.

b) To evaluate a region with pitting, a representative number of pit-couples in the damaged area should be used. If the pitting is uniform, a minimum sample size of ten pit-couples is recommended. If the pitting is non-uniform, additional pit-couple data should be taken.

c) The pit-couple samples used in the assessment should be chosen such that the pit-couples are independent. The following procedure should be followed to select the pit-couples for an assessment.

   1) STEP 1 – Select a minimum of ten pits covering a broad area.

   2) STEP 2 – Select the nearest neighbor to each of these ten pits to create a minimum of ten pit-couples (see Figure 6.11). The pit couple population should not contain repeated pits.

   3) STEP 3 – Complete the assessment using paragraph 6.4.

d) The orientation of the pit-couple in a biaxial stress field is used only in the Level 2 assessment. These data typically do not improve the assessment results; unless the pitting damage is preferential (e.g. the pitting damage is concentrated along a longitudinal, circumferential, or spiral weld seam). Therefore, the extra effort and work associated with obtaining this information should be balanced with the potential increase in remaining strength it could demonstrate.

e) To determine the effects that additional pit-couples would have on the assessment results, additional independent pit-couples can be included in the sample size, and the assessment can be repeated. This procedure will provide a measure of the sensitivity of the data with regard to assessment results (see Part 2, paragraph 2.4.3.1). Alternatively, distributions can be developed for the parameters that define a pit-couple (i.e. diameter and depth of each pit, and the distance between the pit centers), and a probabilistic analysis (see Part 2, paragraph 2.4.3.2) can be performed using the assessment model of paragraph 6.4.

f) An overview of the required information for a Level 2 Assessment is shown below.

   1) The specific information required for a Level 2 Assessment is given in paragraph 6.4.3.2. The form shown in Table 6.1 can be used to record this information.

   2) The parameters s and c using the CTP procedure described in Part 5and shown in Figure 6.13 shall be determined if the pitting damage is localized or confined to a localized region of metal loss (see Figure 6.14).

6.3.3.3 The information required to perform a Level 3 Assessment depends on the analysis method utilized. A limit load procedure using a numerical technique should be used to establish acceptable operating conditions. A description of the pitting, similar to that required for a Level 2 Assessment, should be obtained along with the material yield strength and stress-strain curve.

6.3.3.4 The future Pitting Progression Rate (PPR) should be estimated. This is not a straightforward procedure because pits can increase in size (depth and diameter), increase in density, and a region of local pitting may increase in size. All pit dimensions used in the assessments in this Part should be based on the best estimate of future size. The determination of a remaining life for a component with pitting damage is discussed in paragraphs 6.2.4 and 6.5

6.3.4 Recommendation for Inspection Technique and Sizing Requirements

6.3.4.1 Precise measurement of pitting is difficult. Care should be taken to ensure that the correct dimensions are measured because pits often have irregular shapes as shown in Figure 6.12 or are filled with scale. Pit gauges are used to measure pit depth and rulers or calipers to measure pit diameter and the distance between pits. Ultrasonic methods can also be used to measure the wall thickness of pits with large diameters and the average plate thickness in non-pitted areas adjacent to the pitting.

6.3.4.2 It is difficult to detect small diameter pits or to measure the depth of pits using ultrasonic methods. Radiography (RT) may also be used to characterize the damage in pitted regions.

6.3.4.3 If the surface is scaled, dirty or has a damaged coating, cleaning (e.g. sandblasting) may be required in order to obtain accurate pit measurements.

6.3.4.4 Inspection techniques that characterize pitting damage from the opposite surface should only be used when they have sufficient resolution and coverage to ensure that significant damage cannot be overlooked.

6.4 Assessment Techniques and Acceptance Criteria

6.4.1 Overview

6.4.1.1 If the depth of all of the pits is less than the specified corrosion/erosion allowance and adequate thickness is available for future pitting damage (see paragraph 6.5.1), no further action is required other than to record the data; otherwise, an assessment is required.

6.4.1.2 An overview of the assessment levels is provided in Figure 6.1.

a) Level 1 Assessments shall be limited to components with one-sided widespread pitting damage designed to a recognized code or standard using an equation that specifically relates pressure (or liquid fill height for tanks) to a required wall thickness. The only load considered is internal pressure. Level 2 assessments can be used to evaluate components that do not meet Level 1 assessment criteria.

b) The Level 2 Assessment procedures are used to evaluate all four categories of pitting: widespread pitting, localized pitting, pitting within a locally thin area, and a locally thin area in a region of widespread pitting. The Level 2 Assessment rules provide a better estimate of the structural integrity of a component because a measure of the actual damage parameter, the pit-couple, is directly used in the assessment. The Level 2 assessment should be used when the pitting damage occurs on both sides of the component. Level 3 assessments can be used to evaluate components that are not covered by, or do not pass a Level 1 or Level 2 Assessment.

c) The Level 3 Assessment procedures are intended to evaluate more complex regions of pitting, loading conditions, and/or components with details where only limited design rules are provided in the original construction code or standard. Detailed stress analysis techniques should be utilized in a Level 3 Assessment.

6.4.2 Level 1 Assessment

6.4.2.1 The Level 1 Assessment technique utilizes standard pit charts and the maximum pit depth in the area being evaluated to estimate a Remaining Strength Factor, RSF. The surface damage of the pitted region is characterized by making a visual comparison between the actual damage and a standard pit chart. Based on the pit chart that best approximates the present damage, the remaining strength factor can be determined using the measured maximum pit depth.

6.4.2.2 The following assessment procedure can be used to evaluate components that meet the conditions stipulated in paragraph 6.2.5.1. For an atmospheric storage tank, the same procedure can be followed to determine a MFH by replacing the $MAWP$ with the MFH, and determining the MFH using the applicable code equations for a tank shell.

a) STEP 1 – Determine the following parameters: D, FCA, either t_{rd} or t_{nom} and $LOSS$.

b) STEP 2 – Determine the wall thickness to be used in the assessment using Equation (6.1) or Equation (6.2), as applicable.

$$t_c = t_{nom} - LOSS - FCA \tag{6.1}$$

$$t_c = t_{rd} - FCA \tag{6.2}$$

c) STEP 3 – Locate the area on the component that has the highest density of pitting damage based on the number of pits. Obtain photographs (include reference scale), or rubbings of this area to record the amount of surface damage.

d) STEP 4 – Determine the maximum pit depth, $w_{\max}$, in the region of pitting damage being evaluated.

e) STEP 5– Determine the ratio of the remaining wall thickness to the future wall thickness in the pitted region using Equation (6.3). In Equation (6.3), t_{rd} can be replaced by $t_{nom} - LOSS$. If $R_{wt} < 0.2$ the Level 1 assessment criteria are not satisfied.

$$R_{wt} = \frac{t_c + FCA - w_{\max}}{t_c} \tag{6.3}$$

f) STEP 6 – Determine the $MAWP$ for the component (see Annex A, paragraph A.2) using the thickness from STEP 2.

g) STEP 7 – Compare the surface damage from the photographs or rubbings to the standard pit charts shown in Figures 6.3 through 6.10. Select a pit chart that has a measure of surface damage that approximates the actual damage on the component. If the pitting damage is more extensive than that shown in Figure 6.10, then compute the RSF using the following equation and proceed to STEP 9.

$$RSF = R_{wt} \tag{6.4}$$

h) STEP 8 – Determine the RSF from the table shown at the bottom of the pit chart that was chosen in STEP 7 using the value of R_{wt} calculated in STEP 5. Interpolation of the RSF is acceptable for intermediate values of R_{wt}.

i) STEP 9 – If $RSF \geq RSF_a$, then the pitting damage is acceptable for operation at the $MAWP$ determined in STEP 6. If $RSF < RSF_a$, then the region of pitting damage is acceptable for operation at $MAWP_r$, where $MAWP_r$ is computed using the equations in Part 2, paragraph 2.4.2.2. The $MAWP$ from STEP 6 shall be used in this calculation.

6.4.2.3 If the component does not meet the Level 1 assessment requirements, then the following, or combinations thereof, can be considered:

a) Rerate, repair, replace, or retire the component.

b) Adjust the FCA by applying remediation techniques (see Part 4, paragraph 4.6).

c) Conduct a Level 2 or Level 3 Assessment.

6.4.3 Level 2 Assessment

6.4.3.1 The assessment procedure in paragraphs 6.4.3.2 and 6.4.3.3 are used to determine the acceptability of the circumferential and longitudinal stress directions, respectively. A Level 2 assessment provides a better estimate of the Remaining Strength Factor for pitting damage in a component subject to pressure loading, and supplemental loading for cylindrical, and conical shells. This procedure accounts for the orientation of the pit-couple with respect to the maximum stress direction. Guidance for conducting an assessment for the four categories of pitting described in paragraph 6.2.1 is shown in Figure 6.2. The procedure in this Part or the pitting charts in Level 1 can be used to determine the acceptability of a component at a future date when an estimate on the pitting progression rate can be determined (See 6.3.3.4).

6.4.3.2 The following assessment procedure can be used to evaluate components when conditions described in paragraph 6.2.5.1 are met. If the flaw is found to be unacceptable, the procedure can be used to establish a reduced $MAWP$. For an atmospheric storage tank, the same procedure can be followed to determine a MFH by replacing the $MAWP$ with the MFH, and determining the MFH using the applicable code equations for a tank shell.

a) STEP 1 – Determine the following parameters: D, FCA, either t_{rd} or t_{nom} and $LOSS$.

b) STEP 2 – Determine the wall thickness to be used in the assessment using Equation (6.1) or Equation (6.2), as applicable.

c) STEP 3 – Determine the pit-couple sample for the assessment (see 6.3.3.2), and the following parameters for each pit-couple, k, $d_{i,k}$, $d_{j,k}$, P_k, $w_{i,k}$ and $w_{i,k}$. In addition, determine the orientation of the pit-couple measured from the direction of the σ_2 stress component, θ_k (see Figure 6.11); for a conservative analysis set $\theta_k = 0.0$ degrees.

d) STEP 4 – Determine the depth of each pit below t_c in all pit-couples, $w_{i,k}$ and $w_{j,k}$ (see Figure 6.11.b) and compute the average pit depth, w_{avg}, considering all readings. In Equation (6.5), the subscript k represents a calculation for pit-couple k.

$$w_{avg,k} = \frac{\left(w_{i,k} + w_{j,k}\right)}{2} \tag{6.5}$$

e) STEP 5 – Calculate the components of the membrane stress field, σ_1 and σ_2 (see Figure 6.11). Membrane stress equations for shell components are included in Annex A.

f) STEP 6 – Determine the MAWP for the component (see Annex A, paragraph A.2) using the thickness from STEP 2.

g) STEP 7 – For pit-couple k, calculate the Remaining Strength Factor:

1) *Single Layer Analysis* – This analysis can be used when the pitting occurs on one side of the component (see Figure 6.11).

$$RSF_k = 1 - \frac{w_{avg,k}}{t_c} \cdot \left(1 - E_{avg,k}\right) \tag{6.6}$$

where, $w_{avg,k}$ is from STEP 4 and,

$$E_{avg,k} = \min\left[\frac{\Phi_k}{\sqrt{\Psi_k}},\ 1.0\right] \tag{6.7}$$

$$\Phi_k = \mu_{avg,k} \cdot \max\left[\ |\rho_{1,k}|,\ |\rho_{2,k}|,\ |\rho_{1,k} - \rho_{2,k}|\ \right] \tag{6.8}$$

$$\Psi_k = \left(\begin{array}{l}\left(\cos^4\theta_k + \sin^2 2\theta_k\right)\left(\rho_{1,k}\right)^2 - \dfrac{3\left(\sin^2 2\theta_k\right)\rho_{1,k}\rho_{2,k}}{2} + \\ \left(\sin^4\theta_k + \sin^2 2\theta_k\right)\left(\rho_{2,k}\right)^2\end{array}\right) \tag{6.9}$$

$$\rho_{1,k} = \frac{\sigma_1}{\mu_{avg,k}} \tag{6.10}$$

$$\rho_{2,k} = \frac{\sigma_2}{\mu_{avg,k}} \tag{6.11}$$

$$\mu_{avg,k} = \frac{P_k - d_{avg,k}}{P_k} \tag{6.12}$$

$$d_{avg,k} = \frac{d_{i,k} + d_{j,k}}{2} \tag{6.13}$$

2) *Multiple Layer Analysis* – This analysis is used to account for pitting on both sides of the component (see Figure 6.15). In this analysis, $E_{avg,k}$, is calculated for each pit-couple using Equations (6.7) through (6.13). The value of $E_{avg,k}$ is then used along with the thickness of all layers that the pit-couple penetrates to calculate a value of RSF_k for the pit couple. The selection of the number of layers, N, is based on the depth of pits on both sides of the component. The component thickness is divided into layers based on the pitting damage (see Figure 6.15), and the $E_{avg,k}$ is computed using Equation (6.14) considering all layers containing the pit-couple. Each layer thickness, t_L, is determined by the depth of the deeper of the two pits in the pit-couple that establishes the layer. For layers where a pit-couple does not penetrate the layer, and the solid layer for all pit couples, $E_{avg,k}$ in Equation (6.14) equals 1.0. The $MAWP$ used with this expression should be based on t_c. If the pitting damage is overlapped from both surfaces (Figure 6.15), it is not acceptable per Level 2. A Level 3 assessment or the recommendations provided in paragraph 6.4.3.5 can be used.

$$RSF_k = 1 - \sum_{L=1}^{N}\left(\frac{t_L}{t_c}\right)\left(1 - E_{avg,k}\right)_L \tag{6.14}$$

h) STEP 8 – Repeat STEP 7 for all pit-couples, n, recorded at the time of the inspection. Determine the average value of the Remaining Strength Factors, RSF_k, found in STEP 7 and designate this value as RSF_{pit} for the region of pitting.

$$RSF_{pit} = \frac{1}{n} \cdot \sum_{k=1}^{n} RSF_k \tag{6.15}$$

i) STEP 9 - Evaluate results based on the type of pitting damage (see Figure 6.2):

1) Widespread Pitting – For widespread pitting that occurs over a significant region of the component, if $RSF_{pit} \geq RSF_a$, then the pitting damage is acceptable for operation at the MAWP determined in STEP 6. If $RSF_{pit} < RSF_a$, then the region of pitting damage is acceptable for operation at MAWPr, where MAWPr is computed using the equations in Part 2, paragraph 2.4.2.2. The MAWP from STEP 6 shall be used in this calculation.

2) *Localized Pitting* – If the pitting damage is localized, then the damaged area is evaluated as an equivalent region of localized metal loss (LTA, see Part 5 and Figure 6.13). The meridional and circumferential dimensions of the equivalent LTA should be based on the physical bounds of the observed pitting. The equivalent thickness, t_{eq}, for the LTA can be established using the following equation. To complete the analysis, the LTA is then evaluated using the Level 1 or Level 2 assessment procedures in Part 5 with $t_{mm} = t_{eq}$, where t_{eq} is given by Equation (6.16).

$$t_{eq} = RSF_{pit} \cdot t_c \tag{6.16}$$

3) *Region Of Local Metal Loss Located In An Area Of Widespread Pitting* – If a region of local metal loss (LTA) is located in an area of widespread pitting, then a combined Remaining Strength Factor can be determined using the following equation.

$$RSF_{comb} = RSF_{pit} \cdot RSF_{lta} \tag{6.17}$$

If $RSF_{comb} \geq RSF_a$, then the pitting damage is acceptable for operation at the $MAWP$ determined in STEP 6. If $RSF_{pit} < RSF_a$, then the region of pitting damage is acceptable for operation at $MAWP_r$, where $MAWP_r$ is computed using the equations in Part 2, paragraph 2.4.2.2. The $MAWP$ from STEP 6 shall be used in this calculation.

4) *Pitting Confined Within A Region Of Localized Metal Loss* – If the pitting damage is confined within a region of localized metal loss (see Figure 6.14), then the results can be evaluated using the methodology in subparagraph 3) above.

j) STEP 10 – Check the recommended limitations on the individual pit dimensions:

1) *Pit Diameter* – If the following equation is not satisfied for an individual pit, then the pit should be evaluated as a local thin area using the assessment methods of Part 5 The size of the local thin area is the pit diameter and the remaining thickness ratio is defined below. This check is required for larger pits to ensure that a local ligament failure at the base of the pit does not occur.

$$d \leq Q\sqrt{D \cdot t_c} \tag{6.18}$$

The value of Q in Equation (6.18) shall be determined using Part 4, Table 4.5 and is a function of the remaining thickness ratio, R_t, for each pit as given by either of the following equations where $w_{i,k}$ is the depth of the pit under evaluation.

$$R_t = \left(\frac{t_c + FCA - w_{i,k}}{t_c} \right) \tag{6.19}$$

2) *Pit Depth* – The following limit on the remaining thickness ratio is recommended to prevent a local failure characterized by pinhole type leakage. The criterion is expressed in terms of the remaining thickness ratio as follows:

$$R_t \geq 0.20 \tag{6.20}$$

6.4.3.3 The assessment procedures in this paragraph should be used to determine the acceptability of the longitudinal stress direction in a cylindrical or conical shell or pipe with pitting damage subject to pressure and/or supplemental loads. The acceptability of the circumferential stress direction is evaluated using paragraph 6.4.3.2.

a) *Supplemental Loads* – These types of loads may result in a net section axial force, bending moment, torsion, and shear being applied to the cross section containing the flaw (paragraph Annex A, A.2.6). The supplemental loads included in the assessment should include loads that produce both load-controlled and strain controlled effects. Therefore, the net-section axial force, bending moment, torsion, and shear should be computed for two load cases, weight and weight plus thermal (see Part 5, paragraph 5.4.3.3.a).

b) *Special Requirements For Piping Systems* – Requirements in Part 5, paragraph 5.4.3.3.b are required because of the relationship between the component thickness, piping flexibility or stiffness, and resulting stress.

c) *Assessment For Widespread Pitting* – The following procedure should be used to evaluate the permissible membrane, bending and shear stresses resulting from pressure and supplemental loads.

1) STEP 1 – Determine the following parameters: D, D_o, FCA, either t_{rd} or t_{nom} and $LOSS$.

2) STEP 2 – Determine the wall thickness to be used in the assessment using Equation (6.1) or Equation (6.2), as applicable.

3) STEP 3 – Determine the remaining strength factor, RSF, the allowable remaining strength factor, RSF_a, the permissible maximum allowable working pressure, $MAWP_r$, and supplemental loads on the circumferential plane. The remaining strength factor, allowable remaining strength factor, and the permissible maximum allowable working pressure for the region with pitting damage can be established using the procedures in paragraph 6.4.3.2. The supplemental loads are determined in accordance with paragraphs 6.4.3.3.a and 6.4.3.3.b.

4) STEP 4 – Compute the equivalent thickness of the cylinder with pitting damage.

$$t_{eq} = B \cdot t_c \tag{6.21}$$

$$B = \min\left[\frac{RSF}{RSF_a},\ 1.0\right] \tag{6.22}$$

5) STEP 5 – For the supplemental loads determined in STEP 3, compute the components of the resultant bending moment and torsion. This should be done for the weight and the weight plus thermal load cases.

6) STEP 6 – Compute the maximum circumferential stress.

$$\sigma_{cm} = \frac{MAWP_r}{RSF \cdot \cos\alpha}\left(\frac{D}{D_o - D} + 0.6\right) \tag{6.23}$$

7) STEP 7 – Compute the maximum section longitudinal membrane stress and the shear stress for both the weight and the weight plus thermal load cases. All credible load combinations should be considered in the calculation. The section properties required for the calculations are provided in Table 6.2.

$$\sigma_{lm} = \frac{1}{E_C \cdot \cos\alpha}\left[\frac{A_a}{A_m}\left(MAWP_r\right) + \frac{F}{A_m} \pm \frac{Ma}{I_x}\right] \tag{6.24}$$

$$\tau = \frac{M_T}{2A_t t_{eq}} + \frac{V}{A_m} \tag{6.25}$$

8) STEP 8 – Compute the equivalent membrane stress for the weight and the weight plus thermal load cases.

$$\sigma_e = \left[\sigma_{cm}^2 - \sigma_{cm}\sigma_{lm} + \sigma_{lm}^2 + 3\tau^2\right]^{0.5} \tag{6.26}$$

9) STEP 9 – Evaluate the results as follows:

i) The following relationship should be satisfied for either a tensile and compressive longitudinal stress for both the weight and the weight plus thermal load cases:

$$\sigma_e \le H_f\left(\frac{S_a}{RSF_a}\right) \tag{6.27}$$

ii) If the maximum longitudinal stress computed in STEP 7 is compressive, then this stress should be less than or equal to the allowable compressive stress computed using the methodology in Annex A, paragraph A.4.4 or the allowable tensile stress, whichever is smaller. When using this methodology to establish an allowable compressive stress, an average thickness representative of the region of pitting damage in the compressive stress zone should be used in the calculations.

10) STEP 10 – If the equivalent stress criterion of STEP 9 is not satisfied, the $MAWP$ and/or supplemental loads determined in STEP 3 should be reduced, and the evaluation outlined in STEPs 1 through 9 should be repeated. Alternatively, a Level 3 Assessment can be performed.

d) *Assessment For Localized Pitting* – If the flaw is categorized as localized pitting, a LTA located in a region of widely scattered pitting, or pitting confined within a region of an LTA, the assessment procedure in Part 5, paragraph 5.4.3.3 can be used once an equivalent LTA has been derived using the procedures in paragraph 6.4.3.2.i).

6.4.3.4 The assessment procedure in Part 4, paragraph 4.4.3.3 can be used to evaluate components that do not have a design equation that specifically relates pressure (or liquid fill height for tanks) to a required wall thickness (see Part 4, paragraph 4.3.2.1.g). For this assessment, the remaining wall thickness for the nozzle and vessel can be established using the equations in paragraph 6.4.3.3.c.4.

6.4.3.5 If the component does not meet the Level 2 Assessment requirements, then the following, or combinations thereof, can be considered:

a) Rerate, repair, replace, or retire the component.

b) Adjust the FCA by applying remediation techniques (see Part 4, paragraph 4.6).

c) Conduct a Level 3 Assessment.

6.4.4 Level 3 Assessment

6.4.4.1 The stress analysis techniques discussed in Annex B1 can be utilized to assess pitting damage in pressure vessels, piping, and tankage. The limit load techniques described in Annex B1 are typically recommended for this evaluation.

6.4.4.2 If a numerical computation (e.g. finite element method) is used to evaluate pitting, two alternatives for modeling the pits may be considered. In the first method, the pits can be modeled directly using three dimensional continuum finite elements. This method may be impractical based upon the pit density. In the second method, the reduced stiffness of the plate with pits can be approximated by using effective elastic constants or by developing an equivalent thickness. Effective elastic constants for plates with holes with triangular and rectangular pitch patterns are provided in the ASME B&PV Code, Section VIII, Division 1,Part UHX. Either of these methods will facilitate modeling of pitting damage using either shell or continuum finite elements; however, representative values of the effective elastic constants or equivalent thickness should be validated for use in the assessment. In addition, if a limit analysis is being performed, the validity of the effective elastic constants or equivalent thickness in the plastic regime should also be determined.

6.5 Remaining Life Assessment

6.5.1 The $MAWP$ approach, see Part 4, paragraph 4.5.2, provides a systematic way of determining the remaining life of a pressurized component with pitting. When estimating the remaining life of pitting damage, a Pit Propagation Rate should be determined based on the environmental and operating conditions.

6.5.1.1 Pits can grow in three different modes and suitable estimates for a propagation rate should be established for each mode. In addition to these individual modes, pitting damage can also grow from a combination of these modes.

a) *Increase In Pit Size* – an estimate as to how the pit characteristic diameter and depth will increase with time should be made. For a given pit-couple, as the pit diameter and/or depth increases, the RSF decreases.

b) *Increase In Pit Density* – in addition to existing pits continuing to grow, new pits can form, thus increases the pit density. This decreases the pit spacing distance and the RSF.

c) *Increase In Pit Region Size* – if the pitting is localized, future operation may result in an enlargement of the localized region. The enlargement of a local region with pits has similar effects as the enlargement of an LTA.

6.5.1.2 If an estimate of the propagation rates cannot be made, remediation methods may be used to minimize future pitting damage.

6.5.2 The following procedure should be used to determine the remaining life of a component with pitting using the $MAWP$ approach

a) STEP 1 – Determine the uniform metal loss, *LOSS* in the region with pitting.

a) STEP 2 – Using the procedures described in Level 2, determine the $MAWP$ for a series of increasing time increments using a Pit Propagation Rate applied to the pit depth and diameter. Using a statistical analysis, it is possible to predict the likely depth of the deepest pit that was not measured. The statistical value can then be used as the pit depth in the formulas.

b) STEP 3 – The effective pit size and rate of change in the characteristic dimensions are determined as follows:

$$w_f = w_c + PPR_{pit-depth} \cdot time \tag{6.28}$$

$$d_f = d_c + PPR_{pit-diameter} \cdot time \tag{6.29}$$

d) STEP 4 – If remediation is not performed, an estimate of the future pit density should be made and included in the estimation of the $MAWP$ in STEP 2.

e) STEP 5 – If the pitted region is localized, an estimate of the future enlargement of this region should be made and included in the estimation of the $MAWP$ in STEP 2. If there is an interaction between pitting and a LTA, then this interaction shall also be considered in a $MAWP$ versus time calculation.

f) STEP 6 – Determine the remaining life from a plot of the $MAWP$ versus time. The time at which the $MAWP$ curve intersects the design $MAWP$ for the component is defined as the remaining life of the component. The equipment $MAWP$ is taken as the smallest value of the $MAWP$ for the individual components.

6.5.2.1 This approach may also be applied to tankage; however, in this case, the liquid maximum fill height, MFH, is evaluated instead of the $MAWP$.

6.6 Remediation

The remediation methods for general corrosion provided in Part 4 are typically applicable to pit damage. It is very difficult to properly remediate active pitting because the environment in a pit can be different from the bulk fluid environment; therefore, chemical treatments may not be effective. Coatings may be ineffective because they depend on proper surface preparation which can be difficult when removing scale in pits. Therefore, replacement of component sections or welded strip linings may be the remediation method of choice.

6.7 In-Service Monitoring

The remaining life may be difficult to establish for some services where an estimate of the future metal loss and enlargement of the pitted region cannot be adequately characterized. In these circumstances, remediation alone or with in-service monitoring may be required to qualify the assumptions made to establish the remaining life. It is often difficult to monitor pitting progression non-intrusively with ultrasonic methods. Radiography may be an alternative.

6.8 Documentation

6.8.1 The documentation of the FFS assessment should include the information cited in Part 2, paragraph 2.8

6.8.2 Inspection data including readings and locations used to determine the pitting damage RSF factor should be recorded and included in the documentation. A sample data sheet is provided in Table 6.1 for this purpose.

6.9 Nomenclature

A_m	cylinder metal cross-section.
A_a	cylinder aperture cross-section.
A_t	area used in the torsional shear stress calculation.
a	distance from the centroidal axis to the point where the net-section bending stress is to be computed.
α	cone half apex angle.
D	inside diameter of the cylinder, cone (at the location of the flaw), sphere, or formed head; for the center section of an elliptical head an equivalent inside diameter of $K_c D_c$ is used where D_c inside diameter of the head straight flange and K_c is a factor defined in Annex A, paragraph A.3.6; for the center section of a torispherical head two times the crown radius of the spherical section is used. D shall be corrected for $LOSS$ and FCA, as applicable.
D_f	modified cylinder diameter to account for pitting damage.
D_o	outside diameter of the cylinder, corrected for $LOSS$ and FCA as applicable.
d_c	current characteristic pit diameter.
d_f	estimated future characteristic pit diameter.

$d_{i,k}$	diameter of pit i in pit-couple k.
$d_{j,k}$	diameter of pit j in pit-couple k.
$d_{avg,k}$	average diameter of pit-couple k.
E_C	circumferential weld joint efficiency.
E_L	longitudinal weld joint efficiency.
E_y	modulus of elasticity at the assessment temperature.
F	applied section axial force for the weight or weight plus thermal load case, as applicable.
FCA	*future corrosion allowance* in the region of the pitting.(see Annex A, paragraph A.2.7). FCA is not applied to the depth of the individual pits.
H_f	is a factor depending on the load condition being evaluated; use 1.0 for the weight case and 1.67 for the weight plus thermal load case.
$LOSS$	prior metal loss on the component measured against the furnished thickness.
LTA	local thin area.
I_x	cylindrical shell moment of inertia.
M	applied section bending moment for the weight or weight plus thermal load case, as applicable.
$MAWP$	maximum allowable working pressure of the undamaged component.
$MAWP_r$	reduced permissible maximum allowable working pressure of the damaged component.
MFH	maximum fill height of the tank.
MFH_r	reduced permissible maximum fill height of the tank.
M_T	applied net-section torsion for the weight or weight plus thermal load case, as applicable.
n	number of pits used in the assessment.
N	number of layers in a multiple layer analysis.
P_k	distance between pit centers in pit-couple k.
$PPR_{pit-depth}$	estimated rate of change of pit characteristic depth.
$PPR_{pit-diameter}$	estimated rate of change of the pit characteristic diameter.
Q	factor used to determine the length for thickness averaging based on an allowable Remaining Strength Factor (see Part 2) and the remaining thickness ratio (R_t), (see Part 4, Table 4.5).
R_t	remaining thickness ratio.
R_{wt}	ratio of the remaining wall thickness to the future wall thickness for pitting.
RSF	Remaining Strength Factor.
RSF_a	allowable Remaining Strength Factor.
RSF_{comb}	combined Remaining Strength Factor that includes the effects of pitting damage and a local thin area.
RSF_k	Remaining Strength Factor for pit-couple k.
RSF_{lta}	Remaining Strength Factor for a local thin area computed using the methods provided in Part 5 (note that individual pits should be ignored in this calculation).
RSF_{pit}	Remaining Strength Factor for pitting damage calculated using paragraph 6.4.3.2.f.
S_a	allowable stress from the applicable construction code.
σ_{cm}	maximum circumferential stress, typically the hoop stress from pressure loading for the weight and weight plus thermal load case, as applicable.
σ_e	equivalent membrane stress.

σ_{lm} maximum section longitudinal membrane stress computed for the weight or weight plus thermal load case, as applicable.

σ_1 principle membrane stress in direction 1.

σ_2 principle membrane stress in direction 2.

t_c future corroded thickness.

t_{eq} equivalent thickness.

t_L thickness of a layer.

$t_{\min}$ minimum required wall thickness.

t_{nom} nominal or furnished thickness of the component adjusted for mill under tolerance as applicable.

t_{rd} uniform thickness away from the pitted region established by thickness measurements at the time of the assessment.

θ_k angle between σ_2 direction and the line joining pit 1 and 2 of pit couple k. (See Figure 6.11)

$time$ time allocated for future operation.

τ maximum shear stress for the weight or weight plus thermal load case, as applicable.

V applied net-section shear force for the weight or weight plus thermal load case, as applicable.

$w_{\max}$ maximum pit depth in the region of pitting damage

w_c current characteristic pit depth.

w_f estimated future characteristic pit depth.

$w_{avg,k}$ average pit depth of pit-couple k.

$w_{i,k}$ depth of the pit i in pit-couple k.

$w_{j,k}$ depth of the pit j in pit-couple k.

6.10 References

1. ASM, “Metals Handbook, Ninth Edition, Volume 13, Corrosion,” ASM International, Metals Park, Ohio, 1987, pp. 231-233.
2. ASM, “Metals Handbook, Ninth Edition, Volume 13, Corrosion,” ASM International, Metals Park, Ohio, 1987, pp. 113-122.
3. Daidola, J.C., Parente, J., Orisamolu, I.R., “Strength Assessment Of Pitted Panels”, SSC-394, Ship Structures Committee, D.C., 1997.
4. Gumbel, E.J., “Statistical Theory of Extreme Values”, National Bureau of Standards, AMS 33, 1954.
5. Kowaka, Masamichi, “Introduction to Life Prediction of Industrial Plant Materials – Application of the Extreme Value Statistical Method for Corrosion Analysis”, Allerton Press, Inc., 1994.
6. O’Donnell, W.J. and Porowski, J.S., “Yield Surfaces for Perforated Materials”, Transactions of the ASME, *Journal of Applied Mechanics*, American Society of Mechanical Engineers, N.Y., pp. 263-270, 1973.
7. Porowski, J.S., Osage, D.A. and Janelle, J.A., “Limit Analysis of Shells with Random Pattern of Spread Pits,” ASME PVP, 2002.
8. Porowski, W.J., O’Donnell, J.S., Farr, J.R., “Limit Design of Perforated Cylindrical Shells per ASME Code”, *Journal of Pressure Vessel Technology*, American Society of Mechanical Engineers, N.Y., pp. 646-651, 1977.
9. Porowski, W.J. and O’Donnell, J.S., “Effective Elastic Constants for Perforated Materials”, Transactions of the ASME, *Journal of Pressure Vessel Technology*, American Society of Mechanical Engineers, N.Y., pp. 234-241, 1974.

6.11 Tables and Figures

Table 6.1
Required Data for Assessment of Pitting

Use this form to summarize the data obtained from a field inspection.

Equipment Identification: ____
Equipment Type: _____ Pressure Vessel _____ Storage Tank _____ Piping Component
Component Type & Location: ____

Data Required for Level 2:

Pit-Couple	P_k	θ_k	$d_{i,k}$	$w_{i,k}$	$d_{j,k}$	$w_{j,k}$

Table 6.2
Section Properties for Computation of Longitudinal Stress in a Cylinder with an *LTA*

Pitting Damage on the Inside Surface	Pitting Damage on the Outside Surface
$D_f = D_o - 2t_{eq}$	$D_f = D + 2t_{eq}$
$I_{\bar{X}} = \frac{\pi}{64}\left(D_o^4 - D_f^4\right)$	$I_{\bar{X}} = \frac{\pi}{64}\left(D_f^4 - D^4\right)$
$A_m = \frac{\pi}{4}\left(D_o^2 - D_f^2\right)$	$A_m = \frac{\pi}{4}\left(D_f^2 - D^2\right)$
$A_t = \frac{\pi}{16}\left(D_o + D_f\right)^2$	$A_t = \frac{\pi}{16}\left(D_f + D\right)^2$
$a = \frac{D_o}{2}$	$a = \frac{D_f}{2}$
$A_a = \frac{\pi}{4} D_f^2$	$A_a = \frac{\pi}{4} D^2$

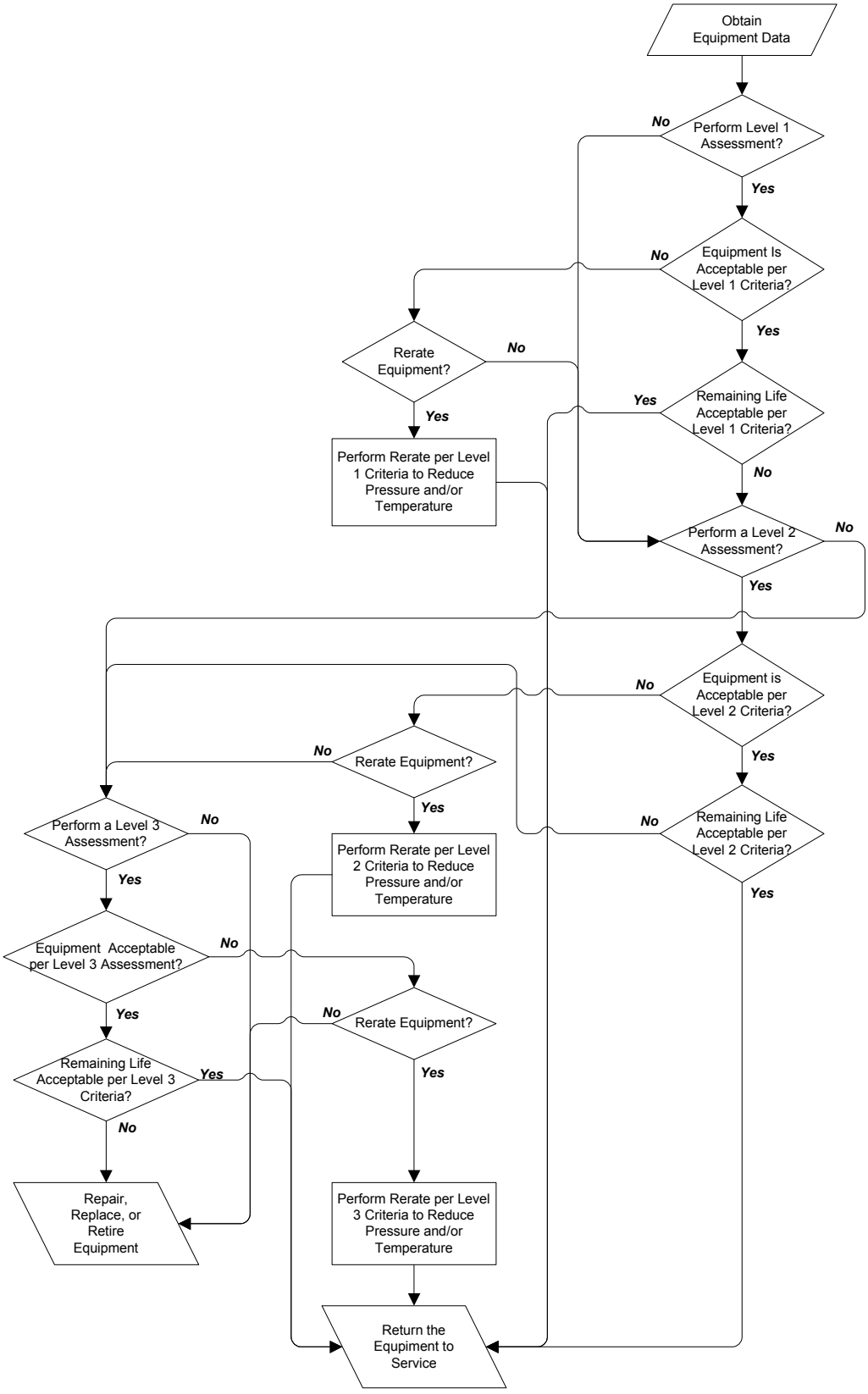

Figure 6.1 – Overview of the Assessment Procedures to Evaluate a Component with Pitting

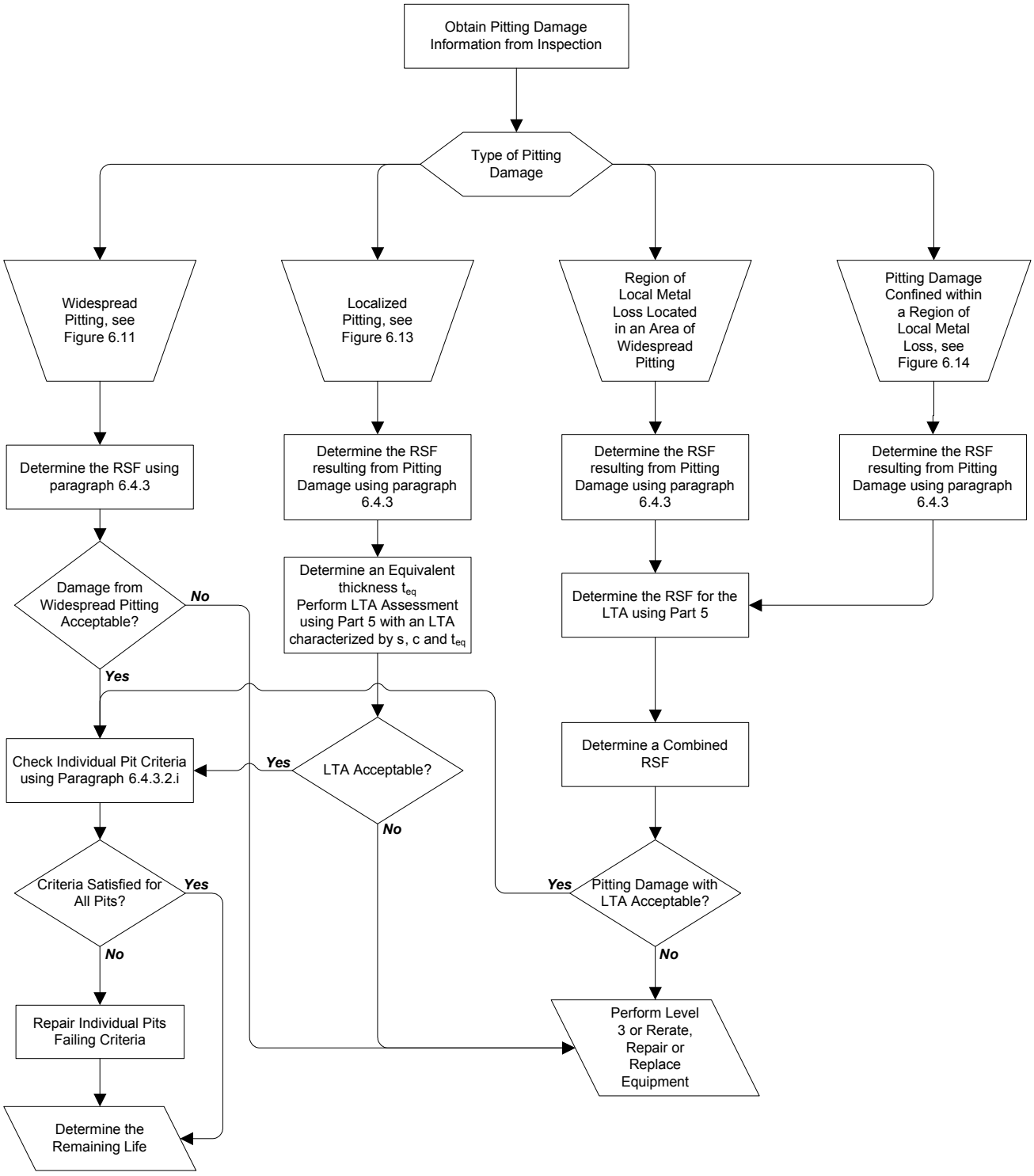

Figure 6.2 – Categories and Analysis Methodology of the Level 2 Pitting Assessment

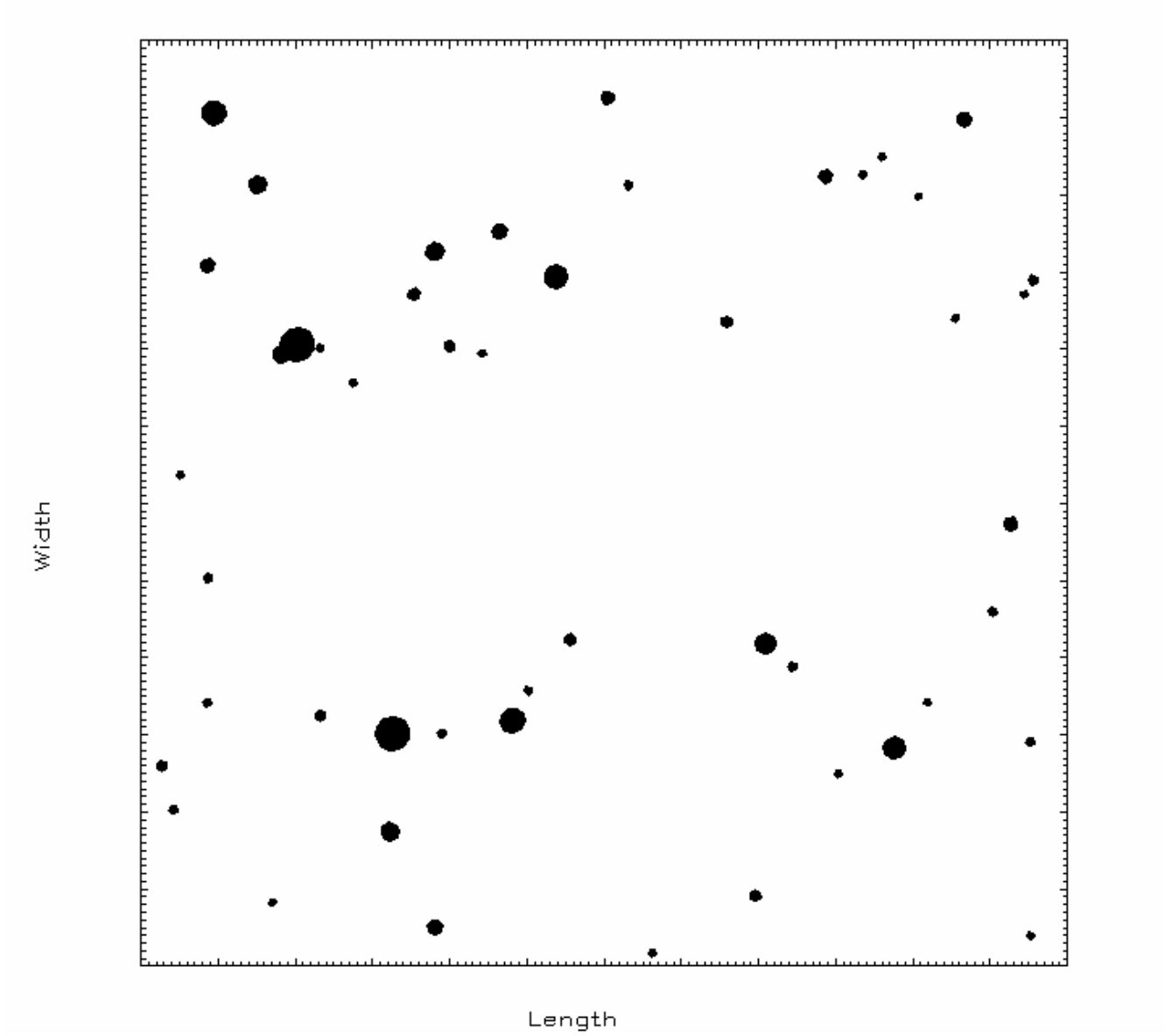

Note: The scale of this figure is 150 mm by 150 mm (6 in by 6 in)

R_{wt}, see Equation (6.3)	Level 1 RSF	
	Cylinder	Sphere
0.8	0.97	0.96
0.6	0.95	0.91
0.4	0.92	0.87
0.2	0.89	0.83

Figure 6.3 – Pitting Chart for Grade 1 Pitting

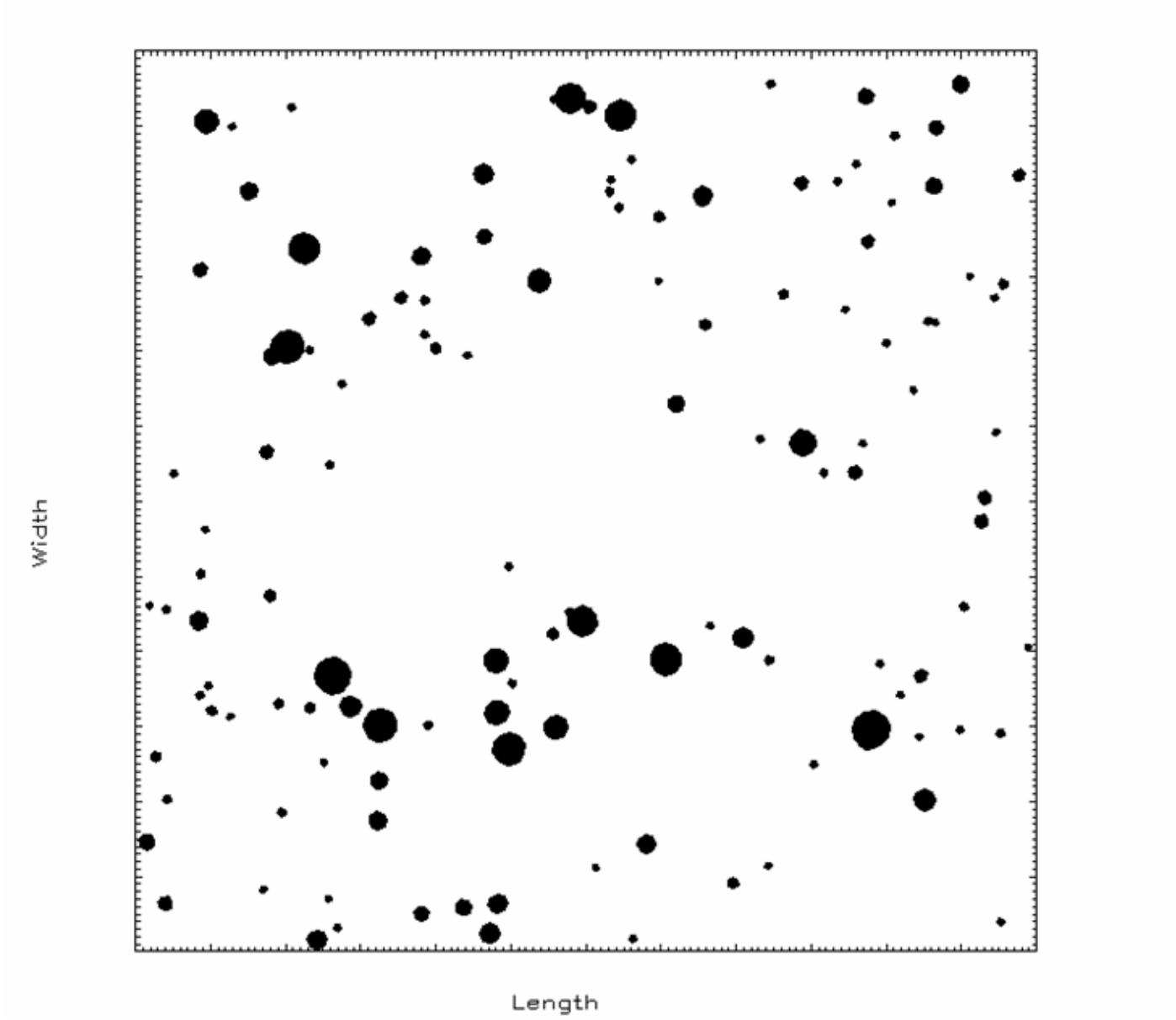

Note: The scale of this figure is 150 mm by 150 mm (6 in by 6 in)

R_{wt}, see Equation (6.3)	Level 1 RSF	
	Cylinder	Sphere
0.8	0.97	0.96
0.6	0.95	0.91
0.4	0.92	0.87
0.2	0.89	0.83

Figure 6.4 – Pitting Chart for Grade 2 Pitting

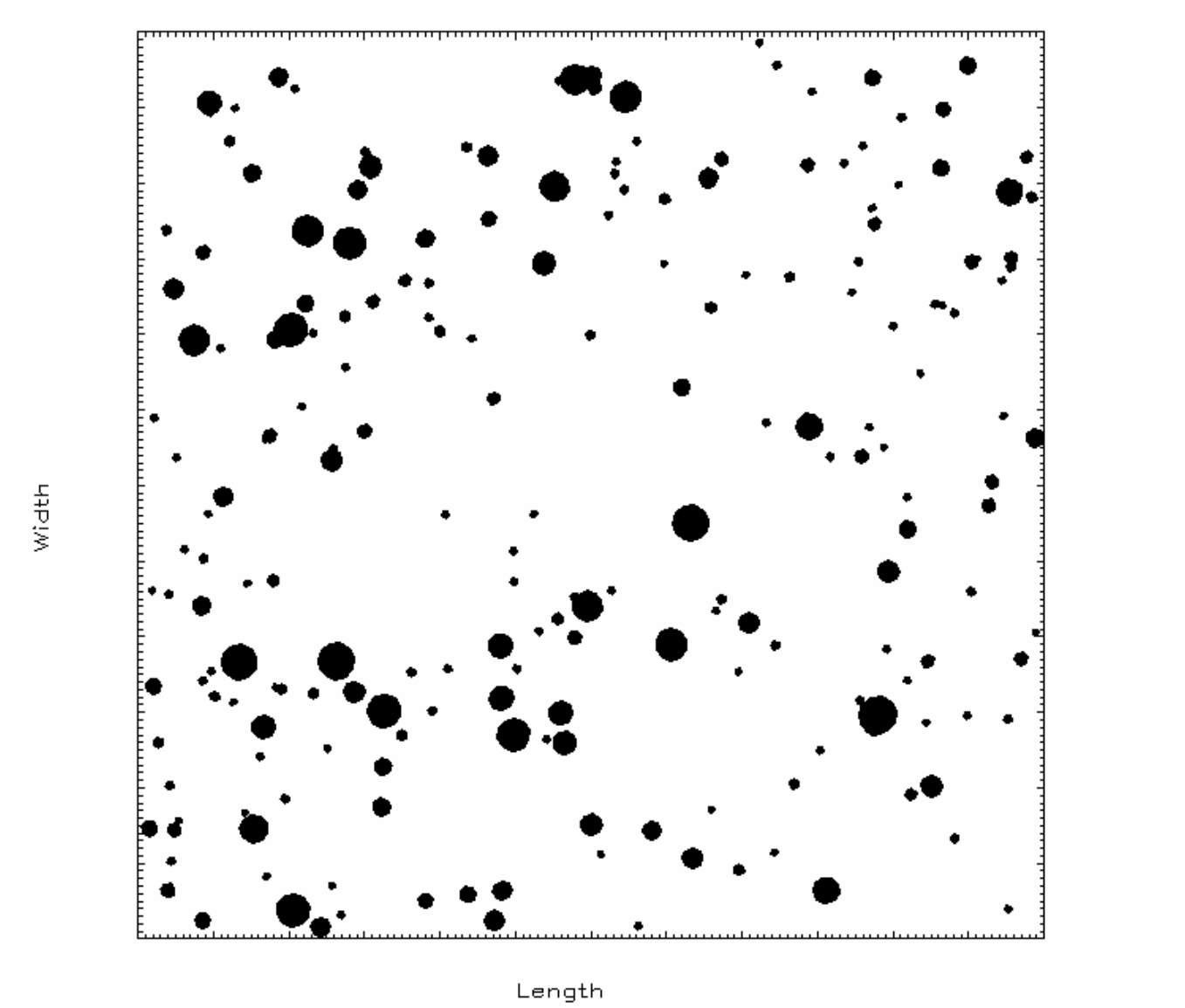

Note: The scale of this figure is 150 mm by 150 mm (6 in by 6 in)

R_{wt}, see Equation (6.3)	Level 1 RSF	
	Cylinder	Sphere
0.8	0.96	0.95
0.6	0.93	0.89
0.4	0.89	0.84
0.2	0.86	0.79

Figure 6.5 – Pitting Chart for Grade 3 Pitting

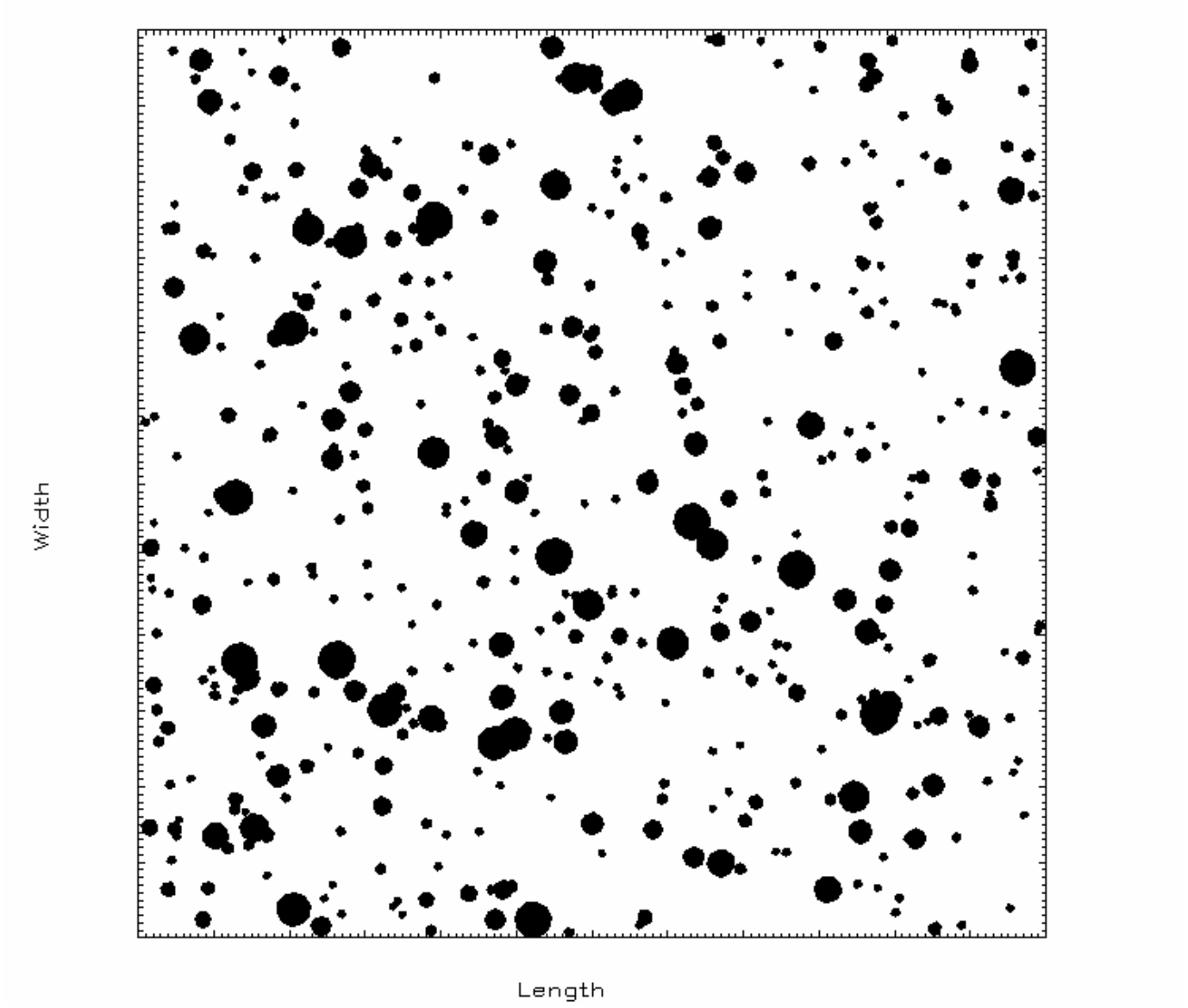

Note: The scale of this figure is 150 mm by 150 mm (6 in by 6 in)

R_{wt}, see Equation (6.3)	Level 1 RSF	
	Cylinder	Sphere
0.8	0.95	0.93
0.6	0.90	0.86
0.4	0.85	0.79
0.2	0.79	0.72

Figure 6.6 – Pitting Chart for Grade 4 Pitting

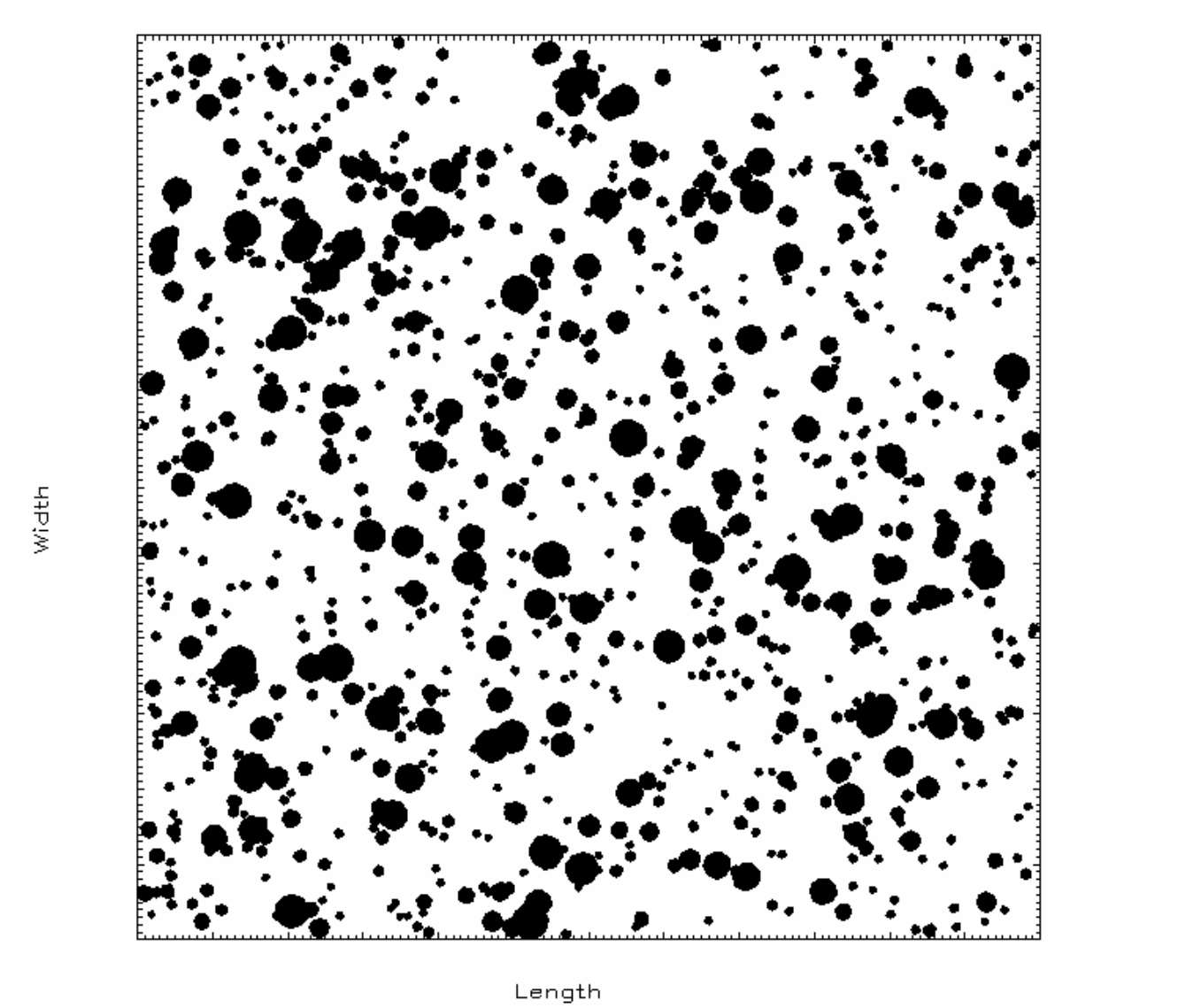

Note: The scale of this figure is 150 mm by 150 mm (6 in by 6 in)

R_{wt}, see Equation (6.3)	Level 1 RSF	
	Cylinder	Sphere
0.8	0.93	0.91
0.6	0.85	0.81
0.4	0.78	0.72
0.2	0.70	0.62

Figure 6.7 – Pitting Chart for Grade 5 Pitting

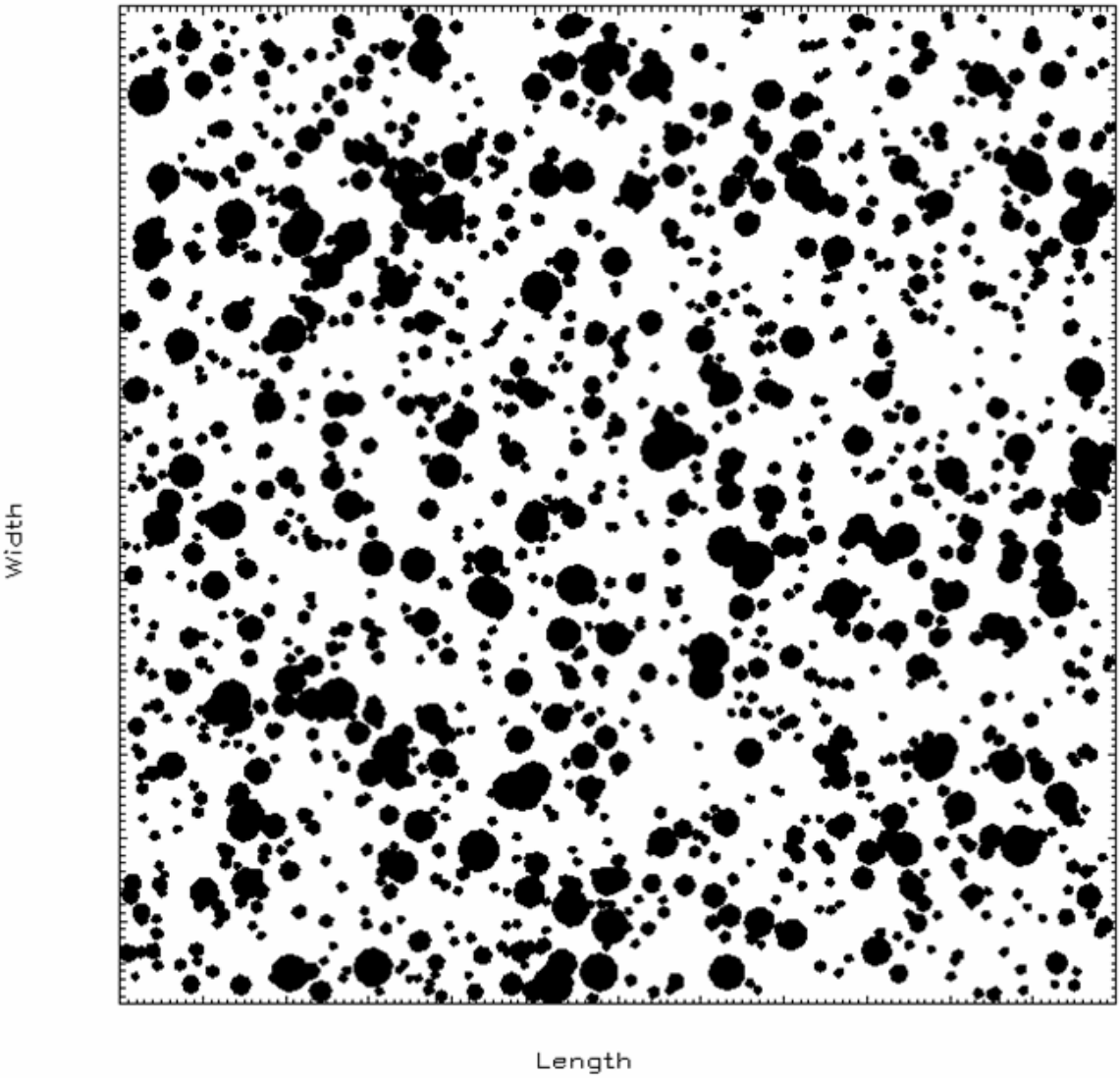

Note: The scale of this figure is 150 mm by 150 mm (6 in by 6 in)

R_{wt}, see Equation (6.3)	Level 1 RSF	
	Cylinder	Sphere
0.8	0.91	0.89
0.6	0.82	0.78
0.4	0.73	0.67
0.2	0.64	0.56

Figure 6.8 – Pitting Chart for Grade 6 Pitting

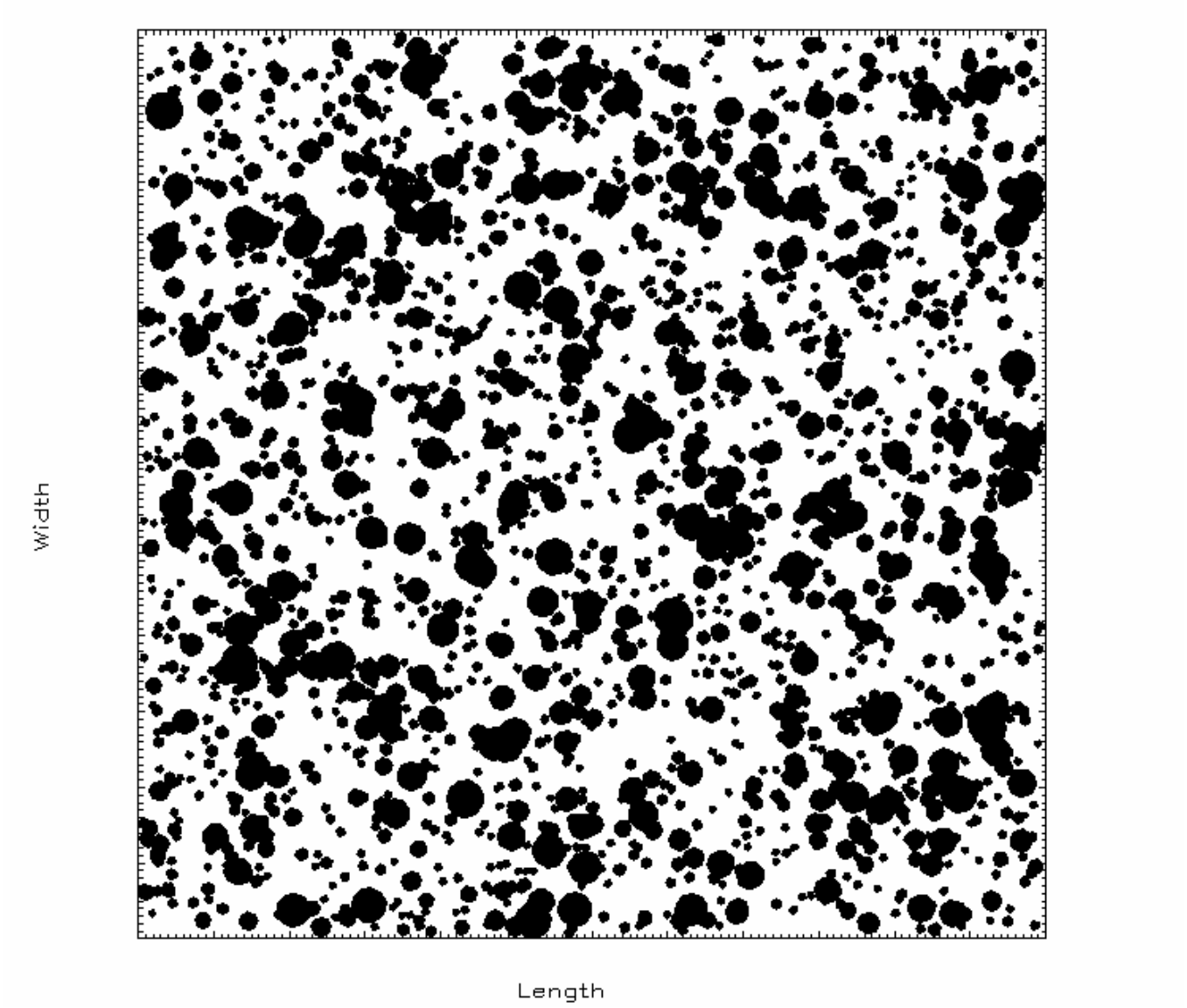

Note: The scale of this figure is 150 mm by 150 mm (6 in by 6 in)

R_{wt}, see Equation (6.3)	Level 1 RSF	
	Cylinder	Sphere
0.8	0.89	0.88
0.6	0.79	0.76
0.4	0.68	0.63
0.2	0.58	0.51

Figure 6.9 – Pitting Chart for Grade 7 Pitting

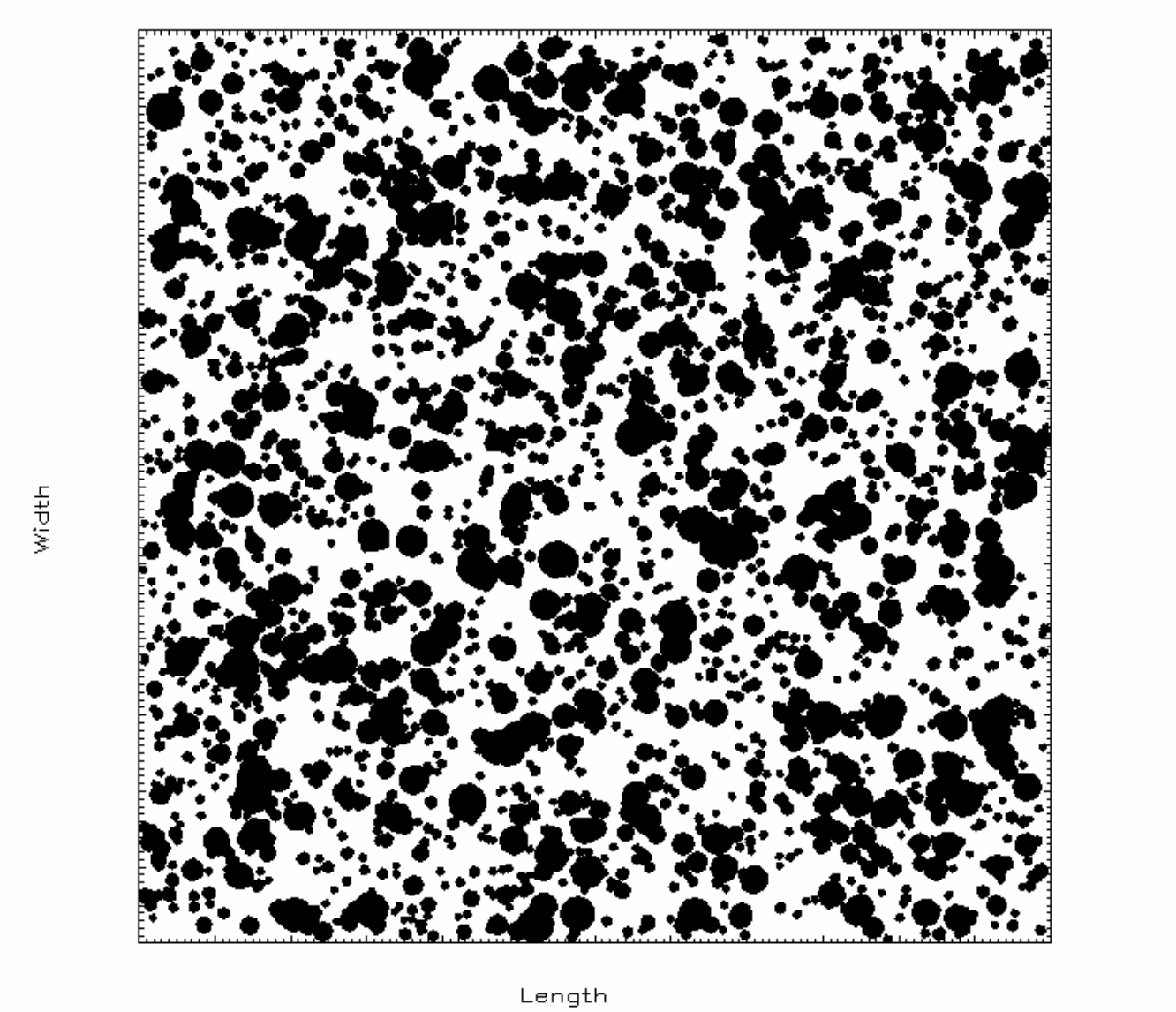

Note: The scale of this figure is 150 mm by 150 mm (6 in by 6 in)

R_{wt}, see Equation (6.3)	Level 1 RSF	
	Cylinder	Sphere
0.8	0.88	0.87
0.6	0.77	0.74
0.4	0.65	0.60
0.2	0.53	0.47

Figure 6.10 – Pitting Chart for Grade 8 Pitting

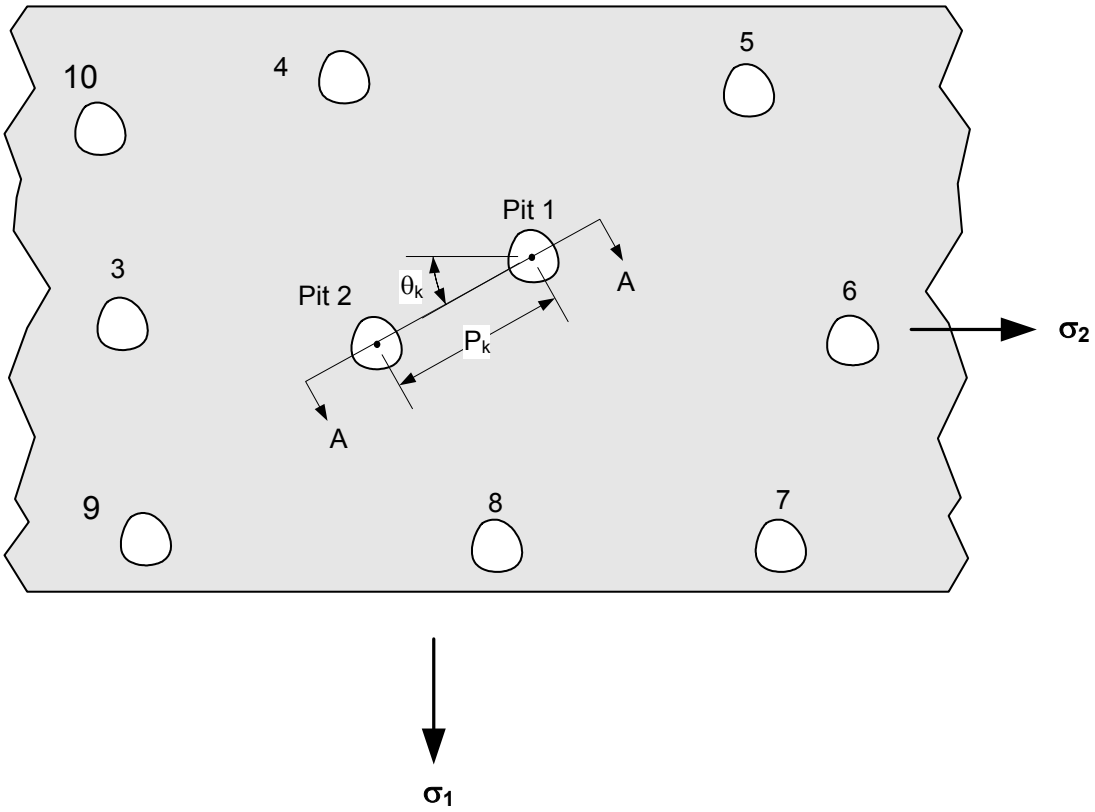

Note: In the example above: $P_k = P_{12}$ and $\theta_k = \theta_{12}$ because the closest pit to pit 1 is pit 2 (i.e. pit 2 is the nearest neighbor to pit 1).

(a) Pit-couple in a Plate Subject to a Biaxial Membrane Stress Field with $\sigma_1 \geq \sigma_2$

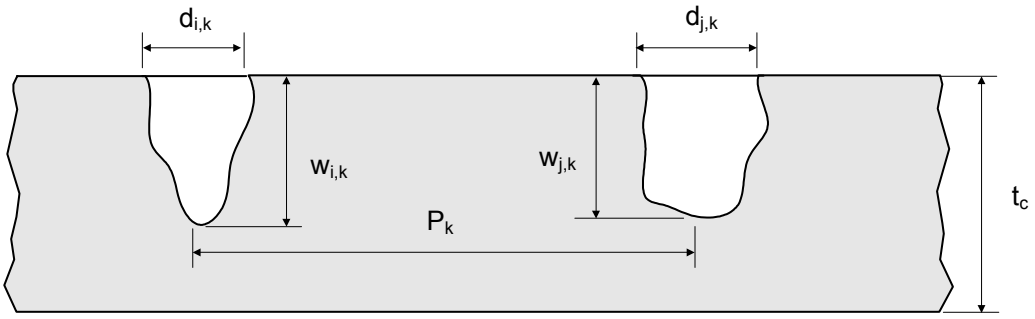

$w_{avg,k} = 0.5(w_{i,k} + w_{j,k})$ $\quad$ $d_{avg,k} = 0.5(d_{i,k} + d_{j,k})$

(b) Section A-A

Figure 6.11 – Parameters for the Analysis of Pits

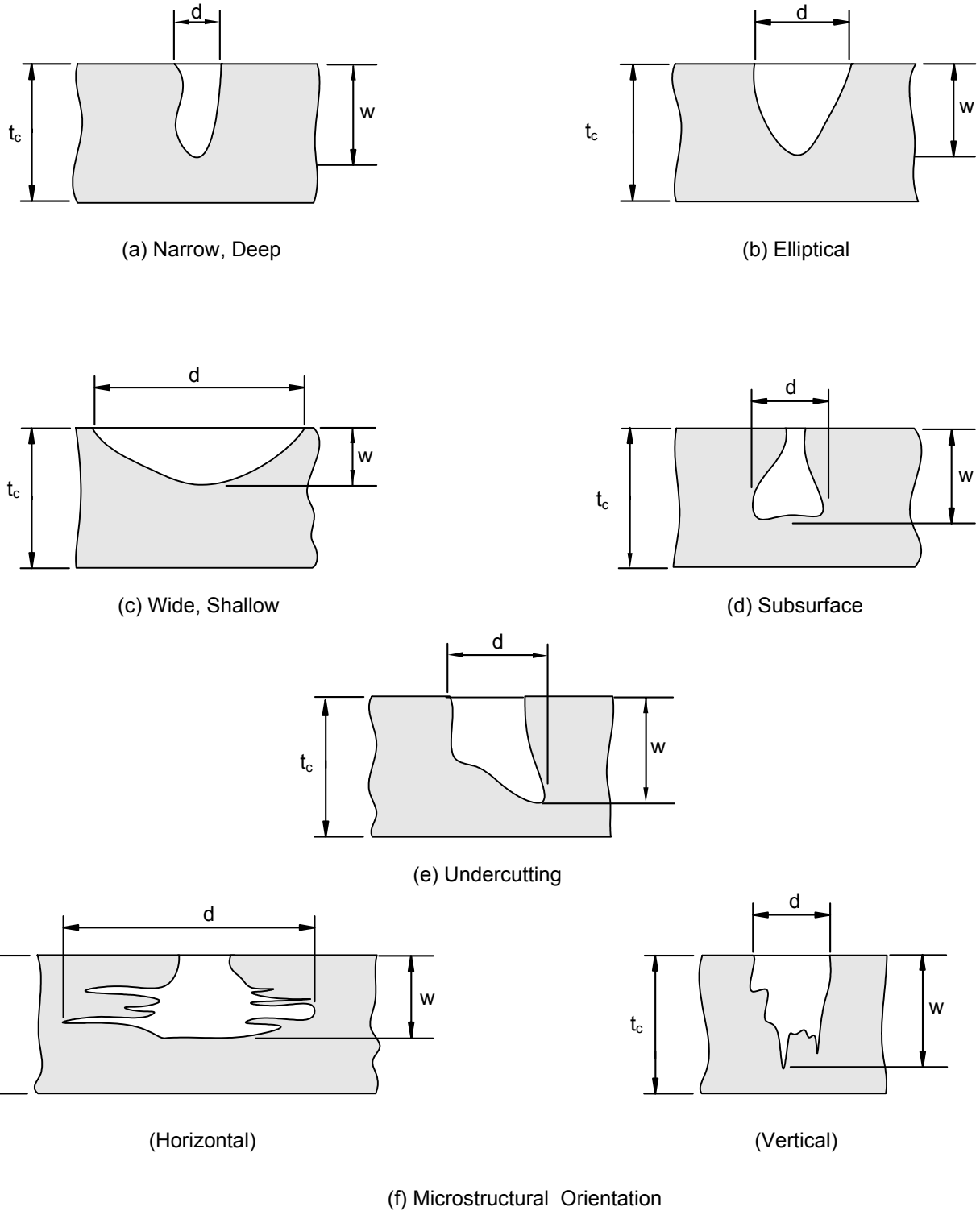

Figure 6.12 – Variation in the Cross Sectional Shapes of Pits

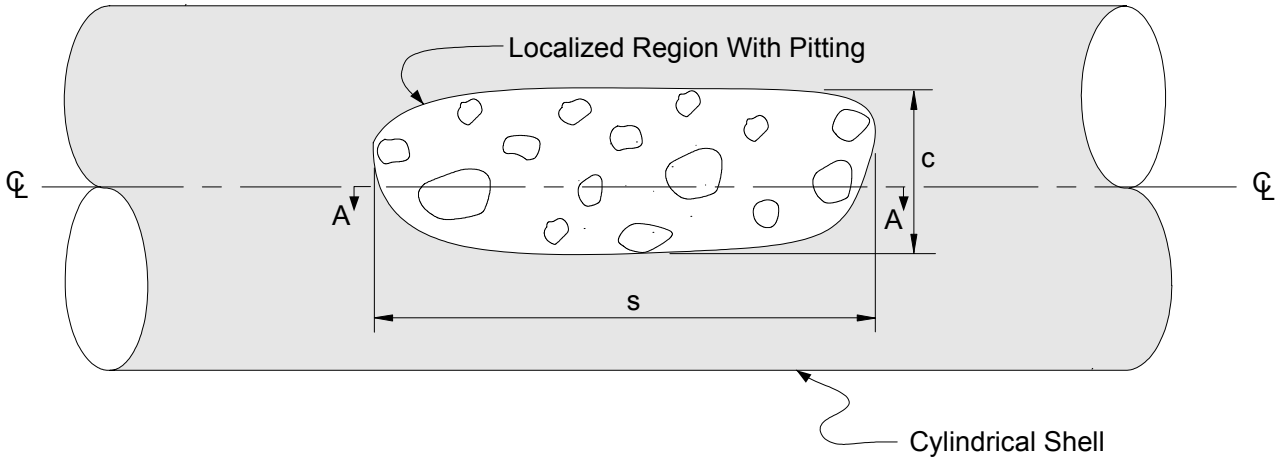

(a) Cylinder With Localized Pitting

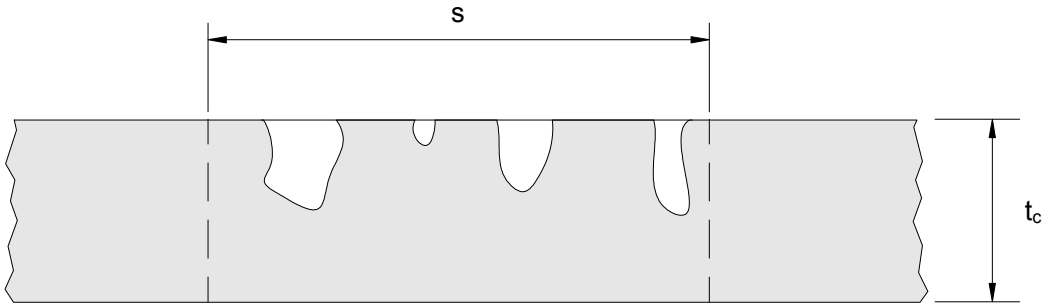

(b) Section A-A

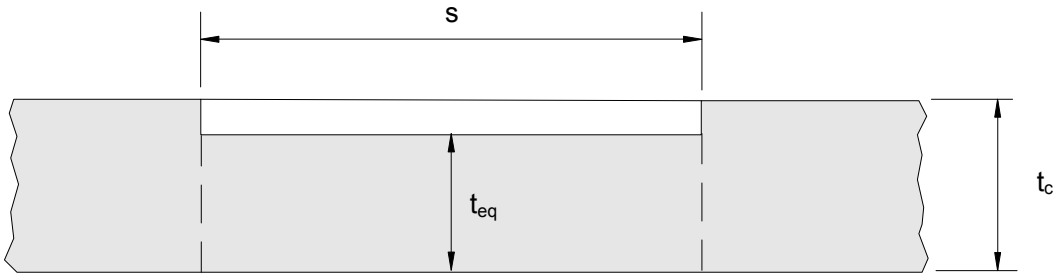

(c) Equivalent Plate Section For LTA Analysis

Figure 6.13 – Additional Parameters for the Analysis of a Localized Region of Pits

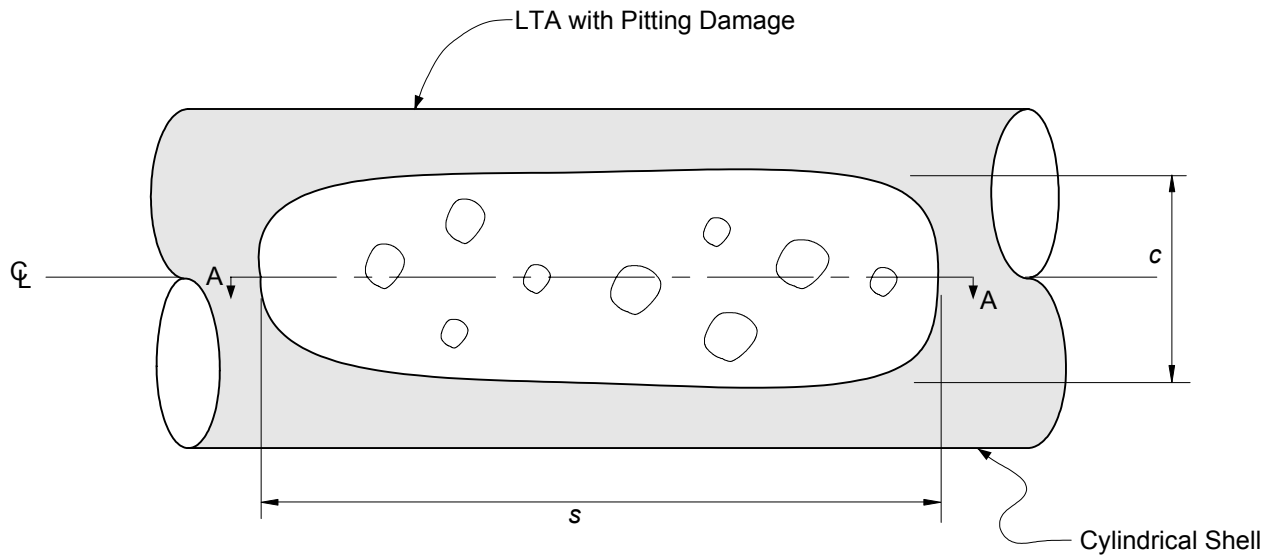

(a) Cylinder With Pitting Damage Confined to an LTA

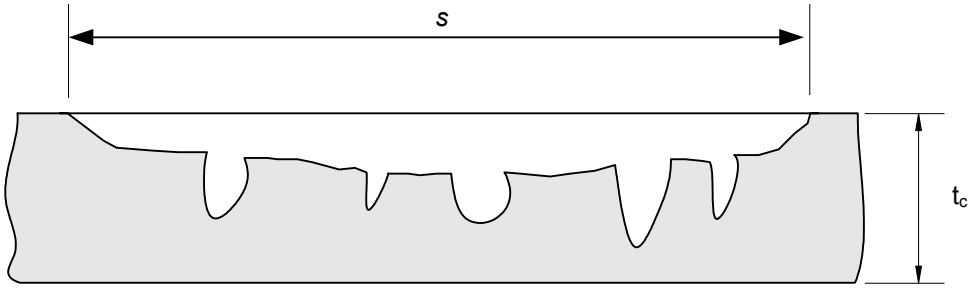

(b) Section A-A

Notes:

1. The dimensions s and c define the region of localized pitting damage.
2. A combined RSF is used in the assessment (see paragraph 6.4.3.2).
3. Section A-A is defined based on the $CTPs$.

Figure 6.14 – Pitting Damage Confined to an LTA

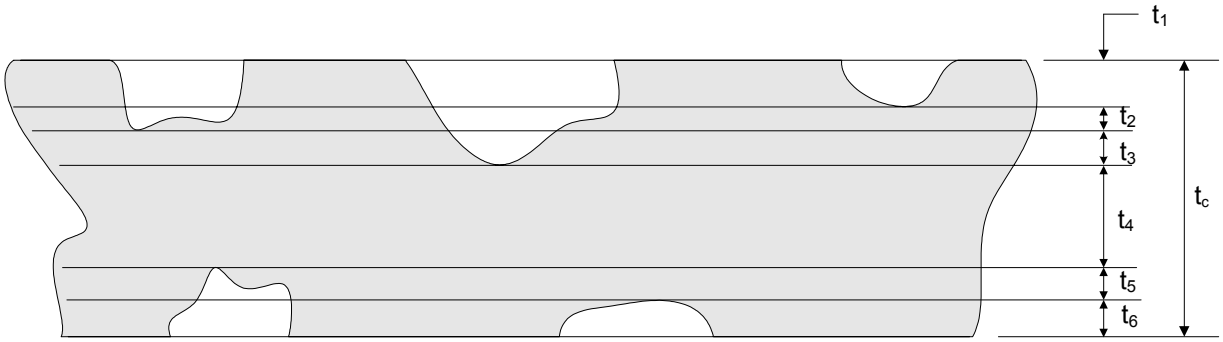

(a) Pit Damage From Both Surfaces Does Not Overlap

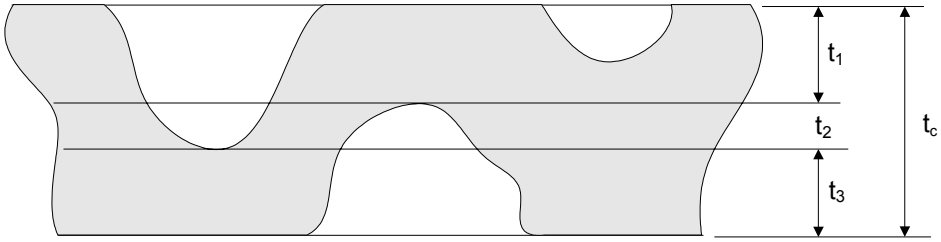

(b) Overlapping Pit Damage From Both Surfaces

Notes:
1. The number of layers used in the assessment is established based on the deepest penetration of the individual pits included in the pit-couple data. A layer is assigned based on the depth of each pit until all pits are accounted for. Using this procedure, a single layer of material will exist (see Detail (a) above) as long as the depth of pitting damage from the inside and outside surface of the component does not overlap (see Detail (b) above).
2. Overlapping pit damage from both surfaces is not acceptable in a Level 2 Assessment.

Figure 6.15 – Layered Shell Model to Evaluate Pitting Damage on Both Surfaces

PART 7

ASSESSMENT OF HYDROGEN BLISTERS AND HYDROGEN DAMAGE ASSOCIATED WITH HIC AND SOHIC

PART CONTENTS

7.1 General

7.1.1 Fitness-For-Service *(FFS)* assessment procedures are provided in this Part for low strength ferritic steel pressurized components with hydrogen induced cracking (HIC) and blisters, and stress oriented HIC (SOHIC) damage. These forms of damage are further described below and in [1]. The assessment procedures for HIC and blister damage are shown in the flow chart contained in Figure 7.1. This Part excludes sulfide stress cracking (SSC) and hydrogen embrittlement of high strength steels which generally occur in steels with hardnesses above Rockwell C 22 (Brinell 237) or with tensile strengths above 793 MPa (115 ksi).

7.1.2 Hydrogen induced cracking (HIC) is characterized by laminar (in-plane) cracking with some associated through-thickness crack linkage. This is sometimes referred to as step-wise cracking, due to its morphology. This type of damage typically occurs in carbon steel plates exposed to an aqueous phase containing hydrogen sulfide, cyanides, hydrofluoric acid, or other species which charge atomic hydrogen into the steel. It is less common in forgings and seamless pipes than in plates. The atomic hydrogen combines at non-metallic inclusions or other imperfections to form hydrogen molecules that are too large to diffuse through the steel. This build-up of internal hydrogen can result in HIC. Typical HIC damage is shown in Figures 7.2 and 7.3.

7.1.3 Stress Oriented HIC (SOHIC) is defined in [1] as follows: "Array of cracks, aligned nearly perpendicular to the stress, that are formed by the link-up of small HIC cracks in steel. Tensile stress (residual or applied) is required to produce SOHIC. SOHIC is commonly observed in the base metal adjacent to the heat-affected zone (HAZ) of a weld, oriented in the through-thickness direction. SOHIC may also be produced in susceptible steels at other high stress points such as from the tip of mechanical cracks and defects, or from the interaction among HIC on different planes in the steel." The hydrogen charging phenomenon is the same as that which causes HIC. Typical SOHIC damage is shown in Figure 7.4.

7.1.4 Hydrogen blistering is characterized by physical bulging of the surface(s) of equipment. It is caused by hydrogen accumulation at imperfections in the steel, such as laminations or inclusions. Atomic hydrogen generated by wet H2S or hydrofluoric acid environments combines at imperfections to form hydrogen molecules that are too large to diffuse through the steel. The hydrogen accumulates and results in the build-up of high pressure that causes local stresses that exceed the yield strength of the material near these imperfections. The yielding of the material and subsequent plastic deformation in the form of bulging due to pressure loading results in a blister. Sometimes cracks can extend from the periphery of a blister and can propagate in a through-wall direction, particularly if the blister is located near a weld. Typical hydrogen blistering is shown in Figures 7.5 through 7.9.

7.1.5 HIC, SOHIC, and blistering are distinct from other forms of damage that may be related to hydrogen in steels which are addressed elsewhere in this document, including:

a) Discrete or singular cracks should be assessed as crack-like flaws per Part 9. This includes hydrogen embrittlement or sulfide stress cracking of high strength or high hardness base metals and weldments.

b) Laminations are planar defects that exist on one or more planes in the equipment, but cause no bulging of the metal surface, have no cracking in the through thickness direction, and are not linked. Laminations may be present in equipment whether or not it is operating in a hydrogen charging environment. Assessment procedures for laminations are covered in Part 13 of this Standard.

7.2 Applicability and Limitations of the Procedure

7.2.1 The *FFS* assessment procedures described below may be used to evaluate the acceptability of HIC, SOHIC, and blisters subject to the limitations in this Part.

7.2.2 Calculation methods are provided to rerate the component if the acceptance criteria in this Part are not satisfied. For pressurized components, the calculation methods can be used to find a reduced $(MAWP)$. For tank components (i.e shell courses), the calculation methods can be used to determine a reduced (MFH).

7.2.3 Unless otherwise specified, this Part is limited to the evaluation of HIC, SOHIC, or blister damage associated with hydrogen charging from the process environment. Other flaw types shall be evaluated in accordance with Part 2, Table 2.1.

7.2.4 The procedures apply to components whose operating temperature is less than 204°C (400°F) for carbon or low alloy steels, or are below the applicable design curve in API 941, whichever is greater. Damage associated with high temperature hydrogen attack is specifically excluded from this assessment.

7.2.5 Specific details pertaining to the applicability and limitations of each of the assessment procedures are discussed below.

7.2.5.1 The Level 1 and Level 2 assessment procedures for HIC and blisters apply only if all of the following conditions are satisfied:

a) The original design criteria were in accordance with a recognized code or standard (see Part 1, paragraphs 1.2.2 or 1.2.3).

b) The material is considered to have sufficient material toughness. If there is uncertainty regarding the material toughness, then a Part 3 (brittle fracture) analysis should be performed. Temperature and/or process conditions that result in material embrittlement are discussed in Annex G of this Standard.

c) The component is not in cyclic service. If the component is subject to less than 150 cycles (i.e. pressure and/or temperature variations including operational changes and start-ups and shut-downs) throughout its history and future planned operation, or satisfies the cyclic service screening procedure in Annex B1, paragraph B1.5.2, then the component is not in cyclic service.

d) The following limitations on component types and applied loads are satisfied:

   1) Level 1 Assessment – Type A Components (see Part 4, paragraph 4.2.5) subject to internal pressure (i.e. supplemental loads are assumed to be negligible).

   2) Level 2 Assessment – Type A or B Components (see Part 4, paragraph 4.2.5) subject to internal pressure, external pressure, supplemental loads (see Annex A, paragraph A.2.7), or any combination thereof.

e) Level 1 and Level 2 Assessments are not provided for SOHIC Damage.

7.2.5.2 A Level 3 assessment for HIC, SOHIC, or blister damage should be performed when the requirements of Level 1 and Level 2 are not satisfied, or if the HIC, SOHIC, or blister damage is located close to a weld seam or a major structural discontinuity. In addition, a Level 3 assessment is required to evaluate a component with a multitude of closely spaced blisters (see Figure 7.9)

7.3 Data Requirements

7.3.1 Original Equipment Design Data

An overview of the original equipment data required for an assessment is provided in Part 2, paragraph 2.3.1.

7.3.2 Maintenance and Operational History

An overview of the maintenance and operational history required for an assessment is provided in Part 2, paragraph 2.3.2.

7.3.3 Required Data/Measurements for a *FFS* Assessment

7.3.3.1 The required data and measurements for assessment of HIC damage are listed below.

a) *HIC Spacing to Nearest HIC or Blister*, L_H and L_{Hs} – Measurements should be made to determine the edge-to-edge spacing between HIC damage and the nearest HIC or blister damage, L_H, (see Figure 7.3). In addition, the longitudinal spacing, L_{Hs}, should also be determined (see Figure 7.3). This information should be detailed and provided on an inspection sketch.

b) *HIC Spacing to Weld Joints,* L_W – Measurements should be made to determine the spacing between the edge of the HIC damage and the nearest weld joint (see Figure 7.3). This information should be detailed and provided on an inspection sketch.

c) *HIC Spacing to Major Structural Discontinuities,* L_{msd} – Measurements should be made to determine the spacing between the edge of the HIC and the nearest major structural discontinuity. This information should be detailed and provided on an inspection sketch.

d) *HIC Through-Thickness Extent of Damage*, w_H – This is the maximum extent of the HIC damage measured in the through-thickness direction of the damaged component (see Figure 7.2).

e) *Minimum Remaining Wall Thickness of Undamaged Metal, Internal Side,* t_{mm-ID} – For subsurface HIC, this is the distance from the HIC to the internal surface of the equipment (see Figure 7.2).

f) *Minimum Remaining Wall Thickness of Undamaged Metal, External Side,* t_{mm-OD} – For subsurface HIC, this is the distance from the HIC to the external surface of the equipment (see Figure 7.2).

g) *Minimum Remaining Wall Thickness of Undamaged Metal, Total,* t_{mm} – For surface breaking HIC, this is the distance from the HIC to the non-damaged surface of the equipment (see Figure 7.2). For subsurface HIC, this is the sum of the distances from the HIC damage to the internal surface, t_{mm-ID}, and from the HIC damage to the external surface, t_{mm-OD}.

h) HIC damage shall be classified as either surface breaking HIC or subsurface HIC. If Equations (7.1) and (7.2) are satisfied (see Figure 7.2), then the HIC damage is classified as subsurface. Otherwise, the HIC damage shall be classified as surface breaking.

$$t_{mm-ID} \geq 0.20 t_c \tag{7.1}$$

$$t_{mm-OD} \geq 0.20 t_c \tag{7.2}$$

i) HIC Damage Dimensions, s and c – The dimensions in the longitudinal and circumferential directions shall be determined as follows.

1) If $L_H \geq 8t_c$, then the HIC damage dimensions, s and c, are taken as the longitudinal and circumferential extent of the damaged zone, respectively. For example, for HIC Damage Zone 1 in Figure 7.3, the HIC damage dimensions, s and c, are given by Equations (7.3) and (7.4).

$$s = s_1 \tag{7.3}$$

$$c = c_1 \tag{7.4}$$

2) If $L_H < 8t_c$, then the HIC damage dimensions, s and c, for HIC Damage Zones 1 and 2 in Figure 7.3 are established using the procedure described in Part 4, Figure 4.7.

7.3.3.2 The required data and measurements for assessment of SOHIC damage are as follows:

a) *SOHIC Spacing to Nearest HIC or Blister*, L_{SH} – Measurements should be made to determine the spacing between SOHIC damage and the nearest HIC or blister damage. This information should be detailed and provided on an inspection sketch.

b) *SOHIC Spacing to Nearest Major Structural Discontinuity,* L_{msd} – Measurements should be made to determine the spacing between the SOHIC and the nearest major structural discontinuity. This information should be detailed and provided on an inspection sketch.

c) *SOHIC Damage Dimensions,* a and $2c$ – The dimensions of the crack-like flaw that will be used to evaluate the SOHIC damage (see Figure 7.4).

7.3.3.3 The required data and measurements for assessment of blister damage are as follows:

a) *Blister Diameter* – The blister dimensions to be recorded depend on the assessment level and are defined below.

1) Level 1 Assessment – The largest dimension in either the longitudinal or circumferential direction, s or c, should be taken as the blister diameter (see Figure 7.5).

2) Level 2 Assessment – The blister dimensions in the longitudinal and circumferential directions, s and c, should be recorded consistent with the method used to characterize a region of localized metal loss in Part 5.

b) *Blister Spacing to Nearest HIC or Blister*, L_B – Measurements should be made to determine the edge-to-edge spacing between a blister and the nearest HIC or blister damage. This information should be detailed and provided on an inspection sketch. If there are multiple blisters in close proximity to one another, the size of the blister to be used in the assessment is established considering the effects of neighboring blisters using the criterion for local metal loss described in Part 4 (see Figure 4.7). In addition, if the distance between two adjacent blisters zones (measured edge-to-edge) is less than or equal to two times the corroded thickness, t_c, the blisters should be combined and evaluated as a single blister.

c) *Bulge Direction and Projection*, B_p – The blister bulge direction, inside or outside of the pressure containing component, and the blister projection above the shell surface (see Figure 7.5) should be recorded.

d) *Minimum Remaining Wall Thickness,* t_{mm} – For an internal blister this is the distance from the outside surface to the blister, and for an external blister, this is the distance from the inside surface to the blister (see Figure 7.5)

e) *Blister Periphery Cracking* – The blister should be examined to determine if there are any cracks extending in the plane of the blister and/or in a through-thickness direction. This type of cracking typically occurs at the periphery of the blister and can lead to cracking in the through thickness direction.

f) *Blister Crown Cracking And Vent Hole Size,* s_c – Cracks or vent holes on the crown of blisters affect the strength calculation; therefore, the dimension s_c should be recorded if cracks or vent holes are present (see Figures 7.6 and 7.7).

g) *Blister Spacing to Weld Joints,* L_W – Measurements should be made to determine the spacing between the blister and the nearest weld joint (see Figure 7.8). This information should be detailed and provided on an inspection sketch.

h) *Blister Spacing To Nearest Major Structural Discontinuity,* L_{msd} – Measurements should be made to determine the spacing between the blister and the nearest major structural discontinuity. This information should be detailed and provided on an inspection sketch.

7.3.3.4 The information in paragraphs 7.3.3.1 and 7.3.3.3 should be recorded in a format similar to the ones shown in Table 7.1 for HIC damage and Table 7.2 for blister damage. In addition, a detailed sketch should be created showing this information. The data format of Part 9 of this Standard may be used to record the information in paragraphs 7.3.3.2.

7.3.4 Recommendations for Detection, Characterization, and Sizing

7.3.4.1 Recommendations For Detection, Characterization, and Sizing of HIC Damage are given below.

a) HIC damage that is open to the surface may be detected by magnetic particle, liquid penetrant, or other methods used to detect surface breaking crack-like flaws, depending on the extent and severity of the damage.

b) HIC damage is, by definition, a three-dimensional array of linear indications. Ultrasonic examination or other suitable techniques must be used to detect HIC damage that is subsurface and to determine the subsurface dimensions of the HIC damage, including the remaining undamaged thickness at the HIC location. Neither radiography nor surface examination methods are sufficient. Figure 7.10 illustrates how ultrasonic examination may be used to assess the dimensions of HIC damage.

c) When HIC damage and/or blisters are present in the proximity of welds, structural discontinuties, or other stress concentrating features, the possibility of stress oriented hydrogen induced cracking (SOHIC) should be considered, and appropriate inspection conducted using UT or other methods. Details regarding this type of cracking and examination techniques are provided in [1].

7.3.4.2 Recommendations For Detection, Characterization, and Sizing of SOHIC Damage are given below.

a) SOHIC damage that is open to the surface may be detected by magnetic particle, liquid penetrant, or other methods used to detect surface breaking crack-like flaws, depending on the extent and severity of the damage. However, SOHIC damage may be entirely subsurface.

b) Sizing of SOHIC damage is a challenge, particularly if there is also HIC damage present. Typically the crack depth can be determined by grinding or by use of angle beam or time of flight diffraction UT methods. Further guidance is given in [1].

7.3.4.3 Recommendations For Detection, Characterization, and Sizing of Blister Damage are shown below.

a) Blisters are usually discovered by visual observation of surface bulging on either the inside or outside of the equipment. During an in-service inspection/monitoring blisters may also be discovered with UT examination.

b) Ultrasonic examination can be used to determine the depth of the blister and remaining thickness at the blister location.

c) The periphery of the blister(s) should be inspected for subsurface and surface breaking cracks. The crown of the blister should also be examined to detect and size any crown cracks. Inspection techniques to identify and size crack-like flaws are covered in Part 9 of this Standard.

7.4 Assessment Techniques and Acceptance Criteria

7.4.1 Overview

7.4.1.1 If the HIC or blister is located within the region of the specified corrosion/erosion allowance, the assessment procedures of this Part should still be followed.

7.4.1.2 An overview of the assessment levels for HIC damage is provided below.

a) The Level 1 assessment procedures provide screening criteria to evaluate HIC damage, considering the damage from the perspective of local metal loss. Steps must be taken to ensure the damage will not propagate.

b) The Level 2 Assessment procedures utilize the methodologies of Part 5 and Part 9 to evaluate the damage zone as a region of local metal loss and as a crack. Steps must be taken to control or periodically monitor the progression of damage. An overview of the Level 2 assessment procedure for HIC is shown in Figure 7.11.

c) The Level 3 assessment procedures are intended to evaluate larger or more complex regions of HIC damage or components that require detailed stress analysis because of complex geometry, complex loading conditions or both.

7.4.1.3 An overview of the assessment levels for SOHIC damage is provided below.

a) The Level 1 and Level 2 assessment procedures are not provided for SOHIC Damage.

b) The Level 3 Assessment procedures utilize the methodologies of Part 9 to evaluate the SOHIC damage as a crack. Steps must be taken to control or periodically monitor the progression of damage.

c) The Level 3 assessment procedures may also be used to evaluate more complex regions of SOHIC damage or components that require detailed stress analysis because of complex geometry, complex loading conditions or both.

7.4.1.4 An overview of the assessment levels for blisters is provided below.

a) The Level 1 assessment procedures provide screening criteria to evaluate blisters.

b) The assessment procedures in Level 2 utilize the methodology of Part 5 to evaluate the blister as an equivalent region of local metal loss. An overview of the Level 2 assessment procedure for blisters is shown in Figure 7.12.

c) The Level 3 assessment procedures are intended to evaluate larger or more complex regions of blister damage or components that require detailed stress analysis because of complex geometry, complex loading conditions or both.

7.4.2 Level 1 Assessment

7.4.2.1 HIC Assessment Procedure

The Level 1 Assessment procedure for determining the acceptability of HIC damage is as shown below.

a) STEP 1 – Determine the information in paragraph 7.3.3.1.

b) STEP 2 – Determine the wall thickness to be used in the assessment using Equation (7.5) or Equation (7.6), as applicable.

$$t_c = t_{nom} - LOSS - FCA \tag{7.5}$$

$$t_c = t_{rd} - FCA \tag{7.6}$$

c) STEP 3 – If all of the following requirements are satisfied, then proceed to STEP 4. Otherwise, the Level 1 Assessment is not satisfied.

1) The planar dimensions of the HIC damage satisfy Equations (7.7) and (7.8).

$$s \le 0.6\sqrt{Dt_c} \tag{7.7}$$

$$c \le 0.6\sqrt{Dt_c} \tag{7.8}$$

2) The through-thickness extent of the damage satisfies Equation (7.9).

$$w_H \le \min\left[\frac{t_c}{3},\ 13\ mm\ (0.5\ in.)\right] \tag{7.9}$$

3) The HIC damage is not surface breaking in accordance with paragraph 7.3.3.1.h (see Equations (7.1) and (7.2)).

4) The distance between the edge of the HIC damage and the nearest weld seam satisfies Equation (7.10)

$$L_w > \max\left[2t_c,\ 25\,mm\ (1.0\,in)\right] \tag{7.10}$$

5) The distance from the edge of the HIC damage to the nearest major structural discontinuity satisfies Equation (7.11).

$$L_{msd} \geq 1.8\sqrt{Dt_c} \tag{7.11}$$

6) Further HIC damage has been prevented by one of the following means:

i) A barrier coating or overlay (e.g. an organic coating, metal spray, weld overlay, etc.) has been applied to prevent contact between the process environment and the metal.

ii) The equipment has been moved or the process environment altered such that no further hydrogen charging of the metal will occur.

d) STEP 4 – The Level 1 Assessment is complete, the component may be returned to service.

7.4.2.2 SOHIC Assessment Procedure

A Level 1 Assessment procedure for determining the acceptability of SOHIC damage is not provided; refer to paragraph 7.4.4.2 for assessment options.

7.4.2.3 Blister Assessment Procedure

The Level 1 Assessment procedure for determining the acceptability of blister damage is shown below.

a) STEP 1 – Determine the information in paragraph 7.3.3.3.

b) STEP 2 – Determine the wall thickness to be used in the assessment using Equation (7.5) or Equation (7.6), as applicable.

c) STEP 3 – If all of the following requirements are satisfied, then proceed to STEP 4. Otherwise, the Level 1 Assessment is not satisfied.

1) The blister diameter and venting requirements meet one of the following criteria.

i) The blister diameter is less than or equal to 50 mm (2 inches), or

ii) The blister is vented and the dimensions satisfy Equations (7.7) and (7.8).

2) The minimum measured undamaged thickness measured from the side that is not bulged (see Figure 7.5) satisfies Equation (7.12).

$$t_{mm} - FCA \geq 0.5t_c \tag{7.12}$$

3) The blister projection satisfies Equation (7.13).

$$B_p \leq 0.10 \cdot \min\left[s,\ c\right] \tag{7.13}$$

4) There are no periphery cracks directed towards the inside or outside surface of the component as shown in Figure 7.5.

5) The distance between the edge of the blister and the nearest weld seam satisfies Equation (7.10).

6) The distance from the blister edge to the nearest major structural discontinuity satisfies Equation (7.11).

d) STEP 4 – The Level 1 Assessment is complete, the component may be returned to service.

7.4.2.4 If the component does not meet the Level 1 Assessment requirements, then the following, or combinations thereof, can be considered:

a) The damaged material may be removed, repaired, or replaced.

b) The damage can be removed by blend grinding as shown in Figure 7.13, and the area evaluated as a local thin area per the assessment procedures of Part 5.

c) A Level 2 or Level 3 Assessment can be conducted.

7.4.3 Level 2 Assessment

7.4.3.1 HIC Assessment Procedure

The Level 2 Assessment procedure for determining the acceptability of HIC damage is shown below. A logic diagram for a Level 2 Assessment is shown in Figure 7.11. The procedure shown below is developed for pressurized components where an $MAWP$ can be determined. For an atmospheric storage tank, the same procedure can be followed to determine a MFH by replacing the $MAWP$ with the MFH, and determining the MFH using the applicable code equations for a tank shell.

a) STEP 1 – Determine the information in paragraph 7.3.3.1.

b) STEP 2 – Determine the wall thickness to be used in the assessment using Equation (7.5) or Equation (7.6).

c) STEP 3 – If the distance between the edge of the HIC damage and the nearest weld seam satisfies Equation (7.10), then proceed to STEP 4. Otherwise, the Level 2 Assessment is not satisfied.

d) STEP 4 – If the distance from the edge of the HIC damage to the nearest major structural discontinuity satisfies Equation (7.11), then proceed to STEP 5. Otherwise, the Level 2 Assessment is not satisfied.

e) STEP 5 – Classify the damage as either subsurface HIC or surface breaking HIC in accordance with paragraph 7.3.3.1.h (see Equations (7.1) and (7.2) and proceed to STEP 6.

f) STEP 6 – Determine the $MAWP$ for the component (see Annex A, paragraph A.2) using the thickness from STEP 2

g) STEP 7 – Calculate the Remaining Strength Factor based on the type of HIC damage. In both cases, the damage parameter for HIC damage shall be set equal to 80%, or $D_H = 0.80$.

1) The Remaining Strength Factor for surface-breaking HIC damage is computed using Equation (7.14). The parameter M_t in Equation (7.14) is determined from Part 5, Table 5.2 using the value of λ given by Equation (7.15).

$$RSF = \frac{1 - \left[\frac{\left(w_H - FCA\right)\cdot D_H}{t_c}\right]}{1 - \frac{1}{M_t}\left[\frac{\left(w_H - FCA\right)\cdot D_H}{t_c}\right]} \qquad (7.14)$$

$$\lambda = \frac{1.285s}{\sqrt{Dt_c}} \qquad (7.15)$$

2) The Remaining Strength Factor for subsurface HIC damage is computed using Equation (7.16). The parameter L_R in Equation (7.16) is given by Equation (7.17) where L_{Hs} is determined in accordance with Figure 7.3.

$$RSF = \frac{2L_R + s\left[1 - \left(\frac{w_H \cdot D_H}{t_c}\right)\right]}{2L_R + s} \tag{7.16}$$

$$L_R = \min\left[\frac{L_{Hs}}{2}, 8t_c\right] \tag{7.17}$$

h) STEP 8 – If $RSF \geq RSF_a$, then the longitudinal extent of the HIC damage satisfes the LTA portion of the assessment at the $MAWP$ determined in STEP 6. . If $RSF < RSF_a$, then the region of local metal loss is acceptable for operation at $MAWP_r$, where $MAWP_r$ is computed using the equations in Part 2, paragraph 2.4.2.2. The $MAWP$ from STEP 6 shall be used in this calculation.

i) STEP 9 – For cylindrical shells, conical shells, and elbows, evaluate the circumferential extent of the HIC damage using an equivalent LTA and the procedures in Part 5 paragraph 5.4.3.4; otherwise, proceed to STEP 10. The equivalent LTA shall have a depth computed using Equation (7.18) and a length equal to the circumferential extent of the HIC damage zone. If the HIC damage is located on the outside surface or is sub-surface, then the equivalent LTA shall be assumed to be on the outside surface. If the HIC is on the inside surface, then the equivalent LTA shall be assumed to be on the inside surface.

$$d_{HIC} = w_H D_H \tag{7.18}$$

j) STEP 10 – Determine whether a fracture assessment is required. If any of the following criteria apply, then proceed to STEP 11; otherwise, proceed to STEP 12.

1) The equipment remains in hydrogen charging service, and hydrogen charging has not been halted by means of a barrier coating, overlay, or process change.

2) The HIC damage is classified as surface-breaking, see paragraph 7.3.3.1.h.

3) The through-wall extent of the HIC damage satisfies Equation (7.19).

$$w_H > \min\left[\frac{t_c}{3}, 13mm\ (0.5\ in.)\right] \tag{7.19}$$

k) STEP 11 – Evaluate the HIC damage as a crack-like flaw in accordance with the procedures of Part 9 in conjunction with the requirements shown below. If the Part 9 assessment is acceptable, then proceed to STEP 12. Otherwise, the Level 2 Assessment is not satisfied.

1) Flaw Size – two crack-like flaw assessments shall be performed, one for the longitudinal direction and one for the circumferential direction.

i) The longitudinal crack-like flaw length shall be set equal to the longitudinal extent of HIC damage, s. The crack-like flaw depth shall be set equal to the maximum extent of HIC damage in the through thickness direction, w_H.

ii) The circumferential crack-like flaw length shall be set equal to the circumferential extent of HIC damage, c. The crack-like flaw depth shall be set equal to the maximum extent of HIC damage in the through thickness direction, w_H.

2) Fracture Toughness – If hydrogen charging of the steel has not been halted by means of a barrier coating, overlay, or process change, then the toughness used in the Part 9 assessment shall include the effects of hydrogen charging, and shall be indexed to the lower bound fracture arrest curve K_{IR} in accordance with the methods specified in Annex F of this Standard.

l) STEP 12 – Confirm that further HIC damage has been either prevented or is limited to a known or verifiable rate by one or more of the following means, then proceed to STEP 13. Otherwise, the Level 2 Assessment is not satisfied.

1) Establishment of a barrier coating (e.g. organic, inorganic, metal spray, etc.)

2) Use of corrosion inhibitors or other process chemicals that reduce the severity of hydrogen charging.

3) Modification of process or operating conditions to reduce the severity of hydrogen charging.

4) Use of devices that monitor hydrogen permeation through the equipment.

5) Review of historical records indicating that HIC damage size and extent is stable, or progressing at a well defined rate.

6) Monitoring of defects at an established interval to ensure growth rates are within expected limits.

m) STEP 13 – The Level 2 Assessment is complete, the component may be returned to service.

7.4.3.2 SOHIC Assessment Procedure

A Level 2 Assessment procedure for determining the acceptability of SOHIC damage is not provided; refer to paragraph 7.4.4.2 for assessment options.

7.4.3.3 Blister Assessment Procedure

The Level 2 Assessment procedure for determining the acceptability of blister damage is given below. A logic diagram for a Level 2 Assessment is provided in Figure 7.12. The procedure shown below is developed for pressurized components where an $MAWP$ can be determined. For an atmospheric storage tank, the same procedure can be followed to determine a MFH by replacing the $MAWP$ with the MFH, and determining the MFH using the applicable code equations for a tank shell.

a) STEP 1 – Determine the information in paragraph 7.3.3.3.

b) STEP 2 – Determine the wall thickness to be used in the assessment using Equation (7.5) or Equation (7.6).

c) STEP 3 – If the distance from the blister edge to the nearest major structural discontinuity satisfies Equation (7.11), then proceed to STEP 4. Otherwise, the Level 2 Assessment is not satisfied.

d) STEP 4 – If the blister has periphery cracks toward either the internal or external surface, then proceed to STEP 5; otherwise, proceed to STEP 6.

e) STEP 5 – If the blister is bulged toward the internal surface and has periphery cracks toward the external surface, or if the the blister is bulged toward the external surface and has periphery cracks toward the internal surface (i.e., periphery cracks are on the opposite side from the bulging), then the blister does not pass the Level 2 assessment. If the periphery cracks are on the same side as the bulging, then proceed to STEP 9.

f) STEP 6 – If the blister does not have a crown crack, then proceed to STEP 7. If the blister has a crown crack, then proceed to STEP 9.

g) STEP 7 – If the blister projection above the surface satisfies Equation (7.13), then proceed to STEP 8. Otherwise, proceed to STEP 9.

h) STEP 8 – If the blister is vented, then go to STEP 10. If the blister is unvented, then proceed to STEP 11. Note that venting is recommended for an unvented blister, except that venting of a blister to the inside surface is not recommended for components in hydrofluoric acid service because of the safety concerns regarding contamination, decontamination, and the potential for corrosion and scale build-up within the blister.

i) STEP 9 – The blister shall be evaluated as an equivalent local thin area using the methods of Part 5. The remaining sound metal thickness to use in the LTA analysis is t_{mm}, as shown in Figures 7.5 – 7.8. The diameter of the local thin area shall be determined using the following criteria.

1) If the blister projection does not satisfy Equation (7.13) and the blister does not have periphery cracks, then the blister diameter shall be used as the size of the region of local metal loss.

2) If the blister projection satisfies equation (7.13) and the blister has only crown cracks, then the blister diameter or the length of the crown crack (see paragraph 7.3.3.3) can be used as the size of the region of local metal loss with a remaining thickness equal to t_{mm} (see Figure 7.6).

3) If the blister has periphery cracks, then the size of local metal loss to use in the assessment is the blister diameter plus any crack growth extension at the periphery.

j) STEP 10 – If the distance between the edge of the blister and the nearest weld seam satisfies Equation (7.10) then go to STEP 12; otherwise go to STEP 11.

k) STEP 11 – An in-service monitoring system should be developed to monitor blister growth while the component is in service, go to STEP 12.

l) STEP 12 – The Level 2 Assessment is complete, the component may be returned to service.

7.4.3.4 If the component does not meet the Level 2 Assessment requirements, then the following, or combinations thereof, can be considered:

a) The equipment may be rerated, and the Level 2 Assessment procedures repeated.

b) The damaged material may be removed, repaired, or replaced.

c) A Level 3 Assessment can be conducted.

7.4.4 Level 3 Assessment

7.4.4.1 HIC Assessment Procedure

The Level 3 Assessment procedure for determining the acceptability of HIC damage is given below.

a) All Level 3 Assessments of HIC damage shall explicitly address the following:

1) Potential for failure due to loss of load bearing capability, and the remaining strength of the equipment

2) Potential for failure due to fracture.

3) The expected future progression (if any) of the damage.

4) Future inspection requirements, including whether in-service monitoring is required.

b) The HIC damage parameter that represents a measure of remaining strength of a HIC damaged Zone may be used in the analysis at a value of less than 80%, or $D_H = 0.80$. If a value less than 80% is utilized, this value shall correspond to inspection information and appropriate correlations between the inspection information and the remaining strength of the HIC Damaged Zone. The final value of the HIC damage parameter utilized in the assessment shall be fully documented and included in the assessment results.

c) If the HIC damage does not satisfy the Level 2 Assessment criteria because of complex component geometry, applied loading, or the damage is close to structural discontinuities, then the Level 3 analysis should include a detailed stress analysis per the techniques discussed in Annex B1 of this Standard.

d) A Level 3 Assessment of HIC damage may be performed using finite element analysis considering explicit modeling of HIC damaged and non-damaged areas. Limit load or elastic plastic analysis in accordance with Annex B1 of this Standard may be performed, but the HIC damaged areas must be modeled as elastic-perfectly plastic material.

e) A fracture mechanics analysis in accordance with Part 9 of this Standard shall be considered for all assessments. If a fracture mechanics assessment is performed, then effects of hydrogen on the fracture toughness of the steel shall be considered unless hydrogen is precluded from entering the steel during operation.

7.4.4.2 SOHIC Assessment Procedure

A Level 3 assessment of SOHIC should be based on the assessment procedures of Part 9, with particular attention given to potential hydrogen effects on future crack growth and fracture toughness.

a) There is currently no accepted method for predicting SOHIC crack growth rate, and therefore no basis for returning actively growing cracks to service. The arrest of SOHIC cracks must be provided by one of the following or comparable means, and must be documented in the analysis:

   1) Reduction and control of the hydrogen flux rate to a level below that which caused the existing damage

   2) Reduction of the crack tip stress intensity that caused the damage

   3) Alteration of the microstructure ahead of the damage zone so as to preclude further crack propagation

b) A fracture assessment is required in accordance with the procedures of Part 9, and the following additional requirements:

   1) Inspection techniques must be applied that can interrogate the affected volume of material, and assess the subsurface extent of the damage. The efficacy of the method(s) used shall be demonstrated specifically for SOHIC damage, including suitable provisions for sizing accuracy.

   2) An analysis must be performed to assess the stress state of the SOHIC damage zone, including primary, secondary, and residual stresses that may affect the crack tip stress intensity. This shall include all stresses which may contribute to the subcritical growth of SOHIC damage, even those that are not normally considered to contribute to brittle fracture.

   3) If the hydrogen charging of the steel has not been halted by means of a barrier coating, overlay, or process change, then the material toughness used in the fracture assessment shall account for the effect of hydrogen charging by indexing to the lower bound fracture arrest curve K_{IR}, in accordance with the methods specified in Annex F of this Standard, or an alternative method that is fully documented.

c) Periodic monitoring can be used to confirm the absence of crack growth. However, when conditions for SOHIC are favorable, crack growth may be so rapid as to render periodic monitoring impractical.

7.4.4.3 Blister Assessment Procedure

A Level 3 Assessment for blisters consists of performing a detailed stress analysis in accordance with the techniques in Annex B1 of this Standard. In addition, if cracks are detected at the blister location by inspection, a fracture mechanics assessment in accordance with Part 9 of this Standard shall be performed. If a component has a multitude of closely spaced blisters (see Figure 7.9), then it is recommended to first use the concepts of this Part to evaluate individual blisters. If the criterion for individual blisters is satisfied, the array of blisters can then be modeled as equivalent pitting damage, and the assessment procedures of Part 6 can be used to evaluate the overall weakening effect due to the blister array.

7.5 Remaining Life Assessment

7.5.1 At the present time, there is no widely accepted method to predict the growth rate of active HIC or SOHIC damage; therefore, a standard method to assess the remaining life of a damaged structure cannot be established. Therefore, unless the determination can be made that the HIC or SOHIC damage is dormant, periodic monitoring is required.

7.5.2 The growth rate and the remaining life of a blister cannot be adequately evaluated using analytical techniques. However, a remaining life evaluation is not required because the presence of blisters in equipment does not have a direct effect on the internal inspection interval except for the special inspection requirements required for in-service monitoring.

7.6 Remediation

7.6.1 Elimination or reduction of hydrogen charging by means of a barrier coating (e.g. organic, metal spray, weld overlay, etc.) or lining, or by changing the process environment is required for Level 1 Assessments of HIC damage (see paragraphs 7.4.2.1), and for Level 3 Assessment of SOHIC damage (see paragraph 7.4.4.2).

7.6.2 Even when not required, the progression of HIC, SOHIC, and blister damage can be reduced or eliminated by controlling the hydrogen charging. Consideration should be given to applying a barrier coating (e.g. organic, metal spray, weld overlay, etc.) or lining to the inside surface of equipment with HIC, SOHIC, or blister damage to prevent further hydrogen charging and damage, particularly in the weld regions. In addition, process changes and/or inhibitor additions that would decrease the hydrogen charging should also be evaluated and considered.

7.6.3 Blisters meeting the acceptance criteria of any assessment level should be considered for venting if the blister is deeper than 3 mm (0.125 inches) from the bulged surface and the blister diameter exceeds 50 mm (2 inches).

a) Venting of blisters may involve risk and all applicable plant safety guidelines should be reviewed and followed. If the component is in-service, additional inspection is required prior to drilling.

b) Venting of blisters can typically be accomplished by drilling a small diameter hole (e.g. 3 mm (0.125 inches)) in the center of the blister from the surface where the bulging is observed. Blisters located on the inside surface of equipment may be vented to the inside, or may be vented from the outside during downtime periods provided:

   1) The blister is parallel to the surface as confirmed by inspection.

   2) The blister is not already vented to the inside by crown or periphery cracking.

   3) The component is not in hydrofluoric acid service.

c) Electric drills should not be used to vent blisters because of the presence of hydrogen in the blister cavity. Air-driven drills should be used, and suitable safety provisions should be made to ensure that ignition of the hydrogen released during the drilling operation does not occur (see [1]). An inert gas and other safety provisions can be utilized to purge the area to help ensure that ignition does not occur.

7.6.4 Blend grinding and weld repair techniques can be used to repair HIC, SOHIC, or blister damage. Caution should be exercised when conducting weld repairs on hydrogen charged steel to prevent crack growth and/or subsequent re-cracking. A hydrogen bakeout should be considered prior to welding or grinding. The application of a suitable coating after blend grinding or weld repairs should be considered. All blend ground areas should be rechecked using either MT or PT examination techniques.

7.6.5 If the material is severely damaged and cannot be accepted per the assessment procedures or repaired, it should be replaced. The metallurgy and design of the replacement material, weld details and weld procedures should be reviewed by a materials engineer and a mechanical engineer (see Part 1, paragraph 1.4.3).

7.6.6 Additional information regarding remediation and repair of HIC and SOHIC damage can be found in [**1**].

7.7 In-Service Monitoring

7.7.1 Periodic monitoring of the process stream for hydrogen charging conditions and/or of the equipment for additional damage should be considered, once HIC, SOHIC, or blister damage has been observed. Monitoring of such damage, particularly damage adjacent to welds that are not vented, is important when the driving force for blister formation and growth (i.e. hydrogen pressure in the blister cavity) has not been relieved.

7.7.2 Various inspection methods can be used to monitor HIC, SOHIC, and blister damage growth. Common methods are straight beam UT for HIC and blisters and angle beam UT for HIC and SOHIC damage. Various forms of hydrogen probes, either internal or external, can be used to monitor hydrogen-charging levels. The inspection monitoring interval can be adjusted based on the measured hydrogen charging levels.

7.7.3 If the HIC, SOHIC, or blister damage is found to grow during the monitoring process, the evaluation procedures in paragraph 7.4 and the remediation guidelines in paragraph 7.6 should be reviewed and implemented based on the severity of the damage that is anticipated.

7.8 Documentation

7.8.1 The documentation of the FFS Assessment should include the information cited in Part 2, paragraph 2.8.

7.8.2 The location, size, spacing and condition of existing HIC, SOHIC, and blister damage should be recorded along with the results of the assessments performed. Sample data sheets for HIC and blister damage are shown in Tables 7.1 and 7.2, respectively. The data sheet for crack-like flaws included in Part 9 can be used for SOHIC damage.

7.8.3 If HIC, SOHIC, or blister damage growth is detected during the monitoring process, the physical dimensions and location of the damage should be recorded along with the time period between measurements. In addition, the associated operating conditions and process stream constituents should be recorded in order to permit an evaluation of the hydrogen-charging environment relative to the operation of the equipment. This information may be valuable in determining suitable process changes in the operation of the equipment, if possible, to mitigate further damage.

7.9 Nomenclature

a	depth a SOHIC crack (see Figure 7.4 and Part 9).
B_p	blister bulge projection.
c	HIC damage or blister dimension in the circumferential direction.
$2c$	length of a SOHIC crack (see Figure 7.4 and Part 9).
c_1	HIC or blister dimension for HIC damage area 1 in the circumferential direction.
c_2	HIC or blister dimension for HIC damage area 2 in the circumferential direction.
d_{HIC}	effective through thickness extent of HIC damage after accounting for the remaining strength of the damaged material.
D	shell inside diameter corrected for $LOSS$ and FCA allowance as applicable.
D_H	HIC Damage parameter that relates the strength of HIC damaged steel to that of undamaged steel. For example, zero percent of HIC damage corresponds to $D_H = 0.0$, 80% HIC damage corresponds to $D_H = 0.80$, and 100% HIC damage corresponds to $D_H = 1.0$. A $D_H = 1.0$ indicates that the HIC damaged area does not have any structural strength.
FCA	future corrosion allowance.
$LOSS$	amount of metal loss at the time of the assessment.

L_B	blister-to-blister or blister-to-HIC spacing.
L_H	edge-to-edge spacing between HIC damage and the nearest HIC or blister damage.
L_{Hs}	HIC-to-HIC or HIC-to-blister spacing in the longitudinal direction.
L_{SH}	SOHIC to HIC or blister damage spacing.
L_R	extent of non-damaged material available for reinforcement of the HIC damaged area.
L_{msd}	spacing to nearest major structural discontinuity.
L_W	spacing to nearest weld joint.
λ	longitudinal flaw length parameter.
$MAWP$	maximum allowable working pressure (see Annex A, paragraph A.2).
$MAWP_r$	reduced permissible maximum allowable working pressure of the damaged component.
MFH	maximum fill height.
M_t	Folias Factor based on the longitudinal or meridional flaw parameter.
RSF	computed remaining strength factor based on the meridional extent of the HIC or blister.
RSF_a	allowable remaining strength factor (see Part 2, paragraph 2.4.2.2).
s	HIC or blister dimension in the longituidinal direction.
s_c	length of a blister crown crack or diameter of a vent hole.
s_1	HIC or blister dimension for HIC damage area 1 in the longituidinal direction.
s_2	HIC or blister dimension for HIC damage area 2 in the longituidinal direction.
t_c	corroded wall thickness, allowing for future corrosion loss.
t_{mm}	minimum measured thickness of undamaged metal at the blister or HIC being evaluated.
t_{mm-ID}	minimum measured thickness of undamaged metal on the internal side of HIC damage.
t_{mm-OD}	minimum measured thickness of undamaged metal on the external side of HIC damage.
t_{nom}	nominal or furnished thickness of the component adjusted for mill undertolerance as applicable.
t_{rd}	uniform thickness away from the local metal loss location established by thickness measurements at the time of the assessment.
w_H	thickness of HIC damage as measured in the through-thickness direction.
W	width of the weld.

7.10 References

1. NACE Standard RP0296-96, “Guidelines for Detection, Repair, and Mitigation of Cracking of Existing Petroleum Refinery Pressure Vessels in Wet H2S Environments”, NACE International, Houston, TX, 2003.
2. Anderson, T.L., Merrick, R.D., Yukawa, S., Bray, D.E., Kaley, L. and Van Scyoc, K., Fitness-For-Service Evaluation Procedures for Operating Pressure Vessels, Tanks, and Piping in Refinery and Chemical Service,” FS-26, Consultants Report, MPC Program on Fitness-For-Service, Draft 5, The Materials Properties Council, New York, N.Y., October, 1995.
3. ASM, “Metals Handbook, Ninth Edition, Volume 13, Corrosion,” ASM International, Metals Park, Ohio, 1987, pp. 1277-1278.
4. Bagnoli, D.L., Yin, H., Walker, S.T. and Milton, D.J., “Fitness For Service Applications For Equipment in Wet H_2S Services”, ASME PVP-Vol. 136, American Society of Mechanical Engineers, New York, 1996, pp. 1-16.
5. Dirham, T.R, Buchheim, G.M., Osage, D.A., Staats, J.C., ”Development of Fitness-For-Service Rules for the Assessment of HIC Damage,” WRC Bulletin in preparation.
6. Osage, D.A., Krishnaswamy, P., Stephens, D.R., Scott, P., Janelle, J., Mohan, R., and Wilkowski, G.M., “Technologies for the Evaluation of Non-Crack-Like Flaws in Pressurized Components – Erosion/Corrosion, Pitting, Blisters, Shell Out-Of-Roundness, Weld Misalignment, Bulges and Dents,” WRC Bulletin 465, Welding Research Council, New York, N.Y., September, 2001.

7.11 Tables and Figures

Table 7.1
Size, Location, Condition, and Spacing for HIC Damage

Enter the data obtained from a field inspection on this form.

Inspection Date: _____

Equipment Identification: _____

Equipment Type: _____ Pressure Vessel _____ Storage Tank _____ Piping Component

Component Type & Location: _____

_____

_____

t_{nom} : _____

LOSS: _____

FCA: _____

t_{rd} : _____

Data Required for Level 1 and Level 2 Assessment					
HIC Identification					
Diameter s (1)					
Dimension c (1)					
Edge-To-Edge Spacing To Nearest HIC or Blister L_H (2)					
Minimum Measured Thickness to Internal Surface t_{mm-ID} (3)					
Minimum Measured Thickness to External Surface t_{mm-OD} (3)					
Minimum Measured Thickness ; Total of Both Sides t_{mm} (3)					
Spacing To Nearest Weld Joint L_W (2)					
Spacing To Nearest Major Structural Discontinuity L_{msd}					

Notes:
1. The HIC-to-HIC spacing may affect the size of the HIC damage to be used in the evaluation (see paragraph 7.3.3.1.i.).
2. See Figure 7.3.
3. See Figure 7.2

Table 7.2
Size, Location, Condition, and Spacing for Blisters

Enter the data obtained from a field inspection on this form.

Inspection Date: _____

Equipment Identification: _____

Equipment Type: _____ Pressure Vessel _____ Storage Tank _____ Piping Component

Component Type & Location: _____

_____

_____

_____

Data Required for Level 1 and Level 2 Assessment

Blister Identification					
Diameter s (1)					
Dimension c (1)					
Edge-To-Edge Spacing To Nearest Blister L_B (1)					
Bulge Direction (inside/ outside)					
Blister Projection B_p					
Minimum Measured Thickness t_{mm}					
Cracking At Periphery (Yes/No)					
Crown Cracking or Venting (Yes/No) (2)					
Length Of Crown Crack or Diameter of Vent Hole s_c (2)					
Spacing To Nearest Weld Joint L_W (3)					
Spacing To Nearest Major Structural Discontinuity L_{msd}					

Notes:

1. The blister-to-blister spacing may affect the size of the blister to be used in the evaluation (see paragraph 7.3.3.3.a & b)
2. If the blister has crown cracks, enter the length of the crack, see dimension s_c in Figure 7.6. If the blister has a vent hole, indicate as such with the diameter of the hole (see Figure 7.7).
3. See Figure 7.8.

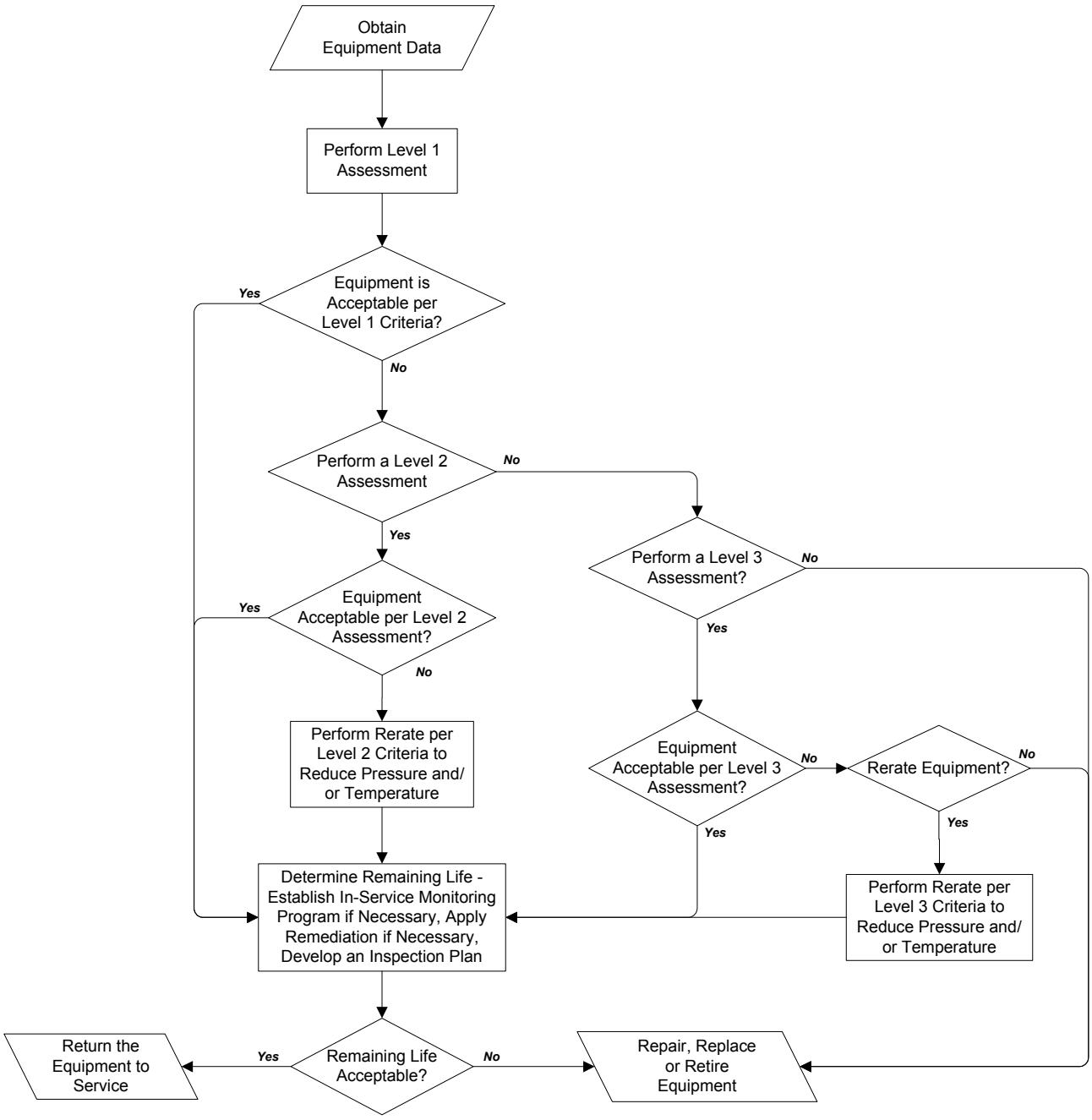

Figure 7.1 – Overview of the Assessment Procedure to Evaluate a Component with HIC or Hydrogen Blisters

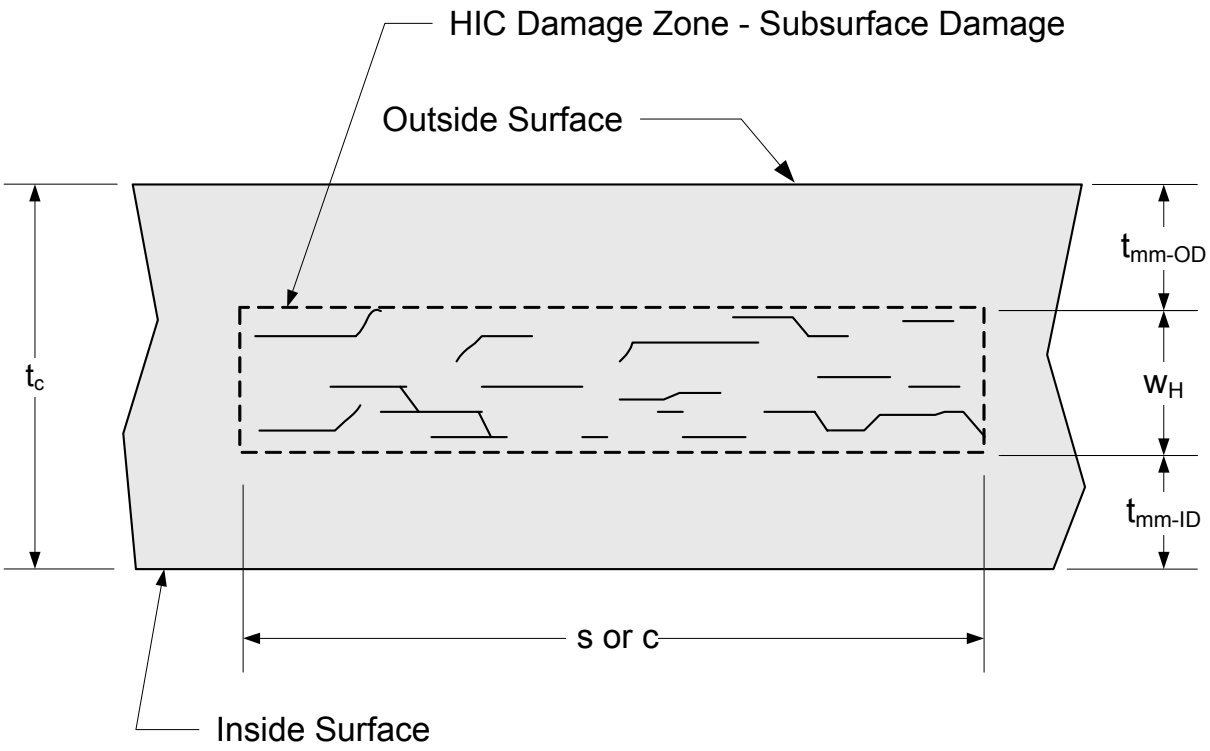

a) Typical Subsurface HIC Damage

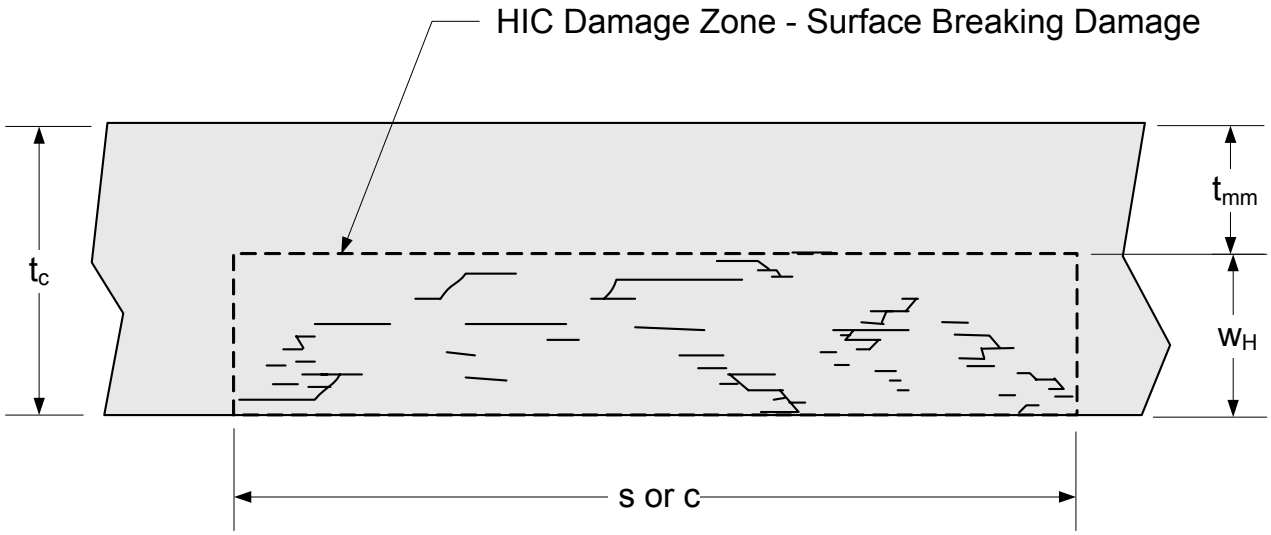

b) Typical Surface Breaking HIC Damage

Figure 7.2 – Surface and Subsurface HIC Damage

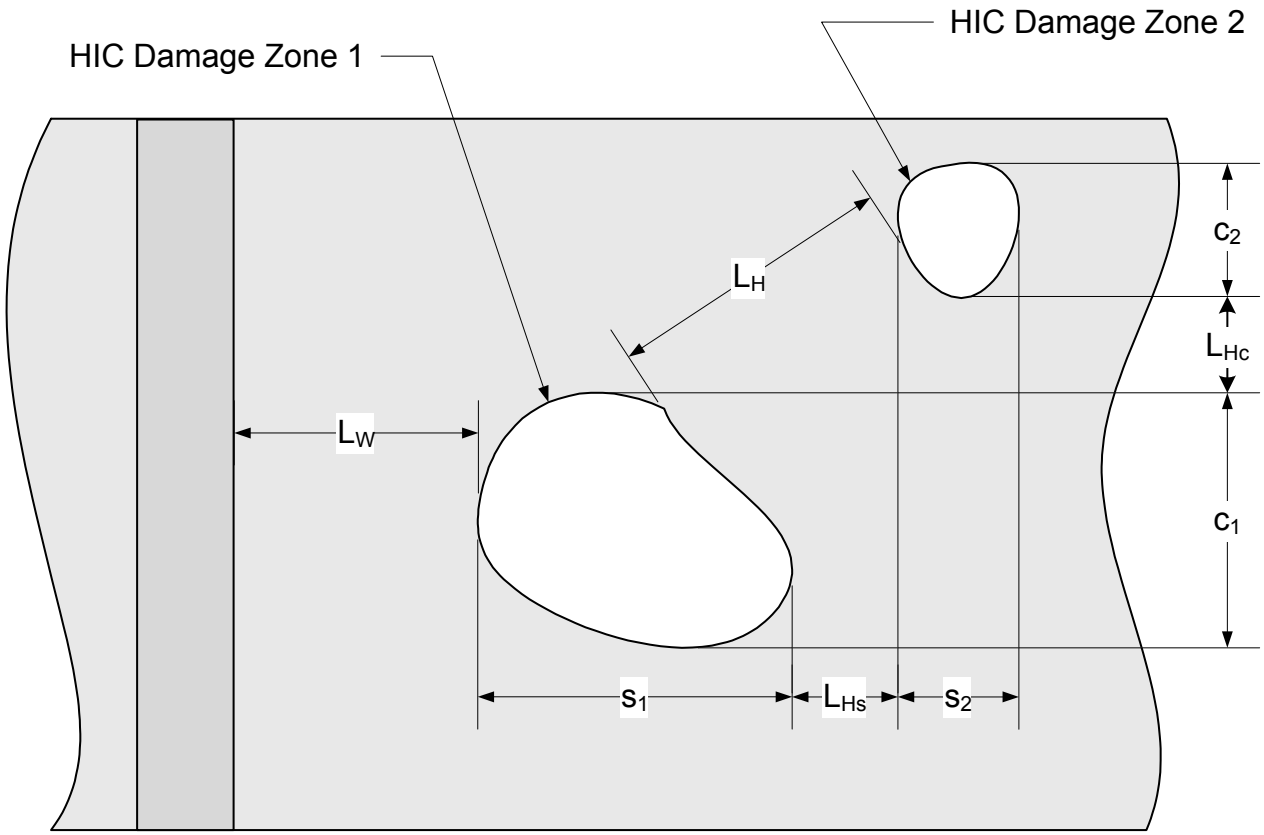

a) Planar View of HIC Damage Close To A Weld Seam And To Other HIC Damaged Zones

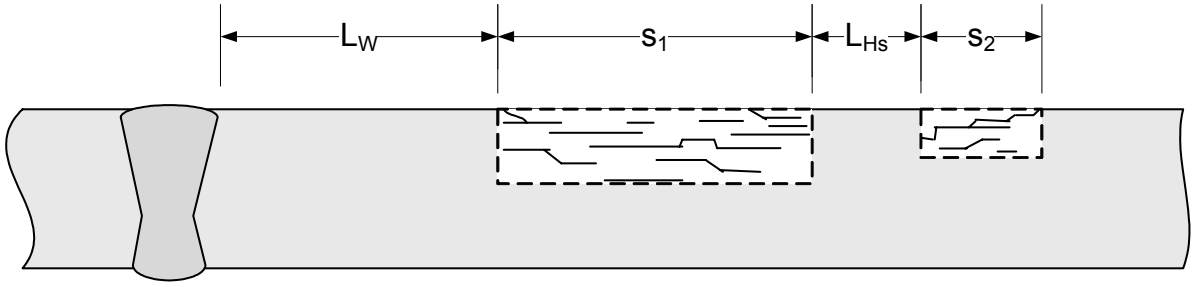

b) Cross Sectional View of HIC Damage Close To A Weld Seam And To Other HIC Damage

Figure 7.3 – HIC Damage in Proximity to a Weld or Other HIC Damage

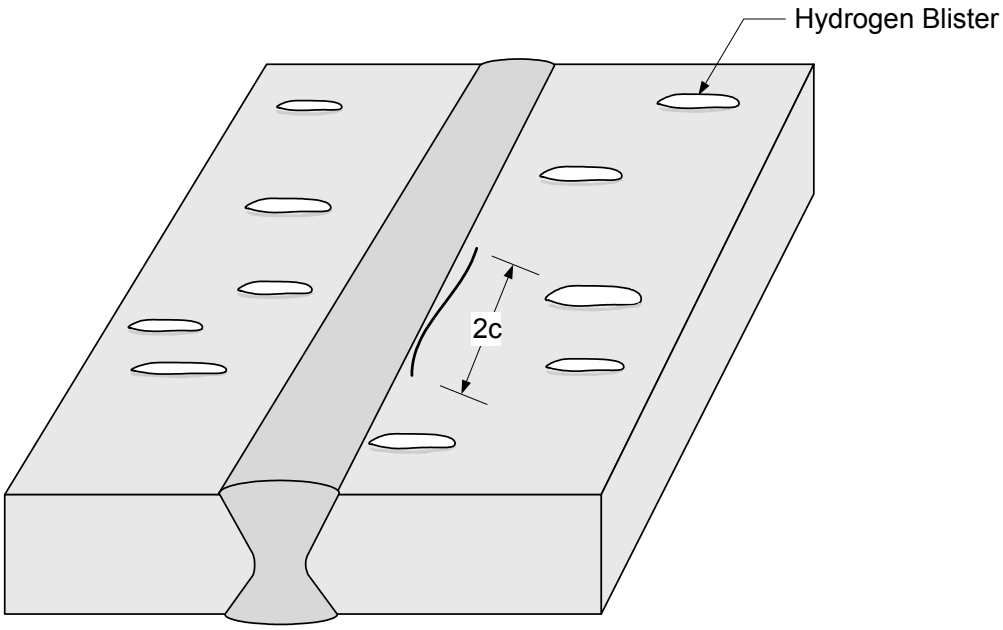

Note: The length of the crack-like flaw should be established using applicable NDE methods. If a series of crack-like flaws are present, the individual flaws shall be combined in accordance with the flaw interaction procedures of Part 9

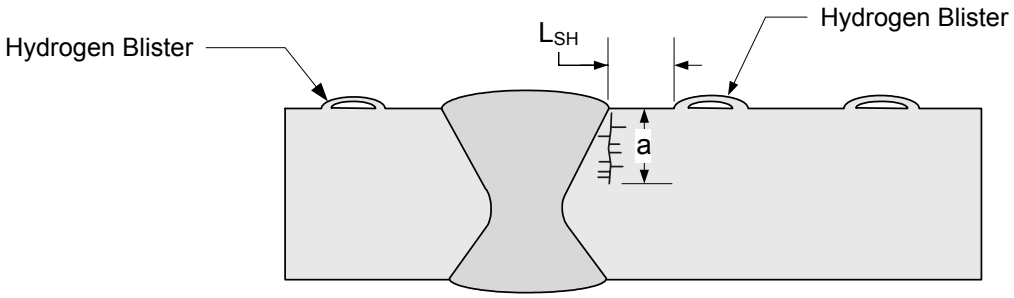

Figure 7.4 – SOHIC Damage

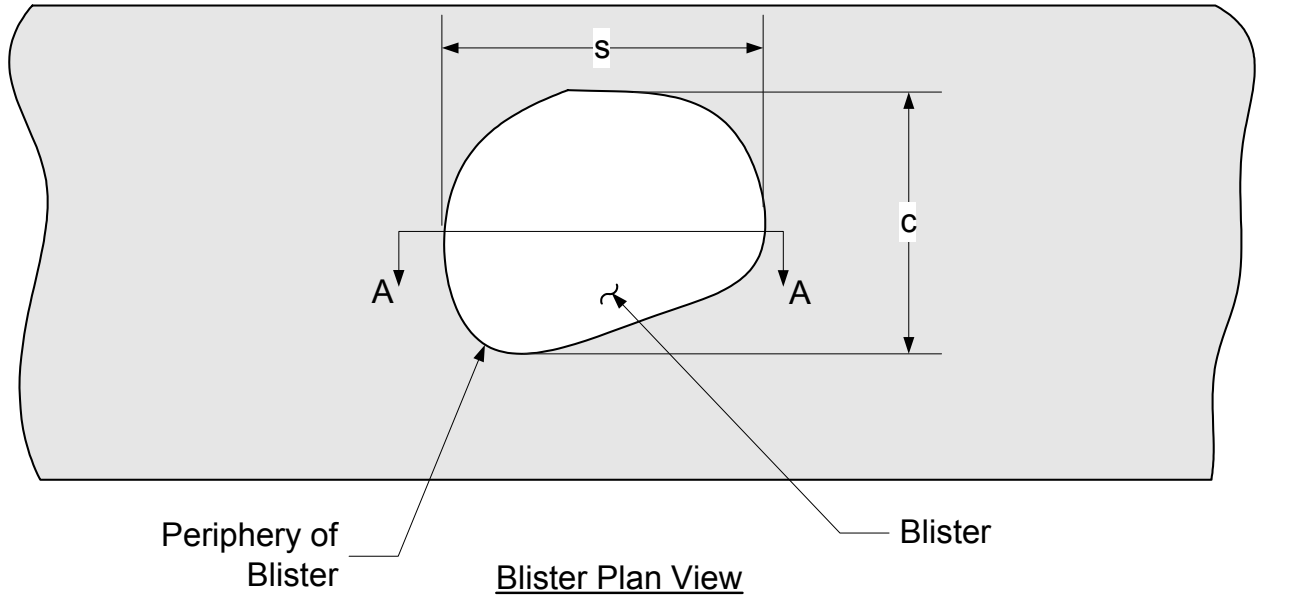

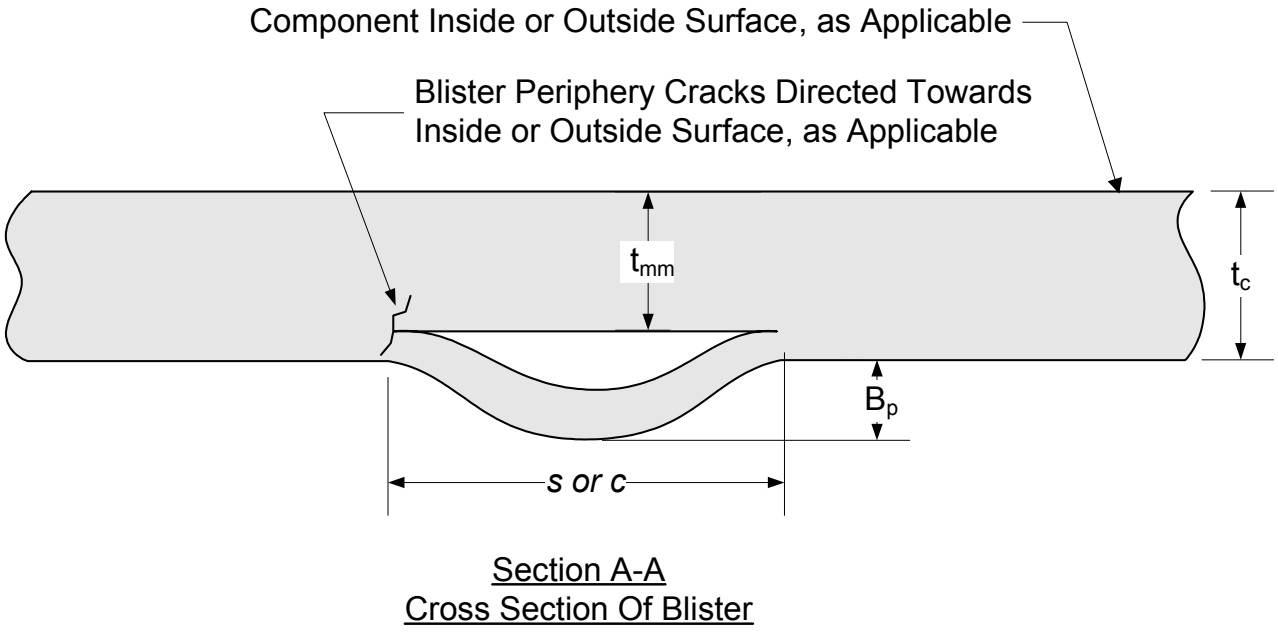

Notes:
1. The blister diameter to be used in the assessment is defined in paragraph 7.3.3.3.a.

Figure 7.5 – Typical Hydrogen Blister

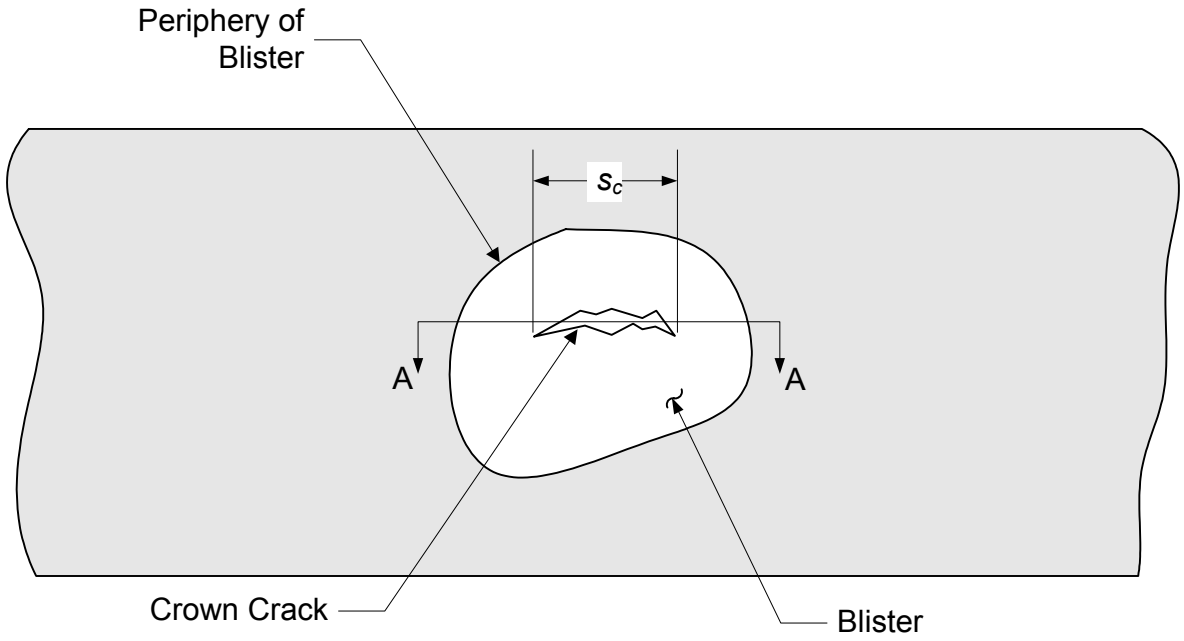

Blister Plan View

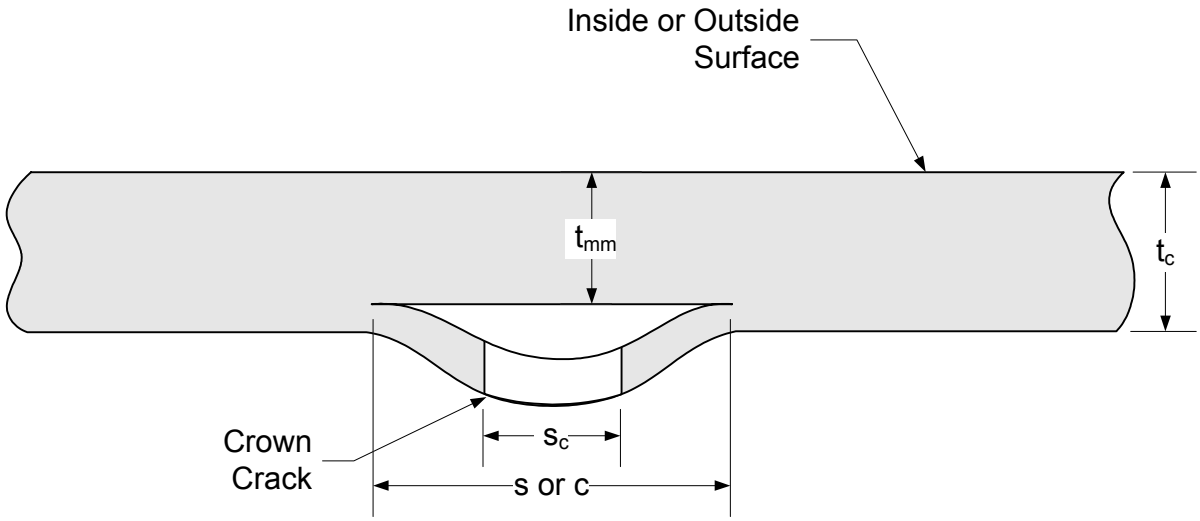

Section A-A
Cross Section of Blister

Notes:
1. The blister diameter to be used in the assessment is defined in paragraph 7.3.3.3.a
2. The dimension s_c can be used to characterize the length of an equivalent LTA for a blister with a crown crack that satisfies the HIC projection criterion; alternatively, the dimension $\max[s, c]$ can be used.

Figure 7.6 – Blister with a Crown Crack

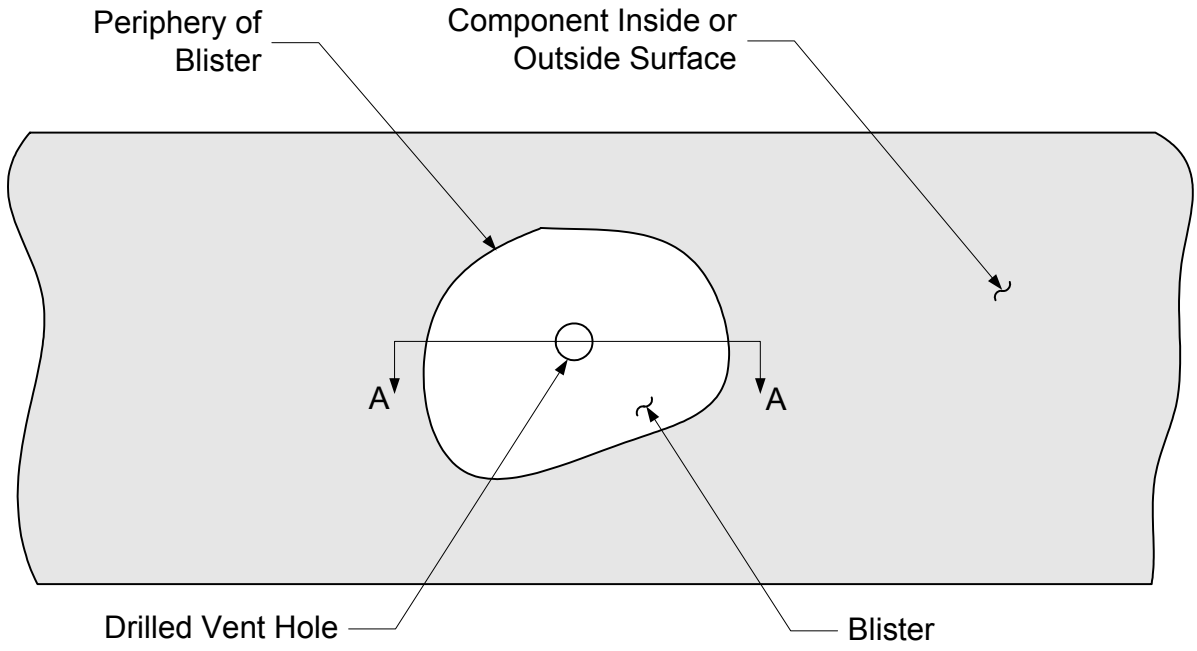

Blister Plan View

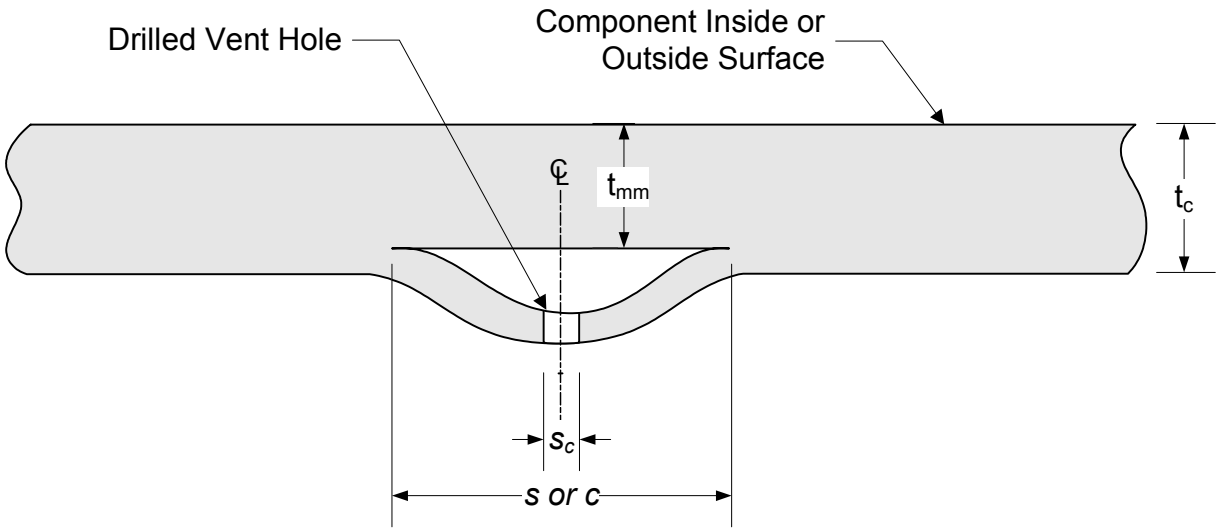

Section A-A
Cross Section of Blister

Notes:
1. The blister diameter to be used in the assessment is defined in paragraph 7.3.3.3.a.

Figure 7.7 - Blister with a Vent Hole

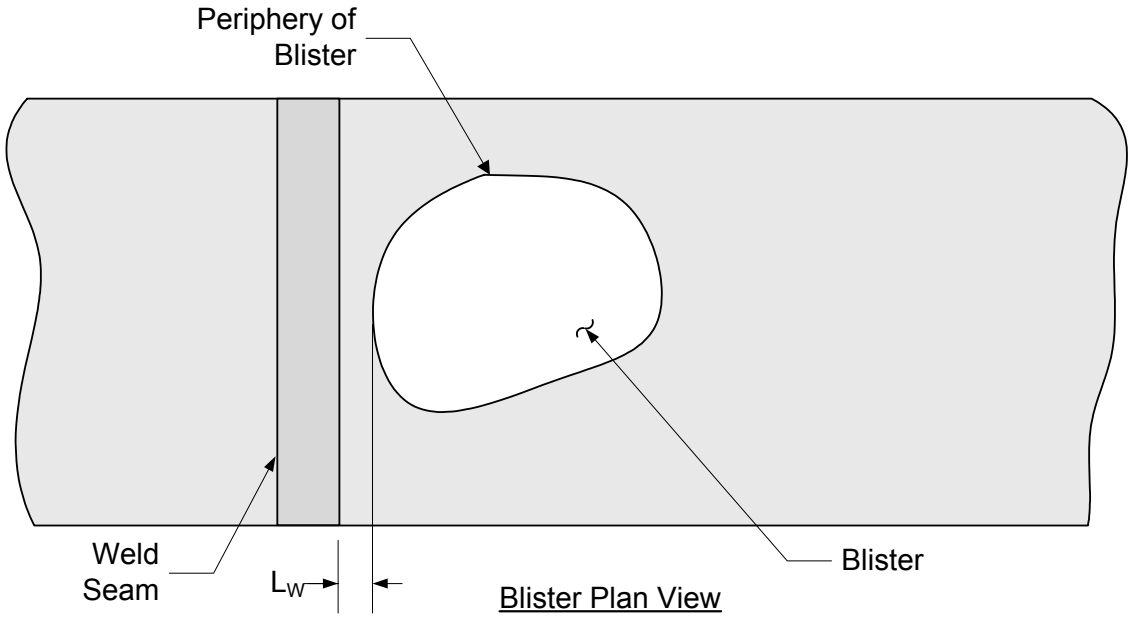

a) Blister Spacing to a Weld Seam

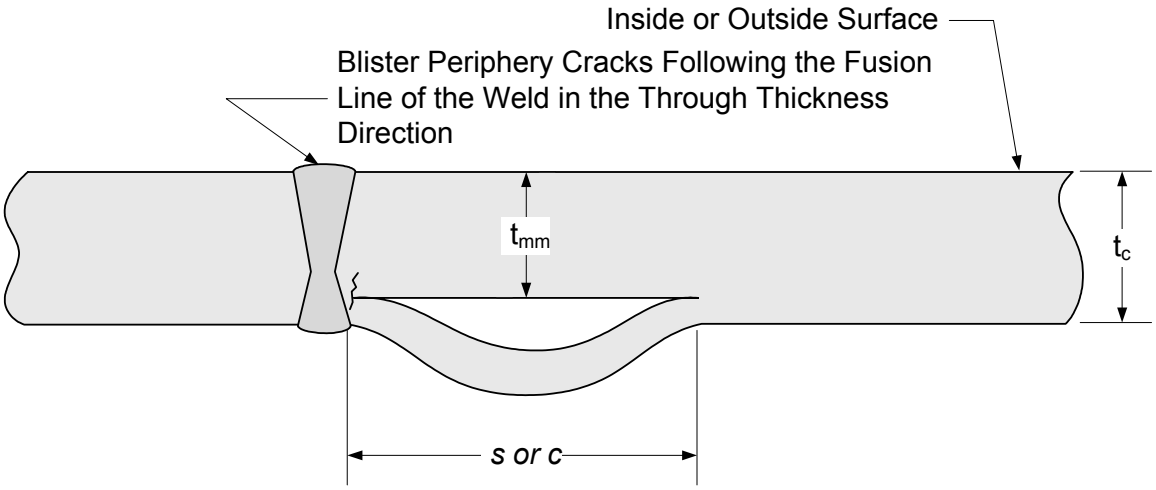

b) Blister Periphery Cracks at the Weld Joint

Notes:

1. The blister is considered to be close to a weld seam if $L_w < \max\left[2t_c,\ 25mm(1.0in)\right]$.
2. The blister diameter to be used in the assessment is defined in paragraph 7.3.3.3.a

Figure 7.8– Blister Periphery Cracks at a Weld

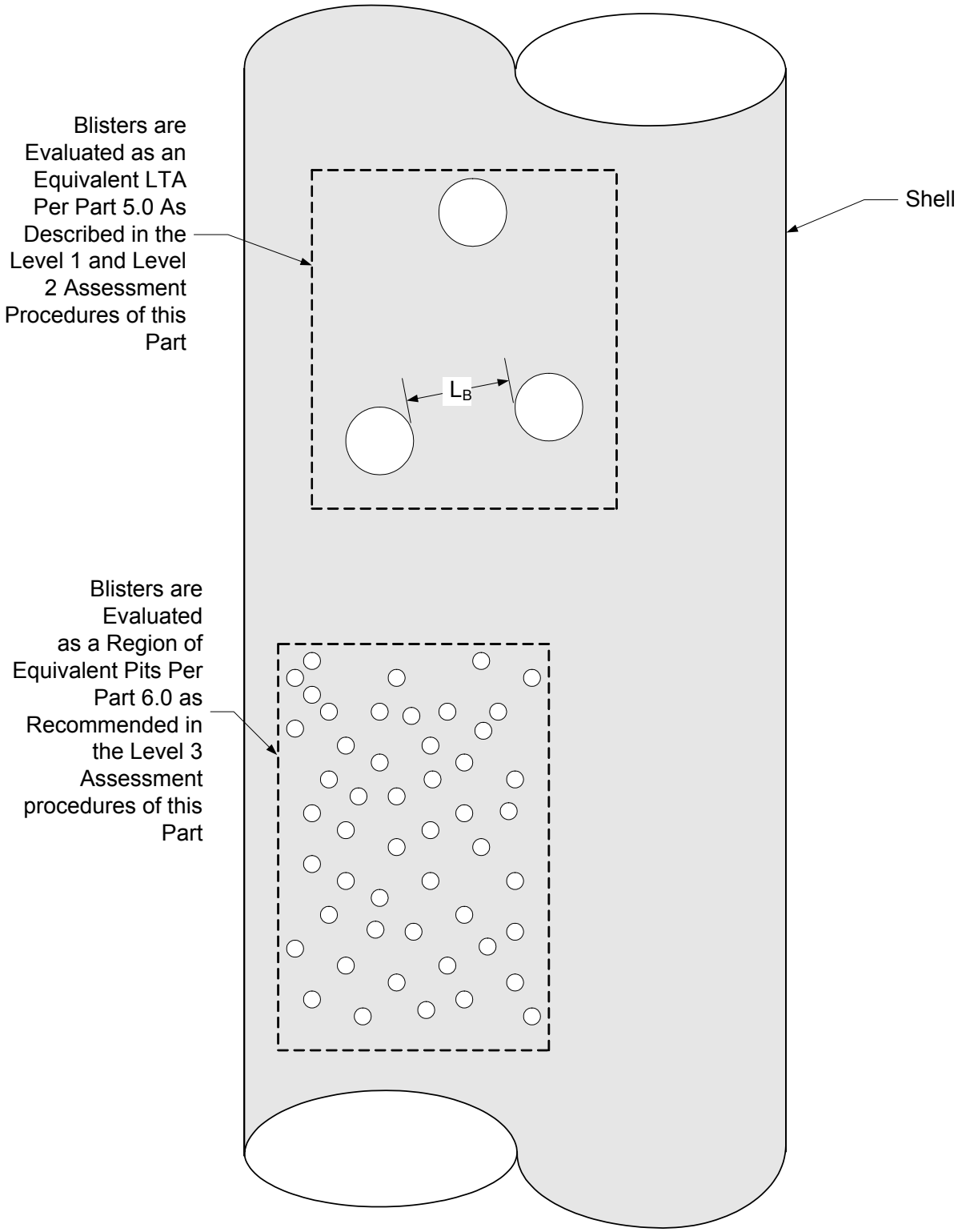

Figure 7.9 – Additional Assessment Requirements for Closely Spaced Blisters

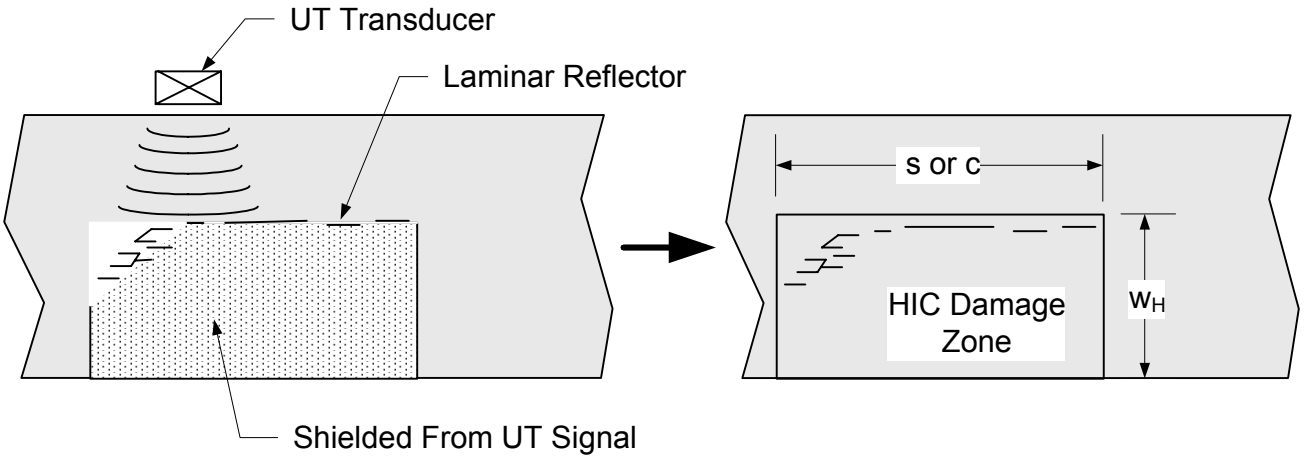

Single Sided UT Exams; if HIC Damage is Found, Treat the Associated Area Shielded From UT Signal as Also Being HIC Damaged.

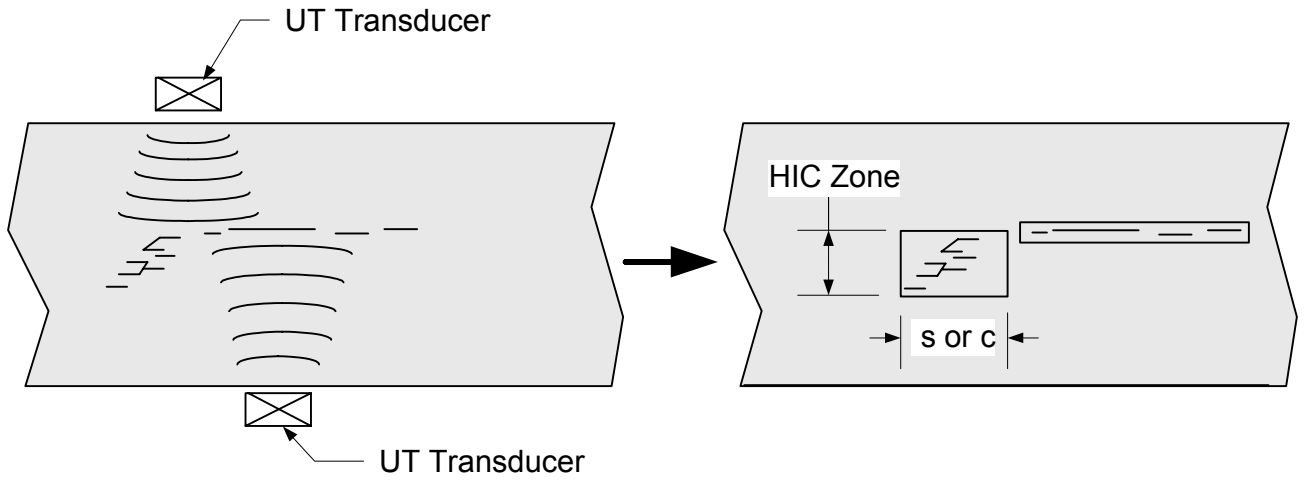

Two sided UT exam: Material under laminar defect can be interrogated. HIC damage size is confirmed to be limited.

Figure 7.10 – Characterization and Sizing of HIC Damage Zones Using Ultrasonic Examination

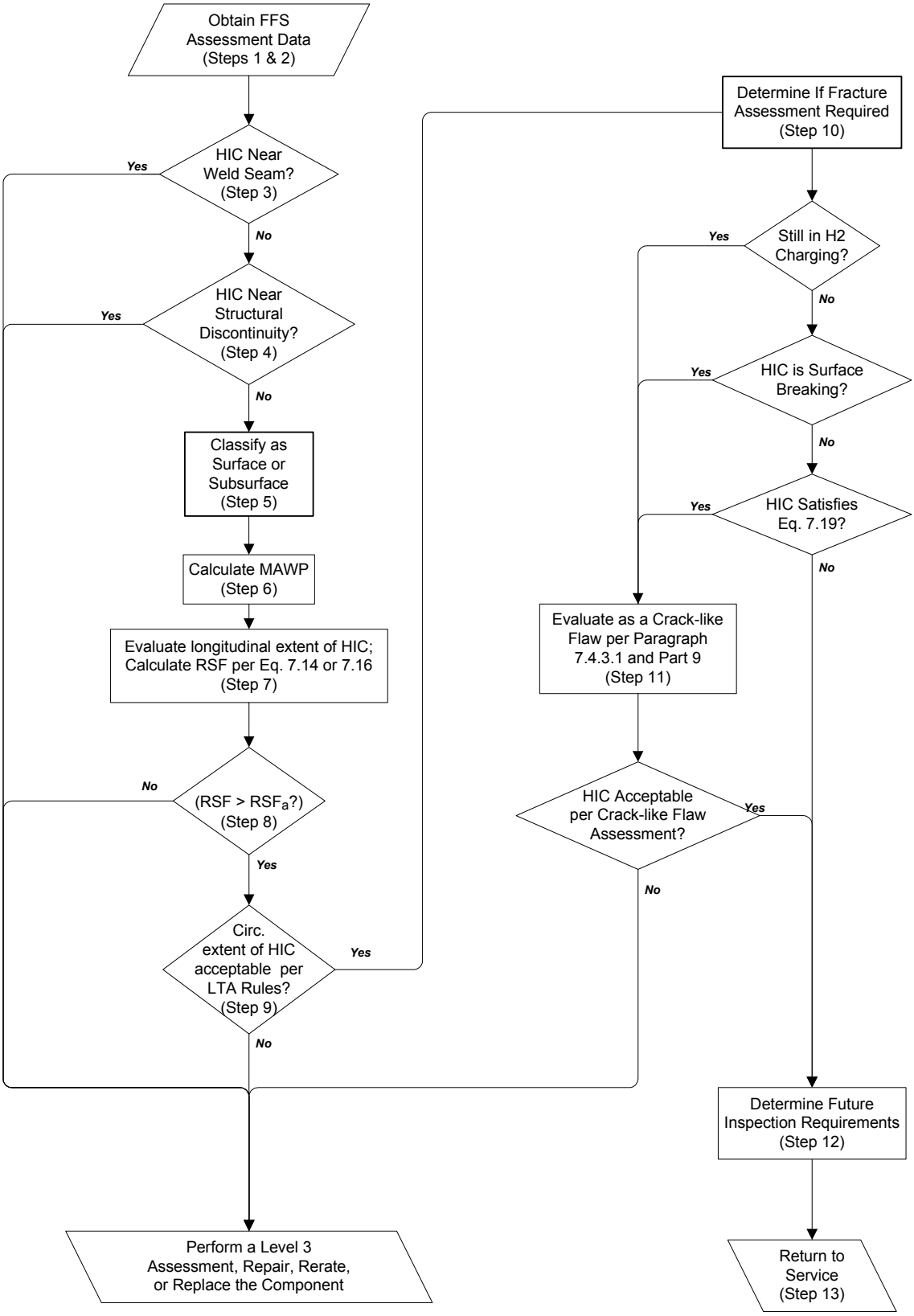

Figure 7.11 – Level 2 Assessment Procedure for HIC Damage

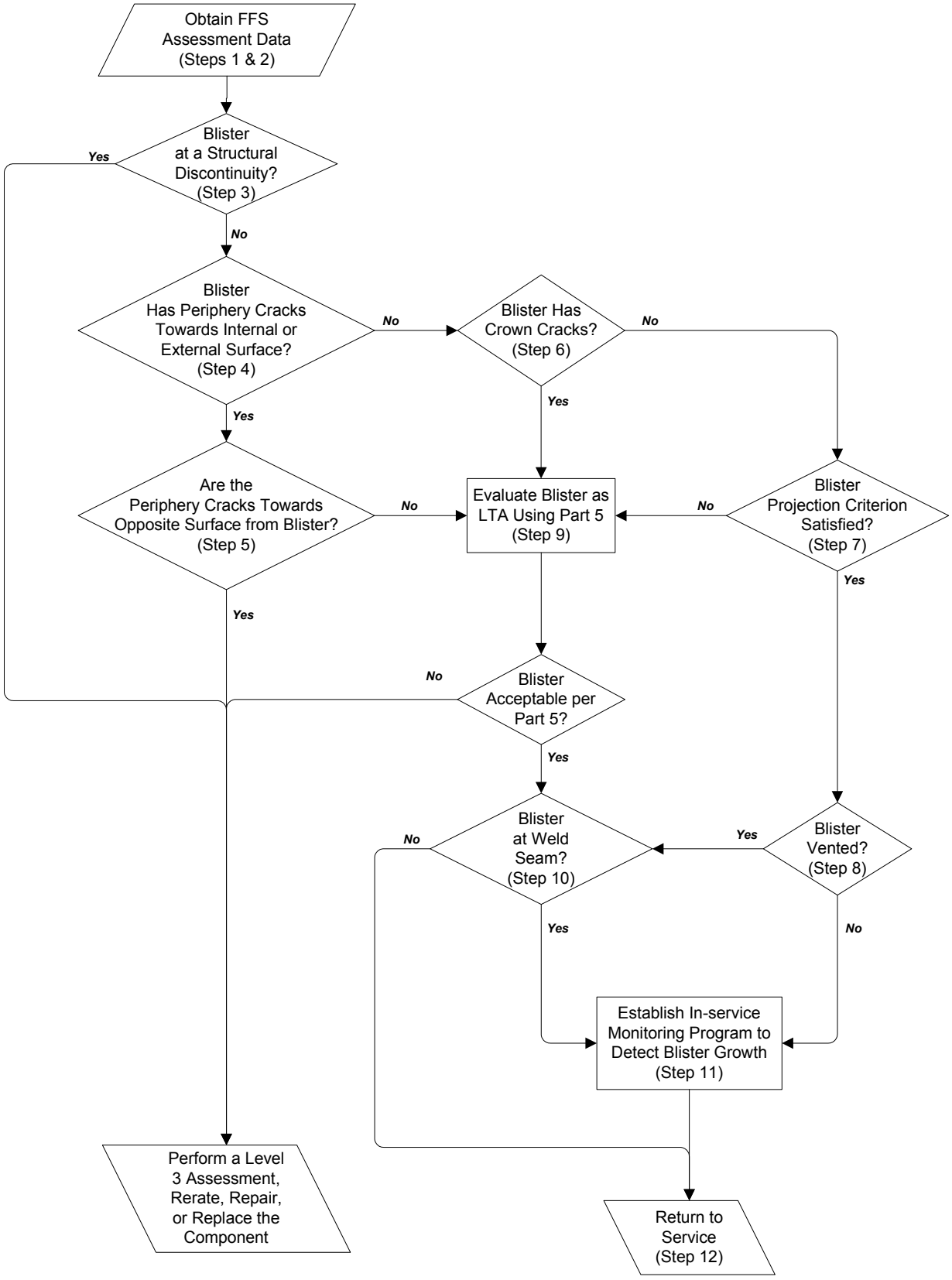

Figure 7.12 – Level 2 Assessment Procedure for Blisters

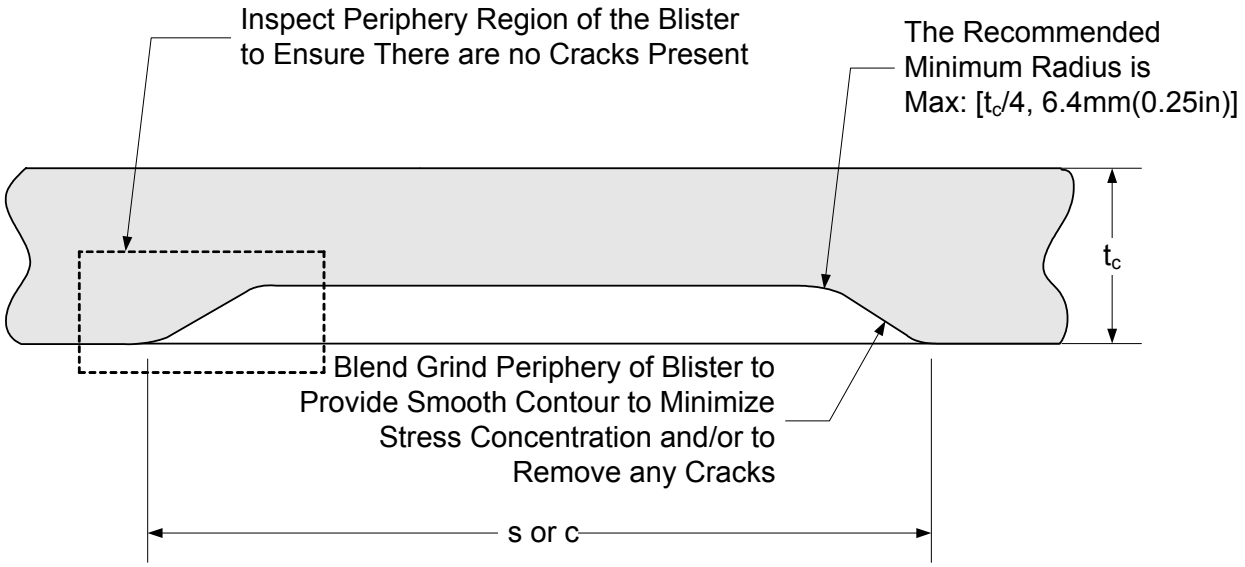

Note: Blisters Removed by Blend Grinding should be Evaluated as an LTA Using the Assessment Procedures in Part 5.

Figure 7.13– Blend Ground Area Remaining After Removal of a HIC Damage Zone or a Blister

PART 8

ASSESSMENT OF WELD MISALIGNMENT AND SHELL DISTORTIONS

PART CONTENTS

8.1 General

Fitness-For-Service (*FFS*) assessment procedures for pressurized components with weld misalignment and shell distortion, including out-of-roundness and bulges, are provided in this part. A flow chart for the evaluation procedure of equipment with a weld misalignment or shell distortion is shown in Figure 8.1.

8.2 Applicability and Limitations of the Procedure

8.2.1 The procedures in this part can be used to assess weld misalignments and shell distortions in components made up of flat plates; cylindrical, conical, and spherical shells; and formed heads. The types of flaws referred to as weld misalignment and shell distortion in this part are defined in the following paragraphs. If the current geometry of a component with a weld misalignment or shell distortion satisfies the original fabrication tolerances only a Level 1 assessment is typically required. Exceptions include components subject to cyclic service and components that have a localized shell distortion such as a bulge.

8.2.1.1 *Weld Misalignment* – Categories covered include centerline offset, angular misalignment (peaking), and a combination of centerline offset and angular misalignment of butt weld joints in flat plates, cylindrical shells and spherical shells (see Figures 8.2 through 8.6).

8.2.1.2 *Shell Distortion* – Categories of shell distortion are defined as follows:

a) General Shell Distortion – A deviation of a shell from an ideal geometry that occurs in the longitudinal and/or circumferential direction and exceeds the deviation permitted by the applicable code or standard. This type of distortion exhibits significant shape variation of the shell (i.e. multiple local curvatures), and typically requires a Level 3 assessment based on a numerical analysis method. Flat spots on a shell are classified as general shell distortion.

b) Out-of-roundness – A deviation of the cross-section of a cylindrical shell or pipe bend from an ideally circular geometry. The out-of-roundness of a cylinder is assumed to be constant in the longitudinal direction (see Figure 8.7 and paragraph 8.2.5.2.d, and either global (oval shape) or arbitrarily shaped in the circumferential direction. The out-of-roundness of a pipe elbow is assumed to be global (oval shape) in the mid-elbow region when the ovality at the end equals 50% of the mid-elbow value.

c) Bulge – An outward deviation of a cross-section of a shell member from an ideal geometry that can be characterized by local radii and angular extent. The local bulge geometry may be either spherical or cylindrical. Flat spots (infinite radius of curvature) are not considered to be bulges; they are classified as general shell distortions. If the bulge occurs at a blister, the analysis procedures in Part 7 should be utilized for the assessment.

8.2.2 Unless otherwise specified, this Part is limited to the evaluation of weld misalignment and shell distortions. Other flaw types shall be evaluated in accordance with Part 2, Table 2.1.

8.2.3 Calculation methods are provided to rerate the component if the acceptance criteria in this part are not satisfied. For pressurized components, the calculation methods determine a reduced maximum allowable working pressure *(MAWP)* and/or coincident temperature. For tank components (shell courses), the calculation methods determine a reduced maximum fill height *(MFH)*.

8.2.4 The assessment procedures only apply to components that are not operating in the creep range; the design temperature is less than or equal to the value in Part 4, Table 4.1. The Materials Engineer should be consulted regarding the creep range temperature limit for materials not listed in this table. Assessment procedures for components operating in the creep range are provided in Part 10.

8.2.5 Specific details pertaining to the applicability and limitations of each of the assessment procedures are discussed below.

8.2.5.1 Level 1 Assessment procedures are based on the criteria in the original construction code. If these criteria are not completely defined by the original construction code and are not in the original owner-user design specification, a Level 2 or Level 3 assessment may be performed. Level 1 Assessment procedures should not be used if the component is in cyclic service. A screening procedure to determine if a component is in cyclic service is provided in Annex B1, paragraph B1.5.2.

8.2.5.2 The Level 2 assessment procedures in this part apply only if all of the following conditions are satisfied:

a) The original design criteria were in accordance with a recognized code or standard (see Part 1, paragraphs 1.2.2 or 1.2.3).

b) The component geometry is one of the following:

   1) Flat plate

   2) Pressure vessel cylindrical or conical shell section

   3) Spherical pressure vessel

   4) Straight section of a piping system

   5) Elbow or pipe bend that does not have structural attachments

   6) Shell course of an atmospheric storage tank

c) The applied loads are limited to pressure and/or supplemental loads (see Annex A) that result in a membrane state of stress in the component, excluding the effects of the weld misalignment and shell distortion (i.e. through-wall bending stresses in the component are a result of the weld misalignment or shell distortion). The assessment procedures can be used to evaluate stresses resulting from both internal and external pressure. Level 2 stability assessment procedures are provided only for cylindrical and conical shells subject to external pressure. The Level 2 stability assessment rules do not apply to cylinders subject to external pressure in combination with supplemental loads that result in significant longitudinal compressive stresses..

d) If the component under evaluation is a cylinder with out-of-roundness, the out-of-roundness is constant along the axis of the cylinder. If local deviations of the cylindrical shell occur in the longitudinal direction, the Level 2 assessment procedure can produce non-conservative results, and the shell distortion should be classified as general shell distortion.

8.2.5.3 A Level 3 assessment may be performed where Level 1 and 2 methods do not apply, such as for the following conditions:

a) Type A, B, or C Components (see Part 4, paragraph 4.2.5) subject to internal pressure, external pressure, supplemental loads, and any combination thereof.

b) Components with a design based on proof testing (e.g. piping tee or reducer produced in accordance with ASME B16.9 where the design may be based on proof testing).

c) The shell distortion is classified as general shell distortion (see paragraph 8.2.1.2).

d) The loading conditions result in significant stress gradients at the location of the weld misalignment or shell distortion.

e) The component is subject to a loading condition that results in compressive stresses where structural stability is a concern. Guidelines for performing a structural stability assessment are provided in Annex B1, paragraph B1.4.

8.3 Data Requirements

8.3.1 Original Equipment Design Data

An overview of the original equipment data required for an assessment is provided in Part 2, paragraph 2.3.1.

8.3.2 Maintenance and Operational History

An overview of the maintenance and operational history required for an assessment is provided in Part 2, paragraph 2.3.2.

8.3.3 Required Data/Measurements for a *FFS* Assessment

8.3.3.1 The information typically used for a Level 1 and Level 2 Assessment is covered in paragraphs 8.4.2 and 8.4.3, respectively. A summary of these data is provided in Table 8.1.

8.3.3.2 The information required to perform a Level 3 Assessment depends on the analysis method utilized. A detailed stress analysis or limit load procedure using a numerical technique can be used to establish acceptable operating conditions. For such analyses, an accurate description of the weld misalignment or shell distortion should be obtained along with the material properties, including the elastic modulus and the yield stress (see Annex F). The description of the weld misalignment or shell distortion should include field measurements that adequately characterize the deformed shape.

8.3.4 Recommendations for Inspection Technique and Sizing Requirements

8.3.4.1 Measurement of the radial (offset) and angular (peaking) misalignment at the weld joint is required to use the assessment procedures for weld misalignment.

a) For flat plates, these two quantities can be established by knowing the plate thicknesses, disposition of the surfaces of the plates in the weld joint (e.g. internal surfaces are flush), the maximum offset between the plate centerlines at the weld joint, and for angular misalignment, the effective height and length used to characterize the deviation.

b) For cylindrical or spherical shells, the radial misalignment can be established by knowing the plate thicknesses and the disposition of the surfaces of the plates in the weld joint (e.g. internal surfaces are flush). The angular misalignment at the joint can be established by using a template as shown in Figure 8.8. The arc length of the template should extend beyond the locally deformed region resulting from the angular misalignment (or the contact point, see Figure 8.8), and should be established using the inside or outside radius of the cylinder, as applicable. The template should be notched as shown in Figure 8.8 so that no part of it is in contact with the area of weld reinforcement (weld cap). Using this technique, the maximum deviation can be calculated using either of the following equations. For a center template,

$$\delta = \frac{(a_1 + a_2)}{2} \tag{8.1}$$

and for a rocked template

$$\delta = \frac{(b_1 + b_2)}{4} \tag{8.2}$$

where a_1, a_2, b_1, and b_2 are defined in Figure 8.8.

8.3.4.2 Measurement of the radius and associated deviation from the mean radius at positions around the circumference are required to use the assessment procedures for circumferential out-of-roundness of cylindrical shells.

a) For the case of global out-of-roundness, the maximum, minimum and mean diameters are required. If these quantities are difficult to measure in the field, the measurement procedure for arbitrary out-of-roundness presented in item (b) below is recommended.

b) An accurate measurement of the cylinder radius at various stations should be made in order to apply the assessment procedures for an arbitrary circumferential out-of-roundness.

1) Radii at an even number of equally spaced intervals around the circumference of the cylinder sufficient to define the profile of the cross section under evaluation should be measured (see Figure 8.9). The recommended minimum number of measurement locations is 24. If access to the inside of the vessel is not possible, an alternative means for measuring the cross section profile will be required. For a vessel that has stiffening rings, the shape deviation of the shell located between the stiffening rings can be measured by placing a level on the outside diameter of the rings and measuring the radial offset to the deformed surface. This method can produce accurate results if the stiffening rings are not significantly out-of-round. For a vessel without stiffening rings, a vertical level or plumb line placed alongside the vessel shell can be used to measure the radial offset (see Part 11, Figure 11.4).

2) In order to determine the deviation from the mean circle, the radius measurements should be corrected for the mean and for the error in positioning the center of measurement. If the radius at i discrete points around the circumference can be represented by the Fourier Series shown in Equation (8.3), then the radius at an angular location, θ, is given by Equation (8.4).

$$R_i = R_m + \sum_{n=1}^{N}\left(A_n \cos\left[\frac{2\pi(i-1)}{M}n\right] + B_n \sin\left[\frac{2\pi(i-1)}{M}n\right]\right) \tag{8.3}$$

$$R(\theta) = R_m + A_1 \cos\theta + B_1 \sin\theta + \varepsilon \tag{8.4}$$

3) The corrected radius and deviation from the mean circle can be calculated using Equations (8.5) and (8.6), respectively.

$$R_i^c = R_i - A_1 \cos\left[\frac{2\pi(i-1)}{M}\right] - B_1 \sin\left[\frac{2\pi(i-1)}{M}\right] \tag{8.5}$$

$$\varepsilon_i = R_i^c - R_m \tag{8.6}$$

4) The mean radius in Equation (8.6) can be calculated using Equation (8.7). The coefficients of the Fourier Series may be determined using Equations (8.8) and (8.9), or the procedure shown in Table 8.2. The parameters A_1 and B_1 in Equation (8.5) are equal to the second value of the sine and cosine terms, respectively, of the computed Fourier coefficients.

$$R_m = \frac{1}{M}\sum_{i=1}^{M} R_i \tag{8.7}$$

$$A_n = \frac{2}{M}\sum_{i=1}^{M} R_i \cos\left[\frac{2\pi(i-1)}{M}n\right] \tag{8.8}$$

$$B_n = \frac{2}{M}\sum_{i=1}^{M} R_i \sin\left[\frac{2\pi(i-1)}{M}n\right] \tag{8.9}$$

8.3.4.3 An estimate of the local radius, R_L, is required to use the assessment procedures for local imperfections in cylindrical shells subject to external pressure. The local radius, R_L, can be estimated using the guidelines shown in Figure 8.10

8.3.4.4 Estimates of the local bulge radii and the bulge angular extent are required to use the assessment procedures for bulges. In addition, if the bulge is caused by local heating, hardness values and other insitu testing should be considered to evaluate the condition of the material.

8.4 Evaluation Techniques and Acceptance Criteria

8.4.1 Overview

An overview of the assessment levels is provided in Figure 8.1.

a) The Level 1 assessment is based on the fabrication tolerances of the original construction code. If the current geometry of the component conforms to the original fabrication tolerances, the Level 1 assessment criteria are satisfied. Additional analysis is not required unless the component is in cyclic service as defined in Annex B1, paragraph B1.5.2, or if a fatigue analysis was conducted as part of the original design; in these cases, a Level 2 or Level 3 assessment is required.

b) Level 2 assessments provide a means to estimate the structural integrity of a component with weld misalignment or shell distortion characterized as out-of-roundness. Level 2 assessments can consider pressure and supplemental loads as well as complicated geometries (e.g. pipes with different wall thickness and locations of welds).

c) Level 3 assessments are intended for the evaluation of components with general shell distortions, complex component geometries and/or loadings. Level 3 assessments involve detailed stress analysis techniques including fracture, fatigue, and numerical stress analysis. Level 3 assessments typically require significant field measurements to characterize the weld misalignment or shell distortion.

8.4.2 Level 1 Assessment

8.4.2.1 The Level 1 assessment procedures are based on the fabrication tolerances provided in the original construction code. Tables 8.3 through 8.7 provide an overview of these tolerances for the following construction codes. For equipment or components designed to other recognized construction codes, standards, or specifications, fabrication tolerances in those documents may also be followed (see paragraph 8.2.5.1).

a) ASME Boiler and Pressure Vessel Code, Section VIII, Division 1 and Division 2 – see Table 8.3

b) ASME B31.3 Piping Code – see Table 8. 4

c) API 620 Standard – see Table 8.5

d) API 650 Standard – see Table 8.6

e) API 653 Standard (reconstructed tanks) – see Table 8.7

8.4.2.2 If the component does not meet the Level 1 Assessment requirements, then a Level 2 or Level 3 Assessment can be conducted.

8.4.3 Level 2 Assessment

8.4.3.1 The Level 2 assessment procedures are computational procedures for assessment of a weld misalignment or shell distortion in a component subject to pressure and supplemental loads. Calculation methods are provided to rerate the component if the acceptance criteria in this part are not satisfied.

8.4.3.2 Weld Misalignment

a) STEP 1 – Identify the component and misalignment type (see Tables 8.8, 8.9, 8.10, and 8.11) and determine the following variables as applicable (see Figures 8.2 through 8.6): A, e, E_y, F, FCA, H_f, L, $LOSS$, M, P, R, S_a, t_1, t_2, t_{nom}, t_{rd}, RSF_a, R_1, R_2, Z, δ, θ_p, and ν.

b) STEP 2 – Determine the wall thickness to be used in the assessment using Equation (8.10) or Equation (8.11), as applicable.

$$t_c = t_{nom} - LOSS - FCA \tag{8.10}$$

$$t_c = t_{rd} - FCA \tag{8.11}$$

c) STEP 3 – Determine the membrane stress from pressure, σ_m, (see Annex A). Note that for cylindrical shells, σ_m^C should be used for misalignment of longitudinal joints, and σ_m^L should be used for misalignment of circumferential joints. For centerline offset in flat plates and circumferential joints in cylindrical shells, determine the resulting longitudinal membrane stress using the following equation if supplemental loads exist.

$$\sigma_{ms} = \frac{F}{A} + \frac{M_{ns}}{Z} \tag{8.12}$$

d) STEP 4 – Calculate the ratio of the induced bending stress to the applied membrane stress using the equations in Tables 8.8, 8.9, 8.10, and 8.11 based on the type of component and weld misalignment, and the thickness determined in STEP 2. This ratio equals zero if no centerline offset or angular misalignment exists. The quantity R_b is the ratio of the induced bending stress to the applied membrane stress resulting from pressure. R_{bs} is the ratio of the induced bending stress to the membrane stress resulting from supplemental loads.

1) Flat Plates (note that a pressure induced bending stress shall be categorized as σ_{ms} and R_{bs} is applicable):

$$R_b = -1.0 \tag{8.13}$$

$$R_{bs} = R_{bs}^{pc} + R_{bs}^{pa} \tag{8.14}$$

2) Cylinders – Circumferential Joints (Longitudinal Stress):

$$R_b = R_b^{ccjc} + R_b^{ccja} \tag{8.15}$$

$$R_{bs} = R_{bs}^{ccjc} + R_{bs}^{ccja} \tag{8.16}$$

3) Cylinders – Longitudinal Joints (Circumferential Stress):

$$R_b = R_b^{cljc} + R_b^{clja} \tag{8.17}$$

$$R_{bs} = -1.0 \tag{8.18}$$

4) Spheres – Circumferential Joints (Circumferential Stress):

$$R_b = R_b^{scjc} + R_b^{scja} \tag{8.19}$$

$$R_{bs} = -1.0 \tag{8.20}$$

e) STEP 5 – Determine the remaining strength factor:

$$RSF = \min\left[\left\{\frac{H_f S_a}{\sigma_m\left(1+R_b\right)+\sigma_{ms}\left(1+R_{bs}\right)}\right\},\ 1.0\right] \tag{8.21}$$

f) STEP 6 – Evaluate the results. If $RSF \geq RSF_a$, then the weld misalignment is acceptable per Level 2; otherwise, refer to paragraph 8.4.3.7

8.4.3.3 Out-Of-Roundness – Cylindrical Shells And Pipe Elbows

a) STEP 1 – Determine the following variables based on the type of out-of-roundness.

1) For Global Out-Of-Roundness (see Figure 8.7), the following parameters are required: θ, C_s, D_m, D_o, $D_{\max}$, $D_{\min}$, E_y, FCA, $LOSS$, t_{nom}, t_{rd}, ν and L_f.

2) For General (Arbitrary Shape) Out-Of-Roundness (see Figure 8.9), the parameter θ and the cross sectional profile of the cylinder at various angles around the vessel circumference when the cylinder is not pressurized are required. The cross sectional profile data can be represented by the Fourier Series in Equation (8.2). The coefficients to this Fourier Series may be determined using the procedure shown in Table 8.2.

b) STEP 2 – Determine the wall thickness to be used in the assessment, t_c, using Equation (8.10) or Equation (8.11), as applicable.

c) STEP 3 – Determine the circumferential membrane stress using the thickness from STEP 2 (see Annex A).

d) STEP 4 – Determine the ratio of the induced circumferential bending stress to the circumferential membrane stress at the circumferential position (denoted by the angle θ) of interest.

1) Global Out-Of-Roundness of a cylinder, θ is measured from the major axis of the oval:

$$R_b^{or}\left(\theta\right) = \frac{1.5\left(D_{\max} - D_{\min}\right)\cos 2\theta}{t_c\left(1+\left[\frac{C_s P\left(1-\nu^2\right)}{E_y}\right]\left[\frac{D_m}{t_c}\right]^3\right)} \tag{8.22}$$

2) General (Arbitrary Shape) Out-Of-Roundness of a cylinder:

$$R_b^{or}\left(\theta\right) = \left(\frac{6}{t_c}\right)\sum_{n=2}^{N}\left\{\frac{\left(A_n\cos(n\theta)+B_n\sin(n\theta)\right)}{1+k_n}\right\} \tag{8.23}$$

where,

$$k_n = \frac{PR^3}{\left(n^2-1\right)D_c} \tag{8.24}$$

$$D_c = \frac{E_y t_c^3}{12\left(1-\nu^2\right)} \tag{8.25}$$

3) Global Out-Of-Roundness Of Long Radius Elbow (note: limitations for the terms of Equation (8.26) are shown in Equations (8.28) and (8.29), see subparagraph 4 if these limitations are not satisfied).

$$R_b^{or}\left(\theta\right) = \frac{C_b \cdot \cos 2\theta}{L_f} \tag{8.26}$$

where,

$$C_b = \left(\begin{array}{l} -0.007281 + 0.05671Y + 0.0008353X + 0.01210XY + \\ 0.00001313X^2 - 0.00008362X^2Y + 0.04889W + 0.1827WY - \\ 0.003201WX - 0.01697WXY - 0.00003506WX^2 - \\ 0.0001021WX^2Y - 0.1386W^2 - 0.09795W^2Y + 0.007906W^2X + \\ 0.004694W^2XY - 0.00003833W^2X^2 + 0.0002649W^2X^2Y \end{array}\right) \tag{8.27}$$

$$W = \frac{1000 \cdot PR}{E_y t_c} \qquad valid\ \ for\ \ 0.045 \le W \le 0.50 \tag{8.28}$$

$$X = \frac{R}{t_c} \qquad valid\ \ for\ \ 20 \le X \le 40 \tag{8.29}$$

$$Y = \frac{100\left(D_{\max} - D_{\min}\right)}{D_o} \tag{8.30}$$

4) Global Out-Of-Roundness Of An Elbow Or Pipe Bend (no limitation on bend radius)

$$R_b^{or}\left(\theta\right) = \frac{\dfrac{3R\cos 2\theta}{t_c L_f}\left(\dfrac{D_{\max} - D_{\min}}{D_o}\right)}{\left[1 + 3.64\left(\dfrac{PR}{E_y t_c}\right)\left(\dfrac{R}{t_c}\right)^2\right]} \tag{8.31}$$

e) STEP 5 – Determine the remaining strength factor using Equation (8.21) with $R_b = abs\left[R_b^{or}\right]$ and $R_{bs} = -1.0$ (the expression abs[x] means the absolute value of x).

f) STEP 6 – Evaluate the results. If $RSF \ge RSF_a$, then the out-of-roundness is acceptable per Level 2; otherwise, refer to paragraph 8.4.3.7.

8.4.3.4 Combined Weld Misalignment and Out-Of-Roundness In Cylindrical Shells Subject To Internal Pressure

a) The ratio of the induced circumferential bending stress to the circumferential membrane stress, R_b, due to weld misalignment can be calculated at the location of the weld using the equations in paragraph 8.4.3.2.. The R_b ratio due to out-of-roundness should be calculated at the location of the longitudinal weld joint (i.e., the position of the weld as defined by θ) using the equations in paragraph 8.4.3.3.

b) The assessment procedure for weld misalignment and out-of-roundness in cylindrical shells subject to internal pressure is as follows:

1) STEP 1 – Determine the wall thickness to be used in the assessment, t_c, using Equation (8.10) or Equation (8.11), as applicable.

2) STEP 2 – Determine the circumferential membrane stress using the thickness from STEP 1 (see Annex A).

3) STEP 3 – Calculate the ratio of the induced bending stress to the applied membrane stress for weld misalignment using paragraph 8.4.3.2, and for circumferential out-of roundness using paragraph 8.4.3.3 (note: when computing R_b^{or} per paragraph 8.4.3.3, do not take the absolute value of the result as indicated in STEP 4).

$$R_b = R_b^{cljc} + R_b^{clja} + R_b^{or} \tag{8.32}$$

4) STEP 4 – Determine the remaining strength factor using Equation (8.21) with the value of R_b determined in STEP 2 and $R_{bs} = -1.0$.

5) STEP 5 – Evaluate the results. If $RSF \geq RSF_a$, then the weld misalignment and out-of-roundness is acceptable per Level 2; otherwise, refer to paragraph 8.4.3.7.

8.4.3.5 Out-Of-Roundness – Cylindrical Shells Subject To External Pressure (Buckling Assessment)

a) Cylindrical shells subject to external pressure should satisfy the stress criteria in paragraph 8.4.3.3 or 8.4.3.4, as applicable, and the buckling criteria set out in this paragraph.

b) The assessment procedure for out-of-roundness for cylindrical and conical shells subject to external pressure is as follows:

1) STEP 1 – Determine the following variables (see Figure 8.10): e_d, E_y, FCA, FS, L, $LOSS$, P, R_o, R_L, t_{nom}, t_{rd}, ν, and σ_{ys}.

2) STEP 2 – Determine the wall thickness to be used in the assessment, t_c, using Equation (8.10) or Equation (8.11), as applicable.

3) STEP 3 – If a conical shell is being evaluated, determine the equivalent length and outside diameter as defined in Annex A, paragraph A.4.8. The equivalent length and equivalent outside radius ($R_o = D_o/2$) are to be used in all subsequent steps.

4) STEP 4 – Find the value of n (the number of waves into which the cylinder will buckle in the circumferential direction to give a minimum value of P_{eL}) for the perfect cylinder ($e_d = 0.0$).

i) Approximate method – determine the value of n using the equations in Annex A, paragraph A.4.2.a.1 with $R_m = R_o$.

ii) Exact method – determine the value of n in the following equation that results in a minimum value of P_{eL}. This calculation assumes the value of n to be a floating point number. Starting with $n = 2$, increase n in increments of 0.10 until a minimum value of P_{eL} is found.

$$P_{eL} = \frac{1}{n^2 + 0.5\lambda^2 - 1}\left(\frac{E_y t_c}{R_o}\right)\left[\frac{\left(n^2 + \lambda^2 - 1\right)^2}{12\left(1 - \nu^2\right)}\left(\frac{t_c}{R_o}\right)^2 + \frac{\lambda^4}{\left(n^2 + \lambda^2\right)^2}\right] \tag{8.33}$$

with,

$$\lambda = \frac{\pi R_o}{L_u} \tag{8.34}$$

5) STEP 5 – Determine the value of the local radius, R_L, of the imperfection using the procedure shown in Figure 8.10 with the measured value of the deviation from the true cylinder, e_d, and the value of n determined in STEP 3.

6) STEP 6 – Substitute R_L for R_o into Equation (8.33) and find a new value of n along with the associated value of the minimum elastic buckling pressure and designate this pressure as P_{ec}. In calculating P_{ec}, start with $n = 2$ and increase n in increments of 0.10 until a minimum value of P_{ec} is found.

7) STEP 7 – Determine the inelastic buckling pressure using Equation (8.35). The parameter F_{hc} in this equation is determined by Annex A paragraph A.4.4.a.3 with the value of F_{he} calculated using Equation (8.36). Note that for materials other than carbon and low alloy steels, the correction described in Annex A paragraph A.4.1.d shall be applied.

$$P_c = \frac{F_{hc} t_c}{R_o} \tag{8.35}$$

$$F_{he} = \frac{P_{ec} R_o}{t_c} \tag{8.36}$$

8) STEP 8 – Determine the permissible external pressure:

$$P_{ext} = \frac{\min\left[P_{ec},\, P_c\right]}{FS} \tag{8.37}$$

9) STEP 9 – Evaluate the results. If $P_{ext} \geq P$, then the component is suitable for continued operation; otherwise, refer to paragraph 8.4.3.7.

8.4.3.6 Bulges

A Level 2 Assessment procedure for determining the acceptability of a bulge is currently not provided; refer to paragraph 8.4.4 for Level 3 Assessment options.

8.4.3.7 Rerating Components

If $RSF \geq RSF_a$, the component is acceptable per Level 2. If this criterion is not satisfied, then the component may be rerated using the equations in Part 2, paragraph 2.4.2.2. It should be noted that in the cases where the R_b factor is a function of pressure, an iterative analysis is required to determine the final $MAWP$.

8.4.3.8 Fatigue Analysis

a) If the component is in cyclic service, or if a fatigue analysis was performed as part of the original design calculations, the fatigue strength including the effects of the weld misalignment or shell distortion should be checked. A screening procedure to determine if a component is in cyclic service is provided in Annex B1, paragraph B1.5.2.

b) The procedure for fatigue assessment that follows may be used to evaluate fatigue in components with weld misalignment, shell out-of-roundness, or a combination of weld misalignment and shell out-of-roundness subject to the restrictions in paragraphs 8.4.3.2, 8.4.3.3, or 8.4.3.4, respectively. A Level 3 Assessment is required for a component with bulges.

1) STEP 1 – Determine the nature of loading, the associated membrane stress (see Annex A), and the number of operating cycles.

2) STEP 2 – Determine the ratio of the induced bending stress to membrane stress, R_b, resulting from weld misalignment, shell out-of-roundness or combination of weld misalignment and shell out-of-roundness, as applicable, using the procedures in paragraphs 8.4.3.2, 8.4.3.3, or 8.4.3.4, respectively.

3) STEP 3 – Using the loading history and membrane stress from STEP 1 and the R_b parameters from STEP 2, calculate the stress range for the fatigue analysis using Table 8.12.

4) STEP 4 – Compute the number of allowed cycles using the stress range determined in STEP 3 using Annex B1, paragraph B1.5.3 or B1.5.5, as applicable.

5) STEP 5 – Evaluate the results. If the computed number of cycles determined in STEP 4 equals or exceeds the number of operating cycles in STEP 1, then the component is acceptable per Level 2.

8.4.3.9 If the component does not meet the Level 2 Assessment requirements, then the following, or combinations thereof, should be considered:

a) Rerate, repair, replace or retire the component.

b) Adjust the FCA by applying remediation techniques (see Part 4, paragraph 4.6).

c) Conduct a Level 3 Assessment.

8.4.4 Level 3 Assessment

8.4.4.1 The stress analysis techniques in Annex B1 can be used to assess the weld misalignment or shell distortion discussed in this part in pressure vessels, piping, and tankage.

8.4.4.2 Linear stress analysis and the stress categorization techniques discussed in Annex B1 , paragraph B1.2.2 can be used to analyze misalignment at weld joints. In the Level 2 Assessment, the induced bending stress resulting from misalignment is considered a secondary bending stress for most applications. In some cases, this stress should be taken as a primary bending stress if elastic follow-up occurs. The limit load techniques described in Annex B1 , paragraph B1.2.3 may be utilized in the analysis to resolve issues pertaining to stress categorization.

8.4.4.3 The non-linear stress analysis techniques described in Annex B1 , paragraph B1.2.4 may be utilized to analyze general shell distortions.

a) Typically, the localized bending stresses resulting from general shell distortion will tend to decrease due to the rounding effect of the shell when subject to internal pressure. This effect is more pronounced in thinner shells and can be directly evaluated using a non-linear analysis that includes the effects of geometric nonlinearity. The rounding effect is introduced in a Level 2 analysis of out-of-roundness through the correction factor, C_f. If material nonlinearity is included in the analysis, the plastic collapse strength of the component can also be determined and used to qualify the component for continued operation.

b) An accurate representation of the deformed shell profile is critical in obtaining accurate analysis results. This is especially important for a shell with significant deviations (or kinks) in the longitudinal and circumferential direction. To obtain an accurate profile of the shell geometry, a grid should be established over the deformed region and measurements taken to determine the actual profile of the shell. The data should then be curve-fit with piece-wise cubic splines to obtain an accurate representation of the deformed shape and ensure that the slope and curvature of the deformed shell profile is continuous.

c) If a kink or sharp bend exists in a shell, traditional shell theory will not provide an accurate estimate of the stress state. In this case, a continuum model including the effects of plasticity is recommended for the evaluation.

d) For shell structures with significant localized distortion resulting from contact with another component or mechanical device, a nonlinear stress analysis to simulate the deformation process should be used to determine the magnitude of permanent plastic strain developed. To simulate the distortion process, perform an analysis that includes geometric and material nonlinearity as well as the contact interaction between the original undeformed shell structure, and the contacting body. The contacting component may be explicitly modeled as a deformable body or as a simple rigid surface. The analysis should include applicable loadings to develop the final distorted configuration of the shell structure. The calculated inelastic strains should be compared to the allowable strain limits given in Annex B1, paragraph B1.3.

8.4.4.4 If the component is subject to a compressive stress field, the nonlinear stress analysis techniques described in Annex B1, paragraph B1.2.4 may be used for the assessment. If geometric non-linearity is included along with material nonlinearity in the assessment, the stability of the component can be evaluated in the same analysis utilized to determine the plastic collapse strength. Alternatively, the stress categorization and structural stability techniques discussed in Annex B1, paragraph B1.2.2 and Annex A, paragraph A.14, respectively, may be utilized in the assessment.

8.4.4.5 If the component is operating in the creep range, a nonlinear analysis that includes both material (plasticity and creep) and geometric nonlinearity should be performed. Stresses due to a localized weld misalignment or shell distortion may not sufficiently relax with time due to the surrounding compliance of the component. In this case, creep strains can accumulate and could result in significant creep damage or cracking. The assessment procedures in Part 10 should be considered.

8.4.4.6 If the component contains a weld misalignment or shell distortion with highly localized stresses, a detailed non-linear stress analysis and assessment should be performed. This assessment should also include an evaluation of the material toughness requirements. Otherwise, repair or replacement of the component is recommended.

8.5 Remaining Life Assessment

8.5.1 A remaining life assessment of components with a weld misalignment or shell distortion generally consists of one of the following three categories:

a) *Metal Loss Resulting From A Corrosive/Erosive Environment* – In this case, adequate protection from a corrosive/erosive environment can be established by setting an appropriate value for the future corrosion allowance. The remaining life as a function of time can be established using the $MAWP$ Approach described in Part 4, paragraph 4.5.2.

b) *Cyclic Loading* – The Level 2 assessment procedures include a fatigue evaluation for weld misalignment and out-of-roundness (see paragraph 8.4.3.8 and Annex B1, paragraph B1.5). The remaining life can be established by combining the results from this analysis with the operational history of the component.

c) *High Temperature Operation* – If the component is operating in the creep regime, the assessment procedures in Part 10 should be utilized to determine a remaining life.

8.5.2 If the component's operation is not within one of the above categories, a detailed Level 3 analysis should be performed to determine the remaining life of the component.

8.6 Remediation

8.6.1 Weld misalignment, out-of-roundness and bulges may be reinforced using stiffening plates and lap patches depending on the geometry, temperature and loading conditions. The reinforcement, if utilized, should be designed using the principles and allowable stresses of the original construction code.

8.6.2 Cylindrical shell sections that are out-of-round can be brought to within original fabrication tolerances or to a shape that reduces the local stress to within acceptable limits by mechanical means. Hydraulic jacks have been used successfully to alter the out-of-round shape of stiffened cylindrical shells. The design of the jacking arrangement and loads should be carefully established and monitored during the shaping process to minimize the potential for damage to the shell and attachments.

8.7 In-Service Monitoring

8.7.1 The weld misalignment and shell distortion covered in this part do not normally require in-service monitoring unless an unusually corrosive environment exists and future corrosion allowance cannot adequately be estimated, or if the component is subject to a cyclic operation and the load history cannot be adequately established. In these cases, the in-service monitoring usually entails visual inspection and field measurements of the components weld misalignment or shell distortion at regular intervals. The type of measurements made depends on the procedure utilized in the assessment.

8.7.2 In-service monitoring is typically required when a Level 3 assessment is performed to qualify a component that contains weld misalignment or shell distortion with a groove-like or crack-like flaw for continued operation.

8.8 Nomenclature

A area of the metal cross section, $2\pi Rt_1$; used for centerline offset of circumferential joints in cylinders when supplemental loads are present.

A_n coefficient of cosine term in the Fourier series used to model arbitrary out-of-roundness of a cylindrical shell.

A_1 correction factor or offset from the center of measurement to the true center of the mean circle (see Figure 8.9).

B_n coefficient of sine term in the Fourier series used to model arbitrary out-of-roundness of a cylindrical shell.

B_1 correction factor or offset from the center of measurement to the true center of the mean circle (see Figure 8.9).

C_f correction factor for angular weld misalignment in the longitudinal joint of a cylindrical shell.

C_s factor to account for the severity of the out-of roundness, use $C_s = 0.5$ for a purely oval shape and $C_s = 0.1$ for shapes which significantly deviate from an oval shape.

C_{ul} factor to account for units in the Equations of Table 8.11. $C_{ul} = 1.0$ if the units of inches are used, and $C_{ul} = 25.4$ if the units of millimeters are used.

D inside diameter corrected for $LOSS$ and FCA as applicable.

D_L cone outside diameter, large end, corrected for $LOSS$ and FCA allowance as applicable.

D_m mean diameter.

$D_{\max}$ maximum outside diameter corrected for $LOSS$ and FCA as applicable.

$D_{\min}$ minimum outside diameter corrected for $LOSS$ and FCA as applicable.

D_o outside diameter of a pipe bend corrected for $LOSS$ and FCA as applicable.

D_S cone outside diameter, small end corrected for $LOSS$ and FCA as applicable.

D_x cone outside diameter at a location within the cone corrected for $LOSS$ and FCA as applicable.

d inward or outward peaking in a cylinder resulting from an angular weld misalignment.

δ height of the angular peaking (see Figures 8.4, 8.5, and 8.6)

ΔS_P range of primary plus secondary plus peak equivalent stress.

$\Delta\sigma_b$ structural bending stress range.

$\Delta\sigma_m$ structural membrane stress range.

E weld joint efficiency.

E_y Young's modulus.

e centerline offset of the plate sections at the welded joint or the maximum inward deviation that occurs within a 2θ arc length when evaluating shells subject to external pressure.

e_d maximum deviation from a true cylinder.

ε deviation from the mean circle at a location defined by θ; see Equation (8.4).

ε_i deviation from the true mean radius at point i; see Equation (8.6).

F net-section axial force; used only for flat plates and for centerline offset of circumferential joints in cylinders.

FCA future corrosion allowance.

FS in-service margin (see Annex A, paragraph A.4.3).

H_f factor dependent on whether the induced stress from the shape deviation is categorized as a primary or secondary stress (see Annex B1); $H_f = 3.0$ if the stress is secondary and $H_f = 1.5$ if the stress is primary.

i index of the current radius measurement point on the cylinder's circumference.

K_c equivalent radius coefficient for an elliptical head.

K_f fatigue strength reduction factor.

L characteristic length used to establish the amount of angular misalignment (see Figures 8.4 and 8.6); the definition of this length is shown in Figure 8.6.

L_f Lorenz factor (see Annex A, paragraph A.5.5.1).

L_u unsupported length of a cylindrical or conical shell used in an external pressure calculation (see Annex A, paragraph A.4.3).

L_{msd} distance from the edge of the bulge under investigation to the nearest major structural discontinuity or adjacent flaw.

$LOSS$ amount of uniform metal loss away from the local metal loss location at the time of the assessment.

λ buckling parameter.

M number of equally spaced measurement locations around the cylinder's circumference, a minimum of 24 points is recommended, M must be an even number.

M_{ns} net section bending moment; used only for flat plates and for centerline offset of circumferential joints in cylinders.

n harmonic number associated with the Fourier series, or the number of waves for a buckled cylindrical shell.

N number of Fourier coefficients used in the calculation equal to $M/2$.

P internal or external design pressure, as applicable.

P_c inelastic buckling pressure of a cylindrical shell subject to external pressure.

P_{ec} minimum elastic buckling pressure of a cylindrical shell subject to external pressure.

P_{eL} elastic buckling pressure of a cylinder.

P_{ext} permissible external pressure.

R mean radius of the cylinder or sphere, measured to mid thickness.

R_b ratio of the induced bending stress to the applied membrane stress in a component that results from pressure.

R_{bs} ratio of the induced bending stress to the applied membrane stress in a component that results from supplemental loads.

R_m average radius.

$R(\theta)$ radius at a location defined by θ corrected for $LOSS$ and FCA as applicable.

R_i measured radius at point i on a cylinder.

R_i^c corrected radius at point i on a cylinder.

R_L local outside radius of imperfect shell (see Figure 8.10) corrected for $LOSS$ and FCA as applicable.

R_o outside radius of the perfect shell (see Figure 8.10) corrected for $LOSS$ and FCA as applicable.

R_1 mean radius of component 1 with a wall thickness of t_1 in the joint (used for centerline offset in circumferential joints of cylinders, see Figure 8.3) corrected for $LOSS$ and FCA as applicable.

R_2 mean radius of component 2 with a wall thickness of t_2 in the joint (used for centerline offset in circumferential joints of cylinders, see Figure 8.3) corrected for $LOSS$ and FCA as applicable.

RSF calculated remaining strength factor for a component.

RSF_a allowable remaining strength factor (see Part 2).

R_{bs}^{pc} R_{bs} factor for a plate, centerline offset.

R_{bs}^{pa} R_{bs} factor for a plate, angular misalignment.

R_b^{ccjc} R_b factor for a cylinder, circumferential joint, centerline offset.

R_b^{ccja} R_b factor for a cylinder, circumferential joint, angular misalignment.

R_{bs}^{ccjc} R_{bs} factor for a cylinder, circumferential joint, centerline offset.

R_{bs}^{ccja} R_{bs} factor for a cylinder, circumferential joint, angular misalignment.

R_b^{cljc} R_b factor for a cylinder, longitudinal joint, centerline offset.

R_b^{clja} R_b factor for a cylinder, longitudinal joint, angular misalignment.

R_b^{scjc} R_b factor for a sphere, circumferential joint, centerline offset.

R_{bs}^{scja} R_b factor for a sphere, circumferential joint, angular misalignment.

R_b^{or} R_b factor for out-of-roundness.

S_a allowable stress for the component at the assessment temperature based on the original construction code.

S_p parameter for misalignment calculation

σ_m membrane stress from pressure.

σ_{ms} membrane stress from supplemental loads.

σ_m^C circumferential membrane stress in a cylindrical shell.

σ_m^L longitudinal membrane stress in a cylindrical shell.

σ_r stress range in a component used in determining the permitted number of cycles in a fatigue analysis.

σ_{ys} yield stress at the assessment temperature (see Annex F) .

T temperature (°C:°F).

t furnished thickness of the component.

t_B minimum local wall thickness in the bulge.

t_c corroded wall thickness.

t_{nom} nominal or furnished thickness of the component adjusted for mill undertolerance as applicable.

t_{rd} uniform thickness away from the local metal loss location established by thickness measurements at the time of the assessment.

t_1 wall thickness of component 1 in the joint where $t_2 \geq t_1$; used for centerline offset weld misalignment in cylindrical shell circumferential weld joints (see Figure 8.3).

t_2 wall thickness of component 2in the joint where $t_2 \geq t_1$; used for centerline offset weld misalignment in cylindrical shell circumferential weld joints (see Figure 8.3).

t_{1c} wall thickness of component 1, adjusted for $LOSS$ and FCA using Equation (8.10) or Equation (8.11), as applicable.

t_{2c} wall thickness of component 2, adjusted for $LOSS$ and FCA using Equation (8.10) or Equation (8.11), as applicable.

θ angle to define the location where the stress will be computed (see Figure 8.5, Figure 8.7, and Figure 8.9)

θ_p angle associated with angular misalignment.

ν Poisson's Ratio.

Z section modulus of the cylindrical shell cross section.

8.9 Documentation

8.9.1 The documentation of the FFS assessment should include the information cited in Part 2, paragraph 2.8.

8.9.2 Inspection data including all field measurements used to determine the extent of the weld misalignment or shell distortion should be included in the documentation of the Fitness-For-Service analysis.

8.10 References

1. Becht IV, C., Cehn, Y., and Lyow, B., “Jacking to Correct Out-Of-Roundness Of A Ring-Stiffened Vessel,” PVP-Vol. 315, Fitness-For-Service and Decisions for Petroleum and Chemical Equipment, ASME, 1995, pp. 447-451.
2. Berge, S., and Myrhe, H., “Fatigue Strength of Misaligned Cruciform and Butt Joints,” Norwegian Maritime Research, No. 1, 1977, pp. 29-39.
3. Bizon, P.T, “Elastic Stresses At A Mismatched Circumferential Joint In A Pressurized Cylinder Including Thickness Changes And Meridional Load Coupling,” NASA TN D-3609, NTIS, Springfield, Va., D.C., September, 1966.
4. Bock, N. and Zeman, J.L., “On Bending Stress at Longitudinal Weld Joints of Cylindrical Shells Due to Peaking,” International Journal of Pressure Vessels & Piping, 60, 1994, pp 103-106.
5. Buchheim, M.B., Osage, D.A., Brown, R.G., and Dobis, J.D., “Failure Investigation of A Low Chrome Long-Seam Weld in a High -Temperature Refinery Piping System,” PVP-Vol. 288, ASME, 1994, pp 363-386.
6. Chuse, R. and Carson, B.E., “The ASME Code Simplified,” 7th Ed., McGraw-Hill, Inc., New York, N.Y., 1993.
7. Connelly, L.M., and Zettlemoyer, N., “Stress Concentrations at Girth Welds of Tubulars with Axial Wall Misalignment,” Tubular Structures, E & FN Spon., 1993.
8. Eiber, R.J., Maxey, W.A., Bert, C.W., and McClure, G.M., “The Effects of Dents on the Failure Characteristics of Line Pipe,” Battelle NG-18 Report No. 125, May 8 , 1981.
9. Hopkins, P., Jones, D.G., and Clyne, A.J., “The Significance Of Dents And Defects In Transmission Pipelines,” C376/049, ImechE, 1989.
10. Haigh, B.P., “An Estimate of Bending Stresses Induced by Pressure in a Tube That is Not Quite Circular,” Appendix IX in the Welding Research Committee Second Report.
11. Hechmer, J.L., “Report 2: Fatigue Strength-Reduction-Factors for Welds Based on NDE,” WRC Bulletin 432, The Welding Research Council, Inc., New York, N.Y., 2003.
12. Johns, R.H. and Orange, T.W., “Theoretical Elastic Stress Distributions Arising From Discontinuities And Edge Loads In Several Shell-Type Structures,” NASA TR R-103, NTIS, Springfield, Va., September, 1966.
13. Kendrick, S., “The Measurement of Shape in Pressure Vessels,” Institute of Mechanical Engineers, C96/80, 1980, pp261-267.
14. Maddox, S.J., “Fatigue Strength of Welded Structures,” 2nd Ed., Abington Publishing, Cambridge, England, 1991.
15. Miller, C.D., “The Effect of Initial Imperfections on the Buckling of Cylinders Subjected to External Pressure,” WRC Bulletin 443, Report No. 1, Pressure Vessel Research Council, New York, N.Y., January, 1995.
16. Morgan, W.C. and Bizon, P.T, “Technical Note D-1200 – Experimental Investigation Of Stress Distributions Near Abrupt Change In Wall Thickness In Thin-Walled Pressurized Cylinders,” NASA TN D-1200, NTIS, Springfield, Va., September, 1966.
17. Morgan, W.C. and Bizon, P.T, “Comparison Of Experimental And Theoretical Stresses At A Mismatch In A Circumferential Joint In A Cylindrical Pressure Vessel,” NASA TN D-3608, NTIS, Springfield, Va., September, 1966.
18. Partanen, T., “Factors Affecting the Fatigue Behavior of Misaligned Transverse Butt Joints in Stiffened Plate Structures,” Engineering Design in Welded Constructions. Proceedings, International Conference, Madrid, Spain, Pergamon Press for the International Institute of Welding (IIW), Oxford, UK, Sept, 1992, pp. 65-72.

19. Ong, L.S., Hoon, K.H., “Bending Stresses at Longitudinal Weld Joints of Pressurized Cylindrical Shells Due to Angular Distortion,” Journal of Pressure Vessel Technology, Vol. 118, ASME, August, 1996, pp. 369-373.

20. Ong, L.S., “Allowable Shape Deviation in a Pressurized Cylinder,” Transactions of the ASME, Vol. 116, August 1994, pp. 274-277.

21. Osage, D.A., Brown, R.G. and Janelle, J.L., “Fitness-For-Service Rules for Shell Distortions and Weld Misalignment in API 579,” PVP-Vol. 411, Service Experience and Fitness-For-Service in Power and Petroleum Processing, ASME, 2000, pp. 191-220.

22. Rodabaugh, E.C. and Pickett, A.G., “Survey Report on Structural Design of Piping Systems and Components,” Report TID-25553, NTIS, December, 1970, pp. 10.3-10.7.

23. Schwarz, M., and Zeman, J.L., “Bending Stresses at Longitudinal Weld Joints of Pressurized Cylindrical Shells Due to Angular Misalignment,” Journal of Pressure Vessel Technology, Vol. 119, ASME, May, 1997, pp. 245-246.

24. Thomas, K., “The Effects of Geometric Irregularities on the Design Analysis of Thin-Walled Piping Elbows,” Journal of Pressure Vessel Technology, Vol. 102, ASME, November, 1980, pp. 410-418.

25. Tooth, A.S., and Ong, L.S., “The Derivation of the Stresses in a Pressurized Pipe or Cylindrical Vessel with Initial Geometric Imperfections,” Strain, February, 1988, pp. 7-13.

26. Zeman, J.L., “Aufdachung an Langsnahten Zylindrischer Schusse,” TU Bd. 34, Nr. 7/8, 1993, pp 292-295.

27. Zeman, J.L., “On the Problem of Angular Misalignment at Longitudinal Weld Joints of Cylinder Shells,” International Journal of Pressure Vessels & Piping, 58, 1994, pp 179-184.

28. Sofronas, A., Fitzgerald, B.J., and Harding, E.M., “The Effect of Manufacturing Tolerances on Pressure Vessels in High Cyclic Service,” PVP Vol. 347, ASME, New York, N.Y.

8.11 Tables and Figures

Table 8.1
Data Required For The Assessment Of A Weld Misalignment Or Shell Distortion

Use this form to summarize the data obtained from a field inspection

Equipment Identification:_____
Equipment Type: _____ Pressure Vessel _____ Storage Tank _____ Piping Component
Component Type & Location:_____

Data required For Level 1 Assessment
Future Corrosion Allowance:_____
Out-Of-Roundness (Cylindrical Shell Subject to internal pressure)
Maximum Measured Internal Diameter (D_{max}):_____
Minimum Measured Internal Diameter (D_{min}):_____
Nominal Diameter:_____
Weld Misalignment
Wall Thickness:_____
Radial Misalignment (e) :_____

Data required For Level 2 Assessment
Temperature: _____
Internal and/or External Pressure:_____
Allowable Stress and Weld Joint Efficiency: _____
Component Inside Diameter (D): _____

Weld Misalignment
Component Wall Thickness (t *or* t_1 *and* t_2): _____
Component Geometry (R *or* R_1 *and* R_2): _____
Measure Of Misalignment (e *or* δ) _____
Characteristic Length (L): _____
Net Section Force, (F) , And Bending Moment (M): _____

Out-Of-Roundness
Component Wall Thickness (t):_____
Mean Radius (R_o): _____
Local Radius (R_L): _____
Young's Modulus (E_y): _____

Bulges
Component Furnished Thickness (t):_____
Minimum Thickness in Bulge (t_b):_____
Bulge Measurements : _____

Distance To Nearest Structural Discontinuity (L_{msd}): _____

Table 8.2
Pseudocode for Computation of Fourier Series Coefficients on a Discrete Range

for Analysis of Out-Of-Roundness Radius Data

```
Fourier (Npoints, RAD, Ncoeff, An, Bn)

Ncoeff = Npoints/2

An(1) = 0.0
Bn(1) = 0.0

sp = 0.0
cp = 1.0
rn = 2.0 / Npoints
arg = 3.14159265*rn
c = cos[arg]
s = sin[arg]

FOR i = 1 TO Npoints
   An(1) = An(1) + RAD(i)
ENDFOR

An(1) = rn * An(1) / 2.0

FOR k = 1 TO Ncoeff
   x = (c * cp) - (s * sp)
   sp = (c * sp) + (s * cp)
   cp = x
   u = 0.0
   v = 0.0

    FOR ii = 2 TO Npoints
        j = np - ii + 2
        w = RAD(j) + (2 * cp * v) - u
        u = v
        v = w
    ENDFOR

    An(k + 1) = rn * (RAD(1) + (cp * v) - u)
    Bn(k + 1) = rn * sp * v
ENDFOR
```

Notes:

1. Definitions of variables
   - Npoints – number of radius reading points
   - RAD – array of radius readings values at a total number of points equal to Npoints
   - Ncoeff – number of Fourier coefficients to be computed
   - An – array of computed coefficients of the cosine portion of the Fourier series
   - Bn – array of computed coefficients of the sine portion of the Fourier series
2. This algorithm may only be used for an even number of equal spacing of readings for a full period or 360°. For example, in Figure 8.9, Npoints=24 readings are indicated with an equal spacing of 15°. The radius readings at 0°, 15°, 30°, …, 345° correspond to RAD(1), RAD(2), RAD(3),…, RAD(Npoints). The radius reading at 360° is assumed to be equal to the reading at 0°.
3. Note that the results from the routine produce Ncoeff Fourier coefficients where An(1), Bn(1) correspond to the A_0 and B_0, An(2), Bn(2) correspond to the A_1 and B_1, and in general, An(k), Bn(k) correspond to the A_{k-1} and B_{k-1}.

Table 8.3
Overview Of Fabrication Tolerances – ASME B&PV Code, Section VIII, Division 1 And Division 2

Fabrication Tolerance	Requirement	Code Reference
Out-Of-Roundness In Cylindrical Shells Under Internal Pressure	$(D_{max} - D_{min})$ shall not exceed 1% of D where: D_{max} Maximum measured internal diameter D_{min} Minimum measured internal diameter D Nominal internal diameter At nozzle openings, this tolerance is increased by 2% of the inside diameter of the opening.	UG-80(a) {AF-130.1}
Out-Of-Roundness In Cylindrical Shells Under External Pressure	The diameter tolerance for internal pressure shall be satisfied. Using a chord length equal to twice the arc length determined from Figure 8.11, the maximum deviation from true circle shall not exceed the value e determined from Figure 8.12. Take measurements on the unwelded plate surface. For shells with a lap joint, increase tolerance by t. Do not include future corrosion allowance in t.	UG-80(b) {AF-130.2}
Shape Of Formed Heads	The inside surface shall not deviate outside the shape by more than 1.25% of the inside diameter nor inside the shape by more than 0.625% of the inside diameter.	UG-81 {AF-135}
Cylindrical Shell-To-Head Attachment Weld	The centerline (radial) misalignment between the shell and the head shall be less than one-half the difference between the actual shell and head thicknesses.	UW-13(b)(3) {AD-420}
Centerline Offset Weld Misalignment – Longitudinal Joints (Category A)	For $t \le$ 13 mm (1/2 in) e = t/4 For 13 mm (1/2 in) < $t \le$ 19 mm (3/4 in) e = 3 mm (1/8 in) For 19 mm (3/4 in) < $t \le$ 38 mm (1-1/2 in) e = 3 mm (1/8 in) For 38 mm (1-1/2 in) < $t \le$ 51 mm (2 in) e = 3 mm (1/8 in) For t > 51 mm (2 in) e = min(t/16, 10 mm) or e = min(t/16, 3/8 in) Where t plate thickness and e allowable centerline offset.	UW-33 {AF-142}
Centerline Offset Weld Misalignment - Circumferential Joints (Category B, C and D)	For $t \le$ 19 mm (3/4 in) e = t/4 For 19 mm (3/4 in) < $t \le$ 38 mm (1-1/2 in) e = 5 mm (3/16 in) For 38 mm (1-1/2 in) < $t \le$ 51 mm (2 in) e = t/8 For t > 51 mm (2 in) e = min(t/8, 19 mm) or e = min(t/8, 3/4 in) Where t plate thickness and e allowable centerline offset.	UW-33 {AF-142}
Angular Weld Misalignment	None stated in Division 1 or Division 2	
Peaking Of Welds (Category A)	The inward or outward peaking dimension, d, shall be measured using a template and included in the fatigue analysis of Division 2 vessels as required. The Manufacturer's Design Report shall stipulate the permitted value.	(AF-136)

Table 8.4
Overview Of Fabrication Tolerances – ASME B31.3

Fabrication Tolerance	Requirement	Code Reference
Out-Of-Roundness In Piping Under Internal Pressure	Default ASTM Standard the pipe was purchased to, for example: • ASTM 530 – For thin wall pipe, the difference in extreme outside diameter readings (ovality) in any one cross-section shall not exceed 1.5% of the specified outside diameter. Thin wall pipe is defined as having a wall thickness of 3% or less of the outside diameter. • ASTM 358 – Difference between major and minor outside diameters, 1% of specified diameter. • ASTM 671 – Difference between major and minor outside diameters, 1% of specified diameter. • ASTM 672 – Difference between major and minor outside diameters, 1% of specified diameter. • ASTM 691 – Difference between major and minor outside diameters, 1% of specified diameter. For wrought steel butt-welding fittings (e.g. elbows, tees, reducers, weld caps), requirements are provided in ASME B16.9.	---
Out-Of-Roundness In Piping Under External Pressure	Same as for internal pressure	---
Centerline Offset Weld Misalignment – Longitudinal Joints	The tolerance defaults to the tolerance of ASTM standard pipe as purchased, or requirement stipulated for centerline offset misalignment of circumferential joints.	328.4.3(b)
Centerline Offset Weld Misalignment - Circumferential Joints	Inside surfaces of components at ends to be joined in girth or miter groove welds shall be aligned within dimensional limits in the WPS and the engineering design.	328.4.3(a)
Angular Weld Misalignment	An angular offset of three degrees (3°) or less is considered acceptable without additional design considerations.	304.2.3

Table 8.5
Overview Of Fabrication Tolerances – API Standard 620

Fabrication Tolerance	Requirement	Code Reference
Out-Of-Plumbness For Tank Shells	Out of plumbness from top of shell to bottom of shell shall not exceed 1/200 of the total tank height.	4.5.2
Out-Of-Roundness For Tank Shells	Maximum allowable out-of-roundness for tank shells, measured as the difference between the maximum and minimum diameters, shall not exceed 1% of average diameter or 300 mm (12 in), whichever is less, except as modified for flat bottom tanks for which the radii measured at 300 mm (12 in) above the bottom corner weld shall not exceed the tolerances shown below. D < 12 m (40 ft) — Tol = 13 mm (1/2 in) 12 m (40 ft) ≤ D < 46 m (150 ft) — Tol = 19 mm (3/4 in) 46 m (150 ft) ≤ D < 76 m (250 ft) — Tol = 25 mm (1 in) D > 76 m (250 ft) — Tol = 32 mm (1-1/4 in) Where D diameter of the tank in meters or feet and Tol tolerance on the radius. Skirts or cylindrical ends of formed tops shall have a maximum difference between maximum and minimum diameters of 1% of the nominal diameter.	4.5.3
Centerline Offset Weld Radial Misalignment – All Butt Joints	For $t \leq$ 6 mm (1/4 in) — e = 2 mm (1/16 in) For $t >$ 6 mm (1/4 in) — e = min [t/4, 3 mm] or e = min [t/4, 1/8 in] Where t plate thickness and e allowable radial misalignment or offset.	4.14
Local Deviations Such As Angular Weld Misalignment (Peaking) And Or Flat Spots	Using a 910 mm (36 in) horizontal sweep board with a radius equal to the nominal radius of the tank, peaking at vertical joints shall not exceed 13 mm (1/2 in) for steel shells and 25 mm (1 in) for aluminum shells (see API 620, Appendix Q). Using a 910 mm (36 in) vertical straight sweep board, banding at horizontal joints shall not exceed 13 mm (1/2 in) for steel shells and 25 mm (1 in) for aluminum shells (see API 620, Appendix Q). Flat spots shall not exceed appropriate flatness and waviness requirements specified in ASTM A6 or ASTM A20 for carbon and alloy steels, ASTM A480 for stainless steels, and Table 3.13 of ANSI H35.2 for aluminum.	4.5.4

Table 8.6
Overview Of Fabrication Tolerances – API Standard 650

Fabrication Tolerance	Requirement	Code Reference
Out-of-Plumbness	The maximum out of plumbness of the top of the shell of revolution to the bottom of the shell shall not exceed 1/200 of the total tank height.	5.5.2
Out-Of-Roundness For Tank Shells	Radii measured at 300 mm (12 in) above the bottom corner weld shall not exceed the tolerances shown below. D < 12 m (40 ft) — Tol = 13 mm (1/2 in) 12 m (40 ft) ≤ D < 46 m (150 ft) — Tol = 19 mm (3/4 in) 46 m (150 ft) ≤ D < 76 m (250 ft) — Tol = 25 mm (1 in) D > 76 m (250 ft) — Tol = 32 mm (1-1/4 in) Where D diameter of the tank in meters or feet and Tol tolerance on the radius.	5.5.3
Centerline Offset Weld Misalignment – Longitudinal Joints	For t ≤ 16 mm (5/8 in) — e = 2 mm (1/16 in) For t > 16 mm (5/8 in) — e = min [t/10, 3 mm] or e = min [t/10, 1/8 in] Where t plate thickness and e allowable radial misalignment or offset.	5.2.3.1
Centerline Offset Weld Misalignment - Circumferential Joints	The upper plate shall not project by more than 20 percent of the thickness of the upper plate, with a maximum projection of 3mm (1/8 in); however, for upper plates less than 8 mm (5/16 in) thick, the maximum projection shall be limited to 2 mm (1/16 in).	5.2.3.2
Local Deviations Such As Angular Weld Misalignment (Peaking) And Or Flat Spots	Using a 910 mm (36 in) horizontal sweep board with a radius equal to the nominal radius of the tank, peaking at vertical joints shall not exceed 13 mm (1/2 in). Using a 910 mm (36 in) vertical straight sweep board, banding at horizontal joints shall not exceed 13 mm (1/2 in). Flat spots shall not exceed appropriate flatness and waviness requirements specified in ASTM A6 or ASTM A20.	5.5.4

Table 8.7
Overview Of Fabrication Tolerances For Reconstructed Tanks – API Standard 653

Fabrication Tolerance	Requirement	Code Reference
Out-of-Plumbness	The maximum out of plumbness of the top of the shell of revolution to the bottom of the shell shall not exceed 1/100 of the total tank height, with a maximum deviation of 130 mm (5 in).	8.5.2.1
Out-Of-Roundness For Tank Shells	Radii measured at 304 mm (12 in) above the bottom corner weld shall not exceed the tolerances shown below. D < 12 m (40 ft) — Tol = 13 mm (1/2 in) 12 m (40 ft) ≤ D < 46 m (150 ft) — Tol = 19 mm (3/4 in) 46 m (150 ft) ≤ D < 76 m (250 ft) — Tol = 25 mm (1 in) D > 76 m (250 ft) — Tol = 32 mm (1-1/4 in) Where D diameter of the tank in meters or feet and Tol tolerance on the radius.	8.5.3
Centerline Offset Weld Misalignment – Longitudinal Joints	For t ≤ 16 mm (5/8 in) — e = 2 mm (1/16 in) For t > 16 mm (5/8 in) — e = min[t/10, 3 mm] or e = min[t/10, 1/8 in] Where t plate thickness and e allowable radial misalignment or offset.	8.4.4.1
Centerline Offset Weld Misalignment - Circumferential Joints	The upper plate shall not project by more than 20 percent of the thickness of the upper plate, with a maximum project of 3 mm (1/8 in); however, for upper plates less than 8 mm (5/16 in) thick, the maximum projection shall be limited to 2 mm (1/16 in).	8.4.4.2
Local Deviations Such As Angular Weld Misalignment (Peaking) And Or Flat Spots	Using a 910 mm (36 in) horizontal sweep board with a radius equal to the nominal radius of the tank, peaking at vertical joints shall not exceed 25 mm (1 in). Using a 910 mm (36 in) vertical straight sweep board, banding at horizontal joints shall not exceed 25 mm (1 in).	8.5.4 & 8.5.5

Table 8.8
Equations For The Ratio Of Induced Bending Stress To Applied Membrane Stress For A Flat Plate With Centerline Offset And Angular Misalignment

Type Of Misalignment	Equations For R_b
Flat Plate – Centerline Offset (see Figure 8.2) (1)	$R_{bs}^{pc} = 1 + \left(\frac{6e}{t_{1c}}\right)\left(1 + \left(\frac{t_{2c}}{t_{1c}}\right)^{1.5}\right)^{-1}$ Limitations: None
Flat Plate – Angular Misalignment (see Figure 8.4) (1)	$R_{bs}^{pa} = \left(\frac{3\delta}{t_c}\right) C_f$ where $C_f = \frac{\tanh\frac{\beta}{2}}{\frac{\beta}{2}}$ *for fixed ends* $C_f = \frac{2\tanh\beta}{\beta}$ *for pinned ends* $\beta = \frac{L}{t_c}\sqrt{\frac{3\sigma_m}{E_y}}$ *(in radians)* $\delta = \frac{L\theta_p}{4}$ Limitations: None

Notes:
1. The equation for R_b and R_{bs} are dimensionless.

Table 8.9
Equations For The Ratio Of Induced Bending Stress To Applied Membrane Stress For The Circumferential Joints Of A Cylinder With Centerline Offset And Angular Misalignment

Type Of Misalignment	Equations For R_b
Centerline Offset (see Figure 8.3) (1)	$R_b^{ccjc} = \text{abs}\left[\frac{12}{R_1 t_{1c}}\left(0.25672 R_2 t_{2c}\left\{\frac{C_1}{C_3}\right\} + \frac{eR_a}{2}\left\{\frac{C_2}{C_3}\right\}\right)\right]$ $R_{bs}^{ccjc} = 1 + \left(\frac{6e}{t_{1c}}\right)\left(1+\rho^{1.5}\right)^{-1}$ where $C_1 = (\rho - 1)\left(\rho^2 - 1\right)$ $C_2 = \rho^2 + 2\rho^{1.5} + 1$ $C_3 = \left(\rho^2 + 1\right)^2 + 2\rho^{1.5}(\rho + 1)$ $\rho = \frac{t_{2c}}{t_{1c}}$ *where* $t_{2c} \geq t_{1c}$ $e = R_1 - R_2$ *where e is a negative number if* $R_2 > R_1$; *otherwise, e is a positive number* $R_a = \frac{R_1 + R_2}{2}$ Limitations: $\frac{R_1}{t_{1c}} \geq 10$, $\frac{R_2}{t_{2c}} \geq 10$, and $0.0 < \frac{e}{t} \leq 1.0$

Table 8.9
Equations For The Ratio Of Induced Bending Stress To Applied Membrane Stress For The Circumferential Joints Of A Cylinder With Centerline Offset And Angular Misalignment

Type Of Misalignment	Equations For R_b
Angular Misalignment (see Figures 8.6) (1)	$R_b^{ccja} = \max\left[\frac{C_1}{C_2}, \frac{C_3}{C_4}\right]$ where $C_1 = \left(\begin{array}{l} 0.023748 - 0.010087\ln\left[S_p\right] + 0.0014571\left(\ln\left[S_p\right]\right)^2 + \\ 11.631\theta_p + 10.476\theta_p^2 - 23.792\theta_p^{\,3} \end{array}\right)$ $C_2 = \left(\begin{array}{l} 1.0 - 0.36581\ln\left[S_p\right] + 0.062036\left(\ln\left[S_p\right]\right)^2 - \\ 0.0044239\left(\ln\left[S_p\right]\right)^3 + 0.20821\theta_p \end{array}\right)$ $C_3 = \left(\begin{array}{l} -0.037285 - 0.0051687\ln\left[S_p\right] + 0.0072395\left(\ln\left[S_p\right]\right)^2 + \\ 14.865\theta_p - 33.1636\theta_p^{\,2} + 91.061\theta_p^{\,3} \end{array}\right)$ $C_4 = \left(\begin{array}{l} 1.0 - 0.35912\ln\left[S_p\right] + 0.065885\left(\ln\left[S_p\right]\right)^2 - \\ 0.0054959\left(\ln\left[S_p\right]\right)^3 + 0.044263\theta_p \end{array}\right)$ $S_p = \sqrt{\frac{12\left(1-\nu^2\right)PR^3}{E_y t_c^3}}$ $\theta_p = \arctan\left(\frac{2\delta}{L}\right) \qquad (in\ radians)$ Note: in the above equations, θ_p is in radians. Equations for R_{bs}^{ccja} are currently under development. Limitations: $10 \le \frac{R}{t_c} \le 500$, $0^o \le \theta_p \le 10^o$, and $0.0 \le S_p \le 67.5$
Notes: 1. The equation for R_b and R_{bs} are dimensionless.	

Table 8.10
Equations For The Ratio Of Induced Bending Stress To Applied Membrane Stress For The Longitudinal Joints Of A Cylinder With Centerline Offset And Angular Misalignment

Type Of Misalignment	Equations For R_b
Centerline Offset (see Figure 8.2) (1)	$R_b^{cljc} = \dfrac{C_1}{C_2}$ with S_p from Table 8.9, and $C_1 = \left(\begin{array}{l} 3.8392\left(10^{-3}\right) + 3.1636\left(\dfrac{e}{t_c}\right) + 1.2377\left(\dfrac{e}{t_c}\right)^2 - \\ 4.0582\left(10^{-3}\right) S_p + 3.4647(10^{-4}) S_p^2 + 3.1205(10^{-6}) S_p^3 \end{array} \right)$ $C_2 = 1.0 + 0.41934\left(\dfrac{e}{t_c}\right) + 9.7390\left(10^{-3}\right) S_p$ Limitations: $10 \le \dfrac{R}{t_c} \le 400$, $0.0 \le \dfrac{e}{t_c} \le 1.0$, and $1.0 \le S_p \le 50.0$
Angular Misalignment, Local Peaking (see Figures 8.4 and 8.5) (1)(2)	$R_b^{clja} = \left(\dfrac{6\delta}{t_c}\right) C_f$ Values of C_f can be determined from Figure 8.13 using S_p from Table 8.9 and δ/R, or by using the series solution provided below: $C_f = 1 - \dfrac{\theta_p}{3\pi} - \dfrac{4}{\pi\theta_p^2}\left(\theta_p - \sin\theta_p\right) - \dfrac{4S_p^2}{\pi\theta_p^2} \sum_{n=2}^{\infty} \dfrac{\left(n\theta_p - \sin n\theta_p\right)}{n^3\left(n^2 - 1 + S_p^2\right)}$ with, $\theta_p = \arccos\left(\dfrac{1}{1+\delta/R}\right) \qquad (in\ radians)$ Limitations: $\dfrac{R}{t_c} \ge 10$ and $0.0 \le S_p \le 30.0$

Table 8.10
Equations For The Ratio Of Induced Bending Stress To Applied Membrane Stress For The Longitudinal Joints Of A Cylinder With Centerline Offset And Angular Misalignment

Type Of Misalignment	Equations For R_b
Angular Misalignment, Global Peaking (see Figures 8.4 and 8.5) (1)(2)	$R_b^{clja} = \left(\frac{6\delta}{t_c}\right) C_f$ with S_p from Table 8.9, and $C_f = 0.5 - \frac{\pi}{2k}\cot k\pi - \frac{k^2-1}{2k^2} + \frac{1}{2k^2-1}$ *for* $S_p^2 < 1$ $C_f = 0.5 + \frac{\pi}{2k}\coth k\pi - \frac{k^2+1}{2k^2} - \frac{1}{k^2+1}$ *for* $S_p^2 \geq 1$ $k^2 = 1 - S_p^2$ *for* $S_p^2 < 1$ $k^2 = S_p^2 - 1$ *for* $S_p^2 \geq 1$

Notes:

1. The equation for R_b is dimensionless.
2. Establish an appropriate cutoff for the series solution for C_f, e.g., the change in C_f is less than .01%.

Table 8.11
Equations For The Ratio Of Induced Bending Stress To Applied Membrane Stress For The Circumferential Joints Of A Sphere With Centerline Offset And Angular Misalignment

Type Of Misalignment	Equations For R_b
Centerline Offset (see Figure 8.2) (1)	$R_b^{scjc} = \left(\begin{array}{l} 9.6291\left(10^{-3}\right) + 3.0791\left(\frac{e}{t_c}\right) - 0.24587\left(\frac{e}{t_c}\right)^2 + 0.025734\left(\frac{e}{t_c}\right)^3 + \\ 0.059281\left(\frac{e}{t_c}\right)^4 - 6.1979\left(10^{-3}\right) S_p + 1.9252\left(10^{-4}\right) S_p^2 + \\ 1.9815\left(10^{-6}\right) S_p^3 - 1.8194\left(10^{-7}\right) S_p^4 + 2.0698\left(10^{-9}\right) S_p^5 \end{array} \right)$ with S_p from Table 8.9. Limitations: $10 \le \frac{R}{t_c} \le 400$, $0.0 \le \frac{e}{t_c} \le 1.0$, and $0.0 \le S_p \le 50.0$
Angular Misalignment (see Figures 8.4 and 8.5) (2)	$R_b^{scja} = \frac{C_1}{C_2}$ with S_p from Table 8.9, and $C_1 = 3.082 + 1.7207(10^{-3}) S_p + 1.3641\psi + 0.062407\psi^2 - 0.033961\psi^3$ $C_2 = 1.0 + 8.9503(10^{-3}) S_p - 2.8724(10^{-4}) S_p^2 + 5.0797(10^{-6}) S_p^3 - 0.21717\psi$ $\psi = \ln\left(\frac{\delta}{C_{ul}}\right)$ Limitations: $10 \le \frac{R}{t_c} \le 300$, $0^o \le \theta_p \le 25^o$ (θ_p is computed using the equation in Table 8.9) and $0.0 \le S_p \le 30.0$

Notes:

1. The equation for R_b is dimensionless.
2. In the equation for R_b, $C_{ul} = 1.0$ if the units of inches are used, and $C_{ul} = 25.4$ if the units of millimeters are used.

Table 8.12
Stress Data Required for a Fatigue Assessment

Type of Fatigue Analysis	Stress Data
Elastic Stress Analysis And Structural Stress Annex B1, paragraph B1.5.5)	Flat Plate – Weld misalignment $\Delta\sigma_m = \sigma_{ms}$ $\Delta\sigma_b = \sigma_{ms}\left(R_b^{pc} + R_b^{pa}\right)$ Cylinder, Circumferential Weld Joint – Weld misalignment $\Delta\sigma_m = \sigma_m + \sigma_{ms}$ $\Delta\sigma_b = \sigma_m\left(R_b^{ccjc} + R_b^{ccja}\right) + \sigma_{ms}\left(R_{bs}^{ccjc} + R_{bs}^{ccja}\right)$ Cylinder, Longitudinal Weld Joint – Weld misalignment and out-of-roundness $\Delta\sigma_m = \sigma_m$ $\Delta\sigma_b = \sigma_m\left(R_b^{cljc} + R_b^{clja} + R_b^{or}\right)$ Spheres, Circumferential Weld Joint – Weld misalignment $\Delta\sigma_m = \sigma_m$ $\Delta\sigma_b = \sigma_m\left(R_b^{scjc} + R_b^{scja}\right)$
Elastic Stress Analysis And Structural Stress Annex B1, paragraph B1.5.5)	Flat Plate – Weld misalignment (1) $\Delta S_P = \sigma_{ms}\left(1 + R_b^{pc} + R_b^{pa}\right)K_f$ Cylinder, Circumferential Weld Joint – Weld misalignment (1) $\Delta S_P = \left[\sigma_m\left(1 + R_b^{ccjc} + R_b^{ccja}\right) + \sigma_{ms}\left(1 + R_{bs}^{ccjc} + R_{bs}^{ccja}\right)\right]K_f$ Cylinder, Longitudinal Weld Joint – Weld misalignment and out-of-roundness (1) $\Delta S_P = \sigma_m\left(1 + R_b^{cljc} + R_b^{clja} + R_b^{or}\right)K_f$ Spheres, Circumferential Weld Joint – Weld misalignment (1) $\Delta S_P = \sigma_m\left(1 + R_b^{scjc} + R_b^{scja}\right)K_f$

Notes:

1. Recommendations for determining the fatigue strength reduction factor, K_f, are provided in Reference 11.

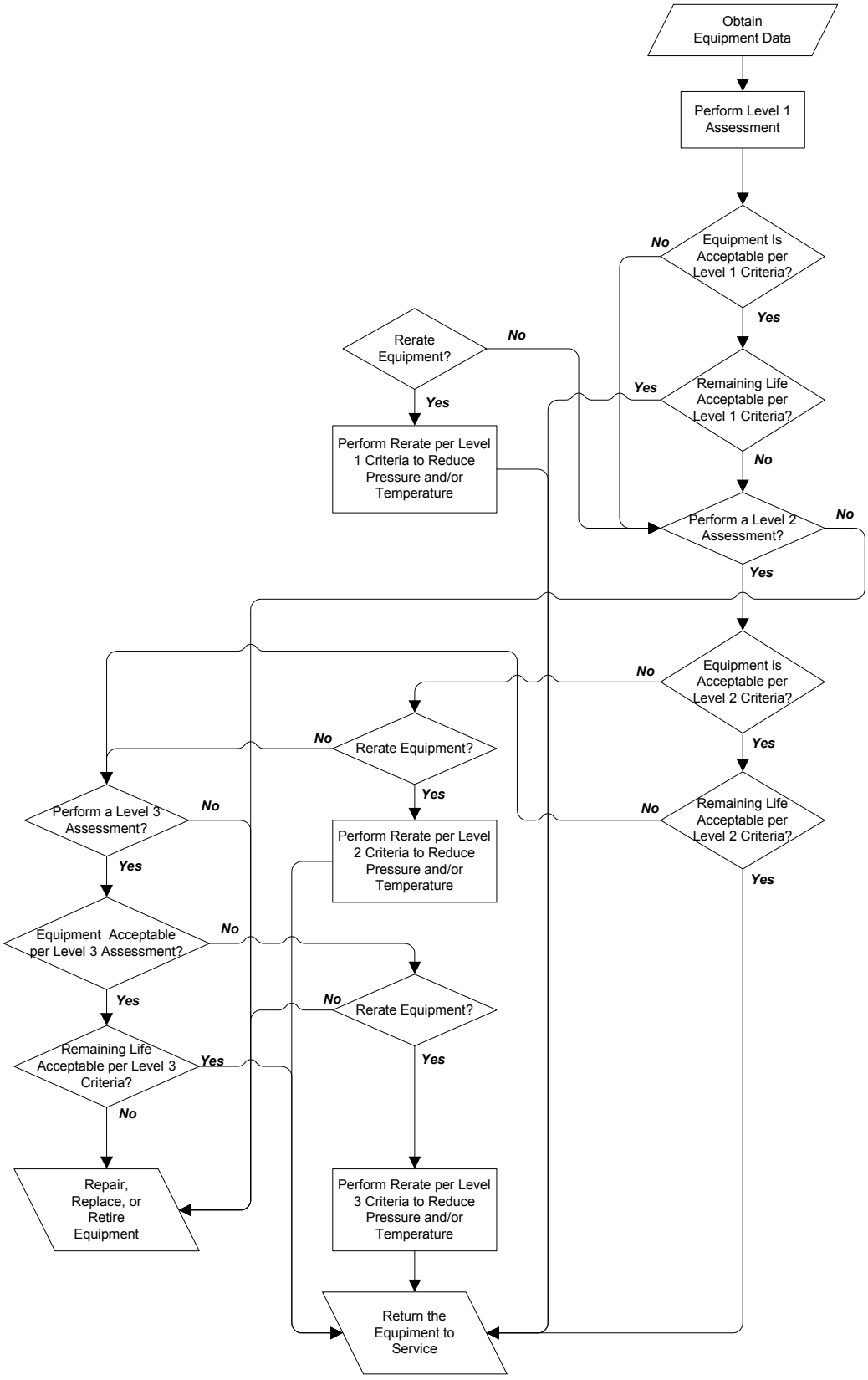

Figure 8.1 – Overview of the Assessment Procedures to Evaluate a Component with a Weld Misalignment or Shell Distortion

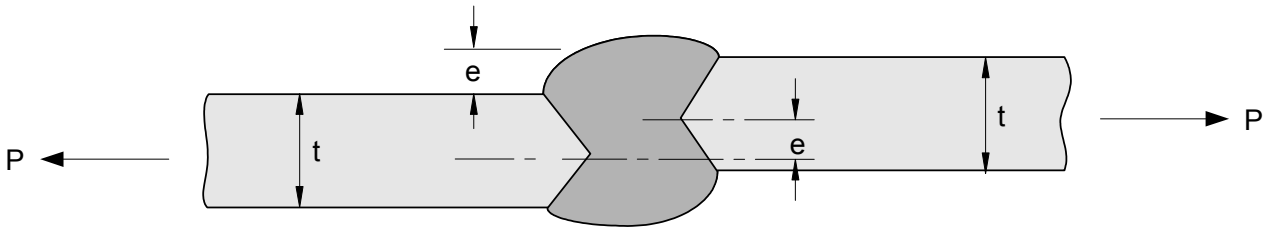

(a) Same Thickness -- Inside and Outside Surfaces Not Aligned

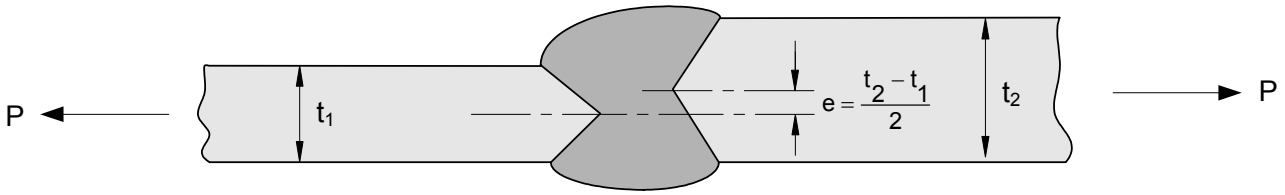

(b) Different Thickness -- Alignment With One Surface

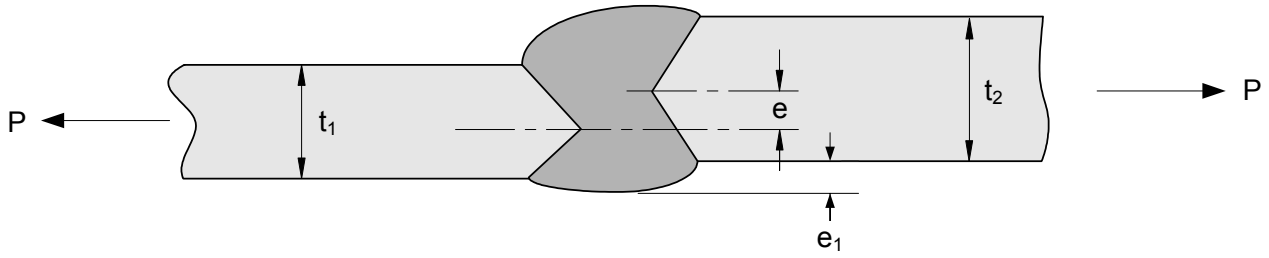

(c) Different Thickness -- Inside and Outside Surfaces Not Aligned

Figure 8.2 – Centerline Offset Weld Misalignment in Butt Weld Joints in Flat Plates

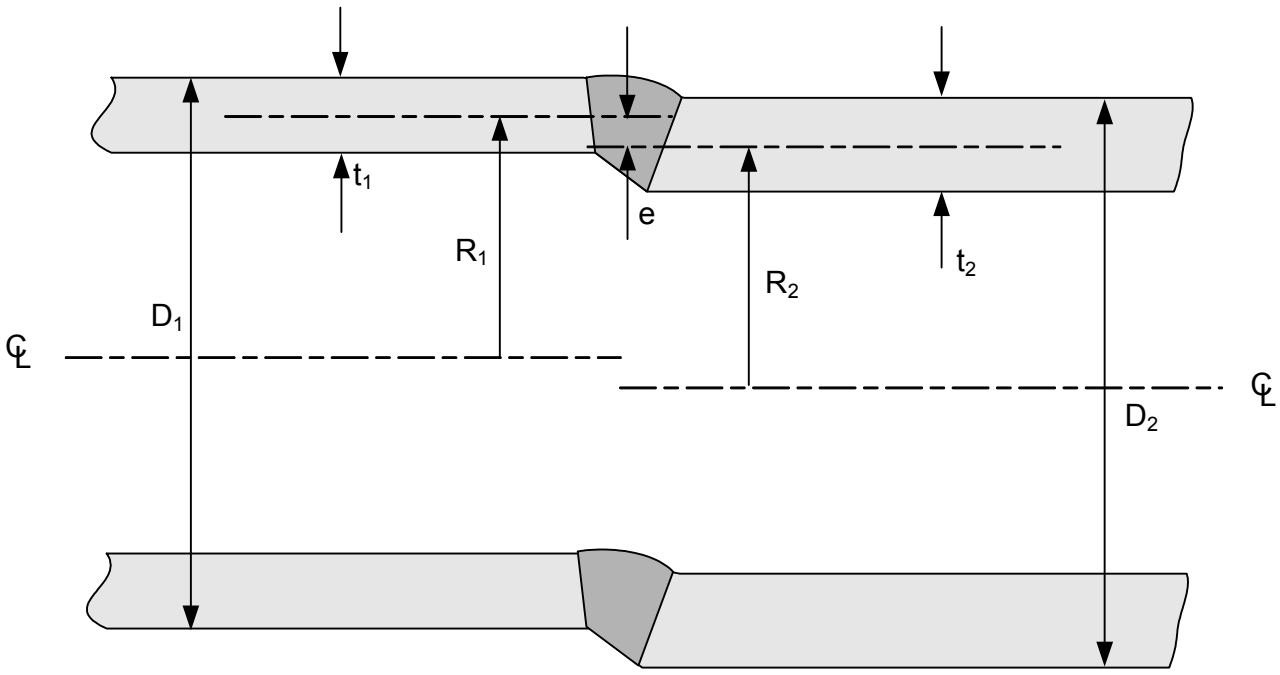

(a) Weld Misalignment - Equal Diameters ($D_1 = D_2$)

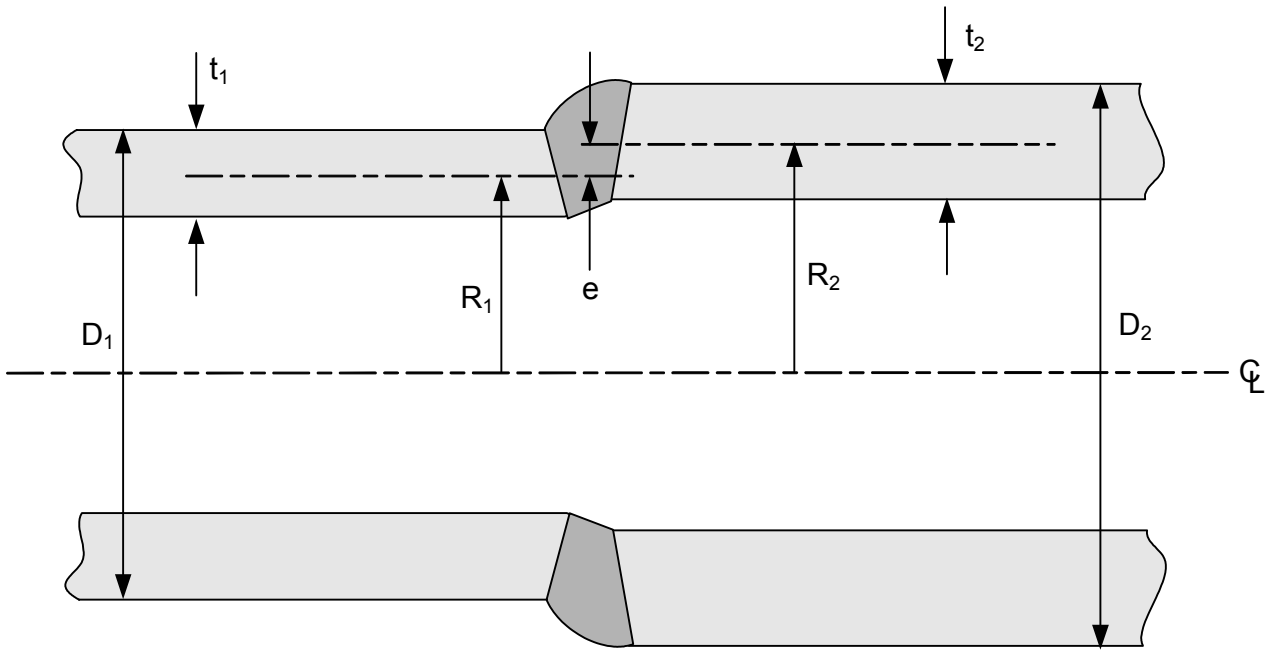

(b) Weld Misalignment - Unequal Diameters ($D_1 \neq D_2$)

Figure 8.3 – Centerline Offset Weld Misalignment in Cylindrical Shell Circumferential Weld Joints

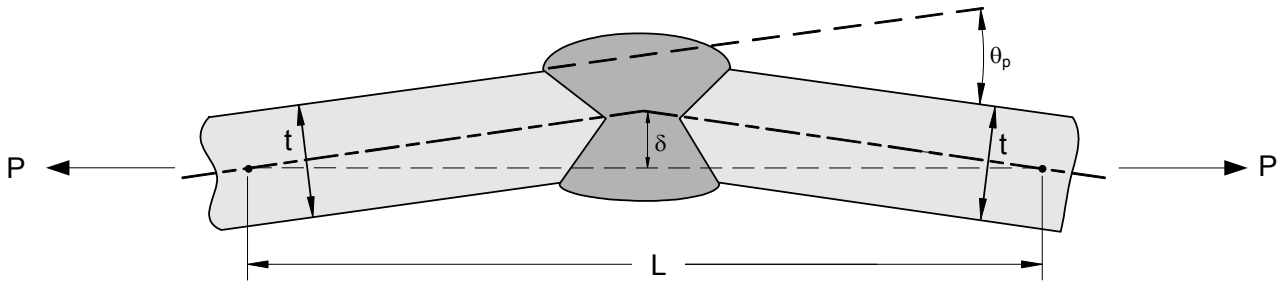

(a) Angular Weld Misalignment

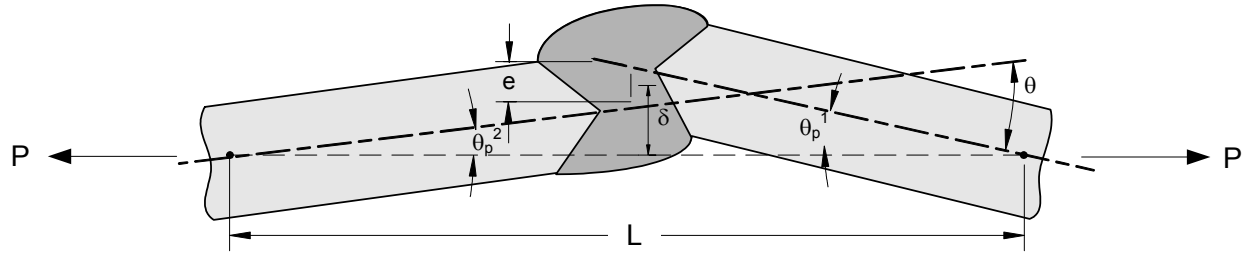

(b) Angular and Centerline Offset Weld Misalignment

Notes: The dimension L is established as shown in Figure 8.6.

Figure 8.4 – Angular Misalignment in Butt Weld Joints in Flat Plates

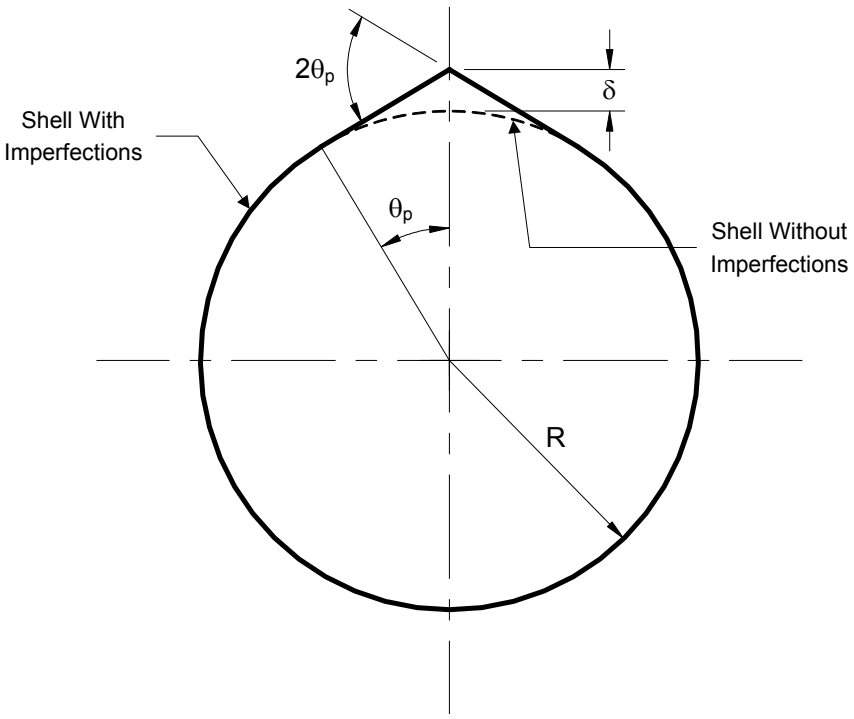

(a) Local Peaking - Cylinder and Sphere

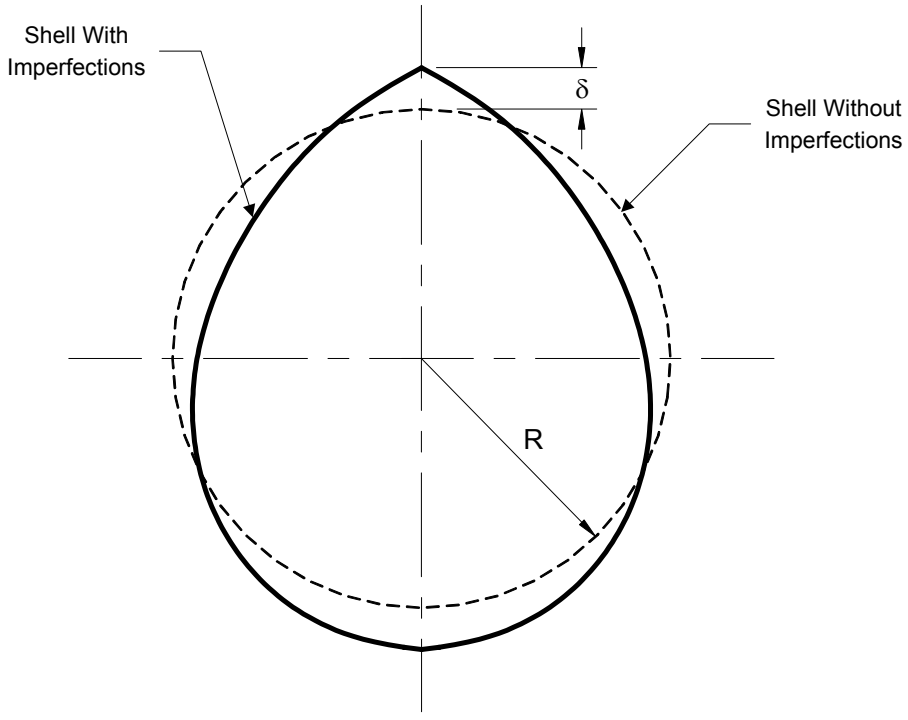

(b) Global Peaking - Cylindrical Shells Only

Figure 8.5 – Angular Misalignment in a Cylindrical Shell Longitudinal Weld and Spherical Shell Circumferential Weld

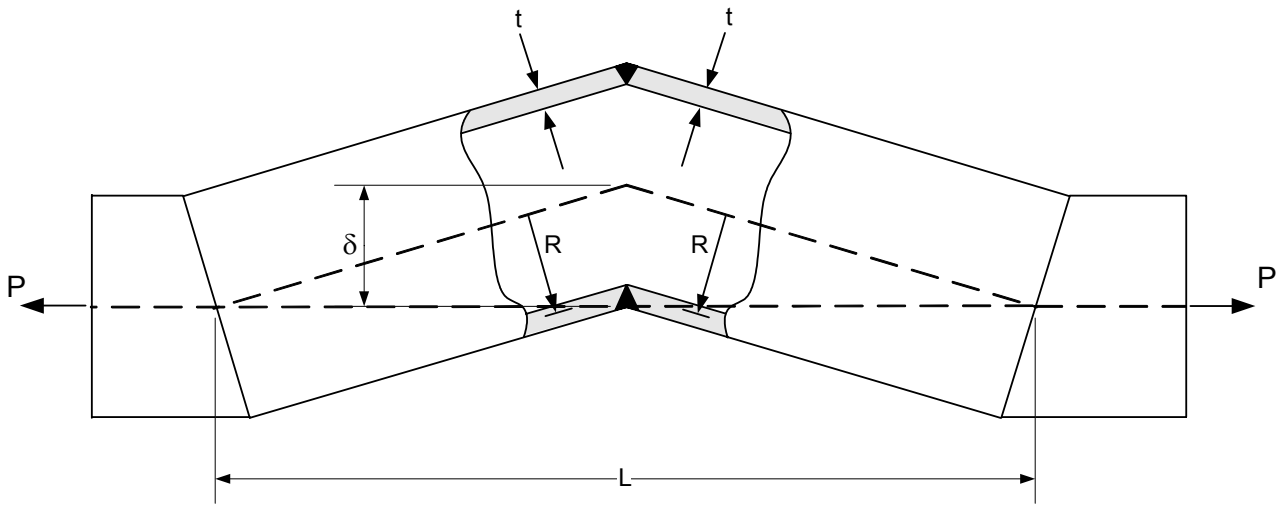

Notes:

1. The dimension L is defined as the length of the base of a triangle whose height is measured from the line of force, P, and whose height equals the angular peaking, δ.
2. Note that as the height of the angular peaking, $\delta \to 0$, $L \to \infty$.

Figure 8.6 – Angular Misalignment in a Cylindrical Shell Circumferential Seam

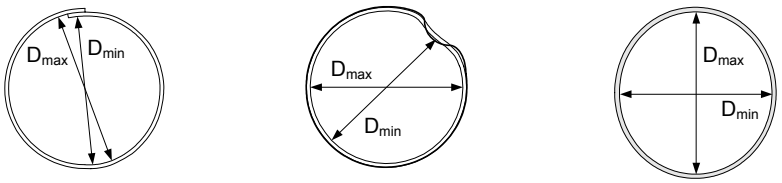

(a) Examples of Differences Between Maximum and Minimum Diameters In Cylindrical, Conical, and Spherical Shells

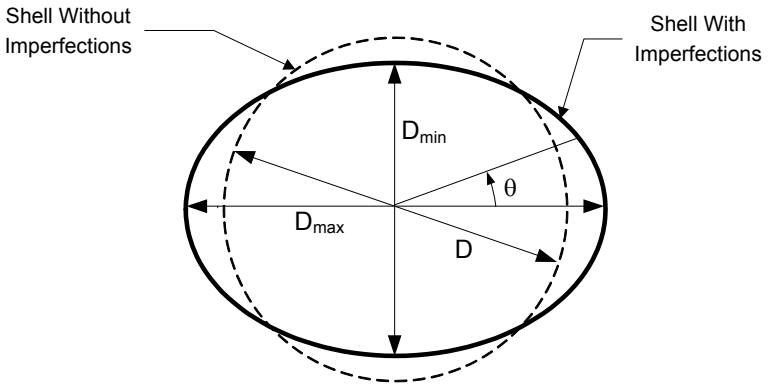

(b) Global Out-Of-Roundness

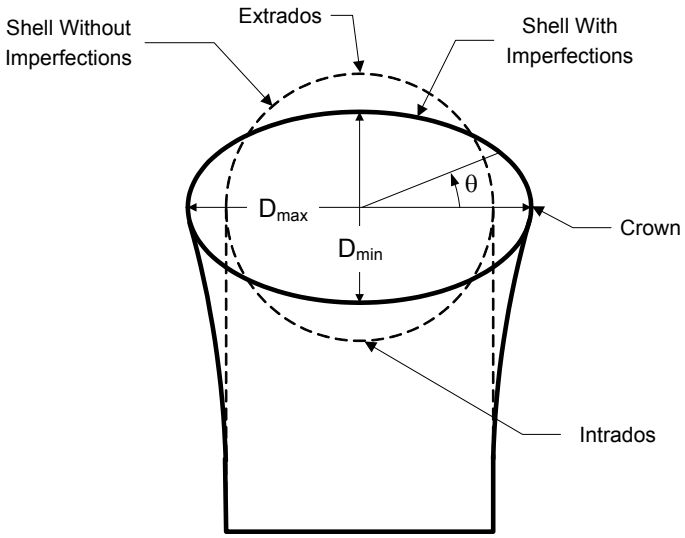

(c) Ovalization of a Pipe Bend

Figure 8.7 – Global Circumferential Out-Of-Roundness

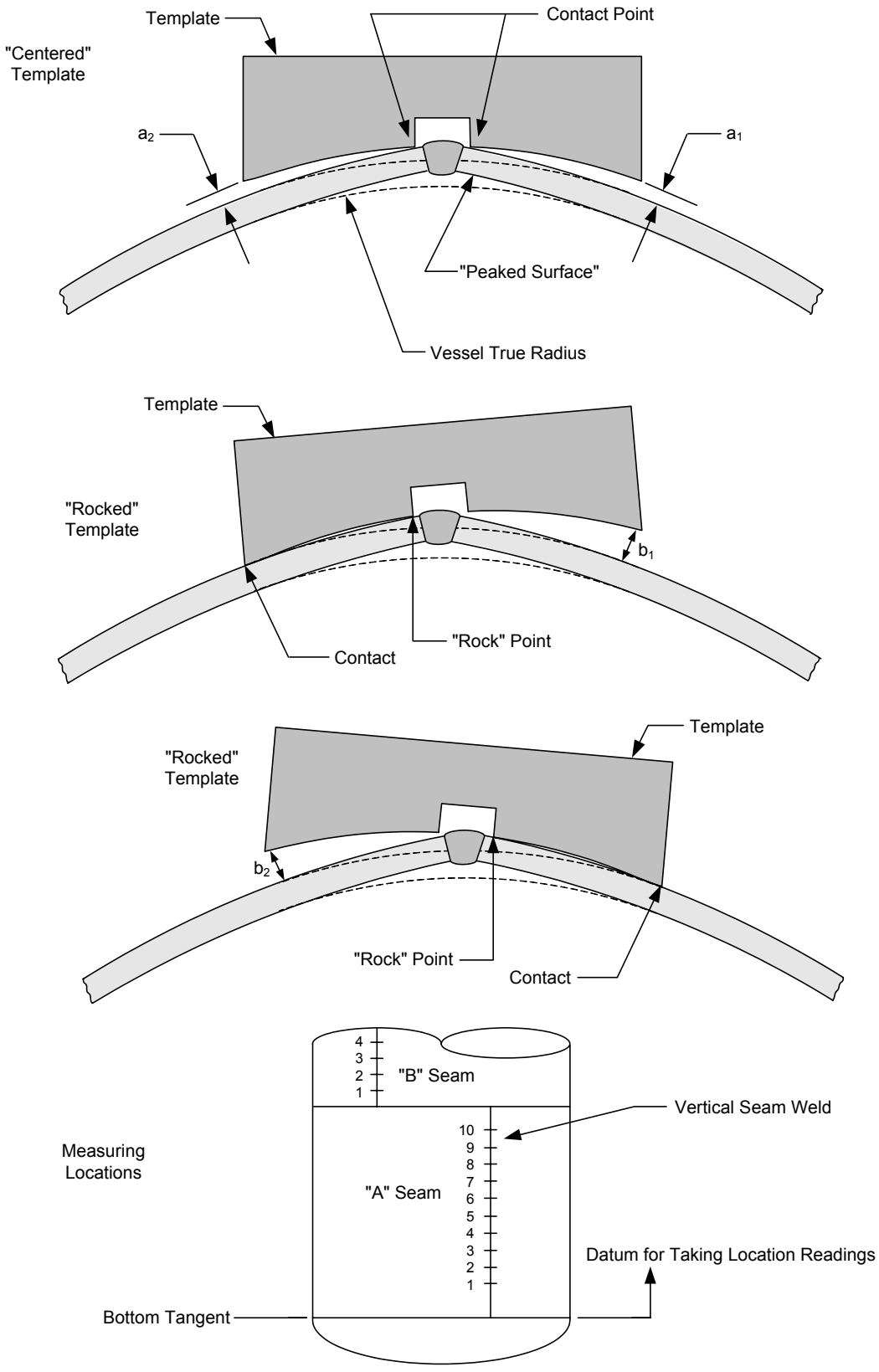

Figure 8.8 – Method of Measurement to Determine the Extent of Peaking in a Shell

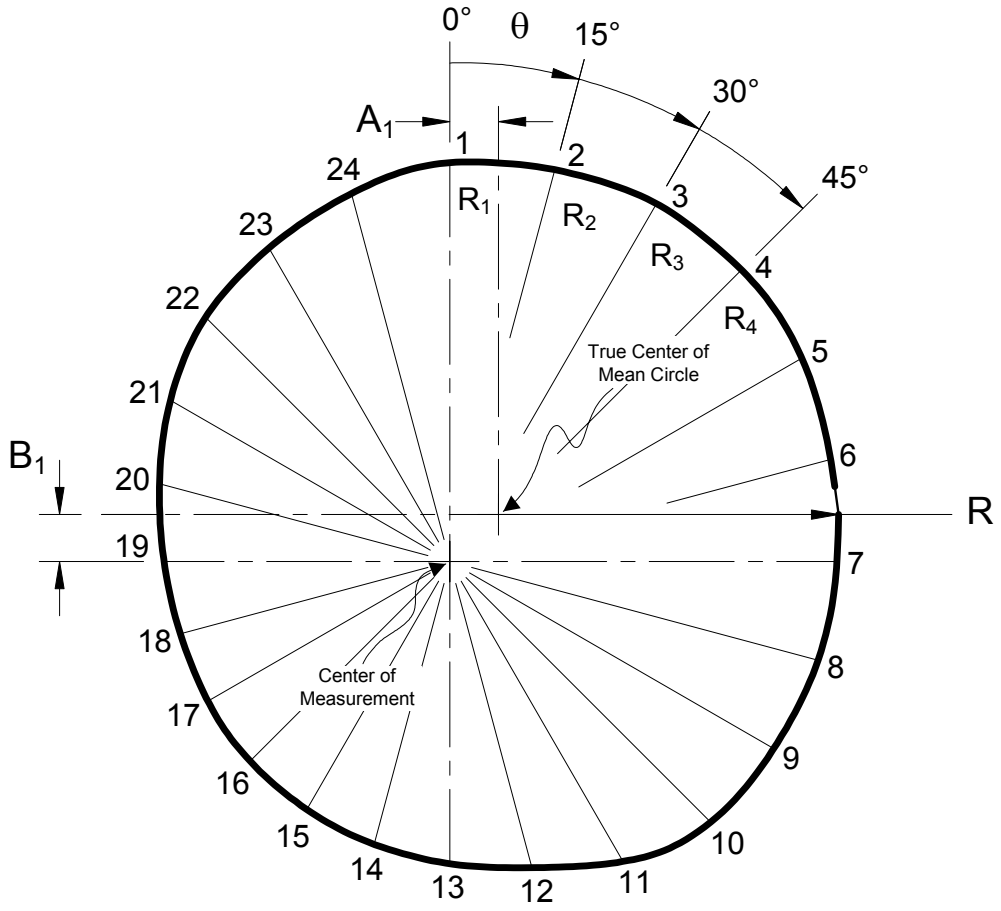

Figure 8.9 – Method of Measurement to Determine the Extent of Out-Of-Roundness in a Cylinder

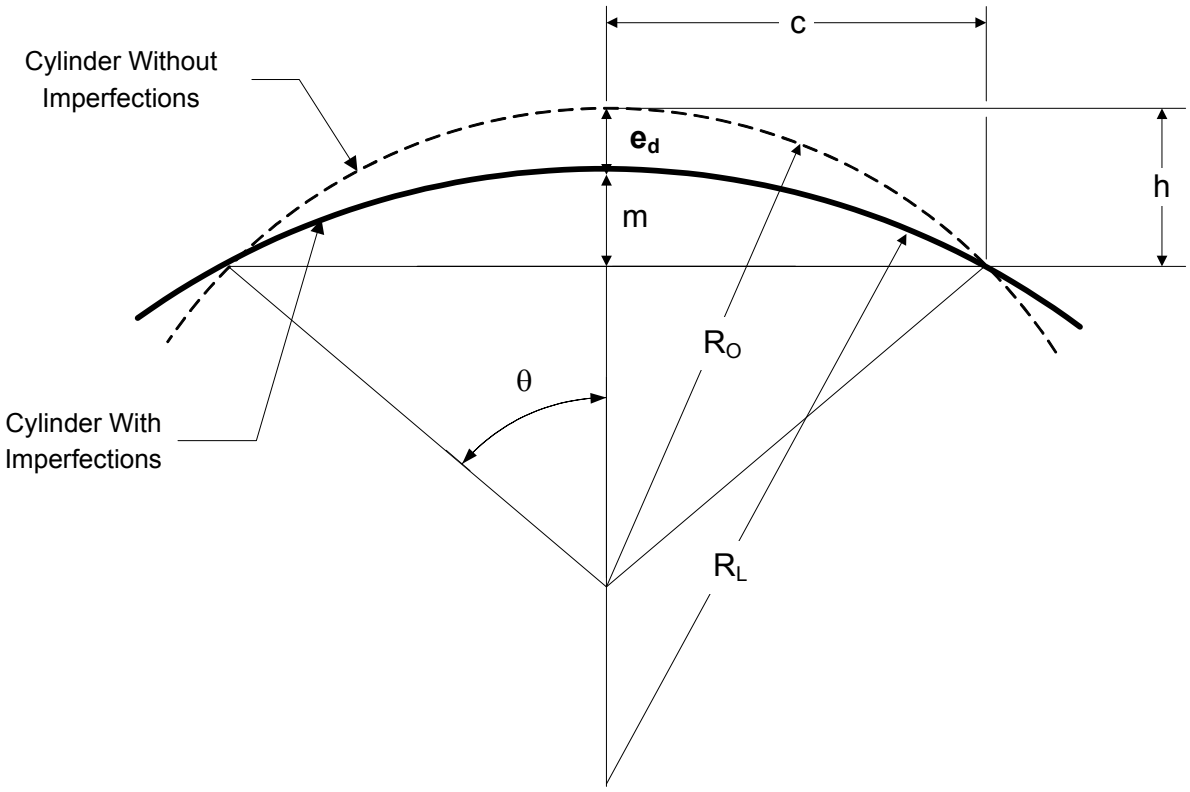

Notes: The following equations can be used to compute the local radius, R_L. The value n is computed using the equations in paragraph 8.4.3.5.b. The maximum deviation from a true cylinder, e_d, is obtained by measurement.

$$\theta = \frac{90}{n} \tag{8.38}$$

$$h = R_o\left(1 - \cos\theta\right) \tag{8.39}$$

$$c = R_o \sin\theta \tag{8.40}$$

$$m = h - e_d \tag{8.41}$$

$$R_L = \frac{m^2 + c^2}{2m} \tag{8.42}$$

Figure 8.10 – Definition of Local Radius Used to Compute the Permissible External Pressure in a Cylindrical Shell with a Geometrical Deviation

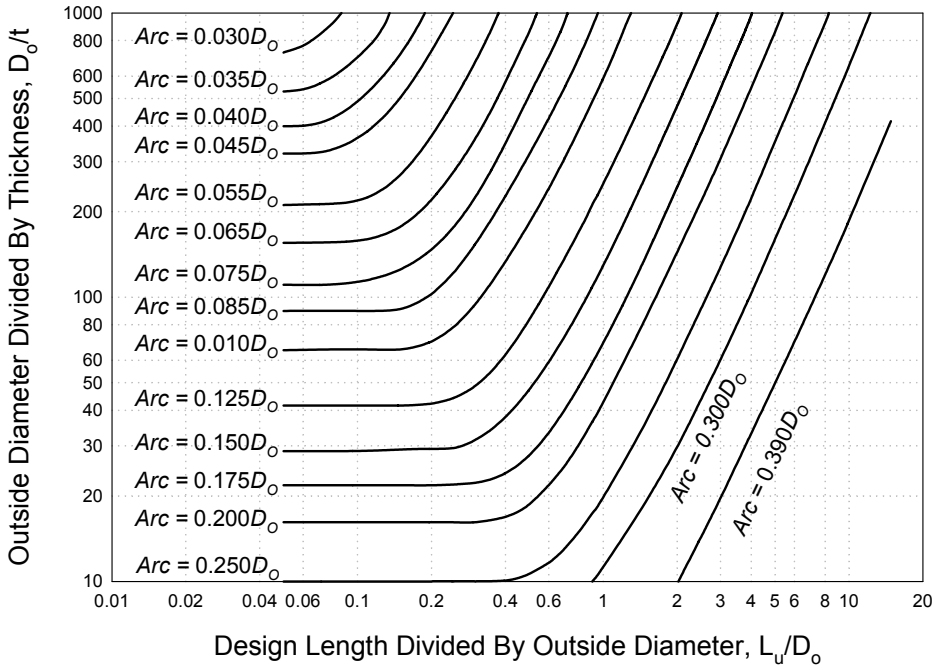

Notes:

1. Cylindrical Shells – L_u unsupported length of the cylinder and D_o outside diameter.
2. Conical Shells – L_u and D_o are established using the following equations for any cross section having a diameter D_x. In these equations D_L and D_S are the cone large end and small end outside diameters, respectively and L unsupported length of the conical section under evaluation.

$$L_{ec} = \left(\frac{L}{2}\right)\left(1+\frac{D_S}{D_L}\right)\left(\frac{D_S}{D_L}\right) \tag{8.43}$$

$$D_o = D_x \tag{8.44}$$

3. Spherical Shell – L_u is one-half of the outside diameter and D_o outside diameter of the sphere.
4. Elliptical Head – L_u is one-half of $K_c D_o$ (see Annex A, paragraph A.3.6.b) and D_o outside diameter of the cylinder at the head attachment point.
5. Torispherical Head – L_u crown radius and D_o outside diameter of the cylinder at the head attachment point.
6. For vessels with butt joints, $t = t_c$. For vessels with lap joints, $t = t_c$ and the permissible deviation is $e + t_c$. Where the shell at any cross section is made from plates of different thicknesses t corroded wall thickness (i.e. including metal loss and future corrosion allowance) of the thinnest plate. For cones and conical sections, t shall be determined using the previous rules except that t shall be replaced by $t/\cos\alpha$.

Figure 8.11 – Maximum Arc of a Shell Used as a Basis to Determine the Deviation From Circular Form

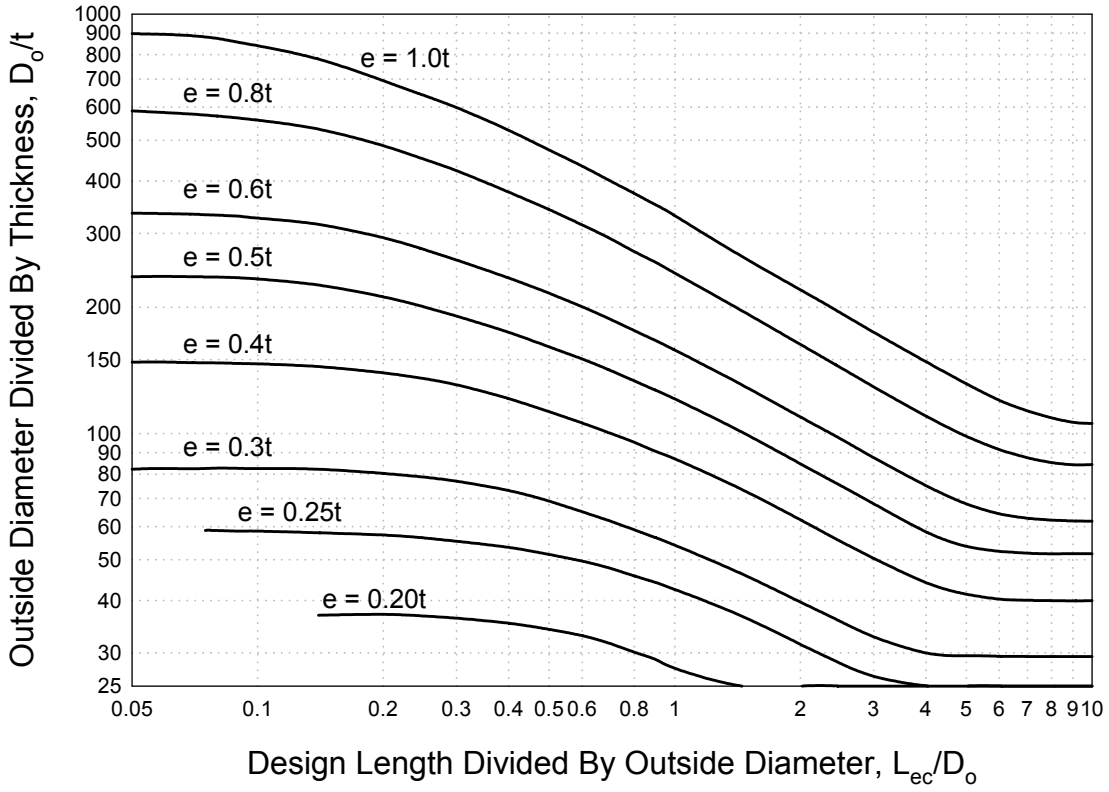

Figure 8.12 – Maximum Permissible Deviation from a Circular Form for Vessels Subject to External Pressure

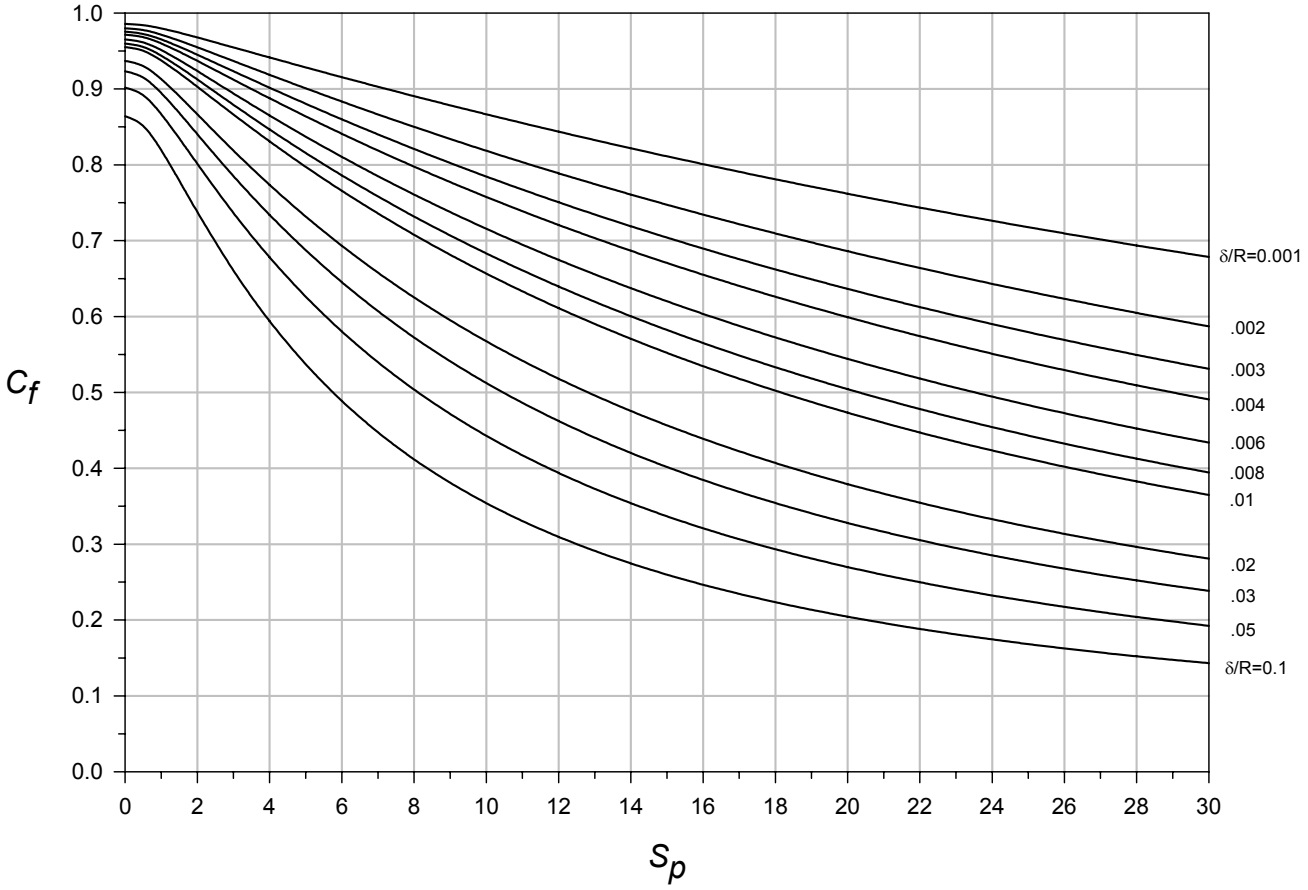

Figure 8.13 – Correction Factor for Angular Weld Misalignment in the Longitudinal Joint of a Cylindrical Shell

PART 9

ASSESSMENT OF CRACK-LIKE FLAWS

PART CONTENTS

9.1 General

9.1.1 Fitness-For-Service (FFS) assessment procedures for evaluating crack-like flaws in components are covered in this Part. These assessment procedures are based on the Failure Assessment Diagram (FAD) method. Details regarding the background and development of the methodology and assessment procedures can be found in [3].

9.1.2 Crack-like flaws are planar flaws that are predominantly characterized by a length and depth, with a sharp root radius. Crack-like flaws may either be surface breaking, embedded, or through-wall. Examples of crack-like flaws include planar cracks, lack of fusion and lack of penetration in welds, sharp groove-like localized corrosion, and branch type cracks associated with environmental cracking.

9.1.2.1 In some cases, it is conservative and advisable to treat volumetric flaws such as aligned porosity or inclusions, deep undercuts, root undercuts, and overlaps as planar flaws, particularly when such volumetric flaws may contain micro-cracks at the root. This is because an NDE examination may not be sensitive enough to determine whether micro-cracks have initiated from the flaw.

9.1.2.2 The assessment procedures in this Part may be used to compare the relative flaw tolerance or evaluate the risk of brittle fracture of an existing component for screening purposes by postulating a standard reference flaw with a depth equal to 25% of the wall thickness and a length equal to six times this depth.

9.1.3 Crack-like flaws may be associated with a wide variety of process environment/material interactions and material damage mechanisms. These environmental/material interactions and the associated damage mechanisms tend to be industry specific; however, the mechanisms associated with similar services (e.g. steam) are common for all industries.

9.1.3.1 An overview of the failure modes and damage mechanisms that are covered by this Standard is given in Annex G. Knowledge of the damage mechanism may affect decisions regarding the following:

a) The choice of material properties to be used in a FFS assessment.

b) The choice of an appropriate crack growth rate.

c) The permissible amount of crack extension prior to the final fracture or the time between inspections.

d) The mode of final failure (e.g. unstable fracture, yielding due to overload of remaining ligament, or leak).

e) The interaction between damage mechanisms (e.g. corrosion and fatigue, creep and fatigue, hydrogen embrittlement and temper-embrittlement, or environmental assisted cracking).

9.1.3.2 Environmental cracks typically occur in multiples and may be branched. The assessment procedures in this Part can be applied to such cracks provided a predominant crack whose behavior largely controls the structural response of the equipment can be identified. The predominant crack in the presence of multiple cracks or branched cracks can be defined through the flaw characterization techniques described in paragraph 9.3.6. When a predominant crack cannot be defined even after re-characterization, more advanced FFS techniques such as damage mechanics (which are outside the scope of this document) are available.

9.2 Applicability and Limitations of the Procedure

9.2.1 The assessment procedures of this Part can be used to evaluate pressurized components containing crack-like flaws. The pressurized components covered include pressure vessels, piping, and tanks that are designed to a recognized code or industry standard.

9.2.2 Specific details pertaining to the applicability and limitations of each of the assessment procedures are discussed below.

9.2.2.1 The Level 1 and 2 Assessment procedures in this Part apply only if all of the following conditions are satisfied:

a) The original design criteria were in accordance with Part 2, paragraph 2.2.2.

b) The component is not operating in the creep range (see Part 4, paragraph 4.2.3.1.b).

c) Dynamic loading effects are not significant (e.g. earthquake, impact, water hammer, etc.).

d) The crack-like flaw is subject to loading conditions and/or an environment that will not result in crack growth. If a flaw is expected to grow in service, it should be evaluated using a Level 3 Assessment, and the remaining life should be evaluated using the procedures of paragraph 9.5.

e) The following limiting conditions are satisfied for a Level 1 Assessment.

1) Limitations on component and crack-like flaw geometries:

i) The component is a flat plate, cylinder, or sphere.

ii) Cylinders and spheres are limited to geometries with $R/t \geq 5$ where R is the inside radius and t is the current thickness of the component.

iii) The wall thickness of the component at the location of the flaw is less than 38 mm (1.5 inches).

iv) The crack-like flaw geometry can be of the surface or through-thickness type, specific limitations for the crack-like flaw depth are included in the Level 1 Assessment procedure (see paragraph 9.4.2). The maximum permitted crack length is 200 mm (8 in).

v) For cylindrical and spherical shell components, the crack-like flaw is oriented in the axial or circumferential direction (i.e. perpendicular to a principal stress direction) and is located at a distance greater than or equal to $1.8\sqrt{Dt}$ from any major structural discontinuity where D is the inside diameter and t is the current thickness of the component. For a flat plate, the crack-like flaw is oriented such that the maximum principal stress direction is perpendicular to the plane of the flaw. If the crack-like flaw is oriented such that it is not perpendicular to a principal stress plane, then the flaw may be characterized by the procedure in paragraph 9.3.6.2.b.

2) Limitations on component loads:

i) The loading on the component is from pressure that produces only a membrane stress field. Pressurized components subject to pressure that result in bending stresses (e.g. head-to-cylinder junction, nozzle intersections, rectangular header boxes on air-cooled heat exchangers) and/or components subject to supplemental loading (see Annex A) shall be evaluated using a Level 2 or Level 3 Assessment.

ii) The membrane stresses during operation are within the design limits of the original construction code.

iii) If a component being evaluated is to be subject to a pressure test, the component's metal temperature shall be above the MAT (see Part 3, paragraph 3.1.4) during the test. After the pressure test, the crack-like flaw shall be re-examined to ensure that the flaw has not grown.

iv) The weld joint geometry is either a Single-V or Double-V configuration; the residual stresses are based on the solutions provided in Annex E.

3) The material meets the following limitations:

i) The material is carbon steel (P1, Group 1 or 2) with an allowable stress in accordance with the original construction code that does not exceed 172 MPa (25 ksi).

ii) The specified minimum yield strength for the base material is less than or equal to 276 MPa (40 ksi), the specified minimum tensile strength for the base material is less than or equal to 483 MPa (70 ksi), and the weldments are made with an electrode compatible with the base material.

iii) The fracture toughness is greater than or equal to the lower bound K_{IC} value obtained from Annex F, paragraph F.4.4.1.c computed using a reference temperature from Annex F, paragraph F.4.4.2. This will be true for carbon steels where the toughness has not been degraded because of environmental damage (e.g., fire damage, over-heating, graphitization, etc.).

9.2.2.2 A Level 3 Assessment should be performed when the Level 1 and 2 methods cannot be applied or produce overly conservative results. Conditions that typically require a Level 3 Assessment include the following.

a) Advanced stress analysis techniques are required to define the state of stress at the location of the flaw because of complicated geometry and/or loading conditions.

b) The flaw is determined or expected to be in an active subcritical growth phase or has the potential to be active because of loading conditions (e.g. cyclic stresses) and/or environmental conditions, and a remaining life assessment or on-stream monitoring of the component is required.

c) High gradients in stress (either primary or secondary), material fracture toughness, or material yield and/or tensile strength exist in the component at the location of the flaw (e.g. mismatch between the weld and base metal).

9.2.3 Assessment procedures to evaluate a notch at the base of a groove-like flaw are covered in Part 12.

9.3 Data Requirements

9.3.1 General

9.3.1.1 The information required for a Level 1 Assessment is shown below:

a) Original Equipment Design Data (see paragraph 9.3.2)

b) Maintenance and Operating History (see paragraph 9.3.3)

c) Material reference temperature (i.e. toughness curve)

d) Flaw Characterization (see paragraph 9.3.6)

9.3.1.2 The information required to perform a Level 2 or Level 3 Assessment is covered in paragraphs 9.3.2 through 9.3.7. The choice of input data should be conservative to compensate for uncertainties if these uncertainties are not accounted for through the use of partial safety factors.

9.3.1.3 The datasheet shown in Table 9.1 should be completed before the FFS assessment is started. This ensures that all of the pertinent factors are considered, communicated, and incorporated into the assessment. The information on this datasheet is used for a Level 1 or Level 2 Assessment. In addition, this information is generally applicable for a Level 3 Assessment. Guidelines for establishing the information to be entered on this datasheet are provided in paragraphs 9.3.2 through 9.3.7.

9.3.2 Original Equipment Design Data

9.3.2.1 An overview of the original equipment data required for an assessment is provided in Part 2, paragraph 2.3.1.

9.3.2.2 Equipment data is required in order to compute the stress intensity factor and reference stress solution based on the geometry of the component at the crack location.

a) For pressure equipment with uniform thickness such as vessels, pipes, and tanks, the important dimensions are the inside diameter and wall thickness.

b) For pressurized equipment with a non-uniform thickness, or where structural discontinuities are involved (e.g. vessel head-to-shell junctions, conical transitions, nozzles, piping tees, and valve bodies) the dimensions required include the diameter, wall thickness, and the local geometric variables required to determine the stress distribution at a structural discontinuity.

9.3.3 Maintenance and Operating History

9.3.3.1 An overview of the maintenance and operating history required for an assessment is provided in Part 2, paragraph 2.3.2.

9.3.3.2 Maintenance and operational input should be provided by personnel familiar with the operational and maintenance requirements of the component containing the crack-like flaw. This data provides a basis for determining the following:

a) The most probable mechanism of the cracking

b) Whether or not the crack is growing

c) Reasonable estimates for the flaw size based on prior records of cracking or experience with other components in a similar service

d) The most probable mechanism of the failure expected

e) Potential remediation measures

9.3.4 Required Data/Measurements for a FFS Assessment – Loads and Stresses

9.3.4.1 Load Cases

The stress distribution at the cracked region of the component should be determined for all relevant loads based on the planned future operating conditions. An overview of the load cases to consider in a stress analysis is provided in Annex A. It is important that the combination of pressure and temperature be determined for all load cases because of the dependence of the material fracture toughness with temperature.

9.3.4.2 Stress Computation

The stress distributions from each load case are calculated based on the uncracked component geometry using loads derived from the future operating conditions.

a) A non-uniform stress distribution may occur through the wall thickness or along the surface of the component. Examples include the through-wall stresses in a pressurized thick wall cylinder, the stress attenuation that occurs at a major structural discontinuity (e.g. nozzle-to-shell and head-to-shell junctions), and the stress distribution caused by a thermal gradient that typically occurs at a skirt-to-vessel attachment. The method used to determine the state of stress in a component should include capabilities to compute stress distributions based on loading conditions and structural configuration.

b) Stress analysis methods based on handbook solutions may be used if these solutions accurately represent the component geometry and loading condition. Otherwise, numerical analysis techniques such as the finite element method shall be used to determine the stress field at the crack location.

c) If it is necessary to linearize computed through-wall stress profiles into membrane and bending stress components to compute a stress intensity factor and reference stress for certain crack geometries and load conditions, then the linearization of the through-wall stress field in the presence of a crack shall be performed in accordance with Annex B1.

d) If it can be verified that the crack-like flaw in the component occurred after application of load, then the stress distribution may be computed using an elastic-plastic analysis.

9.3.4.3 Stress Classification

For each loading condition under consideration, the stress distributions at the cracked region of the component shall be classified into the following stress categories in order to complete a Level 2 Assessment.

a) Primary Stress – The stress distribution developed by the imposed load-controlled loading that is necessary to satisfy the laws of equilibrium (see Annex B1). In addition, the primary stress shall also include any recategorized secondary stresses.

b) Secondary Stress – A secondary stress distribution is developed by the constraint of adjacent parts or by self-constraint of a component (sees Annex B1). If it is uncertain whether a given stress is a primary or secondary stress, it is more conservative to treat it as primary stress. It should be noted that in certain cases secondary stresses that are self-equilibrating over the entire structure or component might still result in plastic collapse in the net-section local to the crack-like flaw. This can occur when the flaw is small compared to the spatial extent of the secondary stress distribution, or there is significant elastic follow-up from the surrounding structure. In these cases, the secondary stress should be treated as a primary stress in the assessment.

c) Residual Stress – Crack extension can occur locally if the crack tip is located in a tensile residual stress field. Therefore, residual stresses resulting from welding shall be included in the assessment. The magnitude and distribution of residual stress shall be determined using Annex E.

9.3.5 Required Data/Measurements for a FFS Assessment – Material Properties

9.3.5.1 Material Yield and Tensile Strength

The yield and tensile strength of the material are required in the FFS assessment to determine the effects of plasticity on the crack driving force, estimate the residual stress, and evaluate the fracture toughness using correlations with other material toughness parameters.

a) If heat-specific yield and tensile strengths for the material and/or weldments are not available, then estimates may be made using the information in Annex F. Otherwise, the specified minimum values of yield stress and tensile stress for the base and weld material shall be used.

b) In general, use of minimum values of yield and tensile strengths will result in a conservative assessment. However, if there are residual stresses in the region of the crack-like flaw, the use of the specified minimum yield strength will tend to under estimate the magnitude of the residual stresses. Therefore, when estimating the magnitude of residual stresses the actual yield strength should be used. If the actual yield strength is not known, the value of the minimum yield strength shall be adjusted using the procedure in Annex E before the residual stresses are computed.

c) The material yield and tensile strength for the regions(s) ahead of the crack tip should be adjusted, as appropriate, to take account of temperature, strain aging, thermal aging, or other prevalent forms of degradation.

d) The material stress-strain curve or Ramberg-Osgood constants are required if a J integral evaluation or elastic-plastic stress analysis is performed as part of the assessment.

9.3.5.2 Material Fracture Toughness

The fracture toughness of the material is a measure of its ability to resist failure by the onset of crack extension to fracture.

a) Guidance for determining fracture toughness for various materials and environments is provided in Annex F.

b) The process environment, service temperature envelope, and any related material/service degradation mechanisms such as embrittlement shall be accounted for when determining the fracture toughness (see Annex F).

c) Local variations in the fracture toughness near the crack tip shall be considered in the assessment.

d) When material specific toughness is not available, then lower bound values shall be used from various correlations (see Annex F).

9.3.5.3 Crack Growth Model

A crack growth model and associated constants are required if an estimate of the remaining life of the component with a crack-like flaw is to be made based on a fracture mechanics approach. An overview of crack growth models is provided in Annex F. The model chosen for the assessment shall account for environmental effects, and may be related to cyclic behavior $\left(da/dN\right)$, time to failure $\left(da/dt\right)$, or both.

9.3.5.4 Material Physical Constants

Material properties such as the elastic modulus, Poisson's ratio, and the thermal expansion coefficient may be required to perform an evaluation. Guidelines for determining these quantities are provided in Annex F.

9.3.6 Required Data/Measurements for a FFS Assessment – Flaw Characterization

9.3.6.1 Overview

The flaw characterization rules allow existing or postulated crack geometry to be modeled by a geometrically simpler one in order to make the actual crack geometry more amenable to fracture mechanics analysis. The nomenclature and idealized shapes used to evaluate crack-like flaws are shown in Figure 9.1. The rules used to characterize crack-like flaws are necessarily conservative and intended to lead to idealized crack geometries that are more severe than the actual crack geometry they represent. These characterization rules account for flaw shape, orientation and interaction.

9.3.6.2 Characterization of Flaw Length

If the flaw is oriented perpendicular to the plane of the maximum principal tensile stress in the component, then the flaw length to be used in calculations (c or $2c$) is the measured length c_m or $2c_m$. If the flaw is not oriented in a principal plane, then an equivalent flaw dimension with a Mode I orientation shall be determined by one of the following options.

a) Option 1 – The flaw dimension, c, to be used in the calculations shall be set equal to the measured length, c_m, irrespective of orientation. For fracture assessments, the plane of the flaw shall be assumed to be normal to the maximum principal tensile stress.

b) Option 2 – The procedure for defining an equivalent Mode I flaw dimension is shown in Figure 9.2.

1) STEP 1 – Project the flaw onto a principal plane. In the case of uniaxial loading, there is only one possible principal plane. When the loading is biaxial (e.g., a pressurized component which is subject to a hoop stress and an axial stress), there is a choice of principal planes on which to project the flaw. In most cases, the flaw should be projected to the plane normal to the maximum principal tensile stress (the σ_1 plane), but there are instances where the σ_2 plane would be more appropriate (e.g., when the angle between the flaw and the principal plane $\left(\alpha\right)$ is greater than 45°).

2) STEP 2 – Compute the equivalent flaw length.

i) For the plane of the flaw projected onto the plane normal to σ_1:

$$\frac{c}{c_m} = \cos^2\alpha + \frac{\left(1-B\right)\sin\alpha\cos\alpha}{2} + B^2\sin^2\alpha \qquad (9.1)$$

ii) For the plane of the flaw projected onto the plane normal to σ_2:

$$\frac{c}{c_m} = \frac{\cos^2\alpha}{B^2} + \frac{(1-B)\sin\alpha\cos\alpha}{2B^2} + \sin^2\alpha \qquad (9.2)$$

In the Equations (9.1) and (9.2), the dimension c corresponds to the half flaw length (or total length for corner or edge cracks) to be used in calculations, c_m is the measured half length for the flaw oriented at an angle α from the σ_1 plane, and B is the biaxiality ratio defined using Equation (9.3). If stress gradients occur in one or more directions, the sum of membrane and bending components shall be used for computing σ_1 and σ_2.

$$B = \frac{\sigma_2}{\sigma_1} \qquad where\ \sigma_1 \geq \sigma_2\ and\ 0.0 \leq B \leq 1.0 \qquad (9.3)$$

Equations (9.1) and (9.2) are only valid when both σ_1 and σ_2 are positive. If σ_2 is compressive or equal to zero, then Equation (9.1) shall be used to compute the equivalent flaw length with $B = 0$, or

$$\frac{c}{c_m} = \cos^2\alpha + \frac{\sin\alpha\cos\alpha}{2} \qquad (9.4)$$

The relationship between c/c_m, α, and the biaxiality stress ratio is shown in Figure 9.3.

9.3.6.3 Characterization of Flaw Depth

The part through-wall depth of a flaw can be considerably more difficult to estimate than the length. Either a default value or a value based on detailed measurements may be used for the flaw depth in the assessment. In services where the owner determines that a leak is not acceptable, the flaw size shall be characterized by actual measurement in accordance with paragraph (b) below.

a) Flaw Depth by Default Values

1) Through-Wall Flaw – If no information is available about the depth of a flaw, a conservative assumption is that the flaw penetrates the wall (i.e., $a = t$ for a surface flaw). In pressurized components, an actual through-wall flaw would most likely lead to leakage, and thus would not be acceptable in the long term. However, if it can be shown that a through-wall flaw of a given length would not lead to brittle fracture or plastic collapse, then the component should be acceptable for continued service with a part-through-wall flaw of that same length. Additional special considerations may be necessary for pressurized components containing a fluid where a leak can result in autorefrigeration of the material near the crack tip, or other dynamic effects.

2) Surface Flaw – Flaw depths less than the full wall may be assumed if justified by service experience with the type of cracking observed. If service experience is not available, then the assumed flaw depth should not be less than the following where length of the flaw is $2c$ (see Figure 9.1(b)).

$$a = \min[t, c] \qquad (9.5)$$

b) Flaw Depth from Actual Measurements

1) The definition of the appropriate depth dimensions (a for a surface flaw, and $2a$ and d for an embedded flaw) when relatively accurate measurements are available is illustrated in Figures 9.1 and 9.4. If the flaw is normal to the surface, the depth dimension, a, is taken as the measured dimension, a_m. However, if the flaw is not normal to the surface (e.g. a lack of fusion flaw that is parallel to the bevel angle or a lamination, see Figure 9.4), the following procedure may be used to compute the depth dimension, a.

i) STEP 1 – Project the flaw onto a plane that is normal to the plate surface, designate this flaw depth as a_m.

ii) STEP 2 – Measure the angle to the flaw, θ, as defined in Figure 9.4, and determine W using the Equations (9.6) and (9.7) or Figure 9.5 where (θ is measured in degrees):

$$W = \max[W_{Theta},\ 1.0] \tag{9.6}$$

$$W_{Theta} = \begin{pmatrix} 0.99999 + 1.0481\left(10^{-5}\right)\theta + 1.5471\left(10^{-4}\right)\theta^2 + \\ 3.4141\left(10^{-5}\right)\theta^3 - 2.0688\left(10^{-6}\right)\theta^4 + 4.4977\left(10^{-8}\right)\theta^5 - \\ 4.5751\left(10^{-10}\right)\theta^6 + 1.8220\left(10^{-12}\right)\theta^7 \end{pmatrix} \tag{9.7}$$

iii) STEP 3 – Multiply a_m by W to obtain the dimension a, which is used in calculations. Note that the dimension d for buried flaws may decrease when the flaw depth is determined using this approach.

2) If the remaining ligament is small, it may be necessary to recategorize the flaw depending on the remaining ligament size. An embedded flaw may be recategorized as a surface flaw and a surface flaw may be recategorized as a through-wall flaw. Rules for flaw recategorization are provided in paragraph 9.3.6.6.

9.3.6.4 Characterization of Branched Cracks

Determination of an idealized flaw is complicated when a branched network of cracks forms in a component because the idealized flaw must be equivalent to the network of cracks from a fracture mechanics approach. The methodology for assessing a network of branched cracks is shown in Figure 9.6. As shown in this figure, the network is idealized as a single planar predominant flaw by means of the following procedure:

a) STEP 1 – Draw a rectangle around the affected region. Define the measured flaw length, $2c_o$, as the length of the rectangle (see Figures 9.6(a) and 9.6(b)).

b) STEP 2 – Rotate the idealized flaw so that it is perpendicular to the maximum principal stress, σ_1. Define an effective length according to the procedure in paragraph 9.3.6.2. (see Figure 9.6(c)). Alternatively, for a conservative estimate of the flaw size, set $c = c_o$

c) STEP 3 – Measure the maximum through-wall depth of the branched network, a_0, (see Figure 9.6(d)). If an actual depth measurement is made, then the flaw depth to be used in the assessment is shown in Figure 9.6(d). Alternatively, the default value defined in paragraph 9.3.6.3.a can be used if accurate measurements are not possible.

9.3.6.5 Characterization of Multiple Flaws

The following procedure applies to multiple discrete flaws that are in close proximity to one another. A branched network of cracks is treated as a single flaw, as discussed in 9.3.6.4.

a) If two or more flaws are close to one another, they can be combined into a single equivalent flaw for the purpose of analysis. If the separation distance is sufficient to avoid interaction, then the flaws can be analyzed independently, and only the worst-case flaw needs to be considered.

b) The procedure for assessing multiple flaws in a local region is illustrated in Figures 9.7 and 9.8 and outlined below:

1) STEP 1 – Rotate each flaw so that it coincides with a principal plane, and determine the effective flaw length according to the procedure in paragraph 9.3.6.2. All flaws in the local region should now be parallel, as illustrated in Figure 9.7(b).

2) STEP 2 – Apply the criteria in Figure 9.8 to check for interaction between parallel flaws. Project all interacting flaws onto a single plane, as illustrated in Figure 9.7(c). Note that some flaws will be combined using this procedure.

3) STEP 3 – Estimate the depth of the flaws with the procedure outlined in paragraph 9.3.6.3. If two or more flaws were combined because of STEP 2 above, define the depth, a, as the width of a rectangle inscribed around the combined flaw, as illustrated in Figure 9.7(d).

4) STEP 4 – Apply the criteria in Figure 9.8 to check for interaction between flaws on a given plane. If interaction exists, the dimensions of the combined flaw are inferred from a rectangle inscribed around the interacting flaws.

c) Multiple flaws do not have to be combined into an equivalent flaw for evaluation if a stress intensity factor and limit load solution can be obtained for the interacting flaw geometries.

9.3.6.6 Recategorization of Flaws

Flaw recategorization is required for two reasons.

a) For an embedded flaw close to the surface or for a deep surface flaw where the remaining ligament is small, the results obtained in the assessment may be overly conservative because the reference stress (see Annex D) in the remaining ligament may over estimate the plasticity effects on the crack driving force resulting in the assessment point falling outside of the failure assessment diagram. Recategorization of an embedded flaw to a surface flaw, or a surface flaw to a through-wall flaw, may result in the associated assessment point being inside of the failure assessment diagram.

b) Most of the stress intensity solutions in Annex C are not accurate for very deep cracks due to high strain/plasticity effects. For example, the commonly published K_I solutions for a semi-elliptical surface flaw are only accurate for $a/t \le 0.8$. Therefore, recategorization to a through-thickness flaw is required to achieve an accurate solution.

c) Flaw Recategorization Guidelines

1) The initial and recategorized crack-like flaws for flaws that experience ligament yielding are shown in Figure 9.9. An embedded or buried flaw can be recategorized as a surface flaw, while a surface flaw can be recategorized as a through-wall flaw. The assumed flaw dimensions are modified as follows.

i) An embedded flaw should be recategorized to a surface flaw when $d/t < 0.2$ (see Figure 9.9(a)). The length and depth of the surface flaw are given by:

$$2c_s = 2c_b + 2d \tag{9.8}$$

$$a_s = 2a_b + d \tag{9.9}$$

ii) A surface flaw should be recategorized as a through-thickness flaw when $a/t > 0.8$ (see Figure 9.9(b)). The length of the through-wall flaw is given by:

$$2c_t = 2c_s + 2\left(t - a_s\right) \tag{9.10}$$

2) Note that the crack length is increased in each case by twice the ligament dimension. When the plastic strain on the remaining ligament is large, the flaw may grow to the free surface by ductile tearing, in which case the flaw is assumed to also extend in the length direction by the same amount on each side.

3) After recategorization, the load ratio, L_r, is determined with the new flaw dimensions. For example, if a deep surface flaw in the axial orientation is found in a component and a local analysis indicates that the computed load ratio is greater than the maximum allowable value (i.e. $L_r > L_{r(\max)}$) the flaw can be recategorized as through-wall, and reanalyzed. Definitions for the computed load ratio and maximum allowable load ratio are provided in Figure 9.20 and Annex D.

d) The recategorized flaw dimensions shall be used in the assessment. In a leak-before-break assessment, the additional requirements in paragraph 9.5.2 shall be satisfied before a leak-before-break can be ensured.

9.3.7 Recommendation for Inspection Technique and Sizing Requirements

9.3.7.1 Reliable sizing of the flaws by nondestructive examination (NDE) is important. Therefore, the choice of the NDE method should be based on its ability to detect and size the depth and length of the flaw.

9.3.7.2 As previously discussed in paragraph 9.3.6, the crack dimensions required as input for an FFS analysis are the crack depth, crack length, crack angle with the plate surface, crack location from the surface, and the spacing between the cracks if the component has multiple cracks.

a) *Surface Cracks* – The crack length, angle relative to the principal stress direction (see Figure 9.2) and distance to other surface cracks may be determined using Magnetic Particle (MT) or Dye Penetrant (PT) examination technique. The depth and angle of the flaw relative to the surface (see Figure 9.4) are typically determined using Ultrasonic (UT) examination techniques.

b) *Embedded Cracks* – The crack depth, length, angle, and distance to other surface breaking or embedded cracks are typically determined using angle beam Ultrasonic (UT) examination techniques (e.g., time-of-flight-diffraction (TOFD) or pulse echo techniques). The calibration settings may need to be more sensitive than are used for new construction weld quality inspections.

9.3.7.3 Accurate sizing of crack-like flaws depends on both the available technology and the skill of the inspector. Parameters to be considered in the uncertainties of flaw sizing include the crack length, depth, flaw orientation, whether or not the flaw is surface breaking, and the number of flaws (i.e. single flaw or multiple flaws). PT or MT should be used to enhance surface breaking flaws prior to determining the crack length. A visual examination should not be used to determine the length of the flaw because the ends of the crack may be closed.

9.3.7.4 Determination of the depth, orientation and position (i.e. the location below the surface for an embedded crack) of a crack-like flaw is usually done by using ultrasonic examination techniques. Radiographic examination techniques may also be used; however, accurate flaw depth and orientation information can be obtained only by moving the component containing the flaw, or moving the source around the component to obtain multiple views. This type of manipulation is typically not possible for many pressure-containing components. A level of qualitative depth and orientation information can sometimes be obtained with electrical resistance (potential drop), magnetic leakage field, and eddy current techniques. The accuracy of the electrical resistance techniques is seriously affected by conditions in the crack (i.e. touching surface and impurities such as oxides). Therefore, ultrasonic examination is the recommended sizing technique for depth and inclination of crack-like flaws.

9.3.7.5 If part of a component is inaccessible for inspection due to the component configuration, materials used, or obstruction by other flaws, and a flaw is suspected in this region because of the surrounding conditions, the possibility of the existence of a flaw the size of the region that cannot be inspected should be considered in the assessment.

9.4 Assessment Techniques and Acceptance Criteria

9.4.1 Overview

9.4.1.1 The Fitness-For-Service assessment procedure used to evaluate crack-like flaws is shown in Figure 9.10. The three assessment levels used to evaluate crack-like flaws are summarized below.

a) Level 1 Assessments are limited to crack-like flaws in pressurized cylinders, spheres or flat plates away from all structural discontinuities.

b) Level 2 Assessments can be used for general shell structures including crack-like flaws located at structural discontinuities. A flow diagram for the Level 2 Assessment is provided in Figure 9.11. In Level 2 Assessments, detailed information on material properties and loading conditions is required, and a stress analysis is required to determine the state of stress at the location of the flaw. The stress analysis at this level may be based on code equations, closed form solutions, or a numerical analysis.

c) Level 3 Assessments can be used to evaluate those cases that do not meet the requirements of Level 1 or Level 2 Assessments. Level 3 Assessments are also required for flaws that may grow in service because of loading or environmental conditions.

9.4.1.2 The assessment levels designated in this document are different from the levels of analysis specified in BS PD6493, BS 7910, and Nuclear Electric R-6 because of the definitions in Part 2.

9.4.2 Level 1 Assessment

9.4.2.1 The Level 1 Assessment is applicable to components that satisfy the limitations in paragraph 9.2.2.1.

9.4.2.2 The following procedure can be used to determine the acceptability of a crack-like flaw using a Level 1 Assessment.

a) STEP 1 – Determine the load cases and temperatures to be used in the assessment based on operating and design conditions (see paragraph 9.3.4). The CET, see Part 3, should be considered in establishing the temperature for the assessment.

b) STEP 2 – Determine the length, $2c$, and depth, a, of the crack-like flaw from inspection data. The flaw should be characterized using the procedure in paragraph 9.3.6.

c) STEP 3 – Determine the Figure from the list below to be used in the assessment based on the component geometry and crack-like flaw orientation with respect to the weld joint.

1) Flat Plate, Crack-Like Flaw Parallel To Joint (Figure 9.12)

2) Cylinder, Longitudinal Joint, Crack-Like Flaw Parallel To Joint (Figure 9.13)

3) Cylinder, Longitudinal Joint, Crack-Like Perpendicular To Joint (Figure 9.14)

4) Cylinder, Circumferential Joint, Crack-Like Flaw Parallel To Joint (Figure 9.15)

5) Cylinder, Circumferential Joint, Crack-Like Flaw Perpendicular To Joint (Figure 9.16)

6) Sphere, Circumferential Joint, Crack-Like Flaw Parallel To Joint (Figure 9.17)

7) Sphere, Circumferential Joint, Crack-Like Flaw Perpendicular To Joint (Figure 9.18)

d) STEP 4 – Determine the screening curve from the Figure selected in STEP 3. The following should be noted when selecting a screening curve.

1) For each Figure in STEP 3, two sets of screening curves, 1/4-t and 1-t crack depths, are provided for three conditions; base metal, weld metal that has been subject to $PWHT$, and weld metal that has not been subject to $PWHT$.

2) If the depth of the flaw can be accurately determined using qualified NDE procedures, then the 1/4-t flaw curve can be used in the assessment based on the criteria in 3) below; otherwise, the 1-t flaw curve should be used.

3) The screening curve to be used in the assessment shall be based on the following criteria.

i) For $t \le 25\,mm\ (1\,in)$:

I) If $a \le t/4$, then the 1/4-t screening curves shall be used.

II) If $a > t/4$, then the 1-t screening curves shall be used.

ii) For $25\,mm\ (1\,in) < t \le 38\,mm\ (1.5\,in)$:

I) If $a \le 6\,mm\ (0.25\,in)$, then the 1/4-t screening curves shall be used.

II) If $a > 6\,mm\ (0.25\,in)$, then the 1-t screening curves shall be used.

4) If the location of the flaw is at the weld, or within a distance of two times the nominal plate thickness measured from the centerline of the weld, then the curves for weld metal should be used; otherwise, the curve for base metal may be used. For flaws located at a weld, the applicable assessment curve is based on heat treatment of the component. If there is question regarding the type and/or quality of $PWHT$, Curve C (i.e. no $PWHT$) should be used.

e) STEP 5 – Determine the reference temperature. Based on the material specification determine the Material Temperature Exemption Curve using Part 3, Table 3.2 and the minimum specified yield strength at ambient temperature based on the original construction code. With the Material Temperature Exemption Curve and the minimum specified yield strength of the material, enter Table 9.2 to determine the reference temperature. If the material is a carbon steel, then the reference temperature is based on the 20 Joule or 15 ft-lb transition temperature. For example, for an A516 grade 70 material, the exemption curve from Part 3, Table 3.2 is B. The minimum specified yield strength for this material is 38 ksi. The material is carbon steel; therefore, is based on the 20 Joule or 15 ft-lb transition temperature. Based on these data, the reference temperature from Table 9.2 is $T_{ref} = 6^{o}C\ (43^{o}F)$.

f) STEP 6 – Determine the maximum permissible crack-like flaw length. Enter the assessment Figure established in STEP 3 with the assessment temperature and reference temperature determined in Steps 1 and 5, respectively, to determine the maximum length of the flaw $(2c)$ using the applicable screening curve.

g) STEP 7 – Evaluate Results – if the permissible flaw size determined in STEP 6 is greater than or equal to the length of the crack-like flaw determined in STEP 2, then the component is acceptable for future operation.

9.4.2.3 The Level 1 Assessment may be based on the Level 2 Assessment calculation procedure subject to the restrictions and requirements stipulated in paragraph 9.2.2.1.

9.4.2.4 If the component does not meet the Level 1 Assessment requirements, then the following actions, or combination thereof, shall be taken:

a) The data used in the analysis can be refined and the Level 1 Assessment can be repeated (i.e. refinement of data entails performing additional NDE to better characterize the flaw dimensions, and determining the future operating conditions accurately to establish the operating temperature envelope).

b) Rerate (e.g. temperature), repair, replace, or retire the component.

c) Conduct a Level 2 or Level 3 Assessment.

9.4.3 Level 2 Assessment

9.4.3.1 The Level 2 Assessment is applicable to components and loading conditions that satisfy the conditions given in paragraph 9.2.2.1. The assessment procedure in Level 2 provides a better estimate of the structural integrity of a component than a Level 1 Assessment with a crack-like flaw. A flow diagram for a Level 2 Assessment is shown in Figure 9.11.

9.4.3.2 The following procedure can be used to determine the acceptability of a crack-like flaw using a Level 2 Assessment. In this procedure, Partial Safety Factors (see Part 2) are applied to the independent variables (i.e. flaw size, material fracture toughness, and stress) to account for uncertainty.

a) STEP 1 – Evaluate operating conditions and determine the pressure, temperature and supplemental loading combinations to be evaluated (see paragraph 9.4.3.1).

b) STEP 2 – Determine the stress distributions (see paragraph 9.4.3.2) at the location of the flaw based on the applied loads in STEP 1 and classify the resulting stresses into the following stress categories (see paragraph 9.3.4.3):

1) Primary stress

2) Secondary stress

3) Residual stress

c) STEP 3 – Determine the material properties; yield strength, tensile strength and fracture toughness (K_{mat}) for the conditions being evaluated in STEP 1 (see paragraph 9.3.5). The yield and tensile strength shall be established using actual values or nominal values defined as the minimum specified values per the applicable material specification. The fracture toughness shall be established based on the actual values, mean values (see Table 9.3, note 6), or a lower-bound estimate.

d) STEP 4 – Determine the crack-like flaw dimensions from inspection data. The flaw should be categorized using the procedure in paragraph 9.3.6.

e) STEP 5 – Modify the primary stress, material fracture toughness, and flaw size using the Partial Safety Factors (PSF). If a given input value is known to be a conservative estimate (e.g. upper-bound stresses, lower-bound fracture toughness, or upper-bound flaw size), then an applicable PSF equal to 1.0 may be used in the assessment.

1) *Primary Membrane and Bending Stress* – Modify the primary membrane and bending stress components determined in STEP 2 (P_m and P_b, respectively) using the PSF for stress (see Table 9.3).

$$P_m = P_m \cdot PSF_s \tag{9.11}$$

$$P_b = P_b \cdot PSF_s \tag{9.12}$$

2) *Material Toughness* – Modify the mean value of the material fracture toughness determined in STEP 3 (K_{mat}) using the PSF for fracture toughness (see Table 9.3).

$$K_{mat} = \frac{K_{mat}}{PSF_k} \tag{9.13}$$

3) *Flaw Size* – Modify the flaw size determined in STEP 4 as shown below using the PSF for flaw size (see Table 9.3). If the modified flaw depth exceeds the wall thickness of the component, then the flaw should be recategorized as a through-wall flaw.

$$a = a \cdot PSF_a \qquad for\ a\ surface\ flaw \tag{9.14}$$

$$2a = 2a \cdot PSF_a \qquad for\ an\ embedded\ flaw \tag{9.15}$$

$$2c = 2c \cdot PSF_a \qquad for\ an\ embedded\ flaw \tag{9.16}$$

f) STEP 6 – Compute the reference stress for primary stresses, σ_{ref}^{P}, based on the modified primary stress distribution and modified flaw size from STEP 5 and the reference stress solutions in Annex D.

g) STEP 7 – Compute the Load Ratio or the abscissa of the FAD using the reference stress for primary loads from STEP 6 and the yield strength from STEP 3.

$$L_r^P = \frac{\sigma_{ref}^P}{\sigma_{ys}} \tag{9.17}$$

h) STEP 8 – Compute the stress intensity attributed to the primary loads, K_I^P, using the modified primary stress distribution and modified flaw size from STEP 5, and the stress intensity factor solutions in Annex C If $K_I^P < 0.0$, then set $K_I^P = 0.0$.

i) STEP 9 – Compute the reference stress for secondary and residual stresses, σ_{ref}^{SR}, based on the secondary and residual stress distributions from STEP 2, the modified flaw size from STEP 5, and the reference stress solutions in Annex D.

j) STEP 10 – Compute the stress intensity attributed to the secondary and residual stresses, K_I^{SR}, using the secondary and residual stress distributions from STEP 2,, the modified flaw size from STEP 5, and the stress intensity factor solutions in Annex C. If $K_I^{SR} < 0.0$, then set $K_I^{SR} = 0.0$. The value of K_I^{SR} should be determined at the same location along the crack front as that used to determine K_I^P.

k) STEP 11 – Compute the plasticity interaction factor, Φ, using the following procedure:

1) STEP 11.1 – If $K_I^{SR} = 0.0$, then set $\Phi = 1.0$ and proceed to STEP 12. Otherwise, compute L_r^{SR} using the following equation with σ_{ref}^{SR} from STEP 9 and σ_{ys} from STEP 3.

$$L_r^{SR} = \frac{\sigma_{ref}^{SR}}{\sigma_{ys}} \tag{9.18}$$

2) STEP 11.2 – Determine ψ and ϕ using Tables 9.4 through 9.7 and compute Φ/Φ_0 using Equation (9.19). The parameter L_r^P used to calculate ψ and ϕ shall be from STEP 7. Alternatively, Φ/Φ_0 can be determined from Figure 9.19.

$$\frac{\Phi}{\Phi_0} = 1 + \frac{\psi}{\phi} \tag{9.19}$$

3) STEP 11.3 – Compute the plasticity interaction factor, Φ.

i) If $0 < L_r^{SR} \le 4.0$, then set $\Phi_0 = 1.0$ and

$$\Phi = 1 + \frac{\psi}{\phi} \tag{9.20}$$

ii) If $L_r^{SR} > 4$, then compute the stress intensity factor for secondary and residual stresses corrected for plasticity effects, K_{Ip}^{SR}, and compute Φ_0 and Φ using Equation (9.21) and Equation (9.22), respectively.

$$\Phi_0 = \frac{K_{Ip}^{SR}}{K_I^{SR}} \tag{9.21}$$

$$\Phi = \Phi_0 \left(1 + \frac{\psi}{\phi} \right) \tag{9.22}$$

The most accurate method to compute K_{Ip}^{SR} is to perform an elastic-plastic finite element analysis of the cracked component with boundary conditions that model the residual stress and secondary loads with all of the primary loads set to zero. Guidelines for performing this analysis are provided in Annex B1. Based on the results from the elastic-plastic analysis, evaluate the J integral and compute K_{Ip}^{SR} from the following equation (see Annex F, paragraph F.4.2.1.a)

$$K_{Ip}^{SR} = \sqrt{\frac{J^{SR} E}{1 - v^2}} \tag{9.23}$$

The following simplified method may be used to compute Φ_0; however, this method may produce overly conservative results.

$$\Phi_0 = \left(\frac{a_{eff}}{a} \right)^{0.5} \tag{9.24}$$

with,

$$a_{eff} = a + \left(\frac{1}{2\pi\tau} \right) \left(\frac{K_I^{SR}}{\sigma_{ys}} \right)^2 \tag{9.25}$$

As an alternative, the methods in Reference [33] may be used to estimate K_{Ip}^{SR}.

l) STEP 12 – Determine toughness ratio or ordinate of the FAD assessment point where K_I^P is the applied stress intensity due to the primary stress distribution from STEP 8, K_I^{SR} is the applied stress intensity due to the secondary and residual stress distributions from STEP 10, K_{mat} is the modified material toughness from STEP 5, and Φ is the plasticity correction factor from STEP 11.

$$K_r = \frac{K_I^P + \Phi K_I^{SR}}{K_{mat}} \tag{9.26}$$

m) STEP 13 – Evaluate results; the FAD assessment point for the current flaw size and operating conditions (stress levels) is defined as $\left(K_r, L_r^P \right)$.

1) STEP 13.1 – Determine the cut-off for the L_r^P-axis of the FAD (see Figure 9.20).

2) STEP 13.2 – Plot the point on the FAD shown in Figure 9.20. If the point is on or inside the FAD (on or below and/or to the left), then the component is acceptable per the Level 2 Assessment procedure. If the point is outside of the FAD (above and/or to the right), then the component is unacceptable per the Level 2 Assessment procedure. Note that the value of K_I^P and K_I^{SR} will vary along the crack front; therefore, the assessment may have to be repeated at a number of points along the crack front to ensure that the critical location is found.

9.4.3.3 A limiting flaw size can be established using the following procedure. Determination of the limiting flaw size may be useful in selecting an appropriate NDE technique for inspection.

a) Increase the crack-like flaw dimensions by a small increment; for a surface flaw compute $a = a_0 + \Delta a$ and $c = c_0 + \Delta c$ where a_o and c_o are the initial flaw sizes found at the time of the inspection. The flaw increments should be proportioned based on the flaw aspect ratio or ratio of the stress intensity factor values at the surface and deepest part of the crack.

b) For the new flaw size, complete the steps in paragraph 9.4.3.2 and determine if the new flaw size is inside of the FAD curve.

c) Continue to increment the flaw size until the calculated assessment point is on the FAD curve. The resulting flaw size is defined as the limiting flaw size. This limiting flaw size should be divided by the partial safety factor in a manner consistent with paragraph 9.4.3.2.e.

9.4.3.4 In certain cases, an acceptable flaw size may be predicted using the Level 2 Assessment procedure although smaller flaw sizes may be unacceptable. This condition, referred to as a "non-unique solution" (see Reference [27]), is a result of the assumptions used for input data and the mathematical form of the equations used in the analytical procedure. Non-unique solutions can also affect the limiting values of other input parameters such as stress results. Non-unique solutions are most likely to occur where stress distributions decrease through the section (e.g. stress gradients associated with a bending stress or stress concentration at the toe of a fillet weld), or where increasing the primary stresses results in increased relaxation of the secondary stress. A sensitivity analysis (see Part 2, paragraph 2.4.3.1) should be performed for these cases to determine acceptability based on a specific situation. In some cases, a more detailed analysis (i.e. Level 3) may need to be performed based on the results of the sensitivity analysis.

9.4.3.5 If the component does not meet the Level 2 Assessment requirements, then the following actions, or combination thereof, shall be taken:

a) The data used in the analysis can be refined and the Level 2 Assessment can be repeated. Refinement of data entails performing additional NDE to better characterize the flaw dimensions, reviewing equipment documentation to justify the use of other than lower bound material properties, and/or determining the future operating conditions and associated stress levels more accurately. If the assessment point lies within the Level 2 FAD after data refinement, the component is acceptable for continued operation.

b) Rerate, repair, replace, or retire the component, and/or

c) A Level 3 Assessment can be performed.

9.4.4 Level 3 Assessment

9.4.4.1 The Level 3 Assessment procedure provides the best estimate of the structural integrity of a component with a crack-like flaw. In addition, this assessment level is required if subcritical crack-growth is possible during future operation. Five methods are permitted in a Level 3 Assessment.

a) *Method A Assessment* – The basis of this method is the Level 2 Assessment procedure except that the FAD in Figure 9.20 is utilized for the acceptance criteria with user specified Partial Safety Factors based on a risk assessment. Alternatively, a probabilistic analysis can be performed.

b) *Method B Assessment* – The basis of this method is the Level 2 Assessment procedure except that the FAD is constructed based on the actual material properties. This method is only suitable for base and weld materials because it requires a specific material dependent stress-strain curve; the method should not be used for assessment of crack-like flaws in the HAZ. The procedure for the assessment is as follows:

1) STEP 1 – Obtain engineering stress-strain data for the material containing the crack-like flaw at the assessment temperature. If a stress-strain curve for the actual material containing the flaw cannot be obtained, a stress-strain curve for a material with the same specification and similar stress-strain response can be used. The 0.2% offset yield strength, tensile strength, and modulus of elasticity should be determined together with sufficient data points to accurately define the stress-strain curve. It is recommended that the engineering stress-strain curve be accurately defined at the following ratios of applied stress to yield stress: $\sigma/\sigma_{ys} = 0.7,\ 0.8,\ 0.98,\ 1.0,\ 1.02,\ 1.1,\ 1.2$ and intervals of 0.1 up to σ_{uts}.

2) STEP 2 – Convert the engineering stress-strain curve obtained in STEP 1 to a true stress-strain curve. The true stress and strain can be computed from the engineering strain as shown in Annex F paragraph F.2.3.2.

3) STEP 3 – Determine the material-specific FAD using the following equation:

$$K_r(L_r^P) = \left(\frac{E\varepsilon_{ref}}{L_r^P \sigma_{ys}} + \frac{\left(L_r^P\right)^3 \sigma_{ys}}{2E\varepsilon_{ref}} \right)^{-1/2} \qquad for\ 0.0 < L_r^P \le L_{r(\max)}^P \tag{9.27}$$

$$K_r(L_r^P) = 1.0 \qquad for\ L_r^P = 0.0 \tag{9.28}$$

4) STEP 4 – Complete the assessment using the Level 2 Assessment procedure except the material-specific FAD is utilized in STEP 13 (see paragraph 9.4.3.2.m). Partial Safety Factors should be used in the assessment. Alternatively, a probabilistic analysis can be performed.

c) *Method C Assessment* – The basis of this method is the Level 2 Assessment procedure except that the FAD is constructed based on the actual loading conditions, component geometry, and material properties. A procedure to construct the geometry and material dependent FAD, and to complete the assessment for a known crack-like flaw is covered in Annex B1, paragraph B1.6.4.3. Partial Safety Factors should be used in the assessment. Alternatively, a probabilistic analysis can be performed.

d) *Method D Assessment* – This method is a ductile tearing analysis where the fracture tearing resistance is defined as a function of the amount of stable ductile tearing. This method should only be used for materials that exhibit stable ductile tearing (e.g. ferritic steels on the upper shelf and austenitic stainless steels). Partial Safety Factors should be used in the assessment. Alternatively, a probabilistic analysis can be performed. The procedure for the assessment is as follows:

1) STEP 1 – Obtain a JR-curve for the material containing the crack-like flaw at the assessment temperature (see Annex F). If a JR-curve for the actual material containing the flaw cannot be obtained, a JR-curve for a material with the same specification and similar ductile tearing response can be used.

2) STEP 2 – Determine a FAD to be used in the assessment from Methods A, B, or C as defined above.

3) STEP 3 – Follow Steps 1 through 13 of the Level 2 Assessment procedure to generate a series of assessment points. For each assessment point, the crack depth, a, is determined by adding a crack depth increment, Δa_j, to the measured or initial crack depth, a_i (i.e. the first point is $a = a_i + \Delta a_1$, the second point is $a = a_i + \Delta a_1 + \Delta a_2$, the third point is $a = a_i + \Delta a_1 + \Delta a_2 + \Delta a_3$, etc.). The magnitude of the crack depth increment, Δa_j, used to generate the series of assessment points can be inferred from the JR-curve. For surface and embedded flaws, the magnitude of crack depth increment should also be applied to the flaw length. The material fracture toughness used for each assessment point is determined from the JR-curve (J can be converted to K using the procedures in Annex F) at the crack depth associated with ductile tearing, a_{JR} (i.e. the first point is $a_{JR} = \Delta a_1$, the second point is $a_{JR} = \Delta a_1 + \Delta a_2$, the third point is $a_{JR} = \Delta a_1 + \Delta a_2 + \Delta a_3$, etc.). Note that for a rising JR Curve, the fracture toughness will increase with the crack depth.

4) STEP 4 – Plot the series of assessment points on the FAD. The three possible outcomes of a tearing analysis are shown on Figure 9.21(b). If all of the assessment points fall inside of the FAD, then unstable crack growth will not occur. If the first few assessment points fall outside of the FAD and subsequent points fall within the FAD, then a finite amount of crack growth or stable ductile tearing will occur. Ductile instability is predicted when all of the assessment points fall outside of the FAD. If the load is fixed, the locus of the assessment typically exhibits a “fish hook” shape where the value of K_r reaches a minimum and then increases. The point of instability occurs when the locus of the assessment points is tangent to the FAD.

e) *Method E Assessment* – The recognized assessment procedures listed below are subject to supplemental requirements that may include the use of Partial Safety Factors or a probabilistic analysis.

1) BS PD6493 or BS 7910 (see Part 1, Table 1.1)

2) Nuclear Electric R-6 (see Part 1, Table 1.1)

3) SAQ/FoU Report 96/08 (see Part 1, Table 1.1)

4) WES 2805 – 1997 (see Part 1, Table 1.1)

5) DPFAD Methodology (see References [6] and [7])

6) EPFM using the J-integral (see References [1], [11] and [12])

7) The J-integral-Tearing Modulus method (see References [1], [19] and [34])

9.4.4.2 It is the responsibility of the Engineer to meet all limitations and requirements imposed by the selected method. In addition, the Engineer must ensure that the method used including all assumptions, analysis parameters, results and conclusions is clearly documented.

9.4.4.3 A sensitivity analysis (see Part 2, paragraph 2.4.3.1) should be performed as part of the assessment regardless of the method chosen.

9.5 Remaining Life Assessment

9.5.1 Subcritical Crack Growth

9.5.1.1 Overview

There is special emphasis in the assessment procedures in this Part for evaluating subcritical crack-growth in pressure containing components. There are a wide variety of process environments and material degradation mechanisms that increase the occurrence of environmentally and service induced cracking (see Annex G).

a) For purposes of this document, in-service crack growth may be categorized into four main types; crack growth by fatigue, crack growth by stress corrosion cracking, crack growth by hydrogen assisted cracking, and crack growth by corrosion fatigue. Details regarding these crack growth mechanisms are covered in Annex F, paragraph F.5.

b) The methodology for crack growth evaluation used in this document is based on fracture mechanics. In this methodology, the growth of a pre-existing crack is controlled by a crack tip stress intensity factor. In addition, it is assumed that the growth of a crack is controlled by a crack growth model for each combination of material, environment, and crack tip stress intensity factor that can be measured or determined independently and applied to a component with a crack-like flaw. An important requirement for this methodology is that the material properties such as yield and flow stress, material toughness, and crack growth model including appropriate coefficients should be determined as closely as possible from conditions that represent the combination of material, equipment age, environment and loading conditions (applied stress intensity level) for the component being evaluated.

c) A major difficulty that must be addressed with environmental cracking data is that crack growth rates can be highly sensitive to changes in the process environment. While the environment is carefully controlled in an experiment, the composition and temperature of an actual process is subject to fluctuations, and the applicability of laboratory data is inappropriate in many cases. Another problem with predicting crack growth rates in structures is that the cracking often occurs as the result of an upset in operating conditions. For example, cracking that is detected after several years of service may have occurred over the space of several hours or days when atypical operating conditions were present; no cracking occurred before or after this upset. An average crack growth rate, obtained by dividing the crack size by the total time in service, would be meaningless in such instances.

d) For cases involving fatigue, or environmentally assisted cracking, new cracks can initiate at other locations in the structure remote from the known cracks being analyzed. This occurs because corrosion, erosion, local cyclic or static stresses or local concentration of the environment is such that threshold values for crack extension are exceeded. Hence, when assessing the significance of known or postulated cracks for in-service crack extension and structural failure, the implications of exceeding such threshold values elsewhere in the structure must be considered.

e) Closed form estimates for the time to reach a limiting flaw size are complicated by random loading, fatigue threshold and retardation effects, and the complexity of the stress intensity solution. Therefore, crack growth is typically done using a numerical algorithm that explicitly increments the crack growth for some repeated block of representative service loading. For complicated loading histories, load blocks may be developed for a representative time period using the rainflow cycle-counting method (see Annex B3).

f) In addition to the complexities described above, sources of error in computing the time to reach a limiting flaw size include uncertainty in sizing the initial defect, variability in material behavior, and oversimplification of the load spectrum. Despite the difficulties of performing crack-growth calculations, estimates of crack-growth time to failure are useful for establishing inspection intervals and prioritizing repairs.

g) All cases in which subcritical crack growth is included in the assessment should be referred to and analyzed by an engineer sufficiently knowledgeable about the interactions between cracks, environment, component (structural) design, and loading history (including cyclic loads) using Level 3 procedures of this document.

h) In cases where subcritical crack growth data is minimal or nonexistent, periodic monitoring of crack growth using appropriate NDE methods is recommended. The incremental growth data resulting from the periodic monitoring can be used as input data to an assessment.

9.5.1.2 Evaluation and Analysis Procedures for Components with Growing Cracks

Analysis of equipment containing growing cracks requires specialized skills, expertise, and experience because of the inherent uncertainties with the methodology. The analysis involves the use of a Level 3 Assessment per paragraph 9.4.4 and the numerical integration of a crack growth model. The overall evaluation methodology for growing cracks is shown in Figure 9.22. Guidance for conducting a crack growth analysis is shown in Figure 9.23. Highlights of the evaluation include the following.

a) STEP 1 – Perform a Level 3 Assessment for the initial crack size. If the component is demonstrated to be acceptable per a Level 3 Assessment, then an attempt to apply remedial measures to prevent further crack growth should be made (see paragraph 9.6).

b) STEP 2 – If effective remedial measures are not possible and slow subcritical crack growth is expected, then determine if a crack growth model and associated data exist for the material and service environment. If a crack growth model and data exist, then a crack growth analysis can be performed. If crack growth data does not exist, it may be determined in accordance with a recognized standard for crack growth testing. The selection of an appropriate crack growth model, the specification of the test conditions that represent the full range of operating conditions the component is subjected to, and selection of the test material are the responsibility of the engineer performing the assessment (see paragraph 9.5.1.1). As an alternative to a subcritical crack growth analysis, a leak-before break analysis may be performed to determine if an acceptable upper bound crack size can be established (see paragraph 9.5.2).

c) STEP 3 – Compute the stress at the flaw based on the future operating conditions. In these calculations, all relevant operating conditions including normal operation, start-up, upset, and shutdown should be considered.

d) STEP 4 – Determine an increment in crack growth based on the previous flaw size (to initialize the process, the previous flaw size is the initial flaw size determined in STEP 1), stress, estimated stress intensity, and the crack growth model. For surface and embedded flaws, the increment of crack growth will have a component in the depth and length dimension. For embedded flaws, the increment of crack growth may also include a component to model the flaw location in the wall thickness direction. The increment of crack growth is established based on the applied stress intensity associated with the component of the crack and the crack growth equation. For example, if a surface flaw is being evaluated, the crack depth is incremented based on the stress intensity factor at the deepest portion of the crack and the length is incremented based on the stress intensity factor at the surface. The flaw size to be used in STEP 5 is the previous flaw size plus the increment of crack growth. A description of methodologies for performing crack growth calculations subject to constant amplitude and variable amplitude loading is contained in References [29], [30], [31], and [34].

e) STEP 5 – Perform a Level 3 Assessment for the current crack size. Demonstrate that for the current crack size, the applied stress intensity factor is less than the critical stress intensity factor for the applicable crack growth mechanism. If the assessment point for the current flaw size is outside of the FAD or the crack is recategorized as a through-wall crack (see paragraph 9.3.6.6), then go to STEP 6; otherwise, go to STEP 4 and continue to grow the crack.

f) STEP 6 – Determine the time or number of stress cycles for the current crack size (a_o, c_o) to reach the limiting flaw size. The component is acceptable for continued operation provided:

1) The time or number of cycles to reach the limiting flaw size, including an appropriate in-service margin, is more than the required operating period.

2) The crack growth is monitored on-stream or during shutdowns, as applicable, by a validated technique.

3) The observed crack growth rate is below the value used in the remaining life prediction as determined by an on-stream monitoring or inspections during shutdowns.

4) Upset conditions in loading or environmental severity are avoidable.

5) If the depth of the limiting flaw size is recategorized as a through-wall thickness crack, the conditions for an acceptable leak-before-break (LBB) criterion should be satisfied (see paragraph 9.5.2).

g) STEP 7 – At the next inspection, establish the actual crack growth rate, and re-evaluate the new flaw conditions per procedures of this Part. Alternatively, repair or replace the component or apply effective mitigation measures.

9.5.2 Leak-Before-Break Analysis

9.5.2.1 Overview

In certain cases, it may be possible to show that a flaw can grow through the wall of a component without causing a catastrophic failure. In such cases, a leak can be detected (taking into consideration the contained fluid and type of insulation) and remedial action could be initiated to avoid a component failure. This type of examination is called a Leak-Before-Break (LBB) analysis. The leak-before-break methodology may be useful to determine an upper bound for a part-through flaw that is growing at an unknown rate; although the remaining life cannot be determined, detection of a leak can serve as an early warning. A leak-before-break analysis begins by re-categorizing the flaw as through-wall, and then evaluating the new geometry according to the procedures in paragraph 9.4.3 or 9.4.4. If the postulated through-wall flaw is acceptable, the existing flaw can be left in service as long as it does not grow through the wall.

9.5.2.2 Limitations of LBB

There are limitations of the leak-before-break methodology. This approach should not be applied to certain situations that are outlined below.

a) The leak should be readily detectable. The LBB approach may not be appropriate if the affected area is covered by insulation, or if the cracking mechanism produces very tight cracks that do not produce leaks when they grow through the wall. The ability to detect a leak may also be influenced by the contained fluid (e.g. liquid or gas).

b) The LBB methodology may not be suitable for flaws near stress concentrations or regions of high residual stress. The pitfalls of LBB in these situations are illustrated in Figure 9.24. When the stresses are higher on the surface than in the interior of the wall, the flaw may grow faster in the surface direction than in the depth direction. In some cases, the flaw can grow virtually around the entire circumference of the vessel before advancing in the depth direction. Therefore, LBB should not be applied to non-post weld heat treated cylindrical shell components with cracks in a circumferential weld joint (e.g. girth seams and head-to-shell junctions) or shell-to-nozzle junctions with circumferential cracks unless it can be shown that the stress distribution will not promote accelerated crack growth at the surface.

c) The LBB approach should not be applied when the crack growth rate could potentially be high. When a leak occurs, adequate time must be available to discover the leak and take the necessary action. This consideration is particularly important when the component is subject to pneumatic pressure.

d) The possible adverse consequences of developing a leak must be considered, especially when the component contains hazardous materials, fluids operating below their boiling point, and fluids operating above their auto-ignition temperature. Pressurized components that contain gas at high pressure can experience pneumatic loading or other dynamic effects at the crack tip making LBB impractical. Pressurized components that contain light hydrocarbon liquids, or other liquids with a low boiling point, can experience autorefrigeration that also make LBB impractical.

9.5.2.3 LBB Procedure

The procedure for assuring that a leak-before-break criterion is satisfied is shown below.

a) STEP 1 – Using methods of paragraph 9.4.3 or 9.4.4 demonstrate that the largest initial flaw size left in the structure will not lead to fracture for all applicable load cases.

b) STEP 2 – Using methods of paragraph 9.4.3 or 9.4.4, determine the largest (critical) crack length of a full through-wall crack below which catastrophic rupture will not occur for all applicable load cases.

c) STEP 3 – Compute the corresponding leak areas associated with the critical crack lengths determined in Step 2.

d) STEP 4 – Determine the leakage rate associated with the crack area computed in STEP 3, and demonstrate that the associated leaks are detectable with the selected leak detection system (see paragraph 9.5.2.5).

9.5.2.4 Flaw Dimensions for LBB

The crack-like flaw dimensions to be used in a LBB analysis are determined as follows:

a) If the component meets all of the conditions outlined in paragraph 9.5.2.2, the assumed LBB flaw can be defined as follows:

$$2c_{LBB} = 2c + 2t \tag{9.29}$$

b) The above equation, which applies to both surface and buried flaws, is more restrictive than the recategorization procedure in paragraph 9.3.6.6. The latter was applied to flaws that experienced ligament yielding. If the current flaw was initially recategorized as a through-wall flaw to account for ligament yielding, the length of the flaw should be redefined using (a) above if a LBB analysis is to be performed.

9.5.2.5 Leak Area Calculations for LBB Analysis

The crack opening area (COA) of a potential through-wall crack-like flaw is required to estimate leakage flow rates. The COA depends on the crack geometry (effective length, shape, orientation, etc.), component geometry, material properties, and the loading conditions. Methods to compute the crack opening area are provided in Annex K of this Standard.

9.5.2.6 Leak Rate Calculations for Through-Wall Cracks

The calculation of the fluid flow or leak rate through a crack-like flaw involves the crack geometry, the flow path length, fluid friction effects, and the thermodynamics of the flow through the crack. A method to compute the leak rate using approximate solutions for isothermal or polytropic flows of gases is provided in Reference [9]. Methods to compute the leak rate for two phase flow of steam/water mixtures are provided in Reference [18].

9.5.2.7 Analysis of Critical Leak Length (CLL) of Through-Wall Cracks

If a leak is expected and acceptable, and if conditions for LBB methodology are met, then the critical length of a through-wall crack for the component under the conditions of the prevalent stresses and material properties shall be performed using paragraph 9.4.3 or 9.4.4. The acceptance criteria of the CLL will depend on the capability and reliability of the in-service monitoring and the leak detection system.

9.6 Remediation

9.6.1 A FFS analysis provides the determination of the remaining life of a component containing a flaw so that operation can be assured until the next scheduled inspection. The remaining life of a component containing crack-like flaws can only be determined if information about the crack growth rate in the service environment is known. Typically, this information is not readily available or established for many of the process environments. Therefore, a combination of analytical techniques (i.e. LBB, see paragraph 9.5.2), in-service monitoring (see paragraph 9.7), and remediation methods may be used to provide assurance that a component can be operated until the next scheduled inspection.

9.6.2 Remediation measures for crack-like flaws generally fall into one of the categories shown below. One or a combination of these methods may be employed.

9.6.2.1 *Remediation Method 1* – Removal or repair of the crack. The crack may be removed by blend grinding. The resulting groove is then repaired using a technique to restore the full thickness of material and the weld repair is subject to $PWHT$ in accordance with the in-service inspection code. Alternatively, repair of the groove is not required if the requirements of FFS assessment procedures in Part 5 are satisfied.

9.6.2.2 *Remediation Method 2* – Use of a crack arresting detail or device. For components that are not a pressure boundary, the simplest form of this method is to drill holes at the end of an existing crack to effectively reduce the crack driving force. For pressurized components, a device can be added to the component to control unstable crack growth (for example, crack arresting devices for pipelines, see Reference [25]).

9.6.2.3 *Remediation Method 3* **–** Performing physical changes to the process stream (see Part 4, paragraph 4.6.3). This method can be used to reduce the crack driving force (reduction in pressure) or to provide an increase in the material toughness at the condition associated with highest stress state. This may involve the introduction of a warm start-up and/or shutdown cycle into equipment operating procedures such that the temperature of the component is high enough to ensure adequate material toughness at load levels associated with the highest state of stress.

9.6.2.4 *Remediation Method 4* – Application of solid barrier linings or coatings to keep the environment isolated from the metal (see Part 4, paragraph 4.6.4). In this method, the flaw is isolated from the process environment to minimize the potential for environmentally assisted subcritical crack growth.

9.6.2.5 *Remediation Method 5* – Injection of water and/or chemicals on a continuous basis to modify the environment or the surface of the metal (see Part 4, paragraph 4.6.5). In this method, the process environment is controlled to minimize the potential for environmentally assisted subcritical crack growth.

9.6.2.6 *Remediation Method 6* – Application of weld overlay (see Part 4, paragraph 4.6.6). In this method, weld overlay is applied to the component surface opposite to the surface containing the cracks to introduce a compressive residual stress field at the location of the crack (for an example, see Reference [9]). The compressive residual stress field should eliminate any future crack growth. This type of repair also increases the structural integrity of the component containing the flaw by the addition of extra wall thickness provided by the weld overlay.

9.6.2.7 *Remediation Method 7* – Use of leak monitoring and leak-sealing devices.

9.7 In-Service Monitoring

9.7.1 In all cases where subcritical in-service crack growth is permitted by the methods of this document, in-service monitoring or monitoring at a shutdown inspection, as applicable, of the crack growth by NDE is required. The applicable NDE method will depend on the specific case.

9.7.2 Before returning the component to service, the monitoring method should be validated to ensure that it could adequately detect the size of the flaw under service conditions. The NDE sensitivity and flaw sizing uncertainty associated with the in-service monitoring procedure should be taken into account when specifying a limiting maximum flaw size for continued operation.

9.8 Documentation

9.8.1 The documentation of the FFS Assessment should include the information cited in Part 2, paragraph 2.8. Additional documentation requirements are essential because of the complexity associated with the assessment. This information should be permanently stored with the equipment record files.

9.8.1.1 The following information should be documented for a structural integrity assessment carried out according to the procedures of this Part.

a) Assessment Level – Any deviations or modifications used at a given level of analysis (Levels 1, 2 and 3).

b) Loading Conditions – normal operation and upset conditions (see Annex A for a summary of loading conditions); additional loads and stresses considered in the assessment (e.g. stresses from supplement loads, thermal gradients and residual stresses); the stress analysis methods (handbook or numerical technique such as finite-element analysis); and categorization of stress results (Levels 1, 2, and 3).

c) Material Properties – The material specification of the component containing the flaw; yield stress, ultimate tensile stress, and fracture toughness at the temperature of interest (including whether the data was obtained by direct testing or indirect means and the source and validity of data); and a description of the process environment including its effect on material properties (Levels 1, 2 and 3).

d) Characterization Of Flaw – The flaw location, shape and size; NDE method used for flaw sizing and allowance for sizing errors; and whether re-characterization of the flaw was required (Levels 1, 2 and 3).

e) Partial Safety Factors – A list of the Partial Safety Factors used in the analysis; in a Level 3 Assessment, a technical summary should be provided if alternative factors are utilized in the assessment (Level 2 and 3).

f) Reference Stress Solution – The source of the reference stress solutions (e.g. handbook solution or finite-element analysis) used in the assessment including whether the local and/or global collapse was considered (Levels 2 and 3).

g) Stress Intensity Factor Solution – The source of stress intensity factor solutions (e.g. handbook solution or finite-element analysis) used in the assessment (Levels 2 and 3).

h) Failure Assessment Diagram – whether the Level 2 recommended curve, a material specific curve (including the source and validity of stress-strain data), or a curve derived from J-analysis is used in the assessment (Level 3).

i) Flaw Growth – whether any allowance is made for crack extension by sub-critical crack growth mechanism (e.g. fatigue or stress corrosion cracking); the crack growth models and associated constants utilized (from technical publication or laboratory measurements) should be summarized (Level 3).

j) In-Service Margins – The results calculated for each loading condition of interest and for each category of analysis undertaken; assessment points should be displayed on the appropriate failure assessment diagram (Level 3).

k) Sensitivity Analysis – A listing of the input parameters used to perform sensitivity studies (e.g. loads, material properties, flaw size, etc.); the results of each individual study should be summarized (Level 3).

9.8.1.2 All assumptions used in the assessment procedures should be documented. In addition, all departures from the procedures in this Part should be reported and separately justified. A separate statement should be made about the significance of potential failure mechanisms remote from the defective areas, if applicable.

9.8.2 If an in-service monitoring system is instituted because of the potential for sub-critical crack growth (see paragraph 9.7) or a leak detection system is installed as the result of a LBB assessment (see paragraph 9.5.2.7), then the following documentation should be kept with the equipment files:

a) Specification for the system

b) Procedures for installation of the system

c) System validation and calibration

d) Procedures for recording data

e) All data readings while the component is in-service readings

9.9 Nomenclature

a	depth of the crack-like flaw.
a_{eff}	effective depth of the crack-like flaw.
a_m	measured depth of the crack-like flaw.
α	angle of the crack measured from the principal plane (see Figure 9.2).
B	biaxial stress ratio.
c_m	measured half length of the crack-like flaw.
c_o	initial half length of the crack-like flaw.
C_u	conversion factor; if the units of K_{mat}^{mean} are $ksi\sqrt{in}$ and σ_{ys} are ksi then $C_u = 1.0$, if the units are $MPa\sqrt{m}$ and MPa then $C_u = 6.275$.
CET	Critical Exposure Temperature (see Part 3 of this Standard).
COA_p	crack opening area of a plate.
COA_s	crack opening area of a shell.
c	half-length of the existing flaw.
$2c$	full length of the existing flaw.
c_{LBB}	half-length of the postulated through-wall flaw.
d	size of the ligament for an embedded flaw (see Figure 9.1.c).
d_m	measured size of the ligament for an embedded flaw (see Figure 9.1.c).
D	inside diameter of the component containing the crack-like flaw including metal loss and future corrosion allowance, as applicable.
E	Young's Modulus.
E'	E for plane stress and $E/\left(1-\nu^2\right)$ for plane strain.
ε_{ref}	reference strain obtained from the true stress-strain curve at a true stress equal to $L_r^P \sigma_{ys}$.
J^{SR}	J interval based on residual stress
K_I^P	stress intensity factor based on primary stresses ($MPa\sqrt{m} : ksi\sqrt{in}$).
K_I^{SR}	stress intensity factor based on secondary and residual stresses ($MPa\sqrt{m} : ksi\sqrt{in}$).
K_{Ip}^{SR}	stress intensity factor based on secondary and residual stresses corrected for plasticity ($MPa\sqrt{m} : ksi\sqrt{in}$)
K_{mat}	value of the material fracture toughness used in the assessment ($MPa\sqrt{m} : ksi\sqrt{in}$).
K_{mat}^{mean}	average value of the material fracture toughness ($MPa\sqrt{m} : ksi\sqrt{in}$).
K_r	toughness ratio.
L_r^P	load ratio based on primary stress.
$L_{r(\max)}^P$	maximum permitted value of L_r^P (see Figure 9.20).
L_r^{SR}	load ratio based on secondary and residual stresses.
ν	Poisson's ratio.
P_m	primary membrane stress.
P_b	primary bending stress.
PSF_a	partial safety factor for the flaw dimensions.

PSF_k partial safety factor for the fracture toughness.

PSF_s partial safety factor for the applied stress.

ψ used in the calculation of plasticity correction factor Φ

R inside radius of the component containing the crack-like flaw including metal loss and future corrosion allowance, as applicable.

S_{srf} secondary and residual stress reduction factor.

σ applied tensile stress.

σ_f flow stress (see Annex F).

σ_{ys} yield strength at the assessment temperature (see Annex F).

σ_{ref}^{P} reference stress based on the primary stress.

σ_{ref}^{SR} reference stress based on the secondary and residual stress from STEP 9.

ϕ parameter used in the calculation of plasticity correction factor Φ.

Φ plasticity correction factor.

t thickness of the component containing the crack-like flaw including metal loss and future corrosion allowance, as applicable.

T_{ref} reference Temperature.

τ factor equal to 1.0 for plane stress and 3.0 for plane strain.

W correction factor for flaw depth.

W_{Theta} parameter used to determine the correction factor for flaw depth.

9.10 References

1. Anderson, T.L., “Fracture Mechanics – Fundamentals and Applications,” 3nd Edition, CRC Press, Boca Raton, Florida, 2005.
2. Anderson, P., Bergman, M., Brickstad, B., Dahlberg, L.“A Procedure for Safety Assessment of Components with Cracks – Handbook,” 3rd Edition, SAQ/FoU-Report 96/08, SAQ Kontroll AB, Sweden, 1997.
3. Anderson, T.L., Merrick, R.D., Yukawa, S., Bray, D.E., Kaley, L. And Van Scyoc, K., “Fitness-For-Service Evaluation Procedures For Operating Pressure Vessels, Tanks, And Piping In Refinery And Chemical Service,” FS-26, Consultants’ Report, MPC Program On Fitness-For-Service, Draft 5, The Materials Properties Council, New York, N.Y., October, 1995.
4. Anderson, T.L. and Osage, D.A., “API 579: A Comprehensive Fitness-For-Service Guide,” International Journal of Pressure Vessels and Piping 77 (2000), pp 953-963.
5. Ainsworth, R.A., “The Treatment of Thermal and Residual Stresses in Fracture Assessments,” *Engineering Fracture Mechanics*, Vol. 24, No. 1, pp. 65-76, 1986.
6. Bloom, J.M., “Deformation Plasticity Failure Assessment Diagram (DPFAD) For Materials With Non-Ramberg-Osgood Stress-Strain Curves,” Journal Of Pressure Vessel Technology, American Society Of Mechanical Engineers, Vol. 117, November 1995.
7. Bloom, J.M., “Deformation Plasticity Failure Assessment Diagram (DPFAD) Approach / A Fitness-For-Purpose Fracture Mechanics Based Methodology for Use in the Petrochemical Industry,” PVP-Vol. 315, Fitness-for-Service and Decisions for Petroleum and Chemical Equipment, ASME, pp. 131-144, 1995.
8. Dong, P., Rahman, S., Wilkowski, G., Brickstad, B., Bergman, M., “Effects Of Weld Residual Stresses On Crack Opening Area Analysis Of Pipes For LBB Applications,” LBB95; Specialist Meeting On Leak-Before-Break In Reactor Piping And Vessels, Lyon, France, October, 1995.
9. Ewing, D.J.F., “Simple Methods For Predicting Gas Leakage Flows Through Cracks,” Paper C376/047 In Proceedings Of International Conference On Pipework Engineering And Operation, I. Mech. E., London, 21-22, Pp. 307-314, February, 1989.
10. Hazelton, W.S., “Technical Report On Material Selection And Processing Guidelines For BWR Coolant Pressure Boundary Piping (Draft Report),” NUREG -0313, Rev. 2, June, 1986.
11. Kumar, V., German, M.D., Shih, C.F., “An Engineering Approach For Elastic-Plastic Fracture Analysis,” EPRI Report NP-1931, EPRI Palo Alto, CA, 1981.
12. Loushin, L.L., “Assessment of Structural Integrity in Pressure Vessels – Predictions and Verification,” PVP Vol. 336, ASME, pp. 97-104, 1996.
13. Langston, D.B., “A Reference Stress Approximation For Determining Crack Opening Displacements In Leak-Before-Break Calculations,” TD/SID/REP/0112, Nuclear Electric Document, 1991.
14. Langston, D.B., Haines, N.F. And Wilson, R., “Development Of A Leak-Before-Break Procedure For Pressurized Components,” CEGB, UK, pp. 287-292.
15. Miller, A.G., “Elastic Crack Opening Displacements And Rotations In Through Cracks In Spheres And Cylinders Under Membrane And Bending Loading,” Engineering Fracture Mechanics, Vol. 23, 1986.
16. Milne, I., Ainsworth, R.A., Dowling, A.R., And Stewart, A.T., “Assessment Of The Integrity Of Structures Containing Defects,” *Int. J. Pres. Vessel & Piping*, 32, 1988, pp. 3-104.
17. Milne, I., Ainsworth, R.A., Dowling, A.R., And Stewart, A.T., “Background To And Validation Of CEGB Report R/H/R6-Revision 3,” *Int. J. Pres. Vessel & Piping*, 32, 1988, pp. 105-196.
18. Paul, D.D., Ahmad, J., Scott, P.M., Flanigan, L.F. And Wilkowski, G.M., “Evaluation And Refinement Of Leak-Rate Estimation Models,” NUREG/CR-5128, Rev. 1, June 1995.
19. Paris, P.C., and Johnson, R.E., “A Method of Application of Elastic-Plastic Fracture Mechanics to Nuclear Vessel Analysis,” Elastic-Plastic Fracture: Second Symposium, Volume II-Fracture Resistance Curves and Engineering Applications, ASTM STP 803, 1983, pp. Ii-4-ii-40.

20. Rahman, S., Brust, F., Ghadiali, N., Choi, Y.H., Krishnaswamy, P., Moberg, F., Brickstad, B. And Wilkowski, G., "Refinement And Evaluation Of Crack Opening Area Analyses For Circumferential Through-Wall Cracks In Pipes," NUREG/CR-6300, 1995.

21. Rahman, S., Ghadiali, Paul, D. And Wilkowski, G., "Probabilistic Pipe Fracture Evaluations For Leak-Rate-Detection Applications," NUREG/CR-6004, April, 1995.

22. Scott, P.M., Anderson, T.L., Osage, D.A., and Wilkowski, G.M., "Review of Existing Fitness-For-Service Criteria for Crack-Like Flaws," WRC Bulletin 430, Welding Research Council, 1998.

23. Sharples, J.K. And Bouchard, P.J., "Assessment Of Crack Opening Area For Leak Rates," LBB95; Specialist Meeting On Leak-Before-Break In Reactor Piping And Vessels, Lyon, France, October, 1995.

24. Smith, E., "The Opening Of Through-Wall Cracks In BWR Coolant Lines Due To The Application Of Severe Overloads," NUREG/CP-0051, August, 1984.

25. Wilkowski, G., Scott, P. And Maxey, W., "Design And Optimization Of Mechanical Crack Arrestors For Pipelines," NG-18 Report No. 134, American Gas Association, July, 1983.

26. Wuthrich, C. "Crack Opening Areas In Pressure Vessels And Pipes*," Engineering Fracture Mechanics*, Vol. 18, No. 5, pp. 1049-1057, 1983.

27. Phaal, R, "Non-unique Solutions in PD6493: 1991 Fracture Assessment Procedures," ASME PVP-Vol. 260, American Society of Mechanical Engineers, pp. 149-155, 1993.

28. Dijkstra, O.D. and Straalen, J.J., van, "Fatigue Crack Growth Program FAFRAM (Fatigue FRActure Mechanics)," TNO Building and Construction Research, Report BI-91-051.

29. Wirsching, P.H. and Mansour, A.E., "Incorporation of Structural Reliability Methods into Fitness-For-Service Procedures," The Materials Properties Council, Inc., May, 1998.

30. Liu, A.F., "Structural Life Assessment Methods," ASM International, Materials Park, Ohio, 1998.

31. Ellyin, F., "Fatigue Damage Crack Growth and Life Prediction," Chapman & Hall, Boundary Row, London 1997.

32. Bockrath, G. and Glassco, J., "Fatigue and Fracture Mechanics of High Risk Parts – Application of LEFM & EMDM Theory," Chapman & Hall, New York, N.Y., 1997.

33. Hooton, G.H. and Budden, P.J., "R6 Developments In The Treatment Of Secondary Stresses," PVP-Vol. 304, ASME, 1995, pp 503-509.

34. Popelar, C.H., "A Tearing Instability Analysis for Strain Hardening Materials," ASTM STP 833, 1984.

35. Farahmand,B., Bockrath, G., and Glassco, J., "Fatigue and Fracture Mechanics of High Risk Parts – Application of LEFM & FMDM Theory," Chapman Hall, New York, N.Y., 1997.

9.11 Tables and Figures

Table 9.1
Data Required for the Assessment of a Crack-Like Flaw

A summary of the data that should be obtained from a field inspection is provided on this form.

Equipment Identification: _____
Equipment Type: _____ Pressure Vessel _____ Storage Tank _____ Piping Component
Component Type & Location: _____

Data Required for Level 1:
Assessment Temperature (typically the minimum temperature at full pressure): _____
Assessment Pressure: _____
Location of Flaw (*Base Metal, Weld Metal or HAZ*): _____
Surface Location (*ID, OD or Through-wall*): _____
Flaw Type (*Surface or Embedded*): _____
Flaw Orientation To Weld Seam (*Parallel or Perpendicular*): _____
Flaw Depth and Length (a *and* $2c$): _____
Flaw Depth Below Surface (d – Embedded Flaw): _____
Axial or Circumferential Crack : _____
Post Weld Heat Treated (*PWHT*): _____
Design Code: _____
Base Material Specification: _____
Weld Material Specification: _____
Wall Thickness: _____
MAWP: _____
Process Environment: _____
Design Pressure & Temperature: _____
Cyclic Loading Conditions: _____
Inspection Method – Flaw Length: _____
Inspection Method – Flaw Depth: _____
Inspection Method – Flaw Depth Below Surface: _____

Additional Data Required for Level 2 (In Addition to the Level 1 Data):
Yield Stress (Base Metal): _____
Tensile Stress (Base Metal): _____
Fracture Toughness (Base Metal): _____
Source Of Material Data (Base Metal): _____
Yield Stress (Weld Metal): _____
Tensile Stress (Weld Metal): _____
Fracture Toughness (Weld Metal): _____
Source Of Material Data (Weld Metal): _____
Yield Stress (HAZ): _____
Tensile Stress (HAZ): _____
Fracture Toughness (HAZ): _____
Source Of Material Data (HAZ): _____
Probability Of Failure Category: _____
Coefficient Of Variation – Loads (COV_s) : _____
Partial Safety Factor – Loads (PSF_s): _____
Partial Safety Factor – Material Fracture Toughness (PSF_s): _____
Partial Safety Factor – Flaw Size (PSF_s): _____

Table 9.2– Reference Temperature for Use in a Level 1 Assessment

Carbon Steels – 20 Joule or 15 ft-lb Transition Temperature for Each ASME Exemption Curve				
MYS (ksi)	ASME Exemption Curve			
	A (ºF)	B (ºF)	C (ºF)	D (ºF)
30	104	66	28	2
32	97	59	21	-5
34	91	53	15	-11
36	86	48	10	-16
38	81	43	5	-21
40	78	40	2	-24
42	74	36	-2	-28
44	71	33	-5	-31
46	68	30	-8	-34
48	66	28	-10	-36
50	63	25	-13	-39
Low Alloy Steels – 27 Joule or 20 ft-lb Transition Temperature for Each ASME Exemption Curve				
MYS (ksi)	ASME Exemption Curve			
	A (ºF)	B (ºF)	C (ºF)	D (ºF)
30	124	86	48	22
32	115	77	39	13
34	107	69	31	5
36	101	63	25	-1
38	96	58	20	-6
40	92	54	16	-10
42	88	50	12	-14
44	85	47	9	-17
46	81	43	5	-21
48	79	41	3	-23
50	76	38	0	-26
52	73	35	-3	-29
54	71	33	-5	-31
56	69	31	-7	-33
58	67	29	-9	-35
60	65	27	-11	-37
62	63	25	-13	-39
64	62	24	-14	-40
66	60	22	-16	-42
68	58	20	-18	-44
70	57	19	-19	-45
72	56	18	-20	-46
74	54	16	-22	-48
76	53	15	-23	-49
78	52	14	-24	-50
80	51	13	-25	-51
Note: MYS minimum specified yield strength of the material.				

Table 9.2M – Reference Temperature for Use in a Level 1 Assessment

Carbon Steels – 20 Joule or 15 ft-lb Transition Temperature for Each ASME Exemption Curve				
MYS (MPa)	ASME Exemption Curve			
	A (ºC)	B (ºC)	C (ºC)	D (ºC)
200	42	21	0	-15
210	38	17	-4	-18
220	36	15	-7	-21
230	33	12	-9	-23
240	31	10	-11	-26
260	27	6	-15	-29
280	24	3	-18	-32
300	22	1	-21	-35
320	19	-2	-23	-37
340	17	-4	-25	-39
360	15	-6	-27	-41
Low Alloy Steels – 27 Joule or 20 ft-lb Transition Temperature for Each ASME Exemption Curve				
MYS (MPa)	ASME Exemption Curve			
	A (ºC)	B (ºC)	C (ºC)	D (ºC)
200	55	33	12	-2
210	50	29	8	-7
220	46	25	4	-11
230	43	22	1	-14
240	40	19	-2	-16
250	38	17	-4	-19
260	36	15	-6	-21
270	34	13	-8	-23
280	32	11	-10	-24
290	31	10	-11	-26
300	30	8	-13	-27
310	28	7	-14	-28
320	27	6	-15	-30
330	26	5	-16	-31
340	25	4	-17	-32
360	23	2	-19	-34
380	21	0	-21	-36
400	19	-2	-23	-37
420	18	-3	-24	-39
440	16	-5	-26	-40
460	15	-6	-27	-42
480	14	-7	-28	-43
500	13	-8	-29	-44
520	12	-9	-30	-45
540	11	-10	-31	-46
560	10	-11	-32	-47
Note: MYS minimum specified yield strength of the material.				

Table 9.3
Partial Safety Factors for the Assessment of Crack-Like Flaws

Shallow Cracks: $a < 5\ mm\ (0.2\ inches)$ (1)								
Probability Of Failure Category (2)	COV_s (3)	R_c (4)	$R_{ky} \le R_c$ (5),(6)			$R_{ky} > R_c$ (5),(6)		
			PSF_s	PSF_k	PSF_a	PSF_s	PSF_k	PSF_a
$p_f = 2.3\left(10^{-2}\right)$ $(\beta = 2.0)$	0.10	1.0	1.20	1.43	1.08	1.25	1.0	1.0
	0.20	1.0	1.30	1.43	1.08	1.50	1.0	1.0
	0.30	1.0	1.55	1.43	1.08	1.75	1.0	1.0
$p_f = 10^{-3}$ $(\beta = 3.09)$	0.10	1.4	1.40	1.43	1.20	1.50	1.0	1.0
	0.20	1.4	1.50	1.82	1.10	2.0	1.0	1.0
	0.30	1.4	2.00	2.0	1.05	2.50	1.0	1.0
$p_f = 10^{-6}$ $(\beta = 4.75)$	0.10	2.0	1.75	2.0	1.35	2.00	1.0	1.0
	0.20	2.0	2.50	2.0	1.50	3.10	1.0	1.0
	0.30	2.0	2.6	2.0	1.50	4.10	1.0	1.0
Deep Cracks: $a \ge 5\ mm\ (0.2\ inches)$ (1)								
Probability Of Failure Category (2)	COV_s (3)	R_c (4)	$R_{ky} \le R_c$ (5),(6)			$R_{ky} > R_c$ (5),(6)		
			PSF_s	PSF_k	PSF_a	PSF_s	PSF_k	PSF_a
$p_f = 2.3\left(10^{-2}\right)$ $(\beta = 2.0)$	0.10	1.8	1.20	1.33	1.10	1.25	1.0	1.0
	0.20	1.3	1.40	1.54	1.10	1.50	1.0	1.0
	0.30	1.1	1.60	1.67	1.10	1.75	1.0	1.0
$p_f = 10^{-3}$ $(\beta = 3.09)$	0.10	1.9	1.40	1.67	1.15	1.50	1.0	1.0
	0.20	1.5	1.80	1.43	1.10	2.0	1.0	1.0
	0.30	1.3	2.30	1.43	1.10	2.50	1.0	1.0
$p_f = 10^{-6}$ $(\beta = 4.75)$	0.10	1.8	1.70	2.0	1.25	2.00	1.0	1.0
	0.20	1.5	2.60	1.82	1.25	3.10	1.0	1.0
	0.30	1.5	3.50	1.67	1.25	4.10	1.0	1.0

Table 9.3
Partial Safety Factors for the Assessment of Crack-Like Flaws

Notes:

1. The flaw depth maximum value measured. The PSFs for flaw depth in this table were established considering flaw size distributions obtained using accurate UT techniques such as time-of-flight diffraction methods (TOFD) or focused beam methods. If the accuracy of the UT technique used to determine the flaw depth is less accurate (i.e. amplitude drop method), then a conservative estimate of the flaw depth should be used in the assessment with the PSF factors in this table.
2. In the Probability Of Failure Category column, p_f probability of failure and β associated safety index.
3. COV_s is the coefficient of variation (standard deviation divided by the mean) used to define the uncertainty in the primary stress distribution. The primary stress to be used in the assessment should be based on the average expected value. Three categories are provided.
   - $COV_s = 0.10$ – The primary loads and corresponding primary stresses in the region of the flaw are computed or measured, and are well known.
   - $COV_s = 0.20$ – The primary loads and corresponding primary stresses in the region of the flaw are computed or measured, and are reasonably well known. The uncertainty in the primary stresses is due to the possible variations in applied loads, or modeling estimates in the stress analysis.
   - $COV_s = 0.30$ – Estimates of the primary stresses are significantly uncertain. The uncertainty in the primary stresses result from the unknown or random nature of applied loading and/or modeling estimates in the stress analysis.
4. R_c is a cut-off value used to define the regions of brittle fracture/plastic collapse and plastic collapse, and the corresponding category of Partial Safety Factors to be used in an assessment.
5. R_{ky} is used in conjunction with R_c to determine the Partial Safety Factors to be used in an assessment (see note 4 above). The definition of R_{ky} is given by the following equation:

$$R_{ky} = \frac{K_{mat}^{mean}}{\sigma_{ys}} C_u$$

6. If the only source of fracture toughness data lower bound estimate in Annex F, paragraph F.4.4, then the mean value of toughness described in paragraph F.4.4.1.f should be used in the assessment. The mean value of fracture toughness is used because the Partial Safety Factors are calibrated against the mean fracture toughness.
7. The background for the Partial Safety Factors is provided in Reference [29].

Table 9.4
Tabular Data for the ψ -Factor

ψ											
L_r^P	L_r^{SR}										
	0.0	0.5	1.0	1.5	2.0	2.5	3.0	3.5	4.0	4.5	≥ 5.0
0.0	0.0	0.000	0.000	0.000	0.000	0.000	0.000	0.000	0.000	0.000	0.000
0.1	0.0	0.020	0.043	0.063	0.074	0.081	0.086	0.090	0.095	0.100	0.107
0.2	0.0	0.028	0.052	0.076	0.091	0.100	0.107	0.113	0.120	0.127	0.137
0.3	0.0	0.033	0.057	0.085	0.102	0.114	0.122	0.130	0.138	0.147	0.160
0.4	0.0	0.037	0.064	0.094	0.113	0.126	0.136	0.145	0.156	0.167	0.180
0.5	0.0	0.043	0.074	0.105	0.124	0.138	0.149	0.160	0.172	0.185	0.201
0.6	0.0	0.051	0.085	0.114	0.133	0.147	0.159	0.170	0.184	0.200	0.215
0.7	0.0	0.058	0.091	0.117	0.134	0.147	0.158	0.171	0.186	0.202	0.214
0.8	0.0	0.057	0.085	0.105	0.119	0.130	0.141	0.155	0.169	0.182	0.190
0.9	0.0	0.043	0.060	0.073	0.082	0.090	0.101	0.113	0.123	0.129	0.132
1.0	0.0	0.016	0.019	0.022	0.025	0.031	0.039	0.043	0.044	0.041	0.033
1.1	0.0	-0.013	-0.025	-0.033	-0.036	-0.037	-0.042	-0.050	-0.061	-0.073	-0.084
1.2	0.0	-0.034	-0.058	-0.075	-0.090	-0.106	-0.122	-0.137	-0.151	-0.164	-0.175
1.3	0.0	-0.043	-0.075	-0.102	-0.126	-0.147	-0.166	-0.181	-0.196	-0.209	-0.220
1.4	0.0	-0.044	-0.080	-0.109	-0.134	-0.155	-0.173	-0.189	-0.203	-0.215	-0.227
1.5	0.0	-0.041	-0.075	-0.103	-0.127	-0.147	-0.164	-0.180	-0.194	-0.206	-0.217
1.6	0.0	-0.037	-0.069	-0.095	-0.117	-0.136	-0.153	-0.168	-0.181	-0.194	-0.205
1.7	0.0	-0.033	-0.062	-0.086	-0.107	-0.125	-0.141	-0.155	-0.168	-0.180	-0.191
1.8	0.0	-0.030	-0.055	-0.077	-0.097	-0.114	-0.129	-0.142	-0.155	-0.166	-0.177
1.9	0.0	-0.026	-0.049	-0.069	-0.086	-0.102	-0.116	-0.129	-0.141	-0.154	-0.162
≥ 2.0	0.0	-0.023	-0.043	-0.061	-0.076	-0.091	-0.104	-0.116	-0.126	-0.137	-0.146

Notes:
1. Equations to determine the ψ -Factor are provided in Table 9.5.
2. Interpolation may be used for intermediate values of L_r^P and L_r^{SR}.

Table 9.5
Equations for Determination of the ψ -Factor (1)

L_r^{SR}	C_1	C_2	C_3	C_4	C_5	C_6	C_7	C_8	C_9	C_{10}
0.0	0.0	0.0	0.0	0.0	0.0	0.0	0.0	0.0	0.0	0.0
0.5	-2.66913E-05	25.6064	0.735321	-96.8583	-1.83570	134.240	1.59978	-83.6105	-0.493497	19.9925
1.0	-4.71153E-07	234.535	9.76896	-802.149	-23.3837	1066.58	19.9783	-648.697	-6.27253	153.617
1.5	-3.75189E-06	66.9192	4.64800	-224.507	-10.9901	288.872	8.92887	-169.271	-2.55693	38.3441
2.0	-1.07886E-05	45.9626	4.06655	-160.787	-10.1655	213.567	8.70602	-128.938	-2.58722	29.9699
2.5	-1.27938E-05	34.0140	3.56530	-126.974	-9.61991	176.724	8.85143	-111.226	-2.78480	26.8421
3.0	-4.62948E-06	27.5781	3.27165	-107.412	-9.20683	154.070	8.85151	-99.6994	-2.90516	24.7475
3.5	8.52189E-07	22.9360	3.03726	-90.9947	-8.63816	131.216	8.37438	-85.1256	-2.76449	21.1760
4.0	1.02755E-04	22.8427	3.04482	-64.9361	-5.39829	93.8627	5.79484	-75.1903	-3.28616	26.1201
4.5	4.44068E-05	19.6562	3.12233	-96.3032	-11.0348	164.591	13.2860	-123.811	-5.35151	35.4213
≥ 5.0	8.19621E-05	21.1804	3.37642	-82.4411	-9.11191	146.507	12.5521	-125.246	-6.70084	42.6723

Notes:

1. The equation to determine ψ -Factor for a given L_r^{SR} is shown below where the coefficients are defined in the table.

$$\psi = \left(\frac{C_1 + C_3 L_r^P + C_5 \left(L_r^P\right)^2 + C_7 \left(L_r^P\right)^3 + C_9 \left(L_r^P\right)^4}{1.0 + C_2 L_r^P + C_4 \left(L_r^P\right)^2 + C_6 \left(L_r^P\right)^3 + C_8 \left(L_r^P\right)^4 + C_{10} \left(L_r^P\right)^5} \right)$$

2. Interpolation may be used for intermediate values of L_r^{SR}.

Table 9.6
Equations for Determination of the ϕ-Factor (1)

ϕ											
L_r^P	L_r^{SR}										
	0.0	0.5	1.0	1.5	2.0	2.5	3.0	3.5	4.0	4.5	≥ 5.0
0.0	0.0	1.0	1.0	1.0	1.0	1.0	1.0	1.0	1.0	1.0	1.0
0.1	0.0	0.815	0.869	0.877	0.880	0.882	0.883	0.883	0.882	0.879	0.874
0.2	0.0	0.690	0.786	0.810	0.821	0.828	0.832	0.833	0.833	0.831	0.825
0.3	0.0	0.596	0.715	0.752	0.769	0.780	0.786	0.789	0.789	0.787	0.780
0.4	0.0	0.521	0.651	0.696	0.718	0.732	0.740	0.744	0.745	0.743	0.735
0.5	0.0	0.457	0.589	0.640	0.666	0.683	0.693	0.698	0.698	0.695	0.688
0.6	0.0	0.399	0.528	0.582	0.612	0.631	0.642	0.647	0.648	0.644	0.638
0.7	0.0	0.344	0.466	0.522	0.554	0.575	0.587	0.593	0.593	0.589	0.587
0.8	0.0	0.290	0.403	0.460	0.493	0.516	0.528	0.533	0.534	0.534	0.535
0.9	0.0	0.236	0.339	0.395	0.430	0.452	0.464	0.470	0.475	0.480	0.486
1.0	0.0	0.185	0.276	0.330	0.364	0.386	0.400	0.411	0.423	0.435	0.449
1.1	0.0	0.139	0.218	0.269	0.302	0.326	0.347	0.367	0.387	0.406	0.423
1.2	0.0	0.104	0.172	0.219	0.256	0.287	0.315	0.340	0.362	0.382	0.399
1.3	0.0	0.082	0.142	0.190	0.229	0.263	0.291	0.316	0.338	0.357	0.375
1.4	0.0	0.070	0.126	0.171	0.209	0.241	0.269	0.293	0.314	0.333	0.350
1.5	0.0	0.062	0.112	0.155	0.190	0.220	0.247	0.270	0.290	0.309	0.325
1.6	0.0	0.055	0.100	0.139	0.172	0.200	0.225	0.247	0.267	0.285	0.301
1.7	0.0	0.048	0.089	0.124	0.154	0.181	0.204	0.224	0.243	0.260	0.276
1.8	0.0	0.042	0.078	0.110	0.137	0.161	0.183	0.202	0.220	0.236	0.250
1.9	0.0	0.036	0.068	0.096	0.120	0.142	0.162	0.180	0.196	0.211	0.225
≥ 2.0	0.0	0.031	0.058	0.083	0.104	0.124	0.141	0.170	0.172	0.186	0.198

Notes:

1. Equations to determine the ϕ-Factor are provided in Table 9.7.
2. Interpolation may be used for intermediate values of L_r^P and L_r^{SR}.

Table 9.7
Equations for Determination of the ϕ-Factor (1)

L_r^S	C_1	C_2	C_3	C_4	C_5	C_6	C_7	C_8
0.0	0.0	0.0	0.0	0.0	0.0	0.0	0.0	0.0
0.5	1.00001	-2.22913	-2.41484	2.93036	1.93850	-2.93471	-0.509730	1.31047
1.0	1.00001	-2.13907	-2.38708	1.90283	1.89948	-1.11292	-0.498340	0.400603
1.5	0.999999	-2.04828	-2.36097	1.45152	1.86492	-0.457048	-0.488331	0.101387
2.0	0.999987	-2.02808	-2.36632	1.30047	1.87918	-0.225165	-0.495719	0.000000
2.5	0.999961	-2.08565	-2.42584	1.34991	1.97702	-0.215801	-0.532519	0.000000
3.0	0.999951	-2.15806	-2.49971	1.43002	2.09759	-0.222316	-0.578002	0.000000
3.5	0.999910	-2.15424	-2.49570	1.41869	2.08859	-0.213589	-0.571688	0.000000
4.0	0.999978	-2.20511	-2.57332	1.42094	2.23701	-0.0755321	-0.636324	-0.0763128
4.5	0.999976	-2.27554	-2.66103	1.48947	2.39550	-0.0340309	-0.699994	-0.101608
≥ 5.0	0.999977	-2.33094	-2.73542	1.54184	2.52395	-0.00694071	-0.750359	-0.119742

Notes:

1. The equation to determine ϕ-Factor for a given L_r^{SR} is shown below where the coefficients are defined in the table.

$$\phi = \left(\frac{C_1 + C_3\left(L_r^P\right)^{0.5} + C_5 L_r^P + C_7\left(L_r^P\right)^{1.5}}{1.0 + C_2\left(L_r^P\right)^{0.5} + C_4 L_r^P + C_6\left(L_r^P\right)^{1.5} + C_8\left(L_r^P\right)^2} \right)$$

2. Interpolation may be used for intermediate values of L_r^{SR}.

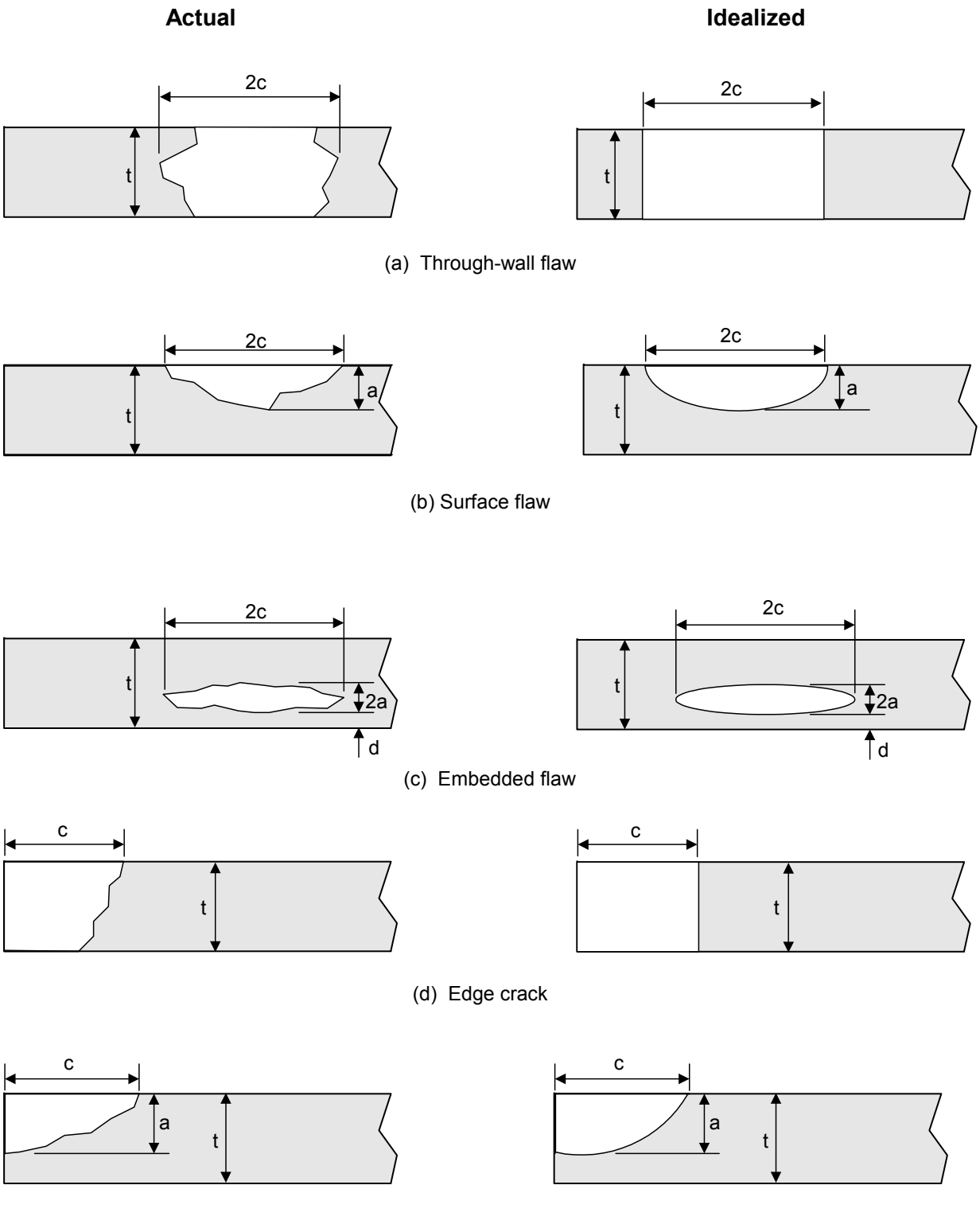

(a) Through-wall flaw

(b) Surface flaw

(c) Embedded flaw

(d) Edge crack

(e) Corner flaw

Figure 9.1 – Nomenclature and Idealized Shapes of Crack-Like Flaws

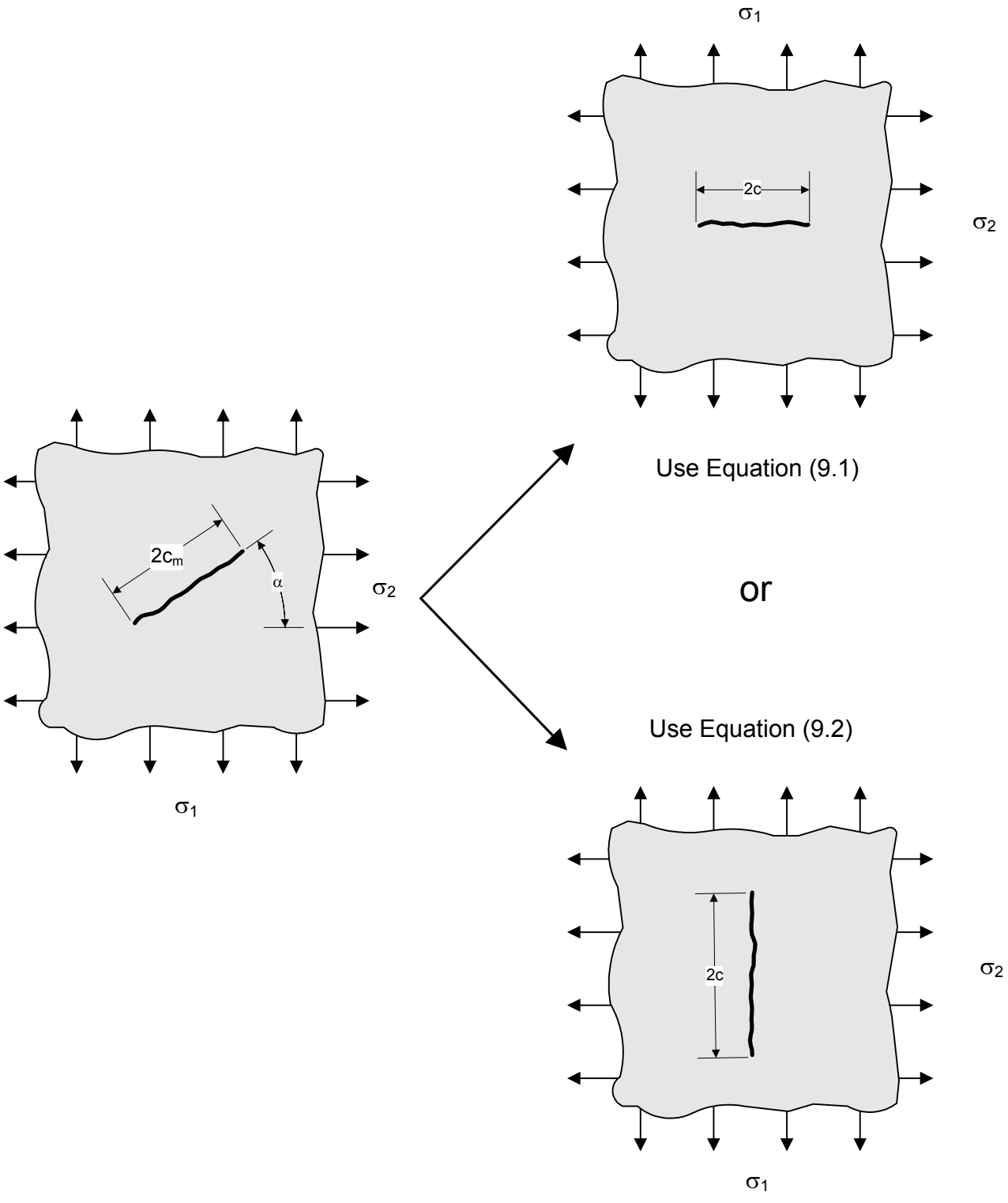

Figure 9.2 – Procedure for Defining an Effective Flaw Length on a Principal Stress Plane

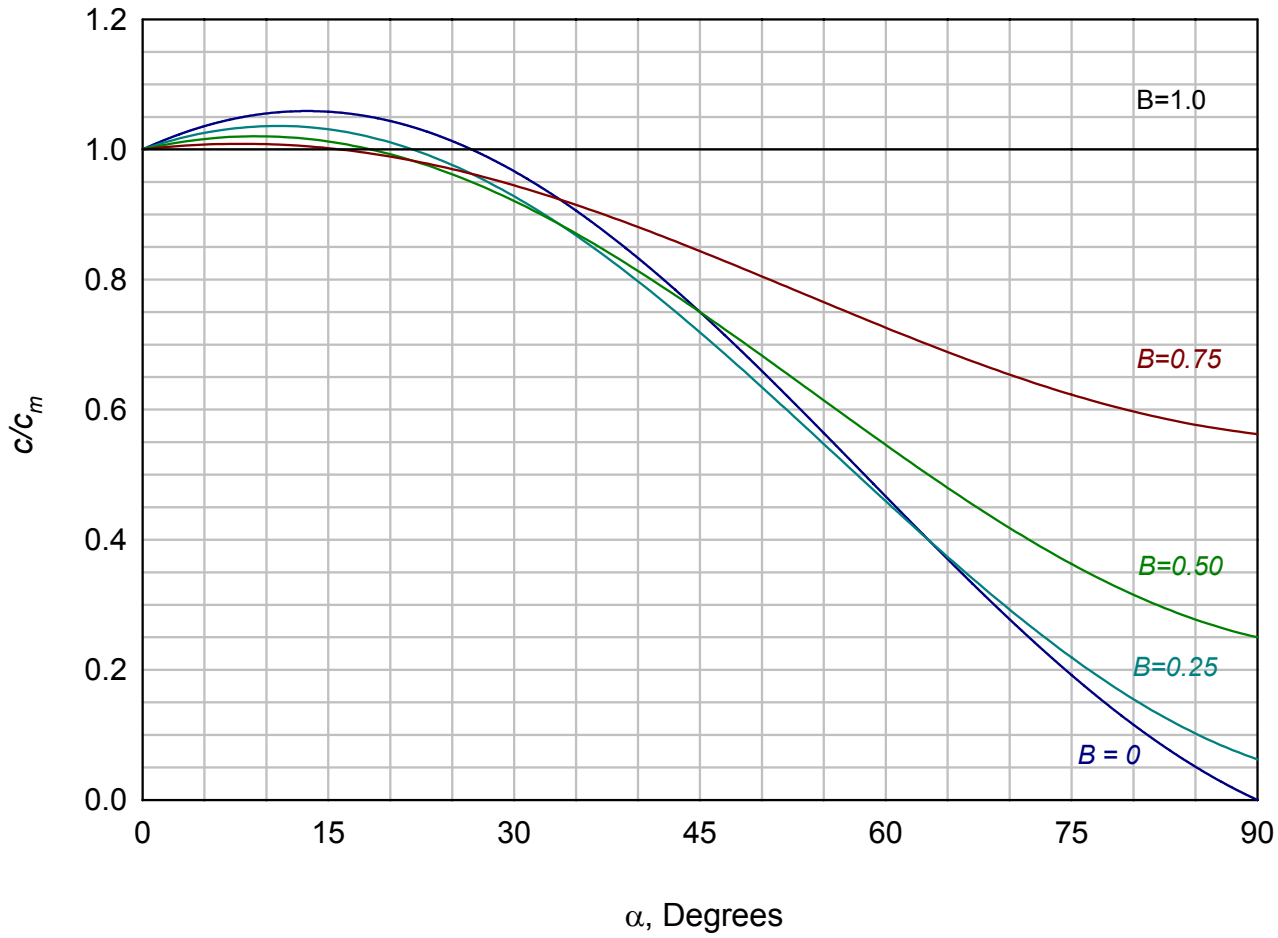

Notes:
1. The figure is a plot of Equation (9.1)
2. B in this figure biaxial stress ratio, see Equation (9.3)

Figure 9.3 – Equivalent Mode I Crack Length as a Function of α and the Stress Biaxiality Ratio

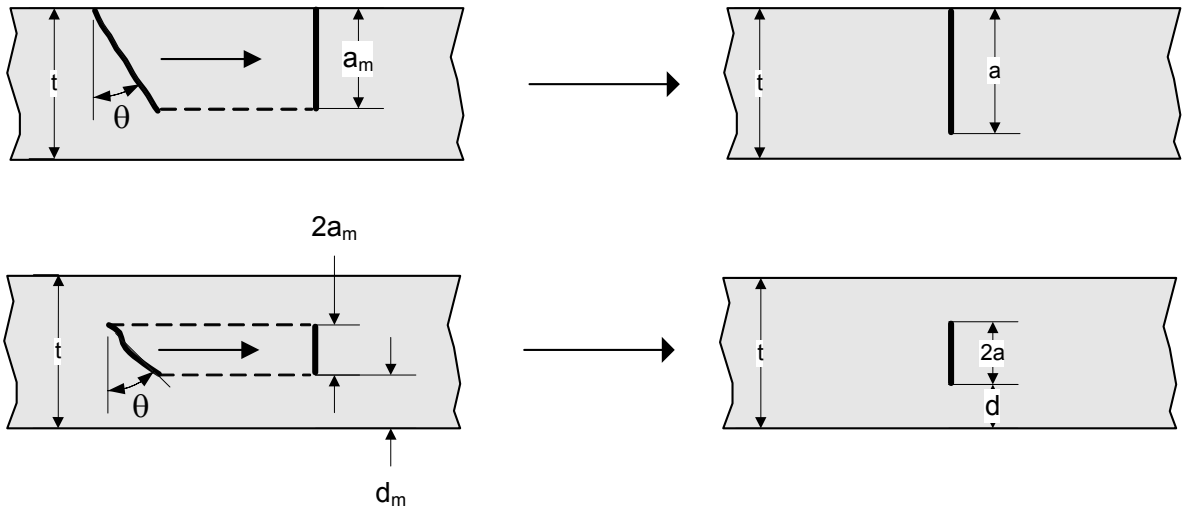

Project the flaw onto the principal plane. $a = Wa_m$, W is determined using Figure 9.5

(a) Planer Crack-Like Flaw

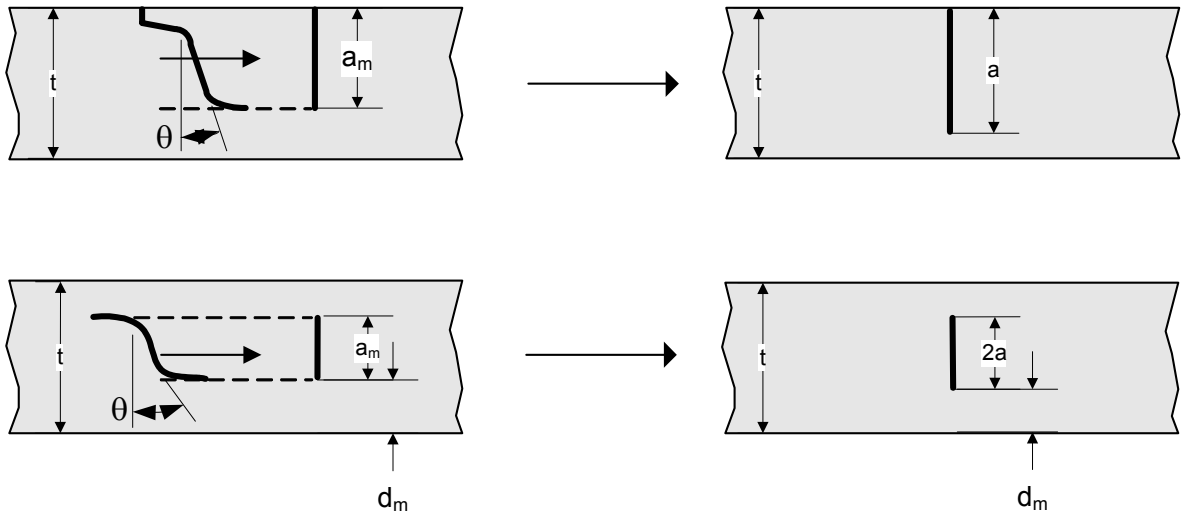

Project the flaw onto the principal plane. $a = Wa_m$, W is determined using Figure 9.5

(b) Stepwise Crack-Like Flaw

Note: For an embedded flaw, d_m and d are the minimum distance from the flaw to the surface

Figure 9.4 – Procedure for Defining the Effective Depth of a Flaw that is Oriented at an Oblique Angle

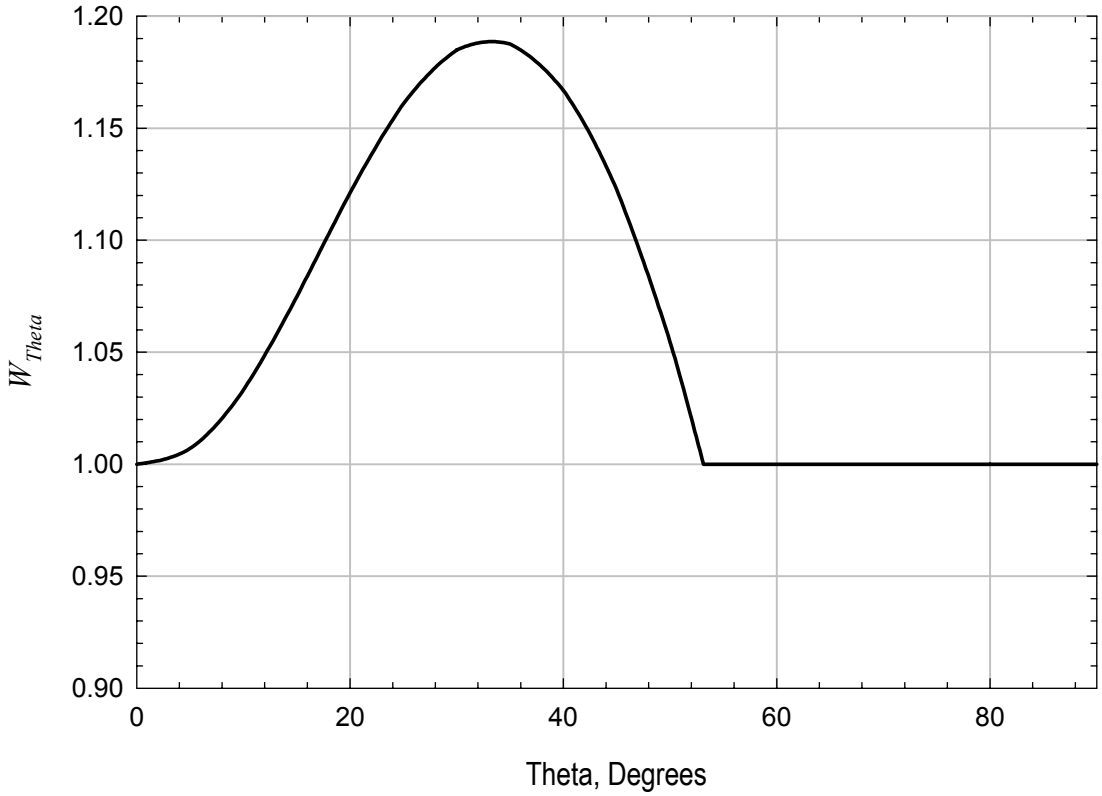

Notes:
1. The figure is a plot of Equation (9.7)
2. Theta in this figure angle of the flaw measured from the normal in the through-thickness direction (see Figure 9.4)

Figure 9.5 – Equivalent Mode I Crack Depth as a Function of the θ Angle

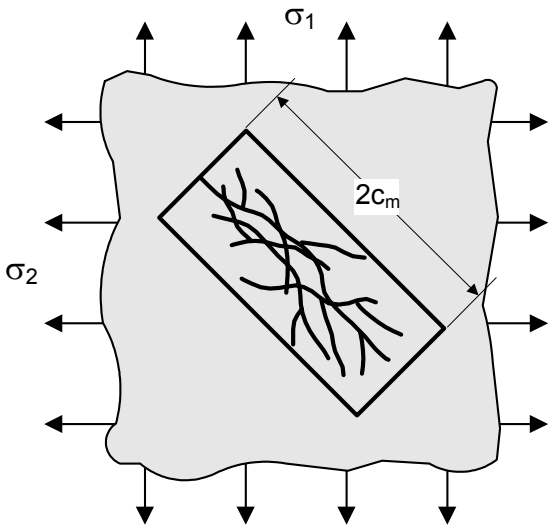

(a) Draw a rectangle around the affected area.

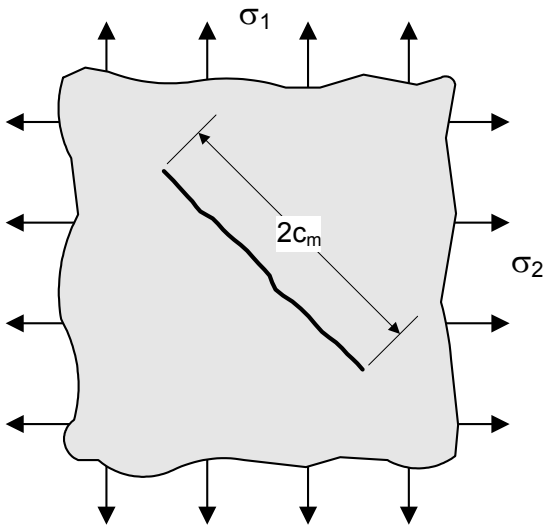

(b) Idealize the area as a planar flaw with length equal to the length of the rectangle.

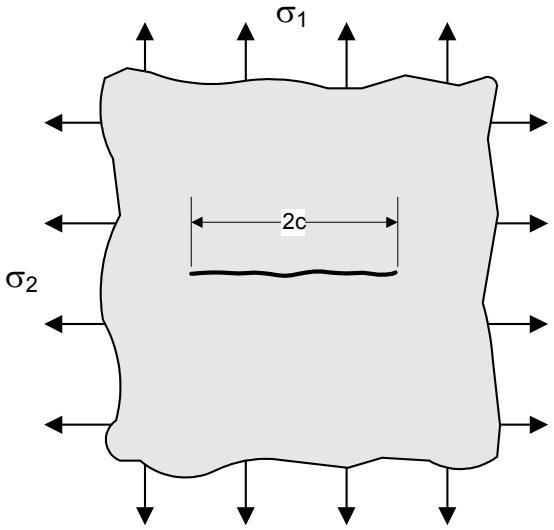

(c) Define an effective flaw length on a principal stress plane. ($\sigma_1 \geq \sigma_2$)

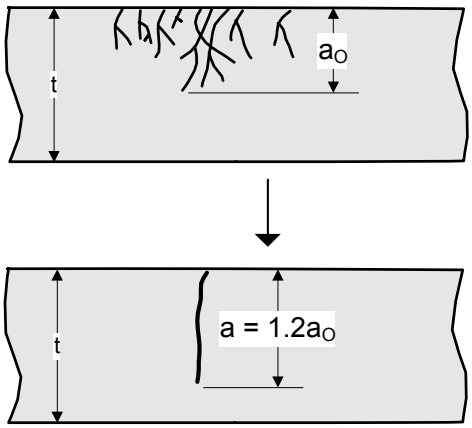

(d) Define the effective flaw depth as 1.2 times the maximum depth of the branched network.

Figure 9.6 – Procedure for Treating Branched Cracking

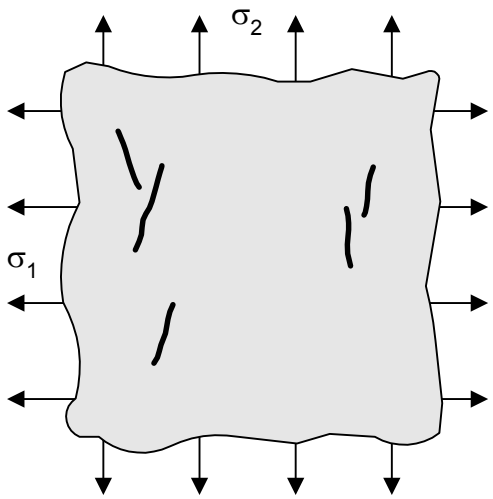

(a) Initial configuration.

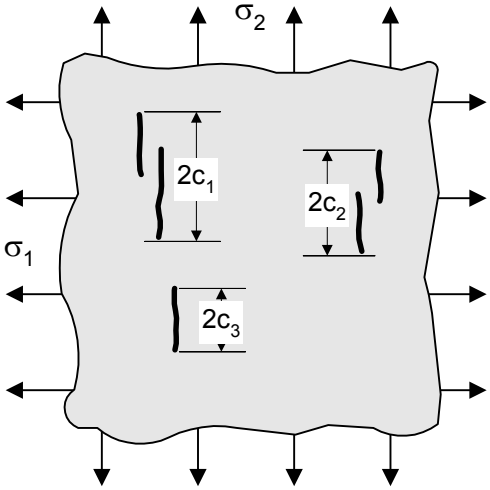

(b) After application of the equivalent flaw length rules in paragraph 9.3.6.2.

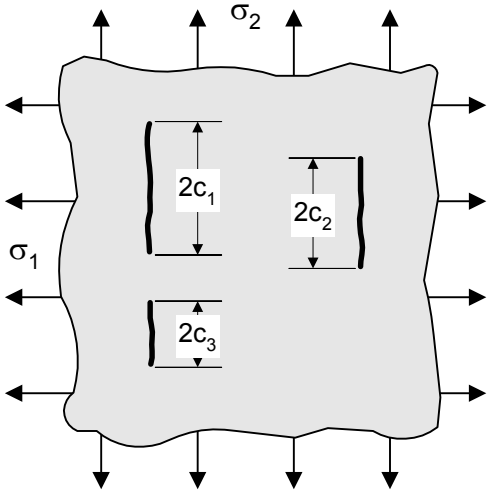

(c) After projecting interacting flaws onto a single plane

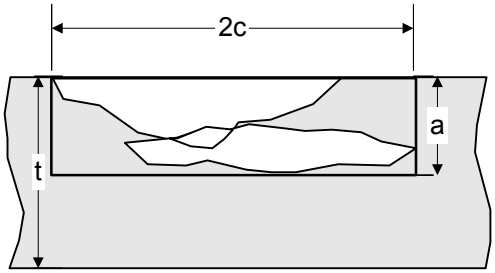

(d) Definition of effective dimensions of flaws that overlap after projection onto a single plane.

Figure 9.7 – Treatment of Multiple Crack-Like Flaws

Multiple Crack-Like Flaw Configuration	Criterion For Interaction	Effective Dimensions After Interaction
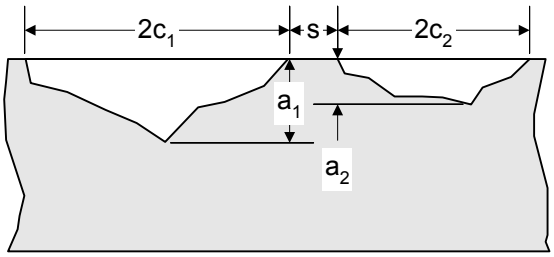	$c_1 + c_2 \geq s$	$2c = 2c_1 + 2c_2 + s$ $a = \max\left[a_1,\ a_2\right]$
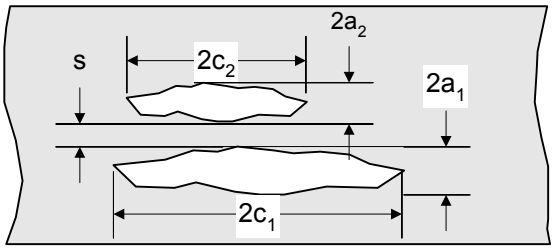	$a_1 + a_2 \geq s$	$2a = 2a_1 + 2a_2 + s$ $2c = \max\left[2c_1,\ 2c_2\right]$
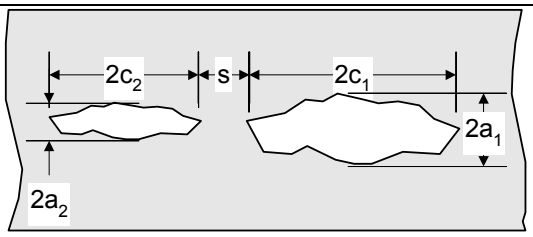	$c_1 + c_2 \geq s$	$2c = 2c_1 + 2c_2 + s$ $2a = \max\left[2a_1,\ 2a_2\right]$
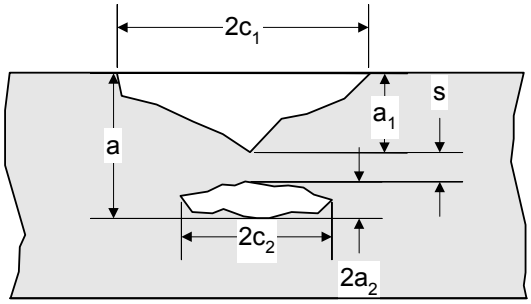	$a_1 + a_2 \geq s$	$a = a_1 + 2a_2 + s$ $2c = \max\left[2c_1,\ 2c_2\right]$

Figure 9.8 – Interaction of Coplanar Flaws

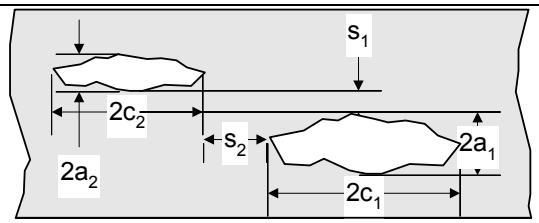	$c_1 + c_2 \geq s_2$ *and* $a_1 + a_2 \geq s_1$	$2c = 2c_1 + 2c_2 + s_2$ $2a = 2a_1 + 2a_2 + s_1$
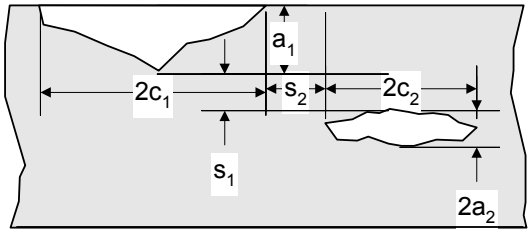	$c_1 + c_2 \geq s_2$ *and* $a_1 + a_2 \geq s_1$	$2c = 2c_1 + 2c_2 + s_2$ $a = a_1 + 2a_2 + s_1$
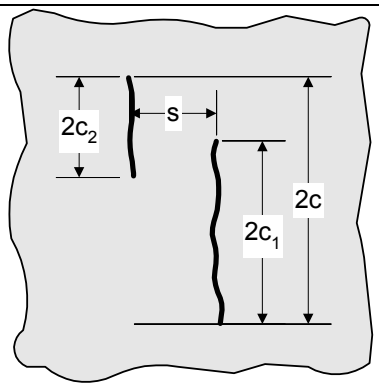	$c_1 + c_2 \geq s$	Project flaws onto the same plane. $2c$ = total length of projection based on cracks defined by $2c_1$ and $2c_2$
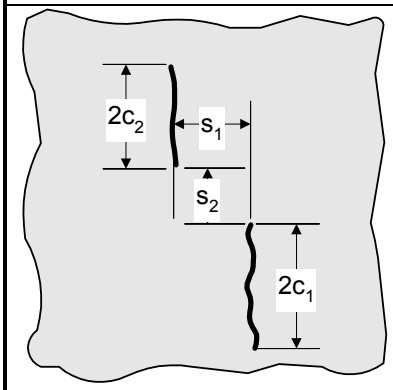	$c_1 + c_2 \geq s_1$ *and* $c_1 + c_2 \geq s_2$	Project flaws onto the same plane. $2c = 2c_1 + 2c_2 + s_2$

Figure 9.8 Continued – Interaction of Coplanar Flaws

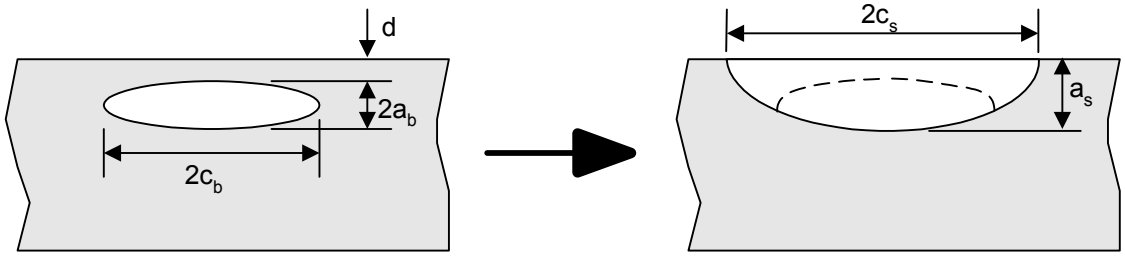

$2c_s = 2c_b + 2d$

$a_s = 2a_b + d$

(a) Embedded flaw recategorized as a surface flaw when $d/t < 0.2$

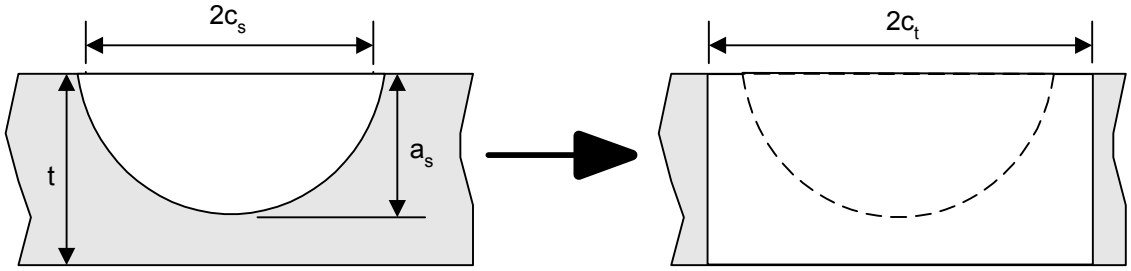

$2c_t = 2c_s + 2(t - a_s)$

(b) Surface flaw recategorized as a through-wall flaw when $a_s/t > 0.8$

Figure 9.9 – Procedure for Re-categorizing Flaws That Experience Ligament Yielding

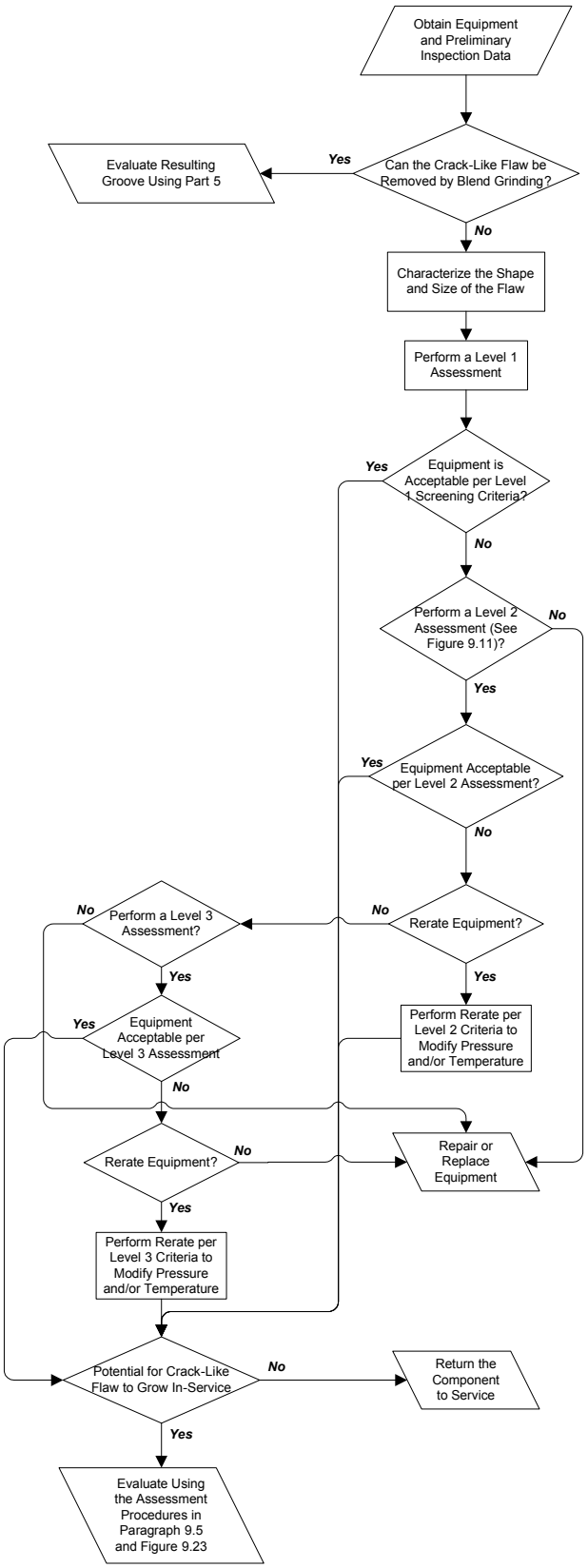

Figure 9.10 – Overview of the Assessment Procedures to Evaluate a Component with Crack-Like Flaws

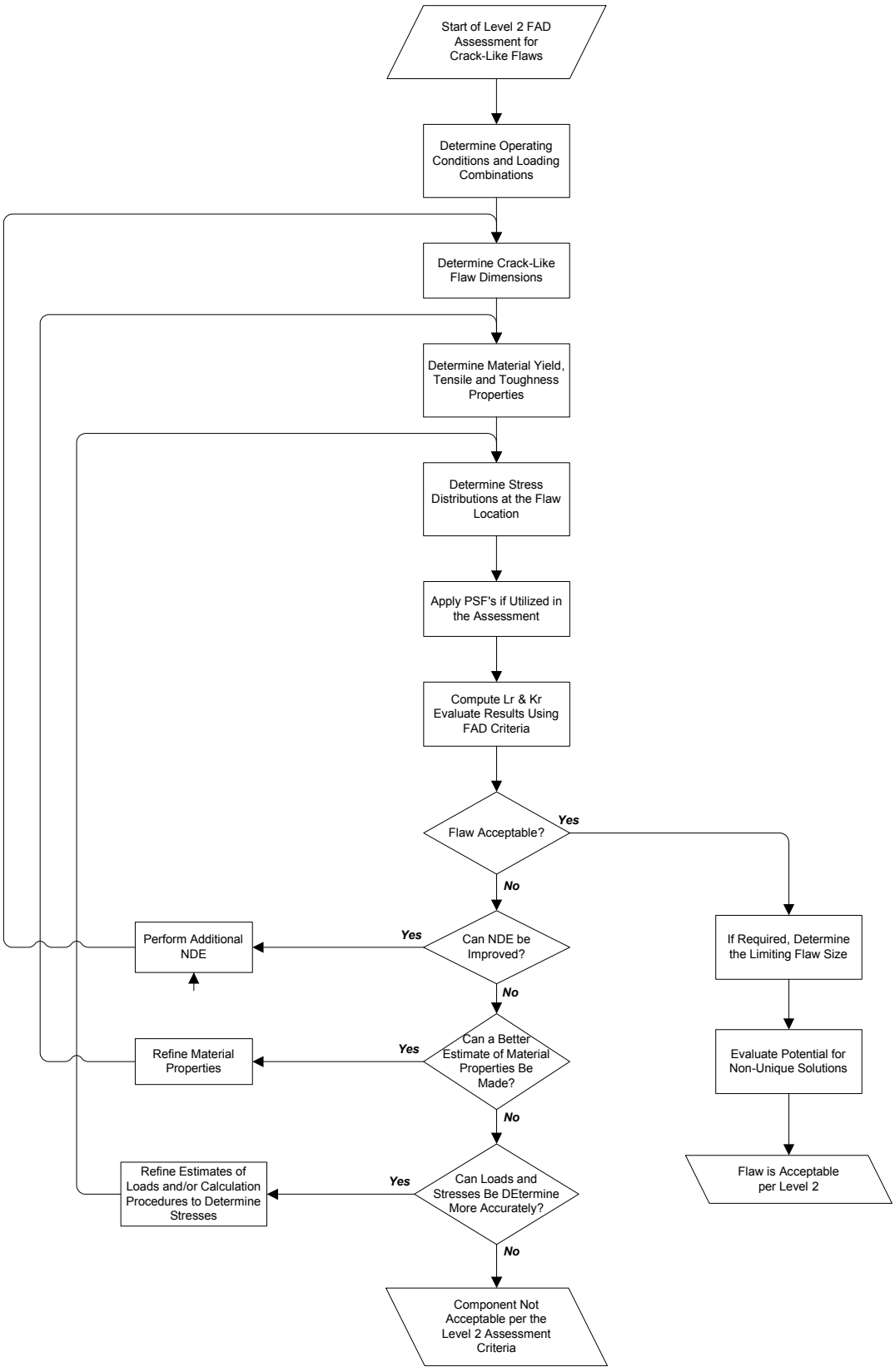

Figure 9.11 – Overview of the Level 2 Assessment Procedure for a Non-Growing Crack-Like Flaw

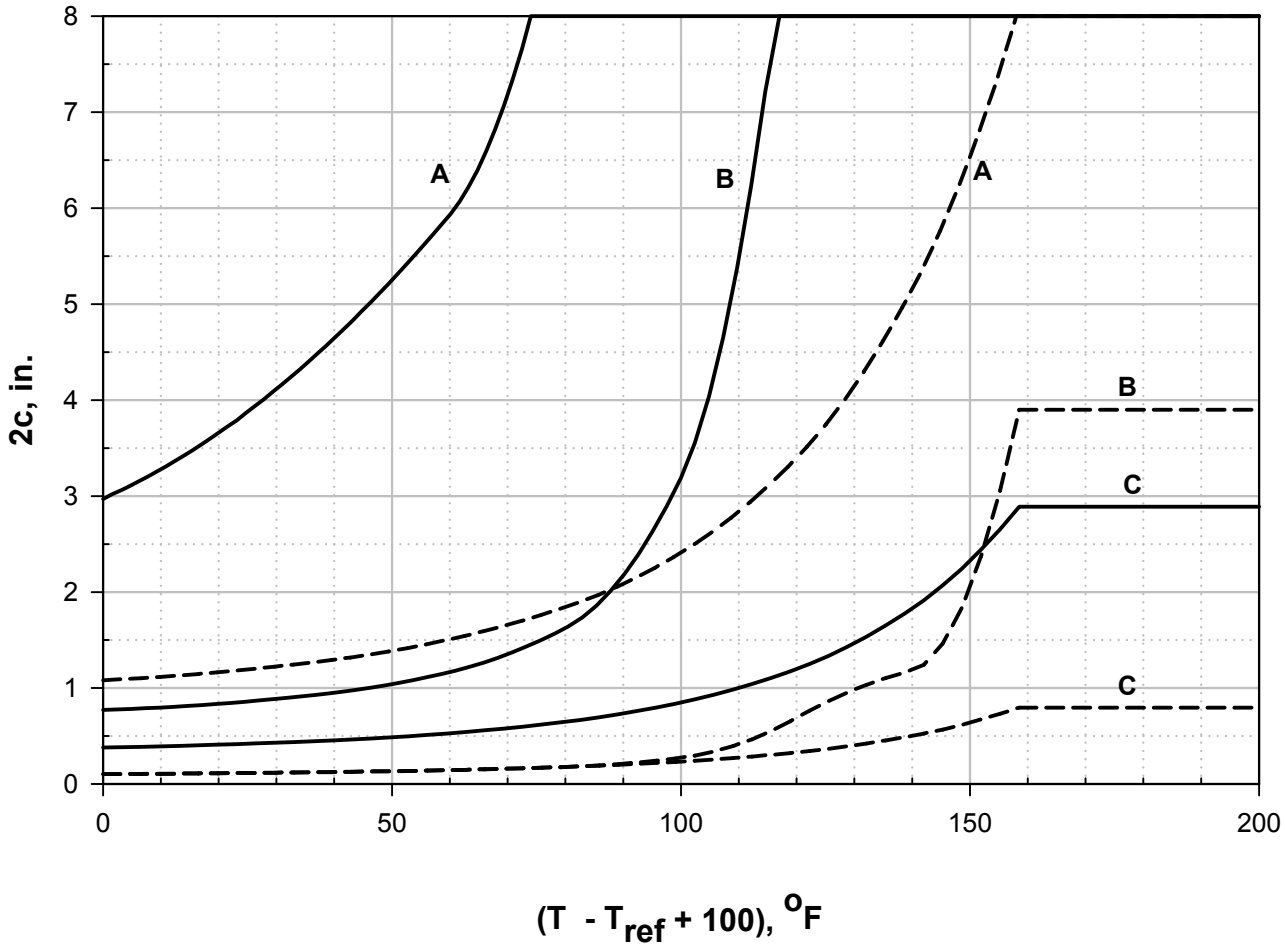

Notes:

1. Definition of Screening Curves (solid line ¼-t flaw, dashed line 1-t flaw):
   - A – Allowable flaw size in base metal.
   - B – Allowable flaw size in weld metal that has been subject to $PWHT$.
   - C – Allowable flaw size in weld metal that has not been subject to $PWHT$.
2. Crack dimension for a 1-t and ¼-t flaw are shown in Annex C, Figures C.1 & C.2.
3. See paragraph 9.2.2.1 for restrictions and limitations.
4. Guidelines for establishing the Reference Temperature, T_{ref} , are covered in paragraph 9.4.2.2.e).
5. The maximum permitted flaw length from this curve is $2c = 8\ in$.

Figure 9.12 – Level 1 Assessment – Flat Plate

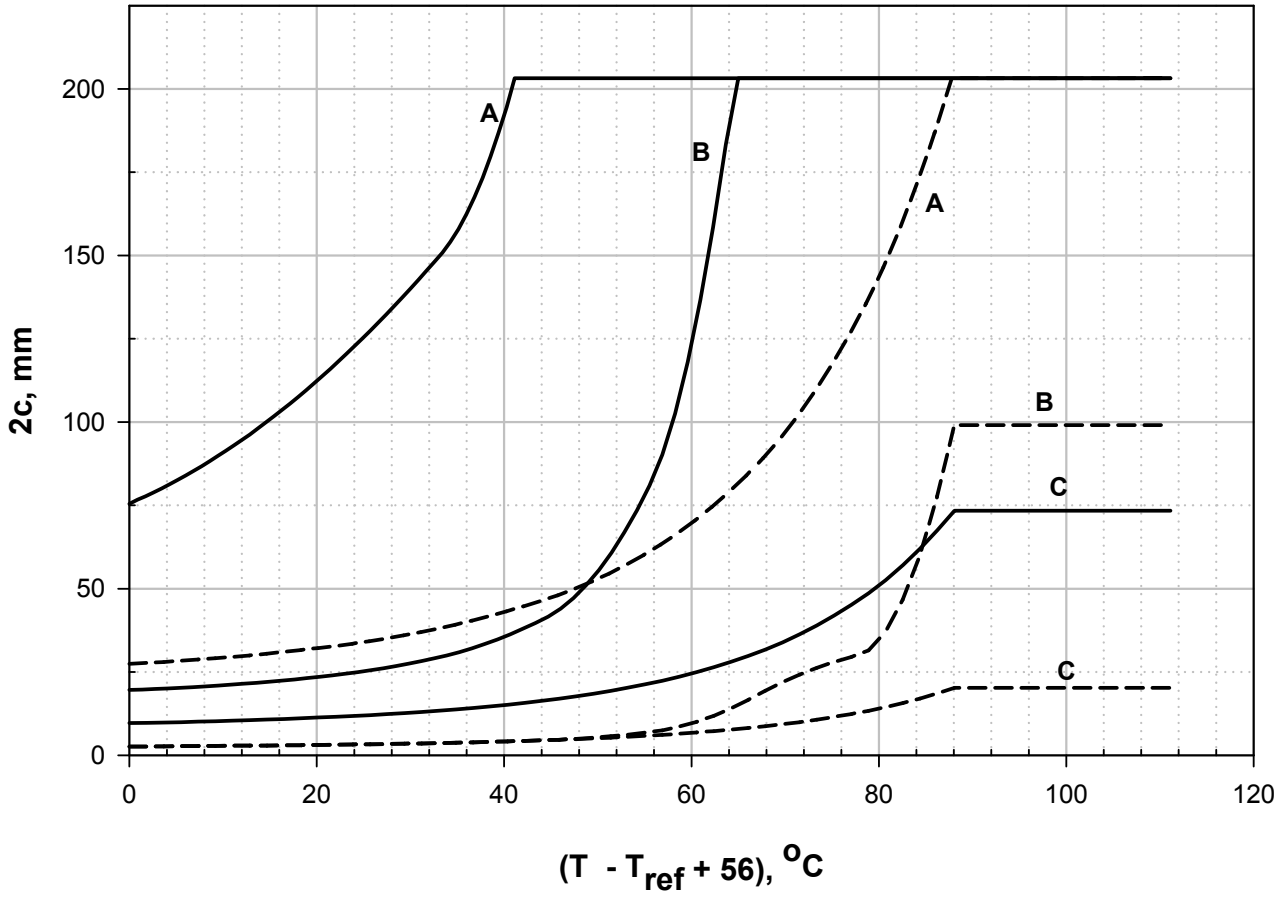

Notes:

1. Definition of Screening Curves (solid line ¼-t flaw, dashed line 1-t flaw):
   - A – Allowable flaw size in base metal.
   - B – Allowable flaw size in weld metal that has been subject to $PWHT$.
   - C – Allowable flaw size in weld metal that has not been subject to $PWHT$.
2. Crack dimension for a 1-t and ¼-t flaw are shown in Annex C, Figures C.1 & C.2.
3. See paragraph 9.2.2.1 for restrictions and limitations.
4. Guidelines for establishing the Reference Temperature, T_{ref} , are covered in paragraph 9.4.2.2.e.
5. The maximum permitted flaw length from this curve is $2c = 200\ mm$.

Figure 9.12 M – Level 1 Assessment – Flat Plate

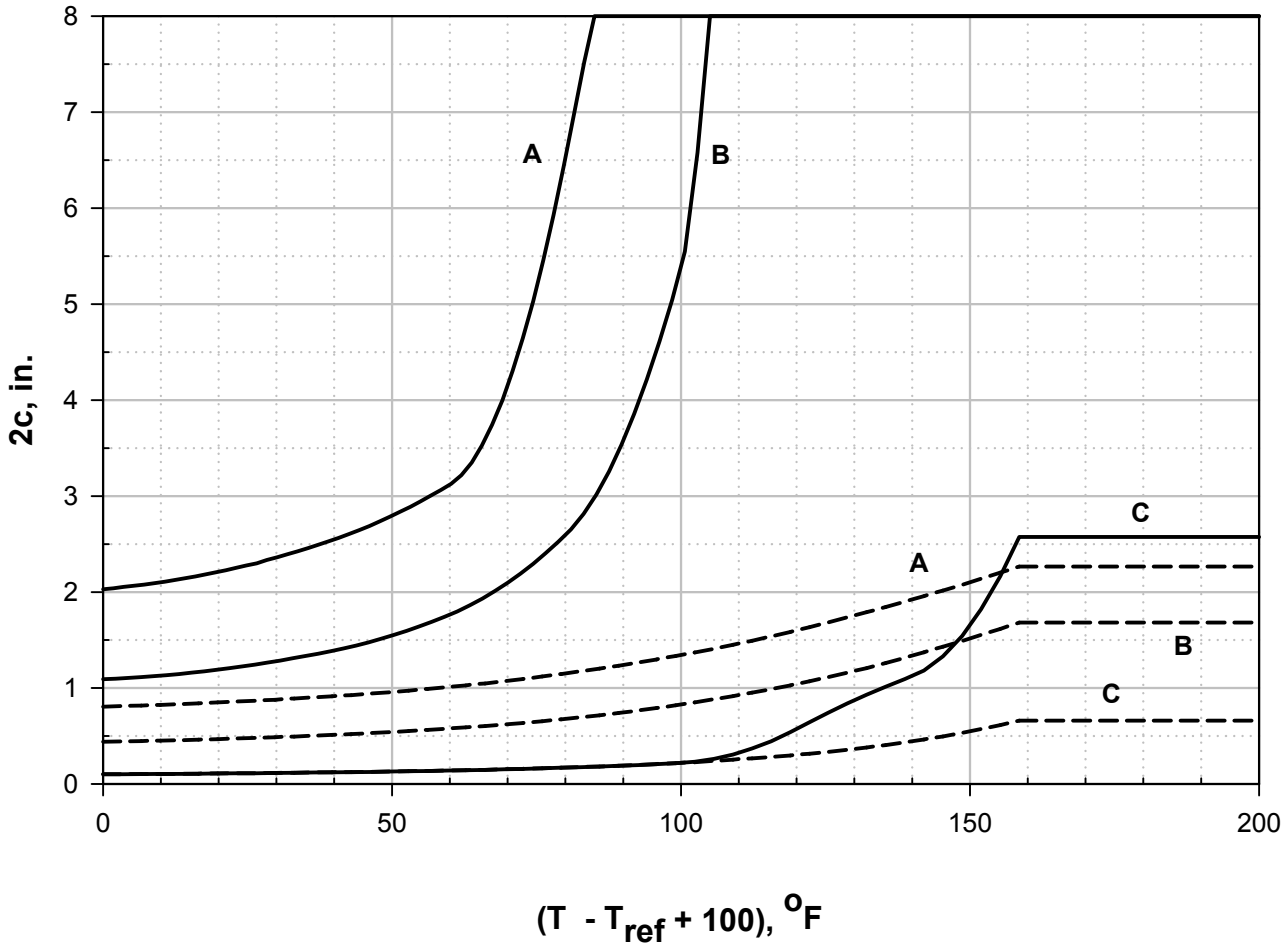

Notes:

1. Definition of Screening Curves (solid line ¼-t flaw, dashed line 1-t flaw):
   - A – Allowable flaw size in base metal.
   - B – Allowable flaw size in weld metal that has been subject to $PWHT$.
   - C – Allowable flaw size in weld metal that has not been subject to $PWHT$.
2. Crack dimension for a 1-t and ¼-t flaw are shown in Annex C, Figures C.10 & C.14.
3. See paragraph 9.2.2.1 for restrictions and limitations.
4. Guidelines for establishing the Reference Temperature, T_{ref} , are covered in paragraph 9.4.2.2.e.
5. The maximum permitted flaw length from this curve is $2c = 8\ in$.

Figure 9.13 – Level 1 Assessment – Cylinder, Longitudinal Joint, Crack-Like Flaw Parallel to the Joint

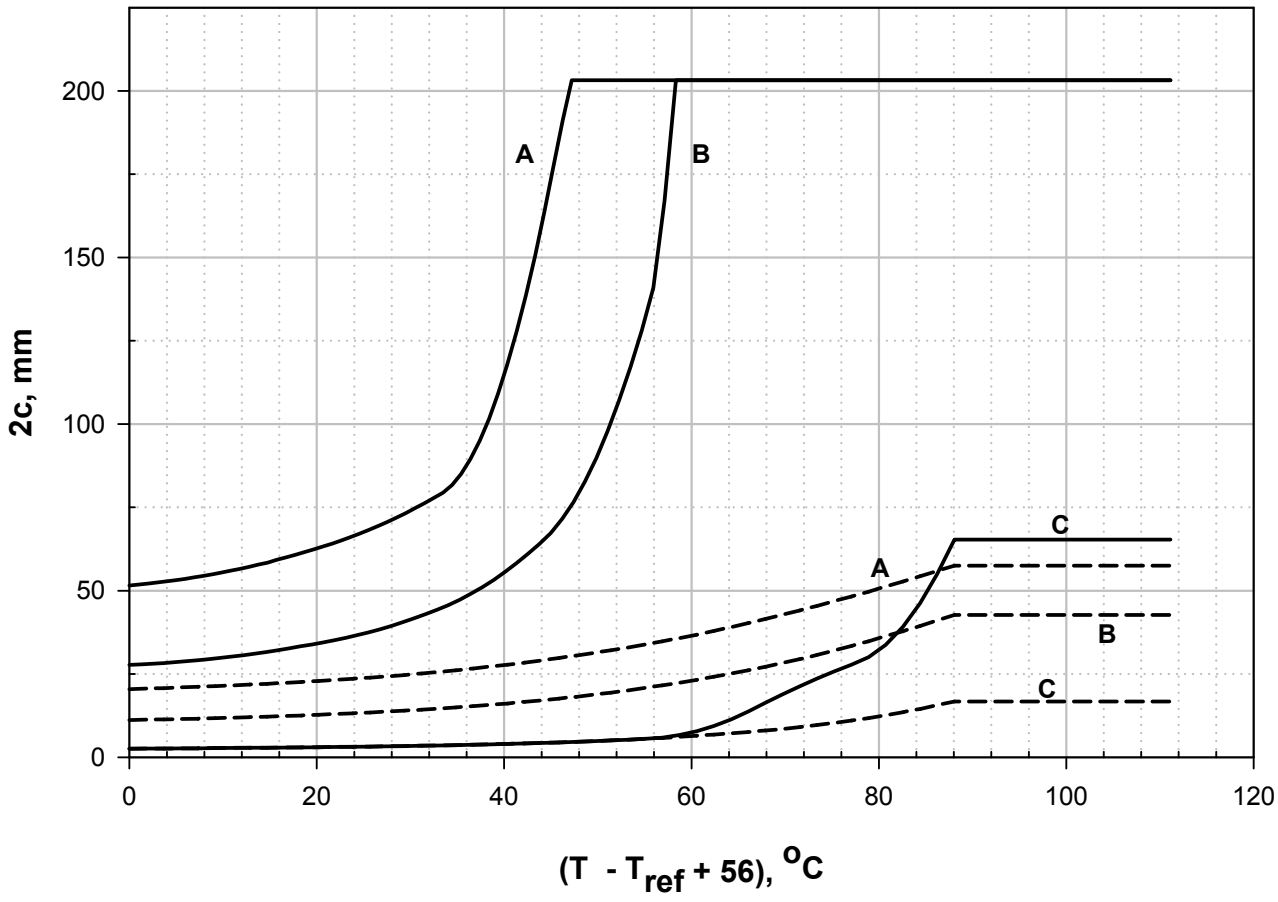

Notes:

1. Definition of Screening Curves (solid line ¼-t flaw, dashed line 1-t flaw):
   - A – Allowable flaw size in base metal.
   - B – Allowable flaw size in weld metal that has been subject to $PWHT$.
   - C – Allowable flaw size in weld metal that has not been subject to $PWHT$.
2. Crack dimension for a 1-t and ¼-t flaw are shown in Annex C, Figures C.10 & C.14.
3. See paragraph 9.2.2.1 for restrictions and limitations.
4. Guidelines for establishing the Reference Temperature, T_{ref} , are covered in paragraph 9.4.2.2.e.
5. The maximum permitted flaw length from this curve is $2c = 200\ mm$.

Figure 9.13M – Level 1 Assessment – Cylinder, Longitudinal Joint, Crack-Like Flaw Parallel to the Joint

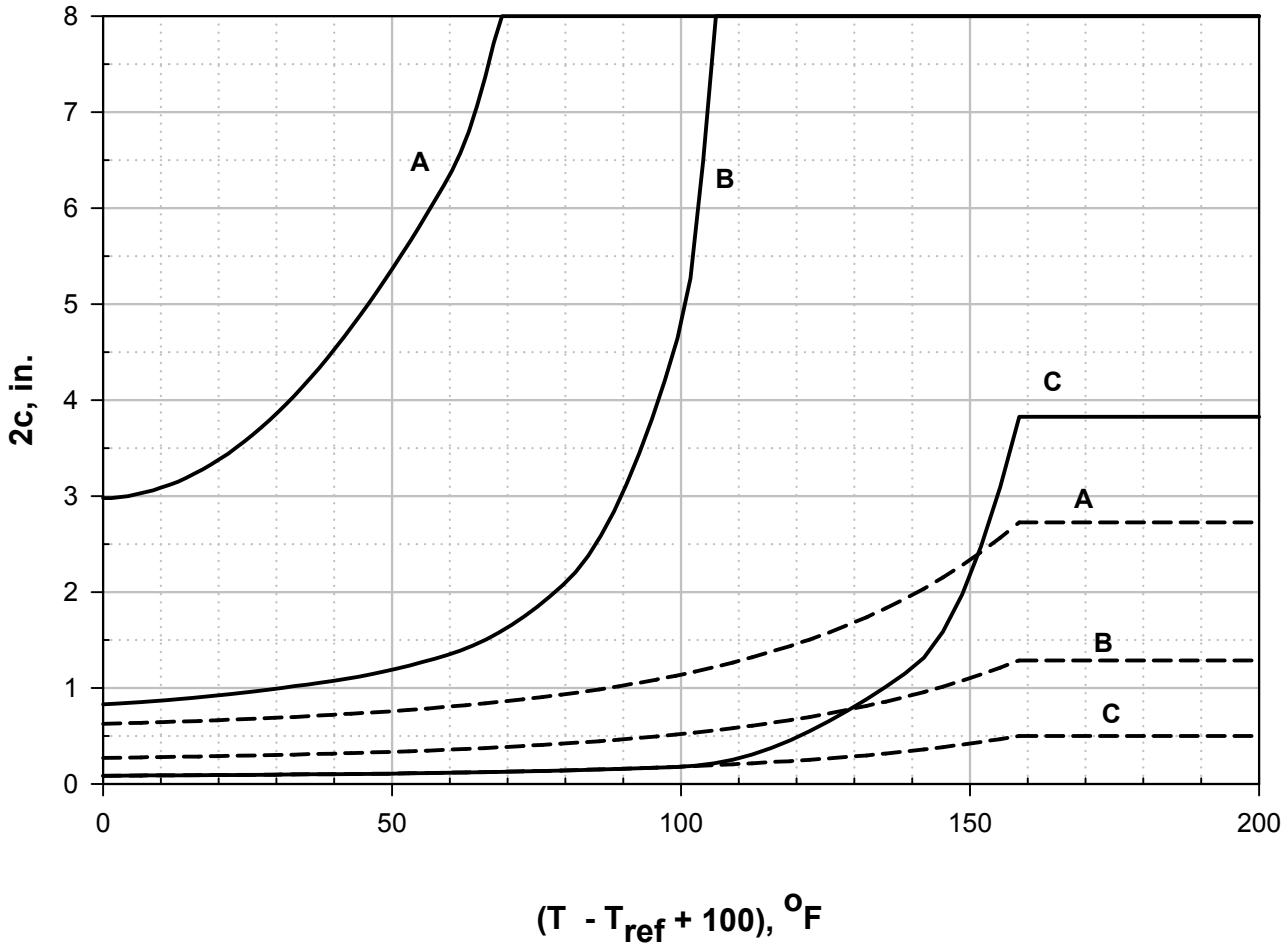

Notes:

1. Definition of Screening Curves (solid line ¼-t flaw, dashed line 1-t flaw):
   - A – Allowable flaw size in base metal.
   - B – Allowable flaw size in weld metal that has been subject to $PWHT$.
   - C – Allowable flaw size in weld metal that has not been subject to $PWHT$.
2. Crack dimension for a 1-t and ¼-t flaw are shown in Annex C, Figures C.11 & C.15.
3. See paragraph 9.2.2.1 for restrictions and limitations.
4. Guidelines for establishing the Reference Temperature, T_{ref} , are covered in paragraph 9.4.2.2.e.
5. The maximum permitted flaw length from this curve is $2c = 8\ in$.

Figure 9.14 – Level 1 Assessment – Cylinder, Longitudinal Joint, Crack-Like Flaw Perpendicular to the Joint

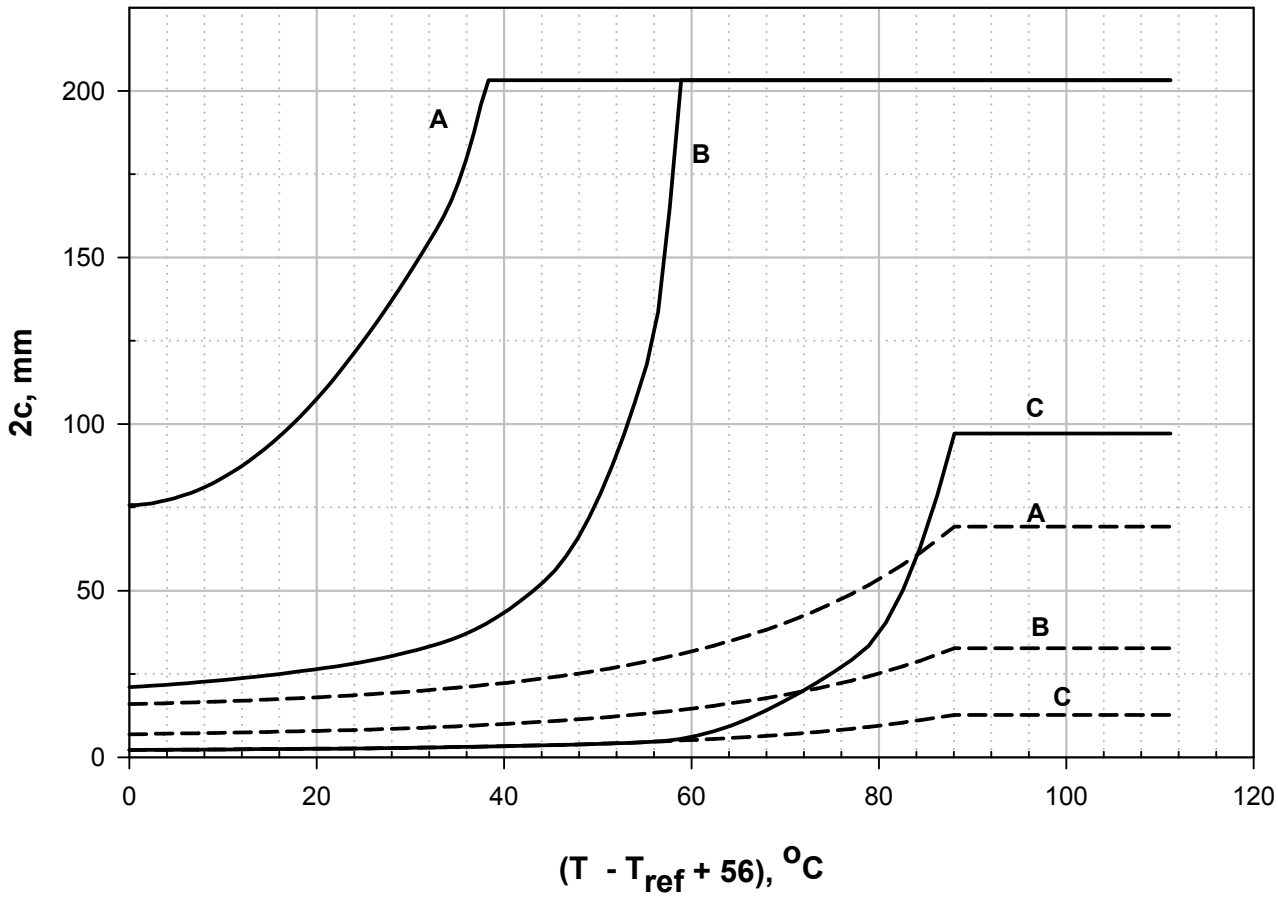

Notes:

1. Definition of Screening Curves (solid line ¼-t flaw, dashed line 1-t flaw):
   - A – Allowable flaw size in base metal.
   - B – Allowable flaw size in weld metal that has been subject to $PWHT$.
   - C – Allowable flaw size in weld metal that has not been subject to $PWHT$.
2. Crack dimension for a 1-t and ¼-t flaw are shown in Annex C, Figures C.11 & C.15.
3. See paragraph 9.2.2.1 for restrictions and limitations.
4. Guidelines for establishing the Reference Temperature, T_{ref} , are covered in paragraph 9.4.2.2.e.
5. The maximum permitted flaw length from this curve is $2c = 200\ mm$.

Figure 9.14M – Level 1 Assessment – Cylinder, Longitudinal Joint, Crack-Like Flaw Perpendicular to the Joint

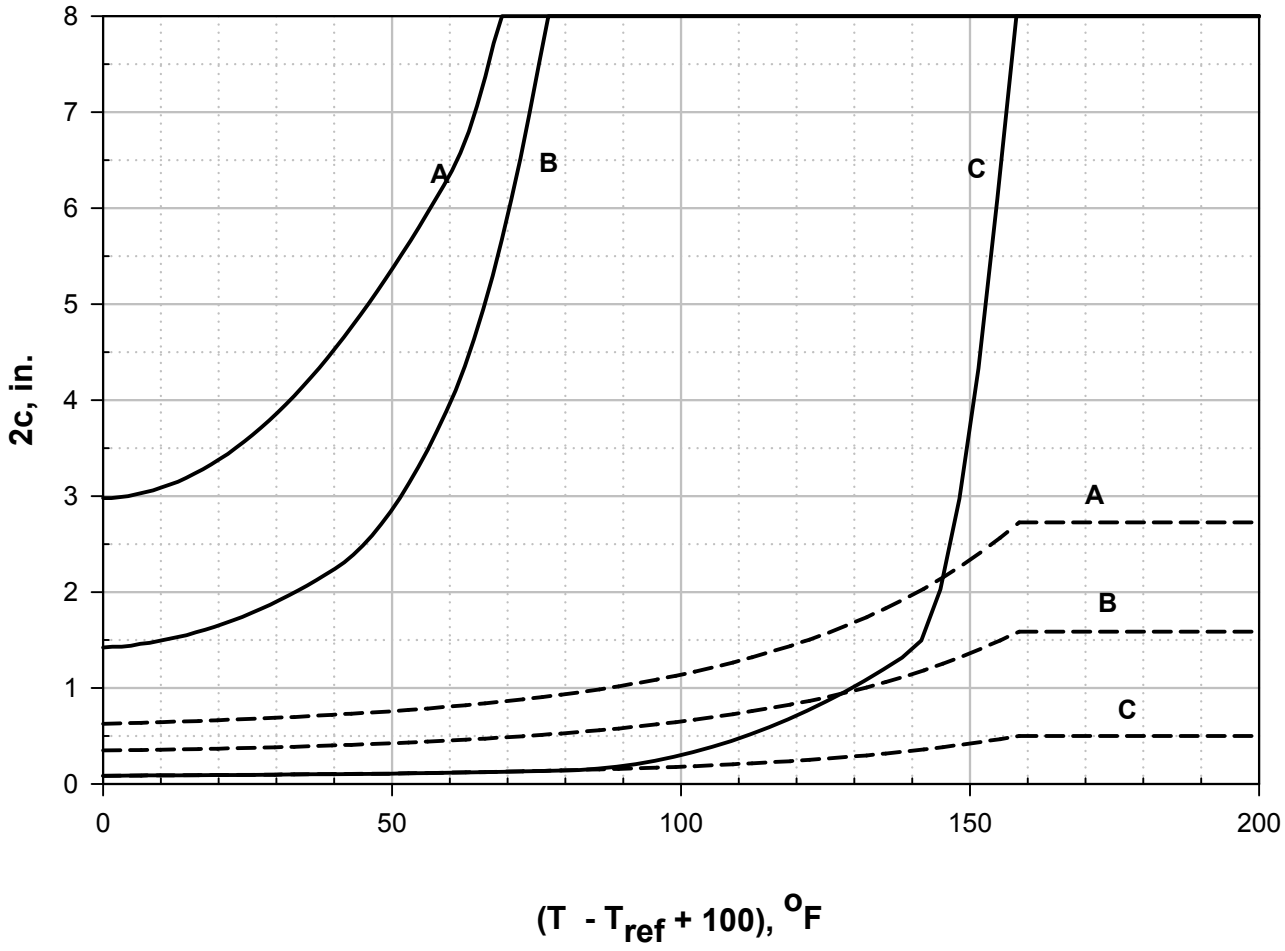

Notes:

1. Definition of Screening Curves (solid line ¼-t flaw, dashed line 1-t flaw):
   - A – Allowable flaw size in base metal.
   - B – Allowable flaw size in weld metal that has been subject to $PWHT$.
   - C – Allowable flaw size in weld metal that has not been subject to $PWHT$.
2. Crack dimension for a 1-t and ¼-t flaw are shown in Annex CFigures C.11 & C.15.
3. See paragraph 9.2.2.1 for restrictions and limitations.
4. Guidelines for establishing the Reference Temperature, T_{ref} , are covered in paragraph 9.4.2.2.e.
5. The maximum permitted flaw length from this curve is $2c = 8\ in$.

Figure 9.15 – Level 1 Assessment – Cylinder, Circumferential Joint, Crack-Like Flaw Parallel to the Joint

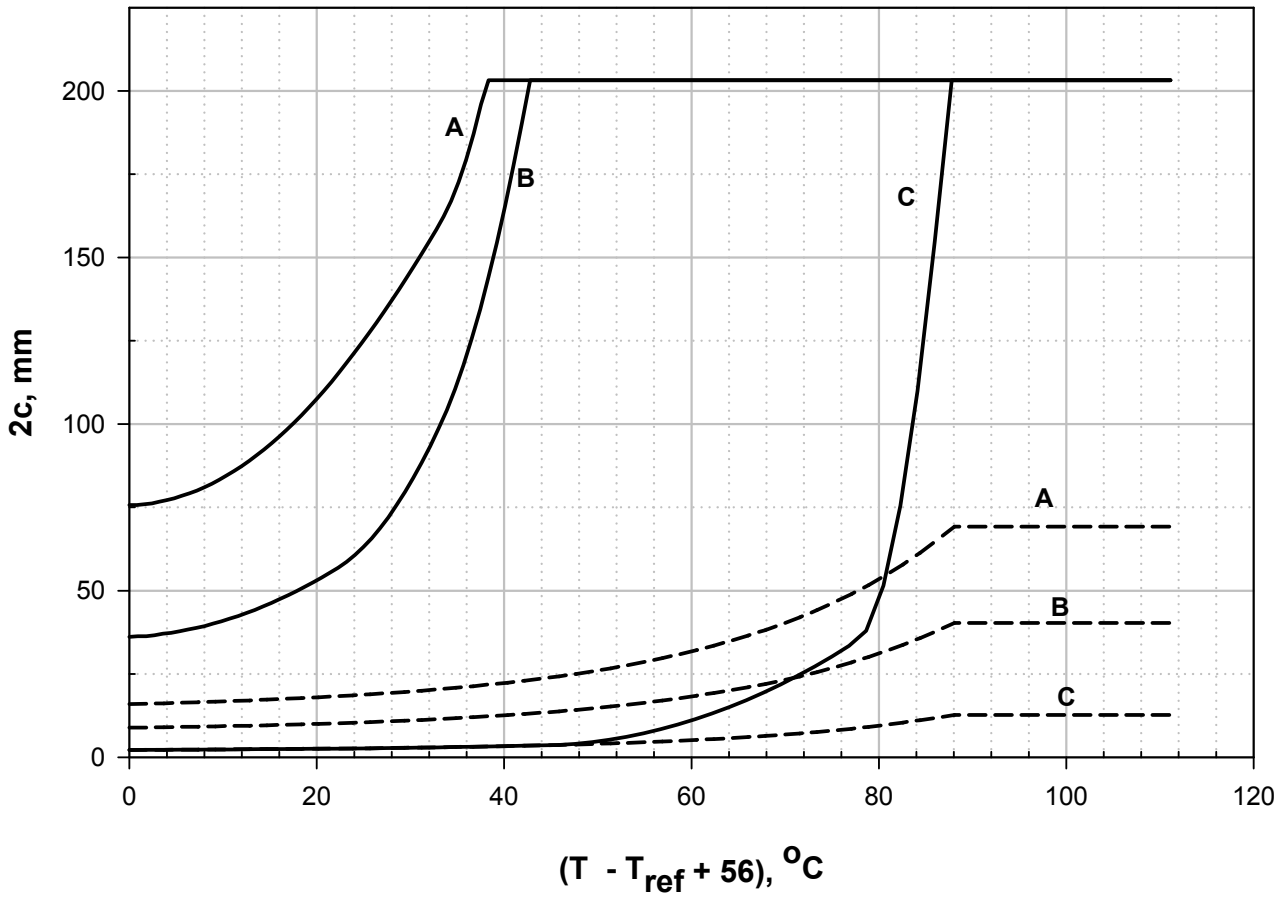

Notes:

1. Definition of Screening Curves (solid line ¼-t flaw, dashed line 1-t flaw):
   - A – Allowable flaw size in base metal.
   - B – Allowable flaw size in weld metal that has been subject to $PWHT$.
   - C – Allowable flaw size in weld metal that has not been subject to $PWHT$.
2. Crack dimension for a 1-t and ¼-t flaw are shown in Annex C, Figures C.11 & C.15.
3. See paragraph 9.2.2.1 for restrictions and limitations.
4. Guidelines for establishing the Reference Temperature, T_{ref} , are covered in paragraph 9.4.2.2.e.
5. The maximum permitted flaw length from this curve is $2c = 200\ mm$.

Figure 9.15M – Level 1 Assessment – Cylinder, Circumferential Joint, Crack-Like Flaw Parallel to the Joint

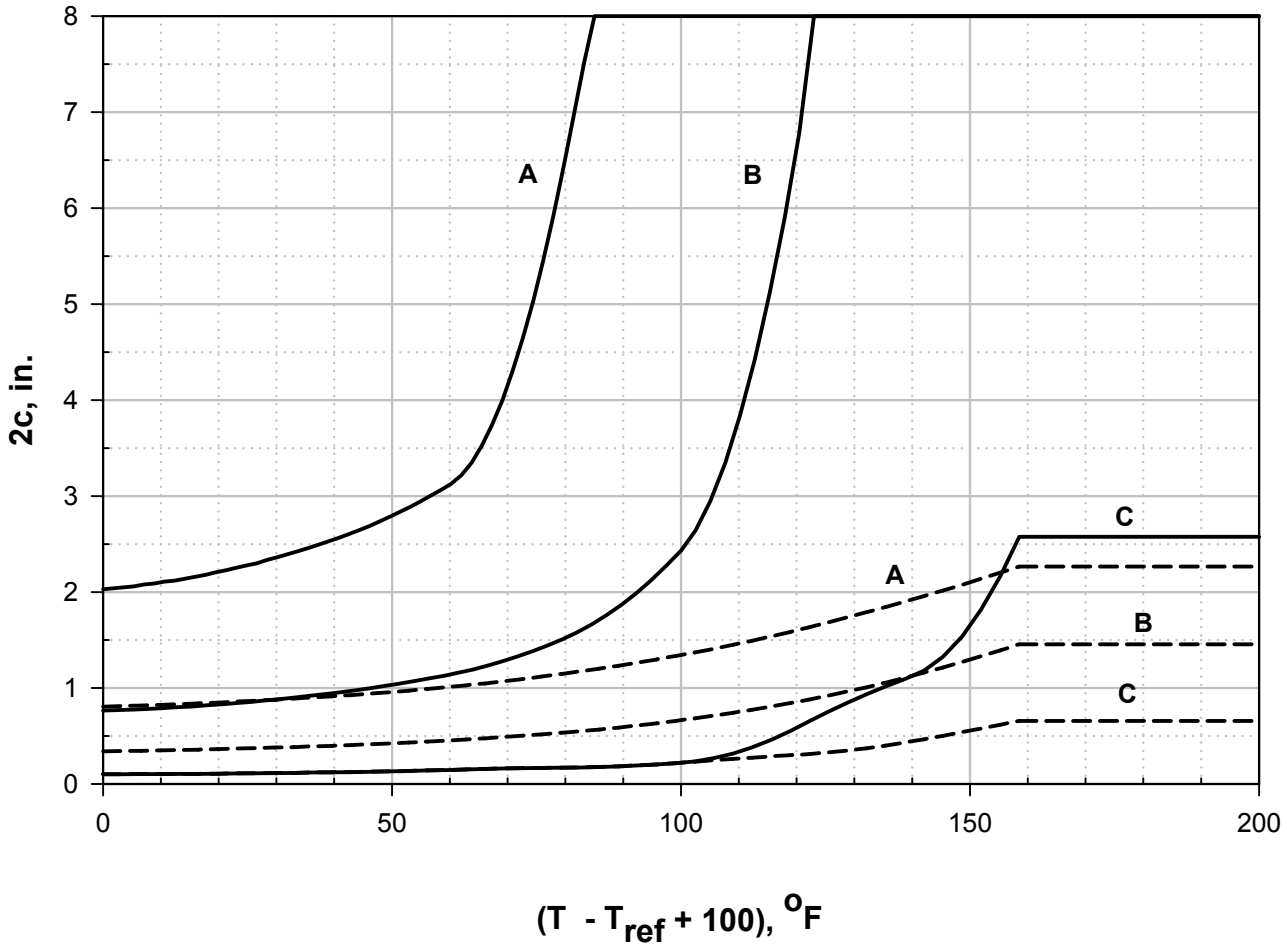

Notes:

1. Definition of Screening Curves (solid line ¼-t flaw, dashed line 1-t flaw):
   - A – Allowable flaw size in base metal.
   - B – Allowable flaw size in weld metal that has been subject to $PWHT$.
   - C – Allowable flaw size in weld metal that has not been subject to $PWHT$.
2. Crack dimension for a 1-t and ¼-t flaw are shown in Annex C, Figures C.10 & C.14.
3. See paragraph 9.2.2.1 for restrictions and limitations.
4. Guidelines for establishing the Reference Temperature, T_{ref} , are covered in paragraph 9.4.2.2.e.
5. The maximum permitted flaw length from this curve is $2c = 8\ in$.

Figure 9.16 – Level 1 Assessment – Cylinder, Circumferential Joint, Crack-Like Flaw Perpendicular to the Joint

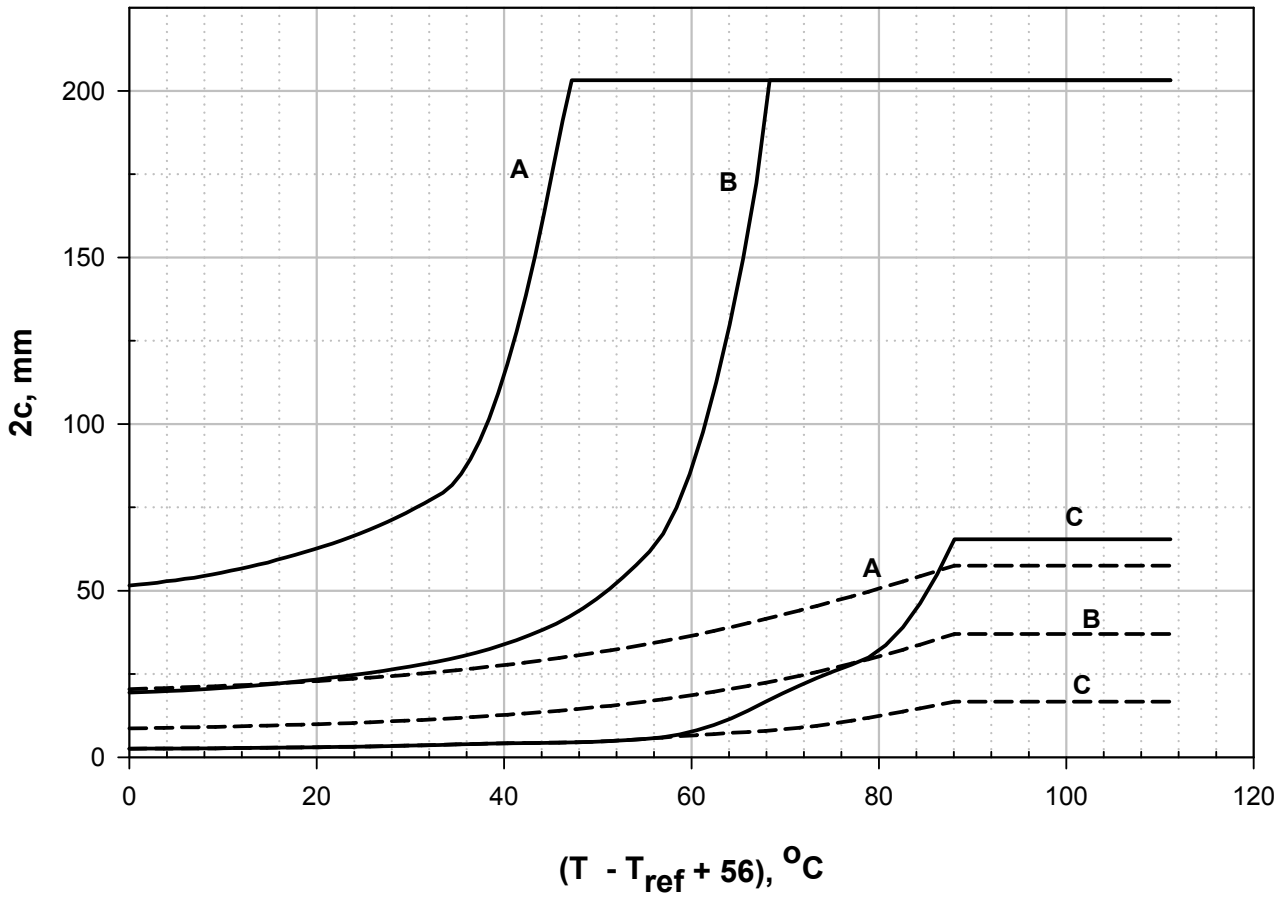

Notes:

1. Definition of Screening Curves (solid line ¼-t flaw, dashed line 1-t flaw):
   - A – Allowable flaw size in base metal.
   - B – Allowable flaw size in weld metal that has been subject to $PWHT$.
   - C – Allowable flaw size in weld metal that has not been subject to $PWHT$.
2. Crack dimension for a 1-t and ¼-t flaw are shown in Annex C, Figures C.10 & C.14.
3. See paragraph 9.2.2.1 for restrictions and limitations.
4. Guidelines for establishing the Reference Temperature, T_{ref} , are covered in paragraph 9.4.2.2.e.
5. The maximum permitted flaw length from this curve is $2c = 200\ mm$.

Figure 9.16M – Level 1 Assessment – Cylinder, Circumferential Joint, Crack-Like Flaw Perpendicular to the Joint

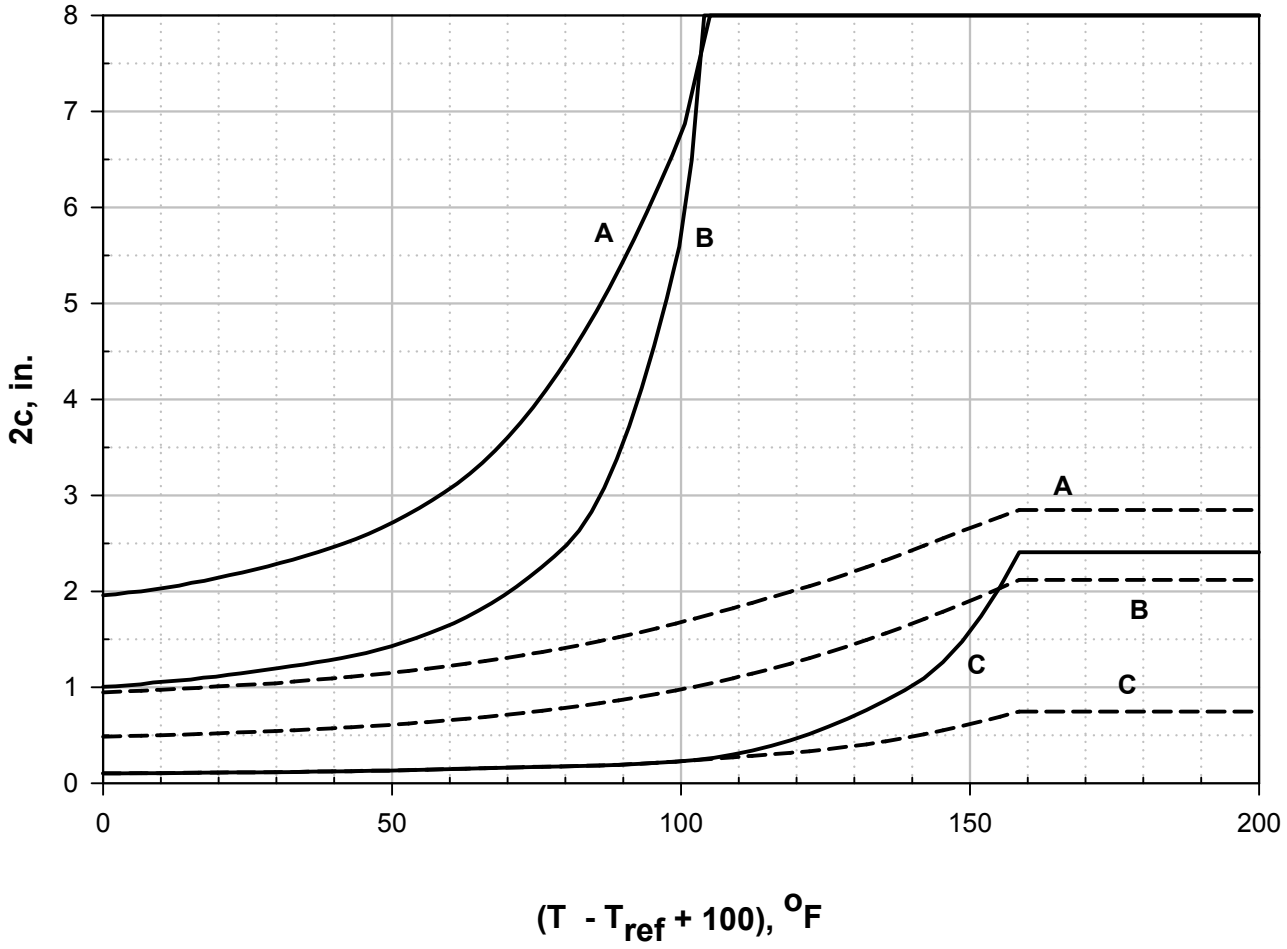

Notes:

1. Definition of Screening Curves (solid line ¼-t flaw, dashed line 1-t flaw):
   - A – Allowable flaw size in base metal.
   - B – Allowable flaw size in weld metal that has been subject to $PWHT$.
   - C – Allowable flaw size in weld metal that has not been subject to $PWHT$.
2. Crack dimension for a 1-t and ¼-t flaw are shown in Annex C, Figures C.20 & C.22.
3. See paragraph 9.2.2.1 for restrictions and limitations.
4. Guidelines for establishing the Reference Temperature, T_{ref}, are covered in paragraph 9.4.2.2.e.
5. The maximum permitted flaw length from this curve is $2c = 8\ in$.

Figure 9.17 – Level 1 Assessment – Sphere, Circumferential Joint, Crack-Like Flaw Parallel to the Joint

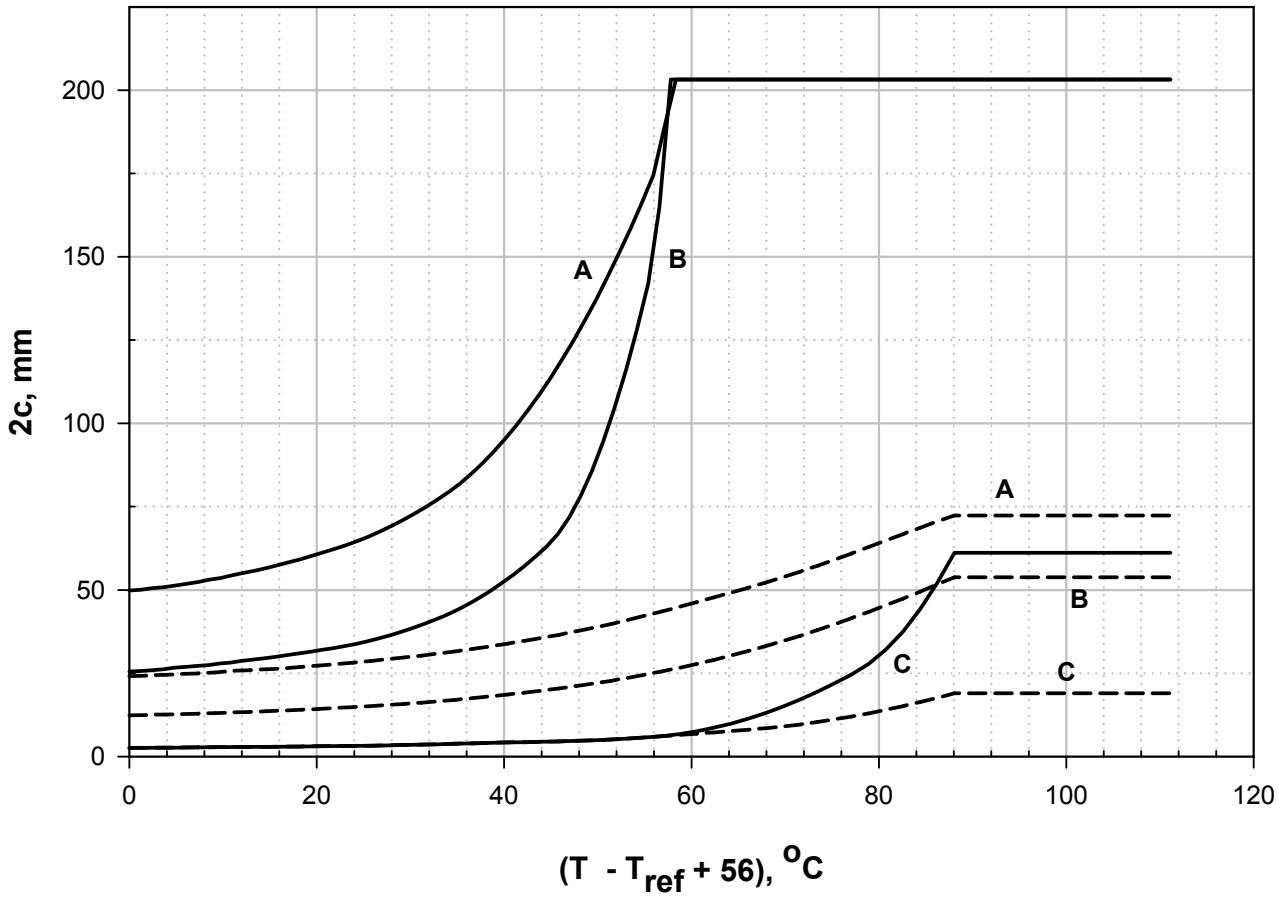

Notes:

1. Definition of Screening Curves (solid line ¼-t flaw, dashed line 1-t flaw):
   - A – Allowable flaw size in base metal.
   - B – Allowable flaw size in weld metal that has been subject to $PWHT$.
   - C – Allowable flaw size in weld metal that has not been subject to $PWHT$.
2. Crack dimension for a 1-t and ¼-t flaw are shown in Annex C Figures C.20 & C.22.
3. See paragraph 9.2.2.1 for restrictions and limitations.
4. Guidelines for establishing the Reference Temperature, T_{ref} , are covered in paragraph 9.4.2.2.e.
5. The maximum permitted flaw length from this curve is $2c = 200\ mm$.

Figure 9.17M– Level 1 Assessment – Sphere, Circumferential Joint, Crack-Like Flaw Parallel to the Joint

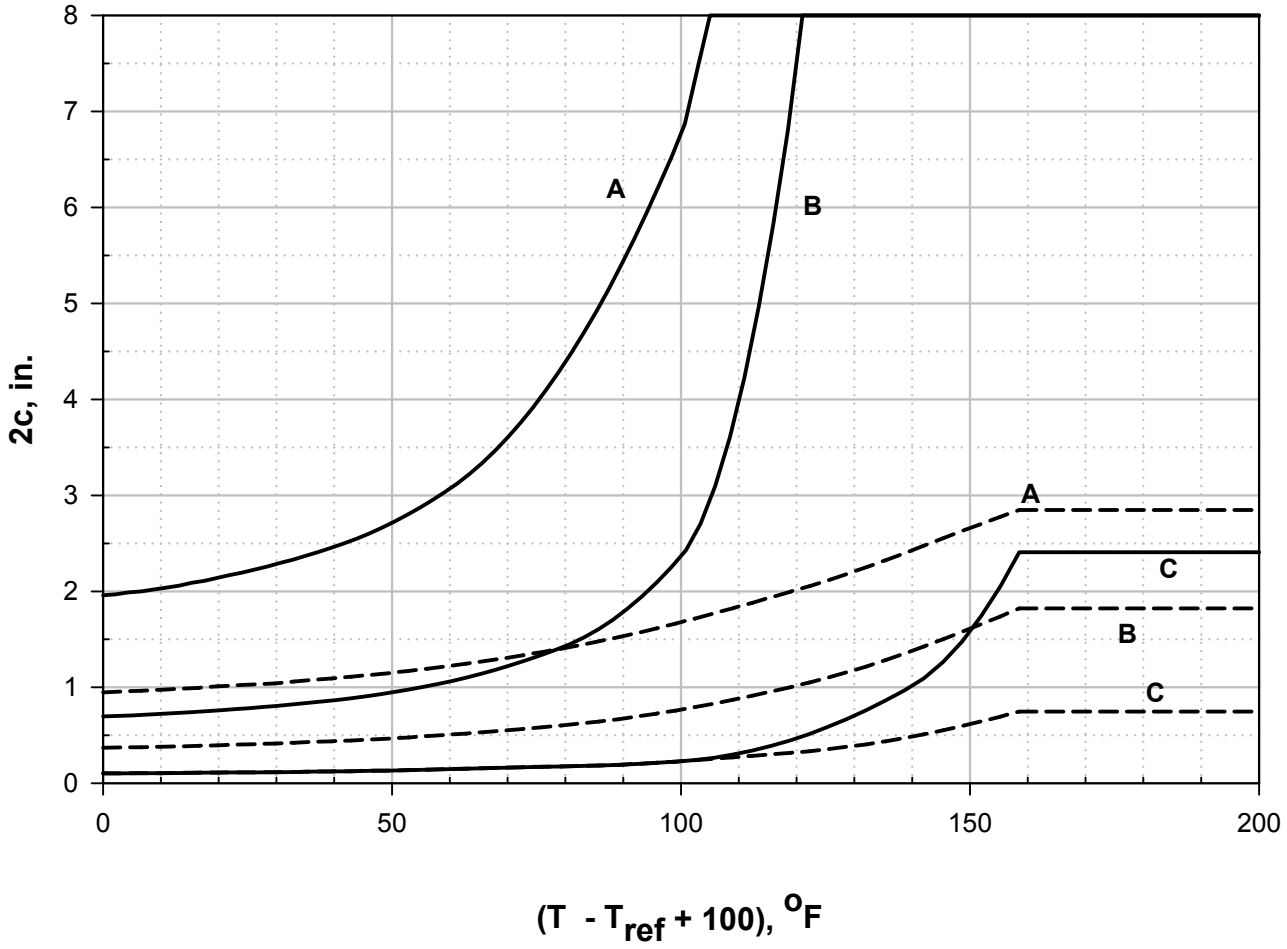

Notes:

1. Definition of Screening Curves (solid line ¼-t flaw, dashed line 1-t flaw):
   - A – Allowable flaw size in base metal.
   - B – Allowable flaw size in weld metal that has been subject to $PWHT$.
   - C – Allowable flaw size in weld metal that has not been subject to $PWHT$.
2. Crack dimension for a 1-t and ¼-t flaw are shown in Annex C, Figures C.20 & C.22.
3. See paragraph 9.2.2.1 for restrictions and limitations.
4. Guidelines for establishing the Reference Temperature, T_{ref}, are covered in paragraph 9.4.2.2.e.
5. The maximum permitted flaw length from this curve is $2c = 8\ in$.

Figure 9.18 – Level 1 Assessment – Sphere, Circumferential Joint, Crack-Like Flaw Perpendicular to the Joint

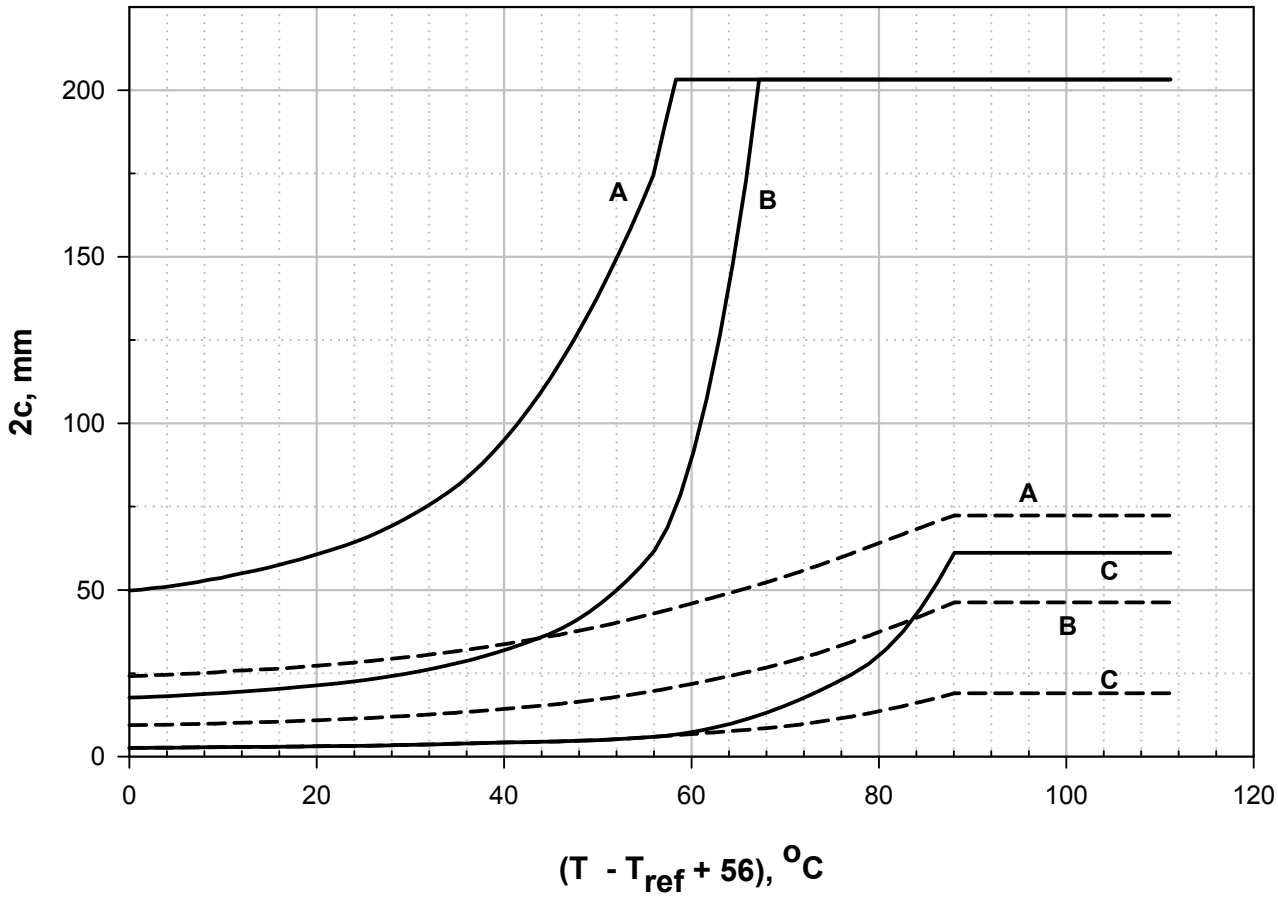

Notes:

1. Definition of Screening Curves (solid line ¼-t flaw, dashed line 1-t flaw):
   - A – Allowable flaw size in base metal.
   - B – Allowable flaw size in weld metal that has been subject to $PWHT$.
   - C – Allowable flaw size in weld metal that has not been subject to $PWHT$.
2. Crack dimension for a 1-t and ¼-t flaw are shown in Annex C, Figures C.20 & C.22.
3. See paragraph 9.2.2.1 for restrictions and limitations.
4. Guidelines for establishing the Reference Temperature, T_{ref} , are covered in paragraph 9.4.2.2.e.
5. The maximum permitted flaw length from this curve is $2c = 200\ mm$.

Figure 9.18M – Level 1 Assessment – Sphere, Circumferential Joint, Crack-Like Flaw Perpendicular to the Joint

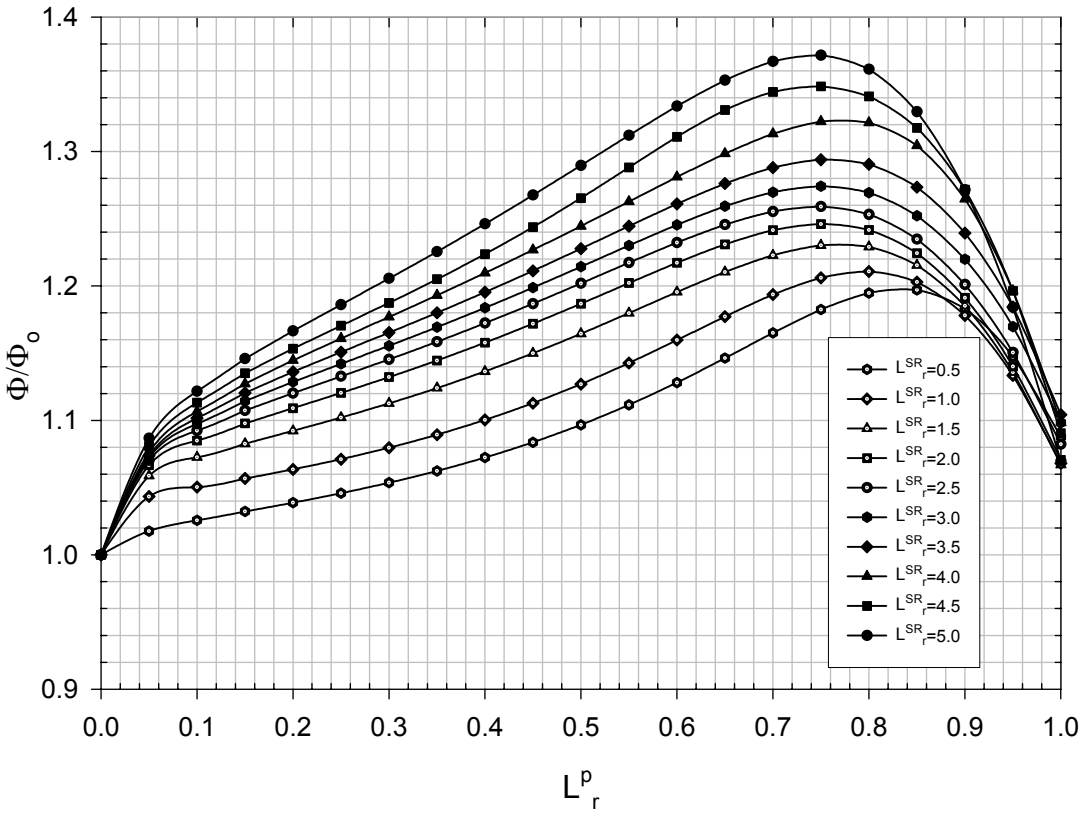

Notes:

1. The plasticity interaction factor, Φ/Φ_o for values of $L_r^P \le 1.0$ are shown in this figure. For value of $L_r^P > 1.0$ greater than 1.0, Φ/Φ_o can be computed using the methodology in paragraph 9.4.3.2.k.
2. Interpolation may be used to determine Φ/Φ_o for intermediate values of L_r^P and L_r^{SR}.

Figure 9.19 – Determination of the Plasticity Interaction Factor

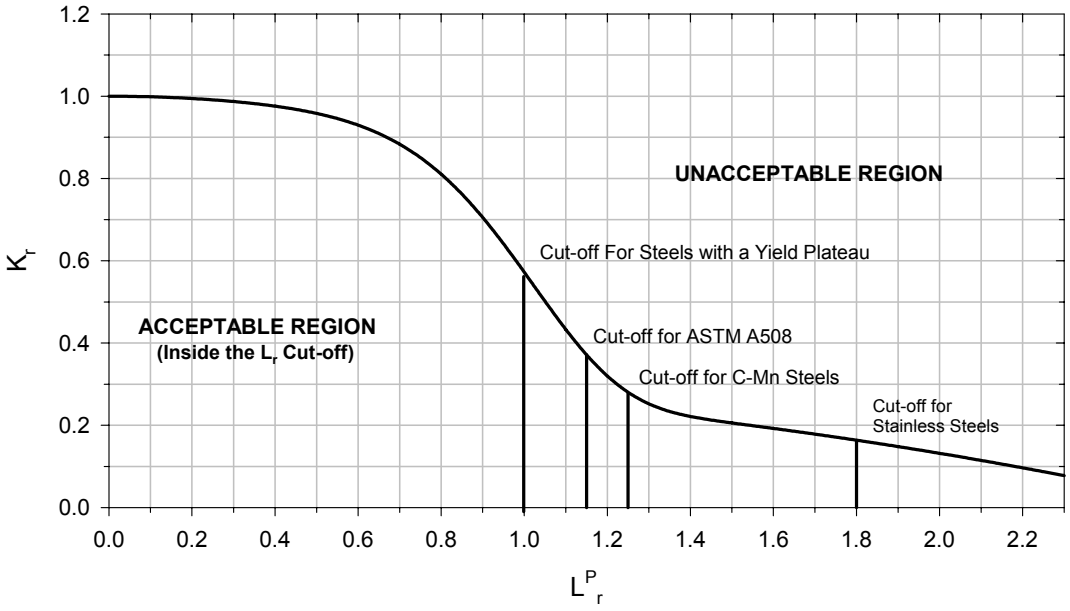

Notes:

1. The FAD is defined using the following equation:

$$K_r = \left(1 - 0.14\left(L_r^P\right)^2\right)\left(0.3 + 0.7\exp\left[-0.65\left(L_r^P\right)^6\right]\right) \quad for \quad L_r^P \le L_{r(\max)}^P \tag{9.30}$$

2. The extent of the FAD on the L_r^P axis is determined as follows:

   a) $L_{r(\max)}^P = 1.00$ for materials with yield point plateau (strain hardening exponent > 15),

   b) $L_{r(\max)}^P = 1.25$ for ASTM A508,

   c) $L_{r(\max)}^P = 1.25$ for C-Mn steels,

   d) $L_{r(\max)}^P = 1.80$ for austenitic stainless steels, and

   e) $L_{r(\max)}^P = \dfrac{\sigma_f}{\sigma_{ys}}$ for other materials where σ_f flow stress (see Annex F) and σ_{ys} yield stress; the flow stress and yield stress are evaluated at the assessment temperature.

   f) $L_{r(\max)}^P = 1.0$ if the strain hardening characteristics of the material are unknown.

3. The value of $L_{r(\max)}^P$ may be increased for redundant components (see Annex D, paragraph D.2.5.2.b).

4. If $L_{r(\max)}^P = 1.0$, then the FAD may be defined using following equation:

$$K_r = \left(1.0 - \left(L_r^P\right)^{2.5}\right)^{0.20} \tag{9.31}$$

Figure 9.20 – The Failure Assessment Diagram

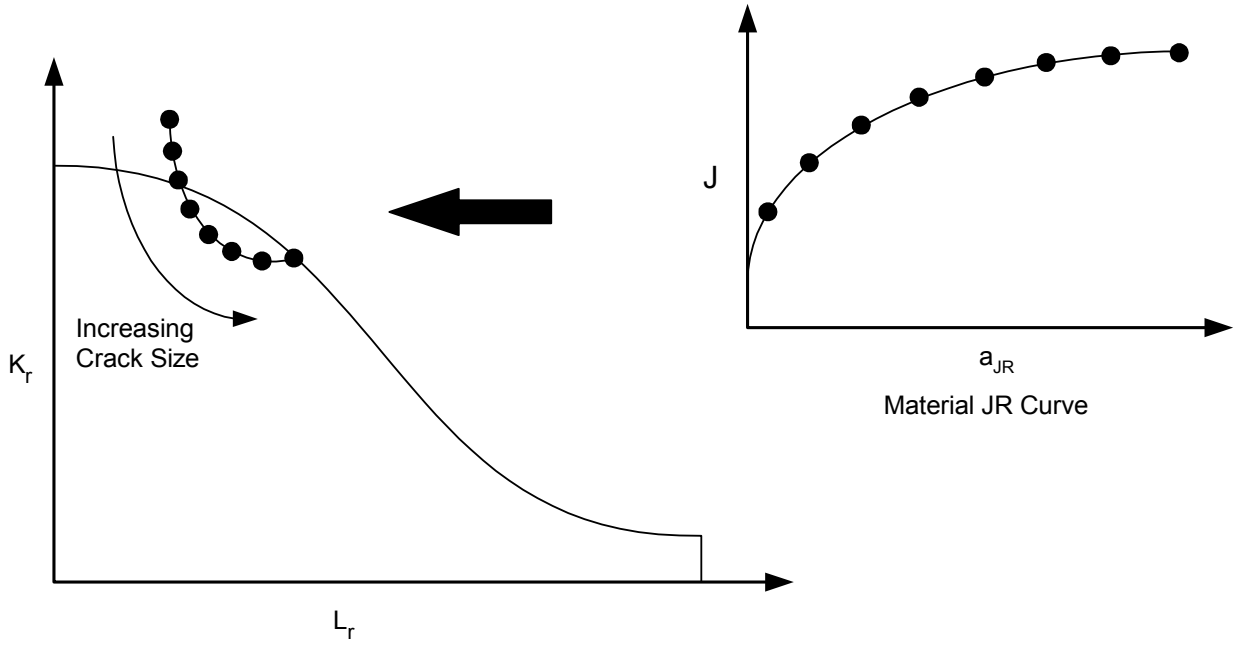

(a) Obtaining a locus of assessment points from a JR-curve

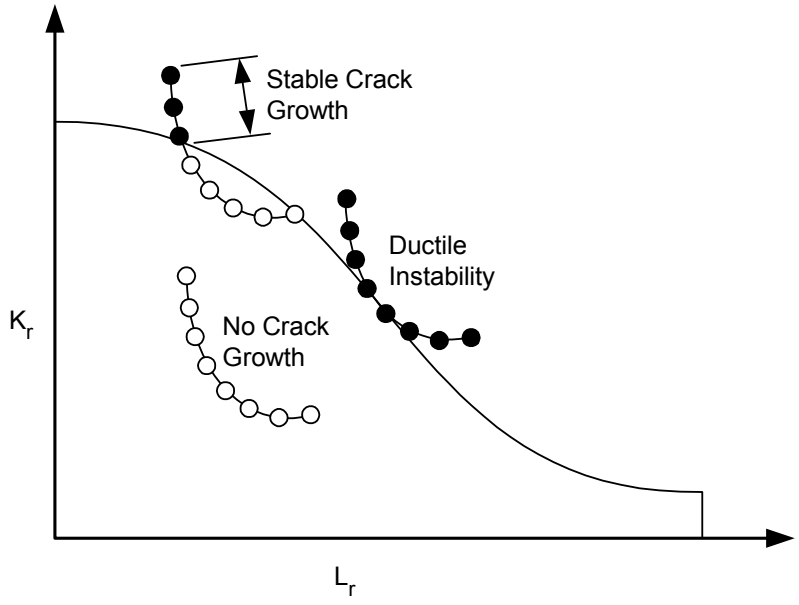

(b) Three possible outcomes of a ductile tearing analysis

Figure 9.21 – Ductile Tearing Analysis

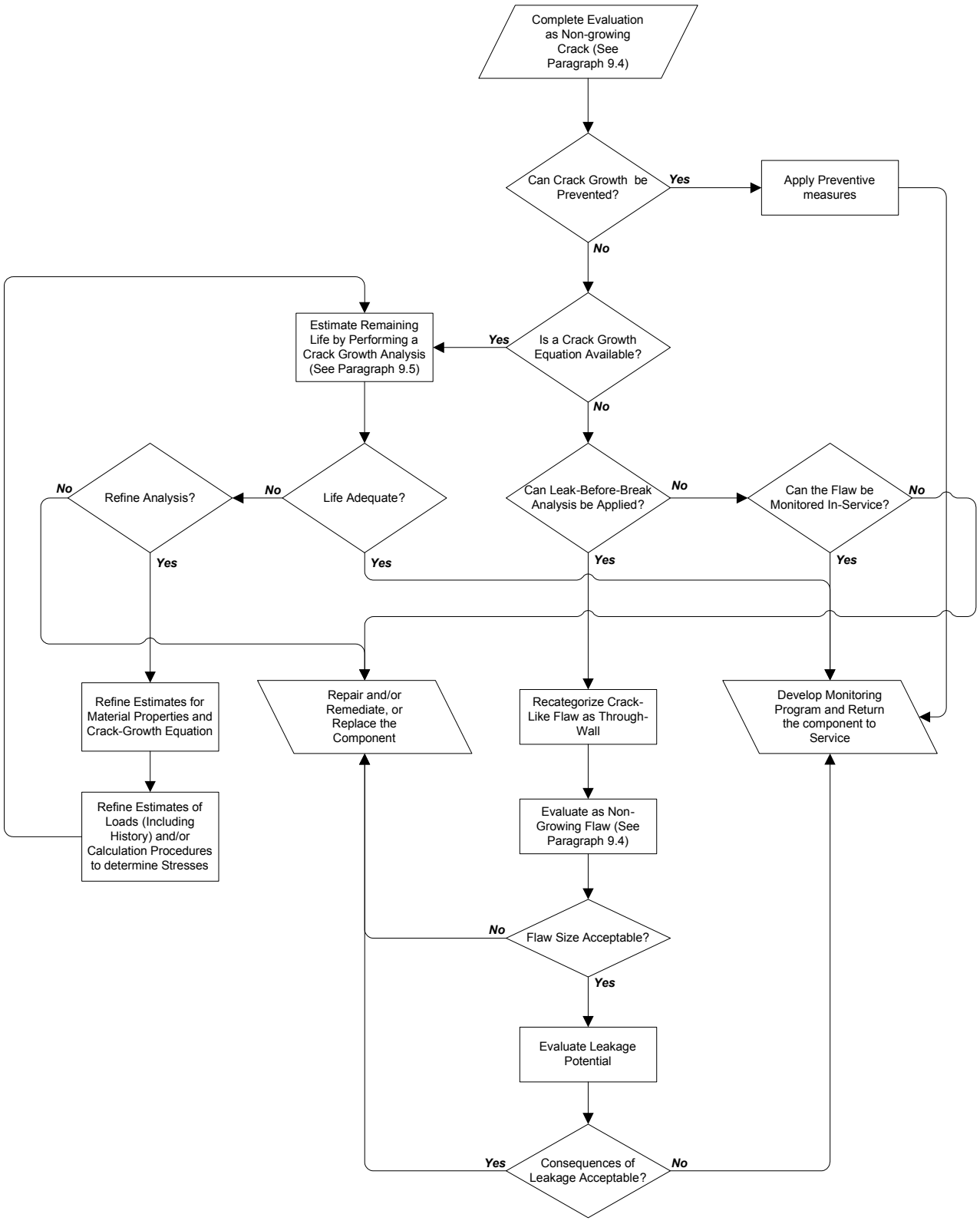

Figure 9.22 – Overview of the Assessment Procedures to Evaluate Growing Crack-Like Flaws

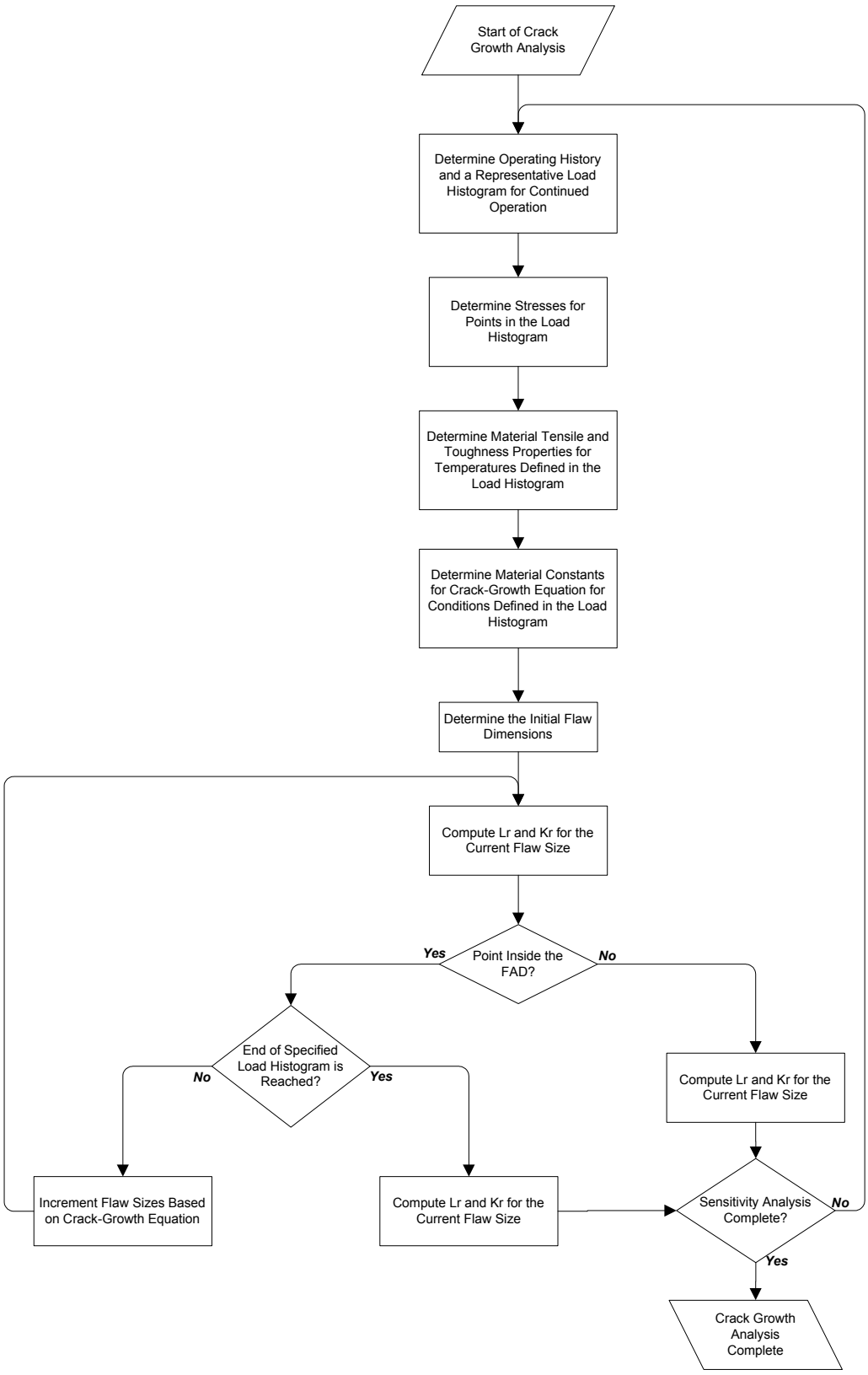

Figure 9.23 – Methodology for Crack Growth Analysis.

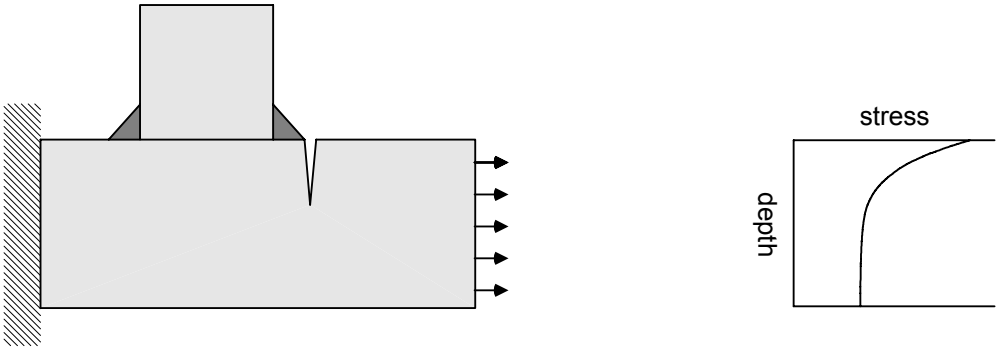

(a) Flaw at a stress concentration

(b) Flaw subject to high residual stresses.

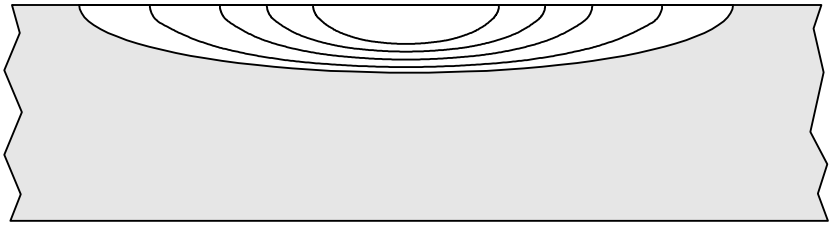

(c) Flaw growth predominantly in the length direction.

Figure 9.24 – Leak-Before-Break for Flaws Near a Stress Concentration

PART 10

ASSESSMENT OF COMPONENTS OPERATING IN THE CREEP RANGE

PART CONTENTS

10.1 General

10.1.1 Fitness-For-Service (FFS) assessment procedures for pressurized components operating in the creep range are provided in this Part. The temperature above which creep needs to be evaluated can be established using a Level 1 Assessment. The procedures in this Part can be used to qualify a component for continued operation or for re-rating. A flow chart for the assessment procedures for components operating in the creep range is shown in Figure 10.1.

10.1.2 The FFS assessment procedure for components operating in the creep range requires an estimate of remaining life. Assessment procedures for determining a remaining life are provided for components with and without a crack-like flaw subject to steady state and cyclic operating conditions. If the component contains a crack-like flaw, and is not operating in the creep range, then Part 9 can be used for the Fitness-For-Service assessment.

10.2 Applicability and Limitations of the Procedure

10.2.1 The assessment procedures in this Part can be used to determine the suitability for continued operation and the remaining life of a component operating in the creep range. The use of these procedures is not normally required for equipment designed to a recognized code or standard that is operating within the original design parameters. However, conditions that may warrant a FFS evaluation for components operating in the creep range include:

a) Operational upsets that result in an operating temperature and pressure, or other loading conditions that may result in creep damage and were not included in the original design.

b) Metal loss in the component beyond that provided for in the original design; metal loss in this category will result in component stress above those originally considered in the original design.

c) Component weldments that have significantly different properties in the weld metal, HAZ, and base metal. Examples include 1.25Cr-0.5Mo, 2.25Cr-1Mo and 9Cr-1Mo-V.

d) Stress concentration regions in the components that were not accounted for in the original design. Examples include out-of-roundness or peaking in long seam welds, notch-like locations such as transition regions with a slope greater than 1:3, and bulges that have occurred in service.

e) Fire damage that can result in a short time heating event.

f) The discovery of a crack-like flaw; both initial fabrication and service induced crack-like flaws should be evaluated.

g) The discovery of an LTA, pitting damage, weld misalignment, out-of-roundness, bulge, dent, or dent-gouge combination that can result in localized creep strain accumulation and subsequent cracking. Both initial fabrication and service-induced flaws should be evaluated.

10.2.2 Specific details pertaining to the applicability and limitations of each of the assessment procedures are discussed below.

10.2.2.1 The Level 1 assessment procedures in this Part apply only if all of the following conditions are satisfied:

a) The original design criteria were in accordance with Part 2, paragraph 2.2.2.

b) The component has not been subject to fire damage or another overheating event that has resulted in a significant change in shape such as sagging or bulging, or excessive metal loss from scaling.

c) The material meets or exceeds the respective minimum hardness and carbon content shown in Table 10.1.

d) The component does not contain:

   1) An LTA or groove-like flaw,

2) Pitting damage,

3) Blister, HIC, or SOHIC damage,

4) Weld misalignment, out-of-roundness, or bulge that exceed the original design code tolerances,

5) A dent or dent-gouge combination,

6) A crack-like flaw, or

7) Microstructural abnormality such as graphitization or hydrogen attack.

10.2.2.2 The Level 2 assessment procedures in this Part apply only if all of the following conditions are satisfied:

a) The original design criteria were in accordance with Part 2, paragraph 2.2.2.

b) A history of the operating conditions and documentation of future operating conditions for the component are available.

c) The component has been subject to less than or equal to 50 cycles of operation including startup and shutdown conditions, or less than that specified in the original design.

d) The component does not contain any of the flaws listed in paragraph 10.2.2.1.d

10.2.2.3 A Level 3 Assessment should be performed when the Level 1 and 2 methods cannot be applied due to applicability and limitations of the procedure or when the results obtained indicate that the component is not suitable for continued service.

a) Conditions that typically require a Level 3 Assessment include the following.

1) Advanced stress analysis techniques are required to define the state of stress because of complicated geometry and/or loading conditions.

2) The component is subject to cyclic operation (see paragraph 10.2.2.2.c).

3) The component contains a flaw listed in paragraph 10.2.2.1.d. A detailed assessment procedure is provided for a crack-like flaw; however, this procedure cannot be used to evaluate crack-like flaws that are caused by stress corrosion, oxide wedging, or similar environmental phenomena.

b) The Level 3 Assessment procedures, with the exception of the procedure for the evaluation of dissimilar metal welds, can be used to evaluate components that contain the flaw types in paragraph 10.2.2.1.d. A separate procedure is provided to evaluate components with crack-like flaws.

c) The assessment procedure provided for dissimilar metal welds is only applicable to 2.25Cr – 1Mo to austenitic stainless steel welds made with stainless steel or nickel-based filler metals. An alternative assessment procedure for this material and other materials that are not currently covered may be used.

10.2.2.4 To perform an evaluation to any of the assessment levels, the material properties for the temperature and stress conditions the component is subject to must be available. For a Level 1 Assessment, the required material properties are included in the material screening curves (see paragraph 10.4.2). For the Level 2 and Level 3 assessments, the required material properties are included for many commonly used materials in Annex F.

10.3 Data Requirements

10.3.1 General

10.3.1.1 The Level 1 Assessment is a screening criterion based on the original design of the component, the past and future planned operating conditions. This assessment can be performed based on the following information.

a) Original Equipment Design Data (see paragraph 10.3.2)

b) Maintenance and Operating History (see paragraph 10.3.3)

10.3.1.2 Significant input data are required to perform a Level 2 or Level 3 Assessment. Details regarding the required data are discussed in paragraphs 10.3.2 through 10.3.6. The accuracy of these data and stress conditions will determine the accuracy of the assessment in this Part.

10.3.2 Original Equipment Design Data

An overview of the original equipment data required for an assessment is provided in Part 2, paragraph 2.3.1.

10.3.3 Maintenance and Operational History

10.3.3.1 An overview of the maintenance and operational history required for an assessment is provided in Part 2, paragraph 2.3.2.

10.3.3.2 The definition of the operating history is required in order to perform a Fitness-For-Service assessment of a component operating in the creep range.

a) The component operating history and future operational conditions are required to perform a remaining life assessment. This information should include an accurate description of operating temperatures, pressures, supplemental loads, and the corresponding time period for all significant events. These events include start-ups, normal operation, upset conditions, and shutdowns. Past operating history may not be required as described in paragraph 10.3.5.2.

b) If an accurate histogram cannot be generated, then an approximate histogram shall be developed based on information obtained from plant personnel. This information shall include a description of all assumptions made, and include a discussion of the accuracy in establishing points on the histogram. A sensitivity analysis (see paragraph 10.5.1.4) shall be included in the FFS assessment to determine and evaluate the effects of the assumptions made to develop the operating history.

c) If past operating conditions are not known or estimated operating conditions have a significant amount of uncertainty, a material test can be performed whereby the creep damage associated with past operation can be evaluated in terms of a material parameter (see paragraph 10.3.5.2).

d) When creating the histogram, the history to be used in the assessment shall be based on the actual sequence of operation.

10.3.4 Required Data for A FFS Assessment – Loads and Stresses

10.3.4.1 A stress analysis is required for a Level 2 or Level 3 Assessment.

a) Level 1 Assessment – Nominal stresses are required. Nominal stress can be computed using code equations (see Annex A).

b) Level 2 and Level 3 Assessments – stress analysis may be performed using the following methods.

   1) Handbook solutions may be used if these solutions accurately represent the component geometry and loading condition.

2) Reference stress solutions that include the effects of stress re-distribution during creep may be used in the assessment if these solutions accurately represent the material creep response, component geometry, and loading conditions.

3) Numerical analysis techniques such as the finite element method can be used to determine the stress state at major structural discontinuities or at the location of a flaw (e.g. crack-like flaw or LTA) where creep damage or creep crack growth is normally manifested. In these cases, it is recommended that this analysis includes the effects of plasticity and creep to account for the redistribution of stresses that occurs in the creep range. This is particularly important because the stresses at major structural discontinuities relax to magnitudes that are significantly less than those computed using an elastic stress calculation. Since the stress results are used directly in the assessment procedure and the remaining life from this procedure is sensitive to the magnitude of stress, the results from an elastic analysis will typically over estimate the creep damage and result in a conservative estimate of remaining life.

4) Guidelines for computing stresses for a tube or elbow in a Level 2 Assessment are provided in paragraph 10.5.2.5.

10.3.4.2 Stress calculations shall be performed for all points included in the load histogram (see paragraph 10.3.3.2) that will be used in the assessment.

10.3.4.3 The stress analysis performed for all assessment levels shall include the effects of service-induced wall thinning (e.g. oxidation).

10.3.4.4 Additional information regarding stress analysis for a component containing a crack-like flaw is provided in Part 9, paragraph 9.3.4.2.

10.3.4.5 Component temperatures used in an assessment should be based on the operating temperatures considering the following.

a) Heat transfer analysis considering thermal conductivity, fluid film coefficients, and transient effects.

b) Insulating effects of scale, other corrosion products, or process products left on the component surfaces.

c) The influence of the process environment on local overheating or cooling.

10.3.5 Required Data for A *FFS* Assessment – Material Properties

10.3.5.1 An overview of the material data required to perform a remaining life assessment is provided in Annex F, paragraph F.7 and summarized below. The material data presented in Annex F are from the MPC Project Omega data that are based on a strain-rate approach, and the creep rupture life data from API Standard 530. Both types of data can be used in the Level 2 or Level 3 Assessment procedures to determine a remaining life. The Project Omega data is required in a Level 3 creep buckling analysis. Material data applicable to service exposed materials from other sources may be used in a Level 3 Assessment.

a) MPC Project Omega Data – data are provided in terms of a damage parameter and strain-rate parameter, a method is suggested to account for minimum and average properties.

b) Creep Rupture Data – data are provided for minimum and average properties in terms of the Larson-Miller Parameter.

10.3.5.2 As previously described, a precise description of the component operating history and future operational conditions is required to perform a remaining life assessment. The future planned operating conditions can be readily defined; however, many times an adequate description of the past operating history cannot be made. To address this problem, the MPC Project Omega Program has developed a testing protocol to evaluate material parameters required for a remaining life assessment. The required tests necessitate removal of a material sample from a location in the component subject to the highest creep damage. This location is typically associated with the highest temperature and/or stress location. When an Omega Test is performed on a material sample from the component, the Omega material parameters are determined, and these parameters include the effects of creep damage associated with past operation. Therefore, by performing an Omega test, the remaining life problem is "shifted" such that the operating conditions up to the time of the test do not need to be evaluated to determine a remaining life (see Figure 10.2). This feature of the MPC Omega Method provides a means to accurately account for creep damage from past operation without having to know how the component was operated.

10.3.5.3 The material data from the MPC Project Omega Program (seeAnnex F, paragraph 7) can be used directly to model creep behavior in an inelastic finite element analysis by implementing the equation shown below. This equation provides a strain-hardening relationship for the creep strain rate (i.e. the current creep strain rate is a function of the current stress, and temperature, and accumulated creep strain) and can be used with finite element computer programs that utilize either an explicit or implicit time integration algorithm for solution of the creep problem. Note that this creep constitutive relationship will need to be implemented in a customized user-subroutine. However, most of the finite element programs that have creep analysis capability provide this option.

$$\dot{\varepsilon}_c = \dot{\varepsilon}_{co} \exp\left[\Omega_m \varepsilon_c\right] \tag{10.1}$$

10.3.5.4 If the component contains a crack-like flaw, parameters for the creep-crack growth equation is required (see Annex F, paragraph F.7). In addition, the fracture toughness is also required because an evaluation of the flaw using the FAD based assessment procedures of Part 9 is required. It should be noted that although unstable crack growth is unlikely at elevated temperature, it may be a possibility during the start-up or shutdown phase of the cycle. In addition, the FAD assessment is required to place a limit on the plastic collapse of a component containing a crack-like flaw.

10.3.6 Required Data for A *FFS* Assessment – Damage Characterization

10.3.6.1 General requirements for all components

a) It shall be verified that the component material conformed to the original specification for the material of construction, or does so now.

b) The remaining sound wall thickness and the extent of corrosion/erosion shall be determined on all surfaces of the component.

c) The existence of flaws or damage described in 10.2.2.1.d shall be determined. If a flaw is found, the extent of the damage shall be documented in accordance with the applicable Parts of this Standard.

d) Local variations in the operating conditions shall be identified. These may result from hot spots, coolant flow patterns, furnace or heater firing condition, etc. Local variations in operating conditions may result in a localized increased rate of wall thinning.

e) Any unusual loading conditions resulting from missing or damaged supports, dead weight loads, etc., shall be noted, and considered in the stress analysis (see paragraph 10.3.4).

f) Environmental interaction such as carburization, decarburization, hydrogen attack, etc., shall be considered and noted accordingly.

g) Where appropriate, and based on the observed metal loss or known reaction rates and the time-temperature history, future reaction rates shall be appropriately accounted for in the assessment.

   1) Where rates of future reactions are not reaction-product thickness limited, the reaction rate may be fit to a form shown in Equation (10.2) based on measurements or literature.

$$R_r = Ae^{-Q/RT} \tag{10.2}$$

2) Where the rate of material thickness change is dependent on the thickness of the reaction product, the reaction rate may be fit to a form shown in Equation (10.3) based on measurements or literature.

$$R_r = B \cdot t^{1/2} \cdot e^{-Q/RT} \tag{10.3}$$

h) If a Level 2 or 3 Assessment is performed, then the grain size, carbon content, and heat treatment conditions should be considered.

i) If a Level 2 or 3 Assessment is performed for a weldment, then the following information should be considered.

1) The weld joint geometry.

2) Composition of the deposit, especially carbon and oxygen contents, and tramp elements and possible resulting embrittlement.

3) Welding process used during fabrication.

4) The effect of creep rate mismatch between the base metal and weld metal or HAZ on the remaining life.

5) The stress concentration at the toe of the weld.

6) The effect of radial (offset) and angular (peaking) misalignment at the weld joint, shell out-of-roundness, and other geometrical imperfections (see Part 8) on the remaining life

7) Inspection records.

8) Post weld heat treatment originally used at the time of construction.

9) Repair history including subsequent $PWHT$ information.

10) Residual stress effects.

11) The effects of precipitates in welds or inclusions on void formation that may result in a reduction in the remaining life.

10.3.6.2 Supplemental requirements for a component with a crack-like flaw

a) A determination should be made whether the crack-like indication is an original fabrication flaw or service damage induced. If the origin of the crack-like indication cannot be established, then it shall be classified as a service-induced flaw.

b) If a crack-like flaw is in the vicinity of a weld, the location of the flaw, in the heat affected zone, at the fusion line, or in the deposit shall be recorded. In addition, the crack-like flaw length and depth, and location from the surface for an embedded flaw shall be established in accordance with Part 9.

10.3.7 Recommendation for Inspection Technique and Sizing Requirements

10.3.7.1 General requirements for all components

Inspection should be performed to establish the component condition and any detectable damage.

a) Wall Thinning – straight beam ultrasonic thickness examination (UT).

b) Crack-Like Flaws (see Part 9, paragraph 9.3.7 for additional information).

1) Surface Cracks – The crack length, angle relative to the principal stress direction (see Part 9, Figure 9.2) and distance to other surface cracks may be determined using Magnetic Particle (MT) or Dye Penetrant (PT) examination technique. The depth and angle of the flaw relative to the surface (see Part 9, Figure 9.4) is typically determined using angle beam Ultrasonic (UT) examination technique.

2) Embedded Cracks – The crack depth, length, angle, and distance to other surface breaking or embedded cracks are typically determined using angle beam Ultrasonic (UT) examination technique (e.g., time-of-flight-diffraction (TOFD) or pulse echo techniques). The calibration settings may need to be more sensitive than are used for new construction weld quality inspections.

c) Bulging – the extent of the bulge shall be measured from a reference plane.

d) Hardness Measurements – may be taken in the field, although measurements made in the laboratory on samples of material in service are more reliable. For measurements in the field, the removal of about 0.5mm (0.02-in.) of material from the surface is recommended. All evidence of oxidation, sulfidation, carburization, nitriding, and decarburization must be removed. All measurements shall be performed in conjunction with the use of calibration blocks in the range of hardness expected.

e) Tube Diameter or Circumference Measurements – Calipers can be used to determine the diameter of a fired heater or boiler tube at orthogonal directions; however, a better method is to measure the circumference of the tube with a strap (flexible measuring tape).

1) Strap measurements should be taken at the highest heat flux areas of tubes. This type of measurement can be related to the swelling and creep in the tube, although complexities arise when there is external oxidation on the tube surface or the tube has ovalized in service due to non-uniform circumferential heating. Therefore, in certain cases, strap measurements are not considered to be a quantitative measure of strain, but are instead performed to provide an indication of overheating or a qualitative measure of creep damage.

2) Strap measurements taken at defined locations on new tubes (baseline measurements) and subsequently at different points in time can provide an indication of creep damage if ovalization or other damage has not occurred.

3) Another way to determine that severe bulging and creep damage has not occurred is to use a set of no-go gauges preset at a given % strain (for example 2%) that can easily be slipped over the tube and slid along the tube length. The location and extent of uneven bulging should be recorded.

4) The level of acceptable strain varies greatly amongst the tube materials and the operating conditions. For heater tubes made of HK alloys, the amount of strain at failure can be as low as 0.5%, so there are limitations to using strapping as a stand-alone method for deciding on when tube replacement is warranted.

10.3.7.2 Nondestructive material examination by means of replication is a metallographic examination method that exposes and replicates the microstructure of the surface material.

a) Method – Portable equipment is typically used for the examination. Surface preparation is conducted by progressive grinding to remove scale, surface carburization, and other surface material. After final grinding, the surface must be polished in the following ways; electrolytic polishing or mechanical polishing using polishing discs and diamond paste (particle size of 1μ to 7μ). After polishing, the surface must be cleaned thoroughly and dried. It is particularly important to thoroughly clean the surface after electro-polishing to prevent corrosion on the newly polished surface by the aggressive electrolyte. A strip of acetate tape is softened in a solvent and pressed against the polished surface. Once the tape dries it is removed and can be viewed under the optical or electron microscope when vapor deposit coated with carbon or gold.

b) Application – The replication method can be used for the examination of all metallic materials. Replication is typically used to establish microstructure of the materials and to determine if cavities or cracks are present. This method is restricted to relatively small areas for examination; however, many replicas can be taken to ensure coverage of a large area. Replication can be used as a follow-up to other detection methods such as magnetic particle or eddy current. Surface cracks can be identified at a much earlier stage using the replication method than with other NDE methods. This early detection allows time to plan repairs and/or replacements thus avoiding unscheduled repairs.

c) Flaw Detection – Because each type of crack has specific characteristics, a damage type determination is usually possible with this method. If further evaluation is desired for metallurgical and microstructural components (such as carbides, cavities, etc.), replicas can be coated with a reflective, conductive material and studied in a scanning electron microscope.

d) Limitations – The replication method can only be used on surfaces that are readily accessible. The surface conditions must be exposed, dry, and at ambient temperature, between about -18°C to 32°C (0°F to 90°F).

10.3.7.3 As an alternative to replication, small samples can be removed from the component to determine composition as well as microstructure. However, it should be noted that repair of this area may be required unless the region can be qualified for continued operation with a Level 3 Assessment.

10.3.7.4 Supplemental requirements for a component with a crack-like flaw

a) Detection and sizing of crack-like flaws originating in creep service requires validation and qualification of procedures and personnel. Service-induced cracks may not be good planar reflectors, and they may not be located in regions easily accessed by shear wave.

b) Surface cracks may be characterized by magnetic particle, dye penetrant, eddy current, or ultrasonic examination, or by replication. Subsurface cracks may be characterized using UT. If crack-like indications are found, the location, length, position relative to surface, and extent must be determined. Position relative to a weld or discontinuity must be recorded.

c) Automated TOFD can be effectively used for rapid screening of aligned clusters of small cavities. High frequency composite transducers may be used for detection of low levels of aligned cavitation. Focus beam transducers may be used for early stage damage characterization, provided the signal responses have been characterized and validated.

10.4 Assessment Techniques and Acceptance Criteria

10.4.1 Overview

The Fitness-For-Service assessment procedures used to evaluate the remaining life of a component operating in the creep range are described below. The three assessment levels used to evaluate creep damage are based on the data and details required for the analysis, whether the component contains a crack-like flaw, the degree of complexity required for a given situation, and the perceived risk (see API RP 580).

a) Level 1 Assessments are based on a comparison with specified time-temperature-stress limits and a simplified creep damage calculation for components subject to multiple operating conditions (i.e. temperature and applied stress combinations). In addition, a check on material properties in terms of hardness or carbon content and a visual examination of the component is made in order to evaluate the potential for creep damage based on component distortion and material characteristics such as discoloration or scaling.

b) Level 2 Assessments can be used for components operating in the creep regime that satisfy the requirements of paragraph 10.2.2.2. The stress analysis for the assessment may be based on closed form stress solutions, reference stress solutions, or solutions obtained from finite element analysis.

c) Level 3 Assessments can be used to evaluate those cases that do not meet the requirements of Level 1 or Level 2 assessments. A detailed stress analysis is required to evaluate creep damage, creep-fatigue damage, creep crack growth, and creep buckling. In addition, a separate procedure is provided to perform a creep-fatigue assessment of a dissimilar-weld joint.

10.4.2 Level 1 Assessment

10.4.2.1 The Level 1 assessment for a component subject to a single design or operating condition in the creep range is provided below.

a) STEP 1 – Determine the maximum operating temperature, pressure, and service time the component is exposed to. If the component contains a weld joint that is loaded in the stress direction that governs the minimum required wall thickness calculation, then 14ºC (25ºF) shall be added to the maximum operating temperature to determine the assessment temperature. Otherwise, the assessment temperature is the maximum operating temperature. The service time shall include past and future planned operation.

b) STEP 2 – Determine the nominal stress of the component for the operating condition defined in STEP 1 using Annex A. The computed nominal stress shall include the effects of service-induced wall thinning.

c) STEP 3 – Determine the material of construction for the component and find the figure with the screening and damage curves to be used for the Level 1 assessment from Figures 10.3 through 10.25.

d) STEP 4 – Determine the maximum permissible time for operation based on the screening curve obtained from STEP 3, the nominal stress from STEP 2, and the assessment temperature from STEP 1. If the time determined from the screening curve exceeds the service time for the component from STEP 1, then the component is acceptable per the Level 1 Assessment procedure. Otherwise, go to STEP 5.

e) STEP 5 – Determine the creep damage rate, R_c and associated creep damage D_c for the operating condition defined in STEP 1 using the damage curve obtained from STEP 3, the nominal stress from STEP 2, and the assessment temperature from STEP 1. The creep damage for this operating condition shall be computed using Equation (10.4) where the service exposure time is determined from STEP 1.

$$D_c^{total} = R_c \cdot t_{se} \tag{10.4}$$

f) STEP 6 – If the total creep damage determined from STEP 5 satisfies Equation (10.5), then the component is acceptable per the Level 1 Assessment procedure. Otherwise, the component is not acceptable and the requirements of paragraph 10.4.2.3 shall be followed.

$$D_c^{total} \le 0.25 \tag{10.5}$$

10.4.2.2 The Level 1 assessment for a component subject to a multiple design or operating conditions in the creep range.

a) STEP 1 – Determine the maximum temperature, pressure, and service time for each operating condition the component is exposed to. Define j as the operating condition number and J as the total number of operating conditions. If the component contains a weld joint that is loaded in the stress direction that governs the minimum required wall thickness calculation, then 14ºC (25ºF) shall be added to the operating temperature to determine the assessment temperature. Otherwise, the operating temperature is the assessment temperature. The service exposure time for each design or operating condition, t_{se}^j, shall include past and future planned operation.

b) STEP 2 – Determine the nominal stress of the component for each of the operating conditions defined in STEP 1 using Annex A The computed nominal stress shall include the effects of service-induced wall thinning.

c) STEP 3 – Determine the material of construction for the component and find the figure with the damage curves to be used for the Level 1 assessment from Figures 10.3 through 10.25.

d) STEP 4 – Determine the creep damage rate, R_c^j and associated creep damage D_c^j for each of the j operating conditions defined in STEP 1 using the damage curve obtained from STEP 3, the nominal stress from STEP 2, and the assessment temperature from STEP 1. The creep damage for each operating condition, j, can be computed using Equation (10.6) where the service exposure time is determined from STEP 1.

$$D_c^j = R_c^j \cdot t_{se}^j \tag{10.6}$$

e) STEP 5 – Determine the creep damage for total number of operating conditions, J, using Equation (10.7).

$$D_c^{total} = \sum_{j=1}^{J} D_c^j \tag{10.7}$$

f) STEP 6 – If the total creep damage determined from STEP 5 satisfies Equation (10.8), then the component is acceptable per the Level 1 Assessment procedure. Otherwise, the component is not acceptable and the requirements of paragraph 10.4.2.3 shall be followed.

$$D_c^{total} \le 0.25 \tag{10.8}$$

10.4.2.3 If the component does not meet the Level 1 Assessment requirements, then the following, or combinations thereof, can be considered:

a) Rerate, repair, replace, or retire the component.

b) Adjust the future operating conditions, the corrosion allowance, or both; note that this does not apply if $D_c^{total} > 0.25$ based on the current operating time.

c) Conduct a Level 2 or a Level 3 Assessment.

10.4.3 Level 2 Assessment

10.4.3.1 The Level 2 assessment procedure shall be performed in accordance with paragraph 10.5.2.3. The temperature of the component used in the assessment is assumed to be uniform for each specific time step.

10.4.3.2 If the component does not meet the Level 2 Assessment requirements, then the following, or combinations thereof, can be considered:

a) Rerate, repair, replace, or retire the component.

b) Adjust the future operating conditions, the corrosion allowance, or both; note that this does not apply if $D_c^{total} > D_c^{allow}$ based on the current operating time.

c) Conduct a Level 3 Assessment.

10.4.4 Level 3 Assessment

10.4.4.1 The Level 3 Assessment procedures are covered in paragraph 10.5. With the exception of the procedure for the evaluation of dissimilar metal welds, these procedures can also be used to evaluate a component containing one or more of the flaws listed in paragraph 10.2.2.1.d. If the flaw is volumetric (i.e. LTA, pitting damage, weld misalignment, out-of-roundness, bulge, dent, or dent-gouge combination), then the stress analysis model used to evaluate the remaining life shall include the flaw so that localized stresses and strains are accounted for. These stress results are then directly used in the assessment. If the component contains a crack-like flaw, then the stress analysis used for remaining life can be based on an uncracked body analysis. The effects of the crack are accounted for in the assessment procedure.

10.4.4.2 If the component does not meet the Level 3 Assessment requirements, then the following, or combinations thereof, can be considered:

a) Rerate, repair, replace, or retire the component.

b) Adjust the future operating conditions, the corrosion allowance, or both; note that this does not apply if $D_c^{total} > D_c^{allow}$ based on the current operating time.

10.5 Remaining Life Assessment

10.5.1 Overview

10.5.1.1 A remaining life calculation is required for all components operating in the creep range. The assessment procedures in paragraph 10.4 are limited to components that are not subject to significant cyclic operation and/or components that do not contain crack-like flaws.

10.5.1.2 The assessment procedures described in this paragraph provide the best estimate of the structural integrity of a component operating at elevated temperature. Five assessment procedures are provided.

a) *Creep Rupture Life* – The assessment procedure is given in paragraph 10.5.2, and is applicable to components that are subject to steady state operation in the creep range which do not have crack-like flaws.

b) *Creep-Fatigue Interaction* – The assessment procedure is given in paragraph 10.5.2, and is used in conjunction with the information in paragraph 10.5.3. This procedure is applicable to components that are subject to cyclic operation in the creep range which do not have crack-like flaws.

c) *Creep Crack Growth* – The assessment procedure is given in paragraph 10.5.4, and is applicable to components that are subject to either steady state or cyclic operation in the creep range which contain crack-like flaws.

d) *Creep Buckling* – The assessment procedure is given in paragraph 10.5.5, and can be used to determine the time at which a component in the creep range may be subject to structural instability due to a compressive stress field. The procedure can be used for a component both with and without a crack-like flaw.

e) *Creep-Fatigue Assessment Of Dissimilar-Weld Joint* – The assessment procedure is given in paragraph 10.5.6, and is applicable to 2.25Cr–1Mo and 2.25Cr–1Mo-V to austenitic stainless steel dissimilar weld joints made with stainless steel or nickel-based filler metals. This procedure is applicable to components that are subject to cyclic operation in the creep range that do not have crack-like flaws. For other types of dissimilar weld joints or for dissimilar weld joints with crack-like flaws, the procedures described above can be used for the assessment. In these cases, the thermal expansion and creep rate differences between the base materials and the weldment shall be considered in the stress analysis.

f) *Microstructural Approaches* – Because of limited applicability and uncertainty of microstructural approaches, these types of assessments are normally used to supplement other techniques. A description of the recognized microstructural approaches is given in paragraph 10.5.7.

10.5.1.3 The recognized assessment procedures listed below may be used as an alternative to the procedures in paragraph 10.5.1.2. Other assessment procedures may be used if the technology used adequately addresses the damage mechanism, a remaining life can be determined, and adequate documentation is provided that discloses all of the assumptions used in the assessment.

a) British Energy R-5 (see Part 1, Table 1.1).

b) BS 7910 (see Part 1, Table 1.1).

c) EPRI *Remaining-Life of Boiler Pressure Parts–Crack Growth Studies* [8].

d) WRC 440 *A Synthesis of the Fracture Assessment methods Proposed in the French RCC-MR Code for High Temperature* [10].

e) ASME Code, Section III, Subsection NH (seePart 1, Table 1.1).

10.5.1.4 A sensitivity analysis (see Part 2, paragraph 2.4.3.1) should be performed as part of the assessment regardless of the method chosen.

a) The assessment procedures in this Part do not contain recommendations for in-service margins that should be applied to the remaining life calculation. It is recommended that the margin be placed on the remaining life prediction rather than the independent variables of the solution (i.e. time in service, applied stress, temperature, etc.).

b) Remaining life estimates in the creep range are sensitive to materials data, applied stresses, and corresponding temperature. Therefore, sensitivity studies should be performed to evaluate the interaction of these variables in regards to the remaining life prediction.

c) Confidence may be gained in the assessment by using a sensitivity analysis when it is possible to demonstrate that small changes in the independent variables do not lead to dramatic reductions in the estimated remaining life of a component. Further confidence is gained when the predictions at the end of an appropriate inspection period indicate that creep damage, or crack growth in the case of a component containing a flaw, is not accelerating in such a way as to lead to imminent failure.

d) Sensitivity analyses should consider the effects of different assumptions on the assessment results. For example, there may be uncertainties in the service loading conditions including temperature and associated time in-service; the extrapolation of materials data to service conditions; the nature, size and shape of the crack-like flaw; and other input variables.

10.5.2 Creep Rupture Life

10.5.2.1 The following analysis procedure can be utilized to evaluate a component operating in the creep range using the results from a stress analysis. The assessment is based on the stresses and strains at a point and through the wall thickness in the component, and the associated operating time and temperature. If an inelastic analysis is used to evaluate the effects of creep, then a material model is required to compute the creep strains in the component as a function of stress, temperature, and accumulated creep strain (strain hardening model, see paragraph 10.3.5.3) or time (time hardening model). If the computed stresses exceed the yield strength of the material at temperature, plasticity should also be included in the material model.

10.5.2.2 The assessment procedure in this paragraph provides a systematic approach for evaluating the creep damage for each operating cycle that is applied to the component. The total creep damage is computed as the sum of the creep damages calculated for each cycle.

10.5.2.3 A procedure to determine the creep damage based upon the results of a stress analysis is shown below.

a) STEP 1 – Determine a load history based on past operation and future planned operation. The load histogram should include all significant operating loads and events that are applied to the component. If there is cyclic operation, the load histogram should be divided into operating cycles as shown in Figure 10.26. Define M as the total number of operating cycles. Note that it is important that the loading conditions in the histogram be analyzed in the same order as the actual sequence of operations even if this entails breaking a loading condition into two or more analysis steps.

b) STEP 2 – For the current operating cycle m, determine the total cycle time, ${}^{m}t$, and divide the cycle into a number of time increments, ${}^{n}t$ as shown in Figure 10.27. Define N as the total number of time increments in operating cycle m.

   1) The time increments used to model the operating cycle should be small enough to capture all significant variations in the operating cycle. The smaller the time increment, the more accurate the remaining life predication.

   2) If the component is subject to corrosion or erosion, the time increments should be set small enough to capture changes in the wall thickness.

c) STEP 3 – Determine the assessment temperature, ${}^{n}T$, for the time increment ${}^{n}t$.

d) STEP 4 – Determine the stress components, ${}^{n}\sigma_{ij}$, for the time increment ${}^{n}t$.

   1) Equations for the principal stresses for cylindrical and spherical shells subject to pressure loading are shown in Table 10.2. Stress calculations for tubes and elbows are discussed in paragraph 10.5.2.5.

   2) The principal stresses can also be computed using a finite element analysis.

e) STEP 5 – Determine if the component has adequate protection against plastic collapse.

1) If the stress components are determined from an elastic analysis, determine the primary load reference stress using Equation (10-.9) and check that the criterion in Equation (10.10) or Equation (10.11) is satisfied. The value of the yield strength, σ_{ys} in this equation is evaluated at temperature ${}^{n}T$ at time increment ${}^{n}t$. If the criterion in Equations (10.10) or (10.11) is satisfied, proceed to STEP 6, otherwise, proceed to STEP 12.

$$ {}^{n}\sigma_{ref}^{p} = \frac{{}^{n}P_b + \left({}^{n}P_b^2 + 9 \cdot {}^{n}P_L^2 \right)^{0.5}}{3} \tag{10.9} $$

$$ {}^{n}\sigma_{ref}^{p} \le \sigma_{ys} \qquad \textit{for austenitic stainless steels} \tag{10.10} $$

$$ {}^{n}\sigma_{ref}^{p} \le 0.75 \cdot \sigma_{ys} \qquad \textit{for all other materials} \tag{10.11} $$

2) If the stress components are based on an inelastic analysis that includes plasticity and creep, protection against plastic collapse can be determined by a limit load or plastic collapse solution in accordance withAnnex B1.

f) STEP 6 – Determine the principal stresses, ${}^{n}\sigma_1$, ${}^{n}\sigma_2$, ${}^{n}\sigma_3$ and the effective stress, ${}^{n}\sigma_e$, using Equation (10.12) for the time increment ${}^{n}t$.

$$ {}^{n}\sigma_e = \frac{1}{\sqrt{2}}\left[\left({}^{n}\sigma_1 - {}^{n}\sigma_2 \right)^2 + \left({}^{n}\sigma_1 - {}^{n}\sigma_3 \right)^2 + \left({}^{n}\sigma_2 - {}^{n}\sigma_3 \right)^2 \right]^{0.5} \tag{10.12} $$

g) STEP 7 - Determine a remaining life at the stress level ${}^{n}\sigma_e$ and temperature ${}^{n}T$ for time increment ${}^{n}t$ by utilizing creep rupture data for the material and designate this value as ${}^{n}L$. The units of measure for use in computing the rupture time in subparagraphs 1) and 2) below are ksi and ${}^{o}F$, the corresponding time to rupture is in $hours$.

1) If MPC Project Omega Data are used in the assessment (see Annex F, paragraph F.7.1.1), then the time to rupture is given by Equation (10.13). If a weld is being analyzed in a Level 2 Assessment, then $\Delta_{\Omega}^{sr} = -0.5$. In a Level 3 Assessment, an alternate value may be assigned based on the weld material composition and other factors.

$$ {}^{n}L = \frac{1}{\dot{\varepsilon}_{co}\Omega_m} \tag{10.13} $$

where

$$ \log_{10}\dot{\varepsilon}_{co} = -\left\{ \left(A_o + \Delta_{\Omega}^{sr} \right) + \left[\frac{1}{460 + {}^{n}T} \right] \left[A_1 + A_2 S_l + A_3 S_l^2 + A_4 S_l^3 \right] \right\} \tag{10.14} $$

$$ \Omega_m = \Omega_n^{\delta_{\Omega}+1} + \alpha_{\Omega} \cdot n_{BN} \tag{10.15} $$

$$ \Omega_n = \max\left[\left(\Omega - n_{BN} \right),\ 3.0 \right] \tag{10.16} $$

$$ \log_{10}\Omega = \left(B_o + \Delta_{\Omega}^{cd} \right) + \left[\frac{1}{460 + {}^{n}T} \right] \left[B_1 + B_2 S_l + B_3 S_l^2 + B_4 S_l^3 \right] \tag{10.17} $$

$$\delta_{\Omega} = \beta_{\Omega}\left(\frac{{}^{n}\sigma_1 + {}^{n}\sigma_2 + {}^{n}\sigma_3}{{}^{n}\sigma_e} - 1.0\right) \tag{10.18}$$

$$n_{BN} = -\left\{\left[\frac{1}{460 + {}^{n}T}\right]\left[A_2 + 2A_3 S_l + 3A_4 S_l^2\right]\right\} \tag{10.19}$$

$$S_l = \log_{10}\left({}^{n}\sigma_e\right) \tag{10.20}$$

2) If creep rupture data are provided in terms of the Larson-Miller parameter (see Annex F, paragraph F.7.1.2), then the time to rupture is given by the equation shown below. Other expressions for creep rupture data that are a function of time and stress level may also be used.

$$\log_{10}{}^{n}L = \frac{1000 \cdot LMP({}^{n}S_{eff})}{\left({}^{n}T + 460\right)} - C_{LMP} \tag{10.21}$$

where

$${}^{n}S_{eff} = {}^{n}\sigma_e \cdot \exp\left[0.24\left(\frac{J_1}{S_s} - 1\right)\right] \tag{10.22}$$

$$J_1 = {}^{n}\sigma_1 + {}^{n}\sigma_2 + {}^{n}\sigma_3 \tag{10.23}$$

$$S_s = \left({}^{n}\sigma_1^2 + {}^{n}\sigma_2^2 + {}^{n}\sigma_3^2\right)^{0.5} \tag{10.24}$$

h) STEP 8 - Repeat STEPS 3 through 7 for each time increment ${}^{n}t$ in the m^{th} operating cycle to determine the rupture time, ${}^{n}L$, for each increment.

i) STEP 9 - Compute the accumulated creep damage for all points in the m^{th} cycle using Equation (10.25). In this equation, ${}^{n}t$ is defined as the time increment where the component is subject to a stress level ${}^{n}\sigma_e$ at a corresponding operating temperature ${}^{n}T$, and ${}^{n}L$ is the permissible life at this temperature based on material data.

$${}^{m}D_c = \sum_{n=1}^{N} \frac{{}^{n}t}{{}^{n}L} \tag{10.25}$$

j) STEP 10 - Repeat STEPS 2 through 9 for each of the operating cycles defined in STEP 1.

k) STEP 11 – Compute the total creep damage for all cycles of operation.

$$D_c^{total} = \sum_{m=1}^{M} {}^{m}D_c \le D_c^{allow} \tag{10.26}$$

l) STEP 12 – The creep damage prediction is complete for this location in the component. The allowable creep damage should be taken as $D_c^{allow} = 0.80$ unless an alternative value can be justified.

1) If the criterion for protection against plastic collapse for any point in the operating history is not satisfied, then the component is not acceptable for continued operation, refer to paragraph 10.4.3.2 or 10.4.4.2, as applicable, for recommended actions.

2) If the total creep damage, D_c^{total}, is less than or equal to the allowable creep damage, D_c^{allow}, then the component is acceptable for continued operation. The remaining life for operation is determined by analyzing additional load cycles and determining the time when $D_c^{total} = D_c^{allow}$.

3) If the total creep damage, D_c^{total}, is greater than the allowable creep damage, D_c^{allow}, then the life of the component is limited to the time corresponding to $D_c^{total} = D_c^{allow}$. If this time is less than the current operating time refer to paragraph 10.4.3.2 or 10.4.4.2, as applicable, for recommended actions.

10.5.2.4 In addition to satisfying the damage criterion in paragraph 10.5.2.3, if the stress components are based on an inelastic analysis that includes plasticity and creep, a limit on the total accumulated inelastic strains should be set to a value that will not limit the operability of the component. The suggested limit for the accumulated strains are provided in Annex B1, paragraph B.3.3.

10.5.2.5 Fired heater and boiler tubes may be evaluated as a special case of the procedure in paragraph 10.5.2.3 if the pressure is approximately constant and temperature is approximately uniform around the circumference of the tube during operation.

a) *Stress Calculations* – recommendations for stress calculations are shown below.

1) Thin Wall Tubes and Elbows Subject to Pressure and Supplemental Loads – For thin wall heater tubes with an outside diameter to thickness ratio greater than six, the thin wall equations for a cylinder based on the mean diameter in Table 10.2 may be used in the assessment. The creep rupture life, life fraction, and cumulative life fraction are evaluated at the equivalent stress. For a straight section of tube, the Lorenz factor is equal to 1.0. The term t_{sl} can be set to zero if the longitudinal stress due to supplementary loads (e.g. weight) is negligible. The resulting stress components for these conditions for the n^{th} operating period are shown below.

$$ {}^{n}\sigma_1 = {}^{n}\sigma_{mean} = \frac{PD_{mean}}{2t_{comp}} \tag{10.27} $$

$$ {}^{n}\sigma_2 = 0.5 \cdot {}^{n}\sigma_{mean} \tag{10.28} $$

$$ {}^{n}\sigma_3 = 0.0 \tag{10.29} $$

$$ {}^{n}\sigma_e = 0.866 \cdot {}^{n}\sigma_{mean} \tag{10.30} $$

2) Thin or Thick Wall Tubes Subject to Pressure – For thin or thick wall heater, the reference stress solutions in Table 10.2 may be used in the assessment. The creep rupture life, life fraction, and cumulative life fraction are evaluated at the reference stress.

3) Thick Wall Tube and Elbow Subject to Pressure – For thick wall heater tubes with an outside diameter to thickness ratio less than six, the steady-state creep solutions in Table 10.2 may be used in the assessment. The creep rupture life, life fraction, and cumulative life fraction are evaluated at the equivalent stress that is computed at the outer diameter, mid-wall, and inner diameter by setting the variable r to R_o, R_{mean}, and R_i, respectively. A realistic value of the Bailey-Norton coefficient n_{BN} shall be used in the stress calculation. This coefficient is a function of the material type, stress, and temperature. An approach that can be used in the stress calculation to arrive at a suitable Bailey-Norton coefficient is to assume a value for n_{BN}, compute σ_1, σ_2, and σ_3 and iterate until a converged value of n_{BN} is obtain using Equation (10.19). Note that although the stresses at the inner surface are typically higher than those at the outside surface, the metal temperature at the outside surface may be higher, and this may result in a corresponding higher value of creep damage on the outside surface. An alternate reasonable approach that can be used is to compute the stress at the mid-wall location and use the outer wall tube metal temperature in the creep damage calculation.

b) *Determination of Rupture Life* – After the stress components for the n^{th} operating period are computed, the corresponding rupture life, ${}^nL$, can be obtained using the MPC Project Omega Method or the Larson-Miller based method (see paragraph 10.5.2.3.g). In the Larson-Miller method, if a thin wall tube is subject to only internal pressure, then the stress for the tube for the n^{th} operating period given by Equation (10.22) reduces to:

$$ {}^nS_{eff} = 0.94 \cdot {}^n\sigma_{mean} \tag{10.31}$$

c) *Life Fraction* – After the rupture life ${}^nL$ for the n^{th} operating period are computed, the life faction for time period n^{th} is computed using Equation (10.32).

$$ {}^nD_c = \frac{{}^nt}{{}^nL} \tag{10.32}$$

d) *Cumulative Life Fraction* The tube life is assumed to be consumed when the cumulative life fraction used for all operating period exceeds D_c^{allow}, the value of D_c^{allow} is typically taken as 1.0. Note that this is similar to the procedure currently used in API Std 530.

$$ D_c^{total} = \sum_{n=1}^{N} {}^nD_c \le D_c^{allow} \tag{10.33}$$

10.5.3 Creep-Fatigue Interaction

10.5.3.1 If there are significant cyclic operations during the operating period, then the effects of combined creep and fatigue damage shall be evaluated. The combination of creep and fatigue damage is may evaluated using the following procedure.

a) STEP 1 – Evaluate the creep and fatigue damage independently. If the assessment procedure in paragraph 10.5.2 is used to evaluate the creep part of the damage, then Equation (10.34) shall be used for the creep damage. If the assessment procedure in Annex B1, paragraph B1.5, is used then Equation (10.35) shall be used for the fatigue damage.

$$ D_c = \sum_{m=1}^{M} {}^mD_c \tag{10.34}$$

$$D_f = \sum_{m=1}^{M} \frac{{}^m n}{{}^m N} \tag{10.35}$$

b) STEP 2 – Determine the acceptable material envelope for creep-fatigue damage based on Figure 10.28 and the material of construction.

c) STEP 3 – Plot the point defined by D_f and D_c calculated in STEP 1 on Figure 10.28 based on the applicable acceptable material envelope for creep-fatigue damage developed in STEP 2. If the point lies on or below the envelope, the component is acceptable for continued operation. If the point lies outside of the envelope, the component is unacceptable for continued operation.

10.5.3.2 In addition to satisfying the damage criterion in paragraph 10.5.3.1, a limit on the total accumulated inelastic strains should be set to a value that will not limit the operability of the component (see paragraph 10.5.2.3).

10.5.4 Creep Crack Growth

10.5.4.1 The following analysis procedure can be utilized to evaluate a component operating in the creep range with a crack-like flaw using the results from a stress analysis. The assessment is based on the stresses and strains at a point and through the wall thickness in the component, and the associated operating time and temperature. If an inelastic analysis is used to evaluate the effects of creep, then a material model is required to compute the creep strains in the component as a function of stress, temperature, and accumulated creep strain (strain hardening model, see paragraph 10.3.5.3) or time (time hardening model). If the computed stresses exceed the yield strength of the material at temperature, plasticity should also be included in the material model.

10.5.4.2 A procedure to determine creep crack growth based upon the results of a stress analysis is shown below.

a) STEP 1 – Determine a load history based on past operation and future planned operation. The load histogram should include all significant operating loads and events that are applied to the component. If there is cyclic operation, the load histogram should be divided into operating cycles. Note that it is important that the loading conditions in the histogram be analyzed in the same order as the actual sequence of operations even if this entails breaking a loading condition into two of more analysis steps.

b) STEP 2 – Determine the material properties; yield strength, tensile strength, fracture toughness (see Part 9, paragraph 9.3.5), and creep properties (see Annex F, paragraph F.7). The yield and tensile strength should be established using nominal values (i.e. minimum specified per the material specification if actual values are unknown), and the toughness should be based on the mean value (see Part 9, Table 9.2, note 6).

c) STEP 3 – Determine the damage in the material ahead of the crack prior to cracking, D_{bc}.

1) If the component is not in cyclic operation, then the damage prior to cracking is the creep damage computed using the procedure in paragraph 10.5.2 . The creep damage is computed using Equation (10.36) where M_{bc} is the total number of operating cycles before the onset of cracking.

$$D_{bc} = \sum_{m=1}^{M_{bc}} {}^m D_c \tag{10.36}$$

2) If the component is subject to cyclic operation, then the damage prior to cracking is the creep-fatigue damage computed using the procedure in paragraph 10.5.2 in conjunction with paragraph 10.5.3.1 . The creep-fatigue damage is computed using Equation (10.37) where M_{bc} is the total number of operating cycles before the onset of cracking.

$$D_{bc} = \sum_{m=1}^{M_{bc}} {}^{m}D_c + \sum_{m=1}^{M_{bc}} \frac{{}^{m}n}{{}^{m}N} \tag{10.37}$$

d) STEP 4 – Determine the initial crack-like flaw dimensions from inspection data, a_o and c_o. The flaw should be categorized using the procedure in Part 9, paragraph 9.3.6.2. Initialize the initial flaw dimension sizes and the starting time for the cycle:

$${}^{i=0}a = a_o \tag{10.38}$$

$${}^{i=0}c = c_o \tag{10.39}$$

$${}^{i=0}t = 0.0 \tag{10.40}$$

$$D_{ac} = 0.0 \tag{10.41}$$

e) STEP 5 – For the current operating cycle m, determine the total cycle time, ${}^{m}t$, and divide the cycle into a number of time periods. Designate the time at the end of each time period ${}^{i}t$. Note that sufficient time periods should be evaluated based on the loading histogram, and the desired accuracy of the final results. A sensitivity analysis may need to be performed in order to evaluate the number of time periods required to achieve the desired accuracy.

f) STEP 6 – Determine the temperature, ${}^{i}T$, and compute the stress components ${}^{i}\sigma_{ij}$ through the wall of the component containing the crack-like flaw at time ${}^{i}t$.

g) STEP 7 – Determine the reference stress, ${}^{i}\sigma_{ref}$, at time ${}^{i}t$ using Annex D based on the crack-like flaw dimensions ${}^{i}a$ and ${}^{i}c$, and the corresponding stress distribution.

h) STEP 8 – Perform a FAD assessment at time ${}^{i}t$ using the procedures in Part 9 based on the crack-like flaw dimensions ${}^{i}a$ and ${}^{i}c$, and the corresponding stress and temperature distribution. If the resulting FAD point is outside of the FAD failure envelope, go to STEP 19; otherwise, go to STEP 9. Note that the FAD assessment at elevated temperatures will essentially result in a plastic collapse check because the fracture toughness will be on the upper shelf. However, at lower temperatures in the histogram, unstable crack growth may occur because of a reduction in the material fracture toughness.

i) STEP 9 – Determine the damage in the material ahead of the crack growth, D_{ac}, at time ${}^{i}t$ based on the crack-like flaw dimensions ${}^{i}a$ and ${}^{i}c$, and the corresponding stress and temperature distribution.

$${}^{i}D_{ac} = {}^{i-1}D_{ac} + \frac{\left({}^{i}t - {}^{i-1}t\right)}{{}^{i}L_{ac}} \tag{10.42}$$

1) If MPC Project Omega Creep Data are used in the assessment, then ${}^{i}L_{ac}$ is evaluated using Equation (10.43) where the parameters Ω_m and $\dot{\varepsilon}_{co}$ are determined using Equations (10.14) through (10.19) with S_l given by Equation (10.44).

$$ {}^{i}L_{ac} = \frac{1}{\Omega_m \dot{\varepsilon}_{co}} \tag{10.43} $$

$$ S_l = \log_{10}\left({}^{i}\sigma_{ref}\right) \tag{10.44} $$

2) If creep rupture data are provided in terms of the Larson-Miller parameter (see Annex F paragraph F.7.1.2), then ${}^{i}L_{ac}$ can be computed using Equation (10.21). Other expressions for creep rupture data that are a function of time and stress level may also be used.

j) STEP 10 – Determine the reference strain rate, ${}^{i}\dot{\varepsilon}_{ref}$, at time ${}^{i}t$ based on the crack-like flaw dimensions, ${}^{i}a$ and ${}^{i}c$, and the corresponding stress and temperature distribution using Equation (10.14) evaluated at the reference stress, or $S_l = \log_{10}\left({}^{i}\sigma_{ref}\right)$.

k) STEP 11 – Determine the stress intensity factor at the deepest point, $K_I^{90}({}^{i}a, {}^{i}c)$, and surface point, $K_I^{0}({}^{i}a, {}^{i}c)$, of the flaw at time ${}^{i}t$ based on the crack-like flaw dimensions ${}^{i}a$ and ${}^{i}c$, and the corresponding stress and temperature distribution using Annex C.

l) STEP 12 – Determine the crack driving force at the deepest point, $C_t^{90}({}^{i}a, {}^{i}c)$, and surface point, $C_t^{0}({}^{i}a, {}^{i}c)$, of the flaw at time ${}^{i}t$ based on the crack-like flaw dimensions ${}^{i}a$ and ${}^{i}c$, and the corresponding stress and temperature distribution using the equations shown below.

$$ C_t^{90}({}^{i}a, {}^{i}c) = C^{*90}({}^{i}a, {}^{i}c) \cdot \left[\left(\frac{t_{relax}^{90}({}^{i}a, {}^{i}c)}{{}^{i}t} \right)^{\left(\frac{n_{BN}-3}{n_{BN}-1}\right)} + 1 \right] \tag{10.45} $$

$$ C^{*90}({}^{i}a, {}^{i}c) = \left(\frac{{}^{i}\dot{\varepsilon}_{ref}}{1 - D_{bc} - {}^{i}D_{ac}} \right) \frac{\left(K_I^{90}({}^{i}a, {}^{i}c)\right)^2}{{}^{i}\sigma_{ref}} \tag{10.46} $$

$$ t_{relax}^{90}({}^{i}a, {}^{i}c) = \frac{0.91\left(K_I^{90}({}^{i}a, {}^{i}c)\right)^2}{\left(n_{BN}+1\right) \cdot E_y \cdot C^{*90}({}^{i}a, {}^{i}c)} \tag{10.47} $$

$$ C_t^{0}({}^{i}a, {}^{i}c) = C^{*0}({}^{i}a, {}^{i}c) \cdot \left[\left(\frac{t_{relax}^{0}({}^{i}a, {}^{i}c)}{{}^{i}t} \right)^{\left(\frac{n_{BN}-3}{n_{BN}-1}\right)} + 1 \right] \tag{10.48} $$

$$ C^{*0}({}^{i}a, {}^{i}c) = \left(\frac{{}^{i}\dot{\varepsilon}_{ref}}{1 - D_{bc} - {}^{i}D_{ac}} \right) \frac{\left(K_I^{0}({}^{i}a, {}^{i}c)\right)^2}{{}^{i}\sigma_{ref}} \tag{10.49} $$

$$t^0_{relax}({}^i a, {}^i c) = \frac{0.91\left(K^0_I({}^i a, {}^i c)\right)^2}{(n_{BN}+1)\cdot E_y \cdot C^{*0}({}^i a, {}^i c)} \tag{10.50}$$

m) STEP 13 – Compute the crack growth rates at time ${}^i t$ using Equations (10.51) and (10.52) based on the crack-like flaw dimensions ${}^i a$ and ${}^i c$, and the corresponding stress and temperature distribution.

$$\frac{{}^i da}{dt} = H_c \cdot \left(C^{90}_t({}^i a, {}^i c)\right)^{\mu} \tag{10.51}$$

$$\frac{{}^i dc}{dt} = H_c \cdot \left(C^{0}_t({}^i a, {}^i c)\right)^{\mu} \tag{10.52}$$

1) If MPC Project Omega creep data are used in the assessment, the constants for the creep crack growth equation are given by Equations (10.53) and (10.54). The units of measure for use in these equations are in, ksi, and ${}^o F$, the corresponding crack growth rate is computed in in/hr. In Equations (10.53) and (10.54) the parameters Ω and n_{BN} are evaluated using Equations (10.17) and (10.19), respectively, with S_l computed using Equation (10.44).

$$H_c = \frac{\Omega}{500} \tag{10.53}$$

$$\mu = \frac{n_{BN}}{n_{BN}+1} \tag{10.54}$$

2) Alternatively, the constants for the creep crack growth equations used in Equations (10.51) and (10.52) can be determined using Annex F.

n) STEP 14 – Compute the time step for integration at time t_i using Equation (10.55). An explicit time integration algorithm is used in this procedure. A suggested value for the explicit time integration parameter is $C_{intg} = 0.005$. A different value may be used based on the specific application. A sensitivity analysis should be used to qualify this value because it is a function of the creep strain rate and crack driving force.

$$\Delta t = \frac{C_{intg} \cdot t_c}{\max\left[\frac{{}^i da}{dt}, \frac{{}^i dc}{dt}\right]} \tag{10.55}$$

o) STEP 15 – Update the flaw dimensions ${}^i a$ and ${}^i c$, and the accumulated time in the cycle, ${}^i t$.

$${}^i a = {}^i a + \frac{{}^i da}{dt} \cdot \Delta t \tag{10.56}$$

$${}^i c = {}^i c + \frac{{}^i dc}{dt} \cdot \Delta t \tag{10.57}$$

$${}^i t = {}^i t + \Delta t \tag{10.58}$$

p) STEP 16 – If the current time in the cycle is less than the total time of the cycle, ${}^{i}t < {}^{m}t$, then go to STEP 5 to continue to grow the crack. Otherwise, proceed to STEP 17.

q) STEP 17 – If the component is subject to cyclic loading, then increment the crack size to account for crack growth from fatigue using the equations shown below. Otherwise, proceed to STEP 19.

$$ {}^{i}a = {}^{i}a + \frac{{}^{m}da}{dN} \tag{10.59}$$

$$ {}^{i}c = {}^{i}c + \frac{{}^{m}dc}{dN} \tag{10.60}$$

where

$$ \frac{{}^{m}da}{dN} = H_f \left({}^{m}\Delta K_{eff}^{90} \cdot \frac{E_{amb}}{E_T} \right)^{\lambda} \tag{10.61}$$

$$ {}^{m}\Delta K_{eff}^{90} = q_0 \left({}^{m}K_{I,\max}^{90} - {}^{m}K_{I,\min}^{90} \right) \tag{10.62}$$

$$ \frac{{}^{m}dc}{dN} = H_f \left({}^{m}\Delta K_{eff}^{0} \cdot \frac{E_{amb}}{E_T} \right)^{\lambda} \tag{10.63}$$

$$ {}^{m}\Delta K_{eff}^{0} = q_0 \left({}^{m}K_{I,\max}^{0} - {}^{m}K_{I,\min}^{0} \right) \tag{10.64}$$

The parameter, q_0, is computed using the following equations where $K_{I,\min}$ and $K_{I,\max}$ are evaluated at the 0° and 90° positions, respectively. The effects of the R-ratio on crack growth given by Equation (10.67) may also be evaluated using an alternative method based on the applicability and availability of crack growth models.

$$ q_0 = 1 \qquad R \geq 0 \tag{10.65}$$

$$ q_0 = \frac{1 - 0.5R}{1 - R} \qquad R \leq 0 \tag{10.66}$$

$$ R = \frac{K_{I,\min}}{K_{I,\max}} \tag{10.67}$$

r) STEP 18 – If this is the last cycle in the histogram, go to STEP 19. Otherwise, go to STEP 5 to continue to grow the crack based on the next cycle of operation.

s) STEP 19 – The crack growth prediction is complete for a location in the component. If another location is to be evaluated, go to STEP 3. If this is the last location in the component, evaluate the crack growth results.

1) If the points on the FAD predicted during crack growth are all within the FAD failure envelope, then the component with the crack-like flaw is acceptable for future operation. The remaining life shall be determined by analyzing additional load cycles, and determining the time at which the FAD assessment point lies on the FAD envelope.

2) If a point on the FAD predicted during crack growth lies on or outside the FAD failure envelope, then the life of the component is limited to the time corresponding to this point. If this time is less than the current operating time, the component should be repaired or retired.

10.5.5 Creep Buckling

10.5.5.1 The in-service margin for protection against collapse from buckling shall be satisfied to avoid buckling of components with a compressive stress field under applied design loads.

a) Time-Independent Buckling – Time-Independent Buckling shall be evaluated in accordance with Annex B1, paragraph B1.4.

b) Time-Dependent Buckling – To protect against load-controlled creep buckling, it shall be demonstrated that instability does not occur within the total operational time for a load histogram obtained by multiplying the specified loadings in paragraph 10.3.3.2 by an in-service margin equal to 1.5. An in-service margin of 1.0 may be used for purely strain-controlled buckling because strain-controlled loads are reduced concurrently with resistance of the structure to buckling when creep is significant.

   1) Load-controlled buckling is characterized by continued application of an applied load in the post-buckling regime, leading to failure, e.g., collapse of a tube under external pressure. Strain-controlled buckling is characterized by the immediate reduction of strain induced load upon initiation of buckling, and by the self-limiting nature of the resulting deformations. The in-service margin applicable to load-controlled buckling shall be used for the combination of load-controlled and strain-controlled loads for conditions under which load-controlled and strain-controlled buckling interact or significant elastic follow-up occurs.

   2) The effects of original fabrication tolerances, geometrical imperfections and other flaw types, as applicable, shall be considered in determining the critical buckling time.

   3) Material properties that may be used in the calculation including isochronous stress-strain curves are provided in Annex F.

   4) If a numerical analysis is performed to determine the buckling load for a component, all possible buckling mode shapes shall be considered in determining the minimum buckling load for the component (see Annex B1, paragraph B1.4.2).

10.5.5.2 The following analysis method can be used to estimate the critical time for creep buckling in the creep range for cylindrical shells subject to external pressure with an $R/t \le 20$. The cylindrical shell cannot contain a major structural discontinuity. If the cylindrical shell contains a major structural discontinuity, then the critical time should be determined using a numerical analysis similar to that described in paragraph 10.5.5.1. In addition, the stress at the applied load adjusted by the in-service margin should be less than 50% of the minimum specified yield strength at the assessment temperature. If the stress is above this value, then primary creep may be a concern and the critical time for creep buckling may be under estimated.

a) The critical time for creep buckling for components subject to a constant loading condition and temperature can be determined using the following procedure.

   1) STEP 1 – Based on the loading history, determine the applied loads, P^L or σ_e^L, and temperature, T, for the assessment.

   2) STEP 2 – Determine the elastic buckling load, P^{cr}, based on the applied loading condition including the effects of imperfections. If the buckling load is a function of more than one load type (e.g. pressure and applied axial force), then compute the stress components and effective stress, σ_e^{cr}, for all of the load types at the critical buckling load.

   3) STEP 3 – Multiply all loads in the applied loading condition by an in-service margin equal to 1.5 and determine the stress components and effective stress, σ_e.

   4) STEP 4 – Determine the effective critical creep strain at the onset of elastic-plastic buckling.

$$\varepsilon_{ce}^{cr} = \frac{\sigma_e}{E_y}\frac{2(1+\nu)}{3}(Q-1) \qquad (10.68)$$

where

$$Q = \frac{P^{cr}}{P^{L}} \tag{10.69}$$

or depending on the applied loads,

$$Q = \frac{\sigma_e^{cr}}{\sigma_e} \tag{10.70}$$

5) STEP 5 – Determine the critical time for creep buckling using Equation (10.71). The parameters Ω_m and $\dot{\varepsilon}_{co}$ in this equation are evaluated using Equations (10.14) through (10.20), and Equation (10.12).

$$t^{cr} = \frac{1 - \exp\left[-\varepsilon_{ce}^{cr}\Omega_m\right]}{\dot{\varepsilon}_{co}\Omega_m} \tag{10.71}$$

b) The critical time for creep buckling for components subject to varying loads and temperatures can be estimated using the procedure described in 10.5.5.2.a for each loading period and the equation shown below. Note that in this equation, the critical time for creep buckling is implicitly defined and can be determined by an iterative procedure.

$$\int_{o}^{t^{cr}} \frac{\varepsilon_{ce}^{cr}\left[P^{L}(t), T(t)\right]}{t^{cr}\left[P^{L}(t), T(t)\right]} dt = \varepsilon_{ce}^{cr}\left[P^{L}(t^{cr}), T(t^{cr})\right] \tag{10.72}$$

10.5.6 Creep-Fatigue Assessment of Dissimilar Weld Joints

10.5.6.1 The metallurgical characteristics of the damage observed in both service and laboratory test samples indicate that creep rupture is the dominant failure mode for Dissimilar Metal Welds (DMW). However, it has also been observed that temperature cycling contributes significantly to damage and can cause failure even when primary stress levels are relatively low. Therefore, a creep-fatigue assessment procedure is required as part of a remaining life calculation. In the assessment of DMW, a creep-fatigue interaction equation is provided to evaluate damage caused by thermal mismatch, sustained primary stresses, and cyclic secondary loads.

10.5.6.2 The damage mechanism of concern is creep damage in the heat-affected zone (HAZ) on the ferritic steel side of the DMW. Damage in this region is expected to occur first because the creep resistance of the material, at the temperatures of interest, is much lower than that of the austenitic base metal or the commonly used filler metals (i.e. stainless steel or nickel-based). The general macroscopic appearance of many failures suggests that failure occurs by a relatively low ductility process and the final fracture surface may show evidence of the weld bead contours. However, detailed examination has shown that failure can occur by one of the following two modes of damage.

a) Mode I – Inter-granular cracking which occurs along prior austenite grain boundaries within the ferritic HAZ adjacent (1 to 2 grains) to the weld metal interface. This mode occurs for DMWs made with austenitic stainless filler metal and sometimes for DMWs made with nickel-based filler metal. The initial inter-granular voiding or cracking develops within the wall of the component, and does not normally initiate either at the inside or outside surfaces. Failure occurs by crack link-up and propagation to the surfaces.

b) Mode II – Interfacial voiding in which voiding and cracking occur along a planar array of coarse globular carbides that form along the ferritic HAZ to weld metal interface. This mode occurs only for DMWs made with nickel-based filler metal, but failure may be accompanied by some Mode I cracking. The initial interfacial voiding again starts from within the wall of the component. Final failure occurs by void link-up and crack propagation to the surfaces.

10.5.6.3 The assessment procedure in this paragraph provides a systematic approach for evaluating the creep-fatigue damage for each operating cycle that is applied to a DMW in a component. The total creep-fatigue damage is computed as the sum of the creep damages calculated for each cycle.

10.5.6.4 The Mode I creep-fatigue damage based on the results of a stress analysis can be computed using the assessment procedure shown below. This mode of failure is only applicable to a DMW made with stainless steel or nickel-based filler metal. Note that the damage equations in this assessment procedure were developed in US Customary Units; therefore, the units of the parameters that must be used in the assessment procedure are shown within parentheses in the applicable steps shown below.

a) STEP 1 – Determine a load history based on past operation and future planned operation. The load histogram should include all significant operating loads and events that are applied to the component. If there is cyclic operation, the load histogram should be divided into operating cycles as shown in Figure 10.26. Define M as the total number of operating cycles (see paragraph10.5.2.3.a).

b) STEP 2 – For the current operating cycle m, divide the cycle into a number of time increments, ${}^{n}t$, as shown in Figure 10.27, and determine the cycle parameters. Define N as the total number of time increments in operating cycle m.

1) The time increments used to model the operating cycle should be small enough to capture all significant variations in the operating cycle. The smaller the time increment, the more accurate the remaining life prediction.

2) If the component is subject to corrosion or erosion, the time increments should be set small enough to capture changes in the wall thickness.

3) The parameters that must be determined for the cycle are:

i) Total time in the cycle, ${}^{m}t$ (hr).

ii) The maximum temperature difference in the cycle, ${}^{m}\Delta T$ (°F).

iii) The difference in the thermal expansion coefficients between the filler and base metal, ${}^{m}\Delta\alpha$, associated with the temperatures used to define ${}^{m}\Delta T$ (1/°F).

iv) The maximum range of axial secondary stress due to applied net-section forces and moments, ${}^{m}\Delta\sigma_s$ (psi).

c) STEP 3 – Determine the following parameters for each time increment, the required units of measure are shown in parentheses.

1) Total time in the increment, ${}^{n}t$ (hr).

2) The temperature in the increment, ${}^{n}T$ (°F).

3) The difference in the thermal expansion coefficients between the filler and base metal, ${}^{n}\Delta\alpha$, associated with the temperatures used to define ${}^{n}T$ (1/°F).

4) Young's Modulus of Elasticity, ${}^{n}E_y$, associated with the temperatures used to define ${}^{n}T$ (psi).

5) The axial primary stress due to pressure and applied net-section forces and moments, ${}^{n}\sigma_p$ (psi).

6) The axial secondary stress due to applied net-section forces and moments, ${}^{n}\sigma_s$ (psi).

d) STEP 4 – Determine the intrinsic creep damage.

$$ {}^{n}D_{Ic} = B_1 \, {}^{n}t \left(\frac{ {}^{n}E_y \cdot {}^{n}\Delta\alpha \cdot \left({}^{n}T - 70 \right)}{2} \right)^{2.7} \cdot 10^{f({}^{n}T)} \tag{10.73} $$

where

$$ f({}^{n}T) = 13.26 - \frac{31032}{\left({}^{n}T + 460 \right)} \tag{10.74} $$

$$ B_1 = 2.5(10)^{-10} \qquad For\ Stainless\ Steel\ Filler\ Material \tag{10.75} $$

$$ B_1 = 0.0 \qquad For\ Nickel - Base\ Material \tag{10.76} $$

e) STEP 5 – Determine the creep damage associated with primary stresses where $f({}^{n}T)$ is determined using Equation (10.74).

$$ {}^{n}D_{Pc} = B_2 \, {}^{n}t \left({}^{n}\sigma_p \right)^{2.7} \cdot 10^{f({}^{n}T)} \tag{10.77} $$

where

$$ B_2 = 2.4(10)^{-7} \qquad For\ Stainless\ Steel\ Filler\ Material \tag{10.78} $$

$$ B_2 = 1.6(10)^{-7} \qquad For\ Nickel - Base\ Material \tag{10.79} $$

f) STEP 6 – Determine the creep damage associated with secondary stresses where $f({}^{n}T)$ is determined using Equation (10.74).

$$ {}^{n}D_{Sc} = 5.5(10)^{-10} \, {}^{n}t \left({}^{n}\sigma_s \right)^{2.7} \cdot 10^{f({}^{n}T)} \tag{10.80} $$

g) STEP 7 - Repeat STEPS 3 through 6 for each time increment ${}^{n}t$.

h) STEP 8 - Compute the accumulated creep damage for all points in the m^{th} cycle.

$$ {}^{m}D_{Ic} = \sum_{n=1}^{N} {}^{n}D_{Ic} \tag{10.81} $$

$$ {}^{m}D_{Pc} = \sum_{n=1}^{N} {}^{n}D_{Pc} \tag{10.82} $$

$$ {}^{m}D_{Sc} = \sum_{n=1}^{N} {}^{n}D_{Sc} \tag{10.83} $$

i) STEP 9 – Compute the intrinsic fatigue damage for the m^{th} cycle.

$$ {}^{m}D_{If} = B_3 \left({}^{m}\Delta\alpha \cdot {}^{m}\Delta T \right)^{0.2} \tag{10.84} $$

where

$$B_3 = 6.8(10)^{-4} \qquad For\ Stainless\ Steel\ Filler\ Material \tag{10.85}$$

$$B_3 = 0.0 \qquad For\ Nickel-Base\ Material \tag{10.86}$$

j) STEP 10 – Compute the fatigue damage associated with secondary stresses for the m^{th} cycle.

$$^{m}D_{Sf} = 1.0(10)^{-2} \cdot \left(^{m}\Delta\sigma_s \right)^{0.2} \tag{10.87}$$

k) STEP 11 – Repeat STEPS 2 through 10 for each of the operating cycles defined in STEP 1.

l) STEP 12 – Compute the total damage for all cycles in the operating history.

$$D_{DMW1}^{total} = \sum_{m=1}^{M} \left[^{m}D_{Ic} + ^{m}D_{Pc} + ^{m}D_{Sc} + ^{m}D_{If} + ^{m}D_{Sf} \right] \le D_{DMW1}^{allow} \tag{10.88}$$

m) STEP 13 – The damage prediction is complete for the DMW in the component. The allowable damage, D_{DMW1}^{allow}, is usually taken as 1.0 unless an alternative value can be justified.

10.5.6.5 The Mode II creep-fatigue damage based upon the results of a stress analysis can be computed using the assessment procedure shown below. This mode of failure is only applicable to a DMW made with nickel-based filler metal. Note that the damage equations in this assessment procedure were developed in US Customary Units; therefore, the units of the parameters that must be used in the assessment procedure are shown within parentheses in the applicable steps shown below.

a) STEP 1 – Determine a load history based on past operation and future planned operation. The load histogram should include all significant operating loads and events that are applied to the component. If there is cyclic operation, the load histogram should be divided into operating cycles as shown in Figure 10.26. Define M as the total number of operating cycles (see paragraph 10.5.2.3.a.).

b) STEP 2 – For the current operating cycle m, divide the cycle into a number of time increments, ^{n}t, as shown in Figure 10.27, and determine the cycle parameters. Define N as the total number of time increments in operating cycle m.

1) The time increments used to model the operating cycle should be small enough to capture all significant variations in the operating cycle. The smaller the time increment, the more accurate the remaining life predication.

2) If the component is subject to corrosion or erosion, the time increments should be set small enough to capture changes in the wall thickness.

3) The parameters that must be determined for the cycle are:

i) Total time in the cycle, ^{m}t (hr).

ii) The maximum range of axial secondary stress due to applied net-section forces and moments, $^{m}\Delta\sigma_s$ (psi).

c) STEP 3 – Determine the following parameters for each time increment, the required units of measure are shown in parentheses.

1) Total time in the increment, ^{n}t (hr).

2) The temperature in the increment, ^{n}T (°F).

3) The axial primary stress due to pressure and applied net-section forces and moments, $^{n}\sigma_p$ (psi).

4) The axial secondary stress due to applied net-section forces and moments, ${}^{n}\sigma_s$ (psi).

d) STEP 4 – Determine the creep damage associated with primary stresses where $f({}^{n}T)$ is determined using Equation (10.74).

$$ {}^{n}D_{Pc} = 6.8(10)^{-8} \cdot {}^{n}t \left(\frac{{}^{n}\sigma_p}{1 - 0.65 \cdot 10^{g({}^{n}T)} \cdot \left({}^{n}t_w + 0.5\,{}^{n}t \right)^{1/3}} \right)^{2.7} \cdot 10^{f({}^{n}T)} \qquad (10.89) $$

where

$$ g({}^{n}T) = 4 - \frac{8555}{\left({}^{n}T + 460 \right)} \qquad (10.90) $$

$$ {}^{n}t_w = {}^{n}\overline{t} \qquad when\ {}^{m,n}\overline{t} \le {}^{n}t_m \qquad (10.91) $$

$$ {}^{n}t_w = 2\,{}^{n}t_m - {}^{n}\overline{t} \qquad when\ {}^{n}t_m < {}^{m,n}\overline{t} \le 2\,{}^{n}t_m \qquad (10.92) $$

$$ {}^{n}t_w = 0.0 \qquad when\ {}^{m,n}\overline{t} > 2\,{}^{n}t_m \qquad (10.93) $$

where

$$ {}^{m,n}\overline{t} = \sum_{j=1}^{(m-1)} \overline{t}^{\,j} + \sum_{k=1}^{n} {}^{k}t \cdot 10^{b} \qquad (10.94) $$

$$ b = 25665 \left[\frac{1}{\left({}^{n}T + 460 \right)} + \frac{1}{\left({}^{k}T + 460 \right)} \right] \qquad (10.95) $$

$$ {}^{n}t_m = 10^{g} \qquad (10.96) $$

$$ g = 38500 \left[\frac{1}{\left({}^{n}T + 460 \right)} - 20 \right] \qquad (10.97) $$

e) STEP 5 – Determine the creep damage associated with secondary stresses where $f({}^{n}T)$ is determined using Equation (10.74), $g({}^{n}T)$ is determined using Equation (10.90), and ${}^{n}t_w$ is determined using Equations (10.91) through (10.97).

$$ {}^{n}D_{Sc} = 8.9(10)^{-9} \cdot {}^{n}t \left(\frac{{}^{n}\sigma_s}{1 - 0.65 \cdot 10^{g({}^{n}T)} \cdot \left({}^{n}t_w + 0.5\,{}^{n}t \right)^{1/3}} \right)^{2.7} \cdot 10^{f({}^{n}T)} \qquad (10.98) $$

f) STEP 6 - Repeat STEPS 3 through 5 for each time increment ${}^{n}t$.

g) STEP 7 - Compute the accumulated creep damage for all points in the m^{th} cycle.

$$ {}^{m}D_{Pc} = \sum_{n=1}^{N} {}^{n}D_{Pc} \tag{10.99} $$

$$ {}^{m}D_{Sc} = \sum_{n=1}^{N} {}^{n}D_{Sc} \tag{10.100} $$

h) STEP 8 – Compute the fatigue damage associated with secondary stresses for the m^{th} cycle.

$$ {}^{m}D_{Sf} = 1.6(10)^{-3} \cdot \left({}^{m}\Delta\sigma_{s} \right)^{0.2} \tag{10.101} $$

i) STEP 9 – Repeat STEPS 2 through 8 for each of the operating cycles defined in STEP 1.

j) STEP 10 – Compute the total damage for all cycles in the operating history.

$$ D_{DMW2}^{total} = \sum_{m=1}^{M} \left[{}^{m}D_{Pc} + {}^{m}D_{Sc} + {}^{m}D_{Sf} \right] \le D_{DMW2}^{allow} \tag{10.102} $$

k) STEP 11 – The damage prediction is complete for the DMW in the component. The allowable damage, D_{DMW2}^{allow}, is usually taken as 1.0 unless an alternative value can be justified.

10.5.7 Microstructural Approach

10.5.7.1 Microstructural Approach Overview

a) Because of limited applicability and uncertainty of microstructural approaches, they are normally used in conjunction with one another and to supplement other techniques. Decisions are usually not made based on a single set of microstructural observations. For example, hardness reduction combined with evidence of cavity coalescence in a material with very coarse grain in a region of high triaxiality or cyclic service may support the finding of advanced damage.

b) Widespread availability, low cost and convenience of microstructural techniques make them a common component of the Fitness-For-Service approach. All critical areas should be sampled and a database of results should be maintained. Changes over time in hardness, appearance, void size or population should be taken as indications of time dependent damage. Thus, microstructural softening occurs in many materials without contributing to the damage rate.

10.5.7.2 Microstructural approaches have been used to estimate the remaining life of a component. The following procedures are recognized.

a) *Hardness Changes* – For certain alloys, tensile strength and hardness are believed to correlate with remaining life. For many other situations, hardness may bear no relation to status with respect to creep damage. However, the absence of a hardness change during service may indicate that the service exposure is unlikely to have caused significant creep damage.

   1) Materials for which hardness is above a reference level indicates that the material is suitable for continued service at nominal design stress levels and temperatures below those indicated in Table 10.3, absent any flaws, etc.

   2) Materials shown in Table 10.4, if known not to have changed in hardness after extended service, are unlikely to have suffered significant creep damage, and are suitable for future service if the future service conditions are not more severe than the past service conditions. The initial hardness readings must be known with certainty to use the information in Table 10.4.

b) *Creep Cavity Evaluation* – Some engineering alloys exhibit creep cavities as precursors to crack initiation and failure. Many alloys do not exhibit such a characteristic. The time to the appearance of detectable creep cavities depend upon stress state, heat treatment, grain size, material cleanliness, embrittlement, and other factors. The numbers, size, and spacing of cavities reported depends on the microscopic techniques, sample preparation, void size and observer experience.

1) Certain circumstances may warrant the development of a calibration curve applicable to specific materials where cavity size and spacing are desired to be used for life assessment. Absent such an application specific calibration curve, the following guidelines may be used.

i) No detectable cavities indicating less than 10% life consumption.

I. High Strength Cr-Mo Alloys (UTS > 110 ksi).
II. High Strength Cr-Mo-V Alloys (UTS > 100 ksi).
III. Submerged arc welds.
IV. Coarse grain heat affected zones in the above.

ii) The presence of multiple cavities of character greater than 1.5μ on most grain boundaries normal to the principal stress or linked cavities appearing as microcracks or fissures is indicative that creep damage exceeds 50% in the area under examination.

2) Sample preparation must be adequate for detection and sizing of cavities by optical and/or electron microscopic techniques.

3) Examinations may be made on shadowed replicas or samples removed from the section of interest. The area to be studied should be free of environmentally caused damage such as oxide penetration. Areas particularly susceptible to cavitation damage include.

i) Coarse grain base metal adjacent to weld fusion line in Cr-Mo and Cr-Mo-V alloys.

ii) Fine grain regions of heat affected zone in base metal or weld metal when surrounded by relatively higher strength material.

iii) Material located in region of high stress concentration in higher strength alloys. Examples include the dovetail of a turbine blade, sharp notches, and changes in the component cross section.

iv) Materials containing regions of coarse precipitate particles such as sigmatized stainless steels or other high alloy materials.

c) *Optical Metallography* – Some guidance as to the creep resistance of materials or the damage state may be obtained from optical microscopy. This information may be useful in modifying the referenced Omega method based strain rate and Omega coefficient equations provided in Annex F. Aside from the cavitation issues noted above, the effects on strain rate and the omega parameter are shown in Table 10.5.

10.6 Remediation

10.6.1 For components that do not contain a crack-like flaw, if the component does not satisfy the creep damage criterion within the required service life, or if the sensitivity analysis indicates unacceptable results, then remedial action is required. One of the following may be considered.

a) Change In Service Parameters – a change in service parameters (load, temperature, service life) may be made and the assessment repeated either to demonstrate acceptance or to estimate at what time replacement will be necessary.

b) Use Of Thermal Linings – conversion of existing hot-wall pressure vessel and piping systems to a cold wall design that utilizes a thermal lining (i.e. refractory) has been performed. In these cases, the thermal lining is designed to reduce the metal temperature to a value below the creep range thereby preventing future creep damage.

10.6.2 For components containing a crack-like flaw, if failure by excessive crack growth is indicated within the required service life, or if the sensitivity analysis indicates unacceptable results, then remedial action is required, such as repair of the component by removing the flaw. Alternatively, a change in service parameters (load, temperature, desired service life) may be made and the assessment repeated either to demonstrate acceptance or to estimate at what time repair will be necessary. Finally, it may be possible to obtain data on the material actually used in the component to remove conservatism in the assessment resulting from the use of bounding data.

10.7 In-Service Monitoring

The most effective tool for in-service monitoring of equipment subject to creep damage is to monitor the temperature and pressure. This information can be used to update the creep remaining life calculation to determine if continued operation is acceptable.

10.8 Documentation

10.8.1 The documentation of the FFS Assessment should include the information cited in Part 2, paragraph 2.8. Additional documentation requirements are essential because of the complexity associated with the assessment. This information should be permanently stored with the equipment record files.

10.8.1.1 The following information shall be documented; the applicable assessment levels are shown within parentheses.

a) *Assessment Level* – Any deviations or modifications used at a given level of analysis (Levels 1, 2 and 3).

b) *Loading Conditions* – a load histogram showing the historical and assumed future start-up, normal, upset, and shut-down conditions should be reported (Levels 1, 2, and 3). In addition, any additional loads and stresses considered in the assessment (e.g. stresses from supplement loads, thermal gradients and residual stresses (Levels 2 and 3)).

c) *Stress Analysis Results* – the stress analysis method (handbook, finite-element or other numerical techniques) and categorization of stress results if required (Levels 1, 2 and 3).

d) *Material Properties* – The material specification of the component; yield strength, ultimate tensile stress, fracture toughness, and creep properties should be reported including whether the data were obtained by direct testing, or indirect means together with the source of the data. If testing is performed to determine material properties, the test results should be included in the documentation. In addition, a description of the process environment including its effect on material properties. If cyclic loads are present, a description of the creep-fatigue interaction rules should be documented (Levels 2 and 3).

e) *Sensitivity Analysis* – A listing of the input parameters used to perform sensitivity studies (e.g. time in service, loads, material properties, flaw size, etc.); the results of each individual study should be summarized (Levels 2 and 3).

10.8.1.2 The following additional information should be documented if a creep crack growth assessment has been performed as part of a Level 3 assessment.

a) *Characterization Of Flaw* – For components with cracks, the flaw location, shape and size; NDE method used for flaw sizing and allowance for sizing errors; and whether re-characterization of the flaw was required (see Part 9).

b) *Partial Safety Factors* – A list of the Partial Safety Factors used in the FAD analysis; a technical summary should be provided if alternative factors are utilized in the assessment.

c) *Reference Stress Solution* – The source of the reference stress solutions (e.g. handbook solution or finite-element analysis) used in the assessment including whether the local and/or global collapse was considered.

d) *Stress Intensity Factor Solution* – The source of stress intensity factor solutions (e.g. handbook solution or finite-element analysis) used in the assessment.

e) *Failure Assessment Diagram (FAD)* – whether the Part 9, Level 2 FAD, a material specific curve (including the source and validity of stress-strain data), or a curve derived from J-analysis is used in the assessment.

f) *Material Properties* – the source and complete description of the creep strain rate and other data used to determine a remaining life should be included.

g) *Creep Crack Growth Equation* – the equation and associated constants used to model creep crack growth, and for components subject to cyclic operation, the equation and associated constants used to model the fatigue crack growth should be summarized (i.e. from technical publication or laboratory measurements).

10.8.1.3 All assumptions used in the assessment procedures should be documented. In addition, all departures from the procedures in this Part should be reported and separately justified. A separate statement should be made about the significance of potential failure mechanisms remote from the defective areas, if applicable.

10.8.1.4 If microstructural approaches are used as part of the assessment, all examination results shall be included in the documentation. If a Creep Cavity Evaluation is made in accordance with paragraph 10.5.7.2.b, then the examination results, cavity sizing procedure and results, and the calibration curve applicable to specific to the component material shall be included in the documentation.

10.8.2 The documentation of the FFS Assessment shall be permanently stored in the equipment record files.

10.9 Nomenclature

a_0	initial crack-like flaw depth.
${}^{i}a$	depth of the crack-like flaw for the i^{th} time step.
A	is a reaction rate parameter.
$A_1 \rightarrow A_4$	material coefficients for the MPC Project Omega strain-rate-parameter, see Annex F, Table F.30.
α_Ω	triaxiality parameter based on the state of stress for MPC Project Omega Life Assessment Model. =3.0 – pressurized sphere or formed head, =2.0 – pressurized cylinder or cone, =1.0 – for all other components and stress states.
B	reaction rate parameter.
$B_1 \rightarrow B_4$	material coefficients for the MPC Project Omega Omega-parameter, see Annex F, Table F.30, or parameters to determine creep damage in a bimetallic weld.
β_Ω	MPC Project Omega parameter to 0.33.
β_1	parameter for creep-fatigue interaction.
β_2	parameter for creep-fatigue interaction.
c_0	initial crack-like flaw half-length.
${}^{i}c$	half-length of the existing flaw for the i^{th} time step
C_F	creep damage fraction used in creep-fatigue interaction.
C_{intg}	explicit time integration parameter.
$C^{*90}({}^{i}a, {}^{i}c)$	crack driving force associated with global steady-state creep at the deepest point of the crack.
$C^{*0}({}^{i}a, {}^{i}c)$	crack driving force associated with global steady-state creep at the surface point of the crack.
C_{LMP}	Larson Miller Constant in Annex F, Table F.31.

$C_t^{90}({}^{i}a, {}^{i}c)$ total crack driving force for creep crack growth at the deepest point of the crack including transient and steady-state creep effects.

$C_t^{0}({}^{i}a, {}^{i}c)$ total crack driving force for creep crack growth at the surface point of the crack including transient and steady-state creep effects.

D_c creep damage.

D_f fatigue damage.

D_{cm} creep damage based material parameter used in creep-fatigue interaction.

D_{fm} fatigue damage based material parameter used in creep-fatigue interaction.

D_c^j creep damage for the j^{th} design or operating condition.

D_{ac}^i local creep damage after the crack initiates, the damage is computed using the reference stress (see Annex D) considering the post-crack loading history.

D_{ac} local creep damage after the crack initiates, the damage is computed using the reference stress (see Annex D) considering the post-crack loading history for the i^{th} time step.

D_{bc} local creep damage before the initiation of the crack, the damage is computed using the net section stress considering the pre-crack loading history.

D_{mean} mean diameter of a cylinder or sphere.

D_c^{allow} allowable creep damage.

D_{DMW1}^{allow} total creep-fatigue Mode I damage in a dissimilar metal weld.

D_{DMW2}^{allow} total creep-fatigue Mode II damage in a dissimilar metal weld.

${}^{m}D_c$ creep damage for the m^{th} operating cycle.

${}^{m}D_{Sc}$ fatigue damage from secondary stresses for the m^{th} operating cycle.

${}^{n}D_c$ creep damage for the n^{th} time period.

D_c^{total} total creep damage considering all operating cycles.

D_{cf}^{total} total creep-fatigue damage considering all operating cycles.

D_{DMW1}^{total} total creep-fatigue mode I damage in a dissimilar metal weld considering all operating cycles.

D_{DMW2}^{total} total creep-fatigue mode II damage in a dissimilar metal weld considering all operating cycles.

${}^{m}D_{Ic}$ total intrinsic creep damage for the m^{th} cycle.

${}^{m}D_{Pc}$ total creep damage from primary stresses for the m^{th} cycle.

${}^{m}D_{Sc}$ total creep damage from secondary stresses for the m^{th} cycle.

${}^{m}D_{If}$ total intrinsic fatigue damage for the m^{th} cycle.

${}^{m}D_{Sf}$ total fatigue damage from secondary stresses for the m^{th} cycle.

${}^{n}D_{Ic}$ intrinsic creep damage for the n^{th} time increment.

${}^{n}D_{Pc}$ creep damage from primary stresses for the n^{th} time increment.

${}^{n}D_{Sc}$ creep damage from secondary stresses for the n^{th} time increment.

${}^{m}\Delta\alpha$ difference in the thermal expansion coefficients between the filler and base metal associated with the temperatures used to define ${}^{m}\Delta T$.

${}^{n}\Delta\alpha$ difference in the thermal expansion coefficients between the filler and base metal associated with the temperatures used to define ${}^{n}T$.

Δt time step.

${}^{m}\Delta T$ maximum temperature difference in the cycle.

${}^{m}\Delta\sigma_s$ maximum range of axial secondary stress due to applied net-section forces and moments.

Δ_{Ω}^{cd} adjustment factor for creep ductility in the Project Omega Model, a range of $+0.3$ for brittle behavior and -0.3 for ductile behavior can be used.

Δ_{Ω}^{sr} adjustment factor for creep strain rate to account for the material scatter band in the Project Omega Model, a range of -0.5 for the bottom of the scatter band to $+0.5$ for the top of the scatter band can be used.

$\frac{{}^{i}da}{dt}$ crack growth rate for the deepest point of a surface flaw for the i^{th} time step.

$\frac{{}^{m}da}{dN}$ increment of fatigue crack growth for the deepest point of a surface flaw for the m^{th} cycle.

$\frac{{}^{i}dc}{dt}$ crack growth rate for the surface point of a surface flaw for the i^{th} time step.

$\frac{{}^{m}dc}{dN}$ increment of fatigue crack growth for the surface point of a surface flaw for the m^{th} cycle.

δ_{Ω} MPC Project Omega parameter.

E_y Young's Modulus evaluated at the mean temperature of the cycle.

${}^{n}E_y$ Young's Modulus for the loading history for the n^{th} time increment.

E_{amb} Young's modulus at ambient temperature.

E_T Young's modulus at the assessment temperature.

ε_c accumulated creep strain.

ε_{ce}^{cr} critical effective creep strain at the onset of elastic creep buckling.

$\dot{\varepsilon}_c$ creep strain rate.

$\dot{\varepsilon}_{co}$ initial creep strain rate at the start of the time period being evaluated based on the stress state and temperature (see Annex F, paragraph F.7.3); note, the units of measure for computing this parameter must be ksi and ${}^{o}F$.

${}^{i}\dot{\varepsilon}_{ref}$ uniaxial strain rate evaluated at the reference stress for the i^{th} time step.

${}^{n}\dot{\varepsilon}_{ref}$ uniaxial strain rate evaluated at the reference stress for the n^{th} time increment.

f exponent in the creep-fatigue damage calculation.

H_c coefficient for the creep crack growth model.

H_f coefficient for the fatigue crack growth model.

j operating condition number or cycle, as applicable.

J total number of operating conditions or cycles, as applicable.

J_1 term used to compute ${}^{n}S_{eff}$.

K total number of operating cycles.

K_{bc} total number of operating cycles before the initiation of the crack.

$K_{I,\max}$ maximum value of the stress intensity.

$K_{I,\min}$ minimum value of the stress intensity.

$K_I^0({}^{i}a, {}^{i}c)$ applied mode I stress intensity factor at the surface point of a surface crack (see Annex C).

$K_I^{90}({}^i a, {}^i c)$ applied mode I stress intensity factor at the deepest point of a surface crack (see Annex C).

${}^m\Delta K_{eff}^0$ effective range of the cyclic applied mode I stress intensity factor at the surface point of a surface crack that occurs in the m^{th} cycle.

${}^m K_{I,\max}^0$ maximum value of the cyclic applied mode I stress intensity factor at the surface point of a surface crack that occurs in the m^{th} cycle (see Annex C).

${}^m K_{I,\min}^0$ minimum value of the cyclic applied mode I stress intensity factor at the surface point of a surface crack that occurs in the m^{th} cycle (see Annex C).

${}^m\Delta K_{eff}^{90}$ effective range of the cyclic applied mode I stress intensity factor at the deepest point of a surface crack that occurs in the m^{th} cycle.

${}^m K_{I,\max}^{90}$ maximum value of the cyclic applied mode I stress intensity factor at the deepest point of a surface crack that occurs in the m^{th} cycle (see Annex C).

${}^m K_{I,\min}^{90}$ minimum value of the cyclic applied mode I stress intensity factor at the deepest point of a surface crack that occurs in the m^{th} cycle (see Annex C).

k current operating cycle.

L_f Lorentz Factor (seeAnnex A, paragraph A.5.5).

L_r load ratio based on primary stress.

${}^n L$ rupture time for the loading history for the n^{th} time increment.

$LMP({}^n S_{eff})$ Larson-Miller parameter at stress S_{eff}^n.

${}^i L_{ac}$ rupture time for the loading history after initiation of the crack applied for time increment ${}^i t$ computed using the reference stress.

λ exponent in the fatigue crack growth equation.

m current operating cycle number.

M total number of operating cycles.

M_{bc} total number of operating cycles before the onset of cracking.

μ exponent in the creep crack growth equation.

N total number of time increments in an operating cycle.

${}^m N$ number of allowable cycles determined from a fatigue curve for the m^{th} cycle.

${}^m n$ number of applications of the m^{th} cycle.

n_{BN} Bailey-Norton coefficient $\left(n_{BN} = -d\log\dot{\varepsilon}_c / d\log\sigma\right)$ evaluated at the reference stress in the current load increment, used in the MPC Project Omega Life Assessment Model.

ν Poisson's ratio.

P pressure inside of a cylinder or sphere.

P_L primary local membrane stress (see Annex B1).

P_b primary bending stress (see Annex B1).

${}^n P_b$ primary bending stress (see Annex B1) for the n^{th} time increment.

P_L primary local membrane stress (see Annex B1).

${}^n P_L$ primary local membrane stress (see Annex B1) for the n^{th} time increment.

P^L generalized applied loading parameter.

$P^L(t)$ generalized applied loading parameter as a function of time.

P^{cr} critical buckling load associated with the generalized loading parameter.

Q loading parameter for a creep buckling analysis, or the activation energy, as applicable.

r radial coordinate in a cylinder or sphere at the location where the stress is being computed.

R universal gas constant.

R_c creep damage rate.

R_c^j creep damage rate for the j^{th} design or operating condition.

R_i inside radius of a cylinder or sphere.

R_{mean} mean radius of a cylinder or sphere.

R_o outside radius of a cylinder or sphere.

R_r reaction rate.

S_l log base 10 of the effective stress.

S_s term used to compute ${}^nS_{eff}$.

${}^nS_{eff}$ effective stress used to compute the remaining life in terms of the Larson-Miller parameter for the n^{th} time increment.

σ_e effective stress.

σ_m meridional stress in a cylinder or sphere stress.

σ_{mean} mean stress for a cylinder subject to internal pressure.

σ_c circumferential stress in a cylinder or sphere.

σ_r radial stress in a cylinder or sphere stress.

σ_{ys} yield strength at the assessment temperature (see Annex F).

σ_e^{cr} critical effective stress associated with the generalized loading parameter at the critical buckling load.

${}^i\sigma_{ij}$ applied stress components for the i^{th} time step.

${}^i\sigma_{ref}$ reference stress for the i^{th} time step (see Annex D).

${}^n\sigma_e$ effective stress for the n^{th} time increment.

${}^n\sigma_{ij}$ applied stress components for the n^{th} time increment.

${}^n\sigma_{mean}$ mean stress for a cylinder subject to internal pressure based on the mean diameter equation for the n^{th} time increment.

${}^n\sigma_p$ axial primary stress due to pressure and applied net-section forces and moments for the n^{th} time increment.

${}^n\sigma_{ref}$ reference stress for the n^{th} time increment (see Annex D).

${}^n\sigma_s$ axial secondary stress due to applied net-section forces and moments for the n^{th} time increment.

${}^n\sigma_1$ principal stress for the n^{th} time increment.

${}^n\sigma_2$ principal stress for the n^{th} time increment.

${}^n\sigma_3$ principal stress for the n^{th} time increment.

t time.

t_c component thickness adjusted for metal loss and future corrosion allowance, as applicable.

t_{se} service exposure time for each design or operating condition.

t_{se}^{j} service exposure time for the j^{th} design or operating condition.

t_{sl} thickness required for supplemental loads (see Annex A).

t_{ac} accumulated creep time in the solution.

T temperature.

$T(t)$ temperature as a function of time.

${}^{i}T$ temperature for the i^{th} time step.

${}^{n}T$ temperature for the n^{th} time increment.

t_{comp} component thickness adjusted for metal loss and corrosion allowance as required.

$t_{relax}^{90}({}^{i}a, {}^{i}c)$ relaxation term in the crack driving force associated with the deepest point of the crack for the i^{th} time step.

$t_{relax}^{0}({}^{i}a, {}^{i}c)$ relaxation term in the crack driving force associated with the surface point of the crack for the i^{th} time step.

${}^{i}t$ cumulative time at the end of the i^{th} time period in the m^{th} cycle.

${}^{m}t$ total time in the m^{th} cycle.

${}^{n}t$ time increment or load duration for use in the damage calculation.

t^{cr} critical time at the onset of elastic-creep buckling.

Y_{B31} coefficient from ASME B31 Piping codes used for determining the pipe wall thickness (See Annex A, Paragraph A.5).

Ω uniaxial Omega damage parameter (see Annex F, paragraph F.7.1.1); note, the units of measure for computing this parameter must be ksi and ${}^{o}F$.

Ω_m multiaxial Omega damage parameter (see Annex F, paragraph F.7.1.1).

Ω_n adjusted uniaxial Omega damage parameter.

10.10 Referenced Publications

1. Anderson, T.L., *Fracture Mechanics – Fundamentals and Applications*, 2nd Edition, CRC Press, Boca Raton, Florida, 1995.
2. Buchheim, G.M., Osage, D.A., Brown, R.G., and Dobis, J.D., “Failure Investigation of a Low Chrome Long-Seam Weld in a High-Temperature Refinery Piping System,” PVP-Vol. 288, ASME, 1994, pp. 363-386.
3. Buchheim, G.M., Becht, C., Nikbin, K.M, Dimopolos, V., Webster, G.A., and Smith D.J., “Influence of Aging on High-Temperature Creep Crack Growth in Type 304H Stainless Steel,” Nonlinear Fracture Mechanics, ASTM STP 995, Volume 1, The American Society of Testing and Materials, Pa, 1988, pp. 153-172.
4. Chern, J.M., “A Simplified Approach to the Prediction of Creep Buckling Time in Structures,” PVP-PB-029, *Simplified Methods in Pressure Vessel Analysis*, ASME, 1978.
5. Chern, J.M., “A Simplified Approach to Creep Buckling of Structures Under Time Varying Loads,” Journal of Pressure Vessel Technology, Vol. 102, ASME, 1980.
6. Huddleston, R.L., “Assessment of an Improved Multiaxial Strength Theory Based on Creep Rupture Data for Inconel 600,” PVP-Vol. 262, *High-Temperature and Time-Dependent Failure*, ASME, 1993.
7. Kraus, H., Creep Analysis, John Wiley & Sons, New York, NY, 1980.
8. Law, P.K. and Saxena, A., “Remaining Life Estimation of Boiler Pressure Parts–Crack Growth Studies,” ERPI CS-4688, Electric Power Research Institute, Palo A lot, CA, July, 1886.

9. McClung, R.C., Chell, G.G., Lee, Y.D., Russell, D.A., and Orient, G.E., “Development of a Practical Methodology for Elastic-Plastic and Fully Plastic Fatigue Crack Growth,” NASA/CR-1999-209428, Marshall Space Flight Center, Alabama, USA, 1999.

10. Moulin, D., Drubay, B., and Laiarinandrasana, “A Synthesis of the Fracture Assessment Methods Proposed in the French RCC-MR Code for High Temperature,” WRC 440, Welding Research Council, New York, NY, 1999.

11. Nikbin, K.M., Smith, D.J., and Webster, G.A., “An Engineering Approach to the Prediction of Creep Crack Growth,” Journal of Engineering Materials and Technology, Vol. 108, The American Society of Mechanical Engineers, pp. 186-191, April 1986.

12. Prager, M., “Development of the MPC Project Omega Method for Life Assessment in the Creep Range,” PVP-Vol. 288, ASME, 1994, pp. 401-421.

13. Prager, M., “Damage Evaluation and Remaining Life Assessment in High Temperature Structural Components by the Omega Method,” Proceedings of 7th Workshop on the Ultra Steel, Ultra Steel: Requirements from New Design of Constructions, June 24 and 25, 2003, pages 150-158.

14. Prager, M., “The Omega Method – An Effective Method for Life and Damage Prediction in Creep Tests and Service,” Oikawa (eds.), Strength of Materials, Japan Institute of Metals, 1994, pp. 571-574.

15. Prager, M., “Proposed Implementation of Criteria for Assignment of Allowable Stresses in the Creep Range,” ASME Journal of Pressure Vessel Technology, May, 1996, Vol. 335, pp. 273-293.

16. Prager, M., “Generation of Isochronous Creep, Tubing Life and Crack Growth Curves Using the MPC Omega Method, Structural Integrity,” NDE, Risk and Material Performance for Petroleum, process and Power, PVP-Vol. 336, ASME, 1996, pp. 303-322.

17. Prager, M. and Ibarra, S., “Approaches to Long Term Life prediction of Furnace and Boiler Tubes,” Fitness For Adverse Environments in Petroleum and Power Equipment, PVP-Vol. 359, ASME, 1997, pp. 339-352.

18. Prager, M. and Ibarra, S., “Approaches To Long Term Life Prediction Of Furnace And Boiler Tubes,” PVP-Vol. 359, Fitness for Adverse Environments in Petroleum and Power Equipment, ASME 1997, pages 339-352.

19. Prager, M., and Osage, D., “Special Topics in Elevated Temperature Life Applications Including Assessment Rules for API 579,”, PVP-Vol. 411, Service Experience and Fitness-For-Service in Power and Petroleum Processing, ASME, 2000, pages 91-104.

20. Ryder, R.H. and Dahms, C.F., “Design Criteria for Dissimilar Metal Welds,” WRC Bulletin 350, Welding Research Council, New York, NY, Jan., 1990.

21. Saxena, A., Han, J., and Banerji, K, “Creep Crack Growth Behavior in Power Plant Boiler and Steam Pipe Steels,” Journal of Pressure Vessel Technology, The American Society of Mechanical Engineers, Vol. 110, pp. 137-146, May, 1988.

22. Saxena, A. Nonlinear Fracture Mechanics for Engineers, CRC Press, Boca Raton, Florida, 1998.

23. Scott, P.M., Anderson, T.L., Osage, D.A., and Wilkowski, G.M., “Review of Existing Fitness-For-Service Criteria for Crack-Like Flaws,” WRC Bulletin 430, Welding Research Council, 1998.

24. Viswanathan, R., “Damage Mechanisms and Life Assessment of High-Temperature Components, ASM International, Metals Park, Ohio, 1989.

25. Webster, G.A., “Lifetime Estimates of Cracked High Temperature Components,” International Journal of Pressure Vessels & Piping, 50, pp. 133-145, 1992.

26. Webster, G.A. and Ainsworth, R.A., High Temperature Component Life Assessment, Chapman & Hall, London, U.K, 1994.

10.11 Tables and Figures

Table 10.1 – Metallurgical Requirements

Material	Brinnell Hardness	Carbon Content
Carbon Steel $\left(UTS \le 414MPa\ (60\ ksi)\right)$	95	---
Carbon Steel $\left(UTS > 414MPa\ (60\ ksi)\right)$	100	---
Carbon Steel – Graphitized	100	---
C-0.5Mo	110	---
1.25Cr-0.5Mo – Normalized & Tempered	130	---
1.25Cr-0.5Mo – Annealed	120	---
2.25Cr-1Mo – Normalized & Tempered	140	---
2.25Cr-1Mo – Annealed	130	---
2.25Cr-1Mo – Quenched & Tempered	150	---
2.25Cr-1Mo-V	180	---
3Cr-1Mo-V	180	---
5Cr-0.5Mo	130	---
7Cr-0.5Mo	130	---
9Cr-1Mo	140	---
9Cr-1Mo-V	180	---
12 Cr	180	---
AISI Type 304 & 304H	---	0.04
AISI Type 316 & 316H	---	0.04
AISI Type 321	---	0.04
AISI Type 321H	---	0.04
AISI Type 347	---	0.04
AISI Type 347H	---	0.04
Alloy 800	---	0.03
Alloy 800H	---	0.04
Alloy 800HT	---	0.05
HK-40	---	0.30

Table 10.2 – Stress Equations for Cylindrical and Spherical Shells

Geometry	Stress Equations
Cylinder or Elbow – Elastic Stress Solution Based on Mean Diameter	$\sigma_1 = \sigma_c = \dfrac{PD_{mean}L_f}{2t_{comp}}$ $\sigma_2 = \sigma_m = \dfrac{PD_{mean}L_f}{4\left(t_{comp} - t_{sl}\right)}$ $\sigma_3 = \sigma_r = 0.0$
Cylinder – Reference Stress Solution	$\sigma_1 = \sigma_c = \dfrac{P\left(1 - \ln\left[R_{r2}\right]\right)}{\ln\left[R_{r1}\right]}$ $\sigma_2 = \sigma_m = \dfrac{P\left(1 - 2\ln\left[R_{r2}\right]\right)}{2\ln\left[R_{r1}\right]}$ $\sigma_3 = \sigma_r = \dfrac{-P\left(\ln\left[R_{r2}\right]\right)}{\ln\left[R_{r1}\right]}$ $R_{r1} = \dfrac{R_o}{R_i}$ $R_{r2} = \dfrac{R_o}{r}$
Cylinder or Elbow – Steady-State Creep Solution	$\sigma_1 = \sigma_c = C\left[1 + \left(\dfrac{2 - n_{BN}}{n_{BN}}\right)\left(\dfrac{R_o}{r}\right)^{\left(\frac{2}{n_{BN}}\right)}\right]L_f$ $\sigma_2 = \sigma_m = C\left[1.0 + \left(\dfrac{1.0 - n_{BN}}{n_{BN}}\right)\left(\dfrac{R_o}{r}\right)^{\left(\frac{2}{n_{BN}}\right)}\right]$ $\sigma_3 = \sigma_r = C\left[1 - \left(\dfrac{R_o}{r}\right)^{\left(\frac{2}{n_{BN}}\right)}\right]$ $C = \dfrac{P}{\left[\left(\dfrac{R_o}{R_i}\right)^{\left(\frac{2}{n_{BN}}\right)} - 1\right]}$

Table 10.2 – Stress Equations for Cylindrical and Spherical Shells

Geometry	Stress Equations
Sphere – Elastic Stress Solution Based on Mean Diameter	$\sigma_1 = \sigma_c = \frac{PD_{mean}}{4t_{comp}}$ $\sigma_2 = \sigma_m = \sigma_c$ $\sigma_3 = \sigma_r = 0.0$
Sphere – Reference Stress Solution	$\sigma_1 = \sigma_c = \frac{P\left(2 - 3\ln\left[R_{r2}\right]\right)}{3\ln\left[R_{r1}\right]}$ $\sigma_2 = \sigma_m = \sigma_c$ $\sigma_3 = \sigma_r = \frac{-P\left(\ln\left[R_{r2}\right]\right)}{\ln\left[R_{r1}\right]}$ $R_{r1} = \frac{R_o}{R_i}$ $R_{r2} = \frac{R_o}{r}$
Sphere – Steady-State Creep Solution	$\sigma_1 = \sigma_c = C\left[1 + \left(\frac{3n_{BN} - 2}{2}\right)\left(\frac{R_o}{r}\right)^{(3n_{BN})}\right]$ $\sigma_2 = \sigma_m = C\left[1 + \left(\frac{3n_{BN} - 2}{2}\right)\left(\frac{R_o}{r}\right)^{(3n_{BN})}\right]$ $\sigma_3 = \sigma_r = C\left[1 - \left(\frac{R_o}{r}\right)^{(3n_{BN})}\right]$ $C = \frac{P}{\left[\left(\frac{R_o}{R_i}\right)^{(3n_{BN})} - 1\right]}$

Notes:

1. The above equations do not include the effect of metal loss or future corrosion allowance. The inside radius, outside radius, and wall thickness should be adjusted accordingly based on service experience.
2. For a cylinder, the Lorentz Factor is $L_f = 1.0$, for an elbow, L_f can be evaluated using Annex A, paragraph A.5.
3. The thick wall stress equations are provided in terms of the Bailey-Norton creep exponent, n_{BN}. This form of the equations will account for the stress redistribution that occurs in the creep range. The elastic solution or Lame equations can be obtained by setting $n_{BN} = 1.0$.

Table 10.3 – Reference Hardness and Temperature Criterion

Material	Reference Hardness, HB	Temperature (˚F)
2.25Cr+Mo, Q+T	190	825
2.25Cr-1Mo-V, Q+T	200	875
3Cr-1Mo-V, Q+T	200	850
9Cr-1Mo-V	200	1075
12Cr-2Mo-V	200	1100

Table 10.3M – Reference Hardness and Temperature Criterion

Material	Reference Hardness, HB	Temperature (˚C)
2.25Cr+Mo, Q+T	190	440
2.25Cr-1Mo-V, Q+T	200	470
3Cr-1Mo-V, Q+T	200	455
9Cr-1Mo-V	200	580
12Cr-2Mo-V	200	595

Table 10.4 – Temperature Criterion for No Change in Hardness During Service that Indicates Creep Damage is Unlikely

Material	Temperature (˚F)
1.25Cr-0.5Mo, Q+T or N+T	850
2.25Cr-1Mo, Q+T or N+T	900
3Cr-1Mo, Q+T or N+T	900
9Cr-1Mo-V	1050
Rotor Steels	875

Table 10.4M – Temperature Criterion for No Change in Hardness During Service that Indicates Creep Damage is Unlikely

Material	Temperature (˚C)
1.25Cr-0.5Mo, Q+T or N+T	455
2.25Cr-1Mo, Q+T or N+T	480
3Cr-1Mo, Q+T or N+T	480
9Cr-1Mo-V	565
Rotor Steels	470

Table 10.5 – Trends Of Strain Rate and Omega Parameter with Microstructure

Microstructure	Strain Rate	Omega
Coarse Grain	Decreases	Increases
Fine Grain	Increases	Decreases
Nodular Graphite	Increases	---
Sigma Formation	---	Increases
Spherodized Carbides	Increases	---
Decarburization	Increases	---
Carburization	Decreases	Increases
Nitriding	Decreases	Increases

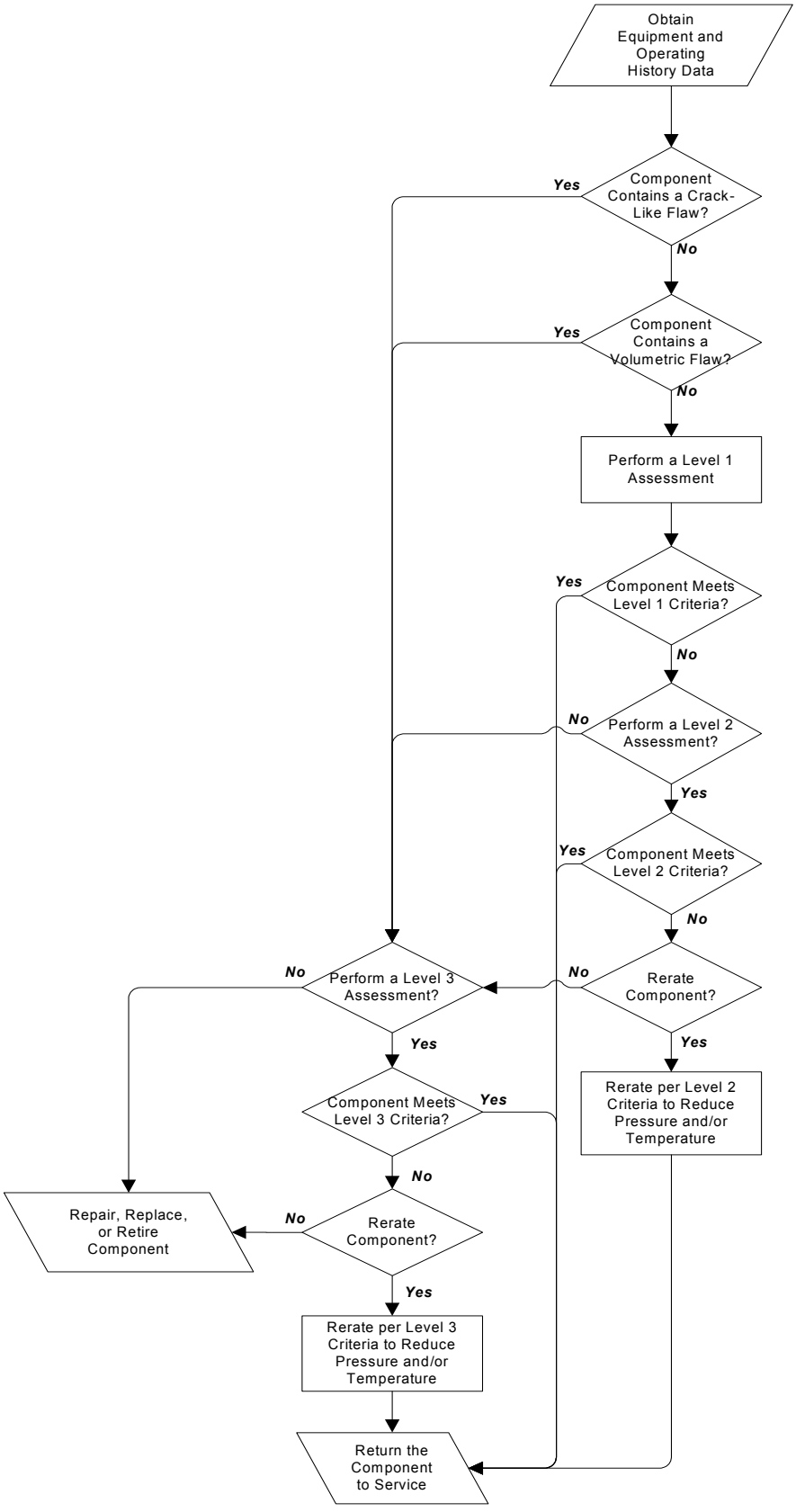

Figure 10.1 – Overview of the Assessment Procedures to Evaluate a Component in the Creep Range

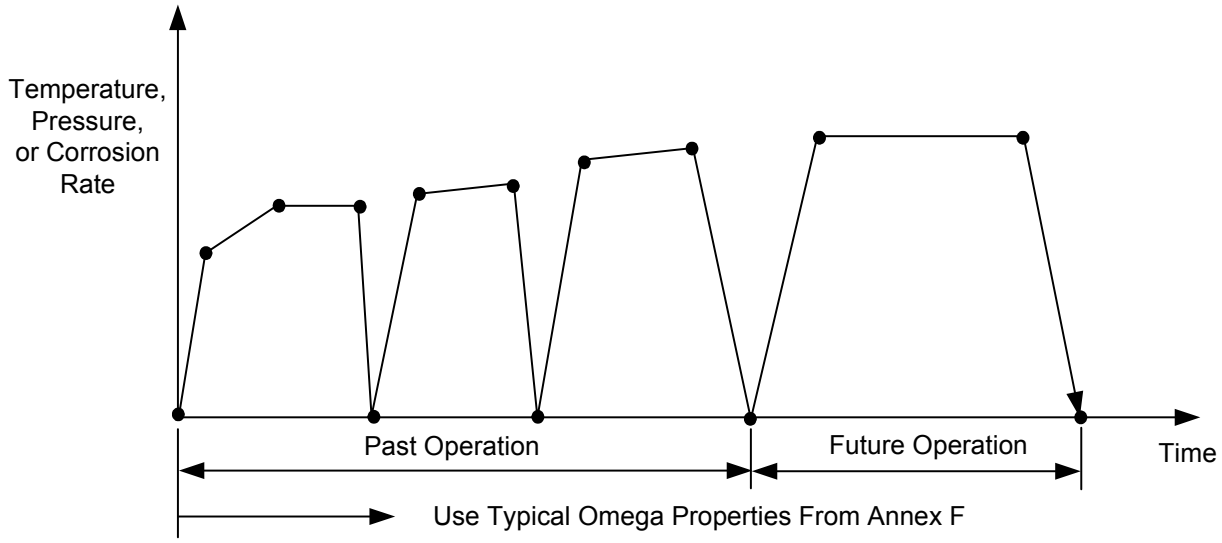

(a) Operating Histogram Showing Past and Future Operation

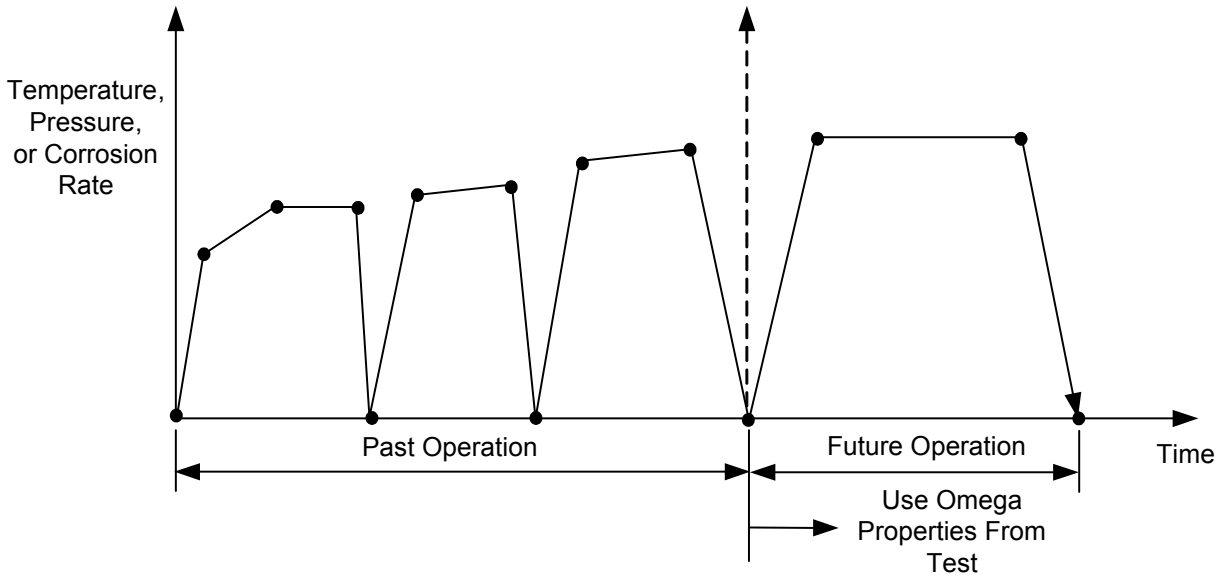

(b) Operating Histogram "Shifted" Based On MPC Project Omega Test

Figure 10.2 – Shifting of the Operating History Based on MPC Project Omega Testing

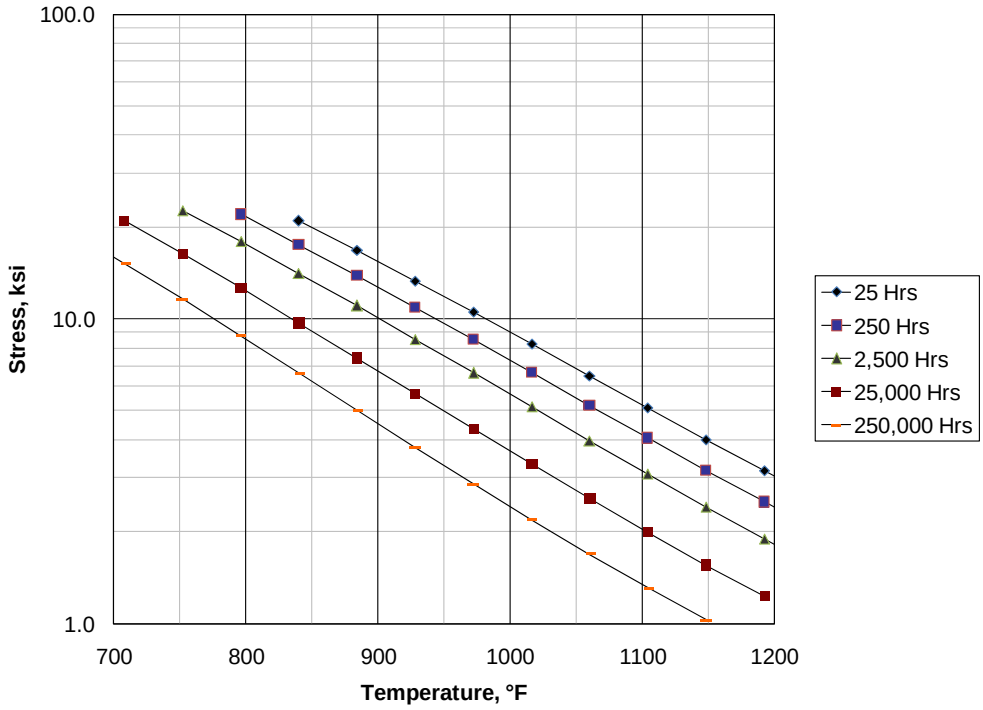

a) Screening Curve

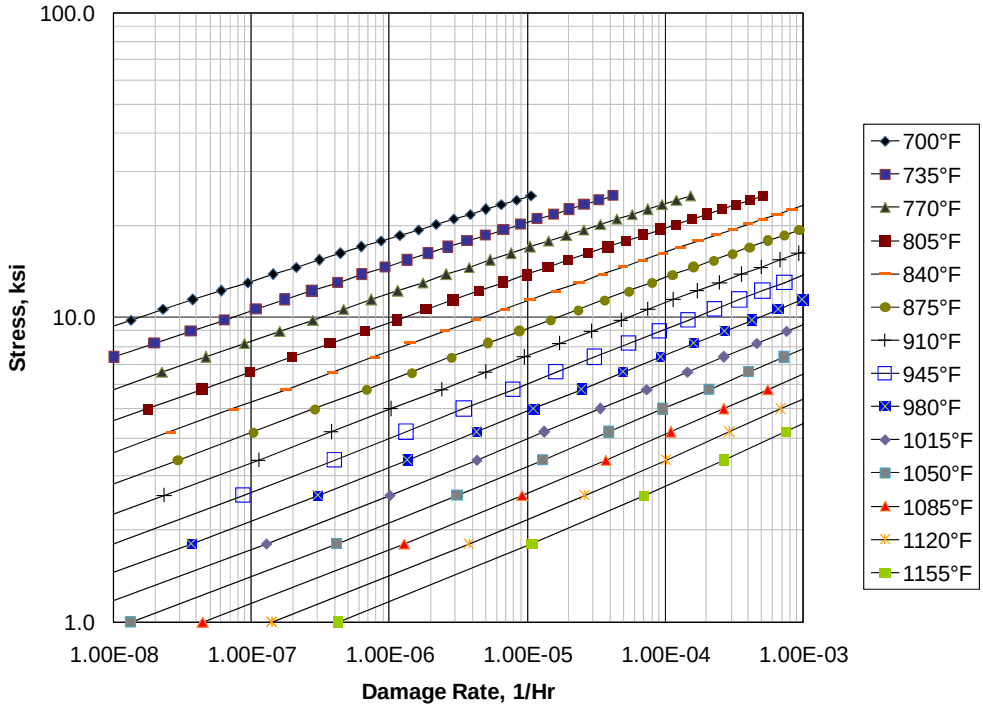

b) Damage Curve

Figure 10.3 – Level 1 Screening Criteria for Carbon Steel

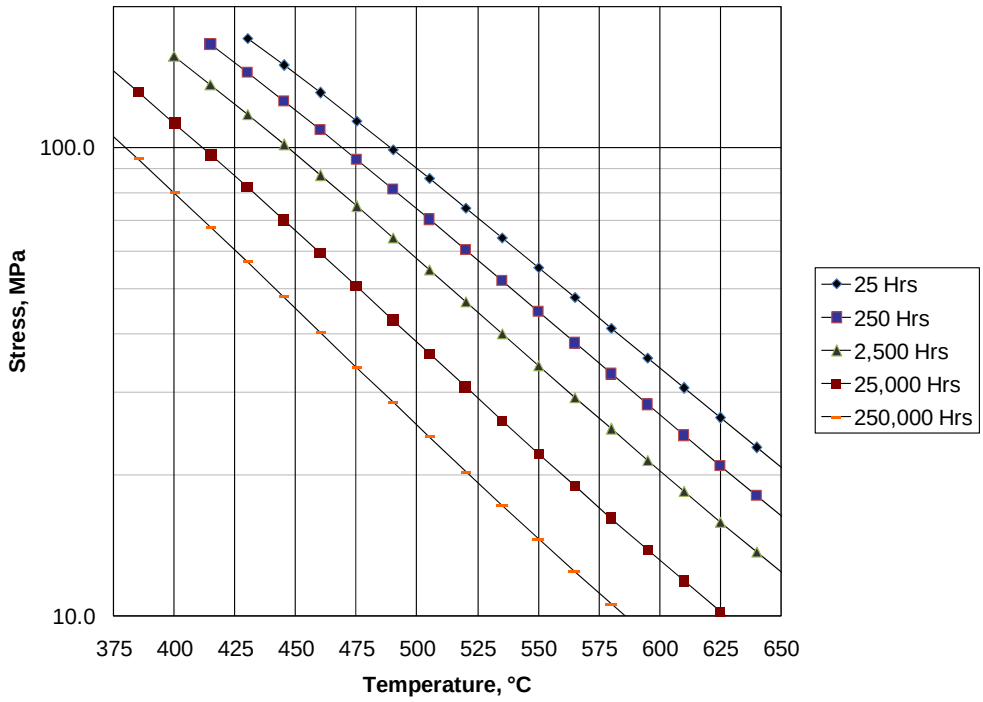

a) Screening Curve

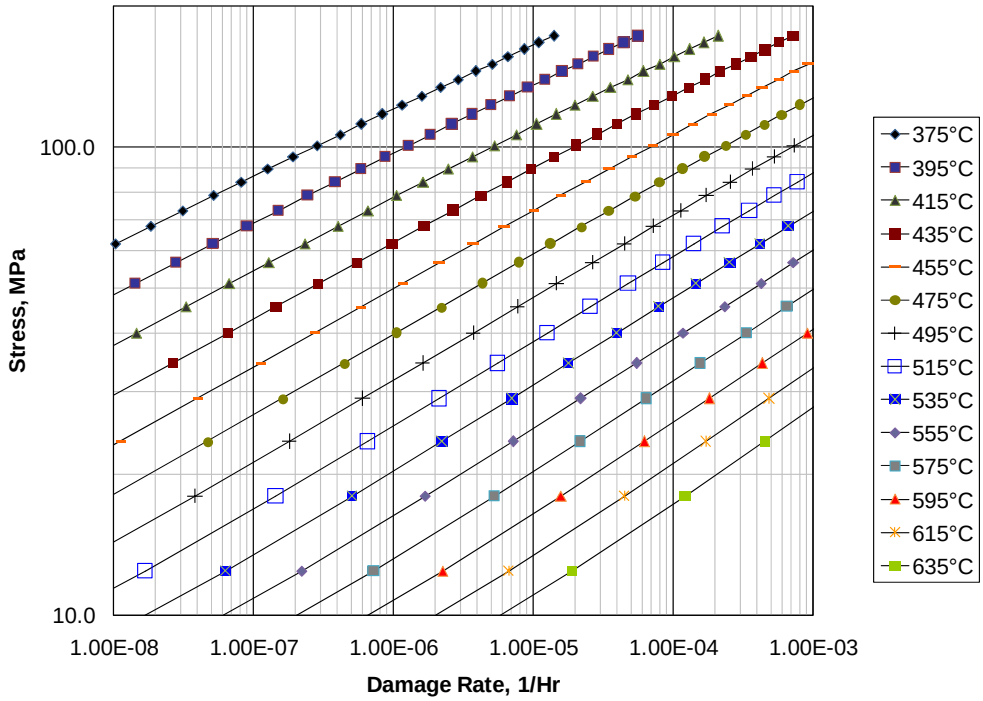

b) Damage Curve

Figure 10.3M – Level 1 Screening Criteria for Carbon Steel

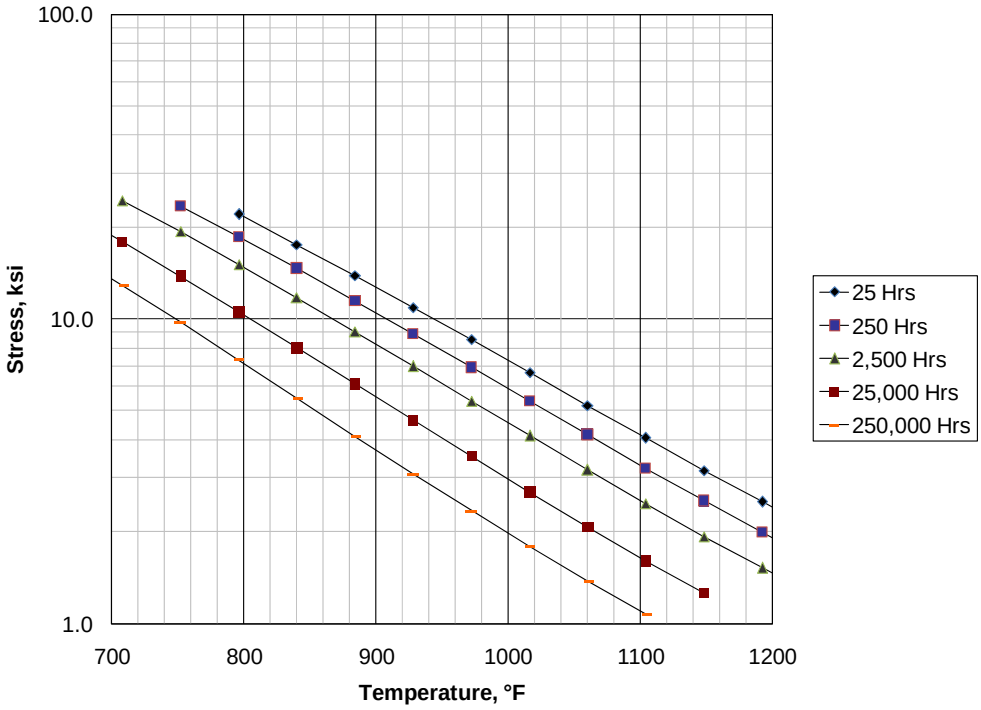

a) Screening Curve

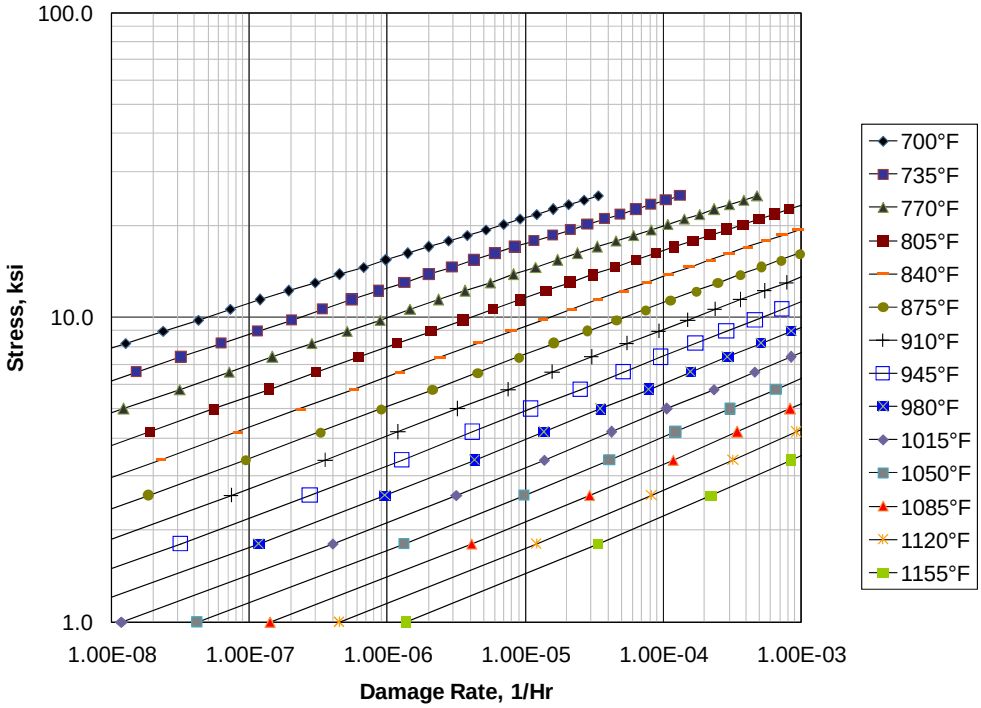

b) Damage Curve

Figure 10.4 – Level 1 Screening Criteria for Carbon Steel – Graphitized

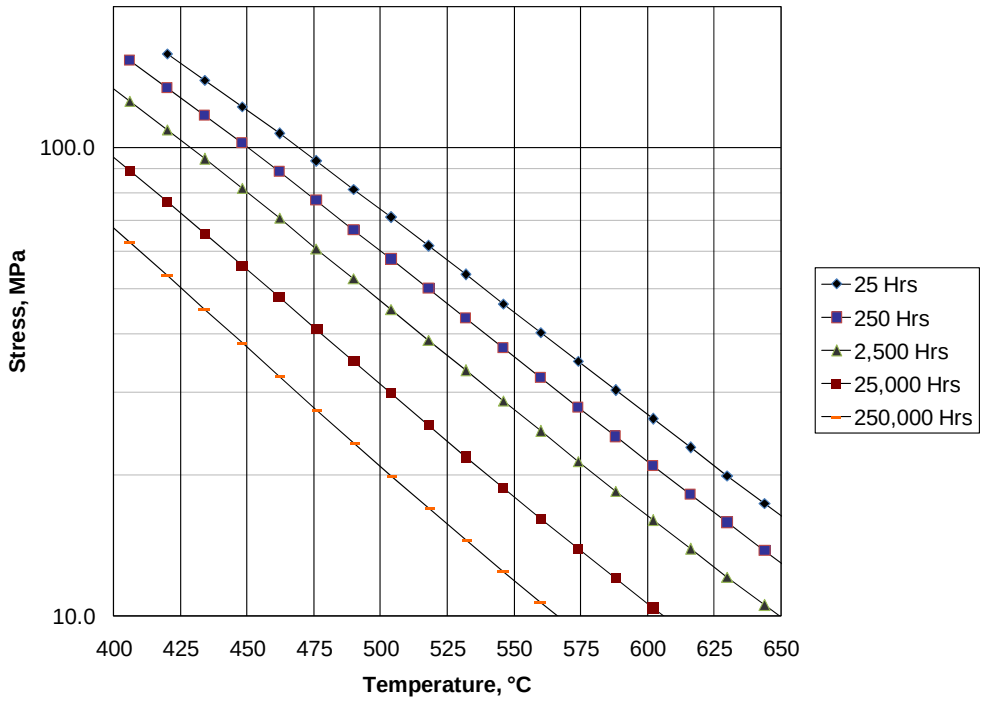

a) Screening Curve

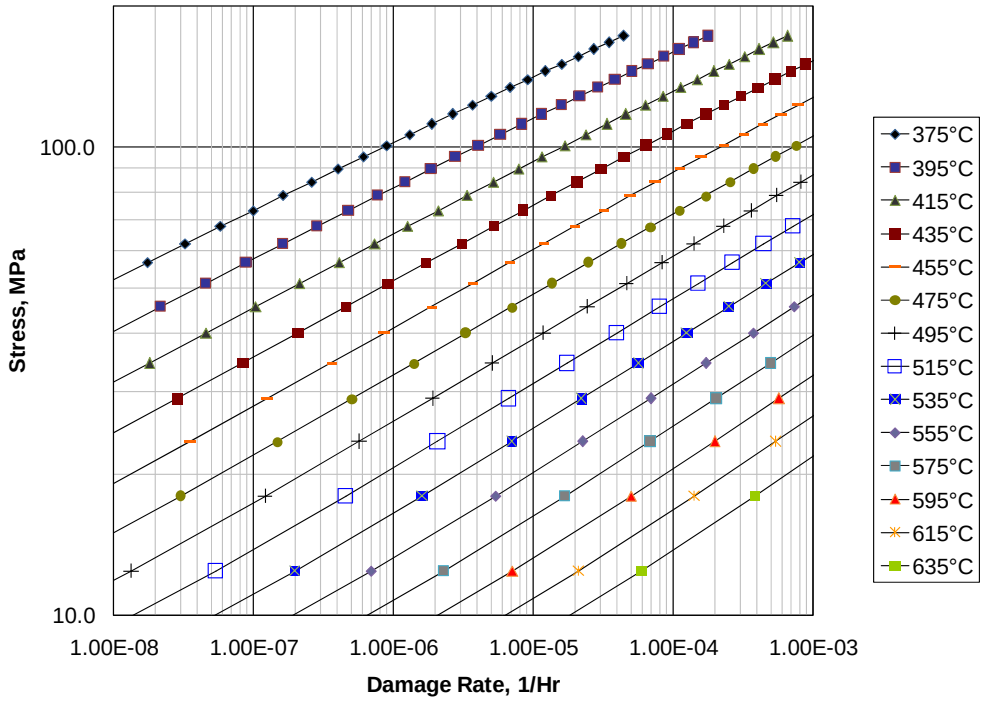

b) Damage Curve

Figure 10.4M – Level 1 Screening Criteria for Carbon Steel – Graphitized

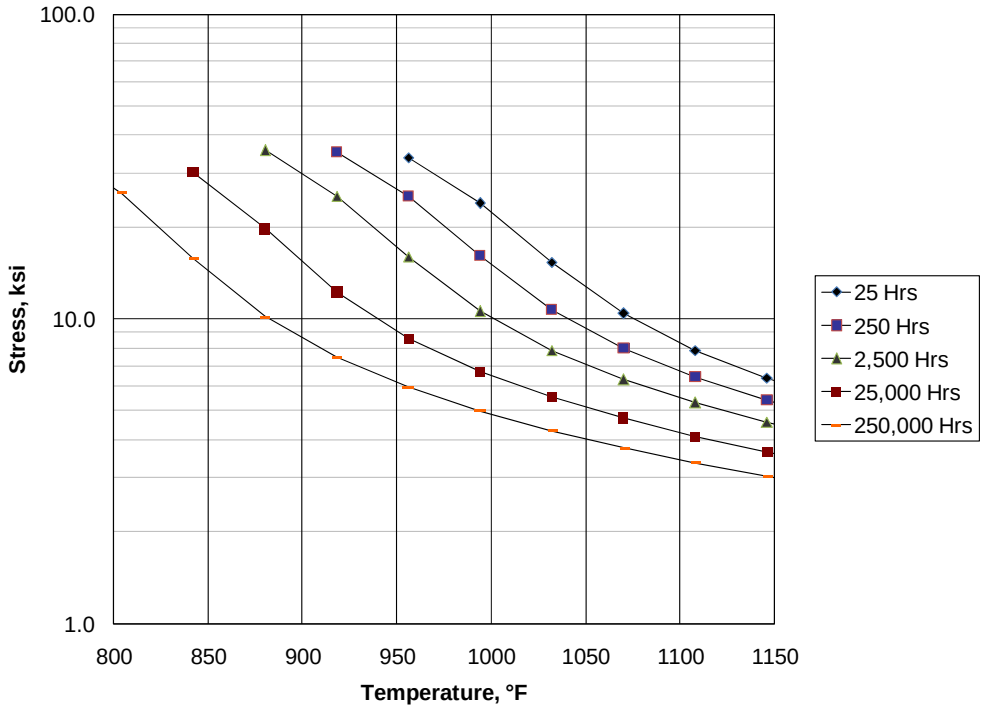

a) Screening Curve

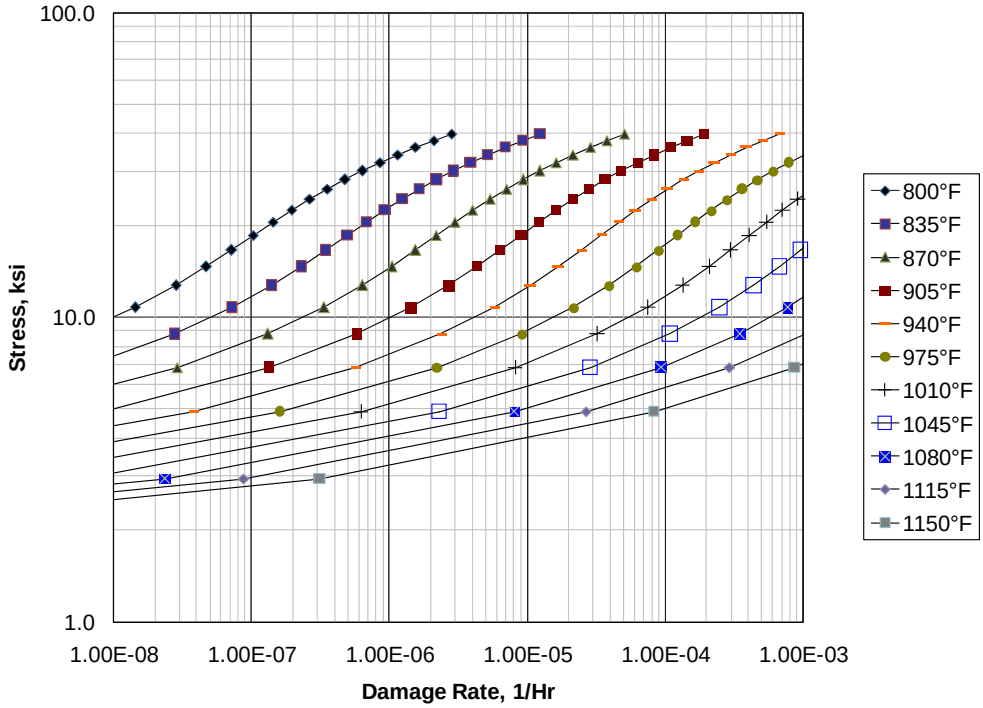

b) Damage Curve

Figure 10.5 – Level 1 Screening Criteria for C-0.5Mo

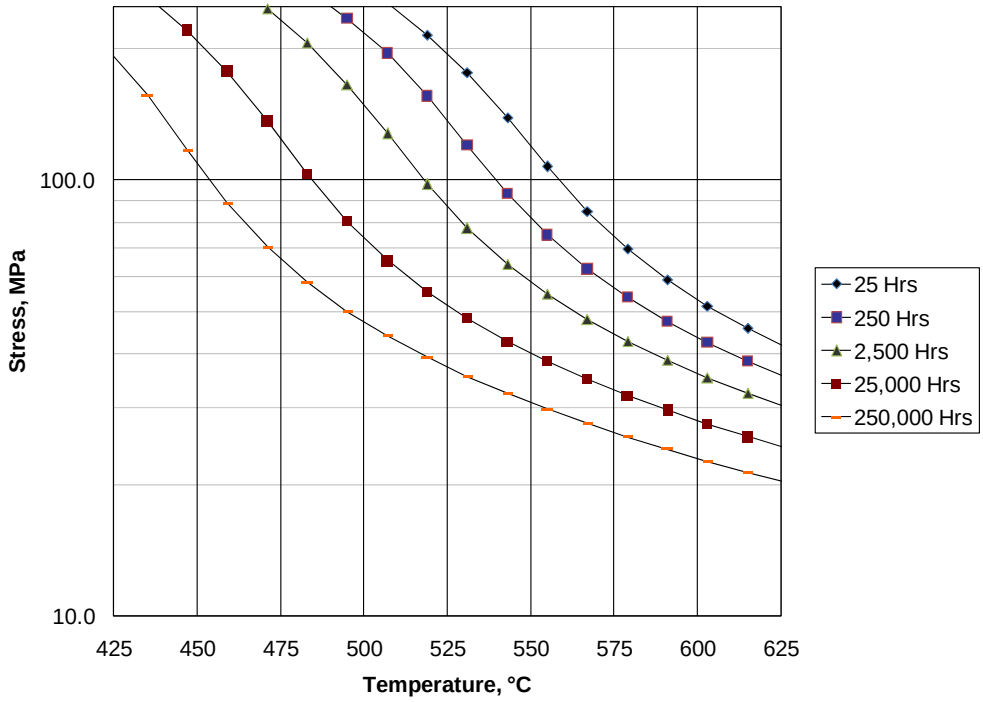

a) Screening Curve

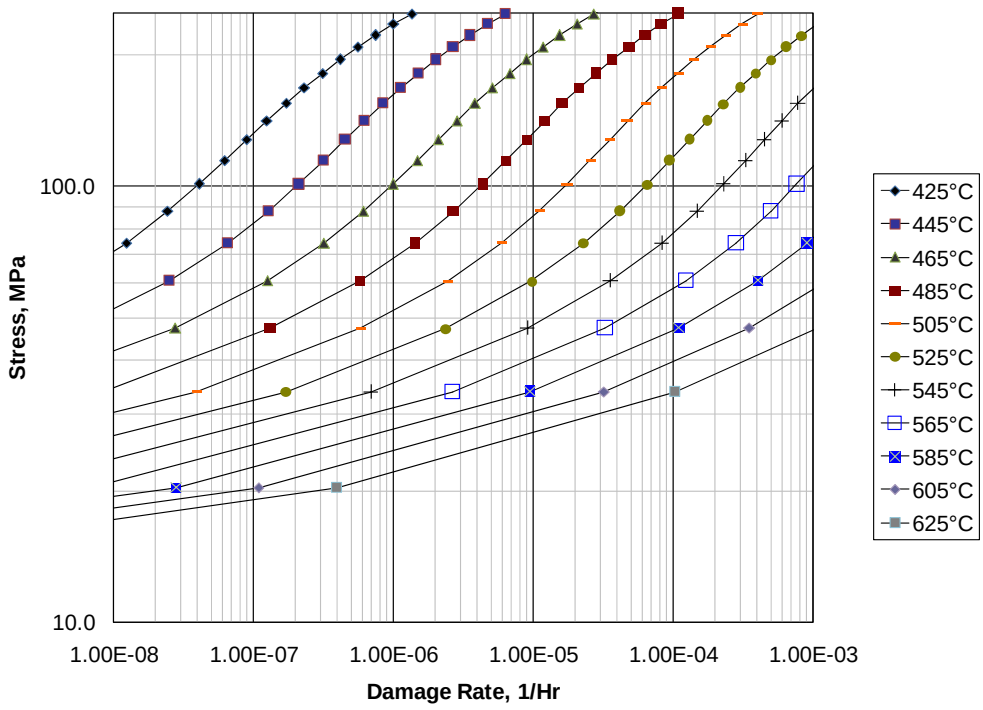

b) Damage Curve

Figure 10.5M – Level 1 Screening Criteria for C-0.5Mo

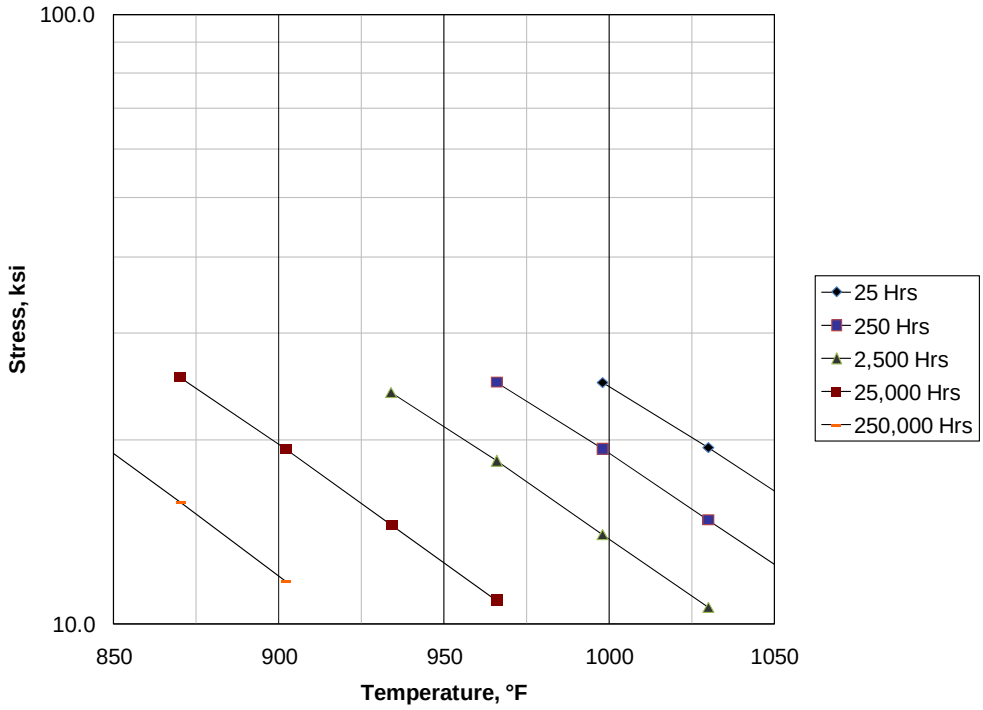

a) Screening Curve

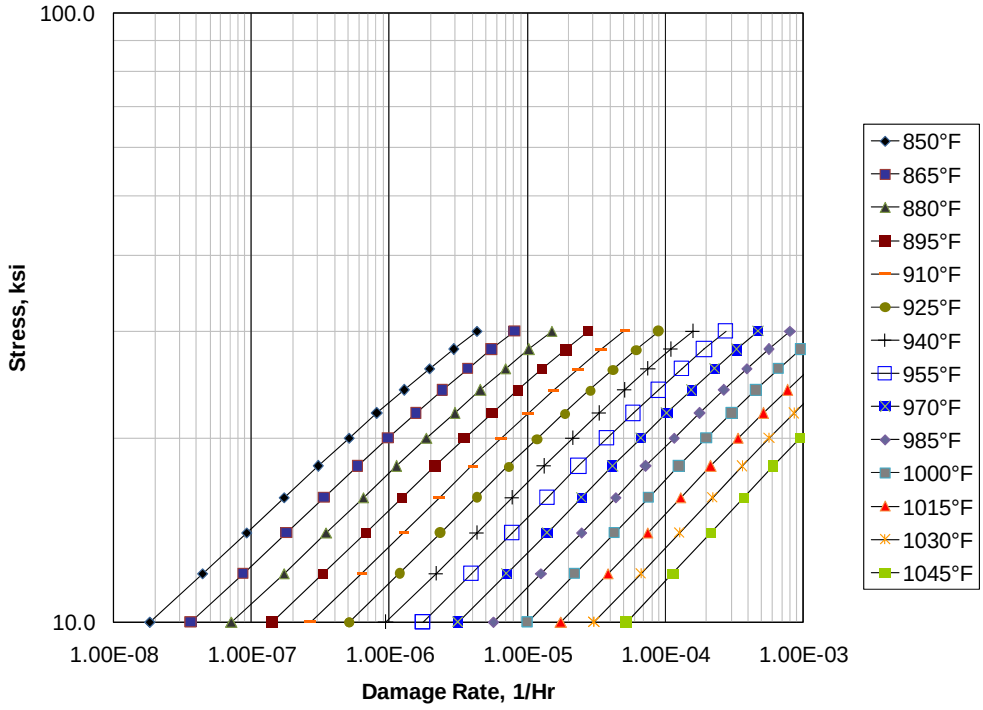

b) Damage Curve

Figure 10.6 – Level 1 Screening Criteria for 1.25Cr-0.5Mo – N&T

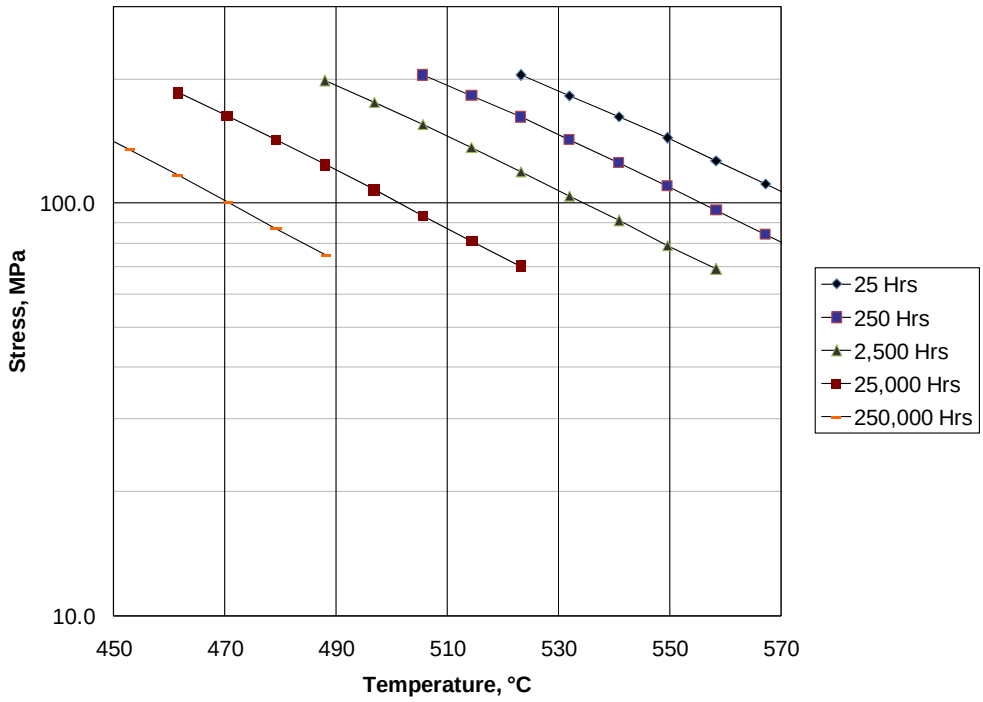

a) Screening Curve

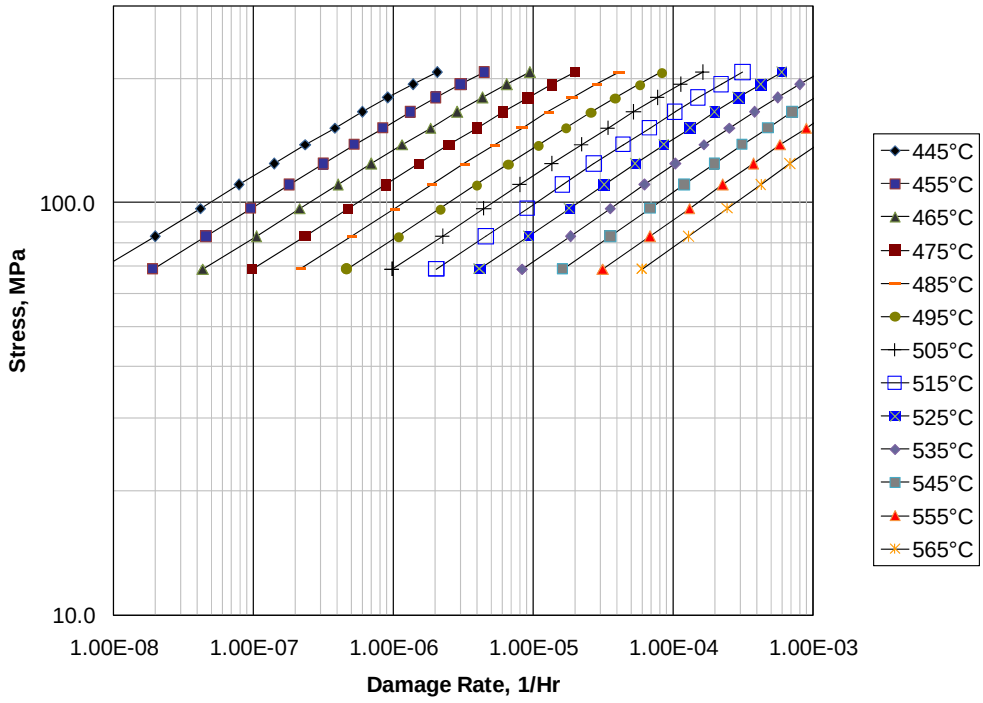

b) Damage Curve

Figure 10.6M – Level 1 Screening Criteria for 1.25Cr-0.5Mo – N&T

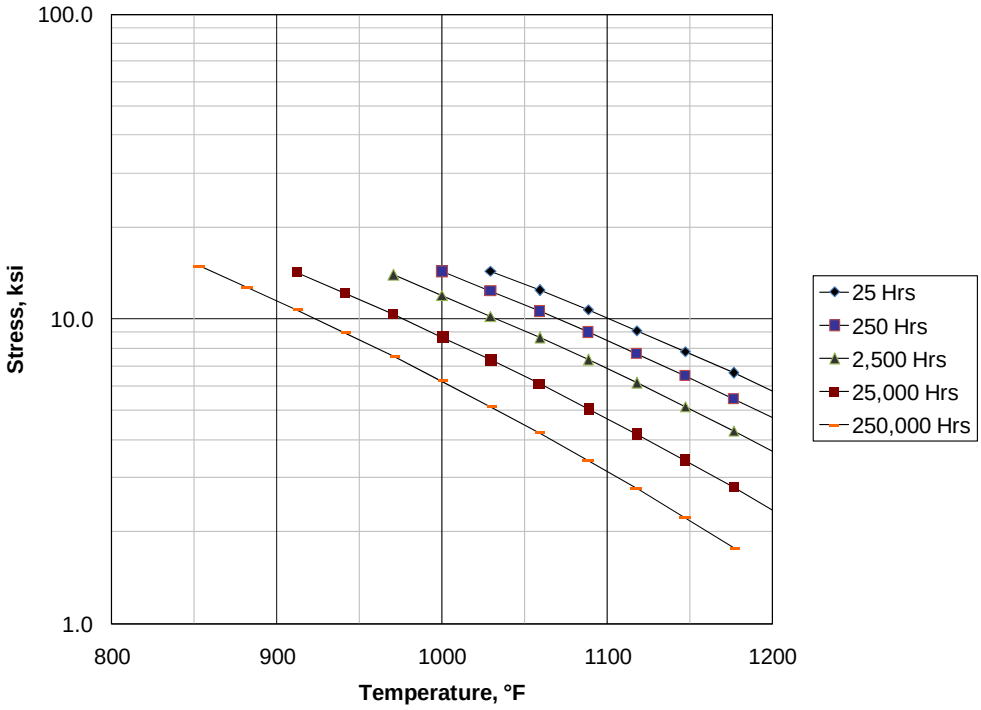

a) Screening Curve

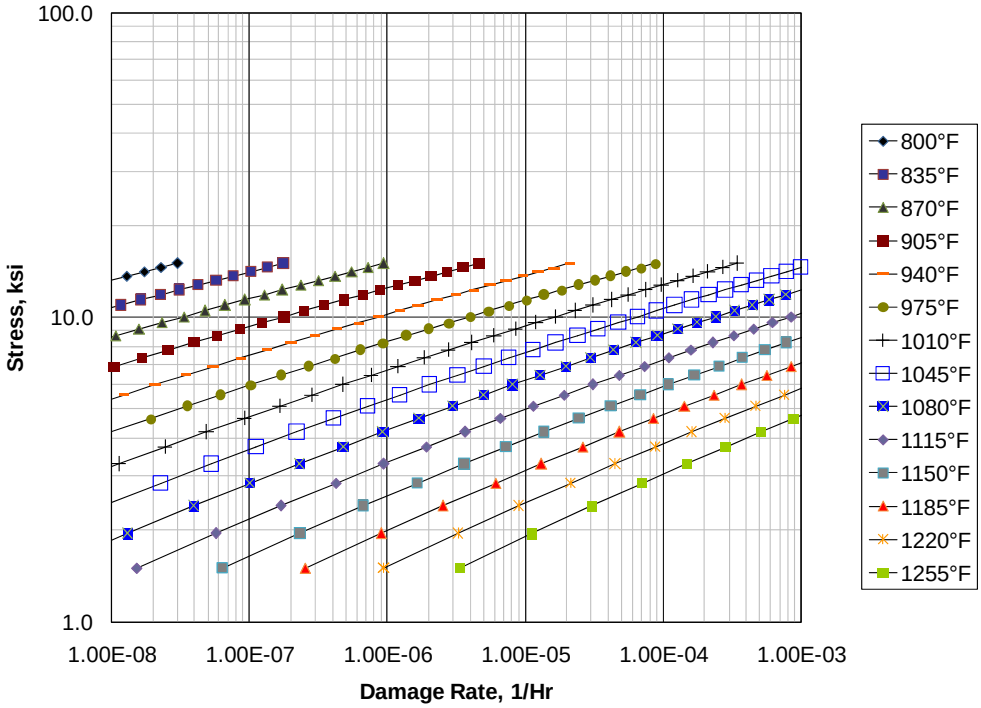

b) Damage Curve

Figure 10.7 – Level 1 Screening Criteria for 1.25Cr-0.5Mo – Annealed

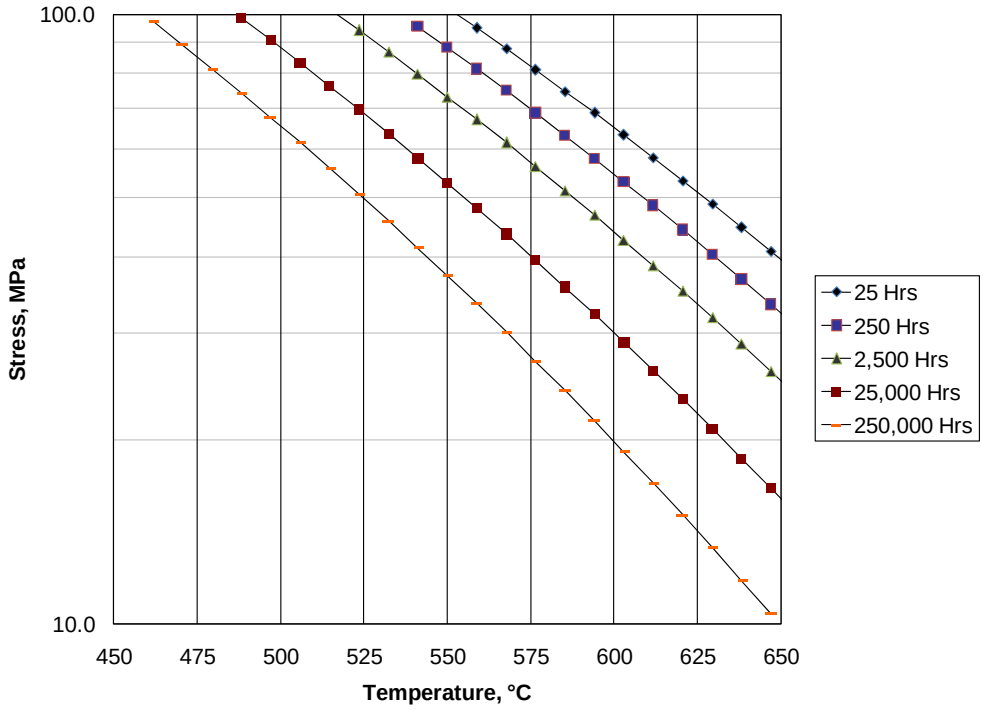

a) Screening Curve

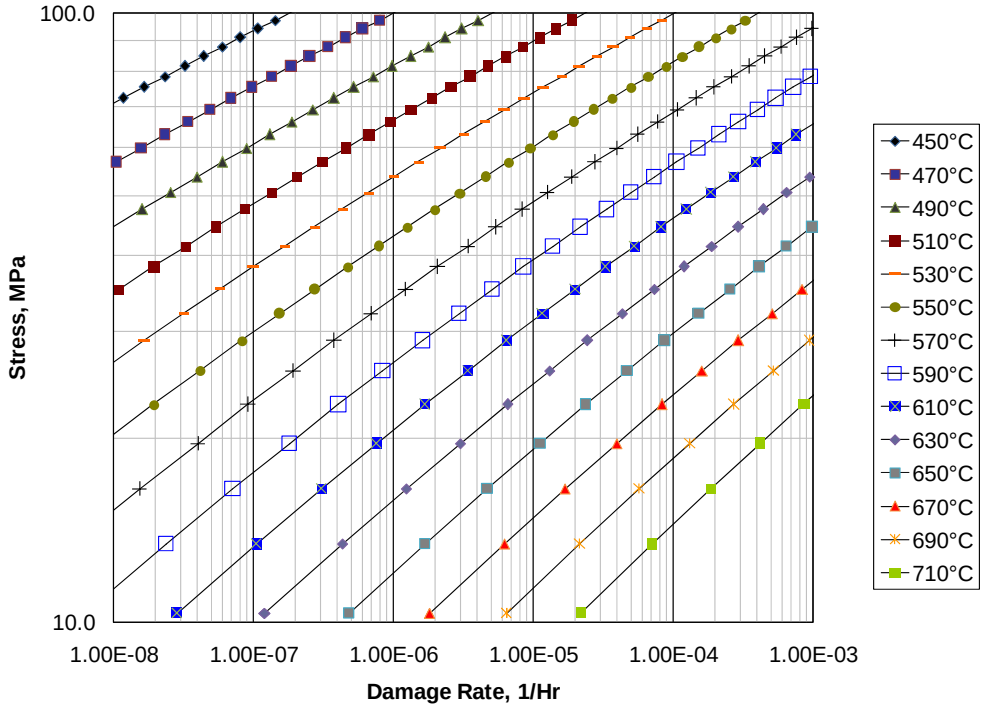

b) Damage Curve

Figure 10.7M – Level 1 Screening Criteria for 1.25Cr-0.5Mo – Annealed

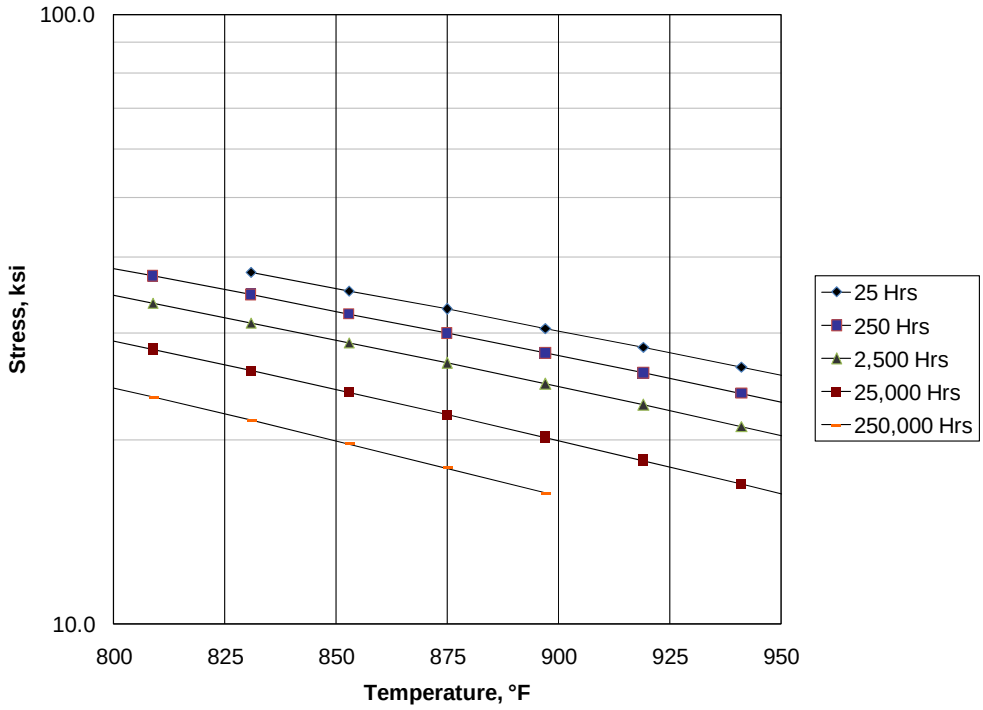

a) Screening Curve

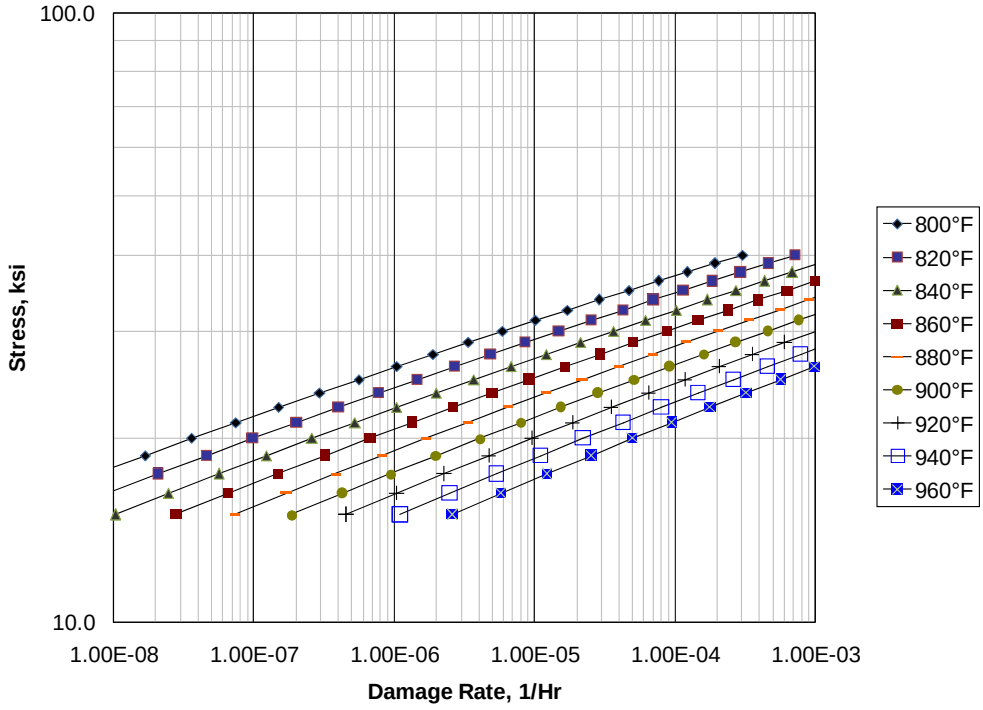

b) Damage Curve

Figure 10.8 – Level 1 Screening Criteria for 2.25Cr-1Mo – N&T

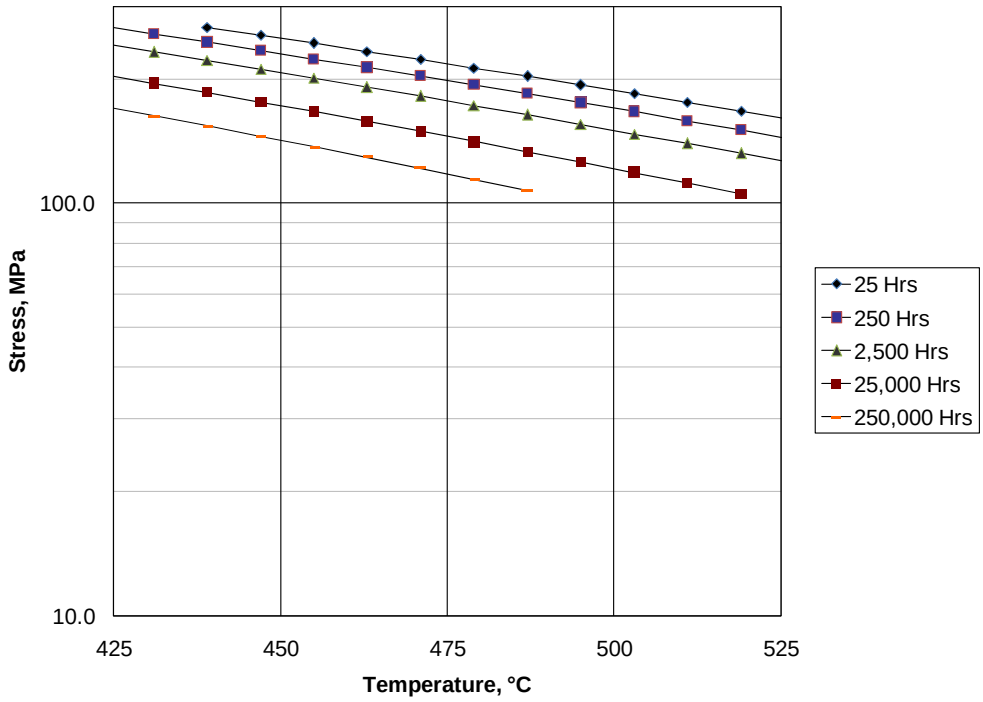

a) Screening Curve

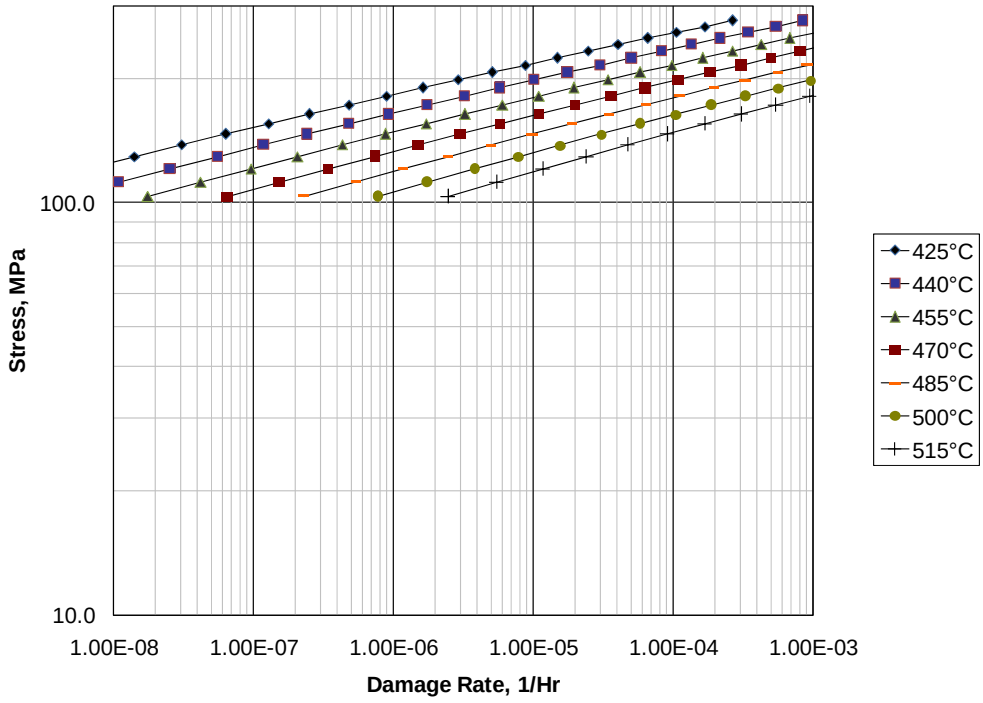

b) Damage Curve

Figure 10.8M – Level 1 Screening Criteria for 2.25Cr-1Mo – N&T

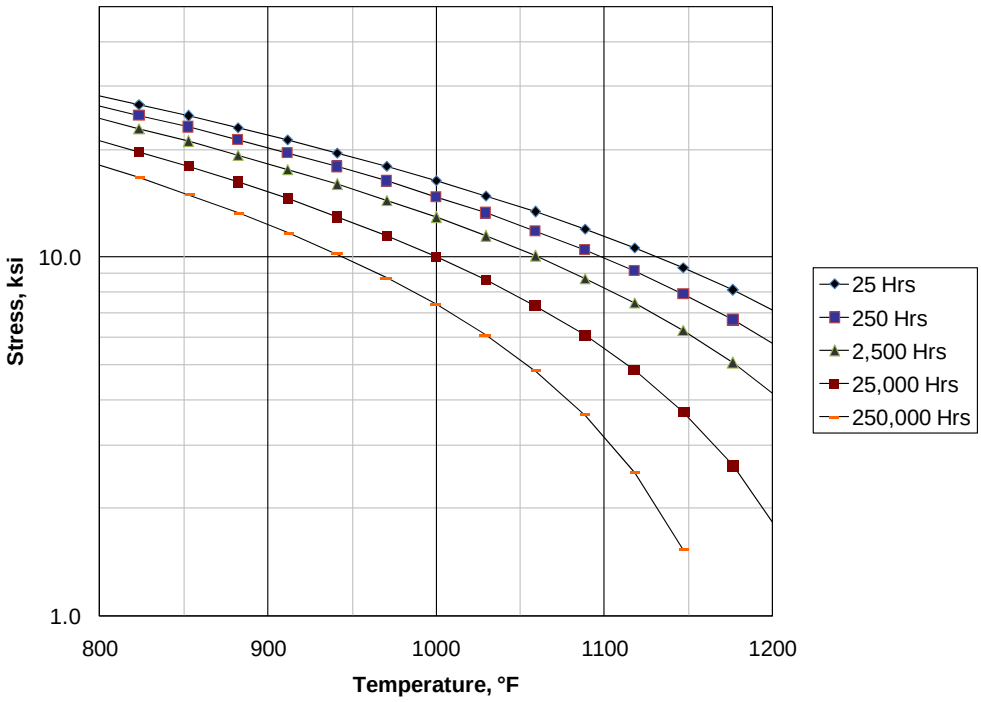

a) Screening Curve

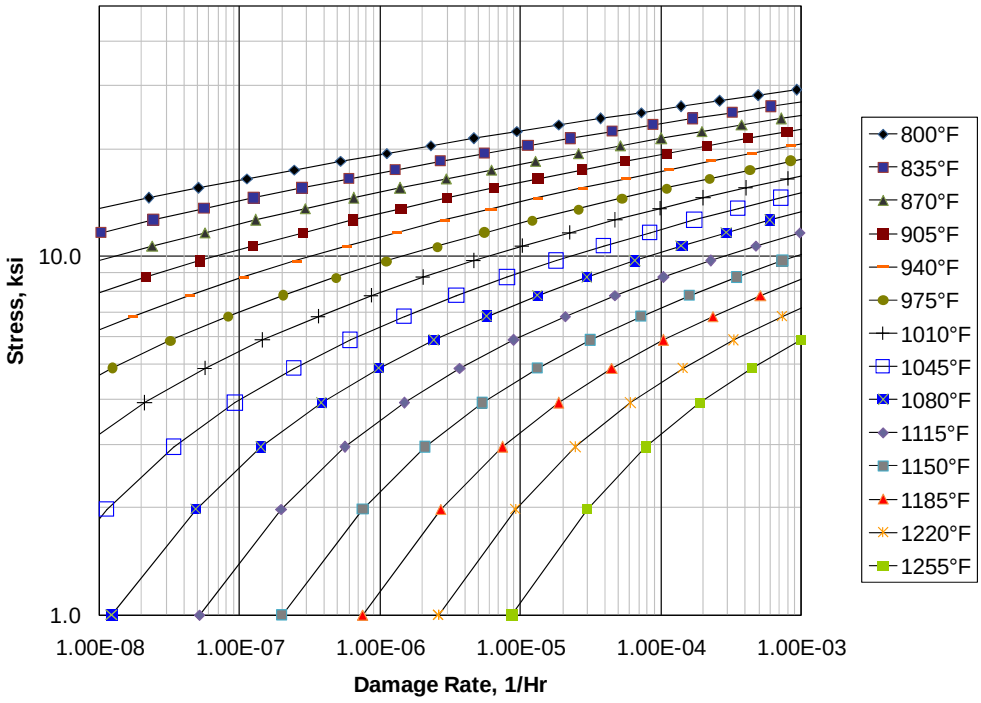

b) Damage Curve

Figure 10.9 – Level 1 Screening Criteria for 2.25Cr-1Mo – Annealed

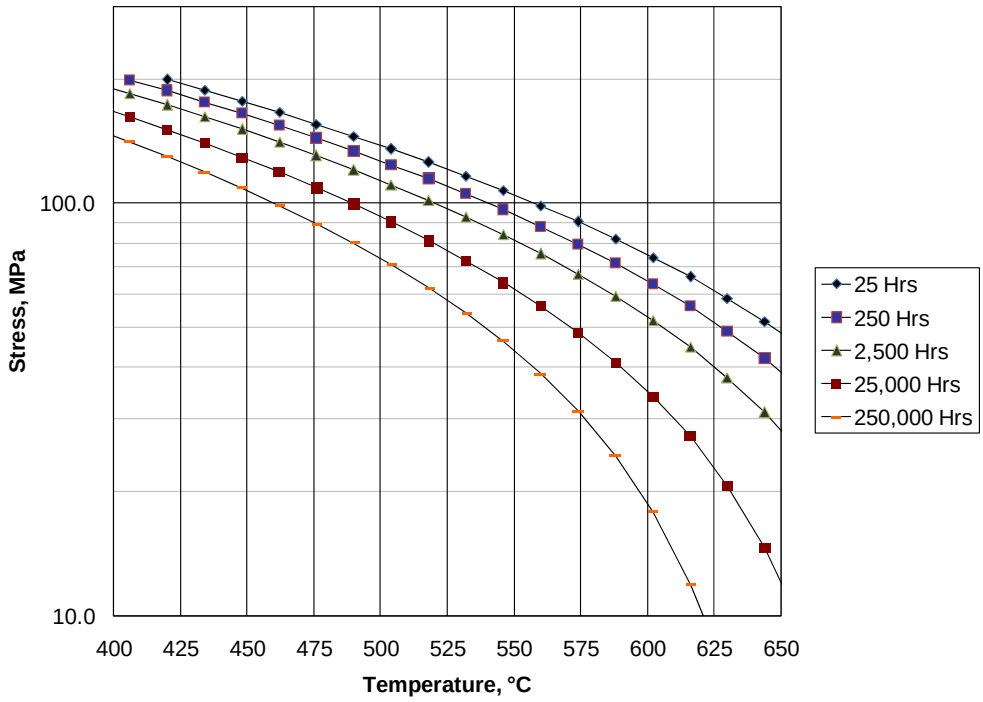

a) Screening Curve

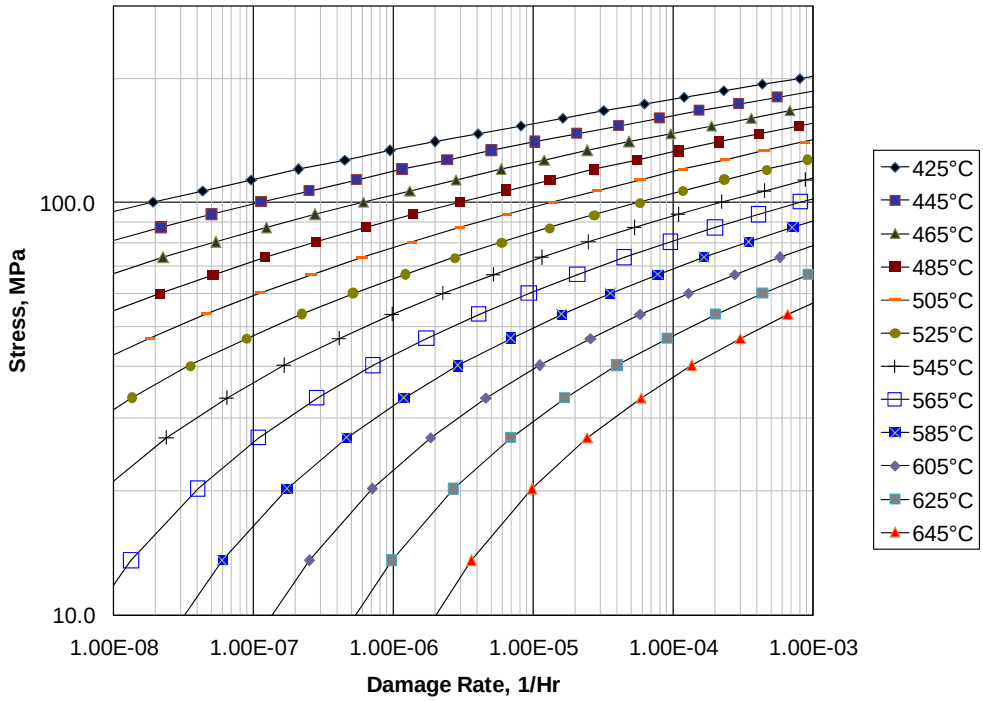

b) Damage Curve

Figure 10.9M – Level 1 Screening Criteria for 2.25Cr-1Mo – Annealed

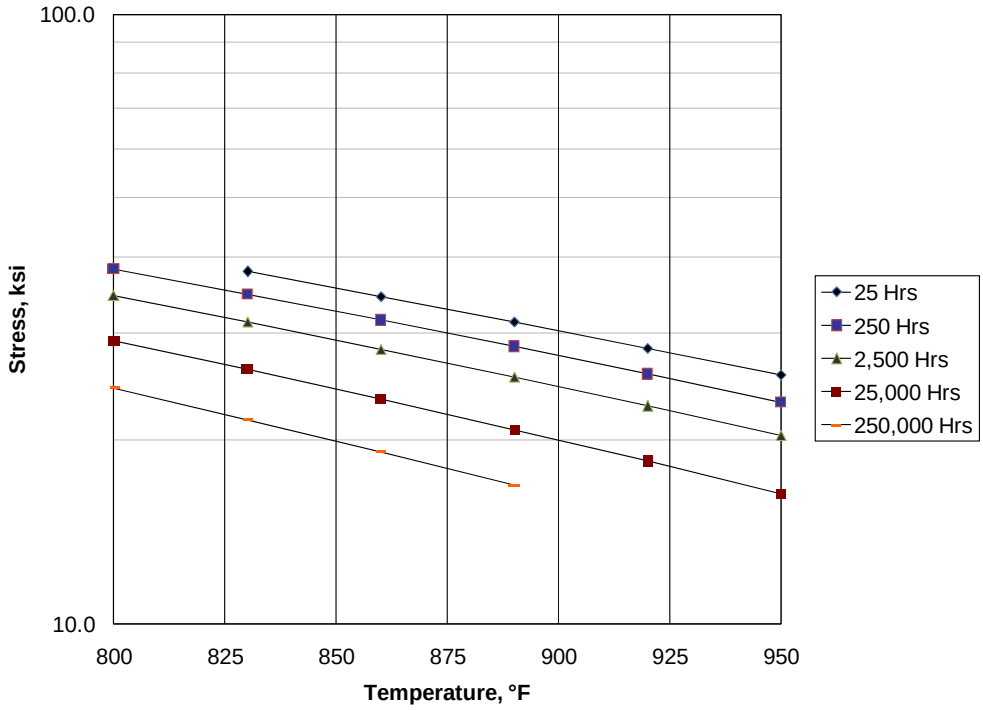

a) Screening Curve

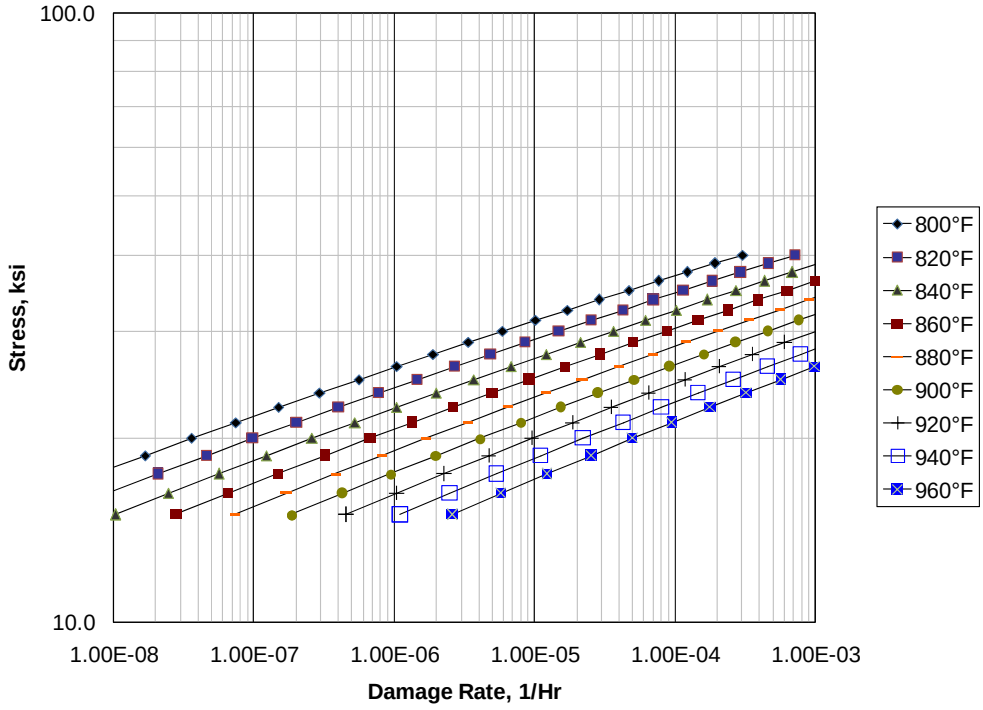

b) Damage Curve

Figure 10.10 – Level 1 Screening Criteria for 2.25Cr-1Mo – Q&T

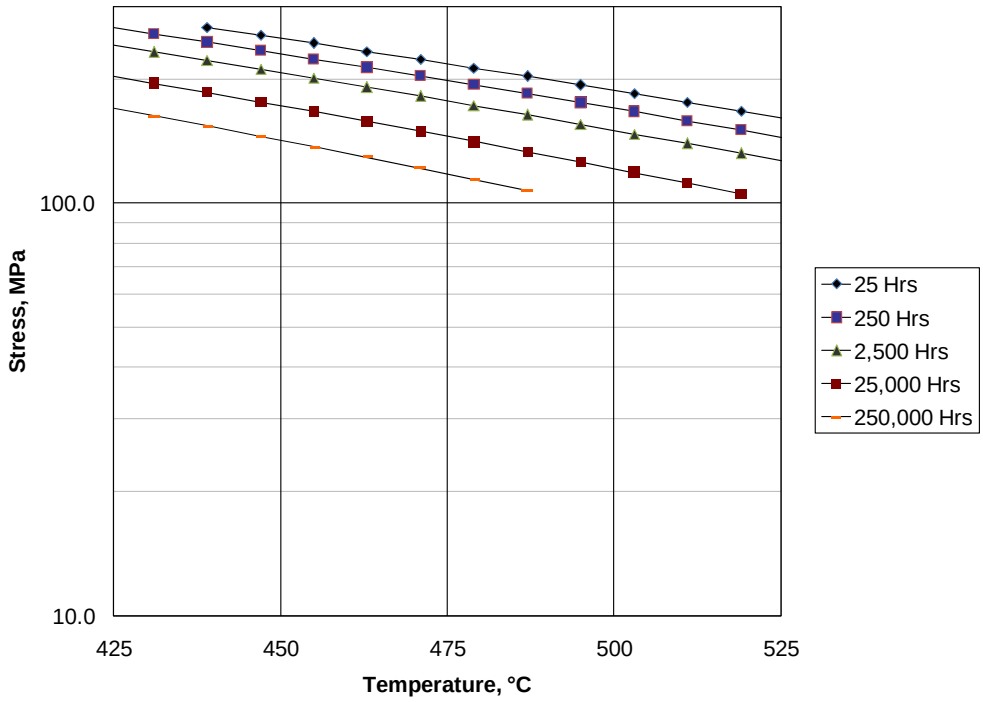

a) Screening Curve

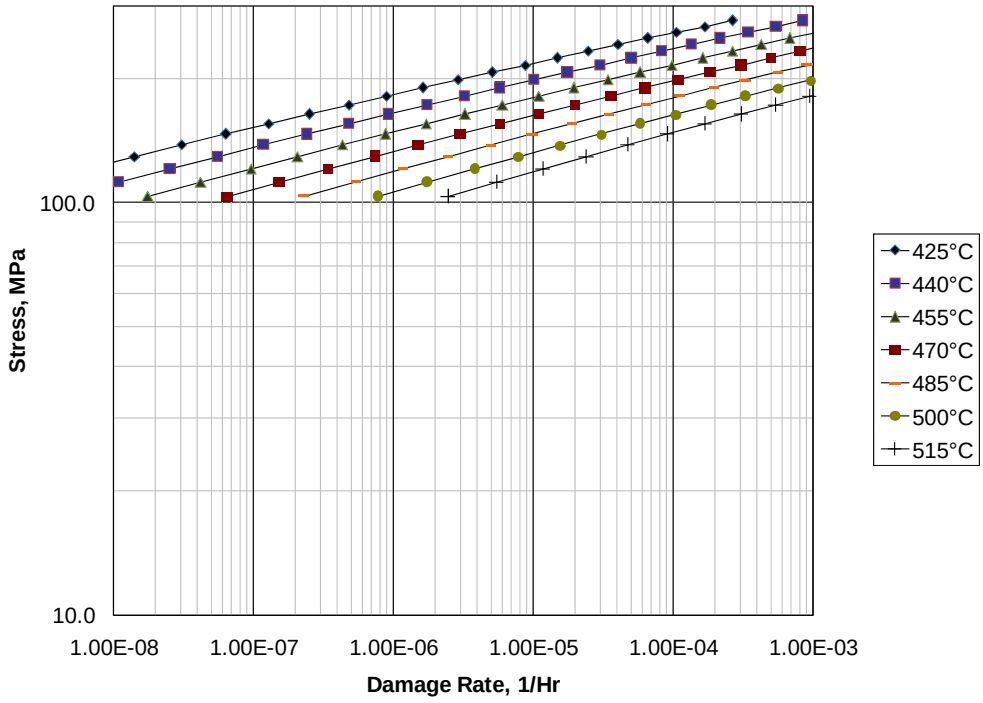

b) Damage Curve

Figure 10.10M – Level 1 Screening Criteria for 2.25Cr-1Mo – Q&T

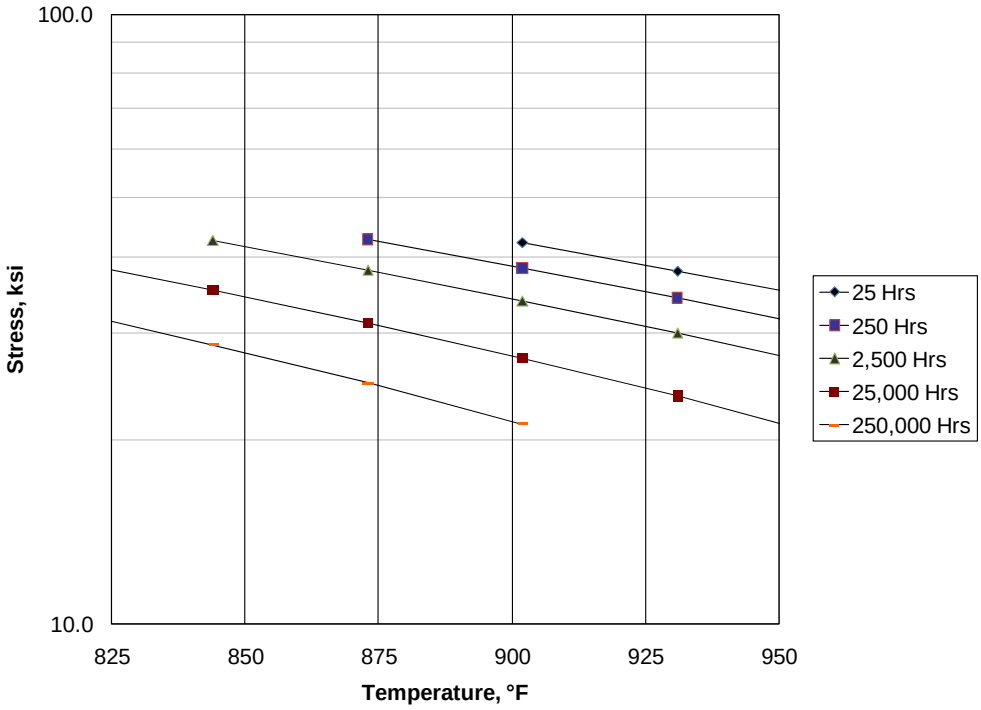

a) Screening Curve

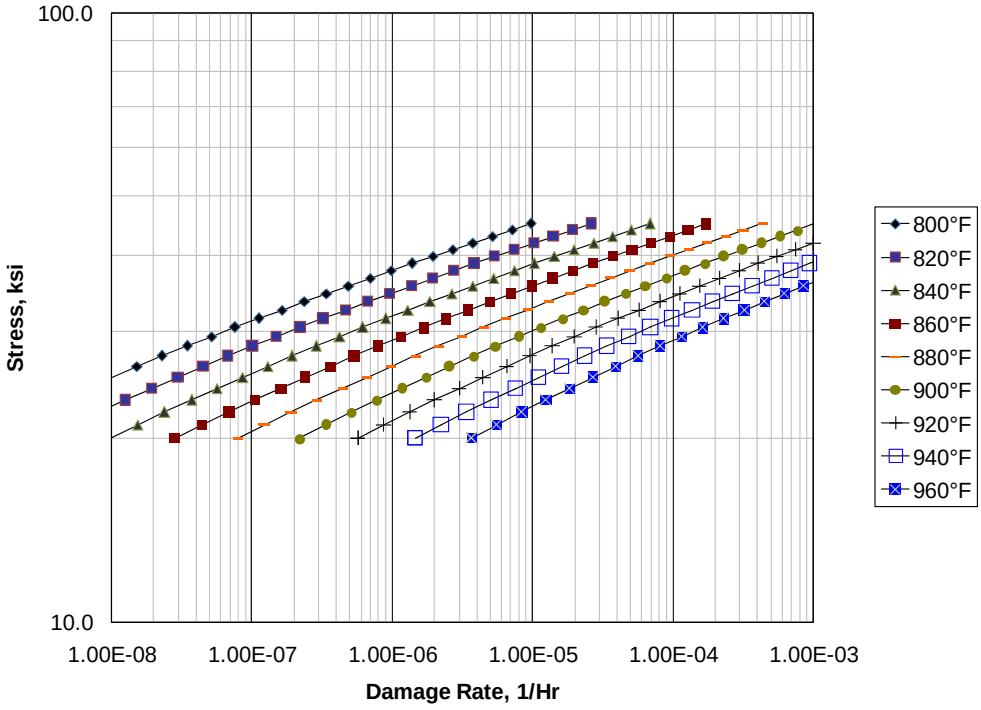

b) Damage Curve

Figure 10.11 – Level 1 Screening Criteria for 2.25Cr-1Mo-V

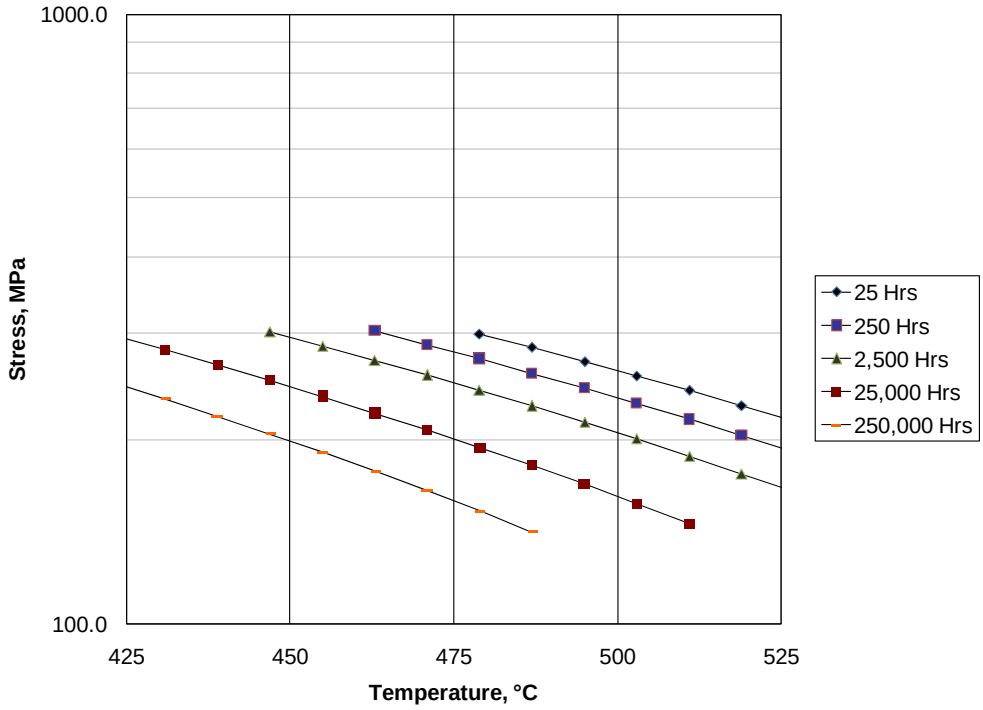

a) Screening Curve

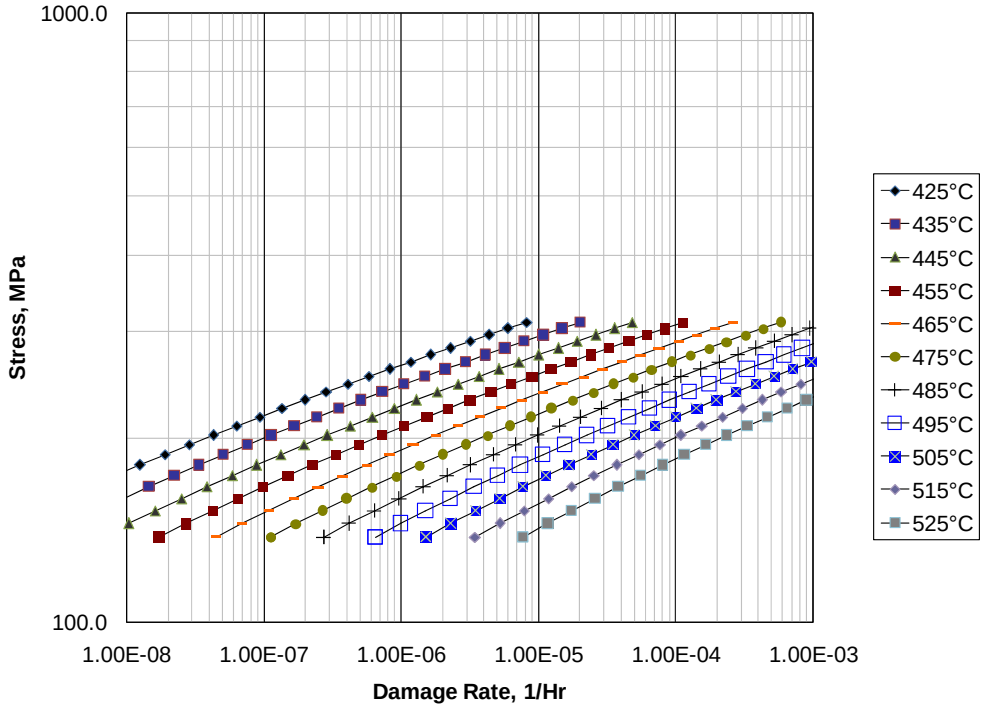

b) Damage Curve

Figure 10.11M – Level 1 Screening Criteria for 2.25Cr-1Mo-V

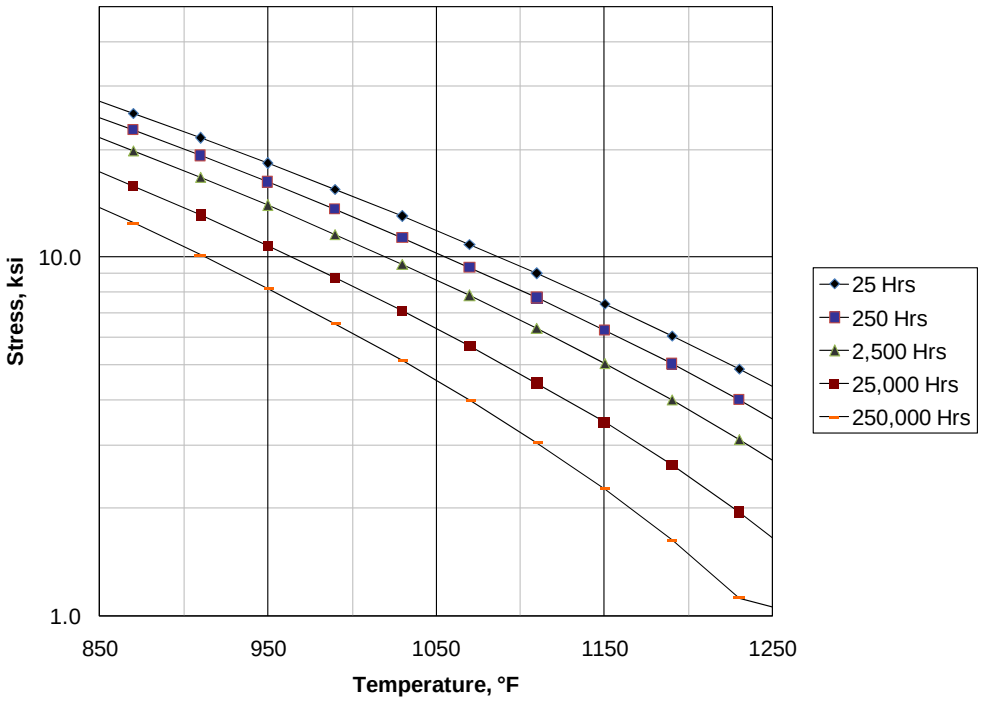

a) Screening Curve

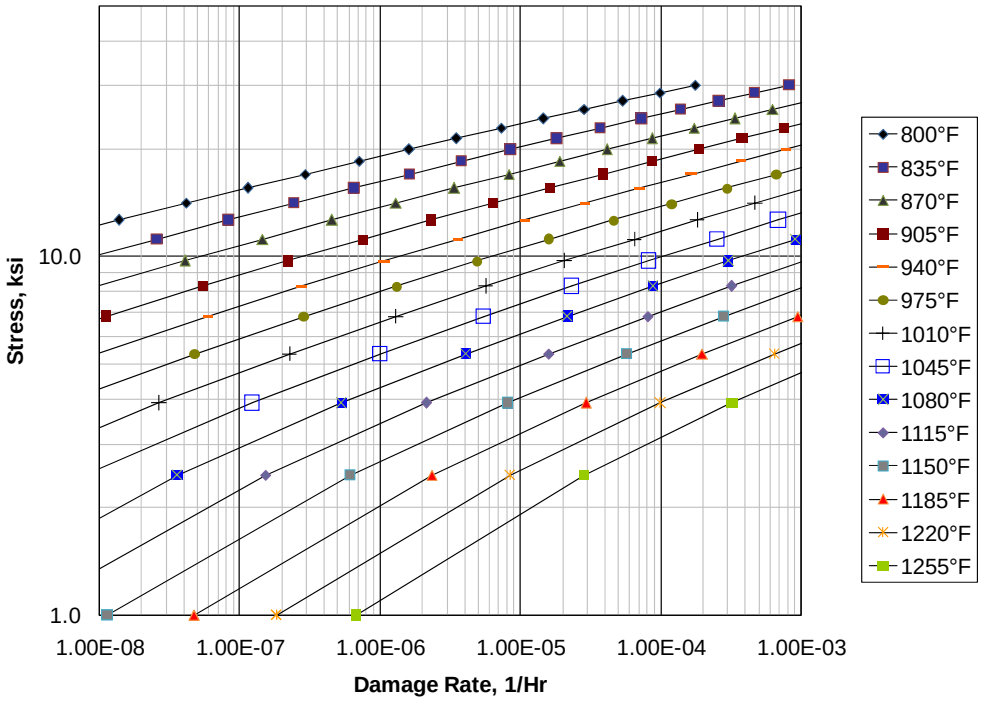

b) Damage Curve

Figure 10.12 – Level 1 Screening Criteria for 5Cr-0.5Mo

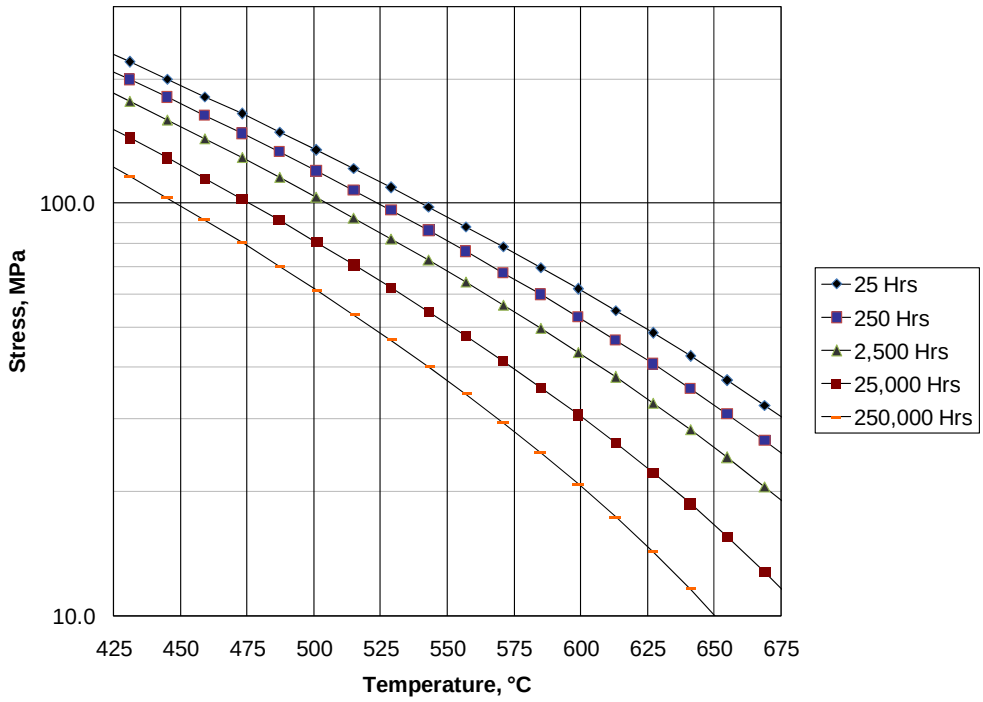

a) Screening Curve

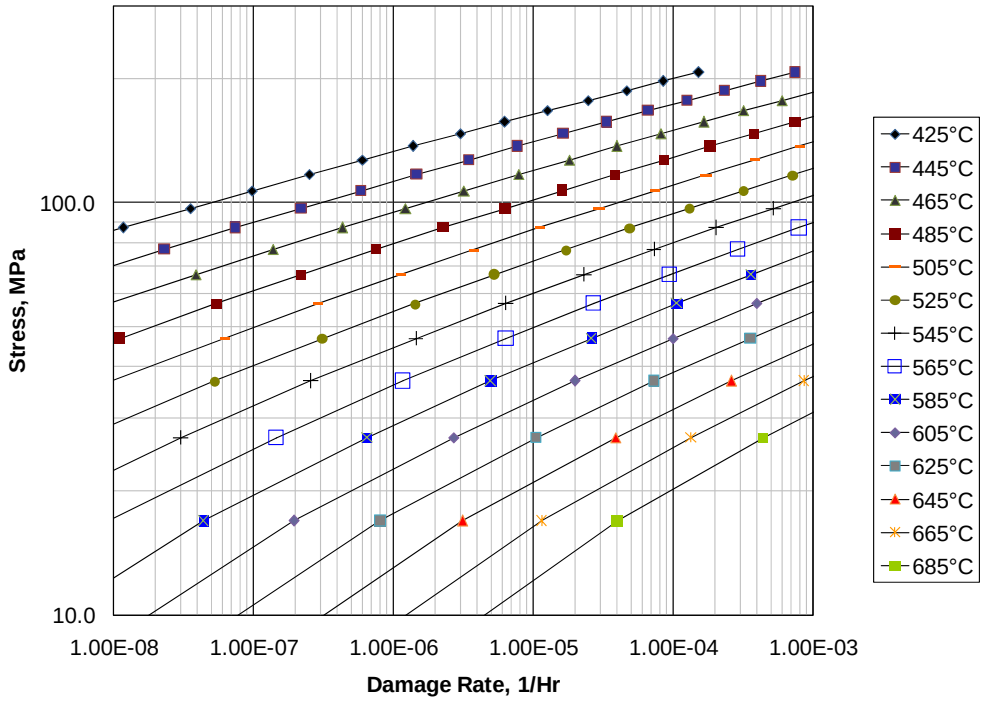

b) Damage Curve

Figure 10.12M – Level 1 Screening Criteria for 5Cr-0.5Mo

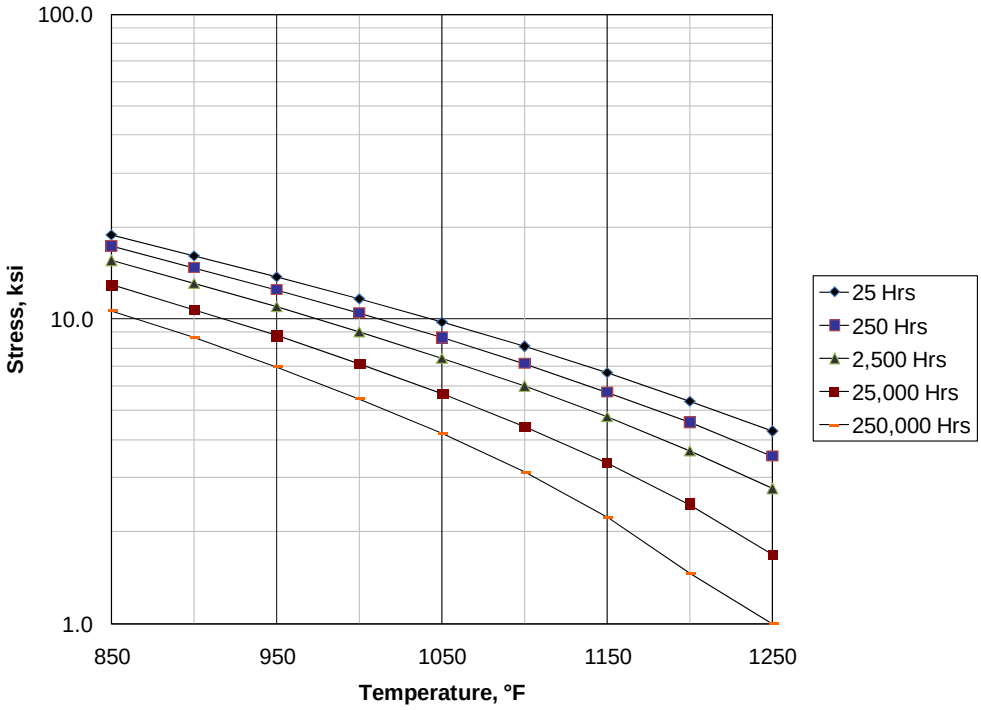

a) Screening Curve

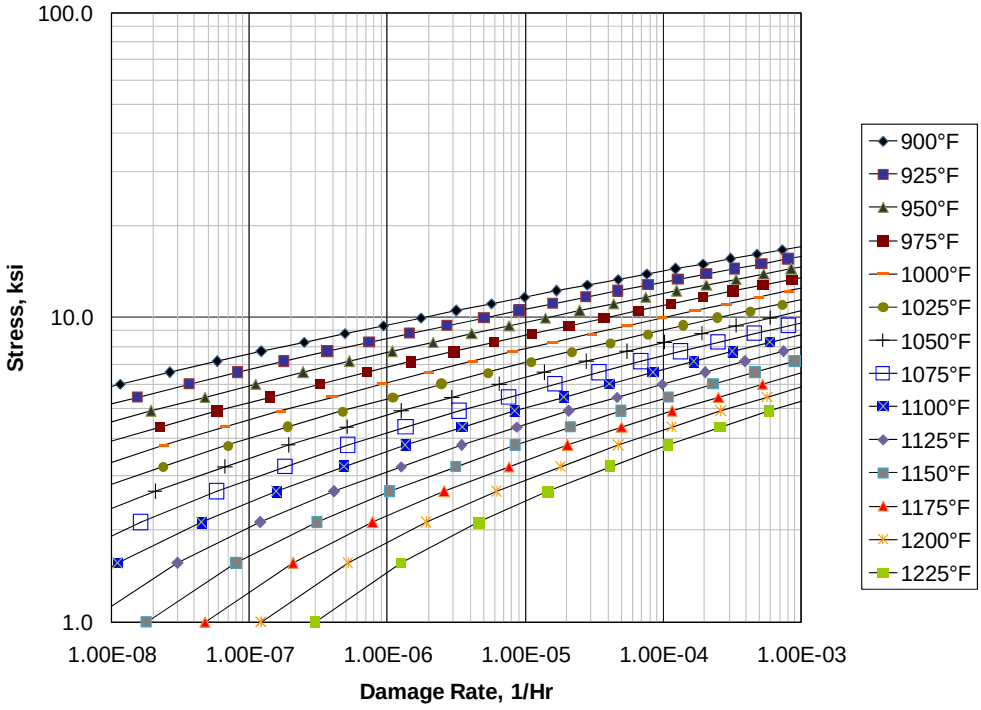

b) Damage Curve

Figure 10.13 – Level 1 Screening Criteria for 9Cr-1Mo

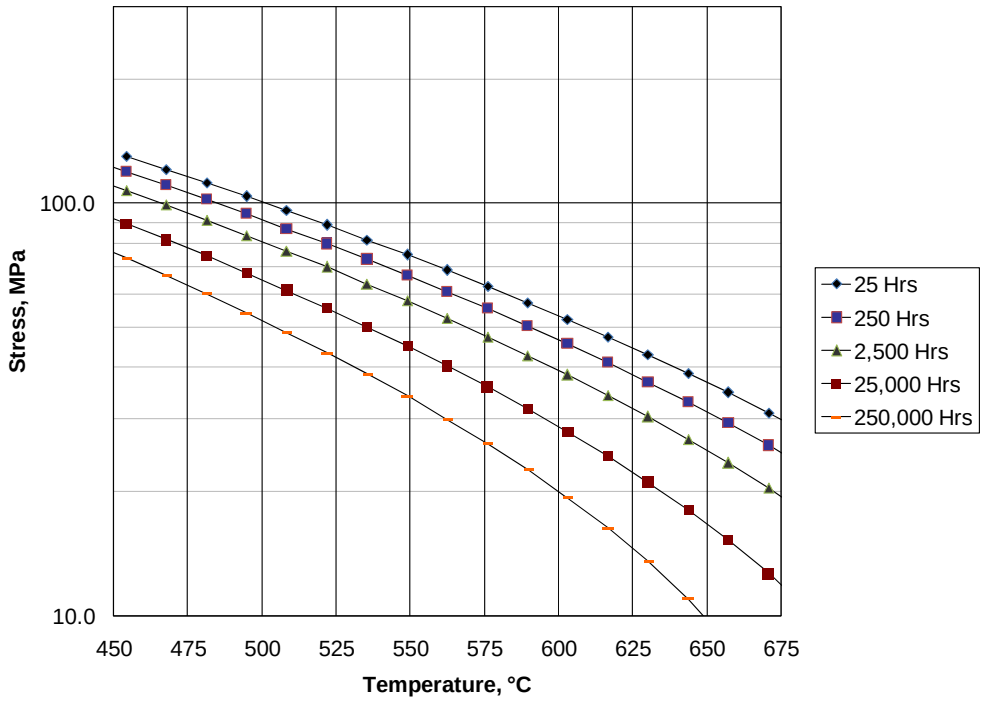

a) Screening Curve

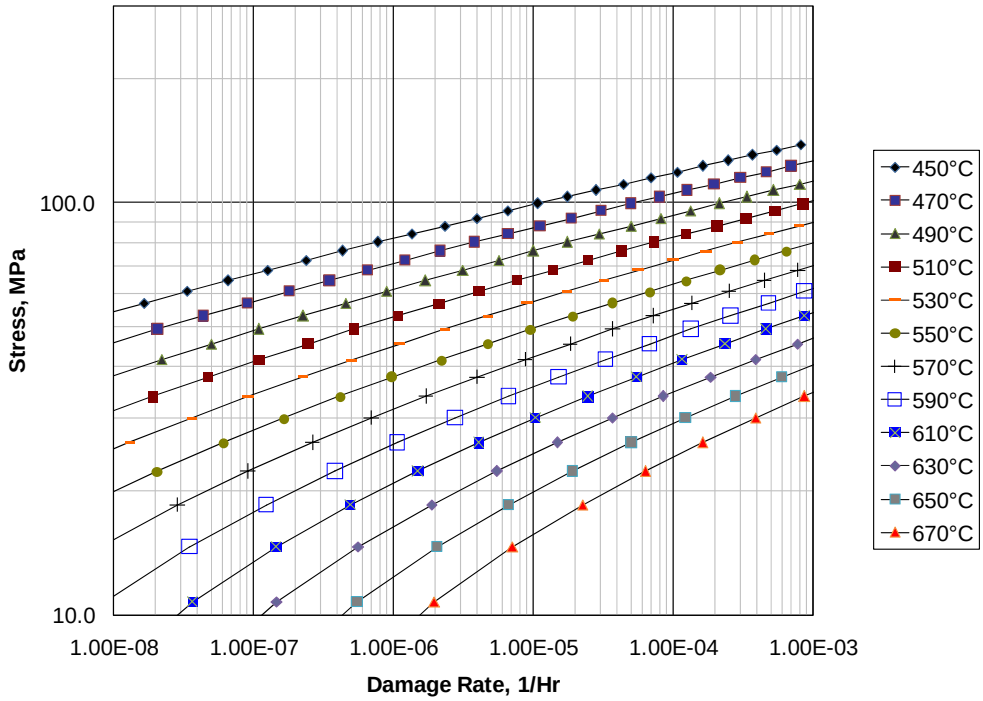

b) Damage Curve

Figure 10.13M – Level 1 Screening Criteria for 9Cr-1Mo

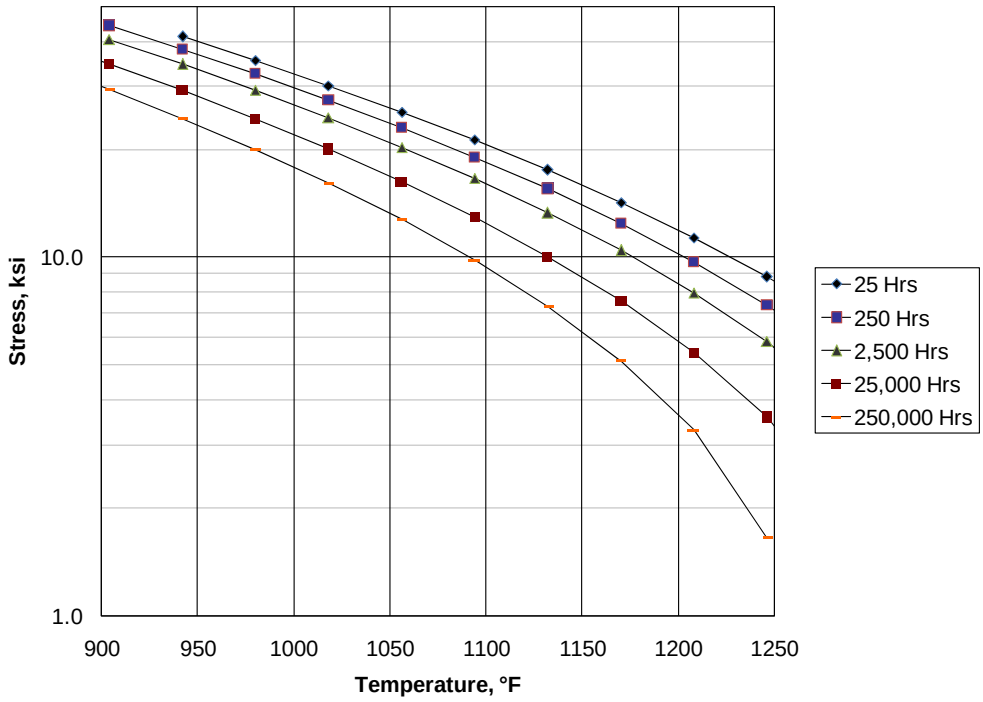

a) Screening Curve

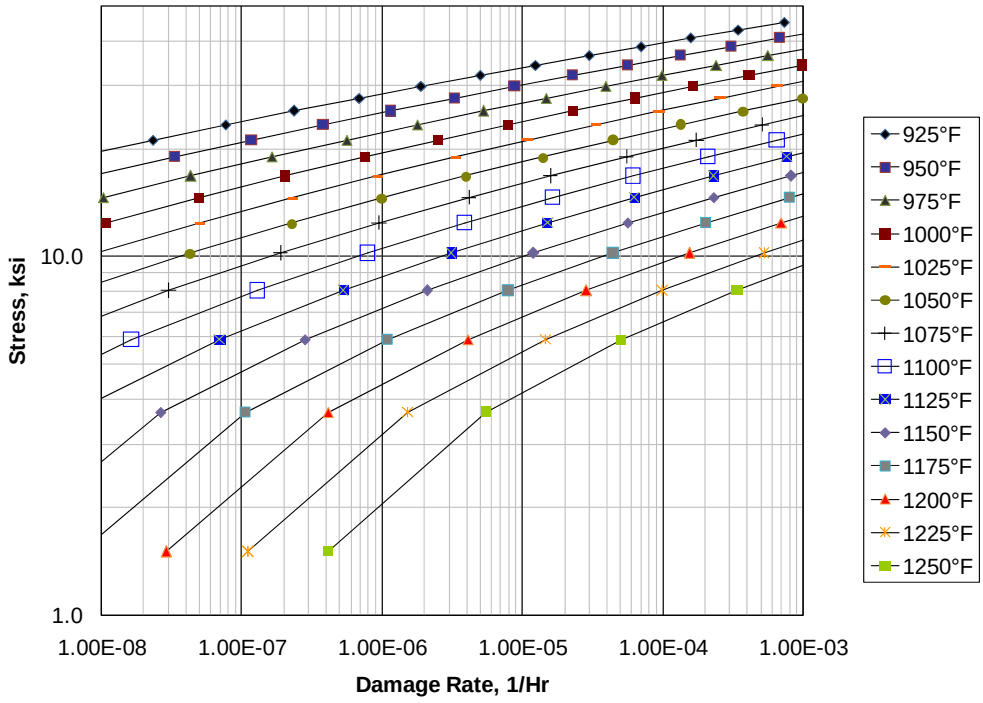

b) Damage Curve

Figure 10.14 – Level 1 Screening Criteria for 9Cr-1Mo-V

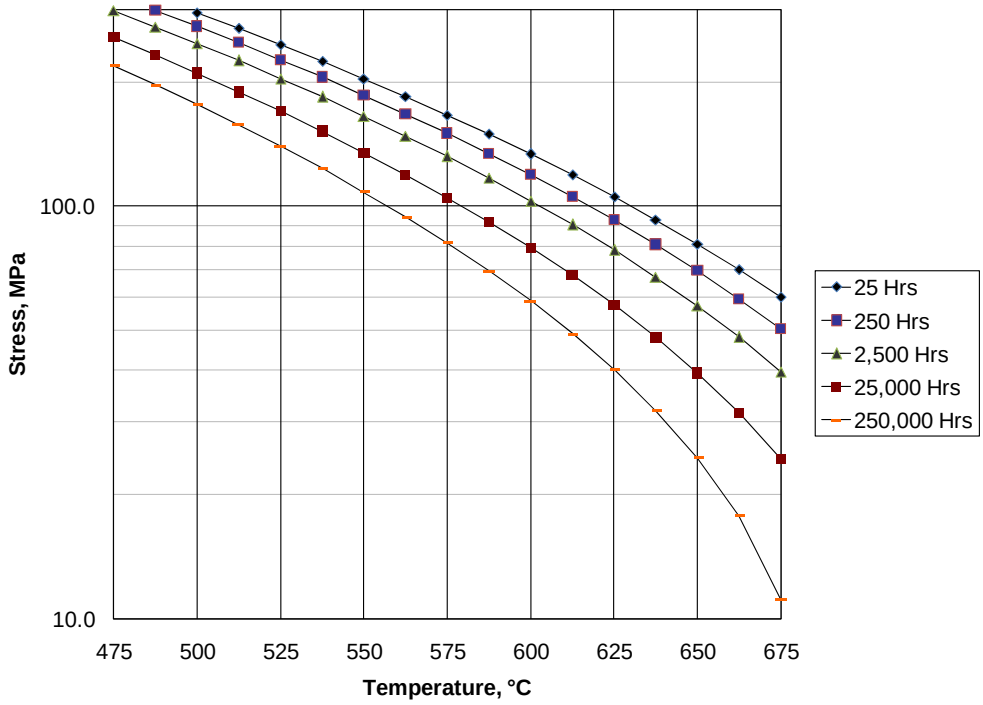

a) Screening Curve

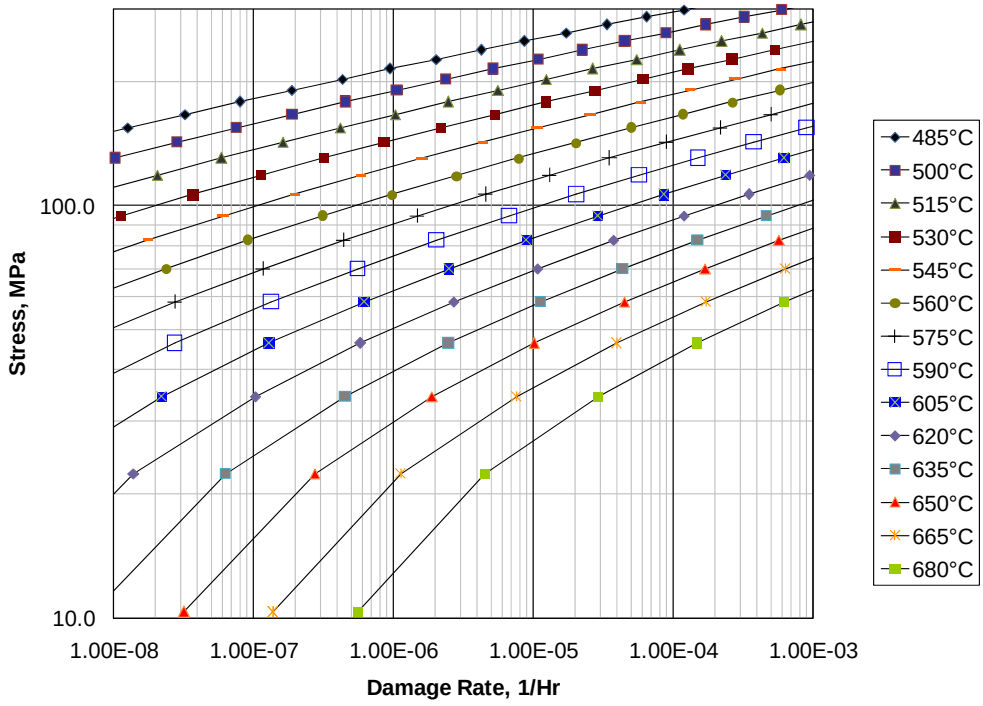

b) Damage Curve

Figure 10.14M – Level 1 Screening Criteria for 9Cr-1Mo-V

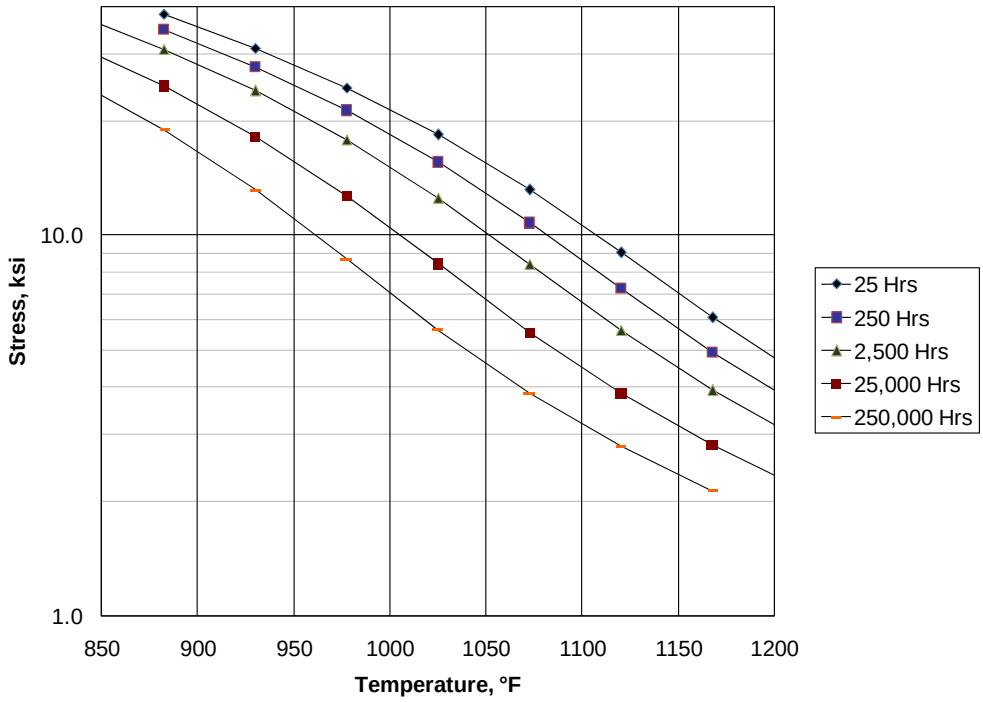

a) Screening Curve

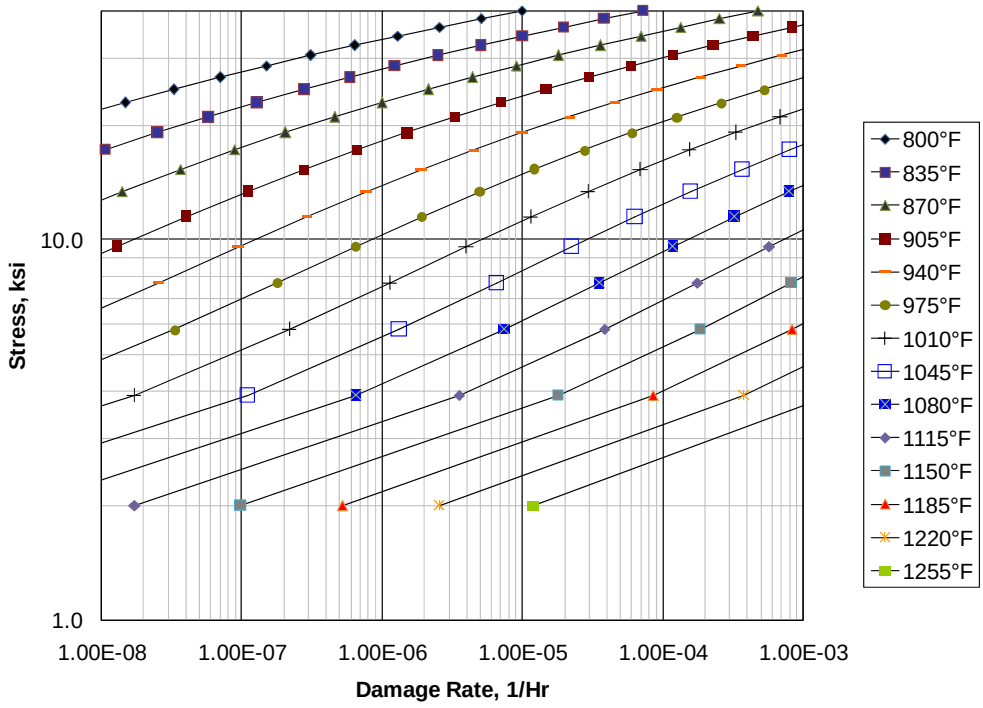

b) Damage Curve

Figure 10.15 – Level 1 Screening Criteria for 12 Cr

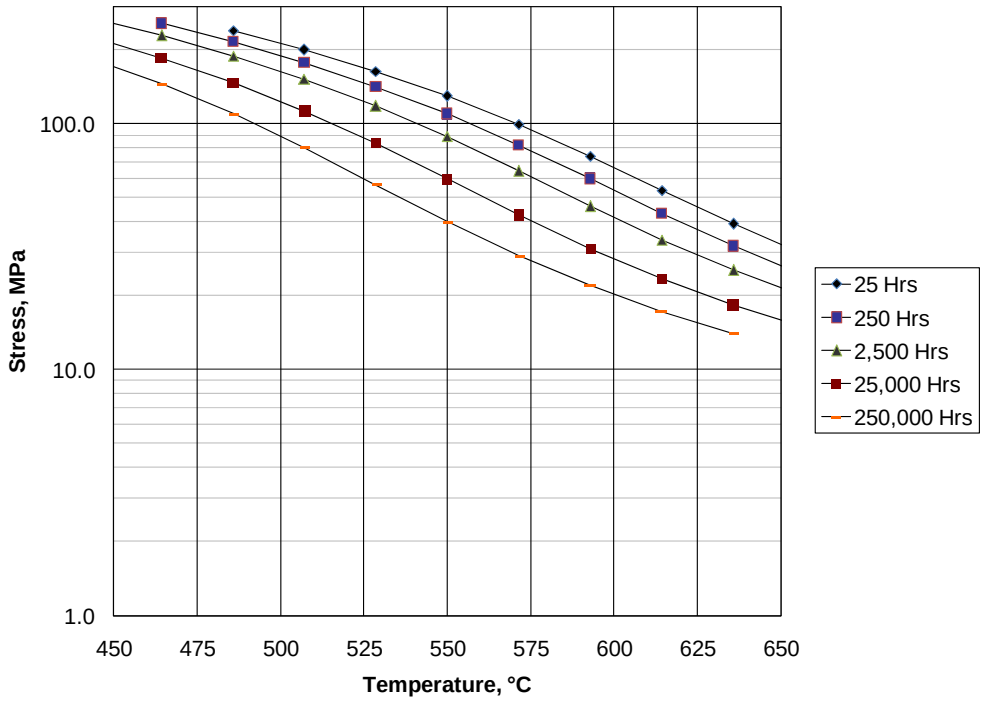

a) Screening Curve

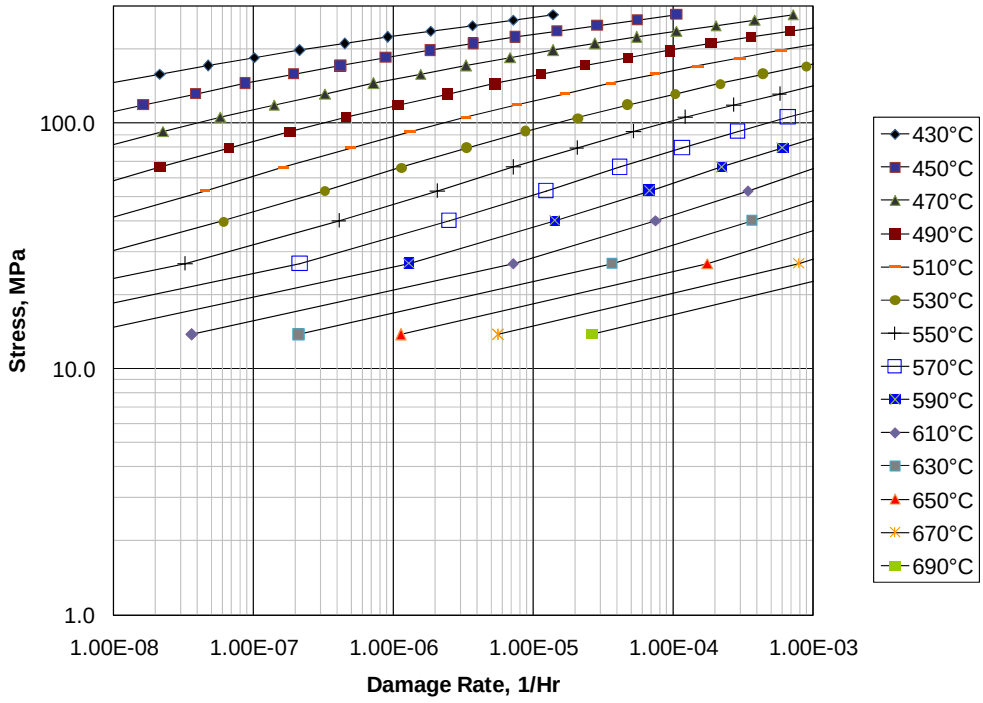

b) Damage Curve

Figure 10.15M – Level 1 Screening Criteria for 12 Cr

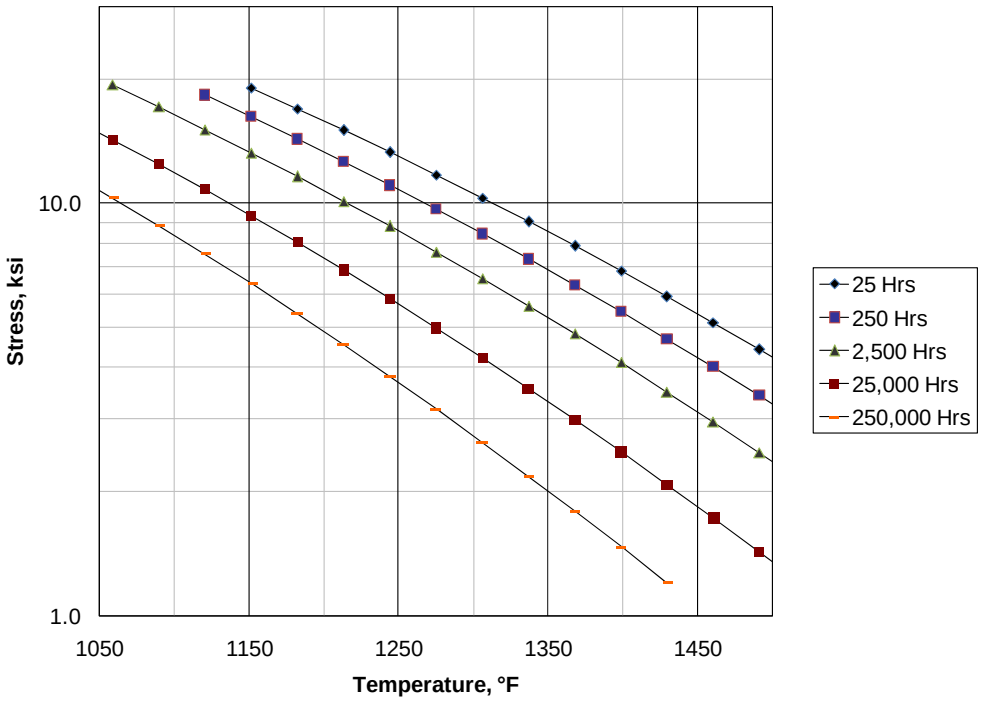

a) Screening Curve

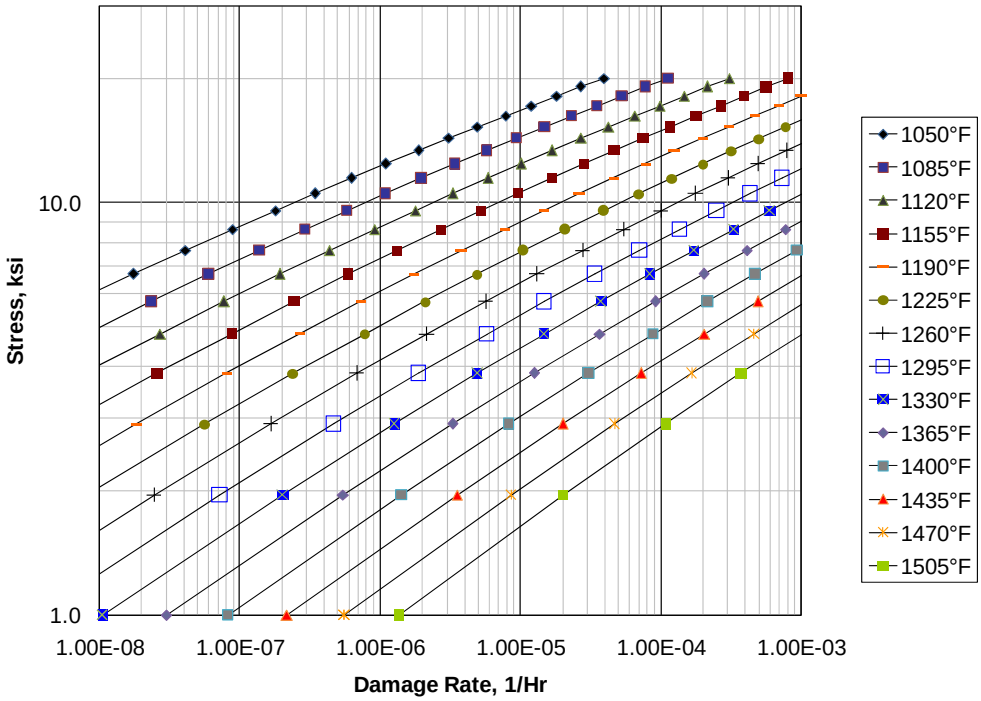

b) Damage Curve

Figure 10.16 – Level 1 Screening Criteria for AISI Type 304 & 304H

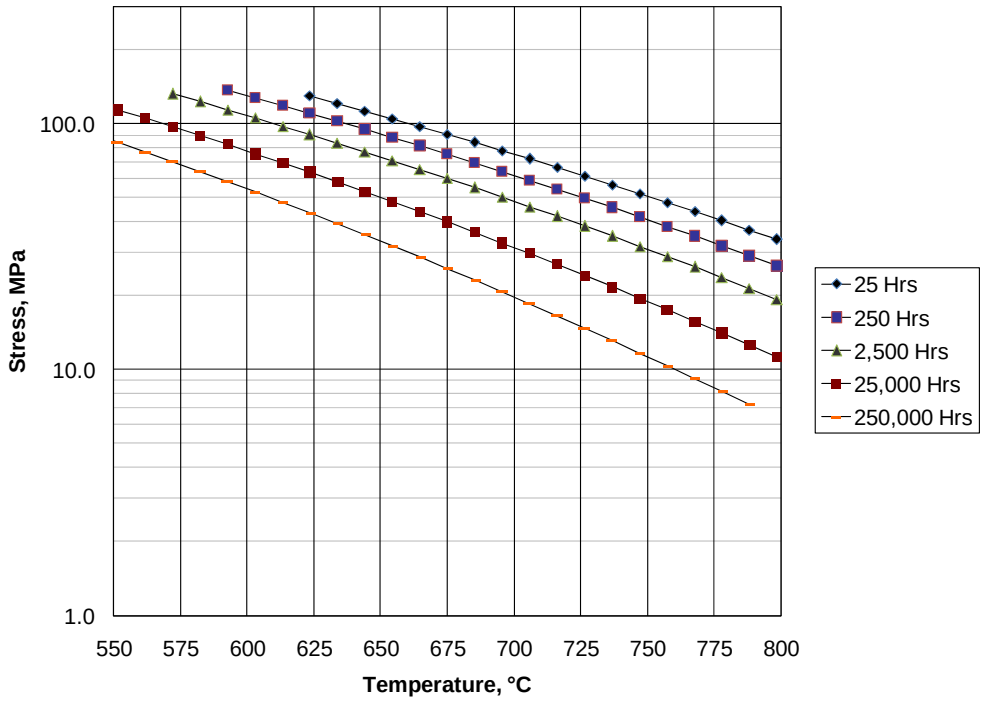

a) Screening Curve

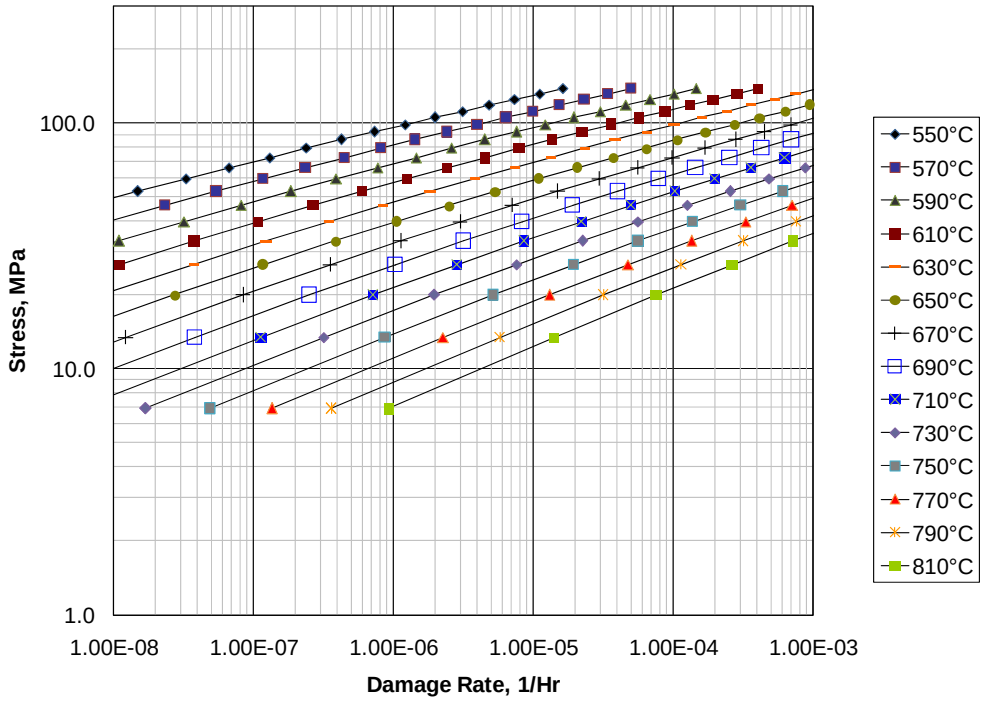

b) Damage Curve

Figure 10.16M – Level 1 Screening Criteria for AISI Type 304 & 304H

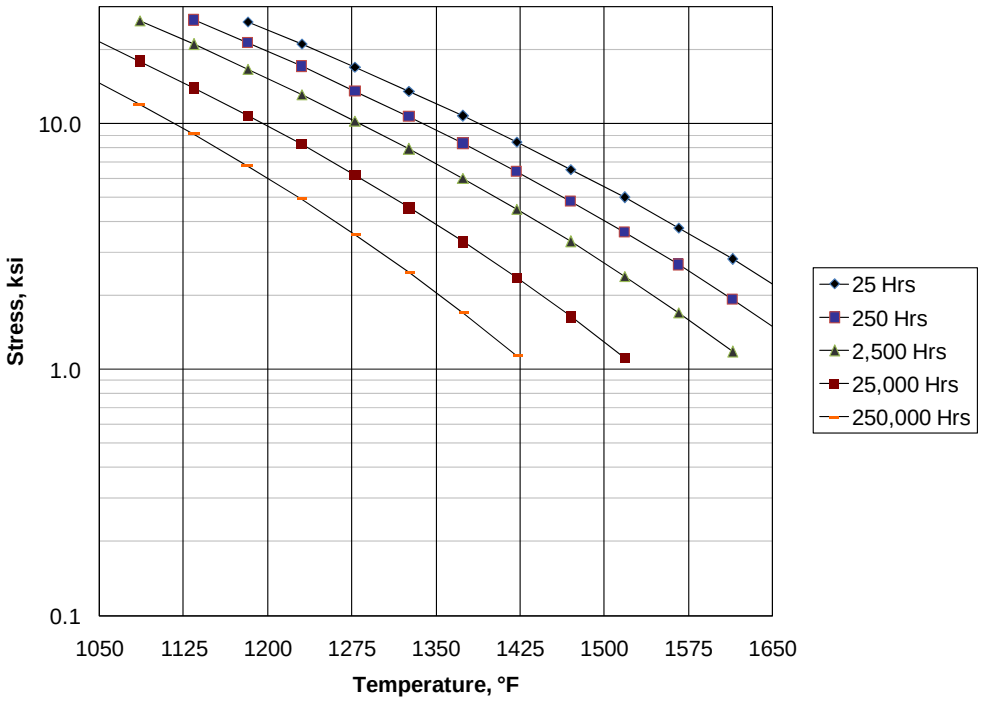

a) Screening Curve

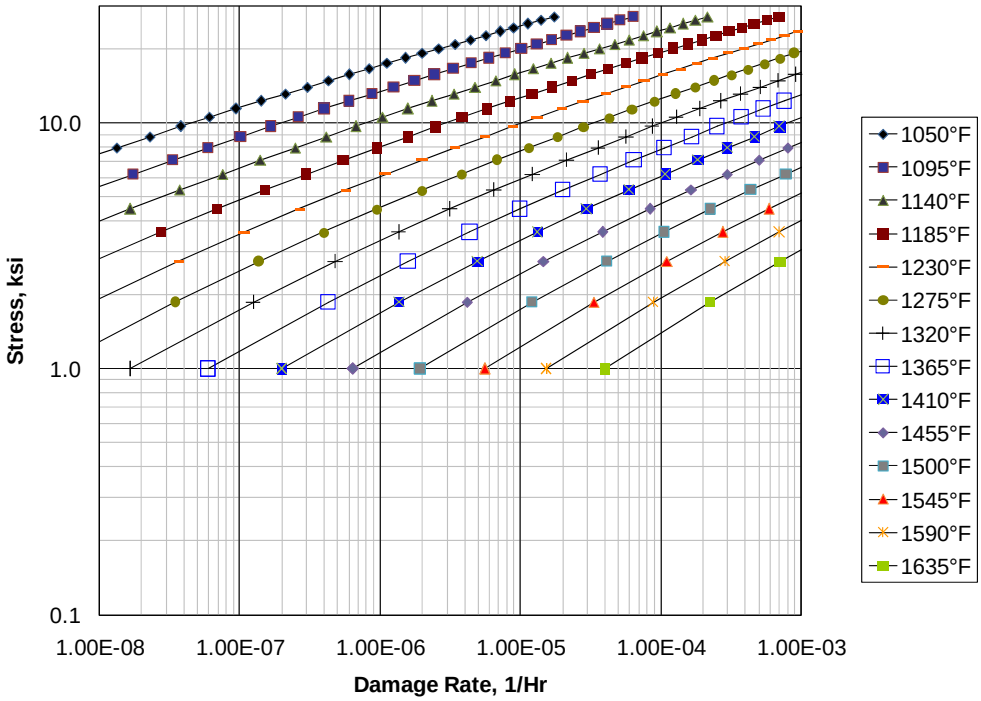

b) Damage Curve

Figure 10.17 – Level 1 Screening Criteria for AISI Type 316 & 316H

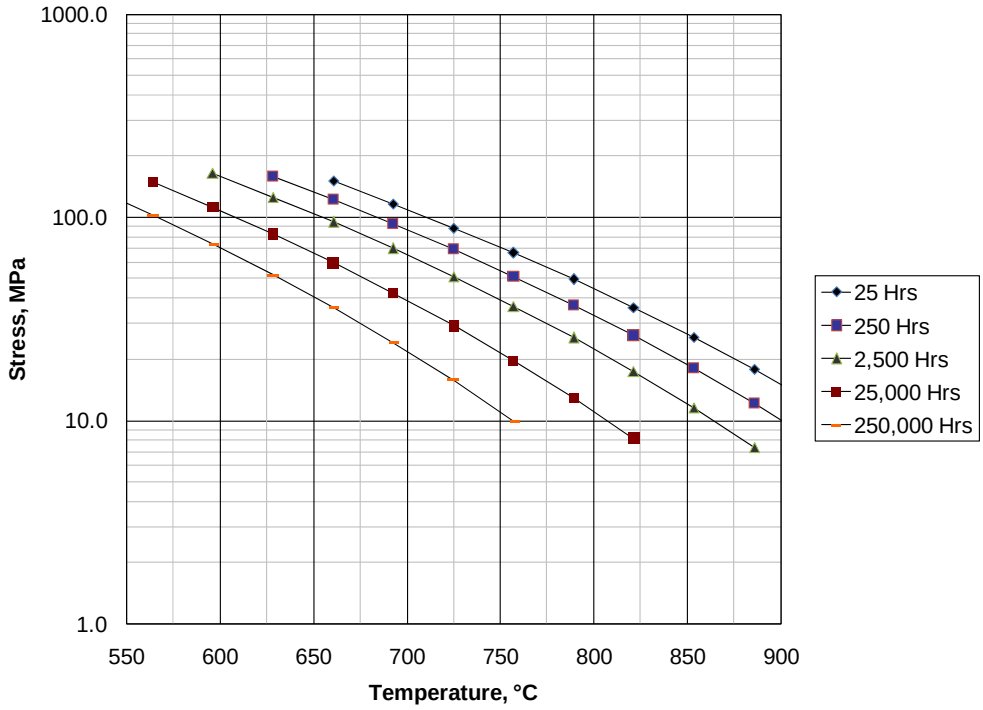

a) Screening Curve

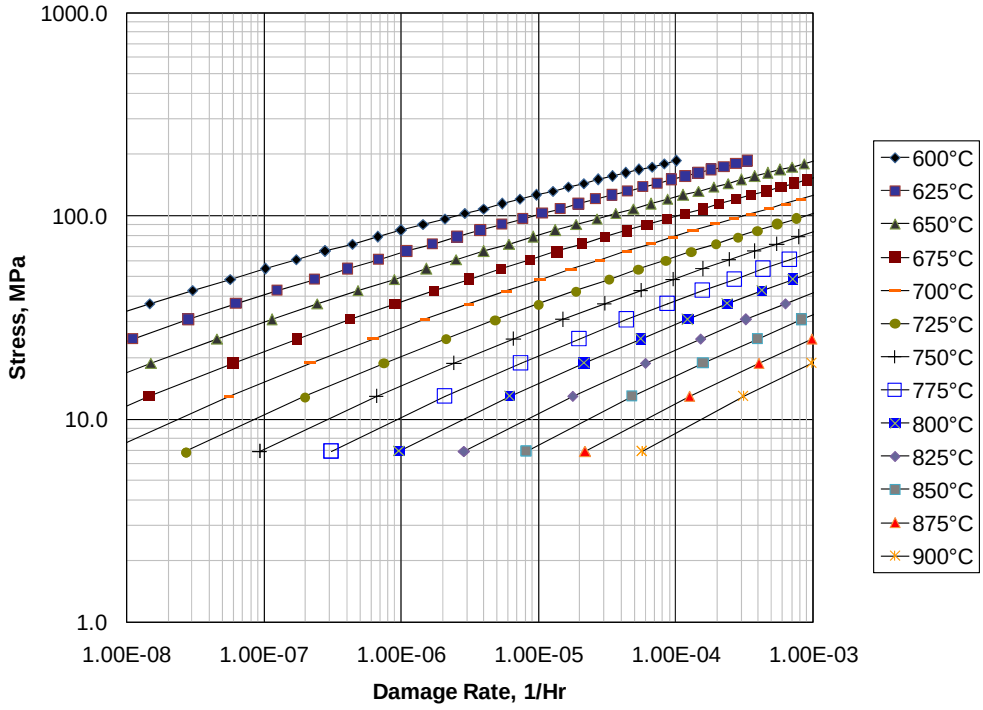

b) Damage Curve

Figure 10.17M – Level 1 Screening Criteria for AISI Type 316 & 316H

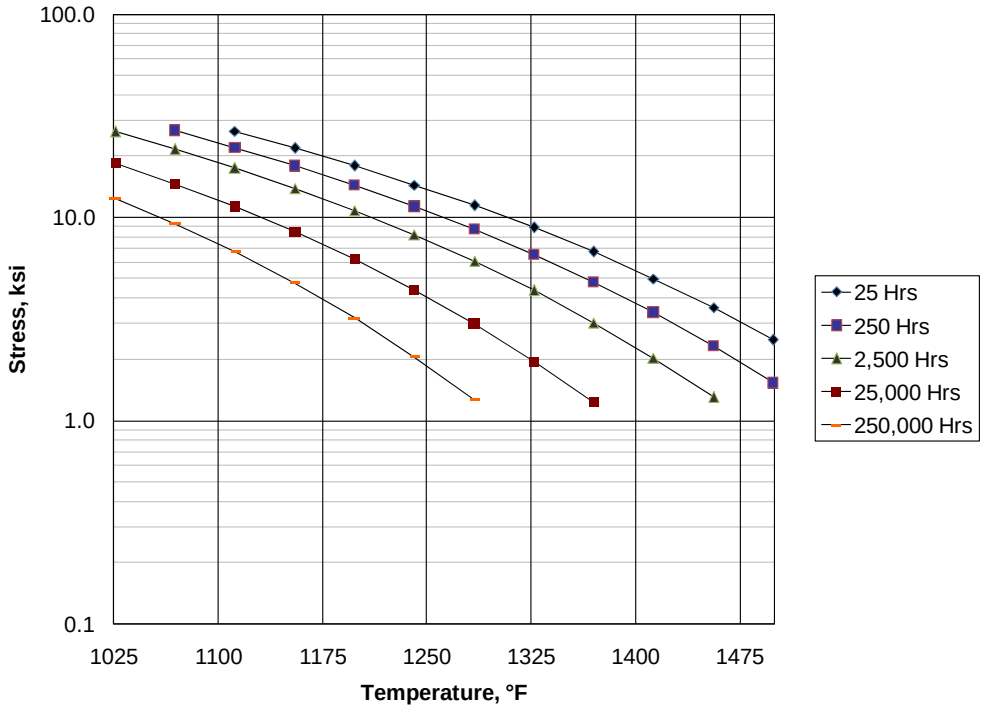

a) Screening Curve

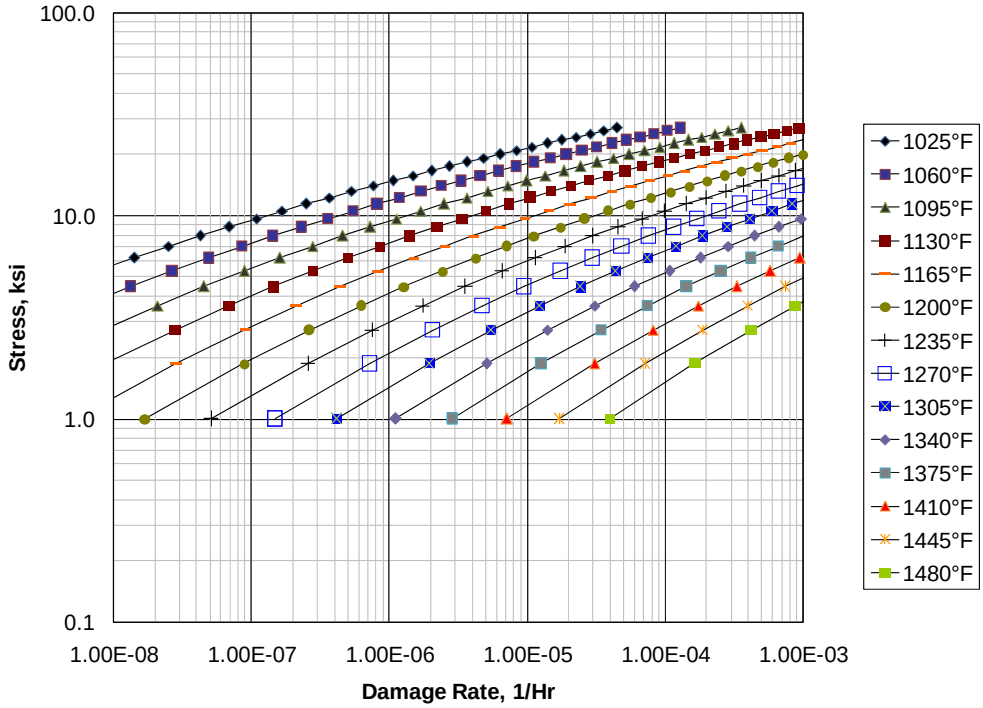

b) Damage Curve

Figure 10.18 – Level 1 Screening Criteria for AISI Type 321

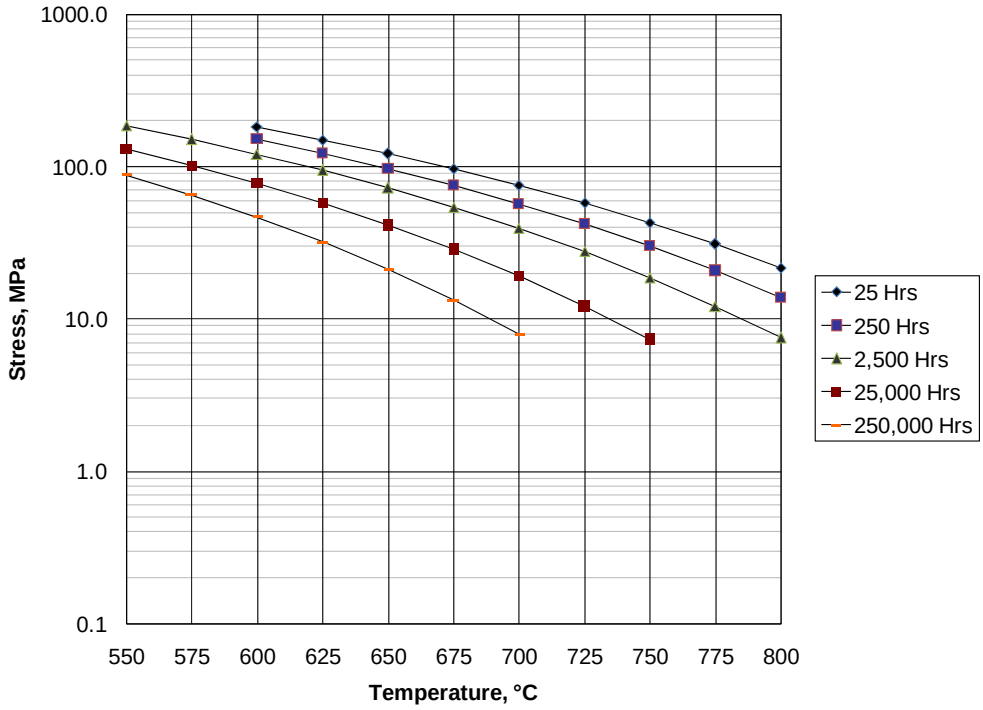

a) Screening Curve

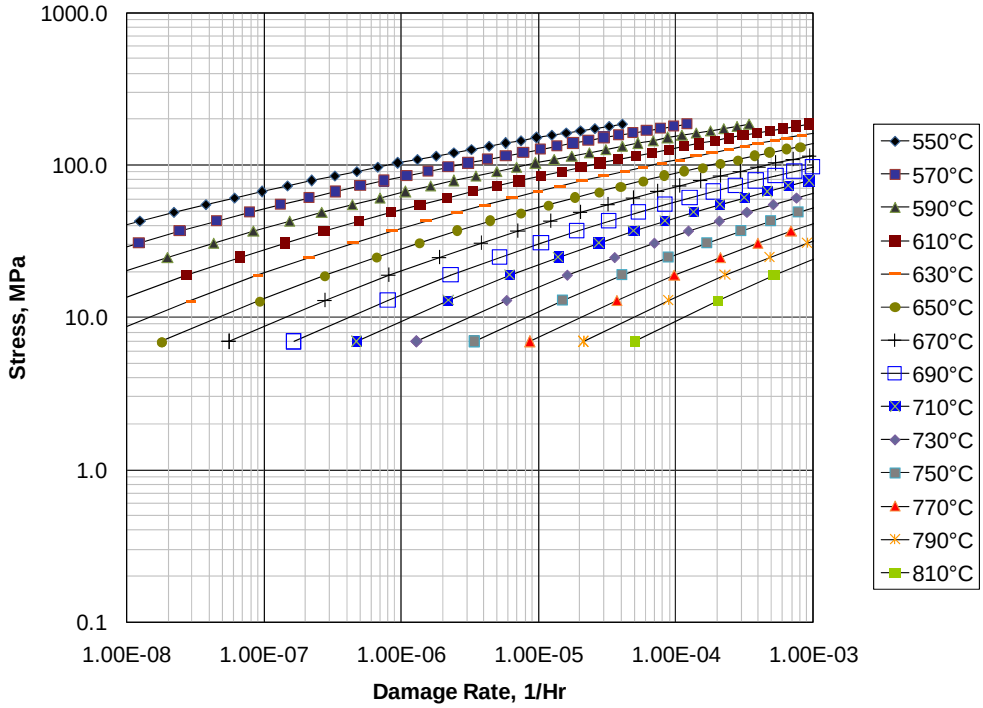

b) Damage Curve

Figure 10.18M – Level 1 Screening Criteria for AISI Type 321

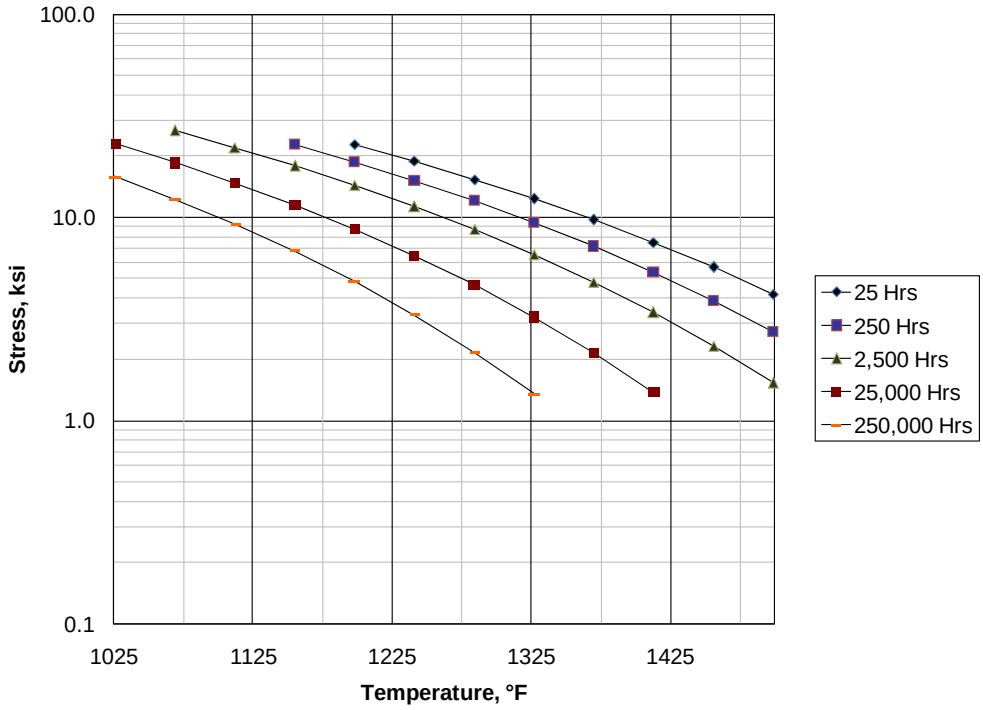

a) Screening Curve

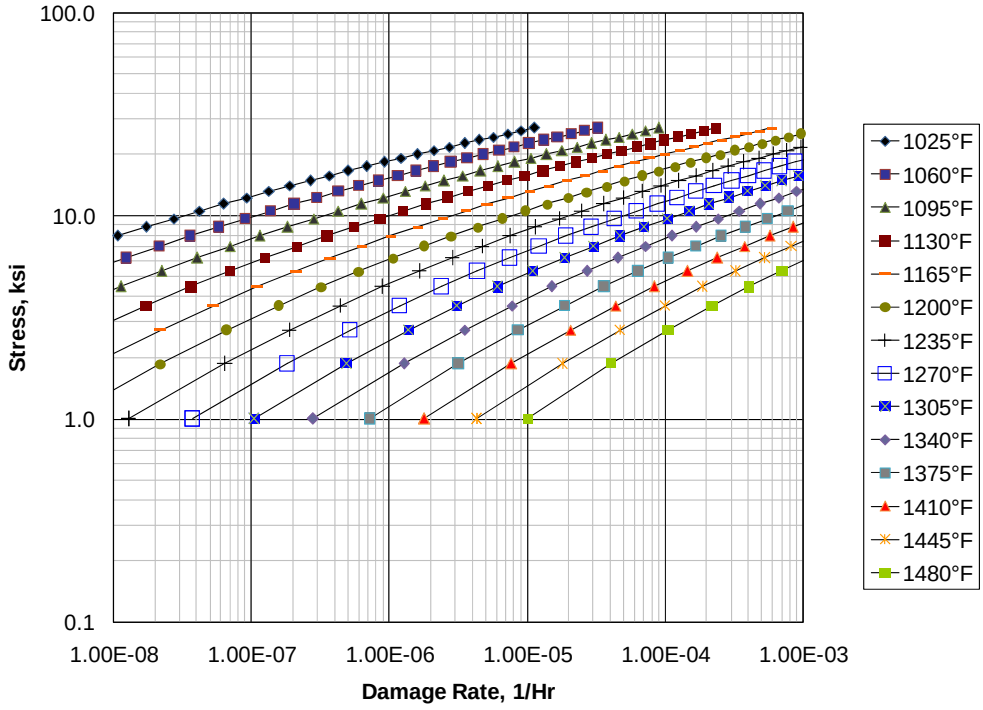

b) Damage Curve

Figure 10.19 – Level 1 Screening Criteria for AISI Type 321H

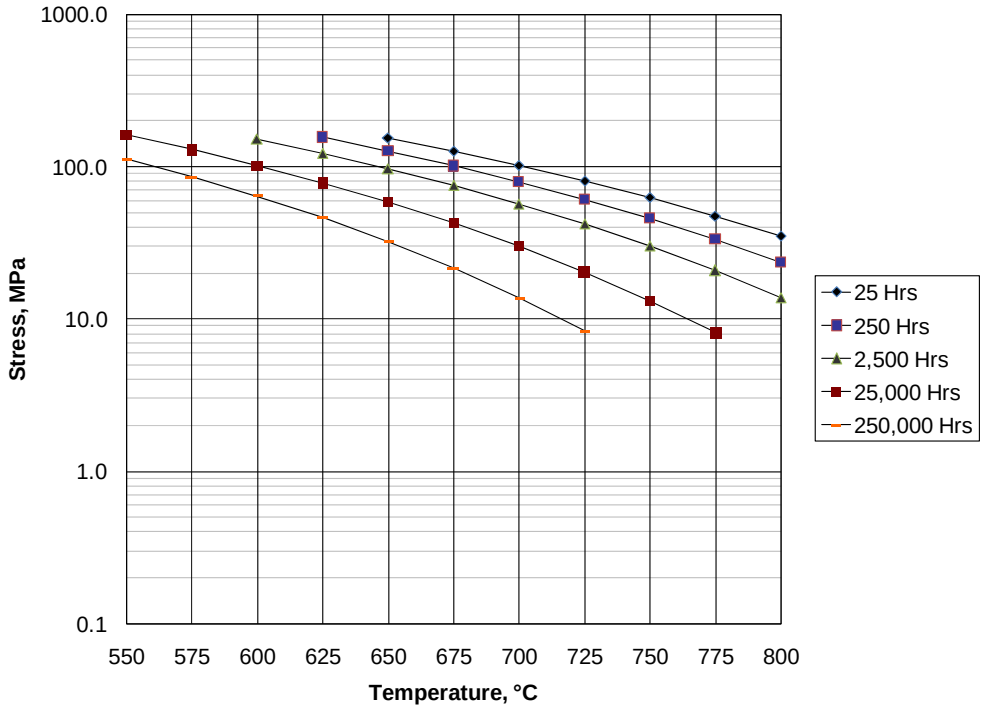

a) Screening Curve

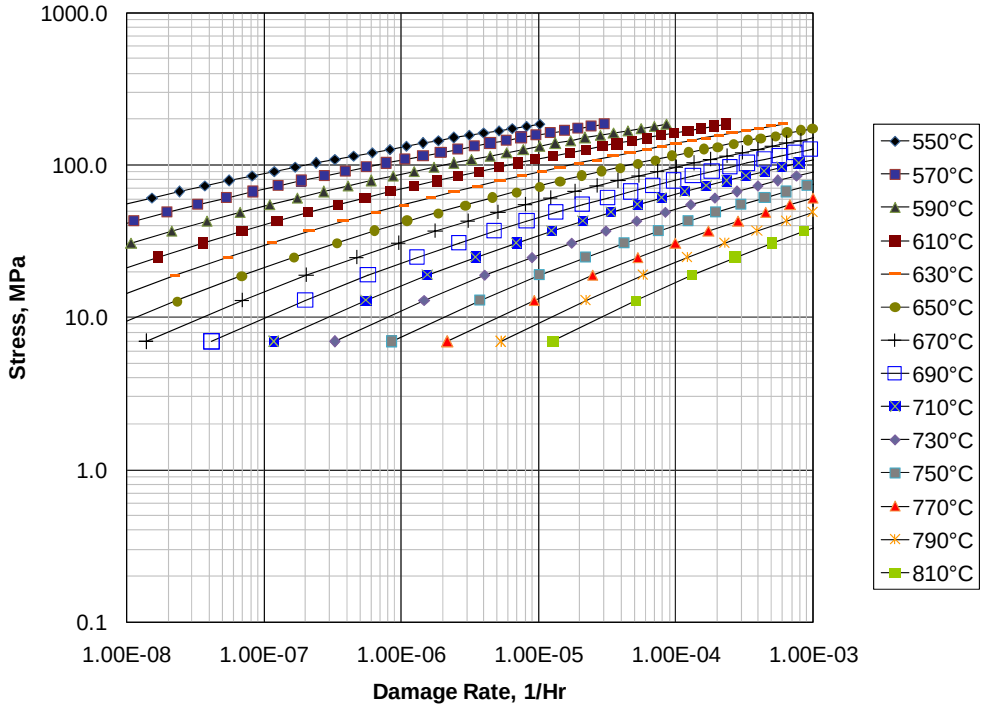

b) Damage Curve

Figure 10.19M – Level 1 Screening Criteria for AISI Type 321H

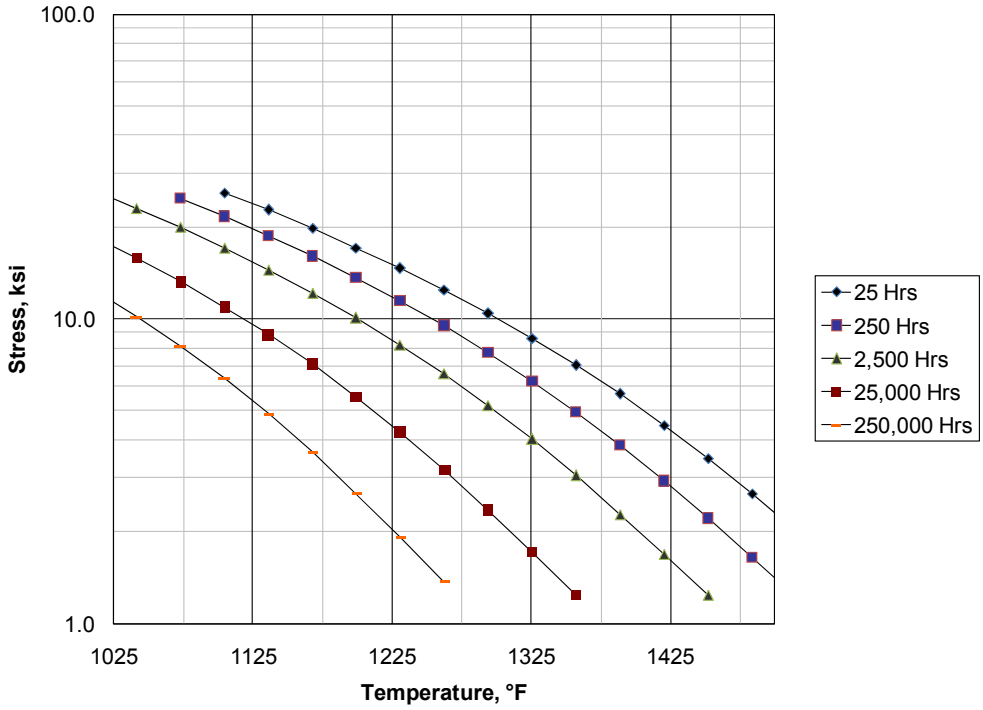

a) Screening Curve

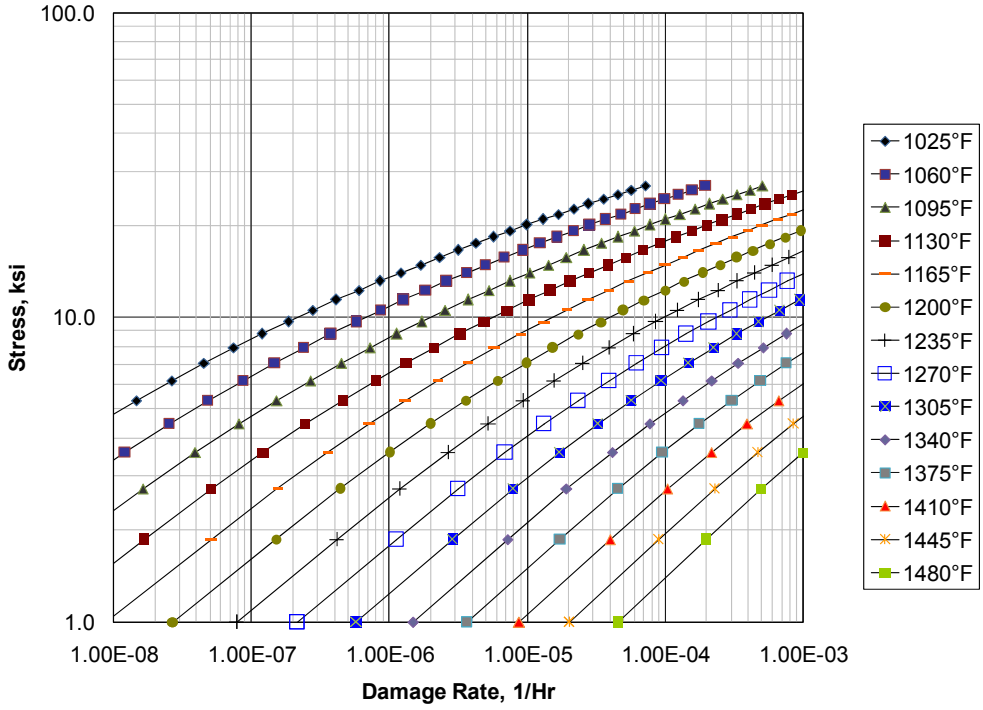

b) Damage Curve

Figure 10.20 – Level 1 Screening Criteria for AISI Type 347

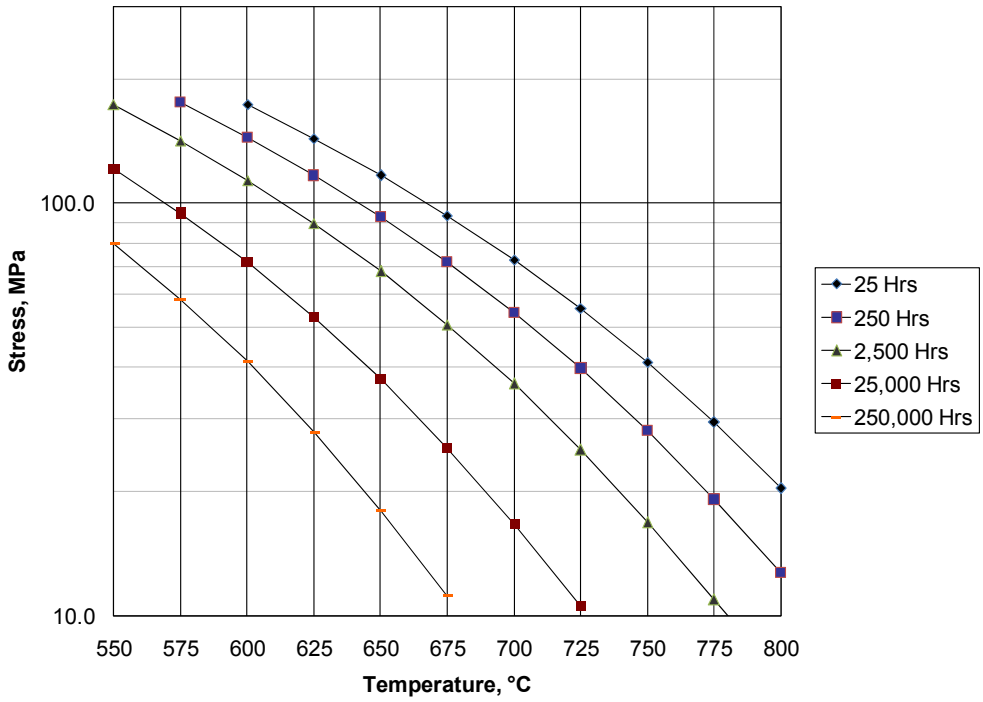

a) Screening Curve

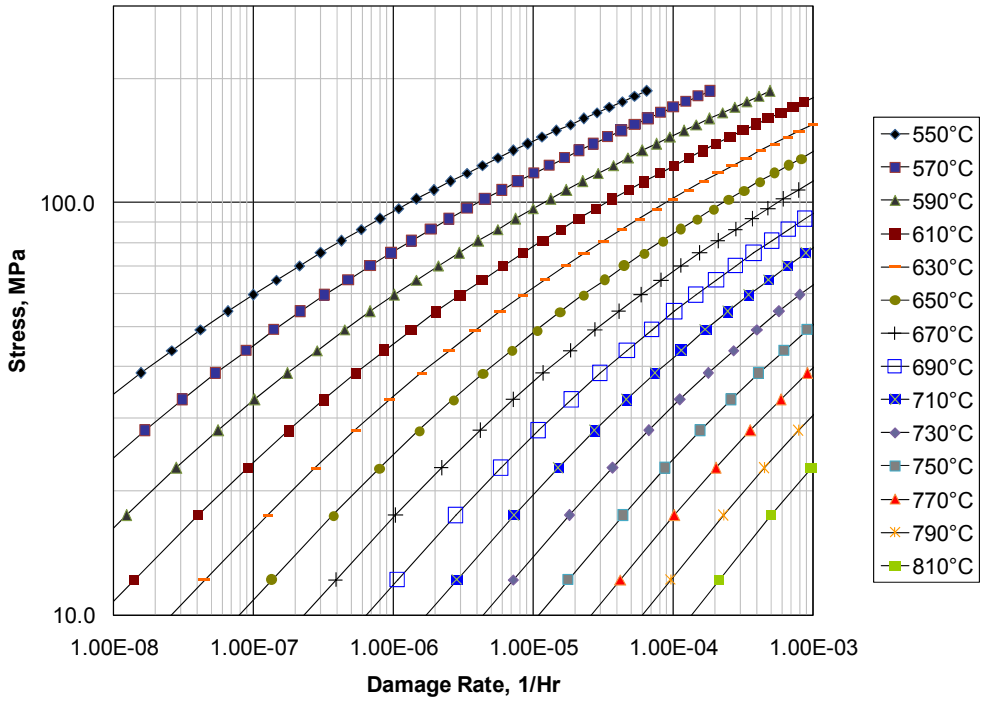

b) Damage Curve

Figure 10.20M – Level 1 Screening Criteria for AISI Type 347

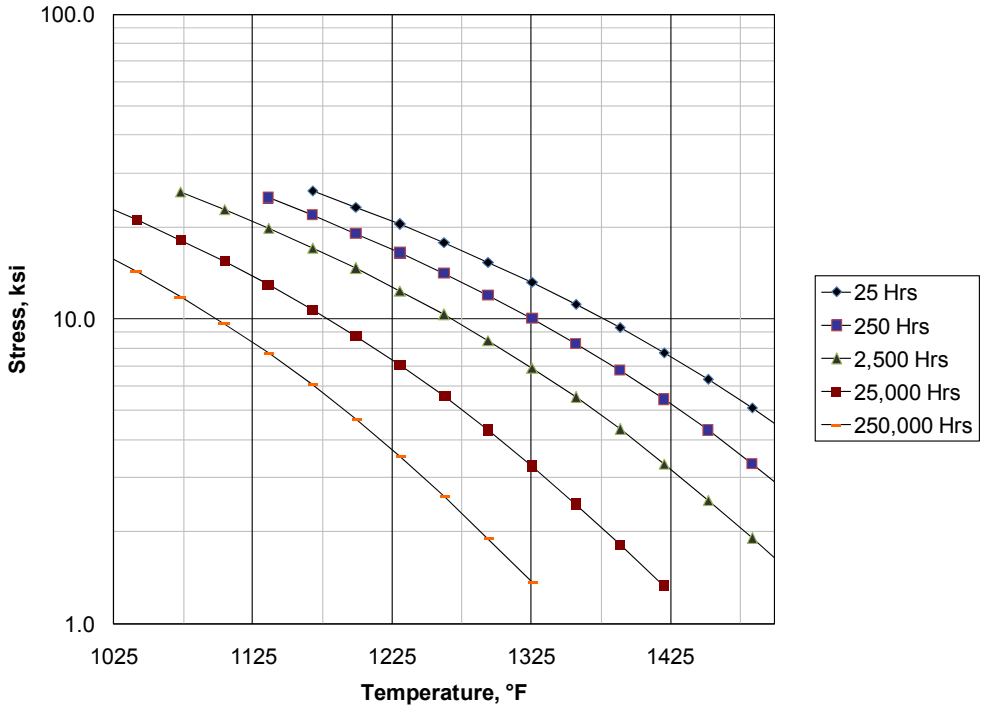

a) Screening Curve

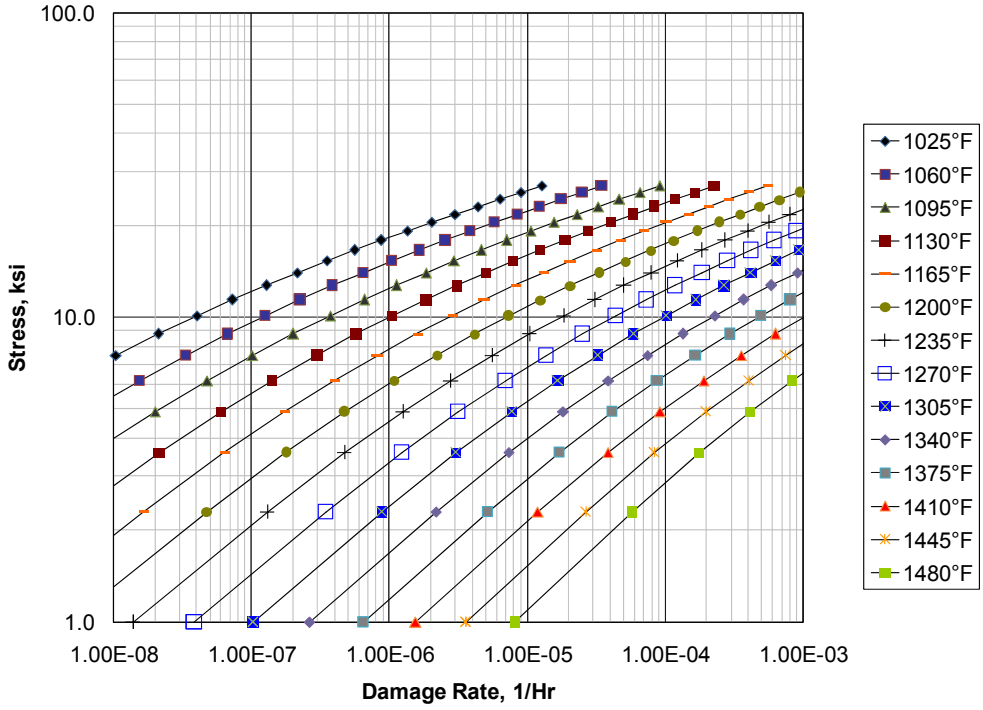

b) Damage Curve

Figure 10.21 – Level 1 Screening Criteria for AISI Type 347H

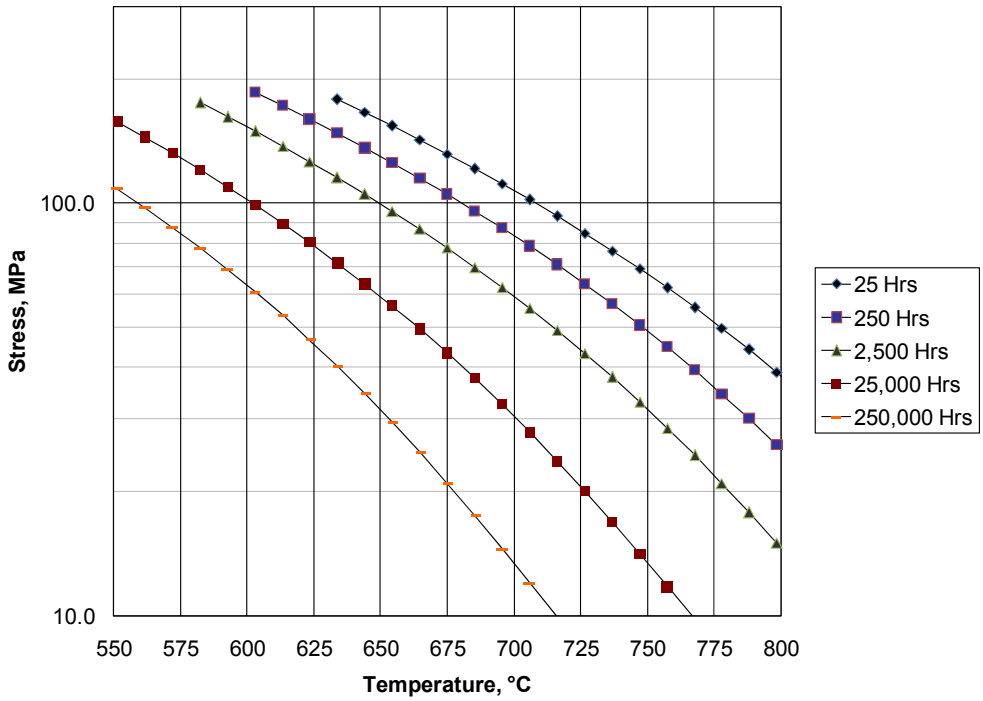

a) Screening Curve

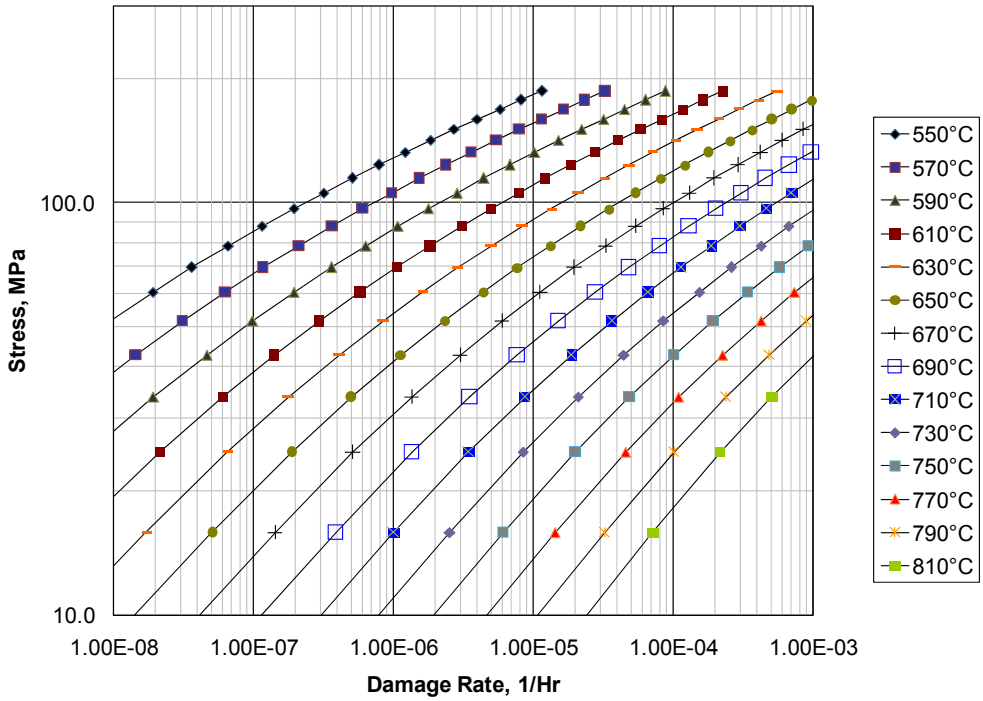

b) Damage Curve

Figure 10.21M – Level 1 Screening Criteria for AISI Type 347H

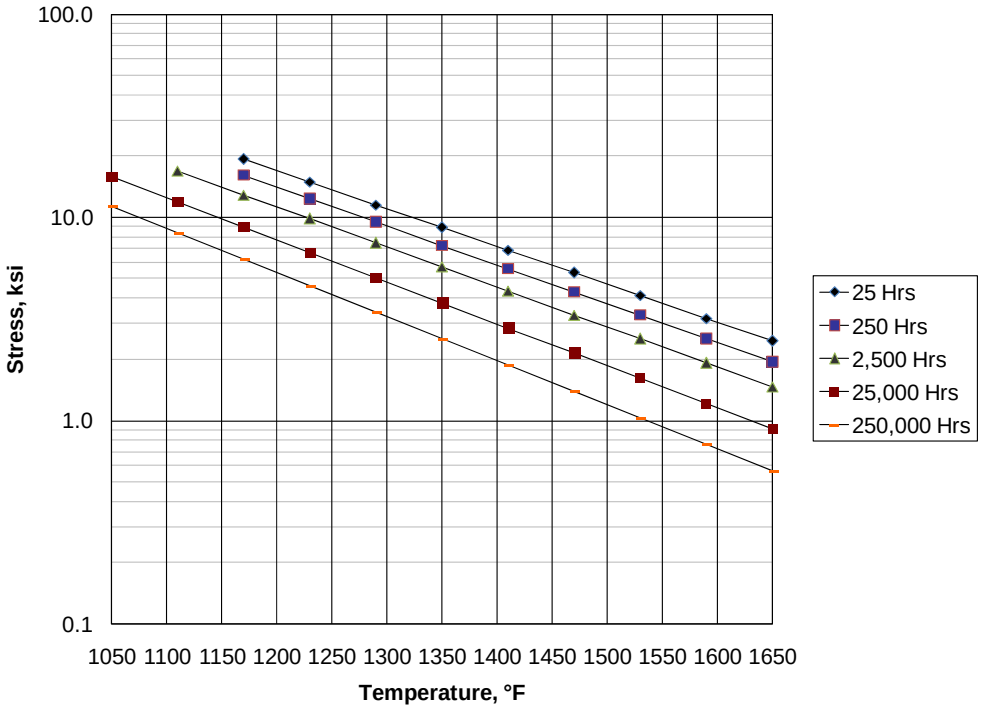

a) Screening Curve

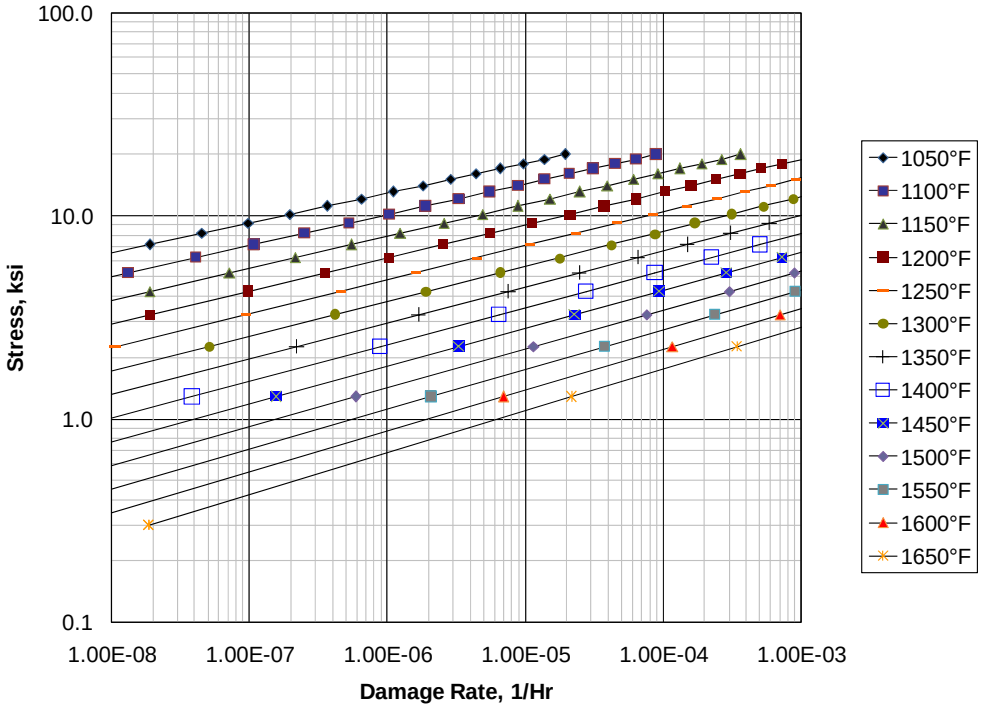

b) Damage Curve

Figure 10.22 – Level 1 Screening Criteria for Alloy 800

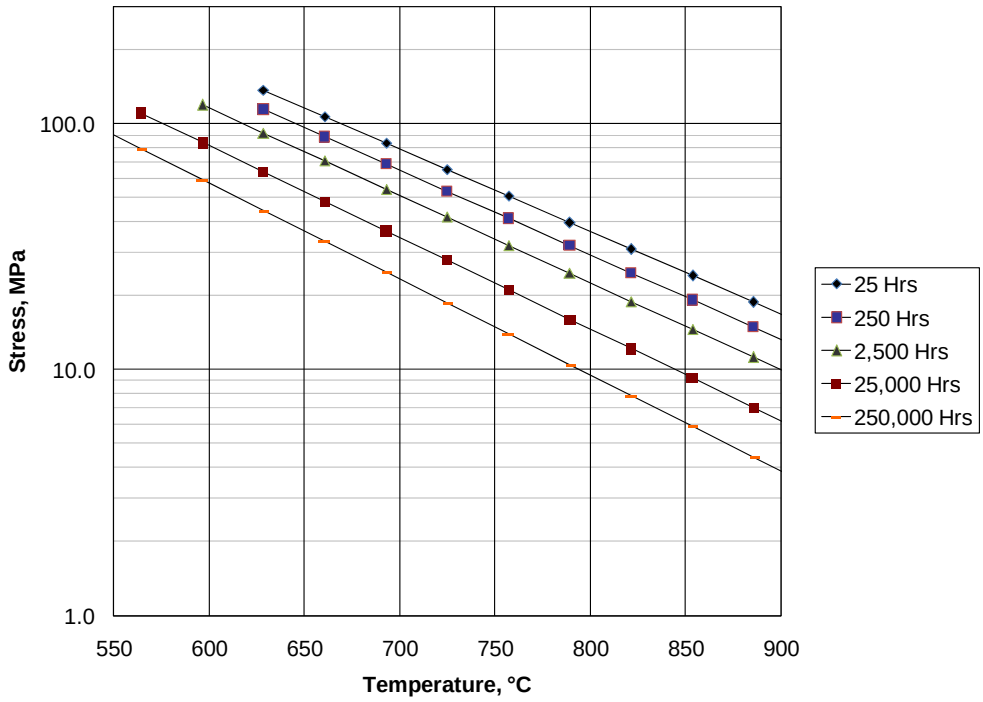

a) Screening Curve

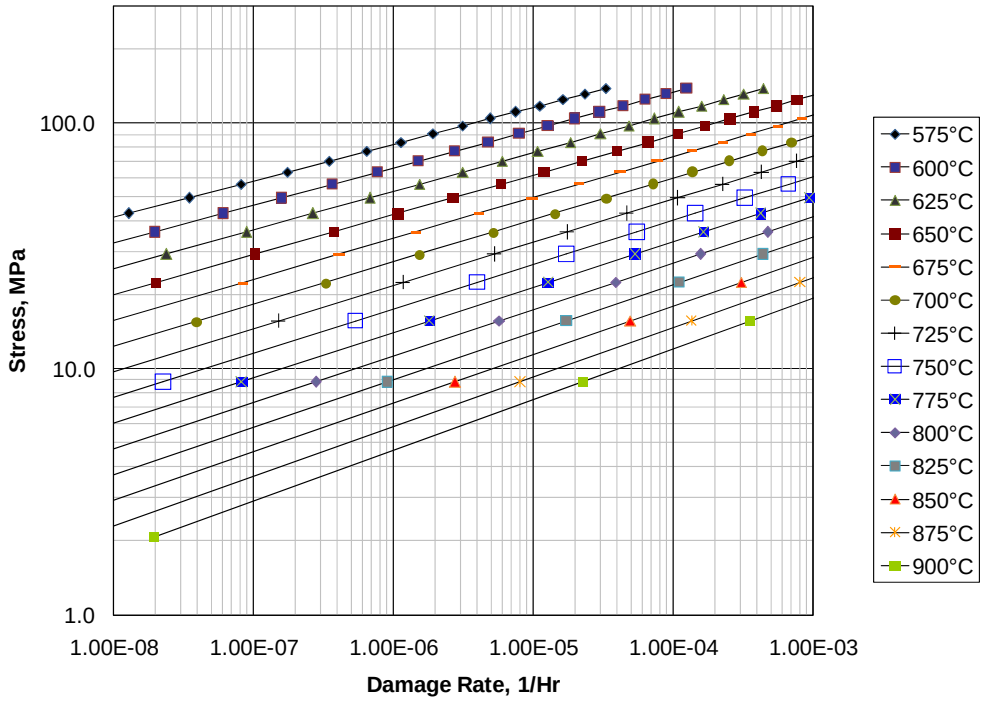

b) Damage Curve

Figure 10.22M – Level 1 Screening Criteria for Alloy 800

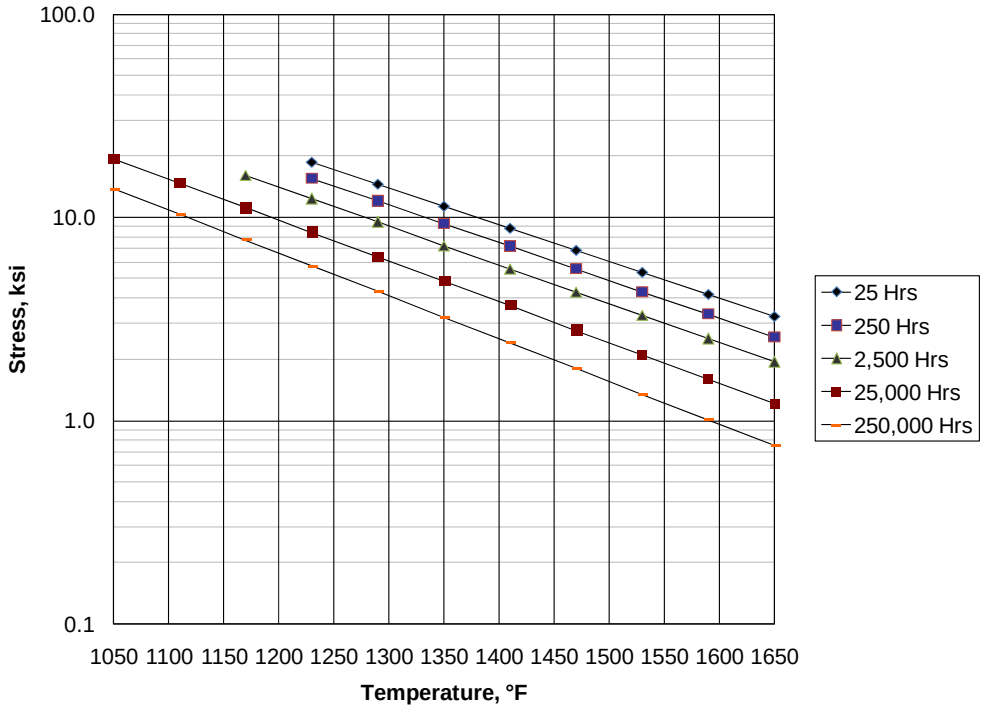

a) Screening Curve

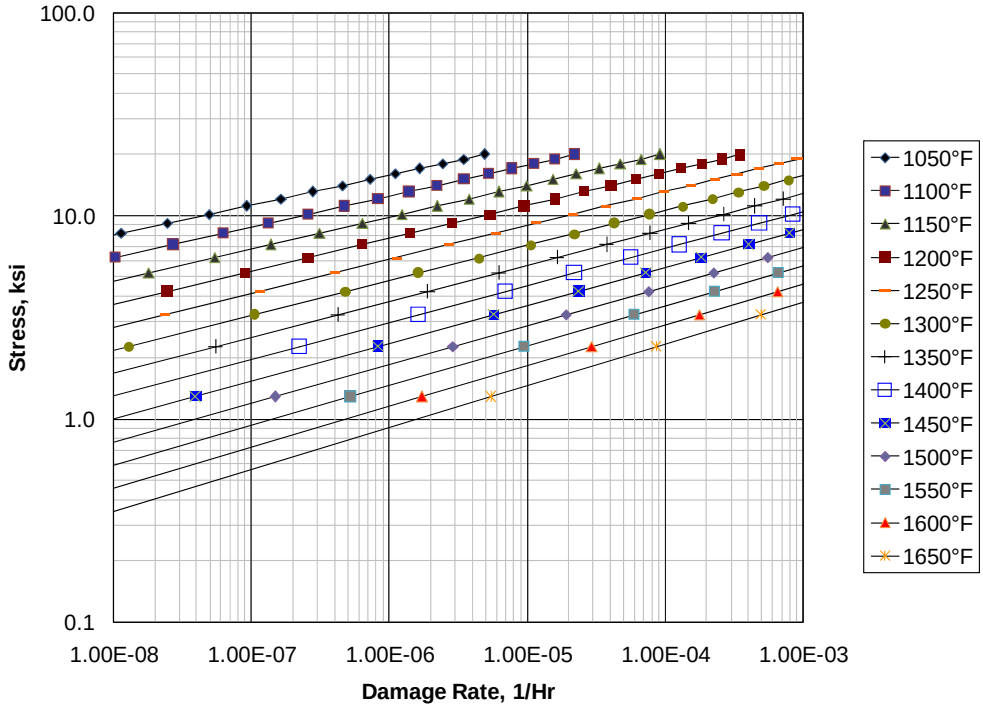

b) Damage Curve

Figure 10.23 – Level 1 Screening Criteria for Alloy 800H

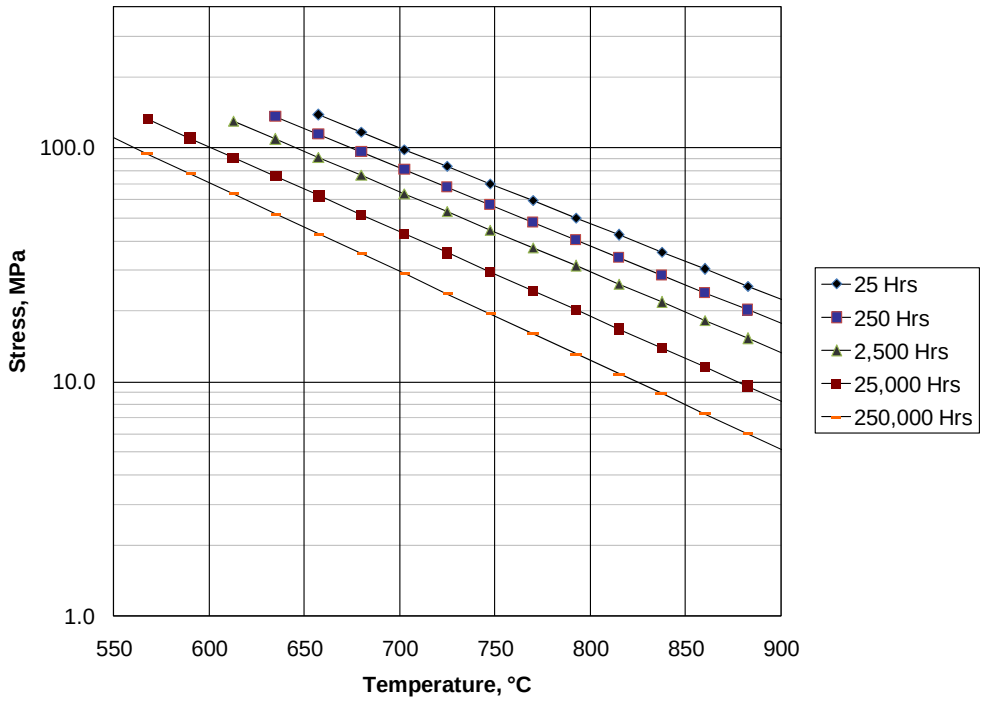

a) Screening Curve

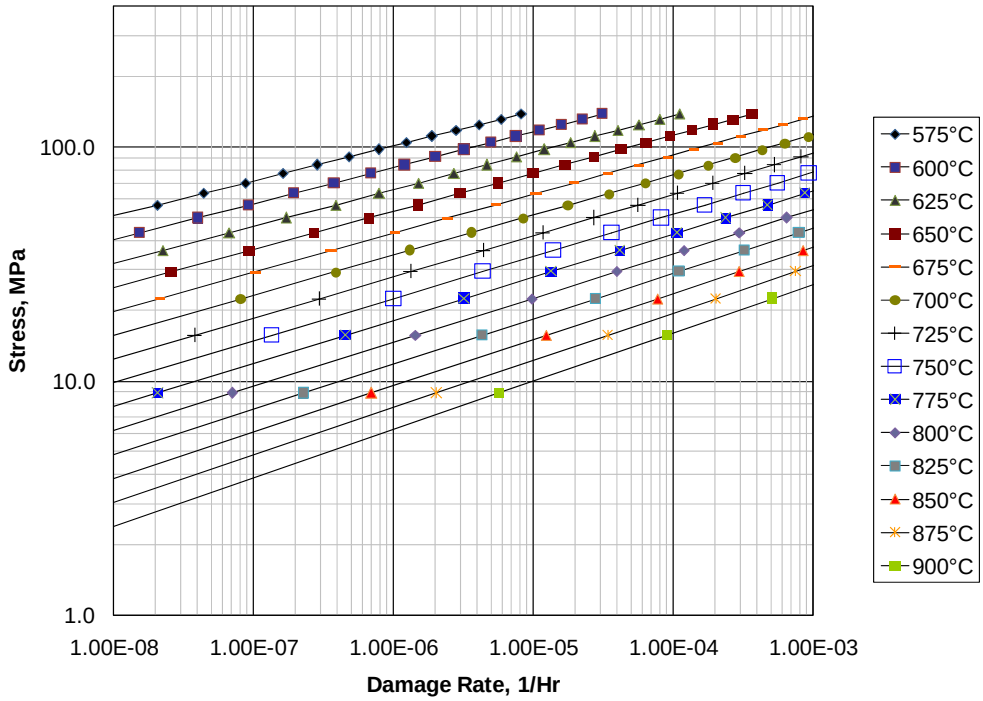

b) Damage Curve

Figure 10.23M – Level 1 Screening Criteria for Alloy 800H

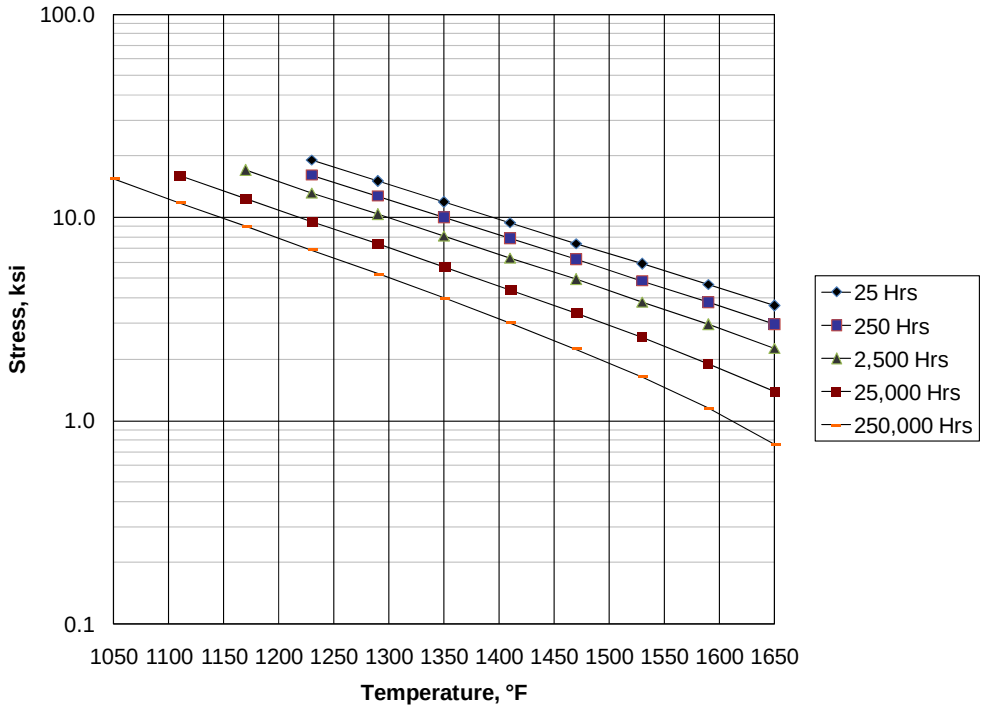

a) Screening Curve

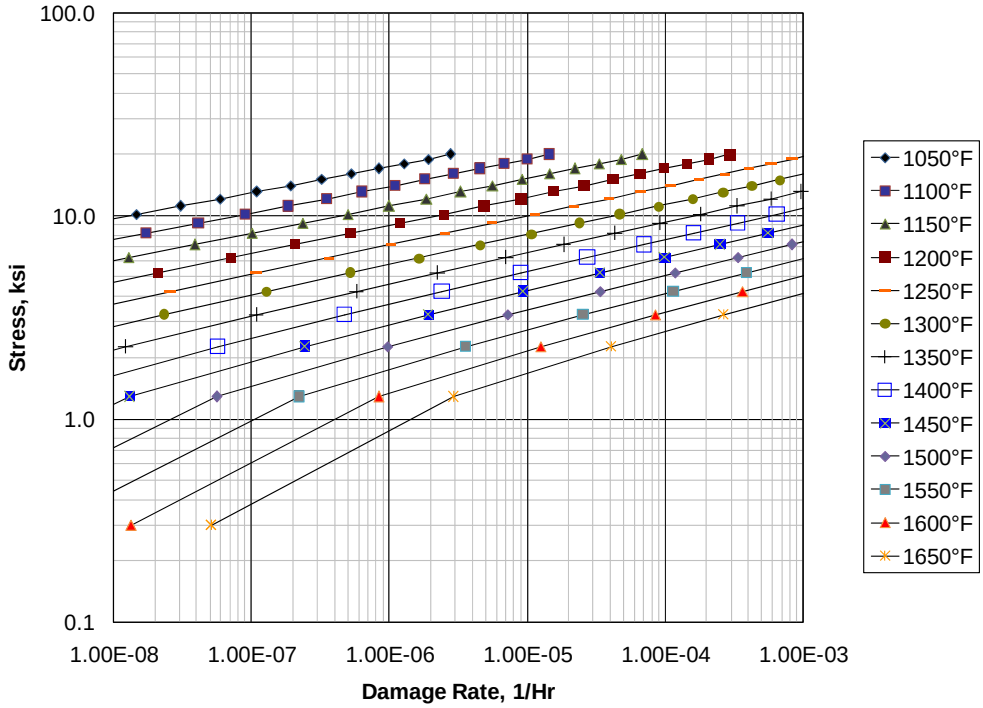

b) Damage Curve

Figure 10.24 – Level 1 Screening Criteria for Alloy 800HT

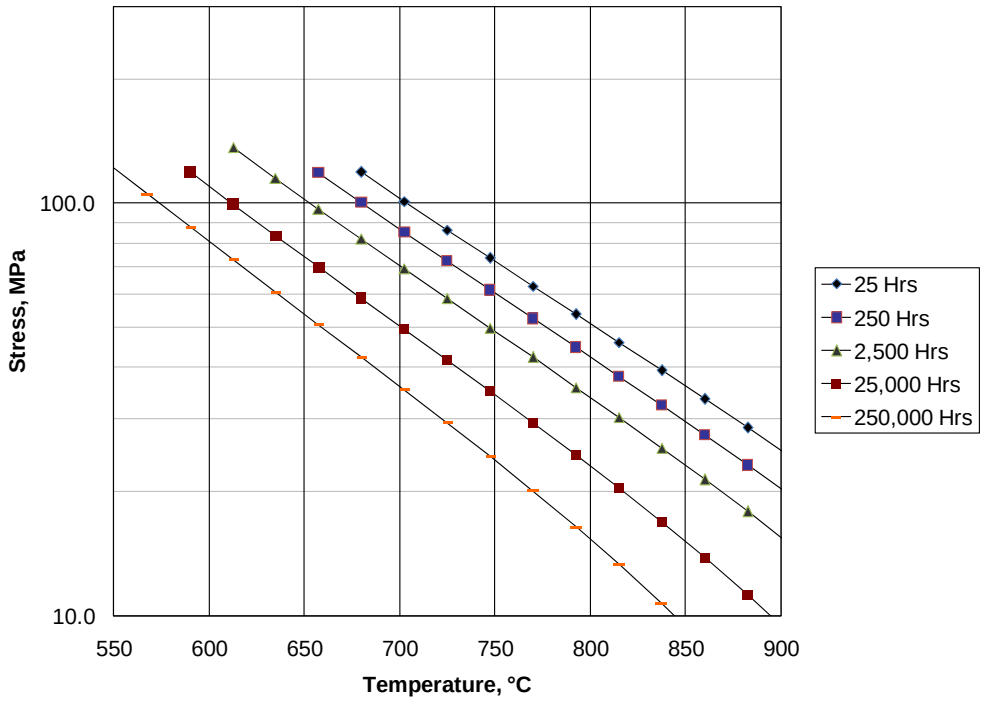

a) Screening Curve

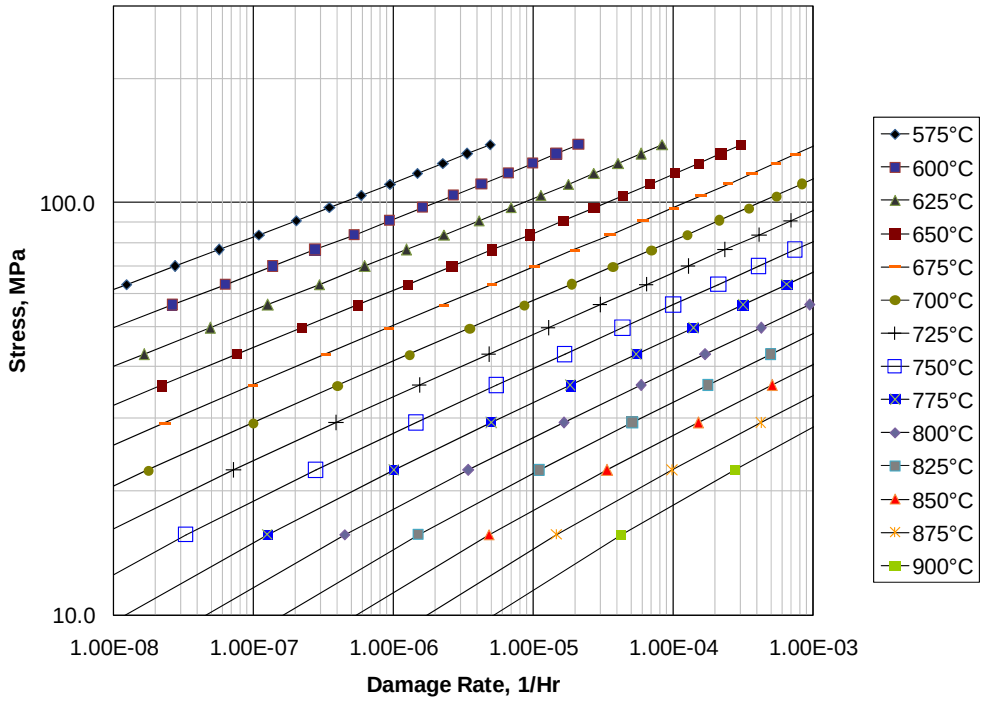

b) Damage Curve

Figure 10.24M – Level 1 Screening Criteria for Alloy 800HT

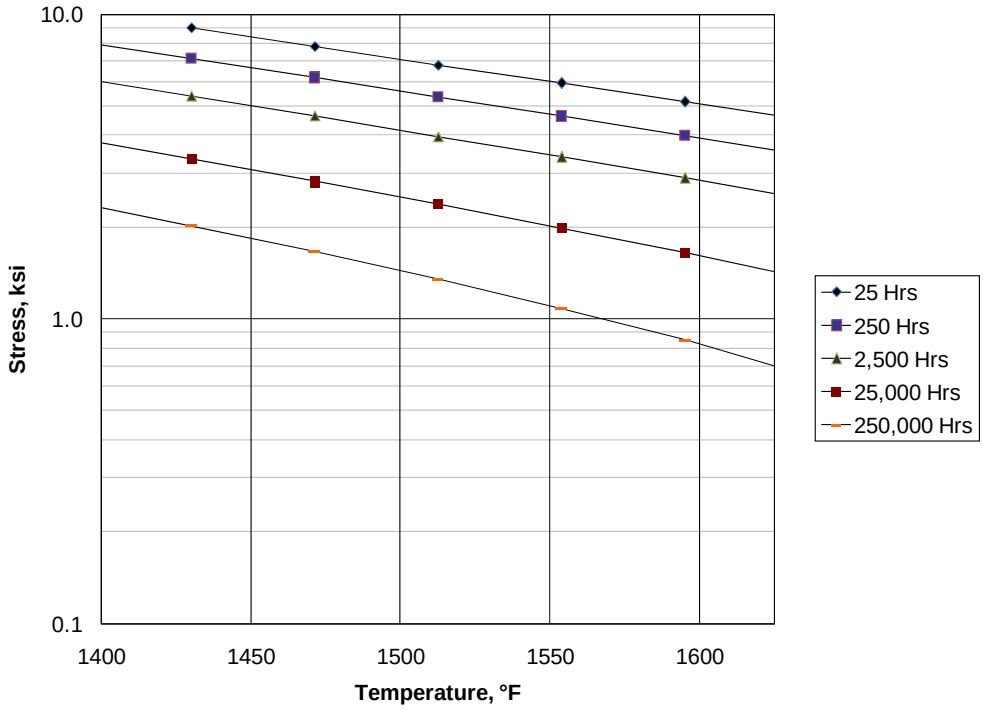

a) Screening Curve

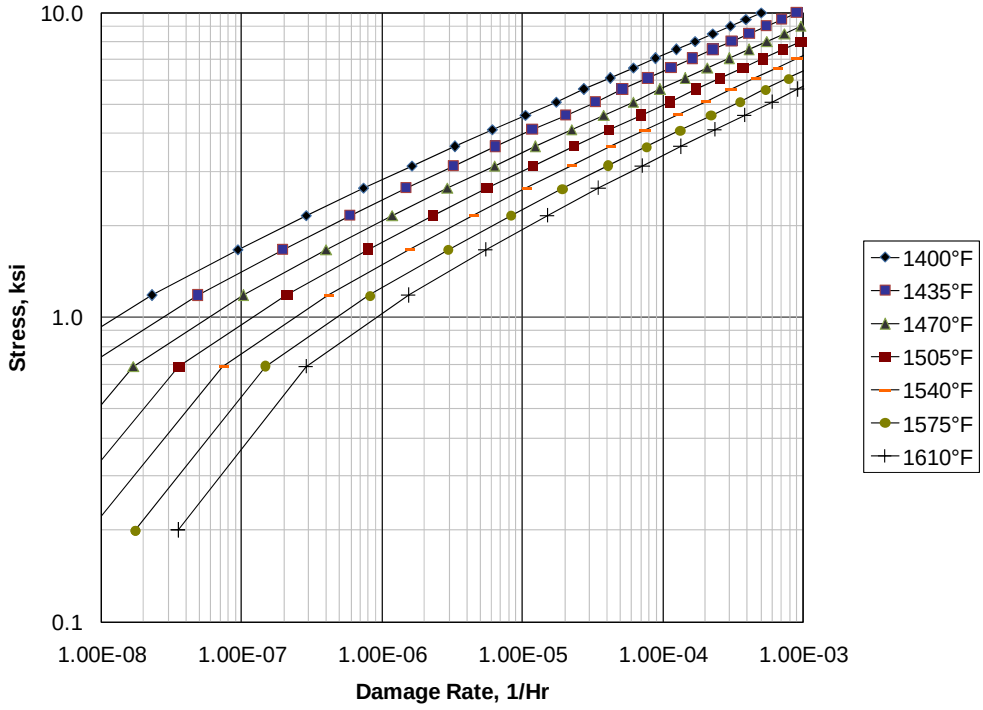

b) Damage Curve

Figure 10.25 – Level 1 Screening Criteria for HK-40

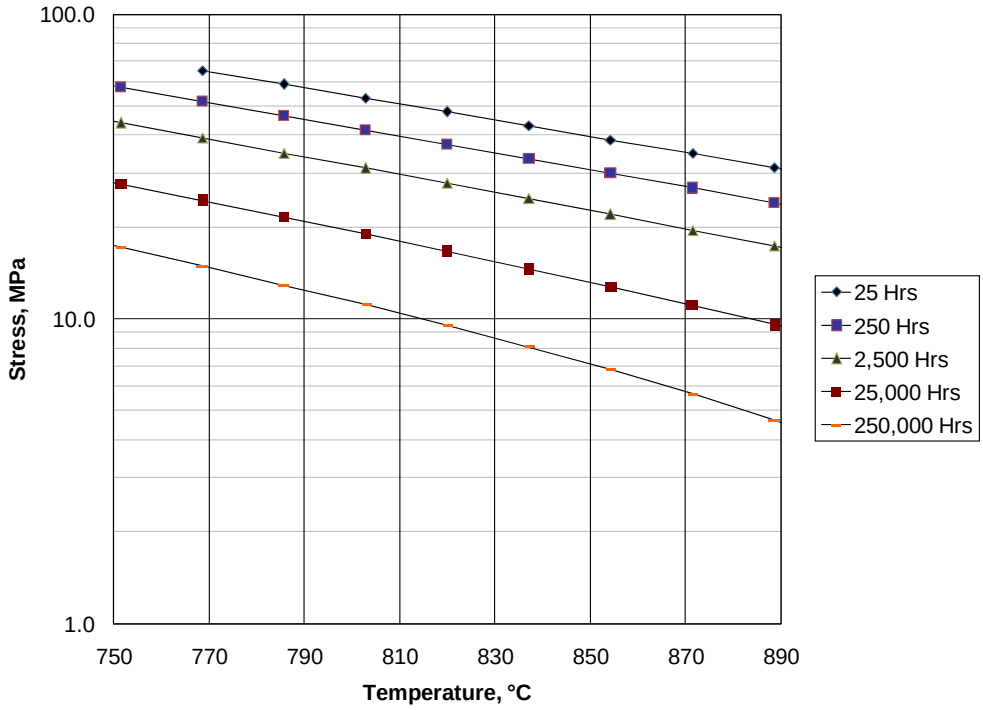

a) Screening Curve

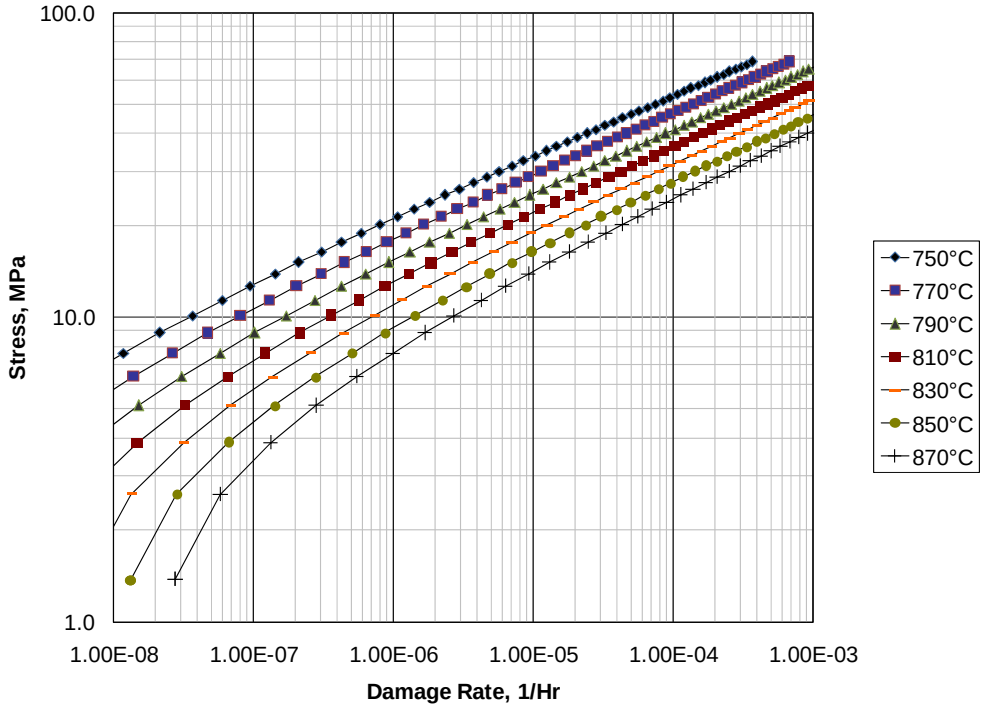

b) Damage Curve

Figure 10.25M – Level 1 Screening Criteria for HK-40

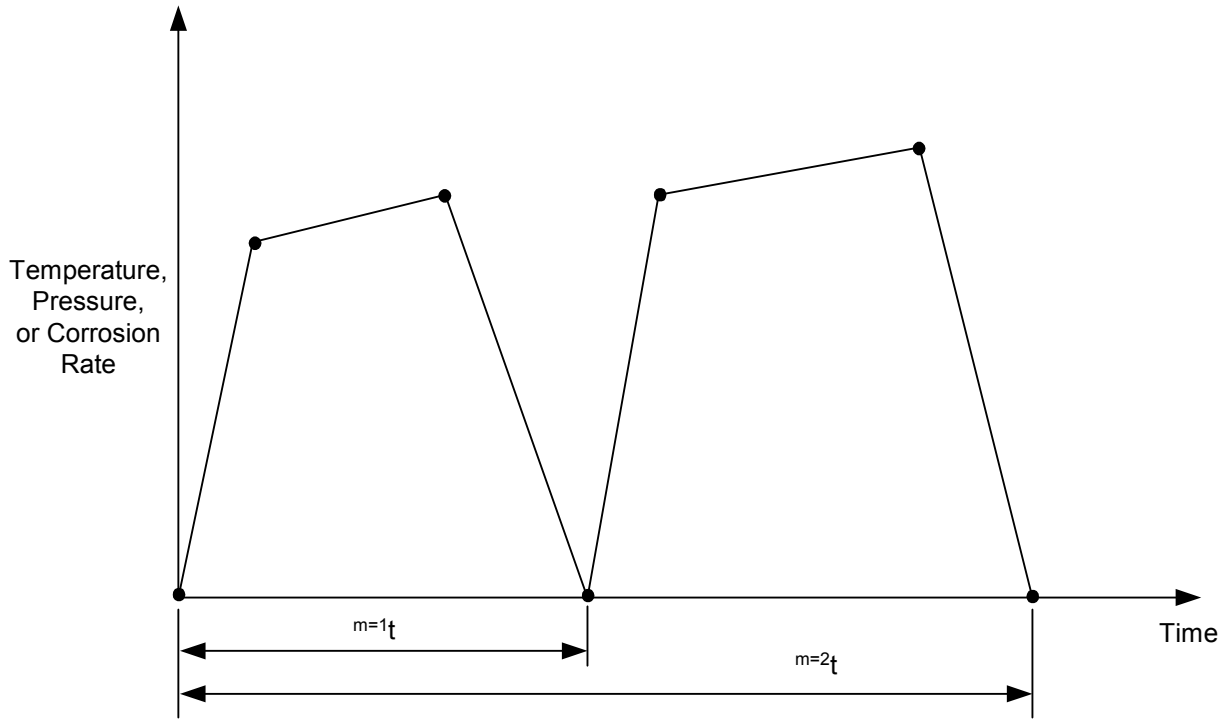

Figure 10.26 – Definition of Multiple Cycles in a Load Histogram

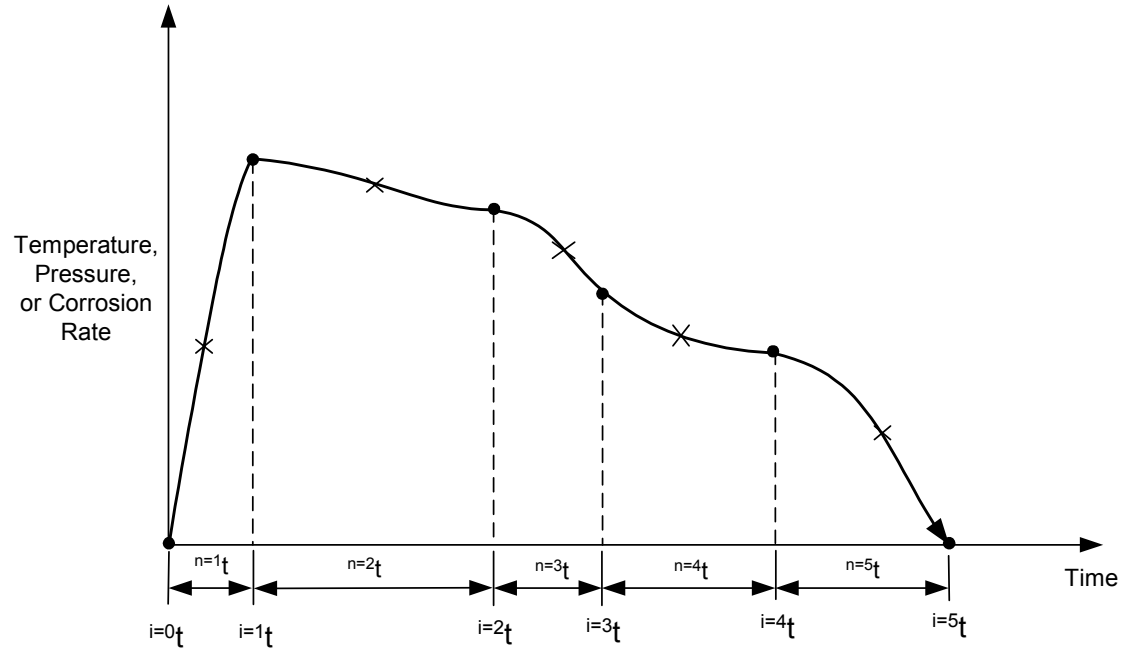

(a) Actual Parameter Variation

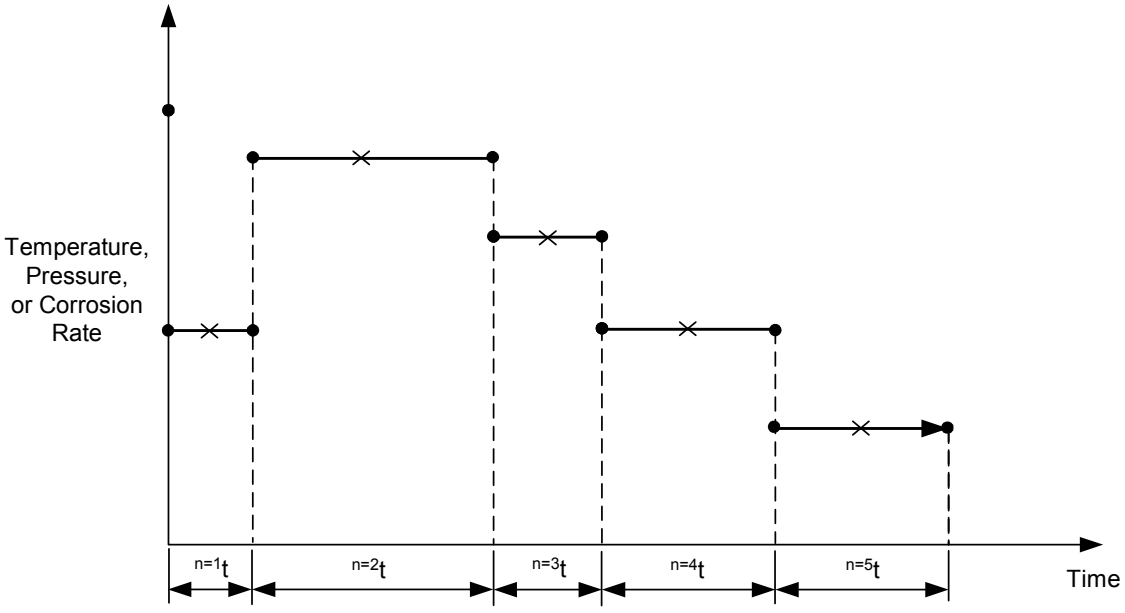

(b) Idealized Parameter Variation Using Average Values Of Parameters

Figure 10.27 – Modeling Of Time Increments In A Cycle For A Remaining Life Calculation

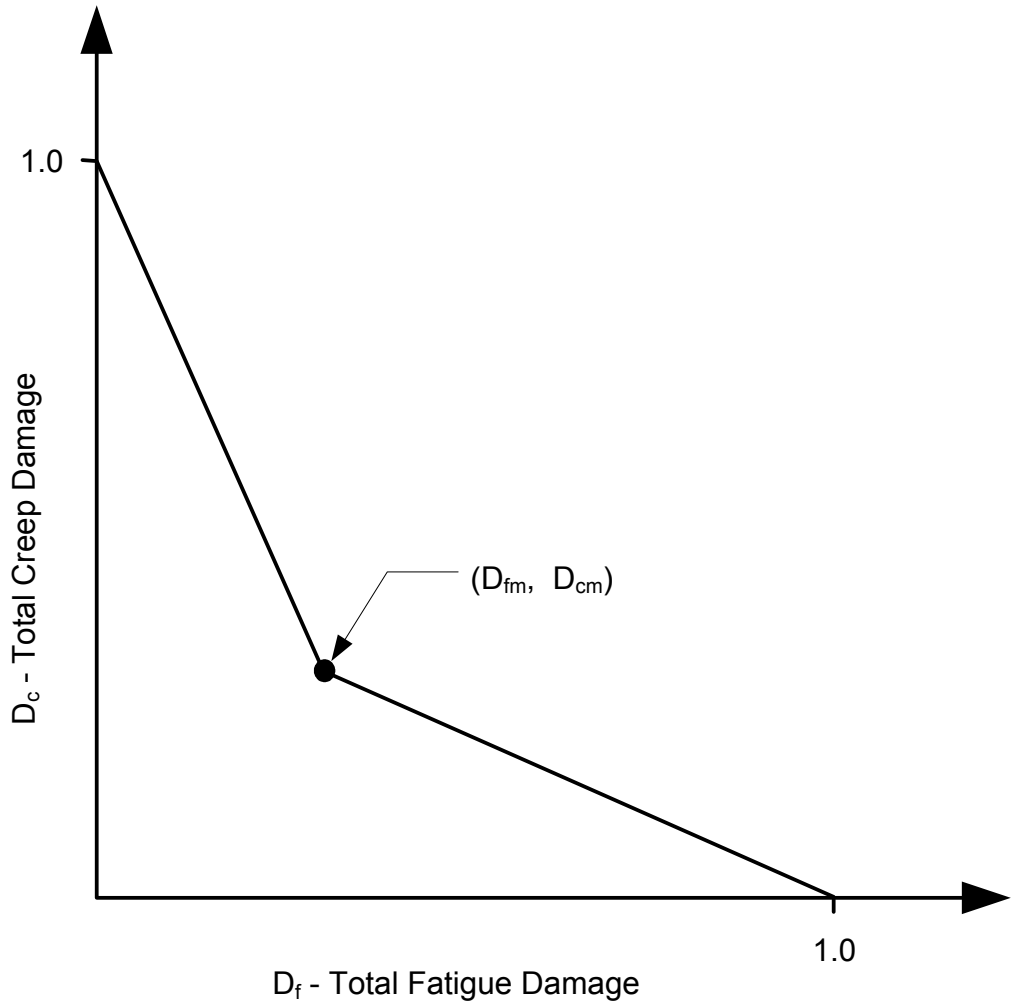

Material Parameters to Define the Acceptable Creep-Fatigue Envelope

Material	D_{fm}	D_{cm}
Carbon Steels	0.15	0.15
Low Alloy Steels	0.15	0.15
Type 304 SS	0.30	0.30
Type 316 SS	0.30	0.30
Alloy 800H	0.15	0.15

Figure 10.28 – Creep Fatigue Damage Acceptance Criterion

PART 11

ASSESSMENT OF FIRE DAMAGE

PART CONTENTS

11.1 General

11.1.1 Fitness-For-Service (FFS) assessment procedures for evaluating pressure vessels, piping and tanks subjected to flame impingement and the radiant heat of a fire are covered in this Part. These assessment procedures address the visually observable structural degradation of components and the less apparent degradation of mechanical properties, such as strength, ductility, and toughness.

11.1.2 This Part provides FFS procedures for pressurized components (i.e. internal and/or external pressure) that are potentially damaged by exposure to a fire. Typically, this is due to a plant fire external to the component. However, these procedures are just as applicable for process upsets due to a chemical reaction within process vessels. Guidelines are given to assist in the identification of components that require a Fitness-For-Service evaluation before being returned to service. Some of these guidelines can assist in rerating components that have been judged to have experienced changes in mechanical properties due to exposure to a fire.

11.1.3 The general forms of damage that should be considered include:

a) Mechanical distortion and structural damage,

b) Degradation of mechanical properties,

c) Degradation of metallurgical microstructure,

d) Degradation in corrosion resistance and susceptibility to environmental cracking and creep damage,

e) Presence of crack-like flaws in the pressure boundary, and

f) Residual stress changes.

11.1.4 If the results of the Fitness-For-Service evaluation indicate that the equipment is not suitable for current design conditions, then one of the following methods may be used.

a) A new maximum allowable working pressure, $MAWP$, (or tank maximum fill height, MFH), maximum design temperature, and/or minimum design metal temperature may be established using the appropriate evaluation procedures contained in other Parts of this standard.

b) Defective sections of the equipment may be repaired or replaced.

c) The equipment may be retired from service.

11.1.5 A flow chart for the assessment procedure for components subject to fire damage or overheating due to a process upset is shown in Figure 11.1.

11.2 Applicability and Limitations of the Procedure

11.2.1 This Part includes procedures that may be used to identify and evaluate components subject to fire damage or overheating due to a process upset.

11.2.2 The pressurized equipment covered in this Part includes all pressure boundary components of pressure vessels, piping, and shell courses of storage tanks. Fitness-For-Service procedures for fixed and floating roofs and bottom plates of storage tanks are covered in Part 2 of API-653.

11.2.3 Structural steel, ladders and platforms are usually distorted during a fire. This Part does not address such non-pressure containing components although information concerning non-pressure components may be helpful in assessing pressurized components. The distortion of equipment extremities such as nozzles and platforms does not necessarily mean that the pressure envelope of the equipment is no longer suitable for continued service. The process fluid inside the vessel could have served as a cooling medium during the fire, thus preventing degradation of mechanical properties.

11.2.4 Instrumentation and wiring are generally destroyed in and around the area affected by a fire. The assessment of instrumentation and wiring are not addressed in this Part.

11.3 Data Requirements

11.3.1 Original Equipment Design Data

An overview of the original equipment data required for an assessment is provided in Part 2, paragraph 2.3.1.

11.3.2 Maintenance and Operational History

An overview of the maintenance and operational history required for an assessment is provided in Part 2, paragraph 2.3.2.

11.3.3 Required Data/Measurements for A *FFS* Assessment

11.3.3.1 Fire Damage Evidence

a) Evidence of fire damage may be collected both during the course of a fire and after the fire is extinguished. The objective of collecting such evidence is twofold:

   1) to determine why the fire occurred, and

   2) to determine the nature and extent of damage so that equipment may be returned to service.

b) Since an accidental fire is a random event, extensive data collection during an accidental fire is seldom possible. However, alert observers can learn significant facts about fires in progress that can help to determine the appropriate boundaries of potential damage

c) Industrial plant fires take many different forms. Some are confined to a rather small area while others are widespread or may have multiple fire sites or sources. The investigator must be alert to such possible variations when studying the fire scene. Flame patterns are often irregular and there may be equipment farther from the flame source that are more severely damaged than equipment closer to the source, because of wind direction, heat flow, insulation differences, fire monitors, etc.

d) Although each fire investigation is unique, data should normally be collected to determine:

   1) The temperature extremes to which various components were subjected,

   2) The nature of the fuel,

   3) The location of ignition source or sources,

   4) The time at temperature, and

   5) The cooling rate.

e) Of the items in (d) above, the first three may typically be obtained without difficulty. The time at temperature can often be deduced from logbooks and fire department records. An estimate of the cooling rate is the most difficult to determine and may only be qualitative for materials that respond to thermal treatment.

f) Where circumstances and manpower permit, a videotape of a fire in progress can be an extremely useful tool for analyzing the nature and extent of fire damage. A fire in progress is always dangerous and could be unpredictable. Videotaping a fire in progress should be supervised by the fire marshal or incident commander in control of the scene. However, when videotape evidence is available, it could be possible to deduce the nature of the fuel, the fire's progression from its ignition source, and temperature extremes from visual evidence on the tape.

g) The initial damage investigation at the fire scene should be thoroughly documented with photographs for later study. Debriefing of plant personnel should occur as soon as possible after the fire is extinguished. Videotaping of the site after the fire offers an excellent technique for recording the overview of the fire-damaged area.

11.3.3.2 Record of the Fire Incident

A record of the fire incident including, but not limited to, the following should be developed to help identify the equipment that needs to be evaluated before being returned to service.

a) A plot plan of the area showing the location of the equipment.

b) The locations of the primary and secondary fire sources, and wind direction during the incident should be shown on the plot plan.

c) The length of time of the incident.

d) The nature of the reactants (fuel) producing the flame in order to estimate flame temperatures and the compatibility of the reactants with the equipment.

e) The temperature, pressure and relief valve release data for the equipment prior to and during the incident. Note that in many instances computer storage of process operating conditions are retained for a limited time; therefore this information should be retrieved as soon as possible.

f) The location, flow directions and the type of water used by fire monitors and hoses to control the incident.

11.3.3.3 Heat Exposure Zones

The Heat Exposure Zone should be defined for each pressure vessel, tank and piping circuit subject to fire damage in order to determine the components that will require an assessment. A description of the Heat Exposure Zones is provided in Table 11.1.

a) A Heat Exposure Zone is established for a component based on the maximum exposure temperature incurred during the fire. This temperature is typically established after the fire is out, and is based on field observations and knowledge of the degradation associated with each exposure zone. The concept of a Heat Exposure Zone implies a physical region that was exposed to a certain temperature. This zone may be limited to only a portion of the equipment affected. The assignment of the Heat Affected Zone helps to screen equipment. However, adjacent components could have been exposed to different levels of heat and therefore suffered varying degree of damage, because one of the components was insulated or fireproofed while the other was not. The goal is to establish the Heat Exposure Zone for the pressure boundary. In the case of completely insulated or fireproofed equipment, the Heat Exposure Zone may be less than that for unprotected components. The Heat Exposure Zone may also be affected by the orientation of horizontal vessels and the shrouding of adjacent equipment.

b) A wide range of temperature-indicating observations may be used to categorize fire-damaged equipment into appropriate Heat Exposure Zones. The basis for these observations is knowledge of the changes of state that take place in materials as temperature increases. Oxidation of polymers and metals, scale formation on metals, melting points, boiling points, and solid-state phase changes are all possible temperature indicators if properly interpreted. Knowledge of the forms of degradation, and an overview of observations associated with fire damage that can be used to deduce the temperature to which a component was exposed are shown in Tables 11.2 through 11.5. Additional information pertaining to temperature indications that can be used to establish a Heat Exposure Zone are provided in Table 11.6. Temperature indicators based on a knowledge of the damage a component exposed to a fire has sustained are provided in Table 11.7.

c) The highest Heat Exposure Zone for a component exposed to more than one fire zone shall be used in the assessment, unless there is a distinct reason to allow for separate assessments, such as with heat exchangers. The component should be assigned to the next most severe fire zone if the information gathered during the investigation is insufficient to adequately categorize a component. As described in paragraph 11.3.3.3.a , adjacent components could have been exposed to varying degrees of heat because of shrouding and differences in insulation and fireproofing. Caution should be exercised before categorizing equipment. For example, it may not be appropriate to categorize all parts of an insulated vessel completely into a low Heat Exposure Zone, since flanges, piping, and other appurtenances that are not insulated could have suffered damage and therefore should be assigned to a higher Heat Exposure Zone. The default categorization of these insulated components should be similar to that of adjacent uninsulated components.

d) Knowledge of the source of the fire can assist in the determination of a Heat Exposure Zone. The damage from fire and its extreme heat usually extends outward from the fuel source and upward (see Figures 11.2 and 11.3). Exceptions are in the cases of high-pressure fuel sources, where a flame jet or torch can be highly directional.

e) Temperatures associated with the fire can also be determined using instrument readings taken during the course of the fire. If videotape is available, temperatures may be estimated based on radiation colors observed on steel surfaces during the fire. Radiation colors corresponding to a range of different temperatures are given in Table 11.8.

f) Knowledge of the nature of the fuel in a fire and the ignition source could be useful in establishing a Heat Exposure Zone.

   1) If the source of the fire is known, the fuel being consumed will often be obvious based on known flammable products in the area. However, this is not always the case, and observers on the scene may be able to characterize the fuel based on the color of the smoke (see Table 11.9).

   2) Ignition sources in refinery and petrochemical plants include electrical sparks, open flames, and exposed hot surfaces. Flammable mixtures of organic vapors and air typically exhibit an autoignition temperature above which the mixture will ignite without a spark or additional energy source. For example, a hot surface with a temperature in excess of the autoignition temperature could be an ignition source. Autoignition temperatures for fuels are shown in Tables 11.10 and 11.11, respectively.

11.3.3.4 Degradation Associated with Heat Exposure

A specific inspection plan should be created for each component subject to fire damage, based on first assigning a Heat Exposure Zone (see paragraph 11.3.3) and then taking into account the following forms of degradation associated with heat exposure as listed in Table 11.6:

a) Softening, sagging (plastic deformation) and over aging of aluminum alloys

b) Softening and sagging (plastic deformation) of copper alloys

c) Hardening and/or tempering of heat treatable steels (e.g. ASTM A193 B7 stud bolts)

d) Grain growth, softening, sagging (plastic deformation), hardening or loss of toughness of carbon and low alloy steels

e) Short term creep and creep rupture

f) Spheroidization of carbon steels after long periods of exposure

g) Stress relieving of stainless steels and nickel alloys (e.g. resulting in tube roll leaks in heat exchangers)

h) Sensitization of stainless steels

i) Halide contamination of austenitic stainless steel or other austenitic alloy surfaces, especially under wet insulation or if salt water is used for fire fighting

j) Liquid metal corrosion or cracking, such as caused by molten zinc dripping on austenitic stainless steel

k) Incipient melting of alloys (e.g. localized melting of low melting point segregation and eutectics),

l) Excessive oxidation of metals leading to wall loss, particularly if the fire or overheat incident exceeds many hours

m) Deterioration of gaskets and valve packing

n) Damage to coating systems, especially coatings applied for under insulation corrosion protection

o) High residual stresses due to distortion, restraint, and loss of supports

p) Cracking of metals due to distortion and restraint, for example, restraint of cooler internal components cracking attachment welds

q) Embrittlement of some grades of steels when cooled through critical temperature ranges

r) Formation of a cast iron structure due to carburization and localized melting of the carbon rich alloy (most likely in furnace tubes processing hydrocarbons)

11.3.3.5 Data and Measurements for Components Subject To Heat Exposure

Collection of the following data and measurements should be considered for components assigned to a Heat Exposure Zone where mechanical property changes and dimensional changes can occur:

a) Diametrical and circumferential variations of cylindrical vessels

b) Dimension profiles of vertical and horizontal vessels

c) Straightness of shell and piping sections

d) Nozzle orientations

e) Vertical plumb measurements

f) Hardness tests of the base metal and welds

g) Removal of coupons for mechanical testing

h) Wall thickness measurements of pressure containing components

i) In-situ metallography and microstructure replication

j) Surface crack detection techniques such as magnetic particle and dye penetrant examination

k) Surface condition of equipment with respect to scale formation, melting, coating damage, insulation condition, and weather barrier construction and condition

11.3.3.6 Evaluation of Mechanical Properties for Components Subject To Heat Exposure

a) Components susceptible to changes in mechanical properties at exposure temperature should be evaluated to determine if the material has retained the necessary strength and toughness properties stipulated in the original construction code. The effects of temperature on mechanical properties of various metals are included in Table 11.6. If mechanical properties have been degraded, the actual strength and toughness properties shall be determined (or estimated) in order to rerate the affected component. In this context, components include:

   1) Pressure Vessels: shell sections, heads, nozzle necks, flanges, vessel supports

   2) Piping Systems: pipe sections, elbows, tees, reducers, flanges and piping supports

   3) Tankage: tank shell courses and nozzle necks

b) Hardness testing is a helpful aid in assessing the loss of tensile strength in carbon and low alloy steels, and loss or extent changes in other material properties such as toughness and ductility. For example, hardness can be measured in areas of a carbon steel pressure vessel known to be in Heat Exposure Zones I through IV (see paragraph 11.3.3.3). These results should be compared to hardness measurements obtained in areas suspected of being exposed to higher temperatures, Zones V and VI.

c) In-situ metallography or replication should be performed on surfaces of components having significantly divergent hardness values or where a certain microstructure is required, such as having a normalized microstructure in carbon steel equipment for notch toughness requirements. In-situ metallography or replication should also be performed in areas shielded from the thermal affects of the fire. These two sets of microstructures should be compared and interpreted by an experienced metallurgical engineer. Proper attention to field procedures is imperative for accurate replicas.

d) In-situ metallography can also be helpful in assessing components if replicas can be obtained from both a fire affected zone and an unaffected zone of the same component. In-situ metallography can also be helpful in assessing sensitized austenitic stainless steel or other alloy microstructures.

e) Hardness testing can sometimes give an indication of a loss of toughness; but there is no direct correlation between hardness and toughness. Softening of steels due to tempering below the lower critical temperature (approximately 720°C (1325°F) for carbon steels) usually results in only small changes in toughness for most materials of construction. Therefore, heat exposure to temperatures below this limit is not normally of a concern; however, long time exposure to the heat of the fire can degrade notch toughness. Heating above the lower critical temperature results in a phase transformation that can dramatically affect toughness. Depending on time of heat exposure, the surface temperature level, and cooling rate, the material may either have the same or a different hardness as the component in the pre-heat exposure condition. In such cases, degradation of toughness cannot be inferred from the results of hardness testing, and field metallography, removal of samples for mechanical testing, or other methods may be required to estimate the toughness. However, hardness testing can often provide useful information about the tensile strength of the material. This method has a better chance of detecting differences in tensile strength if it is done in multiple areas in a component (i.e. a grid pattern). Areas heated above the lower critical temperature will often be bounded by areas of tempering that show low hardness, so an anomalous hardness pattern will result.

f) If hardness readings and in-situ field metallography are inconclusive, then consideration should be given to removing a coupon from the component for destructive testing and evaluation. Destructive evaluation should include tensile tests, metallographic examination of the fire side surface and in a through-thickness direction, and finally fracture mechanics tests.

11.3.4 Recommendations for Inspection Techniques and Sizing Requirements

11.3.4.1 Shell dimensional profiles should be taken for equipment subjected to fire damage. Dimensional profiles of vertical vessels can be obtained by dropping a reference vertical line from the top of the vessel, and measuring the bulges and dents of the shell sections relative to this vertical line at appropriate increments. An example on how to measure a profile for a vertical vessel is illustrated in Figures 11.4 and 11.5. Dimensional profiles of horizontal drums can be taken in a similar way using a horizontal level. Additional methods to determine shell distortions using field measurement techniques are covered in Part 8.

11.3.4.2 Surface preparation is critical for accurate field hardness measurements, especially when microscopic tests, such as Vickers, are used rather than a portable indentation type of hardness tester. When making field hardness measurements at least 0.5 mm (0.02 inches) of metal surface should be removed because of oxide scale and surface carburization or decarburization.

11.3.4.3 Other inspection techniques, such as magnetic particle testing and dye penetrant testing may be needed based on the observed or suspected deterioration mode (see paragraph 11.3.3.4).

11.3.4.4 Non-destructive material examination by means of replication is a metallographic examination method that exposes (or replicates) the microstructure of the surface material (see paragraph 11.3.3.6.c.)

a) *Method* – This method requires the skills and experience of a trained person. Portable equipment is typically used for the examination. Surface preparation requires grinding, sanding, and polishing by mechanical or electrolytic means to a mirror finish, followed by etching. The surface can be viewed directly or a replica can be taken by means of a solvent softened acetate strip applied to the surface. Coating the strip with carbon or gold enhances the features.

b) *Application* – Replication is typically used for the evaluation of microstructures and characterization of crack-like flaws. Creep damage can be identified at a much earlier stage using the replication method than with other NDE methods.

c) *Flaw Detection* – Because each type of crack has specific characteristics, the damage mechanism can be determined using this method.

d) *Limitations* – The replication method can only be used on surfaces that are readily accessible and at metal or ambient temperatures between about -18°C to 32°C (0°F to 90°F).

11.3.4.5 Leak testing of mechanical equipment subject to fire-damage in Heat Exposure Zones IV and higher should be considered prior to returning the equipment to service. The types of equipment included are:

a) Flanged connections,

b) Threaded connections which are not seal-welded,

c) Valves (i.e. both shell and closure test per API 598 should be considered),

d) Gaskets and packing, and

e) Heat exchanger tube sheet rolled joints.

11.4 Assessment Techniques and Acceptance Criteria

11.4.1 Overview

An overview of the assessment levels is provided in Figure 11.1.

a) The Level 1 assessment procedure is a screening criterion where the acceptability for continued service is based on the Heat Exposure Zone and the material of construction. The screening criteria are conservative, and calculations are not required to establish suitability for continued service.

b) The Level 2 assessment procedure determines the structural integrity of a component by evaluating the material strength of a fire-damaged component. Assessment procedures include evaluation methods for flaws and damage incurred during the fire (e.g. local thin areas, crack-like flaws and shell distortions) and a means to rerate the components. These assessment procedures are typically applied to components subject to a Heat Exposure Zone of V and higher, or when dimensional changes are noted during a visual inspection.

c) The Level 3 Assessment procedures may be utilized if the current material strength of the component established using the Level 2 Assessment procedures result in an unacceptable evaluation. Replication or in-situ field metallography, the removal and testing of material samples, and a detailed stress analysis may be utilized in a Level 3 assessment.

11.4.2 Level 1 Assessment

11.4.2.1 The objective of this Level 1 assessment is to gather and document the observations and data used to justify assigning a Heat Exposure Zone to each component. Components do not need a further assessment of mechanical properties if they are assigned to an acceptable Heat Exposure Zone, and there is no mechanical damage or dimensional deviation. The Heat Exposure Zone levels for the materials of construction that are acceptable per a Level 1 assessment are shown in Table 11.12.

11.4.2.2 Gasket inspections and leak checking of flange joints should be included in a startup check list for components passing a Level 1 assessment.

11.4.2.3 Protective coating damage can occur for some components that satisfy the Level 1 acceptance criteria. Protective coatings required for external or internal corrosion resistance must be repaired prior to startup.

11.4.2.4 If the component does not meet the Level 1 Assessment requirements, then the following, or combinations thereof, may be considered:

a) Repair, replace or retire the component,

b) Conduct a Level 2 or Level 3 Assessment, or

c) Rerate the component.

11.4.3 Level 2 Assessment

11.4.3.1 Pressurized components that do not pass a Level 1 Assessment may be evaluated for continued service using a Level 2 Assessment. This evaluation should consider the degradation modes described in paragraph 11.3.3.4.

11.4.3.2 An overview of the Level 2 assessment procedure is provided in Figure 11.6.

a) The first step in the assessment is to conduct dimensional checks on pressure components. The dimensional checks generally take the following forms; overall out-of-plumb or sagging of the component(s) and localized shell distortion. As listed below, the forms of overall out-of-plumbness or sagging are dependent on equipment type whereas local shell distortions such as bulges are common for all equipment types:

   1) Ovality or out-of-roundness,

   2) Sag or bow for horizontal vessels,

   3) Vertical deviations (out-of-plumbness), and

   4) Bulges.

b) Hardness testing is used to estimate the approximate tensile strength of a fire exposed component. The information is subsequently used with the rerating procedures in this document to establish an acceptable $MAWP$. Further evaluation is required to assess specific damage from localized thinning, shell distortions and creep.

c) Components that experience dimensional changes provide insight into the additional evaluations that are required. This insight is based on the observation that carbon steel equipment does not experience a significant reduction in short term high temperature strength properties that would result in a dimension change (i.e. out-of-plumb, sagging or bulging) until a temperature in excess of 425°C (800°F) is reached.

11.4.3.3 The following procedure may be used to evaluate a pressurized component constructed of carbon or low alloy steels for continued operation if the mechanical strength properties are suspected to have been degraded by the fire exposure.

a) STEP 1 – If the component is fabricated from carbon and/or low alloy steel, perform a hardness test on the component (see paragraph 11.3.3.6.b) and convert the resulting hardness value into an estimated ultimate tensile strength using Table F.1 of Annex F. If the component is fabricated from high alloy or nickel base materials, an alternative method is usually required to determine an acceptable stress level for a Fitness-For-Service assessment. Additional materials evaluation may need to be performed depending on the observed severity of damage and future service requirements. This evaluation should include in-situ field metallography to determine the condition of a component. Guidelines for this type of evaluation are provided in Figure 11.7 and paragraph 11.3.3.6.

b) STEP 2 – Determine an allowable stress for the fire damaged component based on the estimated ultimate tensile stress determined in STEP 1 using Equation (11.1). In this equation, the parameter C_{ism} is the in-service margin. The in-service margin may be taken equal to the design margin used on the ultimate tensile strength in the original construction code. If this value is not known, a value of $C_{ism} = 4.0$ is recommended.

$$S_{afd} = \min\left[\left\{\left(\frac{S_{uts}^{ht}}{C_{ism}}\right)\cdot\left(\frac{S_{aT}}{S_{aA}}\right)\right\},\ \{S_{aT}\}\right] \qquad (11.1)$$

c) STEP 3 – Perform the necessary MAWP calculations using the value of allowable stress determined in STEP 2 and the equations in Annex A

d) STEP 4 – If additional forms of damage are present, the $MAWP$ should be further modified using the applicable Parts in this document:

1) General thinning – Part 4

2) Local thinning – Part 5

3) Pitting – Part 6

4) HIC, SOHIC and blister damage – Part 7

5) Shell distortions including out-of-roundness and bulges –Part 8

6) Crack-like flaws – Part 9

7) Dents, gouges, and dent-gouge combinations – Part 12

8) Laminations – Part 13

e) STEP 5 – Evaluate creep damage of the component using Part 10. Normally, components subject to high temperatures during a fire do not experience significant creep damage because the time at temperature is short and significant creep strains and associated damage can not accumulate.

11.4.3.4 Other effects that should be considered in the assessment include the following:

a) Internal attachments that may have been subject to large thermal gradients during a fire should be inspected for cracks on the component surface and at the attachment weld. This inspection is especially important for internal components fabricated from materials with a coefficient of thermal expansion significantly different from that of the shell (e.g. austenitic stainless steel internal attachment support welded to a carbon or low alloy steel shell).

b) Pressure components being rerated because of the reduction in mechanical properties should be assessed if there is a plausible reason to expect a change in the corrosion resistance in the service which the vessel will be exposed (the future corrosion allowance may need to be increased).

11.4.3.5 The beneficial effects of $PWHT$ (stress relief) may have been compromised because of heat exposure. Pressurized components that were subjected to $PWHT$ in accordance with the original construction code (i.e. based on the material and thickness at the weld joint) or for service conditions (e.g. carbon steel subject to caustic SCC or in wet H_2S service) should be evaluated to ascertain whether the benefits of the $PWHT$ have been compromised:

a) For carbon steel, the issue is usually on relief of residual stresses, but sometimes also on tempering hard zones in the microstructure or on improved toughness. Distortion and/or quenching in fire fighting efforts can leave the component with higher residual stresses that could lead to service related cracking.

b) For low alloy steels, the issue is usually on retaining mechanical properties. The original $PWHT$ was conducted to temper a hard microstructure and/or to improve toughness. Heat exposure can lead to a very hard/brittle microstructure in the component that if left in place can lead to premature failure.

11.4.3.6 If the component does not meet the Level 2 Assessment requirements, then the following, or combinations thereof, may be considered:

a) Repair, replace or retire the component,

b) Adjust the future corrosion allowance, FCA, by applying remediation techniques (see Part 4, paragraph 4.6),

c) Adjust the weld joint efficiency factor, E, by conducting additional examination and repeat the assessment (see Part 4, paragraph 4.4.2.2.c), and/or

d) Conduct a Level 3 Assessment.

11.4.4 Level 3 Assessment

11.4.4.1 A Level 3 assessment of a fire damaged component may be performed if the component does not satisfy the Level 1 or Level 2 Assessment criteria. A Level 3 assessment is usually performed for the following reasons.

a) The MAWP calculations associated with a Level 2 Assessment cannot be used to adequately represent the current condition of the component. If the component is severely deformed or shell distortions are located in the region of a major structural discontinuity, then a stress analysis technique from Annex B1 may be utilized in the assessment.

b) The current strength of the material established from a hardness test taken on the material surface is an approximation of the actual tensile strength of the material that in some cases could be conservative, resulting in a reduction of the $MAWP$. In such cases, testing on material samples can be performed to develop a better estimate of the strength of the material.

11.4.4.2 A Level 3 assessment of a known fire-damaged component shall be conducted if an increase in the original $MAWP$ (or temperature) is required. A representative sample of the base metal and weld should be tested to establish an acceptable allowable stress value for use in the rerating calculations. Estimates of changes in mechanical properties based only on hardness measurements and microstructure shall not be used to increase the allowable stress value of a component subject to fire damage.

11.5 Remaining Life Assessment

11.5.1 The applicable Parts of this document may be used to assess remaining life for the damage mechanisms cited in paragraph 11.4.3.3.

11.5.2 Creep damage and the associated remaining life may be calculated using the assessment procedures of Part 10.

11.6 Remediation

11.6.1 Remediation techniques for the damage mechanisms cited in paragraph 11.4.3.3. are covered in the applicable Parts of this document.

11.6.2 In general, badly distorted components should be repaired or replaced. However, if a component cannot be repaired or replaced because of physical limitations or extended replacement schedules, then temporary supports and reinforcement can be added to help reduce stresses associated with the deformed condition. For example, the increased bending stress resulting from out-of-plumbness of a process tower may be acceptable if some form of support is introduced to minimize the bending stress associated with wind loads. Note that added supports should be designed to accommodate thermal expansion of the equipment.

11.7 In-Service Monitoring

Recommendations for in-service monitoring for the damage mechanisms cited in paragraph 11.4.3.3. are covered in the applicable Parts of this document.

11.8 Documentation

11.8.1 The documentation of the FFS assessment shall include the information cited in Part 2, paragraph 2.8.

11.8.2 Information used to assign the Heat Exposure Zones, measurements to quantify component distortions, mechanical property changes, calculations for the $MAWP$, and remaining life calculations should be documented.

11.8.3 All documentation including the calculations used to determine the Fitness-For-Service of a pressurized component should be kept with the inspection records for the component or piece of equipment in the Owner-User inspection department.

11.9 Nomenclature

C_{ism}	in-service margin.
FCA	future corrosion allowance.
S_{afd}	allowable stress for a fire damaged material.
S_{aA}	allowable stress of the original design code or standard at the ambient temperature when the hardness tests are taken.
S_{aT}	allowable stress of the original design code or standard at the specified design temperature
S_{uts}^{ht}	Ultimate tensile strength based on the results from a hardness test.

11.10 References

1. ASM, “Powder Metallurgy,” Metals Handbook, Volume 7, 8th Edition, American Society of Materials, p 133, 1972
2. ASM, “Properties and Selection: Iron and Steels,” Metals Handbook, Volume 1, 9th Edition, American Society of Materials, p 204, 1978
3. Hau, J. L., "Assessment Of Fire Damage To Pressure Vessels In A Refinery Unit", Corrosion, pp 420-437, Vol. 49, No.5, 1993
4. MTI, “Guidelines for Assessing Fire and Explosion Damage,” MTI Publication No. 30, Materials Technology Institute of the Chemical Process Industries, Inc., 1990.
5. MTI, “Guidelines for Preventing Stress-Corrosion Cracking in the Chemical Process Industries,” MTI Publication No. 15, Materials Technology Institute of the Chemical Process Industries, Inc., 1990.
6. Treseder, ed., Corrosion Engineer's Reference Book, National Association of Corrosion Engineers, Houston, TX, p. 177, 1980.
7. Wilson, A. D., Roper, C. R., Orie, K. E., and Fletcher, F. B., Properties and Behavior of Modern A 387 Cr-Mo Steels, PVP-Vol. 239, Seviceability of Petroleum, Process, and Power Equipment, Book No. G00674 – 1992.
8. Orie, Kenneth E. and Upitis, Elmar, The Effect of Post Weld Heat Treatment and Notch Toughness on Welded Joints and on Normalized Base-Metal Properties of A-516 Steel, WRC Bulletin 481 – March 2005.

11.11 Tables and Figures

Table 11.1
Description Of Heat Exposure Zones to Evaluate Fire Damage (1)

Heat Exposure Zone	Description	Thermal Effects On Materials In The Fire Zone
I	Ambient temperature during fire event, no fire exposure	No damaging effects
II	Ambient to 65°C (150 °F); smoke and water exposure	No damaging effects
III	65°C to 205°C (150 °F to 400°F); light heat exposure	Table 11.2
IV	> 205°C to 425°C (>400 °F to 800°F); moderate heat exposure	Table 11.3
V	> 425°C to 730°C (>800 °F to 1350°F); heavy heat exposure	Table 11.4
VI	> 730°C (>1350 °F); severe heat exposure	Table 11.5
Notes: An overview of the damage that is likely to occur in each fire zone is provided in Table 11.6.		

Table 11.2
Guidelines for Observing Fire Damage – Thermal Effects on Materials
Heat Exposure Zone III, 65°C To 205°C (150°F To 400°F)

Temperature (1)		Materials of Construction	Forms or Usage	Thermal Effects
°C	°F			
90	200	Vinyl coatings (3) (4) (5)	Paints on tanks, structural steel, etc	Begins to melt, flow, and bubble; may burn
150	300	Alkyd coatings (6)	Paints on tanks, structural steel, etc.	Color change visible; surface crazing
400	750	Inorganic zinc silicate (10)	Paints on tanks, structural steel, etc.	Begins to melt, flow, and bubble; may burn
205	400	Epoxies & polyurethanes (11)	Paints on tanks, structural steel, etc.	Color change visible; blistering and charring
190	375	UHMW HD Polyethylene (7)	Pipe	Softening and melting
175	350	Elastomers, neoprene (2) (8)	Hose, diaphragms, gaskets	Softening, melting; some burning / charring
180	360	Lead / tin solder	Electrical equipment connectors	Melts
260	500	Baked phenolic (9)	Fiberglass mat binder, micarta tank linings	Surface discoloration; blistering
205	400	Acrylic mastic	Weatherproof coating for insulation	"Mud" cracking; charring

Notes:

1. The temperatures listed in this table are the lower limits of temperature where significant damage is observed. Similar effects may occur at higher temperatures in shorter times
2. Effects of heat vary greatly due to formation of an elastomer and end product. Do not attempt to be too specific based on observations of elastomer condition.
3. The term vinyl can mean two different things when it comes to paint. Solution vinyls are single package paints with polymeric resin dissolved in strong hydrocarbon solvent. The other type of vinyl is similar to latex house paint; these water based paints are typically vinyl acrylic, but they may also be vinyl acetate and other polymer types.
4. Solution vinyl coatings (thermoplastics) have a maximum continuous service temperature of about 60 to 65°C (140 to 150°F) and soften in the 65 to 80°C (150 to 180°F) range; above 90°C (200°F) these coatings will begin to melt and flow, (giving up HCl as a by-product.) They may blister but are generically not good candidates for burning and charring. The significant halogen content stifles burning initially. This will occur with some bubbling which may be a little different than blistering.
5. Vinyl latex paints are also thermoplastic paints but these do not generally contain chlorine or other halogen. Above 90°C (200°F) these materials will begin to melt and flow much like solution vinyls but they burn differently.
6. Alkyds thermoset and as such they have much better temperature resistance than do the vinyls. Alkyds can handle 105 to 120°C (225 to 250°F) continuously for months or years. A good alkyd can handle 150°C (300°F) for several hours. The first symptoms of heat/oxidation damage are yellowing and surface crazing. Different colors mean different pigments and color changes could be important.
7. UHMW and HD polyethylene used as pipe, has a temperature rating of 65 to 70°C (150 to 160°F)

Table 11.2
Guidelines for Observing Fire Damage – Thermal Effects on Materials
Heat Exposure Zone III, 65°C To 205°C (150°F To 400°F)

Temperature (1)		Materials of Construction	Forms or Usage	Thermal Effects
°C	°F			

depending on commodity and pressure. The softening temperature is about 125°C (260°F); it takes some time at temperatures well above 150°C (300°F) to cause appreciable melting. Consider that HDPE pipe is welded at 205 to 260°C (400 to 500°F), depending on the technique.

8. Neoprene has a dry temperature rating of 150 to 175°C (300 to 350°F) depending on formulation specifics. Flame and heat aging/air oxidation resistance are very good for rubber. Neoprene is a type of chlorinated rubber and so it resists burning.
9. Baked phenolics thermoset, typically bake cured in the 165 to 205°C (325 to 400°F) range. Phenolics are typically red, brown, or black initially, so a color change may be difficult to observe. While this generic class may degrade over a range of temperature, the materials would need to be at temperatures close to 260°C (500°F) before major degradation would be observed.
10. For zinc silicate primers, the silicate binders can handle up to about 540°C (1000°F). However, the metallic zinc pigment can be impacted above the melting point near 400°C (750°F).
11. Epoxies and polyurethanes can typically withstand temperatures to about 150°C (300°F) with no significant impact. These paints may begin to blister and/or char once the temperature exceeds 205°C (400°F). As with the alkyd paints, color changes may occur. For example, a common yellow finish color is obtained with hydrated ferric oxide and as the coating gets hot the water of hydration is driven off and the coating starts to turn pink.

Table 11.3
Guidelines For Observing Fire Damage – Thermal Effects On Materials
Heat Exposure Zone IV, greater than 205°C To 425°C (greater than 400°F To 800°F)

Temperature (1)		Material of Construction	Forms or Usage	Thermal Effects
(°C)	(°F)			
205	400	Tempered aluminum alloys	Pipe and tanks of T6 or other temper	Reduced strength (check hardness & electrical conductivity)
230+	450+	Wood – various	Various	Charring, burns
260	500	Steel – machined or polished	Machinery or instrument parts	Develops blue temper color
270	520	Babbitt(2) -- lead based	Sleeve bearings	Melts
280	540	Copper -- cold drawn, bright annealed	Instrument and condenser tubing	Softens, sags, grain coarsening occurs
330	623	Lead (soft)	Lining in pipe and tanks	Melts
390	730	Zinc/aluminum die casting	Small valve handles and instrument parts	Melts
420	790	Zinc	Galvanized coating for steel structures	Melts

Notes:

1. The temperatures listed in this table are the lower limits of temperature where significant damage is observed. Similar effects may occur at higher temperatures in shorter times.
2. Trade Name

Table 11.4
Guidelines For Observing Fire Damage – Thermal Effects On Materials
Heat Exposure Zone V, greater than 425°C To 730°C (greater than 800°F To 1350°F)

Temperature (1)		Material of Construction	Forms or Usage	Thermal Effects
(°C)	(°F)			
480	900	Quenched and Tempered Steels	Springs, fasteners, 4140, etc, (particularly socket head cap screws)	Tempering to lower strength
510	950	Glass	Light bulbs	Distort and melt
540	1000	18-8 Stainless Steel	Vessels, piping etc.	Sensitized (carbide PPT) and reduced corrosion resistance
595	1100	Steel	Vessels and piping	Thermal distortion and creep, some heat scale
620	1150	Precipitation Hardened Stainless Steel	Machinery and valves	Overages -- reduced strength
650	1200	Steel	Vessels, piping, structures	Rapid oxidation -- thick black scale
655	1215	Aluminum	Tanks, piping, accessories	Melts
695	1285	Glass	Windows	Melts
705	1300	Copper	Tubing, pipe, vessels	Rapid oxidation -- black
710	1310	Glass	Pyrex(2) –pipe, sight glass	Melts
730	1350	Silver Solder	Brazed joints on accessories	Melts (may start at lower temperature)

Notes:

1. The temperatures listed in this table are the lower limits of temperature where significant damage is observed. Similar effects may occur at higher temperatures in shorter times.
2. Trade Name

Table 11.5
Guidelines For Observing Fire Damage – Thermal Effects On Materials
Heat Exposure Zone VI, greater than 730°C (greater than 1350°F)

Temperature (1)(2)		Material of Construction	Forms or Usage	Thermal Effects
(°C)	(°F)			
760	1400	Steel	Vessels and piping	Iron carbide (cementite) spheroidizes
815	1500	Steel	All forms -- low alloy most susceptible	Austenitizes -- slow cool equals anneal, fast quench turns hard and brittle
905	1660	Zinc	Galvanizing on steel	Oxidizes to white powder or vaporizes
980	1800	Cellular glass	Thermal insulation	Melts
1095	2000	Copper	Tubing, pipe, etc.	Melts
1305	2385	Alloy C-276	Vessels, pipe	Melts
1400	2550	316 SS – cast	Pumps, valves	Melts
1455	2650	316 SS – wrought	Vessels, pipe	Melts
1515	2760	Steel	Various	Melts
1685	3065	Titanium	Vessels, pipe, etc.	Melts

Notes:

1. The temperatures shown are those in which significant damage begins to occur to the material of construction listed.
2. The temperatures listed in this table are the lower temperatures where heat effects begin. Similar effects may occur at higher temperatures in shorter times.

Table 11.6
Guidelines For Assessing Fire Damage Effects
Description Of The Types Of Damage That May Occur In The Heat Exposure Zone Categories

Heat Exposure Zone	Temperature Range	Heat/Temperature Effects	Observations and Conclusions
ZONE I No evidence of heat, flame, or smoke contact	AMBIENT	Equipment clean. Paint, plastic and elastomer items unaffected.	• No damage, acceptable to operate.
ZONE II Smoke and water contact but no heat exposure	AMBIENT to 65°C (150°F)	Equipment dirty, sooty and wet. No effects on paint, elastomer or plastic items.	• No damage to major equipment. Water and smoke may have damaged insulation, insulation jackets and delicate mechanisms or electronics.(1) • Smoke or fumes from burning chlorinated compounds, i.e. PVC, will release chlorine or HCl, can damage electronics or contaminate insulation.(2)
ZONE III Light heat exposure	Over 65°C (150°F) to 205°C (400°F)	Vinyl and alkyd paints blistered, paints darkened to black, elastomers hardened or charred, plastics charred or melted, lead-tin solder melts.	• No damage to major equipment. Some damage to non-metallics. Check packing and gaskets for heat effects.(3) • Electrical wiring and electronic components damaged.(4) • Belts on machinery drives need replacing. • Check for chlorine or HCl contact from burning organic chlorides. (2)
ZONE IV Medium heat exposure	Over 205°C (400°F) to 425°C (800°F)	Organic coatings blistered or burned off. Plastics and rubber melted or charred. Insulation on electric wiring destroyed. Springs will be tempered and softened. Valves, gauges out of calibration. Cold drawn copper alloys lose strength. Solution annealed copper alloys are less affected.	• Severe general damage to ancillary equipment such as electrical wiring, circuit boards and motors. • All gaskets and packing must be replaced except those made from metallic, spiral or graphite. • Springs in pressure relief valves, check valves etc., will be tempered out of calibration. Rupture discs may also be affected by heat and should be replaced. (5) • Roll joints in heat exchangers might be affected. Sagging tubing joints on instrument tubing might leak. Consult mechanical engineers about copper alloy pressure components if loss of copper alloy strength is observed. (6)

Table 11.6
Guidelines For Assessing Fire Damage Effects
Description Of The Types Of Damage That May Occur In The Heat Exposure Zone Categories

Heat Exposure Zone	Temperature Range	Heat/Temperature Effects	Observations and Conclusions
ZONE IV Medium heat exposure (Continued)	Over 205°C (400°F) to 425°C (800°F)	Aluminum alloys may experience considerable loss in strength due to over-aging and recrystallization. Distortion of aluminum alloys may occur.	• Aluminum equipment often requires replacement. (6)
		Structural steels, stainless steels, solution annealed nickel alloys, non-heat treated titanium and zirconium alloys generally are not affected.	• Usually can be returned to service. (7)
		Possibility of liquid metal embrittlement begins and may affect the integrity of equipment.	• Refurbish susceptible metallic items that have had molten metal dripped on them by repairing damaged areas (by welding and/or grinding) and inspecting for cracking. (8)
ZONE V Severe heat exposure. Direct exposure to flames, no impingement. This is the most important area of fire damage effects. Major equipment has been exposed to severe radiant heat, but not enough to destroy it.	Over 425°C (800°F) to 730°C (1350°F)	Nonmetals destroyed or consumed. Aluminum, pyre and some silver solders melting.	• All ancillary equipment and small piping, tubing, copper materials should be replaced. Concentrate on major equipment. • All gaskets and packing should be replaced.
		The cold-rolled tube ends in heat exchangers may be stress relieved causing leaks.	• Major equipment, including pressure vessels, heat exchangers and rotating equipment should be cleaned, inspected and pressure tested. (9)
		Heat-treated or cold-worked metals may be softened. Check springs on pressure relief valves. Check A193-B7 stud bolts in flanges for softening. Check for localized heating and stressing of steel equipment in critical service.	• In areas of highest temperature, replace all B7 bolts. (10) Pressurized components may need metallurgical sampling to determine exact degree of effects by high-temperature exposure. (13)
		Long exposure to these temperatures may affect grain structure, properties and corrosion resistance of steels and stainless steels.	• Vessel, piping, and tankage components, and associated structural steel supports, that are warped or distorted may require repair or replacement. Regular carbon stainless steels are sensitized, may need replacing. (10)(11)(12)
		Steel starting to oxidize, the thicker the scale the hotter the temperature.	• Remove oxide scale and determine amount of physical damage. (13)
		Copper tubing oxidizing to black scale, softened and distorted.	• Replace copper tubing which has black oxide scale.

Table 11.6
Guidelines For Assessing Fire Damage Effects
Description Of The Types Of Damage That May Occur In The Heat Exposure Zone Categories

Heat Exposure Zone	Temperature Range	Heat/Temperature Effects	Observations and Conclusions
ZONE VI Extreme heat exposure, indicating vicinity of fire source or flame impingement	Over 730°C (1350°F)	Copper and copper alloys destroyed or melted.	• Almost all copper alloys will have to be scrapped. Critical equipment that was protected by insulation, water spray or fire proofing construction will have to be thoroughly inspected and tested.
		Heavily scaled steel may be distorted due to thermal stresses.	• Check areas of severe oxidation. (13)
		Grain growth in fine grained steels.	• Possibility of liquid metal cracking (LMC) is greatest at these temperatures. Check areas exposed to molten metal for LMC. (8)
			• Check piping and vessels in low-temperature service for increase in grain size and loss of toughness. (14)
		Steel that is water quenched may harden and lose ductility. All heat-treated or cold-worked materials may have altered properties.	• Check bolting, vessels and piping components for metallurgical changes. (10)(11)(12)

Notes:

1. Equipment heavily contaminated with smoke and water will require cleaning. Consider the potential effect of chloride-bearing fire water as a source of external stress-corrosion cracking or corrosion under insulation during service at a later date.
2. Consumption of organic chlorides (e.g. vinyl chloride or polyvinyl chloride (PVC)) in the fire may generate chlorine, HCl, or both. These gaseous products will be carried by the smoke and water spray onto the surrounding equipment. If so, decontamination, neutralizing, cleaning, and testing will be required to ensure that HCl corrosion has not and will not damage the equipment. If the fire water has carried acid chlorides onto stainless equipment, rapid external stress corrosion cracking failures could result from further service. A chloride spot check of uninsulated stainless equipment should reveal whether or not decontamination is required.
3. Temperatures in the range of 65°C to 205°C (150°F to 400°F) may begin to melt, char, harden, or change the color of paints, coatings, plastic tubing, and elastomers. Such changes will normally signal the need for replacement or re-coating of such organic components. Flange gaskets, O-ring seals, valve packing, and so forth should be checked for possible deterioration. These items are largely confined, so their deterioration may not be evident on first inspection.
4. As temperatures approach 205°C (400°F) electrical motors may be damaged due to the thermal decomposition of wiring and electrical insulation. Lead-tin solders begin to melt in this temperature range, breaking some electrical connections.
5. Steels of extremely high hardness (tool steels, springs, etc.) are tempered in this temperature range so accidental fire exposure may lower their hardness. Rupture disks, pressure relief valve springs, and pressure gauges may all be out of calibration due to exposure in the 205°C to 425°C (400°F to 800°F) range.

   Since the early 1980s, counterfeit bolts and cap screws have been used in some components and many of these bolts do not meet the strength and alloy requirements of ASTM or Society of Automotive Engineers (SAE) standards. Such substandard bolts may lose substantial strength at temperatures

Table 11.6
Guidelines For Assessing Fire Damage Effects
Description Of The Types Of Damage That May Occur In The Heat Exposure Zone Categories

Heat Exposure Zone	Temperature Range	Heat/Temperature Effects	Observations and Conclusions

where ASTM or SAE standard fasteners are unaffected. For example, SAE low alloy steel with boron additions (and plain carbon steel) has been substituted for SAE grade 8 low alloy steel cap screws. These substandard cap screws will lose substantial strength if exposed to temperatures in excess of about 315°C (600°F) while standard SAE grade 8 cap screws would be completely unaffected by such exposure. Therefore, investigators should be alert to the possibility of lowered strength on flange connections and valve bonnets due to low-temperature tempering of such substandard bolting alloys.

6. Cold-drawn copper and copper alloys lose significant strength due to annealing and recrystalization in the range of 205°C to 425°C (400°F to 800°F). Roll joints in heat exchangers are commonly affected; leak testing and re-rolling will often be necessary. Sagging and deformation of copper instrument tubing will be observed, and tubing joints will often leak.

   Solution-annealed copper alloys suffer relatively little from exposure in the 205°C to 425°C (400°F to 800°F) range; pressurized components should be checked to determine if any observed loss of strength affects the structural integrity.

   Aluminum alloy equipment may suffer considerable loss of strength due to over-aging and recrystallization in the 205°C to 425°C (400°F to 800°F) range. The large thermal expansion of aluminum may cause widespread warping and tensile failures as well. Aluminum equipment exposed in this temperature range will often require replacement.

7. Low carbon structural steels, stainless steels, solution-annealed nickel alloys, non-heat-treated titanium and zirconium alloys are largely unaffected by exposure in the 205°C to 425°C (400°F to 800°F) range and may often be returned to service with no serious damage.

8. Contact of molten tin, lead, zinc and their alloys with structural alloys may seriously affect the integrity of equipment due to liquid metal cracking (LMC). Threshold temperatures and times for cracking are not well established although susceptible combinations of low-melting alloys and structural alloys have been documented (see reference [5]). There is a possibility of LMC in the temperature range 205°C to 425°C (400°F to 800°F); however, the risk of serious damage gets worse as temperatures go up in heat exposure Zones V and VI. If a low-melting alloy has dripped onto a structural item, refurbishment should include a careful and thorough removal of the low-melting alloy and a careful check for intergranular cracking.

9. The onset of many severe metallurgical effects that affect vessel integrity and future service occurs in the range of 425°C to 730°C (800°F to 1350°F). Therefore, equipment exposed in this temperature range will require extra attention from the materials engineer and inspection team. Spheroidization or tempering of carbon and low alloy steels may significantly lower the strength of the materials used in the construction of pressurized components. If there is an evidence of such metallurgical change, tests should be performed on samples removed from the equipment in question to ensure that the properties still meet specification. Stress relief of stainless steel and nickel alloys will begin in this temperature range. In the absence of thermal distortion or sensitization, such stress relief is not a cause for concern. However, rolled joints in shell and tube heat exchangers will often relax and leak, requiring resealing.

10. The normal tempering temperature is approximately 595°C (1100°F) for AISI alloy 4140 stud bolts. These bolts are commonly used in processing plants to ASTM specification A193 Grade B7. If the fire exposes such bolts to temperatures in excess of approximately 665°C (1225°F), the bolts will be softened below their required minimum strength level. Bolts with low strength may yield on re-torquing, producing leaks during unit restart.

    Low carbon steel used for piping and structures will be relatively unaffected by exposure for short times at temperatures in the range 425°C to 730°C (800°F to 1350°F); long-term exposure may lead to strength loss by spheroidization.

    Scaling due to oxidation in air begins on carbon steels in this temperature range. The scale itself is essentially equivalent to the mill scale often encountered on newly delivered steel products. The

Table 11.6
Guidelines For Assessing Fire Damage Effects
Description Of The Types Of Damage That May Occur In The Heat Exposure Zone Categories

Heat Exposure Zone	Temperature Range	Heat/Temperature Effects	Observations and Conclusions

problems of dealing with such heat scale are similar to the problems of dealing with mill scale; such scale may promote pitting and localized attack in service and makes a poor anchor for protective coatings. For these reasons the heat scale should be removed, as mill scale is, by abrasive blasting.

11. Radiant heating or uneven heat flux to a portion of a vessel or pipe can cause severe residual stresses to develop during thermal expansion and contraction. If the various temperature indicators point to localized metal temperatures in excess of 540°C (1100°F), potentially harmful residual stresses should be considered in a Fitness-For-Service assessment. A field stress relief may be needed to reduce uneven or undesirable residual stresses.
12. Sensitization of austenitic stainless steels and other austenitic alloys may occur on exposure to temperatures above 425°C (800°F) and is normally most severe at temperatures around 675°C (1250°F). A sensitized austenitic stainless steel will lose considerable corrosion resistance in many environments; depending on the service such sensitized materials may not be suitable for further use. The mechanical properties of AISI Type 300 stainless steels are not significantly reduced by sensitization.
13. Oxidation of low carbon steel occurs rapidly above 730°C (1350°F) resulting in heavy scale build-up. Damage may be less than it appears initially, since the volume of scale is from seven to 20 times greater than that of the metal from which it formed. Heavily scaled parts should be cleaned of scale, checked for thickness, grain structure, and hardness to facilitate decisions regarding reuse.

    After exposure to temperatures in excess of 730°C (1350°F), hardenable steels may exhibit a wide range of hardness, toughness and grain structure depending on exposure temperature and cooling rate.

    If at temperatures in excess of 730°C (1350°F) is followed by rapid cooling steels may show extremely high hardness and low toughness. Such hardened material is extremely prone to delayed brittle fracture or hydrogen-assisted cracking and therefore must be identified and removed prior to returning the equipment to service.
14. The grain growth that occurs in carbon steels exposed to temperatures above about 815°C (1500°F) is extremely detrimental to toughness. Common structural steels such as ASTM A53 show a gradual coarsening of the grain as temperatures increase; above about 955°C (1750°F), the grain size may be large enough to raise the ductile-to-brittle transition temperature well above the ambient temperature. Fine-grained low-temperature steels such as ASTM A516 and A333 tend to show grain coarsening more abruptly over a narrow range of temperatures beginning at about 1040°C (1900°F). The primary concern for the presence of such coarse grains is the severe loss in toughness. It is seldom practical to refine the grain size of grain-coarsened steels in the field. In some circumstances, a normalization treatment in a heat-treating shop may be used to restore original grain size and toughness.

Table 11.7
Temperature Indicators That Can Be Used To Categorize Fire Damaged Components

Temperature Indicators	Description
Melting, Charring And Ignition	Melting points make excellent temperature indicators, since a piece of melted equipment is easy to identify and the melting ranges of alloys are largely unaffected by time. Only eutectic alloy compositions have a true melting point; all other alloys melt across a range of temperatures (e.g., the lead-based Babbitt frequently used for sliding bearings in pumps and compressors has a solidus temperature of 240°C (465°F), and a liquidus temperature of 270°C (520°F)). The liquidus temperatures for a wide variety of processing plant materials are shown in Table 11.13. Ignition of wood is affected by species, temperature, and time. The ignition temperature for some types of woods is shown in Table 11.14. Glass will melt at high temperature and will crack if subjected to even moderately high cooling rates. Consequently, the condition of sight glasses, flow meters, gauge faces, and other glass items may give useful indications of temperature and cooling rates. Glasses are noncrystalline even at room temperature; their transition to liquid is somewhat different from that of metal alloys. As the temperature of glass increases, it reaches a point where it begins to soften. Higher temperatures produce lower hardness and lower shear strength until, at the "working temperature," the glass is essentially a syrupy liquid. The softening point and working temperatures of many glasses are shown in Table 11.15. The discoloration and charring of some organic materials such as polyurethane foam, phenolics resin, and acrylic resins are also largely controlled by temperature.
Oxidation Of Metals	The onset of high-temperature scaling on carbon steels or stainless steel exposed to air is largely temperature controlled. Below a certain temperature (approximately 540°C (1000°F) for carbon steels, and 845°C (1550°F) for 18Cr-8Ni stainless steels), essentially no high-temperature oxidation will be observed. Above that threshold temperature, a significant oxide scale may form, even in the short-term exposures (15 minutes to several hours) characteristic of accidental fires. The friable nature and logarithmic growth curve of some high-temperature oxides make time or temperature estimates from oxides thickness difficult to interpret. The presence of scale itself is, however, indicative of temperatures at least as high as the threshold. The scaling temperatures for a variety of common processing plant materials are shown in Table 11.16.
Tempering Of Steels	In the range of 205°C to 480°C (400°F to 900°F), cold-worked and heat-treated steels of high hardness begin to lose strength. Bearing assemblies, springs, aircraft-grade fasteners, and other items are affected. The reduction in hardness may be used to estimate time and temperature of exposure based on the tempering curves of the alloy in question. One of the more common bolting materials in processing plants is ASTM A193 Grade B7. Its response to heat exposure is fairly well known and can be used to help assess the heat to which adjacent piping or vessels were subjected. Different tempering temperatures produce different characteristic colors on clean steel surfaces such as pump shafts. (Temper colors will not develop on painted steel or rusty surfaces.) The temper colors commonly observed on steel as a function of temperature are shown in Table 11.17.

Table 11.7
Temperature Indicators That Can Be Used To Categorize Fire Damaged Components

Temperature Indicators	Description
Grain Growth Of Carbon Steel	General purpose carbon steels such as ASTM A53 show a gradual coarsening of the grains as the temperature is increased above the austenitizing temperature. Exposure above about 930°C (1700°F) produces very large grains. The effect of temperature on grain growth of carbon steel is shown in Figure 11.8. Fine-grained carbon steels of high toughness are used for low-temperature service; typical specifications included ASME SA 333 for pipe and SA 350 for flanges. The fine grain size is produced by deoxidizing practice (usually aluminum additions), normalizing, and cooling at a controlled rate. Steels made to fine-grained practice (ASTM 333, 516, etc.) show little grain coarsening between the austenitizing temperature and 1030°C (1900°F). Between 1030°C to 1095°C (1900°F to 2000°F), the grain size increases dramatically.
Grain Growth In Copper And Associated Alloys	In the range of 205°C to 425°C (400°F to 800°F), copper and copper alloys will soften and begin to show grain growth. Laboratory determination of hardness and grain size, when compared with equipment not exposed to the fire, may be useful for estimating the time and temperature of exposure. The effect of temperature on grain growth of cold-drawn, commercially pure copper is shown in Figure 11.9. The effects of temperature on grain size and hardness of cold-drawn admiralty brass are shown in Figures 11.10 and 11.11, respectively.
Spheroidization Of Carbon Steel	Long-term (several hours) exposure to temperatures in the range of 650°C to 730°C (1200°F to 1350°F) may spheroidizes carbon steel if the cooling rate is slow. Spheroidization reduces the strength of the steel.
Sensitization Of Austenitic Stainless Steels	The well-known sensitization reaction of austenitic stainless steels can be a useful temperature indicator. In the temperature range of 425°C to 900°C (800°F to 1650°F) chromium carbide precipitation in the grain boundaries leaves a distinctive ditching pattern when these alloys are examined metallographic ally using the ASTM A262 practice A test. Much of the chromium-nickel austenitic stainless steel produced in recent years is of the low carbon variety, to avoid sensitization during welding. Such low carbon stainless steel may still be sensitized during accidental fires if the time of exposure exceeds approximately 10 hours (See Figure 11.12).
Distortion Of Structural Steel	Gross plastic deformation of low carbon steel I-beams, channel sections, and other structural members is sometimes observed if the temperature is high enough to reduce the yield stress below the applied stress. Above 760°C (1400°F), the yield stress of carbon steel has dropped to only 26 MPa (3750 psi) and gross plastic flow is possible at relatively low stress levels (see Figure 11.13). Therefore, the presence of structural steel grossly deformed by a fire is indicative of temperatures of 760°C (1400°F) or above.
Softening Of Aluminum Alloys	Aluminum alloys rapidly lose strength above about 150°C (300°F) (See Figure 11.14). Sagging or warping of aluminum piping for fittings is suggestive of temperatures at least that high.
Stress Relief Of Austenitic Stainless Steel And Nickel Alloys	Exposure to temperatures above about 480°C (900°F) for more than 15 to 30 minutes will begin to produce significant stress relief of many austenitic stainless steels and nickel alloys. Observations involving stress relief of stainless items include leaking joints in rolled-in heat exchanger tubes, leaking fittings on swaged instrument tubing joints, and softened bourdon tubes on pressure gauges.

Table 11.8
Temperature Of Steel Based On The Visible Radiation Spectrum

Radiation Color During A Fire	Approximate Temperature	
	(°C)	(°F)
Black	540	1000
Faint Dark Red	590	1100
Cherry Red (Dark)	650	1200
Cherry Red (Medium)	700	1300
Red	760	1400
Light Red	815	1500
Reddish-Orange	870	1600
Orange	930	1700
Orange To Pale Orange-Lemon	980	1800
Orange To Pale Orange-Lemon	1040	1900
Orange To Pale Orange-Lemon	1090	2000
Lemon	1150	2100
Light Lemon	1205	2200
Yellow	1260	2300
Light Yellow	1315	2400
Yellowish-Grey: "White"	1370	2500

Table 11.9
Color Of Smoke From Fuel Burned In Air

Fuel	Color Of Smoke
Hay/Vegetable Compounds	White
Phosphorus	White
Benzene	White To gray
Nitro-Cellulose	Yellow To Brownish Yellow
Sulfur	Yellow To Brownish Yellow
Sulfuric Acid, Nitric Acid, Hydrochloric Acid	Yellow To Brownish Yellow
Gunpowder	Yellow To Brownish Yellow
Chlorine Gas	Greenish Yellow
Wood	Gray To Brown
Paper	Gray To Brown
Cloth	Gray To Brown
Iodine	Violet
Cooking Oil	Brown
Naphtha	Brown To Black
Lacquer Thinner	Black
Turpentine	Black
Acetone	Black
Kerosene	Black
Gasoline	Black
Lubricating Oil	Black
Rubber	Black
Tar	Black
Coal	Black
Foamed Plastic	Black
Butadiene	Black

Table 11.10
Ignition Temperature Of Gases

Gas	Temperature	
	(°C)	(°F)
Ammonia (Anhydrous)	650	1200
Butane	405	760
Carbon Monoxide	610	1130
Ethane	515	960
Ethylene	490	915
Hydrogen	400	750
Hydrogen Sulfide	260	500
Methane	540	1005
Natural Gas	480-630	900-1170
Propane	450	840
Propylene	460	860

Table 11.11
Ignition Temperature Of Liquids

Liquid	Flash Point (1)		Autoignition Temperature (2)	
	(°C)	(°F)	(°C)	(°F)
Castor Oil	230	450	450	840
Corn Oil	255	490	395	740
Creosote Oil	75	165	335	635
Denatured Alcohol	15	60	400	750
Ethyl Alcohol, Ethanol	15	55	365	690
Ethyl Ether	-45	-50	160	320
Fuel Oil No. 1	40-75	100-165	210	410
Fuel Oil No. 2	44-90	110-190	255	495
Fuel Oil No. 3	45-110	110-230	260	500
Fuel Oil No. 4	55-65	130-150	265	505
Fuel Oil No. 5	55-65	130-150	NA	NA
Fuel Oil No. 6	65	150	405	765
Gasoline	-45	-45	255	495
Glycerin	160	320	365	690
Kerosene	40-75	100-165	210	410
Lacquer	-20-25	0-80	NA	NA
Linseed Oil	220	430	345	650
Methyl Alcohol	10	50	385	725
Methyl Ethyl Ketene	-5	20	515	960
Naphtha, Safety Solvent	40-60	100-140	235	455
Naphthalene	80	175	525	980
Olive Oil	225	440	345	650
Peanut Oil	280	540	445	835
Soybean Oil	280	540	445	835
Toluene	5	40	480	895
Tong Oil	290	550	455	855
Turpentine	35	95	255	490
Xylem	25-30	80-90	465-530	865-985

Notes:

1. Flash Point – The lowest temperature at which a liquid exposed to air gives off sufficient vapor to form a flammable mixture near the surface of the liquid.
2. Autoignition – The lowest temperature required to cause a self-sustaining combustion, without initiation by a spark or flame, of a flammable material when its vapor is mixed with air in a flammable concentration.

Table 11.12
Heat Exposure Levels For Materials Of Construction Which Satisfy The Level 1 Assessment Criteria

Materials	Typical ASTM Specifications For Pressurized Components	Heat Exposure Zone Levels Which Satisfy The Level 1 Assessment Criteria
Carbon Steels	A36, A53, A105, A106, A131, A139, A181, A216, A234, A266, A283, A285, A333, A350, A352, A420, A515, A516, A537, A671, A672, API 5L	I, II, III, IV
Low Alloy Steels	A182, A217, A234, A335, A336, A387, A691	I, II, III, IV
Austenitic Stainless Steels (1)	A312, A358, A240, A403, A351	I, II, III, IV
Alloy 20	B366, B462, B463, B464, B729, B744	I, II, III, IV
Alloy 400	B127, B164, B165, B366, B564, A494	I, II, III
Duplex Stainless Steels (2) Alloy 2205 Alloy 2507	A182, A240, A789, A790, A815 (UNS S31803, UNS J92205) (2507 – UNS S39275)	I, II
Alloy 800, 800H	B163, B366, B407, B409, B564	I, II, III, IV
Alloy 825	B163, B366, B423, B424, B704, B705	I, II, III, IV
Alloy 600	B163, B168, B366, B564	I, II, III, IV
Alloy 625	B167, B366, B443, B444, B564, A494	I, II, III, IV
Alloy C-276	B366, B575, B622	I, II, III, IV
Copper Alloys	B68, B96, B111, B169, B171, B395, B584	I, II
Aluminum Alloys	B209, B210, B241, B247	I, II
Precipitation Hardened Alloy Steels (3)	17-4PH, 17-7PH	I, II, III

Notes:

1. If the austenitic stainless steel components are insulated, are not coated for under insulation stress corrosion cracking protection, and normally operate between 50°C and 175°C (120°F and 350°F), then preventative maintenance may be required to assure that halide contamination of the insulated surfaces has not occurred. The concern in this case is halide induced stress corrosion cracking of contaminated insulated surfaces after the equipment is returned to service.
2. Above 315°C (600°F), Duplex alloys will undergo a loss of toughness with time and temperature. In addition, severe loss in ductility (sigma phase formation) with short term exposure to 595°C and 925°C (1100°F and 1700°F) can also occur.
3. Precipitation hardened alloys may experience a loss in toughness when heated above 260°C (500°F), and slowly cooled.

Table 11.13
Melting Points Of Metals And Alloys

Material	UNS Number	Melting Point (1)	
		(°C)	(°F)
Commercially Pure Aluminum	A91050	655	1215
Aluminum Alloy	A96061	650	1205
Red Brass	C23000	1025	1880
Yellow Brass	C26800	930	1710
Admiralty Brass	C44300	940	1720
Naval Brass	C46400	900	1650
70/30 Copper Nickel	C71500	1240	2260
Silicon Bronze (2)	C87200	915	1680
Tin Bronze (2)	C90300	1000	1830
2.52% Carbon Gray Iron (2)	F11701	1295	2360
Ductile Iron (2)	F32800	1160	2120
0.15% Carbon Steel	G10150	1525	2780
CA15 (2)	J91150	1510	2750
CD-4Mcu (2)	--	1480	2696
CF-8 (2)	J92600	1425	2595
CF-8M (2)	J92900	1400	2550
CK-20 (2)	J94202	1425	2595
CN-7M (2)	--	1455	2650
1 ¼ Cr – ½ Mo	K11597	1510	2750
2 ¼ Cr – 1 Mo	K21590	1515	2760
5 Cr – ½ Mo	K41545	1510	2755
9 Cr – 1 Mo	K90941	1500	2730
Nickel 200	N02200	1445	2635
Alloy 400 (Model (3))	N04400	1350	2460
Alloy K-500 (Model (3))	N05500	1350	2460
Alloy X (Hostelry (3))	N06002	1315	2400
Alloy G (Hostelry (3))	N06007	1345	2450

Table 11.13
Melting Points Of Metals And Alloys

Material	UNS Number	Melting Point (1)	
		(°C)	(°F)
Alloy 600 (Inconnel (3))	N06600	1415	2580
Alloy 601 (Inconnel (3))	N06601	1370	2495
Alloy 625 (Inconnel (3))	N06625	1350	2460
Alloy 718 (Inconel (3))	N07718	1335	2435
Alloy X-750 (Inconel (3))	N07750	1425	2600
Alloy 20 (20Cb3 (3))	N08020	1425	2600
Alloy 800 (Incoloy (3))	N08800	1385	2525
Alloy 801 (Incoloy (3))	N08801	1385	2525
Alloy 825 (Incoloy (3))	N08825	1400	2550
Alloy 925 (Incoloy (3))	N09925	1365	2490
Alloy C-276 (Hastelloy (3))	N10276	1315	2400
Alloy B-2 (Hastelloy (3))	N10665	1380	2520
17-4 PH	S17400	1440	2625
Type 304	S30400	1450	2640
Type 310	S31000	1450	2640
Type 316	S31600	1400	2550
Type 321	S32100	1425	2595
Type 347	S34700	1425	2595
Titanium Grade 2	R50400	1705	3100
Stellite 6 (3)	W73006	1355	2470
Copper (4)	--	1085	1980
Gold (4)	--	1065	1945
Iron (4)	--	1535	2795
Lead (4)	--	330	620
Magnesium (4)	--	650	1200
Tin (4)	--	230	450
Silver (4)	--	960	1760

Table 11.13
Melting Points Of Metals And Alloys

Material	UNS Number	Melting Point (1)	
		(°C)	(°F)
Zinc (4)	--	420	788
Zirconium (4)	--	1850	3365
95/5 Lead-Tin Solder	54320	310	595
97.5/2.5 Lead-Silver Solder (5)	--	305	580
Lead Babbitt – Alloy 7 (6)	--	270	515

Notes:

1. Pure metals melt at a specific temperature. Metal alloys melt over a temperature range. The temperature shown for alloys is the liquidus temperature; that is, the temperature at which the alloy is completely liquid. The temperature at which the alloy begins to melt (solidus temperature) is somewhat lower
2. Casting
3. Trade Name
4. Pure element
5. ASTM Alloy Grade 2.5S
6. ASTM B23

Table 11.14
Ignition Temperature Of Wood

Type of Wood	Approximate Ignition Temperature	
	(°C)	(°F)
Douglas Fir	260	500
Paper Birch	200	400
Spruce	260	500
Western Red Cedar	190	380
White Oak	200	400
White Pine	260	500

Note: The ordinary ignition temperature of wood is between 230°C and 430°C (450°F and 800°F). The values in the table represent average ignition temperatures for selected wood types.

Table 11.15
Properties Of Commercial Glass

Glass Code	Glass type	Principal Use	Thermal Expansion Coefficient ($^oC^{-1}$)	Modulus Of Elasticity (MPa)	Thermal Shock Resistance			Thermal Stress Resistance (^oC)	Softening Point (^oC)	Working Point (^oC)
					1/8 inch Thick (^oC)	1/4 inch Thick (^oC)	1/2 inch Thick (^oC)			
0010	Potash-soda lead	Lamb tubing	$91(10)^{-7}$	$6.21(10^4)$	65	50	35	19	625	970
0041	Potash-soda-lead	Thermometers	$84(10)^{-7}$	--	70	60	40	19	650	--
0080	Soda-line	Lamp bulbs	$92(10)^{-7}$	$6.76(10^4)$	65	50	35	17	695	1000
0120	Potash-soda-lead	Lamb tubing	$89(10)^{-7}$	--	65	50	35	17	630	975
1710	Hard lime	Cooking utensils	$42(10)^{-7}$	$8.76(10^4)$	135	115	75	29	915	1200
1770	Soda-lime	General	$82(10)^{-7}$	--	70	60	40	19	710	--
2405	Hard red	General	$43(10)^{-7}$	--	135	115	75	36	800	--
2475	Soft-red	Neon signs	$91(10)^{-7}$	--	65	50	35	17	695	--
3321	Hard green sealing	Sealing	$40(10)^{-7}$	--	135	115	75	39	780	--
4407	Soft green	Signal ware	$90(10)^{-7}$	--	65	50	35	17	695	--
6720	Opal	General	$80(10)^{-7}$	--	70	60	40	19	775	--
6750	Opal	Lighting ware	$87(10)^{-7}$	--	65	50	35	18	670	--
6810	Opal	Lighting ware	$69(10)^{-7}$	--	85	70	45	23	770	--
7050	Borosilicate	Series sealing	$46(10)^{-7}$	--	125	100	70	34	705	--
7052	Borosilicate	Kovar sealing	$46(10)^{-7}$	--	125	100	70	34	710	1115
7070	Borosilicate	Low-loss electrical	$32(10)^{-7}$	$4.68(10^4)$	180	150	100	70	---	1100
7250	Borosilicate	Baking Ware	$36(10)^{-7}$	---	160	130	90	43	775	---
7340	Borosilicate	Gauge Glass	$67(10)^{-7}$	$7.93(10^4)$	85	70	45	20	785	---
7720	Borosilicate	Electrical	$36(10)^{-7}$	$6.55(10^4)$	160	130	90	45	755	1110
7740	Borosilicate	General	$32(10)^{-7}$	$6.76(10^4)$	180	150	100	48	820	1220
7760	Borosilicate	Electrical	$34(10)^{-7}$	$6.27(10^4)$	160	130	90	51	780	1210
7900	96% Silica	High Temperature	$8(10)^{-7}$	$6.69(10^4)$	1250	1000	750	200	1500	---
7910	96% Silica	Ultraviolet Transmission	$8(10)^{-7}$	$6.69(10^4)$	1250	1000	750	200	1500	---
7911	96% Silica	Ultraviolet Transmission	$8(10)^{-7}$	$6.69(10^4)$	1250	1000	750	200	1500	---
8870	High Lead	Sealing or Electrical	$91(10)^{-7}$	$5.24(10^4)$	65	50	35	22	580	---
9700	---	Ultraviolet Transmission	$37(10)^{-7}$	---	150	120	80	42	805	1195
9741	---	Ultraviolet Transmission	$39(10)^{-7}$	---	150	120	80	40	705	---

Table 11.16
Scaling Temperatures Of Alloys In Air

Alloy Designation	Composition	Scaling Temperature	
		(°C)	(°F)
Carbon Steel	Fe-0.10C	480	900
Low Alloy Steel	1-1/4Cr-1/2Mo	620	1150
Low Alloy Steel	2-1/4Cr-1Mo	620	1150
Low-Alloy Steel	5Cr-0.5Mo	620	1150
Low Alloy Steel	7Cr-1Mo	650	1200
Low Alloy Steel	9Cr-1Mo	675	1250
Type 410 Stainless Steel	12Cr	760	1400
Type 430 Stainless Steel	17Cr	845	1550
Type 442 Stainless Steel	21Cr	955	1750
Type 446 Stainless Steel	27Cr	1040	1900
Type 304 Stainless Steel Type 321 Stainless Steel Type 347 Stainless Steel	18Cr-8Ni 18Cr-10Ni-Ti 18Cr-10Ni-Cb	900	1650
Type 309 Stainless Steel	23Cr-12Ni	1095	2000
Type 310 Stainless Steel	25Cr-20Ni	1150	2100
Type 316 Stainless Steel	18Cr-8Ni-2Mo	900	1650
Duplex 2205 Duplex 2507	22Cr-5Ni-3Mo 25Cr-7Ni-4Mo	1040	1900
Alloy 600 Alloy 625	72Ni-15Cr-8Fe 60Ni-22Cr-9Mo-3.5Cb	1040	1900
Alloy 800 Alloy 825	33Ni-42Fe-21Cr 42Ni-Fe-21.5Cr-3Mo-2.3Cu	1040	1900
N-155	Fe-based superalloy	1040	1900
S-816	Co-based superalloy	980	1800
M-252	Ni-based superalloy	980	1800
HS-21	Co-based superalloy Cr-based superalloy Ni-based superalloy Cu-based superalloy	1150 900 790 455	2100 1650 1450 850
Brass	70Cu-30Zn	705	1300
Alloy B-2	Ni-based superalloy	760	1400
Alloy C-276	Ni-based superalloy	1150	2100
Alloy X	Ni-based superalloy	1205	2200

Table 11.16
Scaling Temperatures Of Alloys In Air

Alloy Designation	Composition	Scaling Temperature	
		(°C)	(°F)
HW	12Cr-60Ni-bal Fe	1120	2050
HT	15Cr-66Ni-bal Fe	1150	2100
HX	17Cr-66Ni-bal Fe	1150	2100

Notes:

1. The temperature below which the oxidation rate is negligible. Negligible is often defined as less than 0.002 g weight gain per square inch per hour.

Table 11.17
Tempering Colors Of Steel

Temper Color	Approximate Temperature	
	(°C)	(°F)
Pale Yellow	190	380
Straw Yellow	215-225	420-440
Yellowish-Brown	240-250	460-480
Bluish-Purple	260-280	500-540
Violet	280-295	540-560
Pale Blue	295-305	560-580
Blue	315-340	600-640

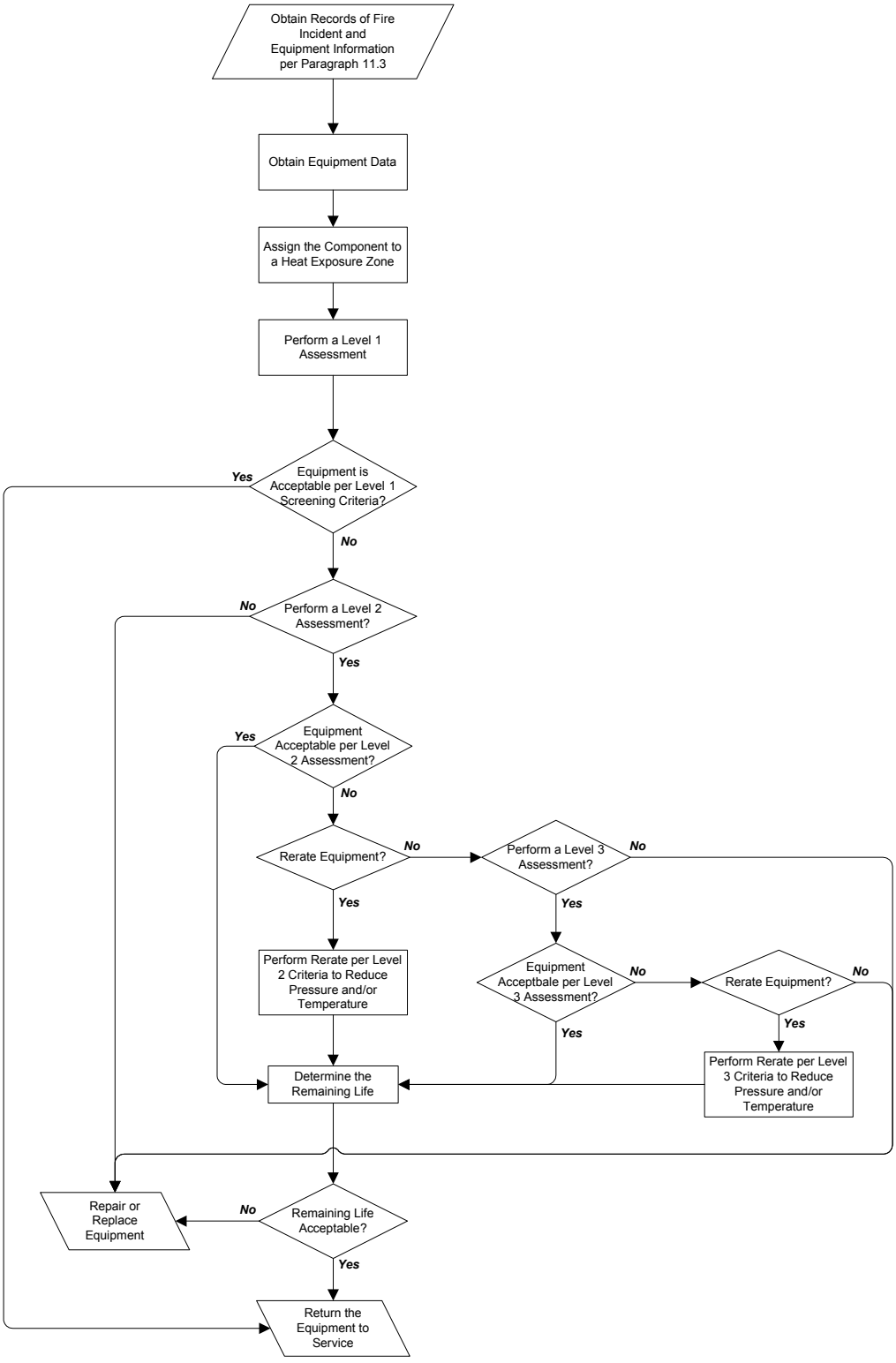

Figure 11.1
Overview of the Procedure to Evaluate a Component with Fire Damage

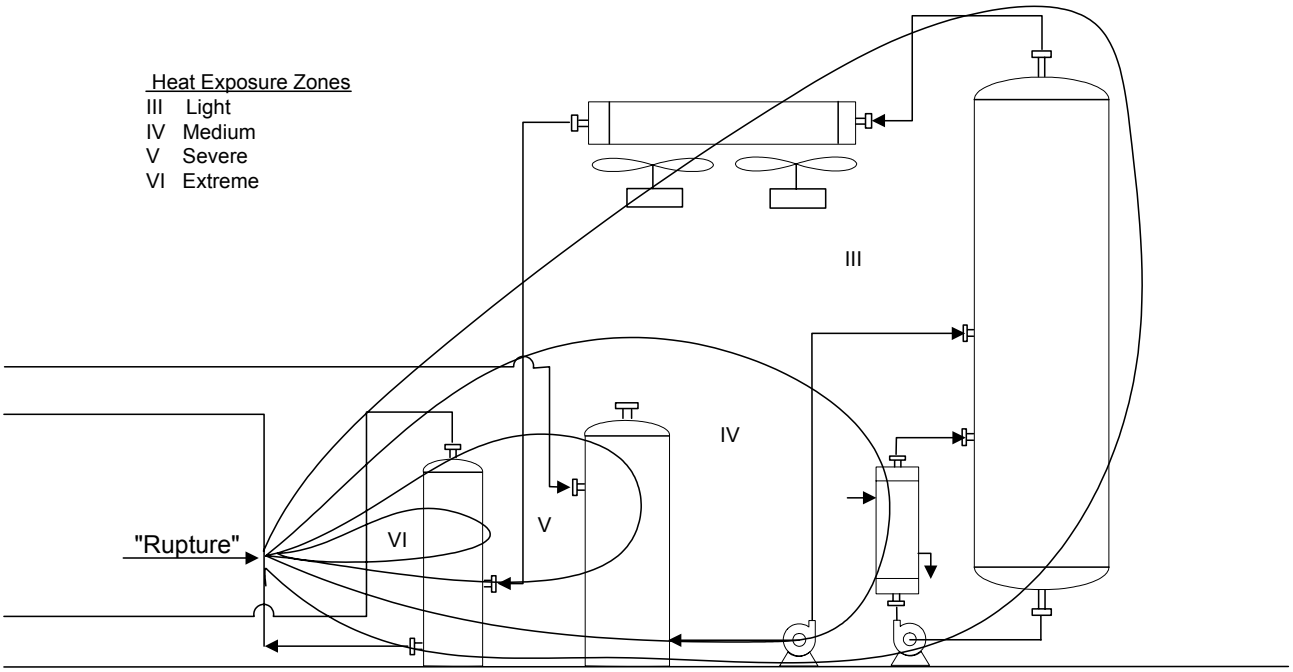

Note: See Table 11.6 for definitions of the Heat Exposure Zones.

Figure 11.2
Idealized Representation of Plant Equipment Exposed To Different Fire (Heat) Zones III through VI

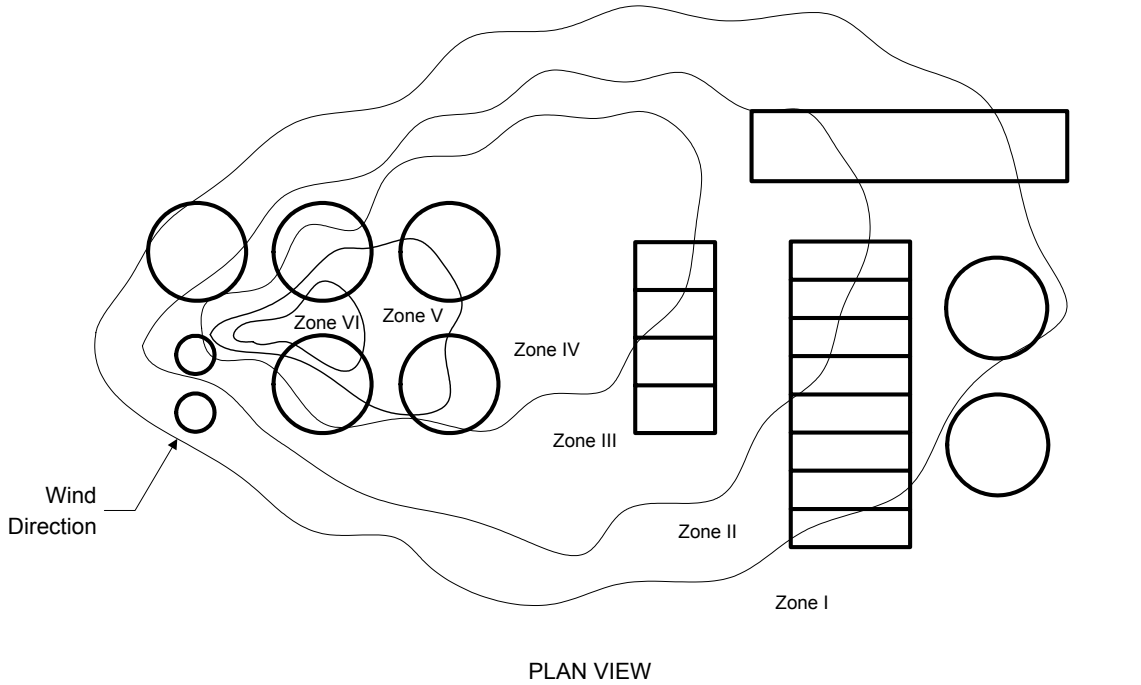

Note: See Table 11.6 for definitions of the Heat Exposure Zones.

Figure 11.3
Idealized Fire (Heat) Pattern and Equipment Exposure with Zones I through VI Shown

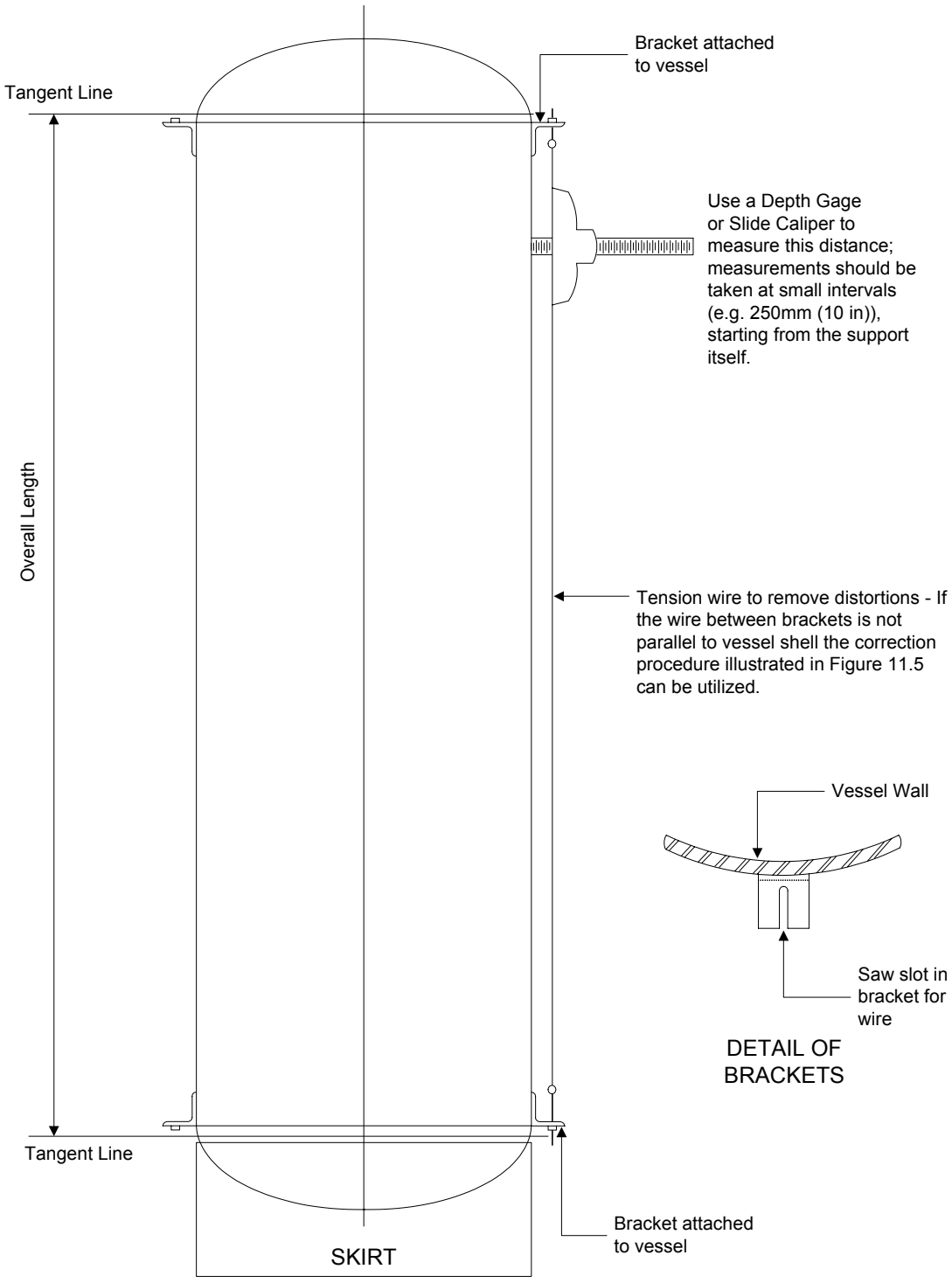

Figure 11.4
Sketch Illustrating the Procedure for Measuring the Vertical Shell Profile to Detect Vessel Distortion

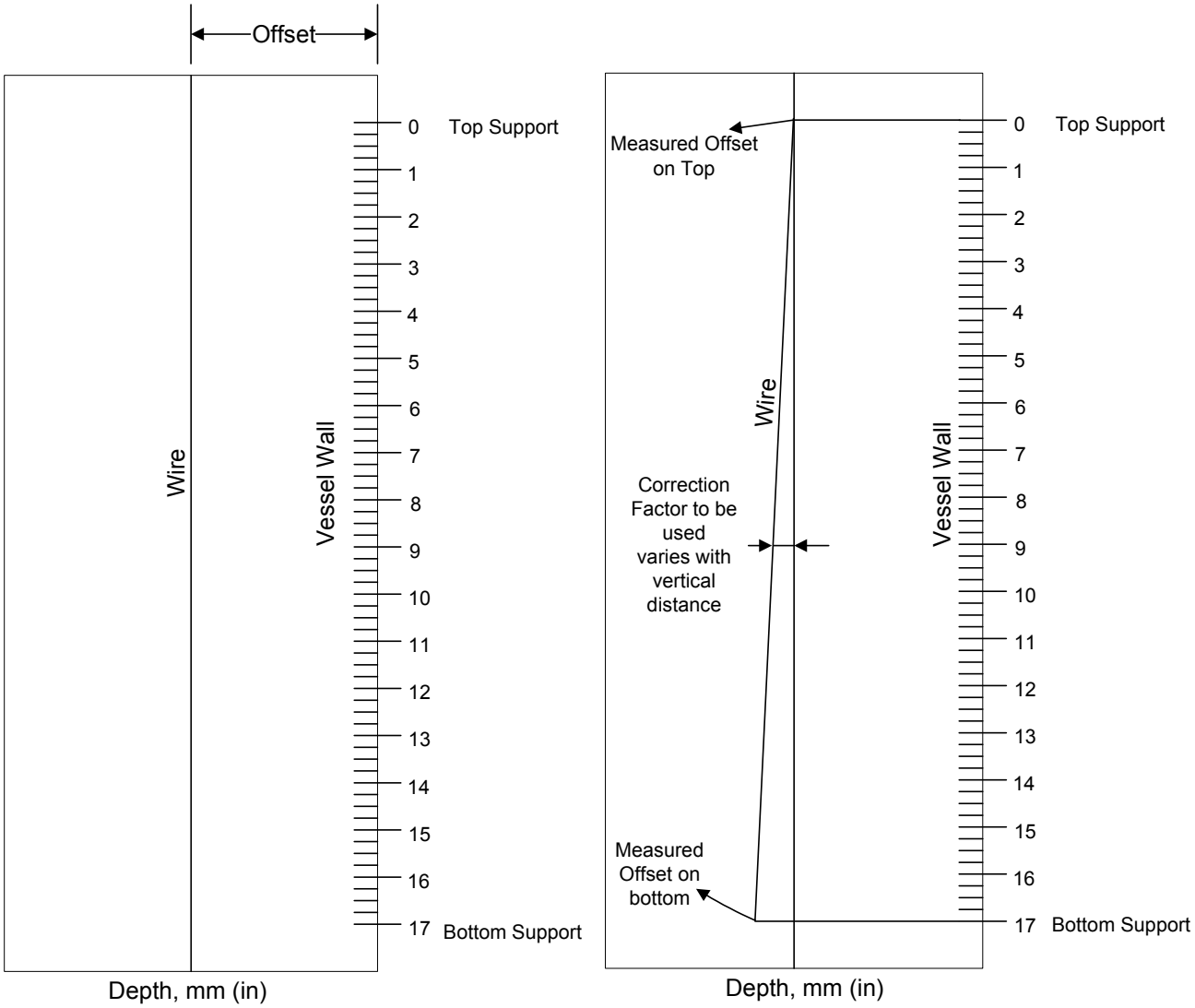

Note: The correction factor is applied to the offset measurements to account for a non-vertical datum (vertical wire used as a reference line)

Figure 11.5
Illustration of Vertical Wire Offset For Measuring Profile for the Ideal Situation and When the String Is Not Parallel To the Vessel

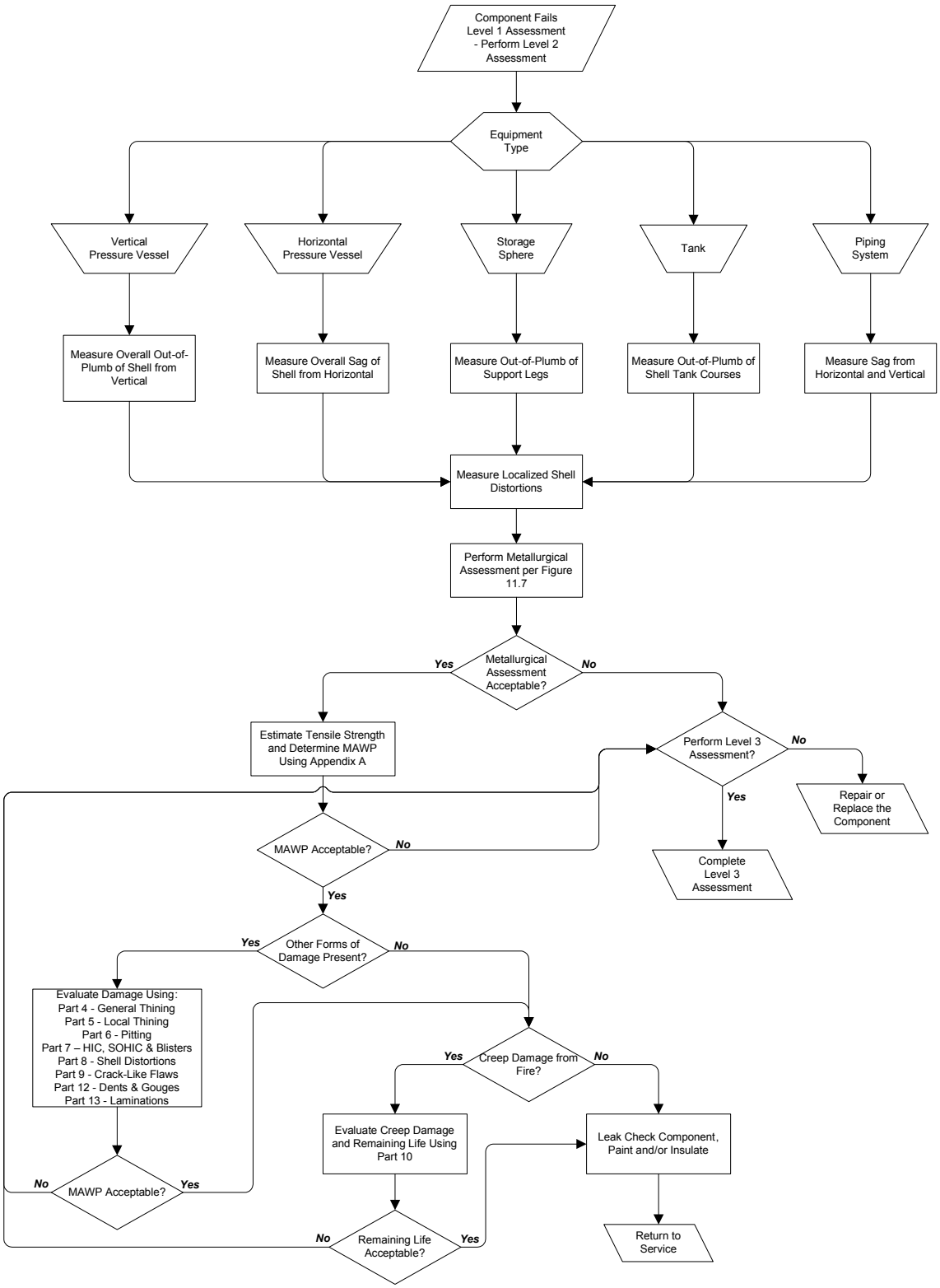

Figure 11.6
Level 2 Assessment Procedure for Fire Damage

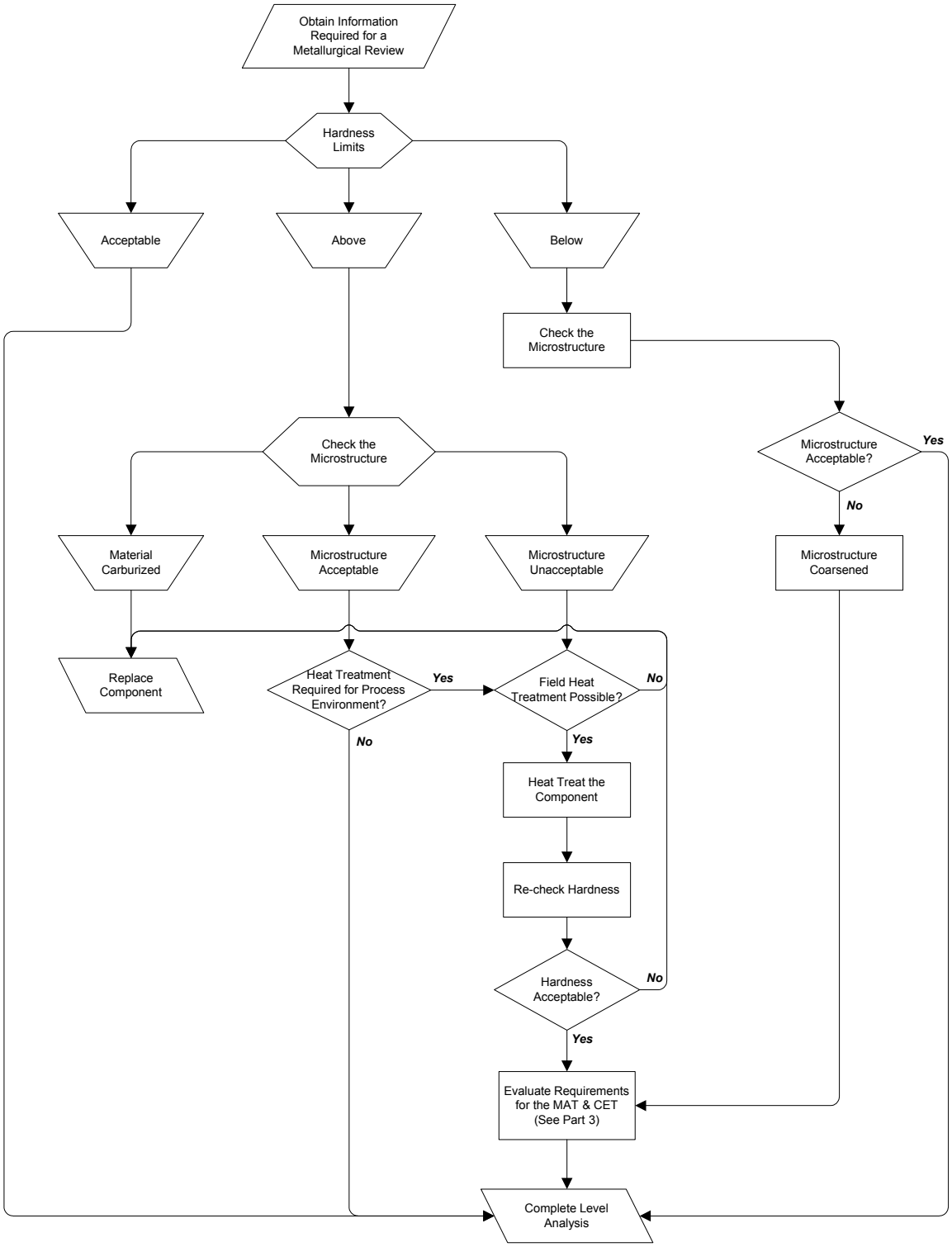

Figure 11.7
Flow Diagram for Metallurgical Assessment of Fire Damage to Carbon and Low Alloy Steels

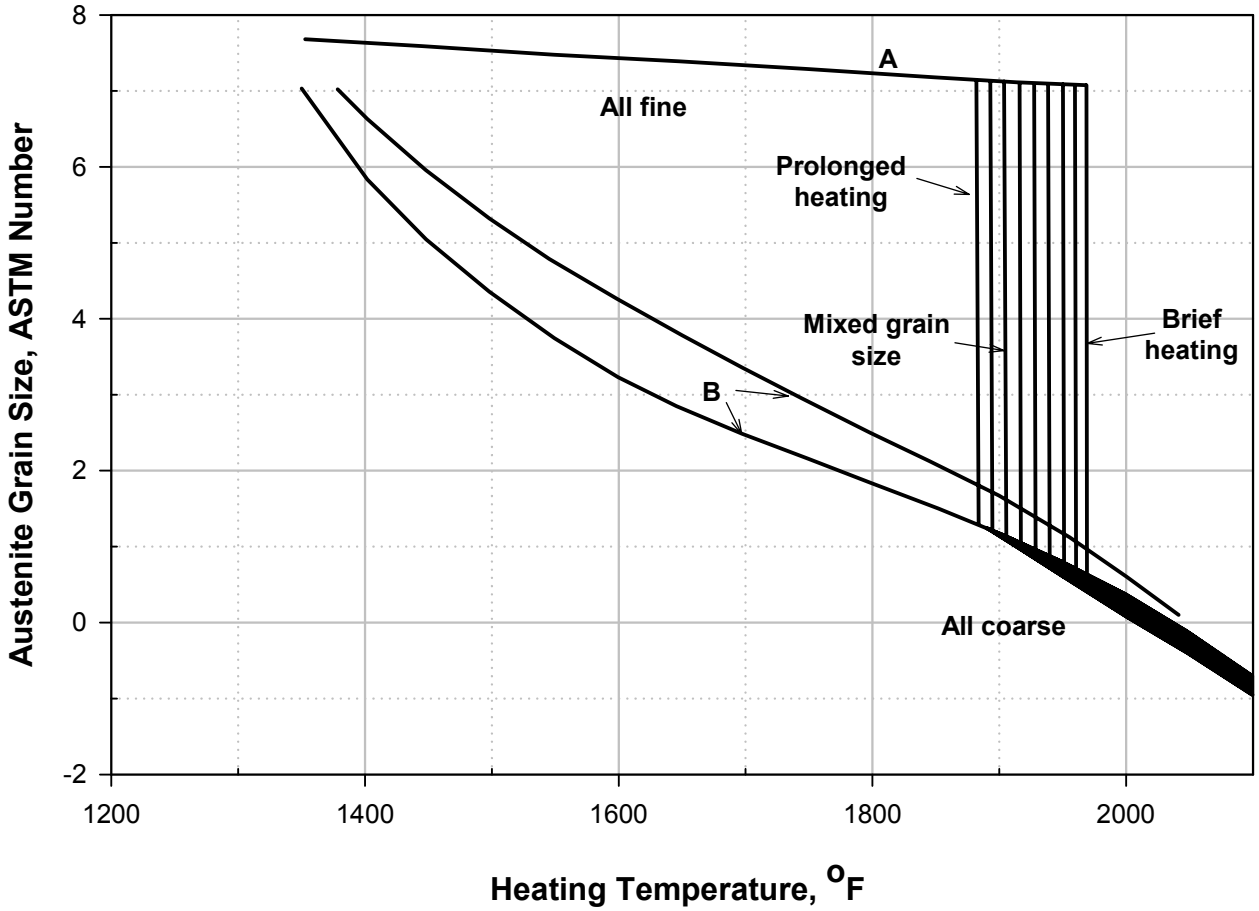

Notes:
1. Curve A – killed steel with a fine austenitic grain size (e.g. ASTM A 516).
2. Curve B – killed steel with a coarse austenitic grain size (e.g. ASTM A 515).

Figure 11.8
Coarsening Behavior of Carbon Steels as a Function of Temperature
(From: ASM Metals Handbook, 1948, ASM International)

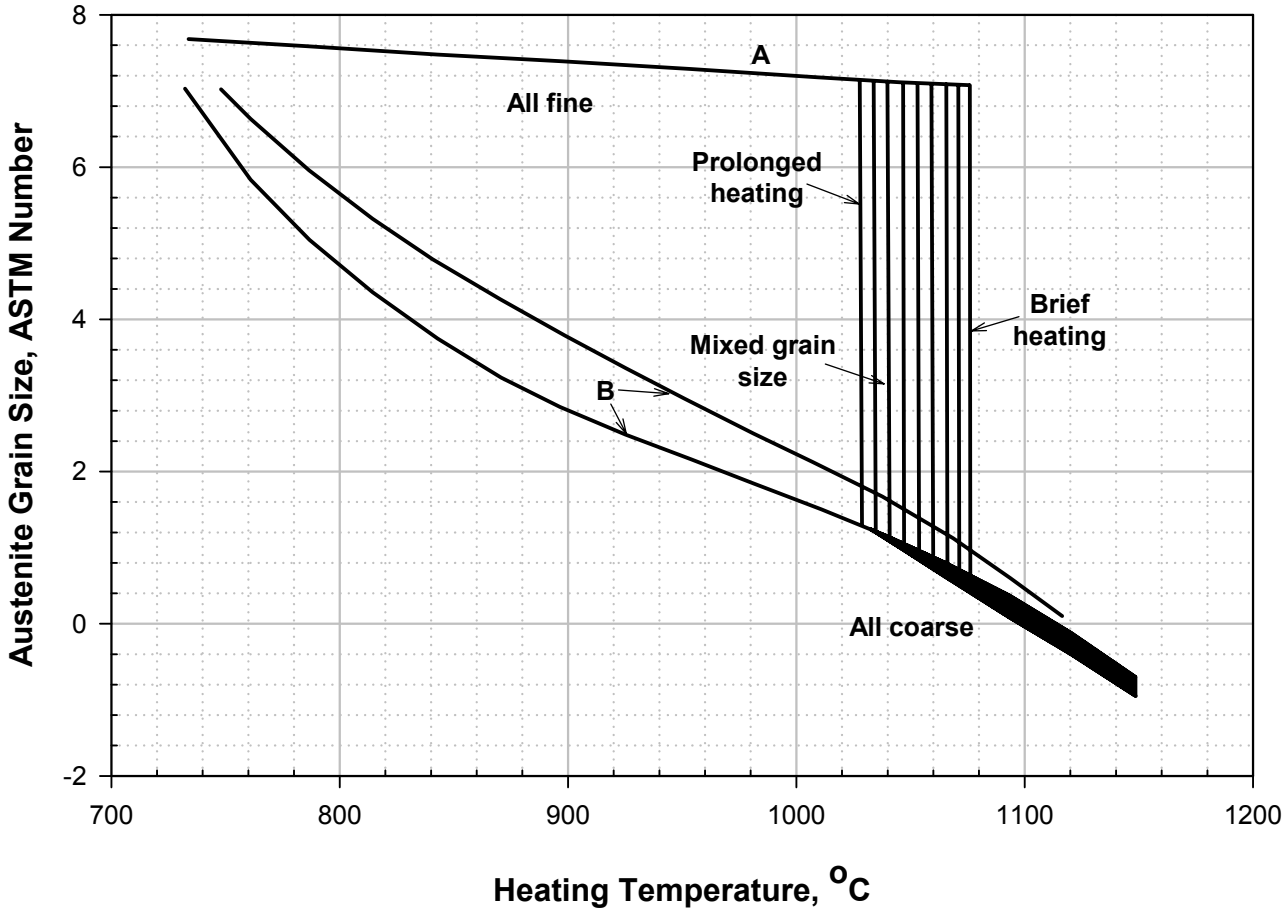

Notes:
1. Curve A – killed steel with a fine austenitic grain size (e.g. ASTM A 516).
2. Curve B – killed steel with a coarse austenitic grain size (e.g. ASTM A 515).

Figure 11.8M
Coarsening Behavior of Carbon Steels as a Function of Temperature
(From: ASM Metals Handbook, 1948, ASM International)

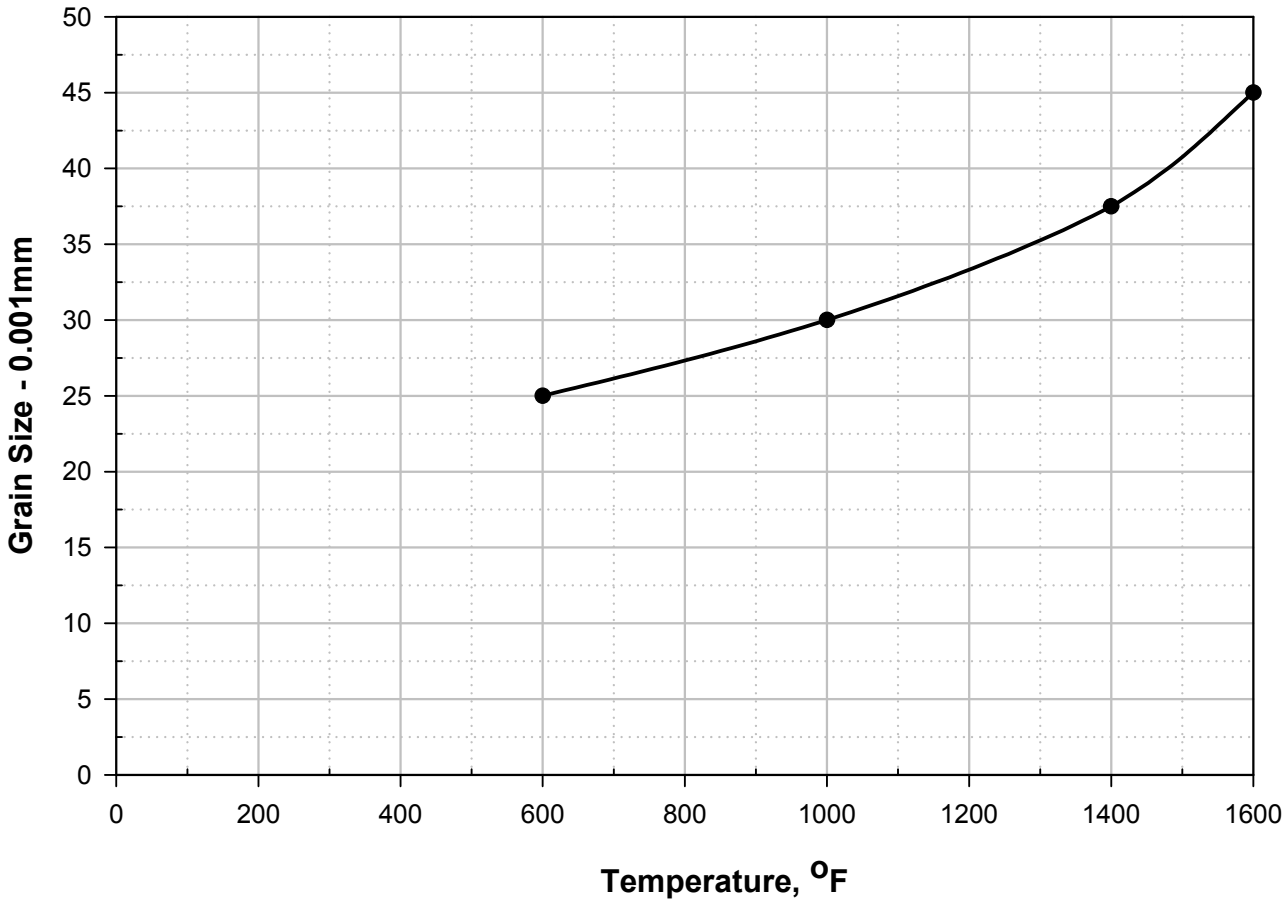

Figure 11.9
Effect of Heat on the Grain Size of Copper

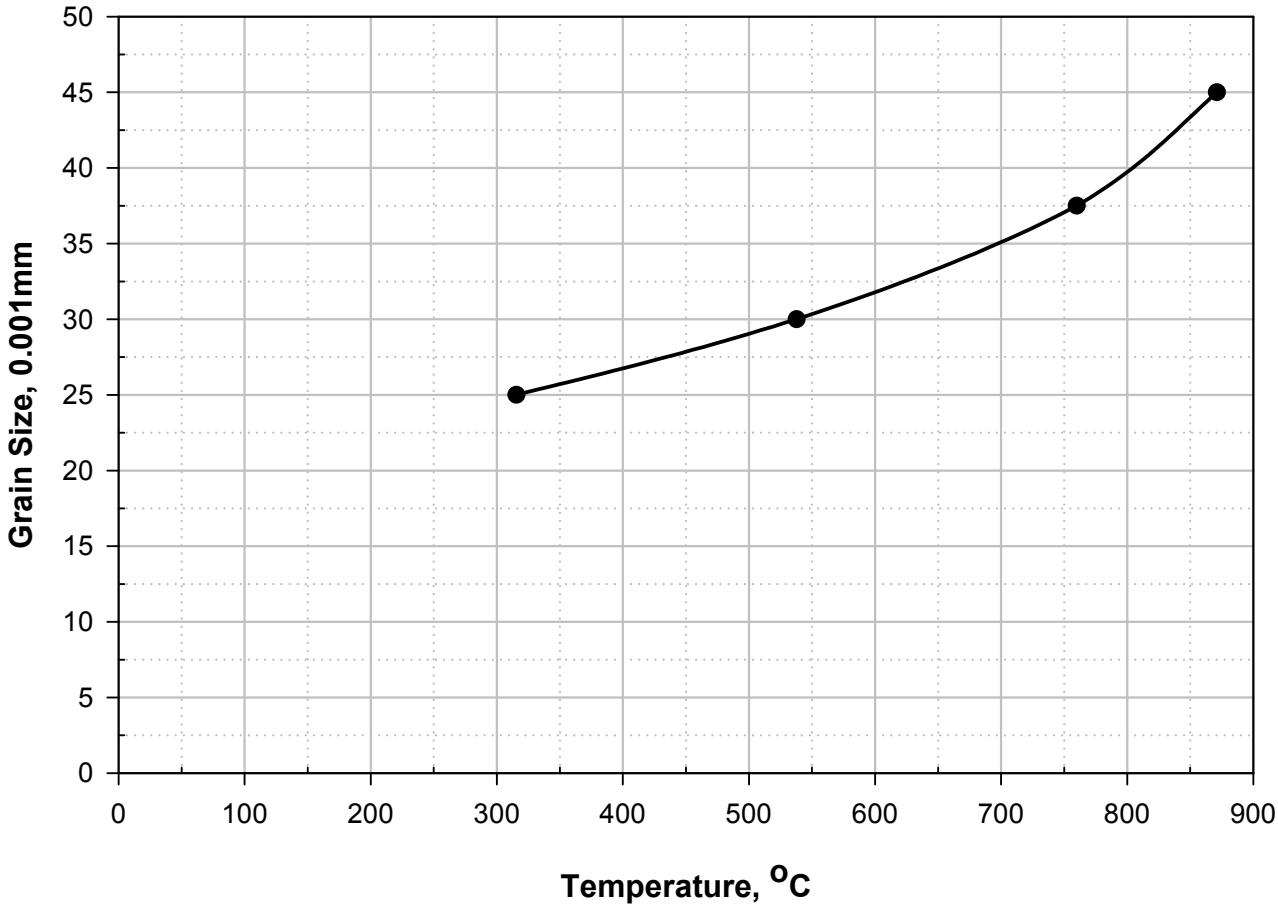

Figure 11.9M
Effect of Heat on the Grain Size of Copper

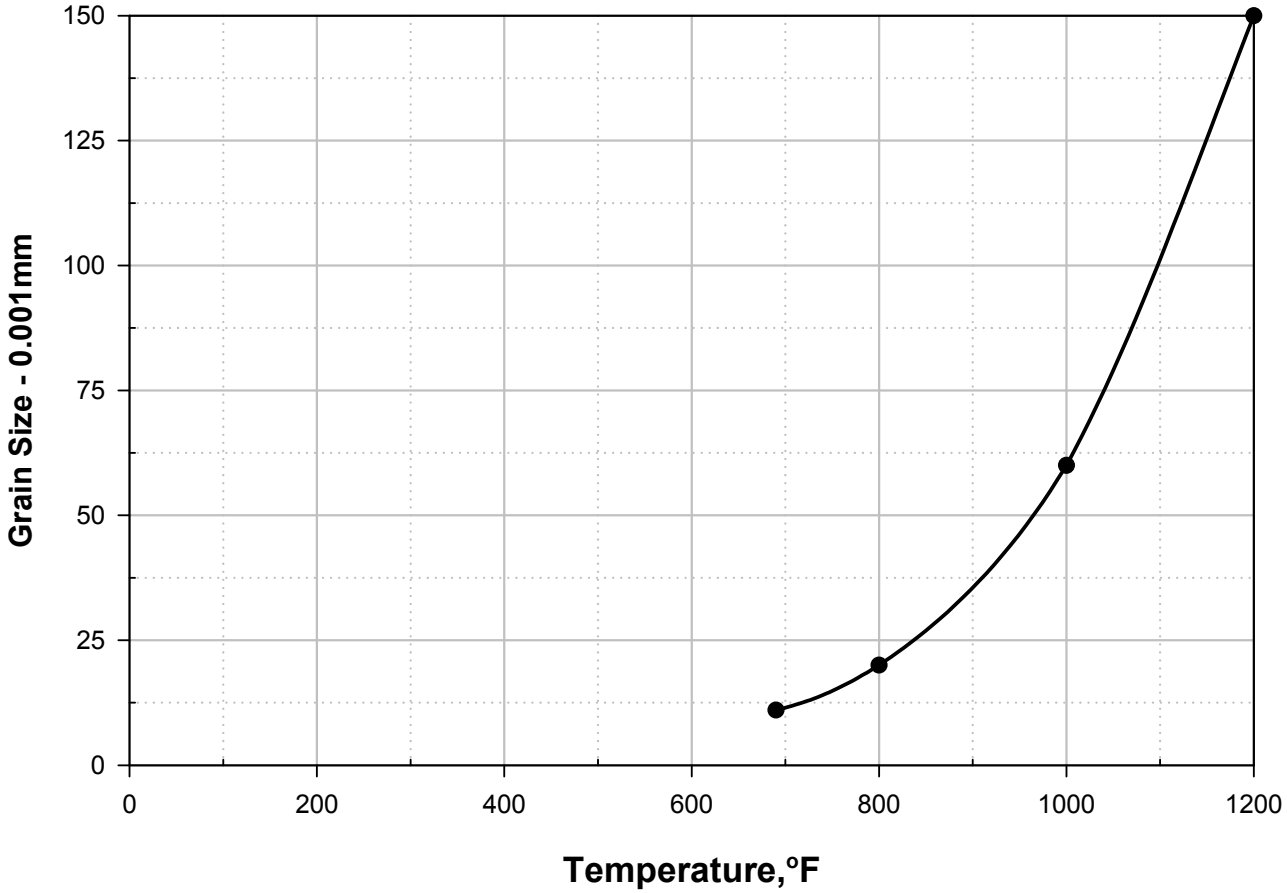

Figure 11.10
Effect of Heat on the Grain Size of Admiralty Brass Tubing Cold Drawn 50%

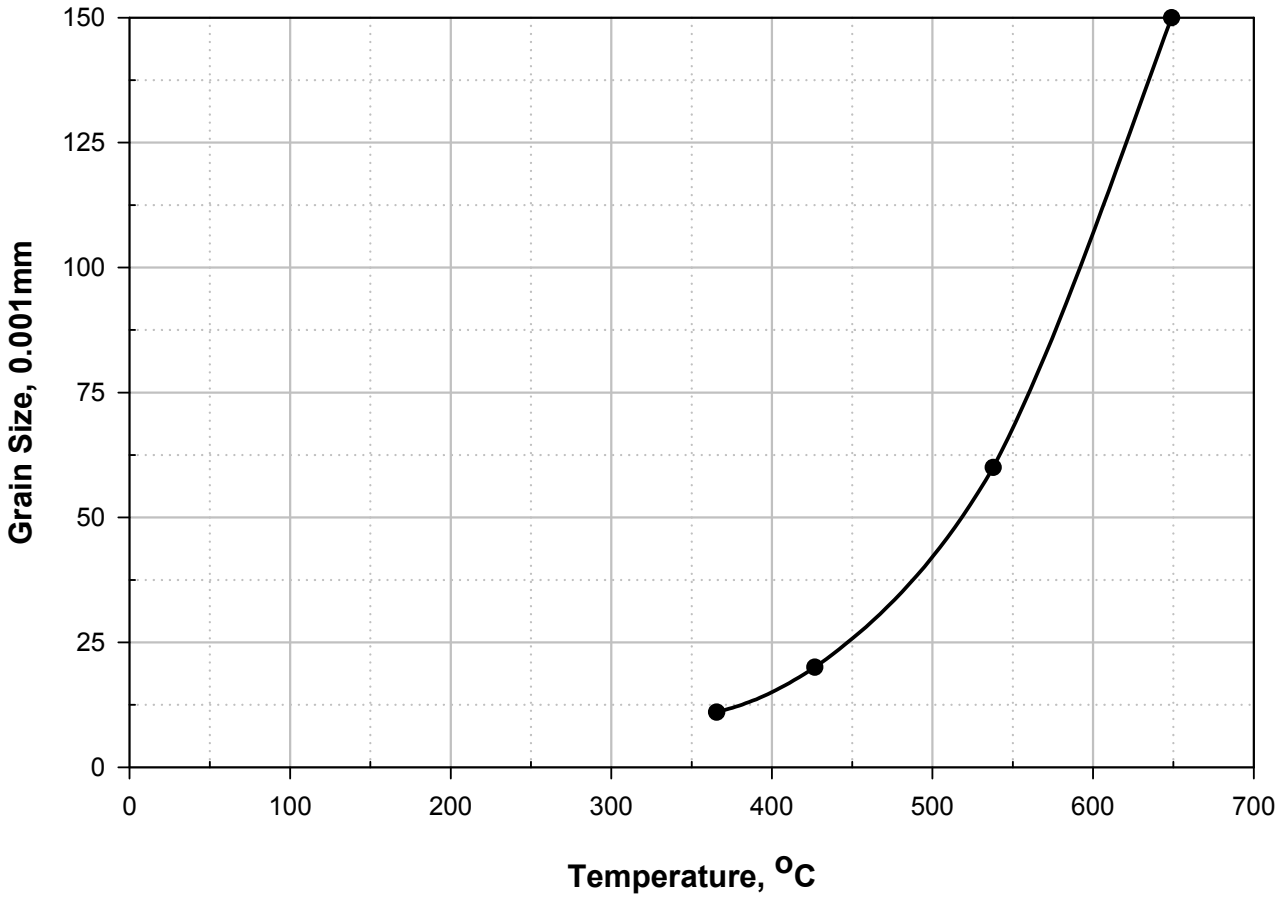

Figure 11.10M
Effect of Heat on the Grain Size of Admiralty Brass Tubing Cold Drawn 50%

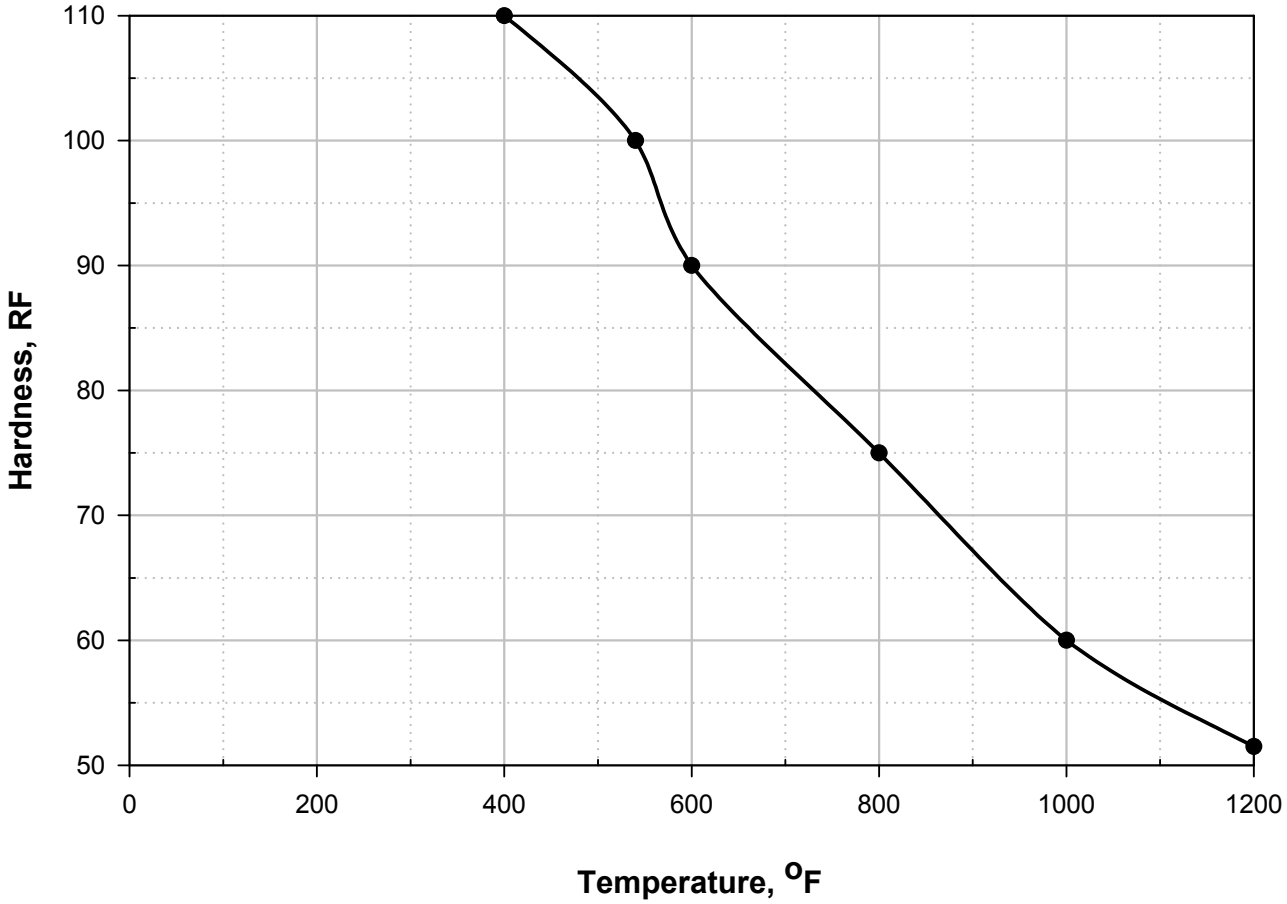

Figure 11.11
Effect ff Heat (Based on a One Hour Exposure) on The Hardness of Admiralty Brass Tubing Cold Drawn 50%

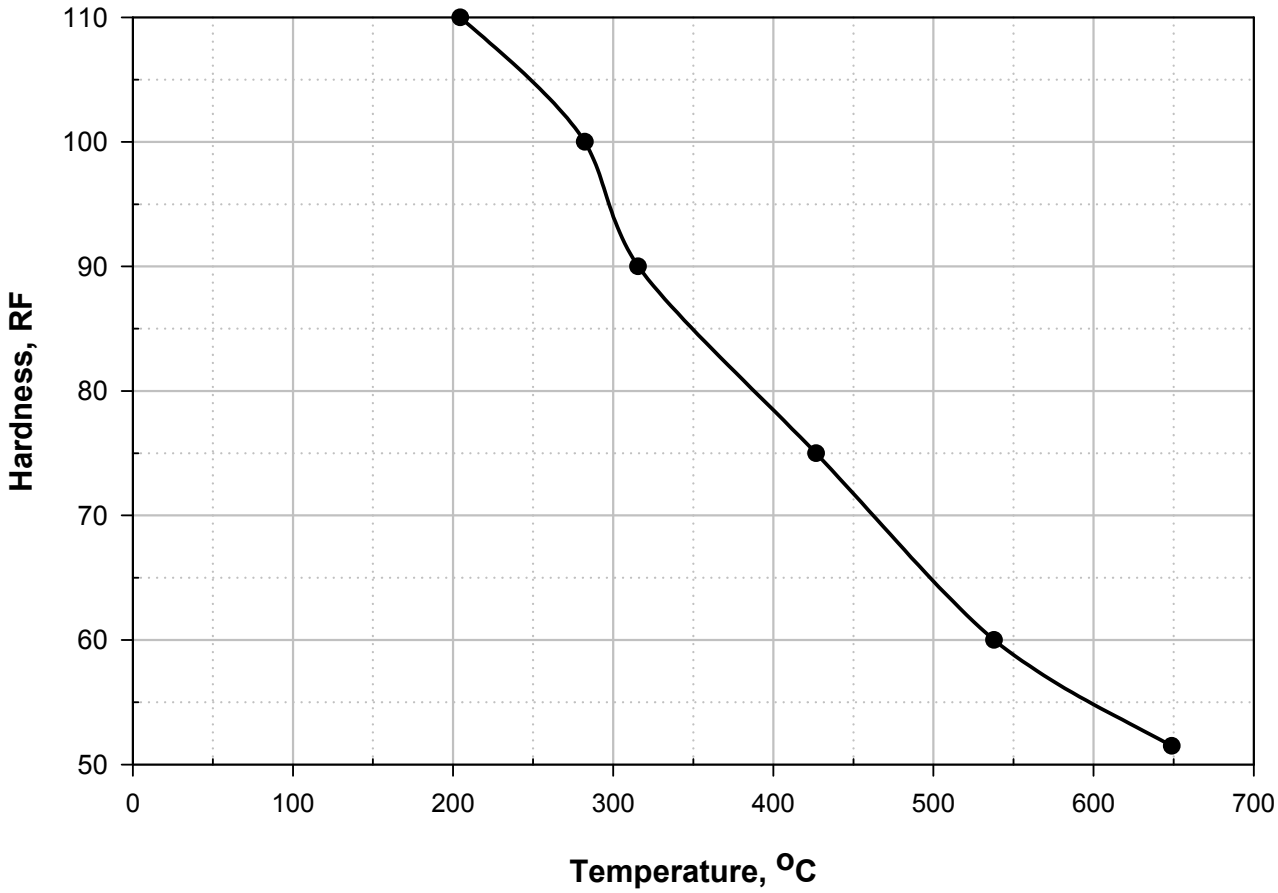

Figure 11.11M
Effect ff Heat (Based on a One Hour Exposure) on The Hardness of Admiralty Brass Tubing Cold Drawn 50%

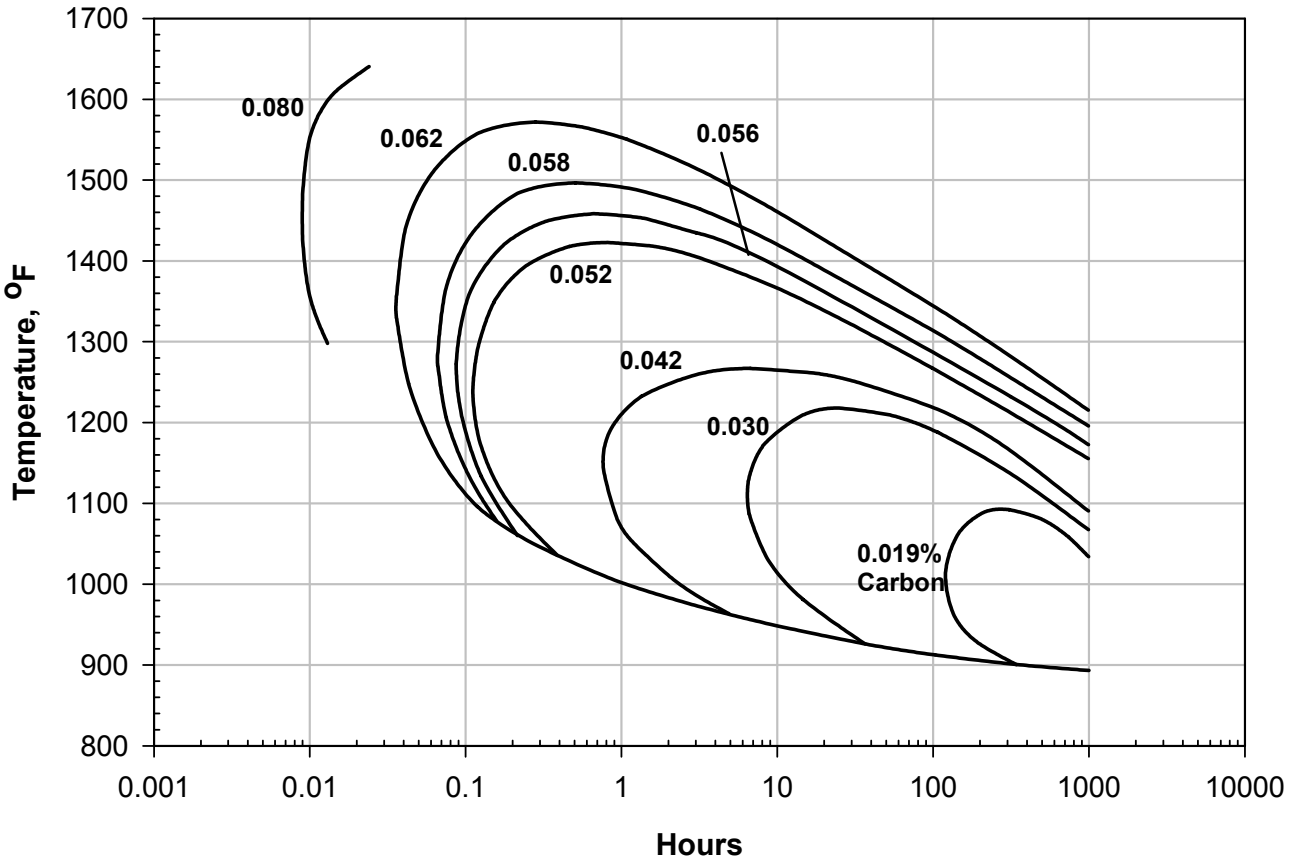

Notes:

1. The time required for formation of carbide precipitation in stainless steels with various carbon contents is shown in the above graph. Carbide precipitation forms in the areas to the right of the various carbon-content curves.
2. Within the time periods applicable to welding, chromium-nickel stainless steels with 0.05% or less carbon would be quite free from grain boundary precipitation.
3. The figure is from *Stainless Steels For Acetic Acid Service*, American Iron And Steel Institute, 1977)

Figure 11.12
Sensitization of Type 300 Series Stainless Steels

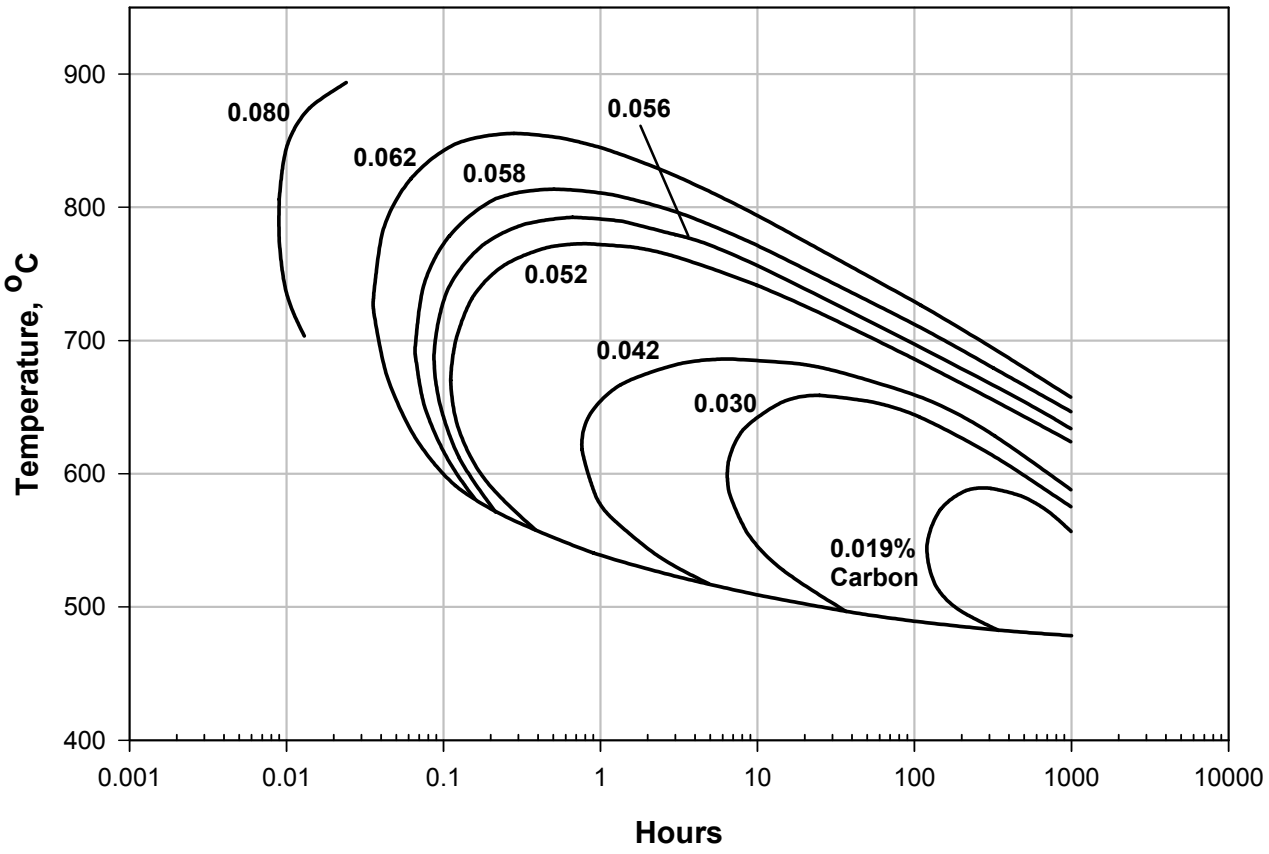

Notes:

1. The time required for formation of carbide precipitation in stainless steels with various carbon contents is shown in the above graph. Carbide precipitation forms in the areas to the right of the various carbon-content curves.
2. Within the time periods applicable to welding, chromium-nickel stainless steels with 0.05% or less carbon would be quite free from grain boundary precipitation.
3. The figure is from *Stainless Steels For Acetic Acid Service*, American Iron And Steel Institute, 1977)

Figure 11.12M
Sensitization of Type 300 Series Stainless Steels

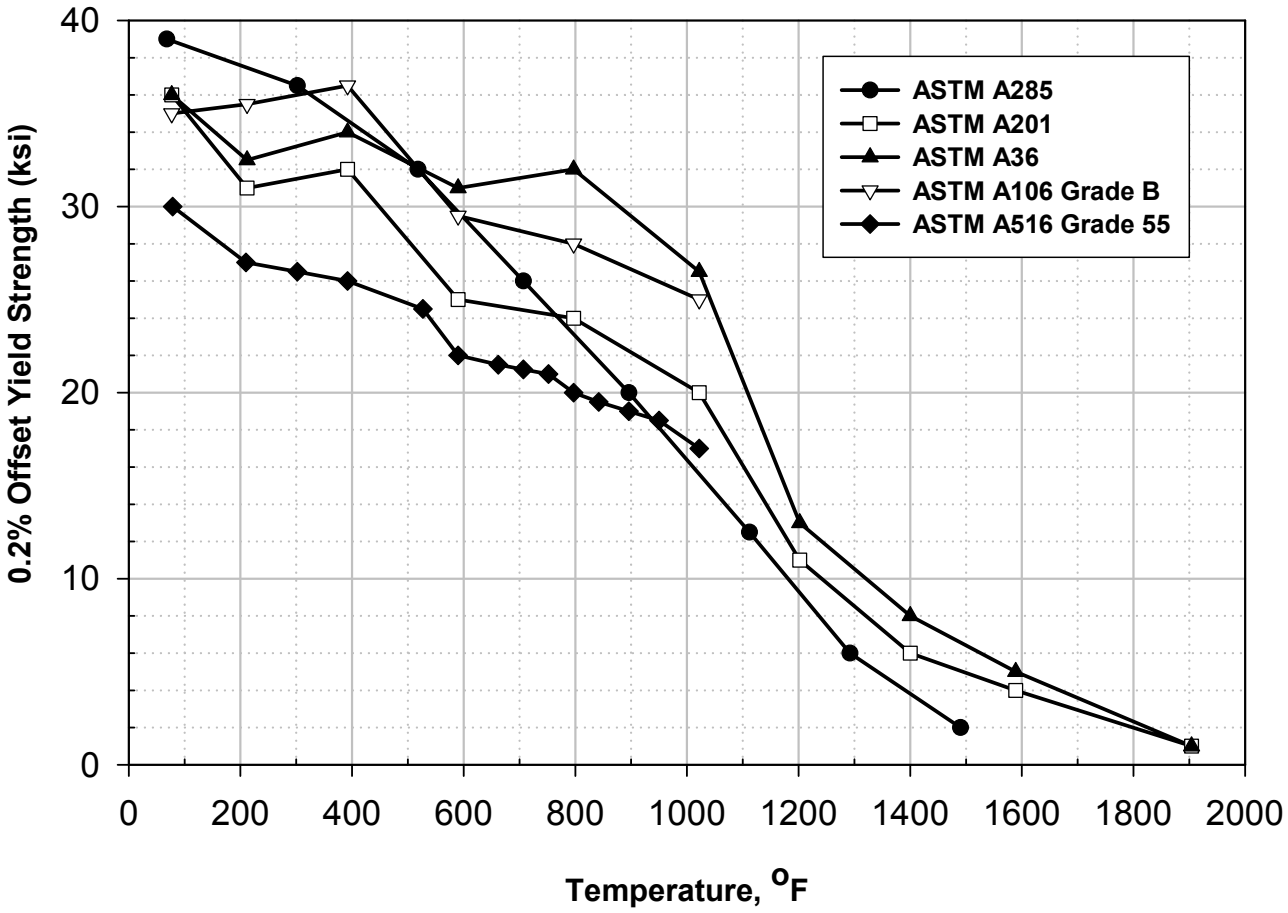

Figure 11.13
High Temperature Yield Strengths of Some Low Carbon Steels

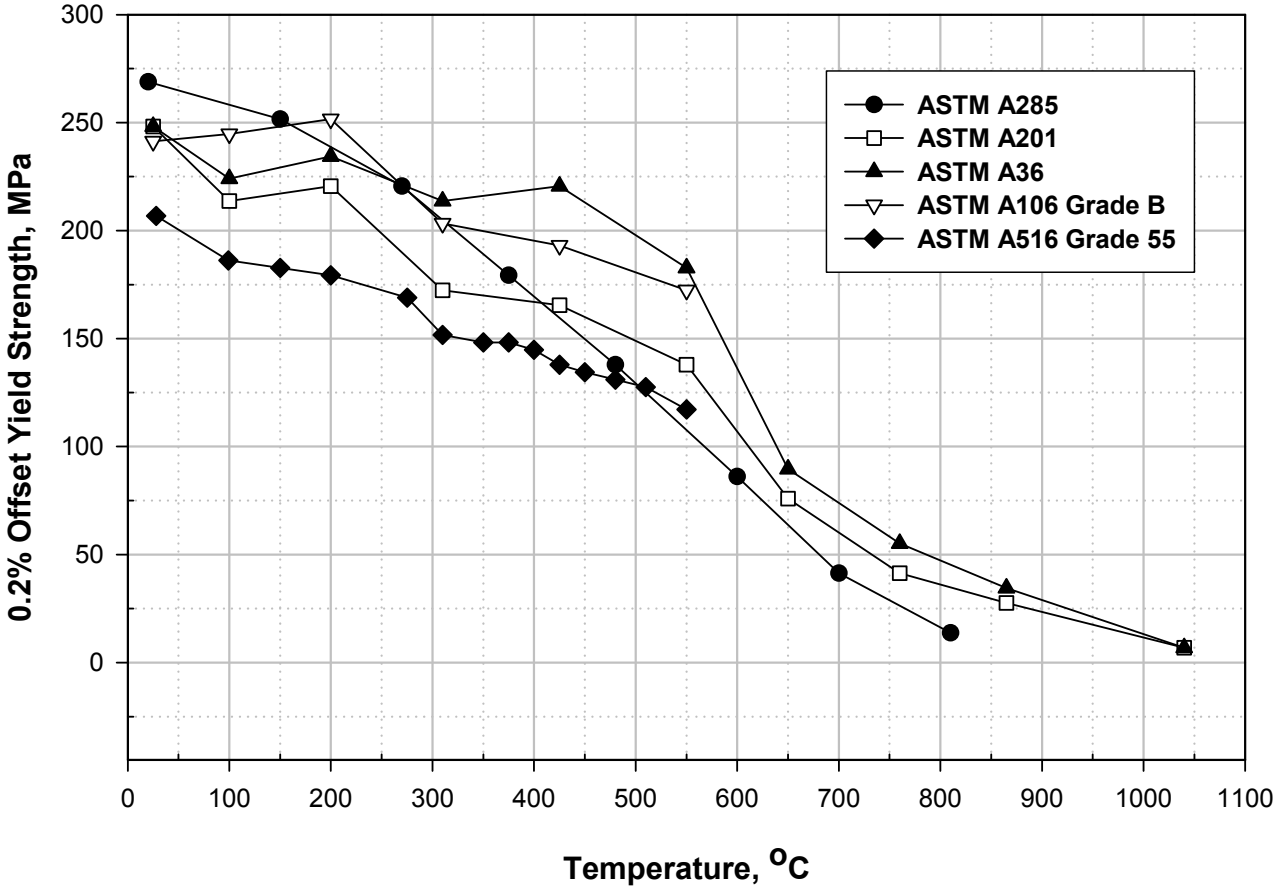

Figure 11.13M
High Temperature Yield Strengths of Some Low Carbon Steels

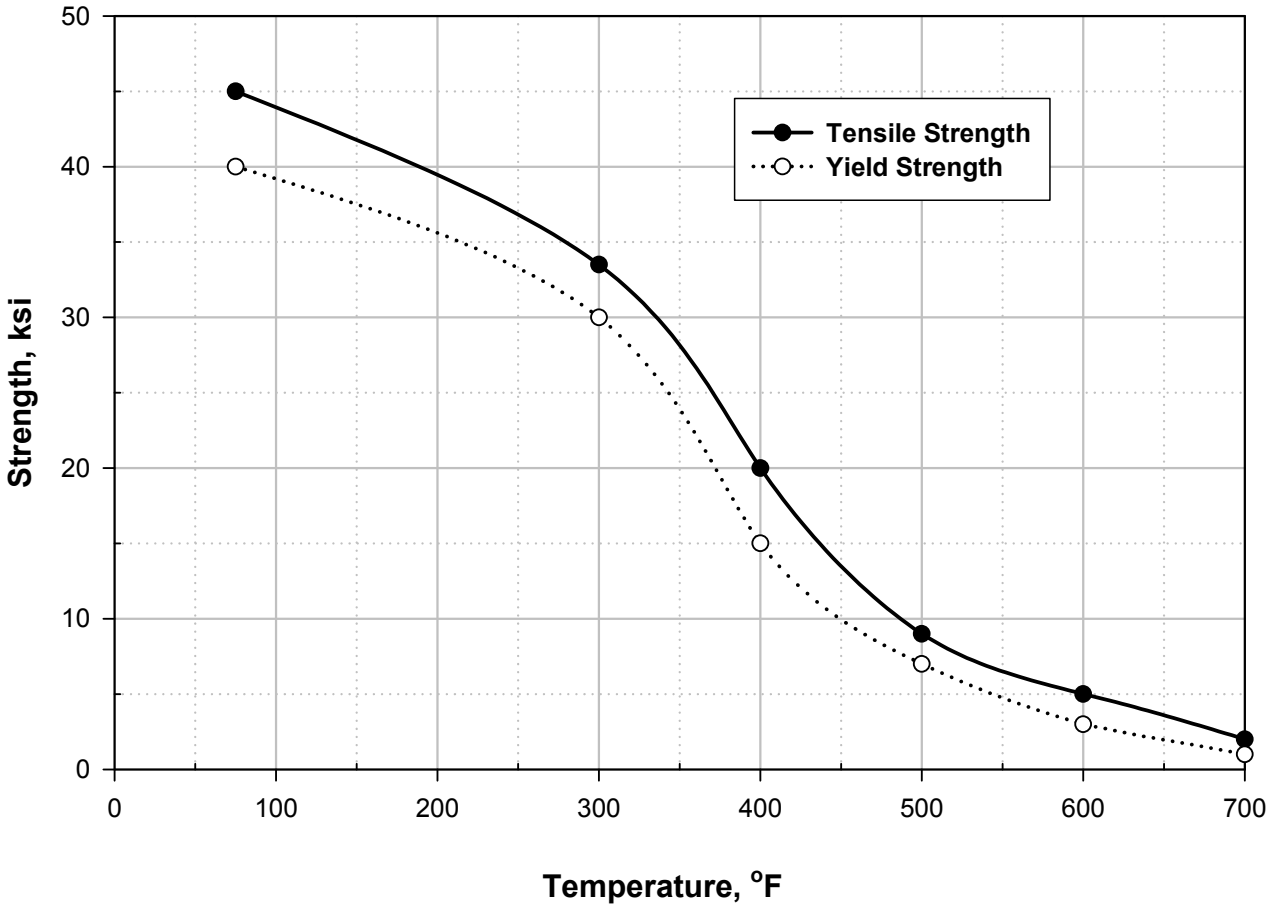

Figure 11.14
Effect of Heat Exposure on The Strength of Aluminum Alloy 6061-T6

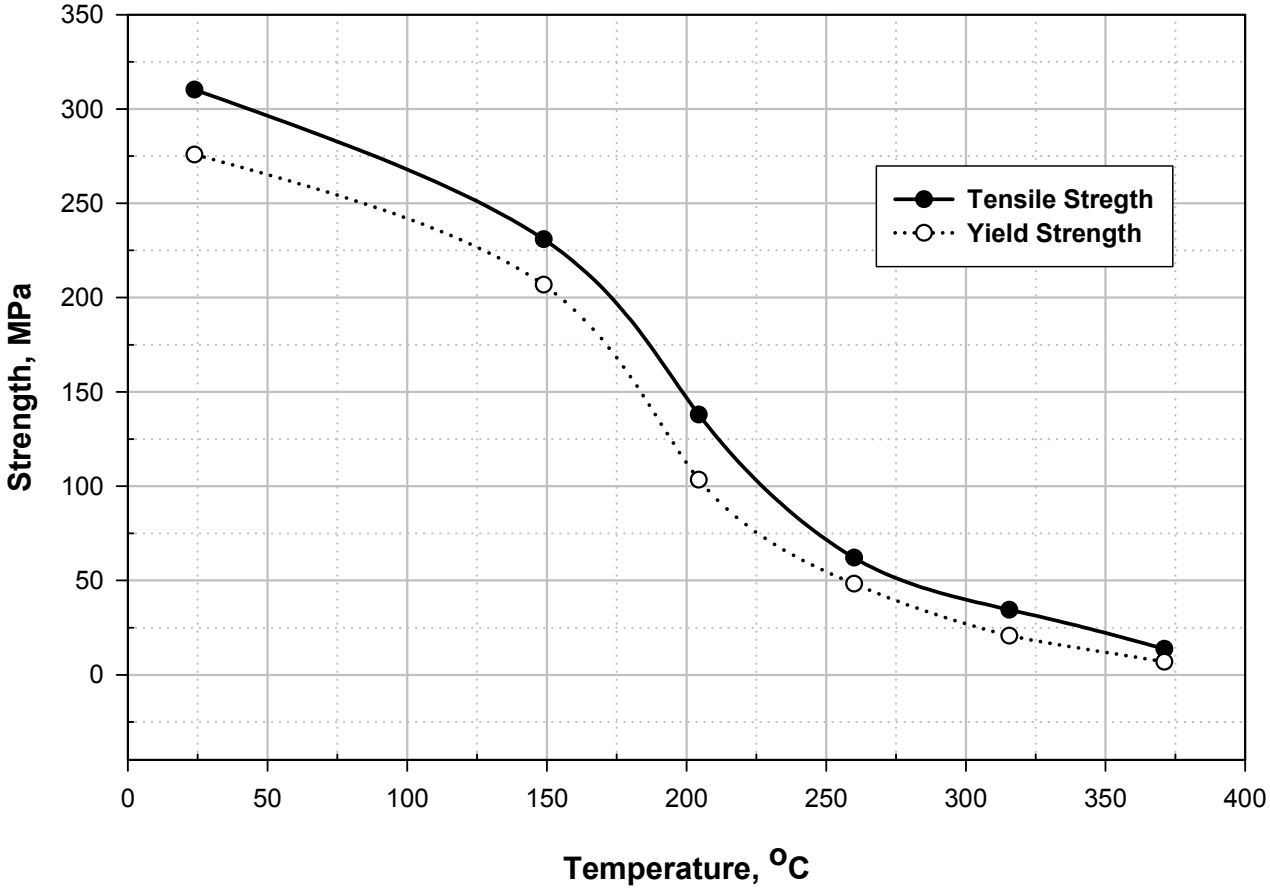

Figure 11.14M
Effect of Heat Exposure on The Strength of Aluminum Alloy 6061-T6

PART 12

ASSESSMENT OF DENTS, GOUGES, AND DENT-GOUGE COMBINATIONS

PART CONTENTS

12.1 General

12.1.1 Fitness-For-Service (FFS) assessment procedures for pressurized components containing dents, gouges, or dent-gouge combinations resulting from mechanical damage are provided in this Part. The procedures can be used to qualify a component for continued operation or for determining a reduced maximum allowable working pressure. A flow chart for the assessment procedures for components containing dents, gouges, or dent-gouge combinations is shown in Figure 12.1.

12.1.2 Assessment procedures for metal loss categorized as a locally thin area or a groove are covered in Part 5, and assessment procedures for other shell distortions such as weld misalignment, out-of-roundness, and bulges are covered inPart 8.

12.2 Applicability and Limitations of the Procedure

12.2.1 The procedures in this Part can be used to evaluate components with dents, gouges, or dent-gouge combinations resulting from mechanical damage as defined below. The dents, gouges, or dent-gouge combinations may occur on the inside or outside of the component.

a) Dent – An inward or outward deviation of a cross-section of a shell member from an ideal shell geometry that is characterized by a small local radius or notch (see Figure 12.2).

b) Gouge – An elongated local removal and/or relocation of material from the surface of a component caused by mechanical means that results in a reduction in wall thickness; the length of a gouge is much greater than the width and the material may have been cold worked in the formation of the flaw. The geometry of a gouge is similar to that of a groove (see Part 5, Figures 5.3 and 5.4). Gouges are typically caused by mechanical damage and often have a work hardened layer of material as a result of the gouging process (e.g. gouging of a section of pipe by mechanical equipment during the excavation of a pipeline). Gouges are frequently associated with dents due to the nature of mechanical damage.

c) Dent-Gouge Combination – A dent with a gouge present in the deformed region (see Figure 12.3).

12.2.2 Calculation methods are provided to determine acceptable $MAWP$ and coincident temperature if the acceptance criteria in this Part are not satisfied. For pressurized components, the calculation methods can be used to find a reduced maximum allowable working pressure. The calculation methods can be used to determine a reduced maximum fill height for tank components (i.e. shell courses).

12.2.3 Unless otherwise specified, this Part is limited to the evaluation of dents, gouges, or dent-gouge combinations. General or uniform corrosion is considered in the assessment procedures. Other flaw types shall be evaluated in accordance with Part 2, Table 2.1.

12.2.4 The assessment procedures only apply to components that are not operating in the creep range; the design temperature is less or equal to the value in Part 4, Table 4.1. The Materials Engineer should be consulted regarding the creep range temperature limit for materials not listed in this table.

12.2.5 Specific details pertaining to the applicability and limitations of each of the assessment procedures are discussed below.

12.2.5.1 The Level 1 or 2 assessment procedures in this Part apply only if all of the following conditions are satisfied.

a) Dents and Dent-Gouge Combinations

1) The original design criteria were in accordance with a recognized code or standard (see Part 1, paragraphs 1.2.2 or 1.2.3).

2) The material is considered to have sufficient material toughness. If there is uncertainty regarding the material toughness, then a Part 3 assessment should be performed. In addition, specific toughness requirements specified in the applicable assessment procedures of this Part shall also be satisfied. If the component is subject to embrittlement during operation due to temperature and/or the process environment (e.g. hydrogen embrittlement), a Level 3 assessment should be performed. Temperature and/or process conditions that result in material embrittlement are discussed in Annex G. One other factor that is unique to dents and gouges is that cold work may be produced by the deformation. This cold worked area may be more susceptible to some forms of mechanical and environmental cracking.

3) The component satisfies the following requirements.

i) The component is a cylindrical shell with a geometry that satisfies Equations (12.1) and (12.2).

$$168\ mm\,(6.625\ in) \le D \le 1050\,mm\,(42\ in) \tag{12.1}$$

$$5\ mm\,(0.20\ in) \le t_c \le 19\,mm\,(0.75\ in) \tag{12.2}$$

ii) The component is subject only to internal pressure (i.e. supplemental loads are assumed to be negligible).

iii) The component material is carbon steel with specified minimum yield strength (SMYS) that satisfies Equation (12.3), and an ultimate tensile strength (UTS) that satisfies Equation (12.4). The limit on SMYS only applies to the static assessment of dent-gouge combinations, and the limit on UTS only applies to the fatigue assessment of dents and dent-gouge combinations.

$$SMYS \le 482\ MPa\,(70\ ksi) \tag{12.3}$$

$$UTS \le 711\ MPa\,(103\ ksi) \tag{12.4}$$

4) The dent or dent-gouge combination is an inward deviation of the shell cross section.

5) The assessment procedures only apply to isolated dents and dent-gouge combinations. In this context, isolated is defined as two times the limit permitted in the assessment procedures for L_{msd}.

b) Gouges

If the material toughness satisfies a minimum criterion, the Level 1 and Level 2 Assessment procedures for gouges are based on the Level 1 and Level 2 Assessment procedures of Part 5, respectively, and the applicability and limitations of the Part 5 assessment procedures shall be used.

12.2.5.2 The Level 1 Assessment procedures are applicable if the component is not in cyclic service. If the component is subject to less than 150 cycles (i.e. pressure and/or temperature variations including operational changes and start-ups and shut-downs) throughout its previous operating history and future planned operating conditions, or satisfies the cyclic service screening procedure in Annex B1, paragraph B1.5.2, then the component is not in cyclic service. In a Level 2 Assessment, if the component is in cyclic pressure service and a fatigue analysis is provided, then the permissible number of cycles shall be determined. Note that if the pressure cycles are complex, or other forms of cyclic stress are present, a Level 3 Assessment is required.

12.2.5.3 A Level 3 Assessment can be performed when the Level 1 and 2 Assessment procedures do not apply, or when these assessment levels produce conservative results (i.e. would not permit operation at the current design conditions). Examples include, but are not limited to the following.

a) Type A, B, or C Components (see Part 4, paragraph 4.2.5) with a geometry that does not satisfy the Level 1 and 2 requirements.

b) The component loading conditions include internal pressure, external pressure, supplemental loads, thermal loads, or any combination thereof.

c) The component material does not satisfy the Level 1 and 2 requirements.

d) Components with a design based on proof testing (e.g. piping tee or reducer produced in accordance with ASME B16.9 where the design may be based on proof testing).

e) Components in cyclic service where the cyclic stresses are a result of complex pressure cycles or other load cycles (supplemental loads and thermal loads).

f) Components operating in the creep range.

g) Components with closely spaced dents, gouges, and/or dent-gouge combinations.

12.3 Data Requirements

12.3.1 Original Equipment Design Data

An overview of the original equipment data required for an assessment is provided in Part 2, paragraph 2.3.1. This data can be entered in the form provided in Part 2, Table 2.2, and Table 12.1 for each component under evaluation.

12.3.2 Maintenance and Operational History

An overview of the maintenance and operational history required for an assessment is provided in Part 2, paragraph 2.3.2.

12.3.3 Required Data/Measurements for a *FFS* Assessment

12.3.3.1 The required data and measurements for assessment of a dent are listed below.

a) *Dent Depth in the Pressurized Condition*, d_{dp}, *and Unpressurized Condition*, d_{d0} – The maximum depth of the dent in the pressurized and the unpressurized condition shall be determined. These values may be measured directly. The Owner-User should consider the risk before increasing the pressure from the current level to measure the depth of the dent in the pressurized condition. Alternatively, if the operating pressure is greater than or equal to 70% of the $MAWP$, then the relationship between the dent depth in the pressurized condition and the dent depth in the unpressurized condition is given by Equation (12.5). Otherwise, the dent depth in the pressurized condition shall be assumed to be equal to the dent depth in the unpressurized condition, or $d_{dp} = d_{d0}$.

$$d_{dp} = 0.70 d_{d0} \tag{12.5}$$

b) *Minimum Specified Ultimate Tensile Strength*, σ_{uts} – The minimum specified ultimate tensile strength may be determined based on the material specification. If the material specification is unknown, then $\sigma_{uts} = 414\ MPa\ (60\ ksi)$ may be used in the assessment. This information is required for a Level 2 Assessment, and may be required for a Level 3 Assessment.

c) *Cyclic Pressure Components*, P_{max} and P_{min} – If the component is in cyclic pressure service that can be represented by a maximum and minimum pressure, the maximum and minimum pressures of the cycle shall be determined. This information is required for a Level 2 Assessment, and may be required for a Level 3 Assessment.

d) *Dent Spacing to Weld Joints,* L_w – Measurements should be made to determine the spacing between the edge of the dent and the nearest weld joint. This information should be detailed and provided on an inspection sketch.

e) *Dent Spacing to Major Structural Discontinuities,* L_{msd} – Measurements should be made to determine the spacing between the edge of the dent and the nearest major structural discontinuity. This information should be detailed and provided on an inspection sketch.

12.3.3.2 The required data and measurements for assessment of a gouge are listed below.

a) *Gouge Dimensions* – The flaw dimensions of the gouge shall be determined using the methods described for a groove inPart 5.

b) *Temperature Corresponding to 40 Joules (30 ft-lbs) of Toughness* – The Level 1 and Level 2 Assessment of Part 5 may be used if one of the following is true.

1) The component is operating at or above the temperature that corresponds to 40 Joules (30 ft-lbs) of CVN toughness, or

2) The gouge is formed by a process that results in a work hardened layer, and the gouge is subsequently dressed to remove this layer and any other defects to obtain a smooth profile.

c) *Material Temperature Exemption Curve* – This data is only required if the temperature that corresponds to 40 Joules (30 ft-lbs) of CVN toughness is estimated based on the material specification and the minimum specified yield strength. Material Temperature Exemption Curves are provided in Part 3, Table 3.2.

d) *Minimum Specified Yield Strength*, σ_{ys} – This data is only required if the temperature that corresponds to 40 Joules (30 ft-lbs) of CVN toughness is estimated based on the material specification and the minimum specified yield strength.

e) *Gouge Spacing to Major Structural Discontinuities,* L_{msd} – Measurements should be made to determine the spacing between the edge of the gouge and the nearest major structural discontinuity. This information should be detailed and provided on an inspection sketch.

12.3.3.3 The required data and measurements for assessment of a dent-gouge combination are listed below.

a) *Dent Depth in the Pressurized Condition*, d_{dp} , *and Unpressurized Condition*, d_{d0} – The maximum depth of the dent in the pressurized and the unpressurized condition shall be determined (see paragraph 12.3.3.1.a).

b) *Gouge Depth* d_g – The maximum depth of the gouge shall be determined using the methods described for a groove inPart 5.

c) *Minimum Specified Yield Strength*, σ_{ys} – The minimum specified yield strength may be determined based on the material specification.

d) *Minimum Specified Ultimate Tensile Strength*, σ_{uts} – The minimum specified ultimate tensile strength may be determined based on the material specification. If the material specification is unknown, then $\sigma_{uts} = 414\ MPa\ (60\ ksi)$ may be used in the assessment. This information is required for a Level 2 Assessment, and may be required for a Level 3 Assessment.

e) *Cyclic Pressure Components*, P_{max} and P_{min} – If the component is in cyclic pressure service that can be represented by a maximum and minimum pressure, the maximum and minimum pressures of the cycle shall be determined. This information is required for a Level 2 Assessment, and may be required for a Level 3 Assessment.

f) *Dent-gouge Combination Spacing to Weld Joints,* L_w – *M*easurements should be made to determine the spacing between the edge of the dent-gouge combination and the nearest weld joint. This information should be detailed and provided on an inspection sketch.

g) *Dent-gouge Combination Spacing to Major Structural Discontinuities,* L_{msd} – *M*easurements should be made to determine the spacing between the edge of the dent-gouge combination and the nearest major structural discontinuity. This information should be detailed and provided on an inspection sketch.

12.3.3.4 The information required to perform a Level 3 Assessment is dependent on the analysis method utilized. In most cases, stress analysis in accordance with Annex B1 will be performed. The stress analysis will typically require a complete description of the geometry, material properties, and loading condition including pressure, supplemental, and thermal loads.

12.3.4 Recommendations for Inspection Technique and Sizing Requirements

12.3.4.1 The maximum depth of the dent may be established using a straight edge along the axis of the cylinder and measuring the offset in the region of the dent. Note that numerous measurements should be taken to establish the dent profile in the axial and circumferential directions if a Level 3 Assessment is to be performed. Only the maximum dent depth is used in the Level 1 and 2 Assessments. The complete dent profile may be used in a Level 3 Assessment.

12.3.4.2 The gouge dimensions may be obtained in accordance with Part 4 and Part 5.

12.3.4.3 The flaw size of the dent-gouge combination may be established using the methods described above.

12.4 Assessment Techniques and Acceptance Criteria

12.4.1 Overview

12.4.1.1 An overview of the assessment levels for the evaluation of a dent is provided below.

a) The Level 1 Assessment is limited to dents in carbon steel cylindrical shells located away from structural discontinuities. The acceptability criterion is based on limiting the maximum dent depth in the component to a percentage of the components outside diameter.

b) The Level 2 Assessment is similar to the Level 1 Assessment. In addition, a fatigue assessment to evaluate the effects of cyclic pressure loading is provided.

c) The Level 3 Assessment rules are intended to evaluate dents in complex geometries subject to general loading conditions. A Level 3 Assessment is also required for materials other than carbon steel. Numerical stress analysis techniques are utilized in a Level 3 assessment.

12.4.1.2 An overview of the assessment levels for the evaluation of a gouge is provided below.

a) The Level 1 and Level 2 Assessment procedures are based on the Level 1 and Level 2 Assessment procedures of Part 5, respectively, if the material has a toughness greater than 40 Joules (30 ft-lbs) or if the gouge is dressed to remove the work hardened layer, which may have been formed during the gouging process, and any other defects to obtain a smooth profile. If the material toughness is unknown, a method to estimate a minimum operating temperature at which 40 Joules (30 ft-lbs) toughness can be expected is provided.

b) Level 3 Assessment rules are intended to evaluate gouges in complex geometries subject to general loading conditions. Numerical stress analysis techniques are utilized in a Level 3 assessment.

12.4.1.3 An overview of the assessment levels for the evaluation of a dent-gouge combination is provided below.

a) The Level 1 Assessment is limited to dent-gouge combinations in carbon steel cylindrical shells located away from structural discontinuities. A screening curve is provided to determine the acceptability for continued operation based on the ratio of the dent depth to cylinder outside diameter and the ratio of the gouge depth to wall thickness.

b) Level 2 Assessment is limited to dent-gouge combinations in carbon steel cylindrical shells located away from structural discontinuities. A remaining strength factor approach is utilized to determine an acceptable $MAWP$ based on the dent depth and gouge depth. In addition, a fatigue assessment to evaluate the effects of cyclic pressure loading is provided.

c) Level 3 Assessment rules are intended to evaluate dent-gouge combinations in complex geometries subject to general loading conditions. A Level 3 Assessment is also required for materials other than carbon steel. Numerical stress analysis techniques are utilized in a Level 3 assessment.

12.4.2 Level 1 Assessment

12.4.2.1 Dent Assessment Procedure

The Level 1 Assessment procedure for determining the acceptability of a dent is shown below.

a) STEP 1 – Determine the parameters in paragraph 12.3.3.1 together with D, FCA, either t_{rd} or t_{nom}, and $LOSS$.

b) STEP 2 – Determine the wall thickness to be used in the assessment using Equation (12.6) or Equation (12.7), as applicable.

$$t_c = t_{nom} - LOSS - FCA \tag{12.6}$$

$$t_c = t_{rd} - FCA \tag{12.7}$$

c) STEP 3 – If Equations (12.8) and (12.9) are satisfied, proceed to STEP 4. Otherwise, the Level 1 Assessment is not satisfied.

$$L_{msd} \geq 1.8\sqrt{Dt_c} \tag{12.8}$$

$$L_w \geq \max\left[2t_c,\ 25\,mm\ (1\ in.)\right] \tag{12.9}$$

d) STEP 4 – If the component is not in cyclic service and Equation (12.10) is satisfied, proceed to STEP 5. Otherwise, the Level 1 Assessment is not satisfied.

$$d_{dp} \leq 0.07D \tag{12.10}$$

e) STEP 5 – Determine the $MAWP$ for the component (see Annex A, paragraph A.2) using the thickness from STEP 2. If the $MAWP$ is greater than or equal to the current design condition, then the component is acceptable for continued operation. Otherwise, the Level 1 Assessment is not satisfied.

12.4.2.2 Gouge Assessment Procedure

The Level 1 Assessment procedure for determining the acceptability of a gouge is as shown below.

a) STEP 1 – Determine the minimum operating temperature and the parameters in paragraph 12.3.3.2.

b) STEP 2 – Determine the toughness (CVN) for the material at the minimum operating temperature. If the toughness is greater than 40 Joules (30ft-lbs) or if the surface of the gouge is dressed to remove the work hardened layer and any other defects to obtain a smooth profile, then proceed to STEP 3. Otherwise, the Level 1 Assessment is not satisfied. Note that if the toughness (CVN) of the material is unknown, then the temperature at which the material can be expected to have a toughness greater than 40 Joules (30ft-lbs) may be obtained from Table 12.2 if an ASME Exemption Curve and the minimum specified yield strength for the material can be established.

c) STEP 3 – The gouge shall be evaluated using the Level 1 Assessment procedures in Part 5.

12.4.2.3 Dent-Gouge Combination Assessment Procedure

The Level 1 Assessment procedure for determining the acceptability of a dent-gouge combination is as shown below.

a) STEP 1 – Determine the parameters in paragraph 12.3.3.3 together with D, FCA, either t_{rd} or t_{nom}, and $LOSS$.

b) STEP 2 – Determine the wall thickness to be used in the assessment using Equation (12.6) or Equation (12.7), and the gouge depth, d_{gc}, to be used in the assessment using Equation (12.11).

$$d_{gc} = d_g + FCA \tag{12.11}$$

c) STEP 3 – If the following requirements are satisfied, proceed to STEP 4. Otherwise, the Level 1 Assessment procedure is not satisfied.

$$t_{mm} - FCA \geq 2.5\ mm\ (0.10\ inches) \tag{12.12}$$

$$L_{msd} \geq 1.8\sqrt{Dt_c} \tag{12.13}$$

$$L_w \geq \max\left[2t_c,\ 25\,mm\ (1\,in.)\right] \tag{12.14}$$

d) STEP 4 – Determine the circumferential stress, σ_m^C, for the component (see Annex A, paragraph A.2) using the thickness from STEP 2.

e) STEP 5 – Determine the gouge depth to wall thickness ratio, d_{gc}/t_c, and the dent depth to component diameter ratio, d_{dp}/D. Enter these data with the circumferential stress, σ_m^C, determined in STEP 4 on Figure 12.4. If the point defined by the intersection of these values is on or below the curve in this figure that corresponds to the circumferential stress in terms of the minimum specified yield strength for the component and the component is not in cyclic service, proceed to STEP 6. Otherwise, the Level 1 Assessment is not satisfied.

f) STEP 6 – Determine the $MAWP$ for the component (see Annex A, paragraph A.2) using the thickness from STEP 2. If the $MAWP$ is greater than or equal to the current design condition, then the component is acceptable for continued operation. Otherwise, the Level 1 Assessment is not satisfied.

12.4.2.4 If the component does not meet the Level 1 Assessment requirements, then the following, or combinations thereof, shall be considered:

a) Repair, replace, or retire the component.

b) Adjust the FCA by applying remediation techniques (see Part 4 paragraph 4.6).

c) Conduct a Level 2 or Level 3 Assessment.

12.4.3 Level 2 Assessment

12.4.3.1 Dent Assessment Procedure

The Level 2 Assessment procedure for determining the acceptability of a dent is as shown below.

a) STEP 1 – Determine the parameters in paragraph 12.3.3.1 together with D, FCA, either t_{rd} or t_{nom}, and $LOSS$.

b) STEP 2 – Determine the wall thickness to be used in the assessment using Equation (12.6) or Equation (12.7).

c) STEP 3 – If the requirements in paragraph 12.4.2.1.c are satisfied, then proceed to STEP 4. Otherwise, the Level 2 Assessment is not satisfied.

d) STEP 4 – If Equation (12.10) is satisfied, proceed to STEP 5. Otherwise, the Level 2 Assessment is not satisfied.

e) STEP 5 – Determine the $MAWP$ for the component (see Annex A, paragraph A.2) using the thickness from STEP 2. If the $MAWP$ is greater than or equal to the current design condition, proceed to STEP 6. Otherwise, the Level 2 Assessment is not satisfied.

f) STEP 6 – If the component is not subject to pressure cycles, the component is acceptable for continued operation and the assessment is complete. If the component is subject to pressure cycles, then determine the acceptable number of cycles as shown below.

1) STEP 6.1 – Determine the circumferential stresses, $\sigma^{C}_{m,max}$ and $\sigma^{C}_{m,min}$, based on P_{max} and P_{min}, respectively, for the component (see Annex A, paragraph A.2) using the thickness from STEP 2.

2) STEP 6.2 – Determine the acceptable number of cycles. If the acceptable number of cycles is greater than or equal to the sum of the past and future anticipated number of cycles, then the component is acceptable for continued operation at the specified conditions. Otherwise, the Level 2 Assessment is not satisfied.

$$N_c = 562.2\left[\frac{\sigma_{uts}}{2\sigma_A K_d K_g}\right]^{5.26} \tag{12.15}$$

$$\sigma_A = \sigma_a\left[1-\left(\frac{\sigma^{C}_{m,max}-\sigma_a}{\sigma_{uts}}\right)^2\right]^{-1} \tag{12.16}$$

$$\sigma_a = \frac{\sigma^{C}_{m,max}-\sigma^{C}_{m,min}}{2} \tag{12.17}$$

$$K_d = 1+C_s\sqrt{\frac{t_c}{D}\left(d_{d0}\cdot C_{ul}\right)^{1.5}} \tag{12.18}$$

$$C_s = 2.0 \qquad for\ smooth\ dents,\ r_d \geq 5t_c \tag{12.19}$$

$$C_s = 1.0 \qquad for\ sharp\ dents,\ r_d < 5t_c \tag{12.20}$$

$$K_g = 1.0 \tag{12.21}$$

12.4.3.2 Gouge Assessment Procedure

The Level 2 Assessment procedure for determining the acceptability of a gouge is as shown below.

a) STEP 1 – Determine the minimum operating temperature and the parameters in paragraph 12.3.3.2.

b) STEP 2 – Determine the toughness (CVN) for the material at the minimum operating temperature. If the toughness is greater than 40 Joules (30ft-lbs) or if the surface of the gouge is dressed to remove the work hardened layer and any other defects to obtain a smooth profile, then proceed to STEP 3. Otherwise, the Level 2 Assessment is not satisfied. Note that if the toughness (CVN) of the material is unknown, then the toughness may be estimated using paragraph 12.4.2.2.b.

c) STEP 3 – The gouge shall be evaluated using the Level 2 Assessment procedures in Part 5.

12.4.3.3 Dent-Gouge Combination Assessment Procedure

The Level 2 Assessment procedure for determining the acceptability of a dent-gouge combination is as shown below.

a) STEP 1 – Determine the parameters in paragraph 12.3.3.3 together with D, FCA, either t_{rd} or t_{nom}, and $LOSS$.

b) STEP 2 – Determine the wall thickness to be used in the assessment using Equation (12.6) or Equation (12.7), and the gouge depth, d_{gc}, to be used in the assessment using Equation (12.11).

c) STEP 3 – If requirements in paragraph 12.4.2.3.c are satisfied, then proceed to STEP 4. Otherwise, the Level 2 Assessment is not satisfied.

d) STEP 4 – If Equations (12.10) and (12.22) are satisfied, proceed to STEP 5. Otherwise, the Level 2 Assessment is not satisfied.

$$d_{gc} \le 0.66 t_c \tag{12.22}$$

e) STEP 5 – Determine the $MAWP$ for the component (see Annex A, paragraph A.2) using the thickness from STEP 2. If the $MAWP$ is greater than or equal to the maximum operating pressure proceed to STEP 6. Otherwise, the Level 2 Assessment is not satisfied.

f) STEP 6 – Determine Remaining Strength Factor (RSF) for the dent-gouge combination.

$$RSF = \frac{2}{\pi}\arccos\left[\exp\left[\frac{-C_1 \cdot C_3}{C_2^2}\right]\right] \cdot \left(1 - \frac{d_{gc}}{t_c}\right) \tag{12.23}$$

$$C_1 = \frac{1.5\pi E_y U_1}{\bar{\sigma}^2 A_{cvn} d_{gc}} \tag{12.24}$$

$$C_2 = Y_1\left(1 - \frac{1.8 d_{d0}}{D}\right) + Y_2\left(\frac{10.2 d_{d0}}{2t_c}\right) \tag{12.25}$$

$$C_3 = \exp\left[\frac{\ln(U_2 \cdot CVN) - 1.9}{0.57}\right] \tag{12.26}$$

$$\bar{\sigma} = 1.15 \cdot \sigma_{ys}\left(1 - \frac{d_{gc}}{t_c}\right) \tag{12.27}$$

$$Y_1 = 1.12 - 0.23\left(\frac{d_{gc}}{t_c}\right) + 10.6\left(\frac{d_{gc}}{t_c}\right)^2 - 21.7\left(\frac{d_{gc}}{t_c}\right)^3 + 30.4\left(\frac{d_{gc}}{t_c}\right)^4 \quad (12.28)$$

$$Y_2 = 1.12 - 1.39\left(\frac{d_{gc}}{t_c}\right) + 7.32\left(\frac{d_{gc}}{t_c}\right)^2 - 13.1\left(\frac{d_{gc}}{t_c}\right)^3 + 14.0\left(\frac{d_{gc}}{t_c}\right)^4 \quad (12.29)$$

g) STEP 7 – If $RSF \geq RSF_a$, then the dent-gouge combination is acceptable for operation at the $MAWP$ determined in STEP 5. If $RSF < RSF_a$, then the dent-gouge combination is acceptable for operation at a reduced $MAWP$ computed using the equations in Part 2, paragraph 2.4.2.2. The $MAWP$ from STEP 5 shall be used in this calculation.

h) STEP 8 – If the component is not subject to pressure cycles, the component is acceptable for continued operation and the assessment is complete. If the component is subject to pressure cycles, then determine the acceptable number of cycles using the procedure in paragraph 12.4.3.1.f. The value of K_g to be used in this calculation is given by Equation (12.30). If the acceptable number of cycles is greater than or equal to the sum of the past and future anticipated number of cycles, then component is acceptable for continued operation at the specified cyclic pressures. Otherwise, the Level 2 Assessment is not satisfied.

$$K_g = 1 + 9\left(\frac{d_{gc}}{t_c}\right) \quad (12.30)$$

12.4.3.4 If the component does not meet the Level 2 Assessment requirements, then the following, or combinations thereof, shall be considered:

a) Rerate, repair, replace, or retire the component.

b) Adjust the FCA by applying remediation techniques (see Part 4, paragraph 4.6).

c) Conduct a Level 3 Assessment.

12.4.4 Level 3 Assessment

12.4.4.1 The Level 3 Assessment procedures for dents, gouges, and dent-gouge combinations involve the evaluation of potential failure modes based on component geometry, material of construction, loading conditions, and operating temperature range.

a) The failure modes listed below shall be considered for dents, gouges, and dent-gouge combinations where the toughness is sufficient to ensure plastic behavior.

   1) Plastic Collapse (see Annex B1, paragraph B1.2)

   2) Local Failure (see Annex B1, paragraph B1.3)

   3) Collapse From Buckling (see Annex B1, paragraph B1.4)

   4) Cyclic Loading (see Annex B1, paragraph B1.5)

   5) Creep or Creep-Fatigue Damage (see Part 10)

b) The failure modes listed in paragraph 12.4.4.1.a and those shown below shall be considered for gouges and dent-gouge combinations with insufficient toughness to ensure plastic behavior.

   1) Crack Stability and Crack Growth (see Part 9)

   2) Creep Crack Stability and Crack Growth (see Part 10)

12.4.4.2 The numerical stress analysis should be performed considering the material as well as geometric non-linearity in order to account for the effect of pressure stiffening on the dent and re-rounding of the shell that occurs under pressure loading.

12.4.4.3 The stress analysis used in the assessment should simulate the deformation process that causes the damage in order to determine the magnitude of permanent plastic strain developed. To simulate the distortion process, an analysis that includes geometric and material nonlinearity as well as the contact interaction between the original undeformed shell structure and the contacting body may be performed. The contacting component may be explicitly modeled as a deformable body or as a simple rigid surface. The analysis should include applicable loadings to develop the final distorted configuration of the shell structure.

12.4.4.4 If a kink or sharp bend exists in a shell, shell theory will not provide an accurate estimate of the stress state. In this case, a continuum model is recommended in the stress analysis described in paragraph 12.4.4.3.

12.4.4.5 For gouges and dent-gouge combinations that are evaluated using the crack-like flaw assessment procedures in Part 9 or Part 10, as applicable, the equivalent crack depth may be taken as the gouge depth and the equivalent crack length may be taken as the gouge length.

12.4.4.6 If the component is operating in the creep range, stresses due to localized geometric irregularities may not sufficiently relax with time due to the surrounding compliance of the component. In this case, creep strains can accumulate and may result in significant creep damage or cracking. The assessment of components that contain dents, gouges, or dent-gouge combinations requires an approach using a stress analysis that incorporates a material model for creep that includes the effects of triaxiality.

12.5 Remaining Life Assessment

12.5.1 A remaining life assessment of components with a dent, gouge, or dent-gouge combination generally consists of one of the following three categories:

a) *Metal Loss Resulting From A Corrosive/Erosive Environment* – In this case, adequate protection from a corrosive/erosive environment can be established by setting an appropriate value for the future corrosion allowance. The remaining life as a function of time can be established using the $MAWP$ Approach described in Part 4, paragraph 4.5.2.

b) *Cyclic Loading* – The Level 2 assessment procedures include a fatigue evaluation for dents and dent-gouge combinations. A Level 3 Assessment is required for a fatigue analysis of a gouge. If a Level 3 Assessment is performed, the fatigue analysis may be based on the S-N approach described inAnnex B1 or a fracture mechanics approach described in Part 9. The remaining life can be established by combining the results from this analysis with the operational history of the component.

c) *High Temperature Operation* – If the component is operating in the creep regime, the assessment procedures in Part 10 should be utilized to determine a remaining life.

12.5.2 If the component's operation is not within one of the above categories, a detailed Level 3 analysis should be performed to determine the remaining life of the component.

12.6 Remediation

12.6.1 A dent or dent-gouge combination represents a very severe flaw type because it is difficult to establish the condition (strength and ductility) at the location of maximum deformation. Therefore, unless the condition of the material can be adequately evaluated, repair or replacement of the component is recommended.

12.6.2 Dents, gouges, and dent-gouge combinations may be reinforced using stiffening plates and lap patches depending on the geometry, temperature, and loading conditions. The reinforcement, if utilized, should be designed using the principles and allowable stresses of the original construction code. Cylindrical shell sections that are out-of-round can be brought to within original fabrication tolerances or to a shape that reduces the local stress to within acceptable limits by mechanical means. Hydraulic jacks have been used successfully to alter the out-of-round shape of stiffened cylindrical shells. The design of the jacking arrangement and loads should be carefully established and monitored during the shaping process to minimize the potential for damage to the shell and attachments.

12.6.2.1 The remediation methods for general corrosion provided in Part 4, paragraph 4.6 are applicable to local metal loss in the vicinity of dents, gouges, and dent-gouge combinations. Because of the localized damage pattern, it may be necessary in some cases to fill deep areas of metal loss with substances such as caulking before the application of a lining.

12.7 In-Service monitoring

12.7.1 The shell distortion associated with dents, gouges, and dent-gouge combinations do not normally require in-service monitoring unless one or more of the following are true.

a) An unusually corrosive environment exists and future corrosion allowance cannot be adequately estimated,

b) The component is subject to a cyclic operation and the load history cannot be adequately established, or

c) The component is operating in the creep range.

12.7.2 If in-service monitoring is performed, it usually entails visual inspection and field measurements of the component's distortion at regular intervals. The type of measurements made depends on the procedure utilized in the assessment.

12.8 Documentation

12.8.1 The documentation of the FFS assessment should include the information cited in Part 2, paragraph 2.8.

12.8.2 Inspection data including all field measurements associated with the dent, gouge, or dent-gouge combination, should be recorded and included in the documentation. A sample data sheet is provided in Table 12.1 for this purpose. A sketch, photograph, or both showing the location and orientation of the dent, gouge, or dent-gouge combination on the component is also recommended.

12.9 Nomenclature

A_{cvn}	fracture area of a 2/3 Charpy specimen; $A_{cvn} = 53.33\ mm^2\ \left(0.083\ in^2\right)$
CVN	Charpy V-notch energy.
C_s	factor used in the fatigue evaluation of dents.
C_{ul}	conversion factor, $C_{ul} = 1.0$ if d_{d0} is in millimeters and $C_{ul} = 25.4$ if d_{d0} is in inches.
C_1	parameter used to compute the RSF for a dent-gouge combination.
C_2	parameter used to compute the RSF for a dent-gouge combination.
C_3	parameter used to compute the RSF for a dent-gouge combination.
d_g	maximum depth of the gouge.
d_{dp}	depth of the dent measured when the component is pressurized.

d_{d0} depth of the dent measured when the component is not pressurized.

d_{gc} depth of the gouge in the corroded condition.

D outside diameter of the cylinder.

E_y modulus of elasticity.

FCA future corrosion allowance.

$LOSS$ amount of uniform metal loss at the time of the assessment.

K_d stress concentration parameter associated with a dent that is used to compute N_c.

K_g stress concentration parameter associated with a gouge that is used to compute N_c.

L_{msd} distance to the nearest major structural discontinuity.

L_w distance to the nearest weld joint.

$MAWP$ maximum allowable working pressure.

MFH maximum fill height.

N_c permissible number of pressure cycles.

P_{max} maximum pressure for cyclic pressure operation.

P_{min} minimum pressure for cyclic pressure operation.

RSF computed remaining strength factor.

RSF_a allowable remaining strength factor (see Part 2, paragraph 2.4.2.2).

r_d radius at the base of the dent.

σ_a cyclic circumferential membrane stress amplitude.

σ_A adjusted cyclic circumferential membrane stress amplitude.

σ_m^C circumferential membrane stress in the cylinder.

$\sigma_{m,max}^C$ maximum circumferential membrane stress associated with P_{max}.

$\sigma_{m,min}^C$ maximum circumferential membrane stress associated with P_{min}.

σ_{ys} minimum specified yield strength.

σ_{uts} minimum specified ultimate tensile strength.

$\overline{\sigma}$ flow stress at the gouge in a dent-gouge combination.

t_c wall thickness in the future corroded condition.

t_{mm} minimum remaining thickness determined at the time of the assessment.

t_{nom} nominal or furnished thickness of the component adjusted for mill undertolerance as applicable.

t_{rd} uniform thickness away from the damage established by thickness measurements at the time of the assessment.

U_1 conversion factor; $U_1 = 113.0$ if E_y and $\overline{\sigma}$ are in MPa, A_{CVN} is in mm^2, and d_{do} is in mm, and $U_1 = 1.0$ if E_y and $\overline{\sigma}$ are in psi, A_{CVN} is in in^2, and d_{do} is in inches.

U_2 conversion factor; $U_2 = 0.738$ for units of $Joules$, and $U_2 = 1.0$ for units of $ft-lbs$.

Y_1 parameter used to compute the RSF for a dent-gouge combination.

Y_2 parameter used to compute the RSF for a dent-gouge combination.

12.10 References

1. Alexander, C., and Keifner, J., “Effects of Smooth and Rock Dents on Liquid Petroleum Pipelines”, API Publication 1156, November 1997.
2. Alexander, C., Keifner, J., “Effects of Smooth and Rock Dents on Liquid Petroleum Pipelines – Phase II”, API Publication 1156 – Addendum, October 1999.
3. Cairns, A., and Hopkins, P., “A Statistical Analysis of Data from Burst Tests on Pipe Containing Dent/Flaw Combinations,” ERS R.2381, October 1981.
4. Corder, I. and Chatain, P., “EPRG Recommendations for the Assessment of the Resistance of Pipelines to External Damage,” Paper Number 12.
5. Corder, I. and Chatain, P., “Towards EPRG Recommendations for the Assessment of the Tolerance and Resistance of Pipelines to External Damage,” Paper Number 13.
6. Eiber, R., and others, “The Effects of Dents on the Failure Characteristics of Line Pipe,” Battelle Columbus Report to A.G.A. NG-18, A.G.A. Catalog No. L51403, May 1981.
7. Eiber, Robert J. and Leis, Brains N., “Line Pipe Resistance To Outside Force,”, Paper Number 14.
8. Shannon, R. W. E., “The Failure Behavior of Linepipe Flaws,” *International Journal of Pressure Vessel and Piping*, pp. 243-255, 1974.
9. Fowler, J. R., and Ayers, R. R., “Acceptability of Plain Dents for Offshore Pipelines,” Paper 35, Proceedings of the PRC/EPRG Ninth Biennial Joint Technical Meeting on Line Pipe Research, Houston, TX, May 1993.
10. Fowler, J.R., Alexander, C.R., Kovach, P.J., and Connelly, L.M., “Cyclic Pressure Fatigue Life of Pipelines with Plain Dents, Dents with Gouges, and Dents with Welds,” AGA Catalog No. L51705, AGA, June, 1994.
11. Hopkins, P., Jones, D.G., Clyne, A.J., “The Significance of Dents and Defects in Transmission Pipelines,” IMechE, C376/049, , 1989.
12. Lancaster, E.R. and Palmer, S.C., “Experimental Study of Strains Caused by Pressurization of Pipes with Dents,” Proceedings of the Fourth (1994) International Offshore and Polar Engineering Conference, Osaka, Japan, April 10-15, 1994, Pages 110-117.
13. Jiao, Guoyang, Sotbert, T., and Bruschi, R., “Probabilistic Assessment of the Wall Thickness Requirement for Pressure Containment of Offshore Pipelines,” 1992 OMAE – Volume V-a, Pipeline Technology, ASME 1992, Pages 249-255.
14. Jones, D. G., “The Significance of Mechanical Damage in Pipelines,” Presented at A.G.A./EPRG Linepipe Research Seminar, Duisburg, W. Germany, ERS E291, September 1981.
15. Kiefner, John F., “Review and Critique of Dent Acceptability Criteria for Offshore Pipelines,” Contract No. PR 218-9119, AGA Report, June 30, 1992.
16. Maxey, W. A., “Topical Report on Outside Force Flaw Behavior,” NG-18 Report 162, Task No. SI-1.1-79, AGA, August 15, 1986.
17. Maxey, W. A., “Outside Force Flaw Behavior,” 7th Symposium on Line Pipe Research, Houston, Texas, Paper 14, October 1986.
18. MSL Engineering Limited, “Appraisal and Development of Pipeline Defect Assessment Methodologies,” Minerals Management Service, US Department of the Interior, Washington, D.C., Contract No. 1435-01-CT-99-50001, DOC REF CH109R001, Rev 0, June 2000.
19. Oguchi, N. and Hagiwara, N., “Fatigue Behavior of Line Pipes Subjected to Severe Mechanical Damage,” Journal of Pressure Vessel Technology, Vol 121, ASME, November 1999, Pages 369-374.

20. Osage, D.A., Krishnaswamy, P., Stephens, D.R., Scott, P., Janelle, J., Mohan, R., and Wilkowski, G.M., *Technologies For The Evaluation Of Non-Crack-like Flaws In Pressurized Components – Erosion/Corrosion, Pitting, Blisters, Shell Out-Of-Roundness, Weld Misalignment, Bulges And Dents*, WRC Bulletin 465, Welding research Council, Inc., September, 2001.

21. Spiekhout, J., Gresnight, A./M., Koning, C., and Wildschut, H., "Calculation Models for the Evaluation of the Resistance Against Mechanical Damage of Pipelines," 3R International , 25, Jahrgang, Heft, 4 April, 1986, pages 198-203.

22. Rooves, P., Bood, R., Galli, M., Marewski, U., Steiner, M., and Zarea, M., "EPRG methods for Assessing the Tolerance and Resistance of Pipelines to External Damage," Proceedings of the 3rd International Pipeline Technology Conference, Volume II, R. Denys (Editor), Brugge, Belgium, Elsevier, 2000.

23. Wang, K.C. and Smith, E.D., "The Effect Of Mechanical Damage On Fracture Initiation In Linepipe Part I – Dents," Metals Technology Laboratories, Report MTL 88-11(TR), January, 1982.

24. Wang, K.C. and Smith, E.D., "The Effect Of Mechanical Damage On Fracture Initiation In Linepipe Part II – Gouges," Metals Technology Laboratories, Report MTL 88-16(TR), March, 1988.

25. Wang, K.C. and Smith, E.D., "The Effect Of Mechanical Damage On Fracture Initiation In Linepipe Part III – Gouge In A Dent," Metals Technology Laboratories, Report PMRL 85-69, December, 1985.

12.11 Tables and Figures

Table 12.1
Data Required for the Assessment of Dents, Gouges, and Dent-Gouge Combinations

Use this form to summarize the data obtained from a field inspection.

Equipment Identification: _____

Equipment Type: _____ Pressure Vessel _____ Storage Tank _____ Piping Component

Component Type & Location: _____

Data Required For A Level 1 And Level 2 Assessment

General Data

Outside Diameter: _____

Nominal Wall Thickness t_{nom}, or Thickness Reading t_{rd}: _____

Metal Loss $LOSS$: _____

Future Corrosion Allowance FCA: _____

Distance to the Nearest Weld Joint L_w: _____

Distance to the Nearest Major Structural Discontinuity L_{msd}: _____

Specific Data for Dents

Dent Depth d_{dp}: _____

Minimum Specified Ultimate Tensile Strength σ_{uts}: _____

Maximum and Minimum Pressure P_{max} and P_{min} (cyclic operation only): _____

Specific Data for Gouges

Temperature Corresponding to a CVN of 40 J (30 ft-lbs): _____

ASME Exemption Curve: _____

Minimum Specified Yield Strength σ_{ys}: _____

Gouge Depth d_g: _____

Gouge Length: _____

Gouge Width: _____

Specific Data for Dent-Gouge Combinations

Dent Depth d_{dp}: _____

Gouge Depth d_g: _____

Minimum Specified Ultimate Tensile Strength σ_{uts}: _____

Maximum and Minimum Pressure P_{max} and P_{min} (cyclic operation only): _____

Table 12.2 – Minimum Temperature Where The Expected Value of the Charpy Impact Energy (CVN) is Above 40 Joules or 30 ft-lbs

SMYS (ksi)	ASME Exemption Curve			
	A (°F)	B (°F)	C (°F)	D (°F)
30	180	142	104	78
32	180	142	104	78
34	180	142	104	78
36	161	123	85	59
38	147	109	71	45
40	138	100	62	36
42	130	92	54	28
44	124	86	48	22
46	119	81	43	17
48	115	77	39	13
50	111	73	35	9
52	107	69	31	5
54	104	66	28	2
56	101	63	25	-1
58	99	61	23	-3
60	96	58	20	-6
62	94	56	18	-8
64	92	54	16	-10
66	90	52	14	-12
68	88	50	12	-14
70	86	48	10	-16
72	84	46	8	-18
74	83	45	7	-19
76	81	43	5	-21
78	80	42	4	-22
80	78	40	2	-24

Note: SMYS specified minimum yield strength of the material.

Table 12.2M – Minimum Temperature Where The Expected Value of the Charpy Impact Energy (CVN) is Above 40 Joules or 30 ft-lbs

SMYS (MPa)	ASME Exemption Curve			
	A (ºC)	B (ºC)	C (ºC)	D (ºC)
200	82	61	40	26
210	82	61	40	26
220	82	61	40	26
230	82	61	40	26
240	78	57	36	22
250	71	49	28	14
260	65	44	23	8
270	61	40	19	4
280	57	36	15	1
290	55	33	12	-2
300	52	31	10	-5
310	50	29	8	-7
320	48	27	6	-9
330	46	25	4	-11
340	44	23	2	-12
360	42	21	-1	-15
380	39	18	-3	-18
400	37	16	-5	-20
420	35	14	-7	-22
440	33	12	-9	-23
460	32	11	-11	-25
480	30	9	-12	-26
500	29	8	-13	-28
520	28	6	-15	-29
540	26	5	-16	-30
560	25	4	-17	-31

Note: SMYS specified minimum yield strength of the material.

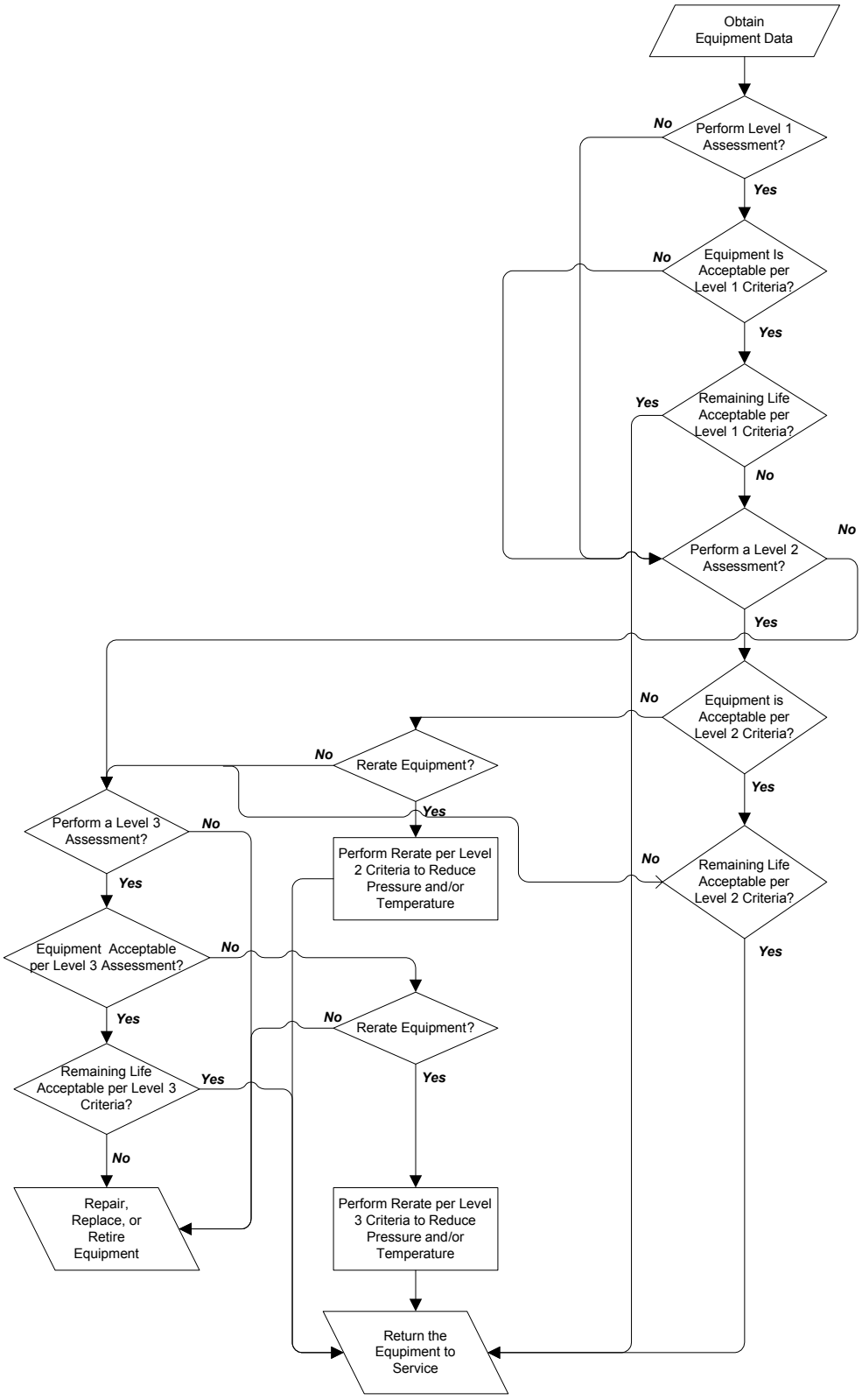

Figure 12.1 – Overview of the Assessment Procedures to Evaluate a Component With a Dent, Gouge, or Dent-Gouge Combination

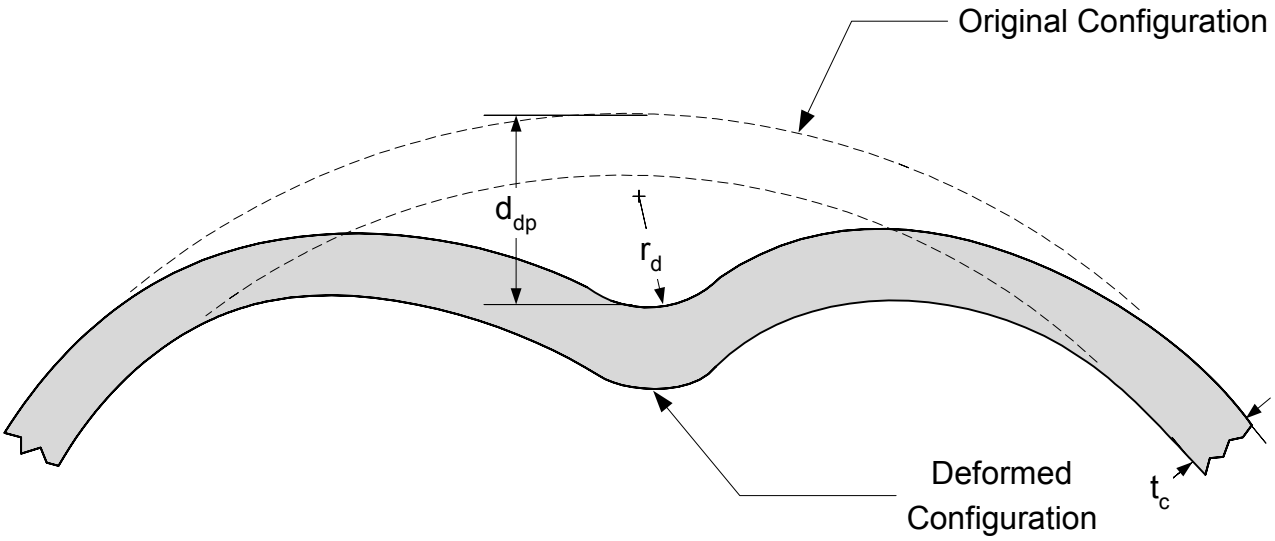

Figure 12.2 – Dent Dimensions

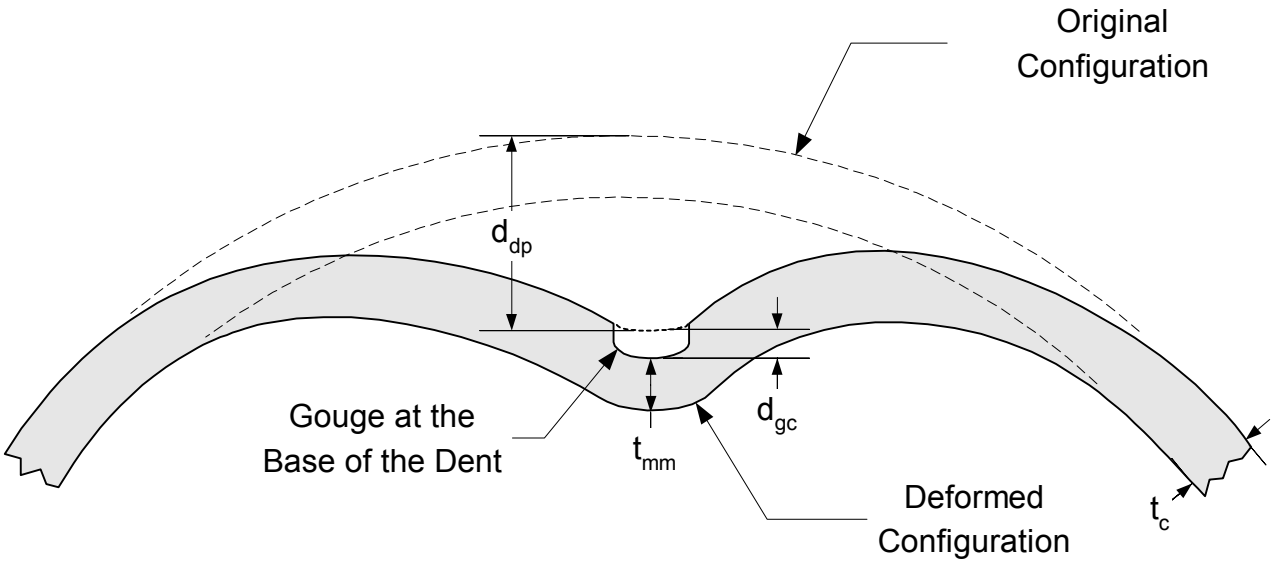

Figure 12.3 – Dent-Gouge Dimensions

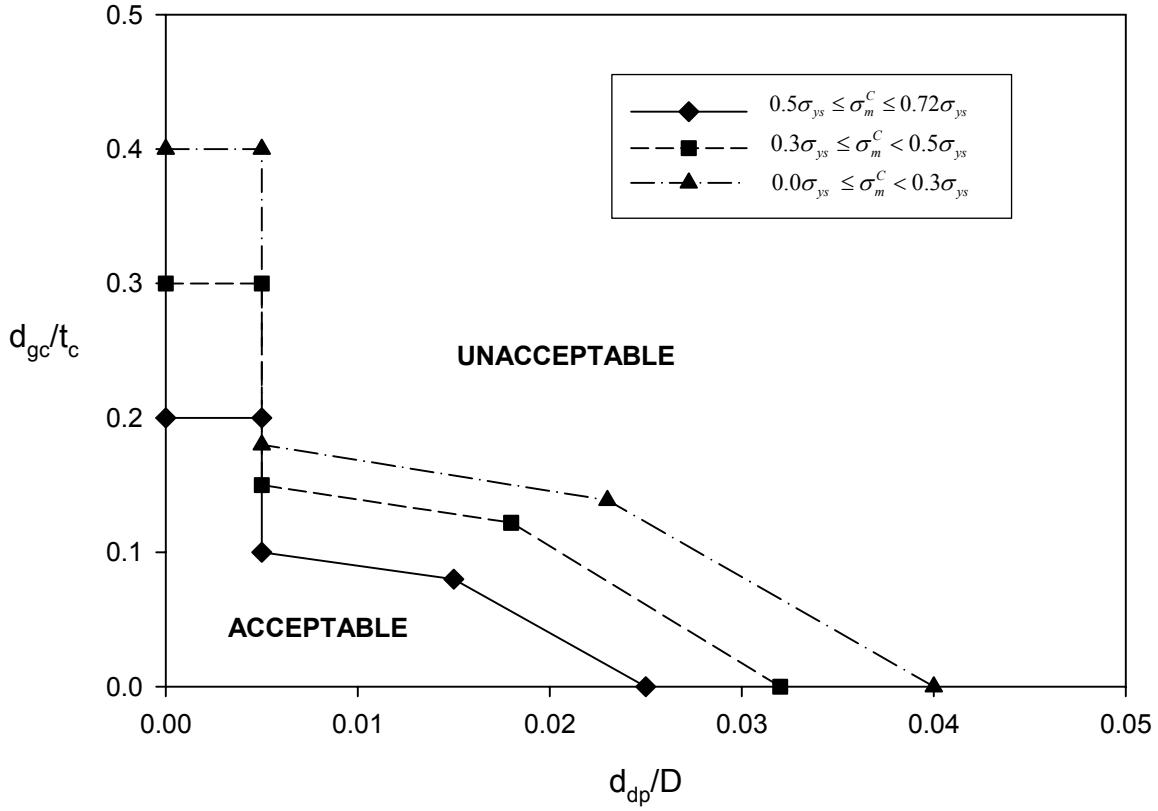

Data Points for Interaction Diagram for Determining the Acceptability of a Dent-Gouge Combination

$0.0\sigma_{ys} \le \sigma_m^C < 0.3\sigma_{ys}$		$0.3\sigma_{ys} \le \sigma_m^C < 0.5\sigma_{ys}$		$0.5\sigma_{ys} \le \sigma_m^C \le 0.72\sigma_{ys}$	
d_{dp}/D	d_{gc}/t_c	d_{dp}/D	d_{gc}/t_c	d_{dp}/D	d_{gc}/t_c
0.0000	0.4000	0.0000	0.3000	0.0000	0.2000
0.0050	0.4000	0.0005	0.3000	0.0005	0.2000
0.0050	0.1800	0.0005	0.1500	0.0005	0.1000
0.0230	0.1387	0.0180	0.1219	0.0150	0.0800
0.0400	0.0000	0.0320	0.0000	0.0250	0.0000

Figure 12.4 – Interaction Diagram for Determining the Acceptability of a Dent-Gouge Combination

PART 13

ASSESSMENT OF LAMINATIONS

PART CONTENTS

13.1 General

13.1.1 Fitness-For-Service (FFS) assessment procedures for pressurized components with laminations, excluding HIC or SOHIC damage, are provided in this Part. The assessment procedures for laminations are shown in the flow chart contained in Figure 13.1.

13.1.2 Laminations are a plane of non-fusion in the interior of a steel plate that results from the steel manufacturing process. Laminations are usually detected during an ultrasonic examination. Laminations affect welding, interfere with ultrasonic examination of welds, and reduce the strength of the plate when the plate is subjected to bending stresses, compressive stresses, or through thickness stresses. Laminations also result in voids to trap hydrogen in components that are in wet hydrogen sulfide service, which may result in blisters. Laminations may not be objectionable if the laminations are parallel to the plate surface, the component is subjected only to tensile membrane stresses from internal pressure, and the laminations are away from structural discontinuities where local bending stresses occur.

13.2 Applicability and Limitations of the Procedure

13.2.1 The FFS assessment procedures described below may be used to evaluate the acceptability of laminations subject to the limitations in this Part. The assessment procedures include analysis methods for laminations that are parallel to the surface of the plate or that have a through-thickness component (i.e. the lamination is not parallel to the surface of the plate).

13.2.2 Calculation methods are provided to determine acceptable $MAWP$ and coincident temperature if the acceptance criteria in this Part are not satisfied. For pressurized components, the calculation methods can be used to find a reduced maximum allowable working pressure. The calculation methods can be used to determine a reduced maximum fill height for tank components (i.e. shell courses).

13.2.3 Unless otherwise specified, this Part is limited to the evaluation of laminations. Other flaw types shall be evaluated in accordance with Part 2, Table 2.1.

13.2.4 The assessment procedures only apply to components that are not operating in the creep range (e.g. the design temperature is less than or equal to the value inPart 4, Table 4.1). A Materials Engineer should be consulted regarding the creep range temperature limit for materials not listed in this table. In the creep range, the lamination shall be evaluated using the Level 3 Assessment method inPart 10.

13.2.5 Specific details pertaining to the applicability and limitations of each of the assessment procedures are discussed below.

13.2.5.1 The Level 1 and 2 assessment procedures for laminations apply only if all of the following criteria are satisfied:

a) The original design criteria were in accordance with a recognized code or standard (see Part 1, paragraphs 1.2.2 or 1.2.3).

b) The material is considered to have sufficient material toughness. If there is uncertainty regarding the material toughness, then a Part 3 assessment should be performed. If the component is subject to embrittlement during operation due to temperature and/or the process environment, a Level 3 assessment should be performed. Temperature and/or process conditions that result in material embrittlement are discussed in Annex G.

c) The component is not in cyclic service, or the component is in cyclic service and adjacent laminations (see Equation (13.1)) are in the same plane and there is no indication of through thickness cracking. If the component is subject to less than 150 cycles (i.e. pressure and/or temperature variations including operational changes and start-ups and shut-downs) throughout its previous operating history and future planned operation, or satisfies the cyclic service screening procedure in Annex B1, paragraph B1.5.2, then the component is not in cyclic service.

d) The component is a Type A Component (see Part 4, paragraph 4.2.5) subject to internal pressure (i.e. supplemental loads are assumed to be negligible).

13.2.5.2 A Level 3 assessment for laminations shall be performed when any of the following is true:

a) The requirements of paragraph 13.2.5.1 are not satisfied.

b) The lamination is located in close proximity to a major structural discontinuity stress, a source of localized bending stress or to a load carrying attachment.

13.3 Data Requirements

13.3.1 Original Equipment Design Data

An overview of the original equipment data required for an assessment is provided in Part 2, paragraph 2.3.1. These data can be entered in the form provided in Part 2, Table 2.2, and Table 13.1 for each component under evaluation.

13.3.2 Maintenance and Operational History

An overview of the maintenance and operational history required for an assessment is provided in Part 2, paragraph 2.3.2.

13.3.3 Required Data/Measurements for a *FFS* Assessment

13.3.3.1 The required data and measurements for a lamination are shown below. This information should be recorded in Table 13.1. In addition, the creation of a sketch at the time of the inspection showing the information in this paragraph is recommended.

a) *Lamination Dimensions* – The largest dimensions in the longitudinal and circumferential direction, s and c, respectively, shall be recorded.

b) *Lamination Height* – The lamination height, L_h, shall be recorded.

c) *Lamination-to-Lamination Spacing,* L_s – Measurements should be made to determine the edge-to-edge spacing between laminations. This information should be detailed and provided on an inspection sketch. If there are multiple laminations in close proximity to one another, the size of the lamination to be used in the assessment is established considering the effects of neighboring laminations using the criterion for local metal loss described in Part 4 (see Figure 4.7). In addition, if the distance between two adjacent laminations (measured edge-to-edge) is less than or equal to two times the corroded plate thickness, t_c, the laminations shall be combined and evaluated as a single lamination.

d) *Lamination Minimum Measured Wall Thickness,* t_{mm} – This is the smallest distance from either surface to the lamination (see Figure 13.2).

e) *Lamination Spacing To Weld Joints,* L_w – Measurements shall be made to determine the spacing of laminations from weld joints. This information is important because if the lamination is close to a weld, through-wall cracking may occur. This information should be detailed and provided on an inspection sketch. A lamination is considered located at a weld seam if it lies within 25 mm (1 inch) or twice the plate thickness from the edge of the weld, whichever is greater (see Figure 13.3). Laminations close to weld seams can propagate along the weld fusion line or in the heat affected zone in the through-thickness direction (see Figure 13.3), particularly if the welds were not originally subject to post weld heat treatment. Therefore, laminations at weld seams should be monitored in-service.

f) *Lamination Spacing To Major Structural Discontinuities,* L_{msd} – Measurements shall be made to determine the location of the lamination with respect to major structural discontinuities. This information should be detailed and provided on an inspection sketch.

g) *Lamination Cracking* – The lamination shall be examined to determine if there are any cracks extending from the plane of the lamination in the through-thickness direction.

13.3.4 Recommendations for Inspection Technique and Sizing Requirements

13.3.4.1 Laminations are usually discovered during an in-service inspection/monitoring UT examination. If any visual observation of surface bulging on either the inside or the outside of the equipment is recorded, then the lamination shall be categorized as a blister and evaluated in accordance with Part 7.

13.3.4.2 Ultrasonic examination can be used to determine the depth of the lamination and remaining plate thickness at the lamination location. UT examination should also be used to ensure that HIC and SOHIC cracking are not present for components in hydrogen service. Details regarding this type of cracking and examination techniques are provided in *NACE Standard RP0296*.

13.4 Assessment Techniques and Acceptance Criteria

13.4.1 Overview

13.4.1.1 The assessment procedures of this Part shall be followed to evaluate the lamination even when the lamination is located within the region of the specified corrosion/erosion allowance

13.4.1.2 An overview of the assessment levels for laminations is provided in Figure 13.1.

a) The Level 1 Assessment procedure is a screening criterion for laminations based on: the lamination size, orientation relative to the surface, and spacing of the lamination to weld joints, structural discontinuities, and other laminations. If the lamination has any evidence of an associated surface bulge, then it shall be evaluated as a blister using the Level 1 blister assessment procedures of Part 7. If there are two or more laminations that are closely spaced at different depths in the wall thickness of the component, then the group of laminations are evaluated as equivalent HIC damage using the Level 1 assessment procedures in Part 7. If the lamination has a through-wall component (i.e. not parallel to the surface), then the through-wall component is evaluated as a equivalent crack-like flaw using the Level 1 assessment procedures of Part 9

b) The Level 2 Assessment procedure is similar to the Level 1 procedure except that the Level 2 assessment procedures of the referenced Parts are used.

c) The Level 3 Assessment procedures are intended to evaluate situations that do not satisfy the Level 1 or Level 2 assessment procedures. Detailed stress analysis techniques are normally required in a Level 3 assessment.

13.4.2 Level 1 Assessment

13.4.2.1 The following procedure shall be used to determine the acceptability of a lamination in a pressurized component:

a) STEP 1 – Determine if there is any surface bulging on either the inside or the outside surface of the component at the location of the lamination. If there is surface bulging, then evaluate the lamination as a blister using the Level 1 Assessment method in Part 7.

b) STEP 2 – Determine the information in paragraph 13.3.3.1.

c) STEP 3 – If there are two or more laminations on the same plane, there is no indication of through thickness cracking, and the spacing does not satisfy Equation (13.1), then the laminations shall be combined into a single larger lamination in the assessment. If there are two or more laminations at different depths in the wall thickness of the component and the spacing does not satisfy Equation (13.1), then the group of laminations shall be evaluated as equivalent HIC damage using the Level 1 Assessment method in Part 7. In applying this criterion, the spacing shall be measured parallel to the wall thickness.

$$L_s > 2t_c \tag{13.1}$$

d) STEP 4 – If Equation (13.2) is satisfied, proceed to STEP 5; otherwise, evaluate the through-thickness component of the lamination as a crack-like flaw using the Level 1 Assessment method in Part 9. In this evaluation, the crack depth shall be equal to $2a = L_h$ and the crack length shall be equal to $2c = \max\left[s,\ c\right]$.

$$L_h \le 0.09 \cdot \max\left[s,\ c\right] \tag{13.2}$$

e) STEP 5 – Determine the wall thickness to be used in the assessment using Equation (13.3) or Equation (13.4), as applicable.

$$t_c = t_{nom} - LOSS - FCA \tag{13.3}$$

$$t_c = t_{rd} - FCA \tag{13.4}$$

f) STEP 6 – If all of the following conditions are satisfied, proceed to STEP 7; otherwise, the lamination is not acceptable per the Level 1 Assessment procedure.

1) There is no indication of through-thickness cracking.

2) The lamination is not surface breaking in accordance with Equation (13.5).

$$t_{mm} \ge 0.10t_c \tag{13.5}$$

3) The distance between any edge of the lamination and the nearest weld seam satisfies Equation (13.6).

$$L_w \ge \max\left[2t_c,\ 25\,mm\ \ (1.0\,in)\right] \tag{13.6}$$

4) The distance from any edge of the lamination to the nearest major structural discontinuity satisfies Equation (13.7).

$$L_{msd} \ge 1.8\sqrt{Dt_c} \tag{13.7}$$

5) If the lamination is in hydrogen charging service, then the planar dimensions of the lamination satisfy Equations (13.8) and (13.9).

$$s \le 0.6\sqrt{Dt_c} \tag{13.8}$$

$$c \le 0.6\sqrt{Dt_c} \tag{13.9}$$

g) STEP 7 – Determine the $MAWP$ for the component (see Annex A, paragraph A.2) using the thickness from STEP 5. The component with the lamination is acceptable for operation at this calculated $MAWP$.

13.4.2.2 If the component does not meet the Level 1 Assessment requirements, then the following, or combinations thereof, can be considered:

a) Repair, replace, or retire the component.

b) Conduct a Level 2 or Level 3 Assessment.

13.4.3 Level 2 Assessment

13.4.3.1 The following procedure shall be used to determine the acceptability of a lamination in a pressurized component.

a) STEP 1 – Determine if there is any surface bulging on either the inside or the outside surface of the component at the location of the lamination. If there is surface bulging, then evaluate the lamination as a blister using the Level 2 Assessment method in Part 7.

b) STEP 2 – Determine the information in paragraph 13.3.3.1.

c) STEP 3 – If there are two or more laminations on the same plane, there is no indication of through thickness cracking, and the spacing does not satisfy Equation (13.1), then the laminations shall be combined into a single larger lamination in the assessment. If there are two or more laminations at different depths in the wall thickness of the component and the spacing does not satisfy Equation (13.1), then the group of laminations shall be evaluated as equivalent HIC damage using the Level 2 Assessment method in Part 7.

d) STEP 4 – If Equation (13.2) is satisfied, then proceed to STEP 5; otherwise, evaluate the through-thickness component of the lamination as a crack-like flaw using the Level 2 Assessment method in Part 9. In this evaluation, the crack depth shall be equal to $2a = L_h$ and the crack length shall be equal to $2c = \max\left[s,\ c\right]$.

e) STEP 5 – Determine the wall thickness to be used in the assessment using Equation (13.3) or Equation (13.4), as applicable.

f) STEP 6 – If all of the following conditions are satisfied, proceed to STEP 7; otherwise, the lamination is not acceptable per the Level 2 Assessment procedure.

   1) There is no indication of through-thickness cracking.

   2) The lamination is not surface breaking in accordance with Equation (13.5).

   3) The distance between any edge of the lamination and the nearest weld seam satisfies Equation (13.6). Laminations that do not satisfy the spacing criteria of Equation (13.6) are acceptable if it is determined that through-thickness cracking does not occur and there is no indication of cracking in the direction towards the inside or outside surface.

   4) The distance from any edge of the lamination to the nearest major structural discontinuity satisfies Equation (13.7).

   5) If the lamination is in hydrogen charging service, then the lamination shall be evaluated as an equivalent local thin area using the methods of Part 5. The remaining sound metal thickness to use in the LTA analysis is the value of $\max\left[\left(t_c - L_h - t_{mm}\right),\ t_{mm}\right]$, and the longitudinal and circumferential extend of the LTA are s and c, respectively (see Figure 13.2).

g) STEP 7 – Determine the $MAWP$ for the component (see Annex A paragraph A.2) using the thickness from STEP 5. The component with the lamination is acceptable for operation at this calculated $MAWP$.

13.4.3.2 If the component does not meet the Level 2 Assessment requirements, then the following, or combinations thereof, can be considered:

a) Repair, replace, or retire the component.

b) Conduct a Level 3 Assessment.

13.4.4 Level 3 Assessment

A Level 3 Assessment for laminations consists of performing a detailed stress analysis using the techniques and acceptance criteria provided in Annex B1. Components subject to external pressure or other loads that result in compressive stresses require continuity through the full thickness to avoid loss of buckling strength. Laminations in components originally designed to resist compressive stresses require a careful evaluation by a competent pressure vessel engineer to ensure that the component has adequate margin against the buckling mode of failure.

13.5 Remaining Life Assessment

A remaining life evaluation is typically not required for shell components under internal pressure loads (i.e. membrane tensile loads) because there is no loss of strength and no associated effect on the internal inspection interval except for the special inspection requirements for in-service monitoring. A remaining life may be required for laminations subject to compressive stresses or bending stresses, or for laminations in components subject to cyclic loads.

13.6 Remediation

Laminations meeting acceptance criteria of any assessment require no further remediation. If the lamination is in hydrogen service, then the remediation provided in Part 7 may be used. If the plate material is severely damaged and cannot be accepted per the assessment procedures, it should be repaired or replaced.

13.7 In-Service Monitoring

Laminations in components in hydrogen charging or other services that may lead to growth of the lamination shall be monitored to determine if there is growth or through-wall cracking occurring, seePart 7, paragraph 7.7. If the lamination is found to grow or cracks are detected during monitoring, then the lamination shall be re-evaluated.

13.8 Documentation

13.8.1 The documentation of the FFS Assessment shall include the information cited in Part 2, paragraph 2.8.

13.8.2 The location, size, spacing and condition of existing laminations should be recorded along with the results of the assessments performed. A sample data sheet is provided in Table 13.1 for this purpose.

13.8.3 If lamination growth is detected during the monitoring process, the physical dimensions and location of the lamination should be recorded along with the time period between measurements. In addition, the associated operating conditions and process stream constituents should be recorded in order to permit an evaluation of the hydrogen-charging environment relative to the operation of the equipment. This information may be valuable in determining suitable process changes in the operation of the equipment, if possible, to mitigate further damage.

13.9 Nomenclature

$2a$	depth of through-wall embedded crack associated with a lamination.
c	lamination dimension in the circumferential direction.
$2c$	length of through-wall embedded crack associated with a lamination.
D	shell inside diameter.
FCA	future corrosion allowance.
L_h	lamination height.
L_{msd}	spacing to the nearest major structural discontinuity.
L_s	lamination-to-lamination spacing.

L_w spacing to the nearest weld joint.

$LOSS$ amount of uniform metal loss at the time of the assessment.

s lamination dimension in the longitudinal direction.

t_c corroded wall thickness, allowing for future corrosion loss.

t_{mm} minimum measured thickness.

t_{nom} nominal or furnished thickness of the component adjusted for mill undertolerance as applicable.

t_{rd} uniform thickness away from the local metal loss location established by thickness measurements at the time of the assessment.

13.10 References

1. NACE Standard RP0296-96, "*Guidelines for Detection, Repair, and Mitigation of Cracking of Existing Petroleum Refinery Pressure Vessels in Wet H2S Environments*", NACE International, Houston, TX, 2003.
2. Osage, D.A., Krishnaswamy, P., Stephens, D.R., Scott, P., Janelle, J., Mohan, R., and Wilkowski, G.M., "Technologies for the Evaluation of Non-Crack-Like Flaws in Pressurized Components – Erosion/Corrosion, Pitting, Blisters, Shell Out-Of-Roundness, Weld Misalignment, Bulges and Dents," WRC Bulletin 465, Welding Research Council, New York, N.Y., September, 2001.

13.11 Tables and Figures

Table 13.1
Size, Location, Condition, And Spacing For Laminations

Enter the data obtained from a field inspection on this form.

Inspection Date: _____

Equipment Identification: _____

Equipment Type: _____ Pressure Vessel _____ Storage Tank _____ Piping Component

Component Type & Location: _____

_____

_____

_____

t_{nom} : _____

LOSS: _____

FCA: _____

t_{rd} : _____

Data Required For Level 1 And Level 2 Assessment					
Lamination Identification					
Dimension s (1)					
Dimension c (1)					
Lamination Height L_h (1)					
Edge-To-Edge Spacing to the nearest lamination L_s (2)					
Minimum Measured Thickness t_{mm} (1)					
Spacing to the Nearest Weld Joint L_w (2)					
Spacing to the Nearest Major Structural Discontinuity L_{msd}					
Through-Wall Cracking (Yes/No)					

Notes:
1. See Figure 13.2.
2. See Figure 13.3.

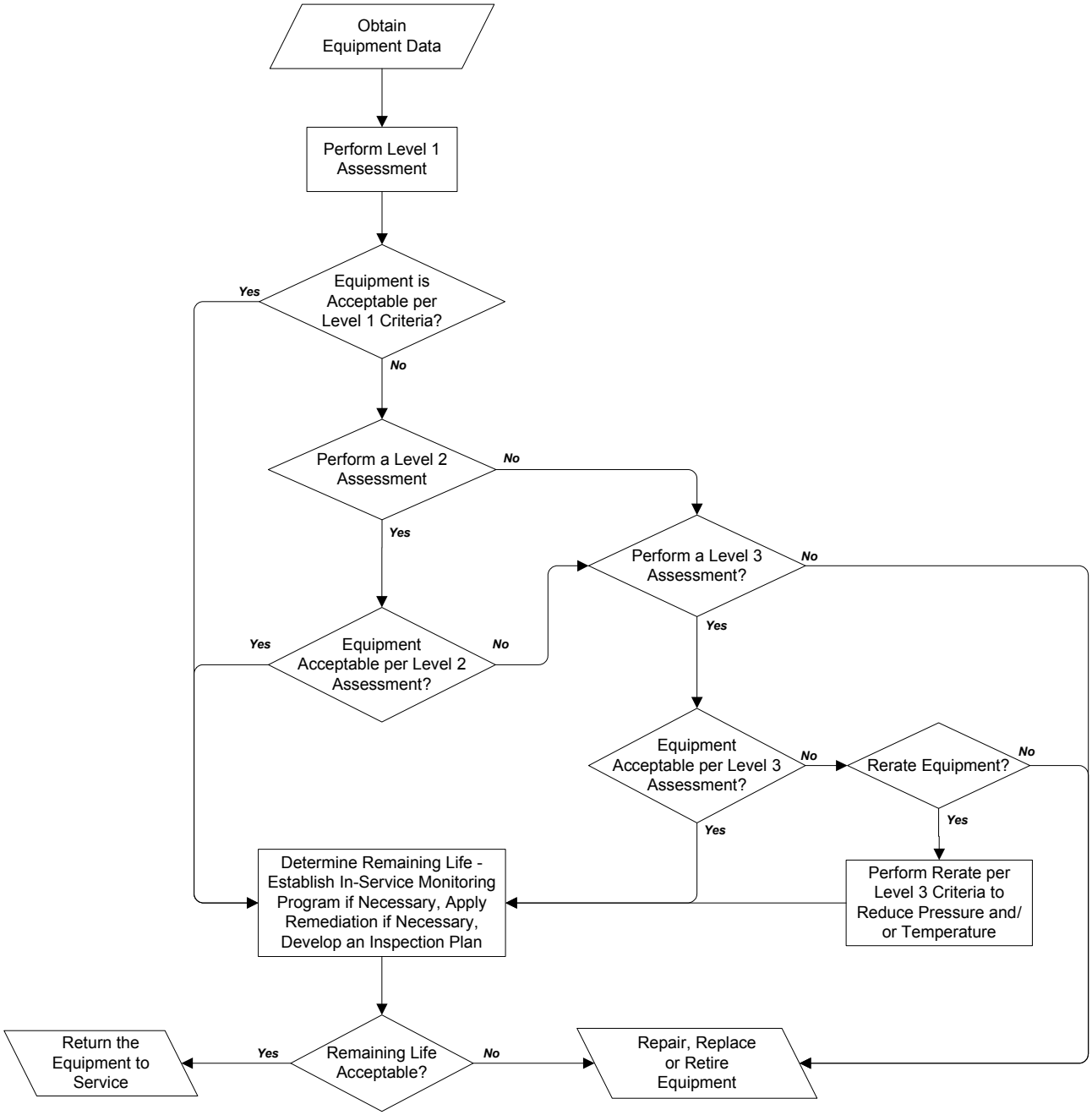

Figure 13.1 – Overview of the Assessment Procedure to Evaluate a Component with Laminations

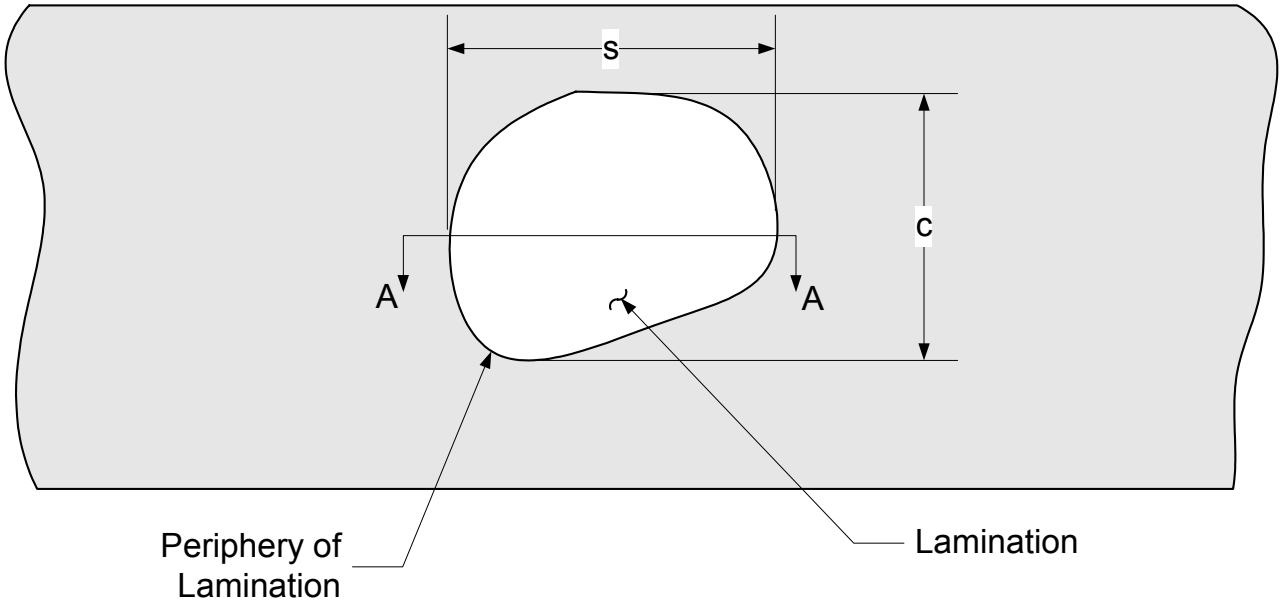

Lamination Plan View

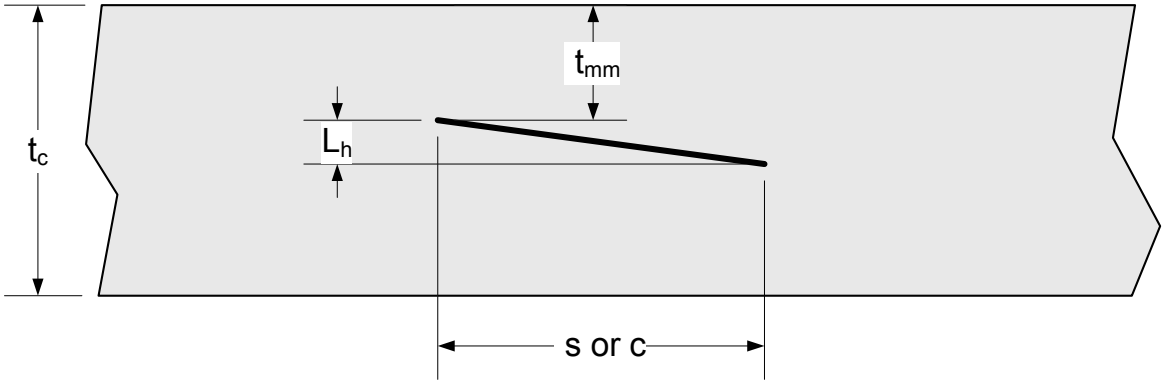

Section A-A
Cross Section Of Lamination

Figure 13.2 – Typical Lamination

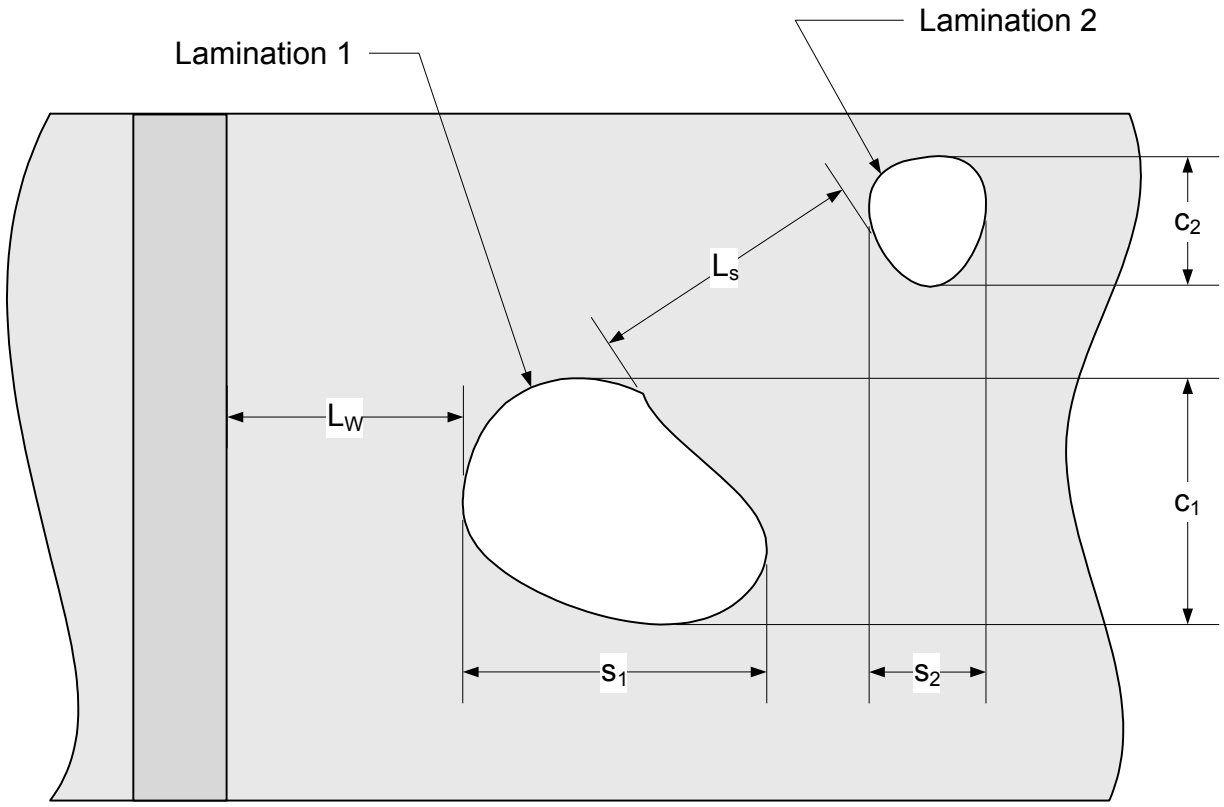

a) Planar View of Laminations Close To A Weld Seam And To Other Laminations

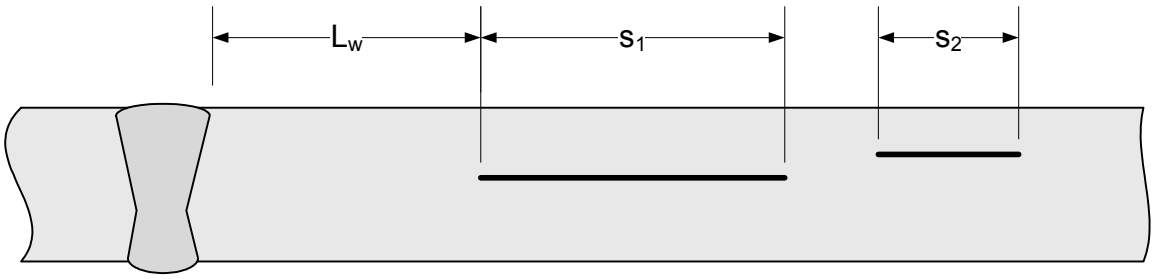

b) Cross Sectional View of Laminations Close To A Weld Seam And To Other Laminations

Figure 13.3 – Weld Joint Spacing and Multiple Laminations

ANNEX A

THICKNESS, MAWP AND STRESS EQUATIONS FOR A FFS ASSESSMENT

(NORMATIVE)

PART CONTENTS

A.1 General

A.1.1 Scope

The minimum required wall thickness, $MAWP$ and membrane stress for common pressure components are required for many of the Level 1 and Level 2 Fitness-For-Service assessments in this document. These parameters may be computed using the appropriate equations and other requirements from the construction code. Equations for thickness, $MAWP$ and membrane stress for internal pressure and external pressure are provided in this annex for easy reference, but they are not intended to replace those of the original construction code. It is the Users' responsibility to ensure that equations and other requirements for the calculation of thickness, $MAWP$, and membrane stress used in a Fitness-For-Service assessment are correct for the code of construction of the equipment. The equations in this annex are based on the following publications: the ASME B&PV Code; Section VIII, Division 1; WRC 406 and ASME B&PV Code Case 2286; and ASME B31.3. The equations are presented in an organized fashion to facilitate use, and are adjusted for metal loss and future corrosion allowance.

A.1.2 MAWP and MFH

In this annex, the safe operating pressure capability of a pressure vessel is described in terms of $MAWP$. This terminology is also used for piping instead of the usual term, maximum allowable operating pressure. For atmospheric storage tanks, the pressure capability is defined in terms of a maximum fill height (MFH).

A.2 Calculation of t_{min}, *MAWP (MFH)*, and Membrane Stress

A.2.1 Overview

Computation of the minimum wall thickness, $MAWP$ and membrane stress for existing equipment typically requires judgment on the part of the user to determine factors and parameters that may significantly affect the final results (e.g. code revisions, determination of allowable stresses for in-service components, weld joint efficiency in corroded regions). Methods to determine these factors and parameters for in-service equipment are provided in Paragraph A.2.

A.2.2 Minimum Required Wall Thickness and *MAWP (MFH)*

a) The minimum wall thickness and the $MAWP$ or MFH of a component can be determined using one of the following options:

1) Option 1 – If the original design conditions have not been changed and $t_{nom} - LOSS - FCA \geq t_{\min}$, then the $MAWP$ or MFH as shown in the original documentation for the equipment may be used. The $MAWP$ for a component may be taken as the design pressure and the MFH for a tank may be taken as the maximum design liquid level. In this case, the minimum required wall thickness may be determined using one of the following alternatives:

i) The minimum required wall thickness as shown in the original documentation for the equipment.

ii) The nominal or furnished thickness t_{nom} minus the original specified corrosion allowance.

2) Option 2 – The $MAWP$, MFH, and minimum required wall thickness may be calculated as follows.

i) The $MAWP$ and minimum required wall thickness for pressure vessel and piping components may be calculated if the design pressure (including liquid head), supplemental loads (see paragraph A.2.7), design temperature, component geometry, current measured thickness, future corrosion allowance, material specification and allowable stress are known.

ii) The MFH and minimum required wall thickness for atmospheric storage tank shell courses may be calculated if the design fill height, fluid specific gravity, supplemental loads (see paragraph A.2.7), design temperature, component geometry, current measured thickness, future corrosion allowance, design temperature, material specification and allowable stress are known.

b) If the component contains a flaw, the $MAWP$ or MFH may be reduced as a function of the Remaining Strength Factor (see Part 2, paragraph 2.4.2.2.b).

A.2.3 Code Revisions

The minimum wall thickness, $MAWP$ (MFH), and membrane stress of a component can be determined using the latest edition of the applicable construction code if the following essential details are known to comply with that code. If any of the essential details do not comply with the latest edition of the code, the minimum thickness, $MAWP$ (MFH), and membrane stress may be established using the edition of the code to which the component was originally constructed. However, an assessment of the component using the latest edition of the code should be made to ensure that the original construction code rules provide an adequate margin of safety.

a) Material specifications

b) Upper and/or lower temperature limits for specific materials

c) Design details (e.g. nozzles, nozzle reinforcement, and conical transitions)

d) Special design requirements for cyclical and/or high temperature design conditions

e) Fabrication details and quality of workmanship

f) Inspection requirements

g) Weld joint efficiency

h) Material toughness (Charpy Impact) requirements

A.2.4 Determination of Allowable Stresses

The allowable stress to be used in the calculation of the minimum required wall thickness and $MAWP$ (MFH) can be determined based on one of the following items.

a) The allowable stress for all components can be based on the original construction code. Recommendations pertaining to the revision of the construction code to use for an assessment are contained in paragraph A.2.3.

b) If a pressure vessel was constructed to the ASME B&PV Code, Section VIII, Division 1 (Code), the allowable stress may be determined from ASME B&PV Section VIII, Division 1, 1999 Addenda and subsequent editions and addenda subject to all of the following:

   1) The pressure vessel was constructed to the 1968 or later edition of the Code,

   2) The essential details listed in paragraph A.2.3 comply with the latest edition of the Code, and

   3) The pressure vessel satisfies one of the assessment levels of Part 3 of this Standard (note that pressure vessels constructed to the 1987 edition of the code, or later edition automatically satisfy this requirement).

c) If a pressure vessel was constructed to the ASME B&PV Code, Section VIII, Division 1 and the flaw is located in the base material of a cylindrical, conical or spherical shell outside of the weld band (see paragraph A.2.5a the allowable stress may be established in accordance with ASME B&PV Code, Section VIII, Division 2. This provision also applies to other construction codes that permit higher design allowable stresses in conjunction with design-by-analysis rules.

d) If the specification for the material of construction cannot be identified, an allowable stress can be estimated based on the material chemistry determined by chemical analysis, methods used for positive materials identification (see API 578), or other physical attributes, e.g. magnetic properties, atmospheric corrosion behavior, hardness, color, etc. This chemistry can then be compared to material specifications and grade in the original construction code. The allowable stress should be based on a specification and grade with a comparable chemistry that results in the lowest value of the code allowable stress at the design temperature.

e) If a component was constructed to more stringent requirements than required by the original construction code, the allowable stress may be established considering the higher quality aspects of the component while taking into account the basis for establishing the design allowable stress in the code. Examples include guaranteed strength properties, increased inspection, design details that minimize stress concentration, and/or material selection to mitigate the effects of environmental damage and/or to provide higher fracture toughness. If the allowable stresses are established based on the enhanced quality of the component, the basis should be documented and included in the assessment records.

A.2.5 Treatment of Weld and Riveted Joint Efficiency, and Ligament Efficiency

The minimum thickness, $MAWP$ (MFH), and membrane stress of a component shall include the appropriate weld or riveted joint or ligament efficiency utilized in the original design unless alternative values for these parameters can be established by stress analysis and/or inspection.

a) For damaged regions (e.g. corrosion/erosion, pitting, etc.) at a weld or riveted joint, the weld or riveted joint efficiency or weld joint quality factor, as applicable, shall be included in the minimum thickness and $MAWP$ calculations. A damaged region is considered to be at a weld or riveted joint if any part of it is located within the weld or riveted joint band. The weld band is defined to be centered on the weld, and has a width of 50.8 mm (2 inches) or twice of the furnished plate thickness, whichever is greater. The riveted joint band is defined to begin at the centerline of the riveted joint and extend 152.4 mm (6 inches) beyond the outermost row of rivets either side of the riveted joint.

b) For damaged regions (e.g. corrosion/erosion, pitting, etc.) outside of the weld or riveted joint band (see subparagraph an above) in components without closely spaced openings, a joint efficiency of 1.0 can be utilized in the minimum thickness and $MAWP$ (MFH) calculations. For components with multiple closely spaced openings, the ligament efficiency associated with the hole pattern shall be utilized in the calculations.

c) The joint efficiency of a riveted lap joint, E, may be determined by the following procedures, or determined by a more detailed stress analysis. Alternatively, for atmospheric storage tanks designed and fabricated to API 12A, paragraph 4.3.4 of API 653 may be used and for atmospheric storage tanks designed to API 650, paragraph 4.3.4 or Table 4-3 of API 653 may be used.

1) STEP 1 – Determine Allowable Stresses: σ_{bp}, σ_{br}, σ_{sr}, and σ_{tp}.

2) STEP 2 – Determine the unit width, w_r, over which the riveted joint efficiency will be determined and the thickness of the plate to be used in the calculation, t_c.

3) STEP 3 – Determine the rivet shear load.

$$P_{rs} = \frac{N_r \pi d_r^2 \sigma_{sr}}{4} \qquad for\ a\ single\ lap\ joint \qquad (A.1)$$

$$P_{rs} = \frac{N_r \pi d_r^2 \sigma_{sr}}{2} \qquad for\ a\ double\ lap\ joint \qquad (A.2)$$

4) STEP 4 – Determine the plate or rivet compressive load

$$P_{rc} = \min\left[\left(N_r d_p t_c \sigma_{bp}\right), \left(N_r d_r t_c \sigma_{br}\right)\right] \qquad (A.3)$$

5) STEP 5 – Determine the plate tension load. The plate tension load shall be computed using Equation (A.4) for the j^{th} row of rivets. The plate tension loads should be calculated for each row of rivets to determine the governing load, this load is designated as $P_{rj,\max}$.

$$P_{rj} = \left(w_r - j \cdot d_p\right) t_c \sigma_{tp} \left(\frac{N_r}{N_r - \sum_{(j-1)} n_{rm}} \right) \tag{A.4}$$

6) STEP 6 – Determine the limiting load

$$P_{rl} = \min\left[P_{rs},\ P_{rc},\ P_{rj,\max} \right] \tag{A.5}$$

7) STEP 7 – Determine the strength of the plate without a riveted joint.

$$P_{rp} = w_r t_c \sigma_{tp} \tag{A.6}$$

8) Step 8 – Determine the riveted joint efficiency

$$E = \frac{P_{rl}}{P_{rp}} \tag{A.7}$$

A.2.6 Treatment of Damage in Formed Heads

If damage (e.g. corrosion/erosion, pitting, etc.) occurs in the center section of an elliptical or torispherical head, the minimum thickness, $MAWP$, and membrane stress can be determined as follows:

a) Elliptical Heads:

1) The minimum thickness and $MAWP$ of the knuckle region for an elliptical head may be calculated by the equations in paragraph A.3.6.

2) The minimum thickness and $MAWP$ of the spherical region of an elliptical head may be calculated by the equation for spherical shells in paragraph A.3.5 using an equivalent radius. The spherical region of an ellipsoidal head is the area located entirely within a circle whose center coincides with the center of the head and whose diameter is equal to 80 percent of the shell diameter. The equivalent radius of the spherical segment is the equivalent spherical radius $K_c D$ where K_c is given in paragraph and D is the inside shell diameter.

b) Torispherical Heads:

1) The minimum thickness and MAWP of the knuckle region for a torispherical head may be calculated by the equations in paragraph A.3.7.

2) The minimum thickness and MAWP of the spherical region of a torispherical head may be calculated by the equation in paragraph A.3.7 with $M = 1.0$.

A.2.7 Thickness for Supplemental Loads

The thickness necessary for supplemental loads shall be considered in the determination of the minimum thickness, $t_{\min}$, $MAWP$ (or MFH), and/or membrane stress.

a) Supplemental loads include, but are not limited to: the weight of the component, contained fluid, insulation or refractory; loads resulting from the constraint of free thermal expansion, thermal gradients or differences in thermal expansion characteristics; occasional loads due to wind, earthquake, snow, and ice; loads due both to environmental and operating conditions; reaction forces from fluid discharges; loads resulting from support displacements; and loads due to process upset conditions.

b) An overview of supplemental loads, loading conditions, and allowances for pressure and/or temperature variations that should be considered in an assessment are shown in Table A.1. Load definitions and load case combinations that shall be considered in an assessment are shown in Annex B1, Tables B1.1 and B1.2, respectively.

c) Supplemental loads may be considered to be negligible if these loads do not effect the minimum required thickness or $MAWP$ (MFH) of a component. Otherwise, these loads are considered to be significant and must be included in an assessment.

d) Typical pressure vessel and piping configurations and flaw locations where the required thickness for supplemental loads may be significant are listed below.

1) Vertical vessels subject to wind or earthquake loading, with flaw located in the lower section of the vessel (see paragraph A.7.2)

2) Horizontal pressure vessels, with the flaw located in the mid-span between saddle support points or close to the saddle (see paragraph A.7.3)

3) Piping systems, with the flaw located at support point locations or in the mid-span of piping sections

A.2.8 Determination of the Future Corrosion Allowance

The Future Corrosion Allowance (FCA) must be established for the intended operating period. This corrosion allowance may be established based upon previous thickness measurements, from corrosion rates on equipment in a similar service, or from information obtained from corrosion design curves. Metal loss on both the inside and outside of a component should be considered when determining a future corrosion allowance.

A.2.9 Required Thickness for Future Operation

The required thickness for future operation can be established from the minimum thickness using the following equation:

$$t_{req} = t_{\min} + FCA \tag{A.8}$$

A.2.10 Treatment of Shell Distortions

While in-service, components may evolve into a configuration that no longer satisfies the fabrication tolerances of the original design code. This distortion in shape may result in areas with high localized stresses, and for components subject to a compressive stress field, a reduction in structural stability. Assessment procedures for shell out-of-roundness and/or shell misalignment are covered in Part 8.

A.3 Pressure Vessels and Boiler Components – Internal Pressure

A.3.1 Overview

The minimum required thickness and $MAWP$ of a pressure vessel component subject to internal pressure may be calculated based on the original construction code. Alternatively, the equations in this section may be utilized in the calculation of these parameters. The equations are based on the ASME B&PV Code, Section VIII, Division 1. The effects of supplemental loads (see paragraphs A.2.7 and A.7) are included in these equations only for cylindrical and conical shells (i.e. longitudinal stress direction) subject to a net section axial force and/or bending moment. The effects of supplemental loads for other component geometries and loading conditions can be evaluated using the stress analysis methods in Annex B1.

A.3.2 Shell Tolerances

The equations presented in this section are valid if the out-of-roundness tolerances for the shell satisfy the tolerances in Part 8, Table 8.3.

A.3.3 Metal Loss

The equations in this paragraph are written in terms of inside diameter of the component with the metal loss and future corrosion allowance applied to the inside surface. If metal loss has only occurred on the outside surface of the component (e.g. corrosion under insulation), the metal loss term in the equations should be set to zero. If metal loss has occurred on both the inside and outside surface, the loss term in the equations should be that for the inside surface.

A.3.4 Cylindrical Shells

The minimum thickness, $MAWP$ and membrane stress equations are as follows.

a) Circumferential Stress when $P \le 0.385SE$ and $t_{\min}^{C} \le 0.5R$ (Longitudinal Joints)

$$t_{\min}^{C} = \frac{PR}{SE - 0.6P} \tag{A.9}$$

$$MAWP^{C} = \frac{SEt_c}{R + 0.6t_c} \tag{A.10}$$

$$\sigma_m^{C} = \frac{P}{E}\left(\frac{R}{t_c} + 0.6\right) \tag{A.11}$$

b) Circumferential Stress when $P > 0.385SE$ or $t_{\min}^{C} > 0.5R$ (Longitudinal Joints)

$$t_{\min}^{C} = R\left(\sqrt{\frac{SE + P}{SE - P}} - 1\right) \tag{A.12}$$

$$MAWP^{C} = SE\left[\left(\frac{R + t_c}{R}\right)^2 - 1\right]\left[\left(\frac{R + t_c}{R}\right)^2 + 1\right]^{-1} \tag{A.13}$$

$$\sigma_m^{C} = \frac{P}{E}\left[\left(\frac{R + t_c}{R}\right)^2 + 1\right]\left[\left(\frac{R + t_c}{R}\right)^2 - 1\right]^{-1} \tag{A.14}$$

c) Longitudinal Stress when $P \le 0.385SE$ and $t_{\min}^{L} \le 0.5R$ (circumferential Joints)

$$t_{\min}^{L} = \frac{PR}{2SE + 0.4P} + t_{sl} \tag{A.15}$$

$$MAWP^{L} = \frac{2SE(t_c - t_{sl})}{R - 0.4(t_c - t_{sl})} \tag{A.16}$$

$$\sigma_m^{L} = \frac{P}{2E}\left(\frac{R}{t_c - t_{sl}} - 0.4\right) \tag{A.17}$$

d) Longitudinal Stress when $P > 0.385SE$ or $t^L_{\min} > 0.5R$ (circumferential Joints)

$$t^L_{\min} = R\left(\sqrt{\frac{P}{SE}+1}-1\right)+t_{sl} \tag{A.18}$$

$$MAWP^L = SE\left\{\left(\frac{R+\left[t_c-t_{sl}\right]}{R}\right)^2-1\right\} \tag{A.19}$$

$$\sigma^L_m = \frac{P}{E}\left\{\left(\frac{R+\left[t_c-t_{sl}\right]}{R}\right)^2-1\right\}^{-1} \tag{A.20}$$

e) Final Values:

$$t_{\min} = \max\left[t^C_{\min},\ t^L_{\min}\right] \tag{A.21}$$

$$MAWP = \min\left[MAWP^C, MAWP^L\right] \tag{A.22}$$

$$\sigma_{\max} = \max\left[\sigma^C_m,\ \sigma^L_m\right] \tag{A.23}$$

A.3.5 Spherical Shell or Hemispherical Head

a) If $P \le 0.665SE$ and $t_{\min} \le 0.356R$, then the minimum thickness, $MAWP$ and membrane stress equations are as follows:

$$t_{\min} = \frac{PR}{2SE-0.2P} \tag{A.24}$$

$$MAWP = \frac{2SEt_c}{R+0.2t_c} \tag{A.25}$$

$$\sigma_m = \frac{P}{2E}\left(\frac{R}{t_c}+0.2\right) \tag{A.26}$$

b) If $P > 0.665SE$ or $t_{\min} > 0.356R$,, then the minimum thickness, $MAWP$ and membrane stress equations are as follows:

$$t_{\min} = R\left(\left[\frac{2\left(SE+P\right)}{2SE-P}\right]^{\frac{1}{3}}-1\right) \tag{A.27}$$

$$MAWP = SE\left[\left(\frac{R+t_c}{R}\right)^3-1\right]\left[\left(\frac{R+t_c}{R}\right)^3+2\right]^{-1} \tag{A.28}$$

$$\sigma_m = \frac{P}{E}\left[\left(\frac{R+t_c}{R}\right)^3 + 2\right]\left[\left(\frac{R+t_c}{R}\right)^3 - 1\right]^{-1} \quad \text{(A.29)}$$

A.3.6 Elliptical Head

The minimum thickness, $MAWP$, and membrane stress equations may be computed using the following procedures (see Figure A.1) if $1.7 \le R_{ell} \le 2.2$, and $D\left(0.44R_{ell} + 0.02\right)/t_{\min} \le 500$ or $D\left(0.44R_{ell} + 0.02\right)/t_c \le 500$, as applicable.

a) Nominal values

$$t_{\min} = \frac{PDK}{2SE - 0.2P} \quad \text{(A.30)}$$

$$MAWP = \frac{2SEt_c}{KD + 0.2t_c} \quad \text{(A.31)}$$

$$\sigma_m = \frac{P}{2E}\left(\frac{DK}{t_c} + 0.2\right) \quad \text{(A.32)}$$

where,

$$K = \frac{1}{6}\left(2.0 + R_{ell}^2\right) \quad \text{(A.33)}$$

b) Values in the center portion of the head – To compute the minimum thickness, $MAWP$, and membrane stress for the center section of an elliptical head (a section within $0.8D$ centered on the head centerline), use K_c instead of K in Equations (A.30), (A.31), and (A.32), respectively.

$$K_c = 0.25346 + 0.13995R_{ell} + 0.12238R_{ell}^2 - 0.015297R_{ell}^3 \quad \text{(A.34)}$$

A.3.7 Torispherical Head

The minimum thickness, $MAWP$, and membrane stress equations may be computed using the following procedures (see Figure A.1) if $0.7 \le C_r/D \le 1.2$, $r_k/D \ge 0.06$, and $C_r/t_{\min} \le 500$ or $C_r/t_c \le 500$, as applicable.

a) Nominal values

$$t_{\min} = \frac{PC_rM}{2SE - 0.2P} \quad \text{(A.35)}$$

$$MAWP = \frac{2SEt_c}{C_rM + 0.2t_c} \quad \text{(A.36)}$$

$$\sigma_m = \frac{P}{2E}\left(\frac{C_rM}{t_c} + 0.2\right) \quad \text{(A.37)}$$

where,

$$M = \frac{1}{4}\left(3.0 + \sqrt{\frac{C_r}{r_k}}\right) \tag{A.38}$$

b) Values in the center or spherical portion of the head – To compute the minimum thickness, $MAWP$, and membrane stress for the center section of a torispherical head, use $M = 1.0$ in Equations (A.35), (A.36), and (A.37), respectively.

A.3.8 Conical Shell

The minimum thickness, $MAWP$, and membrane stress equations may be computed using the following procedures (see Figure A.2).

a) Circumferential Stress (Longitudinal Joints):

$$t_{\min}^{C} = \frac{PD}{2\cos\alpha(SE - 0.6P)} \tag{A.39}$$

$$MAWP^{C} = \frac{2SEt_c\cos\alpha}{D + 1.2t_c\cos\alpha} \tag{A.40}$$

$$\sigma_m^{C} = \frac{P}{2E}\left(\frac{D}{t_c\cos\alpha} + 1.2\right) \tag{A.41}$$

b) Longitudinal Stress (Circumferential Joints):

$$t_{\min}^{L} = \frac{PD}{2\cos\alpha(2SE + 0.4P)} + t_{sl} \tag{A.42}$$

$$MAWP^{L} = \frac{4SE(t_c - t_{sl})\cos\alpha}{D - 0.8(t_c - t_{sl})\cos\alpha} \tag{A.43}$$

$$\sigma_m^{L} = \frac{P}{2E}\left(\frac{D}{2(t_c - t_{sl})\cos\alpha} - 0.4\right) \tag{A.44}$$

c) Final Values

$$t_{\min} = \max\left[t_{\min}^{C},\ t_{\min}^{L}\right] \tag{A.45}$$

$$MAWP = \min\left[MAWP^{C}, MAWP^{L}\right] \tag{A.46}$$

$$\sigma_{\max} = \max\left[\sigma_m^{C},\ \sigma_m^{L}\right] \tag{A.47}$$

d) When determining the minimum thickness or $MAWP$ of a corroded area on a conical shell section, the inside diameter at the location of the minimum thickness reading adjusted for metal loss and corrosion allowance may be used in the above equations instead of maximum cone diameter.

e) Eccentric Cone – The minimum thickness of an eccentric cone shall be taken as the greater of the two thicknesses obtained using both the smallest and largest α in the calculations (see Figure A.3).

A.3.9 Toriconical Head

The minimum thickness, $MAWP$, and membrane stress equations are computed on a component basis (see Figure A.2):

a) Conical Section – The equations in paragraph A.3.8 can be used to compute the minimum required thickness, $MAWP$ and membrane stress of the cone section, designate these values as $t_{\min}^{c}$, $MAWP^{c}$, and σ_{m}^{c}, respectively.

b) Knuckle Section – The following equations can be used to compute the minimum required thickness, $MAWP$ and membrane stress:

$$t_{\min}^{k} = \frac{PL_{kc}M}{2SE - 0.2P} \tag{A.48}$$

$$MAWP^{k} = \frac{2SEt_{kc}}{L_{kc}M + 0.2t_{kc}} \tag{A.49}$$

$$\sigma_{m}^{k} = \frac{P}{2E}\left(\frac{L_{kc}M}{t_{kc}} + 0.2\right) \tag{A.50}$$

where,

$$L_{kc} = \frac{R - r_{k}(1 - \cos\alpha)}{\cos\alpha} \tag{A.51}$$

$$M = \frac{1}{4}\left(3.0 + \sqrt{\frac{L_{kc}}{r_{k}}}\right) \tag{A.52}$$

c) Final Values – Expressions for the minimum required wall thickness, $MAWP$, and membrane stress are provided on a component basis in paragraph A.3.9.a) and A.3.9.b). The values of these quantities to be used in an assessment depend on the location of the flaw. The following equations can be used if a single expression is required for the cone-knuckle configuration.

$$t_{\min} = \max\left[t_{\min}^{c},\, t_{\min}^{k}\right] \tag{A.53}$$

$$MAWP = \min\left[MAWP^{c},\, MAWP^{k}\right] \tag{A.54}$$

$$\sigma_{\max} = \max\left[\sigma_{m}^{c},\, \sigma_{m}^{k}\right] \tag{A.55}$$

A.3.10 Conical Transition

The minimum thickness, $MAWP$ and membrane stress equations are computed on a component basis (see Figure A.3).

a) Conical Section – The equations in paragraph A.3.8 can be used to compute the minimum required thickness, $MAWP$, and membrane stress of the cone section, designate these values as $t_{\min}^{c}$, $MAWP^{c}$, and σ_{m}^{c}, respectively.

b) Knuckle Section (If Used) – Use the following equations to compute the minimum required thickness, $MAWP$, and membrane stress.

$$t_{\min}^{k} = \frac{PL_{kc}M}{2SE - 0.2P} \tag{A.56}$$

$$MAWP^{k} = \frac{2SEt_{kc}}{L_{kc}M + 0.2t_{kc}} \tag{A.57}$$

$$\sigma_{m}^{k} = \frac{P}{2E}\left(\frac{L_{kc}M}{t_{kc}} + 0.2\right) \tag{A.58}$$

where,

$$L_{kc} = \frac{R_L - r_k(1-\cos\alpha)}{\cos\alpha} \tag{A.59}$$

$$M = \frac{1}{4}\left(3 + \sqrt{\frac{L_{kc}}{r_k}}\right) \tag{A.60}$$

c) Flare Section (If Used) – Use the following equations to compute the minimum required thickness, $MAWP$, and membrane stress.

1) Equations based on modification of knuckle equations (see paragraph A.3.10.b)

$$t_{\min}^{f} = \frac{PL_{fc}M}{2SE - 0.2P} \tag{A.61}$$

$$MAWP^{f} = \frac{2SEt_{fc}}{L_{fc}M + 0.2t_{fc}} \tag{A.62}$$

$$\sigma_{m}^{f} = \frac{P}{2E}\left(\frac{L_{fc}M}{t_{fc}} + 0.2\right) \tag{A.63}$$

where,

$$L_{fc} = \frac{R_S + r_f\left(1-\cos\alpha\right)}{\cos\alpha} \tag{A.64}$$

$$M = \frac{1}{4}\left(3 + \sqrt{\frac{L_{fc}}{r_f}}\right) \tag{A.65}$$

2) Equations based on a pressure-area force balance procedure

$$t_{\min}^{f} = \left(\frac{1}{\alpha_r r_f}\right)\left(\frac{P\left[K_1 + K_2 + K_3\right]}{1.5SE} - K_4 - K_5\right) \tag{A.66}$$

$$MAWP^f = 1.5SE\left(\frac{t_{fc}\alpha_r r_f + K_4 + K_5}{K_1 + K_2 + K_3}\right) \quad \text{(A.67)}$$

$$\sigma_m^f = \frac{P\left(K_1 + K_2 + K_3\right)}{1.5E\left(t_{fc}\alpha_r r_f + K_4 + K_5\right)} \quad \text{(A.68)}$$

where,

$$K_1 = 0.125\left(2r_f + D_1\right)^2 \tan\alpha - \frac{\alpha_r r_f^2}{2} \quad \text{(A.69)}$$

$$K_2 = 0.28D_1\left(D_1 t_c\right)^{1/2} \quad \text{(A.70)}$$

$$K_3 = 0.78K_6\left(K_6 t_{cc}\right)^{1/2} \quad \text{(A.71)}$$

$$K_4 = 0.78t_c^c\left(K_6 t_{cc}\right)^{1/2} \quad \text{(A.72)}$$

$$K_5 = 0.55t_c^s\left(D_1 t_c\right)^{1/2} \quad \text{(A.73)}$$

$$K_6 = \frac{D_1 + 2r_f\left(1 - \cos\alpha\right)}{2\cos\alpha} \quad \text{(A.74)}$$

$$\alpha_r = \alpha\left(\frac{\pi}{180}\right) \quad \text{(A.75)}$$

$$D_1 = 2R_s \quad \text{(A.76)}$$

d) Final Values – Expressions for the minimum required wall thickness, $MAWP$, and membrane stress are provided on a component basis in paragraphs A.3.10.a, A.3.10.b, and A.3.10.c. The values of these quantities to be used in an assessment depend on the location of the flaw. The following equations can be used if a single expression is required for the conical transition.

1) Case 1 – The conical transition only contains a cone (Figure A.3(a)).

$$t_{\min} = t_{\min}^c \quad \text{(A.77)}$$

$$MAWP = MAWP^c \quad \text{(A.78)}$$

$$\sigma_{\max} = \sigma_m^c \quad \text{(A.79)}$$

2) Case 2 – The conical transition contains a cone and knuckle (Figure A.3(b)).

$$t_{\min} = \max\left[t_{\min}^c,\ t_{\min}^k\right] \quad \text{(A.80)}$$

$$MAWP = \min\left[MAWP^c,\ MAWP^k\right] \quad \text{(A.81)}$$

$$\sigma_{\max} = \max\left[\sigma_m^c,\ \sigma_m^k\right] \tag{A.82}$$

3) Case 3 – The conical transition contains a cone, knuckle and flare (Figure A.3(c)).

$$t_{\min} = \max\left[t_{\min}^c,\ t_{\min}^k,\ t_{\min}^f\right] \tag{A.83}$$

$$MAWP = \min\left[MAWP^c,\ MAWP^k,\ MAWP^f\right] \tag{A.84}$$

$$\sigma_{\max} = \max\left[\sigma_m^c,\ \sigma_m^k,\ \sigma_m^f\right] \tag{A.85}$$

4) Case 4 – The conical transition contains a knuckle and flare (Figure A.3(d)).

$$t_{\min} = \max\left[t_{\min}^k,\ t_{\min}^f\right] \tag{A.86}$$

$$MAWP = \min\left[MAWP^k,\ MAWP^f\right] \tag{A.87}$$

$$\sigma_{\max} = \max\left[\sigma_m^k,\ \sigma_m^f\right] \tag{A.88}$$

5) Case 5 – The conical transition contains a cone and flare (Figure A.4(d)).

$$t_{\min} = \max\left[t_{\min}^c,\ t_{\min}^f\right] \tag{A.89}$$

$$MAWP = \min\left[MAWP^c,\ MAWP^f\right] \tag{A.90}$$

$$\sigma_{\max} = \max\left[\sigma_m^c,\ \sigma_m^f\right] \tag{A.91}$$

e) The half-apex angle of a conical transition can be computed knowing the shell geometry with the following equations. These equations were developed with the assumption that the conical transition contains a cone section, knuckle, and flare. If the transition does not contain a knuckle or flare, the radii of these components should be set to zero when computing the half-apex angle.

1) If $(R_L - r_k) \geq (R_S + r_f)$

$$\alpha = \phi + \beta \tag{A.92}$$

$$\beta = \arctan\left[\frac{(R_L - r_k) - (R_S + r_f)}{L_c}\right] \tag{A.93}$$

2) If $(R_L - r_k) < (R_S + r_f)$

$$\alpha = \phi - \beta \tag{A.94}$$

$$\beta = \arctan\left[\frac{(R_S + r_f) - (R_L - r_k)}{L_c}\right] \tag{A.95}$$

3) In both cases shown above, the angle ϕ is given by the following equation.

$$\phi = \arcsin\left[\frac{(r_f + r_k)\cos\beta}{L_c}\right] \tag{A.96}$$

A.3.11 Nozzles Connections in Shells

Two procedures are provided, area replacement and limit load. The area replacement procedure must be used for all nozzles in spherical shells or formed heads and for pad reinforced nozzles in cylinders. The limit load procedure may be used for unreinforced nozzles in cylindrical shells. A nozzle weld strength analysis is required for both of these procedures.

a) Required Reinforcement, Area Replacement Method – This assessment procedure is the one used for design of nozzles in the ASME Code, Section VIII, Division 1. The procedure can be used for nozzle connections to most shell types with or without a reinforcing pad. The procedure is known to produce conservative results for small nozzles.

1) Limitations:

i) For openings in cylindrical shells, the opening does not exceed the following; for nozzles that do not meet this criterion, stress analysis techniques using either stress categorization or plastic collapse are recommended to determine an acceptable $MAWP$.

I) For vessels 1524 mm (60 inches) in diameter and less, $\min[D/2,\ 508\ mm\ (20\ in)]$

II) For vessels over 1524 mm (60 inches), $\min[D/3,\ 1016\ mm\ (40\ in)]$

ii) For openings in spherical shells or formed heads there is no restriction on the opening size.

iii) The effects of nozzle loading are not included in either of these procedures. If nozzle loads are significant, a stress analysis must be performed to evaluate the acceptability of the nozzle configuration.

2) The condition required for satisfactory reinforcement of a branch nozzle connection is given by the following:

i) The basic equations for all configurations are shown below.

$$A_r = d_c t_r F + 2t_n t_r F\left(1 - f_{r1}\right) \tag{A.97}$$

$$A_1 = \max\left[\begin{array}{l}\left\{d_c\left(E_1\left(t - c_s\right) - Ft_r\right) - B\right\},\\ \left\{2\left(t + t_n - c_s - c_n\right)\left(E_1\left(t - c_s\right) - Ft_r\right) - B\right\}\end{array}\right] \tag{A.98}$$

$$B = 2\left(t_n - c_n\right)\left(E_1\left(t - c_s\right) - Ft_r\right)\left(1 - f_{r1}\right) \tag{A.99}$$

$$A_3 = \min\left[\begin{array}{l}\left\{5\left(t - c_s\right)\left(t_i - 2c_n\right) f_{r2}\right\},\\ \left\{5\left(t_n - 2c_n\right)^2 f_{r2}\right\},\\ \left\{2h\left(t_i - 2c_n\right) f_{r2}\right\}\end{array}\right] \tag{A.100}$$

$$A_{43} = \left(w_h - c_n\right)^2 f_{r2} \tag{A.101}$$

ii) For nozzles without a reinforcing pad (see Figure A.5 for definition of areas):

$$A_1 + A_2 + A_3 + A_{41} + A_{43} \geq J_r A_r \tag{A.102}$$

$$A_2 = \min\left[\left\{5\left(t_n - c_n - t_{rn}\right) f_{r2}\left(t - c_s\right)\right\},\ \left\{5\left(t_n - c_n - t_{rn}\right) f_{r2}\left(t_n - c_n\right)\right\}\right] \tag{A.103}$$

$$A_{41} = w_n^2 f_{r2} \tag{A.104}$$

iii) For nozzles with a reinforcing pad (see Figure A.5 for definition of areas):

$$A_1 + A_2 + A_3 + A_{41} + A_{42} + A_{43} + A_5 \geq J_r A_r \tag{A.105}$$

$$A_2 = \min\left[\begin{array}{l}\left\{5\left(t_n - c_n - t_{rn}\right) f_{r2}\left(t - c_s\right)\right\}, \\ \left\{2\left(t_n - c_n - t_{rn}\right)\left(2.5\left(t_n - c_n\right) + t_e\right) f_{r2}\right\}\end{array}\right] \tag{A.106}$$

$$A_{41} = w_n^2 f_{r3} \tag{A.107}$$

$$A_{42} = w_p^2 f_{r4} \tag{A.108}$$

$$A_5 = \left[D_p - d_c - 2\left(t_n - c_n\right)\right] t_e f_{r4} \tag{A.109}$$

iv) In the above equations, if $A_1 < 0.0$ use $c_b = LOSS_b + FCA$, or if $A_2 < 0.0$ use $A_2 = 0.0$.

b) Required Reinforcement, Limit Analysis Method – This assessment procedure can be utilized to evaluate nozzles in cylindrical shells subject to internal pressure that do not have a reinforcing pad (see ASME B&PV Code Case 2168-2). The procedure can be used to check a nozzle with a reinforcing pad if the pad is neglected in the analysis. The procedure cannot be used if the nozzle is subject to significant supplemental loading (i.e. applied net section forces and moments from piping loads). Any combination of thicknesses in the nozzle neck or vessel shell is acceptable provided all of the conditions listed below are met. This method is effective for evaluating a region of local metal loss at nozzles where an average thickness is used to represent the metal loss in the nozzle reinforcement zone (see Figures A.6 and A.7, and Part 4, paragraph 4.3.3.4).

1) Limitations – All the following must be satisfied:

i) The temperature limits of Table A.2 are satisfied.

ii) The nozzle and shell are fabricated from a ferrous material with $YS/UTS < 0.80$ where YS is the minimum specified yield strength and UTS is the minimum specified ultimate tensile strength.

iii) The opening does not exceed NPS 24.

iv) The parameters $\left(d_m/D_m\right)$ and $\left(d_m/t\right)$ shall meet the following requirements:

- If $d_m/D_m > 0.5$, then $D_m/t \leq 100$.
- If $d_m/D_m \leq 0.5$, then $D_m/t \leq 250$.

v) The opening is not subject to cyclic loading.

vi) The opening is in a cylindrical vessel and is located a distance of $1.8\sqrt{D_m\left(t - c_s\right)}$ from any major structural discontinuities.

vii) The spacing between the centerlines of the opening and any other opening is more than three times the average diameters of the openings.

viii) The opening is circular in cross section and the nozzle is normal to the surface of the cylindrical vessel. These rules do not apply to laterals or pad reinforced nozzles.

ix) If $L < 0.5\sqrt{d_m t_n}$, then use $t_n = t_p$ in Equations (A.110) and (A.111).

x) $t_n > 0.875 t_{std}$ through an axial length of $L < 0.5\sqrt{d_m t_n}$.

xi) The effects of nozzle loading are not included in either of these procedures. If nozzle loads are significant, a stress analysis must be performed to evaluate the acceptability of the nozzle configuration.

2) Assessment Procedure – The following two equations must be satisfied:

$$\frac{2+2\left(\frac{d_m}{D_m}\right)^{3/2}\left(\frac{t_n-c_n}{t-c_s}\right)^{1/2}+1.25\lambda}{1+\left(\frac{d_m}{D_m}\right)^{1/2}\left(\frac{t_n-c_n}{t-c_s}\right)^{3/2}} \le 2.95\left(\frac{t-c_s}{t_r}\right) \qquad \text{(A.110)}$$

$$\frac{\left[A\left(\frac{t_n-c_n}{t-c_s}\right)^2+228\left(\frac{t_n-c_n}{t-c_s}\right)\left(\frac{d_m}{D_m}\right)+B\right]\lambda+155}{108\lambda^2+\left[228\left(\frac{d_m}{D_m}\right)^2+228\right]\lambda+152} \ge \left(0.93+0.005\lambda\right)\left(\frac{t_r}{t-c_s}\right) \qquad \text{(A.111)}$$

where,

$$\lambda = \left(\frac{d_m}{D_m}\right)\sqrt{\frac{D_m}{t-c_s}} \qquad \text{(A.112)}$$

$$A = 162 \qquad for \qquad \frac{t_n-c_n}{t-c_s} \le 1.0 \qquad \text{(A.113)}$$

$$B = 210 \qquad for \qquad \frac{t_n-c_n}{t-c_s} \le 1.0 \qquad \text{(A.114)}$$

$$A = 54 \qquad for \qquad \frac{t_n-c_n}{t-c_s} > 1.0 \qquad \text{(A.115)}$$

$$B = 318 \qquad for \qquad \frac{t_n-c_n}{t-c_s} > 1.0 \qquad \text{(A.116)}$$

c) Weld Strength Analysis

1) If the nozzle connection is subject to corrosion, the corroded dimensions of the groove and fillet welds should be used in the strength calculations.

2) The following analysis should be used when the nozzle neck is inserted through the vessel wall (set-in nozzle, see Figure A.8); the reinforcement areas to be used in the calculations are defined in paragraph A.8.

i) The required strength is:

$$W = \left[A - A_1 + 2\left(t_n - c_n\right) f_{r1} \left(E_1 \left(t - c_s \right) - F t_r \right) \right] S_v \tag{A.117}$$

$$W_{11} = \left(A_2 + A_{41} + A_{42} + A_5 \right) S_v \tag{A.118}$$

$$W_{22} = \left(A_2 + A_3 + A_{41} + A_{43} + 2\left(t_n - c_n\right)\left(t - c_s\right) f_{r1} \right) S_v \tag{A.119}$$

$$W_{33} = \left(A_2 + A_3 + A_5 + A_{41} + A_{42} + A_{43} + 2\left(t_n - c_n\right)\left(t - c_s\right) f_{r1} \right) S_v \tag{A.120}$$

ii) The computed strength with a reinforcing pad is:

$$W^c = \min\left[W_{11}^c, W_{22}^c, W_{33}^c \right] \tag{A.121}$$

$$W_{11}^c = \frac{\pi}{2} D_p w_p \left(0.49 S_{wp} \right) + \frac{\pi}{2} d_m \left(t_n - c_n \right)\left(0.7 S_n \right) \tag{A.122}$$

$$W_{22}^c = \left(\begin{array}{l} \frac{\pi}{2} d_o w_n \left(0.49 S_{wn} \right) + \frac{\pi}{2} d_o w_{pg} \left(0.74 S_{wpg} \right) + \\ \frac{\pi}{2} d_o w_{ng} \left(0.74 S_{wng} \right) + \frac{\pi}{2} d_o w_h \left(0.49 S_{wh} \right) \end{array} \right) \tag{A.123}$$

$$W_{33}^c = \frac{\pi}{2} D_p w_p \left(0.49 S_{wp} \right) + \frac{\pi}{2} d_o w_{ng} \left(0.74 S_{wng} \right) + \frac{\pi}{2} d_o w_h \left(0.49 S_{wh} \right) \tag{A.124}$$

iii) The computed strength without a reinforcing pad is:

$$W^c = \min\left[W_{11}^c, W_{22}^c \right] \tag{A.125}$$

$$W_{11}^c = \frac{\pi}{2} d_o w_n \left(0.49 S_{wn} \right) + \frac{\pi}{2} d_m \left(t_n - c_n \right)\left(0.7 S_n \right) \tag{A.126}$$

$$W_{22}^c = \frac{\pi}{2} d_o w_n \left(0.49 S_{wn} \right) + \frac{\pi}{2} d_o w_{ng} \left(0.74 S_{wng} \right) + \frac{\pi}{2} d_o w_h \left(0.49 S_{wh} \right) \tag{A.127}$$

$$W_{33}^c = 0.0 \tag{A.128}$$

iv) The acceptance criteria is given by Equation (A.129), or Equations (A.130), (A.131), and (A.132).

$$W^c \geq W \tag{A.129}$$

$$W_{11}^c \geq \min\left[W_{11}, W \right] \tag{A.130}$$

$$W_{22}^{c} \geq \min\left[W_{22}, W\right] \tag{A.131}$$

$$W_{33}^{c} \geq \min\left[W_{33}, W\right] \tag{A.132}$$

3) The following analysis should be used when the nozzle neck abuts the vessel wall (set-on nozzle, see Figure A.9); the reinforcement areas to be used in the calculations are defined in paragraph A.8.

i) The required strength is:

$$W = \left[A - A_1\right] S_v \tag{A.133}$$

$$W_{11} = \left(A_2 + A_5 + A_{41} + A_{42}\right) S_v \tag{A.134}$$

$$W_{22} = \left(A_2 + A_{41}\right) S_v \tag{A.135}$$

ii) The computed strength with a reinforcing pad is:

$$W^{c} = \min\left[W_{11}^{c}, W_{22}^{c}\right] \tag{A.136}$$

$$W_{11}^{c} = \frac{\pi}{2} D_p w_p \left(0.49 S_{wp}\right) + \frac{\pi}{2} d_m w_{ng} \left(0.60 S_{wng}\right) \tag{A.137}$$

$$W_{22}^{c} = \frac{\pi}{2} d_o w_n \left(0.49 S_{wn}\right) + \frac{\pi}{2} d_m w_{ng} \left(0.60 S_{wng}\right) \tag{A.138}$$

iii) The computed strength without a reinforcing pad is:

$$W^{c} = W_{11}^{c} \tag{A.139}$$

$$W_{11}^{c} = \frac{\pi}{2} d_o w_n \left(0.49 S_{wn}\right) + \frac{\pi}{2} d_m w_{ng} \left(0.60 S_{wng}\right) \tag{A.140}$$

$$W_{22}^{c} = 0.0 \tag{A.141}$$

iv) The acceptance criteria is given by Equation (A.142) or Equations (A.143) and (A.144).

$$W^{c} \geq W \tag{A.142}$$

$$W_{11}^{c} \geq \min\left[W_{11}, W\right] \tag{A.143}$$

$$W_{22}^{c} \geq \min\left[W_{22}, W\right] \tag{A.144}$$

4) The reinforcement and weld strength calculations above are given in terms of thicknesses and areas. Therefore, to compute an $MAWP$, an iterative procedure is required. In this procedure, a pressure is assumed and the corresponding wall thicknesses, reinforcement areas, and weld strengths are computed are checked against required values. This process is repeated until a pressure is found that results in satisfaction of all required values. This resulting pressure is the $MAWP$ of the nozzle component.

A.3.12 Junction Reinforcement Requirements at Conical Transitions

For vessels subject to internal pressure, in lieu of a detailed stress analysis, the localized stresses and requirements for a cone-to-cylinder junction stiffening ring can be evaluated using the following procedure. If there is an LTA at cylinder-to-cone junction, an average thickness should be used to represent the metal loss (see Part 4, paragraph 4.3.3.4).

a) The longitudinal membrane and localized membrane plus bending stress requirements should satisfy the following requirements:

1) Determine the membrane stress in the cylindrical shell at the junction due to pressure and applied net section axial force and bending moment.

$$f_x = \frac{PD^2}{D_o^2 - D^2} + \frac{4F}{\pi\left(D_o^2 - D^2\right)} \tag{A.145}$$

$$f_b = \frac{32MD_o}{\pi\left(D_o^4 - D\right)} \tag{A.146}$$

2) Determine the membrane stress in the conical shell at the junction due to pressure and applied net section axial force and bending moment. In these equations, D_o is the outside diameter of the cone at the junction and D_c is the corroded inside diameter of the cone at the junction.

$$f_{xc} = \frac{PD^2}{\left(D_o^2 - D^2\right)\cos\alpha} + \frac{4F}{\pi\left(D_o^2 - D^2\right)\cos\alpha} \tag{A.147}$$

$$f_{bc} = \frac{32MD_o}{\pi\left(D_o^4 - D^4\right)\cos\alpha} \tag{A.148}$$

3) The longitudinal membrane and localized membrane plus bending stress in the cylinder at the junction should satisfy the following requirements:

$$\left(f_x + f_b\right) \le SE \tag{A.149}$$

$$\left(f_x + f_b\right)\left(1 + \frac{0.6t_c\sqrt{D_o\left(t_c + t_{cc}\right)}}{t_c^2}\tan\alpha\right) \le 3SE \tag{A.150}$$

4) The longitudinal membrane and localized membrane plus bending stress in the cone at the junction should satisfy the following requirements:

$$\left(f_{xc} + f_{bc}\right) \le SE \tag{A.151}$$

$$\left(f_{xc} + f_{bc}\right) + \left(\frac{0.6t_c\sqrt{D_o\left(t_c + t_{cc}\right)}}{t_{cc}^2}\tan\alpha\right)\left(f_x + f_b\right) \le 3SE \tag{A.152}$$

5) The circumferential membrane stress in the cylinder at the junction, f_h, should satisfy the following requirements where f_x and f_b are computed using Equations (A.145) and (A.146), and F_{ha} is computed using the equations in the paragraph A.4.4.a with $F_{he} = 0.4tE_y/D$.

$$f_h = 0.45\sqrt{\frac{D_o}{t_c}}\left(f_x + f_b\right)\tan\alpha \qquad \text{(A.153)}$$

$$f_h \le 1.5SE \qquad \textit{for hoop tension} \qquad \text{(A.154)}$$

$$f_h \le F_{ha} \qquad \textit{for hoop compression} \qquad \text{(A.155)}$$

b) If the cone-to-cylinder junction does not satisfy the requirements in the above paragraphs, the junction may be strengthened by increasing the cylinder thickness and/or cone thickness at the junction, or by providing a stiffening ring. The stiffening ring shall be located within a distance $\max\left[t_1,\ 25\,mm\ (1\,in)\right]$ or $\max\left[t_2,\ 25\,mm\ (1\,in)\right]$, as applicable (see Figure A.11.b), from the cone junction.

1) The section properties of the cone stiffening ring shall satisfy the following equations:

$$A_c \ge \frac{tD_o}{S_y}\left(f_x + f_b\right)\tan\alpha \qquad \text{(A.156)}$$

$$I_c \ge \frac{tD_oD_R^2}{8E_y}\left(f_x + f_b\right)\tan\alpha \qquad \text{(A.157)}$$

2) In computing A_c and I_c, the effective length of the shell wall acting as a flange for the composite ring section shall be computed using Equation (A.158) (see Figure A.10):

$$b_e = 0.55\sqrt{D_o t_c} + \sqrt{\frac{D_o t_{cc}}{\cos\alpha}} \qquad \text{(A.158)}$$

A.3.13 Other Components

Calculation procedures for the following components should be evaluated based on the original construction code. References for these components for the ASME Code and TEMA are cited below.

a) Integral tubesheet to cylinder connections (ASME B&PV Code, Section VIII, Division 1,Part UHX),

b) Flat head to cylinder connections (ASME B&PV Code, Section VIII, Division 1, UG-34), and

c) Bolted Flanges (ASME B&PV Code, Section VIII, Division 1, Annex 2).

A.4 Pressure Vessels and Boiler Components – External Pressure

A.4.1 Overview

The minimum thickness and $MAWP$ of a pressure vessel subject to external pressure may be computed based on the original construction code. Alternatively, the equations in the following paragraphs may be utilized in the calculation (see ASME B&PV Code Case 2286-1). These equations are less conservative than the equations in the ASME Code and have been experimentally verified with an extensive testing program. Additional information and requirements for using the equations in this annex are provided below.

a) The buckling strength formulations presented in this section are based on linear structural stability theory that is modified by reduction factors to account for the effects of imperfections, boundary conditions, non-linearity of material properties and residual stresses. The reduction factors are determined from approximate lower bound values of test data of shells with initial imperfections representative of the shell tolerances specified in paragraph A.4.2. Details regarding the derivation and experimental verification of the equations in this section can be found in WRC 406.

b) The equations in this section are applicable to $D_o/t \le 2000$ and $t \ge 5\ mm\ (3/16\ in)$. In developing the equations in this paragraph, the shell section is assumed to be axisymmetric with uniform thickness for unstiffened cylinders and formed heads. Stiffened cylinders and cones are also assumed to be of uniform thickness between stiffeners. Where nozzles with reinforcing plates or locally thickened shell sections exist, the thinnest uniform thickness in the applicable unstiffened or stiffened shell section should be used for the calculation of the allowable compressive stress.

c) The maximum temperature limit permitted for all materials is defined in Table A.2.

d) The allowable compressive stress equations apply directly to shells fabricated from carbon and low alloy steel plate materials given in the ASME B&PV Code, Section II, Part D. For materials other than carbon or low alloy steel, a modification to the allowable stress is required. The procedure for modification of the allowable stress is to calculate the allowable compressive stress based on carbon and low alloy steel plate materials, and then make the following adjustments as described below.

1) For Axial Compression the allowable stress is adjusted as follows. The tangent modulus, E_t, may be determined from Annex F paragraph F.2.3.1.b at a stress equal to F_{xe}.

$$F_{xa} = \frac{F_{xe}}{FS}\frac{E_t}{E_y} \qquad \text{(A.159)}$$

$$F_{ba} = F_{xa} \qquad \text{(A.160)}$$

2) For External Pressure the allowable stress is adjusted as follows. The tangent modulus, E_t, may be determined from Annex F, paragraph F.2.3.1.b at a stress equal to F_{he}.

$$F_{ha} = \frac{F_{he}}{FS}\frac{E_t}{E_y} \qquad \text{(A.161)}$$

3) For Shear the allowable stress is adjusted as follows. The tangent modulus, E_t, may be determined from Annex F, paragraph F.2.3.1.b at a stress equal to F_{ve}.

$$F_{va} = \frac{F_{ve}}{FS}\frac{E_t}{E_y} \qquad \text{(A.162)}$$

e) The effects of supplemental loads may be evaluated using the results from an elastic stress analysis in conjunction with the allowable compressive stress criterion in paragraph A.4.14. Recommendations for elastic stress analysis are provided in Annex B1. Methods for performing a buckling analysis are also provided.

f) Special consideration shall be given to ends of components (shell sections) or areas of load application where stress distribution may be in the inelastic range and localized stresses may exceed those predicted by linear theory..

g) When the localized stresses extend over a distance equal to one-half the length of the buckling mode (approximately $1.2\sqrt{D_o t}$), the localized stresses shall be considered as a uniform stress for the design of the shell section..

h) The allowable stresses are determined by applying an in-service margin, FS, to the predicted buckling stresses. The required values of FS are 2.0 when the buckling stress is elastic and 1.667 when the predicted buckling stress equals the minimum specified yield strength at the design temperature. A linear variation shall be used between these limits. The equations for FS are given below where F_{ic} is the predicted buckling stress that is determined by setting $FS = 1.0$ in the allowable stress equations. For combinations of design loads and earthquake loading or wind loading (see paragraph A.2.7), the allowable stress for F_{bha} or F_{ba} in Equations (A.261), (A.262), (A.263) , (A.266) , (A.267) and (A.268) may be increased by a factor of 1.2.

$$FS = 2.0 \qquad for\ F_{ic} \le 0.55S_y \tag{A.163}$$

$$FS = 2.407 - 0.741\left(\frac{F_{ic}}{S_y}\right) \qquad for\ 0.55S_y < F_{ic} < S_y \tag{A.164}$$

$$FS = 1.667 \qquad for\ F_{ic} \ge S_y \tag{A.165}$$

A.4.2 Shell Tolerances

a) Cylinders and Conical Shells

1) Cylindrical and Conical Shells Subject to External Pressure

The out-of-roundness tolerances shall satisfy the tolerances in Part 8, Table 8.3 except that the maximum deviation from true circular form, e, shall not exceed e_c. The value of e_c is determined by computing e_{c1} from Equation (A.166). If $e_{c1} < 0.2t$, then $e_c = 0.2t$; if $e_{c1} > \min\left[0.0242R_m,\ 2t\right]$, then $e_c = \min\left[0.0242R_m,\ 2t\right]$; otherwise, $e_c = e_{c1}$.

$$e_{c1} = 0.0165t\left(M_x + 3.25\right)^{1.069} \tag{A.166}$$

Measurements to determine e shall be made from a segmental circular template having the design outside radius, and placed on the outside of the shell. The chord length of the template, L_{ec}, shall be determined by Equation (A.167).

$$L_{ec} = 2R_m \sin\left(\frac{\pi}{2n}\right) \tag{A.167}$$

where

$$n = \xi\left(\sqrt{\frac{R_m}{t}} \cdot \frac{R_m}{L}\right)^{\psi} \qquad valid\ for\ 2 \le n \le 1.41\sqrt{\frac{R_m}{t}} \tag{A.168}$$

$$\xi = \min\left[2.28\left(\frac{R_m}{t}\right)^{0.54},\ 2.80\right] \tag{A.169}$$

$$\psi = \min\left[0.38\left(\frac{R_m}{t}\right)^{0.044},\ 0.485\right] \tag{A.170}$$

2) Cylindrical and Conical Shells Subject To Uniform Axial Compression and Axial Compression Due to a Bending Moment

The tolerance requirements in Part 8, Table 8.3 shall be satisfied. In addition, the local inward deviation from a straight line, e, measured along a meridian over gauge length L_x shall not exceed the maximum permissible deviation, e_x, given below:

$$e_x = 0.002R_m \tag{A.171}$$

$$L_x = \min\left[4\sqrt{R_m t},\ L\right] \qquad \textit{for cylindrical shells} \tag{A.172}$$

$$L_x = \min\left[4\sqrt{\frac{R_m t}{\cos\alpha}},\ \frac{L_c}{\cos\alpha}\right] \qquad \textit{for conical shells} \tag{A.173}$$

$$L_x = 25t \qquad \textit{across circumferential welds} \tag{A.174}$$

3) Cylindrical and Conical Shells Subject to External Pressure

The tolerance requirements in Part 8, Table 8.3 shall be satisfied.

b) Spherical Shells and Formed Heads

The tolerance requirements in Part 8, Table 8.3 shall be satisfied. In addition, the maximum local deviation from true circular form, e, for spherical shells and any spherical portion of a formed head shall not exceed the shell thickness. Measurements to determine the maximum local deviation shall be made with a template with a chord length, L_{ec}, given by the following equation.

$$L_{ec} = 3.72\sqrt{R_m t} \tag{A.175}$$

A.4.3 Metal Loss

The equations in this paragraph are written in terms of outside diameter of the component; therefore, the equations do not need to be adjusted for metal loss and future corrosion allowance which occurs on the inside surface. If metal loss has occurred on the outside surface of the component (e.g. corrosion under insulation), the geometry definition terms in the equations (i.e. outside diameter and outside radius) would need to be modified to account for this metal loss. The equations below are based on the future corrosion allowance and metal loss being applied to the inside surface of the shell.

A.4.4 Cylindrical Shell

The minimum required thickness and $MAWP$ equations may be computed using the procedures shown below. In addition, calculation procedures for stiffening rings are also provided.

a) Required Thickness – The required thickness of a cylindrical shell subjected to external pressure loading may be determined using the following procedure.

1) STEP 1 – Assume an initial thickness, t, and unsupported length, L.

2) STEP 2 – Calculate the predicted elastic buckling stress, F_{he}.

$$F_{he} = \frac{1.6C_h E_y t}{D_o} \tag{A.176}$$

$$M_x = \frac{L}{\sqrt{R_o t}} \tag{A.177}$$

$$C_h = 0.55\left(\frac{t}{D_o}\right) \qquad for\ M_x \geq 2\left(\frac{D_o}{t}\right)^{0.94} \tag{A.178}$$

$$C_h = 1.12M_x^{-1.058} \qquad for\ 13 < M_x < 2\left(\frac{D_o}{t}\right)^{0.94} \tag{A.179}$$

$$C_h = \frac{0.92}{M_x - 0.579} \qquad for\ 1.5 < M_x \leq 13 \tag{A.180}$$

$$C_h = 1.0 \qquad for\ M_x \leq 1.5 \tag{A.181}$$

3) STEP 3 – Calculate the predicted inelastic buckling stress, F_{ic}.

$$F_{ic} = S_y \qquad for\ \frac{F_{he}}{S_y} \geq 2.439 \tag{A.182}$$

$$F_{ic} = 0.7S_y\left(\frac{F_{he}}{S_y}\right)^{0.4} \qquad for\ 0.552 < \frac{F_{he}}{S_y} < 2.439 \tag{A.183}$$

$$F_{ic} = F_{he} \qquad for\ \frac{F_{he}}{S_y} \leq 0.552 \tag{A.184}$$

4) STEP 4 – Calculate the value of the in-service margin, FS, per paragraph A.4.1.h.

5) STEP 5 – Calculate the allowable external pressure, P_a

$$P_a = 2F_{ha}\left(\frac{t}{D_o}\right) \tag{A.185}$$

where,

$$F_{ha} = \frac{F_{ic}}{FS} \tag{A.186}$$

6) STEP 6 – If the allowable external pressure, P_a, is less than the design external pressure, increase the shell thickness or reduce the unsupported length of the shell (i.e. by the addition of a stiffening rings) and go to STEP 2. Repeat this process until the allowable external pressure is equal to or greater than the design external pressure.

b) Determination of the $MAWP$ – The $MAWP$ of a cylindrical shell subjected to external pressure loading can be determined by substituting t_c for t in the calculation procedure described in paragraph A.4.4.a.

c) Stiffening Ring Size – The following equations shall be used to determine the size of a stiffening ring.

1) Stiffening Ring Configuration

A combination of large and small stiffening rings may be used along the length of a shell. If a single size stiffener is used, then it shall be sized as a small stiffener. Alternatively, a combination of large and small stiffeners can be used to reduce the size of the intermittent small stiffening rings.

2) Small Stiffening Ring

i) The required moment of inertia of the effective stiffening ring (i.e. actual stiffening ring plus the effective length of shell) shall satisfy Equation (A.187).

$$I_s^C \geq \frac{1.5F_{he}L_sR_{cc}^2t_c}{E_y\left(n^2-1\right)} \tag{A.187}$$

ii) The parameter F_{he} in Equation (A.187) shall be evaluated using the equations in paragraph A.4.4.a.2 with $M_x = L_s \Big/ \sqrt{R_o t_c}$.

iii) The parameter n in Equation (A.187) shall be computed using Equation (A.188). If the computed $n < 2$, then use $n = 2$. If the computed $n > 10$, then use $n = 10$.

$$n = \sqrt{\frac{2D_o^{1.5}}{3L_Bt_c^{0.5}}} \tag{A.188}$$

iv) The actual moment of inertia of the composite section comprised of the small stiffening ring and effective length of the shell about the centroidal axis shall be calculated using Equation (A.189) with L_e based on Equation (A.190).

$$I_S^C = I_S + A_SZ_S^2\left(\frac{L_et_c}{A_S+L_et_c}\right)+\frac{L_et_c^3}{12} \tag{A.189}$$

$$L_e = 1.1\sqrt{D_ot_c} \tag{A.190}$$

3) Large Stiffening Ring or Bulkhead

i) The required moment of inertia of the effective stiffening ring (i.e. actual stiffening ring plus the effective length of shell) shall satisfy Equation (A.191).

$$I_L^C \geq \frac{F_{heF}L_FR_{cc}^2t_c}{2E_y} \tag{A.191}$$

ii) The parameter F_{heF} in Equation (A.191) is the average value of the hoop buckling stress, F_{he}, over length L_F evaluated using the equations in paragraph A.4.4.a.2 with $M_x = L_F \Big/ \sqrt{R_o t_c}$.

iii) The actual moment of inertia of the composite section comprised of the large stiffening ring and effective length of the shell about the centroidal axis shall be calculated using Equation (A.192) with L_e based on Equation (A.193).

$$I_L^C = I_L + A_LZ_L^2\left(\frac{L_et_c}{A_L+L_et_c}\right)+\frac{L_et_c^3}{12} \tag{A.192}$$

$$L_e = 1.1\sqrt{D_ot_c}\left(\frac{A_s+L_st_c}{A_L+L_st_c}\right) \tag{A.193}$$

4) Local Stiffener Geometry Requirements for all Loading Conditions

The following equations shall be met to assure the stability of a stiffening ring.

i) Flat bar stiffener, flange of a tee section and the outstanding leg of an angle stiffener (see Figure A.11)

$$\frac{h_1}{t_1} \le 0.375\left(\frac{E_y}{S_y}\right)^{0.5} \tag{A.194}$$

ii) Web of a tee stiffener or leg of an angle stiffener attached to the shell (see Figure A.11).

$$\frac{h_2}{t_2} \le \left(\frac{E_y}{S_y}\right)^{0.5} \tag{A.195}$$

5) Stiffener Size To Increase Allowable Longitudinal Compressive Stress

Ring stiffeners can be used to increase the allowable longitudinal compressive stress for cylindrical or conical shells subject to uniform axial compression and axial compression due to bending. The required size of the stiffener shall satisfy the following equations. In addition, the spacing of the stiffeners must result in a value of $M_s \le 15$ where M_s is given by Equation (A.199).

$$A_S \text{ and } A_L \ge \left(\frac{0.334}{M_s^{0.6}} - 0.63\right) L_s t_c \tag{A.196}$$

$$A_S \text{ and } A_L \ge 0.06 L_s t_c \tag{A.197}$$

$$I_S^C \text{ and } I_L^C \ge \frac{0.533 L_s t_c^3}{M_s^{1.8}} \tag{A.198}$$

$$M_s = \frac{L_s}{\sqrt{R_o t_c}} \tag{A.199}$$

A.4.5 Spherical Shell or Hemispherical Head

The minimum required thickness and $MAWP$ equations may be computed using the following procedures.

a) Required Thickness – The required thickness of a spherical shell or hemispherical head subjected to external pressure loading may be determined using the following procedure.

1) STEP 1 – Assume an initial thickness, t for the spherical shell.

2) STEP 2 – Calculate the predicted elastic buckling stress, F_{he}.

$$F_{he} = 0.075 E_y \left(\frac{t}{R_o}\right) \tag{A.200}$$

3) STEP 3 – Calculate the predicted inelastic buckling stress, F_{ic}.

$$F_{ic} = S_y \qquad for \quad \frac{F_{he}}{S_y} \ge 6.25 \tag{A.201}$$

$$F_{ic} = \frac{1.31S_y}{\left(1.15 + \frac{F_{he}}{S_y}\right)} \qquad for\ \ 1.6 < \frac{F_{he}}{S_y} < 6.25 \tag{A.202}$$

$$F_{ic} = 0.18F_{he} + 0.45S_y \qquad for\ \ 0.55 < \frac{F_{he}}{S_y} \le 1.6 \tag{A.203}$$

$$F_{ic} = F_{he} \qquad for\ \ \frac{F_{he}}{S_y} \le 0.55 \tag{A.204}$$

4) STEP 4 – Calculate the value of the in-service margin, FS , per paragraph A.4.1.h.

5) STEP 5 – Calculate the allowable external pressure, P_a

$$P_a = 2F_{ha}\left(\frac{t}{R_o}\right) \tag{A.205}$$

where,

$$F_{ha} = \frac{F_{ic}}{FS} \tag{A.206}$$

6) STEP 6 – If the allowable external pressure, P_a, is less than the design external pressure, increase the shell thickness and go to STEP 2. Repeat this process until the allowable external pressure is equal to or greater than the design external pressure.

b) Determination of the $MAWP$ – The $MAWP$ of a spherical shell or hemispherical head subjected to external pressure loading can be determined by substituting t_c for t in the calculation procedure described in paragraph A.4.5.a.

A.4.6 Elliptical Head

The minimum thickness and $MAWP$ for an elliptical head (see Figure A.1) can be determined using the equations for a spherical shell in paragraph A.4.5 by substituting $K_c D_o$ for R_o. An equation for K_c is provided in paragraph A.3.6.

A.4.7 Torispherical Head

The minimum thickness and $MAWP$ for an torispherical head (see Figure A.1) can be determined using the equations for a spherical shell in paragraph A.4.5 by substituting the outside crown radius for R_o.

A.4.8 Conical Shell

The minimum thickness and $MAWP$ equations for a conical shell with a half apex angle of $\alpha \le 60^o$ are as follows (see Figures A.2 to A.6).

a) Determination of the $MAWP$

The $MAWP$ can be determined using the equations for a cylinder in paragraph A.4.4 by making the following substitutions:

1) The value of $0.5\left(D_L + D_S\right)/\cos\alpha$ is substituted for D_o in the equations in paragraph A.4.4.

2) The value of $0.25\left(D_L + D_S\right)/\cos\alpha$ is substituted for R_o in the equations in paragraph A.4.4.

3) The value of $L_c/\cos\alpha$ is substituted for L in the equations in paragraph A.4.4 where L_c is determined as follows:

i) For Sketches (a) and (b) in Figure A.4:

$$L_c = L_{ct} \tag{A.207}$$

ii) For Sketch (c) in Figure A.4:

$$L_c = r_k \sin\alpha + L_{ct} \tag{A.208}$$

iii) For Sketch (d) in Figure A.4

$$L_c = r_f \sin\alpha + L_{ct} \tag{A.209}$$

iv) For Sketch (e) in Figure A.4:

$$L_c = \left(r_k + r_f\right)\sin\alpha + L_{ct} \tag{A.210}$$

b) Determination of a Minimum Thickness

The minimum thickness is determined using the procedure in paragraph A.4.4.b.

c) Intermediate Stiffening Rings

If required, intermediate circumferential stiffening rings within the conical transition can be sized using the equations in paragraph A.4.4.c.2. In these equations, t is the cone thickness, L_s is the average distance to the adjacent rings measured along the cone axis, and F_{he} is the average of the elastic hoop buckling stress computed for the two adjacent bays.

d) Eccentric Cone

The minimum thickness of an eccentric cone shall be taken as the greater of the two thicknesses obtained using both the smallest and largest α in the calculations (see Figure A.3).

A.4.9 Toriconical Head

The minimum thickness and $MAWP$ equations for toriconical heads and transitions can be determined using the procedure of paragraphs A.4.7 and A.4.8.

A.4.10 Conical Transitions

The minimum thickness and MAWP equations for transitions can be determined using the procedure of paragraph A.4.8.

A.4.11 Nozzle Connections in Shells

The reinforcement for openings in single walled shells that do not exceed 25% of the cylinder diameter (or spherical shell or formed head diameter, as applicable) or 80% of the ring spacing into which the opening is placed may be designed in accordance with the rules provided in paragraphs A.4.1 through A.4.10. Openings in shells that exceed these limitations require a special analysis.

a) Reinforcement for nozzle openings in vessels designed for external pressure alone shall be in accordance with paragraph A.3.10.a using $J_r = 0.5$. The required thickness shall be determined using the equations in paragraphs A.4.1 through A.4.10, as applicable.

b) If the cylinder is designed for axial compression (i.e. axial load or bending moment, then the reinforcement of the opening shall satisfy the equations shown below. Note that for these equations to apply, the reinforcement shall be located within a distance of $0.75\sqrt{Rt_c}$ from the edge of the opening. In addition, the reinforcement available in the nozzle neck shall be limited to a thickness that does not exceed the shell thickness at the nozzle attachment, and this reinforcement shall be located within a limit (measured normal to the outside surface of the shell) equal to $\min\left[0.5\sqrt{0.5d_c t_n},\ 2.5t_n\right]$.

$$A_r = 0.0 \qquad for\ d_c \le 0.4\sqrt{Rt_c} \tag{A.211}$$

$$A_r = 0.5dt_r \qquad for\ d_c \le 0.4\sqrt{Rt_c}\ \ and\ \ 0.5d_c\sqrt{Rt_c} \le \left[\frac{1}{291}\left(\frac{R}{t_c}\right)+0.22\right]^2 \tag{A.212}$$

$$A_r = dt_r \qquad for\ d_c \le 0.4\sqrt{Rt_c}\ \ and\ \ 0.5d_c\sqrt{Rt_c} > \left[\frac{1}{291}\left(\frac{R}{t_c}\right)+0.22\right]^2 \tag{A.213}$$

c) If the cylinder is designed for external pressure in combination with axial compression, then the required reinforcement area shall be the maximum of the areas determined in paragraphs A.4.11.a and A.4.11.b.

A.4.12 Junction Reinforcement Requirements at Conical Transitions

For a vessel subject to external pressure – In lieu of a detailed stress analysis, the localized stresses and requirements for a cone-to-cylinder junction stiffening ring can be evaluated using the following procedure.

a) A stiffening ring at the cone to cylinder junction (large end and small end) is not required if $f_h < F_{ha}$ where f_h is the compressive hoop membrane stress in the cone at the junction given by Equation (A.214), and F_{ha} is determined using the equations in paragraph A.4.4 with F_{he} based on $C_h = 0.55\cos\alpha\left(t_c/D_o\right)$. If $t_{cc}\cos\alpha < t_c$, then substitute t_c for t_{cc} to determine f_h.

$$f_h = \frac{PD_o}{2t_{cc}\cos\alpha} \tag{A.214}$$

b) If a stiffening ring at the cone to cylinder junction (large end and small end) is required, the moment of inertia of the composite ring section should satisfy the following equation.

$$I_c \ge \frac{D_o^2}{16E_y}\left(t_c L_1 F_{he} + \frac{t_{cc}L_c F_{hec}}{\cos^2\alpha}\right) \tag{A.215}$$

A.4.13 Other Components

Calculation procedures for the other components are covered in paragraph A.3.12.

A.4.14 Allowable Compressive Stresses and Combined Loadings

a) The rules in this paragraph provide allowable compressive stresses that may be used for the assessment of shells subjected to different loading conditions.

b) Cylindrical Shells

The allowable compressive stresses for cylindrical shells shall be computed using the following rules that are based on loading conditions. The loading conditions are underlined for clarity in the following paragraphs. In addition, common parameters used in each of the loading conditions are summarized in paragraph A.4.14.b.11.

1) External Pressure Acting Alone

The allowable hoop compressive membrane stress of a cylinder subject to external pressure acting alone, F_{ha}, is computed using the equations in paragraph A.4.4.

2) Axial Compressive Stress Acting Alone

The allowable axial compressive membrane stress of a cylinder subject to an axial compressive load acting alone, F_{xa}, is computed using the following equations.

i) For $\lambda_c \le 0.15$ (Local Buckling) where λ_c is given by Equation (A.280):

$$F_{xa} = \min\left[F_{xa1},\ F_{xa2}\right] \tag{A.216}$$

$$F_{xa1} = \frac{S_y}{FS} \qquad for\ \frac{D_o}{t_c} \le 135 \tag{A.217}$$

$$F_{xa1} = \frac{466 S_y}{FS\left(331 + \frac{D_o}{t_c}\right)} \qquad for\ 135 < \frac{D_o}{t_c} < 600 \tag{A.218}$$

$$F_{xa1} = \frac{0.5 S_y}{FS} \qquad for\ 600 \ge \frac{D_o}{t_c} \le 2000 \tag{A.219}$$

$$F_{xa2} = \frac{F_{xe}}{FS} \tag{A.220}$$

$$F_{xe} = \frac{C_x E_y t_c}{D_o} \tag{A.221}$$

$$C_x = \min\left[\frac{409\overline{c}}{\left(389 + \frac{D_o}{t}\right)},\ 0.9\right] \qquad for\ \frac{D_o}{t} < 1247 \tag{A.222}$$

$$C_x = 0.25\overline{c} \qquad for\ 1247 \ge \frac{D_o}{t_c} \le 2000 \tag{A.223}$$

$$\overline{c} = 2.64 \qquad for\ M_x \le 1.5 \tag{A.224}$$

$$\overline{c} = \frac{3.13}{M_x^{0.42}} \qquad for\ 1.5 < M_x < 15 \tag{A.225}$$

$$\overline{c} = 1.0 \qquad for\ \ M_x \ge 15 \tag{A.226}$$

ii) For $\lambda_c > 0.15$ *and* $K_u L_u / r_g < 200$ (Column Buckling) where λ_c is given by Equation (A.280):

$$F_{ca} = F_{xa}\left[1 - 0.74\left(\lambda_c - 0.15\right)\right]^{0.3} \qquad for\ 0.15 < \lambda_c < 1.147 \qquad \text{(A.227)}$$

$$F_{ca} = \frac{0.88F_{xa}}{\lambda_c^2} \qquad for\ \lambda_c \geq 1.147 \qquad \text{(A.228)}$$

3) Compressive Bending Stress

The allowable axial compressive membrane stress of a cylindrical shell subject to a bending moment acting across the full circular cross section F_{ba}, is computed using the following equations..

$$F_{ba} = F_{xa} \qquad for\ 135 \leq \frac{D_o}{t_c} \leq 2000 \qquad \text{(A.229)}$$

$$F_{ba} = \frac{466S_y}{FS\left(331 + \frac{D_o}{t_c}\right)} \qquad for\ 100 \leq \frac{D_o}{t_c} < 135 \qquad \text{(A.230)}$$

$$F_{ba} = \frac{1.081S_y}{FS} \qquad for\ \frac{D_o}{t_c} < 100\ and\ \gamma \geq 0.11 \qquad \text{(A.231)}$$

$$F_{ba} = \frac{S_y\left(1.4 - 2.9\gamma\right)}{FS} \qquad for\ \frac{D_o}{t_c} < 100\ and\ \gamma < 0.11 \qquad \text{(A.232)}$$

$$\gamma = \frac{S_y D_o}{E_y t_c} \qquad \text{(A.233)}$$

4) Shear Stress

The allowable shear stress of a cylindrical shall , F_{va}, is computed using the following equations.

$$F_{va} = \frac{\eta_v F_{ve}}{FS} \qquad \text{(A.234)}$$

$$F_{ve} = \alpha_v C_v E_y \left(\frac{t_c}{D_o}\right) \qquad \text{(A.235)}$$

$$C_v = 4.454 \qquad for\ M_x \leq 1.5 \qquad \text{(A.236)}$$

$$C_v = \left(\frac{9.64}{M_x^2}\right)\left(1 + 0.0239M_x^3\right)^{0.5} \qquad for\ 1.5 < M_x < 26 \qquad \text{(A.237)}$$

$$C_v = \frac{1.492}{M_x^{0.5}} \qquad for\ 26 \le M_x < 4.347\left(\frac{D_o}{t_c}\right) \tag{A.238}$$

$$C_v = 0.716\left(\frac{t_c}{D_o}\right)^{0.5} \qquad for\ M_x \ge 4.347\left(\frac{D_o}{t_c}\right) \tag{A.239}$$

$$\alpha_v = 0.8 \qquad for\ \frac{D_o}{t_c} \le 500 \tag{A.240}$$

$$\alpha_v = 1.389 - 0.218\log_{10}\left(\frac{D_o}{t_c}\right) \qquad for\ \frac{D_o}{t_c} > 500 \tag{A.241}$$

$$\eta_v = 1.0 \qquad for\ \frac{F_{ve}}{S_y} \le 0.48 \tag{A.242}$$

$$\eta_v = 0.43\left(\frac{S_y}{F_{ve}}\right) + 0.1 \qquad for\ 0.48 < \frac{F_{ve}}{S_y} < 1.7 \tag{A.243}$$

$$\eta_v = 0.6\left(\frac{S_y}{F_{ve}}\right) \qquad for\ \frac{F_{ve}}{S_y} \ge 1.7 \tag{A.244}$$

5) Axial Compressive Stress And Hoop Compression

The allowable compressive stress for the combination of uniform axial compression and hoop compression, F_{xha}, is computed using the following equations:

i) For $\lambda_c \le 0.15$; F_{xha} is computed using the following equation with F_{ha} and F_{xa} evaluated using the equations in paragraphs A.4.14.b.1 and A.4.14.b.2.i, respectively.

$$F_{xha} = \left[\left(\frac{1}{F_{xa}^2}\right) - \left(\frac{C_1}{C_2 F_{xa} F_{ha}}\right) + \left(\frac{1}{C_2^2 F_{ha}^2}\right)\right]^{-0.5} \tag{A.245}$$

$$C_1 = \frac{\left(F_{xa}\cdot FS + F_{ha}\cdot FS\right)}{S_y} - 1.0 \tag{A.246}$$

$$C_2 = \frac{f_x}{f_h} \tag{A.247}$$

$$f_x = f_a + f_q \qquad for\ f_x \le F_{xha} \tag{A.248}$$

The parameters f_a and f_q are defined in paragraph A.4.14.b.10.

ii) For $0.15 < \lambda_c \le 1.2$: F_{xha} is computed from the following equation with $F_{ah1} = F_{xha}$ evaluated using the equations in paragraph A.4.14.b.5.i with $f_x = f_a$, and F_{ca} evaluated using the equations in paragraph A.4.14.b.2.ii. As noted, The load on the end of a cylinder due to external pressure does not contribute to column buckling and therefore F_{ah1} is compared with f_a rather than f_x. The stress due to the pressure load does, however, lower the effective yield stress and the quantity in $\left(1 - f_q / S_y\right)$ accounts for this reduction

$$F_{xha} = \min\left[F_{ah1},\ F_{ah2}\right] \tag{A.249}$$

$$F_{ah2} = F_{ca}\left(1 - \frac{f_q}{S_y}\right) \tag{A.250}$$

iii) For $\lambda_c \le 0.15$, the allowable hoop compressive membrane stress, F_{hxa}, is given by the following equation:

$$F_{hxa} = \frac{F_{xha}}{C_2} \tag{A.251}$$

6) Compressive Bending Stress And Hoop Compression

The allowable compressive stress for the combination of axial compression due to a bending moment and hoop compression, F_{bha}, is computed using the following equations.

i) An iterative solution procedure is utilized to solve these equations for C_3 with F_{ha} and F_{ba} evaluated using the equations in paragraphs A.4.14.b.1 and A.4.14.b.3, respectively.

$$F_{bha} = C_3 C_4 F_{ba} \tag{A.252}$$

$$C_4 = \left(\frac{f_b}{f_h}\right)\left(\frac{F_{ha}}{F_{ba}}\right) \tag{A.253}$$

$$C_3^2\left(C_4^2 + 0.6C_4\right) + C_3^{2n} - 1 = 0 \tag{A.254}$$

$$n = 5 - \frac{4F_{ha} \cdot FS}{S_y} \tag{A.255}$$

ii) The allowable hoop compressive membrane stress, F_{hba}, is given by the following equation:

$$F_{hba} = F_{bha}\left(\frac{f_h}{f_b}\right) \tag{A.256}$$

7) Shear Stress And Hoop Compression

The allowable compressive stress for the combination of shear, F_{vha}, and hoop compression is computed using the following equations.

i) The allowable shear stress is given by the following equation with F_{ha} and F_{va} evaluated using the equations in paragraphs A.4.14.b.1 and A.4.14.b.4, respectively.

$$F_{vha} = \left[\left(\frac{F_{va}^2}{2C_5 F_{ha}} \right)^2 + F_{va}^2 \right]^{0.5} - \frac{F_{va}^2}{2C_5 F_{ha}} \qquad \text{(A.257)}$$

$$C_5 = \frac{f_v}{f_h} \qquad \text{(A.258)}$$

ii) The allowable hoop compressive membrane stress, F_{hva}, is given by the following equation:

$$F_{hva} = \frac{F_{vha}}{C_5} \qquad \text{(A.259)}$$

8) Axial Compressive Stress, Compressive Bending Stress, Shear Stress, And Hoop Compression

The allowable compressive stress for the combination of uniform axial compression, axial compression due to a bending moment, and shear in the presence of hoop compression is computed using the following interaction equations.

i) The shear coefficient is determined using the following equation with F_{va} from paragraph A.4.14.b.4.

$$K_s = 1.0 - \left(\frac{f_v}{F_{va}} \right)^2 \qquad \text{(A.260)}$$

ii) For $\lambda_c \le 0.15$; the acceptability of a member subject to compressive axial and bending stresses, f_a and f_b, respectively, is determined using the following interaction equation with F_{xha} and F_{bha} evaluated using the equations in paragraphs A.4.14.b.5.i and A.14.4.b.6.i, respectively.

$$\left(\frac{f_a}{K_s F_{xha}} \right)^{1.7} + \left(\frac{f_b}{K_s F_{bha}} \right) \le 1.0 \qquad \text{(A.261)}$$

iii) For $0.15 < \lambda_c \le 1.2$; the acceptability of a member subject to compressive axial and bending stresses, f_a and f_b, respectively, is determined using the following interaction equation with F_{xha} and F_{bha} evaluated using the equations in paragraphs A.4.14.b.5.ii and A.14.4.b.6.i, respectively.

$$\left(\frac{f_a}{K_s F_{xha}} \right) + \left(\frac{8}{9} \frac{\Delta f_b}{K_s F_{bha}} \right) \le 1.0 \qquad for \quad \frac{f_a}{K_s F_{xha}} \ge 0.2 \qquad \text{(A.262)}$$

$$\left(\frac{f_a}{2K_s F_{xha}} \right) + \left(\frac{\Delta f_b}{K_s F_{bha}} \right) \le 1.0 \qquad for \quad \frac{f_a}{K_s F_{xha}} < 0.2 \qquad \text{(A.263)}$$

$$\Delta = \frac{C_m}{1 - \left(\frac{f_a \cdot FS}{F_e} \right)} \tag{A.264}$$

$$F_e = \frac{\pi^2 E_y}{\left(\frac{K_u L_u}{r_g} \right)^2} \tag{A.265}$$

9) Axial Compressive Stress, Compressive Bending Stress, And Shear

The allowable compressive stress for the combination of uniform axial compression, axial compression due to a bending moment, and shear in the absence of hoop compression is computed using the following interaction equations:

i) The shear coefficient is determined using the equation in paragraph A.4.14.b.8.i with F_{va} from paragraph A.4.14.b.4.

ii) For $\lambda_c \le 0.15$; the acceptability of a member subject to compressive axial and bending stresses f_a and f_b, respectively, is determined using the following interaction equation with, F_{xa} and F_{ba} evaluated using the equations in paragraphs A.4.14.b.2.i and A.4.14.b.3, respectively.

$$\left(\frac{f_a}{K_s F_{xa}} \right)^{1.7} + \left(\frac{f_b}{K_s F_{ba}} \right) \le 1.0 \tag{A.266}$$

iii) For $0.15 < \lambda_c \le 1.2$; the acceptability of a member subject to compressive axial and bending stresses, f_a and f_b, respectively, is determined using the following interaction equation with, F_{ca} and F_{ba} evaluated using the equations in paragraphs A.4.14.b.2.ii and A.4.14.b.3 respectively. The coefficient Δ is evaluated using the equations in paragraph A.4.14.b.8.iii.

$$\left(\frac{f_a}{K_s F_{ca}} \right) + \left(\frac{8}{9} \frac{\Delta f_b}{K_s F_{ba}} \right) \le 1.0 \qquad for \quad \frac{f_a}{K_s F_{ca}} \ge 0.2 \tag{A.267}$$

$$\left(\frac{f_a}{2K_s F_{ca}} \right) + \left(\frac{\Delta f_b}{K_s F_{ba}} \right) \le 1.0 \qquad for \quad \frac{f_a}{K_s F_{ca}} < 0.2 \tag{A.268}$$

10) Buckling Stress Adjustment When Tolerances are Exceeded

The maximum deviation, e may exceed the value of e_x given in paragraph A.4.2 if the maximum axial stress is less than F_{xa} for shells designed for axial compression only, or less than F_{xha} for shells designed for combinations of axial compression and external pressure. The change in buckling stress, F'_{xe}, is given by Equation (A.269). The reduced allowable buckling stress, $F_{xa(reduced)}$, is determined using Equation (A.270) where e is the new maximum deviation, F_{xa} is determined using Equation (A.216), and FS_{xa} is the value of the stress reduction factor used to determine F_{xa}.

$$F'_{xe} = \left(0.944 - \left| 0.286 \log\left[0.0005\left(\frac{e}{e_x} \right) \right] \right| \right)\left(\frac{E_y t}{R} \right) \tag{A.269}$$

$$F_{xa(reduced)} = \frac{F_{xa} \cdot FS_{xa} - F'_{xe}}{FS_{xa}} \tag{A.270}$$

The quantity $0.286 \log\left[0.0005\left(e/e_x \right) \right]$ in Equation (A.269) is an absolute number (i.e. the log of a very small number is negative). For example, if $e = 2e_x$, then the change in the buckling stress computed using Equation (A.269) is $F'_{xe} = 0.086 E_y \left(t/R \right)$.

11) Section Properties, Stresses, Buckling Parameters

Equations for section properties, nominal shell stresses, and buckling parameters that are used in paragraphs A.4.14.b.1 through A.4.14.b.2 are provided below.

$$A = \frac{\pi\left(D_o^2 - D^2 \right)}{4} \tag{A.271}$$

$$S = \frac{\pi\left(D_o^4 - D^4 \right)}{32 D_o} \tag{A.272}$$

$$f_h = \frac{P D_o}{2 t_c} \tag{A.273}$$

$$f_b = \frac{M}{S} \tag{A.274}$$

$$f_a = \frac{F}{A} \tag{A.275}$$

$$f_q = \frac{P \pi D^2}{4A} \tag{A.276}$$

$$f_v = \frac{V \sin \phi_s}{A} \tag{A.277}$$

$$r_g = 0.25\sqrt{D_o^2 + D^2} \tag{A.278}$$

$$M_x = \frac{L}{\sqrt{R_o t_c}} \tag{A.279}$$

$$\lambda_c = \frac{K_u L_u}{\pi r_g}\left(\frac{F_{xa} \cdot FS}{E_y} \right)^{0.5} \tag{A.280}$$

c) Conical Shells

Conical shells shall be evaluated using the equations in paragraph A.4.14.b using the equivalent dimensions defined in paragraph A.4.8. The stress criteria in this paragraph shall be satisfied at all cross-sections along the length of the cone.

d) Spherical Shells and Formed Heads

The allowable compressive stresses are based on the ratio of the biaxial stress state.

1) Equal Biaxial Stresses – The allowable compressive stress for a spherical shell subject to a uniform external pressure, F_{ha}, is given by the equations in paragraph A.4.5.

2) Unequal Biaxial Stresses, Both Stresses Are Compressive – The allowable compressive stress for a spherical shell subject to unequal biaxial stresses, σ_1 and σ_2, where both σ_1 and σ_2 are compressive stresses resulting from the applied loads given by the equations shown below. In these equations, F_{ha} is determined using paragraph A.4.5. F_{1a} is the allowable compressive stress in the direction of σ_1 and F_{2a} is the allowable compressive stress in the direction of σ_2.

$$F_{1a} = \frac{0.6F_{ha}}{1-0.4k} \tag{A.281}$$

$$F_{2a} = kF_{1a} \tag{A.282}$$

$$k = \frac{\sigma_2}{\sigma_1} \qquad where\ |\sigma_1| > |\sigma_2| \tag{A.283}$$

3) Unequal Biaxial Stresses, One Stress Is Compressive And The Other Is Tensile – The allowable compressive stress for a spherical shell subject to unequal biaxial stresses, σ_1 and σ_2, where σ_1 is compressive and σ_2 is tensile resulting from the applied loads given by the equations shown below. In these equations, F_{1a} is the allowable compressive stress in the direction of σ_1, and is the value of F_{ha} determined using paragraph A.4.5 with F_{he} computed using the following equations.

$$F_{he} = \frac{\left(C_o + C_p\right)E_y t_c}{R_o} \tag{A.284}$$

$$C_o = \frac{102.2}{195 + \dfrac{R_o}{t_c}} \qquad for\ \frac{R_o}{t_c} < 622 \tag{A.285}$$

$$C_o = 0.125 \qquad for\ 622 \geq \frac{R_o}{t_c} \leq 1000 \tag{A.286}$$

$$C_p = \frac{1.06}{3.24 + \left(\dfrac{E_y t_c}{\sigma_2 R_o}\right)} \tag{A.287}$$

A.5 Piping Components and Boiler Tubes

A.5.1 Overview

The minimum thickness and $MAWP$ of a straight section or curved section of pipe subject to internal or external pressure with supplemental loads may be computed based on the original construction code. Alternatively, the equations in this section may be utilized in the calculation of these parameters. In addition, a procedure to evaluate branch connections subject to internal pressure is provided. These equations are based upon the ASME B31.3 Piping Code. The effects of supplemental loads (see paragraphs A.2.6 and A.7) are included in these equations only for straight pipe (i.e. longitudinal stress direction) subject to a net-section axial force and/or bending moment. The effects of supplemental loads for other component geometries or loading conditions can be evaluated using the stress analysis methods in Annex B1.

A.5.2 Metal Loss

The equations in paragraph A.5 are written in terms of outside diameter of the pipe, D_o; therefore, the equations do not need to be adjusted for metal loss and future corrosion allowance which occur on the inside surface. If metal loss has occurred on the outside diameter (e.g. corrosion under insulation) D_o would need to be modified to account for this metal loss.

A.5.3 Required Thickness and MAWP – Straight Pipes Subject To Internal Pressure

The minimum thickness and $MAWP$ equations for straight sections of pipe subject to internal pressure are as follows:

a) Circumferential stress (Longitudinal Joints):

$$t_{\min}^{C} = \frac{PD_o}{2\left(SE + PY_{B31}\right)} + MA \tag{A.288}$$

$$MAWP^{C} = \frac{2SE\left(t_c - MA\right)}{D_o - 2Y_{B31}\left(t_c - MA\right)} \tag{A.289}$$

$$\sigma_m^{C} = \frac{P}{E}\left[\frac{D_o}{2\left(t_c - MA\right)} - Y_{B31}\right] \tag{A.290}$$

b) Longitudinal stress (Circumferential Joints):

$$t_{\min}^{L} = \frac{PD_o}{4(SE + PY_{B31})} + t_{sl} + MA \tag{A.291}$$

$$MAWP^{L} = \frac{4SE(t_c - t_{sl} - MA)}{D_o - 4Y_{B31}(t_c - t_{sl} - MA)} \tag{A.292}$$

$$\sigma_m^{L} = \frac{P}{E}\left(\frac{D_o}{4\left(t_c - t_{sl} - MA\right)} - Y_{B31}\right) \tag{A.293}$$

c) Final Values:

$$t_{\min} = \max\left[t_{\min}^{C},\, t_{\min}^{L}\right] \tag{A.294}$$

$$MAWP = \min\left[MAWP^{C},\, MAWP^{L}\right] \tag{A.295}$$

$$\sigma_{\max} = \max\left[\sigma_{m}^{C},\, \sigma_{m}^{L}\right] \tag{A.296}$$

A.5.4 Required Thickness and MAWP – Boiler Tubes

The minimum thickness and $MAWP$ equations for straight sections of pipe and pipe bends subject to internal pressure are shown below. These equations only cover circumferential stress. If longitudinal stresses are significant, the equation in paragraph A.3.4 may be used,

a) Circumferential Stress when $t_c \le 0.5R$ (Longitudinal Joints)

$$t_{\min}^{C} = \frac{PD}{2S+P} + 0.005D + e_t \tag{A.297}$$

$$MAWP^{C} = \frac{2S\left(t_c - 0.005D - e_t\right)}{D - \left(t_c - 0.005D - e_t\right)} \tag{A.298}$$

$$\sigma^{C} = \frac{P\left[D - \left(t_c - 0.005D - e_t\right)\right]}{2\left(t_c - 0.005D - e_t\right)} \tag{A.299}$$

b) Circumferential Stress when $t > 0.5R$ (longitudinal joints) – the equations in paragraph A.3.4.b may be used.

A.5.5 Required Thickness and MAWP – Pipe Bends Subject To Internal Pressure

The results for circumferential stress, and the minimum required thickness and $MAWP$ are shown below for thin wall bends $\left(R_m/t_c \ge 10\right)$. Results for thick wall pipe bends which do not satisfy this criterion can be found in DIN 2413, Parts 1 and 2.

a) Circumferential stress

1) The results for any location defined by the angle θ (see Figure A.14) are given by the following equations.

$$t_{\min}^{C} = \frac{PD_o}{2\left(\dfrac{SE}{L_f} + PY_{B31}\right)} + MA \tag{A.300}$$

$$MAWP^{C} = \frac{2\left(\dfrac{SE}{L_f}\right)\left(t_c - MA\right)}{D_o - 2Y_{B31}\left(t_c - MA\right)} \tag{A.301}$$

$$\sigma_m^C = \frac{PL_f}{E}\left[\frac{D_o}{2(t_c - MA)} - Y_{B31}\right] \tag{A.302}$$

2) In equations shown in paragraph A.5.5.a.1, L_f is the Lorenz factor which is a measure of the stress magnitude in an elbow relative to that in a straight pipe. If $L_f = 1.0$, then equations for stress, minimum required wall thickness and $MAWP$ are the same as those for straight pipe. If the pipe bend contains a flaw, the position defined by the angle θ should coincide with the centerline of the location of the flaw if the flaw is located in the center section or middle one-third of the bend. If the flaw is not located in the center section of the bend, then use L.

i) The Lorenz factor is computed using Equation (A.303).

$$L_f = \left(\frac{\frac{R_b}{R_m} + \frac{\sin\theta}{2}}{\frac{R_b}{R_m} + \sin\theta}\right) \tag{A.303}$$

ii) At the intrados $\left(\theta = -90^o \ or \ \theta = 270^o\right)$ the Lorenz factor is:

$$L_f = \left(\frac{\frac{R_b}{R_m} - 0.5}{\frac{R_b}{R_m} - 1.0}\right) \tag{A.304}$$

iii) and a the extrados $\left(\theta = 90^o\right)$ the Lorenz factor is:

$$L_f = \left(\frac{\frac{R_b}{R_m} + 0.5}{\frac{R_b}{R_m} + 1.0}\right) \tag{A.305}$$

iv) If the bend angle, β, is greater than $2\beta_a$ where β_a is computed in degrees using Equation (A.306), the equations in paragraph A.5.5.a.1 will give the correct value for the maximum circumferential stress. Otherwise, the actual maximum circumferential stress will be less than that given by these equations because of the strengthening effect of the attached straight pipe sections.

$$\beta_a = \left(\frac{121.5R_m}{R_b - R_m}\right)\sqrt{\frac{t}{R_m}} \tag{A.306}$$

b) Longitudinal Stress – The equations in paragraph A.5.3.b can be used.

c) Final Values – The equations in paragraph A.5.3.c can be used.

A.5.6 Required Thickness and MAWP for External Pressure

The minimum thickness and $MAWP$ for straight and curved sections of pipe subject to external pressure can be determined using the methods in paragraph A.4.3.

A.5.7 Branch Connections

Branch connections in piping systems have a thickness dependency and are evaluated in a Level 2 Assessment procedure. The following analysis method based on the area replacement rules in ASME B31.3 may be used for a Level 2 Assessment. The condition for satisfactory reinforcement of a branch nozzle connection is given by Equation (A.307), (see Figure A.13).

$$A_2 + A_3 + A_4 \geq A_r \tag{A.307}$$

where,

$$A_r = t_h d_1 \left(2 - \sin\beta\right) \tag{A.308}$$

$$A_2 = \left(2d_2 - d_1\right)\left(T_h - t_h - c_h\right) \tag{A.309}$$

$$A_3 = \frac{2L_4\left(T_b - t_b - c_b\right)}{\sin\beta} \tag{A.310}$$

$$A_4 = A_{41} + A_{42} + A_{43} \tag{A.311}$$

$$A_{41} = w_n^2 f_w \tag{A.312}$$

$$A_{42} = w_p^2 f_w \tag{A.313}$$

$$A_{43} = \left(D_p - D_b/\sin\beta\right) T_r f_r \tag{A.314}$$

with

$$d_2 = \max\left[d_1,\ \left\{\left(T_b - c_b\right) + \left(T_h - c_h\right) + d_1/2\right)\right\}\right] \tag{A.315}$$

$$L_4 = \min\left[\left\{2.5\left(T_h - c_h\right)\right\},\ \left\{2.5\left(T_b - c_b\right) + T_r\right\}\right] \tag{A.316}$$

$$f_w = \min\left[\left\{\frac{S_w}{S}\right\},\ 1.0\right] \tag{A.317}$$

$$f_r = \min\left[\left\{\frac{S_r}{S}\right\},\ 1.0\right] \tag{A.318}$$

In the above equations, if $A_1 < 0.0$ use $A_1 = 0.0$, and if $A_2 < 0.0$ use $A_2 = 0.0$.

A.6 API 650 Storage Tanks

The equations to evaluate the minimum thickness and maximum fill height of an atmospheric storage tank are covered in Part 2 of API 653.

A.6.1 Overview

The minimum thickness and Maximum Fill Height can be computed by the 1-Foot Method (see paragraph A.6.3) or the Variable Point Method described in API 650.

A.6.2 Metal Loss

The equations in this paragraph are written in terms of the nominal diameter of the tank, D_n; therefore, the diameter does not need to be adjusted for metal loss and future corrosion allowance. The wall thickness is adjusted for metal loss and future corrosion allowance.

A.6.3 Required Thickness and MFH for Liquid Hydrostatic Loading

a) The minimum thickness and MFH in Metric Units are shown below. In these equations, the tank nominal diameter D is in meters, the design fill height H is in meters, the allowable stress S is in MPa, the wall thicknesses $t_{\min}$ and t are in millimeters, and the metal loss $LOSS$ and future corrosion allowance FCA are in millimeters.

$$t_{\min} = \frac{4.9D(H-0.3)G}{S} + FCA \tag{A.319}$$

$$MFH = \frac{(t - LOSS - FCA)S}{4.9G} + 0.3 \tag{A.320}$$

b) The minimum thickness and MFH in US Customary Units are shown below. In these equations, the tank nominal diameter D is in feet, the design fill height H is in feet, the allowable stress S is in psi, the wall thicknesses $t_{\min}$ and t are in inches, and the metal loss $LOSS$ and future corrosion allowance FCA are in inches.

$$t_{\min} = \frac{2.6D(H-1)G}{S} + FCA \tag{A.321}$$

$$MFH = \frac{(t - LOSS - FCA)S}{2.6G} + 1 \tag{A.322}$$

A.7 Thickness Equations for Supplemental Loads

A.7.1 Overview

Supplemental loads (see paragraphs A.2.6) may result in an axial force and/or bending moment being applied to the end of a cylindrical shell, conical shell or pipe section. This type of loading results in longitudinal membrane and bending stresses (stresses acting on a circumferential plane) in addition to the longitudinal and circumferential (hoop) membrane stress caused by pressure loading. The effects of supplemental loads for other loading conditions and/or shell geometries can be evaluated using the stress analysis methods in Annex B1.

A.7.2 Vertical Vessels Subject to Weight and Wind or Earthquake Loads

Use the equations in paragraph A.7.2 with F and M equal to the weight of the tower, attachments, and contents, and the bending moment from the wind or earthquake loading, respectively, above the point of interest. The loads resulting from wind and earthquake load may be calculated using the procedure in ASCE 7.

a) Thick shell:

$$t_{sl} = \frac{2F}{SE\pi\left(D_o + D\right)\cos\alpha} + \frac{16D_oM}{SE\pi\left(D_o + D_c\right)\left(D_o^2 + D^2\right)\cos\alpha} \tag{A.323}$$

b) Thin Shell:

$$t_{sl} = \frac{F}{2SE\pi R_m \cos\alpha} + \frac{M}{SE\pi R_m^2 \cos\alpha} \tag{A.324}$$

A.7.3 Horizontal Vessels Subject to Weight Loads

The following equations can be used to determine the required thickness at the saddle and mid-span locations of the vessel.

a) Saddle Location Without Stiffening Rings

$$t_{sl} = Z_t \left[\frac{\pi\left(\frac{\sin\Delta}{\Delta} - \cos\Delta\right)}{\Delta + \sin\Delta\cos\Delta - 2\frac{\sin^2\Delta}{\Delta}} \right] \tag{A.325}$$

where

$$Z_t = \frac{QL}{4SE\pi R_m^2}\left[\frac{4A}{L}\left(1 - \frac{1 - \frac{A}{L} + \frac{R_m^2 - H^2}{2AL}}{1 + \frac{4H}{3L}}\right)\right] \tag{A.326}$$

$$\Delta = \frac{\pi}{180}\left(\frac{5\theta}{12} + 30\right) \tag{A.327}$$

b) Saddle Location With Stiffening Rings, Z_t is given by Equation (A.326).

$$t_{sl} = Z_t \tag{A.328}$$

c) Mid-span Location

$$t_{sl} = \frac{QL}{4SE\pi R_m^2}\left[\frac{1 + \frac{2\left(R_m^2 - H^2\right)}{L^2}}{1 + \frac{4H}{3L}} - \frac{4A}{L}\right] \tag{A.329}$$

A.8 Nomenclature

A	cross-sectional area of cylinder or the nozzle calculation parameter or the length from the tangent line of the horizontal vessel to the centerline of a saddle support, as applicable.
A_r	required reinforcement area.
A_R	cross-sectional area of the ring stiffener.
A_c	cross sectional area of the conical transition stiffening ring.
A_f	cross-sectional area of a large ring stiffener that acts as a bulkhead.
A_S	cross-sectional area of a small ring stiffener.
A_L	cross-sectional area of a large ring stiffener that acts as a bulkhead.

A_1 available reinforcement area resulting from excess thickness in the shell..

A_2 available reinforcement area resulting from excess thickness in the nozzle or run pipe, as applicable.

A_3 available reinforcement area resulting from excess thickness in the nozzle internal projection or branch pipe, as applicable.

A_4 available reinforcement area provided by the welds and, for piping, the reinforcement pad.

A_5 available reinforcement area provided by a reinforcing pad.

A_{41} available reinforcement area provided by the nozzle to pad or nozzle to pipe attachment welds.

A_{42} available reinforcement area provided by the reinforcement pad attachment welds.

A_{43} available reinforcement area provided by the reinforcement pad.

α_r one-half apex angle of the cone in a conical shell or toriconical head (degrees).

α one-half apex angle of the cone in a conical shell or toriconical head (radians).

α_v compressive stress calculation parameter.

α_1 offset cone angle.

α_2 offset cone angle.

b_e effective length.

B nozzle calculation parameter.

β angle between the axis of the header and branch pipe, or an angle used to compute the geometry of a conical transition with a knuckle and/or flare, as applicable.

β_a angle used to determine the applicability of the Lorentz factor.

c_b $c_b = LOSS_b + FCA$.

c_h $c_h = LOSS_h + FCA$.

c_n $c_n = LOSS_n + FCA$.

c_s $c_s = LOSS_s + FCA$.

C_h shell parameter for the buckling calculation.

C_m coefficient whose value is established as follows:

= 0.85 for compression members in frames subject to joint translation (sidesway).

= $0.6 - 0.4(M_1/M_2)$ for rotationally restrained members in frames braced against joint translation and not subject to transverse loading between their supports in the plane of bending; in this equation, M_1/M_2 ratio of the smaller to large bending moment at the ends of the portion of the member that is unbraced in the plane of bending under consideration (M_1/M_2 is positive when the member is bent in reverse curvature and negative when the member is bent in single curvature).

= 0.85 for compression members in frames braced against joint translation and subject to transverse loading between support points, the member ends are restrained against rotation in the plane of bending.

= 1.0 for compression members in frames braced against joint translation and subject to transverse loading between support points, the member ends are unrestrained against rotation in the plane of bending.

= 1.0 for an unbraced skirt supported vessel.

C_o outside crown radius of a torispherical head corrected for $LOSS$ and FCA as applicable.

C_r inside crown radius of a torispherical head corrected for $LOSS$ and FCA as applicable.

C_v coefficient for the stiffener size calculation based on shear loads.

C_x compressive stress calculation parameter.

C_v compressive stress calculation parameter.

$\overline{c}$ compressive stress calculation parameter.

C_0 compressive stress calculation parameter.

C_p compressive stress calculation parameter.

C_1 compressive stress calculation parameter.

C_2 compressive stress calculation parameter.

C_3 compressive stress calculation parameter.

C_4 compressive stress calculation parameter.

C_5 compressive stress calculation parameter.

D inside shell diameter or the cone diameter at the stiffening ring, corrected for $LOSS$ and FCA as applicable.

D_n tank nominal diameter.

D_L cone outside diameter, large end, corrected for $LOSS$ and FCA as applicable.

D_{LS} cylinder outside diameter, large end, corrected for $LOSS$ and FCA as applicable.

D_{cc} diameter to the centroid of the composite ring section for an external ring; for an internal ring, the inside diameter (see Figure A.10).

D_S cone outside diameter, small end, corrected for $LOSS$ and FCA as applicable.

D_{SS} cylinder outside diameter, small end, corrected for $LOSS$ and FCA as applicable.

D_b outside diameter of the branch pipe corrected for $LOSS$ and FCA as applicable.

D_h outside diameter of the run or header pipe corrected for $LOSS$ and FCA as applicable.

D_m vessel or run pipe mean diameter corrected for $LOSS$ and FCA as applicable.

D_o outside diameter corrected for $LOSS$ and FCA as applicable.

D_p outside diameter of the reinforcing pad.

D_1 diameter used in the flare stress calculation.

d_c diameter of the circular opening, or chord length at the vessel wall mid-surface of a non-radial opening, in the plane under consideration including the effects of metal loss and future corrosion allowance.

d_m nozzle or branch pipe mean diameter corrected for $LOSS$ and FCA as applicable.

d_o outside diameter of the nozzle corrected for $LOSS$ and FCA as applicable.

d_r diameter of the rivet.

d_p diameter of the rivet hole in the plate.

d_1 effective length removed from the pipe at the branch location.

d_2 half-width of reinforcement zone.

Δ parameter in the supplemental thickness calculation for a horizontal vessel or a compressive stress calculation factor, as applicable.

e deviation from a true circle.

e_c parameter to compute the deviation from a true circle.

e_{c1} parameter to compute the deviation from a true circle.

e_x deviation from the meridian of a cylinder or cone.

ψ parameter to compute the deviation from a true circle.

ξ parameter to compute the deviation from a true circle.

e_t parameter used for computing the boiler tube thickness determined as follows: $e_t = 0.0$ for tubes strength-welded to headers and drums, and $e_t = 0.04$ over a length equal to the length of the seat plus 25 mm (1in.) for tubes expanded into tube seats except $e_t = 0.0$ for tubes expanded into tube seats provided the thickness of the tube ends over a length of the seat plus 25 mm (1 in.) is not less than the following:

- 2.41 mm (0.095 in) for tubes 32 mm (1.25 in) OD and smaller,
- 2.67 mm (0.105 in) for tubes above 32 mm (1.25 in) and up to 51 mm (2 in.) inclusive,
- 3.05 mm (0.120 in) for tubes above 51 mm (2 in) and up to 76 mm (3 in.) inclusive,
- 3.43 mm (0.135 in) for tubes above 76 mm (3 in) and up to 102 mm (4 in.) inclusive,
- 3.81 mm (0.150 in) for tubes above 102 mm (4 in) and up to 127 mm (5 in.) inclusive.

E weld joint efficiency or quality factor from the original construction code, if unknown use 0.7.

E_y modulus of elasticity at the assessment temperature.

E_t tangent modulus of elasticity of material at the assessment temperature.

E_1 1.0 when the opening is in solid plate or in a Category B butt joint, otherwise, the joint efficiency of the weld joint the nozzle intersects.

η_v compressive stress calculation parameter.

f_x total axial compressive membrane stress

f_a axial compressive membrane stress resulting from applied axial load.

f_b bending stress.

f_h circumferential stress in the cylinder at the conical transition.

f_q axial compressive membrane stress resulting from the pressure load on the end of the cylinder.

f_v shear stress from applied loads.

f_r weld strength factor.

f_w weld strength factor.

F applied net-section axial force, use a negative value if the axial force produces a compressive stress at the location of the assessment point.

f_{r1} strength reduction factor; $f_{r1} = S_n / S_v$ for a set-in nozzle, $f_{r1} = 1.0$ for a set-on nozzle.

f_{r2} strength reduction factor; $f_{r2} = S_n / S_v$.

f_{r3} strength reduction factor; $f_{r3} = \min\left[S_n, S_p \right] / S_v$.

f_{r4} strength reduction factor; $f_{r4} = S_p / S_v$.

FCA specified future corrosion allowance (see paragraph A.2.7),

FS in-service margin.

F_{ah1} compressive stress calculation parameter.

F_{ah2} compressive stress calculation parameter.

F_{ba} allowable compressive membrane stress of a cylinder subject to a net-section bending moment in the absence of other loads.

F_{ca} allowable compressive membrane stress of a cylinder due to an axial compressive load with $\lambda_c > 0.15$.

F_{bha} allowable axial compressive membrane stress of a cylinder subject due to bending in the presence of hoop compression.

F_{hba} allowable hoop compressive membrane stress of a cylinder in the presence of longitudinal compression due to net-section bending moment.

F_{he} elastic hoop compressive membrane failure stress of a cylinder or formed head subject to external pressure only.

F_{hec} is F_{he} for a cone section treated as an equivalent cylinder.

F_{ha} allowable hoop compressive membrane stress of a cylinder or formed head subject to external pressure only.

F_{heF} average value of the hoop buckling stress, F_{he}, averaged over the length L_F where F_{he} is determined from Equation (A.176).

F_{hva} allowable hoop compressive membrane stress of a cylinder in the presence of shear stress.

F_{hxa} allowable hoop compressive membrane stress of a cylinder in the presence of axial compression.

F_{ic} predicted inelastic buckling stress, which is determined by letting $FS = 1.0$ in the allowable stress equations.

F_{va} allowable shear stress of a cylinder subject to shear loads only.

F_{ve} elastic shear buckling stress of a cylinder subject to shear loads only.

F_{vha} allowable shear stress of a cylinder subject to shear stress in the presence of hoop compression.

F_{xa} allowable compressive membrane stress of a cylinder due to an axial compressive load with $\lambda_c \le 0.15$.

F_{xe} elastic axial compressive failure membrane stress (local buckling) of a cylinder in the absence of other loads.

F_{xha} allowable axial compressive membrane stress of a cylinder subject due to bending in the presence of hoop compression.

G specific gravity of the liquid to be stored in an atmospheric storage tank.

γ buckling parameter.

H height of the horizontal vessel head, or the design liquid level in an atmospheric storage tank, as applicable.

h height of the elliptical head measured to the inside surface or the inside nozzle projection, as applicable.

h_1 ring stiffener dimension (see Figure A.11).

h_2 ring stiffener dimension (see Figure A.11).

j rivet row number.

J_r load factor for external pressure used in the nozzle reinforcement calculation (see paragraph A.4.10 for restrictions).

k compressive stress calculation parameter.

K elliptical head coefficient.

K_c equivalent radius coefficient.

K_s shear coefficient.

$K_1 \rightarrow K_6$ coefficients used in the flare stress calculation.

K_u coefficient based on end conditions of a member subject to axial compression:

= 2.10 for a member with one free end and the other end fixed. In this case, "member" unbraced cylindrical shell or cylindrical shell section as defined in the Nomenclature.
= 1.00 for a member with both ends pinned,
= 0.80 for a member with one end pinned and the other end fixed,
= 0.65 for a member with both ends fixed.

I moment of inertia of the cylinder or cone cross section.

I_c moment of inertia of the conical transition stiffening ring.

I_L actual moment of inertia of the large stiffening ring.

I_L^C actual moment of inertia of the composite section comprised of the large stiffening ring and effective length of the shell about the centroidal axis.

I_S actual moment of inertia of the small stiffening ring.

I_S^C actual moment of inertia of the composite section comprised of the small stiffening ring and effective length of the shell about the centroidal axis.

L axial length of nozzle with thickness t_n, the tangent-to-tangent length of the horizontal vessel or the design length of a vessel section between lines of support, as applicable. A line of support is; a circumferential line on a head (excluding conical heads) at one-third the depth of the head from the tangent line as shown in Figure A.12 or a stiffening ring that meets the requirement of paragraph A.4.4.c.3.

$L, L_1, L_2, \ldots$ design lengths of the unstiffened vessel sections between lines of support (see Figure A.12). A line of support is (1) a circumferential line on a head (excluding conical heads) at one-third the depth of the head measured from the tangent line, (2) a small stiffening rings that meets the requirements of this paragraph, or (3) a tubesheet.

$L_B, L_{B1}, L_{B2}, \ldots$ design lengths of the cylinder between bulkheads or large rings designated to act as bulkheads (see Figure A.12).

L_c axial length of a cone or conical section for an unstiffened cone, or the length from the cone-to-cylinder junction to the first stiffener in the cone for a stiffened cone (see Figure A.3 and A.4).

L_u laterally unbraced length of cylindrical member that is subject to column buckling, equal to zero when evaluating the shell of a vessel under external pressure only.

L_e effective length.

L_{ec} out-of-roundness template chord length.

L_x length used to compute the deviation from a straight line.

L_f Lorentz factor.

L_F one-half of the sum of the distances, L_B, from the center line of a large ring to the next large ring of head line of support on either side of the large ring (see Figure A.12).

L_s one-half of the sum of the distances from the centerline of a small stiffening ring to the next line of support on either side of the ring, measured parallel to the axis of the cylinder (see Figure A.12); a line of support is described in the definition for L.

L_t overall length of vessel as shown in Figure A.12.

L_n dimension to define the height of the reinforcement zone (see Figures A.6 and A.7).

L_v dimension to define the width of the reinforcement zone (see Figures A.6 and A.7).

L_{fc} length for the flare calculation.

L_{kc} length for the knuckle calculation.

L_b height of reinforcement zone.

L_{ct} length of the cone section in a conical transition (see Figure A.4).

λ nozzle calculation parameter.

λ_c slenderness factor for column buckling.

I_{ss} moment of inertia of a large or small ring stiffener plus effective length of shell about centroidal.

$LOSS$ metal loss in the shell prior to the assessment equal to the nominal (or furnished thickness if available) minus the measured minimum thickness at the time of the inspection.

$LOSS_b$ metal loss in the branch pipe from prior periods of operation equal to the nominal (or furnished thickness if available) minus the minimum measured thickness at the time of the inspection.

$LOSS_h$ metal loss in the header pipe from prior periods of operation equal to the nominal (or furnished thickness if available) minus the minimum measured thickness at the time of the inspection.

$LOSS_n$ metal loss in the nozzle from prior periods of operation equal to the nominal (or furnished thickness if available) minus the minimum measured thickness at the time of the inspection.

$LOSS_s$ metal loss in the shell from prior periods of operation equal to the nominal (or furnished thickness if available) minus the minimum measured thickness at the time of the inspection.

M applied net-section bending moment, use a negative value if the bending moment produces a compressive stress at the location of the assessment point. For a formed head M is the knuckle factor.

M_x shell parameter for the buckling calculation.

M_s shell parameter for the buckling calculation.

MA mechanical allowances (thread or groove depth); for threaded components, the nominal thread depth (dimension h of ASME B.1.20.1) shall apply.

$MAWP$ maximum allowable working pressure.

$MAWP^C$ maximum allowable working pressure based on circumferential stress.

$MAWP^L$ maximum allowable working pressure based on longitudinal stress.

$MAWP^c$ maximum allowable working pressure for the cone.

$MAWP^f$ maximum allowable working pressure for the flare.

$MAWP^k$ maximum allowable working pressure for the knuckle.

MFH maximum fill height of the liquid to be stored in an atmospheric storage tank

n number of waves in the shell buckling calculation.

n_{rm} number of rivets.

N_r total number of rivets over the width w_r, for a butt joint, this will encompass one half of the joint pattern.

P internal design pressure.

P_a allowable external pressure in the absence of other loads.

P_{rs} rivet shear load.

P_{rc} minimum compressive load in a riveted joint.

P_{rj} plate tension load for the jth row of rivets in a riveted joint.

$P_{rj,\max}$ governing plate tension load for a riveted joint.

P_{rl} limiting load of a riveted plate.

P_{rp} limiting load of a plate without a rivet.

ϕ angle used to compute the cone geometry.

ϕ_s angle measured around the circumference from the direction of the applied shear force to the point under consideration.

Q saddle reaction resulting from the weight of the vessel and vessel contents.

R inside radius corrected for $LOSS$ and FCA as applicable..

R_{cc} radius to the centroid of the combined ring stiffener and effective length of the shell (see Figure A.11).

R_L inside radius of large cylinder at a conical transition corrected for $LOSS$ and FCA as applicable.

R_S inside radius of small cylinder at a conical transition corrected for $LOSS$ and FCA as applicable.

R_b centerline bend radius (see Figure A.14).

R_{ell} ratio of the major-to-minor axis of an elliptical head (see Figure A.1).

R_m mean radius of shell or pipe; use the large end radius for a conical shell, corrected for $LOSS$ and FCA as applicable.

R_{nc} nozzle inside radius corrected for $LOSS$ and FCA as applicable.

R_o outside radius of shell; use the large end radius for a conical shell, corrected for $LOSS$ and FCA as applicable.

r_f inside radius of the flare at a conical transition, corrected for $LOSS$ and FCA as applicable.

r_g radius of gyration.

r_k inside knuckle radius of a torispherical head, toriconical head, or conical transition, corrected for $LOSS$ and FCA as applicable.

S allowable stress.

S_n allowable stress for the nozzle.

S_p allowable stress for the reinforcing pad.

S_r allowable stress for the reinforcing pad from the original construction code.

S_v allowable stress for the vessel.

S_w allowable stress for the weld metal from the original construction code.

S_y yield stress of material at the assessment temperature.

S_{wh} allowable stress for the nozzle-to-vessel (inside surface) attachment weld.

S_{wn} allowable stress for the nozzle-to-reinforcing pad or nozzle-to-vessel fillet weld.

S_{wp} allowable stress for the shell to reinforcing pad fillet weld.

S_{wpg} allowable stress for the nozzle-to-pad groove weld.

S_{wng} allowable stress for nozzle-to-vessel groove weld.

σ_{bp} allowable bearing stress of plate.

σ_{br} allowable bearing stress of rivets.

σ_{sr} allowable shear stress of rivets.

σ_{tp} allowable tensile stress of plate.

σ_m nominal membrane stress.

σ_m^C nominal circumferential membrane stress for a cylinder or cone, as applicable.

σ_m^L nominal longitudinal membrane stress for a cylinder or cone, as applicable.

σ_m^c maximum stress in the cone.

σ_m^f maximum stress in the flare.

σ_m^k maximum stress in the knuckle.

$\sigma_{\max}$ maximum stress.

σ_1 principal compressive stress in the 1-direction.

σ_2 principal compressive stress in the 2-direction.

T_b nominal or furnished branch pipe thickness.

T_h nominal or furnished header or run pipe thickness.

T_r nominal or furnished thickness of the reinforcing pad.

t nominal or furnished thickness of the shell, the nominal or furnished pipe thickness adjusted for mill tolerance, or cylinder thickness at a conical transition for a junction reinforcement calculation, as applicable.

t_c $t_c = t - LOSS - FCA$.

t_{co} nominal or furnished cone thickness in a conical transition.

t_{cc} $t_{cc} = t_{co} - LOSS - FCA$.

t_b required thickness of the branch pipe, see paragraph A.5.3.

t_e nominal thickness of the reinforcing pad.

t_f nominal or furnished thickness of the flare at a conical transition.

t_{fc} $t_{fc} = t_f - LOSS - FCA$.

t_h required thickness of the header or run pipe, see paragraph A.5.4; for welded pipe, when the branch pipe does not intersect the longitudinal weld on the run pipe, the basic allowable stress for the pipe may be used in determining the required wall thickness. If the branch pipe does intersect the longitudinal weld of the run pipe, then the product of the basic allowable stress and the weld joint efficiency should be used in calculating the required wall thickness.

t_i nominal thickness of the of the internal projection of the nozzle wall.

t_k nominal or furnished thickness of the knuckle.

t_{kc} $t_{kc} = t_k - LOSS - FCA$.

t_r required thickness of the shell.

$t_{\min}$ minimum required thickness.

$t_{\min}^C$ minimum required thickness based on the circumferential membrane stress for a cylinder or cone, as applicable.

$t_{\min}^L$ minimum required thickness based on the longitudinal membrane stress for a cylinder or cone, as applicable.

$t_{\min}^c$ minimum required thickness for the cone.

$t_{\min}^f$ minimum required thickness for the flare.

$t_{\min}^k$ minimum required thickness for the knuckle.

t_n furnished nozzle wall thickness (see Figures A.6 and A.7) – For an integrally reinforced nozzle (see Figure A.7), $t_n = t_p$ if $L < 0.5\sqrt{d_m\left(t_n - c_n\right)}$.

t_p furnished wall thickness of the pipe section for an integrally reinforced nozzle (see Figure A.7).

t_r required thickness of the vessel wall computed with $E = 1.0$.

(1) Cylindrical shell (see paragraphs A.3.3 and A.4.3).
(2) Spherical shell (see paragraphs A.3.4 and A.4.4).
(3) Elliptical head (see paragraphs A.3.5 and A.4.5); for the internal pressure calculation, when the nozzle opening and its reinforcement are completely within a circle the center of that coincides with the center of the head and the diameter of which is 80% of the shell diameter, the required wall thickness shall be determined using K_c instead of K.
(4) Torispherical head (see paragraphs A.3.6 and A.4.6); for the internal pressure calculation, when the nozzle opening is entirely within the spherical of a torispherical head the required wall thickness is computed using M=1.0.
(5) Conical shell (see paragraphs A.3.7 and A.4.7); when the nozzle opening is in a cone, the required wall thickness is determined based on the shell diameter where the nozzle axis intersects the conical shell.

t_{req} required thickness for future operation.

t_{rn} required thickness of a seamless nozzle wall.

t_{sl} supplemental thickness for mechanical loads other than pressure that result in longitudinal stress; this thickness is usually obtained from the results of a weight case in a stress analysis of the piping system (see paragraph A.2.6).

t_{std} nominal thickness of ANSI B36.10 standard weight pipe.

t_1 ring stiffener dimension (see Figure A.11).

t_2 ring stiffener dimension (see Figure A.11).

θ angle of contact of the saddle with the shell or the angle around the elbow circumference where results are to be computed, as applicable.

V net-section shear force.

w_h weld leg size of the nozzle-to-vessel attachment weld on the inside surface of the vessel.

w_n weld leg size of the nozzle-to-vessel or nozzle-to-reinforcing pad (if a pad is used) attachment weld.

w_{ng} depth of nozzle-to-shell groove weld; for a set-on nozzle with a full penetration weld $w_{ng} = (t_n - c_n)$; for a set-in nozzle with a full penetration weld $w_{ng} = (t - c_s)$.

w_p weld leg size of the reinforcing pad-to-vessel attachment weld.

w_r unit width over which the riveted joint efficiency will be determined.

w_{pg} depth of nozzle-to-pad groove weld; for a full penetration weld $w_{pg} = t_p$.

W required weld stress.

W_{11} required weld stress calculation parameter.

W_{22} required weld stress calculation parameter.

W_{33} required weld stress calculation parameter.

W^c computed weld stress.

W_{11}^c computed weld stress calculation parameter.

W_{22}^c computed weld stress calculation parameter.

W_{33}^c computed weld stress calculation parameter.

Y_{B31} coefficient from ASME B31 Piping codes used for determining the pipe wall thickness, the coefficient can be determined from the following table that is valid for $t_{\min} < D_o/6$. The value of Y_{B31} may be interpolated for intermediate temperatures.

Value of Y_{B31}						
Materials	**Temperature °C (°F)**					
	≤ 482 (≤ 900)	**510 (950)**	**538 (1000)**	**566 (1050)**	**593 (1100)**	**≥ 621 (≥ 1150)**
Ferritic Steels	0.4	0.5	0.7	0.7	0.7	0.7
Austenitic Steels	0.4	0.4	0.4	0.4	0.5	0.7
Other Ductile Metals	0.4	0.4	0.4	0.4	0.4	0.4
Cast iron	0.4	---	---	---	---	---

Z_c radial distance from the shell to the stiffening ring centroid.

Z_L radial distance from the centerline of the shell to the centroid of the large ring stiffener.

Z_S radial distance from the centerline of the shell to the centroid of the small ring stiffener.

Z_t parameter in the supplemental thickness calculation for a horizontal vessel.

A.9 References

1. Farr, J.R. and Jawad, M.H., “Guidebook For The Design of ASME Section VIII Pressure Vessels,” ASME, New York, N.Y., 1998.
2. Miller, C.D. and Mokhtarian, K, “A Comparisons of Proposed Alternative Rules with ASME Code Rules for Determining Allowable Compressive Stresses,” The Eight International Conference on Pressure Vessel Technology, Montreal, Canada, July, 1996.
3. Osage, D.A., Buchheim, G.M., Brown, R.G., Poremba, J., “An Alternate Approach For Inspection Scheduling Using the Maximum Allowable Working Pressure for Pressurized Equipment,” PVP-Vol. 288, American Society of Mechanical Engineers, 1994, pp. 261-273.
4. Rodabaugh, E.C., Duffy, A.R., and Atterbury, T.J., “The Internal Pressure Capacity of Butt Welding Elbows,” American Gas Association, NG-18, Report No. 22, September, 1969.
5. WRC, “Review Of Area Replacement Rules for Pipe Connections in Pressure Vessels and Piping,” WRC-335, Welding Research Council, New York, October 1988.
6. WRC, “Proposed Rules for Determining Allowable Compressive Stresses for Cylinders, Cones, Spheres and Formed Heads,” WRC Bulletin 406, Welding Research Council, New York, 1995.
7. Zick, L.P., “Stresses in Large Horizontal Cylindrical Pressure Vessels on Two Saddle Supports,” Welding Research Journal Supplement, September, 1951.
8. Zick, L.P. and Germain, A.R., “Circumferential Stresses in Pressure Vessel Shells of Revolution,” *Journal of Engineering for Industry*, ASME, New York, N.Y., 1963.

A.10 Tables and Figures

Table A.1 – Loads, Load Cases, and Allowable Stresses To Be Considered in a FFS Assessment

Loading Condition	Load Description	Typical Allowable Membrane Stress
Erection	1. Dead load of component less: insulation, fireproofing, piping, all loose internals, catalyst, packing, etc. 2. Temporary loads and forces cased by erection 3. Full wind or earthquake, whichever is greater.	Code of construction design allowable stress as determine in paragraph A.2.4.
Pressure Testing	1. Dead load of component plus insulation, fireproofing, installed internals, platforms and other equipment supported from the component in the installed position. 2. Piping loads including pressure thrust 3. Applicable live loads excluding vibration and maintenance live loads. 4. Pressure and fluid loads (water) for testing and flushing equipment and piping unless a pneumatic test is specified. 5. Wind load for a wind speed of 56.3 Km/hr (35 mph).	Code of construction design allowable stress as determined in paragraph A.2.4. In addition, the following limits may be considered: 1. Tensile membrane stresses shall not exceed 90% of the minimum specified yield strength at 38°C (100°F) multiplied by the applicable weld joint efficiency. 2. Longitudinal compressive membrane stresses shall not exceed the allowable compressive stress calculated at 38°C (100°F).
Normal Operation	1. Dead load of component plus insulation, refractory, fireproofing, installed internals, catalyst, packing, platforms and other equipment supported from the component in the installed position. 2. Piping loads including pressure thrust 3. Applicable live loads. 4. Pressure and fluid loading during normal operation. 5. Thermal loads.	Code of construction design allowable stress as determined in paragraph A.2.4.
Normal Operation plus Occasional (note: occasional loads are usually governed by wind and earthquake; however, other load types such as snow and ice loads may govern, see ASCE-7)	1. Dead load of component plus insulation, refractory, fireproofing, installed internals, catalyst, packing, platforms and other equipment supported from the component in the installed position. 2. Piping loads including pressure thrust 3. Applicable live loads. 4. Pressure and fluid loading during normal operation. 5. Thermal loads 6. Full wind, earthquake or other occasional loads, whichever is greater.	Code of construction design allowable stress as determined in paragraph A.2.4. Load definitions and load case combinations that shall be considered are shown in Annex B1, Tables B1.1 and B1.2, respectively.
Abnormal or Start-up Operation plus Occasional (see note above)	1. Dead load of component plus insulation, refractory, fireproofing, installed internals, catalyst, packing, platforms and other equipment supported from the component in the installed position. 2. Piping loads including pressure thrust 3. Applicable live loads. 4. Pressure and fluid loading associated with the abnormal or start-up conditions 5. Thermal loads 6. Wind load for a wind speed of 35 mph.	Code of construction design allowable stress as determined in paragraph A.2.4 modified as follows: Vessels – Abnormal or start-up operation is considered part of normal operation in the ASME B&PV Code; modification of design allowable stress not permitted. Piping – per Paragraph 302.3.5, limits for occasional loads per Paragraph 302.3.6, allowances for pressure and temperature variations per Paragraph 302.2.4. of the ASME B31.3 Piping Code.

Table A.2 – Temperature Limits For Compressive Stress Equations

ASME B&PV Code Table In Which The Material Is Listed		Temperature Limit	
Section VIII, Division 1	Section VIII, Division 2	°C	°F
UCS-23.1	ACS-1	425	800
UHA-23	AHA-1	425	800
UHT-23	AQT-1	370	700
UNF-23.1	ANF-1.1	150	300
UNF-23.2	ANF-1.2	65	150
UNF-23.3	ANF-1.3	480	900
UNF-23.4	ANF-1.4	315	600
UNF-23.5	---	315	600

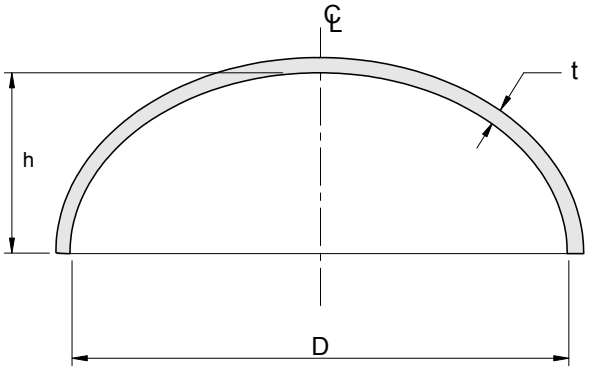

$R_{ell} = D/2h$

(a) Elliptical Head Geometry

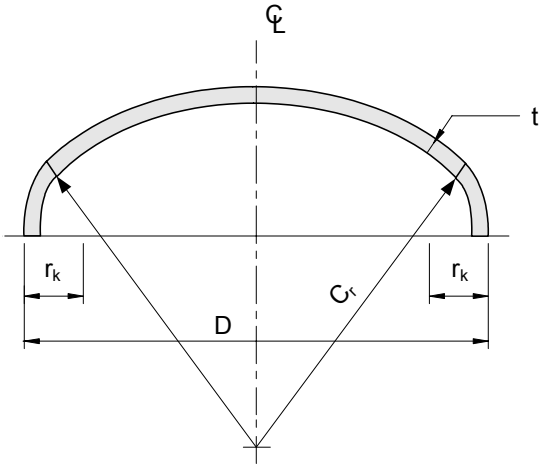

$r_k/C_r \times 100 \geq 6\%$

(b) Torispherical Head Geometry

Figure A.1
Elliptical and Torispherical Head Geometries

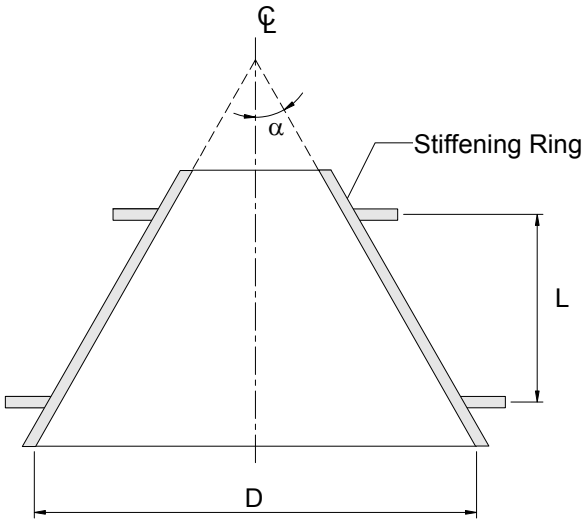

(a) Conical Shell Geometry

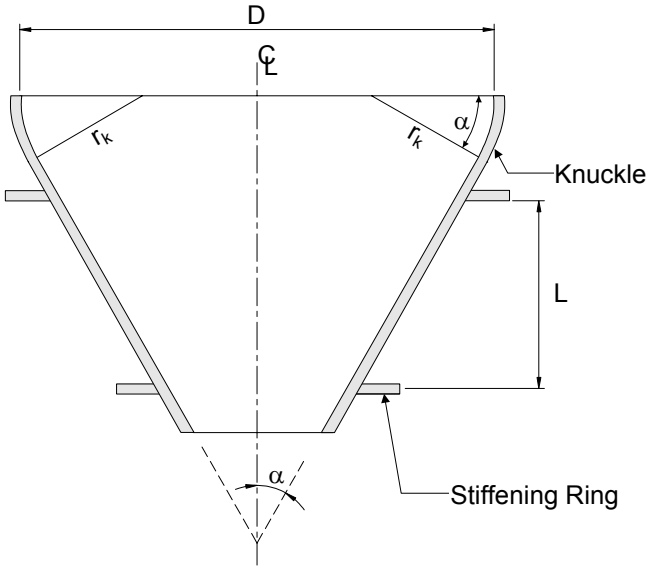

(b) Toriconical Head Geometry

Figure A.2
Conical Shell and Toriconical Head Geometries

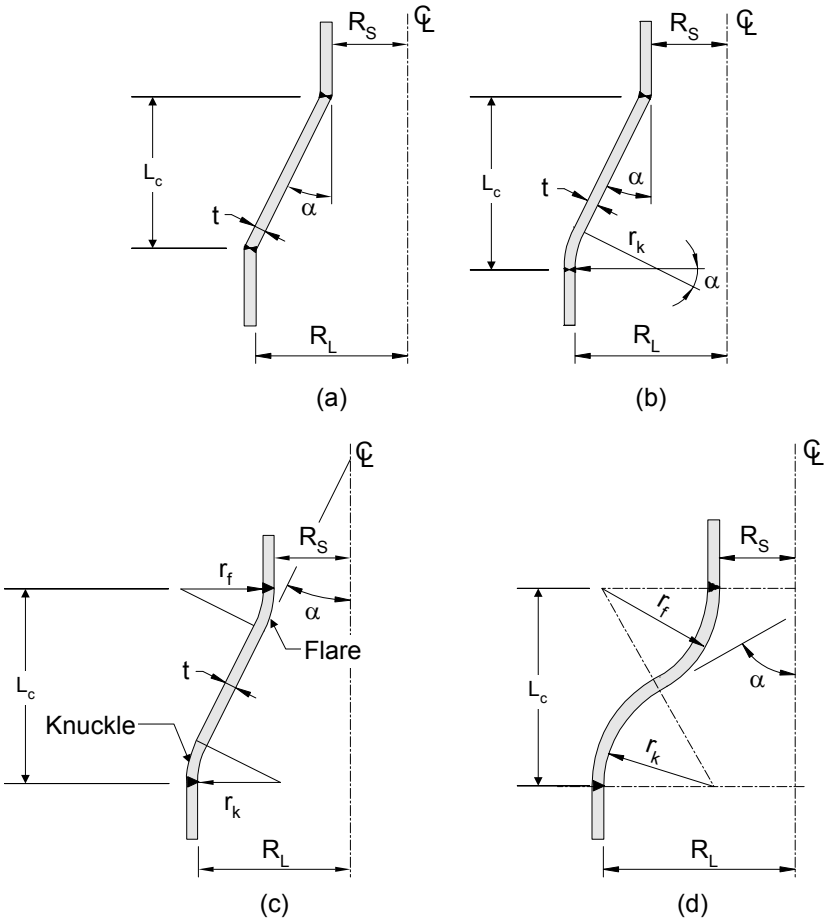

Note: r_k => max[0.12(R_L + t), 3t_c]; R_s has no dimensional requirements.

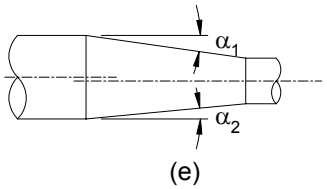

$\alpha_1 > \alpha_2$; Therefore use $\alpha 1$ in design equations.

Figure A.3
Conical Transition Geometries

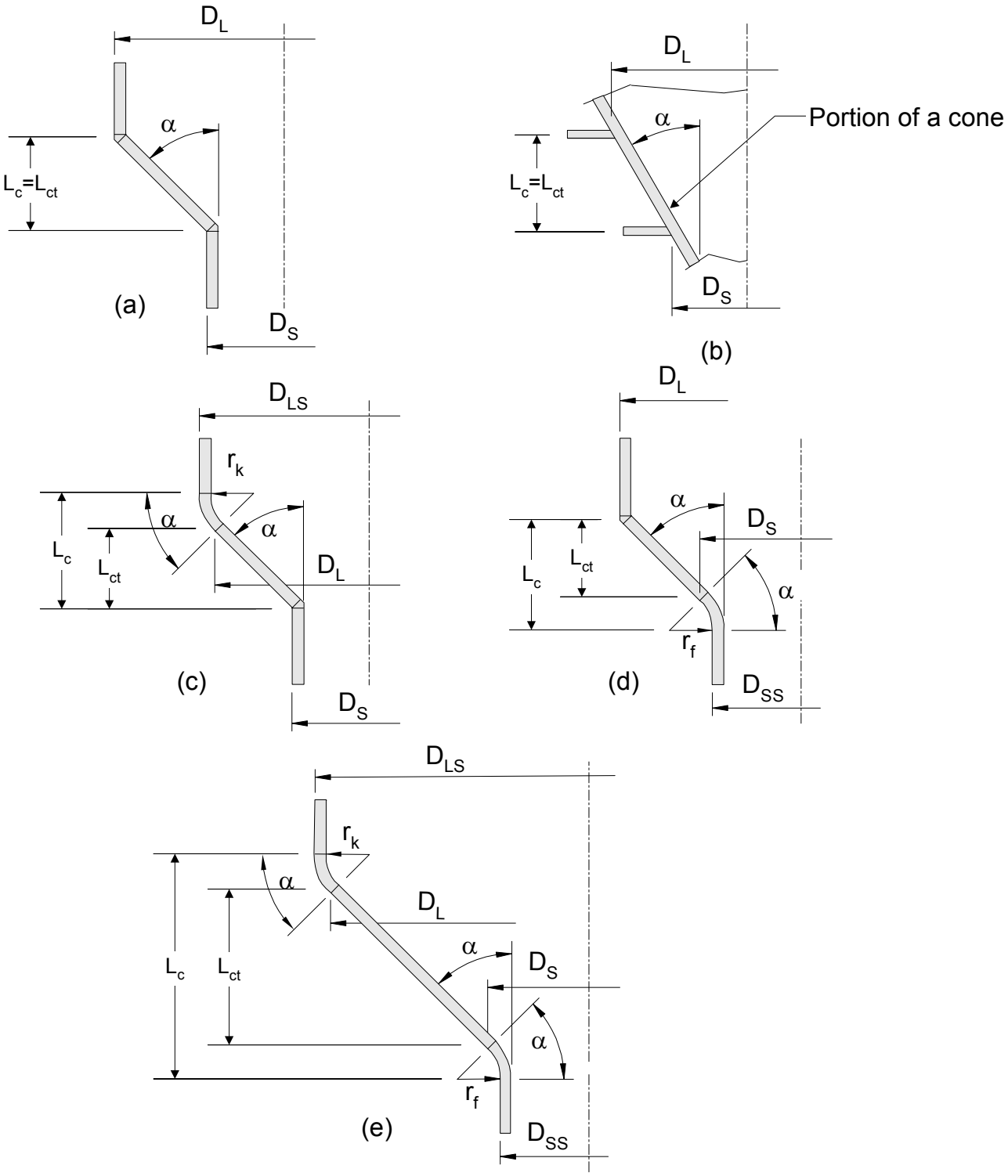

Figure A.4
Unsupported Length for Conical Transitions

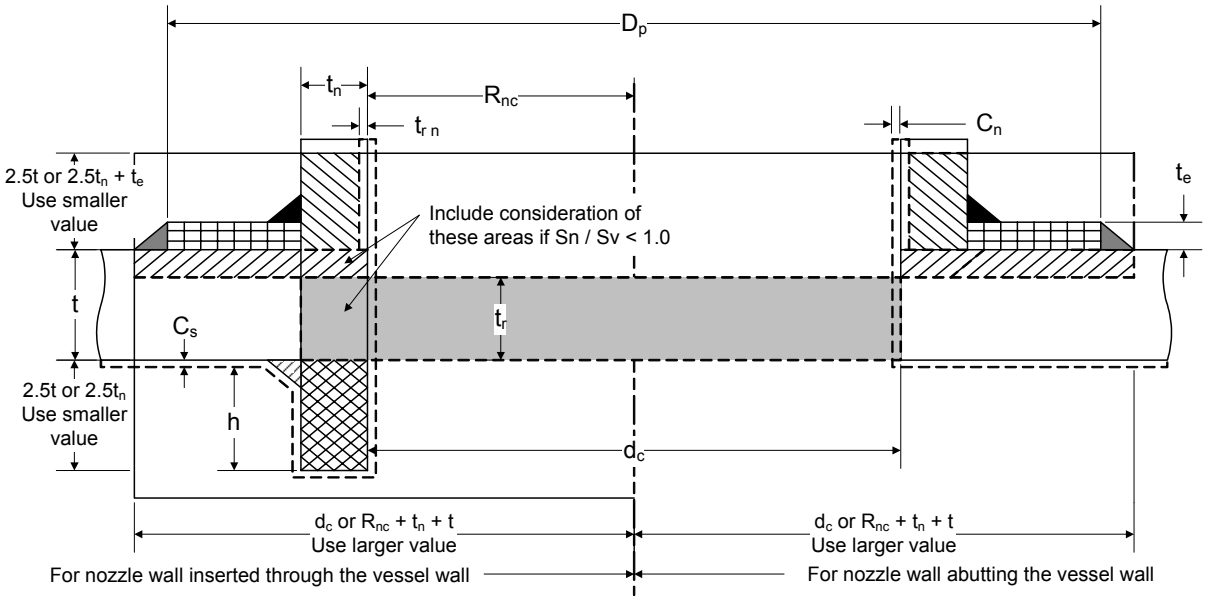

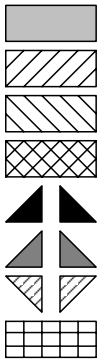

- A_r Required reinforcement area
- A_1 Available reinforcement area in the shell
- A_2 Available reinforcement area in the nozzle
- A_3 Available reinforcement area, inside nozzle projection
- $A_{4\,1}$ Available reinforcement area in the nozzle to pad or vessel weld
- $A_{4\,2}$ Available reinforcement area in the nozzle to weld, inside surface
- $A_{4\,3}$ Available reinforcement area in the reinforcing pad attachment weld
- A_5 Available reinforcement area in the reinforcing pad

Figure A.5
Nozzle Parameters – Area Replacement Method

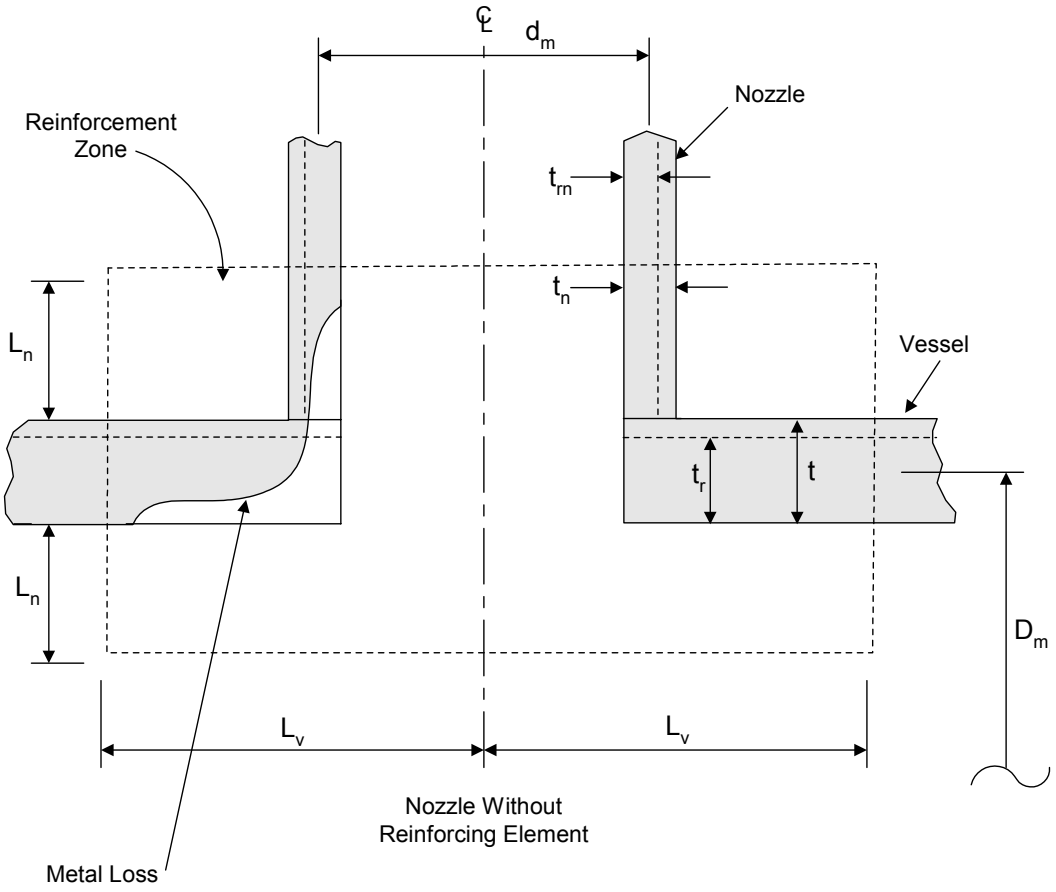

Figure A.6
Nozzle Parameters – Limit Load Analysis

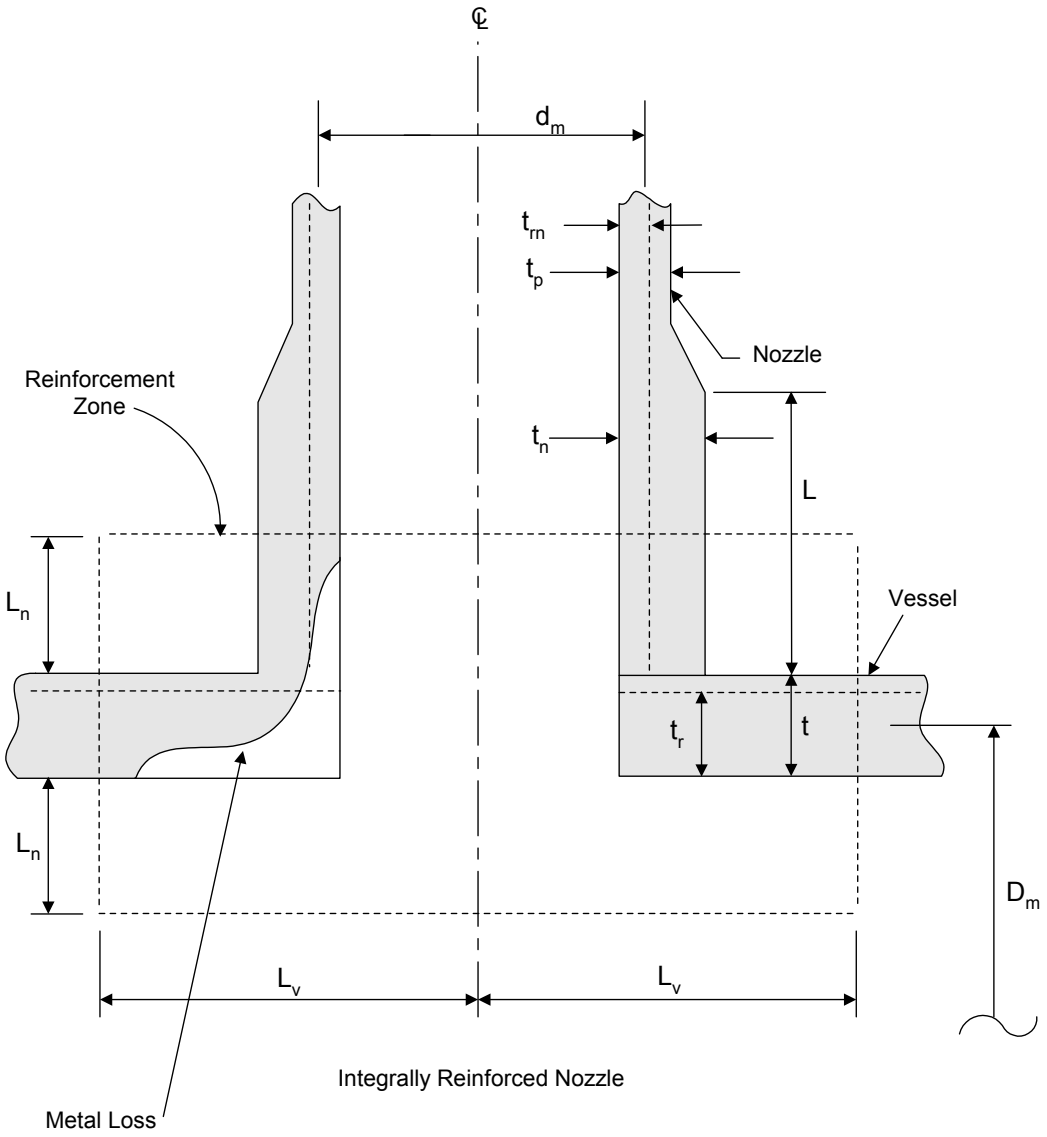

Figure A.7
Nozzle Parameters (Integrally Reinforced Nozzle Neck) – Limit Load Analysis

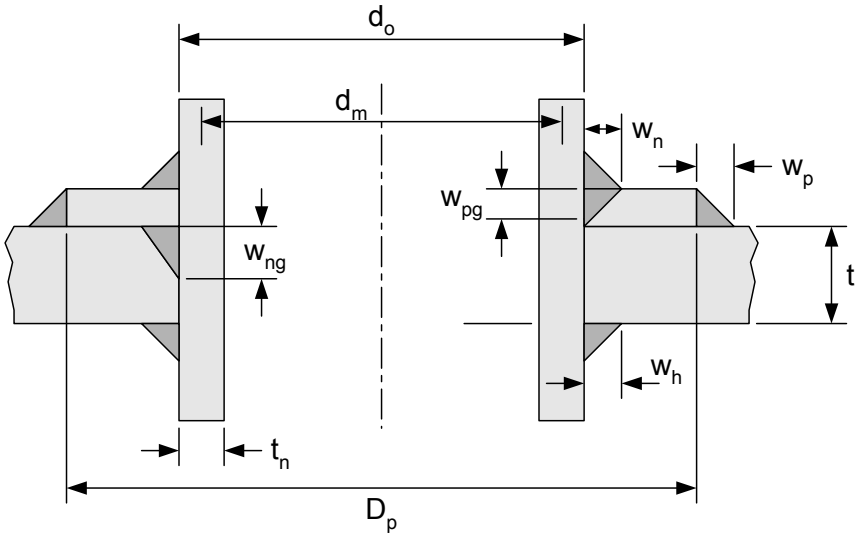

(a) Nozzle and Weld Dimensions

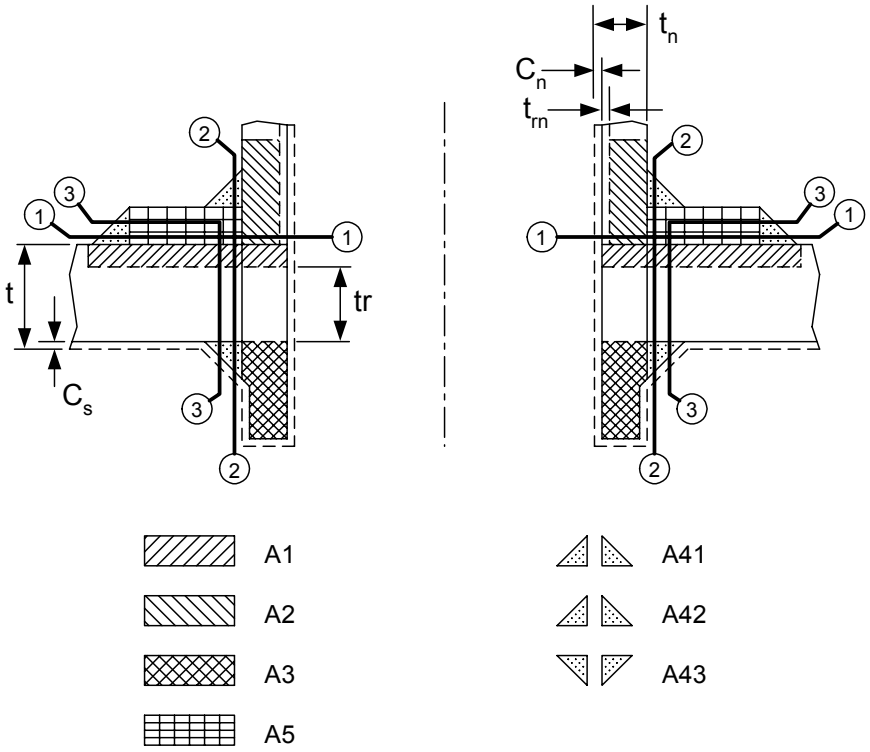

(b) Weld Strength Paths

Figure A.8
Definition of Paths for a Nozzle Weld Strength Analysis – Set-in Nozzle

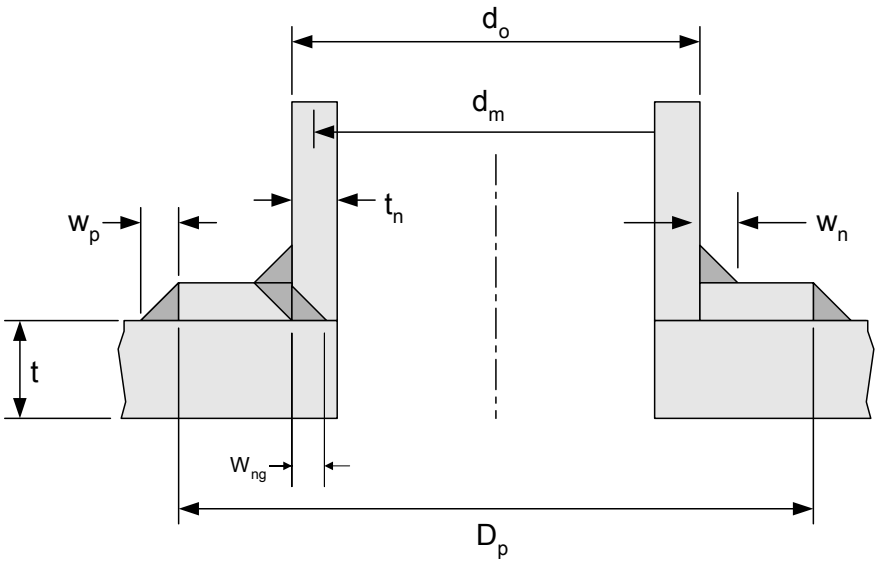

(a) Nozzle and Weld Dimensions

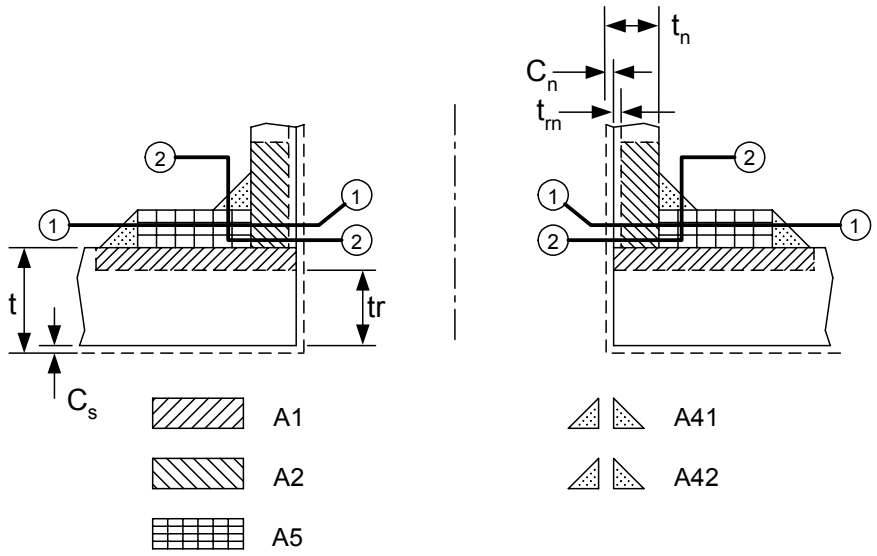

(b) Weld Strength Paths

Figure A.9
Definition of Paths for a Nozzle Weld Strength Analysis – Set-on Nozzle

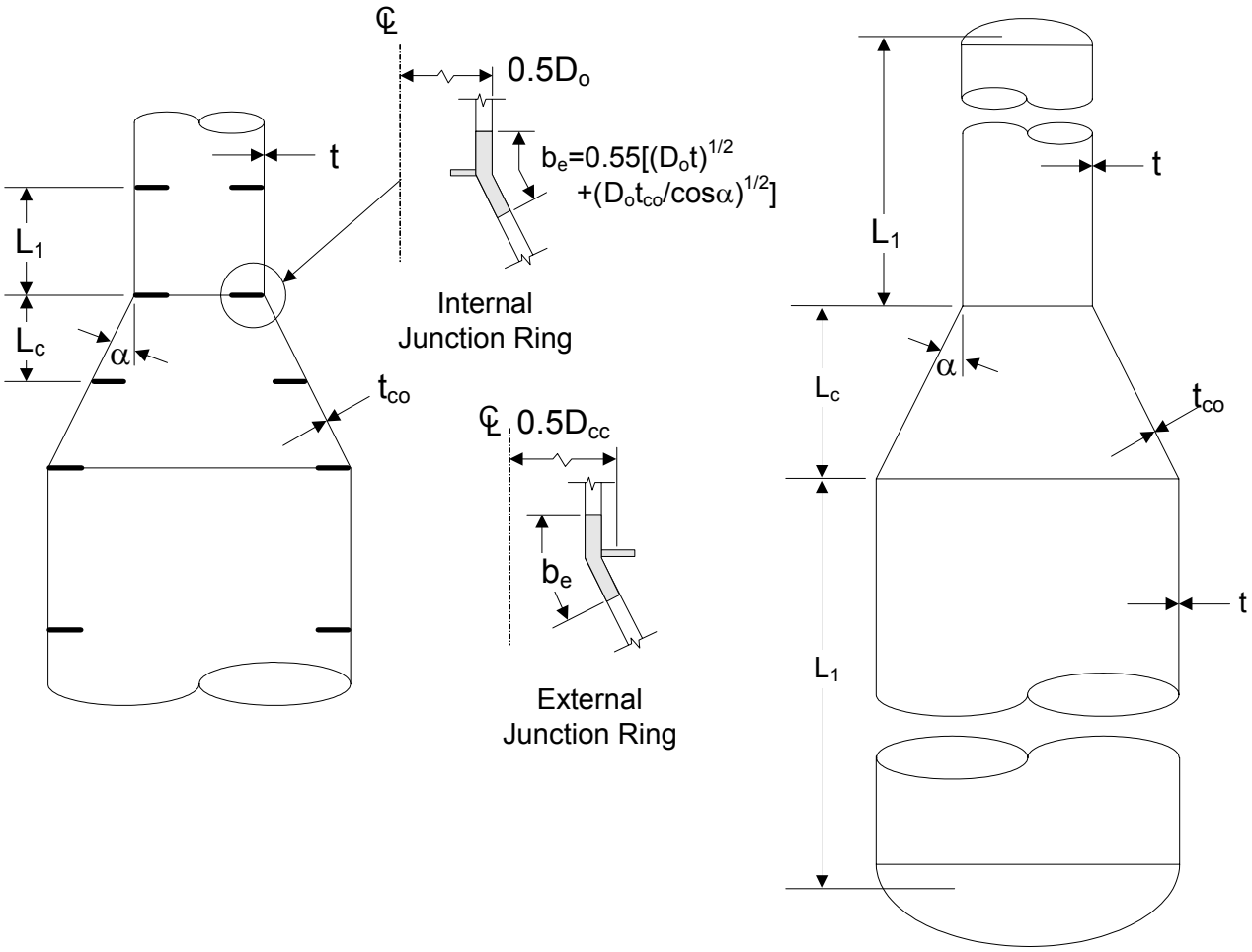

Figure A.10
Definition of Lines of Support for a Conical Transition

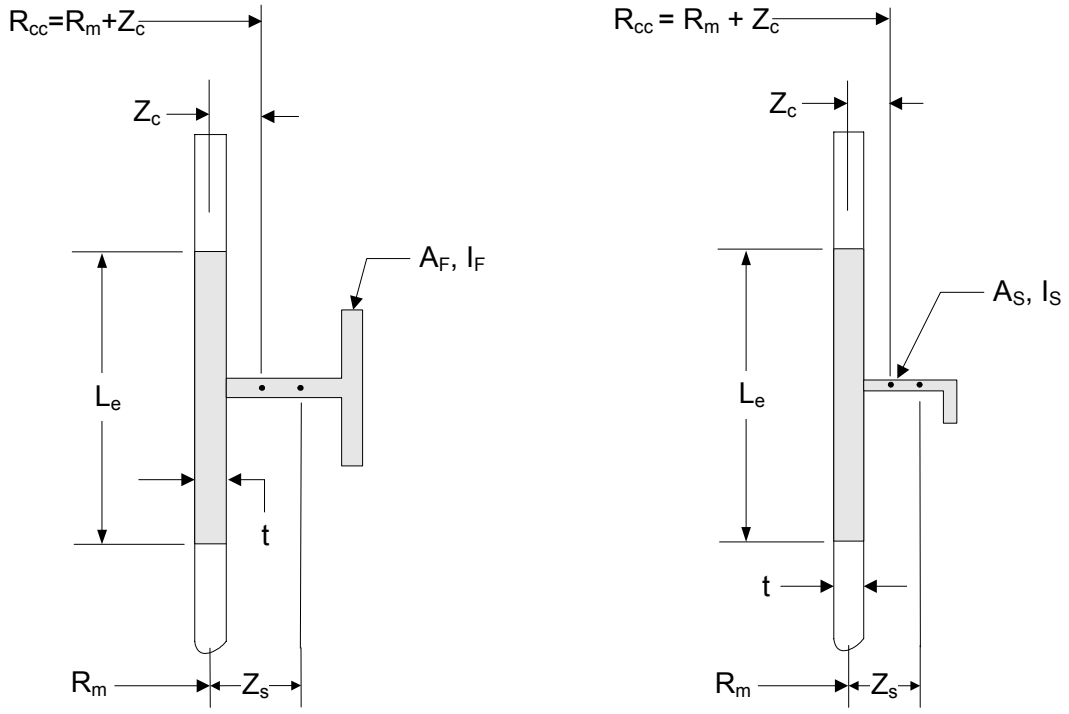

(a-1) Stiffening Ring which Acts as a Bulkhead

(a-2) Small Stiffening Ring

(a) Sections Through Stiffening Rings

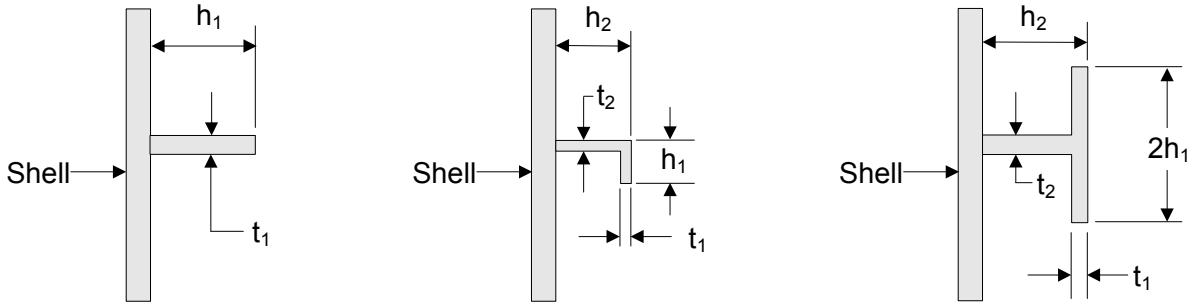

(b) Stiffener Variables for Local Buckling Calculation

Figure A.11
Stiffening Ring Variables

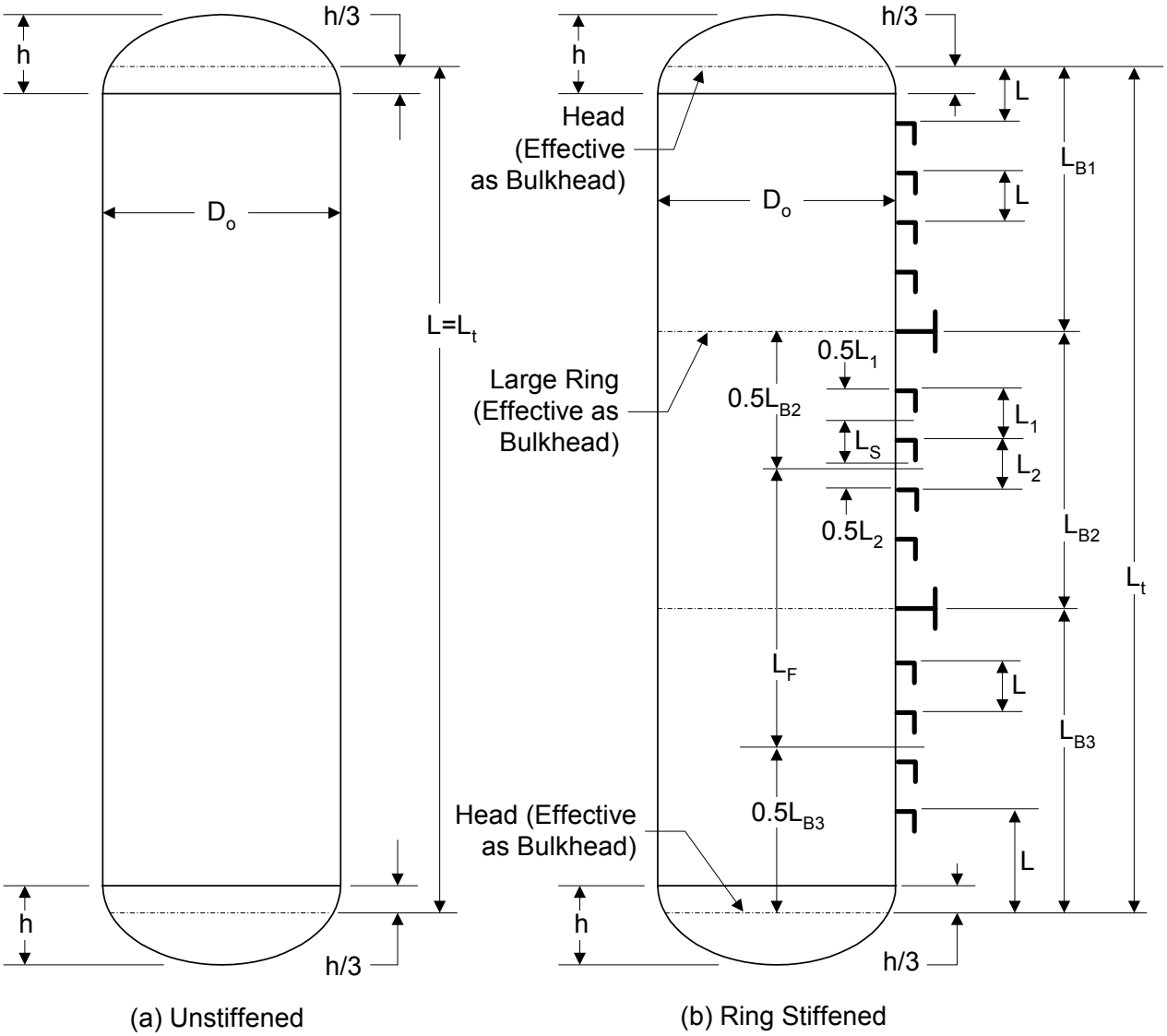

Figure A.12
Definition of Lines of Support for Design of Cylindrical Vessels Subjected to External Pressure

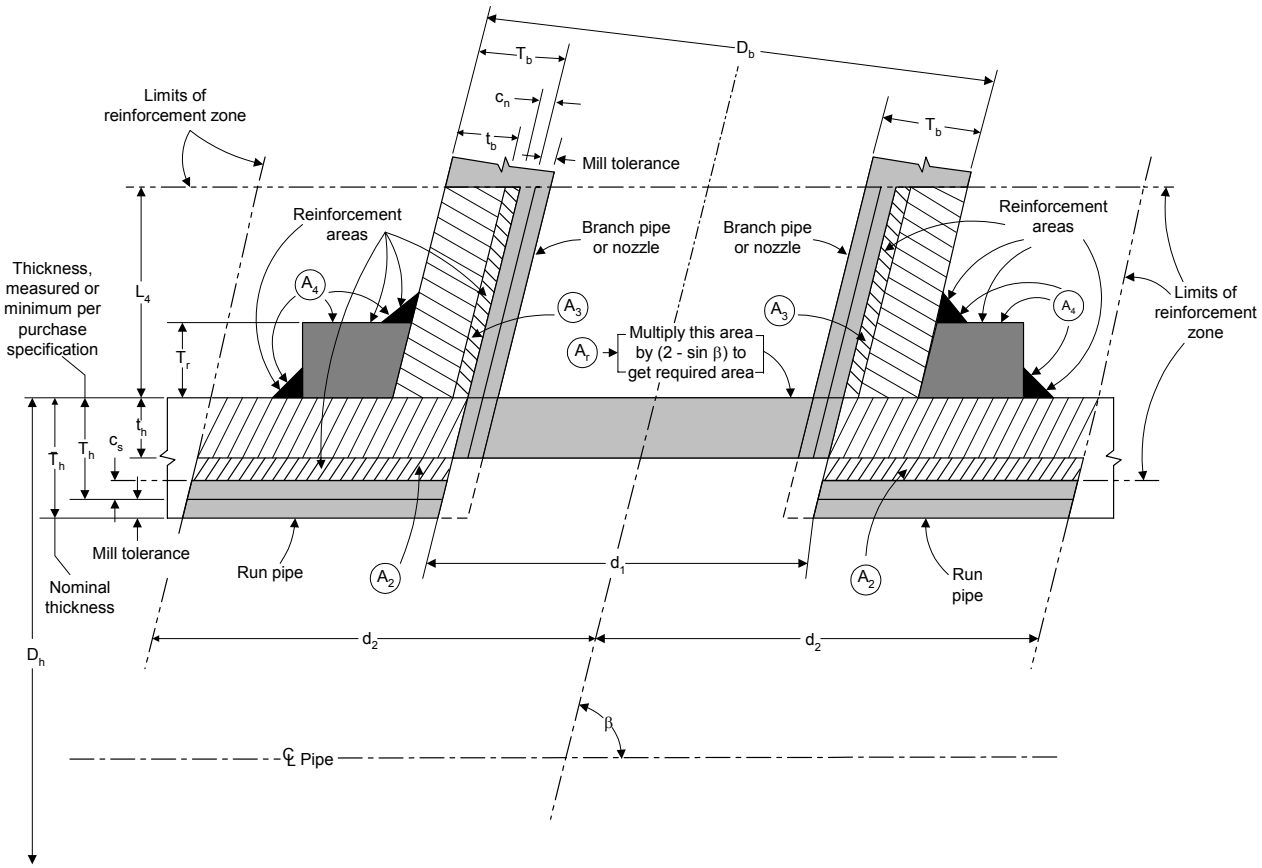

Figure A.13
Definition of Variables for Branch Reinforcement Calculation in Piping Systems

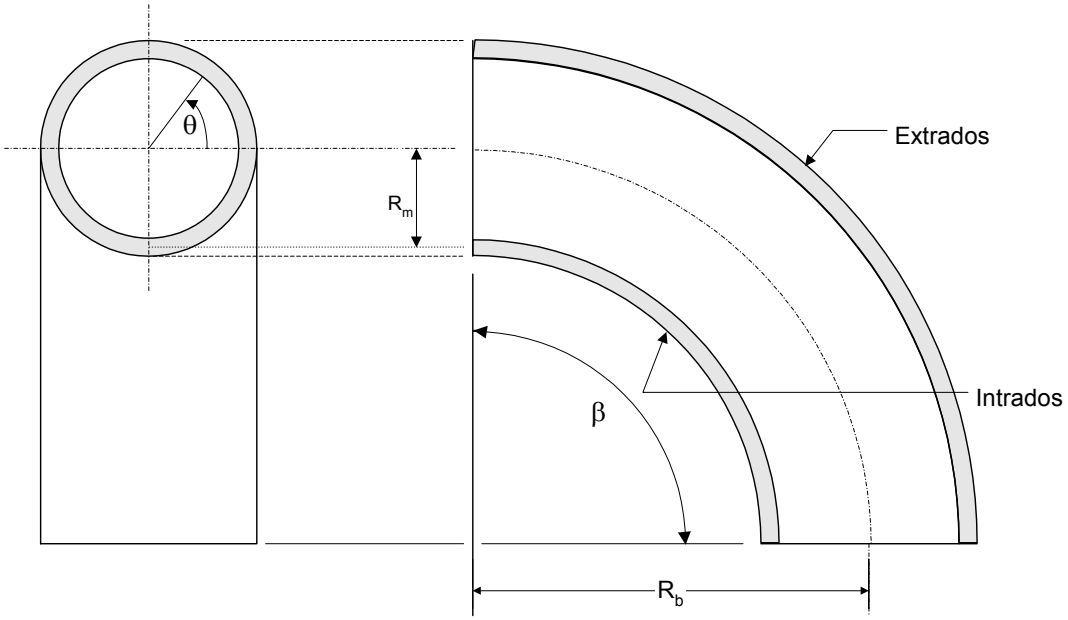

(a) Bend Geometry

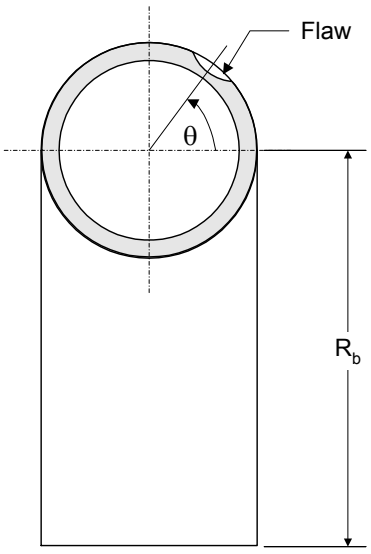

(b) Flaw Location

Figure A.14
Definition of Variables for Piping Bends

ANNEX B1

STRESS ANALYSIS OVERVIEW FOR AN FFS ASSESSMENT

(NORMATIVE)

PART CONTENTS

B1.1 General Requirements

B1.1.1 Scope

B1.1.1.1 The analytical methods contained within this Annex can be used for stress analysis when performing a Fitness-For-Service (FFS) Assessment of a component with a flaw. These methods are typically employed in either a Level 2 or Level 3 assessment. Detailed assessment procedures utilizing the results from a stress analysis are provided to evaluate components for plastic collapse, local failure, buckling, and cyclic loading.

B1.1.1.2 The methods presented in this Annex can be used to evaluate volumetric flaws (i.e. general metal loss, localized metal loss, and shell distortions) and crack-like flaws. Linear or non-linear stress analysis can be used to evaluate volumetric flaws using stress categorization or by determining a plastic collapse load, respectively. The assessment criteria for crack-like flaws can also be based on linear or non-linear stress analysis. If a linear stress analysis is used, the acceptance criteria are based on a two parameter Failure Assessment Diagram (FAD) approach to evaluate the combined effects of fracture and plastic collapse (see Part 9). Alternatively, if an elastic-plastic stress analysis is used, the crack-like flaw can be evaluated directly by using the J-integral. An overview of the assessment requirements for volumetric and crack-like flaws is provided below.

B1.1.1.3 Recommendations are provided on how to perform and utilize results from a stress analysis in a Fitness-For-Service assessment. Procedures for performing linear and non-linear analysis, determination of stress categories and classification of stress results obtained from a linear analysis, and a methodology to perform an elastic-plastic analysis to determine a collapse load or to perform a fatigue evaluation are among the items covered in this Annex.

B1.1.1.4 The analysis requirements for volumetric flaws are organized based on protection against the failure modes listed below. If multiple assessment procedures are provided for a failure mode, only one of these procedures must be satisfied to qualify the component for continued operation. In addition, the component shall be evaluated for each applicable failure mode.

a) Protection Against Plastic Collapse – The requirements of paragraph B1.2 shall be satisfied.
b) Protection Against Local Failure – The requirements of paragraphs B1.3 shall be satisfied.
c) Protection Against Collapse From Buckling – The requirements of paragraph B1.4 shall be satisfied.
d) Protection Against Failure From Cyclic Loading – The requirements of paragraph B1.5 shall be satisfied.
e) Protection Against Creep or Creep-Fatigue Damage – Assessment requirements for components subject to cyclic operation in the creep regime are covered in Part 10.

B1.1.1.5 The analysis requirements for crack-like flaws are organized based on protection against the failure modes listed below. If multiple assessment procedures are provided for a failure mode, only one of these procedures must be satisfied to qualify the component for continued operation. In addition, the component shall be evaluated for each applicable failure mode. The stress analysis methods in paragraph B1.2 and B1.7 may be required for the assessment.

a) Protection Against Failure due to Unstable Crack Growth (Low Temperature) – The assessment requirements for fracture are provided in Part 9
b) Protection Against Failure due to Unstable Crack Growth (High Temperature) – The assessment requirements for creep crack growth are provided in Part 10.
c) Protection Against Collapse From Buckling – The requirements of paragraph B1.4 shall be satisfied.

B1.1.1.6 Annex B is organized into four separate sections to facilitate use and future updates. The sections are defined below.

a) Annex B1 – Contains analytical methods to be used for stress analysis when performing a Fitness-For-Service (FFS) Assessment of a component with a flaw.
b) Annex B2 – Covers recommendations for linearization of stress results for stress classification. Linearization of stress results may be used to evaluate protection against plastic collapse using an elastic stress criterion and may also be used in the assessment of crack-like flaws.
c) Annex B3 – Covers recommendations for histogram development and cycle counting for fatigue analysis.
d) Annex B4 – Contains procedures for the determination of plasticity correction factors and effective alternating stress for elastic fatigue analysis.

B1.1.1.7 The assessment procedures in Annex B may only be used if the allowable stress from the applicable construction code evaluated at the design temperature is governed by time-independent properties unless otherwise noted in a specific design procedure. If the allowable stress from the applicable construction code evaluated at the design temperature is governed by time-dependent properties and the fatigue screening criteria of paragraph B1.5.2.2 are satisfied, the elastic stress analysis procedures in paragraphs B1.2.2, B1.3.2, and B1.6 may be used.

B1.1.2 Numerical Analysis

B1.1.2.1 The assessment methods in this Annex are based on the use of results obtained from a detailed stress analysis of a component. Depending on the loading condition, a thermal analysis to determine the temperature distribution and resulting thermal stresses may also be required.

B1.1.2.2 Procedures are provided for performing stress analyses to determine protection against plastic collapse, local failure, buckling, and cyclic loading. These procedures provide the necessary details to obtain a consistent result with regards to development of loading conditions, selection of material properties, post-processing of results, and comparison to acceptance criteria to determine the suitability of a component.

B1.1.2.3 Recommendations on a stress analysis method, modeling of a component, and validation of analysis results are not provided. While these aspects of the design process are important and shall be considered in the analysis, a detailed treatment of the subject is not provided because of the variability in approaches and design processes. However, an accurate stress analysis including validation of all results shall be provided as part of the design.

B1.1.2.4 The following material properties for use in the stress analysis shall be determined using the data and material models in Annex F.

a) Physical properties – Young's Modulus, thermal expansion coefficient, thermal conductivity, thermal diffusivity, density, Poisson's ratio.
b) Strength Parameters – Allowable stress, minimum specified yield strength, minimum specified tensile strength.
c) Monotonic Stress-Strain Curve – elastic perfectly plastic and elastic-plastic true stress-strain curve with strain hardening.
d) Cyclic Stress-Strain Curve – Stabilized true stress-strain amplitude curve.

B1.1.3 Applicable Loads and Load Case Combinations

B1.1.3.1 All applicable applied loads on the component shall be considered when performing an FFS assessment. Supplemental loads shall be considered in addition to the applied pressure in the form of applicable load cases. An overview of the supplemental loads and loading conditions that shall be considered in a design are shown in Annex A, Table A.1.

B1.1.3.2 Load case combinations shall be considered in the FFS assessment. Typical load definitions are defined in Table B1.1. Load case combinations for elastic analysis, limit load analysis, and elastic plastic analysis are shown in Tables B1.2, B1.3, and B1.4, respectively. In evaluating load cases involving the pressure term, P, the effects of the pressure being equal to zero shall be considered. The applicable load case combinations shall be considered in addition to any other combinations defined by the Owner-User.

B1.1.3.3 If any of the loads vary with time, a loading histogram shall be developed to show the time variation of each specific load.

a) The loading histogram shall include all significant operating temperatures, pressures, supplemental loads, and the corresponding cycles or time periods for all significant events that are applied to the component. The following shall be considered in developing the loading histogram.
   1) The number of cycles associated with each event during the operation life, these events shall include start-ups, normal operation, upset conditions, and shutdowns.
   2) When creating the histogram, the history to be used in the assessment shall be based on the anticipated sequence of operation.
   3) Applicable loadings such as pressure, temperature, supplemental loads such as weight, support displacements, and nozzle reaction loadings.
   4) The relationship between the applied loadings during the time history.
b) If an accurate histogram cannot be generated, then an approximate histogram shall be developed based on information obtained from plant personnel. This information shall include a description of all assumptions made, and include a discussion of the accuracy in establishing points on the histogram. A sensitivity analysis (see Part 2) shall be included in the FFS assessment to determine and evaluate the effects of the assumptions made to develop the operating history.

B1.2 Protection Against Plastic Collapse

B1.2.1 Overview

B1.2.1.1 Three alternative analysis methods are provided for evaluating protection against plastic collapse. A brief description of the analysis methods is provided below.

a) Elastic Stress Analysis Method – Stresses are computed using an elastic analysis, classified into categories, and limited to allowable values that have been conservatively established such that a plastic collapse will not occur.
b) Limit-Load Method – A calculation is performed to determine a lower bound to the limit load of a component. The allowable load on the component is established by applying design factors to the limit load such that the onset of gross plastic deformations (plastic collapse) will not occur.
c) Elastic-Plastic Stress Analysis Method – A collapse load is derived from an elastic-plastic analysis considering both the applied loading and deformation characteristics of the component. The allowable load on the component is established by applying design factors to the plastic collapse load.

B1.2.1.2 For components with a complex geometry and/or complex loading, the categorization of stresses requires significant knowledge and judgment. This is especially true for three-dimensional stress fields. Application of the limit load or elastic-plastic analysis methods in paragraphs B1.2.3 and B1.2.4, respectively, is recommended for cases where the categorization process may produce ambiguous results.

B1.2.1.3 The use of elastic stress analysis combined with stress classification procedures to demonstrate structural integrity for heavy-wall $(R/t \leq 4)$ pressure containing components, especially around structural discontinuities, may produce non-conservative results and is not recommended. The reason for the non-conservatism is that the nonlinear stress distributions associated with heavy wall sections are not accurately represented by the implicit linear stress distribution utilized in the stress categorization and classification procedure. The misrepresentation of the stress distribution is enhanced if yielding occurs. For example, in cases where calculated peak stresses are above yield over a through thickness dimension which is more than five percent of the wall thickness, linear elastic analysis may give a non-conservative result. In these cases, the elastic-plastic stress analysis procedure in paragraphs B1.2.3 and B1.2.4 shall be used.

B1.2.1.4 The structural evaluation procedures based on elastic stress analysis in paragraph B1.2.2 provide an approximation of the protection against plastic collapse. A more accurate estimate of the protection against plastic collapse of a component can be obtained using elastic-plastic stress analysis to develop limit and plastic collapse loads. The limits on the general membrane equivalent stress, local membrane equivalent stress and primary membrane plus primary bending equivalent stress in paragraph B1.2.2 have been placed at a level which conservatively assures the prevention of collapse as determined by the principles of limit analysis. These limits need not be satisfied if the requirements of paragraph B1.2.3 or paragraph B1.2.4 are satisfied.

B1.2.2 Elastic Stress Analysis Method

B1.2.2.1 Overview

To evaluate protection against plastic collapse, the results from an elastic stress analysis of the component subject to defined loading conditions are categorized and compared to an associated limiting value. The basis of the categorization procedure is described below.

a) Basis for Determining Stresses – A quantity known as the equivalent stress is computed at locations in the component and compared to an allowable value of equivalent stress to determine if the component is suitable for the intended design conditions. The equivalent stress at a point in a component is a measure of stress, calculated from stress components utilizing a yield criterion, which is used for comparison with the mechanical strength properties of the material obtained in tests under uniaxial load.

b) The maximum distortion energy yield criterion shall be used to establish the equivalent stress. In this case, the equivalent stress is equal to the von Mises equivalent stress given by Equation (B1.1).

$$S = \sigma_e = \frac{1}{\sqrt{2}}\left[\left(\sigma_1 - \sigma_2\right)^2 + \left(\sigma_2 - \sigma_3\right)^2 + \left(\sigma_3 - \sigma_1\right)^2\right]^{0.5} \qquad \text{(B1.1)}$$

B1.2.2.2 Stress Categorization

The three basic equivalent stress categories and associated limits that are to be satisfied for plastic collapse are defined below. The terms general primary membrane stress, local primary membrane stress, primary bending stress, secondary stress, and peak stress used for elastic analysis are defined in the following paragraphs. The design loads and load combinations to be evaluated and the corresponding allowable membrane stress limits are provided in Tables B1.1 and B1.2, respectively.

a) General Primary Membrane Equivalent Stress (P_m)

1) The general primary membrane equivalent stress (see Figure B1.1) is the equivalent stress, derived from the average value across the thickness of a section, of the general primary stresses produced by the design internal pressure and other specified mechanical loads but excluding all secondary and peak stresses.

2) Examples of this stress category for typical pressure vessel components are shown in Table B1.5.

b) Local Primary Membrane Equivalent Stress (P_L)

1) The local primary membrane equivalent stress (see Figure B1.1) is the equivalent stress, derived from the average value across the thickness of a section, of the local primary stresses produced by the design pressure and specified mechanical loads but excluding all secondary and peak stresses. A region of stress in a component is considered as local if the distance over which the equivalent stress exceeds $1.1S_m$ does not extend in the meridional direction more than $\sqrt{Rt}$.

2) Regions of local primary membrane stress that exceed $1.1S_m$ shall be separated in the meridional direction by a distance greater than or equal to $1.25\left[\left(R_1 + R_2\right)\left(t_1 + t_2\right)\right]^{0.5}$. Discrete regions of local primary membrane stress, such as those resulting from concentrated loads on support brackets, where the membrane stress exceeds $1.1S_m$, shall be spaced so that there is not an overlapping area in which the membrane stress exceeds $1.1S_m$.

3) Examples of this stress category for typical pressure vessel components are shown in Table B1.5.

c) Primary Membrane (General or Local) Plus Primary Bending Equivalent Stress $(P_L + P_b)$

1) The Primary Membrane (General or Local) Plus Primary Bending Equivalent Stress (see Figure B1.1) is the equivalent stress, derived from the highest value across the thickness of a section, of the linearized general or local primary membrane stresses plus primary bending stresses produced by design pressure and other specified mechanical loads but excluding all secondary and peak stresses.

2) Examples of this stress category for typical pressure vessel components are shown in Table B1.5.

B1.2.2.3 Linearization of Stress Results for Stress Categorization

Results from an elastic stress analysis may be used to compute the equivalent linearized membrane and bending stresses for comparison to the limits in paragraph B1.2.2.4 using the methods described in Annex B2.

B1.2.2.4 Assessment Procedure

To determine the acceptability of a component, the computed equivalent stresses given in paragraph B1.2.2.2 shall not exceed specified allowable values. A schematic illustrating the categorization of equivalent stresses and their corresponding allowable values is shown in Figure B1.1. The following procedure is used to compute and categorize the equivalent stress at a point in a component (see paragraph B1.2.2.3), and to determine the acceptability of the resulting stress state.

a) STEP 1 – Determine the types of loads acting on the component. In general, separate load cases are analyzed to evaluate "load-controlled" loads such as pressure and externally applied reactions due to weight effects and "strain-controlled" loads resulting from thermal gradients and imposed displacements. The loads to be considered in the assessment are given in paragraph B1.1.3.

b) STEP 2 – At the point on the vessel that is being investigated, calculate the stress tensor (six unique components of stress) for each type of load. Assign each of the computed stress tensors to one or to a group of the categories defined below. Assistance in assigning each stress tensor to an appropriate category for a component can be obtained by using Figure B1.1 and Table B1.5. Note that the equivalent stresses Q and F do not need to be determined to evaluate protection against plastic collapse. However, these components are required for fatigue and ratcheting evaluations that are based on elastic stress analysis (see paragraphs B1.5.3 and B1.5.6, respectively).

1) General primary membrane equivalent stress – P_m

2) Local primary membrane equivalent stress – P_L

3) Primary bending equivalent stress – P_b

4) Secondary equivalent stress – Q

5) Additional stress produced by a stress concentration or a thermal stress over and above the nominal $(P+Q)$ stress level – F

c) STEP 3 – Sum the stress tensors (stresses are added on a component basis) assigned to each equivalent stress category. The final result is a stress tensor representing the effects of all the loads assigned to each equivalent stress category. Note that when applying STEPs in this paragraph, a detailed stress analysis performed using a numerical method such as finite element analysis typically provides a combination of P_L + P_b and $P_L + P_b + Q$ directly.

1) If a load case is analyzed that includes only "load-controlled" loads (e.g. pressure and weight effects), the computed equivalent stresses shall be used to directly represent the P_m, $P_L + P_b$, or $P_L + P_b + Q$. For example, for a vessel subject to internal pressure with an elliptical head; P_m equivalent stresses occur away from the head to shell junction, and P_L and $P_L + P_b + Q$ equivalent stresses occur at the junction.

2) If a load case is analyzed that includes only "strain-controlled" loads (e.g. thermal gradients), the computed equivalent stresses represent Q alone; the combination $P_L + P_b + Q$ shall be derived from load cases developed from both "load-controlled" and "strain-controlled" loads.

3) If the stress in category F is produced by a stress concentration or thermal stress, the quantity F is the additional stress produced by the stress concentration in excess of the nominal membrane plus bending stress. For example, if a plate has a nominal primary membrane equivalent stress of S, and has a fatigue strength reduction characterized by a factor K_f, then: $P_m = S$, $P_b = 0$, $Q = 0$, and $F = P_m\left(K_f - 1\right)$. The total equivalent stress is $P_m + F$.

d) STEP 4 – Determine the principal stresses of the sum of the stress tensors assigned to the equivalent stress categories, and compute the equivalent stress using Equation (B.1.1).

e) STEP 5 – To evaluate protection against plastic collapse, compare the computed equivalent stress to the corresponding allowable value (see paragraph B1.2.2.5).

$$P_m \le S_m \tag{B1.2}$$

$$P_L \le 1.5 S_m \tag{B1.3}$$

$$\left(P_L + P_b\right) \le 1.5 S_m \tag{B1.4}$$

B1.2.2.5 Allowable Equivalent Stress

The allowable equivalent stress, S_m, to be used in conjunction with paragraph B1.2.2.4 in a FFS assessment is established based on type of equipment.

a) Pressure Vessels– The stress from the applicable pressure vessel construction code shall be used for S_m. Alternatively, for vessels constructed to the ASME B&PV Code, Section VIII, Division 1, S_m may be taken from the ASME B&PV Code, Section VIII, Division 2 for use in a Fitness-For-Service assessment if the component has similar design details and NDE prerequisites as originally required for a Division 2 vessel design (see Annex A, paragraph A.2.4).

b) Piping – The allowable stress from the applicable piping construction code (e.g. ASME B31.3) shall be used for S_m.

c) Tankage – The allowable stress from the applicable tank construction code (e.g. API 650) shall be used for S_m.

B1.2.3 Limit-Load Analysis Method

B1.2.3.1 Overview

a) Limit-load analysis can be used to evaluate the protection against plastic collapse for a component. As defined in the following paragraphs, it provides one option to protect a vessel or component from plastic collapse. It may be applied to single or multiple static loading, applied in any specified order. Limit-load analysis provides an alternative to elastic analysis, stress linearization and categorization, and the satisfaction of primary stress limits in paragraphs B1.2.2.

b) Displacements and strains indicated by a limit analysis solution have no physical meaning. If a limit on such variables is required, the procedures in paragraph B1.2.4 shall be used to satisfy these requirements.

c) Protection against plastic collapse using limit load analysis is based on the theory of limit analysis that defines a lower bound to the limit load of a structure as the solution of a numerical model with the following properties:

1) The material model is elastic-perfectly plastic with a specified yield strength.

2) The strain-displacement relations are those of small displacement theory.

3) Equilibrium is satisfied in the un-deformed configuration.

B1.2.3.2 Limitations

The following limitations apply equally to limit-load analysis and to primary stress limits of paragraph B1.2.2.

a) The effect of strain-controlled loads resulting from prescribed non-zero displacements and temperature fields are not considered.
b) Components that experience a reduction in resistance (weakening) with deformation shall be checked with alternate approaches.

B1.2.3.3 Numerical Analysis

The limit load is obtained using a numerical analysis technique (e.g. finite element method) by incorporating an elastic-perfectly-plastic material model and small displacement theory to obtain a solution. The limit load is the load that causes overall structural instability. This point is indicated by the inability to achieve an equilibrium solution for a small increase in load (i.e. the solution will not converge).

B1.2.3.4 Acceptance Criteria

The acceptability of a component using a limit-load analysis is determined by satisfying the following two criteria.

a) Global Criteria – A global plastic collapse load is established by performing a limit-load analysis of the component subject to the specified loading conditions. The plastic collapse load is taken as the limit load that results in overall structural instability. The concept of Load and Resistance Factor Design (LRFD) is used as an alternative to the rigorous computation of a plastic collapse load to design a component. In this procedure, factored loads that include a design factor to account for uncertainty, and the resistance of the component to these factored loads are determined using a limit load analysis (see Table B1.3).
b) Service Criteria – Service criteria as provided by the Owner/User that limit the potential for unsatisfactory performance shall be satisfied at every location in the component when subject to the design loads. The service criteria shall satisfy the requirements of paragraph B1.2.4.3.b using the procedures in paragraph B1.2.4.

B1.2.3.5 Assessment Procedure

The following assessment procedure is used to determine the acceptability of a component using a limit-load analysis.

a) STEP 1 – Develop a numerical model of the component including all relevant geometry characteristics. The model used for the analysis shall be selected to accurately represent the component geometry, boundary conditions, and applied loads. The model need not be accurate for small details, such as small holes, fillets, corner radii, and other stress raisers, but should otherwise correspond to commonly accepted practice.
b) STEP 2 – Define all relevant loads and applicable load cases. The loads to be considered in the analysis shall include, but not be limited to, those given in Table B1.1.
c) STEP 3 – An elastic-perfectly plastic material model with small displacement theory shall be used in the analysis. The von Mises yield function and associated flow rule should be utilized. The yield strength for the elastic-perfectly plastic model shall be set equal to $1.5S_m$.
d) STEP 4 – Determine the load case combinations to be used in the analysis using the information from STEP 2 in conjunction with Table B1.3. Each of the applicable load cases shall be evaluated. The effects of one or more loads not acting shall be investigated. Additional load cases for special conditions not included in Table B1.3 shall be considered, as applicable.
e) STEP 5 – Perform a limit-load analysis for each of the load case combinations defined in STEP 4. If convergence is achieved, the component is stable under the applied loads for this load case. Otherwise, the component configuration (i.e. thickness or configuration) shall be modified or applied loads reduced and the analysis repeated. Note that if the applied loading results in a compressive stress field within the component, buckling may occur, and an evaluation in accordance with paragraph B1.4 may be required.

B1.2.4 Elastic-Plastic Stress Analysis Method

B1.2.4.1 Overview

a) Protection against plastic collapse is evaluated by determining the plastic collapse load of the component using an elastic-plastic stress analysis. The allowable load on the component is established by applying a design factor to the calculated plastic collapse load.

b) Elastic-plastic stress analysis provides a more accurate assessment of the protection against plastic collapse of a component relative to the criteria in paragraphs B1.2.2 and B1.2.3 because the actual structural behavior is more closely approximated. The redistribution of stress that occurs as a result of inelastic deformation (plasticity) and deformation characteristics of the component are considered directly in the analysis.

B1.2.4.2 Numerical Analysis

The plastic collapse load can be obtained using a numerical analysis technique (e.g. finite element method) by incorporating an elastic-plastic material model to obtain a solution. The effects of non-linear geometry shall be considered in this analysis. The plastic collapse load is the load that causes overall structural instability. This point is indicated by the inability to achieve an equilibrium solution for a small increase in load (i.e. the solution will not converge).

B1.2.4.3 Acceptance Criteria

The acceptability of a component using an elastic-plastic analysis is determined by satisfying the following two criteria.

a) Global Criteria – A global plastic collapse load is established by performing an elastic-plastic analysis of the component subject to the specified loading conditions. The plastic collapse load is taken as the load that results in overall structural instability. The concept of Load and Resistance Factor Design (LRFD) is used to evaluate load combinations on the component. In this procedure, factored loads that include a design factor to account for uncertainty, and the resistance of the component to these factored loads is determined using an elastic-plastic stress analysis (see Table B1.4).

b) Service Criteria – Service criteria as provided by the Owner/User that limit the potential for unsatisfactory performance shall be satisfied at every location in the component when subject to the design loads (see Table B1.4). Examples of service criteria are limits on the rotation of a mating flange pair to avoid possible flange leakage concerns and limits on tower deflection that may cause operational concerns. In addition, the effect of deformation of the component on service performance shall be evaluated at the design load combinations. This is especially important for components that experience an increase in resistance (geometrically stiffen) with deformation under applied loads such as elliptical or torispherical heads subject to internal pressure loading. The plastic collapse criteria may be satisfied but the component may have excessive deformation at the derived design conditions. In this case, the design loads may have to be reduced based on a deformation criterion. Examples of some of the considerations in this evaluation are the effect of deformation on:

   1) piping connections,

   2) misalignment of trays, platforms and other internal or external appurtenances, and

   3) interference with adjacent structures and equipment.

B1.2.4.4 Assessment Procedure

The following assessment procedure is used to determine the acceptability of a component using an elastic-plastic stress analysis.

a) STEP 1 – Develop a numerical model of the component including all relevant geometry characteristics. The model used for the analysis shall be selected to accurately represent the component geometry, boundary conditions, and applied loads. In addition, refinement of the model around areas of stress and strain concentrations shall be considered. The analysis of one or more analytical models may be required to ensure that an accurate description of the stress and strains in the component is achieved.

b) STEP 2 – Define all relevant loads and applicable load cases (see Tables B1.1). The loads to be considered in the design shall include, but not be limited to, those given in Table B1.1.

c) STEP 3 – An elastic-plastic material model shall be used in the analysis. The von Mises yield function and associated flow rule should be utilized if plasticity is anticipated. A material model that includes hardening or softening, or an elastic-perfectly plastic model may be utilized. A true stress-strain curve model that includes temperature dependent hardening behavior is provided in Annex F. When using this material model, the hardening behavior shall be included up to the true ultimate stress and perfect plasticity behavior (i.e. the slope of the stress-strain curves is zero) beyond this limit. . The effects of non-linear geometry shall be considered in the analysis.

d) STEP 4 – Determine the load case combinations to be used in the analysis using the information from STEP 2 in conjunction with Table B1.4. Each of the applicable load cases shall be evaluated. The effects of one or more loads not acting shall be investigated. Additional load cases for special conditions not included in Table B1.4 shall be considered, as applicable.

e) STEP 5 – Perform an elastic-plastic analysis for each of the load cases defined in STEP 4. If convergence is achieved, the component is stable under the applied loads for this load case. Otherwise, the component configuration (i.e. thickness) shall be modified or applied loads reduced and the analysis repeated. Note that if the applied loading results in a compressive stress field within the component, buckling may occur, and an evaluation in accordance with paragraph B1.4 may be required.

B1.3 Protection Against Local Failure

B1.3.1 Overview

B1.3.1.1 In addition to demonstrating protection against plastic collapse as defined in paragraph B1.2, the applicable local failure criteria below shall be satisfied for a component. The strain limit criterion typically does not need to be evaluated if the component design is in accordance with the applicable construction code and the presence of a flaw does not result in a significant strain concentration. If the significance of a strain concentration cannot be established, then the strain limit criterion should be evaluated as part of the assessment.

B1.3.1.2 Two analysis methodologies are provided for evaluating protection against local failure to limit the potential for fracture under applied design loads.

a) The analysis procedures in paragraph B1.3.2 provide an approximation of the protection against local failure based on the results of an elastic analysis.

b) A more accurate estimate of the protection against local failure of a component can be obtained using the elastic-plastic stress analysis procedures in paragraph B1.3.3.

B1.3.2 Elastic Analysis

In addition to demonstrating protection against plastic collapse, the following elastic analysis criterion shall be satisfied for each point in the component. The sum of the local primary membrane plus bending principal stresses shall be used for checking this criterion.

$$\left(\sigma_1 + \sigma_2 + \sigma_3\right) \le 4S_m \qquad \text{(B1.5)}$$

B1.3.3 Elastic-Plastic Analysis

B1.3.3.1 The following procedure can be used to evaluate protection against local failure for a sequence of applied loads.

a) STEP 1 – Perform an elastic-plastic stress analysis based on the load case combinations for the local criteria given in Table B1.4. The effects of non-linear geometry shall be considered in the analysis.

b) STEP 2 – For a location in the component subject to evaluation, determine the principal stresses, σ_1, σ_2, σ_3, the equivalent stress using Equation (B1.1), σ_e, and the total equivalent plastic strain, ε_{peq}.

c) STEP 3 – Determine the limiting triaxial strain, ε_L, using Equation (B1.6). In this equation ε_{Lu}, m_2, and α_{sl} are determined from Table B1.6.

$$\varepsilon_L = \varepsilon_{Lu} \cdot \exp\left[-\left(\frac{\alpha_{sl}}{1+m_2} \right) \left(\left\{ \frac{(\sigma_1 + \sigma_2 + \sigma_3)}{3\sigma_e} \right\} - \frac{1}{3} \right) \right] \quad \text{(B1.6)}$$

d) STEP 4 – Determine the forming strain ε_{cf} based on the material and fabrication method in accordance with the applicable construction code. If heat treatment is performed in accordance with the applicable construction code, the forming strain may be assumed to be zero.

e) STEP 5 – Determine if the strain limit is satisfied. The location in the component is acceptable for the specified load case if Equation (B1.7) is satisfied.

$$\varepsilon_{peq} + \varepsilon_{cf} \le \varepsilon_L \quad \text{(B1.7)}$$

B1.3.3.2 If a specific loading sequence is to be evaluated in accordance with the Owner-user's Specification, a strain limit damage calculation procedure is required. This procedure may also be used in lieu of the procedure in B1.3.3.1. In this procedure, the loading path is divided into k load increments and the principal stresses, $\sigma_{1,k}$, $\sigma_{2,k}$, $\sigma_{3,k}$, equivalent stress, $\Delta\sigma_{e,k}$, and change in the equivalent plastic strain from the previous load increment, $\Delta\varepsilon_{peq,k}$, are calculated for each load increment. The strain limit for the k^{th} load increment, $\varepsilon_{L,k}$, is calculated using Equation (B1.8) where, ε_{Lu}, m_2, and α_{sl} are determined from Table B1.6. The strain limit damage for each load increment is calculated using Equation (B1.9). The strain limit damage from forming, $D_{\varepsilon form}$, is calculated using Equation (B1.10). If heat treatment is performed in accordance with the applicable construction code, the strain limit damage from forming is assumed to be zero. The accumulated strain limit damage is calculated using Equation (B1.11). The location in the component is acceptable for the specified loading sequence if this equation is satisfied.

$$\varepsilon_{L,k} = \varepsilon_{Lu} \cdot \exp\left[-\left(\frac{\alpha_{sl}}{1+m_2} \right) \left(\left\{ \frac{(\sigma_{1,k} + \sigma_{2,k} + \sigma_{3,k})}{3\sigma_{e,k}} \right\} - \frac{1}{3} \right) \right] \quad \text{(B1.8)}$$

$$D_{\varepsilon,k} = \frac{\Delta\varepsilon_{peq,k}}{\varepsilon_{L,k}} \quad \text{(B1.9)}$$

$$D_{\varepsilon form} = \frac{\varepsilon_{cf}}{\varepsilon_{Lu} \cdot \exp\left[-0.67 \left(\frac{\alpha_{sl}}{1+m_2} \right) \right]} \quad \text{(B1.10)}$$

$$D_{\varepsilon} = D_{\varepsilon form} + \sum_{k=1}^{M} D_{\varepsilon,k} \le 1.0 \quad \text{(B1.11)}$$

B1.4 Protection Against Collapse From Buckling

B1.4.1 Design Factors

B1.4.1.1 In addition to evaluating protection against plastic collapse as defined in paragraph B1.2, an in-service margin for protection against collapse from buckling shall be satisfied to avoid structural instability of components with a compressive stress field under applied design loads. The in-service margin or buckling factor to be used in a structural stability assessment is based on the type of buckling analysis performed. The following in-service margins are the minimum recommended for use with shell components when the buckling loads are determined using a numerical solution (i.e. bifurcation buckling analysis or elastic-plastic collapse analysis).

a) Type 1 – If a bifurcation buckling analysis is performed using an elastic stress analysis without geometric nonlinearities in the solution to determine the pre-stress in the component, a minimum buckling factor of $\Phi_B = 2/\beta_{cr}$ shall be used (see paragraph B1.4.1.3). In this analysis, the pre-stress in the component is established based on the loading combinations in Table B1.2.

b) Type 2 – If a bifurcation buckling analysis is performed using an elastic-plastic stress analysis with the effects of non-linear geometry in the solution to determine the pre-stress in the component, a minimum buckling factor of $\Phi_B = 1.667/\beta_{cr}$ shall be used (see paragraph B1.4.1.3). In this analysis, the pre-stress in the component is established based on the loading combinations in Table B1.2.

c) Type 3 – If a collapse analysis is performed in accordance with paragraph B1.2.4, and imperfections are explicitly considered in the analysis model geometry, the buckling factor is accounted for in the factored load combinations in Table B1.4. It should be noted that a collapse analysis may be performed using either elastic or elastic-plastic material behavior. In general it is recommended to use an elastic-plastic material model. If the structure remains elastic when subject to the applied loads, the elastic-plastic material model will provide the required elastic behavior, and the collapse load will be computed based on this behavior. Recommendations on including imperfections in a stability analysis are provided in reference [6].

B1.4.1.2 To account for imperfections, the capacity reduction factors, β_{cr}, shown below shall be used unless alternative factors can be developed from published information.

a) For unstiffened or ring stiffened cylinders and cones under axial compression

$$\beta_{cr} = 0.207 \qquad for \qquad \frac{D_o}{t} \geq 1247 \tag{B1.12}$$

$$\beta_{cr} = \frac{338}{389 + \frac{D_o}{t}} \qquad for \qquad \frac{D_o}{t} < 1247 \tag{B1.13}$$

b) For unstiffened and ring stiffened cylinders and cones under external pressure

$$\beta_{cr} = 0.80 \tag{B1.14}$$

c) For spherical shells and spherical, torispherical, elliptical heads under external pressure

$$\beta_{cr} = 0.124 \tag{B1.15}$$

B1.4.1.3 If the structural stability analysis is based on the results obtained from an elastic stress analysis (see paragraph B1.4.1.1), then the allowable compressive stress criteria in Annex A, paragraph A.4.14 may be used in the assessment.

B1.4.2 Numerical Analysis

If a numerical analysis is performed to determine the buckling load for a component, all possible buckling mode shapes shall be considered in determining the minimum buckling load for the component. Care should be taken to ensure that simplification of the model does not result in exclusion of a critical buckling mode shape. For example, when determining the minimum buckling load for a ring-stiffened cylindrical shell, both axisymmetric and non-axisymmetric buckling modes shall be considered in determination of the minimum buckling load.

B1.4.3 Structural Stability For Components With Flaws

B1.4.3.1 Assessment of the structural stability of a component with flaws should consider growth aspects and remaining life. The location, size and reduced thickness associated with a flaw will affect the structural stability of a component. Therefore, the assessment should be performed for the flaw size at the end of its useful life. For volumetric-type flaws, account should be taken of the possibility of increased metal loss and expansion of the corroded area with time. For crack-like flaws, account should be taken of the possibility of crack growth by fatigue, corrosion-fatigue, stress corrosion cracking and creep.

B1.4.3.2 The significance of planar flaws parallel to a plate or shell surface in the direction of compressive stress (laminations, laminar tears, etc.) should be assessed by checking the buckling strength of each part of the material between the flaw and the component surface. This may be done by calculation as if the individual parts of the material are separate plates of the same area as the flaw using the distance between the flaw and the surface as an effective thickness.

B1.4.3.3 If a flaw occurs parallel to the surface under the weld attaching a stiffener to a shell or plate loaded in compression, it will reduce the effective length over which the stiffener is attached to the plate. If a flaw of this type is located, it should be assessed assuming that the stiffener is intermittently welded to the plate and that the flaw forms a "space" between two welds. Rules for determining the allowable weld spacing for stiffener attachment from the original design code may be used in this evaluation.

B1.4.3.4 The allowable compressive stress for a shell component with a flaw can be established using the compressive stress equations in Annex A, paragraph A.4.14. The thickness to be used in the compressive stress calculation should be the minimum thickness less any future corrosion allowance unless another thickness can be justified.

B1.5 Protection Against Failure From Cyclic Loading

B1.5.1 Overview

B1.5.1.1 A fatigue evaluation shall be performed if the component is subject to cyclic operation. The evaluation for fatigue is made on the basis of the number of applied cycles of a stress or strain range at a point in the component. The allowable number of cycles should be adequate for the specified duration of operation to determine the suitability for continued operation.

B1.5.1.2 Screening criteria are provided in paragraph B1.5.2 that can be used to determine if fatigue analysis is required as part of an assessment. If the component does not satisfy the screening criteria, a fatigue evaluation shall be performed using the techniques in paragraphs B1.5.3, B1.5.4 or B1.5.5.

B1.5.1.3 Fatigue curves are typically presented in two forms: fatigue curves that are based on smooth bar test specimens and fatigue curves that are based on test specimens that include weld details of quality consistent with the fabrication and inspection requirements of the original construction code.

a) Smooth bar fatigue curves may be used for components with or without welds. The welded joint fatigue curves shall only be used for welded joints.
b) The smooth bar fatigue curves are applicable up to the maximum number of cycles given on the curves. The welded joint fatigue curves do not exhibit an endurance limit and are acceptable for all cycles.

c) If welded joint fatigue curves are used in the evaluation, and if thermal transients result in a through-thickness stress difference at any time that is greater than the steady state difference, the number of permissible cycles shall be determined as the smaller of the number of cycles for the base metal established using either paragraph B1.5.3 or B1.5.4, and for the weld established in accordance with paragraph B1.5.5.

B1.5.1.4 Stresses and strains produced by any load or thermal condition that does not vary during the cycle need not be considered in a fatigue analysis if the fatigue curves utilized in the evaluation are adjusted for mean stresses and strains. The design fatigue curves referenced in paragraph B1.5.3 and B1.5.4 are based on smooth bar test specimens and are adjusted for the maximum possible effect of mean stress and strain; therefore, an adjustment for mean stress effects is not required. The fatigue curve referenced in paragraph B1.5.5 is based on welded test specimens and includes explicit adjustments for thickness and mean stress effects.

B1.5.1.5 Under certain combinations of steady state and cyclic loadings there is a possibility of ratcheting. A rigorous evaluation of ratcheting normally requires an elastic-plastic analysis of the component; however, under a limited number of loading conditions, an approximate analysis can be utilized based on the results of an elastic stress analysis, see paragraph B1.5.6.

B1.5.1.6 Protection against ratcheting shall be considered for all operating loads considered in the assessment and shall be performed even if the fatigue screening criteria are satisfied (see paragraph B1.5.1.2). Protection against ratcheting is satisfied if one of the following three conditions is met:

a) The loading results in only primary stresses without any cyclic secondary stresses.
b) Elastic Stress Analysis Criteria – Protection against ratcheting is demonstrated by satisfying the rules of paragraph B1.5.6.
c) Elastic-Plastic Stress Analysis Criteria – Protection against ratcheting is demonstrated by satisfying the rules of paragraph B1.5.7.

B1.5.2 Screening Criteria For Fatigue

B1.5.2.1 Overview

a) The provisions of this paragraph can be used to determine if a fatigue analysis is required as part of the vessel design. The screening options to determine the need for fatigue analyses are described below. If any one of the screening options is satisfied, then a fatigue analysis is not required as part of the vessel design.
    1) Provisions of paragraph B1.5.2.2 – Experience with comparable equipment operating under similar conditions.
    2) Provisions of paragraph B1.5.2.3 – Method A based on the materials of construction (limited applicability), construction details, loading histogram, and smooth bar fatigue curve data.
    3) Provisions of paragraph B1.5.2.4 – Method B based on the materials of construction (unlimited applicability), construction details, loading histogram, and smooth bar fatigue curve data.
b) The fatigue exemption in accordance with this paragraph is performed on a component or part basis. One component (integral) may be exempt, while another component (non-integral) is not exempt. If any one component is not exempt, then a fatigue evaluation shall be performed for that component.
c) If the specified number of cycles is greater than $(10)^6$, then the screening criteria are not applicable and a fatigue analysis is required.

B1.5.2.2 Fatigue Analysis Screening Based On Experience with Comparable Equipment

If successful experience over a sufficient time frame is obtained and documented with comparable equipment subject to a similar loading histogram, then a fatigue analysis is not required as part of the vessel design. When evaluating experience with comparable equipment operating under similar conditions as related to the design and service contemplated, the possible harmful effects of the following design features shall be evaluated.

a) The use of non-integral construction, such as the use of pad type reinforcements or of fillet welded attachments, as opposed to integral construction

b) The use of pipe threaded connections, particularly for diameters in excess of 70 mm (2.75 in.)
c) The use of stud bolted attachments
d) The use of partial penetration welds
e) Major thickness changes between adjacent members
f) Attachments and nozzles in the knuckle region of formed heads
g) Components with a flaw characterized by a Remaining Strength Factor determined in accordance with Part 5, Part 6, Part 7, Part 8, or Part 12

B1.5.2.3 Fatigue Analysis Screening – Method A

The following procedure can only be used for materials with a specified minimum tensile strength that is less than or equal to 552 MPa (80,000 psi).

a) STEP 1 – Determine a load history as defined in paragraph B1.1.3.3. The load history should include all cyclic operating loads and events that are applied to the component.
b) STEP 2 – Based on the load history in STEP 1, determine the expected (design) number of full-range pressure cycles including startup and shutdown, and designate this value as $N_{\Delta FP}$.
c) STEP 3 – Based on the load history in STEP 1, determine the expected number of operating pressure cycles in which the range of pressure variation exceeds 20% of the design pressure for integral construction or 15% of the design pressure for non-integral construction, and designate this value as $N_{\Delta PO}$. Pressure cycles in which the pressure variation does not exceed these percentages of the design pressure and pressure cycles caused by fluctuations in atmospheric conditions do not need to be considered in this evaluation.
d) STEP 4 – Based on the load history in STEP 1, determine the effective number of changes in metal temperature difference between any two adjacent points, ΔT_E, as defined below, and designate this value as $N_{\Delta TE}$. The effective number of such changes is determined by multiplying the number of changes in metal temperature difference of a certain magnitude by the factor given in Table B1.7, and by adding the resulting numbers. In calculating the temperature difference between adjacent points, conductive heat transfer shall be considered only through welded or integral cross sections with no allowance for conductive heat transfer across un-welded contact surfaces (i.e. vessel shell and reinforcing pad). Temperature cycles caused by fluctuations in atmospheric conditions, do not need to be considered in this evaluation.
    1) For surface temperature differences, points are considered to be adjacent if they are within the distance L computed as follows: for shells and dished heads in the meridional or circumferential directions,

$$L = 2.5\sqrt{Rt} \qquad \text{(B1.16)}$$

and for flat plates,

$$L = 3.5a \qquad \text{(B1.17)}$$

    2) For through-the-thickness temperature differences, adjacent points are defined as any two points on a line normal to any surface in the component.
e) STEP 5 – Based on the load history in STEP 1, determine the number of temperature cycles for components involving welds between materials having different coefficients of thermal expansion that causes the value of $(\alpha_1 - \alpha_2)\Delta T$ to exceed 0.00034, and designate this value as $N_{\Delta T\alpha}$.
f) STEP 6 – If the expected number of operating cycles from STEPs 2, 3, 4 and 5 satisfy the criterion in Table B1.8, then a fatigue analysis is not required as part of the vessel design. If this criterion is not satisfied, then a fatigue analysis is required as part of the vessel design. Examples of non-integral attachments are: screwed-on caps, screwed-in plugs, fillet welded attachments, shear ring closures, and breech lock closures. Components with a flaw are characterized by a Remaining Strength Factor, RSF, determined in accordance with Part 5, Part 6, Part 7, Part 8, or Part 12.

B1.5.2.4 Fatigue Analysis Screening – Method B

The following procedure can be used for all materials.

a) STEP 1 – Determine a load history based on the information in paragraph B1.1.3.3. The load histogram should include all significant cyclic operating loads and events that the component will be subjected to. Note, in Equation (B1.18), the number of cycles from the applicable design fatigue curve (see Annex F) evaluated at a stress amplitude of S is defined as $N(S)$. Also in Equations (B1.19) through (B1.23), the stress amplitude from the applicable design fatigue curve (see Annex F) evaluated at N cycles is defined as $S_a(N)$.

b) STEP 2 – Determine the fatigue screening criteria factors, C_1 and C_2, based on the type of construction in accordance with Table B1.9.

c) STEP 3 – Based on the load histogram in STEP 1, determine the design number of full-range pressure cycles including startup and shutdown, $N_{\Delta FP}$. If the following equation is satisfied, proceed to STEP 4; otherwise, a detailed fatigue analysis of the vessel is required.

$$N_{\Delta FP} \le N\left(C_1 S_m\right) \tag{B1.18}$$

d) STEP 4 – Based on the load histogram in STEP 1, determine the maximum range of pressure fluctuation during normal operation, excluding startups and shutdowns, ΔP_N, and the corresponding number of significant cycles, $N_{\Delta P}$. Significant pressure fluctuation cycles are defined as cycles where the pressure range exceeds $S_{as}/3S_m$ times the design pressure. If the following equation is satisfied, proceed to STEP 5; otherwise, a detailed fatigue analysis of the vessel is required.

$$\Delta P_N \le \frac{p}{C_1}\left(\frac{S_a\left(N_{\Delta P}\right)}{S_m}\right) \tag{B1.19}$$

e) STEP 5 – Based on the load histogram in STEP 1, determine the maximum temperature difference between any two adjacent points (see paragraph B1.5.2.3.d) of the vessel during normal operation, and during startup and shutdown operation, ΔT_N, and the corresponding number of cycles, $N_{\Delta TN}$. If the following equation is satisfied, proceed to STEP 6; otherwise, a detailed fatigue analysis of the vessel is required.

$$\Delta T_N \le \left(\frac{S_a\left(N_{\Delta TN}\right)}{C_2 E_{ym}\alpha}\right) \tag{B1.20}$$

f) STEP 6 – Based on the load histogram in STEP 1, determine the maximum range of temperature difference fluctuation, ΔT_R, between any two adjacent points (see paragraph B1.5.2.3.d) of the vessel during normal operation, excluding startups and shutdowns, and the corresponding number of significant cycles, $N_{\Delta TR}$. Significant temperature difference fluctuation cycles for this step are defined as cycles where the temperature range exceeds $S_{as}/2E_{ym}\alpha$. If the following equation is satisfied, proceed to STEP 7; otherwise, a detailed fatigue analysis of the vessel is required.

$$\Delta T_R \le \left(\frac{S_a\left(N_{\Delta TR}\right)}{C_2 E_{ym}\alpha}\right) \tag{B1.21}$$

g) STEP 7 – Based on the load histogram in STEP 1, determine the range of temperature difference fluctuation between any two adjacent points (see paragraph B1.5.2.3.d) for components fabricated from different materials of construction during normal operation, ΔT_M , and the corresponding number of significant cycles, $N_{\Delta TM}$. Significant temperature difference fluctuation cycles for this step are defined as cycles where the temperature range exceeds $S_{as} \Big/ \left[2\left(E_{y1}\alpha_1 - E_{y2}\alpha_2 \right) \right]$. If the following equation is satisfied, proceed to STEP 8; otherwise, a detailed fatigue analysis of the vessel is required.

$$\Delta T_M \le \left(\frac{S_a\left(N_{\Delta TM}\right)}{C_2\left(E_{y1}\alpha_1 - E_{y2}\alpha_2\right)} \right) \qquad \text{(B1.22)}$$

h) STEP 8 – Based on the load histogram in STEP 1, determine the equivalent stress range computed from the specified full range of mechanical loads, excluding pressure but including piping reactions, ΔS_{ML} , and the corresponding number of significant cycles, $N_{\Delta S}$. Significant mechanical load range cycles for this step are defined as cycles where the stress range exceeds S_{as} . If the total specified number of significant load fluctuations exceeds the maximum number of cycles defined on the applicable fatigue curve, the S_{as} value corresponding to the maximum number of cycles defined on the fatigue curve shall be used. If the following equation is satisfied a fatigue analysis is not required; otherwise, a detailed fatigue analysis of the vessel is required.

$$\Delta S_{ML} \le S_a\left(N_{\Delta S}\right) \qquad \text{(B1.23)}$$

B1.5.3 Fatigue Assessment – Elastic Stress Analysis and Equivalent Stresses

B1.5.3.1 Overview

a) The effective total equivalent stress amplitude is used to evaluate the fatigue damage for results obtained from a linear elastic stress analysis. The controlling stress for the fatigue evaluation is the effective total equivalent stress amplitude, defined as one-half of the effective total equivalent stress range $\left(P_L + P_b + Q + F\right)$ calculated for each cycle in the loading histogram.

b) The primary plus secondary plus peak equivalent stress (see Figure B1.1) is the equivalent stress, derived from the highest value across the thickness of a section, of the combination of all primary, secondary, and peak stresses produced by specified operating pressures and other mechanical loads and by general and local thermal effects and including the effects of gross and local structural discontinuities. Examples of load case combinations for this stress category for typical pressure vessel components are shown in Table B1.5.

B1.5.3.2 Assessment Procedure

The following procedure can be used to evaluate protection against failure due to cyclic loading based on the effective total equivalent stress amplitude.

a) STEP 1 – Determine a load history based on the information in paragraph B1.1.1.3 and the methods in Annex B2. The load history should include all significant operating loads and events that are applied to the component. If the exact sequence of loads is not known, alternatives should be examined to establish the most severe fatigue damage, see STEP 6.

b) STEP 2 – For a location in the component subject to a fatigue evaluation, determine the individual stress-strain cycles using the cycle counting methods in Annex B2. Define the total number of cyclic stress ranges in the histogram as M .

c) STEP 3 – Determine the equivalent stress range for the k^{th} cycle counted in STEP 2.

1) If the effective alternating equivalent stress is computed using Equation (B1.30), then determine the stress tensor at the start and end points (time points ${}^{m}t$ and ${}^{n}t$, respectively) for the k^{th} cycle counted in STEP 2, Determine the local thermal stress at time points ${}^{m}t$ and ${}^{n}t$, ${}^{m}\sigma_{ij,k}^{LT}$ and ${}^{n}\sigma_{ij,k}^{LT}$, respectively, as described in Annex B3. The component stress ranges between time points ${}^{m}t$ and ${}^{n}t$ and the effective equivalent stress range for use in Equation (B1.30) are calculated using Equations (B1.24) through (B1.27).

$$\Delta\sigma_{ij,k} = \left({}^{m}\sigma_{ij,k} - {}^{m}\sigma_{ij,k}^{LT}\right) - \left({}^{n}\sigma_{ij,k} - {}^{n}\sigma_{ij,k}^{LT}\right) \tag{B1.24}$$

$$\left(\Delta S_{P,k} - \Delta S_{LT,k}\right) = \frac{1}{\sqrt{2}}\left[\begin{array}{l}\left(\Delta\sigma_{11,k} - \Delta\sigma_{22,k}\right)^2 + \left(\Delta\sigma_{11,k} - \Delta\sigma_{33,k}\right)^2 + \\ \left(\Delta\sigma_{22,k} - \Delta\sigma_{33,k}\right)^2 + 6\left(\Delta\sigma_{12,k}^2 + \Delta\sigma_{13,k}^2 + \Delta\sigma_{23,k}^2\right)\end{array}\right]^{0.5} \tag{B1.25}$$

$$\Delta\sigma_{ij,k}^{LT} = {}^{m}\sigma_{ij,k}^{LT} - {}^{n}\sigma_{ij,k}^{LT} \tag{B1.26}$$

$$\Delta S_{LT,k} = \frac{1}{\sqrt{2}}\left[\left(\Delta\sigma_{11,k}^{LT} - \Delta\sigma_{22,k}^{LT}\right)^2 + \left(\Delta\sigma_{11,k}^{LT} - \Delta\sigma_{33,k}^{LT}\right)^2 + \left(\Delta\sigma_{22,k}^{LT} - \Delta\sigma_{33,k}^{LT}\right)^2\right]^{0.5} \tag{B1.27}$$

2) If the effective alternating equivalent stress is computed using Equation (B.1.35), then determine the stress tensor at the start and end points (time points ${}^{m}t$ and ${}^{n}t$, respectively) for the k^{th} cycle counted in STEP 2, The component stress ranges between time points ${}^{m}t$ and ${}^{n}t$, and the effective equivalent stress range for use in Equation (B1.35) are given by Equations (B1.28) and (B1.29), respectively.

$$\Delta\sigma_{ij,k} = {}^{m}\sigma_{ij,k} - {}^{n}\sigma_{ij,k} \tag{B1.28}$$

$$\Delta S_{P,k} = \frac{1}{\sqrt{2}}\left[\begin{array}{l}\left(\Delta\sigma_{11,k} - \Delta\sigma_{22,k}\right)^2 + \left(\Delta\sigma_{11,k} - \Delta\sigma_{33,k}\right)^2 + \\ \left(\Delta\sigma_{22,k} - \Delta\sigma_{33,k}\right)^2 + 6\left(\Delta\sigma_{12,k}^2 + \Delta\sigma_{13,k}^2 + \Delta\sigma_{23,k}^2\right)\end{array}\right]^{0.5} \tag{B1.29}$$

d) STEP 4 – Determine the effective alternating equivalent stress for the k^{th} cycle using the results from STEP 3.

$$S_{alt,k} = \frac{K_f \cdot K_{e,k} \cdot \left(\Delta S_{P,k} - \Delta S_{LT,k}\right) + K_{v,k} \cdot \Delta S_{LT,k}}{2} \tag{B1.30}$$

1) If the local notch or effect of the weld is accounted for in the numerical model, then $K_f = 1.0$ in Equations (B1.30) and (B1.35). If the local notch or effect of the weld is not accounted for in the analytical model, then a fatigue strength reduction factor, K_f, shall be included. Recommended values for fatigue strength reduction factors for welds are provided in Tables B.10 and B.11.

2) The fatigue penalty factor, $K_{e,k}$, is evaluated using the equations shown below. In these equations, the parameters m and n are determined from Table B1.12, and S_{PS} and $\Delta S_{n,k}$ are defined in paragraph B1.5.6.1. If $K_{e,k} > 1.0$, then the simplified elastic-plastic criteria of paragraph B1.5.6.2 shall be satisfied.

$$K_{e,k} = 1.0 \qquad for\ \Delta S_{n,k} \le S_{PS} \tag{B1.31}$$

$$K_{e,k} = 1.0 + \frac{(1-n)}{n(m-1)}\left(\frac{\Delta S_{n,k}}{S_{PS}} - 1\right) \qquad for\ S_{PS} < \Delta S_{n,k} < mS_{PS} \tag{B1.32}$$

$$K_{e,k} = \frac{1}{n} \qquad for\ \Delta S_{n,k} \ge mS_{PS} \tag{B1.33}$$

3) The Poisson correction factor, $K_{v,k}$ in Equation (B1.30) is computed using Equation (B1.34).

$$K_{v,k} = 0.5 - 0.2\left(\frac{S_{y,k}}{S_{a,k}}\right) \tag{B1.34}$$

4) The Poisson correction factor, $K_{v,k}$, in Equation (B1.34) need not be used if the fatigue penalty factor, $K_{e,k}$, is used for the entire stress range (including $\Delta S_{LT,k}$). In this case, Equation (B1.30) becomes:

$$S_{alt,k} = \frac{K_f \cdot K_{e,k} \cdot \Delta S_{P,k}}{2} \tag{B1.35}$$

e) STEP 5 – Determine the permissible number of cycles, N_k, for the alternating equivalent stress computed in STEP 4. Fatigue curves based on the materials of construction are provided in Annex F.

f) STEP 6 – Determine the fatigue damage for the k^{th} cycle, where the actual number of repetitions of the k^{th} cycle is n_k.

$$D_{f,k} = \frac{n_k}{N_k} \tag{B1.36}$$

g) STEP 7 – Repeat STEPs 3 through 6 for all stress ranges, M, identified in the cycle counting process in STEP 2.

h) STEP 8 – Compute the accumulated fatigue damage using the following equation. The location in the component is acceptable for continued operation if this equation is satisfied.

$$D_f = \sum_{k=1}^{M} D_{f,k} \le 1.0 \tag{B1.37}$$

i) STEP 9 – Repeat STEPs 2 through 8 for each point in the component subject to a fatigue evaluation.

B1.5.3.3 In STEP 4 of paragraph B1.5.3.2, $K_{e,k}$, may be calculated using one of the following methods.

a) Method 1 – The equivalent total strain range from elastic-plastic analysis and the equivalent total strain range from elastic analysis for the point of interest as given below.

$$K_{e,k} = \frac{\left(\Delta\varepsilon_{t,k}\right)_{ep}}{\left(\Delta\varepsilon_{t,k}\right)_{e}} \tag{B1.38}$$

where,

$$\left(\Delta\varepsilon_{t,k}\right)_{ep} = \frac{\sqrt{2}}{3}\left[\begin{array}{l}\left(\Delta e_{11,k} - \Delta e_{22,k}\right)^2 + \left(\Delta e_{22,k} - \Delta e_{33,k}\right)^2 + \\ \left(\Delta e_{33,k} - \Delta e_{11,k}\right)^2 + 1.5\left(\Delta e_{12,k}^2 + \Delta e_{23,k}^2 + \Delta e_{31,k}^2\right)\end{array}\right]^{0.5} \quad \text{(B1.39)}$$

$$\left(\Delta\varepsilon_{t,k}\right)_{e} = \frac{\Delta S_{P,k}}{E_{ya,k}} \quad \text{(B1.40)}$$

The stress range $\Delta S_{P,k}$ is given by Equation (B1.29).

b) Method 2 – The alternate plasticity adjustment factors and alternating equivalent stress may be computed using Annex B4.

B1.5.4 Fatigue Assessment – Elastic-Plastic Stress Analysis and Equivalent Strain

B1.5.4.1 Overview

a) The effective strain range is used to evaluate the fatigue damage for results obtained from an elastic-plastic stress analysis. The Effective Strain Range is calculated for each cycle in the loading histogram using either cycle-by-cycle analysis or the Twice Yield Method. For the cycle-by-cycle analysis, a cyclic plasticity algorithm with kinematic hardening shall be used.

b) The Twice Yield Method is an elastic-plastic stress analysis performed in a single loading step, based on a specified stabilized cyclic stress range-strain range curve and a specified load range representing a cycle. Stress and strain ranges are the direct output from this analysis. This method is performed in the same manner as a monotonic analysis and does not require cycle-by-cycle analysis of unloading and reloading. The Twice Yield Method can be used with an analysis program without cyclic plasticity capability.

c) For the calculation of the stress range and strain range of a cycle at a point in the component, a stabilized cyclic stress-strain curve and other material properties shall be used based on the average temperature of the cycle being evaluated for each material of construction. The cyclic curve may be that obtained by test for the material, or that which is known to have more conservative cyclic behavior to the material that is specified. Cyclic stress-strain curves are also provided in Annex F for certain materials and temperatures. Other cyclic stress-strain curves may be used that are known to be either more accurate for the application or lead to more conservative results.

B1.5.4.2 Assessment Procedure

The following procedure can be used to evaluate protection against failure due to cyclic loading using elastic-plastic stress analysis.

a) STEP 1 – Determine a load history based on the information in paragraph B1.1.1.3 and the methods in Annex B2. The load history should include all significant operating loads and events that are applied to the component.

b) STEP 2 – For a location in the component subject to a fatigue evaluation, determine the individual stress-strain cycles using the cycle counting methods in Annex B2. Define the total number of cyclic stress ranges in the histogram as M .

c) STEP 3 – Determine the loadings at the start and end points of the k^{th} cycle counted in STEP 2. Using these data, determine the loading ranges (differences between the loadings at the start and end points of the cycle).

d) STEP 4 – Perform elastic-plastic stress analysis for the k^{th} cycle. For cycle-by-cycle analysis, constant-amplitude loading is cycled using cyclic stress amplitude-strain amplitude curve (paragraph B1.5.4.1.c). For the Twice Yield Method, the loading at the start point of the cycle is zero and the loading at the end point is the loading range determined in STEP 3. The cyclic stress range-strain range curve or hysteresis loop stress-strain curve (see Annex F, paragraph F.2.4) is used in the analysis. For thermal loading, the loading range in Twice-Yield Method may be applied by specifying the temperature field at the start point for the cycle as an initial condition, and applying the temperature field at the end point for the cycle in a single loading step.

e) STEP 5 – Calculate the effective strain range for the k^{th} cycle.

$$\Delta\varepsilon_{eff,k} = \frac{\Delta S_{P,k}}{E_{ya,k}} + \Delta\varepsilon_{peq,k} \tag{B1.41}$$

where, the stress range $\Delta S_{P,k}$ is given by Equation (B1.29).

$$\Delta\varepsilon_{peq,k} = \frac{\sqrt{2}}{3}\left[\begin{array}{l}\left(\Delta p_{11,k} - \Delta p_{22,k}\right)^2 + \left(\Delta p_{22,k} - \Delta p_{33,k}\right)^2 + \\ \left(\Delta p_{33,k} - \Delta p_{11,k}\right)^2 + 1.5\left(\Delta p_{12,k}^2 + \Delta p_{23,k}^2 + \Delta p_{31,k}^2\right)\end{array}\right]^{0.5} \tag{B1.42}$$

The component stress and plastic strain ranges (differences between the components at the start and end points of the cycle) for the k^{th} cycle are designated as $\Delta\sigma_{ij,k}$ and $\Delta p_{ij,k}$, respectively. However, since a range of loading is applied in a single load step with the Twice Yield Method, the calculated maximum equivalent plastic strain range, $\Delta\varepsilon_{peq,k}$, and the von Mises equivalent stress range $\Delta S_{P,k}$ defined above are typical output variables that can be obtained directly from a stress analysis.

f) STEP 6 – Determine the effective alternating equivalent stress for the k^{th} cycle.

$$S_{alt,k} = \frac{1}{2} E_{yf} \cdot \Delta\varepsilon_{eff,k} \tag{B1.43}$$

g) STEP 7 – Determine the permissible number of cycles, N_k, for the alternating equivalent stress computed in STEP 6. Fatigue curves based on the materials of construction are provided in Annex F.

h) STEP 8 – Determine the fatigue damage for the k^{th} cycle, where the actual number of repetitions of the k^{th} cycle is n_k.

$$D_{f,k} = \frac{n_k}{N_k} \tag{B1.44}$$

i) STEP 9 – Repeat STEPs 3 through 8 for all stress ranges, M, identified in the cycle counting process in STEP 2.

j) STEP 10 – Compute the accumulated fatigue damage using the following equation. The location in the component is acceptable for continued operation if this equation is satisfied.

$$\sum_{k=1}^{M} D_{f,k} \le 1.0 \tag{B1.45}$$

k) STEP 11 – Repeat STEPs 2 through 10 for each point in the component subject to a fatigue evaluation.

B1.5.5 Fatigue Assessment of Welds – Elastic Stress Analysis and Structural Stress

B1.5.5.1 Overview

a) An equivalent structural stress range parameter is used to evaluate the fatigue damage for results obtained from a linear elastic stress analysis. The controlling stress for the fatigue evaluation is the structural stress that is a function of the membrane and bending stresses normal to the hypothetical crack plane. This method is recommended for evaluation of welded joints that have not been machined to a smooth profile. Weld joints with controlled smooth profiles may be evaluated using paragraphs B1.5.3 or B1.5.4.

b) Fatigue cracks at pressure vessel welds are typically located at the toe of a weld. For as-welded joints and weld joints subject to post weld heat treatment, the expected orientation of a fatigue crack is along the weld toe in the through-thickness direction, and the structural stress normal to the expected crack is the stress measure used to correlate fatigue life data. For fillet welded components, fatigue cracking may occur at the toe of the fillet weld or the weld throat, and both locations shall be considered in the assessment. It is difficult to accurately predict fatigue life at the weld throat due to variability in throat dimension, which is a function of the depth of the weld penetration. It is recommended to perform sensitivity analysis where the weld throat dimension is varied.

B1.5.5.2 Assessment Procedure

The following procedure can be used to evaluate protection against failure due to cyclic loading using the equivalent structural stress range.

a) STEP 1 – Determine a load history based on the information in paragraph B1.1.1.3 and the histogram development methods in Annex B2. The load history should include all significant operating loads and events that are applied to the component.

b) STEP 2 – For a location at a weld joint subject to a fatigue evaluation, determine the individual stress-strain cycles using the cycle counting methods in Annex B3. Define the total number of cyclic stress ranges in the histogram as M .

c) STEP 3 – Determine the elastically calculated membrane and bending stress normal to the assumed hypothetical crack plane at the start and end points (time points ${}^{m}t$ and ${}^{n}t$, respectively) for the k^{th} cycle counted in STEP 2. Using this data, calculate the membrane and bending stress ranges between time points ${}^{m}t$ and ${}^{n}t$, and the maximum, minimum and mean stress.

$$\Delta\sigma^{e}_{m,k} = {}^{m}\sigma^{e}_{m,k} - {}^{n}\sigma^{e}_{m,k} \tag{B1.46}$$

$$\Delta\sigma^{e}_{b,k} = {}^{m}\sigma^{e}_{b,k} - {}^{n}\sigma^{e}_{b,k} \tag{B1.47}$$

$$\sigma_{max,k} = \max\left[\left({}^{m}\sigma^{e}_{m,k} + {}^{m}\sigma^{e}_{b,k}\right),\ \left({}^{n}\sigma^{e}_{m,k} + {}^{n}\sigma^{e}_{b,k}\right)\right] \tag{B1.48}$$

$$\sigma_{min,k} = \min\left[\left({}^{m}\sigma^{e}_{m,k} + {}^{m}\sigma^{e}_{b,k}\right),\ \left({}^{n}\sigma^{e}_{m,k} + {}^{n}\sigma^{e}_{b,k}\right)\right] \tag{B1.49}$$

$$\sigma_{mean,k} = \frac{\sigma_{max,k} + \sigma_{min,k}}{2} \tag{B1.50}$$

d) STEP 4 – Determine the elastically calculated structural stress range for the k^{th} cycle, $\Delta\sigma^{e}_{k}$, using Equation (B1.51).

$$\Delta\sigma^{e}_{k} = \Delta\sigma^{e}_{m,k} + \Delta\sigma^{e}_{b,k} \tag{B1.51}$$

e) STEP 5 – Determine the elastically calculated structural strain, $\Delta\varepsilon^{e}_{k}$, from the elastically calculated structural stress, $\Delta\sigma^{e}_{k}$, using Equation (B1.52).

$$\Delta\varepsilon_k^e = \frac{\Delta\sigma_k^e}{E_{ya,k}} \tag{B1.52}$$

The corresponding local nonlinear structural stress and strain ranges, $\Delta\sigma$ and $\Delta\varepsilon$, respectively, are determined by simultaneously solving Neuber's Rule, Equation (B1.53), and a model for the material hysteresis loop stress-strain curve given by Equation (B1.54), see Annex F, paragraph F.2.4.

$$\Delta\sigma_k \cdot \Delta\varepsilon_k = \Delta\sigma_k^e \cdot \Delta\varepsilon_k^e \tag{B1.53}$$

$$\Delta\varepsilon_k = \frac{\Delta\sigma_k}{E_{ya,k}} + 2\left(\frac{\Delta\sigma_k}{2K_{css}}\right)^{\frac{1}{n_{css}}} \tag{B1.54}$$

The structural stress range computed solving Equations (B1.53) and (B1.54) is subsequently modified for low-cycle fatigue using Equation (B1.55).

$$\Delta\sigma_k = \left(\frac{E_{ya,k}}{1-\nu^2}\right)\Delta\varepsilon_k \tag{B1.55}$$

Note: The modification described above is for low-cycle or strain-controlled fatigue. This modification should always be performed because the exact distinction between high-cycle fatigue and low-cycle fatigue cannot be determined without evaluating the effects of plasticity which is a function of the applied stress range and cyclic stress-strain curve. For high cycle fatigue applications, this procedure will provide correct results, i.e. the elastically calculated structural stress will not be modified.

f) STEP 6 – Compute the equivalent structural stress range parameter for the k^{th} cycle using the following equations. In Equation (B1.56), for SI Units, the thickness, t, stress range, $\Delta\sigma_k$, and the equivalent structural stress range parameter, $\Delta S_{ess,k}$, are in mm, MPa, and $MPa/(mm)^{(2-m_{ss})/2m_{ss}}$, respectively, and for US Customary Units, the thickness, t, stress range, $\Delta\sigma_k$, and the equivalent structural stress range parameter, $\Delta S_{ess,k}$, are in $inches$, ksi, and $ksi/(inches)^{(2-m_{ss})/2m_{ss}}$, respectively.

$$\Delta S_{ess,k} = \frac{\Delta\sigma_k}{t_{ess}^{\left(\frac{2-m_{ss}}{2m_{ss}}\right)} \cdot I^{\frac{1}{m_{ss}}} \cdot f_{M,k}} \tag{B1.56}$$

where,

$$m_{ss} = 3.6 \tag{B1.57}$$

$$t_{ess} = 16\ mm\ (0.625\ in.) \qquad for \qquad t \le 16\ mm\ (0.625\ in.) \tag{B1.58}$$

$$t_{ess} = t \qquad for \qquad 16\ mm\ (0.625\ in.) < t < 150\ mm\ (6\ in.) \tag{B1.59}$$

$$t_{ess} = 150\ mm\ (6\ in.) \qquad for \qquad t \ge 150\ mm\ (6\ in.) \tag{B1.60}$$

$$I^{\frac{1}{m_{ss}}} = \frac{1.23 - 0.364R_{b,k} - 0.17R_{b,k}^2}{1.007 - 0.306R_{b,k} - 0.178R_{b,k}^2} \tag{B1.61}$$

$$R_{b,k} = \frac{\left|\Delta\sigma_{b,k}\right|}{\left|\Delta\sigma_{m,k}\right| + \left|\Delta\sigma_{b,k}\right|} \tag{B1.62}$$

$$f_{M,k} = \left(1 - R_k\right)^{\frac{1}{m_{ss}}} \qquad for \quad \begin{vmatrix} \sigma_{mean,k} \geq 0.5 S_{y,k}, \ and \\ R_k > 0, \ and \\ \left|\Delta\sigma_{m,k} + \Delta\sigma_{b,k}\right| \leq 2 S_{y,k} \end{vmatrix} \tag{B1.63}$$

$$f_{M,k} = 1.0 \qquad for \quad \begin{vmatrix} \sigma_{mean,k} < 0.5 S_{y,k}, \ or \\ R_k \leq 0, \ or \\ \left|\Delta\sigma_{m,k} + \Delta\sigma_{b,k}\right| > 2 S_{y,k} \end{vmatrix} \tag{B1.64}$$

$$R = \frac{\sigma_{min,k}}{\sigma_{max,k}} \tag{B1.65}$$

g) STEP 7 – Determine the permissible number of cycles, N_k, based on the equivalent structural stress range parameter for the k^{th} cycle computed in STEP 6. Fatigue curves for welded joints are provided in Annex F.

h) STEP 8 – Determine the fatigue damage for the k^{th} cycle, where the actual number of repetitions of the k^{th} cycle is n_k.

$$D_{f,k} = \frac{n_k}{N_k} \tag{B1.66}$$

i) STEP 9 – Repeat STEPs 3 through 8 for all stress ranges, M, identified in the cycle counting process in STEP 2.

j) STEP 10 – Compute the accumulated fatigue damage using the following equation. The location along the weld joint is suitable for continued operation if this equation is satisfied.

$$D_f = \sum_{k=1}^{M} D_{f,k} \leq 1.0 \tag{B1.67}$$

k) STEP 11 – Repeat STEPs 2 through 10 for each point along the weld joint that is subject to a fatigue evaluation.

B1.5.5.3 Assessment Procedure Modifications

The assessment procedure in paragraph B1.5.5.2 may be modified as shown below.

a) Multiaxial Fatigue – If the structural shear stress range is not negligible, i.e. $\Delta\tau_k > \Delta\sigma_k / 3$, a modification should be made when computing the equivalent structural stress range. Two conditions need to be considered:

1) If $\Delta\sigma_k$ and $\Delta\tau_k$ are out of phase, the equivalent structural stress range $\Delta S_{ess,k}$ in Equation (B1.56) should be replaced by:

$$\Delta S_{ess,k} = \frac{1}{F(\delta)}\left[\left(\frac{\Delta\sigma_k}{t_{ess}^{\left(\frac{2-m_{ss}}{2m_{ss}}\right)} \cdot I^{\frac{1}{m_{ss}}} \cdot f_{M,k}}\right)^2 + 3\left(\frac{\Delta\tau_k^e}{t_{ess}^{\left(\frac{2-m_{ss}}{2m_{ss}}\right)} \cdot I_\tau^{\frac{1}{m_{ss}}}}\right)^2\right]^{0.5} \tag{B1.68}$$

where

$$I_\tau^{\frac{1}{m_{ss}}} = \frac{1.23 - 0.364R_{b\tau,k} - 0.17R_{b\tau,k}^2}{1.007 - 0.306R_{b\tau,k} - 0.178R_{b\tau,k}^2} \tag{B1.69}$$

$$\Delta\tau_k^e = \Delta\tau_{m,k}^e + \Delta\tau_{b,k}^e \tag{B1.70}$$

$$\Delta\tau_{m,k}^e = {}^m\tau_{m,k}^e - {}^n\tau_{m,k}^e \tag{B1.71}$$

$$\Delta\tau_{b,k}^e = {}^m\tau_{b,k}^e - {}^n\tau_{b,k}^e \tag{B1.72}$$

$$R_{b\tau,k} = \frac{\left|\Delta\tau_{b,k}^e\right|}{\left|\Delta\tau_{m,k}^e\right| + \left|\Delta\tau_{b,k}^e\right|} \tag{B1.73}$$

In Equation (B1.68), $F(\delta)$ is a function of the out-of-phase angle between $\Delta\sigma_k$ and $\Delta\tau_k$ if both loading modes can be described by sinusoidal functions, or:

$$F(\delta) = \frac{1}{\sqrt{2}}\left[1 + \left[1 - \frac{12 \cdot \Delta\sigma_k^2 \cdot \Delta\tau_k^2 \cdot \sin^2[\delta]}{\left(\Delta\sigma_k^2 + 3\Delta\tau_k^2\right)^2}\right]^{0.5}\right]^{0.5} \tag{B1.74}$$

A conservative approach is to ignore the out-of-phase angle and recognize the existence of a minimum possible value for $F(\delta)$ in Equation (B1.74) given by:

$$F(\delta) = \frac{1}{\sqrt{2}} \tag{B1.75}$$

2) If $\Delta\sigma_k$ and $\Delta\tau_k$ are in-phase the equivalent structural stress range $\Delta S_{ess,k}$ is given by Equation (B1.68) with $F(\delta) = 1.0$.

b) Weld Quality – If a defect exists at the toe of a weld that can be characterized as a crack-like flaw, i.e. undercut, and this defect exceeds the value permitted by the applicable construction code, then a reduction in fatigue life may be calculated by substituting the value of $I^{1/m_{ss}}$ in Equation (B1.61) with the value given by Equation (B1.76). In this equation, a is the depth of the crack-like flaw at the weld toe. Equation (B1.76) is valid only when $a/t \le 0.1$.

$$I^{\frac{1}{m_{ss}}} = \frac{1.229 - 0.365R_{b,k} + 0.789\left(\frac{a}{t}\right) - 0.17R_{b,k}^2 + 13.771\left(\frac{a}{t}\right)^2 + 1.243R_{b,k}\left(\frac{a}{t}\right)}{1 - 0.302R_{b,k} + 7.115\left(\frac{a}{t}\right) - 0.178R_{b,k}^2 + 12.903\left(\frac{a}{t}\right)^2 - 4.091R_{b,k}\left(\frac{a}{t}\right)} \tag{B1.76}$$

B1.5.6 Ratcheting Assessment – Elastic Stress Analysis

B1.5.6.1 Elastic Ratcheting Analysis Method

a) To evaluate protection against ratcheting the following limit shall be satisfied.

$$\Delta S_{n,k} \le S_{PS} \qquad \text{(B1.77)}$$

b) The primary plus secondary equivalent stress range, $\Delta S_{n,k}$, is the equivalent stress range, derived from the highest value across the thickness of a section, of the combination of linearized general or local primary membrane stresses plus primary bending stresses plus secondary stresses $\left(P_L + P_b + Q\right)$, produced by specified operating pressure and other specified mechanical loads and by general thermal effects. The effects of gross structural discontinuities but not of local structural discontinuities (stress concentrations) shall be included. Examples of this stress category for typical pressure vessel components are shown in Table B1.5.

c) The maximum range of this equivalent stress is limited to S_{PS} . The quantity S_{PS} represents a limit on the primary plus secondary equivalent stress range and is defined in paragraph B1.5.6.1.d. In the determination of the maximum primary plus secondary equivalent stress range, it may be necessary to consider the effects of multiple cycles where the total stress range may be greater than the stress range of any of the individual cycles. In this case, the value of S_{PS} may vary with the specified cycle, or combination of cycles, being considered since the temperature extremes may be different in each case. Therefore, care shall be exercised to assure that the applicable value of S_{PS} for each cycle, or combination of cycles, is used (see paragraph B1.5.3).

d) The allowable limit on the primary plus secondary stress range, S_{PS}, is determined as shown below except that S_{PS} shall be determined by Equation (B1.79) when S_m at the highest temperature in the operational cycle is governed by time-dependent material properties.

$$S_{PS} = \max\left[3S_{m,cycle}\,,\, 2S_{y,cycle}\right] \qquad for\ YS/UTS \le 0.70 \qquad \text{(B1.78)}$$

$$S_{PS} = 3S_{m,cycle} \qquad for\ YS/UTS > 0.70 \qquad \text{(B1.79)}$$

B1.5.6.2 Simplified Elastic-Plastic Analysis

The equivalent stress limit on the range of primary plus secondary equivalent stress in paragraph B1.5.6.1 may be exceeded provided all of the following are true:

a) The range of primary plus secondary membrane plus bending equivalent stress, excluding thermal bending stress, is less than S_{PS} .

b) The value of the alternating stress range in paragraph B1.5.3.2.d is multiplied by the factor $K_{e,k}$ (see Equations (B1.31) through (B1.33), or paragraph B1.5.3.3).

c) The material of the component satisfies $YS/UTS \le 0.80$.

d) The component meets the secondary equivalent stress range requirements of paragraph B1.5.6.3.

B1.5.6.3 Thermal Stress Ratcheting Assessment

The allowable limit on the secondary equivalent stress range from thermal loading to prevent ratcheting, when applied in conjunction with a steady state general or local primary membrane equivalent stress, is determined below. This procedure can only be used with an assumed linear or parabolic distribution of a secondary stress range (e.g. thermal stress).

a) STEP 1 – Determine the ratio of the primary membrane stress to the specified minimum yield strength at the average temperature of the cycle.

$$X = \left(\frac{P_m}{S_y} \right) \tag{B1.80}$$

b) STEP 2 – Compute the secondary equivalent stress range from thermal loading, ΔQ, using elastic analysis methods.

c) STEP 3 – Determine the allowable limit on the secondary equivalent stress range from thermal loading, S_Q.

1) For a secondary equivalent stress range from thermal loading with a linear variation through the wall thickness:

$$S_Q = S_y \left(\frac{1}{X} \right) \qquad for \quad 0 < X < 0.5 \tag{B1.81}$$

$$S_Q = 4.0 S_y \left(1 - X \right) \qquad for \quad 0.5 \le X \le 1.0 \tag{B1.82}$$

2) For a secondary equivalent stress range from thermal loading with a parabolic constantly increasing or decreasing variation through the wall thickness:

$$S_Q = S_y \left(\frac{1}{0.12244 + 0.994437 X^2} \right) \qquad for \quad 0.0 < X < 0.615 \tag{B1.83}$$

$$S_Q = 5.2 S_y \left(1 - X \right) \qquad for \quad 0.615 \le X \le 1.0 \tag{B1.84}$$

d) STEP 4 – To demonstrate protection against ratcheting, the following criteria shall be satisfied.

$$\Delta Q \le S_Q \tag{B1.85}$$

B1.5.6.4 Progressive Distortion of Non-Integral Connections

Screwed-on caps, screwed-in plugs, shear ring closures, and breech lock closures are examples of non-integral connections that are subject to failure by bell-mouthing or other types of progressive deformation. If any combination of applied loads produces yielding, such joints are subject to ratcheting because the mating members may become loose at the end of each complete operating cycle and may start the next cycle in a new relationship with each other, with or without manual manipulation. Additional distortion may occur in each cycle so that interlocking parts, such as threads, can eventually lose engagement. Therefore primary plus secondary equivalent stresses that produce slippage between the parts of a non-integral connection in which disengagement could occur as a result of progressive distortion, shall be limited to the minimum specified yield strength at temperature, S_y, or evaluated using the procedure in paragraph B1.5.7.

B1.5.7 Ratcheting Assessment – Elastic-Plastic Stress Analysis

B1.5.7.1 Overview

To evaluate protection against ratcheting using elastic-plastic analysis, an assessment is performed by application, removal and re-application of the applied loadings. If protection against ratcheting is satisfied, it may be assumed that progression of the stress-strain hysteresis loop along the strain axis cannot be sustained with cycles and that the hysteresis loop will stabilize. A separate check for plastic shakedown to alternating plasticity is not required.

B1.5.7.2 Assessment Procedure

The following assessment procedure can be used to evaluate protection against ratcheting using elastic-plastic analysis.

a) STEP 1 – Develop a numerical model of the component including all relevant geometry characteristics. The model used for the analysis shall be selected to accurately represent the component geometry, boundary conditions, and applied loads.
b) STEP 2 – Define all relevant loads and applicable load cases (see Table B1.1).
c) STEP 3 – An elastic-perfectly plastic material model shall be used in the analysis. The von Mises yield function and associated flow rule should be utilized. The yield strength defining the plastic limit shall be the minimum specified yield strength at temperature. The effects of non-linear geometry shall be considered in the analysis.
d) STEP 4 – Perform an elastic-plastic analysis for the applicable loading from STEP 2 for a number of repetitions of a loading event or, if more than one event is applied, of two events that are selected so as to produce the highest likelihood of ratcheting.
e) STEP 5 – The ratcheting criteria below should be evaluated after application of a minimum of three complete repetitions of the cycle. Additional cycles may need to be applied to demonstrate convergence. If any one of the following conditions is met, the ratcheting criteria are satisfied. If the criteria shown below are not satisfied, the component configuration (i.e. thickness) shall be modified or applied loads reduced and the analysis repeated.
    1. There is no plastic action (i.e. zero plastic strains incurred) in the component.
    2. There is an elastic core in the primary-load-bearing boundary of the component.
    3. There is not a permanent change in the overall dimensions of the component. This can be demonstrated by developing a plot of relevant component dimensions versus time between the last and the next to the last cycles.

B1.6 Supplemental Requirements for Stress Classification in Nozzle Necks

The following classification of stresses shall be used for stress in a nozzle neck. The classification of stress in the shell shall be in accordance with paragraph B1.2.2.2.

a) Within the limits of reinforcement given by Annex A, paragraph A3.11, whether or not nozzle reinforcement is provided, the following classification shall be applied.
    1) A P_m classification is applicable to equivalent stresses resulting from pressure induced general membrane stresses as well as stresses, other than discontinuity stresses, due to external loads and moments including those attributable to restrained free end displacements of the attached pipe.
    2) A P_L classification shall be applied to local primary membrane equivalent stresses derived from discontinuity effects plus primary bending equivalent stresses due to combined pressure and external loads and moments including those attributable to restrained free end displacements of the attached pipe.
    3) A $P_L + P_b + Q$ classification (see paragraph B1.5.2) shall apply to primary plus secondary equivalent stresses resulting from a combination of pressure, temperature, and external loads and moments, including those due to restrained free end displacements of the attached pipe.
b) Outside of the limits of reinforcement given in Annex A, paragraph A3.11, the following classification shall be applied.
    1) A P_m classification is applicable to equivalent stresses resulting from pressure induced general membrane stresses as well as the average stress across the nozzle thickness due to externally applied nozzle axial, shear, and torsional loads other than those attributable to restrained free end displacement of the attached pipe.
    2) A $P_L + P_b$ classification is applicable to the equivalent stresses resulting from adding those stresses classified as P_m to those due to externally applied bending moments except those attributable to restrained free end displacement of the pipe.
    3) A $P_L + P_b + Q$ classification (see paragraph B1.5.2) is applicable to equivalent stresses resulting from all pressure, temperature, and external loads and moments, including those attributable to restrained free end displacements of the attached pipe.

c) Beyond the limits of reinforcement, the S_{PS} limit on the range of primary plus secondary equivalent stress may be exceeded as provided in paragraph B1.5.6.2, except that in the evaluation of the range of primary plus secondary equivalent stress, $P_L + P_b + Q$, stresses resulting from the restrained free end displacements of the attached pipe may also be excluded. The range of membrane plus bending equivalent stress attributable solely to the restrained free end displacements of the attached piping shall be less than S_{PS}.

B1.7 Special Requirements for Crack-Like Flaws

B1.7.1 Overview

a) The Level 2 FAD-based assessment procedures in Part 9 have been developed to make maximum use of existing solutions for crack driving force (i.e., stress intensity factor and reference stress solutions in Annex C and Annex D, respectively). Even in cases where a rigorous closed form solution has not been tabulated, it is often possible to use existing solutions to generate reasonable approximations of the case at hand. The weight function method, for example, enables stress intensity factor solutions to be derived for arbitrary through-wall stress distributions. There are other instances where the problem is sufficiently complex that it is appropriate to perform a detailed stress analysis where the crack-like flaw is explicitly included in the numerical model.

b) Paragraph B1.7.2 describes how to use conventional stress analysis (where the crack is *not* included in the mesh) to assess crack-like flaws. Paragraph B1.7.3 outlines the basic procedures for incorporating a crack into a finite element model. The specific details of the analysis and the way in which the results are used depend on the application. Paragraphs B1.7.4 and B1.7.5 present two alternative approaches for assessing non-growing cracks. Growing cracks are addressed in paragraph B1.7.6.

B1.7.2 Using the Results of a Conventional Stress Analysis

B1.7.2.1 Stress Analysis of the Un-Cracked Configuration

a) Stress analysis results may be used in a crack-like flaw assessment even if the numerical model does not include the crack explicitly. The approach entails post-processing the stress values in such a way as to tie into existing K_I and σ_{ref} solutions in Annex C and Annex D, respectively. This approach is best suited to the case where the geometry can be approximated by simple shapes that are addressed in Annex C and Annex D (e.g., flat plate, cylindrical shell, spherical shell). The stress distribution may either be uniform or non-uniform through the wall thickness at the location of the crack. Several examples are listed below:

b) Cylindrical or spherical shell under pressure loading

c) Cylindrical shell with an internal attachment, which creates a local peak stress.

d) Thermal shock on the inside of a pressure vessel, which creates a highly non-uniform thermal stress distribution.

e) Seam weld with a non-uniform through-wall weld residual stress distribution, obtained from Annex E or from a multi-pass weld simulation.

B1.7.2.2 Linearization of Stress Results

Membrane and bending stresses normal to the plane of the crack can be developed by linearization of the stress components through the wall thickness with the same orientation using the methods in Annex B2. The linearization may be performed on the basis of the crack location within the wall thickness (see Figure B1.2) or the section thickness (see Figure B1.3). The linearization method is not recommended for K_I estimation when the stress distribution is highly non-uniform because significant errors can occur, and more accurate methods are available (see paragraphs B1.7.2.3 and B1.7.2.4 below). Alternatively, the reference stress is controlled by the development of net-section plasticity, so it is less sensitive to local peak stresses. Therefore, an accurate reference stress may be determined from the membrane and bending stresses derived from the linearization of stress results.

B1.7.2.3 Fitting Stress Results to a Polynomial

If the stress distribution normal to the flaw can be represented by a polynomial (4^{th} degree or lower), then the K_I solutions in Annex C may be used if a component geometry and crack geometry can be found to model the actual cracked configuration. Note that a linear approximation of the through-wall stress distribution is merely a special case of the polynomial approach. As is the case with the linearization method, a polynomial fit of the stress distribution can be performed locally at the flaw location or through the entire cross section.

B1.7.2.4 The Weight Function Method

In many cases, a simple polynomial expression does not provide a good fit to stress analysis results. In these cases, it is preferable to use the weight function approach. The weight function method (see Annex C) can compute K_I for an arbitrary through-wall variation of stress normal to the crack plane. The disadvantage of the weight function method is that numerical integration is required.

B1.7.3 Finite Element Analysis of Components with Cracks

The following steps provide general guidelines for numerical analysis of components with cracks. Additional considerations are discussed in paragraphs B1.7.4 and B1.7.5. Incorporating one or more cracks into a finite element model is considered a Level 3 approach, and should be undertaken only by individuals with suitable qualifications.

a) STEP 1 – Develop a finite element model of the component, including all relevant geometry and flaw characteristics. The following provides an overview for mesh design at the crack tip. Further details regarding finite element mesh design can be found in reference [1]. In addition, the user's manual of the finite element program should be consulted.

   1) Two-Dimensional (2D) Small-Strain Analysis – The suggested (but not mandatory) mesh design for the crack tip region is a focused "spider web" mesh with elements concentrated at the crack tip (see Figure B1.4). The first ring of elements is made up of quadrilaterals degenerated to triangles with several nodes coincident at the crack tip. Subsequent rings of elements are quadrilaterals. For elastic analysis, the crack tip nodes should be tied, but the element type should be specified as quadrilateral rather than triangle. The reason is that most commercial finite element programs that evaluate the J-integral will return an error message if triangular elements are in the integration domain. For elastic-plastic analyses, it is important that the crack tip nodes not be tied together, nor merged into a single node. Under load, the nodes that are initially coincident move apart, resulting in a blunted crack. Note that the crack tip opening displacement (CTOD) can be inferred from the deformed mesh in an elastic-plastic analysis. Irrespective of the material model, isoparametric 2D (8-node or 9-node) elements are recommended, but linear (4-node) elements are acceptable, provided the level of mesh refinement is sufficient. One advantage of the degenerated isoparametric elements is that an appropriate strain singularity can be achieved, which improves accuracy. Collapsing (but not tying) the crack tip nodes results in a $1/r$ strain singularity, which is appropriate for elastic-plastic analysis. For elastic analysis, the desired $1/\sqrt{r}$ singularity is achieved by tying the crack tip nodes and moving mid-side nodes of isoparametric elements to the quarter point closest to the crack tip.

   2) Three-Dimensional (3D) Small-Strain Analysis – The recommendations for the 2D analysis are also applicable to 3D analysis. The main difference is that 3D continuum elements are used rather than 2D continuum elements. Either isoparametric (20-node or 27-node) bricks or 8-node bricks may be used, but the number of elements required for an accurate solution is greater for the 8-node bricks. A typical 3D finite model of a surface crack is shown in Figure B1.5. It should be noted that constructing meshes such as depicted in Figure B1.5 can be extremely cumbersome and time consuming. It is recommended that the analyst develop or acquire mesh generation software for this purpose.

3) Two- or Three-Dimensional Large-Strain Analysis – Collapsed elements at the crack tip are not appropriate when large-strain plasticity and a nonlinear geometry kinematic assumption are incorporated into the analysis. In such cases, the crack should be modeled with a finite radius at the tip. The initial crack tip radius should be at least five times smaller than the tip radius in the deformed state. A "keyhole" mesh, which is created by removing the first ring of collapsed elements from a focused "spider web" mesh, can also be used for large-strain, nonlinear geometry analysis, but is less desirable than a mesh with a finite crack tip radius.

b) STEP 2 – Define all relevant loading conditions including pressure, supplemental loads, temperature distributions, and residual stresses (see paragraph B1.1.3 and Annex E). Crack face tractions should also be applied where appropriate. Note that with the FAD-based method (paragraph B1.7.4), primary loads must be considered separately from secondary and residual stresses.

c) STEP 3 – Define the appropriate material properties. An elastic-plastic finite element analysis requires a stress-strain curve for the material of interest. Commercial finite element programs typically accept either a stress-strain data table or a parametric equation such as the Ramberg-Osgood power law (see Annex F). Some finite element codes offer the option of a bilinear stress-strain curve, but that option is not recommended here. If the flaw of interest is in or near a weld, both the weld metal and base metal flow behavior should be modeled in an elastic-plastic analysis.

d) STEP 4 – Perform the finite element analysis and evaluate the results. The type of results and evaluation procedure depend on the application (see paragraphs B1.7.4 to B1.7.5).

B1.7.4 FAD-Based Method for Non-Growing Cracks

B1.7.4.1 Overview

This procedure entails the determination of stress intensity factor and reference stress solutions, as well as the FAD curve, for the configuration of interest and then applying the Level 2 assessment in Part 9. The FAD method requires that loads (or stresses) be categorized as primary, secondary, or residual. If more than one primary load is present (e.g. the component is subject to both a membrane and bending stress), the FAD method assumes that these loads are applied simultaneously. If the primary loads are out of phase with one another (e.g. if the membrane stress is applied first, followed by the bending stress), the FAD approach is not strictly valid. The J driving force method described in paragraph B1.7.5 is better suited to such situations.

B1.7.4.2 Assessment Procedure

The following steps describe the determination of a *J*-based FAD curve for the configuration of interest, followed by an assessment in accordance with the Level 2 procedure in Part 9.

a) STEP 1 – Categorize all loads as primary, secondary, or residual. It is important to point out that stresses that are labeled as secondary in the original design code may not behave as such as far as a crack-like flaw is concerned. The two questions below can be used to determine whether or not a particular load should be categorized as primary or secondary. When in doubt, the load should be treated as primary.

1) Could the load, if its magnitude were sufficiently high, contribute to overload, rupture, or buckling of the component? If the answer is yes, then the load is primary. Thermal expansion loads could lead to rupture or buckling of a piping system, despite these loads being classified as secondary by the design code.

2) Will the stress in question relax if there is net-section yielding in the vicinity of the crack? If so, the stress can be classified as secondary/residual. Weld residual stresses relax with local plastic flow, but long-range thermal expansion loads may not.

b) STEP 2 – Construct an elastic-plastic finite element model of the configuration of interest (see paragraph B1.7.3). Include only the primary loading in the model.

c) STEP 3 – During the finite element analysis, gradually increase the applied primary load(s) and compute the J-integral at each step. If there is more than one primary load, they should be applied proportionately. For example, for combined membrane and bending stress, a constant σ_b^P / σ_m^P ratio should be maintained throughout the analysis. Make sure that there are several output steps at low loads where plastic strains are negligible, and that there are a number of output steps in the fully plastic regime. Specifying the appropriate load values to define the FAD curve may require some trial and error.

d) STEP 4 – At each output step, convert the J-integral to the equivalent stress intensity factor using the following relationship:

$$K_J = \sqrt{\frac{JE_y}{1-\nu^2}} \tag{B1.86}$$

e) STEP 5 – Infer the elastic K_I^P solution for the configuration of interest from the initial slope of the K_J versus applied stress plot (see Figure B1.6.a). Alternatively, perform a separate elastic finite element analysis on the configuration of interest.

f) STEP 6 – Compute the vertical coordinate of the FAD, K_r, at each load step as follows:

$$K_r = \frac{K_I^P}{K_J} \tag{B1.87}$$

g) STEP 7 – Determine the reference stress solution for the configuration of interest and compute the horizontal coordinate of the FAD, L_r, at each K_r value.

1) The load ratio is defined follows:

$$L_r = \frac{\sigma_{ref}}{\sigma_{ys}} \tag{B1.88}$$

2) The K_r at which $L_r = 1$ is given by

$$K_r\big|_{L_r=1} = \left[1 + \frac{0.002E_y}{\sigma_{ys}} + \frac{1}{2}\left(1 + \frac{0.002E_y}{\sigma_{ys}}\right)^{-1}\right]^{-0.5} \tag{B1.89}$$

3) From the K_r values determined in STEP 6, determine the applied stress at which Equation (B1.89) is satisfied. The reference stress is related to the applied primary stress as follows.

$$\sigma_{ref} = F_{ref} \cdot \sigma^P \tag{B1.90}$$

The parameter F_{ref} is the reference stress geometry factor, which is given by:

$$F_{ref} = \frac{\sigma_{ys}}{\sigma^P\big|_{L_r=1}} \tag{B1.91}$$

h) STEP 8 – Plot K_r versus L_r. This is the FAD curve (see Figure B1.6.c).

i) STEP 9 – Compute L_r for the operating loads from Equation (B1.88) and (B1.90).

j) STEP 10 – Compute K_I^P for the operating loads using the elastic solution determined in STEP 5.

k) STEP 11 – Compute K_I^{SR} corresponding to the secondary and residual stresses. Unless the through-wall distribution of secondary and residual stresses is the same as the primary stresses, the elastic solution from STEP 5 is not applicable. Consequently, another elastic solution is needed. This can be accomplished by re-using the finite model created in STEP 2. The crack tip elements should be modified for use with an elastic material model (see paragraph B1.7.3.a.1). There are two common methods for inferring K_I^{SR} from elastic finite element analysis:

1) Method 1 – Apply the secondary and residual normal stress distribution as a crack face traction and compute the resulting stress intensity factor. In order to use this approach, however, the crack face mesh must be sufficiently refined to capture the stress gradients. Errors will result if the traction varies significantly across an element face.

2) Method 2 – If the flaw of interest is a part-through surface crack, the weight function method (see Annex C) can be used to compute K_I^{SR} . The weight function coefficients can be inferred from reference K_I solutions for uniform and linear crack face pressure. These reference solutions can be obtained from the finite element model of the component of interest. Unlike Method 1 above, which entails applying the secondary and residual stress directly as a crack face traction, the weight function method does not require a high degree of crack face refinement to compute K_I^{SR} in the case of steep stress gradients.

l) STEP 12 – Compute the plasticity interaction factor, Φ , according to the procedure outlined in Part 9.

m) STEP 13 – Compute the toughness ratio as follows:

$$K_r = \frac{K_I^P + \Phi K_I^{SR}}{K_{mat}} \qquad \text{(B1.92)}$$

n) STEP 14 – Plot the point $\left(L_r, K_r\right)$ (from STEPs 9 and 13, respectively) on the FAD curve determined in STEP 8.

o) STEP 15 – Evaluate the results. Note that Partial Safety Factors (PSFs) were not prescribed in the above assessment. Uncertainty in the independent variables of the assessment (i.e. load, fracture toughness and flaw size) may be introduced in a variety of manners depending on the application. Examples are given below.

1) For a deterministic Fitness-For-Service assessment of a known crack-like flaw, the flaw size in the finite element analysis may be adjusted by a PSF. Additional PSFs can then be applied to other input parameters in STEPs 9 and 13.

2) For a probabilistic assessment, STEPs 9 to 14 may be repeated numerous times in a Monte Carlo analysis. In order to address uncertainty in flaw size, however, the finite element analysis would have to be performed for a range of flaw dimensions.

3) In order to predict the results of a burst test or to quantify the critical conditions for a failure, the above assessment could be applied deterministically without adjusting the input values with PSFs.

B1.7.5 Driving Force Method for Non-Growing Cracks

B1.7.5.1 Overview

The FAD method suffers from a number of limitations, even if an elastic-plastic finite element solution for the configuration of interest is available. The FAD approach requires stress classification. Moreover, when multiple primary loads are present, they are assumed to increase and decrease in phase with one another. Direct evaluation of the J-integral from an elastic-plastic finite element analysis and comparison with the fracture toughness avoids these difficulties and limitations. Stress classification is unnecessary, and the approach is sufficiently general to handle any load history.

B1.7.5.2 Assessment Procedure

The *J* driving force method is described below. As with the J-based FAD approach (paragraph B1.7.3), the procedure that follows does not incorporate an explicit safety margin. It is the responsibility of the analyst to use these results in a prudent manner.

a) STEP 1 – Construct an elastic-plastic finite element model of the configuration of interest (see paragraph B1.7.3).

b) STEP 2 – Impose loading that is initially present in the component, such as weld residual stresses. There are two common approaches to incorporating weld residual stresses into an elastic-plastic finite element model.

1) Method 1 – Define the thermal expansion properties of the weld metal and base metal in such as way as to mimic weld shrinkage. The simplest way to accomplish this is to set the stress-free reference temperature of the weld metal to a higher value than that of the base metal. The precise temperature difference to achieve a particular residual stress must be determined by trial and error on the specific geometry of interest. As a first guess, however, the following expression may be

used to estimate the temperature difference required to achieve a particular von Mises residual stress:

$$\Delta T \approx \alpha \frac{\sigma^R}{E_y} \tag{B1.93}$$

2) Method 2 – Impose the residual stress distribution computed from a multi-pass weld simulation. In Method 1 above, the modified thermal properties can be applied directly to the finite element model that contains a crack. However a multi-pass weld simulation normally requires a separate analysis. The computed residual stresses can then be mapped onto a mesh that contains a crack. In such cases the crack should be held closed in the first analysis step following the stress mapping. The crack can then be allowed to open after this initial equilibrium iteration.

c) STEP 3 – Impose the loads in the sequence they occur in service, and evaluate the J-integral at each load step. It may be appropriate to take the model through multiple operating cycles to determine if there is ratcheting in the J-integral. The loading history might also include a hydro test or a process upset, depending on the scenario that is being evaluated.

d) STEP 4 – Convert the applied J-integral at each load step to K_J using Equation (B1.86). Compare the crack driving force to the fracture toughness, K_{mat}.

B1.7.6 Assessment of Growing Cracks

B1.7.6.1 Annex F provides examples of crack growth models for various mechanisms. The rate of growth of a crack-like flaw can usually be correlated to a fracture mechanics driving force parameter. Fatigue and environmental cracking are typically correlated to the applied stress intensity factor, while creep crack growth is a function of a time-dependent parameter defined as C_t. The latter parameter can be estimated from K_I and σ_{ref}.

B1.7.6.2 Solutions for K_I and σ_{ref} for a range of geometries are listed in Annex C and Annex D, respectively. When the solutions are not available for the geometry of interest, they can be obtained from finite element analysis. An elastic analysis of the cracked component is sufficient to determine K_I, but an elastic-plastic analysis is required to infer σ_{ref}. The procedure outlined in STEPs 1 through 7 of paragraph B1.7.4.2 should be followed when computing σ_{ref} for a given application.

B1.7.6.3 Remaining life prediction is normally accomplished by integrating the crack growth expression from an initial crack size to a final size. The latter may be based on a failure criterion, such as the assessment point (L_r, K_r) falling outside of the FAD curve, or on a practical crack growth limit (e.g., crack growth through the wall, resulting in a leak).

B1.7.6.4 It is also possible to model a growing crack in a finite element model. Such an analysis requires special modeling capabilities that involve continuous updating of the model to account for crack growth.

B1.8 Definitions

1. Bending Stress – The variable component of normal stress, the variation may or may not be linear across the section thickness.
2. Bifurcation Buckling – The point of instability where there is a branch in the primary load versus displacement path for a structure.
3. Event – The Owner-Users' Specification may include one or more events that produce fatigue damage. Each event consists of loading components specified at a number of time points over a time period and is repeated a specified number of times. For example, an event may be the startup, shutdown, upset condition, or any other cyclic action. The sequence of multiple events may be specified or random.

4. Cycle – A cycle is a relationship between stress and strain that is established by the specified loading at a location in a vessel or component. More than one stress-strain cycle may be produced at a location, either within an event or in transition between two events, and the accumulated fatigue damage of the stress-strain cycles determines the adequacy for the specified operation at that location. This determination shall be made with respect to the stabilized stress-strain cycle.
5. Cyclic Loading – A service in which fatigue becomes significant due to the cyclic nature of the mechanical and/or thermal loads. A screening criteria is provided in paragraph B1.5.2 that can be used to determine if a fatigue analysis should be included as part of the vessel design.
6. Fatigue – The conditions leading to fracture under repeated or fluctuating stresses having a maximum value less than the tensile strength of the material.
7. Fatigue Endurance Limit – The maximum stress below which a material can undergo 10^{11} alternating stress cycles without failure.
8. Fatigue Strength Reduction Factor – A stress intensification factor which accounts for the effect of a local structural discontinuity (stress concentration) on the fatigue strength. It is the ratio of the fatigue strength of a component without a discontinuity or weld joint to the fatigue strength of that same component with a discontinuity or weld joint. Values for some specific cases are empirically determined (e.g. socket welds). In the absence of experimental data, the stress intensification factor can be developed from a theoretical stress concentration factor derived from the theory of elasticity or based on the guidance provided in Tables B1.10 and B1.11.
9. Fracture Mechanics – an engineering discipline concerned with the behavior of cracks in materials. Fracture mechanics models provide mathematical relationships for critical combinations of stress, crack size and fracture toughness that lead to crack propagation. Linear Elastic Fracture Mechanics (LEFM) approaches apply to cases where crack propagation occurs during predominately elastic loading with negligible plasticity. Elastic-Plastic Fracture Mechanics (EPFM) methods are suitable for materials that undergo significant plastic deformation during crack propagation.
10. Gross Structural Discontinuity – A source of stress or strain intensification that affects a relatively large portion of a structure and has a significant effect on the overall stress or strain pattern or on the structure as a whole. Examples of gross structural discontinuities are head-to-shell and flange-to-shell junctions, nozzles, and junctions between shells of different diameters or thicknesses.
11. Local Primary Membrane Stress – Cases arise in which a membrane stress produced by pressure, or other mechanical loading associated with a primary and/or a discontinuity effect would, if not limited, produce excessive distortion in the transfer of load to other portions of the structure. Conservatism requires that such a stress be classified as a local primary membrane stress even though it has some characteristics of a secondary stress.
12. Local Structural Discontinuity – A source of stress or strain intensification which affects a relatively small volume of material and does not have a significant effect on the overall stress or strain pattern, or on the structure as a whole. Examples are small fillet radii, small attachments, and partial penetration welds.
13. Membrane Stress – The component of normal stress that is uniformly distributed and equal to the average value of stress across the thickness of the section under consideration.
14. Normal Stress – The component of stress normal to the plane of reference. Usually the distribution of normal stress is not uniform through the thickness of a part.
15. Operational Cycle – An operational cycle is defined as the initiation and establishment of new conditions followed by a return to the conditions that prevailed at the beginning of the cycle. Three types of operational cycles are considered: the startup-shutdown cycle, defined as any cycle which has atmospheric temperature and/or pressure as one of its extremes and normal operating conditions as its other extreme; the initiation of, and recovery from, any emergency or upset condition or pressure test condition that shall be considered in the design; and the normal operating cycle, defined as any cycle between startup and shutdown which is required for the vessel to perform its intended purpose.
16. Peak Stress – The basic characteristic of a peak stress is that it does not cause any noticeable distortion and is objectionable only as a possible source of a fatigue crack or a brittle fracture. A stress that is not highly localized falls into this category if it is of a type that cannot cause noticeable distortion. Examples of peak stress are: the thermal stress in the austenitic steel cladding of a carbon steel vessel, the thermal stress in the wall of a vessel or pipe caused by a rapid change in temperature of the contained fluid, and the stress at a local structural discontinuity.

17. Primary Stress – A normal or shear stress developed by the imposed loading which is necessary to satisfy the laws of equilibrium of external and internal forces and moments. The basic characteristic of a primary stress is that it is not self-limiting. Primary stresses which considerably exceed the yield strength will result in failure or at least in gross distortion. A thermal stress is not classified as a primary stress. Primary membrane stress is divided into general and local categories. A general primary membrane stress is one that is distributed in the structure such that no redistribution of load occurs as a result of yielding. Examples of primary stress are general membrane stress in a circular cylindrical or a spherical shell due to internal pressure or to distributed live loads and the bending stress in the central portion of a flat head due to pressure. Cases arise in which a membrane stress produced by pressure or other mechanical loading and associated with a primary and/or a discontinuity effect would, if not limited, produce excessive distortion in the transfer of load to other portions of the structure. Conservatism requires that such a stress be classified as a local primary membrane stress even though it has some characteristics of a secondary stress. Finally a primary bending stress can be defined as a bending stress developed by the imposed loading which is necessary to satisfy the laws of equilibrium of external and internal forces and moments.
18. Ratcheting – A progressive incremental inelastic deformation or strain that can occur in a component subjected to variations of mechanical stress, thermal stress, or both (thermal stress ratcheting is partly or wholly caused by thermal stress). Ratcheting is produced by a sustained load acting over the full cross section of a component, in combination with a strain controlled cyclic load or temperature distribution that is alternately applied and removed. Ratcheting causes cyclic straining of the material, which can result in failure by fatigue and at the same time produces cyclic incremental growth of a structure, which could ultimately lead to collapse.
19. Secondary Stress – A normal stress or a shear stress developed by the constraint of adjacent parts or by self-constraint of a structure. The basic characteristic of a secondary stress is that it is self-limiting. Local yielding and minor distortions can satisfy the conditions that cause the stress to occur and failure from one application of the stress is not to be expected. Examples of secondary stress are a general thermal stress and the bending stress at a gross structural discontinuity.
20. Shakedown – Caused by cyclic loads or cyclic temperature distributions which produce plastic deformations in some regions of the component when the loading or temperature distribution is applied, but upon removal of the loading or temperature distribution, only elastic primary and secondary stresses are developed in the component, except in small areas associated with local stress (strain) concentrations. These small areas shall exhibit a stable hysteresis loop, with no indication of progressive deformation. Further loading and unloading, or applications and removals of the temperature distribution shall produce only elastic primary and secondary stresses.
21. Shear Stress – The component of stress tangent to the plane of reference.
22. Stress Concentration Factor – The ratio of the maximum stress to the average section stress or bending stress.
23. Stress Cycle – A stress cycle is a condition in which the alternating stress difference goes from an initial value through an algebraic maximum value and an algebraic minimum value and then returns to the initial value. A single operational cycle may result in one or more stress cycles.
24. Thermal Stress – A self-balancing stress produced by a non-uniform distribution of temperature or by differing thermal coefficients of expansion. Thermal stress is developed in a solid body whenever a volume of material is prevented from assuming the size and shape that it normally should under a change in temperature. For the purpose of establishing allowable stresses, two types of thermal stress are recognized, depending on the volume or area in which distortion takes place. A general thermal stress that is associated with distortion of the structure in which it occurs. If a stress of this type, neglecting stress concentrations, exceeds twice the yield strength of the material, the elastic analysis may be invalid and successive thermal cycles may produce incremental distortion. Therefore this type is classified as a secondary stress. Examples of general thermal stress are: the stress produced by an axial temperature distribution in a cylindrical shell, the stress produced by the temperature difference between a nozzle and the shell to which It is attached, and the equivalent linear stress produced by the radial temperature distribution in a cylindrical shell. A Local thermal stress is associated with almost complete suppression of the differential expansion and thus produces no significant distortion. Such stresses shall be considered only from the fatigue standpoint and are therefore classified as local stresses. Examples of local thermal stresses are the stress in a small hot spot in a vessel wall, the difference between the non-linear portion of

a through-wall temperature gradient in a cylindrical shell, and the thermal stress in a cladding material that has a coefficient of expansion different from that of the base metal.

B1.9 Nomenclature

a radius of hot spot or heated area within a plate or the depth of a crack-like flaw at a weld toe, as applicable.

α thermal expansion coefficient of the material at the mean temperature of two adjacent points, the thermal expansion coefficient of material evaluated at the mean temperature of the cycle, or the cone angle, as applicable.
thermal expansion coefficient of material 1 evaluated at the mean temperature of the cycle.

α_1 thermal expansion coefficient of material 2 evaluated at the mean temperature of the cycle.

α_2 material factor for the multiaxial strain limit.

β Load Factor coefficient.

β_{cr} capacity reduction factor.

C_1 factor for a fatigue analysis screening based on Method B.

C_2 factor for a fatigue analysis screening based on Method B.

C_t time-dependent crack growth parameter.

$D_{f,k}$ fatigue damage for the k^{th} cycle.

D_f cumulative fatigue damage.

D_o outside diameter.

D_ε cumulative strain limit damage.

$D_{\varepsilon form}$ strain limit damage from forming.

$D_{\varepsilon,k}$ strain limit damage for the k^{th} loading condition. $\Delta\varepsilon_k$ strain range at the point under evaluation for the k^{th} cycle.

$\Delta e_{ij,k}$ change in total strain range minus the free thermal strain at the point under evaluation for the k^{th} cycle. Note that shear strains are the engineering strain values (i.e. not tensor strains) that are typically output from a finite element analysis.

$\left(\Delta\varepsilon_{t,k}\right)_e$ equivalent strain range for the k^{th} cycle, computed from elastic analysis, using the total strain less the free thermal strain.

$\left(\Delta\varepsilon_{t,k}\right)_{ep}$ equivalent strain range for the k^{th} cycle, computed from elastic-plastic analysis, using the total strain less the free thermal strain.

$\Delta\varepsilon_k$ local nonlinear structural strain range at the point under evaluation for the k^{th} cycle.

$\Delta\varepsilon_k^e$ elastically calculated structural strain range at the point under evaluation for the k^{th} cycle.

$\Delta\varepsilon_{t,k}$ equivalent strain range for the k^{th} cycle, computed using the total strain less the free thermal strain.

$\Delta\varepsilon_{peq,k}$ equivalent plastic strain range for the k^{th} loading condition or cycle.

$\Delta\varepsilon_{eff,k}$ effective strain range for the k^{th} cycle.

$\Delta p_{ij,k}$ change in plastic strain range at the point under evaluation for the k^{th} loading condition or cycle. Note that the shear strains are the engineering strain values (i.e. not tensor strains) that are typically output from a finite element analysis.

ΔP_N maximum design range of pressure associated with $N_{\Delta P}$.

$\Delta S_{n,k}$ primary plus secondary equivalent stress range.

$\Delta S_{P,k}$ range of primary plus secondary plus peak equivalent stress for the k^{th} cycle.

$\Delta S_{LT,k}$ local thermal equivalent stress for the k^{th} cycle.

$\Delta S_{ess,k}$ range of equivalent structural stress for the k^{th} cycle.

ΔS_{ML} equivalent stress range computed from the specified full range of mechanical loads, excluding pressure but including piping reactions.

ΔQ range of secondary equivalent stress.

ΔT operating temperature range.

ΔT_E effective number of changes in metal temperature between any two adjacent points.

ΔT_M temperature difference between any two adjacent points of the vessel during normal operation, and during startup and shutdown operation with $N_{\Delta TM}$.

ΔT_N temperature difference between any two adjacent points of the vessel during normal operation, and during startup and shutdown operation with $N_{\Delta TN}$.

ΔT_R temperature difference between any two adjacent points of the vessel during normal operation, and during startup and shutdown operation with $N_{\Delta TR}$.

$\Delta\sigma$ local nonlinear structural stress range at the point under evaluation.

$\Delta\sigma_i$ stress range associated with the principal stress in the i^{th}-direction.

$\Delta\sigma_{ij}$ stress tensor range.

$\Delta\sigma_k$ structural stress range at the point under evaluation for the k^{th} cycle.

$\Delta\sigma_k^e$ elastically calculated structural stress range at the point under evaluation for the k^{th} cycle.

$\Delta\sigma_{b,k}^e$ elastically calculated structural bending stress range at the point under evaluation for the k^{th} cycle.

$\Delta\sigma_{ij,k}$ stress tensor range at the point under evaluation for the k^{th} cycle.

$\Delta\sigma_{m,k}^e$ elastically calculated structural membrane stress range at the point under evaluation for the k^{th} cycle.

$\Delta\tau_k^e$ elastically calculated structural shear stress range at the point under evaluation for the k^{th} cycle.

$\Delta\tau_{m,k}^e$ elastically calculated bending component of the structural shear stress range at the point under evaluation for the k^{th} cycle.

$\Delta\tau_{m,k}^e$ elastically calculated membrane component of the structural shear stress range at the point under evaluation for the k^{th} cycle.

δ out-of-phase angle between $\Delta\sigma_k$ and $\Delta\tau_k$ for the k^{th} cycle.

E_y Young's modulus at the assessment temperature.

E_{yf} value of modulus of elasticity on the fatigue curve being utilized.

$E_{ya,k}$ value of modulus of elasticity of the material at the point under consideration, evaluated at the mean temperature of the k^{th} cycle.

E_{y1} Young's Modulus of material 1 evaluated at the mean temperature of the cycle.

E_{y2} Young's Modulus of material 2 evaluated at the mean temperature of the cycle.

E_{ym} Young's Modulus of the material evaluated at the mean temperature of the cycle.

ε_{cf} cold forming strain.

ε_{cf} strain limit associated with the triaxial stress state.
uniaxial strain limit.

$\varepsilon_{L,k}$ limiting triaxial strain.

ε_{peq} total equivalent plastic strain.

$f_{M,k}$ mean stress correction factor for the k^{th} cycle.

F applied net-section axial compression load or the additional stress produced by the stress concentration over and above the nominal stress level resulting from operating loadings.

F_{ref} reference stress geometry factor.

$F(\delta)$ a fatigue modification factor based on the out-of-phase angle between $\Delta\sigma_k$ and $\Delta\tau_k$.

I correction factor used in the structural stress evaluation.

I_τ correction factor used in the structural shear stress evaluation.

J total J solution for the specific flaw and loading condition being evaluated.

K_r equivalent stress ratio.

K_{css} material parameter for the cyclic stress-strain curve model.

K_I stress intensity factor.

K_I^P stress intensity factor associated with primary stress.

K_I^{SR} stress intensity factor associated with secondary and residual stress.

$K_{e,k}$ fatigue penalty factor for the k^{th} cycle.

$K_{v,k}$ plastic Poisson's ratio adjustment for local thermal and thermal bending stresses for the k^{th} cycle.

K_f fatigue strength reduction factor used to compute the cyclic stress amplitude or range .

K_J stress intensity factor derived from J-integral.

K_{mat} material fracture toughness.

L length between points used in the fatigue screening analysis.

L_r load ratio.

M total number of stress ranges at a point derived from the cycle counting procedure, or the applied net-section bending moment, as applicable

m material constant used for the fatigue knock-down factor used in the simplified elastic-plastic analysis

m_{ss} exponent used in a fatigue analysis based on the structural stress.

m_2 strain hardening exponent.

n material constant used for the fatigue knock-down factor used in the simplified elastic-plastic analysis, or a parameter to compute the deviation from a true circle.

n_k actual number of repetitions of the k^{th} cycle.

n_{css} material parameter for the cyclic stress-strain curve model.

N number of cycles.

N_k permissible number of cycles for the k^{th} cycle.

$N\left(C_1 S_m\right)$ number of cycles from the applicable design fatigue curve (see Annex F) evaluated at $C_1 S_m$.

$N\left(S\right)$ number of cycles from the applicable design fatigue curve (see Annex F) evaluated at S.

$N_{\Delta FP}$ design number of full-range pressure cycles including startup and shutdown.

$N_{\Delta P}$ number of significant cycles associated with ΔP_N.

$N_{\Delta PO}$ expected number of operating pressure cycles in which the range of pressure variation exceeds 20% of the design pressure for integral construction or 15% of the design pressure for non-integral construction.

$N_{\Delta S}$ number of significant cycles associated with ΔS_{ML}, significant cycles are those for which the range in temperature exceeds S_{am}.

$N_{\Delta TN}$ number of cycles associated with ΔT_N.

$N_{\Delta TE}$ number of cycles associated with ΔT_E.

$N_{\Delta TM}$ number of significant cycles associated with ΔT_M.

$N_{\Delta TR}$ number of significant cycles associated with ΔT_R.

$N_{\Delta T\alpha}$ number of temperature cycles for components involving welds between materials having different coefficients of expansion.

ν Poisson's ratio.

$p_{ij,k}$ plastic strain tensor for the k^{th} cycle.

P pressure.

P_b primary bending equivalent stress.

P_L local primary membrane equivalent stress.

P_m general primary membrane equivalent stress.

Φ plasticity interaction factor.

Φ_B buckling factor.

Q secondary equivalent stress resulting from operating loadings.

R inside radius measured normal to the surface from the mid-wall of the shell to the axis of revolution, or the ratio of the minimum stress in the k^{th} cycle to the maximum stress in the k^{th} cycle, as applicable.

RA reduction in area.

R_k stress ratio for the k^{th} cycle.

$R_{b,k}$ ratio of the bending stress to the membrane plus bending stress.

$R_{b\tau,k}$ ratio of the bending component of the shear stress to the membrane plus bending component of the shear stress.

RSF computed remaining strength factor.

RSF_a allowable remaining strength factor, see Part 2.

R_1 mid-surface radius of curvature of region 1 where the local primary membrane stress exceeds $1.1S_m$.

R_2 mid-surface radius of curvature of region 2 where the local primary membrane stress exceeds $1.1S_m$.

S	allowable membrane stress from the applicable construction code at the design temperature or the computed equivalent stress or the elastic section modulus of full shell cross section, as applicable.
S_a	alternating stress obtained from a fatigue curve for the specified number of operating cycles.
S_{as}	stress amplitude from the applicable design fatigue curve (see Annex F) evaluated at 1E6 cycles.
$S_{a,k}$	value of alternating stress obtained from the applicable design fatigue curve for the specified number of cycles of the k^{th} cycle.
$S_{alt,k}$	alternating equivalent stress for the k^{th} cycle.
$S_{y,k}$	yield strength of the material evaluated at the mean temperature of the k^{th} cycle.
S_m	allowable stress based on the material of construction and design temperature.
$S_{m,cycle}$	average of the S_m values for the material at the highest and lowest temperatures during the operational cycle.
S_Q	allowable limit on the secondary stress range.
S_{PS}	allowable limit on the primary plus secondary stress range.
S_y	minimum specified yield strength at the design temperature.
$S_{y,cycle}$	average of the values for the material at the highest and lowest temperatures during the operational cycle.
$S_a\left(N\right)$	stress amplitude from the applicable design fatigue curve (see Annex F) evaluated at N.
$S_a\left(N_{\Delta P}\right)$	stress amplitude from the applicable design fatigue curve (see Annex F) evaluated at $N_{\Delta P}$.
$S_a\left(N_{\Delta S}\right)$	stress amplitude from the applicable design fatigue curve (see Annex F) evaluated at $N_{\Delta S}$ cycles.
$S_a\left(N_{\Delta TN}\right)$	stress amplitude from the applicable design fatigue curve (see Annex F) evaluated at $N_{\Delta TN}$ cycles.
$S_a\left(N_{\Delta TM}\right)$	stress amplitude from the applicable design fatigue curve (see Annex F) evaluated at $N_{\Delta TM}$ cycles.
$S_a\left(N_{\Delta TR}\right)$	stress amplitude from the applicable design fatigue curve (see Annex F) evaluated at $N_{\Delta TR}$ cycles.
σ_e	von Mises stress.
$\sigma_{e,k}$	von Mises stress for the k^{th} loading condition.
σ_{ref}	reference stress.
$\sigma_{max,k}$	maximum stress in the k^{th} cycle.
$\sigma_{mean,k}$	mean stress in the k^{th} cycle.
$\sigma_{min,k}$	minimum stress in the k^{th} cycle.
σ_{ys}	yield strength of material at the assessment temperature.
$\sigma_{ij,k}$	stress tensor at the point under evaluation for the k^{th} cycle.
σ_b^p	bending stress from primary loads.
σ_m^p	membrane stress from primary loads.

$\sigma_{ij,k}^{LT}$ stress tensor due to local thermal stress at the location and time point under evaluation for the k^{th} cycle.

${}^{m}\sigma_{ij,k}$ stress tensor at the location under evaluation at time point ${}^{m}t$ for the k^{th} cycle.

${}^{n}\sigma_{ij,k}$ stress tensor at the location under evaluation at time point ${}^{n}t$ for the k^{th} cycle.

${}^{m}\sigma_{ij,k}^{LT}$ stress tensor due to local thermal stress at the location under evaluation at time point ${}^{m}t$ for the k^{th} cycle.

${}^{n}\sigma_{ij,k}^{LT}$ stress tensor due to local thermal stress at the location under evaluation at time point ${}^{n}t$ for the k^{th} cycle.

${}^{m}\sigma_{b,k}^{e}$ elastically calculated bending stress normal to the hypothetical crack plane at the location under evaluation at time point ${}^{m}t$ for the k^{th} cycle.

${}^{n}\sigma_{b,k}^{e}$ elastically calculated bending stress normal to the hypothetical crack plane at the location under evaluation at time point ${}^{n}t$ for the k^{th} cycle.

${}^{m}\sigma_{m,k}^{e}$ elastically calculated membrane stress normal to the hypothetical crack plane at the location under evaluation at time point ${}^{m}t$ for the k^{th} cycle.

${}^{n}\sigma_{m,k}^{e}$ elastically calculated membrane stress normal to the hypothetical crack plane at the location under evaluation at time point ${}^{n}t$ for the k^{th} cycle.

σ^{P} generalized stress from primary loads.

σ^{R} generalized residual stress.

σ_1 principal stress in the 1-direction.

σ_2 principal stress in the 2-direction.

σ_3 principal stress in the 3-direction.

$\sigma_{1,k}$ principal stress in the 1-direction for the k^{th} loading condition.

$\sigma_{2,k}$ principal stress in the 2-direction for the k^{th} loading condition.

$\sigma_{3,k}$ principal stress in the 3-direction for the k^{th} loading condition.

t minimum wall thickness in the region under consideration, or the thickness of the component, as applicable.

t_{ess} structural stress effective thickness.

t_1 minimum wall thickness associated with R_1.

t_2 minimum wall thickness associated with R_2.

${}^{m}t$ time point m for the k^{th} cycle.

${}^{n}t$ time point n for the k^{th} cycle.

$T_{max,k}$ maximum temperature in the k^{th} cycle.

${}^{m}\tau_{b,k}^{e}$ elastically calculated bending component of shear stress parallel to the hypothetical crack plane at the location under evaluation at time point ${}^{m}t$ for the k^{th} cycle.

${}^{n}\tau_{b,k}^{e}$ elastically calculated bending component of shear stress parallel to the hypothetical crack plane at the location under evaluation at time point ${}^{n}t$ for the k^{th} cycle.

${}^{m}\tau_{m,k}^{e}$ elastically calculated membrane component shear stress parallel to the hypothetical crack plane at the location under evaluation at time point ${}^{m}t$ for the k^{th} cycle.

$^{n}\tau^{e}_{m,k}$	elastically calculated membrane component shear stress parallel to the hypothetical crack plane at the location under evaluation at time point ^{n}t for the k^{th} cycle
UTS	minimum specified ultimate tensile strength at room temperature.
X	maximum general primary membrane stress divided by the yield strength.
YS	minimum specified yield strength at room temperature.

B1.10 References

1. Anderson, T.L., *Fracture Mechanics – Fundamentals and Applications*, 3rd Edition, CRC Press, Boca Raton, Florida, 2005.
2. Bannantine, J.A., Comer, J.J., and Handrock, J.L., *Fundamentals of Metal Fatigue Analysis,* Prentice-Hall, Inc., Englewood cliffs, N.J., 1990.
3. Barsom, J.M. and Vecchio, R.S., *Fatigue of Welded Structures*, WRC Bulletin 422, Welding Research Council, New York, 1997.
4. Barsom, J.M., and Vecchio, R.S., "Fatigue Of Welded Components," PVP Vol. 313-1, International Pressure Vessels and Piping Codes and Standards: Volume 1, ASME, 1995.
5. Brown, Robert, G., "Development of Elastic Stress Intensity Factor Solutions and Elastic-Plastic Failure Assessment Diagrams For Fillet Toe Cracks at Ring-Stiffened Cylindrical Shells," Thesis, The University of Akron, December, 1996.
6. Bushnell D., *Computerized Buckling Analysis and Shells*, Kluwer Academic Publishers, Norwell, MA, 1985.
7. Dodds, R.H., Jr. And Vargas, P.M., "Numerical Evaluation of Domain and Contour Integrals for Nonlinear Fracture Mechanics." Report UILU-ENG-88-2006, University of Illinois, Urbana, IL, August 1988.
8. Dong, P., Osage, D.A., and Prager, M., *Master S-N Curve Method for Fatigue Evaluation of Welded Components*, WRC Bulletin 474, Welding Research Council, New York, N.Y., 2002.
9. Dowling, N.E., "Fatigue at Notches and the Local Strain and Fracture Mechanics Approaches," Fracture Mechanics, ASTM STP 677, American Society for Testing and Materials, 1979.
10. Dowling, N.E., *Mechanical Behavior of Materials*, Prentice-Hall, Englewood Cliffs, N.J. 1993.
11. Gerdeen, J.C., Rodabaugh, E.C., and O'Donnell, W.J., *A Critical Evaluation of Plastic Behavior Data and a Unified Definition of Plastic Loads for Pressure Components*, WRC Bulletin 254, Welding Research Council, New York, 1979.
12. Gurney, T.R., *Fatigue of Thin Walled Joints Under Complex Loading*, Abington Publishing, Abington Hall, Abington, Cambridge, England, 1997.
13. Hibbitt, Karlson & Sorensen, Inc., "ABAQUS/Standard User's Manual – Volume 1, Version 5.6," Hibbitt, Karlson & Sorensen, Inc., Pawtucket, RI, 1997.
14. IIW, *Stress Determination for Fatigue Analysis of Welded Components*, Edited by Erkki Niemi, Abington Publishing, Abington Hall, Abington, Cambridge, England, 1995.
15. Maddox, S.J., *Fatigue Strength of Welded Structures*, 2nd Edition, Abington Publishing, Woodhead Publishing Limited, Abington hall, Abington, Cambridge, England, 1991.
16. Miline, I., Ainsworth, R.A., Dowling, A.R., Stewart, A.T., "Assessment of the Integrity of Structures Containing Defects," Int. J. Pres. Ves. & Piping 32, 1988, pp. 66-72.
17. Miller, C.D. and Mokhtarian, K., *Proposed Rules for Determining Allowable Compressive Stresses for Cylinders, Cones, Spheres and Formed Heads*, WRC Bulletin 406, Welding Research Council, New York, 1995.
18. Munse, W.H., *Fatigue of Welded Steel Structures*, Welding Research Council, New York, N.Y., 1964.
19. Nelson, D.V., "Cumulative Fatigue Damage in Metals", Ph.D. Dissertation, Stanford, California: Stanford University, 1978.

20. Osage, D.A., Krishnaswamy, P., Stephens, D.R., Scott, P., Janelle, J., Mohan, R., and Wilkowski, G.M., *Technologies for the Evaluation of Non-Crack-Like Flaws in Pressurized Components – Erosion/Corrosion, Pitting, Blisters, Shell Out-Of-Roundness, Weld Misalignment, Bulges and Dents*, WRC Bulletin 465, Welding Research Council, New York, N.Y., September, 2001.

21. Radaj, D. and Sonsino, C.M., *Fatigue Assessment of Welded Joints by Local Approaches*, Abington Publishing, Woodhead Publishing Limited, Abington hall, Abington, Cambridge, England, 1998.

22. Shih, C.F., Moran, B., and Nakamura, T., "Energy Release Rate Along a Three-Dimensional Crack Front in a Thermally Stressed Body." *International Journal of Fracture*, Vol. 30, 1986, pp. 79-102.

23. Socie, D.F. and Marquis, G.B., *Multiaxial Fatigue*, Society of Automotive Engineers, Inc., Warrendale, PA, 2000.

24. Stephens, R.I., Fatemi, A., Stephens, R.R., and Fuchs, H.O., *Metal Fatigue in Engineering*, 2nd Edition, John Wiley & Sons, Inc., New York, N.Y., 2001.

25. Suresh, S., *Fatigue of Materials*, 2nd Edition, Cambridge University Press, Cambridge, UK, 1998.

26. Wirsching, P.H. and Wu, Y.T., "Probabilistic and Statistical Methods of Fatigue Analysis and Design," Pressure Vessel and Piping Technology – 1985, American Society of Mechanical Engineers, New York, 1985, pp. 793-819.

B1.11 Tables

Table B1.1 – Load Descriptions

Design Load Parameter	Description
P	Internal and external maximum allowable working pressure
P_s	Static head from liquid or bulk materials (e.g. catalyst)
D	Dead weight of the vessel, contents, and appurtenances at the location of interest, including the following: • Weight of vessel including internals, supports (e.g. skirts, lugs, saddles, and legs), and appurtenances (e.g. platforms, ladders, etc.) • Weight of vessel contents under operating and test conditions • Refractory linings, insulation • Static reactions from the weight of attached equipment, such as motors, machinery, other vessels, and piping
L	• Appurtenance Live loading • Effects of fluid momentum, steady state and transient
E	Earthquake loads (see ASCE 7 for the specific definition of the earthquake load, as applicable)
W	Wind Loads
W_{pt}	Is the pressure test wind load case. The design wind speed for this case shall be specified by the Owner-User.
S_s	Snow Loads
T	Is the self-restraining load case (i.e. thermal loads, applied displacements). This load case does not typically affect the collapse load, but should be considered in cases where elastic follow-up causes stresses that do not relax sufficiently to redistribute the load without excessive deformation.

Table B1.2 – Load Case Combinations and Allowable Membrane Stresses for an FFS Assessment Based on Elastic Analysis

Load Case Combination	Allowable General Primary Membrane Stress (1),(2),(3)
1) $P+P_s+D$	S_m
2) $P+P_s+D+L$	S_m
3) $P+P_s+D+S_s$	S_m
4) $0.6D+\left(W\ or\ 0.7E\right)$ (4)	S_m
5) $0.9P+P_s+D+\left(W\ or\ 0.7E\right)$	S_m
6) $0.9P+P_s+D+0.75L+0.75S_s$	S_m
7) $0.9P+P_s+D+0.75\left(W\ or\ 0.7E\right)+0.75L+0.75S_s$	S_m

Notes:

1) The parameters used in the Design Load Combination column are defined in Table B1.1.
2) The term $0.9P$ is considered an operating pressure.
3) S_m is the allowable stress for the load case combination. This value represents the general primary membrane stress limit for "load-controlled" loads. Stress limits for local membrane and bending stresses from "load-controlled" or "strain-controlled" loads are provided in paragraph B.1.2.2.4.
4) This load combination addresses an overturning condition. If anchorage is included in the design, consideration of this load combination is not required.

Table B1.3 – Load Case Combinations and Load Factors for an FFS Assessment Based on Limit Load Analysis

Analysis Conditions	
Criteria	Required Factored Load Combinations
Global Criteria	1) $\{1.5(P+P_s+D)\}\cdot RSF_a$ 2) $\{1.3(P+P_s+D+T)+1.7L+0.54S_s\}\cdot RSF_a$ 3) $\{1.3(P+P_s+D)+1.7S_s+(1.1L \text{ or } 0.86W)\}\cdot RSF_a$ 4) $\{1.3(P+P_s+D)+1.7W+1.1L+0.54S_s\}\cdot RSF_a$ 5) $\{1.3(P+P_s+D)+1.1E+1.1L+0.21S_s\}\cdot RSF_a$
Local Criteria	Per Table B1.4
Serviceability Criteria	Per Owner-user's Specification, if applicable, see Table B1.4.
Hydrostatic Test Conditions	
Global and Local Criteria	$\max\left[1.43, 1.25\left(\frac{S_T}{S}\right)\right]\cdot(P+P_s+D)+1.7W_{pt}$
Serviceability Criteria	Per Owner-user's Specification, if applicable.
Pneumatic Test Conditions	
Global and Local Criteria	$1.15\left(\frac{S_T}{S}\right)\cdot(P+P_s+D)+1.7W_{pt}$
Serviceability Criteria	Per Owner-user's Specification, if applicable.

Notes:

1) The parameters used in the Design Load Combination column are defined in Table B1.1.
2) See paragraph B1.2.3.4 for descriptions of global and serviceability criteria.
3) S is the allowable membrane stress from the applicable construction code at the design temperature.
4) S_T is the allowable membrane stress from the applicable construction code at the pressure test temperature.
5) RSF_a is the allowable Remaining Strength Factor from Part 2.

Table B1.4 – Load Case Combinations and Load Factors for an FFS Assessment Based on Elastic-Plastic Analysis

Analysis Conditions	
Criteria	Required Factored Load Combinations
Global Criteria	1) $\beta\left(P+P_s+D\right)$ 2) $0.86\beta\left(P+P_s+D+T\right)+1.1\beta L+0.36\beta S_s$ 3) $0.86\beta\left(P+P_s+D\right)+1.1\beta S_s+\left(0.71\beta L \text{ or } 0.57\beta W\right)$ 4) $0.86\beta\left(P+P_s+D\right)+1.1\beta W+0.71\beta L+0.36\beta S_s$ 5) $0.86\beta\left(P+P_s+D\right)+0.71\beta E+0.71\beta L+0.14\beta S_s$
Local Criteria	$1.7\left(P+P_s+D\right)\cdot RSF_a$
Serviceability Criteria	Per Owner-user's Specification, if applicable, see paragraph B1.2.4.3.b.
Hydrostatic Test Conditions	
Global and Local Criteria	$\max\left[0.95\beta,\ 0.83\beta\left(\frac{S_T}{S}\right)\right]\cdot\left(P+P_s+D\right)+1.1\beta W_{pt}$
Serviceability Criteria	Per Owner-user's Specification, if applicable.
Pneumatic Test Conditions	
Global and Local Criteria	$0.76\beta\left(\frac{S_T}{S}\right)\cdot\left(P+P_s+D\right)+1.1\beta W_{pt}$
Serviceability Criteria	Per Owner-user's Specification, if applicable.

Table B1.4 – Load Case Combinations and Load Factors for an FFS Assessment Based on Elastic-Plastic Analysis

Notes:

1) The parameters used in the Design Load Combination column are defined in Table B1.1.
2) See paragraph B1.2.4.3 for descriptions of global, local, and serviceability criteria.
3) S is the allowable membrane stress from the applicable construction code at the design temperature.
4) S_T is the allowable membrane stress from the applicable construction code at the pressure test temperature.
5) RSF_a is the allowable Remaining Strength Factor from Part 2.
6) The parameter β is the load factor coefficient based on the factor applied to the ultimate tensile strength used to establish a design allowable stress in the applicable construction code. For example:

Construction Code	β
PD 5500	$2.35 \cdot RSF_a$
EN 13345	$2.4 \cdot RSF_a$
ASME Section VIII, Division 2 and ASME B31.3	$3.0 \cdot RSF_a$
ASME Section VIII, Division 1, post 1999	$3.5 \cdot RSF_a$
ASME Section VIII, Division 1, pre 1999 and ASME B31.1	$4.0 \cdot RSF_a$

Table B1.5 – Examples Of Stress Classification

Vessel Component	Location	Origin of Stress	Type of Stress	Classification
Any shell including cylinders, cones, spheres and formed heads	Shell plate remote from discontinuities	Internal pressure	General membrane Gradient through plate thickness	P_m Q
		Axial thermal gradient	Membrane Bending	Q Q
	Near nozzle or other opening	Net-section axial force and/or bending moment applied to the nozzle, and/or internal pressure	Local membrane Bending Peak (fillet or corner)	P_L Q F
	Any location	Temperature difference between shell and head	Membrane Bending	Q Q
	Shell distortions such as out-of-roundness and dents	Internal pressure	Membrane Bending	P_m Q
Cylindrical or conical shell	Any section across entire vessel	Net-section axial force, bending moment applied to the cylinder or cone, and/or internal pressure	Membrane stress averaged through the thickness remote from discontinuities; stress component perpendicular to cross section	P_m
			Bending stress through the thickness; stress component perpendicular to cross section	P_b
	Junction with head or flange	Internal pressure	Membrane Bending	P_L Q
Dished head or conical head	Crown	Internal pressure	Membrane Bending	P_m P_b
	Knuckle or junction to shell	Internal pressure	Membrane Bending	P_L [note (1)] Q
Flat head	Center region	Internal pressure	Membrane Bending	P_m P_b
	Junction to shell	Internal pressure	Membrane Bending	P_L Q [note (2)]
Perforated head or shell	Typical ligament in a uniform pattern	Pressure	Membrane (averaged through cross section) Bending (averaged through width of ligament., but gradient through plate) Peak	P_m P_b F

Table B1.5 – Examples Of Stress Classification

Vessel Component	Location	Origin of Stress	Type of Stress	Classification
Perforated head or shell	Isolated or atypical ligament	Pressure	Membrane Bending Peak	Q F F
Nozzle (see paragraph B1.6)	Within the limits of reinforcement given by Annex A paragraph A.3.11	Pressure and external loads and moments including those attributable to restrained free end displacements of attached piping	General membrane Bending (other than gross structural discontinuity stresses) averaged through nozzle thickness	P_m P_m
	Outside the limits of reinforcement given by Annex A paragraph A.3.11	Pressure and external axial, shear, and torsional loads including those attributable to restrained free end displacements of attached piping	General Membrane	P_m
		Pressure and external loads and moments, excluding those attributable to restrained free end displacements of attached piping	Membrane Bending	P_L P_b
		Pressure and all external loads and moments	Membrane Bending Peak	P_L Q F
	Nozzle wall	Gross structural discontinuities	Membrane Bending Peak	P_L Q F
		Differential expansion	Membrane Bending Peak	Q Q F
Cladding	Any	Differential expansion	Membrane Bending	F F
Any	Any	Radial temperature distribution [note (3)]	Equivalent linear stress [note (4)] Nonlinear portion of stress distribution	Q F
Any	Any	Any	Stress concentration (notch effect)	F

Notes:

1. Consideration shall also be given to the possibility of wrinkling and excessive deformation in vessels with large diameter-to-thickness ratio.
2. If the bending moment at the edge is required to maintain the bending stress in the center region within acceptable limits, the edge bending is classified as P_b; otherwise, it is classified as Q.
3. Consider possibility of thermal stress ratchet.
4. Equivalent linear stress is defined as the linear stress distribution that has the same net bending moment as the actual stress distribution.

Table B1.6 – Uniaxial Strain Limit for use in Multiaxial Strain Limit Criterion

Material	Maximum Temperature	ε_{Lu} Uniaxial Strain Limit (1), (2), (3)			α_{sl}
		m_2	Elongation Specified	Reduction of Area Specified	
Ferritic Steel	480°C (900°F)	$0.60\left(1.00-R\right)$	$2\cdot\ln\left[1+\frac{E}{100}\right]$	$\ln\left[\frac{100}{100-RA}\right]$	2.2
Stainless Steel and Nickel Base Alloys	480°C (900°F)	$0.75\left(1.00-R\right)$	$3\cdot\ln\left[1+\frac{E}{100}\right]$	$\ln\left[\frac{100}{100-RA}\right]$	0.6
Duplex Stainless Steel	480°C (900°F)	$0.70\left(0.95-R\right)$	$2\cdot\ln\left[1+\frac{E}{100}\right]$	$\ln\left[\frac{100}{100-RA}\right]$	2.2
Super Alloys (4)	480°C (900°F)	$1.90\left(0.93-R\right)$	$\ln\left[1+\frac{E}{100}\right]$	$\ln\left[\frac{100}{100-RA}\right]$	2.2
Aluminum	120°C (250°F)	$0.52\left(0.98-R\right)$	$1.3\cdot\ln\left[1+\frac{E}{100}\right]$	$\ln\left[\frac{100}{100-RA}\right]$	2.2
Copper	65°C (150°F)	$0.50\left(1.00-R\right)$	$2\cdot\ln\left[1+\frac{E}{100}\right]$	$\ln\left[\frac{100}{100-RA}\right]$	2.2
Titanium and Zirconium	260°C (500°F)	$0.50\left(0.98-R\right)$	$1.3\cdot\ln\left[1+\frac{E}{100}\right]$	$\ln\left[\frac{100}{100-RA}\right]$	2.2

Notes:

1. If the elongation and reduction in area are not specified, then $\varepsilon_{Lu}=m_2$. If the elongation or reduction in area is specified, then ε_{Lu} is the maximum number computed from columns 3, 4 or 5, as applicable.
2. R is the ratio of the minimum specified yield strength divided by the minimum specified ultimate tensile strength.
3. E is the elongation in % and RA is the reduction in area in % determined from the applicable material specification.
4. Precipitation hardening austenitic alloys.

Table B1.7 – Temperature Factors For Fatigue Screening Criteria

Metal temperature Differential		Temperature Factor For Fatigue Screening Criteria
°C	°F	
28 or less	50 or less	0
29 to 56	51 to 100	1
57 to 83	101 to 150	2
84 to 139	151 to 250	4
140 to 194	251 to 350	8
195 to 250	351 to 450	12
Greater than 250	Greater than 450	20

Notes:

1. If the weld metal temperature differential is unknown or cannot be established, a value of 20 shall be used.
2. As an example illustrating the use of this table, consider a component subject to metal temperature differentials for the following number of thermal cycles.

Temperature Differential	Temperature Factor Based On Temperature Differential	Number Of Thermal Cycles
28°C (50°F)	0	1000
50°C (90°F)	1	250
222°C (400°F)	12	5

The effective number of thermal cycles due to changes in metal temperature is:

$$N_{\Delta TE} = 1000(0) + 250(1) + 5(12) = 310 \ cycles$$

Table B1.8 – Fatigue Screening Criteria For Method A

Description		
Integral Construction	Attachments and nozzles in the knuckle region of formed heads	$N_{\Delta FP} + N_{\Delta PO} + N_{\Delta TE} + N_{\Delta T\alpha} \le 350$
	All other components that do not contain a flaw	$N_{\Delta FP} + N_{\Delta PO} + N_{\Delta TE} + N_{\Delta T\alpha} \le 1000$
Non-integral construction	Attachments and nozzles in the knuckle region of formed heads	$N_{\Delta FP} + N_{\Delta PO} + N_{\Delta TE} + N_{\Delta T\alpha} \le 60$
	All other components that do not contain a flaw	$N_{\Delta FP} + N_{\Delta PO} + N_{\Delta TE} + N_{\Delta T\alpha} \le 400$
Components with a flaw are characterized by a Remaining Strength Factor, RSF, determined in accordance with Parts Part 5, Part 6, Part 7, Part 8, or Part 12		$N_{\Delta FP} + N_{\Delta PO} + N_{\Delta TE} + N_{\Delta T\alpha} \le 150$

Table B1.9 – Fatigue Screening Criteria Factors For Method B

Description		C_1	C_2
Integral Construction	Attachments and nozzles in the knuckle region of formed heads	$C_1 = 4$	$C_2 = 2.7$
	All other components that do not contain a flaw	$C_1 = 3$	$C_2 = 2$
Non-integral construction	Attachments and nozzles in the knuckle region of formed heads	$C_1 = 5.3$	$C_2 = 3.6$
	All other components that do not contain a flaw	$C_1 = 4$	$C_2 = 2.7$
Integral or Non-Integral Construction	Components with a flaw are characterized by a Remaining Strength Factor, RSF, determined in accordance with Parts Part 5, Part 6, Part 7, Part 8, or Part 12	$C_1 = \frac{3}{RSF}$	$C_2 = \frac{2}{RSF}$

Table B1.10 – Weld Surface Fatigue-Strength-Reduction Factors

Weld Condition	Surface Condition	Quality Levels (see Table B1.11)						
		1	2	3	4	5	6	7
Full penetration	Machined	1.0	1.5	1.5	2.0	2.5	3.0	4.0
	As-welded	1.2	1.6	1.7	2.0	2.5	3.0	4.0
Partial Penetration	Final Surface Machined	NA	1.5	1.5	2.0	2.5	3.0	4.0
	Final Surface As-welded	NA	1.6	1.7	2.0	2.5	3.0	4.0
	Root	NA	1.5	NA	NA	NA	3.0	4.0
Fillet	Toe machined	NA	NA	1.5	NA	2.5	3.0	4.0
	Toe as-welded	NA	NA	1.7	NA	2.5	3.0	3.0–4.0
	Root	NA	NA	NA	NA	NA	3.0	4.0

Table B1.11 – Weld Surface Fatigue-Strength-Reduction Factors

Fatigue-Strength-Reduction Factor	Quality Level	Definition
1.0	1	Machined or ground weld that receives a full volumetric examination, and a surface that receives MT/PT examination and a VT examination.
1.2	1	As-welded weld that receives a full volumetric examination, and a surface that receives MP/PT and VT examination
1.5	2	Machined or ground weld that receives a partial volumetric examination, and a surface that receives MT/PT examination and VT examination
1.6	2	As-welded weld that receives a partial volumetric examination, and a surface that receives MP/PT and VT examination
1.5	3	Machined or ground weld surface that receives MT/PT examination and a VT examination (visual), but the weld receives no volumetric examination inspection
1.7	3	As-welded or ground weld surface that receives MT/PT examination and a VT examination (visual), but the weld receives no volumetric examination inspection
2.0	4	Weld has received a partial or full volumetric examination, and the surface has received VT examination, but no MT/PT examination
2.5	5	VT examination only of the surface; no volumetric examination nor MT/PT examination.
3.0	6	Volumetric examination only
4.0	7	Weld backsides that are non-definable and/or receive no examination.

Notes:

1. Volumetric examination is RT or UT in accordance with the applicable construction code.
2. MT/PT examination is magnetic partial or liquid penetrant examination in accordance with the applicable construction code.
3. VT examination is visual examination in accordance with the applicable construction code.
4. See WRC Bulletin 432 for further information.

Table B1.12 – Fatigue Penalty Factors For Fatigue Analysis

Material	$K_{e,k}$ (1)		$T_{max,k}$ (2)	
	m	n	(^{o}C)	(^{o}F)
Low alloy steel	2.0	0.2	371	700
Martensitic stainless steel	2.0	0.2	371	700
Carbon steel	3.0	0.2	371	700
Austenitic stainless steel	1.7	0.3	427	800
Nickel-chromium-iron	1.7	0.3	427	800
Nickel-copper	1.7	0.3	427	800

Notes:

1. Fatigue penalty factor
2. The fatigue penalty factor should only be used if all of the following are satisfied:
   - The component is not subject to thermal ratcheting, and
   - The maximum temperature in the cycle is within the value in the table for the material.

B1.12 Figures

Stress Category	Primary			Secondary Membrane plus Bending	Peak
	General Membrane	Local Membrane	Bending		
Description (For examples, see Table 5.2)	Average primary stress across solid section. Excludes discontinuities and concentrations. Produced only by mechanical loads.	Average stress across any solid section. Considers discontinuities but not concentrations. Produced only by mechanical loads.	Component of primary stress proportional to distance from centroid of solid section. Excludes discontinuities and concentrations. Produced only by mechanical loads.	Self-equilibrating stress necessary to satisfy continuity of structure. Occurs at structural discontinuities. Can be caused by mechanical load or by differential thermal expansion. Excludes local stress concentrations.	1. Increment added to primary or secondary stress by a concentration (notch). 2. Certain thermal stresses which may cause fatigue but not distortion of vessel shape.
Symbol	P_m	P_L	P_b	Q	F

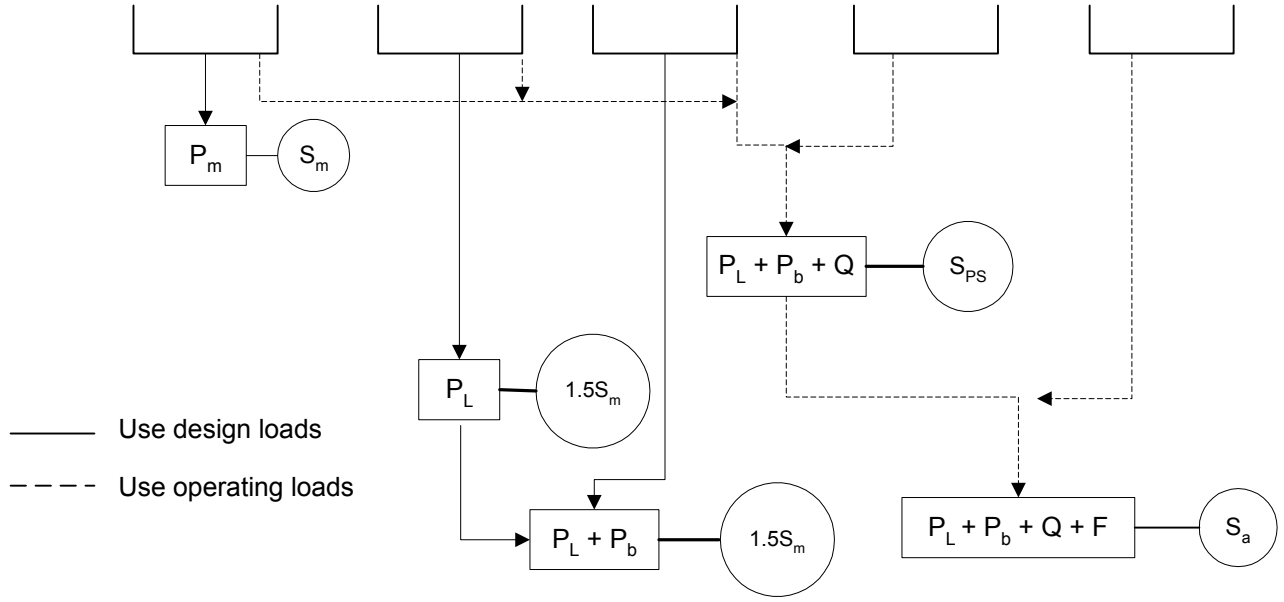

Figure B1.1
Stress Categories and Limits of Equivalent Stress

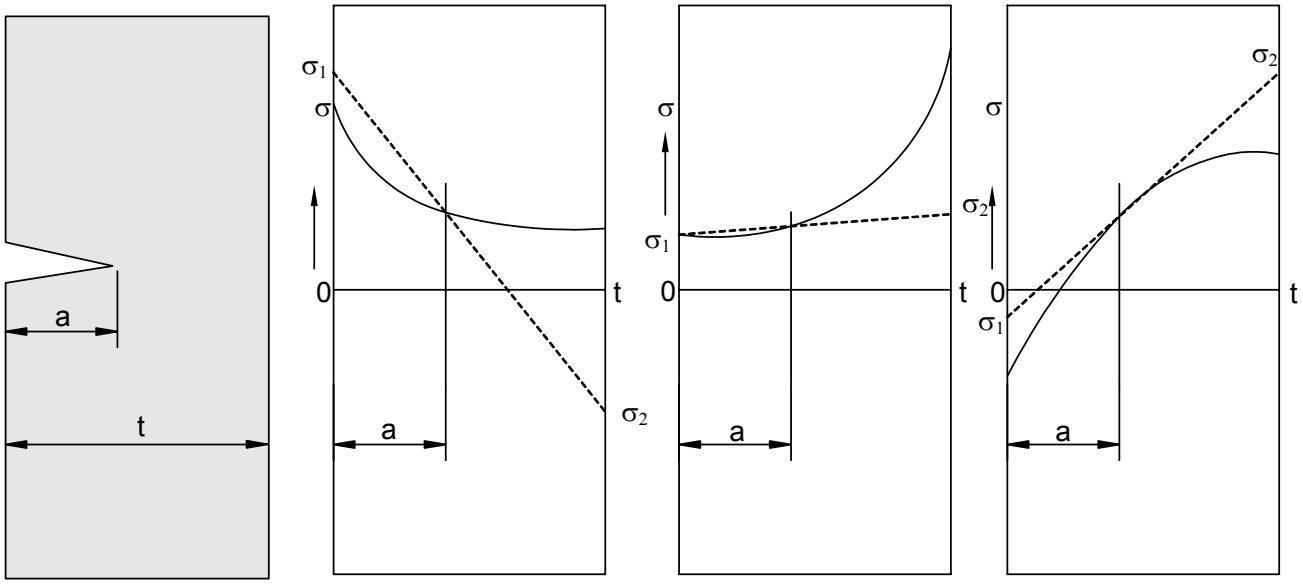

(a) Linearization Over the Defect - Surface Flaw

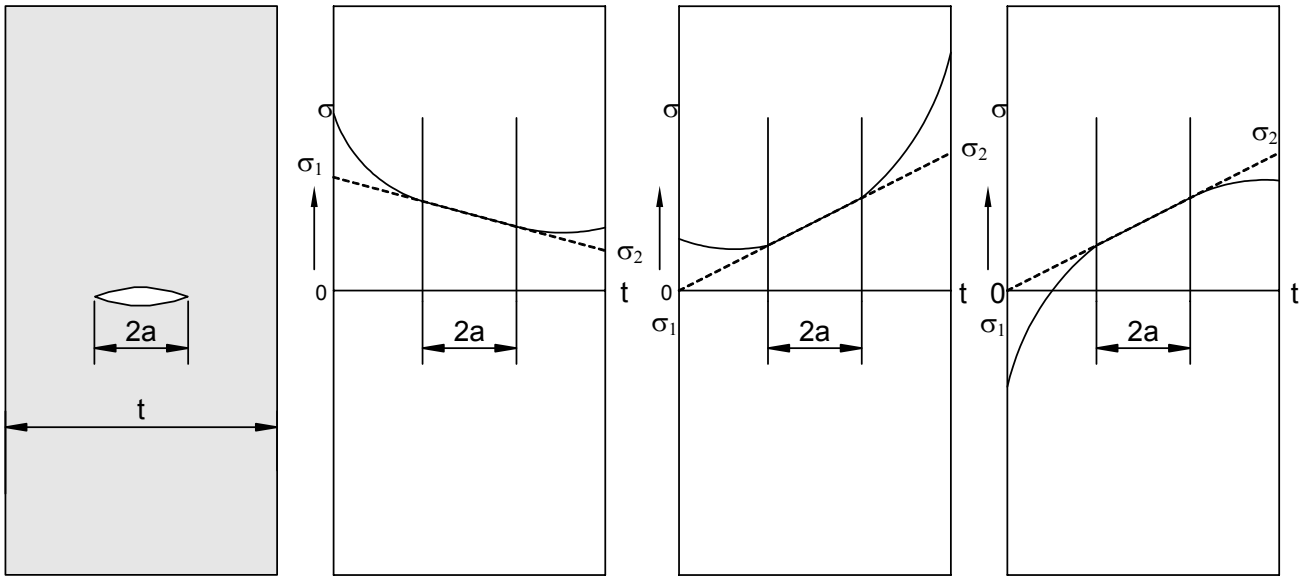

(b) Linearization Over the Defect - Embedded Flaw

Figure B1.2
Stress Linearization Based on the Defect

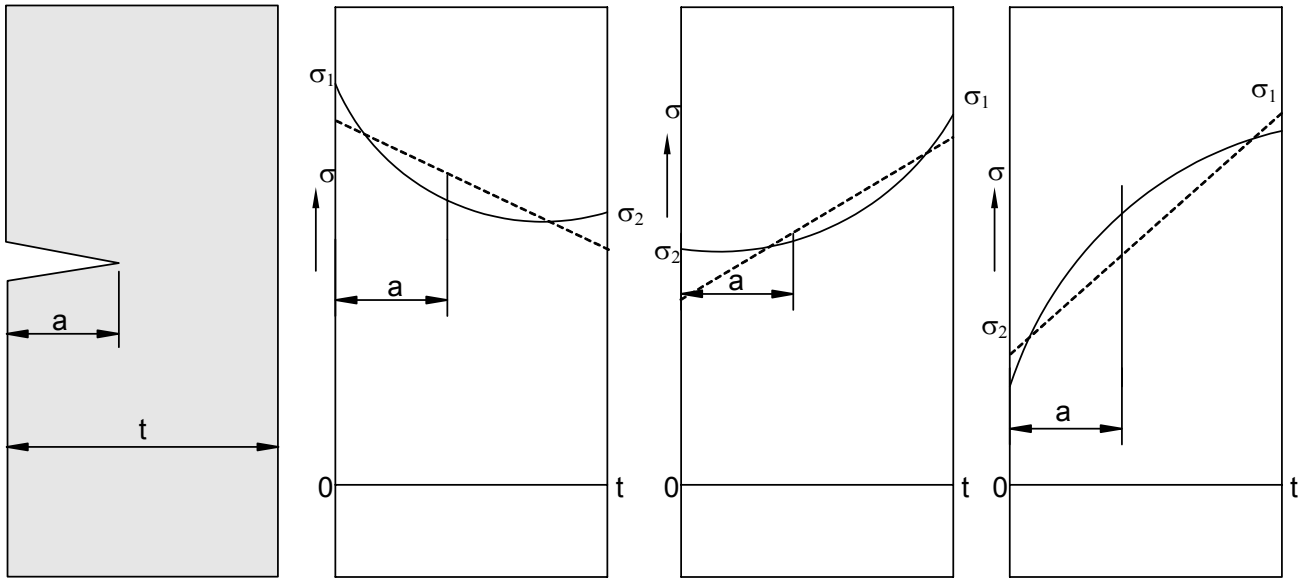

(a) Linearization Over the Cross Section - Surface Flaw

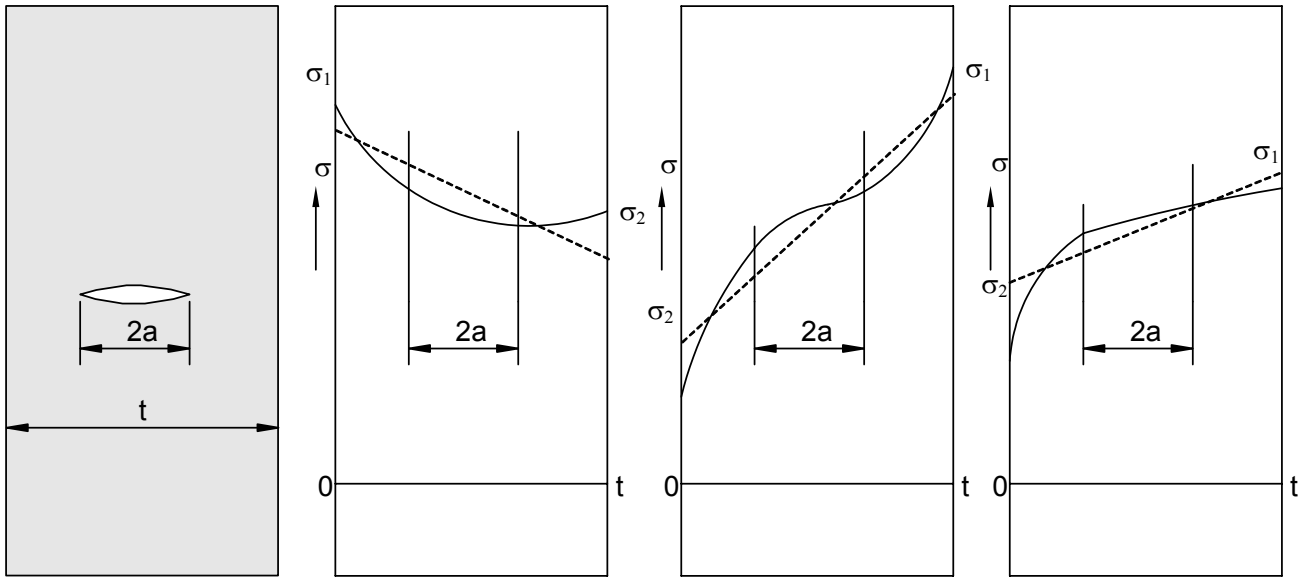

(b) Linearization Over the Cross Section - Embedded Flaw

Figure B1.3
Stress Linearization Based on the Cross Section

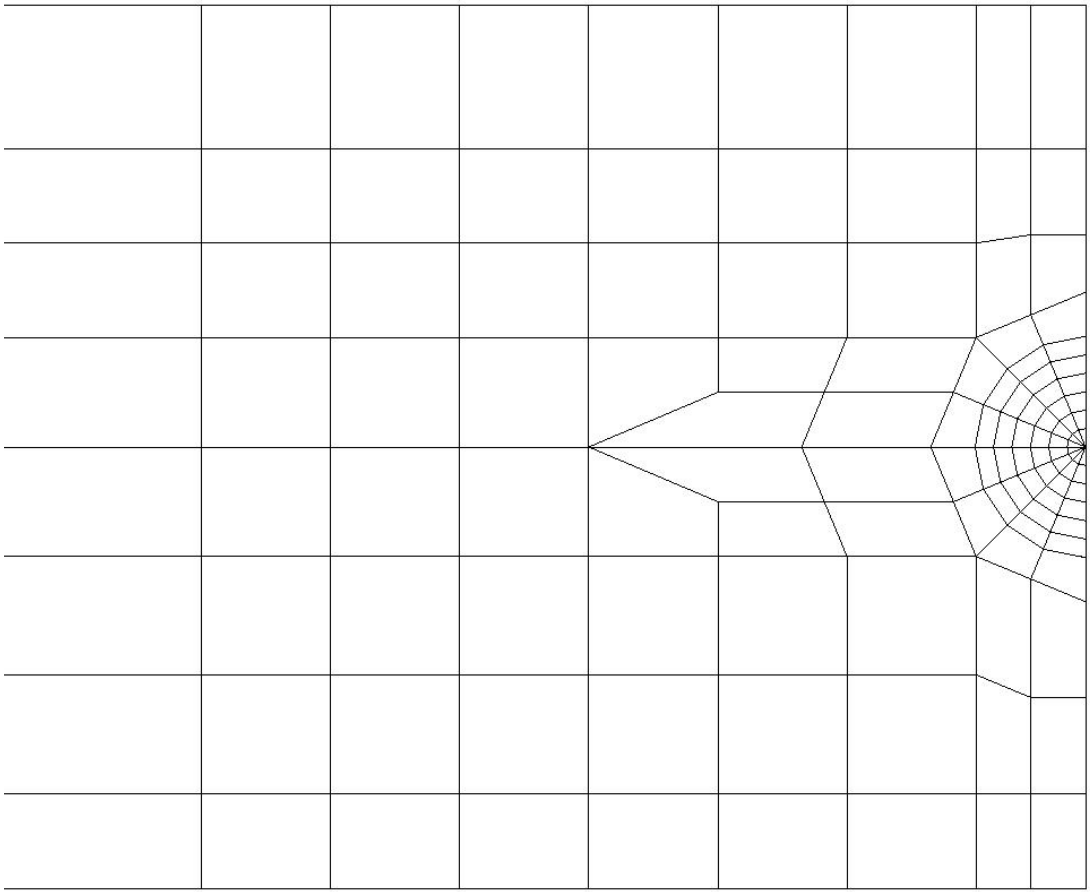

Figure B1.4
***Spider Web* Mesh with Elements Concentrated at the Crack Tip**

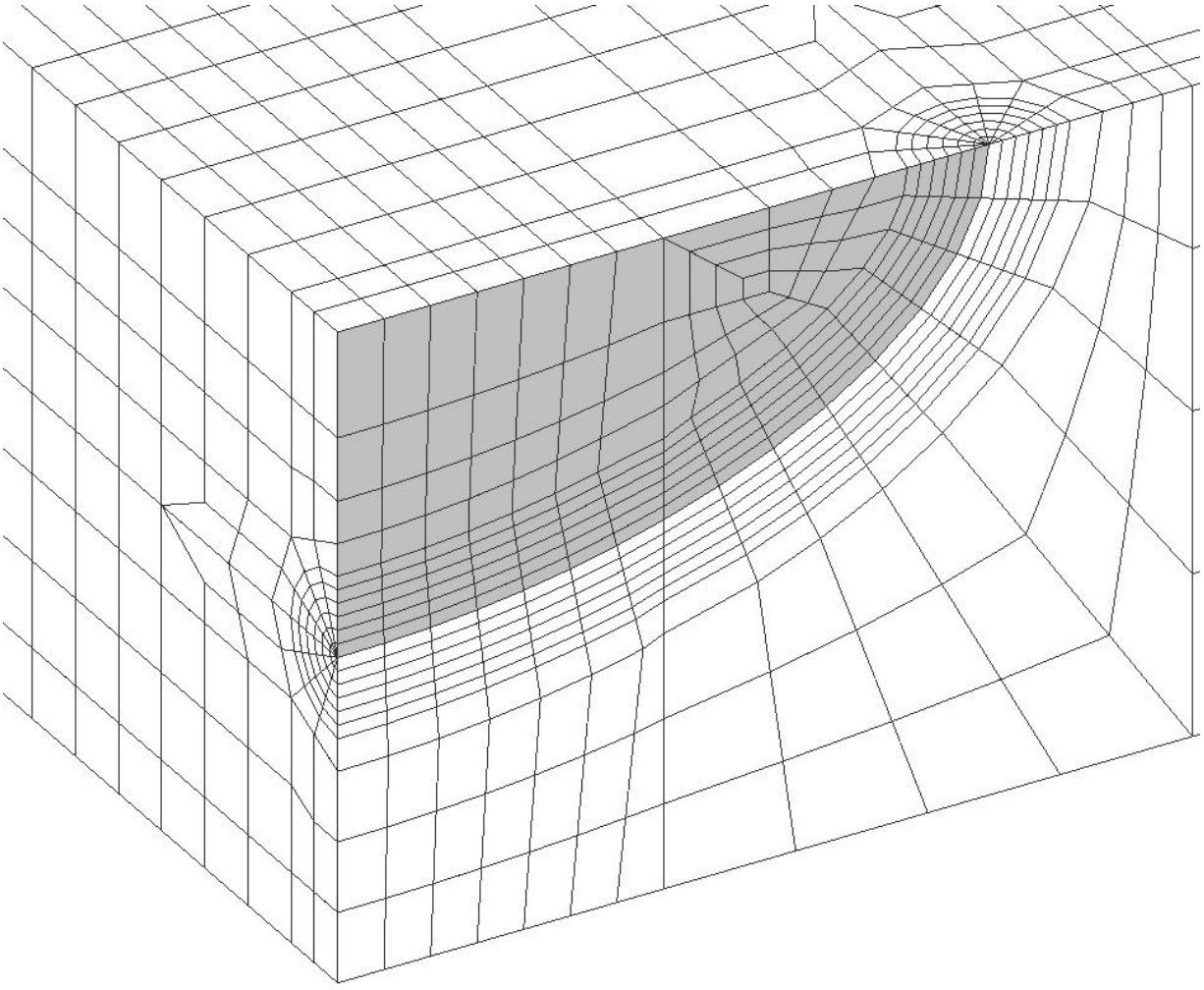

Figure B1.5
Typical 3D Finite Model of a Surface Crack

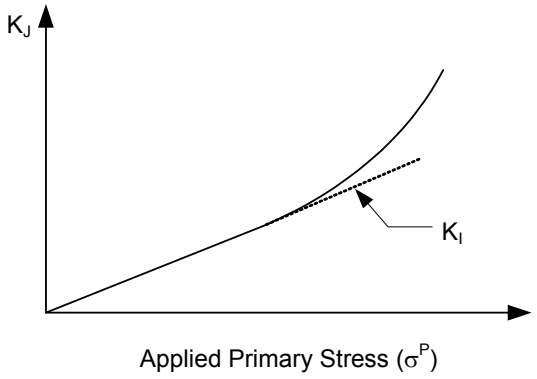

(a) Crack Driving Force (K_J) Versus Primary Stress.

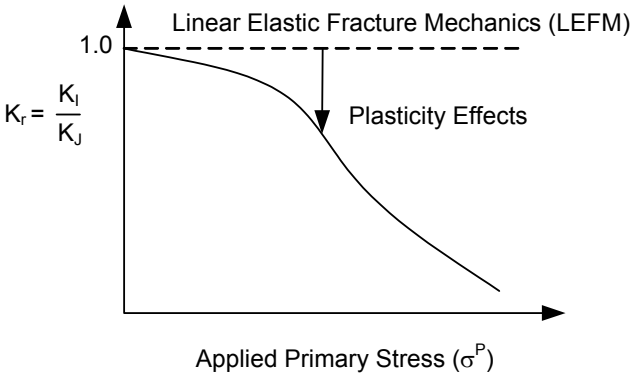

(b) Definition Of The Vertical Axis Of The FAD.

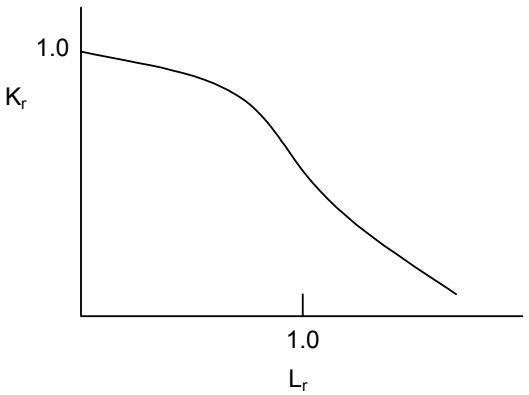

(c) Normalizing The Horizontal Axis With L_r.

Figure B1.6
Derivation of a J-Based FAD Curve

ANNEX B2

RECOMMENDATIONS FOR LINEARIZATION OF STRESS RESULTS FOR STRESS CLASSIFICATION

(NORMATIVE)

PART CONTENTS

B2.1 Scope

This Annex provides recommendations for post-processing of the results from an elastic finite element stress analysis for comparison to the limits in Annex B1.

B2.2 General

a) In the finite element method, when continuum elements are used in an analysis, the total stress distribution is obtained. Therefore, to produce membrane and bending stresses, the total stress distribution shall be linearized on a stress component basis and used to calculate the equivalent stresses. If shell elements (shell theory) are used, then the membrane and bending stresses shall be obtained directly from shell stress resultants.

b) Membrane and bending stresses are developed on cross sections through the thickness of a component. These sections are called stress classification planes (SCPs). In a planar geometry, a Stress Classification Line (SCL) is obtained by reducing two opposite sides of a SCP to an infinitesimal length. SCPs are flat planes that cut through a section of a component and SCLs are straight lines that cut through a section of a component. SCLs are surfaces when viewed in an axisymmetric or planar geometry. Examples of an SCP and SCL are given in Figure B2.1 and Figure B2.2.

c) The following three approaches are provided for linearization of finite element results.

   1) Stress Integration Method – This method can be used to linearize stress results from continuum finite element models [1].

   2) Structural Stress Method Based on Nodal Forces – This method is based on processing of nodal forces, and has been shown to be mesh insensitive and correlate well with welded fatigue data [2].

   3) Structural Stress Method Based on Stress Integration – This method utilizes the Stress Integration Method, but restricts the set of elements that contribute to the line of nodes being processed.

d) The Structural Stress Method based on Stress Integration is recommended unless another method can be shown to produce a more accurate assessment for the given component and loading condition. This method matches the Structural Stress Method Based on Nodal Forces, which is insensitive to mesh refinement. In addition, this method can be performed with post-processing tools typically provided by commercial finite element analysis software.

B2.3 Selection of Stress Classification Lines

a) Pressure vessels usually contain structural discontinuity regions where abrupt changes in geometry, material or loading occur. These regions are typically the locations of highest stress in a component. For the evaluation of failure modes of plastic collapse and ratcheting, Stress Classification Lines (SCLs) are typically located at gross structural discontinuities. For the evaluation of local failure and fatigue, SCLs are typically located at local structural discontinuities.

b) For SCLs that span a material discontinuity (e.g. base metal with cladding), the SCL should include all materials and associated loadings. If one of the materials, such as cladding, is neglected for strength calculations, then only the base metal thickness should be used to calculate the membrane and bending stresses from the linearized forces and moments across the full section for the evaluation of plastic collapse.

c) To most accurately determine the linearized membrane and bending stresses for comparison to Annex B1 elastic stress limits, the following guidelines should be followed. These guidelines can be used as a qualitative means to evaluate the applicability of different SCLs. Failure to comply with any of these criteria may not produce valid membrane and/or bending stresses. Application of the limit load or elastic-plastic analysis methods in Annex B1 is recommended for cases where elastic stress analysis and stress linearization may produce ambiguous results

1) SCLs should be oriented normal to contour lines of the stress component of highest magnitude. However, as this may be difficult to implement, similar accuracy can be obtained by orienting the SCL normal to the mid-surface of the cross section. SCL orientation guidelines are shown in Figure B2.3.a.

2) Hoop and meridional component stress distributions on the SCL should be monotonically increasing or decreasing, except for the effects of stress concentration or thermal peak stresses (see Figure B2.3.b).

3) The distribution of the through-thickness stress should be monotonically increasing or decreasing. For pressure loading, the through-thickness stress should be equal to the compressive pressure on the applied surface, and approximately zero on the other surface defining the SCL (see Figure B2.3.c). When the SCL is not perpendicular to the surfaces, this requirement will not be satisfied.

4) The shear stress distribution should be parabolic and/or the stress should be low relative to the hoop and meridional stresses. Depending on the type of loading, the shear stress should be approximately zero on both surfaces defined by the SCL. Guidelines are provided in Figure B2.3.d.

   i) The shear stress distribution along an SCL will approximate a parabolic distribution only when the inner and outer surfaces are parallel and the SCL is normal to the surfaces. If the surfaces are not parallel or an SCL is not normal to the surfaces, the appropriate shear distribution will not be obtained. However, if the magnitude of shear stress is small as compared to the hoop or meridional stresses, this orientation criterion can be waived.

   ii) When the shear stress distribution is approximately linear, the shear stress is likely to be significant.

5) For pressure boundary components, the hoop or meridional stresses typically are the largest magnitude component stresses and are the dominant terms in the equivalent stress. Typically the hoop or meridional stresses deviate from a monotonically increasing or decreasing trend along an SCL if the SCL is skewed with respect to the interior, exterior, or mid surfaces. For most pressure vessel applications, the hoop or meridional stresses due to pressure should be nearly linear.

B2.4 Stress Integration Method

B2.4.1 Continuum Elements

B2.4.1.1 Overview

Stress results derived from a finite element analysis utilizing two-dimensional or three-dimensional continuum elements may be processed using the stress integration method. Stress components are integrated along SCLs through the wall thickness to determine the membrane and bending stress components. The peak stress components can be derived directly using this procedure by subtracting the membrane plus bending stress distribution from the total stress distribution. Using these components, the equivalent stress shall be computed per Equation (B2.1).

B2.4.1.2 Stress Linearization Procedure

The methods to derive the membrane, bending, and peak components of a stress distribution are shown below, and in Figure B2.4. The component stresses used for the calculations shall be based on a local coordinate system defined by the orientation of the SCL, see Figure B2.2.

a) STEP 1 – Calculate the membrane stress tensor. The membrane stress tensor is the tensor comprised of the average of each stress component along the stress classification line, or:

$$\sigma_{ij,m} = \frac{1}{t}\int_0^t \sigma_{ij} dx \tag{B2.1}$$

b) STEP 2 – Calculate the bending stress tensor.

1) Bending stresses are calculated only for the local hoop and meridional (normal) component stresses, and not for the local component stress parallel to the SCL or in-plane shear stress.

2) The linear portion of shear stress needs to be considered only for shear stress distributions that result in torsion of the SCL (out-of-plane shear stress in the normal-hoop plane, see Figure B2.2).

3) The bending stress tensor is comprised of the linear varying portion of each stress component along the stress classification line, or:

$$\sigma_{ij,b} = \frac{6}{t^2}\int_0^t \sigma_{ij}\left(\frac{t}{2} - x\right) dx \tag{B2.2}$$

c) STEP 3 – Calculate the peak stress tensor. The peak stress tensor is the tensor whose components are equal to:

$$\sigma_{ij,F}(x)\big|_{x=0} = \sigma_{ij}(x)\big|_{x=0} - \left(\sigma_{ij,m} + \sigma_{ij,b}\right) \tag{B2.3}$$

$$\sigma_{ij,F}(x)\big|_{x=t} = \sigma_{ij}(x)\big|_{x=t} - \left(\sigma_{ij,m} - \sigma_{ij,b}\right) \tag{B2.4}$$

d) STEP 4 – Calculate the three principal stresses at the ends of the SCL based on components of membrane and membrane plus bending stresses.

e) STEP 5 – Calculate the equivalent stresses using Equation (B1.1) at the ends of the SCL based on components of membrane and membrane plus bending stresses.

B2.4.2 Shell Elements

B2.4.2.1 Overview

Stress results derived from a finite element analysis utilizing two-dimensional or three-dimensional shells are obtained directly from the analysis results. Using the component stresses, the equivalent stress shall be computed per Equation (B1.1).

B2.4.2.2 Stress Linearization Procedure

The methods to derive the membrane, bending, and peak components of a stress distribution are shown below.

a) The membrane stress tensor is the tensor comprised of the average of each stress component along the stress classification line, or:

$$\sigma_{ij,m} = \frac{\sigma_{ij,in} + \sigma_{ij,out}}{2} \tag{B2.5}$$

b) The bending stress tensor is the tensor comprised of the linear varying portion of each stress component along the stress classification line, or:

$$\sigma_{ij,b} = \frac{\sigma_{ij,in} - \sigma_{ij,out}}{2} \tag{B2.6}$$

c) The peak stress tensor is the tensor whose components are equal to:

$$\sigma_{ij,F} = \left(\sigma_{ij,m} + \sigma_{ij,b}\right)\left(K_f - 1\right) \quad \text{(B2.7)}$$

B2.5 Structural Stress Method Based on Nodal Forces

B2.5.1 Overview

Stress results derived from a finite element analysis utilizing continuum or shell elements may be processed using the Structural Stress Method based on nodal forces. The mesh-insensitive structural stress method provides a robust procedure for capturing the membrane and bending stresses and can be directly utilized in fatigue design of welded joints. With this method, the structural stress normal to a hypothetical cracked plane at a weld is evaluated. For typical pressure vessel component welds, the choice of possible crack orientations is straightforward (e.g. toe of fillet weld). Two alternative calculation procedures for the structural stress method are presented for continuum elements; a procedure based on nodal forces and a procedure based on stress integration. A typical finite element continuum model and stress evaluation line for this type of analysis is shown in Figure B2.5.

B2.5.2 Continuum Elements

a) Stress results derived from a finite element analysis utilizing two-dimensional or three-dimensional continuum elements may be processed using the structural stress method and nodal forces as described below. The membrane and bending stresses can be computed from element nodal internal forces using the equations provided in Table B2.1. The process is illustrated in Figure B2.6. This method is recommended when internal force results can be obtained as part of the finite element output because the results are insensitive to the mesh density.

b) When using three-dimensional continuum elements, forces and moments must be summed with respect to the mid-thickness of a member from the forces at nodes in the solid model at a through-thickness cross section of interest. For a second order element, three summation lines of nodes are processed along the element faces through the wall thickness. The process is illustrated in Figure B2.7.

c) For a symmetric structural stress range, the two weld toes have equal opportunity to develop fatigue cracks. Therefore, the structural stress calculation involves establishing the equilibrium equivalent membrane and bending stress components with respect to one-half of the plate thickness. The equivalent structural stress calculation procedure for a symmetric stress state is illustrated in Figure B2.8.

B2.5.3 Shell Elements

a) Stress results derived from a finite element analysis utilizing shell elements may be processed using the structural stress method and nodal forces. The membrane and bending stresses can be computed from element nodal internal forces using the equations provided in Table B2.2. A typical shell model is illustrated in Figure B2.9.

b) When using three-dimensional shell elements, forces and moments with respect to the mid-thickness of a member must be obtained at a cross section of interest. The process is illustrated in Figure B2.10.

B2.6 Structural Stress Method Based on Stress Integration

As an alternative to the nodal force method above, stress results derived from a finite element analysis utilizing two-dimensional or three-dimensional continuum elements may be processed using the Structural Stress Method Based on Stress Integration. This method utilizes the Stress Integration Method of paragraph B2.3, but restricts the set of elements that contribute to the line of nodes being processed. The elements applicable to the SCL for the region being evaluated shall be included in the post-processing, as is illustrated in Figure B2.11. For a symmetric structural stress range, the integration is performed in the same manner, except that the integration is performed across one-half of the wall thickness, see Figure B2.8.

B2.7 Nomenclature

$\Delta\sigma_s$	structural stress range.
f_i	line force at element location position i.
NF_j	nodal force at node j, normal to the section.
NF_{ij}	nodal force at node j, normal to the section, for element location position .
NM_j	in-plane nodal moment at node j, normal to the section, for a shell element.
F_i	nodal force resultant for element location position i.
K_f	fatigue strength reduction factor.
m_i	line moment at element location position i.
M_i	nodal moment resultant for element location position i.
n	number of nodes in the through-wall thickness direction.
σ_m	membrane stress.
σ_{mi}	membrane stress for element location position i.
σ_b	bending stress.
σ_{bi}	bending stress for element location position i.
σ_{ij}	stress tensor at the point under evaluation.
$\sigma_{ij,m}$	membrane stress tensor at the point under evaluation.
$\sigma_{ij,b}$	bending stress tensor at the point under evaluation.
$\sigma_{ij,F}$	peak stress component.
$\sigma_{ij,in}$	stress tensor on the inside surface of the shell.
$\sigma_{ij,out}$	stress tensor on the outside surface of the shell.
σ_s	structural stress.
r_j	radial coordinate of node j for an axisymmetric element.
s_j	local coordinate, parallel to the stress classification line, that defines the location of nodal force NF_j relative to the mid-thickness of the section.
P	primary equivalent stress.
Q	secondary equivalent stress.
X_L	local X axis, oriented parallel to the stress classification line.
Y_L	local Y axis, oriented normal to the stress classification line.
X_g	global X axis.
Y_g	global Y axis.
t	wall thickness in the region under consideration, or the thickness of the vessel, as applicable.
w	width of the element to determine structural stresses from finite element analysis.
x	through-wall thickness coordinate.

B2.8 References

1. Hechmer, J. L., Hollinger, G. L., “3D Stress Criteria Guidelines For Application,” WRC Bulletin 429, Welding Research Council, New York, N.Y., February, 1998.
2. Dong, P., Hong, Jeong K., Osage, D. A., Prager, M., “Master S-N Curve Method For Fatigue Evaluation Of Welded Components,” WRC Bulletin 474, Welding Research Council, New York, N.Y., August 2002.

B2.9 Tables

Table B2.1 – Structural Stress Definitions for Continuum Finite Elements

Element Type	Membrane Stress	Bending Stress
2D Axisymmetric Second Order (8-Node) Continuum Elements	$\sigma_m = \frac{1}{t}\sum\frac{NF_j}{2\pi r_j}$	$\sigma_b = \frac{6}{t^2}\sum\frac{NF_j \cdot s_j}{2\pi r_j}$
2D Second Order Plane Stress or Plane Strain (8-Node) Continuum Elements	$\sigma_m = \frac{1}{t}\sum\frac{NF_j}{w}$	$\sigma_b = \frac{6}{t^2}\sum\frac{NF_j \cdot s_j}{w}$
3D Second Order (20-Node) Continuum Elements	$\sigma_{mi} = \frac{f_i}{t}$ Note: f_i represents the line force corresponding to the element location positions ($i = 1,2,3$) along the element width (w); position $i = 2$ corresponds to the mid-side of the element (see Figure B2.7): $f_1 = \frac{3(6F_1 + 2F_3 - F_2)}{2w}$ $f_2 = \frac{-3(2F_1 + 2F_3 - 3F_2)}{4w}$ $f_3 = \frac{3(2F_1 + 6F_3 - F_2)}{2w}$ In the above, F_1, F_2 , and F_3 are the nodal force resultants (producing normal membrane stress to Section A-A) through the thickness and along the width (w) of the group of elements $F_i = \sum NF_{ij}$ summed over the nodes from $j = 1, n$ (number of nodes in the through-thickness direction) at Section A-A (see Figure B2.7)	$\sigma_{bi} = \frac{6 \cdot m_i}{t^2}$ Note: m_i represents the line moment corresponding to the element location positions ($i = 1,2,3$) along the element width (w); position $i = 2$ corresponds to the mid-side of the element (see Figure B2.7): $m_1 = \frac{3(6M_1 + 2M_3 - M_2)}{2w}$ $m_2 = \frac{-3(2M_1 + 2M_3 - 3M_2)}{4w}$ $m_3 = \frac{3(2M_1 + 6M_3 - M_2)}{2w}$ In the above, M_1, M_2 , and M_3 are the nodal moment resultants (producing normal bending stress to Section A-A) calculated based on nodal forces with respect to the mid-thickness (s_j) along the width (w) of the group of elements $M_i = \sum NF_{ij} \cdot s_j$ summed over the nodes from $j = 1, n$ (number of nodes in the through-thickness direction) at Section A-A (see Figure B2.7)

Table B2.2 – Structural Stress Definitions for Shell or Plate Finite Elements

Element Type	Membrane Stress	Bending Stress
3D Second Order (8-Node) Shell Elements	$\sigma_{mi} = \frac{f_i}{t}$ Note: f_i represents the force corresponding to the element location positions ($i = 1, 2, 3$) along the element width (w); position $i = 2$ corresponds to the mid-side of the element (see Figure B2.10): $f_1 = \frac{3(6NF_1 + 2NF_3 - NF_2)}{2w}$ $f_2 = \frac{-3(2NF_1 + 2NF_3 - 3NF_2)}{4w}$ $f_3 = \frac{3(2NF_1 + 6NF_3 - NF_2)}{2w}$ In the above, NF_1, NF_2, and NF_3 are the internal nodal forces (in the direction normal to Section A-A) from the shell model along a weld (see Figure B2.10)	$\sigma_{bi} = \frac{6 \cdot m_i}{t^2}$ Note: m_i represents the moment corresponding to the element location positions ($i = 1, 2, 3$) along the element width (w); position $i = 2$ corresponds to the mid-side of the element (see Figure B2.10): $m_1 = \frac{3(6NM_1 + 2NM_3 - NM_2)}{2w}$ $m_2 = \frac{-3(2NM_1 + 2NM_3 - 3NM_2)}{4w}$ $m_3 = \frac{3(2NM_1 + 6NM_3 - NM_2)}{2w}$ In the above, NM_1, NM_2, and NM_3 are the internal nodal moments (producing normal bending stresses to Section A-A) from the shell model along a weld (see Figure B2.10)
3D First Order (4-Node) Shell Elements	$\sigma_{mi} = \frac{f_i}{t}$ Note: f_i represents the force corresponding to the element corner node location positions ($i = 1, 2$) along the element width (w): $f_1 = \frac{2(2NF_1 - NF_2)}{w}$ $f_2 = \frac{2(2NF_2 - NF_1)}{w}$	$\sigma_{bi} = \frac{6 \cdot m_i}{t^2}$ Note: m_i represents the moment corresponding to the element corner node location positions ($i = 1, 2$) along the element width (w): $m_1 = \frac{2(2NM_1 - NM_2)}{w}$ $m_2 = \frac{2(2NM_2 - NM_1)}{w}$
Axisymmetric Linear and Parabolic Shell Finite Element	$\sigma_m = \frac{NF_j}{2\pi r_j t}$	$\sigma_b = \frac{6 \cdot NM_j}{2\pi r_j t^2}$

B2.10 Figures

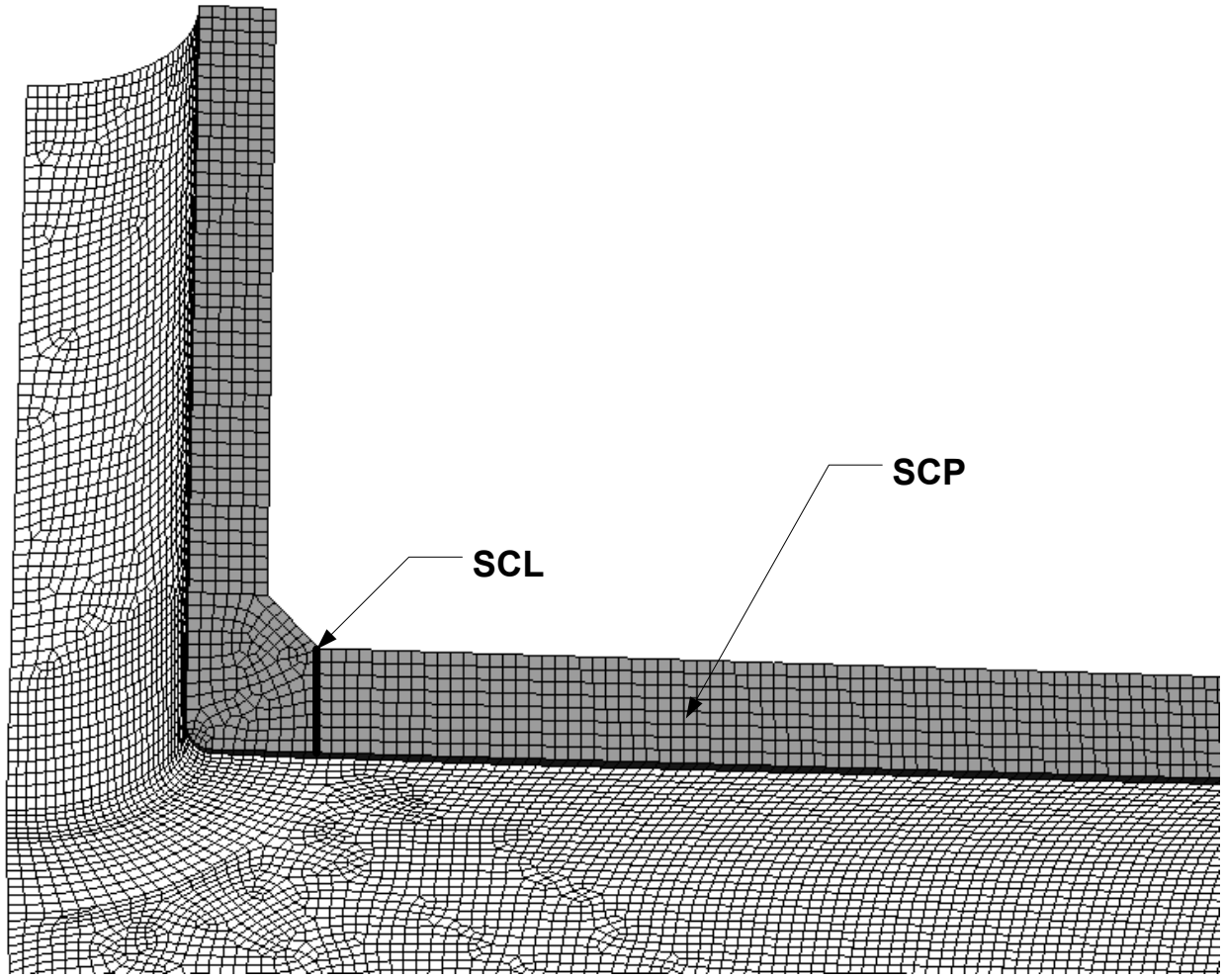

Figure B2.1
Stress Classification Line (SCL) and Stress Classification Plane (SCP)

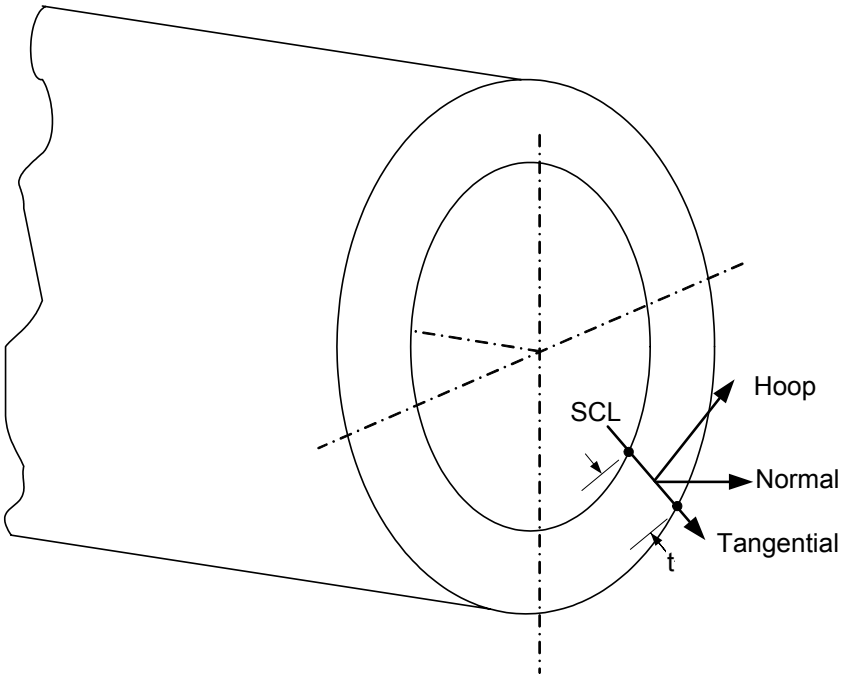

(a) SCL Orientation, Three-Dimensional Model

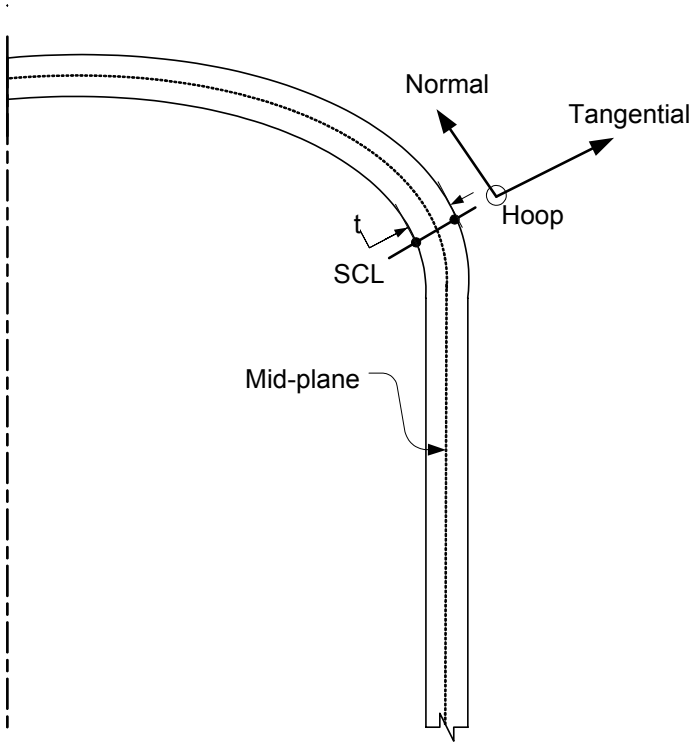

(b) SCL Orientation, Two-Dimensional Model

Figure B2.2
Stress Classification Lines (SCLs)

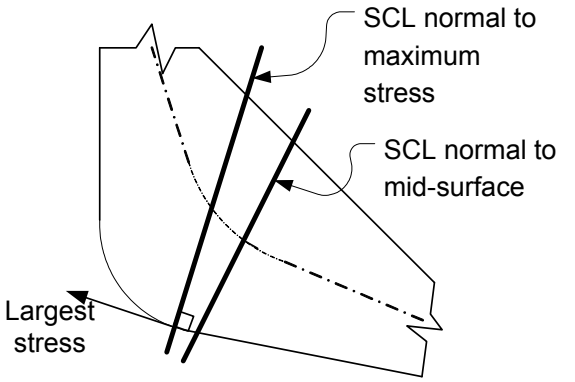

(a) Example of SCL Orientation

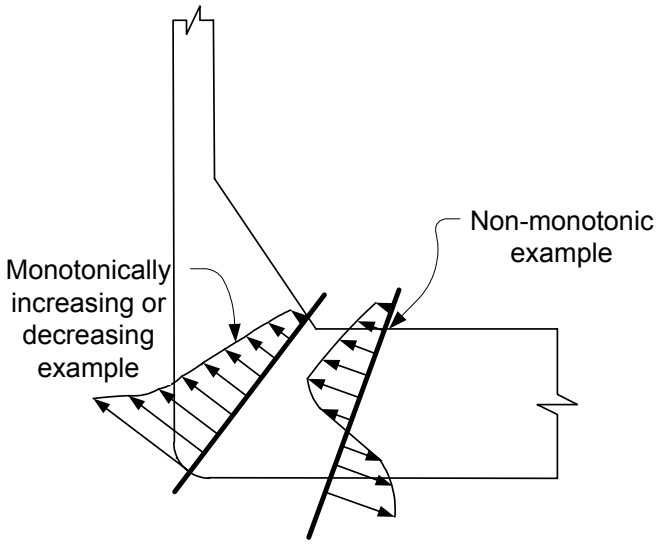

(b) Hoop and Meridional Stress Conditions

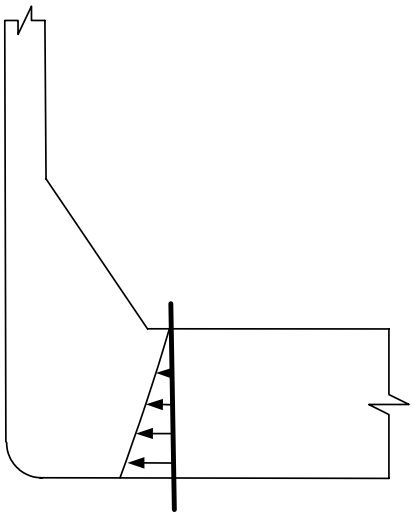

(c) Through-thickness Stress Conditions

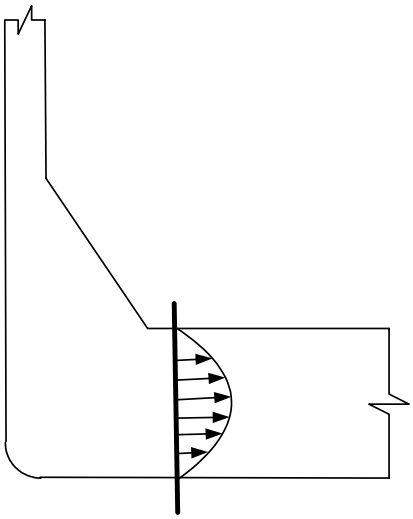

(d) Shear Stress Conditions

Figure B2.3
Stress Classification Line Orientation and Validity Guidelines

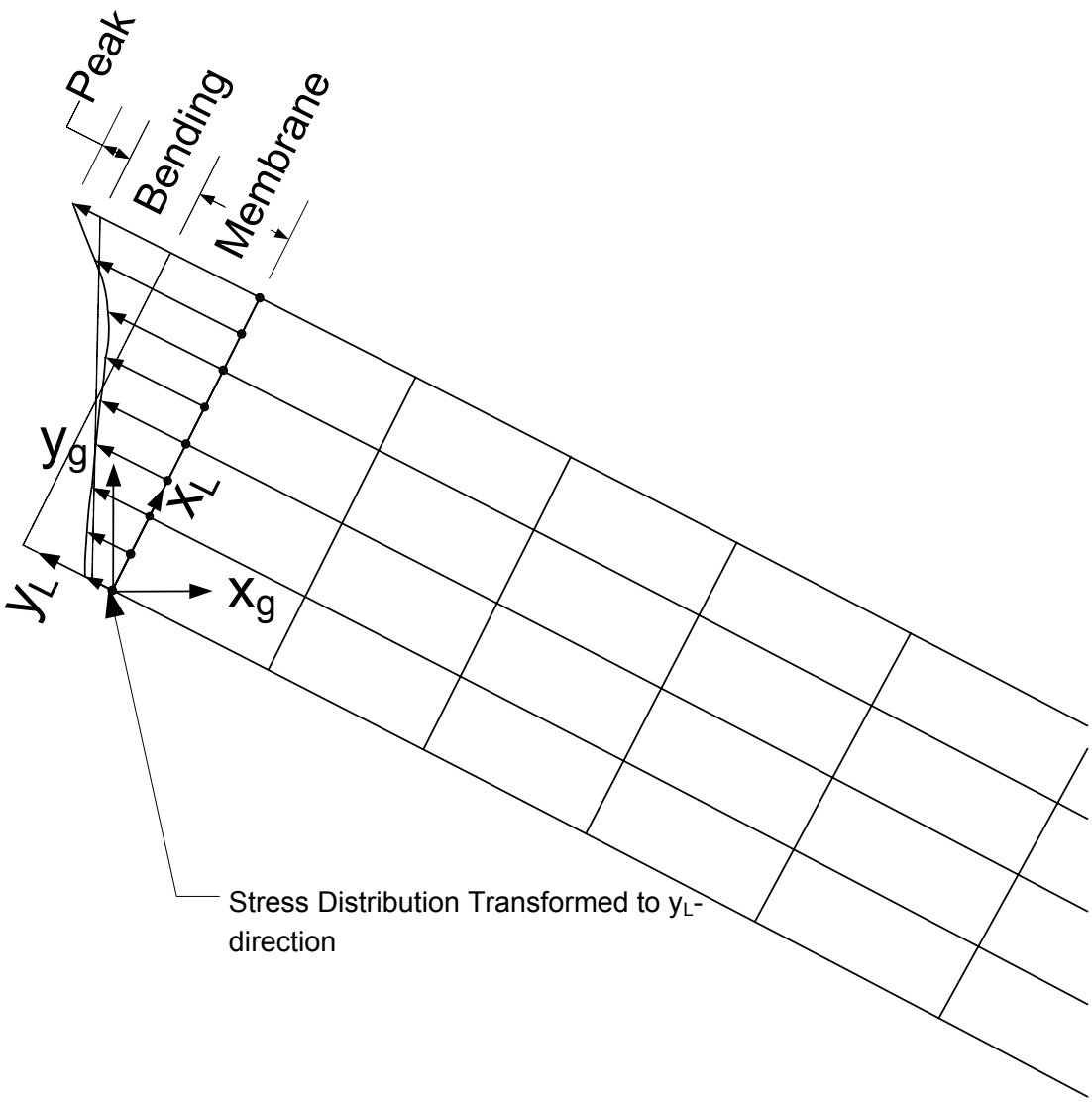

Figure B2.4
Computation of Membrane and Bending Equivalent Stresses by the Stress Integration Method Using the Results from a Finite Element Model with Continuum Elements

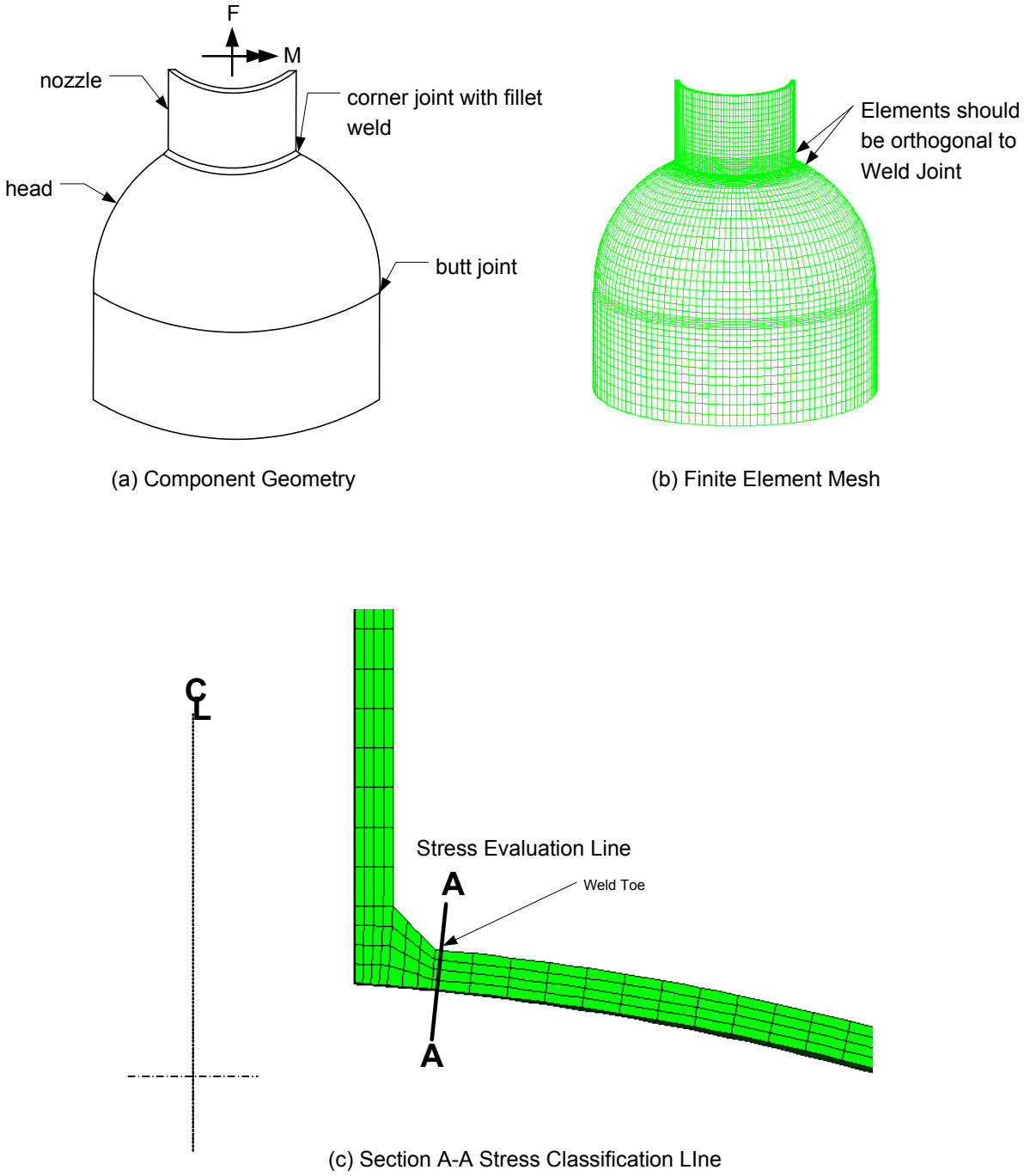

Figure B2.5
Continuum Finite Element Model Stress Classification Line for the Structural Stress Method

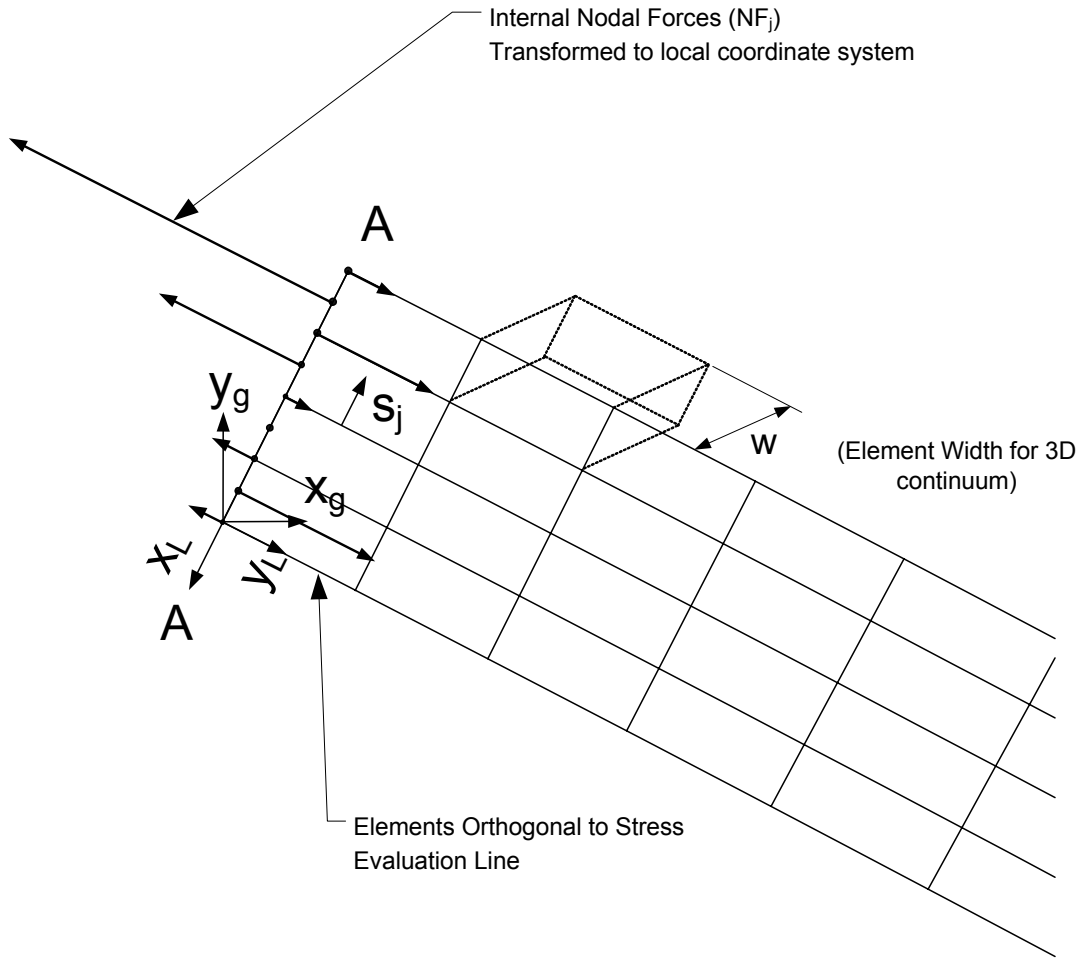

Figure B2.6
Computation of Membrane and Bending Equivalent Stresses by the Structural Stress Method Using Nodal Force Results from a Finite Element Model with Continuum Elements

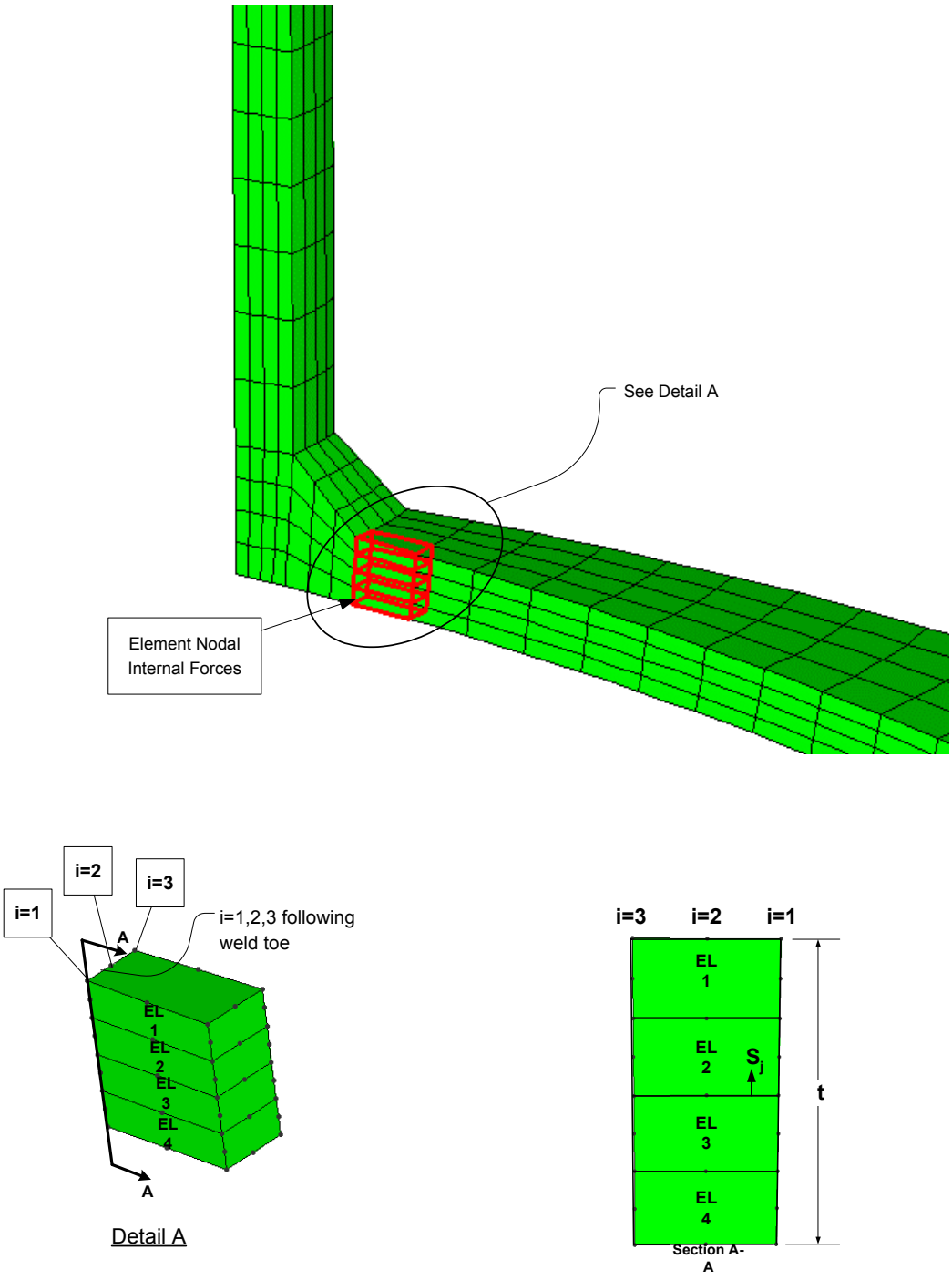

Figure B2.7
Processing Nodal Force Results with the Structural Stress Method Using the Results from a Finite Element Model with Three Dimensional Second Order Continuum Elements

(a) Symmetric Structural Stress State (symmetric joint and symmetric loading)

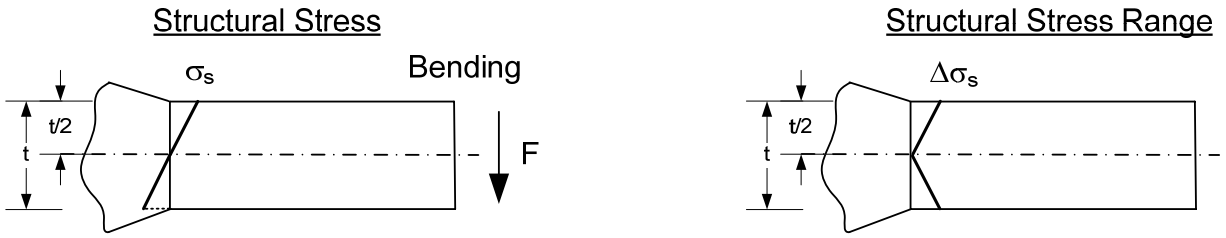

(b) Anti-symmetric Structural Stress State (symmetric joint and anti-symmetric loading)

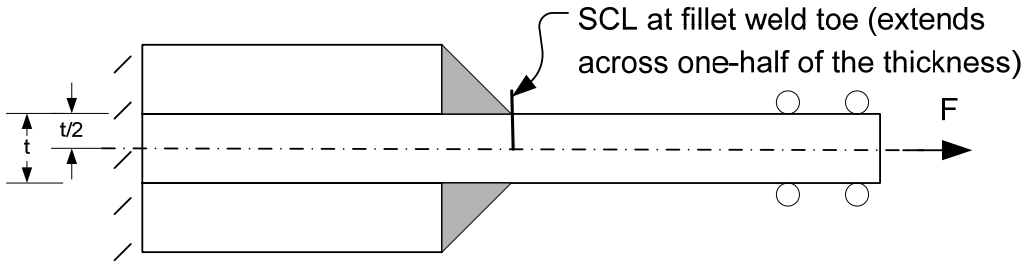

(c) Example of Symmetric Joint (double plate lap fillet weld)

Figure B2.8
Processing Structural Stress Method Results for a Symmetric Structural Stress Range

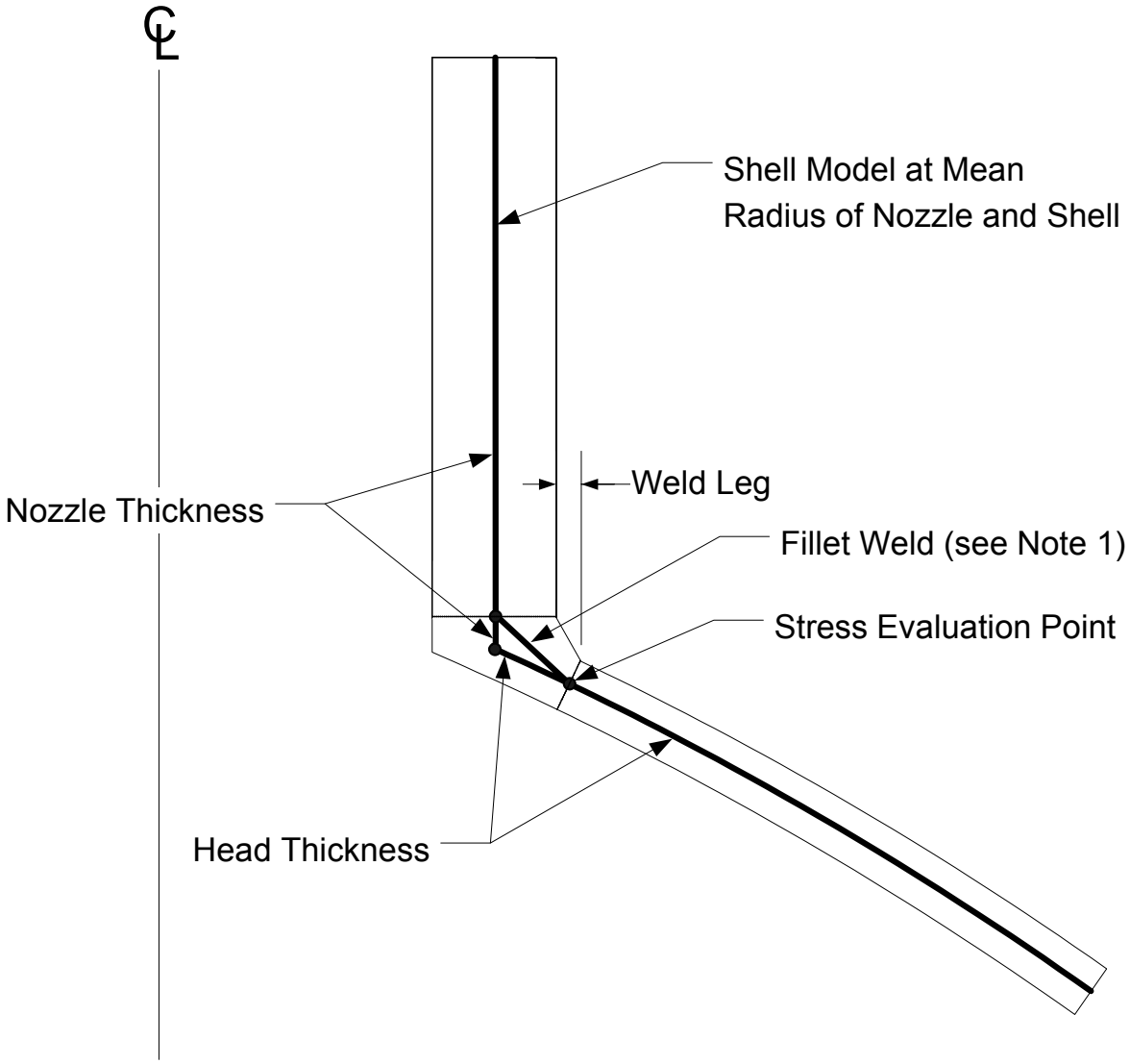

Note 1: The thickness and material properties of the shell element used to model the fillet weld should be established based on producing an equivalent stiffness of the actual fillet weld.

Figure B2.9
Computation of Membrane and Bending Equivalent Stresses by the Structural Stress Method Using the Results from a Finite Element Model with Shell Elements

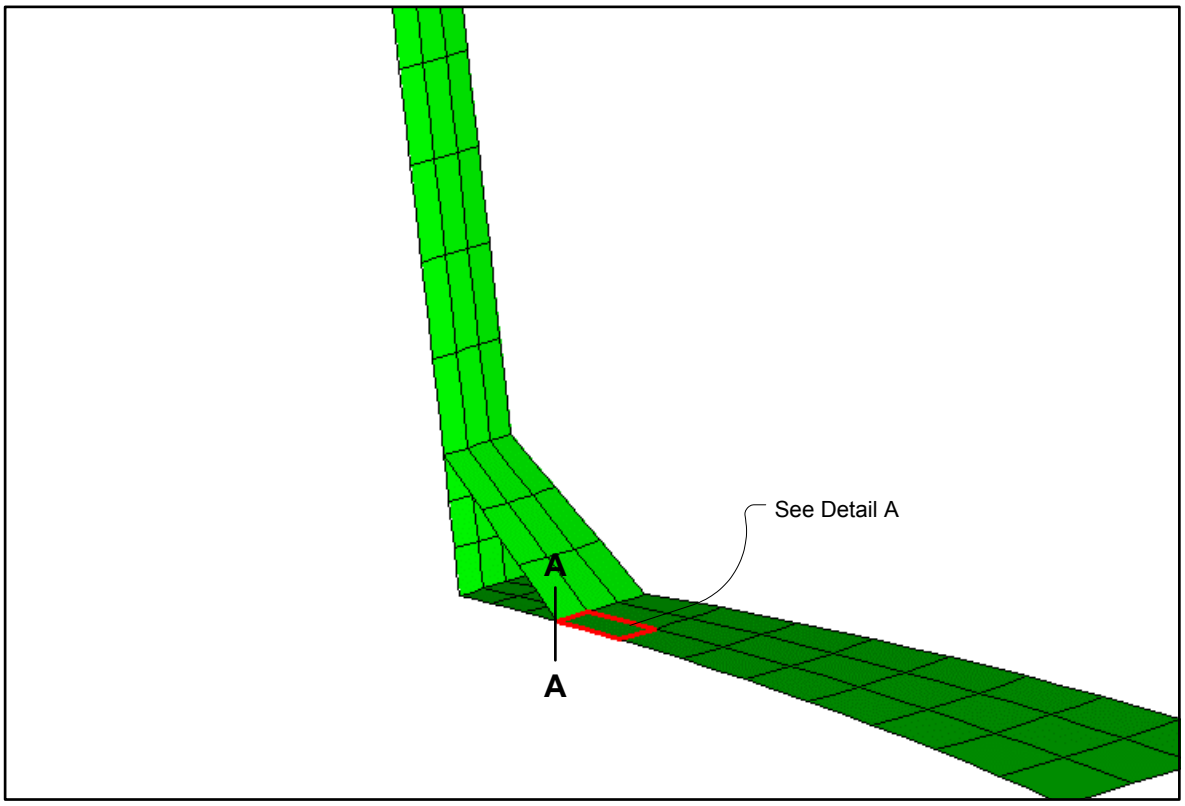

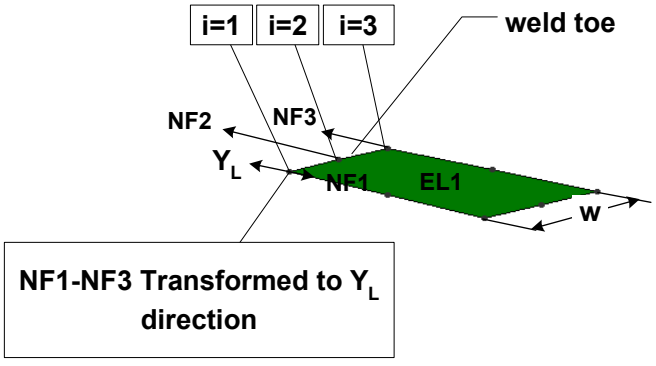

Detail A

Figure B2.10
Processing Nodal Force Results with the Structural Stress Method Using the Results From a Finite Element Model with Three Dimensional Second Order Shell Elements

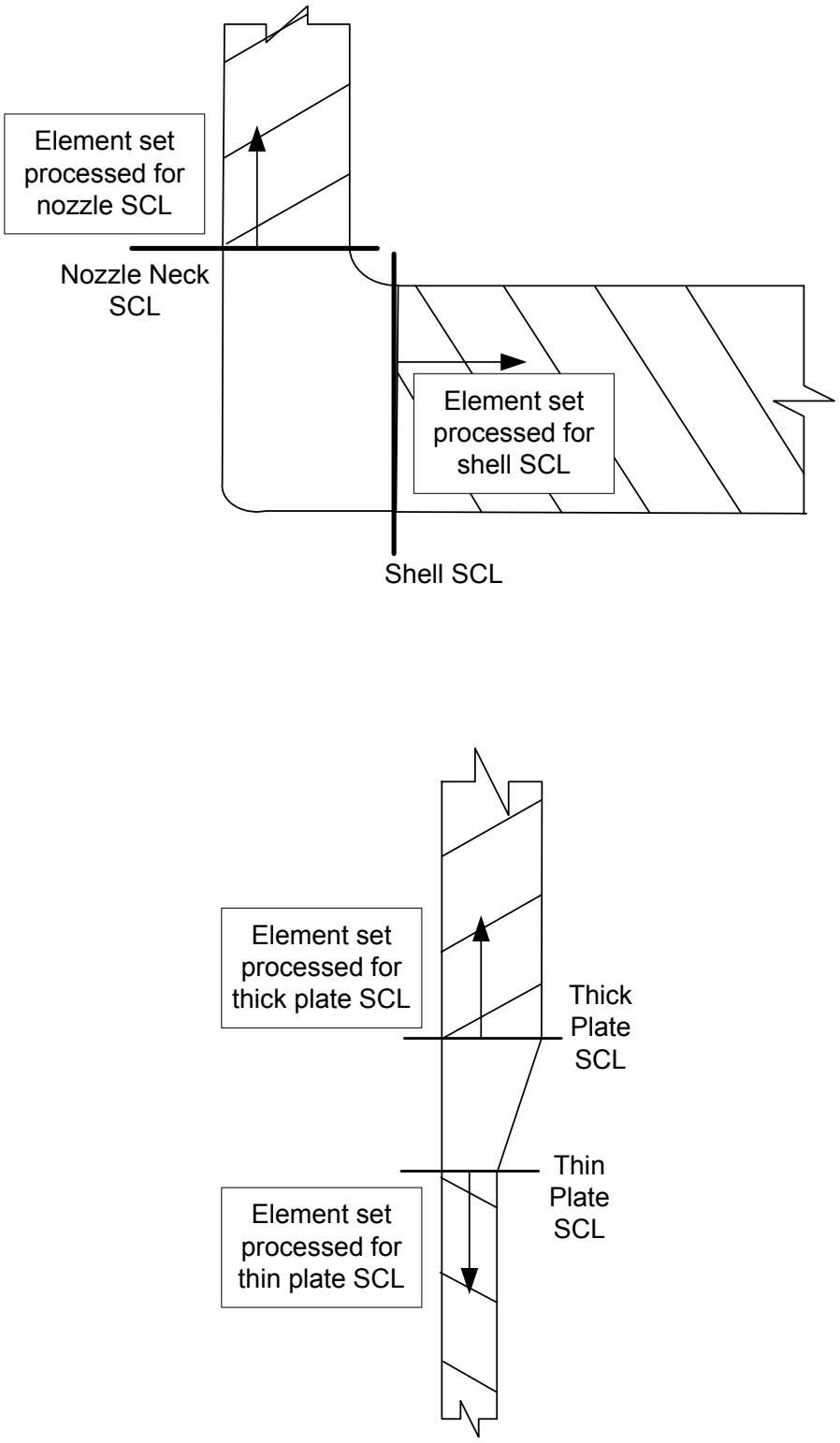

Figure B2.11
Element Sets for Processing Finite Element Nodal Stress Results with the Structural Stress Method Based on Stress Integration

ANNEX B3

HISTOGRAM DEVELOPMENT AND CYCLE COUNTING FOR FATIGUE ANALYSIS

(NORMATIVE)

PART CONTENTS

B3.1 Scope

This Annex contains cycle counting procedures required to perform a fatigue assessment for irregular stress or strain versus time histories. These procedures are used to break the loading history down into individual cycles that can be evaluated using the fatigue assessment rules of Annex B1. Two cycle counting methods are presented in this Annex. An alternative cycle counting method may be used if agreed to by the Owner-User.

B3.2 Definitions

The definitions used in this Annex are shown below.

a) Event – The operating histogram may include one or more events that produce fatigue damage. Each event consists of loading components specified at a number of time points over a time period and is repeated a specified number of times. For example, an event may be the startup, shutdown, upset condition, or any other cyclic action. The sequence of multiple events may be specified or random.

b) Cycle – A cycle is a relationship between stress and strain that is established by the specified loading at a location in a vessel or component. More than one stress-strain cycle may be produced at a location, either within an event or in transition between two events, and the accumulated fatigue damage of the stress-strain cycles determines the adequacy for the specified operation at that location. This determination shall be made with respect to the stabilized stress-strain cycle.

c) Proportional Loading – During constant amplitude loading, as the magnitudes of the applied stresses vary with time, the size of Mohr's circle of stress also varies with time. In some cases, even though the size of Mohr's circle varies during cyclic loading, if the orientation of the principal axes remains fixed, the loading is called proportional. An example of proportional loading is a shaft subjected to in-phase torsion and bending, where the ratio of axial and torsional stress remains constant during cycling.

d) Non-Proportional Loading – If the orientation of the principal axes are not fixed, but change orientation during cyclic loading, the loading is called non-proportional. An example of non-proportional loading is a shaft subjected to out-of-phase torsion and bending, where the ratio of axial and torsional stress varies continuously during cycling.

e) Peak – The point at which the first derivative of the loading or stress histogram changes from positive to negative.

f) Valley – The point at which the first derivative of the loading or stress histogram changes from negative to positive.

B3.3 Histogram Development

The loading histogram should be determined in accordance with Annex B1.

B3.4 Cycle Counting Using The Rainflow Method

B3.4.1 Overview

The Rainflow Cycle Counting Method (ASTM Standard No. E1049) is recommended to determine the time points representing individual cycles for the case of situations where the variation in time of loading, stress, or strain can be represented by a single parameter. This cycle counting method is not applicable for non-proportional loading. Cycles counted with the Rainflow Method correspond to closed stress-strain hysteresis loops, with each loop representing a cycle.

B3.4.2 Procedure for Histogram Development

a) STEP 1 – Determine the sequence of peaks and valleys in the loading histogram. If multiple loadings are applied, it may be necessary to determine the sequence of peaks and valleys using a stress histogram. If the sequence of events is unknown, the worst case sequence should be chosen.

b) STEP 2 – Re-order the loading histogram to start and end at either the highest peak or lowest valley, so that only full cycles are counted. Determine the sequence of peaks and valleys in the loading history. Let X denote the range under consideration, and let Y denote the previous range adjacent to X.

c) STEP 3 – Read the next peak or valley. If out of data, go to STEP 8.

d) STEP 4 – If there are less than 3 points, go to STEP 3; If not, form ranges X and Y using the three most recent peaks and valleys that have not been discarded.

e) STEP 5 – Compare the absolute values of ranges X and Y.

   1) If $X < Y$ go to STEP 3

   2) If $X \geq Y$ go to STEP 6

f) STEP 6 – Count range Y as one cycle; discard the peak and valley of Y. Record the time points and loadings or component stresses, as applicable, at the starting and ending time points of the cycle.

g) STEP 7 – Return to STEP 4 and repeat STEPs 4 to 6 until no more time points with stress reversals remain.

h) STEP 8 – Using the data recorded for the counted cycles perform fatigue assessment in accordance with Annex B1.

B3.5 Cycle Counting Using Max-Min Cycle Counting Method

B3.5.1 Overview

The Max-Min Cycle Counting Method is recommended to determine the time points representing individual cycles for the case of non-proportional loading. The cycle counting is performed by first constructing the largest possible cycle, using the highest peak and lowest valley, followed by the second largest cycle, etc., until all peak counts are used.

B3.5.2 Procedure for Histogram Development

a) STEP 1 – Determine the sequence of peaks and valleys in the loading history. If some events are known to follow each other, group them together but otherwise arrange the random events in any order.

b) STEP 2 – Calculate the elastic stress components σ_{ij} produced by the applied loading at every point in time during each event at a selected location of a vessel. All stress components must be referred to the same global coordinate system. The stress analysis must include peak stresses at local discontinuities.

c) STEP 3 – Scan the interior points of each event and delete the time points at which none of the stress components indicate reversals (peaks or valleys).

d) STEP 4 – Using the stress histogram from STEP 2, determine the time point with the highest peak or lowest valley. Designate the time point as ${}^{m}t$, and the stress components as ${}^{m}\sigma_{ij}$.

e) STEP 5 – If time point ${}^{m}t$ is a peak in the stress histogram, determine the component stress range between time point ${}^{m}t$ and the next valley in the stress histogram. If time point ${}^{m}t$ is a valley, determine the component stress range between time point ${}^{m}t$ and the next peak. Designate the next time point as ${}^{n}t$, and the stress components as ${}^{n}\sigma_{ij}$. Calculate the stress component ranges and the von Mises equivalent stress range between time points ${}^{m}t$ and ${}^{n}t$.

$$ {}^{mn}\Delta\sigma_{ij} = {}^{m}\sigma_{ij} - {}^{n}\sigma_{ij} \tag{B3.1} $$

$$ {}^{mn}\Delta S_{range} = \frac{1}{\sqrt{2}}\left[\begin{array}{l}\left({}^{mn}\Delta\sigma_{11} - {}^{mn}\Delta\sigma_{22}\right)^2 + \left({}^{mn}\Delta\sigma_{22} - {}^{mn}\Delta\sigma_{33}\right)^2 + \\ \left({}^{mn}\Delta\sigma_{33} - {}^{mn}\Delta\sigma_{11}\right)^2 + 6\left({}^{mn}\Delta\sigma_{12}^2 + {}^{mn}\Delta\sigma_{23}^2 + {}^{mn}\Delta\sigma_{13}^2\right)\end{array}\right]^{0.5} \tag{B3.2} $$

f) STEP 6 – Repeat STEP 5, for the current time point, ${}^{m}t$ and the time point of the next peak or valley in the sequence of the stress histogram. Repeat this process for every remaining time point in the stress histogram.

g) STEP 7 – Determine the maximum von Mises equivalent stress range obtained in STEP 5 and record the time points ${}^{m}t$ and ${}^{n}t$ that define the start and end points of the k^{th} cycle.

h) STEP 8 – Determine the event or events to which the time points ${}^{m}t$ and ${}^{n}t$ belong and record their specified number of repetitions as ${}^{m}N$ and ${}^{n}N$, respectively.

i) STEP 9 – Determine the number of repetitions of the k^{th} cycle.

1) If ${}^{m}N < {}^{n}N$: Delete the time point ${}^{m}t$ from those considered in STEP 4, and reduce the number of repetitions at time point ${}^{n}t$ from ${}^{n}N$ to $({}^{n}N - {}^{m}N)$.

2) If ${}^{m}N > {}^{n}N$: Delete the time point ${}^{n}t$ from those considered in STEP 4, and reduce the number of repetitions at time point ${}^{m}t$ from ${}^{m}N$ to $({}^{m}N - {}^{n}N)$.

3) If ${}^{m}N = {}^{n}N$: Delete both time points ${}^{m}t$ and ${}^{n}t$ from those considered in STEP 4.

j) STEP 10 – Return to STEP 4 and repeat STEPs 4 to 10 until no more time points with stress reversals remain.

k) STEP 11 – Using the data recorded for the counted cycles, perform fatigue assessment in accordance with Annex B1 Note that an elastic-plastic fatigue assessment (see Annex B1, paragraph B1.5.4) may be applied if ${}^{mn}\Delta S_{range}$ exceeds the yield point of the cyclic stress range-strain range curve of the material.

B3.6 Nomenclature

$^{mn}\Delta S_{range}$	von Mises equivalent stress range between time points ^{m}t and ^{n}t.
$^{mn}\Delta\sigma_{ij}$	stress component range between time points ^{m}t and ^{n}t.
^{m}N	specified number of repetitions of the event associated with time point ^{m}t.
^{n}N	specified number of repetitions of the event associated with time point ^{n}t.
σ_{ij}	stress tensor at the point under evaluation.
$^{m}\sigma_{ij}$	stress tensor at the point under evaluation at time point ^{m}t.
$^{n}\sigma_{ij}$	stress tensor at the point under evaluation at time point ^{n}t.
^{m}t	time point under consideration with the highest peak or lowest valley.
^{n}t	time point under consideration that forms a range with time point ^{m}t.
X	absolute value of the range (load or stress) under consideration using the Rainflow Cycle Counting Method.
Y	absolute value of the adjacent range (load or stress) to previous X using the Rainflow Cycle Counting Method.

ANNEX B4

ALTERNATIVE PLASTICITY ADJUSTMENT FACTORS AND EFFECTIVE ALTERNATING STRESS FOR ELASTIC FATIGUE ANALYSIS

(NORMATIVE)

PART CONTENTS

B4.1 Scope

This Annex contains procedures for the determination of plasticity correction factors and effective alternating equivalent stress for elastic fatigue analysis. These procedures include a modified Poisson's ratio adjustment for local thermal and thermal bending stresses, a notch plasticity adjustment factor that is applied to thermal bending stresses, and a non-local plastic strain redistribution adjustment that is applied to all stresses except local thermal and thermal bending stresses. These procedures are an alternative to effective alternating stress calculations in Annex B1, paragraph B1.5.3.2.d.

B4.2 Definitions

B4.2.1 Thermal Bending Stress – Thermal bending stress is caused by the linear portion of the through-wall temperature gradient. Such stresses shall be classified as secondary stresses.

B4.2.2 Local Thermal Stress – Local thermal stress is associated with almost complete suppression of the differential expansion and thus produces no significant distortion. Such stresses shall be considered only from the fatigue standpoint and are therefore classified as peak stresses. Examples of local thermal stresses are the stress in a small hot spot in a vessel wall, the non-linear portion of a through-wall temperature gradient in a cylindrical shell, and the thermal stress in a cladding material that has a coefficient of expansion different from that of the base metal. Local thermal stresses are characterized by having two principal stresses that are approximately equal.

B4.3 Effective Alternating Stress for Elastic Fatigue Analysis

B4.3.1 The effective total equivalent stress amplitude is used to evaluate the fatigue damage for results obtained from a linear elastic stress analysis. The controlling stress for the fatigue evaluation is the effective total equivalent stress amplitude, defined as one-half of the effective total equivalent stress range $\left(P_L + P_b + Q + F\right)$ calculated for each cycle in the loading histogram.

B4.3.2 The following procedure can be used to determine plasticity correction factors for elastic fatigue analysis and the effective alternating equivalent stress.

a) STEP 1 – At the point of interest, determine the following stress tensors and associated equivalent stresses at the start and end points (time points ${}^{m}t$ and ${}^{n}t$, respectively) for the k^{th} cycle counted in Annex B1, paragraph B1.5.3.2.b.

1) Calculate the component stress range between time points ${}^{m}t$ and ${}^{n}t$ and compute an equivalent stress range due to primary plus secondary plus peak stress as given below.

$$\Delta\sigma_{ij,k} = {}^{m}\sigma_{ij,k} - {}^{n}\sigma_{ij,k} \tag{B4.1}$$

$$\Delta S_{P,k} = \frac{1}{\sqrt{2}}\left[\begin{array}{l}\left(\Delta\sigma_{11,k} - \Delta\sigma_{22,k}\right)^2 + \left(\Delta\sigma_{11,k} - \Delta\sigma_{33,k}\right)^2 + \\ \left(\Delta\sigma_{22,k} - \Delta\sigma_{33,k}\right)^2 + 6\left(\Delta\sigma_{12,k}^2 + \Delta\sigma_{13,k}^2 + \Delta\sigma_{23,k}^2\right)\end{array}\right]^{0.5} \tag{B4.2}$$

2) Using the linearized stress results due to primary plus secondary stresses, compute the component stress range using Equation (B4.1). Compute the equivalent stress range using Equation (B4.2) and designate this quantity as $\Delta S_{n,k}$.

3) Determine the stress tensor due to local thermal and thermal bending stresses at the start and end points for the k^{th} cycle. It may be difficult to calculate the local thermal stress from stress distributions obtained from numerical methods. If this is the case, the procedure below can be used to calculate the local thermal and thermal bending stresses due to a non-linear temperature distribution. This method is based on calculating a thermal stress difference range associated with the linearized temperature distribution along the SCL for the time steps of interest. Consistent with that method, consider the distribution of the temperature from a numerical method as a function of the local through thickness direction. The temperature distribution for each time step can be separated into three parts.

i) A constant temperature equal to the average of the temperature distribution

$$T_{avg} = \frac{1}{t}\int_0^t T dx \tag{B4.3}$$

ii) The linearly varying portion of the temperature distribution

$$T_b = \frac{6}{t^2}\int_0^t T\left(\frac{t}{2} - x\right)dx \tag{B4.4}$$

iii) The non-linear portion of the temperature distribution

$$T_p = T - \left(T_{avg} + \frac{2T_b}{t}\right) \tag{B4.5}$$

By assuming full suppression of the differential expansion of the cross-section, the associated local thermal stress parallel to the surface for each time step may be calculated as given below where T_p is given by Equation (B4.5).

$$\sigma_{ij,k}^{LT} = \frac{-E\alpha T_p}{1-\nu} \qquad for \quad i = j = 1,2 \tag{B4.6}$$

$$\sigma_{ij,k}^{LT} = 0 \qquad for \quad i \neq j \quad and \quad i = j = 3 \tag{B4.7}$$

4) Using Equations (B4.6) and (B4.7), determine the local thermal component stress range using Equation (B4.1) and designate this quantity as $\Delta\sigma_{ij,k}^{LT}$. The thermal bending component stress range, $\Delta\sigma_{ij,k}^{TB}$, is determined by linearizing the through-wall stress distribution due to thermal effects only. Compute the equivalent stress range due to primary plus secondary plus peak stress minus the local thermal stress using Equations (B4.8) and (B4.9).

$$\Delta\sigma_{ij,k} = \left({}^m\sigma_{ij,k} - {}^m\sigma_{ij,k}^{LT}\right) - \left({}^n\sigma_{ij,k} - {}^n\sigma_{ij,k}^{LT}\right) \tag{B4.8}$$

$$\left(\Delta S_{P,k} - \Delta S_{LT,k}\right) = \frac{1}{\sqrt{2}}\left[\begin{array}{l}\left(\Delta\sigma_{11,k} - \Delta\sigma_{22,k}\right)^2 + \left(\Delta\sigma_{11,k} - \Delta\sigma_{33,k}\right)^2 + \\ \left(\Delta\sigma_{22,k} - \Delta\sigma_{33,k}\right)^2 + 6\left(\Delta\sigma_{12,k}^2 + \Delta\sigma_{13,k}^2 + \Delta\sigma_{23,k}^2\right)\end{array}\right]^{0.5} \tag{B4.9}$$

5) Compute the equivalent stress ranges due to local thermal plus thermal bending stress using Equations (B4.10) and (B4.11).

$$\Delta\sigma_{ij,k} = \left({}^m\sigma_{ij,k}^{TB} + {}^m\sigma_{ij,k}^{LT}\right) - \left({}^n\sigma_{ij,k}^{TB} + {}^n\sigma_{ij,k}^{LT}\right) \tag{B4.10}$$

$$\left(\Delta S_{LT,k}+\Delta S_{TB,k}\right)=\frac{1}{\sqrt{2}}\left[\begin{array}{l}\left(\Delta\sigma_{11,k}-\Delta\sigma_{22,k}\right)^2+\left(\Delta\sigma_{11,k}-\Delta\sigma_{33,k}\right)^2+\\ \left(\Delta\sigma_{22,k}-\Delta\sigma_{33,k}\right)^2+6\left(\Delta\sigma_{12,k}^2+\Delta\sigma_{13,k}^2+\Delta\sigma_{23,k}^2\right)\end{array}\right]^{0.5} \quad \text{(B4.11)}$$

6) If required, see Equation (B4.32), compute the stress tensor due to non-thermal effects (all loadings except local thermal and thermal bending), $\sigma_{ij,k}^{NT}$, at the start and end points for the k^{th} cycle.

b) STEP 2 – Determine the Poisson's ratio adjustment, $K_{v,k}$ to adjust local thermal and thermal bending stresses for the k^{th} cycle based on the equivalent stress ranges in STEP 1 using the following equations (S_{PS} is defined in Annex B1 paragraph B1.5.6.1):

$$K_{v,k}=1.0 \qquad for \qquad \Delta S_{P,k}\le S_{PS} \quad \text{(B4.12)}$$

$$K_{v,k}=0.6\left[\frac{\left(\Delta S_{P,k}-S_{PS}\right)}{\left(\Delta S_{LT,k}+\Delta S_{TB,k}\right)}\right]+1.0 \qquad for \qquad \left|\begin{array}{l}\Delta S_{P,k}>S_{PS} \quad and\\ \left(\Delta S_{LT,k}+\Delta S_{TB,k}\right)>\left(\Delta S_{P,k}-S_{PS}\right)\end{array}\right. \quad \text{(B4.13)}$$

$$K_{v,k}=1.6 \qquad for \qquad \left|\begin{array}{l}\Delta S_{P,k}>S_{PS} \quad and\\ \left(\Delta S_{LT,k}+\Delta S_{TB,k}\right)\le\left(\Delta S_{P,k}-S_{PS}\right)\end{array}\right. \quad \text{(B4.14)}$$

c) STEP 3 – Determine the non-local plastic strain redistribution adjustment, $K_{nl,k}$ to adjust all stresses except local thermal and thermal bending for the k^{th} cycle. In these equations, the parameters m and n are defined in Annex B1 Table B1.12.

$$K_{nl,k}=1.0 \qquad for \qquad \Delta S_{n,k}\le S_{PS} \quad \text{(B4.15)}$$

$$K_{nl,k}=1.0+\frac{(1-n)}{n(m-1)}\left(\frac{\Delta S_{n,k}}{S_{PS}}-1\right) \qquad for \qquad S_{PS}<\Delta S_{n,k}<mS_{PS} \quad \text{(B4.16)}$$

$$K_{nl,k}=\frac{1}{n} \qquad for \qquad \Delta S_{n,k}\ge mS_{PS} \quad \text{(B4.17)}$$

d) STEP 4 – Determine the notch plasticity adjustment factor, $K_{np,k}$ based on the equivalent stress ranges in STEP 1 to adjust thermal bending stresses to account for additional local strain concentration due to a geometric stress riser for the k^{th} cycle. In these equations, the parameters n is defined in Annex B1 Table B1.12.

For numerical results used directly:

$$K_{np,k}=1.0 \qquad for \qquad \left(\Delta S_{P,k}-\Delta S_{LT,k}\right)\le S_{PS} \quad \text{(B4.18)}$$

$$K_{np,k}=\min\left[K_1,\ K_2\right] \qquad for \qquad \left(\Delta S_{P,k}-\Delta S_{LT,k}\right)>S_{PS} \quad \text{(B4.19)}$$

$$K_1 = \left[\left(\frac{\Delta S_{P,k} - \Delta S_{LT,k}}{\Delta S_{n,k}} \right)^{\left(\frac{1-n}{1+n}\right)} - 1.0 \right] \cdot \left[\frac{\left(\Delta S_{P,k} - \Delta S_{LT,k}\right) - S_{PS}}{\left(\Delta S_{P,k} - \Delta S_{LT,k}\right)} \right] + 1.0 \tag{B4.20}$$

$$K_2 = \frac{K_{nl,k}}{K_{v,k}} \tag{B4.21}$$

For numerical results that are adjusted with a stress concentration factor (SCF):

$$K_{np,k} = 1.0 \qquad for \qquad \left(\Delta S_{n,k} \cdot SCF\right) \le S_{PS} \tag{B4.22}$$

$$K_{np,k} = \min\left[K_1,\, K_2\right] \qquad for \qquad \left(\Delta S_{n,k} \cdot SCF\right) > S_{PS} \tag{B4.23}$$

$$K_1 = \left[\left(SCF\right)^{\left(\frac{1-n}{1+n}\right)} - 1.0 \right] \cdot \left[\frac{\left(\Delta S_{n,k} \cdot SCF\right) - S_{PS}}{\left(\Delta S_{n,k} \cdot SCF\right)} \right] + 1.0 \tag{B4.24}$$

$$K_2 = \frac{K_{nl,k}}{K_{v,k}} \tag{B4.25}$$

Note that the SCF and $K_{np,k}$ values may be dependent upon the component stress direction.

e) STEP 5 – Apply the plasticity adjustment factors to the component stresses at the start and end points for the k^{th} cycle.

1) Compute the component stresses including plastic Poisson's ratio and notch plasticity adjustments as given below for time points ${}^{m}t$ and ${}^{n}t$.

For numerical results used directly:

$$\left(\sigma_{ij}^{LT}\right)_{adj} = \sigma_{ij,k}^{LT} \cdot K_{v,k} \tag{B4.26}$$

$$\left(\sigma_{ij}^{TB}\right)_{adj} = \sigma_{ij,k}^{TB} \cdot K_{v,k} \cdot K_{np,k} + \sigma_{ij,k}^{TB} \cdot \left(SCF_{NUM} - 1\right) \cdot K_{np,k} \tag{B4.27}$$

For numerical results that are adjusted with a stress concentration factor (SCF):

$$\left(\sigma_{ij}^{LT}\right)_{adj} = \sigma_{ij,k}^{LT} \cdot K_{v,k} \cdot SCF_{LT} \tag{B4.28}$$

$$\left(\sigma_{ij}^{TB}\right)_{adj} = \sigma_{ij,k}^{TB} \cdot K_{v,k} \cdot K_{np,k} \cdot SCF + \sigma_{ij,k}^{TB} \cdot \left(SCF_{NUM} - 1\right) \cdot K_{np,k} \tag{B4.29}$$

2) Compute the component stresses including non-local plastic strain redistribution adjustment as given below for time points ${}^{m}t$ and ${}^{n}t$.

For numerical results used directly:

$$\left(\sigma_{ij}^{NT}\right)_{adj} = \left[\sigma_{ij,k} - \sigma_{ij,k}^{TB}\left(SCF_{NUM} - 1\right)\right] \cdot K_{np,k} \tag{B4.30}$$

$$SCF_{NUM} = \frac{\left(\Delta S_{p,k} - \Delta S_{LT,k}\right)}{\Delta S_{n,k}} \tag{B4.31}$$

For numerical results that are adjusted with a stress concentration factor (SCF):

$$\left(\sigma_{ij}^{NT}\right)_{adj} = \sigma_{ij,k}^{NT} \cdot K_{nl,k} \cdot SCF \tag{B4.32}$$

f) STEP 6 – Compute the adjusted component stress ranges between time points ${}^{m}t$ and ${}^{n}t$ as given below.

$$\left(\Delta\sigma_{ij,k}\right)_{adj} = \left\{ \begin{array}{l} {}^{m}\left[\left(\sigma_{ij}^{LT}\right)_{adj} + \left(\sigma_{ij}^{NT}\right)_{adj} + \left(\sigma_{ij}^{TB}\right)_{adj}\right] - \\ {}^{n}\left[\left(\sigma_{ij}^{LT}\right)_{adj} + \left(\sigma_{ij}^{NT}\right)_{adj} + \left(\sigma_{ij}^{TB}\right)_{adj}\right] \end{array} \right\} \tag{B4.33}$$

g) STEP 7 – Compute the effective equivalent stress range using the adjusted component stress ranges from STEP 6 and Equation (B4.2). Designate the adjusted effective equivalent stress range as $\left(\Delta S_{P,k}\right)_{adj}$.

h) STEP 8 – Compute the effective alternating equivalent stress for the k^{th} cycle as given below.

$$S_{alt,k} = 0.5\left(\Delta S_{P,k}\right)_{adj} \tag{B4.34}$$

B4.4 Nomenclature

α thermal expansion coefficient of the material at the point under consideration, evaluated at the mean temperature of the k^{th} cycle.

$\Delta S_{n,k}$ primary plus secondary equivalent stress range for the k^{th} cycle.

$\Delta S_{P,k}$ range of primary plus secondary plus peak equivalent stress for the k^{th} cycle.

$\Delta S_{LT,k}$ primary plus secondary plus peak equivalent stress range due to local thermal effects for the k^{th} cycle.

$\Delta S_{TB,k}$ primary plus secondary plus peak equivalent stress range due to thermal bending effects for the k^{th} cycle.

$\Delta S_{NT,k}$ primary plus secondary plus peak equivalent stress range due to non-thermal effects for the k^{th} cycle.

$\left(\Delta S_{P,k}\right)_{adj}$ adjusted range of primary plus secondary plus peak equivalent stress, including non-local strain redistribution, notch plasticity, and plastic Poisson's ratio adjustments for the k^{th} cycle.

$\Delta\sigma_{ij,k}$ stress component range between time points ${}^{m}t$ and ${}^{n}t$ for the k^{th} cycle.

$\Delta\sigma_{ij,k}^{LT}$ stress component range due to local thermal stress between time point ${}^{m}t$ and ${}^{n}t$ for the k^{th} cycle.

$\Delta\sigma_{ij,k}^{TB}$ stress component range due to thermal bending stress between time points ${}^{m}t$ and ${}^{n}t$ for the k^{th} cycle.

$\left(\Delta\sigma_{ij,k}\right)_{adj}$ adjusted stress tensor, including non-local strain redistribution, notch plasticity, and plastic Poisson's ratio adjustments at the location and time point under evaluation for the k^{th} cycle.

E Young's Modulus of the material evaluated at the mean temperature of the cycle.

K_1 parameter used to compute $K_{np,k}$.

K_2 parameter used to compute $K_{np,k}$.

$K_{nl,k}$ non-local strain redistribution adjustment factor for the k^{th} cycle.

$K_{np,k}$ notch plasticity adjustment factor for the k^{th} cycle.

$K_{v,k}$ plastic Poisson's ratio adjustment factor for the k^{th} cycle.

m material constant used for the non-local strain redistribution adjustment factor per Annex B1 Table B1.7.

n material constant used for the non-local strain redistribution adjustment factor per Annex B1 Table B1.7.

ν Poisson's ratio.

$S_{alt,k}$ alternating equivalent stress for the k^{th} cycle.

S_{PS} allowable limit on the primary plus secondary stress range.

SCF stress concentration factor.

SCF_{LT} stress concentration factor applicable for local thermal stress.

SCF_{NUM} stress concentration factor determined from the numerical model.

$\sigma_{ij,k}^{LT}$ stress tensor due to local thermal stress at the location and time point under evaluation for the k^{th} cycle.

$\sigma_{ij,k}^{NT}$ stress tensor due to non-thermal stress at the location and time point under evaluation for the k^{th} cycle.

$\sigma_{ij,k}^{TB}$ stress tensor due to thermal bending stress due to the linearly varying portion of the temperature distribution at the location and time point under evaluation for the k^{th} cycle.

${}^{m}\sigma_{ij,k}$ stress tensor at the point under evaluation at time point ${}^{m}t$ for the k^{th} cycle.

${}^{n}\sigma_{ij,k}$ stress tensor at the point under evaluation at time point ${}^{n}t$ for the k^{th} cycle.

${}^{m}\sigma_{ij,k}^{LT}$ stress tensor due to local thermal stress at the location under evaluation at time point ${}^{m}t$ for the k^{th} cycle.

${}^{n}\sigma_{ij,k}^{LT}$ stress tensor due to local thermal stress at the location under evaluation at time point ${}^{n}t$ for the k^{th} cycle.

${}^{m}\sigma_{ij,k}^{TB}$ stress tensor due to thermal bending stress at the location under evaluation at time point ${}^{m}t$ for the k^{th} cycle.

${}^{n}\sigma_{ij,k}^{TB}$ stress tensor due to thermal bending stress at the location under evaluation at time point ${}^{n}t$ for the k^{th} cycle.

$\left(\sigma_{ij}^{LT}\right)_{adj}$ adjusted stress tensor due to local thermal stress at the location and time point under evaluation for the k^{th} cycle.

$\left(\sigma_{ij}^{NT}\right)_{adj}$ adjusted stress tensor due to non-thermal stress at the location and time point under evaluation for the k^{th} cycle.

$\left(\sigma_{ij}^{TB}\right)_{adj}$ adjusted stress tensor due to thermal bending stress at the location and time point under evaluation for the k^{th} cycle.

t wall thickness.

${}^{m}t$ time point under consideration with the highest peak or lowest valley.

${}^{n}t$ time point under consideration that forms a range with time point ${}^{m}t$.

T temperature distribution.

T_{avg} average temperature component of temperature distribution T.

T_b equivalent linear temperature component of temperature distribution T.

T_p peak temperature component of temperature distribution T.

x position through the wall thickness.

z local coordinate for the temperature distribution.

ANNEX C

COMPENDIUM OF STRESS INTENSITY FACTOR SOLUTIONS

(NORMATIVE)

PART CONTENTS

C.1 General

C.1.1 Overview

C.1.1.1 This Annex contains stress intensity factor solutions for many crack geometries that are likely to occur in pressurized components. Stress intensity factor solutions are used in the assessment of crack-like flaws (see Part 9).

C.1.1.2 A summary of the stress intensity factor solutions is contained in Table C.1. These stress intensity factor solutions are recommended for most applications based on consideration of accuracy, range of applicability and convenience. However, additional cases and improved solutions are being produced for future incorporation into this Annex.

C.1.1.3 Stress intensity factors not included in this annex may be obtained from handbooks (see references [2], [14], [20], [21] and [28]) if the tabulated solutions correspond to the component and crack geometry, and the loading condition. Otherwise, the stress intensity factor should be computed using a numerical approach such as the finite element method.

C.1.1.4 The stress intensity factor solutions for plates can be utilized to approximate the solution for a curved shell (cylinder and sphere) by introduction of a surface correction or bulging factor. This type of solution should only be utilized if a stress intensity factor equation is not listed in the sections covering shell type components.

C.1.1.5 An identifier has been assigned to each stress intensity factor solutions in this annex (see Table C.1). This identifier is a set of alpha-numeric characters that uniquely identifies the component geometry, crack geometry, and loading condition. The identifier can also be used to determine the associated reference stress solution to be used in an assessment of crack like flaws (see Part 9). For example, if a flat plate with a through-wall crack subject to a membrane stress is being evaluated, the stress intensity factor solution to be used is KPTC, and the associated reference stress solution is RPTC. A listing of the reference stress solutions is provided in Annex D.

C.2 Stress Analysis

C.2.1 Overview

C.2.1.1 A stress analysis using handbook or numerical techniques is required to compute the state of stress at the location of a crack. The stress distribution to be utilized in determining the stress intensity factor is based on the component of stress normal to the crack face. The distribution may be linear (made up of membrane and/or bending distributions) or highly nonlinear based on the component geometry and loading conditions.

C.2.1.2 The stress distribution normal to the crack face should be determined for the primary, secondary, and residual stress loading conditions based on the service requirements that the uncracked component geometry is subjected to. If the component is subject to different operating conditions, the stress distribution for each condition should be evaluated and a separate fitness-for-service assessment should be performed for each condition.

C.2.2 Stress Distributions

C.2.2.1 *Overview* – The stress intensity factor solutions in this annex are formulated in terms of the coefficients of a linear stress distribution (membrane and bending) or fourth order polynomial stress distribution, or in terms of a general stress distribution (weight functions). Therefore, if the stress intensity factor required for the assessment is written in terms of coefficients of a stress distribution, it is necessary to derive these coefficients from the results obtained from a stress analysis.

C.2.2.2 *General Stress Distribution* – A general stress distribution through the wall thickness can be obtained from a two or three-dimensional elasticity solution (e.g. Lame solutions for a thick wall cylinder and sphere) or it can be determined using a numerical analysis technique such as the finite element method. In some cases, the stress distribution normal to the crack face may be highly non-linear.

a) Statically equivalent membrane and bending stress components can be determined from the general stress distribution using the following equations; the integration is performed along a line assuming a unit width, see Annex B2.

$$\sigma_{ij,m} = \frac{1}{t}\int_0^t \sigma_{ij}\,dx \tag{C.1}$$

$$\sigma_{ij,b} = \frac{6}{t^2}\int_0^t \sigma_{ij}\left(\frac{t}{2} - x\right)dx \tag{C.2}$$

b) A general stress distribution can be used directly to determine a stress intensity factor by integration of this distribution with a suitable weight function. Weight functions are provided in this annex for a limited number of component and crack geometries.

C.2.2.3 *Fourth Order* Polynomial *Stress Distribution* – The fourth order polynomial stress distribution can be obtained by curve-fitting the general stress distribution. This distribution is utilized to obtain a more accurate representation of the stress intensity for a highly nonlinear stress distribution. Many of the stress intensity factor solutions in this annex have been developed based on a fourth order polynomial stress distribution.

a) The general form of the fourth order polynomial stress distribution is as follows:

$$\sigma(x) = \sigma_o + \sigma_1\left(\frac{x}{t}\right) + \sigma_2\left(\frac{x}{t}\right)^2 + \sigma_3\left(\frac{x}{t}\right)^3 + \sigma_4\left(\frac{x}{t}\right)^4 \tag{C.3}$$

b) The equivalent membrane and bending stress distributions for the fourth order polynomial stress distribution are:

$$\sigma_m = \sigma_0 + \frac{\sigma_1}{2} + \frac{\sigma_2}{3} + \frac{\sigma_3}{4} + \frac{\sigma_4}{5} \tag{C.4}$$

$$\sigma_b = -\frac{\sigma_1}{2} - \frac{\sigma_2}{2} - \frac{9\sigma_3}{20} - \frac{6\sigma_4}{15} \tag{C.5}$$

C.2.2.4 *Fourth Order Polynomial Stress Distribution With Net Section Bending Stress* – This distribution is used to represent a through-wall fourth order polynomial stress and a net section or global bending stress applied to a circumferential crack in a cylindrical shell.

$$\sigma(x, x_g, y_g) = \sigma_o + \sigma_1\left(\frac{x}{t}\right) + \sigma_2\left(\frac{x}{t}\right)^2 + \sigma_3\left(\frac{x}{t}\right)^3 + \sigma_4\left(\frac{x}{t}\right)^4 + \sigma_5\left(\frac{y_g}{R_i + t}\right) + \sigma_6\left(\frac{x_g}{R_i + t}\right) \tag{C.6}$$

C.2.2.5 *Membrane and Through-Wall Bending* – The membrane and bending stress distributions are linear through the wall thickness and represent a common subset of the general stress distribution. These distributions occur in thin plate and shell structures and can be computed using handbook solutions or by using a numerical technique such as finite element analysis. If finite element analysis is utilized in a fitness-for-service assessment, the results from plate and shell elements will directly yield membrane and bending stress distributions. The stress intensity factor solutions in this annex can be used if a membrane and through-wall bending stress distribution is known. For the special case of weld misalignment and shell out-of-roundness, the bending stress solution can be computed using the membrane stress solution and the following equation:

$$\sigma_b = \sigma_m R_b \tag{C.7}$$

C.2.3 Surface Correction Factors

C.2.3.1 Surface correction or bulging factors are used to quantify the local increase in the state of stress at the location of a crack in a shell that occurs because of local bulging. The magnified state of stress is then used together with a reference stress solution for a plate with a similar crack geometry to determine the reference stress for the shell. Surface correction factors are typically only applied to the membrane part of the stress intensity solution because this represents the dominant part of the solution.

C.2.3.2 The surface correction factors for through-wall cracks in cylindrical and spherical shells subject to membrane stress loading are defined in Annex D, paragraph D.2.3.2. The surface correction factors for surface cracks can be approximated using the results obtained for a though-wall crack by using one of the methods discussed in Annex D, paragraph D.2.3.3. The surface correction factor based on net section collapse is recommended for use in this annex.

C.3 Stress Intensity Factor Solutions for Plates

C.3.1 Plate – Through-Wall Crack, Through-Wall Membrane and Bending Stress (KPTC)

C.3.1.1 The Mode I Stress Intensity Factor [1],[35]

$$K_I = \left(\{\sigma_m + p_c\} + M_b \sigma_b\right)\sqrt{\pi c} f_w \tag{C.8}$$

where,

$$M_b = \frac{0.302327 + 70.50193\psi + 110.305\psi^2}{1.0 + 110.960\psi + 98.7089\psi^2 + 0.753594\psi^3} \tag{C.9}$$

$$\psi = \frac{t}{c\sqrt{10}} \tag{C.10}$$

$$f_w = \left[\sec\left(\frac{\pi c}{2W}\right)\right]^{1/2} \tag{C.11}$$

C.3.1.2 Notes:

a) See Figure C.1 for the component and crack geometry.

b) Crack and geometry dimensional limits: $0.0 < c/W < 1.0$.

c) The membrane and bending stress, σ_m and σ_b, can be determined using stress equations based on strength of materials concepts.

C.3.2 Plate – Surface Crack, Infinite Length, Through-Wall Fourth Order Polynomial Stress Distribution (KPSCL1)

C.3.2.1 The Mode I Stress Intensity Factor [40]

$$K_I = \left[G_o \{\sigma_o + p_c\} + G_1\sigma_1\left(\frac{a}{t}\right) + G_2\sigma_2\left(\frac{a}{t}\right)^2 + G_3\sigma_3\left(\frac{a}{t}\right)^3 + G_4\sigma_4\left(\frac{a}{t}\right)^4 \right]\sqrt{\pi a} \qquad \text{(C.12)}$$

C.3.2.2 Notes:

a) See Figure C.2(b) for the component and crack geometry.

b) The coefficients of the stress distribution to be used are defined in paragraph C.2.2.3.

c) The influence coefficients G_0 through G_4 are given by the following equation where the constants C_0 through C_4 are provided in Table C.2.

$$G_i = C_0 + C_1\left(\frac{a}{t}\right)^2 + C_2\left(\frac{a}{t}\right)^4 + C_3\left(\frac{a}{t}\right)^6 + C_4\left(\frac{a}{t}\right)^8 \qquad \text{(C.13)}$$

d) Crack and geometry dimensional limits, $0.0 < a/t \le 0.8$.

e) The solution presented is for the case of no restraint on the ends of the plate.

C.3.3 Plate – Surface Crack, Infinite Length, Through-Wall Arbitrary Stress Distribution (KPSCL2)

C.3.3.1 The Mode I Stress Intensity Factor [3]

The stress intensity factor can be determined using the weight function method (see paragraph C.14.3). The influence coefficients G_0 and G_1 required to compute M_1, M_2, and M_3 can be determined using paragraph C.3.2.2.c.

C.3.3.2 Notes: see paragraph C.3.2.2.

C.3.4 Plate – Surface Crack, Semi-Elliptical Shape, Through-wall Membrane and Bending Stress (KPSCE1)

C.3.4.1 The Mode I Stress Intensity Factor [1]

$$K_I = \left(M_m\{\sigma_m + p_c\} + M_b\sigma_b\right)\sqrt{\frac{\pi a}{Q}} \qquad \text{(C.14)}$$

where,

$$Q = 1.0 + 1.464\left(\frac{a}{c}\right)^{1.65} \quad for \;\; a/c \le 1.0 \qquad \text{(C.15)}$$

$$Q = 1.0 + 1.464\left(\frac{c}{a}\right)^{1.65} \quad for \;\; a/c > 1.0 \qquad \text{(C.16)}$$

The membrane correction factor is given by:

$$M_m = M_s \left\{ M_1 + M_2 \left(\frac{a}{t} \right)^2 + M_3 \left(\frac{a}{t} \right)^4 \right\} g f_\varphi f_w \tag{C.17}$$

where,

$$M_s = 1.0 \tag{C.18}$$

$$f_w = \left\{ \sec\left(\frac{\pi c}{2W} \sqrt{\frac{a}{t}} \right) \right\}^{0.5} \tag{C.19}$$

For $a/c \le 1.0$

$$M_1 = 1.13 - 0.09 \left(\frac{a}{c} \right) \tag{C.20}$$

$$M_2 = \frac{0.89}{0.2 + \left(\frac{a}{c} \right)} - 0.54 \tag{C.21}$$

$$M_3 = 0.5 - \frac{1}{0.65 + \left(\frac{a}{c} \right)} + 14 \left\{ 1 - \left(\frac{a}{c} \right) \right\}^{24} \tag{C.22}$$

$$g = 1 + \left\{ 0.1 + 0.35 \left(\frac{a}{t} \right)^2 \right\} (1 - \sin\varphi)^2 \tag{C.23}$$

$$f_\varphi = \left\{ \left(\frac{a}{c} \right)^2 \cos^2\varphi + \sin^2\varphi \right\}^{0.25} \tag{C.24}$$

For $a/c > 1.0$

$$M_1 = \left(\frac{c}{a} \right)^{0.5} \left\{ 1 + 0.04 \left(\frac{c}{a} \right) \right\} \tag{C.25}$$

$$M_2 = 0.2 \left(\frac{c}{a} \right)^4 \tag{C.26}$$

$$M_3 = -0.11 \left(\frac{c}{a} \right)^4 \tag{C.27}$$

$$g = 1 + \left\{ 0.1 + 0.35 \left(\frac{c}{a} \right) \left(\frac{a}{t} \right)^2 \right\} (1 - \sin\varphi)^2 \tag{C.28}$$

$$f_{\varphi} = \left\{ \left(\frac{c}{a} \right)^2 \sin^2 \varphi + \cos^2 \varphi \right\}^{0.25} \tag{C.29}$$

The bending correction factor is given by:

$$M_b = M_m H \tag{C.30}$$

where,

$$H = H_1 + \left(H_2 - H_1 \right) \sin^q \varphi \tag{C.31}$$

$$H_2 = 1 + G_1 \left(\frac{a}{t} \right) + G_2 \left(\frac{a}{t} \right)^2 \tag{C.32}$$

For $a/c \le 1.0$

$$q = 0.2 + \left(\frac{a}{c} \right) + 0.6 \left(\frac{a}{t} \right) \tag{C.33}$$

$$H_1 = 1 - 0.34 \left(\frac{a}{t} \right) - 0.11 \left(\frac{a}{c} \right) \left(\frac{a}{t} \right) \tag{C.34}$$

$$G_1 = -1.22 - 0.12 \left(\frac{a}{c} \right) \tag{C.35}$$

$$G_2 = 0.55 - 1.05 \left(\frac{a}{c} \right)^{0.75} + 0.47 \left(\frac{a}{c} \right)^{1.5} \tag{C.36}$$

For $a/c > 1.0$

$$q = 0.2 + \left(\frac{c}{a} \right) + 0.6 \left(\frac{a}{t} \right) \tag{C.37}$$

$$H_1 = 1 - \left\{ 0.04 + 0.41 \left(\frac{c}{a} \right) \right\} \left(\frac{a}{t} \right) + \left\{ 0.55 - 1.93 \left(\frac{c}{a} \right)^{0.75} + 1.38 \left(\frac{c}{a} \right)^{1.5} \right\} \left(\frac{a}{t} \right)^2 \tag{C.38}$$

$$G_1 = -2.11 + 0.77 \left(\frac{c}{a} \right) \tag{C.39}$$

$$G_2 = 0.55 - 0.72 \left(\frac{c}{a} \right)^{0.75} + 0.14 \left(\frac{c}{a} \right)^{1.5} \tag{C.40}$$

C.3.4.2 Notes:

a) See Figure C.2(a) for the component and crack geometry.

b) Crack and geometry dimensional limits:

1) $0.0 < a/t \le 0.8 \quad for \quad 0.0 < a/c \le 0.2$

2) $0.0 < a/t \le 1.0 \quad for \quad 0.2 < a/c \le 2.0$

3) $0.0 < a/c \le 2.0$

4) $0.0 < c/W < 1.0$

5) $0 \le \varphi \le \pi$

c) If $c >> a$, the solution approaches that of a plate with an edge crack (see Part 9, Figure 9.1(d)).

d) The solution presented can be used to determine a conservative estimate of the stress intensity factor for cylinders and spheres when $R_i/t > 10$. The following modifications are required:

1) A surface correction factor, M_s, should be used for longitudinal cracks or circumferential cracks in cylinders or circumferential cracks in spheres, see paragraph C.2.3.

2) The finite width correction factor should be set equal to one, $f_w = 1.0$.

3) For internal cracks, the pressure loading on the crack faces should be included in the membrane stress.

e) The stress intensity factor solution presented above may be overly conservative for finite width plates. A more accurate estimate of the stress intensity factor can be obtained by using the following finite width correction factor for the membrane stress in Equation (C.17). The finite width correction factor for the bending stress is given by Equation (C.19) [20].

$$f_{wm} = f_b \left\{ \sec\left[\left(\frac{\pi c}{2W} \right) \cdot \sqrt{\left(\frac{a}{t} \right)\left(1 - 0.6\sin\varphi\right)} \right] \right\}^{0.5} \qquad \text{(C.41)}$$

where

$$f_b = 1 + 0.38\left(\frac{a}{c} \right)\left(\frac{a}{t} \right)\left(\frac{c}{W} \right)^2 \cos\varphi \qquad \text{(C.42)}$$

f) The stresses σ_m and σ_b can be determined using stress equations based on strength of materials concepts.

C.3.5 Plate – Surface Cracks, Semi-Elliptical Shape, Through-Wall Fourth Order Polynomial Stress Distribution (KPSCE2)

C.3.5.1 The Mode I Stress Intensity Factor [3]

$$K_I = \left[G_o\left\{ \sigma_o + p_c \right\} + G_1\sigma_1\left(\frac{a}{t} \right) + G_2\sigma_2\left(\frac{a}{t} \right)^2 + G_3\sigma_3\left(\frac{a}{t} \right)^3 + G_4\sigma_4\left(\frac{a}{t} \right)^4 \right] \sqrt{\frac{\pi a}{Q}} f_w \qquad \text{(C.43)}$$

C.3.5.2 Notes:

a) See Figure C.2(a) for the component and crack geometry.

b) The coefficients of the stress distribution to be used are defined in paragraph C.2.2.3.

c) The influence coefficients G_0 through G_4 are given by the equations shown below. The constants for these equations are provided in Table C.3 for $0.2 \le a/c \le 1.0$. The expressions for the influence coefficients were developed by curve fitting the data provided in Tables A-3320-1 and A-3320-2 of Section XI, Division 1 of the ASME B&PV Code. The curve fit equations cover the full range of data within 3%.

For $\varphi = 0^o$:

$$G_i = \frac{C_0 + C_2\left(\frac{a}{t}\right) + C_4\left(\frac{a}{2c}\right) + C_6\left(\frac{a}{t}\right)^2 + C_8\left(\frac{a}{2c}\right)^2 + C_{10}\left(\frac{a}{t}\right)\cdot\left(\frac{a}{2c}\right)}{1.0 + C_1\left(\frac{a}{t}\right) + C_3\left(\frac{a}{2c}\right) + C_5\left(\frac{a}{t}\right)^2 + C_7\left(\frac{a}{2c}\right)^2 + C_9\left(\frac{a}{t}\right)\cdot\left(\frac{a}{2c}\right)} \qquad \text{(C.44)}$$

For $\varphi = 90^o$:

$$G_i = \begin{pmatrix} C_0 + C_1\left(\frac{a}{t}\right) + C_2\ln\left(\frac{a}{2c}\right) + C_3\left(\frac{a}{t}\right)^2 + C_4\left[\ln\left(\frac{a}{2c}\right)\right]^2 + C_5\left(\frac{a}{t}\right)\cdot\ln\left(\frac{a}{2c}\right) + \\ C_6\left(\frac{a}{t}\right)^3 + C_7\left[\ln\left(\frac{a}{2c}\right)\right]^3 + C_8\left(\frac{a}{t}\right)\cdot\left[\ln\left(\frac{a}{2c}\right)\right]^2 + C_9\left(\frac{a}{t}\right)^2\cdot\left[\ln\left(\frac{a}{2c}\right)\right] \end{pmatrix} \qquad \text{(C.45)}$$

d) If $a/c < 0.2$, the influence coefficients G_0 and G_1 are determined from the solution in paragraph C.3.4 using the equations shown below. The influence coefficients G_2, G_3, and G_4 can be computed using paragraph C.14.3 or C.14.4.

$$G_o = M_m / f_w \qquad \text{(C.46)}$$

$$G_1 = \frac{t}{a}\left(\frac{M_m - M_b}{2}\right)\frac{1}{f_w} \qquad \text{(C.47)}$$

e) The following coefficients have been previously defined:

1) Q by Equations (C.15)

2) f_w by Equation (C.19)

3) M_m by Equation (C17)

4) M_b by Equation (C.30)

f) Crack and geometry dimensional limits:

1) $0.0 < a/t \le 0.8$

2) $0.0 < a/c \le 1.0$

3) $0.0 < c/W < 1.0$

4) $0 \le \varphi \le \pi$

g) See paragraph C.3.4.2.d to determine M_s.

h) The solution in paragraph C.5.11 can be used for a flat plate by setting $t/R_i = 0$.

C.3.6 Plate – Surface Crack, Semi-Elliptical Shape, Through-Wall Arbitrary Stress Distribution (KPSCE3)

C.3.6.1 The Mode I Stress Intensity Factor [6]

$$K_I = \left[\int_0^a h(x,a)\sigma(x)dx\right] f_w \tag{C.48}$$

The parameter $h(x,a)$ is a weight function, $\sigma(x)$ is the stress normal to the crack plane computed when the component is in the uncracked state, x is the through-thickness distance measured from the free surface that contains the crack, and f_w is the finite width correction factor given by Equation (C.19)

The weight function at the deepest point of the crack $(\varphi = \pi/2)$:

$$h_{\varphi=90}(x,a) = \frac{2}{\sqrt{2\pi(a-x)}}\left[1 + M_1\left(1-\frac{x}{a}\right)^{1/2} + M_2\left(1-\frac{x}{a}\right) + M_3\left(1-\frac{x}{a}\right)^{3/2}\right] \tag{C.49}$$

where Q is given by Equation (C.15) and,

$$M_1 = \frac{\pi}{\sqrt{2Q}}(4Y_o - 6Y_1) - \frac{24}{5} \tag{C.50}$$

$$M_2 = 3 \tag{C.51}$$

$$M_3 = 2\left(\frac{\pi}{\sqrt{2Q}}Y_o - M_1 - 4\right) \tag{C.52}$$

$$Y_o = B_o + B_1\left(\frac{a}{t}\right)^2 + B_2\left(\frac{a}{t}\right)^4 \tag{C.53}$$

$$B_o = 1.10190 - 0.019863\left(\frac{a}{c}\right) - 0.043588\left(\frac{a}{c}\right)^2 \tag{C.54}$$

$$B_1 = 4.32489 - 14.9372\left(\frac{a}{c}\right) + 19.4389\left(\frac{a}{c}\right)^2 - 8.52318\left(\frac{a}{c}\right)^3 \tag{C.55}$$

$$B_2 = -3.03329 + 9.96083\left(\frac{a}{c}\right) - 12.582\left(\frac{a}{c}\right)^2 + 5.52318\left(\frac{a}{c}\right)^3 \tag{C.56}$$

$$Y_1 = A_o + A_1\left(\frac{a}{t}\right)^2 + A_2\left(\frac{a}{t}\right)^4 \tag{C.57}$$

$$A_o = 0.456128 - 0.114206\left(\frac{a}{c}\right) - 0.046523\left(\frac{a}{c}\right)^2 \quad \text{(C.58)}$$

$$A_1 = 3.022 - 10.8679\left(\frac{a}{c}\right) + 14.94\left(\frac{a}{c}\right)^2 - 6.8537\left(\frac{a}{c}\right)^3 \quad \text{(C.59)}$$

$$A_2 = -2.28655 + 7.88771\left(\frac{a}{c}\right) - 11.0675\left(\frac{a}{c}\right)^2 + 5.16354\left(\frac{a}{c}\right)^3 \quad \text{(C.60)}$$

The weight function at the free surface of the crack $(\varphi = 0)$:

$$h_{\varphi=0}(x,a) = \frac{2}{\sqrt{\pi x}}\left[1 + N_1\left(\frac{x}{a}\right)^{1/2} + N_2\left(\frac{x}{a}\right) + N_3\left(\frac{x}{a}\right)^{3/2}\right] \quad \text{(C.61)}$$

where,

$$N_1 = \frac{\pi}{\sqrt{4Q}}\left(30F_1 - 18F_o\right) - 8 \quad \text{(C.62)}$$

$$N_2 = \frac{\pi}{\sqrt{4Q}}\left(60F_0 - 90F_1\right) + 15 \quad \text{(C.63)}$$

$$N_3 = -\left(1 + N_1 + N_2\right) \quad \text{(C.64)}$$

$$F_0 = \alpha\left(\frac{a}{c}\right)^{\beta} \quad \text{(C.65)}$$

$$\alpha = 1.14326 + 0.0175996\left(\frac{a}{t}\right) + 0.501001\left(\frac{a}{t}\right)^2 \quad \text{(C.66)}$$

$$\beta = 0.458320 - 0.102985\left(\frac{a}{t}\right) - 0.398175\left(\frac{a}{t}\right)^2 \quad \text{(C.67)}$$

$$F_1 = \gamma\left(\frac{a}{c}\right)^{\delta} \quad \text{(C.68)}$$

$$\gamma = 0.976770 - 0.131975\left(\frac{a}{t}\right) - 0.484875\left(\frac{a}{t}\right)^2 \quad \text{(C.69)}$$

$$\delta = 0.448863 - 0.173295\left(\frac{a}{t}\right) - 0.267775\left(\frac{a}{t}\right)^2 \quad \text{(C.70)}$$

C.3.6.2 Notes:

a) See Figure C.2(a) for the component and crack geometry.

b) Crack and geometry dimensional limits:

1) $0.0 < a/t \le 0.8$

2) $0.1 < a/c \le 1.0$

3) $0.0 < c/W < 1.0$

4) $0 \le \varphi \le \pi$

C.3.7 Plate – Embedded Crack, Infinite Length, Through-Wall Fourth Order Polynomial Stress Distribution (KPECL)

C.3.7.1 The Mode I Stress Intensity Factor [40]

$$K_I = \left[\begin{array}{l} G_o \left\{ \{\sigma_o + p_c\} + \sigma_1 \left(\frac{d_1}{t}\right) + \sigma_2 \left(\frac{d_1}{t}\right)^2 + \sigma_3 \left(\frac{d_1}{t}\right)^3 + \sigma_4 \left(\frac{d_1}{t}\right)^4 \right\} + \\ G_1 \left\{ \sigma_1 + 2\sigma_2 \left(\frac{d_1}{t}\right) + 3\sigma_3 \left(\frac{d_1}{t}\right)^2 + 4\sigma_4 \left(\frac{d_1}{t}\right)^3 \right\} \left(\frac{a}{t}\right) + \\ G_2 \left\{ \sigma_2 + 3\sigma_3 \left(\frac{d_1}{t}\right) + 6\sigma_4 \left(\frac{d_1}{t}\right)^2 \right\} \left(\frac{a}{t}\right)^2 + \\ G_3 \left\{ \sigma_3 + 4\sigma_4 \left(\frac{d_1}{t}\right) \right\} \left(\frac{a}{t}\right)^3 + \\ G_4 \{\sigma_4\} \left(\frac{a}{t}\right)^4 \end{array} \right] \sqrt{\pi a} \qquad \text{(C.71)}$$

C.3.7.2 Notes:

a) See Figure C.3(b) for the component and crack geometry.

b) The coefficients of the stress distribution to be used are defined in paragraph C.2.2.3.

c) The influence coefficients G_1 through G_4 for points A and B are provided in Table C.4.

d) Crack and geometry dimensional limits:

1) $0.1 \le d_1/t \le 0.9$

2) For $d_1/t > 0.5$ use $d_1/t = 1 - d_1/t$ to determine the influence coefficients G_1 through G_4 in Table C.4, and reverse the stress field for the analysis (See note below).

e) The datum for the stress distribution is at $d_1/t = 0.0$ for $d_1/t \le 0.5$ and at $d_1/t = 1.0$ for $d_1/t > 0.5$ (See Figure C.4).

f) The solution presented can be used for cylinders and spheres when $R_i/t \ge 5$. In this case, the finite width correction factor should be set to unity, or $f_w = 1.0$.

C.3.8 Plate – Embedded Crack, Elliptical Shape, Through-Wall Membrane and Bending Stress (KPECE1)

C.3.8.1 The Mode I Stress Intensity Factor [4]

$$K_I = \left(M_m \sigma_{me} + M_b \sigma_{be}\right)\sqrt{\frac{\pi a}{Q}} \tag{C.72}$$

where Q is given by Equation (C.15) . The local membrane and bending stress components acting on the crack face (see Figure C.5) are given by the following equations.

$$\sigma_{me} = \left\{\sigma_m + p_c\right\} + \sigma_b\left(1 - \frac{2d_2}{t}\right) \tag{C.73}$$

$$\sigma_{be} = \sigma_b\left(\frac{2a}{t}\right) \tag{C.74}$$

The membrane correction factor is given by

$$M_m = H_\varphi f_\varphi f_w \tag{C.75}$$

where f_w is given by Equation (C.19), f_φ is given by Equation (C.24), and

$$H_\varphi = \frac{1}{2}\sin^2\varphi\left[H_{90}\left(1+\sin\varphi\right) + H_{270}\left(1-\sin\varphi\right)\right] + H_0\cos^2\varphi \tag{C.76}$$

with,

$$H_{90} = h_1\left(\alpha,\beta_1\right)h_3\left(\alpha,\beta_2\right) \tag{C.77}$$

$$H_0 = h_2\left(\alpha,\beta_1\right)h_2\left(\alpha,\beta_2\right) \tag{C.78}$$

$$H_{270} = h_3\left(\alpha,\beta_1\right)h_1\left(\alpha,\beta_2\right) \tag{C.79}$$

$$h_1\left(\alpha,\beta_i\right) = 1 + \left(-0.04 + \frac{0.085}{0.34+\alpha}\right)\beta_i^2 + \left(0.05 - 0.03\alpha\right)\beta_i^4 \tag{C.80}$$

$$h_2\left(\alpha,\beta_i\right) = 1 + \left(-0.03 + \frac{0.075}{0.3+\alpha}\right)\beta_i^2 + \left(0.08 - \frac{0.024}{0.1+\alpha}\right)\beta_i^4 \tag{C.81}$$

$$h_3\left(\alpha,\beta_i\right) = 1 + \left(-0.06 + \frac{0.07}{0.25+\alpha}\right)\beta_i^2 + \left(0.643 - 0.343\alpha\right)\beta_i^4 \tag{C.82}$$

$$\alpha = \frac{a}{c} \tag{C.83}$$

$$\beta_1 = \frac{a}{d_1} \tag{C.84}$$

$$\beta_2 = \frac{a}{d_2} \tag{C.85}$$

The bending correction factor is:

$$M_b = -\left[0.5 + 0.2591\alpha^{1.5} - 0.09189\alpha^{2.5}\right] f_\varphi f_W f_\beta \sin\varphi \tag{C.86}$$

where terms are defined above, and

$$f_\beta = \frac{f_{270} + f_{90}}{2} - \frac{f_{270} - f_{90}}{2}\sin\varphi \tag{C.87}$$

$$f_{90} = 1 + \exp\left[-1.9249 - 3.9087\alpha^{0.5} + 4.1067\beta_2{}^3\right] \tag{C.88}$$

$$f_{270} = 1 + \exp\left[-1.9249 - 3.9087\alpha^{0.5} + 4.1067\beta_1{}^3\right] \tag{C.89}$$

C.3.8.2 Notes:

a) See Figure C.3(a) for the component and crack geometry.

b) See Figure C.5 for the definition of the membrane and through-wall bending stress components.

c) See Figure C.6 for the sign convention of the bending stress.

d) Crack and geometry dimensional limits:

1) $\left(\frac{d_1 - a}{t}\right) \geq 0.2 \quad when \quad d_1 \leq \frac{t}{2}$

2) $\left(\frac{d_2 - a}{t}\right) \geq 0.2 \quad when \quad d_2 \leq \frac{t}{2}$

3) $0.20 \leq d_1/t \leq 0.80$

4) $0.0 < a/c < 1.0$

5) $0.0 < c/W < 1.0$

6) $0 \leq \varphi \leq 2\pi$

e) The solution presented can be used for cylinders and spheres when $R_i/t \geq 5.0$. In this case, the finite width correction factor should be set to unity, $f_w = 1.0$.

C.3.9 Plate – Embedded Crack, Elliptical Shape, Through-Wall Fourth Order Polynomial Stress Distribution (KPECE2)

C.3.9.1 Mode I Stress Intensity Factor [40]

$$K_I = \left[\begin{array}{l} G_o \left\{ \{\sigma_o + p_c\} + \sigma_1 \left(\frac{d_1}{t}\right) + \sigma_2 \left(\frac{d_1}{t}\right)^2 + \sigma_3 \left(\frac{d_1}{t}\right)^3 + \sigma_4 \left(\frac{d_1}{t}\right)^4 \right\} + \\ G_1 \left\{ \sigma_1 + 2\sigma_2 \left(\frac{d_1}{t}\right) + 3\sigma_3 \left(\frac{d_1}{t}\right)^2 + 4\sigma_4 \left(\frac{d_1}{t}\right)^3 \right\} \left(\frac{a}{t}\right) + \\ G_2 \left\{ \sigma_2 + 3\sigma_3 \left(\frac{d_1}{t}\right) + 6\sigma_4 \left(\frac{d_1}{t}\right)^2 \right\} \left(\frac{a}{t}\right)^2 + \\ G_3 \left\{ \sigma_3 + 4\sigma_4 \left(\frac{d_1}{t}\right) \right\} \left(\frac{a}{t}\right)^3 + \\ G_4 \{\sigma_4\} \left(\frac{a}{t}\right)^4 \end{array} \right] \sqrt{\frac{\pi a}{Q}} f_w \qquad \text{(C.90)}$$

C.3.9.2 Notes:

a) See Figure C.3(a) for the component and crack geometry.

b) The coefficients of the stress distribution to be used are defined in paragraph C.2.2.3

c) The influence coefficients G_0 through G_4 for inside and outside surface cracks can be determined using the following equations.

$$G_0 = A_{0,0} + A_{1,0}\beta + A_{2,0}\beta^2 + A_{3,0}\beta^3 + A_{4,0}\beta^4 + A_{5,0}\beta^5 + A_{6,0}\beta^6 \qquad \text{(C.91)}$$

$$G_1 = A_{0,1} + A_{1,1}\beta + A_{2,1}\beta^2 + A_{3,1}\beta^3 + A_{4,1}\beta^4 + A_{5,1}\beta^5 + A_{6,1}\beta^6 \qquad \text{(C.92)}$$

$$G_2 = A_{0,2} + A_{1,2}\beta + A_{2,2}\beta^2 + A_{3,2}\beta^3 + A_{4,2}\beta^4 + A_{5,2}\beta^5 + A_{6,2}\beta^6 \qquad \text{(C.93)}$$

$$G_3 = A_{0,3} + A_{1,3}\beta + A_{2,3}\beta^2 + A_{3,3}\beta^3 + A_{4,3}\beta^4 + A_{5,3}\beta^5 + A_{6,3}\beta^6 \qquad \text{(C.94)}$$

$$G_4 = A_{0,4} + A_{1,4}\beta + A_{2,4}\beta^2 + A_{3,4}\beta^3 + A_{4,4}\beta^4 + A_{5,4}\beta^5 + A_{6,4}\beta^6 \qquad \text{(C.95)}$$

where,

$$\beta = \frac{2\varphi}{\pi} \qquad \text{(C.96)}$$

The parameters A_{ij} (i.e. the values from the row corresponding to G_i and column A_j) are provided in Table C.5 for $d_1/t = 0.25$ and $d_1/t = 0.50$.

d) The parameter Q is given by Equation (C.15), and f_w is given by Equation (C.19).

e) Crack and geometry dimensional limits:

1) $0.1 \le d_1/t \le 0.9$

2) $0.125 < a/c \le 1.0$

3) $-\pi/2 \le \varphi \le \pi/2$

4) For $d_1/t > 0.5$ use $d_1/t = 1 - d_1/t$ to determine the influence coefficients G_1 through G_4 in Table C.5, and reverse the stress field for the analysis (See note below).

f) The datum for the stress distribution is at $d_1/t = 0.0$ for $d_1/t \le 0.5$ and at $d_1/t = 1.0$ for $d_1/t > 0.5$.

g) The solution presented can be used for cylinders and spheres when $R_i/t \ge 5$. In this case, the finite width correction factor should be set to unity, $f_w = 1.0$ (See Figure C.4).

C.4 Stress Intensity Factor Solutions for Plates with Holes

C.4.1 Plate with Hole – Through-Wall Single Edge Crack, Through-Wall Membrane and Bending Stress (KPHTC1)

C.4.1.1 The Mode I Stress Intensity Factor [2], [12]

$$K_I = M_m \{\sigma_m + p_c\}\sqrt{\pi c} + M_b \sigma_b \sqrt{\pi (R_h + c)} \qquad \text{(C.97)}$$

The membrane correction factor is given by:

$$M_m = F_1 + BF_2 \qquad \text{(C.98)}$$

$$F_1 = \frac{3.3583 + 6.33015\zeta + 3.80461\zeta^2}{1 + 4.012118\zeta + 5.317858\zeta^2} \qquad \text{(C.99)}$$

$$F_2 = \frac{-1.1186 + 0.534114\zeta - 0.0594921\zeta^2}{1 + 2.980567\zeta + 4.253003\zeta^2} \qquad \text{(C.100)}$$

and the bending correction factor is given by

$$M_b = 0.4\left(\frac{19.252\zeta + 173.83\zeta^2 + 60.469\zeta^3}{1.0 + 49.254\zeta + 139.02\zeta^2 + 88.167\zeta^3 - 0.44324\zeta^4}\right) \qquad \text{(C.101)}$$

with,

$$\zeta = \frac{c}{R_h} \qquad \text{(C.102)}$$

C.4.1.2 Notes:

a) See Figure C.7(a) for the component and crack geometry.

b) See Figure C.7(b) for the definition of B;

c) Crack and geometry dimensional limits: $\zeta \ge 0.0$; $R_h <<$ plate width.

d) The stresses σ_m and σ_b can be determined using stress equations based on strength of materials concepts.

C.4.2 Plate with Hole – Through-Wall Double Edge Crack, Through-Wall Membrane and Bending Stress (KPHTC2)

C.4.2.1 The Mode I Stress Intensity Factor [2], [12]

$$K_I = M_m \{\sigma_m + p_c\}\sqrt{\pi c} + M_b \sigma_b \sqrt{\pi (R_h + c)} \tag{C.103}$$

The membrane correction factor is given by Equation (C.98) with:

$$F_1 = \frac{3.3633 + 3.6393\zeta + 0.680967\zeta^2}{1 + 3.54903\zeta + 0.652471\zeta^2} \tag{C.104}$$

$$F_2 = \frac{-1.1152 + 0.176708\zeta - 0.0112175\zeta^2}{1 + 3.220917\zeta + 5.047662\zeta^2} \tag{C.105}$$

The bending correction factor is given by

$$M_b = 0.4\left(\frac{17.739\zeta + 105.05\zeta^2 + 128.16\zeta^3}{1.0 + 35.699\zeta + 95.850\zeta^2 + 130.02\zeta^3 - 0.15592\zeta^4}\right) \tag{C.106}$$

with,

$$\zeta = \frac{c}{R_h} \tag{C.107}$$

C.4.2.2 Notes:

a) See Figure C.8(a) for the component and crack geometry.

b) See Figure C.8(b) for the definition of B.

c) Crack and geometry dimensional limits: $\zeta \geq 0.0$; $R_h <<$ plate width.

d) The stresses σ_m and σ_b can be determined using stress equations based on strength of materials concepts.

C.4.3 Plate with Hole – Surface Crack In Hole, Semi-Elliptical Shape, Through-Wall Membrane Stress (KPHSC1)

C.4.3.1 The Mode I Stress Intensity Factor [1]

$$K_I = M_m \{\sigma_m + p_c\}\sqrt{\frac{\pi a}{Q}} \tag{C.108}$$

where, Q is given by Equation (C.15) or (C.16), and the membrane correction factor is given by

$$M_m = \left[M_1 + M_2\left(\frac{a}{t}\right)^2 + M_3\left(\frac{a}{t}\right)^4\right] g_1 g_2 g_3 f_\varphi f_w \tag{C.109}$$

with,

$$M_2 = \frac{0.05}{0.11 + \left(\frac{a}{c}\right)^{1.5}} \tag{C.110}$$

$$M_3 = \frac{0.29}{0.23 + \left(\frac{a}{c}\right)^{1.5}} \tag{C.111}$$

$$g_1 = 1.0 - \frac{\left(\frac{a}{t}\right)^4 \sqrt{2.6 - 2\left(\frac{a}{t}\right)}}{1.0 + 4\left(\frac{a}{c}\right)} \cos\varphi \tag{C.112}$$

$$g_2 = \frac{1.0 + 0.358\zeta + 1.425\zeta^2 - 1.578\zeta^3 + 2.156\zeta^4}{1.0 + 0.08\zeta^2} \tag{C.113}$$

$$\zeta = \frac{1.0}{1.0 + \left(\frac{c}{R_h}\right)\cos\left(0.9\varphi\right)} \tag{C.114}$$

$$g_3 = 1.0 + 0.1\left(1 - \cos\varphi\right)^2 \left(1 - \frac{a}{t}\right)^{10} \tag{C.115}$$

In the following equation, set $n = 2$ for two cracks and $n = 1$ for one crack (see paragraph C.4.3.2.c)

$$f_w = \sqrt{\sec\left(\frac{\pi R_h}{2W}\right)\sec\left(\frac{\pi\left(2R_h + nc\right)}{4\left(W - c\right) + 2nc} \cdot \sqrt{\frac{a}{t}}\right)} \tag{C.116}$$

For $a/c \le 1.0$, f_φ is given by Equation (C.24) and

$$M_1 = 1.0 \tag{C.117}$$

For $a/c > 1.0$, f_φ is given by Equation (C.29) and

$$M_1 = \sqrt{\frac{c}{a}} \tag{C.118}$$

C.4.3.2 Notes:

a) See Figure C.9 for the component and crack geometry.

b) Crack and geometry dimensional limits:

1) $0.0 < a/t < 1.0$

2) $0.2 \le a/c \le 2.0$

3) $0.5 \le R_h/t \le 2.0$

4) $\left(R_h + c\right)/W < 0.5$

5) $-\pi/2 \le \varphi \le \pi/2$

c) The stress intensity factor solution provided is for two cracks. To estimate the stress intensity factor for one crack, the following equation can be used:

$$K_{1-crack} = \left(\sqrt{\frac{\frac{4}{\pi} + \frac{ac}{2tR_h}}{\frac{4}{\pi} + \frac{ac}{tR_h}}} \right) K_{2-crack} \qquad \text{(C.119)}$$

d) The membrane stress, σ_m, can be determined using stress equations based on strength of materials concepts.

C.4.4 Plate with Hole, Corner Crack, Semi-Elliptical Shape, Through-Wall Membrane and Bending Stress (KPHSC2)

C.4.4.1 The Mode I Stress Intensity Factor [1]

$$K_I = \left(M_m \left\{ \sigma_m + p_c \right\} + M_b \sigma_b \right) \sqrt{\frac{\pi a}{Q}} \qquad \text{(C.120)}$$

where Q is given by Equation (C.15) or (C.16). The membrane correction factor is given by:

$$M_m = \left\{ M_1 + M_2 \left(\frac{a}{t} \right)^2 + M_3 \left(\frac{a}{t} \right)^4 \right\} g_1 g_2 g_3 g_4 f_\varphi f_w \qquad \text{(C.121)}$$

where f_w is given by Equation (C.116), and

$$g_2 = \frac{1.0 + 0.358\zeta + 1.425\zeta^2 - 1.578\zeta^3 + 2.156\zeta^4}{1.0 + 0.13\zeta^2} \qquad \text{(C.122)}$$

$$\zeta = \frac{1.0}{1.0 + \left(\frac{c}{R_h} \right) \cos\left(\mu\varphi \right)} \qquad \text{(C.123)}$$

$$\mu = 0.85 \qquad \text{(C.124)}$$

For $a/c \le 1.0$, f_φ is given by Equation (C.24), and

$$M_1 = 1.13 - 0.09 \left(\frac{a}{c} \right) \qquad \text{(C.125)}$$

$$M_2 = \frac{0.89}{0.2 + \left(\frac{a}{c}\right)} - 0.54 \tag{C.126}$$

$$M_3 = 0.5 - \frac{1}{0.65 + \left(\frac{a}{c}\right)} + 14\left\{1 - \left(\frac{a}{c}\right)\right\}^{24} \tag{C.127}$$

$$g_1 = 1 + \left\{0.1 + 0.35\left(\frac{a}{t}\right)^2\right\}(1 - \sin\varphi)^2 \tag{C.128}$$

$$g_3 = \left[1 + 0.04\left(\frac{a}{c}\right)\right]\left[1 + 0.1(1 - \cos\varphi)^2\right]\left[0.85 + 0.15\left(\frac{a}{t}\right)^{0.25}\right] \tag{C.129}$$

$$g_4 = 1 - 0.7\left[1 - \left(\frac{a}{t}\right)\right]\left[\left(\frac{a}{c}\right) - 0.2\right]\left[1 - \left(\frac{a}{c}\right)\right] \tag{C.130}$$

For $a/c > 1.0$, f_φ is given by Equation (C.29), and

$$M_1 = \left(\frac{c}{a}\right)^{0.5}\left\{1 + 0.04\left(\frac{c}{a}\right)\right\} \tag{C.131}$$

$$M_2 = 0.2\left(\frac{c}{a}\right)^4 \tag{C.132}$$

$$M_3 = -0.11\left(\frac{c}{a}\right)^4 \tag{C.133}$$

$$g_1 = 1 + \left\{0.1 + 0.35\left(\frac{c}{a}\right)\left(\frac{a}{t}\right)^2\right\}(1 - \sin\varphi)^2 \tag{C.134}$$

$$g_3 = \left[1.13 - 0.09\left(\frac{c}{a}\right)\right]\left[1 + 0.1(1 - \cos\varphi)^2\right]\left[0.85 + 0.15\left(\frac{a}{t}\right)^{0.25}\right] \tag{C.135}$$

$$g_4 = 1.0 \tag{C.136}$$

The bending correction factor is given by:

$$M_b = M_m H \tag{C.137}$$

where M_m is evaluated using the above equations with

$$\mu = 0.85 - 0.25\left(\frac{a}{t}\right)^{0.25} \tag{C.138}$$

and,

$$H = H_1 + \left(H_2 - H_1\right)\sin^q \varphi \tag{C.139}$$

$$H_1 = 1 + G_{11}\left(\frac{a}{t}\right) + G_{12}\left(\frac{a}{t}\right)^2 + G_{13}\left(\frac{a}{t}\right)^3 \tag{C.140}$$

$$H_2 = 1 + G_{21}\left(\frac{a}{t}\right) + G_{22}\left(\frac{a}{t}\right)^2 + G_{23}\left(\frac{a}{t}\right)^3 \tag{C.141}$$

For $a/c \le 1.0$

$$q = 0.2 + \left(\frac{a}{c}\right) + 0.6\left(\frac{a}{t}\right) \tag{C.142}$$

$$G_{11} = -0.43 - 0.74\left(\frac{a}{c}\right) - 0.84\left(\frac{a}{c}\right)^2 \tag{C.143}$$

$$G_{12} = 1.25 - 1.19\left(\frac{a}{c}\right) + 4.39\left(\frac{a}{c}\right)^2 \tag{C.144}$$

$$G_{13} = -1.94 + 4.22\left(\frac{a}{c}\right) - 5.51\left(\frac{a}{c}\right)^2 \tag{C.145}$$

$$G_{21} = -1.5 - 0.04\left(\frac{a}{c}\right) - 1.73\left(\frac{a}{c}\right)^2 \tag{C.146}$$

$$G_{22} = 1.71 - 3.17\left(\frac{a}{c}\right) + 6.84\left(\frac{a}{c}\right)^2 \tag{C.147}$$

$$G_{23} = -1.28 + 2.71\left(\frac{a}{c}\right) - 5.22\left(\frac{a}{c}\right)^2 \tag{C.148}$$

For $a/c > 1.0$

$$q = 0.2 + \left(\frac{c}{a}\right) + 0.6\left(\frac{a}{t}\right) \tag{C.149}$$

$$G_{11} = -2.07 + 0.06\left(\frac{c}{a}\right) \quad \text{(C.150)}$$

$$G_{12} = 4.35 + 0.16\left(\frac{c}{a}\right) \quad \text{(C.151)}$$

$$G_{13} = -2.93 - 0.3\left(\frac{c}{a}\right) \quad \text{(C.152)}$$

$$G_{21} = -3.64 + 0.37\left(\frac{c}{a}\right) \quad \text{(C.153)}$$

$$G_{22} = 5.87 - 0.49\left(\frac{c}{a}\right) \quad \text{(C.154)}$$

$$G_{23} = -4.32 + 0.53\left(\frac{c}{a}\right) \quad \text{(C.155)}$$

C.4.4.2 Notes:

a) See Figure C.10 for the component and crack geometry.

b) Crack and geometry dimensional limits:

1) $0.0 < a/t \le 1.0$ for remote tension

2) $0.0 < a/t \le 0.8$ for remote bending

3) $0.2 \le a/c \le 2.0$

4) $0.5 \le R_h/t \le 2.0$

5) $\left(R_h + c\right)/W < 0.5$

6) $0 \le \varphi \le \pi$

c) To estimate the stress intensity factor for one crack, use Equation (C.119).

d) The membrane and bending stress, σ_m and σ_b, can be determined using stress equations based on strength of materials concepts.

C.5 Stress Intensity Factor Solutions for Cylinders

C.5.1 Cylinder – Through-Wall Crack, Longitudinal Direction, Through-Wall Membrane and Bending Stress (KCTCL)

C.5.1.1 The Mode I Stress Intensity Factor [11], [16]

Membrane and Bending Stress:

$$K_I = \left[\left\{\sigma_m + p_c\right\} G_0 + \sigma_b \left(G_0 - 2G_1\right)\right]\sqrt{\pi c} \quad \text{(C.156)}$$

or

$$K_I = \left(\{\sigma_0 + p_c\} G_0 + \sigma_1 G_1\right)\sqrt{\pi c} \tag{C.157}$$

Internal Pressure Only, crack face pressure loading is included:

$$K_I = \frac{pR_o}{t} G_p \sqrt{\pi c} \tag{C.158}$$

C.5.1.2 Notes:

a) See Figure C.11 for the component and crack geometry.

b) The influence coefficients G_0, G_1, and G_p are calculated using the following equations where the constants $A_1 \rightarrow A_6$ are provided in Table C.6 for K_I at the inside surface and in Table C.7 for the outside surface.

$$G_{0,1,p} = \frac{A_0 + A_1\lambda + A_2\lambda^2 + A_3\lambda^3}{1 + A_4\lambda + A_5\lambda^2 + A_6\lambda^3} \tag{C.159}$$

$$\lambda = \frac{1.818c}{\sqrt{R_i t}} \tag{C.160}$$

C.5.2 Cylinder – Through-Wall Crack, Circumferential Direction, Through-Wall Membrane and Bending Stress (KCTCC1)

C.5.2.1 The Mode I Stress Intensity Factor [11], [16]

Membrane and Bending Stress:

$$K_I = \left[\{\sigma_m + p_c\} G_0 + \sigma_b \left(G_0 - 2G_1\right)\right]\sqrt{\pi c} \tag{C.161}$$

or

$$K_I = \left(\{\sigma_0 + p_c\} G_0 + \sigma_1 G_1\right)\sqrt{\pi c} \tag{C.162}$$

Internal Pressure Only, crack face pressure loading is included:

$$K_I = \frac{pR_o^2}{R_o^2 - R_i^2} G_0 \sqrt{\pi c} \tag{C.163}$$

C.5.2.2 Notes:

a) See Figure C.12 for the component and crack geometry.

b) The influence coefficients G_0, and G_1 are calculated using the following equations where the constants $A_1 \rightarrow A_6$ are provided in Table C.8 for inside diameter surface crack and in Table C.9 for outside diameter surface crack.

$$G_{0,1} = \frac{A_0 + A_1\lambda + A_2\lambda^2 + A_3\lambda^3}{1 + A_4\lambda + A_5\lambda^2 + A_6\lambda^3} \tag{C.164}$$

$$\lambda = \frac{1.818c}{\sqrt{R_i t}} \tag{C.165}$$

c) For internal pressure with a net section axial force,

$$\sigma_m = \frac{pR_i^{\,2}}{R_o^{\,2} - R_i^{\,2}} + \frac{F}{\pi\left(R_o^{\,2} - R_i^{\,2}\right)} \tag{C.166}$$

$$\sigma_b = 0.0 \tag{C.167}$$

C.5.3 Cylinder – Through-Wall Crack, Circumferential Direction, Pressure with Net Section Axial Force and Bending Moment (KCTCC2)

C.5.3.1 The Mode I Stress Intensity Factor [16]

Membrane and Bending Stress:

$$K_I = \left[\left\{\sigma_m + p_c\right\} G_0 + \sigma_b \left(G_0 - 2G_1\right) + \sigma_{gb} G_5\right]\sqrt{\pi c} \tag{C.168}$$

Internal Pressure Stress plus Net Section Bending Only, crack face pressure loading is included:

$$K_I = \left[\frac{pR_o^2}{R_o^2 - R_i^2} G_0 + \sigma_{gb} G_5\right]\sqrt{\pi c} \tag{C.169}$$

C.5.3.2 Notes:

a) See Figure C.12 for the component and crack geometry.

b) The influence coefficients G_0, G_1, and G_5 are calculated using the following equations where the constants $A_1 \rightarrow A_6$ are provided in Table C.8 for inside diameter surface crack and in Table C.9 for outside diameter surface crack.

$$G_{0,1,5} = \frac{A_0 + A_1\lambda + A_2\lambda^2 + A_3\lambda^3}{1 + A_4\lambda + A_5\lambda^2 + A_6\lambda^3} \tag{C.170}$$

$$\lambda = \frac{1.818c}{\sqrt{R_i t}} \tag{C.171}$$

c) For internal pressure with a net section axial force, and net-section bending moment

$$\sigma_m = \frac{pR_i^2}{\left(R_o^2 - R_i^2\right)} + \frac{F}{\pi\left(R_o^2 - R_i^2\right)} \tag{C.172}$$

$$\sigma_b = 0.0 \tag{C.173}$$

$$\sigma_{gb} = \frac{MR_o}{0.25\pi\left(R_o^4 - R_i^4\right)} \tag{C.174}$$

C.5.4 Cylinder – Surface Crack, Longitudinal Direction – Infinite Length, Internal Pressure (KCSCLL1)

C.5.4.1 The Mode I Stress Intensity Factor [40]

Inside Surface, crack face pressure loading is included:

$$K_I = \frac{pR_0^2}{R_0^2 - R_i^2}\left[2G_o - 2G_1\left(\frac{a}{R_i}\right) + 3G_2\left(\frac{a}{R_i}\right)^2 - 4G_3\left(\frac{a}{R_i}\right)^3 + 5G_4\left(\frac{a}{R_i}\right)^4\right]\sqrt{\pi a} \qquad \text{(C.175)}$$

Outside Surface:

$$K_I = \frac{pR_i^2}{R_0^2 - R_i^2}\left[2G_o + 2G_1\left(\frac{a}{R_o}\right) + 3G_2\left(\frac{a}{R_o}\right)^2 + 4G_3\left(\frac{a}{R_o}\right)^3 + 5G_4\left(\frac{a}{R_o}\right)^4\right]\sqrt{\pi a} \qquad \text{(C.176)}$$

C.5.4.2 Notes:

a) See Figure C.13 for the component and crack geometry.

b) The influence coefficients G_0 through G_4 are provided in Table C.10.

c) Crack and geometry dimensional limits:

1) $0.0 \le a/t \le 0.8$

2) $0 \le t/R_i \le 1.0$

C.5.5 Cylinder – Surface Crack, Longitudinal Direction – Infinite Length, Through-Wall Fourth Order Polynomial Stress Distribution (KCSCLL2)

C.5.5.1 The Mode I Stress Intensity Factor [40]

$$K_I = \left[G_o\{\sigma_o + p_c\} + G_1\sigma_1\left(\frac{a}{t}\right) + G_2\sigma_2\left(\frac{a}{t}\right)^2 + G_3\sigma_3\left(\frac{a}{t}\right)^3 + G_4\sigma_4\left(\frac{a}{t}\right)^4\right]\sqrt{\pi a} \qquad \text{(C.177)}$$

C.5.5.2 Notes:

a) See paragraph C.5.4.2.

b) The coefficients of the stress distribution to be used are defined in paragraph C.2.2.3.

C.5.6 Cylinder – Surface Crack, Longitudinal Direction – Infinite Length, Through-Wall Arbitrary Stress Distribution (KCSCLL3)

C.5.6.1 The Mode I Stress Intensity Factor

The stress intensity factor can be determined using the weight function method (see paragraph C.14.5). The influence coefficients G_0 and G_1 required to compute M_1, M_2, and M_3 can be determined using paragraph C.5.4.2.b.

C.5.6.2 Notes: see paragraph C.5.4.2.

C.5.7 Cylinder – Surface Crack, Circumferential Direction – 360 Degrees, Pressure With A Net Section Axial Force and Bending Moment (KCSCCL1)

C.5.7.1 The Mode I Stress Intensity Factor

$$K_I = \left[G_o \left\{ \sigma_o + p_c \right\} + G_1 \sigma_1 \left(\frac{a}{t} \right) \right] \sqrt{\pi a} \tag{C.178}$$

where for an inside surface crack,

$$\sigma_0 = \sigma_m - \sigma_b \tag{C.179}$$

$$\sigma_1 = 2\sigma_b \tag{C.180}$$

and for an outside surface crack,

$$\sigma_0 = \sigma_m + \sigma_b \tag{C.181}$$

$$\sigma_1 = -2\sigma_b \tag{C.182}$$

with,

$$\sigma_m = \frac{pR_i^2}{\left(R_o^2 - R_i^2 \right)} + \frac{F}{\pi \left(R_o^2 - R_i^2 \right)} + \frac{2M \left(R_o + R_i \right)}{\pi \left(R_o^4 - R_i^4 \right)} \tag{C.183}$$

$$\sigma_b = \frac{2M \left(R_o - R_i \right)}{\pi \left(R_o^4 - R_i^4 \right)} \tag{C.184}$$

C.5.7.2 Notes:

a) See Figure C.14 for the component and crack geometry.

b) The influence coefficients G_0 and G_1 are provided in Table C.11.

c) Crack and geometry dimensional limits:

1) $0.0 \le a/t \le 0.8$

2) $0.001 \le t/R_i \le 1.0$

d) This solution represents the maximum stress intensity on the cross section at the location of maximum bending stress. The stress intensity factor at other locations can be determined by using the appropriate value of bending stress.

C.5.8 Cylinder – Surface Crack, Circumferential Direction – 360 Degrees, Through-Wall Fourth Order Polynomial Stress Distribution (KCSCCL2)

C.5.8.1 The Mode I Stress Intensity Factor [40]

$$K_I = \left[G_o \left\{ \sigma_o + p_c \right\} + G_1 \sigma_1 \left(\frac{a}{t} \right) + G_2 \sigma_2 \left(\frac{a}{t} \right)^2 + G_3 \sigma_3 \left(\frac{a}{t} \right)^3 + G_4 \sigma_4 \left(\frac{a}{t} \right)^4 \right] \sqrt{\pi a} \tag{C.185}$$

C.5.8.2 Notes:

a) See paragraph C.5.7.2.

b) The coefficients of the stress distribution to be used are defined in paragraph. C.2.2.3

c) The influence coefficients G_0 through G_4 are provided in Table C.11.

C.5.9 Cylinder – Surface Crack, Circumferential Direction – 360 Degrees, Through-Wall Arbitrary Stress Distribution (KCSCCL3)

C.5.9.1 The Mode I Stress Intensity Factor

The stress intensity factor can be determined using the weight function method (see paragraph C.14.5). The influence coefficients G_0 and G_1 required to compute M_1, M_2, and M_3 can be determined using paragraph C.5.7.2.b..

C.5.9.2 Notes: see paragraph C.5.7.2.

C.5.10 Cylinder – Surface Crack, Longitudinal Direction – Semi-Elliptical Shape, Internal Pressure (KCSCLE1)

C.5.10.1 The Mode I Stress Intensity Factor [40]

Inside Surface, crack face pressure loading is included:

$$K_I = \frac{pR_0^{\,2}}{R_0^{\,2} - R_i^{\,2}} \left[2G_o - 2G_1 \left(\frac{a}{R_i} \right) + 3G_2 \left(\frac{a}{R_i} \right)^2 - 4G_3 \left(\frac{a}{R_i} \right)^3 + 5G_4 \left(\frac{a}{R_i} \right)^4 \right] \sqrt{\frac{\pi a}{Q}} \qquad \text{(C.186)}$$

Outside Surface:

$$K_I = \frac{pR_i^{\,2}}{R_0^{\,2} - R_i^{\,2}} \left[2G_o + 2G_1 \left(\frac{a}{R_o} \right) + 3G_2 \left(\frac{a}{R_o} \right)^2 + 4G_3 \left(\frac{a}{R_o} \right)^3 + 5G_4 \left(\frac{a}{R_o} \right)^4 \right] \sqrt{\frac{\pi a}{Q}} \qquad \text{(C.187)}$$

C.5.10.2 Notes:

a) See Figure C.15 for the component and crack geometry.

b) The influence coefficients G_0 and G_1 for inside and outside surface cracks can be determined using the following equations:

$$G_0 = A_{0,0} + A_{1,0}\beta + A_{2,0}\beta^2 + A_{3,0}\beta^3 + A_{4,0}\beta^4 + A_{5,0}\beta^5 + A_{6,0}\beta^6 \qquad \text{(C.188)}$$

$$G_1 = A_{0,1} + A_{1,1}\beta + A_{2,1}\beta^2 + A_{3,1}\beta^3 + A_{4,1}\beta^4 + A_{5,1}\beta^5 + A_{6,1}\beta^6 \qquad \text{(C.189)}$$

where β is given by Equation (C.96) and the parameters A_{ij} (i.e. the values from the row corresponding to G_i and column A_j) are provided in Table C.12 for an inside diameter crack and in Table C.13 for an outside diameter crack. The influence coefficients G_2, G_3, and G_4 can be computed using paragraph C.14.3 or C.14.4.

c) Q is determined using Equation (C.15) or (C.16).

d) Crack and geometry dimensional limits:

1) $0.0 \le a/t \le 0.8$

2) $0.03125 \le a/c \le 2.0$

3) $0 \le \varphi \le \pi$

4) $0.0 \le t/R_i \le 1.0$

e) Influence coefficients are provided in Table C.12 and Table C.13 for values of $0.03125 \le a/c \le 2.0$. For long cracks where $a/c < 0.03125$, the influence coefficients can be determined by interpolation using the values in Table C.12 and Table C.13 and the following values for G_0 and G_1. The influence coefficients for the long flaw or infinite length solution (G_0^L and G_1^L) in these equations can be computed using Table C.10.

$$G_0 = G_0^L \left(\frac{2\varphi}{\pi} \right)^6 \tag{C.190}$$

$$G_1 = G_1^L \left(\frac{2\varphi}{\pi} \right)^6 \tag{C.191}$$

C.5.11 Cylinder – Surface Crack, Longitudinal Direction – Semi-Elliptical Shape, Through-Wall Fourth Order Polynomial Stress Distribution (KCSCLE2)

C.5.11.1 The Mode I Stress Intensity Factor [40]

$$K_I = \left[G_o \{\sigma_o + p_c\} + G_1\sigma_1 \left(\frac{a}{t}\right) + G_2\sigma_2 \left(\frac{a}{t}\right)^2 + G_3\sigma_3 \left(\frac{a}{t}\right)^3 + G_4\sigma_4 \left(\frac{a}{t}\right)^4 \right] \sqrt{\frac{\pi a}{Q}} \tag{C.192}$$

C.5.11.2 Notes:

a) See paragraph C.5.10.2.

b) The coefficients of the stress distribution to be used are defined in paragraph C.2.2.3.

C.5.12 Cylinder – Surface Crack, Longitudinal Direction – Semi-Elliptical Shape, Through-Wall Arbitrary Stress Distribution (KCSCLE3)

C.5.12.1 The Mode I Stress Intensity Factor

The stress intensity factor can be determined using the weight function method (see paragraph C.14.5). The influence coefficients G_0 and G_1 required to compute M_1, M_2, and M_3 can be determined using paragraph. C.5.10.2.b

C.5.12.2 Notes: see paragraph C.5.10.2.

C.5.13 Cylinder – Surface Crack, Circumferential Direction – Semi-Elliptical Shape, Internal Pressure and Net-Section Axial Force (KCSCCE1)

C.5.13.1 The Mode I Stress Intensity Factor [40]

Inside Surface, crack face pressure loading is included:

$$K_I = G_o \left(\frac{pR_o^{\,2}}{R_0^{\,2} - R_i^{\,2}} + \frac{F}{\pi\left(R_0^{\,2} - R_i^{\,2}\right)} \right) \sqrt{\frac{\pi a}{Q}} \tag{C.193}$$

Outside Surface:

$$K_I = G_o \left(\frac{pR_i^{\,2}}{R_0^{\,2} - R_i^{\,2}} + \frac{F}{\pi\left(R_0^{\,2} - R_i^{\,2}\right)} \right) \sqrt{\frac{\pi a}{Q}} \tag{C.194}$$

C.5.13.2 Notes:

a) See Figure C.16 for the component and crack geometry.

b) The influence coefficient, G_0, can be determined using paragraph C.5.14.2.b.

c) The parameter Q is given by Equation (C.15) or (C.16).

d) Crack and geometry dimensional limits are shown in C.5.14.2.

C.5.14 Cylinder – Surface Crack, Circumferential Direction – Semi-Elliptical Shape, Through-Wall Fourth Order Polynomial Stress Distribution with a Net Section Bending Stress (KCSCCE2)

C.5.14.1 The Mode I Stress Intensity Factor [40]

$$K_I = \left[\begin{array}{l} G_o\left\{\sigma_o + p_c\right\} + G_1\sigma_1\left(\frac{a}{t}\right) + G_2\sigma_2\left(\frac{a}{t}\right)^2 + G_3\sigma_3\left(\frac{a}{t}\right)^3 + G_4\sigma_4\left(\frac{a}{t}\right)^4 + \\ G_5\sigma_5 + G_6\sigma_6 \end{array} \right] \sqrt{\frac{\pi a}{Q}} \tag{C.195}$$

C.5.14.2 Notes:

a) See Figure C.16 for the component and crack geometry.

b) The influence coefficients G_0, G_1, G_5, and G_6 for inside and outside surface cracks can be determined using the following equations:

$$G_0 = A_{0,0} + A_{1,0}\beta + A_{2,0}\beta^2 + A_{3,0}\beta^3 + A_{4,0}\beta^4 + A_{5,0}\beta^5 + A_{6,0}\beta^6 \tag{C.196}$$

$$G_1 = A_{0,1} + A_{1,1}\beta + A_{2,1}\beta^2 + A_{3,1}\beta^3 + A_{4,1}\beta^4 + A_{5,1}\beta^5 + A_{6,1}\beta^6 \tag{C.197}$$

$$G_5 = A_{0,5} + A_{1,5}\beta + A_{2,5}\beta^2 + A_{3,5}\beta^3 + A_{4,5}\beta^4 + A_{5,5}\beta^5 + A_{6,5}\beta^6 \tag{C.198}$$

$$G_6 = A_{0,6} + A_{1,6}\beta + A_{2,6}\beta^2 + A_{3,6}\beta^3 + A_{4,6}\beta^4 + A_{5,6}\beta^5 + A_{6,6}\beta^6 \tag{C.199}$$

where β is given by Equation (96) and the parameters A_{ij} (i.e. the values from the row corresponding to G_i and column A_j), are provided in Table C.14 for an inside diameter crack and in Table C.15 for an outside diameter crack. The influence coefficients G_2, G_3, and G_4 can be computed using paragraph C.14.3 or C.14.4.

c) Q is determined using Equation (C.15) or (C.16).

d) Crack and geometry dimensional limits:

1) $0.0 \le a/t \le 0.8$

2) $0.03125 \le a/c \le 2.0$

3) $0 \le \varphi \le \pi$

4) $0.0 \le t/R_i \le 1.0$

e) Influence coefficients are provided in Table C.14 and Table C.15 for values of $0.03125 \le a/c \le 2.0$. For long cracks where $a/c < 0.03125$, the influence coefficients can be determined by interpolation using the values in Table C.14 and Table C.15 and the values for G_0 and G_1 computed using the equations in paragraph C.5.10.2. The influence coefficients for the long flaw or infinite length solution (G_0^L and G_1^L) in these equations can be computed using Table C.11.

f) The coefficients of the stress distribution to be used are defined in paragraph C.2.2.3.

g) The net-section bending stress about the x-axis and y-axis are computed as follows:

$$\sigma_5 = \frac{M_x R_o}{0.25\pi\left(R_o^4 - R_i^4\right)} \qquad \text{(C.200)}$$

$$\sigma_6 = \frac{M_y R_o}{0.25\pi\left(R_o^4 - R_i^4\right)} \qquad \text{(C.201)}$$

h) If the polynomial stress distribution has been derived from the most highly stressed location around the circumference using an analysis that include the net-section bending moments, then the terms with G_5 and G_6 do not need to be included in the calculation of the stress intensity factor using Equation (C.195). It should be noted that this method will provide a conservative solution depending on the orientation of the crack with respect to the applied net-section bending moments.

C.5.15 Cylinder – Surface Crack, Circumferential Direction – Semi-Elliptical Shape, Through-Wall Arbitrary Stress Distribution (KCSCCE3)

C.5.15.1 The Mode I Stress Intensity Factor

The stress intensity factor can be determined using the weight function method (see paragraph C.14.5). The influence coefficients G_0 and G_1 required to compute M_1, M_2, and M_3 can be determined using paragraph C.5.14.2.b.

C.5.15.2 Notes: see paragraph C.5.13.2.

C.5.16 Cylinder – Embedded Crack, Longitudinal Direction – Infinite Length, Through-Wall Fourth Order Polynomial Stress Distribution (KCECLL)

C.5.16.1 The Mode I Stress Intensity Factor solution in paragraph C.3.7 can be used

C.5.16.2 Notes:

a) See Figure C.17 for the component and crack geometry.

b) See paragraph C.3.7.

C.5.17 Cylinder – Embedded Crack, Circumferential Direction – 360 Degrees, Through-Wall Fourth Order Polynomial Stress Distribution (KCECCL)

C.5.17.1 The Mode I Stress Intensity Factor solution in paragraph C.3.7can be used

C.5.17.2 Notes:

a) See Figure C.18 for the component and crack geometry.

b) See paragraph C.3.7.

C.5.18 Cylinder – Embedded Crack, Longitudinal Direction – Elliptical Shape, Through-Wall Fourth Order Polynomial Stress Distribution (KCECLE)

C.5.18.1 The Mode I Stress Intensity Factor solution in paragraph C.3.9 can be used

C.5.18.2 Notes:

a) See Figure C.19 for the component and crack geometry.

b) See paragraph C.3.9.2.

C.5.19 Cylinder – Embedded Crack, Circumferential Direction – Elliptical Shape, Through-Wall Fourth Order Polynomial Stress Distribution (KCECCE)

C.5.19.1 The Mode I Stress Intensity Factor solution in paragraph C.3.9 can be used

C.5.19.2 Notes:

a) See Figure C.20 for the component and crack geometry.

b) See paragraph C.3.9.2..

C.6 Stress Intensity Factor Solutions for Spheres

C.6.1 Sphere – Through-Wall Crack, Through-Wall Membrane and Bending Stress (KSTC)

C.6.1.1 The Mode I Stress Intensity Factor [10], [11]

Membrane and Bending Stress:

$$K_I = \left[\left\{\sigma_m + p_c\right\} G_0 + \sigma_b \left(G_0 - 2G_1\right)\right]\sqrt{\pi c} \qquad \text{(C.202)}$$

or

$$K_I = \left(\left\{\sigma_0 + p_c\right\} G_0 + \sigma_1 G_1\right)\sqrt{\pi c} \qquad \text{(C.203)}$$

Internal Pressure Only, crack face pressure loading is included:

$$K_I = \frac{pR_o^2}{R_o^2 - R_i^2} G_p \sqrt{\pi c} \qquad \text{(C.204)}$$

C.6.1.2 Notes:

a) See Figure C.21 for the component and crack geometry.

b) The influence coefficients G_0, G_1, and G_p are calculated using the following equations where the constants $A_1 \rightarrow A_8$ are provided in Table C.16 for K_I at the inside diameter and in Table C.17 for K_I at the outside diameter.

$$G_{0,1,p} = A_0 + A_1\lambda + A_2\lambda^2 + A_3\lambda^3 + A_4\lambda^4 + A_5\lambda^5 + A_6\lambda^6 + A_7\lambda^7 + A_8\lambda^8 \qquad \text{(C.205)}$$

$$\lambda = \frac{1.818c}{\sqrt{R_i t}} \qquad \text{(C.206)}$$

C.6.2 Sphere – Surface Crack, Circumferential Direction – 360 Degrees, Internal Pressure (KSSCCL1)

C.6.2.1 The Mode I Stress Intensity Factor [40]

Inside Surface, crack face pressure loading is included:

$$K_I = \frac{pR_0^3}{R_0^3 - R_i^3}\left[1.5G_o - 1.5G_1\left(\frac{a}{R_i}\right) + 3G_2\left(\frac{a}{R_i}\right)^2 - 5G_3\left(\frac{a}{R_i}\right)^3 + 7.5G_4\left(\frac{a}{R_i}\right)^4\right]\sqrt{\pi a} \qquad \text{(C.207)}$$

Outside Surface:

$$K_I = \frac{pR_i^3}{R_0^3 - R_i^3}\left[1.5G_o + 1.5G_1\left(\frac{a}{R_o}\right) + 3G_2\left(\frac{a}{R_o}\right)^2 + 5G_3\left(\frac{a}{R_o}\right)^3 + 7.5G_4\left(\frac{a}{R_o}\right)^4\right]\sqrt{\pi a} \qquad \text{(C.208)}$$

C.6.2.2 Notes:

a) See Figure C.22 for the component and crack geometry.

b) The influence coefficients G_0 through G_4 are provided in Table C.18.

c) Crack and geometry dimensional limits:

1) $0.0 < a/t \le 0.8$

2) $0.001 \le t/R_i \le 0.33$

C.6.3 Sphere – Surface Crack, Circumferential Direction – 360 Degrees, Through-Wall Fourth Order Polynomial Stress Distribution (KSSCCL2)

C.6.3.1 The Mode I Stress Intensity Factor [40]

$$K_I = \left[G_o \{\sigma_o + p_c\} + G_1\sigma_1\left(\frac{a}{t}\right) + G_2\sigma_2\left(\frac{a}{t}\right)^2 + G_3\sigma_3\left(\frac{a}{t}\right)^3 + G_4\sigma_4\left(\frac{a}{t}\right)^4 \right]\sqrt{\pi a} \qquad \text{(C.209)}$$

C.6.3.2 Notes:

a) See paragraph C.6.2.2.

b) The coefficients of the stress distribution to be used are defined in paragraph C.2.2.3.

C.6.4 Sphere – Surface Crack, Circumferential Direction – 360 Degrees, Through-Wall Arbitrary Stress Distribution (KSSCCL3)

C.6.4.1 The Mode I Stress Intensity Factor [3]

The stress intensity factor can be determined using the weight function method (see paragraph C.14.5). The influence coefficients G_0 and G_1 required to compute M_1, M_2, and M_3 can be determined using paragraph C.6.2.2.b

C.6.4.2 Notes: see paragraph C.6.2.2.

C.6.5 Sphere – Surface Crack, Circumferential Direction – Semi-Elliptical Shape, Internal Pressure (KSSCCE1)

C.6.5.1 The Mode I Stress Intensity Factor [40]

Inside Surface, crack face pressure loading is included:

$$K_I = \frac{pR_0^{\,3}}{R_0^{\,3} - R_i^{\,3}}\left[1.5G_o - 1.5G_1\left(\frac{a}{R_i}\right) + 3G_2\left(\frac{a}{R_i}\right)^2 - 5G_3\left(\frac{a}{R_i}\right)^3 + 7.5G_4\left(\frac{a}{R_i}\right)^4 \right]\sqrt{\frac{\pi a}{Q}} \qquad \text{(C.210)}$$

Outside Surface:

$$K_I = \frac{pR_i^{\,3}}{R_0^{\,3} - R_i^{\,3}}\left[1.5G_o + 1.5G_1\left(\frac{a}{R_o}\right) + 3G_2\left(\frac{a}{R_o}\right)^2 + 5G_3\left(\frac{a}{R_o}\right)^3 + 7.5G_4\left(\frac{a}{R_o}\right)^4 \right]\sqrt{\frac{\pi a}{Q}} \qquad \text{(C.211)}$$

C.6.5.2 Notes:

a) See Figure C.23 for the component and crack geometry.

b) The influence coefficients G_0 and G_1 for inside and outside surface cracks can be determined using the following equations:

$$G_0 = A_{0,0} + A_{1,0}\beta + A_{2,0}\beta^2 + A_{3,0}\beta^3 + A_{4,0}\beta^4 + A_{5,0}\beta^5 + A_{6,0}\beta^6 \quad \text{(C.212)}$$

$$G_1 = A_{0,1} + A_{1,1}\beta + A_{2,1}\beta^2 + A_{3,1}\beta^3 + A_{4,1}\beta^4 + A_{5,1}\beta^5 + A_{6,1}\beta^6 \quad \text{(C.213)}$$

where β is given by Equation (C.96) and the parameters A_{ij} (i.e. the values from the row corresponding to G_i and column A_j) are provided in Table C.19 for inside diameter cracks and in Table C.20 for outside diameter cracks. The influence coefficients G_2, G_3, and G_4 can be calculated using paragraph C.14.3.or C.14.4

c) The parameter Q is given by Equation (C.15) or (C.16).

d) Crack and geometry dimensional limits:

1) $0.2 \le a/t \le 0.8$

2) $0.03125 \le a/c \le 2.0$

3) $0 \le \varphi \le \pi$

4) $0.0 \le t/R_i \le 0.33$

e) Influence coefficients are provided in Table C.19 and Table C.20 for values of $0.03125 \le a/c \le 2.0$. For long cracks where $a/c < 0.03125$, the influence coefficients can be determined by interpolation using the values in Table C.19 and Table C.20 and the following values for G_0 and G_1 computed using the equations in paragraph C.5.10.2.e. The influence coefficients for the long flaw or infinite length solution (G_0^L and G_1^L) in these equations can be computed using Table C.18.

C.6.6 Sphere – Surface Crack, Circumferential Direction – Semi-Elliptical Shape, Through-Wall Fourth Order Polynomial Stress Distribution (KSSCCE2)

C.6.6.1 The Mode I Stress Intensity Factor [40]

$$K_I = \left[G_o\{\sigma_o + p_c\} + G_1\sigma_1\left(\frac{a}{t}\right) + G_2\sigma_2\left(\frac{a}{t}\right)^2 + G_3\sigma_3\left(\frac{a}{t}\right)^3 + G_4\sigma_4\left(\frac{a}{t}\right)^4 \right]\sqrt{\frac{\pi a}{Q}} \quad \text{(C.214)}$$

C.6.6.2 Notes:

a) See paragraph C.6.5.2.

b) The coefficients of the stress distribution to be used are defined in paragraph C.2.2.3.

C.6.7 Sphere – Surface Crack, Circumferential Direction – Semi-Elliptical Shape, Through-Wall Arbitrary Stress Distribution (KSSCCE3)

C.6.7.1 The Mode I Stress Intensity Factor [3]

The stress intensity factor can be determined using the weight function method (see paragraph C.14.5). The influence coefficients G_0 and G_1 required to compute M_1, M_2, and M_3 can be determined using paragraph C.6.5.2.b..

C.6.7.2 Notes: see paragraph C.6.5.2.

C.6.8 Sphere – Embedded Crack, Circumferential Direction – 360 Degrees, Through-Wall Fourth Order Polynomial Stress Distribution (KSECCL)

C.6.8.1 The Mode I Stress Intensity Factor solution in paragraph C.3.7 can be used.

C.6.8.2 Notes:

a) See Figure C.24 for the component and crack geometry.

b) See paragraph C.3.7.2.

C.6.9 Sphere – Embedded Crack, Circumferential Direction – Elliptical Shape, Through-Wall Fourth Order Polynomial Stress Distribution (KSECCE)

C.6.9.1 The Mode I Stress Intensity Factor solution in paragraph C.3.9 can be used.

C.6.9.2 Notes:

a) See Figure C.25 for the component and crack geometry.

b) See paragraph C.3.9.2.

C.7 Stress Intensity Factor Solutions for Elbows and Pipe Bends

The stress intensity factor solutions for cylinders can be used for elbows and pipe bends if the stress at the location of the crack is determined considering the bend geometry and applied loads. The net-section forces and moments applied to elbow, as well as internal pressure, should be considered when determining the stress at the crack location.

C.8 Stress Intensity Factor Solutions for Nozzles and Piping Tees

C.8.1 Nozzle – Corner Crack, Radial Direction, Quarter-Circular Shape, Membrane Stress at the Corner (KNCC1)

C.8.1.1 The Mode I Stress Intensity Factor [36], [37]

$$K_I = M_f M_b \left(k_{ta}\sigma_{nom} + p_c\right)\frac{2\sqrt{\pi a}}{\pi} \tag{C.215}$$

where

$$M_f = 1.43 - 0.24\left(\sin\varphi + \cos\varphi\right) \tag{C.216}$$

$$M_b = 1 + 0.15\left(\frac{a}{\sqrt{t^2 + t_n^2}}\right)^2 \tag{C.217}$$

$$k_{ta} = 1 + \left(k_{tn} - 1\right)\left(1 + \frac{\pi a\left\{\sin\varphi + \cos\varphi\right\}}{2\left\{d_n - t_n\right\}}\right)^{-B} \tag{C.218}$$

with

$$B = 2 - 2\sqrt{\frac{t_n}{d_n}} \quad (for\ nozzles\ in\ spherical\ shells) \tag{C.219}$$

$$B = 2.7 - 2\sqrt{\frac{t_n}{d_n}} \quad (for\ nozzles\ in\ cylindrical\ shells) \tag{C.220}$$

$$B = 3.3 - 2\sqrt{\frac{t_n}{d_n}} \quad (for\ nozzles\ in\ plates) \tag{C.221}$$

C.8.1.2 Notes:

a) See Figure C.26 (Crack labeled G) and Figure C.27 for the component and crack geometry.

b) The parameter k_{tn} is the theoretical stress concentration factor that can be used to compute the maximum stress at the corner of a nozzle, or

$$k_{tn} = \frac{\sigma_{\max}}{\sigma_{nom}} \tag{C.222}$$

C.8.2 Nozzle – Corner Crack, Radial Direction, Quarter-Circular Shape, Cubic Polynomial Stress at the Corner (KNCC)

C.8.2.1 The Mode I Stress Intensity Factor [40]

$$K_I = \left[0.706\{\sigma_0 + p_c\} + 0.537\left(\frac{2a}{\pi}\right)\sigma_1 + 0.448\left(\frac{a^2}{2}\right)\sigma_2 + 0.393\left(\frac{4a^3}{3\pi}\right)\sigma_3\right]\sqrt{\pi a} \tag{C.223}$$

C.8.2.2 Notes:

a) See Figure C.26 (i.e. the crack labeled G) and Figure C.27 for the component and crack geometry.

b) Crack and geometry dimensional limits (see Figure C.27 for definitions of t and t_n):

1) $0.0 \le a/t \le 0.5$

2) $0.0 \le a/t_n \le 0.5$

3) $\varphi = \pi/4$

c) The coefficients of the stress distribution to be used are defined below.

$$\sigma(x) = \sigma_0 + \sigma_1 x + \sigma_2 x^2 + \sigma_3 x^3 \tag{C.224}$$

C.8.3 Surface Cracks At Nozzles – General Solution

The stress intensity factor solutions shown below can be used for surface cracks at nozzles if the stress distribution normal to the plane of the crack is determined based on the nozzle geometry and applied loads. The stress distribution normal to the plane of the crack, $\sigma(x)$, should be computed for the component in the uncracked state considering the effects of the structural configuration and fillet weld geometry (see Figure C.33(b)). The net-section forces and moments applied to shell and nozzle, as well as internal pressure, should be considered when determining the stress distribution. The use of this method to compute the stress intensity factor will result in a conservative value as long as the geometry of the crack does not significantly reduce the stiffness of the cylinder-to-cylinder connection. If the geometry of the crack does result in a significant loss in stiffness, the resulting deformation will result in a higher value of the stress intensity factor. In these cases, an analysis of the cracked geometry is required to accurately determine the stress intensity factor.

a) Nozzle Neck or Branch (see Figure C.26)

   1) Crack A – Use KCTCC1, KCTCC2, KCSCCL3, KCSCCE3, KCECCL or KCECCE

   2) Crack B – Use KCTCL, KCSCLL3, KCSCLE3, KCECLL or KCECLE

b) Shell or Run Pipe (see Figure C.26)

   1) Crack D & F – Use KPTC, KPSCE3, KPECL, or KPECE2

   2) Crack E & C – Use KPTC, KPSCE3, KPECL, or KPECE2

   3) Crack G – Use KNCC1 or KNCC2

C.9 Stress Intensity Factor Solutions For Ring-Stiffened Cylinders

C.9.1 Ring-Stiffened Cylinder – Surface Crack at the Toe of One Fillet Weld, Circumferential Direction – 360 Degrees, Pressure Loading (KRCSCCL1)

C.9.1.1 The Mode I Stress Intensity Factor [29]

$$K_I = pM_p^{1c}\sqrt{\pi a} \qquad \text{(C.225)}$$

C.9.1.2 Notes:

a) See Figure C.28 for the component and crack geometry.

b) The coefficients, M_p^{1c}, are provided in Table C.21.

c) Crack and geometry dimensional limits:

   1) $0.2 \le a/t \le 0.8$

   2) $1.0 \le A_r/t \le 32.0$

   3) $10 \le R_i/t \le 300$, when $R_i/t < 10$ use $R_i/t = 10$ and when $R_i/t > 300$ use $R_i/t = 300$

d) The effects of the fillet weld on the stress field at the location of the fillet weld are included in the solution; a magnification factor is not required.

e) This solution may be used for W, T, L and I sections attached by fillet welds to the inside of the vessel when the vessel is subject to a positive internal pressure.

f) This solution may also be used for W, T, L, and I sections attached by fillet welds to the outside of the vessel when the vessel is subject to a partial or full vacuum. The results for this configuration and loading will be conservative because the membrane stress field in the vessel is compressive; the only tensile stress is a result of local through-wall bending at the ring to cylinder attachment location.

C.9.2 Ring-Stiffened Cylinder – Surface Crack at the Toe of Both Fillet Welds, Circumferential Direction – 360 Degrees, Pressure Loading (KRCSCCL2)

C.9.2.1 The Mode I Stress Intensity Factor [29]

$$K_I = pM_p^{2c}\sqrt{\pi a} \tag{C.226}$$

C.9.2.2 Notes:

a) See Figure C.28 for the component and crack geometry.

b) The coefficients, M_p^{2c}, are provided in Table C.21.

c) Refer to paragraph C.9.1.2 for other details regarding this solution.

C.10 Stress Intensity Factor Solutions for Sleeve Reinforced Cylinders

The stress intensity factor solutions shown below can be used for surface cracks at sleeve-reinforced cylinders (see Figure C.29) if the stress distribution normal to the plane of the crack is determined based on the component geometry and applied loads. The stress distribution normal to the plane of the crack, $\sigma(x)$, should be computed for the component in the uncracked state considering the effects of the structural configuration and fillet weld geometry (see Figure C.33(b)). The net-section forces and moments applied to cylindrical shell, as well as internal pressure, should be considered when determining the stress distribution. The use of this method to compute the stress intensity factor will result in a conservative value as long as the geometry of the crack does not significantly reduce the stiffness of the sleeve-reinforced cylinder connection. If the geometry of the crack does result in a significant loss in stiffness, the resulting deformation will result in a higher value of the stress intensity factor. In these cases, an analysis of the cracked geometry is required to accurately determine the stress intensity factor.

a) Crack A – Use KCTCC1, KCTCC2, KCSCCL3, KCSCCE3, KCECCL or KCECCE

b) Crack B – Use KCTCL, KCSCLL3, KCSCLE3, KCECLL or KCECLE

C.11 Stress Intensity Factor Solutions for Round Bars and Bolts

C.11.1 Round Bar, Surface Crack – 360 Degrees, Through-Wall Membrane and Bending Stress (KBSCL)

C.11.1.1 The Mode I Stress Intensity Factor [12], [18]

$$K_I = \left(M_m\sigma_m + M_b\sigma_b\right)\sqrt{\pi a} \tag{C.227}$$

where,

$$M_m = \frac{0.50}{\zeta^{1.5}}\left(1 + 0.5\zeta + 0.375\zeta^2 - 0.363\zeta^3 + 0.731\zeta^4\right) \tag{C.228}$$

$$M_b = \frac{0.375}{\zeta^{2.5}}\left(1 + 0.5\zeta + 0.375\zeta^2 - 0.313\zeta^3 + 0.273\zeta^4 + 0.537\zeta^5\right) \tag{C.229}$$

$$\zeta = 1 - \frac{a}{R_o} \tag{C.230}$$

C.11.1.2 Notes:

a) For the component and crack geometry see Figure C.30.

b) Crack geometry dimensional limits: $\zeta < 1.0$.

c) The membrane and bending stress, σ_m and σ_b, can be determined using the following equations:

$$\sigma_m = \frac{F_{bar}}{\pi\left(R_o - a\right)^2} \tag{C.231}$$

$$\sigma_b = \frac{4M_{bar}}{\pi\left(R_o - a\right)^3} \tag{C.232}$$

C.11.2 Round Bar – Surface Crack, Straight Front, Through-Wall Membrane and Bending Stress (KBSCS)

C.11.2.1 The Mode I Stress Intensity Factor [19]

$$K_I = \left(M_m\sigma_m + M_b\sigma_b\right)\sqrt{\pi a} \tag{C.233}$$

where,

$$M_m = 0.926 - 1.771\zeta + 26.421\zeta^2 - 78.481\zeta^3 + 87.911\zeta^4 \tag{C.234}$$

$$M_b = 1.04 - 3.64\zeta + 16.86\zeta^2 - 32.59\zeta^3 + 28.41\zeta^4 \tag{C.235}$$

$$\zeta = \frac{a}{2R_o} \tag{C.236}$$

C.11.2.2 Notes:

a) For the component and crack geometry see Figure C.31.

b) Crack geometry dimensional limits: $0.0625 \le \zeta \le 0.625$.

c) The membrane and bending stress, σ_m and σ_b, can be determined using the following equations:

$$\sigma_m = \frac{F_{bar}}{\pi R_o^2} \tag{C.237}$$

$$\sigma_b = \frac{4M_{bar}}{\pi R_o^3} \tag{C.238}$$

C.11.3 Round Bar, Surface Crack, Semi-Circular, Through-Wall Membrane and Bending Stress (KBSCC)

C.11.3.1 The Mode I Stress Intensity Factor [12]

$$K_I = \left(M_m\sigma_m + M_b\sigma_b\right)\sqrt{\pi a} \tag{C.239}$$

where,

$$M_m = g\left[0.752 + 2.02\zeta + 0.37\left(1-\sin\psi\right)^3\right] \quad \text{(C.240)}$$

$$M_b = g\left[0.923 + 0.199\left(1-\sin\psi\right)^4\right] \quad \text{(C.241)}$$

$$g = \frac{\frac{1.84}{\pi}\left(\frac{\tan\psi}{\psi}\right)^{0.5}}{\cos\psi} \quad \text{(C.242)}$$

$$\zeta = \frac{a}{2R_o} \quad \text{(C.243)}$$

$$\psi = \frac{\pi a}{4R_o} \quad \text{(C.244)}$$

C.11.3.2 Notes:

a) For the component and crack geometry see Figure C.31.

b) Crack geometry dimensional limits: $\zeta \le 0.6$.

c) The membrane and bending stress, σ_m and σ_b, can be determined using stress equations (C.237) and (C.238) respectively.

C.11.4 Bolt, Surface Crack, Semi-Circular or Straight Front Shape, Membrane and Bending Stress (KBSC)

C.11.4.1 The Mode I Stress Intensity Factor [17]

$$K_I = \left(M_m\sigma_m + M_b\sigma_b\right)\sqrt{\pi a} \quad \text{(C.245)}$$

where,

$$M_m = 2.043e^{-31.332\zeta} + 0.6507 + 0.5367\zeta + 3.0469\zeta^2 - 19.504\zeta^3 + 45.647\zeta^4 \quad \text{(C.246)}$$

$$M_b = 0.6301 + 0.03488\zeta - 3.3365\zeta^2 + 13.406\zeta^3 - 6.0021\zeta^4 \quad \text{(C.247)}$$

$$\zeta = \frac{a}{2R_{th}} \quad \text{(C.248)}$$

C.11.4.2 Notes:

a) For the component and crack geometry see Figure C.32; the solution applies to a semi-circular or straight front surface crack.

b) Crack geometry dimensional limits: $0.004 \le \zeta \le 0.5$.

c) The solution provided is for UNF bolts. The solution for the bending stress does not include the effects of the thread.

d) The solution for the membrane stress can be used for round bars if the exponential term is set to zero.

e) The membrane and bending stress, σ_m and σ_b, can be determined using stress equations (C.237) and (C.238) respectively.

C.12 Stress Intensity Factor Solutions for Cracks at Fillet Welds

C.12.1 Cracks at Fillet Welds – Surface Crack at a Tee Joint, Semi-Elliptical Shape, Through-Wall Membrane and Bending Stress (KFWSCE1)

C.12.1.1 The Mode I Stress Intensity Factor [30]

$$K_I = \left(M_{km} M_m \left\{ \sigma_m + p_c \right\} + M_{kb} M_b \sigma_b \right) \sqrt{\frac{\pi a}{Q}} \tag{C.249}$$

Where M_m and M_b are determined using the equations in paragraph C.3.4.1 and Q is determined using Equation (C.15) or (C.16).

The factors M_{km} and M_{kb} are given by the following equations using the appropriate parameters from Table C.22.

$$M_{km} = \max\left[\left(\left(F_1 - F_2 \right) F_4 + F_2 + F_3 \right),\ 1.0 \right] \tag{C.250}$$

$$M_{kb} = \max\left[\left(\left(F_1 - F_2 \right) F_4 + F_2 + F_3 \right),\ 1.0 \right] \tag{C.251}$$

where,

$$F_1 = 1.0 + P_1 \left(\frac{r_w}{t} \right)^g \cdot \sin\left(\alpha \right)^h \cdot \left[1.0 - \exp\left\{ \left(P_6 + P_7 \left\{ \frac{a}{c} \right\} \right) \left(\frac{L}{t} \right) \right\} \right] \cdot \left[1.0 + P_8 \left(\frac{a}{c} \right)^{P_9} \right] \tag{C.252}$$

$$g = P_2 + P_3 \left(\frac{a}{c} \right) \tag{C.253}$$

$$h = P_4 + P_5 \left(\frac{a}{c} \right) \tag{C.254}$$

$$F_2 = F_1 \left[1.0 - P_{10} - P_{11} \left(\frac{a}{c} \right) \right] - P_{12} - P_{13} \left(\frac{a}{c} \right) \tag{C.255}$$

$$F_3 = \left(\begin{array}{l} \left[1.0 + P_{14} \left(\frac{a}{c} \right) + P_{15} \left(\frac{a}{c} \right)^2 + P_{16} \left(\frac{a}{c} \right)^3 + P_{17} \left(\frac{a}{c} \right)^4 \right] \cdot \\ \left[P_{18} \left(\frac{a}{t} \right) + P_{19} \left(\frac{a}{t} \right)^2 + P_{20} \left(\frac{a}{t} \right)^3 + P_{21} \left(\frac{a}{t} \right)^4 \right] \end{array} \right) \tag{C.256}$$

For the deepest point of the crack (Point B):

$$F_4 = \left(\begin{array}{l} P_{22} \cdot \exp\left[-P_{23} \left(\frac{a}{t} \right)^{P_{24}} \right] + \\ P_{25} \left(\frac{a}{c} \right) \cdot \exp\left[-\left(\frac{a}{t} \right)^{P_{24}} \cdot \left(P_{23} + P_{26} \left\{ \frac{a}{c} \right\} \right) \right] + \\ P_{27} \left(\frac{L}{t} \right) \cdot \exp\left[-\left(\frac{a}{t} \right)^{P_{24}} \cdot \left(P_{23} + P_{28} \left\{ \frac{L}{t} \right\} \right) \right] + \\ P_{29} \left(\frac{t}{r_w} \right) \cdot \exp\left[-\left(\frac{a}{t} \right)^{P_{24}} \cdot \left(P_{23} + P_{30} \left\{ \frac{t}{r_w} \right\} \right) \right] + \\ P_{31} \cdot \sin(\alpha) \cdot \exp\left[-\left(\frac{a}{t} \right)^{P_{24}} \cdot \left(P_{23} + P_{32} \cdot \sin(\alpha) \right) \right] \end{array} \right) \quad \text{(C.257)}$$

For the surface point of the crack (Point A):

$$F_4 = \exp\left[-R \cdot \left(\frac{a}{t} \right)^{P_{22}} \right] + \left[P_{35} + P_{36} \left(\frac{a}{c} \right)^{P_{37}} \right] \cdot \left(\frac{a}{t} \right)^{P_{38}} \quad \text{(C.258)}$$

$$R = \left(\begin{array}{l} P_{23} + P_{24} \left(\frac{a}{c} \right)^{P_{25}} + \left[P_{26} + P_{27} \left(\frac{a}{c} \right)^{P_{28}} \right] \left(\frac{L}{t} \right) + \\ \left[P_{29} + P_{30} \left(\frac{a}{c} \right)^{P_{31}} \right] \left(\frac{t}{r_w} \right) + \left[P_{32} + P_{33} \left(\frac{a}{c} \right)^{P_{34}} \right] \cdot \sin(\alpha) \end{array} \right) \quad \text{(C.259)}$$

C.12.1.2 Notes:

a) For the component and crack geometry see Figure C.33.

b) Crack and geometry dimensional limits:

1) $0.0 < a/t < 1.0$

2) $0.0 < a/c \le 1.0$

3) $0.01 \le r_w/t \le 0.07$

4) $\pi/6 \le \alpha \le \pi/3$

5) $0.16 \le L/t \le 4.0$

c) The membrane and bending stress, σ_m and σ_b, can be determined using stress equations based on strength of materials concepts.

C.12.2 Cracks at Fillet Welds In Tee Junctions– General Solution

The stress intensity factor solutions shown below can be used for surface cracks at tee junction fillet welds in pressure containing components (see Figure C.33) if the stress distribution normal to the plane of the crack is determined based on the tee junction geometry and applied loads. The stress distribution normal to the plane of the crack, $\sigma(x)$, should be computed for the component in the uncracked state considering the effects of the structural configuration and fillet weld geometry (see Figure C.33 (b)). The use of this method to compute the stress intensity factor will result in a conservative value as long as the geometry of the crack does not significantly reduce the stiffness of the tee junction connection. If the geometry of the crack does result in a significant loss in stiffness, the resulting deformation will result in a higher value of the stress intensity factor. In these cases, an analysis of the cracked geometry is required to accurately determine the stress intensity factor.

a) Flat Plate Tee Junctions – Use KPTC, KPSCE3, KPECL, or KPECE2

b) Longitudinal Tee Junctions in Cylinders – Use KCTCL, KCSCLL3, KCSCLE3, KCECLL or KCECLE

c) Circumferential Tee Junctions in Cylinders – Use KCTCC1, KCTCC2, KCSCCL3, KCSCCE3, KCECCL or KCECCE

d) Circumferential Tee Junctions in Spheres – Use KSTC, KSSCCL3, KSECCL or KSECCE

C.13 Stress Intensity Factor Solutions Cracks in Clad Plates and Shells

The stress intensity factor solutions in this annex can be use to evaluate clad or weld overlayed plate and shell components if the modulus of elasticity between the clad or weld overlay is within 25% of the base material. If the difference between the elastic modulus is greater, the stress intensity factor should be computed numerically considering the actual properties of the materials. If the thermal expansion coefficients between the cladding and base material is different and the component is subject to a thermal load condition, a steep stress gradient will result at the cladding-to-base material interface. The weight function method (see paragraph C.14) should be used to compute the stress factor for this condition because it is the only method that can effectively capture the effects of the steep stress gradient.

a) Flat Plates – Use KPSCE3

b) Cylinders – KCSCLL3 or KCSCLE3

c) Spheres – Use KSSCCL3 or KSSCCE3

C.14 The Weight Function Method for Surface Cracks

C.14.1 Weight functions provide a means to infer stress intensity factors for nonuniform stress distributions. Consider a surface crack of depth a, subject to a normal stress $\sigma(x)$ that is an arbitrary function of x, where x is oriented in the crack depth direction and is measured from the free surface. The Mode I stress intensity factor for this case is given by the following equation where $h(x,a)$ is the weight function.

$$K_I = \int_0^a h(x,a)\,\sigma(x)\,dx \qquad \text{(C.260)}$$

For the deepest point of a semi-elliptical surface crack $(\varphi = \pi/2 \ or \ 90^o)$, the weight function can be represented by the following equation (see Reference [32]) where M_1, M_2, and M_3 depend on the component geometry and crack size. This equation also applies to an infinitely long surface crack.

$$h_{90} = \frac{2}{\sqrt{2\pi(a-x)}}\left[1 + M_1\left(1-\frac{x}{a}\right)^{1/2} + M_2\left(1-\frac{x}{a}\right) + M_3\left(1-\frac{x}{a}\right)^{3/2}\right] \qquad \text{(C.261)}$$

For the surface point of the crack $(\varphi = 0)$ the weight function can be represented by [32]:

$$h_0 = \frac{2}{\sqrt{\pi x}}\left[1 + N_1\left(\frac{x}{a}\right)^{1/2} + N_2\left(\frac{x}{a}\right) + N_3\left(\frac{x}{a}\right)^{3/2}\right] \tag{C.262}$$

C.14.2 The weight function coefficients M_i and N_i can be inferred from two reference stress intensity factor solutions. Normally, the K_I solutions for uniform and linear loading are used to derive the weight function coefficients. For a uniform stress, σ_0, the stress intensity factor is given by the following equation where G_0 is the influence coefficient, which depends on the component geometry and crack dimensions, and Q is given by Equations. (C.15) or (C.16)

$$K_I = \sigma_o G_0 \sqrt{\frac{\pi a}{Q}} \tag{C.263}$$

For a linear stress distribution defined as

$$\sigma(x) = \sigma_1\left(\frac{x}{t}\right) \tag{C.264}$$

the Mode I stress intensity factor is given by the following expression,

$$K_I = \sigma_1 G_1\left(\frac{a}{t}\right)\sqrt{\frac{\pi a}{Q}} \tag{C.265}$$

At the deepest point of the surface crack, the weight function coefficients are given by the following equations (see Reference [33]) where the influence coefficients from the reference stress intensity factor solution, G_0 and G_1, are evaluated at $\varphi = \pi/2$.

$$M_1 = \frac{2\pi}{\sqrt{2Q}}(3G_1 - G_0) - \frac{24}{5} \tag{C.266}$$

$$M_2 = 3 \tag{C.267}$$

$$M_3 = \frac{6\pi}{\sqrt{2Q}}(G_0 - 2G_1) + \frac{8}{5} \tag{C.268}$$

At the surface point of the surface crack, the weight function coefficients are given by the following equations (see Reference [33]) where the influence coefficients from the reference stress intensity factor solution, G_o and G_1, are evaluated at $\varphi = 0$.

$$N_1 = \frac{3\pi}{\sqrt{Q}}(2G_0 - 5G_1) - 8 \tag{C.269}$$

$$N_2 = \frac{15\pi}{\sqrt{Q}}(3G_1 - G_0) + 15 \tag{C.270}$$

$$N_3 = \frac{3\pi}{\sqrt{Q}}\left(3G_0 - 10G_1\right) - 8 \tag{C.271}$$

C.14.3 The weight function coefficients defined above can be used to obtain a K_I solution for a polynomial stress distribution defined as:

$$\sigma(x) = \sigma_o + \sigma_1\left(\frac{x}{t}\right) + \sigma_2\left(\frac{x}{t}\right)^2 + \sigma_3\left(\frac{x}{t}\right)^3 + \sigma_4\left(\frac{x}{t}\right)^4 \tag{C.272}$$

The stress intensity solution is obtained by invoking the principle of superposition in summing contributions from each term in the polynomial.

$$K_I = \left[\sigma_o G_o + \sigma_1 G_1\left(\frac{a}{t}\right) + \sigma_2 G_2\left(\frac{a}{t}\right)^2 + \sigma_3 G_3\left(\frac{a}{t}\right)^3 + \sigma_4 G_4\left(\frac{a}{t}\right)^4\right]\sqrt{\frac{\pi a}{Q}} \tag{C.273}$$

If the weight function coefficients M_i and N_i are known, it is possible to solve for the influence coefficients, G_i. This is accomplished by substituting Equation (C.261) or Equation (C.262) into Equation (C.260) and integrating with the appropriate power-law stress distribution. The resulting expressions for G_i are given below (see Reference [33]).

For the deepest point of a semi-elliptical surface crack $(\varphi = \pi/2)$:

$$G_2 = \frac{\sqrt{2Q}}{\pi}\left(\frac{16}{15} + \frac{1}{3}M_1 + \frac{16}{105}M_2 + \frac{1}{12}M_3\right) \tag{C.274}$$

$$G_3 = \frac{\sqrt{2Q}}{\pi}\left(\frac{32}{35} + \frac{1}{4}M_1 + \frac{32}{315}M_2 + \frac{1}{20}M_3\right) \tag{C.275}$$

$$G_4 = \frac{\sqrt{2Q}}{\pi}\left(\frac{256}{315} + \frac{1}{5}M_1 + \frac{256}{3465}M_2 + \frac{1}{30}M_3\right) \tag{C.276}$$

The above expressions can also be applied an infinitely long surface crack by setting $Q = 1.0$.

For the surface point of the crack $(\varphi = 0)$:

$$G_2 = \frac{\sqrt{Q}}{\pi}\left(\frac{4}{5} + \frac{2}{3}N_1 + \frac{4}{7}N_2 + \frac{1}{2}N_3\right) \tag{C.277}$$

$$G_3 = \frac{\sqrt{Q}}{\pi}\left(\frac{4}{7} + \frac{1}{2}N_1 + \frac{4}{9}N_2 + \frac{2}{5}N_3\right) \tag{C.278}$$

$$G_4 = \frac{\sqrt{Q}}{\pi}\left(\frac{4}{9} + \frac{2}{5}N_1 + \frac{4}{11}N_2 + \frac{1}{3}N_3\right) \tag{C.279}$$

C.14.4 If the G_0 and G_1 influence coefficients are known for a given position along the crack front defined by the elliptic angle φ, then the complete K_I solution for a polynomial stress distribution defined by Equation (C.272) can be determined by computing the G_2, G_3 and G_4 influence coefficients using the following equations and substituting the results into Equation (C.273) (see Reference [34]). Note that if the K_I solution is required at $\varphi = \pi/2$ or $\varphi = 0$, then the G_2, G_3 and G_4 influence coefficients must be computed using the equations in paragraph C.14.3

$$G_{21} = 108 + 180z + 576z^2 - 864z^3 + \left(1056 + 128M_1\right)\delta z^{2.5} \tag{C.280}$$

$$G_{22} = M_3\left(45\eta + 54\eta z + 72\eta z^2 - 315\omega z^{2.5} + 144\eta z^3\right) \tag{C.281}$$

$$G_2 = \frac{\sqrt{Q}}{945\pi}\left(G_{21} + G_{22}\right) \tag{C.282}$$

$$G_{31} = 880 + 1232z + 2112z^2 + 7040z^3 - 11264z^4 + \left(13056 + 1280M_1\right)\delta z^{3.5} \tag{C.283}$$

$$G_{32} = M_3\left(385\eta + 440\eta z + 528\eta z^2 + 704\eta z^3 - 3465\omega z^{3.5} + 1408\eta z^4\right) \tag{C.284}$$

$$G_3 = \frac{\sqrt{Q}}{13860\pi}\left(G_{31} + G_{32}\right) \tag{C.285}$$

$$G_{41} = \begin{pmatrix} 1820 + 2340z + 3328z^2 + 5824z^3 + 19968z^4 - \\ 33280z^5 + \left(37376 + 3072M_1\right)\delta z^{4.5} \end{pmatrix} \tag{C.286}$$

$$G_{42} = M_3\left(819\eta + 909\eta z + 1040\eta z^2 + 1248\eta z^3 + 1664\eta z^4 - 9009\omega z^{4.5} + 3328\eta z^5\right) \tag{C.287}$$

$$G_4 = \frac{\sqrt{Q}}{45045\pi}\left(G_{41} + G_{42}\right) \tag{C.288}$$

where (note that M_2 and M_4 are only used in paragraph C.14.5)

$$M_1 = \frac{-1050\pi G_1 + 105\pi G_0\left(3 + 7z\right) - 4\sqrt{Q}\left(35 - 70z + 35z^2 + 189\delta z^{0.5} + 61\delta z^{1.5}\right)}{\sqrt{Q}\left(168 + 152z\right)z^{0.5}\delta} \tag{C.289}$$

$$M_2 = \frac{1}{3}\left(M_1 - 3\right) \tag{C.290}$$

$$M_3 = \frac{2\left(-105\pi G_1 + 45\pi G_0 z + \sqrt{Q}\left(28 + 24z - 52z^2 + 44\delta z^{1.5}\right)\right)}{\sqrt{Q}\left(-21 + 2z + 19z^2\right)\eta} \tag{C.291}$$

$$M_4 = \frac{(1+M_3\eta)z}{z-1} \tag{C.292}$$

with,

$$z = \sin\varphi \tag{C.293}$$

$$\delta = \sqrt{1+z} \tag{C.294}$$

$$\omega = \sqrt{1-z} \tag{C.295}$$

$$\eta = \sqrt{\frac{1}{z}-1} \tag{C.296}$$

and Q determined using Equations (C.15) or (C.16).

C.14.5 The weight function method is recommended to compute the stress intensity factor for a through-wall arbitrary stress distribution. The stress distribution through the wall thickness of the component, $\sigma(x)$, can be evaluated using the finite element method. The weight function, $h(x,a)$, is evaluated as follows:

a) For $\varphi = \pi/2$ and all infinitely long cracks, evaluate the influence coefficients G_0 and G_1 for the applicable geometry at $\varphi = \pi/2$ and substitute the results into Equations (C.266), (C.267), and (C.268) to determine M_1, M_2, and M_3, respectively. Substitute M_1, M_2, and M_3 into Equation (C.261) to compute the weight function; note that for an infinitely long crack, $Q = 1$. The stress intensity factor is found by substituting the resulting equation into Equation (C.260) and completing the integration.

b) For $\varphi = 0$, evaluate the influence coefficients G_0 and G_1 for the applicable geometry at $\varphi = 0$ and substitute the results into Equations (C.269), (C.270), and (C.271) to determine N_1, N_2, and N_3, respectively. Substitute N_1, N_2, and N_3 into Equation (C.262) to compute the weight function. The stress intensity factor is found by substituting the resulting equation into Equation (C.260) and completing the integration.

c) For all other values of φ, evaluate the influence coefficients G_0 and G_1 for the applicable geometry at the angle φ and substitute the results into Equations (C.289), (C.290), (C.291) and (C.292) to determine M_1, M_2, M_3 and M_4, respectively. Substitute M_1, M_2, M_3 and M_4 into the following equations to determine the weight functions.

$$h_1(x,a) = \frac{\sqrt{\sin\varphi+1}}{\sqrt{\pi(a\sin\varphi - x)}}\left[1 + M_1\left(1-\frac{x}{a\sin\varphi}\right) + M_2\left(1-\frac{x}{a\sin\varphi}\right)^2\right] \tag{C.297}$$

$$h_2(x,a) = \frac{\sqrt{1-\sin\varphi}}{\sqrt{\pi(x - a\sin\varphi)}}\left[1 + M_3\left(\frac{x}{a\sin\varphi}-1\right)^{1/2} + M_4\left(\frac{x}{a\sin\varphi}-1\right)\right] \tag{C.298}$$

The stress intensity factor can be determined by substituting the resulting equations into the following equation and completing the integration.

$$K_I = \int_0^{a\sin\varphi} h_1(x,a)\sigma(x)dx + \int_{a\sin\varphi}^{a} h_2(x,a)\sigma(x)dx \tag{C.299}$$

C.14.6 Methods for performing the numerical integration of the weight function are provided in references [42] and [43].

C.15 Nomenclature

A_r	cross sectional area of a stiffening or tray support ring.
a	crack depth parameter.
α	fillet weld angle (degrees).
c	crack length parameter.
B	biaxial stress ratio.
β	parameter to compute the stress intensity factor.
d_n	mean nozzle diameter (see Figure C.27)
d_1	distance from plate surface to the center of an embedded elliptical crack (see Figure C.3).
d_2	distance from plate surface to the center of an embedded elliptical crack (see Figure C.3).
F	net-section axial force acting on a cylinder.
F_{bar}	net-section axial force acting on a bar.
K_I	Mode I stress intensity factor.
L	length parameter used for stress intensity factor magnification factors and solutions at fillet weld locations.
M	resultant net section bending moment acting on a cylinder.
M_{bar}	net-section bending moment acting on a bar.
M_x	net section bending moment about the x-axis acting on a cylinder.
M_y	net section bending moment about the y-axis acting on a cylinder.
p	pressure.
p_c	crack face pressure, set $p_c = 0.0$ if pressure is not acting on the crack face.
R_b	ratio of induced bending stress to the applied membrane stress (see Part 8, paragraphs 8.4.3.2, 8.4.3.3 and 8.4.3.4).
R_h	hole radius.
R_i	cylinder inside radius.
R_m	cylinder mean radius.
R_o	cylinder, round bar, or bolt outside radius, as applicable.
R_{th}	root radius of a threaded bolt.
r_w	root radius at the fillet weld.
σ_b	through-wall bending stress component.
σ_{ij}	stress component being evaluated.
$\sigma_{ij,m}$	equivalent membrane stress for a stress component.
$\sigma_{ij,b}$	equivalent bending stress for a stress component.
$\sigma_{\max}$	maximum stress at the nozzle corner where the crack is located.
σ_{nom}	nominal membrane stress away from the nozzle corner; for a spherical or cylindrical shell the membrane stress perpendicular to the crack face away from the nozzle (i.e. hoop stress for a spherical shell or cylindrical shell with a radial corner crack aligned with the longitudinal axis), for a plate, the maximum membrane stress perpendicular to the crack face.
σ_m	membrane stress component.

σ_0 uniform coefficient for polynomial stress distribution.

σ_1 linear coefficient for polynomial stress distribution.

σ_2 quadratic coefficient for polynomial stress distribution.

σ_3 third order coefficient for polynomial stress distribution.

σ_4 fourth order coefficient for polynomial stress distribution.

σ_5 bending stress from the net section bending moment about the x-axis acting on a cylinder.

σ_6 bending stress from the net section bending moment about the y-axis acting on a cylinder.

t plate or shell thickness.

t_n nozzle thickness (see Figure C.27).

θ half-angle of a circumferential crack.

ν Poisson's ratio.

φ elliptic angle, see Figure C.2 for surface cracks in plates and shells, Figure C.3 for embedded flaws, and Figure C.10 for surface cracks at holes, and Figure C.27 for radial corner cracks at nozzles (radians).

W distance from the center of the flaw to the free edge of the plate (see Figure C.1).

x radial local coordinate originating at the internal surface of the component.

x_n Local coordinate for the stress distribution measured from the inside surface of the corner crack radius at an angle of $\varphi = \pi/4$ (see Figure C.27); note that this stress distribution is not normalized with the wall thickness (see paragraph C.2.2.3).

x_g global coordinate for definition of net section bending moment about the x-axis.

y_g global coordinate for definition of net section bending moment about the y-axis.

C.16 References

1. Newman, Jr., J.C., Raju, I.S., *Stress Intensity Factor Equations for Cracks in Three-Dimensional Finite bodies Subject to Tension and Bending Loads*, NASA Technical Memorandum 85793, April, 1984.
2. Rooke, DIP and Cartwright, D.J., "Compendium of Stress Intensity Factors," Her Majesty's Stationary Office (HMSO), London, 1974.
3. Cipolla, R.C., "Technical Basis for the Revised Stress Intensity Factor Equation for Surface Flaws in ASME Section XI Appendix A", PVP-Vol. 313-1, International Pressure Vessels and Piping Codes and Standards: Volume 1 – Current Applications, American Society Of Mechanical Engineers, New York, N.Y., 1995, pp. 105-121.
4. Anderson, T.L., Unpublished Work, 2005.
5. Shen, G. and Glinka G. "Weight Functions for a Surface Semi-Elliptical Crack in a Finite Thickness Plate," *Theoretical and Applied Fracture Mechanics*, Vol 15, 1991, pp. 247-255.
6. Vainshtok, V.A. and Varfolomeyev, I.V., "Stress Intensity Factor Equations for Part-Elliptical Cracks and Their Verification." *Engineering Fracture Mechanics*, Vol 34, 1989, pp. 125-136.
7. Klecker, R., Brust, F.W., and Wilkowski, G., "NRC Leak before Break Analysis Method For Circumferentially Through-Wall Cracked Pipes Under Axial Plus bending Loads," NUREG/CR-4572, U.S. Nuclear Regulatory Commission, May, 1986.
8. Shin, C.S. and Wang, C.M. "Experimental Calibration of Stress Intensity Factors for Piping with Circumferential Through-Wall Crack," *International Journal of Pressure Vessels and Piping*, 60, 1994, pp. 285-296.
9. Anderson, T.L., *Fracture Mechanics – Fundamentals and Applications*, 3rd Edition, CRC Press, Boca Raton, Florida, 2005.

10. Erdogen, F. and Kibler, J.J., “Cylindrical and Spherical Shells with Cracks,” *International Journal of Fracture Mechanics*, 5, 1969, pp. 229-237.

11. Folias, E.S., “On the Effect of Initial Curvature on Cracked Sheets,” *International Journal of Fracture Mechanics*, Vol. 5, No. 4, December, 1969, pp. 327-346.

12. Murakami, Y., “Stress Intensity Factors Handbook,” Pergamon Press, Oxford, 1987, pp. 1356-1358.

13. Eiber, R.J., Maxey, W.A., Duffy, A.R., and Atterbury, T.J., “Investigation of the Initiation and Extent of Ductile Pipe Rupture,” Battelle Report Task 17, June, 1971.

14. Fu, B., Haswell, J.V., Bettess, P., "Weld Magnification Factors for Semi-Elliptical Surface Cracks in Fillet Welded T-Butt Joints," *International Journal of Fracture*, 63, 1993, pp. 155-171.

15. Brust, F.W. and Gilles, P., “Approximate Methods for Fracture Analysis of Tubular Members Subjected to Combined Tensile and Bending Loads,” *Journal of Offshore Mechanics and Arctic Engineering*, Vol. 116, November, 1994.

16. Green, D. and Knowles, J., “The Treatment of Residual Stress in Fracture Assessment of Pressure Vessels,” *Journal of Pressure Vessel Technology*, Vol. 116, American Society Of Mechanical Engineers, November 1994, pp. 345-352.

17. James, L.A. and Mills, W.J., “Review and Synthesis of Stress Intensity Factor Solutions Applicable to Cracks in Bolts,” *Engineering Fracture Mechanics*, Vol. 30, No. 5, 1988, pp. 641-654.

18. Tada, H., Paris, P.C. and Irwin, G.R, “The Stress Analysis Of Cracks Handbook – Second Edition,” Paris Productions Inc., St. Louis, Missouri, 1985.

19. Sih, G.C., “Handbook of Stress Intensity Factors,” Institute of Fracture and Solid Mechanics, Lehigh University, Bethlehem, Pa.

20. Newman, J.C., Reuter, W.G., and Aveline Jr, C.R., “Stress and Fracture Analysis of the Surface Crack,” Fatigue and Fracture Mechanics: 30th Volume, ASTM STP 1360, K.L. Jerina and P.C. Paris, ASTM, Philadelphia, PA, 1999.

21. Niu, X. and Glinka, G., “Theoretical and Experimental Analyses of Surface Fatigue Cracks in Weldments,” Surface-Crack Growth: Models, Experiments, and Structures, ASTM STP 1060, W.G. Reuter, J.H. Underwood, and J.C. Newman Jr., Eds., ASTM, Philadelphia, Pa., 1990, pp. 390-413.

22. Barsoum, R.S., Loomis, R.W., and Stewart, B.D., “Analysis of Through Cracks in Cylindrical Shells by the Quarter-Point Elements,” *International Journal of Fracture*, Vol. 15, No. 3, June 1979, pp. 259-280.

23. Chell,G.G, “Application of the CEGB Failure Assessment Procedure, R6, to Surface Flaws,” Fracture Mechanics: Twenty-First Symposium, ASTM STP 1074, J.P. Gudas, J.A. Joyce, and E.M. Hackett, Eds., ASTM, Philadelphia, 1990, pp. 525-544.

24. Kramer, G.S., Wilkowski, G.M., and Maxey, W.A., “Flaw Tolerance of Spiral Welded Pipe,” Battelle NG-18 Report No. 154, January, 1987

25. Kiefner, J.F. and Vieth, P.H., “Project PR 3-805, A Modified Criterion for Evaluating the Remaining Strength of Corroded Pipe,” Battelle Report to the Pipeline Committee of the American Gas Association, 1989.

26. Fett, T., and Munz, D., “Stress Intensity Factors and Weight Functions,” Computational Mechanics Publications, Southampton, UK, 1997.

27. France, C.F., Green, D., Sharples, J.K., and Chivers, T.C., “New Stress Intensity Factor And Crack Opening Area Solutions For Through-Wall Cracks In Pipes And Cylinders,” PVP-Vol. 350, Fatigue and Fracture, Vol. 1, American Society Of Mechanical Engineers, New York, N.Y., 1997, pp. 143-195.

28. Niu, X. and Glinka, G., “Stress-Intensity Factors For Semi-Elliptical Cracks In Welded Joints,” *International Journal Of Fracture*, Vol. 40, Kluwer Academic Publishers, Netherlands, 1989, pp. 255-270.

29. Brown, Robert, G., “Development of Elastic Stress Intensity Factor Solutions and Elastic-Plastic Failure Assessment Diagrams For Fillet Toe Cracks at Ring-Stiffened Cylindrical Shells,” Thesis, The University of Akron, December, 1996.

30. HSE, “Development of Parametric Equations for MK-Factors for Semi-Elliptic Cracks in T-Butt Welds,” Offshore Technology Report – OTO 98 081, Health & Safety Executive, Research Admin, OSD, Bootle, Merseyside, August, 1998.

31. Forman, R.G., Hickman, J.C., and Shivakumer, V., “Stress Intensity Factors for Circumferential Through Cracks in Hollow Cylinders Subjected to Combined Tension and Bending Loads,” *Engineering Fracture Mechanics*, Vol 21, No. 3, 1985, pp. 563-571.

32. Shen, G. and Glinka, G., “Determination of Weight Functions from Reference Stress Intensity Solutions.” *Theoretical and Applied Fracture Mechanics*, Vol. 15, 1991, pp. 237-245.

33. Zheng, X.J., Kiciak, A., and Glinka, G., “Weight Functions and Stress Intensity Factors for Internal Surface Semi-Elliptical Crack in Thick-Walled Cylinder.” *Engineering Fracture Mechanics*, Vol. 58, 1997, pp. 207-221.

34. Anderson, T.L., private communication to D.A. Osage, 1998.

35. Sih,G.C., “Mechanics Of Fracture 3, Plates and Shells with Cracks,” Noordhoff International Publishing Leydon, The Netherlands, 1977.

36. Guozhong, C. and Qichao, H., “Stress Intensity Factors of Nozzle Corner Cracks,” *Engineering Fracture Mechanics*, Vol. 38, No. 1, pp. 27-35, 1991.

37. Guozhong, C. and Qichao, H., “Approximate Stress-Intensity Factor Solutions for Nozzle Corner Cracks,” *Int. J. Pres. Ves. & Piping*, 42, pp. 75-96, 1990.

38. Fife, A.B., Kobsa, I.R., Riccardella, P.C., and Watanabe, H.T., “Boiling Water Reactor Feedwater Nozzle/Spranger Interim Program Report,” NEDO-21480, 77NED125, Class I, General Electric, San Jose, CA,. July 1977.

39. Fife, A.B., Kobsa, I.R., Riccardella, P.C., and Watanabe, H.T., “Boiling Water Reactor Feedwater Nozzle/Spranger Interim Program Report,” NEDO-21480, 77NED125, Class I, General Electric, San Jose, CA,. July 1977.

40. Anderson, T.L., et. al, *Development of Stress Intensity Factor Solutions for Surface and Embedded Cracks in API 579*, WRC Bulletin 471, Welding Research Council, Inc. New York, NY, May 2002.

41. Anderson, T.L., *Stress Intensity and Crack Growth Opening Area Solutions for Through-Wall Cracks in Cylinders and Spheres*, WRC Bulletin 478, Welding Research Council, Inc. New York, NY, Jan 2003.

42. Anderson, T.L. and Glinka, G., “A Closed-Form Method for Integrating Weight Functions for Part-Through Cracks Subject to Mode I Loading,” Submitted to Engineering Fracture Mechanics, November 2005.

43. Moftakhar, A.A. and Glinka, G., “Calculation of Stress Intensity Factors by Efficient Integration of Weight functions,” Engineering Fracture mechanics, Vol 43, No. 5, pp. 749-756, 1992.

C.17 Tables and Figures

Table C.1
Summary Of Stress Intensity Factor Solutions

Component Geometry	Crack Geometry	Crack Loading	Stress Intensity Factor Solution	Reference Stress Solution
Plate	Through-Wall Crack	Through-Wall Membrane And Bending Stress	KPTC (C.3.1)	RPTC (D.3.1)
	Surface Crack, Infinite Length	Through-Wall Fourth Order Polynomial Stress Distribution	KPSCL1 (C.3.2)	RPSCL (D.3.2)
	Surface Crack, Infinite Length	Through-Wall Arbitrary Stress Distribution	KPSCL2 (C.3.3)	RPSCL (D.3.3)
	Surface Crack, Semi-Elliptical Shape	Through-Wall Membrane And Bending Stress	KPSCE1 (C.3.4)	RPSCE1 (D.3.4)
	Surface Crack, Semi-Elliptical Shape	Through-Wall Fourth Order Polynomial Stress Distribution	KPSCE2 (C.3.5)	RPSCE2 (D.3.5)
	Surface Crack, Semi-Elliptical Shape	Through-Wall Arbitrary Stress Distribution	KPSCE3 (C.3.6)	RPSCE3 (D.3.6)
	Embedded Crack, Infinite Length	Through-Wall Fourth Order Polynomial Stress Distribution	KPECL (C.3.7)	RPECL (D.3.7)
	Embedded Crack, Elliptical Shape	Through-Wall Membrane And Bending Stress	KPECE1 (C.3.8)	RPECE1 (D.3.8)
	Embedded Crack, Elliptical Shape	Through-Wall Fourth Order Polynomial Stress Distribution	KPECE2 (C.3.9)	RPECE2 (D.3.9)
Plate With A Hole	Single Hole, Through-Wall Single Edge Crack	Through-Wall Membrane And Bending Stress	KPHTC1 (C.4.1)	RPHTC1 (D.4.1)
	Single Hole, Through-Wall Double Edge Crack	Through-Wall Membrane And Bending Stress	KPHTC2 (C.4.2)	RPHTC2 (D.4.2)
	Single Hole, Surface Crack, Semi-Elliptical Shape	Membrane Stress	KPHSC1 (C.4.3)	RPHSC1 (D.4.3)
	Single Hole, Corner Crack, Semi-Elliptical Shape	Through-Wall Membrane And Bending Stress	KPHSC2 (C.4.4)	RPHSC2 (D.4.4)
Cylinder	Through-Wall Crack, Longitudinal Direction	Through-Wall Membrane And Bending Stress	KCTCL (C.5.1)	RCTCL (D.5.1)
	Through-Wall Crack, Circumferential Direction	Through-Wall Membrane And Bending Stress	KCTCC1 (C.5.2)	RCTCC1 (D.5.2)
	Through-Wall Crack, Circumferential Direction	Pressure With A Net Section Axial Force And Bending Moment	KCTCC2 (C.5.3)	RCTCC2 (D.5.3)
	Surface Crack, Longitudinal Direction, Infinite Length	Internal Pressure (Lame Stress Distribution)	KCSCLL1 (C.5.4)	RCSCLL1 (D.5.4)
	Surface Crack, Longitudinal Direction, Infinite Length	Through-Wall Fourth Order Polynomial Stress Distribution	KCSCLL2 (C.5.5)	RCSCLL2 (D.5.5)
	Surface Crack, Longitudinal Direction, Infinite Length	Through-Wall Arbitrary Stress Distribution	KCSCLL3 (C.5.6)	RCSCLL3 (D.5.6)
	Surface Crack, Circumferential Direction, 360 Degrees	Pressure With Net Section Axial Force And Bending Moment	KCSCCL1 (C.5.7)	RCSCCL1 (D.5.7)

Table C.1
Summary Of Stress Intensity Factor Solutions

Component Geometry	Crack Geometry	Crack Loading	Stress Intensity Factor Solution	Reference Stress Solution
Cylinder	Surface Crack, Circumferential Direction, 360 Degrees	Through-Wall Fourth Order Polynomial Stress Distribution with Net Section Bending Moments	KCSCCL2 (C.5.8)	RCSCCL2 (D.5.8)
	Surface Crack, Circumferential Direction, 360 Degrees	Through-Wall Arbitrary Stress Distribution	KCSCCL3 (C.5.9)	RCSCCL3 (D.5.9)
	Surface Crack, Longitudinal Direction, Semi-Elliptical Shape	Internal Pressure (Lame Stress Distribution)	KCSCLE1 (C.5.10)	RCSCLE1 (D.5.10)
	Surface Crack, Longitudinal Direction, Semi-Elliptical Shape	Through-Wall Fourth Order Polynomial Stress Distribution	KCSCLE2 (C.5.11)	RCSCLE2 (D.5.11)
	Surface Crack, Longitudinal Direction, Semi-Elliptical Shape	Through-Wall Arbitrary Stress Distribution	KCSCLE3 (C.5.12)	RCSCLE3 (D.5.12)
	Surface Crack, Circumferential Direction, Semi-Elliptical Shape	Internal Pressure (Lame Stress Distribution) With Net Section Axial Force	KCSCCE1 (C.5.13)	RCSCCE1 (D.5.13)
	Surface Crack, Circumferential Direction, Semi-Elliptical Shape	Through-Wall Fourth Order Polynomial Stress Distribution With Net Section Bending Moment	KCSCCE2 (C.5.14)	RCSCCE2 (D.5.14)
	Surface Crack, Circumferential Direction, Semi-Elliptical Shape	Through-Wall Arbitrary Stress Distribution	KCSCCE3 (C.5.15)	RCSCCE3 (D.5.15)
	Embedded Crack, Longitudinal Direction, Infinite Length	Through-Wall Fourth Order Polynomial Stress Distribution	KCECLL (C.5.16)	RCECLL (D.5.16)
	Embedded Crack, Circumferential Direction, 360 Degrees	Through-Wall Fourth Order Polynomial Stress Distribution	KCECCL (C.5.17)	RCECCL (D.5.17)
	Embedded Crack, Longitudinal Direction, Elliptical Shape	Through-Wall Fourth Order Polynomial Stress Distribution	KCECLE (C.5.18)	RCECLE (D.5.18)
	Embedded Crack, Circumferential Direction, Elliptical Shape	Through-Wall Fourth Order Polynomial Stress Distribution	KCECCE (C.5.19)	RCECCE (D.5.19)
Sphere	Through-Wall Crack	Through-Wall Membrane And Bending Stress	KSTC (C.6.1)	RSTC (D.6.1)
	Surface Crack, Circumferential Direction, 360 Degrees	Internal Pressure (Lame Stress Distribution)	KSSCCL1 (C.6.2)	RSSCCL1 (D.6.2)
	Surface Crack, Circumferential Direction, 360 Degrees	Through-Wall Fourth Order Polynomial Stress Distribution	KSSCCL2 (C.6.3)	RSSCCL2 (D.6.3)
	Surface Crack, Circumferential Direction, 360 Degrees	Through-Wall Arbitrary Stress Distribution	KSSCCL3 (C.6.4)	RSSCCL3 (D.6.4)
	Surface Crack, Circumferential Direction, Semi-Elliptical Shape	Internal Pressure (Lame Stress Distribution)	KSSCCE1 (C.6.5)	RSSCCE1 (D.6.5)
	Surface Crack, Circumferential Direction, Semi-Elliptical Shape	Through-Wall Fourth Order Polynomial Stress Distribution	KSSCCE2 (C.6.6)	RSSCCE2 (D.6.6)

Table C.1
Summary Of Stress Intensity Factor Solutions

Component Geometry	Crack Geometry	Crack Loading	Stress Intensity Factor Solution	Reference Stress Solution
Sphere	Surface Crack, Circumferential Direction, Semi-Elliptical Shape	Through-Wall Arbitrary Stress Distribution	KSSCCE3 (C.6.7)	RSSCCE3 (D.6.7)
	Embedded Crack, Circumferential Direction, 360 Degrees	Through-Wall Fourth Order Polynomial Stress Distribution	KSECCL (C.6.8)	RSECCL (D.6.8)
	Embedded Crack, Circumferential Direction, Elliptical Shape	Through-Wall Fourth Order Polynomial Stress Distribution	KSECCE (C.6.9)	RSECCE (D.6.9)
Elbow And Pipe Bend	General Solution	See Discussion in Paragraph C.7.	(C.7)	(D.7)
Nozzle or Piping Tee	Corner Cracks, Radial Direction, Quarter-Circular Shape	Membrane Stress	KNCC1 (C.8.1)	RNCC1 (D.8.1)
	Corner Cracks, Radial Direction, Quarter-Circular Shape	Cubic Polynomial Stress Distribution	KNCC2 (C.8.2)	RNCC2 (D.8.2)
	Surface Cracks At Nozzles – General Solution	See Discussion in Paragraph C.8.	(C.8.3)	(D.8.3)
Ring-Stiffened Cylinder	Surface Crack At The Toe Of One Fillet Weld, Circumferential Direction – 360 Degrees	Pressure (Membrane and Bending Stress)	KRCSCCL1 (C.9.1)	RRCSCCL 1 (D.9.1)
	Surface Crack At The Toe Of Both Fillet Welds, Circumferential Direction – 360 Degrees	Pressure (Membrane and Bending Stress)	KRCSCCL2 (C.9.2)	RRCSCCL 2 (D.9.2)
Sleeve Reinforced Cylinder	General Solution	See Discussion in Paragraph C.10.	(C.10)	(D.10)
Round Bar or Bolt	Round Bar, Surface Crack, 360 Degrees	Membrane And Bending Stress	KBSCL (C.11.1)	RBSCL (D.11.1)
	Round Bar, Surface Crack, Straight Front Shape	Membrane And Bending Stress	KBSCS (C.11.2)	RBSCS (D.11.2)
	Round Bar, Surface Crack, Semi-Circular Shape	Membrane And Bending Stress	KBSCC (C.11.3)	RBSCC (D.11.3)
	Bolt, Surface Crack, Semi-Elliptical Or Straight Front Shape	Membrane And Bending Stress	KBSC (C.11.4)	RBSC (D.11.4)

Table C.1
Summary Of Stress Intensity Factor Solutions

Component Geometry	Crack Geometry	Crack Loading	Stress Intensity Factor Solution	Reference Stress Solution
Cracks At Fillet Welds	Surface Crack, Infinite Length	Membrane And Bending Stress	KFWSCE1 (C.12.1)	RFWSCE1 (D.12.1)
	Cracks At Fillet Welds In Tee Junctions In Pressurized Components - General Solution	See Discussion in Paragraph C.12.2	(C.12.2)	(D.12.2)
Cracks In Clad Or Weld Overlayed Plate	General Solution	See Discussion in Paragraph C.13.	(C.13)	(D.13)

Table C.2
Influence Coefficients For A Infinite Length Surface Crack In A Plate (1)

a/t	G_0	G_1	G_2	G_3	G_4
0.0	1.120000	0.682000	0.524500	0.440400	0.379100
0.1	1.180400	0.702800	0.535200	0.447300	0.383600
0.2	1.358700	0.773200	0.575300	0.474100	0.404300
0.4	2.099000	1.052600	0.728500	0.574100	0.479800
0.6	4.008200	1.745900	1.099800	0.812100	0.652600
0.8	11.827200	4.479200	2.524400	1.706900	1.275400
Influence Coefficients In Equation Form (2)					
	C_0	C_1	C_2	C_3	C_4
G_0	1.1202	6.0061	-1.3891	7.9260	31.914
G_1	0.68109	2.3137	-0.71895	3.1140	10.702
G_2	0.52360	1.3006	-0.56913	2.1463	5.0660
G_3	0.43970	0.86873	-0.52507	1.7131	2.8443
G_4	0.37831	0.64919	-0.28777	0.87481	2.2063

Notes:

1. Interpolation may be used for intermediate values of a/t.
2. See paragraph C.3.2.2.C

Table C.3
Influence Coefficients For A Finite Length Surface Crack In A Plate

Coefficients C_0 Through C_5							
φ	G_i	C_0	C_1	C_2	C_3	C_4	C_5
0	G_0	0.27389	-0.79900	-0.26714	1.4761	3.7226	0.16033
	G_1	0.028002	-1.1022	-0.033521	0.22057	0.52258	0.10846
	G_2	0.012675	-1.1481	-0.015221	-0.082355	0.13759	0.041064
	G_3	7.3602e-3	-1.1544	-6.5361e-3	-0.36173	0.049133	0.044540
	G_4	4.9892e-3	-1.2132	-4.3696e-3	-0.46223	0.020326	0.068641
90	G_0	0.79807	0.041621	-0.55195	0.94721	-0.33668	0.52973
	G_1	0.82407	0.023018	0.14705	0.15481	0.048556	0.16795
	G_2	0.75607	1.8397e-3	0.28788	0.023688	0.12715	0.066900
	G_3	0.68582	-1.6499e-3	0.30738	-0.033522	0.13604	0.029992
	G_4	0.63097	8.4876e-3	0.30584	-0.067862	0.13547	0.025147
Coefficients C_6 Through C_{10}							
φ	G_i	C_6	C_7	C_8	C_9	C_{10}	
0	G_0	0.64383	-1.7330	-2.5867	0.55987	-0.54503	
	G_1	0.065941	-3.1077	-0.93098	2.4443	0.18878	
	G_2	0.019569	-1.9848	-0.22151	2.9522	0.16896	
	G_3	8.9574e-3	-1.4999	-0.081464	3.0826	0.10436	
	G_4	4.1052e-3	-1.1912	-0.033493	3.2003	0.074990	
90	G_0	-0.93391	-0.064536	0.28786	-0.22806	0.0	
	G_1	-0.12109	7.2007e-3	0.093079	-0.094413	0.0	
	G_2	0.012227	0.021628	0.041800	-0.051236	0.0	
	G_3	0.072309	0.022755	0.022788	-0.030355	0.0	
	G_4	0.092532	0.022520	0.015831	-0.029806	0.0	

Table C.4
Influence Coefficients For An Embedded Crack Of Infinite Length In A Plate

d_1/t	a/d_1	Point A				
		G_0	G_1	G_2	G_3	G_4
0.1	0.20	1.037474	-0.525539	0.513530	-0.398121	0.385912
	0.40	1.063196	-0.512793	0.527960	-0.381408	0.393538
	0.60	1.124939	-0.511072	0.549082	-0.375003	0.405314
	0.80	1.292554	-0.539518	0.596937	-0.390045	0.431613
0.25	0.20	1.058534	-0.523445	0.525337	-0.391913	0.392771
	0.40	1.093824	-0.522160	0.533711	-0.391325	0.397355
	0.60	1.195165	-0.533388	0.561563	-0.398093	0.412760
	0.80	1.430213	-0.566890	0.625906	-0.415809	0.446381
0.5	0.20	1.069921	-0.675294	0.528362	-0.447519	0.394956
	0.40	1.172232	-0.721464	0.557197	-0.468248	0.411130
	0.60	1.375565	-0.809178	0.609550	-0.504208	0.437929
	0.80	1.912707	-1.049389	0.756235	-0.606419	0.514699
d_1/t	a/d_1	Point B				
		G_0	G_1	G_2	G_3	G_4
0.1	0.20	1.036385	0.500468	0.513132	0.373235	0.385696
	0.40	1.053488	0.529134	0.525443	0.399017	0.392261
	0.60	1.083573	0.543560	0.538003	0.413163	0.399621
	0.80	1.136074	0.537801	0.552329	0.410923	0.407874
0.25	0.20	1.057198	0.523110	0.525004	0.391746	0.392604
	0.40	1.084672	0.520354	0.531924	0.390650	0.396678
	0.60	1.144249	0.519696	0.548254	0.391129	0.405936
	0.80	1.239721	0.511818	0.573109	0.386992	0.418467
0.5	0.20	1.069921	0.675294	0.528362	0.447519	0.394956
	0.40	1.172232	0.721464	0.557197	0.468248	0.411130
	0.60	1.375565	0.809178	0.609550	0.504208	0.437929
	0.80	1.912707	1.049389	0.756235	0.606419	0.514699

Notes: Interpolation may be used for intermediate values of d_1/t and a/d_1.

Table C.5
Influence Coefficients For An Embedded Crack Of Finite Length In A Plate

a/c	d_1/t	a/d_1	G_i	A_0	A_1	A_2	A_3	A_4	A_5	A_6
0.125	0.1	0.2	G_0	0.451757	-0.019628	2.495707	0.099772	-3.902776	-0.102820	2.019707
			G_1	-0.128988	1.598155	-1.296937	-2.270101	3.567902	1.873744	-2.858515
			G_2	-0.000734	0.001631	0.991292	-0.011837	-0.363824	0.012826	-0.123584
			G_3	-0.131076	1.364160	-2.549776	-1.137281	7.707103	-4.400373	-0.494306
			G_4	-0.003336	0.003606	0.165010	-0.022272	1.023934	0.023901	-0.813902
		0.4	G_0	0.460366	-0.010583	2.496873	0.081071	-3.818983	-0.076257	1.952893
			G_1	-0.135447	1.638110	-1.335614	-2.558541	4.677692	0.519790	-2.321867
			G_2	-0.000277	0.001294	0.997736	-0.003634	-0.355062	0.006336	-0.132659
			G_3	-0.140339	1.467292	-3.056527	0.103836	6.321127	-3.775929	-0.564173
			G_4	-0.003458	0.002738	0.165076	-0.014112	1.038749	0.016176	-0.826233
		0.6	G_0	0.468830	-0.006410	2.567734	0.130953	-3.735015	-0.099825	1.856371
			G_1	-0.184501	2.950391	-12.19661	36.420418	-63.01913	56.703701	-20.18709
			G_2	0.000720	-0.000206	1.011667	0.016177	-0.333706	-0.005057	-0.151861
			G_3	-0.283430	5.478717	-37.08400	123.97631	-211.3322	178.51773	-58.94464
			G_4	-0.003102	0.001262	0.167819	-0.002001	1.055681	0.008512	-0.837895
		0.8	G_0	0.463476	-0.012108	2.815707	0.339275	-3.765860	-0.219999	1.805445
			G_1	0.058943	0.745805	1.114598	-7.658195	11.381283	-4.025517	-1.130897
			G_2	0.003032	-0.004707	1.007313	0.067283	-0.196122	-0.023237	-0.246938
			G_3	-0.126978	1.376576	-2.292749	-3.107293	12.050867	-8.003842	0.490849
			G_4	-0.001258	-0.001153	0.155778	0.018553	1.137586	0.007069	-0.889468
0.125	0.25	0.2	G_0	0.402472	-0.050527	2.904407	0.255471	-4.947331	-0.281718	2.736348
			G_1	-0.002654	0.466214	-0.066963	0.459261	0.146976	-0.440574	-0.080979
			G_2	-0.002028	-0.011522	0.899724	-0.037831	-0.235939	0.058484	-0.195269
			G_3	0.001862	0.008824	-0.096953	0.958686	0.183063	-0.620891	-0.089157
			G_4	-0.003131	0.002178	0.153341	-0.082397	0.942617	0.092908	-0.762958
		0.4	G_0	0.423287	-0.031730	2.755031	0.106003	-4.356325	-0.113844	2.276538
			G_1	-0.004337	0.488376	-0.018798	0.445002	0.042130	-0.442372	-0.023399
			G_2	-0.000113	-0.012149	0.951095	-0.003645	-0.308412	0.015653	-0.149110
			G_3	0.000486	0.002651	-0.049583	1.025268	0.091154	-0.665949	-0.044010
			G_4	-0.002569	-0.001080	0.152314	-0.039286	0.982607	0.044717	-0.778851
		0.6	G_0	0.432989	-0.033577	2.872620	0.027125	-4.359993	-0.064021	2.235058
			G_1	-0.004351	0.486459	-0.027018	0.466641	0.031078	-0.455126	-0.013517
			G_2	0.001550	-0.011965	0.969643	-0.021303	-0.285069	0.024774	-0.171453
			G_3	0.000228	0.002766	-0.049174	1.036901	0.077402	-0.671945	-0.035391
			G_4	-0.001651	-0.000909	0.156156	-0.047470	1.008257	0.048482	-0.797691
		0.8	G_0	0.445542	-0.033047	3.041505	-0.234082	-4.127055	0.097677	2.009092
			G_1	-0.005232	0.488237	-0.017605	0.521073	-0.098628	-0.481469	0.071257
			G_2	0.003887	-0.004975	0.999241	-0.082000	-0.187212	0.044134	-0.245910
			G_3	-0.000904	-0.002210	-0.022680	1.092769	-0.025501	-0.702693	0.022851
			G_4	-0.000593	0.002201	0.155600	-0.064479	1.102858	0.042103	-0.860425

Table C.5
Influence Coefficients For An Embedded Crack Of Finite Length In A Plate

a/c	d_1/t	a/d_1	G_i	A_0	A_1	A_2	A_3	A_4	A_5	A_6
0.125	0.5	0.2	G_0	0.452208	-0.017180	2.496135	0.096821	-3.887236	-0.101879	2.006232
			G_1	0.000000	0.515985	-0.006471	0.418733	0.011986	-0.430803	-0.006741
			G_2	0.000137	-0.010747	0.903078	-0.035133	-0.235300	0.056911	-0.196866
			G_3	0.000000	0.005191	0.000427	1.086222	-0.001351	-0.709040	0.000756
			G_4	0.000042	-0.004570	0.184913	-0.033948	0.832546	0.037795	-0.665999
		0.4	G_0	0.460370	-0.014353	2.597565	0.086983	-3.930644	-0.094323	2.000952
			G_1	0.000000	0.514400	-0.000381	0.431274	0.000350	-0.438897	-0.000183
			G_2	0.000650	-0.011494	0.959328	0.003895	-0.301062	0.011214	-0.157400
			G_3	0.000000	0.004923	0.000370	1.088831	-0.000894	-0.710377	0.000399
			G_4	0.000265	-0.001303	0.151837	-0.022125	1.006405	0.027741	-0.796412
		0.6	G_0	0.470563	-0.014111	2.800145	0.085921	-3.915485	-0.093348	1.914262
			G_1	0.000000	0.511104	-0.000060	0.482732	-0.000416	-0.468649	0.000377
			G_2	0.002665	-0.011945	0.985090	0.005107	-0.243501	0.010583	-0.207033
			G_3	0.000000	0.004476	0.000652	1.106319	-0.001608	-0.718463	0.000880
			G_4	0.000610	-0.001640	0.158429	-0.034545	1.039227	0.042712	-0.820420
		0.8	G_0	0.481246	-0.013836	3.156476	0.084019	-3.534391	-0.091215	1.522475
			G_1	0.000000	0.495527	0.000335	0.688092	-0.000886	-0.571261	0.000469
			G_2	0.006111	-0.009234	1.017397	0.009922	-0.010110	0.001466	-0.376235
			G_3	0.000000	-0.002324	0.000564	1.190456	-0.000937	-0.751321	0.000289
			G_4	0.001439	-0.001644	0.150711	-0.020467	1.217097	0.026434	-0.936694
0.25	0.1	0.2	G_0	0.543830	-0.018226	1.961449	0.106248	-2.979252	-0.116592	1.529536
			G_1	-0.059076	0.980665	-0.386364	0.282151	-3.522104	7.282657	-4.059279
			G_2	0.013002	0.002440	0.988364	-0.018001	-0.371509	0.020915	-0.121371
			G_3	-0.090633	1.259726	-5.744277	15.785514	-23.78830	20.841805	-7.877989
			G_4	-0.000292	0.005436	0.185287	-0.036549	1.020086	0.041743	-0.829832
		0.4	G_0	0.550346	-0.013297	1.992952	0.112146	-2.999669	-0.120607	1.533507
			G_1	-0.071819	1.252497	-2.288259	6.452560	-13.62746	15.381954	-6.579865
			G_2	0.014272	0.003008	0.993339	-0.015090	-0.374424	0.018987	-0.120727
			G_3	-0.088131	1.186256	-5.103721	13.492890	-19.91638	17.759417	-6.944417
			G_4	0.000231	0.005582	0.187745	-0.034926	1.016454	0.040707	-0.827892
		0.6	G_0	0.565826	-0.003439	1.954161	0.116425	-2.695496	-0.094323	1.292502
			G_1	-0.074944	1.201129	-1.653420	4.259352	-9.574872	11.488462	-5.116472
			G_2	0.015208	0.001815	1.023301	0.007534	-0.413574	0.000728	-0.096680
			G_3	-0.081855	0.925982	-2.950680	6.263762	-7.632541	7.354279	-3.488731
			G_4	0.000352	0.003360	0.207288	-0.012266	0.970548	0.017652	-0.790600
		0.8	G_0	0.577437	0.001116	2.071873	0.271810	-2.565633	-0.172724	1.155321
			G_1	-0.053761	0.736998	1.844972	-7.546941	10.118862	-4.034211	-0.489541
			G_2	0.017529	-0.001899	1.029554	0.060207	-0.336252	-0.024479	-0.151637
			G_3	-0.057026	0.382926	1.110874	-7.323463	14.704096	-10.15383	1.748983
			G_4	0.001837	0.000165	0.201862	0.017466	1.024534	0.003410	-0.825770

Table C.5
Influence Coefficients For An Embedded Crack Of Finite Length In A Plate

a/c	d_1/t	a/d_1	G_i	A_0	A_1	A_2	A_3	A_4	A_5	A_6
0.25	0.25	0.2	G_0	0.537696	-0.025921	1.955145	0.120407	-2.938922	-0.125258	1.497329
			G_1	-0.000246	0.564125	-0.002740	0.343556	0.005187	-0.380079	-0.003435
			G_2	0.014281	0.000287	1.050888	-0.015054	-0.569580	0.016957	0.010362
			G_3	-0.000107	0.014103	0.000336	1.109461	-0.000465	-0.725386	-0.000354
			G_4	-0.000703	0.007998	0.251550	-0.055277	0.855937	0.063336	-0.739814
		0.4	G_0	0.547860	-0.027674	1.990139	0.108034	-2.971917	-0.117768	1.510431
			G_1	-0.000456	0.564074	-0.005148	0.343801	0.006167	-0.380055	-0.003335
			G_2	0.011184	0.000755	1.018531	-0.017088	-0.428454	0.018686	-0.087797
			G_3	-0.000212	0.014255	-0.000205	1.107599	-0.001989	-0.724060	0.001017
			G_4	-0.001173	0.005128	0.193131	-0.038389	1.010172	0.042987	-0.826030
		0.6	G_0	0.567565	-0.020461	1.969533	-0.009167	-2.705955	-0.016330	1.293079
			G_1	-0.001061	0.571398	-0.007944	0.342287	-0.010781	-0.382996	0.010056
			G_2	0.015595	0.000916	1.015394	-0.034520	-0.386367	0.029949	-0.118726
			G_3	-0.000456	0.016782	-0.001526	1.109613	-0.009983	-0.727432	0.007257
			G_4	0.000208	0.004933	0.203057	-0.044570	0.998683	0.046036	-0.819681
		0.8	G_0	0.576341	-0.040645	2.158031	-0.161776	-2.691429	0.064515	1.222566
			G_1	-0.003531	0.554035	-0.014173	0.424091	-0.087946	-0.426653	0.063971
			G_2	0.017718	-0.000648	1.042168	-0.079493	-0.354045	0.047244	-0.142868
			G_3	-0.001407	0.012543	0.000852	1.129475	-0.060002	-0.733130	0.039306
			G_4	0.001281	0.004904	0.217941	-0.065569	0.998171	0.050659	-0.817098
0.25	0.5	0.2	G_0	0.544046	-0.014364	1.959109	0.095272	-2.959061	-0.108774	1.512392
			G_1	0.000000	0.565516	-0.001180	0.341811	0.002349	-0.378954	-0.001650
			G_2	0.010169	0.002381	1.014622	-0.015806	-0.427709	0.018051	-0.087045
			G_3	0.000000	0.014335	0.001019	1.109745	-0.001143	-0.725493	0.000032
			G_4	0.000225	0.008198	0.254659	-0.052066	0.850805	0.060585	-0.736277
		0.4	G_0	0.556660	-0.014651	2.024524	0.097216	-3.011443	-0.111038	1.528937
			G_1	0.000000	0.566247	-0.001445	0.343967	0.003157	-0.380215	-0.002221
			G_2	0.014997	0.002695	1.004419	-0.017900	-0.387113	0.020447	-0.115022
			G_3	0.000000	0.014697	0.000740	1.109383	-0.000451	-0.725224	-0.000500
			G_4	0.000297	0.005454	0.193812	-0.036216	1.008950	0.041367	-0.824312
		0.6	G_0	0.581808	-0.008651	2.055696	0.049934	-2.712013	-0.053154	1.266472
			G_1	0.000000	0.574804	-0.000789	0.363279	0.000975	-0.395833	-0.000463
			G_2	0.018124	0.001634	1.042789	-0.009439	-0.409391	0.010048	-0.106126
			G_3	0.000000	0.017797	0.000904	1.120134	-0.002384	-0.733520	0.001419
			G_4	0.001852	0.005267	0.206731	-0.036055	1.009944	0.041703	-0.828698
		0.8	G_0	0.608273	-0.008227	2.345792	0.049047	-2.536023	-0.052853	1.042975
			G_1	0.000000	0.561954	-0.000788	0.539207	0.001266	-0.489579	-0.000686
			G_2	0.024349	0.002521	1.062774	-0.017745	-0.244333	0.020774	-0.230939
			G_3	0.000000	0.013542	0.000593	1.186767	-0.001749	-0.761495	0.001179
			G_4	0.004477	0.004744	0.222326	-0.033388	1.060651	0.039086	-0.862354

Table C.5
Influence Coefficients For An Embedded Crack Of Finite Length In A Plate

a/c	d_1/t	a/d_1	G_i	A_0	A_1	A_2	A_3	A_4	A_5	A_6
0.5	0.1	0.2	G_0	0.723795	-0.009606	0.962843	0.045642	-1.209391	-0.051263	0.546590
			G_1	0.006113	0.510372	1.416684	-3.109819	2.553276	-0.322746	-0.474755
			G_2	0.041317	0.001280	1.082754	-0.011444	-0.631608	0.013425	0.043657
			G_3	-0.022438	0.275294	-0.953070	3.596713	-3.711509	2.043595	-0.798055
			G_4	0.007856	0.008546	0.294270	-0.055677	0.839249	0.064720	-0.746243
		0.4	G_0	0.730634	-0.003824	0.983090	0.048746	-1.232904	-0.055099	0.556618
			G_1	0.009072	0.469831	1.647077	-3.692099	3.315310	-0.824240	-0.343649
			G_2	0.042695	0.002419	1.086193	-0.010224	-0.634982	0.012269	0.044901
			G_3	-0.010476	0.151892	-0.242507	1.775101	-1.295989	0.415667	-0.356559
			G_4	0.008457	0.009001	0.295565	-0.054899	0.837748	0.064070	-0.745598
		0.6	G_0	0.742588	0.008241	1.010447	0.053510	-1.191835	-0.044869	0.504411
			G_1	0.017899	0.268473	2.805206	-7.002515	8.521456	-4.968497	0.947229
			G_2	0.042946	0.003871	1.053218	-0.001034	-0.520261	0.004980	-0.027751
			G_3	-0.020865	0.393952	-2.210344	8.340361	-11.85542	8.633315	-2.839960
			G_4	0.009498	0.006090	0.243537	-0.026462	0.952941	0.030691	-0.796910
		0.8	G_0	0.759296	0.028086	1.080270	0.153567	-1.106818	-0.102163	0.417354
			G_1	-0.004237	0.737200	-0.249942	2.098925	-5.079766	5.253233	-2.125630
			G_2	0.046649	0.006545	1.048513	0.029048	-0.446470	-0.006911	-0.081633
			G_3	-0.005999	0.097661	0.022848	0.673785	1.079177	-1.710968	0.304197
			G_4	0.011465	0.006885	0.232771	-0.013663	1.009411	0.030112	-0.838215
0.5	0.25	0.2	G_0	0.717667	-0.020380	0.936510	0.057695	-1.153295	-0.056218	0.512093
			G_1	0.000134	0.723947	-0.006780	0.071199	0.008381	-0.217568	-0.004205
			G_2	0.035086	-0.001476	1.115370	-0.004442	-0.702698	0.006067	0.087912
			G_3	-0.000314	0.073308	0.002381	1.079510	-0.004861	-0.718140	0.001625
			G_4	0.002950	0.010332	0.287094	-0.071217	0.895005	0.082854	-0.796598
		0.4	G_0	0.730290	-0.015680	0.969475	0.043223	-1.201325	-0.047817	0.535517
			G_1	0.000220	0.726457	-0.006588	0.071565	0.007191	-0.218382	-0.003198
			G_2	0.041978	0.000008	1.088962	-0.011715	-0.643704	0.013340	0.051074
			G_3	-0.000330	0.074159	0.002652	1.079969	-0.005697	-0.718580	0.002201
			G_4	0.007325	0.008144	0.300095	-0.056601	0.830792	0.065468	-0.742353
		0.6	G_0	0.743860	-0.021962	1.005065	0.000002	-1.164803	-0.007235	0.483331
			G_1	-0.001394	0.711649	-0.010184	0.123002	0.005080	-0.252337	-0.000531
			G_2	0.042902	-0.001773	1.055272	-0.016718	-0.523410	0.015064	-0.026169
			G_3	-0.000737	0.058020	-0.001953	1.123562	-0.003418	-0.744614	0.002782
			G_4	0.008153	0.003902	0.251503	-0.034795	0.939929	0.035851	-0.790276
		0.8	G_0	0.760458	-0.048773	1.138436	-0.087284	-1.229980	0.034587	0.494763
			G_1	-0.005280	0.701105	-0.009052	0.189475	-0.067278	-0.291822	0.048830
			G_2	0.046198	-0.003951	1.076766	-0.053235	-0.515871	0.032111	-0.036005
			G_3	-0.002230	0.053570	0.000871	1.149157	-0.045224	-0.759029	0.030020
			G_4	0.010715	0.004107	0.251023	-0.057908	0.964621	0.048232	-0.808843

Table C.5
Influence Coefficients For An Embedded Crack Of Finite Length In A Plate

a/c	d_1/t	a/d_1	G_i	A_0	A_1	A_2	A_3	A_4	A_5	A_6
0.5	0.5	0.2	G_0	0.723987	-0.007139	0.955619	0.044991	-1.192714	-0.052151	0.535845
			G_1	0.000000	0.726564	-0.001605	0.070019	0.000591	-0.217340	-0.000287
			G_2	0.040720	0.001588	1.086529	-0.010068	-0.642235	0.011690	0.051144
			G_3	0.000000	0.074017	0.004101	1.080085	-0.006328	-0.718574	0.002099
			G_4	0.006760	0.008736	0.299516	-0.055454	0.830800	0.064516	-0.741818
		0.4	G_0	0.737303	-0.007298	0.992434	0.045879	-1.233273	-0.053050	0.551960
			G_1	0.000000	0.728397	-0.002109	0.072485	0.002030	-0.219508	-0.001176
			G_2	0.043920	0.001719	1.088827	-0.010917	-0.637685	0.012729	0.046100
			G_3	0.000000	0.074923	0.004527	1.080519	-0.007475	-0.719037	0.002846
			G_4	0.008774	0.008724	0.297714	-0.055392	0.835576	0.064431	-0.744573
		0.6	G_0	0.761395	-0.003760	1.051896	0.022076	-1.190796	-0.023822	0.486506
			G_1	0.000000	0.717045	-0.002967	0.131681	0.005004	-0.258490	-0.002813
			G_2	0.046659	0.001634	1.062532	-0.009691	-0.520306	0.010499	-0.031082
			G_3	0.000000	0.059948	0.000684	1.128646	-0.001600	-0.747943	0.000673
			G_4	0.010802	0.005183	0.249832	-0.030714	0.948557	0.033263	-0.795556
		0.8	G_0	0.801961	0.004280	1.253179	0.010431	-1.203325	-0.022751	0.437555
			G_1	0.000000	0.719005	0.011393	0.251467	-0.029449	-0.328034	0.018079
			G_2	0.054811	0.004299	1.094040	-0.015009	-0.474001	0.013135	-0.071147
			G_3	0.000000	0.059324	0.006812	1.183994	-0.016429	-0.778236	0.009714
			G_4	0.014771	0.006609	0.254211	-0.036096	0.997468	0.038652	-0.832479
1	0.1	0.2	G_0	1.008842	-0.003873	-0.026490	-0.000486	0.067133	0.004703	-0.044090
			G_1	-0.008016	1.141768	-0.828590	2.278116	-3.977550	2.728242	-0.668703
			G_2	0.071551	-0.002282	1.331169	0.008588	-1.081617	-0.009361	0.289110
			G_3	-0.005822	0.261327	-1.240302	5.757250	-6.130161	1.756897	0.121760
			G_4	0.016326	0.010038	0.424243	-0.066394	0.788506	0.077407	-0.768932
		0.4	G_0	1.016320	0.003670	-0.022186	-0.006833	0.059320	0.007309	-0.040149
			G_1	0.008240	1.020147	-0.052904	0.109962	-0.890981	0.532400	-0.049770
			G_2	0.073028	-0.000711	1.332180	0.007930	-1.083415	-0.009371	0.290071
			G_3	-0.010448	0.343200	-1.720344	7.126410	-8.162104	3.264041	-0.319019
			G_4	0.016962	0.010719	0.424641	-0.066580	0.787660	0.077405	-0.768489
		0.6	G_0	1.024956	0.015305	-0.012876	-0.004887	0.057887	0.003855	-0.042762
			G_1	0.006140	1.075353	-0.378046	0.997368	-2.099097	1.342078	-0.263382
			G_2	0.075245	0.001931	1.328710	0.008861	-1.078457	-0.010365	0.287713
			G_3	-0.010082	0.349649	-1.763546	7.256957	-8.353949	3.394182	-0.351107
			G_4	0.018011	0.011859	0.422984	-0.065726	0.786060	0.076553	-0.766612
		0.8	G_0	1.039311	0.049750	0.029510	0.016993	0.034407	-0.011554	-0.024655
			G_1	-0.006057	1.223125	-0.767603	0.777482	0.291398	-1.875451	1.068980
			G_2	0.078837	0.008367	1.324360	0.015487	-1.068531	-0.010793	0.289314
			G_3	-0.021655	0.478740	-2.105338	7.096537	-6.493531	0.873062	0.705701
			G_4	0.019611	0.014993	0.422403	-0.068121	0.770969	0.081155	-0.749821

Table C.5
Influence Coefficients For An Embedded Crack Of Finite Length In A Plate

a/c	d_1/t	a/d_1	G_i	A_0	A_1	A_2	A_3	A_4	A_5	A_6
1	0.25	0.2	G_0	0.998584	-0.015684	-0.036382	0.016835	0.092538	-0.005774	-0.060056
			G_1	0.000250	1.052208	-0.007063	-0.426007	0.007622	0.046894	-0.003511
			G_2	0.063900	-0.005874	1.371599	0.019092	-1.170753	-0.020165	0.346043
			G_3	-0.000595	0.164589	0.005755	1.139653	-0.011252	-0.788627	0.004916
			G_4	0.008863	0.013112	0.408872	-0.091416	0.888747	0.107038	-0.856287
		0.4	G_0	1.015009	-0.007528	-0.030901	0.002447	0.081626	0.003224	-0.054949
			G_1	0.000819	1.057810	-0.005844	-0.429289	0.006556	0.047572	-0.003170
			G_2	0.072202	-0.003136	1.334405	0.009943	-1.090502	-0.010740	0.295820
			G_3	-0.000381	0.166856	0.005973	1.138556	-0.010985	-0.788519	0.004677
			G_4	0.015117	0.009818	0.432485	-0.066636	0.775413	0.077664	-0.761771
		0.6	G_0	1.025429	-0.018899	-0.024098	-0.001328	0.088452	0.008861	-0.064283
			G_1	-0.000546	1.056583	-0.009132	-0.425212	0.007313	0.044664	-0.002488
			G_2	0.075269	-0.005550	1.326501	0.007215	-1.074799	-0.007587	0.285693
			G_3	-0.000931	0.167496	0.004138	1.134758	-0.010558	-0.786476	0.004953
			G_4	0.016556	0.008581	0.430086	-0.067017	0.773639	0.077920	-0.759863
		0.8	G_0	1.042557	-0.064164	-0.020997	-0.026482	0.175951	0.035162	-0.131913
			G_1	-0.004758	1.051391	-0.032160	-0.395132	0.004437	0.028163	0.007076
			G_2	0.079656	-0.015330	1.317765	-0.011036	-1.043202	0.004666	0.266819
			G_3	-0.002593	0.167653	-0.005711	1.137499	-0.019303	-0.787576	0.014316
			G_4	0.018859	0.004686	0.426646	-0.079355	0.777681	0.084825	-0.760303
1	0.5	0.2	G_0	1.007335	0.000870	-0.032838	-0.005828	0.083483	0.006862	-0.055173
			G_1	0.000000	1.055473	-0.000686	-0.425363	-0.007413	0.043747	0.007607
			G_2	0.070700	-0.001362	1.333569	0.008830	-1.089365	-0.010341	0.295376
			G_3	0.000000	0.165942	0.007078	1.139476	-0.012172	-0.788841	0.005131
			G_4	0.014449	0.010548	0.432405	-0.066712	0.775486	0.077462	-0.761576
		0.4	G_0	1.020653	0.000802	-0.024712	-0.005325	0.069424	0.006308	-0.047845
			G_1	0.000000	1.059402	-0.000822	-0.426893	-0.006340	0.043580	0.006645
			G_2	0.073767	-0.001180	1.332171	0.007611	-1.083972	-0.008928	0.291070
			G_3	0.000000	0.167661	0.007030	1.138310	-0.012411	-0.788448	0.005386
			G_4	0.017079	0.010573	0.425339	-0.066981	0.787124	0.077776	-0.767555
		0.6	G_0	1.039108	0.000776	-0.005040	-0.005624	0.064248	0.006872	-0.052375
			G_1	0.000000	1.062759	-0.003182	-0.423205	0.000529	0.041231	0.001284
			G_2	0.078057	-0.001199	1.331264	0.007708	-1.079097	-0.008986	0.287330
			G_3	0.000000	0.170220	0.006127	1.135403	-0.010697	-0.787366	0.004307
			G_4	0.019181	0.010461	0.424202	-0.066392	0.785711	0.077226	-0.766443
		0.8	G_0	1.076678	0.001493	0.055210	-0.009915	0.119255	0.011779	-0.114726
			G_1	0.000000	1.077683	-0.006020	-0.374247	0.012880	0.014321	-0.010548
			G_2	0.086643	-0.001194	1.338314	0.007540	-1.043218	-0.008732	0.260265
			G_3	0.000000	0.177403	0.006432	1.156459	-0.012131	-0.800413	0.005542
			G_4	0.022932	0.010421	0.428579	-0.066205	0.798227	0.077073	-0.775999

Note: Interpolation may be used for intermediate values of a/c, d_1/t, and a/d_1.

Table C.6
Influence Coefficients For A Longitudinal Through-Wall Crack In A Cylinder – Inside Surface

t/R_i	G_i	A_0	A_1	A_2	A_3	A_4	A_5	A_6
0.01	G_0	1.00762	-0.178500	0.161440	0.000000	-0.152520	0.058880	-0.003090
	G_1	0.0003	2.728940	0.424320	1.698480	13.87692	3.712580	0.073810
	G_p	1.01406	2.570610	1.040380	1.308630	2.148980	2.354210	-0.032420
0.01667	G_0	1.00764	0.013520	0.179410	0.000000	0.064370	0.024070	-0.001050
	G_1	0.00155	1.965340	0.176480	1.467290	9.452660	3.829850	0.018860
	G_p	1.0148	0.774270	0.451220	0.470680	0.635190	0.878590	-0.010450
0.05	G_0	1.00848	0.011360	0.194630	0.000000	0.073580	0.027420	-0.001140
	G_1	0.00382	0.784820	-0.285200	0.747730	1.890590	2.274800	-0.004600
	G_p	1.02776	0.014070	0.202280	0.000000	0.111820	0.023890	-0.000930
0.1	G_0	1.00856	0.149340	0.243300	0.000000	0.268710	0.009360	-0.000250
	G_1	0.00353	0.542290	-0.148882	0.419400	1.263990	1.193950	0.005930
	G_p	1.05546	0.166380	0.274280	0.000000	0.353440	0.007500	-0.000160
0.2	G_0	1.00475	0.107380	0.229090	0.000000	0.223980	0.012480	-0.000260
	G_1	0.00012	0.506470	0.246340	0.343420	3.059800	0.794490	0.018660
	G_p	1.096636	0.226909	0.315056	0.000000	0.473274	0.002693	0.000150
0.33333	G_0	1.00566	0.279910	0.286730	0.000000	0.483700	-0.012079	0.001377
	G_1	0.01447	0.179880	0.014630	0.000000	-0.029591	0.005410	0.000000
	G_p	1.12254	0.256880	0.371360	0.000000	0.569940	0.011600	-0.000096
1.0	G_0	0.9944	-0.095100	0.225710	0.000000	0.125240	0.029970	0.002957
	G_1	0.00359	0.137790	0.017440	0.000000	-0.065443	0.016350	0.000310
	G_p	1.32435	0.696980	0.400810	0.015540	1.302680	-0.089300	0.018523

Notes: Interpolation of the influence coefficients, G_i, may be used for intermediate values of R_i/t.

Table C.7
Influence Coefficients For A Longitudinal Through-Wall Crack In A Cylinder – Outside Surface

t/R_i	G_i	A_0	A_1	A_2	A_3	A_4	A_5	A_6
0.01	G_0	1.004540	0.392250	0.086470	0.000000	-0.020700	0.030610	-0.000990
	G_1	0.999510	7.930100	4.196810	1.911150	9.117120	3.412640	0.503310
	G_p	0.999190	0.439200	-0.010021	0.000000	0.221300	-0.028073	0.000880
0.01667	G_0	1.004660	0.481660	0.168680	0.000000	0.124010	0.029580	-0.000250
	G_1	0.995030	2.659410	1.233980	0.250070	3.250500	0.526340	0.070820
	G_p	0.993200	0.767840	0.589870	0.000000	0.697560	0.074080	0.001593
0.05	G_0	0.996830	0.338140	0.091330	0.000000	-0.017405	0.027980	-0.000490
	G_1	0.992850	0.786010	0.490220	0.000000	1.020270	0.108660	0.001550
	G_p	0.980700	0.382500	0.206540	0.000000	0.148410	0.038930	0.000405
0.1	G_0	0.994730	0.510250	0.185410	0.000000	0.168770	0.030030	0.000233
	G_1	0.999220	1.713680	0.612070	0.075550	1.973850	0.142370	0.031160
	G_p	0.959540	0.494400	0.213340	0.000000	0.233840	0.032670	0.001154
0.2	G_0	0.995330	0.585820	0.211280	0.000000	0.230790	0.037440	-0.000130
	G_1	0.998190	0.665590	0.343860	0.000000	0.737420	0.097600	0.000330
	G_p	0.947910	0.478700	0.184790	0.000000	0.187160	0.043710	0.000000
0.33333	G_0	0.996150	1.422090	0.689830	0.000000	1.113750	0.085480	0.000444
	G_1	1.000870	0.928950	0.333800	0.000000	0.956970	0.087980	0.000130
	G_p	0.893150	-1.161606	1.758510	2.949500	-2.178423	4.097810	0.558077
1.0	G_0	0.987790	0.427250	0.048420	0.000000	0.053630	0.012170	0.000553
	G_1	0.998500	0.058340	0.016870	0.000000	-0.051282	0.010850	0.000220
	G_p	0.856150	0.357890	0.000900	0.000000	-0.009800	0.009160	-0.000060

Notes: Interpolation of the influence coefficients, G_i, may be used for intermediate values of R_i/t.

Table C.8
Influence Coefficients For A Circumferential Through Wall Crack In A Cylinder – Inside Surface

t/R_i	G_i	A_0	A_1	A_2	A_3	A_4	A_5	A_6
0.01	G_0	0.993480	-0.047161	0.054090	0.000000	0.000380	-0.000680	0.000000
	G_1	0.029980	0.124380	0.000000	0.000000	-0.075550	0.001750	0.000000
	G_5	0.985590	-0.045610	0.051610	0.000000	-0.002030	-0.000410	0.000000
0.01667	G_0	0.983490	-0.020450	0.044819	0.000000	0.005920	-0.001050	0.000000
	G_1	0.031820	0.123290	0.000000	0.000000	-0.064940	0.001230	0.000000
	G_5	0.971070	-0.013090	0.046740	0.000000	0.020930	-0.001310	0.000000
0.05	G_0	0.973550	0.003040	0.084271	0.000000	0.113040	-0.014110	0.000399
	G_1	0.026150	0.140480	0.000000	0.000000	-0.066830	0.000870	0.000000
	G_5	0.933380	0.043860	0.055860	0.000000	0.106990	-0.013120	0.000417
0.1	G_0	0.943450	-0.023300	0.069755	0.000000	0.032420	0.007170	-0.000740
	G_1	0.025510	0.138400	-0.002950	0.000000	-0.065840	0.000400	0.000000
	G_5	0.867590	-0.171700	0.045540	0.000000	-0.207460	0.035710	-0.001580
0.2	G_0	0.892870	0.042440	0.048300	0.000000	0.062390	-0.010370	0.000000
	G_1	0.009880	0.154550	-0.085610	0.017910	-0.658110	0.177100	-0.010080
	G_5	0.766430	-0.113580	0.037070	0.000000	-0.181100	0.032760	-0.001890
0.33333	G_0	0.845290	-0.032400	0.028444	0.000000	-0.080250	-0.000280	0.000000
	G_1	0.005010	0.181600	0.015110	0.000000	0.248280	-0.055500	0.002400
	G_5	0.639210	-0.041000	0.000000	0.000000	-0.192540	0.009610	0.000000
1.0	G_0	0.684160	-0.042100	0.015715	0.000000	-0.167800	0.007820	0.000000
	G_1	-0.005310	0.100550	-0.004990	0.000000	-0.185520	0.009140	0.000000
	G_5	0.355650	0.007130	0.001360	0.000000	-0.182870	0.009290	0.000000

Notes: Interpolation of the influence coefficients, G_i, may be used for intermediate values of R_i/t.

Table C.9
Influence Coefficients For A Circumferential Through Wall Crack In A Cylinder – Outside Surface

t/R_i	G_i	A_0	A_1	A_2	A_3	A_4	A_5	A_6
0.01	G_0	0.999190	0.439200	-0.010020	0.000000	0.221300	-0.028070	0.000880
	G_1	0.993970	1.590210	-0.060740	0.000000	2.031720	-0.212760	0.006006
	G_5	1.000000	0.276970	-0.022358	0.002353	0.063820	-0.011510	0.000697
0.01667	G_0	1.016350	0.098680	0.000000	0.000000	-0.045340	0.000760	0.000000
	G_1	0.990970	0.107330	0.023480	0.000000	0.216380	-0.006700	0.000077
	G_5	1.003060	-0.025740	0.004704	0.013164	-0.239280	0.070140	-0.000730
0.05	G_0	0.996070	0.069010	-0.005580	0.000000	-0.109370	0.004740	-0.000081
	G_1	0.987530	-0.008000	0.022790	0.000000	0.062310	-0.000900	0.000115
	G_5	1.004290	0.136840	-0.021254	0.000900	-0.041250	-0.005740	0.000393
0.1	G_0	1.009490	0.163660	-0.004640	0.000000	0.009750	-0.004170	0.000000
	G_1	0.986430	0.116390	0.002660	0.000000	0.167370	-0.012940	0.000000
	G_5	1.004690	0.074190	-0.000500	0.000000	-0.068590	0.013030	-0.000750
0.2	G_0	0.988400	0.047990	0.000000	0.000000	-0.068610	-0.000140	0.000000
	G_1	0.989020	-0.032660	0.009220	0.000000	0.014110	-0.005480	0.000000
	G_5	0.997760	-0.277760	0.030970	0.000000	-0.366350	0.056330	-0.002420
0.33333	G_0	0.962510	-0.022768	0.000000	0.000000	-0.146530	0.005950	0.000000
	G_1	0.990490	-0.143270	0.018590	0.000000	-0.104870	0.005070	0.000000
	G_5	1.004950	-0.013450	0.000000	0.000000	-0.062110	0.000000	0.000000
1.0	G_0	0.920180	-0.086731	0.000243	0.000000	-0.225570	0.014210	0.000000
	G_1	0.992110	0.319530	-0.042350	0.000000	0.490910	-0.140260	0.009044
	G_5	0.997020	0.250250	-0.043352	0.000000	0.309300	-0.086700	0.004725

Notes: Interpolation of the influence coefficients, G_i, may be used for intermediate values of R_i/t.

Table C.10
Influence Coefficients For a Longitudinal Infinite Length Surface Crack in a Cylindrical Shell

t/R_i	a/t	Inside Surface					Outside Surface				
		G_0	G_1	G_2	G_3	G_4	G_0	G_1	G_2	G_3	G_4
0.001	0	1.120000	0.682000	0.524500	0.440400	0.379075	1.120000	0.682000	0.524500	0.440400	0.379075
	0.2	1.362669	0.775768	0.577169	0.475763	0.405555	1.362492	0.775430	0.577078	0.475707	0.405320
	0.4	2.107481	1.059637	0.734602	0.578123	0.483688	2.106159	1.059018	0.734066	0.577700	0.483457
	0.6	4.023909	1.759944	1.112458	0.819725	0.660648	4.023909	1.759732	1.112458	0.819832	0.660479
	0.8	11.685450	4.447550	2.518103	1.697986	1.278424	11.909190	4.532179	2.565580	1.730506	1.301380
0.00333	0	1.120000	0.682000	0.524500	0.440400	0.379075	1.120000	0.682000	0.524500	0.440400	0.379075
	0.2	1.357654	0.772719	0.575074	0.474050	0.404119	1.357654	0.772836	0.575120	0.474050	0.404212
	0.4	2.098124	1.055171	0.731561	0.575621	0.481987	2.098131	1.055420	0.731740	0.575826	0.482184
	0.6	3.984819	1.744473	1.103460	0.813729	0.656089	3.988986	1.746621	1.104648	0.814588	0.656975
	0.8	11.431820	4.361182	2.474754	1.671906	1.260057	11.418040	4.356190	2.471838	1.670314	1.258819
0.01	0	1.120000	0.682000	0.524500	0.440400	0.379075	1.120000	0.682000	0.524500	0.440400	0.379075
	0.2	1.355721	0.772039	0.574618	0.473607	0.403962	1.355914	0.772205	0.574709	0.473663	0.404056
	0.4	2.088097	1.051685	0.729765	0.574481	0.481203	2.086534	1.050936	0.729261	0.574252	0.480917
	0.6	3.924228	1.722783	1.091988	0.806497	0.650855	3.923337	1.722585	1.091908	0.806497	0.650876
	0.8	10.554820	4.054112	2.314531	1.572029	1.189801	10.534910	4.046475	2.309298	1.569106	1.187672
0.01667	0	1.120000	0.682000	0.524500	0.440400	0.379075	1.120000	0.682000	0.524500	0.440400	0.379075
	0.2	1.353978	0.771359	0.574252	0.473441	0.403767	1.354559	0.771574	0.574391	0.473496	0.403822
	0.4	2.076759	1.047310	0.727245	0.572880	0.479971	2.075495	1.046684	0.726942	0.572615	0.479723
	0.6	3.857250	1.698243	1.078613	0.797885	0.644619	3.858610	1.698758	1.079099	0.798289	0.644759
	0.8	9.818255	3.796811	2.179989	1.488012	1.131273	9.814990	3.795084	2.177882	1.486756	1.130544
0.025	0	1.120000	0.682000	0.524500	0.440400	0.379075	1.120000	0.682000	0.524500	0.440400	0.379075
	0.2	1.351845	0.770679	0.573795	0.473108	0.403649	1.352815	0.770943	0.573978	0.473214	0.403667
	0.4	2.064088	1.042414	0.724534	0.571046	0.478588	2.058880	1.039137	0.721589	0.568690	0.477008
	0.6	3.780308	1.670205	1.063426	0.788181	0.637578	3.783314	1.671252	1.064248	0.788820	0.637814
	0.8	9.046439	3.526527	2.038831	1.400363	1.069409	9.072502	3.534701	2.042477	1.402231	1.070735
0.05	0	1.120000	0.682000	0.524500	0.440400	0.379075	1.120000	0.682000	0.524500	0.440400	0.379075
	0.2	1.345621	0.768292	0.572560	0.472331	0.402984	1.348153	0.769051	0.572972	0.472583	0.403085
	0.4	2.028188	1.028989	0.717256	0.566433	0.475028	2.028188	1.028734	0.717129	0.566281	0.474824
	0.6	3.573882	1.594673	1.023108	0.762465	0.618437	3.584289	1.598763	1.025243	0.763840	0.619628
	0.8	7.388754	2.946567	1.736182	1.211533	0.936978	7.522466	2.992945	1.760192	1.226597	0.947337
0.1	0	1.120000	0.682000	0.524500	0.440400	0.379075	1.120000	0.682000	0.524500	0.440400	0.379075
	0.2	1.332691	0.763153	0.569758	0.470495	0.401459	1.338976	0.765213	0.570770	0.471069	0.401850
	0.4	1.957764	1.002123	0.702473	0.556857	0.467621	1.964321	1.004607	0.703748	0.557628	0.468296
	0.6	3.223438	1.466106	0.953655	0.718048	0.585672	3.270363	1.483681	0.963144	0.724069	0.590347
	0.8	5.543784	2.300604	1.398958	1.000682	0.789201	5.839919	2.403771	1.452694	1.034485	0.812508
0.2	0	1.120000	0.682000	0.524500	0.440400	0.379075	1.120000	0.682000	0.524500	0.440400	0.379075
	0.2	1.307452	0.753466	0.564298	0.466913	0.398757	1.324199	0.759716	0.567636	0.468987	0.400407
	0.4	1.833200	0.954938	0.676408	0.539874	0.454785	1.861734	0.964913	0.681357	0.542909	0.457058
	0.6	2.734052	1.287570	0.857474	0.656596	0.540720	2.864663	1.335823	0.883295	0.673156	0.553201
	0.8	3.940906	1.739955	1.106210	0.818230	0.661258	4.412961	1.903704	1.191550	0.871484	0.697846
0.33333	0	1.120000	0.682000	0.524500	0.440400	0.379075	1.120000	0.682000	0.524500	0.440400	0.379075
	0.2	1.276782	0.742170	0.558403	0.463081	0.359594	1.310620	0.755011	0.565121	0.467379	0.399359
	0.4	1.697454	0.903713	0.648337	0.521591	0.440820	1.768778	0.930197	0.662576	0.531192	0.447877
	0.6	2.343563	1.146104	0.781532	0.605006	0.505644	2.576840	1.231639	0.827059	0.637486	0.527420
	0.8	3.056124	1.430631	0.944773	0.717096	0.591403	3.652018	1.636477	1.051797	0.783771	0.636126
1.0	0	1.120000	0.682000	0.524500	0.440400	0.379075	1.120000	0.682000	0.524500	0.440400	0.379075
	0.2	1.157242	0.690605	0.523454	0.434683	0.378510	1.285088	0.746435	0.560782	0.459361	0.397605
	0.4	1.323647	0.760150	0.565266	0.463993	0.400866	1.582337	0.860502	0.624683	0.502572	0.429409
	0.6	1.551084	0.854214	0.621423	0.503163	0.430629	2.029092	1.029167	0.717944	0.565019	0.474990
	0.8	1.934272	1.036763	0.740108	0.590819	0.500031	2.778609	1.325214	0.886685	0.681558	0.561924

Note: Interpolation of the influence coefficients, G_i, may be used for intermediate values of t/R_i and a/t.

Table C.11
Influence Coefficients For a Circumferential 360° Surface Crack in a Cylindrical Shell

t/R_i	a/t	Inside Surface					Outside Surface				
		G_0	G_1	G_2	G_3	G_4	G_0	G_1	G_2	G_3	G_4
0.001	0	1.120000	0.682000	0.524500	0.440400	0.379075	1.120000	0.682000	0.524500	0.440400	0.379075
	0.2	1.322217	0.749276	0.557422	0.459379	0.392453	1.322614	0.749276	0.557516	0.459436	0.392373
	0.4	1.985705	0.991993	0.684695	0.537194	0.453928	1.988345	0.992918	0.685270	0.537439	0.454140
	0.6	3.550561	1.553001	0.979529	0.719751	0.589763	3.554007	1.554127	0.980154	0.720115	0.589975
	0.8	7.704234	2.997325	1.722909	1.174144	0.914488	7.714443	3.000386	1.724431	1.175261	0.914895
0.00333	0	1.120000	0.682000	0.524500	0.440400	0.379075	1.120000	0.682000	0.524500	0.440400	0.379075
	0.2	1.326772	0.756593	0.563926	0.464829	0.397395	1.327958	0.756940	0.564112	0.464942	0.397435
	0.4	1.963785	0.994898	0.692884	0.546635	0.460636	1.967788	0.996347	0.693830	0.547114	0.460995
	0.6	3.332548	1.491534	0.957864	0.713772	0.584192	3.340673	1.493877	0.959050	0.714507	0.584442
	0.8	6.166579	2.493763	1.483156	1.041092	0.819169	6.185694	2.499017	1.485806	1.042477	0.819550
0.01	0	1.120000	0.682000	0.524500	0.440400	0.379075	1.120000	0.682000	0.524500	0.440400	0.379075
	0.2	1.328921	0.764758	0.572095	0.471607	0.403497	1.332125	0.754093	0.552893	0.446495	0.394324
	0.4	1.899528	0.981795	0.692586	0.550532	0.463005	1.908312	0.972250	0.672981	0.524206	0.453612
	0.6	3.004384	1.379555	0.898565	0.673759	0.560242	3.023794	1.392928	0.914706	0.693364	0.567059
	0.8	4.812997	2.042848	1.263627	0.915957	0.729154	4.859478	2.057938	1.271054	0.920244	0.731930
0.01667	0	1.120000	0.682000	0.524500	0.440400	0.379075	1.120000	0.682000	0.524500	0.440400	0.379075
	0.2	1.318924	0.760855	0.569883	0.470144	0.402374	1.324190	0.750929	0.551104	0.445314	0.393380
	0.4	1.848413	0.962422	0.681854	0.543524	0.457730	1.862482	0.954704	0.663258	0.517887	0.448742
	0.6	2.813119	1.309799	0.861033	0.649812	0.542690	2.842912	1.326360	0.878647	0.670199	0.549981
	0.8	4.237503	1.841730	1.158696	0.850454	0.683358	4.298510	1.860923	1.167928	0.855764	0.686511
0.025	0	1.120000	0.682000	0.524500	0.440400	0.379075	1.120000	0.682000	0.524500	0.440400	0.379075
	0.2	1.308916	0.756949	0.567677	0.468679	0.401251	1.316699	0.747945	0.549407	0.444194	0.392491
	0.4	1.800221	0.944166	0.671752	0.536926	0.452764	1.820527	0.938621	0.654343	0.512094	0.444266
	0.6	2.649761	1.250285	0.829036	0.629406	0.527751	2.691258	1.270496	0.848362	0.650736	0.535620
	0.8	3.822034	1.696662	1.083009	0.803222	0.650398	3.900213	1.720900	1.094600	0.809896	0.654152
0.05	0	1.120000	0.682000	0.524500	0.440400	0.379075	1.120000	0.682000	0.524500	0.440400	0.379075
	0.2	1.286308	0.748129	0.562711	0.465393	0.398716	1.301318	0.741790	0.545907	0.441883	0.390643
	0.4	1.700591	0.906527	0.650941	0.523329	0.442578	1.738126	0.906946	0.636767	0.500662	0.435407
	0.6	2.354964	1.143036	0.771413	0.592683	0.500911	2.426798	1.172917	0.795410	0.616676	0.510449
	0.8	3.202288	1.480478	0.970278	0.732879	0.601399	3.326522	1.518951	0.988743	0.743640	0.607331
0.1	0	1.120000	0.682000	0.524500	0.440400	0.379075	1.120000	0.682000	0.524500	0.440400	0.379075
	0.2	1.254559	0.735816	0.555784	0.460810	0.395216	1.283010	0.734415	0.541694	0.439092	0.388405
	0.4	1.578769	0.860586	0.625575	0.506771	0.430190	1.646171	0.871503	0.617078	0.487850	0.425443
	0.6	2.054427	1.033913	0.712856	0.555383	0.473720	2.176175	1.080225	0.745040	0.584239	0.486420
	0.8	2.691796	1.302652	0.877596	0.675063	0.561238	2.895260	1.366730	0.908821	0.693565	0.571807
0.2	0	1.120000	0.682000	0.524500	0.440400	0.379075	1.120000	0.682000	0.524500	0.440400	0.379075
	0.2	1.210829	0.718943	0.546312	0.454558	0.390464	1.263202	0.726351	0.537074	0.436025	0.385915
	0.4	1.437161	0.807345	0.596196	0.487609	0.415918	1.554170	0.835957	0.597311	0.474989	0.415406
	0.6	1.764286	0.928708	0.656426	0.519455	0.447584	1.966243	1.002411	0.702694	0.556948	0.466155
	0.8	2.272892	1.156841	0.801593	0.627635	0.528369	2.610699	1.265870	0.855722	0.660227	0.548031
0.33333	0	1.120000	0.682000	0.524500	0.440400	0.379075	1.120000	0.682000	0.524500	0.440400	0.379075
	0.2	1.169540	0.703965	0.537405	0.449080	0.386008	1.249224	0.720455	0.534174	0.434006	0.384331
	0.4	1.324079	0.764679	0.572698	0.472643	0.404510	1.495050	0.812809	0.584087	0.468236	0.408711
	0.6	1.564990	0.856347	0.617396	0.494415	0.429555	1.853386	0.960784	0.679981	0.542489	0.455252
	0.8	2.009679	1.065372	0.754056	0.598012	0.507836	2.500104	1.226225	0.834688	0.646925	0.538501
1.0	0	1.120000	0.682000	0.524500	0.440400	0.379075	1.120000	0.682000	0.524500	0.440400	0.379075
	0.2	1.053111	0.658180	0.511768	0.426327	0.373397	1.232641	0.721461	0.541745	0.447374	0.388116
	0.4	1.080722	0.673434	0.522112	0.434533	0.380077	1.429329	0.798668	0.586170	0.477522	0.410543
	0.6	1.201447	0.731154	0.558343	0.462336	0.402108	1.779101	0.933472	0.662679	0.528892	0.448432
	0.8	1.550182	0.905678	0.670755	0.549661	0.471981	2.592796	1.258791	0.852381	0.658939	0.545948

Note: Interpolation of the influence coefficients, G_i, may be used for intermediate values of t/R_i and a/t.

Table C.12
Influence Coefficients For A Longitudinal Semi-Elliptical Surface Crack In A Cylinder – Inside Surface

t/R_i	a/c	a/t	G_i	A_0	A_1	A_2	A_3	A_4	A_5	A_6
0.0	0.03125	0	G_0	0.1965046	2.9373464	-5.2582823	7.4889153	-6.9282667	3.3673349	-0.6677966
			G_1	0.0051780	0.1750280	2.7718680	-4.6457154	4.6780502	-3.2768090	0.9840994
		0.2	G_0	0.2080760	3.0112422	-5.1048701	7.6348715	-6.8347547	2.7940766	-0.3882688
			G_1	0.0084834	0.2406767	2.4574292	-3.6452421	3.6142837	-2.8451814	0.9270638
		0.4	G_0	0.2357940	3.0822400	-3.5792100	3.9476890	1.9131590	-6.8872200	3.1896800
			G_1	0.0145140	0.4038000	1.6422700	-0.3906100	-0.6480700	-0.2940300	0.2514900
		0.6	G_0	0.2902240	3.6892050	-4.5739100	11.709890	-6.3750000	-5.8894100	4.2452400
			G_1	0.0208890	0.7016780	0.1631840	5.7072160	-8.2075800	3.4561120	-0.4454700
		0.8	G_0	0.5163550	2.5310830	14.712900	-43.621800	101.065700	-116.081000	46.190900
			G_1	0.0825460	0.4971770	4.6064810	-7.3326700	21.148620	-29.345100	12.491400
0.0	0.0625	0	G_0	0.2695332	2.1626001	-1.6551569	-1.2970208	4.5604304	-4.3163876	1.4010655
			G_1	0.0138667	0.1827458	2.5749608	-3.9044679	3.3556301	-2.1772209	0.6420134
		0.2	G_0	0.2845892	2.2264055	-1.4546190	-1.5760719	5.1131083	-4.9485443	1.6207574
			G_1	0.0199077	0.2210874	2.4642047	-3.5898625	3.1624039	-2.2403780	0.6965751
		0.4	G_0	0.3261480	2.5200870	-1.8847000	2.1798740	-1.4597100	-0.1886500	0.2393400
			G_1	0.0294120	0.3699370	1.9220850	-1.2071500	-0.4394000	0.2737550	-0.0395200
		0.6	G_0	0.4166330	3.1566470	-2.6248900	7.7325910	-9.6927800	3.6428700	-0.0892000
			G_1	0.0598460	0.4340740	2.6811560	-3.1936600	4.0753720	-4.6940200	1.8285500
		0.8	G_0	0.6540140	3.4231920	3.8158050	-4.1586900	3.4715330	-10.310400	6.6280000
			G_1	0.1214780	0.6975490	2.9718330	-1.3036500	-0.0754900	-3.0465100	2.1670000
0.0	0.125	0	G_0	0.4065238	0.7772483	3.8861644	-12.573943	16.760207	-11.014593	2.8706957
			G_1	0.0320270	0.1825342	2.2670449	-2.7076615	1.2088194	-0.3777430	0.0763155
		0.2	G_0	0.4242116	1.0089302	3.2973815	-12.159726	17.873386	-12.868668	3.6281712
			G_1	0.0429859	0.2033811	2.2563818	-2.8752160	1.8152558	-1.0512327	0.3181077
		0.4	G_0	0.4917770	1.6592320	-0.1080400	0.1793240	-2.7076100	3.3680620	-1.3489700
			G_1	0.0634270	0.3722500	1.6231670	-0.5306500	-2.0007400	1.8943780	-0.5880300
		0.6	G_0	0.6591820	1.8759140	1.0212600	-1.7698000	-0.5653600	1.2479960	-0.4376600
			G_1	0.1116040	0.4714500	1.7940590	-0.7557600	-1.4901700	1.0852180	-0.2113700
		0.8	G_0	0.9809330	1.8846320	4.8020780	-8.0580200	0.4447850	3.4772660	-1.0567500
			G_1	0.2039950	0.4800150	2.8822430	-2.5890100	-0.9683000	1.5372370	-0.3750200
0.0	0.25	0	G_0	0.6152816	-0.3348694	6.2955620	-15.590618	19.299508	-12.488107	3.3010035
			G_1	0.0703566	0.2828152	1.4036169	-0.6511596	-1.2076596	1.0318656	-0.2423741
		0.2	G_0	0.6385889	-0.3095132	6.5329787	-16.622882	21.056641	-13.850120	3.6988146
			G_1	0.0840059	0.1999367	1.8218113	-1.7756899	0.3757186	-0.0785358	0.0643386
		0.4	G_0	0.7390420	0.0548160	4.0842620	-7.5883100	5.4047530	-1.0146100	-0.3483400
			G_1	0.1164500	0.2479880	1.8282520	-1.7169900	0.1912120	0.1165770	-0.0186100
		0.6	G_0	0.9461210	-0.1858800	5.5867460	-9.8634900	5.9596870	0.1296440	-1.0026100
			G_1	0.1778050	0.2056680	2.0979210	-1.8039500	-0.5558700	1.1461400	-0.4206600
		0.8	G_0	1.2452110	-0.6921900	8.3260620	-14.948000	8.6936910	0.4755790	-1.3926600
			G_1	0.2585640	0.1548890	2.1170240	-0.4910000	-4.6146100	5.4550750	-1.9663300
0.0	0.5	0	G_0	0.8776607	-0.6729719	3.7721411	-6.5209060	6.3377934	-3.7028038	0.9872447
			G_1	0.1277541	0.4368502	0.4904522	1.0427434	-2.9631236	2.0826525	-0.5184313
		0.2	G_0	0.9003948	-0.8850488	5.2743239	-11.267523	13.890755	-9.6373584	2.8183906
			G_1	0.1404409	0.3215397	1.1010666	-1.0257556	0.6943940	-1.0793186	0.5410929
		0.4	G_0	1.0058060	-0.7322600	2.9951940	-1.9459200	-3.2613500	5.1424570	-2.0306200
			G_1	0.1740870	0.3051630	1.2070310	-0.6720500	-1.0651300	1.1445590	-0.3644800
		0.6	G_0	1.1826010	-1.1072500	3.9623640	-2.7781300	-4.3097300	7.2772750	-2.9648200
			G_1	0.2277120	0.1701170	1.5499470	-1.1051200	-0.8333700	1.1717060	-0.4194500
		0.8	G_0	1.3833380	-1.3900300	4.3755780	-3.7372600	-2.5403200	5.3036000	-2.0932400
			G_1	0.2820110	0.0839230	1.7258580	-1.5358100	-0.0635600	0.5006780	-0.1982200

Table C.12
Influence Coefficients For A Longitudinal Semi-Elliptical Surface Crack In A Cylinder – Inside Surface

t/R_i	a/c	a/t	G_i	A_0	A_1	A_2	A_3	A_4	A_5	A_6
0.0	1	0	G_0	1.1977992	-0.5244870	0.1498299	2.3284866	-5.1058499	4.3469049	-1.3487980
			G_1	0.1870117	0.6987352	0.1316900	0.7269255	-2.5259384	2.1756251	-0.6540458
		0.2	G_0	1.2263282	-1.1608467	4.4744783	-11.584231	17.811241	-14.408250	4.6998279
			G_1	0.2154786	0.2441623	2.8107820	-7.6574580	11.171413	-9.0053693	2.9542871
		0.4	G_0	1.2989480	-0.9978000	1.9479540	-1.3002700	-1.4940100	2.8306230	-1.2126000
			G_1	0.2386246	0.1447774	3.3198992	-9.2456599	13.823512	-11.223715	3.6868232
		0.6	G_0	1.3971180	-1.1348400	1.7918740	-0.4202600	-2.8679300	3.7685480	-1.4405000
			G_1	0.2445870	0.5326670	0.5939690	-0.0361800	-2.0163100	2.2167010	-0.7782200
		0.8	G_0	1.5117010	-1.3244800	1.7568350	-0.1337900	-2.8629300	3.2953270	-1.1412400
			G_1	0.2704470	0.5113280	0.5357440	-0.0327300	-1.5570200	1.5570970	-0.5094600
0.0	2	0	G_0	0.8150546	-0.5623828	1.4465771	-4.6778133	8.4192164	-7.9025932	2.9866351
			G_1	0.1359146	0.0702340	3.5558581	-11.034445	16.967724	-14.126991	4.8706612
		0.2	G_0	0.8463715	-1.0011024	4.0052312	-11.937181	19.189548	-16.039296	5.4674371
			G_1	0.1395121	0.0753999	3.1895604	-9.5540932	14.214316	-11.649525	4.0073308
		0.4	G_0	0.8570045	-1.0183085	3.9957306	-11.886878	19.152747	-16.047480	5.4801806
			G_1	0.1436696	0.0544018	3.2816127	-9.8164232	14.610963	-11.942138	4.0907797
		0.6	G_0	0.8839861	-1.0765270	4.0774087	-11.976171	19.173189	-15.996207	5.4501217
			G_1	0.1504185	0.0478401	3.2579960	-9.6921199	14.370843	-11.736129	4.0258411
		0.8	G_0	0.9033134	-0.9619755	2.8501500	-7.6366897	11.596116	-9.4828625	3.2550163
			G_1	0.1458559	0.2313881	1.9882138	-5.5546045	7.4196069	-5.8965053	2.0855563
0.01	0.03125	0	G_0	0.1965046	2.9373464	-5.2582823	7.4889153	-6.9282667	3.3673349	-0.6677966
			G_1	0.0051780	0.1750280	2.7718680	-4.6457154	4.6780502	-3.2768090	0.9840994
		0.2	G_0	0.2149558	2.4720875	-1.2147834	-4.1389650	10.539267	-9.6956094	3.1225660
			G_1	0.0081814	0.2385252	2.4687702	-3.7439973	3.7704530	-2.9529315	0.9589542
		0.4	G_0	0.2371100	3.0647320	-3.4513200	3.3917110	2.7324370	-7.4671300	3.3674100
			G_1	0.0110140	0.4025030	1.6437570	-0.3727600	-0.8119700	-0.0858000	0.1781500
		0.6	G_0	0.2921630	3.6926360	-4.6925300	11.901720	-7.7448000	-3.7999500	3.3544000
			G_1	0.0226600	0.6715900	0.4388550	4.5930610	-6.5549400	2.3178280	-0.1251900
		0.8	G_0	0.5243760	2.2524770	16.793480	-53.803200	114.103600	-119.702000	44.914100
			G_1	0.0833680	0.4665890	4.7440270	-8.4336900	21.115630	-26.684500	10.785300
0.01	0.0625	0	G_0	0.2695332	2.1626001	-1.6551569	-1.2970208	4.5604304	-4.3163876	1.4010655
			G_1	0.0138667	0.1827458	2.5749608	-3.9044679	3.3556301	-2.1772209	0.6420134
		0.2	G_0	0.3011924	1.7811106	0.8562316	-6.9529186	11.339236	-8.4567250	2.3835697
			G_1	0.0198422	0.2079432	2.6052559	-4.3155521	4.6614903	-3.6113853	1.1602564
		0.4	G_0	0.3321630	2.4901340	-1.5629300	0.0711970	3.2088600	-4.5926200	1.7583400
			G_1	0.0275700	0.4338520	1.4670200	0.0742960	-2.3137100	1.6328580	-0.4232800
		0.6	G_0	0.4174310	3.3955340	-4.5683700	12.806250	-16.603400	8.3551170	-1.3349400
			G_1	0.0592490	0.4942840	2.2111170	-1.9453300	2.2241680	-3.3126700	1.4345200
		0.8	G_0	0.6609890	3.4633420	2.8481190	-3.5483900	4.2900100	-10.609700	6.3367900
			G_1	0.1233510	0.6910730	2.8678320	-1.6023100	0.5891520	-3.1647400	2.0037600
0.01	0.125	0	G_0	0.4065238	0.7772483	3.8861644	-12.573943	16.760207	-11.014593	2.8706957
			G_1	0.0320270	0.1825342	2.2670449	-2.7076615	1.2088194	-0.3777430	0.0763155
		0.2	G_0	0.4140502	1.1388823	1.7096208	-6.0970813	7.5806259	-4.7412598	1.1879060
			G_1	0.0486456	0.0159697	3.8996081	-9.0058939	12.464506	-9.7091690	2.9890898
		0.4	G_0	0.4927230	1.5440820	0.6341780	-2.3645300	1.5071740	0.0175250	-0.3190500
			G_1	0.0625230	0.3683750	1.6262050	-0.6018500	-1.8348700	1.7392560	-0.5338200
		0.6	G_0	0.6457970	1.8450060	0.8248110	-1.2027800	-1.6161800	2.2686010	-0.8026800
			G_1	0.1079430	0.4523420	1.7937000	-0.7530100	-1.6009900	1.2810970	-0.2997100
		0.8	G_0	0.9331980	1.8484040	4.0610460	-6.4488400	-1.5508000	5.3526860	-1.8508400
			G_1	0.1900180	0.4493580	2.8240480	-2.7063600	-0.5768000	1.3457950	-0.3958100

Table C.12
Influence Coefficients For A Longitudinal Semi-Elliptical Surface Crack In A Cylinder – Inside Surface

t/R_i	a/c	a/t	G_i	A_0	A_1	A_2	A_3	A_4	A_5	A_6
0.01	0.25	0	G_0	0.6152816	-0.3348694	6.2955620	-15.590618	19.299508	-12.488107	3.3010035
			G_1	0.0703566	0.2828152	1.4036169	-0.6511596	-1.2076596	1.0318656	-0.2423741
		0.2	G_0	0.6241551	-0.2465111	7.0309527	-20.022042	27.911625	-19.682762	5.5162697
			G_1	0.0907721	0.1638762	2.5396012	-5.0799147	6.3011931	-4.8260624	1.4910341
		0.4	G_0	0.7353150	0.0335380	4.1529840	-7.8035600	5.7330000	-1.2513900	-0.2813800
			G_1	0.1163980	0.2222910	1.9859130	-2.2466100	1.0747840	-0.5982800	0.2057500
		0.6	G_0	0.9324150	-0.2341500	5.7957890	-10.643200	7.3266510	-0.9708400	-0.6676100
			G_1	0.1737550	0.1916590	2.1300350	-1.8831100	-0.4807900	1.1395430	-0.4345700
		0.8	G_0	1.2219490	-1.1415500	11.712920	-27.080700	29.834180	-16.937700	4.0600500
			G_1	0.2500840	0.0580650	2.8199190	-3.0313700	-0.1601400	1.7951480	-0.8296700
0.01	0.5	0	G_0	0.8776607	-0.6729719	3.7721411	-6.5209060	6.3377934	-3.7028038	0.9872447
			G_1	0.1277541	0.4368502	0.4904522	1.0427434	-2.9631236	2.0826525	-0.5184313
		0.2	G_0	0.9015490	-1.1113733	6.8843421	-16.342574	21.585452	-15.202444	4.3660359
			G_1	0.1484299	0.1541815	2.2768151	-4.5991695	5.8149262	-4.5777434	1.4654106
		0.4	G_0	0.9995660	-0.7280200	2.9776730	-1.9277500	-3.2709000	5.1505490	-2.0350400
			G_1	0.1726160	0.3087790	1.1425500	-0.3862200	-1.6344200	1.6645600	-0.5412700
		0.6	G_0	1.1705130	-1.1242900	4.0543560	-2.9851600	-4.1166400	7.2299430	-2.9791800
			G_1	0.2234860	0.1766680	1.5051550	-0.9863000	-0.9867500	1.2669540	-0.4418100
		0.8	G_0	1.3565360	-1.3769500	4.3964180	-3.8814500	-2.2095000	5.0187600	-2.0135800
			G_1	0.2754490	0.0635260	1.8760200	-1.9807100	0.6070780	0.0190700	-0.0683400
0.01	1	0	G_0	1.1977992	-0.5244870	0.1498299	2.3284866	-5.1058499	4.3469049	-1.3487980
			G_1	0.1870117	0.6987352	0.1316900	0.7269255	-2.5259384	2.1756251	-0.6540458
		0.2	G_0	1.2108906	-1.2118250	5.0003862	-13.525257	21.096357	-16.993711	5.4692793
			G_1	0.2135613	0.1822719	3.2508209	-9.1159303	13.526088	-10.816272	3.4876265
		0.4	G_0	1.2915440	-0.9860000	1.9198180	-1.2048700	-1.6920600	3.0190640	-1.2778100
			G_1	0.2335267	0.1351331	3.4108405	-9.6049414	14.454580	-11.727329	3.8372073
		0.6	G_0	1.3879210	-1.1637000	2.0681660	-1.2956400	-1.4973800	2.7147660	-1.1246500
			G_1	0.2442110	0.4839940	0.9407500	-1.1541500	-0.1848200	0.7462030	-0.3202300
		0.8	G_0	1.4955530	-1.3298700	1.9626990	-0.8242400	-1.7468100	2.4129690	-0.8712900
			G_1	0.2671290	0.4953350	0.6445810	-0.2740900	-1.3088000	1.4517080	-0.5006200
0.01	2	0	G_0	0.8150546	-0.5623828	1.4465771	-4.6778133	8.4192164	-7.9025932	2.9866351
			G_1	0.1359146	0.0702340	3.5558581	-11.034445	16.967724	-14.126991	4.8706612
		0.2	G_0	0.8108427	-0.9469615	4.0418669	-12.589699	20.713465	-17.423042	5.9097427
			G_1	0.1318838	0.0532545	3.3674428	-10.236137	15.430205	-12.636393	4.3051116
		0.4	G_0	0.8250898	-0.2999988	-0.8021829	3.4774334	-6.2776890	4.9519567	-1.3622968
			G_1	0.1346594	0.0300881	3.4841930	-10.598201	15.982963	-13.033343	4.4132933
		0.6	G_0	0.8505718	-0.3504564	-0.7638086	3.5152228	-6.4354105	5.1178036	-1.4187607
			G_1	0.1449083	0.0226142	3.4683252	-10.495830	15.799002	-12.901367	4.3816709
		0.8	G_0	0.9038677	-0.9803128	3.0688019	-8.3574085	12.791955	-10.493661	3.5981987
			G_1	0.1478039	0.0204313	3.4187237	-10.183273	14.776072	-11.479762	3.7099585
0.01667	0.03125	0	G_0	0.1965046	2.9373464	-5.2582823	7.4889153	-6.9282667	3.3673349	-0.6677966
			G_1	0.0051780	0.1750280	2.7718680	-4.6457154	4.6780502	-3.2768090	0.9840994
		0.2	G_0	0.2148671	2.4723189	-1.2180211	-4.1126757	10.496724	-9.6740573	3.1211775
			G_1	0.0080961	0.2401938	2.4502326	-3.6573824	3.5940475	-2.7881220	0.9010264
		0.4	G_0	0.2372950	3.0566010	-3.3944000	3.1477730	3.1530230	-7.7865200	3.4576600
			G_1	0.0106590	0.4095900	1.6083470	-0.3260900	-0.8035100	-0.1463900	0.2110000
		0.6	G_0	0.2937680	3.5870040	-3.8424000	8.4442010	-1.4600300	-8.9339200	4.9119300
			G_1	0.0220570	0.6740750	0.3474810	4.9629310	-7.3508700	3.1732170	-0.4659300
		0.8	G_0	0.4838350	3.1566150	8.8031170	-27.164800	69.601910	-82.479600	32.682600
			G_1	0.0716700	0.7084130	2.6085960	-1.4257400	9.3653570	-16.640500	7.3940300

Table C.12
Influence Coefficients For A Longitudinal Semi-Elliptical Surface Crack In A Cylinder – Inside Surface

t/R_i	a/c	a/t	G_i	A_0	A_1	A_2	A_3	A_4	A_5	A_6
0.01667	0.0625	0	G_0	0.2695332	2.1626001	-1.6551569	-1.2970208	4.5604304	-4.3163876	1.4010655
			G_1	0.0138667	0.1827458	2.5749608	-3.9044679	3.3556301	-2.1772209	0.6420134
		0.2	G_0	0.2857109	2.0654488	-0.9893799	-1.3807471	2.8006402	-2.0206042	0.4892659
			G_1	0.0194914	0.2150005	2.5598171	-4.1817299	4.4576257	-3.4587288	1.1159282
		0.4	G_0	0.3287840	2.5921570	-2.4132600	3.0634190	-1.9525300	-0.3333000	0.4144600
			G_1	0.0280780	0.4276920	1.4973510	0.0288440	-2.3497300	1.7402640	-0.4758200
		0.6	G_0	0.4176850	3.4074150	-4.6753500	13.078590	-17.041300	8.7888280	-1.5084600
			G_1	0.0574660	0.5499100	1.7774590	-0.5099100	-0.1282100	-1.4365500	0.8552000
		0.8	G_0	0.6582530	3.5128870	2.2828230	-1.9924300	2.2310040	-8.6681700	5.4793000
			G_1	0.1225420	0.7046220	2.7569290	-1.4438200	0.6196850	-3.1640900	1.9357000
0.01667	0.125	0	G_0	0.4065238	0.7772483	3.8861644	-12.573943	16.760207	-11.014593	2.8706957
			G_1	0.0320270	0.1825342	2.2670449	-2.7076615	1.2088194	-0.3777430	0.0763155
		0.2	G_0	0.4141982	1.1344888	1.7439464	-6.2232541	7.7907137	-4.9072442	1.2389750
			G_1	0.0486813	0.0152024	3.9061790	-9.0327670	12.510777	-9.7464081	3.0006990
		0.4	G_0	0.4948480	1.4794440	1.1185270	-4.0444100	4.3282860	-2.2595600	0.3903500
			G_1	0.0625520	0.3656340	1.6407500	-0.6554600	-1.7474400	1.6670140	-0.5089000
		0.6	G_0	0.6409930	1.9652950	-0.1642100	2.2005520	-7.4218400	7.0583030	-2.3230500
			G_1	0.1083560	0.4453160	1.8399940	-0.9086700	-1.3774300	1.1373530	-0.2654300
		0.8	G_0	0.9356790	1.8738760	3.8946700	-6.0693900	-1.9444100	5.6896490	-2.0106100
			G_1	0.1916520	0.4524760	2.8002690	-2.6288800	-0.7144600	1.5221540	-0.4838500
0.01667	0.25	0	G_0	0.6152816	-0.3348694	6.2955620	-15.590618	19.299508	-12.488107	3.3010035
			G_1	0.0703566	0.2828152	1.4036169	-0.6511596	-1.2076596	1.0318656	-0.2423741
		0.2	G_0	0.6254105	-0.2756845	7.2372917	-20.717372	29.086839	-20.644329	5.8190829
			G_1	0.0900509	0.1754701	2.4653292	-4.8609065	5.9734789	-4.5843798	1.4212799
		0.4	G_0	0.7330250	0.0541030	4.0064310	-7.3694700	5.0627260	-0.7345100	-0.4373600
			G_1	0.1161040	0.2203390	2.0004310	-2.3056000	1.1713600	-0.6681400	0.2244900
		0.6	G_0	0.9210290	-0.0465700	4.4521870	-6.3769100	0.5403590	4.3048320	-2.2613700
			G_1	0.1702480	0.2497180	1.7270540	-0.6420800	-2.4041500	2.6026300	-0.8686500
		0.8	G_0	1.2047330	-0.7847600	8.9533120	-17.715200	14.218040	-4.3196500	0.1157300
			G_1	0.2472570	0.1171600	2.3652370	-1.4978600	-2.7028500	3.8489740	-1.4739500
0.01667	0.5	0	G_0	0.8776607	-0.6729719	3.7721411	-6.5209060	6.3377934	-3.7028038	0.9872447
			G_1	0.1277541	0.4368502	0.4904522	1.0427434	-2.9631236	2.0826525	-0.5184313
		0.2	G_0	0.8987625	-1.0615830	6.5352105	-15.173572	19.607233	-13.575646	3.8503478
			G_1	0.1492382	0.1399206	2.3632147	-4.8462524	6.1772411	-4.8415701	1.5410021
		0.4	G_0	0.9959920	-0.6970000	2.8073570	-1.4883600	-3.8580500	5.5420790	-2.1380800
			G_1	0.1731960	0.2880460	1.2897340	-0.8838700	-0.7861600	0.9618990	-0.3169700
		0.6	G_0	1.1640340	-1.0701100	3.7508010	-2.1976100	-5.1415900	7.8804140	-3.1390700
			G_1	0.2222510	0.1801650	1.4936230	-0.9830600	-0.9475900	1.2090310	-0.4178500
		0.8	G_0	1.3532210	-1.4106800	4.6621530	-4.7297600	-0.8479500	3.9686690	-1.7045800
			G_1	0.2729800	0.0878270	1.7214050	-1.5086900	-0.1139000	0.5633750	-0.2302700
0.01667	1	0	G_0	1.1977992	-0.5244870	0.1498299	2.3284866	-5.1058499	4.3469049	-1.3487980
			G_1	0.1870117	0.6987352	0.1316900	0.7269255	-2.5259384	2.1756251	-0.6540458
		0.2	G_0	1.2106055	-1.2105643	4.9943941	-13.508283	21.072293	-16.977692	5.4653669
			G_1	0.2138344	0.1777026	3.2716297	-9.1531646	13.549492	-10.812840	3.4815135
		0.4	G_0	1.2891190	-0.9709000	1.8325120	-0.9414100	-2.1003700	3.3316080	-1.3719500
			G_1	0.2133960	0.5774660	0.6071350	-0.1664100	-1.8486500	2.1386670	-0.7727600
		0.6	G_0	1.3851610	-1.1646000	2.1025010	-1.4262200	-1.2663500	2.5193910	-1.0614400
			G_1	0.2421130	0.5102400	0.7555890	-0.5305800	-1.2337100	1.5984880	-0.5866900
		0.8	G_0	1.4915010	-1.3274700	1.9683410	-0.7813900	-1.8938700	2.5733450	-0.9310100
			G_1	0.2653560	0.5038220	0.6296470	-0.3034500	-1.1613700	1.2707090	-0.4290900

Table C.12
Influence Coefficients For A Longitudinal Semi-Elliptical Surface Crack In A Cylinder – Inside Surface

t/R_i	a/c	a/t	G_i	A_0	A_1	A_2	A_3	A_4	A_5	A_6
0.01667	2	0	G_0	0.8150546	-0.5623828	1.4465771	-4.6778133	8.4192164	-7.9025932	2.9866351
			G_1	0.1359146	0.0702340	3.5558581	-11.034445	16.967724	-14.126991	4.8706612
		0.2	G_0	0.8101916	-0.9412593	4.0126414	-12.507285	20.589007	-17.329107	5.8820015
			G_1	0.1322100	0.0467146	3.4045450	-10.328106	15.540798	-12.698847	4.3180540
		0.4	G_0	0.8245651	-0.3028365	-0.7600170	3.3001602	-5.9433064	4.6607966	-1.2672554
			G_1	0.1339511	0.0389739	3.4338823	-10.459900	15.789207	-12.900150	4.3776714
		0.6	G_0	0.8499410	-0.3556093	-0.7320158	3.4590456	-6.4089179	5.1364574	-1.4338641
			G_1	0.1450687	0.0152402	3.5174526	-10.643316	16.026897	-13.077077	4.4350680
		0.8	G_0	0.9019647	-0.9728613	3.0540609	-8.3490973	12.822350	-10.547233	3.6224835
			G_1	0.1471513	0.0263638	3.3848213	-10.079855	14.616140	-11.359881	3.6753008
0.05	0.03125	0	G_0	0.1965046	2.9373464	-5.2582823	7.4889153	-6.9282667	3.3673349	-0.6677966
			G_1	0.0051780	0.1750280	2.7718680	-4.6457154	4.6780502	-3.2768090	0.9840994
		0.2	G_0	0.2147553	2.4733297	-1.2474542	-4.0148844	10.325431	-9.5295230	3.0755621
			G_1	0.0081488	0.2377645	2.4723890	-3.7475362	3.7575353	-2.9323550	0.9509310
		0.4	G_0	0.2360970	3.0572780	-3.4936200	3.2721920	3.0580130	-7.6615500	3.3859300
			G_1	0.0102200	0.4124020	1.5384150	-0.0617800	-1.3675500	0.4323350	-0.0065400
		0.6	G_0	0.2861060	3.5905940	-4.3735000	9.6484880	-3.3065400	-7.0688300	4.1532600
			G_1	0.0198400	0.6562220	0.3810810	4.5714070	-6.6677400	2.8306200	-0.4505100
		0.8	G_0	0.4596930	2.6805760	10.718030	-36.889800	86.523190	-93.759400	35.081500
			G_1	0.0617560	0.6089050	2.8527370	-3.2715300	12.274680	-17.735900	7.2096800
0.05	0.0625	0	G_0	0.2695332	2.1626001	-1.6551569	-1.2970208	4.5604304	-4.3163876	1.4010655
			G_1	0.0138667	0.1827458	2.5749608	-3.9044679	3.3556301	-2.1772209	0.6420134
		0.2	G_0	0.2859329	2.0653053	-0.9905563	-1.4150031	2.8652343	-2.0661068	0.5016295
			G_1	0.0196037	0.2151084	2.5626289	-4.2011550	4.4798485	-3.4669351	1.1166928
		0.4	G_0	0.3300790	2.5687830	-2.2730100	2.4482290	-0.9061800	-1.1152300	0.6336900
			G_1	0.0272960	0.4545140	1.2940000	0.6585910	-3.3745900	2.5567530	-0.7249800
		0.6	G_0	0.4134110	3.3905790	-4.8820500	13.351920	-17.160600	9.1488940	-1.8015900
			G_1	0.0575670	0.5056840	2.0319140	-1.4822100	1.4954900	-2.5583400	1.1145400
		0.8	G_0	0.6264970	3.5543640	0.7919210	0.3194370	2.0824790	-8.6748200	4.8836700
			G_1	0.1126460	0.7058050	2.3784990	-0.9484300	0.6832120	-2.9086500	1.5439800
0.05	0.125	0	G_0	0.4065238	0.7772483	3.8861644	-12.573943	16.760207	-11.014593	2.8706957
			G_1	0.0320270	0.1825342	2.2670449	-2.7076615	1.2088194	-0.3777430	0.0763155
		0.2	G_0	0.4141745	1.1275356	1.7988949	-6.4537497	8.1885840	-5.2215937	1.3338255
			G_1	0.0487792	0.0133782	3.9204009	-9.0880489	12.590390	-9.7977291	3.0135889
		0.4	G_0	0.4917700	1.5480530	0.5402050	-2.1834600	1.2196150	0.2889000	-0.4136700
			G_1	0.0618810	0.3879900	1.4515410	-0.0167500	-2.8752400	2.6301310	-0.8213900
		0.6	G_0	0.6460050	1.8351450	0.8285700	-1.6608000	-0.4877600	1.3380790	-0.5504100
			G_1	0.1093030	0.4366540	1.9181290	-1.3212300	-0.5731700	0.4753220	-0.0675600
		0.8	G_0	0.9327440	1.9648060	3.1532800	-4.8291100	-1.9134300	5.1126320	-1.9475400
			G_1	0.1921390	0.4872100	2.5183370	-1.9746200	-1.3273800	2.0002740	-0.7177100
0.05	0.25	0	G_0	0.6152816	-0.3348694	6.2955620	-15.590618	19.299508	-12.488107	3.3010035
			G_1	0.0703566	0.2828152	1.4036169	-0.6511596	-1.2076596	1.0318656	-0.2423741
		0.2	G_0	0.6229529	-0.2485784	7.0430049	-20.131994	28.206025	-19.995012	5.6320877
			G_1	0.0905859	0.1617121	2.5472316	-5.1142004	6.3762462	-4.8989319	1.5167184
		0.4	G_0	0.7303090	0.0326040	4.1332170	-7.8985600	6.0159640	-1.5217600	-0.1897900
			G_1	0.1142170	0.2418060	1.8297700	-1.7682600	0.3018070	0.0205930	0.0144400
		0.6	G_0	0.9202510	-0.1540100	5.1619380	-8.8082400	4.5807010	1.1262150	-1.3066500
			G_1	0.1702680	0.2235180	1.8974360	-1.2399100	-1.4028300	1.8129880	-0.6307900
		0.8	G_0	1.2322960	-1.4426500	14.003620	-35.237500	44.199690	-28.746600	7.7018200
			G_1	0.2497100	0.1097790	2.4079700	-1.7073400	-2.2186700	3.4494480	-1.3726200

Table C.12
Influence Coefficients For A Longitudinal Semi-Elliptical Surface Crack In A Cylinder – Inside Surface

t/R_i	a/c	a/t	G_i	A_0	A_1	A_2	A_3	A_4	A_5	A_6
0.05	0.5	0	G_0	0.8776607	-0.6729719	3.7721411	-6.5209060	6.3377934	-3.7028038	0.9872447
			G_1	0.1277541	0.4368502	0.4904522	1.0427434	-2.9631236	2.0826525	-0.5184313
		0.2	G_0	0.8998006	-1.1008716	6.7949974	-16.008148	20.985635	-14.692497	4.2008852
			G_1	0.1482707	0.1526809	2.2809119	-4.6071223	5.8286426	-4.5922291	1.4712639
		0.4	G_0	0.9875950	-0.6604200	2.5904420	-0.9060400	-4.6843400	6.1350420	-2.3065200
			G_1	0.1703150	0.3037660	1.2129670	-0.7351300	-0.9145500	0.9993630	-0.3136400
		0.6	G_0	1.1535210	-1.0846600	3.8853140	-2.6803400	-4.3200500	7.2246270	-2.9406900
			G_1	0.2189650	0.1820740	1.4974930	-1.0467100	-0.7825700	1.0459000	-0.3613100
		0.8	G_0	1.3387940	-1.3846800	4.5947460	-4.6182500	-0.8155300	3.8499650	-1.6650000
			G_1	0.2704200	0.0863940	1.7356660	-1.5215400	-0.1070200	0.5843010	-0.2509500
0.05	1	0	G_0	1.1977992	-0.5244870	0.1498299	2.3284866	-5.1058499	4.3469049	-1.3487980
			G_1	0.1870117	0.6987352	0.1316900	0.7269255	-2.5259384	2.1756251	-0.6540458
		0.2	G_0	1.2091906	-1.2119075	5.0112782	-13.553361	21.141961	-17.036849	5.4856225
			G_1	0.2131357	0.1842366	3.2319216	-9.0396511	13.389696	-10.704130	3.4528991
		0.4	G_0	1.2822600	-0.9719500	1.8928700	-1.1442300	-1.7968400	3.1176240	-1.3148300
			G_1	0.2313746	0.1294187	3.4578251	-9.7497871	14.680574	-11.902752	3.8908182
		0.6	G_0	1.3703740	-1.1028000	1.7930470	-0.4916100	-2.7326500	3.6494690	-1.4011700
			G_1	0.2379550	0.5278330	0.6693230	-0.2931400	-1.5654000	1.8255750	-0.6476900
		0.8	G_0	1.4740600	-1.2903000	1.9333060	-0.7538900	-1.8525600	2.4833110	-0.8912300
			G_1	0.2620950	0.4999820	0.6688010	-0.3352900	-1.2212800	1.3834660	-0.4801300
0.05	2	0	G_0	0.8150546	-0.5623828	1.4465771	-4.6778133	8.4192164	-7.9025932	2.9866351
			G_1	0.1359146	0.0702340	3.5558581	-11.034445	16.967724	-14.126991	4.8706612
		0.2	G_0	0.8405900	-0.9828964	3.9783944	-11.929139	19.232361	-16.107076	5.4985318
			G_1	0.1401448	0.0460755	3.3846820	-10.137821	15.107048	-12.328596	4.2110577
		0.4	G_0	0.8204618	-0.2806825	-0.8637066	3.6013842	-6.4111767	5.0203080	-1.3749797
			G_1	0.1422434	0.0527995	3.3104268	-9.9190612	14.794871	-12.107982	4.1496887
		0.6	G_0	0.8457322	-0.3595145	-0.6426755	3.1612151	-5.9385710	4.7719679	-1.3235536
			G_1	0.1488396	0.0406125	3.3249114	-9.9017635	14.712096	-12.020216	4.1204818
		0.8	G_0	0.8946607	-0.9436510	2.9530039	-8.0365810	12.297855	-10.128340	3.4958489
			G_1	0.1434305	0.2331398	2.0104442	-5.6212616	7.5252202	-5.9911091	2.1206547
0.1	0.03125	0	G_0	0.1965046	2.9373464	-5.2582823	7.4889153	-6.9282667	3.3673349	-0.6677966
			G_1	0.0051780	0.1750280	2.7718680	-4.6457154	4.6780502	-3.2768090	0.9840994
		0.2	G_0	0.2144509	2.4711734	-1.2860169	-3.9437101	10.258246	-9.4874515	3.0628400
			G_1	0.0080221	0.2380830	2.4576921	-3.7039504	3.6653669	-2.8375154	0.9161589
		0.4	G_0	0.2362020	3.0232830	-3.3746300	2.6514220	4.2691070	-8.6980100	3.7198100
			G_1	0.0103150	0.3971020	1.6371740	-0.4826500	-0.6416000	-0.1376700	0.1653300
		0.6	G_0	0.2803270	3.5106810	-4.3633000	9.2831770	-2.7203100	-7.4474300	4.2735200
			G_1	0.0176640	0.6383120	0.3362480	4.6736560	-7.0299900	3.3065000	-0.6400000
		0.8	G_0	0.4108450	2.7858000	7.1999900	-24.966400	63.838540	-72.490500	27.635600
			G_1	0.0459140	0.6441140	1.8109850	0.1500500	5.6303710	-11.329200	4.9191600
0.1	0.0625	0	G_0	0.2695332	2.1626001	-1.6551569	-1.2970208	4.5604304	-4.3163876	1.4010655
			G_1	0.0138667	0.1827458	2.5749608	-3.9044679	3.3556301	-2.1772209	0.6420134
		0.2	G_0	0.2852601	2.0623971	-0.9452314	-1.7155871	3.4690201	-2.5845388	0.6675616
			G_1	0.0195666	0.2161881	2.5579251	-4.2119758	4.4960423	-3.4714625	1.1164625
		0.4	G_0	0.3294820	2.5547280	-2.2095000	1.8316820	0.5378940	-2.4428800	1.0694100
			G_1	0.0290130	0.4029930	1.6912760	-0.7784700	-0.9590600	0.6513490	-0.1510800
		0.6	G_0	0.4058800	3.3662220	-5.1482900	13.513450	-16.655100	8.6671530	-1.7293500
			G_1	0.0569260	0.4451650	2.3945360	-2.9719000	4.1328030	-4.5775200	1.6727700
		0.8	G_0	0.5908720	3.5314460	-0.6929200	3.3140250	-0.2495400	-7.1101300	4.1118800
			G_1	0.1004430	0.7134420	1.8363740	0.1930190	-0.5388500	-1.7508700	0.9917100

Table C.12
Influence Coefficients For A Longitudinal Semi-Elliptical Surface Crack In A Cylinder – Inside Surface

t/R_i	a/c	a/t	G_i	A_0	A_1	A_2	A_3	A_4	A_5	A_6
0.1	0.125	0	G_0	0.4065238	0.7772483	3.8861644	-12.573943	16.760207	-11.014593	2.8706957
			G_1	0.0320270	0.1825342	2.2670449	-2.7076615	1.2088194	-0.3777430	0.0763155
		0.2	G_0	0.4138525	1.1243780	1.7964950	-6.5013714	8.2843111	-5.2897626	1.3521056
			G_1	0.0488254	0.0124168	3.9238498	-9.1173502	12.630693	-9.8176804	3.0170051
		0.4	G_0	0.4900830	1.5797060	0.2456910	-1.4169300	0.1330550	1.0979610	-0.6544400
			G_1	0.0625190	0.3795970	1.5007820	-0.2215400	-2.5534400	2.4056210	-0.7613400
		0.6	G_0	0.6383460	1.8896790	0.1654880	0.1405470	-2.8887800	3.1374330	-1.1431800
			G_1	0.1078790	0.4418060	1.8093490	-1.0600900	-0.9104200	0.7835470	-0.1968000
		0.8	G_0	0.9106040	1.6778320	4.1741310	-7.6274100	2.6957210	2.3283330	-1.6172500
			G_1	0.1827830	0.5316620	2.0011150	-0.7238700	-2.5544000	2.7998200	-1.0318900
0.1	0.25	0	G_0	0.6152816	-0.3348694	6.2955620	-15.590618	19.299508	-12.488107	3.3010035
			G_1	0.0703566	0.2828152	1.4036169	-0.6511596	-1.2076596	1.0318656	-0.2423741
		0.2	G_0	0.6221458	-0.2652412	7.1236921	-20.415683	28.691172	-20.391119	5.7567350
			G_1	0.0893032	0.1771452	2.4437349	-4.8273884	5.9604631	-4.5972261	1.4308564
		0.4	G_0	0.7269240	0.0331400	4.0541080	-7.6758800	5.6254770	-1.1588100	-0.3180200
			G_1	0.1141390	0.2282720	1.9094300	-2.0571800	0.7745000	-0.3425200	0.1223300
		0.6	G_0	0.9136940	-0.1128200	4.7770370	-7.7684000	3.1756140	2.1324410	-1.6080500
			G_1	0.1690410	0.2367980	1.7775820	-0.9219600	-1.8420100	2.1429690	-0.7348800
		0.8	G_0	1.2285610	-1.3887200	13.423440	-33.608900	42.330360	-27.500000	7.2734400
			G_1	0.2605760	-0.1180300	4.1243640	-7.6919700	8.0993900	-4.9636300	1.2276300
0.1	0.5	0	G_0	0.8776607	-0.6729719	3.7721411	-6.5209060	6.3377934	-3.7028038	0.9872447
			G_1	0.1277541	0.4368502	0.4904522	1.0427434	-2.9631236	2.0826525	-0.5184313
		0.2	G_0	0.8939439	-1.0523498	6.4920812	-15.138217	19.688676	-13.725026	3.9161703
			G_1	0.1471464	0.1576874	2.2477033	-4.5209327	5.7119515	-4.5121924	1.4494557
		0.4	G_0	0.9797560	-0.6583400	2.5905960	-0.9807000	-4.5022900	5.9676820	-2.2512600
			G_1	0.1683280	0.3025050	1.2065640	-0.7030600	-0.9925300	1.0836790	-0.3460700
		0.6	G_0	1.1399170	-1.0507000	3.7096220	-2.2768200	-4.7650200	7.4625310	-2.9908600
			G_1	0.2156530	0.1890000	1.4447400	-0.8854600	-1.0301700	1.2393260	-0.4219600
		0.8	G_0	1.3104950	-1.0667900	2.8675320	-0.6020200	-5.1697700	6.1071010	-2.1308200
			G_1	0.2673520	0.1194700	1.5170160	-0.8642000	-1.0371700	1.2474400	-0.4452900
0.1	1	0	G_0	1.1977992	-0.5244870	0.1498299	2.3284866	-5.1058499	4.3469049	-1.3487980
			G_1	0.1870117	0.6987352	0.1316900	0.7269255	-2.5259384	2.1756251	-0.6540458
		0.2	G_0	1.2047909	-1.2012348	4.9676187	-13.426779	20.945504	-16.887172	5.4412264
			G_1	0.2119663	0.1873102	3.2105329	-8.9636386	13.261943	-10.603790	3.4231621
		0.4	G_0	1.2697440	-0.9183700	1.6384390	-0.4675200	-2.7367600	3.7616560	-1.4871500
			G_1	0.2313746	0.1294187	3.4578251	-9.7497871	14.680574	-11.902752	3.8908182
		0.6	G_0	1.3563790	-1.1020000	1.8638360	-0.5992700	-2.7466300	3.7780850	-1.4700900
			G_1	0.2338370	0.5347500	0.6371980	-0.1619900	-1.8137100	2.0426640	-0.7195100
		0.8	G_0	1.4582970	-1.3079100	2.2328620	-1.6002400	-0.6409600	1.6167600	-0.6502600
			G_1	0.2583450	0.5028090	0.6746630	-0.2815000	-1.3831100	1.5504100	-0.5408600
0.1	2	0	G_0	0.8150546	-0.5623828	1.4465771	-4.6778133	8.4192164	-7.9025932	2.9866351
			G_1	0.1359146	0.0702340	3.5558581	-11.034445	16.967724	-14.126991	4.8706612
		0.2	G_0	0.8389023	-0.9910627	4.0593253	-12.185366	19.630219	-16.411826	5.5902596
			G_1	0.1391760	0.0538372	3.3380006	-9.9908862	14.871100	-12.143930	4.1552336
		0.4	G_0	0.8168007	-0.2921048	-0.7346646	3.2014916	-5.8126583	4.5798416	-1.2477748
			G_1	0.1412816	0.0503888	3.3380869	-10.010705	14.949170	-12.238855	4.1935739
		0.6	G_0	0.8387058	-0.3482355	-0.6184382	3.0476208	-5.7528210	4.6253567	-1.2780857
			G_1	0.1473521	0.0388746	3.3532681	-9.9888648	14.848958	-12.132523	4.1580679
		0.8	G_0	0.8878357	-0.9627154	3.2133021	-8.8604927	13.568698	-11.103565	3.7915359
			G_1	0.1419379	0.2284659	2.0631482	-5.7641990	7.7262423	-6.1414207	2.1673189

Table C.12
Influence Coefficients For A Longitudinal Semi-Elliptical Surface Crack In A Cylinder – Inside Surface

t/R_i	a/c	a/t	G_i	A_0	A_1	A_2	A_3	A_4	A_5	A_6
0.2	0.03125	0	G_0	0.1965046	2.9373464	-5.2582823	7.4889153	-6.9282667	3.3673349	-0.6677966
			G_1	0.0051780	0.1750280	2.7718680	-4.6457154	4.6780502	-3.2768090	0.9840994
		0.2	G_0	0.2190748	2.5203290	-2.0236870	-1.2734559	5.7568175	-5.8748904	1.9521817
			G_1	0.0082274	0.2471615	2.3678007	-3.4287724	3.2025223	-2.4520746	0.7939694
		0.4	G_0	0.2316580	3.0174340	-3.6739100	3.3486960	3.4951970	-8.3582900	3.7094000
			G_1	0.0132894	0.2678595	2.5665870	-4.0109437	5.6693993	-5.4751609	1.8921069
		0.6	G_0	0.2637180	3.3055520	-4.3385500	9.7328450	-4.9409500	-4.6514100	3.2218700
			G_1	0.0181909	0.3817362	2.1420212	-2.1977697	5.2001900	-7.0131972	2.7040967
		0.8	G_0	0.3497230	2.1192140	8.0739030	-27.587500	62.883920	-66.409000	24.306100
			G_1	0.0235580	0.5103500	1.5026960	1.4467780	1.4312900	-6.0350600	2.7698500
0.2	0.0625	0	G_0	0.2695332	2.1626001	-1.6551569	-1.2970208	4.5604304	-4.3163876	1.4010655
			G_1	0.0138667	0.1827458	2.5749608	-3.9044679	3.3556301	-2.1772209	0.6420134
		0.2	G_0	0.2852936	2.0689704	-1.0554851	-1.4836567	3.1890944	-2.3859114	0.6080571
			G_1	0.0197715	0.2169234	2.5536862	-4.2430898	4.5441255	-3.4924585	1.1187813
		0.4	G_0	0.3285480	2.4958610	-2.0243000	0.8619950	2.4744750	-4.0617200	1.5606500
			G_1	0.0361263	0.3182238	2.4231181	-3.6890071	4.2893407	-3.7603314	1.2600158
		0.6	G_0	0.3915700	3.2250850	-4.9945400	12.185590	-13.428900	5.6813190	-0.7529300
			G_1	0.0514191	0.4402715	2.1487271	-2.5959155	4.1080561	-4.8381973	1.8044669
		0.8	G_0	0.5261450	3.2405970	-1.3815100	4.1519310	0.5109400	-8.1414300	4.3185000
			G_1	0.0814479	0.6559984	1.5337156	0.4475435	0.0534894	-2.5096346	1.2137430
0.2	0.125	0	G_0	0.4065238	0.7772483	3.8861644	-12.573943	16.760207	-11.014593	2.8706957
			G_1	0.0320270	0.1825342	2.2670449	-2.7076615	1.2088194	-0.3777430	0.0763155
		0.2	G_0	0.4136013	1.1220276	1.7642454	-6.5135424	8.3634912	-5.3510304	1.3676362
			G_1	0.0490163	0.0123967	3.9211133	-9.1581812	12.709183	-9.8748627	3.0337707
		0.4	G_0	0.4909940	1.5098770	0.5876890	-2.8587400	2.8113040	-1.1202600	0.0293200
			G_1	0.0747677	0.0749203	3.9389068	-9.1864777	12.998452	-10.295081	3.1890105
		0.6	G_0	0.6249600	1.8325900	0.0013210	-0.0015000	-1.5020700	1.6414400	-0.6878100
			G_1	0.1105969	0.2637050	2.9884892	-5.4654500	6.9950075	-5.7793135	1.8496103
		0.8	G_0	0.8500710	1.9490000	1.0758800	-0.8402600	-2.2385800	3.1877320	-1.4499300
			G_1	0.1789668	0.2399490	3.8931390	-7.7610872	10.294824	-7.8565698	2.2277937
0.2	0.25	0	G_0	0.6152816	-0.3348694	6.2955620	-15.590618	19.299508	-12.488107	3.3010035
			G_1	0.0703566	0.2828152	1.4036169	-0.6511596	-1.2076596	1.0318656	-0.2423741
		0.2	G_0	0.6159056	-0.2050937	6.6909872	-19.186699	26.862981	-19.027126	5.3580488
			G_1	0.0891128	0.1702221	2.4720008	-4.9324186	6.1223136	-4.7123917	1.4632694
		0.4	G_0	0.7215670	0.0374900	3.9226910	-7.4222400	5.3541510	-0.9786100	-0.3710800
			G_1	0.1202781	0.1074802	2.4970523	-3.7079504	3.0213692	-1.8021829	0.4930615
		0.6	G_0	0.9048380	-0.1315600	4.6654820	-7.6840900	3.5404410	1.6663190	-1.4658800
			G_1	0.1803830	-0.0541023	3.7023114	-7.2913373	8.5546816	-5.9999118	1.7212304
		0.8	G_0	1.1866530	-0.8342800	8.7205780	-18.257500	18.406930	-8.8685700	1.4645500
			G_1	0.2633540	-0.1901259	4.3785426	-8.5606515	9.8591518	-6.4535782	1.6581104
0.2	0.5	0	G_0	0.8776607	-0.6729719	3.7721411	-6.5209060	6.3377934	-3.7028038	0.9872447
			G_1	0.1277541	0.4368502	0.4904522	1.0427434	-2.9631236	2.0826525	-0.5184313
		0.2	G_0	0.8858151	-1.0197403	6.2776913	-14.516668	18.732182	-12.986246	3.6925414
			G_1	0.1453215	0.1594771	2.2306775	-4.4869243	5.6738656	-4.4885955	1.4435985
		0.4	G_0	0.9688850	-0.6841400	2.7358770	-1.4201300	-3.8776500	5.5502200	-2.1443700
			G_1	0.1705287	0.1690974	1.9564466	-3.3798091	3.7905011	-3.0373612	1.0275733
		0.6	G_0	1.1240870	-1.0768400	3.8703920	-2.7987600	-3.8803000	6.7635310	-2.7860400
			G_1	0.2171748	0.0842974	2.2072273	-3.7731258	4.0998144	-3.1122546	1.0079677
		0.8	G_0	1.3125100	-1.3603100	4.4157580	-3.9151500	-1.6021800	4.3666690	-1.8710900
			G_1	0.2804807	-0.0036237	2.1078754	-2.5482535	1.5280380	-0.6890973	0.1306713

Table C.12
Influence Coefficients For A Longitudinal Semi-Elliptical Surface Crack In A Cylinder – Inside Surface

t/R_i	a/c	a/t	G_i	A_0	A_1	A_2	A_3	A_4	A_5	A_6
0.2	1	0	G_0	1.1977992	-0.5244870	0.1498299	2.3284866	-5.1058499	4.3469049	-1.3487980
			G_1	0.1870117	0.6987352	0.1316900	0.7269255	-2.5259384	2.1756251	-0.6540458
		0.2	G_0	1.1957780	-1.1928788	4.9690673	-13.450328	20.984072	-16.917257	5.4506179
			G_1	0.2081893	0.2110738	3.0727215	-8.5670342	12.675874	-10.175528	3.3005282
		0.4	G_0	1.2499210	-0.8835300	1.5685020	-0.3587800	-2.8201600	3.7710640	-1.4756300
			G_1	0.2261821	0.1336704	3.4220588	-9.5448451	14.293730	-11.605247	3.8105474
		0.6	G_0	1.3280790	-1.0422100	1.7783590	-0.6033200	-2.4505600	3.3606510	-1.2970500
			G_1	0.2465393	0.1720577	2.9234104	-7.7004235	11.016864	-8.7581419	2.8432632
		0.8	G_0	1.4295430	-1.2362900	2.0609680	-0.9573800	-1.8135900	2.6148850	-0.9777200
			G_1	0.2736792	0.1461663	2.8913901	-7.2809390	10.022374	-7.6326797	2.3534796
0.2	2	0	G_0	0.8150546	-0.5623828	1.4465771	-4.6778133	8.4192164	-7.9025932	2.9866351
			G_1	0.1359146	0.0702340	3.5558581	-11.034445	16.967724	-14.126991	4.8706612
		0.2	G_0	0.8351796	-0.9975558	4.1493278	-12.445145	19.981918	-16.646781	5.6530002
			G_1	0.1380096	0.0562824	3.3282021	-9.9530116	14.806340	-12.097815	4.1444930
		0.4	G_0	0.8306994	-1.0237591	4.3698748	-13.269111	21.479545	-17.921928	6.0620530
			G_1	0.1376183	0.0406712	3.4210114	-10.313146	15.494157	-12.701908	4.3425313
		0.6	G_0	0.8558483	-1.0505654	4.3124794	-12.845362	20.558401	-17.096036	5.8004744
			G_1	0.1446670	0.0167777	3.5323058	-10.571235	15.816043	-12.923783	4.4101264
		0.8	G_0	0.8664408	-0.8724913	2.8280384	-7.6269457	11.393145	-9.2221390	3.1640805
			G_1	0.1390668	0.1865317	2.4237595	-7.0178287	9.8903995	-7.9357249	2.7360663
0.33333	0.03125	0	G_0	0.1965046	2.9373464	-5.2582823	7.4889153	-6.9282667	3.3673349	-0.6677966
			G_1	0.0051780	0.1750280	2.7718680	-4.6457154	4.6780502	-3.2768090	0.9840994
		0.2	G_0	0.2172042	2.5042847	-2.1152523	-1.0663053	5.5897238	-5.8369981	1.9620413
			G_1	0.0076407	0.2402259	2.3741989	-3.4818023	3.2921834	-2.5081221	0.8062819
		0.4	G_0	0.2213040	3.0865230	-5.3162800	10.104880	-9.4190500	3.0782450	-0.0751300
			G_1	0.0109040	0.2379070	2.7257150	-4.5589100	6.4148690	-5.9564800	2.0227340
		0.6	G_0	0.2326720	3.4536430	-7.5171600	21.602680	-27.456600	15.285850	-3.3080200
			G_1	0.0124870	0.2833310	2.5113570	-3.3810700	6.2551880	-7.1855300	2.6289150
		0.8	G_0	0.2431510	3.7925040	-9.4367000	34.625530	-49.585800	30.877910	-7.4781600
			G_1	0.0129250	0.3526240	1.9977450	-0.5838300	3.0764080	-5.7180400	2.2847340
0.33333	0.0625	0	G_0	0.2695332	2.1626001	-1.6551569	-1.2970208	4.5604304	-4.3163876	1.4010655
			G_1	0.0138667	0.1827458	2.5749608	-3.9044679	3.3556301	-2.1772209	0.6420134
		0.2	G_0	0.2844799	2.0640002	-1.1370689	-1.3784733	3.1901236	-2.4501643	0.6364234
			G_1	0.0196105	0.2162750	2.5422614	-4.2578287	4.5779897	-3.5058747	1.1186308
		0.4	G_0	0.3220940	2.4382140	-1.9837600	0.2441520	4.2246520	-5.9119800	2.2494420
			G_1	0.0302700	0.2690970	2.6242350	-4.3253900	5.2447410	-4.4149200	1.4273430
		0.6	G_0	0.3690150	2.8657790	-3.6714400	7.4894220	-5.1881800	-1.1502800	1.4278360
			G_1	0.0421480	0.3508870	2.4986830	-3.8769000	6.1282230	-6.2831600	2.2006960
		0.8	G_0	0.4274530	3.1943180	-5.0036400	17.183440	-22.134100	11.331200	-2.1369500
			G_1	0.0540340	0.4419180	2.1304980	-1.7669500	3.5006620	-4.6673800	1.6550060
0.33333	0.125	0	G_0	0.4065238	0.7772483	3.8861644	-12.573943	16.760207	-11.014593	2.8706957
			G_1	0.0320270	0.1825342	2.2670449	-2.7076615	1.2088194	-0.3777430	0.0763155
		0.2	G_0	0.4128225	1.1171748	1.7294667	-6.5703783	8.5967302	-5.5789250	1.4430231
			G_1	0.0491457	0.0109153	3.9207133	-9.2000295	12.768245	-9.8975712	3.0345710
		0.4	G_0	0.4999770	1.1122800	3.4080100	-12.831300	19.956770	-15.131900	4.4070790
			G_1	0.0655360	0.2653370	2.2964190	-3.1937600	2.6225790	-1.8132600	0.5497690
		0.6	G_0	0.6175010	1.2257330	4.0319720	-14.566200	24.320440	-19.886800	6.1066340
			G_1	0.0998390	0.2849510	2.6838120	-4.6127100	5.8013200	-4.8420000	1.5330940
		0.8	G_0	0.7920490	1.0127770	6.8668830	-21.954100	36.429260	-29.710200	9.0101920
			G_1	0.1476580	0.2244550	3.5532850	-7.2068400	10.474170	-8.3895400	2.3883100

Table C.12
Influence Coefficients For A Longitudinal Semi-Elliptical Surface Crack In A Cylinder – Inside Surface

t/R_i	a/c	a/t	G_i	A_0	A_1	A_2	A_3	A_4	A_5	A_6
0.33333	0.25	0	G_0	0.6152816	-0.3348694	6.2955620	-15.590618	19.299508	-12.488107	3.3010035
			G_1	0.0703566	0.2828152	1.4036169	-0.6511596	-1.2076596	1.0318656	-0.2423741
		0.2	G_0	0.6151200	-0.2559286	6.9419508	-19.977395	28.061835	-19.892262	5.6000832
			G_1	0.0890045	0.1593445	2.5204791	-5.1000189	6.3764694	-4.8919376	1.5129735
		0.4	G_0	0.7305130	-0.3220800	6.3427310	-15.390600	18.411260	-11.349700	2.8193980
			G_1	0.1265635	0.1445088	2.2324974	-3.0386458	2.2662085	-1.4535727	0.4548018
		0.6	G_0	0.9124330	-0.7665200	9.1561340	-23.081300	29.896950	-19.945600	5.3119440
			G_1	0.1687760	0.1014170	2.6091130	-3.8884800	3.4192270	-2.2010400	0.6120270
		0.8	G_0	1.1626120	-1.3970900	12.596200	-31.856200	42.732810	-29.146600	7.7681640
			G_1	0.2450710	-0.1281000	3.9424300	-7.5372100	9.0064480	-6.0816100	1.5366290
0.33333	0.5	0	G_0	0.8776607	-0.6729719	3.7721411	-6.5209060	6.3377934	-3.7028038	0.9872447
			G_1	0.1277541	0.4368502	0.4904522	1.0427434	-2.9631236	2.0826525	-0.5184313
		0.2	G_0	0.8818313	-1.0917996	6.7441757	-15.991176	21.054792	-14.772037	4.2281725
			G_1	0.1441557	0.1424866	2.3284045	-4.7895448	6.1386818	-4.8362727	1.5452935
		0.4	G_0	0.9407980	-0.4985400	1.9170250	-0.0192500	-4.6370600	5.2166830	-1.8075400
			G_1	0.1711202	0.1668531	1.9267560	-3.2630245	3.5831509	-2.8636537	0.9729171
		0.6	G_0	1.1152890	-1.3442300	5.9458650	-10.097200	8.9327530	-4.0621300	0.7185930
			G_1	0.2163543	0.1549463	1.5248691	-1.5230688	0.7692177	-0.7731253	0.3699490
		0.8	G_0	1.2910080	-1.3463700	4.3601980	-3.7608100	-1.3364900	3.8436030	-1.6693300
			G_1	0.2617850	0.1512610	1.1793570	0.3568580	-2.8439400	2.6019470	-0.8740000
0.33333	1	0	G_0	1.1977992	-0.5244870	0.1498299	2.3284866	-5.1058499	4.3469049	-1.3487980
			G_1	0.1870117	0.6987352	0.1316900	0.7269255	-2.5259384	2.1756251	-0.6540458
		0.2	G_0	1.1843664	-1.1847612	4.9902280	-13.538735	21.119771	-17.017414	5.4794601
			G_1	0.2064638	0.1880635	3.2277985	-9.0382566	13.410536	-10.743271	3.4724686
		0.4	G_0	1.2310867	-1.2996546	5.3458402	-14.297856	22.283375	-18.132719	5.9308732
			G_1	0.2232606	0.1330441	3.4286845	-9.5400946	14.273538	-11.599332	3.8156481
		0.6	G_0	1.3016702	-1.3329884	4.6823879	-11.389326	16.885721	-13.394792	4.3283933
			G_1	0.2440755	0.1533295	3.0387623	-7.9723882	11.374712	-9.0179366	2.9233036
		0.8	G_0	1.4059990	-1.4844400	4.6015830	-9.7191000	12.979170	-9.5963900	2.9604700
			G_1	0.2547770	0.3338937	2.0367399	-5.9096868	9.5170399	-8.2252015	2.7607498
0.33333	2	0	G_0	0.8150546	-0.5623828	1.4465771	-4.6778133	8.4192164	-7.9025932	2.9866351
			G_1	0.1359146	0.0702340	3.5558581	-11.034445	16.967724	-14.126991	4.8706612
		0.2	G_0	0.8291377	-0.9895481	4.1798664	-12.600881	20.280744	-16.914774	5.7445745
			G_1	0.1367171	0.0546432	3.3517976	-10.030368	14.931862	-12.199484	4.1771813
		0.4	G_0	0.8281292	-1.0079708	4.3560940	-13.170690	21.184349	-17.624770	5.9654552
			G_1	0.1383911	0.0271839	3.5221879	-10.559706	15.796147	-12.905023	4.4038513
		0.6	G_0	0.8416824	-1.0386714	4.4633302	-13.408838	21.463769	-17.808130	6.0224184
			G_1	0.1432074	0.0086329	3.6113710	-10.774368	16.083937	-13.122391	4.4757876
		0.8	G_0	0.8492888	-0.8700518	3.1479406	-8.7543723	13.222524	-10.685678	3.6241547
			G_1	0.1360843	0.2203399	2.2144388	-6.1874959	8.3319395	-6.6071612	2.3172922
1.0	0.03125	0	G_0	0.1965046	2.9373464	-5.2582823	7.4889153	-6.9282667	3.3673349	-0.6677966
			G_1	0.0051780	0.1750280	2.7718680	-4.6457154	4.6780502	-3.2768090	0.9840994
		0.2	G_0	0.1980698	2.9376255	-5.7910377	9.0906707	-8.3306142	3.5783634	-0.5294521
			G_1	0.0070114	0.1898240	2.6323945	-4.5352932	4.9970582	-3.7704006	1.1719024
		0.4	G_0	0.2036455	3.0536864	-7.5611329	18.090197	-24.359675	16.165416	-4.2713263
			G_1	0.0065988	0.2295720	2.2203944	-2.9443360	3.0963478	-2.8740561	1.0277332
		0.6	G_0	0.2080664	3.0619705	-7.5661345	21.002357	-30.847102	21.774390	-6.0844006
			G_1	0.0064428	0.2406363	2.0576379	-1.8975150	1.7403919	-2.1313070	0.8401771
		0.8	G_0	0.2151530	2.9278961	-6.4283147	20.746751	-33.454495	26.262895	-8.3376656
			G_1	0.0070182	0.2240701	2.1680770	-1.6985478	1.2764760	-1.0093882	0.0706237

Table C.12
Influence Coefficients For A Longitudinal Semi-Elliptical Surface Crack In A Cylinder – Inside Surface

t/R_i	a/c	a/t	G_i	A_0	A_1	A_2	A_3	A_4	A_5	A_6
1.0	0.0625	0	G_0	0.2695332	2.1626001	-1.6551569	-1.2970208	4.5604304	-4.3163876	1.4010655
			G_1	0.0138667	0.1827458	2.5749608	-3.9044679	3.3556301	-2.1772209	0.6420134
		0.2	G_0	0.2763729	2.1599045	-2.0267891	-0.4243455	4.0187485	-4.3462512	1.4738626
			G_1	0.0188237	0.2016690	2.4587678	-3.9257215	3.7489705	-2.5933327	0.7726676
		0.4	G_0	0.2858545	2.3348186	-3.7198821	6.2320571	-5.4958095	1.6375000	0.0378025
			G_1	0.0210044	0.2212507	2.3212950	-3.5787902	4.1509575	-3.5669022	1.1860134
		0.6	G_0	0.2956428	2.4165048	-4.8367868	12.797170	-16.848053	10.075226	-2.3531530
			G_1	0.0209211	0.2469374	2.1002164	-2.7077936	3.6514117	-3.8371464	1.3784540
		0.8	G_0	0.3105134	2.2645011	-3.9423356	13.526186	-20.565663	14.833318	-4.4921637
			G_1	0.0214507	0.2387578	2.1265824	-2.3702841	3.3403888	-3.1407320	0.8212562
1.0	0.125	0	G_0	0.4065238	0.7772483	3.8861644	-12.573943	16.760207	-11.014593	2.8706957
			G_1	0.0320270	0.1825342	2.2670449	-2.7076615	1.2088194	-0.3777430	0.0763155
		0.2	G_0	0.4121982	0.9809633	2.6642734	-10.718719	16.135987	-11.674891	3.2857406
			G_1	0.0429732	0.1691403	2.4438611	-3.9902340	3.8722617	-2.6848999	0.8103888
		0.4	G_0	0.4477387	1.0237602	2.5276007	-10.532059	17.664760	-14.148208	4.2757268
			G_1	0.0540097	0.1987294	2.2948342	-3.5660648	3.7293777	-2.8871555	0.9059529
		0.6	G_0	0.4794850	1.0122248	2.3746013	-8.9100690	16.499364	-14.722907	4.7771766
			G_1	0.0619259	0.1470564	2.7590146	-5.2500160	7.5725453	-6.5638921	2.1055291
		0.8	G_0	0.5164358	0.7095588	4.0378956	-11.615929	20.536460	-17.590932	5.3195877
			G_1	0.0672847	0.0932846	3.1539168	-6.3939996	10.166896	-8.4828712	2.4189185
1.0	0.25	0	G_0	0.6152816	-0.3348694	6.2955620	-15.590618	19.299508	-12.488107	3.3010035
			G_1	0.0703566	0.2828152	1.4036169	-0.6511596	-1.2076596	1.0318656	-0.2423741
		0.2	G_0	0.6036135	-0.2082404	5.3418705	-13.482957	16.721588	-10.762016	2.8234053
			G_1	0.0807441	0.1552152	1.9842592	-2.3730394	1.0667213	-0.3126002	0.0485609
		0.4	G_0	0.6763719	-0.4084805	6.5633796	-17.017482	22.438807	-15.270974	4.1657228
			G_1	0.1065385	0.1005757	2.2911382	-3.2447754	2.5267606	-1.4981637	0.4070186
		0.6	G_0	0.7671408	-0.7046097	8.0697488	-20.607164	28.506140	-20.412698	5.7488452
			G_1	0.1373930	-0.0362089	3.1839681	-5.9666133	7.3004307	-5.4361461	1.5933357
		0.8	G_0	0.8672181	-1.2149195	10.930135	-27.933404	40.819851	-30.187735	8.4787938
			G_1	0.1654534	-0.1999250	4.2025416	-8.9738747	12.795604	-9.7487687	2.7127496
1.0	0.5	0	G_0	0.8776607	-0.6729719	3.7721411	-6.5209060	6.3377934	-3.7028038	0.9872447
			G_1	0.1277541	0.4368502	0.4904522	1.0427434	-2.9631236	2.0826525	-0.5184313
		0.2	G_0	0.8384152	-0.8875162	5.3791336	-11.842585	14.590479	-9.8103109	2.7410811
			G_1	0.1337606	0.1884846	1.9795808	-3.6849341	4.3785592	-3.4701229	1.1326364
		0.4	G_0	0.8892248	-0.9915286	5.5961603	-12.007246	14.615317	-9.8105244	2.7557195
			G_1	0.1532075	0.1645333	1.9260619	-3.3061701	3.6845481	-2.9312177	0.9808108
		0.6	G_0	1.0018108	-1.2454590	6.2353455	-12.673294	15.354167	-10.487556	2.9891745
			G_1	0.1954366	-0.0015461	2.6948093	-5.1511045	6.2981962	-4.8171117	1.5021162
		0.8	G_0	1.1606771	-1.8418488	8.9468374	-18.899983	24.357274	-16.957160	4.6830625
			G_1	0.2459519	-0.1254368	2.9943167	-5.2476171	6.3302036	-4.6469716	1.3044496
1.0	1	0	G_0	1.1977992	-0.5244870	0.1498299	2.3284866	-5.1058499	4.3469049	-1.3487980
			G_1	0.1870117	0.6987352	0.1316900	0.7269255	-2.5259384	2.1756251	-0.6540458
		0.2	G_0	1.1326072	-1.0340344	4.2775103	-11.199805	17.066873	-13.558691	4.3214476
			G_1	0.1913506	0.2635671	2.7487853	-7.3815015	10.511084	-8.2595738	2.6404137
		0.4	G_0	1.1385905	-1.1163059	4.7874242	-12.494750	18.882546	-14.974863	4.7953969
			G_1	0.1977322	0.2151295	2.9666270	-7.9048037	11.307366	-8.9700271	2.9081089
		0.6	G_0	1.1953788	-1.2239875	4.9961246	-12.297253	17.790842	-13.686167	4.2864193
			G_1	0.2188226	0.1664467	3.0963132	-7.9606720	11.040818	-8.5084906	2.6841250
		0.8	G_0	1.3027014	-1.5187590	6.3057897	-15.064791	21.251358	-15.901718	4.8148656
			G_1	0.2577871	0.0308774	3.8532491	-9.8137504	13.632488	-10.277173	3.1213918

Table C.12
Influence Coefficients For A Longitudinal Semi-Elliptical Surface Crack In A Cylinder – Inside Surface

t/R_i	a/c	a/t	G_i	A_0	A_1	A_2	A_3	A_4	A_5	A_6
1.0	2	0	G_0	0.8150546	-0.5623828	1.4465771	-4.6778133	8.4192164	-7.9025932	2.9866351
			G_1	0.1359146	0.0702340	3.5558581	-11.034445	16.967724	-14.126991	4.8706612
		0.2	G_0	0.7967907	-0.9356917	4.2359839	-13.024751	21.072386	-17.564543	5.9427531
			G_1	0.1286709	0.0672126	3.3363822	-10.050673	15.049986	-12.346706	4.2351011
		0.4	G_0	0.7821266	-0.9351264	4.6041832	-14.351050	23.221650	-19.300309	6.5066994
			G_1	0.1302079	-0.0027689	3.8273524	-11.520981	17.340144	-14.169548	4.8192152
		0.6	G_0	0.7800960	-0.8769273	4.3923941	-13.617935	21.726416	-17.843686	5.9715188
			G_1	0.1287406	0.0493532	3.4929744	-10.398601	15.372631	-12.449585	4.2275445
		0.8	G_0	0.7880845	-0.7631360	3.7695776	-11.376091	17.585100	-14.173237	4.7190746
			G_1	0.1290012	0.1457613	2.9297051	-8.5063451	12.097151	-9.6368174	3.2736298

Notes:

1. Interpolation of the influence coefficients, G_i, may be used for intermediate values of t/R_i, a/c, and a/t.

2. The value of the influence coefficients at the surface point of the crack defined by $\varphi = 0^0$ are equal to: $G_i = A_0$.

3. The value of the influence at the deepest point of the crack defined by $\varphi = 90^0$ are equal to: $G_i = \sum_{n=0}^{6} A_n$.

Table C.13
Influence Coefficients For A Longitudinal Semi-Elliptical Surface Crack In A Cylinder – Outside Surface

t/R_i	a/c	a/t	G_i	A_0	A_1	A_2	A_3	A_4	A_5	A_6
0.0	0.03125	0	G_0	0.1965046	2.9373464	-5.2582823	7.4889153	-6.9282667	3.3673349	-0.6677966
			G_1	0.0051780	0.1750280	2.7718680	-4.6457154	4.6780502	-3.2768090	0.9840994
		0.2	G_0	0.2080760	3.0112422	-5.1048701	7.6348715	-6.8347547	2.7940766	-0.3882688
			G_1	0.0084834	0.2406767	2.4574292	-3.6452421	3.6142837	-2.8451814	0.9270638
		0.4	G_0	0.2357940	3.0822400	-3.5792100	3.9476890	1.9131590	-6.8872200	3.1896800
			G_1	0.0145140	0.4038000	1.6422700	-0.3906100	-0.6480700	-0.2940300	0.2514900
		0.6	G_0	0.2902240	3.6892050	-4.5739100	11.709890	-6.3750000	-5.8894100	4.2452400
			G_1	0.0208890	0.7016780	0.1631840	5.7072160	-8.2075800	3.4561120	-0.4454700
		0.8	G_0	0.5163550	2.5310830	14.712900	-43.621800	101.06570	-116.08100	46.190900
			G_1	0.0825460	0.4971770	4.6064810	-7.3326700	21.148620	-29.345100	12.491400
0.0	0.0625	0	G_0	0.2695332	2.1626001	-1.6551569	-1.2970208	4.5604304	-4.3163876	1.4010655
			G_1	0.0138667	0.1827458	2.5749608	-3.9044679	3.3556301	-2.1772209	0.6420134
		0.2	G_0	0.2845892	2.2264055	-1.4546190	-1.5760719	5.1131083	-4.9485443	1.6207574
			G_1	0.0199077	0.2210874	2.4642047	-3.5898625	3.1624039	-2.2403780	0.6965751
		0.4	G_0	0.3261480	2.5200870	-1.8847000	2.1798740	-1.4597100	-0.1886500	0.2393400
			G_1	0.0294120	0.3699370	1.9220850	-1.2071500	-0.4394000	0.2737550	-0.0395200
		0.6	G_0	0.4166330	3.1566470	-2.6248900	7.7325910	-9.6927800	3.6428700	-0.0892000
			G_1	0.0598460	0.4340740	2.6811560	-3.1936600	4.0753720	-4.6940200	1.8285500
		0.8	G_0	0.6540140	3.4231920	3.8158050	-4.1586900	3.4715330	-10.310400	6.6280000
			G_1	0.1214780	0.6975490	2.9718330	-1.3036500	-0.0754900	-3.0465100	2.1670000
0.0	0.125	0	G_0	0.4065238	0.7772483	3.8861644	-12.573943	16.760207	-11.014593	2.8706957
			G_1	0.0320270	0.1825342	2.2670449	-2.7076615	1.2088194	-0.3777430	0.0763155
		0.2	G_0	0.4242116	1.0089302	3.2973815	-12.159726	17.873386	-12.868668	3.6281712
			G_1	0.0429859	0.2033811	2.2563818	-2.8752160	1.8152558	-1.0512327	0.3181077
		0.4	G_0	0.4917770	1.6592320	-0.1080400	0.1793240	-2.7076100	3.3680620	-1.3489700
			G_1	0.0634270	0.3722500	1.6231670	-0.5306500	-2.0007400	1.8943780	-0.5880300
		0.6	G_0	0.6591820	1.8759140	1.0212600	-1.7698000	-0.5653600	1.2479960	-0.4376600
			G_1	0.1116040	0.4714500	1.7940590	-0.7557600	-1.4901700	1.0852180	-0.2113700
		0.8	G_0	0.9809330	1.8846320	4.8020780	-8.0580200	0.4447850	3.4772660	-1.0567500
			G_1	0.2039950	0.4800150	2.8822430	-2.5890100	-0.9683000	1.5372370	-0.3750200
0.0	0.25	0	G_0	0.6152816	-0.3348694	6.2955620	-15.590618	19.299508	-12.488107	3.3010035
			G_1	0.0703566	0.2828152	1.4036169	-0.6511596	-1.2076596	1.0318656	-0.2423741
		0.2	G_0	0.6385889	-0.3095132	6.5329787	-16.622882	21.056641	-13.850120	3.6988146
			G_1	0.0840059	0.1999367	1.8218113	-1.7756899	0.3757186	-0.0785358	0.0643386
		0.4	G_0	0.7390420	0.0548160	4.0842620	-7.5883100	5.4047530	-1.0146100	-0.3483400
			G_1	0.1164500	0.2479880	1.8282520	-1.7169900	0.1912120	0.1165770	-0.0186100
		0.6	G_0	0.9461210	-0.1858800	5.5867460	-9.8634900	5.9596870	0.1296440	-1.0026100
			G_1	0.1778050	0.2056680	2.0979210	-1.8039500	-0.5558700	1.1461400	-0.4206600
		0.8	G_0	1.2452110	-0.6921900	8.3260620	-14.948000	8.6936910	0.4755790	-1.3926600
			G_1	0.2585640	0.1548890	2.1170240	-0.4910000	-4.6146100	5.4550750	-1.9663300
0.0	0.5	0	G_0	0.8776607	-0.6729719	3.7721411	-6.5209060	6.3377934	-3.7028038	0.9872447
			G_1	0.1277541	0.4368502	0.4904522	1.0427434	-2.9631236	2.0826525	-0.5184313
		0.2	G_0	0.9003948	-0.8850488	5.2743239	-11.267523	13.890755	-9.6373584	2.8183906
			G_1	0.1404409	0.3215397	1.1010666	-1.0257556	0.6943940	-1.0793186	0.5410929
		0.4	G_0	1.0058060	-0.7322600	2.9951940	-1.9459200	-3.2613500	5.1424570	-2.0306200
			G_1	0.1740870	0.3051630	1.2070310	-0.6720500	-1.0651300	1.1445590	-0.3644800
		0.6	G_0	1.1826010	-1.1072500	3.9623640	-2.7781300	-4.3097300	7.2772750	-2.9648200
			G_1	0.2277120	0.1701170	1.5499470	-1.1051200	-0.8333700	1.1717060	-0.4194500
		0.8	G_0	1.3833380	-1.3900300	4.3755780	-3.7372600	-2.5403200	5.3036000	-2.0932400
			G_1	0.2820110	0.0839230	1.7258580	-1.5358100	-0.0635600	0.5006780	-0.1982200

Table C.13
Influence Coefficients For A Longitudinal Semi-Elliptical Surface Crack In A Cylinder – Outside Surface

t/R_i	a/c	a/t	G_i	A_0	A_1	A_2	A_3	A_4	A_5	A_6
0.0	1	0	G_0	1.1977992	-0.5244870	0.1498299	2.3284866	-5.1058499	4.3469049	-1.3487980
			G_1	0.1870117	0.6987352	0.1316900	0.7269255	-2.5259384	2.1756251	-0.6540458
		0.2	G_0	1.2263282	-1.1608467	4.4744783	-11.584231	17.811241	-14.408250	4.6998279
			G_1	0.2154786	0.2441623	2.8107820	-7.6574580	11.171413	-9.0053693	2.9542871
		0.4	G_0	1.2989480	-0.9978000	1.9479540	-1.3002700	-1.4940100	2.8306230	-1.2126000
			G_1	0.2386246	0.1447774	3.3198992	-9.2456599	13.823512	-11.223715	3.6868232
		0.6	G_0	1.3971180	-1.1348400	1.7918740	-0.4202600	-2.8679300	3.7685480	-1.4405000
			G_1	0.2445870	0.5326670	0.5939690	-0.0361800	-2.0163100	2.2167010	-0.7782200
		0.8	G_0	1.5117010	-1.3244800	1.7568350	-0.1337900	-2.8629300	3.2953270	-1.1412400
			G_1	0.2704470	0.5113280	0.5357440	-0.0327300	-1.5570200	1.5570970	-0.5094600
0.0	2	0	G_0	0.8150546	-0.5623828	1.4465771	-4.6778133	8.4192164	-7.9025932	2.9866351
			G_1	0.1359146	0.0702340	3.5558581	-11.034445	16.967724	-14.126991	4.8706612
		0.2	G_0	0.8463715	-1.0011024	4.0052312	-11.937181	19.189548	-16.039296	5.4674371
			G_1	0.1395121	0.0753999	3.1895604	-9.5540932	14.214316	-11.649525	4.0073308
		0.4	G_0	0.8570045	-1.0183085	3.9957306	-11.886878	19.152747	-16.047480	5.4801806
			G_1	0.1436696	0.0544018	3.2816127	-9.8164232	14.610963	-11.942138	4.0907797
		0.6	G_0	0.8839861	-1.0765270	4.0774087	-11.976171	19.173189	-15.996207	5.4501217
			G_1	0.1504185	0.0478401	3.2579960	-9.6921199	14.370843	-11.736129	4.0258411
		0.8	G_0	0.9033134	-0.9619755	2.8501500	-7.6366897	11.596116	-9.4828625	3.2550163
			G_1	0.1458559	0.2313881	1.9882138	-5.5546045	7.4196069	-5.8965053	2.0855563
0.01	0.03125	0	G_0	0.1965046	2.9373464	-5.2582823	7.4889153	-6.9282667	3.3673349	-0.6677966
			G_1	0.0051780	0.1750280	2.7718680	-4.6457154	4.6780502	-3.2768090	0.9840994
		0.2	G_0	0.2138782	2.4750252	-1.2287668	-4.0075659	10.335171	-9.5704005	3.0927956
			G_1	0.0075736	0.2344660	2.4810298	-3.7389842	3.7733192	-2.9707472	0.9655728
		0.4	G_0	0.2324070	3.0534560	-3.4791800	3.6288040	2.8534420	-7.8640400	3.5080100
			G_1	0.0090690	0.3929290	1.6585750	-0.4195300	-0.4687700	-0.4895200	0.3051300
		0.6	G_0	0.2702790	3.6742680	-5.4506000	14.673720	-9.6138800	-3.5469800	3.2402500
			G_1	0.0135480	0.6966430	-0.1423800	6.5888590	-8.9248900	3.9512840	-0.7275400
		0.8	G_0	0.4201630	3.2227600	6.0926870	-21.407000	81.165870	-105.68400	42.304800
			G_1	0.0451780	0.8660820	0.6788660	3.1439070	9.8824090	-22.058800	9.8817900
0.01	0.0625	0	G_0	0.2695332	2.1626001	-1.6551569	-1.2970208	4.5604304	-4.3163876	1.4010655
			G_1	0.0138667	0.1827458	2.5749608	-3.9044679	3.3556301	-2.1772209	0.6420134
		0.2	G_0	0.3009539	1.7912734	0.8670775	-6.9946825	11.455578	-8.5937165	2.4360990
			G_1	0.0194819	0.2065054	2.6293195	-4.3818393	4.7973348	-3.7470555	1.2084547
		0.4	G_0	0.3280520	2.5901900	-2.1894200	2.3456720	-0.3205300	-1.9618200	0.9696200
			G_1	0.0260390	0.4612930	1.2629800	0.8720110	-3.5821100	2.6029280	-0.7233600
		0.6	G_0	0.4103170	3.4373160	-4.7250300	14.025440	-17.047300	7.4350500	-0.8385600
			G_1	0.0550830	0.5361340	1.8981060	-0.6893400	0.8014830	-2.6604000	1.3066300
		0.8	G_0	0.6491600	3.5962240	2.0970240	2.6131640	0.5247410	-14.913300	9.6012600
			G_1	0.1176190	0.7527130	2.4225760	0.9070930	-1.0257200	-4.5224300	3.1016800
0.01	0.125	0	G_0	0.4065238	0.7772483	3.8861644	-12.573943	16.760207	-11.014593	2.8706957
			G_1	0.0320270	0.1825342	2.2670449	-2.7076615	1.2088194	-0.3777430	0.0763155
		0.2	G_0	0.4148168	1.1474441	1.7284441	-6.1319982	7.6187598	-4.7707753	1.1968314
			G_1	0.0483704	0.0169824	3.9147652	-9.0442049	12.537266	-9.7790670	3.0128034
		0.4	G_0	0.4972990	1.5382660	0.9543690	-3.4496900	3.4687010	-1.6986900	0.2430300
			G_1	0.0629740	0.3821060	1.5827310	-0.3922800	-2.1832500	2.0019660	-0.6135000
		0.6	G_0	0.6613540	1.9086020	0.9832580	-1.2632200	-1.3863400	1.7681160	-0.5715500
			G_1	0.1127330	0.4681870	1.8754590	-0.8796100	-1.2883700	0.8847250	-0.1438600
		0.8	G_0	0.9969100	1.9634260	4.8633420	-6.9046400	-1.5148200	4.2963280	-1.0385500
			G_1	0.2105360	0.4661310	3.2282240	-3.3926400	0.4841570	0.0394490	0.1974500

Table C.13
Influence Coefficients For A Longitudinal Semi-Elliptical Surface Crack In A Cylinder – Outside Surface

t/R_i	a/c	a/t	G_i	A_0	A_1	A_2	A_3	A_4	A_5	A_6
0.01	0.25	0	G_0	0.6152816	-0.3348694	6.2955620	-15.590618	19.299508	-12.488107	3.3010035
			G_1	0.0703566	0.2828152	1.4036169	-0.6511596	-1.2076596	1.0318656	-0.2423741
		0.2	G_0	0.6260510	-0.2265274	6.9684962	-19.857860	27.709243	-19.572353	5.4946193
			G_1	0.0907270	0.1716775	2.5085021	-4.9758660	6.1431857	-4.7142903	1.4602442
		0.4	G_0	0.7427500	0.0470470	4.2013450	-7.9240300	5.9197900	-1.4176300	-0.2253900
			G_1	0.1183660	0.2202920	2.0681150	-2.5351300	1.5892970	-1.0403300	0.3487600
		0.6	G_0	0.9567890	-0.1725500	5.6362060	-9.8580500	5.8066120	0.2958180	-1.0611700
			G_1	0.1805700	0.2226460	2.0172020	-1.4629900	-1.1806500	1.6683430	-0.5867200
		0.8	G_0	1.3100100	-1.4349000	14.376600	-35.168100	42.221560	-26.611500	7.0832000
			G_1	0.2658870	0.2474310	1.4942640	1.7915740	-8.5849000	8.6773360	-2.9576800
0.01	0.5	0	G_0	0.8776607	-0.6729719	3.7721411	-6.5209060	6.3377934	-3.7028038	0.9872447
			G_1	0.1277541	0.4368502	0.4904522	1.0427434	-2.9631236	2.0826525	-0.5184313
		0.2	G_0	0.9074272	-1.0994201	6.7673813	-15.863097	20.705328	-14.454389	4.1256769
			G_1	0.1495038	0.1587994	2.2591841	-4.5394919	5.7148362	-4.4982384	1.4410683
		0.4	G_0	1.0125390	-0.7568900	3.1311310	-2.2752700	-2.8387900	4.8667220	-1.9590900
			G_1	0.1753200	0.3073370	1.1980380	-0.6340400	-1.1325100	1.1968380	-0.3793700
		0.6	G_0	1.1956150	-1.1378000	4.1718440	-3.3722900	-3.4456700	6.6512090	-2.7867200
			G_1	0.2292050	0.2061920	1.3306330	-0.4513200	-1.8161600	1.8921330	-0.6245200
		0.8	G_0	1.4139890	-1.4985700	5.0657640	-5.7703800	0.4973700	3.0329120	-1.4197400
			G_1	0.2896610	0.0882030	1.6827580	-1.3490500	-0.4354500	0.8253610	-0.3010300
0.01	1	0	G_0	1.1977992	-0.5244870	0.1498299	2.3284866	-5.1058499	4.3469049	-1.3487980
			G_1	0.1870117	0.6987352	0.1316900	0.7269255	-2.5259384	2.1756251	-0.6540458
		0.2	G_0	1.2219944	-1.2333687	5.0312977	-13.549512	21.104009	-16.993209	5.4694705
			G_1	0.2150830	0.1957502	3.1572284	-8.8200177	13.041658	-10.425024	3.3649964
		0.4	G_0	1.3069770	-1.0234600	2.0351750	-1.4790500	-1.2970400	2.7226080	-1.1890400
			G_1	0.2182770	0.5583990	0.7123630	-0.4628400	-1.4273700	1.8443680	-0.6917100
		0.6	G_0	1.4118930	-1.2128500	2.1731690	-1.4236900	-1.4877900	2.8257990	-1.1874200
			G_1	0.2486310	0.5073370	0.7680320	-0.6344600	-0.9874100	1.3617270	-0.5050000
		0.8	G_0	1.5327350	-1.4057100	2.1493270	-1.2998000	-1.0510400	1.8996060	-0.7187000
			G_1	0.2759430	0.4993180	0.5707200	-0.0960600	-1.5281700	1.5841410	-0.5294400
0.01	2	0	G_0	0.8150546	-0.5623828	1.4465771	-4.6778133	8.4192164	-7.9025932	2.9866351
			G_1	0.1359146	0.0702340	3.5558581	-11.034445	16.967724	-14.126991	4.8706612
		0.2	G_0	0.8182987	-0.9750326	4.0974302	-12.658801	20.765368	-17.441363	5.9109102
			G_1	0.1330319	0.0540205	3.3490248	-10.173407	15.321858	-12.541021	4.2720166
		0.4	G_0	0.8343927	-0.3351370	-0.7134755	3.3094161	-6.0713158	4.8139372	-1.3245293
			G_1	0.1361217	0.0308624	3.4638886	-10.533385	15.878401	-12.946378	4.3843584
		0.6	G_0	0.8600665	-0.3540640	-0.9003047	4.0339274	-7.2855701	5.7801566	-1.6177453
			G_1	0.1467987	0.0215030	3.4602749	-10.477254	15.776469	-12.882015	4.3737291
		0.8	G_0	0.9172330	-1.0076975	3.0568469	-8.2482710	12.624440	-10.377963	3.5671701
			G_1	0.1497781	0.0258058	3.3588241	-10.008896	14.518295	-11.284278	3.6504092
0.01667	0.03125	0	G_0	0.1965046	2.9373464	-5.2582823	7.4889153	-6.9282667	3.3673349	-0.6677966
			G_1	0.0051780	0.1750280	2.7718680	-4.6457154	4.6780502	-3.2768090	0.9840994
		0.2	G_0	0.2137018	2.4716292	-1.1955278	-4.1279147	10.564513	-9.7724089	3.1582282
			G_1	0.0074964	0.2331584	2.4891031	-3.7654612	3.8313393	-3.0295323	0.9870984
		0.4	G_0	0.2306780	3.0388050	-3.4728800	3.6385670	2.9071580	-7.9264700	3.5188400
			G_1	0.0109380	0.4020170	1.5438030	-0.0383700	-1.0428800	-0.0524400	0.1690900
		0.6	G_0	0.2647120	3.6557700	-5.5472500	14.585300	-8.9129600	-4.1661800	3.3668200
			G_1	0.0186290	0.6598410	0.0944350	5.5205580	-6.8688900	2.3000600	-0.2605800
		0.8	G_0	0.3916070	3.5824480	2.4629600	-10.937900	63.878550	-89.418500	36.130200
			G_1	0.0377860	0.9314520	-0.0349700	4.7321390	7.3105530	-18.985500	8.4478500

Table C.13
Influence Coefficients For A Longitudinal Semi-Elliptical Surface Crack In A Cylinder – Outside Surface

t/R_i	a/c	a/t	G_i	A_0	A_1	A_2	A_3	A_4	A_5	A_6
0.01667	0.0625	0	G_0	0.2695332	2.1626001	-1.6551569	-1.2970208	4.5604304	-4.3163876	1.4010655
			G_1	0.0138667	0.1827458	2.5749608	-3.9044679	3.3556301	-2.1772209	0.6420134
		0.2	G_0	0.2852680	2.0769228	-0.9978735	-1.2931167	2.6484224	-1.9164331	0.4609809
			G_1	0.0189931	0.2154011	2.5632146	-4.1568147	4.4288027	-3.4553431	1.1186828
		0.4	G_0	0.3281130	2.3901810	-0.8095800	-1.4210300	4.8415630	-5.4354900	1.8791800
			G_1	0.0292320	0.3424400	2.1206150	-1.8136200	0.6498240	-0.6508300	0.2469300
		0.6	G_0	0.3983790	3.2298950	-3.5609200	11.585980	-14.538900	6.4780230	-0.8574500
			G_1	0.0533250	0.4541290	2.3964770	-2.0990900	2.9773820	-4.2600100	1.7406100
		0.8	G_0	0.6074810	3.5000360	1.9324190	4.0078860	-0.6767400	-14.170400	9.1300900
			G_1	0.1057170	0.7235000	2.3194730	1.3286790	-0.9833400	-4.8384300	3.1575700
0.01667	0.125	0	G_0	0.4065238	0.7772483	3.8861644	-12.573943	16.760207	-11.014593	2.8706957
			G_1	0.0320270	0.1825342	2.2670449	-2.7076615	1.2088194	-0.3777430	0.0763155
		0.2	G_0	0.4148376	1.1488796	1.7244494	-6.1093380	7.5825708	-4.7472976	1.1912448
			G_1	0.0483941	0.0166081	3.9196323	-9.0609034	12.573746	-9.8159555	3.0261057
		0.4	G_0	0.4991930	1.4929330	1.3181360	-4.6222100	5.4026230	-3.2510100	0.7215900
			G_1	0.0638630	0.3577190	1.7903870	-1.1250500	-0.8936300	0.9146490	-0.2640700
		0.6	G_0	0.6594470	1.9513050	0.7037310	-0.1328800	-3.1790500	3.0881030	-0.9571500
			G_1	0.1123460	0.4769800	1.8180370	-0.6167100	-1.6918000	1.1653880	-0.2229600
		0.8	G_0	0.9986260	2.0025290	4.7810950	-6.0706900	-2.3363000	4.2175710	-0.8170400
			G_1	0.2105640	0.5008290	3.0054380	-2.3954100	-1.0374800	1.0415670	-0.0534200
0.01667	0.25	0	G_0	0.6152816	-0.3348694	6.2955620	-15.590618	19.299508	-12.488107	3.3010035
			G_1	0.0703566	0.2828152	1.4036169	-0.6511596	-1.2076596	1.0318656	-0.2423741
		0.2	G_0	0.6300329	-0.2862567	7.3164619	-20.805174	29.055169	-20.534766	5.7677852
			G_1	0.0901070	0.1840622	2.4321564	-4.7467316	5.7958716	-4.4552013	1.3845027
		0.4	G_0	0.7457850	0.0066950	4.5171440	-8.9481000	7.5885640	-2.7405800	0.1792400
			G_1	0.1182950	0.2324830	1.9682530	-2.1456800	0.8739200	-0.4224000	0.1461600
		0.6	G_0	0.9598760	-0.1312600	5.3719100	-8.8692700	4.1076570	1.6665860	-1.4860300
			G_1	0.1817520	0.2311760	1.9819240	-1.3437900	-1.3528700	1.7795640	-0.6136800
		0.8	G_0	1.3010250	-0.8000000	9.5285520	-18.152100	13.249470	-3.0269200	-0.2860500
			G_1	0.2815970	0.0012600	3.4198490	-4.6353300	2.0735050	0.0924150	-0.2850300
0.01667	0.5	0	G_0	0.8776607	-0.6729719	3.7721411	-6.5209060	6.3377934	-3.7028038	0.9872447
			G_1	0.1277541	0.4368502	0.4904522	1.0427434	-2.9631236	2.0826525	-0.5184313
		0.2	G_0	0.9094180	-1.1229795	6.9181225	-16.309875	21.379833	-14.955815	4.2713814
			G_1	0.1505282	0.1451739	2.3390416	-4.7612919	6.0370436	-4.7336784	1.5092378
		0.4	G_0	1.0137270	-0.7517100	3.1226580	-2.2992700	-2.7311100	4.7379060	-1.9093200
			G_1	0.1760030	0.3062100	1.1968010	-0.5997200	-1.2268900	1.2973610	-0.4173000
		0.6	G_0	1.2008330	-1.1467100	4.2107140	-3.4130300	-3.4601300	6.6981550	-2.8074000
			G_1	0.2308490	0.2030300	1.3593140	-0.5530200	-1.6299900	1.7276510	-0.5695300
		0.8	G_0	1.4228920	-1.4437600	4.6822680	-4.5430000	-1.4261800	4.4784380	-1.8377400
			G_1	0.2948140	0.0607990	1.8702520	-1.9379200	0.5080380	0.0785840	-0.0704500
0.01667	1	0	G_0	1.1977992	-0.5244870	0.1498299	2.3284866	-5.1058499	4.3469049	-1.3487980
			G_1	0.1870117	0.6987352	0.1316900	0.7269255	-2.5259384	2.1756251	-0.6540458
		0.2	G_0	1.2229223	-1.2350945	5.0353697	-13.554987	21.107245	-16.993613	5.4693935
			G_1	0.2141793	0.2143843	3.0512609	-8.5440546	12.678058	-10.188549	3.3045727
		0.4	G_0	1.3069170	-0.9903600	1.7866620	-0.6452900	-2.7041200	3.8845890	-1.5614400
			G_1	0.2195930	0.5416490	0.8301860	-0.8579700	-0.7616300	1.3017760	-0.5219100
		0.6	G_0	1.4149780	-1.2145600	2.2099370	-1.6537800	-0.9621000	2.3118750	-1.0052600
			G_1	0.2492340	0.5158650	0.7022660	-0.4092700	-1.3769500	1.6896770	-0.6113900
		0.8	G_0	1.5405510	-1.4286100	2.2553870	-1.5994600	-0.6101900	1.5774700	-0.6256600
			G_1	0.2788740	0.4847010	0.6491960	-0.3234800	-1.1852500	1.3257010	-0.4524700

Table C.13
Influence Coefficients For A Longitudinal Semi-Elliptical Surface Crack In A Cylinder – Outside Surface

t/R_i	a/c	a/t	G_i	A_0	A_1	A_2	A_3	A_4	A_5	A_6
0.01667	2	0	G_0	0.8150546	-0.5623828	1.4465771	-4.6778133	8.4192164	-7.9025932	2.9866351
			G_1	0.1359146	0.0702340	3.5558581	-11.034445	16.967724	-14.126991	4.8706612
		0.2	G_0	0.8182509	-0.9683874	4.0481966	-12.506099	20.531123	-17.266667	5.8604688
			G_1	0.1334825	0.0474146	3.3890896	-10.287120	15.485607	-12.657711	4.3047611
		0.4	G_0	0.8362279	-0.3571232	-0.5678228	2.8372219	-5.3004184	4.2029047	-1.1376264
			G_1	0.1356418	0.0411710	3.4054647	-10.380241	15.670811	-12.805065	4.3460700
		0.6	G_0	0.8628933	-0.3858659	-0.6981090	3.3951106	-6.2590966	4.9745741	-1.3727913
			G_1	0.1469324	0.0235743	3.4453527	-10.434511	15.714005	-12.835899	4.3600722
		0.8	G_0	0.9191929	-1.0122491	3.0710619	-8.2917080	12.689191	-10.419864	3.5764034
			G_1	0.1506695	0.0175076	3.4048063	-10.143058	14.721138	-11.435621	3.6945046
0.05	0.03125	0	G_0	0.1965046	2.9373464	-5.2582823	7.4889153	-6.9282667	3.3673349	-0.6677966
			G_1	0.0051780	0.1750280	2.7718680	-4.6457154	4.6780502	-3.2768090	0.9840994
		0.2	G_0	0.2126857	2.4579374	-1.1427912	-4.2121606	10.672531	-9.8506499	3.1779116
			G_1	0.0070880	0.2281639	2.4965869	-3.7556676	3.8111506	-3.0085539	0.9759280
		0.4	G_0	0.2274500	2.9794860	-3.2917300	3.1593030	3.6533720	-8.4864000	3.6768600
			G_1	0.0070090	0.3783660	1.6174000	-0.2661400	-0.6795200	-0.2841700	0.2120000
		0.6	G_0	0.2533640	3.6313610	-6.2242000	17.316250	-14.595100	1.3727100	1.3897900
			G_1	0.0073650	0.7111170	-0.6229600	8.0627590	-11.551800	6.5540000	-1.7339300
		0.8	G_0	0.3498690	3.6190920	0.1968900	-4.0412300	46.267320	-68.423400	27.621900
			G_1	0.0273550	0.8977570	-0.3675800	5.5541200	3.4269510	-12.911100	5.6559800
0.05	0.0625	0	G_0	0.2695332	2.1626001	-1.6551569	-1.2970208	4.5604304	-4.3163876	1.4010655
			G_1	0.0138667	0.1827458	2.5749608	-3.9044679	3.3556301	-2.1772209	0.6420134
		0.2	G_0	0.2848454	2.0654031	-0.9077591	-1.5276620	3.0161277	-2.2090336	0.5488481
			G_1	0.0187192	0.2128839	2.5716802	-4.1560222	4.4282009	-3.4585236	1.1185246
		0.4	G_0	0.3212960	2.3448030	-0.7426900	-1.4194200	5.0119970	-5.6810200	1.9536500
			G_1	0.0260960	0.3422190	2.0005180	-1.3336400	-0.0578300	-0.1230500	0.0775000
		0.6	G_0	0.3733960	3.1033220	-3.5889700	11.529910	-12.947400	4.6508610	-0.3427200
			G_1	0.0456010	0.3836560	2.5608530	-2.7553700	4.6129230	-5.6717900	2.1083700
		0.8	G_0	0.5226140	3.4234390	-0.6548100	9.7485540	-3.2235900	-13.877600	8.5410000
			G_1	0.0769380	0.7188470	1.2769760	3.5804480	-2.1787000	-4.2928600	2.6987400
0.05	0.125	0	G_0	0.4065238	0.7772483	3.8861644	-12.573943	16.760207	-11.014593	2.8706957
			G_1	0.0320270	0.1825342	2.2670449	-2.7076615	1.2088194	-0.3777430	0.0763155
		0.2	G_0	0.4152094	1.1478676	1.7621671	-6.1869855	7.6894963	-4.8377705	1.2221148
			G_1	0.0483124	0.0191548	3.9027693	-8.9811618	12.436651	-9.7095804	2.9940655
		0.4	G_0	0.4926390	1.5721320	0.6544250	-2.0393900	0.9779030	0.3354330	-0.4067600
			G_1	0.0627280	0.3528700	1.7990370	-1.0437500	-1.0428300	1.0290420	-0.3034100
		0.6	G_0	0.6429920	1.9132270	0.8599370	-0.1649600	-2.3392000	1.7431370	-0.4243800
			G_1	0.1057820	0.4826430	1.7091680	-0.0792900	-2.2797500	1.3984440	-0.2595000
		0.8	G_0	0.9533570	1.8590510	5.3300090	-6.3155200	0.9677320	-0.9493900	1.2538800
			G_1	0.1952550	0.4649740	3.0762920	-2.1340900	-0.3677000	-0.4107900	0.5626800
0.05	0.25	0	G_0	0.6152816	-0.3348694	6.2955620	-15.590618	19.299508	-12.488107	3.3010035
			G_1	0.0703566	0.2828152	1.4036169	-0.6511596	-1.2076596	1.0318656	-0.2423741
		0.2	G_0	0.6316981	-0.2961952	7.4180799	-21.116428	29.573759	-20.968968	5.9077913
			G_1	0.0906535	0.1788838	2.4733841	-4.8681054	5.9984214	-4.6244285	1.4384031
		0.4	G_0	0.7461440	0.0677980	4.1232100	-7.5000100	5.1211920	-0.7514200	-0.4390900
			G_1	0.1175070	0.2670220	1.7514510	-1.4364300	-0.2320500	0.4060910	-0.0954800
		0.6	G_0	0.9707830	-0.1536000	5.7123690	-9.6038400	5.1974000	0.7373360	-1.1792900
			G_1	0.1855560	0.2214630	2.0970730	-1.5522700	-1.0883500	1.5718930	-0.5495800
		0.8	G_0	1.3366720	-0.8115500	10.008990	-18.432900	13.074520	-2.9741300	-0.2298200
			G_1	0.2982610	-0.1094100	4.3991850	-7.5259600	6.7389080	-3.7449200	0.9458400

Table C.13
Influence Coefficients For A Longitudinal Semi-Elliptical Surface Crack In A Cylinder – Outside Surface

t/R_i	a/c	a/t	G_i	A_0	A_1	A_2	A_3	A_4	A_5	A_6
0.05	0.5	0	G_0	0.8776607	-0.6729719	3.7721411	-6.5209060	6.3377934	-3.7028038	0.9872447
			G_1	0.1277541	0.4368502	0.4904522	1.0427434	-2.9631236	2.0826525	-0.5184313
		0.2	G_0	0.9094785	-1.0704029	6.5969031	-15.339481	19.891956	-13.831397	3.9381913
			G_1	0.1511354	0.1498618	2.3171901	-4.6991089	5.9510689	-4.6766956	1.4944878
		0.4	G_0	1.0187560	-0.7252200	2.9510620	-1.6965300	-3.7495300	5.5630180	-2.1679600
			G_1	0.1777910	0.3097340	1.1782720	-0.5207400	-1.3685100	1.4131580	-0.4534400
		0.6	G_0	1.2191680	-1.1624100	4.3039990	-3.4956600	-3.5264500	6.8389740	-2.8685000
			G_1	0.2368950	0.1990950	1.3665370	-0.4508000	-1.9303400	2.0355870	-0.6795900
		0.8	G_0	1.4670860	-1.4874600	4.9131560	-4.8217400	-1.4111900	4.6213220	-1.8973500
			G_1	0.3108650	0.0205500	2.1111910	-2.5101100	1.2177130	-0.3862800	0.0564600
0.05	1	0	G_0	1.1977992	-0.5244870	0.1498299	2.3284866	-5.1058499	4.3469049	-1.3487980
			G_1	0.1870117	0.6987352	0.1316900	0.7269255	-2.5259384	2.1756251	-0.6540458
		0.2	G_0	1.2267227	-1.2309827	4.9938199	-13.435866	20.942460	-16.881717	5.4396233
			G_1	0.2162188	0.2008041	3.1282931	-8.7575323	12.984058	-10.406989	3.3659724
		0.4	G_0	1.3146080	-1.0024200	1.8454760	-0.8744700	-2.2504400	3.4654690	-1.4164400
			G_1	0.2217160	0.5404660	0.8385940	-0.8990200	-0.6786400	1.2271190	-0.4969400
		0.6	G_0	1.4273930	-1.1722500	1.8107740	-0.2671700	-3.3078700	4.2258110	-1.6062100
			G_1	0.2553870	0.4839230	0.9022980	-1.0407000	-0.3630800	0.8909080	-0.3661900
		0.8	G_0	1.5669880	-1.4243900	2.0816990	-1.0406600	-1.4652500	2.2092880	-0.8044400
			G_1	0.2873270	0.4823500	0.6339350	-0.2953100	-1.2046800	1.3245420	-0.4469300
0.05	2	0	G_0	0.8150546	-0.5623828	1.4465771	-4.6778133	8.4192164	-7.9025932	2.9866351
			G_1	0.1359146	0.0702340	3.5558581	-11.034445	16.967724	-14.126991	4.8706612
		0.2	G_0	0.8410025	-1.0986979	4.6833289	-14.254400	23.077894	-19.117803	6.3907936
			G_1	0.1393039	0.0157399	3.5854198	-10.908384	16.465690	-13.405784	4.5256310
		0.4	G_0	0.8552595	-1.1713096	5.0505801	-15.423750	24.918773	-20.491114	6.7824876
			G_1	0.1433068	-0.0051111	3.7018421	-11.315879	17.126325	-13.897780	4.6633443
		0.6	G_0	0.8922163	-1.1791312	4.7085484	-14.194993	22.986733	-19.057873	6.3764561
			G_1	0.1531695	0.0011284	3.5772066	-10.858841	16.387974	-13.348661	4.5099477
		0.8	G_0	0.9462314	-1.6448744	7.4204133	-22.617661	35.895514	-28.367552	8.8839133
			G_1	0.1651920	-0.1064856	4.2963413	-13.173123	19.754851	-15.432417	4.9095345
0.1	0.03125	0	G_0	0.1965046	2.9373464	-5.2582823	7.4889153	-6.9282667	3.3673349	-0.6677966
			G_1	0.0051780	0.1750280	2.7718680	-4.6457154	4.6780502	-3.2768090	0.9840994
		0.2	G_0	0.2114908	2.4425792	-1.0853387	-4.3244076	10.821413	-9.9682430	3.2163776
			G_1	0.0066363	0.2226202	2.5052241	-3.7606471	3.8258183	-3.0282477	0.9830947
		0.4	G_0	0.2246500	2.9397340	-3.0871500	2.4310320	4.8690240	-9.5429900	4.0540600
			G_1	0.0148750	0.3763240	1.5876360	-0.2147600	-0.6979300	-0.3343000	0.2518400
		0.6	G_0	0.2495210	3.4159580	-4.9404800	13.042320	-8.3791000	-3.1660100	2.7863600
			G_1	0.0200470	0.6258430	-0.0433000	5.9592140	-8.1321500	3.8137330	-0.8504100
		0.8	G_0	0.3404240	2.7101300	5.4741060	-20.271800	65.828770	-78.807600	29.760500
			G_1	0.0306660	0.6856860	0.6916680	2.5535420	5.9341450	-13.208000	5.4184600
0.1	0.0625	0	G_0	0.2695332	2.1626001	-1.6551569	-1.2970208	4.5604304	-4.3163876	1.4010655
			G_1	0.0138667	0.1827458	2.5749608	-3.9044679	3.3556301	-2.1772209	0.6420134
		0.2	G_0	0.2834411	2.0560718	-0.8751298	-1.5432422	3.0228355	-2.2245268	0.5558294
			G_1	0.0182016	0.2072911	2.5921978	-4.2023608	4.5304917	-3.5646673	1.1564770
		0.4	G_0	0.3137750	2.3258560	-0.8579900	-0.9040300	4.2766520	-5.1745700	1.8051000
			G_1	0.0243570	0.3072050	2.1814360	-1.9816300	1.1663170	-1.1678700	0.4025600
		0.6	G_0	0.3600610	2.8884850	-2.6105300	8.0008110	-6.6659700	-0.3626000	1.1229800
			G_1	0.0371430	0.4201240	2.0068380	-1.0550900	2.0695720	-3.6421800	1.4368800
		0.8	G_0	0.4694430	3.3305190	-1.8346900	11.806850	-5.5419600	-10.763600	6.8425000
			G_1	0.0598490	0.7065030	0.7632970	4.4319820	-3.1569500	-2.8592200	1.8893100

Table C.13
Influence Coefficients For A Longitudinal Semi-Elliptical Surface Crack In A Cylinder – Outside Surface

t/R_i	a/c	a/t	G_i	A_0	A_1	A_2	A_3	A_4	A_5	A_6
0.1	0.125	0	G_0	0.4065238	0.7772483	3.8861644	-12.573943	16.760207	-11.014593	2.8706957
			G_1	0.0320270	0.1825342	2.2670449	-2.7076615	1.2088194	-0.3777430	0.0763155
		0.2	G_0	0.4146617	1.1413375	1.8316706	-6.3486958	7.9232241	-5.0205478	1.2773760
			G_1	0.0480559	0.0160274	3.9258710	-9.0346145	12.528263	-9.7913648	3.0207677
		0.4	G_0	0.4883450	1.4676440	1.4043140	-4.4990000	5.3634750	-3.4240300	0.8052400
			G_1	0.0579240	0.3954930	1.4085140	0.3793750	-3.3794500	2.8735190	-0.8740400
		0.6	G_0	0.6140930	1.8274410	1.0767420	-0.6119200	-0.6954000	-0.1405600	0.2139800
			G_1	0.0956370	0.4497680	1.7875670	-0.2859900	-1.5203300	0.5472650	0.0260000
		0.8	G_0	0.8606090	1.8707420	3.9998690	-2.2213500	-1.4990000	-1.4366100	1.6902100
			G_1	0.1643640	0.4633370	2.6664580	-1.0454000	-0.4337900	-1.3064500	0.9429600
0.1	0.25	0	G_0	0.6152816	-0.3348694	6.2955620	-15.590618	19.299508	-12.488107	3.3010035
			G_1	0.0703566	0.2828152	1.4036169	-0.6511596	-1.2076596	1.0318656	-0.2423741
		0.2	G_0	0.6292130	-0.2336322	7.0478667	-19.982397	27.848411	-19.690368	5.5375234
			G_1	0.0904740	0.1857128	2.4363430	-4.7462460	5.8199075	-4.5017004	1.4053473
		0.4	G_0	0.7474850	0.0425110	4.3717980	-8.1944800	6.2538030	-1.6898700	-0.1427300
			G_1	0.1180950	0.2484880	1.9064220	-1.9057300	0.5526770	-0.2448400	0.1107400
		0.6	G_0	0.9661540	-0.1353200	5.7466490	-9.3625200	4.9078280	0.7588490	-1.1390900
			G_1	0.1830270	0.2407950	2.0333670	-1.2883400	-1.3714400	1.6503570	-0.5396800
		0.8	G_0	1.3341440	-0.9392800	11.458550	-22.447500	20.248040	-9.5095100	1.9907200
			G_1	0.2907130	0.0222280	3.5382670	-4.2976700	1.5378660	0.1623560	-0.1962600
0.1	0.5	0	G_0	0.8776607	-0.6729719	3.7721411	-6.5209060	6.3377934	-3.7028038	0.9872447
			G_1	0.1277541	0.4368502	0.4904522	1.0427434	-2.9631236	2.0826525	-0.5184313
		0.2	G_0	0.9130594	-1.0743549	6.5855208	-15.182614	19.523051	-13.484513	3.8207058
			G_1	0.1514847	0.1586198	2.2698801	-4.5668494	5.7721280	-4.5599113	1.4645610
		0.4	G_0	1.0280510	-0.7637100	3.1906790	-2.3185400	-2.8532900	4.8911910	-1.9674700
			G_1	0.1796830	0.3127760	1.1588480	-0.4062200	-1.6100500	1.6351940	-0.5292900
		0.6	G_0	1.2334260	-1.1348600	4.1411110	-2.7310000	-4.9657400	8.0561550	-3.2581700
			G_1	0.2434960	0.1656450	1.6261480	-1.2283300	-0.7166800	1.0912900	-0.3930600
		0.8	G_0	1.5039180	-1.5034000	5.1335790	-5.1827000	-1.0213400	4.2817510	-1.7636200
			G_1	0.3214900	0.0504200	1.9574280	-1.9407000	0.2832180	0.3023430	-0.1329900
0.1	1	0	G_0	1.1977992	-0.5244870	0.1498299	2.3284866	-5.1058499	4.3469049	-1.3487980
			G_1	0.1870117	0.6987352	0.1316900	0.7269255	-2.5259384	2.1756251	-0.6540458
		0.2	G_0	1.2309943	-1.2311243	4.9655300	-13.330137	20.774727	-16.757204	5.4042537
			G_1	0.2176088	0.1970437	3.1550798	-8.8500614	13.139627	-10.531333	3.4038623
		0.4	G_0	1.3231870	-0.9921100	1.6993240	-0.3237300	-3.2217300	4.2806730	-1.6779000
			G_1	0.2229300	0.5643960	0.6814060	-0.4239100	-1.4164100	1.7944570	-0.6675800
		0.6	G_0	1.4456210	-1.2064800	2.0156090	-1.0147800	-1.9519200	3.0609460	-1.2264900
			G_1	0.2588090	0.5174240	0.6565440	-0.2305700	-1.7170400	1.9972060	-0.7158800
		0.8	G_0	1.5973980	-1.4150900	1.8672670	-0.2830900	-2.7422700	3.2391740	-1.1212900
			G_1	0.2988890	0.4569940	0.7181120	-0.4164400	-1.2008400	1.4390610	-0.5091100
0.1	2	0	G_0	0.8150546	-0.5623828	1.4465771	-4.6778133	8.4192164	-7.9025932	2.9866351
			G_1	0.1359146	0.0702340	3.5558581	-11.034445	16.967724	-14.126991	4.8706612
		0.2	G_0	0.8430489	-1.1005326	4.6617449	-14.157253	22.899128	-18.964329	6.3406074
			G_1	0.1390871	0.0277092	3.5072974	-10.680541	16.126905	-13.155146	4.4523656
		0.4	G_0	0.8605308	-1.1997836	5.1936578	-15.844548	25.563051	-20.974259	6.9229799
			G_1	0.1443506	-0.0060804	3.7006839	-11.307283	17.100992	-13.865758	4.6492973
		0.6	G_0	0.9003490	-1.2107769	4.8455996	-14.595836	23.611401	-19.532572	6.5152373
			G_1	0.1545839	0.0063848	3.5329882	-10.721392	16.161920	-13.159436	4.4472006
		0.8	G_0	0.9554477	-1.6372153	7.2947649	-22.269116	35.425236	-28.048423	8.7975829
			G_1	0.1681089	-0.1082476	4.2889256	-13.154232	19.720738	-15.394068	4.8931181

Table C.13
Influence Coefficients For A Longitudinal Semi-Elliptical Surface Crack In A Cylinder – Outside Surface

t/R_i	a/c	a/t	G_i	A_0	A_1	A_2	A_3	A_4	A_5	A_6
0.2	0.03125	0	G_0	0.1965046	2.9373464	-5.2582823	7.4889153	-6.9282667	3.3673349	-0.6677966
			G_1	0.0051780	0.1750280	2.7718680	-4.6457154	4.6780502	-3.2768090	0.9840994
		0.2	G_0	0.2114908	2.4425792	-1.0853387	-4.3244076	10.821413	-9.9682430	3.2163776
			G_1	0.0066363	0.2226202	2.5052241	-3.7606471	3.8258183	-3.0282477	0.9830947
		0.4	G_0	0.2200000	2.8881700	-3.0327900	2.7778770	3.3274220	-7.7404800	3.3939800
			G_1	0.0091060	0.3453610	1.7142900	-0.5311700	-0.3691000	-0.5118400	0.3025800
		0.6	G_0	0.2348060	3.2261810	-4.4851300	12.433050	-9.9964600	-0.2169700	1.5875600
			G_1	0.0145190	0.5102980	0.5788380	3.9687320	-5.3534000	1.8233690	-0.2307100
		0.8	G_0	0.2865680	2.4834660	4.1449600	-13.505800	45.152730	-55.423700	21.127000
			G_1	0.0206900	0.6400470	-0.0229200	6.0072670	-3.1147600	-3.7934800	2.1179200
0.2	0.0625	0	G_0	0.2695332	2.1626001	-1.6551569	-1.2970208	4.5604304	-4.3163876	1.4010655
			G_1	0.0138667	0.1827458	2.5749608	-3.9044679	3.3556301	-2.1772209	0.6420134
		0.2	G_0	0.2834411	2.0560718	-0.8751298	-1.5432422	3.0228355	-2.2245268	0.5558294
			G_1	0.0182016	0.2072911	2.5921978	-4.2023608	4.5304917	-3.5646673	1.1564770
		0.4	G_0	0.3052040	2.2875080	-0.9001700	-0.4660500	3.3131160	-4.3118300	1.5291400
			G_1	0.0212020	0.3013800	2.0904460	-1.6420300	0.6344910	-0.7559500	0.2745900
		0.6	G_0	0.3364570	2.8141420	-2.9703500	9.5644040	-9.9622400	2.7107940	0.1081600
			G_1	0.0315690	0.3510610	2.2422160	-1.9023800	3.3988860	-4.5777900	1.6874400
		0.8	G_0	0.4123650	2.9008610	-0.8830500	8.4174560	-2.8151000	-9.6909800	5.5666900
			G_1	0.0418770	0.6018790	0.8247160	3.9811330	-3.2906000	-1.5730100	1.1215000
0.2	0.125	0	G_0	0.4065238	0.7772483	3.8861644	-12.573943	16.760207	-11.014593	2.8706957
			G_1	0.0320270	0.1825342	2.2670449	-2.7076615	1.2088194	-0.3777430	0.0763155
		0.2	G_0	0.4146617	1.1413375	1.8316706	-6.3486958	7.9232241	-5.0205478	1.2773760
			G_1	0.0480559	0.0160274	3.9258710	-9.0346145	12.528263	-9.7913648	3.0207677
		0.4	G_0	0.4703850	1.5541910	0.5461170	-1.3287000	0.1961270	0.6156700	-0.4357400
			G_1	0.0532400	0.3675900	1.5616730	-0.1572400	-2.2528300	1.8144520	-0.5189800
		0.6	G_0	0.5699100	1.7741760	0.8463720	0.1611910	-0.9192500	-0.5062400	0.3641200
			G_1	0.0799060	0.4293480	1.7026530	-0.1213800	-1.2211100	0.0433470	0.1948200
		0.8	G_0	0.7433210	1.8172770	2.7976140	0.2753690	-1.4326200	-3.1035000	2.1815400
			G_1	0.1246100	0.4675080	2.0528940	0.3058490	-0.9948000	-1.4118400	0.9245700
0.2	0.25	0	G_0	0.6152816	-0.3348694	6.2955620	-15.590618	19.299508	-12.488107	3.3010035
			G_1	0.0703566	0.2828152	1.4036169	-0.6511596	-1.2076596	1.0318656	-0.2423741
		0.2	G_0	0.6292130	-0.2336322	7.0478667	-19.982397	27.848411	-19.690368	5.5375234
			G_1	0.0904740	0.1857128	2.4363430	-4.7462460	5.8199075	-4.5017004	1.4053473
		0.4	G_0	0.7429640	0.0378310	4.5014520	-8.4869900	6.8268360	-2.2638700	0.0578800
			G_1	0.1151780	0.2656350	1.7915450	-1.4270300	-0.2561800	0.3997230	-0.0925900
		0.6	G_0	0.9371100	-0.0255800	5.1408380	-7.0247800	1.5138460	3.0365680	-1.7628800
			G_1	0.1726810	0.2717190	1.8711170	-0.6546900	-2.1914600	2.1145170	-0.6484000
		0.8	G_0	1.2624900	-0.7577100	10.593400	-18.988200	16.245730	-7.7399600	1.7098800
			G_1	0.2602900	0.2432630	1.9870650	1.1808940	-6.9845000	6.5125760	-2.0745300
0.2	0.5	0	G_0	0.8776607	-0.6729719	3.7721411	-6.5209060	6.3377934	-3.7028038	0.9872447
			G_1	0.1277541	0.4368502	0.4904522	1.0427434	-2.9631236	2.0826525	-0.5184313
		0.2	G_0	0.9130594	-1.0743549	6.5855208	-15.182614	19.523051	-13.484513	3.8207058
			G_1	0.1514847	0.1586198	2.2698801	-4.5668494	5.7721280	-4.5599113	1.4645610
		0.4	G_0	1.0373150	-0.7658000	3.1866550	-2.0564900	-3.5112000	5.5279200	-2.1906800
			G_1	0.1827690	0.3016120	1.2494690	-0.6550800	-1.2174600	1.3119730	-0.4248500
		0.6	G_0	1.2483210	-1.1273200	4.2620860	-2.9342600	-4.6925200	7.8084440	-3.1741300
			G_1	0.2466090	0.1946990	1.4996030	-0.7717700	-1.4533500	1.6452820	-0.5551900
		0.8	G_0	1.5312830	-1.4214000	4.9906150	-4.3683700	-2.3611100	5.1413420	-1.9602900
			G_1	0.3312580	0.0718170	1.9412430	-1.7261000	-0.1198500	0.5699280	-0.1928500

Table C.13
Influence Coefficients For A Longitudinal Semi-Elliptical Surface Crack In A Cylinder – Outside Surface

t/R_i	a/c	a/t	G_i	A_0	A_1	A_2	A_3	A_4	A_5	A_6
0.2	1	0	G_0	1.1977992	-0.5244870	0.1498299	2.3284866	-5.1058499	4.3469049	-1.3487980
			G_1	0.1870117	0.6987352	0.1316900	0.7269255	-2.5259384	2.1756251	-0.6540458
		0.2	G_0	1.2309943	-1.2311243	4.9655300	-13.330137	20.774727	-16.757204	5.4042537
			G_1	0.2176088	0.1970437	3.1550798	-8.8500614	13.139627	-10.531333	3.4038623
		0.4	G_0	1.3395810	-0.9995200	1.6152160	0.0782660	-3.9906500	4.9599370	-1.9049200
			G_1	0.2275940	0.5608710	0.6867250	-0.4215300	-1.4409800	1.8257330	-0.6796800
		0.6	G_0	1.4732900	-1.2085900	1.8254600	-0.1324400	-3.6681900	4.5929990	-1.7396900
			G_1	0.2660940	0.5279130	0.5952580	-0.0963000	-1.8423700	2.0313860	-0.7086300
		0.8	G_0	1.6447550	-1.4592200	1.9736270	-0.4261600	-2.6988600	3.2947350	-1.1534500
			G_1	0.3140820	0.4390350	0.8206310	-0.7553900	-0.6482700	0.9930760	-0.3665800
0.2	2	0	G_0	0.8150546	-0.5623828	1.4465771	-4.6778133	8.4192164	-7.9025932	2.9866351
			G_1	0.1359146	0.0702340	3.5558581	-11.034445	16.967724	-14.126991	4.8706612
		0.2	G_0	0.8536841	-1.0302392	4.0738131	-12.154325	19.629919	-16.443839	5.6017294
			G_1	0.1415607	0.0595042	3.2739576	-9.8453707	14.709899	-12.038154	4.1204970
		0.4	G_0	0.8704024	-1.0725850	4.1489689	-12.315492	19.879021	-16.632323	5.6546309
			G_1	0.1458020	0.0566824	3.2442161	-9.7698352	14.622301	-11.977784	4.1003749
		0.6	G_0	0.9098344	-1.0776714	3.7795127	-11.056320	17.894031	-15.112464	5.2038813
			G_1	0.1562757	0.0628573	3.1195301	-9.3277071	13.870685	-11.365405	3.9093291
		0.8	G_0	0.9473209	-1.0916848	3.2936932	-9.1104990	14.239343	-11.702777	3.9539503
			G_1	0.1579980	0.1971737	2.1502631	-6.2273300	8.6913835	-6.9646090	2.4150002
0.33333	0.03125	0	G_0	0.1965046	2.9373464	-5.2582823	7.4889153	-6.9282667	3.3673349	-0.6677966
			G_1	0.0051780	0.1750280	2.7718680	-4.6457154	4.6780502	-3.2768090	0.9840994
		0.2	G_0	0.2651746	2.0518539	-0.6576529	-2.2400914	4.0586003	-2.9557373	0.7509004
			G_1	0.0134241	0.2145035	2.4853811	-3.7294986	3.6634951	-2.8206848	0.9110972
		0.4	G_0	0.2068432	2.1289212	0.9488071	-7.9908119	17.527999	-16.818919	5.6744489
			G_1	0.0078550	0.1900840	2.9205940	-4.8299400	6.9364230	-6.4967600	2.2038400
		0.6	G_0	0.2176810	3.1796080	-4.8660500	13.825800	-14.215900	4.4304150	-0.0353400
			G_1	0.0077208	0.1777379	2.8308619	-4.4159417	8.8389790	-9.6804295	3.4134994
		0.8	G_0	0.2214280	3.4544570	-5.7728600	22.240290	-23.041500	5.5717540	0.9588560
			G_1	0.0086700	0.2576810	2.7260750	-3.5453100	10.980120	-13.837700	5.0393470
0.33333	0.0625	0	G_0	0.2695332	2.1626001	-1.6551569	-1.2970208	4.5604304	-4.3163876	1.4010655
			G_1	0.0138667	0.1827458	2.5749608	-3.9044679	3.3556301	-2.1772209	0.6420134
		0.2	G_0	0.2602402	1.9101229	0.6250582	-7.1510682	13.076057	-10.659369	3.2200458
			G_1	0.0149877	0.1955673	2.3230283	-2.9558560	2.2512432	-1.6085747	0.5105227
		0.4	G_0	0.2985878	1.4806070	4.0015159	-15.408972	26.416058	-21.963750	6.8318255
			G_1	0.0217550	0.2019200	2.8740480	-4.6530800	6.0952580	-5.4253400	1.7947570
		0.6	G_0	0.3248620	2.5827580	-1.7974700	4.6268000	-1.0563100	-4.8660300	2.6241440
			G_1	0.0274730	0.2394530	2.9636050	-4.8034000	8.6324210	-9.0423400	3.1584620
		0.8	G_0	0.3581590	2.8096210	-2.2342200	12.128880	-10.705600	-1.3607100	2.4982950
			G_1	0.0328400	0.3062750	2.7758730	-3.5996700	9.5233880	-11.672000	4.2059790
0.33333	0.125	0	G_0	0.4065238	0.7772483	3.8861644	-12.573943	16.760207	-11.014593	2.8706957
			G_1	0.0320270	0.1825342	2.2670449	-2.7076615	1.2088194	-0.3777430	0.0763155
		0.2	G_0	0.3882912	1.0609616	3.1532036	-10.997015	15.435099	-10.732447	2.9280131
			G_1	0.0361643	0.1993991	2.1521281	-2.4393155	1.2426343	-0.7115746	0.2338738
		0.4	G_0	0.4550911	0.6846515	5.9119227	-17.160497	24.468016	-17.877938	5.0878696
			G_1	0.0521360	0.2552780	2.3217540	-2.7072400	2.1186830	-1.7821100	0.6094100
		0.6	G_0	0.5489050	1.2094700	4.6400520	-12.898000	21.506680	-18.882700	6.1124270
			G_1	0.0713480	0.2757420	2.6582020	-3.5129500	4.7941620	-4.9393500	1.7461680
		0.8	G_0	0.6623640	1.1473380	6.6549140	-13.993000	24.090210	-23.773700	8.3646690
			G_1	0.0983440	0.2665520	3.1706930	-4.1673500	7.3879790	-8.2858400	2.9658590

Table C.13
Influence Coefficients For A Longitudinal Semi-Elliptical Surface Crack In A Cylinder –

Outside Surface

t/R_i	a/c	a/t	G_i	A_0	A_1	A_2	A_3	A_4	A_5	A_6
0.33333	0.25	0	G_0	0.6152816	-0.3348694	6.2955620	-15.590618	19.299508	-12.488107	3.3010035
			G_1	0.0703566	0.2828152	1.4036169	-0.6511596	-1.2076596	1.0318656	-0.2423741
		0.2	G_0	0.5813392	0.1754806	4.1064690	-9.6118175	10.697163	-6.3416068	1.5662906
			G_1	0.0754953	0.2165572	1.6757864	-1.2279181	-0.4611587	0.5138881	-0.0998820
		0.4	G_0	0.6898568	-0.0773270	5.4806293	-11.407142	11.633671	-6.3018895	1.3834825
			G_1	0.1094450	0.3008580	1.5214730	-0.4181100	-1.9095700	1.6678210	-0.4669100
		0.6	G_0	0.9181390	-0.5237900	9.0497720	-20.248100	24.464580	-16.157900	4.3547490
			G_1	0.1608860	0.2132020	2.3389990	-2.2357400	0.7909320	-0.5441000	0.2284680
		0.8	G_0	1.1608820	-0.7489100	10.891840	-20.643400	21.820600	-13.976200	3.9263300
			G_1	0.2308100	0.1303460	2.9946080	-2.6118400	0.5931240	-0.3660800	0.1958340
0.33333	0.5	0	G_0	0.8776607	-0.6729719	3.7721411	-6.5209060	6.3377934	-3.7028038	0.9872447
			G_1	0.1277541	0.4368502	0.4904522	1.0427434	-2.9631236	2.0826525	-0.5184313
		0.2	G_0	0.9073955	-0.8971202	5.6296095	-12.600224	16.002537	-11.129631	3.2028664
			G_1	0.1423042	0.1193355	2.5733770	-5.9665543	8.9660776	-7.7527147	2.6068720
		0.4	G_0	1.0227900	-0.4769800	1.8915950	0.6470380	-6.0011600	6.2817830	-2.1144300
			G_1	0.1805320	0.3494360	1.0799180	-0.3980200	-1.2385100	1.0681870	-0.2845100
		0.6	G_0	1.2558880	-1.3007200	5.9836960	-9.1319200	6.5768270	-2.0833900	0.1372010
			G_1	0.2408900	0.2961710	0.9788130	0.6485900	-3.2595400	2.6786820	-0.7609600
		0.8	G_0	1.5064650	-0.9515700	2.1848270	5.0110910	-17.165600	16.231510	-5.1671000
			G_1	0.3183620	0.3380430	0.2332610	3.8880520	-9.0315400	7.3427670	-2.1808400
0.33333	1	0	G_0	1.1977992	-0.5244870	0.1498299	2.3284866	-5.1058499	4.3469049	-1.3487980
			G_1	0.1870117	0.6987352	0.1316900	0.7269255	-2.5259384	2.1756251	-0.6540458
		0.2	G_0	1.2251938	-1.1088782	4.3783822	-11.902054	18.917314	-15.537073	5.0861925
			G_1	0.1967570	0.3750251	2.1938569	-6.3981104	9.8525023	-8.3093790	2.8070520
		0.4	G_0	1.3102610	-0.3521400	-1.8346200	8.5385630	-14.391600	11.108920	-3.2682300
			G_1	0.2225920	0.6936100	0.0198130	1.0770080	-3.0231700	2.5251620	-0.7509200
		0.6	G_0	1.4399700	-0.3693300	-2.7283100	11.493880	-18.862500	14.402850	-4.2113200
			G_1	0.2615940	0.6931840	-0.2579300	1.9715370	-4.3708500	3.5256390	-1.0416400
		0.8	G_0	1.6727600	-1.6027700	3.8701220	-8.1470100	11.569570	-9.1115900	2.9716790
			G_1	0.3252650	0.3406560	1.7824050	-4.4816900	6.1843940	-4.9886800	1.6486210
0.33333	2	0	G_0	0.8150546	-0.5623828	1.4465771	-4.6778133	8.4192164	-7.9025932	2.9866351
			G_1	0.1359146	0.0702340	3.5558581	-11.034445	16.967724	-14.126991	4.8706612
		0.2	G_0	0.8585767	-1.0507299	4.1528538	-12.361065	19.924151	-16.649393	5.6568794
			G_1	0.1410557	0.0851240	3.1023875	-9.3241192	13.898320	-11.411063	3.9302795
		0.4	G_0	0.8774308	-1.0721586	4.0656641	-12.050152	19.486315	-16.340345	5.5670727
			G_1	0.1466187	0.0740623	3.1240530	-9.4156798	14.080011	-11.557896	3.9707854
		0.6	G_0	0.9226380	-1.1036903	3.8099517	-11.072222	17.863569	-15.046439	5.1695991
			G_1	0.1587492	0.0714304	3.0474948	-9.1086668	13.518169	-11.073693	3.8126238
		0.8	G_0	0.9631792	-1.0845228	3.0958067	-8.4948235	13.327750	-11.030577	3.7571770
			G_1	0.1624555	0.1998637	2.1090767	-6.1178471	8.5262697	-6.8263049	2.3672889
1.0	0.03125	0	G_0	0.1965046	2.9373464	-5.2582823	7.4889153	-6.9282667	3.3673349	-0.6677966
			G_1	0.0051780	0.1750280	2.7718680	-4.6457154	4.6780502	-3.2768090	0.9840994
		0.2	G_0	0.1953014	2.8857146	-4.3208302	5.4744132	-4.0134519	0.9410490	0.1172163
			G_1	0.0056317	0.1692495	2.7427976	-4.2364355	4.2523072	-3.2051229	1.0140641
		0.4	G_0	0.1989538	2.7504921	-2.7430002	2.7466218	-0.2786268	-2.2502461	1.1490088
			G_1	0.0055375	0.1725097	2.7251922	-3.8291707	4.4109627	-4.0034918	1.3759626
		0.6	G_0	0.1981511	2.9765550	-3.5428031	7.8099586	-7.7884286	2.3877614	-0.0164607
			G_1	0.0052200	0.1870231	2.6865140	-3.3288768	4.8598000	-5.2514410	1.8763475
		0.8	G_0	0.1991164	3.0698031	-3.1633172	9.8147183	-10.848753	5.1283491	-1.4243053
			G_1	0.0053927	0.1786846	2.8327155	-3.2723302	5.7338892	-5.8194405	1.6811048

Table C.13
Influence Coefficients For A Longitudinal Semi-Elliptical Surface Crack In A Cylinder – Outside Surface

t/R_i	a/c	a/t	G_i	A_0	A_1	A_2	A_3	A_4	A_5	A_6
1.0	0.0625	0	G_0	0.2695332	2.1626001	-1.6551569	-1.2970208	4.5604304	-4.3163876	1.4010655
			G_1	0.0138667	0.1827458	2.5749608	-3.9044679	3.3556301	-2.1772209	0.6420134
		0.2	G_0	0.2715940	2.1024792	-0.8251686	-2.6055393	5.9209240	-5.2455526	1.6548386
			G_1	0.0150303	0.1758222	2.5677841	-3.6074069	3.1408983	-2.2687756	0.7163039
		0.4	G_0	0.2777113	2.0986556	-0.4194664	-1.4260711	3.5011609	-3.8010267	1.3387712
			G_1	0.0155020	0.1836026	2.6006839	-3.5389388	4.0212185	-3.7247058	1.2977739
		0.6	G_0	0.2851041	2.2337177	-0.4669277	0.8347740	0.8911966	-3.1973040	1.4390293
			G_1	0.0157533	0.2014410	2.5657394	-3.0637200	4.4719504	-4.9446888	1.7843463
		0.8	G_0	0.2969615	2.1296733	1.3452081	-1.8273770	5.4502252	-6.5713644	1.9432135
			G_1	0.0164599	0.1880783	2.8160846	-3.4852155	6.3096325	-6.4218489	1.9105821
1.0	0.125	0	G_0	0.4065238	0.7772483	3.8861644	-12.573943	16.760207	-11.014593	2.8706957
			G_1	0.0320270	0.1825342	2.2670449	-2.7076615	1.2088194	-0.3777430	0.0763155
		0.2	G_0	0.4115155	0.9865037	3.3032079	-11.115382	15.618784	-11.008999	3.0590331
			G_1	0.0376572	0.1690832	2.4719152	-3.5008614	3.1003664	-2.2831015	0.7359275
		0.4	G_0	0.4209793	1.2265337	1.7709653	-4.0978290	4.4536450	-3.1148588	0.8818491
			G_1	0.0464776	0.0297565	3.8704434	-8.3559638	12.050090	-9.9545839	3.1515874
		0.6	G_0	0.4608006	1.0040220	4.4900108	-11.185813	16.857163	-14.057447	4.4135613
			G_1	0.0464015	0.1688809	2.8532660	-4.2870329	6.2310777	-6.0886059	2.0869057
		0.8	G_0	0.4993921	0.7249266	7.4797239	-18.027074	29.219795	-24.705288	7.5136262
			G_1	0.0519622	0.1229523	3.4495151	-6.0021006	10.613460	-10.115804	3.1838115
1.0	0.25	0	G_0	0.6152816	-0.3348694	6.2955620	-15.590618	19.299508	-12.488107	3.3010035
			G_1	0.0703566	0.2828152	1.4036169	-0.6511596	-1.2076596	1.0318656	-0.2423741
		0.2	G_0	0.6347999	-0.1607774	5.6251819	-13.301724	15.867112	-10.105998	2.6535645
			G_1	0.0831906	0.1946472	1.9111256	-1.8015115	0.1861535	0.2143122	-0.0715121
		0.4	G_0	0.6952294	-0.1820586	6.3265942	-14.501799	17.774804	-11.951291	3.2923578
			G_1	0.0998812	0.1922155	2.0907416	-2.0375068	0.7166759	-0.4207962	0.1636441
		0.6	G_0	0.7697939	-0.1469814	6.3978662	-12.353237	14.107484	-9.6706471	2.7305217
			G_1	0.1214572	0.1522551	2.6166129	-3.2859685	3.1577678	-2.7413387	0.9261632
		0.8	G_0	0.8549284	-0.0429616	5.3609225	-3.9228684	-0.6231868	1.3341905	-0.5199047
			G_1	0.1433757	0.1557243	2.7487977	-2.8474440	3.2406584	-3.4614388	1.2054315
1.0	0.5	0	G_0	0.8776607	-0.6729719	3.7721411	-6.5209060	6.3377934	-3.7028038	0.9872447
			G_1	0.1277541	0.4368502	0.4904522	1.0427434	-2.9631236	2.0826525	-0.5184313
		0.2	G_0	0.9294839	-0.9123438	5.5572996	-11.795967	14.223313	-9.5254694	2.6703017
			G_1	0.1555159	0.2145010	1.9367664	-3.4071858	3.8812609	-3.0987310	1.0252421
		0.4	G_0	1.0335417	-1.0606830	6.4449852	-13.812882	17.012811	-11.651517	3.3253682
			G_1	0.1850381	0.2102095	1.9946057	-3.4025969	3.8162750	-3.0760695	1.0305943
		0.6	G_0	1.1887896	-1.1658034	6.8988296	-13.846554	16.331316	-11.005122	3.1203439
			G_1	0.2333373	0.1703608	2.2444709	-3.7266435	4.1277307	-3.3104596	1.1012959
		0.8	G_0	1.3877372	-0.9475909	4.6700154	-4.4556599	1.2080060	-0.1660389	0.1766818
			G_1	0.2937515	0.2652325	1.3600245	0.0821899	-2.1979103	1.4912239	-0.3122287
1.0	1	0	G_0	1.1977992	-0.5244870	0.1498299	2.3284866	-5.1058499	4.3469049	-1.3487980
			G_1	0.1870117	0.6987352	0.1316900	0.7269255	-2.5259384	2.1756251	-0.6540458
		0.2	G_0	1.2693391	-1.1398036	4.0929525	-10.448235	16.052389	-12.895137	4.1474100
			G_1	0.2250216	0.3007179	2.4398964	-6.5430462	9.3147828	-7.3698889	2.3712608
		0.4	G_0	1.3659313	-1.2311017	4.1982415	-10.684193	16.596630	-13.510212	4.4050361
			G_1	0.2539687	0.2708452	2.5473120	-6.9142097	10.017430	-8.0212153	2.6057054
		0.6	G_0	1.5194803	-1.3672561	4.1631190	-10.126117	15.450063	-12.405478	3.9897462
			G_1	0.2987540	0.2679897	2.3853287	-6.3190782	8.9496175	-7.0446943	2.2506565
		0.8	G_0	1.7239825	-1.6212092	4.6939965	-11.283773	17.175644	-13.758576	4.4014423
			G_1	0.3593364	0.2027013	2.6155305	-6.9763515	10.009223	-7.8458092	2.4681983

Table C.13
Influence Coefficients For A Longitudinal Semi-Elliptical Surface Crack In A Cylinder – Outside Surface

t/R_i	a/c	a/t	G_i	A_0	A_1	A_2	A_3	A_4	A_5	A_6
1.0	2	0	G_0	0.8150546	-0.5623828	1.4465771	-4.6778133	8.4192164	-7.9025932	2.9866351
			G_1	0.1359146	0.0702340	3.5558581	-11.034445	16.967724	-14.126991	4.8706612
		0.2	G_0	0.8691122	-1.0405377	3.9388218	-11.649707	18.786197	-15.734788	5.3626575
			G_1	0.1438551	0.0856869	3.0743371	-9.2270198	13.705530	-11.205866	3.8447622
		0.4	G_0	0.9010736	-1.0921904	3.8953648	-11.380710	18.368891	-15.430651	5.2755679
			G_1	0.1513258	0.0900491	2.9786555	-8.9541697	13.313710	-10.911266	3.7542123
		0.6	G_0	0.9531807	-1.0938416	3.3782715	-9.5974722	15.411214	-12.953543	4.4476404
			G_1	0.1611774	0.1739086	2.3394389	-6.9260024	9.9623905	-8.1201469	2.8326669
		0.8	G_0	1.0093559	-1.0896106	2.7238032	-7.3224261	11.627824	-9.7907203	3.3922012
			G_1	0.1733516	0.2337410	1.8443004	-5.3563299	7.3448611	-5.8772005	2.0618261

Notes:

1. Interpolation of the influence coefficients, G_i, may be used for intermediate values of t/R_i, a/c, and a/t.

2. The value of the influence coefficients at the surface point of the crack defined by $\varphi = 0^0$ are equal to: $G_i = A_0$.

3. The value of the influence coefficients at the deepest point of the crack defined by $\varphi = 90^0$ are equal to: $G_i = \sum_{n=0}^{6} A_n$.

Table C.14
Influence Coefficients For A Circumferential Semi-Elliptical Surface Crack In A Cylinder – Inside Surface

t/R_i	a/c	a/t	G_i	A_0	A_1	A_2	A_3	A_4	A_5	A_6
0.0	0.03125	0	G_0	0.1965046	2.9373464	-5.2582823	7.4889153	-6.9282667	3.3673349	-0.6677966
			G_1	0.0051780	0.1750280	2.7718680	-4.6457154	4.6780502	-3.2768090	0.9840994
			G_5	0.1965050	2.9373460	-5.2582820	7.4889150	-6.9282670	3.3673350	-0.6677970
			G_6	0.0000000	0.0000000	0.0000000	0.0000000	0.0000000	0.0000000	0.0000000
		0.2	G_0	0.2080760	3.0112422	-5.1048701	7.6348715	-6.8347547	2.7940766	-0.3882688
			G_1	0.0084834	0.2406767	2.4574292	-3.6452421	3.6142837	-2.8451814	0.9270638
			G_5	0.2080760	3.0112422	-5.1048701	7.6348715	-6.8347547	2.7940766	-0.3882688
			G_6	0.0000000	0.0000000	0.0000000	0.0000000	0.0000000	0.0000000	0.0000000
		0.4	G_0	0.2357940	3.0822400	-3.5792100	3.9476890	1.9131590	-6.8872200	3.1896800
			G_1	0.0145140	0.4038000	1.6422700	-0.3906100	-0.6480700	-0.2940300	0.2514900
			G_5	0.2357940	3.0822400	-3.5792100	3.9476890	1.9131590	-6.8872200	3.1896800
			G_6	0.0000000	0.0000000	0.0000000	0.0000000	0.0000000	0.0000000	0.0000000
		0.6	G_0	0.2902240	3.6892050	-4.5739100	11.709890	-6.3750000	-5.8894100	4.2452400
			G_1	0.0208890	0.7016780	0.1631840	5.7072160	-8.2075800	3.4561120	-0.4454700
			G_5	0.2902240	3.6892050	-4.5739100	11.709890	-6.3750000	-5.8894100	4.2452400
			G_6	0.0000000	0.0000000	0.0000000	0.0000000	0.0000000	0.0000000	0.0000000
		0.8	G_0	0.5163550	2.5310830	14.712900	-43.621800	101.06570	-116.08100	46.190900
			G_1	0.0825460	0.4971770	4.6064810	-7.3326700	21.148620	-29.345100	12.491400
			G_5	0.5163550	2.5310830	14.712900	-43.621800	101.06570	-116.08100	46.190900
			G_6	0.0000000	0.0000000	0.0000000	0.0000000	0.0000000	0.0000000	0.0000000
0.0	0.0625	0	G_0	0.2695332	2.1626001	-1.6551569	-1.2970208	4.5604304	-4.3163876	1.4010655
			G_1	0.0138667	0.1827458	2.5749608	-3.9044679	3.3556301	-2.1772209	0.6420134
			G_5	0.2695330	2.1626000	-1.6551570	-1.2970210	4.5604300	-4.3163880	1.4010660
			G_6	0.0000000	0.0000000	0.0000000	0.0000000	0.0000000	0.0000000	0.0000000
		0.2	G_0	0.2845892	2.2264055	-1.4546190	-1.5760719	5.1131083	-4.9485443	1.6207574
			G_1	0.0199077	0.2210874	2.4642047	-3.5898625	3.1624039	-2.2403780	0.6965751
			G_5	0.2845892	2.2264055	-1.4546190	-1.5760719	5.1131083	-4.9485443	1.6207574
			G_6	0.0000000	0.0000000	0.0000000	0.0000000	0.0000000	0.0000000	0.0000000
		0.4	G_0	0.3261480	2.5200870	-1.8847000	2.1798740	-1.4597100	-0.1886500	0.2393400
			G_1	0.0294120	0.3699370	1.9220850	-1.2071500	-0.4394000	0.2737550	-0.0395200
			G_5	0.3261480	2.5200870	-1.8847000	2.1798740	-1.4597100	-0.1886500	0.2393400
			G_6	0.0000000	0.0000000	0.0000000	0.0000000	0.0000000	0.0000000	0.0000000
		0.6	G_0	0.4166330	3.1566470	-2.6248900	7.7325910	-9.6927800	3.6428700	-0.0892000
			G_1	0.0598460	0.4340740	2.6811560	-3.1936600	4.0753720	-4.6940200	1.8285500
			G_5	0.4166330	3.1566470	-2.6248900	7.7325910	-9.6927800	3.6428700	-0.0892000
			G_6	0.0000000	0.0000000	0.0000000	0.0000000	0.0000000	0.0000000	0.0000000
		0.8	G_0	0.6540140	3.4231920	3.8158050	-4.1586900	3.4715330	-10.310400	6.6280000
			G_1	0.1214780	0.6975490	2.9718330	-1.3036500	-0.0754900	-3.0465100	2.1670000
			G_5	0.6540140	3.4231920	3.8158050	-4.1586900	3.4715330	-10.310400	6.6280000
			G_6	0.0000000	0.0000000	0.0000000	0.0000000	0.0000000	0.0000000	0.0000000

Table C.14
Influence Coefficients For A Circumferential Semi-Elliptical Surface Crack In A Cylinder – Inside Surface

t/R_i	a/c	a/t	G_i	A_0	A_1	A_2	A_3	A_4	A_5	A_6
0.0	0.125	0	G_0	0.4065238	0.7772483	3.8861644	-12.573943	16.760207	-11.014593	2.8706957
			G_1	0.0320270	0.1825342	2.2670449	-2.7076615	1.2088194	-0.3777430	0.0763155
			G_5	0.4065240	0.7772480	3.8861640	-12.573943	16.760207	-11.014593	2.8706960
			G_6	0.0000000	0.0000000	0.0000000	0.0000000	0.0000000	0.0000000	0.0000000
		0.2	G_0	0.4242116	1.0089302	3.2973815	-12.159726	17.873386	-12.868668	3.6281712
			G_1	0.0429859	0.2033811	2.2563818	-2.8752160	1.8152558	-1.0512327	0.3181077
			G_5	0.4242116	1.0089302	3.2973815	-12.159726	17.873386	-12.868668	3.6281712
			G_6	0.0000000	0.0000000	0.0000000	0.0000000	0.0000000	0.0000000	0.0000000
		0.4	G_0	0.4917770	1.6592320	-0.1080400	0.1793240	-2.7076100	3.3680620	-1.3489700
			G_1	0.0634270	0.3722500	1.6231670	-0.5306500	-2.0007400	1.8943780	-0.5880300
			G_5	0.4917770	1.6592320	-0.1080400	0.1793240	-2.7076100	3.3680620	-1.3489700
			G_6	0.0000000	0.0000000	0.0000000	0.0000000	0.0000000	0.0000000	0.0000000
		0.6	G_0	0.6591820	1.8759140	1.0212600	-1.7698000	-0.5653600	1.2479960	-0.4376600
			G_1	0.1116040	0.4714500	1.7940590	-0.7557600	-1.4901700	1.0852180	-0.2113700
			G_5	0.6591820	1.8759140	1.0212600	-1.7698000	-0.5653600	1.2479960	-0.4376600
			G_6	0.0000000	0.0000000	0.0000000	0.0000000	0.0000000	0.0000000	0.0000000
		0.8	G_0	0.9809330	1.8846320	4.8020780	-8.0580200	0.4447850	3.4772660	-1.0567500
			G_1	0.2039950	0.4800150	2.8822430	-2.5890100	-0.9683000	1.5372370	-0.3750200
			G_5	0.9809330	1.8846320	4.8020780	-8.0580200	0.4447850	3.4772660	-1.0567500
			G_6	0.0000000	0.0000000	0.0000000	0.0000000	0.0000000	0.0000000	0.0000000
0.0	0.25	0	G_0	0.6152816	-0.3348694	6.2955620	-15.590618	19.299508	-12.488107	3.3010035
			G_1	0.0703566	0.2828152	1.4036169	-0.6511596	-1.2076596	1.0318656	-0.2423741
			G_5	0.6152820	-0.3348690	6.2955620	-15.590618	19.299508	-12.488107	3.3010030
			G_6	0.0000000	0.0000000	0.0000000	0.0000000	0.0000000	0.0000000	0.0000000
		0.2	G_0	0.6385889	-0.3095132	6.5329787	-16.622882	21.056641	-13.850120	3.6988146
			G_1	0.0840059	0.1999367	1.8218113	-1.7756899	0.3757186	-0.0785358	0.0643386
			G_5	0.6385889	-0.3095132	6.5329787	-16.622882	21.056641	-13.850120	3.6988146
			G_6	0.0000000	0.0000000	0.0000000	0.0000000	0.0000000	0.0000000	0.0000000
		0.4	G_0	0.7390420	0.0548160	4.0842620	-7.5883100	5.4047530	-1.0146100	-0.3483400
			G_1	0.1164500	0.2479880	1.8282520	-1.7169900	0.1912120	0.1165770	-0.0186100
			G_5	0.7390420	0.0548160	4.0842620	-7.5883100	5.4047530	-1.0146100	-0.3483400
			G_6	0.0000000	0.0000000	0.0000000	0.0000000	0.0000000	0.0000000	0.0000000
		0.6	G_0	0.9461210	-0.1858800	5.5867460	-9.8634900	5.9596870	0.1296440	-1.0026100
			G_1	0.1778050	0.2056680	2.0979210	-1.8039500	-0.5558700	1.1461400	-0.4206600
			G_5	0.9461210	-0.1858800	5.5867460	-9.8634900	5.9596870	0.1296440	-1.0026100
			G_6	0.0000000	0.0000000	0.0000000	0.0000000	0.0000000	0.0000000	0.0000000
		0.8	G_0	1.2452110	-0.6921900	8.3260620	-14.948000	8.6936910	0.4755790	-1.3926600
			G_1	0.2585640	0.1548890	2.1170240	-0.4910000	-4.6146100	5.4550750	-1.9663300
			G_5	1.2452110	-0.6921900	8.3260620	-14.948000	8.6936910	0.4755790	-1.3926600
			G_6	0.0000000	0.0000000	0.0000000	0.0000000	0.0000000	0.0000000	0.0000000

Table C.14
Influence Coefficients For A Circumferential Semi-Elliptical Surface Crack In A Cylinder – Inside Surface

t/R_i	a/c	a/t	G_i	A_0	A_1	A_2	A_3	A_4	A_5	A_6
0.0	0.5	0	G_0	0.8776607	-0.6729719	3.7721411	-6.5209060	6.3377934	-3.7028038	0.9872447
			G_1	0.1277541	0.4368502	0.4904522	1.0427434	-2.9631236	2.0826525	-0.5184313
			G_5	0.8776610	-0.6729720	3.7721410	-6.5209060	6.3377930	-3.7028040	0.9872450
			G_6	0.0000000	0.0000000	0.0000000	0.0000000	0.0000000	0.0000000	0.0000000
		0.2	G_0	0.9003948	-0.8850488	5.2743239	-11.267523	13.890755	-9.6373584	2.8183906
			G_1	0.1404409	0.3215397	1.1010666	-1.0257556	0.6943940	-1.0793186	0.5410929
			G_5	0.9003948	-0.8850488	5.2743239	-11.267523	13.890755	-9.6373584	2.8183906
			G_6	0.0000000	0.0000000	0.0000000	0.0000000	0.0000000	0.0000000	0.0000000
		0.4	G_0	1.0058060	-0.7322600	2.9951940	-1.9459200	-3.2613500	5.1424570	-2.0306200
			G_1	0.1740870	0.3051630	1.2070310	-0.6720500	-1.0651300	1.1445590	-0.3644800
			G_5	0.9000590	-0.5476000	2.4416770	-1.2688500	-3.3815300	4.7868570	-1.8373900
			G_6	0.0000000	0.0000000	0.0000000	0.0000000	0.0000000	0.0000000	0.0000000
		0.6	G_0	1.1826010	-1.1072500	3.9623640	-2.7781300	-4.3097300	7.2772750	-2.9648200
			G_1	0.2277120	0.1701170	1.5499470	-1.1051200	-0.8333700	1.1717060	-0.4194500
			G_5	1.1826010	-1.1072500	3.9623640	-2.7781300	-4.3097300	7.2772750	-2.9648200
			G_6	0.0000000	0.0000000	0.0000000	0.0000000	0.0000000	0.0000000	0.0000000
		0.8	G_0	1.3833380	-1.3900300	4.3755780	-3.7372600	-2.5403200	5.3036000	-2.0932400
			G_1	0.2820110	0.0839230	1.7258580	-1.5358100	-0.0635600	0.5006780	-0.1982200
			G_5	1.3833380	-1.3900300	4.3755780	-3.7372600	-2.5403200	5.3036000	-2.0932400
			G_6	0.0000000	0.0000000	0.0000000	0.0000000	0.0000000	0.0000000	0.0000000
0.0	1	0	G_0	1.1977992	-0.5244870	0.1498299	2.3284866	-5.1058499	4.3469049	-1.3487980
			G_1	0.1870117	0.6987352	0.1316900	0.7269255	-2.5259384	2.1756251	-0.6540458
			G_5	1.1977990	-0.5244870	0.1498300	2.3284870	-5.1058500	4.3469050	-1.3487980
			G_6	0.0000000	0.0000000	0.0000000	0.0000000	0.0000000	0.0000000	0.0000000
		0.2	G_0	1.2263282	-1.1608467	4.4744783	-11.584231	17.811241	-14.408250	4.6998279
			G_1	0.2154786	0.2441623	2.8107820	-7.6574580	11.171413	-9.0053693	2.9542871
			G_5	1.2263282	-1.1608467	4.4744783	-11.584231	17.811241	-14.408250	4.6998279
			G_6	0.0000000	0.0000000	0.0000000	0.0000000	0.0000000	0.0000000	0.0000000
		0.4	G_0	1.2989480	-0.9978000	1.9479540	-1.3002700	-1.4940100	2.8306230	-1.2126000
			G_1	0.2386246	0.1447774	3.3198992	-9.2456599	13.823512	-11.223715	3.6868232
			G_5	1.2989480	-0.9978000	1.9479540	-1.3002700	-1.4940100	2.8306230	-1.2126000
			G_6	0.0000000	0.0000000	0.0000000	0.0000000	0.0000000	0.0000000	0.0000000
		0.6	G_0	1.3971180	-1.1348400	1.7918740	-0.4202600	-2.8679300	3.7685480	-1.4405000
			G_1	0.2445870	0.5326670	0.5939690	-0.0361800	-2.0163100	2.2167010	-0.7782200
			G_5	1.3971180	-1.1348400	1.7918740	-0.4202600	-2.8679300	3.7685480	-1.4405000
			G_6	0.0000000	0.0000000	0.0000000	0.0000000	0.0000000	0.0000000	0.0000000
		0.8	G_0	1.5117010	-1.3244800	1.7568350	-0.1337900	-2.8629300	3.2953270	-1.1412400
			G_1	0.2704470	0.5113280	0.5357440	-0.0327300	-1.5570200	1.5570970	-0.5094600
			G_5	1.5117010	-1.3244800	1.7568350	-0.1337900	-2.8629300	3.2953270	-1.1412400
			G_6	0.0000000	0.0000000	0.0000000	0.0000000	0.0000000	0.0000000	0.0000000

Table C.14
Influence Coefficients For A Circumferential Semi-Elliptical Surface Crack In A Cylinder – Inside Surface

t/R_i	a/c	a/t	G_i	A_0	A_1	A_2	A_3	A_4	A_5	A_6
0.0	2	0	G_0	0.8150546	-0.5623828	1.4465771	-4.6778133	8.4192164	-7.9025932	2.9866351
			G_1	0.1359146	0.0702340	3.5558581	-11.034445	16.967724	-14.126991	4.8706612
			G_5	0.8150550	-0.5623830	1.4465770	-4.6778130	8.4192160	-7.9025930	2.9866350
			G_6	0.0000000	0.0000000	0.0000000	0.0000000	0.0000000	0.0000000	0.0000000
		0.2	G_0	0.8463715	-1.0011024	4.0052312	-11.937181	19.189548	-16.039296	5.4674371
			G_1	0.1395121	0.0753999	3.1895604	-9.5540932	14.214316	-11.649525	4.0073308
			G_5	0.8463715	-1.0011024	4.0052312	-11.937181	19.189548	-16.039296	5.4674371
			G_6	0.0000000	0.0000000	0.0000000	0.0000000	0.0000000	0.0000000	0.0000000
		0.4	G_0	0.8570045	-1.0183085	3.9957306	-11.886878	19.152747	-16.047480	5.4801806
			G_1	0.1436696	0.0544018	3.2816127	-9.8164232	14.610963	-11.942138	4.0907797
			G_5	0.8570045	-1.0183085	3.9957306	-11.886878	19.152747	-16.047480	5.4801806
			G_6	0.0000000	0.0000000	0.0000000	0.0000000	0.0000000	0.0000000	0.0000000
		0.6	G_0	0.8839861	-1.0765270	4.0774087	-11.976171	19.173189	-15.996207	5.4501217
			G_1	0.1504185	0.0478401	3.2579960	-9.6921199	14.370843	-11.736129	4.0258411
			G_5	0.8839861	-1.0765270	4.0774087	-11.976171	19.173189	-15.996207	5.4501217
			G_6	0.0000000	0.0000000	0.0000000	0.0000000	0.0000000	0.0000000	0.0000000
		0.8	G_0	0.9033134	-0.9619755	2.8501500	-7.6366897	11.596116	-9.4828625	3.2550163
			G_1	0.1458559	0.2313881	1.9882138	-5.5546045	7.4196069	-5.8965053	2.0855563
			G_5	0.9033134	-0.9619755	2.8501500	-7.6366897	11.596116	-9.4828625	3.2550163
			G_6	0.0000000	0.0000000	0.0000000	0.0000000	0.0000000	0.0000000	0.0000000
0.01	0.03125	0	G_0	0.1965046	2.9373464	-5.2582823	7.4889153	-6.9282667	3.3673349	-0.6677966
			G_1	0.0051780	0.1750280	2.7718680	-4.6457154	4.6780502	-3.2768090	0.9840994
			G_5	0.1945594	2.9082634	-5.2062198	7.4147673	-6.8596703	3.3339951	-0.6611852
			G_6	0.0000000	0.0000000	0.0000000	0.0000000	0.0000000	0.0000000	0.0000000
		0.2	G_0	0.2113693	2.4611847	-1.2555276	-3.9099693	10.168733	-9.4308428	3.0497093
			G_1	0.0068482	0.2344833	2.4101824	-3.4675608	3.2634711	-2.5230489	0.8210179
			G_5	0.2091661	2.4386755	-1.2400919	-3.8967307	10.151842	-9.4330385	3.0549558
			G_6	-0.0172100	-0.1521300	-0.1779700	1.9726870	-3.8338100	3.2472630	-1.0388400
		0.4	G_0	0.2291320	2.9276350	-3.0738200	2.7397460	2.9604660	-6.9798300	3.0083400
			G_1	0.0142030	0.2192850	2.0564800	-0.9489600	-1.5132300	1.9636370	-0.8532200
			G_5	0.2301040	2.6100030	-0.9176200	-4.6212100	15.609250	-17.451800	6.3333330
			G_6	-0.0150460	-0.1515480	0.4190890	-1.2072670	2.0290350	-1.3179820	0.2449160
		0.6	G_0	0.2623350	3.2092560	-3.2397400	8.5204270	-5.1220000	-3.7665800	2.8156500
			G_1	0.0248090	0.3513540	2.0700650	-0.5290600	0.0968000	-1.4958200	0.7241300
			G_5	0.2549450	3.0200540	-2.1778100	4.6517170	2.0776470	-10.061700	4.8888890
			G_6	-0.0814700	0.7240650	-11.914200	47.514510	-86.327200	74.653510	-24.569200
		0.8	G_0	0.3835990	1.7034980	12.805120	-35.291100	68.861500	-71.762500	27.102700
			G_1	0.0448690	0.0905890	5.0431910	-7.6013700	13.743680	-16.240200	6.5418600
			G_5	0.3481020	2.1573310	8.3171710	-20.490700	45.834380	-54.400000	22.000000
			G_6	-0.1363650	0.8255990	-8.0969840	10.864975	7.1092090	-19.508310	8.9002660

Table C.14
Influence Coefficients For A Circumferential Semi-Elliptical Surface Crack In A Cylinder – Inside Surface

t/R_i	a/c	a/t	G_i	A_0	A_1	A_2	A_3	A_4	A_5	A_6
0.01	0.0625	0	G_0	0.2695332	2.1626001	-1.6551569	-1.2970208	4.5604304	-4.3163876	1.4010655
			G_1	0.0138667	0.1827458	2.5749608	-3.9044679	3.3556301	-2.1772209	0.6420134
			G_5	0.2668644	2.1411881	-1.6387693	-1.2841792	4.5152772	-4.2736515	1.3871941
			G_6	0.0000000	0.0000000	0.0000000	0.0000000	0.0000000	0.0000000	0.0000000
		0.2	G_0	0.2835264	2.0613640	-0.9368782	-1.5744499	3.1600245	-2.3327183	0.5899882
			G_1	0.0183834	0.2135060	2.5392469	-4.0904290	4.3065189	-3.3356302	1.0756474
			G_5	0.2808325	2.0498352	-0.9507559	-1.5219478	3.1086233	-2.3153897	0.5903314
			G_6	-0.0131300	-0.0756700	0.0857440	-0.1357400	0.5299420	-0.6651500	0.2740030
		0.4	G_0	0.3202080	2.5067530	-2.0649000	2.2278280	-0.8623600	-0.9432700	0.4956600
			G_1	0.0284060	0.2705840	1.9478260	-1.0579900	-0.9504800	1.1065000	-0.4544200
			G_5	0.3129040	2.4365950	-1.6600900	0.5673180	2.6075810	-4.3140000	1.7142860
			G_6	-0.0169490	0.0703960	-0.4886870	0.8510980	-0.5594650	0.2904380	-0.1440920
		0.6	G_0	0.3775210	3.2406620	-4.8245900	14.629680	-20.455900	12.075370	-2.7056900
			G_1	0.0496180	0.3348330	2.5241770	-2.7321800	3.1090090	-3.4203600	1.2509400
			G_5	0.3833880	2.7490360	-0.9162100	0.5336120	4.0711300	-8.2199700	3.7142860
			G_6	-0.0553810	0.2890290	-2.9240160	7.3178900	-7.6884650	3.7874410	-0.7302120
		0.8	G_0	0.5380920	2.7195780	4.0871740	-6.3008300	7.1473380	-10.827600	5.6152700
			G_1	0.0760440	0.4104780	3.1576040	-2.2896400	1.0207330	-2.3974500	1.3565500
			G_5	0.5039970	3.3050780	-0.9443300	10.766270	-20.957800	11.568260	-1.2903200
			G_6	-0.1220240	1.4824240	-11.677130	27.520060	-23.121698	2.7601930	3.1288300
0.01	0.125	0	G_0	0.4065238	0.7772483	3.8861644	-12.573943	16.760207	-11.014593	2.8706957
			G_1	0.0320270	0.1825342	2.2670449	-2.7076615	1.2088194	-0.3777430	0.0763155
			G_5	0.4024990	0.7695525	3.8476871	-12.449449	16.594264	-10.905538	2.8422733
			G_6	0.0000000	0.0000000	0.0000000	0.0000000	0.0000000	0.0000000	0.0000000
		0.2	G_0	0.4133004	1.1321686	1.8045358	-6.4250407	8.1265233	-5.1779761	1.3216183
			G_1	0.0478287	0.0131254	3.9210159	-9.0824041	12.609044	-9.8323116	3.0270205
			G_5	0.4085744	1.1502654	1.6207996	-5.8595868	7.2756359	-4.5530051	1.1438168
			G_6	-0.0219020	0.2358900	-1.0557450	1.2836690	0.4004010	-1.4438580	0.6076390
		0.4	G_0	0.4884630	1.5730830	0.6794250	-2.6942700	2.4688900	-1.0967700	0.1279400
			G_1	0.0721890	0.4196840	1.5725580	-0.5246000	-1.8820000	1.6181090	-0.4302300
			G_5	0.4804120	1.2808740	2.6986570	-9.6391400	14.039630	-10.260700	2.8888890
			G_6	-0.0216650	0.2362600	-1.0550020	1.2674570	0.4586870	-1.5213580	0.6415500
		0.6	G_0	0.6325650	1.9612380	0.2124640	1.0673660	-4.8520900	4.2428280	-1.2187600
			G_1	0.1171020	0.4578330	2.1168020	-1.8894800	0.5759570	-0.8442000	0.4875500
			G_5	0.6084410	1.5560570	2.7315980	-7.6163000	9.3971820	-6.7692300	2.0000000
			G_6	-0.0505070	0.4694550	-2.7933710	5.3874320	-3.3467640	-0.4227780	0.7601120
		0.8	G_0	0.9044670	1.6602910	5.4293610	-7.8741700	-1.3182900	5.4386470	-1.7533200
			G_1	0.1947050	0.4093530	3.3076490	-3.2250800	-0.4973400	1.2925110	-0.2919800
			G_5	0.8217350	1.6023680	4.7339870	-8.0546200	1.4068690	2.8512260	-1.1538500
			G_6	-0.1093090	1.9146030	-15.389770	49.115082	-74.961586	55.324734	-15.905227

Table C.14
Influence Coefficients For A Circumferential Semi-Elliptical Surface Crack In A Cylinder – Inside Surface

t/R_i	a/c	a/t	G_i	A_0	A_1	A_2	A_3	A_4	A_5	A_6
0.01	0.25	0	G_0	0.6152816	-0.3348694	6.2955620	-15.590618	19.299508	-12.488107	3.3010035
			G_1	0.0703566	0.2828152	1.4036169	-0.6511596	-1.2076596	1.0318656	-0.2423741
			G_5	0.6091901	-0.3315535	6.2332297	-15.436255	19.108424	-12.364462	3.2683198
			G_6	0.0000000	0.0000000	0.0000000	0.0000000	0.0000000	0.0000000	0.0000000
		0.2	G_0	0.6246031	-0.2494174	7.0847353	-20.200719	28.227826	-19.960558	5.6093784
			G_1	0.0891236	0.1846386	2.4135204	-4.7013804	5.7368556	-4.4125580	1.3716268
			G_5	0.6161299	-0.2007834	6.8142686	-19.552840	27.443393	-19.500929	5.5094250
			G_6	-0.0541160	0.5971300	-2.1038670	2.5704450	-0.3120010	-1.2674590	0.5757640
		0.4	G_0	0.7329950	0.0996250	3.9573730	-7.2526600	4.9136700	-0.6649300	-0.4401500
			G_1	0.1244530	0.2438230	1.9426520	-2.0609400	0.6954550	-0.3004200	0.1292100
			G_5	0.7190360	-0.1450100	5.7680680	-13.467900	15.388650	-9.1789700	2.2222220
			G_6	-0.0206400	-0.1296000	0.8965700	-2.9862200	4.9277530	-3.8982200	1.2103470
		0.6	G_0	0.9335850	-0.0671400	4.9859720	-8.0099800	3.1444570	2.1751370	-1.5670900
			G_1	0.1861600	0.1872070	2.3208790	-2.4591900	0.4288930	0.3550800	-0.1581000
			G_5	0.8894260	-0.0854300	5.2732800	-9.6837700	6.7449300	-1.1691900	-0.4444400
			G_6	-0.0463100	-0.0874700	0.6337330	-2.4633100	4.4763150	-3.6982600	1.1853050
		0.8	G_0	1.2407050	-0.9832700	11.036350	-24.419000	25.074820	-13.247100	3.0448500
			G_1	0.2685320	0.0687020	2.9242790	-3.1935800	-0.0724900	1.6614580	-0.7248500
			G_5	1.1263020	-0.1935400	5.0577920	-4.8699400	-6.8200300	12.339280	-5.0000000
			G_6	-0.0921700	0.0037710	-0.1514300	0.1417710	0.1176790	0.1210370	-0.1406600
0.01	0.5	0	G_0	0.8776607	-0.6729719	3.7721411	-6.5209060	6.3377934	-3.7028038	0.9872447
			G_1	0.1277541	0.4368502	0.4904522	1.0427434	-2.9631236	2.0826525	-0.5184313
			G_5	0.8689713	-0.6663089	3.7347931	-6.4563426	6.2750426	-3.6661426	0.9774703
			G_6	0.0000000	0.0000000	0.0000000	0.0000000	0.0000000	0.0000000	0.0000000
		0.2	G_0	0.9002026	-1.0448586	6.4415960	-14.919959	19.300130	-13.414233	3.8224907
			G_1	0.1486748	0.1536960	2.2835405	-4.6118436	5.8374817	-4.6007501	1.4736264
			G_5	0.8967218	-1.1174698	6.9898115	-16.817521	22.611071	-16.255963	4.7757560
			G_6	-0.0224350	0.2340860	-0.7934310	0.9301460	-0.1266190	-0.3599330	0.1408310
		0.4	G_0	1.0063880	-0.7425700	3.1260260	-2.1867000	-3.0931200	5.1298930	-2.0520500
			G_1	0.1789440	0.3206900	1.1011660	-0.2780300	-1.7360100	1.6648710	-0.5147200
			G_5	0.9524140	-0.3624700	1.1644200	2.7118250	-9.3779500	9.0697680	-3.0000000
			G_6	-0.0457800	0.2901210	-1.3238400	2.8032230	-2.8108600	1.1635060	-0.0763800
		0.6	G_0	1.1876880	-1.1514600	4.3134430	-3.6414000	-3.2248100	6.5781370	-2.7782500
			G_1	0.2348560	0.1694010	1.5310330	-0.9297400	-1.2048400	1.4747130	-0.5037800
			G_5	1.1359920	-0.9448000	3.4128040	-1.8724600	-4.5753100	6.5909090	-2.5000000
			G_6	-0.0468900	0.1396290	-0.4115500	0.1517870	1.2863330	-2.0159700	0.8966670
		0.8	G_0	1.3768550	-1.1807900	3.4327750	-1.9675000	-3.7422900	5.2586230	-1.8511600
			G_1	0.2827170	0.2258060	0.9136330	0.4871590	-2.5046300	1.9013960	-0.5002900
			G_5	1.3394760	-1.4954100	5.6192840	-7.8528200	4.1462310	-0.0014000	-0.4666700
			G_6	-0.0491000	-0.0672300	0.3961180	-0.0658000	-1.5130700	2.1490470	-0.8499800

Table C.14
Influence Coefficients For A Circumferential Semi-Elliptical Surface Crack In A Cylinder – Inside Surface

t/R_i	a/c	a/t	G_i	A_0	A_1	A_2	A_3	A_4	A_5	A_6
0.01	1	0	G_0	1.1977992	-0.5244870	0.1498299	2.3284866	-5.1058499	4.3469049	-1.3487980
			G_1	0.1870117	0.6987352	0.1316900	0.7269255	-2.5259384	2.1756251	-0.6540458
			G_5	1.1859396	-0.5192941	0.1483465	2.3054327	-5.0552970	4.3038663	-1.3354436
			G_6	0.0000000	0.0000000	0.0000000	0.0000000	0.0000000	0.0000000	0.0000000
		0.2	G_0	1.2067321	-1.7033309	8.4788390	-24.777373	38.683559	-29.873440	8.9989111
			G_1	0.2148016	0.0103054	4.4729009	-13.203805	19.861499	-15.242926	4.5969364
			G_5	1.2015675	-1.7750100	9.0214999	-26.633978	41.941806	-32.712927	9.9697884
			G_6	0.0016670	-0.0510880	0.2392280	-0.2578760	-0.4940620	1.1084580	-0.5456990
		0.4	G_0	1.3064660	-1.0152400	1.9350880	-0.8993700	-2.4736000	3.7825660	-1.5472100
			G_1	0.2235710	0.5338870	0.8263620	-0.7439300	-1.0125200	1.5328880	-0.6019500
			G_5	1.2517400	-0.7808000	1.3235020	-1.0210500	0.3224960	-0.1302300	0.1000000
			G_6	-0.0695000	0.6377210	-3.1510300	7.3922700	-8.6270500	4.7282640	-0.9106700
		0.6	G_0	1.4098990	-1.1943200	2.0682710	-0.9892900	-2.2245400	3.4010710	-1.3594400
			G_1	0.2530760	0.4979500	0.7711470	-0.5373400	-1.2119300	1.5653800	-0.5725000
			G_5	1.3465480	-0.8307100	0.6179530	1.6695920	-4.1552400	3.4418610	-1.0000000
			G_6	-0.0726000	0.6362230	-3.1015700	7.3056020	-8.6578800	4.9164400	-1.0262100
		0.8	G_0	1.5256800	-1.3415100	1.7834550	-0.0964700	-2.9501000	3.3412720	-1.1425600
			G_1	0.2815290	0.4575980	0.7882960	-0.6608400	-0.6979100	0.9575600	-0.3420100
			G_5	1.4505130	-0.9455100	0.4188330	2.2447860	-4.4641100	3.0139540	-0.6000000
			G_6	-0.0615400	0.2712860	-0.7398700	0.9603950	-0.3723600	-0.2362900	0.1783660
0.01	2	0	G_0	0.8150546	-0.5623828	1.4465771	-4.6778133	8.4192164	-7.9025932	2.9866351
			G_1	0.1359146	0.0702340	3.5558581	-11.034445	16.967724	-14.126991	4.8706612
			G_5	0.8069852	-0.5568149	1.4322545	-4.6314980	8.3358574	-7.8243495	2.9570644
			G_6	0.0000000	0.0000000	0.0000000	0.0000000	0.0000000	0.0000000	0.0000000
		0.2	G_0	0.8302318	-1.0537920	4.4849604	-13.681535	22.101428	-18.224902	6.0608442
			G_1	0.1359260	0.0420920	3.4125294	-10.351846	15.495515	-12.528053	4.2082167
			G_5	0.8480320	-1.4983161	7.5823511	-23.990117	39.865852	-33.470869	11.205087
			G_6	-0.0080970	0.1348050	-0.7140660	1.3153720	-0.3896700	-0.9981360	0.6542230
		0.4	G_0	0.8319520	-0.2882200	-0.9010500	3.7444010	-6.6020800	5.1512080	-1.4147000
			G_1	0.1383584	0.0278547	3.4704568	-10.542062	15.886092	-12.940522	4.3759927
			G_5	0.8560852	-1.5581979	7.9297434	-25.174918	42.077867	-35.552139	11.971236
			G_6	-0.0087500	0.0024420	0.0265390	-0.0760000	0.0506630	0.0276830	-0.0225900
		0.6	G_0	0.8587580	-0.3374500	-0.8921600	3.9094140	-7.0178900	5.5638580	-1.5595700
			G_1	0.1446303	0.0649644	3.1736270	-9.6071448	14.265975	-11.457141	3.8295030
			G_5	0.8805204	-1.4629959	6.9298534	-21.719290	35.917812	-29.984188	9.9790906
			G_6	-0.0119500	0.0130590	-0.0189400	-0.0124700	0.0793610	-0.0796600	0.0305960
		0.8	G_0	0.9123970	-0.9512000	2.8284570	-7.6354600	11.693170	-9.6165300	3.3094020
			G_1	0.1527108	0.0144266	3.5158698	-10.739376	15.998316	-12.610069	4.0831981
			G_5	0.9095908	-1.5365253	7.0754050	-21.927254	35.660007	-29.052725	9.3994559
			G_6	-0.0013200	-0.1153700	0.5804610	-0.9632700	0.0238800	1.2630520	-0.7874300

Table C.14
Influence Coefficients For A Circumferential Semi-Elliptical Surface Crack In A Cylinder – Inside Surface

t/R_i	a/c	a/t	G_i	A_0	A_1	A_2	A_3	A_4	A_5	A_6
0.01667	0.03125	0	G_0	0.1965046	2.9373464	-5.2582823	7.4889153	-6.9282667	3.3673349	-0.6677966
			G_1	0.0051780	0.1750280	2.7718680	-4.6457154	4.6780502	-3.2768090	0.9840994
			G_5	0.1932836	2.8891928	-5.1720807	7.3661459	-6.8146889	3.3121328	-0.6568495
			G_6	0.0000000	0.0000000	0.0000000	0.0000000	0.0000000	0.0000000	0.0000000
		0.2	G_0	0.2107226	2.4486536	-1.2264604	-3.9760193	10.233171	-9.4520364	3.0496836
			G_1	0.0065380	0.2344969	2.3813083	-3.3550592	3.0827443	-2.3997909	0.7921590
			G_5	0.2063955	2.4043109	-1.2248880	-3.7768457	9.8578431	-9.1610116	2.9644987
			G_6	-0.0233860	-0.2565980	0.5389610	-1.1493680	1.8990440	-1.2165670	0.2090670
		0.4	G_0	0.2273500	2.8994780	-3.0702800	2.8459110	2.4358760	-6.3016400	2.7411400
			G_1	0.0189660	0.3037490	1.8836920	-0.6354500	-1.9172200	1.9671670	-0.6897400
			G_5	0.1945370	3.4390340	-9.0123200	25.942970	-38.952000	28.576390	-8.4444400
			G_6	-0.0743900	0.4483590	-9.4044900	38.831220	-70.525400	60.346370	-19.621700
		0.6	G_0	0.2595040	3.0460360	-2.3026600	5.1476090	-0.2504900	-7.0606900	3.7296200
			G_1	0.0257180	0.3727920	1.8347760	0.7184340	-1.9586500	-0.5017000	0.7219100
			G_5	0.2403820	2.8369760	-1.9677600	4.5458510	1.2275100	-8.5617300	4.2222220
			G_6	-0.0699260	-1.0245610	2.5586860	-8.4346200	15.170731	-10.826057	2.6247580
		0.8	G_0	0.3125960	3.1791700	-0.9308400	13.409610	-18.125500	3.2248090	2.4979200
			G_1	0.0367700	0.3553180	2.2611080	2.0125800	-1.6502800	-4.7043800	3.2604900
			G_5	0.3097830	1.8631470	8.1257570	-20.264800	43.972520	-50.000000	19.571430
			G_6	-0.1595320	0.0832100	-6.9477040	11.215244	1.0718880	-9.9117040	4.6272810
0.01667	0.0625	0	G_0	0.2695332	2.1626001	-1.6551569	-1.2970208	4.5604304	-4.3163876	1.4010655
			G_1	0.0138667	0.1827458	2.5749608	-3.9044679	3.3556301	-2.1772209	0.6420134
			G_5	0.2651144	2.1271475	-1.6280233	-1.2757584	4.4856689	-4.2456275	1.3780977
			G_6	0.0000000	0.0000000	0.0000000	0.0000000	0.0000000	0.0000000	0.0000000
		0.2	G_0	0.2829580	2.0531713	-0.9203782	-1.6053672	3.1800418	-2.3249558	0.5812694
			G_1	0.0182587	0.2137291	2.5327625	-4.0829513	4.3084495	-3.3473999	1.0827066
			G_5	0.2780593	2.0296062	-0.9496222	-1.4452190	2.9402537	-2.1624704	0.5394203
			G_6	-0.0225510	0.0272330	-0.4402790	0.8540010	-0.5328560	0.2460040	-0.1288840
		0.4	G_0	0.3177200	2.4789580	-2.0636800	2.3534080	-1.2687900	-0.4771100	0.3178800
			G_1	0.0379310	0.3225690	1.7647930	-0.7186000	-1.3796600	1.3640920	-0.4972600
			G_5	0.3081320	2.3588290	-1.4043700	-0.1304100	3.6134100	-5.0155600	1.9047620
			G_6	-0.0349600	-0.2394800	0.2252480	-0.0616800	0.6178930	-0.8596200	0.3526020
		0.6	G_0	0.3731390	3.0298410	-3.6957200	10.933370	-14.841000	8.0528590	-1.5849700
			G_1	0.0514370	0.3466610	2.5069820	-2.5319400	2.3055250	-2.5341400	0.9518700
			G_5	0.3401350	3.4619520	-7.6020900	24.312920	-36.614800	25.009010	-6.6666700
			G_6	-0.0732710	0.1153490	-2.6257100	6.7943630	-6.8870630	3.3544050	-0.6808330
		0.8	G_0	0.5126800	2.5746070	4.1006990	-6.7070900	7.1938800	-9.5294200	4.7148300
			G_1	0.0735390	0.3946950	3.2561800	-2.6515300	1.1069300	-1.9905100	1.1124200
			G_5	0.4933740	2.5442680	3.7776100	-5.6559200	6.3897230	-9.5947100	4.9032260
			G_6	-0.1353150	0.9140800	-9.2209120	21.912621	-17.958429	2.2107340	2.2578890

Table C.14
Influence Coefficients For A Circumferential Semi-Elliptical Surface Crack In A Cylinder – Inside Surface

t/R_i	a/c	a/t	G_i	A_0	A_1	A_2	A_3	A_4	A_5	A_6
0.01667	0.125	0	G_0	0.4065238	0.7772483	3.8861644	-12.573943	16.760207	-11.014593	2.8706957
			G_1	0.0320270	0.1825342	2.2670449	-2.7076615	1.2088194	-0.3777430	0.0763155
			G_5	0.3998597	0.7645062	3.8224564	-12.367813	16.485450	-10.834026	2.8236354
			G_6	0.0000000	0.0000000	0.0000000	0.0000000	0.0000000	0.0000000	0.0000000
		0.2	G_0	0.4127878	1.1288265	1.8044046	-6.4152938	8.1001222	-5.1480835	1.3099846
			G_1	0.0477082	0.0127494	3.9215370	-9.0953666	12.638799	-9.8588153	3.0356787
			G_5	0.4051564	1.1427315	1.5835103	-5.7158859	7.0488009	-4.3781328	1.0910220
			G_6	-0.0257390	0.2239250	-1.0656070	1.3604470	0.3212500	-1.4129050	0.6046200
		0.4	G_0	0.4759910	1.6149290	0.0563100	-0.3881200	-1.8058600	2.7702150	-1.2288200
			G_1	0.0625368	0.2593641	2.1873520	-2.5516862	1.6083652	-1.1599244	0.3987083
			G_5	0.4717020	1.3107280	2.2107570	-7.7795000	10.750680	-7.4960600	2.0000000
			G_6	-0.0223500	-0.2105800	1.0960460	-3.6464900	6.5149560	-5.4848300	1.7532350
		0.6	G_0	0.6041080	1.7018390	1.2976620	-2.3454700	0.0435520	1.1629990	-0.5711700
			G_1	0.0872040	0.3767790	1.9214790	-0.9505800	-1.4252600	1.3537350	-0.4119700
			G_5	0.5935830	1.5018730	2.7019050	-7.3122800	8.7534260	-6.1481500	1.7777780
			G_6	-0.0632820	0.4081240	-2.6842580	5.2395720	-3.1385120	-0.5189860	0.7611220
		0.8	G_0	0.8018190	1.4311660	5.1378870	-7.5900400	-1.7258200	7.0870920	-2.9593700
			G_1	0.1409210	0.3131480	2.9222170	-2.2316000	-2.0494000	3.1817740	-1.2080000
			G_5	0.7692690	2.0175650	0.5872390	6.6193680	-23.272500	22.948860	-7.5000000
			G_6	-0.1237590	1.7115580	-14.359310	46.270554	-71.065247	52.964100	-15.407071
0.01667	0.25	0	G_0	0.6152816	-0.3348694	6.2955620	-15.590618	19.299508	-12.488107	3.3010035
			G_1	0.0703566	0.2828152	1.4036169	-0.6511596	-1.2076596	1.0318656	-0.2423741
			G_5	0.6051954	-0.3293793	6.1923561	-15.335034	18.983123	-12.283384	3.2468882
			G_6	0.0000000	0.0000000	0.0000000	0.0000000	0.0000000	0.0000000	0.0000000
		0.2	G_0	0.6229389	-0.2302666	6.9609935	-19.846329	27.701044	-19.565724	5.4918651
			G_1	0.0895535	0.1742480	2.4773249	-4.8948423	6.0340648	-4.6366707	1.4375883
			G_5	0.6114479	-0.1967060	6.7335744	-19.266510	26.945778	-19.076337	5.3693778
			G_6	-0.0564090	0.5906920	-2.0901230	2.5558090	-0.2933150	-1.2772490	0.5764810
		0.4	G_0	0.7230860	0.0763310	4.1369260	-8.0319300	6.3592360	-1.8637300	-0.0810400
			G_1	0.1028340	0.2539710	1.7163870	-1.3407600	-0.3668600	0.5645940	-0.1731400
			G_5	0.7005410	0.0839330	3.9999050	-7.5446700	5.5694900	-1.2943200	-0.2222200
			G_6	-0.0184500	-0.1333500	0.8293120	-2.5649100	4.1316010	-3.2421900	0.9979890
		0.6	G_0	0.9042470	-0.1856500	5.7291240	-10.550800	7.2888100	-0.9640900	-0.6920700
			G_1	0.1529590	0.2545430	1.6922640	-0.5535900	-2.4335400	2.5965280	-0.8797800
			G_5	0.8762120	-0.1312800	5.4835950	-10.309600	7.7457380	-1.9368700	-0.2222200
			G_6	-0.0323300	-0.0460700	0.3379100	-1.4409300	3.0261620	-2.8138300	0.9690880
		0.8	G_0	1.1316880	-0.4419800	6.7055250	-9.9538700	1.0924880	6.3974110	-3.2902800
			G_1	0.2221580	0.0260020	3.0773420	-3.8563700	1.2228800	0.7572230	-0.5598400
			G_5	1.0907520	-0.0093200	3.5712560	0.1162350	-14.914300	18.767860	-7.0000000
			G_6	-0.0379600	-0.0569500	0.4782960	-2.1563900	4.5710590	-4.2264200	1.4283640

Table C.14
Influence Coefficients For A Circumferential Semi-Elliptical Surface Crack In A Cylinder – Inside Surface

t/R_i	a/c	a/t	G_i	A_0	A_1	A_2	A_3	A_4	A_5	A_6
0.01667	0.5	0	G_0	0.8776607	-0.6729719	3.7721411	-6.5209060	6.3377934	-3.7028038	0.9872447
			G_1	0.1277541	0.4368502	0.4904522	1.0427434	-2.9631236	2.0826525	-0.5184313
			G_5	0.8632731	-0.6619397	3.7103026	-6.4140059	6.2338948	-3.6421023	0.9710607
			G_6	0.0000000	0.0000000	0.0000000	0.0000000	0.0000000	0.0000000	0.0000000
		0.2	G_0	0.9018864	-1.0815324	6.6630598	-15.564973	20.271752	-14.141756	4.0363397
			G_1	0.1485414	0.1543040	2.2745789	-4.5728426	5.7593465	-4.5280704	1.4483622
			G_5	0.8878878	-1.0636710	6.6354133	-15.724941	20.876895	-14.895310	4.3591221
			G_6	-0.0240560	0.2342620	-0.7930600	0.9271080	-0.1130250	-0.3740260	0.1454300
		0.4	G_0	0.9932740	-0.6825600	2.8682700	-1.6035900	-3.8094000	5.5684300	-2.1598500
			G_1	0.1642050	0.3239630	1.1158550	-0.3663200	-1.5456100	1.5216710	-0.4853800
			G_5	0.9529570	-0.5373900	2.2996290	-0.7968700	-3.8415400	4.7720930	-1.7000000
			G_6	-0.0392000	0.2369810	-1.1181100	2.3926150	-2.3616400	0.9338270	-0.0444800
		0.6	G_0	1.1605830	-1.0763200	4.0197890	-3.0320900	-3.8705800	6.9112630	-2.8542800
			G_1	0.2139410	0.1922300	1.4906570	-1.0134500	-0.8145000	1.0597230	-0.3693500
			G_5	1.1232190	-0.9453400	3.4102860	-1.7964200	-4.7823700	6.8148880	-2.5869600
			G_6	-0.0322300	0.0915520	-0.2918800	0.0768490	1.1473990	-1.7748300	0.7831460
		0.8	G_0	1.3292370	-1.1615100	3.6535650	-2.8835300	-2.1241600	3.9940500	-1.5102100
			G_1	0.2555740	0.2241250	1.0529710	-0.0313700	-1.6192400	1.2592140	-0.3482200
			G_5	1.3186170	-1.4388800	5.2944210	-6.8009000	2.4762560	1.2996490	-0.8666700
			G_6	-0.0183200	-0.1070800	0.3822120	0.1708450	-1.9543600	2.4519870	-0.9252900
0.01667	1	0	G_0	1.1977992	-0.5244870	0.1498299	2.3284866	-5.1058499	4.3469049	-1.3487980
			G_1	0.1870117	0.6987352	0.1316900	0.7269255	-2.5259384	2.1756251	-0.6540458
			G_5	1.1781630	-0.5158889	0.1473738	2.2903151	-5.0221475	4.2756443	-1.3266866
			G_6	0.0000000	0.0000000	0.0000000	0.0000000	0.0000000	0.0000000	0.0000000
		0.2	G_0	1.2067109	-1.7065538	8.4979605	-24.835253	38.773155	-29.938748	9.0165829
			G_1	0.2151798	0.0025801	4.5248744	-13.370468	20.129832	-15.451386	4.6591613
			G_5	1.1935265	-1.7624606	8.9646344	-26.472241	41.691618	-32.517152	9.9089114
			G_6	0.0004290	-0.0477510	0.2303150	-0.2454810	-0.4980090	1.1046740	-0.5435480
		0.4	G_0	1.2939070	-0.9414400	1.6531910	-0.3354400	-2.9873500	3.9237560	-1.5227800
			G_1	0.2126570	0.5532720	0.7775530	-0.6949900	-0.9165800	1.3359110	-0.5126100
			G_5	1.2352820	-0.6784900	0.6678180	1.0594200	-3.0185000	2.4930230	-0.7000000
			G_6	-0.0594800	0.5291200	-2.6578000	6.2565790	-7.3052800	4.0245700	-0.7877100
		0.6	G_0	1.3919890	-1.1257400	1.8713870	-0.7440400	-2.1474300	3.0319020	-1.1729300
			G_1	0.2410950	0.5100520	0.7629270	-0.5721800	-1.0394000	1.3548150	-0.4949800
			G_5	1.3305680	-0.7687300	0.2917540	2.6225000	-5.5751700	4.4837210	-1.3000000
			G_6	-0.0589800	0.5290780	-2.6456800	6.3019950	-7.5575800	4.3779900	-0.9468200
		0.8	G_0	1.5025910	-1.3208600	1.9312100	-0.7670100	-1.6111100	2.1187910	-0.7381600
			G_1	0.2659580	0.4894100	0.6971000	-0.4857100	-0.8023900	0.9455810	-0.3278000
			G_5	1.4409720	-1.0211000	1.0122900	0.3944090	-1.5174900	0.7069770	0.1000000
			G_6	-0.0428700	0.1817060	-0.4353100	0.3506660	0.2052460	-0.4440300	0.1845920

Table C.14
Influence Coefficients For A Circumferential Semi-Elliptical Surface Crack In A Cylinder – Inside Surface

t/R_i	a/c	a/t	G_i	A_0	A_1	A_2	A_3	A_4	A_5	A_6
0.01667	2	0	G_0	0.8150546	-0.5623828	1.4465771	-4.6778133	8.4192164	-7.9025932	2.9866351
			G_1	0.1359146	0.0702340	3.5558581	-11.034445	16.967724	-14.126991	4.8706612
			G_5	0.8016934	-0.5531636	1.4228626	-4.6011275	8.2811961	-7.7730423	2.9376738
			G_6	0.0000000	0.0000000	0.0000000	0.0000000	0.0000000	0.0000000	0.0000000
		0.2	G_0	0.8296376	-1.0437460	4.4199921	-13.483074	21.791644	-17.984029	5.9870082
			G_1	0.1357441	0.0451258	3.3972981	-10.320631	15.469959	-12.523598	4.2106689
			G_5	0.8422970	-1.4838582	7.5048455	-23.737340	39.436617	-33.106104	11.082670
			G_6	-0.0107800	0.1729480	-0.9051370	1.6854460	-0.5675240	-1.2190630	0.8440970
		0.4	G_0	0.8330510	-0.3136000	-0.7111000	3.1028630	-5.5335600	4.2965440	-1.1522500
			G_1	0.1386490	0.0238778	3.4915465	-10.596710	15.956852	-12.981046	4.3833101
			G_5	0.8502334	-1.5410277	7.8395219	-24.889211	41.608812	-35.164752	11.843785
			G_6	-0.0106700	0.0046110	0.0099130	0.0110280	-0.1252300	0.1847150	-0.0743700
		0.6	G_0	0.8601800	-0.3659600	-0.7108000	3.3562330	-6.1468900	4.8899160	-1.3568600
			G_1	0.1447870	0.0626517	3.1877176	-9.6465015	14.316634	-11.481536	3.8311770
			G_5	0.8767225	-1.4859068	7.0929349	-22.156518	36.504262	-30.362654	10.070615
			G_6	-0.0137600	0.0097030	0.0035010	-0.0347700	0.0516970	-0.0181900	0.0018220
		0.8	G_0	0.9130140	-0.9678700	2.9212000	-7.8705700	12.007920	-9.8246000	3.3624720
			G_1	0.1525958	0.0156732	3.5151883	-10.748640	16.017066	-12.616239	4.0802810
			G_5	0.9033272	-1.5238135	7.0480421	-21.856801	35.548564	-28.953022	9.3615973
			G_6	-0.0039000	-0.1111000	0.5786670	-0.9589900	0.0079690	1.2854910	-0.7981400
0.05	0.03125	0	G_0	0.1965046	2.9373464	-5.2582823	7.4889153	-6.9282667	3.3673349	-0.6677966
			G_1	0.0051780	0.1750280	2.7718680	-4.6457154	4.6780502	-3.2768090	0.9840994
			G_5	0.1871476	2.7974724	-5.0078876	7.1323000	-6.5983495	3.2069857	-0.6359971
			G_6	0.0000000	0.0000000	0.0000000	0.0000000	0.0000000	0.0000000	0.0000000
		0.2	G_0	0.2088527	2.4208010	-1.2059115	-3.9916735	10.186590	-9.3787430	3.0256184
			G_1	0.0055515	0.2359151	2.2714873	-2.9924979	2.5054847	-1.9490634	0.6549441
			G_5	0.1888984	2.1971707	-1.0372558	-3.4434858	9.1271458	-8.6616597	2.8410064
			G_6	-0.0623950	-0.7595440	1.1369060	-0.9471780	1.3406020	-0.7485480	0.0417860
		0.4	G_0	0.2339070	2.4866970	-0.3945000	-6.0377300	16.359450	-17.005100	6.0273300
			G_1	0.0156410	0.6614120	-0.8893200	8.0005790	-14.175100	10.019390	-2.7245400
			G_5	0.1673880	2.1612950	-2.2506700	3.7611730	-0.3508100	-3.8464100	1.9555560
			G_6	-0.1307900	-1.2357300	-1.7183400	13.994790	-27.356200	25.334110	-8.8878600
		0.6	G_0	0.2321560	3.2617860	-5.3526500	15.411070	-19.370700	9.7641860	-1.6839100
			G_1	0.0211950	0.2857910	2.5545540	-2.8774200	4.4712910	-5.3746700	2.0320100
			G_5	0.1288820	1.8063090	-2.3302600	8.5168820	-4.1140600	-4.8425900	3.0000000
			G_6	-0.1413800	-3.5684800	14.158750	-48.400400	86.154800	-68.333100	20.129870
		0.8	G_0	0.2646800	3.0895480	-2.7973700	16.180300	-26.132600	16.061620	-3.6341300
			G_1	0.0304540	0.3263940	1.7725930	3.2143820	-6.9108900	3.8177560	-0.8392400
			G_5	0.0800320	0.9383230	0.0482620	4.7846610	9.2012790	-20.880000	8.7142860
			G_6	-0.2457100	-2.4802500	0.1589000	-5.9846800	17.191700	-7.7771500	-0.8628100

Table C.14
Influence Coefficients For A Circumferential Semi-Elliptical Surface Crack In A Cylinder – Inside Surface

t/R_i	a/c	a/t	G_i	A_0	A_1	A_2	A_3	A_4	A_5	A_6
0.05	0.0625	0	G_0	0.2695332	2.1626001	-1.6551569	-1.2970208	4.5604304	-4.3163876	1.4010655
			G_1	0.0138667	0.1827458	2.5749608	-3.9044679	3.3556301	-2.1772209	0.6420134
			G_5	0.2566981	2.0596191	-1.5763400	-1.2352581	4.3432667	-4.1108457	1.3343486
			G_6	0.0000000	0.0000000	0.0000000	0.0000000	0.0000000	0.0000000	0.0000000
		0.2	G_0	0.2802768	2.0413508	-0.9577520	-1.4564195	2.9169446	-2.1046670	0.5129783
			G_1	0.0171658	0.2157598	2.4727789	-3.9201614	4.1177933	-3.2563293	1.0723311
			G_5	0.2635526	1.9313264	-0.9120544	-1.2450163	2.5909773	-1.9333722	0.4853760
			G_6	-0.0490380	-0.1795280	-0.2454050	1.0625390	-0.7967470	0.3727910	-0.1617450
		0.4	G_0	0.3083410	2.3855850	-1.9218300	1.9803570	-1.0348400	-0.3750400	0.2365600
			G_1	0.0312820	0.3438540	1.7288400	-0.3368700	-2.3671700	2.0699200	-0.6086600
			G_5	0.2750280	2.1806580	-1.7967800	2.3832970	-1.4992300	-0.3630100	0.3333330
			G_6	-0.0890500	-0.6601200	0.5733550	0.4495970	-0.3843100	0.2417050	-0.1311800
		0.6	G_0	0.4011200	1.1955530	10.285170	-38.432200	67.857840	-57.992600	18.745000
			G_1	0.0423900	0.3548810	2.1404590	-1.3301800	0.7123500	-1.8956100	1.0072600
			G_5	0.2794130	2.7404610	-5.1200600	17.016710	-25.540900	17.136940	-4.5333300
			G_6	-0.1700610	-2.5508870	5.6011110	-17.785271	29.901886	-18.428740	3.4337990
		0.8	G_0	0.5058610	0.6109790	16.922960	-51.708500	81.151730	-66.073300	21.183300
			G_1	0.0609080	0.4408160	2.1634560	0.6206470	-3.8418100	1.9777360	-0.1831400
			G_5	0.3533810	1.7655490	3.4503590	-4.4932500	6.0530510	-8.4681500	3.8709680
			G_6	-0.2539510	-2.2330840	-0.1690700	-10.898011	25.769169	-11.742322	-0.4864810
0.05	0.125	0	G_0	0.4065238	0.7772483	3.8861644	-12.573943	16.760207	-11.014593	2.8706957
			G_1	0.0320270	0.1825342	2.2670449	-2.7076615	1.2088194	-0.3777430	0.0763155
			G_5	0.3871657	0.7402362	3.7011086	-11.975184	15.962102	-10.490089	2.7339962
			G_6	0.0000000	0.0000000	0.0000000	0.0000000	0.0000000	0.0000000	0.0000000
		0.2	G_0	0.4109456	1.1190116	1.7995105	-6.3821558	8.0421594	-5.1022908	1.2974798
			G_1	0.0473201	0.0067330	3.9647433	-9.3001823	13.031398	-10.195338	3.1437780
			G_5	0.3895573	1.0872270	1.5921659	-5.6384454	6.9313961	-4.2887233	1.0619525
			G_6	-0.0437360	0.1565020	-1.0313070	1.5105890	0.1664470	-1.3280550	0.5756200
		0.4	G_0	0.4680620	1.5180720	0.2614540	-0.8297400	-1.2785600	2.4640070	-1.1529200
			G_1	0.0526100	0.3455230	1.5293310	-0.1018700	-2.9746300	2.9400000	-0.9895200
			G_5	0.4431360	1.1850890	2.2362750	-7.6062200	10.527620	-7.4015700	2.0000000
			G_6	-0.0626000	-0.3093300	0.8619540	-2.4811300	4.9979170	-4.4640200	1.4572080
		0.6	G_0	0.5665160	1.5767920	1.2059820	-1.7776200	-1.2400200	2.5899110	-1.1423900
			G_1	0.0817480	0.3504140	2.0140820	-1.2364600	-1.2340500	1.4071190	-0.4663800
			G_5	0.5220930	1.4697450	1.3716660	-2.5367400	0.9215330	0.1851850	-0.2222200
			G_6	-0.0738600	-0.5319700	-0.7208000	8.0693990	-17.681500	16.815880	-5.8771600
		0.8	G_0	0.7146940	1.2725460	4.8660520	-7.4026300	-0.9288800	6.6483200	-3.0994700
			G_1	0.1242820	0.2617840	3.1204770	-3.0471900	-0.5955300	2.1074230	-0.9288200
			G_5	0.6587750	1.3060670	3.7931230	-4.5510100	-3.4868700	7.2543200	-2.9629600
			G_6	-0.1525200	-0.2139800	-1.2315300	2.6729460	0.8828610	-3.6394900	1.6817260

Table C.14
Influence Coefficients For A Circumferential Semi-Elliptical Surface Crack In A Cylinder – Inside Surface

t/R_i	a/c	a/t	G_i	A_0	A_1	A_2	A_3	A_4	A_5	A_6
0.05	0.25	0	G_0	0.6152816	-0.3348694	6.2955620	-15.590618	19.299508	-12.488107	3.3010035
			G_1	0.0703566	0.2828152	1.4036169	-0.6511596	-1.2076596	1.0318656	-0.2423741
			G_5	0.5859829	-0.3189229	5.9957733	-14.848208	18.380484	-11.893435	3.1438124
			G_6	0.0000000	0.0000000	0.0000000	0.0000000	0.0000000	0.0000000	0.0000000
		0.2	G_0	0.6185825	-0.1889201	6.6630201	-18.947461	26.356152	-18.579782	5.2089411
			G_1	0.0888470	0.1766640	2.4509045	-4.8210542	5.9307746	-4.5640652	1.4174542
			G_5	0.5938754	-0.2661124	6.9889172	-20.068484	28.334612	-20.243019	5.7446666
			G_6	-0.0681120	0.5735220	-2.0883730	2.6098630	-0.3016110	-1.3119290	0.5925120
		0.4	G_0	0.7120460	0.0997300	3.7002710	-6.3957600	3.5324360	0.4713570	-0.8227100
			G_1	0.1024360	0.2393730	1.7991830	-1.6574200	0.1547970	0.1715920	-0.0598000
			G_5	0.6716500	-0.0268600	4.4154340	-8.9308000	8.0425260	-3.3808300	0.4444440
			G_6	-0.0437100	-0.1688200	0.9143180	-2.9907700	5.3160000	-4.4544200	1.4273980
		0.6	G_0	0.8701730	-0.2013500	5.4916110	-9.7304200	6.1268500	-0.1308800	-0.9428600
			G_1	0.1469610	0.2300010	1.8005340	-0.9098200	-1.9066500	2.2539830	-0.7998300
			G_5	0.8231710	-0.3648800	6.7247340	-14.567700	15.263370	-8.2323200	1.7777780
			G_6	-0.0748700	-0.0531400	0.1049720	-0.7885500	2.5097000	-2.6722100	0.9740960
		0.8	G_0	1.0661580	-0.6820000	8.2347200	-15.488000	11.384610	-2.4213500	-0.4876600
			G_1	0.2033950	0.1526570	2.0857100	-0.5861000	-4.0788400	4.9762720	-1.8710400
			G_5	0.9994820	-0.4571900	6.5754670	-10.481400	4.0268590	2.8928570	-2.0000000
			G_6	-0.1006100	-0.0290000	-0.0990100	-0.2568100	1.9597170	-2.3010900	0.8268150
0.05	0.5	0	G_0	0.8776607	-0.6729719	3.7721411	-6.5209060	6.3377934	-3.7028038	0.9872447
			G_1	0.1277541	0.4368502	0.4904522	1.0427434	-2.9631236	2.0826525	-0.5184313
			G_5	0.8358676	-0.6409257	3.5925152	-6.2103867	6.0359933	-3.5264800	0.9402333
			G_6	0.0000000	0.0000000	0.0000000	0.0000000	0.0000000	0.0000000	0.0000000
		0.2	G_0	0.8989180	-1.0427963	6.3805369	-14.662910	18.841814	-13.030293	3.6986806
			G_1	0.1482951	0.1559585	2.2564549	-4.5210175	5.6965240	-4.4932156	1.4409953
			G_5	0.8597078	-1.0466621	6.5257761	-15.496160	20.638594	-14.767469	4.3300207
			G_6	-0.0318180	0.2358030	-0.7996340	0.9487470	-0.1184270	-0.3787760	0.1467390
		0.4	G_0	0.9871950	-0.6970100	2.8922470	-1.6963800	-3.5365700	5.2595990	-2.0425800
			G_1	0.1641010	0.3116290	1.1745980	-0.5657200	-1.1954700	1.2303370	-0.3932700
			G_5	0.9152470	-0.5327500	2.2655200	-0.7412600	-3.8680300	4.7720930	-1.7000000
			G_6	-0.0548300	0.2201590	-1.0038000	2.1510600	-2.0964600	0.8311100	-0.0472500
		0.6	G_0	1.1416020	-1.0912600	4.0504810	-3.0974600	-3.6415200	6.6258570	-2.7429800
			G_1	0.2103960	0.1869600	1.4864060	-0.9635100	-0.9174600	1.1604050	-0.4073600
			G_5	1.0665520	-0.8887500	3.1626170	-1.2716000	-5.2179700	6.9104090	-2.5652200
			G_6	-0.0587900	0.1072110	-0.3228800	0.1376970	1.1227310	-1.7342600	0.7482830
		0.8	G_0	1.2858380	-1.0689700	3.0323820	-0.7046000	-5.5956800	6.6774710	-2.3334600
			G_1	0.2474970	0.2175330	1.1026400	-0.1675100	-1.3848400	1.0861840	-0.3080700
			G_5	1.2352800	-1.3022500	4.6326660	-4.9251900	-0.0373500	2.9824560	-1.3333300
			G_6	-0.0540900	-0.0927500	0.3897420	-0.0963800	-1.1396700	1.6443890	-0.6512400

Table C.14
Influence Coefficients For A Circumferential Semi-Elliptical Surface Crack In A Cylinder – Inside Surface

t/R_i	a/c	a/t	G_i	A_0	A_1	A_2	A_3	A_4	A_5	A_6
0.05	1	0	G_0	1.1977992	-0.5244870	0.1498299	2.3284866	-5.1058499	4.3469049	-1.3487980
			G_1	0.1870117	0.6987352	0.1316900	0.7269255	-2.5259384	2.1756251	-0.6540458
			G_5	1.1407610	-0.4995114	0.1426952	2.2176067	-4.8627143	4.1399095	-1.2845695
			G_6	0.0000000	0.0000000	0.0000000	0.0000000	0.0000000	0.0000000	0.0000000
		0.2	G_0	1.2084687	-1.7294060	8.6186987	-25.175578	39.288339	-30.318733	9.1234045
			G_1	0.2163478	-0.0120989	4.6109160	-13.629267	20.529426	-15.746786	4.7419942
			G_5	1.1555075	-1.7008589	8.6393123	-25.454348	40.064649	-31.243623	9.5190147
			G_6	-0.0037710	-0.0489600	0.2447630	-0.2640320	-0.4864590	1.1025000	-0.5433790
		0.4	G_0	1.2913150	-0.9650100	1.8057540	-0.9174900	-1.8241900	2.8527550	-1.1595700
			G_1	0.2112910	0.5710160	0.6556010	-0.3623700	-1.3624500	1.6435020	-0.6006500
			G_5	1.1916900	-0.6676400	0.7450230	0.7992390	-2.5897600	2.1534890	-0.6000000
			G_6	-0.0691400	0.5307620	-2.6457900	6.2996400	-7.4455700	4.1740290	-0.8439300
		0.6	G_0	1.3852290	-1.1470100	1.9194050	-0.7144800	-2.2804400	3.1702690	-1.2274700
			G_1	0.2389740	0.5239180	0.6757630	-0.3719900	-1.2356100	1.4486510	-0.5158900
			G_5	1.2864450	-0.8387500	0.9039760	0.8524830	-2.8879500	2.4465120	-0.7000000
			G_6	-0.0758100	0.5692200	-2.8066600	6.7182820	-8.0668600	4.6803110	-1.0184900
		0.8	G_0	1.4894880	-1.3511400	2.1312770	-1.2578300	-0.8055500	1.4488030	-0.5327000
			G_1	0.2640980	0.4833400	0.7438410	-0.6804900	-0.3832900	0.5727370	-0.2136000
			G_5	1.3900720	-1.0885300	1.7049700	-1.5479000	1.3690280	-1.4232600	0.7000000
			G_6	-0.0635800	0.2164910	-0.5719900	0.7731070	-0.4185400	0.0227330	0.0417860
0.05	2	0	G_0	0.8150546	-0.5623828	1.4465771	-4.6778133	8.4192164	-7.9025932	2.9866351
			G_1	0.1359146	0.0702340	3.5558581	-11.034445	16.967724	-14.126991	4.8706612
			G_5	0.7762429	-0.5356029	1.3776924	-4.4550600	8.0183010	-7.5262791	2.8444143
			G_6	0.0000000	0.0000000	0.0000000	0.0000000	0.0000000	0.0000000	0.0000000
		0.2	G_0	0.8303757	-1.0498204	4.4477334	-13.542741	21.849163	-17.992876	5.9769347
			G_1	0.1354705	0.0543807	3.3359372	-10.128052	15.148588	-12.247389	4.1164665
			G_5	0.8151606	-1.4268649	7.2227537	-22.829526	37.909858	-31.815559	10.649474
			G_6	-0.0090960	0.1261280	-0.6706890	1.2469360	-0.3690640	-0.9602970	0.6306940
		0.4	G_0	0.8330780	-0.3084500	-0.7547200	3.2657440	-5.8159500	4.5465500	-1.2404700
			G_1	0.1377281	0.0408094	3.3855168	-10.277166	15.441270	-12.544940	4.2347369
			G_5	0.8233414	-1.4926311	7.6320418	-24.161868	40.274146	-33.946581	11.407910
			G_6	-0.0134800	-0.0043900	0.0592600	-0.1017500	0.0175090	0.0918390	-0.0489900
		0.6	G_0	0.8595130	-0.3581900	-0.7703600	3.5772760	-6.5251400	5.2235110	-1.4752700
			G_1	0.1441670	0.0764692	3.0963445	-9.3576065	13.828183	-11.044497	3.6744786
			G_5	0.8479635	-1.4134353	6.7655216	-21.067314	34.623427	-28.746902	9.5236582
			G_6	-0.0187500	0.0102610	0.0108250	-0.0443900	0.0620740	-0.0240800	0.0040530
		0.8	G_0	0.9118690	-0.9615800	2.8858030	-7.7145200	11.709760	-9.5193500	3.2371640
			G_1	0.1520131	0.0313966	3.4128759	-10.422563	15.464464	-12.118677	3.9007626
			G_5	0.8750218	-1.4693251	6.8784396	-21.216993	34.321483	-27.816896	8.9556168
			G_6	-0.0101100	-0.1069100	0.5613170	-0.9055800	-0.0257400	1.2574370	-0.7704300

Table C.14
Influence Coefficients For A Circumferential Semi-Elliptical Surface Crack In A Cylinder – Inside Surface

t/R_i	a/c	a/t	G_i	A_0	A_1	A_2	A_3	A_4	A_5	A_6
0.1	0.03125	0	G_0	0.1965046	2.9373464	-5.2582823	7.4889153	-6.9282667	3.3673349	-0.6677966
			G_1	0.0051780	0.1750280	2.7718680	-4.6457154	4.6780502	-3.2768090	0.9840994
			G_5	0.1786409	2.6703146	-4.7802564	6.8081046	-6.2984246	3.0612136	-0.6070882
			G_6	0.0000000	0.0000000	0.0000000	0.0000000	0.0000000	0.0000000	0.0000000
		0.2	G_0	0.2073050	2.4043916	-1.2521489	-3.8112746	9.7691991	-8.9612397	2.8836220
			G_1	0.0043895	0.2579812	1.9801891	-2.0115020	0.9000182	-0.6939037	0.2816436
			G_5	0.1506071	1.8944151	-1.5339682	0.0383312	3.8549836	-5.2088399	1.9521928
			G_6	-0.1211200	-0.9625500	-2.4298600	15.998410	-29.266100	24.850920	-8.0696800
		0.4	G_0	0.2154860	2.8003500	-3.0453900	2.0532160	3.4108590	-6.8487000	2.9779500
			G_1	0.0178580	0.3079160	1.6813980	-0.0166100	-2.6394000	2.2074140	-0.6976200
			G_5	0.0618685	0.5599721	1.3932612	-3.1664766	12.223550	-14.947058	5.3365097
			G_6	-0.1830800	-2.4496400	2.8812760	-1.6867300	-0.6663700	5.6696970	-3.5651500
		0.6	G_0	0.2334930	2.7804350	-2.0696500	2.6579110	1.4535300	-5.8352000	2.8125900
			G_1	0.0205410	0.3888190	1.1499270	2.4877470	-5.7318100	3.6427850	-0.9172600
			G_5	0.0072440	2.4750432	-12.934841	8.6909137	49.990467	-75.967243	29.667058
			G_6	-0.1668800	-3.3581200	10.335090	-37.053200	58.288730	-34.216500	6.1708470
		0.8	G_0	0.2427700	2.8035350	-1.2713700	5.4620650	-6.1361900	1.5108850	0.0547000
			G_1	0.0304720	0.2067440	2.9709670	-3.2573400	4.9739790	-5.4464500	1.8285600
			G_5	-0.2096100	-1.0318800	-4.9809500	12.311260	10.127790	-15.473000	1.5969130
			G_6	-0.1074500	-2.0388700	4.2036950	-20.234800	8.0199980	29.788750	-19.631300
0.1	0.0625	0	G_0	0.2695332	2.1626001	-1.6551569	-1.2970208	4.5604304	-4.3163876	1.4010655
			G_1	0.0138667	0.1827458	2.5749608	-3.9044679	3.3556301	-2.1772209	0.6420134
			G_5	0.2450300	1.9660000	-1.5046882	-1.1791100	4.1458455	-3.9239891	1.2736964
			G_6	0.0000000	0.0000000	0.0000000	0.0000000	0.0000000	0.0000000	0.0000000
		0.2	G_0	0.2779608	2.0193256	-0.9275729	-1.5950891	3.1906437	-2.3502174	0.5991162
			G_1	0.0160185	0.2199692	2.3978435	-3.7534347	3.9341356	-3.1541845	1.0504548
			G_5	0.2419300	1.7627817	-0.7393570	-1.2164716	2.5994393	-2.1071979	0.5817704
			G_6	-0.0845470	-0.4374560	-0.1360350	1.8357670	-1.9350120	1.1367400	-0.3762580
		0.4	G_0	0.3011590	2.2369350	-1.2366000	-0.2270000	2.2512460	-2.8387200	1.0123400
			G_1	0.0201666	0.2827653	2.1695559	-2.9258419	3.5150238	-3.5336170	1.2986040
			G_5	0.2220849	1.6042375	-0.5613839	0.9851166	0.0274225	-1.6054790	0.7445933
			G_6	-0.1378000	-1.3643200	1.4106360	1.0971800	-2.9582600	3.4025980	-1.4500400
		0.6	G_0	0.3224330	2.7848890	-3.9933700	11.326780	-16.755000	10.978200	-2.7831100
			G_1	0.0410830	0.2313980	3.0577560	-4.8777100	6.3133550	-5.7918300	2.0004100
			G_5	0.1875036	1.1459365	0.9632276	-0.2360816	4.0646159	-7.1055726	2.8178537
			G_6	-0.2337900	-1.7348100	1.4149140	-2.0114000	6.7183760	-5.0399700	0.8866800
		0.8	G_0	0.4117650	1.7044180	7.4132840	-24.685800	41.662980	-35.936000	11.838500
			G_1	0.0609440	0.0592690	5.0648580	-10.833900	16.281600	-14.006400	4.5603700
			G_5	0.1284298	0.6557187	2.0158926	-0.7693775	9.0901536	-13.652912	4.9195995
			G_6	-0.3031900	-2.3426000	1.4260850	-4.5266500	13.114480	-7.8324800	0.4643600

Table C.14
Influence Coefficients For A Circumferential Semi-Elliptical Surface Crack In A Cylinder – Inside Surface

t/R_i	a/c	a/t	G_i	A_0	A_1	A_2	A_3	A_4	A_5	A_6
0.1	0.125	0	G_0	0.4065238	0.7772483	3.8861644	-12.573943	16.760207	-11.014593	2.8706957
			G_1	0.0320270	0.1825342	2.2670449	-2.7076615	1.2088194	-0.3777430	0.0763155
			G_5	0.3695673	0.7065891	3.5328764	-11.430857	15.236552	-10.013266	2.6097236
			G_6	0.0000000	0.0000000	0.0000000	0.0000000	0.0000000	0.0000000	0.0000000
		0.2	G_0	0.4073632	1.1141359	1.7772808	-6.3608686	8.0436930	-5.1068311	1.2977650
			G_1	0.0463249	-0.0012662	4.0186652	-9.5730735	13.576928	-10.675057	3.3001718
			G_5	0.3672804	1.0342299	1.4947987	-5.2612250	6.4821928	-4.0450187	1.0109412
			G_6	-0.0690920	0.0713160	-1.0328520	1.8138710	-0.0862930	-1.2722490	0.5814380
		0.4	G_0	0.4570240	1.4083920	0.6887150	-2.2096300	0.8473750	0.9393130	-0.7335500
			G_1	0.0614672	0.0306071	4.1452838	-9.9995542	14.683048	-11.862862	3.7194167
			G_5	0.3967885	1.1376492	1.3272280	-3.7178419	4.3265950	-3.0093646	0.8528040
			G_6	-0.1162600	-0.3861300	0.1981140	0.1738100	1.2304200	-1.7726300	0.6726720
		0.6	G_0	0.5223070	1.5197230	1.2517870	-2.3805700	-0.1906100	1.9556200	-1.0072700
			G_1	0.0681380	0.3470990	1.8482480	-0.6958400	-1.9238800	1.7202440	-0.4798400
			G_5	0.4463316	1.1343342	1.5987945	-1.3817396	-0.9469882	1.1230761	-0.3362630
			G_6	-0.1798400	-0.5774800	-0.0079500	1.1466210	0.6354880	-1.6047100	0.5878760
		0.8	G_0	0.6294930	1.4366510	2.5517550	0.4151700	-14.348200	18.547370	-7.2502400
			G_1	0.0982030	0.3339670	2.3218800	-0.8035400	-3.5908200	4.2249730	-1.5661500
			G_5	0.5067261	0.8959043	2.5894421	3.3629236	-15.995588	16.491438	-5.7967706
			G_6	-0.2496000	-0.6660700	-1.9160800	7.6244820	-6.9942900	2.5337230	-0.3321600
0.1	0.25	0	G_0	0.6152816	-0.3348694	6.2955620	-15.590618	19.299508	-12.488107	3.3010035
			G_1	0.0703566	0.2828152	1.4036169	-0.6511596	-1.2076596	1.0318656	-0.2423741
			G_5	0.5593473	-0.3044264	5.7232382	-14.173289	17.545007	-11.352825	3.0009118
			G_6	0.0000000	0.0000000	0.0000000	0.0000000	0.0000000	0.0000000	0.0000000
		0.2	G_0	0.6203701	-0.2735697	7.1419540	-20.356869	28.489937	-20.172430	5.6739197
			G_1	0.0882439	0.1706464	2.4734911	-4.8946737	6.0398855	-4.6377769	1.4364040
			G_5	0.5619179	-0.2210541	6.4445349	-18.440179	25.960076	-18.524879	5.2543664
			G_6	-0.0833730	0.5360330	-2.0372090	2.5868910	-0.1578860	-1.5207340	0.6820320
		0.4	G_0	0.7051060	-0.0231600	4.3023810	-8.2775600	6.5937550	-1.9480200	-0.0820400
			G_1	0.1030370	0.2479400	1.7027470	-1.3246300	-0.4540100	0.6872710	-0.2195500
			G_5	0.6294410	-0.0696200	4.3250250	-8.6688000	7.8431060	-3.3350300	0.4444440
			G_6	-0.0809800	-0.1333100	0.4934000	-1.7465100	3.7729530	-3.4369900	1.1314340
		0.6	G_0	0.8272440	-0.1473300	4.8311860	-7.7180300	3.1488780	2.0824210	-1.5932300
			G_1	0.1412290	0.2010310	1.9839640	-1.5511200	-0.8183800	1.3484690	-0.5036100
			G_5	0.7434380	-0.3035400	5.9106100	-12.151600	11.934150	-5.9065700	1.1111110
			G_6	-0.1284100	-0.0539300	-0.1516800	-0.1596400	2.2505800	-2.8015900	1.0446610
		0.8	G_0	0.9848890	-0.5919300	7.5198620	-13.510100	8.8164640	-0.4816300	-1.1635500
			G_1	0.1816680	0.2057820	1.6810880	0.6978020	-6.0729600	6.5679730	-2.3864200
			G_5	0.8592330	0.0347720	2.7632420	1.7250280	-14.870100	17.491070	-6.5000000
			G_6	-0.1727300	-0.0102100	-0.5090200	0.5706760	2.0135520	-3.0636700	1.1714020

Table C.14
Influence Coefficients For A Circumferential Semi-Elliptical Surface Crack In A Cylinder – Inside Surface

t/R_i	a/c	a/t	G_i	A_0	A_1	A_2	A_3	A_4	A_5	A_6
0.1	0.5	0	G_0	0.8776607	-0.6729719	3.7721411	-6.5209060	6.3377934	-3.7028038	0.9872447
			G_1	0.1277541	0.4368502	0.4904522	1.0427434	-2.9631236	2.0826525	-0.5184313
			G_5	0.7978736	-0.6117927	3.4292191	-5.9280964	5.7616300	-3.3661855	0.8974955
			G_6	0.0000000	0.0000000	0.0000000	0.0000000	0.0000000	0.0000000	0.0000000
		0.2	G_0	0.8973156	-1.0578646	6.4202252	-14.707694	18.854428	-13.015913	3.6898950
			G_1	0.1474310	0.1597183	2.2167686	-4.3932515	5.4975121	-4.3391504	1.3937659
			G_5	0.8192994	-0.9922420	6.1641760	-14.490390	19.139105	-13.615552	3.9753597
			G_6	-0.0430440	0.2417660	-0.8296330	1.0071940	-0.0903370	-0.4811070	0.1975610
		0.4	G_0	0.9797140	-0.7254800	2.9493190	-1.7803700	-3.3922500	5.1150450	-1.9900700
			G_1	0.1634700	0.3030870	1.1780260	-0.5382100	-1.2620000	1.2960220	-0.4171300
			G_5	0.8704930	-0.5506800	2.3089230	-0.9341600	-3.4657800	4.4325590	-1.6000000
			G_6	-0.0740800	0.2359400	-1.1185600	2.4582730	-2.4457400	1.0596080	-0.1154400
		0.6	G_0	1.1154070	-1.0657300	3.7727200	-2.1008700	-5.1931500	7.7858620	-3.0862200
			G_1	0.2048290	0.1913420	1.4364550	-0.8279000	-1.0808600	1.2687530	-0.4410400
			G_5	1.0037320	-0.9196900	3.4318250	-2.2468600	-3.4458400	5.4314890	-2.1087000
			G_6	-0.0889300	0.1269620	-0.4127300	0.2100800	1.3835970	-2.1123000	0.8933220
		0.8	G_0	1.2431440	-1.1153500	3.3984140	-1.6864300	-3.9663600	5.3741580	-1.9576100
			G_1	0.2383820	0.2082130	1.1743690	-0.3888200	-0.9823300	0.7689770	-0.2240300
			G_5	1.1409380	-1.1250400	3.7327740	-2.1506800	-4.1582500	6.0533330	-2.2666700
			G_6	-0.0964200	-0.0395100	0.1733090	0.2988850	-1.3297300	1.6351950	-0.6417300
0.1	1	0	G_0	1.1977992	-0.5244870	0.1498299	2.3284866	-5.1058499	4.3469049	-1.3487980
			G_1	0.1870117	0.6987352	0.1316900	0.7269255	-2.5259384	2.1756251	-0.6540458
			G_5	1.0889082	-0.4768064	0.1362091	2.1168064	-4.6416818	3.9517318	-1.2261800
			G_6	0.0000000	0.0000000	0.0000000	0.0000000	0.0000000	0.0000000	0.0000000
		0.2	G_0	1.2074332	-1.7377740	8.6237280	-25.122900	39.172348	-30.211985	9.0845561
			G_1	0.2154039	-0.0005543	4.5272627	-13.383481	20.173925	-15.484935	4.6634559
			G_5	1.1036486	-1.6181347	8.2081429	-24.114960	37.929125	-29.571408	9.0059756
			G_6	-0.0108580	-0.0329460	0.1737750	-0.1390550	-0.4552700	0.8873630	-0.4227350
		0.4	G_0	1.2859130	-0.9487500	1.6002530	-0.1814400	-2.9779600	3.7295100	-1.4241300
			G_1	0.2263929	0.2417342	2.6832302	-7.2978158	10.667447	-8.5251084	2.7415796
			G_5	1.1392380	-0.6650100	0.8422340	0.5045500	-2.1156100	1.7906980	-0.5000000
			G_6	-0.0770000	0.5142550	-2.5720700	6.1650010	-7.3245000	4.1561480	-0.8618300
		0.6	G_0	1.3753150	-1.1702100	2.0218150	-1.0181300	-1.5953100	2.4728220	-0.9798400
			G_1	0.2376410	0.5197520	0.6785190	-0.4124500	-1.0682900	1.2661940	-0.4553000
			G_5	1.2278340	-0.8558800	1.2069500	-0.0267600	-1.5232100	1.4046510	-0.4000000
			G_6	-0.0891700	0.5380320	-2.6437600	6.3949370	-7.7668300	4.6065810	-1.0398000
		0.8	G_0	1.4688630	-1.3084700	1.8356310	-0.1796200	-2.4202000	2.6048770	-0.8684600
			G_1	0.2596240	0.5185940	0.5077920	0.0042410	-1.3328100	1.2578320	-0.4221500
			G_5	1.3210180	-1.0737100	1.9343580	-2.1542600	2.3106990	-2.1488400	0.9000000
			G_6	-0.0851000	0.2200410	-0.5637000	0.7256100	-0.2530000	-0.1442400	0.1003900

Table C.14
Influence Coefficients For A Circumferential Semi-Elliptical Surface Crack In A Cylinder – Inside Surface

t/R_i	a/c	a/t	G_i	A_0	A_1	A_2	A_3	A_4	A_5	A_6
0.1	2	0	G_0	0.8150546	-0.5623828	1.4465771	-4.6778133	8.4192164	-7.9025932	2.9866351
			G_1	0.1359146	0.0702340	3.5558581	-11.034445	16.967724	-14.126991	4.8706612
			G_5	0.7409591	-0.5112573	1.3150700	-4.2525573	7.6538327	-7.1841755	2.7151227
			G_6	0.0000000	0.0000000	0.0000000	0.0000000	0.0000000	0.0000000	0.0000000
		0.2	G_0	0.8298834	-1.0367874	4.3513354	-13.223826	21.319908	-17.547855	5.8279870
			G_1	0.1353367	0.1199528	2.8902835	-8.6472179	12.720573	-10.334998	3.5369914
			G_5	0.7789753	-1.3563946	6.8812447	-21.723632	36.036893	-30.217963	10.107456
			G_6	-0.0109630	0.1269130	-0.6713740	1.2490330	-0.3541110	-0.9907030	0.6459300
		0.4	G_0	0.8336540	-0.3330500	-0.6501700	3.0585860	-5.6171400	4.4906380	-1.2539900
			G_1	0.1405870	0.0669674	3.1921749	-9.5752272	14.211132	-11.510350	3.8996689
			G_5	0.7870987	-1.4187641	7.2712138	-22.901623	38.021413	-31.953295	10.715502
			G_6	-0.0151900	0.0158950	-0.0435700	0.1259000	-0.2066400	0.1827200	-0.0591100
		0.6	G_0	0.8590230	-0.3794700	-0.6620500	3.3021610	-6.1317800	4.9676950	-1.4192000
			G_1	0.1440687	0.1439522	2.6262653	-7.7509403	11.130715	-8.8604868	2.9920847
			G_5	0.8109444	-1.3410644	6.4943491	-20.143983	32.968174	-27.261393	8.9973210
			G_6	-0.0211000	0.0117120	-0.0131900	0.0464780	-0.0661000	0.0649330	-0.0227300
		0.8	G_0	0.9093260	-0.9654500	2.8959630	-7.6431200	11.484330	-9.2250600	3.1015570
			G_1	0.1479634	0.1791786	2.3828007	-6.9734350	9.8125456	-7.6664669	2.5487367
			G_5	0.8380323	-1.4012215	6.6971976	-20.575896	33.127834	-26.714540	8.5555764
			G_6	-0.0144800	-0.0979100	0.4954390	-0.7304000	-0.1978400	1.3085810	-0.7633900
0.2	0.0625	0	G_0	0.2695332	2.1626001	-1.6551569	-1.2970208	4.5604304	-4.3163876	1.4010655
			G_1	0.0138667	0.1827458	2.5749608	-3.9044679	3.3556301	-2.1772209	0.6420134
			G_5	0.2246108	1.8021667	-1.3792975	-1.0808508	3.8003583	-3.5969900	1.1675550
			G_6	0.0000000	0.0000000	0.0000000	0.0000000	0.0000000	0.0000000	0.0000000
		0.2	G_0	0.2746613	1.9926330	-0.9344868	-1.6006254	3.1712542	-2.2919293	0.5726679
			G_1	0.0154215	0.2148007	2.2991669	-3.1533248	2.5615750	-1.8272676	0.5911296
			G_5	0.1864580	1.3358788	-0.3565298	-0.6436695	1.7373083	-1.8574034	0.6055380
			G_6	-0.1420850	-0.9134530	0.5073540	1.1718630	-0.2639180	-0.5389720	0.1820820
		0.4	G_0	0.2905060	2.2613840	-2.0236600	2.2348690	-2.0384300	0.8480130	-0.1769400
			G_1	0.0144756	0.3060575	1.7690501	-1.9480031	2.1586426	-2.5707633	1.0419656
			G_5	0.0814338	0.4622342	0.9701344	-0.4170561	4.1954989	-6.6059029	2.5147927
			G_6	-0.2668900	-1.4913300	-2.2572300	13.963520	-23.281800	20.497450	-7.1637200
		0.6	G_0	0.3136790	2.2391710	-0.9686200	0.4644400	0.9116520	-2.1793200	0.9255600
			G_1	0.0185012	0.3155587	1.7412147	-0.9629640	0.4000714	-1.1702488	0.5577101
			G_5	-0.0138148	3.0124244	-21.690366	53.641576	-45.054099	9.4961301	2.0727136
			G_6	-0.3563400	1.0277720	-26.712600	94.035930	-163.57100	145.97540	-50.399100
		0.8	G_0	0.3307580	2.2665800	-0.1922100	0.2251110	0.2049680	-0.1791300	-0.4343900
			G_1	0.0244425	0.2650455	2.3621920	-2.3053317	2.2790075	-1.7977214	0.2912095
			G_5	-0.2289300	-0.7174000	-4.5793300	17.518560	-10.321900	2.8966740	-2.7936800
			G_6	-0.1960400	-2.9545700	6.4418390	-16.738900	-11.887500	57.343800	-32.008700

Table C.14
Influence Coefficients For A Circumferential Semi-Elliptical Surface Crack In A Cylinder – Inside Surface

t/R_i	a/c	a/t	G_i	A_0	A_1	A_2	A_3	A_4	A_5	A_6
0.2	0.125	0	G_0	0.4065238	0.7772483	3.8861644	-12.573943	16.760207	-11.014593	2.8706957
			G_1	0.0320270	0.1825342	2.2670449	-2.7076615	1.2088194	-0.3777430	0.0763155
			G_5	0.3387700	0.6477067	3.2384700	-10.478286	13.966839	-9.1788275	2.3922467
			G_6	0.0000000	0.0000000	0.0000000	0.0000000	0.0000000	0.0000000	0.0000000
		0.2	G_0	0.4029371	1.0915242	1.8053108	-6.5056770	8.3443842	-5.3716087	1.3852674
			G_1	0.0452071	-0.0181395	4.1484326	-10.205731	14.812282	-11.740606	3.6414801
			G_5	0.3199265	0.9054968	1.2979152	-4.2860957	5.1801281	-3.2638264	0.8275216
			G_6	-0.1116150	-0.0781560	-1.0400430	2.3887150	-0.6732360	-1.0034070	0.5242030
		0.4	G_0	0.4333520	1.3570530	0.6442570	-1.6162700	-0.9947800	2.9604760	-1.4598700
			G_1	0.0541970	-0.0089757	4.3466655	-11.070580	16.815488	-13.712564	4.3164728
			G_5	0.2994313	0.8822012	0.9409687	-1.5062580	1.2907743	-1.1458133	0.3877044
			G_6	-0.2041000	-0.6628600	-0.0950100	2.3430480	-1.7270700	0.2829070	0.0630740
		0.6	G_0	0.4778330	1.6381280	-0.4449500	2.2452420	-6.0980400	5.5550270	-1.8235500
			G_1	0.0642112	0.0122041	4.5658760	-12.091301	19.452980	-16.480149	5.3023739
			G_5	0.2628298	0.6788669	1.0548894	1.1760094	-2.8340836	1.2008831	-0.1668244
			G_6	-0.3387500	-0.7171400	-2.0254800	7.4624010	-6.9186200	3.5122470	-0.9746500
		0.8	G_0	0.5678290	1.3699790	2.1829740	-2.2567200	-3.7602900	6.9941040	-3.1800000
			G_1	0.0780259	0.1849201	3.0922070	-4.8798214	5.5329482	-3.9782921	1.0031902
			G_5	0.2162607	0.1399392	3.8003479	-5.9198440	10.409525	-9.7649744	2.8601002
			G_6	-0.4948700	-0.7008400	-5.5432300	15.740690	-13.267000	5.7877350	-1.5224600
0.2	0.25	0	G_0	0.6152816	-0.3348694	6.2955620	-15.590618	19.299508	-12.488107	3.3010035
			G_1	0.0703566	0.2828152	1.4036169	-0.6511596	-1.2076596	1.0318656	-0.2423741
			G_5	0.5127350	-0.2790575	5.2463017	-12.992182	16.082923	-10.406756	2.7508358
			G_6	0.0000000	0.0000000	0.0000000	0.0000000	0.0000000	0.0000000	0.0000000
		0.2	G_0	0.6158704	-0.3044136	7.2958788	-20.842918	29.246345	-20.740650	5.8405190
			G_1	0.0860016	0.1750272	2.4176760	-4.7274150	5.7641284	-4.4067981	1.3617675
			G_5	0.5090451	-0.2459198	6.1850917	-17.727067	25.120721	-18.031279	5.1362957
			G_6	-0.0874650	0.2048870	-0.7877790	-0.1144930	3.4096200	-3.9775920	1.3587750
		0.4	G_0	0.6807090	-0.0181700	4.1010120	-7.7342100	5.7789710	-1.2781400	-0.3020800
			G_1	0.0977220	0.2345930	1.7571400	-1.5032200	-0.1782300	0.4680680	-0.1464000
			G_5	0.5474370	-0.1626600	4.5522900	-9.8670500	10.608220	-5.9592900	1.3333330
			G_6	-0.1429600	-0.1522700	0.3434280	-1.3869700	3.9981410	-4.1031700	1.4438050
		0.6	G_0	0.7643780	-0.1045600	4.6780500	-7.7826000	3.6090570	1.7154280	-1.5165200
			G_1	0.1231500	0.1987760	1.9756880	-1.5470200	-0.7898700	1.3021320	-0.4817700
			G_5	0.5889460	-0.0776600	3.9525530	-6.3655800	3.6415570	0.1212120	-0.6666700
			G_6	-0.2281500	-0.0472900	-0.6334600	1.2719350	1.1658530	-2.6941700	1.1652830
		0.8	G_0	0.9005030	-0.8174000	9.1343790	-18.318900	16.233020	-5.9092800	0.3336100
			G_1	0.1592400	0.1254450	2.2234910	-0.9907000	-3.2169100	4.2541320	-1.6800700
			G_5	0.6683370	-0.5392400	6.5084110	-10.972100	7.8124000	-1.5803600	-0.5000000
			G_6	-0.3136200	-0.0427800	-1.0031500	2.2762370	0.9773960	-3.3646700	1.4705920

Table C.14
Influence Coefficients For A Circumferential Semi-Elliptical Surface Crack In A Cylinder – Inside Surface

t/R_i	a/c	a/t	G_i	A_0	A_1	A_2	A_3	A_4	A_5	A_6
0.2	0.5	0	G_0	0.8776607	-0.6729719	3.7721411	-6.5209060	6.3377934	-3.7028038	0.9872447
			G_1	0.1277541	0.4368502	0.4904522	1.0427434	-2.9631236	2.0826525	-0.5184313
			G_5	0.7313842	-0.5608100	3.1434508	-5.4340883	5.2814942	-3.0856700	0.8227042
			G_6	0.0000000	0.0000000	0.0000000	0.0000000	0.0000000	0.0000000	0.0000000
		0.2	G_0	0.8946047	-1.0880987	6.5367812	-14.977374	19.233142	-13.295577	3.7714422
			G_1	0.1468391	0.1494773	2.2541287	-4.4876841	5.6369940	-4.4388487	1.4200259
			G_5	0.7478801	-0.9261333	5.7417804	-13.425920	17.657798	-12.512022	3.6370309
			G_6	-0.0622140	0.2466480	-0.8549860	1.0627900	-0.0460670	-0.5911190	0.2472580
		0.4	G_0	0.9626500	-0.7111300	2.6613670	-0.7162500	-5.1454300	6.5075390	-2.4213200
			G_1	0.1614640	0.2974800	1.1660860	-0.5087200	-1.2726300	1.2871340	-0.4124100
			G_5	0.7806730	-0.4562300	1.7448190	0.5202550	-5.4270200	5.8139530	-2.0000000
			G_6	-0.1213700	0.4129990	-1.9995500	4.6351640	-5.0019800	2.4723590	-0.3976300
		0.6	G_0	1.0751750	-1.0983200	3.9916560	-2.7880300	-3.9548800	6.7235960	-2.7469000
			G_1	0.1954230	0.1962320	1.3895710	-0.6978800	-1.2117900	1.3183430	-0.4441600
			G_5	0.8810430	-0.8080000	3.0593790	-1.6390900	-3.7057000	5.2727270	-2.0000000
			G_6	-0.1479200	0.2002220	-0.6443400	0.5965410	1.5644630	-2.8569900	1.2880200
		0.8	G_0	1.1727800	-1.0890100	3.5149910	-1.9020000	-3.6889300	5.2643130	-1.9823400
			G_1	0.2227940	0.2349260	1.0309020	0.1224120	-1.7617400	1.3487430	-0.3982000
			G_5	0.9842910	-1.1276100	4.5985580	-5.5036800	1.9508470	0.9992980	-0.7333300
			G_6	-0.1671200	-0.0249100	0.2071610	0.6527170	-2.0799000	2.2037960	-0.7917400
0.2	1	0	G_0	1.1977992	-0.5244870	0.1498299	2.3284866	-5.1058499	4.3469049	-1.3487980
			G_1	0.1870117	0.6987352	0.1316900	0.7269255	-2.5259384	2.1756251	-0.6540458
			G_5	0.9981658	-0.4370725	0.1248583	1.9404058	-4.2548750	3.6224208	-1.1239983
			G_6	0.0000000	0.0000000	0.0000000	0.0000000	0.0000000	0.0000000	0.0000000
		0.2	G_0	1.2042139	-1.7184651	8.3974726	-24.297906	37.843150	-29.181362	8.7698916
			G_1	0.2141530	0.0177548	4.3818976	-12.940794	19.522869	-14.998781	4.5154005
			G_5	1.0104920	-1.4866607	7.5586755	-22.106442	34.708840	-27.030280	8.2196099
			G_6	-0.0226250	-0.0176200	0.1169620	-0.0423700	-0.3894120	0.6553310	-0.3004810
		0.4	G_0	1.2827300	-1.0376300	2.0196040	-1.2981600	-1.1540600	2.2233130	-0.9499300
			G_1	0.2239049	0.2463097	2.6203846	-7.1285809	10.498578	-8.4296199	2.7081472
			G_5	1.0436480	-0.6146200	0.7831210	0.6384640	-2.2283500	1.8139540	-0.5000000
			G_6	-0.1070200	0.6703990	-3.2584800	7.6913240	-8.8678600	4.7415690	-0.8699400
		0.6	G_0	1.3573590	-1.1704500	1.8759680	-0.3400600	-2.5386900	3.0522770	-1.1249500
			G_1	0.2339280	0.5254690	0.5931330	-0.1929100	-1.2290500	1.2994260	-0.4586100
			G_5	1.1254030	-0.9052000	1.9129080	-2.1369000	1.8300790	-1.2418600	0.4000000
			G_6	-0.1281700	0.6899310	-3.2765600	7.8600090	-9.3273600	5.2734440	-1.0912900
		0.8	G_0	1.4394340	-1.3098700	1.7771300	0.3860890	-3.3253800	3.2539520	-1.0700400
			G_1	0.2573740	0.4951230	0.6501790	-0.5490400	-0.1469600	0.1702270	-0.0718800
			G_5	1.1881780	-0.8564700	1.1754060	0.1918800	-1.2135200	0.4744190	0.1000000
			G_6	-0.1307600	0.3275810	-0.9451600	1.7563070	-1.5599400	0.5843160	-0.0323500

Table C.14
Influence Coefficients For A Circumferential Semi-Elliptical Surface Crack In A Cylinder – Inside Surface

t/R_i	a/c	a/t	G_i	A_0	A_1	A_2	A_3	A_4	A_5	A_6
0.2	2	0	G_0	0.8150546	-0.5623828	1.4465771	-4.6778133	8.4192164	-7.9025932	2.9866351
			G_1	0.1359146	0.0702340	3.5558581	-11.034445	16.967724	-14.126991	4.8706612
			G_5	0.6792125	-0.4686525	1.2054808	-3.8981775	7.0160133	-6.5854942	2.4888625
			G_6	0.0000000	0.0000000	0.0000000	0.0000000	0.0000000	0.0000000	0.0000000
		0.2	G_0	0.8358198	-0.9924158	3.9768720	-11.895121	19.092328	-15.767916	5.2807657
			G_1	0.1359403	0.1029899	2.9965678	-8.9811709	13.214205	-10.645384	3.5992645
			G_5	0.7133337	-1.2206448	6.2110937	-19.560635	32.381152	-27.109103	9.0576036
			G_6	-0.0126410	0.1047460	-0.5669950	1.0875330	-0.3104870	-0.8897690	0.5826880
		0.4	G_0	0.8325100	-0.3194100	-0.7533800	3.3629820	-6.0395900	4.8258600	-1.3722100
			G_1	0.1390275	0.0874112	3.0561984	-9.1666723	13.520813	-10.858590	3.6501024
			G_5	0.7154977	-1.2303429	6.3379078	-19.902438	32.964781	-27.668674	9.2758719
			G_6	-0.0193200	-0.0131100	0.1021510	-0.1416000	0.0088670	0.1372810	-0.0742600
		0.6	G_0	0.8584020	-0.3933300	-0.6204500	3.2822090	-6.1804800	5.1102160	-1.5076600
			G_1	0.1440293	0.1448134	2.6171481	-7.7432148	11.073113	-8.6716926	2.8678919
			G_5	0.7385051	-1.1518575	5.6378202	-17.404615	28.376173	-23.390975	7.7010721
			G_6	-0.0312300	0.0232800	-0.0601000	0.1680520	-0.1758700	0.0935340	-0.0176600
		0.8	G_0	0.9059700	-0.9530400	2.7940290	-7.1938500	10.653830	-8.4054600	2.7741360
			G_1	0.1497196	0.1548492	2.5650135	-7.6154978	10.830952	-8.3100088	2.6668419
			G_5	0.7661965	-1.2226050	6.0077780	-18.334715	29.298571	-23.433628	7.4415387
			G_6	-0.0270400	-0.0979600	0.5106690	-0.7699900	-0.0498500	1.1091270	-0.6749600
0.33333	0.125	0	G_0	0.4065238	0.7772483	3.8861644	-12.573943	16.760207	-11.014593	2.8706957
			G_1	0.0320270	0.1825342	2.2670449	-2.7076615	1.2088194	-0.3777430	0.0763155
			G_5	0.3048930	0.5829360	2.9146230	-9.4304573	12.570155	-8.2609448	2.1530220
			G_6	0.0000000	0.0000000	0.0000000	0.0000000	0.0000000	0.0000000	0.0000000
		0.2	G_0	0.3975304	1.0704943	1.8409164	-6.7524995	8.8513103	-5.7966783	1.5167162
			G_1	0.0437487	-0.0379438	4.3032790	-10.979411	16.325212	-13.042939	4.0580042
			G_5	0.2598731	0.7431824	1.0817664	-3.0985122	3.7427052	-2.5608814	0.7055471
			G_6	-0.1560910	-0.1991580	-1.2102800	3.1753640	-1.1892930	-1.0207720	0.6068420
		0.4	G_0	0.4238500	1.1235390	2.5509630	-9.8789800	15.140340	-11.492500	3.3935110
			G_1	0.0497907	-0.0602976	4.7351023	-12.965424	20.468483	-16.831335	5.3096778
			G_5	0.1697435	0.5461098	0.3497346	1.7372481	-2.5772737	0.7601711	0.0073845
			G_6	-0.2516800	-0.8485800	-0.1616800	1.7778520	0.5757210	-1.6402700	0.5486370
		0.6	G_0	0.4556600	0.8736780	4.4545930	-13.785100	19.802200	-14.490000	4.1432600
			G_1	0.0541596	-0.0346110	4.8465458	-14.018203	23.536910	-20.054942	6.4399617
			G_5	0.0446172	0.0047650	1.3276798	-0.2022316	5.0799128	-8.1465781	3.0576874
			G_6	-0.2271900	-1.4977600	2.6245340	-13.151900	32.228690	-29.431700	9.4553330
		0.8	G_0	0.5070500	0.8103760	6.0448070	-18.725500	28.520740	-20.813300	5.5469780
			G_1	0.0626980	0.1915790	2.9204050	-4.4566900	4.6654090	-2.8958000	0.5196150
			G_5	0.0293525	2.3968607	-12.676891	10.733250	36.954925	-59.325311	23.370902
			G_6	-0.3128300	-1.0496800	-0.2836900	-4.0511200	9.2232340	-2.0408400	-1.4850800

Table C.14
Influence Coefficients For A Circumferential Semi-Elliptical Surface Crack In A Cylinder – Inside Surface

t/R_i	a/c	a/t	G_i	A_0	A_1	A_2	A_3	A_4	A_5	A_6
0.33333	0.25	0	G_0	0.6152816	-0.3348694	6.2955620	-15.590618	19.299508	-12.488107	3.3010035
			G_1	0.0703566	0.2828152	1.4036169	-0.6511596	-1.2076596	1.0318656	-0.2423741
			G_5	0.4614615	-0.2511518	4.7216715	-11.692964	14.474631	-9.3660803	2.4757523
			G_6	0.0000000	0.0000000	0.0000000	0.0000000	0.0000000	0.0000000	0.0000000
		0.2	G_0	0.6083440	-0.2904124	7.0896330	-20.176785	28.205837	-19.948430	5.6066871
			G_1	0.0838285	0.1746451	2.3793286	-4.6232641	5.6071472	-4.2823544	1.3235074
			G_5	0.4499786	-0.1852406	4.4943031	-11.145785	14.081722	-9.4097438	2.5683214
			G_6	-0.1219890	0.2306280	-1.2120370	1.2196580	1.6286170	-2.7432500	1.0045930
		0.4	G_0	0.6526970	-0.4837600	7.6611730	-19.998400	26.417930	-17.968700	4.8913320
			G_1	0.0831650	0.2409880	1.6951000	-1.5385200	0.2695350	-0.1584300	0.1162410
			G_5	0.4292630	-0.3106000	5.3124130	-13.181800	17.490330	-12.245600	3.4183450
			G_6	-0.1386700	-0.6159000	1.3198340	-1.3713700	1.0283420	0.0952910	-0.3175300
		0.6	G_0	0.7317460	-0.3303400	5.5440620	-9.4951500	5.7237640	0.0933760	-0.9528500
			G_1	0.1080000	0.2765580	1.2250360	0.9782820	-4.7273400	4.2126330	-1.3066700
			G_5	0.4238890	-0.0841600	2.7845590	-2.2848200	-1.5056400	2.9519690	-1.2352400
			G_6	-0.3162700	0.0983480	-2.3401800	5.2319350	-2.9719700	-0.1371700	0.4353040
		0.8	G_0	0.8402820	-0.8949500	10.595930	-26.628500	34.904410	-23.479700	6.2376480
			G_1	0.1477640	0.0411330	3.1601870	-5.2967700	5.5402620	-3.5864300	0.8821650
			G_5	0.4212720	-0.4648100	5.9023420	-13.138900	18.981120	-14.760300	4.3338570
			G_6	-0.4127500	0.2305260	-3.9773100	9.4936830	-8.5226200	4.1775270	-0.9890500
0.33333	0.5	0	G_0	0.8776607	-0.6729719	3.7721411	-6.5209060	6.3377934	-3.7028038	0.9872447
			G_1	0.1277541	0.4368502	0.4904522	1.0427434	-2.9631236	2.0826525	-0.5184313
			G_5	0.6582458	-0.5047290	2.8291058	-4.8906795	4.7533448	-2.7771030	0.7404338
			G_6	0.0000000	0.0000000	0.0000000	0.0000000	0.0000000	0.0000000	0.0000000
		0.2	G_0	0.8895794	-1.1126308	6.5752022	-14.855752	18.769034	-12.769139	3.5706030
			G_1	0.1451309	0.1469326	2.2308775	-4.3705650	5.4139824	-4.2413440	1.3531815
			G_5	0.6658258	-0.7835355	4.8162796	-10.777119	13.753050	-9.6562727	2.8173218
			G_6	-0.0826750	0.2486620	-0.8714890	1.1120030	-0.0336570	-0.6328160	0.2623350
		0.4	G_0	0.9404760	-0.7171300	2.8683290	-1.9822900	-2.2272100	3.6257200	-1.3881800
			G_1	0.1574600	0.2822130	1.2690630	-0.9471000	-0.3659400	0.4292320	-0.1110700
			G_5	0.6852640	-0.5845700	2.7454920	-2.9660400	0.4623200	1.0854340	-0.5496200
			G_6	-0.1387000	0.0697930	-0.2841400	0.5371760	-0.0906000	-0.1401700	0.0466450
		0.6	G_0	1.0445780	-1.3803400	6.1955220	-10.014600	7.9838570	-2.9309700	0.2857320
			G_1	0.1787820	0.2882640	0.8060020	1.0425460	-3.7076700	3.0209080	-0.8866100
			G_5	0.7517630	-0.9610200	4.7115960	-7.5088500	6.2941800	-2.7984400	0.4781860
			G_6	-0.2099100	0.1853170	-0.7684100	1.1473110	0.1521720	-0.8435900	0.3371120
		0.8	G_0	1.0843000	-0.7460900	1.4321000	6.3082000	-19.305000	19.233000	-6.7012000
			G_1	0.2111800	0.1098200	1.8768000	-2.2163000	1.6060000	-1.0307000	0.2496700
			G_5	0.7720800	-0.5866300	2.0623000	1.3104000	-7.5437000	7.8678000	-2.7908000
			G_6	-0.1930800	0.3869550	-4.3698700	13.210980	-17.895400	12.239770	-3.3793400

Table C.14
Influence Coefficients For A Circumferential Semi-Elliptical Surface Crack In A Cylinder – Inside Surface

t/R_i	a/c	a/t	G_i	A_0	A_1	A_2	A_3	A_4	A_5	A_6
0.33333	1	0	G_0	1.1977992	-0.5244870	0.1498299	2.3284866	-5.1058499	4.3469049	-1.3487980
			G_1	0.1870117	0.6987352	0.1316900	0.7269255	-2.5259384	2.1756251	-0.6540458
			G_5	0.8983493	-0.3933653	0.1123725	1.7463653	-3.8293875	3.2601788	-1.0115985
			G_6	0.0000000	0.0000000	0.0000000	0.0000000	0.0000000	0.0000000	0.0000000
		0.2	G_0	1.2012642	-1.7333005	8.3781140	-24.063822	37.374764	-28.763015	8.6237108
			G_1	0.2153060	-0.0149500	4.5588615	-13.461994	20.337566	-15.605137	4.6842087
			G_5	0.9105186	-1.1384184	5.4097849	-15.339953	24.188520	-19.160345	5.9427986
			G_6	-0.0345160	-0.0167840	0.1297610	-0.0527050	-0.3346670	0.5652860	-0.2567380
		0.4	G_0	1.2353020	-0.4554500	-1.3844300	7.7438190	-13.114500	9.9554010	-2.8936100
			G_1	0.2231273	0.2854589	2.2703165	-5.9312058	8.6225042	-7.0084921	2.2832798
			G_5	0.9136960	-0.2915800	-0.8322300	5.1393320	-8.6812300	6.4245520	-1.8094800
			G_6	-0.0911000	0.0616370	-0.1210900	0.3104310	-0.3007600	0.2039090	-0.0630300
		0.6	G_0	1.2948850	-0.5296600	-1.8164200	9.6512410	-16.061200	12.054080	-3.4771700
			G_1	0.2437058	0.2916478	1.9336493	-4.6996771	6.6474053	-5.3956082	1.7365158
			G_5	0.9663080	-0.3126800	-1.2238000	6.9796950	-11.736700	8.7605150	-2.5098100
			G_6	-0.1230600	0.0274730	0.1438200	-0.4241600	0.8313660	-0.6134200	0.1579830
		0.8	G_0	1.4110710	-1.5153300	3.6940490	-6.1586400	8.0493230	-6.3320300	2.0368880
			G_1	0.2576230	0.3718990	1.5321880	-3.5848900	5.2701160	-4.4872900	1.4628370
			G_5	1.0612560	-1.1039100	3.5230400	-6.9044200	9.8738080	-8.0508200	2.6221170
			G_6	-0.1788800	0.4037560	-2.0916400	6.1449500	-9.2086300	7.2003620	-2.2699200
0.33333	2	0	G_0	0.8150546	-0.5623828	1.4465771	-4.6778133	8.4192164	-7.9025932	2.9866351
			G_1	0.1359146	0.0702340	3.5558581	-11.034445	16.967724	-14.126991	4.8706612
			G_5	0.6112913	-0.4217873	1.0849328	-3.5083598	6.3144120	-5.9269448	2.2399763
			G_6	0.0000000	0.0000000	0.0000000	0.0000000	0.0000000	0.0000000	0.0000000
		0.2	G_0	0.8352781	-0.9846724	3.9006089	-11.598574	18.537951	-15.233685	5.0778570
			G_1	0.1352852	0.1228393	2.8607553	-8.5533030	12.496366	-10.010600	3.3741234
			G_5	0.6470104	-1.0551846	5.3220976	-16.632247	27.466509	-23.033790	7.7267507
			G_6	-0.0142710	0.0762410	-0.4315580	0.8690960	-0.2323740	-0.7815010	0.5099400
		0.4	G_0	0.8387535	-0.9644546	3.6234112	-10.614751	16.935822	-13.909712	4.6383496
			G_1	0.1391285	0.0994766	2.9628455	-8.8586428	12.949581	-10.264284	3.4057784
			G_5	0.6547443	-1.0753542	5.5609093	-17.311471	28.535555	-23.897683	8.0055284
			G_6	-0.0275500	0.0118070	-0.0132100	0.0962120	-0.1684500	0.1535230	-0.0523400
		0.6	G_0	0.8647141	-0.9933994	3.4972128	-9.9646125	15.605175	-12.506693	4.0588148
			G_1	0.1439330	0.1659077	2.4756770	-7.3335082	10.402275	-8.0129443	2.5997844
			G_5	0.6728344	-0.9405580	4.5855658	-13.905932	22.493373	-18.532141	6.1244287
			G_6	-0.0428500	0.0404420	-0.1589900	0.4421460	-0.4883600	0.2585730	-0.0509700
		0.8	G_0	0.8961065	-1.1484363	4.2826404	-12.236817	19.080943	-14.996807	4.7040118
			G_1	0.1518350	0.1503798	2.6001073	-7.7801582	11.113224	-8.4029371	2.6236987
			G_5	0.6973028	-0.9440042	4.5851930	-13.593268	21.493375	-17.216662	5.5090422
			G_6	-0.0425300	-0.0823600	0.4082940	-0.4782200	-0.3499100	1.2189920	-0.6742600

Table C.14
Influence Coefficients For A Circumferential Semi-Elliptical Surface Crack In A Cylinder – Inside Surface

t/R_i	a/c	a/t	G_i	A_0	A_1	A_2	A_3	A_4	A_5	A_6
1.0	0.25	0	G_0	0.6152816	-0.3348694	6.2955620	-15.590618	19.299508	-12.488107	3.3010035
			G_1	0.0703566	0.2828152	1.4036169	-0.6511596	-1.2076596	1.0318656	-0.2423741
			G_5	0.3076408	-0.1674347	3.1477810	-7.7953092	9.6497542	-6.2440535	1.6505017
			G_6	0.0000000	0.0000000	0.0000000	0.0000000	0.0000000	0.0000000	0.0000000
		0.2	G_0	0.5930770	-0.3523725	6.0748396	-14.903322	18.107637	-11.410168	2.9273576
			G_1	0.0712547	0.1933519	1.6561816	-1.3023032	-0.3637505	0.5320498	-0.1336164
			G_5	0.2239270	-0.1112263	2.4629292	-5.2693665	6.6915032	-4.8224735	1.3935162
			G_6	-0.1970730	0.1542920	-1.5815150	2.5137220	0.1487130	-1.6888280	0.6560680
		0.4	G_0	0.5411818	0.4312602	-0.4480726	6.7361856	-15.244232	13.003129	-3.9650896
			G_1	0.0659285	0.2761672	0.8824707	1.0272572	-3.6935597	2.8929461	-0.8034940
			G_5	0.0475054	-0.0268990	0.8181730	-0.5582817	3.7482007	-5.4585911	2.0641956
			G_6	-0.2704900	0.1322780	-2.1311900	2.6783440	1.0000930	-1.8736000	0.4645590
		0.6	G_0	0.5871350	-0.0260138	1.9120535	2.2235230	-11.271614	12.044643	-4.2846949
			G_1	0.0749202	0.2920900	0.5044494	2.9382174	-6.9618287	5.4966899	-1.6303654
			G_5	0.2517416	-3.3362289	34.687578	-148.06228	282.66971	-241.47326	76.005413
			G_6	-0.2103600	-0.0990900	-0.7149500	-2.9829300	5.9605610	-0.4982700	-1.4549600
		0.8	G_0	>360°	>360°	>360°	>360°	>360°	>360°	>360°
			G_1	>360°	>360°	>360°	>360°	>360°	>360°	>360°
			G_5	>360°	>360°	>360°	>360°	>360°	>360°	>360°
			G_6	>360°	>360°	>360°	>360°	>360°	>360°	>360°
1.0	0.5	0	G_0	0.8776607	-0.6729719	3.7721411	-6.5209060	6.3377934	-3.7028038	0.9872447
			G_1	0.1277541	0.4368502	0.4904522	1.0427434	-2.9631236	2.0826525	-0.5184313
			G_5	0.4388304	-0.3364859	1.8860705	-3.2604530	3.1688967	-1.8514019	0.4936224
			G_6	0.0000000	0.0000000	0.0000000	0.0000000	0.0000000	0.0000000	0.0000000
		0.2	G_0	0.8625067	-1.0198663	5.3752626	-10.357891	11.424126	-7.1789304	1.9336593
			G_1	0.1289340	0.3262254	0.7970596	0.2021703	-1.4385249	0.7100078	-0.0492674
			G_5	0.4144878	-0.4873243	2.9443152	-5.9133795	7.1885133	-5.0710122	1.5008093
			G_6	-0.1259910	0.0781930	-0.3101000	0.4708050	-0.0267360	-0.0043400	-0.0799180
		0.4	G_0	0.8896920	-1.5419901	8.3387113	-18.893182	24.270960	-16.715807	4.6911203
			G_1	0.1438484	0.0646092	2.4103393	-4.6951370	5.9210573	-4.6273437	1.4462356
			G_5	0.3729529	-0.5807055	3.5635411	-6.8557227	8.4937473	-6.1987088	1.8514771
			G_6	-0.2380700	0.2739090	-1.0321300	0.1758840	3.6589020	-4.3393000	1.5007980
		0.6	G_0	0.8952409	-1.0044560	3.7014484	-3.2984413	0.9598941	-0.3895844	0.2771066
			G_1	0.1457094	0.3579621	-0.0409513	3.3843829	-6.1116473	3.8786763	-0.8942800
			G_5	0.2935601	-0.4433972	2.5979642	-3.8919565	5.9130979	-5.6114544	1.8951608
			G_6	-0.3260700	0.5935850	-3.6839400	8.4569240	-10.015900	7.4468310	-2.4714700
		0.8	G_0	0.9609348	-1.0583899	2.0399678	6.8041953	-18.346201	16.239607	-5.2152862
			G_1	0.1804784	0.2435281	-0.0730036	5.2178622	-10.214670	7.9142038	-2.4170339
			G_5	0.2192253	-0.5743443	3.2513495	-6.4000389	12.813190	-12.046764	3.7087576
			G_6	-0.3913800	0.4467430	-2.0400500	0.4294660	3.9509510	-2.5582200	0.1624830

Table C.14
Influence Coefficients For A Circumferential Semi-Elliptical Surface Crack In A Cylinder – Inside Surface

t/R_i	a/c	a/t	G_i	A_0	A_1	A_2	A_3	A_4	A_5	A_6
1.0	1	0	G_0	1.1977992	-0.5244870	0.1498299	2.3284866	-5.1058499	4.3469049	-1.3487980
			G_1	0.1870117	0.6987352	0.1316900	0.7269255	-2.5259384	2.1756251	-0.6540458
			G_5	0.5988996	-0.2622435	0.0749149	1.1642433	-2.5529250	2.1734525	-0.6743990
			G_6	0.0000000	0.0000000	0.0000000	0.0000000	0.0000000	0.0000000	0.0000000
		0.2	G_0	1.1962959	-1.1452559	3.5291510	-7.5777475	11.128314	-8.9527860	2.8751356
			G_1	0.2054201	0.3357275	1.9739688	-5.0748308	7.3673907	-6.0040420	1.9329797
			G_5	0.6015408	-0.5523481	2.1581057	-5.0368389	7.6769091	-6.3157685	2.0607100
			G_6	-0.0682010	-0.0332610	0.2349520	-0.1977410	-0.2271960	0.5766970	-0.2854050
		0.4	G_0	1.2132137	-1.6150539	5.5841952	-12.984150	19.693791	-15.781005	4.9513907
			G_1	0.2138716	0.2037226	2.5089995	-6.8941948	10.854520	-9.0166628	2.8693518
			G_5	0.6232694	-0.6781499	2.8895654	-6.4404050	9.8676901	-8.3902167	2.8225737
			G_6	-0.1527200	0.0755060	-0.1419200	0.4184260	-0.4578400	0.4067420	-0.1481900
		0.6	G_0	1.2627345	-1.6295580	4.6318747	-8.8409612	13.348392	-11.477888	3.8404193
			G_1	0.2322829	0.2215096	2.0603956	-5.3654425	8.9950733	-8.0441386	2.6759483
			G_5	0.6300299	-0.6324736	2.3400943	-3.6477219	5.2573815	-4.8971161	1.7446423
			G_6	-0.2155900	0.1224410	-0.5185100	1.1320010	-0.9494200	0.7168970	-0.2878200
		0.8	G_0	1.3465872	-1.7298970	4.5617317	-7.6559188	12.327671	-11.650691	4.1117707
			G_1	0.2676016	0.1731454	2.1267554	-5.4382959	9.9263303	-9.3487174	3.1616003
			G_5	0.6579261	-0.7756153	2.8172996	-3.5373788	4.9146410	-4.7817740	1.6844935
			G_6	-0.2936400	0.2056840	-0.4886300	-0.8910500	3.8333500	-3.0873600	0.7216550
1.0	2	0	G_0	0.8150546	-0.5623828	1.4465771	-4.6778133	8.4192164	-7.9025932	2.9866351
			G_1	0.1359146	0.0702340	3.5558581	-11.034445	16.967724	-14.126991	4.8706612
			G_5	0.4075273	-0.2811914	0.7232885	-2.3389066	4.2096082	-3.9512966	1.4933175
			G_6	0.0000000	0.0000000	0.0000000	0.0000000	0.0000000	0.0000000	0.0000000
		0.2	G_0	0.8387219	-0.8777457	2.9769264	-8.2950369	12.804792	-10.268759	3.3789196
			G_1	0.1347158	0.2251913	2.1433702	-6.2228036	8.5402325	-6.5342242	2.1535653
			G_5	0.4330531	-0.6225768	3.1932288	-9.7713760	15.912281	-13.236253	4.4223001
			G_6	-0.0196270	-0.0038290	-0.0602610	0.3169370	-0.2047170	-0.2432980	0.2147940
		0.4	G_0	0.8290980	-0.9264207	3.0657952	-8.5229086	13.284389	-10.387414	3.2265629
			G_1	0.1335076	0.2546478	1.8583905	-5.6312063	7.8628450	-5.8014323	1.7685426
			G_5	0.4457187	-0.6163440	3.3954053	-10.265957	16.615709	-13.709709	4.5267706
			G_6	-0.0515800	0.0376890	-0.1794100	0.5048450	-0.5265500	0.2669840	-0.0519900
		0.6	G_0	0.8676779	-1.1478841	4.1315127	-11.676695	18.591774	-14.638907	4.4848118
			G_1	0.1495034	0.1675640	2.3779699	-7.4751460	11.183791	-8.4637022	2.5304850
			G_5	0.4641709	-0.5369671	3.0171584	-8.8783034	14.249102	-11.622857	3.7613282
			G_6	-0.0733900	0.0261000	-0.1958400	0.6772550	-0.7605000	0.3928290	-0.0664600
		0.8	G_0	0.9198225	-1.4701866	5.8511769	-16.582454	26.549259	-21.000416	6.4126400
			G_1	0.1729661	0.0000464	3.4303160	-10.833907	16.880575	-13.024162	3.8856451
			G_5	0.4920683	-0.5662915	3.3412229	-9.5502511	15.179702	-12.167664	3.8109332
			G_6	-0.0878200	-0.0702300	0.1175600	0.3135180	-0.9108400	1.1188500	-0.4810400

Notes:

1. Interpolation of the influence coefficients, G_i, may be used for intermediate values of t/R_i, a/c, and a/t.

2. The value of the influence coefficients at the surface point of the crack defined by $\varphi = 0^0$ are equal to:. $G_i = A_0$

3. The value of the influence coefficients at the deepest point of the crack defined by $\varphi = 90^0$ are equal to: $G_i = \sum_{n=0}^{6} A_n$.

Table C.15
Influence Coefficients For A Circumferential Semi-Elliptical Surface Crack In A Cylinder – Outside Surface

t/R_i	a/c	a/t	G_i	A_0	A_1	A_2	A_3	A_4	A_5	A_6
0.0	0.03125	0	G_0	0.1965046	2.9373464	-5.2582823	7.4889153	-6.9282667	3.3673349	-0.6677966
			G_1	0.0051780	0.1750280	2.7718680	-4.6457154	4.6780502	-3.2768090	0.9840994
			G_5	0.1965050	2.9373460	-5.2582820	7.4889150	-6.9282670	3.3673350	-0.6677970
			G_6	0.0000000	0.0000000	0.0000000	0.0000000	0.0000000	0.0000000	0.0000000
		0.2	G_0	0.2080760	3.0112422	-5.1048701	7.6348715	-6.8347547	2.7940766	-0.3882688
			G_1	0.0084834	0.2406767	2.4574292	-3.6452421	3.6142837	-2.8451814	0.9270638
			G_5	0.2080760	3.0112422	-5.1048701	7.6348715	-6.8347547	2.7940766	-0.3882688
			G_6	0.0000000	0.0000000	0.0000000	0.0000000	0.0000000	0.0000000	0.0000000
		0.4	G_0	0.2357940	3.0822400	-3.5792100	3.9476890	1.9131590	-6.8872200	3.1896800
			G_1	0.0145140	0.4038000	1.6422700	-0.3906100	-0.6480700	-0.2940300	0.2514900
			G_5	0.2357940	3.0822400	-3.5792100	3.9476890	1.9131590	-6.8872200	3.1896800
			G_6	0.0000000	0.0000000	0.0000000	0.0000000	0.0000000	0.0000000	0.0000000
		0.6	G_0	0.2902240	3.6892050	-4.5739100	11.709890	-6.3750000	-5.8894100	4.2452400
			G_1	0.0208890	0.7016780	0.1631840	5.7072160	-8.2075800	3.4561120	-0.4454700
			G_5	0.2902240	3.6892050	-4.5739100	11.709890	-6.3750000	-5.8894100	4.2452400
			G_6	0.0000000	0.0000000	0.0000000	0.0000000	0.0000000	0.0000000	0.0000000
		0.8	G_0	0.5163550	2.5310830	14.712900	-43.621800	101.06570	-116.08100	46.190900
			G_1	0.0825460	0.4971770	4.6064810	-7.3326700	21.148620	-29.345100	12.491400
			G_5	0.5163550	2.5310830	14.712900	-43.621800	101.06570	-116.08100	46.190900
			G_6	0.0000000	0.0000000	0.0000000	0.0000000	0.0000000	0.0000000	0.0000000
0.0	0.0625	0	G_0	0.2695332	2.1626001	-1.6551569	-1.2970208	4.5604304	-4.3163876	1.4010655
			G_1	0.0138667	0.1827458	2.5749608	-3.9044679	3.3556301	-2.1772209	0.6420134
			G_5	0.2695330	2.1626000	-1.6551570	-1.2970210	4.5604300	-4.3163880	1.4010660
			G_6	0.0000000	0.0000000	0.0000000	0.0000000	0.0000000	0.0000000	0.0000000
		0.2	G_0	0.2845892	2.2264055	-1.4546190	-1.5760719	5.1131083	-4.9485443	1.6207574
			G_1	0.0199077	0.2210874	2.4642047	-3.5898625	3.1624039	-2.2403780	0.6965751
			G_5	0.2845892	2.2264055	-1.4546190	-1.5760719	5.1131083	-4.9485443	1.6207574
			G_6	0.0000000	0.0000000	0.0000000	0.0000000	0.0000000	0.0000000	0.0000000
		0.4	G_0	0.3261480	2.5200870	-1.8847000	2.1798740	-1.4597100	-0.1886500	0.2393400
			G_1	0.0294120	0.3699370	1.9220850	-1.2071500	-0.4394000	0.2737550	-0.0395200
			G_5	0.3261480	2.5200870	-1.8847000	2.1798740	-1.4597100	-0.1886500	0.2393400
			G_6	0.0000000	0.0000000	0.0000000	0.0000000	0.0000000	0.0000000	0.0000000
		0.6	G_0	0.4166330	3.1566470	-2.6248900	7.7325910	-9.6927800	3.6428700	-0.0892000
			G_1	0.0598460	0.4340740	2.6811560	-3.1936600	4.0753720	-4.6940200	1.8285500
			G_5	0.4166330	3.1566470	-2.6248900	7.7325910	-9.6927800	3.6428700	-0.0892000
			G_6	0.0000000	0.0000000	0.0000000	0.0000000	0.0000000	0.0000000	0.0000000
		0.8	G_0	0.6540140	3.4231920	3.8158050	-4.1586900	3.4715330	-10.310400	6.6280000
			G_1	0.1214780	0.6975490	2.9718330	-1.3036500	-0.0754900	-3.0465100	2.1670000
			G_5	0.6540140	3.4231920	3.8158050	-4.1586900	3.4715330	-10.310400	6.6280000
			G_6	0.0000000	0.0000000	0.0000000	0.0000000	0.0000000	0.0000000	0.0000000

Table C.15
Influence Coefficients For A Circumferential Semi-Elliptical Surface Crack In A Cylinder – Outside Surface

t/R_i	a/c	a/t	G_i	A_0	A_1	A_2	A_3	A_4	A_5	A_6
0.0	0.125	0	G_0	0.4065238	0.7772483	3.8861644	-12.573943	16.760207	-11.014593	2.8706957
			G_1	0.0320270	0.1825342	2.2670449	-2.7076615	1.2088194	-0.3777430	0.0763155
			G_5	0.4065240	0.7772480	3.8861640	-12.573943	16.760207	-11.014593	2.8706960
			G_6	0.0000000	0.0000000	0.0000000	0.0000000	0.0000000	0.0000000	0.0000000
		0.2	G_0	0.4242116	1.0089302	3.2973815	-12.159726	17.873386	-12.868668	3.6281712
			G_1	0.0429859	0.2033811	2.2563818	-2.8752160	1.8152558	-1.0512327	0.3181077
			G_5	0.4242116	1.0089302	3.2973815	-12.159726	17.873386	-12.868668	3.6281712
			G_6	0.0000000	0.0000000	0.0000000	0.0000000	0.0000000	0.0000000	0.0000000
		0.4	G_0	0.4917770	1.6592320	-0.1080400	0.1793240	-2.7076100	3.3680620	-1.3489700
			G_1	0.0634270	0.3722500	1.6231670	-0.5306500	-2.0007400	1.8943780	-0.5880300
			G_5	0.4917770	1.6592320	-0.1080400	0.1793240	-2.7076100	3.3680620	-1.3489700
			G_6	0.0000000	0.0000000	0.0000000	0.0000000	0.0000000	0.0000000	0.0000000
		0.6	G_0	0.6591820	1.8759140	1.0212600	-1.7698000	-0.5653600	1.2479960	-0.4376600
			G_1	0.1116040	0.4714500	1.7940590	-0.7557600	-1.4901700	1.0852180	-0.2113700
			G_5	0.6591820	1.8759140	1.0212600	-1.7698000	-0.5653600	1.2479960	-0.4376600
			G_6	0.0000000	0.0000000	0.0000000	0.0000000	0.0000000	0.0000000	0.0000000
		0.8	G_0	0.9809330	1.8846320	4.8020780	-8.0580200	0.4447850	3.4772660	-1.0567500
			G_1	0.2039950	0.4800150	2.8822430	-2.5890100	-0.9683000	1.5372370	-0.3750200
			G_5	0.9809330	1.8846320	4.8020780	-8.0580200	0.4447850	3.4772660	-1.0567500
			G_6	0.0000000	0.0000000	0.0000000	0.0000000	0.0000000	0.0000000	0.0000000
0.0	0.25	0	G_0	0.6152816	-0.3348694	6.2955620	-15.590618	19.299508	-12.488107	3.3010035
			G_1	0.0703566	0.2828152	1.4036169	-0.6511596	-1.2076596	1.0318656	-0.2423741
			G_5	0.6152820	-0.3348690	6.2955620	-15.590618	19.299508	-12.488107	3.3010030
			G_6	0.0000000	0.0000000	0.0000000	0.0000000	0.0000000	0.0000000	0.0000000
		0.2	G_0	0.6385889	-0.3095132	6.5329787	-16.622882	21.056641	-13.850120	3.6988146
			G_1	0.0840059	0.1999367	1.8218113	-1.7756899	0.3757186	-0.0785358	0.0643386
			G_5	0.6385889	-0.3095132	6.5329787	-16.622882	21.056641	-13.850120	3.6988146
			G_6	0.0000000	0.0000000	0.0000000	0.0000000	0.0000000	0.0000000	0.0000000
		0.4	G_0	0.7390420	0.0548160	4.0842620	-7.5883100	5.4047530	-1.0146100	-0.3483400
			G_1	0.1164500	0.2479880	1.8282520	-1.7169900	0.1912120	0.1165770	-0.0186100
			G_5	0.7390420	0.0548160	4.0842620	-7.5883100	5.4047530	-1.0146100	-0.3483400
			G_6	0.0000000	0.0000000	0.0000000	0.0000000	0.0000000	0.0000000	0.0000000
		0.6	G_0	0.9461210	-0.1858800	5.5867460	-9.8634900	5.9596870	0.1296440	-1.0026100
			G_1	0.1778050	0.2056680	2.0979210	-1.8039500	-0.5558700	1.1461400	-0.4206600
			G_5	0.9461210	-0.1858800	5.5867460	-9.8634900	5.9596870	0.1296440	-1.0026100
			G_6	0.0000000	0.0000000	0.0000000	0.0000000	0.0000000	0.0000000	0.0000000
		0.8	G_0	1.2452110	-0.6921900	8.3260620	-14.948000	8.6936910	0.4755790	-1.3926600
			G_1	0.2585640	0.1548890	2.1170240	-0.4910000	-4.6146100	5.4550750	-1.9663300
			G_5	1.2452110	-0.6921900	8.3260620	-14.948000	8.6936910	0.4755790	-1.3926600
			G_6	0.0000000	0.0000000	0.0000000	0.0000000	0.0000000	0.0000000	0.0000000

Table C.15
Influence Coefficients For A Circumferential Semi-Elliptical Surface Crack In A Cylinder – Outside Surface

t/R_i	a/c	a/t	G_i	A_0	A_1	A_2	A_3	A_4	A_5	A_6
0.0	0.5	0	G_0	0.8776607	-0.6729719	3.7721411	-6.5209060	6.3377934	-3.7028038	0.9872447
			G_1	0.1277541	0.4368502	0.4904522	1.0427434	-2.9631236	2.0826525	-0.5184313
			G_5	0.8776610	-0.6729720	3.7721410	-6.5209060	6.3377930	-3.7028040	0.9872450
			G_6	0.0000000	0.0000000	0.0000000	0.0000000	0.0000000	0.0000000	0.0000000
		0.2	G_0	0.9003948	-0.8850488	5.2743239	-11.267523	13.890755	-9.6373584	2.8183906
			G_1	0.1404409	0.3215397	1.1010666	-1.0257556	0.6943940	-1.0793186	0.5410929
			G_5	0.9003948	-0.8850488	5.2743239	-11.267523	13.890755	-9.6373584	2.8183906
			G_6	0.0000000	0.0000000	0.0000000	0.0000000	0.0000000	0.0000000	0.0000000
		0.4	G_0	1.0058060	-0.7322600	2.9951940	-1.9459200	-3.2613500	5.1424570	-2.0306200
			G_1	0.1740870	0.3051630	1.2070310	-0.6720500	-1.0651300	1.1445590	-0.3644800
			G_5	0.9000590	-0.5476000	2.4416770	-1.2688500	-3.3815300	4.7868570	-1.8373900
			G_6	0.0000000	0.0000000	0.0000000	0.0000000	0.0000000	0.0000000	0.0000000
		0.6	G_0	1.1826010	-1.1072500	3.9623640	-2.7781300	-4.3097300	7.2772750	-2.9648200
			G_1	0.2277120	0.1701170	1.5499470	-1.1051200	-0.8333700	1.1717060	-0.4194500
			G_5	1.1826010	-1.1072500	3.9623640	-2.7781300	-4.3097300	7.2772750	-2.9648200
			G_6	0.0000000	0.0000000	0.0000000	0.0000000	0.0000000	0.0000000	0.0000000
		0.8	G_0	1.3833380	-1.3900300	4.3755780	-3.7372600	-2.5403200	5.3036000	-2.0932400
			G_1	0.2820110	0.0839230	1.7258580	-1.5358100	-0.0635600	0.5006780	-0.1982200
			G_5	1.3833380	-1.3900300	4.3755780	-3.7372600	-2.5403200	5.3036000	-2.0932400
			G_6	0.0000000	0.0000000	0.0000000	0.0000000	0.0000000	0.0000000	0.0000000
0.0	1	0	G_0	1.1977992	-0.5244870	0.1498299	2.3284866	-5.1058499	4.3469049	-1.3487980
			G_1	0.1870117	0.6987352	0.1316900	0.7269255	-2.5259384	2.1756251	-0.6540458
			G_5	1.1977990	-0.5244870	0.1498300	2.3284870	-5.1058500	4.3469050	-1.3487980
			G_6	0.0000000	0.0000000	0.0000000	0.0000000	0.0000000	0.0000000	0.0000000
		0.2	G_0	1.2263282	-1.1608467	4.4744783	-11.584231	17.811241	-14.408250	4.6998279
			G_1	0.2154786	0.2441623	2.8107820	-7.6574580	11.171413	-9.0053693	2.9542871
			G_5	1.2263282	-1.1608467	4.4744783	-11.584231	17.811241	-14.408250	4.6998279
			G_6	0.0000000	0.0000000	0.0000000	0.0000000	0.0000000	0.0000000	0.0000000
		0.4	G_0	1.2989480	-0.9978000	1.9479540	-1.3002700	-1.4940100	2.8306230	-1.2126000
			G_1	0.2386246	0.1447774	3.3198992	-9.2456599	13.823512	-11.223715	3.6868232
			G_5	1.2989480	-0.9978000	1.9479540	-1.3002700	-1.4940100	2.8306230	-1.2126000
			G_6	0.0000000	0.0000000	0.0000000	0.0000000	0.0000000	0.0000000	0.0000000
		0.6	G_0	1.3971180	-1.1348400	1.7918740	-0.4202600	-2.8679300	3.7685480	-1.4405000
			G_1	0.2445870	0.5326670	0.5939690	-0.0361800	-2.0163100	2.2167010	-0.7782200
			G_5	1.3971180	-1.1348400	1.7918740	-0.4202600	-2.8679300	3.7685480	-1.4405000
			G_6	0.0000000	0.0000000	0.0000000	0.0000000	0.0000000	0.0000000	0.0000000
		0.8	G_0	1.5117010	-1.3244800	1.7568350	-0.1337900	-2.8629300	3.2953270	-1.1412400
			G_1	0.2704470	0.5113280	0.5357440	-0.0327300	-1.5570200	1.5570970	-0.5094600
			G_5	1.5117010	-1.3244800	1.7568350	-0.1337900	-2.8629300	3.2953270	-1.1412400
			G_6	0.0000000	0.0000000	0.0000000	0.0000000	0.0000000	0.0000000	0.0000000

Table C.15
Influence Coefficients For A Circumferential Semi-Elliptical Surface Crack In A Cylinder – Outside Surface

t/R_i	a/c	a/t	G_i	A_0	A_1	A_2	A_3	A_4	A_5	A_6
0.0	2	0	G_0	0.8150546	-0.5623828	1.4465771	-4.6778133	8.4192164	-7.9025932	2.9866351
			G_1	0.1359146	0.0702340	3.5558581	-11.034445	16.967724	-14.126991	4.8706612
			G_5	0.8150550	-0.5623830	1.4465770	-4.6778130	8.4192160	-7.9025930	2.9866350
			G_6	0.0000000	0.0000000	0.0000000	0.0000000	0.0000000	0.0000000	0.0000000
		0.2	G_0	0.8463715	-1.0011024	4.0052312	-11.937181	19.189548	-16.039296	5.4674371
			G_1	0.1395121	0.0753999	3.1895604	-9.5540932	14.214316	-11.649525	4.0073308
			G_5	0.8463715	-1.0011024	4.0052312	-11.937181	19.189548	-16.039296	5.4674371
			G_6	0.0000000	0.0000000	0.0000000	0.0000000	0.0000000	0.0000000	0.0000000
		0.4	G_0	0.8570045	-1.0183085	3.9957306	-11.886878	19.152747	-16.047480	5.4801806
			G_1	0.1436696	0.0544018	3.2816127	-9.8164232	14.610963	-11.942138	4.0907797
			G_5	0.8570045	-1.0183085	3.9957306	-11.886878	19.152747	-16.047480	5.4801806
			G_6	0.0000000	0.0000000	0.0000000	0.0000000	0.0000000	0.0000000	0.0000000
		0.6	G_0	0.8839861	-1.0765270	4.0774087	-11.976171	19.173189	-15.996207	5.4501217
			G_1	0.1504185	0.0478401	3.2579960	-9.6921199	14.370843	-11.736129	4.0258411
			G_5	0.8839861	-1.0765270	4.0774087	-11.976171	19.173189	-15.996207	5.4501217
			G_6	0.0000000	0.0000000	0.0000000	0.0000000	0.0000000	0.0000000	0.0000000
		0.8	G_0	0.9033134	-0.9619755	2.8501500	-7.6366897	11.596116	-9.4828625	3.2550163
			G_1	0.1458559	0.2313881	1.9882138	-5.5546045	7.4196069	-5.8965053	2.0855563
			G_5	0.9033134	-0.9619755	2.8501500	-7.6366897	11.596116	-9.4828625	3.2550163
			G_6	0.0000000	0.0000000	0.0000000	0.0000000	0.0000000	0.0000000	0.0000000
0.01	0.03125	0	G_0	0.1965046	2.9373464	-5.2582823	7.4889153	-6.9282667	3.3673349	-0.6677966
			G_1	0.0051780	0.1750280	2.7718680	-4.6457154	4.6780502	-3.2768090	0.9840994
			G_5	0.1965046	2.9373464	-5.2582823	7.4889153	-6.9282667	3.3673349	-0.6677966
			G_6	0.0000000	0.0000000	0.0000000	0.0000000	0.0000000	0.0000000	0.0000000
		0.2	G_0	0.2116559	2.4625298	-1.2086946	-4.0808781	10.512452	-9.7505256	3.1574301
			G_1	0.0073553	0.2248471	2.5465614	-3.9586604	4.1543233	-3.2917455	1.0682038
			G_5	0.2117479	2.4669625	-1.2233443	-4.0356866	10.550152	-9.8518908	3.1982651
			G_6	-0.0150460	-0.1515480	0.4190890	-1.2072670	2.0290350	-1.3179820	0.2449160
		0.4	G_0	0.2267900	2.9874360	-3.3596600	3.3149040	3.3779620	-8.4920000	3.8326500
			G_1	0.0132270	0.4891340	1.4810220	-0.2505600	0.3517190	-2.2787900	1.1808200
			G_5	0.2294300	2.7425010	-1.7305900	-2.0047000	12.170560	-15.530100	6.0000000
			G_6	-0.0279300	-0.4216200	0.5326580	0.4761720	-2.2564800	2.9083470	-1.2111500
		0.6	G_0	0.2451630	3.4073570	-5.1754600	15.029690	-12.238400	-1.0593200	2.7584400
			G_1	0.0374510	0.7790480	-1.1197700	10.267710	-14.396700	7.1767130	-1.3237000
			G_5	0.2385960	3.3073170	-4.6399500	12.795250	-7.6318600	-5.3395100	4.2222220
			G_6	-0.0164590	-1.4702900	8.3251460	-27.317503	43.222664	-31.198496	8.4709110
		0.8	G_0	0.3001970	2.5133470	4.5572250	-10.605300	47.909900	-70.721400	30.714100
			G_1	0.0236690	0.4686529	2.5980287	-4.1635546	22.855996	-32.031979	12.632460
			G_5	0.2652400	3.0910960	-0.7764200	7.0895380	19.882670	-49.200000	24.285720
			G_6	-0.0789050	-0.7973820	3.7213660	-23.342093	50.937027	-44.347210	13.905159

Table C.15
Influence Coefficients For A Circumferential Semi-Elliptical Surface Crack In A Cylinder – Outside Surface

t/R_i	a/c	a/t	G_i	A_0	A_1	A_2	A_3	A_4	A_5	A_6
0.01	0.0625	0	G_0	0.2695332	2.1626001	-1.6551569	-1.2970208	4.5604304	-4.3163876	1.4010655
			G_1	0.0138667	0.1827458	2.5749608	-3.9044679	3.3556301	-2.1772209	0.6420134
			G_5	0.2695332	2.1626001	-1.6551569	-1.2970208	4.5604304	-4.3163876	1.4010655
			G_6	0.0000000	0.0000000	0.0000000	0.0000000	0.0000000	0.0000000	0.0000000
		0.2	G_0	0.2843442	2.0632252	-0.8995815	-1.7002701	3.3771236	-2.5139267	0.6468602
			G_1	0.0193647	0.2110156	2.6078196	-4.3209835	4.6955691	-3.6663355	1.1845300
			G_5	0.2849763	2.0834845	-0.9850383	-1.4461643	3.0094661	-2.2550769	0.5742754
			G_6	-0.0169490	0.0703960	-0.4886870	0.8510980	-0.5594650	0.2904380	-0.1440920
		0.4	G_0	0.3234380	2.5413990	-2.0176200	1.6959050	0.9274120	-3.1662200	1.4358100
			G_1	0.0370330	0.4900840	1.6020220	-0.6385100	-0.7412100	-0.0710100	0.2447400
			G_5	0.3176740	2.5600660	-2.2743400	2.5573490	-0.3247200	-2.3422900	1.2380950
			G_6	-0.0279970	0.0585420	-1.0424680	3.0167250	-4.0103300	2.9378710	-0.9260650
		0.6	G_0	0.3905240	3.2576640	-4.3197100	12.918270	-15.947200	6.8514120	-0.5974600
			G_1	0.0592580	0.5014950	2.3544400	-2.2877200	3.5444420	-5.2408200	2.2860900
			G_5	0.3945880	2.9522020	-1.8265900	3.8511510	-0.2293500	-6.0328700	3.4285710
			G_6	-0.0477040	0.0487110	-1.0141000	0.9246810	2.6287790	-4.2774820	1.7419400
		0.8	G_0	0.5585480	3.0733050	2.7116060	0.1570170	1.1959110	-12.276100	8.1508500
			G_1	0.0998622	0.8721037	0.8806798	7.5243170	-12.931792	5.5339974	-0.1725691
			G_5	0.5311890	3.6060380	-1.6126300	14.376210	-21.813700	5.8796870	2.5806450
			G_6	-0.1319350	1.6593810	-12.837138	29.458530	-22.518377	-0.8027060	5.1521000
0.01	0.125	0	G_0	0.4065238	0.7772483	3.8861644	-12.573943	16.760207	-11.014593	2.8706957
			G_1	0.0320270	0.1825342	2.2670449	-2.7076615	1.2088194	-0.3777430	0.0763155
			G_5	0.4065238	0.7772483	3.8861644	-12.573943	16.760207	-11.014593	2.8706957
			G_6	0.0000000	0.0000000	0.0000000	0.0000000	0.0000000	0.0000000	0.0000000
		0.2	G_0	0.4141304	1.1377070	1.7925852	-6.3816121	8.0611916	-5.1373047	1.3130132
			G_1	0.0487218	0.0175251	3.9073870	-9.0112567	12.465726	-9.7159857	2.9937975
			G_5	0.4141387	1.1728917	1.5879788	-5.7380688	7.0270589	-4.3302414	1.0702122
			G_6	-0.0215100	0.2289000	-1.0183300	1.2001800	0.5002560	-1.5218740	0.6395240
		0.4	G_0	0.4884630	1.5730830	0.6794250	-2.6942700	2.4688900	-1.0967700	0.1279400
			G_1	0.0721890	0.4196840	1.5725580	-0.5246000	-1.8820000	1.6181090	-0.4302300
			G_5	0.4945010	1.2569410	3.1846440	-11.500300	17.519240	-13.417300	4.0000000
			G_6	-0.0326060	0.2599370	-1.2779750	1.6852560	0.2883000	-1.6417090	0.7272120
		0.6	G_0	0.6325650	1.9612380	0.2124640	1.0673660	-4.8520900	4.2428280	-1.2187600
			G_1	0.1171020	0.4578330	2.1168020	-1.8894800	0.5759570	-0.8442000	0.4875500
			G_5	0.6337930	1.7347580	2.0397750	-5.5002600	6.5478530	-5.1994300	1.7777780
			G_6	-0.0510510	0.4679150	-2.8026610	5.4927770	-3.6013470	-0.2141770	0.7157020
		0.8	G_0	0.9044670	1.6602910	5.4293610	-7.8741700	-1.3182900	5.4386470	-1.7533200
			G_1	0.1947050	0.4093530	3.3076490	-3.2250800	-0.4973400	1.2925110	-0.2919800
			G_5	0.8969920	1.8870180	4.1418380	-5.8086600	-1.6246200	3.6711750	-0.6923100
			G_6	-0.1196280	2.1647550	-17.369329	55.455597	-84.446342	61.931057	-17.624773

Table C.15
Influence Coefficients For A Circumferential Semi-Elliptical Surface Crack In A Cylinder – Outside Surface

t/R_i	a/c	a/t	G_i	A_0	A_1	A_2	A_3	A_4	A_5	A_6
0.01	0.25	0	G_0	0.6152816	-0.3348694	6.2955620	-15.590618	19.299508	-12.488107	3.3010035
			G_1	0.0703566	0.2828152	1.4036169	-0.6511596	-1.2076596	1.0318656	-0.2423741
			G_5	0.6152816	-0.3348694	6.2955620	-15.590618	19.299508	-12.488107	3.3010035
			G_6	0.0000000	0.0000000	0.0000000	0.0000000	0.0000000	0.0000000	0.0000000
		0.2	G_0	0.6208898	-0.1664421	6.5968181	-18.807095	26.180692	-18.464818	5.1787192
			G_1	0.0903134	0.1796401	2.4581113	-4.8428461	5.9649997	-4.5970978	1.4302661
			G_5	0.6256175	-0.2460646	7.1786495	-20.690522	29.252069	-20.921801	5.9439866
			G_6	-0.0529280	0.5817080	-2.0439050	2.4908050	-0.3061320	-1.2173360	0.5545260
		0.4	G_0	0.7329950	0.0996250	3.9573730	-7.2526600	4.9136700	-0.6649300	-0.4401500
			G_1	0.1244530	0.2438230	1.9426520	-2.0609400	0.6954550	-0.3004200	0.1292100
			G_5	0.7324580	-0.0790000	5.2132460	-11.267200	11.336950	-5.7116200	1.1111110
			G_6	-0.0724760	0.7545830	-2.6909740	3.3377620	-0.4333620	-1.6647900	0.7776290
		0.6	G_0	0.9335850	-0.0671400	4.9859720	-8.0099800	3.1444570	2.1751370	-1.5670900
			G_1	0.1861600	0.1872070	2.3208790	-2.4591900	0.4288930	0.3550800	-0.1581000
			G_5	0.9308850	-0.2487900	6.4158440	-12.995000	11.662450	-4.8484800	0.6666670
			G_6	-0.0842130	0.8378360	-3.0789330	3.9428740	-0.4659710	-2.2536710	1.1097250
		0.8	G_0	1.2407050	-0.9832700	11.036350	-24.419000	25.074820	-13.247100	3.0448500
			G_1	0.2685320	0.0687020	2.9242790	-3.1935800	-0.0724900	1.6614580	-0.7248500
			G_5	1.2020050	-0.2413600	5.4364160	-5.7446000	-5.6959800	11.276780	-4.5000000
			G_6	-0.0450570	0.4286070	-2.4450330	5.2502870	-4.3532820	0.7113540	0.4546460
0.01	0.5	0	G_0	0.8776607	-0.6729719	3.7721411	-6.5209060	6.3377934	-3.7028038	0.9872447
			G_1	0.1277541	0.4368502	0.4904522	1.0427434	-2.9631236	2.0826525	-0.5184313
			G_5	0.8776607	-0.6729719	3.7721411	-6.5209060	6.3377934	-3.7028038	0.9872447
			G_6	0.0000000	0.0000000	0.0000000	0.0000000	0.0000000	0.0000000	0.0000000
		0.2	G_0	0.9005246	-1.0307386	6.3564034	-14.662730	18.900958	-13.111605	3.7340887
			G_1	0.1490274	0.1602062	2.2439024	-4.4879387	5.6373631	-4.4442698	1.4267720
			G_5	0.9044688	-1.0934309	6.8237929	-16.242399	21.630155	-15.453183	4.5238507
			G_6	-0.0216090	0.2225620	-0.7436250	0.8569840	-0.1124830	-0.3230500	0.1247120
		0.4	G_0	1.0063880	-0.7425700	3.1260260	-2.1867000	-3.0931200	5.1298930	-2.0520500
			G_1	0.1789440	0.3206900	1.1011660	-0.2780300	-1.7360100	1.6648710	-0.5147200
			G_5	0.9827660	-0.5544700	2.1195940	0.3228700	-6.2642600	7.0697670	-2.5000000
			G_6	-0.0330000	0.2558440	-1.2392500	2.7155410	-2.7845300	1.1748480	-0.0894600
		0.6	G_0	1.1876880	-1.1514600	4.3134430	-3.6414000	-3.2248100	6.5781370	-2.7782500
			G_1	0.2348560	0.1694010	1.5310330	-0.9297400	-1.2048400	1.4747130	-0.5037800
			G_5	1.1736920	-1.0985200	4.0914840	-3.4273500	-2.7996400	5.6581030	-2.3260900
			G_6	-0.0241400	0.1054660	-0.3692100	0.1480170	1.3452060	-2.2134300	1.0080860
		0.8	G_0	1.3768550	-1.1807900	3.4327750	-1.9675000	-3.7422900	5.2586230	-1.8511600
			G_1	0.2827170	0.2258060	0.9136330	0.4871590	-2.5046300	1.9013960	-0.5002900
			G_5	1.3852980	-1.4598800	4.8824450	-5.0567200	-0.7333900	3.9649120	-1.6666700
			G_6	-0.0069900	-0.1354100	0.5129600	-0.1715000	-1.4812600	2.0791380	-0.7969500

Table C.15
Influence Coefficients For A Circumferential Semi-Elliptical Surface Crack In A Cylinder – Outside Surface

t/R_i	a/c	a/t	G_i	A_0	A_1	A_2	A_3	A_4	A_5	A_6
0.01	1	0	G_0	1.1977992	-0.5244870	0.1498299	2.3284866	-5.1058499	4.3469049	-1.3487980
			G_1	0.1870117	0.6987352	0.1316900	0.7269255	-2.5259384	2.1756251	-0.6540458
			G_5	1.1977992	-0.5244870	0.1498299	2.3284866	-5.1058499	4.3469049	-1.3487980
			G_6	0.0000000	0.0000000	0.0000000	0.0000000	0.0000000	0.0000000	0.0000000
		0.2	G_0	1.2163255	-1.2105406	4.9378591	-13.277329	20.674347	-16.657341	5.3664988
			G_1	0.2120446	0.2333067	2.9256445	-8.1389620	12.029482	-9.6839968	3.1519185
			G_5	1.2342990	-1.5314671	7.1783779	-20.802459	33.720887	-27.895912	9.1678853
			G_6	-0.0063570	0.0546490	-0.1675720	0.1767300	-0.0347210	-0.0153380	-0.0059650
		0.4	G_0	1.3064660	-1.0152400	1.9350880	-0.8993700	-2.4736000	3.7825660	-1.5472100
			G_1	0.2235710	0.5338870	0.8263620	-0.7439300	-1.0125200	1.5328880	-0.6019500
			G_5	1.2708350	-0.7002200	0.4078220	2.3529450	-5.6716200	5.0139540	-1.6000000
			G_6	-0.0551000	0.5974370	-3.0790700	7.3218950	-8.6144800	4.7584470	-0.9291300
		0.6	G_0	1.4098990	-1.1943200	2.0682710	-0.9892900	-2.2245400	3.4010710	-1.3594400
			G_1	0.2530760	0.4979500	0.7711470	-0.5373400	-1.2119300	1.5653800	-0.5725000
			G_5	1.3784730	-0.9308800	0.8922700	1.1776090	-3.7994200	3.4790700	-1.1000000
			G_6	-0.0532800	0.5783890	-2.9606800	7.0446380	-8.3727000	4.7445190	-0.9808900
		0.8	G_0	1.5256800	-1.3415100	1.7834550	-0.0964700	-2.9501000	3.3412720	-1.1425600
			G_1	0.2815290	0.4575980	0.7882960	-0.6608400	-0.6979100	0.9575600	-0.3420100
			G_5	1.4930550	-1.1540100	1.3584350	-0.4503500	-0.4058400	-0.0186000	0.3000000
			G_6	-0.0356300	0.1933460	-0.5365700	0.5289630	0.1260530	-0.5333200	0.2571630
0.01	2	0	G_0	0.8150546	-0.5623828	1.4465771	-4.6778133	8.4192164	-7.9025932	2.9866351
			G_1	0.1359146	0.0702340	3.5558581	-11.034445	16.967724	-14.126991	4.8706612
			G_5	0.8150546	-0.5623828	1.4465771	-4.6778133	8.4192164	-7.9025932	2.9866351
			G_6	0.0000000	0.0000000	0.0000000	0.0000000	0.0000000	0.0000000	0.0000000
		0.2	G_0	0.8305156	-1.0562168	4.5000068	-13.731088	22.186981	-18.304348	6.0907634
			G_1	0.1355569	0.0490656	3.3708754	-10.235299	15.333651	-12.425096	4.1851932
			G_5	0.8550171	-1.5076606	7.6119033	-24.094325	40.061917	-33.656957	11.274934
			G_6	-0.0073790	0.1254630	-0.6776960	1.2635280	-0.3727710	-0.9851780	0.6488970
		0.4	G_0	0.8365180	-0.3110000	-0.8673900	3.8166980	-6.9326300	5.5500280	-1.5710500
			G_1	0.1387820	0.0213261	3.5079466	-10.649233	16.059172	-13.095865	4.4331795
			G_5	0.8660112	-1.6018348	8.1519012	-25.857651	43.179547	-36.448593	12.261716
			G_6	-0.0053700	0.0119870	-0.0522000	0.0961370	-0.0717500	-0.0085200	0.0297200
		0.6	G_0	0.8647620	-0.3748400	-0.7702800	3.6933770	-6.8531100	5.5382040	-1.5740000
			G_1	0.1453037	0.0535496	3.2458818	-9.8284254	14.629459	-11.772523	3.9396898
			G_5	0.8903262	-1.4861418	7.0094321	-21.999673	36.426386	-30.440664	10.140504
			G_6	-0.0087300	0.0194820	-0.0907000	0.1566490	-0.0749200	-0.0574800	0.0556980
		0.8	G_0	0.9195010	-0.9913000	2.9513880	-7.8747300	11.960150	-9.7994600	3.3736570
			G_1	0.1530620	0.0091124	3.5469729	-10.839841	16.187023	-12.807490	4.1638505
			G_5	0.9218643	-1.5643932	7.1354779	-22.140328	36.077778	-29.456429	9.5508778
			G_6	-0.0021200	-0.1195900	0.5677590	-0.9385300	0.0050640	1.2720990	-0.7846800

Table C.15
Influence Coefficients For A Circumferential Semi-Elliptical Surface Crack In A Cylinder – Outside Surface

t/R_i	a/c	a/t	G_i	A_0	A_1	A_2	A_3	A_4	A_5	A_6
0.01667	0.03125	0	G_0	0.1965046	2.9373464	-5.2582823	7.4889153	-6.9282667	3.3673349	-0.6677966
			G_1	0.0051780	0.1750280	2.7718680	-4.6457154	4.6780502	-3.2768090	0.9840994
			G_5	0.1965046	2.9373464	-5.2582823	7.4889153	-6.9282667	3.3673349	-0.6677966
			G_6	0.0000000	0.0000000	0.0000000	0.0000000	0.0000000	0.0000000	0.0000000
		0.2	G_0	0.2108342	2.4570800	-1.2157061	-4.0236499	10.416307	-9.6803603	3.1375768
			G_1	0.0071744	0.2169830	2.5959489	-4.1234042	4.4149777	-3.4775143	1.1164797
			G_5	0.2106227	2.4544929	-1.2190737	-3.9783189	10.457915	-9.7961980	3.1851951
			G_6	-0.0233720	-0.2625360	0.5660890	-1.2238920	2.0401900	-1.3756660	0.2817280
		0.4	G_0	0.2235430	2.9373900	-3.1994600	2.7809700	4.3738970	-9.3752900	4.1285200
			G_1	0.0153790	0.4262710	1.4374590	-0.0329200	0.1372970	-1.9720300	0.9767200
			G_5	0.2081430	3.1428470	-5.9452100	14.126020	-16.599400	8.7013890	-1.7777800
			G_6	-0.0494000	-0.5534600	0.2919720	1.5669970	-3.5734900	3.7883170	-1.4709400
		0.6	G_0	0.2315580	3.3152690	-5.3487100	15.866400	-14.268900	1.2426960	1.8259100
			G_1	0.0190830	0.6303640	-0.3898700	7.4202930	-10.418700	5.3450100	-1.2464600
			G_5	0.2185180	3.0724260	-4.3389400	12.251530	-6.9322100	-5.4074100	4.0000000
			G_6	-0.0431280	-1.8161870	8.6311060	-27.614206	43.137306	-29.957056	7.6761850
		0.8	G_0	0.2784200	1.6193770	13.249390	-52.219100	129.94510	-142.76800	54.258200
			G_1	0.0274250	-0.4708900	10.876180	-36.906200	79.258380	-78.743200	27.847000
			G_5	0.2018720	2.9940400	-3.6570500	15.285330	6.2359780	-34.960000	18.285720
			G_6	-0.0953020	-1.6854570	6.3336220	-27.809717	49.099262	-33.881794	8.0376910
0.01667	0.0625	0	G_0	0.2695332	2.1626001	-1.6551569	-1.2970208	4.5604304	-4.3163876	1.4010655
			G_1	0.0138667	0.1827458	2.5749608	-3.9044679	3.3556301	-2.1772209	0.6420134
			G_5	0.2695332	2.1626001	-1.6551569	-1.2970208	4.5604304	-4.3163876	1.4010655
			G_6	0.0000000	0.0000000	0.0000000	0.0000000	0.0000000	0.0000000	0.0000000
		0.2	G_0	0.2839701	2.0611223	-0.9023698	-1.6631113	3.3006585	-2.4507567	0.6281212
			G_1	0.0191537	0.2065367	2.6297112	-4.3764448	4.7735576	-3.7182062	1.1967908
			G_5	0.2845863	2.0778513	-0.9742253	-1.4550454	3.0154749	-2.2571717	0.5736301
			G_6	-0.0220090	0.0100440	-0.3065460	0.3744530	0.3410030	-0.5404890	0.1478000
		0.4	G_0	0.3212570	2.5165160	-2.0053400	1.8419650	0.5637890	-2.8167000	1.3130100
			G_1	0.0302880	0.4905940	1.3197410	0.4803190	-2.5162600	1.2803650	-0.1650100
			G_5	0.3153500	2.5119140	-2.0980700	2.0876390	0.4445220	-2.9646400	1.4285710
			G_6	-0.0352400	-0.2058200	-0.0717700	1.1031500	-1.6071400	1.1561240	-0.3393100
		0.6	G_0	0.3766880	3.1807610	-4.3574000	13.458080	-16.961900	7.7325420	-0.9039800
			G_1	0.0464920	0.5054590	1.8272520	-0.3010500	0.3199970	-2.6365000	1.4421600
			G_5	0.3498420	3.6756720	-8.5248700	27.663920	-40.188500	25.940540	-6.4000000
			G_6	-0.0645560	-0.2079890	-0.0562940	-1.9802090	7.4744930	-7.9086160	2.7486360
		0.8	G_0	0.5089370	2.8697610	2.3528320	1.8204240	-0.7866600	-10.843200	7.5884300
			G_1	0.0747990	0.5581130	2.4511290	0.7375290	-0.9973000	-4.1781700	2.9141700
			G_5	0.4963910	2.8883590	1.9568990	2.9262850	-1.2793200	-11.509500	8.0645160
			G_6	-0.1388700	0.6095490	-7.7130700	23.805260	-33.453600	23.682970	-6.7922600

Table C.15
Influence Coefficients For A Circumferential Semi-Elliptical Surface Crack In A Cylinder – Outside Surface

t/R_i	a/c	a/t	G_i	A_0	A_1	A_2	A_3	A_4	A_5	A_6
0.01667	0.125	0	G_0	0.4065238	0.7772483	3.8861644	-12.573943	16.760207	-11.014593	2.8706957
			G_1	0.0320270	0.1825342	2.2670449	-2.7076615	1.2088194	-0.3777430	0.0763155
			G_5	0.4065238	0.7772483	3.8861644	-12.573943	16.760207	-11.014593	2.8706957
			G_6	0.0000000	0.0000000	0.0000000	0.0000000	0.0000000	0.0000000	0.0000000
		0.2	G_0	0.4141030	1.1370353	1.7918721	-6.3657982	8.0276077	-5.1090766	1.3043557
			G_1	0.0486343	0.0164272	3.9099112	-9.0029835	12.437460	-9.6860424	2.9828172
			G_5	0.4143081	1.1612439	1.6725006	-6.0389787	7.5553433	-4.7733918	1.2122682
			G_6	-0.0257390	0.2239250	-1.0656070	1.3604470	0.3212500	-1.4129050	0.6046200
		0.4	G_0	0.4860310	1.6014030	0.4174570	-1.7801100	0.9884490	0.0450910	-0.2110000
			G_1	0.0716230	0.3907820	1.7772010	-1.2379600	-0.5878700	0.4930510	-0.0604600
			G_5	0.4825390	1.5260960	1.0116470	-4.0246700	5.0139140	-3.3630800	0.8888890
			G_6	-0.0202900	-0.2224800	1.2564450	-4.3167000	7.7764130	-6.6030000	2.1296120
		0.6	G_0	0.6270060	1.9158750	0.3750140	0.7243790	-4.3115900	3.7865410	-1.0734300
			G_1	0.1097630	0.4925440	1.7137970	-0.4041900	-1.8971000	1.1354540	-0.1307000
			G_5	0.6308030	1.6413760	2.5244720	-6.8239600	8.5609730	-6.7236500	2.2222220
			G_6	-0.0654530	0.4089380	-2.7275000	5.4276500	-3.4503160	-0.3170070	0.7307650
		0.8	G_0	0.8834920	1.5499750	5.9525350	-9.3777300	1.6582560	2.6247130	-0.7903400
			G_1	0.1827450	0.4170240	3.0645390	-2.2689800	-1.8835600	2.2280410	-0.5460400
			G_5	0.8486090	2.5957920	-2.1629000	17.323570	-41.416700	36.306820	-11.000000
			G_6	-0.0526800	0.0313980	-0.9515500	1.6109290	0.6934160	-2.4678000	1.1362870
0.01667	0.25	0	G_0	0.6152816	-0.3348694	6.2955620	-15.590618	19.299508	-12.488107	3.3010035
			G_1	0.0703566	0.2828152	1.4036169	-0.6511596	-1.2076596	1.0318656	-0.2423741
			G_5	0.6152816	-0.3348694	6.2955620	-15.590618	19.299508	-12.488107	3.3010035
			G_6	0.0000000	0.0000000	0.0000000	0.0000000	0.0000000	0.0000000	0.0000000
		0.2	G_0	0.6268151	-0.2659538	7.2065345	-20.587488	28.869672	-20.486698	5.7761489
			G_1	0.0907196	0.1725963	2.5006366	-4.9586990	6.1276304	-4.7110563	1.4617796
			G_5	0.6251326	-0.2394193	7.1122784	-20.448049	28.825683	-20.563129	5.8286449
			G_6	-0.0564090	0.5906920	-2.0901230	2.5558090	-0.2933150	-1.2772490	0.5764810
		0.4	G_0	0.7331060	0.0986810	3.9472550	-7.1889400	4.7837550	-0.5451500	-0.4819600
			G_1	0.1237230	0.2464690	1.9255840	-2.0144800	0.6420620	-0.2712700	0.1223800
			G_5	0.7315800	-0.0604700	5.0518000	-10.721000	10.434690	-4.9906700	0.8888890
			G_6	-0.0146100	-0.1583700	1.0586750	-3.4445700	5.7766210	-4.7213100	1.5035680
		0.6	G_0	0.9330720	-0.0910200	5.1514030	-8.5062000	3.9372450	1.5522690	-1.3786200
			G_1	0.1835580	0.2173130	2.1201030	-1.8419100	-0.4959200	1.0292210	-0.3502900
			G_5	0.9242220	-0.1379100	5.6239620	-10.482500	7.7246490	-1.8459600	-0.2222200
			G_6	-0.0276100	-0.0847600	0.6326700	-2.4527000	4.7781310	-4.3193100	1.4735860
		0.8	G_0	1.2480880	-1.2667900	13.231880	-31.738500	37.283310	-23.122200	6.1251700
			G_1	0.2617530	0.1907690	1.9836910	0.0718510	-5.5586600	6.0836580	-2.0974100
			G_5	1.1785120	0.2633730	1.5798440	7.4390720	-27.718600	29.000000	-10.000000
			G_6	-0.0372000	0.0294390	-0.3454900	1.0579850	-1.3468700	0.8809930	-0.2388600

Table C.15
Influence Coefficients For A Circumferential Semi-Elliptical Surface Crack In A Cylinder – Outside Surface

t/R_i	a/c	a/t	G_i	A_0	A_1	A_2	A_3	A_4	A_5	A_6
0.01667	0.5	0	G_0	0.8776607	-0.6729719	3.7721411	-6.5209060	6.3377934	-3.7028038	0.9872447
			G_1	0.1277541	0.4368502	0.4904522	1.0427434	-2.9631236	2.0826525	-0.5184313
			G_5	0.8776607	-0.6729719	3.7721411	-6.5209060	6.3377934	-3.7028038	0.9872447
			G_6	0.0000000	0.0000000	0.0000000	0.0000000	0.0000000	0.0000000	0.0000000
		0.2	G_0	0.9022613	-1.0595157	6.5513251	-15.271446	19.858891	-13.849252	3.9547586
			G_1	0.1492632	0.1564498	2.2690315	-4.5619815	5.7476801	-4.5263194	1.4510330
			G_5	0.9029354	-1.0732156	6.6901441	-15.831657	20.969482	-14.922494	4.3567685
			G_6	-0.0240560	0.2342620	-0.7930600	0.9271080	-0.1130250	-0.3740260	0.1454300
		0.4	G_0	1.0074290	-0.7627700	3.2930000	-2.7766500	-2.0930300	4.3235700	-1.8034700
			G_1	0.1810320	0.2833580	1.3218690	-0.8922400	-0.8601000	1.0459710	-0.3429800
			G_5	0.9858560	-0.6144600	2.5659140	-1.2397100	-3.5787400	4.8558140	-1.8000000
			G_6	-0.0338400	0.2387950	-1.1681400	2.5946840	-2.7007500	1.1765800	-0.1073300
		0.6	G_0	1.1851510	-1.1065900	4.0604300	-2.9480500	-4.2109900	7.2804210	-2.9762600
			G_1	0.2335280	0.1829380	1.4758450	-0.8294800	-1.2826600	1.4906960	-0.4992200
			G_5	1.1724980	-1.0832900	4.0212020	-3.3213400	-2.8475900	5.6324110	-2.3043500
			G_6	-0.0275600	0.1023610	-0.3536000	0.1087530	1.4111820	-2.2584400	1.0173030
		0.8	G_0	1.3763340	-1.1705800	3.4426520	-2.1143000	-3.3895100	4.9216180	-1.7364000
			G_1	0.2820140	0.2322400	0.9005230	0.4878420	-2.4663700	1.8500330	-0.4797300
			G_5	1.3815880	-1.3958500	4.5246880	-4.1377600	-1.9430100	4.7522810	-1.8666700
			G_6	-0.0123300	-0.1322000	0.4935200	-0.1065200	-1.5677300	2.1435930	-0.8183300
0.01667	1	0	G_0	1.1977992	-0.5244870	0.1498299	2.3284866	-5.1058499	4.3469049	-1.3487980
			G_1	0.1870117	0.6987352	0.1316900	0.7269255	-2.5259384	2.1756251	-0.6540458
			G_5	1.1977992	-0.5244870	0.1498299	2.3284866	-5.1058499	4.3469049	-1.3487980
			G_6	0.0000000	0.0000000	0.0000000	0.0000000	0.0000000	0.0000000	0.0000000
		0.2	G_0	1.2159041	-1.2019721	4.8943491	-13.164862	20.514432	-16.542122	5.3339888
			G_1	0.2138478	0.2009657	3.1365782	-8.7806790	13.020781	-10.439196	3.3770529
			G_5	1.2336102	-1.5324242	7.1847065	-20.827179	33.758570	-27.923695	9.1765536
			G_6	0.0004290	-0.0477510	0.2303150	-0.2454810	-0.4980090	1.1046740	-0.5435480
		0.4	G_0	1.3057270	-1.0008200	1.8572720	-0.6808000	-2.8231500	4.0709330	-1.6411400
			G_1	0.2250957	0.1870147	3.1086959	-8.6990069	12.827333	-10.126798	3.2062338
			G_5	1.2693430	-0.6672200	0.1805440	3.0628380	-6.8370600	5.9627910	-1.9000000
			G_6	-0.0555600	0.6002060	-3.0806100	7.2729560	-8.4525400	4.5719390	-0.8563900
		0.6	G_0	1.4097520	-1.1958700	2.1136310	-1.1728300	-1.9231000	3.1722290	-1.2928000
			G_1	0.2528090	0.4962060	0.8029830	-0.6609800	-1.0059000	1.4049960	-0.5248000
			G_5	1.3821790	-0.9982800	1.2826480	0.0761910	-2.2401100	2.3906980	-0.8000000
			G_6	-0.0539000	0.5709100	-2.9238200	6.9536840	-8.2458800	4.6543540	-0.9553500
		0.8	G_0	1.5261100	-1.3576900	1.9596150	-0.7444900	-1.8536800	2.4558510	-0.8665000
			G_1	0.2798340	0.4788400	0.6925290	-0.4412500	-0.9713700	1.1277000	-0.3828300
			G_5	1.4934890	-1.1805900	1.5372220	-1.0351600	0.5002050	-0.6976700	0.5000000
			G_6	-0.0364900	0.1772770	-0.4732300	0.4368740	0.1557290	-0.4866500	0.2265000

Table C.15
Influence Coefficients For A Circumferential Semi-Elliptical Surface Crack In A Cylinder – Outside Surface

t/R_i	a/c	a/t	G_i	A_0	A_1	A_2	A_3	A_4	A_5	A_6
0.01667	2	0	G_0	0.8150546	-0.5623828	1.4465771	-4.6778133	8.4192164	-7.9025932	2.9866351
			G_1	0.1359146	0.0702340	3.5558581	-11.034445	16.967724	-14.126991	4.8706612
			G_5	0.8150546	-0.5623828	1.4465771	-4.6778133	8.4192164	-7.9025932	2.9866351
			G_6	0.0000000	0.0000000	0.0000000	0.0000000	0.0000000	0.0000000	0.0000000
		0.2	G_0	0.8303718	-1.0537074	4.4841488	-13.682728	22.110765	-18.246611	6.0741015
			G_1	0.1357357	0.0454828	3.3938622	-10.305120	15.445864	-12.517992	4.2159592
			G_5	0.8545553	-1.5107503	7.6305267	-24.154355	40.161589	-33.739611	11.301885
			G_6	-0.0080940	0.1320720	-0.7037160	1.2969370	-0.3690340	-1.0141950	0.6605490
		0.4	G_0	0.8385880	-0.3494400	-0.6268500	3.1083630	-5.8624300	4.7444070	-1.3320400
			G_1	0.1388141	0.0199458	3.5199209	-10.693028	16.139831	-13.171184	4.4607143
			G_5	0.8648866	-1.5905958	8.0816882	-25.672324	42.927637	-36.279610	12.217855
			G_6	-0.0045600	0.0144990	-0.0770300	0.1717110	-0.1898700	0.0854060	-0.0001600
		0.6	G_0	0.8630510	-0.3484500	-0.9308100	4.1652080	-7.5678400	6.0687740	-1.7269300
			G_1	0.1454406	0.0490957	3.2762981	-9.9197082	14.771504	-11.888335	3.9781433
			G_5	0.8918880	-1.5257631	7.2468282	-22.705998	37.505258	-31.260474	10.386049
			G_6	-0.0086700	0.0226910	-0.1126100	0.2053490	-0.1206900	-0.0422900	0.0562240
		0.8	G_0	0.9207120	-1.0172500	3.1169740	-8.3590500	12.680850	-10.338100	3.5339560
			G_1	0.1532638	0.0041397	3.5793726	-10.934468	16.330683	-12.923367	4.2022735
			G_5	0.9223180	-1.5893812	7.2854088	-22.610593	36.827507	-30.047255	9.7335970
			G_6	-0.0038200	-0.1155400	0.5412020	-0.8878800	-0.0255700	1.2648840	-0.7732900
0.05	0.03125	0	G_0	0.1965046	2.9373464	-5.2582823	7.4889153	-6.9282667	3.3673349	-0.6677966
			G_1	0.0051780	0.1750280	2.7718680	-4.6457154	4.6780502	-3.2768090	0.9840994
			G_5	0.1965046	2.9373464	-5.2582823	7.4889153	-6.9282667	3.3673349	-0.6677966
			G_6	0.0000000	0.0000000	0.0000000	0.0000000	0.0000000	0.0000000	0.0000000
		0.2	G_0	0.2083391	2.4332249	-1.1884009	-3.9755311	10.292250	-9.5789402	3.1062164
			G_1	0.0065178	0.1974121	2.7143430	-4.4411003	4.8704764	-3.8110304	1.2146397
			G_5	0.1997427	2.3264369	-1.1013940	-3.6435752	9.8524559	-9.4316748	3.0993589
			G_6	-0.0625910	-0.7609300	1.1374040	-0.9700630	1.4330310	-0.8787870	0.1043810
		0.4	G_0	0.2126260	2.8183080	-3.0330200	2.7003490	3.8448090	-8.5201400	3.7625700
			G_1	0.0062779	0.1550679	3.1397907	-5.6725343	8.6311078	-7.9698086	2.6560323
			G_5	0.1703620	2.3140590	-2.5633700	3.7786360	2.0860560	-7.4455000	3.4222220
			G_6	-0.1152800	-1.7724100	2.7372250	-2.2958100	0.8232890	2.2788200	-1.6558300
		0.6	G_0	0.2218260	2.6845130	-1.0220600	-1.7085000	16.583430	-23.988200	9.7548700
			G_1	0.0035426	0.1135423	3.3308955	-6.2087481	12.547480	-12.941759	4.3992208
			G_5	0.1081350	2.2058260	-5.6718400	19.053640	-17.725100	4.2901230	0.2222220
			G_6	-0.1613800	-2.9385600	8.4224910	-27.306500	45.537000	-30.693100	7.1400850
		0.8	G_0	0.2334730	2.1926480	2.4092490	-4.8795600	23.225120	-33.519700	13.812200
			G_1	-0.0010039	0.0648251	3.6388741	-7.7669323	20.019952	-21.769540	7.4615512
			G_5	0.0181050	1.8710890	-7.9427300	26.287600	-14.291000	-7.0800000	4.5714290
			G_6	-0.1866490	-2.9656960	5.7981490	-22.657816	24.506548	5.1143480	-9.6122570

Table C.15
Influence Coefficients For A Circumferential Semi-Elliptical Surface Crack In A Cylinder – Outside Surface

t/R_i	a/c	a/t	G_i	A_0	A_1	A_2	A_3	A_4	A_5	A_6
0.05	0.0625	0	G_0	0.2695332	2.1626001	-1.6551569	-1.2970208	4.5604304	-4.3163876	1.4010655
			G_1	0.0138667	0.1827458	2.5749608	-3.9044679	3.3556301	-2.1772209	0.6420134
			G_5	0.2695332	2.1626001	-1.6551569	-1.2970208	4.5604304	-4.3163876	1.4010655
			G_6	0.0000000	0.0000000	0.0000000	0.0000000	0.0000000	0.0000000	0.0000000
		0.2	G_0	0.2823254	2.0534799	-0.8811145	-1.6698150	3.3008195	-2.4575325	0.6309429
			G_1	0.0188087	0.1946355	2.6993220	-4.5348736	4.9477116	-3.7967993	1.2039837
			G_5	0.2797821	2.0418784	-0.9180277	-1.4895340	3.1041398	-2.3826466	0.6237899
			G_6	-0.0486790	-0.1891920	-0.1673130	0.7906470	-0.3121280	-0.0657460	-0.0034250
		0.4	G_0	0.3063080	2.5163740	-2.6301300	4.4511290	-4.0018200	0.9244040	0.1362300
			G_1	0.0257928	0.2227270	2.8558445	-4.6900594	6.1531628	-5.5334459	1.8695561
			G_5	0.2851800	2.5117860	-3.5047600	8.1394150	-10.199500	5.7808220	-1.3333300
			G_6	-0.0885600	-0.7138300	0.9058640	-0.5572300	1.0691100	-0.7296800	0.1143240
		0.6	G_0	0.3496580	2.2502050	1.2825590	-5.6176200	15.285390	-18.227200	7.0634600
			G_1	0.0277182	0.2448111	2.9531717	-3.9581805	6.6052497	-7.4653877	2.7783504
			G_5	0.2821840	2.8317890	-5.3474100	18.238870	-23.947400	12.697300	-2.4000000
			G_6	-0.1526900	-0.9075400	-0.3360500	3.1957760	-3.7192400	3.3890750	-1.4693400
		0.8	G_0	0.4354930	0.5803140	15.809350	-46.076600	82.663310	-77.844000	27.643100
			G_1	0.0176381	0.2811585	2.3799548	0.2769473	2.1722174	-6.8712443	3.3144284
			G_5	0.2913710	2.0067920	0.6126560	7.0477190	-2.6508000	-11.638500	7.5483870
			G_6	-0.2840000	0.0411220	-7.2462300	8.9246250	12.806090	-25.058600	10.816970
0.05	0.125	0	G_0	0.4065238	0.7772483	3.8861644	-12.573943	16.760207	-11.014593	2.8706957
			G_1	0.0320270	0.1825342	2.2670449	-2.7076615	1.2088194	-0.3777430	0.0763155
			G_5	0.4065238	0.7772483	3.8861644	-12.573943	16.760207	-11.014593	2.8706957
			G_6	0.0000000	0.0000000	0.0000000	0.0000000	0.0000000	0.0000000	0.0000000
		0.2	G_0	0.4141975	1.1355682	1.7964913	-6.3267923	7.9329008	-5.0287717	1.2797839
			G_1	0.0482613	0.0194124	3.8693280	-8.7975215	12.040298	-9.3437833	2.8723181
			G_5	0.4124603	1.1555788	1.6454564	-5.9059207	7.3388389	-4.6103126	1.1639931
			G_6	-0.0437600	0.1570090	-1.0325550	1.4917100	0.2508650	-1.4432340	0.6259590
		0.4	G_0	0.4854260	1.4708470	1.1375140	-3.9136300	4.4112120	-2.6701800	0.6201300
			G_1	0.0614100	0.3634290	1.7021770	-0.8033900	-1.2757100	1.0399430	-0.2466000
			G_5	0.4771150	1.3502680	1.9042120	-6.7349300	9.4785330	-6.9606300	2.0000000
			G_6	-0.0625500	-0.2867400	0.7272150	-2.0795100	4.4089060	-4.0660600	1.3587350
		0.6	G_0	0.5975400	1.7337620	1.0590410	-0.9381500	-1.4454000	1.2700200	-0.2491200
			G_1	0.0928190	0.4108880	1.9636550	-1.0589200	-0.6277300	0.0224880	0.2086300
			G_5	0.5842270	1.5377860	2.2724010	-5.3712700	6.6141750	-5.6410300	2.0000000
			G_6	-0.1216800	0.0383230	-2.5834000	8.8415970	-12.590200	9.0060030	-2.5906100
		0.8	G_0	0.7779550	1.3659070	5.9189090	-8.0788400	0.9424640	2.0346540	-0.4382700
			G_1	0.1414370	0.3351560	3.1427840	-2.4175800	-0.8165600	0.9132140	-0.1013800
			G_5	0.7510670	1.4270080	5.0667020	-6.3546600	0.2988000	1.1506170	0.1481480
			G_6	-0.1609000	-0.2162400	-1.2987300	2.6895960	1.3204280	-4.1914600	1.8573060

Table C.15
Influence Coefficients For A Circumferential Semi-Elliptical Surface Crack In A Cylinder – Outside Surface

t/R_i	a/c	a/t	G_i	A_0	A_1	A_2	A_3	A_4	A_5	A_6
0.05	0.25	0	G_0	0.6152816	-0.3348694	6.2955620	-15.590618	19.299508	-12.488107	3.3010035
			G_1	0.0703566	0.2828152	1.4036169	-0.6511596	-1.2076596	1.0318656	-0.2423741
			G_5	0.6152816	-0.3348694	6.2955620	-15.590618	19.299508	-12.488107	3.3010035
			G_6	0.0000000	0.0000000	0.0000000	0.0000000	0.0000000	0.0000000	0.0000000
		0.2	G_0	0.6260632	-0.2355924	7.0084322	-19.936505	27.819799	-19.666590	5.5272065
			G_1	0.0907494	0.1737280	2.4989990	-4.9565466	6.1508242	-4.7530904	1.4807924
			G_5	0.6207464	-0.1740389	6.6462879	-18.975785	26.486146	-18.743280	5.2781587
			G_6	-0.0679890	0.5711840	-2.0794250	2.5966690	-0.2952400	-1.3108420	0.5915290
		0.4	G_0	0.7329360	0.0851660	3.9993920	-7.3274900	5.0490250	-0.7922300	-0.3978000
			G_1	0.1192830	0.2736740	1.7229450	-1.3700900	-0.3250300	0.4357600	-0.0817100
			G_5	0.7256530	-0.0593200	4.9453050	-10.464100	10.199980	-4.9143300	0.8888890
			G_6	-0.0425200	-0.1487000	0.8303450	-2.7784800	5.0546510	-4.3253300	1.4100300
		0.6	G_0	0.9247960	-0.1470300	5.5538350	-9.7985900	6.2555660	-0.4677600	-0.7143100
			G_1	0.1751020	0.2402440	1.9657640	-1.3682400	-1.1130700	1.4068600	-0.4424000
			G_5	0.9099290	-0.2582200	6.4177830	-13.249300	12.657030	-6.0202000	1.1111110
			G_6	-0.0729300	-0.0576300	0.1987110	-1.1582300	3.2150920	-3.3293900	1.2043850
		0.8	G_0	1.1968540	-0.7648200	9.5388220	-18.968400	16.307930	-6.5734600	1.0569200
			G_1	0.2507880	0.0646560	3.0320210	-3.5198100	0.7048460	0.8495480	-0.4370700
			G_5	1.1546950	-0.2482400	5.5468230	-5.9663300	-4.7348200	10.000000	-4.0000000
			G_6	-0.0999700	-0.0107700	-0.1792300	-0.0596600	1.7978730	-2.3389800	0.8907370
0.05	0.5	0	G_0	0.8776607	-0.6729719	3.7721411	-6.5209060	6.3377934	-3.7028038	0.9872447
			G_1	0.1277541	0.4368502	0.4904522	1.0427434	-2.9631236	2.0826525	-0.5184313
			G_5	0.8776607	-0.6729719	3.7721411	-6.5209060	6.3377934	-3.7028038	0.9872447
			G_6	0.0000000	0.0000000	0.0000000	0.0000000	0.0000000	0.0000000	0.0000000
		0.2	G_0	0.9024575	-1.0265565	6.3448697	-14.616034	18.788994	-12.994232	3.6905856
			G_1	0.1492827	0.1640885	2.2385342	-4.4987357	5.6810178	-4.4935522	1.4455306
			G_5	0.9059893	-1.1409542	7.1428296	-17.310642	23.384484	-16.840432	4.9473941
			G_6	-0.0317240	0.2339840	-0.7911240	0.9324040	-0.1062270	-0.3800660	0.1454050
		0.4	G_0	1.0049940	-0.7040200	2.9364040	-1.7198500	-3.7470300	5.6205220	-2.2024400
			G_1	0.1776020	0.3243230	1.0851530	-0.1989300	-1.9311900	1.8735070	-0.5938900
			G_5	0.9745420	-0.5075300	1.8740630	0.8245150	-6.8333300	7.4325590	-2.6000000
			G_6	-0.0532800	0.2868450	-1.3853900	3.1039090	-3.2363300	1.4406240	-0.1563900
		0.6	G_0	1.1816810	-1.0741600	3.9994710	-2.9800900	-3.9897100	7.0547810	-2.9051000
			G_1	0.2303560	0.1966400	1.4525790	-0.8304800	-1.2327600	1.4368850	-0.4815000
			G_5	1.1580110	-0.9930800	3.5342160	-2.0739000	-4.6145900	6.9433470	-2.6956500
			G_6	-0.0535700	0.1269210	-0.4300900	0.2393450	1.4467480	-2.4242500	1.0948900
		0.8	G_0	1.3657570	-1.0371100	2.8879690	-0.7595600	-5.1758900	6.1303710	-2.0679500
			G_1	0.2794450	0.2255490	1.0900980	-0.2597200	-1.1585800	0.7773970	-0.1447000
			G_5	1.3655410	-1.4063200	4.8813510	-5.6719000	0.7791320	2.5557890	-1.2000000
			G_6	-0.0492400	-0.1101500	0.4521470	-0.0943800	-1.3627200	1.8991630	-0.7348300

Table C.15
Influence Coefficients For A Circumferential Semi-Elliptical Surface Crack In A Cylinder – Outside Surface

t/R_i	a/c	a/t	G_i	A_0	A_1	A_2	A_3	A_4	A_5	A_6
0.05	1	0	G_0	1.1977992	-0.5244870	0.1498299	2.3284866	-5.1058499	4.3469049	-1.3487980
			G_1	0.1870117	0.6987352	0.1316900	0.7269255	-2.5259384	2.1756251	-0.6540458
			G_5	1.1977992	-0.5244870	0.1498299	2.3284866	-5.1058499	4.3469049	-1.3487980
			G_6	0.0000000	0.0000000	0.0000000	0.0000000	0.0000000	0.0000000	0.0000000
		0.2	G_0	1.2190691	-1.2245353	5.0563228	-13.673288	21.292042	-17.129807	5.5105091
			G_1	0.2147079	0.1957634	3.1648328	-8.8299606	13.038660	-10.421992	3.3673069
			G_5	1.2323106	-1.5329918	7.1886225	-20.874850	33.839972	-27.983852	9.1956425
			G_6	-0.0035440	-0.0523620	0.2590590	-0.2857470	-0.4830820	1.1203680	-0.5539910
		0.4	G_0	1.3047890	-0.9921900	1.8925730	-0.9100700	-2.4222800	3.7609800	-1.5483900
			G_1	0.2235270	0.1965708	3.0378068	-8.4937162	12.539220	-9.9135650	3.1391235
			G_5	1.2659030	-0.7461000	0.7702550	1.0361650	-3.5093100	3.3395350	-1.1000000
			G_6	-0.0648600	0.6105630	-3.1269700	7.4646540	-8.7857700	4.8446300	-0.9422400
		0.6	G_0	1.4040090	-1.1188500	1.7571000	-0.2160400	-3.4338500	4.3876240	-1.6723000
			G_1	0.2516650	0.4932520	0.8559910	-0.7868600	-0.9283800	1.4229860	-0.5458900
			G_5	1.3698330	-0.9806800	1.3030750	-0.2859600	-1.4911100	1.7581400	-0.6000000
			G_6	-0.0683500	0.5865560	-2.9461100	6.9774480	-8.1882900	4.5482310	-0.9094800
		0.8	G_0	1.5229200	-1.3353800	2.0181060	-1.0374200	-1.5224000	2.3295770	-0.8591600
			G_1	0.2776610	0.4906660	0.6693060	-0.3281100	-1.3001900	1.4734990	-0.5029000
			G_5	1.4721020	-1.0128400	0.5606840	1.8012340	-3.9996100	2.8744190	-0.6000000
			G_6	-0.0559500	0.2195700	-0.6510100	0.9213840	-0.4641700	-0.0948500	0.1250260
0.05	2	0	G_0	0.8150546	-0.5623828	1.4465771	-4.6778133	8.4192164	-7.9025932	2.9866351
			G_1	0.1359146	0.0702340	3.5558581	-11.034445	16.967724	-14.126991	4.8706612
			G_5	0.8150546	-0.5623828	1.4465771	-4.6778133	8.4192164	-7.9025932	2.9866351
			G_6	0.0000000	0.0000000	0.0000000	0.0000000	0.0000000	0.0000000	0.0000000
		0.2	G_0	0.8314774	-1.0666453	4.5748028	-13.981706	22.606222	-18.657217	6.2084870
			G_1	0.1354322	0.0510718	3.3606358	-10.212501	15.321081	-12.446271	4.2036619
			G_5	0.8531681	-1.5115135	7.6197531	-24.136236	40.160863	-33.764166	11.318067
			G_6	-0.0089920	0.1254420	-0.6684330	1.2379590	-0.3507360	-0.9752040	0.6346010
		0.4	G_0	0.8364810	-0.3166000	-0.8197800	3.6598310	-6.6831400	5.3375150	-1.4963800
			G_1	0.1388577	0.0131108	3.5739271	-10.882306	16.486183	-13.496809	4.5805641
			G_5	0.8652411	-1.6446685	8.3920757	-26.621478	44.421021	-37.450368	12.580194
			G_6	-0.0075300	0.0157800	-0.0653600	0.1222650	-0.0886500	-0.0093700	0.0328670
		0.6	G_0	0.8629460	-0.3657900	-0.7831300	3.6718170	-6.7667900	5.4134900	-1.5137300
			G_1	0.1452917	0.0434537	3.3215942	-10.077069	15.070211	-12.191100	4.0976145
			G_5	0.8872276	-1.5214461	7.2033707	-22.690009	37.660813	-31.520822	10.507303
			G_6	-0.0129400	0.0225250	-0.0920100	0.1541220	-0.0464500	-0.0995900	0.0743410
		0.8	G_0	0.9186350	-1.0079400	3.1234490	-8.4794500	12.969650	-10.658800	3.6673810
			G_1	0.1533656	-0.0066478	3.6544321	-11.175413	16.760305	-13.339825	4.3620132
			G_5	0.9176926	-1.6105546	7.3753056	-22.943533	37.443783	-30.611265	9.9345712
			G_6	-0.0030500	-0.1191400	0.5628040	-0.8861500	-0.1023500	1.3745880	-0.8267100

Table C.15
Influence Coefficients For A Circumferential Semi-Elliptical Surface Crack In A Cylinder – Outside Surface

t/R_i	a/c	a/t	G_i	A_0	A_1	A_2	A_3	A_4	A_5	A_6
0.1	0.03125	0	G_0	0.1965046	2.9373464	-5.2582823	7.4889153	-6.9282667	3.3673349	-0.6677966
			G_1	0.0051780	0.1750280	2.7718680	-4.6457154	4.6780502	-3.2768090	0.9840994
			G_5	0.1965046	2.9373464	-5.2582823	7.4889153	-6.9282667	3.3673349	-0.6677966
			G_6	0.0000000	0.0000000	0.0000000	0.0000000	0.0000000	0.0000000	0.0000000
		0.2	G_0	0.2062298	2.4111014	-1.1579831	-3.9618391	10.194552	-9.4698308	3.0669619
			G_1	0.0062688	0.1657744	2.9734268	-5.3001663	6.2503657	-4.8722734	1.5281608
			G_5	0.1707539	2.1495805	-1.7427511	-0.2523829	4.9976467	-6.3918133	2.3496098
			G_6	-0.1132000	-1.3780750	1.7708460	-0.7098550	1.0898820	-0.6591130	0.0017810
		0.4	G_0	0.2070540	2.7537250	-2.8761800	2.2271620	3.9733150	-8.0813400	3.4966400
			G_1	0.0114180	0.3847570	1.2716240	0.3967590	-1.1619600	-0.4328000	0.4535600
			G_5	0.1000570	0.3693550	5.3293420	-19.446200	42.939410	-41.629600	14.000000
			G_6	-0.1983100	-2.4680800	2.4220240	-0.3344800	-3.1190200	8.1947770	-4.4969100
		0.6	G_0	0.2083490	2.8416620	-3.5931900	9.5331750	-7.9036700	-0.4686300	1.6389100
			G_1	0.0179210	0.2958620	1.8278370	-0.7491300	2.2532060	-4.3480500	1.8406900
			G_5	-0.0887000	0.5994810	-8.3268200	33.508100	-42.231900	29.143170	-10.400800
			G_6	-0.1887430	-3.0819190	7.9959810	-30.061684	42.480518	-16.467848	-0.6749710
		0.8	G_0	0.2318420	2.0608840	3.3301360	-9.1692600	24.914970	-29.844100	11.474300
			G_1	0.0250440	0.3295030	1.3777280	1.7151740	-0.1612700	-3.4816300	1.6417600
			G_5	-0.2386600	0.2589480	-13.195300	34.824650	-25.480100	19.604100	-12.816200
			G_6	-0.1232450	-2.1110100	2.1778680	-6.6977480	-34.635532	80.840080	-39.449390
0.1	0.0625	0	G_0	0.2695332	2.1626001	-1.6551569	-1.2970208	4.5604304	-4.3163876	1.4010655
			G_1	0.0138667	0.1827458	2.5749608	-3.9044679	3.3556301	-2.1772209	0.6420134
			G_5	0.2695332	2.1626001	-1.6551569	-1.2970208	4.5604304	-4.3163876	1.4010655
			G_6	0.0000000	0.0000000	0.0000000	0.0000000	0.0000000	0.0000000	0.0000000
		0.2	G_0	0.2806940	2.0374864	-0.8264929	-1.7807353	3.4872503	-2.6298524	0.6904449
			G_1	0.0183868	0.1812388	2.7703041	-4.6792926	5.1145222	-3.9051527	1.2343557
			G_5	0.2694368	1.9612473	-0.8397292	-1.3349670	2.9220021	-2.3881771	0.6601830
			G_6	-0.0842210	-0.4653830	0.0851980	1.0748480	-0.6388330	0.0605260	-0.0279550
		0.4	G_0	0.2914750	2.4030250	-2.1742700	3.0773360	-1.6736600	-1.0254100	0.7639500
			G_1	0.0189582	0.1692677	2.6058681	-3.5933205	4.0083771	-3.5825819	1.2144892
			G_5	0.2473869	1.7676353	-0.4026364	0.2114787	2.4100170	-4.1664108	1.5961656
			G_6	-0.1549900	-1.1945900	0.0000860	5.6600650	-10.284800	9.2054790	-3.2312900
		0.6	G_0	0.2964315	2.0324437	0.1308081	1.2861437	0.9477780	-4.5062364	2.0993887
			G_1	0.0288080	0.2379040	2.4807900	-2.1217300	2.8095710	-3.9330400	1.6059800
			G_5	0.1935424	1.1281848	1.9228156	-3.9287173	14.392040	-17.699290	6.2899615
			G_6	-0.2534700	-1.8722800	1.7439750	-3.6966400	9.2276760	-5.8967600	0.7475020
		0.8	G_0	0.3105210	2.1596820	0.7252700	4.2094560	-2.9669900	-4.8568700	3.3463100
			G_1	0.0552600	0.3259080	1.6878870	2.1616010	-3.0681200	-0.5893900	0.8396800
			G_5	0.0992309	0.2560090	5.1732051	-15.633466	47.627715	-52.134457	17.754855
			G_6	-0.2414000	-2.4089200	1.8354290	-13.989000	32.306850	-21.348100	3.8450590

Table C.15
Influence Coefficients For A Circumferential Semi-Elliptical Surface Crack In A Cylinder – Outside Surface

t/R_i	a/c	a/t	G_i	A_0	A_1	A_2	A_3	A_4	A_5	A_6
0.1	0.125	0	G_0	0.4065238	0.7772483	3.8861644	-12.573943	16.760207	-11.014593	2.8706957
			G_1	0.0320270	0.1825342	2.2670449	-2.7076615	1.2088194	-0.3777430	0.0763155
			G_5	0.4065238	0.7772483	3.8861644	-12.573943	16.760207	-11.014593	2.8706957
			G_6	0.0000000	0.0000000	0.0000000	0.0000000	0.0000000	0.0000000	0.0000000
		0.2	G_0	0.4130806	1.1359250	1.8126683	-6.3619008	7.9833472	-5.0681630	1.2910002
			G_1	0.0478518	0.0217848	3.8356845	-8.6007775	11.633103	-8.9788832	2.7517112
			G_5	0.4079083	1.1498064	1.5975285	-5.6900729	7.0055326	-4.3667746	1.0917928
			G_6	-0.0685020	0.0694090	-1.0205980	1.7915690	-0.0749590	-1.2699890	0.5791410
		0.4	G_0	0.4751460	1.4510040	1.0799110	-3.5387500	3.8108270	-2.2562200	0.5100700
			G_1	0.0507372	0.2672673	1.8729143	-1.2669216	-0.5238020	0.4880615	-0.0939352
			G_5	0.4529101	1.3061296	1.3684453	-3.6852104	4.2372131	-3.0306963	0.8716174
			G_6	-0.1164900	-0.4307100	0.4852870	-0.6401400	2.4648300	-2.7107700	0.9479970
		0.6	G_0	0.5473293	1.4394412	1.7927835	-0.9379253	-2.5499376	2.3507685	-0.6274414
			G_1	0.0742660	0.4355780	1.5411740	0.5590450	-3.5244300	2.5763870	-0.6659400
			G_5	0.5067973	1.3641876	1.3171498	1.2376984	-5.0238384	3.5282012	-0.8790585
			G_6	-0.2011600	-0.3635500	-1.6411400	6.4684860	-7.7232600	4.8110350	-1.3504200
		0.8	G_0	0.6313390	1.7303310	1.8669510	5.4830110	-18.749700	15.989820	-4.4518100
			G_1	0.0982930	0.3504230	2.4625830	0.3541020	-5.2317300	4.3173190	-1.1604400
			G_5	0.5294343	1.2641801	0.7660220	15.705514	-36.095888	29.203245	-8.6137828
			G_6	-0.3348500	-0.0513300	-3.5238900	2.5582000	14.748960	-22.917600	9.5205520
0.1	0.25	0	G_0	0.6152816	-0.3348694	6.2955620	-15.590618	19.299508	-12.488107	3.3010035
			G_1	0.0703566	0.2828152	1.4036169	-0.6511596	-1.2076596	1.0318656	-0.2423741
			G_5	0.6152816	-0.3348694	6.2955620	-15.590618	19.299508	-12.488107	3.3010035
			G_6	0.0000000	0.0000000	0.0000000	0.0000000	0.0000000	0.0000000	0.0000000
		0.2	G_0	0.6246869	-0.1990336	6.7819636	-19.242905	26.763081	-18.884677	5.3025074
			G_1	0.0907982	0.1745008	2.4998733	-4.9503710	6.1385868	-4.7449552	1.4786038
			G_5	0.6084341	0.0392000	5.1847656	-14.417451	19.401392	-13.395311	3.7145503
			G_6	-0.0839210	0.5447980	-2.0690200	2.6644150	-0.3136570	-1.3449380	0.6081850
		0.4	G_0	0.7326180	0.0366070	4.3380400	-8.4916000	7.1162860	-2.5538200	0.1732000
			G_1	0.1166070	0.2554820	1.8570560	-1.8477100	0.5584930	-0.3317600	0.1672700
			G_5	0.7095270	0.1328400	3.4099130	-5.3751600	1.9251720	1.6200170	-1.1111100
			G_6	-0.0801000	-0.1355000	0.5118230	-1.7399900	3.7294580	-3.4507000	1.1649940
		0.6	G_0	0.9058040	-0.1419600	5.5122770	-9.5617500	5.9764900	-0.3592700	-0.7266200
			G_1	0.1633120	0.2600410	1.8259160	-0.9386500	-1.7190000	1.8499160	-0.5803600
			G_5	0.8740860	-0.0414600	4.7396040	-7.6990800	3.8924480	0.6843440	-0.8888900
			G_6	-0.1301100	-0.0183300	-0.2843000	0.1701160	1.9935560	-2.8991100	1.1681810
		0.8	G_0	1.1362950	-0.6322700	8.9930590	-17.154200	13.986480	-5.2792000	0.7778800
			G_1	0.2267910	0.1761450	2.3523390	-1.3128900	-2.6788900	3.3719220	-1.1814200
			G_5	1.0830690	0.0257530	3.7725650	0.1269090	-14.114800	16.892860	-6.0000000
			G_6	-0.1689600	-0.0072400	-0.4675900	0.8092530	1.3871220	-2.5821300	1.0295540

Table C.15
Influence Coefficients For A Circumferential Semi-Elliptical Surface Crack In A Cylinder – Outside Surface

t/R_i	a/c	a/t	G_i	A_0	A_1	A_2	A_3	A_4	A_5	A_6
0.1	0.5	0	G_0	0.8776607	-0.6729719	3.7721411	-6.5209060	6.3377934	-3.7028038	0.9872447
			G_1	0.1277541	0.4368502	0.4904522	1.0427434	-2.9631236	2.0826525	-0.5184313
			G_5	0.8776607	-0.6729719	3.7721411	-6.5209060	6.3377934	-3.7028038	0.9872447
			G_6	0.0000000	0.0000000	0.0000000	0.0000000	0.0000000	0.0000000	0.0000000
		0.2	G_0	0.9002023	-0.9702215	6.0536022	-13.882269	17.810396	-12.331265	3.5110491
			G_1	0.1495747	0.1634833	2.2505843	-4.5297851	5.7083424	-4.4995032	1.4438996
			G_5	0.8999997	-1.0136861	6.3084405	-14.786302	19.506612	-13.927996	4.0990080
			G_6	-0.0424730	0.2353750	-0.7985880	0.9626770	-0.1168940	-0.3848150	0.1473720
		0.4	G_0	1.0018170	-0.6526700	2.7525060	-1.5008000	-3.7179600	5.3983550	-2.0923200
			G_1	0.1773570	0.3012160	1.2765120	-0.8389800	-0.9008500	1.0771530	-0.3564800
			G_5	0.9665280	-0.4473900	1.5183180	1.6545410	-7.9008300	8.1581390	-2.8000000
			G_6	-0.0778300	0.3084970	-1.4829700	3.3510040	-3.5126300	1.6233420	-0.2094200
		0.6	G_0	1.1744170	-1.0266500	3.9235670	-3.0654300	-3.6018500	6.6578170	-2.7725400
			G_1	0.2255660	0.2202280	1.3847150	-0.6930400	-1.4302400	1.6013990	-0.5373200
			G_5	1.1441930	-0.9557800	3.4558090	-2.2783600	-3.9068700	6.2364950	-2.4565200
			G_6	-0.0885200	0.1578950	-0.5316000	0.4087900	1.4498400	-2.5408900	1.1444860
		0.8	G_0	1.3489390	-0.9235200	2.6704340	-0.6902900	-4.7097800	5.4725200	-1.8088900
			G_1	0.2731610	0.2563650	1.0548290	-0.2726400	-1.0807200	0.7012640	-0.1196200
			G_5	1.3439830	-1.3145200	4.6858860	-5.6761600	1.3418740	1.8498250	-0.9333300
			G_6	-0.0873500	-0.0886200	0.3878340	0.1649200	-1.6781300	2.1040180	-0.8026700
0.1	1	0	G_0	1.1977992	-0.5244870	0.1498299	2.3284866	-5.1058499	4.3469049	-1.3487980
			G_1	0.1870117	0.6987352	0.1316900	0.7269255	-2.5259384	2.1756251	-0.6540458
			G_5	1.1977992	-0.5244870	0.1498299	2.3284866	-5.1058499	4.3469049	-1.3487980
			G_6	0.0000000	0.0000000	0.0000000	0.0000000	0.0000000	0.0000000	0.0000000
		0.2	G_0	1.2189520	-1.2097738	5.0035806	-13.570604	21.154946	-17.035957	5.4883898
			G_1	0.2148545	0.1923835	3.2066624	-8.9783210	13.277850	-10.615434	3.4306144
			G_5	1.2348218	-1.5269201	7.1162363	-20.664373	33.524193	-27.770261	9.1475073
			G_6	-0.0092560	-0.0568710	0.2921860	-0.3315290	-0.4709780	1.1501860	-0.5729590
		0.4	G_0	1.3032840	-0.9801200	1.9396690	-1.2179000	-1.8798300	3.3323020	-1.4157700
			G_1	0.2260780	0.1891498	3.1559468	-8.8370736	12.955466	-10.205414	3.2420289
			G_5	1.2591380	-0.7390000	0.7251370	1.1755220	-3.9130200	3.8325580	-1.3000000
			G_6	-0.0778600	0.5780920	-2.8912800	6.8770170	-8.0159800	4.3504740	-0.8204600
		0.6	G_0	1.3998570	-1.0998500	1.8242350	-0.5517400	-3.0050500	4.1670200	-1.6320200
			G_1	0.2485370	0.5078860	0.8346190	-0.7374200	-1.0800000	1.5854580	-0.6001300
			G_5	1.3519740	-0.8505200	0.5388810	1.9241970	-5.0416900	4.6279070	-1.5000000
			G_6	-0.0912600	0.6323660	-3.1077800	7.4058900	-8.7302400	4.8882180	-0.9972000
		0.8	G_0	1.5124900	-1.2482100	1.8172430	-0.7418200	-1.9585100	2.7114870	-0.9820100
			G_1	0.2745170	0.4942760	0.7450050	-0.5511800	-1.1008400	1.4068690	-0.4942200
			G_5	1.4505080	-0.9441200	0.3685860	1.9679090	-4.1014600	2.9209300	-0.6000000
			G_6	-0.0843400	0.2453070	-0.6685400	0.9996230	-0.6106200	0.0423550	0.0762110

Table C.15
Influence Coefficients For A Circumferential Semi-Elliptical Surface Crack In A Cylinder – Outside Surface

t/R_i	a/c	a/t	G_i	A_0	A_1	A_2	A_3	A_4	A_5	A_6
0.1	2	0	G_0	0.8150546	-0.5623828	1.4465771	-4.6778133	8.4192164	-7.9025932	2.9866351
			G_1	0.1359146	0.0702340	3.5558581	-11.034445	16.967724	-14.126991	4.8706612
			G_5	0.8150546	-0.5623828	1.4465771	-4.6778133	8.4192164	-7.9025932	2.9866351
			G_6	0.0000000	0.0000000	0.0000000	0.0000000	0.0000000	0.0000000	0.0000000
		0.2	G_0	0.8318082	-1.0744316	4.6367738	-14.199630	22.984826	-18.988399	6.3228538
			G_1	0.1359368	0.0389874	3.4384062	-10.446088	15.691611	-12.753307	4.3064449
			G_5	0.8564580	-1.5112769	7.5603932	-23.926791	39.860172	-33.596301	11.295662
			G_6	-0.0106640	0.1219130	-0.6449160	1.2065960	-0.3680280	-0.9134070	0.6033690
		0.4	G_0	0.8348640	-0.2936000	-0.9263100	3.9021310	-6.9762200	5.4984440	-1.5244400
			G_1	0.1393714	-0.0045032	3.6949749	-11.266421	17.130648	-14.059458	4.7767704
			G_5	0.8652730	-1.6261381	8.2098099	-26.112774	43.760418	-37.079714	12.518093
			G_6	-0.0145700	0.0176350	-0.0438700	0.0860730	-0.0635500	-0.0193900	0.0376720
		0.6	G_0	0.8612390	-0.3546400	-0.8071600	3.6751250	-6.7152100	5.3181550	-1.4639700
			G_1	0.1456764	0.0206678	3.4832840	-10.595840	15.947484	-12.963085	4.3682056
			G_5	0.8854193	-1.5303165	7.1553070	-22.472768	37.311145	-31.322730	10.487317
			G_6	-0.0216900	0.0302850	-0.0929100	0.1801340	-0.1065400	-0.0528800	0.0635980
		0.8	G_0	0.9156630	-0.9908500	3.0995250	-8.5396400	13.206200	-10.984000	3.8193200
			G_1	0.1530811	-0.0218691	3.7692054	-11.555637	17.436930	-13.982208	4.6031925
			G_5	0.9068474	-1.5066824	6.5832667	-20.426436	33.519921	-27.720880	9.1309784
			G_6	-0.0130600	-0.1144100	0.5959870	-0.9610000	-0.0207700	1.3396050	-0.8263400
0.2	0.0625	0	G_0	0.2695332	2.1626001	-1.6551569	-1.2970208	4.5604304	-4.3163876	1.4010655
			G_1	0.0138667	0.1827458	2.5749608	-3.9044679	3.3556301	-2.1772209	0.6420134
			G_5	0.2695332	2.1626001	-1.6551569	-1.2970208	4.5604304	-4.3163876	1.4010655
			G_6	0.0000000	0.0000000	0.0000000	0.0000000	0.0000000	0.0000000	0.0000000
		0.2	G_0	0.2774908	2.0262553	-0.8133105	-1.7375464	3.4202878	-2.6009946	0.6867850
			G_1	0.0179837	0.1529136	2.9576751	-5.1711648	5.7849984	-4.3571052	1.3519411
			G_5	0.2399928	1.8100037	-0.7426186	-1.4325636	4.3104695	-4.4371558	1.4878002
			G_6	-0.1338400	-1.0002800	0.8073470	0.6262070	0.6560130	-1.7063600	0.7509160
		0.4	G_0	0.2781441	2.1182907	-0.8573663	-0.6940178	4.1137120	-5.3210542	1.9749190
			G_1	0.0170279	0.1270926	3.0978063	-5.1503505	6.6321310	-5.7118949	1.8626268
			G_5	0.1376850	0.8752836	0.9229982	-1.1394534	6.2867597	-8.7023069	3.1746372
			G_6	-0.2668900	-1.4913300	-2.2572300	13.963520	-23.281800	20.497450	-7.1637200
		0.6	G_0	0.2698597	2.1631441	-1.0979827	2.5533805	1.1045698	-5.3720025	2.4755770
			G_1	0.0093374	0.1071110	3.0699264	-4.8291996	8.1014107	-8.2339838	2.8377620
			G_5	0.0387421	0.0943716	-3.8239057	18.474536	-15.996194	3.4545316	-0.2379488
			G_6	-0.3563400	1.0277720	-26.712600	94.035930	-163.57100	145.97540	-50.399100
		0.8	G_0	0.2674593	2.0433452	0.0155220	2.7277592	1.5017795	-6.3715518	2.5965143
			G_1	0.0038165	0.0595955	3.3820597	-5.9553893	12.305288	-12.483753	4.0394895
			G_5	-0.2629900	0.1512970	-10.321900	32.029360	-21.854600	6.6345790	-3.8096300
			G_6	-0.1960400	-2.9545700	6.4418390	-16.738900	-11.887500	57.343800	-32.008700

Table C.15
Influence Coefficients For A Circumferential Semi-Elliptical Surface Crack In A Cylinder – Outside Surface

t/R_i	a/c	a/t	G_i	A_0	A_1	A_2	A_3	A_4	A_5	A_6
0.2	0.125	0	G_0	0.4065238	0.7772483	3.8861644	-12.573943	16.760207	-11.014593	2.8706957
			G_1	0.0320270	0.1825342	2.2670449	-2.7076615	1.2088194	-0.3777430	0.0763155
			G_5	0.4065238	0.7772483	3.8861644	-12.573943	16.760207	-11.014593	2.8706957
			G_6	0.0000000	0.0000000	0.0000000	0.0000000	0.0000000	0.0000000	0.0000000
		0.2	G_0	0.4117875	1.1385881	1.7784942	-6.1639923	7.6448761	-4.8213505	1.2226378
			G_1	0.0470699	0.0295648	3.7396060	-8.1204493	10.711888	-8.1991643	2.5060356
			G_5	0.3971461	1.1200570	1.5332235	-5.2800357	6.4550368	-4.0686358	1.0314054
			G_6	-0.0989900	-0.3971800	0.6515250	-1.4711400	3.9895020	-4.1519400	1.4782250
		0.4	G_0	0.4492521	1.2970887	1.6394114	-4.6101707	5.5388028	-3.8995510	1.1013127
			G_1	0.0584564	0.0847062	3.5928149	-7.0140416	8.9104748	-6.9581901	2.1577698
			G_5	0.3925974	1.1782321	1.0536644	-1.8881185	1.8376671	-1.6477686	0.5450371
			G_6	-0.2041000	-0.6628600	-0.0950100	2.3430480	-1.7270700	0.2829070	0.0630740
		0.6	G_0	0.4881660	1.6507400	0.2050560	2.1433950	-4.5291500	2.1963290	-0.2168300
			G_1	0.0566450	0.3309960	1.9818650	-0.9123500	-0.4442300	-0.4525300	0.4199700
			G_5	0.3466423	1.0235299	0.7336500	4.0764251	-7.4318993	3.9119364	-0.7633649
			G_6	-0.3387500	-0.7171400	-2.0254800	7.4624010	-6.9186200	3.5122470	-0.9746500
		0.8	G_0	0.5121250	1.5704480	2.4143130	0.2498080	-4.3262900	2.1073350	-0.0575300
			G_1	0.0561240	0.3465660	2.3212940	-0.6279400	-1.0469300	-0.2889500	0.4244900
			G_5	0.2408720	0.4224221	3.5982027	-0.5713316	4.0453456	-9.4061812	4.1654423
			G_6	-0.4674500	-1.1687700	0.4132170	-10.223100	34.719670	-34.908100	11.634500
0.2	0.25	0	G_0	0.6152816	-0.3348694	6.2955620	-15.590618	19.299508	-12.488107	3.3010035
			G_1	0.0703566	0.2828152	1.4036169	-0.6511596	-1.2076596	1.0318656	-0.2423741
			G_5	0.6152816	-0.3348694	6.2955620	-15.590618	19.299508	-12.488107	3.3010035
			G_6	0.0000000	0.0000000	0.0000000	0.0000000	0.0000000	0.0000000	0.0000000
		0.2	G_0	0.6271377	-0.2298482	7.0204766	-19.981373	27.955848	-19.841412	5.6004795
			G_1	0.0907652	0.1775295	2.5002998	-4.9548232	6.1690007	-4.7911060	1.4984781
			G_5	0.6267188	-0.2150752	5.9244999	-15.141684	19.361210	-12.962335	3.5399114
			G_6	-0.0730300	-0.1039500	0.3779340	-1.4730700	3.4257760	-3.3001300	1.1464610
		0.4	G_0	0.7243940	0.0982170	3.8649050	-6.8572100	4.4474240	-0.4646900	-0.4610600
			G_1	0.1116160	0.2421110	1.9598510	-2.2366400	1.2671380	-0.9068300	0.3367200
			G_5	0.6870350	0.0387870	3.9170980	-7.1437000	5.1449910	-1.1416500	-0.2222200
			G_6	-0.1429600	-0.1522700	0.3434280	-1.3869700	3.9981410	-4.1031700	1.4438050
		0.6	G_0	0.8591310	0.0156500	4.8410810	-7.6957700	3.5329350	1.1471070	-1.0891600
			G_1	0.1506290	0.2414840	2.0792750	-1.7964600	-0.2806200	0.6982770	-0.2306800
			G_5	0.7980120	-0.1517600	5.6710930	-11.201800	10.646550	-5.3611100	1.1111110
			G_6	-0.2281500	-0.0472900	-0.6334600	1.2719350	1.1658530	-2.6941700	1.1652830
		0.8	G_0	1.0109730	-0.1571000	7.0684530	-11.622100	6.4274650	-0.2949400	-0.5470500
			G_1	0.1949920	0.1486120	2.9915130	-3.4528600	0.9912030	0.3037770	-0.2056700
			G_5	0.8870610	0.3775580	2.2456250	3.9607610	-17.744100	18.035720	-6.0000000
			G_6	-0.3136200	-0.0427800	-1.0031500	2.2762370	0.9773960	-3.3646700	1.4705920

Table C.15
Influence Coefficients For A Circumferential Semi-Elliptical Surface Crack In A Cylinder – Outside Surface

t/R_i	a/c	a/t	G_i	A_0	A_1	A_2	A_3	A_4	A_5	A_6
0.2	0.5	0	G_0	0.8776607	-0.6729719	3.7721411	-6.5209060	6.3377934	-3.7028038	0.9872447
			G_1	0.1277541	0.4368502	0.4904522	1.0427434	-2.9631236	2.0826525	-0.5184313
			G_5	0.8776607	-0.6729719	3.7721411	-6.5209060	6.3377934	-3.7028038	0.9872447
			G_6	0.0000000	0.0000000	0.0000000	0.0000000	0.0000000	0.0000000	0.0000000
		0.2	G_0	0.9018630	-0.9538496	5.9919622	-13.738556	17.612623	-12.191476	3.4725648
			G_1	0.1495608	0.1733747	2.2120339	-4.4335931	5.5703879	-4.4014805	1.4175068
			G_5	0.8989059	-0.9882804	6.1271579	-14.287453	18.780450	-13.406411	3.9549546
			G_6	-0.0705200	0.2567410	-1.2495900	2.8677950	-3.0504600	1.4356940	-0.1896600
		0.4	G_0	1.0019030	-0.6556300	2.8775410	-1.9787200	-3.0003900	4.9257760	-1.9790600
			G_1	0.1738940	0.3355690	1.1270520	-0.4578300	-1.4623100	1.5065800	-0.4867600
			G_5	0.9505460	-0.4598500	1.7330080	0.5011690	-5.6648600	6.2604660	-2.2000000
			G_6	-0.1213700	0.4129990	-1.9995500	4.6351640	-5.0019800	2.4723590	-0.3976300
		0.6	G_0	1.1589040	-0.9119700	3.6019430	-2.5613200	-4.0414800	6.8676550	-2.8162900
			G_1	0.2195810	0.2504100	1.3344200	-0.6342900	-1.5137700	1.6844020	-0.5678100
			G_5	1.1041200	-0.8565000	3.1614520	-2.0800900	-3.6322300	5.7885380	-2.2826100
			G_6	-0.1479200	0.2002220	-0.6443400	0.5965410	1.5644630	-2.8569900	1.2880200
		0.8	G_0	1.3175280	-0.7714200	2.5794970	-1.1653400	-3.4376600	4.2682690	-1.4121500
			G_1	0.2602210	0.3199750	0.9492120	-0.1839400	-1.1009900	0.6684550	-0.0987300
			G_5	1.2740170	-1.1637300	4.5095380	-6.0754300	2.7026250	0.4828070	-0.4666700
			G_6	-0.1671200	-0.0249100	0.2071610	0.6527170	-2.0799000	2.2037960	-0.7917400
0.2	1	0	G_0	1.1977992	-0.5244870	0.1498299	2.3284866	-5.1058499	4.3469049	-1.3487980
			G_1	0.1870117	0.6987352	0.1316900	0.7269255	-2.5259384	2.1756251	-0.6540458
			G_5	1.1977992	-0.5244870	0.1498299	2.3284866	-5.1058499	4.3469049	-1.3487980
			G_6	0.0000000	0.0000000	0.0000000	0.0000000	0.0000000	0.0000000	0.0000000
		0.2	G_0	1.2208938	-1.2041917	5.0334698	-13.741887	21.435583	-17.257339	5.5625096
			G_1	0.2144977	0.2060705	3.1319639	-8.7325400	12.853217	-10.282493	3.3370053
			G_5	1.2350971	-1.5079685	6.9553573	-20.208191	32.816115	-27.245603	9.0067094
			G_6	-0.0828200	0.6613920	-3.3269100	7.7832260	-8.6558500	4.1418630	-0.5209000
		0.4	G_0	1.2974480	-0.8978500	1.5464860	-0.0684400	-3.8891500	5.0715000	-1.9856700
			G_1	0.2279963	0.2557041	2.7316895	-7.3765941	10.510743	-8.3256498	2.7071280
			G_5	1.2392890	-0.7267700	0.7939140	0.5894400	-2.7996000	2.9069770	-1.0000000
			G_6	-0.1070200	0.6703990	-3.2584800	7.6913240	-8.8678600	4.7415690	-0.8699400
		0.6	G_0	1.3902670	-1.0526700	1.8671080	-0.9437600	-2.5011700	3.9208390	-1.5891100
			G_1	0.2440310	0.5137240	0.8974300	-0.8785500	-1.0881800	1.7286490	-0.6657300
			G_5	1.3181210	-0.7998800	0.4938380	1.5489800	-4.2573600	3.9953490	-1.3000000
			G_6	-0.1281700	0.6899310	-3.2765600	7.8600090	-9.3273600	5.2734440	-1.0912900
		0.8	G_0	1.4978360	-1.1640500	1.8344600	-1.1167700	-1.6062200	2.6731730	-1.0165300
			G_1	0.2690770	0.5138280	0.7713690	-0.5894800	-1.2981100	1.6877650	-0.5889500
			G_5	1.4113850	-0.9874900	1.0715580	-0.7321800	0.2206270	-0.3814000	0.4000000
			G_6	-0.1307600	0.3275810	-0.9451600	1.7563070	-1.5599400	0.5843160	-0.0323500

Table C.15
Influence Coefficients For A Circumferential Semi-Elliptical Surface Crack In A Cylinder – Outside Surface

t/R_i	a/c	a/t	G_i	A_0	A_1	A_2	A_3	A_4	A_5	A_6
0.2	2	0	G_0	0.8150546	-0.5623828	1.4465771	-4.6778133	8.4192164	-7.9025932	2.9866351
			G_1	0.1359146	0.0702340	3.5558581	-11.034445	16.967724	-14.126991	4.8706612
			G_5	0.8150546	-0.5623828	1.4465771	-4.6778133	8.4192164	-7.9025932	2.9866351
			G_6	0.0000000	0.0000000	0.0000000	0.0000000	0.0000000	0.0000000	0.0000000
		0.2	G_0	0.8319739	-1.0737151	4.6490836	-14.283121	23.181415	-19.212560	6.4181218
			G_1	0.1367829	0.0195825	3.5727027	-10.883865	16.435739	-13.397326	4.5265031
			G_5	0.8587201	-1.5078217	7.4605134	-23.602425	39.397717	-33.324166	11.250246
			G_6	-0.0013600	0.0067490	-0.0078600	0.0154990	-0.0227600	0.0006890	0.0090320
		0.4	G_0	0.8306360	-0.2783600	-0.9579000	3.8962200	-6.8631100	5.3033590	-1.4257900
			G_1	0.1414167	-0.0083138	3.7265323	-11.341965	17.307508	-14.334310	4.9200146
			G_5	0.8651941	-1.6414372	8.2119118	-26.195706	44.070198	-37.499897	12.710196
			G_6	-0.0204200	0.0175040	-0.0184100	0.0563730	-0.0617800	0.0082410	0.0185040
		0.6	G_0	0.8556570	-0.3568100	-0.6900000	3.2047690	-5.8960900	4.5761710	-1.1943900
			G_1	0.1450802	0.0389886	3.3678594	-10.170959	15.319892	-12.658323	4.3602413
			G_5	0.8781226	-1.5169522	6.9468106	-21.892973	36.571741	-30.949926	10.451527
			G_6	-0.0301300	0.0314260	-0.0707200	0.1957270	-0.1994100	0.0478270	0.0252810
		0.8	G_0	0.9091900	-1.0214700	3.4711980	-9.9203800	15.637600	-13.142700	4.5753490
			G_1	0.1478586	0.0682866	3.1625977	-9.5415913	14.299739	-11.806182	4.0649234
			G_5	0.8923217	-1.4448983	6.0075154	-18.631958	30.794580	-25.802121	8.6362697
			G_6	-0.0234000	-0.1198900	0.6560330	-0.9660400	-0.2436600	1.6734190	-0.9764600
0.33333	0.125	0	G_0	0.4065238	0.7772483	3.8861644	-12.573943	16.760207	-11.014593	2.8706957
			G_1	0.0320270	0.1825342	2.2670449	-2.7076615	1.2088194	-0.3777430	0.0763155
			G_5	0.4065238	0.7772483	3.8861644	-12.573943	16.760207	-11.014593	2.8706957
			G_6	0.0000000	0.0000000	0.0000000	0.0000000	0.0000000	0.0000000	0.0000000
		0.2	G_0	0.4099613	1.1334144	1.8167755	-6.1933976	7.6194214	-4.7676610	1.1972653
			G_1	0.0462103	0.0340256	3.6705315	-7.7292467	9.9287487	-7.5175409	2.2859463
			G_5	0.3781184	1.0782386	1.3896969	-4.4300255	5.1708948	-3.2094344	0.8003934
			G_6	-0.1440800	-0.5237500	0.4347310	-0.2173300	2.3742060	-3.1240500	1.2002700
		0.4	G_0	0.4533770	1.0766900	3.5058010	-11.549900	17.918540	-14.316700	4.4298660
			G_1	0.0523522	0.0848838	3.4278771	-6.1023514	7.1456705	-5.4439258	1.6695382
			G_5	0.3133139	0.9747113	0.6917682	0.6225195	-1.5943871	0.3406017	0.0734211
			G_6	-0.2907100	-0.8909900	-0.1971000	2.5029520	-0.4154300	-1.2933500	0.5846360
		0.6	G_0	0.4709970	0.7906930	6.3141400	-17.458100	26.655280	-21.459500	6.6178750
			G_1	0.0462130	0.1791657	2.8322826	-3.4762634	3.7158317	-3.6187167	1.3051475
			G_5	0.1771076	0.3899173	2.3204598	-1.4538642	6.0522140	-9.3757919	3.6701943
			G_6	-0.4185600	-1.1827300	-0.9627800	2.7897690	1.8354460	-2.5019400	0.4407850
		0.8	G_0	0.4435980	1.2520030	3.3031060	-2.6255800	2.8823370	-4.6559200	1.9668050
			G_1	0.0347263	0.1941740	2.8167869	-2.0526330	2.2452322	-3.3744831	1.3721332
			G_5	0.1067768	-1.1059070	1.9184730	12.339821	-15.038255	4.2343108	-0.1594022
			G_6	-0.3502400	-1.8200500	-2.3187300	0.8497210	14.129590	-14.707700	4.2173670

Table C.15
Influence Coefficients For A Circumferential Semi-Elliptical Surface Crack In A Cylinder – Outside Surface

t/R_i	a/c	a/t	G_i	A_0	A_1	A_2	A_3	A_4	A_5	A_6
0.33333	0.25	0	G_0	0.6152816	-0.3348694	6.2955620	-15.590618	19.299508	-12.488107	3.3010035
			G_1	0.0703566	0.2828152	1.4036169	-0.6511596	-1.2076596	1.0318656	-0.2423741
			G_5	0.6152816	-0.3348694	6.2955620	-15.590618	19.299508	-12.488107	3.3010035
			G_6	0.0000000	0.0000000	0.0000000	0.0000000	0.0000000	0.0000000	0.0000000
		0.2	G_0	0.6247110	-0.1841775	6.7646437	-19.122556	26.490065	-18.633480	5.2176726
			G_1	0.0902680	0.1863897	2.4580412	-4.8000656	5.9136117	-4.5969548	1.4420194
			G_5	0.6188062	-0.2124520	5.8656185	-14.966741	19.138738	-12.819133	3.5001285
			G_6	-0.1133700	0.0386090	-0.7483700	1.8940110	-1.3915000	0.2087770	0.1118400
		0.4	G_0	0.7285570	-0.1787800	5.9836260	-13.655900	15.406530	-9.1372500	2.2140220
			G_1	0.1068720	0.2817480	1.6735290	-1.1790200	-0.6310000	0.7077640	-0.1838800
			G_5	0.6544370	-0.1552600	5.2209810	-11.650100	13.030050	-7.7164200	1.8592460
			G_6	-0.2193000	0.0425450	-1.3544600	3.7675290	-3.2851000	1.1023660	-0.0535800
		0.6	G_0	0.8443080	-0.5795400	9.6687260	-23.049300	28.167150	-18.272400	4.8614220
			G_1	0.1391010	0.2003860	2.4182470	-2.4894900	0.4710610	0.2306300	-0.0993900
			G_5	0.7034360	-0.4721000	7.8058200	-17.653700	21.157630	-13.776400	3.6887940
			G_6	-0.3396100	0.0377040	-1.9404100	5.1897370	-3.6971200	0.3704200	0.3792770
		0.8	G_0	0.9520760	-0.1754800	7.5423420	-13.331500	11.885240	-6.9538200	2.0803610
			G_1	0.1701480	0.2848700	2.1734480	-1.0215800	-1.7757000	1.4765150	-0.2998500
			G_5	0.7201900	-0.1035200	5.4180790	-7.7404000	5.9504530	-4.0595900	1.5230280
			G_6	-0.4790200	0.0451970	-2.0762300	3.9884540	1.1847190	-4.8004700	2.1373500
0.33333	0.5	0	G_0	0.8776607	-0.6729719	3.7721411	-6.5209060	6.3377934	-3.7028038	0.9872447
			G_1	0.1277541	0.4368502	0.4904522	1.0427434	-2.9631236	2.0826525	-0.5184313
			G_5	0.8776607	-0.6729719	3.7721411	-6.5209060	6.3377934	-3.7028038	0.9872447
			G_6	0.0000000	0.0000000	0.0000000	0.0000000	0.0000000	0.0000000	0.0000000
		0.2	G_0	0.9066169	-1.0098809	6.4500448	-15.276412	20.122076	-14.176827	4.0826731
			G_1	0.1492778	0.1842512	2.1734412	-4.3450372	5.4492142	-4.3195528	1.3970909
			G_5	0.8914928	-0.9078192	5.6229793	-12.889289	16.743862	-11.930113	3.5383034
			G_6	-0.0731700	-0.0019200	0.1112140	-0.3517100	0.7595710	-0.6537100	0.2097210
		0.4	G_0	0.9745940	-0.2537500	0.9422670	2.4134430	-8.0311500	7.6591860	-2.5119400
			G_1	0.1677910	0.3861730	0.9608550	-0.2805400	-1.3649300	1.1990170	-0.3335200
			G_5	0.9236760	-0.3872800	1.4642830	0.6726050	-5.2981700	5.6675470	-1.9567300
			G_6	-0.1336400	-0.0061900	0.2483910	-0.7804100	1.6547940	-1.4364400	0.4535040
		0.6	G_0	1.1489090	-0.9628100	4.7197790	-7.2385800	4.7190150	-0.8600300	-0.2218800
			G_1	0.2074750	0.3710920	0.7536550	0.8750530	-3.5617500	3.0181320	-0.8916700
			G_5	1.0605150	-0.9384600	4.2401570	-6.3570900	3.8804030	-0.3727100	-0.3571700
			G_6	-0.2088100	0.1861540	-0.5969000	1.1076490	-0.1339800	-0.7782600	0.4241420
		0.8	G_0	1.2919860	-0.5742900	1.7855010	2.6509560	-11.664400	11.851350	-3.9241400
			G_1	0.2520800	0.4019340	0.4065200	2.4606020	-6.6673200	5.7443690	-1.7758300
			G_5	1.1599780	-0.5682200	1.3649980	3.1291180	-11.561500	11.451800	-3.7613000
			G_6	-0.2744400	0.1898780	-0.4285700	0.7415200	0.4312720	-1.1716300	0.5119770

Table C.15
Influence Coefficients For A Circumferential Semi-Elliptical Surface Crack In A Cylinder – Outside Surface

t/R_i	a/c	a/t	G_i	A_0	A_1	A_2	A_3	A_4	A_5	A_6
0.33333	1	0	G_0	1.1977992	-0.5244870	0.1498299	2.3284866	-5.1058499	4.3469049	-1.3487980
			G_1	0.1870117	0.6987352	0.1316900	0.7269255	-2.5259384	2.1756251	-0.6540458
			G_5	1.1977992	-0.5244870	0.1498299	2.3284866	-5.1058499	4.3469049	-1.3487980
			G_6	0.0000000	0.0000000	0.0000000	0.0000000	0.0000000	0.0000000	0.0000000
		0.2	G_0	1.2220417	-1.2014542	5.0931939	-14.015936	21.882198	-17.611726	5.6790779
			G_1	0.2144011	0.2076611	3.1479697	-8.7880102	12.919129	-10.335990	3.3611678
			G_5	1.2320744	-1.5110742	6.9601667	-20.284073	32.929016	-27.327658	9.0387452
			G_6	-0.0490800	-0.0266200	0.3507710	-1.0858100	1.7945020	-1.4605800	0.4768160
		0.4	G_0	1.2493780	-0.1807200	-2.1512500	9.0872720	-15.619500	12.451940	-3.7683100
			G_1	0.2277520	0.2442248	2.8502573	-7.7013661	10.911804	-8.6055298	2.8003299
			G_5	1.1860660	-0.1633600	-2.5846400	10.208460	-17.192400	13.660050	-4.1506700
			G_6	-0.0847200	-0.0130400	0.4450670	-1.3612100	2.2705210	-1.8636500	0.6070300
		0.6	G_0	1.3282800	-0.1805500	-2.6139900	10.483400	-17.872600	14.215520	-4.2781900
			G_1	0.2244930	0.7671250	-0.4475100	2.7627880	-6.2712500	5.3388310	-1.6303400
			G_5	1.2510160	-0.2335300	-2.7704000	10.674610	-17.843000	14.118660	-4.2549700
			G_6	-0.1229000	0.0987760	-0.0510800	0.0753380	0.2033960	-0.3948100	0.1912830
		0.8	G_0	1.4785910	-1.2353000	3.6180340	-8.2725500	10.979570	-8.0343800	2.5668670
			G_1	0.2647100	0.4116600	1.8029290	-4.2515600	5.0019550	-3.7691200	1.2975750
			G_5	1.3832810	-1.3901800	4.0196220	-10.087000	14.697690	-11.393300	3.7011250
			G_6	-0.1828100	0.6153590	-3.1104800	9.4475170	-14.736200	11.582900	-3.6163100
0.33333	2	0	G_0	0.8150546	-0.5623828	1.4465771	-4.6778133	8.4192164	-7.9025932	2.9866351
			G_1	0.1359146	0.0702340	3.5558581	-11.034445	16.967724	-14.126991	4.8706612
			G_5	0.8150546	-0.5623828	1.4465771	-4.6778133	8.4192164	-7.9025932	2.9866351
			G_6	0.0000000	0.0000000	0.0000000	0.0000000	0.0000000	0.0000000	0.0000000
		0.2	G_0	0.8331327	-1.0983961	4.8310919	-14.895078	24.214240	-20.089273	6.7122349
			G_1	0.1374607	0.0008167	3.6998791	-11.290852	17.125293	-14.000885	4.7362430
			G_5	0.8590462	-1.4944677	7.2901818	-23.037515	38.516128	-32.701232	11.093104
			G_6	-0.0046700	0.0180740	-0.0638400	0.1222610	-0.0829200	-0.0216300	0.0327160
		0.4	G_0	0.8283100	-0.2747400	-0.9278400	3.7320330	-6.5492300	4.9873730	-1.2999200
			G_1	0.1426112	-0.0204439	3.8267365	-11.671861	17.925207	-14.972682	5.1786686
			G_5	0.8690036	-1.7119175	8.5353824	-27.203901	45.752326	-38.936187	13.200079
			G_6	-0.0276200	0.0342780	-0.0751100	0.1858580	-0.1916200	0.0577570	0.0164540
		0.6	G_0	0.8508740	-0.3486600	-0.6430600	2.9213950	-5.3199000	3.9848080	-0.9604400
			G_1	0.1448686	0.0284442	3.4562322	-10.447804	15.869466	-13.299505	4.6445600
			G_5	0.8707662	-1.5022966	6.7207535	-21.298542	35.863052	-30.637128	10.444495
			G_6	-0.0400200	0.0397750	-0.0574200	0.1528560	-0.1187200	-0.0270400	0.0505700
		0.8	G_0	0.9042450	-1.0486000	3.8207860	-11.291000	18.161500	-15.468300	5.4125140
			G_1	0.1453857	0.0854754	3.0581116	-9.1833308	13.836217	-11.703621	4.1461877
			G_5	0.8788989	-1.4042484	5.5584708	-17.279835	28.790156	-24.426973	8.2965772
			G_6	-0.0362200	-0.1136800	0.6936160	-1.0067200	-0.3158000	1.8522520	-1.0734500

Table C.15
Influence Coefficients For A Circumferential Semi-Elliptical Surface Crack In A Cylinder – Outside Surface

t/R_i	a/c	a/t	G_i	A_0	A_1	A_2	A_3	A_4	A_5	A_6
1.0	0.25	0	G_0	0.6152816	-0.3348694	6.2955620	-15.590618	19.299508	-12.488107	3.3010035
			G_1	0.0703566	0.2828152	1.4036169	-0.6511596	-1.2076596	1.0318656	-0.2423741
			G_5	0.6152816	-0.3348694	6.2955620	-15.590618	19.299508	-12.488107	3.3010035
			G_6	0.0000000	0.0000000	0.0000000	0.0000000	0.0000000	0.0000000	0.0000000
		0.2	G_0	0.6325077	-0.1237835	5.4933139	-13.354203	16.158098	-10.342658	2.7213600
			G_1	0.0837357	0.2118914	1.8184383	-1.5588154	-0.2764673	0.6310913	-0.2035715
			G_5	0.5759298	-0.1208515	4.9251769	-11.934902	14.764921	-9.7777680	2.6609175
			G_6	-0.1790600	-0.2668400	1.1582240	-4.6894500	10.493520	-9.8097800	3.2933910
		0.4	G_0	0.6444073	0.7365248	-0.8635726	9.4953524	-20.751270	17.472484	-5.3129659
			G_1	0.0884386	0.5329509	-0.4272183	6.1382654	-12.251001	9.3705550	-2.6598529
			G_5	0.5212637	-0.1038323	4.8086459	-10.700635	13.751600	-10.014017	2.9558428
			G_6	-0.3658800	-0.0236700	-1.5538400	3.5756560	-0.5229400	-2.3014900	1.1921600
		0.6	G_0	0.7228476	0.4610828	1.8630770	5.0820470	-16.991943	15.831398	-5.1173098
			G_1	0.1081128	0.4515473	0.5218137	4.4136428	-10.314107	8.0880026	-2.3243612
			G_5	0.3785959	0.0502413	3.6547418	-4.8375232	5.6776718	-5.5022599	2.0033432
			G_6	-0.5086100	-0.3272600	-0.2676300	-1.6452800	10.271870	-11.634900	4.1117840
		0.8	G_0	0.7383878	0.2039050	5.9795014	-2.2071247	-7.2949484	7.5815045	-2.3858270
			G_1	0.1051410	0.4105167	1.6026304	2.9671893	-8.4475408	6.2704340	-1.6829015
			G_5	0.1484157	0.3722983	1.7072168	4.8086967	-7.2713509	1.1773589	0.8440161
			G_6	-0.6470100	-0.3391800	-1.6737900	1.4222280	7.7580450	-9.8400600	3.3197590
1.0	0.5	0	G_0	0.8776607	-0.6729719	3.7721411	-6.5209060	6.3377934	-3.7028038	0.9872447
			G_1	0.1277541	0.4368502	0.4904522	1.0427434	-2.9631236	2.0826525	-0.5184313
			G_5	0.8776607	-0.6729719	3.7721411	-6.5209060	6.3377934	-3.7028038	0.9872447
			G_6	0.0000000	0.0000000	0.0000000	0.0000000	0.0000000	0.0000000	0.0000000
		0.2	G_0	0.9032830	-0.7690152	5.0361326	-10.897229	13.116758	-8.7063469	2.4273611
			G_1	0.1491342	0.2432235	1.8461335	-3.2318681	3.5420769	-2.7768926	0.9219431
			G_5	0.8678274	-0.8559667	5.3435989	-12.280319	15.763974	-10.980834	3.1691822
			G_6	-0.1257700	0.0631880	-0.1814800	0.4340110	-0.1505400	-0.1187000	0.0792820
		0.4	G_0	0.9855457	-0.7398563	5.5164526	-13.651852	18.653027	-13.538430	3.9793425
			G_1	0.1775106	0.2299572	2.1216706	-4.2782717	5.2687845	-4.1124186	1.3150474
			G_5	0.9069722	-0.9108825	5.8333286	-14.136478	18.977528	-13.667987	4.0529308
			G_6	-0.2305200	0.1029790	-0.1704000	0.5834450	-0.2659400	-0.1046800	0.0851140
		0.6	G_0	1.0985374	-0.1190387	1.3832042	-0.3432214	-1.4589578	0.6531219	0.1785308
			G_1	0.2073151	0.5068511	0.2806012	1.7189911	-3.9720102	2.5637933	-0.5185999
			G_5	0.9428059	-0.7773982	5.3084480	-12.832244	17.470947	-13.044983	4.0414480
			G_6	-0.3471300	0.2460140	-0.6173600	1.2365450	0.3228370	-1.6567900	0.8158790
		0.8	G_0	1.2369365	0.6616268	-4.3347561	22.938065	-44.060391	35.750791	-10.551909
			G_1	0.2530239	0.7369240	-1.4471062	9.1382491	-17.909751	14.237263	-4.1335904
			G_5	0.9785273	-0.5458577	4.4489211	-9.0291409	9.9288853	-6.7512644	2.1631102
			G_6	-0.4628100	0.3277880	-0.6575600	1.3001460	0.8846790	-2.6056800	1.2134270

Table C.15
Influence Coefficients For A Circumferential Semi-Elliptical Surface Crack In A Cylinder – Outside Surface

t/R_i	a/c	a/t	G_i	A_0	A_1	A_2	A_3	A_4	A_5	A_6
1.0	1	0	G_0	1.1977992	-0.5244870	0.1498299	2.3284866	-5.1058499	4.3469049	-1.3487980
			G_1	0.1870117	0.6987352	0.1316900	0.7269255	-2.5259384	2.1756251	-0.6540458
			G_5	1.1977992	-0.5244870	0.1498299	2.3284866	-5.1058499	4.3469049	-1.3487980
			G_6	0.0000000	0.0000000	0.0000000	0.0000000	0.0000000	0.0000000	0.0000000
		0.2	G_0	1.2250711	-1.0352593	4.0953534	-10.822370	16.379424	-12.977198	4.1750887
			G_1	0.2131187	0.2915441	2.6210725	-6.9226429	9.5199489	-7.3960772	2.3934692
			G_5	1.0287490	-0.1318900	-2.0388300	8.0097800	-13.425600	10.628180	-3.2206400
			G_6	-0.0828100	0.0760420	-0.1217900	0.2588570	-0.1280800	-0.0973900	0.0951740
		0.4	G_0	1.2491832	-0.8678901	3.2771207	-9.1246075	14.319328	-11.650852	3.8252562
			G_1	0.2146704	0.4336763	1.7811506	-4.5706210	5.9588122	-4.7290996	1.6140138
			G_5	1.2338652	-1.4662611	6.3124028	-18.437296	29.313320	-23.885910	7.8510224
			G_6	-0.1423600	0.1103720	-0.0334200	0.1731450	-0.1238200	-0.0504000	0.0664720
		0.6	G_0	1.3433125	-0.7609708	2.5763713	-7.0807324	10.742997	-8.7974661	3.0249807
			G_1	0.2404262	0.4683598	1.5454449	-3.5434398	3.8745212	-3.0227777	1.1390920
			G_5	1.2602827	-1.3512525	5.2299090	-15.484682	24.683800	-20.201017	6.7131491
			G_6	-0.1985700	0.1701430	-0.0423500	0.3134580	-0.3752400	0.0790070	0.0535520
		0.8	G_0	1.4673569	-0.8602312	2.9003430	-6.8719917	8.2221651	-5.8912426	2.0852466
			G_1	0.2739808	0.4255563	1.7002625	-3.2773673	2.5281146	-1.7589452	0.8057502
			G_5	1.3042768	-1.3208070	4.4817682	-12.713695	19.112321	-15.129005	5.0323084
			G_6	-0.2523200	0.1478750	0.3944010	-0.0049400	-1.6452900	2.5117740	-1.1515000
1.0	2	0	G_0	0.8150546	-0.5623828	1.4465771	-4.6778133	8.4192164	-7.9025932	2.9866351
			G_1	0.1359146	0.0702340	3.5558581	-11.034445	16.967724	-14.126991	4.8706612
			G_5	0.8150546	-0.5623828	1.4465771	-4.6778133	8.4192164	-7.9025932	2.9866351
			G_6	0.0000000	0.0000000	0.0000000	0.0000000	0.0000000	0.0000000	0.0000000
		0.2	G_0	0.8439707	-1.0394462	4.3792885	-13.370814	21.805844	-18.442155	6.3309092
			G_1	0.1386553	0.0352450	3.4783655	-10.516386	15.937350	-13.285808	4.6190201
			G_5	0.8470136	-1.5329876	7.4251137	-23.586513	39.607024	-33.741501	11.473551
			G_6	-0.0285800	0.0362540	-0.0880100	0.1808850	-0.1128000	-0.0453600	0.0576170
		0.4	G_0	0.8178056	-0.7710138	2.7565514	-8.8298754	15.216819	-13.639983	4.9131276
			G_1	0.1206118	0.2902900	1.8227079	-5.6518526	8.5954589	-7.7602419	2.9554246
			G_5	0.8569685	-1.8407787	9.1603542	-29.549672	50.138836	-42.897101	14.578505
			G_6	-0.0485800	0.0664020	-0.1365400	0.3269440	-0.3183300	0.0779280	0.0321760
		0.6	G_0	0.8392619	-0.7402002	2.4961630	-8.2786779	14.738638	-13.694325	5.0781817
			G_1	0.1244695	0.3009364	1.7573836	-5.5119837	8.6117810	-8.1228867	3.1930430
			G_5	0.8481463	-1.6950631	7.7337421	-25.082442	42.782429	-36.711701	12.498541
			G_6	-0.0659400	0.0804830	-0.0875000	0.2388800	-0.2429700	0.0295500	0.0474870
		0.8	G_0	0.8713709	-0.8403753	2.8895120	-9.2850042	16.056477	-14.745171	5.4576140
			G_1	0.1319829	0.2422569	2.0859439	-6.4113812	10.032682	-9.4553773	3.7027605
			G_5	0.8423023	-1.5825792	6.4312159	-20.800596	35.393650	-30.235702	10.247249
			G_6	-0.0678300	-0.1164900	0.9749320	-1.5131000	-0.2480700	2.4117980	-1.4412500

Notes:

1. Interpolation of the influence coefficients, G_i, may be used for intermediate values of t/R_i, a/c, and a/t.

2. The value of the influence coefficients at the surface point of the crack defined by $\varphi = 0^0$ are equal to:. $G_i = A_0$

3. The value of the influence coefficients at the deepest point of the crack defined by $\varphi = 90^0$ are equal to: $G_i = \sum_{n=0}^{6} A_n$.

Table C.16
Influence Coefficients For A Circumferential Through Wall Crack In A Sphere – Inside Surface

t/R_i	G_i	A_0	A_1	A_2	A_3	A_4
0.01	G_0	0.996176140	-0.136758833	0.287370688	-0.021281327	0.001614339
	G_1	0.044812392	0.259340393	0.002323025	0.015757981	-0.001236315
	G_p	1.004221696	-0.167942026	0.292305595	-0.022174673	0.001329751
0.01667	G_0	0.991485916	-0.123995291	0.258774210	-0.003234973	-0.003037501
	G_1	0.044449377	0.329870565	-0.080013831	0.043185458	-0.004430561
	G_p	1.007412943	-0.122314488	0.207938107	0.027876580	-0.011026831
0.05	G_0	0.972086762	-0.160593405	0.322770004	-0.046962649	0.009841309
	G_1	0.005444054	0.500718442	-0.407095219	0.257589713	-0.064153363
	G_p	1.016842538	-0.124612983	0.192323868	0.029228099	-0.010429496
0.1	G_0	0.942279944	-0.099201862	0.204585843	0.024467655	-0.009996340
	G_1	0.002573686	0.205082631	0.057545268	0.002773726	-0.000044775
	G_p	1.003333955	-0.099987188	0.145978848	0.052933686	-0.016655808
0.2	G_0	0.906931687	-0.135342636	0.113534642	0.245624518	-0.167632893
	G_1	0.001981728	0.195681690	0.078164645	-0.006180974	0.000733825
	G_p	1.031155982	-0.675755928	1.239084081	-0.741013347	0.250332573
0.33333	G_0	0.852357575	0.022535087	-0.543973921	1.124441452	-0.716813516
	G_1	-0.001766453	0.265994715	-0.214958095	0.279847270	-0.134380666
	G_p	1.037606706	-1.065302487	2.222552179	-1.657623100	0.630449841
t/R_i	G_i	A_5	A_6	A_7	A_8	---
0.01	G_0	-0.000042228	0.000000000	0.000000000	0.000000000	---
	G_1	0.000032495	0.000000000	0.000000000	0.000000000	---
	G_p	-0.000003796	-0.000001208	0.000000000	0.000000000	---
0.01667	G_0	0.000453864	-0.000017696	0.000000000	0.000000000	---
	G_1	0.000151378	0.000000000	0.000000000	0.000000000	---
	G_p	0.001260660	-0.000044986	0.000000000	0.000000000	---
0.05	G_0	-0.001237926	0.000082018	-0.000002120	0.000000000	---
	G_1	0.008073071	-0.000494471	0.000011706	0.000000000	---
	G_p	0.001403746	-0.000083815	0.000001882	0.000000000	---
0.1	G_0	0.001470499	-0.000092852	0.000002178	0.000000000	---
	G_1	0.000004322	0.000000000	0.000000000	0.000000000	---
	G_p	0.002250674	-0.000138201	0.000003223	0.000000000	---
0.2	G_0	0.052005435	-0.008216050	0.000637070	-0.000019115	---
	G_1	0.000000000	0.000000000	0.000000000	0.000000000	---
	G_p	-0.042638069	0.003496156	-0.000109049	0.000000000	---
0.33333	G_0	0.228690564	-0.038335412	0.003210444	-0.000105495	---
	G_1	0.032990268	-0.003923423	0.000177997	0.000000000	---
	G_p	-0.119933248	0.010997535	-0.000385651	0.000000000	---

Note: Interpolation may be used for intermediate values of R_i/t.

Table C.17
Influence Coefficients For A Circumferential Through Wall Crack In A Sphere – Outside Surface

t/R_i	G_i	A_0	A_1	A_2	A_3	A_4
0.01	G_0	1.000081599	0.373644366	0.191913526	-0.067372381	0.009174932
	G_1	0.988670046	-0.084224131	0.181255625	-0.038122523	0.002831900
	G_p	0.990490873	0.379074327	0.117700970	-0.033786795	0.002265847
0.01667	G_0	0.993366131	0.400052320	0.137082159	-0.039414298	0.003414265
	G_1	0.990851836	-0.141604651	0.258638595	-0.066265614	0.006355895
	G_p	0.999261355	0.352070288	0.140730133	-0.046550905	0.004654802
0.05	G_0	0.994548744	0.264794870	0.328273330	-0.156754808	0.035235794
	G_1	0.999613246	-0.168935301	0.384213423	-0.175389720	0.040401774
	G_p	0.996575908	0.311883656	0.125315390	-0.036745174	0.002252144
0.1	G_0	0.996187434	0.214400912	0.348804428	-0.167469117	0.040060365
	G_1	0.999493403	-0.008575611	0.123480901	-0.032176781	0.003701792
	G_p	0.975810822	0.380142341	0.011074721	0.017934230	-0.011467369
0.2	G_0	0.995213839	0.014598654	0.815870555	-0.616813158	0.241781646
	G_1	1.002745997	-0.078220201	0.229674431	-0.087645986	0.015431840
	G_p	0.951843702	0.586803756	-0.442871291	0.328892014	-0.112749517
0.33333	G_0	0.994134590	-0.111105053	1.066365098	-0.901784563	0.398023204
	G_1	0.999438036	-0.054656134	0.318788668	-0.294466264	0.158987833
	G_p	0.932521476	0.711948724	-0.770560233	0.584183910	-0.209919538

t/R_i	G_i	A_5	A_6	A_7	A_8	---
0.01	G_0	-0.000594291	0.000014130	0.000000000	0.000000000	---
	G_1	-0.000072325	0.000000000	0.000000000	0.000000000	---
	G_p	-0.000047279	0.000000000	0.000000000	0.000000000	---
0.01667	G_0	-0.000107359	0.000000000	0.000000000	0.000000000	---
	G_1	-0.000210459	0.000000000	0.000000000	0.000000000	---
	G_p	-0.000211522	0.000003441	0.000000000	0.000000000	---
0.05	G_0	-0.004290880	0.000260114	-0.000006143	0.000000000	---
	G_1	-0.004958385	0.000301935	-0.000007156	0.000000000	---
	G_p	0.000123218	-0.000023892	0.000000908	0.000000000	---
0.1	G_0	-0.005671383	0.000460140	-0.000019943	0.000000360	---
	G_1	-0.000238211	0.000006200	0.000000000	0.000000000	---
	G_p	0.001989205	-0.000155782	0.000004675	0.000000000	---
0.2	G_0	-0.053716832	0.006690865	-0.000434417	0.000011398	---
	G_1	-0.001330949	0.000042881	0.000000000	0.000000000	---
	G_p	0.018687574	-0.001498727	0.000046390	0.000000000	---
0.33333	G_0	-0.099327539	0.013916145	-0.001018574	0.000030207	---
	G_1	-0.048834246	0.008271172	-0.000719616	0.000025055	---
	G_p	0.037632809	-0.003303607	0.000112568	0.000000000	---

Note: Interpolation may be used for intermediate values of R_i/t.

Table C.18
Influence Coefficients For a Circumferential 360° Surface Crack in a Spherical Shell

t/R_i	a/t	Inside Surface					Outside Surface				
		G_0	G_1	G_2	G_3	G_4	G_0	G_1	G_2	G_3	G_4
0.001	0	1.120000	0.682000	0.524500	0.440400	0.379075	1.120000	0.682000	0.524500	0.440400	0.379075
	0.05	1.024082	0.601169	0.459493	0.387539	0.333594	1.020798	0.602390	0.461317	0.389214	0.335227
	0.1	0.982026	0.555537	0.420873	0.355007	0.305499	0.980903	0.554875	0.420499	0.355007	0.305194
	0.2	0.969389	0.484180	0.351367	0.294234	0.250941	0.969389	0.484342	0.351591	0.294144	0.251071
	0.4	1.584413	0.640551	0.375023	0.262572	0.253033	1.586151	0.641165	0.375198	0.262821	0.253176
	0.6	2.990095	1.039894	0.508081	0.285484	0.291371	2.993602	1.040903	0.508425	0.285546	0.291477
	0.8	6.751458	2.106236	0.886556	0.388222	0.392172	6.760196	2.108414	0.887591	0.388560	0.392167
0.00333	0	1.120000	0.682000	0.524500	0.440400	0.379075	1.120000	0.682000	0.524500	0.440400	0.379075
	0.05	1.070867	0.635287	0.486127	0.408884	0.351531	1.067923	0.637431	0.488495	0.411111	0.353835
	0.1	1.075365	0.625130	0.475100	0.399249	0.342505	1.075365	0.624542	0.474658	0.398986	0.342035
	0.2	1.133792	0.611639	0.451255	0.374918	0.320027	1.134948	0.611982	0.451429	0.375058	0.320071
	0.4	1.746727	0.796624	0.510245	0.378227	0.345428	1.752724	0.808879	0.528579	0.401085	0.354033
	0.6	3.051466	1.234450	0.721692	0.496415	0.434741	3.059194	1.236715	0.722661	0.496943	0.435008
	0.8	5.772142	2.124837	1.136853	0.715883	0.602916	5.789161	2.129462	1.138928	0.716981	0.603212
0.01	0	1.120000	0.682000	0.524500	0.440400	0.379075	1.120000	0.682000	0.524500	0.440400	0.379075
	0.05	1.098440	0.655289	0.501637	0.421894	0.362018	1.097580	0.655129	0.501846	0.422044	0.362062
	0.1	1.112300	0.654809	0.498490	0.417996	0.358862	1.114656	0.655369	0.498700	0.418247	0.358839
	0.2	1.208823	0.673259	0.500433	0.414909	0.354317	1.212723	0.674660	0.501219	0.415415	0.354658
	0.4	1.775773	0.870581	0.593351	0.462736	0.398785	1.786084	0.874039	0.595117	0.463840	0.399489
	0.6	2.860047	1.249167	0.783061	0.572346	0.484799	2.879549	1.255034	0.785848	0.573872	0.485592
	0.8	4.638121	1.877737	1.107159	0.768207	0.632040	4.684553	1.891310	1.113538	0.771869	0.633612
0.01667	0	1.120000	0.682000	0.524500	0.440400	0.379075	1.120000	0.682000	0.524500	0.440400	0.379075
	0.05	1.103967	0.660076	0.505804	0.425190	0.364742	1.104537	0.660076	0.505596	0.425066	0.364628
	0.1	1.123564	0.664117	0.505907	0.424102	0.364056	1.127294	0.665538	0.506736	0.424720	0.364446
	0.2	1.226490	0.690153	0.514444	0.426569	0.364299	1.232890	0.692392	0.515615	0.427307	0.364810
	0.4	1.756462	0.875239	0.600383	0.468847	0.406373	1.772076	0.884482	0.610136	0.479525	0.410645
	0.6	2.712860	1.220200	0.783173	0.582943	0.491062	2.742675	1.229196	0.787404	0.585487	0.492297
	0.8	4.126269	1.735804	1.057964	0.755031	0.620864	4.178392	1.750103	1.064146	0.758412	0.621879
0.025	0	1.120000	0.682000	0.524500	0.440400	0.379075	1.120000	0.682000	0.524500	0.440400	0.379075
	0.05	1.106720	0.662931	0.508081	0.427061	0.366476	1.108710	0.663406	0.508287	0.427159	0.366458
	0.1	1.129154	0.669390	0.510348	0.427798	0.367156	1.134717	0.671581	0.511580	0.428533	0.367796
	0.2	1.233528	0.699216	0.522388	0.433221	0.370142	1.243062	0.702548	0.524143	0.434370	0.370900
	0.4	1.727851	0.875389	0.607334	0.478073	0.412216	1.750478	0.886408	0.616977	0.487689	0.416505
	0.6	2.575276	1.185079	0.773736	0.583393	0.490483	2.616709	1.197704	0.779703	0.586830	0.492296
	0.8	3.748132	1.624554	1.013576	0.737098	0.607492	3.814046	1.642621	1.021248	0.741180	0.608762
0.05	0	1.120000	0.682000	0.524500	0.440400	0.379075	1.120000	0.682000	0.524500	0.440400	0.379075
	0.05	1.109939	0.666405	0.510964	0.429585	0.368611	1.115692	0.667977	0.511785	0.429951	0.368718
	0.1	1.132866	0.675010	0.515361	0.432069	0.370909	1.143927	0.679194	0.517596	0.433524	0.372045
	0.2	1.232890	0.707311	0.530660	0.440666	0.376746	1.251895	0.713993	0.534207	0.442923	0.378290
	0.4	1.654952	0.864381	0.612924	0.489863	0.417989	1.694893	0.877783	0.619735	0.494049	0.420723
	0.6	2.313398	1.108205	0.743888	0.572346	0.481359	2.384504	1.130006	0.754394	0.578425	0.484579
	0.8	3.170440	1.445533	0.935159	0.698728	0.579813	3.277447	1.475174	0.948252	0.705919	0.582125
0.1	0	1.120000	0.682000	0.524500	0.440400	0.379075	1.120000	0.682000	0.524500	0.440400	0.379075
	0.05	1.108615	0.667506	0.512195	0.430804	0.369757	1.123378	0.671737	0.514240	0.431826	0.370189
	0.1	1.129154	0.676718	0.517697	0.434370	0.373018	1.151243	0.684964	0.522238	0.437260	0.375197
	0.2	1.214669	0.706198	0.532683	0.443396	0.379499	1.252314	0.719666	0.539728	0.447812	0.382744
	0.4	1.548235	0.833006	0.600820	0.485289	0.414232	1.622130	0.858289	0.613780	0.493332	0.419680
	0.6	2.033355	1.018225	0.702908	0.551016	0.465383	2.152844	1.055420	0.720965	0.561704	0.471242
	0.8	2.688413	1.290690	0.862710	0.659519	0.552344	2.865317	1.341520	0.885964	0.672615	0.557628
0.2	0	1.120000	0.682000	0.524500	0.440400	0.379075	1.120000	0.682000	0.524500	0.440400	0.379075
	0.05	1.103301	0.666719	0.512400	0.431194	0.370190	1.124218	0.677493	0.519316	0.436202	0.374625
	0.1	1.115127	0.673609	0.516886	0.434249	0.373337	1.156245	0.688402	0.524943	0.439534	0.376947
	0.2	1.177157	0.695982	0.528877	0.441915	0.378829	1.249587	0.722068	0.542782	0.450731	0.385211
	0.4	1.415271	0.789345	0.580161	0.474188	0.405897	1.546794	0.834422	0.603652	0.488737	0.415653
	0.6	1.758950	0.926020	0.657926	0.525343	0.446501	1.953068	0.987620	0.688199	0.543506	0.456957
	0.8	2.297752	1.162919	0.801303	0.624584	0.528260	2.574511	1.243062	0.837873	0.645142	0.537022

Table C.18
Influence Coefficients For a Circumferential 360° Surface Crack in a Spherical Shell

t/R_i	a/t	Inside Surface					Outside Surface				
		G_0	G_1	G_2	G_3	G_4	G_0	G_1	G_2	G_3	G_4
0.33333	0	1.120000	0.682000	0.524500	0.440400	0.379075	1.120000	0.682000	0.524500	0.440400	0.379075
	0.05	1.094572	0.664481	0.512071	0.430731	0.369999	1.133297	0.680394	0.520747	0.436776	0.374992
	0.1	1.093356	0.667271	0.513708	0.432827	0.372573	1.160379	0.689942	0.525766	0.440225	0.378198
	0.2	1.137977	0.684117	0.523336	0.439239	0.376944	1.253402	0.725103	0.548614	0.454180	0.387225
	0.4	1.326360	0.753316	0.562372	0.463844	0.398192	1.503800	0.820848	0.598058	0.486976	0.414096
	0.6	1.574222	0.863314	0.626650	0.510734	0.433284	1.845450	0.950648	0.670079	0.533337	0.448895
	0.8	2.058835	1.084679	0.763446	0.602847	0.513638	2.448941	1.201019	0.817044	0.632677	0.528476

Note: Interpolation of the influence coefficients, G_i, may be used for intermediate values of t/R_i and a/t.

Table C.19
Influence Coefficients For A Circumferential Semi-Elliptical Surface Crack In A Sphere – Inside Surface

t/R_i	a/c	a/t	G_i	A_0	A_1	A_2	A_3	A_4	A_5	A_6
0.0	0.03125	0.0	G_0	0.1965046	2.9373464	-5.2582823	7.4889153	-6.9282667	3.3673349	-0.6677966
			G_1	0.0051780	0.1750280	2.7718680	-4.6457154	4.6780502	-3.2768090	0.9840994
		0.2	G_0	0.2080760	3.0112422	-5.1048701	7.6348715	-6.8347547	2.7940766	-0.3882688
			G_1	0.0084834	0.2406767	2.4574292	-3.6452421	3.6142837	-2.8451814	0.9270638
		0.4	G_0	0.2357940	3.0822400	-3.5792100	3.9476890	1.9131590	-6.8872200	3.1896800
			G_1	0.0145140	0.4038000	1.6422700	-0.3906100	-0.6480700	-0.2940300	0.2514900
		0.6	G_0	0.2902240	3.6892050	-4.5739100	11.709890	-6.3750000	-5.8894100	4.2452400
			G_1	0.0208890	0.7016780	0.1631840	5.7072160	-8.2075800	3.4561120	-0.4454700
		0.8	G_0	0.5163550	2.5310830	14.712900	-43.621800	101.06570	-116.08100	46.190900
			G_1	0.0825460	0.4971770	4.6064810	-7.3326700	21.148620	-29.345100	12.491400
0.0	0.0625	0.0	G_0	0.2695332	2.1626001	-1.6551569	-1.2970208	4.5604304	-4.3163876	1.4010655
			G_1	0.0138667	0.1827458	2.5749608	-3.9044679	3.3556301	-2.1772209	0.6420134
		0.2	G_0	0.2845892	2.2264055	-1.4546190	-1.5760719	5.1131083	-4.9485443	1.6207574
			G_1	0.0199077	0.2210874	2.4642047	-3.5898625	3.1624039	-2.2403780	0.6965751
		0.4	G_0	0.3261480	2.5200870	-1.8847000	2.1798740	-1.4597100	-0.1886500	0.2393400
			G_1	0.0294120	0.3699370	1.9220850	-1.2071500	-0.4394000	0.2737550	-0.0395200
		0.6	G_0	0.4166330	3.1566470	-2.6248900	7.7325910	-9.6927800	3.6428700	-0.0892000
			G_1	0.0598460	0.4340740	2.6811560	-3.1936600	4.0753720	-4.6940200	1.8285500
		0.8	G_0	0.6540140	3.4231920	3.8158050	-4.1586900	3.4715330	-10.310400	6.6280000
			G_1	0.1214780	0.6975490	2.9718330	-1.3036500	-0.0754900	-3.0465100	2.1670000
0.0	0.125	0.0	G_0	0.4065238	0.7772483	3.8861644	-12.573943	16.760207	-11.014593	2.8706957
			G_1	0.0320270	0.1825342	2.2670449	-2.7076615	1.2088194	-0.3777430	0.0763155
		0.2	G_0	0.4242116	1.0089302	3.2973815	-12.159726	17.873386	-12.868668	3.6281712
			G_1	0.0429859	0.2033811	2.2563818	-2.8752160	1.8152558	-1.0512327	0.3181077
		0.4	G_0	0.4917770	1.6592320	-0.1080400	0.1793240	-2.7076100	3.3680620	-1.3489700
			G_1	0.0634270	0.3722500	1.6231670	-0.5306500	-2.0007400	1.8943780	-0.5880300
		0.6	G_0	0.6591820	1.8759140	1.0212600	-1.7698000	-0.5653600	1.2479960	-0.4376600
			G_1	0.1116040	0.4714500	1.7940590	-0.7557600	-1.4901700	1.0852180	-0.2113700
		0.8	G_0	0.9809330	1.8846320	4.8020780	-8.0580200	0.4447850	3.4772660	-1.0567500
			G_1	0.2039950	0.4800150	2.8822430	-2.5890100	-0.9683000	1.5372370	-0.3750200
0.0	0.25	0.0	G_0	0.6152816	-0.3348694	6.2955620	-15.590618	19.299508	-12.488107	3.3010035
			G_1	0.0703566	0.2828152	1.4036169	-0.6511596	-1.2076596	1.0318656	-0.2423741
		0.2	G_0	0.6385889	-0.3095132	6.5329787	-16.622882	21.056641	-13.850120	3.6988146
			G_1	0.0840059	0.1999367	1.8218113	-1.7756899	0.3757186	-0.0785358	0.0643386
		0.4	G_0	0.7390420	0.0548160	4.0842620	-7.5883100	5.4047530	-1.0146100	-0.3483400
			G_1	0.1164500	0.2479880	1.8282520	-1.7169900	0.1912120	0.1165770	-0.0186100
		0.6	G_0	0.9461210	-0.1858800	5.5867460	-9.8634900	5.9596870	0.1296440	-1.0026100
			G_1	0.1778050	0.2056680	2.0979210	-1.8039500	-0.5558700	1.1461400	-0.4206600
		0.8	G_0	1.2452110	-0.6921900	8.3260620	-14.948000	8.6936910	0.4755790	-1.3926600
			G_1	0.2585640	0.1548890	2.1170240	-0.4910000	-4.6146100	5.4550750	-1.9663300
0.0	0.5	0.0	G_0	0.8776607	-0.6729719	3.7721411	-6.5209060	6.3377934	-3.7028038	0.9872447
			G_1	0.1277541	0.4368502	0.4904522	1.0427434	-2.9631236	2.0826525	-0.5184313
		0.2	G_0	0.9003948	-0.8850488	5.2743239	-11.267523	13.890755	-9.6373584	2.8183906
			G_1	0.1404409	0.3215397	1.1010666	-1.0257556	0.6943940	-1.0793186	0.5410929
		0.4	G_0	1.0058060	-0.7322600	2.9951940	-1.9459200	-3.2613500	5.1424570	-2.0306200
			G_1	0.1740870	0.3051630	1.2070310	-0.6720500	-1.0651300	1.1445590	-0.3644800
		0.6	G_0	1.1826010	-1.1072500	3.9623640	-2.7781300	-4.3097300	7.2772750	-2.9648200
			G_1	0.2277120	0.1701170	1.5499470	-1.1051200	-0.8333700	1.1717060	-0.4194500
		0.8	G_0	1.3833380	-1.3900300	4.3755780	-3.7372600	-2.5403200	5.3036000	-2.0932400
			G_1	0.2820110	0.0839230	1.7258580	-1.5358100	-0.0635600	0.5006780	-0.1982200

Table C.19
Influence Coefficients For A Circumferential Semi-Elliptical Surface Crack In A Sphere – Inside Surface

t/R_i	a/c	a/t	G_i	A_0	A_1	A_2	A_3	A_4	A_5	A_6
0.0	1	0.0	G_0	1.1977992	-0.5244870	0.1498299	2.3284866	-5.1058499	4.3469049	-1.3487980
			G_1	0.1870117	0.6987352	0.1316900	0.7269255	-2.5259384	2.1756251	-0.6540458
		0.2	G_0	1.2263282	-1.1608467	4.4744783	-11.584231	17.811241	-14.408250	4.6998279
			G_1	0.2154786	0.2441623	2.8107820	-7.6574580	11.171413	-9.0053693	2.9542871
		0.4	G_0	1.2989480	-0.9978000	1.9479540	-1.3002700	-1.4940100	2.8306230	-1.2126000
			G_1	0.2386246	0.1447774	3.3198992	-9.2456599	13.823512	-11.223715	3.6868232
		0.6	G_0	1.3971180	-1.1348400	1.7918740	-0.4202600	-2.8679300	3.7685480	-1.4405000
			G_1	0.2445870	0.5326670	0.5939690	-0.0361800	-2.0163100	2.2167010	-0.7782200
		0.8	G_0	1.5117010	-1.3244800	1.7568350	-0.1337900	-2.8629300	3.2953270	-1.1412400
			G_1	0.2704470	0.5113280	0.5357440	-0.0327300	-1.5570200	1.5570970	-0.5094600
0.0	2	0.0	G_0	0.8150546	-0.5623828	1.4465771	-4.6778133	8.4192164	-7.9025932	2.9866351
			G_1	0.1359146	0.0702340	3.5558581	-11.034445	16.967724	-14.126991	4.8706612
		0.2	G_0	0.8463715	-1.0011024	4.0052312	-11.937181	19.189548	-16.039296	5.4674371
			G_1	0.1395121	0.0753999	3.1895604	-9.5540932	14.214316	-11.649525	4.0073308
		0.4	G_0	0.8570045	-1.0183085	3.9957306	-11.886878	19.152747	-16.047480	5.4801806
			G_1	0.1436696	0.0544018	3.2816127	-9.8164232	14.610963	-11.942138	4.0907797
		0.6	G_0	0.8839861	-1.0765270	4.0774087	-11.976171	19.173189	-15.996207	5.4501217
			G_1	0.1504185	0.0478401	3.2579960	-9.6921199	14.370843	-11.736129	4.0258411
		0.8	G_0	0.9033134	-0.9619755	2.8501500	-7.6366897	11.596116	-9.4828625	3.2550163
			G_1	0.1458559	0.2313881	1.9882138	-5.5546045	7.4196069	-5.8965053	2.0855563
0.01	0.03125	0.0	G_0	0.1965046	2.9373464	-5.2582823	7.4889153	-6.9282667	3.3673349	-0.6677966
			G_1	0.0051780	0.1750280	2.7718680	-4.6457154	4.6780502	-3.2768090	0.9840994
		0.2	G_0	0.2054741	2.5611013	-2.9596332	3.1954661	-2.6645031	1.2439888	-0.3032678
			G_1	0.0054195	0.2246517	2.4896120	-3.8089914	3.8104646	-2.9072861	0.9224626
		0.4	G_0	0.2294240	2.9738130	-3.3635100	3.3893400	2.1700680	-6.5149000	2.9153700
			G_1	0.0154010	0.2512660	1.9593420	-0.8526500	-1.4031000	1.6657830	-0.7008700
		0.6	G_0	0.2674970	3.1773150	-2.7738500	6.3229130	-1.1128000	-6.8512500	3.6651000
			G_1	0.0165544	0.4538318	1.5394249	0.5061319	0.6658622	-3.7799579	1.8704652
		0.8	G_0	0.3747330	2.0063460	10.399280	-28.789300	59.058120	-62.102200	23.033300
			G_1	0.0434670	0.1280210	4.7021650	-6.7931300	12.190040	-13.929700	5.3401500
0.01	0.0625	0.0	G_0	0.2695332	2.1626001	-1.6551569	-1.2970208	4.5604304	-4.3163876	1.4010655
			G_1	0.0138667	0.1827458	2.5749608	-3.9044679	3.3556301	-2.1772209	0.6420134
		0.2	G_0	0.2759680	2.0225739	-0.6996063	-2.1721721	3.8653975	-2.7105955	0.6601162
			G_1	0.0166925	0.2164200	2.5114777	-4.0903645	4.4164183	-3.4801215	1.1319557
		0.4	G_0	0.3202990	2.5245970	-2.1779500	2.4733910	-1.2325400	-0.6552000	0.4148000
			G_1	0.0279540	0.2953030	1.7740760	-0.5112500	-1.8441100	1.8025300	-0.6586400
		0.6	G_0	0.3823290	3.2747250	-4.8976100	14.499560	-20.205300	11.981390	-2.7101200
			G_1	0.0411270	0.3611160	2.3656710	-2.1931200	2.0455880	-2.4365800	0.9174400
		0.8	G_0	0.5540600	2.8620620	3.5774670	-5.4505700	6.1537190	-9.4586500	4.8515500
			G_1	0.0836030	0.4318770	3.2512220	-2.7789000	1.7943750	-2.7518800	1.3433300
0.01	0.125	0.0	G_0	0.4065238	0.7772483	3.8861644	-12.573943	16.760207	-11.014593	2.8706957
			G_1	0.0320270	0.1825342	2.2670449	-2.7076615	1.2088194	-0.3777430	0.0763155
		0.2	G_0	0.4048264	1.1578449	1.6197884	-5.7295006	6.9227475	-4.2148411	1.0309624
			G_1	0.0464705	0.0041545	4.0262527	-9.5703182	13.562839	-10.666035	3.2973390
		0.4	G_0	0.4791840	1.3870110	1.5742300	-5.0231600	5.7521780	-3.4899500	0.8181900
			G_1	0.0511420	0.2534930	1.9906620	-1.3981400	-0.6794600	0.9027200	-0.3071400
		0.6	G_0	0.6096530	1.7754120	0.7329590	0.2126290	-5.2166300	6.0034300	-2.2092100
			G_1	0.0912660	0.2790100	2.6496090	-3.3562600	2.5558220	-1.8436100	0.5793000
		0.8	G_0	0.8402230	1.5177340	5.2378910	-8.4186300	-0.2464500	5.9346420	-2.6149000
			G_1	0.1513260	0.3150260	3.0469360	-2.6913700	-1.2904100	2.5995700	-1.0407500

Table C.19
Influence Coefficients For A Circumferential Semi-Elliptical Surface Crack In A Sphere – Inside Surface

t/R_i	a/c	a/t	G_i	A_0	A_1	A_2	A_3	A_4	A_5	A_6
0.01	0.25	0.0	G_0	0.6152816	-0.3348694	6.2955620	-15.590618	19.299508	-12.488107	3.3010035
			G_1	0.0703566	0.2828152	1.4036169	-0.6511596	-1.2076596	1.0318656	-0.2423741
		0.2	G_0	0.6001162	0.1425199	4.5757413	-12.857132	17.390660	-12.106120	3.3854502
			G_1	0.0826855	0.2816842	1.7854964	-2.9045659	3.1646698	-2.6210713	0.8899897
		0.4	G_0	0.7214580	0.1033650	3.9806460	-7.6039800	5.7251550	-1.3917500	-0.2178800
			G_1	0.1022410	0.2585340	1.6925330	-1.2923900	-0.4045500	0.5652840	-0.1652700
		0.6	G_0	0.8959000	0.0229790	4.2765850	-6.0386200	0.2589510	4.3815880	-2.2677400
			G_1	0.1546700	0.2341080	1.8505670	-1.1247800	-1.4402800	1.7689870	-0.6143800
		0.8	G_0	1.0846360	0.6183170	-1.7905600	20.153400	-50.372100	48.289670	-16.326200
			G_1	0.2163400	0.1783190	1.8690990	0.2361760	-5.3445000	5.7549830	-2.0155900
0.01	0.5	0.0	G_0	0.8776607	-0.6729719	3.7721411	-6.5209060	6.3377934	-3.7028038	0.9872447
			G_1	0.1277541	0.4368502	0.4904522	1.0427434	-2.9631236	2.0826525	-0.5184313
		0.2	G_0	0.8843656	-0.8825526	5.4237760	-11.876360	14.769862	-10.169874	2.9324829
			G_1	0.1435544	0.2047681	1.9196249	-3.4935583	4.1718932	-3.4276657	1.1625408
		0.4	G_0	0.9897010	-0.6737700	2.9314480	-2.0870300	-2.7294800	4.5595390	-1.8183600
			G_1	0.1647140	0.3010190	1.2635350	-0.8087200	-0.8819100	1.0349150	-0.3461100
		0.6	G_0	1.1473540	-0.8992000	3.2669790	-2.0093700	-3.6942100	5.5965600	-2.1518600
			G_1	0.2127700	0.2268860	1.4293980	-1.0538200	-0.6404000	0.8730140	-0.2917800
		0.8	G_0	1.3239080	-1.0764400	3.1315630	-1.3594100	-4.3926100	5.6756190	-2.0025500
			G_1	0.2534620	0.2515530	0.8944120	0.4182770	-2.2677700	1.7287360	-0.4840800
0.01	1	0.0	G_0	1.1977992	-0.5244870	0.1498299	2.3284866	-5.1058499	4.3469049	-1.3487980
			G_1	0.1870117	0.6987352	0.1316900	0.7269255	-2.5259384	2.1756251	-0.6540458
		0.2	G_0	1.2070754	-1.2221997	5.1111900	-13.966446	22.144836	-18.212527	5.9900420
			G_1	0.2126878	0.1592439	3.4016275	-9.6610590	14.631958	-11.939360	3.9249291
		0.4	G_0	1.2866950	-0.9149800	1.6025020	-0.4064800	-2.6297800	3.5109270	-1.3680900
			G_1	0.2348060	0.1500424	3.2918536	-9.1682940	13.723214	-11.151448	3.6625083
		0.6	G_0	1.3875130	-1.1342100	1.9912280	-1.1972200	-1.3615400	2.3898410	-0.9730700
			G_1	0.2384520	0.5247780	0.6991270	-0.4392000	-1.1781000	1.4236780	-0.5076100
		0.8	G_0	1.4863980	-1.2449000	1.6321080	-0.1886400	-2.0854400	2.2312950	-0.7176800
			G_1	0.2607040	0.5186780	0.5832820	-0.3285000	-0.7939400	0.7881120	-0.2472200
0.01	2	0.0	G_0	0.8150546	-0.5623828	1.4465771	-4.6778133	8.4192164	-7.9025932	2.9866351
			G_1	0.1359146	0.0702340	3.5558581	-11.034445	16.967724	-14.126991	4.8706612
		0.2	G_0	0.8004572	-0.9423051	3.8677945	-11.733659	19.085447	-16.027877	5.4594536
			G_1	0.1279139	0.0638427	3.2498718	-9.8213966	14.739825	-12.074165	4.1253194
		0.4	G_0	0.8282738	-0.2914582	-0.8469581	3.5453417	-6.2544427	4.8659458	-1.3264716
			G_1	0.1412848	0.0553372	3.2844423	-9.8782715	14.769556	-12.077829	4.1273126
		0.6	G_0	0.8574827	-0.3584410	-0.7392613	3.4427023	-6.2878270	4.9979448	-1.3881873
			G_1	0.1482679	0.0191704	3.4720530	-10.498316	15.789419	-12.865211	4.3570473
		0.8	G_0	0.9080987	-0.9400711	2.7958615	-7.5701151	11.657561	-9.6444073	3.3336215
			G_1	0.1513719	0.0242499	3.4636042	-10.591832	15.792927	-12.472688	4.0477749
0.01667	0.03125	0.0	G_0	0.1965046	2.9373464	-5.2582823	7.4889153	-6.9282667	3.3673349	-0.6677966
			G_1	0.0051780	0.1750280	2.7718680	-4.6457154	4.6780502	-3.2768090	0.9840994
		0.2	G_0	0.2052101	2.5533693	-2.9267157	3.0534719	-2.4121435	1.0357930	-0.2362885
			G_1	0.0052759	0.2286923	2.4404265	-3.6371264	3.5390118	-2.7186132	0.8760317
		0.4	G_0	0.2189337	3.1279004	-5.3775994	11.531042	-12.856477	6.2795553	-1.1577653
			G_1	0.0114659	0.2526547	2.5727508	-3.7773155	5.1638660	-5.1014550	1.8020600
		0.6	G_0	0.2636630	3.0068190	-1.7595700	2.2584030	5.4483910	-11.617400	4.9994800
			G_1	0.0264910	0.3382800	2.1916910	-0.7796200	0.6936340	-2.5355000	1.2872700
		0.8	G_0	0.3210130	2.8196340	2.3419320	-1.8680300	11.537550	-20.523200	9.1151800
			G_1	0.0459550	0.3427560	2.3730470	0.8057490	0.7883340	-5.8950700	3.1843100

Table C.19
Influence Coefficients For A Circumferential Semi-Elliptical Surface Crack In A Sphere – Inside Surface

t/R_i	a/c	a/t	G_i	A_0	A_1	A_2	A_3	A_4	A_5	A_6
0.01667	0.0625	0.0	G_0	0.2695332	2.1626001	-1.6551569	-1.2970208	4.5604304	-4.3163876	1.4010655
			G_1	0.0138667	0.1827458	2.5749608	-3.9044679	3.3556301	-2.1772209	0.6420134
		0.2	G_0	0.2755463	2.0190847	-0.7102131	-2.1466612	3.8346488	-2.6931885	0.6576969
			G_1	0.0166594	0.2184216	2.4941038	-4.0488103	4.3570043	-3.4386099	1.1217193
		0.4	G_0	0.3189630	2.5036380	-2.1918000	2.5893110	-1.5926000	-0.2460600	0.2646500
			G_1	0.0288524	0.2884400	2.3985840	-3.2802142	3.5681601	-3.2862980	1.1551067
		0.6	G_0	0.3798610	3.1009390	-3.9959800	11.503410	-15.719300	8.9415330	-1.9392700
			G_1	0.0445670	0.3566430	2.5396620	-2.7728300	2.6905830	-2.7764600	1.0050600
		0.8	G_0	0.5255960	2.8068730	2.7604390	-3.3079300	2.6131920	-5.3475400	2.9814200
			G_1	0.0798310	0.4515320	3.0733190	-2.3711000	0.9991140	-1.7909000	0.9239300
0.01667	0.125	0.0	G_0	0.4065238	0.7772483	3.8861644	-12.573943	16.760207	-11.014593	2.8706957
			G_1	0.0320270	0.1825342	2.2670449	-2.7076615	1.2088194	-0.3777430	0.0763155
		0.2	G_0	0.4044209	1.1520573	1.6383619	-5.7992049	7.0395445	-4.3026142	1.0557168
			G_1	0.0463551	0.0048175	4.0171926	-9.5540173	13.544104	-10.652816	3.2935742
		0.4	G_0	0.4742270	1.4486540	0.9441430	-2.7830300	1.8682280	-0.2627600	-0.2064200
			G_1	0.0684887	0.0711241	3.9201925	-8.9540416	12.651466	-10.126277	3.1705597
		0.6	G_0	0.6007740	1.7794800	0.4132540	1.2838500	-7.0074700	7.5056630	-2.6984600
			G_1	0.0919660	0.2738720	2.6953680	-3.5387900	2.7558210	-1.9110000	0.5789800
		0.8	G_0	0.8236880	1.4243800	5.4504410	-9.3568100	1.7122670	4.4942090	-2.3085900
			G_1	0.1501480	0.3110770	3.0739110	-2.9209300	-0.8651500	2.3593210	-1.0179600
0.01667	0.25	0.0	G_0	0.6152816	-0.3348694	6.2955620	-15.590618	19.299508	-12.488107	3.3010035
			G_1	0.0703566	0.2828152	1.4036169	-0.6511596	-1.2076596	1.0318656	-0.2423741
		0.2	G_0	0.6006412	0.1200883	4.6889410	-13.147636	17.760233	-12.331467	3.4379468
			G_1	0.0823805	0.2845653	1.7595773	-2.8182477	3.0142764	-2.4926028	0.8479623
		0.4	G_0	0.7168180	0.1385890	3.6456880	-6.4571300	3.8053530	0.1619780	-0.7025200
			G_1	0.1180703	0.1215398	2.4566849	-3.4891053	2.6628686	-1.5512395	0.4242018
		0.6	G_0	0.8876110	0.0006320	4.3344170	-6.2527900	0.6754690	4.0262590	-2.1571000
			G_1	0.1534930	0.2234680	1.9335370	-1.4780100	-0.7810300	1.2056120	-0.4326300
		0.8	G_0	1.0714710	0.5124440	-1.0787600	17.590810	-45.713000	44.368040	-15.098000
			G_1	0.2165780	0.0967650	2.4940140	-1.9755700	-1.5151400	2.6158670	-1.0374400
0.01667	0.5	0.0	G_0	0.8776607	-0.6729719	3.7721411	-6.5209060	6.3377934	-3.7028038	0.9872447
			G_1	0.1277541	0.4368502	0.4904522	1.0427434	-2.9631236	2.0826525	-0.5184313
		0.2	G_0	0.8797856	-0.8189753	5.0106624	-10.648831	12.938939	-8.8379105	2.5566038
			G_1	0.1429203	0.2118953	1.8692102	-3.3358064	3.9194259	-3.2278570	1.1008228
		0.4	G_0	0.9858350	-0.6539200	2.7563870	-1.4880900	-3.7182700	5.3443380	-2.0581100
			G_1	0.1752744	0.1759213	1.9448935	-3.3090927	3.6614977	-2.9372114	0.9971908
		0.6	G_0	1.1386810	-0.8767800	3.1183900	-1.5659500	-4.3491900	6.0771430	-2.2920100
			G_1	0.2098120	0.2475400	1.3012030	-0.6895000	-1.1717600	1.2614220	-0.4043400
		0.8	G_0	1.3083680	-1.0202700	2.7808040	-0.2523900	-6.0662600	6.9210510	-2.3716800
			G_1	0.2498370	0.2674650	0.7878510	0.7536720	-2.7696800	2.0998750	-0.5937600
0.01667	1	0.0	G_0	1.1977992	-0.5244870	0.1498299	2.3284866	-5.1058499	4.3469049	-1.3487980
			G_1	0.1870117	0.6987352	0.1316900	0.7269255	-2.5259384	2.1756251	-0.6540458
		0.2	G_0	1.2056440	-1.2177859	5.0817914	-13.869274	21.990752	-18.094492	5.9547617
			G_1	0.2121530	0.1654877	3.3487320	-9.4747450	14.317893	-11.685705	3.8460630
		0.4	G_0	1.2854180	-0.9345000	1.7077280	-0.6641200	-2.2863700	3.2735540	-1.3019700
			G_1	0.2341252	0.1481234	3.3101935	-9.2393973	13.855454	-11.264661	3.6985698
		0.6	G_0	1.3804330	-1.0926500	1.7268520	-0.3443200	-2.7397100	3.4824740	-1.3117200
			G_1	0.2377410	0.5177690	0.7425160	-0.5650700	-0.9866000	1.2847770	-0.4700800
		0.8	G_0	1.4791920	-1.2508200	1.7403820	-0.5515300	-1.4528000	1.7023130	-0.5518600
			G_1	0.2596210	0.5100840	0.6508110	-0.5404300	-0.4458500	0.5142900	-0.1661100

Table C.19
Influence Coefficients For A Circumferential Semi-Elliptical Surface Crack In A Sphere – Inside Surface

t/R_i	a/c	a/t	G_i	A_0	A_1	A_2	A_3	A_4	A_5	A_6
0.01667	2	0.0	G_0	0.8150546	-0.5623828	1.4465771	-4.6778133	8.4192164	-7.9025932	2.9866351
			G_1	0.1359146	0.0702340	3.5558581	-11.034445	16.967724	-14.126991	4.8706612
		0.2	G_0	0.8000774	-0.9446252	3.8893952	-11.802689	19.194938	-16.111926	5.4842920
			G_1	0.1277364	0.0659659	3.2316806	-9.7467461	14.591103	-11.934479	4.0760751
		0.4	G_0	0.8278456	-0.3064661	-0.7104847	3.0736923	-5.4721608	4.2460084	-1.1379080
			G_1	0.1412063	0.0537972	3.2925671	-9.8930279	14.775749	-12.067699	4.1195287
		0.6	G_0	0.8563095	-0.3647863	-0.6828579	3.2780595	-6.0457187	4.8229046	-1.3386430
			G_1	0.1478074	0.0209242	3.4681015	-10.494533	15.786300	-12.857397	4.3516213
		0.8	G_0	0.9071520	-0.9586397	2.9370213	-7.9787493	12.257472	-10.076715	3.4546072
			G_1	0.1508950	0.0261778	3.4556040	-10.564756	15.743394	-12.423987	4.0289121
0.05	0.03125	0.0	G_0	0.1965046	2.9373464	-5.2582823	7.4889153	-6.9282667	3.3673349	-0.6677966
			G_1	0.0051780	0.1750280	2.7718680	-4.6457154	4.6780502	-3.2768090	0.9840994
		0.2	G_0	0.2063002	2.4348208	-1.6792669	-2.0521935	6.7328132	-6.5230628	2.1312083
			G_1	0.0046542	0.2627118	2.0457223	-2.3629875	1.5974738	-1.2915665	0.4682223
		0.4	G_0	0.2223780	2.8577860	-3.2804700	3.2986700	1.3072070	-5.0730500	2.3355800
			G_1	0.0166560	0.3647680	1.5986630	-0.8164400	0.8155950	-2.1386000	1.0593800
		0.6	G_0	0.2428340	2.9680040	-2.7123500	4.2276280	1.9716580	-8.4856900	4.0759500
			G_1	0.0217110	0.4843760	0.7385220	3.7350680	-7.3827500	4.9965730	-1.4675300
		0.8	G_0	0.2902570	2.3196210	4.2465490	-13.689800	31.500160	-34.075400	12.499100
			G_1	0.0274960	0.2852170	2.3927440	-0.4558000	0.7192520	-2.5606000	1.0195300
0.05	0.0625	0.0	G_0	0.2695332	2.1626001	-1.6551569	-1.2970208	4.5604304	-4.3163876	1.4010655
			G_1	0.0138667	0.1827458	2.5749608	-3.9044679	3.3556301	-2.1772209	0.6420134
		0.2	G_0	0.2737872	2.0048135	-0.7265377	-2.1376005	3.8183170	-2.6580856	0.6426073
			G_1	0.0159227	0.2244459	2.4125747	-3.8360214	4.0737272	-3.2611907	1.0825973
		0.4	G_0	0.3132520	2.4121650	-1.9883100	1.7361320	-0.2765900	-1.1091800	0.4834300
			G_1	0.0243370	0.3319760	1.8759790	-0.8794800	-1.6338700	1.6356670	-0.5085300
		0.6	G_0	0.3487740	2.9277140	-3.9144400	10.759540	-15.166200	9.7091670	-2.5697200
			G_1	0.0369750	0.3228750	2.4958380	-2.7866100	3.2162240	-3.7181600	1.4702100
		0.8	G_0	0.4409800	2.4409310	2.1913290	-4.0767400	5.8623460	-6.4414300	2.3701600
			G_1	0.0518150	0.3919640	2.4879240	-1.1766000	-0.0382500	-0.7649400	0.3544400
0.05	0.125	0.0	G_0	0.4065238	0.7772483	3.8861644	-12.573943	16.760207	-11.014593	2.8706957
			G_1	0.0320270	0.1825342	2.2670449	-2.7076615	1.2088194	-0.3777430	0.0763155
		0.2	G_0	0.4023356	1.1416026	1.6015250	-5.7067883	6.9115457	-4.2052659	1.0280524
			G_1	0.0461385	-0.0013993	4.0568875	-9.7684931	13.957243	-11.003908	3.4062359
		0.4	G_0	0.4731020	1.4598250	0.6686580	-2.4313900	1.4392340	0.3170760	-0.4982700
			G_1	0.0539600	0.3468750	1.5149680	-0.1187500	-2.9767700	2.9842000	-1.0116100
		0.6	G_0	0.5768930	1.6736950	0.5839020	-0.4166100	-2.9284700	3.8129030	-1.5216800
			G_1	0.0873860	0.3718430	1.9316280	-1.1754100	-1.1865200	1.3307430	-0.4408300
		0.8	G_0	0.7476330	1.5255190	3.4911010	-5.9067000	0.6609760	3.8597640	-2.1647600
			G_1	0.1350910	0.3555410	2.6415380	-2.4037300	-0.4893400	1.6644630	-0.8079800
0.05	0.25	0.0	G_0	0.6152816	-0.3348694	6.2955620	-15.590618	19.299508	-12.488107	3.3010035
			G_1	0.0703566	0.2828152	1.4036169	-0.6511596	-1.2076596	1.0318656	-0.2423741
		0.2	G_0	0.5995216	0.0745184	4.9157036	-13.844652	18.839744	-13.140826	3.6737383
			G_1	0.0813168	0.2876417	1.7176699	-2.7024974	2.8342997	-2.3477094	0.8026856
		0.4	G_0	0.7102380	0.0439840	3.9902400	-7.4695900	5.3742220	-1.0152600	-0.3583400
			G_1	0.1036140	0.2398990	1.7711840	-1.5881000	0.0239240	0.2836080	-0.0909500
		0.6	G_0	0.8668440	-0.1853500	5.2094010	-9.0092600	5.1296440	0.6287600	-1.1777900
			G_1	0.1484450	0.2501360	1.6315370	-0.4506700	-2.5744500	2.7430720	-0.9382000
		0.8	G_0	1.0904790	-0.8801900	9.5612400	-20.310000	20.023580	-9.4224700	1.5940800
			G_1	0.2092240	0.2051490	1.6130080	0.9488890	-6.5225500	6.9995060	-2.5512200

Table C.19
Influence Coefficients For A Circumferential Semi-Elliptical Surface Crack In A Sphere – Inside Surface

t/R_i	a/c	a/t	G_i	A_0	A_1	A_2	A_3	A_4	A_5	A_6
0.05	0.5	0.0	G_0	0.8776607	-0.6729719	3.7721411	-6.5209060	6.3377934	-3.7028038	0.9872447
			G_1	0.1277541	0.4368502	0.4904522	1.0427434	-2.9631236	2.0826525	-0.5184313
		0.2	G_0	0.8775005	-0.8675711	5.2847489	-11.413044	14.009496	-9.5615193	2.7437562
			G_1	0.1415696	0.2121724	1.8544551	-3.2969631	3.8715613	-3.1962335	1.0916526
		0.4	G_0	0.9746810	-0.6764800	2.7817250	-1.4704600	-3.7922100	5.4145200	-2.0805200
			G_1	0.1609320	0.3221510	1.0828040	-0.2783200	-1.6569600	1.5946140	-0.5042700
		0.6	G_0	1.1219930	-1.0618100	3.8706440	-2.6144100	-4.3263600	7.1328260	-2.8953300
			G_1	0.2049110	0.2110230	1.3108450	-0.4293200	-1.7417300	1.7933410	-0.5985300
		0.8	G_0	1.2840520	-1.3687200	4.7660190	-4.9287800	-0.3916900	3.5649270	-1.6220800
			G_1	0.2543300	0.0523300	2.0496430	-2.5303100	1.5985850	-0.7631200	0.1387500
0.05	1	0.0	G_0	1.1977992	-0.5244870	0.1498299	2.3284866	-5.1058499	4.3469049	-1.3487980
			G_1	0.1870117	0.6987352	0.1316900	0.7269255	-2.5259384	2.1756251	-0.6540458
		0.2	G_0	1.2002994	-1.2236777	5.1305529	-13.994650	22.171398	-18.221125	5.9865275
			G_1	0.2108241	0.1630844	3.3655746	-9.5404779	14.447016	-11.795107	3.8786410
		0.4	G_0	1.2775500	-0.9717200	1.9465790	-1.3327300	-1.2496000	2.4601150	-1.0533700
			G_1	0.2271050	0.1554666	3.2762813	-9.2008474	13.878254	-11.301080	3.7032258
		0.6	G_0	1.3630880	-1.1355900	2.0377550	-1.1421700	-1.5764700	2.6001810	-1.0483700
			G_1	0.2340870	0.5037420	0.8243890	-0.7879300	-0.6213500	0.9879850	-0.3791600
		0.8	G_0	1.4588610	-1.2829700	1.9411540	-0.5400700	-2.1595700	2.6385470	-0.9299900
			G_1	0.2575880	0.4907760	0.7196260	-0.4754300	-0.8587700	1.0287600	-0.3729500
0.05	2	0.0	G_0	0.8150546	-0.5623828	1.4465771	-4.6778133	8.4192164	-7.9025932	2.9866351
			G_1	0.1359146	0.0702340	3.5558581	-11.034445	16.967724	-14.126991	4.8706612
		0.2	G_0	0.7973196	-0.9381424	3.8909617	-11.830984	19.234526	-16.118679	5.4755183
			G_1	0.1274597	0.0631239	3.2547584	-9.8153123	14.686785	-11.990357	4.0857813
		0.4	G_0	0.8219489	-0.2688351	-0.9012045	3.6405439	-6.3491321	4.9311895	-1.3509729
			G_1	0.1368187	0.0344331	3.4352335	-10.428022	15.682372	-12.738140	4.2956725
		0.6	G_0	0.8502963	-0.3657363	-0.5930920	2.9905584	-5.6109214	4.5263371	-1.2674956
			G_1	0.1462277	0.0307414	3.4084485	-10.285583	15.400473	-12.485259	4.2107194
		0.8	G_0	0.8970583	-0.9194808	2.8028991	-7.5318379	11.471860	-9.3822670	3.2124529
			G_1	0.1489320	0.0377374	3.4059416	-10.404290	15.449222	-12.125448	3.9093420
0.1	0.03125	0.0	G_0	0.1965046	2.9373464	-5.2582823	7.4889153	-6.9282667	3.3673349	-0.6677966
			G_1	0.0051780	0.1750280	2.7718680	-4.6457154	4.6780502	-3.2768090	0.9840994
		0.2	G_0	0.2056151	2.3876240	-1.2594709	-3.9600494	10.263090	-9.4728811	3.0615394
			G_1	0.0055285	0.2220479	2.2722444	-2.9582870	2.2834250	-1.6416281	0.5311764
		0.4	G_0	0.2092293	2.9825394	-4.9329850	8.8533505	-8.2951024	2.9215984	-0.1801457
			G_1	0.0086354	0.2230926	2.5017267	-3.5679613	4.2965576	-3.9848117	1.3716472
		0.6	G_0	0.2156946	3.3194024	-6.7127312	17.752305	-22.219396	12.305863	-2.6343514
			G_1	0.0095494	0.2722523	2.2990303	-2.5229292	3.9759245	-4.8178097	1.8171860
		0.8	G_0	0.2106541	4.0693503	-12.314028	43.297719	-67.899601	49.749656	-14.453951
			G_1	0.0052008	0.5131981	0.2825660	5.8237240	-9.7973928	6.2698867	-1.7971248
0.1	0.0625	0.0	G_0	0.2695332	2.1626001	-1.6551569	-1.2970208	4.5604304	-4.3163876	1.4010655
			G_1	0.0138667	0.1827458	2.5749608	-3.9044679	3.3556301	-2.1772209	0.6420134
		0.2	G_0	0.2734455	1.9681289	-0.6332429	-2.4507798	4.3416872	-3.0780568	0.7761721
			G_1	0.0152751	0.2288569	2.3378606	-3.6783066	3.9024648	-3.1657268	1.0624553
		0.4	G_0	0.3069420	2.2661960	-1.4011000	-0.1823600	2.5876020	-3.1790500	1.0989000
			G_1	0.0170970	0.3974880	1.2707560	0.7398430	-3.5913300	2.7604580	-0.7723900
		0.6	G_0	0.3252810	2.9110250	-5.0383200	13.339660	-17.918400	11.117430	-2.8068700
			G_1	0.0321510	0.2670050	2.7738640	-4.2188800	5.4231930	-4.8925100	1.5974400
		0.8	G_0	0.4029060	2.5130770	-0.8265200	2.0036310	0.8442140	-4.1326900	1.7303900
			G_1	0.0410260	0.4369650	1.6388160	0.3340340	-1.6643000	0.8372800	-0.3914600

Table C.19
Influence Coefficients For A Circumferential Semi-Elliptical Surface Crack In A Sphere – Inside Surface

t/R_i	a/c	a/t	G_i	A_0	A_1	A_2	A_3	A_4	A_5	A_6
0.1	0.125	0.0	G_0	0.4065238	0.7772483	3.8861644	-12.573943	16.760207	-11.014593	2.8706957
			G_1	0.0320270	0.1825342	2.2670449	-2.7076615	1.2088194	-0.3777430	0.0763155
		0.2	G_0	0.3993741	1.1157939	1.7168739	-6.1865447	7.7474504	-4.8620610	1.2242468
			G_1	0.0455353	-0.0135463	4.1419231	-10.167325	14.710359	-11.641060	3.6088361
		0.4	G_0	0.4617530	1.4622820	0.2156210	-0.8812900	-1.3328400	2.7878940	-1.3388300
			G_1	0.0536630	0.3276020	1.6209140	-0.4541700	-2.5278500	2.6497620	-0.8945800
		0.6	G_0	0.5380720	1.6213820	0.4653070	-0.5397900	-2.4739000	3.7359840	-1.6506700
			G_1	0.0753350	0.3637430	1.7925290	-0.8305100	-1.4751600	1.3895700	-0.4213100
		0.8	G_0	0.6628870	1.4047270	2.7816950	-4.1401700	-0.3587800	4.2499960	-2.4267700
			G_1	0.1086010	0.3364230	2.3178370	-1.7185200	-0.6824300	1.5432330	-0.8117800
0.1	0.25	0.0	G_0	0.6152816	-0.3348694	6.2955620	-15.590618	19.299508	-12.488107	3.3010035
			G_1	0.0703566	0.2828152	1.4036169	-0.6511596	-1.2076596	1.0318656	-0.2423741
		0.2	G_0	0.5946315	0.1630558	4.1726937	-11.442887	15.001336	-10.166362	2.7840781
			G_1	0.0799165	0.3122584	1.5121304	-2.0502690	1.8012664	-1.5552403	0.5688688
		0.4	G_0	0.7002690	-0.0112900	4.0839410	-7.7072400	5.6977540	-1.1953700	-0.3271800
			G_1	0.1044360	0.2092790	1.9497990	-2.2166900	1.0304150	-0.4828700	0.1377200
		0.6	G_0	0.8327810	-0.1429600	4.6335640	-7.4550200	3.1278560	1.9985630	-1.5759000
			G_1	0.1447420	0.2143310	1.8268530	-1.1379500	-1.4219100	1.8413810	-0.6692300
		0.8	G_0	1.0408980	-1.0572400	10.765920	-25.160500	29.563410	-17.485000	4.0117800
			G_1	0.2090000	-0.0738100	3.7135650	-6.3740300	6.0799340	-3.2263400	0.5888100
0.1	0.5	0.0	G_0	0.8776607	-0.6729719	3.7721411	-6.5209060	6.3377934	-3.7028038	0.9872447
			G_1	0.1277541	0.4368502	0.4904522	1.0427434	-2.9631236	2.0826525	-0.5184313
		0.2	G_0	0.8763580	-0.8696069	5.2444797	-11.291330	13.885305	-9.5329867	2.7563560
			G_1	0.1414533	0.2149777	1.8065139	-3.1255644	3.5946509	-2.9851198	1.0299591
		0.4	G_0	0.9628790	-0.7184100	2.9189220	-1.8029700	-3.2999000	5.0465790	-1.9741800
			G_1	0.1596580	0.3006910	1.1779510	-0.5684100	-1.1982000	1.2462930	-0.4026600
		0.6	G_0	1.0967370	-1.1070900	4.0513750	-3.0267600	-3.6936500	6.6464720	-2.7585600
			G_1	0.1997760	0.1953150	1.3974000	-0.7646900	-1.0876900	1.2196840	-0.4138900
		0.8	G_0	1.2424830	-1.3001900	4.2941430	-3.2969300	-2.7560400	5.3099170	-2.1723700
			G_1	0.2473640	0.0819390	1.8270490	-1.8506300	0.6823350	-0.1218100	-0.0558100
0.1	1	0.0	G_0	1.1977992	-0.5244870	0.1498299	2.3284866	-5.1058499	4.3469049	-1.3487980
			G_1	0.1870117	0.6987352	0.1316900	0.7269255	-2.5259384	2.1756251	-0.6540458
		0.2	G_0	1.2005677	-1.2230016	5.0985217	-13.837672	21.890898	-17.988267	5.9105357
			G_1	0.2113782	0.1664234	3.3274422	-9.4052634	14.236208	-11.632675	3.8277229
		0.4	G_0	1.2638600	-0.9614100	1.8822030	-1.1747600	-1.3442200	2.4305450	-1.0245000
			G_1	0.2282186	0.1489274	3.2665130	-9.0686011	13.608451	-11.071798	3.6294031
		0.6	G_0	1.3385050	-1.0805500	1.6851940	0.0595880	-3.4485600	4.0132490	-1.4715700
			G_1	0.2286090	0.5343970	0.6085790	-0.1308700	-1.5964100	1.7241660	-0.6053000
		0.8	G_0	1.4306440	-1.2636300	1.9100820	-0.1800600	-2.8031200	3.1532600	-1.1039200
			G_1	0.2524840	0.5095760	0.6303900	-0.2703000	-1.0026900	1.0556480	-0.3754900
0.1	2	0.0	G_0	0.8150546	-0.5623828	1.4465771	-4.6778133	8.4192164	-7.9025932	2.9866351
			G_1	0.1359146	0.0702340	3.5558581	-11.034445	16.967724	-14.126991	4.8706612
		0.2	G_0	0.8037855	-0.9092929	3.7353895	-11.416378	18.639255	-15.682327	5.3485818
			G_1	0.1286222	0.0914525	3.0868205	-9.2893804	13.840605	-11.320690	3.8796337
		0.4	G_0	0.8174447	-0.2826820	-0.7753340	3.3044722	-5.9069786	4.6666813	-1.2969702
			G_1	0.1396265	0.0763945	3.1512330	-9.3939695	13.870673	-11.246516	3.8300230
		0.6	G_0	0.8412020	-0.3463883	-0.6219701	3.0678735	-5.7507939	4.6839414	-1.3382006
			G_1	0.1457296	0.0728417	3.1174048	-9.2123878	13.483161	-10.858611	3.6845393
		0.8	G_0	0.8871849	-0.9132745	2.8983617	-7.7749672	11.739486	-9.4660625	3.1911523
			G_1	0.1406352	0.2552970	1.8998084	-5.2594318	6.8575162	-5.2828773	1.8237938

Table C.19
Influence Coefficients For A Circumferential Semi-Elliptical Surface Crack In A Sphere – Inside Surface

t/R_i	a/c	a/t	G_i	A_0	A_1	A_2	A_3	A_4	A_5	A_6
0.2	0.0625	0.0	G_0	0.2695332	2.1626001	-1.6551569	-1.2970208	4.5604304	-4.3163876	1.4010655
			G_1	0.0138667	0.1827458	2.5749608	-3.9044679	3.3556301	-2.1772209	0.6420134
		0.2	G_0	0.2737585	2.0989557	-1.3366600	-2.0216133	5.7609793	-5.3164212	1.7002530
			G_1	0.0172389	0.1931788	2.4328584	-3.5131947	2.8778096	-1.8716576	0.5553443
		0.4	G_0	0.2942695	1.6309557	1.9282841	-10.599320	19.044288	-15.839499	4.9002661
			G_1	0.0197789	0.1838190	2.5736443	-4.1164538	4.6841392	-3.8087419	1.2237021
		0.6	G_0	0.3582710	1.1316670	8.9981080	-39.164000	74.850940	-66.338200	21.892300
			G_1	0.0252680	0.5624700	-0.0774500	5.6321440	-11.573200	9.2788790	-2.9259400
		0.8	G_0	0.3499740	2.2914350	-0.2831900	-2.4992200	9.7923300	-11.123300	3.7094100
			G_1	0.0264840	0.4051970	1.5865810	-0.3364900	-0.3696500	0.1769020	-0.3491600
0.2	0.125	0.0	G_0	0.4065238	0.7772483	3.8861644	-12.573943	16.760207	-11.014593	2.8706957
			G_1	0.0320270	0.1825342	2.2670449	-2.7076615	1.2088194	-0.3777430	0.0763155
		0.2	G_0	0.4084458	0.9728544	2.9451362	-11.032946	16.077444	-11.435539	3.1901555
			G_1	0.0385061	0.2062311	2.1039263	-2.6035551	1.5672811	-0.9370389	0.3033573
		0.4	G_0	0.4430160	1.3487560	0.6778660	-2.4532700	1.0000460	1.1820340	-0.8966900
			G_1	0.0452250	0.3516930	1.3572720	0.1641320	-3.1358400	2.8585510	-0.8900400
		0.6	G_0	0.4939730	1.6106370	-0.4741100	1.0725300	-2.4838600	2.2320220	-0.8679600
			G_1	0.0599710	0.4327900	1.0944060	0.8406750	-3.5251900	2.8446460	-0.8879300
		0.8	G_0	0.5703130	1.5331780	0.1960790	1.6381490	-5.1731200	6.2059300	-2.9109200
			G_1	0.0836110	0.3426920	1.8504940	-1.1043800	-0.5459400	1.3182020	-0.8771200
0.2	0.25	0.0	G_0	0.6152816	-0.3348694	6.2955620	-15.590618	19.299508	-12.488107	3.3010035
			G_1	0.0703566	0.2828152	1.4036169	-0.6511596	-1.2076596	1.0318656	-0.2423741
		0.2	G_0	0.6133907	-0.2635319	5.9754897	-15.245175	19.397444	-12.868262	3.4777552
			G_1	0.0815379	0.1197957	2.3185388	-3.4598086	2.9385877	-1.8712161	0.5393793
		0.4	G_0	0.6835090	-0.0762400	4.1822090	-8.0663800	6.2903700	-1.5521400	-0.2711800
			G_1	0.1004930	0.2132070	1.8019670	-1.6633100	-0.0824400	0.5789510	-0.2348900
		0.6	G_0	0.7811640	-0.1443900	4.5779910	-7.7709400	4.0234850	1.3759920	-1.4785900
			G_1	0.1308160	0.2114970	1.7861730	-1.1092300	-1.3132500	1.7043170	-0.6271500
		0.8	G_0	0.9516200	-1.0914200	10.564350	-24.138600	28.221470	-16.194300	3.3940700
			G_1	0.1855060	-0.0949900	3.7286180	-6.5150900	6.8116510	-3.9697800	0.7915400
0.2	0.5	0.0	G_0	0.8776607	-0.6729719	3.7721411	-6.5209060	6.3377934	-3.7028038	0.9872447
			G_1	0.1277541	0.4368502	0.4904522	1.0427434	-2.9631236	2.0826525	-0.5184313
		0.2	G_0	0.8742248	-0.9052377	5.2670077	-11.045503	13.195491	-8.8422731	2.5138892
			G_1	0.1403924	0.2163568	1.7349237	-2.8428627	3.1113750	-2.5977594	0.9110634
		0.4	G_0	0.9401030	-0.7451800	2.9664560	-1.9749400	-2.8932700	4.6449810	-1.8344300
			G_1	0.1555140	0.2970190	1.1574570	-0.5681000	-1.0965000	1.1098090	-0.3486700
		0.6	G_0	1.0537880	-1.1093600	4.0579950	-3.1632500	-3.1381200	6.0141240	-2.5319500
			G_1	0.1922940	0.1879200	1.3801410	-0.6746200	-1.2045000	1.2997450	-0.4403500
		0.8	G_0	1.1884610	-1.2911700	4.2898150	-3.0135200	-3.0823600	5.6399870	-2.3739300
			G_1	0.2380870	0.1010080	1.6081810	-1.0026700	-0.6465600	0.9578210	-0.4255000
0.2	1	0.0	G_0	1.1977992	-0.5244870	0.1498299	2.3284866	-5.1058499	4.3469049	-1.3487980
			G_1	0.1870117	0.6987352	0.1316900	0.7269255	-2.5259384	2.1756251	-0.6540458
		0.2	G_0	1.2019274	-1.2495893	5.1046981	-13.602601	21.368497	-17.519717	5.7503733
			G_1	0.2123063	0.1600851	3.3211697	-9.3446295	14.144479	-11.559200	3.7991746
		0.4	G_0	1.2422470	-0.9714600	1.8852790	-0.9908600	-1.6585700	2.6485320	-1.0881700
			G_1	0.2218584	0.1625068	3.1510566	-8.7140941	13.119255	-10.711408	3.5113447
		0.6	G_0	1.3046120	-1.0790500	1.7356360	0.0128460	-3.1861400	3.6339400	-1.3238800
			G_1	0.2222060	0.5241130	0.6543980	-0.3228700	-1.0897200	1.2192770	-0.4395200
		0.8	G_0	1.3908420	-1.2477800	1.9896800	-0.1664500	-2.7059000	2.9650450	-1.0478600
			G_1	0.2488650	0.5058520	0.6232410	-0.2059600	-0.9627500	0.9695670	-0.3598300

Table C.19
Influence Coefficients For A Circumferential Semi-Elliptical Surface Crack In A Sphere – Inside Surface

t/R_i	a/c	a/t	G_i	A_0	A_1	A_2	A_3	A_4	A_5	A_6
0.2	2	0.0	G_0	0.8150546	-0.5623828	1.4465771	-4.6778133	8.4192164	-7.9025932	2.9866351
			G_1	0.1359146	0.0702340	3.5558581	-11.034445	16.967724	-14.126991	4.8706612
		0.2	G_0	0.8250975	-0.9438687	3.8105923	-11.470951	18.537512	-15.482925	5.2571666
			G_1	0.1356047	0.0746798	3.1854379	-9.5353120	14.124071	-11.450020	3.8901899
		0.4	G_0	0.8139942	-0.3159698	-0.4999519	2.5090342	-4.7632356	3.9015300	-1.1103420
			G_1	0.1380121	0.0952916	3.0412294	-9.0460679	13.258399	-10.660849	3.6064159
		0.6	G_0	0.8300414	-0.3394132	-0.5415102	2.8491907	-5.4748640	4.5771074	-1.3522891
			G_1	0.1429879	0.0961143	2.9878547	-8.7967602	12.736287	-10.120997	3.3946646
		0.8	G_0	0.8729867	-0.8783754	2.8952584	-7.7169371	11.500786	-9.0803442	2.9911160
			G_1	0.1400092	0.2554510	1.9392782	-5.3577221	6.9103675	-5.1468324	1.7079398
0.33333	0.125	0.0	G_0	0.4065238	0.7772483	3.8861644	-12.573943	16.760207	-11.014593	2.8706957
			G_1	0.0320270	0.1825342	2.2670449	-2.7076615	1.2088194	-0.3777430	0.0763155
		0.2	G_0	0.4020000	0.9853595	2.7043980	-10.513668	15.464532	-11.026411	3.0760461
			G_1	0.0372110	0.2063396	2.0679496	-2.5708822	1.5350316	-0.8956604	0.2859264
		0.4	G_0	0.4353513	1.0074059	2.9587394	-11.549309	18.119891	-13.752999	4.0097223
			G_1	0.0491893	0.1999997	2.2616203	-3.1204287	2.5261383	-1.7193112	0.5223301
		0.6	G_0	0.6536134	-0.3960714	3.9021296	1.1836114	-14.440087	16.822912	-6.2583556
			G_1	0.0893580	0.2902339	-0.1501292	7.0452471	-14.749314	11.977710	-3.6847679
		0.8	G_0	0.5730046	-0.2848721	11.935635	-34.590748	49.744679	-33.654577	8.2066323
			G_1	0.0918762	-0.2872288	5.8672732	-13.319779	17.442403	-11.198133	2.4320312
0.33333	0.25	0.0	G_0	0.6152816	-0.3348694	6.2955620	-15.590618	19.299508	-12.488107	3.3010035
			G_1	0.0703566	0.2828152	1.4036169	-0.6511596	-1.2076596	1.0318656	-0.2423741
		0.2	G_0	0.6051739	-0.2720363	5.8549634	-14.849672	18.753613	-12.354730	3.3228649
			G_1	0.0797227	0.1133642	2.3119122	-3.4664732	2.9490005	-1.8638300	0.5327646
		0.4	G_0	0.7512788	-1.7015711	13.690661	-35.526023	47.428484	-32.325665	8.8198002
			G_1	0.1009842	0.0938557	2.2987210	-3.1266301	2.3590792	-1.4947249	0.4568768
		0.6	G_0	0.8342864	-1.9526111	15.450960	-40.564748	55.579185	-38.728413	10.698090
			G_1	0.1312765	-0.0059848	2.9477834	-4.8816998	5.1202114	-3.5854913	1.0355862
		0.8	G_0	0.8805576	-1.3233844	12.321751	-32.489275	46.108417	-32.487421	8.6957482
			G_1	0.1723697	-0.1621971	4.0976228	-8.5360647	11.331973	-8.0070418	2.0432026
0.33333	0.5	0.0	G_0	0.8776607	-0.6729719	3.7721411	-6.5209060	6.3377934	-3.7028038	0.9872447
			G_1	0.1277541	0.4368502	0.4904522	1.0427434	-2.9631236	2.0826525	-0.5184313
		0.2	G_0	0.8637041	-0.9579411	5.5193636	-11.685961	14.029918	-9.3776725	2.6483366
			G_1	0.1375681	0.2020794	1.7847423	-2.9704902	3.2909875	-2.7216072	0.9438583
		0.4	G_0	1.0748010	-3.1343180	15.652793	-35.787158	45.096152	-29.974302	8.1420931
			G_1	0.1585619	0.1298599	1.7627391	-2.4097712	2.4267576	-2.2345607	0.8527975
		0.6	G_0	1.1434265	-3.2071828	16.049409	-36.939714	47.156679	-31.706900	8.6657124
			G_1	0.1911418	0.0566092	1.9186548	-2.2593205	1.6495597	-1.3251807	0.4935857
		0.8	G_0	1.1547897	-1.8109612	8.1002548	-15.155969	17.051101	-10.542865	2.6030956
			G_1	0.2421556	-0.0724574	2.5190224	-3.7734438	4.0569536	-2.9162745	0.7860745
0.33333	1	0.0	G_0	1.1977992	-0.5244870	0.1498299	2.3284866	-5.1058499	4.3469049	-1.3487980
			G_1	0.1870117	0.6987352	0.1316900	0.7269255	-2.5259384	2.1756251	-0.6540458
		0.2	G_0	1.1875625	-1.2432639	5.0281758	-13.245081	20.748463	-17.004471	5.5764820
			G_1	0.2082564	0.1715823	3.2203073	-9.0303758	13.686914	-11.208961	3.6846903
		0.4	G_0	1.4876625	-4.5324977	19.641221	-46.607296	62.182534	-43.493509	12.383858
			G_1	0.2385240	-0.0937573	4.2543566	-11.186814	16.198364	-12.669420	3.9990332
		0.6	G_0	1.5000661	-4.1947739	17.489127	-40.328659	52.861248	-36.481471	10.252286
			G_1	0.2511561	-0.0152239	3.5438994	-8.7733020	12.271038	-9.4722234	2.9534289
		0.8	G_0	1.3390263	-1.3241238	3.2298761	-4.6387878	5.7003012	-4.6556451	1.5695068
			G_1	0.2576932	0.3305364	1.4832349	-3.0035476	4.2515862	-3.7224290	1.2347530

Table C.19
Influence Coefficients For A Circumferential Semi-Elliptical Surface Crack In A Sphere – Inside Surface

t/R_i	a/c	a/t	G_i	A_0	A_1	A_2	A_3	A_4	A_5	A_6
0.33333	2	0.0	G_0	0.8150546	-0.5623828	1.4465771	-4.6778133	8.4192164	-7.9025932	2.9866351
			G_1	0.1359146	0.0702340	3.5558581	-11.034445	16.967724	-14.126991	4.8706612
		0.2	G_0	0.8183590	-0.9202621	3.7119207	-11.153624	17.978556	-14.963095	5.0641776
			G_1	0.1336155	0.0946846	3.0589552	-9.1310235	13.436743	-10.839985	3.6743713
		0.4	G_0	0.8271021	-0.9666760	3.9511559	-11.593058	18.251495	-14.828350	4.9121211
			G_1	0.1363643	0.1116181	2.9365323	-8.6680634	12.529636	-9.9279173	3.3204599
		0.6	G_0	0.8340322	-0.9307282	3.6181955	-10.368517	16.099398	-12.941929	4.2608708
			G_1	0.1413107	0.1037118	2.9507169	-8.6545394	12.400986	-9.6678730	3.1751898
		0.8	G_0	0.8474108	-0.8443446	2.9324673	-7.7308789	11.239031	-8.5582060	2.7123537
			G_1	0.1412033	0.2357192	2.1073932	-5.8766063	7.6722573	-5.5747592	1.7604674

Notes:

1. Interpolation of the influence coefficients, G_i, may be used for intermediate values of t/R_i, a/c, and a/t.

2. The value of the influence coefficients at the surface point of the crack defined by $\varphi = 0^0$ are equal to: $G_i = A_0$.

3. The value of the influence coefficients at the deepest point of the crack defined by $\varphi = 90^0$ are equal to: $G_i = \sum_{n=0}^{6} A_n$.

Table C.20
Influence Coefficients For A Circumferential Semi-Elliptical Surface Crack In A Sphere – Outside Surface

t/R_i	a/c	a/t	G_i	A_0	A_1	A_2	A_3	A_4	A_5	A_6
0.0	0.03125	0.0	G_0	0.1965046	2.9373464	-5.2582823	7.4889153	-6.9282667	3.3673349	-0.6677966
			G_1	0.0051780	0.1750280	2.7718680	-4.6457154	4.6780502	-3.2768090	0.9840994
		0.2	G_0	0.2080760	3.0112422	-5.1048701	7.6348715	-6.8347547	2.7940766	-0.3882688
			G_1	0.0084834	0.2406767	2.4574292	-3.6452421	3.6142837	-2.8451814	0.9270638
		0.4	G_0	0.2357940	3.0822400	-3.5792100	3.9476890	1.9131590	-6.8872200	3.1896800
			G_1	0.0145140	0.4038000	1.6422700	-0.3906100	-0.6480700	-0.2940300	0.2514900
		0.6	G_0	0.2902240	3.6892050	-4.5739100	11.709890	-6.3750000	-5.8894100	4.2452400
			G_1	0.0208890	0.7016780	0.1631840	5.7072160	-8.2075800	3.4561120	-0.4454700
		0.8	G_0	0.5163550	2.5310830	14.712900	-43.621800	101.06570	-116.08100	46.190900
			G_1	0.0825460	0.4971770	4.6064810	-7.3326700	21.148620	-29.345100	12.491400
0.0	0.0625	0.0	G_0	0.2695332	2.1626001	-1.6551569	-1.2970208	4.5604304	-4.3163876	1.4010655
			G_1	0.0138667	0.1827458	2.5749608	-3.9044679	3.3556301	-2.1772209	0.6420134
		0.2	G_0	0.2845892	2.2264055	-1.4546190	-1.5760719	5.1131083	-4.9485443	1.6207574
			G_1	0.0199077	0.2210874	2.4642047	-3.5898625	3.1624039	-2.2403780	0.6965751
		0.4	G_0	0.3261480	2.5200870	-1.8847000	2.1798740	-1.4597100	-0.1886500	0.2393400
			G_1	0.0294120	0.3699370	1.9220850	-1.2071500	-0.4394000	0.2737550	-0.0395200
		0.6	G_0	0.4166330	3.1566470	-2.6248900	7.7325910	-9.6927800	3.6428700	-0.0892000
			G_1	0.0598460	0.4340740	2.6811560	-3.1936600	4.0753720	-4.6940200	1.8285500
		0.8	G_0	0.6540140	3.4231920	3.8158050	-4.1586900	3.4715330	-10.310400	6.6280000
			G_1	0.1214780	0.6975490	2.9718330	-1.3036500	-0.0754900	-3.0465100	2.1670000
0.0	0.125	0.0	G_0	0.4065238	0.7772483	3.8861644	-12.573943	16.760207	-11.014593	2.8706957
			G_1	0.0320270	0.1825342	2.2670449	-2.7076615	1.2088194	-0.3777430	0.0763155
		0.2	G_0	0.4242116	1.0089302	3.2973815	-12.159726	17.873386	-12.868668	3.6281712
			G_1	0.0429859	0.2033811	2.2563818	-2.8752160	1.8152558	-1.0512327	0.3181077
		0.4	G_0	0.4917770	1.6592320	-0.1080400	0.1793240	-2.7076100	3.3680620	-1.3489700
			G_1	0.0634270	0.3722500	1.6231670	-0.5306500	-2.0007400	1.8943780	-0.5880300
		0.6	G_0	0.6591820	1.8759140	1.0212600	-1.7698000	-0.5653600	1.2479960	-0.4376600
			G_1	0.1116040	0.4714500	1.7940590	-0.7557600	-1.4901700	1.0852180	-0.2113700
		0.8	G_0	0.9809330	1.8846320	4.8020780	-8.0580200	0.4447850	3.4772660	-1.0567500
			G_1	0.2039950	0.4800150	2.8822430	-2.5890100	-0.9683000	1.5372370	-0.3750200
0.0	0.25	0.0	G_0	0.6152816	-0.3348694	6.2955620	-15.590618	19.299508	-12.488107	3.3010035
			G_1	0.0703566	0.2828152	1.4036169	-0.6511596	-1.2076596	1.0318656	-0.2423741
		0.2	G_0	0.6385889	-0.3095132	6.5329787	-16.622882	21.056641	-13.850120	3.6988146
			G_1	0.0840059	0.1999367	1.8218113	-1.7756899	0.3757186	-0.0785358	0.0643386
		0.4	G_0	0.7390420	0.0548160	4.0842620	-7.5883100	5.4047530	-1.0146100	-0.3483400
			G_1	0.1164500	0.2479880	1.8282520	-1.7169900	0.1912120	0.1165770	-0.0186100
		0.6	G_0	0.9461210	-0.1858800	5.5867460	-9.8634900	5.9596870	0.1296440	-1.0026100
			G_1	0.1778050	0.2056680	2.0979210	-1.8039500	-0.5558700	1.1461400	-0.4206600
		0.8	G_0	1.2452110	-0.6921900	8.3260620	-14.948000	8.6936910	0.4755790	-1.3926600
			G_1	0.2585640	0.1548890	2.1170240	-0.4910000	-4.6146100	5.4550750	-1.9663300
0.0	0.5	0.0	G_0	0.8776607	-0.6729719	3.7721411	-6.5209060	6.3377934	-3.7028038	0.9872447
			G_1	0.1277541	0.4368502	0.4904522	1.0427434	-2.9631236	2.0826525	-0.5184313
		0.2	G_0	0.9003948	-0.8850488	5.2743239	-11.267523	13.890755	-9.6373584	2.8183906
			G_1	0.1404409	0.3215397	1.1010666	-1.0257556	0.6943940	-1.0793186	0.5410929
		0.4	G_0	1.0058060	-0.7322600	2.9951940	-1.9459200	-3.2613500	5.1424570	-2.0306200
			G_1	0.1740870	0.3051630	1.2070310	-0.6720500	-1.0651300	1.1445590	-0.3644800
		0.6	G_0	1.1826010	-1.1072500	3.9623640	-2.7781300	-4.3097300	7.2772750	-2.9648200
			G_1	0.2277120	0.1701170	1.5499470	-1.1051200	-0.8333700	1.1717060	-0.4194500
		0.8	G_0	1.3833380	-1.3900300	4.3755780	-3.7372600	-2.5403200	5.3036000	-2.0932400
			G_1	0.2820110	0.0839230	1.7258580	-1.5358100	-0.0635600	0.5006780	-0.1982200

Table C.20
Influence Coefficients For A Circumferential Semi-Elliptical Surface Crack In A Sphere – Outside Surface

t/R_i	a/c	a/t	G_i	A_0	A_1	A_2	A_3	A_4	A_5	A_6
0.0	1	0.0	G_0	1.1977992	-0.5244870	0.1498299	2.3284866	-5.1058499	4.3469049	-1.3487980
			G_1	0.1870117	0.6987352	0.1316900	0.7269255	-2.5259384	2.1756251	-0.6540458
		0.2	G_0	1.2263282	-1.1608467	4.4744783	-11.584231	17.811241	-14.408250	4.6998279
			G_1	0.2154786	0.2441623	2.8107820	-7.6574580	11.171413	-9.0053693	2.9542871
		0.4	G_0	1.2989480	-0.9978000	1.9479540	-1.3002700	-1.4940100	2.8306230	-1.2126000
			G_1	0.2386246	0.1447774	3.3198992	-9.2456599	13.823512	-11.223715	3.6868232
		0.6	G_0	1.3971180	-1.1348400	1.7918740	-0.4202600	-2.8679300	3.7685480	-1.4405000
			G_1	0.2445870	0.5326670	0.5939690	-0.0361800	-2.0163100	2.2167010	-0.7782200
		0.8	G_0	1.5117010	-1.3244800	1.7568350	-0.1337900	-2.8629300	3.2953270	-1.1412400
			G_1	0.2704470	0.5113280	0.5357440	-0.0327300	-1.5570200	1.5570970	-0.5094600
0.0	2	0.0	G_0	0.8150546	-0.5623828	1.4465771	-4.6778133	8.4192164	-7.9025932	2.9866351
			G_1	0.1359146	0.0702340	3.5558581	-11.034445	16.967724	-14.126991	4.8706612
		0.2	G_0	0.8463715	-1.0011024	4.0052312	-11.937181	19.189548	-16.039296	5.4674371
			G_1	0.1395121	0.0753999	3.1895604	-9.5540932	14.214316	-11.649525	4.0073308
		0.4	G_0	0.8570045	-1.0183085	3.9957306	-11.886878	19.152747	-16.047480	5.4801806
			G_1	0.1436696	0.0544018	3.2816127	-9.8164232	14.610963	-11.942138	4.0907797
		0.6	G_0	0.8839861	-1.0765270	4.0774087	-11.976171	19.173189	-15.996207	5.4501217
			G_1	0.1504185	0.0478401	3.2579960	-9.6921199	14.370843	-11.736129	4.0258411
		0.8	G_0	0.9033134	-0.9619755	2.8501500	-7.6366897	11.596116	-9.4828625	3.2550163
			G_1	0.1458559	0.2313881	1.9882138	-5.5546045	7.4196069	-5.8965053	2.0855563
0.01	0.03125	0.0	G_0	0.1965046	2.9373464	-5.2582823	7.4889153	-6.9282667	3.3673349	-0.6677966
			G_1	0.0051780	0.1750280	2.7718680	-4.6457154	4.6780502	-3.2768090	0.9840994
		0.2	G_0	0.2077867	2.2749380	0.1405830	-8.1883567	16.585201	-14.085844	4.3580585
			G_1	0.0058829	0.2123600	2.6447168	-4.3435807	4.7836038	-3.7532574	1.1949871
		0.4	G_0	0.2228150	2.9734920	-3.4283200	3.3930740	3.7873140	-9.1100500	4.0601300
			G_1	0.0112870	0.4802660	1.4073800	0.0510890	-0.0972200	-1.8992500	1.0371600
		0.6	G_0	0.2282140	3.5166310	-6.8236400	20.411300	-20.304700	5.6194120	0.3783500
			G_1	0.0183830	0.7773130	-1.4752300	11.278750	-15.823300	8.6430980	-1.9893500
		0.8	G_0	0.2615290	2.7339220	1.5901460	-6.4403200	48.322670	-70.868000	29.356500
			G_1	0.0220870	0.8779500	-2.0000400	11.244490	-3.7584200	-9.8042500	5.5705000
0.01	0.0625	0.0	G_0	0.2695332	2.1626001	-1.6551569	-1.2970208	4.5604304	-4.3163876	1.4010655
			G_1	0.0138667	0.1827458	2.5749608	-3.9044679	3.3556301	-2.1772209	0.6420134
		0.2	G_0	0.2769613	2.0258789	-0.6462394	-2.3171130	4.1211301	-2.9457279	0.7405852
			G_1	0.0177280	0.2145484	2.5823250	-4.3171184	4.8055429	-3.8182428	1.2440577
		0.4	G_0	0.3198770	2.5511570	-2.0536700	1.7976150	1.0661150	-3.4940800	1.5768700
			G_1	0.0352270	0.5096780	1.4381240	-0.0647700	-1.5756000	0.5058010	0.0840900
		0.6	G_0	0.3724790	3.3785840	-5.5275400	17.226590	-21.828900	10.689630	-1.6511000
			G_1	0.0528640	0.5448000	1.8813540	-0.5637400	1.1153130	-3.5764200	1.8037600
		0.8	G_0	0.5171860	3.0210280	1.8715830	3.6003150	1.4454340	-16.702800	10.241500
			G_1	0.0816830	0.6467690	2.0872710	2.2894120	-2.1269000	-4.5735100	3.3312900
0.01	0.125	0.0	G_0	0.4065238	0.7772483	3.8861644	-12.573943	16.760207	-11.014593	2.8706957
			G_1	0.0320270	0.1825342	2.2670449	-2.7076615	1.2088194	-0.3777430	0.0763155
		0.2	G_0	0.4061772	1.1680061	1.5950075	-5.6041264	6.7047751	-4.0556730	0.9877657
			G_1	0.0474966	0.0088231	4.0171999	-9.5055990	13.434246	-10.567935	3.2711539
		0.4	G_0	0.4850880	1.4332010	1.5839620	-5.0901000	6.1655090	-4.1166300	1.1040100
			G_1	0.0731420	0.3638050	1.8984620	-1.4040100	-0.4493800	0.3771280	-0.0065100
		0.6	G_0	0.6328180	1.9450870	0.3228000	1.9973750	-7.5429500	6.9968300	-2.2307700
			G_1	0.1186200	0.4314880	2.3144430	-2.1725900	0.7855010	-0.9041900	0.4760100
		0.8	G_0	0.9239180	1.7165070	5.8526200	-7.9882200	-0.8312700	4.0567570	-1.0070400
			G_1	0.2017510	0.4407840	3.3328700	-2.8052100	-1.1192100	1.4485860	-0.2278300

Table C.20
Influence Coefficients For A Circumferential Semi-Elliptical Surface Crack In A Sphere – Outside Surface

t/R_i	a/c	a/t	G_i	A_0	A_1	A_2	A_3	A_4	A_5	A_6
0.01	0.25	0.0	G_0	0.6152816	-0.3348694	6.2955620	-15.590618	19.299508	-12.488107	3.3010035
			G_1	0.0703566	0.2828152	1.4036169	-0.6511596	-1.2076596	1.0318656	-0.2423741
		0.2	G_0	0.6034886	0.1249569	4.7121854	-13.217504	17.879255	-12.438871	3.4748076
			G_1	0.0832497	0.2943416	1.7190774	-2.6924810	2.8266885	-2.3624724	0.8135845
		0.4	G_0	0.7329190	0.1074600	4.0675530	-7.6739500	5.6676310	-1.3115800	-0.2299100
			G_1	0.1240140	0.2681570	1.8177580	-1.6805900	0.1395580	0.0835500	0.0274100
		0.6	G_0	0.9370040	0.0230720	4.5541080	-6.4470500	0.4628380	4.3635300	-2.2615500
			G_1	0.1861970	0.2475700	1.9590760	-1.2692500	-1.4877100	1.8549340	-0.6173600
		0.8	G_0	1.2073610	0.2919720	1.0067710	12.275230	-38.970100	39.620240	-13.603400
			G_1	0.2727130	0.1608730	2.1939320	-0.2432300	-5.2756800	5.8457490	-1.9946000
0.01	0.5	0.0	G_0	0.8776607	-0.6729719	3.7721411	-6.5209060	6.3377934	-3.7028038	0.9872447
			G_1	0.1277541	0.4368502	0.4904522	1.0427434	-2.9631236	2.0826525	-0.5184313
		0.2	G_0	0.8872475	-0.8816683	5.4321461	-11.914421	14.854353	-10.257839	2.9661420
			G_1	0.1439007	0.2201219	1.8303174	-3.2294108	3.7691815	-3.1256488	1.0743502
		0.4	G_0	1.0045010	-0.7016800	3.0089200	-1.9772600	-3.2633100	5.1698220	-2.0441700
			G_1	0.1806240	0.3006750	1.2260040	-0.5849200	-1.3514400	1.4305690	-0.4612300
		0.6	G_0	1.1836260	-0.9309300	3.2905090	-1.6010900	-4.8402800	6.7524960	-2.5536700
			G_1	0.2368250	0.2146190	1.4242410	-0.8414500	-1.1900400	1.3808530	-0.4493600
		0.8	G_0	1.3992290	-1.1131100	2.9649560	-0.3065100	-6.5225200	7.4276460	-2.4919100
			G_1	0.2922820	0.2075630	1.0263870	0.1996680	-2.0883700	1.5772350	-0.3978900
0.01	1	0.0	G_0	1.1977992	-0.5244870	0.1498299	2.3284866	-5.1058499	4.3469049	-1.3487980
			G_1	0.1870117	0.6987352	0.1316900	0.7269255	-2.5259384	2.1756251	-0.6540458
		0.2	G_0	1.2100415	-1.2196778	5.0851813	-13.887803	22.015976	-18.111977	5.9617039
			G_1	0.2140206	0.1547905	3.4287820	-9.7373187	14.739129	-12.020076	3.9511125
		0.4	G_0	1.3056570	-0.9840700	1.8094060	-0.6734700	-2.5826300	3.7122980	-1.4919000
			G_1	0.2232750	0.5449490	0.7738700	-0.6566600	-1.0193200	1.4561880	-0.5611700
		0.6	G_0	1.4183740	-1.2135500	2.1993510	-1.4933300	-1.2218900	2.4847680	-1.0514900
			G_1	0.2551250	0.5019830	0.7547510	-0.5639900	-1.0363700	1.3526400	-0.4940600
		0.8	G_0	1.5326420	-1.3065800	1.5838410	0.2543670	-3.0285100	3.0930990	-0.9974000
			G_1	0.2830950	0.4811650	0.6674890	-0.5045900	-0.6068900	0.6856470	-0.2173300
0.01	2	0.0	G_0	0.8150546	-0.5623828	1.4465771	-4.6778133	8.4192164	-7.9025932	2.9866351
			G_1	0.1359146	0.0702340	3.5558581	-11.034445	16.967724	-14.126991	4.8706612
		0.2	G_0	0.8028980	-0.9650666	3.9970040	-12.122017	19.696606	-16.510345	5.6097792
			G_1	0.1301047	0.0878063	3.0990196	-9.3341391	13.946577	-11.459553	3.9447497
		0.4	G_0	0.8356296	-0.3224289	-0.7985231	3.5989904	-6.5651593	5.2488556	-1.4769852
			G_1	0.1402778	0.0513398	3.3153847	-10.032609	15.088369	-12.371071	4.2273204
		0.6	G_0	0.8661064	-0.3731907	-0.7988330	3.7602432	-6.9074912	5.5440593	-1.5664796
			G_1	0.1500634	0.0351369	3.3528083	-10.075993	15.097091	-12.363741	4.2277521
		0.8	G_0	0.9207020	-0.9736206	2.8107240	-7.4869514	11.444939	-9.4620056	3.2859159
			G_1	0.1497823	0.1241355	2.7412325	-8.1567935	11.844592	-9.4737292	3.1871348
0.01667	0.03125	0.0	G_0	0.1965046	2.9373464	-5.2582823	7.4889153	-6.9282667	3.3673349	-0.6677966
			G_1	0.0051780	0.1750280	2.7718680	-4.6457154	4.6780502	-3.2768090	0.9840994
		0.2	G_0	0.2072100	2.2706177	0.1180275	-8.0757534	16.419765	-13.978696	4.3309594
			G_1	0.0056314	0.2083374	2.6523526	-4.3557964	4.7921966	-3.7396344	1.1821048
		0.4	G_0	0.2187800	2.9201170	-3.2541400	2.7790300	4.9355160	-10.096300	4.3752100
			G_1	0.0097590	0.3943140	1.5573730	-0.5245700	1.0871590	-2.7010000	1.1644800
		0.6	G_0	0.2221170	3.2864290	-5.6165700	15.962040	-13.285800	0.6263510	1.7133900
			G_1	0.0094710	0.6041920	-0.2782800	6.3200750	-7.7901100	3.2903430	-0.7791200
		0.8	G_0	0.2135000	3.4928720	-5.7522600	17.914470	2.5583030	-28.453500	14.547300
			G_1	0.0113070	0.7637710	-1.1723500	8.1834960	-3.4020600	-4.7874200	2.3849100

Table C.20
Influence Coefficients For A Circumferential Semi-Elliptical Surface Crack In A Sphere – Outside Surface

t/R_i	a/c	a/t	G_i	A_0	A_1	A_2	A_3	A_4	A_5	A_6
0.01667	0.0625	0.0	G_0	0.2695332	2.1626001	-1.6551569	-1.2970208	4.5604304	-4.3163876	1.4010655
			G_1	0.0138667	0.1827458	2.5749608	-3.9044679	3.3556301	-2.1772209	0.6420134
		0.2	G_0	0.2766818	2.0225220	-0.6355478	-2.3051909	4.0699208	-2.8921145	0.7209720
			G_1	0.0174385	0.2100226	2.6007574	-4.3532124	4.8533251	-3.8493461	1.2507471
		0.4	G_0	0.3147650	2.5291720	-2.0919000	2.1143120	0.5588770	-3.1232700	1.4632900
			G_1	0.0279520	0.4902460	1.2476560	0.8350840	-3.0553800	1.6809190	-0.2943900
		0.6	G_0	0.3554270	3.1691060	-4.7808200	15.069000	-17.990700	7.6081440	-0.7807800
			G_1	0.0396470	0.4761990	1.8210230	-0.2332000	0.8740410	-3.4309000	1.7059100
		0.8	G_0	0.4441620	2.8737710	0.2861520	8.2262140	-3.4495800	-13.232100	8.8135400
			G_1	0.0514840	0.5532200	1.6197540	3.3442680	-2.5539000	-4.3338700	3.0434300
0.01667	0.125	0.0	G_0	0.4065238	0.7772483	3.8861644	-12.573943	16.760207	-11.014593	2.8706957
			G_1	0.0320270	0.1825342	2.2670449	-2.7076615	1.2088194	-0.3777430	0.0763155
		0.2	G_0	0.4064707	1.1624907	1.6426210	-5.7433231	6.9198224	-4.2203447	1.0363847
			G_1	0.0473528	0.0100264	4.0034731	-9.4376443	13.307126	-10.460898	3.2369598
		0.4	G_0	0.4821610	1.4369770	1.5439830	-4.8198600	5.6391460	-3.6557100	0.9473000
			G_1	0.0716470	0.3226950	2.1748350	-2.3167400	1.1718590	-1.0086300	0.4403100
		0.6	G_0	0.6240930	1.8391850	1.0572030	-0.2916400	-3.4030700	3.3740640	-1.0492000
			G_1	0.1102270	0.4453490	2.0731700	-1.1859400	-0.7675400	0.2583820	0.1253900
		0.8	G_0	0.8805760	1.7866630	4.9018830	-3.9261500	-6.4686100	7.4680620	-1.8176000
			G_1	0.1837080	0.4424260	3.1186980	-1.8691400	-2.0596300	1.6779760	-0.1873200
0.01667	0.25	0.0	G_0	0.6152816	-0.3348694	6.2955620	-15.590618	19.299508	-12.488107	3.3010035
			G_1	0.0703566	0.2828152	1.4036169	-0.6511596	-1.2076596	1.0318656	-0.2423741
		0.2	G_0	0.6023257	0.1545741	4.5360513	-12.711785	17.157905	-11.940369	3.3414681
			G_1	0.0835309	0.2906933	1.7444852	-2.7644188	2.9354101	-2.4449975	0.8380360
		0.4	G_0	0.7331250	0.0894980	4.3048780	-8.5018200	7.0726920	-2.4545500	0.1249100
			G_1	0.1237180	0.2606840	1.8820280	-1.8520000	0.3848460	-0.0889900	0.0727300
		0.6	G_0	0.9357390	0.0600830	4.4065180	-5.8388500	-0.5866500	5.1893780	-2.5117500
			G_1	0.1846200	0.2541920	1.9652450	-1.3196500	-1.2886700	1.5996390	-0.5141500
		0.8	G_0	1.2001780	0.5721990	-0.8532500	18.991280	-50.389900	48.780140	-16.417100
			G_1	0.2722260	0.1802680	2.1304200	0.0968830	-5.8603400	6.2649050	-2.1059800
0.01667	0.5	0.0	G_0	0.8776607	-0.6729719	3.7721411	-6.5209060	6.3377934	-3.7028038	0.9872447
			G_1	0.1277541	0.4368502	0.4904522	1.0427434	-2.9631236	2.0826525	-0.5184313
		0.2	G_0	0.8861552	-0.8475972	5.2281796	-11.342469	14.043389	-9.6947405	2.8144567
			G_1	0.1437180	0.2270616	1.7877516	-3.0976685	3.5596526	-2.9618029	1.0245128
		0.4	G_0	1.0082480	-0.7456300	3.3510180	-3.0347700	-1.6027300	3.8799180	-1.6527200
			G_1	0.1796900	0.3205770	1.1071750	-0.2040000	-1.9598000	1.9027500	-0.6035800
		0.6	G_0	1.1877360	-0.9200100	3.2830680	-1.5231900	-5.0470300	6.9575050	-2.6253200
			G_1	0.2384060	0.2050470	1.5138910	-1.1176800	-0.7473400	1.0264950	-0.3388600
		0.8	G_0	1.4129910	-1.1463200	3.3006820	-1.3233100	-4.9730900	6.2362190	-2.1281100
			G_1	0.2966970	0.1915670	1.1787620	-0.3009000	-1.2516400	0.8833770	-0.1739600
0.01667	1	0.0	G_0	1.1977992	-0.5244870	0.1498299	2.3284866	-5.1058499	4.3469049	-1.3487980
			G_1	0.1870117	0.6987352	0.1316900	0.7269255	-2.5259384	2.1756251	-0.6540458
		0.2	G_0	1.2109353	-1.2177397	5.0743805	-13.865698	21.990202	-18.097614	5.9594076
			G_1	0.2130552	0.1755510	3.3026352	-9.3689236	14.181057	-11.600284	3.8274381
		0.4	G_0	1.3107300	-1.0156000	1.9707500	-1.0039900	-2.2721700	3.6010860	-1.4904600
			G_1	0.2235330	0.5550130	0.6959270	-0.3676800	-1.5233900	1.8742770	-0.6944500
		0.6	G_0	1.4219950	-1.1738900	1.9016680	-0.4274700	-3.0901900	4.0467930	-1.5502100
			G_1	0.2575680	0.4881880	0.8193810	-0.6793500	-0.9509600	1.3387320	-0.5011100
		0.8	G_0	1.5441710	-1.3325300	1.7019960	0.0066410	-2.7889800	2.9926440	-0.9845900
			G_1	0.2855800	0.4863980	0.6356880	-0.4253800	-0.6903700	0.7139070	-0.2145800

Table C.20
Influence Coefficients For A Circumferential Semi-Elliptical Surface Crack In A Sphere – Outside Surface

t/R_i	a/c	a/t	G_i	A_0	A_1	A_2	A_3	A_4	A_5	A_6
0.01667	2	0.0	G_0	0.8150546	-0.5623828	1.4465771	-4.6778133	8.4192164	-7.9025932	2.9866351
			G_1	0.1359146	0.0702340	3.5558581	-11.034445	16.967724	-14.126991	4.8706612
		0.2	G_0	0.8028351	-0.9568446	3.9434949	-11.975192	19.497930	-16.382699	5.5792085
			G_1	0.1279559	0.0702782	3.2025280	-9.6672580	14.491084	-11.886655	4.0727789
		0.4	G_0	0.8380589	-0.3513714	-0.6291162	3.1142671	-5.8512931	4.7228055	-1.3233607
			G_1	0.1419656	0.0558979	3.2758482	-9.8563050	14.756640	-12.102671	4.1493773
		0.6	G_0	0.8665287	-0.3612175	-0.8863819	4.0316038	-7.3391614	5.8802748	-1.6679659
			G_1	0.1509178	0.0382471	3.3253185	-9.9492109	14.852138	-12.164336	4.1704975
		0.8	G_0	0.9224303	-0.9753725	2.8158522	-7.5259514	11.536233	-9.5573301	3.3229496
			G_1	0.1476854	0.1915534	2.2701951	-6.5794718	9.2487344	-7.4444819	2.5829071
0.05	0.03125	0.0	G_0	0.1965046	2.9373464	-5.2582823	7.4889153	-6.9282667	3.3673349	-0.6677966
			G_1	0.0051780	0.1750280	2.7718680	-4.6457154	4.6780502	-3.2768090	0.9840994
		0.2	G_0	0.2033833	2.5286342	-1.8283974	-2.6930570	9.3707942	-9.5463774	3.2538037
			G_1	0.0049452	0.1952030	2.6898536	-4.3708930	4.7450394	-3.6789217	1.1613232
		0.4	G_0	0.2089810	2.8283000	-3.1998500	3.1505100	3.4039130	-8.3689700	3.7588300
			G_1	0.0080440	0.2694800	1.9433080	-0.3471100	-2.3907600	2.4438430	-0.9810100
		0.6	G_0	0.2055460	3.1555140	-5.5955300	15.954450	-15.825500	4.1143530	0.5020900
			G_1	0.0082470	0.3030350	1.9668890	-1.9390600	6.1885430	-8.7757300	3.4765000
		0.8	G_0	0.2369010	2.2074040	2.8793440	-8.9851400	32.279360	-41.393400	16.253700
			G_1	0.0090710	0.5351660	-0.0295000	5.5371600	-3.5366700	-2.5110100	1.5982100
0.05	0.0625	0.0	G_0	0.2695332	2.1626001	-1.6551569	-1.2970208	4.5604304	-4.3163876	1.4010655
			G_1	0.0138667	0.1827458	2.5749608	-3.9044679	3.3556301	-2.1772209	0.6420134
		0.2	G_0	0.2777401	2.0228942	-0.3762730	-3.9243880	7.6606230	-6.2555801	1.8583009
			G_1	0.0167530	0.1966749	2.6687417	-4.4807588	4.9742054	-3.8877324	1.2453071
		0.4	G_0	0.2949710	2.4263270	-1.9374800	1.8505470	1.3048900	-3.9403500	1.7452900
			G_1	0.0204430	0.2543760	2.4978040	-3.4240000	4.3019290	-4.0825600	1.3571300
		0.6	G_0	0.2932040	2.9237900	-4.9116200	15.281750	-17.518100	7.3210470	-0.8963700
			G_1	0.0226050	0.2234740	2.8903570	-3.8473800	6.1195550	-6.2676700	2.0574300
		0.8	G_0	0.3122360	2.4798240	-1.4430000	9.7299330	-3.1601800	-10.668500	6.2696700
			G_1	0.0313670	0.3920770	1.1522490	3.1467290	-1.8541600	-2.8779900	1.6154400
0.05	0.125	0.0	G_0	0.4065238	0.7772483	3.8861644	-12.573943	16.760207	-11.014593	2.8706957
			G_1	0.0320270	0.1825342	2.2670449	-2.7076615	1.2088194	-0.3777430	0.0763155
		0.2	G_0	0.4060953	1.1644812	1.6385609	-5.6458829	6.7482434	-4.1123639	1.0134083
			G_1	0.0467212	0.0112075	3.9795496	-9.2799411	13.005505	-10.210942	3.1584278
		0.4	G_0	0.4637710	1.6245020	0.4824070	-1.9574400	1.8537600	-1.0826800	0.2160800
			G_1	0.0559820	0.3663650	1.7297660	-0.8434800	-0.9789500	0.6140790	-0.0788100
		0.6	G_0	0.5549300	1.8055790	0.9321470	-0.3578800	-0.5307800	-0.8350500	0.6371000
			G_1	0.0767100	0.4575490	1.5658320	0.4829420	-2.5380200	1.0860880	-0.0526300
		0.8	G_0	0.6787290	1.7207550	3.5024190	-0.7988100	-2.6258600	-1.5230200	2.0523400
			G_1	0.1083820	0.4007860	2.5476580	-0.5622500	-0.9045000	-1.2453500	1.0278300
0.05	0.25	0.0	G_0	0.6152816	-0.3348694	6.2955620	-15.590618	19.299508	-12.488107	3.3010035
			G_1	0.0703566	0.2828152	1.4036169	-0.6511596	-1.2076596	1.0318656	-0.2423741
		0.2	G_0	0.6336200	-0.2241448	6.0145553	-15.177593	19.245817	-12.833947	3.4982967
			G_1	0.0857951	0.1479275	2.2281138	-3.0764070	2.3359025	-1.4641332	0.4360045
		0.4	G_0	0.7210140	0.2079740	3.8695370	-7.2148900	5.1589060	-1.0561100	-0.2846700
			G_1	0.1159200	0.2797270	1.8006830	-1.5262400	-0.0969100	0.2472200	-0.0259400
		0.6	G_0	0.9203340	-0.0146700	5.6709480	-9.9731200	6.6568860	-1.0393900	-0.4792100
			G_1	0.1729310	0.2700710	1.9969270	-1.2725900	-1.2286900	1.3793560	-0.4054400
		0.8	G_0	1.2153540	-0.4744400	9.0911160	-15.761900	10.345020	-2.2431500	-0.0760500
			G_1	0.2558270	0.1978370	2.4511390	-0.7909400	-4.1058800	4.5470700	-1.5064400

Table C.20
Influence Coefficients For A Circumferential Semi-Elliptical Surface Crack In A Sphere – Outside Surface

t/R_i	a/c	a/t	G_i	A_0	A_1	A_2	A_3	A_4	A_5	A_6
0.05	0.5	0.0	G_0	0.8776607	-0.6729719	3.7721411	-6.5209060	6.3377934	-3.7028038	0.9872447
			G_1	0.1277541	0.4368502	0.4904522	1.0427434	-2.9631236	2.0826525	-0.5184313
		0.2	G_0	0.8960862	-0.8110788	4.9563363	-10.433624	12.562793	-8.5356654	2.4644908
			G_1	0.1473772	0.2208319	1.8261603	-3.1801479	3.6631029	-3.0395570	1.0501901
		0.4	G_0	1.0097830	-0.6874900	3.2330140	-2.5544100	-2.5969400	4.7905890	-1.9612600
			G_1	0.1799730	0.3053860	1.2909090	-0.7459300	-1.1007400	1.2104980	-0.3861300
		0.6	G_0	1.2068900	-1.0128100	3.9596390	-2.3313200	-5.6495000	8.6313880	-3.4362100
			G_1	0.2394390	0.1895050	1.5832110	-1.0518100	-0.9937500	1.2574080	-0.4225600
		0.8	G_0	1.4575620	-1.3492700	4.9831730	-4.9881500	-1.4061800	4.6648170	-1.8907900
			G_1	0.3110330	0.0849830	1.9084200	-1.7754200	0.0212320	0.4653100	-0.1625300
0.05	1	0.0	G_0	1.1977992	-0.5244870	0.1498299	2.3284866	-5.1058499	4.3469049	-1.3487980
			G_1	0.1870117	0.6987352	0.1316900	0.7269255	-2.5259384	2.1756251	-0.6540458
		0.2	G_0	1.2317647	-1.2668535	5.2719942	-14.375480	22.713640	-18.634068	6.1234149
			G_1	0.2185075	0.1721631	3.3030368	-9.3243704	14.064573	-11.498670	3.7993477
		0.4	G_0	1.3280650	-1.0067200	1.8840770	-0.4718700	-3.3649000	4.5608980	-1.8016300
			G_1	0.2288730	0.5425330	0.7718760	-0.5272300	-1.2930700	1.6853270	-0.6337000
		0.6	G_0	1.4498840	-1.2061500	2.1605180	-1.0888200	-2.2230600	3.4522760	-1.3820700
			G_1	0.2647910	0.4868560	0.8402780	-0.6830900	-0.9740800	1.3518340	-0.5012700
		0.8	G_0	1.5986470	-1.4400100	2.2795920	-1.2360400	-1.6646800	2.6100510	-0.9686900
			G_1	0.3004770	0.4631460	0.7203190	-0.3884500	-1.1395400	1.2722420	-0.4237800
0.05	2	0.0	G_0	0.8150546	-0.5623828	1.4465771	-4.6778133	8.4192164	-7.9025932	2.9866351
			G_1	0.1359146	0.0702340	3.5558581	-11.034445	16.967724	-14.126991	4.8706612
		0.2	G_0	0.8261869	-0.9760945	3.9159333	-11.828914	19.270954	-16.254170	5.5646493
			G_1	0.1343782	0.0647996	3.2358020	-9.7518926	14.621269	-12.017040	4.1281758
		0.4	G_0	0.8404268	-0.3327374	-0.7716352	3.4961782	-6.3579059	5.0391431	-1.3957126
			G_1	0.1443070	0.0426802	3.3560498	-10.087084	15.121007	-12.419980	4.2634049
		0.6	G_0	0.8721260	-0.3774122	-0.8225068	3.8259304	-6.9952612	5.5798197	-1.5623326
			G_1	0.1521311	0.0386765	3.3191844	-9.9331613	14.859339	-12.233733	4.2193345
		0.8	G_0	0.9313062	-1.0113444	2.9977317	-8.1240616	12.547051	-10.425995	3.6200006
			G_1	0.1491534	0.2059118	2.1482404	-6.1418067	8.5120738	-6.9013685	2.4416991
0.1	0.03125	0.0	G_0	0.1965046	2.9373464	-5.2582823	7.4889153	-6.9282667	3.3673349	-0.6677966
			G_1	0.0051780	0.1750280	2.7718680	-4.6457154	4.6780502	-3.2768090	0.9840994
		0.2	G_0	0.2137025	1.4325421	4.1167565	-19.216759	33.344440	-26.945303	8.2464142
			G_1	0.0052475	0.1259041	2.6736467	-4.5590793	5.2686292	-4.1357154	1.3041985
		0.4	G_0	0.1979150	1.9340145	1.4781131	-9.2801878	19.142396	-17.924063	6.0232196
			G_1	0.0040005	0.1461665	2.5347969	-3.8021141	5.3553730	-5.2227792	1.8176331
		0.6	G_0	0.1860194	2.5432457	-2.3392398	6.5940454	-5.3262654	-0.8960931	1.3680747
			G_1	0.0020990	0.1774103	2.3394685	-2.7383263	5.4523448	-6.6666842	2.4847314
		0.8	G_0	0.1754774	2.9957430	-5.6326095	23.665960	-34.288886	21.521790	-5.5542454
			G_1	0.0002774	0.1921685	2.1887636	-1.5273413	5.0483569	-7.1411578	2.5874760
0.1	0.0625	0.0	G_0	0.2695332	2.1626001	-1.6551569	-1.2970208	4.5604304	-4.3163876	1.4010655
			G_1	0.0138667	0.1827458	2.5749608	-3.9044679	3.3556301	-2.1772209	0.6420134
		0.2	G_0	0.2890499	0.9219896	6.0096997	-21.937629	33.946446	-25.339866	7.3108326
			G_1	0.0147811	0.1328586	2.5982425	-3.8907259	3.5562726	-2.4471215	0.7260215
		0.4	G_0	0.2873059	1.3052621	4.6012131	-17.084571	28.947144	-23.791473	7.3353113
			G_1	0.0155072	0.1448568	2.6766011	-3.9466405	4.8914663	-4.4048681	1.4680245
		0.6	G_0	0.2809744	1.7401393	2.2988686	-7.7235391	17.385265	-18.152842	6.3604835
			G_1	0.0126043	0.1465942	2.7615205	-4.0810736	7.2809390	-7.7678947	2.7177283
		0.8	G_0	0.2695106	1.9636065	1.2283002	-0.8213441	9.9420209	-15.935439	6.3440991
			G_1	0.0084372	0.1053328	3.0865264	-5.1047572	11.797139	-12.904792	4.3973960

Table C.20
Influence Coefficients For A Circumferential Semi-Elliptical Surface Crack In A Sphere – Outside Surface

t/R_i	a/c	a/t	G_i	A_0	A_1	A_2	A_3	A_4	A_5	A_6
0.1	0.125	0.0	G_0	0.4065238	0.7772483	3.8861644	-12.573943	16.760207	-11.014593	2.8706957
			G_1	0.0320270	0.1825342	2.2670449	-2.7076615	1.2088194	-0.3777430	0.0763155
		0.2	G_0	0.4043512	1.1681039	1.6434561	-5.5687394	6.5838903	-3.9846901	0.9756456
			G_1	0.0458647	0.0143495	3.9367213	-9.0232258	12.498287	-9.7735425	3.0170109
		0.4	G_0	0.4325510	1.7019350	-0.0540700	-0.2710400	-0.2974000	0.1894200	-0.0856700
			G_1	0.0452780	0.3334410	1.8205130	-1.1453300	-0.2249300	-0.0767900	0.1196500
		0.6	G_0	0.4662460	1.8462810	0.1188260	1.8951460	-2.2287300	-0.6467800	0.7465300
			G_1	0.0515130	0.3627920	1.9453630	-0.8198300	0.0320510	-1.0330000	0.5409500
		0.8	G_0	0.5004200	1.5655730	2.1869090	2.2008540	-2.1879200	-4.1459300	2.8744500
			G_1	0.0509260	0.3210580	2.0764570	0.5519790	-0.7578200	-2.1663300	1.3044300
0.1	0.25	0.0	G_0	0.6152816	-0.3348694	6.2955620	-15.590618	19.299508	-12.488107	3.3010035
			G_1	0.0703566	0.2828152	1.4036169	-0.6511596	-1.2076596	1.0318656	-0.2423741
		0.2	G_0	0.6350228	-0.2119641	5.9568028	-14.916184	18.776502	-12.456735	3.3832587
			G_1	0.0856903	0.1511286	2.2237294	-3.0557324	2.3214261	-1.4731351	0.4439542
		0.4	G_0	0.6987930	0.3447790	3.4424380	-6.0517700	3.6043320	-0.0452500	-0.5532900
			G_1	0.1077030	0.2651880	2.0013730	-2.2123900	1.2433410	-0.9817400	0.3852200
		0.6	G_0	0.8589440	0.2633150	4.5097920	-6.4207300	1.9301370	1.8839450	-1.2009200
			G_1	0.1525220	0.2760100	2.0850880	-1.4562900	-0.6710600	0.7275950	-0.1720400
		0.8	G_0	1.0845520	-0.2782000	9.0855350	-15.543200	12.287140	-5.7702200	1.4420300
			G_1	0.2113300	0.2542150	2.3848150	-0.4194600	-3.8790000	3.6488360	-1.0778800
0.1	0.5	0.0	G_0	0.8776607	-0.6729719	3.7721411	-6.5209060	6.3377934	-3.7028038	0.9872447
			G_1	0.1277541	0.4368502	0.4904522	1.0427434	-2.9631236	2.0826525	-0.5184313
		0.2	G_0	0.9089240	-0.9470277	5.8122694	-12.939505	16.332513	-11.352074	3.2913303
			G_1	0.1487903	0.2149757	1.8829219	-3.3561626	3.9304025	-3.2399641	1.1093948
		0.4	G_0	1.0029850	-0.5759600	2.9821620	-1.8309800	-3.8190200	5.7887660	-2.2760500
			G_1	0.1771680	0.3219970	1.2553580	-0.4865100	-1.6480100	1.6936600	-0.5453300
		0.6	G_0	1.2064040	-0.9321800	4.1240170	-2.7832100	-5.1249600	8.3127460	-3.3621500
			G_1	0.2383680	0.2030160	1.6282540	-0.9652900	-1.3505200	1.6296530	-0.5561200
		0.8	G_0	1.4594660	-1.1444900	4.7732460	-4.1451600	-2.9602200	5.8139350	-2.1977000
			G_1	0.3122420	0.1024290	2.0857110	-2.0834200	0.2839790	0.3119550	-0.1176700
0.1	1	0.0	G_0	1.1977992	-0.5244870	0.1498299	2.3284866	-5.1058499	4.3469049	-1.3487980
			G_1	0.1870117	0.6987352	0.1316900	0.7269255	-2.5259384	2.1756251	-0.6540458
		0.2	G_0	1.2380657	-1.2701768	5.2914711	-14.476169	22.897148	-18.796156	6.1822911
			G_1	0.2194837	0.1768071	3.2996872	-9.3618333	14.167089	-11.612517	3.8461643
		0.4	G_0	1.3427420	-1.0146600	2.0436160	-0.7478200	-3.1748800	4.5270860	-1.8145100
			G_1	0.2328790	0.5209850	0.9293030	-0.9415700	-0.6268200	1.1262530	-0.4527700
		0.6	G_0	1.4757130	-1.2047200	2.2963490	-1.2790300	-2.2758700	3.6916080	-1.4981600
			G_1	0.2721640	0.4674680	0.9709180	-0.9130500	-0.7725000	1.2665250	-0.4901300
		0.8	G_0	1.6389960	-1.3600900	2.0178020	-0.3744100	-3.2533700	3.9560490	-1.3889300
			G_1	0.3141930	0.4470660	0.8433550	-0.6042100	-0.9836700	1.2289950	-0.4219000
0.1	2	0.0	G_0	0.8150546	-0.5623828	1.4465771	-4.6778133	8.4192164	-7.9025932	2.9866351
			G_1	0.1359146	0.0702340	3.5558581	-11.034445	16.967724	-14.126991	4.8706612
		0.2	G_0	0.8297052	-0.9932212	3.9945197	-12.078107	19.703504	-16.637981	5.6988875
			G_1	0.1348860	0.0624776	3.2528748	-9.8245409	14.775725	-12.179089	4.1921695
		0.4	G_0	0.8458749	-0.3594010	-0.6577823	3.1889098	-5.9152513	4.6977129	-1.2859128
			G_1	0.1452270	0.0359473	3.4048512	-10.271104	15.480348	-12.777595	4.4006315
		0.6	G_0	0.8760954	-0.3601463	-0.9648929	4.2085152	-7.5094681	5.8890448	-1.6240482
			G_1	0.1537017	0.0238822	3.4227047	-10.295342	15.522205	-12.858919	4.4503340
		0.8	G_0	0.9390036	-1.0262914	3.0604601	-8.3936234	13.086182	-10.973664	3.8361075
			G_1	0.1509371	0.1981818	2.1987908	-6.3405515	8.9157835	-7.3314460	2.6167416

Table C.20
Influence Coefficients For A Circumferential Semi-Elliptical Surface Crack In A Sphere – Outside Surface

t/R_i	a/c	a/t	G_i	A_0	A_1	A_2	A_3	A_4	A_5	A_6
0.2	0.0625	0.0	G_0	0.2695332	2.1626001	-1.6551569	-1.2970208	4.5604304	-4.3163876	1.4010655
			G_1	0.0138667	0.1827458	2.5749608	-3.9044679	3.3556301	-2.1772209	0.6420134
		0.2	G_0	0.2846891	0.9259643	5.9103335	-21.460325	33.126452	-24.702238	7.1191407
			G_1	0.0133598	0.1259805	2.6073541	-3.8908359	3.6033838	-2.5215410	0.7547302
		0.4	G_0	0.2766488	1.6110281	2.3516100	-10.341186	18.921547	-16.540412	5.3013624
			G_1	0.0118367	0.1575003	2.5745703	-3.6857687	4.6301169	-4.2961611	1.4533059
		0.6	G_0	0.2689968	1.9034093	0.6472840	-2.3491353	8.1436603	-10.667333	4.1167079
			G_1	0.0087301	0.1497819	2.6774334	-3.9694008	7.0437495	-7.5002452	2.6245395
		0.8	G_0	0.2554783	2.0468462	-0.0822131	3.4213664	0.6981926	-6.5421021	2.9676454
			G_1	0.0045719	0.1110321	2.9583143	-5.0077730	11.197636	-11.755968	3.8272846
0.2	0.125	0.0	G_0	0.4065238	0.7772483	3.8861644	-12.573943	16.760207	-11.014593	2.8706957
			G_1	0.0320270	0.1825342	2.2670449	-2.7076615	1.2088194	-0.3777430	0.0763155
		0.2	G_0	0.4014872	1.1741907	1.5646730	-5.0362060	5.5615994	-3.1453683	0.7160267
			G_1	0.0443453	0.0224028	3.8206837	-8.4139316	11.339663	-8.7979577	2.7081857
		0.4	G_0	0.3823340	1.7459190	-0.0828300	-0.5504300	1.0904920	-1.5202200	0.5548400
			G_1	0.0316780	0.3226130	1.5266340	0.6253550	-3.9114300	3.3310290	-1.0507400
		0.6	G_0	0.3795700	1.9588500	-1.1419500	4.1575230	-2.7423400	-1.7343300	1.2469000
			G_1	0.0220180	0.4043780	1.1228810	1.4114680	-2.2682000	0.0447910	0.3250500
		0.8	G_0	0.3743020	1.7350230	-0.3704600	7.0142130	-6.6994400	0.1724090	0.6283300
			G_1	0.0075720	0.4255330	0.6869830	3.4008880	-3.5933800	0.2812360	0.1435500
0.2	0.25	0.0	G_0	0.6152816	-0.3348694	6.2955620	-15.590618	19.299508	-12.488107	3.3010035
			G_1	0.0703566	0.2828152	1.4036169	-0.6511596	-1.2076596	1.0318656	-0.2423741
		0.2	G_0	0.6359717	-0.1946895	5.9248092	-14.774025	18.556654	-12.309769	3.3437575
			G_1	0.0852188	0.1622272	2.1678098	-2.8437025	1.9809989	-1.2197689	0.3704304
		0.4	G_0	0.6548070	0.4906810	3.4735670	-6.8787000	5.9955580	-2.6086300	0.3784600
			G_1	0.0918840	0.3012510	1.8673950	-1.7219200	0.7157350	-0.7857800	0.3675700
		0.6	G_0	0.7367620	0.5329010	4.0652760	-5.6789800	2.7020960	-0.0771700	-0.3437600
			G_1	0.1127050	0.3293460	1.9238500	-0.8550500	-1.1357300	0.7270230	-0.1169400
		0.8	G_0	0.8235610	0.0496050	8.0660590	-12.067200	10.889570	-7.8621300	2.6614300
			G_1	0.1336310	0.1468590	3.2572260	-2.8593100	1.4996830	-1.7545100	0.7932100
0.2	0.5	0.0	G_0	0.8776607	-0.6729719	3.7721411	-6.5209060	6.3377934	-3.7028038	0.9872447
			G_1	0.1277541	0.4368502	0.4904522	1.0427434	-2.9631236	2.0826525	-0.5184313
		0.2	G_0	0.9111832	-0.8704236	5.4253176	-11.903328	14.866815	-10.312652	3.0008184
			G_1	0.1497822	0.2268838	1.8393043	-3.2327001	3.7365317	-3.0918831	1.0662371
		0.4	G_0	0.9872480	-0.4453000	3.1245470	-2.4761100	-2.8171500	5.0194640	-2.0491500
			G_1	0.1679190	0.3768860	1.1273070	-0.0344600	-2.3343800	2.1644560	-0.6727400
		0.6	G_0	1.1816730	-0.7620000	4.3929080	-3.4235600	-4.4982000	7.9816110	-3.3045700
			G_1	0.2253530	0.2659600	1.5824750	-0.6755000	-1.8341300	1.9429500	-0.6350900
		0.8	G_0	1.4137870	-0.9166800	5.7849410	-6.8719200	1.0910810	2.4108090	-1.0690500
			G_1	0.2953760	0.1751530	2.2894570	-2.3905100	0.6532250	-0.1021700	0.0564000
0.2	1	0.0	G_0	1.1977992	-0.5244870	0.1498299	2.3284866	-5.1058499	4.3469049	-1.3487980
			G_1	0.1870117	0.6987352	0.1316900	0.7269255	-2.5259384	2.1756251	-0.6540458
		0.2	G_0	1.2459636	-1.2684630	5.3227950	-14.672901	23.252766	-19.096733	6.2858919
			G_1	0.2223172	0.1610842	3.4145518	-9.6936477	14.621415	-11.929534	3.9388987
		0.4	G_0	1.3688960	-1.0440800	2.5361260	-1.8901400	-1.7813900	3.6257870	-1.5804900
			G_1	0.2392750	0.5323640	0.8557990	-0.4613200	-1.4868900	1.7868370	-0.6475000
		0.6	G_0	1.5187010	-1.1782100	2.5603360	-1.6965000	-2.2170100	3.9633910	-1.6481800
			G_1	0.2836700	0.4844930	0.9316080	-0.5572500	-1.4804500	1.8386220	-0.6623700
		0.8	G_0	1.7061150	-1.2868800	2.2454580	-0.7754000	-3.3317500	4.3578560	-1.5589200
			G_1	0.3325930	0.4674090	0.8587280	-0.3981100	-1.5912000	1.7969810	-0.6017500

Table C.20
Influence Coefficients For A Circumferential Semi-Elliptical Surface Crack In A Sphere – Outside Surface

t/R_i	a/c	a/t	G_i	A_0	A_1	A_2	A_3	A_4	A_5	A_6
0.2	2	0.0	G_0	0.8150546	-0.5623828	1.4465771	-4.6778133	8.4192164	-7.9025932	2.9866351
			G_1	0.1359146	0.0702340	3.5558581	-11.034445	16.967724	-14.126991	4.8706612
		0.2	G_0	0.8328850	-0.9992018	4.0086624	-12.151398	19.883977	-16.849142	5.7890893
			G_1	0.1355167	0.0583355	3.2799736	-9.9261053	14.984541	-12.404007	4.2843881
		0.4	G_0	0.8514779	-0.3260458	-0.8924282	3.7884421	-6.6921368	5.1564980	-1.3771960
			G_1	0.1471213	0.0328202	3.4336651	-10.388789	15.742019	-13.094220	4.5426268
		0.6	G_0	0.8852158	-0.3912028	-0.7878178	3.5577693	-6.3491249	4.8462272	-1.2556058
			G_1	0.1565145	-0.0057907	3.6253156	-10.968973	16.711109	-13.958826	4.8532715
		0.8	G_0	0.9511352	-1.0642903	3.3097711	-9.3699961	14.892041	-12.642730	4.4397097
			G_1	0.1534693	0.1916966	2.2421706	-6.5009981	9.2612620	-7.7751453	2.8260643
0.33333	0.125	0.0	G_0	0.4065238	0.7772483	3.8861644	-12.573943	16.760207	-11.014593	2.8706957
			G_1	0.0320270	0.1825342	2.2670449	-2.7076615	1.2088194	-0.3777430	0.0763155
		0.2	G_0	0.3999453	1.1378099	1.8837409	-5.9120772	6.9147328	-4.2124418	1.0410171
			G_1	0.0432523	0.0215395	3.7904607	-8.1289447	10.763741	-8.3129980	2.5551138
		0.4	G_0	0.4296335	1.0041041	3.8959378	-12.057383	18.412611	-14.408772	4.3022733
			G_1	0.0397925	0.1879821	2.4341024	-2.9044672	2.6267076	-2.3395968	0.8089253
		0.6	G_0	0.4270492	0.9372419	4.6774304	-12.816229	22.136585	-19.630950	6.3060701
			G_1	0.0324591	0.1435626	2.7929483	-3.9397629	5.9961920	-6.0796339	2.0851337
		0.8	G_0	0.3995502	0.7593599	5.9836408	-15.132435	30.500061	-29.316818	9.5533887
			G_1	0.0161665	0.0491796	3.4935697	-6.7094610	13.737725	-13.713995	4.4513954
0.33333	0.25	0.0	G_0	0.6152816	-0.3348694	6.2955620	-15.590618	19.299508	-12.488107	3.3010035
			G_1	0.0703566	0.2828152	1.4036169	-0.6511596	-1.2076596	1.0318656	-0.2423741
		0.2	G_0	0.6381645	-0.2547494	6.5598868	-16.785781	21.683987	-14.680561	4.0404689
			G_1	0.0852630	0.1512639	2.2794720	-3.1334300	2.3872418	-1.5138985	0.4543945
		0.4	G_0	0.7229440	-0.1327500	5.9623940	-13.044300	14.489110	-8.6605800	2.1226270
			G_1	0.1014390	0.3149520	1.5304960	-0.5374400	-1.5532000	1.2896360	-0.3327000
		0.6	G_0	0.8056090	-0.5534700	10.013880	-23.141800	29.129710	-19.917800	5.5198320
			G_1	0.1214770	0.2249700	2.3876170	-2.0864300	0.3425960	-0.1442200	0.1042080
		0.8	G_0	0.8320670	0.2103690	5.3637430	-5.4363900	4.4211560	-5.5005100	2.5690920
			G_1	0.1229720	0.4233740	1.3543830	1.8448010	-4.2606800	1.6752550	0.0117770
0.33333	0.5	0.0	G_0	0.8776607	-0.6729719	3.7721411	-6.5209060	6.3377934	-3.7028038	0.9872447
			G_1	0.1277541	0.4368502	0.4904522	1.0427434	-2.9631236	2.0826525	-0.5184313
		0.2	G_0	0.9167822	-0.8329923	5.2670130	-11.483170	14.269534	-9.8883620	2.8823826
			G_1	0.1519046	0.2243972	1.8954464	-3.4222778	4.0428864	-3.3359097	1.1424959
		0.4	G_0	1.0084180	-0.2094500	0.8034380	3.1162370	-9.2606100	8.5893620	-2.7802200
			G_1	0.1751170	0.4253180	0.8135250	0.2323860	-2.1952900	1.8341110	-0.5239700
		0.6	G_0	1.2023400	-0.8461300	4.4196170	-5.8060400	2.2669380	0.9670340	-0.7423700
			G_1	0.2222170	0.4177690	0.6748910	1.2429340	-4.1524200	3.4107350	-0.9888200
		0.8	G_0	1.3694060	-0.2562400	0.7922660	6.8643940	-18.758400	17.024640	-5.3342900
			G_1	0.2738310	0.5220650	0.0389670	3.9695460	-9.2012700	7.5724070	-2.2613100
0.33333	1	0.0	G_0	1.1977992	-0.5244870	0.1498299	2.3284866	-5.1058499	4.3469049	-1.3487980
			G_1	0.1870117	0.6987352	0.1316900	0.7269255	-2.5259384	2.1756251	-0.6540458
		0.2	G_0	1.2554619	-1.2705280	5.3824723	-14.954811	23.731001	-19.481595	6.4118814
			G_1	0.2245665	0.1648418	3.4055159	-9.6584362	14.530510	-11.851660	3.9206556
		0.4	G_0	1.3026300	-0.1578200	-2.5260000	10.182540	-17.165300	13.533850	-4.0656700
			G_1	0.2187120	0.7561160	-0.2289500	1.9239160	-4.7376100	4.0820740	-1.2574500
		0.6	G_0	1.4126140	-0.0936900	-3.3743500	12.583770	-20.843800	16.338280	-4.8785500
			G_1	0.2479600	0.8009420	-0.6180700	3.1142740	-6.6660300	5.5667210	-1.6809600
		0.8	G_0	1.5053276	-0.4119768	0.8465948	-6.1807564	14.714118	-14.632260	5.3209771
			G_1	0.3021350	0.4630840	1.5275970	-3.6089400	4.0734720	-3.0503100	1.0770470

Table C.20
Influence Coefficients For A Circumferential Semi-Elliptical Surface Crack In A Sphere – Outside Surface

t/R_i	a/c	a/t	G_i	A_0	A_1	A_2	A_3	A_4	A_5	A_6
0.33333	2	0.0	G_0	0.8150546	-0.5623828	1.4465771	-4.6778133	8.4192164	-7.9025932	2.9866351
			G_1	0.1359146	0.0702340	3.5558581	-11.034445	16.967724	-14.126991	4.8706612
		0.2	G_0	0.8376294	-1.0150330	4.0796464	-12.398254	20.340898	-17.278075	5.9462878
			G_1	0.1365429	0.0531598	3.3094628	-10.022244	15.161783	-12.584481	4.3568636
		0.4	G_0	0.8578558	-0.3356978	-0.8868820	3.7430432	-6.5595632	4.9671659	-1.2850147
			G_1	0.1173823	0.5937733	-0.0584056	0.7822906	-2.9803324	2.5765209	-0.6281954
		0.6	G_0	0.8935993	-0.4091679	-0.6966760	3.1316414	-5.4783764	3.9792295	-0.9268708
			G_1	0.1252608	0.5771663	-0.0010861	0.6133328	-2.6701696	2.2230706	-0.4717927
		0.8	G_0	0.9611381	-1.0777619	3.4192395	-10.046519	16.437777	-14.263452	5.0697660
			G_1	0.1520218	0.1854095	2.5856063	-7.9036293	11.911110	-10.256157	3.7281358

Notes:

1. Interpolation of the influence coefficients, G_i, may be used for intermediate values of t/R_i, a/c, and a/t.

2. The value of the influence coefficients at the surface point of the crack defined by $\varphi = 0^0$ are equal to: $G_i = A_0$.

3. The value of the influence coefficients at the deepest point of the crack defined by $\varphi = 90^0$ are equal to: $G_i = \sum_{n=0}^{6} A_n$.

Table C.21
Coefficients For One And Two Cracks At The Toe Of A Fillet Weld Of A Ring Stiffened Cylinder Subject To Internal Pressure

R_i/t	A_r/t	a/t	M_p^{1c}	M_p^{2c}
10	1	0.1	11.106	10.707
		0.2	10.428	9.564
		0.4	11.463	9.438
		0.6	13.562	10.255
		0.8	16.369	12.590
	2	0.1	12.717	12.261
		0.2	11.659	10.689
		0.4	12.328	10.134
		0.6	14.174	10.736
		0.8	16.691	12.900
	4	0.1	15.156	14.644
		0.2	13.452	12.425
		0.4	13.474	11.326
		0.6	14.740	11.640
		0.8	16.789	13.533
	8	0.1	16.514	15.941
		0.2	14.560	13.486
		0.4	14.041	12.001
		0.6	14.854	12.083
		0.8	16.423	13.613
	16	0.1	17.276	16.862
		0.2	14.826	14.080
		0.4	13.902	12.488
		0.6	14.359	12.526
		0.8	15.789	13.970
	32	0.1	17.649	17.440
		0.2	14.860	14.532
		0.4	13.486	12.956
		0.6	13.607	12.938
		0.8	14.808	14.193
20	1	0.1	19.269	18.769
		0.2	18.759	17.561
		0.4	22.239	18.858
		0.6	28.552	21.683
		0.8	36.175	26.663
	2	0.1	22.159	21.552
		0.2	21.068	19.680
		0.4	24.104	20.277
		0.6	30.009	22.710
		0.8	36.920	27.288
	4	0.1	27.603	26.846
		0.2	25.406	23.693
		0.4	27.389	23.099
		0.6	32.190	24.732
		0.8	37.716	28.528
	8	0.1	31.262	30.328
		0.2	28.564	26.601
		0.4	29.584	25.029
		0.6	33.343	25.978
		0.8	37.377	27.814

Table C.21
Coefficients For One And Two Cracks At The Toe Of A Fillet Weld Of A Ring Stiffened Cylinder Subject To Internal Pressure

R_i/t	A_r/t	a/t	M_p^{1c}	M_p^{2c}
20	16	0.1	34.441	33.532
		0.2	30.598	28.778
		0.4	30.707	26.632
		0.6	33.518	27.214
		0.8	36.815	29.750
	32	0.1	36.535	35.879
		0.2	31.740	30.526
		0.4	30.505	28.082
		0.6	31.891	25.247
		0.8	34.014	30.330
30	1	0.1	27.137	26.548
		0.2	26.846	25.383
		0.4	33.060	28.564
		0.6	44.379	34.219
		0.8	58.493	42.370
	2	0.1	30.669	30.098
		0.2	30.063	28.385
		0.4	35.781	30.696
		0.6	46.776	35.734
		0.8	59.767	43.291
	4	0.1	38.831	37.948
		0.2	36.414	34.273
		0.4	40.976	34.996
		0.6	50.576	38.833
		0.8	61.329	45.094
	8	0.1	44.710	43.574
		0.2	41.641	39.072
		0.4	44.887	38.289
		0.6	52.987	40.955
		0.8	61.249	45.531
	16	0.1	50.589	49.352
		0.2	45.798	43.140
		0.4	47.902	41.291
		0.6	54.624	43.252
		0.8	61.231	47.163
	32	0.1	54.929	53.818
		0.2	48.707	46.566
		0.4	48.797	44.041
		0.6	53.038	45.271
		0.8	56.949	48.127
50	1	0.1	42.373	41.659
		0.2	42.679	40.812
		0.4	54.728	48.412
		0.6	77.789	61.044
		0.8	108.432	77.271
	2	0.1	47.993	47.208
		0.2	47.448	45.328
		0.4	59.055	51.864
		0.6	81.723	63.725
		0.8	111.144	78.974

Table C.21
Coefficients For One And Two Cracks At The Toe Of A Fillet Weld Of A Ring Stiffened Cylinder Subject To Internal Pressure

R_i/t	A_r/t	a/t	M_p^{1c}	M_p^{2c}
50	4	0.1	60.278	59.142
		0.2	57.556	54.808
		0.4	67.696	59.067
		0.6	88.740	68.963
		0.8	113.738	81.561
	8	0.1	70.395	69.008
		0.2	66.013	62.587
		0.4	75.063	65.135
		0.6	94.910	73.402
		0.8	116.860	83.943
	16	0.1	81.194	79.428
		0.2	74.987	71.097
		0.4	82.216	71.569
		0.6	99.803	78.017
		0.8	117.931	86.566
	32	0.1	90.505	88.764
		0.2	82.141	78.609
		0.4	86.581	77.296
		0.6	99.968	82.189
		0.8	112.846	89.028
100	1	0.1	79.179	78.162
		0.2	81.194	78.532
		0.4	108.832	99.108
		0.6	164.902	134.456
		0.8	252.502	178.701
	2	0.1	88.154	87.030
		0.2	88.966	86.077
		0.4	116.236	105.308
		0.6	173.060	140.138
		0.8	259.063	182.328
	4	0.1	108.924	107.511
		0.2	106.530	102.873
		0.4	132.464	119.117
		0.6	187.884	150.595
		0.8	264.764	187.021
	8	0.1	128.327	126.560
		0.2	123.176	118.394
		0.4	148.108	132.338
		0.6	203.026	161.154
		0.8	274.309	192.685
	16	0.1	151.741	149.243
		0.2	143.372	137.502
		0.4	166.274	147.919
		0.6	218.889	173.102
		0.8	282.962	199.688
	32	0.1	174.828	171.926
		0.2	162.498	156.236
		0.4	182.044	163.057
		0.6	228.983	184.588
		0.8	280.464	205.977

Table C.21
Coefficients For One And Two Cracks At The Toe Of A Fillet Weld Of A Ring Stiffened Cylinder Subject To Internal Pressure

R_i/t	A_r/t	a/t	M_p^{1c}	M_p^{2c}
200	1	0.1	150.420	148.849
		0.2	156.308	152.523
		0.4	216.593	201.874
		0.6	347.722	293.750
		0.8	587.259	419.471
	2	0.1	164.425	162.944
		0.2	168.545	164.634
		0.4	228.814	212.712
		0.6	361.852	304.020
		0.8	601.956	427.103
	4	0.1	198.318	196.602
		0.2	197.859	193.131
		0.4	257.233	237.679
		0.6	390.600	325.449
		0.8	619.002	437.690
	8	0.1	232.986	230.791
		0.2	228.011	221.767
		0.4	287.511	263.983
		0.6	423.357	348.986
		0.8	640.233	450.670
	16	0.1	279.311	276.031
		0.2	269.046	263.426
		0.4	326.872	298.360
		0.6	463.529	378.446
		0.8	670.028	468.110
	32	0.1	330.530	326.493
		0.2	313.114	303.480
		0.4	369.008	335.703
		0.6	502.465	409.708
		0.8	685.282	485.817
300	1	0.1	219.626	217.842
		0.2	229.605	224.306
		0.4	322.659	304.104
		0.6	532.144	460.036
		0.8	955.006	691.338
	2	0.1	238.716	237.289
		0.2	246.132	241.842
		0.4	340.143	320.429
		0.6	553.121	475.768
		0.8	976.452	703.323
	4	0.1	282.843	281.077
		0.2	284.925	279.572
		0.4	378.344	354.437
		0.6	594.759	507.204
		0.8	1006.246	720.786
	8	0.1	330.278	327.755
		0..2	326.495	319.091
		0.4	421.111	392.473
		0.6	644.305	543.771
		0.8	1047.281	743.266

Table C.21
Coefficients For One And Two Cracks At The Toe Of A Fillet Weld Of A Ring Stiffened Cylinder Subject To Internal Pressure

R_i/t	A_r/t	a/t	M_p^{1c}	M_p^{2c}
300	16	0.1	397.141	393.356
		0.2	386.084	376.539
		0.4	480.278	444.954
		0.6	708.066	591.154
		0.8	1098.128	772.214
	32	0.1	475.863	471.069
		0.2	454.952	443.355
		0.4	547.772	505.320
		0.6	778.832	645.850
		0.8	1140.055	804.194

Note: Interpolation may be used for intermediate values of R_i/t, A_r/t, and a/t.

Table C.22
Parameters for Mk-Factors – Surface Crack At A Tee Joint, Semi-Elliptical Shape, Through-Wall Membrane and Bending Stress

Function	Parameter	Deepest point of the crack (Point B)		Surface point of the crack (Point A)	
		M_{km}	M_{kb}	M_{km}	M_{kb}
F_1	P_1	1.04424	1.19137	0.47722	0.52011
	P_2	-0.09627	-0.14198	-0.46228	-0.36027
	P_3	0.03790	0.038086	0.19046	0.12547
	P_4	0.54616	0.86676	0.39777	0.54940
	P_5	-0.12508	-0.24951	0.22176	-0.098759
	P_6	-2.43313	-2.03967	-3.25447	-2.80066
	P_7	-0.07251	0.20231	-0.63489	-0.71090
	P_8	0.18353	0.40094	2.85835	1.50561
	P_9	0.87051	0.94855	1.95878	1.86540
F_2	P_{10}	0.99924	1.00095	0.40489	0.96775
	P_{11}	0.04125	0.10217	0.34526	-0.21496
	P_{12}	-0.75765	-0.95780	-0.29917	-0.82377
	P_{13}	-0.000426	-0.075004	-0.77810	-0.25998
F_3	P_{14}	-0.05692	-0.68779	41.72046	-8.77203
	P_{15}	1.19362	-8.67636	-78.8175	24.27778
	P_{16}	-1.43325	16.16166	34.10390	-28.1240
	P_{17}	0.61335	-8.14948	2.73640	11.4415
	P_{18}	1.05721	-0.152293	0.030034	2.64087
	P_{19}	-2.4052	-0.148843	-0.13126	-10.4940
	P_{20}	2.61759	1.77150	0.11538	12.8098
	P_{21}	-0.98207	-1.27776	0.040551	-5.98773
F_4	P_{22}	1.06748	1.78291	0.53107	0.78365
	P_{23}	7.74090	8.37239	0.26223	-0.24718
	P_{24}	0.47714	0.41021	-0.24730	1.55530
	P_{25}	-0.21542	-0.95097	12.2781	0.049054
	P_{26}	-1.08081	1.64652	-0.059328	0.040332
	P_{27}	-0.002871	3.52508	-0.002740	-0.000146
	P_{28}	0.89122	31.9326	1.04175	-2.41618
	P_{29}	0.008454	0.000011	0.050788	0.002455
	P_{30}	0.14155	0.010084	-0.039354	0.013053
	P_{31}	0.48533	0.93093	1.39315	0.57026
	P_{32}	-2.12357	-2.52809	-10.8442	0.40172
	P_{33}	---	---	16.6945	0.35095
	P_{34}	---	---	0.12542	0.55589
	P_{35}	---	---	-1.39604	0.047656
	P_{36}	---	---	1.21456	0.042067
	P_{37}	---	---	0.69694	1.07535
	P_{38}	---	---	0.42960	-0.48462

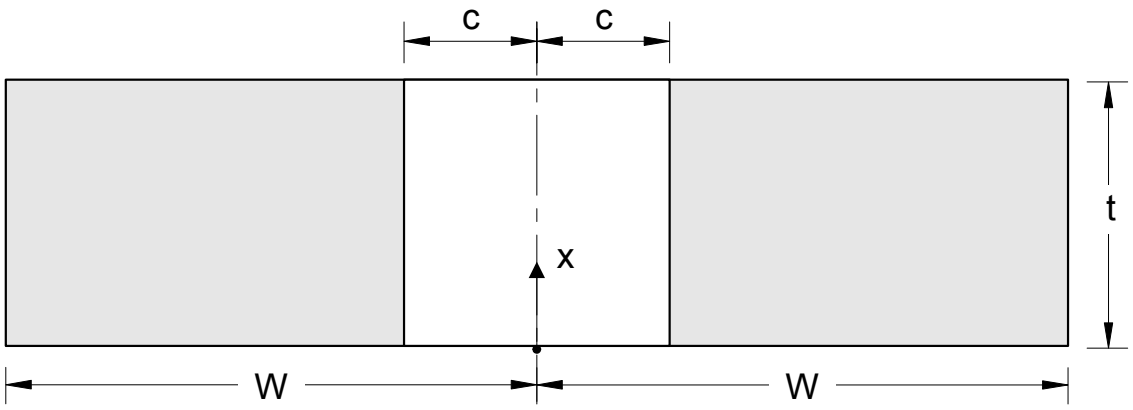

Figure C.1
Plate – Through Wall Crack

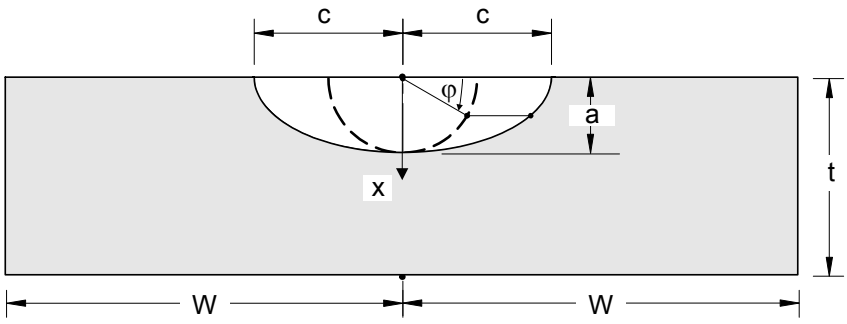

(a) Finite Length Surface Crack

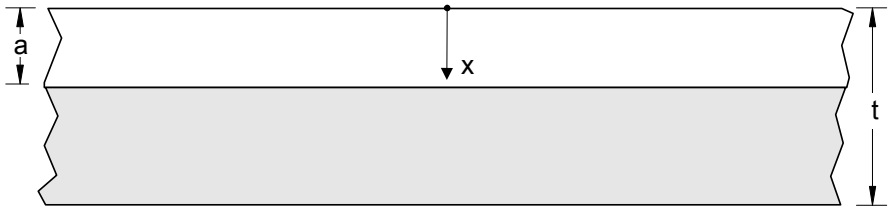

(b) Infinitely Long Surface Crack (c>>a)

Figure C.2
Plate – Surface Crack, Semi-Elliptical Shape

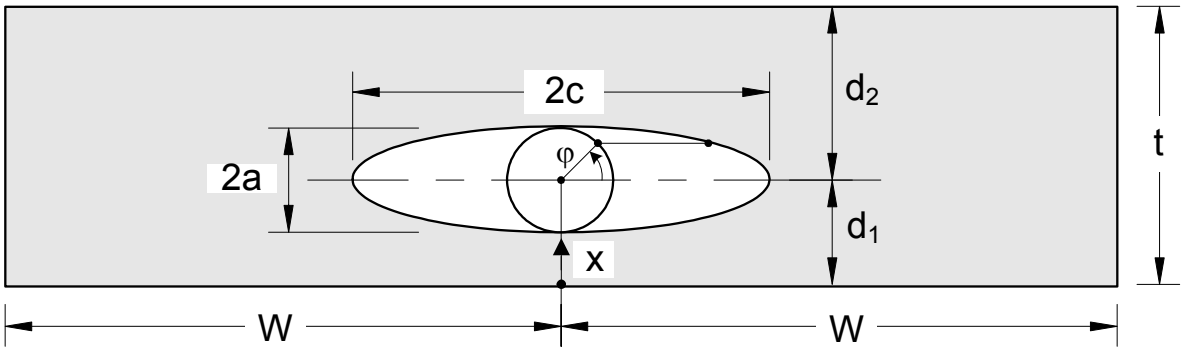

(a) Finite Length Embedded Crack

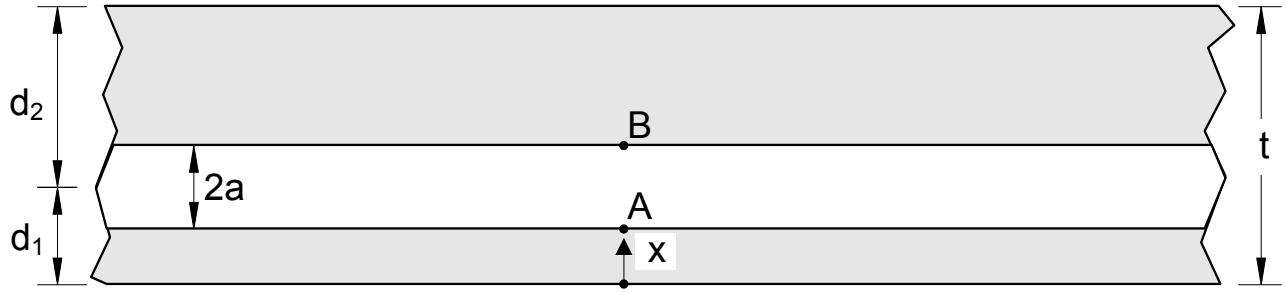

(b) Infinitely Long Embedded Crack (c>>a)

Figure C.3
Plate – Embedded Crack, Elliptical Shape

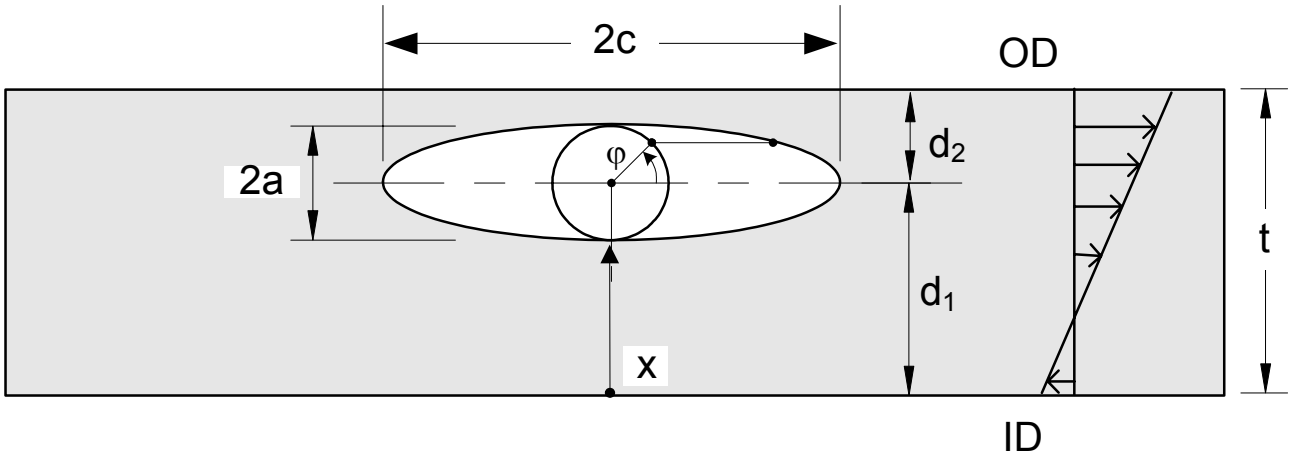

a) Actual Embedded Flaw ($d_1/t>0.5$)

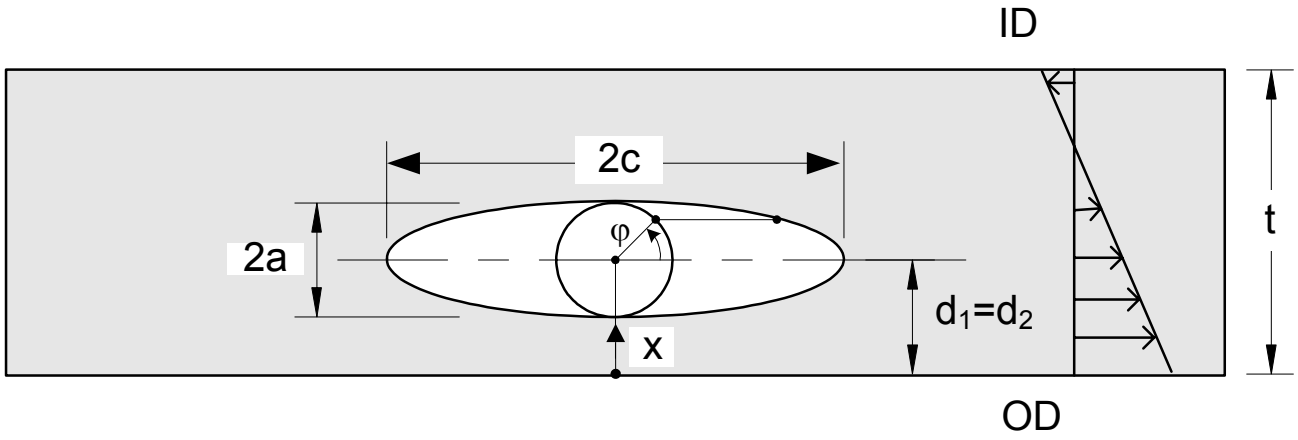

b) Re-characterization of an embedded flaw with reversed stress field

Figure C.4
Plate – Embedded Crack Re-characterization

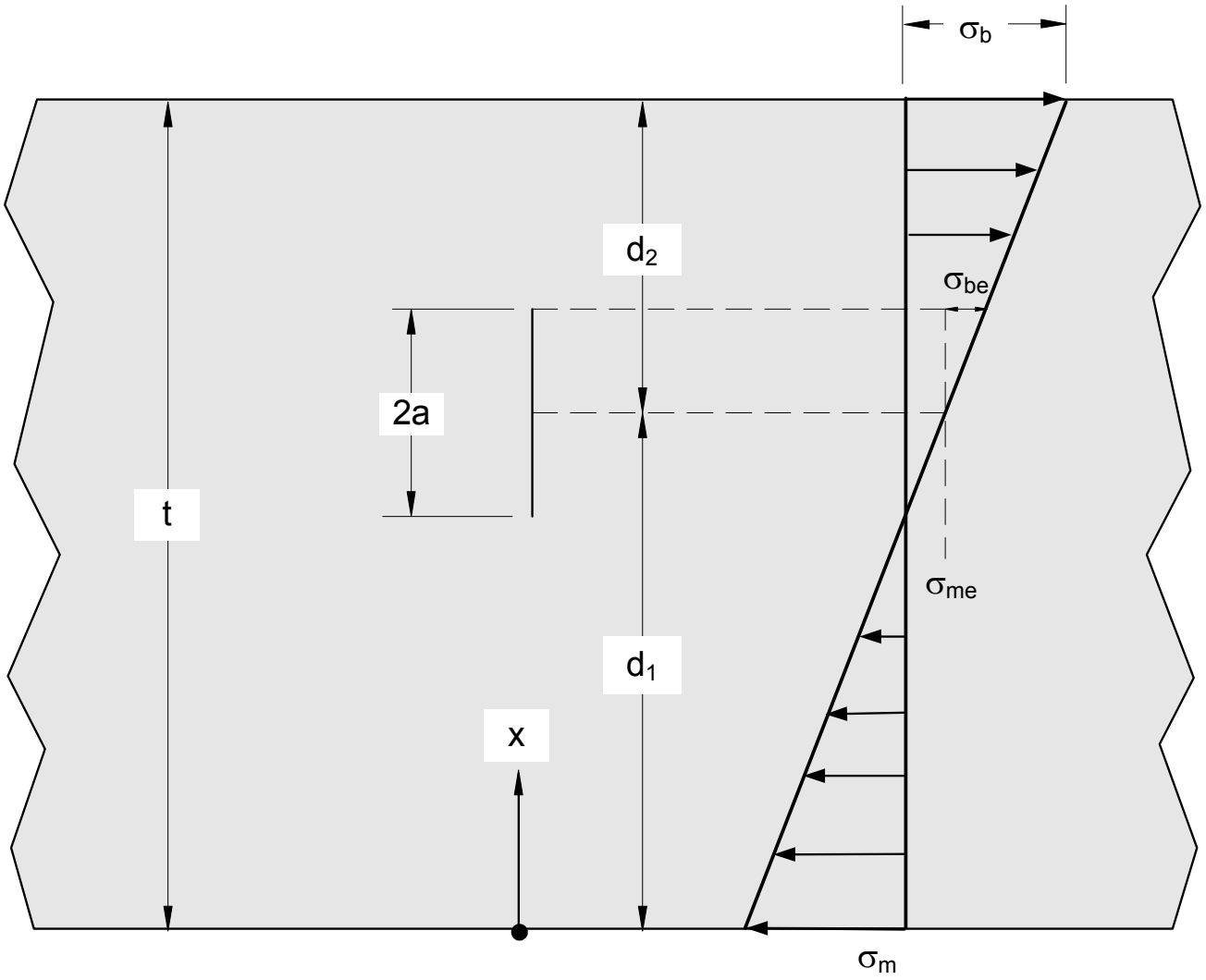

Note: The membrane and bending stress acting on the crack face can be computed using the equations in paragraph C.3.7.1.

Figure C.5
Plate – Embedded Crack, Definition of Membrane and Bending Stress

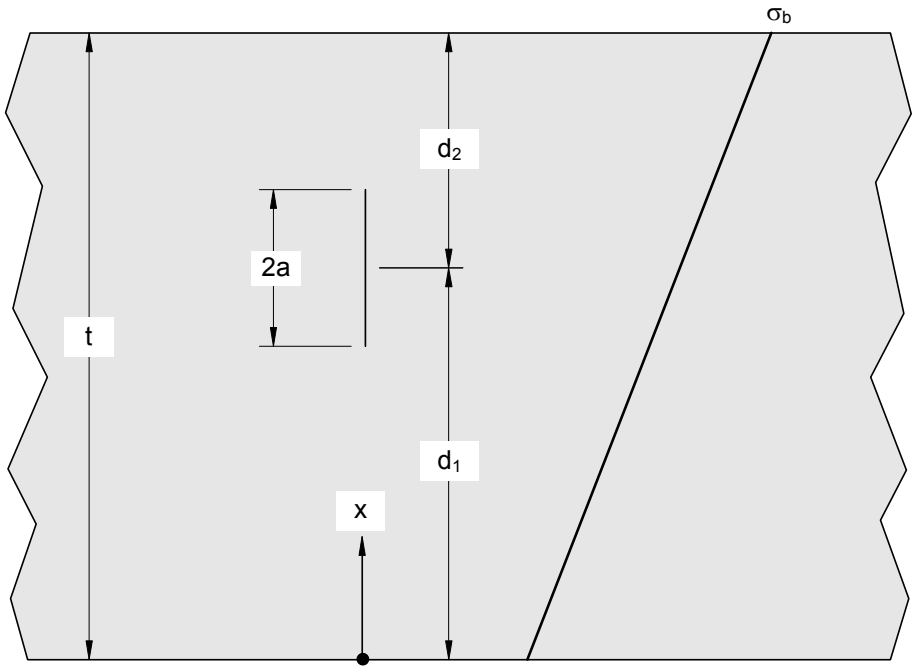

(a) Positive σ_b

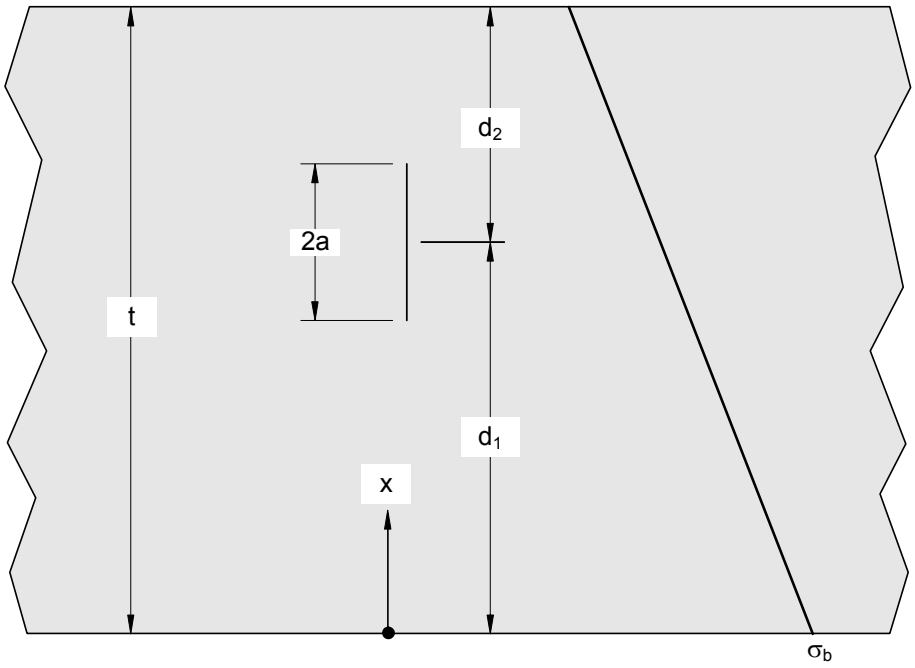

(b) Negative σ_b

Figure C.6
Plate – Embedded Cracks, Sign Convention for Bending Stress Distribution

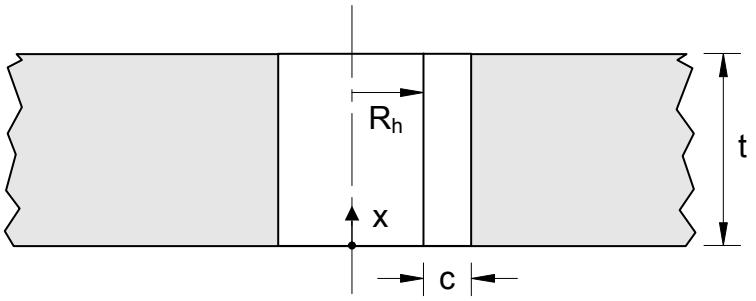

(a) Through-Wall Single Edge Crack

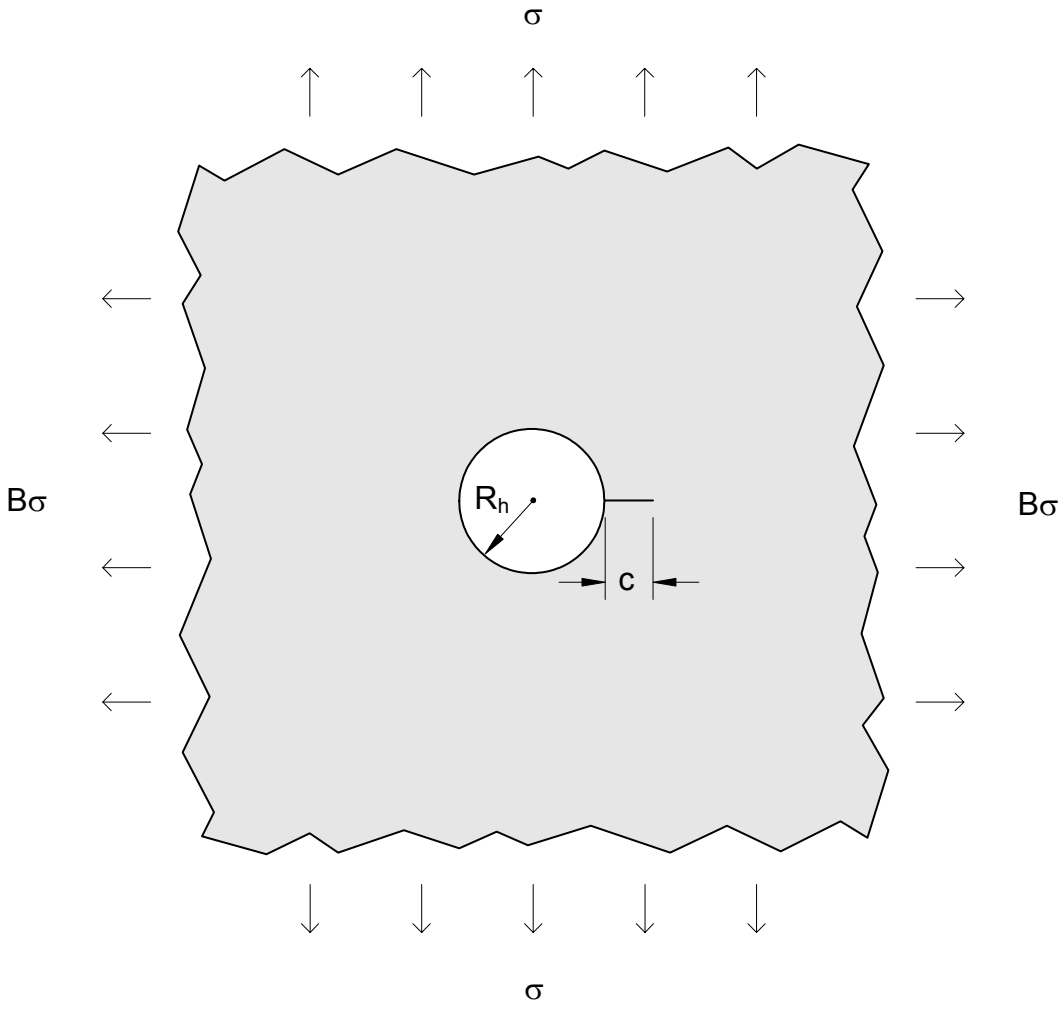

(b) Biaxial Loading

Figure C.7
Plate With Hole – Through-wall Single Edge Crack

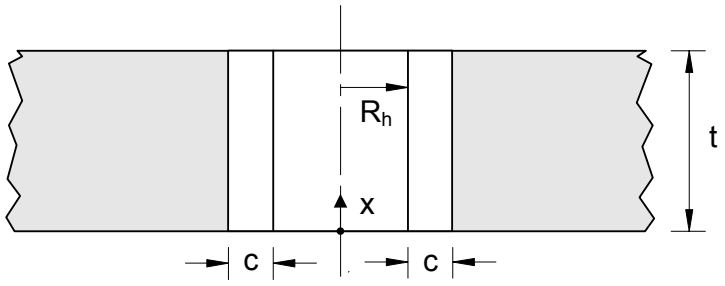

(a) Through-Wall Double Edge Crack

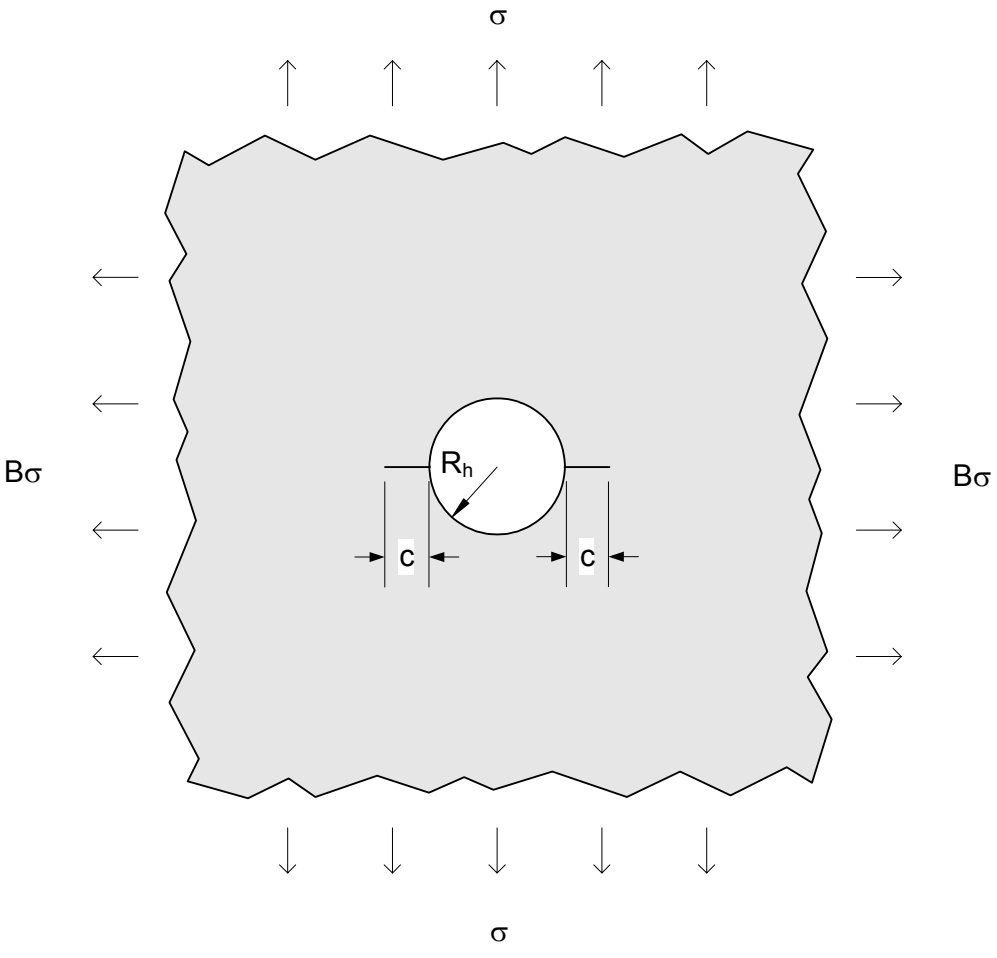

(b) Biaxial Loading

Figure C.8
Plate With Hole – Through-wall Double Edge Crack

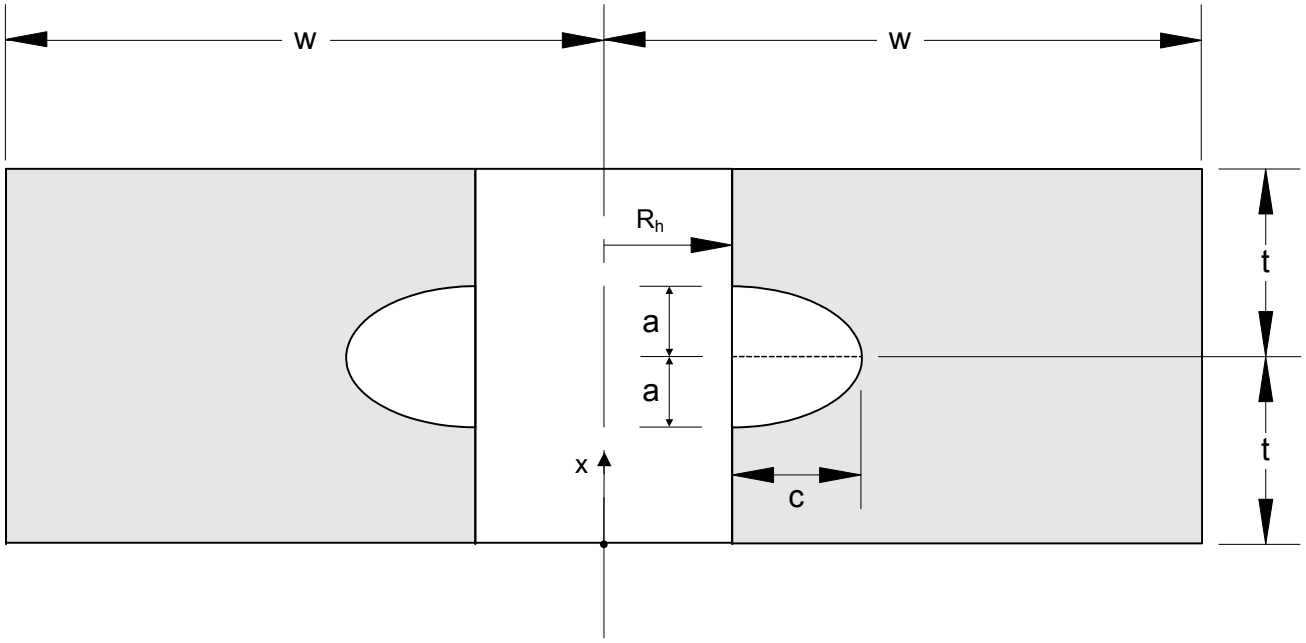

Figure C.9
Plate With Hole – Surface Crack, Semi-Elliptical Shape

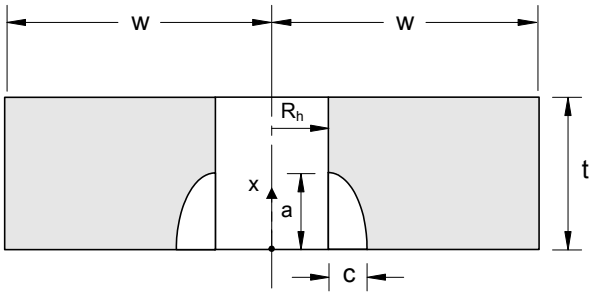

(a) Crack Geometry

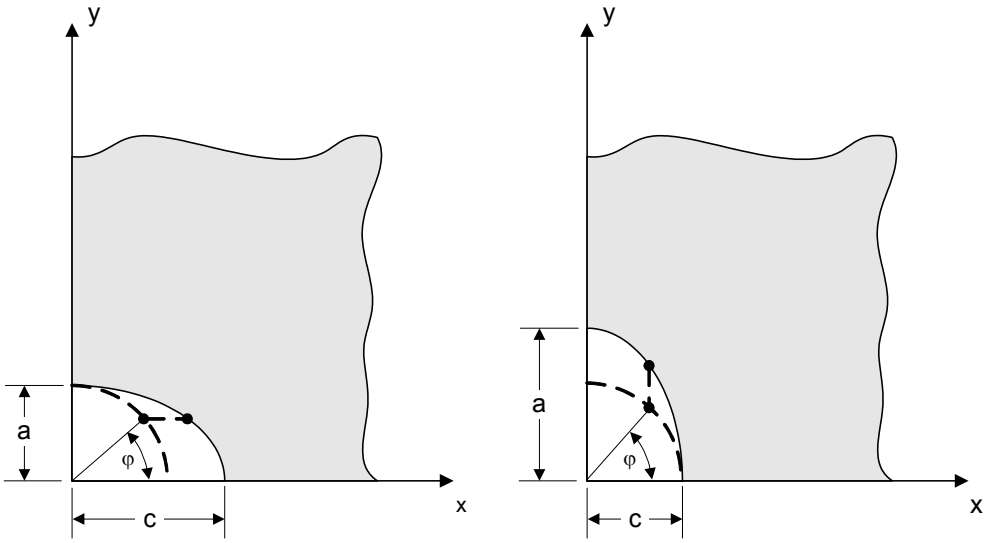

(a) $a/c \leq 1$ (b) $a/c > 1$

(b) Coordinate System Used to Define the Parametric Angle

Figure C.10
Plate With Hole – Corner Crack, Semi-Elliptical Shape

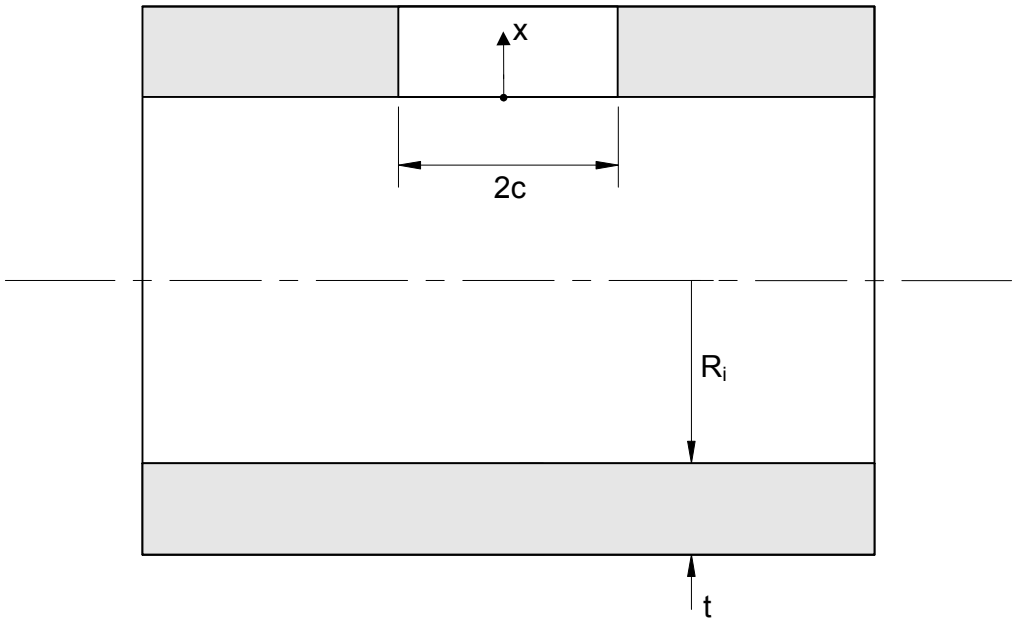

Figure C.11
Cylinder – Through-wall Crack, Longitudinal Direction

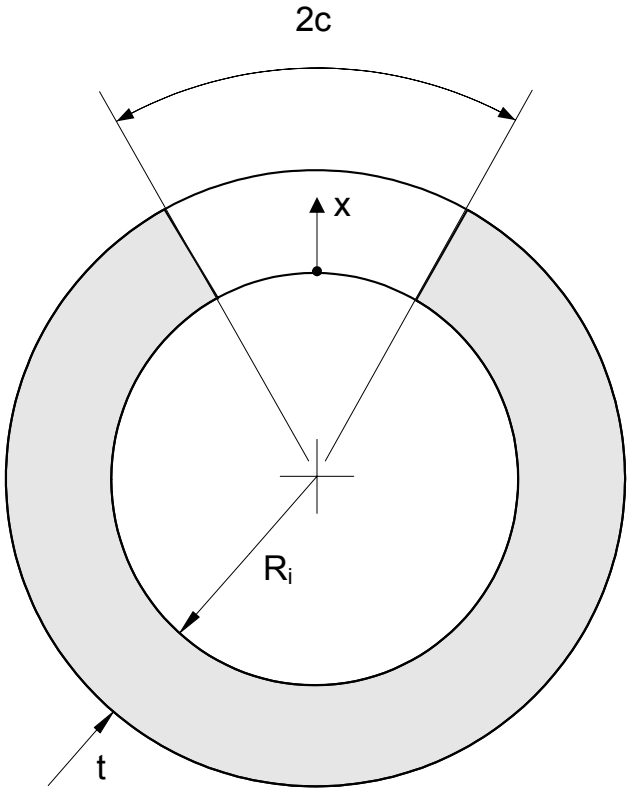

Figure C.12
Cylinder – Through-wall Crack, Circumferential Direction

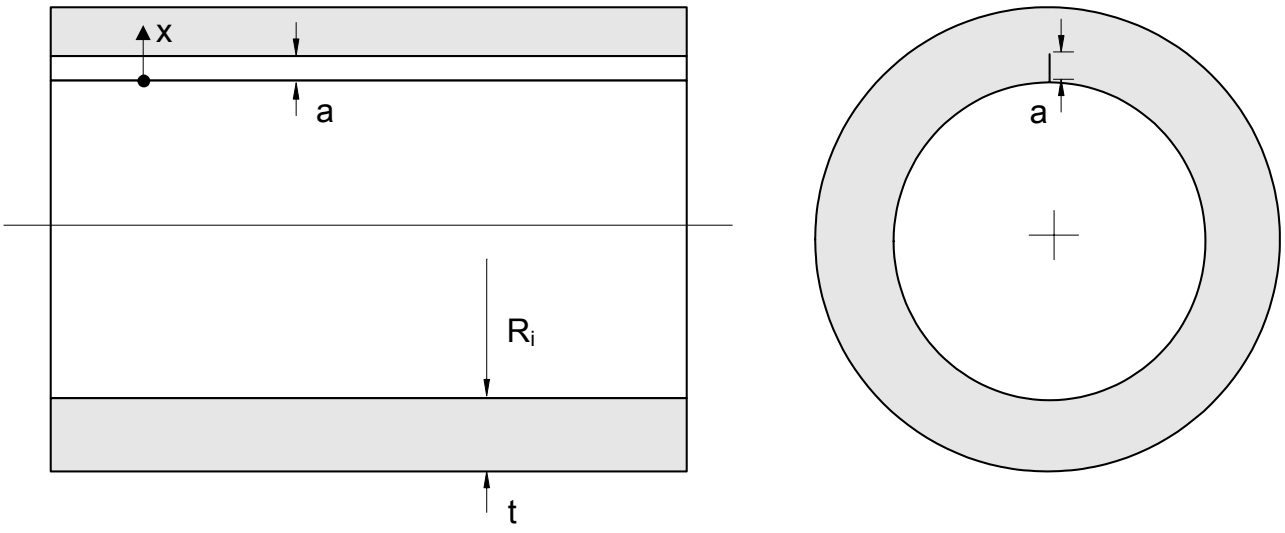

(a) Inside Surface

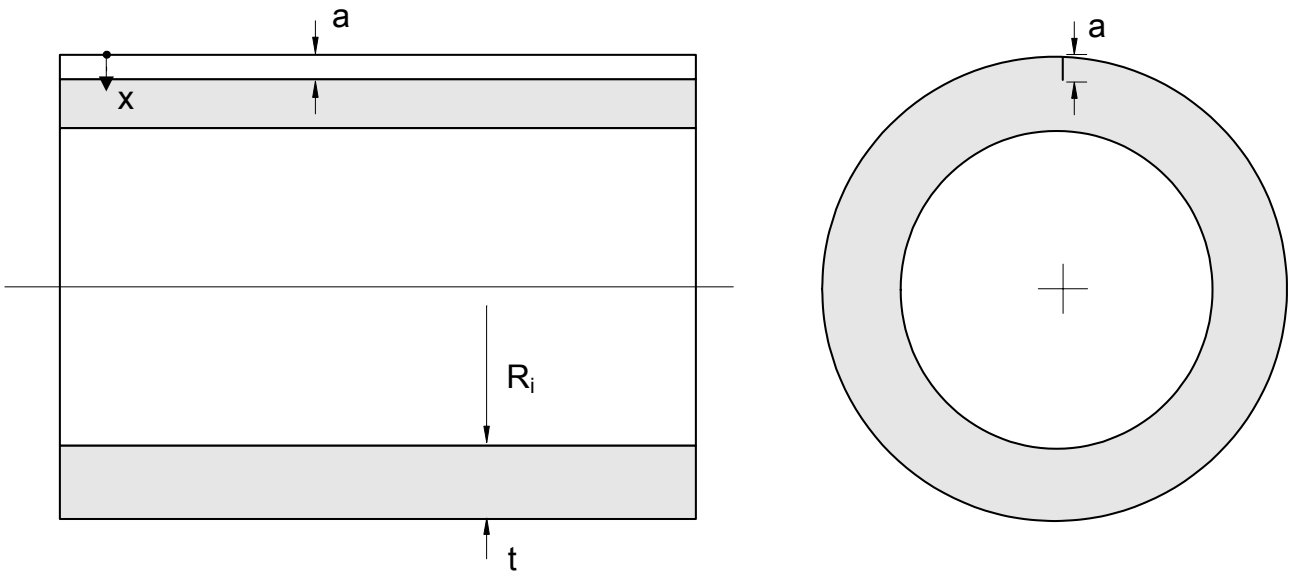

(b) Outside Surface

Figure C.13
Cylinder – Surface Crack, Longitudinal Direction, Infinite Length

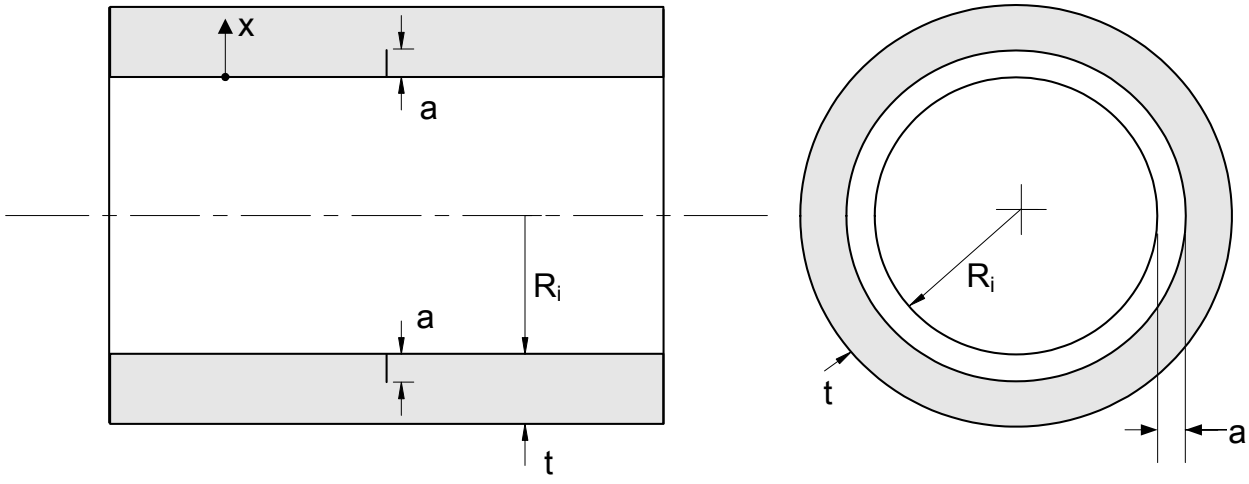

(a) Inside Surface

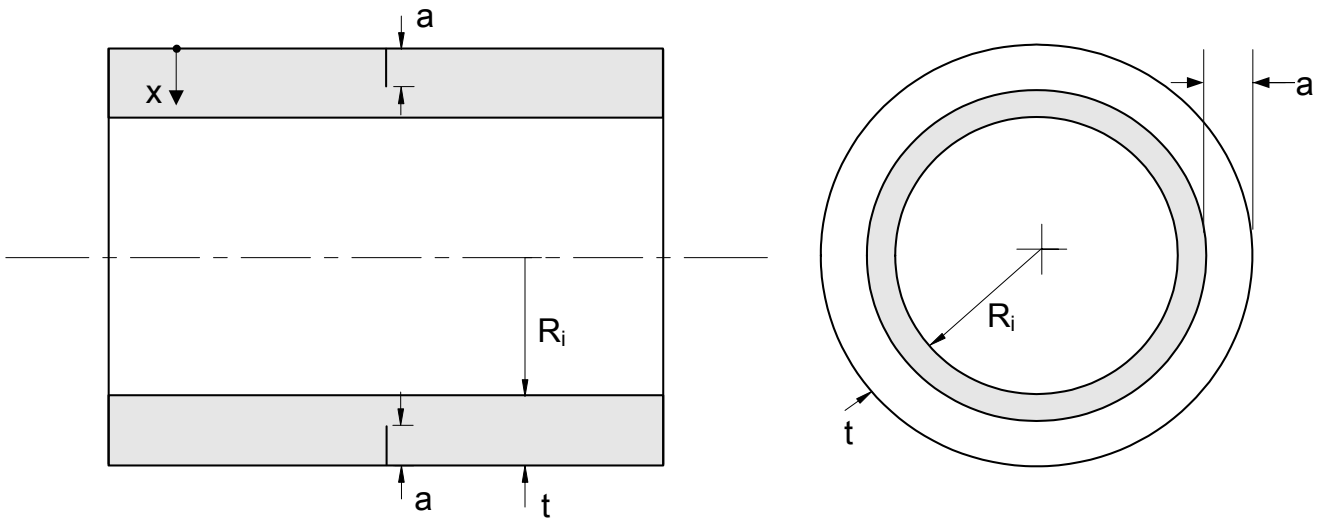

(b) Outside Surface

Figure C.14
Cylinder – Surface Crack, Circumferential Direction, 360 Degrees

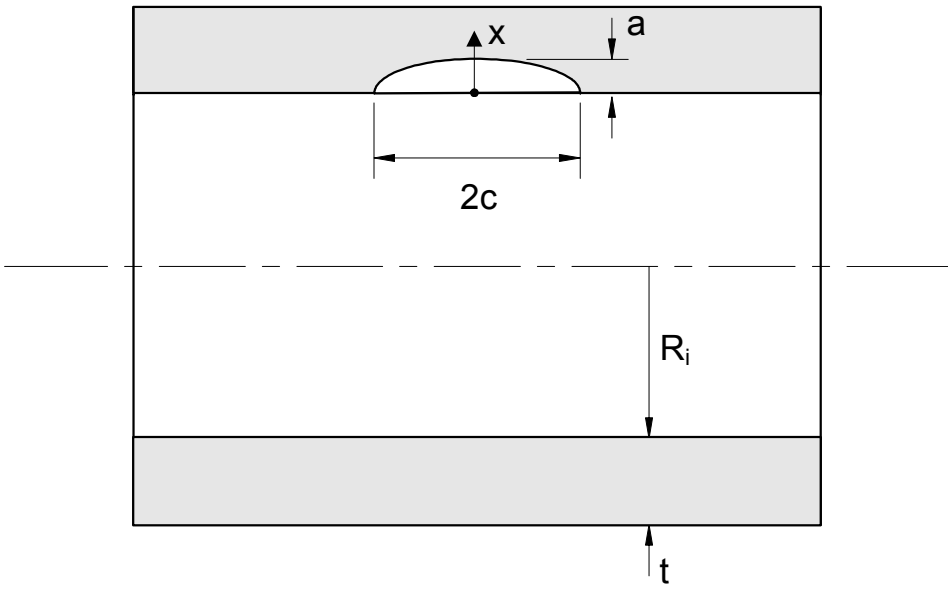

(a) Inside Surface

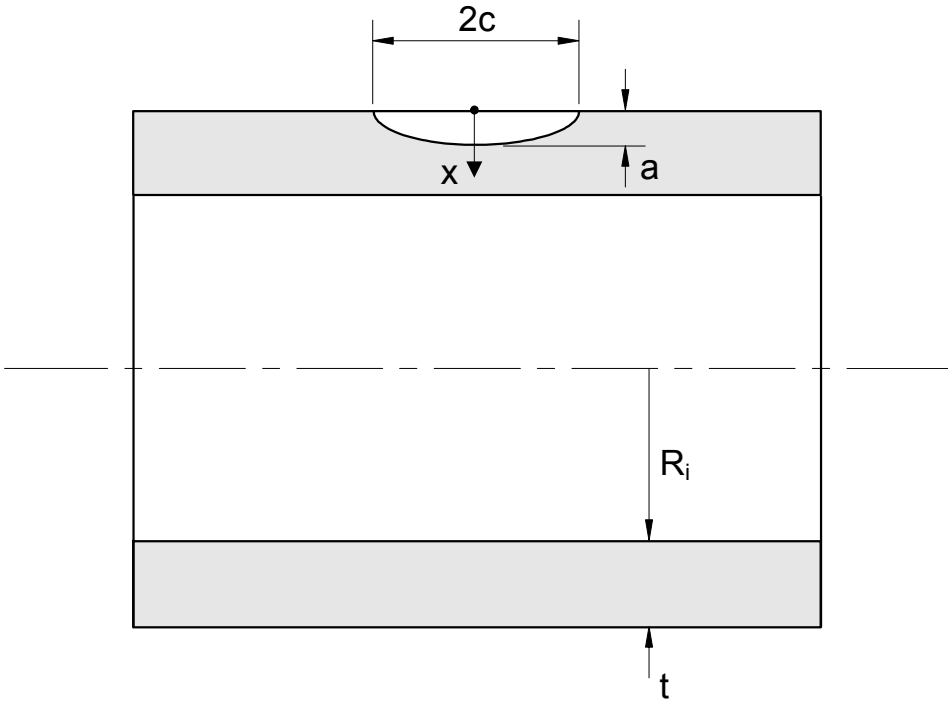

(b) Outside Surface

Figure C.15
Cylinder – Surface Crack, Longitudinal Direction – Semi-elliptical Shape

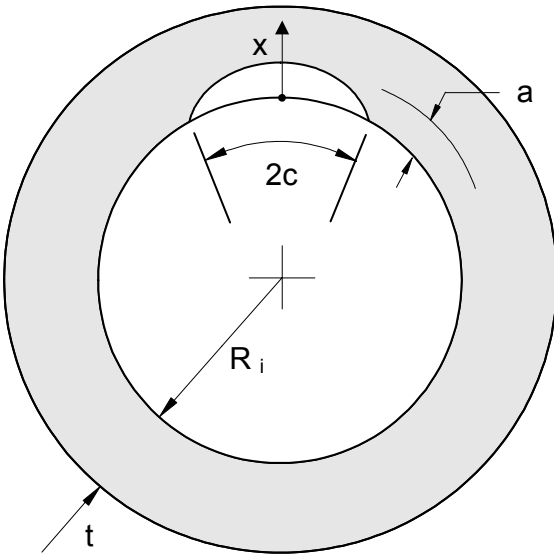

(a) Inside Surface

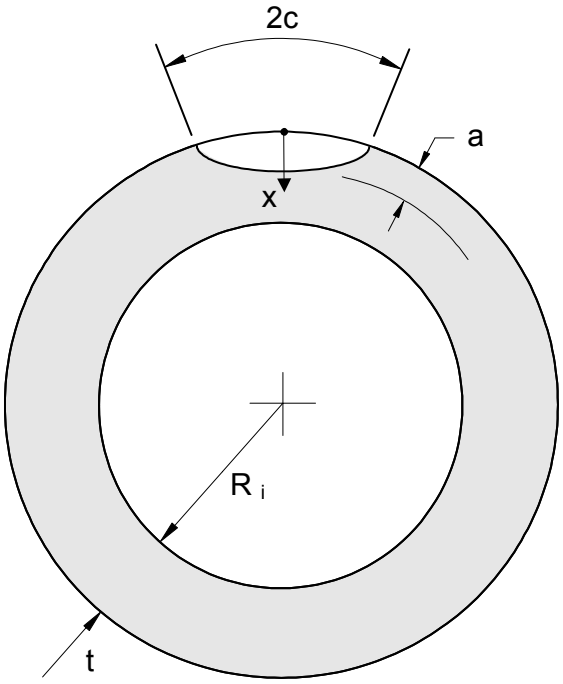

(b) Outside Surface

Figure C.16
Cylinder – Surface Crack, Circumferential Direction, Semi-elliptical Shape

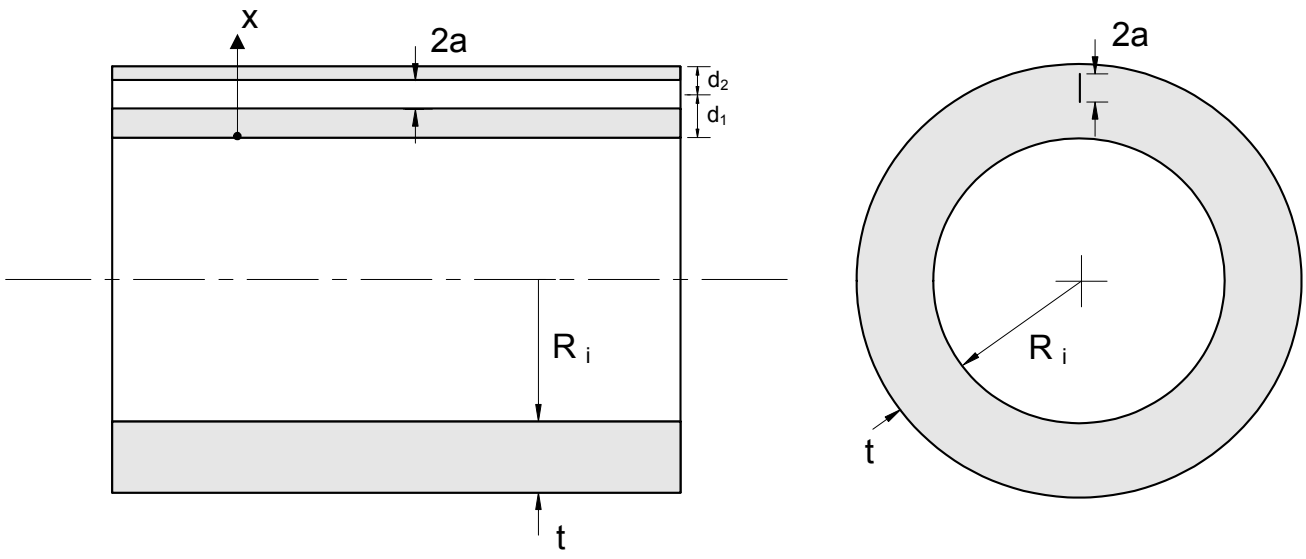

Figure C.17
Cylinder – Embedded Crack, Longitudinal Direction, Infinite Length

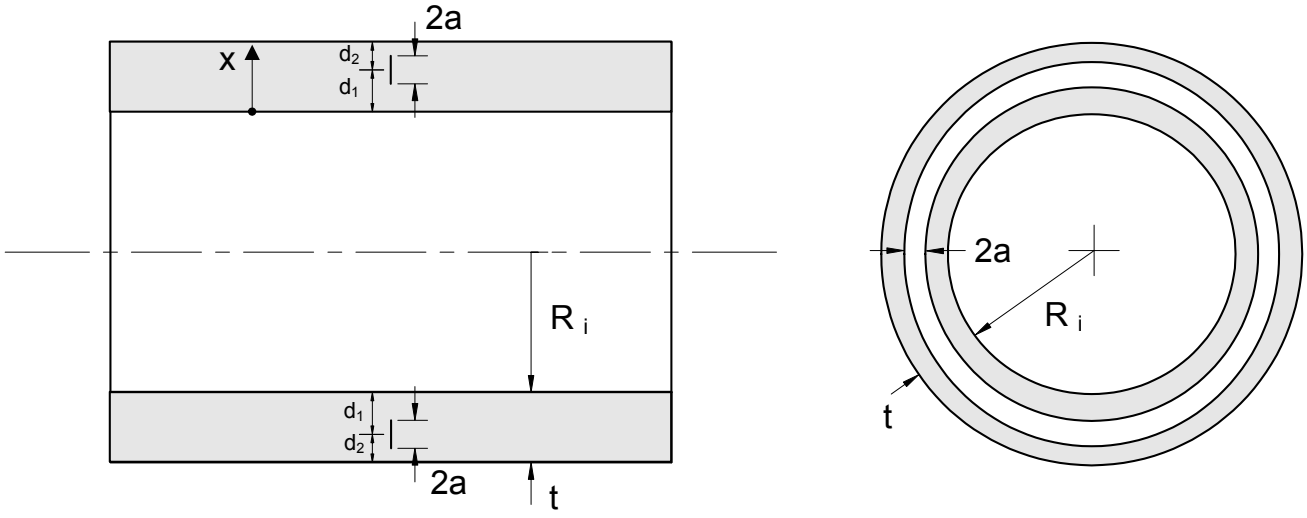

Figure C.18
Cylinder – Embedded Crack, Circumferential Direction – 360 Degrees

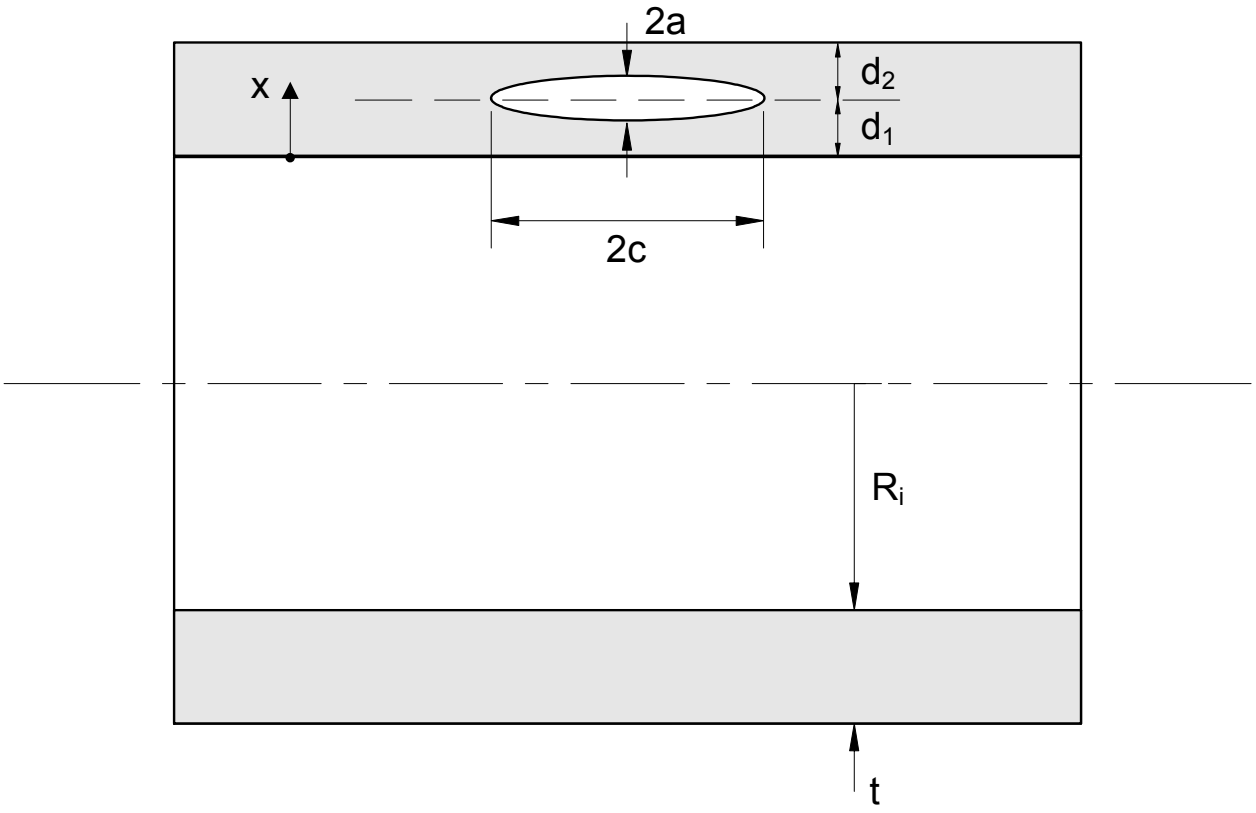

Figure C.19
Cylinder – Embedded Crack, Longitudinal Direction, Elliptical Shape

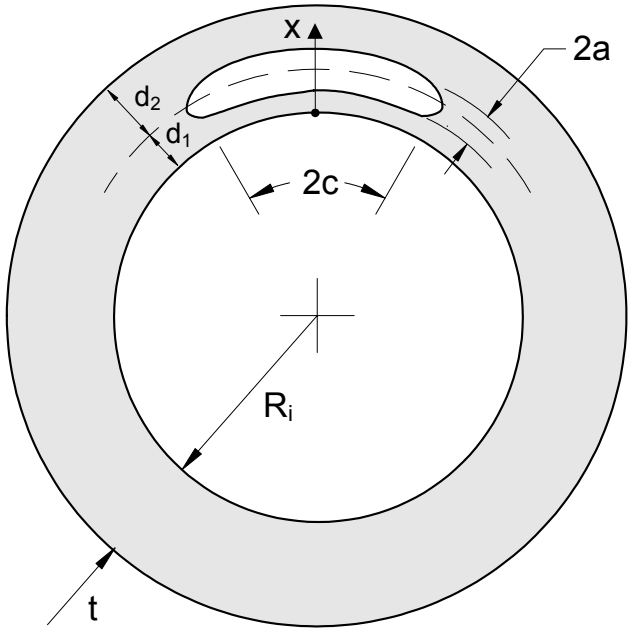

Figure C.20
Cylinder – Embedded Crack, Circumferential Direction, Elliptical Shape

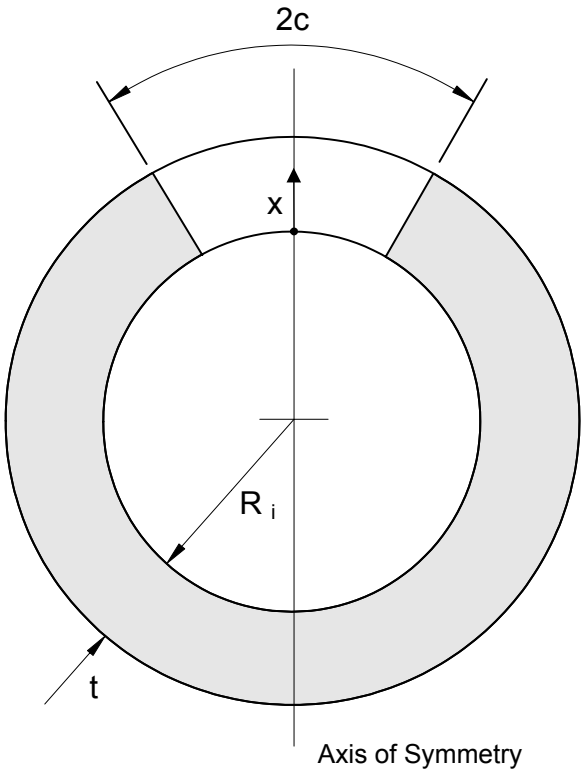

Figure C.21
Sphere – Through-wall Crack

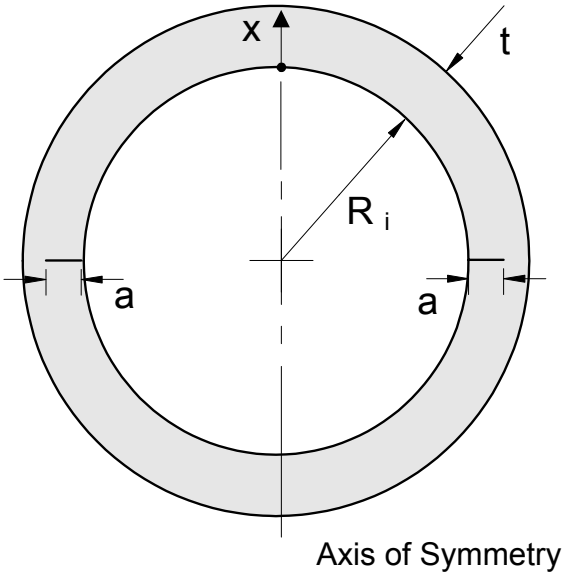

(a) Inside Surface

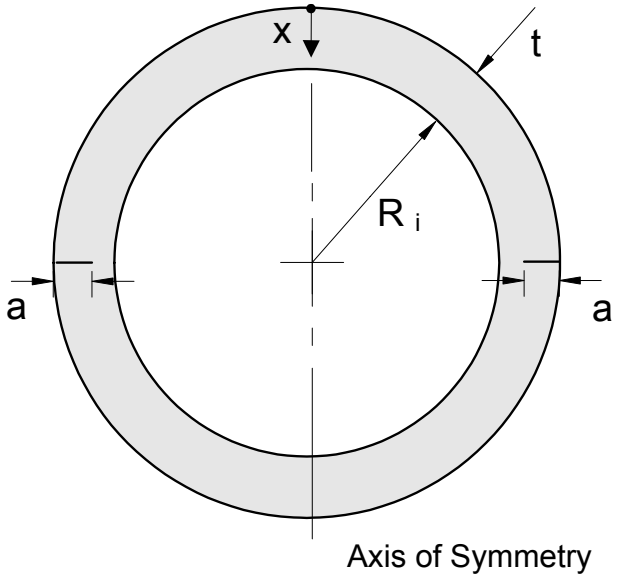

(b) Outside Surface

Figure C.22
Sphere – Surface Crack, Circumferential Direction, 360 Degrees

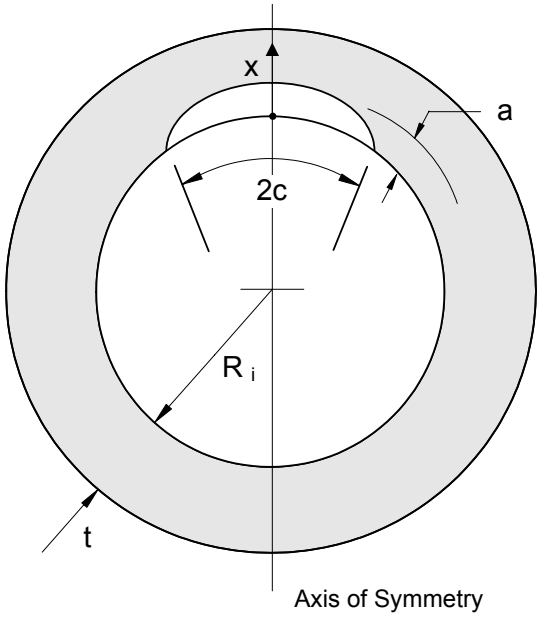

(a) Inside Surface

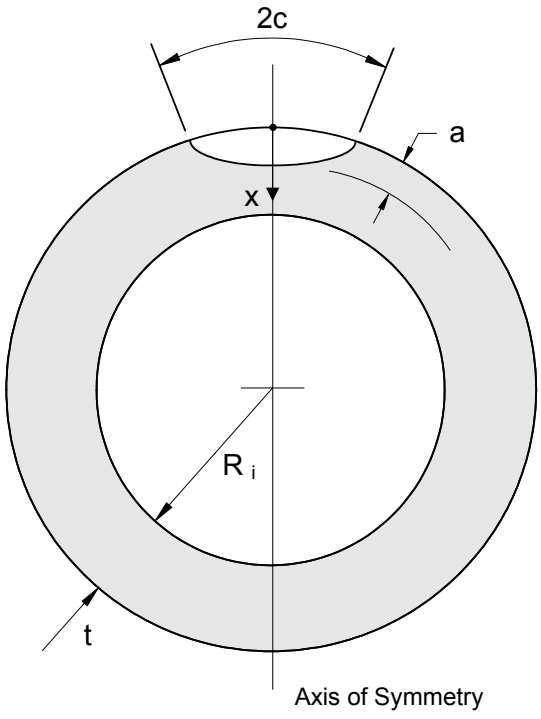

(b) Outside Surface

Figure C.23
Sphere – Surface Crack, Circumferential Direction, Semi-Elliptical Shape

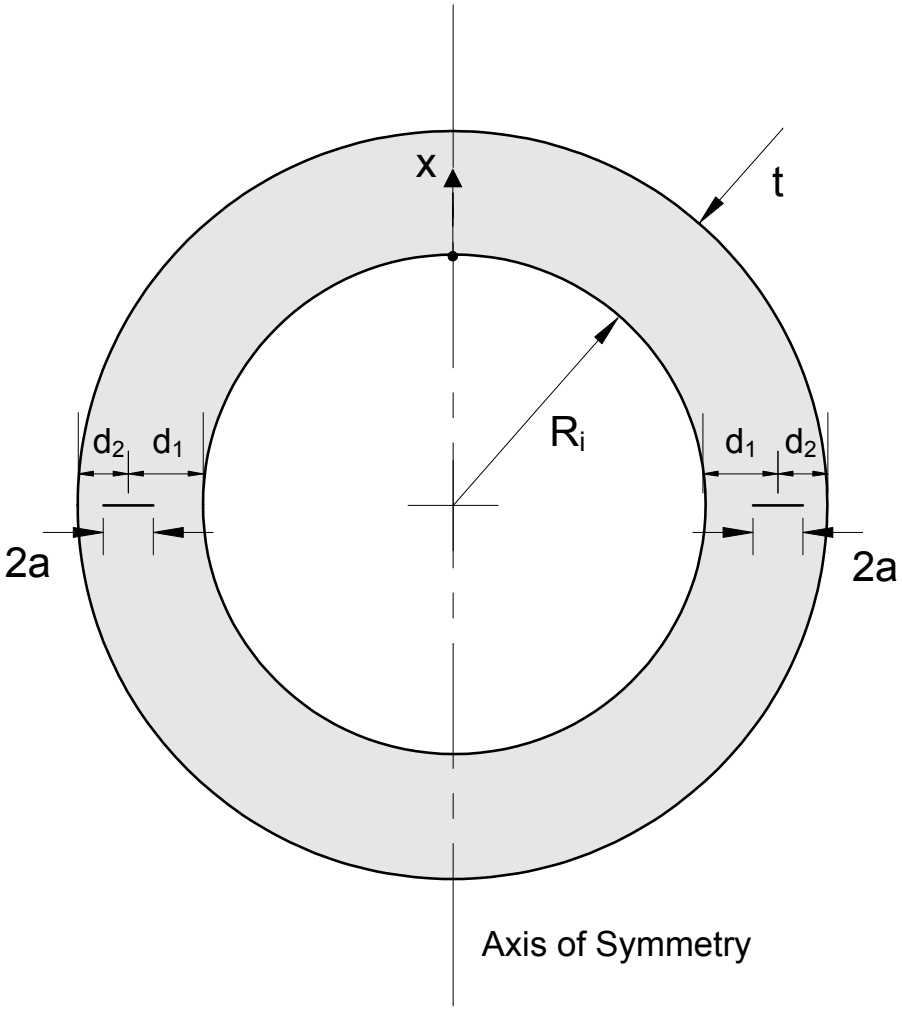

Figure C.24
Sphere – Embedded Crack, Circumferential Direction, 360 Degrees

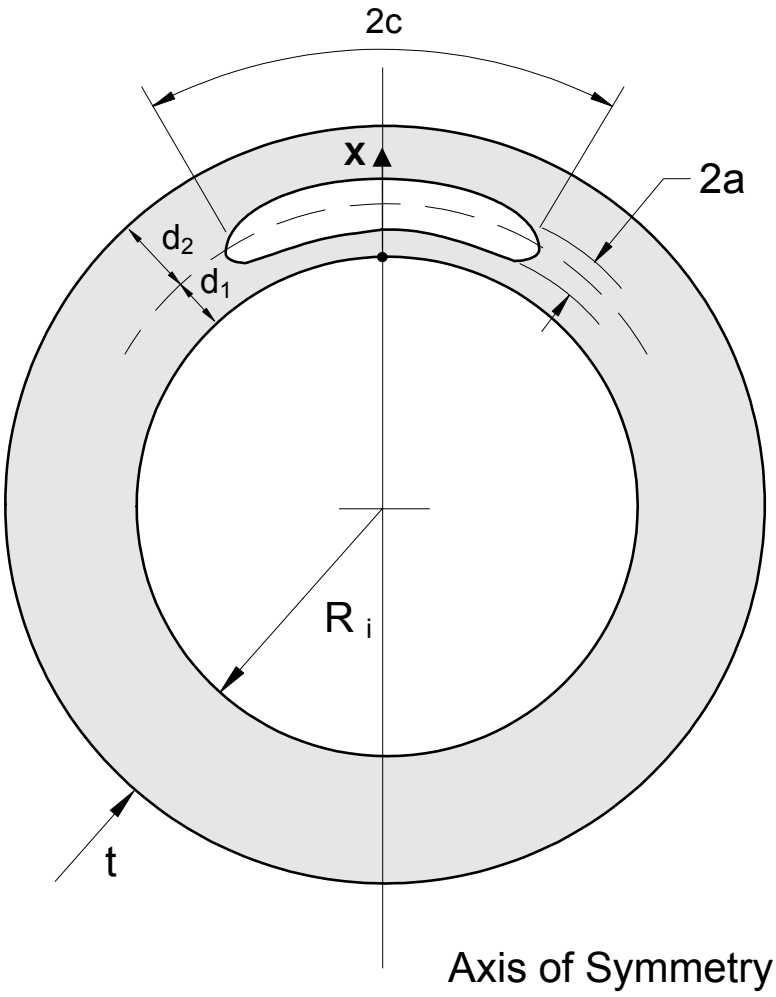

Figure C.25
Sphere – Embedded Crack, Circumferential Direction, Elliptical Shape

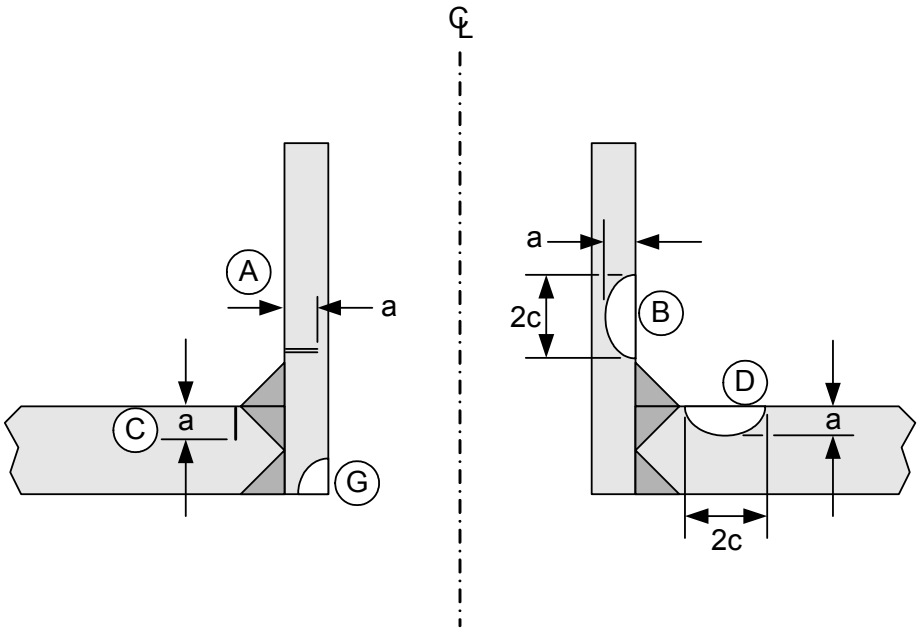

(a) Nozzle or Branch Connection

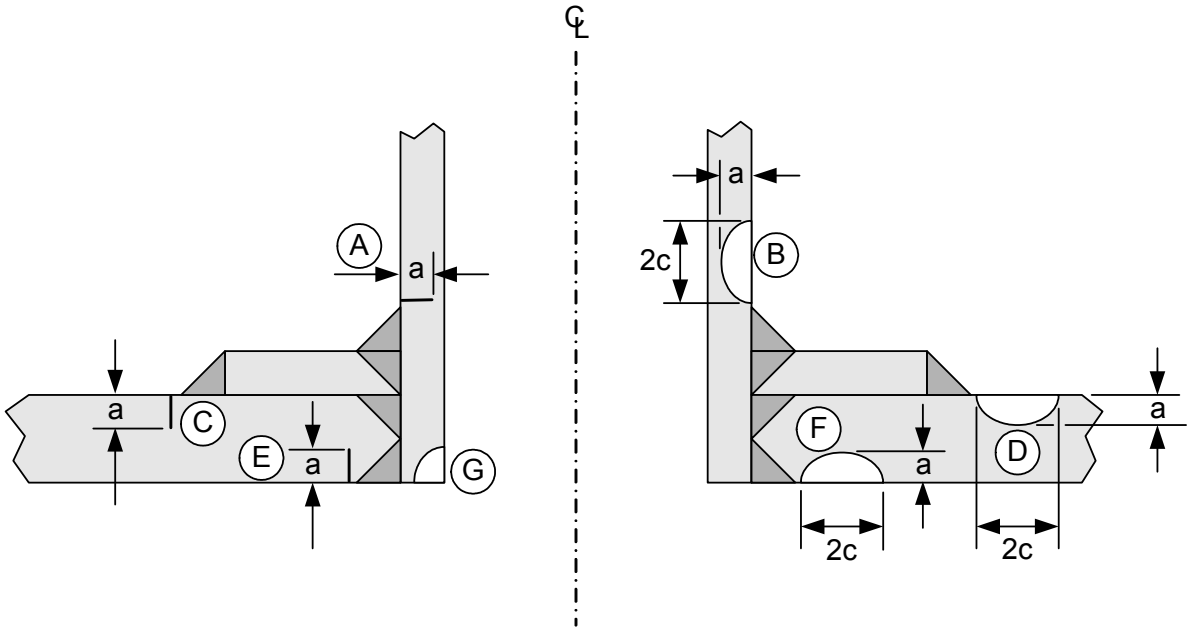

(b) Nozzle or Branch Connection with a Reinforcing Pad

Figure C.26
Cracks At Nozzles And Piping Branch Connections

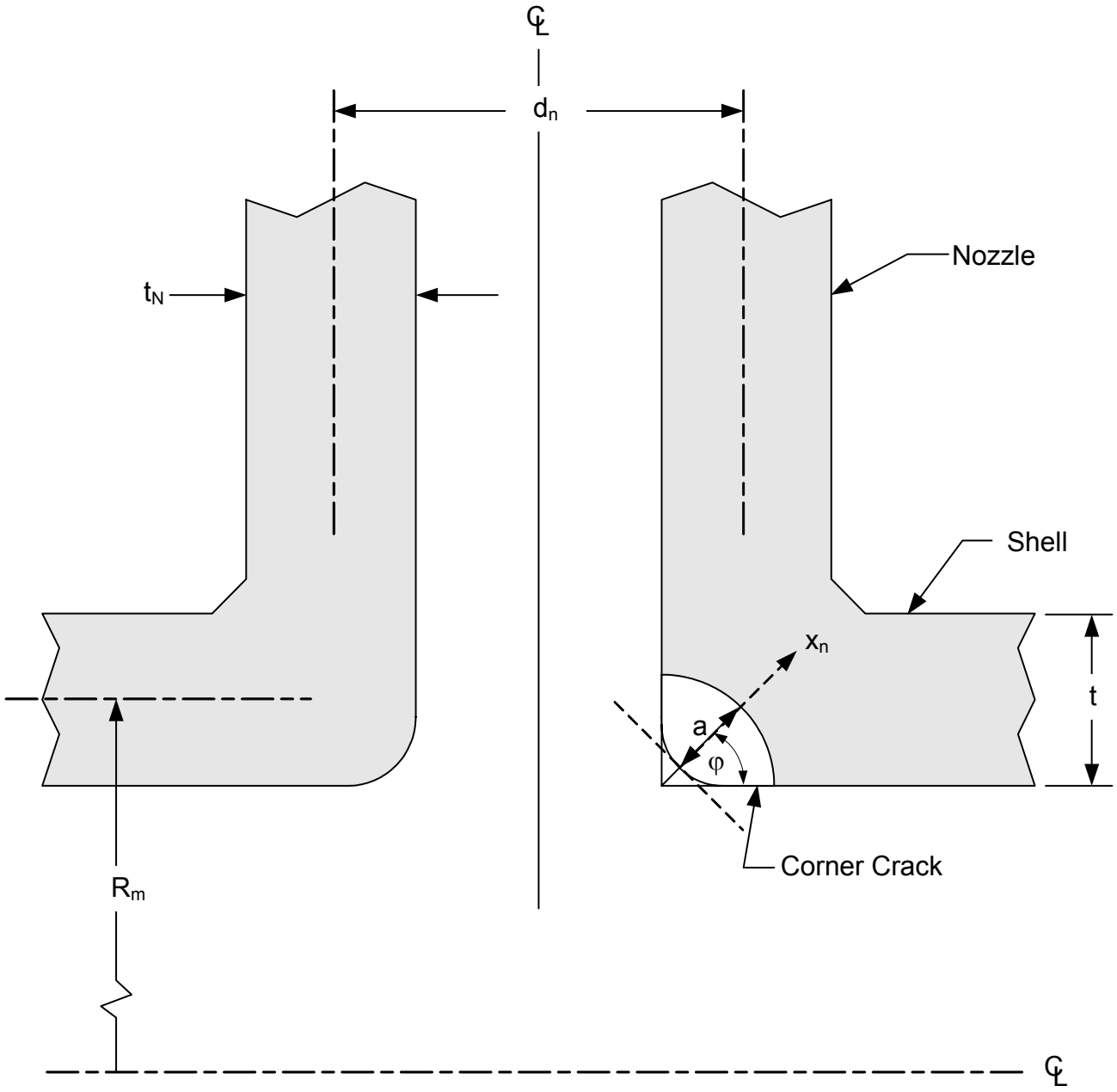

Figure C.27
Nozzle Corner Cracks

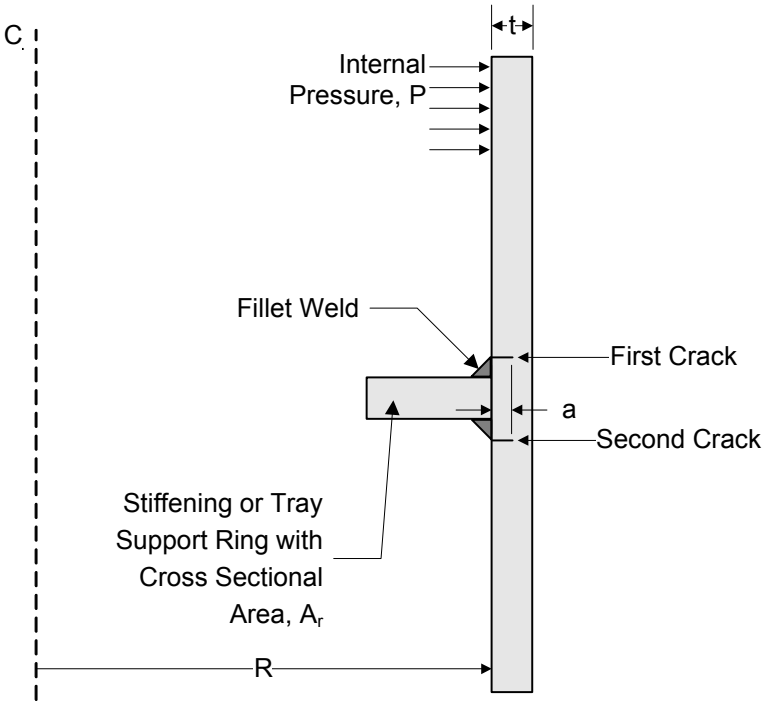

(a) Internal Ring, Internal Pressure

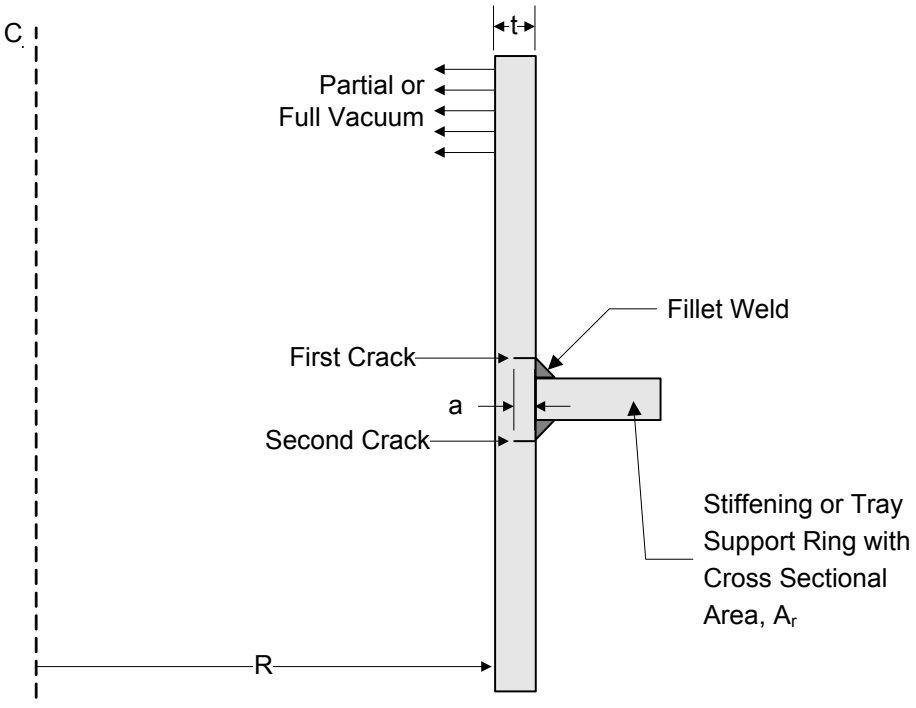

(b) External Ring, Partial or Full Vacuum

Figure C.28
Ring Stiffened Cylinders – Edge Cracks At Fillet Welds

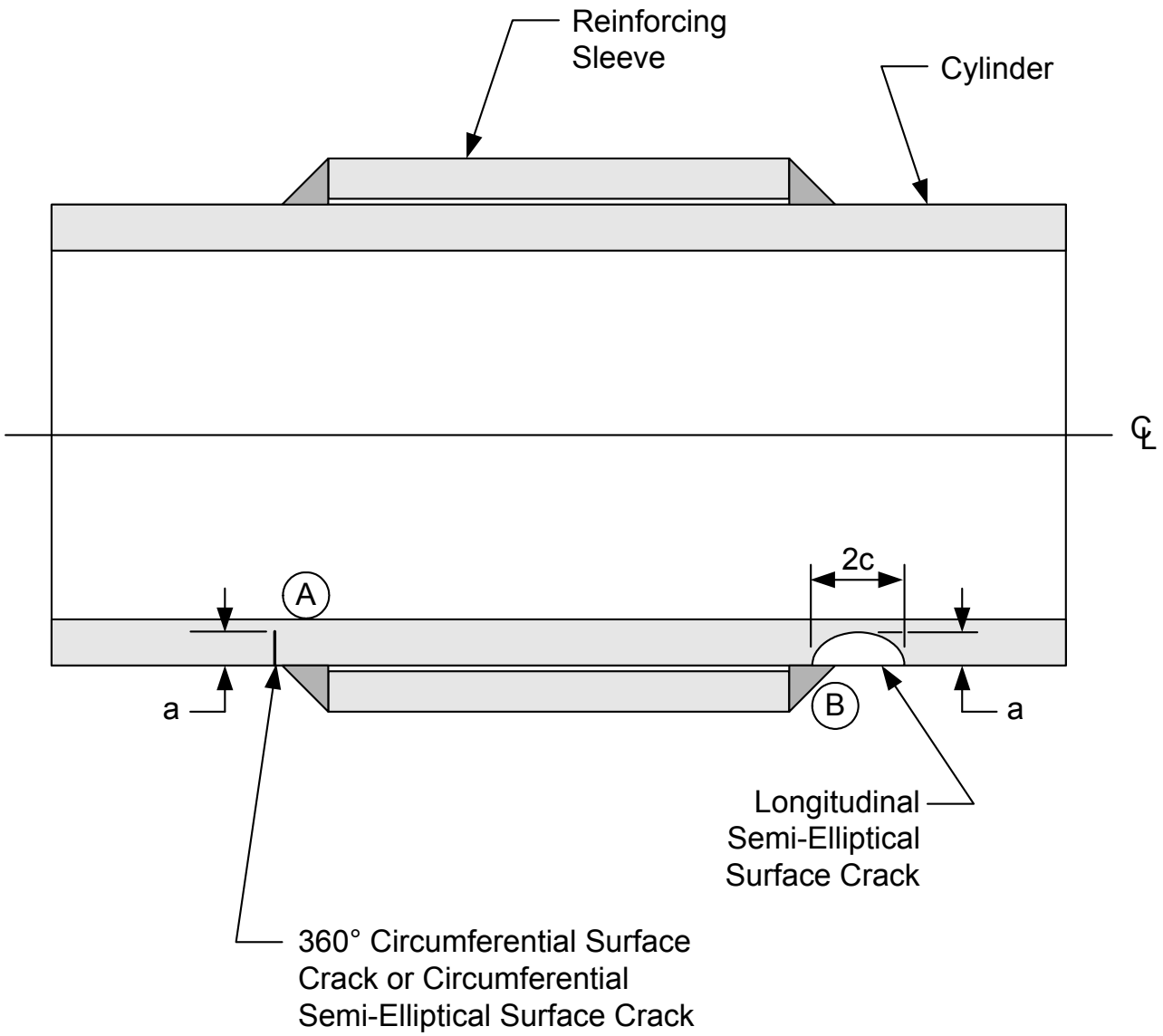

Figure C.29
Cracks At Sleeve Reinforced Cylinders

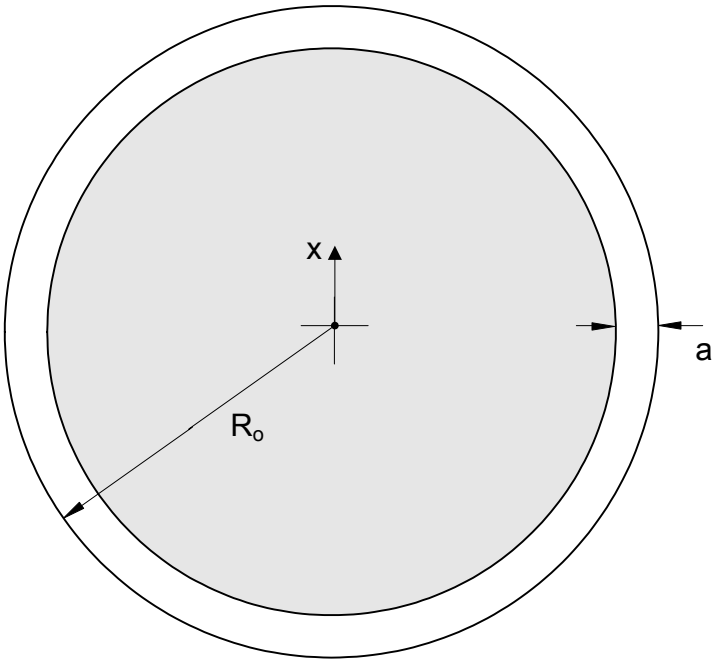

Figure C.30
Round Bar – Surface Crack, 360 Degrees

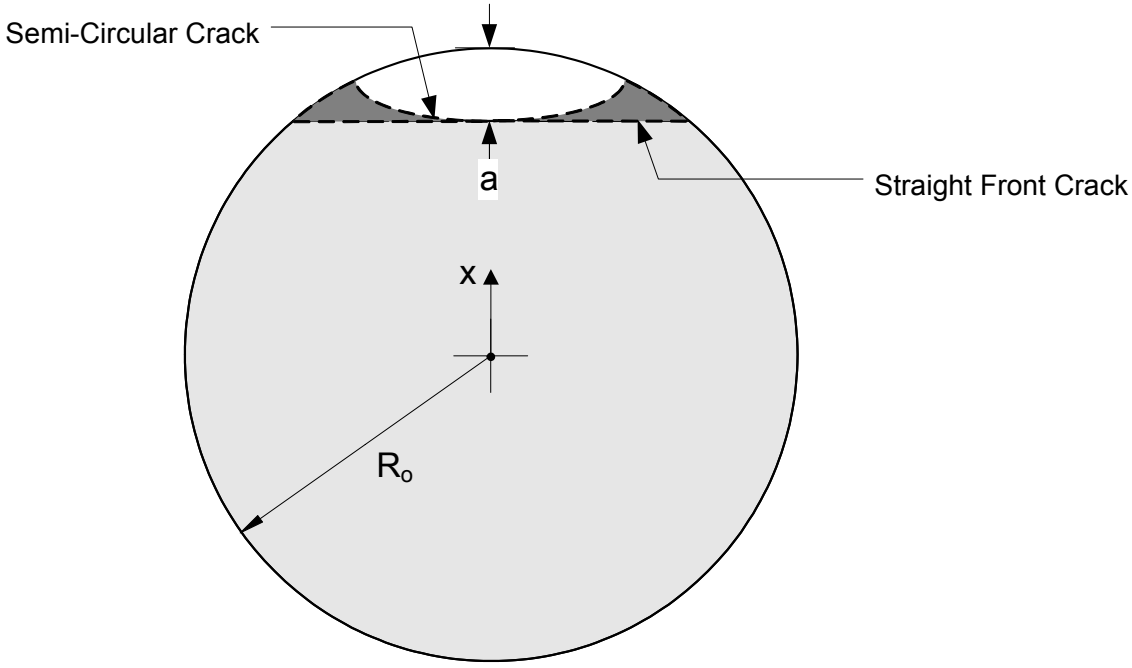

Figure C.31
Round Bar – Surface Crack

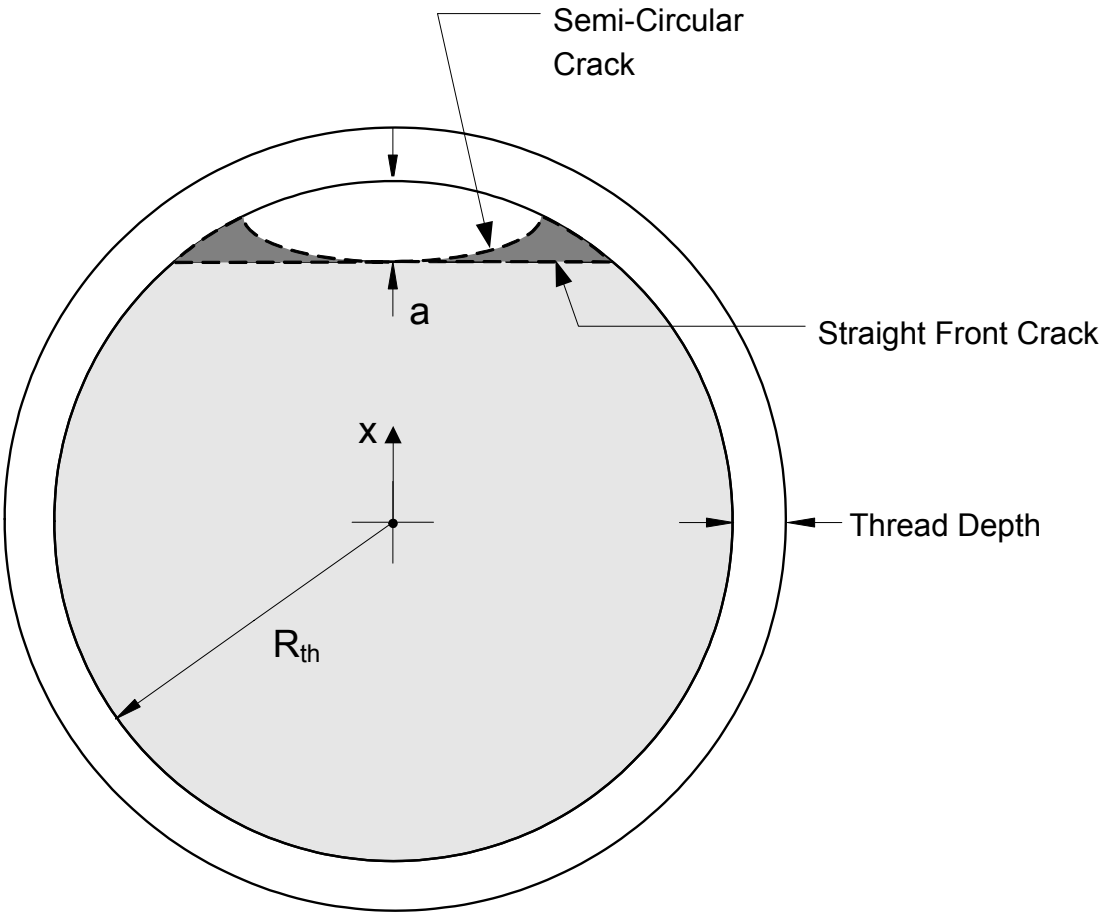

Figure C.32
Bolt – Surface Crack

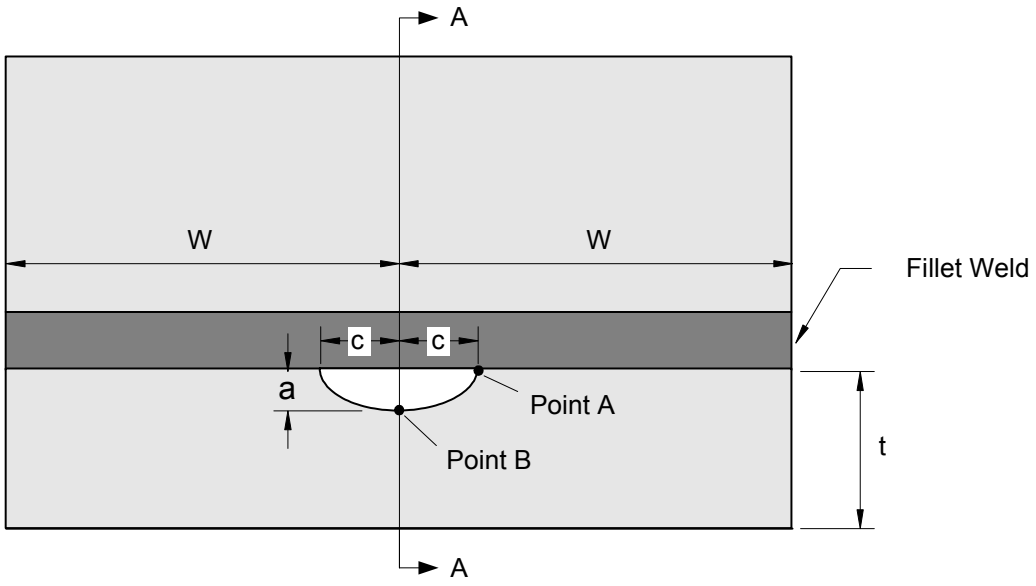

(a) Tee-Joint -- End View

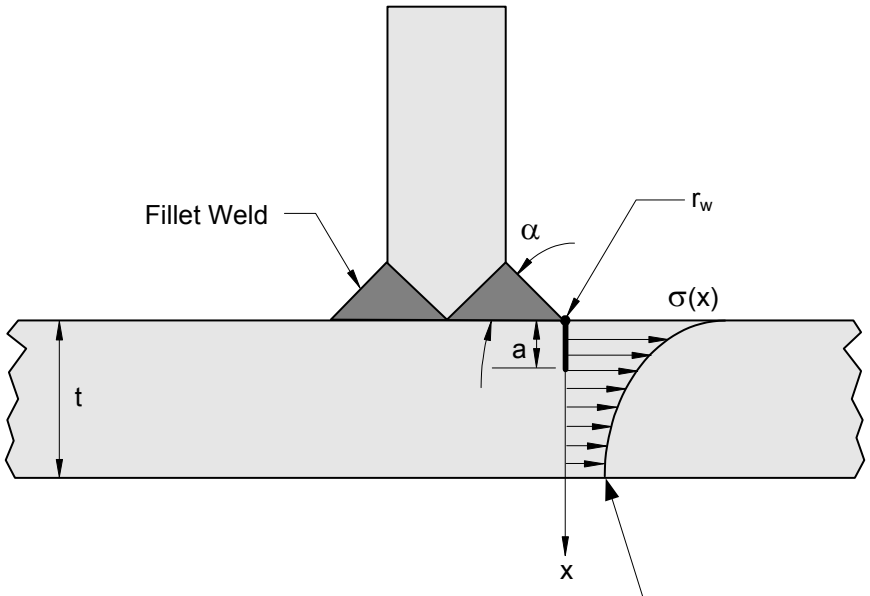

(b) Section A-A

Stress distribution at the location of the crack acting normal to the crack plane determine based on the structural configuration including the effects of the fillet weld geometry

Figure C.33
Crack At Fillet Weld – Surface Crack, Semi-Elliptical Shape

ANNEX D

COMPENDIUM OF REFERENCE STRESS SOLUTIONS FOR CRACK-LIKE FLAWS

(NORMATIVE)

PART CONTENTS

D.1 General

D.1.1 Overview

D.1.1.1 This Annex contains reference stress solutions for many crack geometries that are likely to occur in pressurized components. Reference stress solutions are used in the assessment of crack-like flaws (see Part 9).

D.1.1.2 A summary of the reference stress solutions in this annex is contained in Table C.1 of Annex C. These reference stress solutions are recommended for most applications based on consideration of accuracy, range of applicability, and convenience.

D.1.1.3 Reference stress solutions not included in this annex may be obtained from publications (for example, see references [1] and [2]) if the tabulated solutions correspond to the component and crack geometry, and the loading condition. Otherwise, the reference stress should be computed using a numerical approach such as the finite element method.

D.1.1.4 The reference stress solutions for plates can be used to approximate the solutions for cylinders and spheres by introducing a surface correction (Folias or bulging) factor. This is an approximation that is supported by experimental results.

D.1.1.5 An identifier has been assigned to each reference stress solution in this annex (see Table C.1 of Annex C). This identifier consists of a series of alpha-numeric characters that uniquely identifies the component geometry, crack geometry, and loading condition. The identifier is used to determine the associated stress intensity factor solution to be used in an assessment of crack like flaws (see Part 9). For example, if a flat plate with a through-wall crack subject to a membrane stress and/or bending stress is being evaluated, the reference stress solution is RPTC and the associated stress intensity factor solution is KPTC.

D.2 Stress Analysis

D.2.1 Overview

D.2.1.1 A stress analysis using handbook or numerical techniques is required to compute the state of stress at the location of a crack. The stress distribution to be utilized in determining the stress intensity factor is based on the component of stress normal to the crack face. The distribution may be linear (made up of membrane and/or bending distributions) or highly nonlinear depending on the component geometry and loading conditions.

D.2.1.2 The stress distribution normal to the crack face resulting from primary loads should be determined based on service loading conditions and the uncracked component geometry. If the component is subject to different operating conditions, the stress distribution should be evaluated and a separate fitness-for-service assessment should be performed for each condition.

D.2.1.3 In this annex, the variable P is used in place of σ to signify that the stress distributions used to determine the reference stress and the L_r ratio for the assessment of a crack-like flaw using the FAD (see Part 9) are categorized as primary stress (see Annex B1). The reference stress based on the secondary and residual stress distributions is also required to determine the plasticity interaction factor, Φ, used in the assessment of crack-like flaws (see Part 9). In this case, the variable P may be used to represent the secondary and/or residual stress.

D.2.2 Stress Distributions

D.2.2.1 Overview

The reference stress solutions in this annex are formulated in terms of the coefficients of a linear stress distribution (membrane and bending stress). Therefore, it is necessary to derive these coefficients from the results obtained from a stress analysis.

D.2.2.2 General Stress Distribution

A stress distribution through the wall thickness at the location of a crack-like flaw can be determined using a handbook solution or a numerical analysis technique such as the finite element method. In some cases, the stress distribution normal to the crack face may be highly non-linear. Statically equivalent membrane and bending stress components can be determined from the general stress distribution using the following equations; the integration is performed along a line assuming a unit width (see Annex B2).

$$P_{ij,m} = \frac{1}{t}\int_0^t P_{ij}\,dx \tag{D.1}$$

$$P_{ij,b} = \frac{6}{t^2}\int_0^t P_{ij}\left(\frac{t}{2} - x\right)dx \tag{D.2}$$

D.2.2.3 Fourth Order Polynomial Stress Distribution

The fourth order polynomial stress distribution can be obtained by curve-fitting a general stress distribution to obtain the coefficients of the best-fit fourth order polynomial. The equivalent membrane and bending stress distributions for use in the reference stress solutions in this annex can be obtained directly from the coefficients of this polynomial.

a) The general form of the fourth order polynomial stress distribution is as follows:

$$P(x) = P_o + P_1\left(\frac{x}{t}\right) + P_2\left(\frac{x}{t}\right)^2 + P_3\left(\frac{x}{t}\right)^3 + P_4\left(\frac{x}{t}\right)^4 \tag{D.3}$$

b) The equivalent membrane and bending stress distributions for the fourth order polynomial stress distribution are:

$$P_m = P_0 + \frac{P_1}{2} + \frac{P_2}{3} + \frac{P_3}{4} + \frac{P_4}{5} \tag{D.4}$$

$$P_b = -\frac{P_1}{2} - \frac{P_2}{2} - \frac{9P_3}{20} - \frac{6P_4}{15} \tag{D.5}$$

D.2.2.4 Fourth Order Polynomial Stress Distribution with Net Section Bending Stress

This distribution is used to represent a through-wall fourth order polynomial stress and a net section or global bending stress applied to a circumferential crack in a cylindrical shell.

$$P(x, x_g, y_g) = P_o + P_1\left(\frac{x}{t}\right) + P_2\left(\frac{x}{t}\right)^2 + P_3\left(\frac{x}{t}\right)^3 + P_4\left(\frac{x}{t}\right)^4 + P_5\left(\frac{x_g}{R_i + t}\right) + P_6\left(\frac{y_g}{R_i + t}\right) \tag{D.6}$$

D.2.2.5 Membrane and Through-Wall Bending Stress Distribution

The membrane and bending stress distribution is linear through the wall thickness and represents a common subset of the general stress distribution (see paragraph D.2.2.2). Attributes of this stress distribution are discussed in Annex C, paragraph C.2.2.5. The components of this stress distribution can be used directly in the reference stress solutions in this annex.

D.2.3 Surface Correction Factor for Shells

D.2.3.1 Overview

A surface correction (also referred to as the Folias or bulging factor) is used to quantify the local increase in the state of stress at the location of a crack in a shell type structure that occurs because of local bulging. The magnified state of stress is then used together with a reference stress solution for a plate with similar crack geometry to determine the reference stress for the shell. Surface correction factors are typically only applied to the membrane part of the reference stress because this represents the dominant part of the solution.

D.2.3.2 Surface Correction Factors for Through-wall Cracks

The surface correction factors for through-wall cracks in cylindrical and spherical shells subject to membrane stress loading are shown below. The surface correction factors are normally defined in terms of a single shell parameter, λ, given by the following Equation (D.7). However, recent work indicates that the surface correction factors for cylindrical shells are also a function of the shell radius-to-thickness ratio [9].

$$\lambda = \frac{1.818c}{\sqrt{R_i t}} \tag{D.7}$$

a) Cylindrical shell – Longitudinal through-wall crack

1) Data fit from references [10] and [11] (recommended for use in all assessments):

$$M_t = \left(\frac{1.02 + 0.4411\lambda^2 + 0.006124\lambda^4}{1.0 + 0.02642\lambda^2 + 1.533(10^{-6})\lambda^4} \right)^{0.5} \tag{D.8}$$

2) Approximate expression from references [12] and [13]:

$$M_t = \left(1 + 0.3797\lambda^2 - 0.001236\lambda^4\right)^{0.5} \qquad for \quad \lambda \le 9.1 \tag{D.9}$$

$$M_t = 0.01936\lambda^2 + 3.3 \qquad for \quad \lambda > 9.1 \tag{D.10}$$

3) Upper bound expression from reference [14]:

$$M_t = \left(1 + 0.4845\lambda^2\right)^{0.5} \tag{D.11}$$

4) A general expression for membrane stress and pressure loading is given by Equations (D.12) and (D.13), respectively, where the coefficients G_0 and G_p are calculated using the equations in Annex C, paragraph C.5.1. These equations include an R_i/t ratio dependency that may be significant.

$$M_t = G_0 \qquad membrane\ stress \tag{D.12}$$

$$M_t = G_p \qquad pressure\ loading \tag{D.13}$$

b) Cylindrical shell – Circumferential through-wall crack

1) Data fit from reference [15] (recommended for use in all assessments):

$$M_t = \left(\frac{1.0078 + 0.10368\lambda^2 + 3.7894(10^{-4})\lambda^4}{1.0 + 0.021979\lambda^2 + 1.5742(10^{-6})\lambda^4} \right)^{0.5} \tag{D.14}$$

2) The general expression for membrane stress and pressure loading is given by Equations (D.12) and (D.14) where the coefficients G_0 and G_p are calculated using the equations in Annex C, paragraph C.5.2.

c) Spheres – Circumferential through-wall crack

1) Data fit from references [10] and [11] (recommended for use in all assessments):

$$M_t = \frac{1.0005 + 0.49001\lambda + 0.32409\lambda^2}{1.0 + 0.50144\lambda - 0.011067\lambda^2} \tag{D.15}$$

2) Approximate expression [16]:

$$M_t = \left(1 + 0.427\lambda^2 + 0.00666\lambda^3\right)^{0.5} \tag{D.16}$$

3) A general expression for membrane stress and pressure loading is given by Equations (D.12) and (D.13), respectively, where the coefficients G_0 and G_p are calculated using the equations in Annex C, paragraph C.6.1.

D.2.3.3 Surface Correction Factors for Surface Cracks

The surface correction factors for surface cracks can be approximated using the results obtained for a through-wall crack by using one of the following methods. In all of these methods, the equations for M_t are provided in paragraph D.2.3.2.

a) Cylindrical or Spherical Shell – The following is an empirical equation which does not produce consistent results when the crack approaches a through-wall configuration, see reference [14]. The factor C in the equation is used to define a model for the cross sectional area of the surface crack to be included in the analysis. A value of $C = 1.0$ corresponds to a rectangular model and a value of $C = 0.67$ is used to model a parabolic shape. Experimental results indicate that a value of $C = 0.85$ provides an optimum fit to the data [7], [8]. The results from this equation are usually associated with a local limit load solution; the superscript L in the following equation designates a local limit load solution.

$$M_s^L = \frac{1 - C\left(\frac{a}{t}\right)\left(\frac{1}{M_t}\right)}{1 - C\left(\frac{a}{t}\right)} \tag{D.17}$$

b) Cylindrical or Spherical Shell – Equation (D.18) is based on a lower bound limit load solution and produces a consistent result as the crack approaches a through-wall configuration, see reference [17].

1) In the following equation, the term $M_t(\lambda_a)$ signifies that M_t is evaluated using the equations cited for a through-wall crack with the λ_a shell parameter as opposed to the λ shell parameter (compare Equation (D.7) with Equation (D.19)). The results from this equation are usually associated with a net section limit load solution; the superscript NS in the following equation designates a net section limit load solution.

$$M_s^{NS} = \frac{1}{1-\frac{a}{t}+\frac{a}{t}\left(\frac{1}{M_t(\lambda_a)}\right)} \tag{D.18}$$

where,

$$\lambda_a = \frac{1.818c}{\sqrt{R_i a}} \tag{D.19}$$

2) In reference [17], the crack area is idealized as an equivalent rectangle with an area equal to the elliptical crack area. In this paragraph, this approximation is not used and the area chosen to evaluate M_t is a rectangular area based on the crack depth and the full length of the crack. If desired, the equivalent elliptical area approximation can be introduced into the assessment by multiplying Equation (D.19) by $\pi/4$.

3) Equation (D.18) is written in terms of the component thickness and maximum depth of the flaw. If the flaw shape is characterized by a nonuniform thickness profile, Equation (D.18) can be written in terms of areas as follows:

$$M_s^{NS} = \frac{1}{1-\frac{A}{A_o}+\frac{A}{A_o}\left(\frac{1}{M_t(\lambda_a)}\right)} \tag{D.20}$$

c) The results from equations (D.17) and (D.18) are approximately the same for flaws up to $a/t \le 0.5$. Above this value, the use of Equation (D.17) to compute M_s will produce values that significantly exceed those obtained using Equation (D.18). This will result in conservatism in the computation of the stress intensity ratio, K_r, if the stress intensity factor is a function of M_s, and the load ratio, L_r, in the FAD assessment for a given material toughness and yield stress. Experimental results indicate that Equation (D.18) produces consistent results for $a/t > 0.5$. Therefore, Equation (D.18) is recommended for use to compute the stress intensity factor (numerator in K_r) and reference stress (numerator in L_r) unless additional conservatism is desired in the assessment. In summary, the following values can be used to compute the surface correction factor:

$$M_s = M_s^L \qquad assessment\ based\ on\ local\ ligament\ criteria \tag{D.21}$$

$$M_s = M_s^{NS} \qquad assessment\ based\ on\ net\ \text{section}\ collapse\ (recommended) \tag{D.22}$$

D.2.4 Load Ratio and Reference Stress

D.2.4.1 Load Ratio

The load ratio is the horizontal coordinate on the failure assessment diagram (see Part 9), and is defined as

$$L_r = \frac{P_l}{P_{ly}} \tag{D.23}$$

Alternatively, the load ratio can be written in terms of a reference stress:

$$L_r = \frac{\sigma_{ref}}{\sigma_{ys}} \tag{D.24}$$

with,

$$\sigma_{ref} = \left(\frac{P_l}{P_{ly}} \right) \sigma_{ys} \tag{D.25}$$

D.2.4.2 Reference Stress Solutions

This Annex contains reference stress solutions for selected crack-like flaw geometries. The reference stress solution in paragraph D.2.4.1 can be converted into a yield load solution by rearranging Equation (D.25). The limit load can be inferred by replacing the yield strength with an appropriate flow stress, see Annex F.

D.2.5 Plastic Collapse in the Assessment of Crack-Like Flaws

D.2.5.1 The position of an assessment point $\left(K_r, L_r\right)$ on the FAD represents a particular combination of flaw size, stresses and material properties. This point can be used to demonstrate whether the flaw is acceptable and an associated in-service margin can be computed based on the location of this point. If the flaw is unacceptable, the location of the assessment point on the FAD can indicate the type of failure that would be expected.

a) The failure assessment diagram can be divided into three zones as illustrated in Figure D.1. If the assessment point lies in Zone 1, the predicted failure mode is predominantly fracture controlled and could be associated with brittle fracture. If the assessment point lies in Zone 3, the predicted failure mode is collapse controlled with extensive yielding resulting in large deformations in the component. If the assessment point lies in a Zone 2 the predicted failure mode is elastic-plastic fracture.

b) The significance of the L_r parameter in a FAD assessment can be described in terms of crack-tip plasticity. If fracture occurs under elastic plastic conditions, the K_r value defined by the failure assessment line at the corresponding L_r value represents the elastic component of the crack driving force. The limiting value of K_r reduces from unity as L_r increases. Thus $\left(1 - K_r\right)$ represents the enhancement of the crack driving force due to plasticity. Therefore, the value of the L_r parameter represents a measure of the crack tip plasticity as long as the L_r parameter is less than the maximum permitted or cut-of value (see paragraph D.2.5.2.b).

D.2.5.2 The value of L_r depends on the type of plastic collapse load solution utilized in the assessment.

a) Plastic collapse solutions can be defined in three ways:

1) *Local Collapse* – Plastic collapse of the remaining ligament adjacent to the flaw being assessed. The reference stress solutions shown for plates in paragraphs D.3 and D.4 are based on a local collapse solution. The reference stress solutions shown for cylinders and spheres that utilize the plate ligament equations (see paragraph D.3) with a surface correction factor, M_s, based on a local limit load (see paragraph D.2.3.3, and paragraph C.2.3.3 of Annex C) are also considered to be local collapse solutions.

2) *Net Section Collapse* – Plastic collapse of the structural section containing the flaw. The reference stress solutions shown for cylinders and spheres that do not utilize the plate ligament formulas of paragraph D.3 are considered to be net section collapse solutions. In addition, the reference stress solutions shown for cylinders and spheres which utilize the plate ligament equations (see paragraph D.3) with a surface correction factor, M_s, based on a global limit load (see paragraph D.2.3.3) are also considered to be net section collapse solutions. The reference stress solutions for bars and bolts in paragraph D.11 are net section collapse solutions.

3) *Gross Collapse* – Plastic collapse of the structure by unconstrained or gross straining throughout the structure. This occurs when a plastic collapse mechanism is formed in the structure and may be unaffected by the presence of the crack.

b) It is acceptable to use the local plastic collapse solution to determine the reference stress when computing the value of L_r. However, this may be excessively conservative for redundant structures. If the structure or component has degrees of redundancy, plasticity at the cracked ligament may be contained by the surrounding structure until conditions for gross collapse are reached. In such cases, it may be possible to use more appropriate estimates of L_r based on modified lower bound collapse solutions that are based on the response of the entire structure. For this approach to be adopted, it is essential to confirm by analysis that the plasticity at the cracked section is contained sufficiently by the remaining structure, so that the use of the standard assessment diagram gives conservative results. In ferritic steels, care must also be exercised to ensure that local constraint conditions are not sufficient to induce brittle fracture by a cleavage mechanism. Where global collapse can be shown to occur after the attainment of $L_{r(\max)}$, the $L_{r(cut-off)}$ can be extended to the value relating to global collapse as described.

c) If the assessment point falls outside the acceptable region, then recategorization of the flaw being evaluated can be undertaken and a reassessment made (see Part 9). In general, the recategorization procedures described in Part 9 will only be effective if the assessment point falls within the elastic plastic fracture controlled zone or beyond $L_{r(\max)}$ (in the collapse controlled zone).

D.2.5.3 The reference stress solutions in this annex are based on the assessment of a single flaw. Multiple flaws which interact should be recategorized according to Part 9. However, multiple flaws that do not interact according to Part 9 may still affect the plastic collapse conditions, and allowances should be made to the collapse solutions to accommodate these effects.

D.2.5.4 It is recommended that a gross collapse assessment be performed to ensure that the applied stresses derived for local conditions do not cause failure of the structure in other regions.

a) In many cases a simple calculation can be performed to identify the highest applied stress condition that will result in the attainment of the flow strength on a significant cross section. In certain structures, gross collapse may occur in regions away from the flaw being assessed because of thinned areas, or where design conditions result in yielding of the general structure prior to collapse of the local regions.

b) To facilitate understanding of the relative importance of local, net section and gross collapse loads, it is useful to calculate the minimum collapse load for regions away from the cracked section, as well as that involving the cracked section and determining the parameter for both conditions. The minimum ratio of the gross collapse load for regions away from the cracked section to the local or net section collapse load at the cracked section represents a maximum value or cut-off on the $L_r - axis$. The cut-off limit may be less than one and in such cases the assessment diagram is effectively restricted by this cut-off. The failure assessment diagram is generally limited at higher values of L_r to a cut-off at $L_{r(\max)}$ that is based on material properties rather than structural behavior. In displacement controlled applications, the assessment diagram may be extended beyond the $L_{r(\max)}$ limit to the structural cut-off limit.

D.3 Reference Stress Solutions for Plates

D.3.1 Plate – Through-Wall Crack, Through-Wall Membrane And Bending Stress (RPTC)

D.3.1.1 The Reference Stress is [3]:

$$\sigma_{ref} = \frac{P_b + \left(P_b^2 + 9P_m^2\right)^{0.5}}{3\left(1-\alpha\right)} \tag{D.26}$$

where,

$$\alpha = \frac{c}{W} \tag{D.27}$$

D.3.1.2 Notes:

a) See Annex C Figure C.1 for the component and crack geometry.

b) See paragraph D.2.2.3 for determination of P_m and P_b.

D.3.2 Plate – Surface Crack, Infinite Length, Through-Wall Fourth Order Polynomial Stress Distribution (RPSCL1)

D.3.2.1 The Reference Stress is given by Equation (D.30) with the following definition of α:

$$\alpha = \frac{a}{t} \tag{D.28}$$

D.3.2.2 Notes:

a) See Annex C Figure C.2(b) for the component and crack geometry.

b) See paragraph D.2.3.3 for determination of P_m and P_b.

D.3.3 Plate – Surface Crack, Infinite Length, Through-wall Arbitrary Stress Distribution (RPSCL2)

D.3.3.1 Reference Stress in paragraph D.3.2 can be used.

D.3.3.2 Notes: see paragraph D.3.2.2.

D.3.4 Plate – Surface Crack, Semi-Elliptical Shape, Through-wall Membrane And Bending Stress (RPSCE1)

D.3.4.1 The Reference Stress is [3], [18]:

a) With bending restraint:

$$\sigma_{ref} = \frac{gP_b + \left[\left(gP_b \right)^2 + 9P_m^2 \left(1-\alpha \right)^2 \right]^{0.5}}{3\left(1-\alpha \right)^2} \tag{D.29}$$

b) With negligible bending restraint (e.g. pin-jointed):

$$\sigma_{ref} = \frac{P_b + 3P_m\alpha + \left[\left(P_b + 3P_m\alpha \right)^2 + 9P_m^2 \left(1-\alpha \right)^2 \right]^{0.5}}{3\left(1-\alpha \right)^2} \tag{D.30}$$

where

$$g = 1 - 20\left(\frac{a}{2c} \right)^{0.75} \alpha^3 \tag{D.31))}$$

$$\alpha = \frac{\frac{a}{t}}{1+\frac{t}{c}} \qquad for \quad W \geq \left(c+t \right) \tag{D.32}$$

$$\alpha = \left(\frac{a}{t} \right)\left(\frac{c}{W} \right) \qquad for \quad W < \left(c+t \right) \tag{D.33}$$

D.3.4.2 Notes:

a) See Annex C Figure C.2(a) for the component and crack geometry.

b) See paragraph D.2.2.3 for determination of P_m and P_b.

c) The normal bending restraint solution can be obtained by setting $g = 1.0$ [18].

d) If $a > c$, compute g based on $a/2c = 0.5$.

D.3.5 Plate – Surface Cracks, Semi-Elliptical Shape, Through-Wall Fourth Order Polynomial Stress Distribution (RPSCE2)

D.3.5.1 The Reference Stress in paragraph D.3.4 can be used.

D.3.5.2 Notes: see paragraph D.3.4.2.

D.3.6 Plate – Surface Crack, Semi-Elliptical Shape, Through-wall Arbitrary Stress Distribution (RPSCE3)

D.3.6.1 The Reference Stress in paragraph D.3.4 can be used.

D.3.6.2 Notes: see paragraph D.3.4.2.

D.3.7 Plate – Embedded Crack, Infinite Length, Through-Wall Fourth Order Polynomial Stress Distribution (RPECL)

D.3.7.1 The Reference Stress is [3]:

$$\sigma_{ref} = \frac{P_b + 3P_m\alpha + \left[\left(P_b + 3P_m\alpha\right)^2 + 9P_m^2\left\{\left(1-\alpha\right)^2 + \frac{4d\alpha}{t}\right\}\right]^{0.5}}{3\left[\left(1-\alpha\right)^2 + \frac{4d\alpha}{t}\right]} \tag{D.34}$$

where,

$$d = d_1 - a \tag{D.35}$$

$$\alpha = \frac{2a}{t} \tag{D.36}$$

D.3.7.2 Notes:

a) See Annex C Figure C.3(b) for the component and crack geometry.

b) See paragraph D.2.2.3 for determination of P_m and P_b.

D.3.8 Plate – Embedded Crack, Elliptical Shape, Through-Wall Membrane and Bending Stress (RPECE1)

D.3.8.1 The Reference Stress is given by Equation (D.34) with following definitions of d and α:

$$d = d_1 - a \tag{D.37}$$

$$\alpha = \frac{\frac{2a}{t}}{1+\frac{t}{c}} \qquad for \quad W \geq \left(c+t\right) \tag{D.38}$$

$$\alpha = \left(\frac{2a}{t}\right)\left(\frac{c}{W}\right) \qquad for \quad W < \left(c+t\right) \tag{D.39}$$

D.3.8.2 Notes:

a) See Annex C Figure C.3(a) for the component and crack geometry.

b) See paragraph D.2.2.3 for determination of P_m and P_b.

D.3.9 Plate – Embedded Crack, Elliptical Shape, Through-Wall Fourth-Order Polynomial Stress Distribution (RPECE2)

D.3.9.1 The Reference Stress in paragraph D.3.8.1 can be used.

D.3.9.2 Notes:

a) See Annex C Figure C.3(a) for the component and crack geometry.

b) See paragraph D.2.2.3 for determination of P_m and P_b.

D.4 Reference Stress Solutions For Plates with Holes

D.4.1 Plate With Hole – Through-Wall Single Edge Crack, Through-Wall Membrane And Bending Stress (RPHTC1)

D.4.1.1 The Reference Stress is given by Equation (D.26) with the following definition of α :

$$\alpha = \frac{at}{t\left(a+t\right)} \tag{D.40}$$

D.4.1.2 Notes:

a) See Annex C Figure C.6(a) for the component and crack geometry.

b) See paragraph D.2.2.3 for determination of P_m and P_b.

D.4.2 Plate With Hole – Through-Wall Double Edge Crack, Through-Wall Membrane And Bending Stress (RPHTC2)

D.4.2.1 The Reference Stress is given by Equation (D.26) with the following definition of α :

$$\alpha = \frac{2at}{t\left(2a+t\right)} \tag{D.41}$$

D.4.2.2 Notes:

a) See Annex C Figure C.7(a) for the component and crack geometry.

b) See paragraph D.2.2.3 for determination of P_m and P_b.

D.4.3 Plate With Hole – Surface Crack, Semi-Elliptical Shape, Through-Wall Membrane Stress (RPHSC1)

D.4.3.1 The Reference Stress is:

$$\sigma_{ref} = \frac{3P_m\alpha + \left[\left(3P_m\alpha\right)^2 + 9P_m^2\left\{\left(1-\alpha\right)^2 + \frac{4d\alpha}{t}\right\}\right]^{0.5}}{3\left[\left(1-\alpha\right)^2 + \frac{4d\alpha}{t}\right]} \tag{D.42}$$

where,

$$d = t - c \tag{D.43}$$

$$\alpha = \frac{\frac{2c}{t}}{1+\frac{t}{a}} \tag{D.44}$$

D.4.3.2 Notes:

a) See Annex C Figure C.8 for the component and crack geometry.

b) See paragraph D.2.2.3 for determination of P_m.

D.4.4 Plate With Hole, Corner Crack, Semi-Elliptical Shape, Through-Wall Membrane and Bending Stress (RPHSC2)

D.4.4.1 The Reference Stress is given by Equation (D.26) with the following definition of α :

$$\alpha = \frac{2ac}{t(2a+t)} \tag{D.45}$$

D.4.4.2 Notes:

a) See Annex C Figure C.9 for the component and crack geometry.

b) See paragraph D.2.2.3 for determination of P_m and P_b.

D.5 Reference Stress Solutions For Cylinders

D.5.1 Cylinder – Through-Wall Crack, Longitudinal Direction, Through-Wall Membrane and Bending Stress (RCTCL)

D.5.1.1 The Reference Stress is [1],[3]:

$$\sigma_{ref} = \frac{P_b + \left(P_b^2 + 9\{M_t \cdot P_m\}^2\right)^{0.5}}{3} \tag{D.46}$$

D.5.1.2 Notes:

a) See Annex C Figure C.10 for the component and crack geometry.

b) See paragraph D.2.2.3 for determination of P_m and P_b. For internal pressure loading:

$$P_m = \frac{pR_i}{t} \tag{D.47}$$

$$P_b = \frac{pR_o^{\,2}}{R_o^{\,2} - R_i^{\,2}}\left[\frac{t}{R_i} - \frac{3}{2}\left(\frac{t}{R_i}\right)^2 + \frac{9}{5}\left(\frac{t}{R_i}\right)^3\right] \tag{D.48}$$

c) See paragraph D.2.3 to determine M_t for a through-wall crack in a cylinder.

D.5.2 Cylinder – Through-Wall Crack, Circumferential Direction, Through-Wall Membrane and Bending Stress (RCTCC1)

D.5.2.1 The Reference Stress is [2]:

$$\sigma_{ref} = \frac{P_b + \left(P_b^2 + 9\left\{Z \cdot P_m \cdot (1-\alpha)^2\right\}^2\right)^{0.5}}{3(1-\alpha)^2} \tag{D.49}$$

where,

$$Z = \frac{\pi\left(R_o^2 - R_i^2\right)}{\left(2-\tau\right)R_o t\left(2\psi - \theta\right)} \tag{D.50}$$

$$\tau = \frac{t}{R_o} \tag{D.51}$$

$$\psi = \arccos\left(\frac{\sin\theta}{2}\right) \tag{D.52}$$

$$\theta = \frac{c}{R_m} \tag{D.53}$$

$$\alpha = \frac{c}{\pi R_m} \tag{D.54}$$

D.5.2.2 Notes:

a) See Annex C Figure C.11 for the component and crack geometry.

b) See paragraph D.2.2.3 for determination of P_m and P_b. For internal pressure with a net section axial force:

$$P_m = \frac{pR_i^2}{R_o^2 - R_i^2} + \frac{F}{\pi\left(R_o^2 - R_i^2\right)} \tag{D.55}$$

$$P_b = 0.0 \tag{D.56}$$

D.5.3 Cylinder – Through-Wall Crack, Circumferential Direction, Pressure With Net Section Axial Force and Bending Moment (RCTCC2)

D.5.3.1 The Reference Stress is [4]:

$$\sigma_{ref} = \left[\frac{M}{2\sigma_{ys}R_m^2 t\left(2\cos\beta - \sin\theta\right) - 2pR_m^3\cos\beta}\right]\sigma_{ys} + \sigma_{ref}^{D.5.2} \tag{D.57}$$

where, $\sigma_{ref}^{D.5.2}$ is the reference stress from paragraph D.5.2, and

$$\beta = \frac{\sigma_{ys}R_m t\theta + \frac{F}{2}}{2\sigma_{ys}R_m t - pR_m^2} \tag{D.58}$$

$$\theta = \frac{c}{R_m} \tag{D.59}$$

D.5.3.2 Notes:

a) See Annex C Figure C.11 for the component and crack geometry.

b) If the net-section bending moment is zero, the solution in paragraph D.5.2 must be used.

D.5.4 Cylinder – Surface Crack, Longitudinal Direction – Infinite Length, Internal Pressure (RCSCLL1)

D.5.4.1 The Reference Stress [1], [3]:

$$\sigma_{ref} = \frac{P_b + \left[P_b^2 + 9\left\{ M_s \cdot P_m \cdot \left(1-\alpha\right)^2 \right\}^2 \right]^{0.5}}{3\left(1-\alpha\right)^2} \tag{D.60}$$

where,

$$M_s = \frac{1.0}{1.0-\alpha} \tag{D.61}$$

$$\alpha = \frac{a}{t} \tag{D.62}$$

D.5.4.2 Notes:

a) See Annex C Figure C.12 for the component and crack geometry.

b) See paragraph D.5.1.2.b for determination of P_m and P_b.

D.5.5 Cylinder – Surface Crack, Longitudinal Direction – Infinite Length, Through-Wall Fourth Order Polynomial Stress Distribution (RCSCLL2)

D.5.5.1 The Reference Stress in paragraph D.5.4 can be used.

D.5.5.2 Notes: see paragraph D.5.4.2.

D.5.6 Cylinder – Surface Crack, Longitudinal Direction – Infinite Length, Through-wall Arbitrary Stress Distribution (RCSCLL3)

D.5.6.1 The Reference Stress in paragraph D.5.4 can be used.

D.5.6.2 Notes: see paragraph D.5.4.2..

D.5.7 Cylinder – Surface Crack, Circumferential Direction – 360 Degrees, Pressure With Net Section Axial Force And Bending Moment (RCSCCL1)

D.5.7.1 The Reference Stress is [5]:

$$\sigma_{ref} = \frac{M_r}{2} + \left(N_r^2 + \frac{M_r^2}{4} \right)^{0.5} \tag{D.63}$$

For an inside surface crack

$$N_r = \frac{P_m \left[R_o^2 - R_i^2 \right]}{\left[R_o^2 - \left(R_i + a \right)^2 \right]} \tag{D.64}$$

$$M_r = P_{bg}\frac{3\pi}{16}\left[\frac{R_o^4 - R_i^4}{R_o^4 - R_i\left(R_i + a\right)^3}\right] \tag{D.65}$$

For an outside surface crack

$$N_r = \frac{P_m\left[R_o^2 - R_i^2\right]}{\left[\left(R_o - a\right)^2 - R_i^2\right]} \tag{D.66}$$

$$M_r = P_{bg}\frac{3\pi}{16}\left[\frac{R_o^4 - R_i^4}{R_o\left(R_o - a\right)^3 - R_i^4}\right] \tag{D.67}$$

D.5.7.2 Notes:

a) See Annex C Figure C.13 for the component and crack geometry.

b) P_m and P_{bg} are determined using the following equations:

$$P_m = \frac{pR_i^2}{\left(R_o^2 - R_i^2\right)} + \frac{F}{\pi\left(R_o^2 - R_i^2\right)} \tag{D.68}$$

$$P_{bg} = \frac{MR_o}{0.25\pi\left(R_o^4 - R_i^4\right)} \tag{D.69}$$

D.5.8 Cylinder – Surface Crack, Circumferential Direction – 360 Degrees, Through-Wall Fourth Order Polynomial Stress Distribution (RCSCCL2)

D.5.8.1 The Reference Stress is [2]:

$$\sigma_{ref} = \frac{P_b + \left(P_b^2 + 9\left\{Z \cdot P_m \cdot \left(1-\alpha\right)^2\right\}^2\right)^{0.5}}{3\left(1-\alpha\right)^2} \tag{D.70}$$

where

$$Z = \left[1 - \alpha\left(\frac{2 - 2\tau + \alpha\tau}{2 - \tau}\right)\right]^{-1} \tag{D.71}$$

$$\tau = \frac{t}{R_o} \tag{D.72}$$

$$\alpha = \frac{a}{t} \tag{D.73}$$

D.5.8.2 Notes:

a) See Annex C Figure C.13 for the component and crack geometry.

b) See paragraph D.2.2.3 for determination of P_m and P_b.

D.5.9 Cylinder – Surface Crack, Circumferential Direction – 360 Degrees, Through-wall Arbitrary Stress Distribution (RCSCCL3)

D.5.9.1 The Reference Stress in paragraph D.5.8 can be used.

D.5.9.2 Notes: see paragraph D.5.8.2.

D.5.10 Cylinder – Surface Crack, Longitudinal Direction – Semi-Elliptical Shape, Internal Pressure (RCSCLE1)

D.5.10.1 The Reference Stress is [3], [6]:

$$\sigma_{ref} = \frac{gP_b + \left[\left(gP_b \right)^2 + 9\left(M_s \cdot P_m \cdot \left(1-\alpha \right)^2 \right)^2 \right]^{0.5}}{3\left(1-\alpha \right)^2} \tag{D.74}$$

where g is given by Equation (D.31) with the following definition of α:

$$\alpha = \frac{\frac{a}{t}}{1+\frac{t}{c}} \tag{D.75}$$

D.5.10.2 Notes:

a) See Annex C Figure C.14 for the component and crack geometry.

b) See paragraph D.5.1.2.b for determination of P_m and P_b.

c) See paragraph D.2.3 to determine M_s for a surface crack in a cylinder.

D.5.11 Cylinder – Surface Crack, Longitudinal Direction – Semi-Elliptical Shape, Through-Wall Fourth Order Polynomial Stress Distribution (RCSCLE2)

D.5.11.1 The Reference Stress in paragraph D.5.10 can be used.

D.5.11.2 Notes: see paragraph. D.5.10.2

D.5.12 Cylinder – Surface Crack, Longitudinal Direction – Semi-Elliptical Shape, Through-wall Arbitrary Stress Distribution (RCSCLE3)

D.5.12.1 The Reference Stress in paragraph D.5.10 can be used.

D.5.12.2 Notes: see paragraph D.5.10.2.

D.5.13 Cylinder – Surface Crack, Circumferential Direction – Semi-Elliptical Shape, Internal Pressure and Net-Section Axial Force (RCSCCE1)

D.5.13.1 The Reference Stress is [2]:

$$\sigma_{ref} = \frac{P_b + \left(P_b^2 + 9\left\{ Z \cdot P_m \cdot \left(1-\alpha\right)^2 \right\}^2 \right)^{0.5}}{3\left(1-\alpha\right)^2} \tag{D.76}$$

where,

$$P_m = \frac{pR_i^2}{R_o^2 - R_i^2} + \frac{F}{\pi\left(R_o^2 - R_i^2\right)} \tag{D.77}$$

$$P_b = 0.0 \tag{D.78}$$

$$Z = \left[\frac{2\psi}{\pi} - \frac{x\theta}{\pi}\left(\frac{2 - 2\tau + x\tau}{2-\tau} \right) \right]^{-1} \tag{D.79}$$

$$\psi = \arccos\left(A \sin\theta \right) \tag{D.80}$$

$$\alpha = \frac{\frac{a}{t}}{1 + \frac{t}{c}} \tag{D.81}$$

$$A = x\left[\frac{\left(1-\tau\right)\left(2-2\tau+x\tau\right) + \left(1-\tau+x\tau\right)^2}{2\left\{1+\left(2-\tau\right)\left(1-\tau\right)\right\}} \right] \tag{D.82}$$

$$\tau = \frac{t}{R_o} \tag{D.83}$$

$$x = \frac{a}{t} \tag{D.84}$$

$$\theta = \frac{\pi c}{4R_i} \qquad \textit{for an internal crack} \tag{D.85}$$

$$\theta = \frac{\pi c}{4R_o} \qquad \textit{for an external crack} \tag{D.86}$$

D.5.13.2 Notes:

a) See Annex C Figure C.15 for the component and crack geometry.

b) This solution can be used for any applied through-wall stress distribution if paragraph D.2.2.3 is used to determine of P_m and P_b.

D.5.14 Cylinder – Surface Crack, Circumferential Direction – Semi-Elliptical Shape, Through-Wall Fourth Order Polynomial Stress Distribution With Net Section Bending Stress (RCSCCE2)

D.5.14.1 The Reference Stress is [2]:

If $(\theta+\beta)\le\pi$, then

$$\sigma_{ref}=\frac{M}{2R_m^2t\left(2\sin\beta-\frac{a}{t}\sin\theta\right)}+\sigma_{ref}^{D.5.13} \tag{D.87}$$

where, $\sigma_{ref}^{D.5.13}$ is the reference stress from paragraph D.5.13, and

$$\beta=\frac{\pi}{2}\left[1-\left(\frac{\theta}{\pi}\right)\left(\frac{a}{t}\right)-\frac{P_m}{\sigma_{ys}}\right] \tag{D.88}$$

$$\theta=\frac{\pi c}{4R_i} \qquad \textit{for an internal crack} \tag{D.89}$$

$$\theta=\frac{\pi c}{4R_o} \qquad \textit{for an external crack} \tag{D.90}$$

If $(\theta+\beta)>\pi$, then

$$\sigma_{ref}=\frac{M}{2R_m^2t\left(2-\frac{a}{t}\right)\sin\beta}+\sigma_{ref}^{D.5.13} \tag{D.91}$$

where, $\sigma_{ref}^{D.5.13}$ is the reference stress from paragraph D.5.13, and

$$\beta=\frac{\pi\left(1-\frac{a}{t}-\frac{P_m}{\sigma_{ys}}\right)}{2-\frac{a}{t}} \tag{D.92}$$

D.5.14.2 Notes:

a) See Annex C Figure C.15 for the component and crack geometry.

b) See paragraph D.2.2.3 for determination of P_m.

c) If the net section bending moment is zero, the solution in paragraph D.5.13 can be used with $F=0.0$ and P_m is equal to the value determined in subparagraph b above.

D.5.15 Cylinder – Surface Crack, Circumferential Direction – Semi-Elliptical Shape, Through-wall Arbitrary Stress Distribution (RCSCCE3)

D.5.15.1 The Reference Stress in paragraph D.5.13.1 can be used.

D.5.15.2 Notes:

a) See Annex C , Figure C.15 for the component and crack geometry.

b) See paragraph D.2.2.3 for determination of P_m and P_b.

D.5.16 Cylinder – Embedded Crack, Longitudinal Direction – Infinite Length, Through-Wall Fourth Order Polynomial Stress Distribution (RCECLL)

D.5.16.1 The Reference Stress in paragraph D.3.7.1can be used.

D.5.16.2 Notes:

a) See Annex C Figure C.16 for the component and crack geometry.

b) See paragraph D.2.2.3 for determination of P_m and P_b.

D.5.17 Cylinder – Embedded Crack, Circumferential Direction – 360 Degrees, Through-Wall Fourth Order Polynomial Stress Distribution (RCECCL)

D.5.17.1 The Reference Stress in paragraph D.3.7.1 can be used.

D.5.17.2 Notes:

a) See Annex C Figure C.17 for the component and crack geometry.

b) See paragraph D.2.2.3 for determination of P_m and P_b.

D.5.18 Cylinder – Embedded Crack, Longitudinal Direction – Elliptical Shape, Through-Wall Fourth Order Polynomial Stress Distribution (RCECLE)

D.5.18.1 The Reference Stress is given by Equation (D.34) with the following definitions for d and α:

$$d = d_1 - a \tag{D.93}$$

$$\alpha = \frac{\frac{2a}{t}}{1+\frac{t}{c}} \tag{D.94}$$

D.5.18.2 Notes:

a) See Annex C Figure C.18 for the component and crack geometry.

b) See paragraph D.2.2.3 for determination of P_m and P_b.

D.5.19 Cylinder – Embedded Crack, Circumferential Direction – Elliptical Shape, Through-Wall Fourth Order Polynomial Stress Distribution (RCECCE)

D.5.19.1 The Reference Stress in paragraph D.5.18.1 can be used.

D.5.19.2 Notes:

a) See Annex C Figure C.19 for the component and crack geometry.

b) See paragraph D.2.2.3 for determination of P_m and P_b.

D.6 Reference Stress Solutions For Spheres

D.6.1 Sphere – Through-Wall Crack, Through-Wall Membrane and Bending Stress (RSTC)

D.6.1.1 The Reference Stress solution in paragraph D.5.1.1 can be used.

D.6.1.2 Notes:

a) See Annex C Figure C.20 for the component and crack geometry.

b) See paragraph D.2.2.3 for determination of P_m and P_b. For internal pressure loading only:

$$P_m = \frac{pR_i^{\,2}}{R_o^{\,2} - R_i^{\,2}} \tag{D.95}$$

$$P_b = \frac{pR_o^{\,3}}{R_o^{\,3} - R_i^{\,3}} \left[\frac{3}{4}\left(\frac{t}{R_i}\right) - \frac{3}{2}\left(\frac{t}{R_i}\right)^2 + \frac{9}{4}\left(\frac{t}{R_i}\right)^3 \right] \tag{D.96}$$

c) See paragraph D.2.3.2 to determine M_t for a through-wall crack in a sphere.

D.6.2 Sphere – Surface Crack, Circumferential Direction – 360 Degrees, Internal Pressure (RSSCCL1)

D.6.2.1 The Reference Stress in paragraph D.5.4.1 can be used.

D.6.2.2 Notes:

a) See Annex C Figure C.21 for the component and crack geometry.

b) See paragraph D.2.2.3 for determination of P_m and P_b.

c) See paragraph D.2.3.3 to determine M_s for a surface crack in a sphere.

D.6.3 Sphere – Surface Crack, Circumferential Direction – 360 Degrees, Through-Wall Fourth Order Polynomial Stress Distribution (RSSCCL2)

D.6.3.1 The Reference Stress in paragraph. D.5.4.1 can be used.

D.6.3.2 Notes: see paragraph D.6.2.2.

D.6.4 Sphere – Surface Crack, Circumferential Direction – 360 Degrees, Through-wall Arbitrary Fourth Order Polynomial Stress Distribution (RSSCCL3)

D.6.4.1 The Reference Stress in paragraph D.5.4.1 can be used.

D.6.4.2 Notes: see paragraph D.6.2.2.

D.6.5 Sphere – Surface Crack, Circumferential Direction – Semi-Elliptical Shape, Internal Pressure (RSSCCE1)

D.6.5.1 The Reference Stress in paragraph D.5.10.1 can be used.

D.6.5.2 Notes:

a) See Annex C Figure C.22 for the component and crack geometry.

b) See paragraph D.6.1.2.b for determination of P_m and P_b.

c) See paragraph D.2.3.3 to determine M_s for a surface crack in a sphere.

D.6.6 Sphere – Surface Crack, Circumferential Direction – Semi-Elliptical Shape, Through-Wall Fourth Order Polynomial Stress Distribution (RSSCCE2)

D.6.6.1 The Reference Stress in paragraph D.5.10.1 can be used.

D.6.6.2 Notes: see paragraph D.6.5.2.

D.6.7 Sphere – Surface Crack, Circumferential Direction – Semi-Elliptical Shape, Through-wall Arbitrary Stress Distribution (RSSCCE3)

D.6.7.1 The Reference Stress in paragraph D.5.10.1 can be used.

D.6.7.2 Notes: see paragraph D.6.5.2.

D.6.8 Sphere – Embedded Crack, Circumferential Direction – 360 Degrees, Through-Wall Fourth Order Polynomial Stress Distribution (RSECCL)

D.6.8.1 The Reference Stress in paragraph D.3.7.1 can be used.

D.6.8.2 Notes:

a) See Annex C Figure C.23 for the component and crack geometry.

b) See paragraph D.2.2.3 for determination of P_m and P_b.

D.6.9 Sphere – Embedded Crack, Circumferential Direction – Elliptical Shape, Through-Wall Fourth Order Polynomial Stress Distribution (RSECCE)

D.6.9.1 The Reference Stress in D.3.8.1 can be used.

D.6.9.2 Notes:

a) See Annex C Figure C.24 for the component and crack geometry.

b) See paragraph D.2.2.3 for determination of P_m and P_b.

D.7 Reference Stress Solutions For Elbows And Pipe Bends

The reference stress solutions for cylinders can be used for elbows and pipe bends if the equivalent membrane and bending stress at the location of the crack is determined considering the bend geometry and applied loads. A discussion regarding the stress analysis for elbows is provided in Annex C , paragraph C.7.

D.8 Reference Stress Solutions For Nozzles And Piping Tees

D.8.1 Nozzle – Corner Crack, Radial Direction, Quarter-Circular Shape, Membrane Stress At The Corner (RNCC1)

D.8.1.1 The Reference Stress is [2]:

$$\sigma_{ref} = P_m \left(\frac{2.5t_n^2 + \{q - r_n\}t}{2.5t_n^2 + \{q - r_n\}t - 0.25\pi a^2} \right) \tag{D.97}$$

where,

$$q = \max\left[2r_n, \{r_n + t_n + t\}\right] \tag{D.98}$$

$$r_n = \frac{d_n - t_n}{2} \tag{D.99}$$

D.8.1.2 Notes:

a) See Annex C Figure C.25 (Crack labeled G) and Annex C Figure C.26 for the component and crack geometry.

b) P_m is the primary membrane stress at the nozzle, the effects of the stress concentration are neglected in the calculation of the reference stress because this stress is localized.

D.8.2 Nozzle – Corner Crack, Radial Direction, Quarter-Circular Shape, Cubic Polynomial Stress Distribution (RNCC2)

D.8.2.1 The Reference Stress is computed using equations in paragraph D.8.1.1 with an equivalent membrane stress.

D.8.2.2 Notes:

a) See Annex C Figure C.25 (Crack labeled G) and Annex C Figure C.26 for the component and crack geometry.

b) See paragraph D.2.2.3 for determination of P_m.

D.8.3 Surface Cracks At Nozzles – General Solution

The reference stress solutions shown below can be used for nozzles if the equivalent membrane and bending stress at the location of the crack is determined considering the nozzle geometry and applied loads. A discussion regarding the stress analysis for nozzles is provided in Annex C, paragraph C.8.

a) Nozzle Neck or Branch (see Annex C Figure C.25)

   1) Crack A – Use RCTCC1, RCTCC2, RCSCCL3, RCSCCE3, RCECCL or RCECCE

   2) Crack B – Use RCTCL, RCSCLL3, RCSCLE3, RCECLL or RCECLE

b) Shell or Run Pipe (see Annex C Figure C.25)

   1) Crack D & F – Use RPTC, RPSCE3, RPECL, or RPECE2

   2) Crack E & C – Use RPTC, RPSCE3, RPECL, or RPECE2

   3) Crack G – Use the solutions in paragraph D.8

D.9 Reference Stress Solutions For Ring-Stiffened Cylinders

D.9.1 Ring-Stiffened Cylinder – Internal Ring, Surface Crack At The Toe Of One Fillet Weld, Circumferential Direction – 360 Degrees, Pressure Loading (RRCSCCL1)

D.9.1.1 The Reference Stress in paragraph D.5.8.1 can be used with an equivalent membrane and bending stress.

D.9.1.2 Notes:

a) See Annex C Figure C.27 for the component and crack geometry.

b) See paragraph A.8.3 of Annex A for determination of the equivalent membrane stress, P_m, and bending stress, P_b, based on the stress results at the inside and outside surface, or

$$P_m = \frac{\sigma_{s,ID} + \sigma_{s,OD}}{2} \qquad \text{(D.100)}$$

$$P_b = \frac{\left|\sigma_{s,ID} - \sigma_{s,OD}\right|}{2} \qquad \text{(D.101)}$$

D.9.2 Ring-Stiffened Cylinder – Internal Ring, Surface Crack At The Toe Of Both Fillet Welds, Circumferential Direction – 360 Degrees, Pressure Loading (RRCSCCL2)

D.9.2.1 The Reference Stress in paragraph D.5.8.1 can be used with an equivalent membrane and bending stress.

D.9.2.2 Notes: see paragraph D.9.1.2.

D.10 Reference Stress Solutions For Sleeve Reinforced Cylinders

The reference stress solutions shown below can be used for sleeve reinforced cylinders (see Annex C Figure C.28) if the stress at the location of the crack is determined considering the actual component geometry and applied loads. A discussion regarding the stress analysis is provided for sleeve reinforced cylinders in Annex C , paragraph C.10.

a) Crack A – Use RCTCC1, RCTCC2, RCSCCL3, RCSCCE3, RCECCL or RCECCE

b) Crack B – Use RCTCL, RCSCLL3, RCSCLE3, RCECLL or RCECLE

D.11 Reference Stress Solutions for Round Bars and Bolts

D.11.1 Round Bar, Surface Crack – 360 Degrees, Membrane and Bending Stress (RBSCL)

D.11.1.1 The Reference Stress is:

$$\sigma_{ref} = \frac{M_r}{2} + \left(N_r^2 + \frac{M_r^2}{4} \right)^{0.5} \qquad \text{(D.102)}$$

where,

$$N_r = \frac{P_m R_o^2}{\left(R_o - a\right)^2} \qquad \text{(D.103)}$$

$$M_r = P_{bg}\frac{3\pi}{16}\left[\frac{R_o^4}{R_o\left(R_o - a\right)^3}\right] \tag{D.104}$$

D.11.1.2 Notes:

a) See Annex C Figure C.29 for the component and crack geometry.

b) The primary membrane and global bending stresses are computed using the following equations:

$$P_m = \frac{F}{\pi R_o^2} \tag{D.105}$$

$$P_{bg} = \frac{4M}{\pi R_o^3} \tag{D.106}$$

D.11.2 Round Bar – Surface Crack, Straight Front, Membrane and Bending Stress (RBSCS)

D.11.2.1 The Reference Stress is [6]:

$$\sigma_{ref} = \frac{\pi P_m}{\frac{\pi}{2} + \frac{1}{2}\sin 2\beta + \beta} + \frac{3\pi P_{bg}}{16\omega} \tag{D.107}$$

where,

$$\beta = \arcsin\left(\frac{R_o - a}{R_o}\right) \tag{D.108}$$

$$\omega = 1.0002 - 3.9927\left(\frac{a}{2R_o}\right)^{1.5} + 5.8491\left(\frac{a}{2R_o}\right)^{2.5} - 2.8550\left(\frac{a}{2R_o}\right)^{3} \tag{D.109}$$

D.11.2.2 Notes:

a) For the component and crack geometry see Annex C Figure C.30.

b) The primary membrane and global bending stresses can be determined using the equations in paragraph D.11.1.2.b.

D.11.3 Round Bar – Surface Crack, Semi-Circular, Membrane and Bending Stress (RBSCC)

D.11.3.1 The Reference Stress in paragraph D.11.2.1 can be used.

D.11.3.2 Notes:

a) See Annex C Figure C.30 for the component and crack geometry.

b) The semi-elliptical flaw is evaluated as an equivalent to a straight front flaw.

D.11.4 Bolt, Surface Crack, Semi-Circular or Straight Front Shape, Membrane and Bending Stress (RBSC)

D.11.4.1 The Reference Stress in paragraph D.11.2.1 can be used by replacing R_o with R_{th}.

D.11.4.2 Notes:

a) See Annex C Figure C.31 for the component and crack geometry.

b) The solution applies to a semi-circular or straight front surface crack.

D.12 Reference Stress Solutions For Cracks At Fillet Welds

D.12.1 Cracks at Fillet Welds – Surface Crack At A Tee Joint, Semi-Elliptical Shape, Through-Wall Membrane and Bending Stress (RFWSCE1)

D.12.1.1 The Reference Stress in paragraph D.3.4.1 can be used with an equivalent membrane and bending stress.

D.12.1.2 Notes:

a) See Annex C Figure C.32 for the component and crack geometry.

b) See paragraph D.2.2.3 for determination of P_m and P_b.

D.12.1.3 Cracks at Fillet Welds of Tee Junctions In Pressurized Components – General Solution

The reference stress solutions shown below can be used for cracks at tee junction fillet welds in pressure containing components (see Annex C , Figure C.33) if the stress at the location of the crack is determined considering the actual component geometry and applied loads. A discussion regarding the stress analysis is provided in Annex C , paragraph C.12.

Flat Plate Tee Junctions – Use RPTC, RPSCE3, RPECL, or RPECE2

a) Longitudinal Tee Junctions in Cylinders – Use RCTCL, RCSCLL3, RCSCLE3, RCECLL or RCECLE

b) Circumferential Tee Junctions in Cylinders – Use RCTCC1, RCTCC2, RCSCCL3, RCSCCE3, RCECCL or RCECCE

c) Circumferential Tee Junctions in Spheres – Use RSTC, RSSCCL3, RSECCL or RSECCE

D.13 Reference Stress Solutions For Cracks In Clad Plates And Shells

The reference stress solutions in this annex can be use to evaluate clad or weld overlayed plate and shell components. A discussion regarding the stress analysis for clad and weld overlayed plate and shell components is provided in Annex C , paragraph C.13.

D.14 Nomenclature

A cross-sectional area of the flaw.

A_o cross-sectional area of the component computed for the flaw length.

a crack depth parameter.

α reference stress parameter.

β reference stress parameter. c crack length parameter.

d reference stress parameter.

d_n mean nozzle diameter (see Annex C , Figure C.26).

d_1 distance from plate surface to the center of an embedded elliptical crack (see Annex C , Figure C.3).

F net section axial force acting on a cylinder.

g is a reference stress bending parameter.

λ shell parameter used to determine the surface correction factors.

M resultant net-section bending moment acting on a cylinder.

M_r bending moment.

M_s surface correction factor for a surface crack.

M_t surface correction factor for a through-wall crack.

N_r force.

ω reference stress parameter.

P_b through-wall primary bending stress component.

P_{bg} primary net-section bending stress.

P_l generalized loading parameter, such as applied stress, bending moment, or pressure.

P_m primary membrane stress component.

P_{ij} primary stress component being evaluated.

$P_{ij,b}$ equivalent primary bending stress for a stress component.

$P_{ij,m}$ equivalent primary membrane stress for a stress component.

P_{ly} value of the generalized loading parameter evaluated for the component with a crack-like flaw at the yield stress.

P_0 uniform coefficient for polynomial primary stress distribution.

P_1 linear coefficient for polynomial primary stress distribution.

P_2 quadratic coefficient for polynomial primary stress distribution.

P_3 third order coefficient for polynomial primary stress distribution.

P_4 fourth order coefficient for polynomial primary stress distribution.

P_5 net-section primary bending stress about the x-axis.

P_6 net-section primary bending stress about the y-axis.

p pressure.

ψ reference stress parameter.

q nozzle reinforcement zone.

r_n nozzle radius.

R_i cylinder inside radius.

R_m cylinder mean radius.

R_o cylinder, round bar, or bolt outside radius, as applicable.

R_{th} root radius of a threaded bolt.

σ_{ref} reference stress.

σ_{ys} yield stress (see Annex F).

$\sigma_{s,ID}$ surface stress on the inside diameter.

$\sigma_{s,OD}$ surface stress on the outside diameter.

t plate or shell thickness.

t_n nozzle thickness (see Annex C, Figure C.26).

τ reference stress parameter.

θ half-angle of the crack.

W distance from the center of the flaw to the free edge of the plate.

x radial local coordinate originating at the internal surface of the component or a reference stress parameter.

x_g global coordinate for definition of net section bending moment about the x-axis.

y_g global coordinate for definition of net section bending moment about the y-axis.

Z reference stress parameter.

D.15 References

1. Miller, A.G., “Review of Limit Loads of Structures Containing Defects,” International Journal of Pressure Vessels & Piping, Vol. 32, 1988.
2. Zahoor, A., "Ductile Fracture Handbook", Electric Power Research Institute, Palo Alto, CA, 1989.
3. Willoughby, A.A. and Davey, T.G., “Plastic Collapse in Part-Wall Flaws in Plates,”Fracture Mechanics: Perspectives and Directions (Twentieth Symposium), ASTM STP 1020, R.P. Wei and R.P. Gangloff, Eds., American Society for Testing and Materials, Philadelphia, 1989, pp. 390-409.
4. Bamford, W.H., Landerman, E.I., and Diaz, E., “Thermal Analysis of Cast Stainless Steel, and its Impact on Piping Integrity,” Circumferential Cracks in Pressure vessels and Piping – Vol. II, ASME PVP – Vol. 95, G.M. Wilkowski, American Society of Mechanical Engineers, 1984, pp. 137-172.
5. Bergman, M., Bjorn, B., Dahlberg, L., Nilsson, F., and Sattari-Far, I., “A Procedure For Safety Assessment of Components with Cracks – Handbook,” SA/FoU-Report 91/01, The Swedish Plant Inspectorate, Stockholm, Sweden, December, 1991.
6. BSI, “Draft Revision to PD6493 Fracture Assessment”, TWI, March, 1996.
7. Kiefner, J.F. and Vieth, P.H., “Project PR 3-805, A Modified Criterion for Evaluating the Remaining Strength of Corroded Pipe,” Battelle Report to the Pipeline Committee of the American Gas Association, 1989.
8. Stephens, D.R., Krishnaswamy, P, Mohan, R., Osage, D.A., Sims, J.R., and Wilkowski, G., “A Review of Analysis Methods and Acceptance Criteria for Local Thinned Areas in Piping and Piping Components,” 1997 Pressure Vessels and Piping Conference, Orlando, Florida, July, 1997.
9. Green, D. and Knowles, J., “The Treatment of Residual Stress in Fracture Assessment of Pressure Vessels,” ASME, *Journal of Pressure Vessel Technology*, Vol. 116, November 1994, pp. 345-352.
10. Folias, E.S., “On the Effect of Initial Curvature on Cracked Sheets,” *International Journal of Fracture Mechanics*, Vol. 5, No. 4, December, 1969, pp. 327-346.
11. Sih, G.C., “Handbook of Stress Intensity Factors,” Institute of Fracture and Solid Mechanics, Lehigh University, Bethlehem, Pa.
12. Kramer, G.S., Wilkowski, G.M., and Maxey, W.A., “Flaw Tolerance of Spiral Welded Pipe,” Battelle NG-18 Report No. 154, January, 1987.
13. Kiefner, J.F. and Vieth, P.H., “Project PR 3-805, A Modified Criterion for Evaluating the Remaining Strength of Corroded Pipe,” Battelle Report to the Pipeline Committee of the American Gas Association, 1989.
14. Eiber, R.J., Maxey, W.A., Duffy, A.R., and Atterbury, T.J., “Investigation of the Initiation and Extent of Ductile Pipe Rupture,” Battelle Report Task 17, June, 1971.
15. Murakami, Y., “Stress Intensity Factors Handbook,” Pergamon Press, Oxford, 1987, pp. 1356-1358.
16. Tada, H., Paris, P.c. and Irwin, G.R, “The Stress Analysis Of Cracks Handbook – Second Edition,” Paris Productions Inc., St. Louis, Missouri, 1985.
17. Chell,G.G, “Application of the CEGB Failure Assessment Procedure, R6, to Surface Flaws,” Fracture Mechanics: Twenty-First Symposium, ASTM STP 1074, J.P. Gudas, J.A. Joyce, and E.M. Hackett, Eds., American Society for Testing and Materials, Philadelphia, 1990, pp. 525-544.
18. Sattari-Far, I., “Finite Element Analysis of Limit Loads For Surface Cracks in Plates*,” Int. J. Pres. Ves. & Pipin*g, 57, 1994, pp. 237-243.

D.16 Tables and Figures

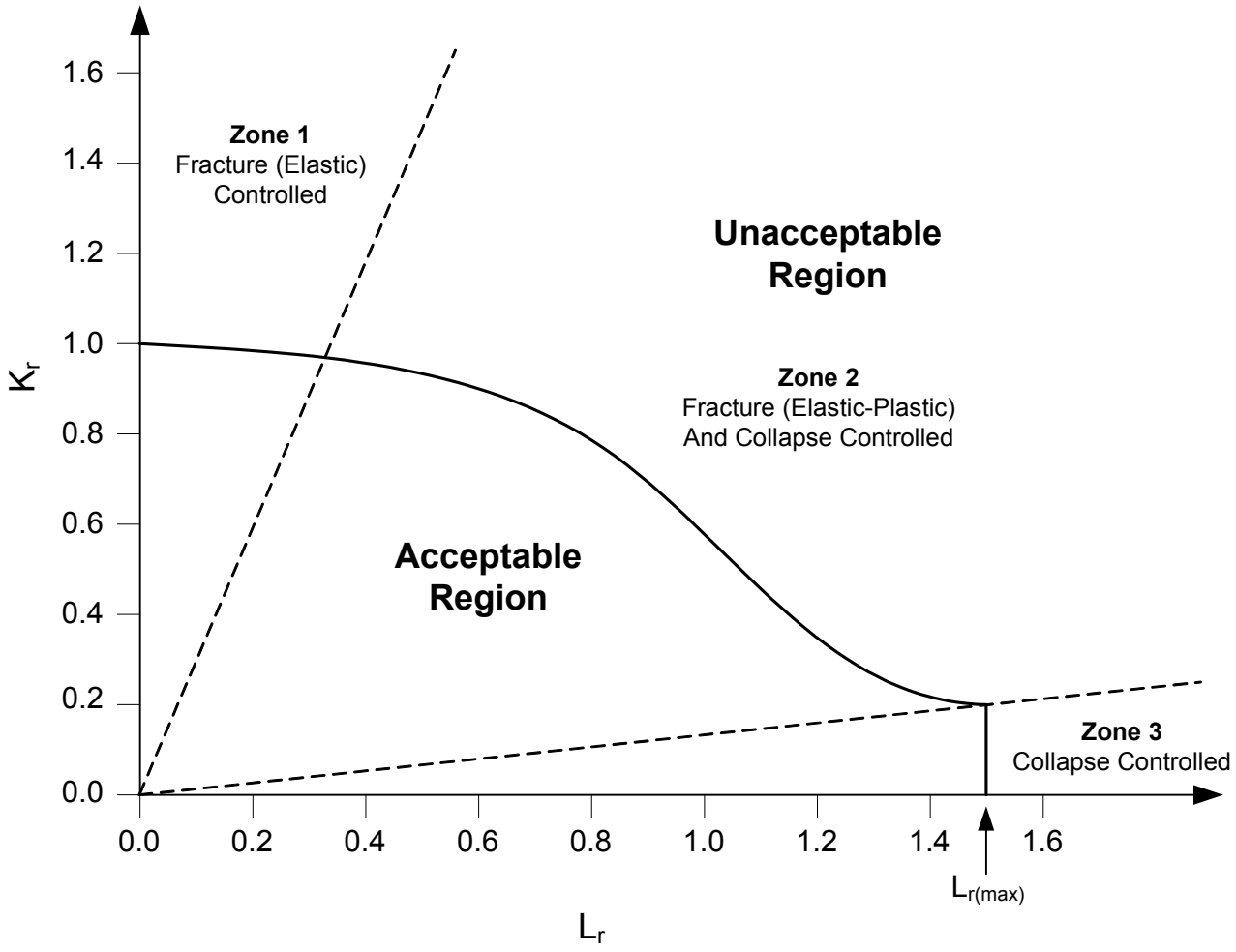

Figure D.1
Failure Regions On The Failure Assessment Diagram

ANNEX E

RESIDUAL STRESSES IN A FITNESS-FOR-SERVICE EVALUATION

(NORMATIVE)

PART CONTENTS

E.1 General

E.1.1 Guidance for determining the magnitude and distribution of residual stresses at a welded joint is provided in this Annex. The residual stress distribution is required as input to perform a fitness-for-service assessment of a component containing a crack-like flaw at a weld joint (see Part 9).

E.1.2 The information from this Annex is used to compute the crack driving force associated with the residual stresses, and also serves as input data for determination of the plasticity interaction factor, Φ, (see Part 9) which quantifies the crack driving force that occurs under situations of combined loading (i.e. primary, secondary and residual stress).

E.2 Applicability and Limitations

E.2.1 The methodology provided herein applies to welded joints located in equipment that has been in-service, as well as to new construction. Residual stress distributions are provided for the following weld joint configurations:

a) Full Penetration Welds in Piping and Pressure Vessel Cylindrical Shells (see paragraph E.4)

b) Full Penetration Welds in Spheres and Pressure Vessel Heads (see paragraph E.5)

c) Full Penetration Welds in Storage Tanks (see paragraph E.6)

d) Full Penetration and Fillet Welds at Corner Joints (see paragraph E.7)

e) Fillet Welds at Tee Joints (see paragraph E.8)

f) Repair Welds (see paragraph E.9)

E.2.2 The residual stress distributions presented in this Annex are based on extensive numerical analyses and a literature survey of published results. The information obtained from the literature survey indicated a substantial scatter in the reported results. Therefore, the residual stress distributions in this Annex were obtained by developing an upper bound solution based on the published results and the results of the numerical analysis. Note that since the residual stress distributions are based on an upper bound solution, they are not necessarily self-equilibrating.

E.2.3 Residual stress distributions are provided for both the as-welded and $PWHT$ conditions. The residual stress distributions for weld joints subject to $PWHT$ are based on a uniform $PWHT$ temperature applied to the component. Uncontrolled and/or local $PWHT$ may result in significantly higher residual stresses. If the type of $PWHT$ cannot be established, the residual stress distribution for the as-welded condition should be used in the assessment. If the weld joint is in a component operating in the creep range (i.e. long-term operation), then the residual stress based on the $PWHT$ condition may be used in the assessment.

E.2.4 Currently, a distinction is not made concerning the material of construction. It is currently recommended that ferritic and stainless steel weldments be assessed using these equations.

E.2.5 The residual stress distributions at a welded joint are sensitive to the restraint condition. The stress distributions in this Annex are not applicable to closure welds where the degree of restraint against shrinkage is not known. In this case, a yield level membrane residual stress distribution should be used in the FFS assessment.

E.2.6 The residual stress distribution is also sensitive to the weld joint geometry. Currently, solutions are provided for single V-Type joints, double V-Type joints, fillet welds, and repair welds. The solutions for the double V-Type joint configuration should be used for joints that are back-gouged but are predominantly welded from one side.

E.2.7 The residual stress distributions provided in this Annex are two-dimensional; the stress distribution is provided through the wall thickness and in the plane of the component. The residual stress in the plane of the component diminishes with increasing distance from the weld joint. The effects of this reduced residual stress may be used in the assessment.

E.2.8 The equations for the residual stress distributions provided in this Annex are referenced from the inside surface (i.e. the local coordinate, x, is referenced from the inside surface). If a surface breaking crack-like flaw is on the outside surface, then the distributions shall be modified so that the local coordinate is defined from the outside surface.

E.2.9 Results from the literature, testing, experimental analysis, or numerical analysis may be used to determine the residual stress at a welded joint as an alternative to the solutions provided in this Annex. For example, residual stresses measured in the field using the depth-controlled hole drilling method can be used to determine the residual stress on the surface of a component. All assumptions used to determine the residual stress distribution by this alternative means should be documented with the assessment results. Residual stress distributions from a single literature source should not be used unless specific information is available to confirm their accuracy.

E.3 Data Requirements and Definition of Variables

E.3.1 Required Data

The following data are required to estimate the residual stress field caused by a welded joint:

a) The material specification,

b) The material specified minimum or actual yield strength,

c) The wall thickness of the component,

d) The heat input used to make the weld,

e) The type of weld (i.e. girth or circumferential joint, longitudinal seam, repair weld, or attachment weld),

f) The weld joint configuration (i.e. single V-groove, double V-groove, corner joint, fillet weld, or repair weld),

g) Whether the weld has been subject to post weld heat treatment in accordance with the original construction code, and

h) Whether the weld has been subject to a pressure test in accordance with the original construction code.

E.3.2 Yield Strength in Residual Stress Calculations

In order to estimate the magnitude of the residual stress distribution at a weld joint, an estimate of the actual yield strength of the material must be made. If actual data do not exist or cannot be determined, the following equations may be used to estimate the magnitude of the yield strength. If the actual value of the yield strength is known, then it may be used in the assessment. The elevation of the effective yield strength above the specified minimum yield strength accounts for the typical elevation of actual properties above minimum requirements. The properties of the base material should be used to determine the specified minimum yield strength.

$$\sigma_{ys}^{r} = \sigma_{ys} + 69 \text{ MPa} \tag{E.1}$$

$$\sigma_{ys}^{r} = \sigma_{ys} + 10 \text{ ksi} \tag{E.2}$$

E.3.3 Surface Residual Stress Distribution

A parametric functional form is used to describe surface residual stress distributions in both longitudinal and transverse directions for both girth and seam welds.

$$\sigma^r(y) = \sigma^r_{ys} \cdot R_r \qquad if \qquad |y| \le \frac{w}{2} \tag{E.3}$$

$$\sigma^r(y) = \left\{ \frac{1 - \left(\frac{|y| - w/2}{c} \right)^2}{1 + \left(\frac{|y| - w/2}{c} \right)^{2n}} \right\} \cdot \sigma^r_{ys} \cdot R_r \qquad if \qquad |y| > \frac{w}{2} \tag{E.4}$$

The local coordinate y for the stress distribution along outer or inner surfaces is measured from the weld center and perpendicular to the weld direction. The distance c is proportional to $\sqrt{rt}$. The parameter n is a constant integer, chosen from 2, 3, 4, or 5, depending on the weld joint type and direction of the residual stress.

E.3.4 Through-Thickness Residual Stress Distribution

a) A parametric functional form is used to describe through-thickness residual stress distributions in both longitudinal and transverse directions for both girth and seam welds.

$$\sigma^r(\zeta) = E \cdot \sigma^r_{ys} \cdot R_r \tag{E.5}$$

$$E = \min\left[D,\ K\right] \qquad for \qquad D \ge 0 \tag{E.6}$$

$$E = \max\left[D,\ -K\right] \qquad for \qquad D < 0 \tag{E.7}$$

$$D = \bar{\sigma}^r_m + \bar{\sigma}^r_b \left(2\zeta - 1\right) + A - B \tag{E.8}$$

$$A = \left(\frac{s^r_o - s^r_i}{2} \right) \left(2\zeta - 1\right)^3 \tag{E.9}$$

$$B = \left(s^r_o + s^r_i \right) \left(\frac{\sin\left[\pi\left(2\zeta - 1\right) + C\right]}{2\sin\left[C\right]} \right) \tag{E.10}$$

$$C = \arctan\left[\frac{5}{\pi} \cdot \left(\frac{s^r_o + s^r_i}{s^r_o - s^r_i} \right) \right] \tag{E.11}$$

$$\zeta = \frac{x}{t} \tag{E.12}$$

$$K = 1.2 \qquad \textit{for residual stresses perpendicular to the weld} \tag{E.13}$$

$$K = 1.5 \qquad \textit{for residual stresses parallel to the weld} \tag{E.14}$$

b) The first and second terms in Equation (E.5) represent the membrane and bending components, respectively. The third and fourth term in this equation represent the self-equilibrating component. The four parameters; $\bar{\sigma}^r_m$, $\bar{\sigma}^r_b$, s^r_o, and s^r_i are determined based on the weld joint and component type.

c) The heat input density parameter, $\hat{Q}$, and the component radius to thickness ratio parameter, $\hat{R}$, are used to correlate the variables $\bar{\sigma}_m^r$ and $\bar{\sigma}_b^r$. The heat input density parameter, $\hat{Q}$, is computed using Equation (E.15) or (E.16). Note that the units of $\hat{Q}$, J/mm^3 , must be used in all parametric equations in this Annex. The component radius to thickness ratio parameter, $\hat{R}$, is computed using Equation (E.17).

$$\hat{Q} = 0.7441\left(\frac{\dot{q}}{t^2}\right) \qquad \left(\frac{J}{mm},\ mm,\ \frac{J}{mm^3}\right) \tag{E.15}$$

$$\hat{Q} = 4.541(10)^{-5}\left(\frac{\dot{q}}{t^2}\right) \qquad \left(\frac{J}{in},\ in,\ \frac{J}{mm^3}\right) \tag{E.16}$$

$$\hat{R} = \frac{r}{t} \tag{E.17}$$

The limitations on the heat input density parameter , $\hat{Q}$, in all parametric equations in this appendix are:

$$\hat{Q} = 1.5 \qquad for \qquad \hat{Q} < 1.5 \tag{E.18}$$

$$\hat{Q} = 25.0 \qquad for \qquad \hat{Q} > 25.0 \tag{E.19}$$

The limitation on the radius to thickness ratio parameter, $\hat{R}$, in all parametric equations in this appendix is:

$$\hat{R} = 30.0 \qquad for \qquad \frac{r}{t} < 30 \tag{E.20}$$

d) In Equations (E.15) and (E.16) , $\dot{q}$ is the linear heat input determined using Equation (E.21) or Equation (E.22).

$$\dot{q} = \frac{I \cdot V \cdot \eta}{u} \qquad \left(amps,\ volts,\ \frac{mm}{\sec},\ \frac{J}{mm}\right) \tag{E.21}$$

$$\dot{q} = \frac{I \cdot V \cdot \eta}{u} \qquad \left(amps,\ volts,\ \frac{in}{\sec},\ \frac{J}{in}\right) \tag{E.22}$$

e) The reference heat input used to establish the reference residual stress relationships in this Annex are based on the parameters shown below. The actual heat input is used to scale the reference residual stress solution to determine the actual residual stress solution.

$$I = 280\ amps \tag{E.23}$$

$$V = 30\ volts \tag{E.24}$$

$$\eta = 0.80 \tag{E.25}$$

$$u = 5\ mm/sec \tag{E.26}$$

f) The heat input defined by Equations (E.21) or (E.22) is the heat input for each pass and is assumed to be equal for all weld passes that encompass the weld.

g) The heat input used in an assessment should be established from the original welding procedure. If the heat input is not known, an average or upper bound may be estimated using Table E.1. If the heat input is determined from this table, then a sensitivity analysis should be performed to determine the significance of the assumption.

E.4 Full Penetration Welds in Piping and Pressure Vessel Cylindrical Shells

E.4.1 Single V-Groove Circumferential (Girth) Welds (see Figures E.1 and E.2)

E.4.1.1 Residual Stress Perpendicular to the Weld Seam (Circumferential Flaw)

a) Surface Residual Stress Distribution – The residual stress distribution for this category of weld made remote from all geometric discontinuities can be approximated using Equations (E.3) or (E.4) for the inner and outer surfaces where c and n are given by the following equations.

$$c = 2\sqrt{rt} \tag{E.27}$$

$$n = 5 \tag{E.28}$$

b) Through-Thickness Residual Stress Distribution – The residual stress distribution for this category of weld made remote from all geometric discontinuities can be approximated using Equation (E.5). The local coordinate x for the stress distribution through the wall thickness is measured from the inside surface. The parameters $\bar{\sigma}_m^r$, $\bar{\sigma}_b^r$, s_o^r and s_i^r are determined using the following equations.

$$\bar{\sigma}_m^r = 0.30 \tag{E.29}$$

$$\bar{\sigma}_b^r = \begin{pmatrix} 1.5161198 - 0.4523099 \cdot \ln\left[\hat{R}\right] - 7.25919(10)^{-2} \cdot \hat{Q} + \\ 5.0417213(10)^{-2} \cdot \left(\ln\left[\hat{R}\right]\right)^2 + 9.2862457(10)^{-4} \cdot \hat{Q}^2 - \\ 1.0999481(10)^{-2} \cdot \hat{Q} \cdot \ln\left[\hat{R}\right] - 2.7500406(10)^{-3}\left(\ln\left[\hat{R}\right]\right)^3 - \\ 2.0566152(10)^{-5} \cdot \hat{Q}^3 - 2.0294677(10)^{-4} \cdot \hat{Q}^2 \cdot \ln\left[\hat{R}\right] + \\ 4.7248503(10)^{-3} \cdot \hat{Q}\left(\ln\left[\hat{R}\right]\right)^2 \end{pmatrix} \tag{E.30}$$

The parameter s_o^r is given by:

$$s_o^r = K - \left|\bar{\sigma}_b^r\right| - \left|\bar{\sigma}_m^r\right| \tag{E.31}$$

The parameter s_i^r is given by:

$$s_i^r = 0.25 s_o^r \tag{E.32}$$

c) Effects of Test Pressure – The reduction in residual stress resulting from the test pressure as a percentage of the residual stress in the as-welded condition may be determined using the equations shown below or Figure E.3.

$$R_r = 1.0 \qquad T_p < 75\% \tag{E.33}$$

$$R_r = \frac{168.5063 - 2.26770T_p + 9.16852(10)^{-3}T_p^2}{100} \qquad 75\% \le T_p \le 110\% \qquad \text{(E.34)}$$

$$R_r = 0.30 \qquad T_p > 110\% \qquad \text{(E.35)}$$

$$T_p = \left(\frac{\sigma_{mc,t}}{\sigma_{ys}^r}\right) \cdot 100 \qquad \text{(E.36)}$$

d) Effects of $PWHT$ – If the weld is known to have been subject to post weld heat treatment per the original construction code, then the residual stress is given by:

$$\sigma^r(x) = 0.2\sigma_{ys}^r \qquad \text{(E.37)}$$

e) The effects of test pressure and $PWHT$ shall be evaluated separately, not in combination.

E.4.1.2 Residual Stress Parallel to the Weld Seam (Longitudinal Flaw)

a) Surface Residual Stress Distribution – The residual stress distribution for this category of weld made remote from all geometric discontinuities can be approximated using Equations (E.3) or (E.4) for the inner and outer surfaces where c and n are given by the following equations.

$$c = 0.5\sqrt{rt} \qquad \text{(E.38)}$$

$$n = 2 \qquad \text{(E.39)}$$

b) Through-Thickness Residual Stress Distribution – The residual stress distribution for this category of weld made remote from all geometric discontinuities can be approximated using Equation (E.5). The local coordinate x for the stress distribution through the wall thickness is measured from the inside surface. The parameters $\bar{\sigma}_m^r$, $\bar{\sigma}_b^r$, s_o^r and s_i^r are determined using the following equations.

$$\bar{\sigma}_m^r = \begin{pmatrix} 0.96552484 - 3.2963068\left(\hat{R}\right)^{-1} + 8.7407683(10)^{-2} \cdot \ln\left[\hat{Q}\right] + \\ 4.1706708\left(\hat{R}\right)^{-2} + 2.5193848(10)^{-2}\left(\ln\left[\hat{Q}\right]\right)^2 - \\ 0.24254479 \cdot \ln\left[\hat{Q}\right]\left(\hat{R}\right)^{-1} - 2.0207082\left(\hat{R}\right)^{-3} - \\ 9.8826285(10)^{-3}\left(\ln\left[\hat{Q}\right]\right)^3 + 0.20952773\left(\ln\left[\hat{Q}\right]\right)^2\left(\hat{R}\right)^{-1} - \\ 0.2086051 \cdot \ln\left[\hat{Q}\right]\left(\hat{R}\right)^{-2} \end{pmatrix} \qquad \text{(E.40)}$$

$$\bar{\sigma}_b^r = \begin{pmatrix} 0.49057581 + 3.6264425\left(\hat{R}\right)^{-1} + 0.10746818 \cdot \ln\left[\hat{Q}\right] - \\ 1.3175842\left(\hat{R}\right)^{-2} - 8.111233(10)^{-2}\left(\ln\left[\hat{Q}\right]\right)^2 - \\ 0.18465977 \cdot \ln\left[\hat{Q}\right]\left(\hat{R}\right)^{-1} - 4.9395089\left(\hat{R}\right)^{-3} - \\ 5.5831999(10)^{-3}\left(\ln\left[\hat{Q}\right]\right)^3 - 0.34858729\left(\ln\left[\hat{Q}\right]\right)^2\left(\hat{R}\right)^{-1} + \\ 1.1980848 \cdot \ln\left[\hat{Q}\right]\left(\hat{R}\right)^{-2} \end{pmatrix} \quad \text{(E.41)}$$

$$s_o^r = K - \left|\bar{\sigma}_b^r\right| - \left|\bar{\sigma}_m^r\right| \quad \text{(E.42)}$$

$$s_i^r = 0.25 s_o^r \quad \text{(E.43)}$$

c) Effects of Test Pressure – The reduction in residual stress resulting from the test pressure as a percentage of the residual stress in the as-welded condition may be determined using paragraph E.4.1.1 c.

d) Effects of $PWHT$ – If the weld is known to have been subject to post weld heat treatment per the original construction code, then the residual stress is given by:

$$\sigma^r(x) = 0.3\sigma_{ys}^r \quad \text{(E.44)}$$

e) The effects of test pressure and $PWHT$ shall be evaluated separately, not in combination.

E.4.2 Double V-Groove Circumferential (Girth) Welds (see Figures E.1 and E.4)

E.4.2.1 Residual Stress Perpendicular to the Weld Seam (Circumferential Flaw)

a) Surface Residual Stress Distribution – The residual stress distribution for this category can be approximated using paragraph E.4.1.1 a.

b) Through-Thickness Residual Stress Distribution – The residual stress distribution for this category of weld made remote from all geometric discontinuities can be approximated using Equation (E.5). The local coordinate x for the stress distribution through the wall thickness is measured from the inside surface. The parameters $\bar{\sigma}_b^r$ and $\bar{\sigma}_m^r$ are given by the following equations, and s_o^r and s_i^r are determined using the equations described in paragraph E.4.1.1 b.

$$\bar{\sigma}_m^r = 0.30 \quad \text{(E.45)}$$

$$\bar{\sigma}_b^r = \begin{pmatrix} 0.76679863 - 0.24776304 \cdot \ln\left[\hat{R}\right] + \\ 3.2846007(10)^{-2} \cdot \hat{Q} + 4.2329418(10)^{-3} \cdot \left(\ln\left[\hat{R}\right]\right)^2 - \\ 1.0168102(10)^{-2} \cdot \hat{Q}^2 + 7.9129197(10)^{-3} \cdot \hat{Q} \cdot \ln\left[\hat{R}\right] + \\ 1.4679998(10)^{-3} \cdot \left(\ln\left[\hat{R}\right]\right)^3 + 2.644861(10)^{-4} \cdot \hat{Q}^3 - \\ 1.6911172(10)^{-4} \cdot \hat{Q}^2 \cdot \ln\left[\hat{R}\right] + 1.5331959(10)^{-3} \cdot \hat{Q} \cdot \left(\ln\left[\hat{R}\right]\right)^2 \end{pmatrix} \quad \text{(E.46)}$$

c) Effects of Test Pressure – The reduction in residual stress resulting from the test pressure as a percentage of the residual stress in the as-welded condition may be determined using paragraph E.4.1.1 c.

d) Effects of $PWHT$ – If the weld is known to have been subject to post weld heat treatment per the original construction code, then the residual stress is given by:

$$\sigma^r(x) = 0.2\sigma^r_{ys} \tag{E.47}$$

e) The effects of test pressure and $PWHT$ shall be evaluated separately, not in combination.

E.4.2.2 Residual Stress Parallel to the Weld Seam (Longitudinal Flaw)

a) Surface Residual Stress Distribution – The residual stress distribution for this category can be approximated using paragraph E.4.1.2 a.

b) Through-Thickness Residual Stress Distribution – The residual stress distribution for this category of weld made remote from all geometric discontinuities can be approximated using Equation (E.5). The local coordinate x for the stress distribution through the wall thickness is measured from the inside surface. The parameters $\bar{\sigma}^r_m$ and $\bar{\sigma}^r_b$ are given by the following equations, and s^r_o and s^r_i are determined using the paragraph E.4.1.2 b.

$$\bar{\sigma}^r_m = \begin{pmatrix} 0.89974213 - 2.4011543\left(\hat{R}\right)^{-1} + 0.13018073\cdot\ln\left[\hat{Q}\right] + \\ 0.95409509\left(\hat{R}\right)^{-2} + 3.5538839(10)^{-2}\cdot\left(\ln\left[\hat{Q}\right]\right)^2 - \\ 0.28525369\cdot\ln\left[\hat{Q}\right]\left(\hat{R}\right)^{-1} + 2.5258852\left(\hat{R}\right)^{-3} - \\ 1.3532583(10)^{-2}\cdot\left(\ln\left[\hat{Q}\right]\right)^3 + 0.16555361\cdot\left(\ln\left[\hat{Q}\right]\right)^2\left(\hat{R}\right)^{-1} + \\ 0.14581755\cdot\ln\left[\hat{Q}\right]\left(\hat{R}\right)^{-2} \end{pmatrix} \tag{E.48}$$

$$\bar{\sigma}^r_b = \begin{pmatrix} 0.25238365 + 4.2390408\left(\hat{R}\right)^{-1} + 6.6851329(10)^{-2}\cdot\ln\left[\hat{Q}\right] - \\ 4.2739426\left(\hat{R}\right)^{-2} + 9.7412539(10)^{-2}\cdot\left(\ln\left[\hat{Q}\right]\right)^2 - \\ 0.50774036\cdot\ln\left[\hat{Q}\right]\left(\hat{R}\right)^{-1} - \\ 5.1902363(10)^{-2}\cdot\left(\ln\left[\hat{Q}\right]\right)^3 - 0.42339085\cdot\left(\ln\left[\hat{Q}\right]\right)^2\left(\hat{R}\right)^{-1} + \\ 1.9315947\cdot\ln\left[\hat{Q}\right]\left(\hat{R}\right)^{-2} \end{pmatrix} \tag{E.49}$$

c) Effects of Test Pressure – The reduction in residual stress resulting from the test pressure as a percentage of the residual stress in the as-welded condition may be determined using paragraph E.4.1.1 c.

d) Effects of $PWHT$ – If the weld is known to have been subject to post weld heat treatment per the original construction code, then the residual stress is given by:

$$\sigma^r(x) = 0.3\sigma^r_{ys} \tag{E.50}$$

e) The effects of test pressure and PWHT shall be evaluated separately, not in combination.

E.4.3 Single V-Groove Longitudinal (Seam) Welds (see Figures E.1 and E.5)

E.4.3.1 Residual Stress Perpendicular to the Weld Seam (Longitudinal Flaw)

a) Surface Residual Stress Distribution – The residual stress distribution for this category can be approximated using paragraph E.4.1.1 a.

b) Through-Thickness Residual Stress Distribution – The residual stress distribution for this category of weld made remote from all geometric discontinuities can be approximated using Equation (E.5). The local coordinate x for the stress distribution through the wall thickness is measured from the inside surface. The parameters $\bar{\sigma}_m^r$ and $\bar{\sigma}_b^r$ are given by the following equations, and s_o^r and s_i^r are determined using paragraph E.4.1.1.b.

$$\bar{\sigma}_m^r = 0.30 \tag{E.51}$$

$$\bar{\sigma}_b^r = \begin{pmatrix} 0.82021316 - 0.21868137 \cdot \ln\left[\hat{R}\right] - 5.0893644(10)^{-2} \cdot \hat{Q} + \\ 2.1924326(10)^{-3} \cdot \left(\ln\left[\hat{R}\right]\right)^2 + 4.3540456(10)^{-4} \cdot \hat{Q}^2 + \\ 1.334161(10)^{-2} \cdot \hat{Q} \cdot \ln\left[\hat{R}\right] \end{pmatrix} \tag{E.52}$$

c) Effects of Test Pressure – The reduction in residual stress resulting from the test pressure as a percentage of the residual stress in the as-welded condition may be determined using the equations shown below or Figure E.6. The parameter T_p in these equations is determined using Equation (E.36).

$$R_r = 1.0 \qquad T_p < 75\% \tag{E.53}$$

$$R_r = \frac{190.67 - 2.4501T_p + 1.07(10)^{-3}T_p^2}{100} \qquad 75\% \le T_p \le 110\% \tag{E.54}$$

$$R_r = 0.506 \qquad T_p > 110\% \tag{E.55}$$

d) Effects of $PWHT$ – If the weld is known to have been subject to post weld heat treatment per the original construction code, then the residual stress is given by:

$$\sigma^r(x) = 0.2\sigma_{ys}^r \tag{E.56}$$

e) The effects of test pressure and $PWHT$ shall be evaluated separately, not in combination.

E.4.3.2 Residual Stress Parallel to the Weld Seam (Circumferential Flaw)

a) Surface Residual Stress Distribution – The residual stress distribution for this category of weld made remote from all geometric discontinuities can be approximated using Equations (E.3) or (E.4) for the inner and outer surfaces where c and n are given by the following equations.

$$c = \sqrt{rt} \tag{E.57}$$

$$n = 3 \tag{E.58}$$

b) Through-Thickness Residual Stress Distribution – The residual stress distribution for this category of weld made remote from all geometric discontinuities can be approximated using Equation (E.5). The local coordinate x for the stress distribution through the wall thickness is measured from the inside surface. The parameters $\bar{\sigma}_b^r$ and $\bar{\sigma}_m^r$ are given by the following equations, and s_o^r and s_i^r are determined using paragraph E.4.1.2 b.

$$\bar{\sigma}_m^r = \begin{pmatrix} 0.92302566 + 0.10179191 \cdot \ln\left[\hat{R}\right] - 0.18818426 \cdot \ln\left[\hat{Q}\right] - \\ 9.2230134(10)^{-2} \cdot \left(\ln\left[\hat{R}\right]\right)^2 + 7.8953222(10)^{-2} \cdot \left(\ln\left[\hat{Q}\right]\right)^2 + \\ 0.20909321 \cdot \ln\left[\hat{Q}\right] \cdot \ln\left[\hat{R}\right] + 6.872986(10)^{-4} \cdot \left(\ln\left[\hat{R}\right]\right)^3 - \\ 1.4513632(10)^{-3} \cdot \left(\ln\left[\hat{Q}\right]\right)^3 - 7.1186886(10)^{-2} \cdot \left(\ln\left[\hat{Q}\right]\right)^2 \cdot \ln\left[\hat{R}\right] + \\ 2.8083317(10)^{-2} \cdot \ln\left[\hat{Q}\right] \cdot \left(\ln\left[\hat{R}\right]\right)^2 \end{pmatrix} \quad \text{(E.59)}$$

$$\bar{\sigma}_b^r = \begin{pmatrix} 0.18322486 + \\ \Psi[\,\hat{R},\ -0.75156308,\ -0.90464916,\ 1.9129297] + \\ \Psi[\,\hat{Q},\ -1.9164004(10)^{-3},\ 4.6535706,\ 8.2161289] + \\ \Psi[\,\hat{R},\ 1.4192901,\ -0.90464916,\ 1.9129297] \cdot \\ \Psi[\,\hat{Q},\ 1.0,\ 4.6535706,\ 8.2161289] \end{pmatrix} \quad \text{(E.60)}$$

The function Ψ in Equation (E.60) is given by:

$$\Psi[C_1, C_2, C_3, C_4] = \frac{4 \cdot C_2 \cdot \exp\left[-\dfrac{C_1 - C_3}{C_4}\right]}{\left(1 + \exp\left[-\dfrac{C_1 - C_3}{C_4}\right]\right)^2} \quad \text{(E.61)}$$

c) Effects of Test Pressure – The reduction in residual stress resulting from the test pressure as a percentage of the residual stress in the as-welded condition may be determined using paragraph E.4.3.1 c.

d) Effects of $PWHT$ – If the weld is known to have been subject to post weld heat treatment per the original construction code, then the residual stress is given by:

$$\sigma^r(x) = 0.3\sigma_{ys}^r \quad \text{(E.62)}$$

e) The effects of test pressure and $PWHT$ shall be evaluated separately, not in combination.

E.4.4 Double V-Groove Longitudinal (Seam) Welds (see Figures E.1 and E.7)

E.4.4.1 Residual Stress Perpendicular to the Weld Seam (Longitudinal Flaw)

a) Surface Residual Stress Distribution – The residual stress distribution for this category can be approximated using paragraph E.4.1.1 a.

b) Through-Thickness Residual Stress Distribution – The residual stress distribution for this category of weld made remote from all geometric discontinuities can be approximated using the Equation (E.5). The local coordinate x for the stress distribution through the wall thickness is measured from the inside surface. The parameters $\bar{\sigma}_b^r$ and $\bar{\sigma}_m^r$ are given by the following equations, and s_o^r and s_i^r are determined using paragraph E.4.1.2 b.

$$\bar{\sigma}_m^r = 0.30 \tag{E.63}$$

$$\bar{\sigma}_b^r = \frac{\left(\begin{array}{l} 0.81461958 + 8.5130064(10)^{-2} \cdot \ln\left[\hat{R}\right] - 0.72126117 \cdot \ln\left[\hat{Q}\right] + \\ 0.15060388 \cdot \left(\ln\left[\hat{Q}\right]\right)^2 - 4.6658082(10)^{-2} \cdot \ln\left[\hat{Q}\right] \cdot \ln\left[\hat{R}\right] \end{array}\right)}{\left(\begin{array}{l} 1 + 0.92134373 \cdot \ln\left[\hat{R}\right] - 0.74641482 \cdot \ln\left[\hat{Q}\right] - \\ 0.10870336 \cdot \left(\ln\left[\hat{Q}\right]\right)^2 - 0.50497004 \cdot \ln\left[\hat{Q}\right] \cdot \ln\left[\hat{R}\right] \end{array}\right)} \tag{E.64}$$

c) Effects of Test Pressure – The reduction in residual stress resulting from the test pressure as a percentage of the residual stress in the as-welded condition may be determined using paragraph E.4.3.1 c.

d) Effects of $PWHT$ – If the weld is known to have been subject to post weld heat treatment per the original construction code, then the residual stress is given by:

$$\sigma^r(x) = 0.2\sigma_{ys}^r \tag{E.65}$$

e) The effects of test pressure and $PWHT$ shall be evaluated separately, not in combination.

E.4.4.2 Residual Stress Parallel to the Weld Seam (Circumferential Flaw)

a) Surface Residual Stress Distribution – The residual stress distribution for this category can be approximated using paragraph E.4.3.2 a.

b) Through-Thickness Residual Stress Distribution – The residual stress distribution for this category of weld made remote from all geometric discontinuities can be approximated using the Equation (E.5). The local coordinate x for the stress distribution through the wall thickness is measured from the inside surface. The parameters $\bar{\sigma}_b^r$ and $\bar{\sigma}_m^r$ are given by the following equations, and s_o^r and s_i^r are determined using paragraph E.4.1.2 b.

$$\bar{\sigma}_m^r = \left(\begin{array}{l} 0.5165368 + 1.7446023\left(\hat{R}\right)^{-1} + 0.66450112 \cdot \ln\left[\hat{Q}\right] - \\ 3.7633844\left(\hat{R}\right)^{-2} - 0.21176553\left(\ln\left[\hat{Q}\right]\right)^2 - \\ 1.0979794 \cdot \ln\left[\hat{Q}\right]\left(\hat{R}\right)^{-1} + 2.388149\left(\hat{R}\right)^{-3} + \\ 2.4044369(10)^{-2}\left(\ln\left[\hat{Q}\right]\right)^3 + 0.17130172\left(\ln\left[\hat{Q}\right]\right)^2\left(\hat{R}\right)^{-1} + \\ 0.37743612 \cdot \ln\left[\hat{Q}\right]\left(\hat{R}\right)^{-2} \end{array}\right) \tag{E.66}$$

$$\bar{\sigma}_b^r = \frac{\left(\begin{array}{l} 0.58635367 - 0.56442049 \cdot \ln\left[\hat{R}\right] - 0.11205157 \cdot \hat{Q} + \\ 2.8191206(10)^{-3} \cdot \hat{Q}^2 - 9.1035381(10)^{-2} \cdot \hat{Q} \cdot \ln\left[\hat{R}\right] \end{array}\right)}{\left(\begin{array}{l} 1 - 2.4459436 \cdot \ln\left[\hat{R}\right] - 0.26775702 \cdot \hat{Q} - \\ 1.7172066(10)^{-2} \cdot \hat{Q}^2 + 0.39450625 \cdot \hat{Q} \cdot \ln\left[\hat{R}\right] \end{array}\right)} \qquad \text{(E.67)}$$

c) Effects of Test Pressure – The reduction in residual stress resulting from the test pressure as a percentage of the residual stress in the as-welded condition may be determined using paragraph E.4.3.1 c.

d) Effects of $PWHT$ – If the weld is known to have been subject to post weld heat treatment per the original construction code, then the residual stress is given by:

$$\sigma^r(x) = 0.3\sigma_{ys}^r \qquad \text{(E.68)}$$

e) The effects of test pressure and $PWHT$ shall be evaluated separately, not in combination.

E.5 Full Penetration Welds in Spheres and Pressure Vessel Heads

E.5.1 Single V-Groove Circumferential Welds (see Figure E.8 and E.9)

E.5.1.1 Residual Stress Perpendicular to the Weld Seam (Circumferential Flaw)

a) Surface Residual Stress Distribution – The residual stress distribution for this category can be approximated using paragraph E.4.1.1 a.

b) Through-Thickness Residual Stress Distribution – The residual stress distribution for this category of weld remote from all geometric discontinuities can be approximated using the equations in paragraph E4.1.1.b, and by replacing r by r_c.

c) Effects of Test Pressure – The reduction in residual stress resulting from the test pressure as a percentage of the residual stress in the as-welded condition may be determined using the equations shown below. The parameter T_p in these equations is determined using Equation (E.36).

$$R_r = 1.0 \qquad T_p < 75\% \qquad \text{(E.69)}$$

$$R_r = \left(\frac{168.5063 - 2.26770T_p + 9.16852(10)^{-3}T_p^2}{100}\right) \cdot \left(\frac{r}{r_c}\right) \qquad 75\% \le T_p \le 110\% \qquad \text{(E.70)}$$

$$R_r = 0.30 \cdot \left(\frac{r}{r_c}\right) \qquad T_p > 110\% \qquad \text{(E.71)}$$

d) Effects of $PWHT$ – If the weld is known to have been subject to post weld heat treatment per the original construction code, then the residual stress is given by:

$$\sigma^r(x) = 0.2\sigma_{ys}^r \qquad \text{(E.72)}$$

e) The effects of test pressure and $PWHT$ shall be evaluated separately, not in combination.

E.5.1.2 Residual Stress Parallel to the Weld Seam (Meridional Flaw)

a) Surface Residual Stress Distribution – The residual stress distribution for this category can be approximated using paragraph E.4.1.2 a.

b) Through-Thickness Residual Stress Distribution – The residual stress distribution for this category of weld remote from all geometric discontinuities can be approximated using the equations in paragraph E.4.1.2 b and by replacing r by r_c.

c) Effects of Test Pressure – The reduction in residual stress resulting from the test pressure as a percentage of the residual stress in the as-welded condition may be determined using paragraph E.5.1.1.c.

d) Effects of $PWHT$ – If the weld is known to have been subject to post weld heat treatment per the original construction code, then the residual stress is given by:

$$\sigma^r(x) = 0.3\sigma^r_{ys} \tag{E.73}$$

e) The effects of test pressure and $PWHT$ shall be evaluated separately, not in combination.

E.5.2 Double V-Groove Circumferential Welds (see Figure E.8 and E.10)

E.5.2.1 Residual Stress Perpendicular to the Weld Seam (Circumferential Flaw)

a) Surface Residual Stress Distribution – The residual stress distribution for this category can be approximated using paragraph E.4.1.1 a.

b) Through-Thickness Residual Stress Distribution – The residual stress distribution for this category of weld remote from all geometric discontinuities can be approximated using the equations in paragraph E.4.1.1.b, and by replacing r by r_c.

c) Effects of Test Pressure – The reduction in residual stress resulting from the test pressure as a percentage of the residual stress in the as-welded condition may be determined using paragraph E.5.1.1.c.

d) Effects of $PWHT$ – If the weld is known to have been subject to post weld heat treatment per the original construction code, then the residual stress is given by:

$$\sigma^r(x) = 0.2\sigma^r_{ys} \tag{E.74}$$

e) The effects of test pressure and $PWHT$ shall be evaluated separately, not in combination.

E.5.2.2 Residual Stress Parallel to the Weld Seam (Meridional Flaw)

a) Surface Residual Stress Distribution – The residual stress distribution for this category can be approximated using paragraph E.4.1.2 a.

b) Through-Thickness Residual Stress Distribution – The residual stress distribution for this category of weld remote from all geometric discontinuities can be approximated using the equations in paragraph E.4.1.2 b, and by replacing r by r_c.

c) Effects of Test Pressure – The reduction in residual stress resulting from the test pressure as a percentage of the residual stress in the as-welded condition may be determined using paragraph E.5.1.1.c.

d) Effects of $PWHT$ – If the weld is known to have been subject to post weld heat treatment per the original construction code, then the residual stress is given by:

$$\sigma^r(x) = 0.3\sigma^r_{ys} \tag{E.75}$$

e) The effects of test pressure and $PWHT$ shall be evaluated separately, not in combination.

E.5.3 Single V-Groove Meridional (Seam) Welds (see Figures E.8 and E.11)

E.5.3.1 Residual Stress Perpendicular to the Weld Seam (Meridional Flaw)

a) Surface Residual Stress Distribution – The residual stress distribution for this category can be approximated using paragraph E.4.1.1 a.

b) Through-Thickness Residual Stress Distribution – The residual stress distribution for this category of weld made remote from all geometric discontinuities can be approximated using the equations in paragraph E.4.1.1.b.

c) Effects of Test Pressure – The reduction in residual stress resulting from the test pressure as a percentage of the residual stress in the as-welded condition may be determined using paragraph E.5.1.1.c.

d) Effects of $PWHT$ – If the weld is known to have been subject to post weld heat treatment per the original construction code, then the residual stress is given by:

$$\sigma^r(x) = 0.2\sigma^r_{ys} \tag{E.76}$$

e) The effects of test pressure and $PWHT$ shall be evaluated separately, not in combination.

E.5.3.2 Residual Stress Parallel to the Weld Seam (Circumferential Flaw)

a) Surface Residual Stress Distribution – The residual stress distribution for this category can be approximated using paragraph E.4.1.2 a.

b) Through-Thickness Residual Stress Distribution – The residual stress distribution for this category of weld made remote from all geometric discontinuities can be approximated using the equations in paragraph E.4.1.2 b, and r is radius of the sphere.

c) Effects of Test Pressure – The reduction in residual stress resulting from the test pressure as a percentage of the residual stress in the as-welded condition may be determined using paragraph E.5.1.1.c.

d) Effects of $PWHT$ – If the weld is known to have been subject to post weld heat treatment per the original construction code, then the residual stress is given by:

$$\sigma^r(x) = 0.3\sigma^r_{ys} \tag{E.77}$$

e) The effects of test pressure and PWHT shall be evaluated separately, not in combination.

E.5.4 Double V-Groove Meridional (Seam) Welds (see Figures E.8 and E.12)

E.5.4.1 Residual Stress Perpendicular to the Weld Seam (Meridional Flaw)

a) Surface Residual Stress Distribution – The residual stress distribution for this category can be approximated using paragraph E.4.1.1 a.

b) Through-Thickness Residual Stress Distribution – The residual stress distribution for this category of weld made remote from all geometric discontinuities can be approximated using the equations in paragraph E.4.1.1.b.

c) Effects of Test Pressure – The reduction in residual stress resulting from the test pressure as a percentage of the residual stress in the as-welded condition may be determined using paragraph E.5.1.1.c.

d) Effects of $PWHT$ – If the weld is known to have been subject to post weld heat treatment per the original construction code, then the residual stress is given by:

$$\sigma^r(x) = 0.2\sigma^r_{ys} \tag{E.78}$$

e) The effects of test pressure and PWHT shall be evaluated separately, not in combination.

E.5.4.2 Residual Stress Parallel to the Weld Seam (Circumferential Flaw)

a) Surface Residual Stress Distribution – The residual stress distribution for this category can be approximated using paragraph E.4.1.2 a.

b) Through-Thickness Residual Stress Distribution – The residual stress distribution for this category of weld made remote from all geometric discontinuities can be approximated using the equations in paragraph E.4.1.2 b.

c) Effects of Test Pressure – The reduction in residual stress resulting from the test pressure as a percentage of the residual stress in the as-welded condition may be determined using paragraph E.5.1.1.c.

d) Effects of $PWHT$ – If the weld is known to have been subject to post weld heat treatment per the original construction code, then the residual stress is given by:

$$\sigma^r(x) = 0.3\sigma^r_{ys} \tag{E.79}$$

e) The effects of test pressure and $PWHT$ shall be evaluated separately, not in combination.

E.6 Full Penetration Welds in Storage Tanks

E.6.1 Single V-Groove Circumferential Welds (see Figure E.2)

The residual stress solutions provided for the single V-groove circumferential weld joint in piping and pressure vessel cylindrical shells in paragraph E.4.1 may be used for the single V-groove circumferential weld joint in storage tanks.

E.6.2 Double V-Groove Circumferential Welds (see Figure E.4)

The residual stress solutions provided for the double V-groove circumferential weld joint in piping and pressure vessel cylindrical shells in paragraph E.4.2 may be used for the double V-groove circumferential weld joint in storage tanks.

E.6.3 Single V-Groove Longitudinal Welds (see Figure E.5)

The residual stress solution provided for the single V-groove longitudinal weld joint in piping and pressure vessel cylindrical shells in paragraph E.4.3 may be used for the single V-groove longitudinal weld joint in storage tanks.

E.6.4 Double V-Groove Longitudinal Welds (see Figure E.7)

The residual stress solution provided for the double V-groove longitudinal weld joint in piping and pressure vessel cylindrical shells in paragraph E.4.4 may be used for the double V-groove longitudinal weld joint in storage tanks.

E.7 Full Penetration Welds at Corner Joints (Nozzles or Piping Branch Connections)

E.7.1 Corner Joint (see Figure E.15, Weld Joint A)

E.7.1.1 Residual Stress Perpendicular to the Weld Seam

a) Surface Residual Stress Distribution

$$\sigma^r(y) = \sigma^r_{ys} \cdot R_r \qquad if \qquad 0 \le y \le w \tag{E.80}$$

$$\sigma^r(y) = \left\{ \frac{1 - \left(\frac{y-w}{c} \right)^2}{1 + \left(\frac{y-w}{c} \right)^{2n}} \right\} \cdot \sigma_{ys}^r \cdot R_r \qquad if \qquad y \geq w \tag{E.81}$$

$$c = 3t_s \tag{E.82}$$

$$n = 2 \tag{E.83}$$

b) Through-Thickness Residual Stress Distribution – The residual stress distribution for this category of weld made remote from all other geometric discontinuities can be approximated using Equation (E.5). The local coordinate x for the stress distribution through the wall thickness is measured from the inside surface. The parameters $\bar{\sigma}_m^r$, $\bar{\sigma}_b^r$, s_o^r and s_i^r are determined using the following equations.

$$\bar{\sigma}_m^r = 0.27 \tag{E.84}$$

$$\bar{\sigma}_b^r = 0.47 \tag{E.85}$$

$$s_o^r = 0.26 \tag{E.86}$$

$$s_i^r = 0.21 \tag{E.87}$$

c) Effects of Test Pressure – The reduction in residual stress resulting from the test pressure is not provided for this weld joint; therefore, $R_r = 1.0$.

d) Effects of $PWHT$ – If the weld is known to have been subject to post weld heat treatment per the original construction code, then the residual stress is given by:

$$\sigma^r(x) = 0.3\sigma_{ys}^r \tag{E.88}$$

E.7.1.2 Residual Stress Parallel to the Weld Seam

a) Surface Residual Stress Distribution – The residual stress distribution for this category can be approximated using paragraph E.7.1.1 a.

b) Through-Thickness Residual Stress Distribution:

$$\sigma^r(x) = \sigma_{ys}^r \tag{E.89}$$

c) Effects of Test Pressure – The reduction in residual stress resulting from the test pressure is not provided for this weld joint; therefore, $R_r = 1.0$.

d) Effects of $PWHT$ – If the weld is known to have been subject to post weld heat treatment per the original construction code, then the residual stress is given by:

$$\sigma^r(x) = 0.3\sigma_{ys}^r \tag{E.90}$$

E.7.2 Nozzle Fillet Weld (see Figure E.15, Weld Joint B)

E.7.2.1 Residual Stress Perpendicular to the Weld Seam

a) Surface Residual Stress Distribution. Note that the origin for the nozzle is O_n and the origin for the shell is O_s, see Figure E.15.

$$\sigma^r(y) = \left\{ \frac{1 - \left(\frac{|y| - w}{c} \right)^2}{1 + \left(\frac{|y| - w}{c} \right)^{2n}} \right\} \cdot \sigma^r_{ys} \cdot R_r \tag{E.91}$$

$$c = 3t_n \tag{E.92}$$

$$n = 2 \tag{E.93}$$

b) Through-Thickness Residual Stress Distribution – The residual stress distribution for this category of weld made remote from all other geometric discontinuities can be approximated using Equation (E.5). The local coordinate x for the stress distribution through the wall thickness is measured from the inside to outside surfaces (see Figure E.15). The parameters $\bar{\sigma}^r_m$, $\bar{\sigma}^r_b$, s^r_o and s^r_i are determined using the following equations.

$$\bar{\sigma}^r_m = 0.27 \tag{E.94}$$

$$\bar{\sigma}^r_b = 0.47 \tag{E.95}$$

$$s^r_o = 0.26 \tag{E.96}$$

$$s^r_i = 0.21 \tag{E.97}$$

c) Effects of Test Pressure – The reduction in residual stress resulting from the test pressure is not provided for this weld joint; therefore, $R_r = 1.0$.

d) Effects of $PWHT$ – If the weld is known to have been subject to post weld heat treatment per the original construction code, then the residual stress is given by:

$$\sigma^r(x) = 0.3\sigma^r_{ys} \tag{E.98}$$

E.7.2.2 Residual Stress Parallel to the Weld Seam

a) Surface Residual Stress Distribution – The residual stress distribution for this category can be approximated using paragraph E.7.1.1 a.

b) Through-Thickness Residual Stress Distribution:

$$\sigma^r(x) = \sigma^r_{ys} \tag{E.99}$$

c) Effects of Test Pressure – The reduction in residual stress resulting from the test pressure is not provided for this weld joint; therefore, $R_r = 1.0$.

d) Effects of $PWHT$ – If the weld is known to have been subject to post weld heat treatment per the original construction code, then the residual stress is given by:

$$\sigma^r(x) = 0.3\sigma^r_{ys} \tag{E.100}$$

E.7.3 Shell Fillet Weld with a Reinforcing Pad (see Figure E.15, Weld Joint C)

The results from paragraph E.81 may be used for this configuration.

E.8 Full Penetration and Fillet Welds at a Tee Joint

E.8.1 Main Plate (see Figures E.16 and E.17)

E.8.1.1 Residual Stress Perpendicular to the Weld Seam

a) Surface Residual Stress Distribution – The residual stress distribution for this category of weld made remote from all other geometric discontinuities can be approximated using the following equations for the top surface. The local coordinate y for the stress distribution along the top surface is measured from the center of the stay plate as shown in Figure E.17.

$$\sigma^r(y) = \sigma^r_{ys} \cdot R_r \qquad if \qquad 0 \le y \le w_t \tag{E.101}$$

$$\sigma^r(y) = \left\{ \frac{1 - \left(\frac{y - w_t}{c} \right)^2}{1 + \left(\frac{y - w_t}{c} \right)^{2n}} \right\} \cdot \sigma^r_{ys} \cdot R_r \qquad if \qquad y > w_t \tag{E.102}$$

$$w_t = \frac{t_2}{2} + w \tag{E.103}$$

$$c = t_1 \qquad if \qquad t_1 \ge 4w \tag{E.104}$$

$$c = 2t_1 \qquad if \qquad t_1 < 4w \tag{E.105}$$

$$n = 2 \tag{E.106}$$

b) Through-Thickness Residual Stress Distribution – The residual stress distribution for this category of weld made remote from all other geometric discontinuities can be approximated using Equation (E.5) if $t_1 \ge 4w$. The local coordinate x for the stress distribution through the wall thickness is measured from the base of the main plate The parameters $\bar{\sigma}^r_m$, $\bar{\sigma}^r_b$, s^r_o and s^r_i are determined using the following equations.

$$\bar{\sigma}^r_m = 0.27 \tag{E.107}$$

$$\bar{\sigma}^r_b = 0.47 \tag{E.108}$$

$$s^r_o = 0.26 \tag{E.109}$$

$$s^r_i = 0.21 \tag{E.110}$$

If $t_1 < 4w$, the residual stress distribution can be determined using the following equations.

$$\sigma^r(\zeta) = \left\{ \zeta + (1-\zeta)\left(\frac{4w - t_1}{3w} \right) \right\} \cdot \sigma_{ys} \cdot R_r \qquad if \qquad w < t_1 < 4w \qquad \text{(E.111)}$$

$$\sigma^r(\zeta) = \sigma_{ys} \cdot R_r \qquad if \qquad t_1 \le w \qquad \text{(E.112)}$$

c) Effects of Test Pressure – The reduction in residual stress resulting from the test pressure is not provided for this weld joint; therefore, $R_r = 1.0$.

d) Effects of PWHT – If the weld is known to have been subject to post weld heat treatment per the original construction code, then the residual stress is given by:

$$\sigma^r(x) = 0.2\sigma^r_{ys} \qquad if \qquad t_1 \ge w \qquad \text{(E.113)}$$

$$\sigma^r(x) = 0.3\sigma^r_{ys} \qquad if \qquad t_1 < w \qquad \text{(E.114)}$$

E.8.1.2 Residual Stress Parallel to the Weld Seam

a) Surface Residual Stress Distribution – The residual stress distribution for this category can be approximated using paragraph E.8.1.1 a.

b) Through-Thickness Residual Stress Distribution – The residual stress distribution for this category can be approximated using paragraph E.8.1.1 b.

c) Effects of Test Pressure – The reduction in residual stress resulting from the test pressure is not provided for this weld joint; therefore, $R_r = 1.0$.

d) Effects of $PWHT$ – If the weld is known to have been subject to post weld heat treatment per the original construction code, then the residual stress is given by paragraph E.8.1.1.d.

E.8.2 Stay Plate (see Figure E.16 and Figure E.18)

E.8.2.1 Residual Stress Perpendicular to the Weld

a) Surface Residual Stress Distribution – The residual stress distribution for this category of weld made remote from all other geometric discontinuities can be approximated using the Equation (E.101) and (E.102) with $w_t = w/2$. The following equations shall be used to determine c and n.

$$c = 2t_2 \qquad \text{(E.115)}$$

$$n = 2 \qquad \text{(E.116)}$$

b) Through-Thickness Residual Stress Distribution – The residual stress distribution for this category of weld made remote from all other geometric discontinuities can be approximated using Equation (E.5). The local coordinate x for the stress distribution through the wall thickness is measured from any surface. The parameters $\bar{\sigma}^r_m$, $\bar{\sigma}^r_b$, s^r_o and s^r_i are determined using the following equations.

$$\bar{\sigma}^r_m = 0.54 + \delta \qquad \text{(E.117)}$$

$$\bar{\sigma}^r_b = 0.0 \qquad \text{(E.118)}$$

$$s^r_o = 0.470 - \delta \qquad \text{(E.119)}$$

$$s_i^r = 0.469 - \delta \tag{E.120}$$

The parameter δ is given by the following equations.

$$\delta = 0.0 \qquad if \qquad t_1 > 3w \tag{E.121}$$

$$\delta = 0.47\left(\frac{3w - t_1}{2w}\right) \qquad if \qquad w \le t_1 \le 3w \tag{E.122}$$

$$\delta = 0.47 \qquad if \qquad t_1 < w \tag{E.123}$$

c) Effects of Test Pressure – The reduction in residual stress resulting from the test pressure is not provided for this weld joint; therefore, $R_r = 1.0$.

d) Effects of $PWHT$ – If the weld is known to have been subject to post weld heat treatment per the original construction code, then the residual stress is given by:

$$\sigma^r(x) = 0.3\sigma_{ys}^r \tag{E.124}$$

E.8.2.2 Residual Stress Parallel to the Weld Seam

a) Surface Residual Stress Distribution – The residual stress distribution for this category can be approximated using paragraph E.8.2.1.a.

b) Through-Thickness Residual Stress Distribution – The residual stress distribution for this category can be approximated using paragraph E.8.2.1.b.

c) Effects of Test Pressure – The reduction in residual stress resulting from the test pressure is not provided for this weld joint; therefore, $R_r = 1.0$.

d) Effects of $PWHT$ – If the weld is known to have been subject to post weld heat treatment per the original construction code, then the residual stress is given by paragraph E.8.2.1.d.

E.9 Repair Welds

E.9.1 Seam Welds (Figure E.19)

E.9.1.1 Residual Stress Perpendicular to the Weld Seam

a) Surface Residual Stress Distribution – The residual stress distribution for this category of weld made remote from all geometric discontinuities can be approximated using the following equations.

$$\sigma^r(y) = \left\{\frac{1 - \left(\frac{y - w/2}{c}\right)^2}{1 + \left(\frac{y - w/2}{c}\right)^{2n}}\right\} \cdot \sigma_{ys}^r \cdot R_r \qquad if \qquad y \le -\frac{w}{2} \tag{E.125}$$

$$\sigma^r(y) = \sigma_{ys}^r \cdot R_r \qquad if \qquad -\frac{w}{2} \le y \le \frac{w}{2} + w_r \tag{E.126}$$

$$\sigma^r(y) = \left\{ \frac{1 - \left(\frac{y - w/2 - w_r}{c} \right)^2}{1 + \left(\frac{y - w/2 - w_r}{c} \right)^{2n}} \right\} \cdot \sigma^r_{ys} \cdot R_r \qquad if \qquad y > \frac{w}{2} + w_r \tag{E.127}$$

$$c = t \tag{E.128}$$

$$n = 2 \tag{E.129}$$

b) Through-Thickness Residual Stress Distribution – The residual stress distribution for this category of weld made remote from all geometric discontinuities can be approximated using Equation (E.5). The local coordinate x for the stress distribution through the wall thickness is measured from the inside surface. The parameters $\bar{\sigma}^r_b$ and $\bar{\sigma}^r_m$ are given by the following equations, and s^r_o and s^r_i are determined using paragraph E.4.1.1.b.

$$\bar{\sigma}^r_m = 0.27\left(1 + \frac{t_w}{t}\right) \tag{E.130}$$

$$\bar{\sigma}^r_b = 0.47 + 0.81\left(\frac{t_w}{t}\right)\left(1 - \frac{t_w^2}{t^2}\right) \tag{E.131}$$

c) Effects of Test Pressure – The reduction in residual stress resulting from the test pressure is not provided for this weld joint; therefore, $R_r = 1.0$.

d) Effects of PWHT – If the weld is known to have been subject to post weld heat treatment per the original construction code, then the residual stress is given by:

$$\sigma^r(x) = 0.3\sigma^r_{ys} \tag{E.132}$$

E.9.1.2 Residual Stress Parallel to the Weld Seam

The residual stress solution provided for the residual stress perpendicular to the Weld Seam in paragraph E.9.1.1 may be used, except that in paragraph E.9.1.1.b, s^r_o and s^r_i are determined using paragraph E.4.1.2.b.

E.9.2 Nozzle Welds

The residual stress for repair of the nozzle-to-shell weld shall be determined on a case-by-case basis considering the original weld and repair weld geometry and welding parameters.

E.10 Nomenclature

Note that the SI units described for each variable must be used in the equation of this Annex. Conversion of the stress distribution to US Customary units, if required, should be performed after the distribution is computed in MPa.

A	parameter used to determine the self equilibrating part of the through-wall stress distribution.
B	parameter used to determine the self equilibrating part of the through-wall stress distribution.
C	parameter used to determine the self equilibrating part of the through-wall stress distribution.
D	parameter used to determine the self equilibrating part of the through-wall stress distribution.

E parameter used to determine the self equilibrating part of the through-wall stress distribution.

$C_1 \rightarrow C_4$ parameters used to fit the Ψ function.

c characteristic length parameter , c is proportional to $\sqrt{rt}$ for pipe joints and to thickness for plate joints.

I welding current used.

ID inside diameter or internal surface (see Figures E.2, E.4, E.5, E.7, E.9, E.10, E.11, E.12, E.13, and E.14).

K residual stress factor.

n an integer chosen from 2, 3, 4, or 5 (see paragraph E.3.3).

OD outside diameter or external surface (see Figures E.2, E.4, E.5, E.7, E.9, E.10, E.11, E.12, E.13, and E.14).

O_N nozzle origin (see Figure E.15).

O_S shell origin (see Figure E.15).

$\dot{q}$ linear heat input to the weld.

$\hat{Q}$ heat input density .

r mean radius of the pipe, cylindrical, or spherical shell, as applicable.

r_c chord length of the spherical shell.

R_r reduction in the residual stress.

$\hat{R}$ radius to thickness ratio parameter.

s_i^r portion of residual stress at the inner surface excluding both bending and membrane components, $s_i^r = \sigma_i^r - \sigma_b^r - \sigma_m^r$.

s_o^r portion of residual stress at the outer surface excluding both bending and membrane components, $s_o^r = \sigma_o^r - \sigma_b^r - \sigma_m^r$.

t nominal wall thickness of the component.

t_n wall thickness of the nozzle (see Figure E.15).

t_s wall thickness of the shell (see Figure E.15).

t_1 wall thickness of the main plate (see Figure E.17 and E.18).

t_2 wall thickness of the stay plate (see Figure E.17 and E.18).

t_w repair weld depth.

T_p nominal circumferential membrane stress in a cylinder or sphere during the pressure test as a percentage of the yield strength.

u welding travel speed.

V welding voltage used.

w weld width.

w_r width of the repair weld that exceeds the original weld width (see Figure E.19)

x local coordinate defined through the wall thickness of the component to define the residual stress distribution.

y local coordinate defined along the surface of the component to define the residual stress distribution.

Ψ mathematical function.

ζ normalized local coordinate defined through the wall thickness of the component to define the residual stress distribution, $\zeta = x/t$.

η welding arc efficiency.

$\sigma_{mc,t}$ nominal circumferential membrane stress in a cylinder or sphere stress during the pressure test.

σ_{para} residual stress parallel to the weld joint.

σ_{perp} residual stress perpendicular to the weld joint.

σ_{ys} specified minimum yield strength.

σ_{ys}^{r} magnitude of the effective yield strength to be used to estimate the residual stress at a welded joint

σ^{r} residual stress distribution either through thickness or along surface.

σ_{i}^{r} residual stress at the inner surface.

σ_{o}^{r} residual stress at the outer surface.

$\overline{\sigma}_{b}^{r}$ normalized bending component of the residual stress.

$\overline{\sigma}_{m}^{r}$ normalized membrane component of the residual stress.

E.11 References

1. Dong, P., Cao, Z., and Hong, J.K., “Investigation of Weld Residual Stresses and Local Post-Weld Heat treatment to PVRC Joint Industry Project (JIP) Sponsors”, Battelle Report, February, 2005.
2. Dong, P., Cao, Z., and Hong, J.K. et al, “Recent Progress in Analysis of Welding Residual Stresses”, Welding Research Council (WRC) Bulletin 455, September 2000.
3. Dong, P., and Hong, J.K., “Recommendation for Determining Residual Stresses in Fitness-for-Service Assessment”, Welding Research Council (WRC) Bulletin 476, November 2002.
4. Dong, P., “Residual Stresses and Distortions in Welded Structures: A Perspective for Engineering Applications”, Science and Technology of Welding and Joining, Vol. 10, N.4, 2005, pp.389-398.
5. Dong, P., “Modeling of Weld Residual Stresses and Distortions: Advanced Computational Procedures and practical Applications,” Keynote Lecture – Proceeding of The Sixth International Conference on Residual Stresses (ICRS-6), Oxford, United Kingdom, July 10-12, 2000, pp.1223-1335.
6. Dong, P., “A Mechanics Based Parametric Description of Residual Stress Profiles for Fracture and Fatigue Assessment,” Proceeding of ASME PVP Conference, Denver, Colorado, USA, July 17-21, 2005.
7. Dong, P. and Cao, Z., “The Mechanics Basis of Residual Stress Profiles in Proposed API 579 Annex E,” Proceeding of PVP2006-ICPVT-11, 2006 ASME Pressure vessels and Piping Division Conference, Vancoucer, BC, Canada, July 23-27, 2006.
8. Bradford, R., “Through-Thickness Distributions of Welding Residual Stresses in Austenitic Steel Cylindrical Butt Welds,” Proceeding of The Sixth International Conference on Residual Stresses (ICRS-6), Oxford, United Kingdom, July 10-12, 2000, pp.1373-1381.
9. Bouchard, J. and Bradford, C., “Validated Axial Residual Stress Profiles for Fracture Assessment of Austenitic Stainless Steel Pipe Girth Welds,” PVP Vol.422: Fracture and Fitness, Proceeding of ASME PVP Conference, Atlanta, Georgia, USA, July 22-26, 2001.
10. SINTAP (Structural Integrity Assessment Procedures for European Industry) Procedure Final Version: November 1999.
11. SINTAP (Structural Integrity Assessment Procedures for European Industry) Procedure Final Version: February 2003.
12. Anderson, P., Bergman, M., Brickstad, B., Dahlberg, L., Nilsson, F., and Sattari-Far, I., “A Procedure for Safety Assessment of Components with Cracks – Handbook,” SAQ/FoU-Report 96/08, SAQ Kontroll AB, SAQ Inspection Ltd, 1996.
13. Bate, S.K., Green, D. and Buttle, D., “A Review Of Residual Stress Distributions In Welded Joints For The Defect Assessment Of Offshore Structures,” Health and Safety Executive – Offshore Technology Report OTH 482, 1997.
14. Brickstad, Bjorn and Josefson, Lennart, “A Parametric Study of Residual Stresses in Multipass Butt-Welded Stainless Steel Pipes,” SAQ/FoU-Report 96/01, SAQ Kontroll AB, SAQ Inspection Ltd, 1996.
15. BSI, “Guidance For Assessing The Acceptability Of Flaws In Fusion Welded Structures,” PD-6493: 1991, British Standards Institute, Aug. 1991.

16. Burdekin, F.M., “Local Stress Relief of Circumferential Butt Welds in Cylinders,” British Welding Journal, September 1963, pp. 483-490.
17. Downey, J.C., Hood, D.W., and Keiser, D.D., “Shrinkage in Mechanized Welded 16 Inch Stainless Pipe,” Welding Journal, March 1975, pp. 170-175.
18. Dubois, D., Devaux, J., and Leblond, J.B., “Numerical Simulation of a Welding Operation: Calculation of Residual Stresses and Hydrogen Diffusion,“ Fifth International Conference of Pressure Vessel Technology, Vol II, Materials and Manufacturing, ASME, 1984.
19. Finch, D.M. and Burdekin, F.M., “Effects of Welding Residual Stresses on Significance of Defects in Various Types of Welded Joint,” Engineering Fracture Mechanics, Vol. 41, No. 5, pp. 721-735, 1992.
20. Finch, D.M., “Effects of Welding Residual Stresses on Significance of Defects in Various Types of Welded Joint-II,” Engineering Fracture Mechanics, Vol. 42, No. 3, pp. 479-500, 1992.
21. Fujita, Y., Nomoto, T., and Hasegawa, H., “Deformations and Residual Stresses in Butt-Welded Pipes and Spheres,” IIW Doc. X-963-80, April 1980.
22. Fujita, Y., Nomoto, T., and Hasegawa, H., “Welding Deformations and Residual Stresses Due to Circumferential Welds at the Joint Between Cylindrical Drum and Hemispherical Head Plate,” IIW Doc. X-985-81, July 1981.
23. Guan Q., and Liu, J.D., “Residual Stress and Distortion in Cylindrical Shells Caused by a Single-Pass Circumferential Butt Weld – A Discussion with Appropriate Calculation Method,” IIW Document X92979.
24. Health & Safety Executive, “A Review of Residual Stress Distributions in Welded Joints for the Defect Assessment of Offshore Structures,” OTH 482, HSE, 1997.
25. Japan High Pressure Gas Institute as reported by T. Tanaka in "Local PWHT for Pressure Vessels" at the Spring 1991 API Refining Meeting, Nashville, Tennessee.
26. Josefson, B.L., “Residual Stresses and Their Redistribution During Annealing of a Girth-Butt Welded Thin-Walled Pipe,” Transactions of the ASME, Journal of Pressure Vessel Technology, August 1982, pp. 245-250.
27. Josefson, B.L., “Stress Distribution During Annealing of a Multi-Pass Butt Welded Pipe,” Journal of Pressure Vessel Technology, Vol. 105, May 1983, pp. 165-170.
28. Kim, D.S., and Smith, J.D., “Residual Stress Measurements of Tension Leg Platform Tendon Welds,” Offshore Mechanics and Arctic Engineering Conference, Houston, Texas, Vol. III, pp. 31-36, 1994.
29. Kim, D.S., MCFarland, D., Reynolds, J.T., Boswell, R.S.,”FFS Assessment Utilizing Field Measured Residual Stress Measurements”, ASME PVP Vol 315, pp 327-334, 1995.
30. Kirk, M.T., Mohr, W.R., and Michaleris, P., “An Improved Treatment Of residual Stresses In Flaw Assessment of Pipes and Pressure Vessels Fabricated From Ferritic Steels,” PVP-Vol. 359, ASME, pp 37-47, 1997.
31. Koppenhoefer, K., “Incorporation of Residual Stresses Caused By Welding into Fracture Assessment Procedures,” EWI Project No. 40568-CSP, MPC No. FS-II-5, Sept. 15, 1998.
32. Lazor, R.B., Leggatt, R.H., and Glover, A.G., “Experimental Stress Analysis of Pipeline Girth Welds,” American Gas Association Catalog No. L51490, August 1985.
33. Leggatt, R.H., “Residual Stresses at Circumferential Welds in Pipes,” TWI Research Bulletin, June 1982, pp. 181-188.
34. Leggatt, R.H., “Residual Stresses at Girth Welds in Pipes,” Welding in Energy-Related Projects, Welding Institute of Canada, Pergamon Press, 1984.
35. Leung, C.K. and Pick, R.J., “Finite Element Analysis of Multi-Pass Welds,” WRC Bulletin 356, Welding Research Council, New York, N.Y., 1990.
36. Leung, C.K., Pick, R.J., and Mok, D.H., “Finite Element Modeling of a Single Pass Weld,” WRC Bulletin 356, Welding Research Council, New York, N.Y., 1990.
37. Makhnenko, V.I., Shekera, V.M., and L. A. Izbenko, L.A., “Special Features of the Distribution of Stresses and Strains Caused by Making Circumferential Welds in Cylindrical Shells,” Automatic Welding, 1970, No., 12, pp. 43-47.
38. McGaughy, T.H., “Effects of Repair Welding on the Residual Stress Distribution and Fracture Toughness in Pipeline Girth Welds", Pipeline Research Committee final report PR-185-9104, August 1992.
39. McGaughy, T.H., and Boyles, L., “Significance of Changes in Residual Stresses and Mechanical Properties Due to SMAW Repair of Girth Welds in Linepipe,” Pipeline Research Committee final report PR-185-905, October 1990.
40. Michaleris, P., “Incorporation of Residual Stresses into Fracture Assessment Models,” EWI Project No. J7412, Nov. 13, 1996.

41. Michaleris, P., Kirk, M., and Laverty, K. “Incorporation of Residual Stresses into Fracture Assessment Models,” MPC FS-30, Materials Properties Council, August 1996.
42. Mohr, W., “Internal Surface Residual Stresses in Girth butt-Welded Steel Pipes,” Proceeding of ASME Pressure Vessel and Pipe Conference, PVP-Vol. 327, Residual Stresses in Design, Fabrication, Assessment and Repair, 1996.
43. Myers, P.S., Uyehara, O.A., and Borman, G.L., “Fundamentals of Heat Flow in Welding,” WRC Bulletin 123, Welding Research Council, New York, N.Y., 1967.
44. Pavlovski, V.I. and Masubuchi, K., “Research in the USSR on Residual Stresses and Distortion in Welded Structures,” WRC Bulletin 388, Welding Research Council, New York, N.Y., 1994.
45. Roelens, J.B., “Numerical Simulation of Some Multipass Submerged Arc Welding Determination of the Residual Stresses and Comparison with Experimental Measurements,” IIW Document XIII-1549-94.
46. Rybicki, E.F., Groom, J.J., Lemcoe, M.M., Mischler, H.W., Rodebaugh, E.C., Schmuster, D.W., Stonesifer, R.B., and Strenkowski, J.S., “Residual Stresses at Girth-Butt Welds in Pipes and Pressure Vessels,” NUREG Report 0376, November 1977.
47. Rybicki, E.F., Groom, J.J., Lemcoe, M.M., Mishler, H.W., Rodabaugh, E.C., Schmuster, D.W., Stonesifer, R.B., and Strenkowski, J.S., “Residual Stresses at Girth-Butt Welds in Pipes and Pressure Vessels,” NUREG-0376 R5, NTIS, 1977.
48. Scaramangas, A., “Residual Stresses in Cylinder Girth Butt Welds,” OTC 5024, 1985.
49. Scaramangas, A., “Residual Stresses in Girth Butt Welded Pipes,” Ph.D. dissertation, Cambridge University, May 1984.
50. Shack, W.J., “Measurement of Through-wall Residual Stresses in Large-Diameter Type 304 Stainless Steel Piping Butt Weldments,” Work Performed under EPRI Contract No. T114-2, Argon National Laboratory, March 1982.
51. Ueda, Y., Fukuda, K., Nishimura, I., Yuma, H., Chiba, N., and Fukuda, M., “Three Dimensional Cold Bending and Welding Residual Stresses in Penstock of 80 kgf/mm2 Class High Strength Steel Plate,” Transactions of the JWRI, Vol. 12, No. 2, 1983 pp. 117-126.
52. Umemoto, T., and Furuya, S., “A Simplified Approach to Assess Weld Residual Stress Distribution Through Pipe Wall,” Nuclear Engineering and Design, Vol. 111, 1989, pp. 159171.
53. Umemoto, T., and Tanaka, S., “A Simplified Approach to Calculate Weld Residual Stresses in a Pipe,” Ishikawajima-Harima Heavy Industries Engineering Review, Vol. 17, No. 3, 1984.
54. Zhou, R.J., Pense, A.W., Basehore, M.L., and Lyons, D.H., “A Study of Residual Stresses in Pressure Vessel Steels,” WRC Bulletin 302, Welding Research Council, New York, N.Y., 1985.

E.12 Tables and Figures

Table E.1
Heat Input Based On Welding Process

Welding Process	Heat Input (KJ/in)			
	Ferritic Steels		Stainless Steel	
	Average	Upper Bound	Average	Upper Bound
SMAW (1)	28.7	46.7	23.9	33.8
SAW (2)	31.0	49.3	27.4	48.8
GTAW (3)	12.7	25.4	12.7	24.0
GMAW (4)	9.9	18.3	9.9	18.3

Notes

1. Based on 1/8 inch electrode, 6 in/min (0.1 in/sec) travel speed, for carbon steel: average 115A-25V, upper bound 180A-26V, for stainless steel: average 95A-25V, upper bound 130A-26V.
2. Based on 5/32 inch electrode, 35 in/min (0.58 in/sec) travel speed, for carbon steel: average 600A-30V, upper bound 800A-36V, for stainless steel: average 500A-32V, upper bound 750A-38V.
3. Based on 3/32 inch electrode, 6 in/min (0.1 in/sec))travel speed, for carbon steel: average 90A-14V, upper bound 160A-16V, for stainless steel: average 90A-14V, upper bound 150A-16V.
4. Based on 0.35 inch electrode, 12 in/min (0.2 in/sec) travel speed, for carbon steel: average 110A-18V, upper bound 175A-21V, for stainless steel: average 100A-20V, upper bound 160A-23V.

Table E.1M
Heat Input Based On Welding Process

Welding Process	Heat Input (J/mm)			
	Ferritic Steels		Stainless Steel	
	Average	Upper Bound	Average	Upper Bound
SMAW (1)	1130	1840	940	1330
SAW (2)	1220	1940	1080	1920
GTAW (3)	500	1000	500	944
GMAW (4)	390	720	390	720

Notes

1. Based on 3.2 mm electrode, 152 mm/min (2.5 mm/sec) travel speed, for carbon steel: average 115A-25V, upper bound 180A-26V, for stainless steel: average 95A-25V, upper bound 130A-26V.
2. Based on 4 mm electrode, 889 mm/min (15 mm/sec) travel speed, for carbon steel: average 600A-30V, upper bound 800A-36V, for stainless steel: average 500A-32V, upper bound 750A-38V.
3. Based on 2.3 mm electrode, 152 mm/min (2.5 mm/sec) travel speed, for carbon steel: average 90A-14V, upper bound 160A-16V, for stainless steel: average 90A-14V, upper bound 150A-16V.
4. Based on 0.9 mm electrode, 305 mm/min (5 mm/sec) travel speed, for carbon steel: average 110A-18V, upper bound 175A-21V, for stainless steel: average 100A-20V, upper bound 160A-23V.

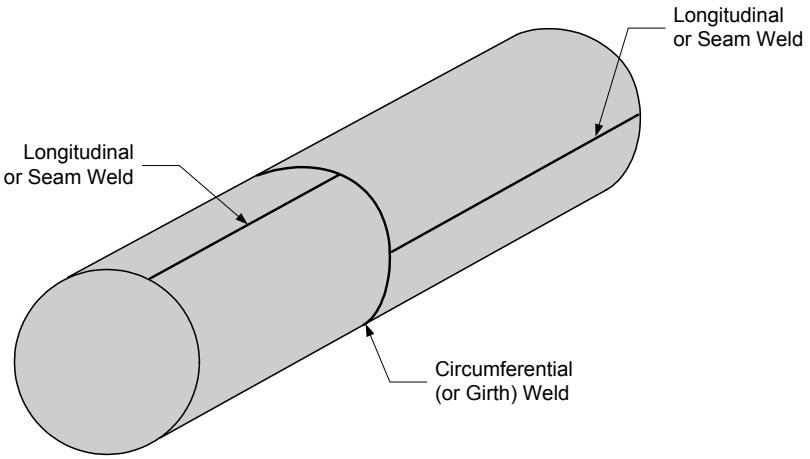

(a) Identification of Welds

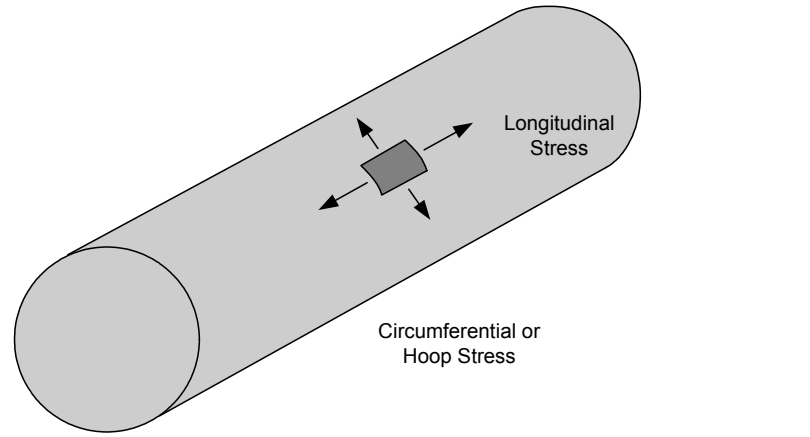

(a) Identification of Stresses

Definition Of Stress Directions

Weld Seam	Stress Component Perpendicular To the Weld Seam	Stress Component Parallel To the Weld Seam
Longitudinal	Circumferential (Hoop) Stress	Longitudinal Stress
Circumferential (Girth)	Longitudinal Stress	Circumferential (Hoop) Stress

Figure E.1
Weld Locations and Stress Directions in a Cylindrical Shell

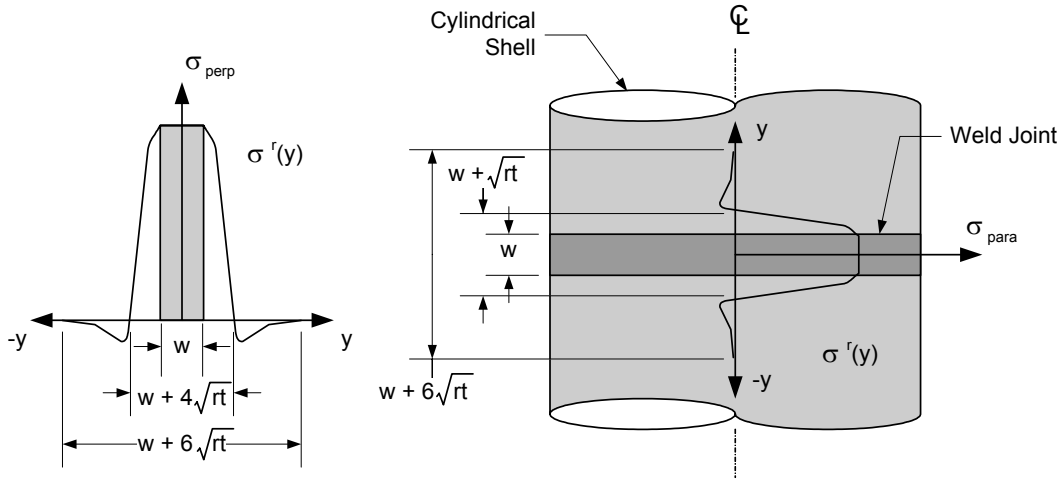

Stress Distribution Perpendicular to Weld (See Paragraph E.4.1.1)

Stress Distribution Parallel to Weld (See Paragraph E.4.1.2)

(a) Surface Stress Distribution

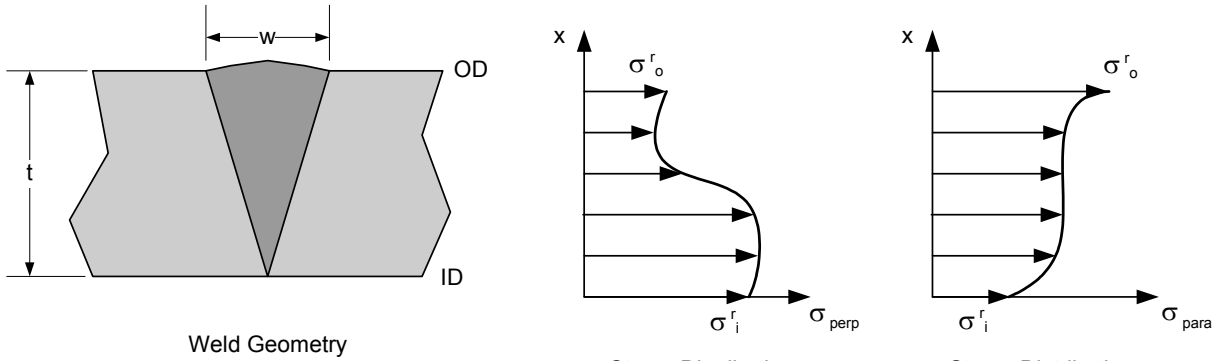

Weld Geometry

Stress Distribution Perpendicular to Weld (See Paragraph E.4.1.1)

Stress Distribution Parallel to Weld (See Paragraph E.4.1.2)

(b) Through-Wall Stress Distribution

Figure E.2
Residual Stress Surface and Through-Wall Distributions for Full Penetration Circumferential Single V-Groove Welds in Piping and Pressure Vessel Cylindrical Shells

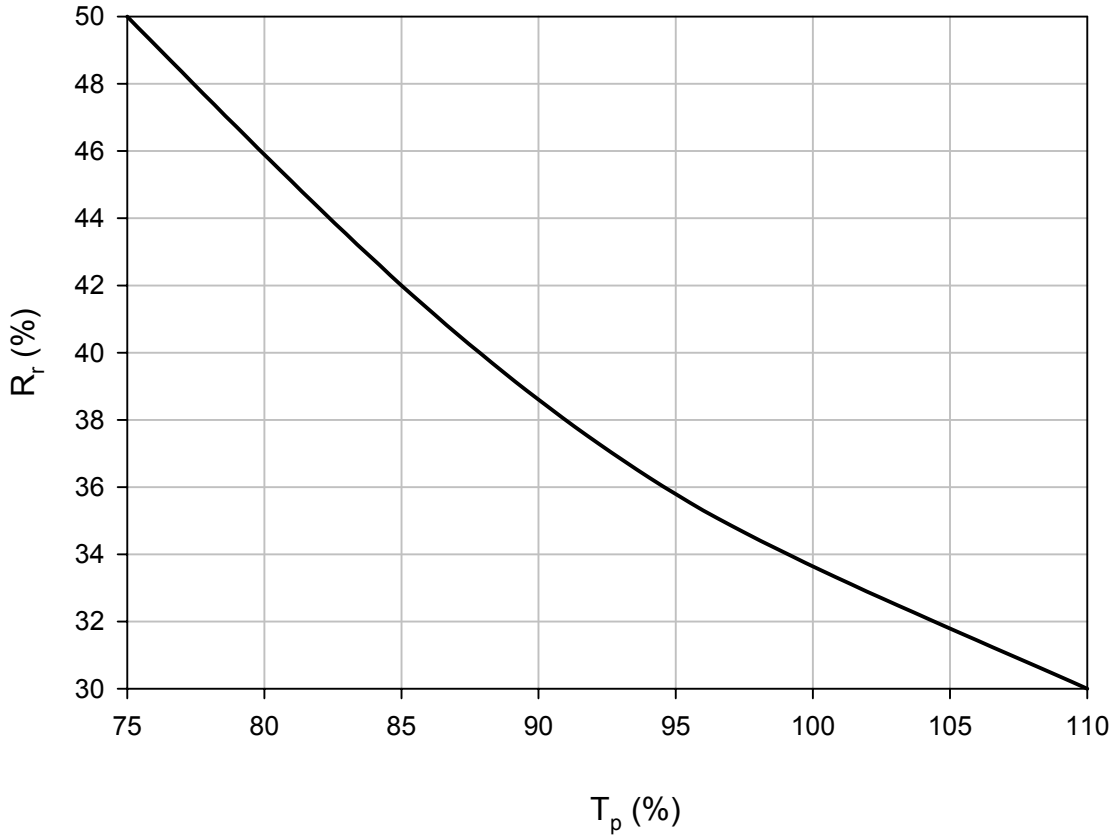

Note: Limitations on R_r are given in paragraphs E.4.1.1.c or paragraph E.5.1.1.c, as applicable.

Figure E.3
Reduction in Residual Stress Based on Test Pressure – Circumferential Joints in Cylinders

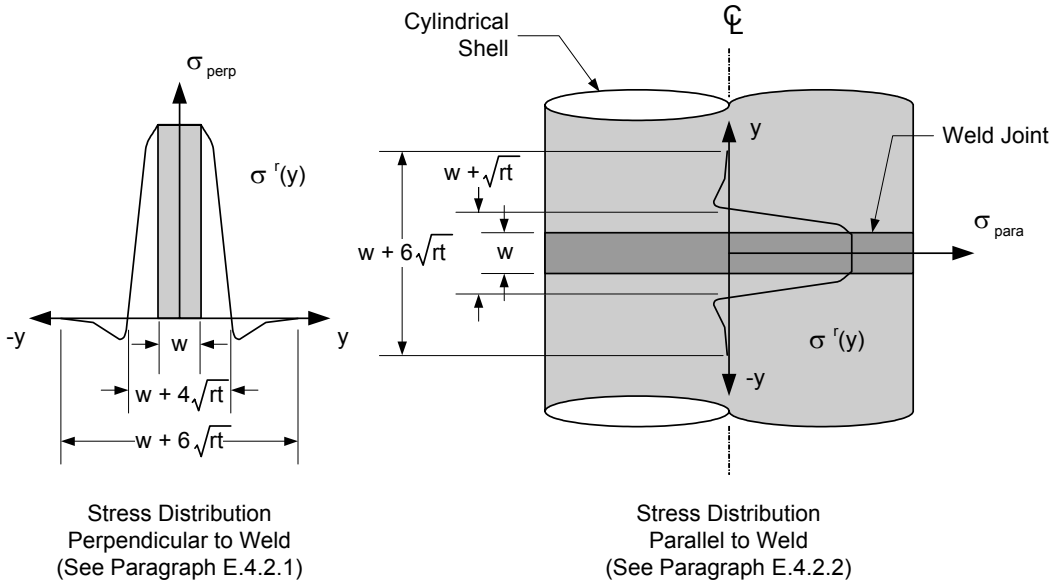

Stress Distribution Perpendicular to Weld (See Paragraph E.4.2.1)

Stress Distribution Parallel to Weld (See Paragraph E.4.2.2)

(a) Surface Stress Distribution

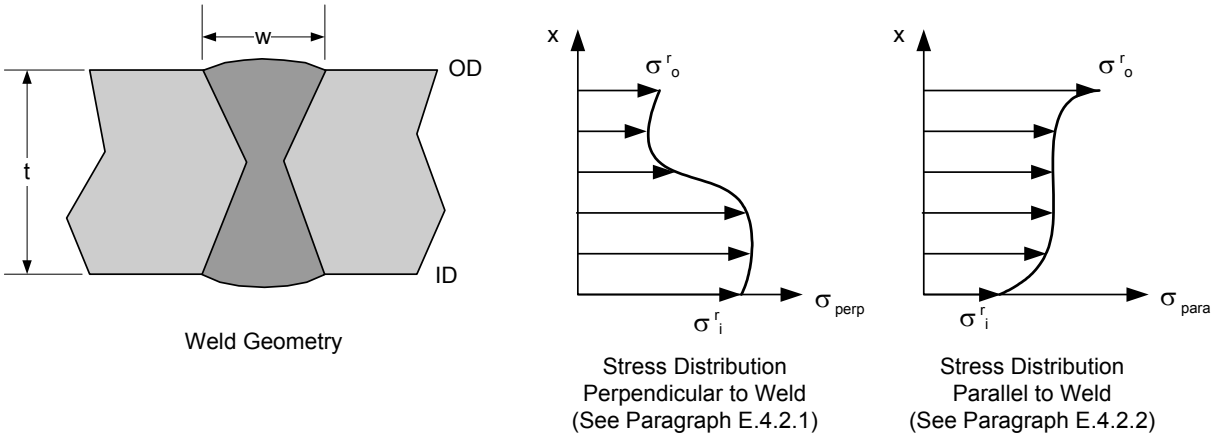

Weld Geometry

Stress Distribution Perpendicular to Weld (See Paragraph E.4.2.1)

Stress Distribution Parallel to Weld (See Paragraph E.4.2.2)

(b) Through-Wall Stress Distribution

Figure E.4
Residual Stress Surface and Through-Wall Distributions for Full Penetration Circumferential Double V-Groove Welds in Piping and Pressure Vessel Cylindrical Shells

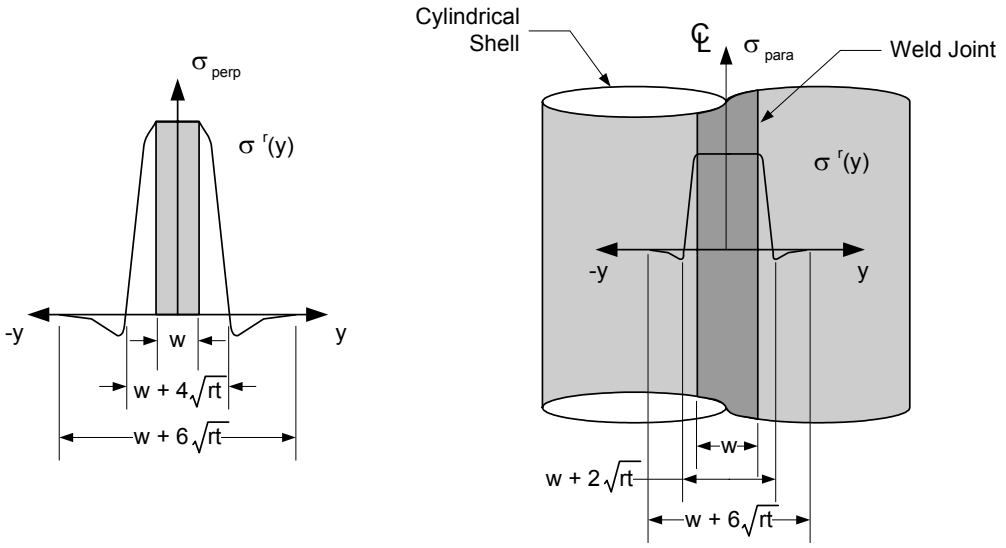

Stress Distribution Perpendicular to Weld (See Paragraph E.4.3.1)

Stress Distribution Parallel to Weld (See Paragraph E.4.3.2)

(a) Surface Stress Distribution

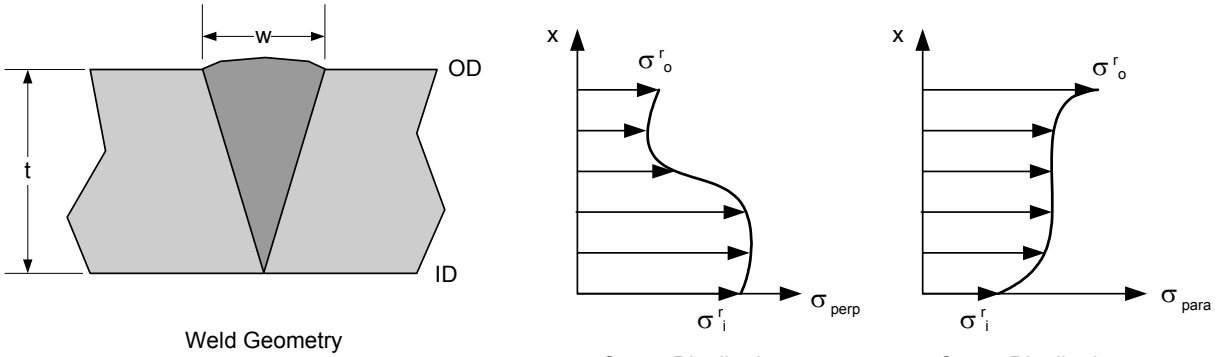

Weld Geometry

Stress Distribution Perpendicular to Weld (See Paragraph E.4.3.1)

Stress Distribution Parallel to Weld (See Paragraph E.4.3.2)

(b) Through-Wall Stress Distribution

Figure E.5
Residual Stress Surface and Through-Wall Distributions for Full Penetration Longitudinal Single V-Groove Welds in Piping and Pressure Vessel Cylindrical Shells

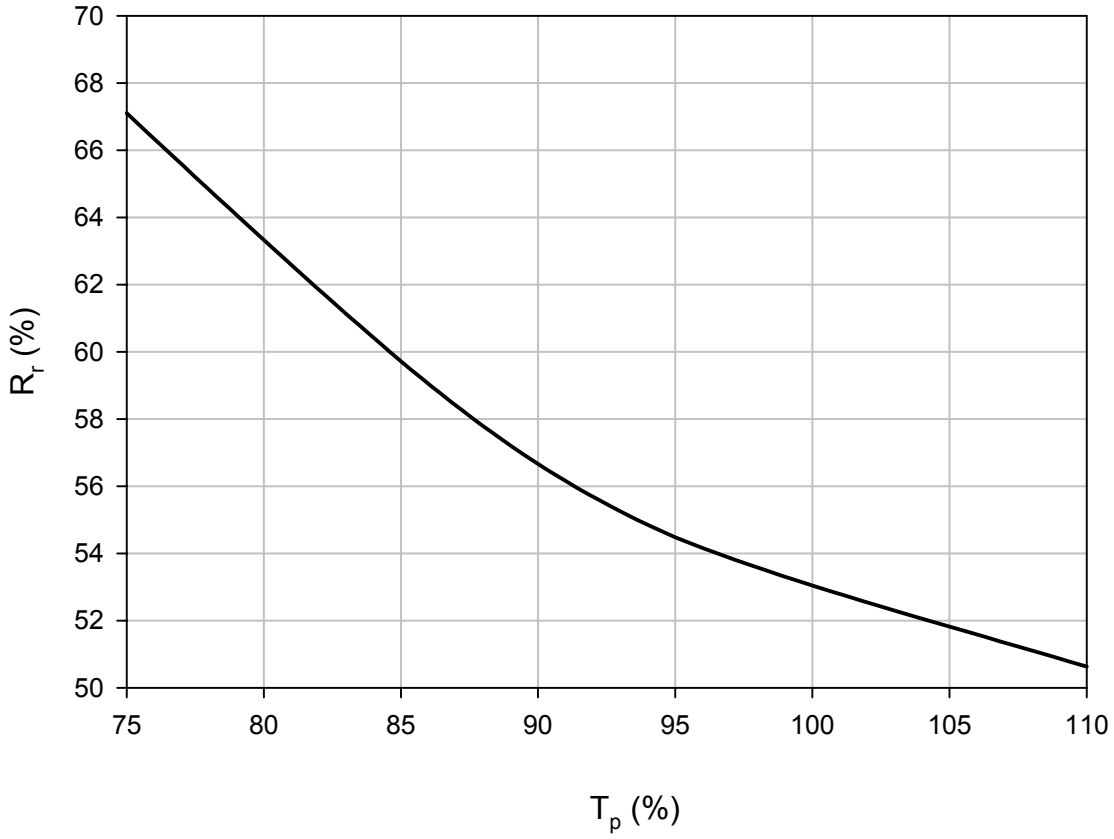

Note: Limitations on R_r are given in paragraph E.4.3.1.c.

Figure E.6
Reduction in Residual Stress Based on Test Pressure – Longitudinal Joints in Cylinders

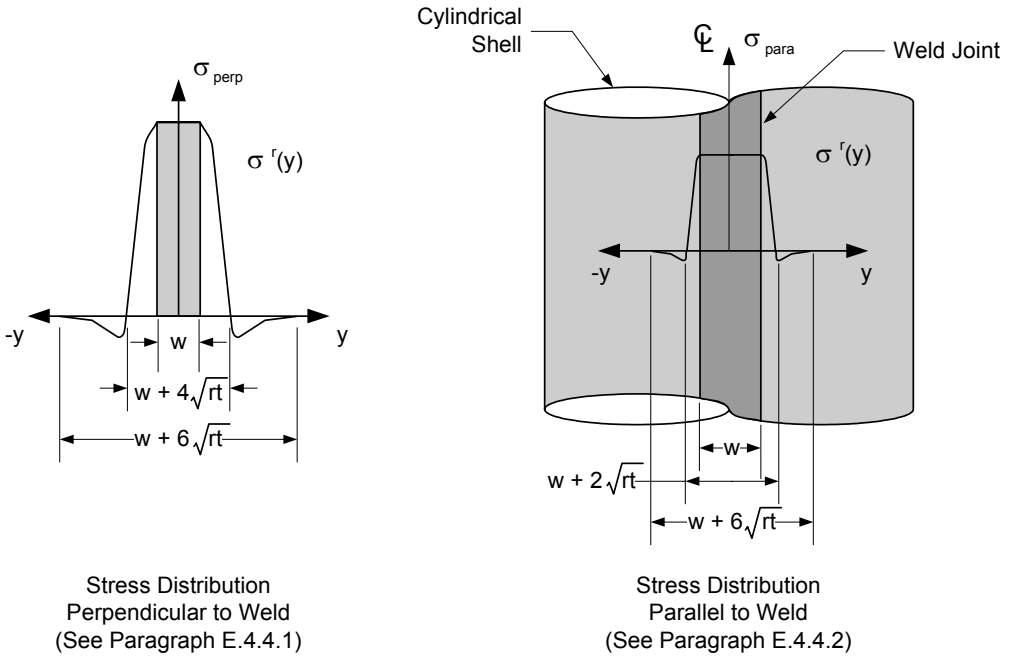

Stress Distribution Perpendicular to Weld (See Paragraph E.4.4.1)

Stress Distribution Parallel to Weld (See Paragraph E.4.4.2)

(a) Surface Stress Distribution

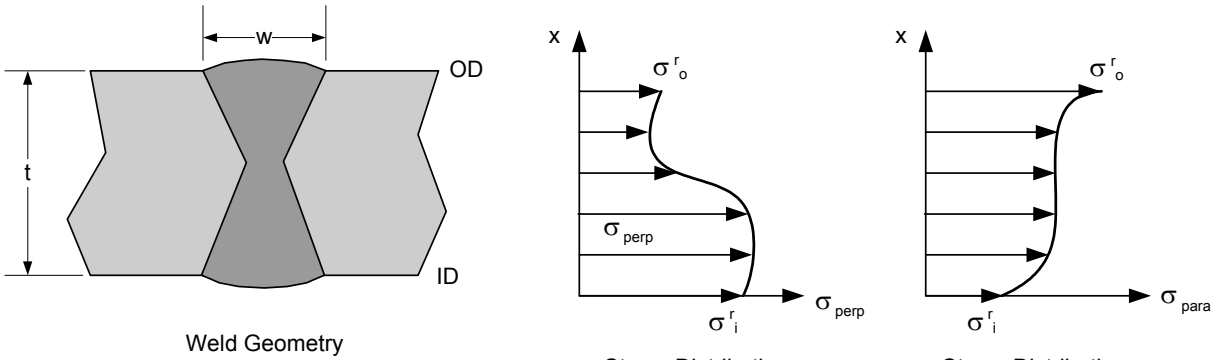

Weld Geometry

Stress Distribution Perpendicular to Weld (See Paragraph E.4.4.1)

Stress Distribution Parallel to Weld (See Paragraph E.4.4.2)

(b) Through-Wall Stress Distribution

Figure E.7
Residual Stress Surface and Through-Wall Distributions for Full Penetration Longitudinal Double V-Groove Welds in Piping and Pressure Vessel Cylindrical Shells

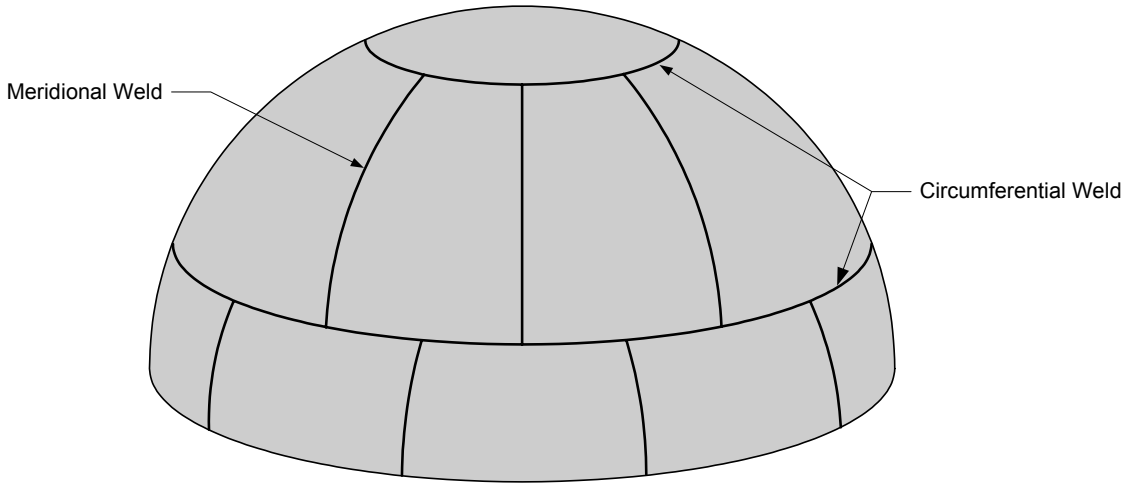

(a) Identification of Welds

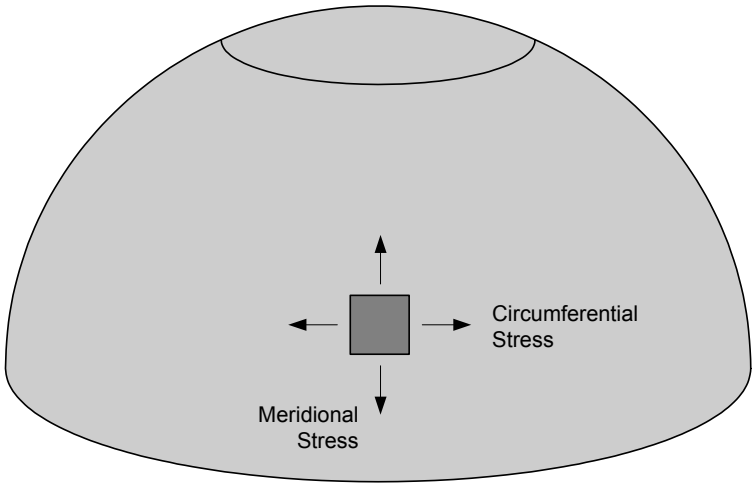

(b) Identification of Stresses

Definition of Stress Directions

Weld Seam	Stress Component Perpendicular To the Weld Seam	Stress Component Parallel To the Weld Seam
Meridional	Circumferential Stress	Meridional Stress
Circumferential	Meridional Stress	Circumferential Stress

Figure E.8
Weld Locations and Stress Directions in a Spherical Shell or Formed Head

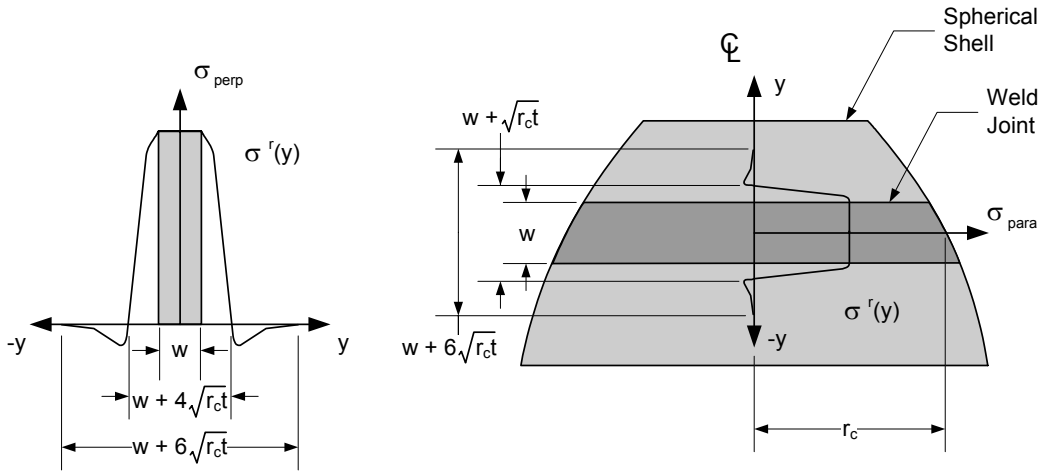

Stress Distribution
Perpendicular to Weld
(See Paragraph E.5.1.1)

Stress Distribution
Parallel to Weld
(See Paragraph E.5.1.2)

(a) Surface Stress Distribution

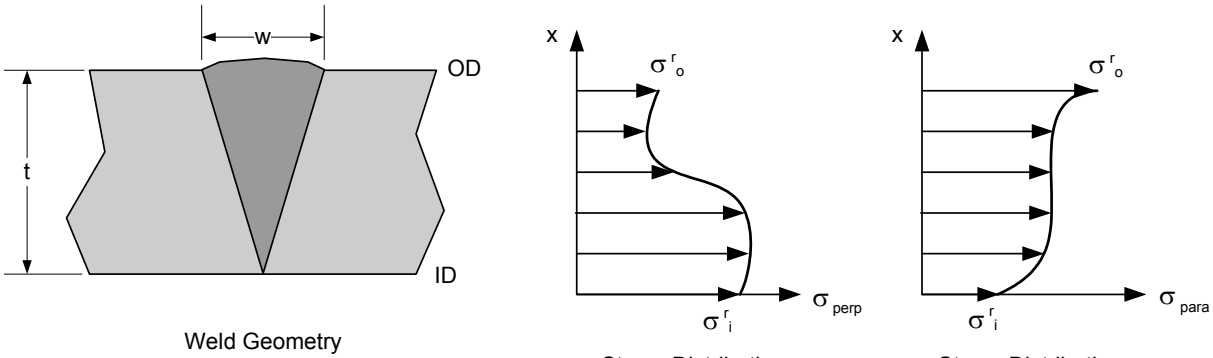

Weld Geometry

Stress Distribution
Perpendicular to Weld
(See Paragraph E.5.1.1)

Stress Distribution
Parallel to Weld
(See Paragraph E.5.1.2)

(b) Through-Wall Stress Distribution

Figure E.9
Residual Stress Surface and Through-Wall Distributions for Full Penetration Circumferential Single V-Groove Welds in Spherical Shells

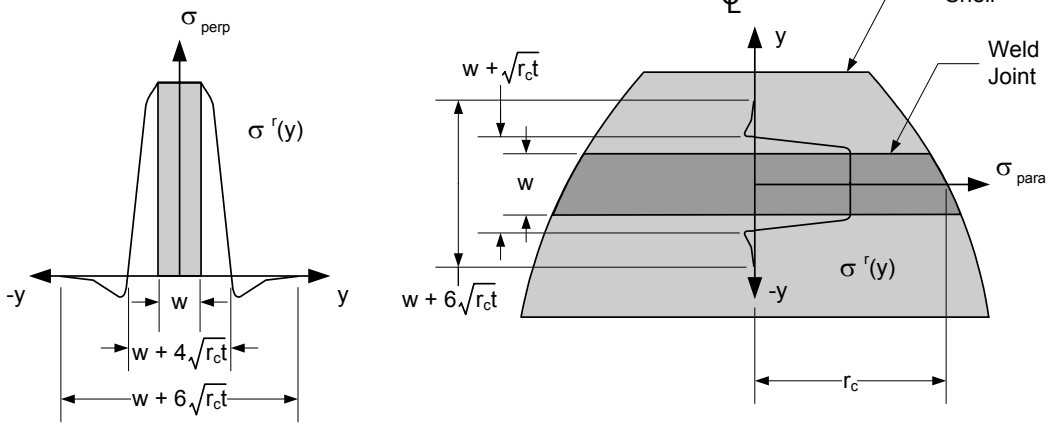

Stress Distribution Perpendicular to Weld (See Paragraph E.5.2.1)

Stress Distribution Parallel to Weld (See Paragraph E.5.2.2)

(a) Surface Stress Distribution

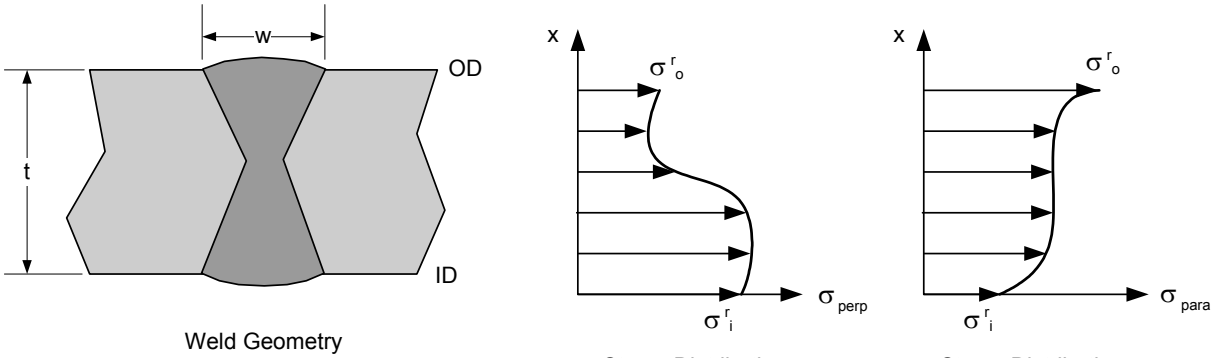

Weld Geometry

Stress Distribution Perpendicular to Weld (See Paragraph E.5.2.1)

Stress Distribution Parallel to Weld (See Paragraph E.5.2.2)

(b) Through-Wall Stress Distribution

Figure E.10
Residual Stress Surface and Through-Wall Distributions for Full Penetration Circumferential Double V-Groove Welds in Spherical Shells

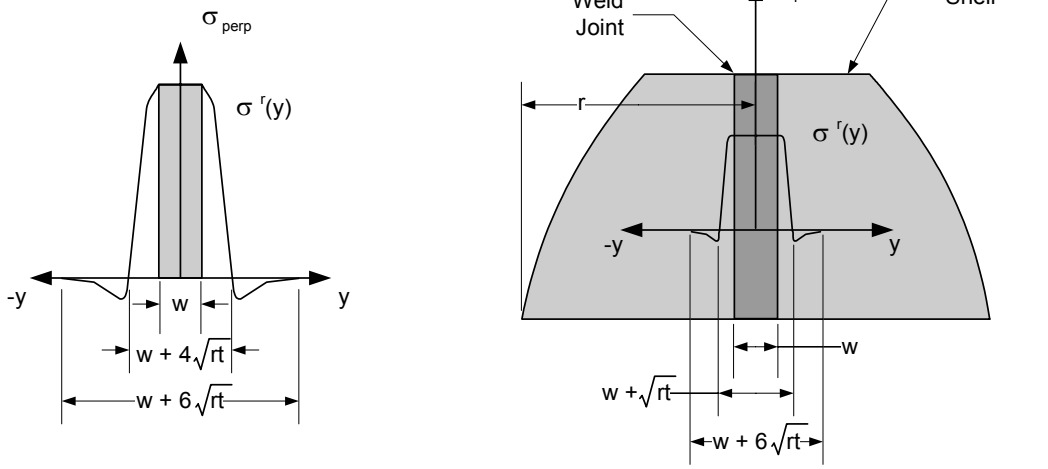

Stress Distribution
Perpendicular to Weld
(See Paragraph E.5.3.1)

Stress Distribution
Parallel to Weld
(See Paragraph E.5.3.2)

(a) Surface Stress Distribution

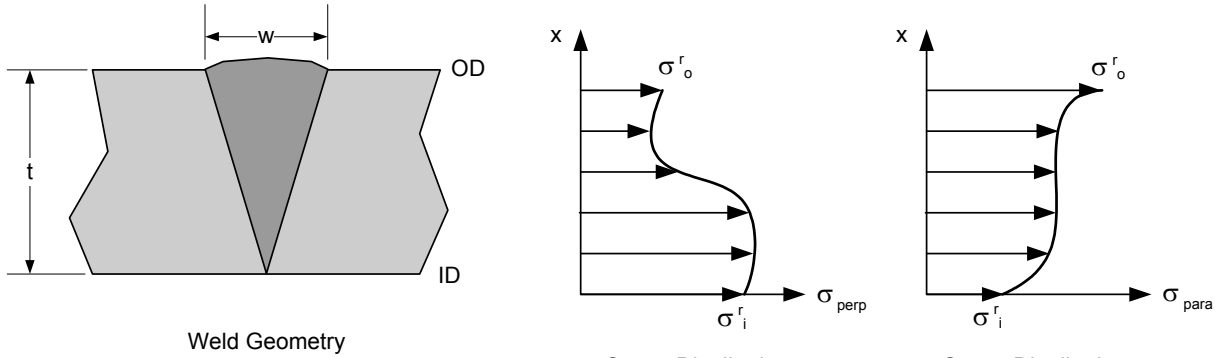

Weld Geometry

Stress Distribution
Perpendicular to Weld
(See Paragraph E.5.3.1)

Stress Distribution
Parallel to Weld
(See Paragraph E.5.3.2)

(b) Through-Wall Stress Distribution

Figure E.11
Residual Stress Surface and Through-Wall Distributions for Full Penetration Meridional Single V-Groove Welds in Spherical Shells

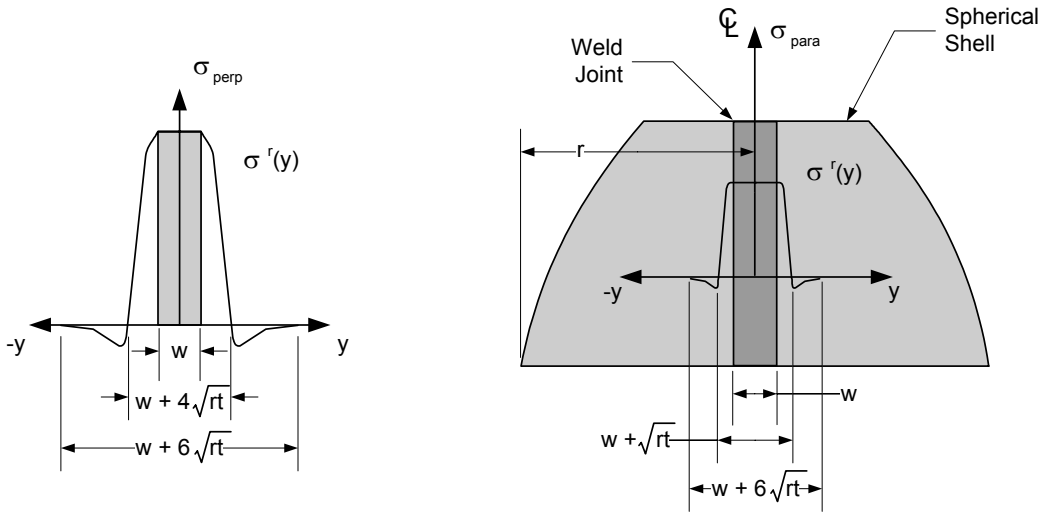

Stress Distribution Perpendicular to Weld (See Paragraph E.5.4.1)

Stress Distribution Parallel to Weld (See Paragraph E.5.4.2)

(a) Surface Stress Distribution

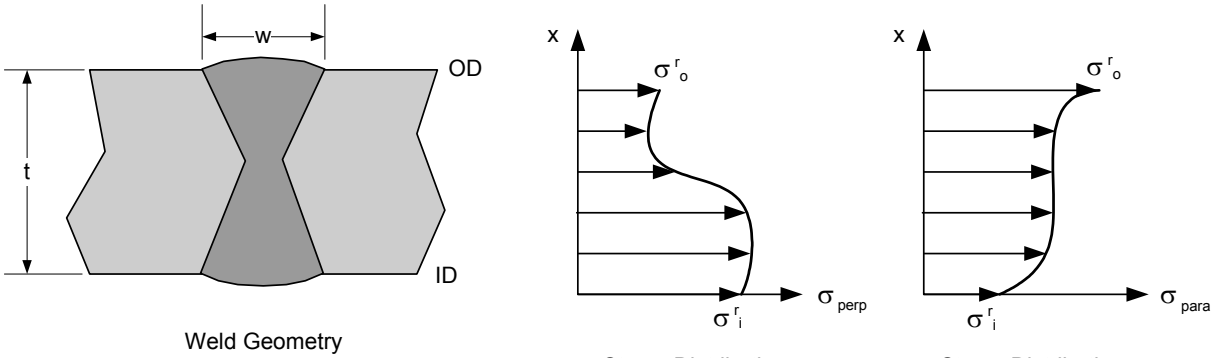

Weld Geometry

Stress Distribution Perpendicular to Weld (See Paragraph E.5.4.1)

Stress Distribution Parallel to Weld (See Paragraph E.5.4.2)

(b) Through-Wall Stress Distribution

Figure E.12
Residual Stress Surface and Through-Wall Distributions for Full Penetration Meridional Double V-Groove Welds in Spherical Shells

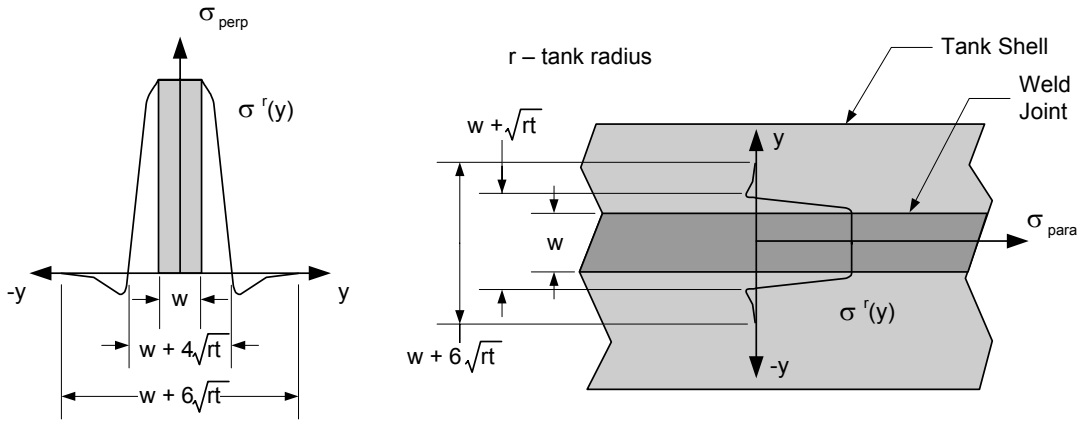

Stress Distribution
Perpendicular to Weld
(See Paragraph E.6.1.1)

Stress Distribution
Parallel to Weld
(See Paragraph E.6.1.2)

(a) Surface Stress Distribution

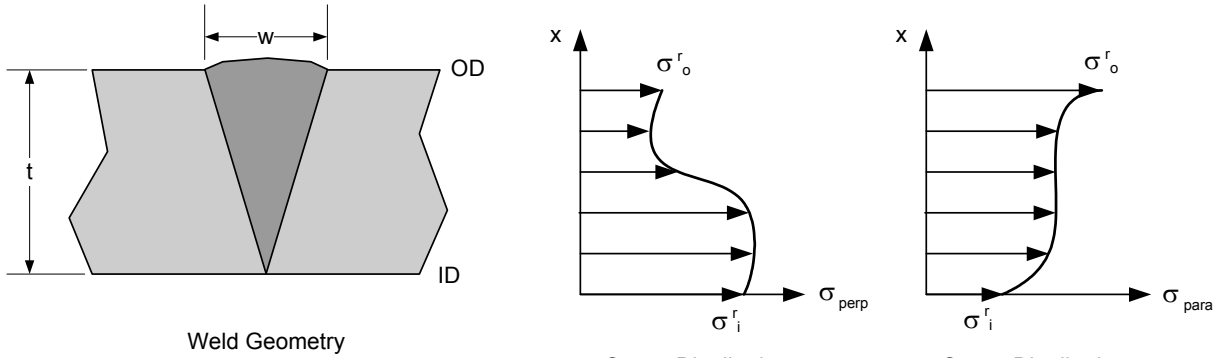

Weld Geometry

Stress Distribution
Perpendicular to Weld
(See Paragraph E.6.1.1)

Stress Distribution
Parallel to Weld
(See Paragraph E.6.1.2)

(b) Through-Wall Stress Distribution

Figure E.13
Residual Stress Surface and Through-Wall Distributions for Full Penetration Circumferential and Longitudinal Single V-Groove Welds in Storage Tanks

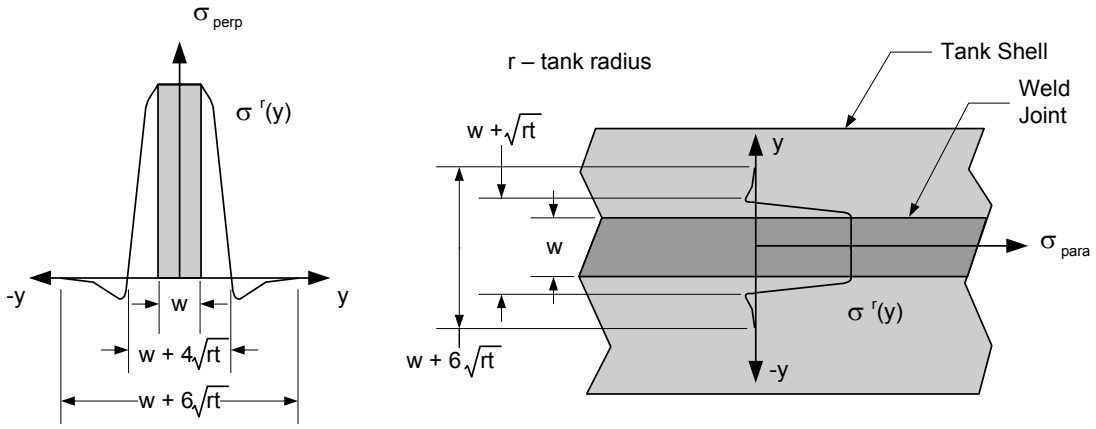

Stress Distribution
Perpendicular to Weld
(See Paragraph E.6.1.1)

Stress Distribution
Parallel to Weld
(See Paragraph E.6.1.2)

(a) Surface Stress Distribution

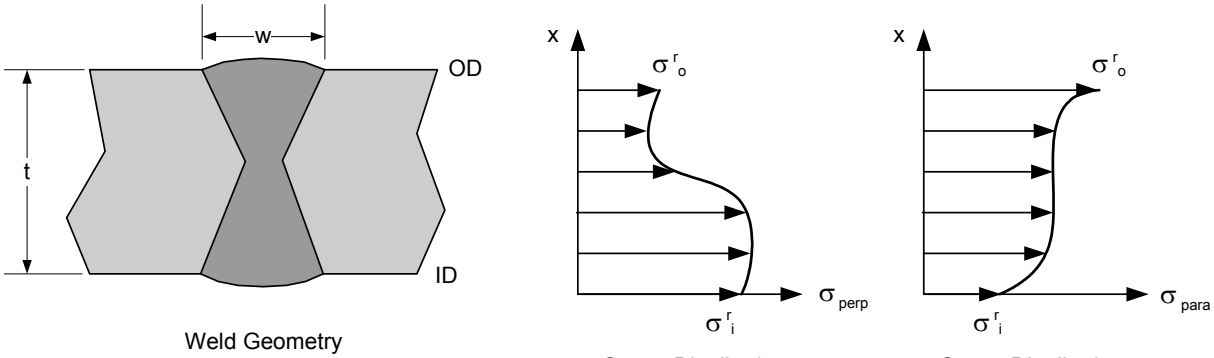

Weld Geometry

Stress Distribution
Perpendicular to Weld
(See Paragraph E.6.1.1)

Stress Distribution
Parallel to Weld
(See Paragraph E.6.1.2)

(b) Through-Wall Stress Distribution

Figure E.14
Residual Stress Surface and Through-Wall Distributions for Full Penetration Circumferential and Longitudinal Double V-Groove Welds in Storage Tanks

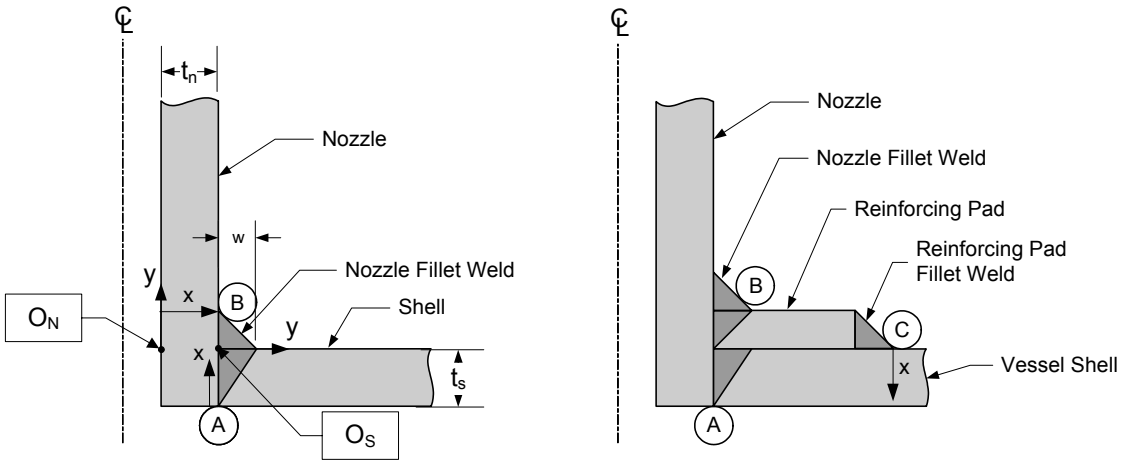

(a) Identification of Welds

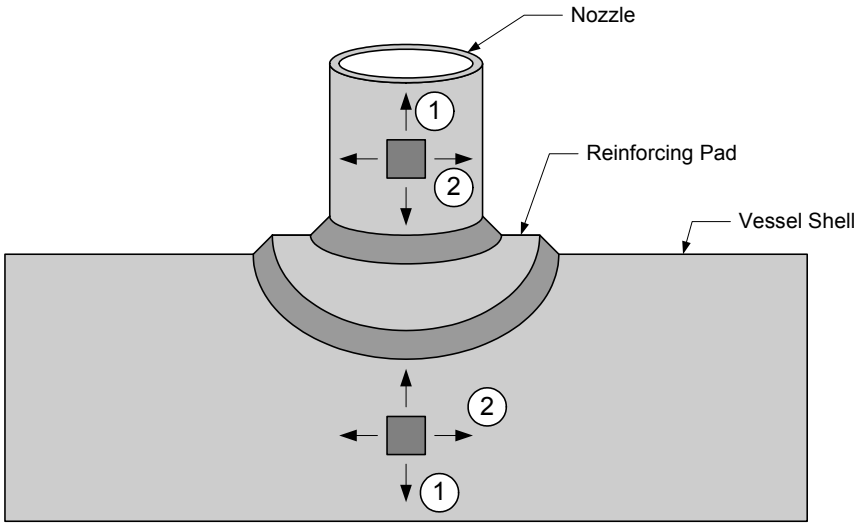

(b) Identification of Stresses

(1) - Stress Perpendicular to the Weld Direction

(2) - Stress Parallel to the Weld Direction

Figure E.15
Weld Locations and Stress Directions in a Corner Joint (Nozzle Attachment)

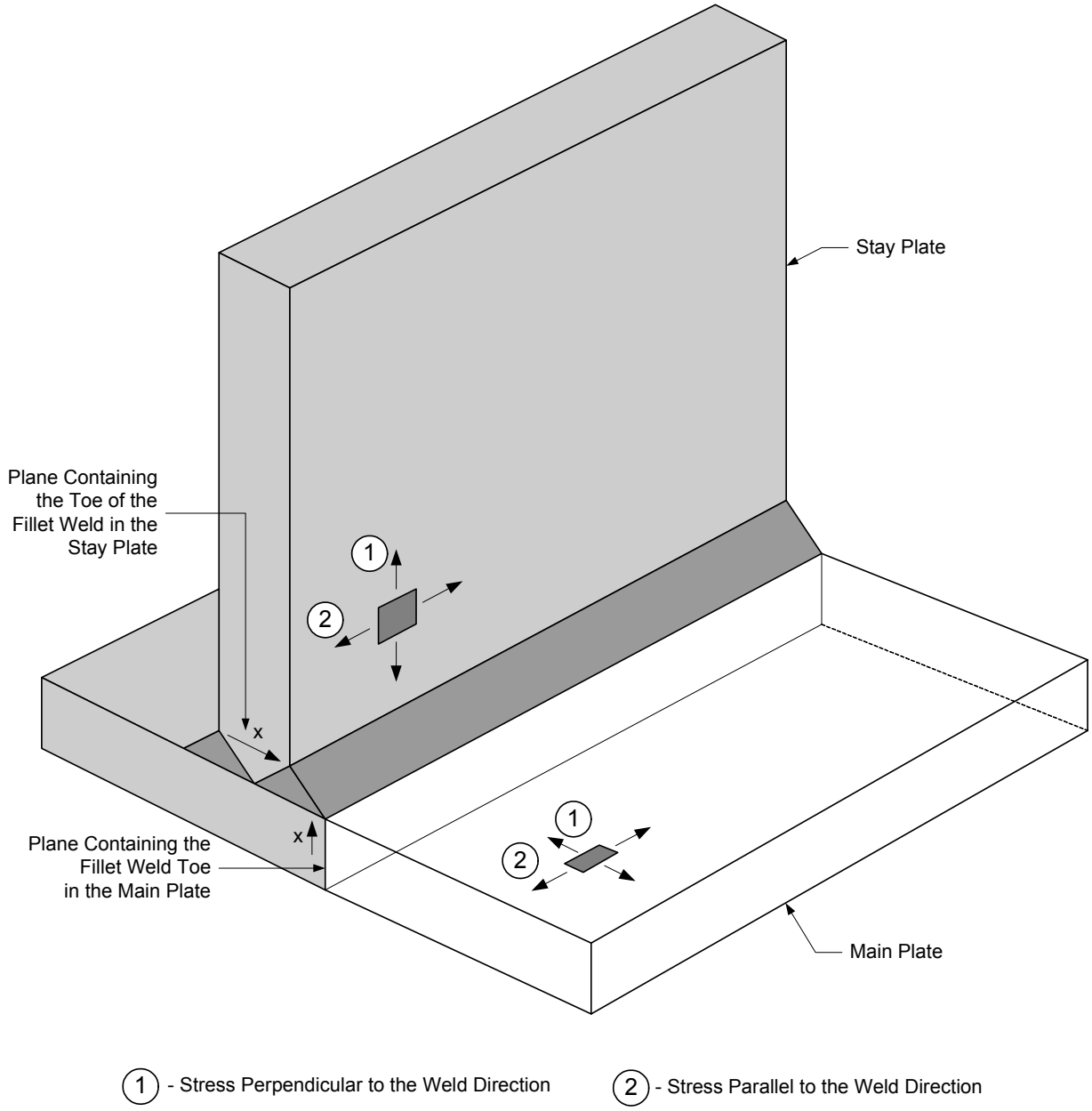

Figure E.16
Weld Locations and Stress Directions in a Tee Joint

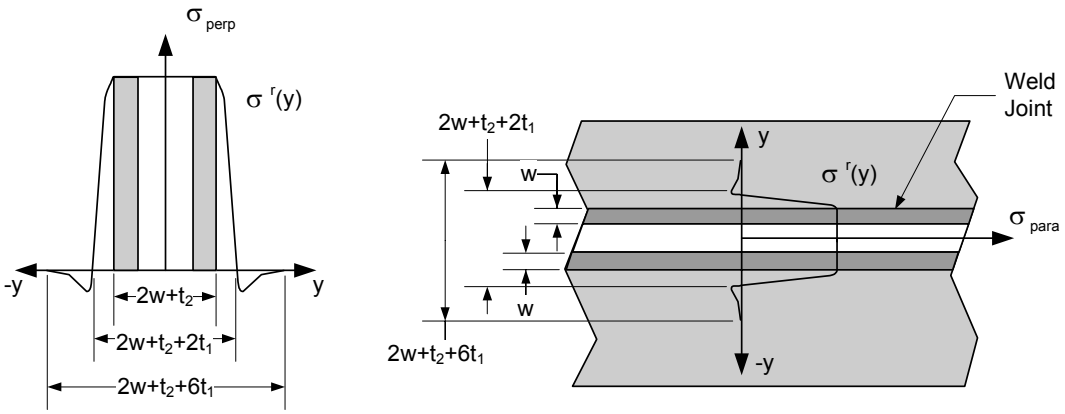

Stress Distribution
Perpendicular to Weld
(See Paragraph E.8.1.1)

Stress Distribution
Parallel to Weld
(See Paragraph E.8.1.2)

(a) Surface Stress Distribution

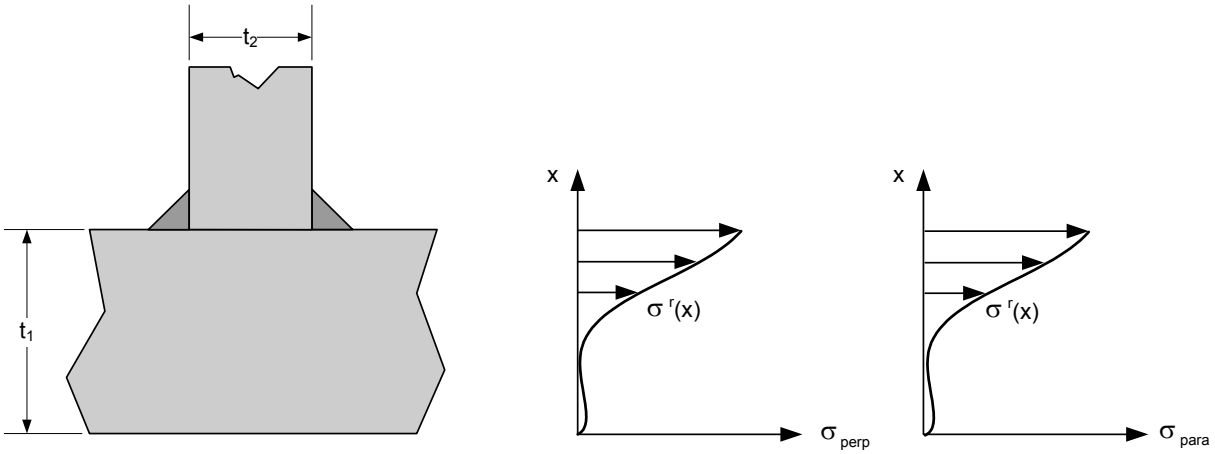

Weld Geometry

Stress Distribution
Perpendicular to Weld
(See Paragraph E.8.1.1)

Stress Distribution
Parallel to Weld
(See Paragraph E.8.1.2)

(b) Through-Wall Stress Distribution

Figure E.17
Residual Stress Surface and Through-Wall Distributions for Joints with Fillet Welds – Main Plate

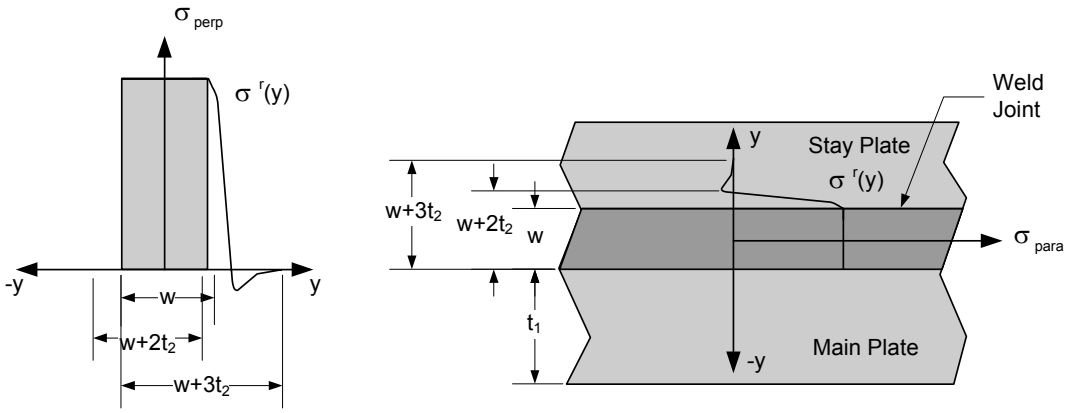

Stress Distribution
Perpendicular to Weld
(See Paragraph E.8.2.1)

Stress Distribution
Parallel to Weld
(See Paragraph E.8.2.2)

(a) Surface Stress Distribution

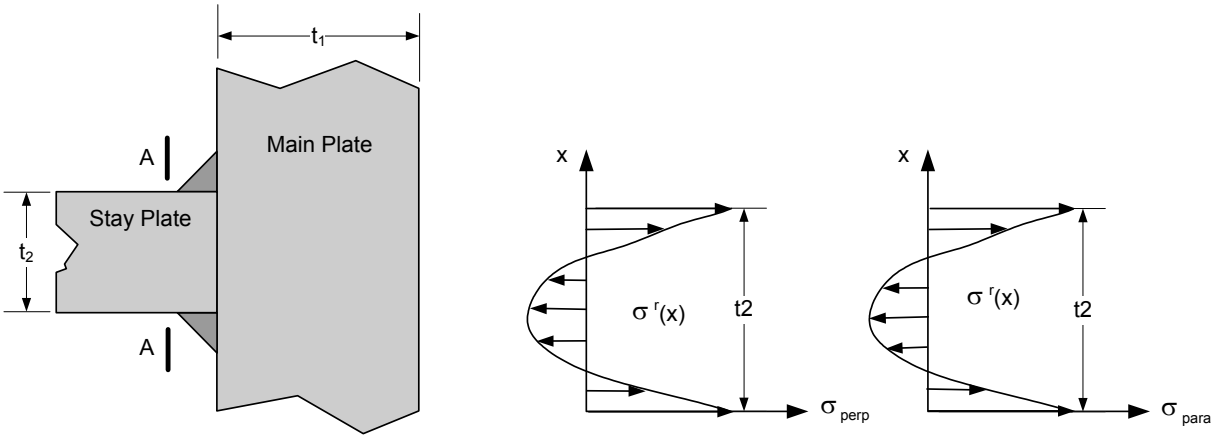

Weld Geometry

Stress Distribution
Perpendicular to Weld
(See Paragraph E.8.2.1)

Stress Distribution
Parallel to Weld
(See Paragraph E.8.2.2)

(b) Through-Wall Stress Distribution

Figure E.18
Residual Stress Surface and Through-Wall Distributions for Joints with Fillet Welds – Stay Plate

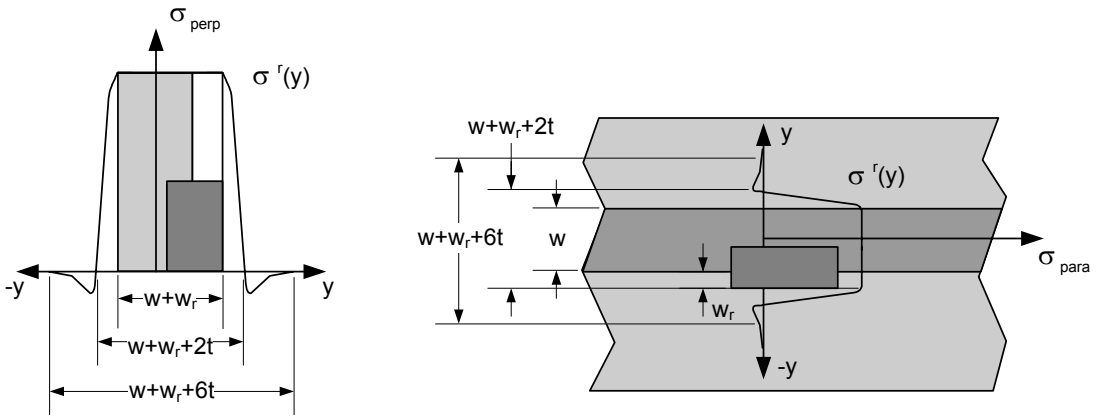

Stress Distribution
Perpendicular to Weld
(See Paragraph E.9.1.1)

Stress Distribution
Parallel to Weld
(See Paragraph E.9.1.2)

(a) Surface Stress Distribution

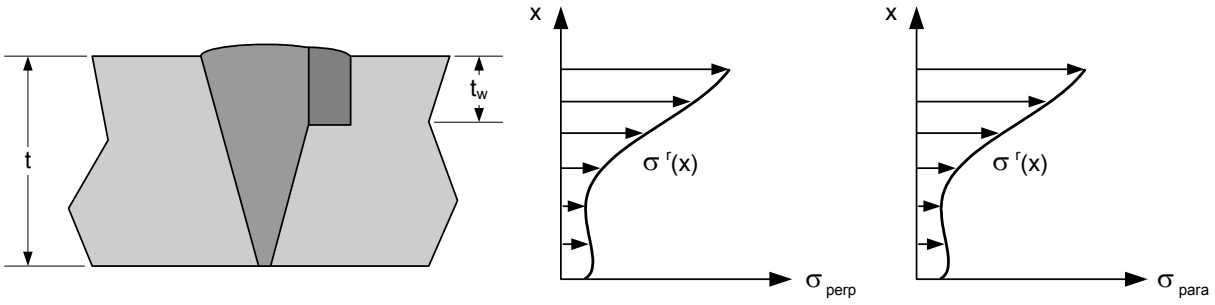

Weld Geometry

Stress Distribution
Perpendicular to Weld
(See Paragraph E.9.1.1)

Stress Distribution
Parallel to Weld
(See Paragraph E.9.1.2)

(b) Through-Wall Stress Distribution

Figure E.19
Residual Stress Surface and Through-Wall Distributions for Repair Welds

ANNEX F

MATERIAL PROPERTIES FOR A *FFS* ASSESSMENT

(NORMATIVE)

PART CONTENTS

F.1 General

F.1.1 The information in this Annex is intended to provide guidance on the materials information required for the *Fitness-For-Service* (*FFS*) assessments covered in this Standard. Specific materials data are provided for many of the assessment methods; however, some of the materials data are provided in terms of references to published sources. To include, and keep up to date, all of the property information required by all of the assessment methods in this Standard would be prohibitive. This is especially true of properties that are affected by the service environment.

F.1.2 The *Fitness-For-Service* assessment procedures in this Standard cover situations involving flaws commonly encountered in pressure vessels, piping and tankage that have been exposed to service for long periods of time. Therefore, when selecting materials properties for an analysis, care must be taken to evaluate these properties in terms of equipment that has been in-service; the properties used in the assessment should reflect any change or degradation, including aging, resulting from the service environment or past operation.

F.2 Strength Parameters

F.2.1 Yield and Tensile Strength

F.2.1.1 Estimates for the material yield strength and tensile strength to be used in a *Fitness-For-Service* assessment can be obtained as follows:

a) It may be necessary to obtain samples from a component and use a standard test procedure to directly determine the yield and tensile strength when accurate estimates of these properties can affect the results of an assessment. The yield strength and ultimate tensile strength for plate and pipe material can be determined in accordance with ASTM A370, ASTM E8, or an equivalent standard method, and reported on a mill test report for the particular heat of steel.

b) Hardness tests can be used to estimate the tensile strength (see Table F.1). The conversions found in this table may be used for carbon and alloy steels in the annealed, normalized, and quench-and-tempered conditions. The conversions are not applicable for cold worked materials, austenitic stainless steels, or for non-ferrous materials.

c) If the temperature for which a *Fitness-For-Service* assessment is to be made differs substantially from the temperature for which the yield and tensile strengths were determined, these values should be modified by a suitable temperature correction factor. The temperature correction factor may be derived from the Materials Properties Council (MPC) material data for the yield strength and ultimate strength given in paragraphs F.2.1.2 and F.2.1.3, respectively.

d) In the absence of heat specific data, mean values for the tensile and yield strength can be approximated using the following equations:

$$\sigma_{uts}^{mean} = \sigma_{uts}^{min} + 69\,MPa \qquad \text{(F.1)}$$

$$\sigma_{uts}^{mean} = \sigma_{uts}^{min} + 10\ ksi \qquad \text{(F.2)}$$

and,

$$\sigma_{ys}^{mean} = \sigma_{ys}^{min} + 69\,MPa \qquad \text{(F.3)}$$

$$\sigma_{ys}^{mean} = \sigma_{ys}^{min} + 10\ ksi \qquad \text{(F.4)}$$

F.2.1.2 Analytical expressions for the minimum specified yield strength as a function of temperature, and the applicable temperature range are provided in Table F.2. The minimum specified yield strength at a temperature is determined by multiplying the value at room temperature by a temperature reduction factor in these tables. The room temperature value of the minimum specified yield strength can be found in the applicable design code. The analytical expressions for the minimum specified yield strength for a limited number of materials are listed in terms of a material pointer, PYS, which can be determined for a specific material of construction using Table F.3.

F.2.1.3 Analytical expressions for the minimum specified ultimate tensile strength as a function of temperature, and the applicable temperature range are provided in Table F.4. The minimum specified ultimate tensile strength at a temperature is determined by multiplying the value at room temperature by a temperature reduction factor in these tables. The room temperature value of the minimum specified ultimate tensile strength can be found in the applicable design code. The analytical expressions for the minimum specified ultimate tensile strength for a limited number of materials are listed in terms of a material pointer, PUS, which can be determined for a specific material of construction using Table F.5.

F.2.1.4 A method to compute the yield and tensile strength as a function of temperature for pipe and tube materials is provided in Table F.6. The data used to develop these equations are from API STD 530.

F.2.1.5 Values for the yield and tensile strength below the creep regime for pressure vessel, piping, and tankage steels can be found in the ASME Code, Section II, Part D. Other sources for yield and tensile strength data for various materials are provided in paragraph F.9. These data sources provide values for the yield and tensile strength that are representative of new materials.

F.2.2 Flow Stress

F.2.2.1 The flow stress, σ_f, can be thought of as the effective yield strength of a work hardened material. The use of a flow stress concept permits the real material to be treated as if it were an elastic-plastic material that can be characterized by a single strength parameter. The flow stress can be used, for example, as the stress level in the material that controls the resistance of a cracked structure to failure by plastic collapse.

F.2.2.2 Several relationships for estimating the flow stress have been proposed which are summarized below. The flow stress to be used in an assessment will be covered in the appropriate Part of this Standard. In the absence of a material test report for plate and pipe, and for weld metal, the specified minimum yield strength and the specified minimum tensile strength for the material can be used to calculate the flow stress.

a) Average of the yield and tensile strengths (recommended for most assessments):

$$\sigma_f = \frac{\left(\sigma_{ys} + \sigma_{uts}\right)}{2} \tag{F.5}$$

b) The yield strength plus 69 MPa (10 ksi):

$$\sigma_f = \sigma_{ys} + 69 \text{ MPa} \tag{F.6}$$

$$\sigma_f = \sigma_{ys} + 10 \text{ ksi} \tag{F.7}$$

c) For austenitic stainless steels, a factor times the average of the yield and tensile strengths:

$$\sigma_f = \frac{1.15 \cdot \left(\sigma_{ys} + \sigma_{uts}\right)}{2} \tag{F.8}$$

d) For ferritic steels and austenitic stainless steels, the maximum allowable stress (S_m) in accordance with the ASME Code, Section VIII, Division 2, multiplied by an appropriate factor:

$$\sigma_f = 2.4 \cdot S_m \qquad \textit{for ferritic steels}$$

$$\sigma_f = 3 \cdot S_m \qquad \textit{for austenitic stainless steels}$$

e) If Ramberg-Osgood parameters are available (see paragraph F.2.3), the flow stress can be computed using the following equation.

$$\sigma_f = \frac{\sigma_{ys}}{2}\left[1 + \frac{\left(\frac{n_{RO}}{0.002}\right)^{n_{RO}}}{\exp\left(n_{RO}\right)}\right] \tag{F.9}$$

F.2.3 Stress-Strain Relationship

F.2.3.1 MPC Model

a) The following model for the stress-strain curve may be used in *Fitness-For-Service* calculations where required by this Standard when the strain hardening characteristics of the stress-strain curve are to be considered.

$$\varepsilon_{ts} = \frac{\sigma_t}{E_y} + \gamma_1 + \gamma_2 \tag{F.10}$$

where

$$\gamma_1 = \frac{\varepsilon_1}{2}\left(1.0 - \tanh\left[H\right]\right) \tag{F.11}$$

$$\gamma_2 = \frac{\varepsilon_2}{2}\left(1.0 + \tanh\left[H\right]\right) \tag{F.12}$$

$$\varepsilon_1 = \left(\frac{\sigma_t}{A_1}\right)^{\frac{1}{m_1}} \tag{F.13}$$

$$A_1 = \frac{\sigma_{ys}\left(1 + \varepsilon_{ys}\right)}{\left(\ln\left[1 + \varepsilon_{ys}\right]\right)^{m_1}} \tag{F.14}$$

$$m_1 = \frac{\ln\left[R\right] + \left(\varepsilon_p - \varepsilon_{ys}\right)}{\ln\left[\frac{\ln\left[1 + \varepsilon_p\right]}{\ln\left[1 + \varepsilon_{ys}\right]}\right]} \tag{F.15}$$

$$\varepsilon_2 = \left(\frac{\sigma_t}{A_2}\right)^{\frac{1}{m_2}} \tag{F.16}$$

$$A_2 = \frac{\sigma_{uts} \exp[m_2]}{m_2^{m_2}} \tag{F.17}$$

$$H = \frac{2\left[\sigma_t - \left(\sigma_{ys} + K\left\{\sigma_{uts} - \sigma_{ys}\right\}\right)\right]}{K\left(\sigma_{uts} - \sigma_{ys}\right)} \tag{F.18}$$

$$R = \frac{\sigma_{ys}}{\sigma_{uts}} \tag{F.19}$$

$$\varepsilon_{ys} = 0.002 \tag{F.20}$$

$$K = 1.5R^{1.5} - 0.5R^{2.5} - R^{3.5} \tag{F.21}$$

The parameters m_2, and ε_p are provided in Table F.7 and σ_t is determined using Equation (F.28).

b) The tangent modulus based on the stress-strain curve model in paragraph F.2.3.1.a is given by Equation (F.22).

$$E_t = \frac{\partial\sigma}{\partial\varepsilon_t} = \left(\frac{\partial\varepsilon_t}{\partial\sigma}\right)^{-1} = \left(\frac{1}{E_y} + D_1 + D_2 + D_3 + D_4\right)^{-1} \tag{F.22}$$

where

$$D_1 = \frac{\sigma^{\left(\frac{1}{m_1}-1\right)}}{2m_1 A_1^{\left(\frac{1}{m_1}\right)}} \tag{F.23}$$

$$D_2 = -\frac{1}{2}\left(\frac{1}{A_1^{\left(\frac{1}{m_1}\right)}}\right)\cdot\left(\sigma^{\left(\frac{1}{m_1}\right)}\left\{\frac{2}{K\left(\sigma_{uts} - \sigma_{ys}\right)}\right\}\left\{1 - \tanh^2[H]\right\} + \frac{1}{m_1}\sigma^{\left(\frac{1}{m_1}-1\right)}\tanh[H]\right) \tag{F.24}$$

$$D_3 = \frac{\sigma^{\left(\frac{1}{m_2}-1\right)}}{2m_2 A_2^{\left(\frac{1}{m_2}\right)}} \tag{F.25}$$

$$D_4 = \frac{1}{2}\left(\frac{1}{A_2^{\left(\frac{1}{m_2}\right)}}\right)\cdot\left(\sigma^{\left(\frac{1}{m_2}\right)}\left\{\frac{2}{K\left(\sigma_{uts} - \sigma_{ys}\right)}\right\}\left\{1 - \tanh^2[H]\right\} + \frac{1}{m_2}\sigma^{\left(\frac{1}{m_2}-1\right)}\tanh[H]\right) \tag{F.26}$$

F.2.3.2 Ramberg-Osgood Model

a) The stress-strain curve of a material can be represented by Equation (F.27) known as the Ramberg-Osgood equation. The exponent used in this equation may be required for a J-integral calculation.

$$\varepsilon_{ts} = \frac{\sigma_t}{E_y} + \left(\frac{\sigma_t}{H_{RO}} \right)^{\frac{1}{n_{RO}}} \tag{F.27}$$

with

$$\sigma_t = \left(1 + \varepsilon_{es}\right)\sigma_{es} \tag{F.28}$$

$$\varepsilon_{ts} = \ln\left(1 + \varepsilon_{es}\right) \tag{F.29}$$

b) If multiple data points for a stress-strain curve are provided, the data fitting constants can be derived using regression techniques. If only the yield and ultimate tensile strength are known, the exponent, n_{RO}, can be computed using Equation (F.30) for the range $0.02 \le \sigma_{ys} / \sigma_{uts} \le 1.0$. The constant H_{RO} is computed using Equation (F.31).

$$n_{RO} = \frac{1 + 1.3495\left(\frac{\sigma_{ys}}{\sigma_{uts}}\right) - 5.3117\left(\frac{\sigma_{ys}}{\sigma_{uts}}\right)^2 + 2.9643\left(\frac{\sigma_{ys}}{\sigma_{uts}}\right)^3}{1.1249 + 11.0097\left(\frac{\sigma_{ys}}{\sigma_{uts}}\right) - 11.7464\left(\frac{\sigma_{ys}}{\sigma_{uts}}\right)^2} \tag{F.30}$$

$$H_{RO} = \frac{\sigma_{uts} \exp\left[n_{RO}\right]}{{n_{RO}}^{n_{RO}}} \tag{F.31}$$

F.2.4 Cyclic Stress Strain Curve

The cyclic stress-strain curve of a material (i.e. strain amplitude versus stress amplitude) may be represented by the Equation (F.32). The material constants for this model are provided in Table F.8.

$$\varepsilon_{ta} = \frac{\sigma_a}{E_y} + \left[\frac{C_{usm}\sigma_a}{K_{css}} \right]^{\frac{1}{n_{css}}} \tag{F.32}$$

The hysteresis loop stress-strain curve of a material (i.e. strain range versus stress range) obtained by scaling the cyclic stress-strain curve by a factor of two is represented by the Equation (F.33). The material constants provided in Table F.8 are also used in this equation.

$$\varepsilon_{tr} = \frac{\sigma_r}{E_y} + 2\left[\frac{C_{usm}\sigma_r}{2K_{css}} \right]^{\frac{1}{n_{css}}} \tag{F.33}$$

F.3 Physical Properties

F.3.1 Elastic Modulus

The elastic or Young's modulus is required to perform stress analysis of a statically indeterminate component. Values for the elastic modulus for a full range in temperatures can be found in WRC 503 or the ASME B&PV Code, Section II, Part D. Additional reference sources for the elastic modulus of various materials are provided in paragraph F.9.

F.3.2 Poisson's Ratio

The value of Poisson's ratio in the elastic range, ν, can normally be taken as 0.3 for steels. Data for specific steels can be found in WRC 503 or the ASME B&PV Code, Section II, Part D.

F.3.3 Coefficient of Thermal Expansion

The coefficient of thermal expansion is required to perform a thermal stress analysis of a component. Values for the thermal expansion coefficient for a full range in temperatures can be found in the WRC 503 or the ASME B&PV Code, Section II, Part D. Additional reference sources for the thermal expansion coefficient of various materials are provided in paragraph F.9

F.3.4 Thermal Conductivity

The thermal conductivity is required to perform a heat transfer analysis of a component. The results from this analysis are utilized in a thermal stress calculation. Values for the thermal conductivity for a full range in temperatures can be found in WRC 503 or the ASME B&PV Code, Section II, Part D.

F.3.5 Thermal Diffusivity

The thermal diffusivity is required to perform a transient thermal heat transfer analysis of a component. The results from this analysis are utilized in a transient thermal stress calculation. Values for the thermal diffusivity for a full range in temperatures can be found in WRC 503 or the ASME B&PV Code, Section II, Part D.

F.3.6 Density

The material density is required to perform a transient thermal heat transfer analysis, and in cases where body force components are to be considered in a stress analysis of a component. The results from this analysis are utilized in a transient thermal stress calculation. Values for the density for a full range in temperatures can be found in WRC 503 or the ASME B&PV Code, Section II, Part D.

F.4 Fracture Toughness

F.4.1 General

F.4.1.1 The fracture toughness of a material measures its ability to resist crack initiation and propagation. Several fracture toughness parameters are available, including critical stress intensity factor $\left(K_{IC}\right)$, the critical value of the J integral $\left(J_{crit}\right)$, and the critical crack tip opening displacement $\left(CTOD \text{ or } \delta_{crit}\right)$. Any one of these parameters can be used for a *Fitness-For-Service* assessment of a component containing crack-like flaws.

F.4.1.2 Ideally, the fracture toughness input to the FFS analysis should come from test data for the specific material of interest. In practice, however, heat-specific fracture toughness data are usually not available for an existing component. Consequently, alternative means must often be employed to obtain conservative estimates of fracture toughness. Guidelines for establishing a fracture toughness to use in a *Fitness-For-Service* assessment are provided in Figures F.1 and F.2. The paragraphs that follow provide details to support the different options in these figures.

F.4.2 Fracture Toughness Parameters

F.4.2.1 For most materials and structures covered by this Standard, it is possible to measure toughness only in terms of J and $CTOD$; valid K_{IC} data can only be obtained for brittle materials or thick sections. It is possible, however, to infer "equivalent" K_{IC} values from J and $CTOD$ data by exploiting the relationships among these three parameters under plane strain linear elastic conditions. The fracture mechanics analysis can be expressed in terms of any one of the three parameters based on the relationships shown below.

a) For small scale yielding an equivalent K_{IC}, denoted as K_{JC}, can be computed from J_{crit} using Equation (F.34).

$$K_{JC} = \sqrt{\frac{J_{crit} \cdot E_y}{1-\nu^2}} \tag{F.34}$$

b) An approximate relationship between the J integral and CTOD is given by Equation (F.35).

$$J_{crit} = m_{CTOD} \cdot \sigma_f \cdot \delta_{crit} \tag{F.35}$$

c) By combining the above equations, the equivalent K_{IC} value (or $K_{\delta C}$) computed from CTOD data is given by Equation (F.36).

$$K_{\delta C} = \sqrt{\frac{m_{CTOD} \cdot \sigma_f \cdot \delta_{crit} \cdot E_y}{1-\nu^2}} \tag{F.36}$$

F.4.2.2 Charpy impact tests can be used to provide a qualitative indication of a material's fracture toughness. The results from these tests cannot be used directly to provide an indication of a material's toughness for use in a *Fitness-For-Service* assessment. However, correlations are available which enable an estimate of fracture toughness to be made based on the results of Charpy impact values (see paragraph F.4.5).

F.4.3 Fracture Toughness Testing

F.1.1.1 Ideally, fracture toughness tests should be heat specific, which necessitates removing specimens from the material under consideration. This can be accomplished in one of three ways:

a) Removal Of A Sample From A Component Currently In Service For Testing – Removal of a material sample from a component is an extreme step, but it is often the only way to obtain heat-specific fracture toughness data for a given structure. The value of component specific toughness data should be assessed versus the potential problems that may result from the procedure required to repair the region where the sample was obtained.

b) Removal Of A Sample From A Retired Component In A Similar Service And Testing – Testing material from a retired component (preferably one that was fabricated from the same material heat) is beneficial because such data provide a relative indication of the toughness of similar vessels. However, these data must be used with caution because a material's fracture toughness data can have significant heat-to-heat variations, and data from one component may not be necessarily applicable to another.

c) Testing A Plate That Was Welded At The Time Of Fabrication – A test weldment will not normally be available for components that have been in service for some time; however, a plate can be produced at the time of fabrication for a new component. The steel in a test plate should come from the same heat as the material used in the actual structure, and it should be welded according to the same procedure and with the same batch of consumables as the structure. If possible, the same welders and equipment should be used for the test plate and structure, and the plate should also have the same PWHT as the structure. Finally, the weld joint should be subject to the same operating conditions if these conditions cause embrittlement.

F.4.3.1 The following items should be noted if testing of a sample is to be performed to determine the fracture toughness of a material for a *Fitness-For-Service* assessment.

a) Test methods for measurement of the K, J, and $CTOD$ fracture toughness parameters are covered in ASTM 1820.

b) It is recommended that a minimum of three specimens be tested for each condition and temperature. If additional test results are available, the equivalent to the minimum of three tests may be used (see Table F.9). If more than ten tests are available, the data may be fitted to the Master Curve (see paragraph F.4.9).

c) Currently, an ASTM Standard covering fracture toughness testing of weldments does not exist. A procedure to test weldments is provided by BS 7448: Part 2.

d) The results from a fracture toughness test can vary significantly. The fracture toughness master curve approach can be used (see paragraph F.4.9) to quantify this variation.

e) The fracture toughness of a material tends to decrease with increasing crack tip triaxiality. Standard laboratory specimens used to determine a material's fracture toughness are usually highly constrained. Therefore, laboratory fracture toughness tests usually underestimate the fracture toughness of structural components of equivalent thickness that contain crack-like flaws, and flaw assessments based on standard fracture toughness data tend to be conservative.

F.4.3.2 Charpy V-Notch Test (CVN) – The standard for CVN testing is ASTM Standard E23. The Charpy specimen is a rectangular bar with cross section measurements of 10 mm x 10 mm and length between end supports of 40 mm. A notch 2 mm deep is machined opposite the impact point with a 0.25 mm notch radius. The axis of the notch is usually oriented in the through-thickness direction with respect to the original material placement. When a component is less than 10 mm thick, "sub-size" specimens are used.

a) The thickness of the CVN specimen can influence both the absorbed energy and the transition temperature as described below (see Figure F.3):

   1) Effect on Absorbed Energy – The reduced cross sectional area of a sub-size CVN specimen reduces its ability to absorb energy. Therefore, the absorbed energy values for sub-size CVN specimens will be less than that characteristic of standard size CVN specimens when both specimens are tested at the same temperature.

   2) Effect on Transition Temperature – The reduced wall thickness of sub-size CVN specimens reduces the tri-axial constraint against plastic flow in comparison with that characteristic of a standard size CVN specimen. This reduced level of constraint makes cleavage fracture less likely to occur in a sub-size CVN specimen than in a standard size CVN specimen when both are tested at the same temperature. Therefore, the fracture mode transition will occur at lower temperatures in sub-sized CVN specimens than in standard CVN size specimens of the same material.

b) For plate materials used in pressure vessels, piping and tankage, the following correlations may be used for the energy and temperature shift. These correlations where derived based on the information in ASTM A370.

$$CVN_{std} = CVN_{ss}\left(\frac{t_{std}}{t_{ss}}\right) \qquad for \quad t_{ss} \le t_{std} \qquad \text{(F.37)}$$

$$TT_{std} = TT_{ss} + \frac{T_{shift}}{1.8} \qquad \left({}^{o}C\right) \qquad \text{(F.38)}$$

$$TT_{std} = TT_{ss} + T_{shift} \qquad \left({}^{o}F\right) \qquad \text{(F.39)}$$

with,

$$T_{shift} = \left[\frac{10.12899 - 9.730841\left(\frac{t_{ss}}{t_{std}}\right)}{1.0 + 0.353215\left(\frac{t_{ss}}{t_{std}}\right)} \right]^2 \qquad \left({}^{o}F\right) \qquad \text{(F.40)}$$

c) The following equation from BS 7910 can also be used to determine the shift in transition temperature for sub-size specimens. A corresponding shift in impact energy is not provided in BS 7910.

$$TT_{std} = TT_{ss} + T_{shift} \qquad \left({}^{o}C\right) \qquad \text{(F.41)}$$

$$TT_{std} = TT_{ss} + 1.8T_{shift} \qquad \left({}^{o}F\right) \qquad \text{(F.42)}$$

with,

$$T_{shift} = 51.4 \ln\left[2\left(\frac{t_{ss}}{10}\right)^{0.25} - 1 \right] \qquad \left({}^{o}C,\ mm\right) \qquad \text{(F.43)}$$

d) For pipeline materials (e.g. API 5L), the following procedure has been used to correlate the impact energies obtained from sub-size and full-size Charpy specimens. The expressions were derived from statistical analysis of data from tests on plain carbon and low alloy steels reported in [3] and [8]. The correlation is not exact because Charpy test data often exhibits scatter, particularly in the transition region. In addition, the use of the correlation may be inappropriate for materials that do not exhibit impact toughness behavior typical of plain carbon and low alloy steels. Note that in the following calculation procedure, the units for the Charpy impact energy are ft-lbs, thickness is in inches, and temperature is in degrees Fahrenheit.

1) STEP 1 – Determine C_A and C_B parameters based upon the size of the Charpy specimen from the table below.

Charpy Specimen Size	1/4	1/3	1/2	2/3	Full
C_A	22	28	36	41	50
C_B	19	24	30	32	33

2) STEP 2 – Obtain the following four quantities from the sub-size specimen (denoted with a subscript "ss") Charpy energy transition curve: CVN_{ss}, CVN_{US-ss}, SA_{ss} and T_{c-ss}. If only two or three of the quantities are available, the unknown quantities can be determined from the following equations. If only one of the quantities is known, the transformation cannot be performed.

$$SA_{ss} = 1.1\left(\frac{CVN_{ss}}{CVN_{US-ss}} - 0.1 \right) \qquad \text{(F.44)}$$

$$CVN_{US-ss} = \frac{CVN_{ss}}{0.9 \cdot SA_{ss} + 0.1} \qquad \text{(F.45)}$$

$$SA_{ss} = \left(1 + \exp\left[-\left\{ \frac{\left(T - T_{c-ss}\right) + C_A}{C_B} \right\} \right] \right)^{-1} \qquad \text{(F.46)}$$

$$T_{c-ss} = T - C_B \cdot \ln\left[\frac{SA_{ss}}{1 - SA_{ss}}\right] + C_A \tag{F.47}$$

3) STEP 3 – Calculate the full size specimen SATT:

$$T_c = T_{c-ss} + 66\left(NWT\right)^{0.55}\left\{\left(t_{ss}\right)^{-0.7} - \left(t_{std}\right)^{-0.7}\right\} \tag{F.48}$$

4) STEP 4 – Calculate the shear area of the full size specimen using the following equation.

$$SA = \left(1 + \exp\left[-\left\{\frac{\left(T - T_c\right) + C_A}{C_B}\right\}\right]\right)^{-1} \tag{F.49}$$

5) STEP 5 – Calculate the upper shelf impact energy for the full size specimen using the following equation.

$$CVN_{US} = CVN_{US-ss}\left(\frac{t_{std}}{t_{ss}}\right) \tag{F.50}$$

6) STEP 6 – Calculate the impact energy for the full size specimen using the Equation (F.51). Note that if CVN_{ss} is on the lower shelf or SA_{ss} is less than five percent, and $t_{ss} < t_c$, the impact energy for the full size specimen can be computed using Equation (F.52).

$$CVN = CVN_{US}\left(0.9 \cdot SA + 0.1\right) \tag{F.51}$$

$$CVN = CVN_{ss}\left(\frac{t_{std}}{t_{ss}}\right) \tag{F.52}$$

F.4.3.3 A measure of the fracture tearing resistance as a function of the amount of stable ductile tearing is provided by determination of a JR curve. Data for some materials are provided in Table F.10. Testing methods for the determination of JR-Curves are covered in ASTM 1820. It should be noted that a JR curve might significantly change depending on loading rate; therefore, dynamic JR curve data should be used in the assessment of components under dynamic loading conditions.

F.4.4 Lower Bound Fracture Toughness

F.4.4.1 When fracture toughness data are not available, an indexing procedure based on a reference temperature can provide a conservative lower-bound estimate of fracture toughness for a ferritic material.

a) The basic premise behind the approach is illustrated schematically in Figure F.4(a). Various ferritic steels, as well as different heats of the same steel, exhibit toughness-temperature curves with similar shapes, but with ductile-brittle transitions at different temperatures. When the toughness is plotted against a temperature relative to a reference transition temperature, these data tend to collapse onto a common trend, albeit with more scatter than in individual data sets. This additional scatter reflects the fact that the indexing temperature removes most, but not all, of the heat-to-heat variation in the fracture toughness curves.

b) The indexing approach was originally developed for nuclear reactor pressure vessel steels, and this methodology is included in Section XI of the ASME Boiler and Pressure Vessel Code. The reference temperature utilized is termed the RT_{NDT}. The RT_{NDT} is defined as the maximum of the nil-ductility transition temperature established by a drop weight test, and the temperature from a Charpy test where the specimen exhibits at least 0.89 mm (35 mils) of lateral expansion and not less that 68 Joules (50 ft-lb) absorbed energy minus 33 ºC (60 ºF).

c) In the late 1960s and early 1970s, a large fracture toughness data set was collected for multiple heats of low alloy pressure vessel steels and was plotted against relative temperature. Two curves were then drawn below the data. The K_{IC} curve is a lower envelope to all of the fracture toughness tests loaded at quasi-static rates. The K_{IR} curve is a lower envelope to all data that include quasi-static initiation, dynamic initiation, and crack arrest toughness results. The K_{IC} and K_{IR} reference curves are shown in Figure F.4(b). The equations for these curves are shown below.

$$K_{IC} = 36.5 + 3.084\exp\left[0.036\left(T - T_{ref} + 56\right)\right] \qquad \left(MPa\sqrt{m},\ ^{o}C\right) \qquad \text{(F.53)}$$

$$K_{IC} = 33.2 + 2.806\exp\left[0.02\left(T - T_{ref} + 100\right)\right] \qquad \left(ksi\sqrt{in},\ ^{o}F\right) \qquad \text{(F.54)}$$

and,

$$K_{IR} = 29.5 + 1.344\exp\left[0.0260\left(T - T_{ref} + 89\right)\right] \qquad \left(MPa\sqrt{m},\ ^{o}C\right) \qquad \text{(F.55)}$$

$$K_{IR} = 26.8 + 1.223\exp\left[0.0144\left(T - T_{ref} + 160\right)\right] \qquad \left(ksi\sqrt{in},\ ^{o}F\right) \qquad \text{(F.56)}$$

d) Although the ASME Section XI reference curves were originally developed for nuclear grade pressure vessel steels, they have also been validated for carbon steel plates and weldments, as well as several heats of 2.25Cr-1Mo steel (see References [2] and [12]).

e) The equations for K_{IC} and K_{IR}, and the curves in Figure F.4(b), should be truncated as follows unless data are available that indicate higher maximum upper shelf toughness.

1) $110\ MPa\sqrt{m}$ $(100\ ksi\sqrt{in})$ should be used for materials with an unknown chemistry.

2) $220\ MPa\sqrt{m}$ $(200\ ksi\sqrt{in})$ can be used for low sulfur carbon steels (0.01 percent or less) or for J_{TE} controlled 2.25Cr-1Mo steels ($J_{TE} \le 150$, see paragraph F.4.7.3).

f) The mean value of the material fracture toughness can be estimated based on the lower bound value as described above using the correlations in Table F.11. The mean value of fracture toughness is used in the assessment of crack-like flaws (see Part 9).

F.4.4.2 The following procedures can be used when fracture toughness data do not exist for a material. These procedures will typically result in a lower bound estimate of the material fracture toughness.

a) Lower Bound Fracture Toughness Based on ASME Section XI Reference Curves – A recommended procedure for determining a lower bound toughness based on ASME Section XI Reference Curves is shown below.

1) STEP 1 – If the RT_{NDT} is known, this value can be used as T_{ref}; therefore, proceed to STEP 4. Otherwise proceed to STEP 2.

2) STEP 2 – Based on the material specification, determine the ASME Exemption Curve using Part 3, Table 3.2, Young's Modulus at ambient temperature, and the minimum specified yield strength at ambient temperature based on the original construction code.

3) STEP 3 – Determine the reference temperature using the following equations. In these equations, CVN should be set at 20 Joules (15 ft-lbs) for carbon steels and 27 Joules (20 ft-lbs) for low alloy steels. The parameter T_0 is determined based on the ASME Exemption Curve using Equations (F.85) to (F.88) and the parameter C is determine from Equation (F.89).

$$T_{ref} = \frac{5}{9}\left(C \cdot \text{atanh}\left[\frac{\frac{\sqrt{640 \cdot CVN \cdot E_y}}{1100 \cdot \left(\sigma_{ys}/C_{us}\right)} - 1.7}{1.7 - \frac{27}{\left(\sigma_{ys}/C_{us}\right)}} \right] + T_0 - 32 \right) \qquad (MPa, {}^{o}C) \qquad \text{(F.57)}$$

$$T_{ref} = C \cdot \text{atanh}\left[\frac{\frac{\sqrt{5000 \cdot CVN \cdot E_y}}{1000 \cdot \sigma_{ys}} - 1.7}{1.7 - \frac{27}{\sigma_{ys}}} \right] + T_0 \qquad (ksi, {}^{o}F) \qquad \text{(F.58)}$$

4) STEP 4 – Compute K_{IC} using Equations (F.53) or (F.54), or K_{IR} using Equations (F.55) or (F.56), as applicable.

b) Lower Bound Fracture Toughness Based on MPC Fracture Toughness Model – A recommended procedure for determining a lower bound toughness based on MPC Fracture Toughness Model is shown below.

5) STEP 1 – Based on the material specification, determine the ASME Exemption Curve using Part 3, Table 3.2 and the minimum specified yield strength at ambient temperature based on the original construction code.

6) STEP 2 – With the ASME Exemption Curve and the minimum specified yield strength of the material, calculate K_{Id} using Equation (F.83), or K_{IC} using Equation (F.84), as applicable.

F.4.4.3 The lower bound curves in paragraph F.4.4.1.c can also be used to estimate the fracture toughness at one temperature based on the value obtained at another temperature. This can be accomplished by calculating the reference temperature from known fracture toughness data using these equations. The fracture toughness at the new temperature can then be computed using the computed reference temperature and these equations. Alternatively, this procedure can be performed graphically by locating the known toughness on the curve in Figure F.4(b) and moving up or down along the curve by the appropriate difference in temperature $\left(T - T_{ref}\right)$ to read the new toughness value. Note that a toughness estimate obtained in this manner may not be a lower bound value.

F.4.5 Assessing Fracture Toughness from Charpy V-Notch Data

F.4.5.1 Although Charpy V-Notch impact test data do not represent true fracture toughness data, these data can be used as a starting point for determining the toughness to use in an assessment. The following provide guidance for estimating the fracture toughness from CVN data.

a) *Lower Bound Fracture Toughness* – The equations in paragraph can be used to establish lower bound fracture toughness based on the value of the reference temperature, T_{ref}. The reference temperature to be used in the calculation is the temperature that corresponds to 20 Joules (15 ft-lb) for carbon steels and 27 Joules (20 ft-lb) for low-alloy steels. This temperature can be determined from the CVN-temperature relationship in subparagraph c).

b) *Fracture Toughness Based On The Master Curve* – The procedure in paragraph F.4.9 can be used to establish fracture toughness based on a reference transition temperature, T_o. A correlation between the reference transition temperature, T_o, and the 27 J (20 ft-lb) Charpy energy transition temperature is provided in paragraph F.4.9.7.

c) *CVN-Temperature Relationship For Multiple Temperatures* – If a Charpy transition temperature curve is provided, then the data can be curve-fit to the hyperbolic tangent equation shown below to determine the relationship between the Charpy impact energy and temperature. The characteristics of this equation are shown in Figure F.5(a). A typical curve-fit to CVN data is shown in Figure F.5(b).

$$CVN = A_{cv} + B_{cv} \tanh\left[\frac{(T - D_{cv})}{C_{cv}}\right] \tag{F.59}$$

F.4.5.2 Charpy V-Notch impact energy can be converted directly to a K_{IC} by using $K_{IC} - CVN$ correlations. The value of the Charpy impact energy to be used with these correlations can be extrapolated, or read directly from a Charpy transition temperature curve (see paragraphs F.4.5.1.c).

a) $K_{IC} - CVN$ Upper Shelf Correlations

1) Rollfe-Novak-Barsom correlation for K_{IC} (see Reference [20])

$$\left(\frac{K_{IC}}{\sigma_{ys}}\right)^2 = 0.64\left(\frac{CVN}{\sigma_{ys}} - 0.01\right) \qquad \left(MPa\sqrt{m},\ MPa,\ J\right) \tag{F.60}$$

$$\left(\frac{K_{IC}}{\sigma_{ys}}\right)^2 = 5\left(\frac{CVN}{\sigma_{ys}} - 0.05\right) \qquad \left(ksi\sqrt{in},\ ksi,\ ft-lb\right) \tag{F.61}$$

2) Lower bound estimate recommend in WRC 265 (see Reference [13]).

$$\left(\frac{K_{IC}}{\sigma_{ys}}\right)^2 = 0.52\left(\frac{CVN}{\sigma_{ys}} - 0.02\right) \qquad \left(MPa\sqrt{m},\ MPa,\ J\right) \tag{F.62}$$

$$\left(\frac{K_{IC}}{\sigma_{ys}}\right)^2 = 4\left(\frac{CVN}{\sigma_{ys}} - 0.1\right) \qquad \left(ksi\sqrt{in},\ ksi,\ ft-lb\right) \tag{F.63}$$

b) $K_{IC} - CVN$ *Transition Region Correlations*

1) Sailors and Corton correlation for static fracture toughness (see Reference [13]).

$$K_{IC} = 14.6\left(CVN\right)^{0.50} \qquad \left(MPa\sqrt{m},\ J\right) \tag{F.64}$$

$$K_{IC} = 15.5\left(CVN\right)^{0.50} \qquad \left(ksi\sqrt{in},\ ft-lb\right) \tag{F.65}$$

2) Lower Bound estimate for static fracture toughness recommended in WRC 265 (see Reference [13]).

$$K_{IC} = 8.47\left(CVN\right)^{0.63} \qquad \left(MPa\sqrt{m},\ J\right) \tag{F.66}$$

$$K_{IC} = 9.35\left(CVN\right)^{0.63} \qquad \left(ksi\sqrt{in},\ ft-lb\right) \tag{F.67}$$

3) Sailors and Corton correlation for dynamic fracture toughness (see Reference [13]).

$$K_{Id} = 15.5\left(CVN\right)^{0.375} \qquad \left(MPa\sqrt{m},\ J\right) \qquad \text{(F.68)}$$

$$K_{Id} = 15.873\left(CVN\right)^{0.375} \qquad \left(ksi\sqrt{in},\ ft-lb\right) \qquad \text{(F.69)}$$

4) Lower Bound estimate for dynamic fracture toughness recommended in WRC 265 (see Reference [13]).

$$K_{Id} = 22.5\left(CVN\right)^{0.17} \qquad \left(MPa\sqrt{m},\ J\right) \qquad \text{(F.70)}$$

$$K_{Id} = 21.6\left(CVN\right)^{0.17} \qquad \left(ksi\sqrt{in},\ ft-lb\right) \qquad \text{(F.71)}$$

5) A two-step procedure for correlating static fracture toughness with Charpy test results in the transition region using a dynamic fracture toughness correlation and temperature shift method may be used (see Reference [13]).

$$K_{Ic}\left(T - \Delta T_s\right) = K_{Id}\left(T\right) \qquad \text{(F.72)}$$

where:

$$K_{Id} = \frac{\sqrt{640 \cdot CVN \cdot E_y}}{1000} \qquad \left(MPa\sqrt{m},\ MPa,\ J\right) \qquad \text{(F.73)}$$

$$\Delta T_s = 119 - 0.12\sigma_{ys} \qquad for\ 250 \le \sigma_{ys} \le 990\,MPa \qquad \left({}^0C, MPa\right) \qquad \text{(F.74)}$$

$$\Delta T_s = 0.0 \qquad for\ \sigma_{ys} > 990\,MPa \qquad \left({}^0C, MPa\right) \qquad \text{(F.75)}$$

$$K_{Id} = \frac{\sqrt{5000 \cdot CVN \cdot E_y}}{1000} \qquad \left(ksi\sqrt{in},\ ksi,\ ft-lb\right) \qquad \text{(F.76)}$$

$$\Delta T_s = 215 - 1.5\sigma_{ys} \qquad for\ 36 \le \sigma_{ys} \le 140\,ksi \qquad \left({}^0F,\ ksi\right) \qquad \text{(F.77)}$$

$$\Delta T_s = 0.0 \qquad for\ \sigma_{ys} > 140\,ksi \qquad \left({}^0F,\ ksi\right) \qquad \text{(F.78)}$$

c) Other $K_{IC} - CVN$ and $K_{Id} - CVN$ correlations may be used depending on the material and region of the transition curve (e.g. lower shelf, transition, and upper shelf), see references [13], [9], and [10].

F.4.5.3 The MPC has developed a Charpy impact energy correlation and a methodology to relate this energy to both the dynamic and static fracture toughness using the model used to develop the ASME Codes, Section VIII, Divisions 1 and 2 Exemption Curves. It should be noted that the ASME exemption curves are independent of the strength of the steel. This is the case even though the driving force for fracture is expected to increase with the applied and residual stresses which in turn are typically related to material strength. The strength independence of the exemption curves lies in assumptions regarding the material property model used when the exemption curves were developed. The main assumption that was used in the development of the exemption curves was that the fracture toughness at the indexing temperature should be proportional to the yield strength of the material and vary with temperature in a strength independent manner. This assumption can be assured through application of yield strength dependent Charpy test requirements. The MPC equations provided herein were developed to provide the connection between the Charpy energy requirement as a function of temperature and the fracture toughness that would be expected when the exemption curves were developed.

a) A two-step procedure for correlating static fracture toughness with Charpy test results in the transition region using a dynamic fracture toughness correlation and temperature shift method may be used.

$$K_{IC}\left(T-\Delta T_s\right)=K_{Id}\left(T\right) \tag{F.79}$$

where:

$$K_{Id}=14\sqrt{CVN} \qquad \left(MPa\sqrt{m},\ J\right) \tag{F.80}$$

$$K_{Id}=15\sqrt{CVN} \qquad \left(ksi\sqrt{in},\ ft-lb\right) \tag{F.81}$$

$$\Delta T_s=42^oC\ \ (75^oF) \tag{F.82}$$

b) The dynamic and static fracture toughness can be related to the ASME Exemption Curves.

$$K_{Id}=\sigma_{ys}\left\{1.7+\left(1.7-\frac{27}{\sigma_{ys}}\right)\cdot\tanh\left[\frac{T-T_0}{C}\right]\right\} \qquad \left(ksi\sqrt{in},\ ksi,\ ^oF\right) \tag{F.83}$$

$$K_{IC}=\sigma_{ys}\left\{1.7+\left(1.7-\frac{27}{\sigma_{ys}}\right)\cdot\tanh\left[\frac{\left(T-75\right)-T_0}{C}\right]\right\} \qquad \left(ksi\sqrt{in},\ ksi,\ ^oF\right) \tag{F.84}$$

where:

$$T_0=114\ ^oF \qquad for\ ASME\ Exemption\ Curve\ A \tag{F.85}$$

$$T_0=76\ ^oF \qquad for\ ASME\ Exemption\ Curve\ B \tag{F.86}$$

$$T_0=38\ ^oF \qquad for\ ASME\ Exemption\ Curve\ C \tag{F.87}$$

$$T_0=12\ ^oF \qquad for\ ASME\ Exemption\ Curve\ D \tag{F.88}$$

$$C=66\ ^oF \tag{F.89}$$

c) Using Equations (F.81) and (F.83), a relationship between the expected temperature for an associated Charpy energy value for materials with an assigned ASME Exemption Curve is shown in Equations (F.90) and (F.91). In these equations, T_0 is determined based on the ASME Exemption Curve using Equations (F.85) to (F.88) and C is determine from Equation (F.90).

$$T = C \cdot \operatorname{atanh}\left[R_{HT}\right] + T_0 \qquad for \qquad R_{HT} < 0.76 \qquad \left(ft-lb,\ ksi,\ ^oF\right) \qquad \text{(F.90)}$$

$$T = C + T_0 \qquad for \qquad R_{HT} \geq 0.76 \qquad \left(ft-lb,\ ksi,\ ^oF\right) \qquad \text{(F.91)}$$

where

$$R_{HT} = \frac{\frac{15\sqrt{CVN}}{\sigma_{ys}} - 1.7}{1.7 - \frac{27}{\sigma_{ys}}} \qquad \left(ft-lb,\ ksi\right) \qquad \text{(F.92)}$$

F.4.5.4 There are two cautions in using Charpy V-Notch data to establish an estimate of the fracture toughness:

a) The Charpy data used to estimate the reference temperature or K_{IC} should be representative of the component being evaluated (i.e. they should be heat and heat treatment specific). These data should also come from a material with a representative microstructure. For example, Charpy data from the base metal may not be applicable when the flaw being evaluated is in the weld metal or in the HAZ.

b) An appropriate temperature must be used to perform the assessment. In cases where the stress varies with temperature (e.g., a pressure vessel that is not fully pressurized until it reaches an elevated temperature) it may be necessary to perform the assessment at several temperatures to identify the worst-case loading.

F.4.6 Fracture Toughness for Materials Subject to In-Service Degradation

F.4.6.1 The inherent fracture toughness of a material can be affected by the service environment. For example, hydrogen can diffuse into the steel and can result in an apparent loss of fracture toughness. Temperature exposure can produce embrittlement, such as strain aging, temper embrittlement, 885-embrittlement, and sigma phase embrittlement. In these cases, a lower fracture toughness that accounts for the loss of toughness resulting from the service environment must be used in the assessment.

F.4.6.2 Hydrogen dissolved in ferritic steel can significantly reduce the apparent fracture toughness of a material (see Figure F.6). Fracture initiation is enhanced when hydrogen diffuses to the tip of a crack. If rapid unstable crack propagation begins, however, diffusing hydrogen cannot keep pace with the growing crack; thus the resistance to rapid crack propagation increases with increasing rate and the rate slows to establish equilibrium between the growth rate and the hydrogen delivery rate. Subcritical growth may then continue at the equilibrium rate. The K_{IR} curve defined by the equation in paragraph is a lower envelope to dynamic initiation and crack arrest toughness data. This curve represents a conservative estimate of the resistance of the material to rapid unstable crack propagation, and can be used to estimate the toughness of steel containing dissolved hydrogen. However, this curve does not provide a threshold against subcritical crack growth.

a) A procedure for inferring the toughness of a hydrogen charged steel against rapid crack propagation is as follows:

1) STEP 1 – Determine the reference temperature, T_{ref} , using paragraphs F.4.4 or F.4.5. Note that if Charpy V-Notch data are available it will normally be for the steel in the uncharged state. Absent of any internal cracking of the steel, the Charpy impact energy is not significantly affected by dissolved hydrogen because of the very high rate of the Charpy test.

2) STEP 2 – Determine a lower-bound K_{IR} toughness by using procedures in paragraph F.4.4.2.

b) Flaws in hydrogen charged materials should be treated with extreme caution. The above procedure does not take account of the following two factors.

1) If a material remains in a hydrogen-charging environment in service, the cracks may grow by what is known as subcritical crack growth. Consequently, a flaw that is acceptable at its current size may grow to a critical size over time. If the applied K is above the threshold stress intensity for crack growth, the flaw will grow until the applied K exceeds a value from the K_{IR} curve, at which time unstable fracture will occur.

2) Long exposure to hydrogen may produce irreversible damage (e.g. microcracks) in the material. The apparent toughness could fall below the K_{IR} curve in such cases.

F.4.6.3 There are several types of metallurgical embrittlement listed below that can reduce the ductility and fracture properties of carbon, alloy, and stainless steels below the K_{IR} curve.

a) Brief descriptions of the types of embrittlement currently encountered in industry are described below.

1) *Strain Age Embrittlement of Carbon and Carbon/Molybdenum Steels* – occurs in the plastic zone at the tip of crack or at a strain concentration. It most typically occurs when a weld is made in close proximity of a crack, causing the material near the crack tip to be strained and heated in the 149°C (300°F) to 260°C (500°F) range. Steels with an aluminum content greater than 0.015 wt % (i.e. killed steels) are not susceptible, and PWHT alleviates the problem for susceptible steels.

2) *Loss Of Toughness with Aging Of* 1.25Cr-0.5Mo *Mo Steel* – can occur in steels that have been in service in the 371°C (700°F) to 593°C (1100°F) temperature range (see Figure F.6). Embrittlement is thought to be related to carbide formation and/or the level of tramp element impurities (i.e. As, P, Sb, and Sn) present in the steel. Factors such as heat treatment condition and microstructure play a role. In many cases, older steels usually are more susceptible than newer generation steels. Toughness may be affected up to 149°C (300°F). In general, steels are more susceptible the higher the carbon content and steels above 0.15 wt% carbon are most susceptible. Although the correlation is not strong, the loss of toughness for 1.25Cr-0.5Mo has been correlated to the $\bar{X}$ factor (see paragraph F.4.7.2).

3) *Temper Embrittlement of* 2.25Cr-1Mo *Steel* – can occur in steels that have been in service in the 343°C (650°F) to 593°C (1100°F) temperature range (see Figure F.6). Embrittlement is related to the level of tramp element impurities (i.e Mn, P, Si, and Sn) present in the steel, and to the heat treatment condition and microstructure. In many cases, older steels usually are more susceptible than newer generation steels. Toughness may be affected up to 149°C (300°F) and more. The degree of susceptibility for 2.25Cr-1Mo has been correlated to the J_{TE} factor (see paragraph F.4.7.3).

4) *885 (F) Embrittlement Of Ferritic Or Duplex Stainless Steels* – can occur if a ferritic or duplex stainless steel is subjected to the temperature range of 371°C (700°F) to 566°C (1050°F). The material toughness for 885 embrittled steels is affected up to 149°C (300°F).

5) *Sigma Phase Embrittlement Of Austenitic Stainless Steels* – sigma phase can form in austenitic stainless steels that contain ferrite in welds and are subject to heat treatment in the 649°C (1200°F) to 760°C (1400°F) temperature range, or irrespective of ferrite content if subjected to a 593°C (1100°F) to 816°C (1500°F) temperature range for prolonged periods. Toughness is affected most at ambient temperatures, but is affected even at operating temperatures.

b) If a material has experienced embrittlement because of the service environment, the toughness can be extremely low. In order to ascertain the toughness, samples may be removed and tests, such as CVN, could be conducted on the material to estimate the toughness. Otherwise, the toughness values may be used based on the relative degree of embrittlement.

F.4.7 Aging Effects on the Fracture Toughness of Cr-Mo Steels

F.4.7.1 The effect of embrittlement due to service conditions on the fracture toughness can be estimated for certain Cr-Mo steels based on chemistry. If the toughness calculated using the following temper embrittlement analyses is higher that that predicted by the methods in paragraphs F.4.2 through F.4.5 for a non-embrittled steel, then the temper embrittlement has no affect on the fracture toughness. However, if the fracture toughness predicted by the following temper embrittlement analyses is lower than that predicted by the methods in paragraph F.4.2 through F.4.5, then temper embrittlement may affect the fracture toughness and the lower value of the estimated fracture toughness should be used in the assessment.

F.4.7.2 The effect of tramp elements on the fracture toughness of 1.25Cr-0.5Mo (see paragraph F.4.6.3.a.2) can be estimated based on knowledge of the material chemistry using a two-step correlation [97].

a) In the first step, the Fracture Appearance Transition Temperature ($FATT$) is estimated based on a material chemistry parameter $\overline{X}$ as shown below. A single correlation is available which corresponds to an upper bound. This correlation applies to both weld metal and base metal. This correlation only considers the effect of tramp elements on toughness. This prediction may be non-conservative if severe carbide embrittlement is possible. In such a case a higher estimated $FATT$ should be used.

$$\overline{X} = \left(10 \cdot \%P + 5 \cdot \%Sb + 4 \cdot \%Sn + \%As\right) \cdot 100 \qquad \text{(F.93)}$$

and,

$$FATT\big|_{upper\ bound} = -87.355 + 11.437\overline{X} - 0.14712\overline{X}^2 \qquad \left(^oC\right) \qquad \text{(F.94)}$$

b) In the second step, the fracture toughness is determined using the equations for K_{IC} or K_{IR} in paragraph F.4.4.1 with $T_{ref} = FATT$. If the material toughness is subject to degradation due to dissolved hydrogen, the fracture toughness should be based on the equation for K_{IR}. Alternatively, the Master Curve relationship (see paragraph F.4.9) can be used to determine the fracture toughness with

$$T_0 = FATT - 75^oC \qquad \text{(F.95)}$$

F.4.7.3 The effect of temper embrittlement on the fracture toughness of 2.25Cr–1Mo (see paragraph F.4.6.3.a.3) can be estimated based on knowledge of the material chemistry using a two-step correlation [97].

a) In the first step, the Fracture Appearance Transition Temperature ($FATT$) is estimated based on a material chemistry parameter J_{TE} as shown below. Three correlations are available corresponding to the mean, 95% confidence limit, and 99% confidence limit. These correlations apply to both weld metal and base metal.

$$J_{TE} = \left(\%Mn + \%Si\right)\left(\%P + \%Sn\right) \cdot 10000 \qquad \text{(F.96)}$$

$$FATT\big|_{mean} = -77.321 + 0.57570 J_{TE} - 5.5147\left(10^{-4}\right) J_{TE}^2 \qquad \left({}^{o}C\right) \tag{F.97}$$

$$FATT\big|_{95\%} = -48.782 + 0.77455 J_{TE} - 8.5424\left(10^{-4}\right) J_{TE}^2 \qquad \left({}^{o}C\right) \tag{F.98}$$

$$FATT\big|_{99\%} = -15.416 + 0.72670 J_{TE} - 8.0043\left(10^{-4}\right) J_{TE}^2 \qquad \left({}^{o}C\right) \tag{F.99}$$

b) In the second step, the fracture toughness is determined using the equations for K_{IC} or K_{IR} in paragraph F.4.4.1 with $T_{ref} = FATT$. If the material toughness is subject to degradation due to dissolved hydrogen, the fracture toughness should be based on the equation for K_{IR}. Alternatively, the Master Curve relationship (see paragraph F.4.9) can be used to determine the fracture toughness with

$$T_0 = FATT - 85^{o}C \tag{F.100}$$

F.4.8 Fracture Toughness of Austenitic Stainless Steel

F.4.8.1 In most cases, austenitic stainless steels do not experience a ductile-brittle transition like ferritic steels. The fracture toughness is usually high, even at low temperatures, provided the material has not experienced degradation in toughness because of exposure to the environment (see paragraph F.4.6.3). However, a toughness transition may occur in austenitic stainless steels with a high ferrite content (i.e. castings).

F.4.8.2 If specific information on the fracture toughness is not available, the following values can be used in an assessment provided the material has not experienced significant thermal degradation and does not exhibit a transition region.

a) Base material: $220\ MPa\sqrt{m}$ $(200\ ksi\sqrt{in})$

b) Weld material: $132\ MPa\sqrt{m}$ $(120\ ksi\sqrt{in})$

F.4.9 Probabilistic Fracture Toughness Distribution

F.4.9.1 The fracture toughness correlations discussed in the previous paragraphs are deterministic and conservative. Since there is a high degree of scatter in fracture toughness data, the actual toughness in a given situation can be considerably higher than the lower-bound curve predicts. Because of this substantial scatter, data should be treated statistically rather than deterministically because the steel does not have a single value of toughness at a particular temperature; rather, the material has a toughness distribution.

F.4.9.2 The ASTM E1921 standard can be used to determine this distribution for the ductile-brittle transition region. This standard utilizes a fracture toughness master curve approach to infer the toughness distribution of a material when fracture toughness data (J or $CTOD$) are available. It may not fit data in the lower shelf very well, and it is totally unsuitable for the upper shelf (the equations in paragraph F.4.9.5 increase without bound with increasing temperature).

F.4.9.3 The ASTM E1921 standard accounts for the temperature dependence of toughness through the use of a fracture toughness master curve (see Figure F.7). A wide range of ferritic steels have a characteristic fracture toughness-temperature curve, and the only difference between different grades and heats of steel is the absolute position of the curve with respect to temperature. Typically, high toughness steels have a low transition temperature and low toughness steels have a high transition temperature.

F.4.9.4 The fracture toughness distribution in ASTM E1921 is defined by a three-parameter Weibull distribution. With the threshold toughness equal to $20\ MPa\sqrt{m}\ \ (18.2\ ksi\sqrt{in})$ the cumulative distribution function is given by the following equation shown below. Note that the thickness of the component, t_{mc} is accounted for in these equations.

$$F_{mc} = 1 - \exp\left[-\frac{L_{mc}}{25.4}\left(\frac{K_{Jc} - 20}{K_0 - 20} \right)^4 \right] \qquad \left(mm,\ MPa\sqrt{m} \right) \tag{F.101}$$

$$F_{mc} = 1 - \exp\left[-L_{mc}\left(\frac{K_{Jc} - 18.2}{K_0 - 18.2} \right)^4 \right] \qquad \left(in,\ ksi\sqrt{in} \right) \tag{F.102}$$

F.4.9.5 The temperature dependence of the median fracture toughness in the transition region can be estimated using the following equation. Note, that at $T = T_0$, the fracture toughness is $100\ MPa\sqrt{m}\ \ (91\ ksi\sqrt{in})$, and K_0 and K_{Jc} correspond to a 25.4 mm (1 inch) crack front length (or a 1 inch fracture toughness specimen).

$$K_{Jc(median)} = 30 + 70\exp[0.0190(T - T_0)] \qquad \left({}^{o}C,\ MPa\sqrt{m} \right) \tag{F.103}$$

$$K_{Jc(median)} = 27 + 64\exp[0.0106(T - T_0)] \qquad \left({}^{o}F,\ ksi\sqrt{in} \right) \tag{F.104}$$

F.4.9.6 The following procedure can be used to develop a fracture toughness distribution for a specific assessment temperature based on K_{Jc} test values (see ASTM E1921 for details).

a) STEP 1 – Perform replicate fracture toughness tests at a constant temperature, the ASTM E1921 standard recommends at least 6 tests. Curve fit these data to the equations in paragraph F.4.9.4 to determine K_0 and $K_{Jc(medium)}$ at the test temperature. Note that this equation has the form of a three-parameter Weibull distribution with two of the three parameters fixed, leaving only one degree of freedom. A distribution that contains only one parameter can be fit with a relatively small sample size. The only fitting parameter in this equation is K_0, which varies with temperature.

b) STEP 2 – Compute T_0 using the following equation obtained by rearranging the equations in paragraph F.4.9.5. The ASTM E1921 standard recommends applying this procedure at several test temperatures in order to obtain more than one estimate of T_0.

$$T_0 = T - \frac{\ln\left[\dfrac{K_{Jc(median)} - 30}{70} \right]}{0.0190} \qquad \left({}^{o}C,\ MPa\sqrt{m} \right) \tag{F.105}$$

$$T_0 = T - \frac{\ln\left[\dfrac{K_{Jc(median)} - 27}{64} \right]}{0.0106} \qquad \left({}^{o}F,\ ksi\sqrt{in} \right) \tag{F.106}$$

c) STEP 3 – Substitute the value of T_0 from STEP 2 into one of the equations in paragraph F.4.9.5 to compute $K_{Jc(median)}$ at the assessment temperature.

d) STEP 4 – Solve for K_0 using the following equation obtained by rearranging the equations in paragraphs F.4.9.4 with $F_{mc} = 0.5$ and using the median fracture toughness from STEP 1.

$$K_0 = \frac{\left(K_{Jc(median)} - 20\right)}{\left(\ln[2]\right)^{0.25}} + 20 \qquad \left(MPa\sqrt{m}\right) \qquad \text{(F.107)}$$

$$K_0 = \frac{\left(K_{Jc(median)} - 18.2\right)}{\left(\ln[2]\right)^{0.25}} + 18.2 \qquad \left(ksi\sqrt{in}\right) \qquad \text{(F.108)}$$

e) STEP 5 – With the computed value of K_0 from STEP 4 and the crack front length, L_{mc}, the fracture toughness distribution is established for a specified assessment temperature using one of the equations shown below. The parameter F_{mc} in these equations represents the probability of at or below the value of K_{Jc}. With this definition, it is possible to compute the median $\left(F_{mc} = 0.5\right)$, upper bound $\left(F_{mc} = 0.95\right)$, and lower-bound $\left(F_{mc} = 0.05\right)$ values for the fracture toughness as a function of assessment temperature (see Figure F.7).

$$K_{Jc} = 20 + \left(\frac{25.4}{L_{mc}} \ln\left[\frac{1}{1 - F_{mc}}\right]\right)^{0.25} \left(K_0 - 20\right) \qquad \left(mm,\ MPa\sqrt{m}\right) \qquad \text{(F.109)}$$

$$K_{Jc} = 18.2 + \left(\frac{1}{L_{mc}} \ln\left[\frac{1}{1 - F_{mc}}\right]\right)^{0.25} \left(K_0 - 18.2\right) \qquad \left(in,\ ksi\sqrt{in}\right) \qquad \text{(F.110)}$$

f) STEP 6 – Repeat STEPs 3 through 5 to determine the fracture toughness distribution for different assessment temperatures.

F.4.9.7 In many applications, Charpy data are the only information available on material toughness. The following procedure can be used to develop a toughness distribution based on Charpy impact test values. Estimates of T_0 obtained from the correlation in this procedure have a standard deviation of 15°C (27°F). This uncertainty can be accounted for by treating T_0 as a random variable in a probabilistic analysis, or adding an appropriate margin to T_0 (i.e. 15°C (27°F) for one standard deviation, 30°C (54°F) for two standard deviations, etc.) in a deterministic analysis.

a) STEP 1 – Determine the 27 Joules (20 ft-lb) transition temperature. If Charpy data are only available for sub-size specimens, then the temperature shift in accordance with paragraph F.4.3.3 should be used when determining this transition temperature.

b) STEP 2 – Estimate T_0 using the following equation.

$$T_0 = T_{27\,Joules} - 18^o C \qquad \text{(F.111)}$$

$$T_0 = T_{20\,ft-lbs} - 32.4^o F \qquad \text{(F.112)}$$

c) STEP 3 – The same as given in paragraph F.4.9.6.c.

d) STEP 4 – The same as given in paragraph F.4.9.6.d.

e) STEP 5 – With the computed value of K_0, and the thickness of the component, t_{mc}, the fracture toughness distribution is known for a specified assessment temperature using Equation (F.109) or (F.110).

f) STEP 6 – Repeat STEPs 3 through 5 to determine the fracture toughness distribution for different assessment temperatures.

F.4.9.8 The master curve approach may produce nonconservative estimates of the fracture toughness in the following cases:

a) Charpy impact specimens exhibit unusual fracture behavior such as fracture path deviation.

b) Splits appear on the fracture surface of fracture toughness specimens due to crystallographic texture (this may give a lower fracture toughness than would be predicted from knowledge of the T_{27J} alone).

c) Through-thickness variation of microstructure and properties and the subsequent difficulty in ensuring that the Charpy specimen represents the same microstructure at the fracture initiation location in the fracture toughness specimen (this is likely to be a problem with weld metals and HAZs, the weld root region could initiate a fracture in a CTOD test but be missed by Charpy testing).

d) Processes such as electron beam or laser welding which lead to narrow welds.

e) Components with weld mis-match induced constraint.

f) Components with cold worked material.

g) Certain high strength steels that exhibit unusual fracture modes such as quasi-cleavage.

F.4.10 Effect of Loading Rate on Toughness

F.4.10.1 Dynamic loading causes the ductile-brittle transition of ferritic steels to occur at higher temperatures relative to quasistatic conditions. When a high rate of loading is present, the corresponding effect on toughness should be taken into account.

F.4.10.2 Three alternative methods are presented below to account for the effects of loading rate on toughness. For materials that do not exhibit a ductile-brittle transition, such as austenitic stainless steel, a loading rate adjustment on toughness is not necessary. Moreover, the upper shelf toughness of ferritic steels need not be adjusted for rate effects.

a) *Method 1 – ASME K_{IR} Curve*: The K_{IR} curve described in paragraph F.4.4 represents a lower bound of dynamic and crack arrest toughness data. Consequently, this curve may be used to estimate toughness in situations where rapid loading occurs. The reference transition temperature, T_{ref}, is used without adjustment.

b) *Method 2 – ASME K_{IC} Curve with Temperature Shift*: When using the lower-bound K_{IC} curve in paragraph F.4.4, a temperature shift should be added to the reference transition temperature, T_{ref}, where T_{ref}^D is the reference transition temperature under dynamic loading.

$$T_{ref}^D = T_{ref} + T_{shift}^D \qquad \text{(F.113)}$$

1) For impact loading, with nominal strain rates on the order of $\dot{\varepsilon} = 10^{-1}/\sec$, the following equations may be used to estimate the temperature shift [20].

$$T_{shift}^D = 119 - 0.12\sigma_{ys} \qquad for\ 250 \le \sigma_{ys} \le 966\,MPa \qquad (MPa : {}^oC) \qquad \text{(F.114)}$$

$$T^D_{shift} = 0.0 \qquad for\ \ \sigma_{ys} > 966\,MPa \qquad (MPa : {}^oC) \qquad \text{(F.115)}$$

$$T^D_{shift} = 215 - 1.5\sigma_{ys} \qquad for\ \ 36 \le \sigma_{ys} \le 140\,ksi \qquad (ksi : {}^oF) \qquad \text{(F.116)}$$

$$T^D_{shift} = 0.0 \qquad for\ \ \sigma_{ys} > 140\,ksi \qquad (ksi : {}^oF) \qquad \text{(F.117)}$$

2) For intermediate loading rates, with nominal strain rates in the range $10^{-3}/\sec \le \dot{\varepsilon} < 10^{-1}/\sec$ the following expressions may be used to adjust the transition temperature [20].

$$T^D_{shift} = \left(83 - 0.081\sigma_{ys}\right)\dot{\varepsilon}^{0.17} \qquad for\ \ \sigma_{ys} \le 966\,MPa \qquad (MPa : {}^oC : s^{-1}) \qquad \text{(F.118)}$$

$$T^D_{shift} = 0.0 \qquad for\ \ \sigma_{ys} > 966\,MPa \qquad (MPa : {}^oC : s^{-1}) \qquad \text{(F.119)}$$

$$T^D_{shift} = \left(150 - \sigma_{ys}\right)\dot{\varepsilon}^{0.17} \qquad for\ \ \sigma_{ys} \le 140\,ksi \qquad (ksi : {}^oF : s^{-1}) \qquad \text{(F.120)}$$

$$T^D_{shift} = 0.0 \qquad for\ \ \sigma_{ys} > 140\,ksi \qquad (ksi : {}^oF : s^{-1}) \qquad \text{(F.121)}$$

c) *Method 3 – Master Curve with Temperature Shift*: If the fracture toughness master curve approach, as described in paragraph F.4.9, is used to infer toughness, then the index temperature, T_0, should be adjusted with the equation below if high or intermediate loading rates are present. The temperature shift, T^D_{shift}, can be estimated using the procedure outlined in paragraph F.4.10.2.b.

$$T^D_0 = T_0 + T^D_{shift} \qquad \text{(F.122)}$$

d) *Method 4 – MPC K_{Id} Curve*: The K_{Id} curve described in paragraph F.4.5.3.b may be used to estimate toughness in situations where rapid loading occurs.

F.4.11 Sources of Fracture Toughness Data

Sources for fracture toughness data for various materials are provided in paragraph F.9.

F.5 Material Data for Crack Growth Calculations

F.5.1 Categories of Crack Growth

F.5.1.1 *Crack Growth by Fatigue* – Crack growth by fatigue occurs when a component is subject to time varying loads that result in cyclic stresses. Each increment of crack extension correlates to a certain increment of stress cycles. Linear elastic fracture mechanics (LEFM) has been validated to relate the crack growth per cycle to the applied stress intensity range through a fatigue crack growth model. The simplest and most common form of fatigue crack growth model is the Paris Equation (see paragraph F.5.2.1). More advanced forms of fatigue crack growth models that take explicit account of such factors as stress ratio, ranges of ΔK, effects of a threshold stress intensity factor, ΔK_{th}, and plasticity-induced crack closure are available for certain materials and environments. These models should be considered in an assessment based on the applied loading, crack configuration, and service environment. The variation of fatigue crack growth rate with cyclic stresses which produce a range of ΔK and the associated fracture mechanisms are shown in Figure F.8. An overview of the fatigue crack growth models and available data are provided in paragraphs F.5.2 and F.5.3, respectively.

F.5.1.2 *Crack Growth by Stress Corrosion Cracking (SCC)* – Stress corrosion cracking results from the combination of a corrosive environment, a static applied or residual tensile stress, and a susceptible material. In the presence of these elements, the passivation, re-passivation and metal dissolution that occur locally at the crack tip are altered such that when the crack tip stress intensity factor exceeds a critical threshold value, SCC will initiate and grow for the specified condition. Active SCC usually accelerates initially until it attains an approximately uniform velocity that is independent of the stress intensity factor, but may be dependent on duration (time), material, temperature, and specific environmental factors. The different type relationships between crack velocity and stress intensity factor that can occur during stress corrosion cracking are shown in Figure F.9(a) for two different environments. The difference in the relationship between the crack velocity and applied stress intensity factor should be noted. An overview of the stress corrosion crack growth models and available data are provided in paragraph F.5.4 and F.5.5, respectively.

F.5.1.3 *Crack Growth by Hydrogen Assisted Cracking (HAC)* – This covers a broad range of crack growth mechanisms that are associated with absorbed hydrogen in the metal. This includes hydrogen embrittlement, hydrogen induced cracking (HIC), stress-oriented hydrogen induced cracking (SOHIC), and sulfide stress cracking. In contrast to the other failure mechanisms, HAC susceptibility is highest at ambient and moderate temperatures and decreasing strain rate.

a) HAC occurs when hydrogen is absorbed by a material during a corrosion process, or by exposure to high-temperature and/or high-pressure hydrogen gas, and diffuses to a pre-existing flaw as atomic hydrogen, and stresses are applied (including residual stresses) to the flaw. The crack will continue to propagate at an increasing subcritical velocity until fracture occurs as long as the stress intensity factor resulting from the applied and residual stresses exceeds a critical threshold value, K_{th}, and a critical concentration of atomic hydrogen is maintained in the vicinity of the crack tip either by continuous absorption of hydrogen from the external surface, or by redistribution of internal lattice hydrogen and internal sources such as hydrogen traps in the material. The rapid, hydrogen accelerated propagation condition is dictated by the value of the material toughness in the presence of absorbed hydrogen at the crack tip. This toughness is designated as K_{IC-H}.

b) Within a LEFM methodology, a HAC crack growth model can be determined from test specimens that relate the crack growth rate to the combined applied and residual stress intensity factor, the material/environment constants, and loading (strain) rate. A simple form of the HAC crack growth curve is shown in Figure F.9 (b). A typical crack growth model for HAC is shown in paragraph F.5.3.7.

F.5.1.4 *Crack Growth by Corrosion Fatigue* – The synergistic effect of combined SCC or HAC with fatigue under cyclic loading in an aggressive environment can produce significantly higher crack growth per cycle compared to an inert environment where SCC or HAC is absent. This interaction can be very complicated, and makes development of a simple crack growth model difficult.

a) Corrosion fatigue crack propagation typically exhibits the three basic types of crack growth rate behavior shown in Figure F.10.

   1) True Corrosion Fatigue (TCF) – describes the behavior when fatigue crack growth rates are enhanced by the presence of aggressive environment at levels of applied K below K_{ISCC} (see Figure F.10 (a)). This behavior is characteristic of materials that do not exhibit stress corrosion (i.e. $K_{ISCC} = K_{IC}$).

   2) Stress Corrosion Fatigue (SCF) – describes corrosion under cyclic loading that occurs whenever the stress in the cycle is greater than K_{ISCC}. This is characterized by a plateau in crack growth (see Figure F.10 (b)) similar to that observed in stress-corrosion cracking.

   3) Combination TCF and SCF – this is the most common type of corrosion fatigue behavior (see Figure F.10 (c)) which is characterized by stress-corrosion fatigue above K_{ISCC}, superimposed on true corrosion fatigue at all stress intensity levels.

b) Equations that describe corrosion fatigue behavior are available for limited stress intensity ranges and material/environment combinations. Therefore, it is advisable to establish and use upper bound crack growth models for such cases.

F.5.2 Fatigue Crack Growth Equations

F.5.2.1 Overview

a) Fatigue crack growth equations that have been used are summarized below. A complete discussion of all aspects of these crack growth models is beyond the scope of this Standard. Further information on fatigue crack growth models can be found in reference [7], [26], [104], [108] and [109].

b) Although experimental data suggest the presence of a threshold condition for fatigue crack growth, fatigue cracking in actual structures with residual stresses may not exhibit fatigue threshold behavior and this should be considered in an analysis.

F.5.2.2 Paris Equation

a) The Paris Equation is the simplest of the fatigue crack growth models (see Figure F.8). The Paris Equation has the form shown below. Note that in this model, the crack growth rate is independent of the load ratio.

$$\frac{da}{dN} = C\left(\Delta K\right)^n \tag{F.123}$$

b) The Paris Equation may also be used in conjunction with a threshold ΔK value. Above the threshold ΔK, the crack growth is given by Equation (F.124), and below the threshold, the crack growth is given by Equation (F.125).

$$\frac{da}{dN} = C\left(\Delta K\right)^n \text{ for } \quad \Delta K > \Delta K_{th} \tag{F.124}$$

$$\frac{da}{dN} = 0.0 \quad \text{for} \quad \Delta K \le \Delta K_{th} \tag{F.125}$$

F.5.2.3 Walker Equation

a) The Walker Equation is a simple but significant generalization of the Paris Equation. The Walker Equation has the form:

$$\frac{da}{dN} = C\left(\Delta K_{eff}\right)^n \quad \text{for} \quad \Delta K > \Delta K_{th} \tag{F.126}$$

where,

$$\Delta K_{eff} = \frac{\Delta K}{(1-R)^m} \tag{F.127}$$

$$R = \frac{K_{\min}}{K_{\max}} \tag{F.128}$$

b) The Walker Equation is the same as the Paris Equation except that ΔK is replaced by an effective value, ΔK_{eff}, that is now dependent on the load ratio. Therefore, while the Paris Equation is only dependent on ΔK, the Walker Equation is dependent on both ΔK and R. The appearance of R in the Walker Equation results in larger crack growth rates being predicted for larger values of R, even if ΔK is held constant. This behavior is intuitive and is also supported by experimental data for numerous metals. The effects of ΔK and $K_{\max}$ are more clearly seen by writing ΔK_{eff} in the following way:

$$\Delta K_{eff} = \Delta K^{(1-m)} K_{\max}^{m} \tag{F.129}$$

or

$$\Delta K_{eff} = \left(1-R\right)^{(1-m)} K_{\max} \tag{F.130}$$

c) The parameter m controls the relative importance of ΔK and $K_{\max}$ on ΔK_{eff}, and thus on the crack growth rate. If $m = 0.0$, then $\Delta K_{eff} = \Delta K$ and the Walker Equation simplifies to the Paris Equation. If $m = 1.0$, then the crack growth is dependent only on $K_{\max}$. The parameter m allows the load ratio dependence of the Walker Equation to be adjusted to fit available experimental data. As a result of this additional parameter, the Walker Equation parameters are slightly more difficult to determine than the Paris Equation parameters.

F.5.2.4 Trilinear and Bilinear Equations

a) The Trilinear and Bilinear Equations reflect another approach to generalization of the Paris Equation. The Trilinear Equation is a combination of three Paris Equations as shown below. The value of ΔK to be used is dependent on the specified transition stress intensity factors, $\Delta K_{tran,1}$ and $\Delta K_{tran,2}$. Note that in the Tilinear Equations, different crack growth rates are predicted at $\Delta K_{tran,1}$ and $\Delta K_{tran,2}$.

$$\frac{da}{dN} = C_1 \left(\Delta K\right)^{n_1} \quad for \quad \Delta K_{th} < \Delta K < \Delta K_{tran,1} \tag{F.131}$$

$$\frac{da}{dN} = C_2 \left(\Delta K\right)^{n_2} \quad for \quad \Delta K_{tran,1} < \Delta K < \Delta K_{tran,2} \tag{F.132}$$

$$\frac{da}{dN} = C_3 \left(\Delta K\right)^{n_3} \quad for \quad \Delta K \geq \Delta K_{tran,2} \tag{F.133}$$

b) The Bilinear Equation is a special case of the Trilinear Equation in that only two Paris equation models are used with a single transition stress intensity factor $\Delta K_{tran,1}$.

F.5.2.5 Modified Forman Equation

a) The Modified Forman Equation is a general crack growth model and can be used to represent the state of crack growth across the full regime of crack propagation (see Figure F.8). The form of the Modified Forman Equation is:

$$\frac{da}{dN} = C\left(1-R\right)^{m}\left(\Delta K\right)^{n}\frac{\left[1-\frac{\Delta K_{th}}{\Delta K}\right]^{p}}{\left[1-\frac{K_{\max}}{K_{IC}}\right]^{q}} \qquad \text{(F.134)}$$

b) The Modified Forman Equation is similar to the Walker Equation in that there is a $\left(1-R\right)^{m}$ factor. However, the constant m in the Modified Forman Equation is not the same as in the Walker Equation due to the term appearing in the numerator, and also due to the $\left(1-R\right)^{m}$ term not being raised to the n power. If p and q are set to zero, then this law becomes equivalent to the Walker Equation with

$$m_F = -m_w \cdot n \qquad \text{(F.135)}$$

c) The terms with the p and q exponents allow the law to accurately represent da/dN vs. ΔK data in the low growth rate (threshold) region, in the mid-range region, and in the high growth rate region ($K_{\max}$ approaching K_{IC}) as shown in Figure F.8. The exponents p and q are in the range of zero to unity and are typically equal to each other. With such values, the factor with the p exponent tends to affect the behavior of the law primarily in the threshold region, while the factor with the q exponent tends to affect the behavior primarily near load levels close to K_{IC}. It should be clear that the p and q exponents have no physical significance, the only real basis for their choice is in making the law fit actual crack growth data.

F.5.2.6 NASGRO Equation

a) The NASGRO Equation represents the most general crack growth model, and except for special purpose models, is the one that would best represent the state of the art in fatigue crack growth relationships. This law also incorporates the effects of fatigue crack closure. The form of the NASGRO Equation is:

$$\frac{da}{dN} = C\left[\left(\frac{1-F}{1-R}\right)\Delta K\right]^{n}\frac{\left[1-\frac{\Delta K_{th}}{\Delta K}\right]^{p}}{\left[1-\frac{K_{\max}}{K_{IC}}\right]^{q}} \qquad \text{(F.136)}$$

b) Details regarding the NASGRO Equation can be found in References [108] and [109].

F.5.2.7 Collipriest Equation

a) The Collipriest Equation was an early attempt at addressing the shortcomings of the Paris and Walker Equations in terms of representing behavior in the threshold and large ΔK regions of the da/dN vs. ΔK plot. The Collipriest Equation tries to compensate for the lack of nonlinear behavior of the simpler models without introducing additional parameters and thus has a rather complicated form:

$$\frac{da}{dN} = C\left(\Delta K_{th}\cdot K_{IC}\right)^{\frac{n}{2}}\cdot\exp\left\{\left(\frac{n}{2}\right)\ln\left(\frac{K_{IC}}{\Delta K_{th}}\right)\cdot a\cdot\tanh\left[\frac{\ln\left[\frac{\left(\Delta K\right)^{2}}{\Delta K_{th}\left(1-R\right)K_{IC}}\right]}{\ln\left[\frac{\left(1-R\right)K_{IC}}{\Delta K_{th}}\right]}\right]\right\} \qquad \text{(F.137)}$$

b) The material parameters of the Collipriest law are the same as for the Paris Equation. This does not imply, however, that one can simply substitute Paris Equation parameters into the Collipriest Equation without verifying that the resulting model provides a reasonable representation of actual material behavior.

F.5.3 Fatigue Crack Growth Data

F.5.3.1 Sources for fatigue crack growth data, da/dN, for various materials and service environments are provided in paragraph F.9. When possible, fatigue crack growth data should be evaluated from test results in a similar environment since this can greatly affect the crack growth rate.

F.5.3.2 The fatigue crack growth equations shown below can be used with the Paris Equation (see paragraph F.5.2.2) in FFS assessments (see Reference [106]). These equations are valid for materials with yield strengths less than or equal to $600\ MPa\ (87\ ksi)$.

a) For ferritic and austenitic steels in air or other non-aggressive service environments at temperatures up to 100°C (212°F):

$$\frac{da}{dN} = 1.65\left(10^{-8}\right)\left(\Delta K\right)^{3.0} \quad for \quad \Delta K > \Delta K_{th} \quad \left(mm/cycle,\ MPa\sqrt{m}\right) \tag{F.138}$$

$$\frac{da}{dN} = 8.61\left(10^{-10}\right)\left(\Delta K\right)^{3.0} \quad for \quad \Delta K > \Delta K_{th} \quad \left(in/cycle,\ ksi\sqrt{in}\right) \tag{F.139}$$

b) For ferritic and austenitic steels in air or other non-aggressive service environments at temperatures operating between 100°C (212°F) and 600°C (1112°F) with cyclic frequencies greater than or equal to 1 Hz:

$$\frac{da}{dN} = 1.65\left(10^{-8}\right)\left(\frac{E_{amb}\cdot\Delta K}{E_{at}}\right)^{3.0} \quad for \quad \Delta K > \Delta K_{th} \quad \left(mm/cycle,\ MPa\sqrt{m}\right) \tag{F.140}$$

$$\frac{da}{dN} = 8.61\left(10^{-10}\right)\left(\frac{E_{amb}\cdot\Delta K}{E_{at}}\right)^{3.0} \quad for \quad \Delta K > \Delta K_{th} \quad \left(in/cycle,\ ksi\sqrt{in}\right) \tag{F.141}$$

c) For ferritic steels operating in a marine environment at temperatures up to 20°C (54°F):

$$\frac{da}{dN} = 7.27\left(10^{-8}\right)\left(\Delta K\right)^{3.0} \quad for \quad \Delta K > \Delta K_{th} \quad \left(mm/cycle,\ MPa\sqrt{m}\right) \tag{F.142}$$

$$\frac{da}{dN} = 3.80\left(10^{-9}\right)\left(\Delta K\right)^{3.0} \quad for \quad \Delta K > \Delta K_{th} \quad \left(in/cycle,\ ksi\sqrt{in}\right) \tag{F.143}$$

d) The following threshold stress intensity value can be used with all of these fatigue crack growth equations in this paragraph.

$$\Delta K_{th} = 2.0\ MPa\sqrt{m} \tag{F.144}$$

$$\Delta K_{th} = 1.8\ ksi\sqrt{in} \tag{F.145}$$

F.5.3.3 The fatigue crack growth equations shown below can be used with the Paris Equation (see paragraph F.5.2.2) in *FFS* assessments (see Reference [104]). These parameters correspond to upper bound crack growth data.

a) For martensitic steels with a yield strength from 552 MPa (80 ksi) to 2068 MPa (300 ksi) at room temperature in air or an other non-aggressive environments:

$$\frac{da}{dN} = 1.36\left(10^{-7}\right)\left(\Delta K\right)^{2.25} \quad for \quad \Delta K > \Delta K_{th} \quad \left(mm/cycle,\ MPa\sqrt{m}\right) \tag{F.146}$$

$$\frac{da}{dN} = 6.60\left(10^{-9}\right)\left(\Delta K\right)^{2.25} \quad for \quad \Delta K > \Delta K_{th} \quad \left(in/cycle,\ ksi\sqrt{in}\right) \tag{F.147}$$

b) For ferritic-pearlite steels at room temperature in air or an other non-aggressive environments:

$$\frac{da}{dN} = 6.89\left(10^{-9}\right)\left(\Delta K\right)^{3.0} \quad for \quad \Delta K > \Delta K_{th} \quad \left(mm/cycle,\ MPa\sqrt{m}\right) \tag{F.148}$$

$$\frac{da}{dN} = 3.60\left(10^{-10}\right)\left(\Delta K\right)^{3.0} \quad for \quad \Delta K > \Delta K_{th} \quad \left(in/cycle,\ ksi\sqrt{in}\right) \tag{F.149}$$

c) For austenitic stainless steels at room temperature in air or an other non-aggressive environments:

$$\frac{da}{dN} = 5.61\left(10^{-9}\right)\left(\Delta K\right)^{3.25} \quad for \quad \Delta K > \Delta K_{th} \quad \left(mm/cycle,\ MPa\sqrt{m}\right) \tag{F.150}$$

$$\frac{da}{dN} = 3.00\left(10^{-10}\right)\left(\Delta K\right)^{3.25} \quad for \quad \Delta K > \Delta K_{th} \quad \left(in/cycle,\ ksi\sqrt{in}\right) \tag{F.151}$$

d) The following threshold stress intensity values can be used with all of the fatigue crack growth equations in this paragraph.

$$\Delta K_{th} = 7\left(1 - 0.85R\right) \quad \left(MPa\sqrt{m}\right) \tag{F.152}$$

$$\Delta K_{th} = 6.37\left(1 - 0.85R\right) \quad \left(ksi\sqrt{in}\right) \tag{F.153}$$

F.5.3.4 The fatigue crack growth equations shown below can be used with the Paris Equation (see paragraph F.5.2.2) in *FFS* assessments (see Reference [104]). These equations are based on data determined from crack propagation testing of as-welded joints.

a) A safe design curve based on a 99% confidence interval of test results is defined by the following equations.

$$\frac{da}{dN} = 2.60\left(10^{-8}\right)\left(\Delta K\right)^{2.75} \quad for \quad \Delta K > \Delta K_{th} \quad \left(mm/cycle,\ MPa\sqrt{m}\right) \tag{F.154}$$

$$\frac{da}{dN} = 1.33\left(10^{-9}\right)\left(\Delta K\right)^{2.75} \quad for \quad \Delta K > \Delta K_{th} \quad \left(in/cycle,\ ksi\sqrt{in}\right) \tag{F.155}$$

$$\Delta K_{th} = 2.0 \quad \left(MPa\sqrt{m}\right) \tag{F.156}$$

$$\Delta K_{th} = 1.82 \qquad \left(ksi\sqrt{in}\right) \qquad \text{(F.157)}$$

b) A mean curve applicable to *Fitness-For-Service* assessments is defined by the following equations.

$$\frac{da}{dN} = 1.45\left(10^{-8}\right)\left(\Delta K\right)^{2.75} \qquad for \qquad \Delta K > \Delta K_{th} \qquad \left(mm/cycle,\ MPa\sqrt{m}\right) \qquad \text{(F.158)}$$

$$\frac{da}{dN} = 7.40\left(10^{-10}\right)\left(\Delta K\right)^{2.75} \qquad for \qquad \Delta K > \Delta K_{th} \qquad \left(in/cycle,\ ksi\sqrt{in}\right) \qquad \text{(F.159)}$$

$$\Delta K_{th} = 2.45 \qquad \left(MPa\sqrt{m}\right) \qquad \text{(F.160)}$$

$$\Delta K_{th} = 2.23 \qquad \left(ksi\sqrt{in}\right) \qquad \text{(F.161)}$$

F.5.3.5 Fatigue crack growth parameters for use with the Bilinear Equation (see paragraph F.5.2.4) are provided below.

a) Fatigue crack growth parameters are provided in Table F.12 for different materials and service environments.

b) The fatigue crack growth equations shown below can be used for pipeline steels (e.g. API 5L) at ambient temperatures in crude oil service (see Reference [111]).

$$\left.\frac{da}{dN}\right|_l = C_l\left(\Delta K + BR\right)^{n_l} \qquad for \qquad \Delta K_{th} < \Delta K < \Delta K_{tran} \qquad \left(mm/cycle,\ MPa\sqrt{m}\right) \qquad \text{(F.162)}$$

$$\left.\frac{da}{dN}\right|_u = C_u\left(\Delta K + BR\right)^{n_u} \qquad for \qquad \Delta K \geq \Delta K_{tran} \qquad \left(mm/cycle,\ MPa\sqrt{m}\right) \qquad \text{(F.163)}$$

1) The parameter B is given by Equation (F.164) and ΔK_{tran} can be computed using Equation (F.165).

$$B = 4.0 \qquad \text{(F.164)}$$

$$\Delta K_{tran} = \left(\frac{C_l}{C_u}\right)^{\left(\frac{1}{n_u - n_l}\right)} \qquad \text{(F.165)}$$

2) The following parameters can be used for sour crude oil (with H_2S). In Equations (F.166) and (F.168) the parameter C_{H_2S} is the concentration of H_2S in ppm.

$$C_l = 7.12\left(10^{-16}\right)\cdot C_{H_2S} + 3.40\left(10^{-13}\right) \qquad \text{(F.166)}$$

$$n_l = 6.40 \qquad \text{(F.167)}$$

$$C_u = 2.50\left(10^{-11}\right)\cdot C_{H_2S} + 1.48\left(10^{-7}\right) \qquad \text{(F.168)}$$

$$n_u = 2.72 \qquad \text{(F.169)}$$

$$\Delta K_{th} = 6\ MPa\sqrt{m} \tag{F.170}$$

3) The following parameters can be used for sweet crude oil (without H_2S):

$$C_l = 1.48\left(10^{-11}\right) \tag{F.171}$$

$$n_l = 4.80 \tag{F.172}$$

$$C_u = 4.00\left(10^{-7}\right) \tag{F.173}$$

$$n_u = 1.90 \tag{F.174}$$

$$\Delta K_{th} = 8\ MPa\sqrt{m} \tag{F.175}$$

F.5.3.6 Fatigue crack growth parameters for use with the NASGRO Equation (see paragraph F.5.2.6) are given in reference [108] for different materials and service environments.

F.5.3.7 ASME Section XI Ferritic Steel Air and Light Water Reactor Equations

a) The fatigue crack growth rate of the material is characterized using Equation (F.176). The material parameters should be based on flaw growth data obtained from specimens of the same material specification and product form, or suitable alternative. Material variability, environment, test frequency, mean stress and other variables that affect the data should be considered.

$$\frac{da}{dN} = C\left(\Delta K\right)^n \qquad for \qquad \Delta K > \Delta K_{th} \qquad \left(in/cycle,\ ksi\sqrt{in}\right) \tag{F.176}$$

b) Air Environment – In the absence of material specific data, the following coefficients may be used.

1) The parameters n and C in Equation (F.176) are given by

$$n = 3.07 \tag{F.177}$$

$$C = 1.99\left(10^{-10}\right)S \tag{F.178}$$

2) If $0 \le R \le 1$, then the parameter S in Equation (F.178) is given by Equation (F.179), and ΔK in Equation (F.176) is given by Equation (F.180).

$$S = 25.72\left(2.88 - R\right)^{-3.07} \tag{F.179}$$

$$\Delta K = K_{\max} - K_{\min} \tag{F.180}$$

3) $R < 0$, then the parameter S in Equation (F.178) is given by Equation (F.181), and ΔK in Equation (F.176) is given by Equations (F.182), (F.183), and (F.184), as applicable. The flow stress, σ_f, in these equations is given by Equation (F.5).

$$S = 1.0 \tag{F.181}$$

$$\Delta K = K_{\max} \qquad for\ -2 \le R < 0\ \ and\ \ \left(K_{\max} - K_{\min}\right) \le 1.12\sigma_f\sqrt{\pi a} \tag{F.182}$$

$$\Delta K = \frac{(1-R)K_{\max}}{3} \qquad for \;\; R < -2 \;\; and \;\; (K_{\max} - K_{\min}) \le 1.12\sigma_f\sqrt{\pi a} \tag{F.183}$$

$$\Delta K = K_{\max} - K_{\min} \qquad for \;\; R < 0 \;\; and \;\; (K_{\max} - K_{\min}) > 1.12\sigma_f\sqrt{\pi a} \tag{F.184}$$

c) Light Water Reactor Environments – In the absence of material specific data, the following coefficients may be used.

1) The parameter ΔK in Equation (F.176) is given by Equation (F.180).

2) The parameters n and C in Equation (F.176) are given by whichever results in the highest fatigue crack growth rate:

- n and C evaluated in accordance with paragraph F.5.3.7.b, or
- n and C evaluated using the method shown below. In evaluating n and C_0 using this method, if $K_{\min} \le 0$, then use $R = 0$.

i) If $\Delta K_{th} < \Delta K < \Delta K_{trans}$, then:

$$n = 5.95 \tag{F.185}$$

$$C = 1.02\left(10^{-12}\right)S \tag{F.186}$$

$$S = 1.0 \qquad for \qquad 0 \le R \le 0.25 \tag{F.187}$$

$$S = 26.9R - 5.725 \qquad for \qquad 0.25 < R \le 0.65 \tag{F.188}$$

$$S = 11.76 \qquad for \qquad 0.65 < R \le 1.0 \tag{F.189}$$

ii) If $\Delta K \ge \Delta K_{trans}$, then:

$$n = 1.95 \tag{F.190}$$

$$C = 1.01\left(10^{-7}\right)S \tag{F.191}$$

$$S = 1.0 \qquad for \qquad 0 \le R \le 0.25 \tag{F.192}$$

$$S = 3.75R + 0.06 \qquad for \qquad 0.25 < R \le 0.65 \tag{F.193}$$

$$S = 2.5 \qquad for \qquad 0.65 < R \le 1.0 \tag{F.194}$$

iii) The parameter ΔK_{trans} above is given by the following equations.

$$\Delta K_{trans} = 17.74 \qquad for \qquad 0 \le R \le 0.25 \tag{F.195}$$

$$\Delta K_{trans} = 17.74\left(\frac{3.75R + 0.06}{26.9R - 5.725}\right)^{0.25} \qquad for \qquad 0.25 < R < 0.65 \tag{F.196}$$

$$\Delta K_{trans} = 12.04 \qquad for \qquad 0.65 \le R \le 1.0 \qquad \text{(F.197)}$$

d) The following threshold stress intensity values can be used for both air and light water reactor environments.

$$\Delta K_{th} = 5 \qquad for\ R < 0 \qquad \left(ksi\sqrt{in}\right) \qquad \text{(F.198)}$$

$$\Delta K_{th} = 5\left(1 - 0.8R\right) \qquad for\ R \ge 0 \qquad \left(ksi\sqrt{in}\right) \qquad \text{(F.199)}$$

F.5.3.8 ASME Section XI Austenitic Stainless Steel Equations For In Air & Water Environments

a) The fatigue crack growth rate of the material is characterized using Equation (F.176). The material parameters should be based on flaw growth data obtained from specimens of the same material specification and product form, or suitable alternative. Material variability, environment, test frequency, mean stress and other variables that affect the data should be considered.

b) Air Environment – In the absence of material specific data, the following coefficients may be used. The parameters n and C in Equation (F.176) are given by the equations shown below. These are valid for temperatures of 427ºC (800ºF) and less.

$$n = 3.3 \qquad \text{(F.200)}$$

$$C = S \cdot 10^{X} \qquad \text{(F.201)}$$

$$X = -10.009 + 8.12(10)^{-4} T_F - 1.13(10)^{-6} T_F^2 + 1.02(10)^{-9} T_F^3 \qquad \text{(F.202)}$$

$$S = 1.0 \qquad for \qquad R \le 0 \qquad \text{(F.203)}$$

$$S = 1.8R + 1.0 \qquad for \qquad 0.0 < R \le 0.79 \qquad \text{(F.204)}$$

$$S = 57.97R - 43.35 \qquad for \qquad 0.79 < R \le 1.0 \qquad \text{(F.205)}$$

c) Light Water Reactor Environments – The fatigue crack growth rates are currently under development.

d) The threshold stress intensity values that can be used for both air and light water reactor environments are given in paragraph F.5.3.7.d.

F.5.4 Stress Corrosion Crack Growth Equations

F.5.4.1 Within the LEFM methodology, a Stress Corrosion Crack (SCC) growth law can be experimentally determined which relates the crack growth rate to the stress intensity factor (K), the material, service environment, and time. This crack growth model can subsequently be used to characterize the crack growth behavior in equipment under a similar combination of stress, material, and service environment to that used in the experiment.

F.5.4.2 An overview of stress corrosion crack growth models is provided in references [7], [26], and [101]. Examples of SCC crack growth models that have been used are shown below.

a) The following three equations have been used to model SCC. In Equation (F.206), the crack growth is a function of the stress intensity factor and associated constants, in Equation (F.207) the crack growth is a function of time and associated constants, and in Equation (F.208) the crack growth rate is a constant and independent of the stress intensity factor and time.

$$\frac{da}{dt} = D_1 \left(K\right)^{n_1} \qquad for \qquad K_{th} \le K \le K_{IC} \tag{F.206}$$

$$\frac{da}{dt} = D_2 \left(t\right)^{n_2} \qquad for \qquad K_{th} \le K \le K_{IC} \tag{F.207}$$

$$\frac{da}{dt} = D_3 \qquad for \qquad K_{th} \le K \le K_{IC} \tag{F.208}$$

b) The following equation is a typical crack growth model for HAC.

$$\frac{da}{dt} = D\left(K\right)^{n} \qquad for \qquad K_{th} \le K \le K_{IC-H} \tag{F.209}$$

F.5.5 Stress Corrosion Crack Growth Data

F.5.5.1 Sources for stress corrosion crack growth data $\left(da/dt\right)$ for various materials are provided in paragraph F.9. When possible, stress corrosion crack growth data should be evaluated from test results in a similar environment. An overview of crack growth mechanisms and rates for several cracking mechanisms commonly observed in materials utilized for petroleum refinery applications is included in reference [101].

F.5.5.2 An upper bound solution for a hydrogen assisted crack growth rate in 2.25Cr-0.5Mo and the associated threshold stress intensity factor is shown below. The tests for the data were conducted in a 500 ppm H_2S solution.

$$\frac{da}{dt} = 2.4\left(10^{-24}\right)\left(K\right)^{11.7} \qquad for \qquad K_{th} \le K \le K_{IC-H} \qquad \left(mm/hour\,,\, MPa\sqrt{m}\right) \tag{F.210}$$

$$K_{th} = 0.0014 \cdot FATT^2 - 0.421 \cdot FATT + 57.0 \qquad \left(MPa\sqrt{m}\right) \tag{F.211}$$

$$\frac{da}{dt} = 2.85\left(10^{-25}\right)\left(K\right)^{11.7} \qquad for \qquad K_{th} \le K \le K_{IC-H} \qquad \left(in/hour\,,\, ksi\sqrt{in}\right) \tag{F.212}$$

$$K_{th} = \frac{0.0014 \cdot FATT^2 - 0.421 \cdot FATT + 57.0}{1.0988} \qquad \left(ksi\sqrt{in}\right) \tag{F.213}$$

F.6 Fatigue Curves

F.6.1 General

F.6.1.1 Fatigue curves are required to evaluate the remaining life of a component subject to cyclic loading conditions. Crack growth for identified or postulated cracks is analyzed using a fracture mechanics analysis.

F.6.1.2 Most of the fatigue curves for crack initiation reported in the literature are based on testing in air at room temperature. There is evidence that these curves may be affected by the environment; an aggressive environment may result in a lowering of the number of cycles to failure. Therefore, if a fatigue curve in the appropriate environment to that which the component is subjected to is available, it should be utilized in the assessment. If a fatigue curve is not available, consideration should be given to the detrimental effects of the environment with regard to fatigue life.

F.6.1.3 Fatigue curves are typically presented in two forms; fatigue curves that are based on smooth bar test specimens and fatigue curves that are based on test specimens that include weld details. In general, the former curves are recommended when the point being evaluated is not at a weld joint, and the latter are recommended when there is a weld joint at the point being evaluated.

F.6.2 Smooth Bar Fatigue Curves

F.6.2.1 For temperatures below the creep range, the allowable number of cycles is provided for the materials shown below in terms of a polynomial function. These fatigue curves are from the ASME B&PV Code, Section VIII, Division 2.

a) Materials – The constants, C_n, to use in Equation (F.215) are provided for different fatigue curves as described below.

1) Carbon, Low Alloy, Series 4xx, and High Tensile Strength Steels for temperatures not exceeding 371°C (700°F) where $\sigma_{uts} \le 552\ MPa\ (80\ ksi)$ (see Table F.13).

2) Carbon, Low Alloy Series 4xx, and High Tensile Strength Steels for temperatures not exceeding 371°C (700°F) where $\sigma_{uts} = 793 - 892\ MPa\ (115 - 130\ ksi)$ (see Table F.14)

3) Series 3xx High Alloy Steels, Nickel-Chromium-Iron Alloy, Nickel-Iron-Chromium Alloy, and Nickel-Copper Alloy for temperatures not exceeding 427°C (800°F) where $S_a > 195\ MPa\ (28.2\ ksi)$ (see Table F.15)

4) Series 3xx High Alloy Steels, Nickel-Chromium-Iron Alloy, Nickel-Iron-Chromium Alloy, and Nickel-Copper Alloy for temperatures not exceeding 427°C (800°F) where $S_a \le 195\ MPa\ (28.2\ ksi)$ (see Table F.16)

5) Wrought 70-30 Copper-Nickel for temperatures not exceeding 232°C (450°F) (see Tables F.17, F.18, and F.19). These data are applicable only for materials with minimum specified yield strength as shown. These data may be interpolated for intermediate values of minimum specified yield strength.

6) Nickel-Chromium-Molybdenum-Iron, Alloys X, G, C-4, And C-276 for temperatures not exceeding 427°C (800°F) (see Table F.20)

7) High strength bolting for temperatures not exceeding 371°C (700°F) (see Table F.21)

b) For temperatures not in the creep range, the allowable number of cycles, N, can be computed from Equation (F.214) or Table F.22 based on the stress amplitude, S_a, in units of ksi or MPa. Methods for computing S_a are covered in Annex B1, paragraph B1.5.

$$N = 10^X \cdot \left(\frac{E_T}{E_{FC}} \right) \qquad \text{(F.214)}$$

where

$$X = \frac{C_1 + C_3\left(\frac{S_a}{C_{us}}\right) + C_5\left(\frac{S_a}{C_{us}}\right)^2 + C_7\left(\frac{S_a}{C_{us}}\right)^3 + C_9\left(\frac{S_a}{C_{us}}\right)^4 + C_{11}\left(\frac{S_a}{C_{us}}\right)^5}{1 + C_2\left(\frac{S_a}{C_{us}}\right) + C_4\left(\frac{S_a}{C_{us}}\right)^2 + C_6\left(\frac{S_a}{C_{us}}\right)^3 + C_8\left(\frac{S_a}{C_{us}}\right)^4 + C_{10}\left(\frac{S_a}{C_{us}}\right)^5} \qquad \text{(F.215)}$$

F.6.2.2 For temperatures in the creep range, the allowable number of cycles is provided for the materials shown below in terms of a polynomial function.

a) Materials – The constants, C_n, to use in Equation (F.217) are provided for different fatigue curves as described below.

1) Type 304 SS (see Table F.23)
2) Type 316 SS (see Table F.24)
3) Alloy 800H (see Table F.25)
4) 2.25Cr-1Mo (see Table F.26)
5) 9Cr-1Mo (see Table F.27)

b) The allowable number of cycles, N, can be computed from Equation (F.216) or Table F.28 based on the strain range, ε_r. Methods for computing ε_r are covered in Annex B1, paragraph B1.5.

$$N = 10^X \tag{F.216}$$

where

$$X = \frac{C_1 + C_3(\varepsilon_r) + C_5(\varepsilon_r)^2 + C_7(\varepsilon_r)^3 + C_9(\varepsilon_r)^4}{1 + C_2(\varepsilon_r) + C_4(\varepsilon_r)^2 + C_6(\varepsilon_r)^3 + C_8(\varepsilon_r)^4} \tag{F.217}$$

F.6.3 Welded Joint Fatigue Curves

F.6.3.1 The welded joint fatigue curves can be used to evaluate welded joints for the following materials and associated temperature limits.

a) Carbon, Low Alloy, Series 4xx, and High Tensile Strength Steels for temperatures not exceeding 371°C (700°F)

b) Series 3xx High Alloy Steels, Nickel-Chromium-Iron Alloy, Nickel-Iron-Chromium Alloy, and Nickel-Copper Alloy for temperatures not exceeding 427°C (800°F)

c) Wrought 70 Copper-Nickel for temperatures not exceeding 232°C (450°F)

d) Nickel-Chromium-Molybdenum-Iron, Alloys X, G, C-4, And C-276 for temperatures not exceeding 427°C (800°F)

e) Aluminum Alloys

F.6.3.2 The allowable number of cycles for the welded joint fatigue curve shall be computed as follows.

a) The number of allowable cycles, N, can be computed from Equation (F.218) based on the equivalent structural stress range parameter, ΔS_{range}. Methods for computing ΔS_{range} are covered in Annex B1, paragraph B1.5. The constants C and h for use in Equation (F.218) are provided in Table F.29.

$$N = \frac{f_I}{f_E}\left(\frac{f_{MT} \cdot C}{\Delta S_{range}}\right)^{\frac{1}{h}} \tag{F.218}$$

b) If a fatigue improvement method is performed, then a fatigue improvement factor, f_I, may be applied. The fatigue improvement factors shown below may be used.

1) For burr grinding in accordance with Figures F.12 and F.13

$$f_I = 1.0 + 2.5 \cdot (10)^q \tag{F.219}$$

2) For TIG dressing

$$f_I = 1.0 + 2.5 \cdot (10)^q \tag{F.220}$$

3) For hammer peening

$$f_I = 1.0 + 4.0 \cdot (10)^q \tag{F.221}$$

4) In the above equations, the parameter q is given by Equation (F.222).

$$q = -0.0016 \cdot \left(\Delta S_{range} \cdot C_{usm} \right)^{1.6} \tag{F.222}$$

c) The allowable number of fatigue cycles given by Equation (F.218) may be modified to account for the effects of environment other than ambient air that may cause corrosion or sub-critical crack propagation. The modification factor, f_E, is typically a function of the fluid environment, loading frequency, temperature, and material variables such as grain size and chemical composition. If information on the environmental factor is not available, then $f_E = 4.0$ shall be used if the environment is mildly aggressive. If aggressive corrosion is anticipated, a higher factor should be used.

d) A temperature adjustment is required to the fatigue curve for materials other than carbon steel and/or temperatures above 21°C (70°F). The temperature adjustment factor is given by Equation (F.223).

$$f_{MT} = \frac{E_{ACS}}{E_T} \tag{F.223}$$

F.7 Material Data for Creep Analysis

F.7.1 Creep Rupture Time

F.7.1.1 MPC Project Omega Data

a) The assessment techniques developed under the MPC Project Omega program provide a methodology for estimating the remaining life of a component operating at high temperature that has been extensively used in the refining and petrochemical industry. The MPC Project Omega Method is a public domain assessment procedure with a proven record and associated property relations covering a wide range of materials used in the refining and petrochemical industry. In this methodology, a strain-rate parameter and multi-axial damage parameter (Omega) are used to predict the rate of strain accumulation, creep damage accumulation, and remaining time to failure as a function of stress state and temperature.

b) The remaining life of a component, L, for a given stress state and temperature can be computed using the following equations. In these equations, stress is in units of ksi, temperature is in degrees Fahrenheit, and the remaining life and time are in hours.

$$L = \frac{1}{\dot{\varepsilon}_{co} \Omega_m} \tag{F.224}$$

where

$$\log_{10} \dot{\varepsilon}_{co} = -\left\{ \left(A_o + \Delta_\Omega^{sr} \right) + \left(\frac{1}{460 + T} \right) \left(A_1 + A_2 S_l + A_3 S_l^2 + A_4 S_l^3 \right) \right\} \tag{F.225}$$

$$\Omega_m = \Omega_n^{\delta_\Omega + 1} + \alpha_\Omega n_{BN} \tag{F.226}$$

$$\Omega_n = \max\left[\left(\Omega - n_{BN}\right),\ 3.0\right] \tag{F.227}$$

$$\log_{10}\Omega = \left(B_o + \Delta_{\Omega}^{cd}\right) + \left(\frac{1}{460+T}\right)\left(B_1 + B_2 S_l + B_3 S_l^2 + B_4 S_l^3\right) \tag{F.228}$$

$$\delta_{\Omega} = \beta_{\Omega}\left(\frac{\sigma_1+\sigma_2+\sigma_3}{\sigma_e} - 1.0\right) \tag{F.229}$$

$$n_{BN} = -\left\{\left(\frac{1}{460+T}\right)\left(A_2 + 2A_3 S_l + 3A_4 S_l^2\right)\right\} \tag{F.230}$$

$$S_l = \log_{10}\left(\sigma_e\right) \tag{F.231}$$

$$\sigma_e = \frac{1}{\sqrt{2}}\left[\left(\sigma_1-\sigma_2\right)^2 + \left(\sigma_1-\sigma_3\right)^2 + \left(\sigma_2-\sigma_3\right)^2\right]^{1/2} \tag{F.232}$$

c) The coefficients for Equations (F.225), (F.230), and (F.228) for different materials are provided in Table F.30.

d) The MPC Project Omega Model for creep currently does not include the effects of primary creep. The effects of primary creep may be important depending on the material, magnitude of applied stress, and exposure temperature. The effects of primary creep may be taken as negligible when the stress from the applied load is less than or equal to 50% of the minimum yield strength at the assessment temperature.

F.7.1.2 API STD 530 Data

a) Creep rupture data may be required to evaluate the remaining life of a component operating at a high temperature. Minimum and average creep rupture data are typically expressed in terms of the Larson-Miller parameter that combines the time to rupture and temperature into a single variable. The Larson-Miller parameter and the time to rupture are computed using Equations (F.233) and (F.234).

$$LMP(\sigma) = \left(T+460\right)\left(C_{LMP} + \mathrm{Log}_{10}\left[L\right]\right)10^{-3} \tag{F.233}$$

$$\log_{10} L = \frac{1000 \cdot LMP(\sigma)}{\left(T+460\right)} - C_{LMP} \tag{F.234}$$

b) The Larson-Miller parameter as a function of stress, $LMP(\sigma)$, which appears in Equations (F.233) and (F.234), for different materials are provided in Table F.31.

F.7.2 Tangent and Secant Modulus

The secant modulus and the tangent modulus can be determined using the MPC Project Omega data. The secant modulus, E_s, and tangent modulus, E_t, can be determined using Equations (F.235) and (F.236), respectively. The parameters for these equations are defined in paragraph F.7.1.1.

$$E_s = \frac{\sigma}{\dfrac{\sigma}{E_y} + \varepsilon_c} \tag{F.235}$$

$$E_t = \left\{\frac{\partial \varepsilon_c}{\partial \sigma}\right\}^{-1} = \left\{\frac{\partial}{\partial \sigma}\left(-\frac{1}{\Omega}\ln\left[1-\dot{\varepsilon}_{co}\Omega t\right]\right)\right\}^{-1} \quad \text{(F.236)}$$

with

$$\varepsilon_c = -\frac{1}{\Omega}\ln\left[1-\dot{\varepsilon}_{co}\Omega t\right] \quad \text{(F.237)}$$

F.7.3 Creep Strain-Rate Data

a) The creep strain rate can be determined using the MPC Project Omega data. The parameters for this equation are defined in paragraph F.7.1.1.

$$\dot{\varepsilon}_c = \dot{\varepsilon}_{co}\exp\left[\Omega_m \varepsilon_c\right] \quad \text{(F.238)}$$

b) Other sources for creep strain rate data are provided in paragraph F.9.

F.7.4 Isochronous Stress-Strain Curves

F.7.4.1 Isochronous stress-strain curves may be calculated using Equation (F.239) obtained by solving the MPC Project Omega expressions in paragraph F.7.1. Since Ω and $\dot{\varepsilon}_{co}$ are functions of the stress and temperature, specification of a time of interest yields a closed form equation for an isochronous stress-strain curve, or

$$\varepsilon_t = \frac{\sigma}{E_y} - \frac{1}{\Omega}\ln\left[1-\dot{\varepsilon}_{co}\Omega t\right] \quad \text{(F.239)}$$

F.7.4.2 Other sources for isochronous stress-strain curves for various materials for components operating at high temperatures are provided in paragraph F.9. Isochronous stress-strain curves may be required to evaluate the remaining life of a component operating at high temperature. These curves are particularly useful in evaluating the creep buckling potential of a component.

F.7.5 Creep Regime Fatigue Curves (Crack Initiation)

Sources for fatigue curves (crack initiation) for various materials for components operating in the creep regime are provided in paragraph F.9.

F.7.6 Creep Crack Growth Data

F.7.6.1 Crack growth data may be required to evaluate the remaining life of a component operating at high temperature containing a crack. The creep crack growth rate can be correlated to the creep fracture mechanics parameter C^* using Equation (F.240). The parameters C_t or $C(t)$ can also be used in this equation.

$$\frac{da}{dt} = D_{cc}(C^*)^{n_{cc}} \quad \text{(F.240)}$$

F.7.6.2 If the crack driving force is in terms of C^*, then Equations (F.241), (F.242), and (F.243) can be used to estimate the crack growth for a wide range of materials where da/dt is in m/hour, C^* is in MPa-m/hour, and ε_f^* is in percentage strain (see Nuclear Electric R-5, Part 1, Table 1.1).

$$\frac{da}{dt} = \frac{0.3\left(C^*\right)^{0.85}}{\varepsilon_f^*} \qquad (plane\ stress) \qquad \text{(F.241)}$$

$$\frac{da}{dt} = \frac{0.03\left(C^*\right)^{0.85}}{\varepsilon_{fLB}^*} \qquad (plane\ stress - Lower\ Bound\ Data) \qquad \text{(F.242)}$$

$$\frac{da}{dt} = \frac{15\left(C^*\right)^{0.85}}{\varepsilon_f^*} \qquad (plane\ strain) \qquad \text{(F.243)}$$

F.7.6.3 Equation (F.241) has been used for remaining life assessment for high temperature components. However, the fracture strain in this model can be difficult to estimate for an in-service component where only limited materials data are available. In addition, the model does not provide a means to consider prior and ongoing damage in the material where the crack will grow. Another creep crack growth relationship, based on MPC Project Omega Methodology that has been used is shown in Equation (F.244). The parameters and use of this equation are fully described in Part 10.

$$\frac{da}{dt} = \frac{\Omega}{500}\left(C_t\right)^{\frac{n_{BN}}{n_{BN}+1}} \qquad \text{(F.244)}$$

F.7.6.4 Data sources for creep crack growth data for C^* and other measures of the crack driving force, C_t or $C(t)$, are provided in paragraph F.9.

F.8 Nomenclature

A	constant in the weld joint fatigue curve equation.
A_{CV}	hyperbolic tangent curve fit coefficient for CVN Transition Range.
A_f	fatigue data constant dependent on the weld class.
A_1	curve fitting constant for the stress-strain curve.
A_2	curve fitting constant for the stress-strain curve.
$A_0 \rightarrow A_5$	curve-fit coefficients for the Yield strength data, the MPC Project Omega creep strain rate parameter, or the Larson Miller Parameter, as applicable.
a	current crack size (mm:in).
α_Ω	parameter based on the state-of-stress for MPC Project Omega Life Assessment Model. = 3.0 – pressurized sphere or formed head, = 2.0 – pressurized cylinder or cone, = 1.0 – for all other components and stress states.
B	exponent in the weld joint fatigue curve equation, or a cyclic crack growth model constant, as applicable.
B_{CV}	hyperbolic tangent curve fit coefficient for CVN Transition Range.
B_l	material parameter for crack growth model, equal to 4 for pipeline steels (API 5L, Grade X60).
$B_0 \rightarrow B_5$	coefficients in K_{mat}^{mean} to K_I relationship or the MPC Project Omega parameter, as applicable.
β_Ω	Prager factor equal to 0.33, for MPC Project Omega Life Assessment Model.
C	material parameter for fracture toughness, crack growth modeling, or the constant for the Master Fatigue Curve, as applicable.

C^* crack driving force associated with global steady-state creep.

C_A & C_B parameters for estimating the impact energy of subsize Charpy specimens.

C_{CV} hyperbolic tangent curve fit coefficient for CVN Transition Range.

C_{H_2S} H_2S concentration in ppm.

C_{LMP} Larson Miller Constant.

C_l material parameter.

C_n equation constants used to represent the smooth bar fatigue curves.

C_{us} conversion factor, $C_{us} = 1.0$ for units of stress in ksi and $C_{us} = 6.894757$ for units of stress in MPa.

C_{usm} conversion factor, $C_{usm} = 1.0$ for units of stress in MPa and $C_{usm} = 6.894757$ for units of stress in ksi.

C_T coefficient of a material model used in a tearing analysis

C_t crack driving force related to the expansion of the creep zone.

$C(t)$ crack driving force related to the expansion of the creep zone.

C_{tu} constant for units conversion, $C_{tu} = 25.4$ if the thickness is expressed in inches and $C_{tu} = 1.0$ if the thickness is expressed in mm.

C_u material parameter.

$C_0 \rightarrow C_4$ material coefficients for the MPC yield strength, ultimate tensile strength data, or constants in the bilinear or trilinear crack growth equation, as applicable.

CVN Charpy V-notch impact value.

CVN_{ss} Charpy impact energy at the test temperature for the sub-size specimen.

CVN_{US} Charpy upper shelf impact energy for the sub-size specimen.

CVN_{std} corrected Charpy impact energy for a standard size CVN specimen.

D stresss corrosion crack growth coefficient.

$D_1 \rightarrow D_4$ material parameters for bi-linear stress corrosion crack growth model or coefficients used in the tangent modulus calculation, as applicable.

D_c creep damage computed based on the loading history.

D_{cc} coefficient of the creep crack growth equation.

D_{ac} local creep damage after the crack initiates, the damage is computed using the reference stress (see Annex D) considering the post-crack loading history.

D_{bc} local creep damage before the initiation of the crack, the damage is computed using the net section stress considering the pre-crack loading history.

D_{ca} allowable creep damage usually taken as 1.0.

D_{CV} hyperbolic tangent curve fit coefficient for CVN transition range.

Δ_{Ω}^{cd} adjustment factor for creep ductility in the Project Omega Model, a range of $+0.3$ for brittle behavior and -0.3 for ductile behavior can be used.

Δ_{Ω}^{sr} adjustment factor for creep strain rate to account for the material scatter band in the Project Omega Model, a range of -0.5 for the bottom of the scatter band to $+0.5$ for the top of the scatter band can be used.

ΔS_{range} computed equivalent structural stress range parameter from Annex B1.

ΔT_s temperature shift for dynamic to static fracture toughness prediction.

$\frac{da}{dt}$ crack growth rate.

$\frac{da}{dN}$ increment of crack growth for a given cycle.

δ_{Ω} damage parameter exponent for MPC Project Omega Life Assessment Model.

δ_{crit} critical CTOD value.

E_{amb} Young's modulus at ambient temperature.

E_{at} Young's modulus at the assessment temperature.

E_s secant Modulus.

E_t tangent Modulus.

E_y Young's Modulus at the temperature of interest.

E_{yc} Young's Modulus evaluated at the mean temperature of the cycle.

E_{ACS} modulus of elasticity of carbon steel at ambient temperature or 21°C (70°F).

E_{FC} modulus of elasticity used to establish the design fatigue curve

E_T modulus of elasticity of the material under evaluation at the average temperature of the cycle being evaluated.

ε_c creep strain at the end of the time period being evaluated.

$\dot{\varepsilon}_c$ creep strain rate.

ε_{es} engineering strain.

ε_p 0. 2% engineering offset strain for the proportional limit, other values may be used.

ε_{pa} true plastic strain amplitude.

ε_r strain range.

ε_t total strain; elastic, elastic plus plastic, elastic plus creep, elastic plus plastic plus creep, as applicable.

ε_{ta} true total strain amplitude.

ε_{tr} true total strain range.

ε_{ys} 0.2% engineering offset strain.

ε_{ts} true strain.

ε_1 true plastic strain in the micro-strain region of the stress-strain curve.

ε_2 true plastic strain in the macro-strain region of the stress-strain curve.

$\dot{\varepsilon}$ loading strain rate

$\dot{\varepsilon}_{co}$ initial creep strain rate at the start of the time period being evaluated based on the stress state and temperature.

$\dot{\varepsilon}_{ref}$ creep strain rate, $\dot{\varepsilon}_{co}$, evaluated at the reference stress (see paragraph F.7.6.3).

ε_f^* creep ductility based on the state of stress at the crack tip, may be taken to be equal to the uniaxial creep ductility at the reference stress.

ε_{fLB}^* lower bound value for ε_f^*.

F_{mc} cumulative probability for Master Curve.

$FATT$ fracture appearance transition temperature (see paragraph F.4.7.3), note that the temperature is in centigrade for this correlation.

F parameter which reflects the amount of plasticity-induced crack closure that is present in the material.

f_E environmental correction factor to the welded joint fatigue curve.

f_I fatigue improvement method correction factor to the welded joint fatigue curve.

f_{MT} material and temperature correction factor to the welded joint fatigue curve.

G factor used to compute the permissible number of cycles.

γ_1 true strain in the micro-strain region of the stress-strain curve.

γ_2 true strain in the macro-strain region of the stress-strain curve.

h exponent for the Master Fatigue Curve.

H Prager doctor factor.

H_{RO} constant in Ramberg-Osgood Stress Strain Model.

J elastic plastic driving force parameter.

J_{crit} critical J - Integral value.

J_T J - Integral value in a tearing analysis.

J_{TE} material chemistry parameter used to determine the Fracture Appearance Transition Temperature ($FATT$) for 2.25Cr-1Mo.

K elastic crack driving force parameter,stress intensity factor, or a parameter in the MPC stress-strain curve model, as applicable.

ΔK $K_{\max} - K_{\min}$; if $\Delta K > \Delta K_{th}$ crack growth occurs; otherwise, if $\Delta K \le \Delta K_{th}$ crack growth does not occur, or $da/dN = 0.0$.

ΔK_{eff} effective ΔK .

K_{css} material parameter for the cyclic stress-strain curve model.

K_I applied mode I stress intensity factor (see Annex C).

K_{IC} plane-strain fracture toughness.

K_{IC-H} material fracture toughness measured in the hydrogen charging environment.

K_{Id} dynamic plane-strain fracture toughness.

K_{IR} arrest fracture toughness.

$K_{\delta c}$ equivalent fracture toughness derived from CTOD data.

K_{IH} threshold fracture toughness value for a hydrogen environment.

K_{ISCC} threshold fracture toughness value for stress corrosion cracking.

K_{Jc} fracture toughness established by converting J_{crit} to an equivalent K .

$K_{Jc(median)}$ median fracture toughness.

$K_{\max}$ maximum stress intensity for a given cycle.

$K_{\min}$ minimum stress intensity for a given cycle.

ΔK_{th} threshold stress intensity factor.

K_{th} threshold stress intensity factor for the material and environment, above which measurable crack extension will occur.

ΔK_{tran} transition ΔK used to determine the constants in the Bilinear crack growth model.

$\Delta K_{tran,1}$ first transition ΔK used to determine the constants in the Trilinear crack growth model.

$\Delta K_{tran,2}$ second transition ΔK used to determine the constants in the Trilinear crack growth model.

ΔK_{th} threshold stress intensity factor.

K_0 63rd percentile fracture toughness ($F_{mc} = 0.63$ when $K_{Jc} = K_0$).

K_{mat}^{mean} mean value of fracture toughness.

L rupture life (hours).

L_{mc} crack front length used in the Master Curve Model; for a surface crack L_{mc} can be aproximated as the total crack length, for a embedded crack L_{mc} can be approximated as twice the total crack length, and for a through-wall crack L_{mc} can be approximated as twice the component thickness.

$LMP(\sigma)$ Larson-Miller parameter as a function of stress.

m material parameter for crack growth modeling.

m_{CTOD} conversion constant, 1.4 can be used in the absence of more reliable information.

m_F m constant for the Modified Forman Equation.

m_w m constant for the Walker Equation.

m_1 curve fitting exponent for the stress-strain curve equal to the true strain at the proportional limit and the strain hardening coefficient in the large strain region.

m_2 curve fitting exponent for the stress-strain curve equal to the true strain at the true ultimate stress.

N allowable number of cycles.

n material parameter for crack growth modeling.

n_{BN} Bailey Norton coefficient evaluated at the reference stress in the current load increment, use in the MPC Project Omega Life Assessment Model..

n_{cc} exponent of crack growth equation.

n_{css} material parameter for the cyclic stress-strain curve model.

n_l material parameter for crack growth modeling.

n_{RO} material parameter for Ramberg-Osgood stress-strain curve model.

n_T exponent of the material model used in a tearing analysis.

n_u material parameter for crack growth modeling.

n_1 material/environment constant for crack growth modeling.

n_2 material/environment constant for crack growth modeling .

n_3 material/environment constant for crack growth modeling .

NWT nominal wall thickness of the pipe (mm:in).

Ω_m Omega multiaxial damage parameter.

Ω Omega uniaxial damage parameter.

p material parameter for Forman and NASGRO Crack Growth Models.

P_L primary local membrane stress.

P_b primary local bending stress.

$\%As$ weight percent Arsenic.

$\%Mn$ weight percent Manganese.

$\%P$ weight percent Phosphorous.

$\%Sb$ weight percent Antimony.

$\%Si$ weight percent Silicon.

$\%Sn$ weight percent Tin.

q material parameter for Forman and NASGRO Crack Growth Models or the parameter used to determine the effect equivalent structural stress range on the fatigue improvement factor, as applicable.

Q secondary stress.

R $K_{\min}/K_{\max}$ ratio or the ratio of the engineering yield stress to engineering tensile stress evaluated at the assessment temperature, as applicable

R_{HT} parameter used to compute the expected temperature for an associated Charpy energy value for materials with an ASME Exemption Curve

RT_{NDT} maximum of the nil-ductility transition temperature established by a drop weight test, and the temperature from a Charpy test where the specimen exhibits at least 0.89 mm (35 mils) of lateral expansion and not less that 68 Joules (50 ft-lb) absorbed energy minus 33 ºC (60 ºF)

S cyclic crack growth model constant.

S_a stress amplitude.

S_m allowable stress.

SA shear area for the full-size specimen at the test temperature for the sub-size specimen expressed as percent divided by 100.

SA_{ss} shear area for the sub-size specimen at the test temperature for the sub-size specimen expressed as percent divided by 100.

ΔS_{range} equivalent structural stress range.

σ stress or the standard deviation, as applicable.

σ_a total stress amplitude.

σ_r total stress range.

σ_t true stress.

σ_e effective stress.

σ_{es} engineering stress.

σ_f flow stress.

σ_{ref} reference stress (see Annex D).

σ_1 principal stress.

σ_2 principal stress.

σ_3 principal stress.

σ_r applied stress range.

σ_{ys} yield stress at the temperature of interest.

σ_{ysamb} yield stress at ambient temperature.

σ_{uts}^{mean} mean value of the ultimate tensile strength.

$\sigma_{uts}^{\min}$ minimum specified ultimate tensile strength from the original construction code.

σ_{ys}^{mean} mean value of the yield strength.

$\sigma_{ys}^{\min}$ minimum specified yield strength.

σ_{uts} engineering ultimate tensile stress evaluated at the temperature of interest.

T temperature.

T_c 85% SATT for the full-size specimen.

T_F temperature in degrees Fahrenheit.

T_{ref} reference temperature.

T_{ref}^D reference temperature after adjustment for rate dependent loading.

T_{shift} temperature shift (temperature at the midpoint between the lower and upper shelf impact energies).

T_0 reference transition temperature.

T_0^D reference transition temperature after adjustment for rate dependent loading.

$T_{20\,ft-lbs}$ predicted temperature at 20 ft-lbs.

$T_{27\,Joules}$ predicted temperature at 27 Joules.

T_{c-ss} 85% Shear Area Transition Temperature (SATT) for the sub-size specimen.

T_{shift}^D shift in transition temperature due to dynamic loading effects.

TT_{std} transition temperature for the standard size CVN specimen (temperature at the midpoint between the lower and upper shelf impact energies).

TT_{ss} transition temperature for the sub-size CVN specimen (temperature at the midpoint between the lower and upper shelf impact energies).

t time.

t^i time increment or load duration for use in the damage calculation.

t_c component thickness.

t_{relax} relaxation term in the crack driving force.

t_{ss} thickness of sub-sized CVN specimen.

t_{std} thickness of standard size CVN specimen.

ν Poisson's ratio.

X exponent used to compute the permissible number of cycles or the crack growth rate, as applicable.

$\overline{X}$ material chemistry parameter used to determine the Fracture Appearance Transition Temperature ($FATT$) for 1.25Cr-0.5Mo.

F.9 References

Technical References – Fracture Mechanics

1. Anderson, T.L., "Fracture Mechanics – Fundamentals and Applications," 2nd Edition, CRC Press, Boca Raton, Florida, 1995.

2. Anderson, TL, Merrick, R.D., Yukawa, S., Bray, D.E., Kaley, L. and Van Scyoc, K., "Fitness-For-Service Evaluation procedures for Operating Pressure Vessels, Tanks, and Piping in Refinery and Chemical Service," FS-26, Consultants' Report, MPC Program on Fitness-For-Service, Draft 5, The Materials Properties Council, New York, N.Y., October, 1995.

3. Eiber, R.J., "Investigation of the Initiation and Extent of Ductile Pipe Rupture," Battelle Report to USAEC, BMI-1908, June, 1971.

4. EPRI, "Evaluation of Flaws in Austenitic Steel Piping, "EPRI NP-4690-SR, Electric Power Research Institute, Palo Alto, CA, July, 1986.

5. EPRI, "Evaluation of Flaws in Ferritic Piping, "EPRI NP-6045, Electric Power Research Institute, Palo Alto, CA, October, 1988.

6. Farahmand, B., "Fracture Mechanics of Metals, Composites, Welds, and Bolted Joints – Applications of LEFM, EPFM, and FMDM Theory," Kluwer Academic Publishers, MA, 2001.

7. Liu, A.F., "Structural Life Assessment Methods," ASM International, Materials Park, Ohio, 1998.

8. Maxey, W.A., "Brittle Fracture Arrest in Gas Pipelines," AGA Report No. 135, Catalog No. L51436, April, 1983.

9. McNicol, R.C., "Correlation of Charpy Test Results for Standard and Nonstandard Size Specimens," WRC 385, September, 1965.

10. Phaal, R., Macdonald, K.A., and Brown, P.A., "Correlations Between Fracture Toughness and Charpy Impact Energy," Report from the Co-operative Research Programme for Industrial Members Only, TWI Report 504/1994, The Welding Institute, Cambridge, U.K., 1994.

11. PVRC Ad Hoc Group on Toughness Requirments, "PVRC Recommendations on Toughness Requirments for Ferritic Materials," WRC 175, Welding Research Council, New York, N.Y., 1972.

12. Scott, P.M., Anderson, T.L., Osage, D.A., Wilkowski, G.M., "Review of Existing Fitness-For-Service Criteria For Crack-like Flaws," WRC 430, Welding Research Council, New York, N.Y., 1998.

13. Roberts, R. and Newton, C., "Interpretive Report on Small Scale Test Correlations with KIc Data," WRC Bulletin 265, Welding Research Council, New, York, N.Y., February, 1981.

14. WRC, "PVRC/MPC Task Group on Fracture Toughness Properties for Nuclear Components," Final Report, WRC 175, Welding Research Council, New York, N.Y., 1977.

Technical References – Materials

15. API, "Characterization Study of Temper Embrittlement of Chromium-Molybdenum Steels," API Publication 959, American Petroleum Institute, Washington, D.C., 1982.

16. McEvily, Jr., A.J. and Wei, R.P., "Corrosion Fatigue: Chemistry, Mechanics and Microstructure," NACE, 1972, pp. 381-395.

17. Grosse-Wordemann, J. and Dittrich, S., "Prevention of Temper Embrittlement in 2 ¼ Cr -1Mo Weld Metal by metallurgical Actions," Welding Research Supplement, May, 1983, pp. 123-128.

18. Robinovich, M., Osage, D.A. and Prager, M. "Compendium of Temperature-Dependent Physical Properties for Pressure Vessel Materials," WRC 503, Welding Research Council, New York, N.Y., 2005.

19. Stout, R.D., "Weldability of Steels," 4th edition, WRC, New York, N.Y., 1987.

Technical References – Fatigue

20. Barsom, J.M. and Rolfe, S.T., "Fracture and Fatigue Control in Structures, " Third Edition, Prentice Hall, Englewood Cliffs, New Jersey, 1999.

21. Barsom, J.M. and Vecchio, R.S., "Fatigue of Welded Components," WRC Bulletin 422, Welding Research Council, New York, N.Y., June, 1997.

22. Booth, G.S., “Improving the Fatigue Strength of Welded Joints By Grinding,” Metal Construction, 18, (7), 1986, pp 432-437.

23. Bockrath, G. and Glassco, J., “Fatigue and Fracture Mechanics of High Risk Parts – Application of LEFM & EMDM Theory,” Chapman & Hall, New York, N.Y., 1997.

24. Dong, P., Hong, J.K., Osage, D.A., and Prager, M., “Master S-N Curve Method for Fatigue Evaluation of Welded Components,” WRC Bulletin 474, Welding Research Council, New York, N.Y., August, 2002.

25. Dong, P., Hong, J.K, and DeJesus, A.M.P., “Analysis of Recent Fatigue Data Using the Structural Stress Procedure in ASME Div2 Rewrite,” ASME PVP, 2005.

26. Ellyin, F., “Fatigue Damage Crack Growth and Life Prediction,” Chapman & Hall, Boundary Row, London 1997.

27. Engineering Sciences Data, Fatigue Endurance Data Sub-series, 3, Stress Concentrations, ESDU International Ltd., London.

28. Gurney, T.R. and Maddox, S.J., “A Re-Analysis of Fatigue Data for Welded Joints in Steel,” Welding Research Int. 3, (4), 1972.

29. Gurney, T.R., “Fatigue of Welded Structures,” Cambridge University Press, 1979.

30. Harrison, J.D. and Maddox, S.J., “A Critical Examination of Rules for the Design of Pressure Vessels Subject to Fatigue Loading,” Proc. 4th Int. Conf. on Pressure Vessel Technology, I.Mech.E., 1980 (or IIW Doc. XIII-941-80, 1980).

31. IIW, “Fatigue Design Of Welded Joints And Components,” A. Hobbacher, Abington Publishing, Abington Hall, Abington, Cambridge, England, 1996

32. IIW, “Stress Determination For Fatigue Analysis Of Welded Components,” Ed. E. Niemi, Abington Publishing, Abington Hall, Abington, Cambridge, England, 1995.

33. IIW, “Fifth Draft (January 1995) Of Proposed Detailed Fatigue Assessment Method Based On Draft Eurcode 3,” The Welding Institute, Abington Hall, Abington, Cambridge, England, 1995.

34. Maddox, S.J., “Fatigue Strength of Welded Structures,” 2nd Ed., Abington Publishing, Cambridge, England, 1991.

35. Maddox, S.J. and Prager, M., “International Conference on Performance of Dynamically Loaded Welded Structures,” IIW 50th Annual Assembly Conference, WRC, New York, N.Y., 1997.

36. Munse, W.H. and Grover, L., “Fatigue of Welded Structures,” WRC, New York, N.Y., 1964.

37. NRIM, “Fatigue Properties of Engineering Materials Manufactured in Japan – NRIM Fatigue Data Sheets,” National Institute For Materials, Tokyo, Japan.

38. Radaj, D. and Sonsino, C.M., “Fatigue Assessment of Welded Joints by Local Approaches,” Abibgton Publishing, Woodjhead Publishing Limited, Abington Hall, Cambridge, England, 1998.

39. Spence, J., and Tooth, A.S. (Ed), “Pressure Vessel Design, Concept and Principles,” E.& F.N. Spon, London, 1994.

Technical References – High Temperature

40. Buchheim, G.M., Osage, D.A., Brown, R.G., and Dobis, J.D., “Failure Investigation of a Low Chrome Long-Seam Weld in a High-Temperature Refinery Piping System,” PVP-Vol. 288, ASME, 1994, pp. 363-386.

41. Dyson, B., “Use of CDM in Materials Modeling and Component Creep Life Prediction,” ASME, Journal of Pressure Vessel Technology, Vol. 122, August 2000, pages 281-296.

42. Ibarra, S. and Konet, R.R., “Life Assessment of 1 1/4Cr-1/2M0 Steel Catalytic Reformer Furnace Tubes Using the MPC Omega Method,” PVP-Vol. 288, Service Experience and Reliability Improvement: Nuclear, Fossil, and Petrochemical Plants, ASME 1994, pages 387-400.

43. Kim, D.S. and Mead, H.E., “Remaining Life Assessment of Refinery Heater Tubes,” PVP-Vol. 388, Fracture, Design Analysis of Pressure Vessels, Heat Exchangers, Piping Components, and Fitness-For-Service, ASME, 1999, pages 361-366.

44. Klehn, R. and Laughlin, C.A., “Chevron’s Experience Using Omega Method Creep Tests for Life Assessment of Refinery Equipment,” PVP-Vol. 288, Service Experience and Reliability Improvement: Nuclear, Fossil, and Petrochemical Plants, ASME 1994, pages 345-350.

45. Prager, M. and Ibarra, S., “Approaches to Long Term Life prediction of Furnace and Boiler Tubes,” Fitness For Adverse Environments in Petroleum and Power Equipment, PVP-Vol. 359, ASME, 1997, pp. 339-352.

46. Prager, M., “Development of the MPC Project Omega Method for Life Assessment in the Creep Range,” PVP-Vol. 288, ASME, 1994, pp. 401-421.

47. Prager, M., “The Omega Method – An Effective Method for Life and Damage Prediction in Creep Tests and Service,” Oikawa (eds.), Strength of Materials, Japan Institute of Metals, 1994, pp. 571-574.

48. Prager, M., “Proposed Implementation of Criteria for Assignment of Allowable Stresses in the Creep Range,” ASME Journal of Pressure Vessel Technology, May, 1996, Vol. 335, pp. 273-293.

49. Prager, M., “Generation of Isochronous Creep, Tubing Life and Crack Growth Curves Using the MPC Omega Method, Structural Integrity,” NDE, Risk and Material Performance for Petroleum, process and Power, PVP-Vol. 336, ASME, 1996, pp. 303-322.

50. Prager, M. and Ibarra, S., “Approaches To Long Term Life Prediction Of Furnace And Boiler Tubes,”, PVP-Vol. 359, Fitness for Adverse Environments in Petroleum and Power Equipment, ASME 1997, pages 339-352.

51. Prager, M., and Osage, D., “Special Topics in Elevated Temperature Life Applications Including Assessment Rules for API 579,”, PVP-Vol. 411, Service Experience and Fitness-For-Service in Power and Petroleum Processing, ASME, 2000, pages 91-104.

52. Prager, M., “Damage Evaluation and Remaining Life Assessment in High Temperature Structural Components by the Omega Method,” Proceedings of 7th Workshop on the Ultra Steel, Ultra Steel: Requirments from New Design of Constructions, June 24 and 25, 2003, pages 150-158.

Yield Strength, Tensile Strength, Stress-Strain Curve Models

53. ASME, “Boiler and Pressure Vessel Code, Section II, Part D – Properties,” ASME Code Section II, Part D, ASME, New York, N.Y.

54. Boyer, H.E. ed., “Atlas of Stress-Strain Curves, “ ASM, 2nd Edition, 2002.

55. Kim, Y., Huh, N., Kim, Y., Choi, Y., and Yang, J., “On Relevant Ramberg-Osgood Fit to Engineering Nonlinear Fracture Mechanics Analysis,” ASME, Journal of Pressure Vessel Technology, Vol. 126, August, 2004, pages 277-283.

56. Holt, J.M., Mindlin, H., and Ho, C.Y., “Structural Alloys Handbook,” Volumes 1, 2 and 3, CINDAS/Purdue University, Potter Engineering Center, West Lafayette, IN, 1995.

57. Neuber, H., “Theory of Stress Concentrations for Shear Strained Prismatic Bodies with Arbitrary Non-linear Stress-Strain Law,” Trans. ASME Journal of Applied Mechanics, 1969, p. 544.

Creep Rupture Strength and Creep Strain Rate Data

58. ASM, “Atlas of Creep and Stress-Rupture Curves,” ASM International, Metals Park, Ohio, 1988.

59. ASME, “Subsection NH – Class 1 Components in Elevated Temperature Service,” ASME Code Section III, Division 1, ASME, New York, N.Y.

60. ASTM, “An Evaluation of the Elevated Temperature Tensile and Creep-Rupture Properties of Wrought,” ASTM Data Series DS 11S1, American Society for Testing Materials, Philadelphia, Pa., 1970.

61. ASTM, “An Evaluation of the Yield, Tensile, Creep, and Rupture Strengths of Wrought 304, 316, 321, and 347 Stainless Steels at Elevated-Temperatures,” ASTM Data Series DS 5S2, American Society for Testing Materials, Philadelphia, Pa., 1969.

62. ASTM, “Elevated-Temperature Properties of Carbon Steels,” ASTM Special Technical Publication No. 180, American Society for Testing Materials, Philadelphia, Pa., 1955.

63. ASTM, “Evaluation of the Elevated Temperature Tensile and Creep-Rupture Properties of 1/2 Cr – 1/2 Mo, 1 Cr – 1/2 Mo, and 1 1/4 Cr – 1/2 Mo-Si Steels,” ASTM Data Series DS 50, American Society for Testing Materials, Philadelphia, Pa., 1973.

64. ASTM, “Evaluation of the Elevated-Temperature Tensile and Creep Rupture Properties of 3 to 9 Percent Chromium-Molybdenum Steels,” ASTM Data Series DS 58, American Society for Testing Materials, Philadelphia, Pa., 1971.

65. ASTM, “Evaluations of the Elevated Temperature Tensile and Creep-Rupture Properties of C-Mo, Mn-Mo and Mn-Mo-Ni Steels,” ASTM Data Series DS 47, American Society for Testing Materials, Philadelphia, Pa., 1971.

66. ASTM, “Evaluations of the Elevated-Temperature Tensile and Creep Rupture Properties of 12 to 27 Percent Chromium Steels,” ASTM Data Series DS 59, American Society for Testing Materials, Philadelphia, Pa., 1980.

67. ASTM, “Report on Elevated-Temperature Properties of Chromium Steels (12 to 27 percent),” ASTM Special Technical Publication No. 228, American Society for Testing Materials, Philadelphia, Pa., 1958.

68. ASTM, “Report on Elevated-Temperature Properties of Stainless Steels,” ASTM Special Technical Publication No. 124, American Society for Testing Materials, Philadelphia, Pa., 1952.

69. ASTM, “Supplemental report on the Elevated-Temperature Properties of Chromium-Molybdenum Steels,” ASTM Data series DS 6S1, American Society for Testing Materials, Philadelphia, Pa., 1966.

70. ASTM, “Supplemental Report on the Elevated-Temperature Properties of Chromium-Molybdenum Steels (AN Evaluation of 2 1/4 Cr – 1Mo Steel),” ASTM Data series DS 6S2, American Society for Testing Materials, Philadelphia, Pa., 1971.

71. ASTM, “Supplemental Report on the Elevated-Temperature Properties of Chromium-Molybdenum Steels,” ASTM Special Technical Publication No. 151, American Society for Testing Materials, Philadelphia, Pa., 1953.

72. ASTM, “The Elevated-Temperature Properties of Weld-Deposited Metal and Weldments,” ASTM Special Technical Publication No. 226, American Society for Testing Materials, Philadelphia, Pa., 1958.

73. Atkins, D.F. and Schwartzbat, H., “Stress-Rupture Behavior of Welded and Decarburized Tubular 2 1/4 Cr – 1 Mo Steel,” MPC-7, The American Society of Mechanical Engineers, New York, N.Y., 1978, pp. 205-223.

74. Blackburn, L.D., “Isochronous Stress-Strain Curves for Austenitic Stainless Steels," The Generation of Isochronous Stress-Strain Curves, American Society of Mechanical Engineers, New York, N.Y., 1972.

75. Booker, M.K., “An Analytical Treatment of the Creep and Creep-Rupture Behavior of Alloy 800H,” MPC-7, The American Society of Mechanical Engineers, New York, N.Y., 1978, pp. 1-27.

76. Booker, M.K., “Use of Generalized Regression Models for the Analysis of Stress-Rupture Data,” Characterization of Materials for Service at Elevated Temperatures,” MPC-7, The American Society of Mechanical Engineers, New York, N.Y., 1978, pp. 459-499.

77. Ellis, F.V., “Time-Temperature Parameter Based Incremental Creep Equation for Finite Element Analysis,” MPC-7, The American Society of Mechanical Engineers, New York, N.Y., 1978, pp. 29-49.

78. Jaske, C.E., “Consideration of Experimental Techniques Used in the Development of Long-Term Properties of Pressure Vessel and Piping Alloys,” MPC-7, The American Society of Mechanical Engineers, New York, N.Y., 1978, pp. 129-144.

79. MEP, “High Temperature Design Data for Ferritic Pressure Vessel Steels,” The Creep of Steels Working Party of the Institute of Mechanical Engineers, Mechanical Engineering Publications, Ltd, London, .

80. Sikka, V.K., Booker, M.K., and Brinkman, C.R., “Relationships Between Short-And Long-Term Mechanical Properties of Several Austenitic Stainless Steels,” MPC-7, The American Society of Mechanical Engineers, New York, N.Y., 1978, pp. 51-82.

81. Schill, T.V. and Bassfor, T.H., “Extrapolation of Incoloy Alloy 800 Creep-Rupture Data at 500°C to 650°C,” MPC-7, The American Society of Mechanical Engineers, New York, N.Y., 1978, pp. 95-105.

82. USS, “Steels for Elevated Temperature Service”, United States Steel Corporation.

83. VanEcho, J.A. and Roach, D.B., “Investigation of Mechanical, Physical, and Creep Rupture Properties of Reformer Materials,” Battelle Technical Report on Materials for Steam Reformer Furnaces, Battelle, Columbus, Ohio, 1973.

84. Viswanathan, R. and Gandy, D.W., “A Review of High Temperature Performance Trends and Design Rules for Cr-Mo Steel Weldments,” EPRI, Palo Alto, CA, 1998, TR-110807.

Physical Properties

85. Avallone, E.A., and Baumeister, T, “Marks’ Standard Handbook for Mechanical Engineers,” Ninth Edition, McGraw-Hill, New York, N.Y., 1978.

86. ASME, “Boiler and Pressure Vessel Code, Section II, Part D – Properties,” ASME Code Section II, Part D, ASME, New York, N.Y.

87. ASME, “Subsection NH – Class 1 Components in Elevated Temperature Service,” ASME Code Section III, Division 1, ASME, New York, N.Y.

88. Holt, J.M., Mindlin, H., and Ho, C.Y., “Structural Alloys Handbook,” Volumes 1, 2 and 3, CINDAS/Purdue University, Potter Engineering Center, West Lafayette, IN, 1995.

89. USS, “Steels for Elevated Temperature Service”, United States Steel Corporation.

Fracture Toughness Data

90. Holt, J.M., Mindlin, H., and Ho, C.Y., “Structural Alloys Handbook,” Volumes 1, 2 and 3, CINDAS/Purdue University, Potter Engineering Center, West Lafayette, IN, 1995.

91. Hudson, C.M. and Ferrainolo, J.J., “A Compendium of Sources of Fracture Toughness and Fatigue Crack Growth Data for Metallic Alloys – Part IV”, International Journal of Fracture, 48, 1991.

92. Hudson, C.M. and Seward, S.K., “A Compendium of Sources of Fracture Toughness and Fatigue Crack Growth Data for Metallic Alloys”, International Journal of Fracture, 14, 1978.

93. Hudson, C.M. and Seward, S.K., “A Compendium of Sources of Fracture Toughness and Fatigue Crack Growth Data for Metallic Alloys – Part II”, International Journal of Fracture, 20, 1982.

94. Hudson, C.M. and Seward, S.K., “A Compendium of Sources of Fracture Toughness and Fatigue Crack Growth Data for Metallic Alloys – Part III”, International Journal of Fracture, 39, 1989.

95. NASA, “Derivation of Crack Growth Properties of Materials for NASA/FLAGRO 2.0,” Volumes I, II, and III, JSC-26254, National Aeronautics and Space Administration, Houston, Texas, 1994.

96. NASA, “fatigue Crack Growth Computer Program NASGRO Version 3.00,” Revision B, JSC-22267B, National Aeronautics and Space Administration, Houston, Texas, September, 1998.

97. Iwadate, T., “Pressurization Temperature Of Pressure Vessels Made Of Cr-Mo Steels,” PVP-Vol. 288, ASME, 1994, pg. 155-163.

98. Yukawa, S., “Review and Evaluation of the Toughness of Austenitic Steels and Nickel Alloys After Long-Term Elevated Temperature Exposure,” WRC 378, The Welding Research Council, New York., N.Y., 1993.

99. Zahoor, A., “Ductile Fracture Handbook Review – Volume 3,” Electric Power Research Institute, Palo Alto, CA, 1991.

100. Orth, F.C. and Mohr, W.C., "Storage Tanks: Correlations Between Charpy Absorbed Energy and The Fracture Toughness of Storage Tank Steels," EWI Project No. J6117, EWI, December 4, 1995.

Fatigue and Stress Corrosion Crack Growth Data

101. Cayard, M.S. and Kane, R.D., “Fitness-For-Service Methodologies for the Assessment of Equipment Containing Corrosion Induced Damage,” Plenary Lecture at the 2nd NACE Latin American Region Corrosion Congress, Rio de Janeiro, Brazil, September, 1996.

102. ASM, “Atlas of Fatigue Curves,” American Society for Metals, Metals Park, Ohio, 1986.

103. ASM, “Atlas of Stress Corrosion and Corrosion Fatigue Curves,” ASM International, Metals Park, Ohio, 1990.

104. Barsom, J.M., “Fatigue Behavior of Pressure-Vessel Steels,” WRC Bulletin 194, Welding Research Council, New York, N.Y., May, 1974.

105. BSI, “Guidance on Methods for Assessing the Acceptability of Flaws in Fusion Welded Structures,” BS PD6493, British Standards Institute, 1991.

106. BSI, “Guide on Methods For Assessing the Acceptability of Flaws in Structures,” BS 7910, British Standards Institute, 1999.

107. Mukherjee, B. and Vanderglas, M.L., “Fatigue Threshold Stress Intensity and Life Estimation of ASTM A 106B Piping Steel,” Vol. 201, Transactions of the ASME, ASME, New York, N.Y., August, 1980, pp. 294-302.

108. NASA, “Derivation of Crack Growth Properties of Materials for NASA/FLAGRO 2.0,” Volumes I, II, and III, JSC-26254, National Aeronautics and Space Administration, Houston, Texas, 1994.

109. NASA, “Fatigue Crack Growth Computer Program NASGRO Version 3.00,” Revision B, JSC-22267B, National Aeronautics and Space Administration, Houston, Texas, September, 1998.

110. Woollin, P. and Tubby, P.J., “Fatigue Crack Propagation in C-Mn Steel HAZ Microstructures Tested in Air and Seawater,” TWI, 526/1995, Abington Hall, Abington, Cambridge, UK, November, 1995.

111. Vosikovsky, O., Macecek, M. and Ross, D.J., “Allowable Defect Sizes in a Sour Crude Oil Pipeline for Corrosion Fatigue Conditions”, International Journal of Pressure Vessels & Piping, 13, pp. 197-226, 1983.

112. Iwadate, T., Watanabe, J., and Tanaka, Y., “Prediction of the Remaining Life of High-Temperature/Pressure Reactors Made of Cr-Mo Steels,” Transactions of the ASME, Vol. 107, ASME, New York, N.Y., August, 1985, pp. 230-238.

113. Woollin, P. and Tubby, P.J., “Fatigue Crack Propagation in C-Mn Steel HAZ Microstructures Tested in Air and Seawater,” TWI Report 526/1995, TWI, Cambridge, UK, November, 1995.

114. Parkins, R.N. and Foroulis, Z.A., “The SCC of Mild Steel in Monoethanolamine Solutions,” Corrosion/87, Paper No. 188, NACE International, March, 1987.

115. Parkins, R.N., “Slow Strain Rate Testing – 25 Years Experience,” Slow Strain Rate Testing for Evaluation of Environmentally Induced Cracking: Research and Engineering Applications, Ed. R.D. Kane, STP 1210, ASTM, W. Conshohocken, PA, 1993, pp. 7-21.

116. Saiolu, F. and Doruk, M., “Correlation Between Yielding Fracture Mechanics Parameters and the Crack Growth Rate of Low Strength Steel in 2N(NH4)2CO3 at 75 C,” International Congress of Metallic Corrosion, Vol. 1, 1984.

117. Slater, J.E., “An Approach to Reliability Analysis of Cracked Continuous Digesters,” Corrosion/82, Paper No. 92, NACE International, March, 1982.

118. Speidel, M.O., “Stress Corrosion Cracking of Stainless Steels in NaCl Solutions,” Metallurgical Transactions, Vol. 12A, ASM International, May, 1981, pp. 779-789.

119. Iwadate, T., “Hydrogen Effect on Remaining Life of Hydroprocessing Reactors,” Corrosion, Vol. 44, NACE International, February, 1988, pp. 103-112.

120. Cayard, M.S. and Kane, R.D., Kaley, L., and Prager, M., “Research Report on Characterization and Monitoring of Cracking in Wet H_2S Service,” Publication 939, American Petroleum Institute, October, 1994.

121. Kane, et al., Slow Strain Rate Testing for Evaluation of Environmentally Induced Cracking: Research and Engineering Applications, Ed. R.D. Kane, STP 1210, ASTM, W. Conshohocken, PA, 1993, pp. 181-192.

Creep Crack Growth Data

122. BSI, “Guide on Methods For Assessing the Acceptability of Flaws in Structures,” BS 7910, British Standards Institute.

123. Buchheim, G.M., Becht, C., Nikbin, K.M, Dimopolos, V., Webster, G.A., and Smith D.J., “Influence of Aging on High-Temperature Creep Crack Growth in Type 304H Stainless Steel,” Nonlinear Fracture Mechanics, ASTM STP 995, Volume 1, The American Society of Testing and Materials, Pa, 1988, pp. 153-172.

124. Dimopulos, V., Nikbin, K.M., and Webster, G.A., “Influence of Cyclic to Mean Load Ratio on Creep/Fatigue Crack Growth,” Metallurgical Transactions A, Volume 19A, pp. 873-880, May 1988.

125. Hollstein, T and Voss, B., “Experimental Determination of the High-Temperature Crack Growth Behavior of Incoloy 800H,” Nonlinear Fracture Mechanics, ASTM STP 995, Volume 1, The American Society of Testing and Materials, Pa, 1988, pp. 195-213.

126. Konosu, S. and Maeda, K., “Creep Embrittlement Susceptibility and Creep Crack Growth Behavior in Low-Alloy Steels: An Assessment of the Effects of Residual Impurity Elements and Postweld Heat Treatment Condition on Creep Ductility and Crack Growth,” Nonlinear Fracture Mechanics, ASTM STP 995, Volume 1, The American Society of Testing and Materials, Pa, 1988, pp. 127-152.

127. Liaw, P.K., Rao, G.V., and Burke, M.G., “Creep Fracture Behavior of 2 1/4 Cr – 1 Mo Welds from a 31-Year-Old Fossil Power Plant,” Materials Science and Engineering, A131, pp. 187-201, 1991.

128. Liaw, P.K., Saxena, A., and Schaefer, J., “Estimating Remaining Life of Elevated-Temperature Steam Pipes-Part I. Materials Properties,” Engineering Fracture Mechanics, Vol. 32, No. 5, pp. 675-708, 1989.

129. Nikbin, K.M., Smith, D.J., and Webster, G.A., “An Engineering Approach to the Prediction of Creep Crack Growth,” Journal of Engineering Materials and Technology, Vol. 108, The American Society of Mechanical Engineers, pp. 186-191, April 1986.

130. Sadananda, K. and Shahinian, P, “Effect of Specimen Thickness on Crack Growth Behavior in Alloy 718 Under Creep and Fatigue Conditions,” MPC-7, The American Society of Mechanical Engineers, New York, N.Y., 1978, pp. 107-127.

131. Saxena, A., Han, J., and Banerji, K, “Creep Crack Growth Behavior in Power Plant Boiler and Steam Pipe Steels,” Journal of Pressure Vessel Technology, The American Society of Mechanical Engineers, Vol. 110, pp. 137-146, May, 1988.

132. Webster, G.A., “Lifetime Estimates of Cracked High Temperature Components,” International Journal of Pressure Vessels & Piping, 50, pp. 133-145, 1992.

133. Fatigue Curves (Crack Initiation) for Components Operating in the Creep Regime

134. Austin, T.S.P. and Webster, G.A., “Application of a Creep-Fatigue Crack Growth Model to Type 316 Stainless Steel”, ESIS Publication 15, Behavior of Defects at High Temperatures, Mechanical Engineering Publications Limited, London, 1993.

135. Okazaki, M., Hashimoto, M., and Mochizuki, T., “Creep-Fatigue Strength of Long-Term Post-Service 2 1/4 Cr – 1 Mo Steel and Remaining Life Estimation,” Journal of Pressure Vessel Technology, Vol. 119, The American Society of Mechanical Engineers, pp. 549-555, 1991.

F.10 Tables and Figures

Table F.1 – Approximate Equivalent Hardness Number and Tensile Strength for Carbon and Low Alloy Steels in the Annealed, Normalized, and Quenched-and-Tempered Conditions

Brinell Hardness No. (3000 kg load)	Vickers Hardness No.	Approximate Tensile Strength	
		(MPa)	(ksi)
441	470	1572	228
433	460	1538	223
425	450	1496	217
415	440	1462	212
405	430	1413	205
397	420	1372	199
388	410	1331	193
379	400	1289	187
369	390	1248	181
360	380	1207	175
350	370	1172	170
341	360	1131	164
331	350	1096	159
322	340	1069	155
313	330	1034	150
303	320	1007	146
294	310	979	142
284	300	951	138
280	295	938	136
275	290	917	133
270	285	903	131
265	280	889	129
261	275	876	127
256	270	855	124
252	265	841	122
247	260	827	120
243	255	807	117
238	250	793	115
233	245	779	113
228	240	765	111
219	230	731	106
209	220	696	101
200	210	669	97
190	200	634	92
181	190	607	88
171	180	579	84
162	170	545	79
152	160	517	75
143	150	490	71
133	140	455	66
124	130	427	62
114	120	393	57

Table F.2 – Minimum Specified Yield Strength as a Function of Temperature

Material Pointer (PYS)	Temperature (°F)		$\sigma_{ys} = \sigma_{ys}^{rt} \cdot \exp\left[C_0 + C_1 T + C_2 T^2 + C_3 T^3 + C_4 T^4 + C_5 T^5 \right] \quad \left({}^{o}F, ksi \right)$					
	Min	Max	C_0	C_1	C_2	C_3	C_4	C_5
1	70	1100	7.32895590E-02	-1.17762521E-03	2.38047105E-06	-3.41856446E-09	2.30957367E-12	-6.50662295E-16
2	70	1100	6.74115307E-02	-1.14022133E-03	2.93774604E-06	-4.04287814E-09	3.37044043E-12	-1.42534965E-15
3	70	1100	8.64892939E-02	-1.46822432E-03	4.43698029E-06	-7.48574857E-09	6.52970740E-12	-2.49641702E-15
4	70	1500	1.15119384E-01	-1.64008687E-03	1.40737810E-06	-6.87419020E-10	4.10067600E-13	-2.28537801E-16
5	70	1500	6.54193489E-02	-9.16571466E-04	1.97469205E-07	9.82045387E-11	3.83196021E-13	-3.00033395E-16
6	70	1500	1.29553432E-01	-1.83405205E-03	1.90867347E-06	-7.72504653E-10	-2.35102806E-13	1.49090484E-16
7	70	1500	7.22867367E-02	-1.18789668E-03	2.93345768E-06	-4.65145193E-09	3.62287974E-12	-1.09404474E-15
8	70	1500	5.02134175E-02	-7.23768917E-04	4.55342493E-07	-9.74792542E-10	1.21882955E-12	-5.03459802E-16
9	70	1500	1.71228796E-01	-2.75036658E-03	5.44467782E-06	-6.11640012E-09	3.62507062E-12	-8.78106064E-16

Table F.2M – Minimum Specified Yield Strength as a Function of Temperature

Material Pointer (PYS)	Temperature (°C)		$\sigma_{ys} = \sigma_{ys}^{rt} \cdot \exp\left[C_0 + C_1 T + C_2 T^2 + C_3 T^3 + C_4 T^4 + C_5 T^5 \right] \quad \left({}^{o}C, MPa \right)$					
	Min	Max	C_0	C_1	C_2	C_3	C_4	C_5
1	21	593	3.79335351E-02	-1.86385965E-03	6.69470079E-06	-1.82518378E-08	2.31521177E-11	-1.22947065E-14
2	21	593	3.38037095E-02	-1.73554380E-03	8.32638097E-06	-2.11471664E-08	3.29874954E-11	-2.69329508E-14
3	21	593	4.38110535E-02	-2.17153985E-03	1.21747825E-05	-3.89315704E-08	6.43532344E-11	-4.71714972E-14
4	21	816	6.40556561E-02	-2.79373298E-03	4.35401064E-06	-3.71656211E-09	3.92086989E-12	-4.31837715E-15
5	21	816	3.62948800E-02	-1.62644958E-03	6.77655338E-07	8.40865268E-10	3.51869766E-12	-5.66933503E-15
6	21	816	7.27926926E-02	-3.08574021E-03	5.93930041E-06	-4.67184681E-09	-2.21760045E-12	2.81716608E-15
7	21	816	3.71292469E-02	-1.82515595E-03	8.12857283E-06	-2.44881384E-08	3.61939674E-11	-2.06727194E-14
8	21	816	2.74884019E-02	-1.25543600E-03	1.19583839E-06	-4.80520518E-09	1.19491660E-11	-9.51321531E-15
9	21	816	8.85957654E-02	-4.35640722E-03	1.58095415E-05	-3.30171850E-08	3.65796603E-11	-1.65924112E-14

Table F.3 – Material Description for the Minimum Specified Yield Strength

PYS	**Applicable Materials**
1	Carbon Steel (YS<40ksi)
2	C-1/2Mo, 1-1/4Cr-1/2Mo Annealed, 2-1/4Cr-1Mo Annealed, 3Cr-1Mo, 5Cr-1/2Mo, 9Cr-1Mo
3	1-1/4Cr-1/2Mo N&T, 2-1/4Cr-1Mo N&T, 2-1/4Cr-1Mo Q&T, 2-1/4Cr-1Mo -V, 9Cr-1Mo-V
4	Type 304, Type 316
5	Type 310, Type 321, Type 347
6	Type 316L
7	Alloy 800
8	Alloy 800H, Alloy 800HT
9	HK-40

Table F.4 – Minimum Specified Ultimate Tensile Strength as a Function of Temperature

Material Pointer	Temperature (°F)		$\sigma_{uts} = \sigma_{uts}^{rt} \cdot \exp\left[C_0 + C_1 T + C_2 T^2 + C_3 T^3 + C_4 T^4 + C_5 T^5 \right] \quad \left({}^{o}F, ksi \right)$					
(PUS)	Min	Max	C_0	C_1	C_2	C_3	C_4	C_5
1	70	1100	4.96592236E-02	-3.77753186E-04	-2.22995759E-06	9.37412910E-09	-1.08177336E-11	3.38063139E-15
2	70	1100	1.03059502E-01	-1.50239969E-03	1.23729610E-06	2.88144828E-09	-3.79884518E-12	7.81749069E-16
3	70	1100	6.32622065E-02	-9.67153551E-04	1.22766678E-06	8.18123287E-10	-2.12906253E-12	5.21468764E-16
4	70	1500	1.32974273E-01	-2.10253189E-03	4.12208906E-06	-4.23720525E-09	2.51092690E-12	-7.88154028E-16
5	70	1500	1.34525275E-01	-2.14511512E-03	4.94560236E-06	-5.06503095E-09	2.39919595E-12	-5.62207065E-16
6	70	1500	1.05691876E-01	-1.63492458E-03	2.65859303E-06	-1.24506534E-09	-3.85312660E-13	1.68156273E-16
7	70	1500	1.31877934E-01	-2.43123502E-03	9.41969068E-06	-1.70606702E-08	1.47018626E-11	-4.92753399E-15
8	70	1500	1.41247151E-01	-2.64436746E-03	1.08241364E-05	-2.09316450E-08	1.90667084E-11	-6.59569764E-15
9	70	1500	1.63465185E-01	-2.70857567E-03	5.77561099E-06	-5.13107773E-09	1.83255377E-12	-2.70855733E-16

Table F.4M – Minimum Specified Ultimate Tensile Strength as a Function of Temperature

Material Pointer	Temperature (°C)		$\sigma_{uts} = \sigma_{uts}^{rt} \cdot \exp\left[C_0 + C_1 T + C_2 T^2 + C_3 T^3 + C_4 T^4 + C_5 T^5 \right] \quad \left({}^{o}C, MPa \right)$					
(PUS)	Min	Max	C_0	C_1	C_2	C_3	C_4	C_5
1	21	593	3.55835868E-02	-8.87531986E-04	-4.52108819E-06	4.67964163E-08	-1.07882077E-10	6.38793289E-14
2	21	593	5.63401650E-02	-2.54673855E-03	4.83029306E-06	1.40154694E-08	-3.85657189E-11	1.47716803E-14
3	21	593	3.35950169E-02	-1.59542267E-03	4.19028077E-06	3.21310030E-09	-2.14741795E-11	9.85350689E-15
4	21	816	6.97780335E-02	-3.33253782E-03	1.20867754E-05	-2.28840524E-08	2.50349101E-11	-1.48927063E-14
5	21	816	7.07824139E-02	-3.31892068E-03	1.44954873E-05	-2.77818452E-08	2.42415074E-11	-1.06232848E-14
6	21	816	5.60554916E-02	-2.64356837E-03	8.21908457E-06	-7.53881321E-09	-3.76242022E-12	3.17742712E-15
7	21	816	6.31803836E-02	-3.38199124E-03	2.55006790E-05	-8.88172175E-08	1.46057908E-10	-9.31091055E-14
8	21	816	6.70451917E-02	-3.62422838E-03	2.89321732E-05	-1.08234025E-07	1.89076439E-10	-1.24630192E-13
9	21	816	8.25387660E-02	-4.23802883E-03	1.71532015E-05	-2.85726267E-08	1.87824828E-11	-5.11800326E-15

Table F.5 – Material Descriptions for the Minimum Ultimate Tensile Strength

PUS	**Applicable Materials**
1	Carbon Steel (YS<40ksi)
2	C-1/2Mo, 1-1/4Cr-1/2Mo Annealed, 2-1/4Cr-1Mo Annealed, 3Cr-1Mo, 5Cr-1/2Mo, 9Cr-1Mo
3	1-1/4Cr-1/2Mo N&T, 2-1/4Cr-1Mo N&T, 2-1/4Cr-1Mo Q&T, 2-1/4Cr-1Mo -V, 9Cr-1Mo-V
4	Type 304, Type 347
5	Type 310, Type 316, Type 321
6	Type 316L
7	Alloy 800
8	Alloy 800H, Alloy 800HT
9	HK-40

Table F.6 – Minimum Yield and Tensile Strength Values from API STD 530 (1) (2)

Material	Temperature Limits and Room Temperature Strength Parameters (3) (4)	Yield Strength: σ_{ys} (3)		Tensile Strength: σ_{uts} (4)	
Low Carbon Steel (Figure 4A) A161 A192	$T_{min} = 149^o C\ (300^o F)$ $T_{max} = 621^o C\ (1150^o F)$ $\sigma_{ys}^{T_{min}} = 157\ MPa\ (22.8\ ksi)$ $\sigma_{uts}^{T_{min}} = 298\ MPa\ (43.2\ ksi)$	A_0	1.6251089E+00	B_0	1.1720989E+00
		A_1	-3.3124966E-03	B_1	-2.0580032E-03
		A_2	5.0904910E-06	B_2	7.6239020E-06
		A_3	-3.3374441E-09	B_3	-9.9459690E-09
		A_4	4.9690402E-13	B_4	3.7189699E-12
		A_5	0.0	B_5	0.0
Medium Carbon Steel (Figure 4B) A53 Grade B A106 Grade B A210 Grade A-1	$T_{min} = 149^o C\ (300^o F)$ $T_{max} = 621^o C\ (1150^o F)$ $\sigma_{ys}^{T_{min}} = 210\ MPa\ (30.5\ ksi)$ $\sigma_{uts}^{T_{min}} = 379\ MPa\ (55.0\ ksi)$	A_0	1.6434698E+00	B_0	1.1872106E+00
		A_1	-3.5201715E-03	B_1	-2.2083065E-03
		A_2	5.8080277E-06	B_2	8.0934859E-06
		A_3	-4.2398160E-09	B_3	-1.0510434E-08
		A_4	8.7536764E-13	B_4	3.9529036E-12
		A_5	0.0	B_5	0.0
C-0.5Mo (Figure 4C) A 161 T1 A 209 T1 A 335 P1	$T_{min} = 149^o C\ (300^o F)$ $T_{max} = 621^o C\ (1150^o F)$ $\sigma_{ys}^{T_{min}} = 186\ MPa\ (27.0\ ksi)$ $\sigma_{uts}^{T_{min}} = 395\ MPa\ (57.3\ ksi)$	A_0	1.0875314E+00	B_0	-8.3107781E-02
		A_1	-2.1270293E-04	B_1	6.7591546E-03
		A_2	-4.4780776E-07	B_2	-1.3556423E-05
		A_3	8.4688943E-10	B_3	1.1122871E-08
		A_4	-5.6614129E-13	B_4	-3.5429684E-12
		A_5	0.0	B_5	0.0
1.25Cr-0.5Mo (Figure 4D) A 213 T11 A 335 P11 A 200 T11	$T_{min} = 149^o C\ (300^o F)$ $T_{max} = 621^o C\ (1150^o F)$ $\sigma_{ys}^{T_{min}} = 183\ MPa\ (26.5\ ksi)$ $\sigma_{uts}^{T_{min}} = 379\ MPa\ (55.0\ ksi)$	A_0	1.1345901E+00	B_0	1.7526113E+00
		A_1	-4.8648764E-04	B_1	-7.0066393E-03
		A_2	3.9401132E-08	B_2	2.3037863E-05
		A_3	4.2209296E-10	B_3	-3.2685799E-08
		A_4	-3.8709072E-13	B_4	2.0963053E-11
		A_5	0.0	B_5	-5.2442438E-15
2.25Cr-1Mo (Figure 4E) A 213 T22 A 335 P22 A 200 T22	$T_{min} = 149^o C\ (300^o F)$ $T_{max} = 732^o C\ (1350^o F)$ $\sigma_{ys}^{T_{min}} = 186\ MPa\ (27.0\ ksi)$ $\sigma_{uts}^{T_{min}} = 364\ MPa\ (52.8\ ksi)$	A_0	1.2398072E+00	B_0	2.0398036E+00
		A_1	-1.5494280E-03	B_1	-7.5239262E-03
		A_2	3.2430371E-06	B_2	1.7967199E-05
		A_3	-2.3756026E-09	B_3	-1.6168512E-08
		A_4	3.1331338E-13	B_4	4.6189330E-12
		A_5	0.0	B_5	0.0

Table F.6 – Minimum Yield and Tensile Strength Values from API STD 530 (1) (2)

Material	Temperature Limits and Room Temperature Strength Parameters (3) (4)	Yield Strength: σ_{ys} (3)		Tensile Strength: σ_{uts} (4)	
3Cr-1Mo (Figure 4F) A 213 T5 A 335 P5 A 200 T5	$T_{min} = 149^o C\ (300^o F)$ $T_{max} = 732^o C\ (1350^o F)$ $\sigma_{ys}^{T_{\min}} = 179\ MPa\ (26.0\ ksi)$ $\sigma_{uts}^{T_{\min}} = 393\ MPa\ (57.0\ ksi)$	A_0	1.3109507E+00	B_0	1.2922744E+00
		A_1	-1.8522910E-03	B_1	-1.7583742E-03
		A_2	3.3285320E-06	B_2	3.5081428E-06
		A_3	-2.1885193E-09	B_3	-2.9914715E-09
		A_4	2.7268140E-13	B_4	6.7845610E-13
		A_5	0.0	B_5	0.0
5Cr-0.5Mo (Figure 4G) A 213 T5 A 335 P5 A 200 T5	$T_{min} = 149^o C\ (300^o F)$ $T_{max} = 732^o C\ (1350^o F)$ $\sigma_{ys}^{T_{\min}} = 175\ MPa\ (25.4\ ksi)$ $\sigma_{uts}^{T_{\min}} = 362\ MPa\ (52.5\ ksi)$	A_0	1.1392352E+00	B_0	1.2563698E+00
		A_1	-1.3518395E-03	B_1	-1.9619215E-03
		A_2	4.3886534E-06	B_2	5.1583250E-06
		A_3	-5.1308445E-09	B_3	-5.4836935E-09
		A_4	1.6914766E-12	B_4	1.7207470E-12
		A_5	0.0	B_5	0.0
5Cr-0.5Mo-Si (Figure 4H) A 213 T5b A 335 P5b	$T_{min} = 149^o C\ (300^o F)$ $T_{max} = 732^o C\ (1350^o F)$ $\sigma_{ys}^{T_{\min}} = 186\,MPa\ (27.0\ ksi)$ $\sigma_{uts}^{T_{\min}} = 356\,MPa\ (51.7\ ksi)$	A_0	1.2324252E+00	B_0	1.2773067E+00
		A_1	-1.6940271E-03	B_1	-2.3196405E-03
		A_2	4.3681713E-06	B_2	6.5893951E-06
		A_3	-4.8983328E-09	B_3	-7.2379937E-09
		A_4	1.6079702E-12	B_4	2.3466718E-12
		A_5	0.0	B_5	0.0
7Cr-0.5Mo (Figure 4I) A 213 T7 A 335 P7 A 200 T7	$T_{min} = 149^o C\ (300^o F)$ $T_{max} = 732^o C\ (1350^o F)$ $\sigma_{ys}^{T_{\min}} = 172\,MPa\ (25.0\ ksi)$ $\sigma_{uts}^{T_{\min}} = 400\,MPa\ (58.0\ ksi)$	A_0	6.9288533E-01	B_0	9.9596073E-01
		A_1	3.4867283E-03	B_1	2.4796284E-05
		A_2	-1.3498948E-05	B_2	3.3129703E-07
		A_3	2.2065464E-08	B_3	-1.4772664E-09
		A_4	-1.6085361E-11	B_4	6.5165864E-13
		A_5	4.1090437E-15	B_5	0.0
9Cr-1Mo (Figure 4J) A 213 T9 A 335 P9 A 200 T9	$T_{min} = 149^o C\ (300^o F)$ $T_{max} = 732^o C\ (1350^o F)$ $\sigma_{ys}^{T_{\min}} = 179\,MPa\ (26.0\ ksi)$ $\sigma_{uts}^{T_{\min}} = 370\,MPa\ (53.6\ ksi)$	A_0	1.3645782E+00	B_0	1.6002250E+00
		A_1	-2.4184891E-03	B_1	-3.8196855E-03
		A_2	5.3798831E-06	B_2	8.1545162E-06
		A_3	-5.0826095E-09	B_3	-7.4536524E-09
		A_4	1.4540216E-12	B_4	2.1749553E-12
		A_5	0.0	B_5	0.0

Table F.6 – Minimum Yield and Tensile Strength Values from API STD 530 (1) (2)

Material	Temperature Limits and Room Temperature Strength Parameters (3) (4)	Yield Strength: σ_{ys} (3)		Tensile Strength: σ_{uts} (4)	
9Cr-1Mo-V (Figure 4K) A 213 T91 A 335 P91 A 200 T91	$T_{min} = 149^o C\ (300^o F)$ $T_{max} = 660^o C\ (1220^o F)$ $\sigma_{ys}^{T_{min}} = 379\,MPa\ (55.0\ ksi)$ $\sigma_{uts}^{T_{min}} = 538\,MPa\ (78.0\ ksi)$	A_0	1.1559737E+00	B_0	1.3561147E+00
		A_1	-1.3027523E-03	B_1	-2.5814516E-03
		A_2	3.6718335E-06	B_2	6.4611130E-06
		A_3	-3.9082343E-09	B_3	-6.6563640E-09
		A_4	1.1136278E-12	B_4	2.0875274E-12
		A_5	0.0	B_5	0.0
Type 304 & 304H (Figure 4L) A 213 Type 304&304H A 271 Type 304&304H A 312 Type 304&304H A 376 Type 304&304H	$T_{min} = 204^o C\ (400^o F)$ $T_{max} = 843^o C\ (1550^o F)$ $\sigma_{ys}^{T_{min}} = 143\,MPa\ (20.8\ ksi)$ $\sigma_{uts}^{T_{min}} = 414\,MPa\ (60.0\ ksi)$	A_0	1.6894159E+00	B_0	1.2907427E+00
		A_1	-3.3500871E-03	B_1	-1.8958334E-03
		A_2	6.0887433E-06	B_2	4.2634694E-06
		A_3	-6.3277196E-09	B_3	-3.7649126E-09
		A_4	3.4413453E-12	B_4	9.8390933E-13
		A_5	-7.8762940E-16	B_5	0.0
Type 316 & 316H (Figure 4M) A 213 Type 316&316H A 271 Type 316&316H A 312 Type 316&316H A 376 Type316&316H	$T_{min} = 204^o C\ (400^o F)$ $T_{max} = 843^o C\ (1550^o F)$ $\sigma_{ys}^{T_{min}} = 148\,MPa\ (21.4\ ksi)$ $\sigma_{uts}^{T_{min}} = 452\,MPa\ (65.5\ ksi)$	A_0	1.3224680E+00	B_0	1.2454373E+00
		A_1	-8.7683155E-04	B_1	-1.6314830E-03
		A_2	-1.3646107E-07	B_2	3.7350778E-06
		A_3	8.9906963E-10	B_3	-3.3393727E-09
		A_4	-4.2098578E-13	B_4	8.7044694E-13
		A_5	0.0	B_5	0.0
Type 316L (Figure 4N) A 213 Type 316L A 312 Type 316L	$T_{min} = 204^o C\ (400^o F)$ $T_{max} = 688^o C\ (1270^o F)$ $\sigma_{ys}^{T_{min}} = 119\,MPa\ (17.3\ ksi)$ $\sigma_{uts}^{T_{min}} = 391\,MPa\ (56.7\ ksi)$	A_0	1.6764367E+00	B_0	1.4209808E+00
		A_1	-2.7911113E-03	B_1	-2.3830395E-03
		A_2	3.5200992E-06	B_2	4.6717029E-06
		A_3	-2.0849191E-09	B_3	-3.7247428E-09
		A_4	3.9274747E-13	B_4	9.0385624E-13
		A_5	0.0	B_5	0.0
Type 321 (Figure 4O) A 213 Type 321 A 271 Type 321 A 312 Type 321 A 376 Type 321	$T_{min} = 204^o C\ (400^o F)$ $T_{max} = 843^o C\ (1550^o F)$ $\sigma_{ys}^{T_{min}} = 142\,MPa\ (20.6\ ksi)$ $\sigma_{uts}^{T_{min}} = 430\,MPa\ (62.4\ ksi)$	A_0	1.6512149E+00	B_0	1.1069812E+00
		A_1	-2.5517760E-03	B_1	2.4195844E-04
		A_2	2.7303828E-06	B_2	-3.4616380E-06
		A_3	-1.0524840E-09	B_3	7.9148731E-09
		A_4	3.6127158E-14	B_4	-6.6204087E-12
		A_5	0.0	B_5	1.7648940E-15

Table F.6 – Minimum Yield and Tensile Strength Values from API STD 530 (1) (2)

Material	Temperature Limits and Room Temperature Strength Parameters (3) (4)	Yield Strength: σ_{ys} (3)		Tensile Strength: σ_{uts} (4)	
Type 321H (Figure 4P) A 213 Type 321H A 271 Type 321H A 312 Type 321H A 376 Type 321H	$T_{min} = 204^o C\ (400^o F)$ $T_{max} = 843^o C\ (1550^o F)$ $\sigma_{ys}^{T_{\min}} = 142\,MPa\ (20.6\ ksi)$ $\sigma_{uts}^{T_{\min}} = 427\,MPa\ (62.0\ ksi)$	A_0	1.5939147E+00	B_0	1.1972163E+00
		A_1	-2.2764479E-03	B_1	-3.3091580E-04
		A_2	2.3000206E-06	B_2	-2.1198718E-06
		A_3	-7.7700412E-10	B_3	6.4820833E-09
		A_4	-2.6637614E-14	B_4	-5.9046170E-12
		A_5	0.0	B_5	1.6286232E-15
Type 347 & 347H (Figure 4Q) A 213 Type 347&347H A 271 Type 347&347H A 312 Type 347&347H A 376 Type 347&347H	$T_{min} = 204^o C\ (400^o F)$ $T_{max} = 843^o C\ (1550^o F)$ $\sigma_{ys}^{T_{\min}} = 165\,MPa\ (24.0\ ksi)$ $\sigma_{uts}^{T_{\min}} = 387\,MPa\ (56.2\ ksi)$	A_0	1.3337499E+00	B_0	1.5437300E+00
		A_1	-7.4852863E-04	B_1	-2.4368121E-03
		A_2	-8.1021768E-07	B_2	3.3229020E-06
		A_3	1.8974804E-09	B_3	-1.5387323E-09
		A_4	-8.3958005E-13	B_4	3.9373670E-14
		A_5	0.0	B_5	0.0
Alloy 800H (Figure 4R) B407 Alloy 800H	(see Note 5)	---	(see Note 5)	---	(see Note 5)
HK-40 (Figure 4S) A608 Grade HK-40	(see Note 5)	---	(see Note 5)	---	(see Note 5)

1. Data for tensile and yield strength in this table are from Figures 4A through 4S of API STD 530 *Calculation of Heater Tube Thickness in Petroleum Refineries.*
2. Units for the equations in this table are as follows: σ_{ys} and σ_{uts} are in ksi and the temperature, T, is in degrees Fahrenheit (see notes 3 and 4).
3. σ_{ys} is the value of the yield stress at temperature where $\sigma_{ys}^{T_{\min}}$ is the value of the yield stress (minimum, average, or maximum as applicable) at the minimum temperature limit defined in this table.

$$\sigma_{ys} = \sigma_{ys}^{T_{\min}} \cdot \left(A_0 + A_1 T + A_2 T^2 + A_3 T^3 + A_4 T^4 + A_5 T^5 \right)$$

4. σ_{uts} is the value of the ultimate tensile stress at temperature where $\sigma_{uts}^{T_{\min}}$ is the value of the ultimate tensile stress (minimum, average, or maximum as applicable) at the minimum temperature limit defined in this table.

$$\sigma_{uts} = \sigma_{uts}^{T_{\min}} \cdot \left(B_0 + B_1 T + B_2 T^2 + B_3 T^3 + B_4 T^4 + B_5 T^5 \right)$$

5. Data for Figures 4R and 4S are not provided in API STD 530.

Table F.7 – Stress-Strain Curve Parameters

Material	Temperature Limit	m_2 (2)	ε_p
Ferritic Steel	480°C (900°F)	$0.60(1.00-R)$	2.0E-5
Stainless Steel and Nickel Base Alloys	480°C (900°F)	$0.75(1.00-R)$	2.0E-5
Duplex Stainless Steel	480°C (900°F)	$0.70(0.95-R)$	2.0E-5
Super Alloys (1)	540°C (1000°F)	$1.90(0.93-R)$	2.0E-5
Aluminum	120°C (250°F)	$0.52(0.98-R)$	5.0E-6
Copper	65°C (150°F)	$0.50(1.00-R)$	5.0E-6
Titanium and Zirconium	260°C (500°F)	$0.50(0.98-R)$	2.0E-5

Notes:
1. Precipitation hardening austenitic alloys
2. R is the ratio of the engineering yield stress to engineering tensile stress evaluated at the assessment temperature, see Equation (F.19).

Table F.8 – Cyclic Stress-Strain Curve Data

Material Description	Temperature (°F)	n_{css}	C_{css} (ksi)
Carbon Steel (0.75 in. – base metal)	70	0.128	109.8
	390	0.134	105.6
	570	0.093	107.5
	750	0.109	96.6
Carbon Steel (0.75 in. – weld metal)	70	0.110	100.8
	390	0.118	99.6
	570	0.066	100.8
	750	0.067	79.6
Carbon Steel (2 in. – base metal)	70	0.126	100.5
	390	0.113	92.2
	570	0.082	107.5
	750	0.101	93.3
Carbon Steel (4 in. – base metal)	70	0.137	111.0
	390	0.156	115.7
	570	0.100	108.5
	750	0.112	96.9
1Cr–1/2Mo (0.75 in. – base metal)	70	0.116	95.7
	390	0.126	95.1
	570	0.094	90.4
	750	0.087	90.8
1Cr–1/2Mo (0.75 in. – weld metal)	70	0.088	96.9
	390	0.114	102.7
	570	0.085	99.1
	750	0.076	86.9
1Cr–1/2Mo (2 in. – base metal)	70	0.105	92.5
	390	0.133	99.2
	570	0.086	88.0
	750	0.079	83.7
1Cr–1Mo–1/4V	70	0.128	156.9
	750	0.128	132.3
	930	0.143	118.2
	1020	0.133	100.5
	1110	0.153	80.6
2-1/4Cr–1/2Mo	70	0.100	115.5
	570	0.109	107.5
	750	0.096	105.9
	930	0.105	94.6
	1110	0.082	62.1

Table F.8 – Cyclic Stress-Strain Curve Data

Material Description	Temperature (°F)	n_{css}	C_{css} (ksi)
9Cr–1Mo	70	0.177	141.4
	930	0.132	100.5
	1020	0.142	88.3
	1110	0.121	64.3
	1200	0.125	49.7
Type 304	70	0.171	178.0
	750	0.095	85.6
	930	0.085	79.8
	1110	0.090	65.3
	1290	0.094	44.4
Type 304 (Annealed)	70	0.334	330.0
800H	70	0.070	91.5
	930	0.085	110.5
	1110	0.088	105.7
	1290	0.092	80.2
	1470	0.080	45.7
Aluminum (Al–4.5Zn–0.6Mn)	70	0.058	65.7
Aluminum (Al–4.5Zn–1.5Mg)	70	0.047	74.1
Aluminum (1100-T6)	70	0.144	22.3
Aluminum (2014-T6)	70	0.132	139.7
Aluminum (5086)	70	0.139	96.0
Aluminum (6009-T4)	70	0.124	83.7
Aluminum (6009-T6)	70	0.128	91.8
Copper	70	0.263	99.1

Table F.8M – Cyclic Stress-Strain Curve Data

Material Description	Temperature (°C)	n_{css}	C_{css} (MPa)
Carbon Steel (20 mm – base metal)	20	0.128	757
	200	0.134	728
	300	0.093	741
	400	0.109	666
Carbon Steel (20 mm – weld metal)	20	0.110	695
	200	0.118	687
	300	0.066	695
	400	0.067	549
Carbon Steel (50 mm – base metal)	20	0.126	693
	200	0.113	636
	300	0.082	741
	400	0.101	643
Carbon Steel (100 mm – base metal)	20	0.137	765
	200	0.156	798
	300	0.100	748
	400	0.112	668
1Cr–1/2Mo (20 mm – base metal)	20	0.116	660
	200	0.126	656
	300	0.094	623
	400	0.087	626
1Cr–1/2Mo (20 mm – weld metal)	20	0.088	668
	200	0.114	708
	300	0.085	683
	400	0.076	599
1Cr–1/2Mo (50 mm – base metal)	20	0.105	638
	200	0.133	684
	300	0.086	607
	400	0.079	577
1Cr–1Mo–1/4V	20	0.128	1082
	400	0.128	912
	500	0.143	815
	550	0.133	693
	600	0.153	556
2-1/4Cr–1/2Mo	20	0.100	796
	300	0.109	741
	400	0.096	730
	500	0.105	652
	600	0.082	428

Table F.8M – Cyclic Stress-Strain Curve Data

Material Description	Temperature (°C)	n_{css}	C_{css} (MPa)
9Cr–1Mo	20	0.177	975
	500	0.132	693
	550	0.142	609
	600	0.121	443
	650	0.125	343
Type 304	20	0.171	1227
	400	0.095	590
	500	0.085	550
	600	0.090	450
	700	0.094	306
Type 304 (Annealed)	20	0.334	2275
800H	20	0.070	631
	500	0.085	762
	600	0.088	729
	700	0.092	553
	800	0.080	315
Aluminum (Al–4.5Zn–0.6Mn)	20	0.058	453
Aluminum (Al–4.5Zn–1.5Mg)	20	0.047	511
Aluminum (1100-T6)	20	0.144	154
Aluminum (2014-T6)	20	0.132	963
Aluminum (5086)	20	0.139	662
Aluminum (6009-T4)	20	0.124	577
Aluminum (6009-T6)	20	0.128	633
Copper	20	0.263	683

Table F.9 – Equivalent to the Minimum of Three Tests

Number of Fracture Toughness Tests	Equivalent To The Minimum Of Three Tests
$3 \rightarrow 5$	Lowest value
$6 \rightarrow 10$	Second Lowest Value
$11 \rightarrow 15$	Third Lowest Value
$16 \rightarrow 20$	Fourth Lowest Value
$21 \rightarrow 25$	Fifth Lowest Vale
$26 \rightarrow 30$	Sixth Lowest Value

Table F.10 – J-R Tearing Resistance Curve Data

Material	Temperature (^{o}F)	Thickness (in)	J_T (in-lb/in^2)	C_T (in-lb/in^2)	n_T	Reference
Generic CS-1	550	1.0	350	1808	0.277	99
Generic CS-2	550	1.0	600	2563	0.274	99
Generic CS-3	550	1.0	1050	5400	0.344	99
T 304 SS	75	1.0	6500	32758	0.519	99
Generic SS/SMAW	550	1.0	990	6033	0.391	99
Generic SS/SAW	550	1.0	650	4448	0.431	99
A508 Cl3	550	1.378	446	3443	0.329	99
A106 Gr B (NPS 8 inch Pipe)	120	0.54	2900	13008	0.334	99
TP 304 SS (NPS 4 inch pipe)	75	0.34	8000	33642	0.435	99

Notes:

1. The values in this table represent typical values for the stated temperature and wall thickness, actual values should be used when available.
2. The equation for the J-R curve is:

$$J_T = C_T \left(\Delta a\right)^{n_T}$$

Table F.11 – Correlations for the Mean-to-Lower Bound Fracture Toughness Ratio (1)

Correlation	Sigma (1)	B_0	B_1	B_2	B_3	B_4	B_5
K_{mat}^{mean}/K_{IC}	0	0.49920	-1.2103E-4	1.7924E-5	3.8591E-8	4.6627E-11	2.9800E-13
	1	0.61401	2.2142E-4	2.1050E-5	5.9334E-8	8.3068E-11	2.9452E-13
	2	0.74203	7.6452E-4	2.4899E-5	8.5761E-8	1.3869E-10	2.8014E-13
	3	0.87961	1.5415E-4	2.9888E-5	1.1822E-7	2.1613E-10	2.7970E-13
K_{mat}^{mean}/K_{IR}	0	0.36138	-1.2356E-3	6.1556E-6	3.8345E-9	-3.6769E-11	5.2537E-14
	1	0.44397	-1.2400E-3	6.2434E-6	7.6693E-9	-4.0941E-11	5.1749E-14
	2	0.53624	-1.1253E-3	6.1389E-6	1.1337E-8	-3.8371E-11	3.9580E-14
	3	0.63577	-8.6564E-4	6.0413E-6	1.4613E-9	-3.0080E-11	5.8440E-14

Notes:

1. The number of standard deviations from the mean. The mean trend of the fracture toughness is taken as the medium master curve. The standard deviation on temperature used to determine the coefficients in this table is given in paragraph F.4.9.7.
2. The equation for the mean-to-lower bound toughness ratio is:

$$\left.\frac{K_{mat}^{mean}}{K_I}\right|_{sigma} = \left(\frac{1.0}{B_0 + B_1\Delta T + B_2\Delta T^2 + B_3\Delta T^3 + B_4\Delta T^4 + B_5\Delta T^5}\right)$$

where

$$\Delta T = T - T_{ref}$$

3. The data in this table is valid for $-200^o F \le \left(T - T_{ref}\right) \le 400^o F$.

Table F.12 – Fatigue Crack Growth Data for Use With the Bilinear Equation

Service Environment	R	Lower Stage of Crack Growth Curve		Upper Stage of Crack Growth Curve		ΔK Transition Between Lower and Upper Curves
		C	n	C	n	
Mean Data						
Steels with $\sigma_{ys} \le 101.5\ ksi$	$R < 0.5$	1.79E-15	8.16	4.29E-10	2.88	9.07
Operating in air or other non-aggressive environments at temperatures up to 212°F	$R \ge 0.5$	1.37E-11	5.10	6.32E-10	2.88	4.14
Steels with $\sigma_{ys} \le 87\ ksi$	$R < 0.5$	2.20E-10	3.42	5.04E-7	1.30	28.6
Operating in a freely corroding marine environment temperatures up to 68°F	$R \ge 0.5$	3.94E-10	3.42	1.15E-6	1.11	21.5
Mean Data $+2\sigma$						
Steels with $\sigma_{ys} \le 101.5\ ksi$	$R < 0.5$	6.45E-15	8.16	7.31E-10	2.88	9.07
Operating in air or other non-aggressive environments at temperatures up to 212°F	$R \ge 0.5$	5.97E-11	5.10	1.39E-9	2.88	4.14
Steels with $\sigma_{ys} \le 87\ ksi$	$R < 0.5$	6.27E-10	3.42	7.66E-7	1.30	28.6
Operating in a freely corroding marine environment temperatures up to 68°F	$R \ge 0.5$	1.26E-9	3.42	1.47E-6	1.11	21.5

Notes:

1. Units for crack growth data are: $\left(in/cycle,\ ksi\sqrt{in}\right)$.
2. The threshold stress intensity factor may be taken as $1.82\ ksi\sqrt{in}$ for use with these data.
3. The conversion factor for fracture toughness is $1.098843\ MPa\sqrt{m} = 1.0\ ksi\sqrt{in}$.
4. In the above table, $R = K_{\min}/K_{\max}$, where $K_{\max}$ and $K_{\min}$ are the maximum and minimum stress intensity for a given cycle.

Table F.12M – Fatigue Crack Growth Data for Use With the Bilinear Equation

Service Environment	R	Lower Stage of Crack Growth Curve		Upper Stage of Crack Growth Curve		ΔK Transition Between Lower and Upper Curves
		C	n	C	n	
Mean Data						
Steels with $\sigma_{ys} \le 700MPa$ Operating in air or other non-aggressive environments at temperatures up to 100°C	$R < 0.5$	2.10E-14	8.16	8.32E-9	2.88	9.96
	$R \ge 0.5$	2.14E-10	5.10	1.22E-8	2.88	4.55
Steels with $\sigma_{ys} \le 600MPa$ Operating in a freely corroding marine environment temperatures up to 20°C	$R < 0.5$	4.05E-9	3.42	1.13E-5	1.30	31.4
	$R \ge 0.5$	7.24E-9	3.42	2.62E-5	1.11	23.7
Mean Data $+2\sigma$						
Steels with $\sigma_{ys} \le 700MPa$ Operating in air or other non-aggressive environments at temperatures up to 100°C	$R < 0.5$	7.59E-14	8.16	1.41E-8	2.88	9.96 (9.07)
	$R \ge 0.5$	9.38E-10	5.10	2.70E-8	2.88	4.55
Steels with $\sigma_{ys} \le 600MPa$ Operating in a freely corroding marine environment temperatures up to 20°C	$R < 0.5$	1.15E-8	3.42	1.72E-5	1.30	31.4
	$R \ge 0.5$	2.32E-8	3.42	3.37E-5	1.11	23.7

Notes:

1. Units for crack growth data are: $\left(mm/cycle,\ MPa\sqrt{m}\right)$
2. The threshold stress intensity factor may be taken as $2.0\ MPa\sqrt{m}$ for use with these data.
3. The conversion factor for fracture toughness is $1.098843\ MPa\sqrt{m} = 1.0\ ksi\sqrt{in}$.
4. In the above table, $R = K_{\min}/K_{\max}$, where $K_{\max}$ and $K_{\min}$ are the maximum and minimum stress intensity for a given cycle.

Table F.13 – Coefficients for Fatigue Curve 110.1 – Carbon, Low Alloy, Series 4XX, High Alloy Steels, and High Tensile Strength Steels for Temperatures not Exceeding 371°C (700°F) – $\sigma_{UTS} \le 552MPa(80ksi)$

Coefficients – C_i	$48 \le S_a < 214(MPa)$ $7 \le S_a < 31(ksi)$	$214 \le S_a \le 3999(MPa)$ $31 \le S_a \le 580(ksi)$
1	2.254510E+00	7.999502E+00
2	-4.642236E-01	5.832491E-02
3	-8.312745E-01	1.500851E-01
4	8.634660E-02	1.273659E-04
5	2.020834E-01	-5.263661E-05
6	-6.940535E-03	0.0
7	-2.079726E-02	0.0
8	2.010235E-04	0.0
9	7.137717E-04	0.0
10	0.0	0.0
11	0.0	0.0
Note: $E_{FC} = 195E3\ MPa\ (28.3E3\ ksi)$		

Table F.14 – Coefficients for Fatigue Curve 110.1 – Carbon, Low Alloy, Series 4XX, High Alloy Steels, and High Tensile Strength Steels for Temperatures not Exceeding 371°C (700°F) – $\sigma_{uts} = 793 - 892\,MPa\ (115 - 130\,ksi)$

Coefficients – C_i	$77.2 \le S_a \le 296(MPa)$ $11.2 \le S_a \le 43(ksi)$	$296 < S_a \le 2896(MPa)$ $43 < S_a \le 420(ksi)$
1	1.608291E+01	8.628486E+00
2	-4.113828E-02	-1.264052E-03
3	-1.023740E+00	-1.605097E-04
4	3.544068E-05	-2.548491E-03
5	2.896256E-02	-1.409031E-02
6	1.826072E-04	8.557033E-05
7	3.863423E-04	5.059948E-04
8	0.0	6.913396E-07
9	0.0	-2.354834E-07
10	0.0	0.0
11	0.0	0.0
Note: $E_{FC} = 195E3\ MPa\ (28.3E3\ ksi)$		

Table F.15 – Coefficients for Fatigue Curve 110.2.1 – Series 3XX High Alloy Steels, Nickel-Chromium-Iron Alloy, Nickel-Iron-Chromium Alloy, and Nickel-Copper Alloy for Temperatures not Exceeding 427°C (800°F) Where $S_a > 195\ MPa\ (28.2\,ksi)$

Coefficients – C_i	$195 \le S_a \le 4881(MPa)$ $28.3 \le S_a \le 708(ksi)$
1	2.114025E+01
2	1.536993E-01
3	4.487599E-01
4	3.651302E-04
5	-8.981314E-05
6	0.0
7	0.0
8	0.0
9	0.0
10	0.0
11	0.0
Notes: $E_{FC} = 195E3\ MPa\ (28.3E3\ ksi)$	

Table F.16 – Coefficients for Fatigue Curve 110.2.2 – Series 3xx High Alloy Steels, Nickel-Chromium-Iron Alloy, Nickel-Iron-Chromium Alloy, and Nickel-Copper Alloy for Temperatures not Exceeding 427°C (800°F) Where $S_a \le 195\ MPa\ (28.2\,ksi)$

Coefficients – C_i	Curve A $163 \le S_a \le 194 (MPa)$ $23.7 \le S_a \le 28.2 (ksi)$	Curve B $114 \le S_a \le 194 (MPa)$ $16.5 \le S_a \le 28.2 (ksi)$	Curve C $94 \le S_a \le 194 (MPa)$ $13.6 \le S_a \le 28.2 (ksi)$
1	1.785872E+01	5.856886E+00	1.891543E+01
2	-4.973162E-02	-1.774051E-01	1.478023E-01
3	-2.264248E+00	-1.070324E+00	-2.436005E+00
4	-4.356560E-03	1.033285E-02	-6.369796E-02
5	9.567759E-02	6.513423E-02	-6.908655E-02
6	3.327393E-04	-1.879553E-04	5.379540E-03
7	-1.347445E-03	-1.320281E-03	1.957898E-02
8	-5.717269E-06	-5.633339E-07	-1.391592E-04
9	0.0	0.0	-6.506543E-04
10	0.0	0.0	0.0
11	0.0	0.0	0.0

Notes:

1. $E_{FC} = 206E3\ MPa\ (30E3\ ksi)$
2. Thermal bending stresses resulting from either axial or through-wall gradients are not included in Q.
3. Curve A is to be used with inelastic analysis.
4. The maximum effect of retained mean stress is included in Curve C.
5. The criterion to select a curve is shown in the following table.

Curve	Elastic Analysis Of Material Other Than Welds And Heat Effected Zones	Elastic Analysis of Welds and Heat Effected Zones
A	$(P_L + P_b + Q)_{range} \le 188\ MPa\ (27.2\,ksi)$	…
B	$(P_L + P_b + Q)_{range} > 188\ MPa\ (27.2\,ksi)$ and S_a is corrected for applied mean stress	$(P_L + P_b + Q)_{range} \le 188\ MPa\ (27.2\,ksi)$
C	$(P_L + P_b + Q)_{range} > 188\ MPa\ (27.2\,ksi)$ and S_a is not corrected for applied mean stress	$(P_L + P_b + Q)_{range} > 188\ MPa\ (27.2\,ksi)$

Table F.17 – Coefficients for Fatigue Curve 110.3 – Wrought 70 Copper-Nickel for Temperatures not Exceeding 371°C (700°F) – $\sigma_{ys} = 134\,MPa\ (18\,ksi)$

Coefficients – C_i	$83 \le S_a \le 359\,(MPa)$ $12 \le S_a \le 52\ (ksi)$	$359 < S_a \le 1793\,(MPa)$ $52 < S_a \le 260\ (ksi)$
1	5.854767E+00	4.940552E+00
2	-1.395072E-01	1.373308E-02
3	-9.597118E-01	-1.385148E-02
4	4.028700E-03	-6.080708E-05
5	4.377509E-02	-1.300476E-05
6	2.487537E-05	0.0
7	-6.795812E-04	0.0
8	-1.517491E-06	0.0
9	1.812235E-06	0.0
10	0.0	0.0
11	0.0	0.0
Note: $E_{FC} = 138E3\ MPa\ (20E3\ ksi)$		

Table F.18 – Coefficients for Fatigue Curve 110.3 – Wrought 70 Copper-Nickel for Temperatures not Exceeding 371°C (700°F) – $\sigma_{ys} = 207\,MPa\ (30\,ksi)$

Coefficients – C_i	$62 \le S_a \le 1793\,(MPa)$ $9 \le S_a \le 260\ (ksi)$
1	1.614520E+01
2	7.084155E-02
3	-3.281777E-03
4	3.171113E-02
5	3.768141E-02
6	-1.244577E-03
7	5.462508E-03
8	1.266873E-04
9	2.317630E-04
10	1.346118E-07
11	-3.703613E-07
Notes: $E_{FC} = 138E3\ MPa\ (20E3\ ksi)$	

Table F.19 – Coefficients for Fatigue Curve 110.3 – Wrought 70 Copper-Nickel for Temperatures not Exceeding 371°C (700°F) – $\sigma_{ys} = 310\,MPa\ (45\,ksi)$

Coefficients – C_i	$34 \le S_a \le 317\,(MPa)$ $4 \le S_a \le 46\,(ksi)$	$317 < S_a \le 1793\,(MPa)$ $46 < S_a \le 260\ (ksi)$
1	-5.420667E+03	1.016333E+01
2	-3.931295E+02	5.328436E-02
3	-4.778662E+01	-6.492899E-02
4	7.981353E+01	-6.685888E-05
5	2.536083E+02	2.120657E-03
6	1.002901E+00	7.140325E-06
7	2.014578E+00	0.0
8	0.0	0.0
9	0.0	0.0
10	0.0	0.0
11	0.0	0.0
Note: $E_{FC} = 138E3\ MPa\ (20E3\ ksi)$		

Table F.20 – Coefficients for Fatigue Curve 110.4 – Nickel-Chromium-Molybdenum-Iron, Alloys X, G, C-4, And C-276 for Temperatures not Exceeding 427°C (800°F)

Coefficients – C_i	$103 \le S_a \le 248\,(MPa)$ $15 \le S_a \le 36\,(ksi)$	$248 < S_a \le 4881\,(MPa)$ $36 < S_a \le 708\,(ksi)$
1	5.562508E+00	1.554581E+01
2	-1.014634E+01	6.229821E-02
3	-5.738073E+01	-8.425030E-02
4	7.152267E-01	-8.596020E-04
5	4.578432E+00	1.029439E-04
6	3.584816E-03	8.030748E-06
7	0.0	1.603119E-05
8	0.0	5.051589E-09
9	0.0	-7.849028E-09
10	0.0	0.0
11	0.0	0.0
Note: $E_{FC} = 195E3\ MPa\ (28.3E3\ ksi)$		

Table F.21 – Coefficients for Fatigue Curve 120.1 – High Strength Bolting for Temperatures not Exceeding 371°C (700°F)

Coefficients – C_i	$Maximum\ Nominal\ Stress \le 2.7S_M$ $93 \le S_a \le 7929(MPa)$ $13.5 \le S_a \le 1150(ksi)$	$Maximum\ Nominal\ Stress \le 3.0S_M$ $37 \le S_a \le 7929(MPa)$ $5.3 \le S_a \le 1150(ksi)$
1	1.083880E-02	1.268660E+01
2	-4.345648E-01	1.906961E-01
3	1.108321E-01	-8.948723E-03
4	6.215019E-02	-6.900662E-02
5	2.299388E-01	1.323214E-01
6	4.484842E-04	5.334778E-02
7	9.653374E-04	2.322671E-01
8	7.056830E-07	9.260755E-04
9	1.365681E-07	2.139043E-03
10	0.0	1.171078E-06
11	0.0	0.0
Note: $E_{FC} = 206E3\ MPa\ (30E3\ ksi)$		

Table F.22 – Data for Fatigue Curves in Table F.13 Through F.21

Number of Cycles	Fatigue Curve Table (1)					
	F.13	F.14	F.15	F.16 Curve A	F.16 Curve B	F.16 Curve C
1E1	580	420	708	---	---	---
2E1	410	320	512	---	---	---
5E1	275	230	345	---	---	---
1E2	205	175	261	---	---	---
2E2	155	135	201	---	---	---
5E2	105	100	148	---	---	---
8.5E2 (2)	---	---	---	---	---	---
1E3	83	78	119	---	---	---
2E3	64	62	97	---	---	---
5E3	48	49	76	---	---	---
1E4	38	38	64	---	---	---
1.2E4 (2)	---	43	---	---	---	---
2E4	31	36	55.5	---	---	---
5E4	23	29	46.3	---	---	---
1E5	20	26	40.8	---	---	---
2E5	16.5	24	35.9	---	---	---
5E5	13.5	22	31.0	---	---	---
1E6	12.5	20	28.3	28.2	28.2	28.2
2E6	---	---	---	26.9	22.8	22.8
5E6	---	---	---	25.7	19.8	18.4
1E7	11.1	17.8	---	25.1	18.5	16.4
2E7	---	---	---	24.7	17.7	15.2
5E7	---	---	---	24.3	17.2	14.3
1E8	9.9	15.9	---	24.1	17.0	14.1
1E9	8.8	14.2	---	23.9	16.8	13.9
1E10	7.9	12.6	---	23.8	16.6	13.7
1E11	7.0	11.2	---	23.7	16.5	13.6

Table F.22 – Data for Fatigue Curves in Table F.13 Through F.21

Number of Cycles	Fatigue Curve Table (1)					
	F.17	F.18	F.19	F.20	F.21 (3)	F.21 (4)
1E1	260	260	260	708	1150	1150
2E1	190	190	190	512	760	760
5E1	125	125	125	345	450	450
1E2	95	95	95	261	320	300
2E2	73	73	73	201	225	205
5E2	52	52	52	148	143	122
8.5E2 (2)	---	---	46	---	---	---
1E3	44	44	39	119	100	81
2E3	36	36	24.5	97	71	55
5E3	28.5	28.5	15.5	76	45	33
1E4	24.5	24.5	12	64	34	22.5
1.2E4 (2)	---	---	---	---	---	---
2E4	21	19.5	9.6	56	27	15
5E4	17	15	7.7	46.3	22	10.5
1E5	15	13	6.7	40.8	19	8.4
2E5	13.5	11.5	6	35.9	17	7.1
5E5	12.5	9.5	5.2	26.0	15	6
1E6	12.0	9.0	5	20.7	13.5	5.3
2E6	---	---	---	18.7	---	---
5E6	---	---	---	17.0	---	---
1E7	---	---	---	16.2	---	---
2E7	---	---	---	15.7	---	---
5E7	---	---	---	15.3	---	---
1E8	---	---	---	15	---	---
1E9	---	---	---	---	---	---
1E10	---	---	---	---	---	---
1E11	---	---	---	---	---	---

Notes:
1. Fatigue data are stress amplitude in ksi.
2. These data are included to provide accurate representation of the fatigue curves at branches or cusps
3. Maximum Nominal Stress (MNS) less than or equal to 2.7Sm
4. Maximum Nominal Stress (MNS) less than or equal to 3Sm

Table F.23 – Fatigue Coefficients for High Temperature Assessments – 304 SS

Coefficients – C_i	38°C (100°F)	427°C (800°F)	482°C (900°F)	538°C (1000°F)
1	1.949600E+02	2.345130E+01	1.982813E+01	1.580919E+01
2	3.266939E+04	2.994078E+03	2.525505E+03	1.948976E+03
3	1.142239E+05	8.885427E+03	6.743732E+03	4.710013E+03
4	1.546511E+06	1.269148E+05	9.925291E+04	7.326199E+04
5	-1.378146E+05	0.0	0.0	0.0
6	0.0	0.0	0.0	0.0
7	0.0	0.0	0.0	0.0
8	0.0	0.0	0.0	0.0
9	0.0	0.0	0.0	---
Coefficients – C_i	**593°C (1100°F)**	**649°C (1200°F)**	**704°C (1300°F)**	---
1	1.332639E+01	1.713751E+01	1.958334E+01	---
2	1.575541E+03	2.809912E+03	4.317931E+03	---
3	3.252683E+03	6.061109E+03	1.133469E+04	---
4	5.196564E+04	1.113861E+05	3.815248E+05	---
5	0.0	0.0	1.272626E+05	---
6	0.0	0.0	0.0	---
7	0.0	0.0	0.0	---
8	0.0	0.0	0.0	---
9	0.0	0.0	0.0	---

Table F.24 – Fatigue Coefficients for High Temperature Assessments – 316 SS

Coefficients – C_i	38°C (100 F)	427°C (800 F)	482°C (900 F)	538°C (1000 F)
1	3.619178E+01	2.135379E+01	1.415720E+01	4.839628E+01
2	6.462144E+03	3.389764E+03	2.216677E+03	1.373783E+04
3	2.370925E+04	1.190586E+04	7.678915E+03	4.493997E+04
4	3.524086E+05	1.989906E+05	1.864740E+05	1.211982E+06
5	0.0	0.0	3.202364E+04	1.740509E+05
6	0.0	0.0	0.0	0.0
7	0.0	0.0	0.0	0.0
8	0.0	0.0	0.0	0.0
9	0.0	0.0	0.0	---
Coefficients – C_i	**649°C (1200°F)**	**704°C (1300°F)**	---	---
1	4.839628E+01	1.366903E+01	---	---
2	1.373783E+04	2.126552E+03	---	---
3	4.493997E+04	3.964792E+03	---	---
4	1.211982E+06	7.588549E+04	---	---
5	1.740509E+05	-3.788228E+04	---	---
6	0.0	0.0	---	---
7	0.0	0.0	---	---
8	0.0	0.0	---	---
9	0.0	0.0	0.0	---

Table F.25 – Fatigue Coefficients for High Temperature Assessments – Alloy 800H

Coefficients – C_i	**427°C (800°F)** $\varepsilon_r < 0.00644$	**538°C (1000°F)** $\varepsilon_r < 0.00409$	**649°C (1200°F)** $\varepsilon_r < 0.00327$	**760°C (1400°F)** $\varepsilon_r < 0.00309$
1	4.689018E+02	1.049801E+00	3.103295E-01	2.643782E+00
2	4.744092E+04	-4.281680E+02	-6.316422E+02	-5.907023E+02
3	1.166065E+05	-1.187157E+03	-1.626079E+03	-1.820215E+03
4	9.668756E+05	-1.789420E+04	-2.961098E+04	6.644026E+04
5	-6.064285E+05	0.0	0.0	3.351655E+05
6	0.0	0.0	0.0	8.823527E+06
7	0.0	0.0	0.0	7.451754E+05
8	0.0	0.0	0.0	0.0
9	0.0	0.0	0.0	0.0
Coefficients – C_i	**427°C (800°F)** $\varepsilon_r \geq 0.00644$	**538°C (1000°F)** $\varepsilon_r \geq 0.00409$	**649°C (1200°F)** $\varepsilon_r \geq 0.00327$	**760°C (1400°F)** $\varepsilon_r \geq 0.00309$
1	1.591947E+01	-1.695365E-01	1.167072E+00	3.068432E+01
2	1.020212E+03	-2.146260E+03	-1.231285E+03	2.253684E+03
3	-3.897240E+02	-3.108909E+03	-3.733410E+03	-4.161959E+04
4	-1.825239E+05	1.401598E+06	-3.295415E+03	-4.564710E+06
5	-3.233094E+05	3.214994E+06	0.0	1.719350E+07
6	0.0	-2.937963E+08	0.0	2.252762E+09
7	0.0	-8.311417E+08	0.0	-1.628228E+09
8	0.0	0.0	0.0	-2.808947E+11
9	0.0	0.0	0.0	0.0

Table F.26 – Fatigue Coefficients for High Temperature Assessments – 2.25Cr-1Mo

Coefficients – C_i	**427°C (800°F)** $\varepsilon_r \le 0.00361$	**482°C (900°F)** $\varepsilon_r \le 0.003311$	**593°C (1100°F)** $\varepsilon_r \le 0.003311$	---
1	3.995798E+01	5.778010E+01	5.778010E+01	---
2	6.990107E+03	5.027539E+03	5.027539E+03	---
3	1.841288E+04	3.311636E+03	3.311636E+03	---
4	1.550651E+05	2.899535E+05	2.899535E+05	---
5	0.0	8.784559E+05	8.784559E+05	---
6	0.0	8.423550E+06	8.423550E+06	---
7	0.0	-6.117400E+06	-6.117400E+06	---
8	0.0	0.0	0.0	---
9	0.0	0.0	0.0	---
Coefficients – C_i	**427°C (800°F)** $\varepsilon_r > 0.00361$	**482°C (900°F)** $\varepsilon_r \le 0.003311$	**593°C (1100°F)** $\varepsilon_r \le 0.003311$	---
1	4.694408E+00	7.679900E+00	7.679900E+00	---
2	-2.707903E+02	-9.961664E+02	-9.961664E+02	---
3	-1.017308E+03	-8.269672E+03	-8.269672E+03	---
4	7.238326E+04	3.733534E+05	3.733534E+05	---
5	2.389872E+05	3.763790E+06	3.763790E+06	---
6	2.768600E+06	1.118880E+08	1.118880E+08	---
7	0.0	7.679900E+00	7.679900E+00	---
8	0.0	0.0	0.0	---
9	0.0	0.0	0.0	---

Table F.27 – Fatigue Coefficients for High Temperature Assessments – 9Cr-1Mo-V

Coefficients – C_i	**427°C (1000°F)** $0.0012 \le \varepsilon_r < 0.0019$	---	---	---
1	2.287031E+02	---	---	---
2	0.0	---	---	---
3	-5.769674E+05	---	---	---
4	0.0	---	---	---
5	5.666126E+08	---	---	---
6	0.0	---	---	---
7	-2.476048E+11	---	---	---
8	0.0	---	---	---
9	4.031465E+13	---	---	---
Coefficients – C_i	**427°C (1000°F)** $0.0019 \le \varepsilon_r < 0.0039$	---	---	---
1	4.952550E+00	---	---	---
2	-5.137604E+02	---	---	---
3	-3.268620E+03	---	---	---
4	-7.629416E+04	---	---	---
5	0.0	---	---	---
6	0.0	---	---	---
7	0.0	---	---	---
8	0.0	---	---	---
9	0.0	---	---	---
Coefficients – C_i	**427°C (1000°F)** $0.0039 \le \varepsilon_r \le 0.028$	---	---	---
1	8.632532E+00	---	---	---
2	0.0	---	---	---
3	0.0	---	---	---
4	1.906960E+05	---	---	---
5	3.833305E+05	---	---	---
6	0.0	---	---	---
7	0.0	---	---	---
8	5.737621E+08	---	---	---
9	3.154726E+08	---	---	---

Table F.28 – Data for Fatigue Curves in Table F.23 Through F.27

Table F.23 – Type 304 SS							
Number of Cycles	Strain Range at Temperature (Cyclic Strain Rate 1.0E-3 in/in/sec)						
	100°F	800°F	900°F	1000°F	1100°F	1200°F	1300°F
1.0E+01	5.10E-02	5.00E-02	4.65E-02	4.25E-02	3.82E-02	3.35E-02	2.97E-02
2.0E+01	3.60E-02	3.45E-02	3.15E-02	2.84E-02	2.50E-02	2.17E-02	1.86E-02
4.0E+01	2.63E-02	2.46E-02	2.22E-02	1.97E-02	1.70E-02	1.46E-02	1.23E-02
1.0E+02	1.80E-02	1.64E-02	1.46E-02	1.28E-02	1.10E-02	9.30E-03	7.70E-03
2.0E+02	1.42E-02	1.25E-02	1.10E-02	9.60E-03	8.20E-03	6.90E-03	5.70E-03
4.0E+02	1.13E-02	9.65E-03	8.45E-03	7.35E-03	6.30E-03	5.25E-03	4.43E-03
1.0E+03	8.45E-03	7.25E-03	6.30E-03	5.50E-03	4.70E-03	3.85E-03	3.33E-03
2.0E+03	6.70E-03	5.90E-03	5.10E-03	4.50E-03	3.80E-03	3.15E-03	2.76E-03
4.0E+03	5.45E-03	4.85E-03	4.20E-03	3.73E-03	3.20E-03	2.63E-03	2.30E-03
1.0E+04	4.30E-03	3.85E-03	3.35E-03	2.98E-03	2.60E-03	2.15E-03	1.85E-03
2.0E+04	3.70E-03	3.30E-03	2.90E-03	2.56E-03	2.26E-03	1.87E-03	1.58E-03
4.0E+04	3.20E-03	2.87E-03	2.54E-03	2.24E-03	1.97E-03	1.62E-03	1.38E-03
1.0E+05	2.72E-03	2.42E-03	2.13E-03	1.88E-03	1.64E-03	1.40E-03	1.17E-03
2.0E+05	2.40E-03	2.15E-03	1.90E-03	1.67E-03	1.45E-03	1.23E-03	1.05E-03
4.0E+05	2.15E-03	1.92E-03	1.70E-03	1.50E-03	1.30E-03	1.10E-03	9.40E-04
1.0E+06	1.90E-03	1.69E-03	1.49E-03	1.30E-03	1.12E-03	9.80E-04	8.40E-04

Table F.24 – Type 316 SS							
Number of Cycles	Strain Range at Temperature (Cyclic Strain Rate 1.0E-3 in/in/sec)						
	100°F	800°F	900°F	1000°F	1200°F	1300°F	---
1.0E+01	5.07E-02	4.38E-02	3.78E-02	3.18E-02	3.18E-02	2.14E-02	---
2.0E+01	3.57E-02	3.18E-02	2.51E-02	2.08E-02	2.08E-02	1.49E-02	---
4.0E+01	2.60E-02	2.33E-02	1.81E-02	1.48E-02	1.48E-02	1.05E-02	---
1.0E+02	1.77E-02	1.59E-02	1.23E-02	9.74E-03	9.74E-03	7.11E-03	---
2.0E+02	1.39E-02	1.25E-02	9.61E-03	7.44E-03	7.44E-03	5.51E-03	---
4.0E+02	1.10E-02	9.56E-03	7.61E-03	5.74E-03	5.74E-03	4.31E-03	---
1.0E+03	8.18E-03	7.16E-03	5.71E-03	4.24E-03	4.24E-03	3.28E-03	---
2.0E+03	6.43E-03	5.81E-03	4.66E-03	3.39E-03	3.39E-03	2.68E-03	---
4.0E+03	5.18E-03	4.76E-03	3.81E-03	2.79E-03	2.79E-03	2.26E-03	---
1.0E+04	4.03E-03	3.76E-03	3.01E-03	2.21E-03	2.21E-03	1.86E-03	---
2.0E+04	3.43E-03	3.16E-03	2.56E-03	1.86E-03	1.86E-03	1.62E-03	---
4.0E+04	2.93E-03	2.73E-03	2.21E-03	1.61E-03	1.61E-03	1.44E-03	---
1.0E+05	2.45E-03	2.26E-03	1.82E-03	1.36E-03	1.36E-03	1.21E-03	---
2.0E+05	2.13E-03	1.96E-03	1.59E-03	1.21E-03	1.21E-03	1.08E-03	---
4.0E+05	1.88E-03	1.73E-03	1.39E-03	1.09E-03	1.09E-03	9.54E-04	---
1.0E+06	1.63E-03	1.51E-03	1.18E-03	9.63E-04	9.63E-04	8.34E-04	---

Table F.28 – Data for Fatigue Curves in Table F.23 Through F.27

Table F.25 – 800H							
Number of Cycles	Strain Range at Temperature (Cyclic Strain Rate 1.0E-3 in/in/sec)						
	800°F	1000°F	1200°F	1400°F	---	---	---
1.0E+01	5.00E-02	4.24E-02	3.41E-02	2.84E-02	---	---	---
2.0E+01	3.62E-02	2.74E-02	2.20E-02	1.83E-02	---	---	---
4.0E+01	2.70E-02	1.85E-02	1.48E-02	1.23E-02	---	---	---
1.0E+02	1.84E-02	1.16E-02	9.32E-03	7.74E-03	---	---	---
2.0E+02	1.42E-02	8.49E-03	6.78E-03	5.62E-03	---	---	---
4.0E+02	1.13E-02	6.60E-03	5.33E-03	4.69E-03	---	---	---
1.0E+03	8.41E-03	5.15E-03	4.17E-03	3.88E-03	---	---	---
2.0E+03	6.85E-03	4.54E-03	3.66E-03	3.49E-03	---	---	---
3.0E+03	6.44E-03	4.33E-03	3.47E-03	3.09E-03	---	---	---
4.0E+03	5.72E-03	4.09E-03	3.27E-03	2.70E-03	---	---	---
1.0E+04	4.52E-03	2.93E-03	2.34E-03	2.12E-03	---	---	---
2.0E+04	3.92E-03	2.43E-03	1.97E-03	1.83E-03	---	---	---
4.0E+04	3.43E-03	2.12E-03	1.75E-03	1.64E-03	---	---	---
1.0E+05	2.88E-03	1.94E-03	1.55E-03	1.49E-03	---	---	---
2.0E+05	2.54E-03	1.86E-03	1.47E-03	1.40E-03	---	---	---
4.0E+05	2.29E-03	1.78E-03	1.40E-03	1.32E-03	---	---	---
1.0E+06	2.00E-03	1.69E-03	1.31E-03	1.22E-03	---	---	---
Table F.26 – 2.25Cr-1Mo							
Number of Cycles	Strain Range at Temperature (Cyclic Strain Rate 1.0E-3 in/in/sec)						
	800°F	900°F	1100°F	---	---	---	---
1.0E+01	5.60E-02	4.00E-02	4.00E-02	---	---	---	---
4.0E+01	2.30E-02	1.63E-02	1.63E-02	---	---	---	---
1.0E+02	1.30E-02	9.70E-03	9.70E-03	---	---	---	---
2.0E+02	9.40E-03	7.00E-03	7.00E-03	---	---	---	---
4.0E+02	7.00E-03	5.60E-03	5.60E-03	---	---	---	---
1.0E+03	5.20E-03	4.20E-03	4.20E-03	---	---	---	---
2.0E+03	4.40E-03	3.90E-03	3.90E-03	---	---	---	---
4.0E+03	4.00E-03	3.50E-03	3.50E-03	---	---	---	---
1.0E+04	3.20E-03	2.65E-03	2.65E-03	---	---	---	---
2.0E+04	2.60E-03	2.15E-03	2.15E-03	---	---	---	---
4.0E+04	2.30E-03	1.82E-03	1.82E-03	---	---	---	---
1.0E+05	1.95E-03	1.58E-03	1.58E-03	---	---	---	---
2.0E+05	1.73E-03	1.42E-03	1.42E-03	---	---	---	---
4.0E+05	1.55E-03	1.30E-03	1.30E-03	---	---	---	---
1.0E+06	1.37E-03	1.18E-03	1.18E-03	---	---	---	---

Table F.28 – Data for Fatigue Curves in Table F.23 Through F.27

Table F.27 – 9Cr-1Mo-V							
Number of Cycles	Strain Range at Temperature (Cyclic Strain Rate 1.0E-3 in/in/sec)						
	1000°F	---	---	---	---	---	---
1.0E+01	2.80E-02	---	---	---	---	---	---
2.0E+01	1.90E-02	---	---	---	---	---	---
4.0E+01	1.38E-02	---	---	---	---	---	---
1.0E+02	9.50E-03	---	---	---	---	---	---
2.0E+02	7.50E-03	---	---	---	---	---	---
4.0E+02	6.20E-03	---	---	---	---	---	---
1.0E+03	5.00E-03	---	---	---	---	---	---
2.0E+03	4.40E-03	---	---	---	---	---	---
4.0E+03	3.90E-03	---	---	---	---	---	---
1.0E+04	2.90E-03	---	---	---	---	---	---
2.0E+04	2.40E-03	---	---	---	---	---	---
4.0E+04	2.10E-03	---	---	---	---	---	---
1.0E+05	1.90E-03	---	---	---	---	---	---
2.0E+05	1.76E-03	---	---	---	---	---	---
4.0E+05	1.70E-03	---	---	---	---	---	---
1.0E+06	1.63E-03	---	---	---	---	---	---
2.0E+06	1.55E-03	---	---	---	---	---	---
4.0E+06	1.48E-03	---	---	---	---	---	---
1.0E+07	1.40E-03	---	---	---	---	---	---
2.0E+07	1.32E-03	---	---	---	---	---	---
4.0E+07	1.25E-03	---	---	---	---	---	---
1.0E+08	1.20E-03	---	---	---	---	---	---

Table F.29 – Coefficients for the Welded Joint Fatigue Curves

Statistical Basis	Ferritic and Stainless Steels		Aluminum	
	C	h	C	h
Mean Curve	1408.7	0.31950	247.04	0.27712
Upper 68% Prediction Interval $(+1\sigma)$	1688.3	0.31950	303.45	0.27712
Lower 68% Prediction Interval (-1σ)	1175.4	0.31950	201.12	0.27712
Upper 95% Prediction Interval $(+2\sigma)$	2023.4	0.31950	372.73	0.27712
Lower 95% Prediction Interval (-2σ)	980.8	0.31950	163.73	0.27712
Upper 99% Prediction Interval $(+3\sigma)$	2424.9	0.31950	457.84	0.27712
Lower 99% Prediction Interval (-3σ)	818.3	0.31950	133.29	0.27712

Note: In US Customary Units, the equivalent structural stress range parameter, ΔS_{range}, in paragraph F.6.3.2 and the structural stress effective thickness, t_{ess}, defined in Annex B1, paragraph B1.5.5 are in $ksi/(inches)^{(2-m_{ss})/2m_{ss}}$ and $inches$, respectively. The parameter m_{ss} is defined in Annex B1,paragraph B1.5.5.

Table F.29M – Coefficients for the Welded Joint Fatigue Curves

Statistical Basis	Ferritic and Stainless Steels		Aluminum	
	C	h	C	h
Mean Curve	19930.2	0.31950	3495.13	0.27712
Upper 68% Prediction Interval $(+1\sigma)$	23885.8	0.31950	4293.19	0.27712
Lower 68% Prediction Interval (-1σ)	16629.7	0.31950	2845.42	0.27712
Upper 95% Prediction Interval $(+2\sigma)$	28626.5	0.31950	5273.48	0.27712
Lower 95% Prediction Interval (-2σ)	13875.7	0.31950	2316.48	0.27712
Upper 99% Prediction Interval $(+3\sigma)$	34308.1	0.31950	6477.60	0.27712
Lower 99% Prediction Interval (-3σ)	11577.9	0.31950	1885.87	0.27712

Note: In SI Units, the equivalent structural stress range parameter, ΔS_{range}, in paragraph F.6.3.2 and the structural stress effective thickness, t_{ess}, defined in Annex B1,paragraph B1.5.5 are in $MPa/(mm)^{(2-m_{ss})/2m_{ss}}$ and mm, respectively. The parameter m_{ss} is defined in Annex B1,paragraph B1.5.5.

Table F.30 – MPC Project Omega Creep Data

Material	Notes	Strain Rate Parameter – $\dot{\varepsilon}_0$		Omega Parameter Ω	
Carbon Steel	• See Notes 1 and 2	A_0	-16.3	B_0	-1.0
		A_1	38060	B_1	3060.0
		A_2	-9165	B_2	135.0
		A_3	1200	B_3	-760.0
		A_4	-600	B_4	247.0
Carbon Steel – Graphitized	• See Notes 1 and 2	A_0	-16.8	B_0	-1.0
		A_1	38060	B_1	3060.0
		A_2	-9165	B_2	135.0
		A_3	1200	B_3	-760.0
		A_4	-600	B_4	247.0
C-0.5Mo	• See Notes 1 and 2	A_0	-19.50	B_0	-1.30
		A_1	61000.0	B_1	4500.0
		A_2	-49000.0	B_2	2000.0
		A_3	33000.0	B_3	-4500.0
		A_4	-8000.0	B_4	2000.0
1.25Cr-0.5Mo – N&T	• See Notes 1 and 2 • Use only below 538ºC (1000ºF) and stresses above (69 MPa) 10 ksi	A_0	-23.35	B_0	-4.40
		A_1	62070.0	B_1	14510.0
		A_2	-47520.0	B_2	-24671.0
		A_3	43800.0	B_3	29384
		A_4	-14790.0	B_4	-10630.0
1.25Cr-0.5Mo – Annealed	• See Notes 1 and 2 • Use only for service softened material • Use only for stresses below (69 MPa) 10 ksi	A_0	-23.5	B_0	-2.65
		A_1	52610	B_1	6110.0
		A_2	-4500	B_2	3000.0
		A_3	-5190	B_3	-4440.0
		A_4	825	B_4	1375.0
2.25Cr-1Mo – N&T	• See Notes 1 and 2 • Use only below 510ºC (950ºF) and stresses above (103 MPa) 15 ksi	A_0	-21.56	B_0	-1.12
		A_1	55518.0	B_1	5032.0
		A_2	-10910.0	B_2	-360.0
		A_3	-1705	B_3	-2320.0
		A_4	0.0	B_4	1210.0

Table F.30 – MPC Project Omega Creep Data					
Material	**Notes**	**Strain Rate Parameter – $\dot{\varepsilon}_0$**		**Omega Parameter Ω**	
2.25Cr-1Mo – Annealed	• See Notes 1 and 2	A_0	-21.86	B_0	-1.85
		A_1	50205	B_1	7205.0
		A_2	-5436	B_2	-2436.0
		A_3	500	B_3	0.0
		A_4	-3400	B_4	0.0
2.25Cr-1Mo – Q&T	• See Notes 1 and 2 • Use only below 510ºC (950ºF) and stresses above (103 MPa) 15 ksi	A_0	-21.56	B_0	-1.12
		A_1	55518.0	B_1	5032.0
		A_2	-10910.0	B_2	-360.0
		A_3	-1705	B_3	-2320.0
		A_4	0.0	B_4	1210.0
2.25Cr-1Mo – V	• See Notes 1 and 2 • Use only below 510ºC (950ºF) and stresses above (138 MPa) 20 ksi	A_0	-25.0	B_0	-2.53
		A_1	50315.0	B_1	9000.0
		A_2	5358.06	B_2	-3500.0
		A_3	-7580.0	B_3	225.0
		A_4	0.0	B_4	0.0
5Cr-0.5Mo	• See Notes 1 and 2	A_0	-22.40	B_0	-1.40
		A_1	51635.0	B_1	5035.0
		A_2	-7330.0	B_2	-1330.0
		A_3	-2577.0	B_3	423.0
		A_4	0.0	B_4	0.0
9Cr-1Mo	• See Notes 1 and 2	A_0	-20.85	B_0	-1.10
		A_1	49672.0	B_1	5400.0
		A_2	-6038.0	B_2	-1600.0
		A_3	-6178.0	B_3	-1000.0
		A_4	0.0	B_4	0.0
9Cr-1Mo – V	• See Notes 1 and 2	A_0	-34.0	B_0	-2.00
		A_1	73201.8	B_1	7200.0
		A_2	-2709.0	B_2	-1500.0
		A_3	-4673.0	B_3	0.0
		A_4	-569.0	B_4	0.0

Table F.30 – MPC Project Omega Creep Data					
Material	**Notes**	**Strain Rate Parameter – $\dot{\varepsilon}_0$**		**Omega Parameter Ω**	
12 Cr	• See Notes 1 and 2	A_0	-30.29	B_0	-3.298
		A_1	67110.0	B_1	6508.0
		A_2	-21093.0	B_2	3016.0
		A_3	14556.0	B_3	-2784.0
		A_4	-5884.0	B_4	480.0
Type 304 & 304H	• See Notes 1 and 2	A_0	-19.17	B_0	-3.40
		A_1	53762.4	B_1	11250.0
		A_2	-13442.4	B_2	-5635.8
		A_3	3162.6	B_3	3380.4
		A_4	-1685.2	B_4	-993.6
Type 316 & 316H	• See Notes 1 and 2	A_0	-18.9	B_0	-4.163
		A_1	57190.0	B_1	17104.762
		A_2	-18060.0	B_2	-12620.0
		A_3	2842.213	B_3	3949.151
		A_4	200.2	B_4	400.0
Type 321	• See Notes 1 and 2	A_0	-19	B_0	-3.4
		A_1	49425	B_1	10625
		A_2	-7417	B_2	-3217
		A_3	1240	B_3	1640
		A_4	-1290	B_4	-490
Type 321H	• See Notes 1 and 2	A_0	-18.4	B_0	-3.4
		A_1	49425	B_1	10625
		A_2	-7417	B_2	-3217
		A_3	1240	B_3	1640
		A_4	-1290	B_4	-490
Type 347	• See Notes 1 and 2	A_0	-18.3	B_0	-3.5
		A_1	47140.0	B_1	10000.0
		A_2	-5434.0	B_2	-800.0
		A_3	500.0	B_3	-100.0
		A_4	-1128.0	B_4	100.0

Table F.30 – MPC Project Omega Creep Data					
Material	**Notes**	**Strain Rate Parameter – $\dot{\varepsilon}_0$**		**Omega Parameter Ω**	
Type 347H	• See Notes 1 and 2	A_0	-17.70	B_0	-3.65
		A_1	47140.0	B_1	10000.0
		A_2	-5434.0	B_2	-800.0
		A_3	500.0	B_3	-100.0
		A_4	-1128.0	B_4	100.0
Alloy 800	• See Notes 1 and 2	A_0	-19.4	B_0	-3.6
		A_1	55548	B_1	11250
		A_2	-15877	B_2	-5635
		A_3	3380	B_3	3380
		A_4	-993	B_4	-993
Alloy 800H	• See Notes 1 and 2	A_0	-18.8	B_0	-3.6
		A_1	55548	B_1	11250
		A_2	-15877	B_2	-5635
		A_3	3380	B_3	3380
		A_4	-993	B_4	-993
Alloy 800HT	• See Notes 1 and 2	A_0	-20.25	B_0	-3.4
		A_1	59415.0	B_1	11250
		A_2	-13677.0	B_2	-5635
		A_3	-1009.0	B_3	3380
		A_4	625.0	B_4	-993
HK-40	• See Notes 1 and 2	A_0	-14.80	B_0	-4.40
		A_1	47065.0	B_1	13000.0
		A_2	-7170.0	B_2	-400.0
		A_3	-2962.0	B_3	0.0
		A_4	1145.0	B_4	0.0

Notes:

1. Coefficients in this table are estimates of the typical material behavior (center of scatter band) based on the MPC Project Omega Materials data from service-aged materials at design stress levels.
2. The coefficients in this table are intended to describe material behavior in the range of the ASME Code design allowable stress for a given material at a specified temperature. These coefficients may be used to estimate the stress relaxation resulting from creep over a similar stress range.

Table F.31 – Minimum and Average Larson-Miller Parameters as a Function of Stress Based on API STD 530

Material	Equation (Note 3)	Parameters	Minimum Larson-Miller Parameter – LMP_m	Average Larson-Miller Parameter – LMP_a
Low Carbon Steel (Figure 4A) A161 A192	1	A_0	3.9472132E+01	3.9793713E+01
		A_1	-1.7555884E-01	-1.5443414E-01
		A_2	0.0	0.0
		A_3	-2.5495581E+00	-2.6260065E+00
		C_{LMP}	20.0	20.0
Medium Carbon Steel (Figure 4B) A53 Grade B A106 Grade B A210 Grade A-1	1	A_0	4.0588307E+01	4.1406114E+01
		A_1	-1.7712679E-01	-9.4412373E-02
		A_2	0.0	-8.1630012E-04
		A_3	-2.6062117E+00	-2.8222989E+00
		C_{LMP}	20.0	20.0
C-0.5Mo (Figure 4C) A 161 T1 A 209 T1 A 335 P1	1	A_0	4.0572407E+01	4.1235292E+01
		A_1	4.6810884E-02	3.7759486E-02
		A_2	-1.7428803E-03	-1.1188817E-03
		A_3	-2.4287545E+00	-2.4403636E+00
		C_{LMP}	20.0	20.0
1.25Cr-0.5Mo (Figure 4D) A 213 T11 A 335 P11 A 200 T11	1	A_0	4.1444290E+01	4.2605250E+01
		A_1	-1.6608091E-03	0.0
		A_2	0.0	0.0
		A_3	-2.5842632E+00	-2.6236052E+00
		C_{LMP}	20.0	20.0
2.25Cr-1Mo (Figure 4E) A 213 T22 A 335 P22 A 200 T22	2	A_0	4.3981719E+01	4.3494159E+01
		A_1	-8.4656117E-01	-6.0165638E-01
		A_2	-4.0483005E+01	-2.8040471E+01
		A_3	2.6236081E-01	2.0644229E-01
		A_4	1.5373650E+01	1.0982290E+01
		A_5	4.9673781E-02	2.8393767E-02
		A_6	6.6049429E-01	3.6067024E-01
		C_{LMP}	20.0	20.0
3Cr-1Mo (Figure 4F) A 213 T5 A 335 P5 A 200 T5	1	A_0	4.4051838E+01	4.4786113E+01
		A_1	0.0	0.0
		A_2	0.0	0.0
		A_3	-3.4764953E+00	-3.5012470E+00
		C_{LMP}	20.0	20.0

Table F.31 – Minimum and Average Larson-Miller Parameters as a Function of Stress Based on API STD 530

Material	Equation (Note 3)	Parameters	Minimum Larson-Miller Parameter – LMP_m	Average Larson-Miller Parameter – LMP_a
5Cr-0.5Mo (Figure 4G) A 213 T5 A 335 P5 A 200 T5	1	A_0	4.4060307E+01	4.5561570E+01
		A_1	0.0	0.0
		A_2	0.0	0.0
		A_3	-3.8832654E+00	-3.9292158E+00
		C_{LMP}	20.0	20.0
5Cr-0.5Mo-Si (Figure 4H) A 213 T5b A 335 P5b	1	A_0	4.3412435E+01	4.5193964E+01
		A_1	6.0084603E-04	0.0
		A_2	0.0	0.0
		A_3	-4.0873944E+00	-4.0637419E+00
		C_{LMP}	20.0	20.0
7Cr-0.5Mo (Figure 4I) A 213 T7 A 335 P7 A 200 T7	1	A_0	4.4585981E+01	4.5795478E+01
		A_1	0.0	0.0
		A_2	0.0	0.0
		A_3	-4.4159080E+00	-4.4250128E+00
		C_{LMP}	20.0	20.0
9Cr-1Mo (Figure 4J) A 213 T9 A 335 P9 A 200 T9	1	A_0	4.3440090E+01	4.4713375E+01
		A_1	0.0	0.0
		A_2	0.0	0.0
		A_3	-3.1274348E+00	-3.1087353E+00
		C_{LMP}	20.0	20.0
9Cr-1Mo-V (Figure 4K) A 213 T91 A 335 P91 A 200 T91	1	A_0	5.8775488E+01	6.0293151E+01
		A_1	6.3030427E-01	2.9164576E-01
		A_2	4.3080961E+01	2.0624046E+01
		A_3	-4.2138473E-02	8.1446975E-03
		C_{LMP}	-5.8181139E+00	-1.3816921E+00
Type 304 & 304H (Figure 4L) A 213 Type 304 & 304H A 271 Type 304 & 304H A 312 Type 304 & 304H A 376 Type 304 & 304H	1	A_0	1.3056690E-03	1.2791388E-04
		A_1	2.8215429E-01	6.5750485E-02
		A_2	30.0	30.0
		A_3	4.1604481E+01	4.3167974E+01
		C_{LMP}	0.0	0.0

Table F.31 – Minimum and Average Larson-Miller Parameters as a Function of Stress Based on API STD 530

Material	Equation (Note 3)	Parameters	Minimum Larson-Miller Parameter – LMP_m	Average Larson-Miller Parameter – LMP_a
Type 316 & 316H (Figure 4M) A 213 Type 316 & 316H A 271 Type 316 & 316H A 312 Type 316 & 316H A 376 Type 316 & 316H	1	A_0	4.0727285E+01	4.1474655E+01
		A_1	0.0	0.0
		A_2	0.0	0.0
		A_3	-3.3777142E+00	-3.3744962E+00
		C_{LMP}	15.0	15.0
Type 316L (Figure 4N) A 213 Type 316L A 312 Type 316L	1	A_0	4.0013821E+01	4.0734498E+01
		A_1	0.0	-3.7185119E-03
		A_2	0.0	0.0
		A_3	-3.2795068E+00	-3.2327975E+00
		C_{LMP}	15.0	15.0
Type 321 (Figure 4O) A 213 Type 321 A 271 Type 321 A 312 Type 321 A 376 Type 321	1	A_0	3.7886814E+01	3.9898092E+01
		A_1	0.0	0.0
		A_2	0.0	0.0
		A_3	-3.1045579E+00	-3.1231396E+00
		C_{LMP}	15.0	15.0
Type 321H (Figure 4P) A 213 Type 321H A 271 Type 321H A 312 Type 321H A 376 Type 321H	1	A_0	4.0463845E+01	4.2128555E+01
		A_1	0.0	0.0
		A_2	0.0	0.0
		A_3	-3.8251065E+00	-3.8415837E+00
		C_{LMP}	15.0	15.0
Type 347 & 347H (Figure 4Q) A 213 Type 347 & 347H A 271 Type 347 & 347H A 312 Type 347 & 347H A 376 Type 347 & 347H	1	A_0	4.0978191E+01	4.1681564E+01
		A_1	0.0	0.0
		A_2	0.0	0.0
		A_3	-3.3967083E+00	-3.3844260E+00
		C_{LMP}	15.0	15.0
Alloy 800H (Figure 4R) B407 Alloy 800H	1	A_0	4.2984876E+01	4.3972044E+01
		A_1	1.0453205E-02	1.1049396E-02
		A_2	0.0	0.0
		A_3	-4.4907290E+00	-4.4942889E+00
		C_{LMP}	15.0	15.0

Table F.31 – Minimum and Average Larson-Miller Parameters as a Function of Stress Based on API STD 530

Material	Equation (Note 3)	Parameters	Minimum Larson-Miller Parameter – LMP_m	Average Larson-Miller Parameter – LMP_a
HK-40 (Figure 4S) A608 Grade HK-40	1	A_0	4.4347806E+01	4.5201670E+01
		A_1	-2.0236623E-01	-1.6593352E-01
		A_2	0.0	0.0
		A_3	-3.7794033E+00	-3.8011626E+00
		C_{LMP}	15.0	15.0

Notes:

1. Data for the minimum and average Larson-Miller parameters in this table are from Figures 4-A through 4-S of API STD 530 *Calculation of Heater Tube Thickness in Petroleum Refineries.*
2. Units for the equations in this table are as follows: σ are in ksi.
3. The general form of Equations 1 and 2 are as follows:

   Equation 1: $LMP_{m,a} = A_o + A_1\sigma + A_2\sigma^2 + A_3 \ln \sigma$

   Equation 2: $LMP_{m,a} = \dfrac{A_o + A_2\sqrt{\sigma} + A_4\sigma + A_6\sigma^{1.5}}{1 + A_1\sqrt{\sigma} + A_3\sigma + A_5\sigma^{1.5}}$

4. LMP_m is the minimum Larson-Miller parameter based on minimum stress to rupture data.
5. LMP_a is the average Larson-Miller parameter based on average stress to rupture data.

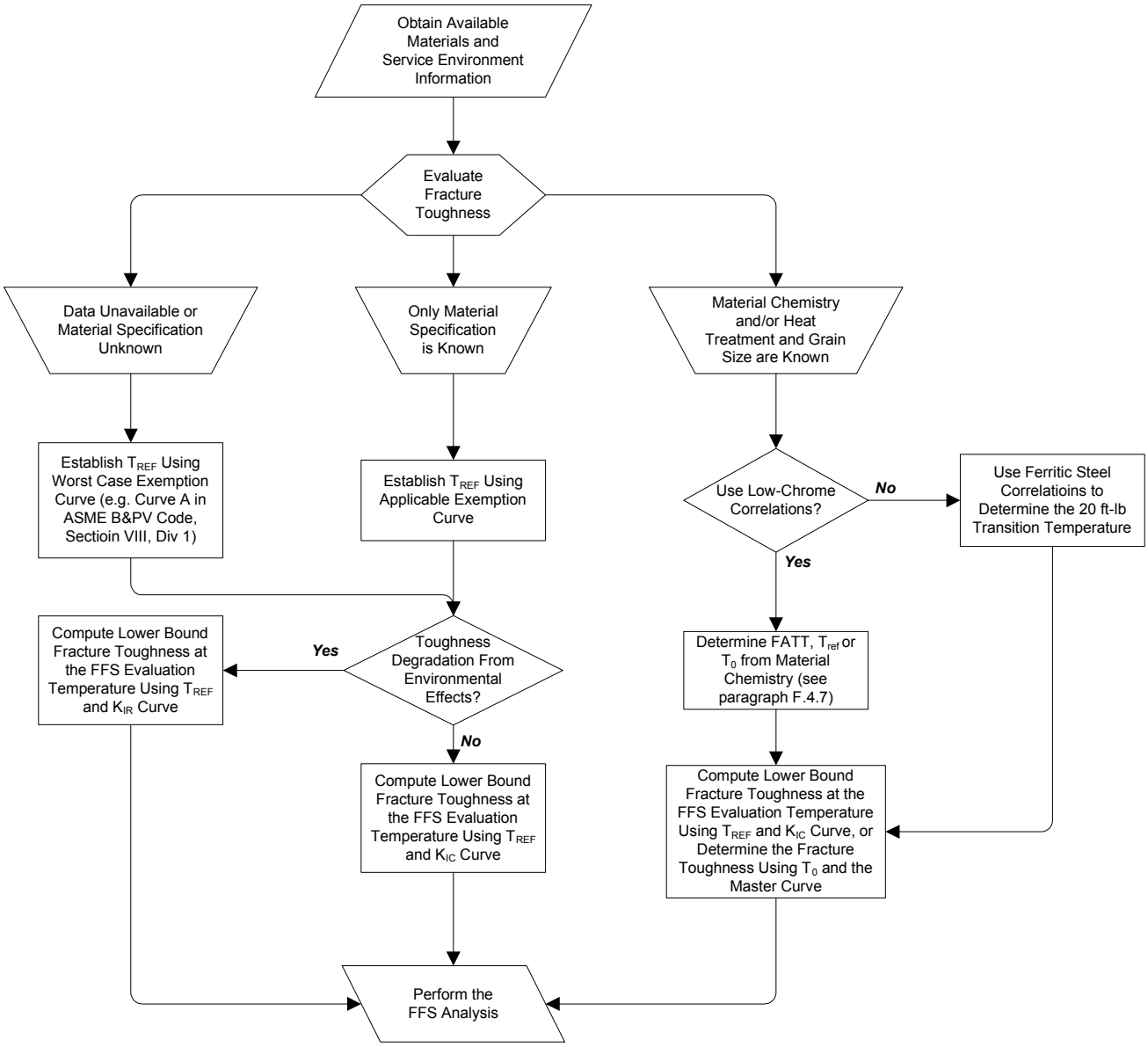

Figure F.1 – Guidelines for Establishing Fracture Toughness in a *FFS* Assessment (Toughness Data Unavailable)

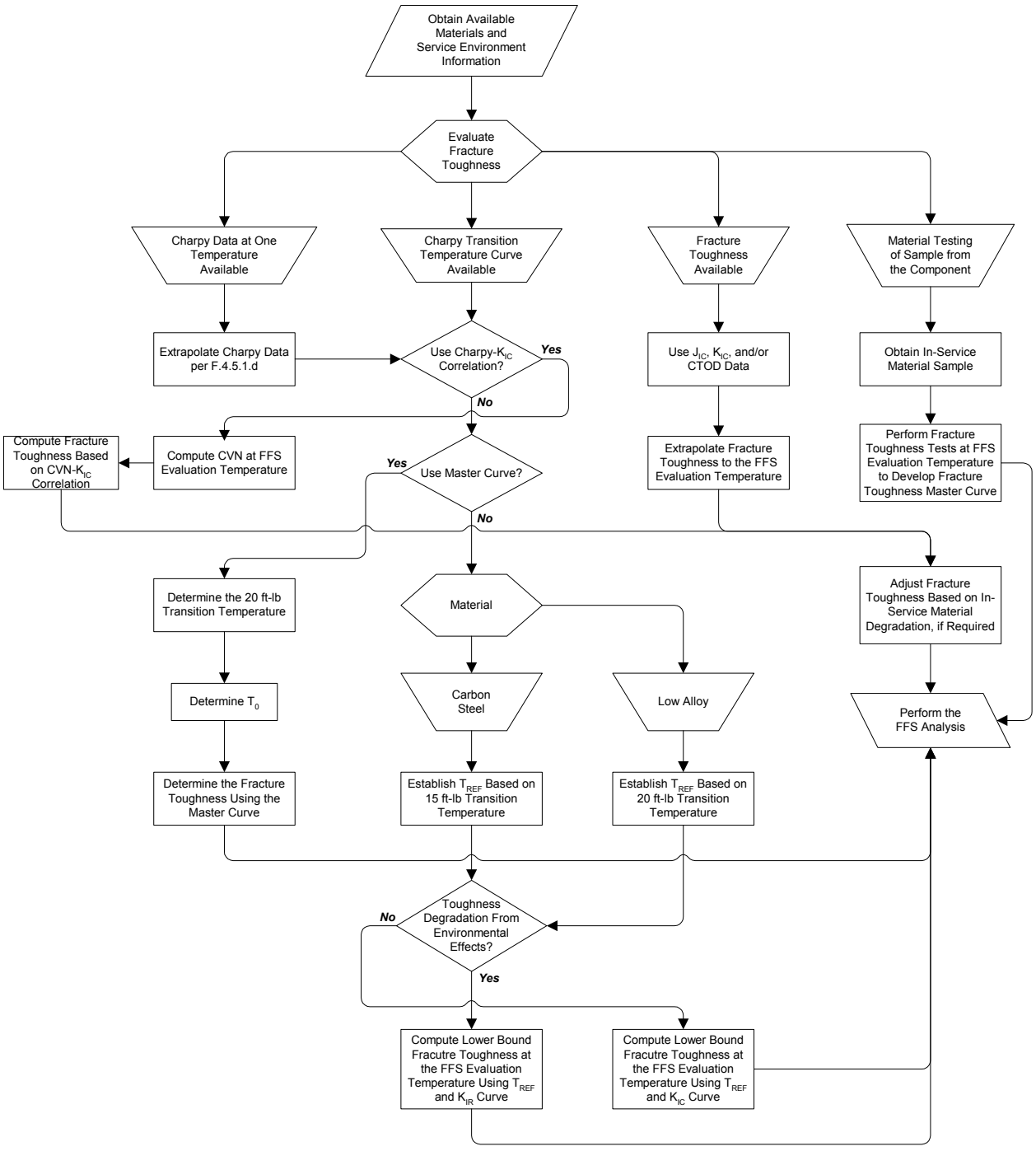

Figure F.2 – Guidelines for Establishing Fracture Toughness in a *FFS* Assessment (Toughness Data Available)

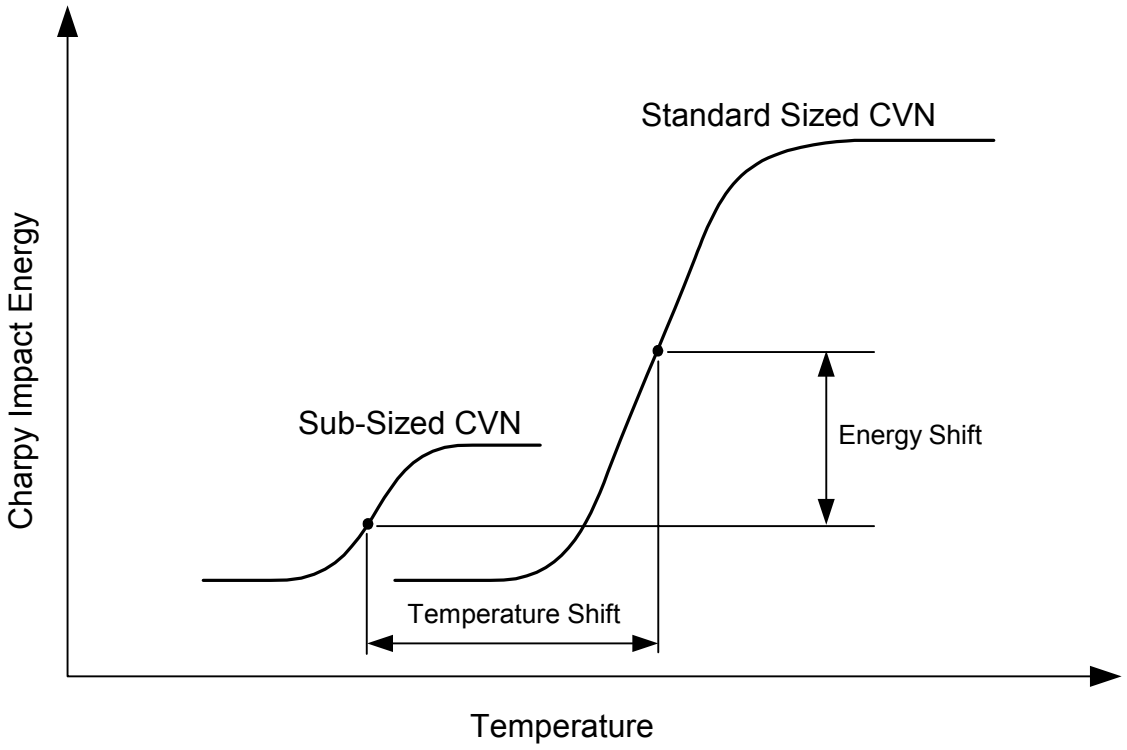

Figure F.3 – Difference in CVN Transition Curve Generated Using Standard Size and Sub-Size Specimens

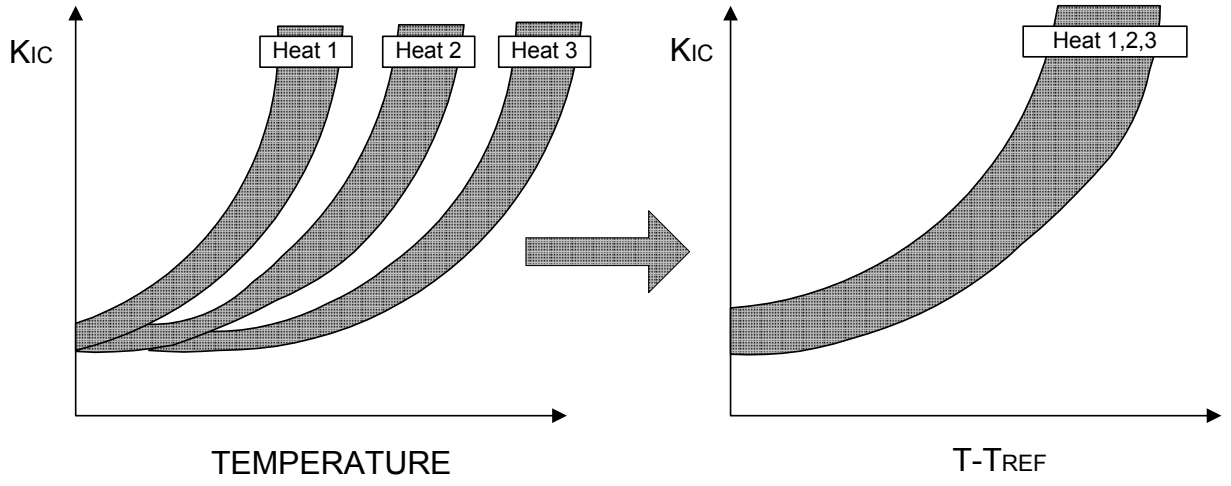

(a) Concept of Fracture Toughness Indexing

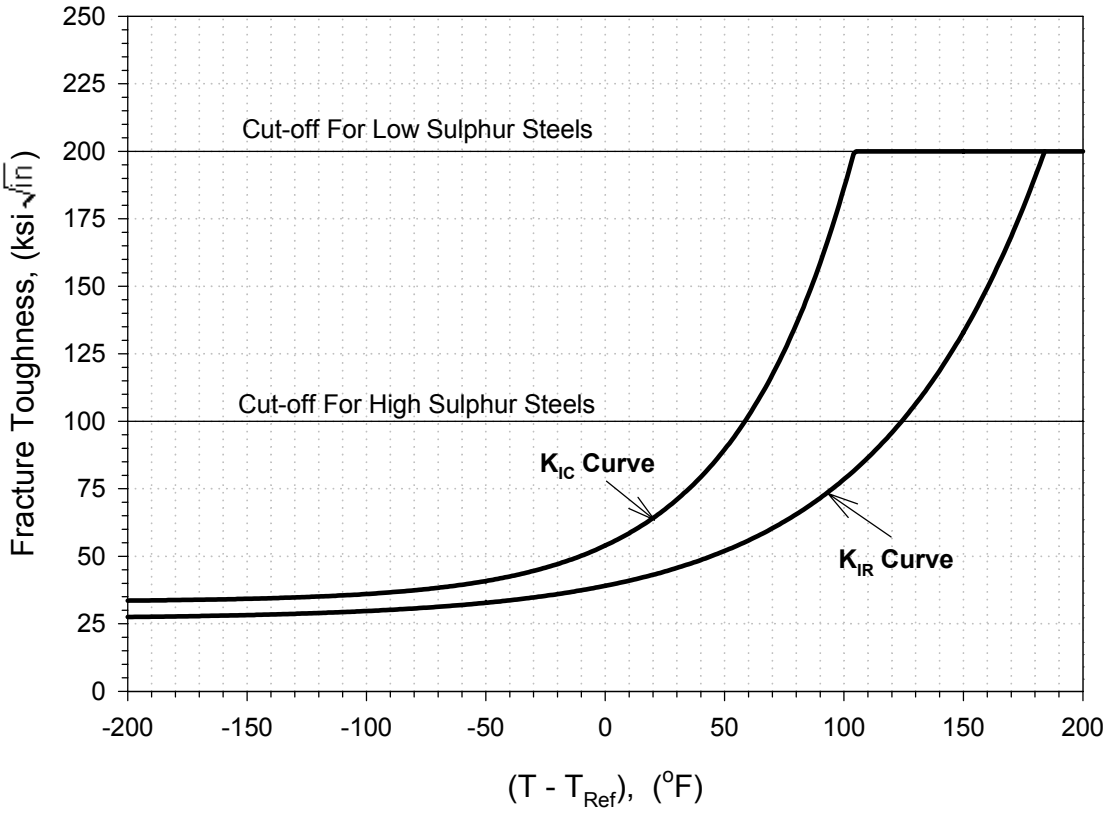

(b) Lower-Bound Fracture Toughness Curves for Ferritic Steels

Figure F.4 – The Fracture Toughness Indexing Approach

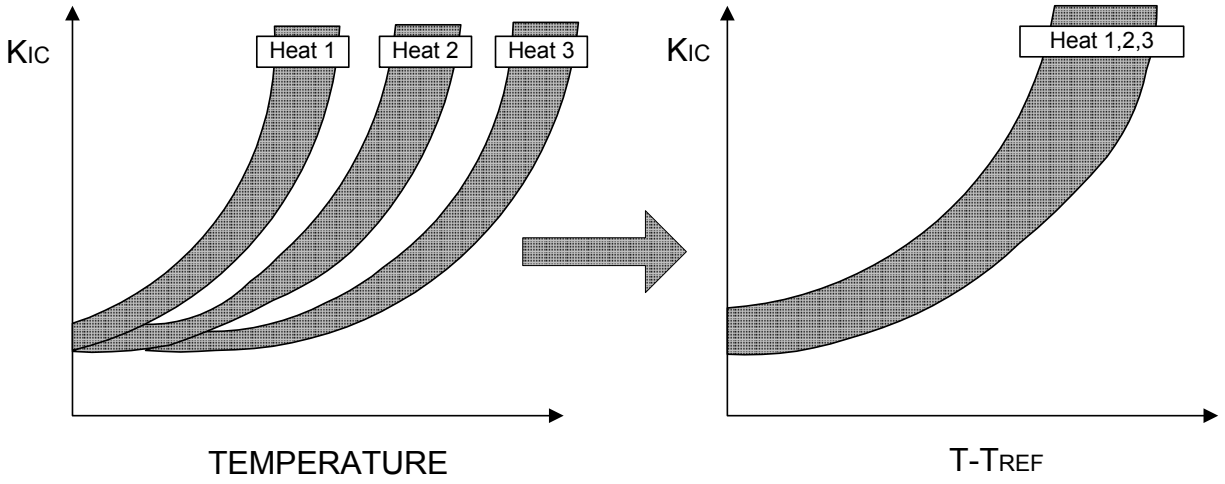

(a) Concept of Fracture Toughness Indexing

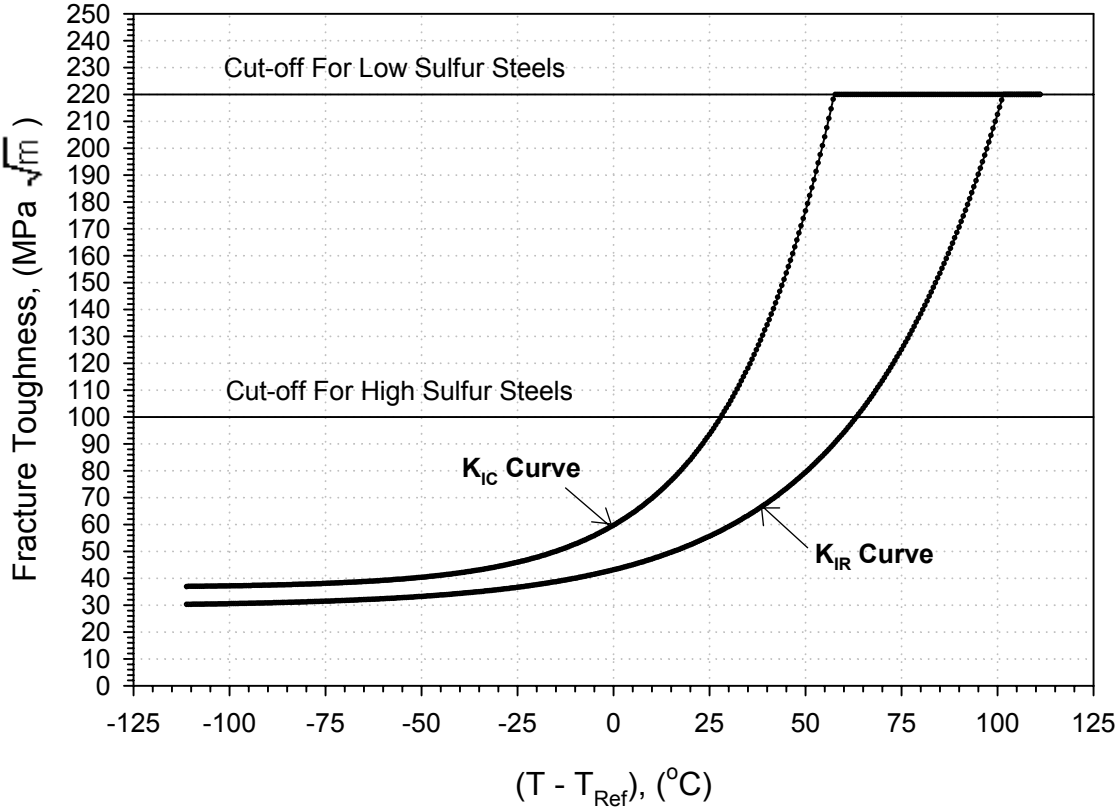

(b) Lower-Bound Fracture Toughness Curves for Ferritic Steels

Figure F.4M – The Fracture Toughness Indexing Approach

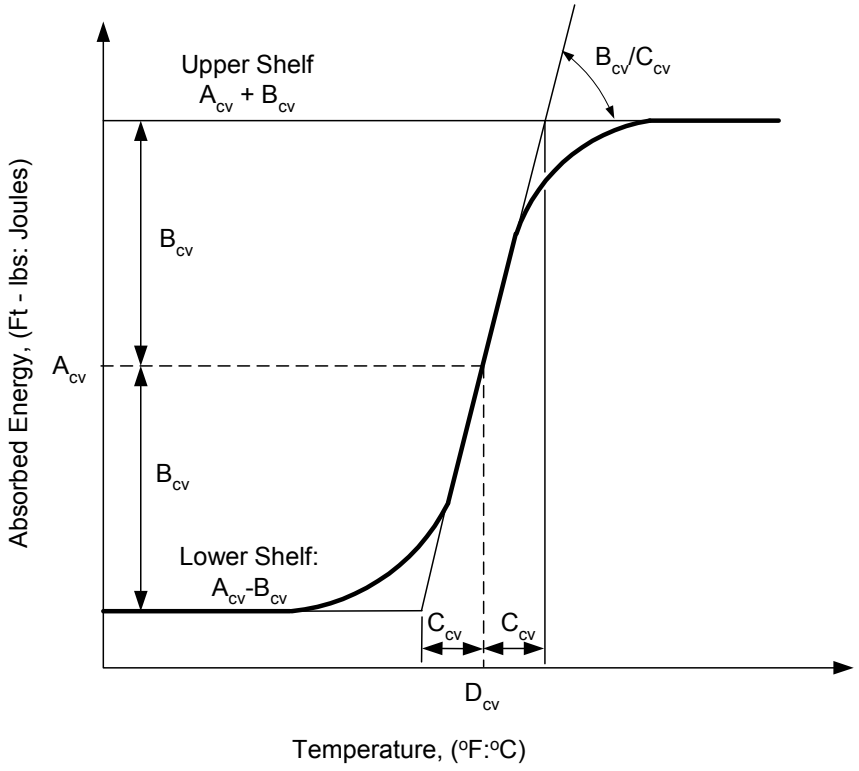

(a) Characteristics of the Hyperbolic Tangent Function

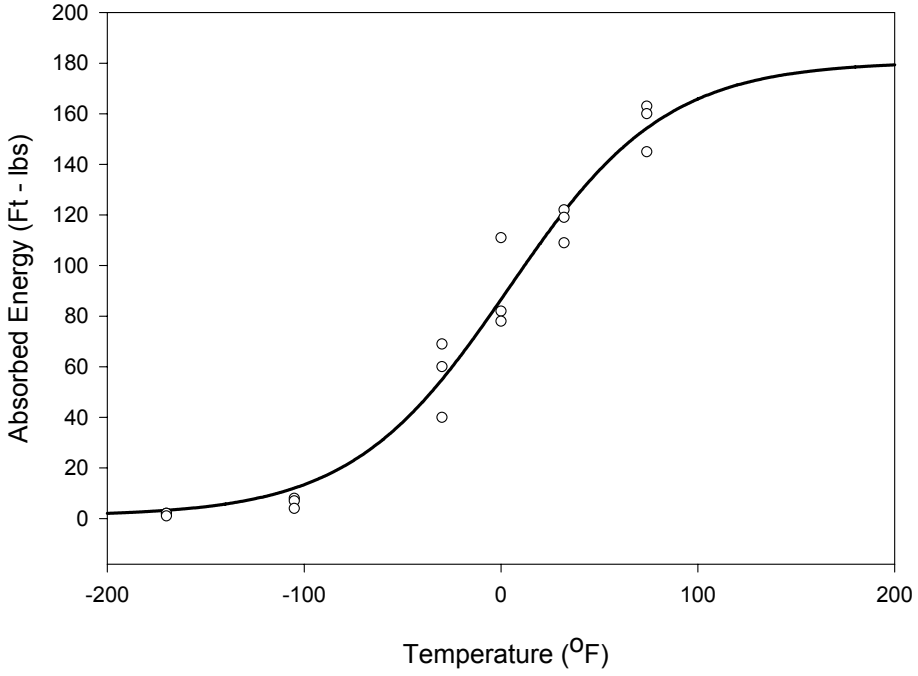

(b) Typical Hyperbolic Tangent Function Curve Fit to CVN data

Figure F.5 – Curve Fitting of Charpy Data

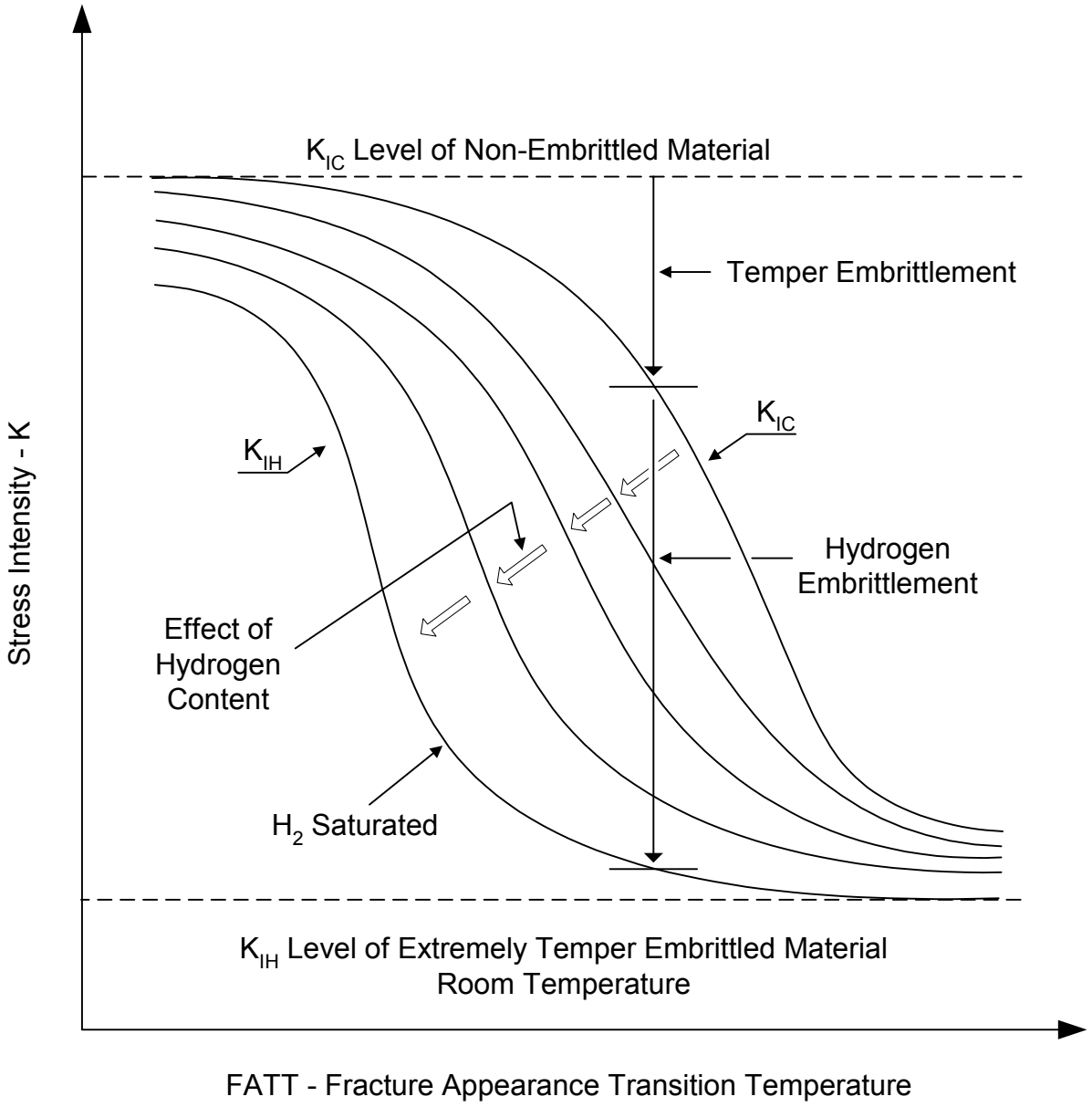

Figure F.6 – Effect of Temper Embrittlement and Hydrogen on the Toughness of 2.25Cr-1Mo Steel

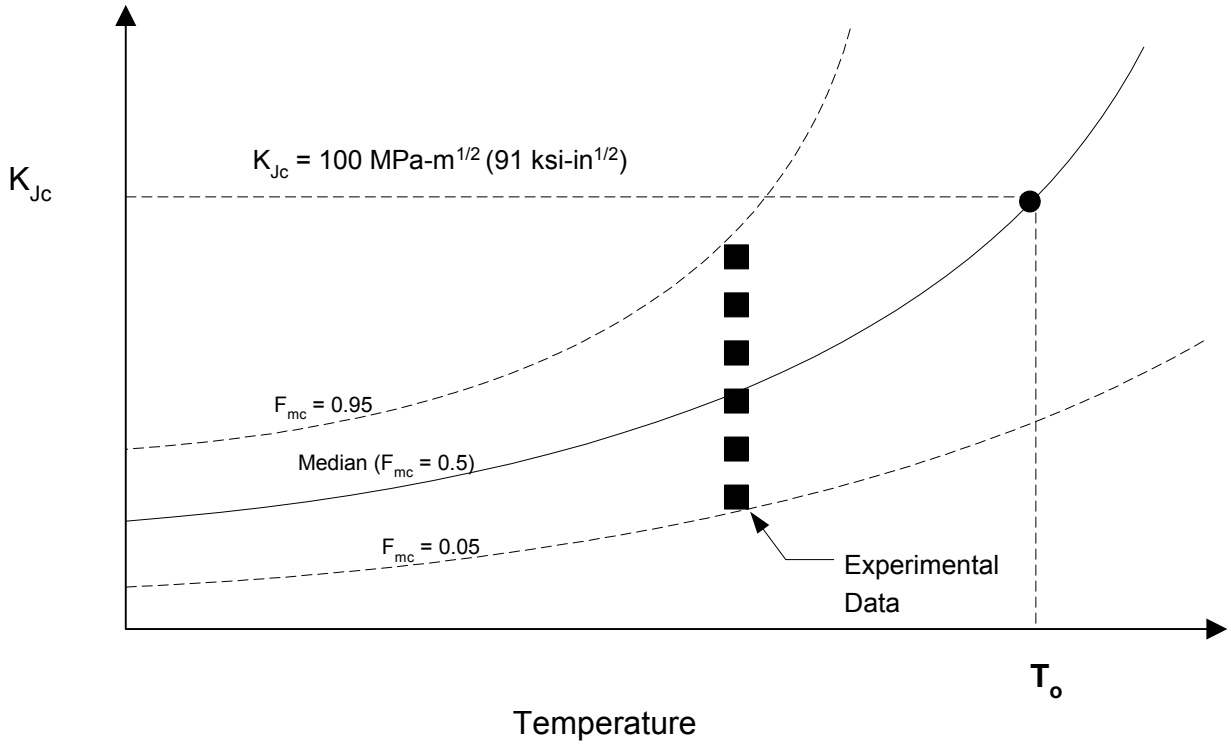

Notes:

1. F_{mc} is the cumulative probability.
2. K_{Jc} is the fracture toughness.
3. T_0 is the temperature at which $K_{Jc} = 100\ MPa\sqrt{m}$.

Figure F.7 – Fracture Toughness Master Curve

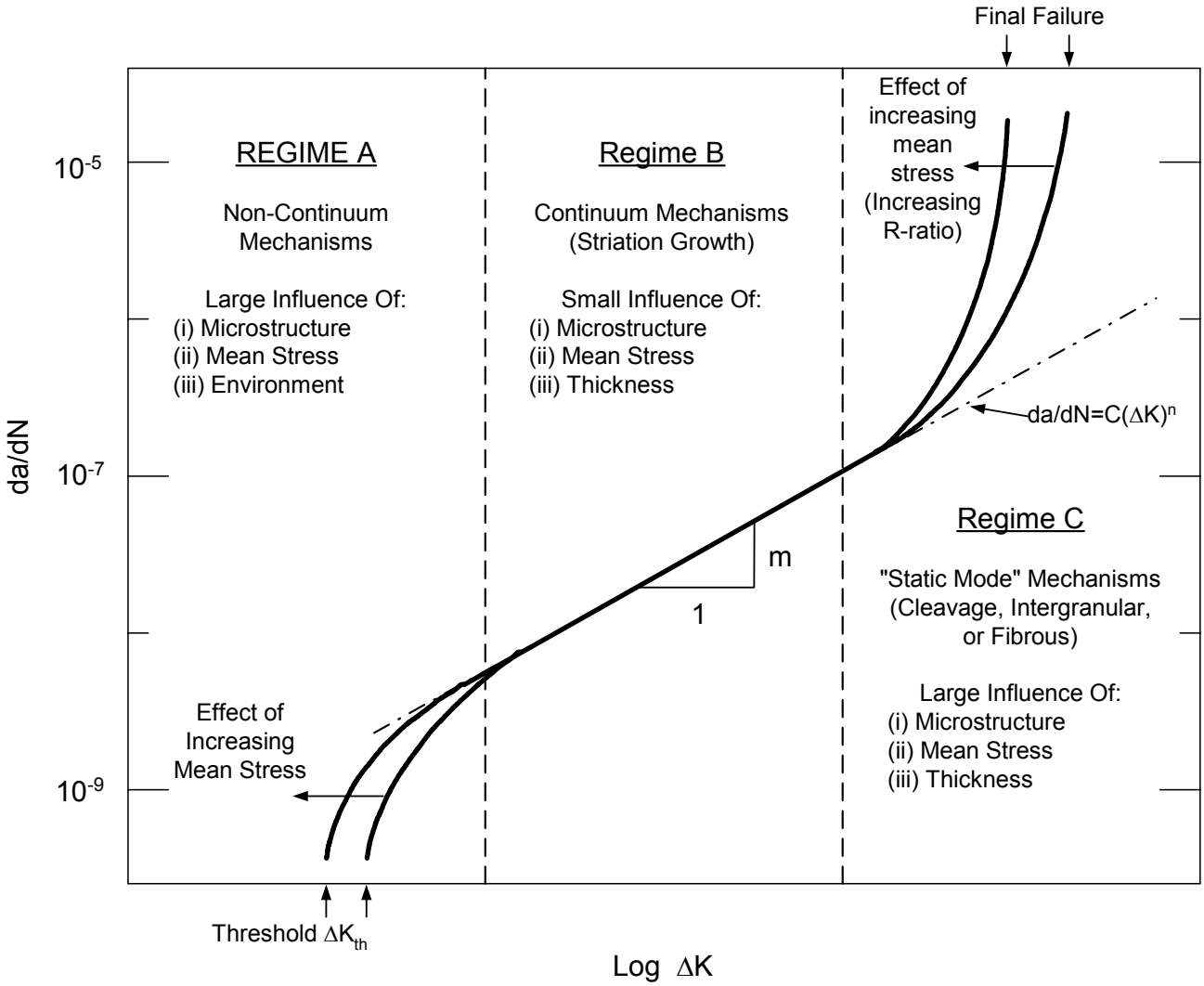

Figure F.8 – Crack Growth Behavior – Fatigue

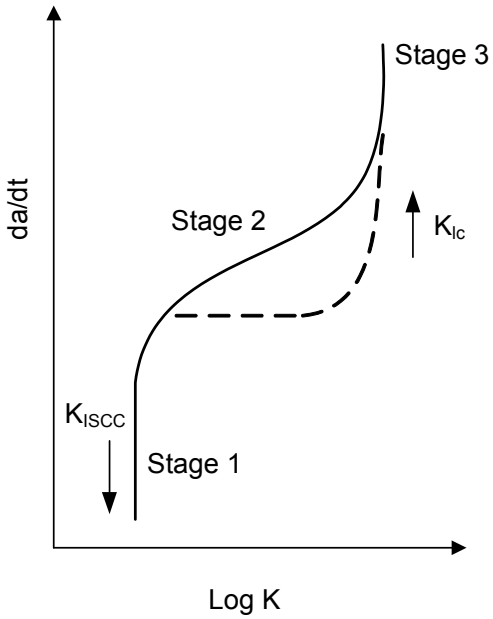

(a) Crack Growth Rate and Stress Intensity Factor Relationship for Two Enviornments

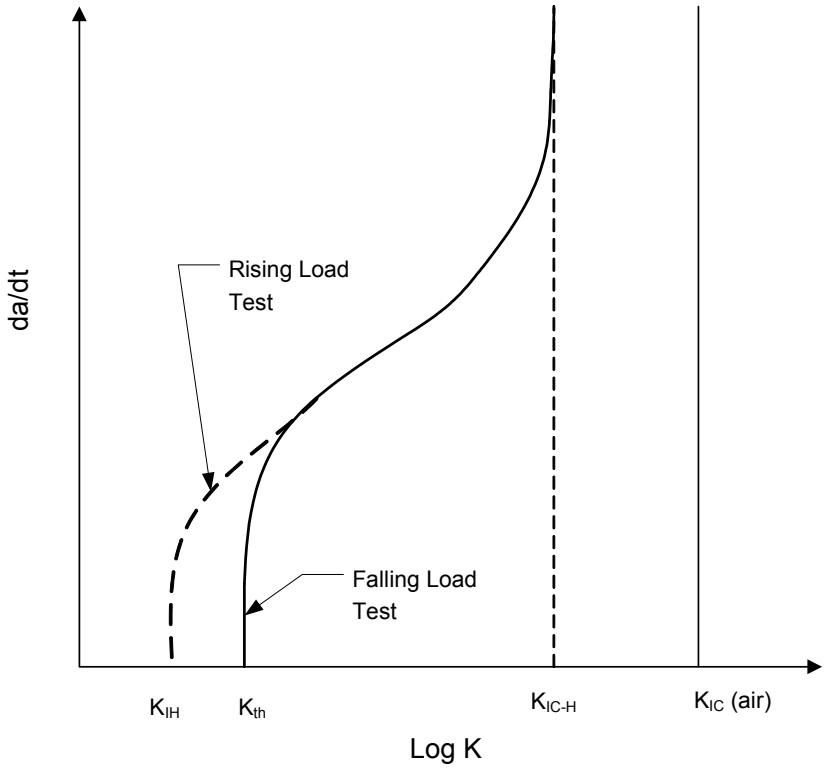

(b) Hydrogen Assisted Crack (HAC) Growth Curve

Figure F.9 – Crack Growth Behavior – Stress Corrosion Cracking and HAC

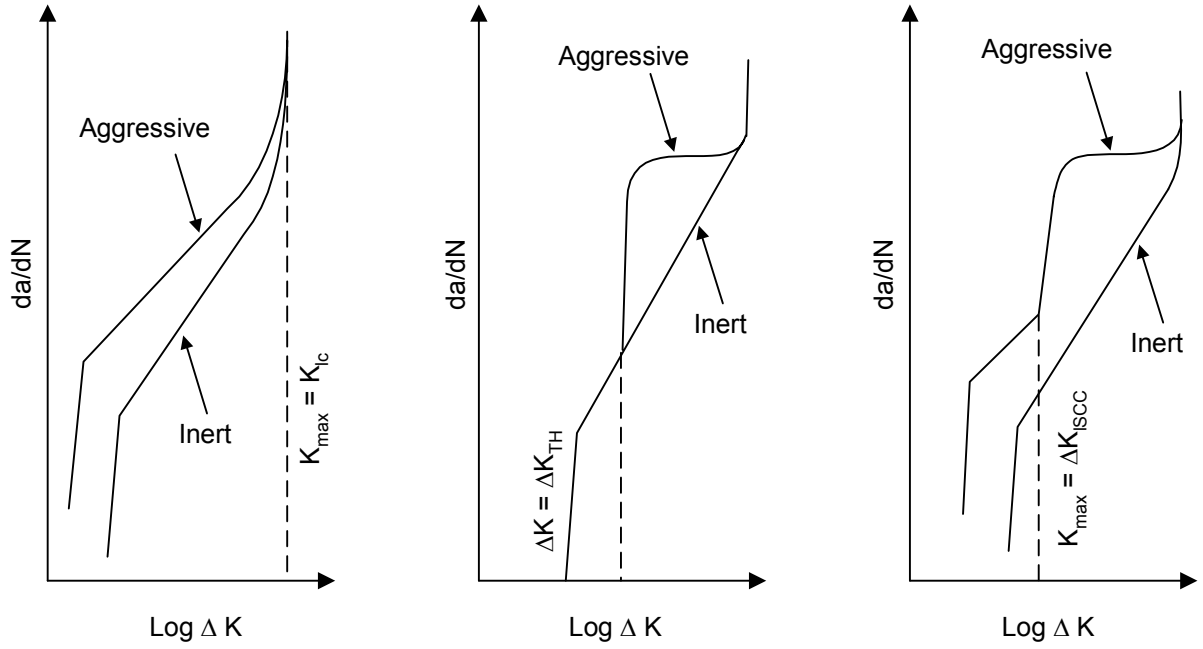

Figure F.10 – Crack Growth Behavior – Corrosion Fatigue

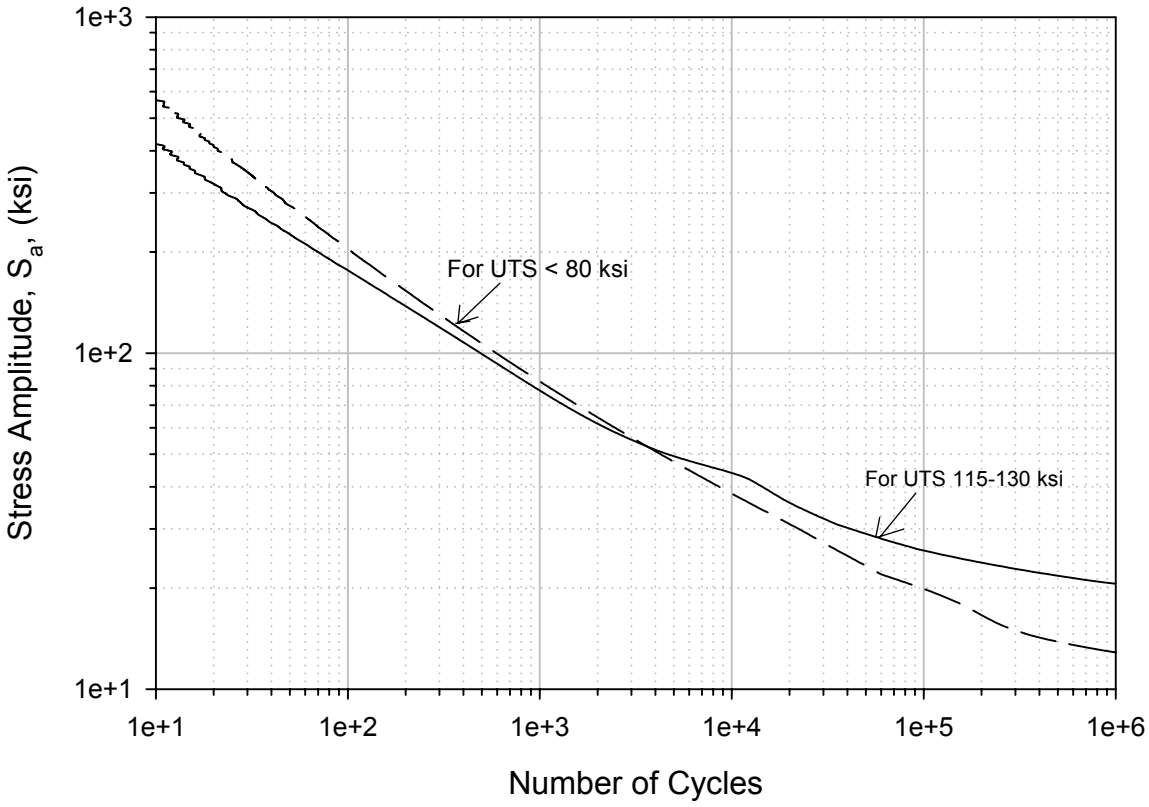

Figure F.11 – Fatigue Curves Based on Smooth Bar Test Specimens

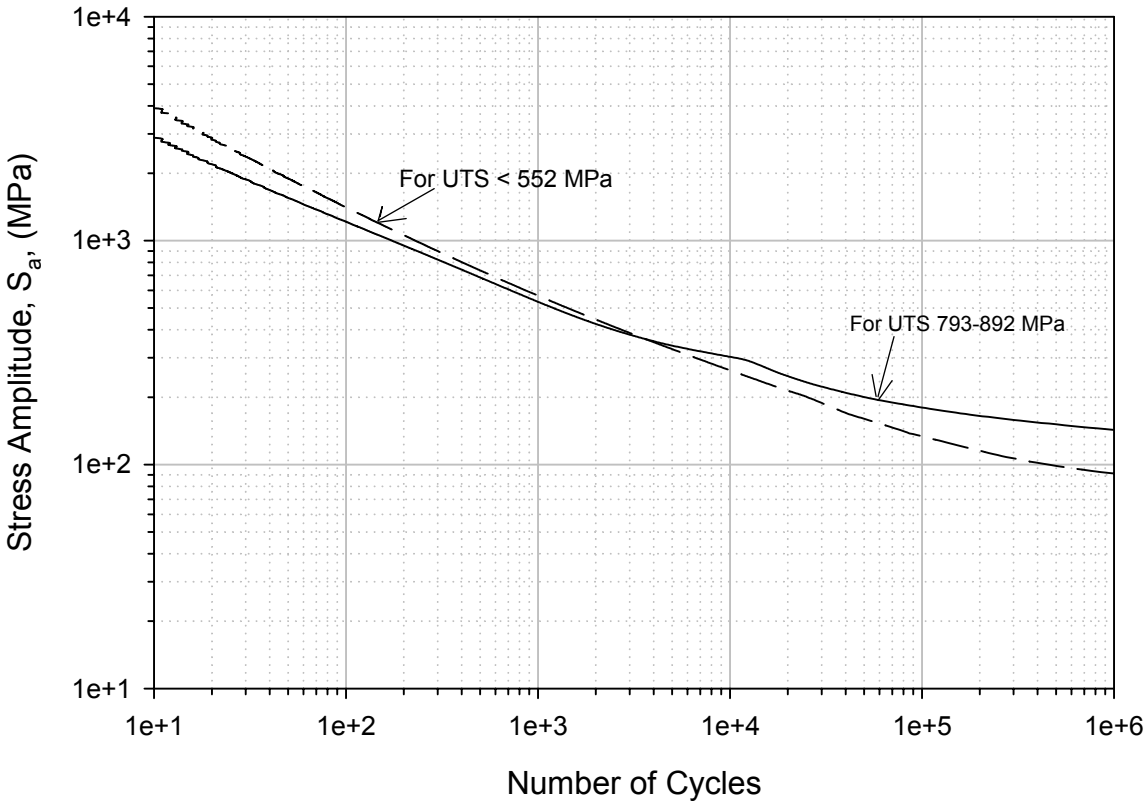

Figure F.11M – Fatigue Curves Based on Smooth Bar Test Specimens

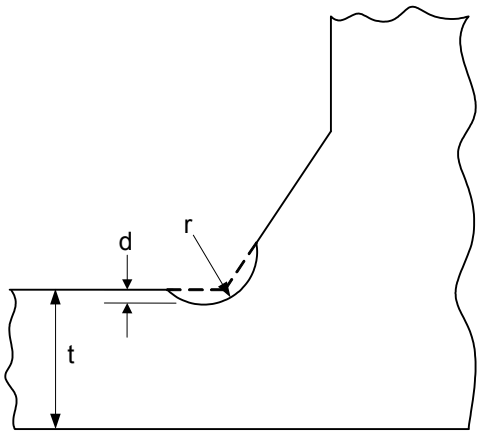

d = 0.5 below undercut

r/t > 0.25

r/d > 4

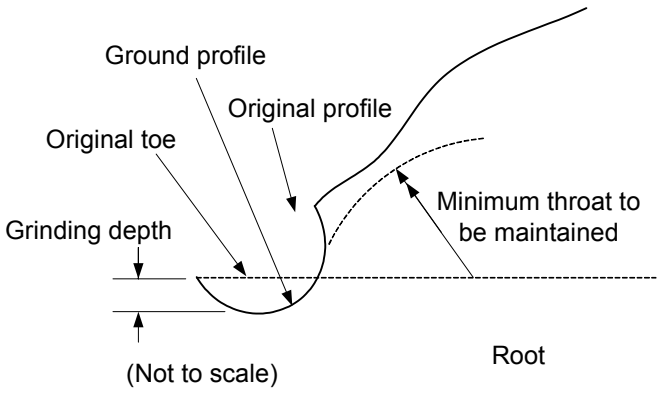

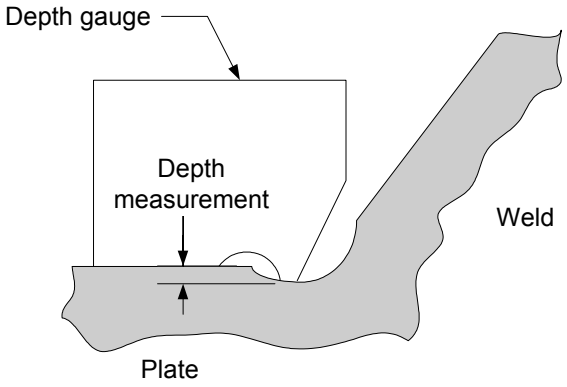

Note: Recommendations for weld toe grinding are shown in Figure F.13

Figure F.12 – Dressing of a Fillet Weld to Increase Fatigue Life

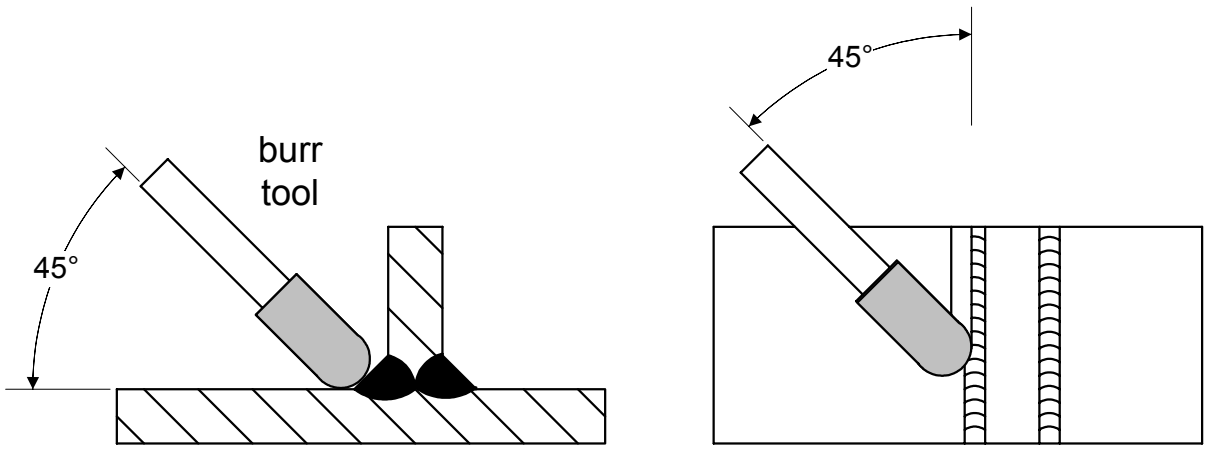

(a) Method of burr grinding

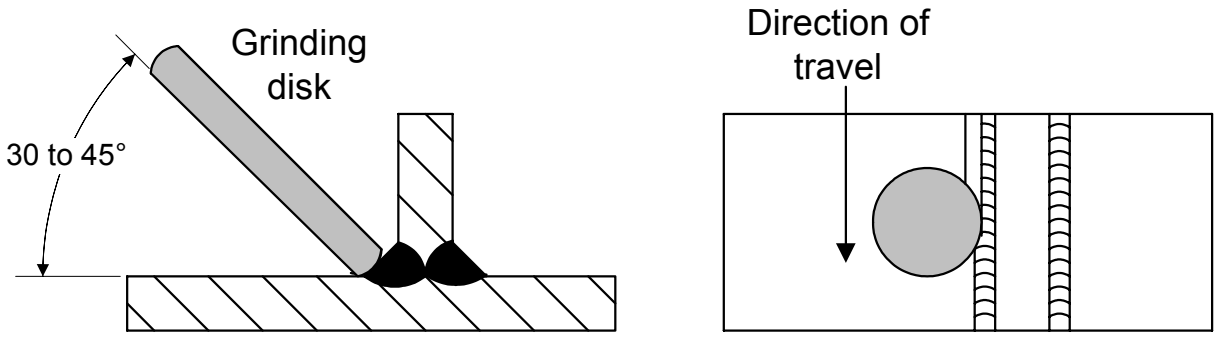

(b) Method of disk grinding

Figure F.13 – Grinding Method for Dressing of Fillet Welds

ANNEX G

DAMAGE MECHANISMS

(NORMATIVE)

PART CONTENTS

G.1 Deterioration and Failure Modes

G.1.1 This annex provides a general overview of the types of flaws and damage observed, concentrating on service-induced damage mechanisms. It also provides general information about mitigation and monitoring methods. A more complete overview of the damage mechanisms that occur in the following industries are shown below.

a) API RP 571 *Damage Mechanisms Affecting Fixed Equipment In The Refining Industry*

b) WRC 489 *Damage Mechanisms Affecting Fixed Equipment In The Refining Industry*

c) WRC 488 *Damage Mechanisms Affecting Fixed Equipment In The Pulp And Paper Industry*

d) WRC 490 *Damage Mechanisms Affecting Fixed Equipment In Fossil Electric Power Industry*

G.1.2 When conducting a FFS assessment, it is very important to determine the cause(s) of the damage or deterioration observed to date and the likelihood and degree of further damage that might occur in the future. Flaws and damage that are discovered during an in-service inspection can be the result of a preexisting condition before the component entered service and/or could be service-induced. The root causes of deterioration could be due to inadequate design considerations including materials selection and design details, or the interaction with aggressive environments/conditions that the equipment is subjected to during normal service or during transient periods.

G.2 Pre-Service Deficiencies

G.2.1 The types of pre-service deficiencies that can be present before equipment enters service are:

a) *Material Production Flaws* – Flaws which occur during production including laminations and laps in wrought products, and voids, segregation, shrinks, cracks, and bursts in cast products.

b) *Welding Related Flaws* – Flaws which occur as a result of the welding process including lack of penetration, lack of fusion, delayed hydrogen cracking, porosity, slag, undercut, weld cracking, and hot shortness.

c) *Fabrication Related Flaws* – Imperfections associated with fabrication including out-of-roundness, forming cracks, grinding cracks and marks, dents, gouges, dent-gouge combinations, and lamellar tearing.

d) *Heat Treatment Related Flaws Or Embrittlement* – Flaws associated with heat treatment including reheat cracking, quench cracking, sensitization, 475°C (885°F) embrittlement, and sigma phase embrittlement. Similar flaws are also associated with in-service elevated temperature exposure.

e) *Wrong Material of Construction* – Due to either faulty materials selection, poor choice of a specification break (i.e. a location in a component where a change in material specification is designated), or due to the inadvertent substitution of a different alloy or heat treatment condition due to a lack of positive material identification (PMI), the installed component does not have the expected resistance or needed properties to the service or loading.

G.2.2 In most instances, one or more of these pre-service deficiencies do not lead to an immediate failure. Usually, only gross errors cause a failure during a pre-service hydrostatic or pneumatic test.

G.2.3 Flaws or damage associated with pre-service deficiencies or damage are often only discovered during an In-Service Inspection (*ISI*), because in many cases the *ISI* techniques used are more sensitive or the inspection scope is wider than the inspection techniques or extent of inspection used during the original construction. Some damage can be classified relatively easily as pre-service, based on its characteristics and location (e.g. void in the interior of a weld is porosity). However, some pre-service damage is indistinguishable from service-induced damage (e.g. delayed hydrogen cracking and sulfide stress cracking). Therefore, the key decision that needs to be made is whether the flaw and associated deterioration (regardless of its origin) is likely to progress in the future based on the material, stress, service conditions, and flaw size.

G.3 In-Service Deterioration and Damage

G.3.1 Overview

G.3.1.1 Once equipment enters service, it is subjected to operating and/or downtime conditions that can deteriorate or damage the equipment. One factor that complicates a *FFS* analysis is that material/environmental condition interactions are extremely varied; many plants contain numerous processing units, each having its own combination of aggressive process streams and temperature/pressure conditions. In general, the following types of damage are encountered in process equipment:

a) General and local metal loss due to corrosion and/or erosion

b) Surface connected cracking

c) Subsurface cracking

d) Microfissuring/microvoid formation

e) Metallurgical changes

G.3.1.2 Each of these general types of damage is caused by a multitude of damage mechanisms, which are specific types of corrosion (e.g. naphthenic acid corrosion of carbon steel), stress corrosion cracking (SCC – e.g. polythionic acid stress corrosion cracking of sensitized austenitic stainless steels (PSCC)), or types of embrittlement (e.g. temper embrittlement of 2-1/4 Cr -1 Mo alloy steel). Each of the damage mechanisms occurs under very specific combinations of materials, process environments, and operating conditions.

G.3.1.3 The following sections of this Annex describe each of the damage types and provide some typical examples of damage mechanisms and potential mitigation methods. These sections are intended to introduce the concepts of service-induced deterioration and failure modes to the non-specialist in corrosion/metallurgy. The user is urged to consult with engineers familiar with damage modes and to refer to publications such as API RP571 and WRC Bulletins 488, 489, and 490 that provide a more detailed description of damage mechanisms in various industries (see paragraph G.1.1)

G.3.1.4 When performing a *FFS* assessment it is important that the potential for further damage is considered or that steps are taken to preclude further damage from occurring by means of mitigation methods. A list of the types of information needed for a specialist to judge whether, and at what rate, further damage is likely to occur is provided in Table G.1.

G.3.2 General Metal Loss Due to Corrosion and/or Erosion

G.3.2.1 General metal loss is defined as relatively uniform thinning over a significant area of the equipment (see Part 4). . Examples of general corrosion for carbon steel and low alloy steels are sulfidation in crude units, H_2/H_2S corrosion in hydrotreaters, and sour water corrosion in moderate velocity situations in sour water strippers.

G.3.2.2 A corrosion rate can usually be calculated from past and current thickness readings, for example see API 510, API 570, and API 653. The corrosion rate can also be predicted from standard corrosion curves/references, such as the modified McConomy Curves for sulfidation of carbon and low alloy steels (these curves are a function of temperature and sulfur content versus alloy). The measured or calculated rate, or a modified rate if conditions have changed, can be factored into a FFS assessment to evaluate future operation.

G.3.2.3 Remediation and monitoring methods for general metal loss are described in Part 4.

G.3.3 Localized Metal Loss Due to Corrosion and/or Erosion

G.3.3.1 Unlike general metal loss, localized metal loss rates can vary significantly within a given area of equipment. Examples of localized metal loss are under deposit corrosion in crude unit overhead systems, naphthenic acid corrosion, injection point corrosion, and corrosion under insulation. Localized corrosion can take many forms, such as pitting resulting in numerous surface cavities, selective galvanic corrosion in the region between two electrochemically different metals, selective corrosion attack along a weld heat affected zone (HAZ), corrosion attack in crevices resulting from the concentration of aggressive chemical specie(s), or local grooving due to impingement. In general, the more resistant an alloy is to general corrosion, the more likely it is that corrosion, if it occurs, will be localized.

G.3.3.2 When localized metal loss is detected, it is important to locate and characterize all of the locally thinned areas and obtain accurate measurements to calculate a metal loss rate. Predicting a localized corrosion rate is difficult, since the damage may only occur under very specific operating conditions (temperatures, chemical species, flow velocity) and is more of an on/off situation and usually does not occur at a steady constant pace. Since localized corrosion rates are extremely sensitive to minor variations in process conditions/materials it is difficult to find applicable reference sources of corrosion data.

G.3.3.3 Remediation and monitoring methods for local metal loss are described in Part 5.

G.3.4 Surface Connected Cracking

G.3.4.1 Most service-induced cracking mechanisms initiate at the surface of the component. Examples of service-induced surface cracking are mechanical and thermal fatigue and various forms of Stress Corrosion Cracking (SCC), such as polythionic acid stress corrosion cracking (PASCC) or chloride SCC of austenitic stainless steels, amine type cracking of carbon steels, and sulfide stress cracking of carbon and low alloy steels. Fatigue cracking data is available from a number of reference sources (see Annex F) and future crack growth rate can be calculated if the stresses can be characterized.

G.3.4.2 The occurrence of SCC requires that a combination of three conditions to be present: a susceptible material or material condition, a chemically aggressive environment, and a sufficiently high tensile stress. Since three factors are involved, generalizations about environments that can cause SCC are difficult even when restricted to a specific class of material. However, experiments and service experience have identified environments that can or have caused SCC in carbon and low alloy steels, and these have been tabulated and described in API RP571.

G.3.4.3 The metallurgical condition of the material is an important determinant of the severity of the SCC problem. For example, high hardness and strength make steel, particularly the HAZ of welds, more susceptible to sulfide stress cracking. Another material condition is sensitization of austenitic steels (chromium-rich carbide precipitation at grain boundaries) that is necessary for PASCC. The environmental and operating conditions of the component are also important. For example, there is a threshold level of caustic concentration and temperature that must be exceeded before carbon steel is susceptible to caustic cracking. In general, the greater the concentration of the causative agent, Cl, ammonia, H_2S, CN, etc., the greater the likelihood of SCC. For some mechanisms, increasing temperature increases susceptibility, while for others it decreases susceptibility. Concentration of the causative agents due to boiling, crevices, etc. can lead to problems where bulk stream composition would not predict susceptibility. Tensile stress is the third required ingredient for SCC. High tensile stresses, both applied and residual, increase the severity of the problem.

Residual stress estimation is very important, because many cracks in practice arrest when they enter a lower residual stress field.

G.3.4.4 Surface cracks often are found by surface inspection techniques, such as visual, PT and MT, although UT methods and AET are also used to detect cracks. Sizing surface connected cracking, in particular SCC, is very difficult, because in many cases the cracks are branched. PT or MT examination methods can be used to determine the length of surface cracks and UT examination methods can be used to determine the depth of cracking. Crack depth can also be determined by destructive grinding.

G.3.4.5 Predicting crack growth rates for SCC is also very difficult, because of a lack of relevant data and lack of precise knowledge of the environmental conditions near the crack tip, which can be different from the bulk stream composition. SCC is also more of an on/off damage type, i.e. cracks can grow very rapidly if all the conditions are conducive, but it can also be dormant for a very long time.

G.3.4.6 Mitigation methods to slow/prevent further SCC without removing cracks are somewhat limited. Strip lining the area and possibly coating the area if the cracks are tight is possible. Other methods are to alter the environment by means of chemical treatments, changing the temperature, or removing contaminants. Monitoring methods consist of periodic UT measurements or continuous passive AET monitoring. Stream sampling/analysis and process variable monitoring to predict when conditions conducive to SCC are present can also be used.

G.3.4.7 If cracks are removed, additional mitigation options are available, such as PWHT or heat treatment to remove residual stresses and/or improve the metallurgical condition such as grain refining, and weld overlays and coatings to isolate the susceptible material from the environment.

G.3.5 Subsurface Cracking and Microfissuring/Microvoid Formation

G.3.5.1 Service-induced damage that is not surface connected or initiates subsurface falls into the general class of low-temperature hydrogen related phenomena or high temperature mechanisms such as creep and hydrogen attack. Hydrogen damage consisting of blistering, HIC, and SOHIC is primarily encountered in carbon steels operating in wet H_2S or HF environments. Much of refinery equipment is subject to wet H_2S charging conditions during service or shutdown conditions. For example, deethanizers in fluid catalytic cracking light ends units typically have an environment with a high pH and cyanides that causes severe hydrogen charging leading to damage. Low-temperature hydrogen related damage occurs because of a local surface corrosion reaction that allows hydrogen atoms to diffuse into the steel. Once the hydrogen charging reaches a threshold concentration, damage can occur. Subsurface service-induced hydrogen damage can also eventually connect with the surface or this type of damage can initiate because of surface cracks, such as sulfide stress cracking.

G.3.5.2 This mechanism is similar to SCC in that susceptible material and an aggressive environment must be present. Hydrogen blistering and HIC are however not stress related, but SOHIC is. Hydrogen damage often is an on-off mechanism, occurring under very specific environmental conditions that may be present only during upsets and startup/shutdowns. Damage often occurs very quickly at first and once surface films buildup they inhibit further damage, although if films are disturbed in service or intentionally during inspections accelerated damage can recur. Since hydrogen charging normally only occurs from the process side of the equipment, the hydrogen concentration decreases through the wall and in practice many cracks arrest mid-wall and blisters are less prevalent on the external surfaces.

G.3.5.3 Metallurgical and microstructural details (e.g. the sulfur impurity level of the steel) affect the susceptibility to damage or threshold level for damage by a certain level of hydrogen charging. Environmental variables, such as pH, temperature, CN, H_2S content, and stream velocity influence the level of hydrogen charging. Applied and residual stresses also influence SOHIC susceptibility. Much of the equipment that will be evaluated for FFS will contain hydrogen damage. It is recommended that an expert in this field be consulted because it is very important to assess the future potential and rate of hydrogen damage. Reference publications that can be used in this assessment are: ANSI/ API RP571; NACE Publications 8X194, 8X294, and RP0296; and API 939.

G.3.5.4 Finding subsurface hydrogen damage is normally accomplished by visual inspection and various UT methods. Assessing the damage is very difficult because this is more a damage mechanics than fracture mechanics problem, since there often is no discreet single crack, cracks may be interconnected, and stacked in arrays. Various UT methods are used to characterize the damage.

G.3.5.5 Mitigation for low temperature hydrogen damage can consist of chemical treatment and/or water washing to minimize hydrogen charging, strip lining or coatings to isolate the steel from the environment, and venting for blisters to relieve the internal stress. If properly performed, PWHT may also reduce the propensity for SOHIC cracking by lowering the residual stress. Monitoring methods consist of hydrogen probes that measure hydrogen flux and periodic UT inspections to monitor damage extent.

G.3.5.6 Creep and/or high temperature hydrogen attack (HTHA) are mechanisms that form voids and fissuring only during latter stages of damage. These mechanisms can be either surface-connected or initiate subsurface. The variables that affect creep damage are the creep strength and strain capability of the material and the exposure conditions (stress and temperature). The variables that affect hydrogen attack are similar, but in addition the hydrogen partial pressure in the process stream and the alloy chemistry are very important. Subsurface creep and hydrogen attack damage that is detectable with UT methods, indicates that the component is at late stages of life for most common alloys. Creep and hydrogen attack damage rates can only be reduced by lowering the severity of the operating conditions. Field metallography may be effective for monitoring creep; however, the best monitoring method involves removing samples and conducting destructive tests while recording the temperature and pressure of the process.

G.3.6 Metallurgical Changes

G.3.6.1 Metallurgical properties, such as strength, ductility, toughness, and corrosion resistance can change while a component is in-service due to microstructural changes because of thermal aging at elevated temperatures. In addition, properties can also change because of hydrogen charging. Examples of embrittlement are shown below.

a) Carbon steels can strain age embrittle, spheroidize, or graphitize

b) Ferritic, austenitic, and duplex stainless steels may form sigma phase or can sensitize

c) Ferritic and duplex stainless steels may experience 475°C (885°F) embrittlement

d) 2.25 Cr-1Mo Steel may experience temper embrittlement

G.3.6.2 These changes in properties are often difficult to detect, since damage may not have occurred yet. Sometimes inferences can be made from examining samples or surface replicas. Steel composition and microstructure, operating temperature, and accumulated strain are the most important factors that determine susceptibility to metallurgical changes. Often an equilibrium state of change is reached and further changes will not occur. Hydrogen charging, even without material damage, will typically lower the ductility and possibly even the toughness of the material. Hydrogen charging is a reversible reaction and if it does not cause damage, has no permanent effect.

G.3.6.3 Once the metallurgical properties are changed in-service, they usually are not recoverable. Heat treatment can be effective, although this often is only a temporary solution. To prevent further damage or degradation to metallurgical properties, the operating conditions can be adjusted to a lower severity. If the degradation in properties is known, then operating precautions such as start-up and shutdown procedures can be altered to prevent damage from occurring despite the degraded physical properties.

G.3.6.4 As previously discussed, loss of toughness can occur in service because of the process environment and service conditions. This form of metallurgical damage will have significant impact on the structural integrity of a component containing a crack-like flaw. In addition, experimental evidence indicates that loss of toughness may also have an effect on the structural integrity of components with blunt flaws that are typically associated with localized corrosion, groove-like flaws or pitting. Some of the service and materials combinations that may be susceptible to loss of toughness are listed below. An evaluation of the materials toughness may be required depending on the flaw type, the severity of the environment, and the operating conditions.

a) Carbon steel in wet H_2S service and hydrofluoric acid service (hydrogen embrittlement)

b) Carbon steel and C-0.5 Mo between 149°C -316°C (300°F – 600° F) (strain age embrittlement)

c) Carbon steel above 427°C (800°F) (graphitization)

d) Carbon steel, low alloy steels (i.e. 0.5 Cr to 9 Cr), and 12 Cr in fire situation when temperatures exceed 704°C (1300°F) (various damage mechanisms, seePart 11)

e) Alloy steels (0.5 Cr – 9 Cr) above 593°C (1100 °F) (carburization)

f) 1.25 Cr-0.5 Mo above 482°C (900°F) (reheat cracking/creep embrittlement)

g) 2.25 Cr-1 Mo above 399°C (750°F) (temper embrittlement)

h) 12 Cr above 371°C (700°F) (475°C (885°F) embrittlement)

i) Austenitic stainless steel above 593°C (1100°F) (sigma phase embrittlement)

G.4 References

1. API, *Research Report on Characterization and Monitoring of Cracking in Wet H_2S Service*, API Publication 939, American Petroleum Institute, Washington D.C., 2003.
2. API, *Damage Mechanisms Affecting Fixed Equipment in The Refining Industry*, API Publication 571, American Petroleum Institute, Washington D.C., 2003.
3. Dobis, J.D. and Prager, M., *Damage Mechanisms Affecting Fixed Equipment in The Pulp And Paper Industry*, WRC Bulletin 488, Welding Research Council, 2004.
4. Dobis, J.D. and Prager, M., *Damage Mechanisms Affecting Fixed Equipment in The Refining Industry*, WRC Bulletin 489, Welding Research Council, 2004.
5. Dobis, J.D. and Prager, M., *Damage Mechanisms Affecting Fixed Equipment in Fossil Electric Power Industry*, WRC Bulletin 490, Welding Research Council, 2004.
6. Logan, H.L., *The Stress Corrosion of Metals,* Wiley, 1966.
7. McConomy, H.F., "High Temperature Sulfuric Corrosion in Hydrogen Free Environments," Proc. API, Vol. 43 (III), pp. 78-96, 1963.
8. NACE, *Guidelines for Detection, Repair, and Mitigation of Cracking of Existing Petroleum Refinery Pressure Vessels in Wet H_2S Environments*, NACE Publication RP0296, National Association of Corrosion Engineers, Houston, TX, 1996.
9. NACE, *Materials and Fabrication Practices for New Pressure Vessels Used in Wet H_2S Refinery Service*, NACE Publication 8X194, National Association of Corrosion Engineers, Houston, TX, 1994.
10. NACE, *Review of Published Literature on Wet H_2S Cracking of Steels Through 1989,* NACE Publication 8X194, National Association of Corrosion Engineers, Houston, TX, 1994.

G.5 Tables and Figures

Table G.1 – Damage Mechanisms Affecting Fixed Equipment

General Information	Data		
Processing Unit/Item			
Year of Construction			
Material Specification			
Material Chemical Composition			
PWHT (Yes/No)			
Lining/Coating Material			
Item (1)	**Operating Information (2)**		
	Normal	**Start-Up /Shutdown**	**Upset**
Crude Fraction Sulfur Content (%)			
Crude Fraction Neut Number			
Water Content (%/pH)			
H_2S (ppm in water)			
NH_3 (ppm in water)			
NH_3 (%)			
H_2S (%)			
HCl (%)			
Chlorides (%)			
Sulfuric Acid (%)			
HF Acid (%)			
Amine Type (MEA/DEA/etc.)			
Amine Concentration (%)			
Amine Loading (mole H_2S & CO_2/mole amine)			
Caustic Concentration (%)			
H_2S Partial Pressure (bar:psia)			
H_2 Partial Pressure (bar:psia)			
Cyanides (Yes/No)			
Water Wash/Injection (Yes/No)			
Polysulfide Injection (Yes/No)			
Neutralizing Amine Injection (Yes/No)			
Filming Amine Injection (Yes/No)			
Caustic Injection (Yes/No)			
Hydrogen Absorption Injection Inhibitor			
Temperature (°C:°F)			
Pressure (bar:psig)			
Flow Velocity (m/sec:ft/sec)			

Notes:
1. Other process stream constituents or operating parameters that may affect the Fitness-For-Service assessment can be entered at the end of this list.
2. Values for the process stream constituents and operating parameters for the start-up, shutdown, and upset conditions, as well as the normal operating condition, need to be defined because significant damage may occur during these phases of operation.

ANNEX H

TECHNICAL BASIS AND VALIDATION

(NORMATIVE)

PART CONTENTS

H.1 Overview

This annex provides an overview of the technical basis and validation that support the Fitness-For-Service (FFS) assessment procedures provided in this standard. Due to the complexity of the assessment procedures and the validation studies performed, only a brief overview is provided herein. Specific details may be found in the cited references.

The initial technical basis document used for the development of API 579-1/ASME FFS-1 was developed by the Joint Industry Project on Fitness-For-Service sponsored by The Materials Properties Council, Inc. This document [3] provided an overview of the current status of Fitness-For-Service methods being utilized in the refining and petrochemical industry at the time of its writing, and served as the foundation for future FFS technology development.

H.2 Assessment of Existing Equipment for Brittle Fracture

The assessment procedures for prevention of brittle fracture for pressure vessel and piping components in Part 3 are based on the design requirements contained in the ASME B&PV Code, Section VIII, Division 1. The technical basis to these rules is presented in references [11], [21], [30], and [54]. A comparison of other international pressure vessel codes to the ASME rules is provided in reference [23]. The use of the ASME toughness rules for evaluation of in-service equipment is described in references [18] and [27]. The assessment procedure for prevention of brittle fracture for tank components in Part 3 is based on the rules in API 653. The technical basis to these rules is provided in reference [28].

H.3 Assessment of General and Local Metal Loss

The technical basis and validation of the assessment procedures for general metal loss and local metal loss contained in Part 4 and Part 5 are provided in references [22], [36] and [37]. In each of these references, a comparison is made between the assessment methods in this Standard and the assessment methods contained in other standards. A comparison of assessment methodologies for the pipeline industry (i.e. B31G, RSTRENG, BS7910) is provided in reference [19]. However, in the comparison of methods for the assessment of local thin areas, the methods in API 579-1/ASME FFS-1 were not considered in reference [19]. In order to provide a complete comparison of the methodologies currently being used for the assessment of local thin areas, the Materials Properties Council Joint Industry Project on Fitness-For-Service commissioned an additional study. The results of this comparison are provided in reference [22]. In addition, a new assessment method that results in less scatter when compared to experimental results than all other methods is presented in reference [22]. This reference also presents recommendations for setting the allowable remaining strength factor for a Fitness-For-Service assessment based on the original construction code and a specified margin against a predicted burst pressure relative to the calculated maximum allowable working pressure.

H.4 Assessment of Pitting Damage

The technical basis of the assessment procedures for pitting damage in Part 6 is provided in references [37] and [40]. The limit analysis used to develop the assessment procedures described in reference [40] was also used to develop the rules for the design of perforated plates included in the ASME Code, Section VIII, Division 2, Appendix 4 and Section III, Division 1, Article-8000, and Non-mandatory Appendix A. The pitting damage assessment procedures could not be compared to experimental results because of lack of data. However, these rules have been used extensively in the industry without incident, and have been proven to provide acceptable results.

H.5 Assessment of HIC/SOHIC and Blister Damage

The technical basis of the assessment procedures for blister damage in Part 7 is provided in references [6], [3] and [37]. The blister damage assessment procedures could not be compared to experimental results because of lack of data. However, these rules have been used extensively in the industry without incident, have been proven to provide acceptable results, and are consistent with NACE guidelines [32]. The technical basis of the assessment procedures for HIC/SOHIC damage in Part 7 is provided in reference [12]. The development of a remaining strength factor approach, similar to that used for local thin areas, and experiments to validate the approach are described in this publication. The rules in Part 7 requiring a crack-like flaw check are based on Part 9 and the validation work for Part 9.

H.6 Assessment of Weld Misalignment and Shell Distortions

The technical basis of the assessment procedures in Part 8 for weld misalignment and shell distortions (i.e. out-of-roundness) is provided in references [35] and [37]. Reference [37] provides an overview of the method and reference [35] provides the basis for the development of the equations for the R_b-factor defined as the ratio of the induced bending stress to the applied membrane stress.

The predominant mode of failure associated with weld misalignment and shell distortions for components in cyclic operation is fatigue. Three methods for fatigue assessment are provided in Annex B1. Two of these methods utilize a fatigue curve derived from smooth bar test specimens while the third method utilizes a fatigue curve based on test specimens that include weld details. The fatigue assessment method and smooth bar fatigue curves are based on the ASME B&PV Code, Section VIII, Division 2. The fatigue assessment method that utilizes the fatigue curves based on welded joint test specimens is described in references [13] and [14].

H.7 Assessment of Crack-Like Flaws

An overview of the assessment procedures in Part 9 for the evaluation of crack-like flaws is provided in reference [4]. The evaluation of crack-like flaws in Part 9 is based on the failure assessment diagram (FAD) approach. This approach has gained wide acceptance throughout the world and has been adopted in a number of prominent codes and standards, including BS 7910 [8], the Nuclear Electric R6 Method [34], The Swedish Plant Inspectorate [50], the Structural Integrity Assessment procedures for European Industry (SINTAP) [55], and ASME Section XI, Article H-4000. Although there are subtle differences among the FAD-based approaches in the various codes and standards, the overall concept is consistent throughout the world. A detailed comparison of various codified approaches for assessing crack-like flaws is provided in [53].

A FAD-based evaluation of a component with a crack-like flaw is described in Part 9 and entails computing a toughness ratio, K_r, and a load ratio, L_r. An assessment point with coordinates $\left(K_r, L_r\right)$ is compared with the FAD curve, which represents the failure locus. The toughness ratio stems directly from linear elastic fracture mechanics [1] and the load ratio provides a plasticity correction. A rigorously correct FAD curve for a given structural component with a crack can be derived from an elastic-plastic J-integral solution of the cracked component, as described in Annex B1 and reference [1]. The Level 2 FAD curve in Part 9 is an approximation of the true elastic-plastic crack driving force. However, provided that the combined primary stresses are less than the yield strength, the outcome of a crack-like flaw assessment is insensitive to the shape of the FAD curve [53].

The FAD-based approach has been extensively validated with burst tests and wide plate tests, see references [2], [5], [9], [10], [34], [51], and [59]. The approach is conservative, provided that a conservative estimate of the key input parameters (toughness, flaw size, primary stress, residual stress) is used. When assessment points are computed from the full-scale tests, such points fall outside of the FAD when conservative assumptions for input parameters are used. When mean estimates for input parameters are used, however, assessment points for full-scale tests fall both inside and outside of the FAD, with roughly a 50:50 split [2]. This indicates that the FAD method provides a good estimate of the mean failure conditions when all conservatism is removed from input parameters.

The uncertainty in the independent variables in a FAD analysis (i.e. stress, flaw size, and fracture toughness) may be accounted for by choosing conservative estimates for each of these parameters. Alternatively, mean values of these parameters may be used with Partial Safety Factors. The Partial Safety Factors in Part 9 are based on work reported in references [38], [56], [57], and [58].

H.8 Assessment of Creep Damage

The elevated temperature life assessment methods in Part 10 are based on traditional concepts, such as linear life summing rules, and also recognize the material properties and documented approaches developed by MPC under the heading of the Omega Method. The original and most complete exposition of the Omega Method is found in reference [41]. It has been summarized in other papers by Prager et al. in references [42] and [48], Zamrik in reference [61], et. al., and Dyson in reference [15]. The Omega Method is widely reported by industrial and academic investigators in literature in Japan by Prager and many others in references [43], [16], [17], [38], [47], [60], and also by the European Creep Collaborative Committee in reference [29]. The method evolved from examination of experimental data that was then converted to parametric expressions for ease of use and extrapolation as described in reference [41]. Application to complex geometries, creep crack growth and other complex stress states, especially for tubular components, was first reported in reference [7]. The parametric approaches applied in the Omega Method are also used for generation of ASME code allowable stresses at elevated temperatures and material modeling as reported in references [45] and [44], respectively. The techniques were applied to life assessment as an alternative to the methods in API 530 starting about 1988, well before the publication of reference [41], and have been in use since then by the petroleum and power industries. Case histories using the Omega Method for assessment of components may be found in references [20], [24], [25], and [46].

The technical basis for the creep crack growth method in Part 10 is described in references [48] and [53]. Additional technical basis and validation are provided in reference [52]. International approaches that were also reviewed during the development of Part 10 are provided in references [31] and [33].

H.9 Assessment of Fire Damage

The basic principles used to develop the assessment procedures in Part 11 for fire damage are provided in reference [26]. These principles are combined with the relevant assessment procedures from the other Parts of this standard (i.e. Part 4 for the assessment of thinning, Part 9 for the assessment of crack like flaws, and Part 10 for the assessment of creep damage) to provide an overall evaluation procedure for fire damage.

H.10 Assessment of Dents, Gouges, and Dent-Gouge Combinations

The technical basis and validation of the assessment procedures in Part 12 for dents, gouges and dent-gouge combinations are provided in reference [49].

H.11 Assessment of Laminations

The technical basis of the assessment procedures in Part 13 for laminations is provided in references [6] and [37].

H.12 References

1. Anderson, T.L., “Fracture Mechanics – Fundamentals and Applications,” 3rd Edition, CRC Press, Boca Raton, Florida, 2005.
2. Anderson, T.L., “Preliminary Validation of the MPC Fitness-for-Service Guidelines.” PVP Vol. 315, *Fitness-for-Service and Decisions for Petroleum and Chemical Equipment*, July 1995, pp. 123-129.
3. Anderson, T.L., Merrick, R.D., Yukawa, S., Bray, D.E., Kaley, L. and Van Scyoc, K., “Fitness-For-Service Evaluation Procedures for Operating Pressure Vessels, Tanks, and Piping in Refinery and Chemical Service,” FS-26, Consultants Report, MPC Program on Fitness-For-Service, Draft 5, The Materials Properties Council, New York, N.Y., October, 1995.
4. Anderson, T.L. and Osage, D.A., “API 579: A Comprehensive Fitness-For-Service Guide,” International Journal of Pressure Vessels and Piping 77 (2000), pp 953-963.

5. Bhuyan, G.S., Sperling, E.J., Shen, G., Yin, H. and Rana, M.D., “Prediction of Failure Behavior of a Welded Pressure Vessel Containing Flaws During a Hydrogen Charged Burst Test,” Transactions of the ASME, Vol. 121, August 1999.
6. Buchheim, G.M., “Fitness-For-Service Hydrogen Blistering and lamination Assessment Rules in API 579,” PVP Vol. 411, Service Experience and Fitness-For-Service in Power and Petroleum Processing, ASME, 2000, pp. 177-190..
7. Buchheim, G.M., Osage, D.A., Brown, R.G., and Dobis, J.D., “Failure Investigation of a Low Chrome Long-Seam Weld in a High-Temperature Refinery Piping System,” PVP-Vol. 288, ASME, 1994, pp. 363-386.
8. BSI, Guide on Methods for Assessing the Acceptability of Flaws in Metallic Structures, BS 7910, British Standards Institute, 1999.
9. Challenger, N.V., Phaal, R. and Garwood, S.J., “Fracture Mechanics Assessment of Industrial Pressure Vessel Failures”, Int. J. Pres. Ves. & Piping 61, 1995, pp 433-456.
10. Challenger, N.V., Phaal, R. and Garwood, S.J., “Appraisal of PD6493:1991 Fracture Assessment Procedures, Part I: TWI Data”, TWI, Abington Hall, UK, June, 1995.
11. Corten, H.T., “Fracture Toughness Considerations Underpinning New Toughness Rules in Section VIII, Division 1, of the ASME Code,” unpublished work.
12. Dirham, T.R, Buchheim, G.M., Osage, D.A., Staats, J.C., ”Development of Fitness-For-Service Rules for the Assessment of HIC Damage,” WRC Bulletin in preparation.
13. Dong, P., Hong, J.K., Osage, D.A., and Prager, M., “Master S-N Curve Method for Fatigue Evaluation of Welded Components,” WRC Bulletin 474, Welding Research Council, New York, N.Y., August, 2002.
14. Dong, P., Hong, J.K, and DeJesus, A.M.P., “Analysis of Recent Fatigue Data Using the Structural Stress Procedure in ASME Div2 Rewrite,” ASME PVP2005-71511, Proceedings of PVP2005, Denver, Colorado, ASME, New York, N.Y., 2005.
15. Dyson, B., “Use of CDM in Materials Modeling and Component Creep Life Prediction,” ASME, Journal of Pressure Vessel Technology, Vol. 122, August 2000, pages 281-296.
16. Endo, T., Park, K.S. and Masuyama, F. “Creep Modeling and Life Evaluation of Long-Term Aged Modified 9 Cr-1Mo Steel,” Symposium on Integrity and Failures in Industry, Milan, Italy, Sept. 1-Oct. 1, 1999, organised by the Italian Group on Fracture and ENEL Research (Milan - I) Editors: V. Bicego, A. Nitta, J. W. H. Price and R. Viswanathan. ISBN 1 901537 15 3 (1999)
17. Endo, T., and Shi, J., “Factors Affecting the Creep Rate and Creep Life of a 2.25Cr-1Mo Steel Under Constant Load,” Strength of Materials, Oikawa et al. ed., ICSMA 10 Sendai, The Japan Institute for Metals, 1994, pp 665-668.
18. Findlay, M., McLaughlin, J.E., and Sims, J.R., “Assessment of Older Cold Service Pressure Vessels for Brittle Fracture During Temperature Excursions Below the Minimum Design Temperature,” ASME PVP-Vol. 288, American Society of Mechanical Engineers, New York, N.Y., pp. 297-305.
19. Fu B., Stephens, D., Ritchie, D. and Jones, C.L., “Methods for Assessing Corroded Pipeline – Review, Validation and Recommendations,” Catalog No. L5878, Pipeline Research Council International, Inc. (PRCI), 2002.
20. Ibarra, S. and Konet, R.R., “Life Assessment of 1 1/4Cr-1/2M0 Steel Catalytic Reformer Furnace Tubes Using the MPC Omega Method,” PVP-Vol. 288, Service Experience and Reliability Improvement: Nuclear, Fossil, and Petrochemical Plants, ASME 1994, pages 387-400.
21. Jacobs, W.S., “ASME Code Material Toughness Requirements for Low Temperature Operation, Section VIII, Division 1 & Division 2, 1998 Edition, 1999 Addenda,” PVP-Vol. 407, Pressure Vessel and Piping Codes and Standards - 2000, ASME 2000, pages 23 through 38.
22. Janelle, J.A. and Osage, D.A., “An Overview and Validation of the Fitness-For-Service Assessment Procedures for Local Thin Areas in API 579,” WRC Bulletin 505, Welding Research Council, New York, N.Y., 2005.
23. Kent, L., “Comparison of Pressure Vessel Codes Requirements for Brittle Fracture Prevention,” Proc. ICPVT-9, 1992, pp 970-990.

24. Kim, D.S. and Mead, H.E., “Remaining Life Assessment of Refinery Heater Tubes,” PVP-Vol. 388, Fracture, Design Analysis of Pressure Vessels, Heat Exchangers, Piping Components, and Fitness-For-Service, ASME, 1999, pages 361-366.
25. Klehn, R. and Laughlin, C.A., “Chevron’s Experience Using Omega Method Creep Tests for Life Assessment of Refinery Equipment,” PVP-Vol. 288, Service Experience and Reliability Improvement: Nuclear, Fossil, and Petrochemical Plants, ASME 1994, pages 345-350.
26. McIntyre, D.R. and Ashbaugh, W.G., “Part 1, Assessment of Fire and Explosion damage to Chemical Plant Equipment,” MTI Publication No. 30, Guidelines for Assessing Fire and Explosion damage, The materials technology Institute of the Chemical process Industries, Inc., 1990.
27. McLaughlin, J.E., Sims, J.R., "Assessment of Older Equipment for Risk of Brittle Fracture," ASME PVP-Vol. 261, American Society of Mechanical Engineers, New York, N.Y., 1993, pp. 257-264.
28. McLaughlin, J.E., "Preventing Brittle Fracture of Aboveground Storage Tanks – Basis for the Approach Incorporated in API 653," Proceedings Case Studies: Sessions III and IV of the IIW Conference, Fitness-For-Purpose of Welded Structures, Key Biscayne, Florida, USA, October 23-24, 1991.
29. Merckling G., “The European Creep Collaborative Committee,” International Symposium on NIMS Creep Data Sheet, National Institute for Materials Science in Japan, March 16, 2004, pp.25-52.
30. Mooney, J.L., “Application of the New ASME Section VIII, Division 1 Toughness Requirements to a Typical Vessel,” Mechanical Engineering, ASME, New York, N.Y., March 1999, pp. 99-101.
31. Moulin, D., Drubay, B. and Laiarinandrasana, L., “A Synthesis of the Fracture Assessment Methods Proposed in the French RCC-MR Code for High Temperature,” WRC 440, The Welding Research Council, New York, N.Y., 1999.
32. NACE Standard RP0296-96, “Guidelines for Detection, Repair, and Mitigation of Cracking of Existing Petroleum Refinery Pressure Vessels in Wet H2S Environments”, NACE International, Houston, TX, 2003.
33. Nuclear Electric, *Assessment Procedure for High Temperature Response of Structures*, Nuclear Electric R-5, Nuclear Electric, Issue 3, 2003.
34. Nuclear Electric, *Assessment of the Integrity of Structures Containing Defects*, Nuclear Electric R-6, Nuclear Electric, Revision 4, 2001.
35. Osage, D.A., Brown, R.G. and Janelle, J.L., “Fitness-For-Service Rules for Shell Distortions and Weld Misalignment in API 579,” PVP-Vol. 411, Service Experience and Fitness-For-Service in Power and Petroleum Processing, ASME, 2000, pp. 191-220.
36. Osage, D.A., Janelle, J. and Henry, P.A., “Fitness-For-Service Local Metal Loss Assessment Rules in API 579,” PVP Vol. 411, Service Experience and Fitness-For-Service in Power and Petroleum Processing, ASME, 2000, pp. 143-176.
37. Osage, D.A., Krishnaswamy, P., Stephens, D.R., Scott, P., Janelle, J., Mohan, R., and Wilkowski, G.M., “Technologies for the Evaluation of Non-Crack-Like Flaws in Pressurized Components – Erosion/Corrosion, Pitting, Blisters, Shell Out-Of-Roundness, Weld Misalignment, Bulges and Dents,” WRC Bulletin 465, Welding Research Council, New York, N.Y., September, 2001.
38. Osage, D.A., Shipley, K.S., Wirsching, P.H. and Mansour, A.E., “Application of Partial Safety Factors for Pressure Containing Equipment,” PVP Vol. 411, Service Experience and Fitness-For-Service in Power and Petroleum Processing, ASME, 2000, pp. 121-142.
39. Park, K.S., Masuyama F. and Endo, T. “Creep Modeling for Life Evaluation of Heat-resistant Steel with a Martensitic Structure,” ISIJ International, Vol. 41 (2001), Supplement, pp S86-S90.
40. Porowski, J.S., Osage, D.A. and Janelle, J.A., “Limit Analysis of Shells with Random Pattern of Spread Pits,” ASME PVP, 2002.
41. Prager, M., “Development of the MPC Project Omega Method for Life Assessment in the Creep Range,” PVP-Vol. 288, ASME, 1994, pp. 401-421.
42. Prager, M., “Damage Evaluation and Remaining Life Assessment in High Temperature Structural Components by the Omega Method,” Proceedings of 7th Workshop on the Ultra Steel, Ultra Steel: Requirements from New Design of Constructions, June 24 and 25, 2003, pages 150-158.
43. Prager, M., “The Omega Method – An Effective Method for Life and Damage Prediction in Creep Tests and Service,” Oikawa (eds.), Strength of Materials, Japan Institute of Metals, 1994, pp. 571-574.

44. Prager, M., “Proposed Implementation of Criteria for Assignment of Allowable Stresses in the Creep Range,” ASME Journal of Pressure Vessel Technology, May, 1996, Vol. 335, pp. 273-293.

45. Prager, M., “Generation of Isochronous Creep, Tubing Life and Crack Growth Curves Using the MPC Omega Method, Structural Integrity,” NDE, Risk and Material Performance for Petroleum, process and Power, PVP-Vol. 336, ASME, 1996, pp. 303-322.

46. Prager, M. and Ibarra, S., “Approaches to Long Term Life prediction of Furnace and Boiler Tubes,” Fitness For Adverse Environments in Petroleum and Power Equipment, PVP-Vol. 359, ASME, 1997, pp. 339-352.

47. Prager, M. and Masuyama, F., “Examination of the Effects of Materials Variables in Advanced Alloys by Studying Creep Deformation Behavior,” Strength of Materials, Oikawa et al. ed., ICSMA 10 Sendai, The Japan Institute for Metals, 1994, pp 575-578.

48. Prager, M., and Osage, D., “Special Topics in Elevated Temperature Life Applications Including Assessment Rules for API 579,”, PVP-Vol. 411, Service Experience and Fitness-For-Service in Power and Petroleum Processing, ASME, 2000, pages 91-104.

49. Roovers, P., Bood, R., Galli, M., Marewski, U., Steiner, M. and Zarea, M., “EPRG Methods for Assessing the Tolerance and Resistance of Pipelines to External Damage,” Pipeline Technology, Volume II, R. Denys (Editor), Elsevier Science B.V., 2000.

50. SAQ/FoU, *A Procedure for Safety Assessment of Components with Cracks – Handbook*, SAQ/FoU-Report 96/08, 1997.

51. Sattari-Farr, I. and Nilsson, F., “Validation of a Procedure for Safety Assessment of Cracks,’ SA/FoU Report 91/19, 2nd Edition Revised, The Swedish Plant Inspectorate, 1991.

52. Saxena, A. and Yoon, D., “Creep Crack Growth Assessment of Defects in High Temperature Components,” WRC 483, The Welding Research Council, New York, N.Y., 2003.

53. Scott, P.M., Anderson, T.L., Osage, D.A., and Wilkowski, G.M. A Review Of Existing Fitness-For-Service Criteria For Crack-Like Flaws, WRC Bulletin 430, The Welding Research Council, New York, N.Y., April, 1998.

54. Selz, A, “New Toughness Rules in Section VIII, Division 1 of the ASME Boiler and Pressure Vessel Code,” 88-PVP-8, ASME.

55. Webster, S. and Bannister, A., “Structural Integrity Assessment Procedure for Europe – of the SINTAP Programme Overview,” Engineering Fracture Mechanics (67) 2000, pp. 481-514.

56. Wirsching, P.H. and Mansour, A.E., “Incorporation of Structural Reliability methods into Fitness for Service Procedures,” Mansour Engineering, Inc., Report to The Materials Properties Council, Inc., May 1998.

57. Wirsching, P.H. and Mansour, A.E., “Incorporation of Structural Reliability methods into Fitness for Service Procedures,” Mansour Engineering, Inc., Report to The Materials Properties Council, Inc., Supplement No. 1, April 1999.

58. Wirsching, P.H. and Mansour, A.E., “Incorporation of Structural Reliability methods into Fitness for Service Procedures,” Mansour Engineering, Inc., Report to The Materials Properties Council, Inc., Supplement No. 2, May 1999.

59. Yin, H. and Bagnoli, D.L., “Case Histories Using Fitness For Service Methods,” PVP-Vol. 288, Service Experience and Reliability Improvement: Nuclear, Fossil, and Petrochemical Plants, ASME, 1994.

60. Yokobori Jr. A.T. and Prager M., “Proposal for a new Concept on Creep Fracture Remnant Life for a Pre-cracked Specimen”, Materials at High Temperatures, 16(3), 1999. pp 137-141.

61. Zamrik, S.Y. and Annigeri, R., “Creep Damage Models for Elevated Temperature Design,” Proc. ICPVT-10 July 7-10, 2004.

ANNEX I

GLOSSARY OF TERMS AND DEFINITIONS

(NORMATIVE)

This Annex contains definitions of terms that are used in this Standard, or terms that may be found elsewhere in documents related to Fitness-For-Service evaluation.

I.1 Abs[a] or |a| – The definition of a mathematical function that indicates that the absolute value of the arguments, a, is to be computed.

I.2 AET – Acoustic Emission Testing.

I.3 Alteration – The definition depends on the equipment type and in-service code as shown below.

a) Pressure vessels (API 510) – A physical change in any component having design implications that affect the pressure-containing capability of a pressure vessel beyond the scope of the items described in existing data reports. It is not intended that any comparable or duplicate replacement, such as the addition of any reinforced nozzle equal to or less than the size of existing reinforced nozzles, the addition of nozzles not requiring reinforcement, or rerating be considered an alteration.

b) Piping Systems (API 570) – A physical change in any component or pipe routing (including support system modifications), which have design implications affecting the pressure-containing capability of the piping system, including the pressure vessels, tanks, and/or equipment it services. For example, an alteration that involves the installation of a heavy valve near a vessel nozzle may have design implications for the pressure vessel as well as the piping system itself.

c) Storage tanks (API 653) – Any work on a tank involving cutting, burning, welding, or heating operations that change the overall physical dimensions and/or configuration of a tank.

d) Pressure Vessels (NB-23) – Any change in the item described in the original Manufacturer's Data Report that affects the pressure containing capability of the pressure retaining item. Non-physical changes such as an increase in the maximum allowable working pressure (internal or external) or design temperature of a pressure retaining item shall be considered an alteration. A reduction in minimum temperature such that additional mechanical tests are required shall also be considered an alteration.

I.4 ASCC (Alkaline Stress Corrosion Cracking) – The cracking of a metal produced by the combined action of corrosion in an aqueous alkaline environment containing H2S, CO2, and tensile stresses (residual or applied). The cracking is branched and intergranular in nature, and typically occurs in carbon steel components that have not been subjected to PWHT. This form of cracking has often been referred to as carbonate cracking when associated with alkaline sour waters, and as amine cracking when associated with alkanolamine treating solutions.

I.5 Bending Stress – The variable component of normal stress, the variation may or may not be linear across the section thickness (see Annex B1).

I.6 CET (Critical Exposure Temperature) – Critical Exposure Temperature is defined as the lowest (coldest) metal temperature derived from either the operating or atmospheric conditions at the maximum credible coincident combination of pressure and supplemental loads that result in primary stresses. Note that operating conditions include startup, shutdown and upset conditions. The CET may be a single temperature at the maximum credible coincident combination of pressure and primary supplemental loads if that is also the lowest (coldest) metal temperature for all other combinations of pressure and primary supplemental loads. If lower (colder) temperatures at lower pressures and supplemental loads are credible, the CET should be defined by an envelope of temperatures and pressures (see Part 3).

I.7 Coefficient Of Variation (COV) – A statistical measure of a distribution defined as the ratio of the standard deviation of the distribution to the mean of the distribution.

I.8 Corrosion – The deterioration of metal caused by chemical or electrochemical attack as a result of its reaction to the environment (see Part 4).

I.9 Crack-Like Flaw – A flaw that may or may not be the result of linear rupture, but which has the physical characteristics of a crack when detected by an NDE technique (see Part 9).

I.10 Creep – The special case of inelasticity that characterizes the stress induced time-dependent deformation under load, usually occurring at elevated temperatures (see Part 10).

I.11 Creep Damage – In polycrystalline materials (e.g. metals) creep damage results from the motion of dislocations within grains, grain boundary sliding and microstructural diffusion processes within the crystalline lattice. The resultant grain boundary voids, or grain and grain boundary distortions (damage), generally impairs the materials strain hardening capability (see Part 10).

I.12 Creep Rupture – An extension of the creep process to the limiting condition of gross section failure (frequently termed creep fracture). The stress that will cause creep fracture at a given time in a specified environment is the creep rupture strength (see Part 10 and Annex F).

I.13 Cyclic Service – A service in which fatigue becomes significant due to the cyclic nature of mechanical and/or thermal loads. A screening criteria is provided in Annex B1, paragraph B1.5.2 which can be used to determine if a fatigue analysis should be included as part of a Fitness-For-Service assessment.

I.14 Damage Mechanism – A phenomenon that induces deleterious micro and/or macro changes in the material conditions that are harmful to the material condition or mechanical properties. Damage mechanisms are usually incremental, cumulative, and unrecoverable. Common damage mechanisms are associated with chemical attack, creep, erosion, fatigue, fracture, embrittlement, and thermal aging (see Part 2 and Annex G).

I.15 Ductility – The ability of a material to plastically deform without fracturing. Ductility is measured as either the reduction in area or elongation in a tensile test specimen.

I.16 Erosion – The destruction of metal by the abrasive action of a liquid or vapor (see Part 4).

I.17 $\exp[x]$ **–** The mathematical function e^x

I.18 FAD – The Failure Assessment Diagram (FAD) used for the evaluation of crack-like flaws in components (see Part 2 and Part 9).

I.19 Fatigue – The damage mechanism resulting in fracture under repeated or fluctuating stresses having a maximum value less than the tensile strength of the material (see Annex B1).

I.20 Fatigue Endurance Limit – Fatigue Endurance Limit or Endurance Limit is the highest stress or range of stress that can be repeated indefinitely without failure of the material.

I.21 Fatigue Strength – The maximum cyclic stress a material can withstand for a given number of cycles before failure occurs (see Annex F).

I.22 Fatigue Strength Reduction Factor – A stress intensification factor that accounts for the effect of a local structural discontinuity (stress concentration) on the fatigue strength. Values for some specific cases are empirically determined (e.g. socket welds). In the absence of experimental data, the stress intensification factor can be developed from a theoretical stress concentration factor derived from the theory of elasticity.

I.23 FCA (Future Corrosion Allowance) – The corrosion allowance required for the future operational period of a component.

I.24 Fillet Weld – A weld of approximately triangular cross section joining two surfaces approximately at right angles to each other in a lap joint, tee joint, or corner joint.

I.25 Fitness-For-Service Assessment – A methodology whereby flaws or a damage state in a component is evaluated in order to determine the adequacy of the component for continued operation (see Part 2).

I.26 Flaw – A discontinuity, irregularity, or defect that is detected by inspection.

I.27 Fracture Mechanics – An engineering discipline concerned with the behavior of cracks in materials. Fracture mechanics models provide mathematical relationships for critical combinations of stress, crack size and fracture toughness that lead to crack propagation. Linear Elastic Fracture Mechanics (LEFM) approaches apply to cases where crack propagation occurs during predominately elastic loading with negligible plasticity. Elastic-Plastic Fracture Mechanics (EPFM) methods are suitable for materials that undergo significant plastic deformation during crack propagation (see Part 9)**.**

I.28 Girth Weld – A butt weld joining plate sections along the circumferential direction of a cylinder or cone.

I.29 Gouge – An elongated local mechanical removal and/or relocation of material from the surface of a component, causing a reduction in wall thickness at the defect; the length of a gouge is much greater than the width and the material may have been cold worked in the formation of the flaw. Gouges are typically caused by mechanical damage, for example, denting and gouging of a section of pipe by mechanical equipment during the excavation of a pipeline (see Part 12).

I.30 Groove – A local elongated thin spot caused by directional erosion or corrosion; the length of the metal loss is significantly greater than the width (see Part 5).

I.31 Gross Structural Discontinuity – Another name for a Major Structural Discontinuity (see paragraph I.47).

I.32 Groove-Like Flaw – A surface flaw with a small, but finite, tip (or frontal) radius wherein the flaw length is very much greater than its depth. Groove-like flaws are categorized as either a groove or gouge (see Part 5and Part 12).

I.33 Heat-Affected Zone (HAZ) – A portion of the base metal adjacent to a weld that has not been melted, but whose metallurgical microstructure and mechanical properties have been changed by the heat of welding, usually with undesirable effects.

I.34 HIC (Hydrogen-Induced Cracking) – Stepwise internal cracks that connect adjacent hydrogen blisters on different planes in the metal, or to the metal surface. No externally applied stress is needed for the formation of HIC. In steels, the development of internal cracks (sometimes referred to as blister cracks) tends to link with other cracks by a transgranular plastic shear mechanism because of internal pressure resulting from the accumulation of hydrogen. The link-up of these cracks on different planes in steels has been referred to as stepwise cracking to characterize the nature of the crack appearance. HIC is commonly found in steels with (a) high impurity levels that have a high density of large planar inclusions, and/or (b) regions of anomalous microstructure produced by segregation of impurity and alloying elements in the steel (see Part 7).

I.35 Hydrogen Blistering – The formation of subsurface planar cavities, called hydrogen blisters, in a metal resulting from excessive internal hydrogen pressure. Growth of near-surface blisters in low-strength metals usually results in surface bulges. Hydrogen blistering in steel involves the absorption and diffusion of atomic hydrogen produced on the metal surface by the sulfide corrosion process. The development of hydrogen blisters in steels is caused by the accumulation of hydrogen that recombines to form molecular hydrogen at internal sites in the metal. Typical sites for the formation of hydrogen blisters are large nonmetallic inclusions, laminations, or other discontinuities in the steel. This differs from the voids, blisters, and cracking associated with high-temperature hydrogen attack (see Part 7).

I.36 Inclusion – A discontinuity in a material, usually consisting of a non-metallic compound (oxides, silicate, etc.) encapsulated in a metallic matrix as unintentional impurity.

I.37 Incomplete Fusion – Lack of complete melting and coalescence (fusion) of some portion of the metal in a weld joint.

I.38 Incomplete Penetration – Partial penetration of the weld through the thickness of the joint.

I.39 In-Service Margin – In terms of applied loads, the ratio of the load that will produce a limiting condition to the applied load in the assessed condition. Similar definitions may be developed for parameters other than load. For example, the safety margin on fracture toughness (see Part 9) is defined as the ratio of the fracture toughness of the material being assessed to the fracture toughness to produce a limiting condition.

I.40 Jurisdiction – A legally constituted government administration that may adopt rules relating to pressurized components.

I.41 Limit Analysis – Limit Analysis is a special case of plastic analysis in which the material is assumed to be ideally plastic (non-strain-hardening). In limit analysis the equilibrium and flow characteristics at the limit state are used to calculate the collapse load (see Annex B1).

I.42 Limit Analysis Collapse Load – The methods of limit analysis are used to compute the maximum load a structure made of an ideally plastic material can carry. The deformations of an ideally plastic structure increase without bound at this load, which is termed the collapse load (see Annex B1).

I.43 Local Primary Membrane Stress – A membrane stress produced by pressure, or other mechanical loading associated with a primary and/or a discontinuity effect would, if not limited, produce excessive distortion in the transfer of load to other portions of the structure. Conservatism requires that such a stress be classified as a local primary membrane stress even though it has some characteristics of a secondary stress (see Annex B1).

I.44 Local Structural Discontinuity – A source of stress or strain intensification that affects a relatively small volume of material and does not have a significant effect on the overall stress or strain pattern, or on the structure as a whole. Examples are small fillet radii, small attachments, and partial penetration welds (see Annex B1).

I.45 Longitudinal Weld – A full penetration butt weld joining plate sections along the longitudinal axis of a cylinder or cone.

I.46 LTA – Locally Thin Area (see Part 5).

I.47 Major Structural Discontinuity – A source of stress or strain intensification that affects a relatively large portion of a structure and has a significant effect on the overall stress or strain pattern of the structure as a whole. Examples are: head-to-shell and flange-to-shell junctions, nozzles, and, junctions between shells of different diameters or thicknesses (see Annex B1).

I.48 MAT (Minimum Allowable Temperature) – The lowest permissible metal temperature for a given material at a specified thickness based on its resistance to brittle fracture. It may be a single temperature, or an envelope of allowable operating temperatures as a function of pressure. The MAT is derived from mechanical design information, materials specifications, and/or materials data (see Part 3).

I.49 MAWP (Maximum Allowable Working Pressure) – The maximum gauge pressure adjusted for liquid head for a component in its operating position at the design temperature, based on calculations using the current minimum thickness, exclusive of thickness required for future corrosion allowance and supplemental loads. Note that this term is also applied to piping components. For components containing a flaw, the MAWP is also a function of the Remaining Strength Factor (see Part 2)**.**

I.50 Max[a1,a2,a3,..,ai] – The definition of a mathematical function that indicates that the maximum value of all of the arguments, ai, is to be computed.

I.51 Membrane Stress – The mean value of normal stress acting on a cross section (see Annex B1).

I.52 MFH (Maximum Fill Height) – The maximum height permitted for a liquid with a given specific gravity in an atmospheric storage tank at the design temperature based on calculations using the current minimum thickness for all critical shell elements, exclusive of thickness required for future corrosion allowance and supplemental loads. For components containing a flaw, the MFH is also a function of the Remaining Strength Factor (see Part 2).

I.53 Min[a1,a2,a3,..,ai] – The definition of a mathematical function that indicates that the minimum value of all of the arguments, ai, is to be computed.

I.54 Minimum Allowable Thickness – The thickness required for each element of a vessel based on calculations considering temperature, pressure, and all loadings (see Annex A).

I.55 Minimum Design Metal Temperature (MDMT) – The lowest temperature at which a significant load can be applied to a pressure vessel as defined by the ASME Code, Section VIII, Division 1 (see Part 3).

I.56 MT – Magnetic particle examination.

I.57 NDE – Non-destructive examination.

I.58 Nil-Ductility Temperature – A temperature at which an otherwise ductile material subject to a load, cracks in a manner characteristic of a brittle fracture.

I.59 Normal Stress – The component of stress normal to the plane of reference (this is also referred to as a direct stress). Usually the distribution of normal stress is not uniform through the thickness of a part, so this stress may be considered to be made up of two components. One stress component is uniformly distributed and equal to the average value of stress across the thickness of the section under consideration, and the other stress component varies with the location across the section thickness.

I.60 Notch Sensitivity – A measure of the reduction in the strength of a metal caused by the presence of a stress concentration.

I.61 Notch Toughness – The ability of a material to resist brittle fracture under conditions of high stress concentration, such as impact loading in the presence of a notch.

I.62 On-Stream Inspection – The use of any of a number of nondestructive examination procedures to establish the suitability of a pressurized component for continued operation. The pressurized component may, or may not, be in operation while the inspection is performed.

I.63 Operational Cycle – An operational cycle is defined as the initiation and establishment of new conditions followed by a return to the conditions that prevailed at the beginning of the cycle. Three types of operational cycles are considered: the startup-shutdown cycle, defined as any cycle that has atmospheric temperature and/or pressure as one of its extremes and normal operating conditions as its other extreme; the initiation of, and recovery from, any emergency or upset condition that must be considered in the design; and the normal operating cycle, defined as any cycle between startup and shutdown that is required for the vessel to perform its intended purpose**.**

I.64 Peak Stress – The basic characteristic of a peak stress is that it does not cause any noticeable distortion and is objectionable only as a possible source of a fatigue crack or a brittle fracture. A stress that is not highly localized falls into this category if it is of a type, which cannot cause noticeable distortion (see Annex B1). Examples of peak stress are: the thermal stress in the austenitic steel cladding of a carbon steel vessel, the thermal stress in the wall of a vessel or pipe caused by a rapid change in temperature of the contained fluid, and the stress at a local structural discontinuity.

I.65 Pitting – Localized corrosion in the form of a cavity or hole such that the surface diameter of the cavity is on the order of the plate thickness (see Part 6).

I.66 Plastic Analysis – A stress analysis method where the structural behavior of a component under load is computed considering the plasticity characteristics of the material including strain hardening and stress redistribution (see Annex B1).

I.67 Plastic Instability Load – The plastic instability load for a structure under predominantly tensile or compressive loading is defined as the load at which unbounded plastic deformation can occur without further load increase. At the plastic tensile instability load, the true stress in the material increases faster than the strain hardening can accommodate (see Annex B1).

I.68 Plasticity – A general characterization of material behavior in which the material undergoes time independent non-recoverable deformation (see Annex B1).

I.69 POD (Probability Of Detection) – A measure of the ability to detect a flaw or indication in a component using a standard NDE technique on a consistent basis.

I.70 Primary Stress – A normal or shear stress developed by the imposed loading that is necessary to satisfy the laws of equilibrium of external and internal forces and moments. The basic characteristic of a primary stress is that it is not self-limiting. Primary stresses that considerably exceed the yield strength will result in failure or at least in gross distortion. A thermal stress is not classified as a primary stress. Primary membrane stress is divided into general and local categories. A general primary membrane stress is one that is distributed in the structure such that no redistribution of load occurs as a result of yielding. Examples of primary stress are general membrane stress in a circular cylindrical or a spherical shell due to internal pressure or to distributed live loads and the bending stress in the central portion of a flat head due to pressure. Cases arise in which a membrane stress produced by pressure or other mechanical loading and associated with a primary and/or a discontinuity effect would, if not limited, produce excessive distortion in the transfer of load to other portions of the structure. Conservatism requires that such a stress be classified as a local primary membrane stress even though it has some characteristics of a secondary stress. A primary bending stress can be defined as a bending stress developed by the imposed loading that is necessary to satisfy the laws of equilibrium of external and internal forces and moments (see Annex B1).

I.71 PSF (Partial Safety Factor) – A deterministic parameter (derived from statistical considerations) that represents a level of uncertainty or importance for a specific field variable. For example, in a fracture mechanics analysis, distinct PSF's may be applied to each of the loading, material toughness and crack sizing variables. In combination these factors yield a desired level of confidence (i.e. degree of safety) in the calculated fracture assessment result. Where the method is prescribed, tabulations are provided that map the required (or critical) analysis variables to a user selected risk level and the associated PSF multiplier. As an application example, the PSF methodology is well established in the Load and Resistance Factor Design Manual of the American Institute of Steel Construction (see Part 2).

I.72 PT – Liquid penetrant examination.

I.73 PWHT (Postweld Heat Treatment) – Uniform heating of a weldment to a temperature below the critical range to relieve the major part of the welding residual stresses, followed by uniform cooling in still air.

I.74 Ratcheting – Progressive incremental inelastic deformation or strain that can occur in a component subjected to variations of mechanical stress, thermal stress, or both (thermal stress ratcheting is partly or wholly caused by thermal stress, see Annex B1).

I.75 Recognized Code or Standard – A term used to define a code or standard that is recognized by a local jurisdiction (see Part 1, paragraphs 1.2.2 and 1.2.3).

I.76 Reference Stress – A quantity that is used to account for plasticity effects in the FAD method. It is computed by multiplying the primary stress by a dimensionless factor that is a function of the component geometry and crack dimensions (see Annex D). Traditionally, the reference stress has been defined from yield load solutions, such that the net cross section is fully plastic when the reference stress is equal to the yield strength. An alternative definition of the reference stress is based on an elastic-plastic J-integral analysis (see Annex B1). This newer definition is more technically sound because it greatly reduces geometry effects in the FAD curve.

I.77 Repair – Restoration of a pressure containing component, the definition is dependent on the equipment type as shown below:

a) Pressure vessels (API 510) – The work necessary to restore a vessel to a condition suitable for safe operation at the design conditions. Repairs also include the addition or replacement of pressure or non-pressure parts that do not change the rating of a vessel.

b) Piping systems (API 570) – The work necessary to restore a piping system to a condition suitable for safe operation at the design conditions. Such repairs are typically completed in compliance with the schedule and pressure class requirements of the piping system. Repairs resulting in schedule/class deviations (e.g. use of lower pressure class fittings) may impact the system design conditions.

c) Storage tanks (API 653) – Any work on a tank necessary to restore a tank to a condition suitable for safe operation.

d) Pressure Vessels (NB-23) – The work necessary to restore pressure retaining items to a safe and satisfactory operating condition.

I.78 Rerating – A change in either or both the temperature rating and the maximum allowable working pressure rating of a vessel (see Part 2).

I.79 RSF (Remaining Strength Factor) – The ratio of the collapse pressure of a damaged component (e.g. cylinder containing an LTA) to the collapse pressure of the undamaged component (see Part 2).

I.80 RT – Radiographic examination.

I.81 Secondary Stress – A normal stress or a shear stress developed by the constraint of adjacent parts or by self-constraint of a structure. The basic characteristic of a secondary stress is that it is self-limiting. Local yielding and minor distortions can satisfy the conditions that cause the stress to occur and failure from one application of the stress is not to be expected (see Annex B1). Examples of secondary stress are a general thermal stress and the bending stress at a gross structural discontinuity.

I.82 Sensitivity Analysis – A statistical or parametric process of varying the independent variables (or inputs) in order to determine the response (or sensitivity) of the dependent variables (or outputs). For example, in a Fitness-For-Service analysis, determination of the maximum permissible crack length may have a strong sensitivity to temperature variation if the material fracture toughness (a material property) is also strongly influenced by temperature (see Part 2).

I.83 Shakedown – Shakedown of a structure occurs if, after a few cycles of load applications, ratcheting ceases. The subsequent structural response is elastic, or elastic-plastic, and progressive incremental inelastic deformation is absent. Elastic shakedown is the case in which the subsequent response is elastic (see Annex B1).

I.84 Shear Stress – The component of stress tangent to the plane on which forces act See Annex B1).

I.85 Shock Chilling – Shock chilling is a rapid decrease in metal temperature caused by the sudden contact of liquid or a two-phase (gas/liquid) fluid with a metal surface when the liquid or two phase fluid is colder than the metal temperature at the instant of contact (seePart 3).

I.86 SOHIC (Stress-Oriented Hydrogen-Induced Cracking) – Arrays of cracks that are aligned nearly perpendicular to the applied stress, which are formed by the link-up of small HIC cracks in steel. Tensile stress (residual or applied) is required to produce SOHIC. SOHIC is commonly observed in the base metal adjacent to the heat-affected zone (HAZ) of a weld, oriented in the through-thickness direction. SOHIC may also be produced in susceptible steels at other high stress points such as from the tip of mechanical cracks and defects, or from the interaction between HIC on different planes in the steel (see Part 7).

I.87 Strain Limiting Load – The load associated with a given strain limit (see Annex B1).

I.88 Stress Concentration Factor – A multiplying factor applied stress equal to the ratio of the maximum stress to the average section stress (see Annex B1).

I.89 Stress Cycle – A stress cycle is a condition in which the alternating stress difference goes from an initial value through an algebraic maximum value and an algebraic minimum value and then returns to the initial value. A single operational cycle may result in one or more stress cycles (see Annex B1 and Annex B3).

I.90 Stress Intensity Factor – A measure of the stress-field intensity near the tip of an ideal crack in a linear elastic medium when deformed so that the crack faces are displaced apart, normal to the crack plane (i.e. crack opening mode or Mode I deformation). The Mode I stress intensity factor (KI) is directly proportional to the applied load and depends on specimen geometry (see Part 9 and Annex C).

I.91 Sulfide Stress Cracking (SSC) – Cracking of a metal under the combined action of tensile stress and corrosion in the presence of water and H2S (a form of hydrogen stress cracking). SSC involves hydrogen embrittlement of the metal by atomic hydrogen that is produced by the sulfide corrosion process on the metal surface. The atomic hydrogen can diffuse into the metal and produce embrittlement. SSC usually occurs more readily in high-strength steels or in hard weld zones of steels.

I.92 Tensile Strength – The maximum load per unit of original cross sectional area that a tensile test specimen of a material sustains prior to fracture. The tensile strength may also be identified as the ultimate tensile strength (see Annex F).

I.93 Thermal Stress – A self-balancing stress produced by a nonuniform distribution of temperature or by differing thermal coefficients of expansion. Thermal stress is developed in a solid body whenever a volume of material is prevented from assuming the size and shape that it normally should under a change in temperature. For the purpose of establishing allowable stresses, two types of thermal stress are recognized, depending on the volume or area in which distortion takes place. A general thermal stress that is associated with distortion of the structure in which it occurs. If a stress of this type, neglecting stress concentrations, exceeds twice the yield strength of the material, the elastic analysis may be invalid and successive thermal cycles may produce incremental distortion. Therefore this type is classified as a secondary stress. Examples of general thermal stress are: the stress produced by an axial temperature distribution in a cylindrical shell, the stress produced by the temperature difference between a nozzle and the shell to which it is attached, and the equivalent linear stress produced by the radial temperature distribution in a cylindrical shell. A Local thermal stress is associated with almost complete suppression of the differential expansion and thus produces no significant distortion. Such stresses shall be considered only from the fatigue standpoint and are therefore classified as local stresses. Examples of local thermal stresses are the stress in a small hot spot in a vessel wall, the difference between the actual stress and the equivalent linear stress resulting from a radial

temperature distribution in a cylindrical shell, and the thermal stress in a cladding material that has a coefficient of expansion different from that of the base metal (see Annex B1).

I.94 Toughness – The ability of a material to absorb energy and deform plastically before fracturing (see Annex F).

I.95 Transition Temperature – The temperature at which a material fracture mode changes from ductile to brittle (see Annex F).

I.96 Undercut – An intermittent or continuous groove, crater or channel that has melted below, and thus undercut, the surface of the base metal adjacent to the toe of a weld and is left unfilled by weld metal.

I.97 UT – Ultrasonic examination.

I.98 Volumetric Flaw – A flaw characterized by a loss of material volume or by a shape imperfection. Examples include general and local corrosion, pitting, blisters, out-of-roundness, bulges, dents, gouges, and dent-gouge combinations, and weld misalignment.

I.99 Weld – A localized coalescence of metal wherein coalescence (i.e. fusion) is produced by heating to suitable temperatures, with or without the application of pressure, and with or without the use of filler metal. If a filler metal is used, it typically has a melting point approximately the same as that of the base metal.

I.100 Yield Strength – The stress at which a material exhibits a specified deviation from the linear proportionality of stress versus strain (see Annex F).

ANNEX J

CURRENTLY NOT USED

ANNEX K

CRACK OPENING AREAS

(NORMATIVE)

PART CONTENTS

K.1 Introduction

The equations for the Crack Opening Areas (COA) in this Annex have been derived for both elastic and plastic conditions for cylinders and spheres with membrane and/or bending stresses based on Reference [1]. Alternative methods to compute the COA are covered in References [2], [3], [4], [5], and [6].

K.2 Overview of Crack Opening Area Calculations

K.2.1 The solutions for cylinders and spheres effectively assume that the cracks are in the center of an infinite body and away from structural discontinuities. For most geometries this will be a reasonable approximation. However, if the crack is close to a major structural discontinuity (e.g. a pipe nozzle intersection) then local stress effects will influence the COA. The COA solutions in this annex may be used to estimate the COA at a structural discontinuity if the membrane and bending stresses are computed using a stress analysis model that considers the structural discontinuity.

K.2.2 Mean material properties should be used to provide a best estimate of the COA. These properties should be relevant to the expected condition of the component; time dependent changes in properties, such as degradation, relaxation and redistribution processes must be taken into consideration. The variation in material properties at welds, the influence of the weld preparation angle, and the presence of residual welding stresses may affect the COA.

K.2.3 Through-wall bending stresses can induce elastic crack face rotations that reduce the effective crack opening area. If complete crack closure occurs, a LBB analysis cannot be justified. Significant local through-wall bending stresses may be present in thick wall shells subject to internal pressure or shells subject to membrane and bending stresses associated with geometric discontinuities and/or thermal gradients. The COA solutions in this annex can be used to determine the taper associated with the though-wall crack by computing the COA on the inside and outside surface. Typically, other models used to determine the COA provide solutions at the shell mid-surface position, and do not account for the crack taper resulting from through-wall bending loads. A method to account for crack taper is discussed in Reference [7].

K.2.4 The effects on crack face rotations due to welding residual stresses should be evaluated (see Reference [8]).

K.2.5 The orientation of the net-section bending moment with respect to the through-wall crack should be considered when determining the COA in a cylindrical shell. The orientation of the net-section bending moment may cause an asymmetric crack opening, partial crack closure, or complete crack closure if the crack is located entirely on the compressive side of the shell section.

K.3 Crack Opening Areas (COA) for Cylinders and Spheres

K.3.1 Longitudinal Cracks in Cylinders

K.3.1.1 For internal pressure, the crack opening area is given by

$$COA = H_p \left(\frac{pR_o}{t} \right) \left(\frac{2\pi c^2}{E} \right) \tag{K.1}$$

The parameter H_p for inside and outside surface is given in Tables K.1 and K.2, respectively. The limiting values of the parameter H_p for inside and outside surfaces are:

$$\lim_{c \to 0} \left[H_{p(OD)} \right] = \left(\frac{R_o^{\,2} + R_i^{\,2}}{R_o^{\,2} - R_i^{\,2}} \right) \left(\frac{t}{R_o} \right) \tag{K.2}$$

$$\lim_{c\to 0}\left[H_{p(ID)}\right]=\left(\frac{2R_o^{\,2}}{R_o^{\,2}-R_i^{\,2}}\right)\left(\frac{t}{R_o}\right) \tag{K.3}$$

K.3.1.2 For a uniform and linear through-wall stress distribution, the crack opening area is given by the following equation where σ_0 and σ_1 are determined in accordance with Annex C.

$$COA=\left(H_o\sigma_o+H_1\sigma_1\right)\frac{2\pi c^2}{E} \tag{K.4}$$

In terms of a membrane and bending stress, Equation (K.4) can be written as:

$$COA=\left[\sigma_m H_o+\sigma_b\left(H_o-2H_1\right)\right]\frac{2\pi c^2}{E} \tag{K.5}$$

The parameters H_0 and H_1 for the inside and outside surface are given in Tables K.1 and K.2, respectively. The limiting values of the parameters H_0 and H_1 for inside and outside surfaces are:

$$\lim_{c\to 0}\left[H_{o(ID)}\right]=1 \tag{K.6}$$

$$\lim_{c\to 0}\left[H_{o(OD)}\right]=1 \tag{K.7}$$

$$\lim_{c\to 0}\left[H_{1(OD)}\right]=1 \tag{K.8}$$

$$\lim_{c\to 0}\left[H_{1(ID)}\right]=0 \tag{K.9}$$

K.3.2 Circumferential Cracks in Cylinders

K.3.2.1 For internal pressure, the crack opening area is given by

$$COA=H_o\left(\frac{pR_o^{\,2}}{R_o^{\,2}-R_i^{\,2}}\right)\left(\frac{2\pi c^2}{E}\right) \tag{K.10}$$

The parameter H_0 for inside and outside surface is given in Tables K.3 and K.4, respectively. The limiting values of the parameter H_p for inside and outside surfaces are:

$$\lim_{c\to 0}\left[H_{o(OD)}\right]=1 \tag{K.11}$$

$$\lim_{c\to 0}\left[H_{o(ID)}\right]=\left(\frac{R_i}{R_o}\right)^2 \tag{K.12}$$

K.3.2.2 For a uniform and linear through-wall stress distribution, the crack opening area is given by the following equation where σ_0 and σ_1 are determined in accordance with Annex C.

$$COA = \left(H_o \sigma_o + H_1 \sigma_1\right) \frac{2\pi c^2}{E} \tag{K.13}$$

In terms of a membrane and bending stress, Equation (K.13) can be written as:

$$COA = \left[\sigma_m H_o + \sigma_b \left(H_o - 2H_1\right)\right] \frac{2\pi c^2}{E} \tag{K.14}$$

The parameters H_0 and H_1 for the inside and outside surface are given in Tables K.3 and K.4, respectively. The limiting values of the parameters H_0 and H_1 for inside and outside surfaces are:

$$\lim_{c \to 0}\left[H_{o(OD)}\right] = 1 \tag{K.15}$$

$$\lim_{c \to 0}\left[H_{o(ID)}\right] = \left(\frac{R_i}{R_o}\right)^2 \tag{K.16}$$

$$\lim_{c \to 0}\left[H_{1(OD)}\right] = 1 \tag{K.17}$$

$$\lim_{c \to 0}\left[H_{1(ID)}\right] = 0 \tag{K.18}$$

K.3.2.3 For the global bending moment, the crack opening area is:

$$COA = H_5 \left[\frac{M_x R_o}{\frac{\pi}{4}\left(R_o{}^4 - R_i{}^4\right)}\right]\left(\frac{2\pi c^2}{E}\right) \tag{K.19}$$

The parameter H_5 for inside and outside surface is given in Tables K.3 and K.4, respectively. The limiting values of the parameter H_5 for inside and outside surfaces are:

$$\lim_{c \to 0}\left[H_{5(OD)}\right] = 1 \tag{K.20}$$

$$\lim_{c \to 0}\left[H_{5(ID)}\right] = \left(\frac{R_i}{R_o}\right)^3 \tag{K.21}$$

K.3.3 Meridional Cracks in Spheres

K.3.3.1 For internal pressure, the crack opening area is given by

$$COA = H_p \left(\frac{pR_o^{\,2}}{R_o^{\,2} - R_i^{\,2}} \right) \left(\frac{2\pi c^2}{E} \right) \tag{K.22}$$

The parameter H_p for inside and outside surface is given in Tables K.5 and K.6, respectively. The limiting values of the parameter H_p for inside and outside surfaces are:

$$\lim_{c \to 0} \left[H_{p(OD)} \right] = \left(\frac{R_o^{\,3} + 0.5R_i^{\,3}}{R_o^{\,3} - R_i^{\,3}} \right) \left(\frac{R_o^{\,2} - R_i^{\,2}}{R_o^{\,2}} \right) \tag{K.23}$$

$$\lim_{c \to 0} \left[H_{p(ID)} \right] = \frac{1.5R_i^{\,2} \left(R_o^{\,2} - R_i^{\,2} \right)}{R_o \left(R_o^{\,3} - R_i^{\,3} \right)} \tag{K.24}$$

K.3.3.2 For a uniform and linear through-wall stress distribution, the crack opening area is given by the following equation where σ_0 and σ_1 are determined in accordance with Annex C.

$$COA = \left(H_o \sigma_o + H_1 \sigma_1 \right) \frac{2\pi c^2}{E} \tag{K.25}$$

In terms of a membrane and bending stress, Equation (K.25) can be written as:

$$COA = \left[\sigma_m H_o + \sigma_b \left(H_o - 2H_1 \right) \right] \frac{2\pi c^2}{E} \tag{K.26}$$

The parameters H_0 and H_1 for the inside and outside surface are given in Tables K.5 and K.6, respectively. The limiting values of the parameters H_0 and H_1 for inside and outside surfaces are given by Equations

$$\lim_{c \to 0} \left[H_{o(OD)} \right] = 1 \tag{K.27}$$

$$\lim_{c \to 0} \left[H_{o(ID)} \right] = \left(\frac{R_i}{R_o} \right)^2 \tag{K.28}$$

$$\lim_{c \to 0} \left[H_{1(OD)} \right] = 1 \tag{K.29}$$

$$\lim_{c \to 0} \left[H_{1(ID)} \right] = 0 \tag{K.30}$$

K.4 Plasticity Correction for the COA

The crack opening areas in paragraph K.3 are based on linear elastic fracture mechanics. For elastic-plastic conditions, the crack opening areas in paragraph K.3 shall be modified as follows:

$$COA = \gamma_p \cdot COA_{elastic} \tag{K.31}$$

The plasticity modifier, γ_p, is determined using the following equation

$$\gamma_p = 1.008 - 0.33015\left(L_r\right)^2 + 5.53696\left(L_r\right)^4 - 3.96974\left(L_r\right)^6 + 2.00844\left(L_r\right)^8 \qquad \text{(K.32)}$$

The above equation is valid for $0 \le L_r \le 1.2$. The load ratio L_r is computed using the procedures in Part 9.

K.5 Nomenclature

c	crack length parameter.
COA	crack opening area
E	modulus of elasticity.
γ_p	plasticity correction factor for the crack opening area.
H_p	pressure loading crack parameter for determining the COA.
H_0	membrane stress crack parameter for determining the COA.
H_1	through-wall bending stress crack parameter for determining the COA.
H_5	net-section bending stress crack parameter for determining the COA.
$H_{p(ID)}$	H_p parameter for the inside surface of the shell.
$H_{p(OD)}$	H_p parameter for the outside surface of the shell.
$H_{0(ID)}$	H_0 parameter for the inside surface of the shell.
$H_{0(OD)}$	H_0 parameter for the outside surface of the shell.
$H_{1(ID)}$	H_1 parameter for the inside surface of the shell.
$H_{1(OD)}$	H_1 parameter for the outside surface of the shell.
$H_{5(ID)}$	H_5 parameter for the inside surface of the shell.
$H_{5(OD)}$	H_5 parameter for the outside surface of the shell.
L_r	load ratio.
λ	through-wall crack shell parameter.
M_x	net-section bending moment about the x-axis acting on a cylinder, see Annex C.
p	pressure.
R_i	inside radius.
R_o	outside radius.
σ_b	through-wall bending stress component.
σ_m	membrane stress component.
σ_0	uniform coefficient for polynomial stress distribution.
σ_1	linear coefficient for polynomial stress distribution.
t	shell thickness

K.6 References

1. Anderson, T.L.., “Stress Intensity And Crack Growth Opening Area Solutions For Through-wall Cracks In Cylinders And Spheres,” WRC Bulletin 478, Welding Research Council, January, 2003.
2. Langston, D.B., “A Reference Stress Approximation For Determining Crack Opening Displacements In Leak-Before-Break Calculations,” TD/SID/REP/0112, Nuclear Electric Document, 1991.
3. Paul, D.D., Ahmad, J., Scott, P.M., Flanigan, L.F. And Wilkowski, G.M., “Evaluation And Refinement Of Leak-Rate Estimation Models,” NUREG/CR-5128, Rev. 1, June 1995.
4. Rahman, S., Brust, F., Ghadiali, N., Choi, Y.H., Krishnaswamy, P., Moberg, F., Brickstad, B. And Wilkowski, G., “Refinement And Evaluation Of Crack Opening Area Analyses For Circumferential Through-Wall Cracks In Pipes,” NUREG/CR-6300, 1995.
5. Scott, P.M., Anderson, T.L., Osage, D.A., and Wilkowski, G.M., “Review of Existing Fitness-For-Service Criteria for Crack-Like Flaws,” WRC Bulletin 430, Welding Research Council, 1998.
6. Sharples, J.K. And Bouchard, P.J., “Assessment Of Crack Opening Area For Leak Rates,” LBB95; Specialist Meeting On Leak-Before-Break In Reactor Piping And Vessels, Lyon, France, October, 1995.
7. Miller, A.G., “Elastic Crack Opening Displacements And Rotations In Through Cracks In Spheres And Cylinders Under Membrane And Bending Loading,” Engineering Fracture Mechanics, Vol. 23, 1986.
8. Dong, P., Rahman, S., Wilkowski, G., Brickstad, B., Bergman, M., “Effects Of Weld Residual Stresses On Crack Opening Area Analysis Of Pipes For LBB Applications,” LBB95; Specialist Meeting On Leak-Before-Break In Reactor Piping And Vessels, Lyon, France, October, 1995.

K.7 Tables

Table K.1
Fitting Coefficients For Non-dimensional COA For A Through-Wall Axial Crack In A Cylinder – Inside Surface

H	$\frac{R_i}{t}$	A_o	A_1	A_2	A_3	A_4	A_5	A_6	A_7
H_p	1	1.3285E+00	-2.0500E-02	2.9616E-01	7.1300E-03	6.0958E-01	-4.5900E-02	5.0461E-03	0.0000E+00
	3	1.1325E+00	6.3690E-01	3.1021E-01	0.0000E+00	1.1955E+00	-2.3526E-01	1.5132E-02	0.0000E+00
	5	1.0939E+00	-1.3430E-01	2.6375E-01	0.0000E+00	1.4787E-01	-3.7400E-03	7.2150E-05	0.0000E+00
	10	1.0561E+00	-1.0080E-01	2.5285E-01	0.0000E+00	1.2380E-01	-4.3000E-03	1.0480E-04	0.0000E+00
	20	1.0309E+00	-9.9600E-02	2.2706E-01	0.0000E+00	6.4060E-02	8.6700E-04	-8.8150E-05	0.0000E+00
	60	1.0253E+00	-1.0020E-01	2.0975E-01	0.0000E+00	2.2530E-02	5.1530E-03	-2.9210E-04	0.0000E+00
	100	1.0118E+00	-1.5890E-01	1.7653E-01	0.0000E+00	-1.1020E-01	2.7880E-02	-1.5922E-03	0.0000E+00
H_0	1	1.0006E+00	-1.4839E-01	2.2231E-01	0.0000E+00	2.0398E-01	-3.4400E-03	1.6426E-03	0.0000E+00
	3	1.0102E+00	-1.0250E-01	2.3144E-01	0.0000E+00	1.3604E-01	-4.3400E-03	2.3506E-04	0.0000E+00
	5	1.0096E+00	-1.6138E-01	2.0773E-01	0.0000E+00	8.1700E-03	1.1710E-02	-5.4290E-04	0.0000E+00
	10	1.0080E+00	-9.0320E-02	2.3175E-01	0.0000E+00	8.8590E-02	-1.4300E-03	1.5395E-05	0.0000E+00
	20	1.0086E+00	-1.0869E-01	2.1726E-01	0.0000E+00	3.5190E-02	4.7500E-03	-2.6170E-04	0.0000E+00
	60	1.0062E+00	-8.0880E-02	2.2574E-01	0.0000E+00	6.0020E-02	6.7000E-04	-1.0720E-04	0.0000E+00
	100	1.0057E+00	-6.8770E-02	2.3517E-01	0.0000E+00	6.5400E-02	1.6000E-03	-2.4480E-04	0.0000E+00
H_1	1	0.0000E+00	2.9294E-01	3.0686E-01	1.5597E-01	3.0619E+00	9.9880E-02	1.0369E-02	2.0034E-03
	3	0.0000E+00	4.5779E-01	6.0330E-02	2.5004E-01	1.7604E+00	4.4082E-01	-2.5522E-02	1.0270E-03
	5	0.0000E+00	5.0958E-01	-1.5290E-01	3.6275E-01	7.9176E-01	1.0117E+00	-8.6835E-02	3.2753E-03
	10	0.0000E+00	8.3007E-01	6.2430E-02	3.6629E-01	3.0214E+00	3.3320E-01	-1.0162E-02	2.3810E-04
	20	0.0000E+00	1.1904E+00	5.4410E-02	5.3063E-01	4.1730E+00	5.5928E-01	-3.2950E-02	1.1460E-03
	60	0.0000E+00	2.2472E+00	2.2038E-01	6.3774E-01	8.5083E+00	-4.8485E-01	9.6235E-02	-3.9870E-03
	100	0.0000E+00	3.0857E+00	3.4730E-01	3.1003E-01	1.2352E+01	-3.5319E+00	5.4458E-01	-2.7082E-02

Notes:

1. H_p, H_0, and H_1 are computed as a function of c, R_i, t, and the coefficients in this table using the following equations.
2. For $R_i/t > 100$, use $R_i/t = 100$ for determining H_p, H_0, and H_1.

$$H_{p,0,1} = \frac{A_0 + A_1\lambda + A_2\lambda^2 + A_3\lambda^3}{1 + A_4\lambda + A_5\lambda^2 + A_6\lambda^3 + A_7\lambda^4}$$

where

$$\lambda = \frac{1.818c}{\sqrt{R_i t}}$$

Table K.2
Fitting Coefficients For Non-dimensional COA For A Through-Wall Axial Crack In A Cylinder – Outside Surface

H	$\frac{R_i}{t}$	A_o	A_1	A_2	A_3	A_4	A_5	A_6	A_7
H_p	1	8.4566E-01	3.2057E-01	5.3890E-02	0.0000E+00	-5.8500E-02	6.2480E-03	1.6910E-04	0.0000E+00
	3	8.9368E-01	3.3349E+00	8.4789E-01	7.2986E-01	2.8505E+00	3.9278E-01	-5.7363E-03	0.0000E+00
	5	9.2511E-01	9.9959E+00	2.5503E+00	2.3599E+00	9.5370E+00	1.0363E+00	-1.2140E-02	0.0000E+00
	10	9.7884E-01	2.2825E-01	1.6445E-01	0.0000E+00	-1.0300E-02	5.2870E-03	-1.6050E-04	0.0000E+00
	20	9.8548E-01	1.5869E-01	1.6186E-01	0.0000E+00	-5.8600E-02	1.2954E-02	-5.3460E-04	0.0000E+00
	60	9.9507E-01	2.7326E-01	3.0251E-01	0.0000E+00	1.5427E-01	-7.5700E-03	1.9570E-04	0.0000E+00
	100	9.9156E-01	5.6846E-01	5.0043E-01	0.0000E+00	5.0579E-01	-4.9210E-02	2.0737E-03	0.0000E+00
H_0	1	1.0008E+00	4.0232E+00	9.3771E-01	4.4196E-01	3.2624E+00	1.0241E-01	9.4544E-03	1.9540E-03
	3	1.0000E+00	4.7679E+00	1.5757E+00	1.3700E+00	3.8236E+00	1.2494E+00	-7.5746E-02	2.8130E-03
	5	1.0011E+00	8.6861E-01	8.0009E-01	9.0884E-01	2.1182E-01	1.4194E+00	-1.2576E-01	4.7020E-03
	10	1.0115E+00	2.1754E-01	1.6257E-01	0.0000E+00	-1.6400E-02	5.9600E-03	-1.8540E-04	0.0000E+00
	20	1.0109E+00	1.2351E-01	1.5247E-01	0.0000E+00	-8.7500E-02	1.6830E-02	-7.0310E-04	0.0000E+00
	60	1.0083E+00	2.7650E-01	2.8587E-01	0.0000E+00	1.3697E-01	-6.8300E-03	1.9226E-04	0.0000E+00
	100	1.0075E+00	5.8706E-01	4.4485E-01	0.0000E+00	4.6436E-01	-5.1030E-02	2.3824E-03	0.0000E+00
H_1	1	1.0016E+00	4.7767E+00	2.0223E-01	4.3078E-01	4.2867E+00	2.7910E-01	7.5547E-03	3.5696E-03
	3	1.0004E+00	5.7661E+00	1.7726E+00	1.5125E+00	5.2299E+00	3.3364E+00	-2.1697E-01	7.5483E-03
	5	1.0000E+00	2.8753E+00	1.6731E+00	1.0874E+00	2.6982E+00	2.9318E+00	-2.4959E-01	9.2830E-03
	10	1.0041E+00	1.3792E-01	3.0920E-01	0.0000E+00	4.8762E-01	-2.4170E-02	6.0590E-04	0.0000E+00
	20	1.0044E+00	4.4300E-01	4.5137E-01	0.0000E+00	1.0648E+00	-9.2470E-02	3.3787E-03	0.0000E+00
	60	9.9975E-01	2.8059E+00	9.1254E-01	4.1162E-01	4.2700E+00	1.6323E-01	-9.1160E-05	0.0000E+00
	100	1.0001E+00	3.1285E+00	1.2271E+00	2.5375E-01	5.0417E+00	-2.3327E-01	1.7392E-02	0.0000E+00

Notes:

1. H_p, H_0, and H_1 are computed as a function of c, R_i, t, and the coefficients in this table using the following equations.

2. For $R_i/t > 100$, use $R_i/t = 100$ for determining H_p, H_0, and H_1.

$$H_{p,0,1} = \frac{A_0 + A_1\lambda + A_2\lambda^2 + A_3\lambda^3}{1 + A_4\lambda + A_5\lambda^2 + A_6\lambda^3 + A_7\lambda^4}$$

where

$$\lambda = \frac{1.818c}{\sqrt{R_i t}}$$

Table K.3
Fitting Coefficients For Non-dimensional COA For A Through-Wall Circumferential Crack In A Cylinder – Inside Surface

H	$\frac{R_i}{t}$	A_o	A_1	A_2	A_3	A_4	A_5
H_0	1	2.5679E-01	-7.6590E-02	8.0900E-03	-3.9071E-01	5.4545E-02	-2.5887E-03
	3	5.7995E-01	-9.5710E-02	1.9180E-02	-1.8178E-01	1.3878E-02	-5.1270E-04
	5	7.1328E-01	-2.9910E-02	2.8760E-02	4.5300E-04	-1.2001E-02	4.6022E-04
	10	8.4104E-01	-2.8570E-02	4.2970E-02	3.1681E-02	-7.7060E-03	1.2773E-04
	20	9.1639E-01	-1.2106E-01	4.1570E-02	-1.0001E-01	3.2437E-03	-2.8080E-05
	60	9.7316E-01	-5.3280E-02	4.0970E-02	-8.0600E-03	-4.7620E-03	1.5812E-04
	100	9.8234E-01	-9.1150E-02	3.5500E-02	-7.6050E-02	1.4295E-03	9.2293E-06
H_1	1	8.9000E-04	3.1810E-02	-2.2300E-03	-2.1446E-01	1.1953E-02	0.0000E+00
	3	3.4300E-03	1.6963E-01	1.8504E-02	6.6176E-01	-1.3716E-01	6.3978E-03
	5	4.9200E-03	3.1458E-01	6.7112E-02	1.5293E+00	-2.3140E-01	8.3724E-03
	10	5.3490E-02	9.6620E-02	0.0000E+00	-8.9140E-02	1.7150E-03	0.0000E+00
	20	7.8390E-02	-1.3060E-02	4.3040E-03	-8.3850E-02	1.6960E-03	0.0000E+00
	60	7.7190E-02	1.0374E-01	0.0000E+00	-9.3820E-02	2.3390E-03	0.0000E+00
	100	7.3460E-02	1.0618E-01	0.0000E+00	-1.0334E-01	2.8380E-03	0.0000E+00
H_5	1	1.2750E-01	1.3160E-03	-1.2000E-04	-2.0852E-01	1.1501E-02	0.0000E+00
	3	4.2775E-01	-1.7090E-02	1.0353E-02	-9.9150E-02	9.2990E-04	0.0000E+00
	5	5.8083E-01	-9.3130E-02	1.5425E-02	-2.1415E-01	2.2591E-02	-9.5390E-04
	10	7.5405E-01	-4.1230E-02	3.5941E-02	-2.6160E-02	3.3975E-03	-3.3130E-04
	20	8.6656E-01	-8.1980E-02	2.9441E-02	-8.9350E-02	2.4262E-03	-7.7230E-06
	60	9.5446E-01	-4.5710E-02	4.2358E-02	7.3090E-03	-5.8760E-03	1.8060E-04
	100	9.7167E-01	-6.4890E-02	4.0249E-02	-2.8960E-02	-3.8160E-03	1.6380E-04

Notes:

1. H_0, H_1, and H_5 are computed as a function of c, R_i, t, and the coefficients in this table using the following equations.

2. For $R_i/t > 100$, use $R_i/t = 100$ for determining H_0, H_1, and H_5.

$$H_{0,1,5} = \frac{A_0 + A_1\lambda + A_2\lambda^2}{1 + A_3\lambda + A_4\lambda^2 + A_5{}^3}$$

where

$$\lambda = \frac{1.818c}{\sqrt{R_i t}}$$

Table K.4
Fitting Coefficients For Non-dimensional COA For A Through-Wall Circumferential Crack In A Cylinder – Outside Surface

H	$\frac{R_i}{t}$	A_o	A_1	A_2	A_3	A_4	A_5
H_0	1	9.9891E-01	-5.3550E-02	2.5360E-02	-2.8100E-02	-2.2115E-02	1.6721E-03
	3	9.9970E-01	1.5021E-01	8.7700E-03	1.0150E-01	-4.1762E-02	2.2694E-03
	5	9.9545E-01	6.9580E-02	1.2140E-02	-2.4630E-02	-1.1780E-02	6.0617E-04
	10	1.0047E+00	3.3570E-02	1.5700E-02	-7.4960E-02	1.1228E-03	-1.5110E-05
	20	1.0135E+00	-2.1130E-02	2.4020E-02	-1.2421E-01	5.4938E-03	-8.3540E-05
	60	1.0020E+00	-3.4100E-02	5.9000E-04	-1.8029E-01	1.1321E-02	-2.4220E-04
	100	1.0001E+00	1.3090E-02	7.0500E-03	-1.3201E-01	6.0185E-03	-8.9900E-05
H_1	1	1.0204E+00	-1.9110E-01	4.4396E-02	1.3990E-02	-1.9467E-02	1.0366E-03
	3	1.0225E+00	1.2294E-01	1.2724E-02	4.4502E-01	-1.0201E-01	4.9602E-03
	5	1.0099E+00	2.6856E-01	1.5057E-02	6.3403E-01	-1.1177E-01	4.4571E-03
	10	9.8708E-01	1.7136E-01	4.5114E-02	4.9503E-01	-5.7289E-02	1.4503E-03
	20	9.9143E-01	-3.5580E-01	3.6745E-02	-5.3770E-02	5.7210E-03	-2.8500E-04
	60	9.7469E-01	8.2480E-02	4.9754E-02	3.8322E-01	-4.3263E-02	1.1589E-03
	100	9.9100E-01	1.0069E+00	6.1993E-02	1.8451E+00	-2.2699E-01	6.9875E-03
H_5	1	1.0044E+00	-2.1929E-01	4.0998E-02	-1.6870E-01	2.1505E-02	-1.2516E-03
	3	9.9290E-01	5.0980E-02	1.3548E-02	5.6730E-02	-2.4037E-02	9.9160E-04
	5	9.9190E-01	-1.6194E-01	1.9518E-02	-2.3093E-01	2.4630E-02	-1.0109E-03
	10	9.9715E-01	5.2434E-02	2.3549E-02	-2.1830E-02	-2.3400E-04	-1.2520E-04
	20	1.0027E+00	-1.6640E-02	1.3537E-02	-1.2529E-01	5.6843E-03	-8.8230E-05
	60	9.9920E-01	-2.0840E-02	5.0330E-03	-1.5207E-01	8.6274E-03	-1.7380E-04
	100	9.9936E-01	1.9795E-01	2.6089E-02	8.4923E-02	-1.8846E-02	6.5230E-04

Notes:

1. H_0, H_1, and H_5 are computed as a function of c, R_i, t, and the coefficients in this table using the following equations.

2. For $R_i/t > 100$, use $R_i/t = 100$ for determining H_0, H_1, and H_5.

$$H_{0,1,5} = \frac{A_0 + A_1\lambda + A_2\lambda^2}{1 + A_3\lambda + A_4\lambda^2 + A_5{}^3}$$

where

$$\lambda = \frac{1.818c}{\sqrt{R_i t}}$$

Table K.5
Fitting Coefficients For Non-dimensional COA For A Through-Wall Meridional Crack In A Sphere – Inside Surface

H	$\frac{R_i}{t}$	A_o	A_1	A_2	A_3	A_4	A_5	A_6	A_7	A_8
H_p	3	6.3820E-01	5.2320E-01	-2.1590E+00	2.8049E+00	-1.6082E+00	4.8428E-01	-7.8246E-02	6.3921E-03	-2.0640E-04
	5	7.5650E-01	3.6733E-01	-1.3556E+00	1.6151E+00	-8.0953E-01	2.1603E-01	-3.1080E-02	2.2633E-03	-6.4980E-05
	10	8.6265E-01	1.8085E-01	-3.2998E-01	2.9748E-01	-7.0830E-02	8.8890E-03	-5.2107E-04	1.2029E-05	0.0000E+00
	20	9.3328E-01	3.7654E-01	-1.3090E+00	1.6340E+00	-7.8345E-01	1.8948E-01	-2.3612E-02	1.4482E-03	-3.4460E-05
	60	9.7959E-01	4.4481E-02	-1.5300E-02	1.5209E-01	-3.3080E-02	3.5060E-03	-1.1791E-04	0.0000E+00	0.0000E+00
	100	9.8904E-01	-2.4740E-02	1.3751E-01	5.7876E-02	-8.2800E-03	8.2800E-04	-2.0828E-05	0.0000E+00	0.0000E+00
H_0	3	5.5951E-01	5.9326E-01	-2.1874E+00	2.8054E+00	-1.6045E+00	4.8297E-01	-7.8045E-02	6.3775E-03	-2.0600E-04
	5	6.9651E-01	4.5017E-01	-1.4391E+00	1.6642E+00	-8.2580E-01	2.1915E-01	-3.1424E-02	2.2834E-03	-6.5470E-05
	10	8.3787E-01	-1.9300E-02	1.1321E-01	-1.5380E-02	3.1976E-02	-8.9500E-03	1.1625E-03	-6.9610E-05	1.5908E-06
	20	9.1363E-01	3.8633E-01	-1.3057E+00	1.6258E+00	-7.7882E-01	1.8830E-01	-2.3461E-02	1.4388E-03	-3.4240E-05
	60	9.7615E-01	1.0130E-01	-8.9080E-02	1.7366E-01	-3.0280E-02	1.9610E-03	0.0000E+00	0.0000E+00	0.0000E+00
	100	9.8823E-01	8.9840E-03	9.8248E-02	7.3648E-02	-1.1120E-02	1.0640E-03	-2.8430E-05	0.0000E+00	0.0000E+00
H_1	3	4.0800E-03	5.1657E-01	-1.1727E+00	1.3634E+00	-7.4432E-01	2.1677E-01	-3.3997E-02	2.6922E-03	-8.3880E-05
	5	4.2850E-03	5.6616E-01	-9.6738E-01	9.6474E-01	-4.5722E-01	1.1864E-01	-1.6803E-02	1.2119E-03	-3.4580E-05
	10	6.5070E-03	5.3228E-01	-4.1931E-01	2.3174E-01	-5.0090E-02	5.8649E-03	-3.3100E-04	7.4162E-06	0.0000E+00
	20	2.1112E-02	6.4770E-01	-5.9407E-01	3.4358E-01	-8.0100E-02	9.8780E-03	-5.8880E-04	1.3688E-05	0.0000E+00
	60	2.2701E-02	9.1335E-01	-9.5929E-01	5.3652E-01	-1.1614E-01	1.1010E-02	-3.5870E-04	0.0000E+00	0.0000E+00
	100	1.7394E-02	8.1190E-01	-6.3608E-01	2.9564E-01	-4.9270E-02	3.6997E-03	-9.4170E-05	0.0000E+00	0.0000E+00

Notes:

1. H_p, H_0, and H_1 are computed as a function of c, R_i, t, and the coefficients in this table using the following equations.

2. For $R_i/t > 100$, use $R_i/t = 100$ for determining H_p, H_0, and H_1.

$$H_{p,0,1} = A_o + A_1\lambda + A_2\lambda^2 + A_3\lambda^3 + A_4\lambda^4 + A_5\lambda^5 + A_6\lambda^6 + A_7\lambda^7 + A_8\lambda^8$$

where

$$\lambda = \frac{1.818c}{\sqrt{R_i t}}$$

Table K.6
Fitting Coefficients For Non-dimensional COA For A Through-Wall Meridional Crack In A Sphere – Outside Surface

H	$\frac{R_i}{t}$	A_o	A_1	A_2	A_3	A_4	A_5	A_6	A_7	A_8
H_p	3	9.1492E-01	1.4629E+00	-3.5770E+00	4.3639E+00	-2.4612E+00	7.3545E-01	-1.1832E-01	9.6396E-03	-3.1070E-04
	5	9.3705E-01	1.1282E+00	-2.0467E+00	2.1926E+00	-1.0661E+00	2.8028E-01	-4.0008E-02	2.9006E-03	-8.3070E-05
	10	9.6831E-01	4.9451E-01	-3.5850E-02	3.5690E-02	2.4577E-02	-8.5900E-03	1.1958E-03	-7.3770E-05	1.7134E-06
	20	9.8208E-01	8.1052E-01	-1.3304E+00	1.6135E+00	-7.7555E-01	1.8861E-01	-2.3603E-02	1.4521E-03	-3.4630E-05
	60	9.9722E-01	5.2138E-01	-1.4522E-01	1.9683E-01	-4.1820E-02	4.3080E-03	-1.4379E-04	0.0000E+00	0.0000E+00
	100	1.0001E+00	3.5564E-01	1.3783E-01	4.0415E-02	-4.4100E-03	5.2700E-04	-1.2930E-05	0.0000E+00	0.0000E+00
H_0	3	9.9959E-01	1.4933E+00	-3.7141E+00	4.4908E+00	-2.5169E+00	7.4877E-01	-1.2010E-01	9.7641E-03	-3.1430E-04
	5	1.0044E+00	1.1086E+00	-2.0715E+00	2.2219E+00	-1.0785E+00	2.8300E-01	-4.0332E-02	2.9207E-03	-8.3570E-05
	10	1.0133E+00	4.6529E-01	-2.3780E-02	3.3565E-02	2.4623E-02	-8.5500E-03	1.1897E-03	-7.3410E-05	1.7056E-06
	20	1.0075E+00	8.2707E-01	-1.4411E+00	1.7429E+00	-8.3913E-01	2.0397E-01	-2.5511E-02	1.5686E-03	-3.7390E-05
	60	1.0080E+00	4.3694E-01	-2.0270E-02	1.1892E-01	-1.9150E-02	1.2980E-03	0.0000E+00	0.0000E+00	0.0000E+00
	100	1.0067E+00	3.4149E-01	1.4671E-01	3.6530E-02	-3.8000E-03	5.0700E-04	-1.4040E-05	0.0000E+00	0.0000E+00
H_1	3	1.0012E+00	2.7649E-01	-1.0546E+00	1.3698E+00	-7.4319E-01	2.0942E-01	-3.1154E-02	2.2851E-03	-6.3660E-05
	5	1.0023E+00	1.3664E-01	-7.0664E-01	9.6719E-01	-5.0371E-01	1.3677E-01	-1.9867E-02	1.4556E-03	-4.1970E-05
	10	1.0074E+00	-2.8973E-01	4.2467E-01	-1.7623E-01	6.0568E-02	-1.1265E-02	1.1763E-03	-6.2404E-05	1.3198E-06
	20	1.0077E+00	-4.5888E-01	6.5971E-01	-2.7309E-01	7.1320E-02	-9.1840E-03	5.8770E-04	-1.4413E-05	0.0000E+00
	60	9.9121E-01	-6.6101E-01	9.6480E-01	-4.0660E-01	8.8452E-02	-8.0150E-03	2.5722E-04	0.0000E+00	0.0000E+00
	100	9.8931E-01	-6.1407E-01	7.7232E-01	-2.4905E-01	4.3340E-02	-3.0320E-03	7.5979E-05	0.0000E+00	0.0000E+00

Notes:

1. H_p, H_0, and H_1 are computed as a function of c, R_i, t, and the coefficients in this table using the following equations.

2. For $R_i/t > 100$, use $R_i/t = 100$ for determining H_p, H_0, and H_1.

$$H_{p,0,1} = A_o + A_1\lambda + A_2\lambda^2 + A_3\lambda^3 + A_4\lambda^4 + A_5\lambda^5 + A_6\lambda^6 + A_7\lambda^7 + A_8\lambda^8$$

where

$$\lambda = \frac{1.818c}{\sqrt{R_i t}}$$

1220 L Street, NW
Washington, DC 20005-4070
USA

202.682.8000

Additional copies are available through IHS
Phone Orders: 1-800-854-7179 (Toll-free in the U.S. and Canada)
303-397-7956 (Local and International)
Fax Orders: 303-397-2740
Online Orders: global.ihs.com

Information about API Publications, Programs and Services
is available on the web at **www.api.org**

ISBN 0-7918-3102-7

A16407

API Product No: C57902